JAMES A. KATOWITZ
WILLIAM R. KATOWITZ
EDITORS

Pediatric Oculoplastic Surgery

Second Edition

Springer

Pediatric Oculoplastic Surgery

James A. Katowitz • William R. Katowitz
Editors

Pediatric Oculoplastic Surgery

Second Edition

Forewords by Linton A Whitaker MD and
Geoffrey E. Rose, DSc, FRCS, FrCOpht

Krystyna Srodulski, CMI
Medical Illustrator

This book was supported by funds from
The Edwin and Fannie Gray Hall Center for Human Appearance
at The Children's Hospital of Philadelphia and
The University of Pennsylvania Perelman School of Medicine

Springer

Editors
James A. Katowitz, MD, FACS
Professor Emeritus of Ophthalmology and
Director of Oculoplastic and Orbital Surgery
The Children's Hospital of Philadelphia and
The Edwin and Fannie Gray Hall Center for
Human Appearance
Perelman School of Medicine at the
University of Pennsylvania
Philadelphia, PA
USA

William R. Katowitz, MD
Associate Professor of Clinical Ophthalmology
and Director of the Oculoplastic and Orbital
Surgery Fellowship Program
The Children's Hospital of Philadelphia and
The Edwin and Fannie Gray Hall Center for
Human Appearance
Perelman School of Medicine at the
University of Pennsylvania
Philadelphia, PA
USA

ISBN 978-3-319-60812-9 ISBN 978-3-319-60814-3 (eBook)
https://doi.org/10.1007/978-3-319-60814-3

Library of Congress Control Number: 2017959646

© Springer International Publishing AG 2002, 2018
This work is subject to copyright. All rights are reserved by the Publisher, whether the whole or part of the material is concerned, specifically the rights of translation, reprinting, reuse of illustrations, recitation, broadcasting, reproduction on microfilms or in any other physical way, and transmission or information storage and retrieval, electronic adaptation, computer software, or by similar or dissimilar methodology now known or hereafter developed.
The use of general descriptive names, registered names, trademarks, service marks, etc. in this publication does not imply, even in the absence of a specific statement, that such names are exempt from the relevant protective laws and regulations and therefore free for general use.
The publisher, the authors and the editors are safe to assume that the advice and information in this book are believed to be true and accurate at the date of publication. Neither the publisher nor the authors or the editors give a warranty, express or implied, with respect to the material contained herein or for any errors or omissions that may have been made. The publisher remains neutral with regard to jurisdictional claims in published maps and institutional affiliations.

Printed on acid-free paper

This Springer imprint is published by Springer Nature
The registered company is Springer International Publishing AG
The registered company address is: Gewerbestrasse 11, 6330 Cham, Switzerland

To Carol and Nicole: for their ever-present love and support and to our children and grandchildren for the special joy they also bring to our lives.

Foreword

The title is symbolic of the inevitable trend, the maturing of a subspecialty area, the crystallization of a field by defining it with the written word, and a direction unchanged by managed care and forces attempting to reorganize the way medicine is practiced in the United States. James Katowitz, by dint of his personal philosophy, persistence, and exceptional ability, has helped to influence and define the new field. In contrast to present trends in medical care, the contributors to this book describe ever-increasing levels of specialization, excellence, and expertise. Patients and physicians demand it because it is possible to do it. With inquiring minds and the constant search for answers to unsolved problems, along with an incessantly rising level of expectation by the public, the direction is inevitable. Thus, while ophthalmology and plastic surgery are mature specialties, oculoplastic surgery develops and gives birth to pediatric oculoplastic surgery. The birthing process is not easy and becomes a defined being only by a limited number of individuals making it happen. That, in essence, is what this book and these individuals are about.

Concepts and techniques common to plastic surgery and ophthalmology originated with the need for repair in the oculo-orbital region, with vaguely conceived techniques ultimately giving rise to the specialty designations. By the twentieth century, specialty lines had been drawn in several areas of surgery, resulting in the founding of the American Board of Ophthalmology in 1916 and the American Board of Plastic Surgery in 1936. Perhaps the first person to bridge the specialties in a way defined in writing was John C. Mustarde in Scotland, an ophthalmologist and a plastic surgeon, resulting in his book about a new specialty, published in 1966 [1]. He bridged the worlds of plastic surgery and ophthalmology perhaps better than anyone else before or since. Of particular importance was his relationship with Paul Tessier, which led to extraordinarily creative surgical methods for orbital problems. Combined with an increasing emphasis on appearance and cosmetically superior outcomes of surgery, new possibilities for reconstructive and aesthetic surgery emerged. The American Society of Ophthalmic Plastic and Reconstructive Surgery came into being in 1969, and J.C. Mustarde became an honorary member. As an honorary member since 1984, I have had the good fortune to observe firsthand a maturing of the field.

In 1979, Iliff, Iliff, and Iliff published *Oculoplastic Surgery* [2]. In their preface, the authors described ophthalmic reconstructive surgery as "a new sub-specialty having emerged." This had been preceded by *Surgery of the Eyelids and Lacrimal System* by Jones and Wobig [3], which had not defined the emerging field of oculoplastic surgery as precisely. In 1972, before either of these publications appeared, Paul Tessier brought about the beginning of craniofacial surgery at our institution. Since then, James Katowitz and I worked together closely for 30 years. The demands of cranio-orbital surgery required constant and ready collaboration between craniofacial plastic surgery and ophthalmology. This became the foundation of a working relationship and, because cranio-orbital surgery has increasingly focused on pediatric malformations, the evolution of this book. Initially, medial and lateral canthopexies and ptosis procedures were done by the plastic surgery service, while lacrimal drainage procedures were done by the ophthalmology service. As a consequence of regular conferences and discussions that ultimately resulted in a collaboration in adults in the Center for Human Appearance at Penn, and after developing an understanding of what each of us did best, we created divisions

among ourselves. I understood that if I did ptosis procedures, I would need to take care of the problems of the cornea and the eye. Jim Katowitz understood that canthopexies involved the skeletal structure. Consequently, I did the majority of the latter, and he the majority of the former as well as drainage procedures. We both did cosmetic procedures. The two began to overlap, and we continued to have an ongoing relationship that was beneficial to both of us. In our medical center, the plastic surgeons have continued to do procedures oriented to the bone in the orbital area, building on Tessier's pioneering works of the 1960s, and in the purely cosmetic soft tissue areas. Although each group will define its own method of handling the crossovers, the need to work together is of critical importance and is illustrated by the breadth of specialties represented in this book. Of primary importance is the understanding that has evolved that function and appearance cannot be separated. While in the orbital region function may dominate, appearance is never far behind. In fact, they usually enhance one another. This understanding is critical for all specialties performing surgery in this area.

James Katowitz has made a substantial contribution by his postgraduate training program, a capacity to work and think with others, and setting a high standard that is defined by this book. All of these factors keep him at the leading edge. With the philosophies of form and function working together and teamwork between specialties, an important concept continues and is increasingly clarified.

References

1. Mustarde JC. Repair and reconstruction in the orbital region. Edinburgh: Livingstone; 1966.
2. Iliff CE, Iliff WJ, Iliff NT. Oculoplastic surgery. Philadelphia: WB Saunders; 1979.
3. Jones LT, Wobig JL. Surgery of the eyelids and lacrimal system. Birmingham: Aesculapius; 1976.

Linton A. Whitaker, MD
Professor and Chief of Plastic Surgery Emeritus
Founder and Director: Edwin and Fannie Gray Hall
Center for Human Appearance
The Children's Hospital of Philadelphia and
The University of Pennsylvania Perelman School of Medicine
Philadelphia, PA, USA

Preface

This book represents a personal effort to summarize more than 50 years of experience in managing oculoplastic problems in children. Many of the contributors are individuals who have trained as oculoplastic surgery fellows at the Children's Hospital of Philadelphia (CHOP) as approved by the American Society of Ophthalmic Plastic and Reconstructive Surgery (ASOPRS). The remainder represent affiliated subspecialists and international colleagues who share our team management approach to patient care.

We have been particularly fortunate to have been associated with this unique institution (the oldest pediatric hospital in the Western hemisphere) and to work with so many individuals of world renown. These gifted physicians and surgeons have always been graciously available for consultation, often without a scheduled appointment.

What is presented in each chapter of this book is not an encyclopedic representation of every surgical pediatric condition, but rather a logical approach to the evaluation and management of a wide spectrum of oculoplastic problems as encountered in children. Our philosophy has been one involving a cooperative team approach to patient care, utilizing the expertise of related disciplines for the benefit of the patient.

We have tried to highlight useful diagnostic approaches and provide the reader with specific steps in management that have proven successful in our hands. In some instances, the management steps may seem either too radical or not aggressive enough when compared to similar problems in adults. It is important to stress, however, that children are not just "little adults." Pediatric specialists require special skills: patience and compassion in relating to children and their family members, as well as diagnostic and surgical acumen and an intuitive "feel" for creative problem-solving. Although we have reached definitive solutions in many areas, others remain frustratingly elusive. It is our collective hope, however, that these chapters may provide new insights for improving the reader's appreciation and skills in the diagnosis and management of pediatric oculoplastic problems.

Philadelphia, PA, USA

James A. Katowitz, MD, FACS
William R. Katowitz, MD

Foreword to the Second Edition

In the presence of the superb and comprehensive parent edition of *Pediatric Oculoplastic Surgery*, it is a real challenge to eclipse the "gold-standard" first edition. As editors for this new work, James and William Katowitz have undoubtedly succeeded, both by assembling a large group of distinguished and experienced authors and by exploring exciting areas of recent change that would not normally appear in an oculoplastic textbook.

Throughout the work, it is very evident that "a child is not just a small adult." The work – a treasure trove of "gems" – covers the development of childhood periocular tissues, details of the way childhood tissues heal after surgery (injury), and the special "tricks" for assessment of the child with adnexal disease. Knowledge of the development of tissues and structures in childhood is particularly important in its relation to the outcomes for surgery: Unlike adults, during growth, children will have many years of developmental change, which will inevitably alter the final result in terms of both structure and function; failure to anticipate these changes will lead to unexpected long-term surgical outcomes.

Unusual for specialist textbooks on oculoplastic surgery, the editors are to be congratulated on incorporating authoritative chapters on subjects like pediatric anesthesia, neuro-ophthalmology, systemic diseases, otorhinolaryngology, and general plastic surgery. Likewise, chapters covering the psychology of the child, care of the child's mental health, and aesthetic rehabilitation are particularly welcome – as is the emphasis on functional and visual development in these children. Although perhaps somewhat daunting to the clinician, coverage of the rapidly changing fields of genetics, molecular biology, and pathology is included, and these chapters provide valuable insight into the future of the diagnosis – and possible treatments – of these diseases.

The clinical chapters are both comprehensive and spectacular – addressing all areas of eyelid, lacrimal, orbital, and socket disease and surgery. The work truly is a mine of information that can happily be used both as a reference text and as a resource to dip into for the reader's enjoyment. I personally would regard this wonderful resource as one that should rightly find pride-of-place on the desk of any pediatric ophthalmologist or reconstructive surgeon interested in pediatric oculoplastic disorders.

Geoffrey E. Rose, DSc, FRCS, FRCOphth
Moorfields Eye Hospital, London, UK

NIHR Biomedical Research Centre,
Institute of Ophthalmology, London, UK

Acknowledgments

We would like to express our deep appreciation to the Trustees of the Edwin and Fannie Gray Hall Trust – Richard B. Goldbeck, William T. Luskus, Esquire, and Robert E. Curran, Esquire – for their dedication and support in helping in the care and rehabilitation of so many children. This book would not have been possible without their support through the Edwin and Fannie Gray Hall Center for Human Appearance (CHA). We would also like to thank Ardis Ryder for her assistance in this work at CHA.

Of primary importance, also, has been Linton A. Whitaker, MD, who was not only instrumental in founding and developing the CHA, but has also been a colleague, mentor, and friend to both of us, beginning with the development of our Craniofacial Surgical Team at The Children's Hospital of Philadelphia (CHOP) in 1972. The evolution of a new subspecialty, pediatric oculoplastic surgery, would not have been possible without his foresight and insight, appreciating the overlap of surgical skills in our multidisciplinary team, and providing the leadership for such a smooth and noncompetitive interaction that has been one of the most gratifying and unique attributes of the CHA.

The challenge of writing this book would not have been possible without the dedication and assistance of a great many individuals. First and foremost are the oculoplastic fellows who have contributed so much, not only to the evolution of this book but also to the evolving new subspecialty of pediatric oculoplastic surgery. This book also reflects an evolutionary partnership which has included so many of our colleagues at CHOP and others both nationally and internationally who have shared in the exploration of new pediatric diagnostic and surgical techniques.

We would especially like to thank N. Scott Adzick, MD, who, as Chairman of the Department of Surgery at CHOP, has been so supportive of our oculoplastic fellowship program. Similarly, much appreciation goes to the administrative leaders at CHOP led by Madeline Bell, President and CEO, for their continuing support and encouragement of this fellowship program.

We would very much like to thank our friend and colleague, Monte Mills, MD, who as Chairman of the Division of Ophthalmology at CHOP, has continued to support the evolution of this new subspecialty. Our thanks go as well to David Schaffer, MD, who was instrumental in developing the Pediatric Ophthalmology Division at CHOP as well as our oculoplastic fellowship program. Our appreciation also goes to Joan O'Brien, MD, Chairman of the Department of Ophthalmology at the Scheie Eye Institute and the University of Pennsylvania Perelman School of Medicine, who has been a strong supporter of our oculoplastic program as well.

Our office staff, which has helped guide patients and their families through often difficult decisions, deserves special thanks. A long chain of individuals form links in this process, beginning with our Division Manager, Jenny Bartelle, our surgical schedulers, Carol Lanni and Nicole DeCicco as well as the many ophthalmic technicians and patient-care coordinators who have contributed over the years. Special thanks must go to Sonia Zhu who has managed our photographic imaging databases over the past two decades.

We are especially indebted to our secretarial support staff, and especially, Suzanne McCullough, who has provided editorial assistance. Our operating room nursing staff has also been wonderful in so many ways. Beginning with the development of our craniofacial surgery team, oculoplastic specialty nursing was improved under the tutelage of Ivy Fenton Kuhn, who

also deserves much praise and admiration for her organizational skills and tireless efforts in her current role as a Divisional Nurse Practitioner, offering compassionate care and support to so many oculoplastic patients and their families.

We would also like to acknowledge our many friends for their support, and in particular, Gregory G. Alexander, not only for assisting in the development and evolution of the CHA, but for being such a special friend. Likewise, we also want to thank his associate, Stanley A. Pelli, for his efforts in assisting the Hall Trustees in support of our work at CHA.

In addition, we would like to thank a number of individuals from Springer International Publishing AG: First and foremost, our Developmental Editor, Connie Walsh, for her extraordinary editing skills and for so patiently pulling together all of the many facets of production in a timely fashion. We also would like to thank Rebekah Collins, the Senior Editor in charge of this project as well as Asja Parrish, our Assistant Editor. And last but not least, the production team from **SPi Global**, led by Jayashree Dhakshnamoorthy and Sivakumar Krishnamoorthy, for creating such an exciting layout as well as keeping the entire production effort on schedule.

Most importantly, we would also like to express our gratitude and admiration to Krystyna Srodulski, our illustrator, whose work is truly remarkable. Oculoplastic surgery is essentially a visual specialty, and her work not only illuminates the text but also guides the reader to a much better understanding of the surgical steps required for managing pediatric oculoplastic problems than would otherwise have been possible.

James A. Katowitz, MD, FACS
William R. Katowitz, MD

Contents

Part I General and Subspecialty Overviews

1 Genetic Considerations in Oculoplastic Disorders 3
Elizabeth Bhoj, Emma Bedoukian, Lama Khatib, and Bart Peter Leroy

2 Embryology and Anatomy of the Developing Face 17
Lama Khatib, Elizabeth Bhoj, and Bart Peter Leroy

3 Updates in Fetal Wound Healing and Scar Prevention 45
Lama Khatib, Darrell L. Cass, and N. Scott Adzick

4 Basic Principles, Techniques, and Instruments 59
Sarah M. Jacobs, Christopher B. Chambers, and Kenneth V. Cahill

5 Anesthetic Management for Pediatric Oculoplastic Surgery 81
Ian Yuan and Scott D. Cook-Sather

6 Pediatric Dermatology and the Oculoplastic Patient 105
Albert C. Yan

7 Plastic Surgical Considerations in Pediatric Dermatologic Abnormalities 121
David W. Low and Oksana A. Jackson

8 Advanced Plastic Surgical Techniques: Facial Prosthetic Considerations, Periorbital Free Flaps, Reanimation, and Corneal Sensory Restoration 145
Oksana A. Jackson, David W. Low, Phuong D. Nguyen, and Kenneth Kent

9 Pediatric Otolaryngologic Considerations 169
Adva Buzi and Mark Rizzi

10 Evaluation of Vision and Motility in Children 183
Lloyd Bender and Graham E. Quinn

11 Pediatric Extraocular Muscle Surgery and Oculoplastic Disorders 193
Brian J. Forbes and Graham E. Quinn

12 Pediatric Conjunctival and Intraocular Malignancies 207
Peter D. Fries

13 Oncologic Management for Liquid and Solid Tumors in Pediatric Oculoplastic Surgery 223
Naomi J. Balamuth, Tamara P. Miller, and Karuna Shekdar

14 Neuro-Ophthalmic Considerations in Pediatric Orbital and Oculoplastic Disease 237
Pavle Doroslovački, Grant T. Liu, and Robert A. Avery

15 Neuro-Oncologic Considerations in Pediatric Oculoplastic Surgery 247
Peter de Blank, Michael D. Coffey, and Michael J. Fisher

16 Molecular Pathology of Pediatric Oculoplastic Disorders 261
Vivian Lee, Tatyana Milman, and Ralph C. Eagle Jr

17 Genomic Applications for Pediatric Orbital Tumours 273
Timothy John Sullivan

18 Aesthetic Considerations in Pediatric Oculoplastic Surgery 279
Jill A. Foster and Femida Kherani

19 Psychosocial Issues in Pediatric Oculoplastic Conditions 291
Leanne Magee

20 Clinical Research Strategies in Oculoplastic Surgery 297
Gil Binenbaum

Part II Eyelids

21 Developmental Eyelid Abnormalities 311
Karen E. Revere, Jill A. Foster, William R. Katowitz, and James A. Katowitz

22 Pediatric Ptosis 359
William R. Katowitz and James A. Katowitz

23 Benign Pediatric Eyelid Tumors 411
William R. Katowitz, Christiana Eva Munroe, and James A. Katowitz

24 Malignant Pediatric Eyelid Tumors 445
Lama Khatib, Peter D. Fries, and William R. Katowitz

25 Pediatric Eyelid and Adnexal Trauma 453
Jordan E. Hollsten, Scott M. Goldstein, Donald A. Hollsten, and James A. Katowitz

Part III The Nasolacrimal System

26 Evaluation of Tearing in Children 469
Maryam Nazemzadeh and Yasmin S. Chambers

27 Initial Management of Pediatric Lower System Problems: Probing and Silicone Stents and Balloons 479
William R. Katowitz, Maryam Nazemzadeh, and James A. Katowitz

28 Management of Pediatric Lower System Problems: Dacryocystorhinostomy 501
William R. Katowitz, Yasmin S. Chambers, and Maryam Nazemzadeh

29 Management of Pediatric Upper System Problems: Punctal and Canalicular Surgery 519
Sarah M. Jacobs, Christopher B. Chambers, William R. Katowitz, and James A. Katowitz

30 Management of Pediatric Upper System Problems: Conjunctivodacryocystorhinostomy 529
Scott M. Goldstein and James A. Katowitz

Part IV The Orbit

31 Classification and Evaluation of Orbital Disorders in Children 543
William R. Katowitz and Peter D. Fries

32 Imaging of the Pediatric Orbit 551
Larissa T. Bilaniuk, Ann P. Murchison, and Jurij R. Bilyk

33 Pediatric Orbital and Periocular Infections 623
Scott M. Goldstein, Jill A. Foster, and James A. Katowitz

34 Pediatric Orbital Inflammatory Disorders 639
Katherine A. Lane, Melissa A. Lerman, and Jurij R. Bilyk

35 Benign Pediatric Orbital Tumors 667
William R. Katowitz, Peter D. Fries, and Michael Kazim

36 Malignant Pediatric Orbital Tumors 743
William R. Katowitz and Peter D. Fries

37 Surgical Approaches to the Pediatric Orbit 771
Michael Kazim, William R. Katowitz, and James A. Katowitz

38 Congenital Craniofacial Deformities: Ophthalmologic Considerations 801
Karen E. Revere, Brian J. Forbes, William R. Katowitz, and James A. Katowitz

39 Management of the Microphthalmic Orbit 831
Karen E. Revere, James A. Katowitz, Maryam Nazemzadeh, and William R. Katowitz

40 Oculoplastic Considerations in Pediatric Craniofacial Surgery 875
Sanjay Naran, Michael F. Spadola, Phillip B. Storm, and Scott P. Bartlett

41 Pediatric Enucleation, Evisceration, and Exenteration Techniques 913
Femida Kherani, Sonul Mehta, and James A. Katowitz

42 Pediatric Orbital Trauma 927
Jordan E. Hollsten, Patrick A. Gerety, Jesse A. Taylor, and Donald A. Hollsten

Index 957

Contributors

N. Scott Adzick, MD Department of Pediatric Surgery, The Center for Fetal Diagnosis and Treatment, The Children's Hospital of Philadelphia, University of Pennsylvania School of Medicine, Philadelphia, PA, USA

Robert A. Avery, DO, MSCE Division of Ophthalmology, Children's Hospital of Philadelphia, Philadelphia, PA, USA

Naomi J. Balamuth, MD Pediatrics, Children's Hospital of Philadelphia, Philadelphia, PA, USA

Scott P. Bartlett, MD Division of Plastic and Reconstructive Surgery, Children's Hospital of Philadelphia, Philadelphia, PA, USA

Emma Bedoukian, BScH, MS Individualized Medical Genetics Center, Children's Hospital of Pennsylvania, Philadelphia, PA, USA

Lloyd Bender, MBChB, MD, FRCOphth Ophthalmology, Children's Hospital of Philadelphia, Philadelphia, PA, USA

Elizabeth Bhoj, MD, PhD Pediatrics and Genetics, Children's Hospital of Philadelphia, Philadelphia, PA, USA

Larissa T. Bilaniuk, MD, FACR Radiology, Perelman School of Medicine at University of Pennsylvania, Philadelphia, PA, USA

Department of Radiology, The Children's Hospital of Philadelphia, Philadelphia, PA, USA

Jurij R. Bilyk, MD Ophthalmology, Skull Base Division, Neuro-Ophthalmology Service, Wills Eye Hospital, Philadelphia, PA, USA

Gil Binenbaum, MD, MSCE Research, Division of Ophthalmology, The Children's Hospital of Philadelphia, Philadelphia, PA, USA

Adva Buzi, MD Division of Otolaryngology, Children's Hospital of Philadelphia, Philadelphia, PA, USA

Department of Otolaryngology, University of Pennsylvania, Philadelphia, PA, USA

Kenneth V. Cahill, MD Ophthalmology/Eye Clinic, Nationwide Children's Hospital, Columbus, OH, USA

Darrell L. Cass, MD Michael E. DeBakey Department of Surgery, Departments of Pediatrics and Obstetrics and Gynecology, Baylor College of Medicine, Texas Children's Fetal Center, Texas Children's Hospital, Houston, TX, USA

Christopher B. Chambers, MD Department of Ophthalmology, University of Washington, Seattle, WA, USA

Yasmin S. Chambers, MD Ophthalmology, The Everett Clinic, Seattle, WA, USA

Michael D. Coffey, MD Radiology, University Hospitals Cleveland Medical Center, Cleveland, OH, USA

Scott D. Cook-Sather, MD Anesthesia, Children's Hospital of Philadelphia, University of Pennsylvania Perelman School of Medicine, Philadelphia, PA, USA

Peter de Blank, MD, MSCE Pediatrics, Division of Oncology, Cincinnati Children's Hospital Medical Center, Cincinnati, OH, USA

Pavle Doroslovački, MD Department of Ophthalmology, MedStar Washington Hospital Center, Washington, DC, USA

Ralph C. Eagle Jr, MD Department of Pathology, Wills Eye Hospital, Philadelphia, PA, USA

Michael J. Fisher, MD Department of Pediatrics, Perelman School of Medicine at the University of Pennsylvania, Philadelphia, PA, USA

Neurofibromatosis Program, Neuro-Oncology Section, Center for Childhood Cancer Research, Division of Oncology, The Children's Hospital of Philadelphia, Philadelphia, PA, USA

Brian J. Forbes, MD, PhD Ophthalmology, University of Pennsylvania/Children's Hospital of Philadelphia, Philadelphia, PA, USA

Jill A. Foster, MD, FACS Ophthalmology, The Ohio State University, Oculoplastics, Nationwide Children's Hospital, Plastic Surgery Ohio, Columbus, OH, USA

Peter D. Fries, MD Eye Surgeons Associates, PC, Bettendorf, IA, USA

Patrick A. Gerety, MD Department of Surgery, University of Indiana & Riley Hospital for Children, Indianapolis, IN, USA

Scott M. Goldstein, MD Oculoplastic Service, Wills Eye Hospital, Ophthalmology, Jefferson Medical College, Perelman School of Medicine, University of Pennsylvania, Philadelphia, PA, USA

Oculo-Facial Plastic Surgery, Tri-County Eye Physicians & Surgeons, Southampton, PA, USA

Donald A. Hollsten, MD, FACS Ophthalmology, Plastic and Reconstructive Surgery, University of Texas Health Science Center at San Antonio, San Antonio, TX, USA

Jordan E. Hollsten, MD Ophthalmology, University of Texas Health Science Center at San Antonio, San Antonio, TX, USA

Oksana A. Jackson, MD Surgery, Division of Plastic Surgery, Perelman School of Medicine at the University of Pennsylvania, The Children's Hospital of Philadelphia, Philadelphia, PA, USA

Sarah M. Jacobs, MD Department of Ophthalmology, University of Washington, Seattle, WA, USA

James A. Katowitz, MD, FACS The Children's Hospital of Philadelphia and The Edwin and Fannie Gray Hall Center for Human Appearance, University of Pennsylvania, Philadelphia, PA, USA

William R. Katowitz, MD The Children's Hospital of Philadelphia and The Edwin and Fannie Gray Hall Center for Human Appearance, University of Pennsylvania, Philadelphia, PA, USA

Michael Kazim, MD Ophthalmology & Surgery, Columbia University, New York, NY, USA

Kenneth Kent, DMD Restorative Dentistry, Removable Prosthodontics, Preventive and Restorative Sciences, University of Pennsylvania School of Dental Medicine, Philadelphia, PA, USA

Lama Khatib, MD Pediatric Ophthalmology, Oculoplastic & Orbital Surgery, Ophthalmology Division, Children's Hospital of Philadelphia, Philadelphia, PA, USA

Femida Kherani, MD, FRCSC Department of Surgery, University of Calgary, Calgary, Canada

Department of Ophthalmology, University of British Columbia, Vancouver, BC, Canada

Katherine A. Lane, MD Ophthalmic Consultants of Vermont, South Burlington, VT, USA

Vivian Lee, MD Ophthalmology, University of Pennsylvania – Scheie Eye Institute, Philadelphia, PA, USA

Melissa A. Lerman, MD Division of Rheumatology, The Children's Hospital of Philadelphia, Philadelphia, PA, USA

Bart Peter Leroy, MD, PhD Department of Ophthalmology, Ghent University Hospital, Ghent, East-Flanders, Belgium

Division of Ophthalmology, The Children's Hospital of Philadelphia, Philadelphia, PA, USA

Grant T. Liu, MD Division of Ophthalmology, Children's Hospital of Philadelphia, Philadelphia, PA, USA

David W. Low, MD Surgery, Division of Plastic Surgery, Perelman School of Medicine at the University of Pennsylvania, The Children's Hospital of Philadelphia, Philadelphia, PA, USA

Leanne Magee, PhD Division of Plastic and Reconstructive Surgery, Department of Child and Adolescent Psychiatry and Behavioral Sciences, The Children's Hospital of Philadelphia, Philadelphia, PA, USA

Sonul Mehta, MD Division of Oculo-Facial Plastic and Reconstructive Surgery, Department of Ophthalmology, Hospital of the University of Pennsylvania, Philadelphia, PA, USA

Tamara P. Miller, MD, MSCE Division of Oncology, Department of Pediatrics, The Children's Hospital of Philadelphia, Philadelphia, PA, USA

Tatyana Milman, MD Pathology and Laboratory Medicine, Hospital of the University of Pennsylvania, Philadelphia, PA, USA

Christiana Eva Munroe, MD Oculoplastic and Orbital Surgery, The Children's Hospital of Philadelphia, Philadelphia, PA, USA

Ann P. Murchison, MD, MPH Wills Eye Emergency Department, Oculoplastic and Orbital Surgery, Wills Eye Hospital, Thomas Jefferson University, Philadelphia, PA, USA

Sanjay Naran, MD Craniofacial Surgery, Division of Plastic Surgery, Children's Hospital of Philadelphia, University of Pennsylvania, Philadelphia, PA, USA

Maryam Nazemzadeh, MD Oculofacial Plastic and Reconstructive Surgery, Rostami Oculo-facial Plastic Consultants, Sanctuary Cosmetic Center, Reston, VA, USA

Phuong D. Nguyen, MD Division of Plastic and Reconstructive Surgery, Children's Hospital of Philadelphia, Perelman School of Medicine at University of Pennsylvania, Philadelphia, PA, USA

Graham E. Quinn, MD, MSCE Ophthalmology, Perelman School of Medicine, University of Pennsylvania, Ophthalmology, The Children's Hospital of Philadelphia, Philadelphia, PA, USA

Karen E. Revere, MD Oculoplastics and Orbital Surgery, Ophthalmology, The Children's Hospital of Philadelphia, Philadelphia, PA, USA

Mark D. Rizzi, MD Clinical Otolaryngology – Head and Neck Surgery, Children's Hospital of Philadelphia, Philadelphia, PA, USA

Geoffrey E. Rose, DSc, FRCS, FRCOphth Moorfields Eye Hospital, NHS Foundation Trust, London, UK

Karuna Shekdar, MD Clinical Radiology, Perelman School of Medicine, University of Pennsylvania, Philadelphia, PA, USA

Radiology, The Children's Hospital of Philadelphia, Philadelphia, PA, USA

Michael F. Spadola, BA Neurosurgery, The Children's Hospital of Philadelphia, Philadelphia, PA, USA

Phillip B. Storm, MD Division of Neurosurgery, Children's Hospital of Philadelphia, University of Pennsylvania Perelman School of Medicine, Philadelphia, PA, USA

Timothy John Sullivan, FRANZCO, FRACS, FRCOphth Department of Ophthalmology, School of Medicine, University of Queensland, Royal Brisbane and Women's Hospital, Lady Cilento Children's Hospital, Brisbane, QLD, Australia

Jesse A. Taylor, MD Plastic Surgery and Craniofacial Surgery, Department of Surgery, Children's Hospital of Philadelphia, Philadelphia, PA, USA

Albert C. Yan, MD Pediatrics and Dermatology, Perelman School of Medicine at the University of Pennsylvania, Section of Pediatric Dermatology, Children's Hospital of Philadelphia, Philadelphia, PA, USA

Ian Yuan, MD, MEng Anesthesiology and Critical Care Medicine, The Children's Hospital of Philadelphia, Perelman School of Medicine at the University of Pennsylvania, Philadelphia, PA, USA

Part I

General and Subspecialty Overviews

Genetic Considerations in Oculoplastic Disorders

1

Elizabeth Bhoj, Emma Bedoukian, Lama Khatib, and Bart Peter Leroy

Manifestations of Genetic Disorders

Disorders that have a genetic basis can be broadly classified into one of three main categories: (1) single-gene disorders, (2) chromosomal disorders, or (3) multifactorial disorders. All of these categories are represented among oculoplastic disorders [1, 2].

Single-gene disorders, also called Mendelian disorders, are caused by an error in a single gene. This error may involve one or both copies of that single gene. This may result in transmission of the erroneous genetic information, with a 50% chance of transmission if one gene has an error and a 100% chance of transmission if both genes have errors. Disorders that are based on a single-gene mutation usually demonstrate characteristic pedigree (family history) patterns. Neurofibromatosis type I, due to a mutation in the *NF1* gene, is an example of a single-gene disorder.

In chromosomal disorders, the genetic error can either be additional or missing genetic material, referred to as duplication and deletion, respectively. The deletion or duplication may affect a single gene, multiple genes, or an entire chromosome. For example, 22q11.2 deletion syndrome, formerly known as DiGeorge syndrome (dysmorphic features, congenital heart disease, immunologic abnormalities, and behavioral abnormalities), is due to a small deletion in the long arm of chromosome 22. Down syndrome, on the other hand, is the result of an entire extra copy of chromosome 21 [3].

Multifactorial disorders are more complex. Imprinted disorders, such as Prader-Willi syndrome, will not always follow a classic pedigree and will be covered in more depth later [4]. The combination of genetic and environmental factors results in a phenotype, and it can be difficult to determine how much genetics has contributed to the disease [5]. These disorders tend to show familial patterns, but do not follow the classic pedigrees of single-gene disorders.

In general, characteristic features in a patient and a family member should raise the suspicion for a genetic syndrome. Typically, when a condition affects multiple family members, at unusually early ages or with varying degrees of severity, further inquiry should be prompted. A three-generation pedigree is usually sufficient, but in rare diseases an extended pedigree to include ancestors or extended family members is recommended. If the patient has multiple anomalies or dysmorphic features that cannot be explained by another cause (such as fetal alcohol syndrome), he or she should be referred for a full genetic examination (Fig. 1.1).

As mentioned earlier, the expression of a gene in an organism is called a phenotype. If one copy of the gene is required for the phenotypic trait to be expressed (heterozygous state), the gene is termed dominant. If two copies of a gene are required for phenotypic expression (homozygous state), the gene is called recessive.

The chromosomes that determine the sex of the individual are the X and the Y chromosome. Genetically, an individual with an X and a Y (an XY individual) will be male, and an individual with two X chromosomes (an XX individual) will be female. Mutations expressed in an allele on the X chromosome are usually more severe in males than females, because males have only one copy of the X chromosome, while females have two copies. In other words, when females have a mutation involving one allele on one X chromosome,

E. Bhoj (✉)
Pediatrics and Genetics,
Children's Hospital of Philadelphia, Philadelphia, PA, USA
e-mail: bhoje@email.chop.edu

E. Bedoukian
Individualized Medical Genetics Center,
Children's Hospital of Pennsylvania, Philadelphia, PA, USA

L. Khatib
Pediatric Ophthalmology, Oculoplastic and Orbital Surgery,
Ophthalmology Division, Children's Hospital of Philadelphia,
Philadelphia, PA, USA

B.P. Leroy
Department of Ophthalmology, Ghent University Hospital,
Ghent, East-Flanders, Belgium

Division of Ophthalmology, The Children's Hospital
of Philadelphia, Philadelphia, PA, USA

© Springer International Publishing AG 2018

J.A. Katowitz, W.R. Katowitz (eds.), *Pediatric Oculoplastic Surgery*, https://doi.org/10.1007/978-3-319-60814-3_1

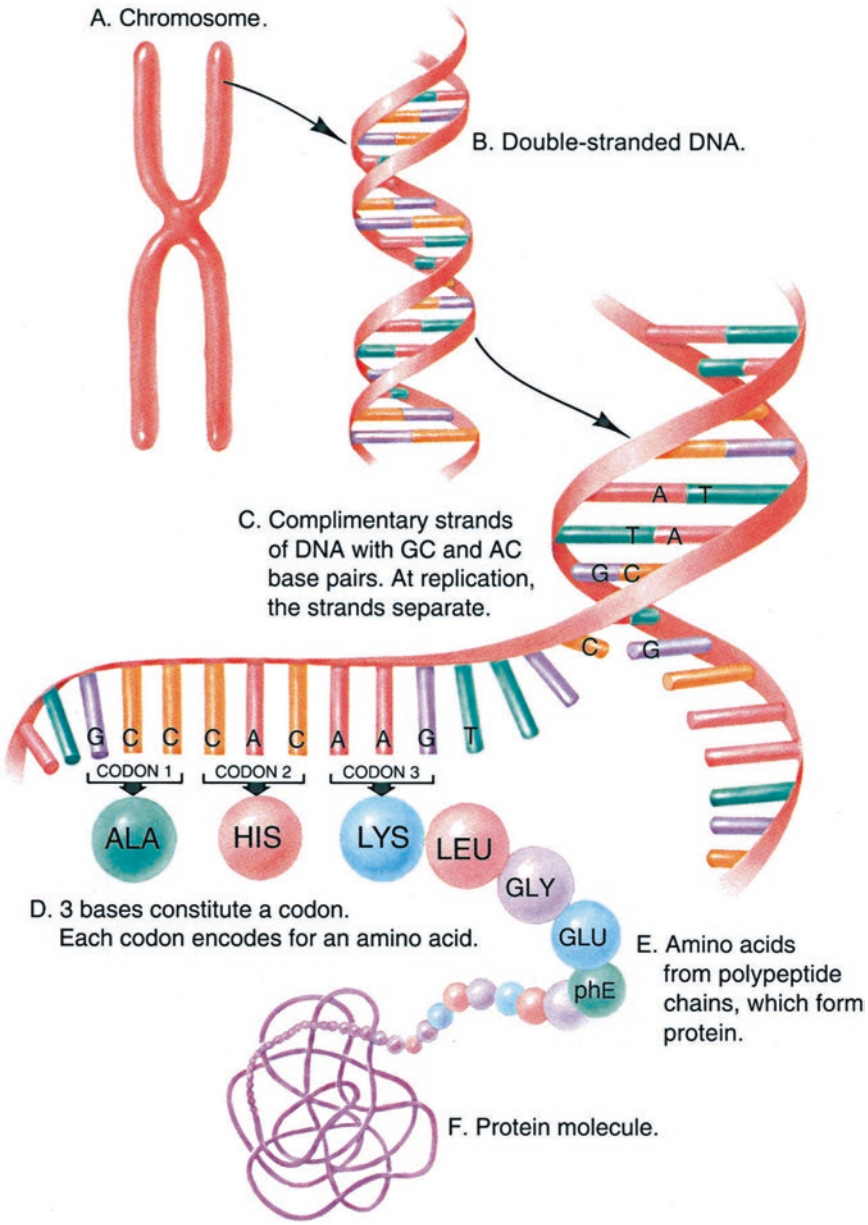


Fig. 1.1 From chromosome to protein

the paired allele on the other X chromosome may produce enough of its product if not mutated, whereas an XY individual does not have an additional copy of the X chromosome in reserve. Rare variations of the genetic constitution exist with some individuals having an XXY or XXXY genome. These individuals are phenotypically male due to the presence of the Y chromosome, with extra copies of the X chromosome.

The translation of genetic code into functional products is quite complex and beyond the scope of this introductory chapter. In summary, start and stop codons regulate the transcription of a gene, and various forms of RNA are involved in this process (tRNA for translational RNA, mRNA for messenger RNA, etc.), in addition to other types of interactive genes. A gene will not entirely get translated into a protein; exons are those stretches of a gene that are ultimately expressed in a protein, and introns are those intervening genetic sequences that are removed before protein translation. Roughly 25–38% of the total DNA is spanned by genes; however only 1.1–1.4% of DNA consists of exons. The function of the rest of human DNA is yet unknown and is an area of active research.

Two important sets of genes that deserve a brief mention are suppressor and anti-suppressor genes [6]. A suppressor

gene's function is to suppress the phenotypic expression of another gene. An anti-suppressor's function is to suppress the suppressor gene. The interaction and balance are extremely complex, yet exquisitely elegant. It should be noted that many genes are solely expressed, or activated, in certain tissue types. Thus a mutated gene will only cause disease in a particular tissue in which it is producing the product or diseased protein. One of the most studied cancers to date is retinoblastoma. The expression of retinoblastomas is due to the inactivation of a tumor suppressor gene affecting the retina [6–8]. Normal function of the suppressor gene is to inhibit the retinoblastoma gene from functioning. Loss of this suppressive factor allows the retinoblastoma gene to become active and produce a tumor.

Genetic changes that cause an abnormal phenotype in an individual are termed "pathogenic variants" and are also called mutations; these affect the gene in which they are found. Other changes will have no effect at all and are termed "benign variants" or polymorphisms. It can be very difficult to predict how some variants are going to affect the patient's phenotype, and these are termed "variants of uncertain significance." Additional functional studies on the particular variant may determine if it is pathogenic or benign. Generally, variants that are found in exons are more likely to be pathogenic if they result in a codon that translates into a different amino acid or a stop codon that truncates the protein product.

Another way to categorize variants of genetic changes is by structure. Point mutations change just one nucleotide, but can cause either a missense or nonsense variant. A missense variant changes just one codon in the sequence and may be tolerated by the gene or not. A nonsense mutation is very often pathogenic as it causes a premature stop codon to be inserted and prevents translation of the rest of the protein. Frameshift mutations are also often pathogenic, as they result from the addition or subtraction of nucleotides in such a way that the reading frame of the rest of the gene is disrupted, resulting in incorrect amino acids in the protein product. A splice site mutation results in insertion, deletion, or changes in the number of nucleotides in the specific site at which splicing of RNA takes place and can change the way the exons assemble. Inheritance patterns should be taken into account when interpreting each variant. Mutations that are not found in the parents are termed spontaneous or de novo and are more likely to cause sporadic disease. A database of variant alleles, collected from both affected and healthy individuals, allows an estimate of the allele frequency in the population. This measure allows for some prediction about the pathogenicity of a variant, as common variants are unlikely to cause rare diseases.

Genes and Environmental Influences

Environmental factors play an important role in genetics, but it is very difficult to determine how much of a disorder is due to genetic error and how much of it is due to environmental influences. For instance, monozygotic twins originate from a single fertilized egg and therefore contain virtually the same genetic makeup. However, if these genetically identical individuals are raised in different environments, they become different individuals with different medical conditions. These differences would be mainly due to environmental factors and not genetic differences. Conversely, just as two genetically identical individuals may develop differently in different environments, genetically different individuals may develop similarly in the same environment.

The timing of an environmental influence or insult plays a significant role on its effect to an individual. Environmental factors that have no influence on one developmental stage may cause drastic results in a different stage. A developing embryo is typically sensitive to temperature and toxins during embryogenesis (3–8 weeks of gestational age), whereas these influences may have little or no effect at all later on. A mature organism is the consequence of the sum and timing of these genetic and environmental interactions.

Genotype and Phenotype

The term genotype describes the genetic constitution of an individual organism or the complete set of genes inherited by that individual. The phenotype of an individual is the set of observable characteristics resulting from the interaction of its genotype with the environment [5].

Penetrance and Expressivity

Penetrance is the probability that a specific gene will have any phenotypic expression at all. When calculating penetrance, the phenotype is considered either present or absent, regardless of varying clinical presentations. It is empirically calculated by dividing the number of people who have both the genotype and phenotype by the total number of people with the genotype alone. When the gene is expressed, but the phenotype differs in individuals with the same genotype, the phenotype has variable expressivity. Many disorders demonstrate variability in the spectrum and severity of abnormalities. For example, in neurofibromatosis type I, every person with an *NF1* pathogenic mutation will show symptoms, but the manifestation and severity will differ from person to person.

Anatomy of the Human Genome

The human genome typically consists of 23 pairs of chromosomes: 22 paired autosomes and 1 pair of sex chromosomes (X and Y chromosomes). Genetic material is stored in the form of deoxyribonucleic acid (DNA), and this message is relayed when the DNA is transcribed to ribonucleic acid (RNA). RNA in turn is translated into the functional products, the polypeptides, or proteins. The building blocks or monomers of DNA and RNA are the nucleotides. There are four nucleotides in DNA, two purines, adenine (A) and guanine (G), and two pyrimidines, thymine (T) and cytosine (C). The formation and operation of the entire human body are encoded by the sequence of these four nucleotides. There is additional genetic material in the mitochondria, which is not part of these 23 pairs of chromosomes.

The information contained in the DNA is translated by the genetic code. The genetic code consists of three adjacent nucleotide bases. The adjacent nucleotides together are called a codon. Each codon corresponds to a particular amino acid. For example, if cytosine, guanine, and adenine were sequential nucleotides (CGA), the corresponding codon corresponds to the amino acid arginine. Three letters summarize each of the 20 amino acids. A series of codons produces a sequence of amino acids that constitute the genetic message. This sequence in turn may translate into the polypeptide chain of a protein molecule. This collection of codons that are transcribed together in a coordinated manner is called a gene; humans have about 20,000 genes.

A specific location on a chromosome is called a locus, which provides the chromosomal address of a gene. Since there are two copies of each of the 23 chromosomes, there are two copies of each gene (an exception is the X and Y chromosomes in males). Variations of the same gene are called alleles. If the two alleles present on each of the two chromosomes are identical, they are homozygous; if the alleles are different, they are heterozygous. Most genes are very complex and comprise multiple alleles for a specific locus.

Modes of Inheritance

With the rapid expansion of the knowledge on genetic disorders, it is essential to have a fundamental understanding of the common inheritance patterns. This helps the clinician have an improved understanding of the disease and therefore more accurately counsel families with regard to diagnosis, prognosis, and recurrence risk. Failure to inform the patient of the inheritance risks has been the cause of much litigation [9–12]. One of the most effective ways of presenting genetic information about a family is through a pedigree. A pedigree usually involves at least three generations back from the patient (proband) and includes information on the age, health, relationships, and previous genetic testing in the family. Using pedigrees allows for patterns consistent with common modes of inheritances to be easily demonstrated (see Fig. 1.2 for common pedigree symbols).

Autosomal Dominant Inheritance

In autosomal dominant inheritance, offspring who are affected can either be the first in their family (if the mutation is de novo) or can have an affected parent who carries at least one copy of the affected gene (while the other parent has two normal alleles) (Fig. 1.3). If a child's parent is a carrier, then they would have a 50% chance of receiving the affected parent's abnormal allele, termed *A*, and a 50% chance of receiving the normal allele, *a*. The other allele, obtained from the normal parent, would be normal. Therefore, the overall risk

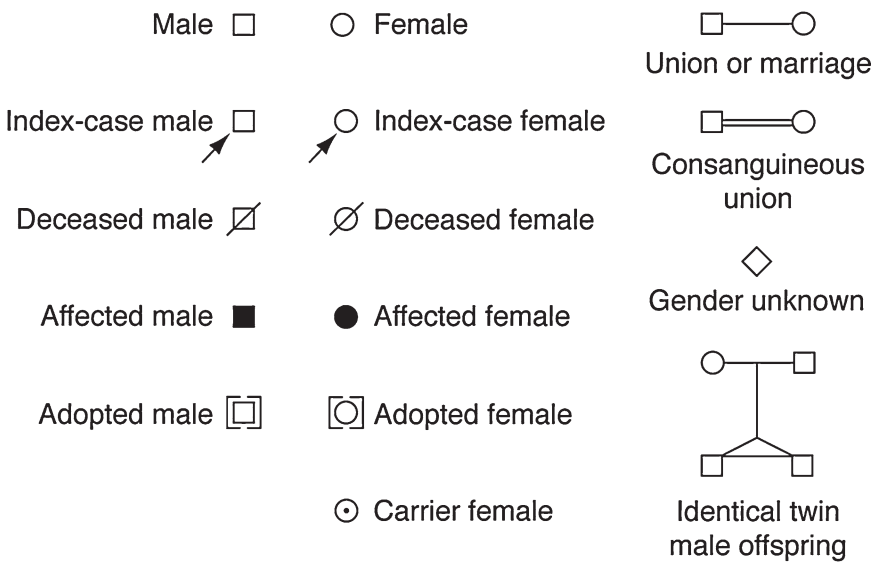


Fig. 1.2 Standard pedigree nomenclature. © 2016 American Academy of Ophthalmology

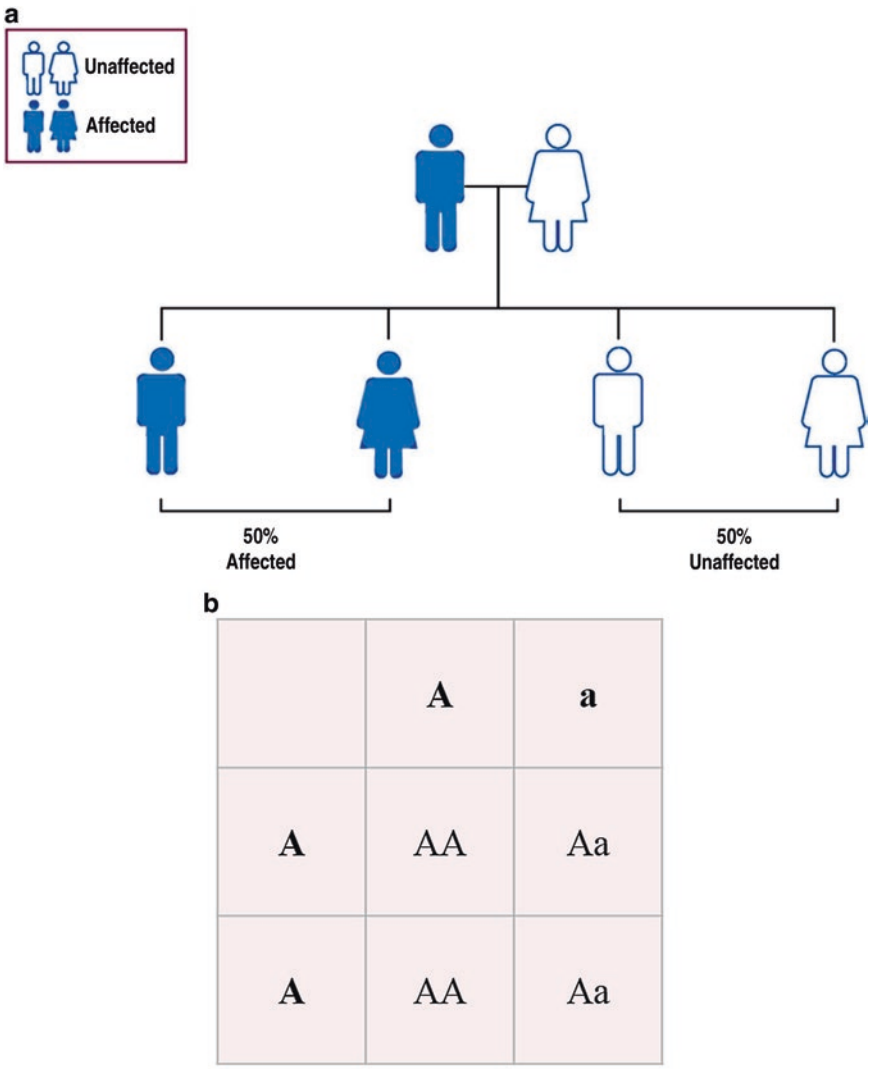


Fig. 1.3 Autosomal dominant inheritance with one parent affected. (**a**) Diagram (Illustration from Genetic Counseling Aids, 6th Edition, Copyright 2013, permission for use granted by Greenwood Genetic Center). (**b**) Punnett square showing possible combinations of alleles; affected (Aa), unaffected (AA)

of disease for each pregnancy would be 50%. Statistically, each pregnancy is an independent event unaffected by previous pregnancies.

An example of an autosomal dominant disorder is neurofibromatosis type I [13, 14]. This disease occurs in approximately one in 4000 births. There is a very high spontaneous or new mutation (de novo) rate [15]. Thus, when seeing an affected individual for the first time, the possibility that the disorder is due to a new mutation must be considered. That is, there might not always be a family history. If the proband is affected with a de novo mutation, then they have the chance to pass it on in their future pregnancies (50% per pregnancy), but the risk of disease to their siblings is low (<1%, not zero due to the possibility of germline mosaicism).

Another example of an autosomal dominant condition is BPES (blepharophimosis, ptosis, and epicanthus inversus syndrome) (Fig. 1.4).

Autosomal Recessive Inheritance

In autosomal recessive disorders, the affected individuals are homozygous for the mutant gene (Fig. 1.5, aa). Typically one mutant allele is acquired from each parent. Both unaffected parents of an affected individual are heterozygote carriers of the disease (Fig. 1.5, Aa). Therefore, the offspring's risk of inheriting two mutant alleles, one from each parent, is one in four (25%). Males and females are equally affected.

If a carrier (Aa) mates with an affected individual (aa), 50% of the offspring would be carriers and 50% would manifest the mutation (Fig. 1.6). Without close examination of the family pedigree, this could be confused with autosomal dominant transmission.

If a carrier of the recessive disease (phenotypically normal and heterozygous for the mutation, Rr) had offspring with a genetically normal individual (RR), all the offspring

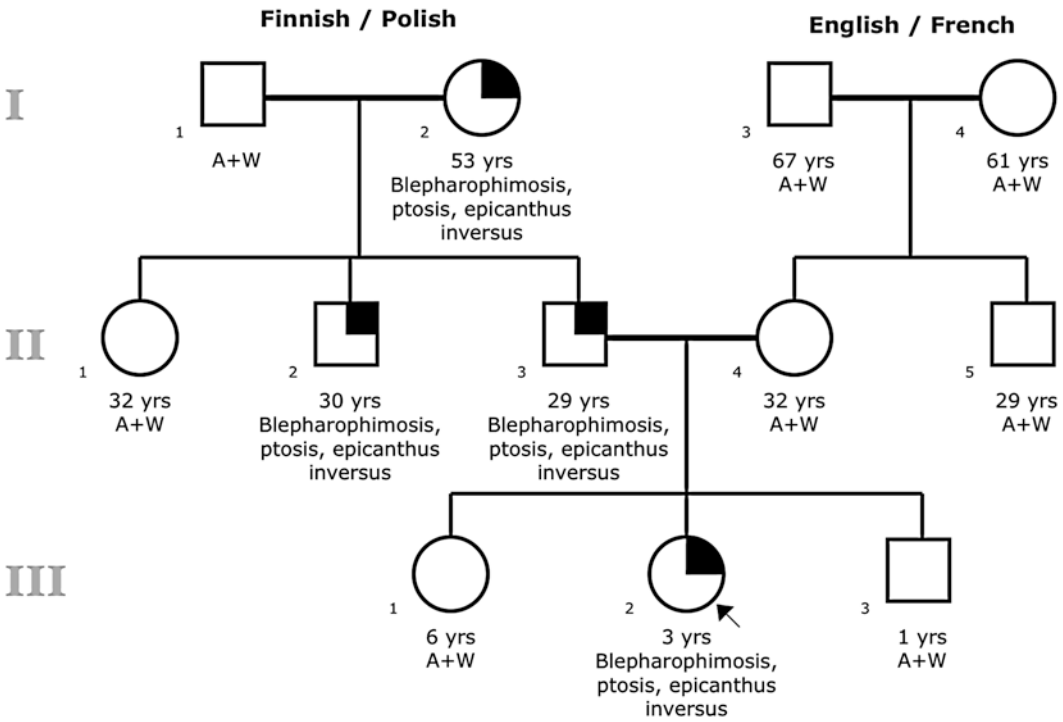
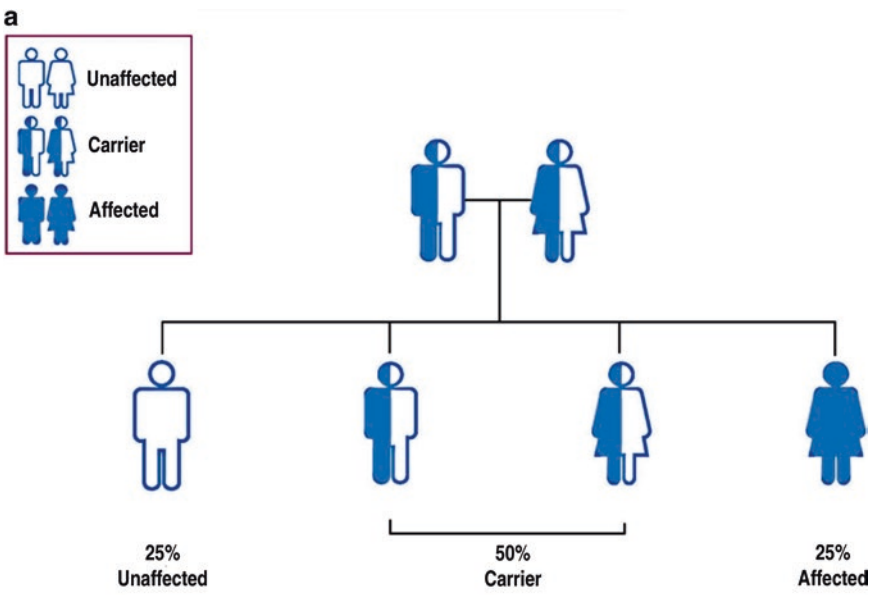


Fig. 1.4 Pedigree for family with BPES illustrates an example of autosomal dominant inheritance



b

	A	a
A	AA	Aa
a	Aa	aa

Fig. 1.5 Autosomal recessive inheritance with both parents carriers. (**a**) Diagram (Illustration from Genetic Counseling Aids, 6th Edition, Copyright 2013, permission for use granted by Greenwood Genetic Center). (**b**) Punnett square showing possible combinations of alleles; affected (aa), unaffected (Aa, aa)

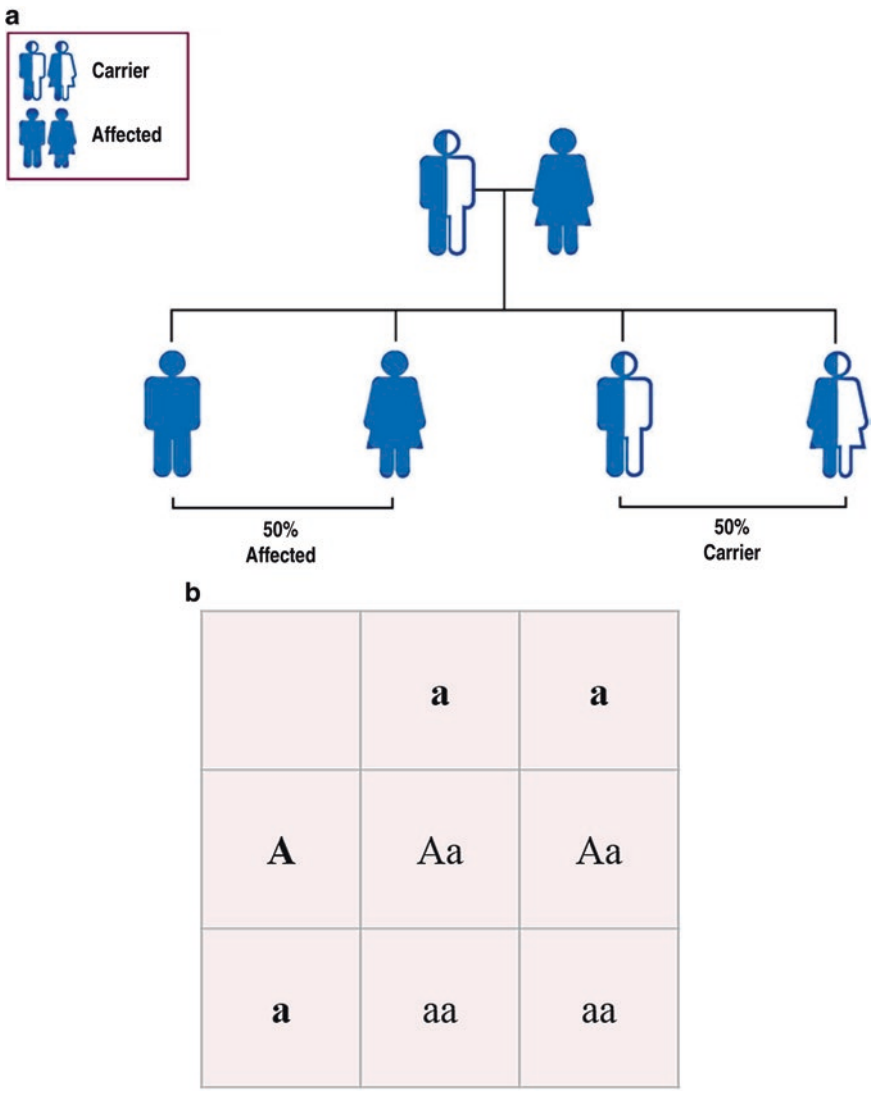


Fig. 1.6 Autosomal recessive inheritance with one parent affected and one parent a carrier for the same disease. (**a**) Diagram (Illustration from Genetic Counseling Aids, 6th Edition, Copyright 2013, permission for use granted by Greenwood Genetic Center). (**b**) Punnett square showing possible combinations of alleles; carrier (Aa) and affected (aa)

would be phenotypically normal, but 50% of the individuals would be carriers of the disease (Fig. 1.7).

If two affected individuals (rr) have offspring, 100% of the offspring will have the disorder (Fig. 1.8).

Patterns of Inheritance Involving the Sex Chromosomes

As previously stated, the genes that generally determine genetic sex are the X and Y chromosomes. Males have one X chromosome and one Y chromosome. Females have two X chromosomes. However, when comparing the quantity of the product formed by a single allele in both the male and female, the amount is nearly equivalent. Mary Lyon eventually explained this in the Lyon hypothesis of X inactivation. The Lyon hypothesis has three main points: (1) in the somatic cells of females (any cell other than the reproductive cells), only one of the X chromosomes is active; (2) this inactivation of one of the X chromosomes occurs early in embryonic life, during the first embryonic week; and (3) inactivation is entirely random, but once a specific X chromosome has been inactivated, that inactivation is permanent, and all of the descendants of that cell line will have the same inactive X chromosome.

The inactivation of an X chromosome in women allows for equalization of gene expression between females, with two X chromosomes, and males, with one X chromosome. This equalization is referred to as "dosage compensation." The inactivation of an X chromosome also leads to variability within and between women. That is, in heterozygous females there is variability in the phenotypic expression of an X-linked gene, depending on the X-inactivation pattern which is random. Since this occurs very early on in embryonic development, females have varying proportions of cells in which a particular allele is active or inactive and in turn will lead to varying phenotypes [16]. A heterozygous female can be entirely normal and have the full disease phenotype or any variation in between. Having two essentially different cell populations within one individual is called mosaicism, so all women are mosaic with respect to the expression of their X chromosomes. This variability translates to

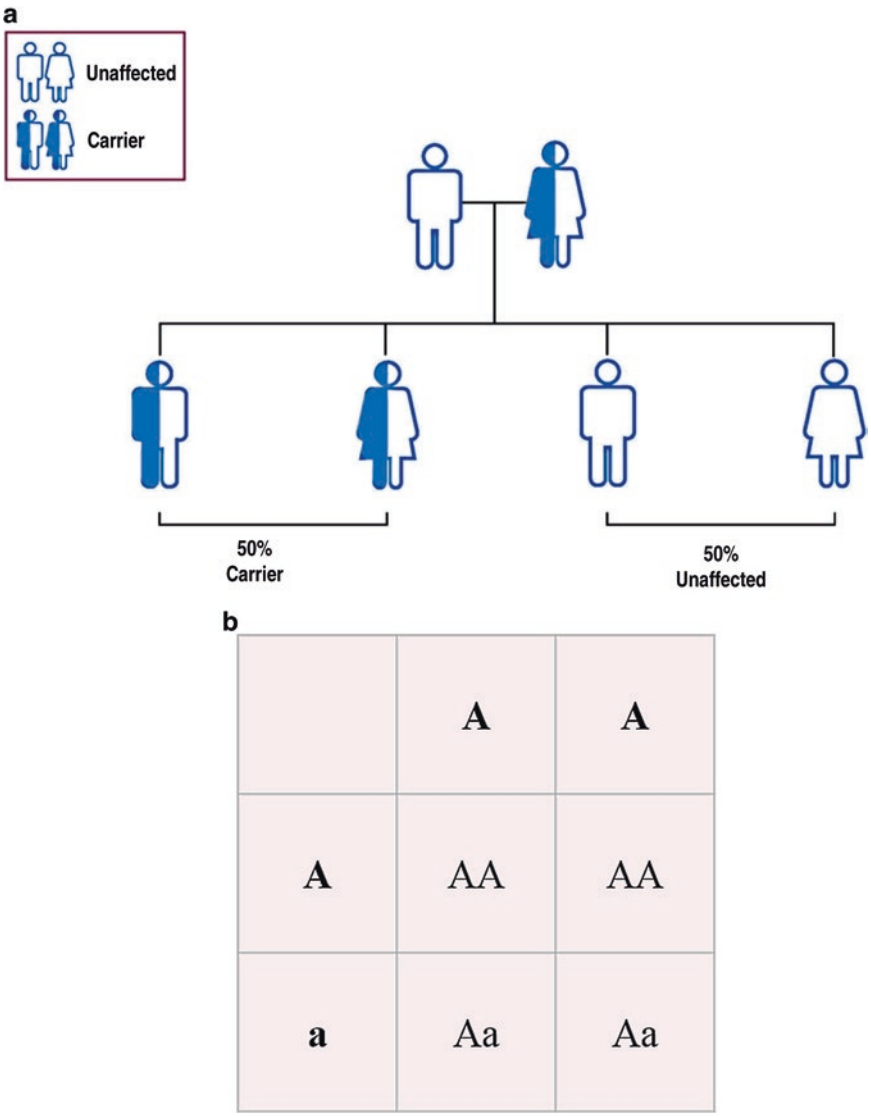


Fig. 1.7 Autosomal recessive inheritance with one parent a carrier and the other not a carrier and unaffected. (**a**) Diagram (Illustration from Genetic Counseling Aids, 6th Edition, Copyright 2013, permission for use granted by Greenwood Genetic Center). (**b**) Punnett square showing possible combinations of alleles; all individuals are unaffected, carrier (Aa) or noncarrier (AA)

differences between individuals as well, since phenotype depends on the proportion of cells or tissues affected by expression of the mutated gene.

X-linked recessive disorders are generally expressed in males, with the rare exception of the female heterozygote that has an extremely high proportion of the inactivated X chromosome. X-linked disorders are transmitted from an affected male to all of his daughters, who become unaffected carriers (if the mother is unaffected). Each male offspring from a normal phenotype carrier female has a 50% chance of inheriting the gene (Fig. 1.9). X-linked genes cannot be transmitted directly from father to son, as the mother transmits the X chromosome and the father transmits the Y chromosome (Fig. 1.10).

Only a few disorders are X-linked dominant. All the offspring produced from affected males and normal females will be normal males and affected daughters. The dominant X-linked gene of the father would be passed to all of his daughters.

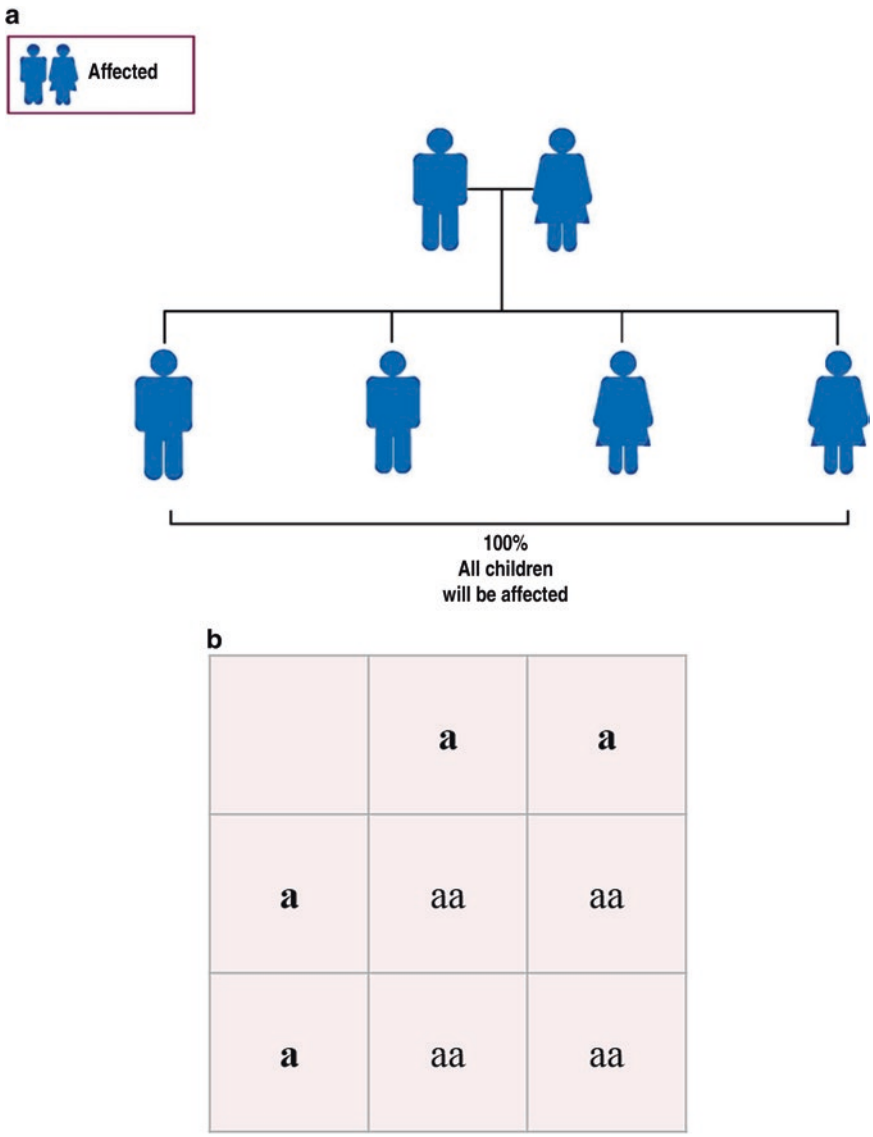


Fig. 1.8 Autosomal recessive inheritance with both parents affected. (**a**) Diagram (Illustration from Genetic Counseling Aids, 6th Edition, Copyright 2013, permission for use granted by Greenwood Genetic Center). (**b**) Punnett square showing possible combinations of alleles; all individuals are affected (aa)

Any X-linked gene inherited by sons must be inherited from a normal mother as the Y chromosome is inherited from the father. A mother with an X-linked dominant disorder will pass the diseased chromosome to 50% of her daughters or sons. When transmission occurs, the phenotype is expressed in both females and males, but may be more severe in males. Females may have a less severe form due to the Lyon principle and the mosaic nature of the cells lines.

Mitochondrial DNA Inheritance

In addition to the classic nuclear chromosomal gene inheritance patterns, there are other modes of inheritance and reasons for genetic disorders. As mentioned previously, in addition to nuclear DNA contained in the traditional chromosomes, there is also DNA in the mitochondria of cells. Mitochondrial DNA (mtDNA) is packaged into a circular chromosome and replicates within the mitochondrion.

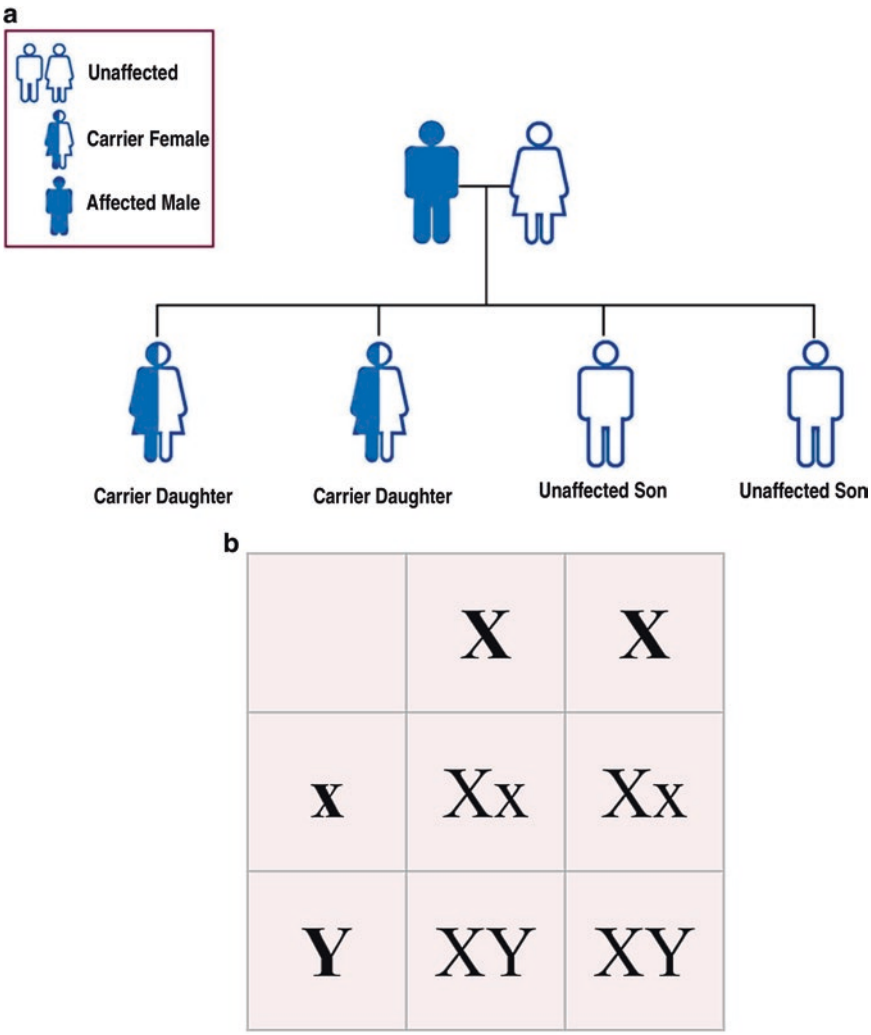


Fig. 1.9 Illustration of X-linked inheritance with father affected and mother a noncarrier. (**a**) Diagram (Illustration from Genetic Counseling Aids, 6th Edition, Copyright 2013, permission for use granted by Greenwood Genetic Center). (**b**) Punnett square, females all carriers (Xx), males all unaffected (XY)

There are multiple copies of mtDNA per mitochondrion and thousands of mitochondria per cell. This multitude of mtDNA copies allows for mutations to occur in just some of the copies of the mtDNA. When a cell with a mixture of normal and mutant mtDNA divides, the daughter cells may contain all normal mtDNA, all mutant mtDNA, or a mixture of both. Like X chromosome activation mosaicism in females, the expression of a mutation of mtDNA depends on the ratio and tissue-specific location of normal and abnormal mtDNA. Mitochondrial DNA is exclusively inherited from the mother. This pattern is seen because the ovum is amply supplied with mitochondria, but the sperm contains only a few, and these do not persist in the offspring. Thus, the mother is the source of all her offspring's mtDNA. Kearns-Sayre syndrome (external ophthalmoplegia, retinal degeneration, heart block) and Leber hereditary optic atrophy are examples of mitochondrially inherited disorders; there are many others as well (see Table 1.1 for additional examples).

Genomic Imprinting

In the past, little attention was given to whether the sex of the parent with the defective gene had any influence on the expression of the gene in the offspring. Now, with the technology available to determine which copy of a gene came from which parent, it has been uncovered that in a number of disorders, the severity of expression is influenced by the parental origin of the gene. Maternal- and paternal-inherited chromosomes can result in different phenotypic expression of the disease. This is one example of genomic imprinting, a form of epigenetics. Epigenetics is an area of study that focuses on changes to structures other than nucleotides that have an effect on nucleotide transcription and translation. For example, the autosomal dominant disorder, neurofibromatosis type I, appears to be more severe with maternal transmission as opposed to paternal transmission. In a more common example, Prader-Willi syndrome can be caused by mutations or deletions in seven

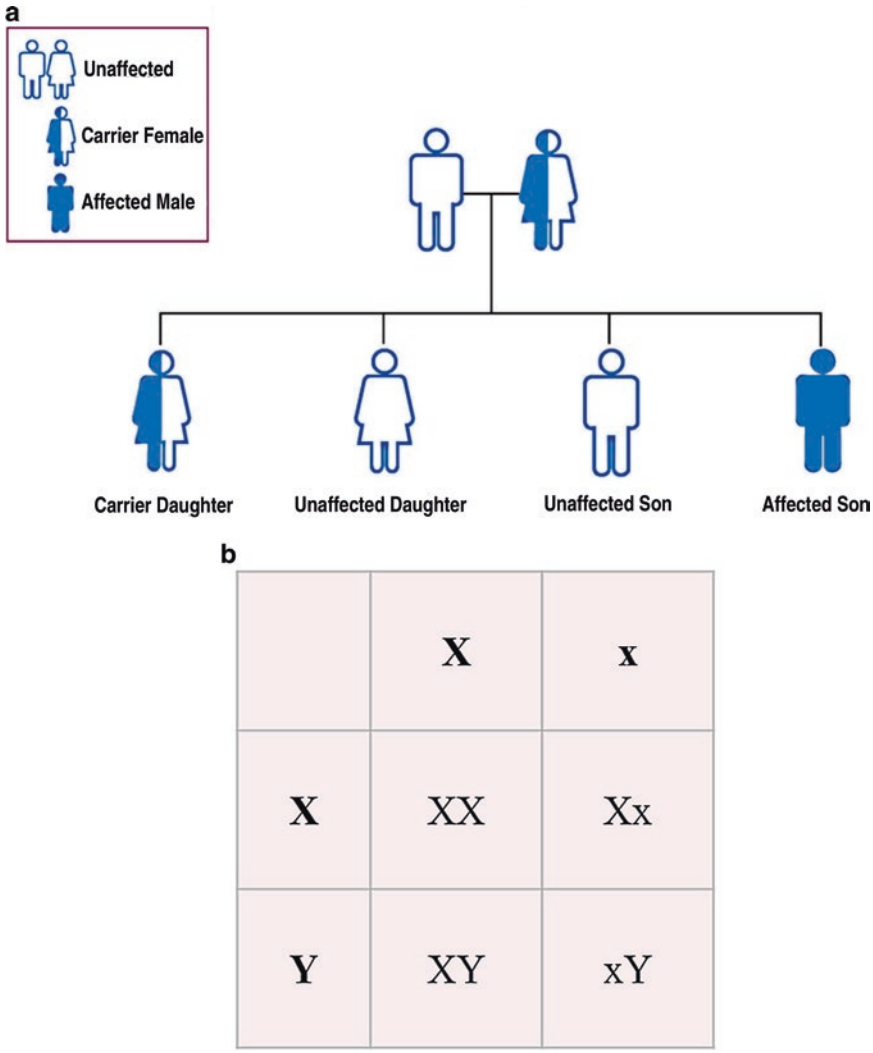


Fig. 1.10 Illustration of X-linked inheritance with mother a carrier and father unaffected. (**a**) Diagram (Illustration from Genetic Counseling Aids, 6th Edition, Copyright 2013, permission for use granted by Greenwood Genetic Center). (**b**) Punnett square, female noncarrier (XX) or carrier (Xx), males unaffected (XY) or affected (xY)

Table 1.1 Categories of genetic conditions and examples

Disorder category	Example disorder	Gene examples	Inheritance	OMIM number
Syndromic craniosynostosis	Crouzon	*FGFR2*	AD	123500
	Saethre-Chotzen	*TWIST1*	AD	101400
	Other	*ALPL, SKI, CD96, ZIC1, IFT43. RUNX2, WDR19, WDR35, SPECC1L, RECQL4, TCF12, IFT122, MSX2, POR, ERF, FGFR1, FGFR3,*		
Mandibular dysostoses	Treacher Collins	*TCOF, POLR1C, POLR1D*	AD	154500
	Other	*EFTUD2, POLR1A*		
Ptosis	Noonan	*PTPN11, RAF1, SOS1, KRAS, BRAF, HRAS, NRAS, CBL, SHOC2, MAP2K2, MAP2K1, SPRED1*	AD	163950
	Kearns-Sayre syndrome	Mitochondrial DNA deletion	Mitochondrial	530000
	Myotonic dystrophy	*DM, DM2*	AD, with anticipation	160900, 602668
	Blepharophimosis, ptosis, and epicanthus inversus syndrome	*FOXL2*	AD	110100
	Other	*AGRN, ALG14, ALG2, C10orf2, CHAT, CHRNA1, CHRNB1, CHRND, CHRNE, COLQ, DNM2, DOK7, DPAGT1, GFPT1, KIF21A, LRP4, MTM1, MUSK, POLG, POLG2, PREPL, RAPSN, RRM2B, RYR1, SLC25A4, TUBB3*		

(continued)

Table 1.1 (continued)

Disorder category	Example disorder	Gene examples	Inheritance	OMIM number
Anophthalmia/ microphthalmia	Lenz	*BCOR*	XLD	300485
	Other	*ALDH1A3, BMP4, RAX, SIX6, SOX2, STRA6, VSX2, TENM3, FOXE3, GDF6, OTX2, SMOC1*		
Aniridia	Aniridia	*PAX6*	XLD	607108
	Wilms' tumor, aniridia, genitourinary anomalies, retardation (WAGR) syndrome	*11p13 deletion (includes PAX6 gene)*	AD	194072
	Other	*ELP4*	AD	606985
Cryptophthalmos	Fraser	*FRAS1, FREM2, GRIP1,*	AR	219000
	Ablepharon-macrostomia syndrome	*TWIST2*	AD	200110
	Other	*SOX2, STRA6*		
Other	CHARGE	*CHD7*	AD	214800
	22q11.2 microdeletion syndrome (formerly DiGeorge syndrome)	22q11.2 microdeletion	AD	602054
	Mitochondrial myopathies	Mutations or deletions in multiple nuclear or mitochondrial genes	AD/AR/XL Mitochondrial	251900

genes on chromosome 15 in the paternal allele [4]. If the maternally derived genetic material from the same region is affected instead, the sister Angelman syndrome is the result due to epigenetic factors.

Aneuploidy

Numerous other problems with the chromosomes themselves can cause genetic disorders [16]. There can be an abnormal number of chromosomes, either too many or too few. There can also be structural problems in the chromosomes.

Aneuploidy is an abnormal number of chromosomes and is virtually always associated with abnormal development. It occurs in an estimated 3–4% of all recognized pregnancies. The most common conditions are trisomy (three copies of a chromosome) and monosomy (one copy of a chromosome). Trisomy is possible for any chromosome; however an extra chromosome is often not compatible with life. Down syndrome is an example of a trisomy compatible with life; full trisomy of chromosome 21 is found in 94% of these individuals. Therefore they have 47 chromosomes (e.g., 47, XX, +21) instead of the usual 46 chromosomes [3].

Monosomy for an entire chromosome is nearly always lethal. An exception is Turner syndrome (45, X), caused by a monosomy or single copy of the X chromosome. Individuals with this syndrome are female (as they have no Y chromosome), but have only 45 chromosomes instead of the usually 46 [17].

Chromosomal Deletions, Duplications, and Other Rearrangements

Occasionally deletions affect specific segments of chromosomes during the replication process, leading to missing genetic information. The clinical manifestations depend on the amount and type of genetic information lost. Deletions can occur at the ends of the chromosome (terminal) or centrally (interstitial). For example, 9p–syndrome (craniosynostosis, midface hypoplasia, shallow orbits, and up-slanted palpebral fissures) is due to a deletion of the distal portion of the short arm of chromosome 9 [18].

Many other structural abnormalities may occur, such as duplications, ring chromosomes, isochromosomes, inversions, and balanced rearrangements. The phenotypes produced depend on the genetic material that has been lost or manipulated. Often an affected individual may be phenotypically normal, but is at risk for the generation of abnormal gametes that can cause severe phenotypes in the next generation. This is one of the reasons it is important to test the unaffected parents of affected children, as they may be silent carriers of genetic abnormalities.

Beyond these single-gene and chromosomal disorders, most disease processes are multifactorial. Many diseases cannot be attributed to a single cause, but to an interaction of many influences. For most illnesses, we still have a poor understanding of how the genetic and environmental components interact. Advances in our knowledge of this interaction could lead to an exciting form of interventional medicine.

For example, smoking has been linked to an increase in lung cancer. By avoiding this environmental factor, an individual significantly decreases the likelihood of developing the disease. By altering the environmental factors, the risk of illness can be decreased. This is true even for classic Mendelian disorders, where specific environmental triggers, such as UV light or ionizing radiation, may lead to exacerbation of the syndrome.

Options for Genetic Testing

Genetic testing provides valuable information even when a diagnosis may be possible based on clinical findings and family history alone. The ability to know the exact molecular or cytogenetic diagnosis allows for more appropriate diagnosis, prognosis, therapy, reproductive counseling for the patient and family members, screening for associated medical conditions, and research opportunities.

There are many different types of genetic tests, for example, gene sequencing, which includes single-gene sequencing, gene panels, exome sequencing, and genome sequencing, or chromosomal-based tests, which include karyotype and chromosomal microarray analysis.

Genetic testing can have various results. They may be positive or negative, or they may need more interpretation so cannot be classified either way at the time of testing. Samples from other family members may be needed to interpret results. Ambiguous results may be reclassified as positive or negative in the future as knowledge of the genetic basis of disease increases.

Sometimes a medical condition due to a change in a specific gene is suspected. If that is the case, then just that particular gene can be sequenced. This is called single-gene sequencing. This process reads through the nucleotides of the gene to see if there are any mutations.

There are also conditions that share a phenotype so they may be caused by one of many genes. If that is the case, then that group of genes can be sequenced simultaneously. This is called a gene panel. This is a faster and more cost-effective approach than sequencing each of those genes one by one.

Sometimes a phenotype is strongly suggestive of a genetic condition in general, but one specific gene or a group of genes cannot be pinpointed. In cases like this, the entire exome can be sequenced; this type of genetic test is called "exome sequencing." The exome is the coding portion of the genome; it includes over 20,000 genes. The exome is the minority of genetic information in the genome, but it represents the majority of disease-causing mutations.

The genome can also be sequenced entirely, called "genome sequencing." Genome sequencing is not readily clinically available at this time.

Aside from these sequencing tests, there are also the chromosomal-based tests. As mentioned above, the two main chromosome tests are karyotype and chromosomal microarray. A karyotype is a visual representation of the chromosomes within a single cell. It is most useful for detecting large abnormalities either in the structure or the number of the chromosomes, such as translocations, aneuploidy, or large deletions and duplications. It is often ordered for families with multiple miscarriages or in children with multiple congenital abnormalities, potentially caused by disruption of a large number of genes.

A chromosomal microarray analysis, also called simply microarray or array, is a type of genetic test that looks for "deletions" or "duplications" within a chromosome. These deleted or duplicated regions may include one or multiple genes, but they are too small to be identified in a traditional karyotype. In addition it can provide information about how closely related the parents of the patient are and can show other valuable information such as uniparental disomy (UPD) in a SNP microarray.

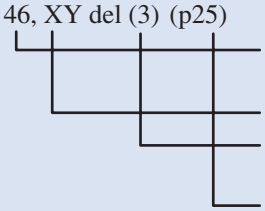
Other chromosomal-based tests include fluorescent in situ hybridization (FISH) or multiplex ligation-dependent probe amplification (MPLA). FISH uses fluorescent probes that bind to those parts of a chromosome with a high degree of sequence complementarity and allows for detection and localization of the presence or absence of specific DNA sequences. MLPA detects small deletions and duplications in a specific region and is useful when a particular genetic region is suspected and copy number variations are a common cause of disease, such as the 22q11.2 deletion syndrome.

Sequencing and chromosomal-based tests can also be categorized into directed testing and agnostic testing. Directed testing is when clinical suspicion is high for a certain disorder or group of disorders. Agnostic testing is when, though genetic involvement in a disorder is suspected, the symptoms do not point toward a precise gene or group of genes.

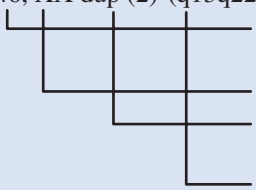
Here is a scenario example to demonstrate the use of genetic testing in a child with microphthalmia. The clinician sees a patient with microphthalmia and suspects Lenz microphthalmia syndrome. They could test the single gene *BCOR* individually, or they could do a microphthalmia panel with many genes known to cause microphthalmia if the diagnosis was not as clear. If directed testing is negative, then agnostic testing, like exome sequencing, could be the next step.

The nomenclature illustrated in Table 1.1 uses the «short system,» which is the most commonly used system of cytogenetic shorthand in the literature [19, 20].

Example 1.1 Male with a Partial Monosomy for the Short arm of Chromosome 3

46, XY del (3) (p25) 	Number of chromosomes, 46 = normal
	XY = Male
	Deletion of part of chromosome 3
	The deletion is on the short arm (p) of the chromosome on band number 25

Example 1.2 Female with a Partial Trisomy for the Long Arm of Chromosome 2

46, XX dup (2) (q13q22) 	Number of chromosomes, 46 = normal
	XX = Female
	Duplication of part of chromosome 2
	The duplication is on the long arm (q) and extends from the 13 band to the 22 band

Example 1.3 Patient with a Missense Mutation in *SPECC1L* Gene

SPECC1L c.1258G > A:p. E420K	The name of the gene with the mutation is stated first The "c." refers to the location of the mutation in the DNA The "p." refers to the location of the mutation in the protein structure (often the amino acids are shortened into their three-or one-letter abbreviations as in this case) *SPECC1L* mutation that is a substitution of a guanine to adenosine at the 1258 position of the DNA, which leads to a substitution at the 420th amino acid in the protein of a glutamic acid (E) for a lysine (K)

Genetic Causes of Common Oculoplastic Disorders

Table 1.1 includes different categories of conditions that may come to the attention of an oculoplastic surgeon. There are examples provided within each disorder group; however this is not an exhaustive list. In the "Important Genetic Resources" section, there are websites that may be helpful to deduce the differential diagnosis for a patient, for example, the Online Mendelian Inheritance in Man database (www.omim.org).

Important Genetic Resources

Online Mendelian Inheritance in Man (OMIM): www.omim.org

GeneTests: www.genetests.org

Genetic Testing Resource: Nextgxdx.com

National Institutes of Health Clinical Trials Database: www.clinicaltrials.gov

GeneReviews: www.genereviews.org

National Organization for Rare Disorders: www.rarediseases.org

Acknowledgement to and in memory of: **Kenneth L. Piest**

References

1. Allen RC. Proliferation and arrest: the genetics of orbital disorders. Curr Opin Ophthalmol. 2015;26(5):382–91.
2. Allen RC. Hereditary disorders affecting the lacrimal system. Curr Opin Ophthalmol. 2014;25(5):424–31.
3. Jones KL. Down syndrome. In: Jones KL, editor. Smith's recognizable patterns of human malformation. Philadelphia: WB Saunders; 1988. p. 10–2.
4. Jones KL. Prader-Willi syndrome. In: Jones KL, editor. Smith's recognizable patterns of human malformation. Philadelphia: WB Saunders; 1988. p. 170–1.
5. King RC. A dictionary of genetics. 2d ed. New York: Oxford University Press; 1974.
6. Sager R. Tumor suppressor genes: the puzzle and the promise. Science. 1990;246:1406–12.
7. Vogal F. Genetics of retinoblastoma. Hum Genet. 1979;52:1–54.
8. Yandell DW, Campbell TA, Dayton SH, et al. Identification of oncogenic point mutations in the human retinoblastoma gene and application to genetic counseling. N Engl J Med. 1989;321:1689–95.
9. Miller DM, Blume S, Borst M, et al. Oncogenes, malignant transformation, and modern medicine. Am J Med Sci. 1990;300:59–69.
10. Ponder B. Inherited predisposition to cancer. Trends Genet. 1990;6:213–8.
11. Weinberg RA. The genetic basis of cancer. Arch Surg. 1990;125:257–60.
12. Bishop JM. The molecular genetics of cancer. Science. 1987;235:308–11.
13. National Institutes of Health consensus development conference statement on neurofibromatosis. Arch Neurol. 1988;45:575–93.
14. Riccardi VM, Eichner JE. Neurofibromatosis: phenotype, natural history, and pathogenesis. Baltimore: Johns Hopkins University Press; 1986.
15. Barker D, Wright E, Nguyen K, et al. Gene for von Recklinghausen neurofibromatosis is in the pericentromeric region of chromosome 17. Science. 1987;236:1100–4.
16. Emery AEH, Rimoin DL. Principles and practice of medical genetics. 2d ed. Edinburgh: Churchill Livingstone; 1990.
17. Jones KL. Turner syndrome. In: Jones KL, editor. Smith's recognizable patterns of human Malformation. Philadelphia: WB Saunders; 1988. p. 74–5.
18. Jones KL. 9p monosomy syndrome. In: Jones KL, editor. Smith's recognizable patterns of human malformation. Philadelphia: WB Saunders; 1988. p. 46–7.
19. The National Foundation-March of Dimes. Paris Conference: Standardization in Human Genetics. White Plains, BD: OAS VIII; 1972.
20. The National Foundation-March of Dimes. Paris Conference Supplement: Standardization in Human Cytogenetics. White Plains, NY: OAS XI; 1975.

Embryology and Anatomy of the Developing Face

2

Lama Khatib, Elizabeth Bhoj, and Bart Peter Leroy

The anatomy of the head and facial structures is best appreciated by understanding the basic steps of embryologic and human morphologic development [1–5]. The following chapter will review embryologic development of the human face at three main levels: the molecular level, the cellular level, and the developmental field level. Developmental field levels are those parts or systems of the embryo in which the process of development obeys a spatially ordered, temporally synchronized hierarchy. The impact of altered development on craniofacial and orbital anatomy will also be discussed in the context of potential surgical intervention.

Levels of Embryological Development

Early *Molecular* interactions occur at the genetic level, the details of which are discussed in Chap. 1. At the *cellular* level, the spermatozoon (male gamete) fertilizes the ovum (female gamete), and a single diploid cell or zygote is formed. The nuclear material of the zygote consists of a combination of genetic material from both parents. The simple zygote then begins to divide, in a process called cleavage to initiate the developmental process. Once a critical mass of about 16–32 cells is reached, the solid sphere of cells called a morula becomes more compact, and the differentiation process begins, as cleavage continues. Differentiation is the process by which cells and tissues acquire features unique to their location and function in an organ system. Intracellular messengers mediate the differentiation and growth process by dictating cellular behavior and growth pattern. As cleavage and differentiation continue, a blastocyst is then formed and implanted in the uterus. The germinal stage is the developmental process that the zygote goes through until implantation. Embryogenesis covers the first 8 weeks of development from the zygote stage until a fetus is formed.

As multiplying cells start forming units, they begin to function as a *developmental field*, also referred to as a functional matrix. A developmental field is a morphogenetic unit that can induce organogenesis through the hierarchal processes of determination, induction, and differentiation, respectively. In other words, as groups of cells differentiate and begin to develop, they will influence the development of subsequent stages within that same unit and that of neighboring units. An error that occurs at one stage will have an influence on successive stages and possibly affect the development of other systems that depend on the development of that specific unit. The successful development of the entire organism depends on the successful development of the different parts in a specific sequence.

Cytogenesis and Morphogenesis

As the organism begins to increase in mass, two distinct processes are occurring: growth and differentiation. Growth is an increase in cell mass due to cellular multiplication. The organism becomes larger in size because of an increase in the number of cells. These cells, however, would all be identical unless a second developmental process took place. Differentiation is the process by which cells acquire distinctive cytological and biochemical features. Cytogenesis is the

L. Khatib (✉)
Pediatric Ophthalmology, Oculoplastic and Orbital Surgery, Ophthalmology Division, Children's Hospital of Philadelphia, Philadelphia, PA, USA
e-mail: lamahkhatib@gmail.com

E. Bhoj
Pediatrics and Genetics, Children's Hospital of Philadelphia, Philadelphia, PA, USA

B.P. Leroy
Department of Ophthalmology, Ghent University Hospital, Ghent, East-Flanders, Belgium

Division of Ophthalmology, The Children's Hospital of Philadelphia, Philadelphia, PA, USA

© Springer International Publishing AG 2018

J.A. Katowitz, W.R. Katowitz (eds.), *Pediatric Oculoplastic Surgery*, https://doi.org/10.1007/978-3-319-60814-3_2

acquisition of the differentiated state by the individual cell. Morphogenesis on the other hand is the change in the shape and position of the cells that results in the appearance of the various tissues and organ systems. Thus, differentiation occurs both at the cellular level, referred to as cytogenesis, and at the organ level, referred to as morphogenesis. Both are essential components of development. For example, for proper lacrimal gland function, secretory cells need to undergo cytogenesis to produce the chemical components of tears, and the tissue must undergo morphogenesis to form the lacrimal gland ductules that allow for delivery of the tears to the ocular surface. Failure of either of these steps to occur could result in inadequate tear production, which could negatively impact the health of the eye [6].

Craniofacial Morphogenesis

The critical period for structural development of the head and face occurs during 4 and 8 weeks of gestation. By 8 weeks gestational age (GA), facial features are recognizable in the embryo, resembling those of an adult human face.

As the embryo begins to develop, it forms a relatively planar structure. Longitudinally, through the center of the flat embryonic plate, a primitive groove forms, which later develops into the neural groove (Fig. 2.1). On the lateral aspects of the neural groove, cellular proliferations take place and the neural folds are formed. Along the lateral margins of the embryonic neural folds, a special population of cells arises, called the neural crest cells. A large portion of facial tissues is derived from ectodermal neural crest tissue. As the neural folds begin to fuse to form the neural tube around day 22 GA, the neural crest cells located along the crest of each neural fold lose their epithelial affinity and form a flattened middle layer between the neural tube and the overlying surface ectoderm (Fig. 2.1). They migrate from this area and give rise to a diverse array of structures in the mature face, including nearly all of the connective tissues and adnexal structures of the eye (Fig. 2.2).

Neural crest cell migration depends on multiple intricate developmental events. Alteration of any step in this developmental sequence can produce fundamentally different but often superficially similar malformations [7]. Typically, cells with longer pathways are more prone to malformations. For example, as the embryo undergoes three-dimensional development, and midbrain flexure occurs, neural crest cells only need to migrate a short path to reach their final destination (Fig. 2.2). This may explain why structures derived from the frontonasal neural crest tissue have a lower incidence of deformities than structures derived from neural crest cells with longer pathways.

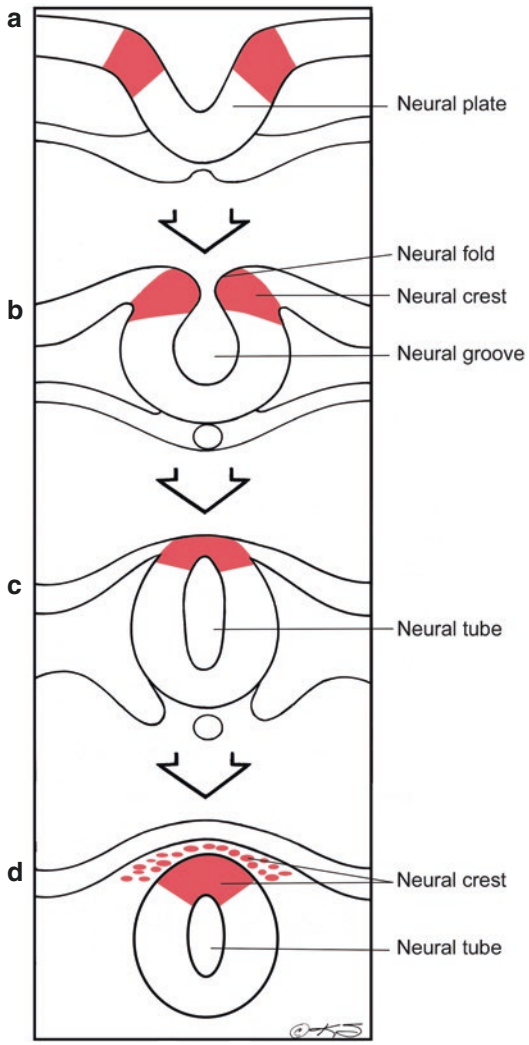


Fig. 2.1 Neural crest cell migration as the neural fold develops into the neural tube. (**a**) Primitive groove formation. (**b**) Neural crest cells arise at the margin of the neural folds. (**c**) Neural fold fusion and neural tube formation. (**d**) Neural crest cells lose affinity to surface ectoderm

Pharyngeal Arches

Pharyngeal or branchial arches begin to form distal to the frontonasal prominence early in the fourth week. Humans have five pairs of arches, numbered 1, 2, 3, 4, and 6 in a cranial to caudal sequence (Fig. 2.3). Arch 5 does not develop in humans or even if initially present regresses rapidly. They consist of visible layers of tissue outgrowth arising from

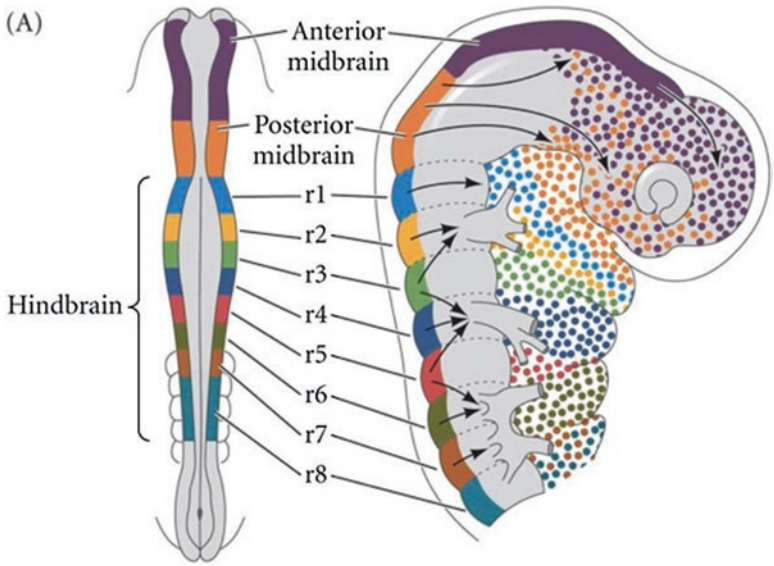


Fig. 2.2 Midbrain flexure and neural crest cell migration. The neural crest cells in the forebrain area do not have to migrate far because they are transported forward by the forward flexion of the embryo. The vertical numbers r1–r8 indicate rhombomeres 1–8 (From: Scott F. Gilbert: Developmental Biology, Ninth Edition. 2010:384. © Sinauer Associates, Inc. Reprinted with permission)

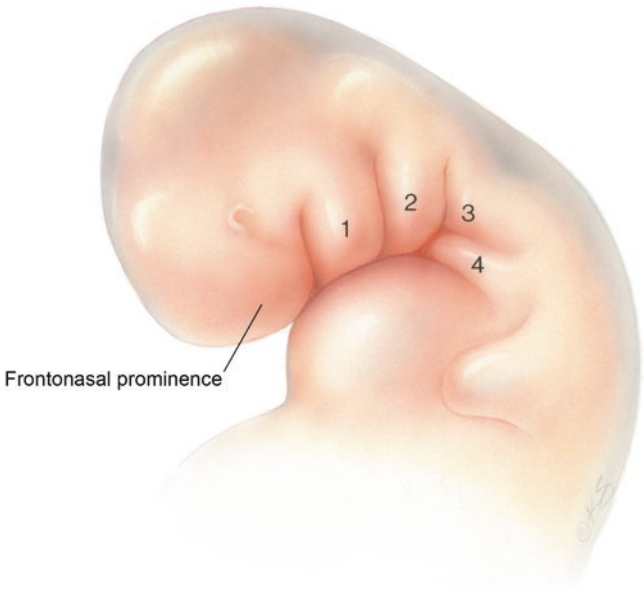


Fig. 2.3 Pharyngeal arches. Pharyngeal arches 1 through 4 are visible prominences in the embryo; pharyngeal arch 6 is detectable histologically but does not manifest as a prominent or exophytic structure

underneath the early brain and frontonasal prominence. These primitive embryonic structures contribute greatly to the formation of the head and neck [8]. Congenital anomalies in these regions may occur during the transformation of these structures into their adult derivatives. For example, the first arch contributes to the development of the face. The second arch forms the muscles of facial expression. The fourth and sixth arches contribute to the tongue and larynx. Pharyngeal arches are derived from all three germ cell layers: endoderm, mesoderm, and ectoderm. The neural crest cells also contribute to the formation of the pharyngeal arches (Fig. 2.2).

Facial Development

Pharyngeal arch 1 is the main contributor to lower facial prominences and structures and the main one of relevance to this chapter. Early during the fourth week, the paired segments of arch 1 begin to grow, and each divides into a maxillary process and a mandibular process (Fig. 2.4a, b). The cranial limb produces the maxillary prominence, and the caudal limb produces the mandibular prominence. Facial prominences are swellings that appear in the fourth week of embryologic development. Five main facial prominences contribute to facial development (Fig. 2.4a).

Facial formation involves the union of prominences by either one of two distinct processes: merging and fusion. Merging is the process by which two adjacent prominences are united by an upheaval of the separating valley (Fig. 2.5a). Fusion on the other hand is the process by which two adjacent prominences contact each other while trapping a double layer sheet of epithelial cells (Fig. 2.5b).

A single frontonasal prominence develops ventral to the forebrain around the same time as the paired maxillary and mandibular prominences. It is derived from neural crest cells that migrate from the ectodermal folds to invade the space

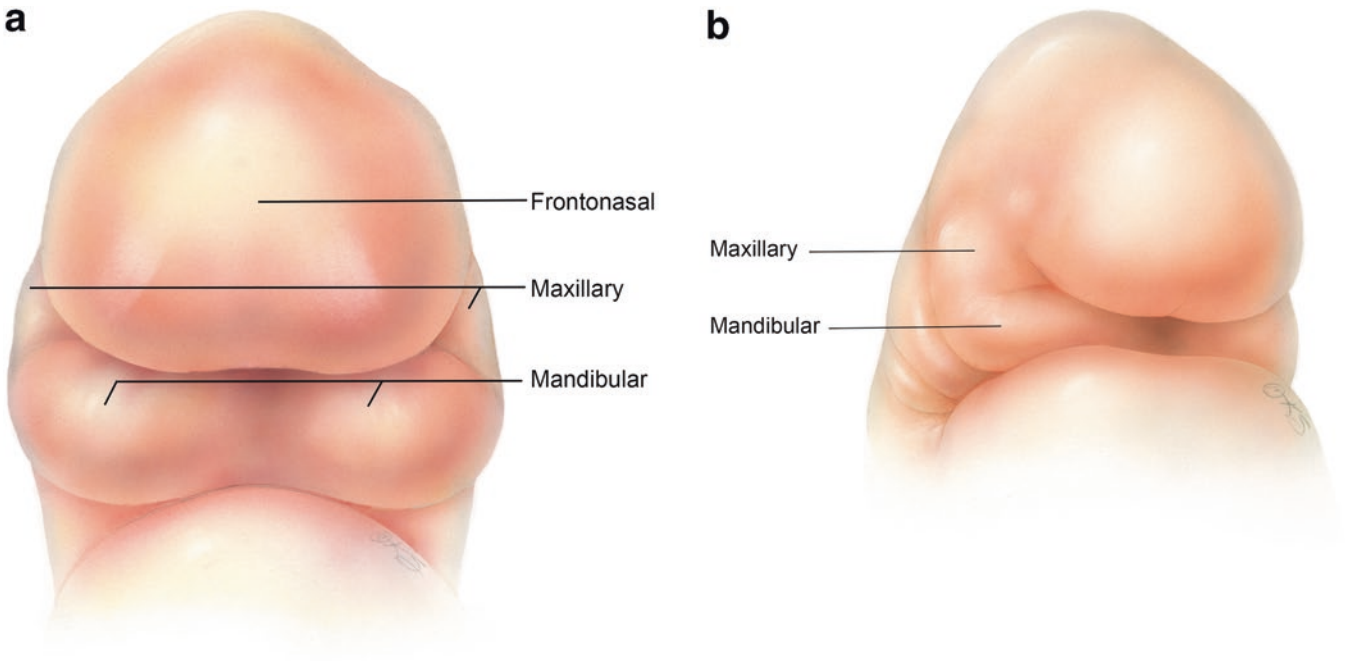


Fig. 2.4 Five main facial prominences (**a**) Frontal view: one frontonasal, two maxillary, two mandibular. (**b**) Fronto-lateral view

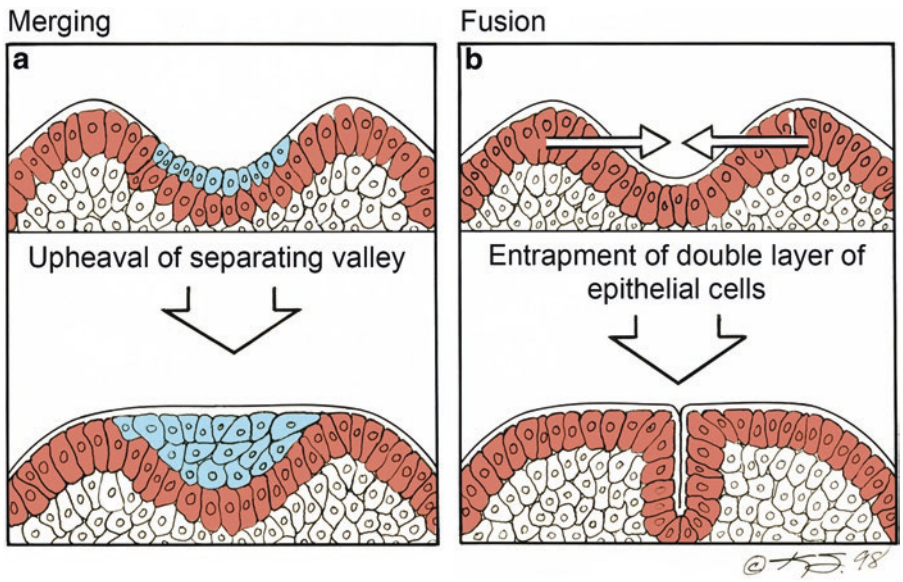


Fig. 2.5 (**a**) Merging vs. (**b**) fusion in facial development

that will form the frontonasal prominence. The five facial prominences constitute the major building blocks of the face and all five appear by the end of the fourth week. Facial development will then be a process of proliferation of cells within prominences, division, merging, and fusion of these prominences [9].

During the fifth week, the nasal placodes form. These are paired areas of thickened surface ectoderm on the ventrolateral aspect of the frontonasal prominence (Figs. 2.6a and 2.7a). In the sixth week, each nasal placode divides into medial and lateral components (Figs. 2.6b and 2.7b).

Around the same time during the sixth week, the upper jaw begins to form. The medial nasal and maxillary prominences merge to form the upper jaw. The two adjacent medial nasal prominences then merge across the midline to form the philtrum, middle segment of the upper jaw, and the tip of the nose. All five prominences contribute to the formation of the nose. The nasal bridge is formed by the frontonasal prominence. The tip and crest of the nose are formed by the merged medial nasal prominences, as mentioned above. The sides of the nose (alae) are formed by the lateral nasal prominences (Figs. 2.8 and 2.9).

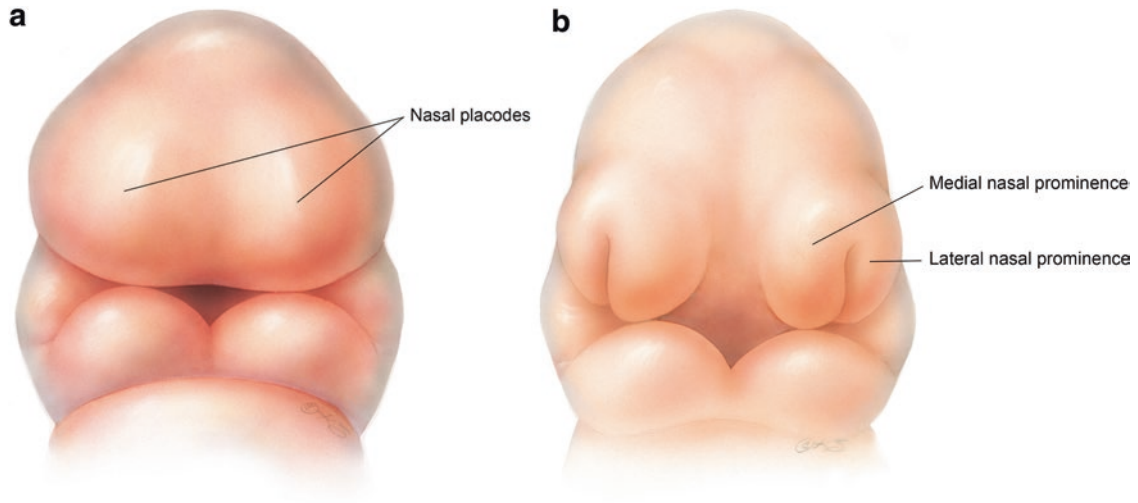


Fig. 2.6 (**a**) Embryo week 5: Nasal placode formation. The paired nasal placodes arise from a thickened area of surface ectoderm from the ventrolateral aspect of the frontal process. (**b**) Embryo week 6: The nasal placodes divide to form the medial and lateral nasal prominences

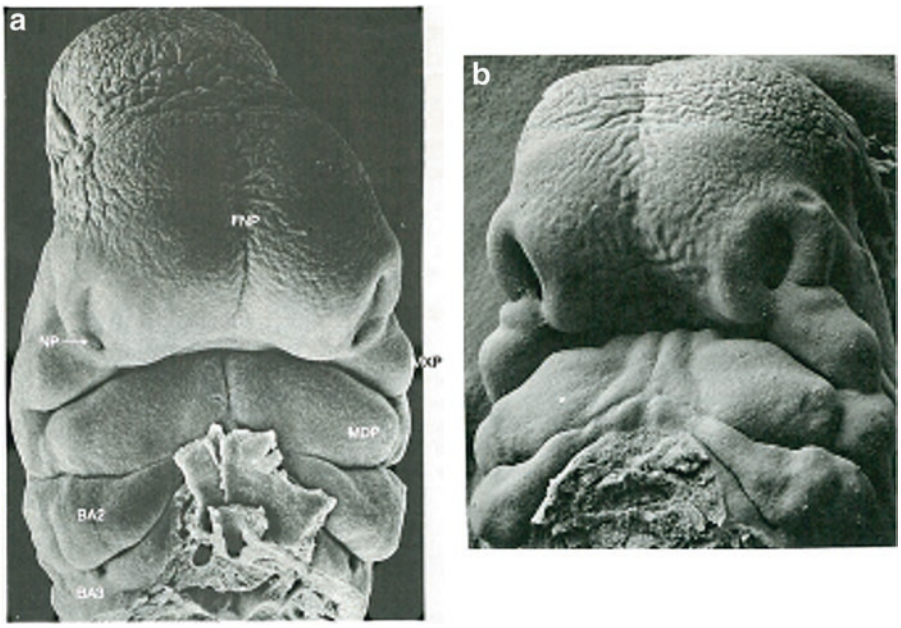


Fig. 2.7 Scanning electron micrograph of a 4- to 5-week-old human embryo in a frontal view: (**a**) Nasal placodes form on the ventrolateral aspect of the frontonasal prominence. Nasal pits (NP) form as small depressions in the nasal placodes bilaterally. (**b**) The nasal placodes give rise to the medial and lateral nasal prominences around the nasal pits (From Henrichsen [42] Reprinted with permission)

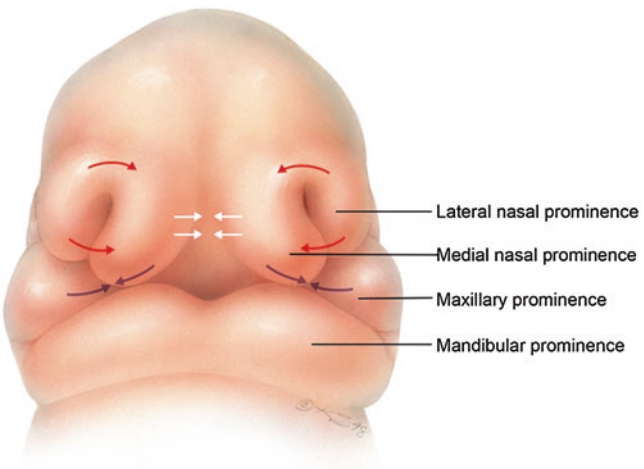


Fig. 2.8 Nasal and midface formation from five prominences. The nose is formed by the merging of the medial nasal prominences (*white arrows*) joining together across the midline forming the philtrum, the central segment of the upper jaw, and the tip of the nose. The lateral nasal prominences (*red arrows*) merge with the superior and inferior aspects of the medial nasal prominences. The upper jaw is formed by the merging of the medial nasal prominences and the maxillary prominences (*purple arrows*)

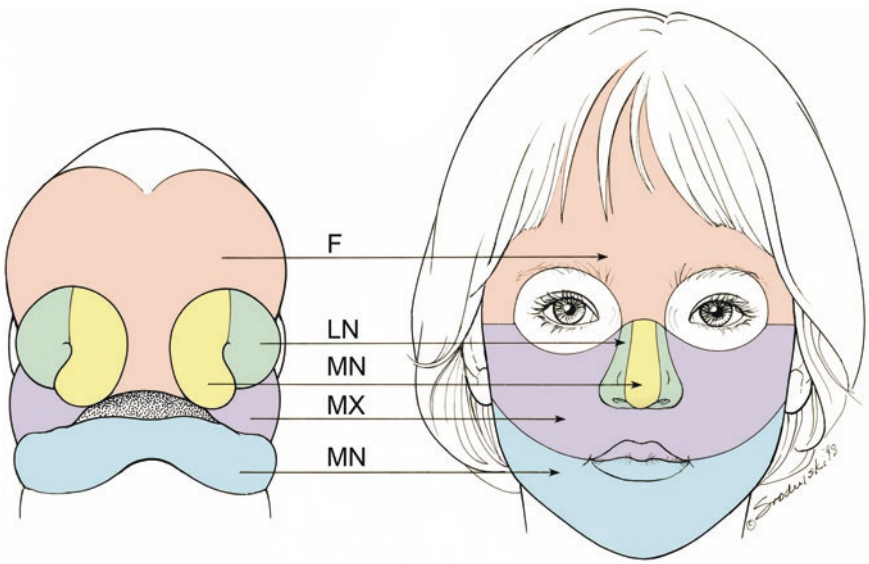


Fig. 2.9 The child's face derivation from facial prominences: Frontonasal prominence (*F*), lateral nasal prominence (*LN*), medial nasal prominence (*MN*), maxillary prominence (*MX*), mandibular prominence (*MN*)

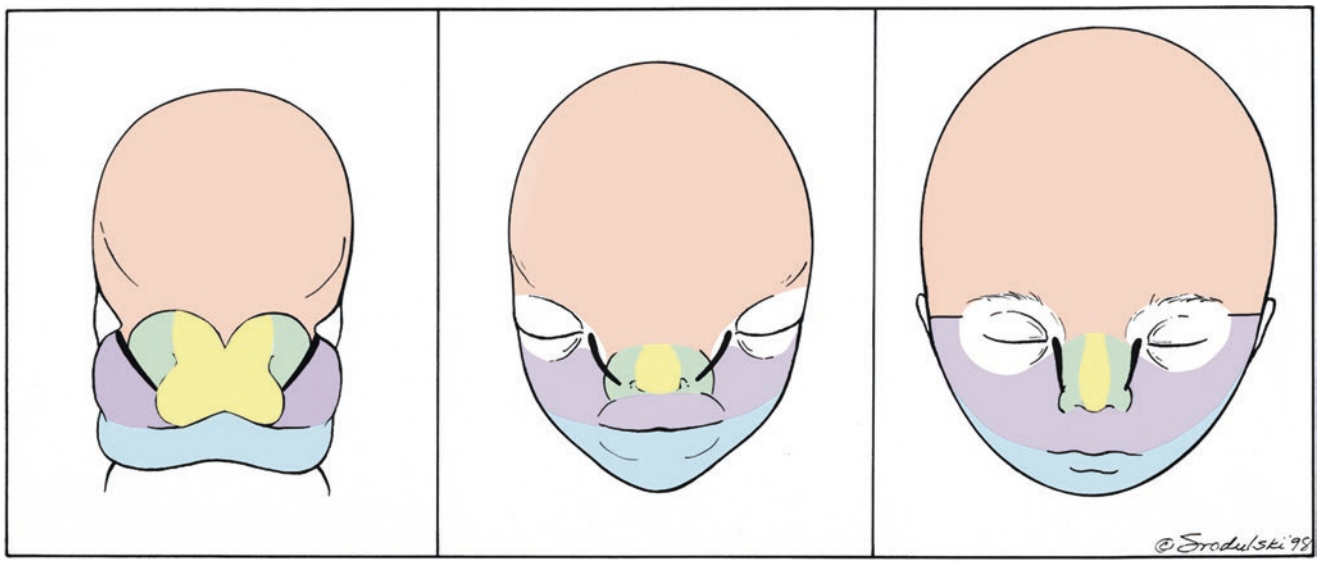


Fig. 2.10 Nasolacrimal duct formation: begins as a furrow between the lateral nasal prominence and the maxillary prominence. Fusion occurs around the groove trapping a double layer of epithelial cells. As the face develops, this cord of cells, which was horizontal in orientation originally, assumes its mature vertical position. This cord of epithelial cells later canalizes to form the lacrimal outflow system

The cheeks and the maxillae are derived from the maxillary prominences. The maxillary prominences enlarge considerably to develop the majority of the midface area in the mature human face (Fig. 2.9) [10].

The distal nasolacrimal lacrimal system is formed by the fusion of the lateral nasal prominence and the maxillary prominence and starts as a nasolacrimal furrow (Fig. 2.10). As these two prominences fuse, a double layer of epithelium is trapped between them. At first, this cord of epithelial cells is in a relatively horizontal orientation as depicted in Fig. 2.10, but as the maxillary prominences develop and the midface enlarges, this cord of cells assumes a more mature vertical position (Fig. 2.10). Near birth or soon after, this solid cord of cells canalizes and forms the nasolacrimal duct [11].

Mandibulofacial dysostosis syndrome, also known as Treacher Collins syndrome, is a good example of how insults at the embryonic stage can result in craniofacial deformities. This condition can be induced when a 9-day-old mouse embryo (approximately equal to a 4-week human embryo) is treated with retinoic acid. This produces a cell deficiency in the proximal aspect of the maxillary and mandibular prominences (Fig. 2.11). This early embryonic cell deficiency is manifested in the mature infant as the hypoplastic midface and jaw area seen in this syndrome [12–14].

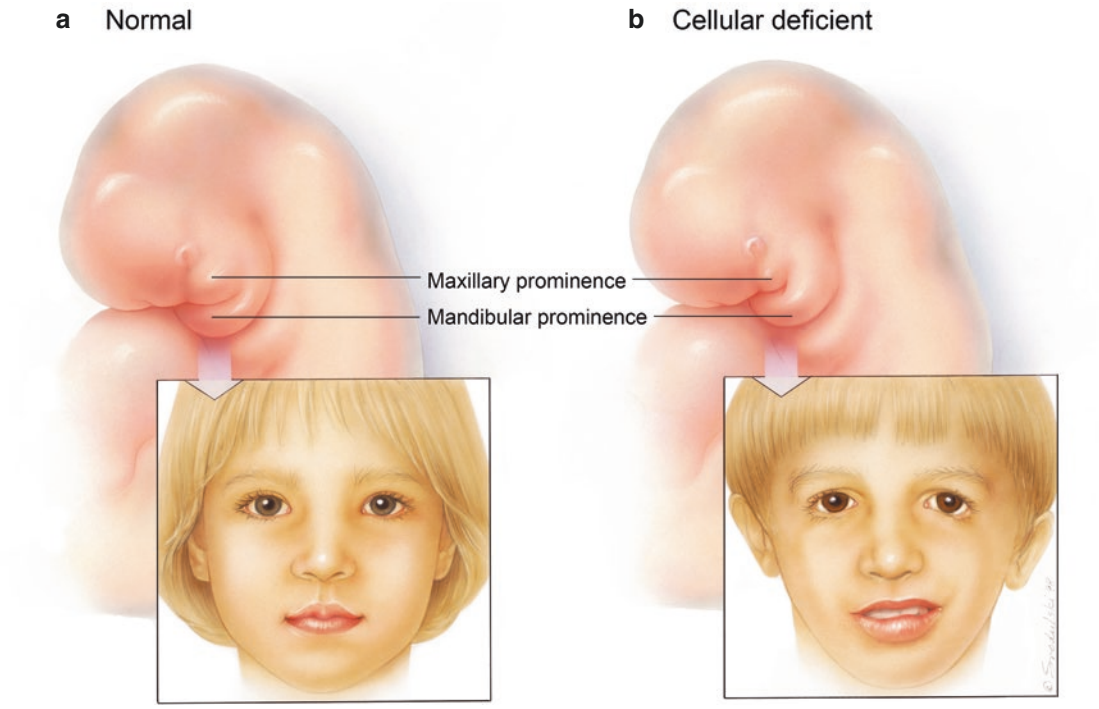


Fig. 2.11 Mandibulofacial dysostosis (MFD): cell deficiency and result. In MFD there is a cellular deficiency in the area of the maxillary and mandibular prominence. (**a**) A normal maxillary prominence produces normal midface area. (**b**) Cellular deficient maxillary and mandibular prominences produce hypoplastic midface and mandibular areas

Development of the Skull

The skull consists of two major portions, the cranial base and the calvarium, both of which derive from neural crest mesenchyme. The cranial base derives from the chondrocranium, also known as the cartilaginous neurocranium. The latter arises from the fusion of several cartilaginous centers surrounding the notochord in the cranial portion of the embryo. Its development is quite complex, as the formation of the cranial base should allow for the formation of the numerous foramina for the transit of nerves and vessels in and out of the skull. The bones of the cranial base derive from cartilage and ossify by a process called endochondral ossification. The skull base consists of the sphenoid bones, the sella turcica (saddle shaped depression in the body of the sphenoid bone), the ethmoid bones, the nasal concha bones, and the nasal septum. The membranous neurocranium on the other hand forms the cranial vault or the calvaria. Mesenchyme surrounds the sides and the top of the brain. This subdivides into an inner and outer layer. The inner layer forms the pia and arachnoid coverings of the brain. The outer layer divides into the dura and the cranial bones of the skull. Ossification centers develop in the outer layer of the mesenchyme to form the individual calvarial bones. Sutures are areas of dense connective tissue that separate cranial bones from one another. They allow for the overlapping of neonatal cranial bones for head passage through the birth canal. Areas where sutures meet are called fontanelles in infants. There are six membrane-covered fontanelles including one anterior, one posterior, two sphenoid, and two mastoid fontanelles (Fig. 2.12). Sutures, fontanelles, and growth plates at the edges of the calvarial bones allow for skull growth resulting from expansive forces of the growing brain [15] (Fig. 2.13).

The posterior fontanelle usually closes around 3 months of postnatal life, whereas the anterior fontanelle remains open until about 18 months of age. Palpation of the anterior fontanelle is useful for detecting increased intracranial pressure or dehydration and is routinely performed by pediatricians during physical exams to check for premature closure. The fetal and newborn skulls are large in proportion to the rest of the body. Increase in calvarial size is greatest during the first 2 years of life, which coincides with the most rapid period of brain growth. The skull continues to increase in size until the mid-teenage years and then increases slightly in size for 3 or 4 more years due to thickening of the bones. Craniosynostosis results from the premature fusion of the calvarial sutures. The type and severity of skull deformity depend on which and how many sutures have closed prematurely [16, 17]. Craniosynostosis is covered in detail in Chaps. 38 and 40. Growth defects in the cranial base also lead to morphological deformities and mainly exorbitism

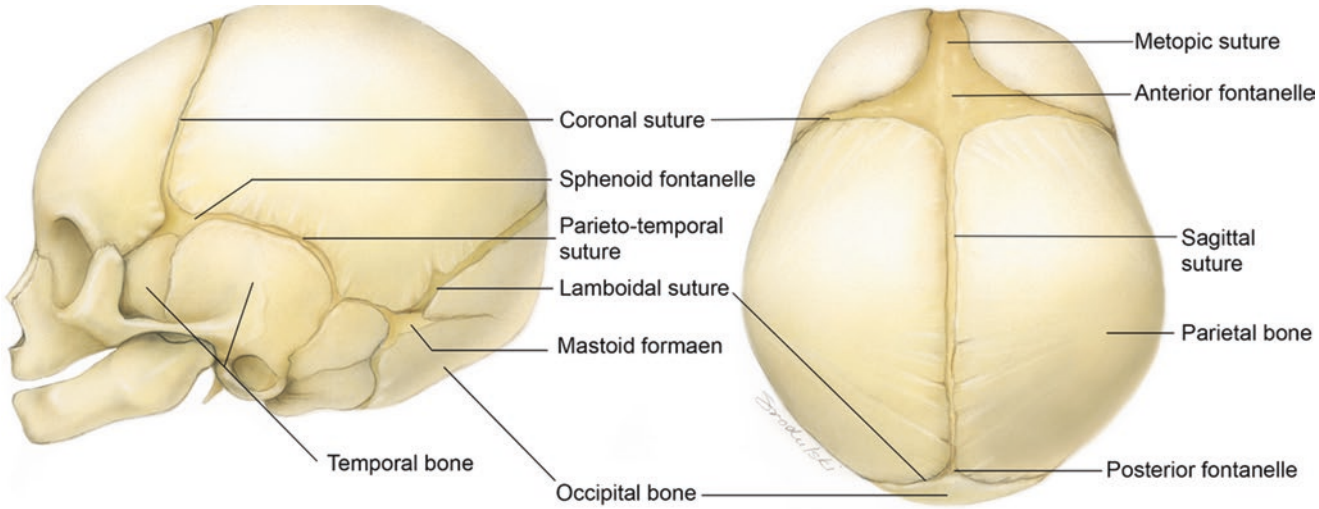


Fig. 2.12 Lateral (*left*) and superior (*right*) view of the skull fontanelles and sutures. Note the larger size of the anterior fontanelle as compared to the posterior

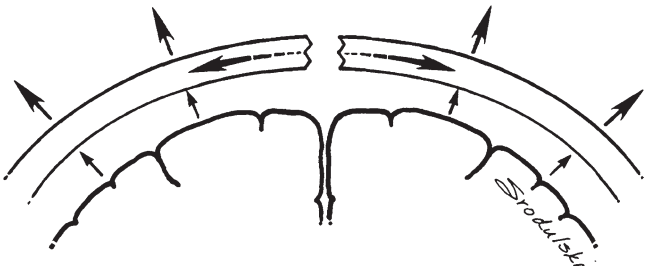


Fig. 2.13 Growth of the skull is a combination of factors: cellular proliferation in the suture areas, surface apposition and resorption, and the expanding forces from the growing brain

(shallow orbits), skull deformities, and midface hypoplasia [18]. Since the cranial base involves cartilaginous growth, disturbances in cartilage growth can also produce skull and facial abnormalities, such as in achondroplasia and Down syndrome.

The face is also relatively small when compared to the size of the skull in the newborn period. This is due to the small size of the mandibular and midface areas and the underdevelopment of the paranasal sinuses. There is rapid growth of the face and jaw with the eruption of the primary teeth during early childhood and again at the time of the secondary teeth eruption. In addition, growth and aeration of the sinuses contribute greatly to the maturation of the facial area (Fig. 2.14). The maxillary sinuses are the largest sinuses in the adult human face, and their pneumatization leads to growth of the midface area. The ethmoidal sinuses are located in between the orbits, and their pneumatization leads to an increase in the intercanthal distance.

Eyelid and Orbital Development

Eyelid formation is closely related to the development of the eye. The eyes begin their development as swellings called the optic placodes on the sides of the embryo's forebrain early in the fourth week of gestational age (Fig. 2.15a). Optic placodes later give rise to the optic vesicles, which project from the sides of the forebrain. The optic vesicles' surface layer then invaginates to form the optic cups. As the optic cup begins its indentation, the overlying ectoderm thickens and forms the lens placode. The surrounding edges of the optic cup continue to migrate forward, and the lens placode is pinched off internally and migrates to become the ocular lens (Fig. 2.15b, c). The ectoderm overlying the optic cup later becomes the cornea. During the sixth week, small folds of surface ectoderm appear cranial and caudal to the developing cornea, with a mesenchymal core (Fig. 2.16). These two folds give rise to the upper and lower eyelids. They continue to grow toward each other, until they meet and fuse together between weeks 8 and 10. They remain fused until the fifth to seventh month, at which time they separate again (Fig. 2.17). During this period, muscle cells originating from the mesenchyme begin to form the circular orbicularis muscle around the palpebral fissure.

Cryptophthalmos is a rare congenital condition caused by anomalous eyelid development. It usually occurs in association with systemic malformations, in which case the condition is referred to as Fraser syndrome. In this condition, the eyelid folds do not develop or fail to separate; the surface of the globe is covered by epithelial tissue fused to the surface, leading to underdevelopment of the cornea and microphthalmia [19, 20]. Cryptophthalmos can be partial or complete, where no eyelids can be identified.

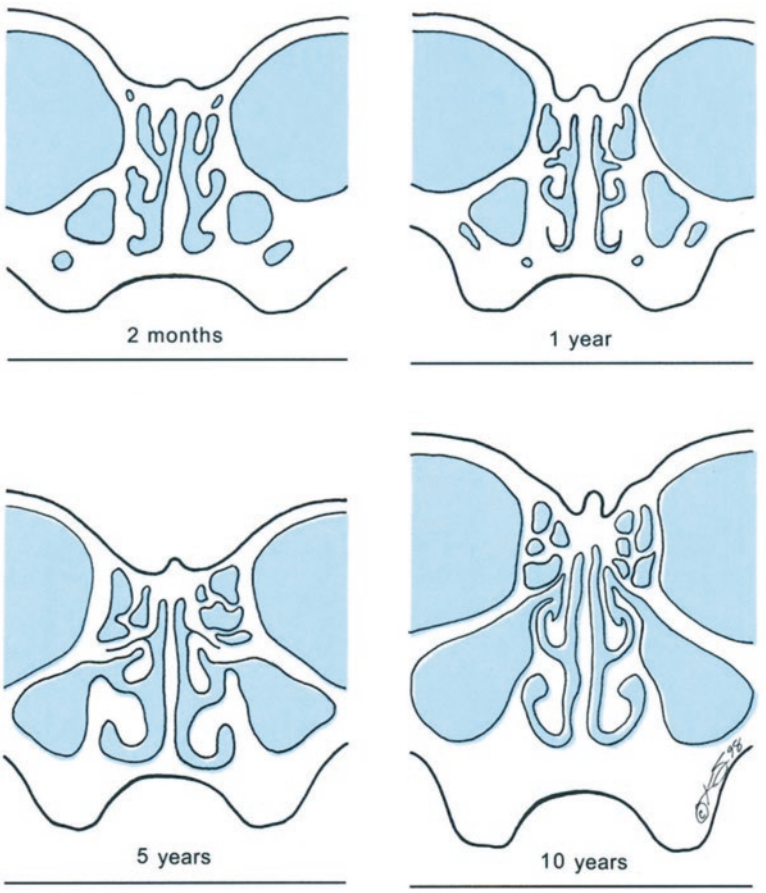


Fig. 2.14 Sinus development and aeration. Coronal view depicting ethmoidal and maxillary sinus development at 2 months (*top left*), 1 year (*top right*), 5 years (*bottom left*), and 10 years of age (*bottom right*)

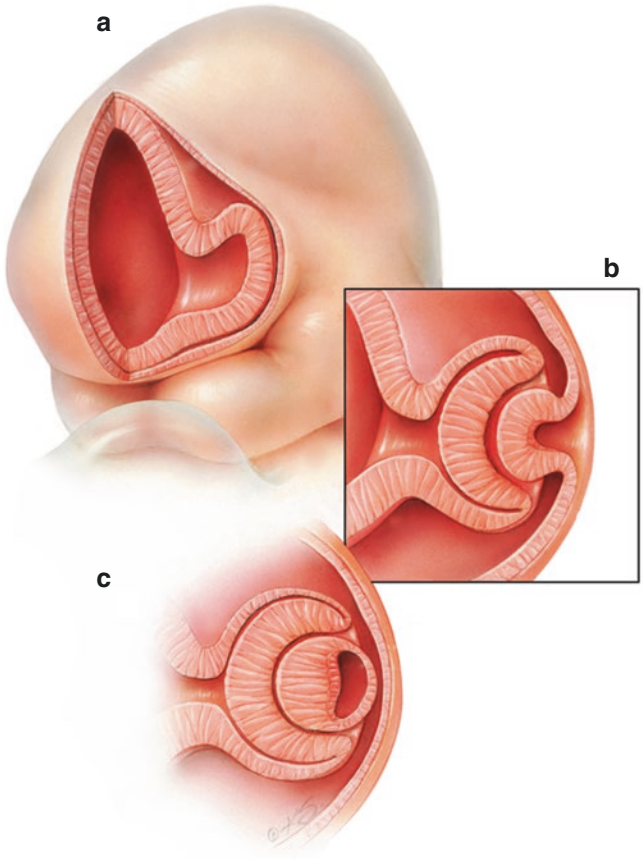


Fig. 2.15 Embryo week 4: optic vesicle formation. (**a**) As seen through a cutout diagram, the optic vesicle forms from an evagination from the prosencephalon. (**b**, **c**) The optic vesicle invaginates to form a bilayered optic cup. The surface ectoderm invaginates into the optic cup and separates from the surface, forming the lens placode

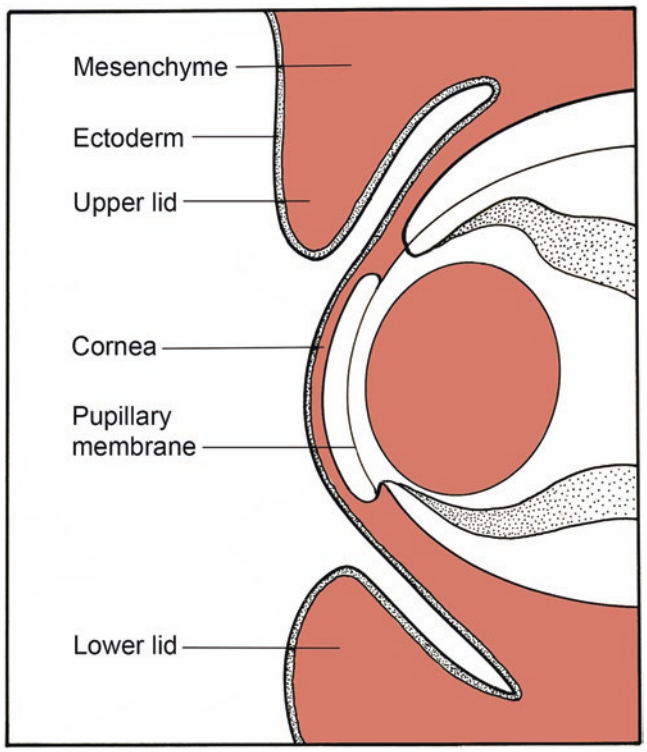


Fig. 2.16 Embryo week 6 – eyelid formation. The upper and lower eyelids form from folds of surface ectoderm with a core of mesenchymal tissue

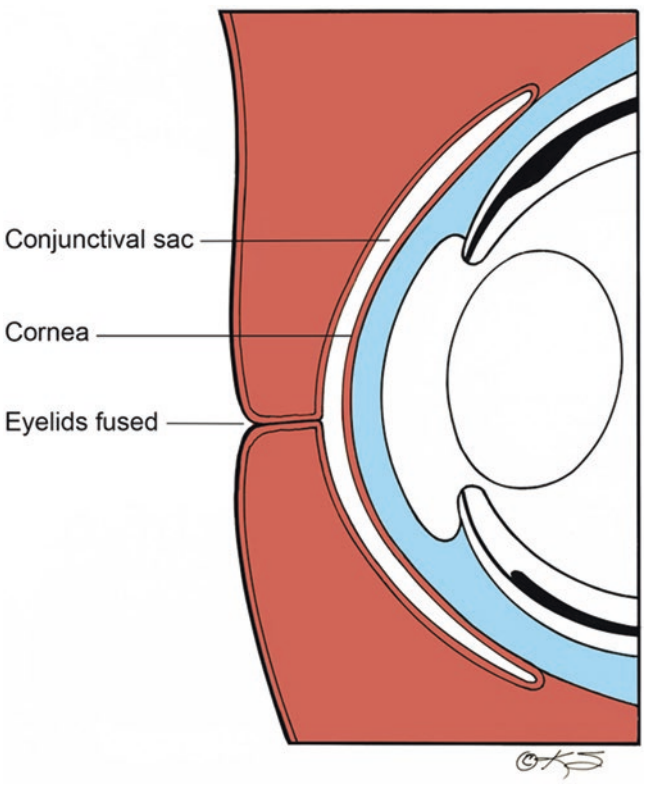


Fig. 2.17 Embryo weeks 8–10: eyelid fusion. The eyelids meet and fuse together. While the eyelids are fused, a closed conjunctival sac exists. The eyelids separate later during the second trimester

Normal orbital development is dependent on a complex array of factors that includes normal eye development. The orbital development is influenced by the formation and normal evolution of the optic cup, and the limits of the orbital walls are determined by the optic cup. Neural crest cells migrate to surround the optic cup and ultimately give rise to the bony orbital walls. As mentioned earlier, the skull base development also has an influence on the orbital shape and size, as the sphenoid and ethmoid bones contribute to the orbital walls. The maxillary process contributes to the floor and the lateral wall. During the third month, the orbital bones become differentiated. As the face and cranium of the embryo develop, the angle between the two orbital axes as seen on an axial view begins to decrease. The orbital angle starts at 180°, reduces to 105° at 3 months GA, and is 71° around birth. It will decrease slightly more after birth until reaching the adult angle of about 68° (Fig. 2.18) [21].

During early childhood, orbital volume increases in a linear fashion, achieving 77% of its final adult volume at around 5 years of age. There is a total increase in the size of orbital volume by a factor of 1.7–1.8 by age 15. However, the total growth of the maxillary and mandibular area overcomes that of the orbital area; hence, the eyes take up more surface area in the infant's face as compared to that of the adult [22].

Anatomy

Orbital Bones and Fissures

The human orbit is cone shaped, with its narrow apex situated posteriorly and wider opening formed by the orbital rims situated anteriorly. There are no distinct sharp demarcations between the walls of the orbit because of variations in bony curvatures among individuals. However for practcial purposes, the bony orbit is clinically and anatomically subdivided into four walls: medial, lateral, floor, and roof. The periosteal lining of the orbit is loosely adherent to the bone and can easily be dissected off surgically, except at certain areas where it becomes tightly adherent such as bony sutures, fissures, canals, the trochlear fossa, and the optic nerve canal where it fuses with the dura of the brain. The term periorbital soft tissue refers to any soft tissue adjacent to or surrounding the orbit.

Four bones contribute to the medial orbital wall (Fig. 2.19): the frontal process of the maxilla, the lacrimal bone, the ethmoidal bone, and the lesser wing of the sphenoidal bone, listed from anterior to posterior. The lacrimal sac is situated in a deep groove in the lacrimal bone delineated anteriorly by the anterior lacrimal crest (an extension of the maxillary process) and posteriorly by the posterior lacrimal crest (part of the lacrimal bone). Posterior to the lacrimal bone is the ethmoid bone, a paper-thin bony layer overlying the ethmoidal air cells, also referred to as the lamina papyracea. The anterior and posterior ethmoidal foramina are important anatomic landmarks.

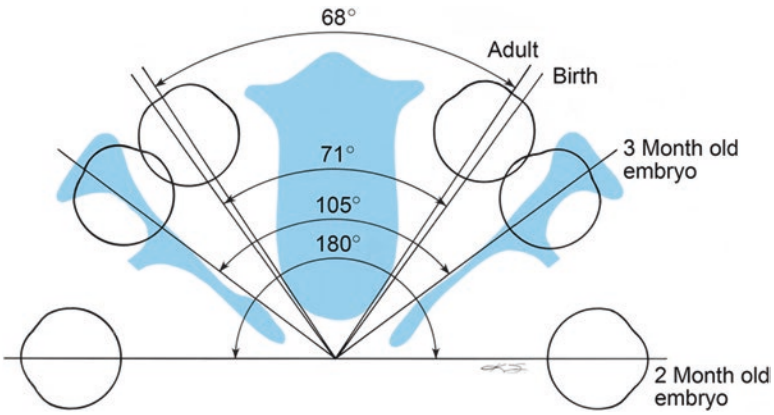


Fig. 2.18 Axial view drawing depicting the change in orbital position and convergence with increasing age

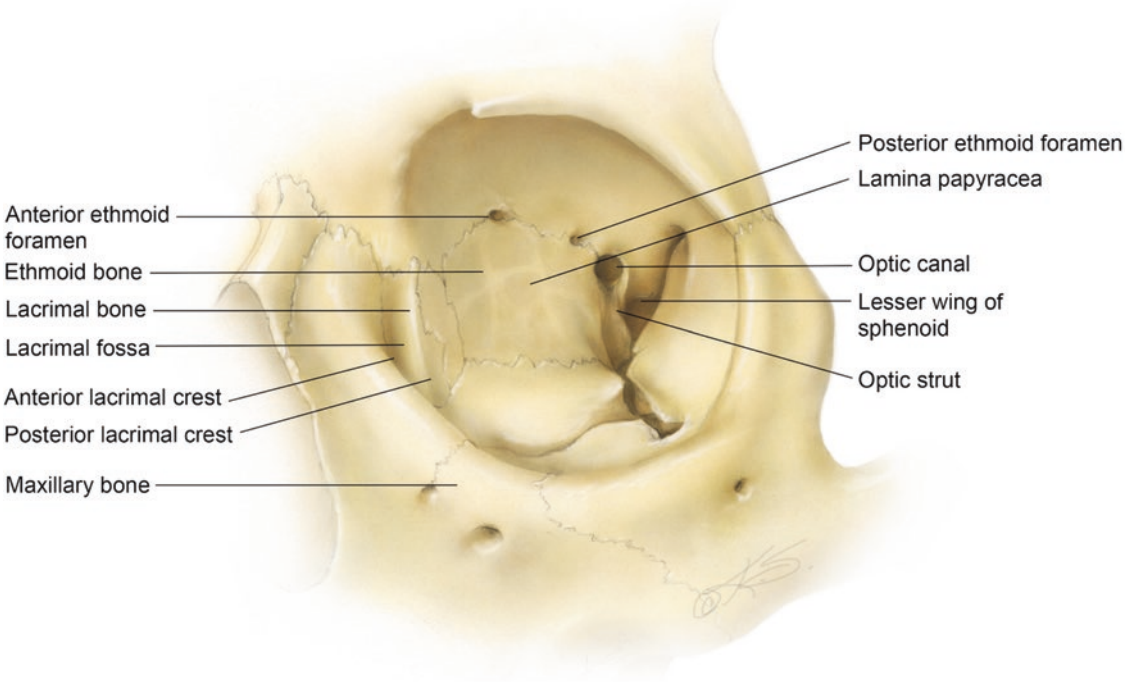


Fig. 2.19 Medial orbital wall

The anterior and posterior ethmoidal arteries, which are branches of the ophthalmic artery, and the nasociliary nerve, enter the orbit through these foramina. They are located at the frontoethmoidal suture approximately 20 and 35 mm respectively, posterior from the anterior lacrimal crest. These foramina are believed to be the culprit in orbital cellulitis in children via hematogenous spread. The cribriform plate (horizontal plate) is located just above the frontoethmoidal suture. A fracture of the cribriform plate can result in cerebrospinal fluid leak into the nose and anosmia, or loss of the sense of smell.

The ethmoidal-maxillary suture delineates the inferior border of the medial orbital wall and beginning of the orbital floor medially (Fig. 2.20). The orbital plate of the maxilla contributes to the majority of the orbital floor. Two other bones that contribute to the floor are the zygomatic bone and the minute orbital process of the palatine bone. The thinnest portion of the orbital floor is the posteromedial portion, which is also the roof of the maxillary sinus, where blowout fractures can result in inferior rectus muscle entrapment. The infraorbital fissure delineates the orbital floor laterally. The infraorbital groove is located medial to the infraorbital fissure and near the middle posterior surface of the orbital floor. The infraorbital canal is a continuation of the infraorbital groove as it dives into the middle of the orbital floor and serves as a conduit to the infraorbital neurovascular bundle. The infraorbital neurovascular bundle exits the canal at the infraorbital foramen along the medial side of the inferior orbital rim. Injury to the infraorbital nerve is often associated with orbital floor fractures or repairs, leading to hypoesthesia of the ipsilateral superior cheek area.

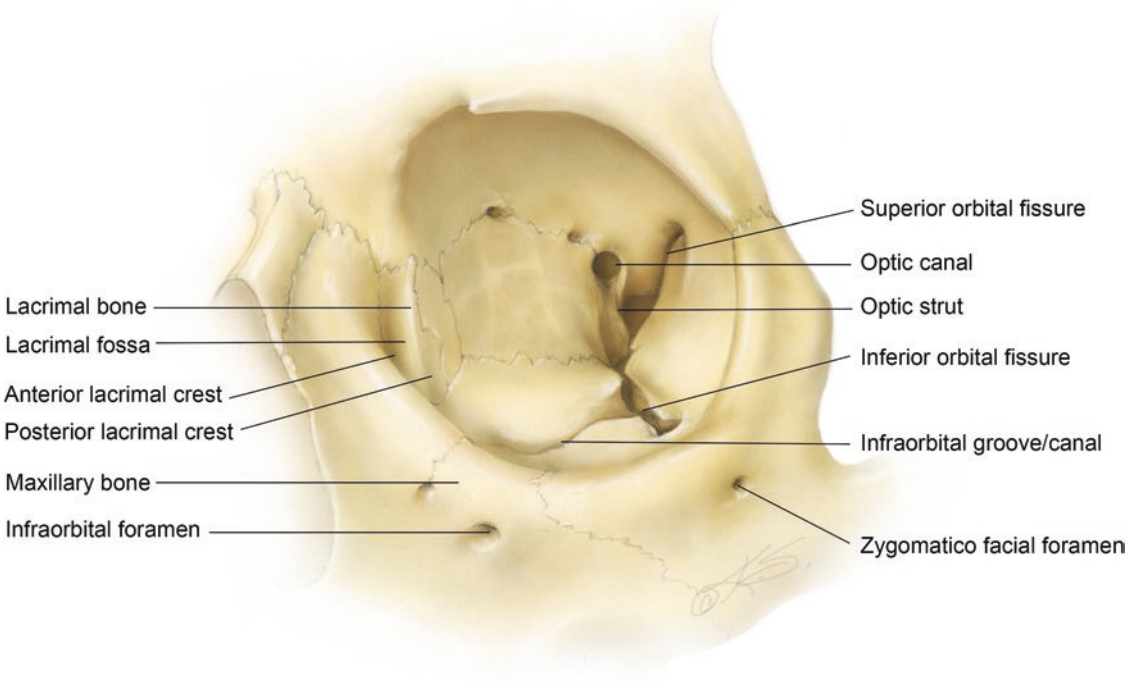


Fig. 2.20 Orbital floor

Table 2.1 Major neurovascular structures that enter/exit the orbital apex through the optic canal, the superior orbital fissure (SOF), and the inferior orbital fissure (IOF)

Optic canal	SOF	IOF
Optic nerve	Cranial nerves CN III, IV, and VI	Infraorbital nerve
Ophthalmic artery	Lacrimal nerve	Zygomatic nerve
Ophthalmic vein	Frontal nerve	Parasympathetics to lacrimal gland
	Nasociliary nerve	Infraorbital artery
	Orbital branch of middle meningeal artery	Infraorbital vein
	Recurrent branch of lacrimal artery	Inferior ophthalmic vein branch to pterygoid plexus
	Superior orbital vein	
	Superior ophthalmic vein	

The lateral wall consists of the zygoma anteriorly and the greater wing of the sphenoid posteriorly. The superior and inferior orbital fissures demarcate the superior and inferior borders of the lateral orbital wall. They serve as a conduit for major neurovascular structures in and out of the orbit. The major nerves and vessels enter the orbit through three openings: the superior orbital fissure (SOF), the inferior orbital fissure (IOF), and the optic canal (Table 2.1). The lateral orbital wall is the thickest, making it the most resilient, which is relevant since it is the most exposed and at risk for injury. The lateral orbital tubercle is a small prominence on the orbital side of the zygoma about 3–4 mm posterior from the lateral orbital rim. It serves as an anchor for the attachments of the lateral canthal tendon, levator aponeurosis fascia, superior transverse ligament, and inferior suspensory ligament (Fig. 2.21).

The frontal bone is the main contributor to the orbital roof, with a small posterior contribution from the lesser wing of the sphenoid near the apex. Superior to the roof is the frontal sinus anteriorly and the anterior cranial fossa posteriorly. In the medial aspect of the orbital roof lies the supratrochlear notch anteriorly (a small groove) 5 mm inside of the orbital rim. The supratrochlear notch houses the trochlea, a cartilaginous ring that serves as a pulley for the superior oblique muscle as it passes through it. The trochlea is the only cartilaginous structure found within the orbit. Lateral to the supratrochlear notch is the supraorbital notch. It is closed in 25% of individuals to form the supraorbital foramen, which transmits the supraorbital nerve and vessels. Laterally in the orbital roof lies the lacrimal gland fossa, a small depression in the frontal bone that houses the orbital portion of the lacrimal gland (Fig. 2.22).

Fig. 2.21 Lateral orbital wall

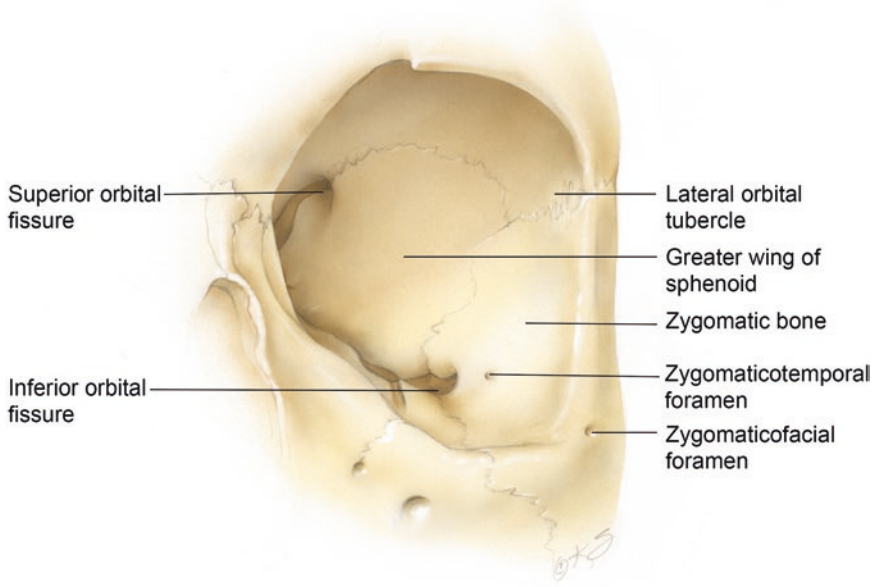
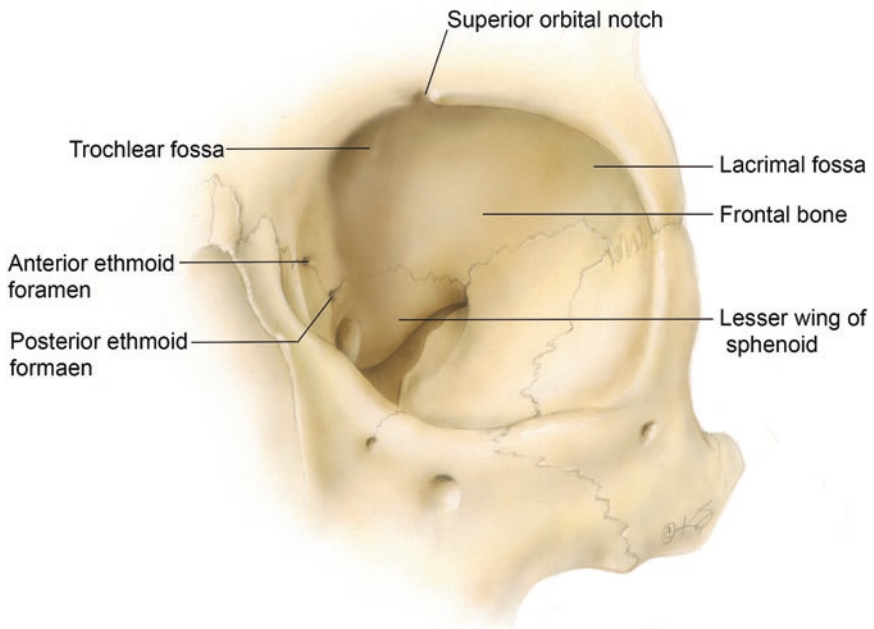


Fig. 2.22 Orbital roof



Anatomy of the Eyelids and Adnexa

The anatomy of the eyelids, adnexa, and periorbital soft tissues is quite complex. Despite representing a small surface area of the face, the periorbital/adnexal area is elegantly designed to provide both a functional purpose and protection to the visual system. The following section covers some of the most pertinent anatomical points but is not meant, however, to provide a comprehensive anatomical review [23–28].

Surface Anatomy

The eyelid structures allow for both protection of the eye and distribution of the tear film over the ocular surface. In the wakeful state, the upper lid rests just below the superior limbus and the lower lid at the inferior limbus. The highest point of curvature of the upper lid margin is situated just nasal to the pupil. The lowest point of the lower lid is just temporal to the lateral limbus. The upper lid crease is commonly present at the superior border of the tarsus and results from the

attachment of levator aponeurosis fibers to the skin. In the Asian eyelid, however, the crease is often much lower and related to an epicanthal tarsalis fold. The lid crease can be absent in congenital ptosis due to abnormal levator muscle development and attachments. It can also be abnormally elevated in conditions where a dehiscence of the aponeurosis has occurred as seen with involutional ptosis or trauma from a forceps delivery. The area between the upper lid crease and the superior orbital rim represents the superior sulcus. The lateral canthus is usually at an equal level or slightly higher than the medial canthus (Fig. 2.23) [29, 30]. An extra fold of upper lid tissue may be present in the medial canthal area and often obscures a portion of the medial canthus. This is referred to as an epicanthal fold and be classified into one of four types: supraciliaris, tarsalis, palpebris, and inversus (Fig. 2.24). Epicanthal folds may be a normal variant of eyelid anatomy, but may also associated with certain syndromes such as trisomy 21. When an epicanthal fold arises from the lower lid skin or crease instead, the condition is referred to as epicanthus inversus and is pathognomonic for the blepharophimosis-ptosis-epicanthus inversus syndrome (BPES).

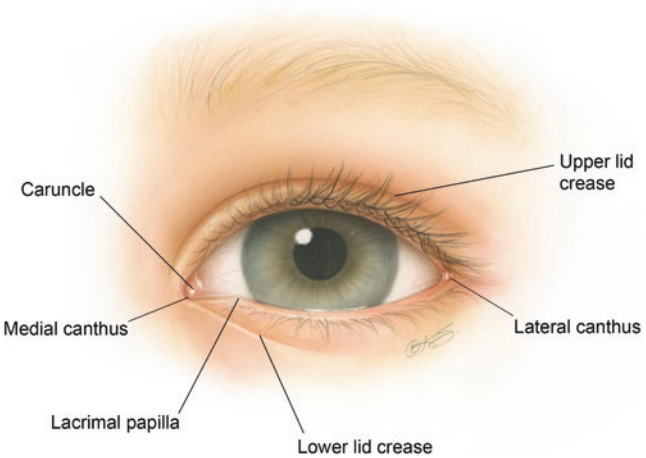


Fig. 2.23 Surface eyelid anatomy



Fig. 2.24 Types of epicanthal folds. (**a**) Supraciliaris, (**b**) tarsalis, (**c**) palpebris, and (**d**) inversus

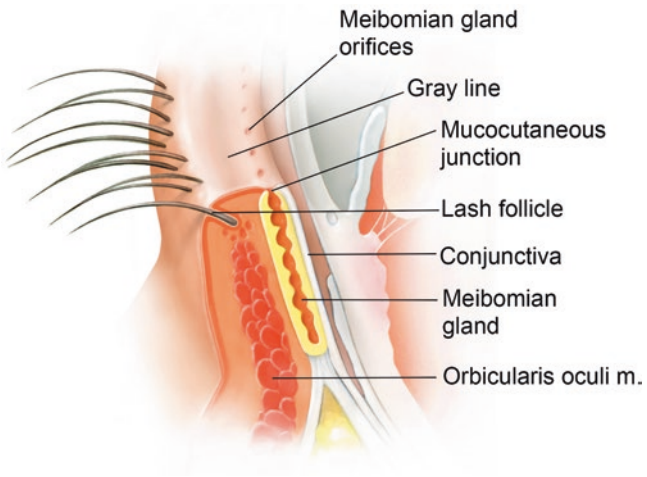


Fig. 2.25 Lower lid margin cross-section anatomy

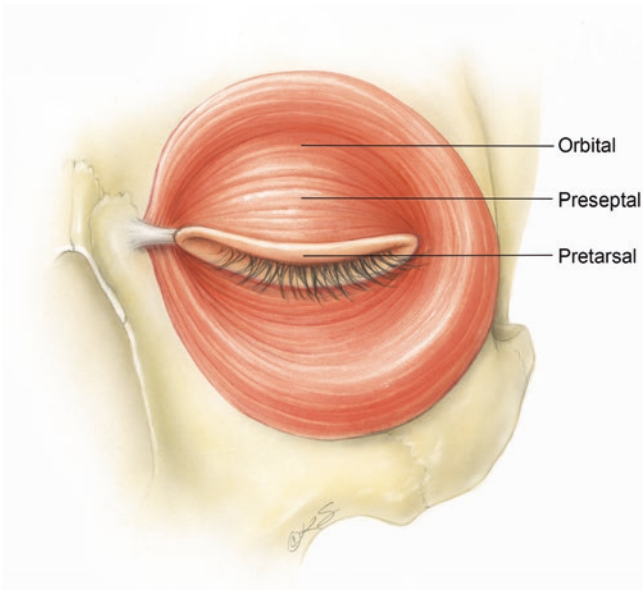


Fig. 2.26 Orbicularis oculi muscle

The Eyelid and the Eyelid Margin

The eyelid skin is the thinnest in the human body. The transition to thick skin that occurs around the orbital rim is abrupt. Four layers make up the eyelid from anterior to posterior lamella: (1) thin skin with sparse subcutaneous tissue; (2) the orbicularis oculi muscle, which is firmly adherent to the underlying layer; (3) a dense fibrous tarsus; and (4) the innermost layer, the conjunctiva, which is also tightly adherent to the tarsus [31]. A full-thickness laceration in the eyelid at the tarsal level typically involves some or all four layers mentioned above, depending on its depth, and may or may not be associated with a ruptured globe. A laceration above the upper eyelid tarsus on the other hand, as demarcated by the upper lid crease, may enter the orbit if the orbital septum is compromised. The layers from anterior to posterior at 10 mm above the upper lid crease are (1) the skin, (2) preseptal orbicularis muscle, (3) orbital septum, (4) orbital fat, (5) levator aponeurosis, and (6) Müller's muscle. On occasion, with a deep laceration, the superior rectus can also be affected.

The eyelid margin refers to the edge of the eyelid and includes from anterior to posterior: the lash line, the gray line, and the openings of the Meibomian glands (Fig. 2.25). The gray line is used to define anterior and posterior lamellae of the eyelid. The eyelid margin is frequently involved in eyelid lacerations. It can also be involved with certain skin tumors. For this reason, a thorough understanding of eyelid anatomy is crucial for proper surgical management. Proper re-approximation of the eyelid margin in lacerations and wedge resections for skin tumors is crucial to prevent postoperative eyelid notching or scarring.

Orbicularis Oculi Muscle

The orbicularis oculi muscle is anatomically divided into three sections representing the underlying structures beneath it: pretarsal, preseptal, and orbital (Fig. 2.26). Its primary function is closure of the eyelids, with its palpebral portion responsible for the involuntary blinking function and its orbital portion responsible for the forceful voluntary closure of the eyelids [32]. The orbicularis oculi also plays important roles in both the lateral and medial canthal areas where it attaches to the orbital bones via tendons. In the lateral canthal area, the pretarsal muscle attaches to Whitnall's tubercle; this helps keep the lower eyelid tautly apposed to the globe. This attachment may become more lax with aging thereby contributing to horizontal lower lid laxity observed in involutional lower lid ectropion.

In the medial canthal area, the muscle tapers alongside of the medial canthal tendon or medial palpebral ligament, which is about 4 mm in length and 2 mm in width to attach to the orbital rim. Its anterior portion attaches to the anterior lacrimal crest (frontal process of the maxilla). The posterior portion of the medial pretarsal muscle and tendon travels posterior to the lacrimal sac and inserts onto the posterior lacrimal fascia and then onto the posterior lacrimal crest. It is sometimes referred to as Horner's muscle or Tensor tarsi. The lacrimal fascia provides a strong aponeurotic lamina that expands around the lacrimal sac. This arrangement of the different portions of the muscle inserting on the lacrimal fascia and the anterior and posterior lacrimal crests forms the lacrimal pump mechanism (Fig. 2.27) (see Chap. 26). With increased laxity of the orbicularis muscle or loss of tone such as in facial palsy, the lacrimal pumping mechanism is compromised and may result in epiphora.

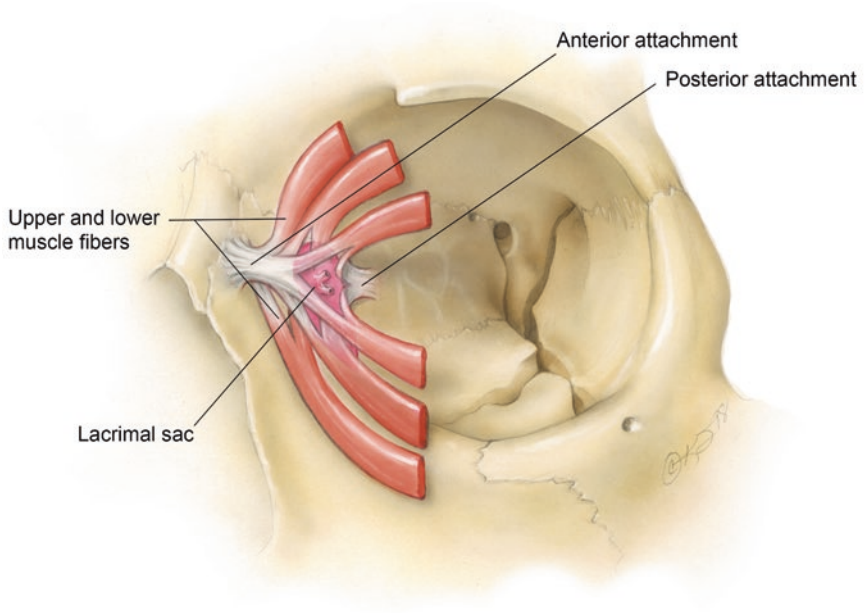


Fig. 2.27 Medial canthal tendon insertions permitting a lacrimal pump effect with opening and closing the eyelids

Tarsus and Canthal Tendons

The tarsus consists of dense fibrous tissue and not cartilage. It provides structural integrity and stability to the eyelids. The tarsus measures about 10 mm in vertical height in the upper eyelid and roughly half that size at 4–5 mm in the lower eyelid. Medially and laterally the tarsus is attached to the orbital rims via canthal tendons, firmly holding the eyelids to the orbital rims maintaining the lids in the proper taut position against the globe. The tarsal-medial canthal tendon attachment to the lacrimal crest and fascia of the lacrimal sac parallels the attachments of the orbicularis muscle, as previously described, and thus contributes to the lacrimal pump function (Fig. 2.27). Negative pressure is created within the lacrimal sac with opening and closing of the eyelids, and this helps pull the tears into the canaliculi from the ocular surface [33] (see also Chap. 26). The lateral canthal tendon attaches the lateral border of the tarsus and orbicularis muscle to Whitnall's tubercle within the lateral orbital rim (Fig. 2.28).

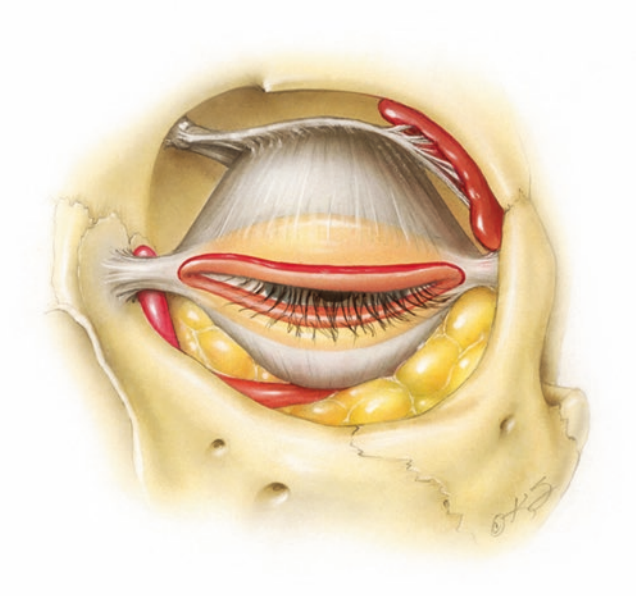


Fig. 2.28 Eyelid anatomy with fat pads removed demonstrating the fascial and tendon attachments

Conjunctiva and Accessory Lacrimal Glands

The conjunctiva consists of nonkeratinized epithelial tissue that lines the surface of the eye (referred to as bulbar conjunctiva) and inner aspect of the eyelids (referred to as palpebral conjunctiva). The palpebral conjunctiva is very firmly attached to underlying tarsus as opposed to bulbar conjunctiva that can be freely moved or separated from the underlying sclera. The bulbar and palpebral conjunctival surfaces meet in the upper and lower eyelid sulci, referred to as upper and lower fornix. The conjunctiva contains several of the accessory lacrimal glands, considered ectopic portions of the lacrimal gland tissue (Fig. 2.29) [34]. All of these glands produce tears of the same composition onto the conjunctival surface. Krause glands are located in the upper and lower fornices, with about 40 glands in the upper fornix and 6–8 in the lower fornix. The main lacrimal gland ducts open in the superotemporal upper conjunctival cul-de-sac. The glands of Wolfring are small accessory glands located in the midtarsal conjunctiva. The glands of Henle, on the other hand, are not true glands, but mere invaginations of epithelial conjunctival tissue near the marginal tarsal area (Fig. 2.29). Adequate conjunctival tissue

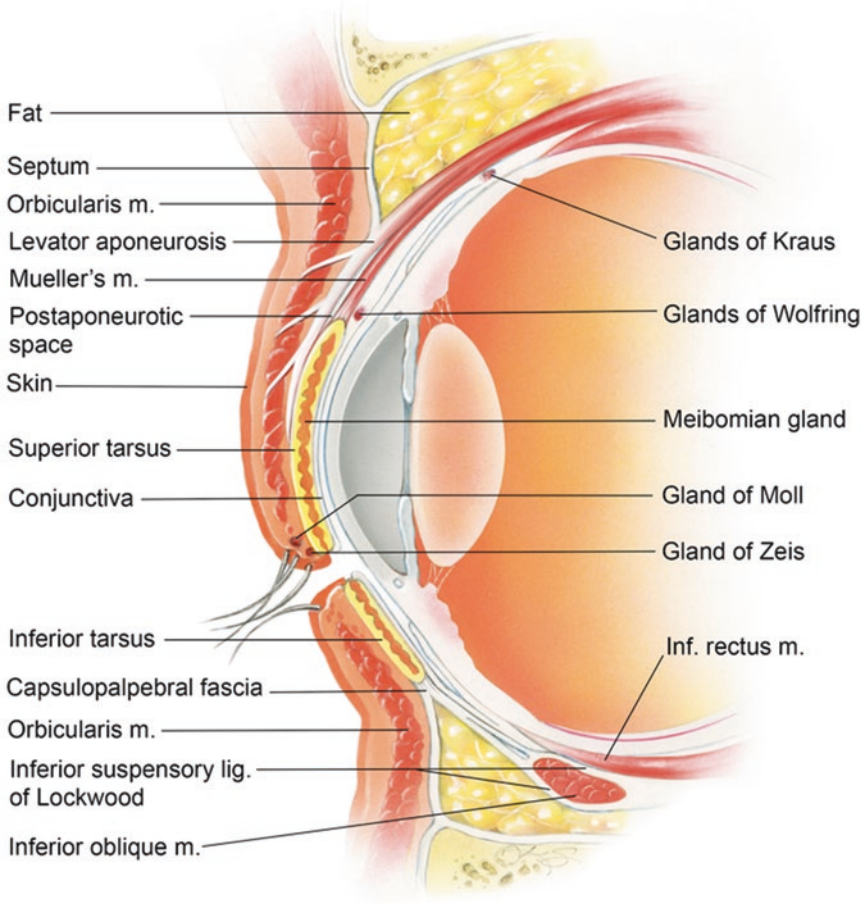


Fig. 2.29 Cross-section of lids and conjunctiva with accessory lacrimal glands

is essential for the health and function of the eye and socket. Conjunctival inflammation and scarring may occur in HSV infections or following strabismus surgery and may lead to adhesions between conjunctival tissue and eyelid skin, a condition referred to as symblepharon. Loss of conjunctival tissue or its elasticity can lead to restrictive strabismus or an entropion with inward rotation of the lid margin and lashes.

Orbital Septum

The orbital septum is a membranous structure that delineates the anterior boundary of the orbit. It originates from the periosteum of the orbital rim where the outer and inner periosteal layers meet, forming the arcus marginalis of the orbital septum. In the Caucasian upper eyelid, the septum fuses with the levator aponeurosis and inserts onto the superior tarsal border approximately 10 mm above the upper lid margin. In the Asian eyelid, the septum inserts much lower on the aponeurosis, such that the orbital fat is displaced forward, often obscuring or obliterating the upper lid crease (Fig. 2.30). In the lower lid, the septum inserts directly on the inferior tarsus [35].

Orbital Fat

Orbital fat lies posterior to the orbital septum. It comprises anterior fat pads and posterior orbital intraconal fat that surrounds the optic nerve and extraocular muscles. This is most visible in the coronal plane, where the intermuscular septum (a membrane connecting all four recti muscles) forms a ring that divides orbital fat into the intraconal fat and the extraconal (anterior) fat pads. The anterior orbital fat pads lie immediately deep to the orbital septum. There are two anterior fat pads in the upper lid and three in the lower lid (Fig. 2.31). In the upper lid, the central preaponeurotic fat pad is the largest and is yellow in color, medial to it is the smaller medial fat pad and is lighter in color. Loss of anterior orbital fat can lead to the sunken eye appearance seen in trauma or aging. Intraconal orbital fat can also herniate into the subconjunctival superotemporal quadrant, and this is typically seen in elderly, obese men. This type of fat herniation should not be confused with lacrimal gland prolapse, which can also occur temporally. Differentiation of orbital fat from lacrimal gland tissue is crucial during any orbital fat repositioning/resection procedures. Orbital fat is softer and

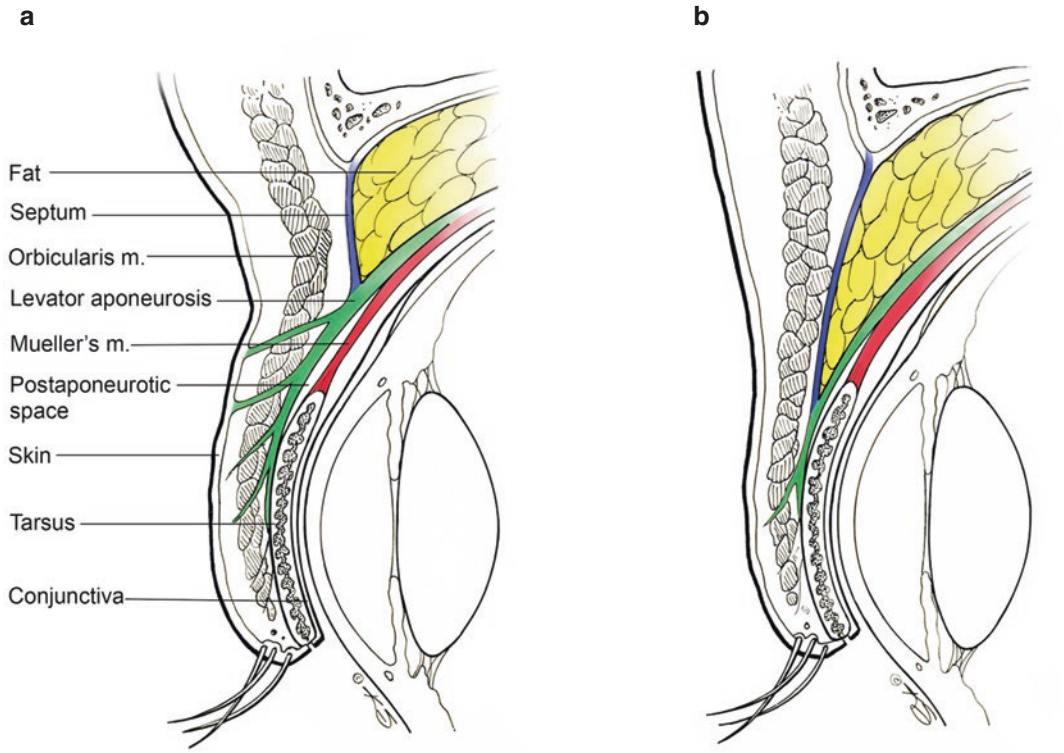


Fig. 2.30 Orbital septum. (**a**) Insertion in the Caucasian upper eyelid. (**b**) Insertion in the Asian upper eyelid

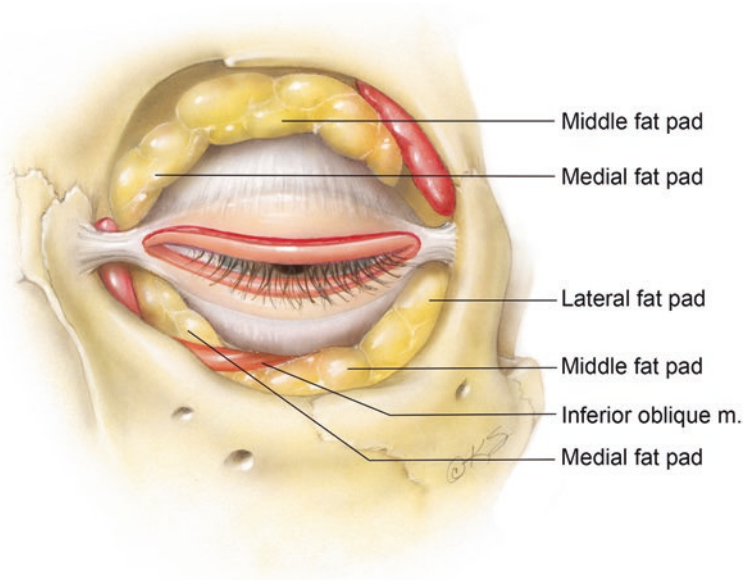


Fig. 2.31 Postseptal fat pads. Note: the lacrimal gland replaces an otherwise upper lateral fat pad, and the inferior oblique muscle separates the medial and central lower fat pads

more yellow in color as opposed to the rubbery consistency and more gray-pink color of the lacrimal gland.

In the lower eyelid, three fat pads are present: medial, central, and lateral. The inferior oblique muscle separates the medial and central lower fat pads. Fascia attachments from the inferior oblique muscle separate the central and medial pads (Fig. 2.31). The upper and lower medial fat pads also house terminal branches of the ophthalmic artery, and hence cautious manipulation of these structures is warranted during surgery.

Levator Palpebrae Superioris, Ligament of Whitnall, and Muller's Muscle

The levator palpebrae muscle is a skeletal muscle that serves to elevate and retract the upper eyelid. It arises from the lesser wing of the sphenoid above the optic foramen and annulus of Zinn and courses anteriorly just above the superior rectus muscle and below the roof of the orbit (see below, *extraocular muscles*). Upon reaching the inner aspect of the superior orbital rim, the levator muscle crosses the fibrous superior transverse ligament, also known as the ligament of Whitnall. This ligament primarily provides suspensory support to the upper eyelid and superior orbital tissues and additionally acts as a fulcrum for the levator muscle. Medially the ligament of Whitnall inserts onto connective tissue surrounding the trochlea, and laterally it forms septations through the orbital lobe of the lacrimal gland prior to inserting on the inner surface of the lateral orbital wall above the lateral orbital tubercle [36]. Upon traversing this ligament, the levator muscle changes in structure to become a fibrous aponeurotic sheath and changes direction from horizontal to vertical. The levator aponeurosis fans out at this point to become a broad sheet with a loose medial horn that inserts onto posterior lacrimal crest and a strong lateral horn that divides the lacrimal gland into orbital and palpebral lobes prior to inserting onto the lateral orbital tubercle. The horns are important in ptosis surgery, as their release can facilitate levator advancement or resection. The aponeurosis then divides into anterior and posterior portions prior to insertion. The anterior aponeurosis sends out fine strands to the pretarsal orbicularis muscle and skin. The most superior of these strands are responsible for formation of the upper lid crease, which is seen dynamically upon contraction of the levator muscle (Fig. 2.32). Folding of the upper lid skin occurs at the site of the uppermost attachments of the aponeurosis resulting in overhanging of the superiorly situated orbicularis and skin. The posterior aponeurosis inserts onto the lower half of the anterior surface of the tarsus. The levator muscle is innervated by the superior division of the oculomotor nerve (CN III). Dehiscence or disinsertion of the aponeurosis at this level, such as seen in trauma or senescence, results in ptosis (Fig. 2.32).

Arising from the underside of the levator muscle at the level of Whitnall's ligament is the muscle of Müller, also known as the superior tarsal muscle. It travels along the posterior surface of the levator aponeurosis and inserts onto the superior border of the tarsus (Fig. 2.32). This muscle provides an overall functional elevation of the upper eyelid up to 2 mm. Müller's muscle receives separate innervation from the sympathetic system; when its innervation is compromised such as in Horner's syndrome, mild ptosis may result.

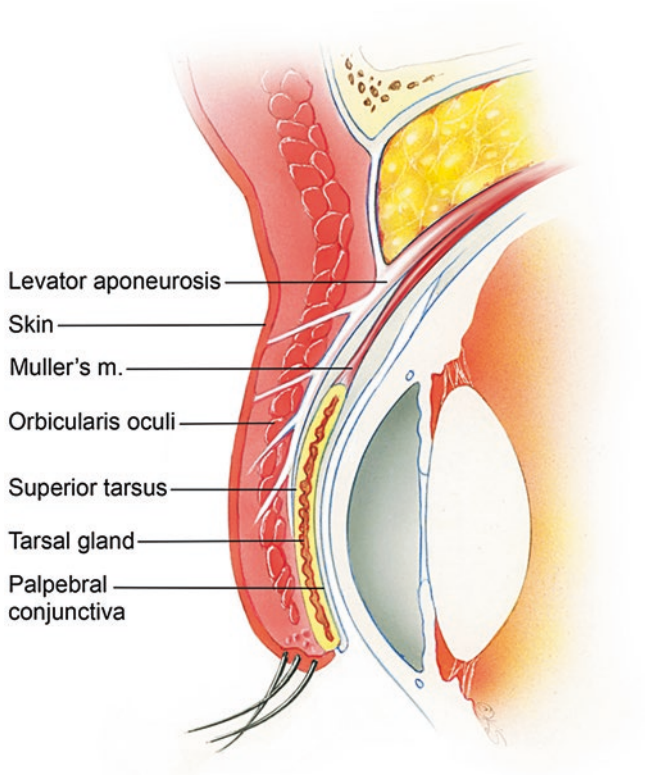


Fig. 2.32 Upper eyelid anatomy: Cross-section demonstrating the levator aponeurosis insertion on the lower one-third of the tarsus with filaments passing up through the orbicularis muscle to the skin. It also demonstrates the origin of Muller's superior tarsal muscle from the levator muscle as well as its insertion into the superior edge of the tarsus

Lower Lid Retractor Complex and Lockwood Ligament

The anatomy of the lower eyelid is similar to that of the upper eyelid; however it is much less complex. The vertical height of the lower tarsus is roughly half that of the upper tarsus and features about half the number of eyelashes and Meibomian glands (Figs. 2.25 and 2.29). The inferior orbital septum inserts directly onto the inferior tarsus.

The suspensory ligament of Lockwood serves as the main hammock suspending the eyeball. Arising from thickened Tenon's capsule, it inserts onto check ligaments medially and laterally and encloses the inferior rectus and inferior oblique muscles. It plays a role in lower eyelid retraction as it contributes to the anterior layer of the lower lid retractor complex.

From the inferior rectus muscle arises the capsulopalpebral fascia, the equivalent of the levator aponeurosis in the upper lid. Along with contribution from Lockwood ligament, this forms the anterior layer of the lower lid retractors and continues to insert onto the anterior lamella [37]. A posterior dense layer contains sympathetic smooth muscle, the inferior tarsal muscle, inserting onto the inferior tarsus. The latter constitutes the main contractile component of the lower

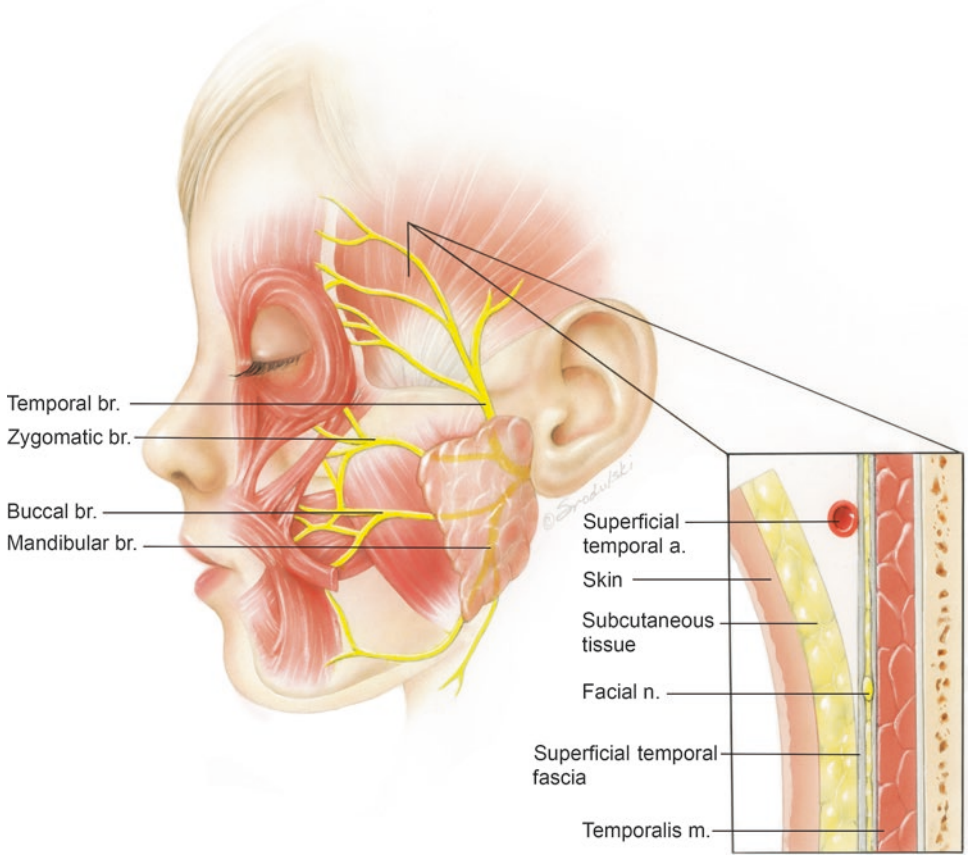


Fig. 2.33 Branches of the facial nerve. (*Inset*) Cross-section of anatomical plane

eyelid retractors. Together these structures comprise the lower lid retractor complex. The vertical movement of the lower lid is much less than that of the upper lid. Thus, while much of the anatomy and function of the lower lid are similar to that of the upper lid, it is much less pronounced.

The Facial Nerve and Musculature

The facial nerve (CN VII) supplies motor innervation for facial expression. The motor part of the nerve arises from the facial nucleus in the pons and then has an intracranial course running anteriorly in the posterior cranial fossa. It crosses the subarachnoid space to the internal auditory canal in the petrous temporal bone. It then runs a tortuous course in the facial canal within the temporal bone (labyrinthine, tympanic and mastoid segments) and exits the skull through the stylomastoid foramen [38, 39]. It travels only 0.5–1.5 cm extracranially before it enters the parotid gland. It is within the parotid gland that the different branches of the facial nerve arise. The branching pattern is complex and varies widely among individuals. Most commonly, the facial nerve divides into five main branches: temporal, zygomatic, buccal, marginal mandibular, and cervical. The temporal and zygomatic branches cross over the zygomatic arch approximately midway between the tragus and the lateral canthus. Superior to the arch, the nerve lies in the plane of the superficial temporalis fascia (Fig. 2.33). This is the same plane in which the superficial temporal artery travels. The temporal branch of the nerve provides motor innervation to the orbicularis oculi, frontalis, procerus, and corrugator muscles. The zygomatic branch also provides the orbicularis oculi muscle with additional innervation.

Nasolacrimal System

The lacrimal drainage system provides a conduit for the tears from the ocular surface into the nasal cavity. It comprises several components, and from proximal to distal, they are the puncta, the canaliculi (vertical and horizontal), the common canaliculus, the lacrimal sac, and the nasolacrimal duct (Fig. 2.34) [40]. The entire length of the drainage system from puncta to meatal opening of the nasolacrimal duct ranges from 25 mm in the newborn to about 35 mm in the adult.

Each eyelid, upper and lower, has a punctum in its medial tarsal aspect. It is a small opening, 0.3 mm in diameter that arises out of a raised lacrimal papilla. This circular opening

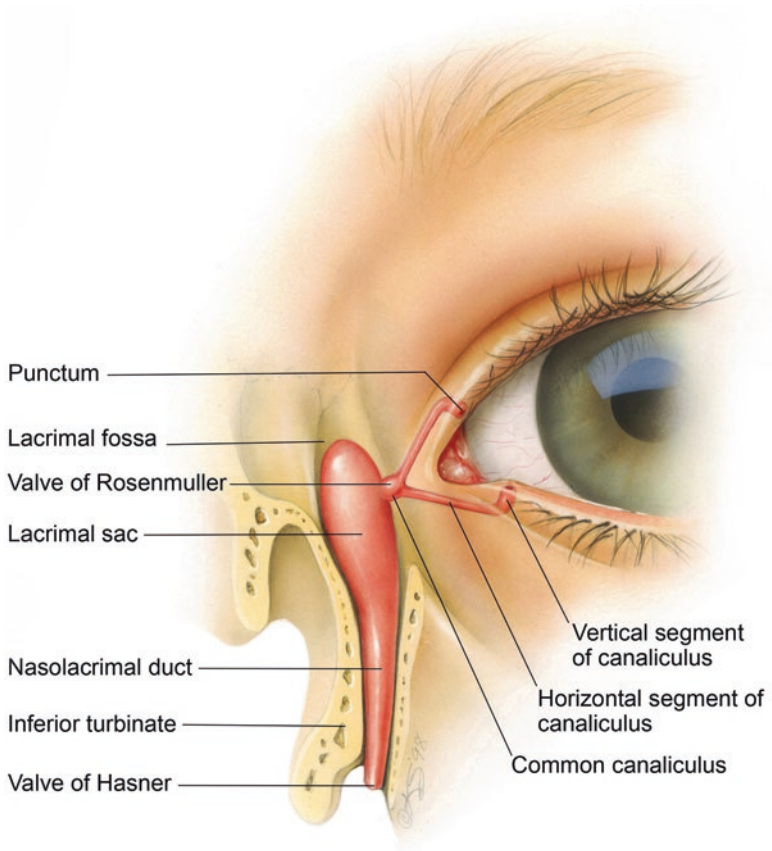


Fig. 2.34 Nasolacrimal drainage system

is made up of connective and elastic tissue that allows for easy dilation of the puncta during probing procedures. Each punctum is directed posteriorly against the surface of the globe and is best visualized by everting the eyelid. This is important for proper tear drainage, as a punctal ectropion may result in epiphora. Punctae are relatively avascular compared to the surrounding structures, and this allows for the relatively bloodless punctal snip procedures (see Chap. 29). The lacrimal punctae open into vertical canaliculi. The canaliculi are the smaller drainage canals of the lids; they course through the eyelids and open into the lacrimal sac. Each canaliculus consists of a short, vertical 2 mm segment and a more distal horizontal 8 mm segment. The upper and lower canaliculi usually join to form a common canaliculus (internal punctum) just prior to entering the lacrimal sac. The common canaliculus enters the sac on its lateral surface in a superior, posterior location. However, variations can occur as each of the upper and lower canaliculi may enter the sac individually.

The lacrimal sac lies in the lacrimal sac groove of the lacrimal bone in the medial wall of the orbit, between the anterior and posterior lacrimal crests. The lacrimal sac is roughly oval in shape with a fundus superiorly and a body inferiorly. It measures approximately 10–15 mm in length with 2–5 mm of its body length lying above the level of the medial canthal tendon and 10 mm below. The lacrimal sac is enclosed by lacrimal fascia emanating from the posterior lacrimal crest periosteum and receives attachments from the superficial and deep portions of the medial canthal tendon, as well as attachments from the orbicularis muscle. As mentioned earlier, blinking of the eyelids is responsible for the lacrimal pump mechanism, by inducing negative pressure within the lacrimal sac that helps suck up the tears from the ocular surface.

The lacrimal sac opens into the nasolacrimal duct. Both structures are composed of the same stratified columnar epithelium with mucus-secreting goblet cells and surrounding connective tissue. The lacrimal sac is surrounded by soft tissue structures laterally and the bony lacrimal fossa medially. The nasolacrimal duct is surrounded by the bone for about 12 mm of its length. Upon its entry into the inferior meatus of the nose, it may extend an additional 2–5 mm. The lacrimal sac and proximal portion of the nasolacrimal duct may be easily dissected off the bone; however, the distal segment of the nasolacrimal duct is tightly adherent to the adjacent bone. Nasolacrimal duct stenosis is commonly seen in craniofacial syndromes and typically results in reduced

outcomes following probing procedures. The duct opens into the inferior meatus under the inferior turbinate. The intranasal space is typically crowded in children, and the inferior turbinate may impinge on the opening of the duct. Inferior turbinate infracture is a procedure commonly performed by lacrimal surgeons to allow for less crowding of structures at the inferior meatus and the valve of Hasner, in an effort to improve tear drainage.

Several valves can be identified within the nasolacrimal system. These are typically located at points of entry into a different tissue type. The valve of Rosenmuller is located at the junction of the common canaliculus and the lacrimal sac. It consists of a fold of mucosal tissue that prevents tear reflux. The valve of Krause, located at the junction between lacrimal sac and duct, is formed by an indentation of the periosteum and orbicularis muscle. The distal portion of the nasolacrimal duct opens into the nasal cavity at the valve of Hasner. This valve consists of a mucosal fold and is commonly the cause of congenital nasolacrimal duct obstruction. It remains imperforate in about 70% of newborns, but usually opens in the first month of life. Spontaneous opening may still occur in the first 6–12 months of life.

Lacrimal Gland

The lacrimal gland lies in the lacrimal fossa on the inner aspect of the frontal bone and in the superior aspect of the lateral orbital wall [41]. It is responsible for secretion of the aqueous portion of the tear film, the oily portion being produced by the Meibomian glands. The gland can be grossly divided into two lobes by the levator aponeurosis prior to its attachment to the lateral orbital tubercle. The smaller palpebral lobe lies close to the lateral portion of the upper eyelid and conjunctiva and functions as a conduit for the tears to the ocular surface. The larger orbital lobe lies deeper within the orbit. It consists of many lobules that contain serous secreting acini. The lobules open into fine interlobular ducts that join to form 3–5 main excretory ducts. The excretory ducts then branch out to form 5–7 ducts in the palpebral portion and open into the superior, temporal fornix of the conjunctiva beneath the upper eyelid. The superior transverse ligament of Whitnall inserts into the lacrimal gland fascia, forming the lobular septations within the gland. The gland receives its neurovascular supply on its posterior surface, which can be damaged in an orbital dissection. Inflammation of the lacrimal gland, called dacryoadenitis, is commonly seen in autoimmune and infectious diseases, or as part of the idiopathic orbital inflammatory syndrome (IOIS). Lacrimal gland biopsy is warranted in these instances for proper diagnosis. Biopsy of the orbital portion is recommended, to avoid injury to the ducts of the palpebral portion, which may result in ocular dryness.

Orbital Fascia

The orbital fascia consists of an extensive network of connective tissue (Fig. 2.35). It can be divided into three main groups: the fascia covering the globe, the fascia surrounding the extraocular muscles, and the orbital fascial compartments. Tenon's

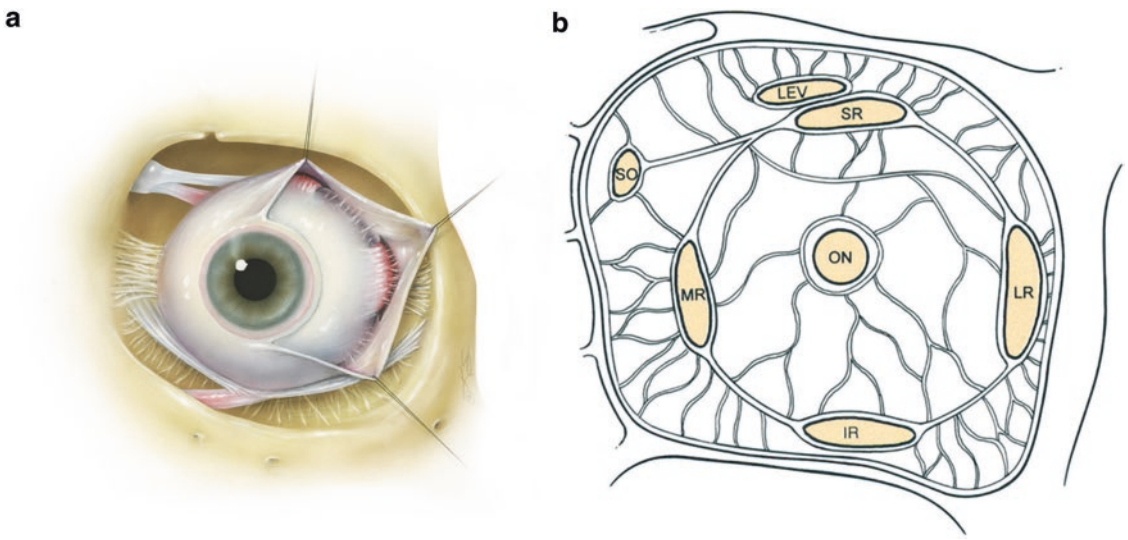


Fig. 2.35 (**a**) Anterior fascial connections within the orbit. (**b**) Posterior fascial connections within the orbit. Conjunctiva and Tenon's capsule reflected to demonstrate rectus muscle check ligaments and other anterior orbital fascial connections (medial check ligament, lateral check ligament, Lockwood's suspensory ligament) (Based on Koorneef [43]) A complicated fascial network surrounds and supports structures within the orbit including the extraocular muscles, peripheral nerves, blood vessels, optic nerve, and the globe. A ringlike structure, the intermuscular septa, also connects the rectus muscles. Fine septa divide the orbital space into compartments that attach to the periorbita over the orbital bony surface. Because of these fascial relationships, orbital wall fractures can result in diplopia even without actual muscle entrapment. (*ON* optic nerve, *SO* superior oblique, *MR* medial rectus, *LR* lateral rectus, *IR* inferior rectus, *SR* superior rectus, *LEV* levator muscle) (Based on Koorneef [44])

fascia is the fascia that covers the globe, beginning just posterior to the limbus and extending to the optic nerve. Each extraocular muscle is also encased in a fascial sheath. The fascia extends between each muscle and forms check ligaments that attach to the periorbita. Within the orbit, fine fascial septa divide the orbital soft tissue contents into various compartments. The fascia acts as a supporting structure and framework for the orbital contents including orbital fat, arteries, and veins as well as the extraocular muscles.

Extraocular Muscles

There are six extraocular muscles: four recti muscles and two oblique muscles. All the extraocular muscles originate from the orbital apex, with the exception of the inferior oblique (Fig. 2.36). The inferior oblique originates from the orbital floor on the lateral aspect of the posterior lacrimal crest. It courses beneath the inferior rectus muscle and inserts onto the posterior globe lateral to the macula. The four recti muscles arise from the annulus of Zinn. The annulus of Zinn is a fibrous ring in the apex of the orbit overlying the optic foramen and the central portion of the superior orbital fissure. It is attached to the dura posteriorly and to the greater and lesser wings of the sphenoid. Four structures pass though the annulus of Zinn (superior to inferior): superior division of the oculomotor nerve (CN III), the nasociliary nerve (branch of the ophthalmic nerve), inferior division of the oculomotor nerve (CN III), and the abducens nerve (CN VI). The recti muscles insert at varying distance from the limbus: with the medial rectus at about 5.5 mm, inferior rectus at 6.5 mm, lateral rectus at 7.0 mm, and superior rectus at 7.5 mm (this increasing distance of insertion is referred to as the spiral of Tillaux and may vary widely among individuals). The superior oblique muscle arises from the lesser wing of the sphenoid. It courses anteriorly along the medial orbit and passes through the trochlea, changes direction, and continues beneath the superior rectus muscle to insert on the globe (Fig. 2.36).

All the recti muscles course very close to their respective orbital walls. Fractures involving an orbital wall may lead to extraocular muscle entrapment. However, mere incarceration of fascial tissue surrounding the muscles may produce muscle restriction as well, mistaken for entrapment. Restriction of extraocular movement warrants radiological investigation and possible need for surgical intervention.

Nerves of the Orbit

The Optic Nerve

The optic nerve represents an extension of the central nervous system (Fig. 2.36). The nerve leaves the globe 3 mm nasal and 1 mm below the most posterior point of the globe. Its diameter measures about 3 mm at its exit from the globe. The intraorbital portion of the nerve measures 24 mm in length. About 6 mm of nerve is slack allowing the globe to rotate freely without undo tension on the nerve. The ophthalmic artery pierces the dura of the optic nerve 8–15 mm behind the globe on the inferonasal aspect of the nerve. The ciliary ganglion is located about 15 mm posterior to the globe on the temporal side of the nerve. The same layers surround brain tissue and optic nerve, and these are the pia, arachnoid, and dura, with additional Tenon's tissue covering the outermost

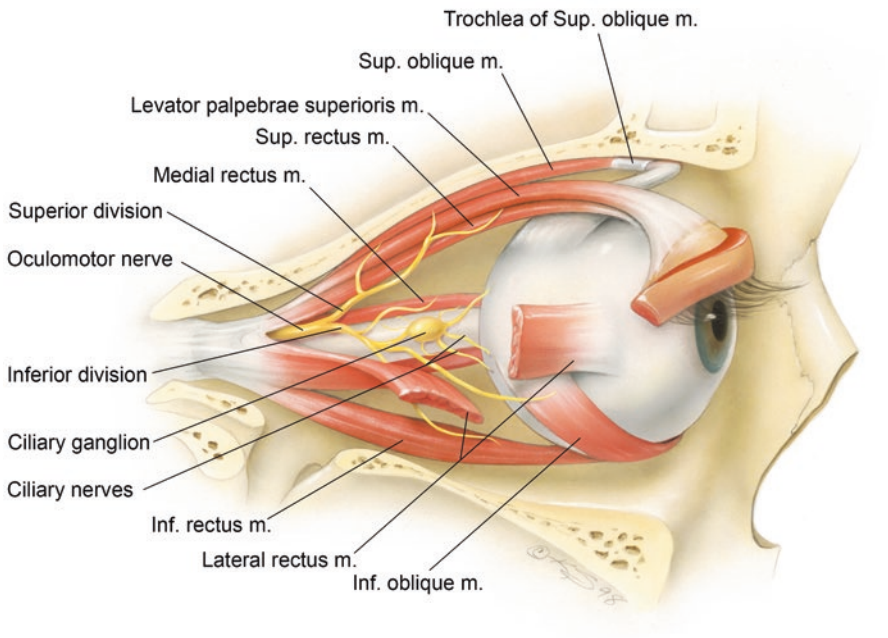


Fig. 2.36 Cross-sectional lateral view of the orbit. The superior, inferior, medial, and lateral recti arise from the annulus of Zinn. The superior oblique muscle arises immediately above and medial to the superior rectus muscle from the lesser wing of the sphenoid. The levator muscle arises from the lesser wing of the sphenoid above the annulus of Zinn and courses anteriorly just above the superior rectus

portion of the nerve. In the subarachnoid space, the cerebrospinal fluid (CSF) connects with ventricles and CSF of the central nervous system. The nerve enters the optic canal on the medial aspect of the orbit and travels 5–8 mm within the optic canal. This intracanalicular segment of the nerve adheres tightly to the surrounding bone. The optic nerve exits the optic canal and travels an additional 10 mm to enter the optic chiasm. Nerve fibers from the opposite optic nerve (representing the superolateral visual field) extend several millimeters anterior to the chiasm along the contralateral optic nerve; this is referred to as Von Willebrand's knee. Thus, in prophylactic resection of an optic nerve glioma, for example, several millimeters need to be spared anterior to the chiasm in order to avoid creating a visual field deficit in the other eye.

Other Nerves

In addition to the optic nerve, there are additional motor and sensory nerves coursing through the orbit. Table 2.1 summarizes additional nerves that enter and exit the orbital apex (see also Fig. 2.36). The ciliary ganglion is another important surgical landmark. It sits lateral to the optic nerve and is a way station for connecting sympathetic and parasympathetic fibers of the eye and orbit. The postganglionic short ciliary nerves provide innervation to the sphincter pupillae muscle (resposible for miosis) and the ciliaris muscle (resposible for accomodation) (Fig. 2.36).

The Ocular Globe and Vascular Supply

The eye is located in the anterior aspect of the orbit and occupies approximately one-fifth of the total orbital volume. It sits slightly closer to the lateral and superior walls than to the medial wall and floor. The globe is more exposed on its lateral aspect due to the recessed position of the lateral orbital rim. The mature ocular globe diameter measures on average 24 mm in its anteroposterior axis. The globe volume is about 6.5 ml and weighs about 7.5 g.

Arterial blood supply to the eye derives from the central retinal artery and anterior and posterior ciliary arteries, all of which arise from the ophthalmic artery. The ophthalmic artery is the first branch of the internal carotid artery and enters the orbit with the optic nerve through the optic canal. It travels with the optic nerve anteriorly and gives off the central retinal artery, in the most posterior part of the orbit which in turn pierces the dura of the optic nerve 8–15 mm posterior to the globe on the inferonasal aspect of the nerve and then runs in the central aspect of the nerve to supply the inner retinal layers. One to five posterior ciliary arteries branch off of the ophthalmic artery in the posterior part of the orbit, each giving a short and long posterior ciliary to a respective choroidal area in the posterior part of the globe. Superior and inferior muscular branches of the ophthalmic artery give rise to the anterior ciliary arteries which supply the extraocular muscles (two for each muscle and one for the lateral rectus). The anterior ciliary system provides vascular supply to the anterior segment of the eye; hence, no more than two extraocular muscles must be disinserted at a time during strabismus surgery so as not to precipitate anterior segment ischemia.

The venous drainage of the globe consists of the vortex veins, the anterior ciliary veins, and the posterior ciliary veins. The vortex system drains nearly all of the choroids and portions of the ciliary body and iris. About five to eight vortex veins are usually located in the oblique quadrants between the extraocular muscles. Their location ranges from 13.75 to 25 mm posterior to the limbus. However, the number and location can vary widely. The anterior ciliary system drains much of the anterior segment of the globe, including the aqueous humor, and part of the ciliary body. The posterior ciliary system drains a portion of the posterior sclera. The venous system is one of the routes for intraocular tumor metastasis.

The inferior ophthalmic vein receives branches from the inferior vortex veins and the pterygoid plexus upon exit through the inferior orbital fissure. It also enters the cavernous sinus.

Arterial Supply to the Eyelids and Orbit

The eyelids and orbit receive their arterial supply from both the external and internal carotid systems. The ophthalmic artery is the first branch of the internal carotid artery. It supplies the orbit, eyelids, and forehead from its branches: supraorbital, supratrochlear, lacrimal, and dorsal nasal (Figs. 2.37 and 2.38). In the upper eyelid, two vascular arcades are formed: the marginal and deep peripheral. They are formed by anastomoses between the dorsal nasal and lacrimal arteries. The marginal arcade in the upper lid is approximately 2 mm above the lid margin between the superficial surface of the tarsus and the orbicularis. The deep peripheral arcade is located at the superior border of the tarsus between the levator aponeurosis and Muller's muscle. In the lower lid, a less-developed double arcade is present as well.

From the external carotid artery, the facial artery crosses under the ramus of the mandible and then over the body of the mandible to the angle of the mouth and then ascends along the side of the nose. As it travels closer to the medial corner of the eye, it becomes the angular artery, which is the

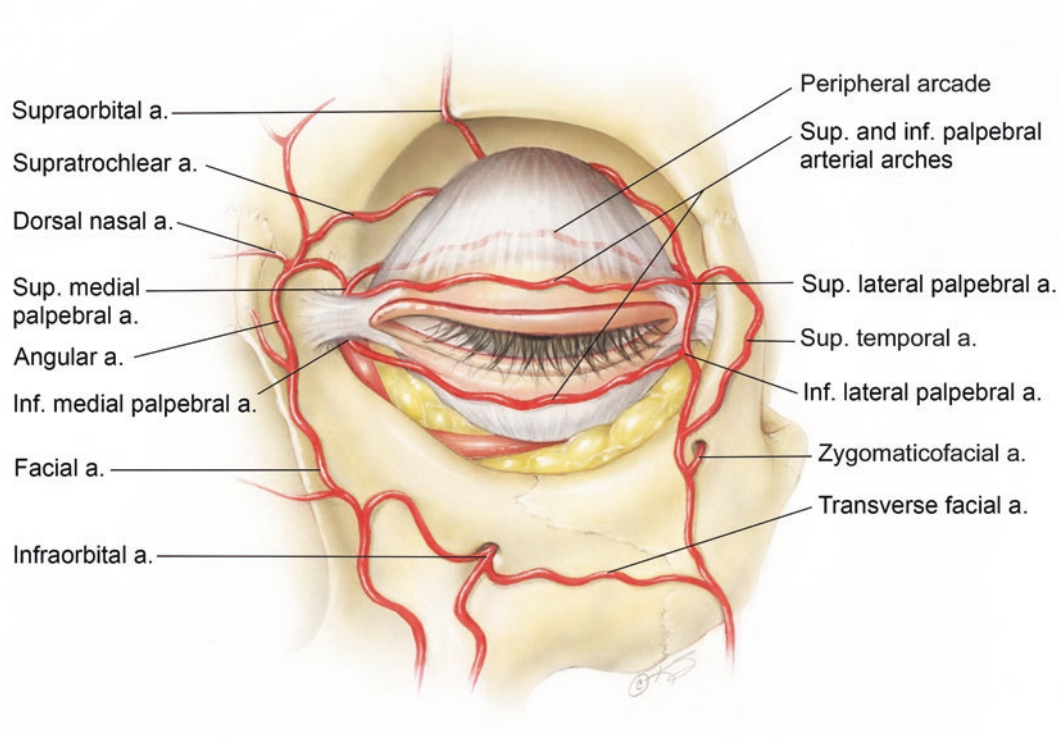


Fig. 2.37 Arterial arcades of the eyelids (frontal view)

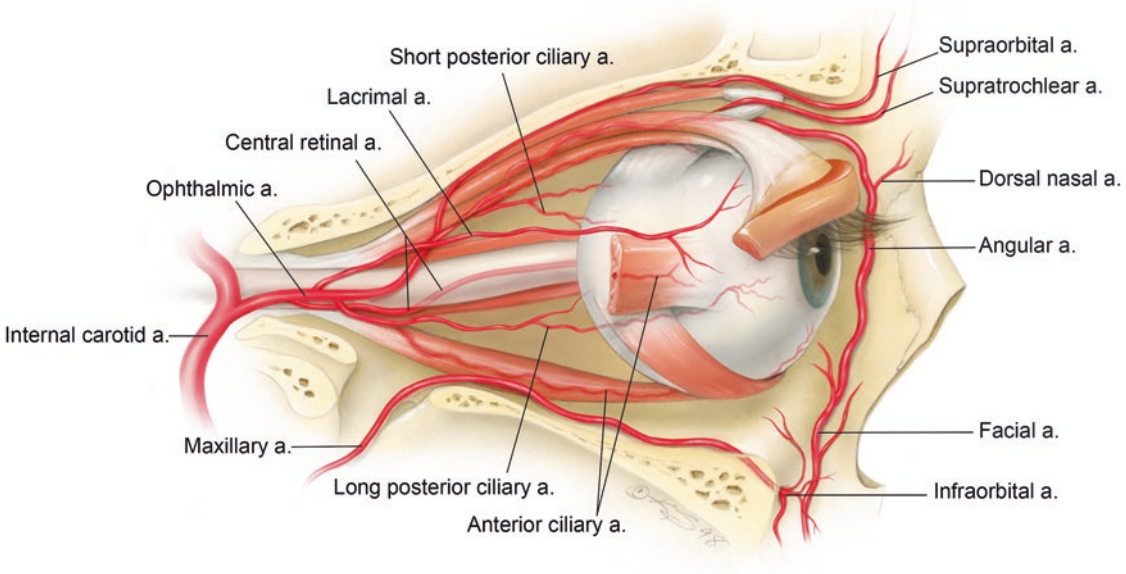


Fig. 2.38 Arterial supply of the orbit (lateral view). The ophthalmic artery is the first branch of the internal carotid artery. It enters the orbit through the optic foramen, inferolateral to the optic nerve. Its branches are the central retinal artery (CRA); the lacrimal artery (LA); one to five posterior ciliary arteries (PCAs), each branching into a long and a short posterior ciliary (LPCA and SPCA); superior and inferior muscular branches that terminate as the anterior ciliary arteries (ACA); the supraorbital artery (SOA); ethmoidal arteries (not pictured in this drawing); medial palpebral arteries (see Fig. 2.37); and terminal branches, the supratrochlear and dorsal nasal arteries

terminal branch of the facial artery. It lays 6–8 mm medial to the medial canthus just below the orbicularis muscle. The location of the artery is important when performing lacrimal surgery. It anastomoses with the dorsal nasal branch of the ophthalmic artery. The superficial temporal artery is the smaller of two terminal branches that bifurcate superiorly from the external carotid artery. It is a major artery of the head and also supplies the lateral eyelid area. The infraorbital artery is a branch from the internal maxillary artery of the external carotid. It runs along the infraorbital groove with the infraorbital nerve and exits the orbit through the infraorbital foramen. Within the canal it gives off orbital branches (to the inferior rectus, inferior oblique, and lacrimal sac).

Venous Drainage from the Eyelids and Orbit

Rich anastomoses characterize the eyelid and orbital venous drainage systems. The facial vein is the main superficial vein draining the angular and medial palpebral veins. It has anastomoses with the deep pterygoid venous plexus and the cavernous sinus (Figs. 2.39 and 2.40).

In the orbit, the superior vortex veins and ethmoidal, lacrimal, central retinal, and ciliary veins empty into the superior ophthalmic vein. The superior ophthalmic vein begins in the upper nasal portion of the orbit and leaves the orbit through the superior orbital fissure above the annulus of Zinn and enters the cavernous sinus (Fig. 2.40). The inferior

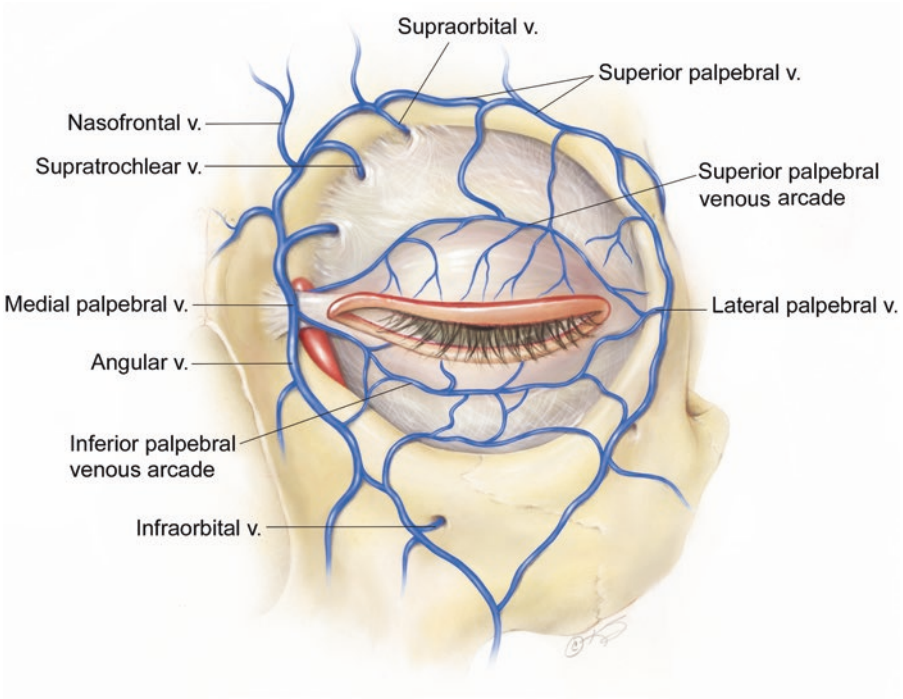


Fig. 2.39 Venous drainage from the eyelids (frontal view)

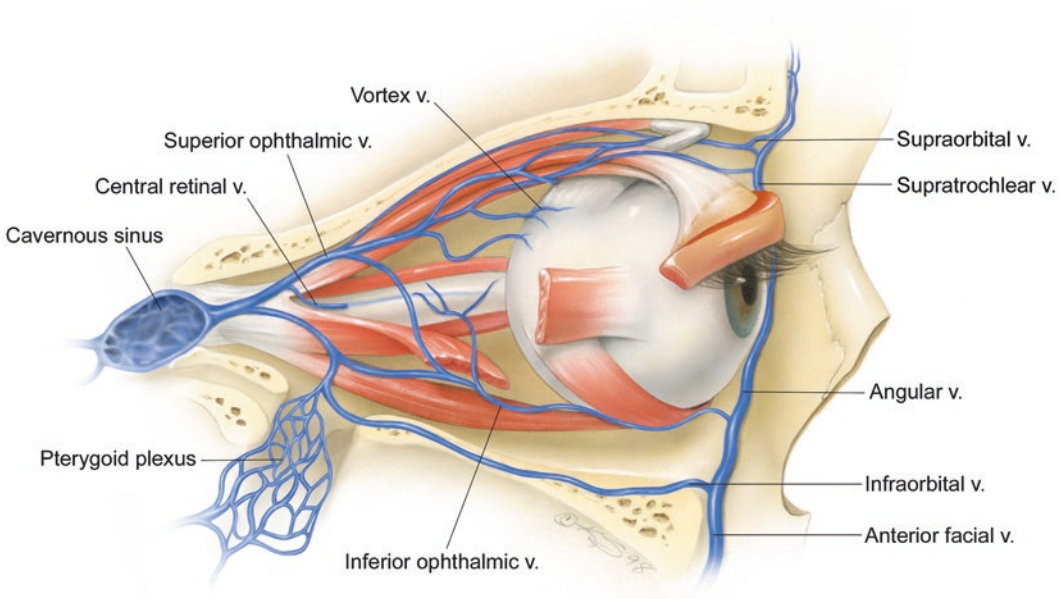


Fig. 2.40 Venous drainage from the orbit (lateral view)

ophthalmic vein receives contributions from the inferior vortex veins and pterygoid plexus upon its exit through the inferior fissure as previously discussed. It often joins the superior ophthalmic vein and also enters the cavernous sinus (Figs. 2.39 and 2.40).

Sinuses

The medial, inferior, and superior walls of the orbit are surrounded by the ethmoidal, maxillary, and frontal sinuses, respectively. The sphenoid sinus is located posterior to the ethmoidal sinuses adjacent to the orbital apex. Any pathology involving the sinuses can directly extend to the orbit (Fig. 2.14).

The maxillary sinuses are the largest in the human face and the first to develop. They begin to form in embryonic weeks 10–11 and are usually present at birth. They continue to grow until the descent of the secondary teeth. The roof of the maxillary sinus is the floor of the orbit.

The sphenoid sinus begins its development in the fourth prenatal month. Growth and pneumatization continue into adulthood. The optic canal can be reached by a transsphenoidal approach for surgical decompression. Just above the sphenoid sinus in a coronal plane lies the cavernous sinus, containing major structures such as the internal carotid artery, the oculomotor nerve (CN3), the trochlear nerve (CN4), and the branches 1 (ophthalmic) and 2 (maxillary) of the trigeminal nerve. Cavernous sinus syndrome is caused by cavernous sinus thrombosis and typically manifests with eyelid and conjunctival edema and cranial nerve palsy.

The ethmoid sinuses begin their development during the fifth month of fetal formation. Growth and aeration continue until puberty. Instead of a single large space, as is the case with the maxillary sinus, the ethmoids form smaller individual air cells. The cells above the middle turbinate are the posterior ethmoidal air cells and those below the middle turbinate are referred to as the anterior ethmoids. The orbit lies lateral to the ethmoidal air cells, and their paper-thin dividing wall is referred to as the lamina papyracea. Infections of the ethmoid sinus can produce an orbital cellulitis, by direct spread through the anterior and posterior ethmoidal foramina.

The frontal sinus is the last to develop. It is not until around the sixth year of life that this sinus becomes evident and its expansion continues well into adulthood.

Any sinus pathology may potentially have a direct impact on the orbit. Such pathologies may include, but are not limited to, sinusitis precipitating preseptal cellulitis or true orbital cellulitis, invasive sinus malignancies and mucoceles spreading to the orbit, and silent sinus syndrome resulting in enophthalmos from maxillary sinus contraction.

References

1. England MA. Color atlas of life before birth: normal fetal development. Chicago: Year Book Medical; 1983.
2. Larsen WJ. Human Embryology. New York: Churchill Livingston; 1993.
3. Moore KL, Persaud TVN. The developing human. 5th ed. Philadelphia: WB Saunders; 1993.
4. Patten BM. The normal development of the facial region. In: Pruzansky S, editor. Congenital anomalies of the face and associated structures. Springfield, IL: Charles C Thomas; 1961. p. 11–45.
5. Vig KWL, Burdi AR, Ferrara A. Editors. *Craniofacial Morphogenesis and Dysmorphogenesis. Monograph 21: Craniofacial Growth Series*. Ann Arbor: The University of Michigan; 1987.
6. Burdi AR. Biological forces which shape the human midface before birth. In: McNamara JA, editor. Factors affecting the growth of the Midface. Monograph 6: craniofacial growth series. Ann Arbor: The University of Michigan; 1976. p. 9–37.
7. Johnson MC. The neural crest abnormalities of the face and brain. Birth Defects. 1975;11:416–40.
8. Poswillo D. The pathogenesis of the first and second branchial arch syndromes. Oral Surg. 1973;35:302–23.
9. Sulik KK. Craniofacial development. In: Turvey TA, Vig KWL, Fonseca RJ, editors. Facial clefts and Craniosynostosis. Philadelphia: WB Saunders; 1996. p. 3–27.
10. Sperber GH. The facial skeleton. In: Craniofacial embryology. Chicago: Year Book Medical; 1976. p. 88–97.
11. Whitaker LA, Katowitz JA, Randall P. The nasolacrimal apparatus in congenital facial anomalies. J Maxillo Facial Surg. 1974;2:59–63.
12. Pruzansky S. Clinical investigation of the experiments of nature. In: ASHA report 8, orofacial anomalies: clinical and research implications. Washington, DC: American Speech and Hearing Association; 1973. p. 62–94.
13. Posnick JC, et al. Cranio-orbito-zygomatic measurements from standard CT scans in unoperated Treacher Collins syndrome patients: comparison with normal controls. Cleft Palate Craniofac J. 1995;32:20–4.
14. Sulik KH, Johnson MC, Smiley SJ, et al. Mandibulofacial dysostosis (Treacher Collins syndrome): a new proposal for its pathogenesis. Am J Med Genet. 1987;27:359–72.
15. Van Limborgh J. Clinical alteration of the growing face. In: McNamara JA, Ribbens KA, Howe RP, editors. Monography 14: craniofacial growth series. Ann Arbor: The University of Michigan; 1982. p. 6–15.
16. Schendel SA, Tessier P, Tulasne JF. Facial clefting disorders and craniofacial synostoses: skeletal considerations. In: Turvey TA, Vig KWL, Fonseca RJ, editors. Facial clefts and Craniosynostosis. Philadelphia: WB Saunders; 1996. p. 3–27.
17. Babler WJ. Effects of multiple suture closure on the craniofacial growth in rabbits. In: KWL V, Burdi AR, Ferrara A, editors. Craniofacial morphogenesis and Dysmorphogenesis. Monograph 21: craniofacial growth series. Ann Arbor: The University of Michigan; 1987. p. 73–89.
18. Marsh JL, Vannier MW. Computo-assisted imaging in the diagnosis, management, and study of dysmorphic patients. In: KWL V, Burdi AR, Ferrara A, editors. Craniofacial morphogenesis and Dysmorphogenesis. Monograph 21: craniofacial growth series. Ann Arbor: The University of Michigan; 1987. p. 109–25.
19. Duke-Elder S, Cook C. Normal and abnormal development, part 2: congenital deformities. In: Duke-Elder S, editor. System, of Ophthalmology. St. Louis: CV Mosby; 1963. p. 829–34.
20. Conlon MR, Sutula FC. Congenital eyelid anomalies. In: Albert DM, Jakobiec FA, editors. Principles and practice of Ophthalmology. Philadelphia: WB Saunders; 1994. p. 1693–4.
21. Duke-Elder S, Cook C. Normal and abnormal development, part 1: embryology. In: Duke-Elder S, editor. System of Ophthalmology. St. Louis: CV Mosby; 1963. p. 215–6.

22. Bentley RP, Sgouros S, Natarajan K, Dover MS, Hockley AD. Normal changes in orbital volume during childhood. J Neurosurg. 2002;96(4): 742–6.
23. McCotter RE, Fralick FB, Henderson JW. A comprehensive description of the orbit, orbital content, and associated structures with Clinical applications. San Francisco: American Academy of Ophthalmology; 1949.
24. Reeh MJ, Wobig JL, Wirtschafter JD. Ophthalmic anatomy. San Francisco: American Academy of Ophthalmology; 1981.
25. Lemke BN. Anatomy of the ocular adnexa and orbit. In: Smith BC, Della Rocca RC, Nesi FA, Lisman RD, editors. Ophthalmic Plastic and reconstructive surgery. St. Louis: CV Mosby; 1987. p. 3–74.
26. Rootman J, Stewart B, Goldberg RA. Orbital anatomy. In: Orbital surgery: a conceptual approach. Philadelphia: Lippincott-Raven; 1995. p. 79–149.
27. Lebeau J. Orbital anatomy. In: van der Meulen JC, Gruss JS, editors. Ocular Plastic surgery. London: Mosby-Wolfe; 1996. p. 1–8.
28. Zide BM, Jelks GW. Surgical anatomy of the orbit. New York: Raven; 1985.
29. Broadbent TR, Mathews VL. Artistic relationships in surface anatomy of the face: application to reconstructive surgery. Plast Reconstr Surg. 1957;20:1–17.
30. Gonzalez-Ulloa M. Quantitative principles in cosmetic surgery of the face (profileplasty). Plast Reconstr Surg. 1962;29:186–98.
31. Werb A. The upper lid: structure and restructure. Orbit. 1992;2:63–73.
32. Patrinely JR, Anderson RL. Anatomy of the orbicularis oculi and other facial muscles. Adv Neurol. 1988;49:15–23.
33. Takahashi Y, et al. Anatomy of anterior ethmoidal foramen, medial canthal tendon, and lacrimal fossa for transcutaneous anterior ethmoidal nerve block in Japanese individuals. Ophthal Plast Reconstr Surg. 2014;30(5):431–3.
34. Jordan DR, Anderson RB, Mamalis N. Accessory lacrimal glands. Ophthalmic Surg. 1990;21(2):146–7.
35. Stasior GO, Lemke BN, Wallow IH, Dortzbach RK. Levator aponeurosis elastic fiber network. Ophthal Plast Reconstr Surg. 1993;9(1):1–10.
36. Codère F, Tucker NA, Renaldi B. The anatomy of Whitnall ligament. Ophthalmology. 1995;102(12):2016–9.
37. Hirohiko Kakizaki MD, et al. The lower eyelid retractor consists of definite double layers. Ophthalmology. 2006;113(12):2346–50.
38. Myckatyn TM, Mackinnon SE. A review of facial nerve anatomy. Semin Plast Surg. 2004;18(1):5–12.
39. Monkhouse WS. The anatomy of the facial nerve. Ear Nose Throat J. 1990;69(10):677–83. 686-7
40. Örge FH, Boente CS. The lacrimal system. Pediatr Clin North Am. 2014;61(3):529–39.
41. Obata H. Anatomy and histopathology of the human lacrimal gland. Cornea. 2006;25(10 Suppl 1):S82–9.
42. Henrichsen K. The early development of morphology and patterns of the face in the human embryo. In: Advances in anatomy, embryology and cell biology, vol. 98. New York: Springer; 1985.
43. Koorneef L. Orbital septa, anatomy and functions. Ophthalmology. 1979;86:876.
44. Koorneef L. New insights in the human orbital connective tissue. Arch Ophthalmol. 1977;95:1272.

Updates in Fetal Wound Healing and Scar Prevention

3

Lama Khatib, Darrell L. Cass, and N. Scott Adzick

An understanding of basic wound-healing processes and scar formation is essential to the pediatric and oculoplastic surgeon. In children, just as in adults, when the periocular tissue or skin is wounded or surgically incised, it heals with inflammation, collagen deposition, wound contraction, and scarring. These wound-healing processes lead to rapid restoration of tissue integrity. However, occasionally these wound-healing events work ineffectively or abundantly, resulting in incomplete repair or excessive scarring. In periocular tissues, impaired wound healing or excessive scarring can result in devastating clinical consequences, including psychosocial repercussions due to disfigurement, ptosis (loss of normal function), and visually threatening eyelid retraction (loss of movement) due to corneal exposure and potentially amblyogenic compromise of the visual axis. Surgeons should understand basic wound-healing processes in order to prevent and reduce scarring occurrence.

In contrast to the child or adult, the early-gestation fetus, before 24 weeks gestational age (GA), has the ability to heal wounds without inflammation and scar formation and instead with regeneration of epithelial and mesenchymal tissues and restoration of normal tissue architecture [1, 2]. Insights into these remarkable repair characteristics have been gained largely from developments in the field of fetal surgery, in which congenital fetal anomalies are surgically treated before birth. Currently, fetal surgery is employed to treat life-threatening birth defects (Fig. 3.1) and open neural tube defects, a non-life-threatening disorder [3, 4]. As prenatal diagnosis and treatment technologies improve, indications for fetal surgery may expand to include other nonlethal congenital disorders such as craniofacial malformations, including eyelid colobomas and microphthalmia. Fetal correction of these anomalies may permit restoration of normal periorbital adnexal development without limitations from postsurgical scarring which typically results from postnatal treatment of these conditions.

In this chapter we review basic pediatric and adult wound-healing mechanisms and then discuss those unique characteristics of scarless fetal wound healing that are known to date.



Fig. 3.1 Hand of a 22-week human fetus during fetal surgery for a life-threatening congenital cystic adenomatoid malformation associated with hydrops.

L. Khatib (✉)
Pediatric Ophthalmology, Oculoplastic and Orbital Surgery, Ophthalmology Division, Children's Hospital of Philadelphia, Philadelphia, PA, USA
e-mail: lamahkhatib@gmail.com

D.L. Cass
Michael E. DeBakey Department of Surgery and Departments of Pediatrics and Obstetrics and Gynecology, Baylor College of Medicine, Houston, TX, USA

Texas Children's Fetal Center, Texas Children's Hospital, Houston, TX, USA

N.S. Adzick
Department of Pediatric Surgery, The Center for Fetal Diagnosis and Treatment, The Children's Hospital of Philadelphia, University of Pennsylvania School of Medicine, Philadelphia, PA, USA

© Springer International Publishing AG 2018

J.A. Katowitz, W.R. Katowitz (eds.), *Pediatric Oculoplastic Surgery*, https://doi.org/10.1007/978-3-319-60814-3_3

Overview of Postnatal and Adult Wound Healing

In both children and adults, wound repair proceeds in a cascade of four overlapping major stages: hemostasis, inflammation, proliferation (fibroplasia, angiogenesis, formation of granulation tissue), and scar maturation [5, 6]. In all postnatal animals (except certain amphibians), synthesis and remodeling of the new extracellular matrix in wounds lead to scarring (Table 3.1).

Hemostasis is the first phase of the postnatal or adult wound-healing response. Whether caused by a scalpel or burn, tissue injury leads to vascular disruption and extravasation of red blood cells, platelets, and plasma. Tissue thromboplastin and activated factor XII cause activation of the coagulation cascades and formation of a hemostatic platelet-fibrin plug (Fig. 3.2). Within the wound plug, aggregated platelets become activated after binding to fibronectin, collagen, and other wound proteins [7]. Platelets then degranulate and release proteases, vasoactive amines, and adhesive glycoproteins, such as fibrinogen and fibronectin. In addition, platelets release a cadre of biologically active growth factors, such as platelet-derived growth factor (PDGF), transforming growth factor-beta-1 (TGF-β1), and insulin-like growth factor-1 (IGF-1). Aside from limiting blood loss, the platelet-fibrin clot also forms a protective scab. Furthermore, fibrin and fibronectin within the clot form a provisional matrix that provides a scaffold for monocyte, fibroblast, and keratinocyte deposition [8].

In the inflammatory/migratory phase of adult repair, white blood cells enter the area of injury [5, 9]. Neutrophils are recruited first via chemotactic stimulus to scavenge cellular debris, dirt, and bacteria. Neutrophils are the most predominant cell type during the first 48 h after injury in adults (Fig. 3.2). However, it has been shown that the absence of neutrophils does not prevent healing. In fact, mice studies have shown that neutrophils are not essential to the wound-healing process [10]. The expression of adhesion molecules is upregulated to facilitate passage of leukocytes from the blood stream into the wound [11]. Subsequently, cellular degradation products attract monocytes to the wound, and, along with macrophages, they synthesize a plethora of growth factors [PDGF, TGF-β, fibroblast growth factors (FGF), and transforming growth factor-alpha (TGF-α)]. These growth factors attract and activate local fibroblasts, endothelial cells, and epithelial cells to initiate their respective roles in the wound-repair process. As opposed to neutrophils, tissue macrophages are essential in wound repair. Not only do macrophages remove debris, they also secrete collagenases and other enzymes that break down necrotic tissue [12]. Macrophages provide the signaling cascade that initiates angiogenesis and fibroblasts to regenerate the dermis. Further, macrophages can and do produce many of the matrix elements and matrix-remodeling metalloproteinases [13, 14].

Table 3.1 Comparison of adult and fetal skin wound-healing characteristics

Characteristics of wound healing	Adult	Fetus
Scar and scab	Present	Absent
Speed to closure	Slow	Fast
Acute inflammation	Greater	Lesser
Oxygen tension	Higher	Lower
Sterile environment	Absent	Present
Keratinization	Present	Immature
Epithelialization	Slower	Faster
Angiogenesis	Greater	Lesser
Interleukins	Increased IL-6 and IL-8 (pro-inflammatory)	Increased IL-10 (anti-inflammatory), leads to decreased IL-6 and IL-8
Platelets	Higher degranulation and release of PDGF, TGF-β1, TGF-β2	Less degranulation, aggregation, and release of PDGF, TGF-β1, TGF-β2
TGF-β levels	High levels of TGF-β1, TGF-β2	Low levels of TGF-β1, TGF-β2, increased TGF-β3
HA/HASA	Low levels lead decreased cellular migration	Higher levels promote cellular migration and trap water
ECM metalloproteinase	Low levels favor accumulation of collagen	Higher levels promote matrix turnover and remodeling
Matrix deposition	Slower, disorganized	Faster, organized
Collagen content	Predominance of type I: provides tensile strength and rigidity	Predominance of type III: promotes cellular migration and regeneration
Fibronectin	Late deposition: disorganized tissue structure	Early deposition: organized tissue structure
Tenascin C	Late appearance	Early appearance
Decorin	High, binds and entraps growth factors	Low, growth factors appear transiently and are not stored
Adhesion proteins	Low levels, leading to slow cellular migration	Rapid upregulation, leading to faster cellular migration
Stem cells (progenitor cells)	Absent	Inherently present, capable of regenerative repair
Integrin upregulation	Slower	Faster

Abbreviations: *HA* hyaluronic acid, *HASA* hyaluronic acid-stimulating activity, *TGF-β* transforming growth factor-beta, *bFGF* basic fibroblast growth factor, *ECM* extracellular matrix, *IL-6* Interleukin-6, *IL-8* Interleukin-8, *IL-10* Interleukin-10

In the proliferative and synthetic phases of wound healing, growth of new tissue occurs. During this phase, granulation tissue formation, angiogenesis, epithelialization, and fibroplasia restore tissue integrity and function. Within hours of skin injury, epidermal cells at the wound margin acquire a flattened phenotype and pseudopodia in preparation for wound contrac-

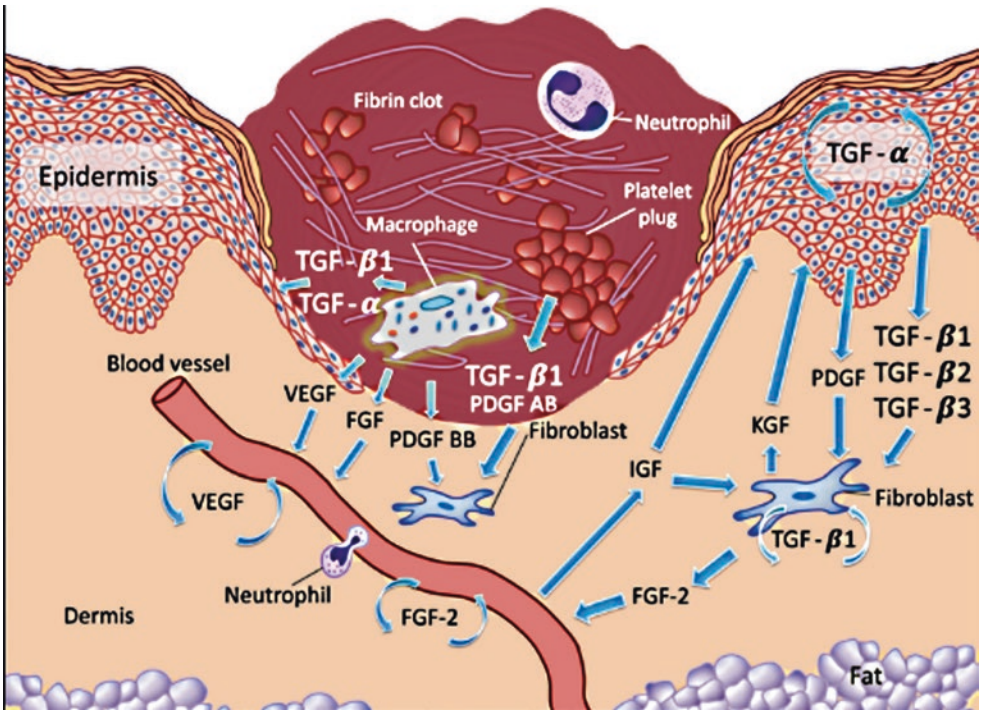


Fig. 3.2 Early phases of wound healing: Hemostasis and inflammation. Growth factors thought to be necessary for cell movement into the wound as shown. Abbreviations: Transforming growth factor β1, $-\beta$2, and -β3 (TGF-β1, TGF-β2, TGF-β3), transforming growth factor-alpha (TGF-α), fibroblast growth factors (FGF), platelet-derived growth factor (PDGF), platelet-derived growth factor-AB (PDGF-AB), platelet-derived growth factor-BB (PDGF-BB), insulin-like growth factor-1 (IGF-1), and keratinocyte growth factor (KGF) (Figure reproduced with permission of TICEBA GmbH. Source: http://www.ticeba.com)

tion and migration across the tissue defect [15]. In addition, migrating keratinocytes upregulate expression of specific cell surface receptors that bind to extracellular molecules within the wound matrix, such as hyaluronic acid, fibronectin, fibrin, and collagens [16–18]. Growth factors regulate reepithelialization [5, 15, 19]. TGF-β and epidermal growth factor (EGF) stimulate keratinocyte migration and synthesis of fibronectin. EGF and TGF-α appear to mediate epidermal cell proliferation at the wound margin [20]. Once epithelial integrity is restored, basement membrane proteins (laminin, collagen) reappear, and keratinocytes reform hemidesmosomes and other cell-cell and cell-matrix attachments.

Angiogenesis is the formation of new blood vessels, or neovascularization. It occurs in concert with reepithelialization and granulation tissue formation [5, 9, 21]. Endothelial cells at the tip of injured capillaries form new capillary buds and migrate into the wound in response to several factors (fibronectin, heparin, PDGF, basic FGF, and vascular endothelial growth factor (VEGF)). Low oxygen tension, lactic acid, and biogenic amines further potentiate angiogenesis. Basic FGF and heparin act in synergy to enhance new vessel growth.

Within 48–72 h after injury, granulation tissue begins to form during the proliferative phase of wound healing. Granulation tissue consists of a tissue matrix hosting a variety of cell types. Fibroblasts from the surrounding tissue migrate into the wound, proliferate, and begin to synthesize extracellular matrix molecules by excreting collagen and fibronectin [5, 21]. Macrophage-derived growth factors, such as TGF-β, stimulate fibroblast proliferation and increased synthesis of collagen, elastin, and proteoglycans. During wound remodeling, fibroblasts secrete hyaluronidase to break down and replace the provisional hyaluronate-rich matrix with larger sulfated glycosaminoglycans. With further wound remodeling, type I collagen gradually replaces type III collagen as the primary collagen in scarring.

Subpopulations of fibroblasts may serve different functions in the wound-repair process. Myofibroblasts are specialized mesenchymal cells that share functional and structural characteristics of both fibroblasts and smooth muscle cells. They express a type of actin called α-smooth muscle actin, a cytoskeletal microfilament that functions in smooth muscle type contraction using the myosin-actin complex [22–24]. Myofibroblasts are naturally found in some subepithelial mucosal surfaces such as the gastrointestinal or genitourinary tract. They provide support and have paracrine function. They were first described in granulation tissue and appear transiently to mediate wound contraction, collagen synthesis, and scar formation. They help speed up wound repair by contracting the edges of the wound. After wound healing is complete, and during the maturation phase, collagen is realigned along tension lines, and myofibroblasts undergo apoptosis; however they may occasionally persist and contribute to the formation of keloids or hypertrophic scars. Myofibroblasts additionally persist in many fibrotic diseases, such as hepatic cirrhosis, renal and pulmonary fibrosis, Dupuytren contracture, and neoplasia-induced desmoplastic reactions. Understanding the signals that regulate myofibroblast apoptosis may contribute to our understanding of hypertrophic scars and how to prevent their formation.

In newborn and adult animals alike, matrix synthesis and remodeling invariably lead to scar formation [5, 9, 21]. Although scar remodeling occurs for months to years after

the initial injury, complete restoration of the normal extracellular matrix architecture is never achieved [6]. Mature scars restore only 70% of the tensile strength of normal skin, and normal function is never completely recovered [25]. In general, scarring refers to alteration in the normal composition and organization of a tissue. Scarring is perhaps best characterized in skin, where it refers to a disruption in the pattern of collagen and other extracellular proteins of the dermis. A mature scar is a relatively acellular, avascular area with abundant parallel bundles of collagen, a lack of elastin, and an absence of dermal appendages such as sweat glands and hair follicles. The size of a scar depends on the extent of tissue injury, the degree of wound contamination, the inflammatory response, and the overall nutritional status of the host [9]. A clean surgical incision in which the wound edges are carefully reapproximated heals with minimal scarring. Larger, contaminated wounds result in larger scars.

In contrast, the embryo and early gestation fetus can heal skin wounds without scarring and with regeneration of dermal appendages and restoration of a normal pattern of collagen and extracellular matrix that is indistinguishable from the surrounding, unwounded skin. Although many differences between fetal and adult wound repair have been described, the key mechanisms that mediate scarless fetal repair remain unclear. In the next sections of this chapter, we review those unique characteristics of the fetus that may contribute to scarless repair as well as some new advents in the field.

Fetal Skin and the Fetal Environment

Several fundamental differences exist between fetal and adult skin that may be at the origin of the scar-free fetal tissue repair. Understanding skin embryogenesis can provide insights into the major differences between fetal and adult scarring. In the human embryo, a primitive epidermis first appears at gestational day 20. During 4–8 weeks of gestation, the human primitive epidermis develops into two layers, the periderm and the basal cell layer. Epidermal stratification begins by 9 weeks, and epidermal keratinization begins by 21 weeks. By 16 weeks, fetal skin has many of the adult skin components such as a basal cell layer, an intermediate layer, sweat glands, hair follicles, and follicular keratinization. By 24 weeks gestation, human fetal skin has all the features of mature adult skin, and at birth neonatal skin is histologically indistinguishable from adult skin [26–28].

Scarring in adult wounds occurs mainly at the dermal level. The fetal dermis similarly undergoes morphologic and biochemical changes during the healing process however without major structural alterations [26]. Early in gestation, the fetal dermis is thin and cellular with a paucity of extracellular matrix. As development proceeds, dermal collagen is deposited, and sulfated glycosaminoglycans replace hyaluronic acid and other non-sulfated glycosaminoglycans. The rapid growth rate of fetal skin and the loose, hyaluronic acid-rich composition of the extracellular matrix provide a conducive environment for scarless fetal repair. Scarless fetal wound healing was first described about three decades ago [29]. It was demonstrated by the repair model of full-thickness eyelid colobomas produced in midgestational fetal sheep (Fig. 3.3). The same occurs in humans before 24 weeks GA [2].

It has been suggested that differences between the fetal and adult wound environments may influence wound repair. Fetal wounds are bathed in warm, sterile amniotic fluid that is rich in growth factors and certain adhesion molecules, such as fibronectin and hyaluronic acid [30]. Furthermore, fetal subcutaneous tissue is relatively hypoxemic as compared to the adult counterpart. However, early evidence suggests that the fetal environment is neither sufficient nor necessary for scarless fetal repair as fetal skin outside the uterine environment also heals without scar as demonstrated by experiments on the newborn opossum [31, 32]. At birth, the opossum remains fetal-like, both physiologically and anatomically, and remains attached to the mother's nipple for 4–5 weeks. Despite their extrauterine location, incisional wounds in early pouch young reepithelialize within 2 days, synthesize collagen within 24 h, and heal scarlessly [31]. In contrast, wounds in older pouch young heal more slowly and with scarring. Furthermore, human fetal skin transplanted subcutaneously to an immuno-incompetent mouse, such as the athymic nude mouse, retains its developmental characteristics [27] and heals scarlessly [33]. Thus, scarless repair capabilities appear to be intrinsic to the fetal tissue itself, rather than dependent on the sterile, in utero amniotic environment. On the other hand, adult skin in the fetal environment heals with scarring. When adult sheep skin is transplanted into 60-day-gestation fetal sheep (before term which is 145 days and before the fetal immune system has developed sufficiently to reject the allografts), incisional wounds in the adult grafts heal with scarring [34]. Thus, scar formation appears to be intrinsic to adult skin, and neither the amniotic fluid environment nor perfusion by fetal blood prevented scarring. Late gestation fetuses have been observed to heal with scarring despite remaining within the amniotic environment. Primate fetuses demonstrate these developmental changes in their repair response [35]. Full-thickness, upper lip wounds in fetal rhesus monkeys at 75 days GA (165 days being full term) heal scarlessly with regeneration of hair follicles and a dermal collagen pattern that is indistinguishable from unwounded tissue (Fig. 3.4). Conversely, similar wounds in fetuses at 107 days GA or older heal with scarring. Interestingly, wounds made in 85–100 day gestation fetuses heal with intermediate, transitional repair morphology. Fetal wound-healing studies in rodents [36], opossum [32], and sheep [37] demonstrate a similar

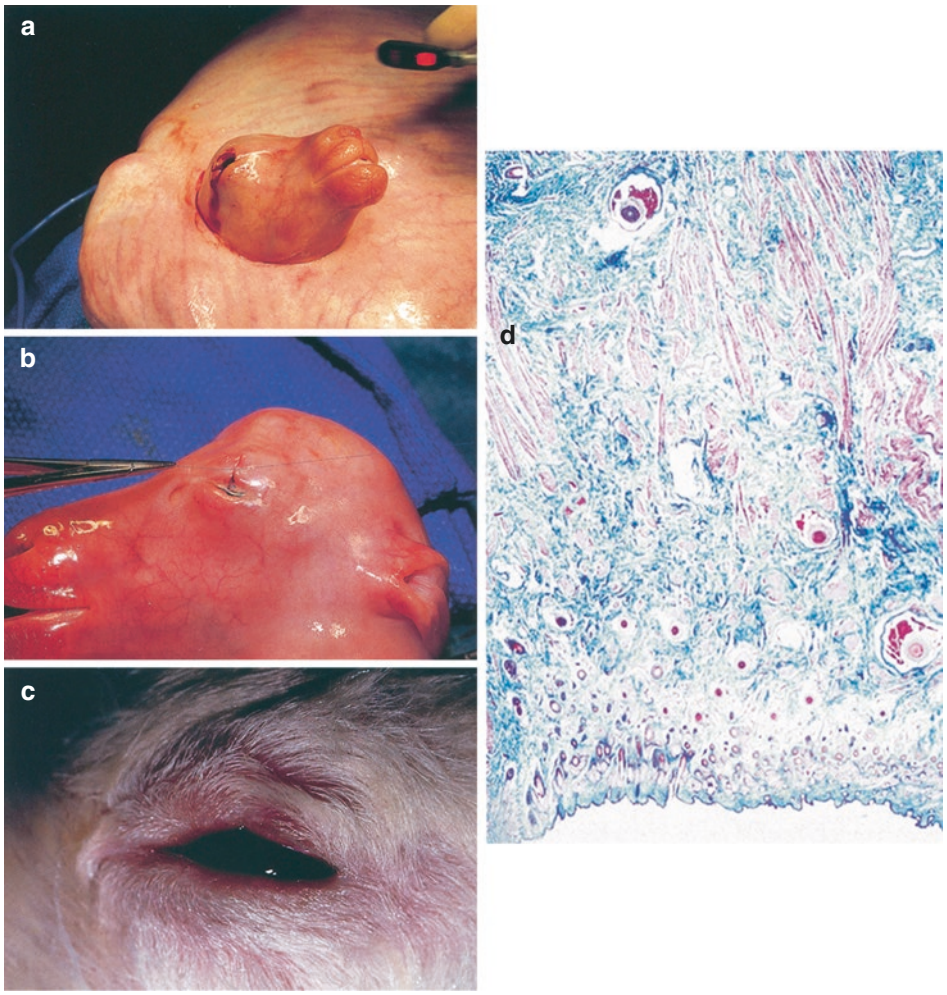


Fig. 3.3 Scarless repair of a fetal sheep eyelid. (**a**) Full-thickness left upper eyelid coloboma (one-half lid length) produced in 90-day-midgestational fetal sheep. (Observe fetal head protruding from maternal uterus.) (**b**) Repaired eyelid coloboma before fetal head replacement into maternal uterus. (**c**) Repaired eyelid coloboma at term. (**d**) Masson's trichrome stain of repaired eyelid coloboma. Note normal follicles and muscle architecture without any evidence of scarring (Courtesy of Michael A. Johnson, MD, James A. Katowitz, MD, and Timothy G. Crombleholme, MD)

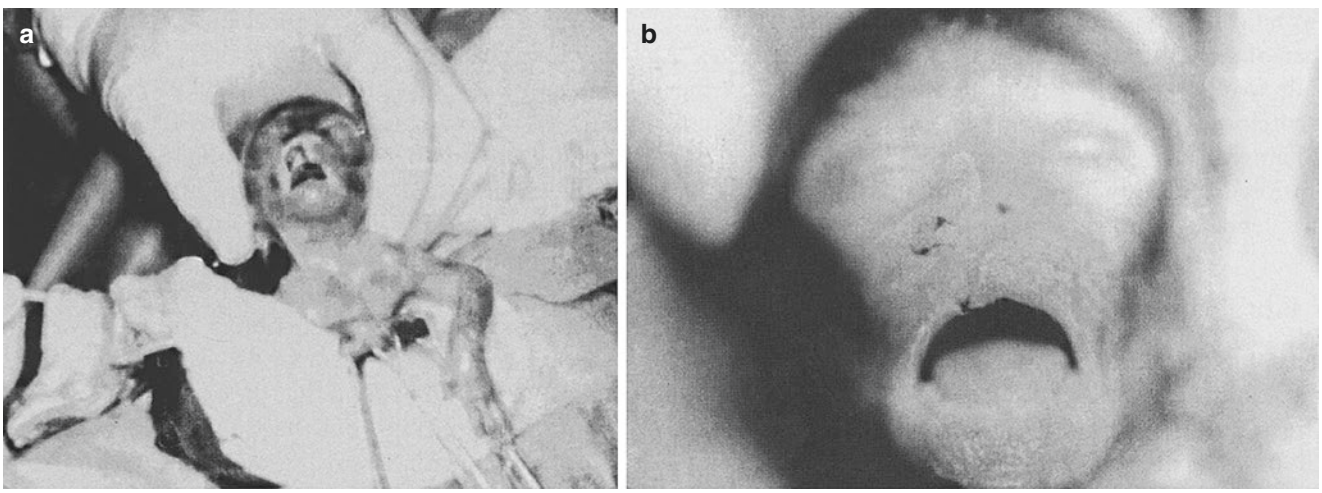


Fig. 3.4 Scarless repair of a lip wound in a fetal rhesus monkey. (**a**) A full-thickness upper lip wound was made in a midgestation fetal rhesus monkey. (The back and hindquarters of the fetus remain within the uterus. Babcock clamps secure the fetal membranes at the cut edge of the uterus). (**b**) Scarlessly healed fetal wound 14 days later. The healed wound is marked by sutures but otherwise is indistinguishable from the surrounding tissue

developmental transition from scarless to scar-type repair. Thus, there is more to the mechanisms of scarless fetal repair than the sterile, growth factor-rich amniotic environment.

Not all fetal organ systems heal scarlessly. Whereas fetal skin, bone, and cartilage can regenerate, fetal nerve tissue, diaphragm, stomach, and peritoneum scar [30, 38–41]. Additionally, scarring is positively correlated with wound size, and while small fetal wounds heal scarlessly, large fetal wounds scar [42]. The unique characteristics of fetal tissue repair appear to be intrinsic to fetal skin and the cells and extracellular matrix that compose it.

Characteristics of Fetal Wound Healing

Fetal-type wound healing is most remarkable for its regenerative speed and the absence of scarring, even at the histologic level. All primary histologic structures (hair follicles and sweat glands) are restored in the process. Studies reveal that the differences between fetal and adult type of wound repair lie mainly in the inflammatory and proliferative phases [33]. Additionally, differences are noted both at the intracellular level and extracellular level/matrix (Table 3.1).

At the Cellular Level

Hemostatic Plug and Platelet Function

Differences between fetal and adult platelets may contribute to differences in the wound inflammatory response. Platelet counts, structure, alpha granules, and other organelle content are similar between fetus and adult pigs [43, 44]. However, fetal platelets show decreased aggregation to ADP and collagen compared to older fetuses or adults [43]. Additionally, serum growth factor levels in the youngest fetuses were approximately one-third to one-half those in the adult. Since nearly all serum PDGF and 90% of TGF-β is derived from platelets, a more limited inflammatory response might result from less platelet aggregation or a limited release of platelet-derived cytokines at the wound.

Inflammatory Phase and Cellular Mediators

The fetal immune system is functionally immature relative to its adult counterpart [45–49]. Fetal cells are in fact capable of mounting an inflammatory response; however this response is not elicited in the repair of early fetal wounds, and the reason behind this remains unclear. Immunoglobulin deposition is absent in lamb and mouse fetal wounds [37, 50]. Lymphocytes and polymorphonuclear leukocytes are conspicuously absent in fetal rabbit wounds [46, 51]. However, when polyvinyl alcohol (PVA) dipped, adult implanted sponges are subsequently transplanted subcutaneously into fetal rabbits, they will induce fetal neutrophil migration [48]. This suggests that adult wound chemoattractants can induce fetal leukocyte migration to the wound site. Similarly, when bacteria (live or irradiated)-rich sponges are implanted subcutaneously in fetal rabbits, or when turpentine (solvent) or carrageenan (food additive) is injected into the skin of fetal lambs, neutrophils, macrophages, and lymphocytes are recruited to the wound [52, 53].

Macrophages

In adults, macrophages synthesize matrix metalloproteinases and their inhibitors as previously described, and coordinate wound healing. The acute inflammatory infiltrate in the fetal wound consists mainly of macrophages and almost no leukocytes or lymphocytes [54], and hence the low phagocytic activity leads to less neutrophilic infiltration. Wound macrophages participate in coordination of fetal repair as they do in the adult [5, 9, 55]; however they are present in lower numbers than in the adult [56]. Fetal macrophages express a number of growth factors, just as adult macrophages do [57]. Because fetal skin repair is characterized by the restoration of a normal extracellular matrix, an essential regulatory role for fetal macrophages seems likely.

Fetal Fibroblasts

The fetal fibroblast deposits collagen and other extracellular matrix in an organized, scar-free pattern and likely plays a leading role in scarless wound repair. Therefore, it is crucial to compare the early-gestation fetal fibroblast to the late-gestation and adult fibroblast to uncover differences between fetal and adult wound-repair mechanisms. In vitro, fetal fibroblasts demonstrate several fundamental differences when compared to adult fibroblasts with regard to collagen production and the response to and production of TGF-β. Human fetal fibroblasts demonstrate greater prolyl hydroxylase activity, greater collagen synthesis [58], and higher levels of TGF-β than adult fibroblast cells in normoxic conditions [59]. However in response to hypoxia, fetal fibroblasts decrease TGF-β transcription, as opposed to adult fibroblasts. In addition, fetal fibroblasts increase synthesis of both type I and type III collagen in response to TGF-β2 as opposed to adult cells [60]. Whereas adult and neonatal fibroblast migration is stimulated by TGF-β1, human fetal fibroblast migration appears to be inhibited [61]. Studies on fetal rabbit fibroblasts suggest that TGF-β receptor density decreases with advancing gestational age [62]. In addition, fetal rabbit fibroblasts have a two- to fourfold greater number of cell surface hyaluronic acid receptors (CD44) than adult cells [63]. Thus, there appear to be fundamental differences between fetal and adult fibroblasts in the regulation and synthesis of collagen, their response to growth factors, and the expression of cell surface receptors.

At the Extracellular Level

Hyaluronic Acid

Proteoglycans are a heterogeneous group of large, polyanionic molecules that consist of a protein core covalently bound to one or many polysaccharide side chains (glycosaminoglycans). Proteoglycans likely play an important role in fetal repair. Hyaluronic acid (HA), a high molecular weight glycosaminoglycan, is present in high concentrations during embryogenesis and during periods of rapid tissue proliferation. Because of a large number of hydrophilic residues, HA gives fetal tissue a loose, porous nature. The extracellular matrix of fetal skin is rich in glycosaminoglycans, of which nearly 95% is hyaluronic acid [64]. With advancing fetal age, HA and total glycosaminoglycan content decreases, whereas the relative concentrations of sulfated glycosaminoglycans, including dermatan sulfate, heparan sulfate, and chondroitin sulfate, increase [64–66]. Along with a decrease in HA, there is a similar decrease in the water content of fetal skin, from nearly 93% in fetal lambs at 90 days gestation to 76% by term [63]. Meyer and Stern have measured total HA content in human skin from 28 weeks fetal gestation through 88 years of age [67]. Unlike previous reports, they found that the actual HA content was similar in all age groups but that HA was less bioavailable with advancing age, presumably from increased association with HA-binding proteins. Changes in glycosaminoglycan composition and the flexibility/pliability of the extracellular matrix, in association with a higher number of HA receptors on fetal fibroblasts, may account for differences in the ability of fetal cells to move efficiently through the wound environment and to effect rapid repair. Hyaluronic acid accumulates rapidly in both fetal and adult wounds or PVA sponges. In adults these levels rapidly return to baseline after 3 days, but in the fetus, elevated levels persist until 21 days after the insult [68]. Unlike adult repair, these sustained fetal HA levels are associated with elevated levels of hyaluronic acid-stimulating activity and low levels of hyaluronidase [69, 70]. A prolonged presence of HA, facilitated by fetal and amniotic hyaluronic acid-stimulating activity and low levels of hyaluronidase, provides an environment that is conducive to scarless repair.

Collagen

Collagen comprises nearly 77% of the fat-free dry weight of the skin [71]. There are differences in the content and collagen composition between fetal and adult skin and between fetal and adult wounds. In fetal skin, total collagen content increases with advancing gestational age and increased skin development. Human fetal skin collagen content more than triples between 19 and 40 weeks gestation [72]. Early-gestation fetal skin has a predominance of type III collagen rather than late-gestation fetal or adult skin. In humans the ratio of type I to type III collagen is nearly 1 at midgestation and 2.7 at term [73]. This preponderance of type I collagen persists throughout postnatal life [73]. Scar tissue is morphologically represented by disruption of the normal dermal spatial composition of collagen. Since type III collagen has a smaller, reticular structure and has a greater propensity to cross-link than type I collagen, it may contribute to the regeneration of the fine collagen network after wounding. Type I collagen in postnatal wounds provides more strength and rigidity to the skin; however this may impede the regenerative process by haltering cellular migration. Similar to unwounded skin, scar tissue shows a difference in its collagen composition, whereby collagen type I is predominant in adult wounds and type III is predominant in fetal wounds [74]. Rapid fetal repair and collagen deposition have been demonstrated in multiple animal models [2, 37, 50, 56]. Nath and colleagues compared the levels of type I collagen expression between fetal and adult rabbits [75]. Whereas fetal wounds showed increased collagen expression by 3 days after wounding and only a modest increase in wound cellularity (1.5-fold), adult wounds did not show increased collagen expression until 7 days after wounding, and there was a much greater early increase in wound cellularity (6.3-fold). Fetal wounds showed a rapid but modest increase in collagen synthesis above an already high level of constitutive expression. In contrast, adult wounds showed a delayed but marked increase in collagen synthesis that reflected tremendous influx of new wound-specific fibroblasts and marked induction of collagen synthesis in native dermal fibroblasts. Scar-free repair in the fetus seems to involve relatively small injury-related changes to an already revved-up system. Wound-breaking strength seems to be similar between fetal and adult animal models; however fetal wounds regain tensile strength more rapidly than adult wounds [76, 77]. The mechanisms underlying this phenomenon are unknown but probably relate to differences in the type of collagen structure.

Fibromodulin

Fibromodulin is a member of the family of small interstitial leucine-rich proteoglycans (SLRP) that also include decorin. It is encoded by the gene FMOD [78]. Fibromodulin participates in the assembly of the collagen fibers of the extracellular matrix. It binds to the same site on the collagen type I molecule as lumican [79] and inhibits fibrillogenesis of collagen type I and collagen type III in vitro [80, 81]. It also regulates TGF-beta activities by sequestering TGF-beta into the extracellular matrix. Sequence variations in this gene may be associated with the pathogenesis of high myopia. Fibromodulin is found in the epidermis of human skin and is expressed by skin cells (keratinocytes) in culture. Fibromodulin knockout mice have very fragile skin [82], abnormal tails, and Achilles tendons and manifest several clinical features of Ehlers-Danlos syndrome [83]. The collagen fiber bundles in these tendons are

scarcer and disorganized. The levels of lumican increased fourfold in the tail tendons of the FMOD-knockout mice. Liposomal-based delivery of the fibromodulin gene was investigated in a rat model with Achilles tendon injury. Encouraging results were observed that may provide new clinical therapeutic strategies [84]. In a recent study using loss- and gain-of-function rodent fetal wound models, fibromodulin was found to be essential for scarless wound healing. In particular, the loss of fibromodulin can eliminate the ability of early-gestation fetal rodents to heal without a scar. Administration of the protein alone was capable of restoring scarless healing in late-gestation rat fetal wounds, with dermal appendage restoration and organized collagen deposition that were virtually indistinguishable from those in controls with unwounded skin. High fibromodulin levels correlated with decreased transforming growth factor (TGF)-β1 expression and scarless repair, while low levels correlated with increased TGF-β1 expression and scar formation. Hence the FM-TGF-β1 nexus potentially plays a crucial role in fetal-type scarless skin repair [85].

Cell Adhesion Molecules

In the early stages of adult wound repair, fibronectin, fibrin, and other plasma proteins are deposited into the wound bed [5, 8, 9]. These proteins promote hemostasis and form a provisional wound matrix for keratinocyte and fibroblast migration. Differences in the structure of the provisional wound matrix between the fetus and the adult may contribute to the more rapid reepithelialization and scarless fetal repair (Fig. 3.5).

Fibronectins belong to a family of glycoproteins that are present in plasma and widely distributed in connective tissue matrices. During adult wound repair, fibronectin mediates cell adhesion and serves as a substratum for cell migration [8, 86]. Fibronectin appears earlier in fetal rabbit wounds, at 4 h as compared to 24 h in the adult [87]. Whitby et al. studied the synthesis of fibronectin isoforms in upper lip wounds in fetal mice [88]. Fetal wounds increased expression of all fibronectin isoforms between 6 and 24 h, whereas in adult wounds expression was delayed until 5 days post-wounding. In the fetus, early expression of fibronectin may provide an earlier wound scaffold on which keratinocytes and fibroblasts can migrate to rapidly repair the wound.

Tenascin is an extracellular matrix glycoprotein that mediates cell migration and inhibits cell attachment to fibronectin. Tenascin is expressed widely throughout development and in adult wound repair [89]. The temporal appearance of tenascin in fetal wounds in both mice and sheep correlates with the faster rate of epithelialization [50, 90]. In fetal lamb incisional wounds, tenascin appeared within 4 h, whereas it was not seen until 8 h in older fetuses and not until 24 h in the adult ewes [90]. These wounds reepithelialized in 48 h, 72 h, and 7 days, respectively. Given that the appearance of tenascin corresponds to cell migration, it is reasonable to hypothesize that tenascin mediates rapid cell migration in the fetal wound and early reepithelialization.

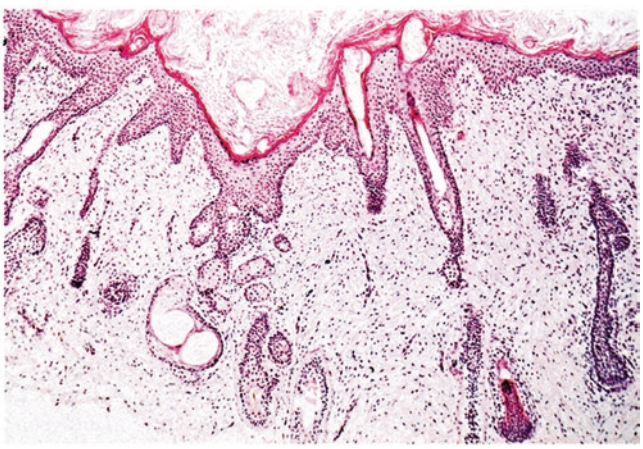


Fig. 3.5 Scarless human fetal skin repair. A model of scarless fetal repair has been developed in which human fetal skin is transplanted to an immuno-incompetent mouse (does not reject the xenograft), allowed to engraft, and then wounded. In this model human fetal skin heals rapidly and scarlessly with restoration of perfect tissue architecture

Fetal Wound Contraction

Injured tissue heals either by contraction of surrounding tissue or synthesis of new tissue. In embryonic wound repair, Martin et al. have shown that excisional wounds close by nearly equal contributions from wound contraction and cell proliferation [91, 92]. Epithelial cells at the wound margin release mesenchymal attachments and form a circumferential actin cable that appears to close the wound by a regeneration of new tissue in a purse stringlike action. In contrast to adult wound contraction which is due in great deal to the physical contraction of the myofibroblasts, the fetal wound has virtually no myofibroblasts and undergoes contraction by regeneration [93]. Fetal rabbit wounds behave differently, and a notable lack of myofibroblasts results in deficient wound contraction [94]. Hence myofibroblasts may be required but are not sufficient for scar formation in fetal wound repair. Myofibroblasts are present in fetal wounds in midgestation fetal sheep at 3 and 7 days after wounding, but by 14 days myofibroblasts are relatively absent in wounds that heal scarlessly, whereas they remain abundant in wounds that scar.

The role of wound contraction in other fetal animal models is less clear [95, 96]. Unless covered, excisional wounds in fetal rabbits gape open and increase in size as the fetus grows. Fetal rabbit wounds close only to the extent to which they are covered by a silastic or biobrane membrane [97, 98], suggesting that the covering is required to exclude amniotic fluid or to serve as a template for cell migration. Both rabbit and human amniotic fluids inhibit both fetal and adult human

fibroblast contraction in collagen lattices (FPCL) [99]. Conversely, sheep amniotic fluid has been shown to stimulate fetal and adult fibroblast contraction in FPCL [100]. Identification of the putative factors in amniotic fluid that inhibit or stimulate wound closure may provide a possible treatment for pathologic wound contracture.

Growth Factors and Cytokines

Growth factors play a key role in all aspects of adult wound repair from activation of the coagulation cascade to scar remodeling [19]. Growth factors are also important in fetal development by directing cell migration, proliferation, and differentiation. It ensues that growth factors (or their relative absence) contribute to regulation of fetal wound repair.

The spatial and temporal expression of growth factors in healing lip wounds of fetal and adult mice was examined by Whitby and Ferguson [101]. PDGF appeared at the wound surface within 1 h in both fetal and adult wounds; it disappeared by 48 h in the fetus compared to 72 h in the adult. Expression of bFGF and TGF-β was increased in adult wounds, but not in fetal wounds. Several studies have demonstrated that fetal wound repair can be modulated by the exogenous addition of growth factors. PDGF is a potent stimulator of mitogenesis, migration, and collagen synthesis. PDGF is a dimeric glycoprotein that can be composed of two A subunits (PDGF-AA), two B subunits (PDGF-BB), or one of each (PDGF-AB). PDGF-AB or BB causes a 1.5- to twofold increase in proliferation and collagen synthesis in fetal fibroblasts in vitro [102]. When either PDGF or TGF-β is applied to PVA sponge implants in fetal rabbits, there is a dose-dependent increase in inflammation and fibrosis [102, 103]. Similarly, when TGF-β is delivered to healing human fetal skin wounds by a slow-release disk, there is a dose-dependent increase in the amount of scar formation. EGF enhances reepithelialization in fetal rabbit wounds, which normally do not heal unless excluded from amniotic fluid [104]. Epidermal growth factor receptors are expressed in developing human fetal skin [105], and EGF may play a role in reepithelialization in human fetal wounds.

Tremendous focus was also shed on TGF-β as multiple studies attempted at uncovering its role in human and other animal wound healing models. The TGF-β isoforms are chemoattractants for monocytes, fibroblasts, and inflammatory cells and are involved in all steps of the wound-repair process and have different effects on scar formation and wound healing. In scarless fetal wounds, TGF-β1 and TGF-β2 expression is unchanged, whereas TGF-β3 expression is increased [106–108]. Conversely, TGF-β1 expression is increased and TGF-β3 expression is decreased in scarring fetal wounds. Insertion of TGF- β1 containing PVA sponges into fetal wounds leads to scar formation in fetal mice models [103]. Paradoxically, in a fetal lamb model, Siebert and colleagues found increased expression of TGF-β1, -β2, and -β3, as well as their receptors, at the wound margin by 3 days after wounding [109]. The authors suggest that differences between fetal and adult wound repair may be mediated by differences in growth factor effect rather than by differences in upregulation or downregulation. Furthermore, in mouse embryo wounds, Martin et al. showed a transient induction of TGF-β1 at 1 h after wounding, but levels returned to baseline by 18 h [110], as opposed to adult wounds, that showed a more sustained increase in TGF-β1 and TGF-β2 expression [106–108]. Treatment of adult wounds with exogenous TGF-β3 reduces scar formation [111]. Similarly, treatment of adult rat wounds with neutralizing antibodies to TGF-β1 and TGF-β2 reduces scar formation [108, 111]. Hence, the relative proportion of TGF-β isoforms, and not the absolute amount of any one isoform, may determine whether tissue regenerates with or without scar formation.

Interleukins are a group of cytokines that play a role in chemotaxis and activation of inflammatory cell mediators. Lymphocytes, monocytes, macrophages, and endothelial cells synthesize interleukins. Interleukin-6 and interleukin-8 are pro-inflammatory [112, 113]. The addition of interleukin-6 to fetal wounds produces scar in normally scarless wounds. Interleukin-10 has an anti-inflammatory function through downregulation of interleukin-6 and interleukin-8. Skin grafts from Interleukin-10 knockout mice that are transplanted onto syngeneic adult mice heal with significant inflammation and scar [113]. In adult mice subsequently treated with an interleukin-10 adenoviral vector, inflammation was reduced, and scarless healing occurred.

Modulators in in Postnatal Wound Healing

With our increased understanding of wound repair and growth factor biology, various therapeutic agents are currently under investigation in an effort to modulate wound healing in both normal and healing-impaired animal models and humans. Of the many growth factors that participate in wound repair, TGF-β has been the most widely studied so far [114]. Early paradoxical effects of TGF-β in wound-healing models are now recognized to be due to the different effects of the different isoforms [115–121]. TGF-β isoforms 1 and 2 promote collagen synthesis and scar formation, whereas isoform 3 promotes better wound healing and scar prevention [122, 123]. Using an antibody to TGF-β1 and TGF-β2, Shah et al. were able to diminish scarring in adult rat wounds [124]. The wounds treated with neutralizing antibody had normal tensile strength and a nearly normal dermal architecture compared with untreated wounds. This salutary effect is accompanied by deposition of less collagen and fibronectin and infiltration by fewer macrophages and blood vessels. Application of neutralizing antibodies at the time of wounding (and not later) was essential to reduce active TGF-β levels, prevent autoinduction of TGF-β1 and -β2 mRNA, and limit macrophage infiltration and further TGF-β release. Administration of TGF-β3 in the

same rat model reduced the TGF-β1 and TGF-β2 levels and reduced scarring in a dose-dependent fashion. Human recombinant active TGF-β3 (avotermin) has been studied for the prevention and reduction of human scarring. Despite successful early trials, it failed to prove as an effective treatment modality [125]. Administration of either TGF-β1 antiserum or decorin to neutralize TGF-β biologic activity in a glomerulonephritis model suppresses the deposition of the pathologic matrix, which leads to fibrosis in this disease entity [126]. Hence, modulation of the TGF-β isoform profile or proportions within a healing wound can alter the cellularity and extracellular architecture of the repair process.

Although injection of cytokine antibodies into wounds has limited clinical potential because of antigenicity problems, there are other alternatives to reduce wound levels of TGF-β1 and TGF-β2. Hypothetical treatment modalities in counteracting TGF-β1 and TGF-β2 activity may include flooding the wound with soluble receptors to compete with cellular binding sites and potential targeted gene therapy to add antisense oligonucleotides to reduce TGF-β gene expression. Inhibitors of TGF-β may be important future drugs in the treatment of wounds and fibrosis. Other agents under investigation include but are not limited to: VEGF, bFGF (basic fibroblast growth factor), hepatocyte growth factor, mannose-6-phosphate, IL-10, prostaglandin E-2, and antihistamines [127].

Current Modalities for Prevention and Treatment of Scars

As the research in the field of scar prevention is ongoing, treatment for established or hypertrophic scars has also evolved over the last decades. Several newer technologies (such as laser) and drug agents have been investigated thoroughly for potential value in scar reduction and treatment. They are hereby presented in brief.

CO2 Laser Resurfacing

Carbon dioxide (CO2) laser was first introduced in 1964 and has been widely used in industrial and medical settings. It is highly absorbed by water and water-containing biological tissues, and hence useful in medical and surgical settings. In surgical settings it can be used in cutting and hemostasis. The use of CO2 laser in skin resurfacing or photorejuvenation first started in 1995 [128]. It functions by removing (dermabrading) vertical layers of skin tissue in a fractionated manner, in other words columns of skin are treated, leaving the interval skin intact to aid in skin healing and collagen deposition. It is used in treatment of scars, fine and deep wrinkles, skin discoloration, skin laxity, and structural irregularities. The skin is left red, inflamed, and takes about 1–21 days to heal. Great results have been reported with CO2 laser resurfacing of the skin for treatment of scars. Antibiotics, antivirals, and steroids may be prescribed beforehand or after the treatment has been completed. Recently, CO2 laser has been used for the treatment of pediatric hypertrophic burn scars with promising results [129]. This new treatment modality constitutes a promising new alternative for children who are psychosocially affected by their scars [130].

Another type of laser treatment is erbium laser resurfacing. The advantage is minimal burn to surrounding tissues, thus causing less discomfort, less swelling, bruising, and redness.

Miscellaneous Agents Under Investigation (Table 3.2)

Table 3.2 Miscellaneous newer agents are under investigation for hypertrophic and keloid scars, some with promising results and some still under scrutiny [127, 131]

Agent	Drug class/mechanism of action	Effect on scar prevention/treatment
Mitomycin C	Antineoplastic antibiotic with antiproliferative effect on fibroblasts (affects TGF-β1)	Mixed results
Tamoxifen citrate	Selective estrogen receptor modulator (decreases TGFB1 expression)	Improved scarring, prospective studies required
Methotrexate	Dihydrofolate reductase inhibitor, anti-inflammatory action in low doses	Successful prevention of keloid recurrence
Imiquimod and resiquimod	Topical immunomodulators. Induce production of interferon alpha (antifibrotic cytokine)	Mixed results
Retinoids	Reduce human fibroblast proliferation, inhibit type I collagen expression by human fibroblasts	Slight reduction in size and symptoms of keloids
Tacrolimus	Calcineurin inhibitor, immunosuppressive agent	Under investigation (great for eczema and keloid due to atopic dermatitis)
Sirolimus	Regulates collagen expression and decreases ECM deposition	Under investigation
Polydeoxyribonucleotide (PDRN)	Stimulates wound healing by improving angiogenesis and increasing fibroblast growth rates	Found to speed healing of wounds caused by laser, more studies required to prove its role in scar prevention and treatment

Conclusion

As much as we have learned from the impeccable model of early fetal wound repair, a great deal of knowledge and ensuing treatment modalities have yet to be uncovered. We could hypothesize different strategies to manipulate wound healing in children and adults from observing the early fetal model. We can inhibit the wound inflammatory response by blocking inflammatory cytokines, adding exogenous proteins to modulate extracellular matrices, or altering keratinocyte and fibroblast function. As umbilical cord blood sampling and stem cell banking have become widely available, we could potentially transplant stem cells to the adult wound site. Although all these potential therapeutic strategies remain hypothetical and require further investigation, it does not seem impossible to alter wound-healing mechanisms toward a scar-free, fetal-like phenotype. Such strategies will likely advance the practice of pediatric oculoplastic surgery and the practice of surgery as a whole. Alternatively, as fetal surgery becomes more widely performed, we may take advantage of the scarless wound-repair capacity of the fetus and treat ocular and adnexal abnormalities before birth. These developments may be the new frontiers of pediatric oculoplastic surgery.

Potential Strategies to Minimize Scarring in Postnatal Wounds

- Neutralizing antibodies to block an exuberant growth factor response
- Administration of antiscarring cytokines (TGF-β3) or proteins (fibromodulin)
- Stem cell transplantation
- Antisense oligonucleotides to inhibit growth factor synthesis
- Flooding wound with soluble receptor to inhibit growth factor effect
- Gene therapy to enhance integrin expression and reepithelialization
- Administration of extracellular matrix molecules (hyaluronic acid, fibronectin, tenascin) to enhance cell migration and wound closure

References

1. Larson BJ, Longaker MT, Peter Lorenz H. Scarless fetal wound healing: a basic science review. Hagey Plast Reconstr Surg. 2010;126(4):1172–80. doi:10.1097/PRS.0b013e3181eae781.
2. Adzick NS, Longaker MT, editors. Fetal wound healing. New York: Elsevier Scientific; 1992.
3. Harrison MR. Fetal surgery. Am J Obstet Gynecol. 1996;174:1255–64.
4. Adzick NS, Thom EA, Spong CY, et al. A randomized trial of prenatal versus postnatal repair of myelomeningocele. N Engl J Med. 2011;364:993–1004.
5. Kirsner RS, Eaglstein WH. The wound healing process. Dermatol Clin. 1993;11:629–40.
6. Colwell AS, Phan TT, Kong W, et al. Hypertrophic scar fibroblasts have increased connective tissue growth factor expression after transforming growth factor-beta stimulation. Plast Reconstr Surg. 2005;116:1387–90.
7. Terkeltaub RA, Ginsberg MH. Platelets and response to injury. In: Clark RAF, Henson PM, editors. Molecular and cellular biology of wound repair. New York: Plenum; 1988. p. 35–55.
8. Clark RAF, Lanigan JM, DellaPelle P, et al. Fibronectin and fibrin provide a provisional matrix for epidermal cell migration during reepithelialization. J Invest Dermatol. 1982;79:264–9.
9. Jennings RW, Hunt TK. Overview of postnatal wound healing. In: Adzick NS, Longaker MT, editors. Fetal wound healing. New York: Elsevier Scientific; 1992. p. 25–52.
10. Martin P, et al. Wound healing in the PU.1 null mouse – tissue repair is not dependent on inflammatory cells. Curr Biol. 2003;13(13):1122–8.
11. Tonnesen MG, Anderson DC, Springer TA, et al. Adherence of neutrophils to cultured human microvascular endothelial cells stimulated by chemotactic peptides and lipid mediators and dependence upon the Mac-1, LFA-1, p150,95, glycoprotein family. J Clin Invest. 1989;83:637–46.
12. Werner S, Grose R. Regulation of wound healing by growth factors and cytokines. Physiol Rev. 2003;83(3):835–70.
13. Lucas T, et al. Differential roles of macrophages in diverse phases of skin repair. J Immunol. 2010;184(7):3964–77.
14. Yates C, Hebda P, Wells A. Skin wound healing and scarring: fetal wounds and regenerative restitution. Birth Defects Res C Embryo Today. 2012;96(4):325–33.
15. Grinnell F. Wound repair, keratinocyte activation and integrin modulation. J Cell Sci. 1992;101:1–5.
16. Oksala O, Salo T, Tammi R, et al. Expression of proteoglycans and hyaluronan during wound healing. J Histochem Cytochem. 1995;43:125–35.
17. Savani RC, Khalil N, Turley EA. Hyaluronan receptor antagonists alter skin inflammation and fibrosis following injury. Proc West Pharmacol Soc. 1995;38:131–6.
18. Juhasz I, Murphy GF, Yan HY, et al. Regulation of extracellular matrix proteins and integrin cell substratum adhesion receptors on epithelium during cutaneous human wound healing in vivo. Am J Pathol. 1993;143:1458–69.
19. Falanga V. Growth factors and wound healing. Dermatol Clin. 1993;11:667–75.
20. Carpenter G, Cohen S. Epidermal growth factor. Annu Rev. 1979;48:193–216.
21. Clark RAF. Biology of dermal repair. Dermatol Clin. 1993;11:647–66.
22. Schmitt-Graff A, Desmouliére A, Gabbiani G. Heterogeneity of myofibroblast phenotypic features: an example of fibroblastic cell plasticity. Virchows Arch. 1994;425:3–24.
23. Grinnell F. Fibroblasts, myofibroblasts, and wound contraction. J Cell Biol. 1994;124:401–4.
24. Desmoulière A. Factors influencing myofibroblast differentiation during wound healing and fibrosis. Cell Biol Int. 1995;19:471–6.
25. Madden JW, Peacock EE. Studies on the biology of collagen during wound healing: dynamic metabolism of scar collagen and remodeling of dermal wounds. Ann Surg. 1971;174:511–20.
26. Holbrook KA, Hoff MS. Structure of the developing human embryonic and fetal skin. Semin Dermatol. 1984;3:185–202.
27. Lane AT, Scott GA, Day KH. Development of human fetal skin transplanted to the nude mouse. J Invest Dermatol. 1989;93:787–91.

28. Coolen NA, Schouten KC, Middelkoop E, et al. Comparison between human fetal and adult skin. Arch Dermatol Res. 2010;302(1):47–55.
29. Rowlatt U. Intrauterine wound healing in a 20 week human fetus. Virchows Arch A Pathol Anat Histol. 1979;381(3):353–61.
30. Adzick NS, Lorenz HP. Cells, matrix, growth factors, and the surgeon: the biology of scarless fetal wound repair. Ann Surg. 1994;220:10–8.
31. Block M. Wound healing in the newborn opossum. Nature. 1960;187:340–1.
32. Armstrong JR, Ferguson MWJ. Ontogeny of the skin and the transition from scar free to scarring phenotype during wound healing in the pouch young of the marsupial Monodelphis domestica. Dev Biol. 1995;169:242–60.
33. Lorenz HP, Longaker MT, Perkocha LA, et al. Scarless wound repair: a human fetal skin model. Development. 1992;114:253–9.
34. Longaker MT, Whitby DJ, Ferguson MWJ, et al. Adult skin wounds in the fetal environment heal with scar formation. Ann Surg. 1994;219:65–72.
35. Lorenz HP, Whitby DJ, Longaker MT, et al. Fetal wound healing: the ontogeny of scar formation in the non-human primate. Ann Surg. 1993;217:391–6.
36. Ihara S, Motobayashi Y, Nagao E, et al. Ontogenetic transition of wound healing pattern in rat skin occurring at the fetal stage. Development. 1990;110:671–80.
37. Longaker MT, Whitby DJ, Adzick NS, et al. Studies in fetal wound healing, VI: second and early third trimester fetal wounds demonstrate rapid collagen deposition without scar formation. J Pediatr Surg. 1990;25:63–9.
38. Longaker MT, Moelleken BRW, Cheng JC, et al. Fetal fracture healing in a lamb model. Plast Reconstr Surg. 1992;90:161–73.
39. Goss AN. Intra-uterine healing of fetal rat oral mucosal, skin and cartilage wounds. J Oral Pathol. 1977;6:35–43.
40. Meuli-Simmen C, Meuli M, Yingling CD, et al. Failure of the fetal sciatic nerve to regenerate at midgestation. Surg Forum. 1995;46:689–91.
41. Longaker MT, Whitby DJ, Jennings RW, et al. Fetal diaphragmatic wounds heal with scar formation. J Surg Res. 1991;50:375–85.
42. Cass DL, Bullard KM, Sylvester KG, et al. Wound size and gestational age modulate scar formation in fetal wound repair. J Pediatr Surg. 1997;32(3):411–5.
43. Olutoye OO, Alaish SM, Carr ME, et al. Aggregatory characteristics and expression of the collagen adhesion receptor in fetal porcine platelets. J Pediatr Surg. 1995;30:1649–53.
44. Olutoye OO, Yager DR, Cohen IK, et al. Lower cytokine release by fetal porcine platelets: a possible explanation for reduced inflammation after fetal wounding. J Pediatr Surg. 1996;31:91–5.
45. Jennings RW, Adzick NS, Longaker MT, et al. Ontogeny of fetal sheep polymorphonuclear leukocyte phagocytosis. J Pediatr Surg. 1991;26:853–5.
46. Adolph VR, DiSanto SK, Bleacher JC, et al. The potential role of the lymphocyte in fetal wound healing. J Pediatr Surg. 1993;28:1316–20.
47. Dixon JB. Inflammation in the foetal and neonatal rat: the local reactions to skin burns. J Pathol Bact. 1960;80:73–82.
48. Mast BA, Krummel TM. Acute inflammation in fetal wound healing. In: Adzick NS, Longaker MT, editors. Fetal wound healing. New York: Elsevier Scientific; 1992. p. 227–40.
49. Schwartz LW, Osburn BI. An ontogenic study of the acute inflammatory reaction in the fetal rhesus monkey. Lab Investig. 1974;31:441–53.
50. Whitby DJ, Ferguson MWJ. The extracellular matrix of lip wounds in fetal, neonatal and adult mice. Development. 1991;112:651–68.
51. Dillon PW, Keefer K, Blackburn JH, et al. The extracellular matrix of the fetal wound: hyaluronic acid controls lymphocyte adhesion. J Surg Res. 1994;57:170–3.
52. Frantz FW, Bettinger DA, Haynes JH, et al. Biology of fetal repair: the presence of bacteria in fetal wounds induces an adult-like healing response. J Pediatr Surg. 1993;28:428–34.
53. Kumta S, Ritz M, Hurley V, et al. Acute inflammation in foetal and adult sheep: the response to subcutaneous injection of turpentine and carrageenan. Br J Plast Surg. 1994;47:360–8.
54. Hopkinson-Woolley J, Hughes D, Gordon S, Martin P. Macrophage recruitment during limb development and wound healing in the embryonic and foetal mouse. J Cell Sci. 1994;107(Pt 5):1159–67.
55. Diegelmann RF, Cohen IK, Kaplan AM. The role of macrophages in wound repair: a review. Plast Reconstr Surg. 1981;68:107–13.
56. Adzick NS, Harrison MR, Glick PL, et al. Comparison of fetal, newborn, and adult wound healing by histologic, enzyme-histochemical and hydroxyproline determinations. J Pediatr Surg. 1985;20:315–9.
57. Longaker MT, Bouhana KS, Roberts AB, et al. Regulation of fetal wound healing. Surg Forum. 1991;42:654–5.
58. Duncan BW, Qian J, Liu X, et al. Regulation of prolyl hydroxylase activity in fetal and adult fibroblasts. In: Adzick NS, Longaker MT, editors. Fetal wound healing. New York: Elsevier Scientific; 1992. p. 303–16.
59. Chang J, Longaker MT, Lorenz HP, et al. Fetal and adult sheep fibroblast TGF-β1 gene expression in vitro: effects of hypoxia and gestational age. Surg Forum. 1993;44:720–2.
60. Lorenz HP, Chang J, Longaker MT, et al. Transforming growth factors β1 and β2 synergistically increase collagen gene expression in fetal fibroblasts but not in adult fibroblasts. Surg Forum. 1993;44:723–5.
61. Moriarty KP, Crombleholme TM. Differential fibroblast chemotaxis in fetal, neonatal, and adult cell lies in response to TGF-β1 and fetal bovine serum. Surg Forum. 1995;46:679–81.
62. Durham LA, Krummel TM, Cawthorn JW, et al. Analysis of transforming growth factor beta receptor binding in embryonic, fetal, and rabbit fibroblasts. J Pediatr Surg. 1989;24:784–8.
63. Alaish SM, Yager D, Diegelmann RF, et al. Biology of fetal wound healing: hyaluronate receptor expression in fetal fibroblasts. J Pediatr Surg. 1994;29:1040–3.
64. Freund RM, Siebert JW, Cabrera RC, et al. Serial quantitation of hyaluronan and sulfated glycosaminoglycans in fetal sheep skin. Biochem Mol Biol Int. 1993;29:773–83.
65. DePalma RL, Krummel TM, Durham LA, et al. Characterization and quantitation of wound matrix in the fetal rabbit. Matrix. 1989;9:224–31.
66. Knight KR, Horne RS, Leporre DA, et al. Glycosaminoglycan composition of uninjured skin and of scar tissue in fetal, newborn and adult sheep. Res Exp Med. 1994;194:119–27.
67. Meyer LJM, Stern R. Age-dependent changes of hyaluronan in human skin. J Invest Dermatol. 1994;102:385–9.
68. Estes JM, Adzick NS, Harrison MR, et al. Hyaluronate metabolism undergoes an ontogenic transition during fetal development: implications for scar-free wound healing. J Pediatr Surg. 1993;28:1227–31.
69. Bertolami CN, Donoff RB. Hyaluronidase activity during open wound healing in rabbits: a preliminary report. J Surg Res. 1978;25:256–9.
70. Longaker MT, Chiu ES, Adzick NS, et al. Studies in fetal wound healing, V: a prolonged presence of hyaluronic acid characterizes fetal wound fluid. Ann Surg. 1991;213:292–6.
71. Siebert JW, Burd AR, McCarthy, et al. Fetal wound healing: a biochemical study of scarless healing. Plast Reconstr Surg. 1990;85:495–504.
72. Epstein EH. [α1(III)] human skin collagen. J Biol Chem. 1974;249:3225–31.
73. Merkel JR, DiPaolo BR, Hallock GG, et al. Type I and type III collagen content of healing wounds in fetal and adult rats. Proc Soc Exp Biol Med. 1988;187:493–7.
74. Chesney J, Metz C, Stavitsky AB, Bacher M, Bucala R. Regulated production of type I collagen and inflammatory cytokines by peripheral blood fibrocytes. J Immunol. 1998;160(1):419–25.

75. Nath RK, Parks WC, Mackinnon SE, et al. The regulation of collagen in fetal skin wounds: mRNA localization and analysis. J Pediatr Surg. 1994;29:855–62.
76. Burd DAR, Longaker MT, Adzick NS, et al. Fetal wound healing in a large animal model: the deposition of collagen is confirmed. Br J Plast Surg. 1990;43:571–7.
77. Frantz FW, Mast BA, Diegelmann RF, et al. Rapid restoration of breaking strength in healing fetal rabbit wounds. Surg Forum. 1991;42:661–3.
78. Sztrolovics R, Chen XN, Grover J, Roughley PJ, Korenberg JR. Localization of the human fibromodulin gene (FMOD) to chromosome 1q32 and completion of the cDNA sequence. Genomics. 1995;23(3):715–7.
79. Halper J. Proteoglycans and diseases of soft tissues. Adv Exp Med Biol. 2014;802:49–58.
80. Ezura Y, Chakravarti S, Oldberg A, Chervoneva I, Birk DE. Differential expression of lumican and fibromodulin regulate collagen fibrillogenesis in developing mouse tendons. J Cell Biol. 2000;151(4):779–88.
81. Kalamajski S, Oldberg A. Fibromodulin binds collagen type I via Glu-353 and Lys-355 in leucine-rich repeat 11. J Biol Chem. 2007;282(37):26740–5.
82. Smith MM, Melrose J. Proteoglycans in normal and healing skin. Adv Wound Care. 2015;4(3):152–73.
83. Juneja SC, Veillette C. Defects in tendon, ligament, and enthesis in response to genetic alterations in key proteoglycans and glycoproteins: a review. Arthritis. 2013;2013:154812.
84. Delalande A, Gosselin MP, Suwalski A, Guilmain W, Leduc C, Berchel M, Jaffrès PA, Baril P, Midoux P, Pichon C. Enhanced Achilles tendon healing by fibromodulin gene transfer. Nanomed Nanotechnol Biol Med. 2015;11(7):1735–44.
85. Zheng Z, Zhang X, Dang C, Beanes S, Chang GX, Chen Y, Li CS, Lee KS, Ting K, Soo C. Fibromodulin is essential for fetal-type scarless cutaneous wound healing. Am J Pathol. 2016;186(11):2824–32. pii: S0002–9440(16)30307–8
86. Ffrench-Constant C, Van DeWater L, Dvorak HF, et al. Reappearance of an embryonic pattern of fibronectin splicing during wound healing in the adult rat. J Cell Biol. 1989;109:903–14.
87. Longaker MT, Whitby DJ, Ferguson MW, et al. Studies in fetal wound healing, III: early deposition of fibronectin distinguishes fetal from adult wound healing. J Pediatr Surg. 1989;24:799–805.
88. Whitby DJ, Longaker MT, Brown L, et al. Expression of alternatively spliced fibronectin mRNA during fetal wound healing. Surg Forum. 1995;46:644–6.
89. Mackie EJ, Halfter W, Liverani KD. Induction of tenascin in healing wounds. J Cell Biol. 1988;107:2757–67.
90. Whitby DJ, Longaker MT, Adzick NS, et al. Rapid epithelialization of fetal wounds is associated with the early deposition of tenascin. J Cell Sci. 1991;99:583–6.
91. Martin P, Lewis J. Actin cables and epidermal movement in embryonic wound healing. Nature. 1992;360:179–82.
92. Martin P, Nobes C, McCluskey J, et al. Repair of excisional wounds in the embryo. Eye. 1994;8:155–60.
93. Darby I, Skalli O, Gabbiani G. α-Smooth muscle actin is transiently expressed by myofibroblasts during experimental wound healing. Lab Invest. 1990;63:21–9.
94. Haynes JH, Krummel TM, Schatzki PF, et al. Histology of the open fetal rabbit wound. Surg Forum. 1989;40:558–60.
95. Longaker MT, Burd DAR, Gown AM, et al. Midgestational fetal lamb excisional wounds contract in utero. J Pediatr Surg. 1991;26:942–8.
96. Krummel TM, Ehrlich HP, Nelson JM, et al. In vitro and in vivo analysis of the inability of fetal rabbit wounds to contract. Wound Repair Regen. 1993;1:15–21.
97. Somasundaram K, Prathap K. The effect of exclusion of amniotic fluid on intrauterine healing of skin wounds in rabbit foetuses. J Pathol. 1972;107:127–30.
98. Ledbetter MS, Morykwas MJ, Ditesheim JA, et al. The effects of partial and total amniotic fluid exclusion on excisional fetal rabbit wounds. Ann Plast Surg. 1991;27:139–45.
99. Wider TM, Yager JS, Rittenberg T, et al. The inhibition of fibroblast-populated collagen lattice contraction by human amniotic fluid: a chronologic examination. Plast Reconstr Surg. 1993;91:1287–93.
100. Rittenberg T, Longaker MT, Adzick NS, et al. Sheep amniotic fluid has a protein which stimulates human fibroblast populated collagen lattice contraction. J Cell Physiol. 1991;149:444–50.
101. Whitby DH, Ferguson MWJ. Immunohistochemical localization of growth factors in fetal wound healing. Dev Biol. 1989;147:207–15.
102. Gould LJ, Diegelmann RF, Yager D, et al. The differential effects of platelet-derived growth factor (PDGF) isoforms on fetal wound healing. Surg Forum. 1993;44:728–9.
103. Krummel TM, Michna BA, Thomas BL, et al. Transforming growth factor beta (TGF-β) induces fibrosis in a fetal wound model. J Pediatr Surg. 1988;23:647–52.
104. DeLozier J, Nanney LB, Hagan K, et al. Epidermal growth factor enhances fetal epithelialization. Surg Forum. 1986;37:623–6.
105. Nanney LB, Stoscheck CM, King LE, et al. Immunolocalization of epidermal growth factor receptors in normal developing human skin. J Invest Dermatol. 1990;94:742–8.
106. Lin RY, Sullivan KM, Argenta PA, et al. Exogenous transforming growth factor-beta amplifies its own expression and induces scar formation in a model of human fetal skin repair. Ann Surg. 1995;222:146–54.
107. Sullivan KM, Lorenz HP, Meuli M, et al. A model of scarless human fetal wound repair is deficient in transforming growth factor beta. J Pediatr Surg. 1995;30:198–203.
108. Nath RK, La Regina M, Markham H, et al. The expression of transforming growth factor type beta in fetal and adult rabbit skin wounds. J Pediatr Surg. 1994;29:416–21.
109. Siebert JW, Sung JJ, Zirn J, et al. Immunohistochemical localization of TGF-β1, -β2, and -β3 isoforms during fetal wound healing. Surg Forum. 1995;46:646–8.
110. Martin P, Dickson MC, Millan FA, et al. Rapid induction and clearance of TGFβ1 is an early response to wounding in the mouse embryo. Dev Genet. 1993;14:225–38.
111. Shah M, Foreman DM, Ferguson MWJ. Neutralisation of TGF-β1 and TGF-β2 or exogenous addition of TGF-β3 to cutaneous rat wounds reduces scarring. J Cell Sci. 1995;108:985–1002.
112. Liechty KW, Crombleholme TM, Cass DL, Martin B, Adzick NS. Diminished interleukin-8 (IL-8) production in the fetal wound healing response. J Surg Res. 1998;77(1):80–4.
113. Liechty KW, Kim HB, Adzick NS, et al. Fetal wound repair results in scar formation in interleukin-10 deficient mice in a syngeneic murine model of scarless fetal wound repair. J Pediatr Surg. 2000;35:866–72.
114. Roberts AB. Transforming growth factor-β: activity and efficacy in animal models of wound healing. Wound Repair Regen. 1995;3:408–18.
115. Mustoe TA, Pierce GF, Thomason A, et al. Accelerated healing of incisional wounds in rats induced by transforming growth factor-beta. Science. 1987;237:1333–6.
116. Pierce GF, Mustoe TA, Lingelbach J, et al. Transforming growth factor beta reverses the glucocorticoid-induced wound-healing deficit in rats: possible regulation in macrophages by platelet-derived growth factor. Proc Natl Acad Sci USA. 1989;86:2229–33.
117. Beck LS, DeGuzman L, Lee WP, et al. One systemic administration of transforming growth factor-beta 1 reverses age- or glucocorticoid-impaired wound healing. J Clin Invest. 1993;92:2841–9.

118. Curtsinger LJ, Pietsch JD, Brown GL, et al. Reversal of adriamycin-impaired wounds: importance of transforming growth factor-beta. Surg Gynecol Obstet. 1989;168:517–22.
119. Cromack DT, Porras-Reyes B, Purdy JA, et al. Acceleration of tissue repair by transforming growth factor beta 1: identification of in vivo mechanism of action with radiotherapy-induced specific healing deficits. Surgery. 1993;113:36–42.
120. Grant MB, Khaw PT, Schultz GS, et al. Effects of epidermal growth factor, fibroblast growth factor, and transforming growth factor-beta on corneal cell chemotaxis. Invest Ophthalmol Vis Sci. 1992;33:3292–301.
121. Smiddy WE, Glaser BM, Thompson JT, et al. Transforming growth factor-beta 2 significantly enhances the ability to flatten the rim of subretinal fluid surrounding macular holes: preliminary anatomic results of a multicenter prospective randomized study. Retina. 1993;13:296–301.
122. Walraven M, Beelen RH, Ulrich MM. Transforming growth factor-β (TGF-β) signaling in healthy human fetal skin: a descriptive study. J Dermatol Sci. 2015;78(2):117–24.
123. Lichtman MK, et al. Transforming growth factor beta (TGF-β) isoforms in wound healing and fibrosis. Wound Repair Regen. 2016;24(2):215–22.
124. Shah M, Foreman DM, Ferguson MWJ. Control of scarring in adult wounds by neutralizing antibody to transforming growth factor beta. Lancet. 1992;339:213–4.
125. Little JA, et al. TGF β 3 immunoassay standardization: comparison of NIBSC reference preparation code 98/608 with avotermin lot 205-0505-005. J Immunoassay Immunochem. 2012;33(1):66–81.
126. Border WA, Noble NA, Yamamoto T, et al. Natural inhibitor of transforming growth factor-β protects against scarring in experimental kidney disease. Nature. 1992;360:361–4.
127. Viera M, et al. Innovative therapies in the treatment of keloids and hypertrophic scars. J Clin Aesthet Dermatol. 2010;3(5):20–6.
128. Roberts, Thomas L III. The emerging role of the CO2 laser in aesthetic plastic surgery. Presented at the XIII Congress of the International Society for Aesthetic Plastic Surgery, New York, NY, Sept 28–Oct 1, 1995.
129. Zadkowski T, et al. A new CO2 laser technique for the treatment of pediatric hypertrophic burn scars: an observational study. Medicine. 2016;95(42):e5168.
130. Krakowski AC, et al. Scar management in the pediatric and adolescent populations. Pediatrics. 2016;137(2):e20142065.
131. Yu M, et al. Polydeoxyribonucleotide improves wound healing of fractional laser resurfacing in rat model. J Cosmet Laser Ther. 2017;19(1):43–8.

Basic Principles, Techniques, and Instruments

4

Sarah M. Jacobs, Christopher B. Chambers, and Kenneth V. Cahill

To achieve predictable and optimal results, the surgeon must adhere to sound diagnostic and therapeutic principles, be skilled in basic surgical techniques, and have proper instrumentation [1]. The principles, techniques, and instruments described in this chapter for pediatric ophthalmic plastic and reconstructive surgery are readily applicable in the ophthalmic surgeon's practice, minimizing complications or the need for secondary procedures.

Preoperative Considerations

When meeting with a child and his/her family, it is useful for the surgeon to not only evaluate the physical findings on the child but also the family's motives, expectations, and insight into the desired surgery. The pediatric patient often presents an interesting set of challenges in this regard.

Patient and Family Expectations

Emotional stability of the pediatric patient and his/her parents may assume even greater importance if cosmetic surgery is requested. While the teenager may express direct concerns about appearance, in younger children such concerns are usually expressed by parents and grandparents. These concerns may or may not be realistic, and it is important for the surgeon to be patient and not to dismiss the family's distress. A careful explanation of surgical realities must be given, never promising more than doing one's best within these surgical realities.

S.M. Jacobs • C.B. Chambers (✉)
Department of Ophthalmology,
University of Washington, Seattle, WA, USA
e-mail: cbc108@uw.edu

K.V. Cahill
Ophthalmology/Eye Clinic, Nationwide Children's Hospital,
Columbus, OH, USA

Children who are about to enter school may be poised to experience heightened social traumas. Experience has demonstrated that families can often shelter and protect a child, especially those with major craniofacial deformities, preserving a positive sense of self. However, upon entering school, other children can be quite direct and even cruel in their social interactions. The surgeon must always remember to think of the child as a whole person, not just a surgical problem to solve, and to consider the whole family constellation in this regard. Suggestions for genetic and psychological counseling, as well as for family support groups, are important considerations, particularly for serious syndromes or deformities.

History

An appropriate history and examination (both systemic and ophthalmic) is mandatory for each patient, even when the diagnosis and indicated treatment appear obvious to the surgeon. Taking a careful history will also afford the doctor an opportunity to increase rapport with the patient and family before surgery, gaining a fuller sense of their needs and expectations.

From a systemic standpoint, information should be sought on medical conditions that may significantly influence the intraoperative risks or the surgical outcome. In trauma-related cases, specific details about time, place, and accompanying circumstances are particularly important, as a later preoccupation with secondary gain may distort the facts. Every effort should be made to obtain outside records from the child's pediatrician, as well as any other subspecialists involved in treatment. Obtaining an accurate history regarding bleeding disorders, medications, and allergies is mandatory.

From an ophthalmic standpoint, a history of prior eye care, refractions, and eye patching all provide valuable clues to preoperative visual impairment and should be noted in the patient's record. Specific questions about previous ocular or craniofacial surgery should be pursued.

© Springer International Publishing AG 2018

J.A. Katowitz, W.R. Katowitz (eds.), *Pediatric Oculoplastic Surgery*, https://doi.org/10.1007/978-3-319-60814-3_4

Physical Exam

With young children, playful interaction will usually permit useful observation even without touching the patient. After a time, the child may relax and feel comfortable enough to allow elements of the exam requiring physical contact.

Preoperative photographs are useful as a learning aid for the surgeon, as verification for insurance purposes, and in refreshing the memory about details of the patient during surgery. For easy comparison, preoperative and postoperative photographs should be taken at the same distance and from the same perspective. Older photographs of the patient are often helpful, along with previous operative notes and pathology reports.

Consent

The surgeon must make a recommendation based on an honest, objective view of the findings but should resist the temptation to rush the patient's decision. It is often helpful after the initial interview to give the patient and family some time alone to think about what has been discussed. Sometimes that will mean a return visit to the office, while in other cases, a few minutes alone in a quiet, private area will be sufficient. This time gives the patient and family the opportunity to weigh alternatives and bring matters to the surface that may have been difficult to express initially. With elective procedures, it is imperative that the patient and parents, not the surgeon, make the actual decision to proceed with surgery.

Serious complications can occur during any surgical procedure, so the surgeon, patient, and family should view all surgical procedures with an appropriate measure of caution and respect. An operative permit specifically mentioning the remote possibility of blindness during the course of surgery is particularly helpful in properly preparing the patient and family for surgery. Descriptive terms that might be used to put the patient and family at ease—such as "routine," "simple," and "minor"—should be avoided, because they imply a guarantee of success without any complications. Reading, understanding, and signing the operative permit should be completed in the relaxed atmosphere of the office when the surgery is scheduled, not left until the day of surgery. Taking care of this matter in the office also allows patients and families the opportunity to discuss with the surgeon any questions they may have regarding the permit or the procedure. The preoperative evaluation, surgical indications, recommendations, and discussion of risks and alternative treatment should be clearly documented in the patient's record.

Preoperative Planning

Pediatric ophthalmic plastic surgery requires not only planning but also flexibility. The surgeon should begin each operation with a basic plan and with alternative plans should circumstances during surgery so dictate. The ultimate purpose of this planning is to bring about the best possible result in the most efficient manner. Preoperative planning minimizes operating time, tissue exposure, and anesthesia time, which in turn helps to minimize the overall risk to the patient.

Intraoperative Considerations: Instruments, Needles, and Suture Materials

Instruments must be kept in good repair to avoid needless tissue damage. A variety of forceps, skin hooks, scalpels, scissors, and sutures are useful in ophthalmic plastic surgery and should be readily available for every case. Specific instrument and suture choices are determined by the type of the tissue being handled or repaired [2]. The instrument tray is not a recommended place to economize. The surgeon should purchase the best quality instruments available.

Forceps and Skin Hooks

Forceps may be either toothed or smooth. Toothed forceps are used to handle the tissue. Non-toothed (smooth) forceps are designed to hold and tie sutures. Smooth forceps should not be used for handling the tissue, as they tend to crush the tissue which can delay wound healing or make histopathologic examination difficult.

Regular ophthalmic forceps (e.g., 0.5 mm) are usually the most appropriate for ophthalmic plastic procedures. The toothed forceps used in general plastic surgery are generally too heavy for eyelid and orbital work, and they risk damaging these delicate tissues. The fine forceps (e.g., 0.12 mm) used for cataract, cornea, and glaucoma surgery are generally too weak to adequately grasp periocular tissue. In pediatric surgery, operating on a smaller child does not necessarily entail using forceps with smaller teeth.

Smooth, fine-tipped jeweler's forceps are particularly useful for suture removal and epilation of abnormal cilia. Bishop-Harmon and Adson forceps have teeth set at right angles, permitting secure stabilization of tissue between the teeth. The ends of the forceps are free of barbs or rough surfaces, helping to prevent damage to tissue in front of the forceps, which is important in intraocular surgery. Castroviejo

forceps have forward-angled teeth, permitting greater ease in grasping and manipulating tissues in ophthalmic plastic surgery. A tying platform can be added to toothed forceps, so that the same set of forceps can be used to hold and tie sutures as well as to grasp tissue.

Small, double-pronged skin hooks have wide application in ophthalmic plastic surgery. Hooks can strongly engage skin flaps to retract and elevate them while causing only pinpoint piercing-type damage to the tissue, whereas forceps in the same situation may distribute a broader crushing or tearing injury to the tissue. Multipronged rakes (e.g., the 4-pronged Blair rake) are also appropriate in a number of circumstances for tissue retraction and stabilization.

Scissors

Scissors may be straight, curved, sharp pointed, or blunt tipped. They may be standard cross-acting scissors with ring handles or have a spring action that is squeezed between the fingers. A variety of scissors may be used during every procedure and should always be available on the surgical tray. The choice of scissors is often a matter of personal experience and preference, but some general concepts are worth keeping in mind. The curve of the scissors should follow the curve of the proposed incision or the concavity or convexity of the tissue surface. Separating tissue planes by spreading is usually best accomplished with blunt-tipped scissors with ring handles, minimizing the risk of perforation and bleeding. Tiny, short-nosed, sharp-tipped scissors are especially useful in removing sutures and small lesions from the lids.

Scissors, like all instruments, must be carefully maintained. Dull or misaligned blades can crush or macerate tissue, causing damage that impedes good operative outcomes. The surgeon should have them routinely serviced, with sharpening by a skilled technician. When sharpening no longer restores proper function, the scissors should be replaced.

Blades

Razor blades, or their more common replacement, the so-called supersharp blades, make excellent cutting edges for ophthalmic plastic procedures. Traditional curved or straight scalpel blades are also useful. In general, pointed blades are used for penetrating, dagger-like incisions, as in incising a chalazion for curettage or in manually shaving off a lid margin lesion. The No. 15 Bard-Parker blade is often the appropriate choice for external eyelid and periocular incisions.

Needle Drivers

Needle holders come in a variety of sizes. The shape of the jaw into which the needle is loaded may be curved or straight. Spring-loaded needle holders such as the Castroviejo are more typically convenient for oculoplastic surgery than needle drivers with a traditional ring handle design such as the Webster. Choice is dictated by the size of the needle required for the repair and by the surgeon's preference. Needle holders designed to be used with delicate ophthalmic needles will be damaged if they are used with larger needles. A locking mechanism is usually incorporated in a needle holder used for ophthalmic plastic surgery. The lock is typically engaged or released by gently squeezing the finger-grip surface. This locking feature permits the needle to be securely loaded and held between suture passes. A properly functioning lock will not compromise smooth and accurate needle passage.

Suture Needles

Suture needles consist of a head, a shaft, and an eye (Fig. 4.1). The head is the tip and cutting edge, which may be shaped as a taper, cutting point, reverse cutting point, or spatulated point.

The taper point is used when tissue resistance is low and tissue cutting by the point is to be minimized. Taper-point needles are recommended for superior rectus bridle sutures, microvascular anastomoses, and closure of conjunctival flaps in glaucoma filtration surgery. Because the tapered point stretches the tissue around it as it passes, rather than cutting the tissue, the hole created by the pass is as compact and watertight as possible. Tapered points are at a disadvantage in thicker skin and soft tissue, as it may take significantly more force to push the needle through the pass compared to a cutting needle.

The cutting and reverse cutting needles pass through tissue much more easily because they cut a larger track. On each of these needles, the point is shaped like the prow of a boat and acts as a tiny blade to slice through the tissue as the leading edge of the needle contacts it. For a classic cutting needle, the cutting surface is oriented toward the interior curve of the needle. On a reverse cutting needle, the cutting surface is oriented toward the outer curvature, making it less likely to inadvertently cut back through the tissue ("cheese wire") if the needle is pulled toward the surgeon. Reverse cutting needles are the most frequently used needles in ophthalmic plastic surgery.

Spatulated needle points also pass with minimal resistance. They have a cutting surface at the lateral sides of the needle head, but are smooth along the inner and outer curva-

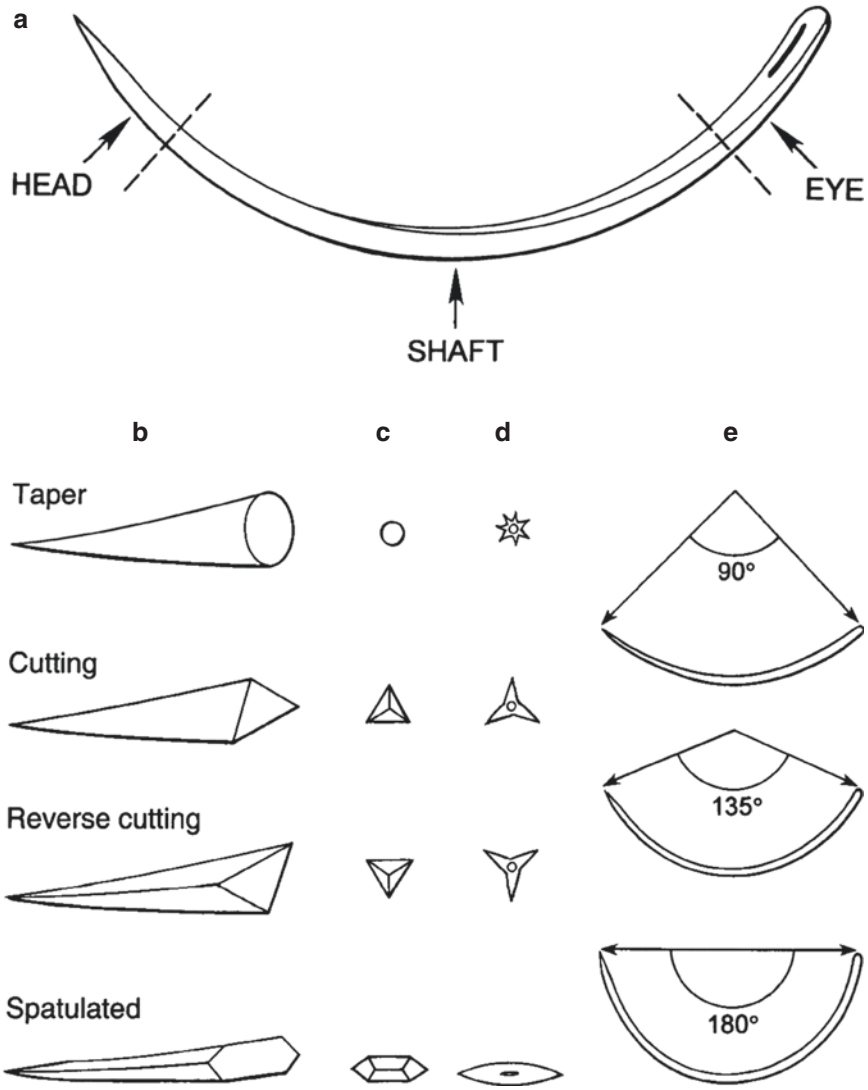


Fig. 4.1 Suture needles used in ophthalmic plastic surgery. (**a**) Structural zones of a surgical needle. (**b**) Various types of needle points. (**c**) Schematic cross section of each needle point. (**d**) Schematic cross section of tissue tracks created by each needle design shown above. (**e**) Examples of curvatures commonly used for surgical needles (Adapted from Cahill and Carroll [1])

ture of the needle. As such, they cut a horizontal tract and are utilized when a suture is to be passed through a thin, flat tissue. For example, spatulated needles are invaluable for scleral sutures in strabismus surgery, securing a mucous membrane graft over the cornea, partial-thickness tarsal sutures in ptosis surgery, and securing cartilage or hard palate grafts in eyelid reconstruction surgery.

The shaft of the needle typically has a partly flattened profile to permit secure fixation in the jaws of a needle holder. The surgeon should take care to grasp the needle at its flat shaft rather than near its head (which dulls the point) or its rounded base (which allows the needle to roll and rotate within the needle driver).

The eye of the needle is now typically replaced by a "swedged-on suture" in which the suture material has been attached by the manufacturer by means of crimping it into the back end of the needle rather than threading the material through an opening or the eye in the needle.

The needles used in ophthalmic plastic surgery are most often curved, commonly with an arc that is 3/8 of a circle (135°). Some spatulated needles used for making straight passes through the tarsus or sclera have an arc that is 1/4 of a circle (90°). Sutures that must be passed in extremely tight spaces or with a deep-yet-short course, such as those used in canalicular laceration repairs, may be provided with a stiff needle that is 1/2 of a circle (180°).

Although the curvature of a needle assists the surgeon in making different shapes of suture tracts, the path through which the needle point is directed is the ultimate determinant of the shape of the suture tract. This can be influenced by tissue traction and by the torsional force applied to the needle holder. Regardless of the curvature of the needle, the length of the needle should always be greater than the desired course of the suture, so that the needle shaft can be grasped by the needle holder during both insertion and removal. Attempting long passes with short needles can

result in burial of the entire needle beneath the soft tissue, making it difficult to retrieve.

Suture Materials

Suture materials commonly used in ophthalmic plastic surgery are gut, polyglactin (Vicryl, Dexon), silk, nylon, and polypropylene (Prolene).

Gut can be obtained in plain, fast-absorbing, or chromic forms. Plain gut has relatively low tensile strength and dissolves over time. Standard plain gut can take several weeks to fully absorb and frequently leaves suture tract scars on the skin. A fast-absorbing plain gut has been developed for skin sutures that do not have to be removed (Ethicon 1916G). It absorbs within a week so that an epithelialized suture tract is unlikely to form. Chromic gut is chemically treated to resist breakdown, so it absorbs even more slowly than plain gut. It provides tensile strength for approximately 2 weeks and can be used for buried sutures to close tarsal plate, orbicularis muscle, and the subcuticular tissue plane. 5-0 chromic gut can provide a good material for temporary tarsorrhaphy sutures after enucleation surgery if it is placed from gray line to gray line (i.e., suture is externalized through the lid margin and tied, rather than through the skin of the anterior lamella), holding the lid closed for ~2 weeks without the need for suture removal thereafter.

Polyglactin is a synthetic, absorbable, braided multifilament suture material. It has high tensile strength for approximately 3 weeks. The tensile strength is then gradually lost over the next month. It is used for sutures in the tarsal plate, for orbicularis muscle closure, buried deep sutures to take tension off of wound closure, and in repairs of the canthal tendons that are not under excessive tension. Because of its slow breakdown time, it should not be left in place as a skin closure, as this will lead to visible scarred suture tracts.

Silk is a multifilament suture material with high tensile strength. It is an easy suture to use because it is fairly pliable and ties easily, but it does not absorb. It is not used often for buried sutures because it occasionally causes a suture granuloma or becomes a site of infection. 6-0 black silk can be used for eyelid skin sutures, which are typically removed after 5 days. When used for lid margin repairs, 6-0 black silk can be left for 8–12 days without creating suture scars.

Nylon and polypropylene are nonabsorbable synthetic monofilament suture materials with high tensile strength. Nylon degrades over several years, while polypropylene is virtually permanent. Polypropylene is used for canthal tendon surgery if a permanent suture is needed. Either of these materials can be used for skin sutures where a "slick," easily removed suture is desired. Because nylon and polypropylene are monofilament materials, they can be placed in running fashion with less resistance to passage through tissue during removal than a multifilament suture material. Polypropylene has less tissue resistance than nylon and is the most "wiry" suture material, which makes it more difficult to handle. Because of their slick and wiry properties, polypropylene and nylon sutures are more likely to unravel if knots are not tied secure and square with multiple throws and long tails.

Intraoperative Techniques: Incision, Dissection, and Traction

Incision Location

Faulty placement or execution of an incision may result in a functional success but cosmetic disaster [2]. Incisions in adults are usually planned preoperatively to follow the normal skin creases and folds, often enabling planned incisions to be hidden or camouflaged (Fig. 4.2). These folds occur along relaxed skin tension lines (RSTL), which correspond to the directional pull existing in relaxed skin. In children the surgeon may have to imagine where these lines will be in later life, as they have not yet formed. However, some lines are formed by deeper skin attachment to facial muscles so that a crease or dimple may be seen with smiling or other forms of expression. Polaroid or digital pictures can help to remind the surgeon of the location of such lines and the possible use of these for surgical incision.

Marking

Incision lines should be marked prior to injecting local anesthesia to avoid blurring anatomic landmarks and misplacing



Fig. 4.2 Relaxed Skin Tension Lines (RSTL) in children represent future *wrinkle lines*

the incision. If the marks are to be drawn prior to skin preparation, the skin should first be gently wiped with an alcohol swab and dried. This permits the ink to penetrate the skin so that the scrub will not remove it.

Protecting the Eye

Prior to creating incisions near the eye, a plastic protective shell lubricated with ointment may be placed on the globe both for protection from blades, needles, and instruments. The shell also keeps the operating room light from bothering the patient under local anesthesia.

Creating the Incision

It is helpful to begin cutting at the lowest gravity-dependent part of the incision to keep blood from obscuring the advancing incision line. With rare exceptions (i.e., incisions within the eyebrow), incisions should be made perpendicular to the skin's surface, keeping the skin taut to avoid beveling the incision and subsequent poor wound closure secondary to overlapping wound edges. The skin incision should be made through the epidermis and dermis, which is the thinnest in the eyelid and the thickest immediately above the brow. The depth of the incision can be judged by looking at the cut edges. They will begin to spread once the full thickness of the dermis is cut in taut skin.

To minimize tissue trauma, either skin hooks or fine-toothed forceps should be used to handle the wound edges. If forceps are used, the finest instrument that will accomplish the task is usually chosen. This applies mostly to the final skin closure. When working with larger or heavier flaps, a larger, toothed forceps is useful to avoid tearing the tissue from the weight or tension created by pulling or supporting such flaps. Brow tissue, for example, may require heavier forceps (e.g., Adson or Adson-Brown), whereas fine 0.5 mm Castroviejo forceps may be more appropriate for delicate eyelid skin.

Dissection

A variety of scissors are useful in ophthalmic plastic surgery. Spring action scissors such as Westcott, and direct action scissors such as Iris or Kaye, should be kept immediately available on the instrument tray. In general, gently curved, sharp-pointed scissors are most satisfactory in completing a curved incision. The curve of the instrument should correspond to the directional curve of the incision. Blunt-tipped, curved scissors (e.g., Stevens Tenotomy) are of particular value in undermining. The blunt tip allows the surgeon to push into the tissue plane and spread the blades with minimal risk of "buttonholing" the overlying eyelid skin. Delicate, sharply pointed, fine-tipped scissors are especially useful in surgery near the lacrimal apparatus.

Traction and Countertraction

Placing skin and soft tissue on stretch enables finer incision lines, better view of dissection planes, optimized access for cautery without injury to surrounding tissue, and improved exposure within deep incisions or in the orbit. Depending upon the situation, traction can be achieved with the assistance of cotton-tipped applicators, atraumatic smooth retractors (e.g., Desmarres or Ragnell for the eyelid, or malleable ribbons within the orbit), toothed retractors such as skin hooks or rakes to firmly engage the elevated tissue, or specialized eyelid forceps (e.g., Von Graefe) which provide ridges for traction but a broad platform to distribute the force less traumatically.

Traction sutures may also be placed through the upper or lower eyelid margin and then held in place by an assistant or a hemostat affixed to the drape. For eyelid margin traction sutures, the plane of the gray line is utilized. A 4-0 black silk suture with a reverse cutting needle is introduced into the gray line in a vertical direction, while the lid is kept on stretch horizontally. After the needle penetrates 2 mm, it is turned so that the curvature of the needle is followed parallel to the plane of the lid until the point of the needle emerges in the gray line. This suture can be left in place and used postoperatively as a Frost suture, if indicated.

Intraoperative Techniques: Hemostasis

The benefits of meticulous hemostasis are apparent during surgery, but carry forward into the postoperative period as well. Hemostasis aids visualization, which permits accurate tissue identification, dissection, and wound closure. At the conclusion of the case, it eliminates the need for elaborate dressings. Postoperatively, it promotes optimum wound healing, as blood clots trapped in a wound can retard healing, increase scarring, and serve as a nidus for microorganism growth.

The use of a local anesthetic containing epinephrine (1:100,000–1:200,000), even when the patient is under general anesthesia, is a worthwhile first step in achieving good hemostasis. The anesthesiologist should be consulted prior to local epinephrine use so that cardiac and blood pressure changes can be anticipated.

Manual pressure with cotton-tipped applicators or a gauze sponge is frequently sufficient to obtain hemostasis from pinpoint bleeding sources during eyelid surgery. Most bleeding in the eyelids is adequately handled with a disposable thermal cautery unit or monopolar or bipolar electrocoagulation.

The Colorado needle (Colorado Biomedical, Evergreen, CO 80439) is particularly useful. It is a very fine, reusable, monopolar cautery tip that can be used in modes for cutting and cautery.

When working deep within a cavity, such as when performing a dacryocystorhinostomy, the ophthalmic surgeon should consider using the combined suction-electrocautery unit popular with neurosurgeons. Pharmaceutical adjuncts such as cotton pledgets soaked in 1:100,000 epinephrine solution or a 1:1 mixture of 4% cocaine and oxymetazoline (Afrin), an absorbable gelatin sponge soaked in thrombin, or microfibrillar collagen hemostat powder (Avitene) are occasionally useful for orbital and lacrimal surgeries, or within the oral cavity after graft harvest.

Patients, families, and the general pediatricians managing their systemic care should be asked about anticoagulant usage, with specific attention to warfarin, heparin, clopidogrel, aspirin, and other NSAIDs, but also non-prescription supplements such as fish oil and gingko [3]. If at all medically possible, anticoagulants should be stopped for an appropriate time interval before surgery in order to minimize the risk of bleeding. Optimal coagulation is especially important in children, both to decrease blood loss during surgery and to reduce the risk of postoperative hemorrhage. Lower circulating volume means that intraoperative blood loss has a higher relative hemodynamic impact on smaller patients. Furthermore, it is often difficult to maintain activity restrictions postoperatively in young children, which raises the risk of hemorrhage after surgery due to prematurely straining, bending, or rubbing the wound.

Intraoperative Techniques: Wound Closure

If a wound is contaminated, cleansing should be the first step in management. This is usually done by thoroughly irrigating the wound with sterile saline or antibiotic solutions. In addition, the wound must be carefully searched for foreign bodies that could interfere with wound healing and give rise to a draining fistula tract. Foreign bodies or dirt trapped in the subcutaneous tissue or skin may leave tattoo marks that are most difficult to manage satisfactorily once healing has occurred.

While extensive debridement in the eyelids should be avoided, frankly necrotic tissue should be carefully trimmed prior to suturing. Any trimming of the wound edges, however, should be done with extreme care, especially if the wound crosses the relaxed skin tension lines. A straight scar from a wound that has been carelessly trimmed may ultimately be more disfiguring than the scar from a carefully closed jagged, irregular laceration.

Closing Deep Tissue

"Dead space," which is an open cavity in the internal recesses of the incision, can serve as a reservoir for hematoma and microorganisms, prevent accurate wound closure, and impair wound healing. Properly placed deep sutures should not only eliminate dead space in the depths of the wound but also relieve tension from the cutaneous suture line, thereby minimizing postoperative widening of the wound.

For deep closure, absorbable sutures are popular (e.g., 4-0 or 5-0 chromic gut or polygalactin on a spatulated needle or reverse cutting needle). The knots of the subcutaneous sutures are usually buried to avoid interference with skin closure and decrease the risk of postoperative erosion of the knot through the wound surface (Fig. 4.3). To ensure that the knot does in fact assume the desired buried position in the depths of the wound, the surgeon must be sure that both ends of the suture are on the same side of the loop before tying the suture and must then pull the ends of the suture in a direction along the length of the incision while tightening the knot. Tarsal sutures are a specific exception to burying the knot

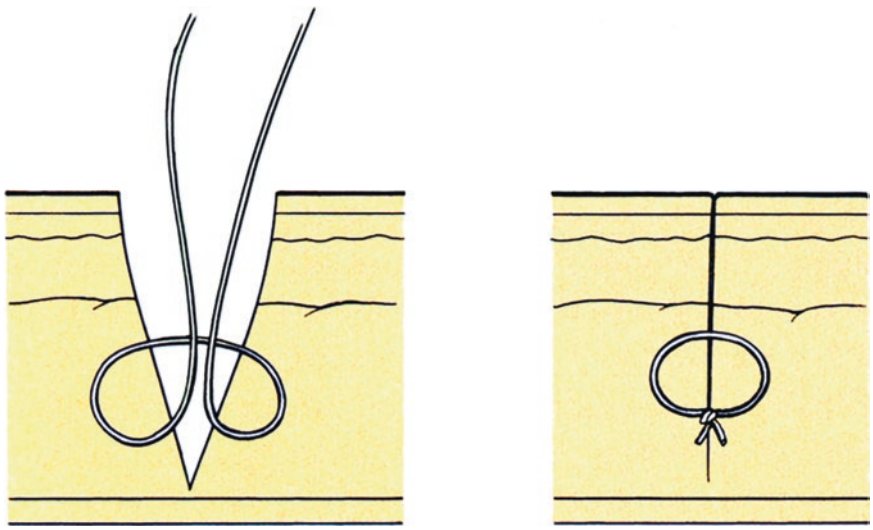


Fig. 4.3 Technique of buried suture placement. The knots of subcutaneous sutures should lie in the base of the incision (Adapted from Cahill and Carroll [1])

of a subcutaneous suture, as erosion through the conjunctiva may cause corneal ulceration. Instead, the knot for deep tarsal sutures should be oriented toward the anterior (orbicularis) surface rather than the posterior (conjunctival) surface.

Closing Skin

There is room for personal preference regarding the suture material (silk, nylon, fast-absorbing gut, etc.) and the method of suturing (interrupted, running, subcuticular, etc.). However, there are baseline principles to be followed every time in order to minimize the final scar:

- *Choose a needle holder that is appropriate to the size of the needle*, allowing a controlled movement which follows the curve of the needle as it passes through the tissue.
- *Use the smallest caliber suture that will accomplish the specific task*. Size 6-0 or 7-0 sutures on atraumatic cutting or reverse cutting needles are commonly used for closure of thin skin on the eyelids. Size 5-0 or 6-0 sutures may be used above the brow or beyond the nasojugal fold.
- *Skin tension should be minimized* in order to prevent widening of the scar as the incision heals. This is accomplished by orienting incisions appropriately and by using appropriate supportive deep sutures. Some types of wounds require special tension-relieving sutures for skin closure, such as the vertical and horizontal mattress suture or the near/far-far/near suture (Fig. 4.4). The vertical mattress suture lies perpendicular to the wound edges and is most useful in the heavier tissues of the eyebrow, cheek, and temple or when closing the donor site for a dermis-fat graft taken from the buttock. This suture can be used to reduce the number of buried subcutaneous sutures and therefore help minimize "suture reaction." To eliminate inturning of the wound edges, the vertical mattress suture should not be used to bring the skin edges completely together; rather, an interrupted or running suture should be used for this purpose after the vertical mattress sutures have been placed. The horizontal mattress suture finds specific application in closing the tips of triangular flaps and in closing unequal wound edges. The near/far-far/near suture is occasionally useful in relieving tension on snug eyelid margin closures.
- *Wound edges must be aligned without overlap or rolling under* of the skin edge. The edge opposite the surgeon should be grasped with either fine-toothed forceps (e.g., Bishop-Harmon, Manhattan, Castroviejo) or a skin hook directly in line with the suture needle. This helps maintain a pass perpendicular to the wound edge. In thin eyelid skin with a tendency to roll under at the incision edge, the tooth of the forceps can be used to unscroll the edge and then maintain it in everted position during the suture pass.
- *Everting the wound edges is essential* in preventing late depression of the resulting scar. This is especially important in the thicker skin of the brow and cheek. In cross section, the sutures should assume a trapezoid configuration where slightly more deep tissue is included in the suture, thereby forcing the wound edges outward when the knot is tied.
- *Suture knots must be tied with appropriate tension*. Faulty suture tension can give rise to necrosis of the wound edges if the sutures are tied too tightly; an unsightly wide scar may result if they are tied too loosely. In tying sutures, the surgeon can obtain the desired tension with an initial "double throw," or two wraps, of the suture material. Additional single-wrap throws are then placed as square knots to secure this tension. Usually two additional throws are sufficient with monofilament sutures, particularly if there is any weight or tension. Occasionally, an initial triple throw is useful to avoid slippage when the closure is under tension. The surgeon should resist the common tendency to increase suture tension with the second throw, as this can result in distortion of the wound edges and subsequent unnecessary scarring. To prevent a bothersome loop of suture in the attempt to tie a knot, it is helpful to pull the suture far enough through the wound so that the end of the suture can be grasped with the needle holder or tying forceps. This also saves suture material. Another valuable point is to work with an appropriate length of suture. Although one wishes not to waste material, 18 inches of suture only gets in the way of efficiency. One should trim the excess as needed.
- *The sutures should be removed or absorbed as soon as incisional healing allows*. Sutures which remain in place too long can lead to local reactions, scars, or epithelialized suture tracts. To minimize scarring, skin sutures that have little or no tension on them should be removed in 3–5 days. If necessary, the wound edges can then be reinforced with 1/8-inch or 1/4-inch Steristrips (3 M Medical-Surgical Division, St. Paul, MN) for an additional 3–5 days. If vertical mattress sutures have been used in closing the wound, they are removed in 7 days. Lid margin sutures are usually removed in 8–12 days.

Traction Sutures and Tarsorrhaphy Sutures

Traction sutures placed through the gray line of the lids may be useful to ensure corneal protection and/or to keep lid tissues on stretch. A Frost suture can be used to stretch one lid (Fig. 4.5a). An intermarginal suture brings both lids together, but may limit visualization of the ocular surface depending on placement (Fig. 4.5b, c). The serpentine intermarginal suture brings both lids together and can be loosened to permit inspection of the ocular surface (Fig. 4.5d).

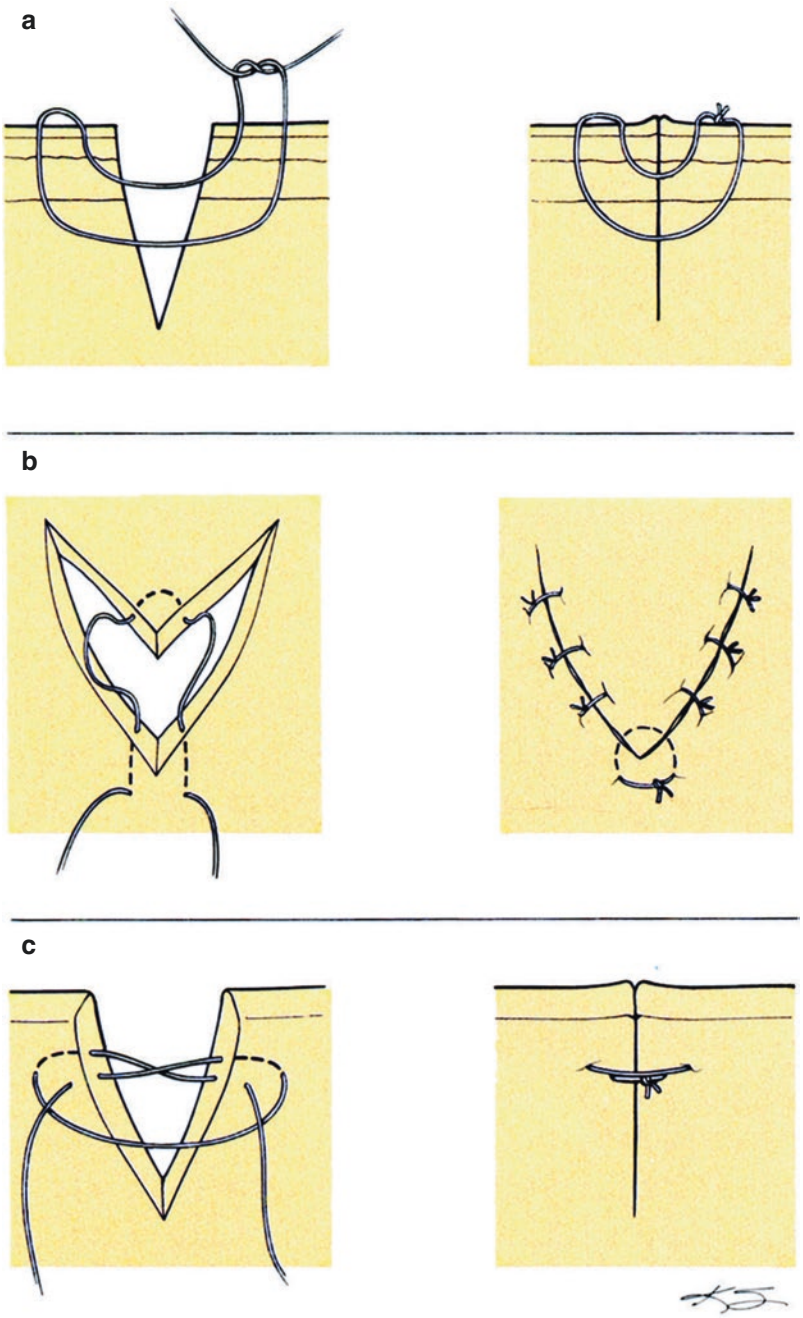


Fig. 4.4 Tension-relieving sutures. (**a**) The vertical mattress suture, (**b**) the horizontal mattress suture, and (**c**) the near/far-far/near suture (Adapted from Cahill and Carroll [1])

As an added consideration in children, postoperative suture removal can be traumatic, at times even requiring a return to the operating room for removal under anesthesia if the child will not permit safe removal in the clinic. Thus, although nonabsorbable materials are often used for skin closure in adults, using absorbable sutures in children eliminates the need for suture removal.

A rapidly dissolving 6-0 fast gut suture is available for suturing skin (e.g., Ethicon 1916G). This rarely causes epithelialized suture tracts or skin inflammation, which can result from the use of regular gut sutures. It allows more flexibility in the timing of postoperative visits. Because the rapidly dissolving gut suture has less tensile strength than other sutures of the same caliber, it must be used only for skin alignment and not for closing wounds under tension. Additional throws may be placed on the knots since the decreased tensile strength may *prevent the knot from being cinched as tightly as stronger sutures.* For supporting wounds under tension, beige-colored Vicryl or Dexon (Davis & Geek, Inc., Manati, Puerto Rico) can be effective. The 7-0 Dexon can be used as an interrupted stitch for skin closure to supplement a running fast-absorbing gut. It is also very useful for small flaps and Z-plasties as in epicanthal fold repairs.

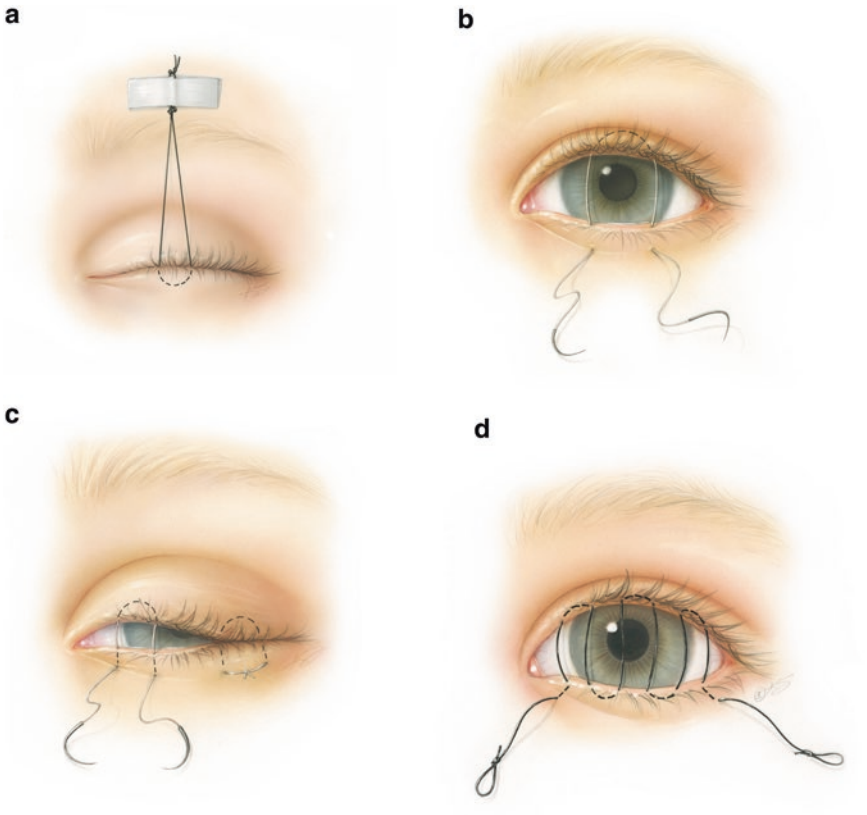


Fig. 4.5 Gray line sutures. (**a**) A Frost gray line suture can be taped to the skin for tension and loosened to inspect the globe. (**b**) An intermarginal gray line suture keeps the ocular surface protected but does limit visualization of the globe unless tied with a slipknot. (**c**) The intermarginal suture technique can be done in any combination of central, lateral, and/or medial as dictated by the clinical situation. The sutures can be secured with or without a bolster. (**d**) An intermarginal serpentine gray line suture can also provide a reversible lid method of closure. The ends may be taped in place and loosened for visualization as needed. The serpentine suture can remain in place for 2–3 weeks

Postoperative Dressings and Wound Care

Bandages can be avoided after many ophthalmic plastic procedures, particularly in the pediatric patient. In children, dressings tend to become an annoyance that leads to more picking and wound manipulation. Meticulous intraoperative attention to hemostasis and wound closure results in sutured incisions that do not need postoperative dressings. However, there are times when a dressing should be utilized: After surgery of anophthalmic sockets and some orbital cases, a dressing may be necessary in order to protect the site, apply pressure, or decrease the risk of postoperative hemorrhage. Bolster dressings may be needed after lid reconstructive cases with skin grafts in order to improve graft adherence and survival. Tegaderm dressings are particularly useful for fat graft harvest wounds on the buttock, providing protection in children wearing diapers. If there is concern of disrupting the eyelid wound during sleep, the patient may be asked to wear a protective metal or plastic shield to bed.

When such bandages are required, the use of elbow restraints is often very useful in young or developmentally delayed pediatric patients. These allow the child to play, but not be able to reach hands to face. Masking of signs and symptoms, injury to delicate eyelid tissue, and blindness have been reported following the use of "pressure" patches, so their use should be monitored appropriately.

For postoperative swelling and ecchymosis, cold packs or preferably several gauze pads soaked in ice water can be used intermittently for a total of 15 min out of each waking hour on the day of surgery for their vasoconstrictive effect in minimizing postoperative edema. Warm packs for 10 min every 3 h may be started 24 h after surgery to promote vasodilation and absorption of the edema that has occurred. The use of these may, however, be difficult in the pediatric age group. Excessive straining, which may cause venous congestion, increased swelling, and bleeding, should be avoided as much as possible.

The family should be specifically instructed on how to keep the area clean (e.g., gentle, twice-daily wiping with a clean, moist cloth or cotton ball, followed by the application of a small amount of ophthalmic antibiotic ointment). Some patients have difficulty attending to this wound hygiene because of their fear of "hurting something." Instructions regarding baths or showers must be individualized. Prolonged soaking of the wound disrupts the healing process.

Wound Healing

Wound healing is a continuum initiated by a traumatic or surgical event that may continue for years [4]. This process can be divided into four overlapping phases: inflammatory, fibroblastic, wound contraction, and scar maturation. This is covered in more detail in Chap. 3.

Inflammatory Phase

In uncontaminated wounds, the inflammatory phase may last 4–6 days. This phase is initiated by vasoconstriction and deposition of fibrin platelet clots that help control bleeding. Vasodilation follows and is accompanied by the release of chemotactic substances that attract leukocytes and macrophages to the wound. These cells cleanse the wound of debris. Epithelial cells also migrate into the wound to bridge the edges and serve as a barrier to infection. Proper wound hygiene, along with careful tissue handling, can shorten the inflammatory phase of wound healing. In contaminated wounds with retained foreign bodies, the inflammatory phase will be prolonged and may result in a chronic inflammatory reaction. A good tension-relieving subcutaneous suture closure is all the more important in light of the fact that skin sutures are usually removed during the inflammatory phase of wound healing when little actual wound strength has been formed.

Fibroblastic Phase

Toward the end of the inflammatory phase and continuing for 2–4 weeks, fibroblasts that have migrated into the wound begin laying down collagen fibrils in a rather disorganized manner. Initially, an excessive amount of collagen is produced, accounting for the prominent scars patients sometime exhibit during this period. In most patients, however, an equilibrium is soon established between collagen production and collagenolysis.

Wound Contraction Phase

Wound contraction is a normal phase of wound healing that occurs along with the fibroblastic phase. In anticipation of this contraction, it is important to strive for everted wound edges at the time of suturing to avoid depressed scars in the late postoperative period. Free grafts should be approximately one-third larger than their recipient beds, also in anticipation of this normal contraction. Steroids can inhibit wound contraction, but they can also interfere with the proliferation of fibroblasts and collagen synthesis, thereby decreasing the strength of the wound.

Scar Maturation Phase

The scar maturation phase begins about 1 month following the trauma or surgery and may continue for years. During the early part of the phase, fibroblasts begin leaving the area. Thereafter, organization and dehydration of the collagen fibrils occur, serving to strengthen and refine the wound.

Hypertrophic Scars and Keloids

Hypertrophic scars involve only the tissue of the wound, and these scars usually become paler, softer, and less visible with the passage of time. Keloids are tumorlike overgrowths that invade surrounding tissue and may take years to reach their maximum size. Both hypertrophic scars and keloids are characterized by tissue responses that exceed the physiologic needs of the wound healing. Both have a predilection for dark-skinned children and young adults.

Treatment of hypertrophic scars includes massage, steroid ointment, and steroid injections into the scar. A 30-gauge needle on a 1 mL syringe is used to inject 1/10 mL of triamcinolone diacetate (Kenalog 10 mg/mL: Apothecon-Bristol Meyers, Squibb, Princeton, NJ) directly into the scar. The injections can be repeated every 2 weeks as needed. Atrophy and depigmentation may result if more concentrated suspensions are used or if the steroid is injected intradermally. Radiation, cryotherapy, surgical excision, and other modalities (e.g., vitamin E oil applied topically or taken orally) have been used with limited success in the treatment of keloids. Prolonged patching with silicone sheets may also help.

Scar Revision

Scars can be minimized by planning incisions carefully, closing wounds accurately, understanding the principles of wound healing, and monitoring postoperative progress attentively [4, 5]. However, there are many other factors over which the surgeon often has little control, including the following:

- Relationship of the wound to the relaxed skin tension lines
- Cause of the wound (e.g., elective incision vs. dog bite)
- Region involved (e.g., lid with thin dermis vs. brow with thick dermis)
- Depth of the wound
- Length of the wound
- Shape of the wound (e.g., trapdoor, stellate)
- Tissue loss
- Individual factors (e.g., age, race, general health, predilection to keloid formation)
- Previous treatment (e.g., surgery, radiation)

Scars are never exactly the same. Every scar deserves careful analysis, and every scar revision deserves careful planning before the patient is taken to surgery. Factors that may significantly influence the result of scar revision must be discussed in detail preoperatively, and often the surgeon must spend considerable time dispelling common misconceptions. For example, it is not unusual for the patient to regard “plastic surgery” as a magical removal or erasure of a

scar, whereas scar revision is in fact an attempt to replace a less desirable scar with a more acceptable scar. The optimal appearance of a scar may take years to achieve. The patient must have a realistic notion of what can and cannot be accomplished by the recommended treatment. The patient must understand that the best possible result may not be entirely satisfactory, even with the most carefully executed surgery. In this way, misunderstandings and postoperative disappointment can be minimized.

The first step when approaching scar revision is to assess the relationship of the scar to the relaxed skin tension lines. RSTL correspond to the directional pull existing in relaxed skin. This directional pull is determined by underlying structures such as the muscle and bone. Incisions that parallel the RSTL tend to remain narrow. Incisions perpendicular to the RSTL are referred to as antitension line (ATL) incisions. These tend to gape and result in more prominent scarring. Generally, the closer the incision or wound follows the RSTL, the better the cosmetic and functional result. As previously discussed, RSTL orientation can be more difficult to determine in children due to a lack of wrinkles. Furthermore, the skin has greater elasticity or resistance to stretch in pediatric patients, making skin closure or scar revision more difficult compared to the same procedure in adults.

Revisions of scars in which there has been no tissue loss can usually be improved by one or more of the three linear scar revision techniques: fusiform excision, Z-plasty, or W-plasty. Which technique or combination of techniques the surgeon uses to deal with a particular scar is again based on knowledge of the RSTL. The fusiform excision is the most useful for revision of scars that follow the RSTL. W-Plasty finds its greatest application in ATL scars of the eyebrow, forehead, temples, and cheeks, but single or multiple Z-plasties are usually preferred for all other ATL scars. In lengthy irregular scars, it is not uncommon to combine all of these techniques during a single procedure. The overall objective in scar revision is to hide or camouflage the scar. The linear scar revision techniques accomplish this objective by breaking scars into smaller segments and redirecting the original scar into a more favorable relationship with RSTL.

Fusiform

The fusiform excision involves resection of the tissue that includes the scar paralleling the RSTL (Fig. 4.6). This places the tension on the ends of the wound, which tends to promote closure of the wound. If the fusiform excision is perpendicular to the RSTL, the tissue tension would be at the center and would pull on the incision line, resulting in a broader scar. The angles of the fusiform excision apices should be 30° or less to ensure smooth closure. Once the fusiform strip is removed, the wound edges are undermined, creating two sliding flaps that are moved in to cover the defect. The subcutaneous tissue is then closed with supportive deep sutures in order to allow skin approximation without tension.

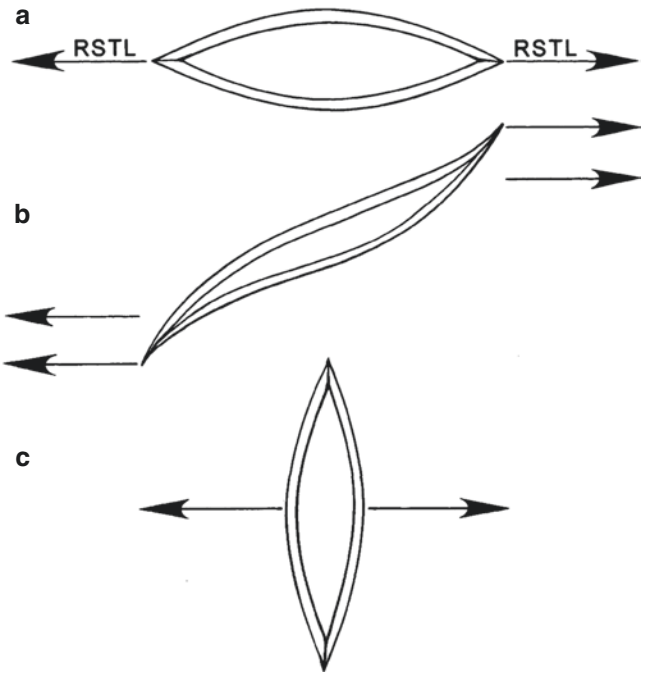


Fig. 4.6 Fusiform excision. (**a**) Fusiform excisions should follow the relaxed skin tension lines (*RSTL*). The tension will then be lengthwise along the fusiform excision, facilitating wound closure. (**b**, **c**) If the tension is on the skin edges, a widened scar is more likely to result (Adapted from Cahill and Carroll [1])

Z-Plasty

A Z-plasty utilizes two adjoining triangular flaps created by a Z-shaped incision. The central limb of the Z should be placed along the line of contracture. A transverse diagonal line drawn perpendicular to the central limb then allows the surgeon to consider two sets of triangles (Fig. 4.7). One pair of triangles is usually more suitable than the other pair as determined by assessment of the surrounding tissues and the relationship of the final incision lines to the RSTL. Once the configuration of the Z is determined, each flap is incised, undermined, elevated, and transposed into its partner's bed (Fig. 4.7b, c). If there is cutaneous scar over the line of contracture, it can be removed in a fusiform excision along the central limb (Fig. 4.7d).

The amount of lengthening achieved by a Z-plasty depends on the angles of the flaps and the length of the arms. Except in unusual circumstances, the angles should be between 50 and 60°. Smaller angles progressively lessen the amount of lengthening achieved, while angles greater than 60° become increasingly difficult to transpose.

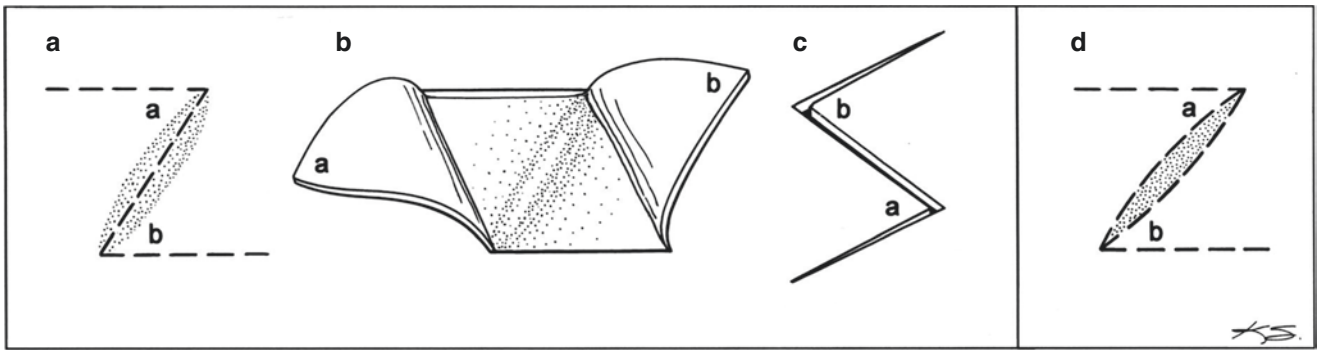


Fig. 4.7 Z-Plasty. (**a**) The central limb of the Z overlies the contraction line and allows the construction of two sets of flaps: one using a and b as arms and the other using the *dotted lines* as arms. (**b**) Any subcutaneous traction band must be released. (**c**) The flaps are transposed. (**d**) Example of a fusiform excision combined with a Z-plasty (Adapted from Cahill and Carroll [1])

The surgeon must remember to completely incise or excise the subcutaneous traction bands once the flaps of the Z-plasty are elevated. Failure to do this compromises the effect of the revision. Keeping the flaps of sufficient thickness and the flap angles between 50 and 60° helps avoid ischemic necrosis of the tips of the flaps. This complication is most likely to occur if the base of the flap is too narrow, if the flap is constructed in scar tissue, or if the sutures are placed in such a way as to cut off the blood supply to the tips of the flaps. The surgeon should consider using the previously described horizontal mattress suture to avoid compromising the vascular supply to the tips of the flaps.

W-Plasty

A variation or extension of the Z-plasty, the W-plasty, is a zigzag incision using short, acutely angulated incisions that are closed by advancement without rotation of tissue. The W-plasty finds its greatest use in ATL scars in the eyebrow, forehead, temple, and cheek areas. Some tissue must necessarily be sacrificed in using the W-plasty, so the procedure is contraindicated when the tissue cannot be spared. A simple variation of the W-plasty can occasionally be used in upper eyelid blepharoplasty and in closing elliptical incisions.

Ancillary measures such as eyeglasses, cosmetics, shave excisions, and dermabrasions should also be considered in planning scar revisions and camouflage. Newer techniques, such as injectable collagen, appear to provide only temporary improvement when used to change skin contour. Injectable collagen has been avoided in the eyelids because of a report of visual loss from retinal artery occlusion following eyelid treatment. Another promising modality is the application of cosmetic resurfacing lasers in scar management (see Chap. 7).

Grafts

Grafts have found widespread application in ophthalmic plastic surgery. Autologous tissues (e.g., skin, fascia lata, ear cartilage, mucous membrane, dermis fat, hard palate mucosa) are those which are placed on the same patient from whom they were obtained. Homologous grafts (e.g., donor sclera, banked fascia lata) are obtained from a separate donor, processed to decrease the risk of rejection or communicable disease and then placed in a patient. Autologous tissues can be further subcategorized as free grafts versus flaps. A free graft is completely detached from its donor site and therefore has no blood supply of its own. In contrast, a flap remains partly attached to its donor site by a pedicle, thereby maintaining a blood supply.

Skin Grafts

Skin grafts may be either full thickness or split thickness, depending on whether all or only part of the dermis is included in the graft. Poor color match and contraction of split-thickness grafts often preclude their use in eyelid surgery. Full-thickness skin grafts are frequently used for scar revisions, repair of cicatricial ectropion, and eyelid reconstruction. While the skin from the contralateral upper eyelid is the best match for repair of an upper eyelid defect, in children this source is rarely able to provide adequate harvestable surface area. Furthermore, the surgeon must consider the asymmetric postoperative appearance that may result when this donor site is used. Postauricular skin is a desirable donor site for lower eyelid defects and in practice is also a common donor site for repair of upper eyelid defects (Fig. 4.8).

To achieve optimal functional and cosmetic results, the recipient bed must be properly prepared. The graft itself must be obtained, sized, placed, and sutured with meticulous technique. Attentive postoperative care is essential. The

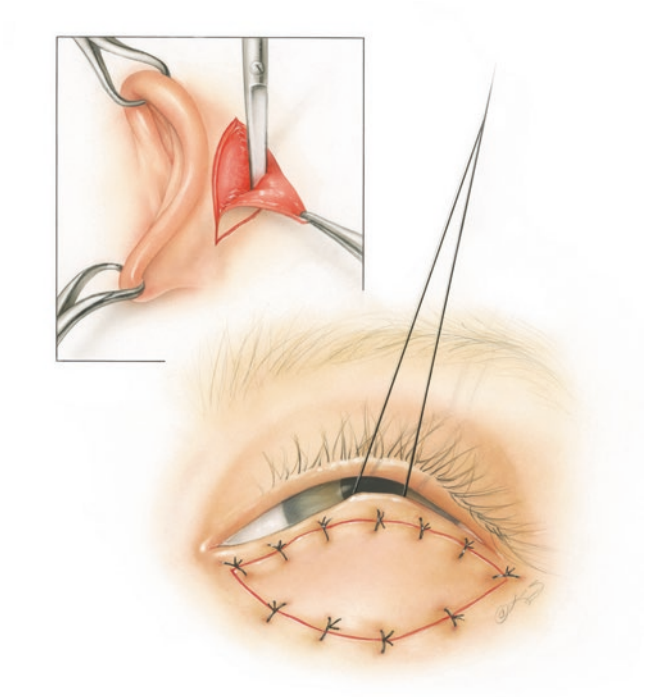


Fig. 4.8 A retroauricular full-thickness skin graft being harvested and then sutured in the lower eyelid for a repair of a cicatricial retraction

basic steps in obtaining and placing a full-thickness postauricular skin graft are as follows:

1. All scar tissue is incised or excised as appropriate in the recipient area.
2. The recipient bed must be free of blood and other debris that may interfere with vascularization of the graft.
3. The size of the defect is measured. A template may be helpful.
4. To obtain the graft, the head is turned, and the external ear is brought forward toward the cheek with a 4-0 silk traction suture.
5. The proposed donor site is inspected to ensure that it is hairless.
6. A marking pen is used to outline the proposed graft so that it is at least one-third larger than the previously measured recipient bed. This is most important because the reflection of the external ear places the retroauricular skin on stretch. The proposed graft is positioned so that the midline of the graft falls along the crease, with half of the graft skin on the posterior aspect of the ear and half overlying the bony skull.
7. Lidocaine 1% or 2% with epinephrine is injected subdermally, hydrodissecting the tissue planes and providing hemostasis.
8. The marked incision line is incised with a scalpel.
9. The graft is then removed using a combination of sharp and blunt scissors dissection.
10. The graft is placed in saline-moistened gauze.
11. After establishing hemostasis, the donor area is closed with a running suture (e.g., 4-0 silk, nylon, or chromic gut) or with interrupted simple mattress sutures. For a running closure, it is helpful to leave the ear traction suture in place until the postauricular suture has been completely threaded. After the traction suture is released, the running postauricular suture is tightened to remove any laxity and then tied.
12. All subcutaneous tissue is meticulously removed from the graft to eliminate this potential barrier to vascularization of the graft. This is most easily performed with Westcott scissors, while the graft is on a saline-moistened 4 × 4in. gauze stretched over the index finger of the surgeon's nondominant hand.
13. The graft is then placed in the recipient bed and sutured using multiple interrupted 6-0 silk sutures to align its cardinal points. It is helpful to suture one edge in place before making any final modifications in the shape or size of the graft. At least four of the interrupted sutures are left long, for later use securing the bolster. A running suture of fast-absorbing 6-0 plain gut and/or 7-0 Dexon can be used to maintain alignment of the skin edges between the silk sutures. It is useful to engage the graft first with the needle/suture and then the recipient bed, to pull the graft toward the recipient bed in the process of passing the suture.
14. A piece of Telfa is cut to the shape of the graft and placed over the graft. A moistened cotton roll is used to form a pledget, which is placed over the Telfa. This bolster is secured with the long ends of the interrupted 6-0 sutures and kept in place 5–7 days.
15. In some cases, a lid margin suture is also used to keep the operated area flat and immobile during the initial postoperative period. Amblyopia is a concern with prolonged patching.
16. Silk sutures are removed at 5–7 days postoperatively. Steristrips (1/4inch width) are sometimes used to reinforce the edges of the graft for an additional 2–3 days after the suture removal.
17. The patient is asked to wear an eye shield to bed for 2 weeks following surgery to protect the graft. The patient is also instructed to avoid excessive sun exposure for 4–6 weeks postoperatively to minimize color changes in the graft.

Fascia Lata Grafts

A fascia lata graft can be used when tensile strength is needed, such as frontalis suspension ptosis repair. It can also be used as a smooth barrier, such as covering a rough-surfaced orbital implant after enucleation, or in repairing an

early extrusion of an orbital implant. Banked fascia lata is commercially available, but if it is possible to obtain the tissue from the patient, then autogenous fascia lata is felt to be superior. Musculoskeletal development is usually considered sufficient to permit the harvest of an adequate fascia lata graft in children of age 4 years and older but can often be successfully done even below age 2 (Fig. 4.9) (see also Chap. 22 on Pediatric Ptosis).

The basic steps in obtaining fascia lata graft tissue are as follows:

1. The leg should be internally rotated for this procedure. Identify the lateral tibial condyle and the tubercle of the iliac crest, and mark a 3–4 cm incision line superior to the knee joint along the imaginary line passing between these bony landmarks [4] (Fig. 4.9).
2. Incise skin with a scalpel. Blunt and sharp dissection through subcutaneous fat will expose the white, glistening fascia lata. Use long, narrow scissors to bluntly dissect between the fascia and subcutaneous fat as far superiorly as possible. Retract the skin and subcutaneous fat to widely expose the fascia inferiorly.
3. Make two longitudinal parallel incisions through the fascia 4–8 mm apart, beginning at the most inferior exposed aspect and following the vertical orientation of the fascial fibers. Extend these incisions as far superiorly as the exposure permits. Undermine the fascia with blunt scissors dissection, separating it from underlying muscle as well as the overlying skin and subcutaneous tissues. Carry this as far superiorly as possible.
4. Cut between the two parallel incisions at their inferior extent. Pass this free end of the fascia through the stripper mechanism, and grasp it securely with one or two Kocher clamps. Pass the stripper as far superiorly as possible (at least 10 cm) and sever the fascia.
5. The fascial defect does not require closure. After establishing hemostasis, subcutaneous tissue should be closed securely with 4-0 Vicryl. The skin may be closed with sutures or staples.
6. The fascia should be cleaned of extraneous connective tissue. For ptosis surgery, strips that are 2 mm in width are usually adequate. These strips can be started with scissors, cutting parallel to the collagen fibers. The strips can usually then be pulled apart for the remainder of the length [6].
7. If a rectangular piece of fascia lata is required, it can be harvested using a similar technique without the need for the fascia stripper.

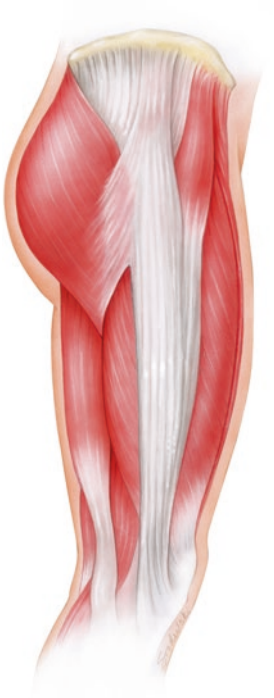


Fig. 4.9 Anatomy of the lateral thigh illustrating the iliotibial tract component of fascia lata

Oral Mucous Membrane Grafts

Oral mucous membrane is an effective substitute for the conjunctiva and is used in the reformation of conjunctival cul-de-sacs (Fig. 4.10) (see also Chap. 39: "Management of the Microphthalmic Orbit").

Steps taken to obtain full-thickness mucous membranes are as follows:

1. The length and height of the conjunctival defect are measured. An ellipse is then drawn with surgical marking pen inside the lower lip. The ellipse is sized approximately 20% larger than the desired dimension to compensate for

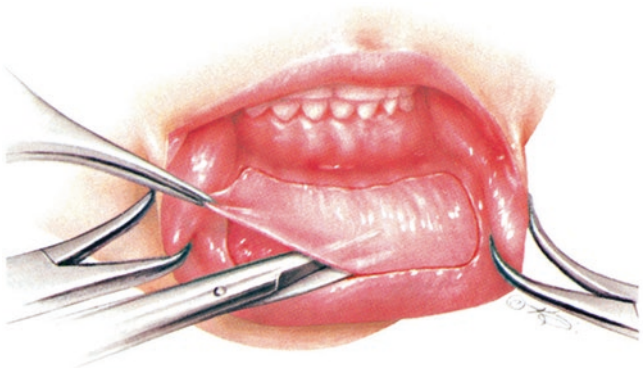


Fig. 4.10 Retracted lower lip. The anesthetized, retracted lower lip is an excellent source of mucous membrane for eyelid reconstruction. The margin of the lip and the gingiva should be avoided. The graft can be carefully dissected after marking size needed with methylene *blue*

the stretching of the lip. The margin of the lip and the gingiva should be avoided. Alternatively, the ellipse can be drawn on the buccal mucosa inside the cheek with its long axis anteroposterior, taking care to avoid the salivary duct or Stensen's duct located abutting the first upper molar.
2. The oral mucosa is injected with the local anesthetic mixture in the submucosal plane. The injection is used even if the patient is under general anesthesia because the epinephrine in the anesthetic improves hemostasis. The injection should balloon the mucous membrane for ease of dissection.
3. After 5–7 min have elapsed to allow the epinephrine to constrict blood vessels, two towel clips are applied to the lip for use as retractors (Fig. 4.10).
4. A No. 15 blade is used to incise the mucosa on the lower lip as an assistant retracts the lip outward (Fig. 4.10).
5. Westcott scissors and forceps are used to excise the graft. The dissection is performed carefully to avoid taking submucosal tissue with the graft.
6. After the graft has been excised, a small piece of Gelfoam soaked in thrombin should be pressed against the bare tissue surface for hemostasis. The area may ooze somewhat throughout the remainder of the procedure. Cautery should be avoided to lessen the chance of soreness and contraction.
7. The graft is draped over the surgeon's finger on the nondominant hand, mucosal side down, and any subcutaneous tissue is excised with Westcott scissors.

Hard Palate Mucosa Grafts

Hard palate mucosa can be used to add surface area to the palpebral conjunctiva [7]. Unlike buccal mucosa, the hard palate has some structural resiliency, allowing it to supplement the support of the tarsal plate or in some cases to replace part of the tarsus. There have been cases in which the coarse mucosa of the hard palate has caused corneal surface irritation. For this reason, it is often avoided in the upper lid but quite appropriate in the lower lid. Placing it inferior to the lower lid, the tarsus further guards against corneal irritation. In children, hard palate mucosal grafts can be used in cases of severe cicatricial entropion, lower lid retraction resulting from tight lower lid retractors, and reconstruction of full-thickness lid defects (Fig. 4.11).

The basic steps in obtaining a hard palate mucosal graft are as follows:

1. A bite block or dental retractor is inserted between the upper and lower molar teeth. The length and height of the defect are measured, and 1–2 mm is added to allow for shrinkage. The desired graft is marked with a skin marker on the hard palate between the gingiva and the palatine raphe, orienting the long axis of the graft anteroposterior and avoiding the midline (Fig. 4.11).
2. The submucosal plane is injected with the anesthetic mixture diffusely or by a greater palatine block.
3. After 5–7 min have elapsed, a No. 15 blade is used to incise the mucosa on the hard palate.
4. Westcott scissors and forceps are used to excise the graft, while the periosteum is left intact. The surgeon must diligently avoid the tendency to go progressively deeper/thicker with the graft harvest at its more posterior edge. Deep incisions will bleed more, cause more pain, and take longer to heal. Briskly bleeding vessels are cauterized.
5. A piece of oxidized regenerated cellulose is placed on the palate defect. The bite block or retractor is removed.
6. Mild discomfort at the donor site lasts about 1 week and is usually well tolerated. Postoperative care can

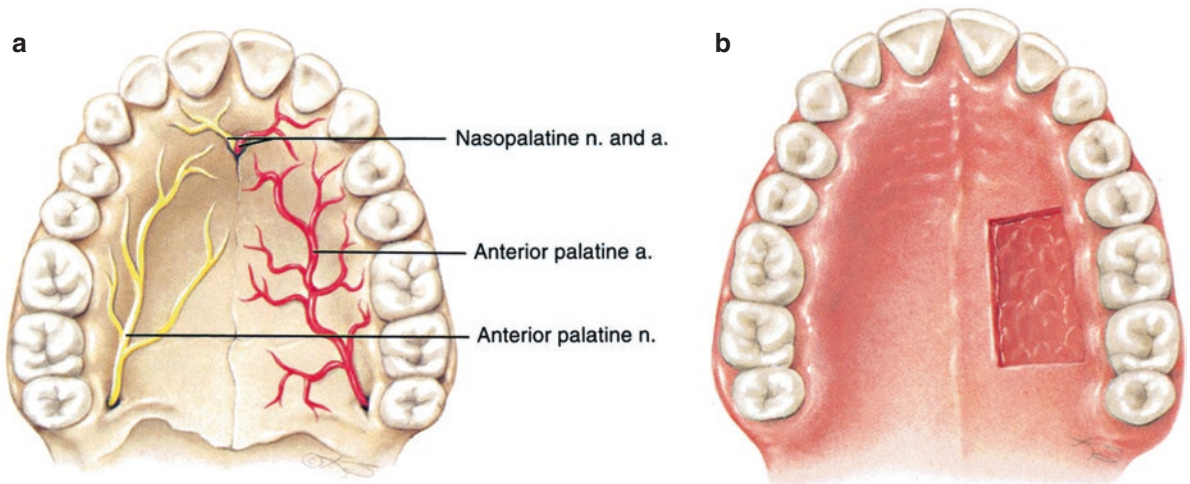


Fig. 4.11 Hard palate mucosal grafts. (**a**) Hard palate mucosal grafts should be harvested so as to avoid the gingiva, the palatine raphe, the nasopalatine foramen, and the greater palatine foramen through which pass corresponding nerves and vessels. (**b**) The graft site can be lightly cauterized for hemostasis as needed

include rinses with 0.5% hydrogen peroxide twice daily. Topical lidocaine gel can also be applied. The donor site will usually reepithelialize in 3 weeks. Molded stents or slates are sometimes used to facilitate donor site healing [8, 9] but are usually unnecessary.

Ear Cartilage Grafts

Ear cartilage can be used as a rigid substitute for the tarsus in eyelid reconstruction [10]. It is best to cover the cartilage with palpebral conjunctiva to expedite healing and to minimize ocular irritation (Fig. 4.12).

The basic steps in obtaining ear cartilage grafts are as follows:

1. Measure the size of the ear cartilage graft required; a template may be helpful.
2. A skin incision of the length of the desired graft is marked on the posterior aspect of the ear parallel to the helix and approximately 5 mm from its edge.
3. Local anesthesia with epinephrine is injected subcutaneously anterior and posterior to the cartilage.
4. The ear is reflected anteriorly with digital traction, 4-0 silk traction sutures, or towel clamps.
5. The skin is incised with a No. 15 Bard-Parker blade. Scissors are used to dissect subcutaneous tissue off of the cartilage (Fig. 4.12).
6. The graft shape is drawn on the exposed cartilage, leaving a minimum width of 4 mm of the cartilage along the edge to prevent subsequent deformity of the helix.
7. The cartilage is incised partial thickness with the No. 15 Bard-Parker blade. Stevens scissors are used to complete the incision so that the skin of the anterior surface of the ear is not buttonholed. Scissors are also used to separate the cartilage from anterior subcutaneous tissue to fully free the graft, taking care not to bend or stress the cartilage as this may result in cracks.
8. Complete hemostasis is achieved. The ear tissue is highly vascular and prone to postoperative hematoma formation unless very thorough care is taken at this step.
9. There is no need for deep closure or tension-relieving sutures. The incision is closed with skin sutures such as 6-0 fast-absorbing plain gut.
10. If desired, moistened cotton gauze can be used to form dressings that conform to the anterior and posterior surface of the ear. These can be held firmly in place with a mattress suture of 4-0 silk which passes through the ear. Many surgeons forego this step, but it can help prevent postoperative hematoma formation and deformity of the helix.
11. The harvested cartilage may be treated with a cartilage crusher or lightly scored with Colorado needle cautery to create a thinner graft with better contour.
12. The cartilage graft is placed into the recipient bed and sutured into place with buried 6-0 Vicryl. The use of a spatulated needle is recommended, as cutting needles tend to split or shred the cartilage tissue.

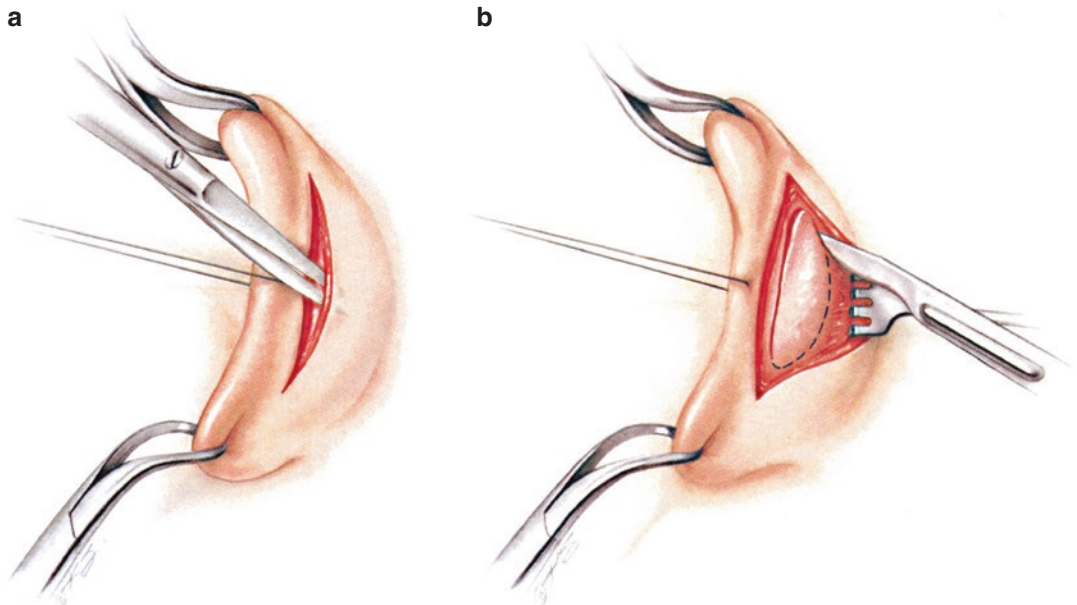


Fig. 4.12 . (**a**) Ear cartilage grafts are most readily harvested through a posterior skin incision parallel to the helix. (**b**) An elliptical piece of the cartilage can be harvested and scored with a scalpel or light cautery for improved flexibility

Dermis-Fat Grafts

Dermis-fat grafts (DFG) are an excellent source of tissue volume for the anophthalmic socket [11, 12]. The dermis facilitates vascular ingrowth to enhance graft survival, while the fat provides volume and a positive trophic influence on the growing bony orbit. The dermis epithelializes and can add surface area to the socket lining. Of note, the dermis alone can also be harvested for usage correcting facial contour defects.

The best donor sites for DFG in adults are the lower abdomen and the flank. In children the buttock is usually used (Fig. 4.13). Although this site is more prone to postoperative suture line stress with slower healing, it still provides the best source for sufficient fast in the pediatric age group. Wound contamination from soiled diapers is also a concern. Tegaderm dressings are helpful in this regard. A football-shaped graft scaled to fit the orbit of the children can usually provide ample tissue and can be closed easily.

The basic steps for obtaining a DFG are as follows:

1. Mark the skin with the desired graft outline.
2. Incise the skin superficially with a scalpel in several areas to maintain outline after prepping.
3. With the surrounding skin placed on stretch, the epidermal layer can be mechanically dermabraded with a dia-

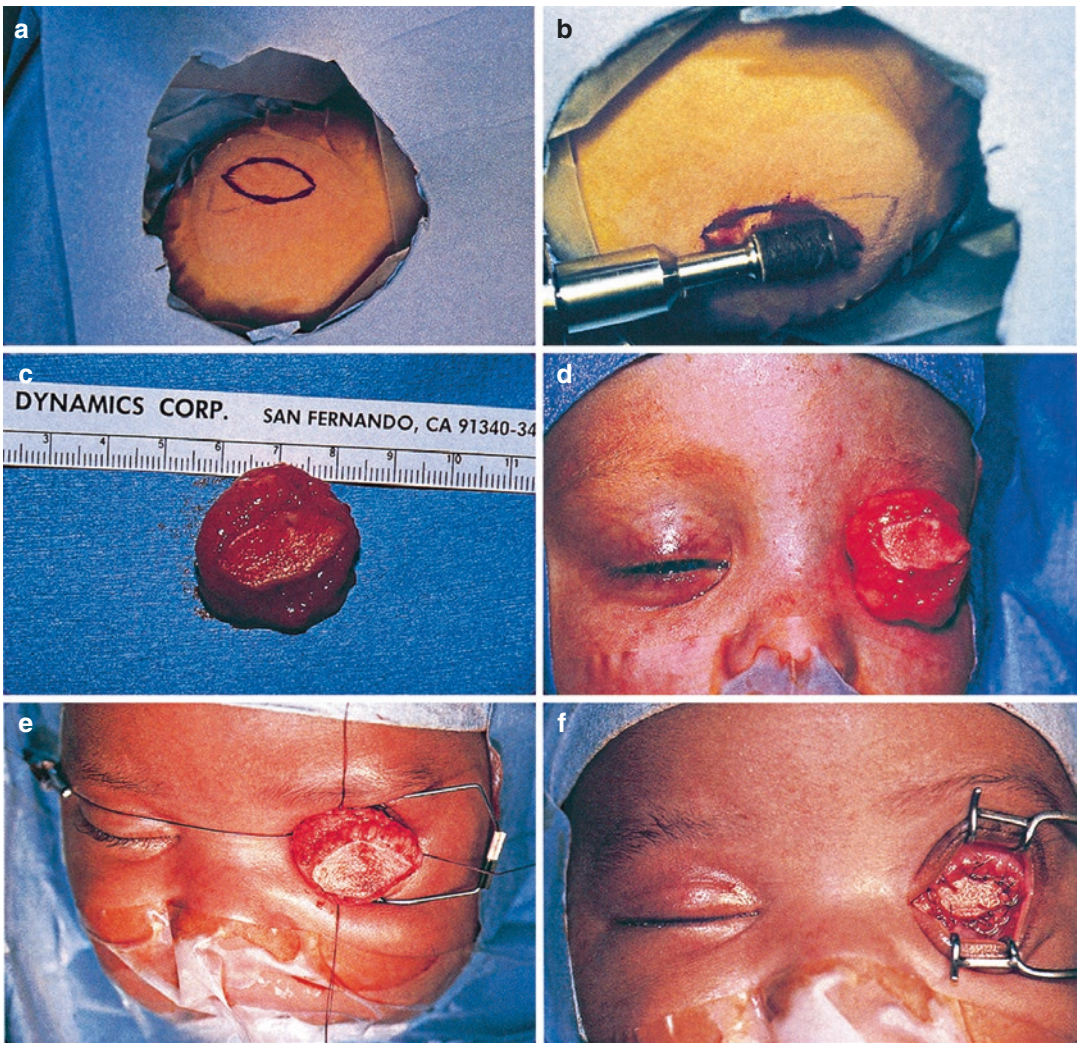


Fig. 4.13 Dermis-fat graft as orbital implant. (**a**) Dermis-fat donor site outlined on the buttock. (**b**) Multiple superficial stab incisions are used to outline the graft edges; a dermabrader is used to remove the epithelium down to the dermis. (**c**) The fat component of the dermis-fat graft is larger in all dimensions than the skin component. (**d**) Graft is placed over left orbit. (**e**) Rectus muscles isolated and sutured to dermal edge and then back through Tenon's capsule and the conjunctiva; excess fat is trimmed. (**f**) Multiple interrupted 5-0 polyglactin sutures are used to prevent fat prolapse, and a clear conformer is placed over the graft

mond burr and drill. If this is not available, then the epidermis can be excised in a lamellar fashion using forceps and a No. 10 Bard-Parker blade, leaving the underlying dermis in place. This step tends to dull the blade and may be necessary to change blades one or more times to complete the task. The exposed dermis will give a uniform spotted appearance of exposed vessels when the proper thickness of the epidermis has been excised. The excision is too deep if fat is visualized.

4. The dermis and fat are then incised together, perpendicular to the skin surface, with a No. 10 blade for a depth of 2 cm (if the child's fat layer is thick enough to permit that depth). For use as an enucleation implant, a wider border of fat should be excised around the dermis border in order to provide increased volume for the orbit. The dermis and fat are lifted up with a forceps and excised from the base with scissors. Complete hemostasis should be established. The graft may be stored in saline-moistened cotton gauze.
5. The donor site is closed using 3-0 or 4-0 polygalactin sutures with buried knots to approximate the fat layer and close the dead space. The dermis is then further closed with horizontal mattress sutures using the same suture material. The skin is closed with sutures of sufficient strength placed in a running subcuticular fashion.
6. Dermabond glue is then applied and covered with Telfa, and a Tegaderm bandage is kept in place during the first post-op week. The area should not be immersed in water for 1–2 weeks after surgery. As such, sponge baths rather than tub baths are recommended.

Flaps

By definition, flaps have at least one pedicle connecting them to adjacent tissue. Thus, unlike grafts, flaps do not depend solely on their recipient bed for nourishment [13]. This means they can be used more successfully than grafts in areas with a compromised blood supply (e.g., previously irradiated tissue, traumatic defects down to bare bone, etc.). Because skin flaps usually include subcutaneous tissue, they are also useful when bulk is needed to fill a defect. Underlying muscle can be included in the flap, forming a myocutaneous flap with more bulk and an even more robust blood supply.

Flaps most frequently used in eyelid surgery are local, open, and single. This means that they are taken from a neighboring area (local), placed flat in a recipient bed (open), and have a single pedicle (single). Flaps may also be classified according to their blood supply as either random or axial. The random flap, far more frequently used, receives its blood supply from segmental, anastomotic, or axial arteries, which lie deep below the muscle layer under the flap. These vessels send perpendicular, perforating, musculocutaneous arteries to the interconnecting dermal plexae of the flap. The axial flap, on the other hand, receives its blood supply through a direct cutaneous artery, which lies above the muscle layer in the flap. The midline or paramedian forehead flap, based on the frontal branch of the ophthalmic artery, is probably the most common example of an axial flap used in eyelid surgery.

Local flaps may also be classified as sliding, advancement, rotation, or transposition (Fig. 4.14).

- *Sliding flaps:* After an elliptical excision, the two wound edges are undermined, creating two sliding flaps that are each pulled toward the midline of the defect and sutured together to cover the defect.
- *Advancement flap*: A single area of adjacent tissue, usually rectangular in shape, is undermined and then moved directly into a defect without any rotation or lateral movement.
- *Rotation and transposition flaps*: The flap is undermined and then rotated about a pivot point to fill the defect. These may be classified as either a simple rotation flap (rotated into an adjacent tissue defect) or a transposition flap (rotated into a nonadjacent defect). The Tenzel semicircular flap is an example of a simple rotation flap, whereas the midline forehead flap is often used as a transposition flap.

Gentle, atraumatic technique is particularly important in dealing with flaps. The tissue is best handled with skin hooks rather than forceps, with special care given to the tips of the flaps to avoid compromising their delicate blood supply. Other sources of ischemia are poorly placed or carelessly tied sutures and kinking of the pedicle of the flap. The flap should flow smoothly from the donor to the recipient site, with no tendency for the pedicle to fold back on itself.

O-Defects

After excising a lesion, the surgeon must often deal with a circular or oval-shaped defect, referred to as an O-defect. If the area is small, it can usually be converted to a small fusiform excision, undermined to permit sliding, and sutured closed as a linear defect. As described in the fusiform incision section earlier in this chapter, the angle formed at each apex of the wound should be no greater than 30°. Wider angles result in standing cone deformities or "dog ears," due to excess bunching of the skin at the end of a wound closure (These are discussed in the next section).

If the lesion is large, it is often still possible to convert the defect to a fusiform shape. To limit the resulting scar length and avoid the removal of a large amount of normal tissue, yet

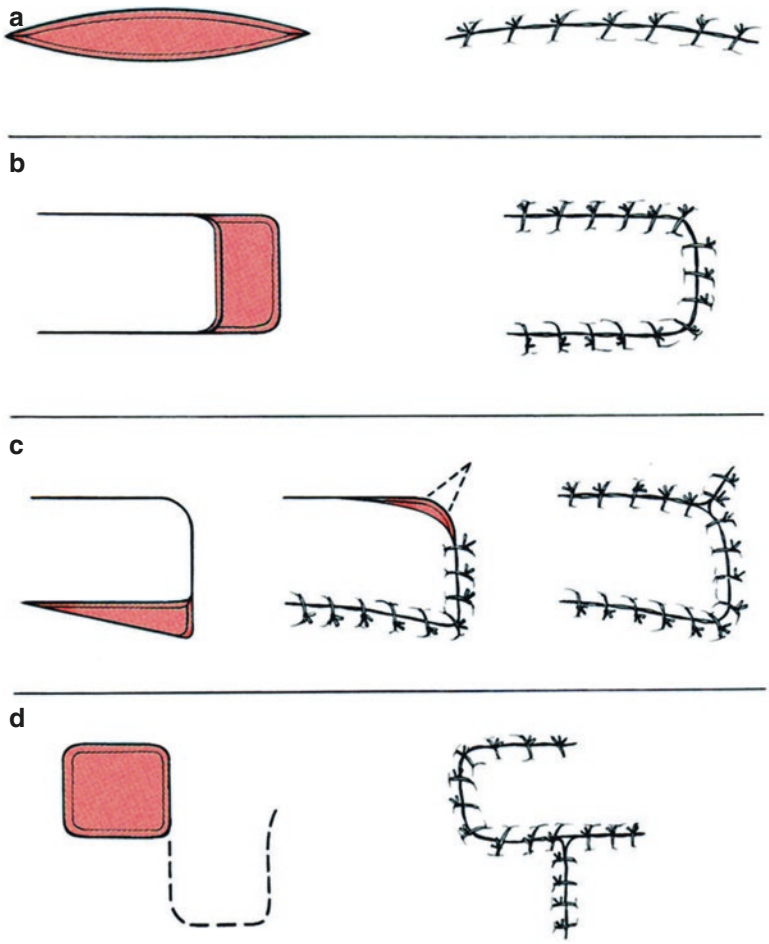


Fig. 4.14 The types of flaps most commonly used in ophthalmic plastic surgery. (**a**) Sliding, (**b**) advancement, (**c**) rotation, and (**d**) transposition (Adapted from Cahill and Carroll [1])

still maintain 30° corner angles, M- and W-plasties can be utilized (Fig. 4.15a). In other situations, it may be more advantageous to use single or multiple triangular island flaps [14]. These flaps are maintained on a subcutaneous pedicle, slid into the O-defect, and sutured (Fig. 4.15b). Another technique for closing large, round defects employs two curvilinear incisions that create two triangular Z-plasty-type flaps (Fig. 4.15c). These flaps, however, are not transposed; they are simply widely undermined and rotated into the defect. To avoid dog ears at the distant corners, it may be necessary to excise small triangles. Finally, the O-defect may be converted into a rectangular defect and closed by advancement rectangular flaps or by a rhomboid flap [15] (Fig. 4.15d, e). The rhomboid flap is especially useful in the lateral canthal area.

Dog-Ear Deformities

A dog-ear deformity can occur in a variety of situations. Most commonly, it results when the surgeon attempts to close a round or broad ellipse directly or when one side of an ellipse is longer than the other. Simply lengthening the incision in an attempt to smooth out the redundant tissue ("chasing the dog ear") is ineffective, as the excess tissue will still be bunched up at the newly extended tip of the incision. For example, in upper lid blepharoplasty, a dog ear at the nasal end of the incision may be "chased" into the thicker nasal skin and subsequently cause an unsightly web scar. Deliberate excision of the redundant tissue is therefore desirable (Fig. 4.16). Various triangular excisions are frequently used in skin closure to avoid and eliminate the dog-ear deformity.

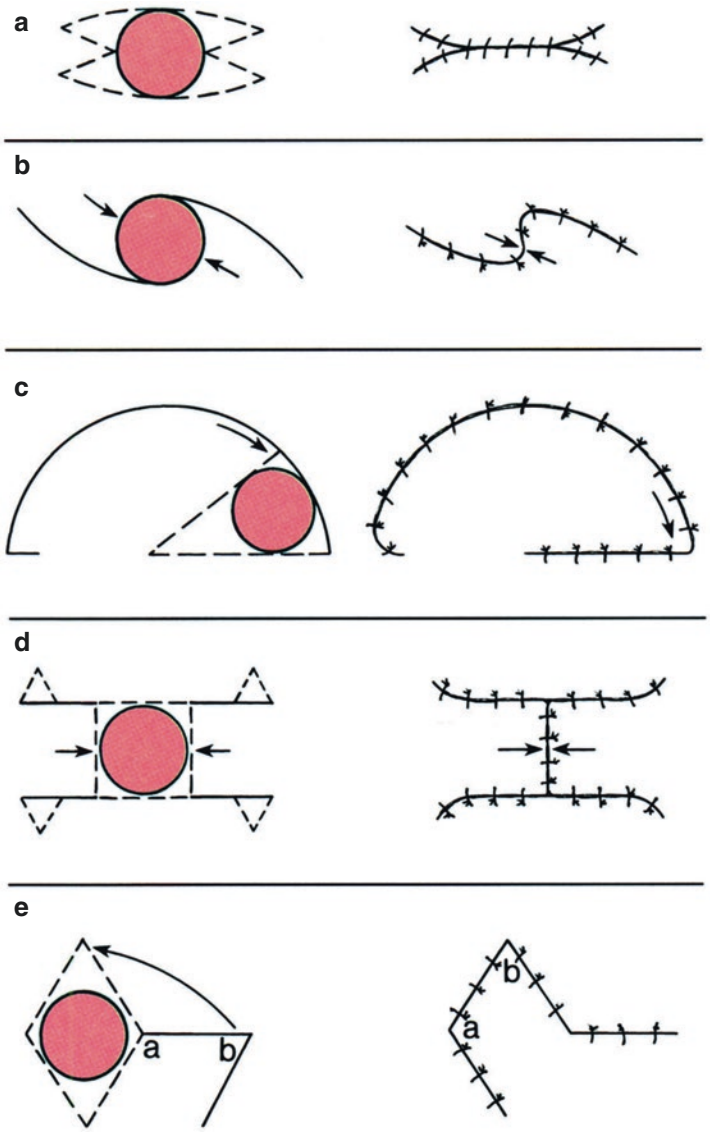


Fig. 4.15 Closure of an O-defect. Closure may be accomplished in many instances by a full-thickness skin graft. A variety of flaps can also be utilized depending on the extent and location of the defect. (**a**) M-Plasty. This technique sacrifices less tissue than an ellipse with a shorter incision length. (**b**) O-Plasty to Z-plasty. Curvilinear incisions can be made to run along relaxed skin tension lines (RSTL), but scars from this technique can be very noticeable in the midface. (**c**) Rotation flaps can work well when the skin is less tightly attached and more flexible such as in the cheek area of the face. They can be particularly useful for large defects involving the lower lid. (**d**) Sliding or advancement flap. These can be single or double for larger defects. The length-to-width ratios depend on adequate blood supply. The triangles at the ends of each incision represent dog ears which when removed slightly extend the incision while also flattening them out. (**e**) Rhomboid flaps. These flaps are very useful for small circular defects, particularly in the canthal areas. All sides of the triangles created to encompass the circular defect are equal in length to each other. The length of each side of the adjacent parallelogram developed for rotation into the defect should also be of equal length to the sides of the triangles

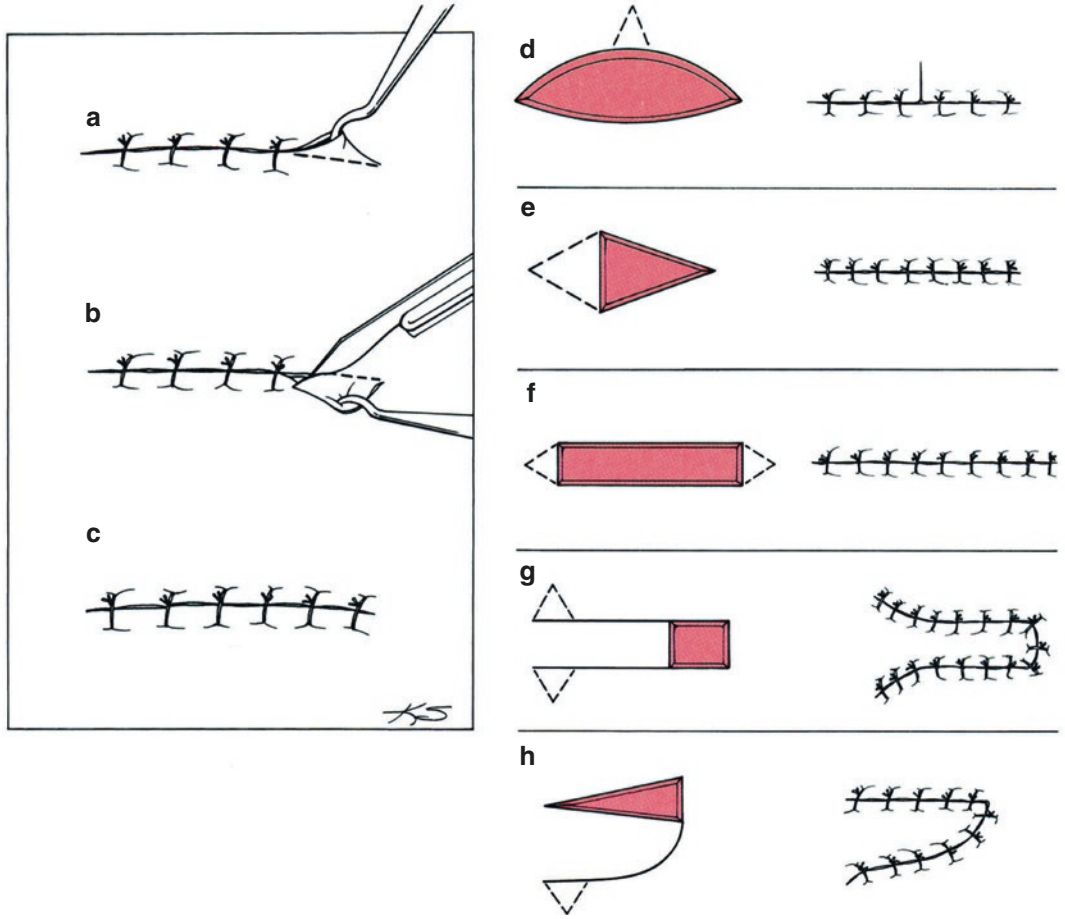


Fig. 4.16 Technique for eliminating a troublesome "dog ear" at the end of an incision. (**a**) The dog ear is elevated with a skin hook. (**b**) Scissors or a scalpel blade is used to incise one side of the dog ear following the incision line. (**c**) The flat triangle of the skin is elevated and cut along its base and then suturing is completed. (**d**–**h**) Dog ears can often be avoided by incorporating small, triangular excisions into the wound closure (Adapted from Cahill and Carroll [1])

References

1. Cahill KV, Carroll RP. Principles, techniques, and instruments. In: Stewart WB, editor. Surgery of the eyelid, orbit, and Lacrimal system, vol. 1. San Francisco: American Academy of Ophthalmology; 1993. p. 2–25.
2. Eisner G. Eye surgery: an introduction to operative technique. 2d ed. New York: Springer; 1990.
3. Kent TL, Custer PL. Bleeding complications in both anticoagulated and nonanticoagulated surgical patients. Ophthal Plast Reconstr Surg. 2013;29(2):113–7.
4. Wilkins RB, Kulwin DR. Wound healing. Ophthalmology. 1979;86:507–10.
5. Borges AF. Elective incisions and scar revision. Boston: Little, Brown; 1973.
6. Jordan DR, Anderson RL. Obtaining fascia lata. Arch Ophthalmol. 1987;105:1139–40.
7. Cohen MS, Shorr N. Eyelid reconstruction with hard palate mucosa grafts. Ophthalmic Plast Reconstr Surg. 1992;8:183–95.
8. Mauriello JA, Wasserman B, Allee S, et al. Molded acrylic mouthguard to control bleeding at the hard palate graft site after eyelid reconstruction. Am J Ophthalmol. 1992;113:342–4.
9. Shorr N, Enzer YR. Molded acrylic mouthguard to control bleeding of the hard palate graft site after eyelid reconstruction. Am J Ophthalmol. 1992;114:779–80.
10. Bayliss HI, Rosen N, Neuhaus RW. Obtaining auricular cartilage for reconstructive surgery. Am J Ophthalmol. 1982;93:709–12.
11. Smith B, Petrelli R. Dermis-fat graft as a movable implant within the muscle cone. Am J Ophthalmol. 1978;85:62–6.
12. Quaranta-Leoni FM, Sposato S, Raglione P, Mastromarino A. Dermis-fat graft in children as primary and secondary orbital implant. Ophthal Plast Reconstr Surg. 2016;32(3):214–9.
13. Grabb WC, Myers MB. Skin Flaps. Boston: Little, Brown; 1975.
14. Saunders DH, Shannon GM. Subcutaneous-based triangular skin flaps. Ophthalmic Surg. 1980;11:437–9.
15. Custer PL, Neimkin M. Lower eyelid reconstruction with combined sliding tarsal and rhomboid skin flaps. Ophthalmic Plast Reconstr Surg. 2016;32(3):230–2.

Anesthetic Management for Pediatric Oculoplastic Surgery

5

Ian Yuan and Scott D. Cook-Sather

Introduction

Even the healthiest of infants and children provide challenges for the anesthesiologist, and many who present for oculoplastic surgery have associated syndromes that add particular complexity to anesthetic management. This chapter covers the fundamentals of pediatric anesthesia for oculoplastic surgery. We begin with preoperative assessment, patient preparation, and an expanded section on anesthetic risk. A review of basic intraoperative anesthetic technique follows with emphasis on airway management. Pediatric oculoplastic and specifically major craniofacial and orbital procedures with significant anesthetic implications are discussed. A final section on postoperative considerations examines nausea/vomiting, pain management, emergence delirium, and general discharge criteria. Several excellent texts are available that discuss anesthesia for pediatric patients overall [1–3].

Preoperative Assessment and Preparation

The goals of preoperative preparation are to determine whether the child is medically optimized for surgery and to prepare the child and family for the process of undergoing surgery and anesthesia [4]. For healthy infants and children undergoing routine day surgery procedures, preoperative assessment can be initiated with a short telephone interview in advance and completed by the anesthesiologist on the day of surgery. For more complicated patients or procedures, a visit to the anesthesia preoperative assessment clinic allows an opportunity for completion of the history and physical examination and necessary tests and consultations. Infants and children with major craniofacial syndromes, those with significant comorbidities (e.g., congenital heart disease, hypertension, or adrenal insufficiency), and those to undergo procedures with anticipated blood loss requiring transfusion should be seen in the anesthesia clinic two or more days prior to surgery. This arrangement assures optimal medical management, facilitates the development of a comprehensive anesthetic management plan, and minimizes the likelihood of cancellation on the day of surgery [5].

Past Medical History

Medical histories for pediatric surgical patients should emphasize issues that could affect anesthetic management, such as neurological development, airway anomalies, cardiac and respiratory function, gastroesophageal reflux disease, endocrine disorders, anemia, and coagulation history [4]. A detailed neonatal history is most important for children less than a year of age and for former premature infants. In infants and children presenting for oculoplastic procedures, craniofacial syndromes with patient-specific variations and manifestations must be understood in depth. Many such syndromes are associated with difficult airway (Table 5.1) and also pose challenges in patient positioning and intravascular access [6].

Past Surgical and Anesthetic History

Prior surgeries should be reviewed paying particular attention to those patients with syndromes requiring serial procedures. Though many patients will carry a diagnosis of difficult airway through their entire lives, airway conditions for some may change over time. For example, patients who have had mandibular distractors placed and who have had significant interval growth may have improved airway

I. Yuan (✉) • S.D. Cook-Sather
Anesthesiology and Critical Care Medicine, The Children's Hospital of Philadelphia, Perelman School of Medicine at the University of Pennsylvania, Philadelphia, PA, USA
e-mail: yuani@email.chop.edu

© Springer International Publishing AG 2018

J.A. Katowitz, W.R. Katowitz (eds.), *Pediatric Oculoplastic Surgery*, https://doi.org/10.1007/978-3-319-60814-3_5

Table 5.1 Common craniofacial syndromes associated with difficult pediatric airways

Syndrome	Airway-associated features	Difficult mask ventilation?	Difficult intubation?
Apert (acrocephalosyndactyly)	Midface hypoplasia, soft palate against posterior pharyngeal wall, narrow palate ± cleft	Due to upper airway obstruction	Potential difficult intubation
Cornelia de Lange	Microcephaly, high-arched palate		Potential difficult intubation
Crouzon (craniofacial dysostosis)	Maxillary hypoplasia, soft palate against posterior pharyngeal wall	Due to upper airway obstruction	Potential difficult intubation
Down (trisomy 21)	Small oral cavity in relation to normal tongue size, obstructive sleep apnea, possible atlanto-occipital instability	Due to upper airway obstruction	Potential difficult intubation due to small mouth opening. May require head neutral position during intubation
Goldenhar (oculoauriculovertebral dyplasia)	Micrognathia, facial hypoplasia, and limited cervical neck mobility		Very difficult intubation
Hallermann-Streiff (oculomandibulodyscephaly)	Mandibular and malar hypoplasia, small mouth, faulty dentition, anteriorly displaced temporomandibular joints	May be difficult to open mouth and perform jaw thrust	Potential difficult intubation with small mouth
Robin sequence (Pierre-Robin syndrome)	Micrognathia, glossoptosis, cleft palate, upper airway obstruction	Upper airway obstruction due to large tongue	Very difficult intubation
Treacher Collin (mandibulofacial dysostosis)	Malar and mandibular hypoplasia, cleft palate, incompetent soft palate	Due to hypoplastic mandible making mask seal and jaw thrust difficult	Very difficult intubation

anatomy now amenable to routine direct laryngoscopy intubation technique. While the most recent anesthetic record may be the most relevant for current planning, older records may reveal sequential changes and/or best practice. All available anesthetic records should be scrutinized for documentation of untoward reactions, challenging vascular access, difficult mask ventilation or tracheal intubation, and variation from expected tracheal tube size. Techniques that have been successful should be included in the development of the anesthetic plan. Evidence of postoperative complications such as prolonged emergence, inadequate pain control, nausea and vomiting, extended supplemental oxygen requirement, and unanticipated hospital admission should be sought. When asked, parents of children with syndromes and/or chronic illness requiring repeated anesthetics will often identify techniques that have resulted in improved (or worse) recovery.

Medications

A list of medications and the conditions for which they are prescribed is essential. Most prescribed medications should be administered on the morning of surgery and may be taken with a small sip of water. Longstanding antihypertensive regimens should be continued. Children with asthma should be treated the night before and morning of surgery with inhaled bronchodilators and with steroids as advised by their pediatrician or pulmonologist for those with moderate to severe disease. Over-the-counter and herbal medicine and, in particular, aspirin should be stopped at least 1 week prior to surgery, unless there is a specific reason to continue them [4]. Other nonsteroidal anti-inflammatory drugs, such as ibuprofen, may be allowed up to 3 days prior to surgery.

Allergies

A history of allergies to medications and other items found in the operating room such as latex, betadine, or chlorhexidine should be noted. Specific adverse reactions to medications should be listed because some, such as diarrhea with a particular antibiotic, do not constitute true allergy. Only 10–15% of patients who report penicillin allergy are found to have actual IgE-mediated allergy upon testing [7, 8]. In patients with proven penicillin allergy, 2.5% will develop an allergy to the cephalosporins commonly used for surgical site infection prophylaxis, while in patients simply reporting penicillin allergy, only 1% are cross-reactive. The incidence of cross-reactivity is substantially lower with third- and fourth-generation cephalosporins [9, 10]. Vancomycin, administered to patients positive for methicillin-resistant *Staphylococcus aureus* (MRSA), may cause flushing and pruritis "red man syndrome" when infused too rapidly; this does not represent a true allergy and is generally prevented by administration times of an hour or more [11]. Children with myelomeningocele, bladder exstrophy, or cerebral palsy with ventriculoperitoneal shunts may be at increased risk of latex allergy [12–14], which may lead to life-threatening anaphylactic reactions. However, latex-allergic children can be safely anesthetized if exposure to latex in the medical environment is avoided and prophylactic medications appear to be unnecessary [15]. With the increased use of non-latex products overall,

anaphylactic reactions to latex in the operating room have declined significantly in the past two decades and are now rare events.

Review of Systems

Important areas include general health, development, and exercise tolerance. Prematurity and the presence of associated reactive airway disease and/or bronchopulmonary dysplasia may predispose to perioperative respiratory complications. Recent upper respiratory infection (URI), bronchiolitis, or previous episodes of croup are of particular concern. URI with active symptoms or with symptoms less than 2 weeks prior to surgery is associated with a twofold increase of perioperative respiratory adverse events, such as bronchospasm, laryngospasm, and airway obstruction [16]. In patients with congenital cardiac disease, understanding the nature of the lesion, its correction or palliation, and the current functional status is essential. Consultation with the patient's cardiologist and repeat echocardiography may be prudent if there have been no such recent evaluations, or the patient's cardiopulmonary symptoms or exercise tolerance has changed, or the planned procedure is expected to place unusual demands on the heart. For those infants and children with residual complex cardiac disease, such as those with hypoplastic left heart syndrome, management by anesthesiologists with subspecialty training in pediatric cardiac anesthesia is prefered. Renal and hepatic diseases affect drug disposition and metabolism. Anesthetic management is also affected by neurologic disease and autism spectrum disorders, including convulsive disorders, cognitive impairment, and neuromuscular disease.

Family History

A family history suggestive of possible malignant hyperthermia (MH), pseudocholinesterase deficiency (succinylcholine sensitivity), neuromuscular disease, or coagulation disorder deserves detailed exploration [17]. MH has an incidence of 1:5000 to 1:50,000–100,000 with a higher prevalence in males [17, 18]. The incidence of pseudocholinesterase deficiency is 1:3200–5000 [19]. While several laboratory tests may be useful in determining risk for these disorders, comprehensive genetic testing remains under development.

Physical Examination

Age, Weight, Height, and Vital Signs

Patient age affects the approach to induction, need for preanesthetic medication, and anesthetic risk. Children less than 1 year of age have an increased risk of complications, especially children in the first 2 months of life [20]. If possible, procedures that are entirely elective should be postponed until after 6 months of age. The weight of the child affects the dose of medications administered and reflects the child's general state of health. Significant medical problems often result in growth failure. A determination of BMI and ideal body weight are essential for dosing in overweight/obese patients. Heart rate, blood pressure, and temperature should be determined prior to induction of anesthesia. Pulse oximetry (SpO2) is measured prior to transfer to the operating room in order to rule out unanticipated lower respiratory tract system or cardiac pathology.

Physical Examination

The examination of the airway focuses on mask fit, mouth opening, neck mobility, tongue size, thyromental distance, and mandibular size. Patients who are less than a year old, weigh less than 10 kg, have short thyromental distance, and have preexisting airway or craniofacial abnormalities are at risk for difficult intubation [21–24]. Examination of mouth opening in the uncooperative infant may be facilitated by removing and inserting a pacifier and observing the extent of opening. The modified Mallampati grading system for mouth opening divides patients into four groups: Class 1: the soft palate, uvula, fauces, and pillars can all be visualized; Class 2: the soft palate, uvula, and fauces are visible; Class 3: the soft palate and base of uvula are visible; and Class 4: only the hard palate is visible [25, 26]. If the Mallampati score can be obtained, higher incidences of difficult laryngoscopy are seen in patients with Mallampati scores 3 and 4 [23].

Protruding or loose teeth (especially in children aged 5–9 years) should be noted to assess whether in the former case they may interfere with laryngoscopy or whether in the latter case they should be removed to minimize pulmonary aspiration risk. Adequate neck mobility is important in the alignment of the oropharyngeal and tracheal axis for the best laryngoscopic view.

The chest examination should include observations on the symmetry of chest excursion, ease of respiratory effort, and auscultatory findings. Elective procedures should be postponed if rhonchi are heard, indicating active bronchitis or pneumonia. Mild to moderate wheezing may be treated with a bronchodilator in advance of induction to see if it improves and to prepare the airway for the stimulus of intubation. The cardiac examination should note the color of the extremities and the quality of peripheral pulses. Heart murmurs are most commonly innocent functional murmurs, but can be indicative of serious undiagnosed pathology. Functional murmurs are soft systolic murmurs that are best heard along the left sternal border, change with respiratory cycle and patient position, and have no diastolic component or clicks. If the child's pediatrician has noted the murmur on

previous examinations and believes it to be innocent, no additional workup is generally needed. Cardiology is consulted if the patient is symptomatic or if there is any doubt about murmur type.

Preoperative Testing

Routine preoperative laboratory testing for healthy patients is unnecessary. Determination of the patient's hemoglobin level is needed only if anemia is suspected or for operations where substantial blood loss is anticipated, such as craniofacial reconstruction. Similarly, in asymptomatic patients, coagulation studies are reserved only for procedures associated with large blood loss. All menstruating girls are screened for pregnancy with an urine or serum ß-HCG level.

Preoperative Preparation

A child's fear of strangers, needles, pain, foreign environments, and separation from parents must be addressed [27]. Having informed, calm parents is the best way to ensure that the child will be calm and relaxed on the day of surgery. A visit to the hospital prior to the planned surgery allows the child and parents to have their questions answered in a relaxed setting and provides the information necessary for the parents to prepare their child for the day of surgery. This visit has shown to reduce parental anxiety on the day of surgery [28]. Telephone interviews, brochures, and web resources are alternatives when a preoperative hospital visit is not possible.

In an age-appropriate manner, children should be informed about what to expect on the day of surgery, using an honest, positive, and non-threatening approach. They should know that they will be in a deep sleep brought on by medicines and will not awaken until after the operation is over. They should be informed of the plan for separation from their parents, induction of anesthesia, and postsurgical process, including staying in the recovery room and management of postoperative pain.

Risks of Anesthesia

Although anesthesia is generally considered very safe for healthy children, the preoperative meeting with the family should still include a discussion on the potential risks and complications of anesthesia. Some common adverse reactions to anesthesia include postoperative nausea and vomiting (6%) and sore throat. Less common complications include respiratory complications such as airway obstruction (1.1%), laryngospasm (1.7%), bronchospasm (0.2%), aspiration (0.04%), and allergic reactions (0.01–0.1%) [29–32]. Severe complications, such as cardiac arrests that are attributed to anesthesia, are rare (0.65–1.4:10,000 procedures) [33, 34]. The incidence of both respiratory complications and cardiac arrest are much higher in children under 1 year old and especially children under 1 month old.

Neurotoxicity

Recent investigations have raised concern about the potential harm of anesthetic exposure to a developing child's brain. Animal studies, including several in nonhuman primates, demonstrate that many general anesthetic agents used in human clinical practice can be neurotoxic to the developing brain. The issue was brought to scientific attention in 1999 when Ikonomidou et al. showed that blockade of N-methyl-D-aspartate (NMDA) glutamate receptors for only a few hours during late fetal or early neonatal life triggered widespread apoptotic neurodegeneration in the developing rat brain [35]. Early exposure to ethanol, which blocks NMDA glutamate receptors and activates gamma-aminobutyric acid (GABAA) receptors, results in similar pathology [36]. Neonatal rats exposed to a combination of midazolam (GABA-agonist), isoflurane (combined GABA-agonist and NMDA-antagonist), and nitrous oxide (NMDA-antagonist) maintained at a surgical depth of anesthesia experienced both immediate brain cell loss and impaired long-term neurocognitive function [37]. A variety of neurotoxic effects, including acute neuronal cell loss, altered dendritic architecture, reduced synaptic density, decreased levels of neurotrophic factors, mitochondrial degeneration, destabilization of the cytoskeleton, and cell cycle abnormalities, have been described following exposure to standard anesthetics and sedatives in a broad range of immature animal species [38].

Whether these findings translate to human risk remains unclear. There is no accepted unified mechanistic theory to explain the neurotoxic effects, and the pathologies themselves vary across animal species. Many of the animal studies utilize anesthetic agents in doses and durations that far exceed clinical equivalents for humans [39]. Furthermore, anesthetic management is less controlled in experimental neonatal animal models than in humans; the neonatal animal's small size precludes continuous hemodynamic monitoring, assessment of acid-base status, and glucose levels, all of which normally dictate changes in anesthetic management of a human neonate [38]. Unrecognized hypotension, hypercarbia, metabolic acidosis, and hypoglycemia associated with anesthesia in a neonatal rodent could lead to pathology and neurologic deficits without direct biochemical neurotoxicity [38–42].

Several large retrospective human cohort studies evaluating behavioral and cognitive effects of anesthetic exposure in the developing brain have been completed. Researchers from the Mayo Clinic compared standardized aptitude test score in 5357 students, out of which 593 had general anesthesia before age 4 with their unexposed peers. In a follow-up

study, 350 children who were exposed to anesthesia before age 2 were matched to 700 unexposed controls. Both studies showed there were no differences in test scores between children who were unexposed and children who had had a single anesthetic exposure. However, in both studies, children who had multiple anesthetic exposures did incrementally worse than their peers who received none [43, 44]. A study consisting of 2689 Danish children who had surgery in infancy were age-matched to a control group of 14,575 children who did not. Academic tests scores at ninth grade showed no differences between these groups [45]. Using the Western Australian Pregnancy Cohort Study data, consisting of 2608 children with 321 of them exposed to anesthesia before 3 years old, Ing et al. found some associations between anesthetic exposure and language, cognitive function, motor skills, and behavior outcomes at age 10 y [46]. However, the results were neither consistent within nor across modalities: one language test, the Clinical Evaluation of Language Fundamentals, showed clear differences in receptive language ability, whereas no differences were seen in the Peabody Picture Vocabulary assessment and no differences in visual tracking and attention (Symbol Digit Modality Test), fine and gross motor function (McCarron Assessment of Neuromuscular Development), or behavior (Child Behavior Checklist) related to exposure status.

Although the results of these retrospective cohort studies have not been conclusive, in aggregate they suggest that a brief, single anesthetic exposure is not associated with future learning disability and/or lower test scores. For outcome differences that are suggested in these nonrandomized studies, the child's underlying pathology or surgery itself may confound effects otherwise attributable to anesthesia [38].

Researchers conducting the large multinational prospective trial, General Anesthesia versus Spinal (GAS Study), sought to more definitively answer the neurotoxicity question. The study design minimized the confounding effects of surgery by comparing only infants who had a single surgery – inguinal hernia repair. Subjects were randomized to general or regional anesthesia, the latter generally acknowledged being non-neurotoxic. Cognitive development at 2 y of age using the Bayley Scales of Infant Development III test were no different between the two groups when <1 hr of sevoflurane anesthesia was administered [47]. A 5-year follow-up intelligence test is planned.

Although these results were reassuring, there are still many important concerns and questions that cannot be answered by the GAS study. Brain function is very complex and cannot be fully measured with a single cognitive test. How does exposure to anesthetics affect the development of other functions such as memory, language, motor skills, and emotional development? Do these effects change when multiple anesthetic drugs are combined? Are the results the same for procedures other than hernia repair? Animal and epidemiological data suggest that the risk of anesthetics to the developing brain increases with longer duration exposure or multiple exposures. Is this true for children? Further research will be required to address these questions [48].

At present, however, healthcare providers may best be advised to follow and share the consensus statement released by SmartTots.org, a partnership between the US Food and Drug Administration (FDA) and the International Anesthesia Research Society (IARS), which states the following [48, 49]:

> …It is not yet possible to know whether anesthetic drugs are safe for children in a single short duration procedure…Concerns regarding the unknown risk of anesthetic exposure to the child's brain development must be weighed against the potential harm associated with cancelling or delaying a needed procedure. Each child must be evaluated individually based on age, the type of procedure, level of urgency, and other health factors...

Preoperative Fasting

The purpose of the fast is to decrease the risk of aspiration of gastric contents after the patient undergoes anesthesia. The volume of gastric contents depends on continuous gastric secretion, swallowed saliva, ingested solids and liquids, and rate of gastric emptying. Gastric contents empty at a variable rate depending on the volume and constituents of the content. The most recent fasting recommendations are outlined in Table 5.2.

Clear Liquids

Clear liquids, including water, oral electrolyte solution (Pedialyte®), juices without pulp, carbohydrate drinks, and coffee or tea without milk, move rapidly out of the stomach; the 50% emptying time is 12 min [50]. Two hours after a clear liquid drink, most individuals' gastric volume will be similar to someone who had completed an overnight fast [51–54]. Therefore, most pediatric anesthesiologists allow healthy children to drink clear liquids up to 2 hr prior to induction, which appear to be safe and has other benefits [55]. Children are less irritable, less thirsty and hungry, and tolerate the preoperative wait better if they are allowed to drink. They are also less likely to be hypoglycemic.

Table 5.2 Preoperative fasting recommendations for healthy patients undergoing elective procedures

Ingested material	Minimum fast (hr)
Clear liquids	2
Breast milk	4
Infant formula	6
Nonhuman milk	6
Meal (toast and clears)	6
Other meal	>8

Milk and Formula

A minimum of a 4-hr fast is advisable after breast milk and 6 hr after nonhuman milk or infant formula [56–59]. Healthy infants <6 mo of age may be eligible for formula fasts relaxed to 4 hr [60]. Scheduling surgery early in the day helps minimize the waiting period and avoids some of the feeding problems for young infants.

Solids

Solid meals have linear gastric emptying patterns with the mean half-time of emptying of approximately 5 hr for a filling meal [55]. Based on current evidence, it is recommended to fast for 6 hr after a light meal and 8 hr after a full meal [61]. Chewing gum is considered equivalent to drinking clear liquids, as it generates saliva and stimulates gastric secretion. However, swallowing chewing gum would be considered as solid intake and delay the procedure for 6 hr [62].

Patient compliance is a potential problem for children, regardless of preoperative instructions. Explicit written instruction for patients and their families helps avoid feeding policy violations, and these instructions should be reinforced during preoperative visits or phone calls. On the day of surgery, the anesthesiologist should also verify the patient's PO intake status.

Reduction of Anxiety During Induction

Up to 60% of young children undergoing anesthesia and surgery experience significant anxiety [63, 64]. Some of the risk factors associated with the development of preoperative anxiety include age (highest with children between 1–5 years), temperament and baseline anxiety, past medical encounters, and parental anxiety [65]. Anxiety is not only psychologically stressful for the patient and family, it has also been linked to significantly higher postoperative pain, delayed hospital discharge, and higher incidence of emergence delirium, sleep disturbances, and other maladaptive behavioral changes that last up to a few weeks following surgery [66, 67]. Given the negative consequences of preoperative anxiety, several approaches have been used to reduce anxiety in the child and to some extent the parent. Some common methods include parental presence during induction, distraction techniques using toys or electronic devices, eliciting the help of child-life specialists, and sedative premedications.

Parental Presence

The idea that a parent could lessen the anxiety of anesthetic induction is not new, and although parental presence at induction (PPIA) is used at many institutions, often at the request of the parent, the evidence of its effectiveness is mixed. Earlier studies indicate that children will be calmer with a parent present, while some other studies showed no effect to the child, but a reduction in anxiety of the parents [63, 68, 69]. A recent Cochrane review showed that parental presence made no difference in the child's anxiety and was far less effective than premedication [70]. Of note, children of anxious parents do not benefit by having their parents present during induction. The ultimate choice of whether or not to include the parent rests with the anesthesiologist and the institution. If a PPIA is chosen, it is important to mentally prepare the parents who are about to witness the physiological changes of their child during the induction of anesthesia.

Preoperative Sedation

Compared to PPIA, sedative premedication may lower children's preoperative anxiety and improve compliance with face mask on induction [71]. At present the most commonly used medication is oral midazolam (0.5 mg/kg to 10–15 mg maximum doses). Midazolam is a short-acting benzodiazepine, where an oral dose of 0.5–0.75 mg/kg permits satisfactory separation in 15–30 min and results in 45–60 min of sedation [72]. Oral midazolam is generally well tolerated although some children may refuse it and rare adverse reactions such as disinhibition and dysphoria have been recorded [73]. Midazolam may also be administered intranasally at a dose of 0.3 mg/kg.

Although not commonly used, ketamine is an effective preanesthetic medication at an oral dose of 6–8 mg/kg [74, 75]. Sedation begins in approximately 20–25 min after administration, and almost all patients are calm at the time of induction. Oral ketamine (3 mg/kg) can also be added to oral midazolam (0.5 mg/kg) to supplement inadequate sedation or to heavily sedate a difficult patient. For patients with severe behavioral problems, such as autism, 4–5 mg/kg intramuscular ketamine can be extremely effective. Regardless of its route of administration, ketamine stimulates the secretion of saliva and should be given in conjunction with an antisialagogue, such as glycopyrrolate or atropine. Although ketamine has been associated with hallucinations in adults, the incidence was not significant in the pediatric population and may be countered by concomitant midazolam administration [76].

Operative Management

General Anesthetic Induction Techniques

Inhalation and intravenous induction are the most common techniques for the induction of general anesthesia. An inhalational induction is often chosen for fasted healthy children

without preexisting intravenous lines. However, if a child requires an emergency procedure under general anesthesia and is not appropriately fasted, a rapid sequence intravenous induction is usually indicated. Children with complicated medical conditions such as a known or suspected difficult airway, cardiac disease, and severe gastroesophageal reflux require special induction strategies.

Inhalation Anesthetics

Inhalation induction of anesthesia may be facilitated by either preoperative sedative administration or parental presence. Distraction techniques such as singing songs, playing a movie or game on a tablet, and using flavors to disguise the smell of the anesthetic all help to smooth the induction process. Of the many inhalation anesthetics, only nitrous oxide, sevoflurane, isoflurane, and desflurane remain commonly used in the United States. Nitrous oxide is not a potent agent and is typically used to supplement the potent inhalation agents or intravenous anesthetics. The minimum alveolar concentration (MAC) is the alveolar concentration at which 50% of patients do not move to skin incision and is the standard measure for potency of an anesthetic gas [77]. MAC increases with age, reaching a maximum value in infants 1–6 months of age, and gradually decreases through adulthood [78–80] (Table 5.3). Despite having a higher MAC than older children, neonates and infants are more susceptible to myocardial depression from the inhalation agents and are more prone to cardiac arrest secondary to overdose [29, 34, 81, 82].

Sevoflurane has become the anesthetic of choice for inhalation induction, as it is the least irritating agent to the airway and provides excellent cardiovascular stability [83, 84]. These qualities plus its insolubility make anesthetic induction very rapid and also readily allow tracheal intubation without the use of muscle relaxants [85, 86]. For most healthy children without cardiovascular disease, an inhalational induction can be safely performed with sevoflurane up to 8%, mixed with nitrous oxide 70% and oxygen 30%. Desflurane is the newest inhalational agent, introduced 2 years after sevoflurane in 1992. Although it is associated with a rapid emergence and recovery due to its low blood solubility [87], it is highly irritating to the upper airway and is not recommended as an induction agent [88]. Furthermore, unlike other inhalation agents that have bronchodilation effects, desflurane can cause bronchoconstriction at levels above 1 MAC [89]. Isoflurane was introduced in the 1980s and is characterized by its higher blood solubility [90]. It is also irritating to the airway and is therefore not recommended for inhalation induction, but can be used for maintenance of anesthesia. It is significantly less expensive than either sevoflurane or desflurane.

Table 5.3 Inhalation anesthetics: effect of age on potency

		Minimum alveolar concentration (MAC)				
Agent	$\lambda_{B/G}$	Neonate	1–6 mo	1–3 y	3–10 y	Adult
Nitrous oxide	0.46	…	…	…	…	104
Isoflurane	1.3	1.6	1.8	1.6	1.6	1.2
Desflurane	0.42	9.2	9.9	8.6	8.0	7.0
Sevoflurane	0.66	3.3	3.2	2.5	2.5	2.1

MAC = The alveolar concentration in percent of volume at which 50% of patients do not move on skin incision
$\lambda_{B/G}$ = blood/gas partition coefficient
… = MAC values for this age group is not available

Intravenous Anesthetics

Intravenous induction may be chosen as a technique to manage a known or suspected difficult airway, or if there is concern about aspiration risk, or because an intravenous line is already in place. Compared to an inhalation induction, it provides a faster induction but is also more likely to result in patient apnea [91]. For patients who do not have an established intravenous catheter, several techniques may facilitate catheter placement. Cutaneous analgesia can be achieved with the topical application of an eutectic mixture of local anesthetics (EMLA 5% cream, Astra Pharmaceuticals) or lidocaine 4% ointment (ELA-Max) 30–60 min prior to placing the catheter [92]. Unfortunately, EMLA may cause significant cutaneous vasoconstriction, making cannulation more difficult [93]. Application of 50% nitrous oxide in oxygen by face mask provides effective analgesia within 2–3 min and is commonly practiced. Prior to venous cannulation, local infiltration of 1% lidocaine with a small (30 gauge) needle may further decrease discomfort. This approach has been shown to be superior to EMLA by one set of investigators [94].

Propofol, ketamine, and etomidate are viable choices for intravenous induction of anesthesia. Propofol dominates current practice due to its rapid induction of anesthesia, fast recovery profile, and low incidence of nausea and vomiting. The usual induction dose for children ranges between 2.5 and 3.0 mg/kg [95], but infants may require higher doses [96]. Intravenous injection of propofol may cause a localized burning sensation. Injecting 2% lidocaine (1 mg/kg) immediately prior to propofol administration can help minimize this. Ketamine, an NMDA receptor antagonist, is not commonly used as an induction agent in oculoplastic patients due to drug-induced nystagmus and, at high doses, increased intraocular pressure [97, 98]. Its use is typically reserved for patients who are unable to cooperate or sedate by other means (intramuscular ketamine as described above), or in patients with a difficult airway where preserving spontaneous respiration is important. The usual induction dose is 2–4 mg/kg IV [74, 75, 99]. Etomidate is a GABA receptor agonist and is typically reserved for patients who are hemodynamically unstable or in patients with congenital heart disease where it is important to maintain systemic blood pressure.

Propofol infusions (50–100 mcg/kg/min) can be used for sedation during procedures performed under local or

regional anesthesia. The level of sedation is readily adjusted to the patient's needs, and it dissipates rapidly after short-term infusions are discontinued. Higher propofol infusion rates (100–300 mcg/kg/min) may be used in place of inhalation agents for general anesthesia. When combined with ultrashort-acting intravenous agents such as remifentanil, total intravenous anesthesia (TIVA) can replace the need for inhalational agents. TIVA is particularly useful when inhalational agents are to be avoided, such as in patients who are at risk or have a history of malignant hyperthermia. A recent comparative study in pediatric strabismus surgery, however, showed no significant differences in incidences of postoperative hypoxemia, vomiting, and time to PACU and hospital discharge between intravenous and inhalation techniques [100]. A study in adults, however, showed that the TIVA technique compared to inhalational agents was associated with a lower incidence of postoperative nausea and vomiting [101].

Although not an induction agent, dexmedetomidine is a valuable adjunct agent used to supplement the effects of other anesthetic agents. It is an alpha-2 adrenergic agonist and causes sedation, anxiolysis, and analgesia, without the respiratory depression associated with propofol. Dexmedetomidine can be used alone to provide sedation or with other agents to decrease the total anesthetic requirement [102]. One of the drug's common side effects is bradycardia [103].

Muscle Relaxants

Muscle relaxants may be used to facilitate tracheal intubation and/or to maintain paralysis during surgery. The specific choice of neuromuscular blocking agent is based on the duration of surgery and the patient's needs (Table 5.4). The volume of distribution and the plasma concentration of these agents are related to the patient's age and other comorbidities, which the anesthesiologist must be attuned to. Several reviews detail the pharmacology of these agents [104, 105].

Table 5.4 Properties of common neuromuscular relaxants

Drug	Intubation dose (mg/kg)	Onset time (min)	Recovery time to 25% twitch height (min)
Depolarizing			
Succinylcholine	1–2 IV 4 IM	1	4 10–20
Non-depolarizing			
Rocuronium	0.6 IV 0.9 IV 1.2 IV 1.8 IM	1–1.5 1–1.25 1 2.5–3.7	27–37 53 73 89
Atracurium	0.5 IV	1.5	33
Cisatracurium	0.1 IV	1.7	31
Vecuronium	0.1 IV	1.3	24
Pancuronium	0.1 IV	2.5	60–90

Succinylcholine is the only depolarizing relaxant regularly used today. It has the fastest onset of any of the muscle relaxants but is associated with numerous side effects, some of which are of particular interest to the surgeon. It increases intraocular pressure and should be used with caution depending on the nature of the proposed procedure (open eye wound or eye pressure measurement). After a single dose of succinylcholine, increased intraocular pressure peaks at 25 mmHg after 90 s and returns to baseline (15 mmHg) in 5 min [106]. Anecdotes of extrusion of ocular contents from succinylcholine have been reported, but recent reviews on this issue do not substantiate this risk [107]. Of greater concern, succinylcholine can trigger malignant hyperthermia in susceptible individuals and life-threatening hyperkalemia in patients with myopathies, recent burns, or major trauma. Having earned a black box warning from the Food and Drug Administration in 1993, succinylcholine is currently indicated for rapid sequence induction and treatment of laryngospasm, and it remains the only drug recommended for intramuscular administration in emergency circumstances.

Non-depolarizing agents do not increase intraocular pressure. Rocuronium has a rapid onset of action and may be used as part of a rapid sequence induction for emergency surgery. Should early reversal of its associated neuromuscular blockade be required, a new agent, sugammadex, may be used. Vecuronium and cisatracurium are intermediate in onset and duration and are appropriate choices for many ophthalmologic procedures. Pancuronium is an older, inexpensive drug and remains an appropriate choice for surgical procedures that exceed 45–60 min. In general, the effects of non-depolarizing muscle relaxants may be reversed with neostigmine after the neuromuscular junction begin to recover. This reversal is preceded by a dose of an anticholinergic drug such as atropine or glycopyrrolate to prevent bradycardia associated with neostigmine administration. Because many of the non-depolarizing agents require 20 min or longer to reach the point of being reversible, the anesthesiologist should be kept informed of the estimated surgical duration to assure administration of the appropriate type and dose of non-depolarizing agent.

Intraoperative Monitoring and Operating Room Environment

Basic monitoring for pediatric patients consists of pulse oximetry, electrocardiography, automated noninvasive blood pressure cuff, capnography, temperature monitoring, and agent-specific gas analysis. For brief procedures, such as nasolacrimal duct probing, an intravenous catheter may not be essential, but it may be beneficial for administration of intravenous fluids and medications to reduce the risk of nausea and vomiting, and management of pain and postoperative agitation.

Infants and children can rapidly cool in the operating room environment. The room temperature during induction and emergence should be appropriately warm; young infants should be kept warm with an underbody and overhead warmer. A warm blanket helps diminish heat loss during the procedure, as does a heat moisture exchanger in the anesthesia circuit [108]. For longer cases, the addition of a forced warm air blanket that covers or surrounds the child helps minimize the risks of either hypothermia or hyperthermia.

Airway Management

General anesthesia can be maintained either via face mask, laryngeal mask airway (LMA), or tracheal tube. The type of procedure, experience of the anesthesiologist, and age and comorbidities of the patient will determine the choice of appropriate airway.

Face Mask

Pediatric face masks come in many different sizes to fit patients of all ages. It should readily conform to the face and allow the anesthesiologist to visualize the mouth and nose. In patients who have upper airway obstruction after induction of anesthesia, an oral or nasal airway can help relieve the obstruction. Short procedures such as probing and irrigation of blocked nasolacrimal ducts can be done with a face mask, but LMAs are often preferred for better surgical access and control of secretions.

Laryngeal Mask Airway

Developed in the 1980s, the LMA has become an essential device for both routine and difficult airway management. Several designs and models are available (Fig. 5.1). The LMA provides a direct route for oxygen and anesthetic gases to reach the trachea without the need for visualization of the larynx or insertion of a tube into the trachea. The tip of the LMA tip sits in the esophageal inlet; the cuff extends to the base of the tongue and forms a low-pressure seal around the larynx. A fenestrated opening surrounds the larynx with a semirigid tube connecting to a circuit or ventilator outside the mouth. The LMA is included in the American Society of Anesthesiologists difficult airway algorithm and can be lifesaving in the "cannot ventilate, cannot intubate" scenario [109]. Seven sizes based on the weight of the patient are available ranging from newborn to large adult. Although investigators have reported excellent success with the smallest LMA size [110], many are more reluctant to use the #1 LMA for maintenance of anesthesia in infants and reserve it for brief procedures or as an emergency airway device. The occasional failure of the #1 LMA is thought to be due to the neonate's relatively larger and more flaccid epiglottis blocking the LMA inlet [111].

The LMA should be thought of as a mask and not a tracheal tube. Laryngospasm and aspirations of regurgitated gastric contents can occur with the LMA in place if an adequate depth of anesthesia is not maintained. On the other hand, the LMA protects the airway from secretions from above the larynx, such as injected methylene blue or fluorescein dye



Fig. 5.1 Comparisons of different laryngeal mask airways (LMA). From *top* clockwise, trademarked brands are in () low-profile flexible LMA (Ambu), LMA with gastric suction port (LMA Supreme), intubating LMA (Cookgas Air-Q), regular LMA (Ambu)

administration during probing and irrigation of blocked nasolacrimal ducts [112]. It allows the surgeon complete access to the eye and nose for probing of blocked nasolacrimal ducts, silastic intubation, examination under anesthesia, strabismus repair, chalazion drainage, and other minor oculoplastic procedures. The shaft of a flexible LMA may be taped closely to the patient's chin, maintaining a low airway profile, thereby further increasing surgical work space.

Anesthetic maintenance can be conducted with an LMA using spontaneous or controlled ventilation. The LMA "leaks" when the peak inflating pressure exceeds 15–20 cm H_2O. When used with controlled ventilation, the LMA can be used in conjunction with neuromuscular blocking agents, though many practitioners view the necessity to control ventilation as an indication for tracheal intubation. At the end of the procedure, the LMA may be removed while the patient is still anesthetized ("deep removal") or fully awake. The decision is based on the anesthesiologist's experience, patient characteristics, and recovery area standard practices. A recent systematic review showed that the safety profile is similar for either approach; coughing was less frequent with deep removal, and airway obstruction was less frequent with awake removal [113].

Tracheal Intubation

Tracheal intubation is the most definitive method for airway management in children. As with LMAs, a variety of tracheal tubes are available to meet specific needs (Fig. 5.2). A number of systems have been used to predict the appropriate tracheal tube size for infants and children. Cole's formula (age (yr) /4 + 4) correctly predicts the correct uncuffed tube size approximately 60% of the time and 95% of the time is within 0.5 mm of the correct size [114]. Uncuffed tracheal tubes have traditionally been recommended for infants and children until the age of 8–10 years, in order to mitigate against post-extubation stridor. This concept has been refuted in studies showing that the incidence of post-extubation stridor is the same between uncuffed and cuffed tracheal tubes [115]. Furthermore, using cuffed tubes resulted in fewer tube exchanges due to leaks around the tube, lower fresh gas flow usage, and less waste gas contamination [116]. As a result, most pediatric anesthesiologists use cuffed tubes downsized 0.5–1.0 mm ID from uncuffed ones unless there are strong reasons not to [117]. To ensure that the tube fits properly, the pressure at which gas leaks around the tube is measured (leak test) and the cuffed filled to allow a leak between 15 and 25 cm H_2O [118].

For many pediatric oculoplastic procedures, it is convenient to use a tracheal tube with a preconfigured bend, such as the oral RAE tube (Ring-Adair-Elwyn, Mallinckrodt). These tubes are inherently less secure, especially in the smaller sizes, but allow the anesthesia circuit to remain out of the way of the surgeon. Care must be taken during positioning not to dislodge the tube. Flexion and extension of the head in infants may move the distal tip of a tracheal tube by ±1.7 cm and may lead to unintended endobronchial intubation or extubation [119]. Wire reinforced (anode) tubes provide an alternative to the oral RAE tube. They allow more precise positioning of the tip of the tube since they do not have a preformed bend and will not kink or occlude when the head is repositioned. Anesthesiologists should continuously monitor airway pressures and breath sounds for signs of endobronchial intubation or tracheal tube obstruction during surgery.

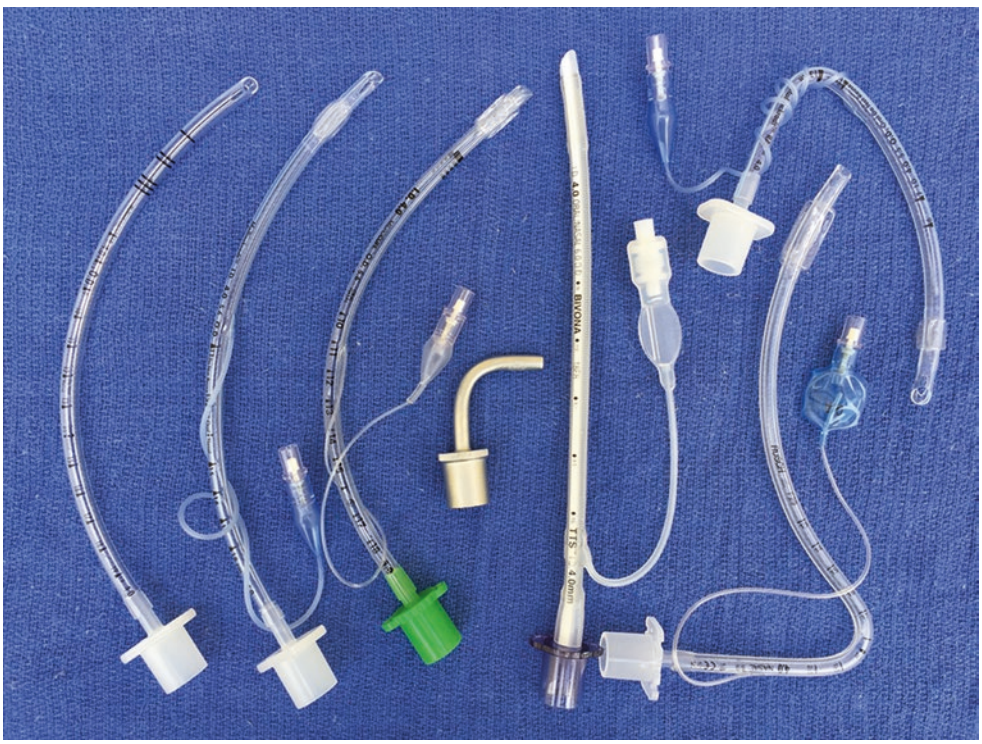


Fig. 5.2 Comparison of different endotracheal tubes. From *left to right*, trademarked brands are in (): uncuffed tracheal tube (Mallinckrodt); cuffed tracheal tube (Mallinckrodt); microcuffed tracheal tube (Halyard Microcuff); tracheal tube adapter used to connect to a shortened tube; wire-enforced flexible tracheal tube (Bivona); bottom, curved nasal RAE tube (Rusch); top, curved oral RAE tube (Mallinckrodt)

The Difficult Pediatric Airway

Normal Anatomy and Physiology

The anatomic differences between the normal pediatric and the normal adult airway present several challenges for the anesthesiologist. The child's larynx is more cephalad and has an anterior tilt compared to that of the adult, making visualization by direct laryngoscopy more difficult. Furthermore, the infant's larger tongue in proportion to the oral aperture and floppy omega-shaped epiglottis can also make intubation more challenging.

To support a higher basal metabolic rate of 7–8 mL O_2/kg/min compared to 3.5 mL O_2/kg/min in the adult, infants and young children must increase their minute ventilation by doubling respiratory rate. This places a greater physiologic demand on the airway. Functional residual capacity (FRC), which provides oxygen storage, is approximately the same on a per kilogram basis in infants and adults. During intubation, the anesthesiologist relies on the FRC to provide oxygen while the patient is apneic. Because of the doubled oxygen consumption and the fixed per kilogram FRC, the anesthesiologist has a shorter amount of time to secure the infant airway before oxygen desaturation begins [120].

Because of the major morbidity and mortality associated with airway loss in any patient, anesthesiologists are always concerned with the nature of a patient's airway. Concern is heightened for those pediatric patients with congenital syndromes or abnormal airways, where additional factors may preclude straightforward ventilation and/or intubation.

Airway Evaluation

Evaluation of the airway begins during the preoperative assessment. The patient's medical history, past anesthetics with particular reference to airway management, and airway examination are vital in this process. A patient's ability to lie flat and sleep without substantial airway obstruction suggests that the patient may be safely anesthetized prior to insertion of a tracheal tube. Induction techniques used in the past, specific nature of the airway difficulty (mask ventilation versus intubation), and airway equipment used (nasal or oral airways, laryngeal mask airway, type of laryngoscope blade, fiber-optic bronchoscope, smaller tracheal tube size) should be noted. Since the airway may change with time, the most recent anesthetic record will likely provide the most useful information. If several years have elapsed since the last anesthetic and signs and symptoms have changed, an entirely new approach to the airway may be required. The anesthesiologist should review the records, perform a thorough airway examination, and discuss the proposed anesthetic with the patient and family. Induction of anesthesia should take place in a setting where the anesthesiologist will have access to all necessary equipment and the assistance of other experienced anesthesiologists and consulting otolaryngology surgeons.

Management of the Difficult Airway

The American Society of Anesthesiologists (ASA) developed the difficult airway algorithm as a set of guidelines for the management of the recognized and unrecognized difficult airway [109]. This algorithm was designed for use in adults and presents a general airway management algorithm with an emphasis on planning, preparing, and having multiple backup strategies. Among its recommendations are availability of experienced personnel and equipment, recognizing the likelihood and clinical impact of difficult mask ventilation, supraglottic airway (LMA) placement, laryngoscopy, intubation, and surgical access, and supplemental oxygen delivery during management (Fig. 5.3).

While many parts of the ASA difficult airway algorithm have their place in pediatric practice, there are some aspects that may not easily apply to infants and children. Most importantly, awake/sedated intubation and tracheostomy facilitated by local anesthesia and sedation play prominent roles in the management of adult patients with difficult airways, but have limited application in children. Pediatric patients who are not expected to present difficulties with mask ventilation may undergo an inhalation induction with O_2/N_2O/sevoflurane. Spontaneous ventilation offers a margin of safety during induction and may be more difficult to achieve using intravenous agents. Although an intravenous induction may not be chosen, it is extremely helpful to have a working intravenous line in place prior to managing the difficult airway in order to administer antisialogues, sedatives, or emergency medications. To maintain a patent airway, the anesthesiologist may need to apply continuous positive airway pressure (CPAP) between 5 and 15 cm H_2O and relieve airway obstruction from the tongue with a jaw thrust maneuver or an oral airway. If ventilation can be controlled with bag and mask or LMA, then the use of muscle relaxants may be considered prior to attempting tracheal intubation [121].

Equipment used for difficult adult airways such as the video laryngoscope, LMA, and fiber-optic bronchoscope all have roles in managing difficult pediatric airways. The efficacy and safety of the video laryngoscope has been well validated [122–124]. Video laryngoscopy, compared to direct laryngoscopy, results in more successful intubations on first attempt (93% vs. 84%) and shorter time to intubation (33 s vs. 46 s), without difference in complication rates [124].

The importance of the LMA is reflected in its prominence within the difficult airway algorithm. It can be used on the awake intubation pathway as a conduit for fiber-optic intubation, on the nonemergency pathway as a definitive airway or as a fiber-optic conduit, or on the emergency anesthetized pathway as both a lifesaving ventilation device and as a conduit [125]. In patients with Pierre-Robin syndrome or other airway abnormalities, the LMA can be inserted in the awake or sedated patient to allow for inhalation induction [126].

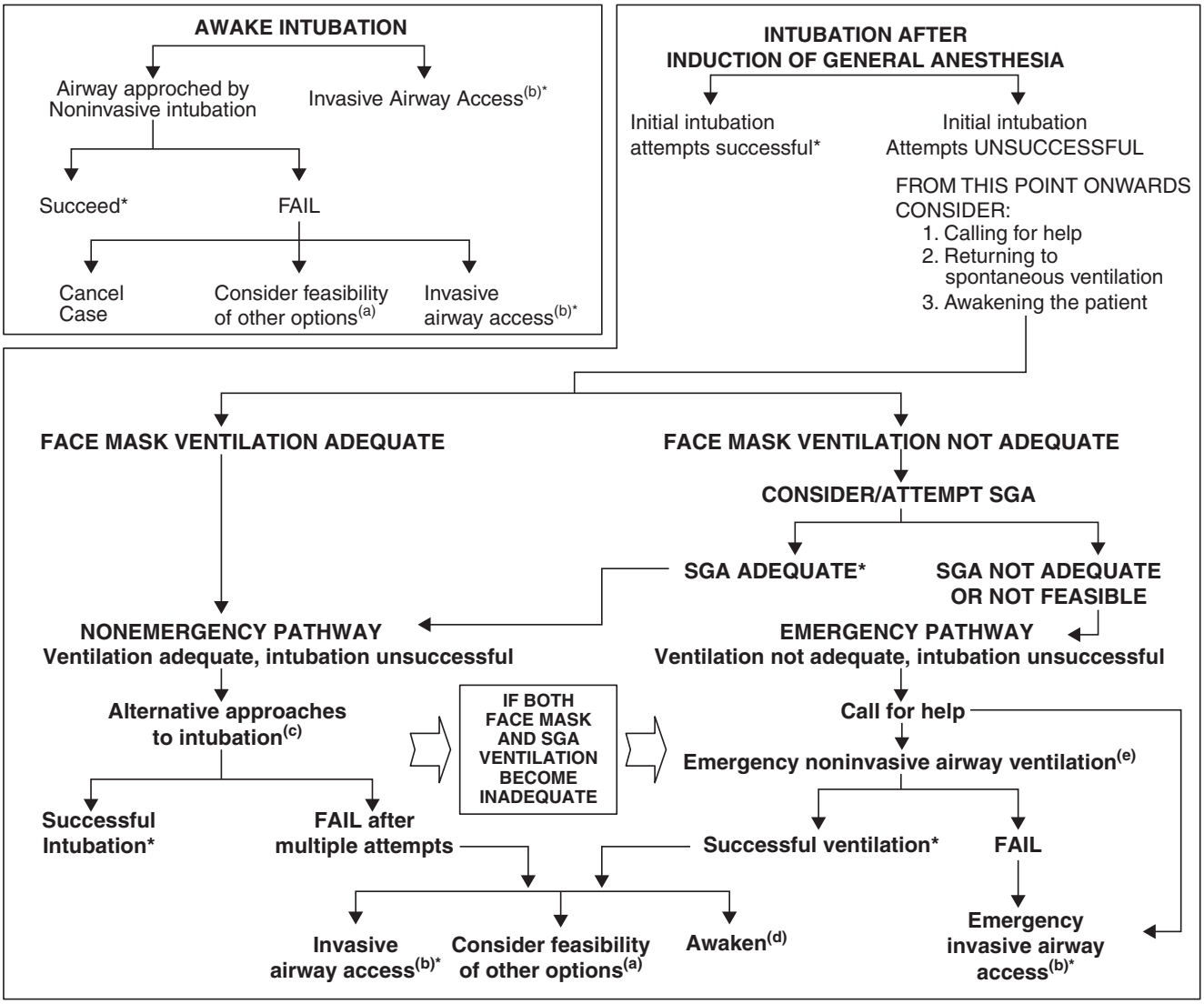


Fig. 5.3 Difficult airway algorithm. Decision points to consider: 1. Awake intubation vs. intubation after induction of general anesthesia. 2. Noninvasive technique vs. invasive techniques for the initial approach to intubation. 3. Video-assisted laryngoscopy as an initial approach to intubation. 4. Preservation vs. ablation of spontaneous ventilation. a. Other options include (but are not limited to) surgery utilizing face mask or supraglottic airway (SGA) anesthesia (e.g., LMA), local anesthesia infiltration, or regional nerve blockade. b. Invasive airway access includes surgical or percutaneous airway, jet ventilation, and retrograde intubation. c. Alternative difficult intubation approaches include (but are not limited to) video-assisted laryngoscopy, alternative laryngoscope blades, SGA (e.g., LMA or ILMA) as an intubation conduit (with or without fiber-optic guidance), fiber-optic intubation, intubating stylet or tube changer, light wand, and blind oral or nasal intubation. d. Consider re-preparation of the patient for awake intubation or canceling surgery. e. Emergency noninvasive airway ventilation consists of a SGA (Adapted from Apfelbaum et al. [109], with permission from Wolters Kluwer Health, Inc.)

The fiber-optic bronchoscope can be useful in securing the difficult pediatric airway and may be used to directly guide a tracheal tube or to insert a guide wire into the trachea and facilitate tracheal intubation. Often the fiber-optic bronchoscope is inserted through the nares, which provides the most direct approach to the larynx. An oropharynx devoid of blood and excess secretions is essential to successfully use this technique. Unfortunately, the smaller fiber-optic bronchoscopes used in small infants do not have a suction port to remove secretions or insufflate oxygen to expand the oropharynx.

The following devices may also be useful in the difficult pediatric airway: nasopharyngeal airway, lighted stylet, and Jackson anterior commissure laryngoscope. Preparation, personnel, skill, experience, and flexibility remain the keys to successful management of the difficult airway. Recent findings from the pediatric difficult intubation registry show that most complications were associated with more than two tracheal intubation attempts and three direct laryngoscopy attempts before an indirect technique [24]. This demonstrates that if the first laryngoscopy attempt is unsuccessful,

backup personnel and other approaches should be considered before attempting another laryngoscopy using an identical approach. As long as the patient can be ventilated, there is time to attempt alternate intubation strategies or even to awaken the patient and postpone the case. It is the "cannot intubate, cannot ventilate" scenario which is the most terrifying and demands immediate action such as emergency cricothyroidotomy or tracheostomy.

Intraoperative Complications

Complications that are of significance to the surgeon and anesthesiologist taking care of pediatric oculoplastic patients are highlighted here: laryngospasm, oculocardiac reflex, local anesthetic systemic toxicity, and airway fire.

Laryngospasm

Laryngospasm, defined as involuntary vocal cord contraction causing partial or complete airway obstruction, is a serious concern to all pediatric anesthesiologists. It occurs in 1.7% of children under 9 year of age and is a common cause of anesthesia emergencies [127, 128]. It typically occurs during the critical periods of induction, emergence, and extubation. Prompt diagnosis is key, and treatments consist of chin lift, jaw thrust, and continuous positive airway pressure with face mask. Intravenous propofol may be used to relieve partial obstruction in patients who are not hypoxic. In patients who have complete laryngospasm, impending hypoxia, and/or bradycardia, additional help should be summoned, and succinylcholine IV or IM should be given without delay [129]. Atropine (0.02 mg/kg IV) may be used to treat succinylcholine-associated bradycardia, especially in younger patients or when a second dose is required.

Oculocardiac Reflex

Eye muscle traction, particularly on the medial rectus, can trigger the oculocardiac (trigeminovagal) reflex. This reflex can also be caused by traction on the eyelid, pressure on the eye, or an acute increase in intraocular pressure from hematoma or glaucoma. The incidence and magnitude of this reflex have decreased with the replacement of halothane by modern volatile anesthetics. Sinus bradycardia is the most common dysrhythmia, but other more severe dysrhythmias have been noted including junctional rhythm, premature atrial or ventricular beats, ventricular fibrillation, and even sinus arrest. Gentle slow traction reduces the incidence by almost half, and the reflex tends to extinguish with time [130]. Discontinuation of the stimulus is the first line of treatment for severe bradycardia. Prophylactic intravenous atropine (0.02 mg/kg) or glycopyrrolate (0.01 mg/kg) is no longer common; and atropine administration is largely limited to those cases when bradycardia is associated with hypotension [131].

Local Anesthetic Systemic Toxicity

Local anesthetic systemic toxicity (LAST) is rare, difficult to treat, and potentially fatal. In the awake patient, the first typical early signs of LAST are central nervous changes such as seizures, headaches, confusion, and perioral paresthesia [132]. In the anesthetized child, however, presenting signs may include muscular rigidity, hypoxemia, tachycardia, dysrhythmias, or even cardiovascular collapse [1]. Children may be at increased risk of LAST due to their higher cardiac output and increased systemic uptake of local anesthetic. In advance of any local anesthetic administration, both the surgeon and anesthesiologist must calculate maximum allowable dose: lidocaine plain 5 mg/kg, with epinephrine 7 mg/kg; bupivacaine 3 mg/kg, with and without epinephrine; and ropivacaine 3 mg/kg [1]. Other steps to prevent LAST include minimum effective dose usage, careful aspiration prior to incremental injection, and use of intravascular markers (epinephrine) for larger doses [133]. LAST is an emergency and additional help should be summoned. Treatment focuses on supporting hemodynamics, resuscitation, and IV lipid emulsion therapy [134].

Airway Fire

Fortunately, airway fires are rare occurrences (~100 cases/year in the United States), but they can cause severe morbidity and even mortality [135, 136]. Three elements, known as the "fire triad," must be present to initiate a fire: (1) heat or an ignition source such as electrocautery; (2) fuel, such as volatile antiseptic preparatory solutions, surgical drapes, or the patient's polyvinylchloride endotracheal tube; and (3) an oxidizer, oxygen or nitrous oxide. The risk of airway fire may be reduced in several ways. If using an alcohol-based preparatory solution, one should wait for the solution to dry completely before applying the surgical drapes. For oculoplastic surgery where there will be extensive use of cautery or laser, it is advisable to use a metal-enforced endotracheal tube. Cuffed endotracheal tubes are also preferred over uncuffed ones to minimize the amount of gas leak around the tube. Finally, to reduce the source of oxidizer, nitrous oxide should be avoided during the case, and the fractional inspired oxygen should be lowered to <0.3 as allowed by patient need and response. In the event of an airway fire, additional help should be summoned immediately. Measures should be taken to put out the fire by disconnecting the oxygen supply, flooding the field with saline, and removing the endotracheal tube. Re-intubation with a new tracheal tube may be required to provide oxygenation and ventilation. Antibiotics and corticosteroids do not influence survival rates and should not be routinely administered [135].

Specific Procedures

Examination Under Anesthesia

Many children require general anesthesia for intraocular pressure measurement and eye examination. Anesthetic technique can affect intraocular pressure and should be taken into account when developing the anesthetic plan. Succinylcholine increases intraocular pressure by 10 mmHg for 5 min, while non-depolarizing relaxants have the opposite effect. Virtually all other anesthetics including the inhalation anesthetics are reported to decrease intraocular pressure in a dose-dependent manner. Tracheal intubation on the other hand increases intraocular pressure 140% above baseline pressure for approximately 2 min [137, 138]. Conversely, insertion of the LMA does not affect pressure. When an operative procedure is to be performed pending the result of the eye examination, we prefer to use a mask or LMA for the duration of the examination. We wait to perform tracheal intubation, if necessary, until after the examination is completed.

Obstruction of Nasolacrimal System

The LMA allows the surgeon full access to the eye and nose and therefore represents a major improvement over face mask anesthesia for probing of blocked nasolacrimal ducts. Furthermore, it readily deflects injected dye away from the larynx, decreasing the likelihood of adverse airway events. Prolonged procedures such as dacryocystorhinostomy (DCR) may best be performed with controlled ventilation through a tracheal tube. Because of the potential for increased bleeding that can obstruct the surgical field during DCR, patient blood pressure is maintained in the low normal range. This is usually accomplished simply by increasing the depth of the inhalation anesthetic.

Eyelid Surgery

Simple eyelid procedures such as removal of a chalazion removal can be easily performed using inhalation anesthesia and an LMA. Ptosis repair is best performed using an oral RAE tube and neuromuscular blockade. Any of the inhalation or intravenous anesthetics are reasonable choices for these procedures and basic monitoring techniques should suffice. For prolonged procedures, care must be taken to adequately cushion the head to prevent excess pressure on the occiput and potential alopecia. We use foam headrests either alone or in combination with U-shaped sandbags that limit lateral mobility. Some employ a 10° head-up bed position to minimize the pooling of blood, which may otherwise obscure the operative site.

Strabismus Repair

The anesthetic requirements for strabismus repair are relatively straightforward. The airway may be maintained with either an LMA or an oral RAE tube. Because of the delicacy of the procedure, ensuring patient immobility is a high priority, and many anesthesiologists employ neuromuscular blockade and controlled ventilation. Multimodal low-dose intravenous opioid (fentanyl, 0.5–1 mcg/kg, or morphine, 25–50 mcg/kg), intravenous ketorolac 0.5 mg/kg (administered at the procedure's end), and several drops of topical 1% ophthalmic tetracaine provide for excellent postoperative analgesia. Postoperative vomiting is common after strabismus surgery (60–80%), and the procedure itself is an independent risk factor for postoperative vomiting [139]. Full intravenous fluid replacement of an 8-h deficit and dual antiemetic prophylaxis with ondansetron and dexamethasone are warranted. A detailed discussion on the prevention and treatment of postoperative vomiting can be found in the postoperative management section. Bradycardia associated with the oculocardiac reflex may occur with traction on the extraocular muscles as discussed above.

Major Craniofacial and Orbital Procedures

Preoperative Evaluation

The preanesthetic history and physical examination should be conducted with attention to uncommon syndromes and diseases, especially those associated with difficult airways (see Table 5.1). It is estimated that between 40 and 50% of infants with syndromic craniosynostosis have clinical features of obstructive sleep apnea [140]. Some patients with craniosynostosis will have elevated intracranial pressure (ICP) suggested by nausea and vomiting, lethargy, diplopia, and headache. The incidence of increased ICP is higher in syndromic craniosynostosis, with 50% of patients having fundoscopic evidence of papilledema [141]. In patients with elevated ICP, opioids should be given with caution to reduce the risk of hypoventilation, hypercarbia, and further increases in ICP.

Laboratory evaluation should include a complete blood count, and depending on the procedure, typed and crossed blood for 0.5–2 blood volumes (one blood volume = 70–80 mL/kg) should be available. In older adolescent patients, an autologous donation may be appropriate. Units of directed donor blood may also be available and should be noted at the preoperative visit. Depending on the availability, whole blood is an ideal replacement choice for infants or smaller patients. A platelet count may be helpful to estimate the need for intraoperative platelet transfusion should blood loss exceed one blood volume. In an otherwise healthy child with no clinical signs of coagulopathy, a coagu-

lation panel (prothrombin time PT and partial thromboplastin time PTT) is not routinely ordered, since these may lead to false positives, often because of clinically insignificant viral inhibitors.

Anesthetic Induction and Monitoring

Either inhalation or intravenous induction of anesthesia are appropriate with due consideration for the difficult airway. For most patients without intravenous access, we advocate an inhalation induction with O_2/N_2O/sevoflurane. After placement of an intravenous catheter, and following administration of a non-depolarizing muscle relaxant and fentanyl (1–5 μg/kg), we intubate the trachea with an oral RAE tracheal tube. Because of repeat movements of the head during the procedure, the tracheal tube should be secured with benzoin and tape or wired in place by the surgeon.

We advocate having at least two intravenous catheters, one large (22 gauge minimum in infants) catheter for rapid volume replacement and one for maintenance fluid and medication administration. A blood warmer should be primed with either saline or blood depending on the preoperative hemoglobin and patient size. In addition to standard monitoring, an arterial catheter is recommended as it allows for continuous blood pressure measurement and blood sampling during the case. A central venous catheter is not routinely placed unless adequate peripheral intravenous access could not be obtained. One study showed that routine central venous pressure (CVP) monitoring was not associated with a decreased incidence and duration of hypotension in patients experiencing massive hemorrhage and that a significant decrease in CVP was not usually associated with hypotension [142]. A bladder catheter prevents bladder distension and provides a measure of adequate fluid replacement. Final preparation includes lubrication of the eyes and, depending upon the procedure, taping the eyelids closed. Positioning and padding are important to prevent nerve injuries and pressure necrosis given the typical length of the procedures (4–12 h). Slight head elevation may improve surgical exposure and decrease venous bleeding.

Intraoperative Maintenance

We typically use a volatile anesthetic agent for maintenance of anesthesia. For pain control, we administer fentanyl 5–10 μg/kg at the beginning of the case and 1–2 μg/kg/hr. as needed throughout. While muscle relaxation is not essential for this procedure, it ensures patient immobility for the more exacting parts of surgical reconstruction and allows the anesthesiologist to use lower concentrations of potent inhalation anesthetics. In patients without a history of hypercoagulability, antifibrinolytic agents can help decrease the amount of blood loss during the procedure. At our institution, we administer a bolus of 100 mg/kg ε-aminocaproic acid (EACA) at the start of the case followed by an infusion that continues for the duration of the procedure. This has shown to decrease the estimated blood loss (82 ± 43 vs. 106 ± 63 ml/kg, P = 0.01) and lower surgical drain output in the first postoperative 24 h (28 ml/kg vs. 37 ml/kg, P = 0.001) [143].

Intraoperative Fluid Management

Careful fluid replacement is one of the most important components of successful anesthetic management for craniofacial surgery. In general, crystalloids such as Ringer's lactate are sufficient for early volume replacement and replenishment of fluid deficits. Maintenance requirements with crystalloids are based on body weight and may be calculated using the "4-2-1 rule," where 4 mL/kg/hr. intravenous fluid is administered for the first 10 kg, 2 mL/kg/hr. for the next 10 kg, and 1 mL/kg/hr. for each additional kilogram. Preoperative fluid deficits should be replenished in the first 3 h of the procedure: 1/2 in the first hour and 1/4 in each subsequent hour. Ongoing third-space loss may be as much as 5–10 mL/kg/hour and must be included in replacement calculations. If blood loss is replaced by crystalloid, it should be done in a 3:1 of fluid to blood loss ratio. Colloid infusions (5% albumin) should be given with caution, as they have been shown to increase the incidence of postoperative coagulation derangements and administration of hemostatic blood products (odds ratio 5.9 [95% CI, 2.2–15.7, P 0.001], 2.8[95% CI, 1.2–6.5, P 0.016], respectively) [144]. In smaller infants, due to a small circulating blood volume and hemodilution caused by even small amounts of crystalloids, many anesthesiologists start blood product transfusion early. Some start with packed red blood cells (PRBCs), while others transfuse PRBCs and fresh frozen plasma (FFP) together, with the idea of simulating reconstituted whole blood. Infusion of 10 ml/kg PRBCs increases the hemoglobin concentration by 2.5–3 g/dL. In small infants, when available from the blood bank, we prefer fresh whole blood 1:1 to replenish blood loss.

The anesthesiologist must be vigilant to avoid hypovolemia. In major craniofacial procedures, hypotension indicates hypovolemia until proven otherwise. Although blood loss is generally slow and continuous in these procedures, a rare acute arterial or dural sinus bleed may lead to sudden rapid blood loss. Accurate estimated blood loss is difficult as some of the blood loss does not end up in suction canisters, but instead is trapped in the drapes or drips onto the floor. Therefore, we rely on serial hemoglobin/hematocrit measurements to guide transfusion. One retrospective study showed that although 43.4% of patients lost less than one

blood volume, 46.5% lost between one and two blood volumes ($N = 159$). In this same population, all patients were transfused PRBCs, with an average volume of 51 ml/kg of PRBCs, 20 ml/kg of FFP, and 16 ml/kg of platelets transfused [144]. Clearly, blood loss can be substantial and transfusion is common, though much of it is dependent on the specific procedure and skill of the surgical team. It generally takes 45–60 min to prepare additional blood products, so forethought is required to maintain an adequate available blood reserve in the operating room.

Coagulopathies may arise from dilution thrombocytopenia or decreased coagulation factor concentration as the replaced blood loss approaches 1–2 blood volumes. Platelet counts, PT, and PTT lab values are necessary to determine whether platelet or fresh frozen plasma (FFP) transfusion is required. Alternatively, thromboelastography can help diagnose developing coagulopathies. When initial platelet counts are less than 150,000/mm^3, the patient may require exogenous platelets after one blood volume is lost; however, patients with normal or above normal counts and normal platelet function may not require exogenous platelet therapy until over two blood volumes have been lost [145]. Transfusion of 0.2 U/kg raises the platelet count by approximately 50,000/mm^3. FFP is often administered in 10–20 mL/kg boluses to maintain adequate coagulation factor levels (above 30% normal).

When large volumes of blood products containing plasma (whole blood, fresh frozen plasma and platelets) are transfused rapidly, citrate accumulation may lead to profound hypocalcemia [146]. Ionized calcium levels will recover spontaneously over 5–10 min if transfusion is stopped. If the blood pressure decreases or fails to respond to adequate volume replacement during transfusion, then hypocalcemia should be suspected. Although serial ionized calcium measurements can help guide therapy, during rapid transfusion we typically give calcium gluconate 100 mg for every 100 ml of blood products transfused to prevent hypocalcemia.

Whole blood and packed red blood cells that are stored for over a week may cause clinically significant hyperkalemia and even cardiac arrest, especially in young infants. The plasma potassium averages <20 mmol/L in stored blood less than a week old and >40 mmol/L for blood older than 2 weeks [147]. Children requiring more than one blood volume, particularly if the transfusion is sudden and large, may be at risk. Since the treatment of hyperkalemia includes calcium and bicarbonate infusion, it is doubly important to maintain normal or near normal ionized calcium levels if massive transfusion is required.

Temperature

Infants and children have proportionally larger head surface area compared to adults, and during craniofacial reconstruction in a cool operating room, may lose significant amounts of heat. Core temperature should be measured using a rectal or esophageal probe and maintained near 37 ° C. In addition to standard measures to maintain temperature, a forced warm air device with a lower-body warming blanket should be routinely used, and all intravenous products should be administered through a fluid warmer.

Complications

In addition to massive blood loss and coagulopathy discussed above, several other complications may occur during craniofacial surgery. Metabolic acidosis related to hypovolemia and blood loss is also common, as is kinking and occlusion of the tracheal tube, endobronchial displacement, and accidental extubation from movement of the head during surgery. Sudden bradycardia and/or asystole associated with a trigeminal-vagal reflex (elicited from any of the three divisions of the trigeminal nerve) are less common events and can be caused by the surgeon compressing the eyes or face [148]. Venous air embolism and sudden cardiac arrest have been described even in the supine position and are rare events [149]. To minimize the risk of entraining air from the surgical field, it is recommended that the mean arterial pressure be maintained above 55–60 mmHg.

Anesthetic Emergence and Postoperative Recovery

At the conclusion of the case, the anesthesiologist in conjunction with the surgical team must decide if it is safe to extubate the patient. After long procedures, or when significant volumes of fluid have been administered, or if the procedure involved extensive work in the mouth or airway, it may be best to leave the trachea intubated. Additional time in the pediatric intensive care unit will allow for the child to awaken and for physicians to make more careful assessments of the patient's potential to maintain a natural airway. Following extubation, laryngospasm, vocal cord paralysis, and subglottic edema may complicate airway management [150]. Subglottic edema and post-extubation croup may be more common in children undergoing craniofacial surgery because of their younger age, long duration of intubation, and frequent repositioning of the head and neck during surgery [151]. Proper equipment and personnel for potential re-intubation should be made ready. In children who continue to experience significant subglottic edema, but do not require re-intubation, nebulized racemic epinephrine and steroids may be therapeutic.

In addition to assuring airway patency and adequate ventilation, the intensive care staff should closely monitor the

patient's neurologic examination, replace fluids, and administer medications to control postoperative pain. Worsening neurological exams may indicate an intracranial hemorrhage, a need for emergent head CT scan, and a potential surgical re-exploration. Serial hemoglobin measurements will help guide continued blood loss replacement. Pain is generally controlled with incremental intravenous boluses of fentanyl (1–2 μg/kg) or MSO4 (50–100 μg/kg). Opioid infusions and patient-controlled analgesia may be appropriate depending upon the nature of the surgery and the cognitive age and ability of the child.

Postoperative Management

Criteria for Discharge After Day Surgery

Most patients undergoing oculoplastic surgery will be discharged the same day of their surgery. Recovery is usually a two-stage process, split between phase I postanesthesia care unit (PACU) and phase II predischarge day surgical unit (DSU). Parents may be included in either or both units depending on hospital policy.

Discharge criteria vary across institutions and are based on available resources. Many institutions utilize a physiological-based criteria (Table 5.5) that incorporates an objective scoring system, such as the modified Aldrete Score (Aldrete) or postanesthesia discharge scoring system [152, 153]. These scoring systems are more time and resource-efficient than time-based discharge criteria, particularly for ambulatory surgery [154].

Requiring patients to drink liquids prior to discharge is no longer recommended as it has been shown to increase the risk of PACU/DSU vomiting by 50% and delay discharge from the hospital but not increase the likelihood of readmission for treatment of post-discharge dehydration [155]. Since many children drink little or nothing prior to hospital discharge, however, they should receive intravenous fluids equivalent to 6–8 times their hourly maintenance prior to discharge from the hospital in order to mitigate dehydration risk.

Table 5.5 Medically fit for discharge criteria

Phase I Recovery (for both inpatients and day surgery (DS) patients)
Routine "medically fit for discharge" (MFFD) criteria for all American Society of Anesthesiologists (ASA) physical status (PS) I–III patients
1. Awake or easily arousable or back to baseline consciousness (PACU score ≥ 5)
2. Maintaining patent airway with protective reflexes
3. Adequate ventilation; normal respiratory rate; no evidence of respiratory distress
4. Arterial oxygen hemoglobin saturation ≥ 92% in room air, asleep; ≥95%, awake
5. Temperature, heart rate, and blood pressure within normal limits or at baseline
6. Pain well controlled
(a) With no IV opioids in the last 20 min
(b) With no epidural boluses in the last 30 min
7. No active vomiting
8. No excessive surgical site drainage
9. Laboratory/radiographic studies completed/reviewed by ordering MD (or designee)
10. Appropriate postoperative physician orders in chart
Phase II Recovery (DS patients)
Routine MFFD criteria
1. All Phase I criteria continue to be met
2. Adequate hydration
3. No more than 2 emetic episodes (in Phase II)
4. Postoperative instructions given including hospital and personnel phone numbers
5. No further questions for surgeons or anesthesiologists
6. Appropriate prescriptions and/or medications given
7. Parent, legal guardian, or official designate to escort patient home

Postoperative Nausea and Vomiting

Postoperative nausea and vomiting (PONV) is a common side effect of anesthesia and surgery and can be especially common following strabismus repair. Although rarely life threatening, PONV can lead to aspiration, dehydration, and distress among the patient and family. Many young children may have never experienced nausea and are unable to verbalize the sensation, making it difficult for them to warn the PACU staff that they are nauseated or about to vomit [2]. Four independent predictors are associated with PONV in the pediatric population: duration of surgery ≥ 30 min, age 3 ≥ yrs., strabismus surgery, and history of PONV in the patient or family. When 0, 1, 2, 3, or 4 of the independent predictors are present, the corresponding risk for PONV is approximately 10%, 10%, 30%, 55%, or 70%, respectively [139].

Many antiemetics are available to decrease postoperative emesis (Table 5.6) [156–159]. Systematic reviews have shown that 5-HT3 antagonist (ondansetron) or dexamethasone alone is effective in preventing PONV with a relative risk reduction of 50–60%. When combined together, the relative risk reduction may be as high as 80% [160]. Thus, children who are at moderate or high risk for PONV are recommended to receive combination therapy with at least two prophylactic medications from different classes [161]. In our practice, we routinely administer ondansetron and dexamethasone to high-risk patients such as those having strabismus repair unless there are contraindications. For prolonged or intractable PONV despite first-line antiemetic medications, a drug from a different class may be more beneficial than repeated doses of the same drug, as it will target

Table 5.6 Commonly used intravenous antiemetic medications

Drug	Class (receptor antagonist)	Side effects	Dosage
Ondansetron	Serotonin 5-HT_3 receptor antagonist in the GI tract and central nervous system	Prolonged QT interval	50 μg/kg (maximum 4 mg) q 6 h
Dexamethasone	Corticosteroid	Hyperglycemia	150 μg/kg up to 5 mg IV
Metoclopramide	Benzamide (D2 dopaminergic receptor antagonist and 5-HT_3 antagonist at high doses)	Sedation, dyskinesia, or extrapyramidal symptoms reversed with diphenhydramine	0.15 mg/kg (max 10 mg, may be repeated prior to discharge)
Droperidol	Butyrophenone (dopaminergic receptor antagonist)	Sedation, prolonged QT, dyskinesia, or extrapyramidal symptoms	50–75 μg/kg
Dimenhydrinate	Combination of diphenhydramine (antihistamine) and 8-chlorotheophylline (methylxanthine)	Sedation	0.5 mg/kg up to 25 mg
Lorazepam	Benzodiazepine	Sedation	10 μg/kg

different receptors in the chemoreceptor trigger zone and potentially work synergistically.

Postoperative Pain Management

Adequate control of postoperative pain is one of the most important factors in determining patient and parental satisfaction in the perioperative period. The preoperative visit with the patient and family should include a discussion on postoperative pain, including what to expect after surgery and the available treatment options. Since the child's pain may fluctuate greatly in the immediate postoperative period, the potency and dose of analgesia should match the patient's current level of pain, which may be challenging to assess in the infant population; it is often difficult to differentiate between pain, anxiety, emergence delirium, and other causes of stress.

Pain Assessment

Several age and behavioral pain assessment scales have been created and validated. For young infants or patients who are unable to communicate their pain, the observational FLACC scale has been used extensively [162]. It assigns a score of 0, 1, or 2, to each of the criteria: face, legs, activity, cry, and consolability, with a score range of 0–10. The Children's Hospital of Eastern Ontario Pain Scale (CHEOPS) is another observational scoring system used in this population [163]. It assigns points to the following categories: cry, facial, child verbal, torso, touch, and legs, with a total score range of 4–13. In children who are older than three and verbal, the Wong-Baker FACES pain rating scale is another option [164]. It is a self-reporting scale that allows the patient to rate their pain using numbers (0–10) that are matched with pictures of faces, with each face depicting progressively worse pain. Finally, in older children and adolescent, numerical pain scores such as the visual analog score (VAS) score have be used, where the patient rates their pain from 0 (no pain) to 10 (worse pain).

Outpatients

Acetaminophen, or paracetamol outside of the United States, is an effective analgesic for low-grade pain and may be adequate for many outpatient procedures. It is not associated with nausea, sedation, pruritus, and ileus that can be caused by opioids, or gastritis, renal toxicity, and diminished platelet function that are associated with nosteroidal anti-inflammatory drugs (NSAIDS). It can be given by mouth (PO), by rectal (PR), or intravenously (IV). The usual PO dose of 10–15 mg/kg every 4 h may not be appropriate for the patient who cannot take oral medications in the postoperative period. Rectally administered acetaminophen (20–40 mg/kg) lasts longer than the oral form but can take 2 h to reach peak effect, making it less practical for many outpatient surgeries [165]. Finally, IV acetaminophen (15 mg/kg) provides a faster onset and shorter duration of action than the PR route, but is more expensive [166]. When administering acetaminophen caution must be exercised over potential overdosing, which can lead to acute liver toxicity. A dose reduction may be warranted in the neonatal population due to decreased clearance drug from unconjugated hyperbilirubinemia [167].

Nonsteroidal anti-inflammatory agents (NSAIDS) provide effective postoperative relief for moderate pain without the side effects of opioids. However, these agents may cause gastritis, renal insufficiency, and platelet dysfunction. For patients who are able to take oral medications, ibuprofen PO 10 mg/kg q 6 h is an excellent choice. An IV NSAID, ketorolac, is also available and can be given 0.5 mg / kg q8h. Although earlier studies have linked ketorolac to a higher incidence of bleeding following tonsillectomy and adenoidectomy [168], a later systematic review for the same procedure showed that ketorolac was associated with a higher incidence of reoperation, but not intraoperative or postoperative blood loss or hospital admission [169]. Another systematic review including 27 double-blinded, randomized, controlled studies showed that postoperative bleeding was not significantly higher in the ketorolac group compared to placebo (2.5% vs. 2.1%) [170].

Opioids may be used for patients in moderate to severe pain. In the PACU, IV morphine 25 μg–50 μg/kg q 10–20 min, hydromorphone 5 μg–10 μg/kg q 10–20 min, or IV fentanyl 0.5 μg–1 μg/kg q 5–10 min may be titrated to the patient's comfort level. In patients who are able to take oral medications, oxycodone 50–150 μg/kg q 4–6 h offers longer-lasting analgesia. The side effects of opioids include respiratory depression, sedation, nausea, vomiting, pruritus, hives, ileus, and constipation. The treatments for these symptoms are described below in the inpatient section.

Regional nerve blocks are not commonly used for pediatric oculoplastic surgery; however, topical anesthetics can be used by the surgeon to supplement PO or IV anesthetics. A randomized control trial comparing topical amethocaine to placebo in 41 patients showed a significant difference in pain scale at 120 min postoperative [171]. We frequently instill 1% tetracaine in the operative eye before and immediately after strabismus surgery.

Inpatients

For infants and children who are admitted to the hospital due to more extensive surgery or medical history, additional pain treatment options are available. Surgical services may order postoperative parenteral analgesics, or in more complex cases, the inpatient anesthesia pain management may be consulted.

Patients with severe pain and are NPO generally require either parenteral opioid boluses or infusions. Patient-controlled analgesia (PCA) provides excellent pain control for children ≥ 7 years of age with on-demand boluses of opioid administered by pressing a button. The bolus frequency, amount in mg, and hourly maximum are programmed in the PACU and can be adjusted based on patient need. The number of bolus attempts and actual deliveries are electronically recorded and may be retrieved to inform clinicians in making further adjustments. As an important rule to prevent overdosing, the patient's family or caregivers are informed that only the patient should press the button for boluses. Typical settings for a morphine PCA include (1) a 15–20 μg/kg/dose, (2) an 8–15 min lockout, (3) a 0–20 μg/kg/hr. basal infusion rate, and (4) a 100 μg/kg/hr. hourly maximum.

In patients who are too young or unable to use a PCA, an opioid infusion with rescue boluses administered by the nursing staff may be used. Standard morphine infusions at our institution range from 15 to 30 μg/kg/hr. with rescue doses of 50–100 μg/kg IV q 3 h. Vital signs, including pain scores, should be recorded at least every 4 h, and because of the risk of respiratory depression, continuous cardiorespiratory monitoring such as a pulse oximeter is essential. Depending on the institution, this level of monitoring may only be available in the intensive care unit, and a pain management consult is typically required to follow these patients.

Given the longer duration of exposure to parental opioids, the inpatient population is more likely to experience opioid side effects such as pruritus, nausea and vomiting, urinary retention, ileus, and respiratory depression. Pruritis may be treated with nalbuphine 50 μg/kg IV q 3 h PRN, and consideration should be given to changing the infusion drug to a different type of opioid or to nalbuphine itself if the pain is moderate and pruritus persists. Nausea or vomiting is discussed in an earlier section and may be relieved by ondansetron 50–100 μg/kg IV q 6–8 h PRN. Urinary retention may be secondary to the opioid analgesics or the general anesthetic gases and may require nalbuphine 50 μg/kg IV, naloxone 1–5 μg/kg IV, or urinary catheter placement. Ileus may be minimized by reducing the infusion rate if feasible and by encouraging early patient ambulation. Respiratory depression may be mild and only require decreasing the opioid infusion rate and bolus dose, or severe and require stopping the infusion, stimulating the patient, or administration of naloxone 1–5 μg/kg IV or 5–10 μg/kg IM. In most severe cases, temporary support of ventilation with an anesthesia bag and mask or even tracheal intubation may be required.

Emergence Delirium

Emergence delirium (ED) usually manifests as crying, screaming, thrashing, and disorientation. Although the presentation may appear similar to pain, the patient is not consolable and unable to recognize their caregivers and may experience it even after a non-painful procedure (e.g., MRI scan) [2]. It was first described in the 1960s by Eckenhoff et al. [172] and was common in the era of ether and cyclopropane, but its incidence waned with the introduction of halothane. With the newer short-acting volatile anesthetics sevoflurane and desflurane, however, the problem of ED reappeared [173, 174]. To better define this issue, several assessment scores have been developed, such as the Watcha, Pediatric Anesthesia Emergence Delirium (PAED), and Cravero scales [175–177]. Comparisons among these three metrics showed that they correlated well with each other in ED detection, but the Watcha score was a simpler tool to use in clinical practice and may have a higher overall sensitivity and specificity [178]. Although the cause of ED remains unknown, several risk factors have been associated with it including rapid emergence from anesthesia, use of short-acting volatile anesthetic agents, postoperative pain, surgery type, age, preoperative anxiety, and child temperament [173]. Propofol, dexmedetomidine, midazolam, ketamine, and fentanyl have all been shown to have a prophylactic effect in preventing ED, which may not be specifically related to analgesic properties [179, 180]. Pain itself can contribute to ED and must be treated primarily. Most cases of ED are self-limiting and will resolve without intervention overtime. However, it is important to prevent the child from injuring themselves or others during this phase

and occasionally "rescue" medications such as boluses of fentanyl IV 1–2 mcg/kg, propofol IV 0.5–1 mg/kg, midazolam 0.02–0.1 mg/kg, or dexmedetomidine 0.5mcg/kg can be given to effectively treat ED [173].

Summary

Anesthesia practice for pediatric oculoplastic surgery has evolved to incorporate some of the best evidence-based practices and latest short-acting, easily titrated agents. This continues to make our practice safer, and the recent introduction of subspecialty board certification of pediatric anesthesia further recognizes the importance of specialty care for pediatric patients. Even with these recent advances, basic preoperative evaluation and planning remain essential to the conduct of safe anesthesia, and particular attention must be directed to those infants and children with syndromes known to include the difficult airway. Throughout the perioperative period, continued communication between the anesthesiologist and surgeon maximizes the quality of patient care.

References

1. Davis PJ, Cladis FP, Motoyama EK. Smith's anesthesia for infants and children: expert consult premium. London: Elsevier Health Sciences; 2010.
2. Cote CJ, Lerman J, Todres ID. A practice of anesthesia for infants and children: expert consult: online and print. London: Elsevier Health Sciences; 2012.
3. Gregory GA, Andropoulos DB. Gregory's pediatric anesthesia. Oxford: Wiley-Blackwell; 2012.
4. Anesthesiology SO, Medicine P, Goldschneider KR, Cravero JP, Anderson C, Bannister C, et al. The pediatrician's role in the evaluation and preparation of pediatric patients undergoing anesthesia. Pediatrics. American Academy of Pediatrics. 2014;134:634–41.
5. Evaluation and preparation of pediatric patients undergoing anesthesia. American Academy of Pediatrics. Section on Anesthesiology. Pediatrics. 1996;98:502–8.
6. Jones KL, Jones MC, Del Campo M. Smith's recognizable patterns of human malformation. Philadelphia: Elsevier Saunders, cop; 2013.
7. Gadde J, Spence M, Wheeler B, Adkinson NF. Clinical experience with penicillin skin testing in a large Inner-City STD clinic. JAMA. 1993;270:2456–63.
8. Mendelson LM, Ressler C, Rosen JP, Selcow JE. Routine elective penicillin allergy skin testing in children and adolescents: study of sensitization. J Allergy Clin Immunol. Mosby. 1984;73:76–81.
9. Campagna JD, Bond MC, Schabelman E, Hayes BD. The use of cephalosporins in penicillin-allergic patients: a literature review. J Emerg Med. Elsevier. 2012;42:612–20.
10. Park MA, Solensky R, Khan DA, Castells MC, Macy EM, Lang DM. Patients with positive skin test results to penicillin should not undergo penicillin or amoxicillin challenge. J Allergy Clin Immunol. Elsevier. 2015;135:816–7.
11. Polk RE, Healy DP, Schwartz LB, Rock DT, Garson ML, Roller K. Vancomycin and the red-man syndrome: pharmacodynamics of histamine release. J Infect Dis. 1988;157:502–7.
12. Dormans JP, Templeton JJ, Edmonds C. Intraoperative anaphylaxis due to exposure to latex (natural rubber) in children. J Pediatr Orthop. 1995;15:411.
13. Holzman RS. Latex allergy: an emerging operating room problem. Anesth Analg. 1993;76:635–41.
14. Landwehr LP, Boguniewicz M. Current perspectives on latex allergy. J Pediatr. 1996;128:305–12.
15. Holzman RS. Clinical management of latex-allergic children. Anesth Analg. 1997;85:529–33.
16. von BS US, Boda K, Chambers NA, Rebmann C, Johnson C, Sly PD, et al. Risk assessment for respiratory complications in paediatric anaesthesia: a prospective cohort study. Lancet. Elsevier. 2010;376:773–83.
17. Brady JE, Sun LS, Rosenberg H, Li G. Prevalence of malignant hyperthermia due to anesthesia in New York state, 2001–2005. Anesth Analg. 2009;109:1162–6.
18. Rosenberg H, Davis M, James D, Pollock N, Rosenberg H, Stowell K. Malignant hyperthermia. Google Scholar. Orphanet J Rare Dis. 2007;2:21.
19. NIH. Pseudocholinesterase Deficiency [Internet]. Pseudocholinesterase-deficiency. [cited 2016 Apr 30]. Available from: https://ghr.nlm.nih.gov/condition/pseudocholinesterase-deficiency#.
20. Tiret L, Nivoche Y, Hatton F, Desmonts JM, Vourc'h G. Complications related to anaesthesia in infants and children. A prospective survey of 40240 anaesthetics. Br J Anaesth. 1988;61:263–9.
21. Bai W, Golmirzaie K, Burke C, Van Veen T, Christensen R, Voepel Lewis T, et al. Evaluation of emergency pediatric tracheal intubation by pediatric anesthesiologists on inpatient units and the emergency department. Lerman J, editor. Paediatr Anaesth. 2016;26:384–91.
22. Graciano AL, Tamburro R, Thompson AE, Fiadjoe J, Nadkarni VM, Nishisaki A. Incidence and associated factors of difficult tracheal intubations in pediatric ICUs: a report from National Emergency Airway Registry for children: NEAR4KIDS. Intensive Care Med. 2014;40:1659–69.
23. Heinrich S, Birkholz T, Ihmsen H, Irouschek A, Ackermann A, Schmidt J. Incidence and predictors of difficult laryngoscopy in 11.219 pediatric anesthesia procedures. Paediatr Anaesth. 2012;22:729–36.
24. Fiadjoe JE, Nishisaki A, Jagannathan N, Hunyady AI, Greenberg RS, Reynolds PI, et al. Airway management complications in children with difficult tracheal intubation from the pediatric difficult intubation (PeDI) registry: a prospective cohort analysis. Lancet Respir med. Elsevier. 2016;4:37–48.
25. Mallampati SR. Clinical sign to predict difficult tracheal intubation (hypothesis). Can Anaesth soc J. Springer. 1983;30:316–7.
26. Lee A, Fan LTY, Gin T, Karmakar MK, Ngan Kee WD. A systematic review (meta-analysis) of the accuracy of the mallampati tests to predict the difficult airway. Anesth Analg. 2006;102:1867–78.
27. McGraw T. Preparing children for the operating room: psychological issues. Can J Anaesth. Springer. 1994;41:1094–103.
28. Fortier MA, Kain ZN. Treating perioperative anxiety and pain in children: a tailored and innovative approach. Morton N, editor. Paediatr Anaesth. 2015;25:27–35.
29. Cohen MM, Cameron CB, Duncan PG. Pediatric anesthesia morbidity and mortality in the perioperative period. Anesth Analg. 1990;70:160.
30. Warner MA, Warner ME, Warner DO, Warner LO, Warner JE. Perioperative pulmonary aspiration in infants and children. Anesthesiology. The American Society of Anesthesiologists. 1999;90:66–71.
31. Murat I, Constant I, Maud'huy H. Perioperative anaesthetic morbidity in children: a database of 24165 anaesthetics over a 30-month period. Paediatr Anaesth. 2004;14:158–66.

32. Mertes PM, Tajima K, Regnier-Kimmoun MA, Lambert M, Iohom G, Guéant-Rodriguez RM, et al. Perioperative anaphylaxis. Med Clin North Am. 2010;94:761–89.
33. Flick RP, Sprung J, Harrison TE, Gleich SJ, Schroeder DR, Hanson AC, et al. Perioperative cardiac arrests in children between 1988 and 2005 at a tertiary referral center: a study of 92,881 patients. Anesthesiology. 2007;106:226–37–quiz413–4.
34. Morray JP, Geiduschek JM, Ramamoorthy C, Haberkern CM, Hackel A, Caplan RA, et al. Anesthesia-related cardiac arrest in children initial findings of the pediatric perioperative cardiac arrest (POCA) registry. Anesthesiology. The American Society of Anesthesiologists. 2000;93:6–14.
35. Ikonomidou C, Bosch F, Miksa M, Bittigau P, Vöckler J, Dikranian K, et al. Blockade of NMDA receptors and apoptotic neurodegeneration in the developing brain. Science. American Association for the Advancement of Science. 1999;283:70–4.
36. Ikonomidou C, Bittigau P, Ishimaru MJ, Wozniak DF, Koch C, Genz K, et al. Ethanol-induced apoptotic neurodegeneration and fetal alcohol syndrome. Science. American Association for the Advancement of Science. 2000;287:1056–60.
37. Jevtovic-Todorovic V, Hartman RE. Early exposure to common anesthetic agents causes widespread neurodegeneration in the developing rat brain and persistent learning deficits. J Neurosci. 2003;23:876.
38. Lin EP, Soriano SG, Loepke AW. Anesthetic neurotoxicity. Anesthesiol ClinElsevier. 2014;32:133–55.
39. Paule MG, Li M, Allen RR, Liu F, Zou X, Hotchkiss C, et al. Ketamine anesthesia during the first week of life can cause long-lasting cognitive deficits in rhesus monkeys. Neurotoxicol Teratol. 2011;33:220–30.
40. Stratmann G, May L, Sall JW. Effect of hypercarbia and isoflurane on brain cell death and neurocognitive dysfunction in 7-day-old rats. Anesthesiology. 2009;110:849.
41. Loepke AW, McCann JC, Kurth CD, McAuliffe JJ. The physiologic effects of isoflurane anesthesia in neonatal mice. Anesth Analg. 2006;102:75–80.
42. McCann ME, Soriano SG. Perioperative central nervous system injury in neonates. Br J Anaesth. Oxford University Press. 2012;109(Suppl 1):i60–7.
43. Wilder RT, Flick RP, Sprung J. Early exposure to anesthesia and learning disabilities in a population-based birth cohort. Anesthesiology. 2009;110:796.
44. Flick RP, Katusic SK, Colligan RC, Wilder RT, Voigt RG, Olson MD, et al. Cognitive and behavioral outcomes after early exposure to anesthesia and surgery. Pediatrics. 2011;128:e1053–61.
45. Hansen TG, Pedersen JK, Henneberg SW, Pedersen DA, Murray JC, Morton NS, et al. Academic performance in adolescence after inguinal hernia repair in infancy a nationwide cohort study. Anesthesiology. The American Society of Anesthesiologists. 2011;114:1076–85.
46. Ing C, DiMaggio C, Whitehouse A, Hegarty MK, Brady J, von BS US, et al. Long-term differences in language and cognitive function after childhood exposure to anesthesia. Pediatrics. American Academy of Pediatrics. 2012;130:e476–85.
47. Davidson AJ, Disma N, de Graaff JC, Withington DE, Dorris L, Bell G, et al. Neurodevelopmental outcome at 2 years of age after general anaesthesia and awake-regional anaesthesia in infancy (GAS): an international multicentre, randomised controlled trial. Lancet. 2016;387:239–50.
48. Suresh, H. Important questions remain on the effects of anesthetics on neurodevelopment in infants [Internet]. httpsmarttots.orgwp-contentuploadsCSsupplement...pdf. 2015 [cited 2016 Apr 30]. Available from: http://smarttots.org/wp-content/uploads/2015/11/CSsupplement11.9.2015.pdf.
49. SaferAnesthesia. Consensus Statement On the Use of Anesthetic and Sedative Drugs in Infants and Toddlers [Internet]. [cited 2016 Apr 30]. Available from: http://smarttots.org/about/consensus-statement.
50. Hunt JN. Some properties of an alimentary osmoreceptor mechanism. J Physiol. 1956;132:267–88.
51. Maltby JR, Sutherland AD, Sale JP, Shaffer EA. Preoperative oral fluids: is a five-hour fast justified prior to elective surgery? Anesth Analg. 1986;65:1112.
52. Schreiner MS, Triebwasser A, Keon TP. Ingestion of liquids compared with preoperative fasting in pediatric outpatients. Anesthesiology. 1990;72:593–7.
53. Splinter WM, Schaefer JD. Ingestion of clear fluids is safe for adolescents up to 3 H before anaesthesia. Br J Anaesth. Oxford University Press. 1991;66:48–52.
54. Crawford M, Lerman J, Christensen S, Farrow-Gillespie A. Effects of duration of fasting on gastric fluid pH and volume in healthy children. Anesth Analg. 1990;71:400.
55. Nicolson SC, Schreiner MS. Feed the babies. Anesth Analg. 1994;79:407.
56. Cavkll B. Gastric emptying in infants fed human milk or infant formula. Acta Paediatr. Blackwell Publishing Ltd. 1981;70:639–41.
57. Tomomasa T, Hyman PE, Itoh K, Hsu JY, Koizumi T, Itoh Z, et al. Gastroduodenal motility in neonates: response to human milk compared with cow's milk formula. Pediatrics. American Academy of Pediatrics. 1987;80:434–8.
58. Van der Walt JH, Foate JA, Murrell D, Jacob R, Bentley M. A study of preoperative fasting in infants aged less than three months. Anaesth Intensive Care. 1990;18:527–31.
59. Litman RS, Wu CL, Quinlivan JK. Gastric volume and pH in infants fed clear liquids and breast milk prior to surgery. Anesth Analg. 1994;79:482.
60. Cook-Sather SD, Litman RS. Modern fasting guidelines in children. Best Pract Res Clin Anaesthesiol. Elsevier. 2006;20:471–81.
61. NA. Practice guidelines for preoperative fasting and the use of pharmacologic agents to reduce the risk of pulmonary aspiration: application to healthy patients undergoing elective procedures: an updated report by the American Society of Anesthesiologists Committee on standards and practice parameters. Anesthesiology. 2011;114:495–511.
62. Ouanes J-PP, Bicket MC, Togioka B, Tomas VG, Wu CL, Murphy JD. The role of perioperative chewing gum on gastric fluid volume and gastric pH: a meta-analysis. J Clin Anesth. Elsevier. 2015;27:146–52.
63. Kain ZN, Mayes LC, O'Connor TZ. Preoperative anxiety in children: predictors and outcomes. Arch Pediatr Adolesc Med. 1996;150:1238.
64. Kain ZN, Wang SM, Mayes LC, Caramico LA, Hofstadter MB. Distress during the induction of anesthesia and postoperative behavioral outcomes. Anesth Analg. 1999;88:1042–7.
65. Kain ZN, Caldwell-Andrews AA. Preoperative psychological preparation of the child for surgery: an update. Anesthesiol Clin North Am. 2005;23:597–614.
66. Kain ZN. Postoperative maladaptive behavioral changes in children: incidence, risks factors and interventions. Acta Anaesthesiol Belg. 2000;51:217–26.
67. Kain ZN, Caldwell-Andrews AA, Maranets I, McClain B, Gaal D, Mayes LC, et al. Preoperative anxiety and emergence delirium and postoperative maladaptive behaviors. Anesth Analg. 2004;99:1648–54–tableofcontents.
68. Hannallah RS, Rosales JK. Experience with parents' presence during anaesthesia induction in children. Can Anaesth Soc J. 1983;30:286–9.
69. Kain ZN, Mayes LC, Wang SM, Caramico LA, Krivutza DM, Hofstadter MB. Parental presence and a sedative premedicant for children undergoing surgery: a hierarchical study. Anesthesiology. 2000;92:939–46.
70. Manyande A, CYNA AM, Yip P, Chooi C, Middleton P. Non-pharmacological interventions for assisting the induction of

anaesthesia in children. Cochrane Database Syst Rev. CYNA AM, editor. Chichester, UK: John Wiley & Sons, Ltd. 2015;7:CD006447.
71. Kain ZN, Mayes LC, Wang SM, Caramico LA, Hofstadter MB. Parental presence during induction of anesthesia versus sedative premedication: which intervention is more effective? Anesthesiology. 1998;89:1147–56–discussion9A–10A.
72. Weldon BC, Watcha MF, White PF. Oral midazolam in children: effect of time and adjunctive therapy. Anesth Analg. 1992;75:51–5.
73. Ullyot SC. Paediatric premedication. Can J Anaesth. Springer. 1992;39:533–6.
74. Gutstein HB, Johnson KL, Heard MB, Gregory GA. Oral ketamine preanesthetic medication in children. Anesthesiology. 1992;76:28–33.
75. Turhanoğlu S, Kararmaz A, Ozyilmaz MA, Kaya S, Tok D. Effects of different doses of oral ketamine for premedication of children. Eur J Anaesthesiol. 2003;20:56–60.
76. Cho HK, Kim KW, Jeong YM, Lee HS, Lee YJ, Hwang SH. Efficacy of ketamine in improving pain after tonsillectomy in children: meta-analysis. PLoS One. Hashimoto K, editor Public Library of Science. 2014;9:e101259.
77. Eger EI, Saidman LJ, Brandstater B. Minimum alveolar anesthetic concentration: a standard of anesthetic potency. Anesthesiology. 1965;26:756–63.
78. Lerman J, Robinson S, Willis MM, Gregory GA. Anesthetic requirements for halothane in young children 0-1 month and 1-6 months of age. Anesthesiology. 1983;59:421–4.
79. Lerman J, Sikich N, Kleinman S, Yentis S. The pharmacology of sevoflurane in infants and children. Anesthesiology. 1994;80:814–24.
80. Mapleson WW. Effect of age on MAC in humans: a meta-analysis. Br J Anaesth. 1996;76:179–85.
81. Keenan RL, Shapiro JH, Kane FR, Simpson PM. Bradycardia during anesthesia in infants. An epidemiologic study. Anesthesiology. 1994;80:976–82.
82. Keenan RL, Shapiro JH, Dawson K. Frequency of anesthetic cardiac arrests in infants: effect of pediatric anesthesiologists. J Clin Anesth. 1991;3:433–7.
83. Holzman RS, van der Velde ME, Kaus SJ, Body SC, Colan SD, Sullivan LJ, et al. Sevoflurane depresses myocardial contractility less than halothane during induction of anesthesia in children. Anesthesiology. 1996;85:1260–7.
84. Wodey E, Pladys P, Copin C, Lucas MM, Chaumont A, Carre P, et al. Comparative hemodynamic depression of sevoflurane versus halothane in infants: an echocardiographic study. Anesthesiology. 1997;87:795–800.
85. Inomata S, Watanabe S, Taguchi M, Okada M. End-tidal sevoflurane concentration for tracheal intubation and minimum alveolar concentration in pediatric patients. Anesthesiology. 1994;80:93–6.
86. Politis GD, Tobin JR, Morell RC, James RL, Cantwell MF. Tracheal intubation of healthy pediatric patients without muscle relaxant: a survey of technique utilization and perceptions of safety. Anesth Analg. 1999;88:737–41.
87. Taylor RH, Lerman J. Minimum alveolar concentration of desflurane and hemodynamic responses in neonates, infants, and children. Anesthesiology. 1991;75:975–9.
88. Zwass MS, Fisher DM, Welborn LG, Cote CJ, Davis PJ, Dinner M, et al. Induction and maintenance characteristics of anesthesia with desflurane and nitrous oxide in infants and children. Anesthesiology. 1992;76:373–8.
89. Dikmen Y, Eminoglu E, Salihoglu Z, Demiroluk S. Pulmonary mechanics during isoflurane, sevoflurane and desflurane anaesthesia. Anaesthesia. 2003;58:745–8.
90. Terrell RC. The invention and development of enflurane, isoflurane, sevoflurane, and desflurane. Anesthesiology. The American Society of Anesthesiologists. 2008;108:531–3.
91. Thwaites AJ, Edmends S, Tomlinson AA, Kendall JB, Smith I. Double-blind comparison of sevofluran vs propofol and succinylcholine for tracheal intubation in children. Br J Anaesth. 1999;83:410–4.
92. Kleiber C, Sorenson M, Whiteside K, Gronstal BA, Tannous R. Topical anesthetics for intravenous insertion in children: a randomized equivalency study. Pediatrics. 2002;110:758–61.
93. Gajraj NM, Pennant JH, Watcha MF. Eutectic mixture of local anesthetics (EMLA) cream. Anesth Analg. 1994;78:574–83.
94. Vetter TR. A comparison of EMLA cream versus nitrous oxide for pediatric venous cannulation. J Clin Anesth. 1995;7:486–90.
95. Manschot HJ, Meursing AE, Axt P, Byttebier GO, Erdmann W. Propofol requirements for induction of anesthesia in children of different age groups. Anesth Analg. 1992;75:876–9.
96. Westrin P. The induction dose of propofol in infants 1-6 months of age and in children 10-16 years of age. Anesthesiology. 1991;74:455–8.
97. Nagdeve NG, Yaddanapudi S, Pandav SS. The effect of different doses of ketamine on intraocular pressure in anesthetized children. J Pediatr Ophthalmol Strabismus. 2006;43:219–23.
98. Radant AD, Bowdle TA, Cowley DS, Kharasch ED, Roy-Byrne PP. Does ketamine-mediated N-methyl-D-aspartate receptor antagonism cause schizophrenia-like oculomotor abnormalities? Neuropsychopharmacology. Nature Publishing Group. 1998;19:434–44.
99. Green SM, Hummel CB, Wittlake WA, Rothrock SG, Hopkins GA, Garrett W. What is the optimal dose of intramuscular ketamine for pediatric sedation? Acad Emerg Med. 1999;6:21–6.
100. Davis PJ, Lerman J, Suresh S, McGowan FX, Cote CJ, Landsman I, et al. A randomized multicenter study of remifentanil compared with alfentanil, isoflurane, or propofol in anesthetized pediatric patients undergoing elective strabismus surgery. Anesth Analg. 1997;84:982–9.
101. Visser K, Hassink EA, Bonsel GJ, Moen J, Kalkman CJ. Randomized controlled trial of total intravenous anesthesia with propofol versus inhalation anesthesia with isoflurane-nitrous oxide: postoperative nausea with vomiting and economic analysis. Anesthesiology. 2001;95:616–26.
102. Koroglu A, Teksan H, Sagir O, Yucel A, Toprak HI, Ersoy OM. A comparison of the sedative, hemodynamic, and respiratory effects of dexmedetomidine and propofol in children undergoing magnetic resonance imaging. Anesth Analg. 2006;103:63–7–tableofcontents.
103. Hammer GB, Drover DR, Cao H, Jackson E, Williams GD, Ramamoorthy C, et al. The effects of dexmedetomidine on cardiac electrophysiology in children. Anesth Analg. 2008;106:79–83–tableofcontents.
104. Fisher DM. Neuromuscular blocking agents in paediatric anaesthesia. Br J Anaesth. 1999;83:58–64.
105. Brandom BW, Fine GF. Neuromuscular blocking drugs in pediatric anesthesia. Anesthesiol Clin North Am. 2002;20:45–58.
106. Kelly RE, Dinner M, Turner LS, Haik B, Abramson DH, Daines P. Succinylcholine increases intraocular pressure in the human eye with the extraocular muscles detached. Anesthesiology. 1993;79:948–52.
107. Vachon CA, Warner DO, Bacon DR. Succinylcholine and the open globe. Tracing the teaching. Anesthesiology. 2003;99:220–3.
108. Bissonnette B, Sessler DI. Passive or active inspired gas humidification increases thermal steady-state temperatures in anesthetized infants. Anesth Analg. 1989;69:783–7.
109. Apfelbaum JL, Hagberg CA, Caplan RA, Nickinovich DG, Benumof JL, Berry FA, et al. Practice guidelines for management of the difficult airway: an updated report by the American Society of Anesthesiologists Task Force on Management of the Difficult Airway. Anesthesiology. The American Society of Anesthesiologists. 2013;118:251–70.
110. Dubreuil M, Laffon M, Plaud B, Penon C, Ecoffey C. Complications and fiberoptic assessment of size 1 laryngeal mask airway. Anesth Analg. 1993;76:527–9.

111. Patel B, Bingham R. Laryngeal mask airway and other supraglottic airway devices in paediatric practice. Contin Educ Anaesth Crit Care Pain. 2009;9:6–9.
112. John RE, Hill S, Hughes TJ. Airway protection by the laryngeal mask. A barrier to dye placed in the pharynx. Anaesthesia. 1991;46:366–7.
113. Mathew PJ, Mathew JL. Early versus late removal of the laryngeal mask airway (LMA) for general anaesthesia. Cochrane Database Syst Rev. Mathew PJ, editor. Chichester, UK: John Wiley & Sons, Ltd. 2015;8:CD007082.
114. King BR, Baker MD, Braitman LE, Seidl-Friedman J, Schreiner MS. Endotracheal tube selection in children: a comparison of four methods. Ann Emerg Med. 1993;22:530–4.
115. Weiss M, Dullenkopf A, Fischer JE, Keller C, Gerber AC, European Paediatric Endotracheal Intubation Study Group. Prospective randomized controlled multi-centre trial of cuffed or uncuffed endotracheal tubes in small children. Br J Anaesth. Oxford University Press. 2009;103:867–73.
116. Khine HH, Corddry DH, Kettrick RG, MARTIN TM, McCloskey JJ, ROSE JB, et al. Comparison of cuffed and uncuffed endotracheal tubes in young children during general anesthesia. Anesthesiology. 1997;86:627–31–discussion27A.
117. Litman RS, Maxwell LG. Cuffed versus uncuffed endotracheal tubes in pediatric anesthesia: the debate should finally end. Anesthesiology. The American Society of Anesthesiologists. 2013;118:500–1.
118. Finholt DA, Henry DB, Raphaely RC. Factors affecting leak around tracheal tubes in children. Can Anaesth Soc J. 1985;32:326–9.
119. Sugiyama K, Yokoyama K. Displacement of the endotracheal tube caused by change of head position in pediatric anesthesia: evaluation by fiberoptic bronchoscopy. Anesth Analg. 1996;82:251–3.
120. Kinouchi K, Tanigami H, Tashiro C, Nishimura M, Fukumitsu K, Takauchi Y. Duration of apnea in anesthetized infants and children required for desaturation of hemoglobin to 95%. The influence of upper respiratory infection. Anesthesiology. 1992;77:1105–7.
121. Mayhew JF. Use of neuromuscular relaxants in a child with an abnormal anatomy. Anesthesiology. The American Society of Anesthesiologists. 1993;78:797–7.
122. Redel A, Karademir F, Schlitterlau A, Frommer M, Scholtz LU, Kranke P, et al. Validation of the glidescope video laryngoscope in pediatric patients. Paediatr Anaesth. Blackwell Publishing Ltd. 2009;19:667–71.
123. Fiadjoe JE, Stricker PA, Hackell RS, Salam A, Gurnaney H, Rehman MA, et al. The efficacy of the Storz miller 1 video laryngoscope in a simulated infant difficult intubation. Anesth Analg. 2009;108:1783–6.
124. Aziz MF, Dillman D, Fu R, Brambrink AM. Comparative effectiveness of the C-MAC video laryngoscope versus direct laryngoscopy in the setting of the predicted difficult airway. Surv Anesthesiol. 2013;57:46–7.
125. Campo SL, Denman WT. The laryngeal mask airway: its role in the difficult airway. Int Anesthesiol Clin. 2000;38:29.
126. Markakis DA, SCS S, Schreiner MS. Insertion of the laryngeal mask airway in awake infants with the robin sequence. Anesth Analg. 1992;75:822.
127. Olsson GL, Hallen B. Laryngospasm during anaesthesia. A computer-aided incidence study in 136 929 patients. Acta Anaesthesiol Scand. Blackwell Publishing Ltd. 1984;28:567–75.
128. Schleelein LE, Vincent AM, Jawad AF, Pruitt EY, Kreher GD, Rehman MA, Goebel TK, Cohen DE, Cook-Sather SD. Pediatric perioperative adverse events requiring rapid response: a retrospective case–control study. Paediatr Anaesth. 2016;26:734–41. doi:10.1111/pan.12922.
129. Orliaguet GA, Gall O. Case scenario perianesthetic management of laryngospasm in children. Anesthesiology. 2012;116:458.
130. Blanc VF, Hardy J-F, Milot J, Jacob J-L. The oculocardiac reflex: a graphic and statistical analysis in infants and children. Can Anaesth Soc J. Springer. 1983;30:360–9.
131. Meyers EF, Tomeldan SA. Glycopyrrolate compared with atropine in prevention of the oculocardiac reflex during eye-muscle surgery. Anesthesiology. The American Society of Anesthesiologists. 1979;51:350–1.
132. Wolfe JW, Butterworth JF. Local anesthetic systemic toxicity: update on mechanisms and treatment. Curr Opin Anaesthesiol. 2011;24:561–6.
133. Mulroy MF, Hejtmanek MR. Prevention of local anesthetic systemic toxicity. Reg Anesth Pain Med. 2010;35:177–80.
134. Hoegberg LCG, Bania TC, Lavergne V, Bailey B, Turgeon AF, Thomas SHL, et al. Systematic review of the effect of intravenous lipid emulsion therapy for local anesthetic toxicity. Clin Toxicol. Taylor & Francis. 2016;54:167–93.
135. Akhtar N, Ansar F, Baig MS, Abbas A. Airway fires during surgery: management and prevention. J Anaesthesiol Clin Pharmacol. Medknow Publications. 2016;32:109–11.
136. Rinder CS. Fire safety in the operating room. Current Opinion in Anesthesiology. 2008;21:790–5.
137. Watcha MF, White PF, Tychsen L, Stevens JL. Comparative effects of laryngeal mask airway and endotracheal tube insertion on intraocular pressure in children. Anesth Analg. 1992;75:355.
138. Lamb K, James MF, Janicki PK. The laryngeal mask airway for intraocular surgery: effects on intraocular pressure and stress responses. Br J Anaesth. 1992;69:143–7.
139. Eberhart LHJ, Geldner G, Kranke P, Morin AM, Schäuffelen A, Treiber H, et al. The development and validation of a risk score to predict the probability of postoperative vomiting in pediatric patients. Anesth Analg. 2004;99:1630–7–tableofcontents.
140. Pijpers M, Poels PJP, Vaandrager JM, de Hoog M, van den Berg S, Hoeve HJ, et al. Undiagnosed obstructive sleep apnea syndrome in children with syndromal craniofacial synostosis. J Craniofac Surg. 2004;15:670–4.
141. Bannink N, Joosten KFM, van Veelen M-LC, Bartels MC, Tasker RC, van Adrichem LNA, et al. Papilledema in patients with Apert, Crouzon, and Pfeiffer syndrome: prevalence, efficacy of treatment, and risk factors. J Craniofac Surg. 2008;19:121–7.
142. Stricker PA, Lin EE, Fiadjoe JE, Sussman EM, Pruitt EY, Zhao H, et al. Evaluation of central venous pressure monitoring in children undergoing craniofacial reconstruction surgery. Anesth Analg. 2013;116:411–9.
143. Hsu G, Taylor JA, Fiadjoe JE, Vincent AM, Pruitt EY, Bartlett SP, et al. Aminocaproic acid administration is associated with reduced perioperative blood loss and transfusion in pediatric craniofacial surgery. Acta Anaesthesiol Scand. 2016;60:158–65.
144. Stricker PA, Shaw TL, Desouza DG, Hernandez SV, Bartlett SP, Friedman DF, et al. Blood loss, replacement, and associated morbidity in infants and children undergoing craniofacial surgery. Paediatr Anaesth. Blackwell Publishing Ltd. 2010;20:150–9.
145. Cote CJ, Liu LM, Szyfelbein SK, Goudsouzian NG, Daniels AL. Changes in serial platelet counts following massive blood transfusion in pediatric patients. Anesthesiology. 1985;62:197–201.
146. Denlinger JK, Nahrwold ML, Gibbs PS, Lecky JH. Hypocalcaemia during rapid blood transfusion in anaesthetized man. Br J Anaesth. 1976;48:995–1000.
147. Brown KA, Bissonnette B, MacDonald M, Poon AO. Hyperkalaemia during massive blood transfusion in paediatric craniofacial surgery. Can J Anaesth. Springer. 1990;37:401–8.
148. Blanc VF. Trigeminocardiac reflexes. Can J Anaesth. Springer. 1991;38:696–9.
149. Harris MM, Strafford MA, Rowe RW, Sanders SP, Winston KR, Rockoff MA. Venous air embolism and cardiac arrest during craniectomy in a supine infant. Anesthesiology. 1986;65:547–50.

150. Hartley M, Vaughan RS. Problems associated with tracheal extubation. Br J Anaesth. 1993;71:561–8.
151. Koka BV, Jeon IS, Andre JM, MacKay I, Smith RM. Postintubation croup in children. Anesth Analg. 1977;56:501–5.
152. Aldrete JA. The post-anesthesia recovery score revisited. J Clin Anesth. 1995;7:89–91.
153. Marshall SI, Chung F. Discharge criteria and complications after ambulatory surgery. Anesth Analg. 1999;88:508–17.
154. Armstrong J, Forrest H, Crawford MW. Erratum to: a prospective observational study comparing a physiological scoring system with time-based discharge criteria in pediatric ambulatory surgical patients. Can J Anaesth. Springer US. 2015;62:1363–3.
155. Schreiner MS, Nicolson SC, Martin T, Whitney L. Should children drink before discharge from day surgery? Anesthesiology. 1992;76:528–33.
156. Watcha MF, White PF. Postoperative nausea and vomiting. Its etiology, treatment, and prevention. Anesthesiology. 1992;77:162–84.
157. Rose JB, Martin TM. Posttonsillectomy vomiting. Ondansetron or metoclopramide during paediatric tonsillectomy: are two doses better than one? Paediatr Anaesth. Blackwell Publishing Ltd. 1996;6:39–44.
158. Lerman J, Eustis S, Smith DR. Effect of droperidol pretreatment on postanesthetic vomiting in children undergoing strabismus surgery. Anesthesiology. 1986;65:322–5.
159. Khalil SN, Berry JM, Howard G, Lawson K, Hanis C, Mazow ML, et al. The antiemetic effect of lorazepam after outpatient strabismus surgery in children. Anesthesiology. 1992;77:915–9.
160. Engelman E, Salengros J-C, Barvais L. How much does pharmacologic prophylaxis reduce postoperative vomiting in children? Calculation of prophylaxis effectiveness and expected incidence of vomiting under treatment using Bayesian meta-analysis. Anesthesiology. The American Society of Anesthesiologists. 2008;109:1023–35.
161. Gan TJ, Diemunsch P, Habib AS, Kovac A, Kranke P, Meyer TA, et al. Consensus guidelines for the management of postoperative nausea and vomiting. Anesth Analg. 2014;118:85–113.
162. Merkel SI, Voepel-Lewis T, Shayevitz JR, Malviya S. The FLACC: a behavioral scale for scoring postoperative pain in young children. Pediatr Nurs. 1997;23:293–7.
163. Beyer JE, McGrath PJ, Berde CB. Discordance between self-report and behavioral pain measures in children aged 3-7 years after surgery. J Pain Symptom Manag. 1990;5:350–6.
164. Wong D, Baker C. Wong-Baker FACES® Pain Rating Scale [Internet]. 2015 [cited 2016 Apr 30]. Available from: (http://wongbakerfaces.org/).
165. Anderson BJ, Woolard GA, Holford NH. Pharmacokinetics of rectal paracetamol after major surgery in children. Paediatr Anaesth. 1995;5:237–42.
166. Capici F, Ingelmo PM, Davidson A, Sacchi CA, Milan B, Sperti LR, et al. Randomized controlled trial of duration of analgesia following intravenous or rectal acetaminophen after adenotonsillectomy in children. Br J Anaesth. 2007;100:251–5.
167. Palmer GM, Atkins M, Anderson BJ, Smith KR, Culnane TJ, McNally CM, et al. I.V. Acetaminophen pharmacokinetics in neonates after multiple doses. Br J Anaesth. 2008;101:523–30.
168. Strom BL, Berlin JA, Kinman JL, Spitz PW, Hennessy S, Feldman H, et al. Parenteral ketorolac and risk of gastrointestinal and operative site bleeding. A postmarketing surveillance study. JAMA. 1996;275:376–82.
169. Møiniche S, Rømsing J, Dahl JB, Tramèr MR. Nonsteroidal antiinflammatory drugs and the risk of operative site bleeding after tonsillectomy: a quantitative systematic review. Anesth Analg. 2003;96:68–77–tableofcontents.
170. Gobble RM, Hoang HLT, Kachniarz B, Orgill DP. Ketorolac does not increase perioperative bleeding: a meta-analysis of randomized controlled trials. Plast Reconstr Surg. 2014;133:741–55.
171. Carden SM, Colville DJ, Davidson AJ, McKenzie IM, Mackey DA, McKenzie J, et al. Adjunctive intra-operative local anaesthesia in paediatric strabismus surgery: a randomized controlled trial. Aust N Z J Ophthalmol. 1998;26:289–97.
172. Eckenhoff JE, Kneale DH, Dripps RD. The incidence and etiology of postanesthetic excitment. A clinical survey. Anesthesiology. 1961;22:667–73.
173. Vlajkovic GP, Sindjelic RP. Emergence delirium in children: many questions, few answers. Anesth Analg. 2007;104:84–91.
174. Holzki J, Kretz FJ. Changing aspects of sevoflurane in paediatric anaesthesia: 1975-99. Paediatr Anaesth. 1999;9:283–6.
175. Watcha MF, Ramirez-Ruiz M, White PF, Jones MB, Lagueruela RG, Terkonda RP. Perioperative effects of oral ketorolac and acetaminophen in children undergoing bilateral myringotomy. Can J Anaesth. Springer. 1992;39:649–54.
176. Sikich N, Lerman J. Development and psychometric evaluation of the pediatric anesthesia emergence delirium scale. Anesthesiology. 2004;100:1138–45.
177. Cravero J, Surgenor S, Whalen K. Emergence agitation in paediatric patients after sevoflurane anaesthesia and no surgery: a comparison with halothane. Paediatr Anaesth. 2000;10:419–24.
178. Bajwa SA, Costi D, Cyna AM. A comparison of emergence delirium scales following general anesthesia in children. Paediatr Anaesth. 2010;20:704–11.
179. Dahmani S, Stany I, Brasher C, Lejeune C, Bruneau B, Wood C, et al. Pharmacological prevention of sevoflurane- and desflurane-related emergence agitation in children: a meta-analysis of published studies. Br J Anaesth. 2010;104:216–23.
180. Costi D, Cyna AM, Ahmed S, Stephens K, Strickland P, Ellwood J, et al. Effects of sevoflurane versus other general anaesthesia on emergence agitation in children. Cochrane Database Syst Rev. COSTI D, editor. Chichester, UK: John Wiley & Sons, Ltd. 2014;9:CD007084.

Pediatric Dermatology and the Oculoplastic Patient

6

Albert C. Yan

Pigmented Lesions

Congenital Melanocytic Nevus

Congenital melanocytic nevi (i.e., those present at birth or shortly thereafter) are present in at least 1% of all newborns [1]. Congenital nevi have been divided into three principal groups based on predicted adult size: small lesions with a diameter of less than 1.5 cm, intermediate or medium-sized lesions with a diameter of between 1.5 and 20 cm, and large lesions that are greater than 20 cm in diameter (some include a distinction for those greater than 50 cm as being so-called giant). For large and giant lesions, the malignant potential in large congenital nevi may be as high as 4–6% in a lifetime [2], with most malignant change occurring before puberty [3]. Large and giant nevi are more likely to demonstrate mutations in NRAS which controls with a low frequency of BRAF mutations [4]. The NRAS gene provides instructions for making a protein called N-Ras that is involved primarily in regulating cell division and belongs to a class of genes known as oncogenes. When mutated, oncogenes have the potential to cause normal cells to become cancerous. The BRAF gene provides instructions for making a protein that helps transmit chemical signals from outside the cell to the cell's nucleus regulating growth and division of cells. The malignant potential of small and medium congenital nevi appears to be very low [5], with the change most likely occurring after puberty. Small and medium congenital nevi harbor mutations in BRAF or NRAS [4]. At some point, congenital nevi will likely be defined more accurately by genotype rather than by phenotype as additional genetic markers are identified and further elucidated [6].

Congenital melanocytic nevi can arise on the eyelid and conjunctiva. They often initially present as tan macules or as papules that may have mottled freckling. With time they may become elevated and darker in color. The divided nevus (Fig. 6.1) is a rare congenital nevus that involves adjacent areas of the upper and lower eyelids. The nevus appears as a single lesion when the eyes are closed and thus seems to have been present in the fetus before a gestational age of 24 weeks, at which time the fused eyelids begin to separate. Besides their malignant potential, these lesions are cosmetically disfiguring and may affect visual development. The increased bulk of the upper lid can create a mechanical ptosis that interferes with vision [7]. Divided nevi may require surgical intervention in early infancy if they begin to affect visual development. Dermabrasion has been attempted in some reported cases, but regrowth of the lesion often recurs due to the persistence of nevus cells within the dermis that migrate to the surface.



Fig. 6.1 Congenital divided nevus

A.C. Yan
Pediatrics and Dermatology, Perelman School of Medicine at the University of Pennsylvania, Philadelphia, PA, USA

Section of Pediatric Dermatology, Children's Hospital of Philadelphia, Philadelphia, PA, USA
e-mail: yana@email.chop.edu

© Springer International Publishing AG 2018

J.A. Katowitz, W.R. Katowitz (eds.), *Pediatric Oculoplastic Surgery*, https://doi.org/10.1007/978-3-319-60814-3_6

Nevus of Ota (Oculodermal Melanocytosis)

Oculodermal melanocytosis, known historically as the nevus of Ota, represents a disorder defined by the presence of melanocytes within the dermis which gives these lesions their characteristically bluish-gray or blue-brown color. The pigmentation occurs most likely as a mosaic phenomenon and has been associated in some cases with somatic activating mutation in genes encoding G-proteins such as GNAQ and GNA11 [8]. Nevus of Ota is most commonly seen in the Japanese population, although it does occur in other individuals. Women are affected two [9] to five times as frequently as men [10].

The eye is involved in approximately two-thirds of cases [9]. Approximately 95% of cases are unilateral. In the affected eye, the sclera is blue and the conjunctiva is brown. The episclera and iris are most commonly affected, followed by involvement of the anterior chamber angle and the choroid [9]. Pigmentation may also occur on the eyelids, cornea, and optic disk. The pigmentation may be present at birth but usually manifests itself later in childhood, becoming progressively darker and persisting into adulthood. The condition may manifest itself in three different patterns. In one pattern, the skin and the eye are involved (Fig. 6.2). Other patients may have just skin involvement, while a small number of patients have only ocular involvement.

Children who present with oculodermal melanocytosis should have a full skin evaluation for coexisting capillary malformations (port wine stains) as part of the syndrome, phakomatosis pigmentovascularis.

Ocular complications include intraocular hypertension and, rarely, malignant melanoma [11–13]. Malignant transformation has been seen most commonly in patients with light-colored skin types, less so in darker-skinned patients, and least among patients of Asian background [12].

Ophthalmologic management consists primarily of periodic eye examinations to monitor for development of glaucoma and ocular melanoma. Treatment, where desired, can be performed with nanosecond or picosecond lasers (Q-switched ruby, Nd:YAG, alexandrite) [14] and typically requires multiple serial interventions. While earlier intervention may be associated with better response rates, eventual recurrence following laser treatment is commonplace. Dermabrasion and cryotherapy have also been reported although these modalities are accompanied by higher rates of post-therapy dyspigmentation.



Fig. 6.2 Nevus of Ota (oculodermal melanocytosis) (Courtesy of the Section of Dermatology at the Children's Hospital of Philadelphia, used with permission)

Ocular Melanoma

Only 1% of all ocular melanomas occur in the pediatric population, and pediatric melanoma, in general, is fortunately rarely encountered [15]. These may arise from preexisting congenital melanocytic nevi or oculodermal melanocytosis and arise as metastatic disease from elsewhere, or in the context of predisposition to malignancy, such as xeroderma pigmentosum [16]. The presence of ocular nevi can be associated with both increased risk of ocular and cutaneous melanoma; additionally, those with atypical cutaneous nevi appear to be at higher risk of ocular melanoma [17]. Some estimates indicate that the lifetime risk of ocular melanoma in the context of oculodermal melanocytosis is approximately 1 in 400 affected patients [18]. Congenital ocular melanoma is an extremely rare event, with only three cases previously reported [19–21].

Cystic Lesions

Dermoid Cysts

Dermoid cysts manifest as non-tender, firm, smooth, subcutaneous nodules (Fig. 6.3). Initially mobile, they may become fixed on palpation. They are the most common cystic tumors of the orbit in childhood, accounting for more than a third of all orbital lesions. Although dermoid cysts are present at



Fig. 6.3 Dermoid cyst, commonly seen on lateral eyebrow area

birth, less than 25% of the lesions are evident at birth. These lesions are presumed to arise as the result of tissue sequestration at lines of embryonic closure during fetal development. As a result, dermoid cysts are most commonly found on the upper temporal quadrant, superonasally, and occasionally in the epibulbar or intraorbital locations. Histologically, dermoid cysts contain keratin and sebaceous material with a surrounding epithelial lining that can contain sebaceous glands, hair follicles, apocrine glands, and eccrine glands.

Midline lesions may represent sites of underlying cranial dysraphism [22]. Often, these lesions on the superonasal area manifest as a dimpled area, sometimes with small protruding hairs. Patients with midline lesions should undergo brain imaging to evaluate the extent of underlying cranial dysraphism and communication with the central nervous system.

Untreated lesions may leak contents resulting in local inflammatory subcutaneous tissue changes, and the pressure from the cyst can cause erosion of underlying bone. Prophylactic excision of identified cysts can prevent progression to these reported complications.

Epidermal Cysts

Epidermal (inclusion) cysts present as flesh-colored or slightly yellowish, raised, firm, slightly compressible, 0.5–5 cm dermal or subcutaneous nodules. A small black overlying punctum may be observed. They arise most commonly on the face including the periorbital area, neck, shoulders, and chest. Being slow growing and asymptomatic, some epidermal cysts may leak contents and become inflamed. When they break down, cheesy off-white and often foul-smelling material may be extruded. Histologically, these consist of a cyst wall of keratinizing epithelium filled with keratinaceous material. While some inflamed cysts may be ameliorated with intralesional steroid injection, definitive excision is typically required as these cysts recur if residual cyst lining is left behind.

Milia

Presenting as either a single or multiple small 1–2 mm yellow-white papules, milia are commonly encountered in the periorbital region. Essentially small epidermal cysts, milia consist of small cystic accumulations of keratin within the pilosebaceous unit of vellus hair follicles.

Milia are frequently encountered during the neonatal period, but may arise at any age. In children, milia tend to spontaneously regress, while in adults, lesions may be more persistent.

Milia arise at sites of trauma and are often noted following cutaneous burns, during the healing of blistered areas in mechanobullous disorders such as epidermolysis bullosa or metabolic disorders such as porphyria. Periorbital milia may be a sign of allergic rhinoconjunctivitis in association with frequent intermittent rubbing of the eyes. Milia may also be an indicator of an underlying syndromic association.

Treatment consists of either simple incision and extraction of the keratinaceous contents or therapy with a topical retinoid for lesions outside the immediate periorbital area to hasten resolution, as long as topical agents can be kept from getting into the conjunctival space and irritating the eye.

Conditions Associated with Facial Milia
Anhidrotic ectodermal dysplasia
Basal cell nevus syndrome
Basan-Baird syndrome
Bazex syndrome
Brooke-Spiegler syndrome
Congenital atrichia with papules
Epidermolysis bullosa (especially the dystrophic variety)
Hereditary trichodysplasia (Marie-Unna hypotrichosis)
Oral-facial-digital syndrome, types I and IX
Rombo syndrome

Tumors

Basal Cell Carcinoma

Basal cell carcinoma (BCC) has been occasionally reported on the eyelids in children and young adults, though this condition is more commonly seen in middle-aged and older adults who have experienced lifetime significant sun damage [23–26]. Rare reports have documented congenital presentation [27].

Clinically, early BCC lesions classically present as small pearly appearing, dome-shaped papules that are often accompanied by small overlying telangiectasias. As lesions evolve, ulceration and crusting may occur. Rarely metastatic, BCC can be locally destructive as a result of local invasion into underlying soft tissues and bone.

When encountered in the pediatric population, BCC may arise from an underlying lesion predisposed to malignant transformation (such as a nevus sebaceous), in the context of a predisposing genetic condition such as xeroderma pigmentosum or basal cell nevus syndrome, or related to a history of significant radiation exposure (as with radiation therapy or iatrogenic photosensitivity related to voriconazole administration) [28].

When arising as singular, isolated lesions, surgical excision with adequate margins is advised to minimize risk of recurrence. This is often performed using Mohs micrographic surgery followed by oculoplastic surgical repair and reconstruction. In cases that are not amenable to surgical excision, alternatives such as topical imiquimod application, radiation therapy, cryotherapy, or photodynamic therapy may be considered.

Hemangiomas

Hemangiomas are benign tumors characterized by the proliferation of vascular endothelial cells. While only approximately 2.5% of hemangiomas are present at birth, 90% of them are noted during the first month of life. After a rapid growth period of 3–6 months, hemangiomas stabilize and then go through a process of involution. Fifty percent of hemangiomas reach their maximal involution by 5 years of age and 90% by 9 years of age. Some residua such as telangiectasias, fibrofatty tissue, and atrophic skin may persist indefinitely once a hemangioma has involuted in between up to 2/3 of patients [29]. Hemangiomas may present on any part of the body and are most worrisome when they occur around vital structures such as the eyes.

Hemangiomas in and around the orbit can cause amblyopia due to obstruction of the visual axis, strabismus, or anisometropia. Prompt ophthalmologic evaluation should be accompanied by consideration of appropriate strategies for intervention. During the proliferative phase, hemangiomas are highly responsive to pharmacologic therapy. Due to their favorable safety profile and degree of efficacy, beta-blockers have largely supplanted systemic corticosteroid as the mainstay of therapy. Beta-blockers are thought to exert their effect through vasoconstriction, inhibition of vascular endothelial growth factor, and induction of apoptosis [30]. Propranolol was approved by the FDA in 2014 for the treatment of infantile hemangioma in full-term infants 5 weeks and older, at a gradually up-titrated target dosage of 3.4 mg/kg/day divided twice daily for 6 months [31]. Approximately 90% of hemangiomas show a rapid and favorable response [32], and early treatment responses may be seen within 3 days of initiation. Patients treated with propranolol must be monitored for blood pressure and heart rate as well as signs and symptoms of hypoglycemia and bronchoconstriction. Variations in dosage and duration are not uncommon since the drug has been used extensively off-label since 2008 when the efficacy of propranolol was initially reported [33]. Other systemic beta-blockers have also been reported as effective – including atenolol and nadolol, though their use remains off-label [34, 35]. Topical beta-blocker therapy also shows promise for thin, superficial hemangiomas. Topical timolol which is available in an ophthalmologic formulation can be applied two to three times daily and can slow, arrest, or even regress proliferating hemangiomas. The gel-forming solution is commonly used for this purpose until the proliferation and plateau period has ended.

The diagnosis and management of hemangiomas occurring around the eyes is also discussed in Chaps. 7, 23 and 35.

Mastocytosis

Mastocytosis is a condition characterized by the accumulation of mast cells in the skin and sometimes other organs. In children, three principal types of cutaneous lesions are usually present: urticaria pigmentosa, solitary mastocytomas, and diffuse cutaneous mastocytosis.

Urticaria pigmentosa is the most common form of this disorder. It is characterized by numerous yellow to reddish-brown macules or papules that usually display a positive Darier's sign, the development of urticaria, or blistering upon stroking the lesion. The lesions usually appear on the trunk but may be found on any part of the body, including the eyelids.

Solitary mastocytomas are reddish-tan, brown, or yellow-orange cutaneous nodules (Fig. 6.4). They also display a positive Darier's sign in which stroking the lesion elicits urtication. They are present at birth or during early infancy with most lesions regressing within several years. Mastocytomas usually present on the arms, neck, and trunk. Blistering may occur, especially before 2 years of age. There are scant three case reports in the literature of a solitary mastocytoma involving the eyelid [36–38]. The lesion was present at birth and excised without recurrence. Solitary mastocytomas almost always regress, so excision is unnecessary except in cases where the diagnosis is in doubt, as it was in the congenital eyelid lesion.

Diffuse cutaneous mastocytosis is a very rare cutaneous variant of mastocytosis characterized by indistinct diffuse skin infiltration with mast cells. The skin has a rippled, boggy, thickened appearance with doughy consistency.



Fig. 6.4 Urticaria pigmentosa: lesions are common on the forehead and periocular areas (Courtesy of the Section of Dermatology at the Children's Hospital of Philadelphia, used with permission)

These patients can be quite ill, with extensive bulla formation, flushing attacks, fainting, and diarrhea.

The symptoms and cosmetic changes of mastocytosis disappear with time. Residual pigmentation may remain if the lesions are extensive. When faced with a lesion suggestive of mastocytosis, the lesion should be stroked in an attempt to elicit Darier's sign. Biopsy of a suspected lesion would typically show evidence of mast cells with Giemsa or other appropriate mast cell stain. In cases where one mastocytoma is identified, a total body examination to look for similar lesions is advised.

Nasal Glioma

The nasal glioma is a benign lesion that may be considered a sequestered encephalocele, consisting of neuroectodermal tissue that herniates through the nasofrontal fontanelle during early fetal development and is not retracted at the time of craniofrontal suture closure [39–41]. Nasal glioma presents as a congenital lesion on the lateral aspect of the nasal bridge or occasionally as polypoid lesions within the nose or pharynx (Fig. 6.5). Typically red to purple, firm, dome-shaped nodules, nasal gliomas, measure up to approximately 3 cm in diameter though some have been larger and will grow with the child. These lesions may grow to obstruct local structures such as the ipsilateral lacrimal apparatus or, when large enough, may compromise vision [41]. Internal nasal gliomas present as polypoid lesions in the nose or pharynx.

Nasal gliomas do not transilluminate the way fluid-filled encephaloceles do, and this may be a useful diagnostic feature. That being said, because nasal gliomas may also resemble deep hemangiomas, dermoid cysts, as well as encephaloceles [22, 42], radiologic imaging studies are often needed to define the nature and extent of the lesion prior to any surgical intervention [43].

Pilomatrixoma

Common hair follicle tumors, pilomatricomas manifest most often as solitary, firm dermal or subcutaneous nodules that often have a bluish hue. Palpation reveals a jagged, irregular border and often a stony-hard consistency due to associated calcification. Pressure to one lateral edge of the lesion produces elevation of the opposite side in what is referred to as the "teeter totter sign." Lesions are often located on the face, including the periorbital area where the upper eyelid is more commonly seen than the lower eyelid [44, 45], as well as the neck, or upper extremity, and show gradual growth over time. Untreated lesions may ulcerate, or extrude calcium material (Fig. 6.6). Rarely, malignant transformation to a pilomatrix carcinoma has been reported.

Children who have multiple pilomatricomas may have an associated underlying disorder that predisposes to their



Fig. 6.5 Nasal glioma



Fig. 6.6 Pilomatrixoma. Note the early extrusion of calcified material

formation. Since pilomatricomas generally persist, have the potential to ulcerate and scar, and have a low but potential for malignant change, prophylactic surgical removal is advised.

Conditions Associated with Multiple pilomatricomas
Gardner syndrome
Myotonic dystrophy
Rubinstein-Taybi syndrome
Turner syndrome
Trisomy 9
21-hHydroxylase deficiency
Familial Sotos syndrome
Gliomatosis cerebri
Glioblastoma multiforme

Pyogenic Granuloma

Pyogenic granulomas are bright red to brownish-red, raised, vascular-appearing papules or nodules, with a collarette of epidermis at the base (Figs. 6.7 and 6.8). They may be pedunculated or sessile and may grow to 10 mm in diameter. Pyogenic granulomas are common in children and may present on any cutaneous surface, although they most commonly occur on the face, forearms, and hands. Patients usually present with complaints of a rapidly growing lesion with recurrent bleeding.



Fig. 6.7 Pyogenic granuloma (Courtesy of the Section of Dermatology at the Children's Hospital of Philadelphia, used with permission)

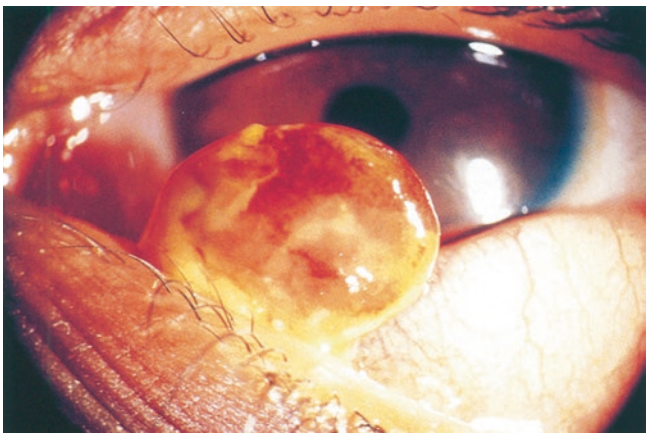


Fig. 6.8 Pyogenic granuloma on the conjunctiva (Courtesy of Sylvia Kodsi, MD)

When near the orbit, pyogenic granulomas occur most commonly on the eyelids, with a preference for the lower lids [46, 47]. Pyogenic granulomas have also been reported on the fornix [48], palpebral and bulbar conjunctiva [49, 50], lacrimal sac [51], and, rarely, the cornea [52]. Their cause is unknown, although many believe them to be a reactive lesion, as a response to antecedent trauma or inflammation. A study of 100 cases of pyogenic granulomas around the eyes found that 87% were associated with a predisposing factor such as chalazion, ocular or adnexal surgery, or accidental trauma [53]. This is in contrast to pyogenic granulomas occurring in other locations where a clear history of preceding trauma is rarely elicited.

Treatment includes curettage with gentle cautery. Larger lesions typically require excision. If the feeder vessel remains, there is a chance for recurrence. All lesions should be sent for histopathologic diagnosis, because the clinical differential diagnosis includes malignancies including but not limited to amelanotic melanoma, carcinomas, and sarcomas.

Squamous Cell Carcinoma

Persistently scaly or crusted papules or erosions may rarely indicate a squamous cell carcinoma. These lesions are extremely rare in children and are typically associated with underlying predispositions to malignancy as might be seen with DNA repair disorders (xeroderma pigmentosum) [54] or from severe photosensitivity related to medications (as seen with voriconazole) [37]. Because of the potential for metastasis, prophylactic surgical excision with clear margins is advised. Mohs micrographic surgery in conjunction with oculoplastic surgical repair and reconstruction may be necessary when the periocular area is involved.

Syringoma

Syringomas are benign adnexal tumors that derive from eccrine duct structures. Presenting as multiple, small, 1–3 mm, monomorphic skin-colored to yellowish papules, syringomas are most commonly seen on the periorbital and especially lower eyelid areas (Fig. 6.9). When considering this diagnosis, identifying similar lesions on the neck, trunk, abdomen, and genitalia can help corroborate the diagnosis of syringoma. Patients with Down syndrome [55] have an increased risk for developing syringomas. While benign and generally asymptomatic, patients may wish to pursue treatment for persistent lesions for cosmetic purposes. Treatments include topical retinoid therapy, cryotherapy, electrodesiccation, or local excision.

Trichoepithelioma

Trichoepitheliomas manifest as benign, firm, skin-colored, slightly translucent papules that typically range in size from 2 to 5 mm, although some can grow as large as 3 cm. Lesions tend to appear on the face especially along the nasolabial folds, central face, and eyelids. Trichoepitheliomas tend to arise during the second or third decades. Lesions may be solitary or multiple and, when multiple, may arise as part of an autosomal-dominant disorder referred to epithelioma adenoides cysticum. When cylindromas are also present on the scalp in conjunction with trichoepitheliomas, Brooke-Spiegler syndrome should be considered. Clinically, trichoepitheliomas may resemble syringomas or non-ulcerated basal cell carcinomas. Rarely, trichoepitheliomas may devolve into basal cell carcinoma. While shave techniques may allow for histologic sampling, residual lesions tend to regrow and treatment typically involves excision of the lesion.



Fig. 6.9 Syringomas

Xanthelasma

Xanthelasma or xanthoma palpebrarum are yellowish papules or plaques that are commonly found on the upper eyelids around the inner canthus. They are generally bilateral and symmetrical. While rare in children, when present, they may indicate familial hypercholesterolemia, hyperapo B syndrome, or phytosterolemia, and affected children should therefore be evaluated for an underlying lipid metabolism disorder [56]. Xanthoma disseminatum, a proliferation of non-x histiocytes that resembles xanthelasma, may rarely occur on the eyelids along with disseminated skin and visceral disease [57]. Adults may also develop lesions resembling xanthelasma in response to filler injections [58]. Treatment modalities include trichloroacetic acid chemical peeling, destruction with cautery, laser ablation, or excision.

Granulomatous Lesions

Granuloma Annulare

Granuloma annulare (GA) is a benign cutaneous disorder characterized by dermal granulomas that present clinically as papules or nodules in an annular configuration. The lesions usually begin at sites predisposed to trauma such as the dorsum of the hands and feet, but can occur at any site, including the eyelids (Fig. 6.10). Seventy-nine percent of cases of nodular granuloma annulare occur in people under 25 years of age [59]. While the condition is more common in



Fig. 6.10 Granuloma annulare, near medial canthus (Courtesy of the Section of Dermatology at the Children's Hospital of Philadelphia, used with permission)

childhood, adults may be more predisposed to the more generalized form of the disorder. Variations in presentation include plaques, annular plaques, perforating papules, and subcutaneous nodules. Although their exact etiology is unknown, lesions may arise as an idiosyncratic response to trauma. Unlike in adults, this condition is rarely associated with diabetes mellitus in children.

The nodular or subcutaneous form of GA is also known as pseudorheumatoid nodules because of their histologic resemblance to nodules seen in patients with rheumatoid arthritis. Seventy-nine percent of cases of nodular GA occur in people under 25 years of age. The lesions in nodular granuloma annulare most commonly occur on the extensor surface of the extremities, the dorsum of the hands and feet, the scalp, buttocks, and the eye. Nodules have been reported on the eyelid, periorbital area, lateral canthus, medial canthus, episclera, orbit, and lateral rectus muscle.

In the absence of other cutaneous lesions indicative of GA, nodules presenting in the periorbital area should be evaluated further with either imaging or biopsy. The differential diagnosis includes epidermal cysts, dermoids, neurofibromas, leukemia, lymphoma, pilomatrixomas, syringomas, sarcoidosis, and other granulomatous processes.

Most lesions do not require treatment as they typically resolve within months to years, if left untreated. Some lesions spontaneously resolve after being biopsied.

If treatment is desired, topical agents such as calcineurin inhibitors (pimecrolimus or tacrolimus) have been used successfully to hasten resolution of GA [59, 60].

Sarcoidosis

Sarcoidosis is a granulomatous disorder of unknown etiology and rarely presents during childhood. When present, it may occur in preschool-aged children, generally those of ages 4 years or younger. The presentation at this age, often referred to as Blau syndrome, is characterized by polyarthritis, uveitis, and multiple cutaneous lesions that include flesh-colored, yellow, or red infiltrated papules, reddish-brown confluent plaques, and eczematous lesions (Fig. 6.11). The infiltrated lesions may occur in the periorbital area. Other ocular findings in children include conjunctival and lacrimal gland involvement, keratitis, retinitis, and glaucoma. The chest x-ray in affected children is usually normal. A complete physical examination should be done to look for cutaneous lesions elsewhere. Sarcoidal lesions can also appear psoriasiform and lupus erythematosus-like or present as small follicular papules. A biopsy of these lesions will reveal typical sarcoidal granulomas. Sampling of the conjunctivae frequently yields sarcoidal granulomas histologically.

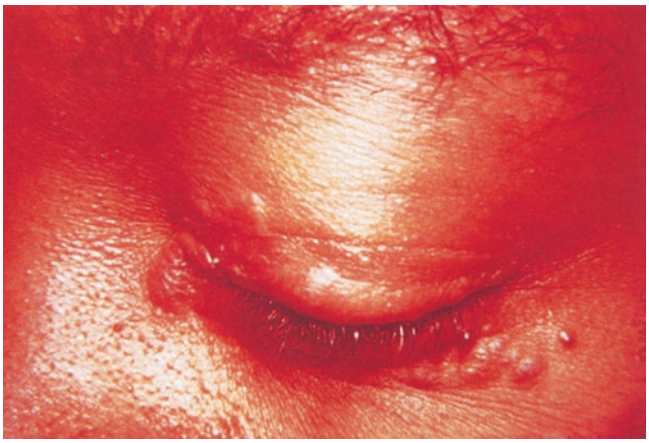


Fig. 6.11 Sarcoidosis

Histiocytic Disorders

Juvenile Xanthogranuloma

Juvenile xanthogranuloma *(JXG)* is a benign cutaneous disease of infants and children. It is now classified as a non-Langerhans cell histiocytosis and is characterized clinically by the development of one or more red to yellow-orange papules with a rubbery consistency. Lesions generally measure between 1 and 10 mm in diameter. JXGs usually develop within the first 9 months of life although 20% are present at birth. JXGs are commonly located on the face, scalp, and neck, but can also be seen on the upper trunk and proximal portions of the upper extremities (Fig. 6.12). Although JXGs usually remain localized to the skin, there are reports of extracutaneous lesions involving the eye, lungs, pericardium, testes, liver, spleen, and central nervous system.

The eye is the most common extraocular site affected. Ocular involvement was first reported in 1949 [61]. Since that time, a number of cases of juvenile xanthogranuloma involving the eyelid, conjunctiva, cornea, sclera, limbus, retina, orbit, and optic nerve have been reported. A macronodular variant, where the lesions can measure several centimeters in diameter, has been reported on the eyelid [62]. There is great variation in the color of the ocular lesions, thereby creating a large differential diagnosis and making clinical diagnosis difficult. Ocular lesions have been reported to occur in up to 10% of patients with cutaneous lesions. Juvenile xanthogranulomas of the iris are the most common, followed by eyelid involvement. Eighty-five percent of patients with intraocular involvement present during the first year of life [63]. These patients present with spontaneous hyphemas and glaucoma [64, 65]. Most lesions regress after a year, although some may persist for longer periods.

Histologically, mature lesions are characterized by a granulomatous infiltrate containing foam cells, foreign body

giant cells, Touton giant cells, histiocytes, lymphocytes, and eosinophils. The Touton giant cell is characterized by a "wreath" of nuclei surrounded by foamy cytoplasm and is quite typical for juvenile xanthogranuloma. Treatment, when indicated, includes corticosteroids, excision, and radiotherapy (see Chap. 12).

Benign Cephalic Histiocytosis

Benign cephalic histiocytosis is a self-limiting disease that develops between 2 months and 3 years of life. The disease presents with 2–5 mm red to reddish-brown papules on the face (Fig. 6.13), scalp, or neck and may spread to involve the trunk and upper extremities. On occasion the lesions may initially present on the eyelids. The eruption tends to heal without scarring in 4–9 years.

Histopathologically, the lesions are characterized by a dermal infiltrate of non-Langerhans cell histiocytes. Electron microscopic examination shows that up to 30% of the cells contain comma-shaped bodies and coated vesicles. No treatment is necessary for this self-limited condition.



Fig. 6.12 Juvenile xanthogranuloma (Courtesy of Ruggero Caputo, MD)



Fig. 6.13 Benign cephalic histiocytosis (Courtesy of Ruggero Caputo, MD)



Fig. 6.14 Xanthoma disseminatum (Courtesy of Ruggero Caputo, MD)

Xanthoma Disseminatum

Xanthoma disseminatum is a xanthomatous histiocytic disorder affecting the skin and mucous membranes of the eyes, upper respiratory tract, and the central nervous system, leading to diabetes insipidus. The disorder is seen most frequently in young males. Thirty percent of the cases develop before the age of 15 years.

The skin lesions are characterized by numerous red-brown to yellow-brown papules, plaques, and nodules that symmetrically involve the face, trunk, and proximal extremities as well as in the flexures and folds of the neck, extremities, and groin. On the face, periorbital and eyelid involvement is common (Fig. 6.14). Lesions are also found on the mucous membranes of the mouth, larynx, and pharynx, as well as the conjunctiva and cornea. Upper respiratory involvement may lead to respiratory difficulty. Meningeal involvement at the base of the brain leads to diabetes insipidus in up to 40% of cases. The disease is self-limiting but may persist for many years. The differential diagnosis includes Langerhans cell histiocytosis, xanthomas, and juvenile xanthogranulomas.

Genodermatoses

Basal Cell Nevus Syndrome

The basal cell nevus syndrome, also known as Gorlin syndrome, is an autosomal-dominant disorder characterized by

the early development of multiple basal cell carcinomas and hamartomas associated with numerous other abnormalities. These are caused by mutations in genes within the hedgehog signaling pathway.

These other abnormalities include odontogenic jaw cysts, rib and vertebral anomalies, frontal bossing, broad nasal root, calcification of the falx cerebri, agenesis of the corpus callosum, palmar and plantar pits, and the development of other tumors, including medulloblastoma, ovarian fibromas, and cardiac fibromas.

The head, including the eyelids, and neck are the most common sites for development of basal cell carcinomas. Other ocular findings associated with the syndrome include cataracts, glaucoma, colobomas, hypertelorism, dystopia canthorum, microphthalmia, and strabismus [66–68]. A basal cell carcinoma in any child or adolescent should warrant a workup for the possibility of the basal cell nevus syndrome.

Early recognition and identification can aid in avoidance of ionizing radiation, screening for underlying tumors, and appropriate treatment of the basal cell neoplasms. Treatment of these neoplasms includes excision, curettage and electrodesiccation, cryotherapy, laser ablation, photodynamic therapy, imiquimod, and, in severe cases, systemic vismodegib.

Colobomas

A coloboma is a congenital or acquired notch, gap, or fissure that can occur in any of the ocular structures. Colobomas indicate the incomplete closure of the embryonic fissure. Colobomas present to the pediatric ophthalmologist in patients who have chromosomal abnormalities, single-gene disorders with multisystem involvement, and malformation syndromes. Colobomas are discussed in more detail in Chaps. 17 and 34.

Coloboma Syndromes with a Dermatologic Component

Amniotic band syndrome
Basal cell nevus syndrome
Branchiooculofacial syndrome
Encephalocraniocutaneous syndrome
Epidermal nevus syndrome/linear nevus sebaceous (Schimmelpenning) syndrome
Focal dermal hypoplasia (Goltz) syndrome
Goldenhar syndrome
Heminasal agenesis
Monosomy 13
Neuroocular cutaneous syndrome
Oculocerebrocutaneous (Delleman) syndrome
Zunich neuroectodermal (CHIME) syndrome

Epidermal Nevus Syndrome/Nevus Sebaceous Syndrome

Epidermal nevi are hamartomatous growths that are characterized by hyperplasia of the epidermis and adnexal structures in a localized area of skin. The verrucous epidermal nevus is characterized by verrucous papules that coalesce into a curvilinear configuration. The lesion may be localized or diffuse, with a pattern of whorls and swirls. The nevus sebaceous presents as a hairless yellow plaque on the scalp (Fig. 6.15). It may be found on the face, neck, or trunk. At puberty, the lesion becomes verrucous and may develop benign or malignant tumors, such as syringocystadenoma papilliferum and basal cell carcinoma.

The epidermal nevus syndrome is a genetic RASopathy disorder in which an epidermal nevus is associated with abnormalities of the skin, eyes, central nervous system, and cardiovascular and urogenital systems. These syndromes arise as a result of somatic mutations in HRAS or, occasionally, KRAS. A wide range of deformities have been reported within each of these systems. Ocular abnormalities that have been reported in association with the epidermal nevus syndrome include the epidermal nevus itself extending onto the eyelid, conjunctiva, or sclera; lipodermoids of the upper lid and conjunctiva; colobomas of the eyelid, iris, choroid, and retina; and corneal opacity and pannus formation, cataracts, ptosis, optic nerve hypoplasia, nystagmus, and cortical blindness [69, 70]. Hypophosphatemic rickets is an important association seen in a subset of these affected patients [71].

Epidermolysis Bullosa

Epidermolysis bullosa (EB) is the name given to a heterogeneous group of inherited disorders characterized by varying degrees of skin fragility and blistering of the skin and at times the mucosa. Epidermolysis bullosa is divided into four



Fig. 6.15 Nevus sebaceus

main categories (EB simplex, junctional EB, dystrophic EB, and Kindler syndrome) which correlate with the level of blistering within the epidermis or dermis. Within each category there are different subtypes that are differentiated by the clinical course and the inherited molecular genetic defect. The ocular abnormalities in patients with epidermolysis bullosa are related to fragility of the ocular mucosa [72].

EB simplex is associated with defects of keratin filaments characterized by blisters that occur within the epidermis and heal without scarring. Of all the different subtypes of EB simplex, the Dowling-Meara subtype has been associated with ocular involvement that has included corneal abrasions and eyelid blisters [72].

Junctional EB is associated with defects occurring within the basement membrane region of the epidermis, specifically the lamina lucida and lamina densa. These patients have more extensive blistering on the skin and have dysplastic nails and teeth. Ocular abnormalities in this type include corneal blisters, abrasions, and scars; eyelid scars; ectropion; conjunctival blisters [73–75]; and, in one case, lens subluxation [76].

In dystrophic EB the blisters are subepidermally located, forming below the lamina densa, with either absent or reduced numbers of anchoring fibrils. The underlying genetic abnormality is a defect in type VII collagen formation. Dystrophic EB is a scarring form of EB of which there is a dominant dystrophic and recessive dystrophic type. Patients with the dominant dystrophic type are usually less severely affected, and children are generally in good health. Ocular findings reported in dominant dystrophic EB include corneal pannus, eyelid blisters, and scars [77, 78]. Patients with recessive dystrophic EB show more severe and extensive involvement of the hair, skin, nails, and mucosa. A significant number of these patients develop ocular problems that include corneal abrasions and scars and, less commonly, corneal pannus, symblepharon, eyelid blisters and scars, and ectropion.

Kindler syndrome is a rare, autosomal recessive blistering disorder characterized by photosensitivity and resulting poikiloderma. Ocular findings seen in children with Kindler syndrome have included keratoconjunctivitis, symblepharon, ectropion, corneal erosions, and blindness [77, 78].

Lipoid Proteinosis

Lipoid proteinosis, also known as hyalinosis cutis et mucosae and Urbach-Wiethe syndrome, is an autosomal recessive disorder caused by mutations in ECM1, an extracellular matrix glycoprotein involved in tissue homeostasis [79]. The disorder is characterized by the abnormal deposition of hyaline material into the skin, oral and laryngeal mucosa, and viscera. Patients initially present at birth or shortly thereafter with hoarseness and a low-pitched cry secondary to laryngeal involvement [80, 81]. The oral mucous membranes become extensively infiltrated. Infiltration into the tongue produces a woody thickening that makes tongue protrusion difficult. The skin develops yellow-ivory-colored papules that become confluent on the face, neck, axillae, and hands. Vesicular lesions may occur, leaving atrophic or varioliform scars. The elbows and knees develop thickened, hyperkeratotic lesions. The skin eventually becomes diffusely thickened. Intracranial calcifications also occur. The eyelid margins develop a string of bead-like yellowish papules (Fig. 6.16), known as moniliform blepharosis, that in some patients lead to loss of cilia. In the absence of curative therapy, treatments for lipoid proteinosis are directed at the clinical problems: laryngeal deposits may be addressed with microlaryngoscopic excision, ablative laser therapy, or tracheostomy, isolated case reports have suggested that systemic retinoids such as etretinate or acitretin may moderate some of the vocal cord symptoms, and seizures may be managed with anticonvulsant medications.

Neurofibromatosis

Neurofibromatosis is a heterogeneous disorder of eight different subtypes, the most common being neurofibromatosis type 1 (NF-l). Neurofibromatosis in the past was traditionally included in a group of disorders known as the phakomatoses, although it is now clear that each of those disorders is unique and caused by different genetic mutations.

NF-l is another RASopathy and is transmitted as an autosomal-dominant trait with incomplete penetrance and variable expressivity. The disease is caused by mutations in the Ras/MAPK pathway and, specifically, the gene encoding neurofibromin on chromosome 17. Other genes in this pathway can be affected and cause phenotypes resembling neurofibromatosis, as is seen with Legius syndrome, caused by



Fig. 6.16 Lipoid proteinosis (Courtesy of Elyse Rafal, MD)

mutations in SPRED1, downstream from neurofibromin. Legius syndrome, however, has a less severe phenotype that those with neurofibromatosis, type 1.

The clinical criteria for NF-l include the presence of two or more of the following: six or more cafe-au-lait macules over 5 mm in greatest diameter in prepubertal individuals and over 15 mm in greatest diameter in postpubertal individuals, axillary or inguinal freckling, two or more neurofibromas of any type or one plexiform neurofibroma, two or more Lisch nodules, an optic glioma, a distinctive osseous lesion such as sphenoid dysplasia or thinning of the long bone cortex with or without pseudoarthrosis, and a first-degree relative with NF-l by the above criteria [82].

Three of the above diagnostic criteria – Lisch nodules, optic glioma, and sphenoid dysplasia – involve ocular structures, while cafe-au-lait macules and plexiform neurofibromas can present in the periorbital and orbital areas. Cafe-au-lait macules may be seen on the eyelids and conjunctivae. Lisch nodules are melanocytic hamartomas of the iris, which are present in greater than 97% of postpubertal patients with NF-l. They vary greatly in size, number, and pigmentation. Optic gliomas are seen with a greatly increased frequency in patients with neurofibromatosis, especially in patients with associated macrocephaly. There is no consensus on what treatment, if any, should be used for asymptomatic optic gliomas [83]. Meningiomas of the optic nerve sheath are also more common in children with neurofibromatosis, requiring surgical intervention due to their aggressiveness. There is also an increased incidence of choroidal melanoma in patients with neurofibromatosis.

Plexiform neurofibromas are the most common eyelid lesion (Fig. 6.17). They are usually unilateral and in the temporal portion of the lid. Early lesions present as drooping and thickening of the upper eyelid. They can grow and extend into the surrounding structures, leading to significant facial disfigurement. Plexiform neurofibromas of the eyelid are accompanied by ipsilateral congenital glaucoma in about 50% of cases [84, 85]. The incidence of congenital or acquired glaucoma without an associated plexiform neurofibroma is also increased in neurofibromatosis and is usually treated surgically. Rarely, plexiform neurofibromas evolve into a neurofibrosarcoma, fibrosarcoma, or a malignant schwannoma. Lesions that interfere with vision or cause significant lid disfigurement may benefit from surgical debulking. Unfortunately, there is a high recurrence rate. Other methods, including radiotherapy, are not effective. More detailed discussion regarding the management of plexiform neurofibromas involving the eyelids and periorbital soft tissues can be found in Chaps. 17 and 31.



Fig. 6.17 Plexiform neurofibroma

Evaluation of patients suspected of having neurofibromatosis or a related disorder should undergo appropriate molecular diagnostic testing for mutations in neurofibromin with reflex testing for mutations in SPRED1 for Legius syndrome.

Xeroderma Pigmentosum

Xeroderma pigmentosum is a rare autosomal recessive disorder characterized by defective DNA excision repair induced by UV radiation leading to photosensitivity; pigmentary changes of the skin, eye, and mucous membranes; and the early development of malignancies in those areas. There is clinical and genetic heterogeneity, with ten genetic complementation groups (A-I, XP variant) being recognized. Symptoms develop in 75% of affected patients between the ages of 6 months and 3 years. Most cases that begin in early childhood reach the tumor stage before age 20. The most common malignancies are basal cell carcinomas, squamous cell carcinomas, and melanomas.

Ocular changes that develop in patients with xeroderma pigmentosum include photophobia, conjunctivitis, keratitis, symblepharon, corneal opacification, conjunctival nevi, and epibulbar and lid neoplasms [86, 87]. The eyelid skin shows pigmentary changes (including freckles), atrophy, loss of lids and lashes, and ectropion [86, 87]. The changes are much more common on the lower lid than the upper lid [88]. Basal cell carcinomas and squamous cell carcinomas can develop on the eyelids. Ocular surface neoplasms, including BCC, SCC, and melanomas, when present, tend to occur in the limbal area. Management of these patients includes avoidance of UV radiation, the use of sunscreens and sunglasses, and close follow-up with early excision of suspicious lesions.

Infections

Molluscum Contagiosum

Molluscum contagiosum is a viral disorder of the skin and mucous membranes caused by a DNA virus of the

poxvirus family. The lesions produced are characterized by 2–5 mm, flesh-colored, umbilicated papules that may present as single or multiple lesions. Although they can present at any age, they commonly appear between the ages of 3 and 16. As the name implies, the disease is contagious, with an incubation period estimated at 14 days to 6 months [89]. In children the lesions usually appear on the face, trunk, and extremities. Lesions on the face commonly occur in the periorbital area and may appear on the eyelids (Fig. 6.18). When they are seen on the eyelids, there may be an associated chronic follicular conjunctivitis in up to 50% of patients. The conjunctivitis may be followed by a superficial punctate keratitis that in very rare cases progresses to the development of a pannus in the upper part of the cornea [90].

Patients with an underlying immune deficiency such as DOCK8, on immunosuppressive therapy, or infected with human immunodeficiency virus are at risk of developing widespread lesions that may be quite large [91–94]. Molluscum contagiosum infection is self-limited, with most cases resolving within 6–18 months, although some lesions persist for up to 4 years [95, 96].

Treatments for molluscum contagiosum include cryotherapy, curettage, excision, chemical ablatives, oral immune stimulators (namely, cimetidine), or cautery. Cantharidin treatment is generally avoided around the eyelid due to unpredictable and often excessive resulting blistering. There is no general consensus as to the therapeutic approach of periocular molluscum contagiosum. Toxic conjunctivitis associated with molluscum contagiosum does not usually resolve until the lesions at or near the lid margins are eradicated. The asymptomatic child with periocular molluscum contagiosum need not be treated unless there are other compelling circumstances that account for the need for a procedure under anesthesia.



Fig. 6.18 Molluscum contagiosum

Warts

Warts are caused by the human papillomavirus (HPV), of which there are over 170 types. Warts present in four principal ways: the common wart, plane or planar wart, plantar wart, and condyloma acuminatum. Warts can occur on any part of the body, with different HPV types more common in some areas than others. Common warts can present around the eye or on the eyelids, usually with a digitate, or filiform, appearance. When warts present on the conjunctiva, they have a cauliflower-like appearance and are often associated with a low-grade papillary conjunctivitis or punctate epithelial keratitis [88].

Children with multiple flat warts on the face that have more generalized presentations and that are recalcitrant to therapy or continue to recur frequently despite therapy may benefit from histologic confirmation to rule out other types of warts such as epidermodysplasia verruciformis, as well as other diagnostic entities such as basal cell nevus syndrome. Epidermodysplasia verruciformis is an autosomal recessive genodermatosis caused by mutations in the EVER1 or EVER2 genes. Affected patients are at risk for malignant transformation as well as recurrent and recalcitrant warts.

Treatment of warts includes excision, liquid-nitrogen cryotherapy, bichloroacetic acid, trichloroacetic acid, cantharidin (not recommended for use on the eyelids or close to the eye), topical immunomodulatory agents (imiquimod and sinecatechins), and ablative laser for large, recalcitrant warts.

Miscellaneous

Amniotic Bands

Amniotic band syndrome, or amniotic rupture malformation sequence, is a collection of fetal malformations brought about by the early rupture of the amniotic sac, leading to the formation of mesodermal bands causing entanglement or attachment of amniotic remnants [97, 98]. Interestingly, the bands themselves are not usually present at the time of birth, with one series reporting their presence in only 13% of cases [99]. The resulting anomalies tend to be grouped into three different categories: limb defects being the most common, followed by craniofacial and visceral defects. Defects in the different categories can occur in the same patient.

Limb defects are thought to be associated with amniotic rupture later in pregnancy. The most common type of limb anomaly is the constriction anomaly, which in its severest form leads to amputation. Craniofacial defects include encephalocele, anencephaly, and facial clefting. Lip and palate clefts may result from swallowing of fibrous bands. Visceral defects include gastroschisis and omphalocele.

Ocular anomalies tend to occur with other craniofacial defects (see Chaps. 17 and 34). The ocular defects include eyelid colobomas, unilateral uveal colobomas, hypertelorism, strabismus, anophthalmia, and microphthalmia [100–103]. In one study the most common ocular malformations were congenital corneal leukomas, corneal opacities secondary to exposure, and eyelid colobomas [103].

Mycoplasma-Associated Mucositis, Stevens-Johnson Syndrome, and Toxic Epidermal Necrolysis

Stevens-Johnson syndrome, also known as erythema multiforme major, is a syndrome most commonly caused by infectious agents and drugs.

The infectious agent most commonly associated is *Mycoplasma pneumoniae*, and in affected patients, this is often referred to as mycoplasma-associated mucositis since the patients present typically with severe mucositis (oral, ocular, genital) and relatively little cutaneous or systemic involvement [104].

By contrast, Stevens-Johnson syndrome is often traditionally reserved for drug-induced presentations and exists on a spectrum with toxic epidermal necrolysis. It is characterized by the development of a widespread cutaneous bullous eruption and involvement of two or more mucous membranes. Patients are ill-appearing, with high fever and constitutional symptoms. The mucous membranes of the lips, mouth, eyes, nose, genitalia, and rectum may develop bullae that develop hemorrhagic crusts, as well as superficial erosions and ulcerations. The lungs and urinary tract may also be involved.

In the acute phase, eye changes include conjunctivitis that may be purulent, corneal ulcerations, keratitis, uveitis, and panophthalmitis. In the healing phase, the ocular complications include symblepharon, synechiae, trichiasis, corneal opacities or scarring, pannus formation, and permanent blindness (Fig. 6.19). Blindness may occur in up to 3–10% of cases. Early intervention with adjuvant amniotic membrane transplantation is helpful in preventing corneal haze, limbal stem cell deficiency, symblepharon, ankyloblepharon, and lid-related complications [105]. Although data remains conflicting, systemic administration of intravenous immunoglobulin or infliximab may also be helpful in a subset of patients [106, 107].

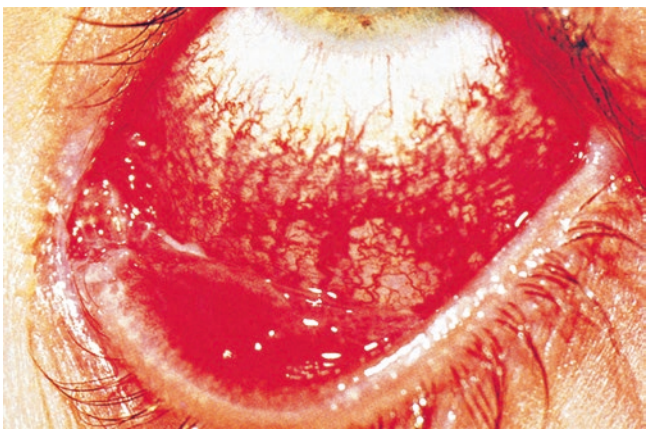


Fig. 6.19 Stevens-Johnson syndrome (Courtesy of Sylvia Kodsi, MD)

Acknowledgments The author gratefully acknowledges the original chapter written by Leonard Kristal and Paul J. Honig upon which this chapter revision is based.

References

1. Osburn K, Schosser RH, Everett MA. Congenital pigmented and vascular lesions in newborn infants. J Am Acad Dermatol. 1987;16:788–92.
2. Lorentzen M, Pers M, Brettville JG. The incidence of malignant transformation in giant pigmented nevi. Scand J Plast Reconstr Surg. 1977;11:163–7.
3. Quaba AA, Wallace AF. Incidence of malignant melanoma rising in large congenital nevocellular nevi. Plast Reconst Surg. 1986;78:174–87.
4. Charbel C, Fontaine RH, Malouf GG, et al. NRAS mutation is the sole recurrent somatic mutation in large congenital melanocytic nevi. J Invest Dermatol. 2014;134:1067–74.
5. Roh MR, Eliades P, Gupta S, Tsao H. Genetics of melanocytic nevi. Pigment Cell Melanoma Res. 2015;28(6):661–72.
6. Illig L, Weidner F, Hundeiker M, et al. Congenital nevi less than 10 cm as precursors to melanoma. Arch Dermatol. 1985;121:1274–81.
7. McDonnell PJ, Mayou B. Congenital divided nevus of the eyelids. Br J Ophthalmol. 1988;72:198–201.
8. Van Raamsdonk CD, Fitch KR, Fuchs H, et al. Effects of G-protein mutations on skin color. Nat Genet. 2004;36(9):961–8.
9. Teekhasaenee C, Ritch R, Rutnin U, et al. Ocular findings in oculodermal melanocytosis. Arch Ophthalmol. 1990;108:1114–20.
10. Hidano A, Kajima H, Ikeda S, et al. Natural history of nevus of Ota. Arch Dermatol. 1967;85:187–95.
11. Jay B. Malignant melanoma of the orbit in a case of oculodermal melanocytosis (nevus of Ota). Br J Ophthalmol. 1965;49:359.
12. Dutton JJ, Anderson RL, Schelper RL, et al. Orbital malignant melanoma and oculodermal melanocytosis: report of 2 cases and review of the literature. Ophthalmology. 1984;91:497–507.
13. Sang DN, Albert DM, Sober AJ. Nevus of Ota with contralateral cerebral melanoma. Ophthalmology. 1985;20:176–8.
14. Levin MK, Ng E, Bae YS, et al. Treatment of pigmentary disorders in patients with skin of color with a novel 755 nm picosecond, Q-switched ruby, and Q-switched Nd:YAG nanosecond lasers: a retrospective photographic review. Lasers Surg Med. 2016;48(2):181–7.
15. Stanford DG, Hart R, Thompson JF. Ocular melanoma in childhood. Aust NZ J Surg. 1993;63:729–31.
16. Vivian AJ, Ellison DW, McGill JI. Ocular melanomas in xeroderma pigmentosum. Br J Ophthalmol. 1993;77(9):597–8.
17. Bataille V, Sasieni P, Cuzick J, et al. Risk of ocular melanoma in relation to cutaneous and iris naevi. Int J Cancer. 1995;60(5):622–6.
18. Sheilds CL, Kaliki S, Livesey M, et al. Association of ocular and oculodermal melanocytosis with the rate of uveal melanoma metastasis: analysis of 7872 consecutive eyes. JAMA Ophthalmol. 2013;131(8):993–1003.
19. Broadway D, Lang S, Harper J, et al. Congenital malignant melanoma of the eye. Cancer. 1991;67:2642–52.

20. Greer CH. Congenital melanoma of the anterior uvea. Arch Ophthalmol. 1966;76(1):77–8.
21. Colenbrander MC. A cystic eye with a congenital melanoma. Ophthalmologica. 1968;156(1):83–5.
22. Paller AS, Pensler JM, Tomita T. Nasal midline masses in infants and children: dermoids, encephaloceles, and gliomas. Arch Dermatol. 1991;127:362–6.
23. Murray JE, Cannon B. Basal-cell cancer in children and young adults. N Engl J Med. 1960;262:440.
24. Stein HL, Webster GV. Basal cell carcinoma in children. Am J Surg. 1958;96:445.
25. Milstone EB, Helwig EB. Basal cell carcinoma in children. Arch Dermatol. 1973;108:523–7.
26. Comstock J, Hansen RC, Korc A. Basal cell carcinoma in a 12-year-old boy. Pediatrics. 1990;86:460–3.
27. Ledwig PA, Paller AS. Congenital basal cell carcinoma. Arch Dermatol. 1991;127:1066–7.
28. Khosravi H, Schmidt B, Huang JT. Characteristics and outcomes of nonmelanoma skin cancer (NMSC) in children and young adults. J Am Acad Dermatol. 2015;73(5):785–90.
29. Bauland CG, Lüning TH, Smit JM, et al. Untreated hemangiomas: growth pattern and residual lesions. Plast Reconstr Surg. 2011;127(4):1643–8.
30. Storch C, Hoeger PH. Propranolol for infantile haemangiomas: insights in to the molecular mechanisms of action. Br J Dermatol. 2010;163(2):269–74.
31. Hemangeol prescribing information. https://www.accessdata.fda.gov/drugsatfda_docs/label/2014/205410s000lbl.pdf. Last accessed 8 Aug 2016.
32. Léauté-Labrèze C, Hoeger P, Mazereeuw-Hautier J, et al. A randomized, controlled trial of oral propranolol in infantile hemangioma. N Engl J Med. 2015;372(8):735–46.
33. Léauté-Labrèze C, Dumas de la Roque E, Hubiche T, et al. Propranolol for severe hemangiomas of infancy. N Engl J Med. 2008;358(24):2649–51.
34. Abarzúa-Araya A, Avarrete-Dechent CP, Heusser F, et al. Atenolol versus propranolol for the treatment of infantile hemangiomas: a randomized controlled study. J Am Acad Dermatol. 2014;70(6):1045–9.
35. Randhawa HK, Sibbald C, Garcia Romero MT, Pope E. Oral nadolol for the treatment of infantile hemangiomas: a single-institution retrospective cohort study. Pediatr Dermatol. 2015;32(5):690–5.
36. Scheck O, Horny HP, Ruck P, et al. Solitary mastocytoma of the eyelid: a case report with special reference to the immunocytology of human tissue mast cells, and a review of the literature. Virchows Arch. 1987;412:31–6.
37. Naysan J, Kodsi SR, Kristal L. Solitary mastocytoma of the eyelid. J AAPOS. 2013;17(4):443–4.
38. Ma SP, Hardy TG. Solitary mastocytoma of the eyelid in an adult patient with prolidase deficiency. Ophthal Plast Reconstr Surg. 2015;33(1):e10–3.
39. Hughes GB, Shapiro G, Hunt W, et al. Management of the congenital midline nasal masses: a review. Head Neck Surg. 1980;2:222–3.
40. Whitaker SR, Sprinkle PM, Chou SM. Nasal glioma. Arch Otolaryngol. 1981;107:550–4.
41. Thompson HG, Al-Qattan MM, Becker LE. Nasal glioma: Is dermis involvement significant? Ann Plast Surg. 1995;34:168–72.
42. Levine MR, Kellis A, Lash R. Nasal glioma masquerading as a capillary hemangioma. Ophthal Plast Reconstr Surg. 1993;9:132–4.
43. Kennard CD, Rasmussen JE. Congenital midline nasal masses: diagnosis and management. J Dermatol Surg Oncol. 1990;16:1025–36.
44. Boniuk M, Zimmerman LE. Pilomatrixoma (benign calcifying epithelioma) of the eyelids and eyebrows. Arch Ophthalmol. 1963;70:399–406.
45. O'Grady RB, Spoerl G. Pilomatrixoma (benign calcifying epithelioma of Malherbe). Ophthalmology. 1981;88:1196–7.
46. Friedman AH, Henkind P. Granuloma pyogenicum of the palpebral conjunctiva. Am J Ophthalmol. 1971;71:868–72.
47. Duke-Elder S. Textbook of Ophthalmology, vol. 5. London: Kimpton; 1952. p. 4839.
48. Sen DK. Granuloma pyogenicum of the palpebral conjunctiva. J Pediatr Ophthalmol Strabismus. 1982;19:112–4.
49. Ferry AP, Zimmerman LE. Granuloma pyogenicum of limbus simulating recurrent squamous cell carcinoma. Arch Ophthalmol. 1965;74:229–30.
50. Mohan H, Gupta AN. Granuloma pyogenicum. Am J Ophthalmol. 1968;65:619–20.
51. Asiyo MN, Stefani FH. Pyogenic granulomas of the lacrimal sac. Eye. 1992;6:97–101.
52. Minckler D. Pyogenic granuloma of the cornea simulating squamous cell carcinoma. Arch Ophthalmol. 1979;97:516–7.
53. Ferry AP. Pyogenic granulomas of the eye and ocular adnexa: a study of 100 cases. Trans Am Ophthalmol Soc. 1989;87:327–47.
54. Hertle RW, Durso F, Metzler JP, et al. Epibulbar squamous cell carcinomas in brothers with xeroderma pigmentosa. J Pediatr Ophthalmol Strabismus. 1991;28:350–3.
55. Butterworth T, Strean LP, Beerman H, et al. Syringoma and mongolism. Arch Dermatol. 1964;90:483–7.
56. Haber C, Kwiterovich PO Jr. Dyslipoproteinemia and xanthomatosis. Pediatr Dermatol. 1984;1:261–80.
57. Ozcelik U, Dogru D, Akcoren Z, et al. Xanthoma disseminatum: a child with respiratory system involvement and bronchiectasis. Pediatr Pulmonol. 2005;39(1):84–7.
58. Or L, Eviatar JA, Massry GG. Xanthelasma-like reaction to filler injections. Ophthal Plast Reconstr Surg. 2016. [Epub ahead of print].
59. Rigopoulos D, Prantsidis A, Christofidou E, et al. Pimecrolimus 1% cream in the treatment of disseminated granuloma annulare. Br J Dermatol. 2005 Jun;152(6):1364–5.
60. Jain S, Stephens CJ. Successful treatment of disseminated granuloma annulare with topical tacrolimus. Br J Dermatol. 2004;150(5):1042–3.
61. Blank H, Eglick JG, Beerman H. Nevoxanthoendothelioma with ocular involvement. Pediatrics. 1949;4:349–54.
62. Schwartz TL, Carter KD, Judisch GF, et al. Congenital macronodular juvenile xanthogranuloma of the eyelid. Ophthalmology. 1991;98:1230–3.
63. Zimmerman LE. Ocular lesions of juvenile xanthogranuloma: nevoxanthoendothelioma. Trans Am Acad Ophthalmol Otolaryngol. 1965;69:412–42.
64. Sanders TE. Intraocular juvenile xanthogranuloma. Am J Ophthalmol. 1962;53:455.
65. Brenkman RF, Oosterhuis JA, Manschot WA. Recurrent hemorrhage in the anterior chamber caused by a (juvenile) xanthogranuloma of the iris in an adult. Doc Ophthalmol. 1977;42:329–33.
66. Gorlin RJ, Goltz RW. Multiple nevoid basal cell epithelioma, jaw cysts and bifid rib syndrome. N Engl J Med. 1960;262:908–12.
67. Gorlin RJ. Nevoid basal cell carcinoma syndrome. Medicine (Baltimore). 1987;66:99–109.
68. Evans DGR, Ladusans EJ, Rimmer S, et al. Complications of the naevoid basal cell carcinoma syndrome: results of a population based study. J Med Genet. 1993;30:460–4.
69. Insler MI, Davlin L. Ocular findings in linear sebaceous nevus syndrome. Br J Ophthalmol. 1987;71:268–72.
70. Ho VCY, McLean D. Epidermal nevus syndrome. In: Fitzpatrick TB, Eisen AZ, Wolff K, Freedberg M, Austen KF, editors. Dermatology in general Medicine. New York: McGraw-Hill; 1993. p. 863–5.
71. Lim YH, Ovejero D, Sugarman JS, et al. Multilineage somatic activating mutations in HRAS and NRAS cause mosaic cutaneous and skeletal lesions elevated FGF23, and hypophosphatemia. Hum Mol Genet. 2014;23(2):397–407.
72. Lin AN, Murphy F, Brodie SE, et al. Review of ophthalmic findings in 204 patients with epidermolysis bullosa. Am J Ophthalmol. 1994;118:384–90.

73. Hammerton ME, Turner TW, Pyne RJ. A case of junctional epidermolysis bullosa (Herlitz-Pearson) with corneal bullae. Austr J Ophthalmol. 1984;12:45–8.
74. McDonnell PJ, Schofield OMV, Spalton DJ, et al. Eye involvement in junctional epidermolysis bullosa. Arch Ophthalmol. 1989;107:1635–7.
75. Nakar S, Ingber A, Kremer I, et al. Late-onset localized junctional epidermolysis bullosa and mental retardation: a distinct autosomal recessive syndrome. Am J Med Genet. 1992;43:776.
76. Gans LA. Eye lesions of epidermolysis bullosa: clinical features, management, and prognosis. Arch Dermatol. 1988;124:762–4.
77. Signes-Soler I, Rodriguez-Prats JL, Carbonell S, et al. Corneal erosion and Kindler syndrome. Optom Vis Sci. 2013;90(1):e9–10.
78. El Hachem M, Diociaiuti A, Proto V, et al. Kindler syndrome with severe mucosal involvement in a large Palestinian pedigree. Eur J Dermatol. 2015;25(1):14–9.
79. Hamada T, McLean WH, Ramsay M, et al. Lipoid proteinosis maps to 1q21 and is caused by mutations in the extracellular matrix protein 1 gene (ECM1). Hum Mol Genet. 2002;11(7):833–40.
80. McGrath JA. Lipoid proteinosis. Handb Clin Neurol. 2015;132:317–22.
81. Vahidnezhad H, Youssefian L, Uitto J. Lipoid proteinosis. In: Pagon RA, Adam MP, Ardinger HH, et al., editors. GeneReviews®. Seattle (WA): University of Washington, Seattle; 2016. p. 1993–2016.
82. National Institutes of Health Consensus Development Conference Statement. July 13–15, 1987. Neurofibromatosis. https://consensus.nih.gov/1987/1987Neurofibramatosis064html.htm Last accessed 8 Aug 2016.
83. Hoffman HJ, Humphreys RP, Drake JM, et al. Optic pathway/hypothalamic gliomas: a dilemma in management. Pediatr Neurosurg. 1993;19:186–95.
84. Yanoff M, Fine BS. Ocular pathology: a text and atlas. 2d ed. Philadelphia: Harper & Row; 1982. p. 33–9.
85. Little JM, Brownstein S. Ocular neurofibromatosis. Ophthalmology. 1983;91:1595–9.
86. Goyal JL, Rao VA, Srinivasan R, et al. Oculocutaneous manifestations in xeroderma pigmentosa. Br J Ophthalmol. 1994;78:295–7.
87. Kraemer KH, Lee MM, Scotto J. Xeroderma pigmentosum - cutaneous, ocular and neurologic abnormalities in 830 published cases. Arch Dermatol. 1987;123:241–50.
88. Miller DM, Brodell RT, Levine MR. The conjunctival wart: report of a case and review of treatment options. Ophthalmic Surg. 1994;25:545–8.
89. Lynch PJ, Minkin W. Molluscum contagiosum of the adult: probably venereal transmission. Arch Dermatol. 1969;98:141–3.
90. Mathur SP. Ocular complications in molluscum contagiosum. Br J Ophthalmol. 1960;44:572–3.
91. Lombardo P. Molluscum contagiosum and the acquired immunodeficiency syndrome [letter]. Arch Dermatol. 1985;121:834–5.
92. Chen X, Anstey AV, Bugert JJ. Molluscum contagiosum virus infection. Lancet Infect dis. 2013;13(10):877–88.
93. Cotton DWK, Cooper C, Barrett DF, et al. Severe atypical molluscum contagiosum infection in an immunocompromised host. Br J Dermatol. 1987;116:871–6.
94. Kohn SR. Molluscum contagiosum in patients with the acquired immunodeficiency syndrome [letter]. Arch Ophthalmol. 1987;105:458.
95. Robinson MR, Udell IJ, Garber PF, et al. Molluscum contagiosum of the eyelids in patients with acquired immune deficiency syndrome. Ophthalmology. 1992;99:1745–7.
96. Overfield TM, Brody JA. An epidemiologic study of molluscum contagiosum in anchorage. Alaska J Pediatr. 1966;69:640–2.
97. Torpin R. Amniochorionic mesoblastic fibrous strings and amnion bands: associated constricting fetal malformation or fetal death. Am J Obstet Gynecol. 1965;91:65–75.
98. Torpin R. Fetal malformations caused by amnion rupture during gestation. Charles C. Thomas: Springfield; 1968.
99. Seeds JW, Cefalo RC, Herbert WNP. Amniotic band syndrome. Am J Obstet Gynecol. 1982;144:243–8.
100. Braude L, Miller MT, Cuttone J. Ocular abnormalities in the amniogenic band syndrome. Br J Ophthalmol. 1981;65:299.
101. BenEzra D, Frucht Y. Uveal coloboma associated with amniotic band syndrome. Can J Ophthalmol. 1983;18:136–8.
102. Tower P. Coloboma of lower lid and choroid, with facial defects and deformity of hand and forearm. Arch Ophthalmol. 1953;50:333.
103. Miller MT, Deutsch TA, Cronin C, et al. Amniotic bands as a cause of ocular anomalies. Am J Ophthalmol. 1987;104:270–9.
104. Canavan TN, Mathes EF, Frieden I, Shinkai K. Mycoplasma pneumonia-induced rash and mucositis as a syndrome distinct from Stevens-Johnson syndrome and erythema multiforme: a systematic review. J Am Acad Dermatol. 2015;72(2):239–45.
105. Sharma N, Thenarasun SA, Kaur M, et al. Adjuvant role of amniotic membrane transplantation in acute ocular Stevens-johnson syndrome: a randomized control trial. Ophthalmology. 2016;123(3):484–91.
106. Robert MC, Crnej A, Shen LQ, et al. Infliximab after Boston keratoprosthesis in Stevens-Johnson syndrome: an update. Ocul Immunol Inflamm. 2016;25:1–5. Epub ahead of print. 114.
107. Barron SJ, Del Vecchio MT, Aronoff SC. Intravenous immunoglobulin in the treatment of Stevens-Johnson syndrome and toxic epidermal necrolysis: a meta-analysis with meta-regression of observational studies. Int J Dermatol. 2015;54(1):108–15.

Plastic Surgical Considerations in Pediatric Dermatologic Abnormalities

7

David W. Low and Oksana A. Jackson

Cutaneous and subcutaneous anomalies of the periorbital region are usually noted in the neonatal period or within the first few months of life, and because of their highly visible nature, concerned parents are often referred to a pediatric dermatologist for initial evaluation and then to a pediatric plastic or oculoplastic surgeon for possible definitive management.

An understanding of the nature of each specific lesion, with particular regard to its potential for progressive growth and distortion, possible impairment of visual acuity, possible later malignant degeneration, and possible permanent disfigurement, is essential to the plastic and oculoplastic surgeon to allow accurate counseling and appropriate treatment recommendations.

This chapter deals with a potpourri of dermatologic and subcutaneous conditions, including hemangiomas, vascular malformations, congenital nevi, dermoid cysts, and periorbital scars. Clinical diagnosis, appropriate testing, and initial management strategies are discussed, followed by a description of possible reconstructive techniques.

Hemangiomas and Vascular Malformations

Hemangiomas are the most common benign tumor of infancy, occurring in 10% of full-term white infants and up to 30% of premature infants weighing less than a kilogram. The incidence is believed to be lower in African Americans and Asians. Sixty percent of hemangiomas occur in the head and neck area, and therefore a significant number may involve the periorbital region.

The clinician must have a clear understanding of the difference between hemangiomas and all other vascular anomalies, since only hemangiomas have the potential to spontaneously involute. Unfortunately, to this day, many physicians continue to lump all vascular anomalies under the category of "hemangiomas," leading to inaccurate diagnoses and recommendations. Many parents are erroneously advised to wait patiently for involution of a vascular malformation that has no capacity to regress. Even more importantly, the periorbital region is one of the few areas where the natural growth and slow involution of hemangiomas often cannot be tolerated, and medical intervention becomes mandatory.

Current reviews of vascular anomalies emphasize a classification scheme based on the biological activity of the lesion. *Vascular tumors* are characterized by true neoplastic blood vessel growth, whereas *vascular malformations* are composed of abnormally formed vessels with normal endothelial cell turnover. These vessels may be composed of capillaries, arteries, veins, lymphatics, or combinations of vessel types. The 2014 meeting of the International Society for the Study of Vascular Anomalies further divided vascular tumors into benign, locally aggressive or borderline, and malignant tumors. Vascular malformations were categorized by vessel type, by combinations of vessels, by associated named syndromes, and occasionally by the named vessel that is abnormal [1].

The most common benign tumor during the first year of life is a hemangioma. Hemangiomas are the only vascular tumors that undergo initial proliferation and growth, followed by slow regression. In contrast, vascular malformations tend to grow proportionately with the growth of the child, without capacity for spontaneous regression. Therefore, physicians who label all vascular birthmarks as "hemangiomas" will not only offer inaccurate prognostic information to the parents of their patients but also run the risk of providing inappropriate and potentially dangerous care. A litigious situation may develop if the parents feel inadequate care was provided in a difficult clinical situation that results in impaired vision and permanent facial disfigurement.

D.W. Low (✉) • O.A. Jackson
Division of Plastic Surgery, Perelman School of Medicine at the University of Pennsylvania, Philadelphia, PA, USA

The Children's Hospital of Philadelphia, Philadelphia, PA, USA
e-mail: david.low@uphs.upenn.edu

© Springer International Publishing AG 2018

J.A. Katowitz, W.R. Katowitz (eds.), *Pediatric Oculoplastic Surgery*, https://doi.org/10.1007/978-3-319-60814-3_7

Hemangiomas

History

In the majority of cases, the diagnosis of a hemangioma is straightforward and can be made on the basis of an accurate medical history, which is then confirmed on physical examination. The typical infantile hemangioma is not present at birth, but appears in the first few weeks of life. Most parents describe a small red patch that they presumed was a small scratch, but that failed to resolve and then began to enlarge disproportionately in comparison to the child's growth. In addition to circumferential enlargement, hemangiomas commonly will thicken and protrude (Fig. 7.1). Intradermal hemangiomas are bright strawberry red, whereas subcutaneous hemangiomas are blue. Some patients will have both a dermal and an underlying subcutaneous component.

In contrast, a capillary vascular malformation (port-wine stain) involving the V1 distribution of the trigeminal nerve is present at birth and enlarges proportionately (Fig. 7.2). During infancy a port-wine stain is usually flat, but hypertrophy can occur as the child matures.

Hemangiomas will generally grow until 6–12 months of age and then undergo a prolonged regression period over an average of 5 years. During involution the vessels shut down, the color lightens, and the mass softens. While many hemangiomas will significantly improve, some will leave behind fibrofatty bulky tissue and/or redundant skin. On the other hand, if the history indicates continued growth beyond the first year of life, one may be dealing with a slowly expanding venous, lymphatic, venolymphatic, or arteriovenous malformation. A plexiform neurofibroma may also present as a slowly expanding mass that fails to involute, and the correct diagnosis may be suggested by a positive family history of neurofibromatosis and other physical stigmata of this condition. If the parents or pediatrician reports a rapidly enlarging and intermittently bleeding "hemangioma" in a child well past the first year of life, it is more likely a pyogenic granuloma rather than a classic infantile hemangioma.



Fig. 7.2 Port-wine stain. This capillary vascular malformation was present at birth and involves the V1 division of the right trigeminal nerve. Such patients require ophthalmologic examination to rule out glaucoma; a CT scan may be warranted if a seizure history suggests Sturge–Weber syndrome



Fig. 7.1 Partially obstructing bulky hemangioma of the left upper eyelid. This patient was treated with steroid therapy in 2003, prior to the advent of beta blocker therapy in 2008

Interestingly, although hemangiomas are far more common than vascular malformations, the majority of vascular anomalies associated with syndromic newborns are *not* hemangiomas [2]. The majority are macular stains (stork bite) that tend to fade with time. Hemangiomas have been associated with a handful of midline defects (sternal clefting, midabdominal raphe, right-sided coarctation of the aorta, sacral and genitourinary defects), and large plaque-like facial hemangiomas have been associated with Dandy–Walker and other posterior fossa malformations (PHACES syndrome – posterior cranial fossa cerebellar cysts, hemangiomas, arterial abnormalities, cardiac abnormalities and coarctation, eye findings such as microphthalmia and cataract, and sternal clefting) [3].

Physical Examination

The physical examination usually confirms the diagnosis, particularly if the hemangioma is located in the dermis layer of the skin. Superficial hemangiomas display a classic strawberry red pigmentation. However, hemangiomas in the subcutaneous tissue appear bluish and have been mislabeled "cavernous" with the presumption that they contain dilated venules, but microscopic examination reveals proliferating capillaries identical to the dermal type. It is simply the deeper location that renders a bluish hue. In contrast, true venous vascular malformations tend to be softer and more compressible and may significantly expand when the head is held in a dependent position. In the older child, a venous malformation may also contain hard nodules (phleboliths), or they may show rapid painful enlargement and prolonged tenderness if rupture of the fragile ectatic vessels results in a transient hematoma.

Hemangiomas are often mixed lesions that have both a dermal and a subcutaneous component, with potential submuscular extension into the orbit. One will commonly see a central island of protruding bright red tissue atop a mound of bluish-tinted skin. It is the superficial component that is more likely to result in ulceration and permanent dermal scarring. Overdistention of the skin envelope may also result in atrophic skin redundancy, and incomplete resolution of the mass may result in residual fibrofatty tissue that will benefit from later judicious debulking. Purely subcutaneous and intramuscular hemangiomas may also expand the overlying skin, but there is greater potential for normal skin tone and texture following involution if the integrity of the dermis has not been violated. Twenty percent of infants will have more than one hemangioma, which may grow and regress at different rates and may differ in maximum size and degree of involution.

Hemangiomas in the periorbital region may involve either the upper or lower eyelid, the brow, the forehead, the paranasal regions and nasal dorsum, the cheek, or the temple. The orbit itself may be involved. Massive hemangiomas may involve all of these areas simultaneously.

Particular attention should be given to determining whether the hemangioma already obstructs vision or if continued growth will result in potential obstruction of the visual field. Extensive involvement of the head may also be associated with subglottic involvement, and any evidence of stridor or respiratory compromise warrants immediate otorhinolaryngology evaluation. Infants with large plaque-like facial hemangiomas and evidence of macrocephaly, enlarging head circumference, or unusual ophthalmologic findings (choroidal hemangioma, cryptophthalmos, microphthalmus, exophthalmos, and cataract) may have associated Dandy–Walker malformations (hypoplasia or absence of the cerebellar vermis and posterior fossa cysts) (Fig. 7.3). These patients may also display apnea, vomiting, posturing, developmental delay, and hemiparesis. The diagnosis can be confirmed with a computed tomography (CT) or a magnetic resonance imaging (MRI) scan [4].



Fig. 7.3 An infant with extensive facial hemangioma and PHACES syndrome that included coarctation of the aorta. She was treated with systemic steroid therapy to suppress the hemangiomas because of threatened visual obstruction

Lab and Imaging Studies

The majority of hemangiomas will not require radiologic studies for confirmation, but the extent of periorbital hemangiomas is best determined with MRI and magnetic resonance angiography (MRA). Gadolinium-enhanced MRI scanning demonstrates progressive and total filling of intraorbital vascular lesions. Distortion of the globe and orbital walls from mass effect can be appreciated. This will also help to distinguish a hemangioma from a venous or lymphatic malformation or a high-flow arteriovenous malformation. While contrast-enhanced CT scans will also show the extent of hemangiomas, the ability of MR scanning to demonstrate flow characteristics and the lack of radiation exposure makes it preferable to CT scanning in the vast majority of patients.

Arteriography is not necessary, although it has been described in the management of problematic hepatic hemangiomas associated with high-output cardiac failure, where embolization is a potential treatment option. Plane films are generally not useful. Hemangiomas rarely

show bony distortion, although there may be some orbital enlargement from the expanding mass. In contrast, vascular malformations may show skeletal overgrowth or, in high-flow situations, bone destruction. The presence of a phlebolith would favor a venous or venolymphatic malformation instead of a hemangioma as the proper diagnosis. Ultrasound has been utilized to monitor hepatic hemangiomas and to scan the body for other vascular anomalies.

In the rare event that a biopsy is performed, typical infantile hemangiomas will demonstrate high immunoreactivity for glucose transporter protein 1 [5]. Tissue that is GLUT1 positive is considered diagnostic of classic hemangiomas, whereas the less common rapidly involuting congenital hemangioma (RICH) and non-involuting congenital hemangioma (NICH) are GLUT1 negative.

Clinical Course

The stimulus for angiogenesis usually persists until 6–12 months of age, but may extend to 18 months. As the hemangioma reaches the slow involutional phase, a plateau in growth is noted, the thrombosis and sclerosis of the tiny capillary vessels results in patchy gray pigmentation, and tissue turgor begins to diminish.

The average hemangioma takes about 5 years to fully involute, although some may take several years more. It is estimated that about 70% of hemangiomas will regress satisfactorily enough so as to need no intervention [6]. However, that still leaves at least 30% of patients who will have significant residual deformity (Fig. 7.4).

Additionally, there are certain regions of the body where the risk of unacceptable scarring and residual deformity requiring reconstructive surgery is more likely, particularly when the lips, cheeks, and periorbital regions are involved. Additionally, since obstruction of the visual axis by an enlarging hemangioma for as little as 1 week during the first year of life can result in deprivation amblyopia, periorbital hemangiomas must be regarded as a potential ophthalmologic emergency (Fig. 7.5). There is a linear corelation between the duration of complete eye obstruction and the loss of visual acuity. Refractive errors can result from the mass effect of an adjacent hemangioma on the globe or cornea (anisometropic amblyopia), and hemangiomas involving the extraocular muscles can result in strabismus due to distortion and scarring of the muscles despite later involution. Retrobulbar hemangiomas can also compress the optic nerve.

The plastic surgeon who deals with hemangiomas should have a close working relationship with a multidisciplinary team of specialists familiar with all vascular anomalies. In addition to an interventional radiologist, dermatologist, and nursing coordinator, other team members may include a hematologist–oncologist, an orthopedic surgeon, and, when the periorbital region is involved, an oculoplastic surgeon and/or ophthalmologist.



Fig. 7.4 Bulky pedunculated hemangioma that is composed of redundant skin and fibrofatty tissue. Surgical debulking was recommended to remove the obstructing soft tissue mass



Fig. 7.5 Right periorbital hemangioma with both a dermal and subcutaneous component, with potential obstruction of the right eye

Nonoperative Treatment of Periorbital Hemangiomas

While the plastic surgeon may choose to primarily manage the patient, any infant with a hemangioma that already does or may eventually obstruct even part of the visual field

should be immediately evaluated by an ophthalmologist or oculoplastic surgeon. Thomson et al. [7] reviewed 51 patients with eyelid hemangiomas. Of these, 17 patients who had normal vision had only partial eyelid obstruction (smaller or more localized hemangiomas) that involuted at an earlier age (2.8 years) compared with patients with ultimately compromised vision. These favorable hemangiomas occupied only one-third of the lid margin, did not extend beyond the region of the eyelid, and/or involved only the lower lid.

Seven patients with isolated anisometropic (astigmatic) amblyopia had larger and bulkier lesions that took longer to resolve (4 years). Fifteen patients with deprivation amblyopia had large hemangiomas extending beyond the eyelid region that completely obstructed the eye for variable periods and, on average, took 4.5 years to resolve. They recommended measures to splint the affected eye open while patching the dominant eye. Lesions that were refractory to conservative measures were candidates for surgical excision if frequent ophthalmologic examinations showed developing amblyopia.

At our institution, the diagnosis of amblyopia secondary to an enlarging hemangioma in an infant is suggested by an abnormal Teller preferential looking test. A consultation between the pediatric ophthalmologist or oculoplastic surgeon and the plastic surgeon determines the need for a patching schedule for the contralateral side, and strong consideration is given for the immediate institution of suppressive antiangiogenic therapy.

Prior to 2008, intralesional or systemic steroids were the treatment of choice for problematic hemangiomas [8–11]. Oral steroid therapy was highly effective in up to 90% of patients, and regression was often observed within a week of steroid institution. However, the common side effects of steroids which included irritability, growth suppression, gastrointestinal upset, and hypertension prompted ophthalmologists to try intralesional injection with a combination of a rapid-acting steroid such a betamethasone and a long-acting steroid such as triamcinolone.

Intralesional steroid injection was promoted for the treatment of periorbital hemangiomas as early as 1978 by Mazzola [12], who treated 11 patients, with rapid benefit noted in 7 patients after 1 or 2 injections. Kushner was a strong proponent of intralesional steroid therapy in the ophthalmologic literature [13], citing the ease of administration, speed of action, paucity of side effects, and repeatability of injections. Using both a rapid-acting (betamethasone) and a long-acting (triamcinolone) steroid combination, visible change (blanching) was noted in as early as 1–2 days and dramatic results by 1 week. Doses ranged from 40 to 80 mg triamcinolone and 6 to 12 mg betamethasone per injection, delivered through 27-gauge needles. Most patients received two injections a month apart. In a later report, Kushner [14] limited his injections to 40 mg triamcinolone and 6 mg betamethasone because of potential complications of higher doses in small infants.

The safety of intralesional therapy for periorbital hemangiomas has been questioned [15, 16], with concerns noted regarding the use of general anesthesia during injection, the development of cholestrin plaques at the site of injection, and potential hematoma development and localized necrosis and scarring of the skin where concentrations of steroid might be heavy. Fat atrophy can also occur, with subsequent soft tissue contour abnormalities. Kushner himself noted the theoretical possibility of retinal artery occlusion with injections into retrobulbar or nasal mucosal hemangiomas. Furthermore, steroid injection into a vascular mass probably does not totally avoid systemic dosing, and the beneficial effect may not be due entirely to local effects.

Bilyk et al. [17] provide a comprehensive overview of treatment options for periorbital hemangiomas of infancy, again listing the risks and benefits of intralesional versus systemic steroid therapy. Other treatment options of historical interest include cryotherapy, which can cause skin scarring and hypopigmentation; surgical ligation of the feeding arteries, which has equivocal results on involution; radiation, which can cause damage to the lens, retina, periorbital bone, and overlying skin; sclerosing agents, which can cause significant destruction and scarring of local tissues; and embolization, which risks infarction of critical local tissues. While embolization has been reported, retinal artery occlusion and blindness is a significant risk. Embolization appears to have a more appropriate role in the treatment of high-output cardiac failure associated with visceral hemangiomas or as an adjunct to excision of high-flow arteriovenous malformations.

Interferon [18–20] is also of mostly historical interest, having received a great deal of enthusiasm in the 1990s as an alternative to steroid therapy, but its many significant side effects including neurologic sequelae restricted its use to the most serious life- and vision-threatening situations where steroids were ineffective. With the advent of beta blocker therapy in 2008, both steroids and interferon have taken a back seat in the treatment of problematic hemangiomas.

Beta Blocker Therapy for Infantile Hemangiomas

Leauté-Labréze et al. reported 11 patients treated with propranolol who showed significant hemangioma regression [21]. The mechanism of action may be related to vasoconstriction, suppression of vascular endothelial growth factor and basic fibroblast growth factor, and stimulation of capillary endothelial cell apoptosis. At the Children's Hospital of Philadelphia, propranolol has replaced steroids as first-line therapy for problematic hemangiomas, including those involving the periorbital area and airway. Initially, because of the potential cardiovascular, pulmonary, and hypoglycemic effects of beta blocker therapy, the propranolol protocol required hospital admission for blood pressure, heart rate, and glucose monitoring, while children were gradually administered therapeutic levels. Both inpatient and outpatient propranolol administra-

tion were directed by our dermatology colleagues. Currently, the dermatology protocol follows the FDA guideline that children of 45 weeks gestation or older are candidates for outpatient propranolol therapy if they have a normal EKG. Blood pressure and heart rate are monitored for 1–2 h during an initial partial dose administration and again the following week when the full dose is administered. Propranolol appears to have fewer adverse side effects and may even be more effective than steroids in suppressing hemangiomas and causing them to involute more rapidly (Figs. 7.6 and 7.7).



Fig. 7.6 (**a**, **b**) Periorbital and forehead hemangioma treated with propranolol with excellent suppression and regression within 4 months (Courtesy James Treat, MD)

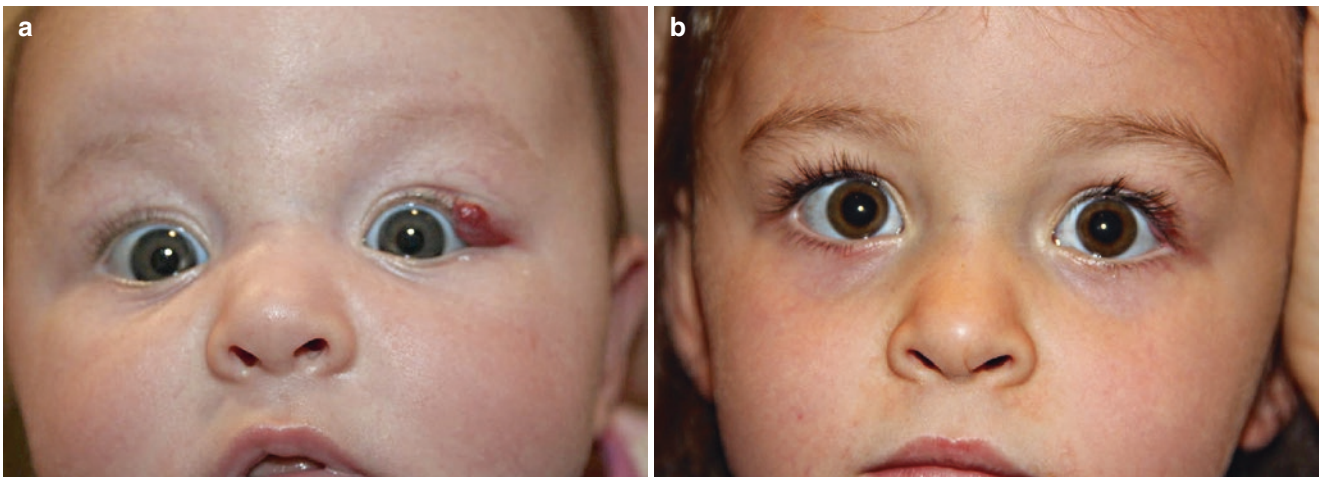


Fig. 7.7 (**a**, **b**) Lateral eyelid hemangioma treated with propranolol with excellent regression (Courtesy James Treat, MD)

A review of 100 patients with periocular hemangiomas treated with propranolol revealed it was the first-line treatment in the majority, with improvement in 96% of patients and minimal side effects. The most common dose was 2 mg/kg/day [22].

Topical beta blocker in the form of timolol maleate gel, 0.25% applied twice daily, may also be effective and is easily applied by parents [23].

Laser Therapy for Periorbital Hemangiomas

Historically, a variety of vascular lesion lasers have been used for the treatment of undesirable cutaneous blood vessels [24–29]. All operate on the principle that blood (oxyhemoglobin) absorbs certain wavelengths of light preferentially, thereby allowing selective or semiselective destruction of blood vessels by heating the blood inside. These have included argon (wavelength 488,515 nm; blue-green light), KTP (wavelength 532 nm, green light), pulsed yellow dye (current wavelength 595 nm, yellow light), tunable yellow dye (wavelength 577–630 nm, usually tuned to 585 nm), and copper vapor (wavelength 578 nm, yellow light) lasers. The pulsed yellow dye laser delivers a high-energy pulse of laser light that causes rapid expansion and rupture of the blood vessels, resulting in purpura. All of the other lasers cause vascular coagulation and blanching. None of the lasers can penetrate more than 1–2 mm into the skin, and therefore treatment is limited to thin cutaneous lesions. Neodymium:YAG lasers (wavelength 1064) will penetrate 5–6 mm, but the light is not specifically absorbed by blood. It will cause nonspecific deep thermal coagulation, and therefore has potential in treating highly vascular lesions, but at the risk of significant thermal damage to surrounding tissue.

The pulsed yellow dye laser has become well accepted as the laser of choice for pediatric port-wine stains, because of its low risk of scarring, favorable results, and rapidity and ease of delivery [30]. It may be very effective in aborting small flat hemangiomas, but in many cases, rebound growth may warrant repeated laser treatments until the hemangioma undergoes permanent regression. In such cases, interim oral propranolol or topical application of timolol may help to suppress rebound growth.

In general, thick hemangiomas do not appear to respond well to laser because of the limited depth of penetration. They may lose their bright red surface pigmentation without decreasing in size and may still require surgical debulking in the case of an obstructing hemangioma.

The pulsed dye laser is best used for early flat hemangiomas or for those that have regressed but have left persistent vascular pigmentation in the dermis (Fig. 7.8).



Fig. 7.8 In addition to treating early hemangiomas, the pulsed yellow dye laser is useful for residual vascular pigmentation after hemangiomas have involuted. In this case, redundant skin and scar tissue from prior ulceration will be excised, while the peripheral hemangioma is treated with the laser. Note the protective corneal shield

Operative Therapy for Periorbital Hemangiomas

Small hemangiomas can be excised or debulked using standard surgical techniques. If the surgeon has the luxury of being able to stay away from the hemangioma, the dissection is through normal tissue planes, and bleeding is minimal. Usually there are 1–2 feeding vessels, and vascular control and hemostasis are straightforward. Ideally, incisions are placed inconspicuously or along natural expression lines, but this is not always possible depending on the size and location of the hemangioma (Fig. 7.9).

Certain problematic periorbital hemangiomas, however, are not amenable to complete excision, and debulking becomes necessary to prevent or relieve visual obstruction. In such cases, incisions must be made within the hypervascular tissue, and hemostasis may be difficult. Electric cautery, particularly the bipolar cautery, is extremely useful to shrink and seal off engorged capillary vessels, and the bipolar forceps can even be used to dissect through the hemangioma by pinching the tissue with the tips of the forceps. Standard cautery tends to be less hemostatic, but may be useful for making initial incisions. Vaporization with a CO_2 laser can also prove useful, but the laser does not coagulate as well as other lasers that target oxyhemoglobin. After removing the necessary bulk of the hemangioma, residual raw edges must be meticulously cauterized or oversewn to avoid a hematoma. Suture closure with a tapered needle is preferable to a cutting needle, to avoid further bleeding.

Regressed hemangiomas that have left redundant skin and fibrofatty tissue as well as persistent vascular pigmentation may be treated by a combination of excision and pulsed yellow dye laser photocoagulation (Fig. 7.10).

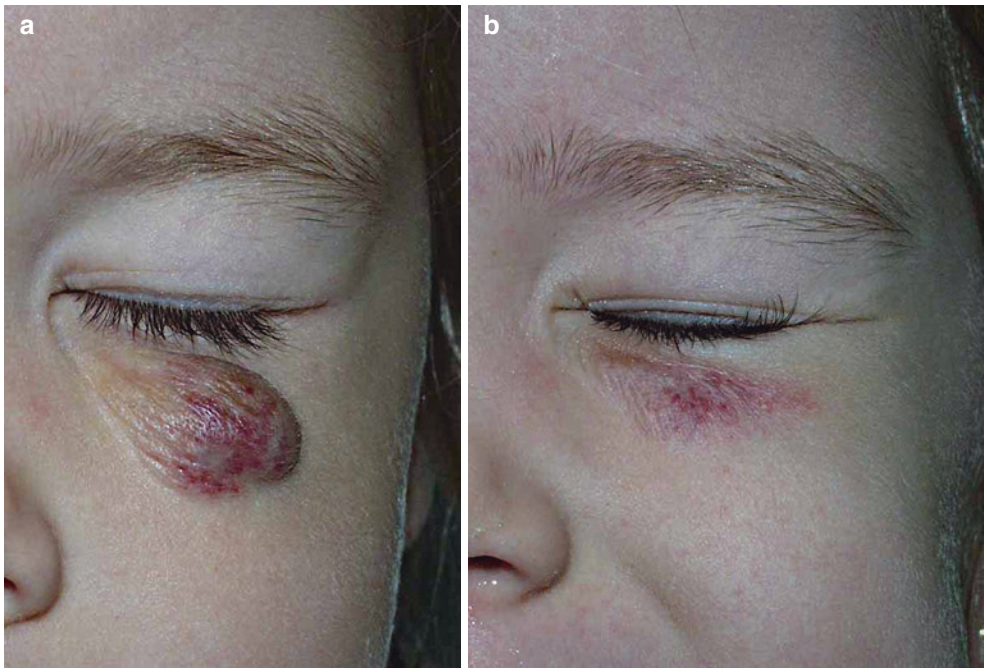


Fig. 7.9 (**a**) Redundant lower eyelid skin and fibrofatty subcutaneous tissue after hemangioma regression. (**b**) In this case, it was not possible to remove all involved skin without placing excessive traction on the lower lid



Fig. 7.10 Upper lid hemangiomas often leave redundant skin due to their tissue expansive effect. Excess skin and soft tissue can be debulked using a blepharoplasty-type pattern

Other Vascular Lesions

Pyogenic Granulomas

Pyogenic granulomas are neither pyogenic nor are they granulomas, but this misnomer appears to be forever entrenched in our medical terminology. More accurately termed lobular capillary hemangiomas, these are truly proliferative vascular lesions that may occur throughout childhood and adulthood. The history of a rapidly enlarging and engorged vascular lesion with periodic bleeding, in a patient that is usually beyond infancy, is almost diagnostic. By the time the child presents to a plastic or oculoplastic surgeon, he/she has usually been to the emergency room for troublesome bleeding, and one usually observes a Band-Aid in place and some localized black staining secondary to prior attempts at silver nitrate cauterization (Fig. 7.11).

Patrice et al. [31] reviewed 178 cases of pyogenic granulomas, of which two-thirds were located on the head and neck, including 9% involving the lips or eyelids. A thin and easily traumatized epidermal covering over a protruding and often pedunculated vascular mass characterizes these lesions, which, in fact, are neither pyogenic nor granulomas. Microscopically, there are lobules of proliferating capillaries, of which the pericyte rather than the endothelial cell is the major hyperplastic cellular component. The etiology is unclear, but may be associated with minor trauma, an insect bite, localized viral infections, underlying port-wine stains (capillary vascular malformations), or other underlying dermatologic disorders that may result in an angiogenic stimulus.

While some pyogenic granulomas may spontaneously disappear, they are usually problematic enough because of their annoyingly frequent bleeding episodes to warrant interventional therapy. Since the vessels usually penetrate into the deep dermis, shave excision alone or superficial laser or cautery may not be sufficient to obliterate the dermal component. Direct surgical excision is probably the most expeditious



Fig. 7.11 (**a**) Pyogenic granuloma. A typical pyogenic granuloma exhibiting crusting and silver nitrate staining in the area of ulceration and bleeding. There is also adhesive residue on the skin, the "positive Band-Aid sign." (**b**) Pyogenic granulomas that have not ulcerated have a fragile epidermal layer overlying a red nodule of proliferating capillaries

and the safest way to remove eyelid pyogenic granulomas. Shave excision followed immediately by cauterization or laser photocoagulation of the base has a high rate of success in other areas, but may risk thermal injury of the delicate eyelid tissues. Removed tissue should always be sent for pathologic confirmation. Protective eyeshields should always be used if a laser is involved.

Capillary Vascular Malformations (Port-Wine Stains)

Capillary vascular malformations occur in 3 out of every 1000 births. Most commonly called port-wine stains, they are composed of dilated ectatic dermal capillaries. Unlike hemangiomas, they are present at birth and grow proportionately with the child. Many appear to roughly follow a dermatome distribution, which supports the theory that improper neuronal influence during development leads to a lack of sympathetic vasomotor control. Unlike macular stains, which are commonly located in the glabellar, central forehead, and nape of the neck areas, capillary vascular malformations do not lighten with time. In fact, it may be difficult to clinically distinguish a macular stain from a port-wine stain, but a history of gradual spontaneous fading favors the former diagnosis. In contrast, many pale childhood port-wine stains will gradually darken with time and develop some bulky nodularity as the small capillaries and venules gradually dilate in adulthood.

Parents should be advised that these malformations will not disappear with time. They can be reassured that they are nonhereditary in nature and that the pattern of vascular pigmentation will not spread to uninvolved areas.

Capillary vascular malformations involving the V1 distribution of the trigeminal nerve have special significance for the physician, since these patients may have associated neuro-ocular symptoms. Sturge–Weber syndrome is characterized by a facial capillary vascular malformation involving at least a portion of the V1 cutaneous area, with ipsilateral leptomeningeal vascular anomalies, and possible ipsilateral choroidal vascular lesions with glaucoma. The neurologic symptoms may include childhood seizures, hemiparesis or hemiplegia, gyriform intracranial calcifications, and cerebral atrophy [32]. All of these tissues are derivatives of the neurectodermal germ layer, suggesting a morphogenetic error arising in a limited part of the cephalic neural crest. Patients with capillary vascular malformations involving the V1 distribution should have repeated ophthalmologic examinations to rule out glaucoma and a CT or an MRI scan to rule out ocular–CNS involvement.

Unlike capillary vascular malformations on the trunk and extremities, facial port-wine stains are highly visible. Although cover makeup can help to camouflage the vascular pigmentation, it requires daily application and tends to give the skin a thick opaque texture. Hypertrophic malformations with a nodular surface cannot be easily hidden by makeup.

Laser photocoagulation is now considered to be the standard of care for pediatric and adult capillary vascular malformations (Fig. 7.12). Previous modalities such as staged excision, excision with skin grafting, and tattoo pigmentation are no longer appropriate for pediatric capillary vascular malformations. Surgical treatments will leave permanent surgical scars and are best reserved for adolescent or adult



Fig. 7.12 (**a**) Extensive facial capillary vascular malformation. (**b**) Multiple pulsed dye laser treatments spanning 4 years have lightened the vascular pigmentation; however, the light cannot penetrate deeply enough to photocoagulate all of the vessels

port-wine stains that have developed significant hypertrophy and excessive soft tissue redundancy that is unresponsive to laser therapy. It is unusual to see hypertrophic periocular skin in children, unless a particularly dark port-wine stain is present, suggesting that there is a dense network of dilated capillaries and venules that gradually engorges with time. The goal of serial laser treatments is to not only lighten the vascular pigmentation but also prevent future hypertrophy and soft tissue distortion.

The pulsed yellow dye laser has become the most popular laser for pediatric and adult capillary vascular malformations. The yellow dye energy (595 nm wavelength) is well absorbed by oxyhemoglobin, resulting in highly specific injury to the dermal vessels, termed selective photothermolysis. Unlike lasers that deliver a continuous beam of light that causes coagulation and blanching of the dilated vessels, the pulsed dye laser delivers high-energy light bursts of very short duration (1.5 milliseconds). This results in less heat transfer to the surrounding skin and a very low risk of scar formation. Most commonly the largest spot size (10 mm) is utilized, but around the eye, one may choose one of the smaller diameter handpieces that deliver the energy in 5- or 7-mm circular spots. This results in blood vessel rupture, temporary purpuric staining, and then gradual lightening of the vessels. Although an early report by Tan et al. [30] suggested complete clearing in all 35 patients in about 7 treatment sessions, most patients will show lightening, but very few stains will actually completely clear. This may be due to the presence of deep dermal vessels that cannot be reached by the laser light.

When treating the periocular capillary vascular malformation, an opaque metal eyeshield is lubricated and placed directly on the cornea. This allows treatment of the eyelid itself, and in most infants and children, a starting power density of 6 J/cm^2 can be used. The laser will singe eyelashes and eyebrows, so the clinician may choose to mask these structures with an opaque, nonreflective barrier. The patient will immediately develop dark purpuric spots that take about 2 weeks to fade. Significant eyelid edema will develop for 2–3 days, which may be partially obstructive. Lightening of the stain may be observed within 2–3 months. Multiple treatment sessions are necessary for optimum results, and parents are repeatedly reminded not to expect complete fading. The power density of the laser can be cautiously increased if prior settings have not caused any crusting or blisters. The laser sessions, which are routinely done under general anesthesia when treating the periocular area, are discontinued when no further lightening is observed. The current fourth-generation Candela pulsed yellow dye Perfecta VBeam laser (Wayland, MA) will achieve a power density as high as 20 joules/cm^2, but most patients will demonstrate unacceptable crusting and potential scarring before reaching that fluence.

Parkes–Weber syndrome involves a cutaneous capillary vascular malformation with an underlying high-flow arteriovenous malformation. Laser treatment may lighten the cutaneous stain, but most patients will gradually exhibit increasing soft tissue warmth and bulk and sometimes an obvious pulsatile quality to the involved area. In these difficult situations, a multidisciplinary approach may involve a diagnostic MRI/MRA scan, palliative or preoperative embolization, surgical debulking, and possible flap reconstruction.

Macular stains (stork bite) that lighten but do not completely disappear spontaneously are excellent candidates for laser therapy. Unlike typical port-wine stains, which require multiple laser sessions and usually persist to some degree, macular stains do appear to virtually disappear within a couple of laser treatment sessions. Since it is not understood why they naturally fade, their accelerated response to laser therapy is also not understood. The vessels may be located in the superficial dermis making them very responsive to the laser light.



Fig. 7.13 Spider angioma of the right cheek below the eyelid. The central feeding arteriole is surrounded by radiating peripheral branches. Treatment options include laser therapy and electrodessication

Spider Angiomas

These common vascular malformations consist of a central feeding arteriole with multiple radiating branches (Fig. 7.13). They are often located on the malar eminence and lower eyelids of children and usually slowly increase in size as additional peripheral vessels are recruited. On rare occasions, the protruding central feeding vessel may ulcerate and bleed. Treatment includes electrodessication of the central feeding vessel, but long-standing angiomas may persist even if the central vessel is destroyed. Lasers usually provide complete cure, with minimal risk of residual scarring. The pulsed dye laser is least likely to cause any dermal scarring and is therefore the laser of choice.

Venous Vascular Malformations

Periorbital venous vascular malformations are composed of dilated venules and veins that gradually engorge, causing increasing soft tissue contour deformity. They may not be clinically obvious at birth, but over time become evident as the vascular spaces engorge (Fig. 7.14). Trauma may result in transient painful hematoma formation, but usually discomfort is minimal. Positional changes will commonly cause a fluctuation in size, with an obvious increase in size and firmness when the head is in a dependent position.

MRI/MRA scanning will best determine the extent and confirm the low-flow pattern of these malformations. If the lesions are small with well-defined margins, cure can be attempted by direct surgical excision using standard techniques. Laser therapy is usually not an option, because laser light will not penetrate to the depths of the malformation without burning the thin eyelid skin. This is in contrast to venous malformations of the lips and oral mucosa, where lasers can be used routinely to shrink or obliterate venous malformations, either by transcutaneous or intralesional light delivery, without prohibitive scarring.

Another treatment option is intravenous sclerotherapy using ultrasound and fluoroscopic guidance, performed by an interventional radiologist. Multiple injection sessions, delivered with a general anesthetic, may be necessary. Absolute alcohol (95% ethanol), sodium tetradecyl sulfate (Sotradecol®, Mylan Institutional, Galway, Ireland), and polidocanol (Asclera®, Merz Aesthetics, Chemische Fabrik Kreussler & Co, Wiesbaden, Germany) are available in this country. Care must be taken to avoid extravasation of the sclerosant, which can cause skin ulceration and scarring. Bleomycin is also used as a sclerosant. Although it may be less effective than ethanol, the risk of skin necrosis is significantly lower [33]. Superficial venous malformations may be more safely sclerosed with polidocanol (Asclera). For unresectable venous malformations, repeated sclerotherapy sessions may provide significant palliation, with a significant improvement in contour.

The neurosurgical and ophthalmological literature describes orbital cavernous angiomas as being the most common benign lesion of the orbital cavity. Rather than proliferative hemangiomas, these are vascular malformations with low flow that gradually expand, causing exophthalmos, potential compression of the optic nerve, and a loss of visual acuity. Intralesional or extralesional hemorrhage may also cause a symptomatic mass effect. MRI or CT scan provides a reliable diagnosis, and excision has been approached by anterior, lateral, medial, and even a transcranial approach [34]. En bloc resection has been recommended to decrease

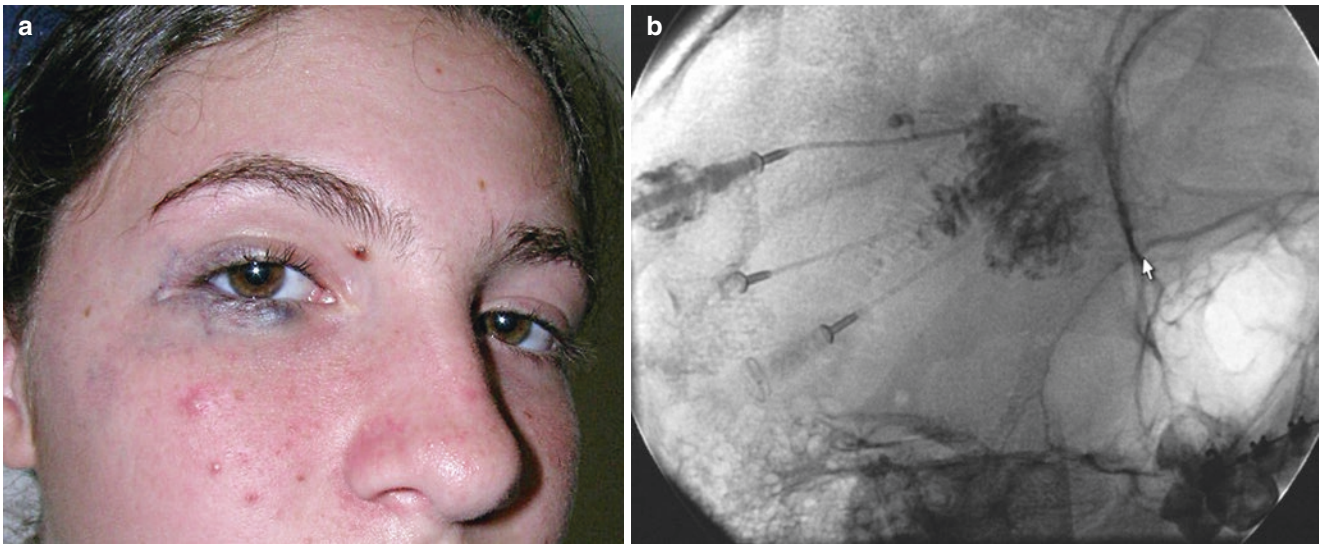


Fig. 7.14 (**a**) Venous vascular malformation involving the lower eyelid. (**b**) Sclerotherapy was performed under fluoroscopic guidance

the risk of recurrence. There may be a role for medical therapy in the form of sirolimus (rapamycin), which is becoming increasingly popular as a very viable option for the treatment of challenging lymphatic and venolymphatic malformations.

Lymphatic and Venolymphatic Malformations

These are among the most difficult vascular malformations to treat the head and neck area, because the abnormal vessels permeate normal structures. The abnormal lymphatics may also communicate with dermal lymphatics, resulting in cutaneous vesicle formation, ulceration, and crusting. Often the vesicles are dark purple as blood pigment from associated abnormal veins enters the lymphatics. Cutaneous or mucosal ulceration may lead to repeated episodes of cellulitis. Small, isolated patches may be amenable to excision, but larger areas may only be candidates for palliative cauterization of the symptomatic vesicles and partial excision of the deeper component [35]. Attempts at surgical debulking are usually far from rewarding and are reserved for cases of extreme contour distortion. Often the underlying bone is also distorted, and sophisticated craniofacial or orthognathic surgery may be necessary as part of the overall reconstruction. The danger to facial muscles and nerves is significant. In a review of 17 patients with large cervicofacial lymphatic malformation who underwent soft tissue excision by Padwa et al. [36], 76% had facial nerve and 24% had hypoglossal nerve injuries following surgery.

If significant periorbital lymphatic involvement causes soft tissue distortion, debulking may be indicated. An MRI/MRA or a CT scan is advisable to document the extent of the malformation and to confirm the diagnosis. Although exposure can be provided by supratarsal fold and lower lid incisions, excellent exposure can be obtained with a bicoronal incision, which permits a subperiosteal dissection of the brow and superior, medial, and lateral orbit (Fig. 7.15). Complete excision is usually not feasible, and parents must understand that continued enlargement and the need for future intervention are highly likely.

Nonoperative intervention in the form of sclerotherapy using bleomycin has received considerable attention and some success around the world [37, 38]. Results are better for patients with macrocystic lesions that communicate well with each other, as this permits easier intralesional delivery and dispersal of the sclerosant. Unfortunately, macrocystic lymphatic malformations are more common in the neck than in the periorbital area, making most patients with periorbital involvement less than ideal candidates for sclerotherapy.

Recently there has been a great deal of enthusiasm for the use of sirolimus (rapamycin) in the treatment of complicated vascular anomalies [39]. The activation of the P13K/AKT/mTor pathway in angiogenesis and lymphangiogenesis is inhibited by sirolimus, making it a significant treatment option for patients with vascular anomalies with a significant lymphatic component. Particularly patients with a microcystic component not amenable to sclerotherapy may be effectively controlled with sirolimus. In the future, antiangiogenic therapy will likely play an increasingly important role in the treatment of challenging vascular anomalies, particularly when the risk/benefit ratio associated with surgery and sclerotherapy is unfavorable.

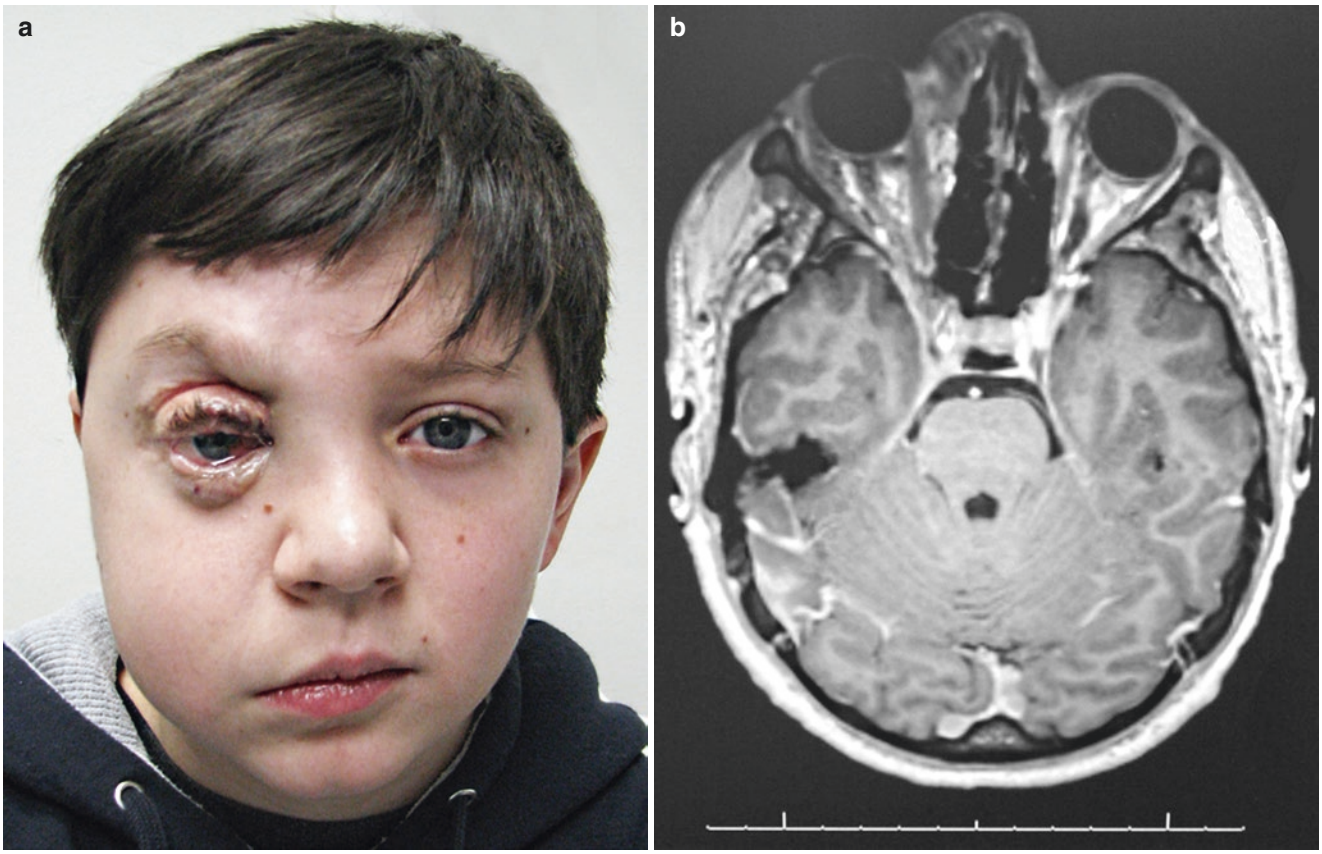


Fig. 7.15 (**a**) Venolymphatic vascular malformation involving the right periorbital region and the right cheek. (**b**) The scan confirms extensive periorbital and intraorbital involvement, making complete excision impossible

Arteriovenous Malformations and Arterial Aneurysms

As described earlier, arteriovenous malformations of the head and neck may present with associated cutaneous capillary vascular malformations (Parkes–Weber syndrome) or as isolated malformations without a cutaneous component. Clinical findings may include increased skin temperature, a visible soft tissue contour enlargement, a visible or palpable pulsatile mass, an audible bruit, a complaint of tinnitus, and a history of noticeable enlargement at puberty.

An MRI/MRA scan is the diagnostic procedure of choice to confirm the high-flow pattern, determine the source of the feeding vessels, and document the extent of the lesion, which may not necessarily correspond to the cutaneous component. An arteriogram is reserved for therapeutic preoperative embolization and is not part of the initial diagnostic workup.

It is now well recognized that simple ligation or embolic occlusion of the feeding vessels is absolutely contraindicated, because this will result in only temporary palliation. The malformation will rapidly reacquire high-flow perfusion from other sources, making future management more difficult. The best chance for cure is complete excision, commonly preceded by preoperative selective embolization. Reconstruction with well-vascularized tissue rather than a skin graft is recommended, to decrease the stimulus of an ischemic bed to open up additional arteriovenous shunts. This may require a microvascular flap transfer, and a two-team approach may optimize operative efficiency, because the flap can be harvested while the malformation is being resected.

In unresectable arteriovenous malformations, superselective embolization on a periodic basis has been described as a palliative approach (and in some cases may even be curative), but care should be taken to avoid simple occlusion of the major feeding artery, since this will make future attempts at selective embolization more difficult, particularly if the malformation is stimulated to acquire flow from the contralateral external carotid or the internal carotid arteries.

Traumatic injuries to the head may result in pseudoaneurysms, aneurysms, or traumatic AV fistulas. These can be treated by embolization or direct surgical ligation and excision with high success rates as they are more localized (Fig. 7.16).

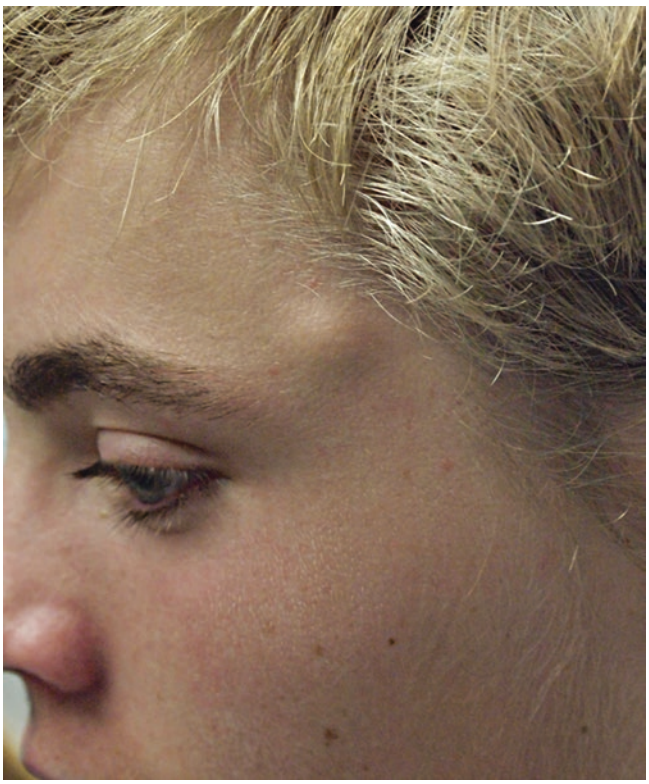


Fig. 7.16 This teenager developed a traumatic arterial pseudoaneurysm after blunt trauma to his lacrosse helmet. The pulsatile lesion was treated by surgical excision



Fig. 7.17 Congenital epidermal nevus of the left upper and lower eyelid and cheek. Although the malignant potential is negligible, these nevi may become increasingly verrucous over time

Congenital Nevi

Nevi are discussed elsewhere, along with a review of pediatric dermatology. This section discusses surgical strategies in those patients choosing interventional options.

The risk of malignant transformation in an epidermal linear nevus is almost negligible, and therefore options include no treatment, partial removal, or attempts at excision where feasible (Fig. 7.17). Since the lesions protrude above the surface of the skin, palliative maneuvers, such as shave excision, dermabrasion, or carbon dioxide laser vaporization, can help to flatten the contour and lighten the pigmentation. Regrowth may occur in time, but large nevi that cannot be easily excised can be treated with these technically straightforward measures. If surgical scars can be placed in cosmetically acceptable locations and in favorable directions, direct full-thickness skin excision will prevent recurrence.

In the typical pigmented congenital nevus that may or may not be hair-bearing, nevus cells not only are located at the dermal–epidermal junction but may also be deeply located within the dermis along hair follicles and other skin appendages. The malignant potential of these nevi is probably less than 1% over the patient's entire lifetime and virtually nonexistent prior to age 11. Since complete removal can be accomplished only by full-thickness excision, patients and parents must be counseled regarding the risks and benefits of observation only, surgical excision with direct closure, and excision combined with skin grafting, local flaps, and/or skin expansion for larger lesions (Figs. 7.18 and 7.19).

At the current time, laser therapy cannot be recommended for the treatment of these congenital nevi. Although melanin can be targeted by several available wavelengths, such as the argon and Q-switched ruby lasers, complete obliteration of the nevus cells is not assured. While it has been shown anecdotally that the color and a significant number of pigmented nevus cells can be removed with laser therapy, the risk of melanoma theoretically remains as long as some cells persist. The light may be unable to reach the deep dermis where some of these cells are located, and it may not be able to destroy the hair follicles whose roots extend to the subcutaneous tissue layer. While it is unlikely that the available lasers will stimulate malignant transformation, being visible rather than ultraviolet light, there is also the concern that it may be more difficult to diagnose a new melanoma. Since color change is one of the hallmarks of a suspicious nevus, depigmentation by laser therapy may remove that important diagnostic feature. Long-term studies are necessary to prove the efficacy and safety of laser therapy for congenital nevi. It is possible in the future



Fig. 7.18 Congenital nevus of the medial canthal region and brow

that laser therapy will become a viable alternative to treat nevi in difficult areas such as the eyelid and periorbital region if the risk of future malignant degeneration is shown to be negligible, since currently available methods of surgical reconstruction may leave significant surgical scars and deformity.

Dermoid Cysts

Dermoid cysts are benign cysts derived from ectodermal tissue that is trapped beneath normal skin along embryonic lines of fusion. Composed of normal skin elements, these cysts contain oil and hair units and can grow anywhere in the body. Periorbital dermoid cysts are usually adherent to the periosteum and may cause a bony indentation (Fig. 7.20). It is extremely rare for brow, orbital, and midline cysts superior to the nasofrontal suture to penetrate intracranially, and therefore CT scans of these dermoids are not usually necessary for treatment planning [40]. Conversely, any midline nasal dermoid cysts that lie caudal to the nasofrontal suture warrant either CT or MRI scan to rule out an intracranial extension which would require neurosurgical collaboration to completely excise (Fig. 7.21). Dermoid cysts of the greater wing of the sphenoid bone lateral to the orbit may rarely penetrate intracranially as well, making diagnosis and treatment challenging.

Our preferred approach to lateral orbital/brow dermoids is through a supratarsal fold incision rather than an infra-brow incision. The scar is usually imperceptible compared to a brow scar that can damage eyebrow hair roots.

Hemangiomas in the brow region may mimic dermoid cysts, in which case an MRI scan will demonstrate the vascular nature of these lesions. Lipoblastomas in the periorbital region may also mimic dermoid cysts and hemangiomas, and MRI scanning may help in the diagnosis.

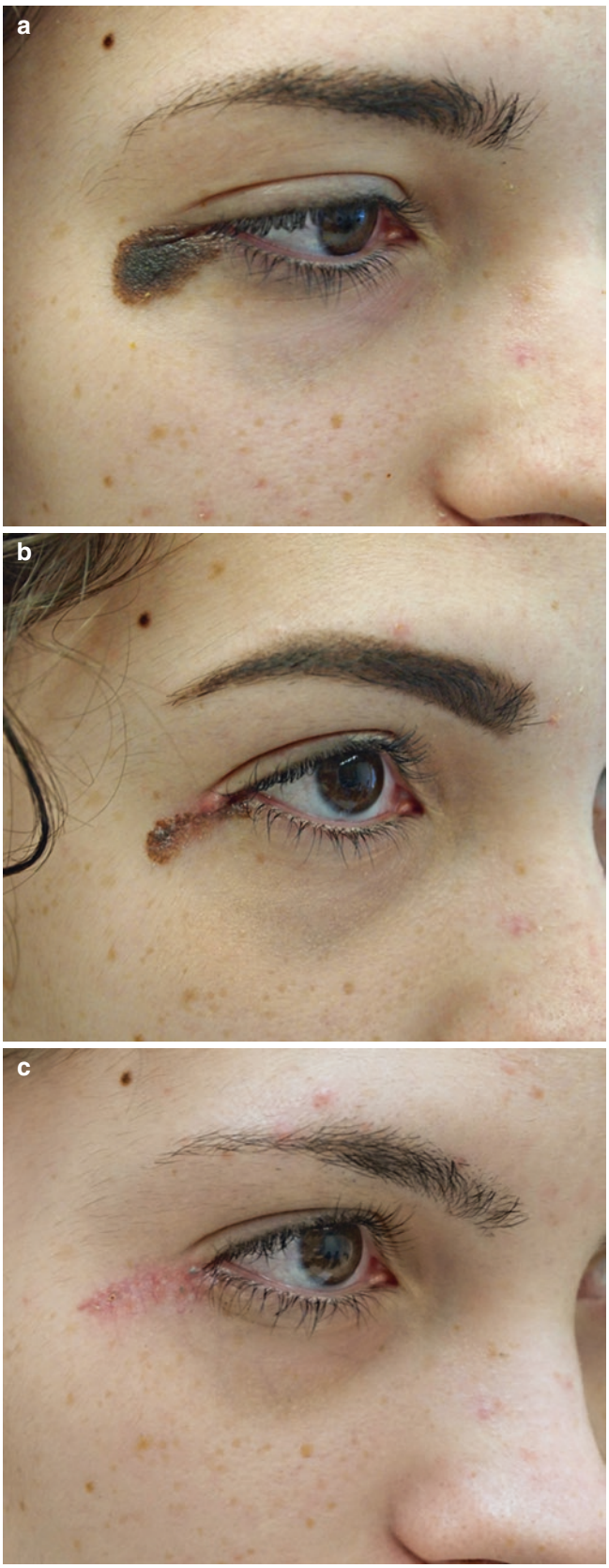


Fig. 7.19 (**a**–**c**) Serial excision of a lateral canthal nevus with the final scar following the natural skin expression lines

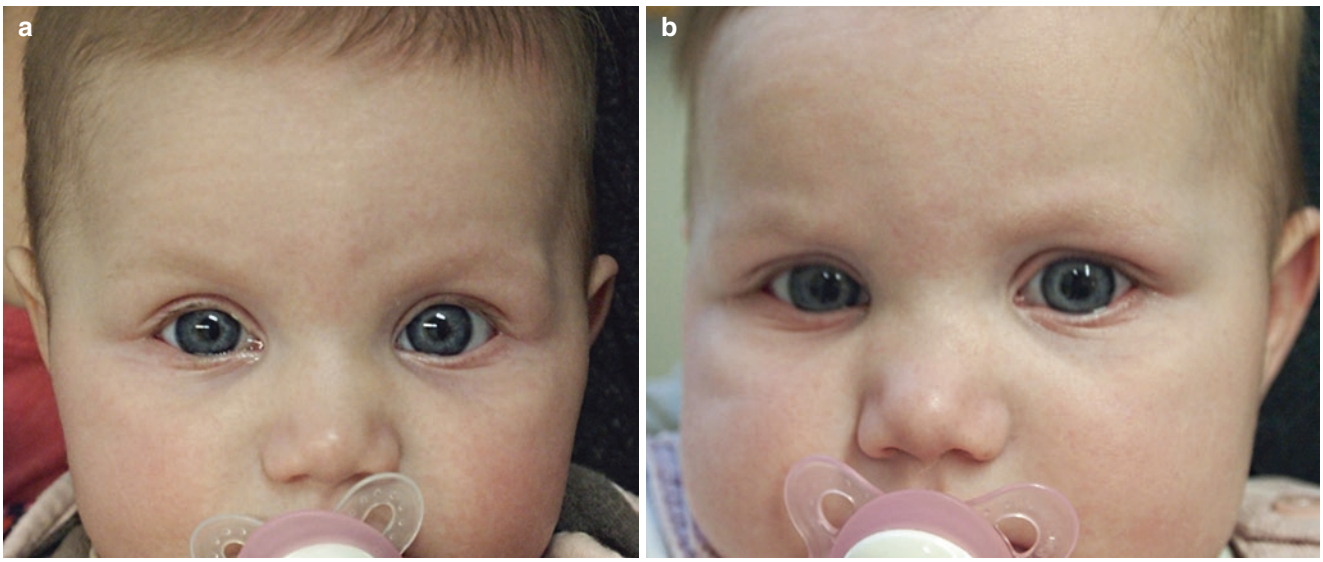


Fig. 7.20 (**a**) Typical left lateral brow dermoid cyst adherent to the periosteum of the orbital rim. (**b**) A supratarsal fold incision leaves an imperceptible scar and is favored over a brow incision

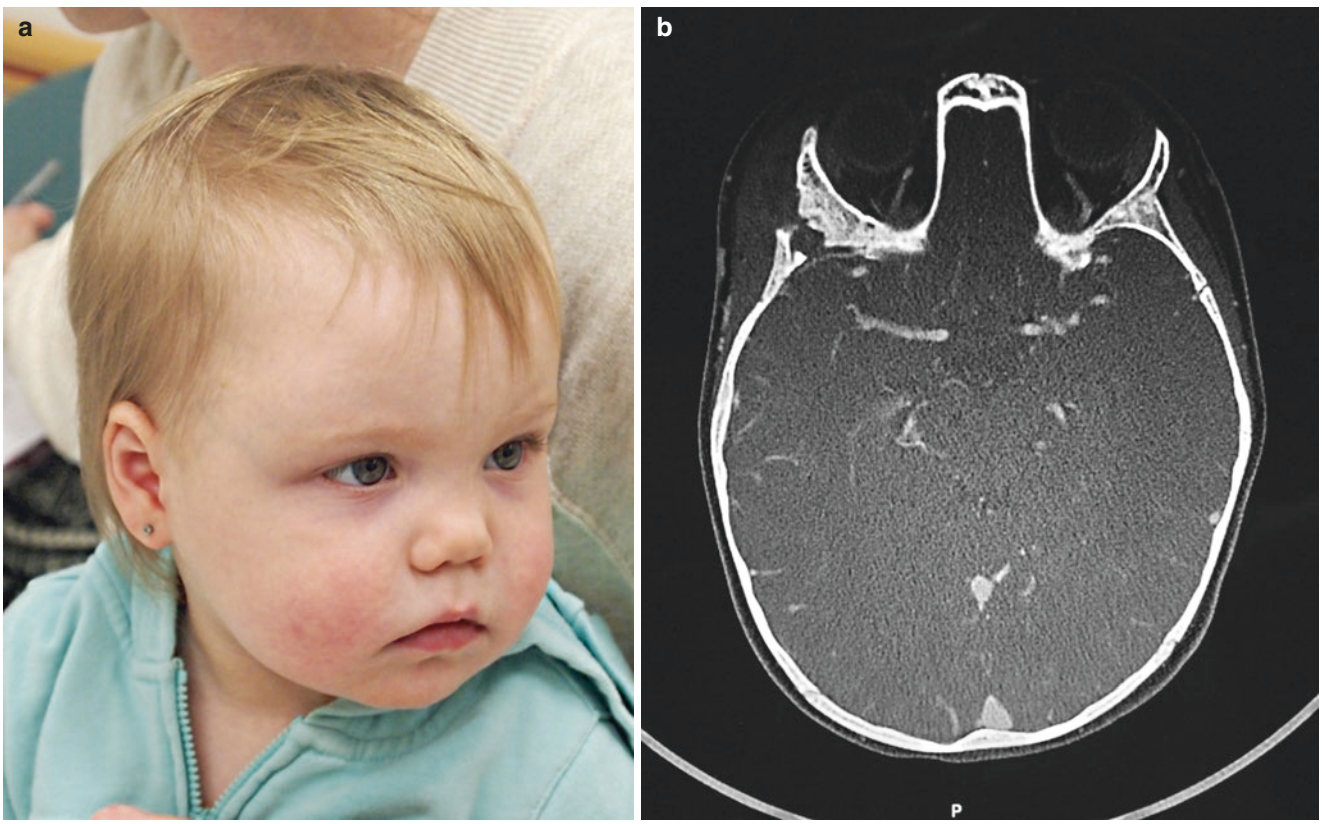


Fig. 7.21 (**a**, **b**) There was only mild soft tissue swelling associated with this infected right sphenoid cyst, but the CT scan demonstrated full-thickness penetration through the sphenoid bone to the dura. It was treated by complete excision

Reconstructive Strategies in the Periorbital Area

A discussion of the myriad techniques for complex eyelid reconstruction is beyond the scope of this chapter. The following section focuses on superficial soft tissue reconstruction, specifically methods for obtaining satisfactory skin and subcutaneous tissue coverage and eyelash and eyebrow reconstruction. The restoration of normal skin tone and texture is not always an attainable goal, and patients must be carefully counseled to formulate realistic expectations and avoid disappointment. The restoration of hair may be a critical part of the overall reconstructive process. Camouflage techniques such as cover makeup and micropigmentation (tattoo pigmentation) may further optimize the end result.

Skin Coverage

The oft-described reconstructive ladder begins with direct primary closure of a surgical wound, followed by the use of skin grafts or composite grafts, local flaps, distant pedicled flaps, and, finally, microvascular-free tissue transfer. In many cases, the more complex option will yield a superior functional and cosmetic result and should be chosen in favor of the simpler options.

Reconstruction following hemangioma or nevus excision is usually a matter of satisfactory skin closure and subcutaneous tissue contouring, without involvement of the deeper structures. However, in the area of the eyelid, nose, and lips, the surgeon may also have to deal with cartilage and muscle reconstruction if these have been previously distorted by the hemangioma. Attenuated and atrophic tissue may require full-thickness wedge excision with layered closure.

Small hemangiomas that leave protruding or pedunculated fibrofatty tissue and atrophic skin can usually be excised and closed primarily. Any residual patent vessels can be readily cauterized or laser coagulated at the time of excision. Bulky subcutaneous fat can be judiciously trimmed. An ellipse oriented along the natural skin expression lines will result in a straight-line scar, and parents should be advised that the scar will be longer than the diameter of the hemangioma.

Hemangiomas or nevi that are too large for complete excision may be candidates for serial excision, with at least 3 months between operations to allow the adjacent normal skin to soften and stretch. Many hemangiomas act like tissue expanders, and there is actually an excess of skin that must be tailored to improve symmetry. A surprisingly large amount of involved atrophic tissue may be removed in many patients without creating undue tension on the suture lines.

Another option is skin grafting after the scarred skin is removed, but the choice of donor site skin is critical. Grafts from the trunk or lower extremities have a high likelihood of resulting in a color mismatch. Parents must also understand that the skin graft may not have a completely normal or smooth texture, and there will be a scar around the border where it is sewn to the adjacent skin. The concept of grafting an entire aesthetic unit may decrease the prominence of these peripheral scars. Ideally, a full-thickness skin graft will have a better color and texture and be less likely to contract significantly when compared with a split-thickness skin graft (Fig. 7.22).

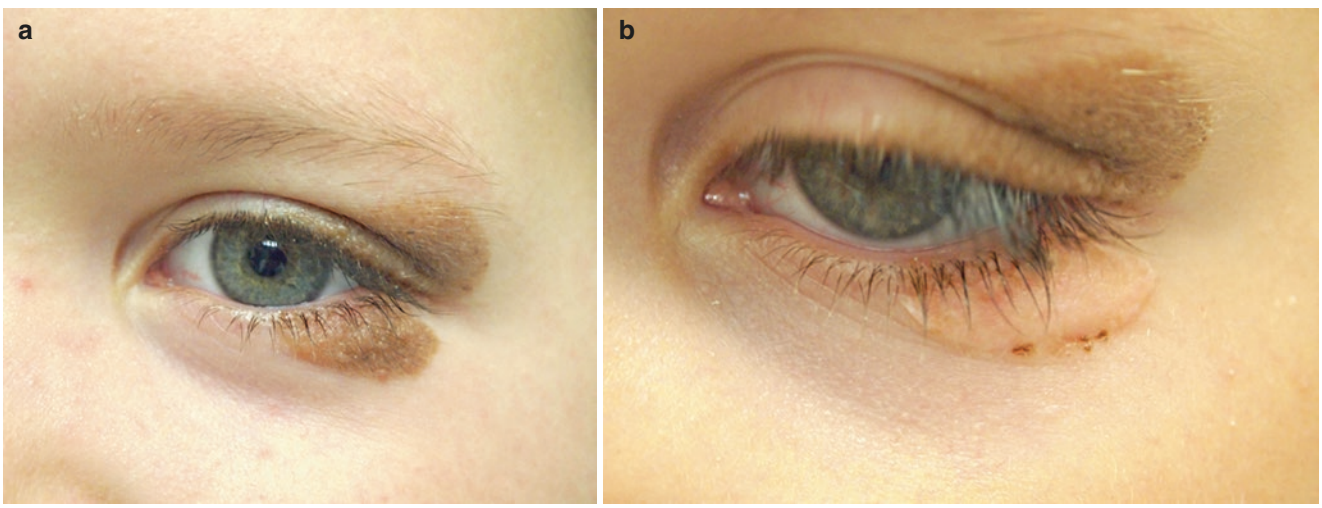


Fig. 7.22 (**a**, **b**) Nevus excision from the lower lid. The defect was reconstructed with a full-thickness skin graft to decrease the risk of graft contracture and ectropion

Traditionally, the postauricular region has provided the best source of full-thickness skin for grafting, since the donor site is well hidden and the color match is excellent. However, the amount of available skin may be limited, especially when a large aesthetic unit is to be covered.

Tissue expansion is most commonly used to generate additional skin adjacent to a large scar deformity [41]. Preoperative expansion may also precede excision of a large nevus to facilitate wound closure (Fig. 7.23). The forehead and cheek provide the best sources of expandable skin for periorbital skin coverage, but patients and parents must fully understand the morbidity of the expansion process. In addition to an operation for expander insertion, patients must tolerate weekly injections, the temporary discomfort of pressure and tight skin following each injection, and risks that include expander infection, erosion and extrusion, inadequate skin production, and the very significant contour distortion associated with expansion. An expanded forehead flap provides the options of simple advancement or rotation based on the supratrochlear vessels with facilitated donor site closure, which, in a child, would otherwise be technically quite difficult.

Other regional rotation flaps can be based on the superficial temporal vessels [42]. These include hair-bearing scalp and non-hair-bearing forehead skin for eyebrow and eyelid reconstruction, temporoparietal fascia flaps combined with skin grafts for the restoration of thin lining, pericranial flaps for restoring soft tissue bulk, and temporary scalping flaps, which provide soft tissue coverage over exposed bone in preparation for later skin grafting. The temporal muscle has been used to fill the orbit following enucleation for neoplasia or trauma.

Microvascular-free tissue transfer for stable soft tissue coverage is more commonly used in the setting of significant orbital trauma or neoplasm excision. It can bring healthy and pliable tissue to a heavily scarred or irradiated area. Potential flaps include the radial forearm, the thoracodorsal artery perforator (TAP flap), the transverse scapular and parascapular fasciocutaneous flaps, and, in thin patients, the anterolateral thigh flap, most commonly anastomosed to the superficial temporal or facial vessels. Muscle flaps and vascularized fascial flaps will readily support a skin graft, which is routinely placed after the microvascular flap has been inset. This is discussed in detail in another chapter.

Eyebrow and Eyelash Reconstruction

In addition to an obvious cosmetic function, the eyelashes and eyebrows provide a protective function in the process of vision by preventing foreign material from entering the eye. Congenital or acquired absence or distortion of these structures therefore has both aesthetic and functional implications. For most plastic and oculoplastic surgeons, the deformity is an acquired one, secondary to trauma such as burns or facial injuries. Periorbital hemangiomas can also obliterate or distort the eyelashes or eyebrows secondary to scarring of the dermis and subcutaneous tissues. Nevus or neoplasm excision may also remove hair-bearing skin in the brow region. In the case of a hairy nevus that includes the eyebrow region, a compromise option is to excise only part of the nevus, leaving the nevus that falls within the normal eyebrow contour. The patient must understand that the residual nevus still has malignant potential, but it is probably less than 1% over the patient's lifetime, similar to other nevi of comparable size. If any suspicious changes occur within the eyebrow region, the remaining nevus warrants excision at that time.

Eyelash and eyebrow loss can also be due to a variety of medical conditions, most conveniently divided into nonscarring, scarring, and miscellaneous causes [43]. Nonscarring causes, such as alopecia areata, alterations in the hair growth cycle, endocrinopathies, inflammatory dermatoses, and some systemic diseases such as lupus, may be reversible, in which case treatment should initially be conservative. Scarring causes, such as severe infections (leprosy, tertiary syphilis, lupus vulgaris, dissecting cellulitis, herpes simplex) or dermatoses (discoid lupus erythematosus, scleroderma), usually result in permanent hair loss. Probably the most common cause of eyebrow loss in adults is overplucking, a form of trichotillomania. Restoration of hair or the semblance of hair can dramatically improve the end result of a complex reconstruction, whether it be for congenital deformity, hemangioma scarring, burn scarring, or postexcisional or posttraumatic deformity.

Micropigmentation (Medical Tattooing)

Conservative forms of camouflage hair restoration include eyebrow pencil and eyeliner, mascara to thicken residual lashes, and adhesive application of artificial lashes or eyebrows. Patients who tire of the daily application of eyebrow pencil and eyeliner may be candidates for "permanent" pigment tattooing. While physicians may elect to apply tattoo pigmentation themselves, many have recruited professional tattoo artists who have the experience and skill to recreate eyebrows, apply eyeliner, camouflage scars, and restore lost pigment in patients with vitiligo (Figs. 7.24, 7.25, and 7.26).

Patients should be advised preoperatively that there may be significant lightening as pigment in the epidermis will be shed, leaving the underlying dermal pigment. Also, exposure to sunlight will potentially cause significant lightening of even the dermal pigment. "Permanent" may be a misleading description, since gradual fading may warrant periodic retreatment. However, patients should also be aware that it may be difficult to remove pigment if they are unhappy with the result. The available tattoo lasers may gradually remove the pigment, but there may also be some paradoxical darkening of the pigment as the iron oxide particles turn black.



Fig. 7.23 (**a**–**c**) This patient had a large congenital nevus of the forehead. Tissue expanders were used to generate additional normal skin which permitted excision of the majority of the nevus and closure with adjacent skin flap advancement



Fig. 7.24 (**a**, **b**) Micropigmentation (tattoo) for alopecia (Courtesy of Mandy Sauler, University of Pennsylvania)

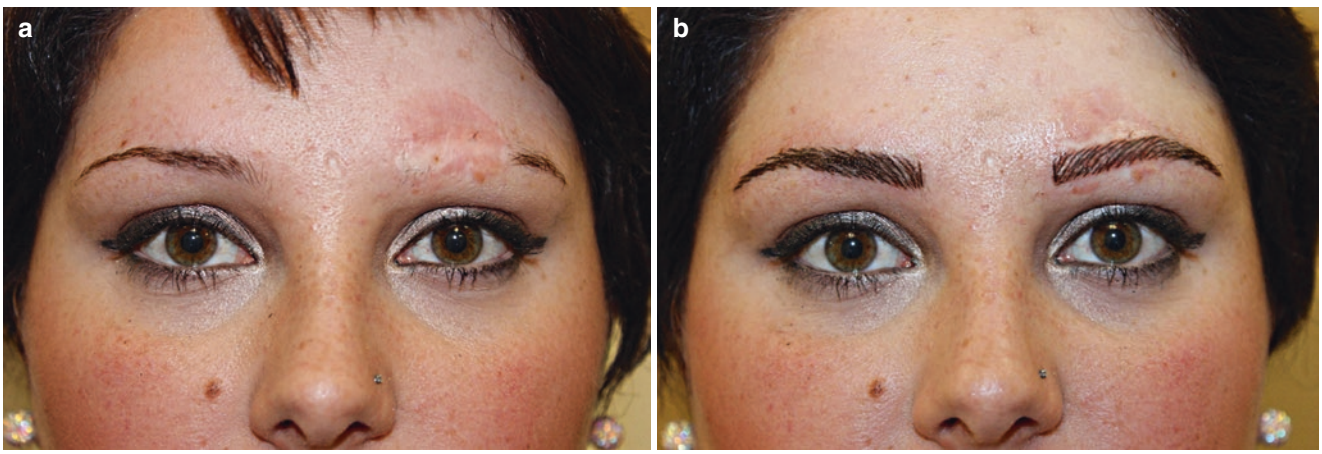


Fig. 7.25 (**a**, **b**) Micropigmentation (tattoo) for traumatic absence of the eyebrow (Courtesy of Mandy Sauler, University of Pennsylvania)

Hair Transplantation for Eyebrow and Eyelash Restoration

Successful transplantation of viable hair follicles is the basis of surgical hair replacement for male pattern baldness, but these techniques are also applicable to eyebrow, eyelash, and mustache reconstruction. The hair must be transplanted with a surrounding cuff of skin and an intact papilla (the hair follicle). Plucked hairs are not viable donor material. The surgeon must also be cognizant of hair color, texture, thickness, curl, and donor site, since these will also impact upon the final result.

Eyebrow and eyelash hair differ from scalp hair in growth rate and growth potential. Scalp hair grows much more quickly and will grow to a significantly longer length during its growth cycle. Transplanted hair will maintain its previous growth characteristics, a concept known as "donor dominance." This means that scalp hair transplanted to the eyelid or brow area will still grow like scalp hair, and patients must be advised that frequent trimming will be necessary to maintain an optimal appearance.

It is best to transplant hair that has limited growth potential, with the same density and length as the contralateral side. Proper direction is also important, to avoid corneal irritation by transplanted hairs and to mimic the natural tangential orientation of eyebrow hairs. The medial eyebrow hairs are directed superolaterally. The lateral eyebrow hairs tend to run inferolaterally. A darker ridge of overlapping hairs is created by the confluence of these clashing hairs.



Fig. 7.26 (**a**, **b**) Vitiligo can be camouflaged with matching skin pigments. Patients should be advised that sun exposure will create seasonal fluctuation in their normal pigment which may affect the color match with areas that have been tattooed (Courtesy of Mandy Sauler, University of Pennsylvania)

Composite grafting, using contralateral eyelid tissue to restore a lid margin, is a well-recognized oculoplastic technique. Usually, the cilia are lost, but in at least 14% of patients, hairs may survive the transplant [44]. This raises the possibility of using the contralateral eye for donor hair grafts, but the low rate of successful growth would seem to make this method prohibitively risky.

Brent [45] has successfully harvested a strip of eyebrow hair to create a lash line with "auto-limited" hair. Extreme care must be taken to incise parallel to the hair follicles to avoid destroying the roots. The composite graft is then sandwiched in a pocket created by filleting the border of the eyelid.

Hata and Matsuka [46] ingeniously transplanted nasal vibrissae to create eyelashes that had a superb length and color match to existing eyelash hairs. Transplanting single hairs is significantly more tedious despite recent innovations in instrumentation to simplify the process [47]. The eyelid is so thin that accurate placement of individual hairs in a well-organized row is much more difficult compared with a thinly sliced strip of hairs. The eyebrow, however, does well with micrografting, standard punch grafting, strip grafting, and, as described earlier, reconstruction with an island of hair-bearing scalp based on the superficial temporal vessels.

Micrografting usually involves harvesting a strip of scalp with hair of suitable color and texture. The natural angle of the hairs with respect to the skin is less important, since the strip will be sliced into individual grafts containing 1–3 hairs per graft. The hairs are then placed into slits or hypodermic needle puncture marks. Care is taken to insert the needles at a very tangential angle to the skin. The grafts will usually be stable because the fibrin naturally glues the grafts in place, but collodion or cyanoacrylate can be used to further stabilize the grafts. The main advantage of micrografting is the absence of obvious "cornrow" or "doll's head" hair distribution associated with punch grafts, the absence of peripheral scars around strip grafts, and the ability to feather the borders with a graded hair density. There is also the option of gradually thickening the reconstructed eyebrow with subsequent transplantation sessions (Fig. 7.27).

Alternatively, strips of scalp as wide as 4 mm and as long as necessary can be harvested and transplanted without dividing them into smaller grafts. Like standard 4-mm round punch grafts, the tissue first survives by diffusion of oxygen until the surrounding vessels connect or grow into the graft. Grafts wider than 4 mm may result in central hair loss due to ischemia. When constructing a thick eyebrow, two-strip grafts can be used, preserving a narrow strip of native brow skin between the two grafts to provide an adequate blood and oxygen supply. After several months, the non-hair-bearing strip can be excised, with or without additional grafting. With strip grafting, hair direction and angle of growth from the skin is important. Hair from the temples or occiput is more tangential than hair on the top of the head.

More recently, the NeoGraft™ Hair Restoration system has been promoted as having the ability to harvest individual hair follicle grafts from the back of the scalp with minimal trauma. A handheld device harvests and inserts individual hair follicles



Fig. 7.27 (**a**, **b**) A patient undergoing burn reconstruction had micrografting to his right eyebrow. More sessions are necessary to create optimal hair density. The hairs were harvested from his scalp and therefore require frequent trimming to maintain a suitable length

which are reportedly very consistent in quality, and it avoids the scalp scars associated with punch or strip harvesting.

With any type of hair transplantation, most hairs go into telogen for about 3 months, and patients must realize that the success of the operation cannot be determined prior to that time. Patients must also be aware of the possible need for multiple transplant sessions, particularly when micrografts or punch grafts are used. Lastly, it cannot be overemphasized that scalp donor hairs will still grow like scalp hair, obligating the patient to a lifetime of trimming. Patients may find micropigmentation (tattoo) to be far less demanding in terms of personal maintenance.

References

1. Wassef M, Blei F, Adams D, Alomari A, Baselga E, Berenstein A, Burrows P, Frieden IJ, Garzon MC, Lopez-Gutierrez JC, Lord DJE, Mitchel S, Powel J, Prendiville J, Vikkula M. Vascular anomalies classificiation: recommendations from the International Society for the Study of vascular anomalies. Pediatrics. 2015;136(1):1–12.
2. Burns AJ, Kaplan LC, Mulliken JB. Is there an association between hemangioma and syndromes with dysmorphic features? Pediatrics. 1991;88:1257–67.
3. Reese V, Frieden IJ, Paller AS, et al. Association of facial hemangiomas with Dandy–Walker and other posterior fossa malformations. J Pediatr. 1993;122:379–84.
4. Aspestrand F, Kolbenstvedt A. Vascular mass lesions and hypervascular tumors in the head and neck: characteristics at CT, MR imaging and angiography. Acta Radiol. 1995;36:136–41.
5. North PE, Waner M, Mizeracki A, Mihm MC. GLUT1: a newly discovered immunohistochemical marker for juvenile hemangiomas. Hum Pathol. 2000;31(1):11–22.
6. Bowers RE, Graham EA, Tomlinson KM. The natural history of the strawberry nevus. Arch Dermatol. 1960;82:667–80.
7. Thomson HG, Ward CM, Crawford JS, et al. Hemangiomas of the eyelid: visual complications and prophylactic concepts. Plast Reconstr Surg. 1979;63:641–7.
8. Zarem HA, Edgerton MT. Induced resolution of cavernous hemangiomas following prednisolone therapy. Plast Reconstr Surg. 1967;39:76–83.
9. Brown SH, Neerhout RC, Fonkalsrud EW. Prednisone therapy in the management of large hemangiomas in infants and children. Surgery. 1972;71:168–73.
10. Enjolras O, Riche MC, Merland JJ, et al. Management of alarming hemangiomas in infancy: a review of 25 cases. Pediatrics. 1990;85:491–8.
11. Sadan N, Wolach B. Treatment of hemangiomas of infants with high doses of prednisone. J Pediatr. 1996;128:141–6.
12. Mazzola RF. Treatment of haemangiomas in children by intralesional injections of steroids. Chir Plastica (Berl). 1978;4:161.
13. Kushner BJ. Intralesional corticosteroid injection for infantile adnexal hemangioma. Am J Ophthalmol. 1982;93:496–506.
14. Kushner BJ. The treatment of periorbital infantile hemangioma with intralesional corticosteroid. Plast Reconstr Surg. 1985;76:517–24.
15. Edgerton MT. Discussion of Kushner BJ: the treatment of periorbital infantile hemangioma with intralesional corticosteroid. Plast Reconstr Surg. 1985;76:525–6.
16. Sloan GM, Reinisch JF, Nichter LS, et al. Intralesional corticosteroid therapy for infantile hemangiomas. Plast Reconstr Surg. 1989;83:459–66.
17. Bilyk JR, Adamis AP, Mulliken JB. Treatment options for periorbital hemangioma of infancy. Int Ophthalmol Clin. 1992;32:95–109.
18. Ezekowitz RAB, Mulliken JB, Folkman J. Interferon alpha-2a therapy for life-threatening hemangiomas of infancy. N Engl J Med. 1992;326:1456–63.
19. Ricketts RR, Hatley RM, Corden BJ, et al. Interferon-alpha-2a for the treatment of complex hemangiomas of infancy and childhood. Ann Surg. 1994;219:605–14.
20. MacArthur CJ, Senders CW, Katz J. The use of interferon alpha-2a for life-threatening hemangiomas. Arch Otolayngol Head Neck Surg. 1995;121:690–3.

21. Leauté-Labréze C, Dumas de la Roque E, Hubiche T, Boralevi F. Propranolol for severe hemangiomas of infancy. NEJM. 2008;358:2649–51.
22. Spiteri Cornish K, Reddy AR. The use of propranolol in the management of periocular capillary haemangioma – a systemic review. Eye. 2011;25(10):1277–83.
23. Chambers CB, Katowitz WR, Katowtiz JA. A controlled study of topical 0.25% Timolol maleate gel in the treatment of cutaneous infantile capillary hemangioma. Ophthal Plast Reconstr Surg. 2012;28:103–6.
24. Hobby LW. Further evaluation of the potential of the argon laser in the treatment of strawberry hemangiomas. Plast Reconstr Surg. 1983;71:481–9.
25. Achauer BM, Vander Kam VM. Capillary hemangioma (strawberry mark) of infancy: comparison of argon and Nd:YAG laser treatment. Plast Reconstr Surg. 1989;84:60–70.
26. Achauer BM, Vander Kam VM. Strawberry hemangioma of infancy: early definitive treatment with an argon laser. Plast Reconstr Surg. 1991;88:486–9.
27. Garden JM, Bakus AD, Paller AS. Treatment of cutaneous hemangiomas by the flashlamp-pumped dye laser: prospective analysis. J Pediatr. 1992;120:555–60.
28. Landthaler M, Hohenleutner U, El-Raheem TA. Laser therapy of childhood haemangiomas. Br J Dermatol. 1995;133:275–81.
29. Geronemus RG, Kauver AN. The pulsed-dye laser for infantile hemangiomas. Plast Reconstr Surg. 1996;97:1302–3.
30. Tan OT, Sherwood K, Gilchrest BA. Treatment of children with port-wine stains using the flashlamp-pulsed tunable dye laser. N Engl J Med. 1989;320:416–21.
31. Patrice SJ, Wiss K, Mulliken JB. Pyogenic granuloma (lobular capillary hemangioma): a clinicopathologic study of 178 cases. Pediatr Dermatol. 1991;8:267–76.
32. Enjolras O, Riche MC, Merland JJ. Facial port-wine stains and Sturge–Weber syndrome. Pediatrics. 1985;76:48–51.
33. Zhang J, Li HB, Zhou SY, Chen KS, Niu CQ, Tan XY, Jiang YZ, Lin QQ. Comparison between absolute ethanol and bleomycin for the treatment of venous malformation in children. Exp Ther Med. 2013;16(2):305–9.
34. Missori P, Tarantino R, Delfini R, et al. Surgical management of orbital cavernous angiomas: prognosis for visual function after removal. Neurosurgery. 1994;35:34–8.
35. Bauer BS, Kernahan DA, Hugo NE. Lymphangioma circumscriptum: a clinicopathologic review. Ann Plast Surg. 1981;7:318–26.
36. Padwa BL, Hayward PG, Ferraro NF, Mulliken JB. Cervicofacial lymphatic malformation: clinical course, surgical intervention, and pathogenesis of skeletal hypertrophy. Plast Reconstr Surg. 1995;95:951–60.
37. Sung MW, Chang SO, Choi JH, et al. Bleomycin sclerotherapy in patients with congenital lymphatic malformation in the head and neck. Am J Otolaryngol. 1995;16:236–41.
38. Mathur NN, Rana I, Bothra R, Dhawan R, Kathuria G, Pradhan T. Bleomycin sclerotherapy in congenital lymphatic and vascular malformations of head and neck. Int J Pedatr Otorhinolayngol. 2005;69(1):75–80.
39. Adams DM, Trenor CC, Hammill AM, Vinks AA, Patel MN, Chaudry G, Wentzel MS, Mobberley-Schuman PS, Campbell LM, Brookbank C, Gupta A, Chute C, Eile J, McKenna J, Merrow AC, Fei L, Hornung L, Seid M, Dasgupta AR, Dickie BH, Elluru RG, Lucky AW, Weiss B, Azizkhan RG. Efficacy and safety of sirolimus in the treatment of complicated vascular anomalies. Pediatrics. 2016;137(2):e20153257.
40. Bartlett SP, Lin KY, Grossman R. The surgical management of orbitofacial dermoids in the pediatric patient. Plast Reconstr Surg. 1993;91(7):1208–15.
41. Tse DT, McCafferty LR. Controlled tissue expansion in periocular reconstructive surgery. Ophthalmology. 1993;100:260–8.
42. Matsuba HM, Hakki AR, Romm S, et al. Variations on the temporoparietal fascial flap. Laryngoscope. 1990;100:1236–40.
43. Draelos ZK, Yeatts RP. Eyebrow loss, eyelash loss, and dermatochalasis. Dermatol Clin. 1992;10:793–8.
44. Werner MS, Olson JJ, Putterman AM. Composite grafting for eyelid reconstruction. Am J Ophthalmol. 1993;116:11–6.
45. Brent B. Reconstruction of the eyebrow and eyelashes with free grafts. In: Brent B, editor. The artistry of reconstructive surgery. St. Louis: Mosby; 1987. p. 199–202.
46. Hata Y, Matsuka K. Eyelash reconstruction by means of strip skin grafting with vibrissae. Br J Plast Surg. 1992;45:163–4.
47. Choi YC, Kim JC. Single hair transplantation using the Choi hair transplanter. J Dermatol Surg Oncol. 1992;18:945–8.

8 Advanced Plastic Surgical Techniques: Facial Prosthetic Considerations, Periorbital Free Flaps, Reanimation, and Corneal Sensory Restoration

Oksana A. Jackson, David W. Low, Phuong D. Nguyen, and Kenneth Kent

Successful periorbital reconstruction in the pediatric population presents many challenges. Periorbital defects can be secondary to trauma, neoplasm, radiation therapy, and autoimmune disease or be associated with a variety of congenital or developmental anomalies. Reconstruction may involve replacement of all periorbital tissues, including bone and soft tissue, removal of the globe itself, placement of craniofacial implants, or contouring of the periorbital area in cases of relative deficiency. Often an ocular or orbital prosthesis is an integral component of the reconstructive rehabilitation (Fig. 8.1).

Although similar principles apply for defects in both children and adults, reconstruction in children is further compounded by expected growth and the need to achieve lasting symmetry. Free microvascular tissue transfer to the periorbital area can satisfy a diverse range of reconstructive needs and is necessary for stable reconstruction of most larger and complex defects. In this chapter we draw on pediatric as well as adult examples to emphasize common principles of reconstruction and rehabilitation.

O.A. Jackson (✉) • D.W. Low
Division of Plastic Surgery, Perelman School of Medicine at the University of Pennsylvania, The Children's Hospital of Philadelphia, Philadelphia, PA, USA
e-mail: jacksono@email.chop.edu

P.D. Nguyen
Division of Plastic and Reconstructive Surgery, Children's Hospital of Philadelphia, Perelman School of Medicine at University of Pennsylvania, Philadelphia, PA, USA

K. Kent
Restorative Dentistry, Removable Prosthodontics, Preventive and Restorative Sciences, University of Pennsylvania School of Dental Medicine, Philadelphia, PA, USA

Reconstructive Considerations

The optimal management of periorbital defects is best accomplished through a team approach with collaboration between the pediatric ophthalmologist, the reconstructive surgeon, the prosthodontist/prosthetist, and the patient. Appropriate planning needs to consider the following: (1) the magnitude of the defect, (2) the quality of the adjacent hard and soft tissues, (3) other tissues and materials available for reconstruction and restoration, (4) mechanisms available for achieving stability and retention for anticipated prostheses, (5) functional and aesthetic requirements, (6) emerging technologies to retain a prosthesis and restore movement and vision where possible, (7) the patient's ability to tolerate the procedures and (8) patient and family expectations. With appropriate planning and collaboration, optimal results can be achieved and enable rehabilitated patients to lead normal lives without significant psychosocial stigma.

After comprehensive evaluation and assessment, the decision must be made to provide exclusively surgical repair, prosthetic rehabilitation, or a combination of the two modalities. Prosthetic options include ocular, orbital, and facial prostheses. The selection of treatment modalities is determined by the characteristics of the defect and the available reconstructive options and is influenced by patient age, comorbidities, and patient preference. Notable facial differences and, in particular, absence of the ocular globe can be difficult to conceal and lead to significant psychosocial distress, especially in children. Every effort should be made to optimize the aesthetics of the reconstruction, minimize visible facial scarring, and utilize an ocular prosthesis whenever possible in this population age group.

Surgical restoration of the bony and soft tissue components of the defect with autogenous tissue is always preferred as successful surgical repair can provide a stable, long-lasting reconstruction and can eliminate the inconveniences

© Springer International Publishing AG 2018

J.A. Katowitz, W.R. Katowitz (eds.), *Pediatric Oculoplastic Surgery*, https://doi.org/10.1007/978-3-319-60814-3_8



Fig. 8.1 (**a**) Well-healed orbital exenteration defect lined with a split-thickness skin graft. (**b**) Orbital prosthesis fabricated with a custom methyl methacrylate ocular component integrated into a silicone orbital prosthesis, which is retained with skin adhesives. (**c**) Excellent foundation for an orbital prosthesis provided by graft. (**d**) Unfortunately most orbital prostheses are static, while the remaining lids and globe retain significant function and movement. Use of tinted and magnified lenses (**e**, **f**) may help to provide optical illusion of symmetry and function for the static orbital prosthesis. Corrective lenses also provide protection, and mask margins, of the orbital prosthesis

associated with a facial prosthesis. Prostheses must be removed and cleaned on a daily basis. Often the supporting tissues must be left uncovered for 6–10 hours per day to allow adequate recovery. This interval is a time of compromise and embarrassment for many. Patients may have difficulty placing the prosthesis in the proper orientation or have difficulty tolerating the chemical irritation of adhesives. Static prostheses must be remade or revised as the patient grows. The average material life of a prosthetic rehabilitation prior to material degradation ranges from to 2 to 5 years.

Prosthetic rehabilitation does have advantages for certain patients. Patients with compromised medical status or inadequate donor tissues are poor candidates for surgical intervention. Patients who have had high-dose radiotherapy to the orbit are at increased risk for tissue compromise, notably osteoradionecrosis, restricted growth, or fibrosis. Some patients who have had periorbital neoplasms resected are advised to maintain an obvious surgical defect to allow adequate visualization and monitoring of the tumor bed. Other patients may prefer to avoid additional surgical interventions altogether. Additionally, children treated with tumoricidal doses of radiotherapy to immature growth centers may also exhibit developmental retardation with resultant deformities.

The magnitude of the facial defect, including size as well as type of tissue components missing, is the next important

consideration in reconstructive planning. Autologous tissue reconstruction requires an appreciation for the three-dimensional aspects of the orbital defect, and the prosthetic requirement will dictate the type of reconstruction needed [1]. A small soft tissue defect is often easier to repair, surgically or prosthetically, than a large facial defect involving multiple tissue components. For smaller defects, restoration of form and aesthetics more readily can be achieved with a well-made prosthesis or local flap repair. The casual observer may be unaware that the patient has had surgery and is using a facial prosthesis. However, unfortunately, it is still not possible to provide a prosthesis that can restore vision or undergo normal physiologic color change such as blushing or tanning.

The condition of the local tissues is another important consideration in planning periorbital reconstruction. Scarring and tissue damage from previous surgical procedures, traumatic injury, or radiation treatments can limit local flap options and necessitate free tissue transfer even for smaller defects. In addition, these same conditions can make free tissue transfer procedures more challenging, lengthy, and invasive due to lack of adequate donor vessels in close proximity to the defect. Under these adverse conditions, however, successful free tissue reconstruction can optimize outcomes by bringing well-vascularized, healthy tissues to the irradiated or scarred periorbital environment, allowing for improved healing and enabling stable prosthetic restoration when jointly planned.

Prosthetic Considerations

When the globe is absent and the child is capable of utilizing an ocular prosthesis, the goal of reconstruction should focus on creating an adequate socket to accept an ocular prosthesis. Preservation of functional eyelids and mobile orbital contents facilitates the use of an ocular prosthesis that can provide normal iris and scleral appearance and the illusion of relatively normal ocular motion.

When possible, it is best to use local tissues for eyelid and periorbital reconstruction because of their similar tissue texture and color match. When the lids are preserved, the size of the ocular prosthesis is limited by the ocular aperture. If a larger prosthesis is required to supplement soft and hard tissue deficiencies, most patients find an orbital prosthesis preferable to an excessively large ocular prosthesis. A very large ocular prosthesis may be difficult or impossible to insert between the lids. In this situation, the best option is to surgically augment the defect to allow fabrication of a reasonable size ocular prosthesis. Often local tissues are not available, or the complexity of periorbital defect and the requirements for appropriate prosthetic use exceed the limits of regional flaps, and free tissue transfer is needed.

A larger defect extending beyond the confines of the orbit is more difficult to restore. Patients who have had a full orbital exenteration often must rely on a facial prosthesis for the most aesthetic restoration. Basic requirements must be met for prosthetic success, which foremost include adequate space for placement of the prosthesis. Placement of a prosthesis on a bulky flap that projects beyond the confines of normal facial contours will attract attention and is less satisfactory than no restoration (Fig. 8.2).

A slightly retruded prosthesis is less noticeable than one that is prominent. Magnification in corrective lenses worn over an orbital prosthesis can help to mask an over- or undercontoured prosthesis (Fig. 8.3).

It is difficult to achieve acceptable aesthetics and prosthesis durability with an orbital prosthesis less than 1 cm in thickness because a thin prosthesis is likely to tear during application, removal, or cleaning.

The quality of the supporting and marginal tissues is critical to prosthetic success. As with any prosthesis, a stable and immobile base is preferred. With newer, flexible silicone materials, some movement of marginal tissues can be tolerated. It is, however, very difficult to make a prosthesis that can move with adjacent tissues. If function or facial expression causes movement of the tissues adjacent to or underneath the prosthesis, it will become dislodged or displaced. Initially this is evidenced by the margins of the prosthesis breaking away from the supporting tissue. Surgical undermining of soft tissues along the margin of the defect and placement of split-thickness skin grafts at the margin will provide an immobile base and improve the integrity of the prosthetic rehabilitation. Prosthetic rehabilitation with split-thickness skin grafts can be successful long term but can be subject to breakdown from previous radiation for tumor management (Fig. 8.4).



Fig. 8.2 Patient with rectus myocutaneous flap reconstruction for orbitomaxillary defect

Communications between the orbital defect and the upper aerodigestive tract should be eliminated if possible. Without bony separation of the potential air spaces, the flap will vibrate or substantially move, causing displacement of the prosthesis. Air pressure from respiration can cause movement of the flap or the prosthesis. Additionally, respiratory moisture can cause failure of the adhesive used to retain the prosthesis. If the patient has nasal reflux through the defect, the retention and hygiene maintenance of the prosthesis can be further compromised. It may be necessary to add a secondary prosthesis such as a superiorly based obturator to provide separation of the defect

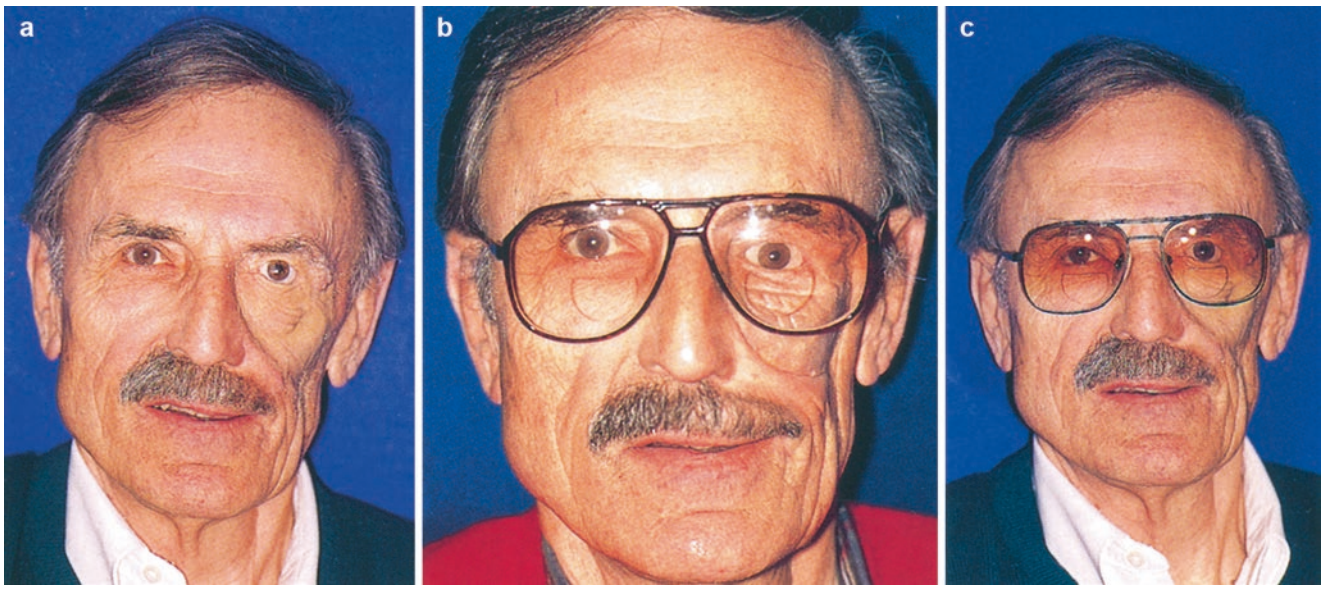


Fig. 8.3 Use of corrective lenses to mask facial asymmetry. (**a**) Following a radical maxillectomy in continuity with an orbital exenteration and postoperative radiation therapy, a significant surgical removal of skeletal support and muscle atrophy has resulted in depression of the right side of the face. A facial prosthesis was to match the depressed facial contours. (**b**) Corrective lenses with additional magnification of the lens over the prosthesis provide a more desirable aesthetic result. (**c**) Corrective lenses with tinting of the superior half of both lenses can further mask margins and improve appearance

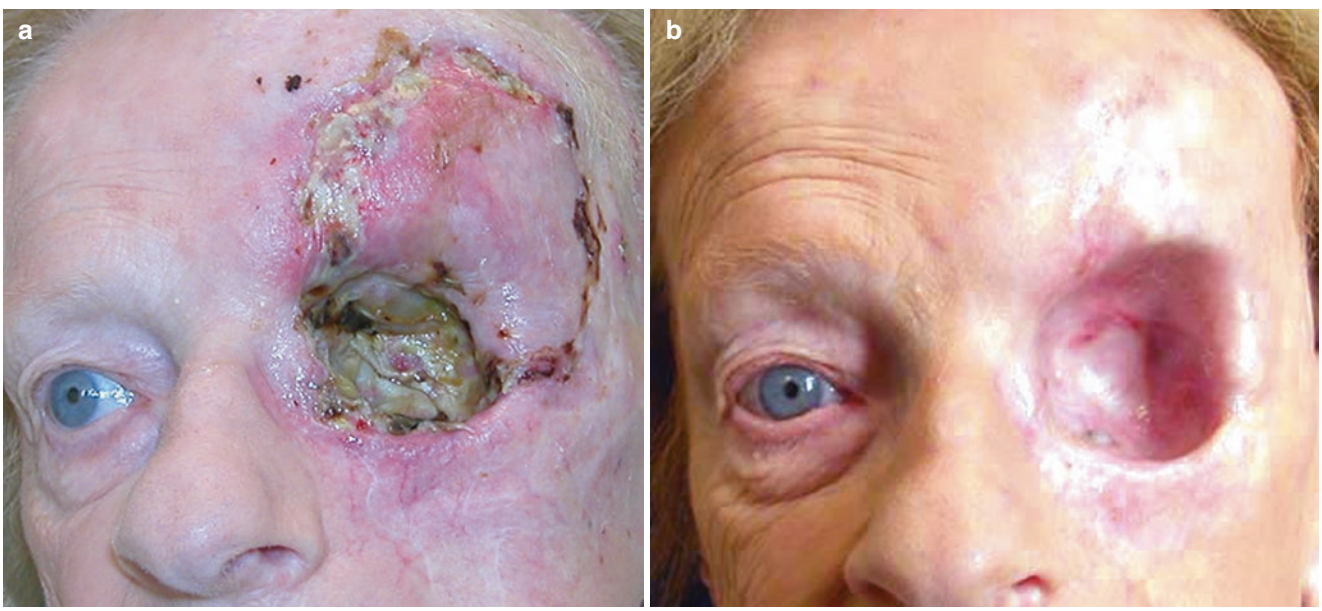


Fig. 8.4 (**a**) Split-thickness skin graft used to line an orbital defect after 1 week of healing. (**b**) Fully healed split-thickness skin graft used to line an orbital defect providing excellent quality keratinized immobile tissue to support an orbital prosthesis. (**c**) An orbital prosthesis blended in to surrounding tissues of the split-thickness skin graft. (**d**) The same defect, more than 5 years after prosthetic rehabilitation, developed an osteoradionecrosis which responded well to hyperbaric oxygen therapy and limited debridement, while the patient was able to continue with the same orbital prosthesis

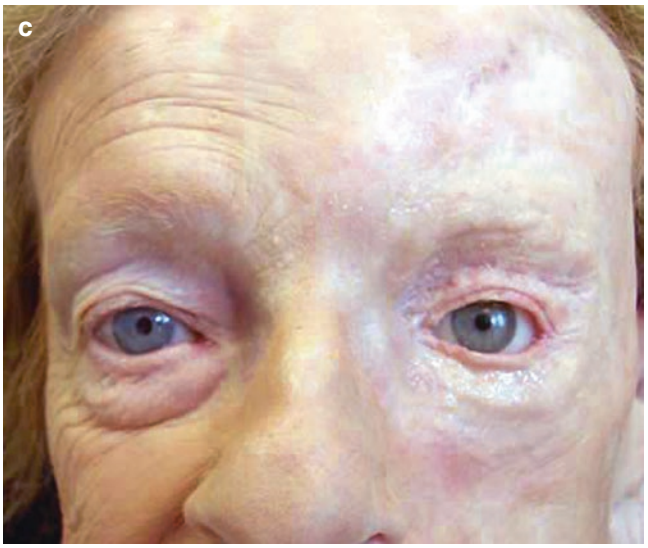




Fig. 8.4 (contiuned)

from the airway and minimize movement secondary to speech or respiration.

Orbital Prostheses

If the goal is to utilize an orbital prosthesis, then the reconstructive efforts should be focused on developing adequate hard and soft tissue support and retentive capability for the prosthesis. Considerations should include preservation of a bony socket with good bone stock for potential osseointegration. Soft tissue coverage of the prosthetic bearing area should be keratinized epithelium. A split-thickness skin graft lining the defect provides an excellent base for an orbital prosthesis. If an osseointegrated implant retention is to be used for the prosthesis, the underlying skin or mucosal bed should be contoured to provide a total maximum thickness of 2–3 mm. If conventional prosthetic adhesives instead of craniofacial implants are to be used for retention, the soft tissue must be thick enough to block out substantial soft tissue and bony undercuts and to withstand the load of the prosthesis and tension associated with removal of the adhesive retained prosthesis. Limited undercuts can aid in the mechanical retention of a prosthesis. Excessive undercuts often lead to trauma of the marginal tissues as the prosthesis is inserted and removed.

If a prosthetic rehabilitation of the orbit is to be retained with osseointegrated craniofacial implants, adequate bone stock and a very thin soft tissue envelope are most helpful. This may require bony osteotomies, if one is adding bone, and, if necessary, a debulking procedure or skin graft in the future. If the goal is to avoid prosthetic rehabilitation, the reconstructive plan should focus on obliterating the cavity with a well-vascularized, bulky flap providing good soft tissue fill (Fig. 8.5). If the patient's lids are resected, it is difficult to place and contour a soft tissue flap that will recreate

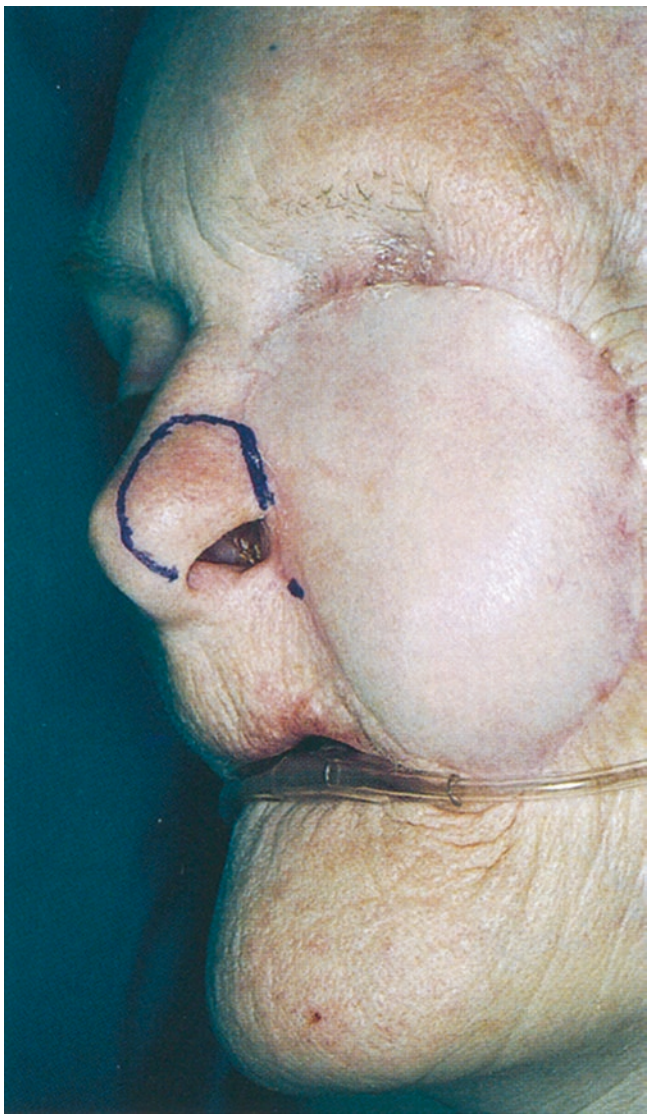


Fig. 8.5 Latissimus dorsi flap for orbitomaxillary reconstruction

natural appearing eyelids to retain an ocular prosthesis. When the lids have been excised, a better cosmetic result is usually achieved with an orbital prosthesis.

Ocular Prostheses

Many enucleations leave a patient with adequate soft tissues and orbital bone requiring only ocular prosthetic intervention. A custom ocular prosthesis can be fabricated to fill the enucleation defect with an excellent cosmetic result (see Chap. 41). Historically, ocular prostheses were fabricated of individually blown glass. Currently, most ocular prostheses are fabricated of methyl methacrylate polymers that are cast to fit a mold of the defect. Each prosthesis is hand colored to match the remaining eye. Methyl methacrylate ocular prostheses can also be shaped to provide support for a drooping upper eyelid (Fig. 8.6).

A well-adapted ocular prosthetic shell placed in an ocular socket overlying functional extraocular muscles can appear to track movement in concert with the remaining eye. This movement may be enhanced by integrating the prosthetic shell with a post connected to a porous ocular implant within the muscle cone, but this is usually reserved for the adult population. Any patient who has had an orbital enucleation or exenteration should be encouraged to wear protective lenses to minimize risk of injury or loss of the remaining, functional eye. The eyeglass lens for the defect side can be tinted, clouded, or opaqued to help mask the residual deformity. The lens may also be made to match any corrections required to improve normal vision in the remaining eye. Cosmesis is improved when both corrective lenses are balanced to match. The corrective lens, however, can include magnification to mask postsurgical depression of the defect or postradiation atrophy of the periorbital structures (Figs. 8.1 and 8.3).

Attempts at reconstruction of the eyelids and socket are not always successful, however. Fabrication of an ocular prosthesis may provide less desirable results than surgical preparation of a defect suitable for an orbital prosthesis (Fig. 8.7).

Orbital prosthetic replacements should not be attached to or retained with eyeglasses. Patients do not want to remove their facial prostheses every time they have to clean or remove their eyeglasses. As eyewear slips during normal activities, it is very embarrassing to have the prosthesis become dislodged. Adhesive or implant retention eliminates the need to retain a prosthesis by attaching it to eyeglasses.

Socket expansion is sometimes necessary to provide an adequate space for an ocular prosthesis. Expansion has long been used as a treatment in patients with periorbital defects. For young patients, custom methyl methacrylate conformers of increasing size can be placed as the child grows. This will help to preserve the contours of the ocular defect to retain a prosthesis. Use of ocular conformers of increasing size can also aid in stimulating normal growth of the periorbital bone and soft tissues and minimize the need for surgical expansion of the periorbital area. On occasion, however, multiple osteotomies with the use of either free bone grafts or vascularized free flaps are necessary [2, 3] (see Chap. 39). Numerous free flaps have been advocated to restore or replace destroyed periorbital tissues and are described in more detail within this chapter [4–19].

The most severe deformity usually exists in patients who have undergone enucleation at an early age, followed by radiation therapy for retinoblastoma or other malignant orbital tumors (Fig. 8.8).

These patients often have considerable contraction of the socket and hypoplasia of the orbital bone and periorbital soft tissues. For these patients, the conventional skin graft or mucosal graft is not effective because of the poor vascularity

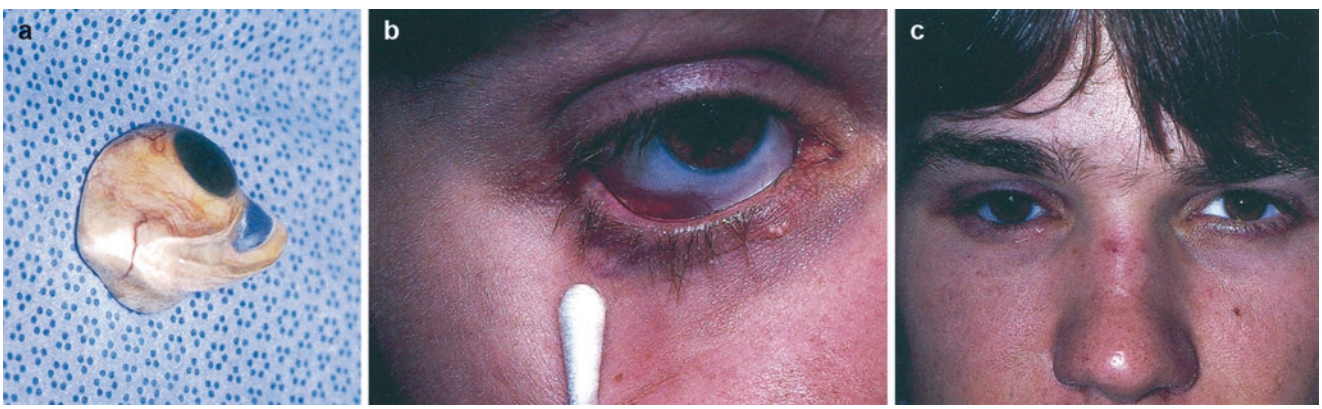


Fig. 8.6 Ocular prosthetics. A custom methyl methacrylate ocular prosthesis provides nonsurgical restoration of enucleation defects. (**a**) The prosthesis can be modified to provide support for a ptotic eyelid. The acrylic can be contoured with flanges or shelves to provide improved positioning of the lids. (**b**) A shelf provides support for the lower lid. (**c**) An acceptable aesthetic result achieved with a modified ocular prosthesis, but over the long-term surgical repair of the ptotic lid may be preferable

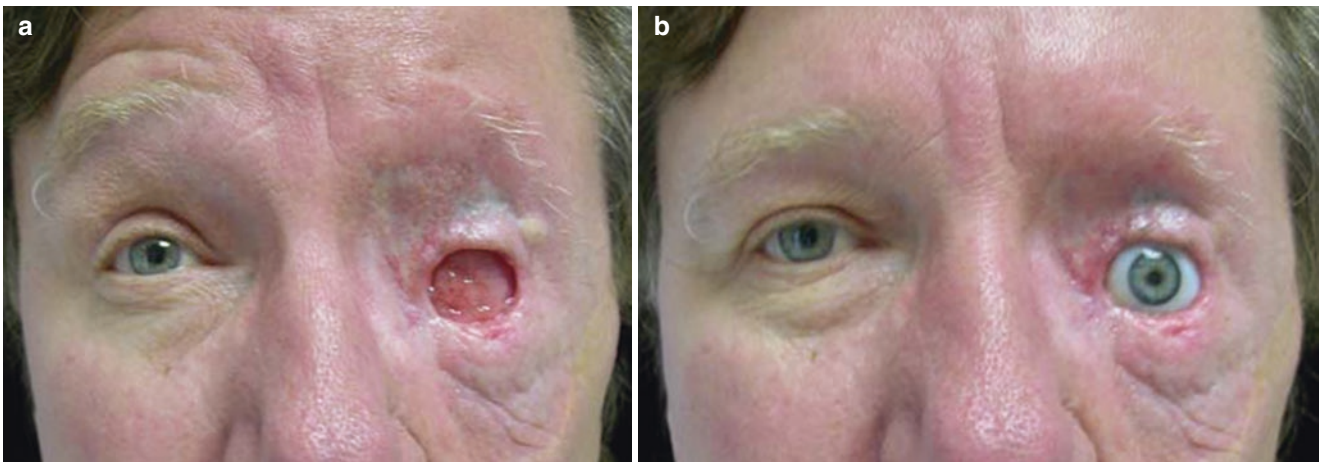


Fig. 8.7 (**a**) Severe trauma from a motorcycle accident resulting in orbital fractures with loss of the left globe and eyelid structures. (**b**) Post additional reconstruction with an ocular prosthetic. An orbital prosthesis may have provided a much better aesthetic result minimizing the number of surgical procedures to reach this endpoint



Fig. 8.8 Bilateral enucleations followed by radiation for retinoblastomas. Radiation therapy to the orbit at an early age produced severe deformities of the orbits

of the region. Furthermore, the depression is too severe to fill in with local skin flaps alone. Free soft tissue transfer will improve the vascular supply to this region and avoid postoperative contracture. When prosthetic rehabilitation is anticipated, an immobile base of tissue must be prepared that is suitable to withstand skin adhesives or allow placement of osseointegrated implants.

Osseointegrated craniofacial implants closely resemble those used intraorally to support dental restorations [20]. The implant fixtures are fabricated of medical-grade titanium and usually have a threaded, screw-type design. There are two major differences between intraoral and craniofacial implants. Craniofacial implants are short, usually 3–5 mm in length. They also have a flange about the top of the fixture to limit the depth of implant placement and maximize contact of the fixture to the bone surface (Fig. 8.9).

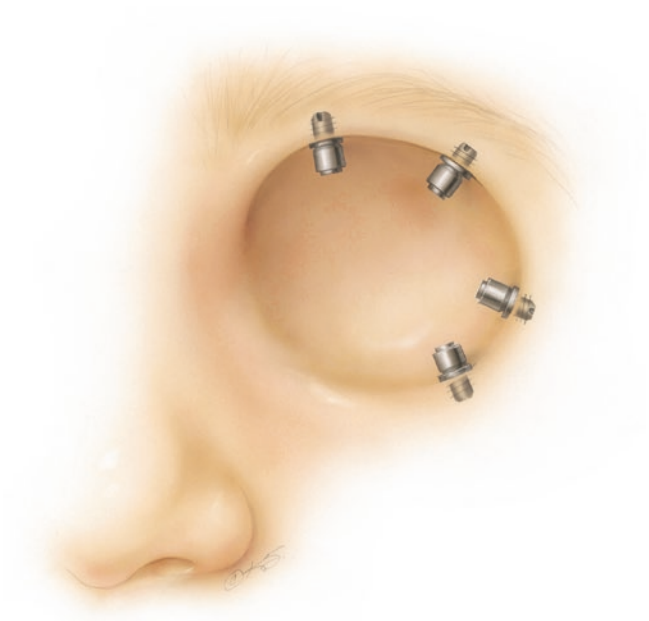


Fig. 8.9 Titanium craniofacial implant placed with flange countersunk in cortical bone to resist displacement

Each implant is placed in a receptor hole that has been drilled and tapped at very low speeds with copious irrigation to minimize heating and injury of the bone. Fixtures are not loaded and are usually kept submerged below the epithelium for 4–6 months to allow maximal healing of the surrounding bone against the implant.

After an appropriate healing period, the implant fixtures are exposed, and abutment connections are placed (Fig. 8.10). A cast gold alloy or titanium suprastructure is fabricated to connect the fixtures and incorporate magnets, snaps, or clips for retention of the prosthesis (Fig. 8.11). The

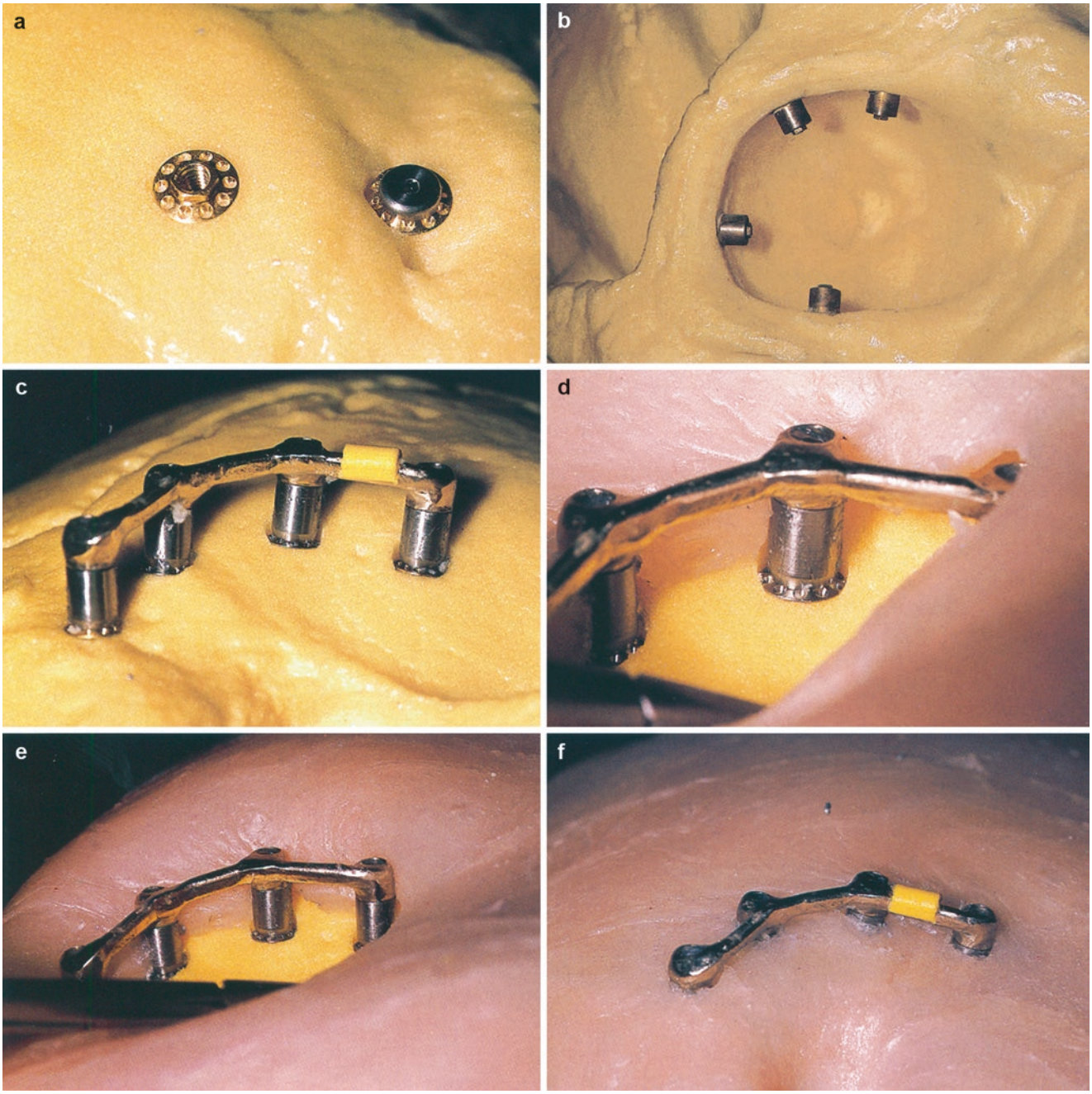


Fig. 8.10 Craniofacial implants used to anchor facial prosthesis. (**a**) Craniofacial implant placed in bone with flange flush or countersunk in cortical bone. The fixture on the right demonstrates a sealing screw, which is left in place for the first 4–6 months, while the implant is buried to allow osseointegration. The sealing screw prevents bone growth into the internal threads visualized on the left. (**b**) Implants should be strategically placed in the residual bone of the orbital rim. Specific site selection should be performed preoperatively by the surgeon and maxillofacial prosthodondist. (**c**–**e**) Implant abutments have been attached to the implants to serve as transmucosal connectors of the implants to the implant bar (shown with one retentive clip in place). The abutment height should be selected to allow the top of the abutment to be immediately above the level of the epithelium. (**f**) The final implant bar should be above the level of the epithelium to allow proper hygiene and home care (shown with one retentive clip in place)

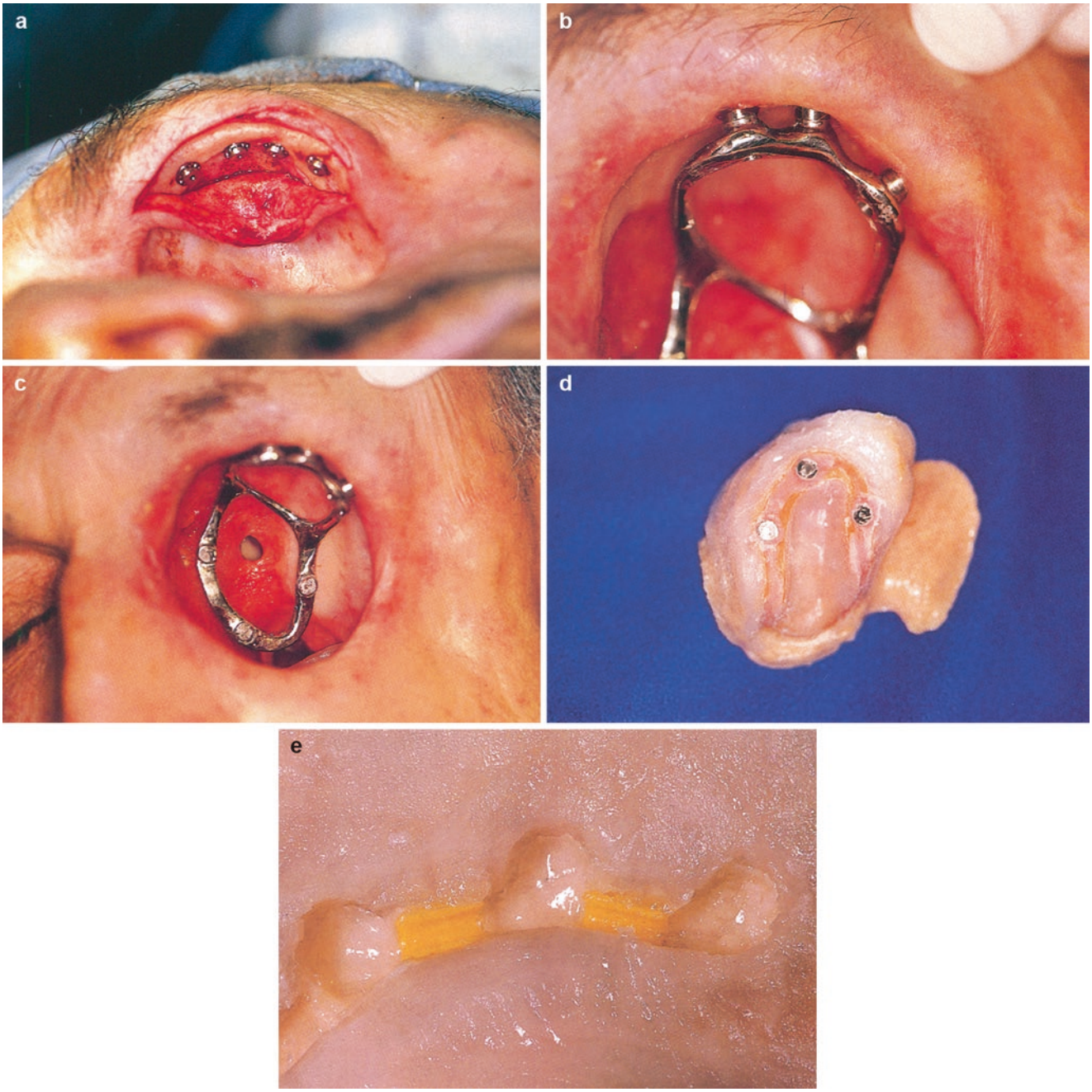


Fig. 8.11 Craniofacial implants placed within the orbital rim anchor a cast metal bar with magnetic keepers or configuration for retaining clips or snaps. The magnets, clips, or snaps are incorporated into the facial prosthesis to provide positive retention and eliminate the need for adhesives to retain the prosthesis. (**a**) Titanium craniofacial implants can be positioned in available bone of the superior and lateral orbital rim. (**b**) Transcutaneous connectors join the craniofacial implants to a cast metal suprastructure. (**c**) Three magnetic keepers are incorporated into the cast metal implant suprastructure. (**d**) Magnets are incorporated into the tissue surface of the facial prosthesis to provide a positive seat and retention. (**e**) A bar with retentive clips can be used instead of magnets. Retentive clips are demonstrated in the facial prosthesis

patient must maintain meticulous daily hygiene about the transcutaneous implant connections to prevent tissue irritation and inflammation.

The orbital prosthesis is fabricated using a combination of methyl methacrylate and silicone polymers. An impression of the defect, implant suprastructure, and surrounding tissues is made and used to fabricate a reinforced gypsum cast. A prefabricated or custom-made ocular prosthesis is incorporated into a wax or clay sculpture defining the contours, extent, and texture of the final prosthesis. The prosthesis is fabricated using a "lost-wax" casting technique. Natural color is accomplished using intrinsic and extrinsic stains to complement the natural surrounding tissues.

Reconstructive Options

Prior to the advent of microsurgical techniques, a variety of regional flaps were used for periorbital reconstruction [4]. These included pedicled flaps such as the sternomastoid platysma flap, the deltopectoral flap, the temporalis flap, and pedicled vascularized cranial bone flaps (Fig. 8.12). These flaps are still useful today, but are often affected by a hostile environment such as in radiation injury or the composite tissue requirement from a severe trauma or congenital absence. Microsurgical tissue transfer techniques can offer a variety of tissues for the appropriate replacement. Furthermore, microsurgical reconstruction can provide a number of composite flaps in a single operation without the need for staging. This chapter emphasizes both the use of microsurgery in reconstructing the periorbital region in children and the surgical preparation of the facial defect for a facial prosthesis.

Most studies reporting on free tissue reconstruction of periorbital defects involve adults; fewer have specifically addressed techniques and results in the pediatric population. Pediatric microsurgery in general, however, is now routinely performed at most large pediatric institutions. Several studies have reported successful outcomes, demonstrating that vessel size, even in young children, is sufficient for successful free tissue transfer [21–26] (Fig. 8.13).



Fig. 8.12 Orbital evisceration. (**a**) Young boy after orbital enucleation from a retinoblastoma. Orbital defect due to skin graft breakdown following irradiation. (**b**) Lateral view. (**c**) Temporalis muscle flap through zigzag coronal incision. (**d**) Note the use of the anterior half of the muscle to fill the orbital defect. The posterior temporalis is rotated anteriorly to fill the donor-site defect. (**e**) Muscle transposed into orbital defect can provide a vascular bed for a skin graft or even a dermis fat graft for additional volume

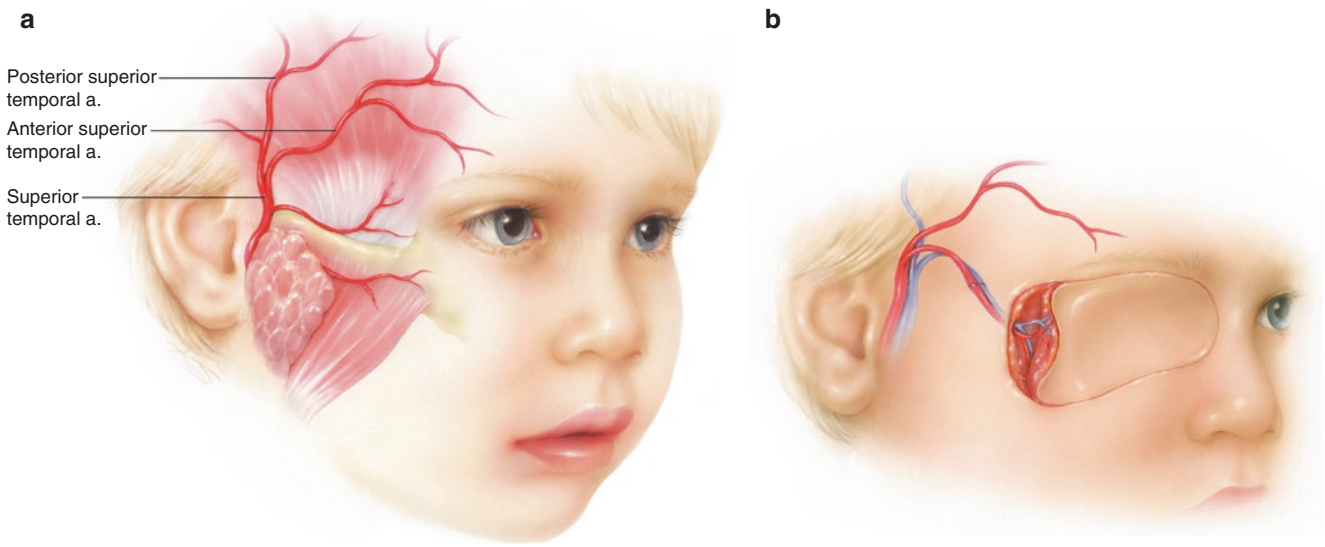


Fig. 8.13 Preauricular incision. (**a**) Illustration of recipient vessel which can be approached through a facelift or preauricular incision. (**b**) Placement of radial forearm flap into orbital defect with associated vessels demonstrated

Numerous free flaps have been advocated to restore or replace destroyed periorbital tissues [4–7, 10]. In the past, the more commonly used free flaps included the temporoparietal fascial flap, the radial forearm flap, the dorsalis pedis flap, the parascapular or scapular osteocutaneous flap, the latissimus dorsi flap, as well as the fibular osteocutaneous or osseous flap and the free iliac bone flaps [8, 9, 11–13]. The popularity of perforator flaps has increased the choice of thin fasciocutaneous flaps for orbital and periorbital soft tissue coverage and depending upon body habitus may include anterolateral thigh flaps and thoracodorsal artery perforator flaps [27–30]. Both of these flaps have long vascular pedicles and may include a portion of vastus lateralis or latissimus muscle if needed. When a large quantity of bone is needed, the free fibula is the best choice; other flaps that can provide adequate bone for periorbital reconstruction incorporate iliac crest bone, scapular bone, or radial bone with or without their soft tissue components.

The anastomoses for free transfer to the periorbital region are ideally performed to the superficial temporal vessels because of their close proximity (Fig. 8.14). For improved appearance, access to the vessels can be obtained through a facelift-type preauricular incision. A subcutaneous tunnel with anastomosis to the facial vessels is an alternative when the superficial temporal vessels are not available or are inadequate.

If the flap pedicle is too short to reach the facial vessels, or further targets are required, an arteriovenous loop is often necessary which involves sewing a saphenous vein graft from the target vessels to the flap vessels (Fig. 8.15). This is not infrequently the case when patients have undergone radiation or multiple previous procedures.

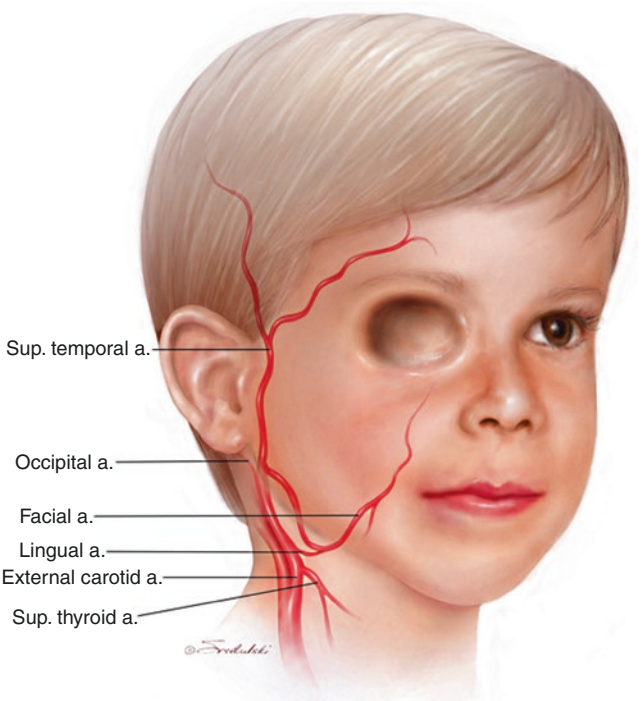


Fig. 8.14 Arterial circulation for free flaps: the superficial temporal and the facial artery are the most commonly used vessels, but any suitable branch off the external carotid may be used

Congenital hypoplasia of the periorbital region requires augmentation rather than replacement. Therefore, the type of flaps needed for augmentation are usually soft tissue free flaps. In addition, osseointegration is usually not required in these patients.

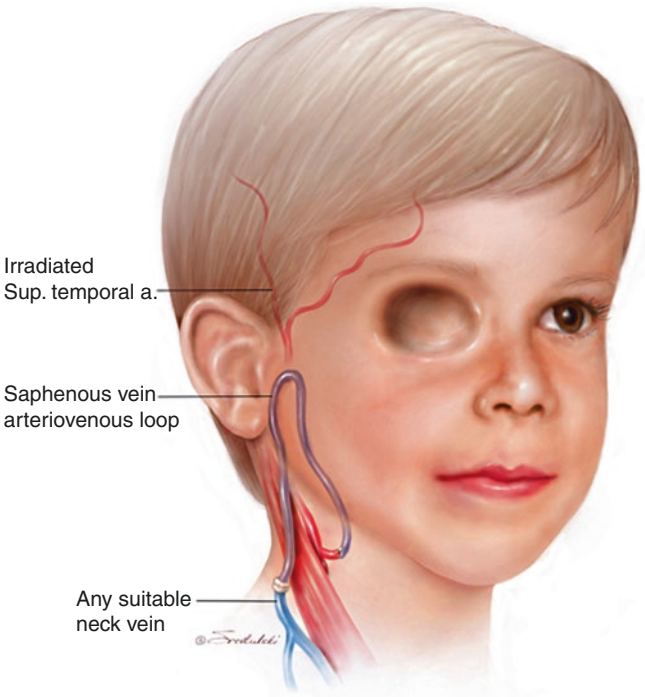


Fig. 8.15 A saphenous vein graft can be used to extend a short pedicle, or it can be fashioned as an arteriovenous loop to provide both arterial inflow and venous outflow for the microvascular free flap. A venous coupler can facilitate the multiple venous anastomoses required

Preparation of the Socket with Free Tissue Transfer

Multiple reports exist on utilizing various free flaps for eye socket reconstruction [14–19]. If the bony orbit is adequate but complicated by radiation changes to the soft tissues, then a well-vascularized, thin soft tissue flap is needed. The parascapular, dorsalis pedis, and radial forearm free flap have historically been ideal choices [14]. Advances in microsurgery had added perforator flaps to the armamentarium including the anterolateral thigh flap. All of these flaps have variable donor-site morbidity and ease of harvest. Flaps harvested from the back may require a change of position. Overweight patients may have thick subcutaneous deposits making flaps from the back or leg difficult to inset in the periorbital region and require significant later revision.

The radial forearm flap is the ideal thin flap for simple soft tissue changes. It is a reliable flap that can be thinned and skin grafted at a later date, if necessary. In addition, it provides a large amount of soft tissue area to correct the deformity in one stage. The radial forearm flap has a long vascular pedicle, which can easily access the superficial temporal or facial vessels (Fig. 8.16).

If modest bony augmentation is necessary, up to one-third of the radius bone can be utilized without a significant

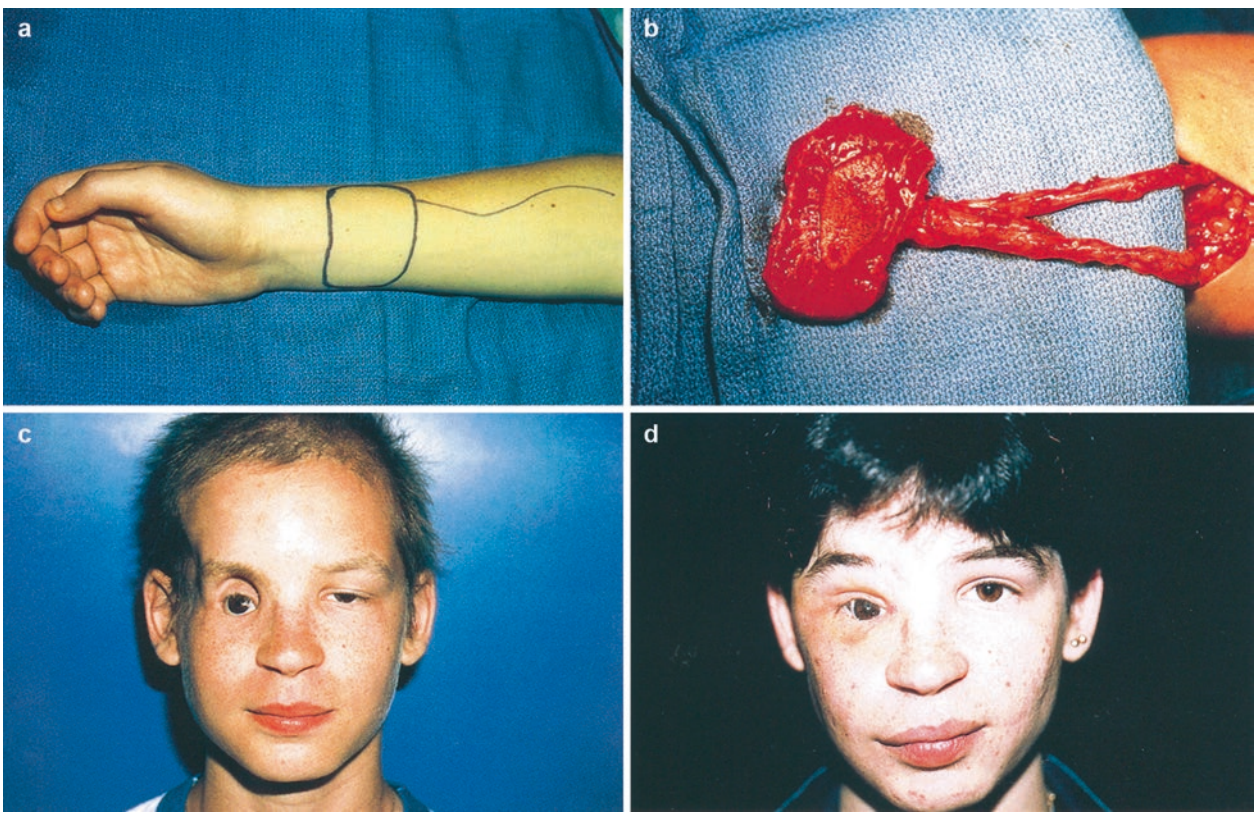


Fig. 8.16 Microvascular free flap. (**a**) Radial forearm flap outlined in methylene blue. (**b**) Graft harvested, demonstrating isolated artery and vein anastomosis with temporal vessels. (**c**) Patient with long-standing problem retaining prosthetic shell. Note severe atrophy of periorbital soft tissues and temporalis muscle secondary to radiation following enucleation for retinoblastoma. (**d**) Two years postoperative radial forearm free flap (Courtesy of Scott Bartlett, MD)

donor-site defect, and this composite flap has been used successfully for orbital reconstruction [31]. Radius bone instability or fracture is associated with significant morbidity; thus patients should be casted for up to 6 weeks postoperatively to prevent pathologic fracture of the donor arm. The one significant disadvantage of the radial forearm flap is the unsightly donor site left on the visible area of the medial distal forearm for sizeable flaps. The donor-site appearance can be improved with judicious closure of the donor site and the use of a full-thickness rather than a split-thickness skin graft over the exposed underlying tendons (Fig. 8.17).

Alternative thin flaps for socket coverage include the parascapular flap and the thoracodorsal artery perforator flap, although these often require intraoperative positional changes for harvesting, as well as the anterolateral thigh perforator flap as examples of reconstruction using these flaps and are illustrated in Figs. 8.26 and 8.27. These flaps, however, can be thicker than desired in some patients. A series of successful reconstruction with small anterolateral thigh flaps in pediatric patients has recently been reported [32].

An additional choice in thinner patients is the use of the fibula flap with its surrounding skin paddle (Figs. 8.18 and 8.19). The advantage of the fibula is the ability to make multiple osteotomies for the purposes of bone contouring, particularly in the inferior portion where the skin paddle can be rotated to the appropriate place to allow for soft tissue fill. This flap often is slightly thicker than the radial forearm in thin patients and will require thinning and skin grafting in the future. Other advantages of the fibula are the ease of harvest and low donor-site morbidity.

Partial fibular resection does not seem to give significant morbidity in the pediatric patient, although valgus deformities and ankle instability have been reported [33, 34]. Complex reconstructive cases may be simplified by computer-aided design/computer-aided manufacturing (CAD/CAM)-assisted surgical planning by prefabrication of cutting guides for the fibula and the periorbital region. This technology has become more popular in both adult and pediatric mandibular reconstructions and has been applied to many other regions of the craniofacial skeleton [35–38].

Patients who have had orbital exenteration in continuity with a maxillectomy have special problems (Figs. 8.20, 8.21, and 8.22). Adequate soft tissue fill of the defect without bony support will still reveal movement of the tissue with respiration and deglutition. Fabrication of a maxillary obturator is much more difficult if a soft tissue flap is used to obliterate the oral-antral communication resultant from the maxillectomy. Often the flap provides inadequate support for a

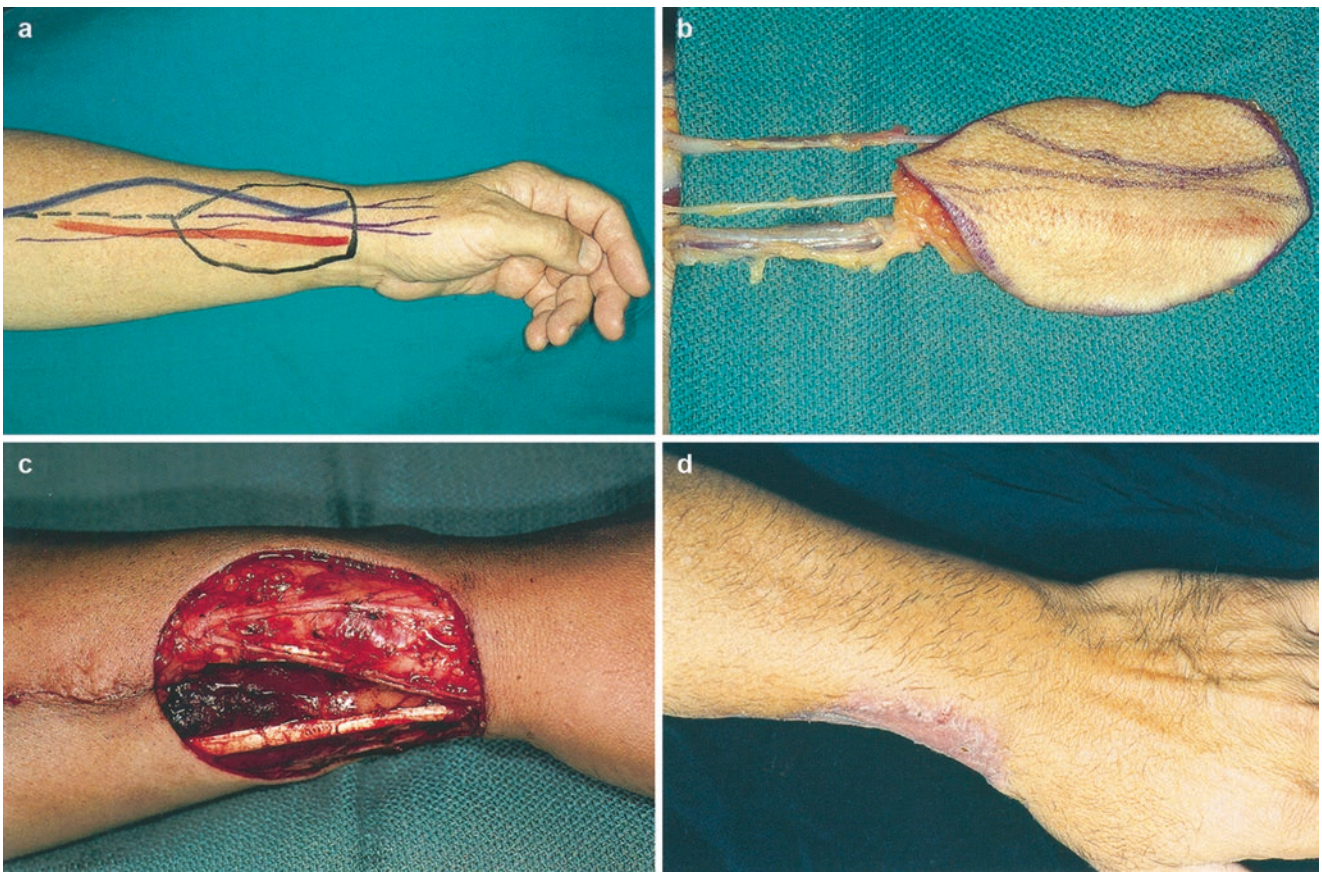


Fig. 8.17 Radial forearm flap. (**a**) Markings for radial forearm flap with radial artery in red, cephalic vein in blue, cutaneous nerve in dashed line. (**b**) Forearm flap with artery, vein, and preserved nerve. (**c**) Donor-site defect. (**d**) Healed donor site with full-thickness defect closed

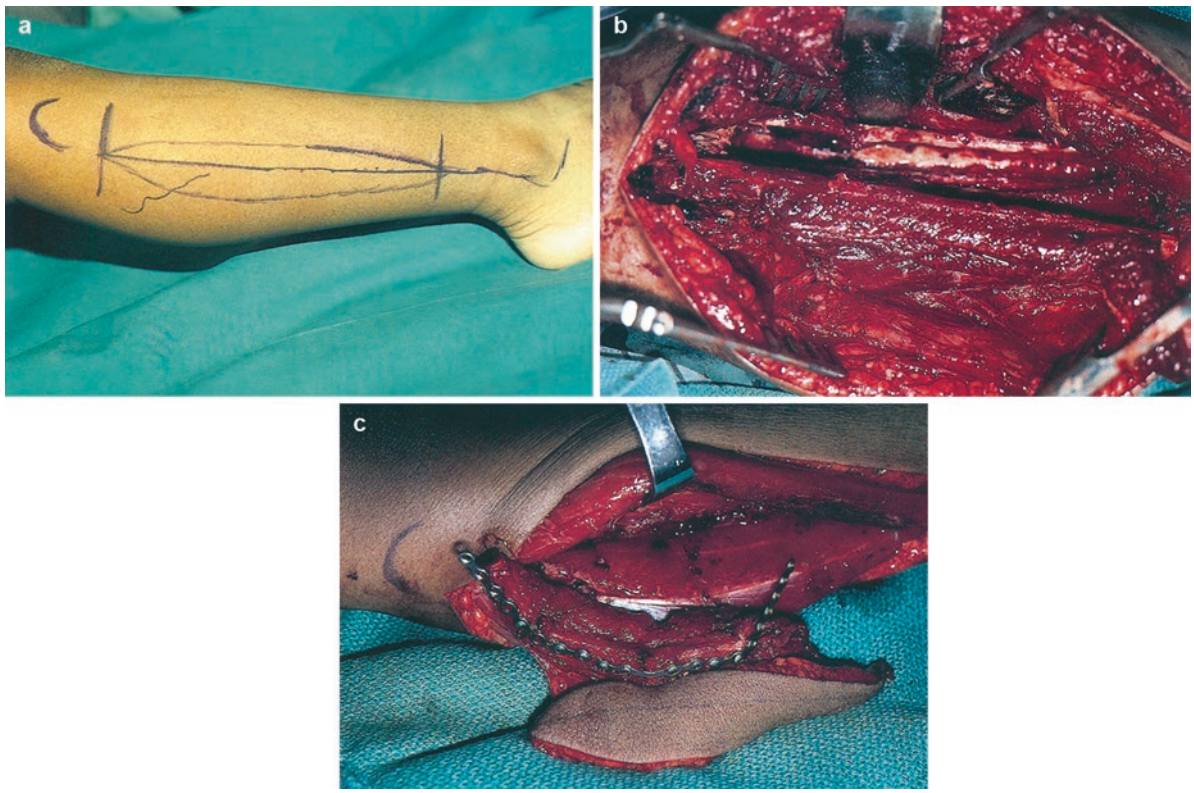


Fig. 8.18 Fibula flap. (**a**) Drawing of proposed fibula free flap with skin paddle. (**b**) Fibula exposed in situ prior to osteotomies. (**c**) Fibula with osteotomies and skin paddle

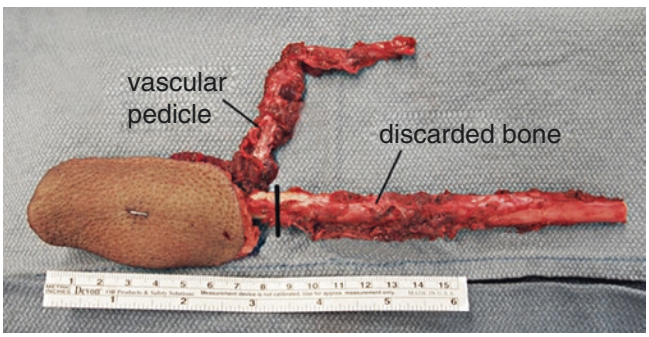


Fig. 8.19 Free fibula osteocutaneous flap. The peroneal vascular pedicle of the fibula osteocutaneous flap can be lengthened significantly by discarding the proximal bone

prosthesis, and the prosthesis can become dislodged during normal function. The best results are achieved when the maxillectomy defect can be reconstructed with a bony bridge. If bony support cannot be provided for the flap between the oral cavity and the orbital defect, many patients are more comfortable using a conventional obturator to restore the deficient maxillary structures. If an obturator is used to restore the maxillary defect, then the facial defect can be restored separately with surgery and/or a prosthesis.

Periorbital Reconstruction

In patients with the globe present, the usual goal of reconstruction is to recreate missing anatomic structures using autologous tissue or custom fabricated craniofacial implants, thereby creating symmetry with the contralateral globe and periorbital structures.

With a normal-appearing globe, efforts should be made to reconstruct periorbital soft tissues and bone, if at all possible, to protect the eye and improve appearance. A composite osteofasciocutaneous radial forearm flap is an excellent choice for reconstruction of the inferior orbital rim in postablative defects. This flap not only restores both hard and soft tissues but is thick enough to allow for a prosthesis and future osseointegration. As the bony requirements increase, the fibula, iliac crest, and scapula flaps are excellent and quite amenable for osseointegration. Several studies have demonstrated the importance of using vascularized bone flaps for placement of osseointegrated implants. When there is communication with the maxilla, both bulk and a strong bone buttress are required. In this situation, the iliac crest and scapula are appropriate; however, the fibula offers the best option due to the quantity and quality of bone it provides, as well as adequate soft tissue for most orbital defects. The



Fig. 8.20 Considerations in the obliteration of the exenteration defect with flaps. (**a**) Donor tissue for flap or graft reconstruction of the exenteration defect should be selected from a site that closely matches the tissues adjacent to the recipient site. If the flap has excessive surface vascularity or the tissue was harvested from a distant site with different pigmentation, a poor color match will compromise the result. (**b**) An excellent color match was achieved with a flap repair of the defect. The resultant temporal depression was acceptable to the patient. (**c**) Unfortunately, during mastication, swallowing, and speech, the flap movement is noticeable. (**d**, **e**) Flaps used to close maxillectomy defects, which are in continuity with orbital defects, often provide unsuitable support for a prosthesis to replace teeth. These flaps often occupy the space where tooth replacements would be positioned, preventing the patient from having a functional dental prosthesis, which is essential to proper mastication, speech, and appearance. Frequently, a patient will function better with a well-designed and well-constructed maxillary obturator prosthesis than with a bulky flap placed to obliterate the maxillectomy defect

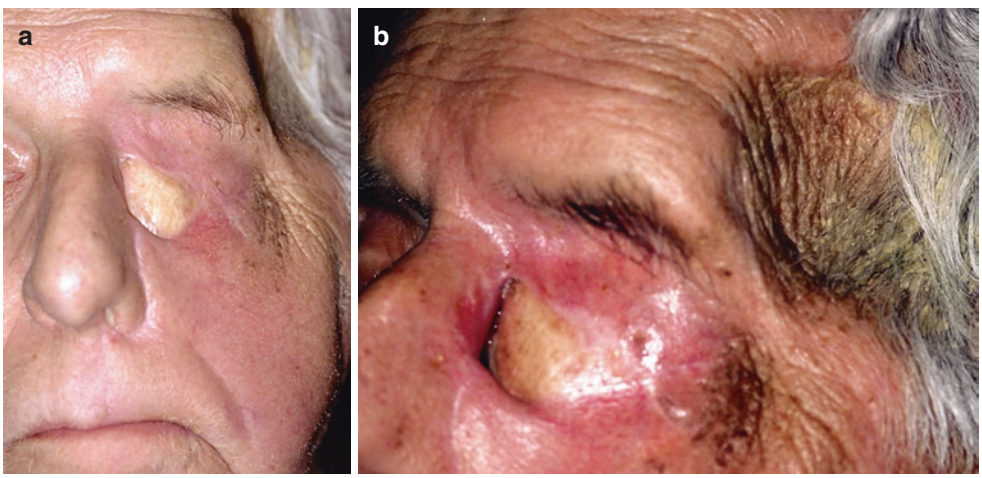


Fig. 8.21 (**a**, **b**) Soft tissue flaps without bony support placed over orbital defects which communicate with the upper airway will inflate and deflate with respiration and speech. This type of mobile flap does not provide adequate support for a facial prosthesis

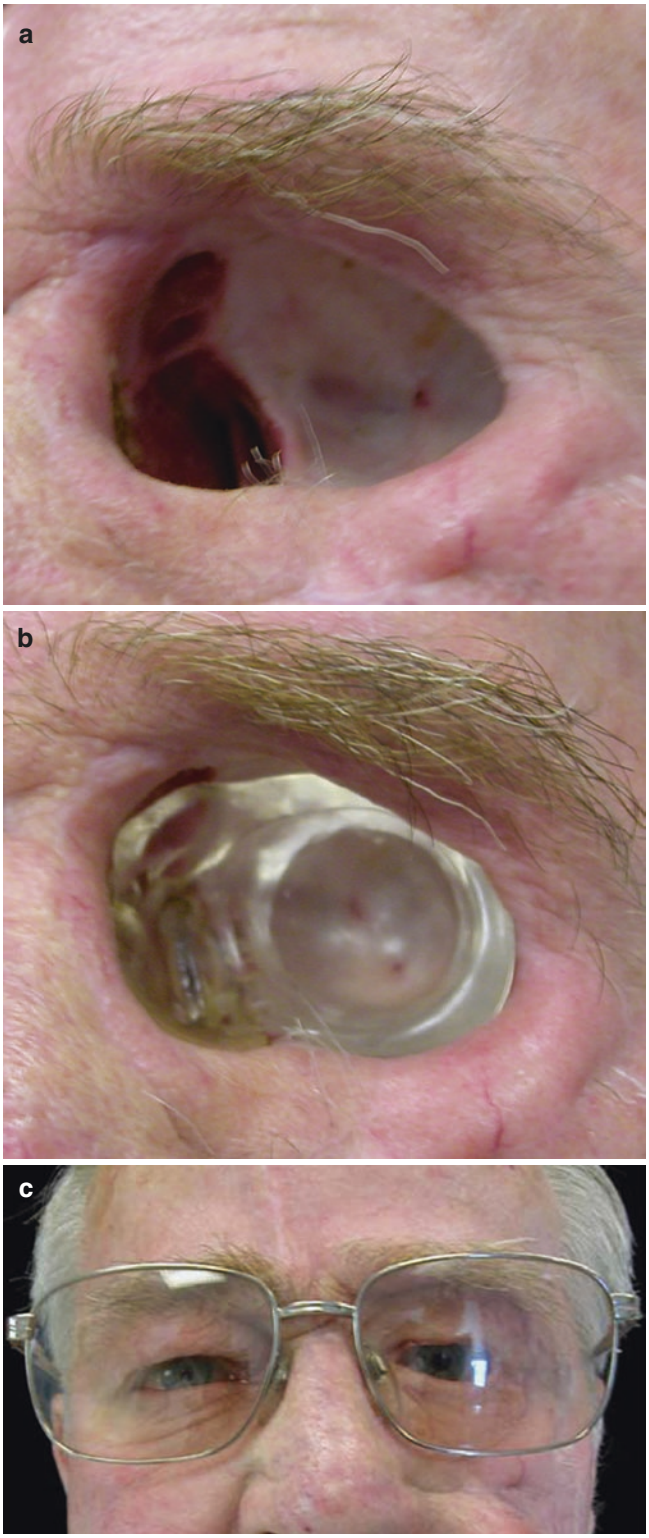


Fig. 8.22 (**a**–**c**) A superiorly based prosthetic obturator may be fabricated to provide separation of the upper airway from an orbital defect to prevent movement of the prosthesis during respiration or phonation

limiting factor to the fibula is the relative shortness of the vascular pedicle. This can be improved by removing several centimeters of proximal fibular bone, which will increase the pedicle length enough to reach the facial vessels if necessary.

If the globe is preserved, but is no longer of normal appearance, prosthetic rehabilitation can still provide an excellent cosmetic result (see Chap. 39). If there is a corneal scar, cataract, or a defect in the iris or pupil, and if the sclera is normal, a cosmetic soft contact lens or custom scleral shell may be used. If there are abnormalities of the sclera, the eye is nonfunctional, or the iris is malpositioned or oversized, a custom scleral shell should be fabricated. Scleral shells can be made very thin to conform to the globe and to match the opposite eye. If the globe moves normally, a well-contoured scleral shell will appear to track and move naturally. However, if corneal sensation does not permit a scleral shell to be tolerated, then an oral mucous membrane graft can be used to cover the cornea and allow continuous wear [15].

If ocular prosthetic rehabilitation is not possible, then filling the soft tissue defect and the maxilla itself can be done with a large muscle flap such as the latissimus dorsi or rectus myocutaneous flap (Fig. 8.5). These are preferred over fasciocutaneous flaps because of their reliability and their bulk and the improved donor site. Absence of the orbital roof or medial orbital wall in the irradiated patient presents a risk of intracranial and nasopharyngeal communication. Dural and mucosal injuries should be repaired but then must be covered with well-vascularized hard and/or soft tissue to prevent cerebral spinal fluid leak and to minimize the chance of meningitis and extradural abscess. These patients have a need for well-vascularized flaps with good-quality soft tissue to separate the orbit from the nasopharyngeal and intracranial spaces.

Contouring

The pediatric population is also unique because of the contouring requirements associated with children with craniofacial deformities. Certain clinical situations are amenable to the use of free flaps for contouring of the periorbital region. Patients with hemifacial microsomia, Romberg disease, and Treacher Collins syndrome, for example, demonstrate deficiencies in all of the layers from bone to skin. Previously, many of these children have received free bone grafts as part of their reconstruction. However, soft tissue transfer using vascularized flaps has improved the results in patients with hemifacial microsomia and Romberg disease [39]. Fasciocutaneous free flaps, in addition to free bone grafts, are helpful in reconstructing severe facial contour irregularities in these patients

[10]. Muscle flaps, such as the latissimus flap, have been used and are easy to harvest with good pedicle length. However, denervation of the muscle can result in atrophy and make the adequacy of the augmentation difficult to gauge. The parascapular flap and its modification, the inframammary extended circumflex scapular flap, have been used extensively due to the fact that there is less atrophy (Figs. 8.23, 8.24, and 8.25).

An additional perforator flap popular currently with less potential to atrophy is the thoracodorsal artery perforator flap [11]. These flaps are replacing the scapular flaps in many instances because there are easier to harvest. They can be used to fill large orbital defects after exenteration (Fig. 8.26), as well as for situations with a seeing eye such as orbital fat atrophy with enophthalmos following radiation (Fig. 8.27).

An additional option is the anterolateral thigh flap which allows for harvest in the supine position and a well-hidden scar on the thigh. The advantages of these perforator flaps are that they can be customized to provide variable tissue depths and that they are more reliable and less bulky than muscle flaps. In addition, more predictable results are obtainable without accompanying muscle atrophy. Often, overcorrection is performed, and revisionary surgery is needed 3–6 months postoperatively. In addition, the majority of these cases can be satisfactorily reconstructed with soft tissue alone. If bone is needed, then scapula can be harvested with the flap as well.

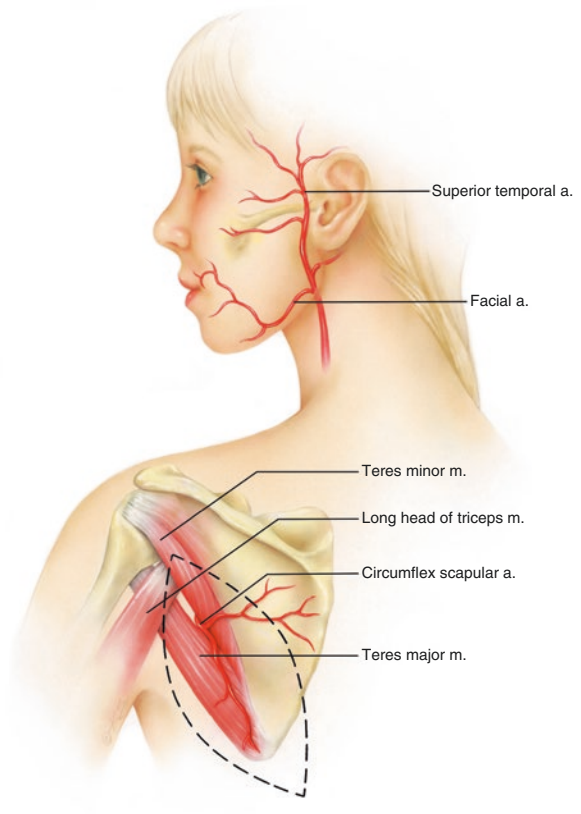


Fig. 8.23 Illustration of scapular flap anatomy, including two common facial arterial recipient sites

Reanimation and Sensory Restoration

In recent years, there have been exciting developments in grafting nerves for the restoration of both motor and sensory function. Cross nerve transfer for facial palsy and corneal sensory reconstruction have been two exciting examples that involve facial and ocular structures.

Cross face nerve grafting for facial rehabilitation utilizing direct stimulus of the contralateral facial nerve has been well established as a primary means of reconstruction for acquired or congenital unilateral facial palsy. Though the majority of attention has been directed toward reanimating the midface and smile functions, dynamic reconstitution of the upper and lower lid and periorbital deformities remains a significant challenge. Traditional interventions included static therapies such as gold weight placements to the upper lid and tarsorrhaphies, while dynamic options have included muscle transfers and direct neurotization. Most commonly, these include temporalis muscle transpositions, cross face nerve grafting to a free gracilis muscle transfer, or direct neurotization of the orbicularis oculi [38, 39]. Unfortunately, a universal consensus does not yet exist as results have remained suboptimal.

While motor nerve restoration has been well established, there are new significant developments in sensory restoration, utilizing similar principles. Up to now, there has been no primary treatment for neurotrophic cornea, which causes amblyopia, ulceration, scarring, and vision loss in young children. Corneal sensation is essential for maintenance of epithelial integrity and limbal stem cell function.

Corneal anesthesia may have congenital or acquired etiologies. In acquired cases, this most commonly results from trigeminal neuropathy following herpes infection. However, it may also be seen after posterior fossa tumor resection, trauma, and stroke. Any of these etiologies may damage the ophthalmic division of the trigeminal nerve resulting in neurotrophic keratopathy. Congenital causes may be sporadic or syndromic. With the absence of protective sensation and feedback, much like a diabetic foot, repetitive injury leads to scarring, ulceration, and, ultimately, vision loss. Furthermore, corneal sensory denervation leads to the formation of non-healing epithelial defects that may ulcerate and perforate. In addition,

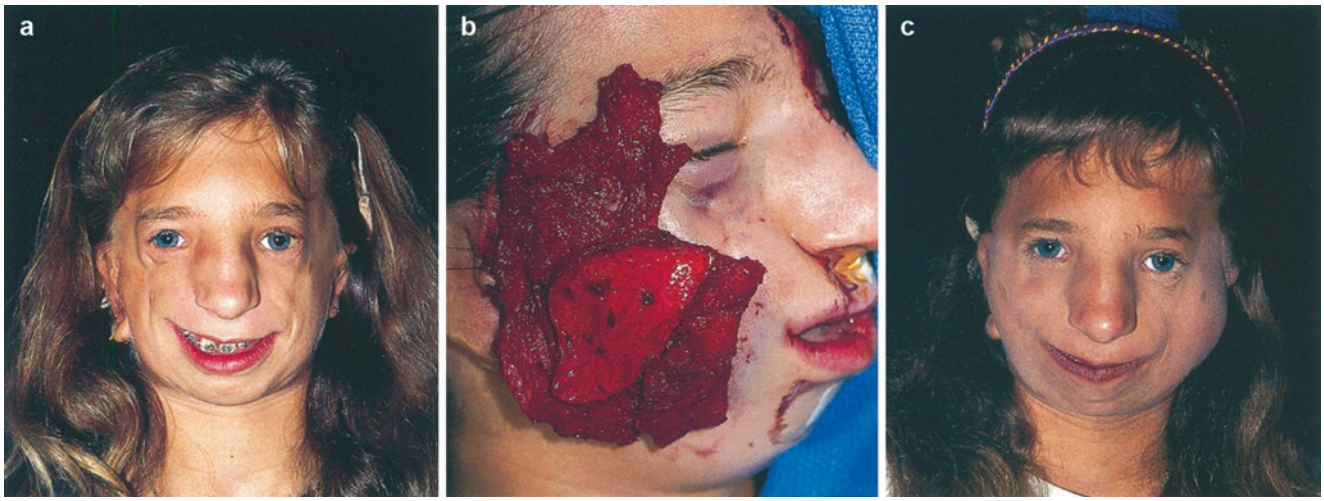


Fig. 8.24 (**a**) An 11-year-old female with Treacher Collins syndrome prior to bilateral facial augmentation with a scapular facial free flap. (**b**) Right scapular flap prior to insetting. Note variable augmentation within flap. (**c**) Four months post bilateral scapular flap augmentation



Fig. 8.25 (**a**) A 17-year-old male with hemifacial microsomia prior to facial augmentation. (**b**) Proposed left scapular free flap drawings. (**c**) Scapular free flap prior to subscapular pedicle division. (**d**) Planning for recipient flap on left face. Note preparation for anastomosis to temporal vessels. (**e**) Four months post left scapular free flap transfer

deficiency may not be isolated to the ophthalmic division of the trigeminal nerve, as patients may also suffer from lagophthalmos, strabismus, or paralytic ectropion depending on the original etiology and involvement of other cranial nerves. Current therapies have been less than optimal and have aimed at mechanically protecting the cornea through permanent lateral tarsorrhaphy. Corneal transplantation may be required in cases of corneal perforation. However, this has proven to be



Fig. 8.26 Patient with history of rhabdomyosarcoma s/p orbital exenteration and adjuvant therapy. This patient was initially reconstructed with a chimera flap to orbit and maxillary sinus consisting of a thoracorsal artery flap with a small segment of latissimus dorsi muscle, then subsequently a rectus muscle free flap was also performed when additional vascularized tissue was needed to obliterate her irradiated sinuses and orbit. (**a**) Preoperative irradiated orbit, (**b**) surgical plan to use latissimus muscle and independent thoracodorsal artery skin island, (**c**) flap inset using superficial temporal vessels, (**d**) superomedial wound dehiscence due to residual open sinus,



Fig. 8.26 (contiuned) (**e**) rectus muscle free flap connected to facial vessels, and (**f**) final result showing stable well-healed reconstruction

ineffective, as the etiology of the corneal anesthesia has not been addressed, and repeat injury continues. Furthermore, there is a substantial reduction in corneo-limbal stem cells in the neurotrophic cornea, and grafted corneas do not heal well leading to limited visual prognosis.

The concept of neurotization utilizes the transfer of a healthy donor nerve to a separate tissue to establish motor or sensory function. This technique has been well described in other arenas including upper extremity and facial palsy. The first description of direct neurotization of the insensate cornea was by Terzis et al. in adults in unilateral facial paral-



Fig. 8.27 Adolescent patient with history of malar Ewing's sarcoma treated with excision, chemotherapy, and radiation and initially reconstructed with a titanium prosthesis that became infected. Secondary free tissue reconstruction to augment the malar area was accomplished with a thoracodorsal artery perforator flap anastomosed to facial vessels. (**a**) Appearance after removal of infected custom made titanium zygoma prosthesis, (**b**) markings for thoracodorsal artery perforator flap,

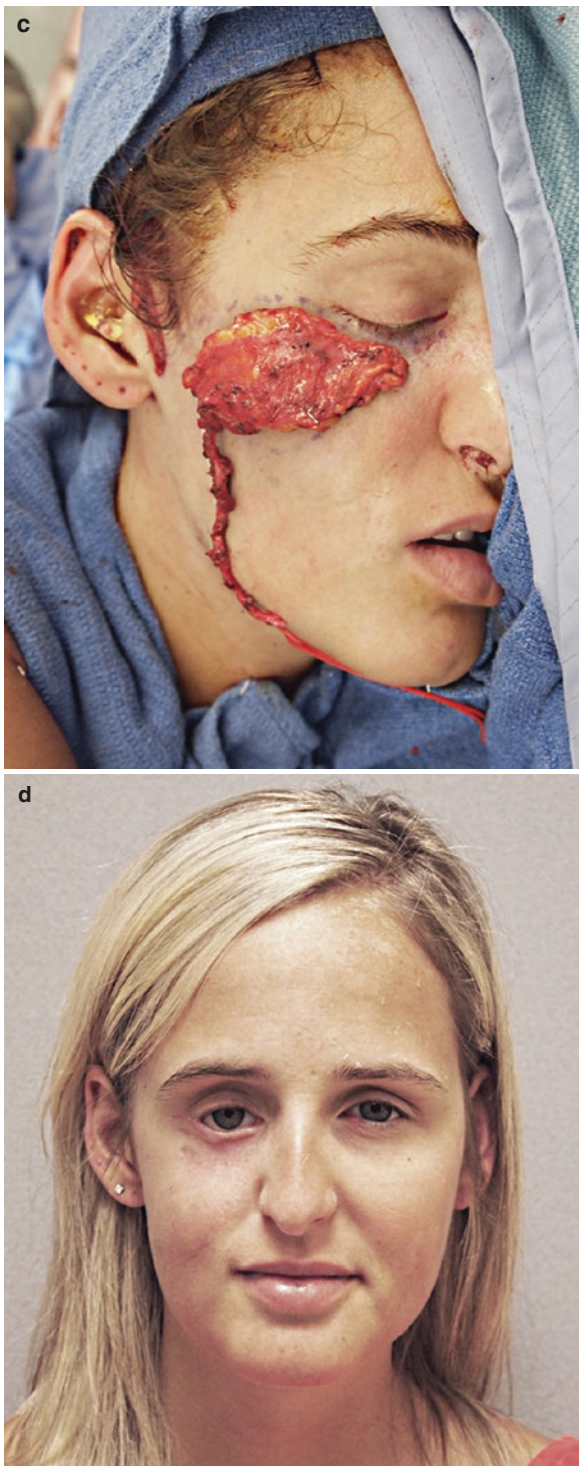


Fig. 8.27 (contiuned) (**c**) de-epithelialized flap prior to pedicle tunneling, (**d**) postoperative appearance with improved malar contour. She later underwent additional Medpor cheek augmentation once she had stable soft tissue coverage provided by the flap

ysis [40]. This method utilized a bicoronal incision, with harvesting of the contralateral supraorbital and supratrochlear nerves such that they were pedicled with the distal ends directly coapted to the insensate corneal limbus. Though significant in its ingenuity drawbacks included donor-site morbidity of loss of sensation to the forehead and scalp, as well as a large scar burden. In this report, all patients showed improvement of corneal health and sensibility with subjective sensibility between 6 months and 1 year and objective sensibility at 2.8 years. Subsequently, this technique has been refined and applied to the pediatric population. The team of Borschel, Zuker, and Ali at the Hospital for Sick Children in Toronto, Canada, developed a minimally invasive method of corneal neurotization and has reported early success [41, 42]. Preoperatively, forehead sensation is assessed using a Semmes-Weinstein monofilament. Next, a sural nerve graft is harvested through two to three small incisions using the proximal sural nerve and a blunt nerve harvester. Subsequently, the contralateral supratrochlear nerve is identified and dissected out through a medial upper lid incision. The supraorbital nerve is spared unless there is anatomic deficiency of the supratrochlear nerve. A subcutaneous tunnel is created through the glabellar area, and a matching medial upper lid incision is created on the affected side. The sural nerve graft is reversed in orientation and is brought in through an incision at the superior fornix using a Wright needle. The nerve is then separated into its terminal fascicles (normally between 4 and 5) and, with the use of a microscope, tunneled subconjunctivally into four quadrants around the limbus (Fig. 8.28). In our experience, we have adjusted the technique by performing scleral tunnels and directly coapting the nerve endings to the sclera. The sural nerve is then coapted directly end to end to the contralateral supratrochlear nerve with epineural sutures. A temporary tarsorrhaphy is performed on the affected eye and kept in place for 1 week. The patient undergoes monthly follow-up for assessment of corneal sensation with a Cochet-Bonnet esthesiometer and assessment of corneal nerve density with confocal microscopy. By approximately 3 months postoperatively, patients report sensation in the distribution of the contralateral forehead when the cornea is stimulated, with protective sensation of the cornea occurring at 6 months. Patients should be advised that discomfort may be expected when sensation begins to return as the formerly insensate corneal surface now registers new mechanical stimulation. As the scarred ocular surface begins to heal, this discomfort subsides. Neural plasticity allows for the distribution of sensation to migrate from the forehead to the affected cornea.

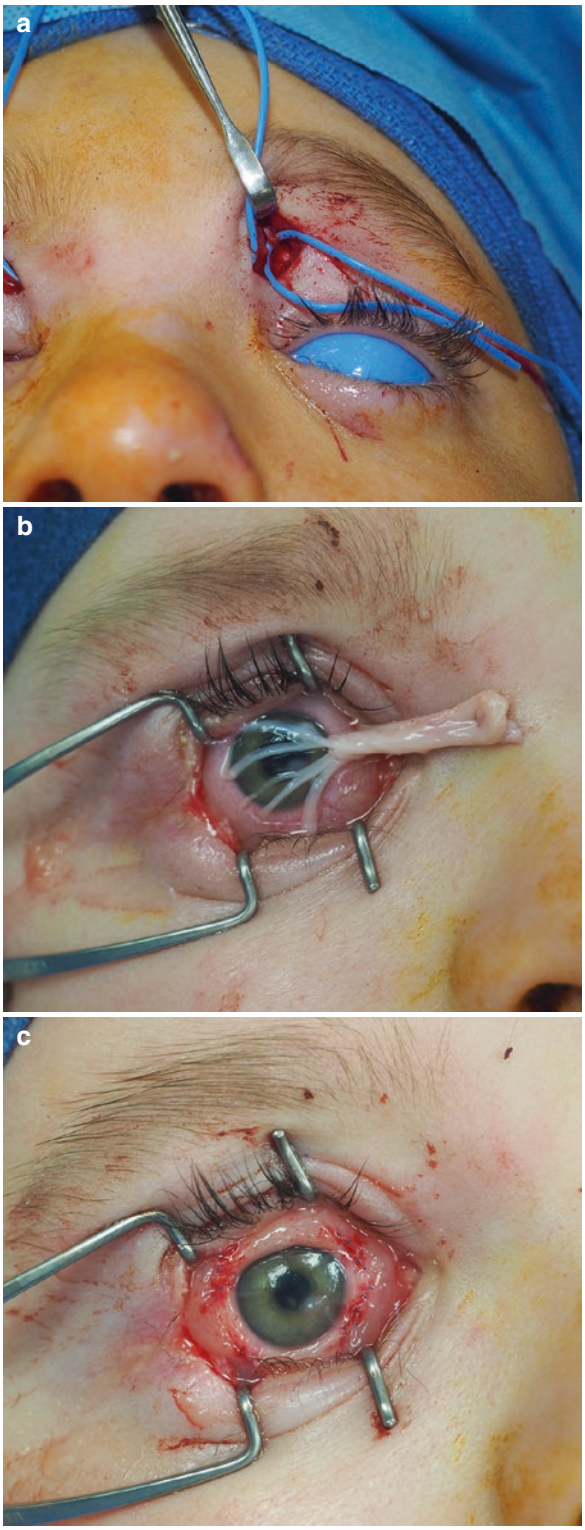


Fig. 8.28 Six-year-old male with right corneal anesthesia following traumatic brain injury. Patient underwent corneal neurotization with sural nerve graft. (**a**) Exposed contralateral supratrochlear nerve. (**b**) Sural nerve dissected into individual fascicles. (**c**) Closed scleral incisions after subconjunctival tunneling of sural nerve

In addition to restored sensation, the neurotized scarred corneal epithelium has also been observed to thicken and heal postoperatively. This exciting new treatment continues to develop as we gain more data and understanding of the physiology of this technique.

Summary

Orbital deformities, especially when associated with an absence of the ocular globe, are difficult to conceal and often cause profound difficulties in children. Successful rehabilitation of periocular or orbital defects usually requires surgical preparation of the defect. Particular tissue requirements depend on whether prosthetic rehabilitation is needed, and the specifics of prosthetic rehabilitation are also quite important. Fortunately, microsurgical techniques are now available that can provide multiple tissue sources to reconstruct the periorbital region and aid in the management of these difficult cases.

Microsurgical techniques can also utilize nerve grafts to assist in facial reanimation and the restoration of corneal sensation. With appropriate collaboration, improvements in appearance and in many instances function as well can be achieved so that rehabilitated patients can be better able to lead normal lives with minimal psychological stigma.

References

1. Weng CJ. Periorbital soft-tissue and socket reconstruction. Ann Plast Surg. 1995;34(5):457–62; discussion 62–4
2. Funk GF, Laurenzo JF, Valentino J, McCulloch TM, Frodel JL, Hoffman HT. Free-tissue transfer reconstruction of midfacial and cranio-orbito-facial defects. Arch Otolaryngol Head Neck Surg. 1995;121(3):293–303.
3. McLoughlin PM, Gilhooly M, Phillips JG. Reconstruction of the infraorbital margin with a composite microvascular free flap. Br J Oral Maxillofac Surg. 1993;31(4):227–9.
4. Mustoe TA, Corral CJ. Soft tissue reconstructive choices for craniofacial reconstruction. Clin Plast Surg. 1995;22(3):543–54.
5. Yamamoto Y, Minakawa H, Sugihara T, Shintomi Y, Nohira K, Yoshida T, et al. Facial reconstruction with free-tissue transfer. Plast Reconstr Surg. 1994;94(3):483–9.
6. Brent B, Upton J, Acland RD, Shaw WW, Finseth FJ, Rogers C, et al. Experience with the temporoparietal fascial free flap. Plast Reconstr Surg. 1985;76(2):177–88.
7. Rose EH, Norris MS. The versatile temporoparietal fascial flap: adaptability to a variety of composite defects. Plast Reconstr Surg. 1990;85(2):224–32.
8. Guyuron B, Labandter HP, Berlin AJ. Fasciocutaneous flap, secondary axial pattern flap, and microvascular free flap in socket reconstruction. Ophthalmology. 1984;91(1):94–101.
9. Siebert JW, Longaker MT, Angrigiani C. The inframammary extended circumflex scapular flap: an aesthetic improvement of the parascapular flap. Plast Reconstr Surg. 1997;99(1):70–7.

10. Siebert JW, Longaker MT. Microsurgical correction of asymmetry in hemifacial microsomia. Operative Techniques. Plast Reconstr Surg. 1994;1:93–8.
11. Tahara S, Susuki T. Eye socket reconstruction with free radial forearm flap. Ann Plast Surg. 1989;23(2):112–6.
12. Asato H, Harii K, Yamada A, Ueda K. Eye socket reconstruction with free-flap transfer. Plast Reconstr Surg. 1993;92(6):1061–7.
13. Heher KL, Katowitz JA. Oral mucous membrane grafts for corneal protection to permit prosthetic shell wear. Ophthal Plast Reconstr Surg. 1997;13(1):40–7.
14. Colen SR. Selective microvascular procedures in oculoplastic surgery. Clin Plast Surg. 1988;15(2):283–7.
15. Brown JS. Deep circumflex iliac artery free flap with internal oblique muscle as a new method of immediate reconstruction of maxillectomy defect. Head Neck. 1996;18(5):412–21.
16. Potparic Z, Starovic B. Reconstruction of extensive defects of the cranium using free-tissue transfer. Head Neck. 1993;15(2):97–104.
17. Schusterman MA, Reece GP, Miller MJ. Osseous free flaps for orbit and midface reconstruction. Am J Surg. 1993;166(4):341–5.
18. Frodel JL Jr, Funk GF, Capper DT, Fridrich KL, Blumer JR, Haller JR, et al. Osseointegrated implants: a comparative study of bone thickness in four vascularized bone flaps. Plast Reconstr Surg. 1993;92(3):449–55; discussion 56–8
19. Serletti JM, Schingo VA Jr, Deuber MA, Carras AJ, Herrera HR, Reale VF. Free tissue transfer in pediatric patients. Ann Plast Surg. 1996;36(6):561–8.
20. Upton J, Guo L. Pediatric free tissue transfer: a 29-year experience with 433 transfers. Plast Reconstr Surg. 2008;121(5):1725–37.
21. Organek AJ, Klebuc MJ, Zuker RM. Indications and outcomes of free tissue transfer to the lower extremity in children: review. J Reconstr Microsurg. 2006;22(3):173–81.
22. Ghert M, Colterjohn N, Manfrini M. The use of free vascularized fibular grafts in skeletal reconstruction for bone tumors in children. J Am Acad Orthop Surg. 2007;15(10):577–87.
23. Aboelatta YA, Aly HM. Free tissue transfer and replantation in pediatric patients: technical feasibility and outcome in a series of 28 patients. J Hand Microsurg. 2013;5(2):74–80.
24. Yildirim S, Calikapan GT, Akoz T. Reconstructive microsurgery in pediatric population-a series of 25 patients. Microsurgery. 2008;28(2):99–107.
25. Wong CH, Wei FC. Anterolateral thigh flap. Head Neck. 2010;32(4):529–40.
26. Sever C, Uygur F, Kulahci Y, Karagoz H, Sahin C. Thoracodorsal artery perforator fasciocutaneous flap: a versatile alternative for coverage of various soft tissue defects. Indian J Plast Surg. 2012;45(3):478–84.
27. Ayhan S, Tuncer S, Demir Y, Kandal S. Thoracodorsal artery perforator flap: a versatile alternative for various soft tissue defects. J Reconstr Microsurg. 2008;24(4):285–93.
28. Kuo YR, Seng-Feng J, Kuo FM, Liu YT, Lai PW. Versatility of the free anterolateral thigh flap for reconstruction of soft-tissue defects: review of 140 cases. Ann Plast Surg. 2002;48(2):161–6.
29. Silverman DA, Przylecki WH, Shnayder Y, Tsue TT, Girod DA, Andrews BT. Expanding the utilization of the osteocutaneous radial forearm free flap beyond mandibular reconstruction. J Reconstr Microsurg. 2016;32(5):361–5.
30. Hynes SL, Forrest CR, Borschel GH. Use of the anterolateral thigh flap for reconstruction of the pediatric anophthalmic orbit. J Plast Reconstr Aesthet Surg. 2016;69(1):84–90.
31. Nathan SS, Hung-Yi L, Disa JJ, Athanasian E, Boland P, Cordeiro PG, et al. Ankle instability after vascularized fibular harvest for tumor reconstruction. Ann Surg Oncol. 2005;12(1):57–64.
32. Schwarz GS, Disa JJ, Mehrara BJ, Healey JH, Cordeiro PG. Reconstruction of oncologic tibial defects in children using vascularized fibula flaps. Plast Reconstr Surg. 2012;129(1):195–206.
33. Gougoutas AJ, Bastidas N, Bartlett SP, Jackson O. The use of computer-aided design/manufacturing (CAD/CAM) technology to aid in the reconstruction of congenitally deficient pediatric mandibles: a case series. Int J Pediatr Otorhinolaryngol. 2015;79(12):2332–42.
34. Matros E, Albornoz CR, Rensberger M, Weimer K, Garfein ES. Computer-assisted design and computer-assisted modeling technique optimization and advantages over traditional methods of osseous flap reconstruction. J Reconstr Microsurg. 2014;30(5):289–96.
35. Tahiri Y, Taylor JA. In support of using computer-aided design and modeling for periorbital osteotomies. J Craniofac Surg. 2015;26(1):100–3.
36. Rodby KA, Turin S, Jacobs RJ, Cruz JF, Hassid VJ, Kolokythas A, et al. Advances in oncologic head and neck reconstruction: systematic review and future considerations of virtual surgical planning and computer aided design/computer aided modeling. J Plast Reconstr Aesthet Surg. 2014;67(9):1171–85.
37. Longaker MT, Siebert JW. Microvascular free-flap correction of severe hemifacial atrophy. Plast Reconstr Surg. 1995;96(4):800–9.
38. Frey M, Giovanoli P, Tzou CH, Kropf N, Friedl S. Dynamic reconstruction of eye closure by muscle transposition or functional muscle transplantation in facial palsy. Plast Reconstr Surg. 2004;114(4):865–75.
39. Terzis JK, Karypidis D. The outcomes of dynamic procedures for blink restoration in pediatric facial paralysis. Plast Reconstr Surg. 2010;125(2):629–44.
40. Terzis JK, Dryer MM, Bodner BI. Corneal neurotization: a novel solution to neurotrophic keratopathy. Plast Reconstr Surg. 2009;123(1):112–20.
41. Bains RD, Elbaz U, Zuker RM, Ali A, Borschel GH. Corneal neurotization from the supratrochlear nerve with sural nerve grafts: a minimally invasive approach. Plast Reconstr Surg. 2015;135(2):397e–400e.
42. Elbaz U, Bains R, Zuker RM, Borschel GH, Ali A. Restoration of corneal sensation with regional nerve transfers and nerve grafts: a new approach to a difficult problem. JAMA Ophthalmol. 2014;132(11):1289–95.

Pediatric Otolaryngologic Considerations

9

Adva Buzi and Mark Rizzi

Introduction

The close proximity of the orbit to the nose and paranasal sinuses often results in an intersection between the fields of ophthalmology and otolaryngology. Conditions of the orbit and lacrimal system may originate within the boundaries of the nasal cavity, sinuses, and nasopharynx. Conversely, orbital infections and masses may extend to involve surrounding sinuses and paranasal tissues. Management of these patients may require consultation with multiple surgical services.

Recent advances in endoscopic sinus surgery have also led to an alternative approach to the orbit. What once may have required an external surgical approach can now often be treated in a less-invasive manner. Open procedures, however, remain essential for several ophthalmologic indications. This chapter focuses on ophthalmologic or otolaryngologic pathologies of the orbit and paranasal regions and the associated problems that may be encountered by pediatric ophthalmologists, oculoplastic surgeons, and otolaryngologists. Various surgical techniques from endoscopic to open approaches are also reviewed.

A. Buzi
Division of Otolaryngology, Children's Hospital of Philadelphia, Philadelphia, PA, USA

Department of Otolaryngology, University of Pennsylvania, Philadelphia, PA, USA

M. Rizzi (✉)
Division of Otolaryngology, Children's Hospital of Philadelphia, Philadelphia, PA, USA

Department of Otolaryngology, University of Pennsylvania, Philadelphia, PA, USA

Clinical Otolaryngology – Head and Neck Surgery, Children's Hospital of Philadelphia, Philadelphia, PA, USA
e-mail: rizzim@email.chop.edu

Embryology and Anatomy of the Nose and Paranasal Sinuses

The sinuses have distinctive patterns of growth throughout childhood and adolescence. Diminutive maxillary and ethmoid sinuses are present at birth and continue to grow through childhood. The sphenoid sinuses begin to develop at approximately the age of four through involution of marrow fat and subsequent pneumatization of the sphenoid bone. They are consistently visible in children over the age of seven. The frontal sinuses develop as an evagination of the anterior ethmoids and may take up to 10 years to emerge [1]. In children, the ethmoids are the most commonly affected sinuses during upper respiratory tract infections. Infection or tumor can spread laterally from here into the medial orbit through the thin-walled lamina papyracea and associated natural dehiscences in this region [2, 3]. Pathological processes may also extend from the frontal sinus inferiorly to the eye and superiorly to the dura and cranial cavity. Infectious extension may occur through direct bone destruction, osteomyelitis, or venous thrombosis (Fig. 9.1).

Nasal Examination

Nasal examination in children can be performed with simple tools available to most clinicians. The child is seated on a chair or the lap of a parent, while the skin and vestibule of the nose are inspected for presence of drainage, adequate airflow, or excoriations and skin irritations. Simply tilting the head up and gently lifting the tip of the nose upward with the examiners thumb and using a penlight will usually give an adequate view of the inferior turbinate and anterior septum (Fig. 9.2). An otoscope with a speculum may be used to view the region of the anterior nasal cavity for masses, signs of crusting, bleeding, and suspected foreign bodies.

An examiner may also use oxymetazoline spray prior to examination to shrink the engorged nasal turbinates. After 5–10 min, the vasoconstriction is complete, and a more

© Springer International Publishing AG 2018

J.A. Katowitz, W.R. Katowitz (eds.), *Pediatric Oculoplastic Surgery*, https://doi.org/10.1007/978-3-319-60814-3_9

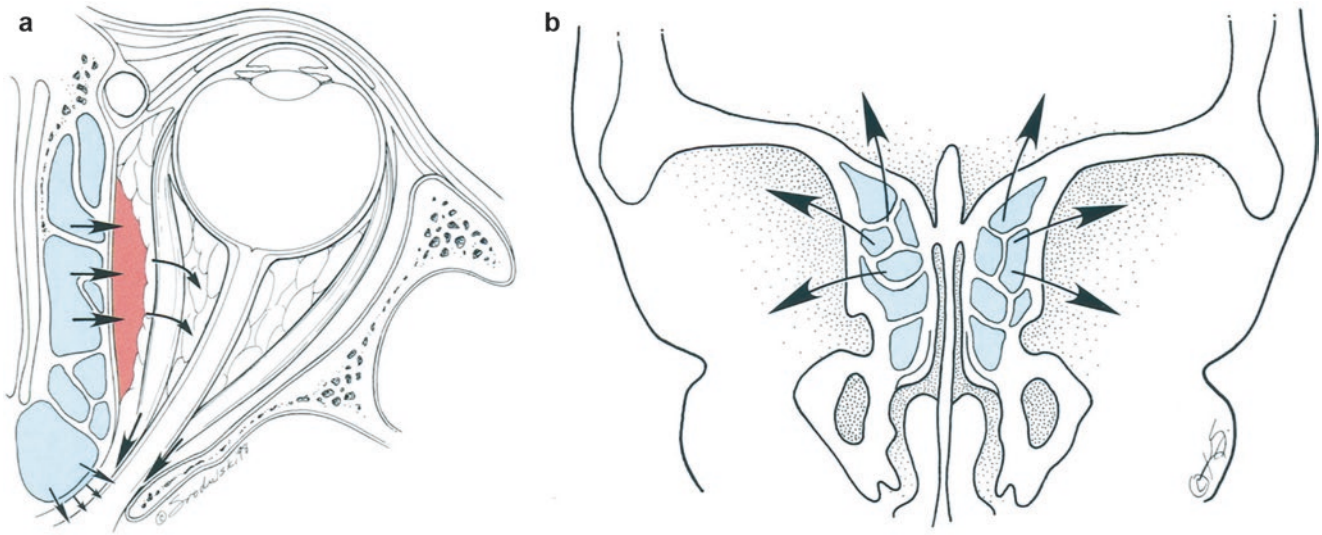


Fig. 9.1 Infection and tumor spread. (**a**) Axial view: routes of infection and tumor spread from the paranasal sinuses to the orbit, brain, and cavernous sinus. (**b**) Coronal view: route of spread upward from frontal sinus cavity through posterior bony wall to the dura or brain parenchyma

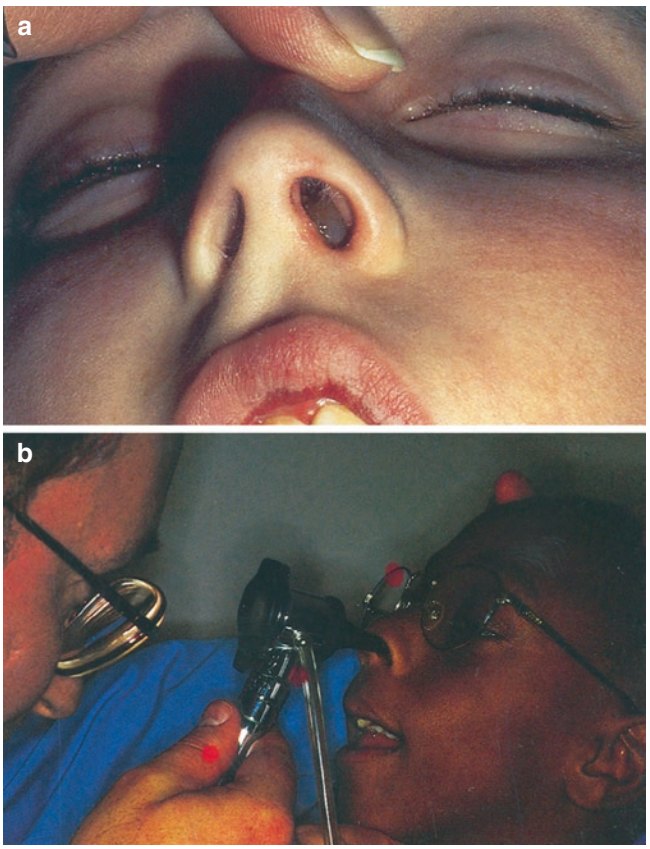


Fig. 9.2 Anterior nasal exam. (**a**) Anterior nasal exam performed with headlight. Note the polyp growing from the left nasal cavity. (**b**) Examination performed with large ear speculum

detailed anterior examination is possible. Vasoconstriction with resulting reduction in turbinate size and decreased bleeding are critical factors in successful intraoperative endoscopic office examination procedures. Nasal endoscopy using a small fiber-optic scope allows for the evaluation of

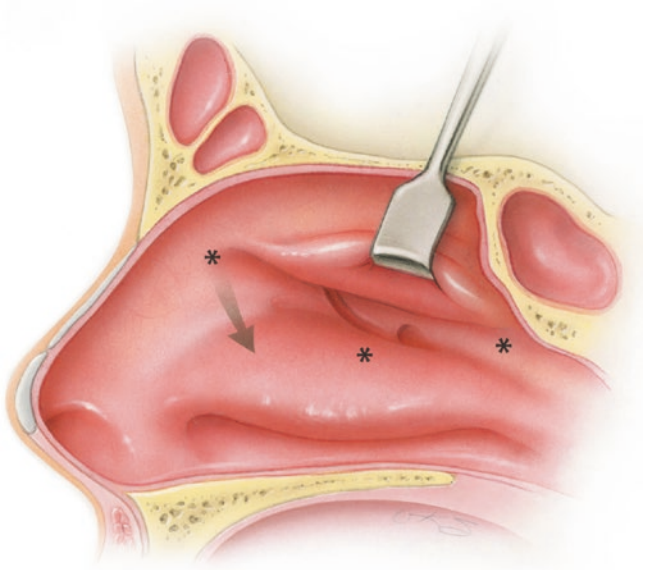


Fig. 9.3 Lateral nasal wall. Lateral nasal wall with usual sites of injection for endoscopic surgical procedures (*). *Large arrow* shows usual course of nasolacrimal duct

areas of the nose and pharynx that are not seen on anterior rhinoscopy alone. The use of topical 4% lidocaine in addition to oxymetazoline can facilitate this exam. A medical allergy history should be reviewed prior to the application of the lidocaine.

While general anesthesia facilitates surgery and examination, it increases blood flow to the nasal cavities. Precise local infiltration of lidocaine and epinephrine is, therefore, essential in minimizing blood loss for enhanced visualization during surgery. Key points of this technique include injecting the multiple areas illustrated, keeping the beveled edge below the nasal mucosa, observing blanching, and reinserting the needle if the agent begins to leak out into the nasal cavity (Fig. 9.3).

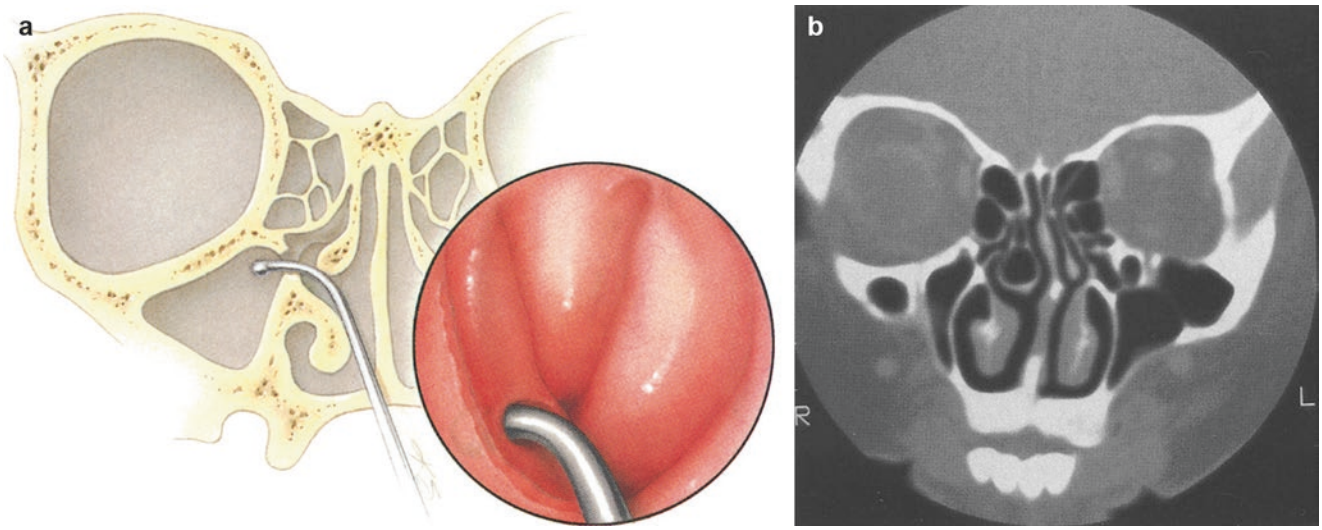


Fig. 9.4 Coronal view of the ostium. (**a**) Coronal view of the ostium of the maxillary sinus. Insert shows a probe entering and enlarging the sinus ostium. Region of maxillary, ethmoid, and frontal sinus drainage termed the OMC (*). (**b**) Coronal CT scan showing maxillary ostia and relation to the middle turbinates

The ostiomeatal complex (OMC) and associated maxillary sinus ostium are illustrated in Fig. 9.4. This region lies lateral to the middle turbinate. The nasolacrimal duct is anterior to the ostium of the maxillary sinus.

Ophthalmic Complications of Sinusitis

Pediatric Acute Rhinosinusitis Complicated by Orbital Infection

Children may have less specific complaints of facial pain and headache associated with acute or chronic sinusitis than adults. Nasal symptoms of purulent discharge, congestion, and associated chronic cough with high fever or if lasting more than 10 days may indicate a sinus infection [4]. The ethmoid and maxillary sinuses are commonly affected in pediatric sinusitis. Infection may spread to the eye from the ethmoid sinus through the thin and permeable lamina papyracea (so named for its paper-thin nature) that separates these two compartments. Once infection breaches this bone, the periosteum and the orbital septum with which it is continuous anteriorly serve as the next barrier in protecting the eye. Additionally, the absence of valves within nasal and ophthalmic veins may permit hematogenous spread of infection within these compartments as well as intracranially. Chandler et al. have described the clinical stages of inflammatory lesions encountered in the orbit [5]. This classification provides a description of the progression of infection to the eye from the ethmoid sinuses (Table 9.1).

Children with facial infections, trauma, and prolonged intubation in the intensive care setting are also at risk for orbital infections [6]. Severe blunt facial trauma with fractures extending into the skull base may expose the contents of the orbit and cranium to sinus mucosa. Penetrating and lacerating injuries from bites or foreign objects around the orbit and maxilla may become infected.

Table 9.1 Classification scheme devised by Chandler et al. to describe the progression of orbital involvement by complicated acute rhinosinusitis

Group I	Preseptal cellulitis
Group II	Postseptal (orbital) cellulitis
Group III	Subperiosteal abscess
Group IV	Orbital abscess
Group V	Cavernous sinus thrombosis

Adapted from [5]

Periorbital Cellulitis and Subperiosteal Orbital Abscess

Preseptal cellulitis in children 6–18 months of age usually follows a recent URI. If diagnosed promptly, this condition may be treated with outpatient antibiotics in compliant families. Subperiosteal orbital abscess (SPOA) is less common and requires inpatient admission for medical and possible surgical therapy [7, 8].

Diagnosis

The diagnosis of periorbital or orbital infections is based on the practitioner's index of suspicion and the general condition of the child. Proptosis, chemosis, loss of visual acuity, and restriction of ocular movement may be present with cellulitis, abscess, and cavernous sinus thrombosis. Infectious processes can threaten vision by direct extension, through pressure on



Fig. 9.5 A 16-year-old girl with left sphenoid sinusitis (*), left-sided V2 and V3 hypesthesia, and decreased visual acuity. Note the proximity of the sinus inflammation and the cavernous sinus (*arrows*)

the optic nerve and optic chiasm, or by direct extension into the cavernous sinus, which contains cranial nerves 3, 4, 6, and trigeminal V2 and V3 [9]. Figure 9.5 is a magnetic resonance image (MRI) revealing inflammation of the right side of the sphenoid sinus. Despite the lack of lateral extension noted on this scan, the patient experienced loss of sensation along the ipsilateral V2 and V3 branches. Progressive cranial nerve involvement, seizures, mental obtundation, hemiparesis, and meningeal signs may occur in conjunction with orbital infections and signal an ominous intracranial extension.

CT scans may be used as an adjunctive diagnostic procedure in children who present with equivocal symptoms or have had minimal therapeutic benefit from medical therapy. With suspected periorbital abscess or intracranial progression, CT with contrast provides accurate anatomical information for the surgical team by localizing both periorbital and intracranial pathologies. MRI with fat suppression techniques is less desirable than CT because of the lack of bone detail, but it does have some advantage in differentiating cellulitis and abscess. MRI is also superior to CT in detecting cerebritis and dural inflammation (Fig. 9.6) [10].

While many consider the CT scan to be the "gold standard" in diagnosing subperiosteal abscesses, CT findings may be equivocal despite moderate-to-severe clinical findings. The timing of CT scanning may influence these results. An immature abscess may be diagnosed as a subperiosteal phlegmon in the very early course of treatment [11].

Medical Management

The presence of subperiosteal abscess is not in itself an absolute indication for surgery, and multiple studies have reported that some patients with this condition can be successfully treated with medicine alone [12, 13]. The initiation of broad spectrum antibiotics as early as possible is necessary to reduce the morbidity and possible mortality of this condition [14]. Studies of bacteriology of acute pediatric sinusitis show that these infections are often polymicrobial, with Streptococcal species, Haemophilus influenza, Moraxella catarrhalis, and anaerobes frequently cultured [15]. Initiating antibiotics with coverage of β-lactamase-producing or penicillin-resistant bacterial strains, such as ceftriaxone or ampicillin-sulbactam in addition to covering anaerobes with metronidazole or clindamycin, is recommended. Decongestants, both topical oxymetazoline and systemic pseudoephedrine, are sometimes used to promote sinus drainage. Vigilant ophthalmologic and neurologic examinations are essential over the first 24 h of hospitalization in patients to observe for changes in visual acuity or motility [16].

Surgical Management

Prompt drainage should be considered if the patient's condition worsens or is not apparently improved with antibiotic therapy over an observation period of 24–36 h. The indications for immediate surgical management of periorbital abscesses are:

Exploration is, therefore, based on the general condition of the patient and may be recommended in children with equivocal CT scans but who exhibit worsening orbital symptoms (Figs. 9.6 and 9.7). Various authors have reported that patients are more likely to fail a trial of medical management for SPOA if they present with significant proptosis (>2 mm), are older (≥9 years), have large abscesses (width >4 mm), have elevated intraocular pressure (>20 mmHg), chemosis, or gaze restriction [17–19]. In a review article of the available literature, Bedwell and Choi recommended prompt surgery as the primary treatment modality for patients with impaired visual acuity, elevated IOP, ophthalmoplegia, proptosis ≥5 mm, and abscess width >10 mm [13]. Patients with less severe findings may improve with conservative management.

Surgical drainage of SPOA can be accomplished via either an endoscopic or open approach and sometimes necessitates a combination of the two. The majority can be drained via an endoscopic approach. In these procedures, the maxillary sinus is drained via removal of the uncinate process. The anterior and posterior ethmoid sinuses are then opened

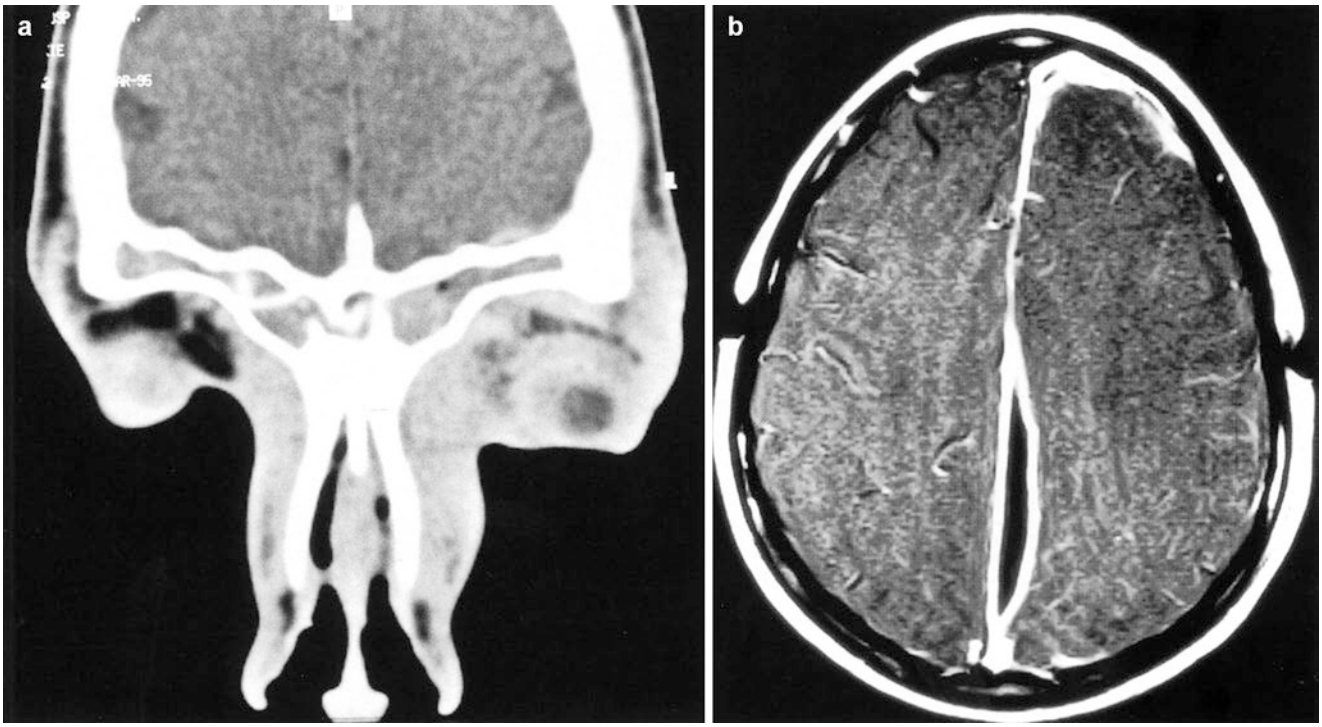


Fig. 9.6 Frontal sinus. (**a**) CT scan of the frontal sinus with complete opacification of the sinus. (**b**) MRI of the same patient showing intracranial abscess and cerebritis

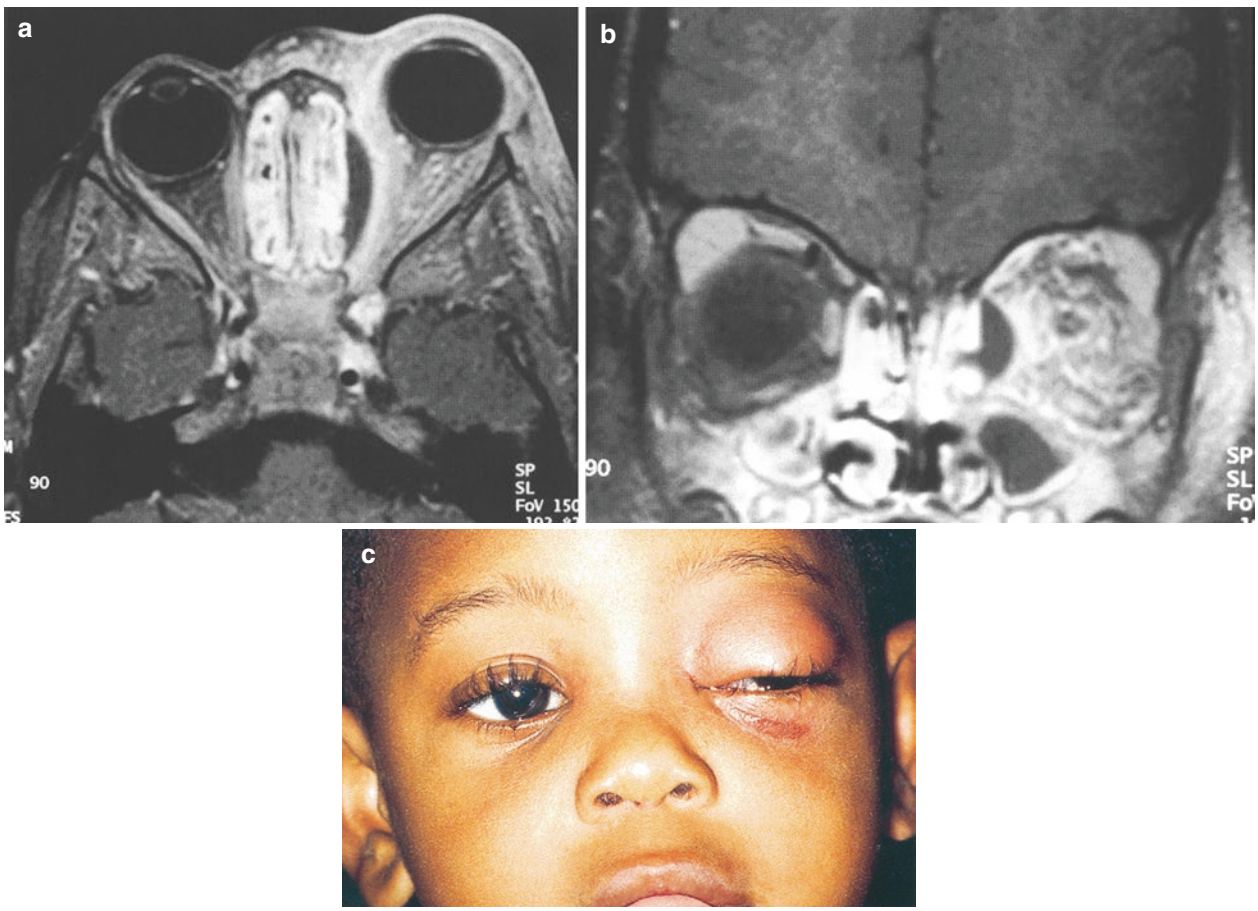


Fig. 9.7 Periorbital abscess. (**a**) MRI axial view of the orbit showing periorbital abscess (*). (**b**) Same patient coronal view. (**c**) Photo of patient with periorbital abscess

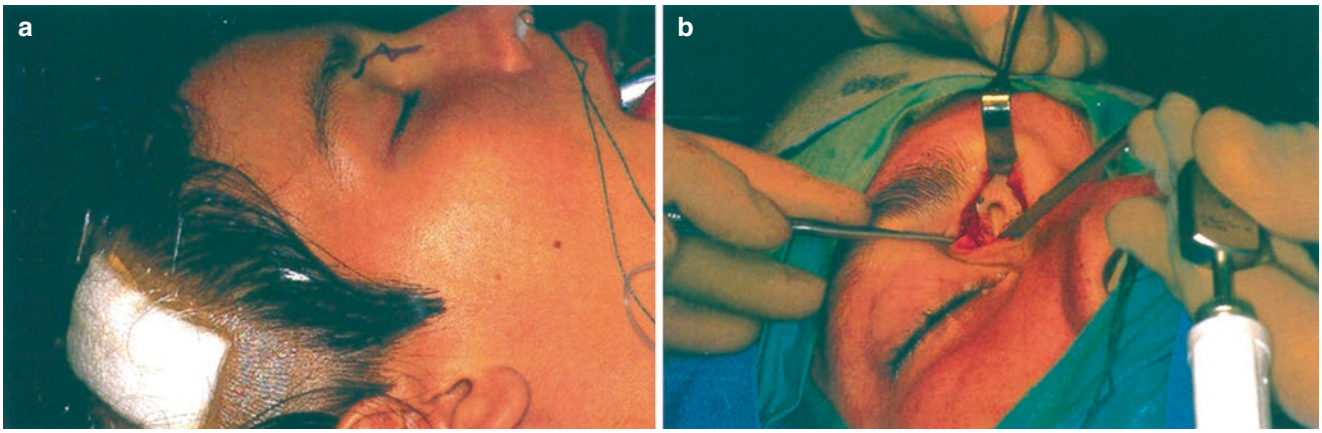


Fig. 9.8 Lynch incision. (**a**) A Lynch incision may be made midway between the medial canthus and nasal dorsum. Z-plasty is recommended to decrease scar retraction. Note previous burr hole site. (**b**) Patient undergoing frontal sinus trephine through a Lynch incision. Thick purulent material is suctioned from sinus cavity (*)

allowing drainage of what is likely the primary site of infection. If there is an obvious dehiscence in the lamina papyracea in continuity with the infected ethmoid, the procedure can be deemed complete at this point. Otherwise, the lamina can be opened to evacuate the SPOA into the nose. The use of image guidance, which correlates intraoperative surgical landmarks to the patient's preoperative CT data, can be used to enhance safety and accuracy [20]. Endoscopic drainage may be difficult when the surgeon encounters limitations to surgical exposure secondary to severe intranasal cellulitis, edema, and bleeding brought about by the acute sinusitis. Also, the child's nasal cavities are smaller, further limiting the visual workspace and increasing the possible risks of intracranial and orbital injury. Pre- or intraoperative use of dexamethasone, reverse Trendelenburg positioning, and meticulous hemostasis through topical vasoconstrictive agents all may aid in facilitating safe endoscopic surgery. Nevertheless, in cases where surgical access is difficult or when the abscess is in a more superior location, an open approach may be necessary. The Lynch incision offers an excellent external approach to the orbit, the ipsilateral ethmoid, and frontal sinuses (Fig. 9.8). During this procedure, the lamina papyracea is opened widely to offer drainage of the abscess into the ethmoid sinuses. The ethmoid and other affected sinuses should be opened and able to drain into the nasal cavity. A rubber band drain is placed in the external incision and removed in 2–3 days. Intracranial, orbital, and sinus infectious processes should be treated during the same setting for optimal recovery [21–23].

Indications for Exploration and Drainage of Periorbital Abscess

Evidence of intracranial involvement
Visual acuity less than 20/60
Worsening visual acuity
Worsening ocular motility
Ophthalmoplegia
Failure to clinically improve after 36–48 h
Immunocompromised patients

Fungal Sinusitis

Invasive fungal sinusitis may also be included in the category of inflammatory and highly destructive periorbital lesions. Immunocompromised children, including diabetic and transplant patients, are at risk for a fulminant destructive fungal infection from aspergillus, rhizopus, and mucormycosis [24]. These children require prompt diagnosis, systemic antifungal agents, and appropriate debridement of the avascular nasal and sinus tissue [25]. Progressive visual disturbances and particularly blindness are ominous signs of skull base fungal invasion.

Noninvasive fungal sinusitis, such as fungal ball or allergic fungal rhinosinusitis, can sometimes cause expansion of the orbit with resulting proptosis and facial disfigurement (Fig. 9.9). Wide ventilation of involved sinuses, coupled with meticulous removal of fungal elements and eosinophilic mucin, is the treatment of choice. Follow-up should consist of periodic sinus CT examinations with repeat endoscopies.

The use of systemic antifungal agents and long-term steroid therapy is controversial [24–26]. The long-term use of oral steroids in children with fungal sinusitis is problematic. The risks of long-term oral steroid therapy include increased capillary fragility, myopathy, disruption of the adrenopituitary axis, gastric bleeding, and premature closure of the epiphyseal growth plates. Topical nasal steroids may increase the risk of nasal hemorrhage and worsen preexisting glaucoma.

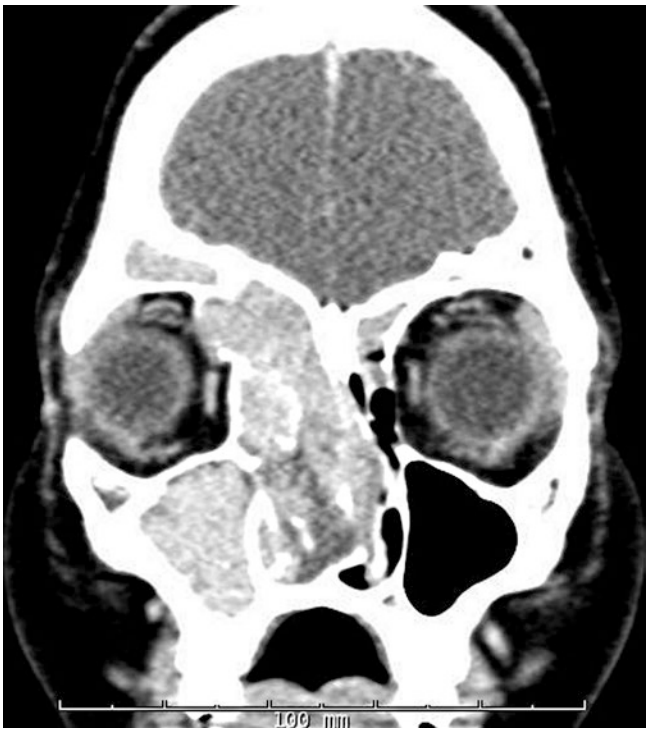


Fig. 9.9 Coronal CT scan of a 12-year-old girl with allergic fungal rhinosinusitis with compression of the orbit and consequent proptosis. Note areas of hyperattenuation that are characteristic of the presence of noninvasive fungal elements

Tumors and Congenital Masses

Physical Exam and History

Pathological findings associated with tumors and expanding intranasal masses of the upper airway and surrounding structures of the orbit may lead the physician to obtain an otolaryngology consultation. The nasal exam in the office, emergency department, or intensive care unit should begin with observation of alar and midnasal symmetry, dorsum swelling, or a protruding nasal mass. Airflow reduction from a nasopharyngeal or paranasal sinus mass may produce mouth breathing, hyponasal speech, snoring, and sometimes sleep apnea. Nasal endoscopy is advised in the workup of abnormal masses causing obstruction (Fig. 9.10). Signs of serious pathology include reduced visual acuity, trismus, hypesthesia of the cheek, and swelling of the nose, face, and orbital rim [27]. Orbital findings such as chemosis, proptosis, and/or extraocular muscle immobility may occur during the process of extension of tumor from the nose and paranasal sinuses into the orbit [28]. Children may not exhibit orbital symptoms for an extended period of time if the tumor originates in the deeper parts of the skull base or nasal cavities. Unilateral chronic rhinorrhea should be considered to be a sign of nasal tumor or foreign body until proven otherwise.

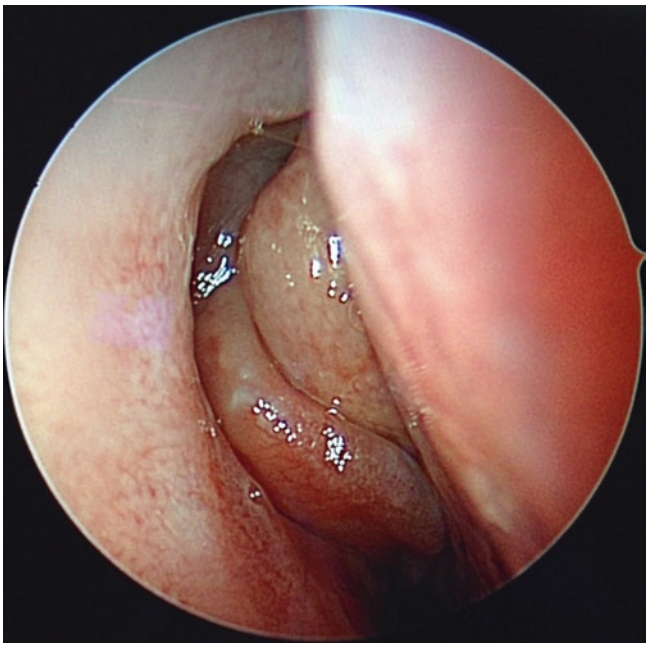


Fig. 9.10 Nasal endoscopic view of an osteoma involving the right middle meatus and medial orbital wall

Pediatric epistaxis may have various causes such as local inflammation and trauma of the normal nasal and sinus vasculature or angioblastic growth and necrosis of various tumors, such as juvenile angiofibromas. Systemic causes may include a blood dyscrasia or hereditary conditions such as hereditary telangiectasia [29].

Imaging

After careful history and physical examination have been performed, management of the pediatric patient with a suspected orbital or skull base lesion should be directed toward obtaining appropriate radiologic imaging studies. Due to the vascularity associated with certain tumors and the possibility of direct intracranial extension, imaging must be performed prior to any surgical intervention, including biopsy. The combination of both high-resolution CT and MRI is ideal in imaging the bony and soft tissue details of nasal tumors. CT is ideal for evaluating bone erosion, and MRI is the ideal modality to differentiate benign sinus obstruction with inspissated mucus from tumor. Both examinations are useful in identifying tumor type, extension, and vascularity [30].

Neoplastic Lesions and Anatomic Location

Various benign and malignant tumors may originate outside of the orbit but grow to invade the orbit and its contents.

Tumor Types and Anatomical Location

Sinus tumors
Benign
- Mucocele
- Fibrous dysplasia
  - Monostotic
  - Polyostotic
  - McCune Albright syndrome
- Juvenile active ossifying fibroma
- Melanotic neuroectodermal tumor of infancy
- Eosinophilic granuloma/histiocytosis x

Malignant
- Rhabdomyosarcoma
- Lymphoma
- Esthesioneuroblastoma

Nasal tumors
Benign
- Polyps
- Papillomas
- Hemangiopericytoma
- Dermoid
- Wegener granulomatosis
- Meningioma
- Esthesioneuroblastoma
- Mixed tumors
- Inverting papilloma
- Nasolacrimal duct cysts

Malignant
- Midline malignant reticulosis
- Lymphoma
- Ewing sarcoma

Nasopharyngeal tumor
Benign
- Angiofibroma
- Teratoma
- Chordoma[a]
- Hemangioma

Malignant
- Nasopharyngeal carcinoma
- Rhabdomyosarcoma
- Lymphomas

[a]Malignant potential exists

Malignant Neoplasms

Tumors affecting the orbit, adnexa, and optic nerve may originate in the nasopharynx, sphenoid sinus, pituitary gland, and anterior cranial skull base. Nearly one-third of all pediatric head and neck carcinomas occur in the nasopharynx [31]. The most common type of malignant tumor in younger children is rhabdomyosarcoma, whereas nasopharyngeal carcinoma occurs more frequently in adolescents [32]. Ophthalmologic complications are common to invasive neoplastic disorders of the nasopharynx due to the proximity of the cavernous sinus, skull base, and the relative lack of barriers to the spread of neoplasia in this region. Tom et al. reported that compression of the foramen lacerum with nasopharyngeal carcinoma produced abducens and trigeminal cranial nerve palsies in 44% of children [33]. Direct orbital invasion by nasopharyngeal carcinoma is rare but may occur in up to 3% of cases and is associated with a poor prognosis [34]. Rhabdomyosarcoma is the most common primary orbital malignancy of childhood and may erode through an orbital pathway into the nasal cavity, causing stuffiness and epistaxis [35].

Esthesioneuroblastomas are neuroectodermal tumors that originate from the olfactory epithelium in the anterior skull base. Ethmoid sinus extension is common, while ophthalmic involvement is a late finding [36]. These tumors are extremely fibrous, easily invade healthy periorbita, and often extend into the anterior skull base.

Meningiomas and peripheral nerve sheath tumors (neurofibromas) may also originate in surrounding sinuses and spread to invade the orbit, nose, adjacent sinuses, and cranial cavity [37]. Figure 9.11 details the extent of a meningioma causing proptosis and nasal obstruction, which required an intracranial approach for removal.

Mucoceles and Benign Tumors

Mucoceles are obstructed paranasal sinuses that continue to produce secretions and consequently expand. The infected form is called a mucopyocele. Previous sinus surgery or trauma causing scarring and poor drainage can lead to their development [38]. Frontal and anterior ethmoid sinus mucoceles can present with diplopia and frontal, facial, and orbital deformation from the slow expansion that occurs to the orbital wall. This destructive process may take many years to develop, and most pediatric mucoceles are found on incidental sinus CT examinations. Diagnosis is usually obtained before ocular damage occurs (Fig. 9.12).

Juvenile angiofibromas develop in preadolescent males from the vascular region in the area of the sphenopalatine foramen (Fig. 9.13). These children present with long-standing nasal obstruction and bouts of severe epistaxis. Orbital invasion may occur in up to 30% of patients [39], and proptosis may be seen in 10% of patients [40]. The mass gains entrance into the orbit from traversing the pterygopalatine fossa, then moving upward through the inferior orbital fissure.

Osseous lesions may encroach upon the sinuses, the orbit, and its contents. Monostotic fibrous dysplasia is the most

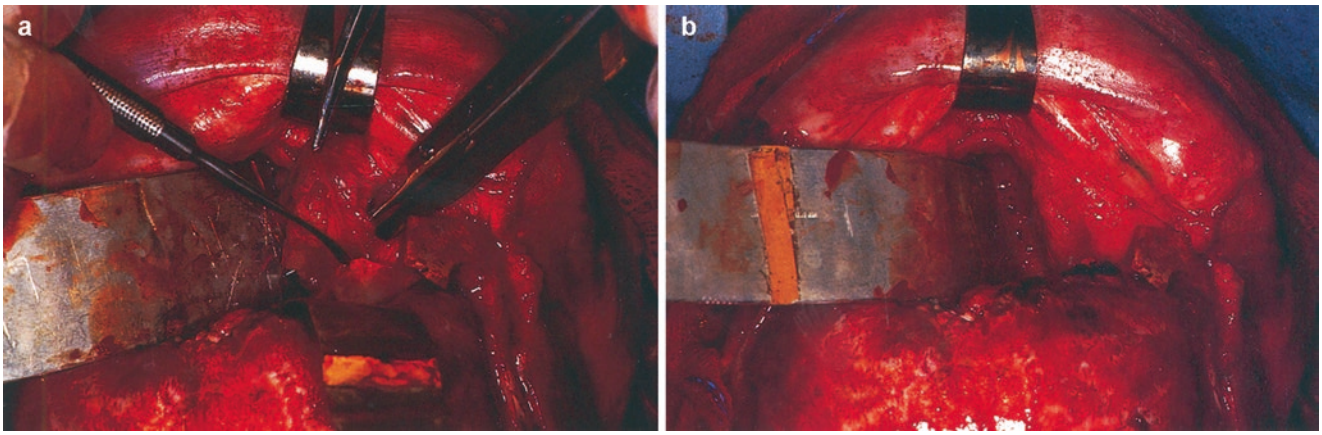


Fig. 9.11 Frontal sinus meningioma. (**a**) Frontal sinus meningioma of a 5-year-old requiring an anterior cranial approach. The tumor is being removed from the periorbitae and nasal cavity. (**b**) Postoperative cavity after complete tumor removal

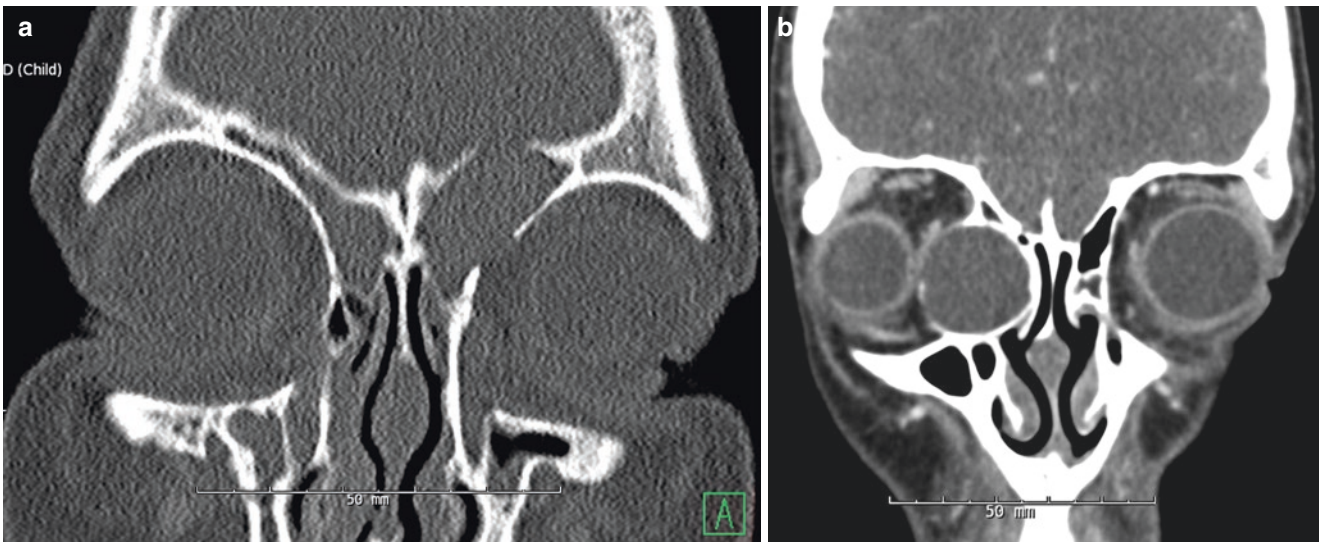


Fig. 9.12 Mucoceles. (**a**) Left frontoethmoidal mucocele with associated erosion of the superomedial orbital wall and posterior table of the inferior frontal sinus. (**b**) Right ethmoidal mucocele expanding into the orbit

common fibro-osseous disorder that involves the orbit and paranasal structures (Fig. 9.14a) [41]. Polyostotic fibrous dysplasia (Albright syndrome) is associated with multiple bony lesions, precocious puberty, and skin lesions and usually does not affect the orbit or facial skeleton. Ossifying fibromas have a more aggressive growth pattern and a more sclerotic bone pattern than fibrous dysplasia [42]. Osteomas may occur in the orbit or paranasal sinuses, usually in developed frontal sinuses, causing headaches or frontal sinus blockage (Fig. 9.14b).

Management

After the appropriate imaging studies are reviewed by the surgical team, the next step is to ascertain the pathology of the lesion in question and formulate a treatment. Often incisional biopsies at the time of initial surgical exposure are required due to the location, size, and vascular nature of the pathology.

Approaches to both benign and malignant pediatric tumors should be performed with a concern for achieving maximum exposure with minimum cosmetic deformity. Benign tumors may recur and cause damage years later if not completely excised. If surgically feasible, meningiomas, fibrous dysplasia, ossifying fibromas, angiofibromas, and hemangiopericytomas are best controlled by complete removal. Some tumor types, such as inverted papillomas, have a propensity to become malignant, increasing the need for total excision [43]. Fortunately, most benign lesions tend to gradually push the periorbital contents forward, causing remarkable clinical exophthalmos without actual involvement of the orbital tissues.

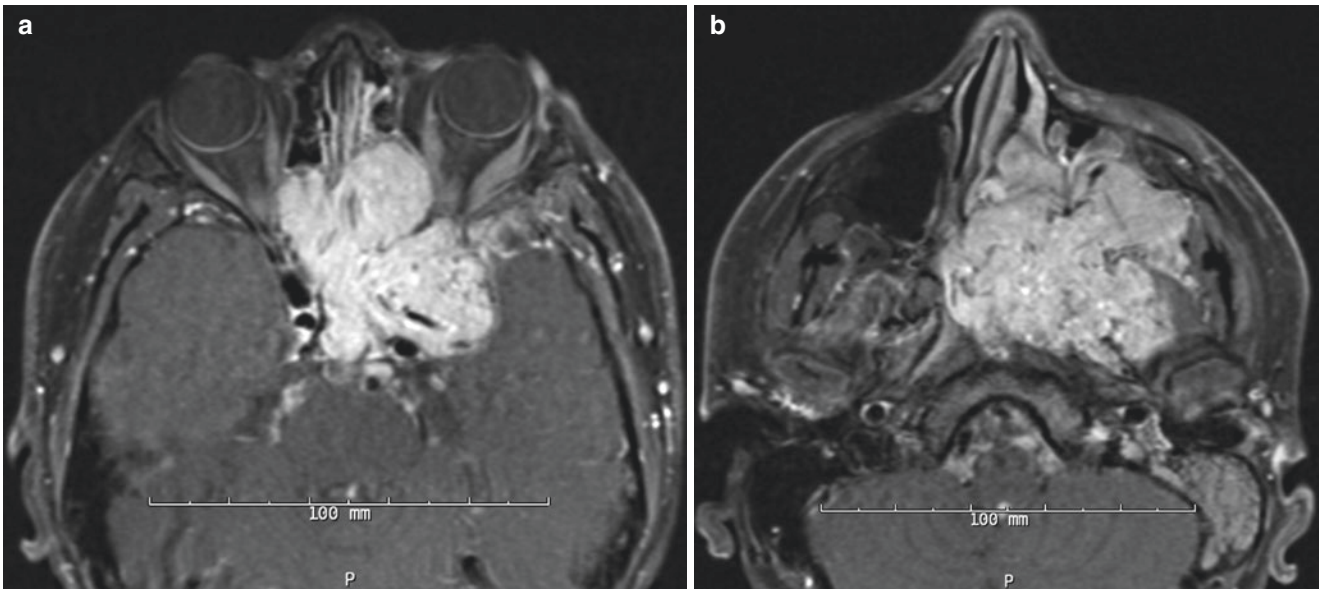


Fig. 9.13 (**a**, **b**) Juvenile nasopharyngeal angiofibroma. Two axial T1-weighted, gadolinium-enhanced views of a large angiofibroma in a 13-year-old male. Note the avid gadolinium enhancement of this very vascular tumor as well as displacement of the orbital wall

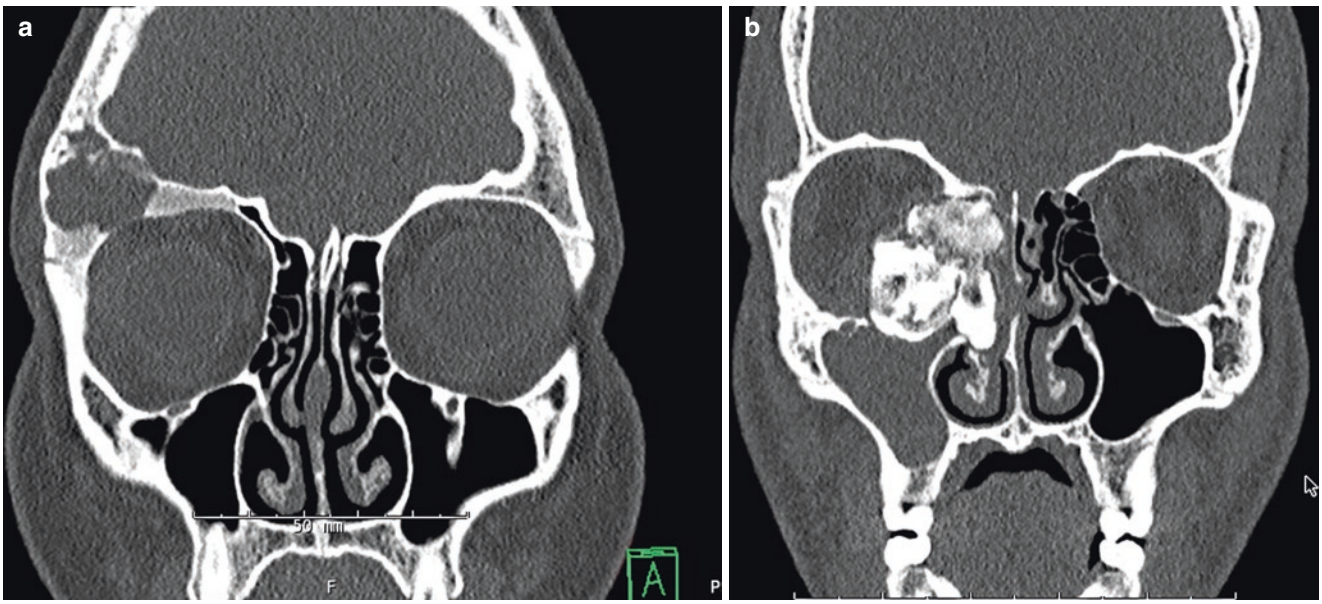


Fig. 9.14 Fibro-osseous lesions. (**a**) Coronal CT revealing a fibro-osseous lesion involving the right superior orbit. Pathology was consistent with fibrous dysplasia. (**b**) Coronal CT image of an osteoma involving the medial orbital wall with associated proptosis

Polyps of the sinuses and nasal cavities, although easily removed, have the propensity to recur. With each recurrence, the chances of intraoperative orbital or intracranial damage increase as normal landmarks become obscure.

Malignant tumors of the orbit may also invade the periorbita, indicating the need for removal of orbital contents. Histologic types that may require orbital exenteration include squamous cell carcinoma, adenocarcinoma, esthesioneuroblastoma, and adenocystic carcinoma, the latter of which has a particular tendency toward perineural invasion [44].

Rhabdomyosarcoma in any head and neck site may be an aggressive and rapidly expanding destructive tumor. Chemotherapy and radiotherapy remain the mainstay of initial treatment after staging biopsies are performed [45, 46]. Aggressive craniofacial surgery is utilized only after medical therapy has failed. Extranodular lymphomas and leukemic infiltrates are also best treated with chemotherapy and radiation.

Complete surgical excision is recommended for both aggressive ossifying fibroma and the slower-growing fibrous dysplasia if possible. In diffuse facial bone involvement, conservative shaving is recommended. Each case must be

individually analyzed for the appropriate choice of approaches. Surgeons encountering large periorbital fibromas must keep in mind that these disorders are not malignant and that an orbit and functioning globe should be spared injury with conservative resection whenever possible.

Surgical Procedures

Endoscopic Surgery

Advances in technology and experience have allowed for endoscopic nasal surgery to become the primary treatment modality for a wide array of sinonasal and orbital pathologies in the pediatric population [47]. The development of angled telescopes coupled with advances in high definition optic technology has allowed for improved exposure and superior visualization when compared with open approaches for many sinonasal lesions. Techniques such as orbital decompression and dacryocystorhinostomy can be routinely accomplished without external incisions in selected patients. Endoscopic techniques are feasible in accessing structures in the orbit that are medial to the optic nerve [48].

Lateral Rhinotomy

Lateral rhinotomy allows excellent exposure to the anterior and posterior skull bases, sinuses, and orbit (Fig. 9.15). Tumors with minimum intracranial involvement may also be approached with this incision. Medial maxillectomy can be added to open the posterior exposure to the apex of the orbit, sphenoid, and inferior orbit [49].

Midfacial Degloving

Midfacial degloving offers excellent exposure to the sinuses and orbits from below without visible incisions [50]. Its usefulness is limited, however, in those lesions located very anterior (ethmoids) and those with intracranial extensions. Complications of degloving may include saddle deformity of the nose and stenosis of the nasal vestibule.

Iatrogenic Complications

Complications involving the orbit from endoscopic sinus surgery are rare and usually minor [51]. Ohnishi et al. have identified the following high-risk areas: lamina papyracea, anterior ethmoid artery, cribriform plate, posterior ethmoid artery, and the region between the sphenoid and posterior ethmoid air cells [52]. Specific types of injury may occur, depending on the location (Table 9.2).

Complications may arise during sinus and skull base surgery that require immediate ophthalmologic consultation. Serious ophthalmic complications include blindness from direct optic nerve trauma or retrobulbar hematoma, damage to the extraocular muscles, and damage to the ophthalmic division of the trigeminal nerve resulting in corneal anesthesia [3]. Direct trauma to the optic nerve is rare [53]. Orbital hemorrhage has been described to occur less than 1% of the time [54, 55]. Surgeons should be aware of the location of the lamina papyracea and ethmoid vessels and palpate the globe during surgery to observe for evidence of herniation of orbital contents into the nose. Chemosis, proptosis,

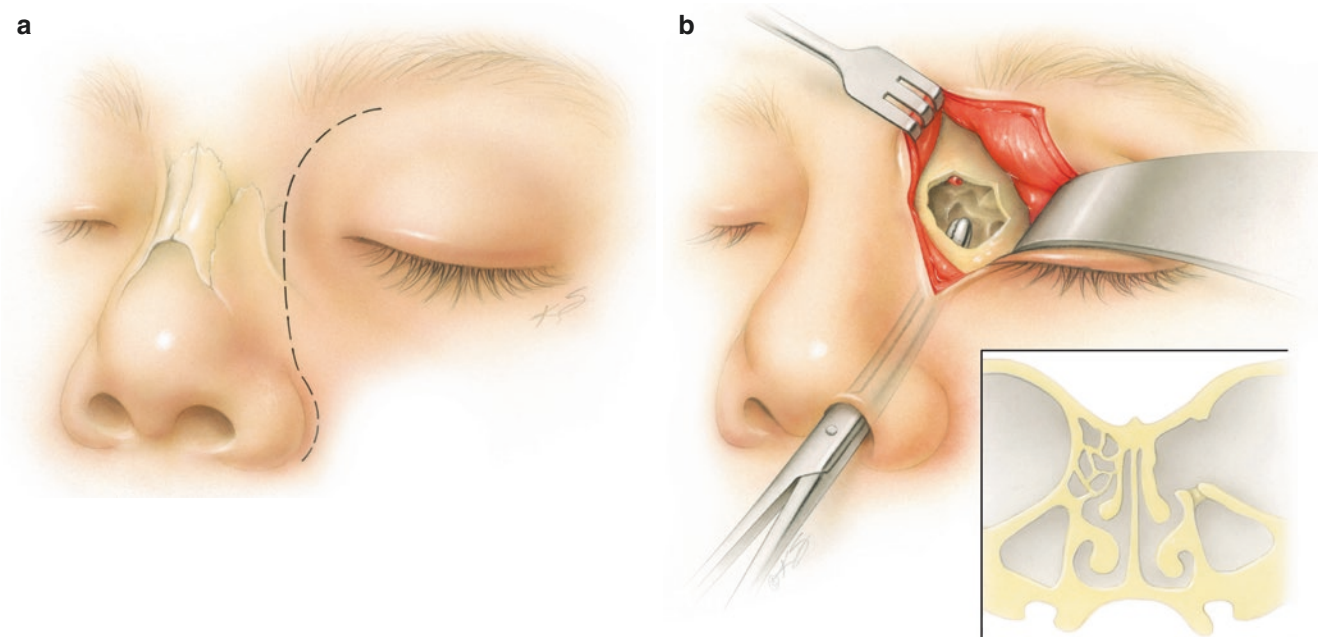


Fig. 9.15 Lateral rhinotomy and ethmoidectomy. (**a**) A lateral rhinotomy may begin with a Lynch incision. The periorbita is carefully elevated off the lamina papyracea. (**b**) Postoperative view following external ethmoidectomy. Clamp in nasal cavity illustrates the adequate sinus drainage offered by this approach when combined with the removal of the ethmoid air cells

Table 9.2 Anatomical variations and pathophysiological/surgical considerations

Dehiscent lamina papyracea	Route of infection/tumor/orbital contents damaged
Variable roof of ethmoid	Risk of intracranial injury/CSF leak/ethmoid artery damage
Infraorbital ethmoid cell	Increased risk of sinus infection/orbital (Haller cell) and lacrimal injury
Sphenoethmoid cell	Increased risk of injury to optic nerve (onodi cell)

Source: Adapted from Stammberger [61]

and lid edema should prompt the surgeon to obtain immediate ophthalmologic consultation. Management of optic nerve trauma and retrobulbar hematoma is outlined below [56]. Mobility disturbances can also occur due to direct trauma to the medial and superior rectus and superior oblique muscles. Scar tissue formation and myositis have also been described secondary to surgical interruption of the integrity of the lamina papyracea and resulting orbital muscle fixation [56].

Minor orbital complications include orbital emphysema, edema, and epiphora from lacrimal duct damage. Ophthalmologic consultation should also be obtained if visual or motility problems are noted postoperatively.

Lacrimal damage may be unavoidable during large resections, especially with medial maxillectomies and many transfacial approaches. Dacryocystorhinostomy or marsupialization may be necessary to prevent long-lasting lacrimal blockage, synechiae, and epiphora. The lacrimal system, however, may be able to tolerate trauma better than previously expected. Bolger et al. have reported that a substantial number of lacrimal duct injuries may occur during endoscopic surgery without any resulting clinical symptoms [57].

Complications of Skull Base Tumors and Surgery

Nasal
- Epistaxis
- Packing

Airway

Orbital
- Retrobulbar hematoma
- Motility disorders
- Optic nerve
- Lacrimal system
- Orbital emphysema

Intracranial

CSF leak

Management of Orbital Complications

Orbital nerve trauma (normal intraocular pressure)

Medical
- Steroids
- Postoperative CT

Surgical
- Consider intracanalicular nerve decompression

Retrobulbar hematoma (elevated intraocular pressure)

Medical
- Remove nasal packs
- Mannitol (1–2 gm/kg over 20–30 min)
- Acetazolamide (500-mg IV bolus)
- Dexamethasone (10-mg IV bolus)

Surgical (if no medical response)
- Lateral canthotomy
- Superior and inferior cantholysis

Medial orbital wall decompression
- Control anterior and posterior ethmoid arteries

Source: Adapted from Neuman et al. [56]

Epistaxis

Epistaxis secondary to nasal tumors or trauma may require nasal endoscopy, cauterization (chemical or electrical), and anterior and posterior packing. Most cases of epistaxis in children originate from the anterior septum. Simple gentle pinching of the sides of the nose may help to control initial and recurrent bleeding. Oxymetazoline nasal spray will often cause appropriate topical vasoconstriction and greatly assist in the reduction of bleeding. This technique is commonly recommended by otolaryngologists to their patients if bleeding is encountered after sinus or nasal surgery.

Prolonged bleeding, longer than 10 min, should be reported to the surgeon. Nasal packing may be necessary in those patients with prolonged and recurrent episodes. Children who require packing while awake in an emergency department are often anxious and frightened by the visible blood. Topical anesthetic agents such as 2% lidocaine simply sprayed into the nasal cavities may aid in the reduction of discomfort prior to instrumentation or packing of the nose.

Agents used in packing may include those that dissolve and do not require removal and fiber materials that must be removed. Gelfoam, Avitene, and Surgicel have excellent hemostatic properties, with the added advantages of soft textures, ease of handling, and the tendency to dissolve with the applications of saline nasal sprays. Merocel sponges or cotton ribbon packing may be necessary if simple measures

prove inadequate. Correct placement requires knowledge of the bleeding site and nasal anatomy. Rough or incorrect placement of these materials may cause lacerations to the mucosa of the nasal cavities and further bleeding. Applications of antibiotic ointment to the fiber or sponge packing ease the insertion and removal and reduce bacterial growth in the sinus or nasal cavities.

Packing is not without both local and systemic concerns. Toxic shock syndrome has been reported after nasal surgery with the use of both Merocel sponges and Gelfoam [58]. Additionally, nasal packing may worsen the consequences of an expanding retro-orbital hematoma as noted previously. Prevention of these issues is best avoiding packing altogether when possible.

Posterior nasal bleeding is extremely rare in children. Delayed cases of severe bleeding have occurred a few days to years after trauma to the skull base and surrounding vasculature [59]. Mauer et al. described a triad of massive epistaxis, unilateral blindness, and orbital fracture with a posttraumatic aneurysm located in the cavernous sinus portion of the internal carotid artery [60].

Angiography has a vital role in the treatment of a patient with intractable bleeding or suspected vascular trauma. Interventional radiologists may be consulted to perform angiography with the intention of embolizing the targeted vessel with Gelfoam, polyvinyl alcohol, and/or wire springs in areas where surgical entry may prove difficult or too destructive. Preoperative embolization may assist in the reduction of intraoperative blood loss during surgery of highly vascular tumors.

Airway Concerns

Craniofacial resections may require observation in the intensive care unit and prolonged intubation. Tracheostomy may be considered if the resection is significant and the patient's upper airway remains edematous for prolonged periods. Cranial nerve dysfunction can also contribute to airway obstruction.

Summary

Infections and tumors of the nose and paranasal sinuses occurring in the pediatric population may encroach upon the orbit and its contents and require cooperative ophthalmic and otolaryngologic treatment. The otolaryngologist skilled in pediatric skull base and endoscopic surgical techniques may assist the ophthalmologist by obtaining biopsies, gaining access to tumors, and treating severe sinus disorders affecting the orbit and adnexa. Orbital complications that may arise during sinus and skull base surgeries require prompt recognition and ophthalmologic consultation.

References

1. Wald ER. In: Bluestone CD, Stool SE, editors. Rhinitis and acute and chronic sinusitis. 2nd ed. Philadelphia: WB Saunders; 1990. p. 729–44.
2. Ritter FN. The paranasal sinuses: anatomy and surgical technique. St. Louis, MO: Mosby; 1973.
3. Wilson JL, Dreshler DG, Kaplan MJ, Pillsbury HC. Complications of cranial base surgery. In: Weissler MC, Pillsbury HC, editors. Complications of head and neck surgery. New York: Thieme Medical; 1995. p. 336–51.
4. Wald ER, Applegate KE, Bordley C, Darrow DH, Glode MP, Marcy SM, Nelson CE, Rosenfeld RM, Shaikh N, Smith MJ, Williams PV, Weinberg ST. Clinical practice guideline for the diagnosis and management of acute bacterial sinusitis in children aged 1 to 18 years. Pediatrics. 2013;132(1):e262–80.
5. Chandler JR, Langenbrunner DJ, Stevens ER. The pathogenesis of orbital complications in acute sinusitis. Laryngoscope. 1970;80:1414–28.
6. Johnson DL, Markle BM, Weiderman BL, Hanahan L. Treatment of intracranial abscesses associated with sinusitis in children and adolescents. J Pediatr. 1988;113:15–23.
7. Erickson BP, Lee WW. Orbital cellulitis and subperiosteal abscess: a 5-year outcomes analysis. Orbit. 2015;34:115–20.
8. Hornblass A, Hershorn BJ, Stern K, Grimes C. Orbital abscess. Surv Ophthalmol. 1984;29:661–6.
9. Patt BS, Manning SC. Blindness resulting from orbital complications of sinusitis. Otolaryngol Head Neck Surg. 1991;104:789.
10. Mafee MF. Modern imaging of paranasal sinuses and the role of limited sinus computerized tomography; considerations of time cost and radiation. ENT J. 1994;73:532–46.
11. Towbin R, Bokyung RH, Kaufmann RA, Burke M. Postseptal cellulitis: CT in diagnosis and management. Radiology. 1986;158:735–7.
12. Garcia GH, Harris GJ. Criteria for nonsurgical management of subperiosteal abscess of the orbit: analysis of outcomes 1988–1998. Ophthalmology. 2000;107:1454–6.
13. Bedwell JR, Choi SS. Medical versus surgical management of pediatric orbital subperiosteal abscesses. Laryngoscope. 2013;123:2337–8.
14. Rubenstein JB, Handler SD. Orbital and periorbital cellulitis. Head Neck Surg. 1982;5:15–21.
15. Brook I. Microbiology and choice of antimicrobial therapy for acute sinusitis complicated by subperiosteal abscess in children. Int J Pediatr Otorhinolaryngol. 2016;84:21–6.
16. Souliere CR, Antione GA, Martin MP, Blumberg AI, Isaacson G. Selective non-surgical management of subperiosteal abscess of indication for surgical drainage. Int J Pediatr Otolaryngol. 1990;19:109–19.
17. Rahbar R, Robson CD, Petersen RA, DiCanzio J, Rosbe KW, McGill TJ, et al. Management of orbital subperiosteal abscess in children. Arch Otolaryngol Head Neck Surg. 2001;127:281–6.
18. Oxford LE, McClay J. Medical and surgical management of subperiosteal orbital abscess secondary to acute sinusitis in children. Int J Pediatr Otorhinolaryngol. 2006;70:1853–61.
19. Ryan JT, Preciado DA, Bauman N, Pena M, Bose S, Zalzal GH, et al. Management of pediatric orbital cellulitis in patients with radiographic findings of subperiosteal abscess. Otolaryngol Head Neck Surg. 2009;140:907–11.
20. Parikj SR, Cuellar J, Sadoughi B, Aroniadis O, Fried MP. Indications for image-guidance in pediatric sinonasal surgery. Int J Pediatr Otorhinolaryngol. 2009;73:351–6.
21. Hoyt DJ, Fisher SR. Otolaryngologic management of patients with subdural empyema. Laryngoscope. 1991;101:20–4.
22. Gurucharri MJ, Lazar RH, Younis RT. Current management and treatment of complications of sinusitis in children. ENT J. 1993;70:107–12.

23. Lusk RP, Tychen L, Park TS. Complications of sinusitis. In: Lusk RP, editor. Pediatric sinusitis. New York: Raven; 1992. p. 127–46.
22. Lusk RP. Surgical management of chronic sinusitis. In: Lusk RP, editor. Pediatric sinusitis. New York: Raven; 1992. p. 77–125.
23. Turner WJ, Davidson TM. Endoscopic management of acute frontal sinusitis. ENT J. 1994;73:594–7.
24. Washburn RG, Kennedy DW, Begley MG, Henderson DK, Bennet JE. Chronic fungal sinusitis in apparently normal hosts. Medicine. 1988;67:231–47.
25. Goodwin WJ. Infectious and inflammatory diseases of the orbit. Otolaryngol Clin N Am. 1998;21:65–75.
26. Hartwick RW, Batsakis JG. Pathology consultation: sinus aspergillosis and allergic fungal sinusitis. Ann Otol Rhinol Laryngol. 1991;100:427–30.
27. Stanievich JF, Lore JM. Tumors of the nose, paranasal sinuses, and nasopharynx. In: Bluestone CD, Stool S, Scheetz MD, editors. Pediatric otolaryngology. 2nd ed. Philadelphia: WB Saunders; 1990.
28. Calcaterra TC, Trapp LK. Unilateral proptosis. Otolaryngol Clin N Am. 1988;21:53–63.
29. Petruson B. Epistaxsis in childhood. Rhinology. 1979;17:83–90.
30. Mosesson RE, Som PM. The radiographic evaluation of sinonasal tumors: an overview. Otolaryngol Clin N Am. 1995;28:1097–115.
31. Cunningham MJ, Myers EN, Bluestone CD. Malignant tumors of the head and neck: a twenty year review. Int J Pediatr Otorhinolaryngol. 1987;13:270–92.
32. Canalis RF, Jenkins HA, Hemenway WG. Nasopharyngeal rhabdomyosarcoma: a clinical perspective. Arch Otolaryngol. 1982;104:424–40.
33. Tom LWC, Anderson GJ, Womer RB, et al. Nasopharyngeal malignancies in children. Laryngoscope. 1992;102:509–14.
34. Hsu WM, Wang AG. Nasopharyngeal carcinoma with orbital invasion. Eye. 2004;18:833–8.
35. Stefanyszyn MA, Handler SD, Wright JE. Pediatric orbital tumors. N Am Clin Otolaryngol. 1988;21:103–18.
36. Jackson IT, Somers P, Marsh WR. Esthesioneuroblastoma: treatment of skull base recurrence. Plast Reconstr Surg. 1995;76:195–200.
37. Robitaille Y, Seemayer TA, El Deiry A. Peripheral nerve tumors involving paransal sinuses: a case report and review of the literature. Cancer. 1975;35:1257–68.
38. Bordley JE, Bosly WR. Mucoceles of the frontal sinus: causes and treatment. Ann Otol. 1973;82:696–702.
39. Cruz AA, Atique JM, Melo-Filho FV, Elias J. Orbital involvement in juvenile nasopharyngeal angiofibroma: prevalence and treatment. Ophthal Plast Reconstr Surg. 2004;20:296–300.
40. Neel HB. Juvenile angiofibroma. In: Blitzer A, Lawson W, Freidman WH, editors. Surgery of the paranasal sinuses. Philadelphia: WB Saunders; 1985. p. 247–59.
41. Moore AT, Bunic JR, Munro IR. Fibrous dysplasia of the orbit in childhood. Ophthalmology. 1985;92:12–20.
42. Margo CE, Ragsdale BD, Perman KI, et al. Psammatoid ossifying fibroma of the orbit. Ophthalmology. 1985;92:150–9.
43. Batsakis JG. Nasal papillomas. Ann Otol Rhinol Laryngol. 1980;90:190.
44. Kimmelman CP, Korovin GW. Management of paranasal sinus neoplasms invading the orbit: orbital surgery for head and neck surgeons. N Am Clin North America. 1988;21:77–92.
45. Wharam M, Foulkes M, Lawrence W, et al. Soft tissue sarcoma of the head and neck in childhood: nonorbital and nonparameningeal sites. Cancer. 1984;53:1016.
46. Sutlow W, Montague E. Pediatric tumors. In: MacComb W, Fletcher G, editors. Cancer of the head and neck. Baltimore: Williams & Wilkins; 1967. p. 428–46.
47. Rastatter JC, Snyderman CH, Gardner PA, Alden TD, Tyler-Kabara E. Endoscopic surgery for sinonasal skull base lesions in the pediatric population. Otolaryngol Clin N Am. 2015;48:77–99.
48. Tepedino MS, Pinhiero-Neto CD, Bezerra TF, Gardner PA, Snyderman CH, Voegels RL. Endonasal identification of the orbital apex. Larynogscope. 2016;126:33–8.
49. Weisman R. Lateral rhinotomy and medial maxillectomy. Otolaryngol Clin N Am. 1995;28:1145–56.
50. Maniglia AJ, Phillips DA. Midfacial degloving for the management of nasal, sinus, and skull base neoplasms. Otolaryngol Clin N Am. 1995;28:1127–43.
51. Seredyka-Burduk M, Burduck PK, Wierzchowska M, Kaluzny B, Malukiewicz G. Ophthalmic complications of endoscopic sinus surgery. Braz J Otorhinolaryngol. 2016;S1808-8694(16):30084–2. https://doi.org/10.1016/j.bjorl.2016.04.00 (epub).
52. Ohnishi T, Tachibana T, Kaneko Y, Esaki S. High risk areas in endoscopic sinus surgery and prevention of complications. Laryngoscope. 1993;103:1181–5.
53. Buus DR, Tse DT, Farris BK. Ophthalmic complications of sinus surgery. Ophthalmology. 1990;97:612–9.
54. Batti MT, Stankiewicz JA. Ophthalmic complications of endoscopic sinus surgery. Br J Ophthalmol. 2001;85:598–603.
55. Stankiewicz JA, Chow JM. Two faces of orbital hematoma inintranasal (endoscopic) sinus surgery. Otolaryngol Head NeckSurg. 1999;120:841–7.
56. Neuman TR, Turner WJ, Davidson TM. Complications of endoscopic surgery. ENT J. 1994;73:585–90.
57. Bolger WE, Parsons DS, Mair TEA, et al. Lacrimal drainage system injury in functional endoscopic sinus surgery. Incidence, analysis, and prevention. Arch Otolaryngol. 1992;118:1179–84.
58. Thomas SW, Baird IM, Frazier RW. Toxic shock syndrome following submucous resection and rhinoplasty. JAMA. 1982; 247:2402–3.
59. Cusick B, Casler JD, David C. Traumatic aneurysm of the cavernous carotid artery: management of delayed massive epistaxis. Am J Rhinol. 1992;6:165–8.
60. Mauer JJ, Mills M, Berman WJ. Triad of unilateral blindness orbital fracture and massive epistaxis after head injury. J Neurosurg. 1961;18:837–40.
61. Stammberger H. Functional endoscopic sinus surgery: the Messerklinger technique. Philadelphia: Decker; 1991.

Evaluation of Vision and Motility in Children

10

Lloyd Bender and Graham E. Quinn

Introduction

The assessment of vision and ocular motility and alignment in infants and young children presents many challenges for the clinician. In this chapter we highlight the techniques found most useful in assessing visual function for each age group.

The techniques of visual acuity and motility assessment vary little from those utilized in adults, and the primary aim of the examination remains the detection of decreased visual function or strabismus. Early detection of abnormalities will provide the child with the best opportunity for optimum visual development in each eye and the highest probability of normal binocular function.

Assessment of Visual Function: Visual Acuity Clinical Examination

Initial assessment of visual acuity involves the clinical examination of the child using standard techniques. There is no substitute for careful observation of visual behavior as this may be the only tool available in some children.

Fixation preference continues to be one of the simplest, most reliable ways of detecting amblyopia in the strabismic patient, even in infants as young as 5–6 months. This technique is based on the premise that an eye with amblyopia will not maintain fixation on an accommodative target if the fellow eye is sound. The strabismic child who does not have amblyopia in either eye will alternate fixation freely or at least hold fixation for an extended period with either eye during binocular viewing. In contrast, the strabismic child with amblyopia will show a strong preference for fixation with the sound eye and poor fixation ability with the amblyopic eye. Zipf [1] reported that fixation preference was reliable for detecting moderate to severe amblyopia in deviations of greater than 10 prism diopters (PD). He also reported poor reliability of this method for detecting amblyopia in the child with a small-angle strabismus.

Wright et al. [2, 3] developed a technique of assessment of fixation preference (useful in children with a small-angle strabismus or orthotropia) that involves inducing a vertical deviation with a 10-PD prism placed in front of the eye (see Fig. 10.1). The child is asked or induced to fixate on a distant accommodative target, and the prism is introduced in front of one eye; fixation preference is assessed while the child has this induced vertical misalignment. The child is then asked (or induced) to fixate during a smooth pursuit with the prism in front of one eye. Using this technique, Wright et al. divided fixation preference patterns into five categories that suggest the presence or absence of amblyopia. As shown in Table 10.1, children who freely alternate fixation or hold fixation *through a smooth pursuit* in each eye for at least 5 seconds, or through a blink, are not likely to have moderate or severe amblyopia in either eye. Children who show a strong fixation preference should be suspected of being amblyopic in the non-preferred eye. The 10-PD technique can be difficult in children with ptosis, which may obstruct easy visualization of the upward movement of the eye.

An alternative is assessing the fixation response to placing a 20PD base out prism in front of each eye sequentially and assessing eso-deviation of the eye under prism to take up fixation. This test relies on peripheral fusion and may be used as a marker for fixation preference and potential amblyopia [4].

L. Bender (✉)
Children's Hospital of Philadelphia, Philadelphia, PA, USA
e-mail: lloydbender@icloud.com; lloydbender@doctors.org.uk

G.E. Quinn
Perelman School of Medicine, University of Pennsylvania, Philadelphia, PA, USA

The Children's Hospital of Philadelphia, Philadelphia, PA, USA

© Springer International Publishing AG 2018

J.A. Katowitz, W.R. Katowitz (eds.), *Pediatric Oculoplastic Surgery*, https://doi.org/10.1007/978-3-319-60814-3_10

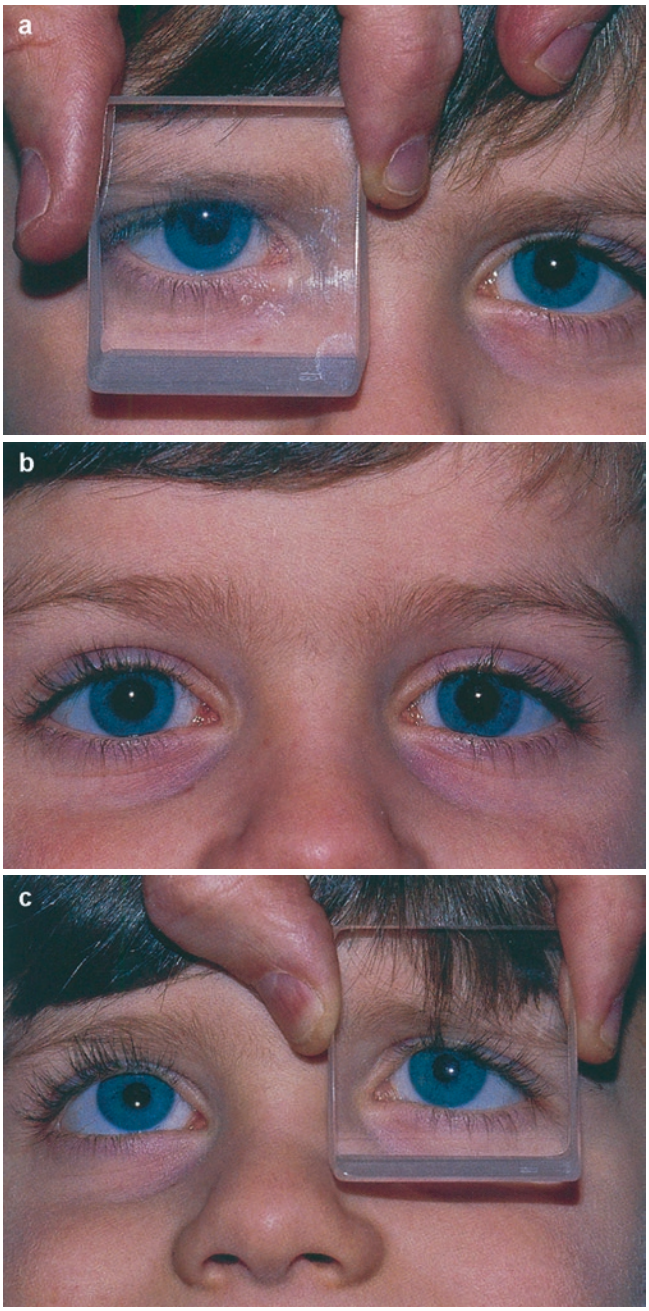


Fig. 10.1 The 10-prism base down test for amblyopia. As described by Wright et al. [2], the 10-prism base down test for amblyopia is useful in children with straight eyes. The child with straight eyes (**b**) is asked to fixate a distant target after the prism is placed in front of the right eye (**a**) and then left eye (**c**). Since the image is slightly blurred with the prism, the fact that the child elevates both eyes to fixate with the left eye in (**c**) strongly suggests amblyopia of the right eye

Table 10.1 Fixation preference in patients with small-angle strabismus or straight eyes

	Fixation pattern	Definition
Equal ocular preference	Alternates fixation Holds well	Freely alternates Holds fixation in non-preferred eye for at least 5 s through a smooth pursuit
Strong fixation preference	Holds briefly Holds momentarily Will not hold	Holds for 3 s before refixation Holds only 1–2 s before refixation Immediate re-fixation to preferred eye

Source: Adapted from data in Wright et al. [3]

Quantitative Methods of Acuity Testing

Quantitative visual acuity tasks in young children are divided into three basic types of acuity assessment: detection acuity, resolution acuity, and recognition acuity. Detection acuity tasks involve detecting the presence of a stimulus against a standard background [5]. Several different techniques have been used, such as the Bock candy bead test where small candy nonpareils are presented to the child (and the task of finding the candy pieces is reinforced by allowing the child to eat them). Other tasks involved finding white balls on a black background, black wires of various widths, and black dots on a white field. The tasks also tend to involve movement of the stimulus in front of the subject. None of these tasks has been successfully incorporated into a routine clinical setting.

Resolution acuity techniques rely on the subject's ability to discriminate a stimulus pattern, typically a black and white grating, when presented against a luminance-matched, homogeneous gray background. Three basic methods are employed in testing resolution acuity in infants: (1) preferential looking, which depends on the looking behavior of the child when regarding a pattern stimulus; (2) optokinetic nystagmus, which depends on generation of involuntary eye movements in response to large moving stimuli of varying spatial frequency; and (3) visual evoked response, which determines the electrophysiologic response of the visual cortex to visual targets. All of these techniques have been incorporated into clinical settings for testing of very young children.

Preferential looking procedures were developed from work in the 1950s and 1960s by Fantz [6, 7] and are based on the observation that infants prefer to look at a grating pattern instead of a plain background. Fantz observed the duration of the infant's looking behavior at a patterned stimulus, compared to a plain stimulus, and judged that the child could discriminate between the two stimuli if the duration of looking at the patterned stimulus was significantly longer than the duration of looking at the plain stimulus.

Teller and coworkers [8, 9] modified the preferential looking procedure by requiring that an observer present the patterned stimulus to the child's right and left side and then, without knowledge of the location of the patterned stimulus, evaluate, based on the child's looking behavior, whether the

child could discriminate the grating. Acuity could then be estimated from the highest spatial frequency grating that the infant was reliably judged to see (usually based on a criterion of 75% correct). This "forced-choice preferential looking" procedure was relatively quick and was further adapted for use in clinical settings.

The Cardiff acuity cards are picture cards that utilize the same principle of preferential looking but using pictures and not gratings. This may be more engaging for preverbal toddlers [10–12].

The Teller Acuity Card Procedure

The acuity card procedure [13, 14] was developed to shorten the time needed to obtain an estimate of acuity for an individual infant and thus enable preferential looking procedures to be incorporated into clinical settings. It consists of a series of gray cards (Fig. 10.2) 25.5 × 51.0 cm, with a black and white grating (measuring 12.5 × 12.5 cm) located on one side of a central peephole.

The observer or tester, who is masked to the location of the grating (striped pattern), presents the card to the infant enough times to determine with confidence whether the child can distinguish stripes on one card before presenting the card with the next narrower pattern on it. Increasingly, narrow gratings are presented until the tester determines that the child can no longer resolve the gratings. The infant's threshold acuity is determined by the smallest stripes (highest spatial frequency) that it can resolve at the testing distance. Efficiency of the acuity card procedure is enhanced by the subjective judgments that the tester makes concerning the infant's looking behavior, thus shortening the time necessary to reach threshold acuity. As shown in Fig. 10.3, the acuity card procedure maximizes the child's interest in the task by allowing the tester to interact with the infant between presentations. In addition, the threshold acuity obtained using the acuity card procedure is in good agreement with those obtained using traditional methods of preferential looking procedures. However, there are also limitations of the acuity card procedure, including potential tester bias and artifacts in the cards themselves [13].

Early clinical studies of preferential looking techniques showed high success rates for monocular testing, usually better than 90% in infants older than 6 months [15].

Incorporation of the acuity card procedure into clinical practice requires knowledge of the normal range and the development of grating acuity in infants and young children (Fig. 10.4). Mayer et al. [16] provided normative values for monocular testing using rigorous standardized techniques of subjects from 1 month to 4 years. The acuity card procedure has been used in various clinical conditions, in addition to ROP, such as cataracts and aphakia, Leber's congenital amaurosis, macular colobomas, nystagmus, and various central nervous system abnormalities, such as periventricular leukomalacia and delayed visual maturation. In strabismic amblyopia, it appears that amblyopic eyes show greater acuity deficits when tested using recognition acuity tests compared to acuity results of grating acuity tests. In addition, a fixation preference for one eye may not be reflected by decreased grating acuity in the fellow amblyopic eye [16].

Interpretation of acuity values obtained in infants and young children using resolution acuity methods must be carefully reported and interpreted. A key consideration is that resolution acuity values are not necessarily equivalent to

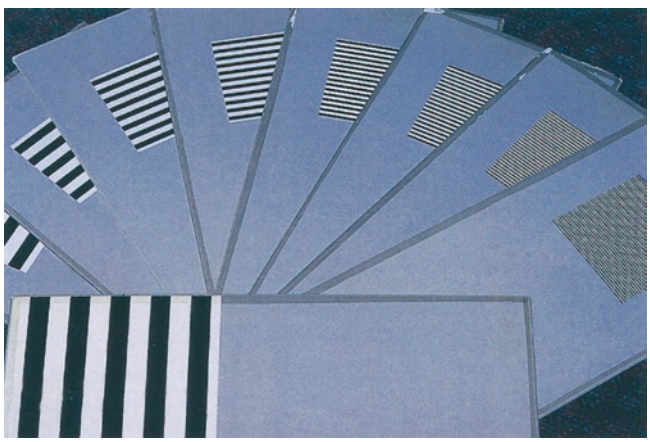


Fig. 10.2 The Teller acuity card set. The Teller acuity card set consists of 17 cards with 12.5 × 12.5-cm patches of evenly spaced black and white stripes in half-octave steps, including a blank card and a "low vision" card on which the stripes occupy half of the acuity card and each stripe measures 2.3 cm



Fig. 10.3 Tester interaction. The Teller acuity card procedure allows for tester interaction so that the tester can be certain of the child's looking patterns and attention as part of the procedure

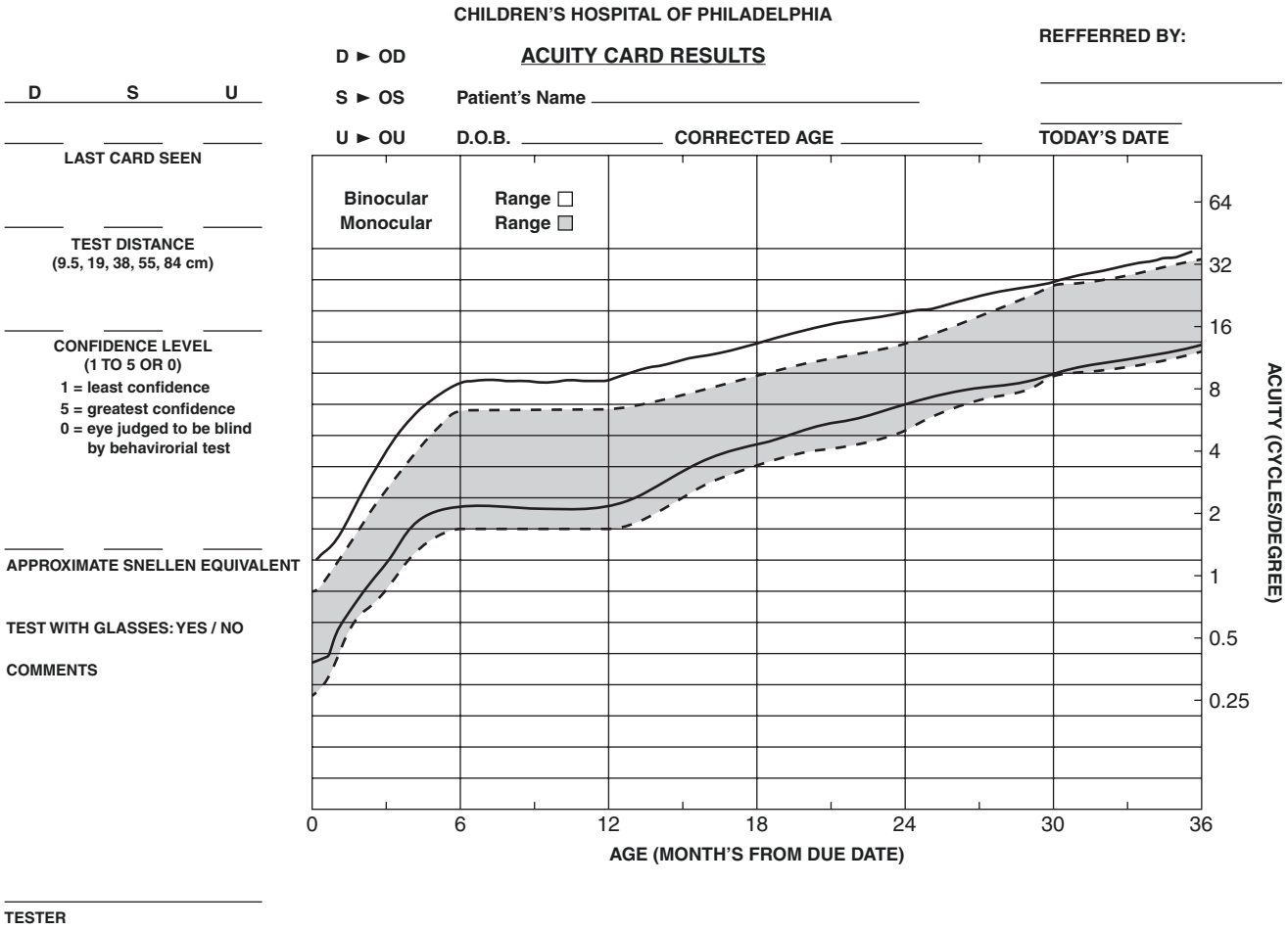


Fig. 10.4 Grating acuity. Grating acuity results are recorded in terms of the last card the tester thought the child saw at a particular distance. A "confidence" level is provided to indicate whether the tester thought the test provided an accurate assessment of the child's grating acuity. Finally, the results are recorded on a graph that has the 95% confidence intervals for children with no known ocular or central nervous system disorders

recognition acuity [17] and there are, as yet, no methods for assessing recognition acuity in infants and very young children. However, several studies in older children and adults suggest that measures of recognition acuity and measures of resolution acuity give similar values. The largest to date is from the CRYO-ROP study [18] that compares results of letter acuity testing, using a crowded HOTV chart and results of grating acuity testing, using the acuity card procedure. Visual acuity scores were obtained from 1694 eyes at age 3½ years to 2101 eyes at 4½ years. There was a significant correlation between letter acuity and grating acuity in young children with birth weights of less than 1251 g, whether or not the eyes had ROP residua. Eyes that had acuity below 20/150 generally showed better grating acuity than letter acuity, and it was possible to provide the 90% confidence intervals for letter acuity scores for specific grating acuity results (see Table 10.2).

The clinician must remember that resolution acuity results will often underestimate the degree of visual loss present in a child that may be documented when a more standard recognition acuity measure can be obtained. As Kushner [17] suggests, care must be taken in reporting grating acuity values in terms of Snellen acuity values, especially to agencies making determination of need for visual services. It is also important to remember that an acuity in the normal range at an early age does not necessarily predict normal acuity at a later stage later.

Incorporation of the acuity card procedure into a busy clinical practice requires adaptations and individuals responsible for testing must be trained in the technique. A well-lit quiet

Table 10.2 Estimation of recognition acuity from grating acuity measured with Teller acuity card procedure in 3½- to 4½-year-old children

	Predicted recognition acuity (crowded HOTV)			
	Normal eyes (N = 2487)		Eyes with abnormalities (N = 1308)	
Grating acuity (cycles/deg)	Median (n)	90% confidence	Median (n)	90% confidence
≥45	20/20 (18)	–	20/20 (5)	–
32 to <45	20/20 (57)	20/25 to 20/16	20/20 (15)	–
23 to <32	20/20 (565)	20/30 to 20/16	20/25 (164)	20/30 to 20/16
16 to <23	20/25 (1265)	20/40 to 20/20	20/25 (514)	20/40 to 20/20
11 to <16	20/25 (453)	20/40 to 20/20	20/30 (284)	20/60 to 20/20
8 to <11	20/40 (104)	20/80 to 20/25	20/50 (157)	20/164 to 20/25
5.6 to <8	20/55 (18)	–	20/100 (73)	20/342 to 20/40
4 to <5.6	20/80 (5)	–	20/125 (39)	20/640 to 20/60
2.8 to <4	(1)	–	20/200 (19)	–
2 to <2.8	(0)	–	20/400 (15)	–
<2	(1)	–	20/320 (23)	20/955 to 20/110

Source: Adapted from Dobson et al. [27]

space should be provided for testing, and one should also be wary of bias, since in a clinical setting the same tester may test a child several times and remember which is the "bad" eye and which is the "good" one [19]. The tester must also be familiar with nonstandard techniques needed to test the child with low vision, nystagmus, and visual field abnormalities [20].

Visual Evoked Potential Techniques

The Visual Evoked Potential (VEP) (recorded at the occipital region of the scalp) can be elicited with varying stimuli and has a correlation with visual acuity. Checkerboards and gratings of varying spatial frequency are the most common stimuli used in recording pattern visual evoked potentials (PVEP). In normal children, an estimate of visual acuity may be based on the amplitude of the PVEP although it is not realistic to expect a direct correlation [21, 22]. A recordable PVEP to a 50′ or smaller check size indicates good vision, while a flash VEP response with no recordable PVEP suggests rudimentary vision. PVEPs may be useful for serial monitoring and interocular comparisons in infancy [23]. Sweep VEP techniques allow rapid acquisition of responses to a stimulus that varies in spatial frequency and may provide a more easily acquired estimation of acuity [24, 25].

In addition to estimating acuity, serial VEP monitoring may be helpful in detecting early optic nerve dysfunction in children with craniofacial anomalies at risk of raised intracranial pressure [23, 26].

The technique for measuring visual evoked potential requires intense interaction between the tester and the subject with the tester ensuring that the child is attending the test patterns. This interaction between subject and tester is especially important since the computer equipment, electrodes placed on the head, and eye patches can be very intimidating for the young patient.

Comparisons of the results of VEP estimated acuity to measured acuity with letter recognition tests show the same underestimation of an acuity deficit using VEP techniques. This is similar to results comparing recognition acuity tests to grating acuity tests and is likely due to the simpler task of resolving grating patterns compared to the higher order form discrimination task of letter recognition.

ISCEV (International Society for Clinical Electrophysiology of Vision) sets the technical standards for visual electrophysiological testing. Each laboratory however must develop its own normative database and maintain high-quality control over data collection and interpretation. As this technology becomes more user-friendly and widely available, it is reasonable to expect increasing widespread clinical use of these techniques [28].

Recognition Acuity Tests

Recognition acuity tests rely on the form recognition of symbols, pictures, or letters of decreasing spatial frequency to determine the threshold acuity. Many optotypes in various arrangements have been proposed and several are in widespread use.

The Landolt C has been designated as the standard optotype for recognition acuity testing by the World Health Organization and the National Research Council of the National Academy of Science. However, no test has been designated standard for use in verbal, preschool children. The Allen and Snellen picture charts, which have simple recognizable pictures, tumbling E, crowded HOTV, and Snellen letters, have all been used for very young children, along with numerous variations of numbers of symbols per line and spatial relation of the symbols [29]. Lea symbols were introduced in 1980 and provide similar results to the Landolt C acuity testing and are now in widespread use [30]. Kay pictures provide comparable acuity assessment to logMAR acuity testing but may underestimate amblyopia in children with lower acuity [31].

Sprague et al. [29] found that isolation of symbols was required more frequently for logMAR charts than for standard charts and that young children had slightly worse acuity scores using logMAR charts than when tested with standard charts.

As shown in Fig. 10.5, for testing with the HOTV chart, the child performs a pretest in which he/she is presented with the individual letters, H, O, T, and V and is asked to identify the letter by pointing it out on a lap board. By matching the symbols, the child can provide a recognition acuity without actually "reading" the letters. Even if the child is unsuccessful in completing testing initially, two copies of the letters can be sent home with the child for practice. Sprague et al. [25] reported that 84% of 3-year-olds and 94% of 4-year-old children were able to complete testing using HOTV optotypes at 10 feet at the first or second screening, compared to 59% at 3 years and 88% at 4 years for the E chart. Investigators in the VIP study found a test distance of 5 feet more effective with younger children [32].

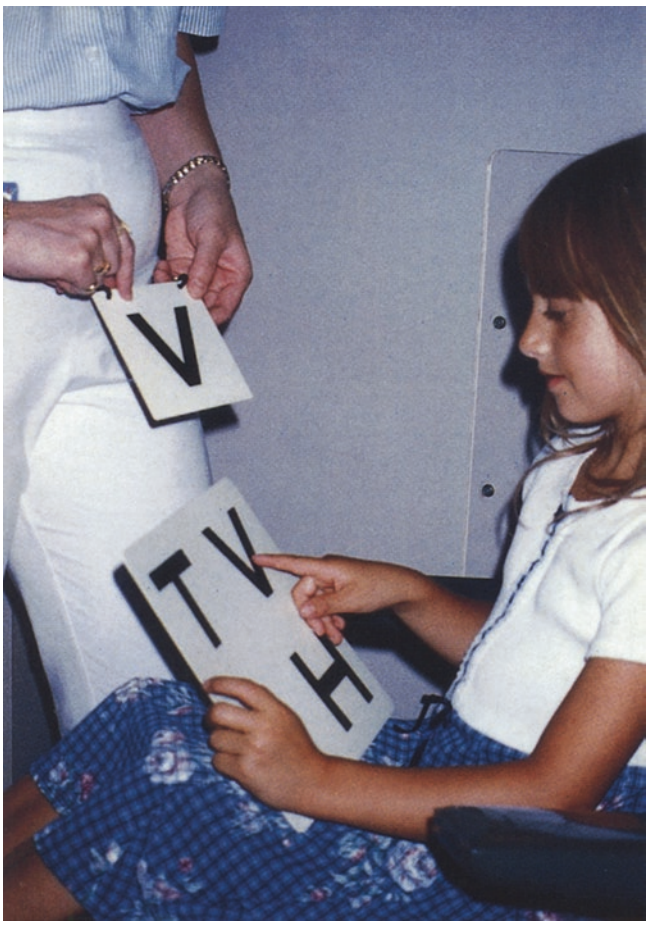


Fig. 10.5 Letter matching. The child is given a lap board with the four letters H, O, T, and V, and the tester shows the child a flip chart to determine whether the child can match or otherwise identify the four letters accurately

The primary aim for testing visual acuity in very young children is the detection of poor acuity, in particular amblyopia. The tests for recognition acuity should therefore maximize detection of amblyopia. Jenkins et al. [33] reported a comparison of the Allen picture chart, Snellen pictures, tumbling E, and the HOTV chart. The Allen picture chart was remarkably poor at detecting a two-line difference between the sound eye and the amblyopic eye, while the HOTV chart and Snellen pictures detected a two-line difference in over 90% of the patients with amblyopia.

It should be noted that amblyopic eyes tend to have better visual acuity tested with single letters or figures than when tested with lines or arrays of letters [34, 35]. The crowding effect is an important consideration and crowded or blocked acuity should be performed whenever possible.

Other Assessments of Visual Function

Visual Field

Quantitative assessment of visual field extent in infants and young children is technically challenging, is often tedious, and remains largely a research tool. Double-arc perimeters with large central and peripheral targets, described by Mohn and van Hof-van Duin [36] and Schwartz et al. [37] and a hemispheric perimeter using small LEDs as stimuli described by Mayer et al. [38] have been used to define visual field development in infants and young children. Both techniques have been useful in detecting visual field abnormalities in children with hydrocephalus [31] and periventricular leukomalacia [39, 40] as well as visual field deficits due to ocular disorders such as ROP [41].

Quantitative assessment of visual fields is, however, practical in children as young as 3½ to 4 years using kinetic targets with standard perimeters, such as the Goldmann or Humphrey apparatus. However, special attention must be given to making the procedure ergonomically feasible for the child. Make sure that the chin rest is comfortable and that the child feels stable in the apparatus. Very young children may have difficulty understanding when to press the buzzer. We have found a very high correlation of visual field extent measured using the buzzer press as the endpoint compared to using a looking response toward the peripheral target as the endpoint measure [42]. It is also useful to ask the child to perform trial runs to become familiar with the procedure. In addition, we suggest that kinetic perimetry using the Goldmann perimeter is easier to perform in very young children than threshold testing in any apparatus currently available.

Color Vision

Congenital color vision defects are not known to occur more commonly in patients with oculoplastic abnormalities. Therefore, routine surveillance is warranted, such as screening using pseudo isochromatic plates that are portable, easy to use, and low in cost [43]. However, damage to the optic nerve or retina from trauma, vascular disease, inflammation, or metabolic disorders may result in acquired defects in the pediatric oculoplastics patient. Testing for acquired defects is extremely difficult in young children, with high false-positive and false-negative tests [44, 45].

Retinal Function/Electrophysiological Testing

The ocular abnormalities in patients with oculoplastic disorders frequently require assessment of retinal function. In disorders such as unilateral microphthalmia, it is important to determine retinal function in the "sound" eye as part of the overall management plan.

Electroretinographic testing is relatively simple in children under 12–14 months of age, at least, in part because the 30-min period of dark adaptation leaves the child subdued. Testing does, however, require patience and time to overcome resistance to lens insertion and manipulation. Recording the ERG with skin electrodes is routinely performed in some centers. Although the ERG recorded with a skin electrode is 12–15% of the amplitude of the ERG recorded with corneal electrode, it is substantial and reliable [46, 47].

Motility Assessment

Cover Testing

The foundation of strabismus diagnosis and quantification is clinical-cover, alternate-cover, and simultaneous prism-cover testing. All these tests are performed with the patient's best corrected acuity fixated on an accommodative target. Cover testing is performed by covering one eye repeatedly and observing both the covered and uncovered eye. After a short time, this is repeated for the fellow eye. If movement is detected during this test, then a constant or intermittent *tropia* is present. If no ocular movement is detected with cover testing, then the cover is switched alternately between right and left eyes without a delay and without allowing bifixation. If movement is detected only during this test, a *phoria* is diagnosed. The total amount of deviation (phoria plus tropia) is measured by neutralizing the deviation with prisms during alternate-cover testing. The tropia is measured alone when neutralizing the deviation using the simultaneous prism-cover test (performed by simultaneously occluding the fixing eye while placing a prism over the deviating eye until no movement is observed).

Cardinal Positions of Gaze

The full ocular deviation (phoria plus tropia) should be determined straight ahead in the distance (primary position), 30° right, left, up, and down gaze (secondary positions) and 30° up and down, to the right and left, as well as up and down (tertiary positions), in addition to an accommodative target at near with and without an add of +3.00 diopters.

Corneal Reflection Tests

Younger children and infants often are not cooperative enough to perform the above standard of strabismus assessment, and corneal reflection tests are valuable in this situation. Hirschberg first suggested the use of corneal reflections to assess ocular deviation and maintained that for each 1 mm of displacement of the corneal reflection, the visual axes are misaligned by 7 °. In several later studies, this conversion factor was revised to closer to 12 ° per mm of corneal reflection displacement [48–50].

Krimsky later described placing increasing power prisms in front of the fixing eye sufficient to allow centration of the corneal reflection in the non-fixing eye [51]. A variation is to place the prism in front of the non-fixing eye to centralize the corneal reflection. This can be less accurate as assessing the corneal reflection through a prism can be difficult. Kushner found that even with experienced strabismologists, these tests had a high rate of error, and if possible cover testing should always be relied on for surgical planning [52]. Notwithstanding, corneal reflection tests can be a valuable method of obtaining an approximate measurement of the angle of strabismus in children unable to cooperate with cover testing.

Versions/Ductions

Binocular (versions) and monocular (ductions) movements of the eyes should be assessed and graded in all positions of gaze. Bielchowsky maintained that a study of the versions is of more value than the ductions as it is easier to overcome a mild weakness of a muscle action with a powerful innervation impulse during ductions. Assessing ocular movement with one eye occluded can be challenging in young children, and therefore assessing versions is potentially easier and may be more informative.

Sensory Testing

Assessing binocular function is mostly limited to older children as there are currently no clinical tools for assessing binocular vision in preverbal infants. The Worth 4 dot test is useful for assessing sensory fusion and suppression and has been adapted for near and distance fixation. It however has a high mean age of failure and us rarely administered to children under 5 years of age [53]. Stereo tests such as the Titmus test rely on dissociated viewing while the Frisby test allows non-dissociated binocular viewing. Other stereo tests in use include the Lang, TNO, and random dot stereogram tests. Randot stereograms may be more useful in determining stereoacuity in children age 3–5 [54].

Incidence of Strabismus in Pediatric Oculoplastic Patients

Strabismus is more common in children with oculoplastic disorders, with the highest incidence noted in those patients with craniofacial syndromes [55–57]. Table 10.3 provides the prevalence of strabismus seen in patients examined in the craniofacial clinic at the Children's Hospital of Philadelphia. The highest incidence of strabismus is seen in patients with craniosynostosis and the lowest incidence in patients with tumors of the orbit.

In general, the decision for surgical intervention for strabismus in patients with oculoplastic conditions should be made based on the visual development of the child and the child's potential for binocularity. Delaying strabismus surgery for other surgical procedures is not always necessary. Previous experience in our clinic and in others has shown that craniofacial surgical procedures do not usually affect the type or extent of strabismus.

Table 10.3 Prevalence of strabismus and abnormal refractive errors among patients with craniofacial abnormalities

	Percentage with strabismus	Percentage with significant refractive error[a]
Craniosynostosis (n = 163)	56	76
Clefting syndromes (n = 82)	45	70
Trauma (n = 12)	50	66
Tumor (n = 9)	22	42
Other isolated anomalies (n = 56)	42	86
Overall (n = 322)	51	72

Source: Based on 322 patients seen in the craniofacial clinic at the Children's Hospital of Philadelphia and data from Katowitz et al. [57]
[a]Defined as greater than +2.00 or −1.50 diopter sphere or +1.50 diopter cylinder.

Refractive Errors

Refractive errors are also common in the pediatric oculoplastic patient, with the highest incidence in patients with craniofacial abnormalities. As shown in Table 10.3, the majority of patients seen in a craniofacial clinic have ametropia, which could certainly lead to amblyopia during the period of visual development.

Amblyopia

Amblyopia in the context of pediatric oculoplastic disorders may be deprivational, refractive, or strabismic. The treatment of amblyopia should follow established guidelines with treatment of the underlying cause where possible and prompt and appropriate occlusion therapy with appropriate monitoring [58].

Where occlusion is not possible, the use of Atropine penalization is accepted as equally efficacious even in moderate to severe amblyopia [59].

Acknowledgment We would like to acknowledge the invaluable contributions made by Richard W. Hertle and David B. Schaffer in the previous edition of this chapter.

References

1. Zipf RF. Binocular fixation pattern. Arch Ophthalmol (Chicago, Ill.: 1960). 1976;94:401–5.
2. Wright KW, Walonker F, Edelman P. 10-Diopter fixation test for amblyopia. Arch Ophthalmol (Chicago, Ill.: 1960). 1981;99:1242–6.
3. Wright KW, Edelman PM, Walonker F, Yiu S. Reliability of fixation preference testing in diagnosing amblyopia. Arch Ophthalmol (Chicago, Ill.: 1960). 1986;104:549–53.
4. Kaban T, Smith K, Beldavs R, Cadera W, Orton RB. The 20-prism-dioptre base-out test: an indicator of peripheral binocularity. Can J Ophthalmol (Journal Canadien d'ophtalmologie). 1995;30:247–50.
5. McDonald MA. Assessment of visual acuity in toddlers. Surv Ophthalmol. 1986;31:189–210.
6. Fantz RL. Pattern vision in newborn infants. Science. 1963;140(3564):296–7.
7. Fantz RL, Fagan JF. Early visual selectivity. In:Infant perception: from sensation to cognition. Elsevier. 1975.
8. McDonald MA, Dobson V, Sebris SL, Baitch L, Varner D, Teller DY. The acuity card procedure: a rapid test of infant acuity.Invest Ophthalmol Vis Sci. 1985;26(8):1158–62.
9. Teller DY, McDonald MA, Preston K, Sebris SL, Dobson V. Assessment of visual Acuity in infants and children: the acuity card procedure. Dev Med Child Neurol. 1986;28:779–89.
10. Adoh TO, Woodhouse JM. The Cardiff acuity test used for measuring visual acuity development in toddlers. Vis Res. 1994;34:555–60.
11. Jackson AJ, Saunders KJ. The optometric assessment of the visually impaired infant and young child. Ophthalmic Physiol Opt. 1999;19(Suppl 2):S49–62.
12. Woodhouse JM, et al. New acuity test for toddlers. Ophthalmic Physiol Opt. 1992;12:249–51.

13. Dobson V. Visual acuity testing by preferential looking techniques. In: The eye in infancy. St Louis: C. V. Mosby; 1994.
14. Dobson V, et al. Acuity card assessment of visual function in the cryotherapy for retinopathy of prematurity trial. Invest Ophthalmol Vis Sci. 1990;31:1702–8.
15. Preston KL, McDonald M, Sebris SL, Dobson V, Teller DY. Validation of the acuity card procedure for assessment of infants with ocular disorders. OPHTHA. 1987;94:644–53.
16. Mayer DL, et al. Monocular acuity norms for the Teller Acuity cards between ages one month and four years. Invest Ophthalmol Vis Sci. 1995;36:671–85.
17. Kushner BJ, et al. Arch Ophthalmol (Chicago, Ill.: 1960). 1994;112:1030–1.
18. Dobson V, Quinn GE, Tung B, Palmer EA, Reynolds JD. Comparison of recognition and grating acuities in very-low-birth-weight children with and without retinal residua of retinopathy of prematurity. Cryotherapy for Retinopathy of Prematurity Cooperative Group. Invest Ophthalmol Vis Sci. 1995;36:692–702.
19. Quinn GE, Berlin JA, James M. The Teller acuity card procedure. Three Testers in a Clinical Setting. Ophthalmology. 1993;100:488–94.
20. Trueb L, Evans J, Hammel A, Bartholemew P, Dobson V. Assessing visual acuity of visually impaired children using the Teller acuity card procedure. Am Orthopt J. 1992;42149–154.
21. Sokol S. Measurement of infant visual acuity from pattern reversal evoked potentials. Vis res. 1978;18:33–9.
22. Allen D, Tyler CW, Norcia AM. Development of grating acuity and contrast sensitivity in the central and peripheral visual field of the human infant. Vis Res. 1996;36:1945–53.
23. Liasis A, Thompson DA, Hayward R, Nischal KK. Sustained raised intracranial pressure implicated only by pattern reversal visual evoked potentials after cranial vault expansion surgery. Pediatr Neurosurg. 2003;39:75–80.
24. Tyler CW, Apkarian P, Levi DM, Nakayama K. Rapid assessment of visual function: an electronic sweep technique for the pattern visual evoked potential. Invest Ophthalmol Vis Sci. 1979;18:703–13.
25. Norcia AM, Tyler CW, Hamer RD, Wesemann W. Measurement of spatial contrast sensitivity with the swept contrast VEP. Vis Res. 1989;29:627–37.
26. Liasis A, Nischal KK, Walters B. Monitoring visual function in children with syndromic craniosynostosis: a comparison of 3 methods. Arch Ophthalmo. 2006;124(8):1119–26.
27. Dobson V, et al. Grating visual acuity in eyes with retinal residua of retinopathy of prematurity. The Cryotherapy for Retinopathy of Prematurity Cooperative Group. Arch Ophthalmol. 1995;113:1172–7.
28. Gottlob I, et al. Visual Acuity measurements by swept spatial frequency Visual-Evoked-Cortical Potentials (VECPs): clinical application in children with various visual disorders. J Pediatr Ophthalmol Strabismus. 1990;27:40–7.
29. Sprague JB, Stock LA, Connett J, Bromberg J. Study of chart designs and optotypes for preschool vision screening—I. Comparability of Chart Designs. J Pediatr Ophthalmol Strabismus. 1989;26:189–97.
30. Gräf MH, Becker R, Kaufmann H. Lea symbols: visual acuity assessment and detection of amblyopia. Graefes Arch Clin Exp Ophthalmol. 2000;238:53–8.
31. Elliott MC, Firth AY. The logMAR Kay picture test and the logMAR acuity test: a comparative study. Eye. 2009;23:85–8.
32. Vision in Preschoolers Study Group. Preschool vision screening tests administered by nurse screeners compared with lay screeners in the vision in preschoolers study. Invest Ophthalmol Vis Sci. 2005;46:2639–48.
33. Jenkins PF, Prager T, Mazow ML. Preliterate vision screening: a comparative study. Am Orthopt J. 1983;33:91–8.
34. Simons K. Preschool vision screening: rationale, methodology and outcome. Surv Ophthalmol. 1996;41:3–30.
35. Rodier DW, Mayer DL, Fulton AB. Assessment of young Amblyopes: Array vs single picture acuities. Ophthalmology. 1985;92:1197–202.
36. van Hof-van Duin J, Mohn G. Visual field measurements, optokinetic nystagmus and the visual threatening response: normal and abnormal development. Detect Measur Vis Impair Pre-Verbal Child. 1986;45:305–15.
37. Schwartz TL, Dobson V, Sandstrom DJ, van Hof-van Duin J. Kinetic perimetry assessment of binocular visual field shape and size in young infants. Vis Res. 1987;27:2163–75.
38. Mayer DL, Fulton AB, Cummings MF. Visual fields of infants assessed with a new perimetric technique. Invest Ophthalmol Vis Sci. 1988;29:452–9.
39. Scher MS, Dobson V, Carpenter NA, Guthrie RD. Visual and neurological outcome of infants with periventricular Leukomalacia. Dev Med Child Neurol. 1989;31:353–65.
40. Luna B, Dobson V, Scher MS, Guthrie RD. Grating acuity and visual field development in infants following perinatal asphyxia. Dev Med Child Neurol. 1995;37:330–44.
41. Luna B, Dobson V, Carpenter NA, Biglan AW. Visual field development in infants with stage 3 retinopathy of prematurity. Invest Ophthalmol Vis Sci. 1989;30:580–2.
42. Quinn GE, Fea AM, Minguini N. Visual fields in 4- to 10-year-old children using Goldmann and double-arc perimeters. J Pediatr Ophthalmol Strabismus. 1991;28:314–9.
43. Hardy LH, Rand G, Rittler MC. Tests for detection and analysis of color blindness; an evaluation of the Ishihara test. Arch Ophthalmol (Chicago, Ill.: 1929). 1945;34:295–302.
44. Hill AR, Heron G, Lloyd M, Lowther P. An evaluation of some colour vision tests for children. Doc Ophthalmol Proc Ser. 1982;33:183–7.
45. Verriest, G., et al. "Colour vision tests in children." Doc Ophthalmol Proc Ser33. 1982:175–8.
46. Bradshaw K, Hansen R, Fulton A. Comparison of ERGs recorded with skin and corneal-contact electrodes in normal children and adults. Doc Ophthalmol. 2004;109:43–55.
47. Esakowitz L, Kriss A, Shawkat F. A comparison of flash electroretinograms recorded from Burian Allen, JET, C-glide, gold foil, DTL and skin electrodes. Eye (Lond). 1993;7(Pt 1):169–71.
48. Brodie SE. Photographic calibration of the Hirschberg test. Invest Ophthalmol Vis Sci. 1987;28:736–42.
49. DeRespinis PA, Naidu E, Brodie SE. Calibration of Hirschber test photographs under clinical conditions. Ophthalmology. 1989; 96:944–9.
50. Eskridge JB, Perrigin DM, Leach NE. The Hirschberg test: correlation with corneal radius and axial length. Optom Vis Sci. 1990;67:243–7.
51. Krimsky E. The binocular examination of the young child. Am J Ophthalmol. 1943;26:624.
52. Choi RY, Kushner BJ. The accuracy of experienced strabismologists using the Hirschberg and Krimsky tests. Ophthalmology. 1998;105(7):1301–6.
53. Morale SE, et al. Preschool worth 4-shape test: testability, reliability, and validity. YMPA. 2002;6:247–51.
54. Birch E, Williams C, Hunter J, Lapa MC. Random dot stereoacuity of preschool children. ALSPAC 'Children in Focus' Study Team. J Pediatr Ophthalmol Strabismus. 1997;34:217–22– quiz 247–8.
55. Hertle RW, Quinn GE, Minguini N, Katowitz JA. Visual loss in patients with craniofacial synostosis. J Pediatr Ophthalmol Strabismus. 1991;28:344–9.
56. Hertle RW, Quinn GE, Katowitz JA. Ocular and adnexal findings in patients with facial Mierosomias. Ophthalmology. 1992;99:114–9.
57. Katowitz JA, Hertle RW, Quinn GE. Ophthalmic management of craniofacial syndromes. In: Duane's clinical ophthalmology. Philadelphia: Lippincott; 1993.
58. Wu C, Hunter DG. Amblyopia: diagnostic and therapeutic options. Am J Ophthalmol. 2006;141:175–84.e2.
59. Repka MX, et al. Two-year follow-up of a 6-month randomized trial of atropine vs patching for treatment of moderate amblyopia in children. Arch Ophthalmol. 2005;123:149–57.

Pediatric Extraocular Muscle Surgery and Oculoplastic Disorders

11

Brian J. Forbes and Graham E. Quinn

Oculomotor system abnormalities are commonly associated with disorders of the lids and orbits [1–6]. Disturbances of extraocular muscle function are associated with both primary pathology and iatrogenic manipulation of lid and orbital tissues. Disruption of extraocular muscle function is particularly important in the pediatric population because of the vulnerability of associated compromises to visual acuity such as amblyopia and binocular coordination including fusion and stereopsis [7, 8].

Extraocular muscle dysfunction is generally due to either of two mechanisms: interference with "supranuclear" function including disease above the level of the ocular motor nuclei or infranuclear function including disease below the level of the ocular motor nuclei (Fig. 11.1). Most forms of primary childhood strabismus are due to supranuclear abnormalities of the oculomotor system. Most forms of strabismus associated with lid and orbital disease are due to infranuclear disease. Abnormalities of the oculomotor nuclei, the nerve fascicle, nerve bundle, neuromuscular junction, and extraocular muscle are infranuclear disorders and manifest clinically as incomitant strabismus. The two broad categories of infranuclear strabismus are restrictive and paralytic. Most strabismus associated with disorders of the lids and orbits is due to restriction or weakness of the extraocular muscles, malrotation of the orbits, or some combination.

The above classification of associated extraocular muscle dysfunction can assist with a diagnosis of lid or orbital disorders, such as paralytic strabismus associated with ptosis in cranial nerve disease and restrictive strabismus associated with proptosis or lid retraction in thyroid ophthalmopathy. Neuropathic or myopathic processes may first present as orbital or lid abnormalities and only later, or on careful examination, reveal associated extraocular muscle dysfunction.

Separate examination of both sensory and motor systems in children with lid and orbital disease is necessary for accurate diagnosis and treatments. A routine examination of the visual sensory system and ocular motor system should be part of the initial and subsequent ophthalmic evaluation in children with lid and orbital pathology.

Education of patients and families regarding associated extraocular muscle dysfunction, its clinical consequences, and probable treatments is necessary for complete care in these children. Staging of medical and surgical treatments requires cooperation between the various ophthalmic subspecialists involved in the care of these patients.

To understand the pathophysiologic relationship in children between lid and orbital disorders and extraocular muscle dysfunction, an appreciation of developmental anatomy is needed. Embryologic development of the mesenchymal process destined to become the extraocular muscles is intimately related to the development of neighboring structures. The developing extraocular muscle complexes arise simultaneously with and are connected to important lid and orbital structures [9–12]. The superior extraocular muscle complex begins as a condensation of mesenchyme in the superior orbit at the 5-mm stage of gestation [13]. The persistence of some embryologic attachments between the superior rectus and levator muscles after full development is evident as attachments between the horn of the levator aponeurosis and the superior rectus. A more permanent anatomic relationship exists between the inferior orbital extraocular muscles and the muscles of the lower lid (Fig. 11.2). The lower lid retractors, inferior rectus, and inferior oblique muscle join to form a condensation of tissues that is the central part of Lockwood's ligament. Surgery on either the lower lid retractors or the inferior rectus alone may result in a malposition of the other with resulting strabismus or lid malposition.

B.J. Forbes (✉) • G.E. Quinn
University of Pennsylvania/Children's Hospital of Philadelphia, Philadelphia, PA, USA

Perelman School of Medicine, University of Pennsylvania, Philadelphia, PA, USA
e-mail: forbesb@email.chop.edu

© Springer International Publishing AG 2018

J.A. Katowitz, W.R. Katowitz (eds.), *Pediatric Oculoplastic Surgery*, https://doi.org/10.1007/978-3-319-60814-3_11

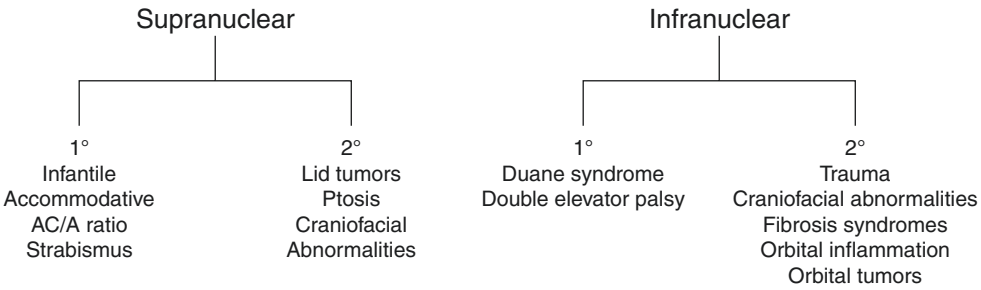


Fig. 11.1 Diagnostic pathway. Diagnostic pathway and classification of extraocular muscle dysfunction in pediatric patients with oculoplastic disorders

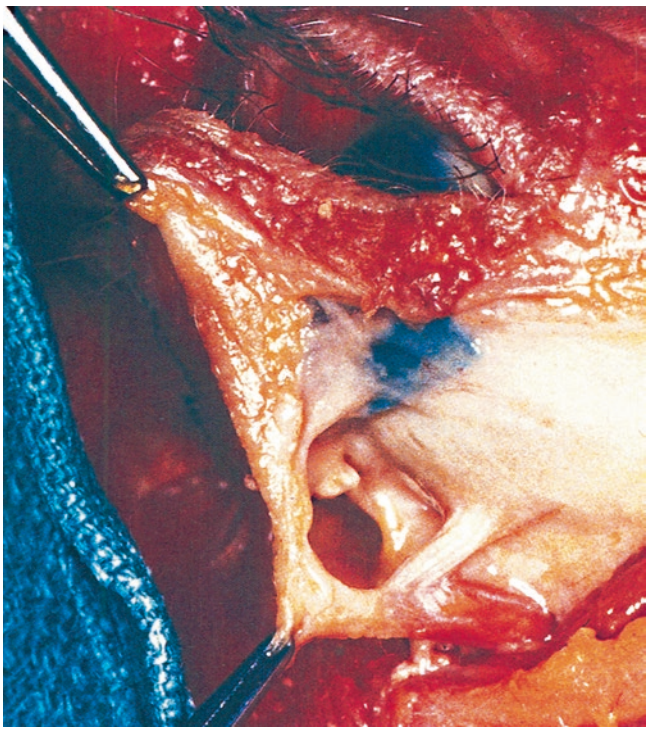


Fig. 11.2 Cadaveric orbital dissection. Cadaveric orbital dissection illustrating the anatomic relationship of the lower lid retractors, head of the capsulo-palpebral fascia, and the inferior rectus

Developmental anomalies of the orbits (microphthalmia, anophthalmia, orbital hypoplasia, and retrusion), especially those occurring with major craniofacial malformations, often have associated abnormalities of extraocular muscle function [14–19]. This may be due to associated primary maldevelopment of the muscles and tendons or a secondary effect of abnormal supporting orbital structures [1–3, 18, 19]. Perimuscular orbital structures allow for smooth coordinated movements of the extraocular muscles. Lid movements have voluntary and involuntary static and dynamic functions. The relative positions of the lids to the eye are held constant due to complex neuromechanical control mechanisms. Interruptions of normal lid and orbital functional interrelationships can be due to many mechanisms from disturbances at the level of the central nervous system to the extraocular muscles alone.

Classification of Strabismus and Oculoplastic Disorders

Strabismus and extraocular muscle dysfunction in the pediatric population most often occurs without any associated disorders of the lids and orbits. When strabismus does occur in association with pediatric oculoplastic disorders, it can be classified as that which is directly due to the oculoplastic disorder (secondary strabismus), that which causes the oculoplastic disorder (primary strabismus), and that which occurs simultaneously and has no etiologic connection to the oculoplastic disorder (associated strabismus) (Fig. 11.1).

Secondary Strabismus Types

These disorders of extraocular muscle dysfunction are directly due to disturbances of the orbits, lid, and adnexa. Anomalous development of the lids and orbits occurs frequently with craniofacial disorders and genetic syndromes [1, 4, 16–19]. The major craniofacial anomalies include craniosynostoses and clefting syndromes (see Chap. 38). Extraocular muscle disorders occur very commonly in these patients and are due to both supranuclear and infranuclear abnormalities in the ocular motor system [16–20]. Typical childhood strabismus syndromes, such as infantile esotropia and exotropia, accommodative esotropia, and incomitant strabismus, can occur alone or in combination with absent and maldeveloped extraocular muscles. Genetic syndromes and chromosomal abnormalities are frequently associated with strabismus and extraocular muscle dysfunction.

Trauma is very common in childhood and is a major etiology of visual system damage in children [21]. Extraocular muscle dysfunction is secondary to related damage involving surrounding orbital bones and sinuses. These include soft tissue or muscle entrapment, nerve damage, or secondary restrictive strabismus associated with orbital hemorrhage and scarring. Lastly, bony damage can result in displacement of the orbit with secondary misalignment of the visual axis.

Inflammatory disorders of the orbit commonly result in secondary extraocular muscle dysfunction [22]. The most common orbital inflammations in childhood include

infectious cellulitis, idiopathic orbital pseudotumor or myositis, and those orbital tumors with some associated inflammation (rhabdomyosarcoma, capillary and cavernous hemangiomas, lymphangioma, and blood dyscrasia) [22, 25]. Orbital infiltrative processes result in a clinical picture of extraocular muscle dysfunction consistent with intranuclear or incomitant strabismus due to changes in the contractility (strength) or length-tension characteristics (stiffness) of the muscles. This results from a combination of factors, such as stretching from proptosis and direct extraocular muscle or nerve infiltration with cells, edema, abnormal extracellular matrix, or tumor tissue.

Primary Strabismus

Many primary extraocular muscle disorders in childhood have secondary orbital and/or lid anomalies. Anomalous development of the extraocular muscles can be due to intrauterine toxins, infections, and chromosomal disorders [9–13]. The incidence of developmental malformations in general is reported to be between 2% and 4% at birth [22, 23]. However, the incidence rises to 6% or 7% if abnormalities that manifest later in life are included [22, 23]. Severe developmental abnormalities of the orbit such as anophthalmos, microphthalmos, cryptophthalmos, craniostenoses, and clefting syndromes have both primary and secondary abnormalities of the extraocular muscle and orbits and are discussed more fully in Chap. 5 [10, 29, 30].

Primary hypoplasia and dysplasia of the extraocular muscles are often associated with abnormalities of the levator and lid retractor muscles, resulting in congenital lid malpositions (ptosis, entropion, ectropion, etc.) (Fig. 11.3). These abnormalities of the orbital extraocular muscles can be associated with canthal dystopia and epicanthal skin abnormalities (Fig. 11.4). Severe forms of congenital dysplasia of the extraocular muscles such as the fibrosis syndromes result in severe associated orbital and lid deformations (Fig. 11.5) [24].

Trauma resulting in disorders of the extraocular muscle function is mainly due to interruption of infranuclear oculomotor pathways. This can occur in the central nervous system (brain stem, interpeduncular space), the cavernous sinus, or orbit. Classification of traumatic disorders is the same as elsewhere in the body (e.g., blunt vs. sharp, penetrating vs. nonpenetrating). Traumatic disruption of extraocular muscle function in infancy and childhood is often associated with lid and orbital involvement [9, 12]. The high incidence of associated involvement of these structures has unique implications in this age group [11, 25, 26]. Acquired strabismus, ptosis, and orbital deformities interrupt the normal developmental physiology of vision, including binocularity, refractive development, and orbital growth [27]. This results in amblyopia, persistent loss of binocularity, and continued cosmetic and functional asymmetries in the lids and orbits. The evaluation of trauma in the child is often very difficult, and a complete examination is difficult and can be accomplished only under anesthesia. The potential long-term functional and cosmetic implications of extraocular muscle, lid, and orbital trauma in the pediatric patient require prompt diagnosis and treatment with reversal of amblyogenic factors and restoration of anatomy and symmetry.



Fig. 11.3 Unilateral ptosis and strabismus. Patient with congenital unilateral ptosis and combination restrictive/paralytic strabismus due to congenital unilateral complete third cranial nerve palsy associated with hemiatrophy of the ipsilateral brain stem



Fig. 11.4 Primary hypertelorism. Patient with primary hypertelorism displaying numerous canthal disturbances and strabismus



Fig. 11.5 Unilateral fibrosis syndrome. Patient with left congenital unilateral fibrosis syndrome with restrictive strabismus, ptosis, lid lag, and lagophthalmos

Primary inflammatory disorders of the extraocular muscles occur commonly in the pediatric population and often present with a clinical picture due to associated orbital inflammation. Division into infectious and noninfectious inflammatory disorders is important for treatment and prognosis. Infectious myositis is usually associated with contiguous orbital cellulitis but can occur in isolation due to metastatic septic emboli. Noninfectious myositis is usually part of the spectrum of orbital inflammatory pseudotumor, although Graves's thyroid orbitopathy can also present in childhood. In children, infectious vs. noninfectious myositis and/or orbital cellulitis are often difficult to distinguish clinically because both can present with fever, lethargy, lid and orbital edema, proptosis, orbital pain, and headache. A more complete physical exam (including temperature, ear, nose, and throat, with associated laboratory studies such as complete blood cell count, erythrocyte sedimentation rate, etc. as well as radiologic testing such as computer-assisted tomography [CT] scan and magnetic resonance imaging [MRI]) is needed to differentiate these processes.

Tumors involving the extraocular muscles in infants and children are rare. In a study of computed tomography features of nonthyroid extraocular muscle enlargement, primary or locally invasive neoplasms accounted for 26% of all cases, and 20% of cases were attributable to metastases [23]. Rhabdomyosarcoma and hematologic malignancies are the most common primary neoplasias that involve extraocular muscles. Numerous primary and secondary orbital tumors in childhood (discussed in Chaps. 23 and 24) can invade the extraocular muscles. Regardless of the tumor type, position, or size, the resultant interference with extraocular muscle function clinically appears as either restrictive or paralytic strabismus or a combination of these two forms.

Diagnostic Techniques

Examination techniques are the most important part of strabismic diagnosis, whether occurring primarily or associated with lid and orbital disorders. The general examination of binocular and extraocular muscle systems involves both sensory (afferent) and motor (efferent) systems. Sensory system examination includes measurement of central visual acuity, fusion, and stereopsis. Like many subjective tests in the pediatric population, accuracy and consistency can be a problem clinically. Vision and visual acuity measurement are discussed fully in Chap. 10. Worth 4-dot testing provides information regarding the child's binocular status and, if there is a deviation, whether the child is able to alternately suppress either eye. A test of "fine" fusion or stereopsis using stereograms such as Titmus Fly and Random Dot is also given prior to the motor examination to assess the presence of stereopsis in the visual cortex. Although a primary absence or malfunction of cortical fusion may be responsible for many forms of childhood strabismus, disruption of the extraocular muscle system due to orbital disease in infancy can interfere with full development and potential of cortical fusion [28, 29].

Measurement of the ocular deviation is important for several reasons. Accurate measurement of the angle of strabismus in all positions of gaze is an important step in diagnosis of ocular motor system dysfunction. If the deviation is comitant, then dysfunction is likely due to disease above (supranuclear) the level of the ocular motor nuclei (e.g., infantile esotropia). If the strabismic deviation is incomitant, then this is most likely due to disease at or below the level of the ocular motor nuclei (infranuclear), for example, sixth cranial nerve palsy.

Cover–uncover testing, alternate cover testing, and simultaneous prism/cover testing are the standard clinical tests for determining a tropia, tropia plus phoria, and total tropic deviation, respectively. If possible, this should be determined in primary, secondary, and tertiary (oblique) positions of gaze at distance and near with best corrected acuity to an accommodative target. Recording this information in a standard diagram is often helpful for future reference and clinical decision-making (Fig. 11.6).

If the deviation is incomitant, which is likely in those situations in which one eye has a weak or restricted muscle, then these differences along with clinical versions (ocular rotations with both eyes open) and ductions (ocular rotations with one eye covered) testing are noted. There are many ways of recording versions and ductions. We prefer to use a scale of −4 to +4, with 0 being normal. A −4 version would be a lack of rotation to midline horizontally or vertically with both eyes open (Fig. 11.7). If a restriction is suspected, intraocular pressure in the limited field of gaze may be increased.

Special testing is available and is often helpful in diagnosis and quantification of strabismus associated with oculoplastic disorders. These tests may be difficult to perform on infants and young children, although older children are usually compliant. These special tests include forced ductions, forced generations, diplopic fields, and electrooculography. Forced duction and forced generation testing are clinical adjuncts useful in differentiating a "weakness" from a restriction. After instillation of topical anesthetic, the patient is asked to move the eye in the affected direction (Fig. 11.8). The examiner then attempts to manually move the eye further in the same direction. Resistance to further movement of the eye is considered a positive forced duction and is indicative of restrictive disease. When performing forced generation, the eye is grasped at the limbus anterior to the muscle insertion affected; then the patient is asked to move the eye in the field of action of the muscle, while the tester attempts to hold the eye against the patient's movements (Fig. 11.9). In this way the examiner can "feel" the force generated by voluntary innervation of this muscle. The information obtained after performing these two clinical maneuvers is important for both diagnosis and treatment since approach to treatment of paralytic versus restrictive strabismus is quite different.

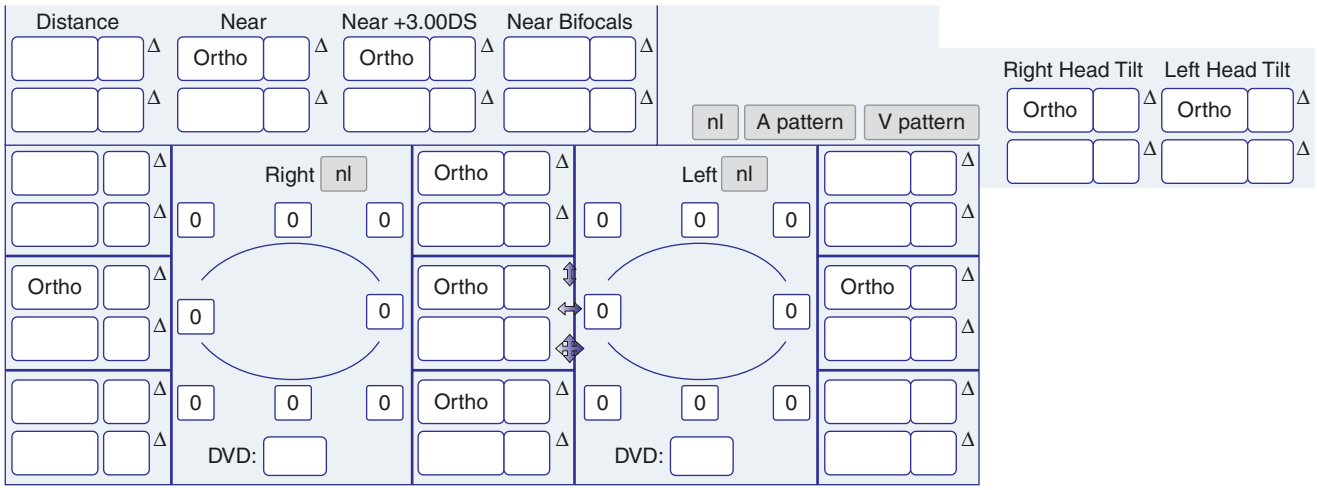


Fig. 11.6 Ocular motility examination diagram. Ocular motility examination diagram with spaces for recording the patient's versions and deviation in primary, secondary, and near deviations

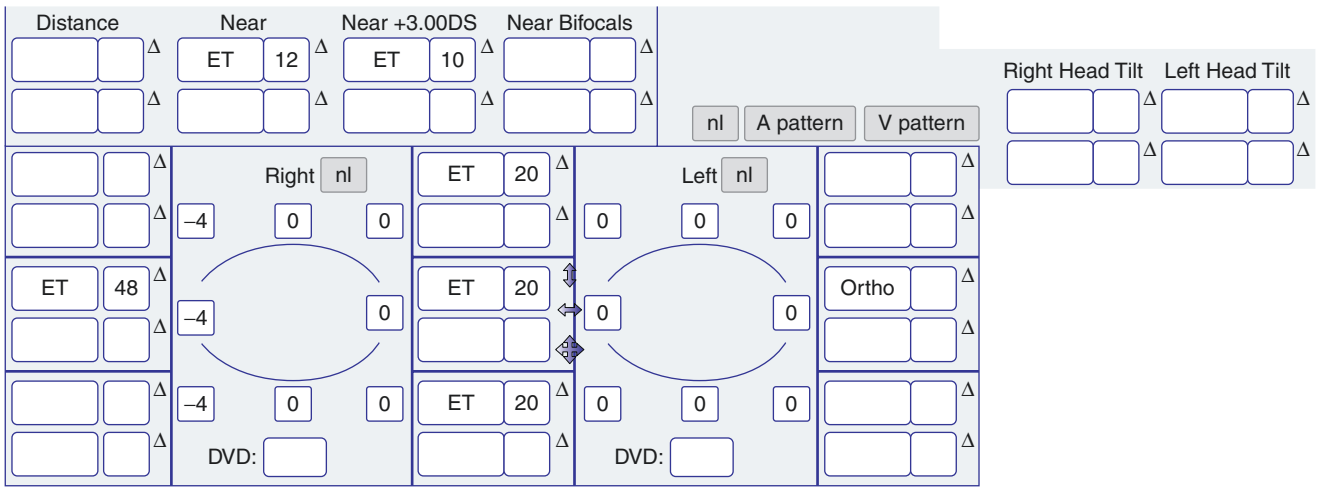


Fig. 11.7 Ocular motility examination diagram. Ocular motility examination diagram illustrating recording of a patient with paralytic strabismus due to a right sixth nerve palsy

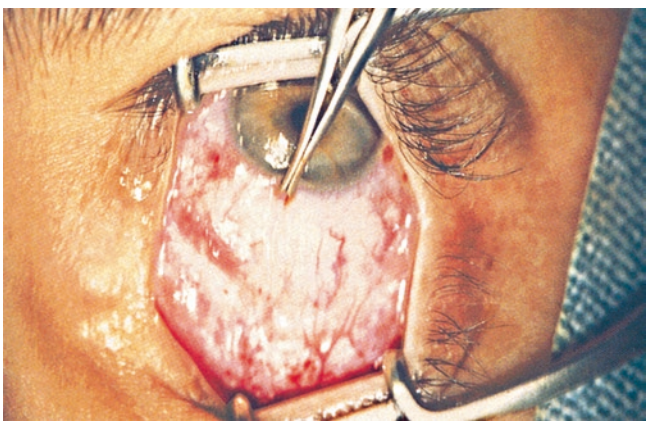


Fig. 11.8 Intraoperative forced duction of an inferior restriction. The eye is grasped at the inferior limbus and the globe is gently pulled out of the orbit and rotated superiorly



Fig. 11.9 A forced generation test. A forced generation test can be performed in the office with a cotton tip applicator after anesthetizing the eye and holding it against attempted movements in the field of decreased duction, as in this patient with a right sixth nerve palsy

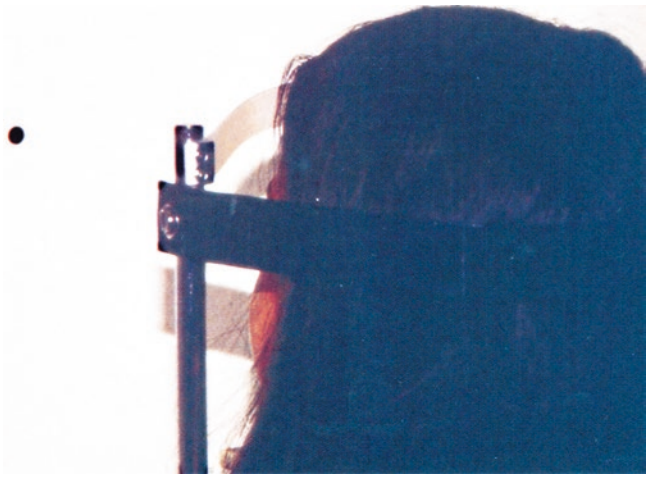


Fig. 11.10 Child placed in Goldmann perimeter. Child placed binocularly with the forehead in the middle of the viewing aperture of the Goldmann perimeter in preparation for determination of her field of singular binocular vision

In patients who complain of diplopia, quantification of their field of single binocular vision (SBV) is important preoperative information. In general, oculoplastic disorders associated with extraocular muscle dysfunction leading to diplopia can be effectively treated. Surgical or medical treatment results in either restoring some SBV or expanding the patient's field of SBV, but often do not return their field to 100% normal. The diplopic field can be evaluated using the Goldmann perimeter where the patient is placed in the perimeter with the head straight and both eyes open. The examiner's view places the bridge of the patient's nose in the patient's viewing circle by appropriately positioning the chin rest (Fig. 11.10). Isopters are determined dynamically using a target of threshold size and width (e.g., I2c, I4e). The target is presented first centrally or within the center of the patient's field of SBV. The target is then moved along each meridian until the patient reports edge blurring or frank diplopia. This is marked on a standard perimetric data collection sheet outlined with the normal field of SBV (Fig. 11.11).

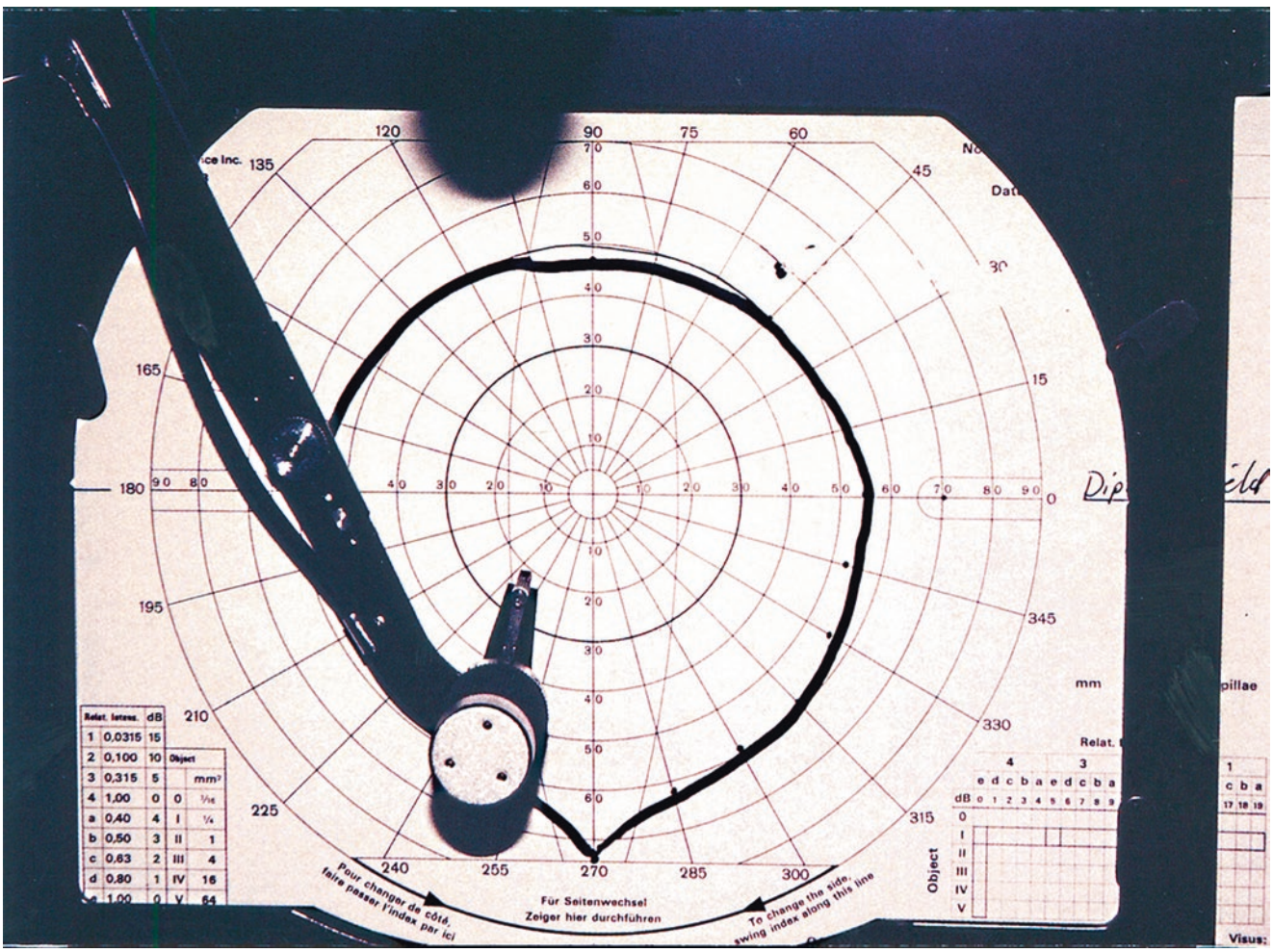


Fig. 11.11 Tester's view of Goldmann perimetric binocular field measurement. Also displayed is a previously marked normal field of single binocular vision

Imaging techniques are often used when evaluating lid, orbital, and adnexal disease. If the patient has associated extraocular muscle dysfunction, additional diagnostic information can be simultaneously obtained. In addition to obvious structural disease of the extraocular muscles, CT scans and MRI can now be used to assess dynamic function by incorporating cinematic effects. These dynamic imaging techniques can be performed on infants and children and assist with diagnosis of muscle position, weakness, or restriction. Additionally, electrooculography, a noninvasive method of analysis of both the supranuclear and infranuclear ocular motor systems can be utilized. This apparatus uses infrared light to detect motion of the eyes from which an electric signal is generated and analyzed via chart recorders or computer software programs (Fig. 11.12). With oculography a definite diagnosis of restriction versus paresis and quantification of amount of muscle function can be accomplished (Fig. 11.13).

Laboratory studies evaluating blood and biopsied tissue are helpful in diagnosis of those oculoplastic disorders associated with systemic diseases and atypical clinical presentations. They are most helpful in diagnosing infections, autoimmune inflammations, and tumors. Testing can broadly be defined as screening tests, such as complete blood cell count, erythrocyte sedimentation rate, antinuclear antibody test, or specific tests, such as cultures and histopathology.

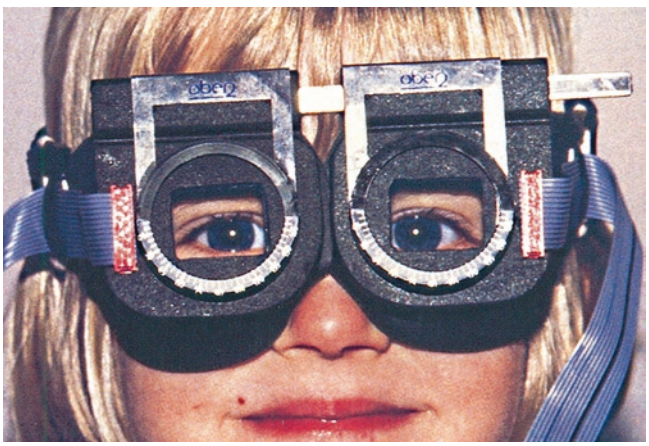


Fig. 11.12 Infrared oculographic goggles. Child with infrared oculographic goggles in position for recording

Treatment Approaches

In general, treatment of extraocular muscle abnormalities associated with oculoplastic disorders requires accurate diagnosis and cooperation with planned oculoplastic intervention. The two categories of treatment are medical and surgical. Medical treatments include those topical and systemic agents used to treat the primary etiology, for example, antimicrobials, anti-inflammatories, and antineoplastics. These treatments take precedence over surgical treatment, because they may alone result in effective elimination of the extraocular muscle dysfunction. Other medical treatments of extraocular muscle dysfunction involve spectacles, botulinum toxin, and occasionally topical drops. Spectacles with and without prisms can treat associated refractive errors and diplopia. Botulinum may restore ocular muscle balance by temporally paralyzing muscles antagonistic to those with acquired paresis or restriction [30–37]. This prevents contracture of the antagonist muscle during recovery of nerve

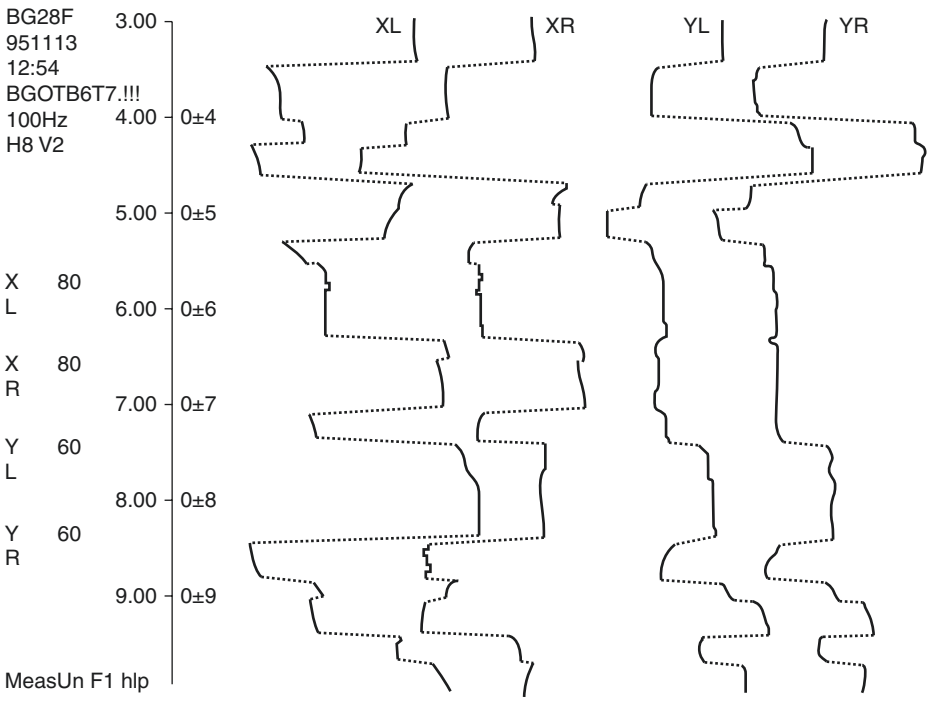


Fig. 11.13 Oculographic recording. Oculographic recording showing normal conjugate, symmetric horizontal and vertical saccadic activity. Seconds on Y axis. XL = OS horizontal, XR = OD horizontal with *rightward* and *leftward* deflections for this axis representing *rightward* and *leftward* movements, respectively. YL = OS vertical and YR = OD vertical with *rightward* and *leftward* deflections representing *upward* and *downward* movements, respectively

function in the affected muscle with a greater chance of restoration of extraocular muscle balance after recovery. Topical drops, such as anticholinesterases, may help with esotropic deviations which are greater at near than distance.

An important associated condition of extraocular muscle dysfunction associated with pediatric visual oculoplastic disorders is amblyopia, an ever-present threat to the vision of infants and children with strabismus due to any etiology. Amblyopia can occur quickly and does so in about 50% of patients. Thus, the vigilant search for amblyopia and institution of treatment can prevent unnecessary visual loss in this population of patients and aid in treatment of their extraocular muscle dysfunction.

Extraocular muscle surgery is an alternative treatment approach when the deviation of the visual axis is greater than 8–12 prism diopters and is unsuccessfully treated medically. A primary preoperative consideration is maximum visual rehabilitation prior to surgical correction. This includes clearing the visual axis, optical correction, and amblyopia treatment. General surgical principles include performing extraocular muscle surgery after major orbital reconstruction procedures but before lid positioning procedures, releasing restrictions if present, matching any duction defect if full ductions cannot be restored and, if possible, using an adjustable suture approach [38, 39].

Accurate evaluation and diagnosis of the strabismic disorder is an important requirement for a successful procedure. This should be accomplished as much as possible preoperatively, although many times a definitive diagnosis is not made until the operative procedure. This should be communicated to the patient and their family with the idea that definitive procedures will not be known until surgery [25, 37, 40, 41].

In summary, the extraocular muscle abnormality is either coincidental to the oculoplastic disorder, causes the oculoplastic disorder, or results from the oculoplastic disorder. Next is the determination as to whether the strabismus is supranuclear (comitant) or infranuclear (incomitant) and, if infranuclear, whether paralytic, restrictive, or a combination of both. When the vision is corrected and the deviation is stable over an appropriate period of time (from 2 to 12 months, depending on the patient's age), and medical treatment is either ineffective or not indicated, surgery can then be planned.

As mentioned previously, strabismus surgery should be performed after major reconstructive surgery on the orbits and periocular tissues, but usually before lid repositioning procedures as severe ptosis will require immediate attention. The patient's age and symptoms may also aid in determining when surgery should be performed. In a visually immature child, correction of strabismus will insure the highest probability of continued normal visual and binocular development, whereas in the visually mature child, restoration of already established normal visual and binocular functions is the major goal; thus, more rapid correction is usually required for infants and younger children.

The surgical decisions generally follow those used in typical childhood strabismus. Surgical formulas are useful as guidelines from which to plan the procedure [25, 33]. Evaluating extraocular muscles on the MRI preoperatively (as well as CT axials and coronals/ultrasound) and intraoperatively can be very helpful in craniofacial patients though interpretation can be difficult to get done well if unfamiliar with necessary techniques. The 3D US can yield an acceptably accurate anatomic picture of the eye muscles though it is less valuable as a tool for determining variations in muscle position. Preoperative knowledge of such variations may provide additional information to the surgeon planning the procedure. This especially holds true in the craniosynostosis population in which a muscle that the surgeon was intending to operate on may be absent, malformed, or located in an aberrant position. Occasionally, an absent or anomalous muscle may change the surgical plan. The amount of recession, resection, myotomy, tenotomy, or transposition is modified by the preoperative measurements, the intraoperative findings, and the surgeon's experience [42–44]. Some general surgical principles are helpful and can also be used as a foundation for surgical planning. Operating to first release restrictions and second to match duction deficits helps restore comitancy. Operating on the minimal number of muscles and operating on previously unoperated muscles using recessions rather than resections have been preferable in our experience. Additionally, in those cases in which use of standard formulas are not applicable, adjustable suture techniques in compliant children can increase the likelihood of postoperative success [39, 42–44].

Orbital and ocular excyclorotation can cause pseudo inferior oblique overaction, superior oblique underaction, and V patterns as the medial rectus adducts and elevates. To treat pseudo inferior oblique overaction with a V pattern, one can transpose the medial rectus down and +/− the lateral rectus up which treats hypertropias in side gaze and V pattern but can worsen extorsion which in a patient with fusion can be problematic [45]. Alternatively, inferior oblique weakening +/− superior oblique strengthening (tuck) can be performed which treats hypertropias in side gaze and V pattern and improves extorsion [46]. Additionally, anteriorization of the inferior oblique can be performed which reduces overelevation in adduction and helps eliminate or reduce divergence of the eyes in upgaze, but esodeviation may persist in downgaze [45, 46]. This procedure is most effective in absence of the superior oblique tendon.

Surgical Techniques

General anesthesia is nearly always required for strabismus surgery in infants and children. This is accomplished using standard endotracheal intubation or the newer technique using laryngeal mask anesthesia. A combination of an orbital

block and additional local infiltration during surgery can occasionally provide successful anesthesia and akinesia in unilateral extraocular muscle surgery in cooperative older children.

Standard instruments required for strabismus surgery include extraocular muscle hooks, toothed and non-toothed forceps, and Stevens tenotomy, Wescott, and Aebli scissors to assist with blunt and sharp dissection and myotomy/tenotomy, respectively. It is important to select a spatulated needle (e.g., S-29 or S-14 Ethicon) for passing a suture through the sclera. Commonly used suture sizes are 5–0 and 6–0, and material includes Vicryl (Ethicon) for reattachment of the muscles to sclera, noncoated absorbable gut for closing conjunctival tissues, and Prolene (Ethicon) for muscle-sharing procedures and permanent implants (e.g., the silicone band spacer in superior oblique surgery) [47–51]. Perioperative adjuncts may include a mixture of Decadron (4 mg/mL) and gentamicin (40 mg/mL) used for immediate postoperative subtenons irrigation in reoperations and adjustable suture surgery and hyaluronic acid (Healon) injected between the muscles placed on an adjustable suture and the insertion site to decrease postoperative adjustment friction [52].

Surgery on the extraocular muscles is performed in an attempt to normalize infranuclear forces responsible for positioning and rotating the eyes. This type of surgery involves three concepts. First, manipulation of any individual or group of extraocular muscle affects the function of that muscle primarily and other extraocular muscles secondarily. Second, muscle action can be modified in only two ways: A muscle or group of muscles can be manipulated to increase (strengthen) or to decrease (weaken) the effect of the muscles in primary position or in their field of action. Third, transposition and/or sharing of muscle tendons can create motion in a direction previously limited due to restrictions and pareses. The extraocular muscles are approached surgically through an incision in the conjunctival fornix or through a limbal incision. All six muscles can be approached through two fornix incisions (superior-nasal and inferior-temporal) (Fig. 11.14). A limbal approach is frequently preferred when performing reoperations and major muscle-sharing procedures.

Extraocular muscle strengthening procedures include resections, tucks, and plications. Resections are usually performed on the recti after the muscle is isolated. A section of muscle from 3 to 15 mm is removed, and the cut end is reattached to the original insertion site. Resections will result immediately in limited ductions in the opposite direction from the resected muscle and usually produce more inflammation and patient discomfort than recessions. The shortened muscle will undergo relaxation and elongation in the weeks following surgery. The histologic explanation of this phenomenon is an increase in sarcomere length [37, 39]. If a large resection is performed in a nonfixing eye or across from a weak antagonist, a permanent limitation of duction may result. A resected muscle can be placed directly on an adjustable suture at the original insertion site or by overresecting the muscle and allowing it to suspend back from the original insertion.

The reflected portion of the superior oblique tendon is the most common muscle to be tucked. This involves shortening the muscle at the tendon by folding or doubling over

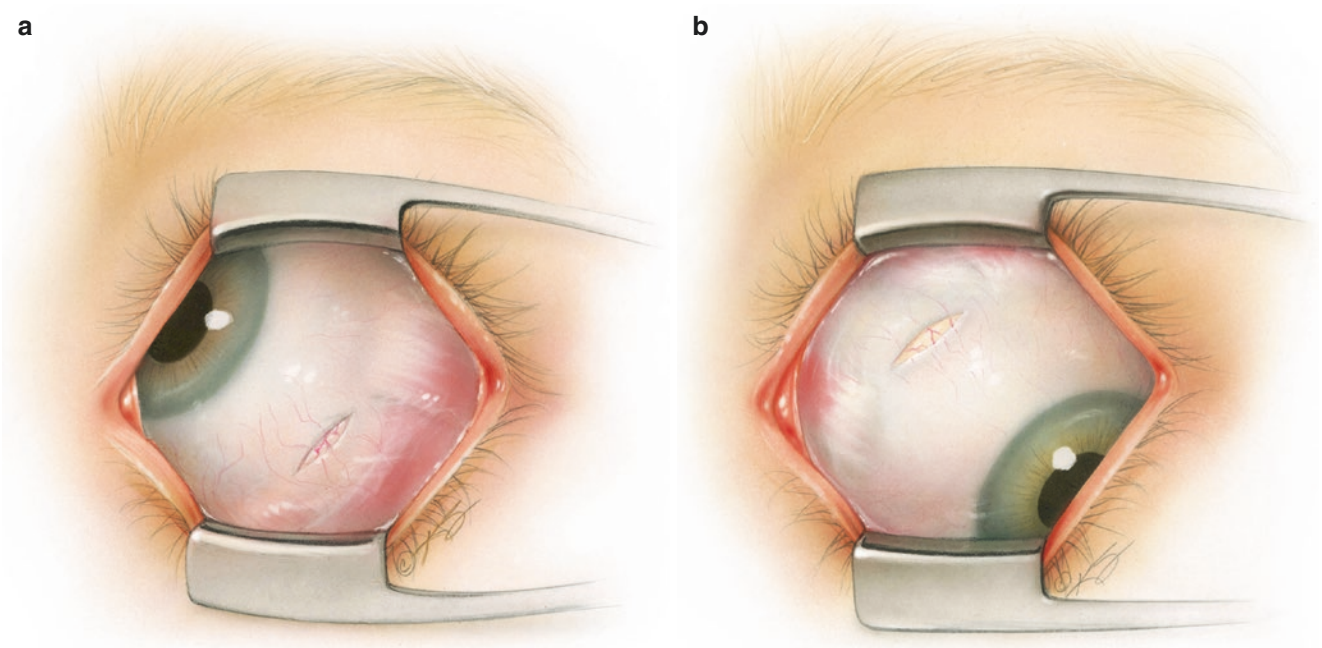


Fig. 11.14 Forniceal incisions for strabismus surgery. All six muscles can be isolated from these two incisions. (**a**) Infero-temporal incision: isolates the lateral rectus, inferior rectus, and inferior oblique muscles. (**b**) Superonasal incision: isolates the medial rectus, superior rectus, and superior oblique muscles

the tendon upon itself using a nonabsorbable suture [1, 10, 25, 38, 49–51]. This does not directly increase the action of this muscle, but creates a restriction of its direct antagonist (e.g., it decreases inferior oblique overaction and the resulting hypertropia). Tucks on the superior oblique tendon are less predictable than resection surgery on the recti. Excessive tucking of a muscle can result in restriction and overcorrection.

Extraocular muscle weakening procedures include recessions, myotomies, myectomies, tenotomies, and tenectomies. These procedures generally affect muscle function by temporarily reducing rotation of the globe in the field of action of that muscle and by promoting the "pullover" effect of the ipsilateral antagonist. A weakening procedure is more effective the greater the function of its ipsilateral antagonist, for example, a recession performed across from a paralyzed antagonist will be minimally effective in repositioning the globe or increasing its ductions. As with resections, we use a fornix approach whenever possible, preferring to use the limbal approach for reoperations and transposition procedures as needed. When a recession is performed in an attempt to reduce a restricted duction, it is important to perform intraoperative forced ductions of the eye before and after removal of the muscle from the globe [40, 52, 53]. If, after disinsertion of the muscle, forced duction testing reveals continued restriction, a diagnosis of an orbital restrictive component that is contributing to the strabismus must be considered. If disinsertion of the muscle results in completely freeing rotations of the globe, then the restriction is caused by the muscle.

Conventional recessions of the extraocular muscles include all those procedures in which the recessed muscle is sutured directly to the sclera in the desired position. Placement of the rectus muscles is usually from 3.0 to 9.0 mm posterior to the original insertion and can be displaced (transposed) away from the original insertion to assist with treatment of alphabet incomitance (A, V, Y, and X patterns) or to redistribute extraocular muscle forces (full transpositions or sharing procedures) [34, 44, 48]. The inferior oblique muscle is routinely recessed to near the lateral border or insertion of the inferior rectus [54–58]. A recession of the superior oblique is difficult and less predictable and seldom done at this point in time. The amount of conventional extraocular muscle recession performed is variable and depends on many clinical factors. Tables of suggested recession amounts have been published by several authors, and these numbers are useful as a foundation for a surgical approach [25, 38, 43, 44]. Any one surgeon's results become reproducible with experience and are dependent on preoperative and intraoperative clinical findings.

Recessions that allow the muscle to suspend from a place on the sclera anteriorly are called suspension recessions and include adjustable suture surgery nonadjustable hang-back and hemi-hang-back procedures [42, 43, 45, 46, 59]. A suspension recession is accomplished by passing the suture needles through the original insertion of the extraocular muscle and allowing the muscle to slide posterior to a desired or predetermined amount of recession. If the sutures are tied and cut, this constitutes a nonadjustable hang-back procedure. If a slip or bowknot is tied around the suture ends temporarily for later adjustment when the patient is awake and cooperative, this constitutes an adjustable hang-back procedure. If the needles are placed through sclera posterior to the original insertion and additional recession is obtained by further leaving the muscle suspended from this position, it is a hemi-hang-back procedure (HHB). The HHB can be useful when performing large initial or re-recessions of the extraocular muscles (14.0–25.0 mm from the limbus).

The use of tenotomy and/or tenectomy is generally limited to the reflected portion of the superior oblique. By severing this portion of the tendon, its function as an intorter, depressor, and abductor is decreased [50, 51]. The tendon can be approached either temporal or nasal to the superior rectus muscle. Unpredictable weakening can be obtained when a tenectomy or complete tenotomy is performed in this manner, resulting in a clinical picture of a superior oblique palsy in as many as 20% of patients [25, 50], leading to modification of this technique by suturing varying lengths of a #240 retinal band between the cut ends of the tendon (superior oblique tendon spacer) [51].

A myotomy or myectomy is commonly performed on the inferior oblique muscle [54–58]. An inferior oblique myectomy is a useful procedure for treatment of superior oblique palsy [54–58]. The portion of inferior oblique that is removed extends from its insertion on the globe to its penetration through posterior tenons capsule [55]. It is important to put a hemostatic suture through the remaining muscle stump and cauterize it to prevent postoperative orbital hemorrhage. More recently, a simple recession to the Parks position has become the procedure of choice [57, 58].

Preventing Lid Malpositions

Due to the anatomic relationships between vertically acting muscles and the muscles that control lid position, a brief discussion of lid malpositions associated with surgery on the vertically acting muscles is appropriate [60]. A change in eyelid position can occur frequently with vertical rectus muscle surgery. In a study, superior rectus recessions caused 91% of patients to develop upper lid retraction using lid margin to pupillary reflex distance measurements pre- and postoperatively [61]. With inferior rectus recessions, up to 94% of patients can develop lower lid retraction [61]. In this same study, an inferior rectus resection caused almost all patients to develop some evidence of lower lid advancement and flattening. Due to these and previous clinical observations,

attempts should be made to perform some of the following maneuvers during surgery, specifically on the superior and inferior recti [62, 63].

All attempts should be made to carefully dissect free all of the intermuscular membranes and fascial attachments around the superior rectus muscle, especially those connecting the superior rectus muscle to the horn of the levator and the underlying superior oblique. This is especially important when performing recessions of more than 5 mm or any resections. If this is not done, when recessing the muscle posteriorly, the superior rectus attachments to the horn of the levator will cause upper lid retraction. In resections the levator is moved anteriorly with the potential for ptosis.

During surgery on the inferior rectus muscle, it is important to identify the head of the capsulo-palpebral fascia, because this is a more tenacious attachment between the lower lid retractors and inferior recti. If the inferior rectus is recessed 5 mm or greater, or resected at all, then the head of the capsulo-palpebral fascia needs to be identified and treated in one of two following manners. Blunt dissection of the head of the capsulo-palpebral fascia off the inferior rectus using a wet cotton tip applicator is very effective at allowing the capsular palpebral fascia to be placed in its normal anatomic location, approximately 14–15 mm posterior to the inferior limbus. This is useful for infants or patients undergoing small recessions. In adults or children with lid problems or restricted extraocular muscle disease such as thyroid ophthalmopathy, it is important to reattach the head of the capsulo-palpebral fascia in its normal anatomic location. This can be accomplished by placing a 6–0 Vicryl suture with a spatulated S29 Ethicon needle through the head of the capsulo-palpebral fascia in a double whip-lock fashion, much the same as through the tendon of an extraocular muscle (Fig. 11.15). After placement of the inferior rectus at its recessed position, the sutures connected to the head of the capsulo-palpebral fascia can be used to reattach this at 14–15 mm posterior to the limbus, often on the tendon of the recessed inferior rectus muscle or posteriorly on the muscle belly itself (Figs. 11.16 and 11.17). These sutures can also be brought out medial and lateral to the inferior rectus and on an adjustable suture either alone or along with the inferior rectus. By using these intraoperative steps, some lid malpositions associated with surgery on the vertically acting extraocular muscles can be prevented.

Indications for surgery on the extraocular muscles in patients with lid and adnexal disorders are generally the same as those in patients who are having surgical treatment for strabismus alone. The chance of one surgical treatment correcting the alignment of the extraocular muscles is approximately 75–80% [11, 28, 38, 39, 42, 43, 47, 48, 59]. This does not

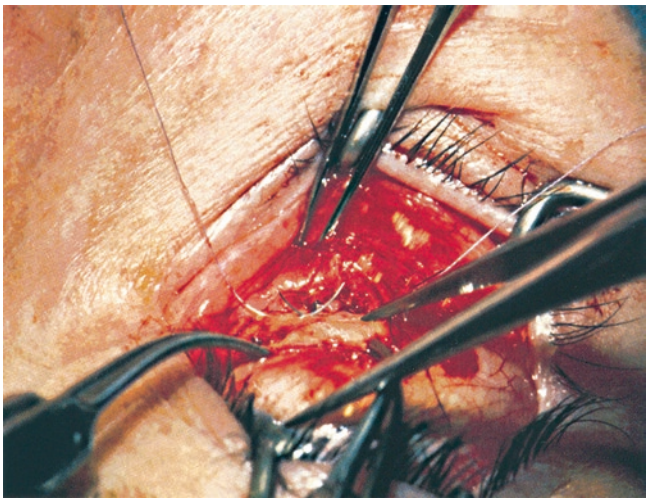


Fig. 11.16 Head of CPF being replaced on sclera anterior to recessed IR. The *arrow* shows the suture of the CPF

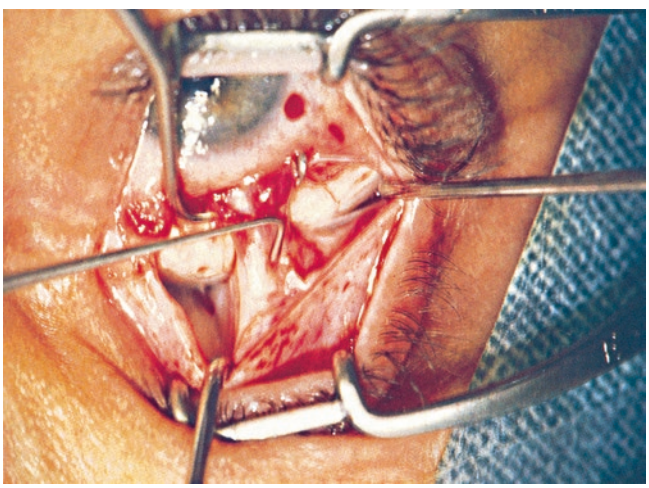


Fig. 11.15 Capsulo-palpebral fascia and inferior rectus. Surgical photograph of the head of the capsulo-palpebral fascia prior to suture placement and disinsertion from the inferior rectus

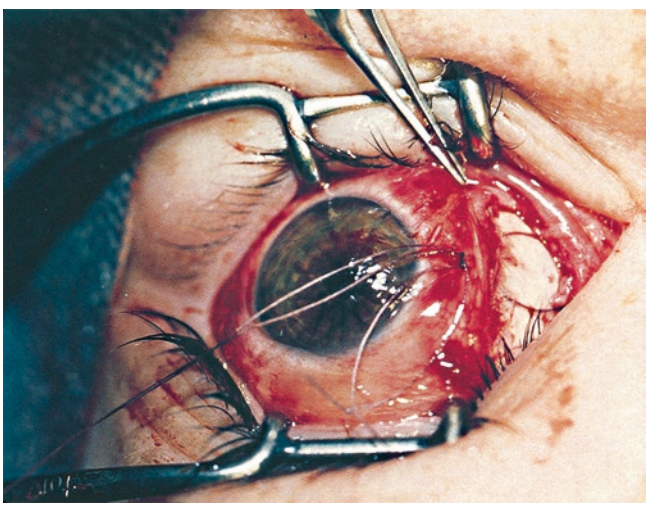


Fig. 11.17 Adjustable recession technique illustrated through the conjunctival fornix

mean that a patient's strabismus is cured or extraocular muscle function is normal. Success is defined in a variety of ways by different investigators, most simply as a deviation under 10 prism diopters in primary position or as complicated as restoration of full comitancy, fusion, and full field of singular binocular vision. The minimum definition for success in children is alignment of the visual axis with some binocular function, thus reducing amblyopic potential. Restoration of a full field of single binocular vision and full comitancy in patients who present with incomitant strabismus due to either restrictions or paralysis is often unobtainable. A realistic outcome includes a small angle or no residual deviation both in primary position and at near with at least some single binocular vision or binocular function in those positions. Full restoration of clinical comitancy is not necessary to prevent amblyopia. Routine and consistent communication with patients and their families should emphasize that surgical treatment of strabismus in patients with lid and oculoplastic disorders is not a cure, but that it is a form of aggressive treatment and is effective in almost all patients.

Complications specific to strabismus surgery are rare in patients with oculoplastic disorders, but strabismic surgical complications, in general, occur with a frequency of 1 in 10,000 and include orbital and/or intraocular hemorrhage, infection, secondary orbital inflammation with restrictions, and extraocular surface problems such as exposure keratitis due to lid malpositions and lagophthalmos.

In summary, treatment of extraocular muscle dysfunction in children with oculoplastic disorders is generally successful, providing that all the steps are taken to accurately diagnose and treat associated visual disorders. There are two forms of success in these patients. The first one is subjective and includes no diplopia, with the eyes appearing straight and moving together. The second is objective and includes either creation or expansion of the field of single binocular vision to a more functional level, increased comitancy, and the release of any restrictions without interfering with lid function. The principles of strabismus treatment in children with oculoplastic abnormalities are generally the same as those in children without these disorders, although the association of these problems often makes solutions more complicated. Perioperative attention to clinical diagnosis, special testing, and communication with plastic and reconstructive surgeons will enhance the chances for good visual and cosmetic results in these patients.

References

1. Miller MT. Ocular abnormalities in craniofacial malformation. Int Ophthalmol Clin. 1984;24:143.
2. Morax S, Beaumont C. Relationship between motor defects of the eyes and cranio-orbito facial malformation. Transaction of the 4th International Symposium on Orbital Disorders, Amsterdam, 1–4 September 1981.
3. Tokumaru AM, Barkovich AJ, Ciricillo SF, Edwards MS. Skull Base and Calverial deformities association with intracranial changes in craniofacial syndromes. Am J Neuroradiol. 1996;17:619–30.
4. Whitaker L, Katowitz J. Facial anomalies involving the nasolacrimal apparatus. In: Tessier P, Callahan A, Mustarde J, et al., editors. Symposium on plastic surgery in the orbital region. St. Louis: Mosby; 1974.
5. Whitaker LA, Katowitz JA, Jacobs WE. Ocular adnexal problems in craniofacial deformities. J Maxillofac Surg. 1979;7:55.
6. Diamond GR, Katowitz JA, Whitaker LA, et al. Ocular and adnexal complication of unilateral orbital advancement for plagiocephaly. Arch Ophthalmol. 1987;105:381.
7. Hertle RW, Quinn GE, Katowitz JA. Ocular and adnexal findings in patients with facial microsomias. Ophthalmology. 1992;99:144.
8. Hertle RW, Quinn GE, Katowitz JA, et al. Visual abnormalites and strabismus in craniofacial clinic. Ophthalmology (Suppl). 1990;97:150.
9. Apt L. An anatomical reevaluation of rectus muscle insertions. Trans Am Ophthalmol Soc. 1980;38:365.
10. Kushner BJ. Anatomical considerations in strabismus surgery. Int Ophthalmol Clin. 1985;25:1.
11. Swan KC, Wilkins JH. Extraocular muscle surgery in early infancy—anatomical factors. J Pediatr Ophthalmol Strabimus. 1984;21:44.
12. Demer JL. Pivotal role of orbital connective tissues in binocular alignment and strabismus. Investig Ophthalmol Vis Sci. 2004;45:729–38.
13. Gilbert PW. The origin and development of the human extrinsic ocular muscles. Contrib Embryol Carnegie Inst. 1957;36:59–78.
14. Cohen MM Jr. An etiologic and nonsologic overview of craniosynostosis syndromes. Birth Defects. 1975;11:137.
15. Wisnicki HJ, Repka MX, Guyton DL. Reoperation rate in adjustable strabismus surgery. J Pediatr Ophthalmol Strabismus. 1988;25:112.
16. Parks MM, Costenbader FO. Craniofacial dysostosis (Crouzon's disease). Am J Ophthalmol. 1950;33:77.
17. Diamond GR, Katowitz JA, Whitaker LA, et al. Ocular alignment after craniofacial reconstruction. Am J Ophthalmol. 1980;90:248.
18. Diamond GR, Whitaker LA. Ocular motility in craniofacial reconstruction. Plast Reconstr Surg. 1984;73:31.
19. Diamond GR, Katowitz JA, Whitaker LA, et al. Variations in extraocular muscle and structure in craniofacial dysostosis. Am J Ophthalmol. 1980;90:416.
20. Fries PD, Katowitz JA. Congenital craniofacial anomalies of ophthalmic importance. Surv Ophthalmol. 1990;35:87.
21. Grin TR, Nelson LB, Jeffers JB. Eye injuries in childhood. Pediatrics. 1987;80:13–9.
22. Jacobs D, Galetta S. Diagnosis and management of orbital pseudotumor. Curr Opin Ophthalmol. 2002;12:347–51.
23. Shields JA, editor. Diagnosis and management of orbital tumors. Philadelphia: WB Saunders; 1989.
24. Hertle RW, Katowitz JA, Young TL, Quinn GE, Farber MG. Congenital unilateral fibrosis, blepharoptosis, and enophthalmos syndrome. Ophthalmology. 1992;3:347–55.
25. Parks MM. Atlas of strabismus surgery. Philadelphia: Harper & Row; 1983.
26. Plager DA, Parks MM. Recognition and repair of the "lost" rectus muscle. Ophthalmology. 1990;97:136.
27. Hertle RW, Quinn GE, Minguini N, Katowitz JA. Visual loss in patients with craniofacial synostosis. J Pediatr Ophthalmol Strabismus. 1991;28:344.
28. Fells P. Management of paralytic strabismus. Br J Ophthalmol. 1974;58:255.
29. Preston KI, McDonald M, Sebris SL, et al. Validation of the acuity card procedure for assessment of infants with ocular disorders. Ophthalmology. 1987;94:644.

30. Elston JS, Lee JP. Paralytic strabismus: the role of botulinum toxin. Br J Ophthalmol. 1985;69:891.
31. Gammon JA, Gemmill M, Tigges J, Lerman S. Botulinum chemodenervation treatment of strabismus. J Pediatr Ophthalmol Strabismus. 1985;22:221.
32. Magoon EH. Botulinum chemodenervation for strabismus and other disorders. Int Ophthalmol Clin. 1986;25:149.
33. Kowal L, Wong E, Yahalom C. Botulinum toxin in the treatment of strabismus. A review of its use and effects. Disabil Rehabil. 2007;29:1823–31.
34. Rosenbaum A, Kushner BJ, Kirschen D. Vertical rectus muscle transposition and botulinum toxin (oculinum) to medial rectus for abducens palsy. Arch Ophthalmol. 1989;107:820.
35. Scott AB. Botulinum toxin injection into extraocular muscles as an alternative to strabismus surgery. Ophthalmology. 1980;87:1044.
36. Scott AB. Botulinum toxin injection of eye muscles to correct strabismus. Trans am Ophthalmol Soc. 1981;79:734.
37. Scott AB, Kraft SP. Botulinum toxin injection in the management of lateral rectus paresis. Ophthalmology. 1985;92:676.
38. Guyton DL. Strabismus surgery. In: Rice TA, Michels RG, Stark WJ, editors. Ophthalmic surgery. 4th ed. St. Louis: Mosby; 1984.
39. Engel JM, Guyton DL, Hunter DG. Adjustable suture surgery in children. J Am Assoc Pediatr Ophthalmol Strabismus. 2014;18:278–84.
40. Guyton DL. Exaggerated traction test for the oblique muscles. Ophthalmology. 1981;88:1035.
41. Kushner BJ. Evaluation of the posterior fixation plus recession operation with saccadic velocities. J Pediatr Ophthalmol Strabismus. 1983;20:202.
42. Keech RV, Scott WE, Christensen LE. Adjustable suture strabismus surgery. J Pediatr Ophthalmol Strabismus. 1987;24:97.
43. Rosenbaum AL, Metz HS, Carlson M, Jampolsky AJ. Adjustable rectus muscle recession surgery. Arch Ophthalmol. 1977;95:817.
44. Wright KW. Practical aspects of the adjustable suture technique for strabismus surgery. Int Ophthalmol Clin. 1989;29:10.
45. Coats DK, Paysse EA, Stager DA. Surgical management of V-pattern strabismus and oblique dysfunction in craniofacial dysostosis. JAAPOS. 2000;4(6):338–42.
46. Holmes JM, Hatt SR, Leske DA. Superior oblique tucks for apparent inferior oblique overaction and V-pattern strabismus associated with craniosynostosis. Strabismus. 2010;3:111–5.
47. Cline RA, Scott WE. Long-term follow-up of Jensen procedures. J Pediatr Ophthalmol Strabismus. 1988;25:264.
48. Helveston EM. Muscle transpostion procedures. Surv Ophthalmol. 1971;16:92.
49. Parks MM. Surgery for Brown's syndrome. In: Symposium on strabismus: transactions of the New Orleans academy of ophthalmology. St. Louis: Mosby; 1978. p. 157.
50. Parks MM. Management of overaction superior oblique muscles. In: Pediatric olphthalmology and strabismus: transactions of the New Orleans academy of ophthalmology. New York: Raven; 1986. p. 409.
51. Wright KW. Superior oblique silicone expander for Brown's syndrome and superior oblique overaction. J Pediatr Ophthalmol Strabismus. 1991;28(2):101–7.
52. Granet DB, Hertle RW, Ziylan S. The use of hyaluronic acid during adjustable suture surgery. J Pediatr Ophthalmol Strabismus. 1994;31:287–9.
53. Guyton D. Torsion and elevation under general anesthesia and during voluntary eyelid closure (bell phenomenon): discussion. J Pediatr Ophthalmol Strabismus. 1984;21:78.
54. Apt L, Call NB. Inferior oblique muscle recession. Am J Ophthalmol. 1978;95:95.
55. Del Monte M, Parks M. Denervation and extirpation of the inferior oblique: an improved weakening procedure for marked overaction. Ophthalmology. 1983;90:1178.
56. Elliott L, Nankin J. Anterior transposition of the inferior oblique. J Pediatr Ophthalmol Strabismus. 1981;18:35.
57. Mims JL, Wood RC. Bilateral anterior transposition of the inferior obliques. Arch Ophthalmol. 1989;107:41–4.
58. Whitaker LA, Katowitz JA, Randall P. The nasolacrimal apparatus in congenital facial anomalies. J Maxillofac Surg. 1974;2:59.
59. Repka MX, Guyton DL. Comparison of hang-back, medial rectus recession with conventional recession. Ophthalmology. 1988;95:782.
60. Hawes MJ, Dortzback RK. The microscopic anatomy of the lower eyelid retractors. Arch Ophthalmol. 1982;100:1313.
61. Pacheco EM, Guyton DL, Repka MX. Changes in eyelid position accompanying vertical rectus muscle surgery and prevention of lower lid retraction with adjustable surgery. J Pediatr Ophthalmol Strabismus. 1992;29:265–72.
62. Kushner BJ. A surgical procedure to minimize lower eyelid retraction with inferior rectus recession. Arch Opthalmol. 1992;110:1011–5.
63. Legreze WA, Gerling J, Staubach F. Changes of the lid fissure after surgery on the horizontal Extraocular muscles. Am J Ophthalmol. 2005;140:1145–6.

Pediatric Conjunctival and Intraocular Malignancies

12

Peter D. Fries

Introduction

Now, nearly 15 years after the first edition of *Pediatric Oculoplastic Surgery* was published, pediatric conjunctival and ocular malignancies still are rare conditions that some ophthalmologists may never encounter in their practice. Although the rarity has changed, for some conditions, such as retinoblastoma, radical changes in the genetics, treatment, and prognosis have occurred. Still, the clinical presentation and evaluation of these lesions require a similar process as in the past with the oculoplastic physician more likely to play a secondary or tertiary role in the care of these cases requiring some basic knowledge of treatment options, prognosis, and counseling for the family when deciding on potential procedures or alternative therapies for that patients' particular condition, stage, and preference. Other chapters in this text delve in depth regarding lid and orbital processes, including benign and malignant varieties, and, therefore, these will not be covered in this chapter. What lies between these anatomic areas is the conjunctiva and globe having separate conditions that may involve oculoplastics for certain treatment options that we will attempt to elucidate.

Conjunctival Malignancies

Epibulbar tumors in children are rare and malignancies of this tissue rarer still. Several series of pediatric conjunctival lesions and their pathologic features have been reported over the last 29 years [1–3]. All series demonstrate a consistent frequency of tissue-type lesions that are grouped as being melanocytic, choristomatous, vascular, epithelial variants, xanthomatous, or reactive. These three series identified only seven malignant lesions: three non-Hodgkin's lymphomas, one botryoid rhabdomyosarcoma, two melanomas, and one squamous carcinoma that arose in a child with xeroderma pigmentosa. Melanocytic lesions accounted for over 50% of the biopsied lesions.

Clinical features may help distinguish benign from malignant lesions especially with melanocytic lesions. Called upon to evaluate, excise, or biopsy, these lesions require some forethought as to what part to biopsy and what tissue studies and stains may be needed, will immunohistochemistry be helpful in deciphering these lesions, and what additional repair or grafting may be necessary (see Chap. 16).

Ocular Melanosis

Melanosis is the presence of excessive melanocytic pigmentation. It is classified based on two considerations: whether it is congenital or acquired and whether it is intraepithelial or subepithelial. A cutaneous area of epithelial congenital melanosis is more popularly known as an ephelis or freckle. Presentation in the conjunctival epithelium shows a similar picture with a distinct area of dark pigmentation that is not adherent to the underlying Tenon's capsule or episcleral tissues. Subepithelial congenital melanosis has a distinctly different clinical picture with the abnormal melanin-containing cells situated in the sclera and episclera producing a slate blue appearance (Fig. 12.1). This external finding coupled with increased uveal melanocytes is termed ocular melanocytosis. No distinct conjunctival pigmentation is observed in this condition, but it is included here due to its frequent confusion as a pigmented conjunctival lesion.

Ocular melanocytosis is a congenital lesion often visible in the first few weeks of life as irregular areas of unilateral episcleral pigmentation, heterochromia iridis, and increased choroidal pigmentation. It may first become visible when the patient achieves puberty. Increased size and numbers of melanocytes in these areas account for this appearance. If this process carries over to the surrounding dermis with resultant patchy skin pigmentation, one can diagnose this as oculodermal melanocytosis or nevus of Ota (Fig. 12.2).

P.D. Fries, MD
Eye Surgeons Associates, PC, Bettendorf, IA, USA
e-mail: pfries@eyesurgeonspc.com

© Springer International Publishing AG 2018

J.A. Katowitz, W.R. Katowitz (eds.), *Pediatric Oculoplastic Surgery*, https://doi.org/10.1007/978-3-319-60814-3_12

While ocular melanocytosis is almost always unilateral, nevus of Ota can be bilateral but asymmetric. A proclivity toward Asian (especially Japanese) and Black patients is consistent; nevus of Ota occurs 50–75 times more frequently among patients of Japanese extraction compared with American Blacks [4]. The incidence of nevus of Ota in Caucasians is approximately five times less than in Blacks. Ocular melanocytosis occurs more commonly in Caucasians.

Since the conjunctiva itself has no involvement, no conjunctival pigmented malignancies arise in these forms of ocular melanosis. Due to the pigmentary abnormalities arising in the uvea, episcleral, and orbital tissues, intraocular and orbital melanomas have arisen in both ocular melanocytosis and nevus of Ota [5–8]. In the first edition of this text, a note was made of the shortage of data and studies as to the risk of developing melanoma and metastases in these individuals with oculo(dermal) melanocytosis. Newer studies, particularly retrospective evaluations in children and adolescents with melanocytosis and melanoma, give a clearer picture of these risks. Several retrospective studies mostly from the large melanoma population at the Wills' Ocular Oncology Service have revisited and recalculated incidence and metastases of intraocular melanoma in children and teenagers [9–11]. In Singh et al. 2000's review of this population of pediatric patients with intraocular melanoma, it was estimated that an iris, ciliary body, or choroidal melanoma in children under the age of 20 was nine times more common in patients with oculo(dermal) melanocytosis [9]. An additional review of this cohort was published by Shields et al. in 2013 identifying 122 children and teenagers with uveal melanoma finding 4 patients (3%) with ocular melanocytosis but no case of nevus of Ota [10]. Nevus of Ota is unusual in that uveal melanoma is unknown in the pediatric age group with the earliest reported case in a 34-year-old White female [4]. A further retrospective follow-up study of this expanding cohort of intraocular pediatric melanomas by Kaliki et al. performed a matched retrospective cohort study evaluating the influence of age on these younger patients versus adults which focused on iris, ciliary, and choroidal melanomas and the incidence of metastasis [11]. Using Kaplan-Meier analysis, this study found a significantly lower risk of metastatic disease at 3, 5, and 10 years post-diagnosis in children than adults supporting the importance of early evaluation and follow-up of children with ocular melanocytosis and oculodermal melanocytosis.

Finally, Shields et al. reported on the specific association of rate of metastases in patients with oculo(dermal) melanocytosis-related uveal melanoma in their cohort of 7282 uveal melanomas [12]. A total of 230 patients in this cohort had oculo(dermal) melanocytosis and showed a twofold greater rate of metastases at 10 years posttreatment. This led to the recommendation of twice yearly dilated exams and OCT enabling earlier diagnosis of uveal melanomas in these patients.

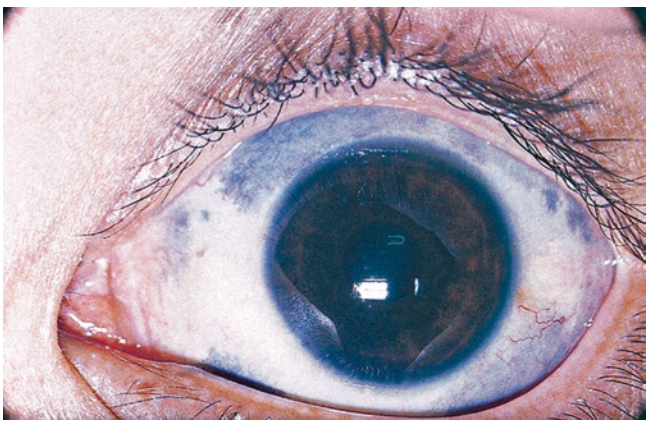


Fig. 12.1 External photograph showing bluish scleral coloration typical for ocular melanocytosis

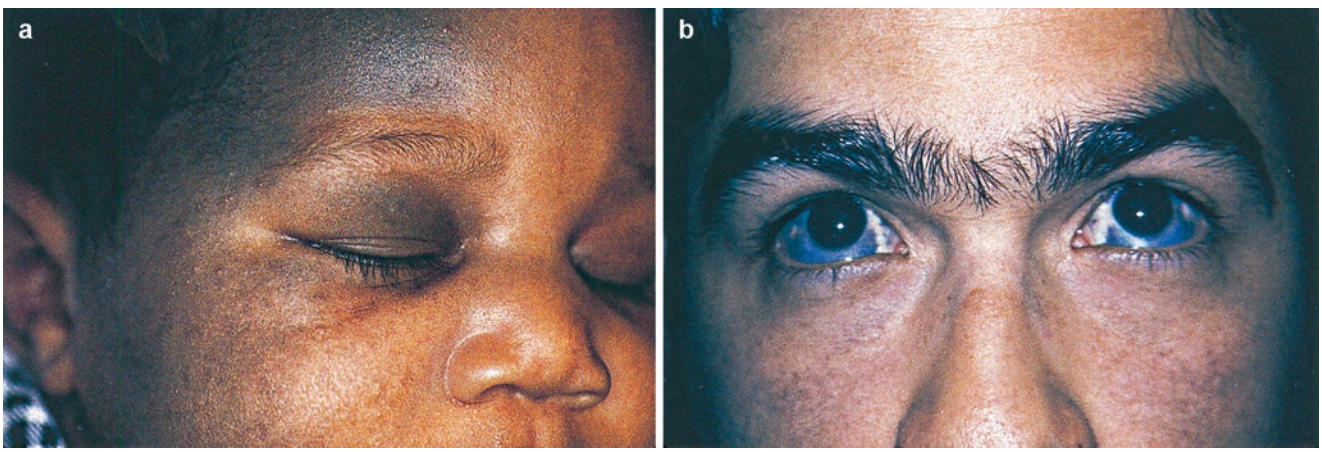


Fig. 12.2 Oculodermal melanocytosis. (**a**) Periocular facial pigmentation observed with oculodermal melanocytosis. (**b**) Unusual case of bilateral oculodermal melanocytosis

Conjunctival Nevi/Melanoma

Conjunctival nevi are not uncommon in the pediatric population. An exact incidence is unknown, but when conjunctival nevi do arise, 43% are apparent by 10 years of age, and another 22% are seen by age 20 [13]. Most appear on the bulbar conjunctiva frequently near the limbus. Approximately 14% are seen on the caruncle or semilunar fold but are unusual to arise in the tarsal or lid margin conjunctiva [2]. The majority are seen in Caucasians with much less frequency in Asians and Blacks.

Three histopathological subtypes classify conjunctival nevi: junctional, compound, and subepithelial. This classification is the same as that used for cutaneous nevi. Melanocytic nevus cells derive from epithelial melanocytes or their neural crest precursors. Collections of these cells are called nevi. Junctional nevus cells are located entirely within the epithelium of the conjunctiva and account for approximately 19% of all pediatric conjunctival nevi. Subepithelial nevi are the largest group accounting for 73% of pediatric nevi [14]. Compound nevi are the least frequent (8%) and have epithelial and subepithelial rests of cells. The clinical appearance of pediatric conjunctival nevi is similar to that in adults – a variable pigmented, isolated, flat lesion usually near the limbus without significant vascularity or inflammatory signs (Fig. 12.3a).

Junctional nevi often have cysts within the pigmented portion of the lesion that purport the benign nature of the nevus (Fig. 12.3b). Clinically scattered pigmentation throughout the epibulbar tissue denotes melanosis rather than nevus. This can be racial pigmentation as seen in very dark-skinned Blacks or melanocytosis if other ocular tissues are involved as previously discussed. Gradually increasing or changing pigmentation or lesion enlargement, especially near puberty, is not unusual and does not typically denote malignant transformation.

The diagnosis of conjunctival melanoma in the pediatric age group is decidedly rare [15]. Review of a large cohort of conjunctival tumors in childhood found melanocytic lesions to have less than a 1% chance of conversion to malignancy [1]. A large study evaluating the clinical appearance of conjunctival nevi and their pathological diagnosis and therapeutic outcome found no clinical features that were consistent with malignant transformation as all specimens were benign on histopathologic examination [16]. Clinical features suspicious for melanomatous transformation in conjunctival nevi have included rapid enlargement, marked pigmentary changes, nodular enlargement within the nevus, and the development of "feeder" vessels. These features were present in multiple specimens in the previously cited reference, but no melanoma was found on pathology. What other clinical features should one use as being suspicious for melanoma resulting in the decision for surgical intervention? The largest series to date evaluating the relationship of conjunctival melanocytic lesions and melanoma did not include data regarding patent age [17]. However, the clinical information regarding the presentation of these reported melanomas features a consistent theme: a pigmented lesion noticed for several years, not evident at birth, which suddenly and rapidly began to change in size and/or pigmentation. This would insinuate that these malignant transformations occurred de novo rather than arising from melanocytic changes in the conjunctiva which is somewhat supported by histopathologic slides lacking signs of nevus cells at the base of these malignancies [17]. Two authors report conjunctival melanomas that presented with ulceration prior to excision and indicate that ulceration was an important prognosticator for local control and survival for these lesions [18, 19]. Tumor thickness was also an important prognosticator as well [18]. Presence of the lesion arising on non-bulbar conjunctiva was considered to be a risk for melanomatous transformation in one case report (Fig. 12.4) [19]. One large observational

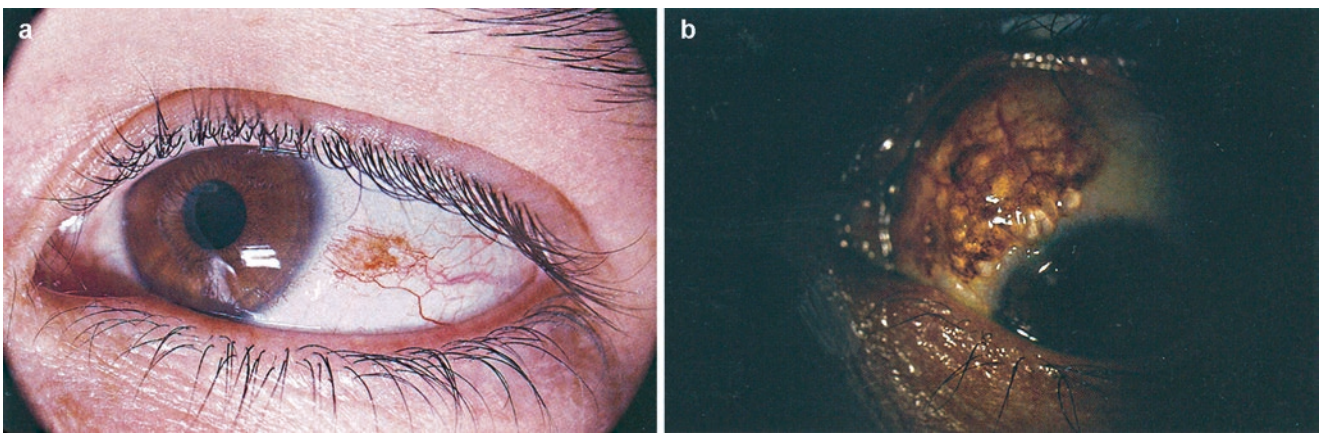


Fig. 12.3 Conjunctival nevi. (**a**) Bulbar conjunctival nevus with *brownish*, wispy conjunctival pigmentation. (**b**) Larger conjunctival nevus with multiple cysts

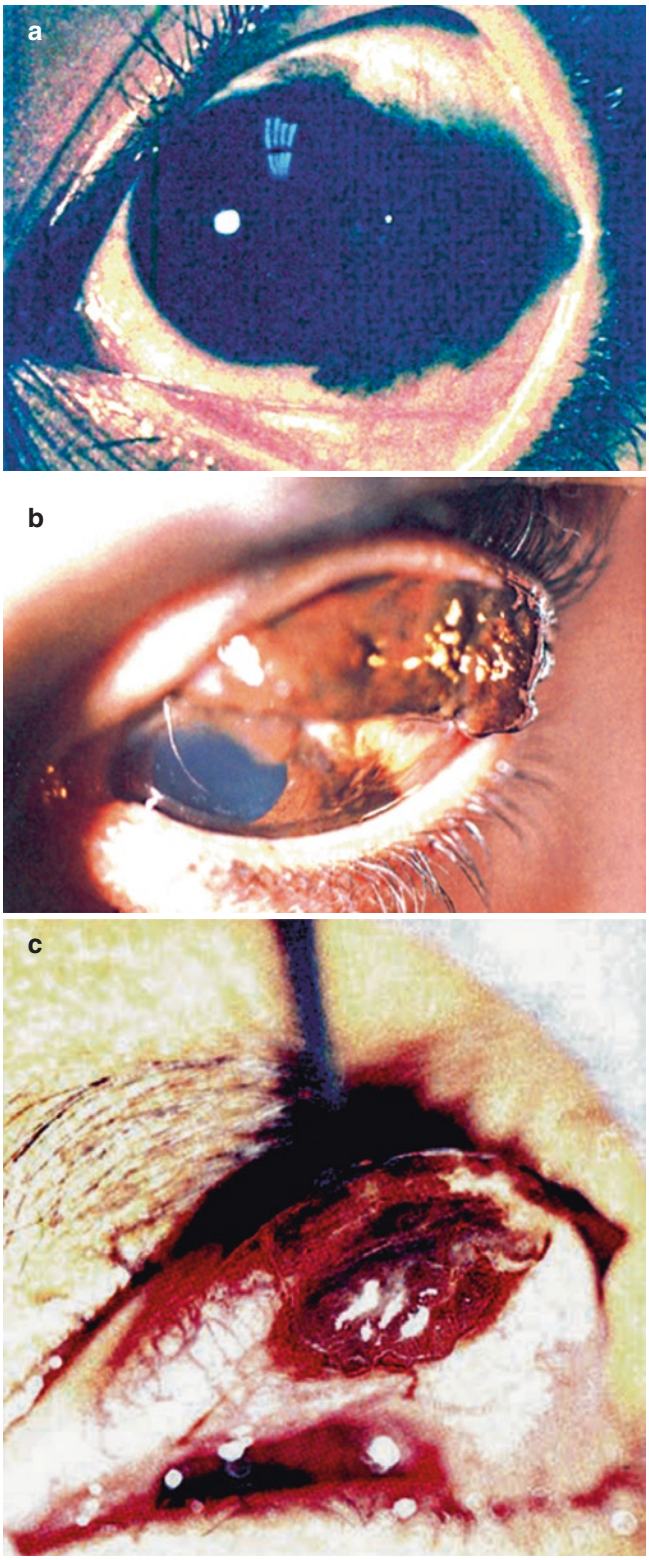


Fig. 12.4 (**a**) Polaroid photograph of large, congenital bulbar conjunctival pigmented lesion in a 12-year-old female. Surgical excision was performed and the pathology report indicated a nevus. (**b**) Clinical appearance 1 year later demonstrating bulbar and palpebral recurrence of pigmented masses that on biopsy are malignant melanoma. (**c**) Double eversion of the upper lid shows supra-tarsal tumor

study of 410 patients with conjunctival nevi found three patients transforming to melanoma (two compound nevi and one blue nevus), but all of these three were adults [20].

It is difficult to arrive at any solid clinical criteria that signal malignant transformation of childhood nevi primarily because so few cases have been reported. A pigmented lesion present for several years, not present at birth, with sudden change in size, pigmentation, thickness, and ulceration or arising from palpebral conjunctiva should alert the clinician to possible transformation.

What should be the next step: biopsy or excision? In children, strong consideration should be given to complete excision with 3 mm margins and submission for fixation and evaluation for tumor type and tumor thickness and whether the margins are free of tumor [13]. Frozen section analysis is fraught with difficulties including obscuration of cells by pigment and distortion of cell morphology. Pathology is very important in establishing the tumor type, marginal involvement, and grade for staging purposes. General agreement among pathologists has emerged regarding the features of atypia in grading conjunctival melanocytic lesions [21, 22].

Still, some lesions defy easy classification resulting in the pursuit of immunohistochemical markers to achieve more definitive diagnostic certainty for the classification of benign, carcinoma in situ and melanomatous lesions of the conjunctiva [23–25]. Here again, the vast majority of these conjunctival melanomas occur in adults, most of which arise from primary acquired melanosis which are exceedingly rare in children and which dominate this research in immunohistochemical analysis as an avenue of better identification for differentiating equivocal melanotic specimens as benign or malignant. Despite the adult predilection, the expression of certain cell antigens could possibly be expected from any melanocytic lesion with the potential of malignant transformation. Jakobiec et al., in a study of immunohistochemical analysis of atypical conjunctival melanocytic lesions (blue nevus, granular cell nevus, epithelioid nevus, and balloon cell nevus), demonstrated that Ki-67 expression was very low (<1%) in these benign variants, whereas this same expression in conjunctival melanomas is usually greater than 10% in nuclear positivity among all cells counted in these specimens [23, 24]. The consideration of immunohistochemical analysis should be utilized in any atypical melanocytic conjunctival lesion where clinical features do not reveal a clear-cut diagnosis.

Faced with these limitations, one must still consider the rate of recurrence after resection and the potential for metastatic spread. Adjuvant treatment with topical mitomycin C, interferon alpha-2b, or 5-fluorouracil may control future recurrence with positive margins seen on pathologic specimens as a secondary treatment based on final pathology findings [18]. As with adult conjunctival melanoma, clinical

recurrence may be difficult to assess if pigmentation is not present. Consideration of conjunctival biopsies for any suspicious area of conjunctival erosion, hypervascularity, spotty pigmentation, or amelanotic thickening is warranted. The potential role of topical adjuvant treatment in superficial recurrence or de novo melanomatous change would seem advantageous in these circumstances. It warrants reinforcement that palpebral conjunctiva needs to be adequately visualized in the follow-up of these patients.

Finally, with clear marginal resection, what should be done to monitor for future systemic disease? Only two case reports of metastatic disease in children with conjunctival malignant melanoma have found their way into the literature [15, 26]. Both cases had a history of rapid recurrence after initial and subsequent surgical resection. Folberg et al., with their clinicopathologic review of conjunctival melanosis and melanoma in adults, reported both pathologic and clinical entities that indicate the likelihood of future metastatic or local recurrence: tumor extending to the margin or base of the specimen, orbital extension, a common pagetoid growth pattern, involvement of the caruncle, the full thickness of the epithelium simulating an in situ carcinoma, the absence of an inflammatory response to the invasive component of the lesion, tumor thickness greater than 0.8 mm, and the presence of five or more mitotic figures per ten high-power fields [17]. One could certainly add rapid recurrence after resection to this list which, individually or in multiples, would be a good reason for the involvement of a pediatric oncologist for short-term metastatic assessment and long-term monitoring. The role of the oculoplastic physician will undoubtedly be integral to the original surgical resection and repair of postsurgical defects as well as the possible role of exenteration as a life-sparing technique in hopes of surgical tumor control. The above reference of orbital extension harboring worsening prognosis for survival is based on the clinical findings that approximately 90% of patients at the time of exenteration are already manifesting systemic metastases making exenteration of little use except for pain or mass effect control.

Other Conjunctival Malignancies

A variety of rare conjunctival tumors have been described in the pediatric population. While most practitioners are unlikely to encounter these entities, an awareness of their presentation is essential when evaluating a suspicious conjunctival mass.

Conjunctival Rhabdomyosarcoma

Periocular rhabdomyosarcoma typically not only arises as an intraorbital tumor but can also originate in other sites (lids, iris, and periorbital subcutaneous tissues) and as a conjunctival mass [27]. The conjunctival clinical features are typically



Fig. 12.5 Conjunctival embryonal rhabdomyosarcoma in a 9-year-old female

a pinkish multilobulated/papillary epibulbar lesion with prominent feeder vessels with rapid growth (Fig. 12.5) [28].

Other pediatric conjunctival lesions have similar appearances and include juvenile xanthogranuloma, squamous papilloma, leukemia, lymphoma, and neurofibroma [29]. The clustering multilobulated appearance is the origin of its name, botryoid rhabdomyosarcoma. While the tumor appears to arise from the conjunctiva, it is a subconjunctival mass that can have the episcleral, lid, or anterior orbital tissues as its site of origin.

Clinical series reporting on primary ocular rhabdomyosarcoma place the conjunctiva as the least likely site of origin in the periocular region. One series found only one case in the 33 patients with primary ocular rhabdomyosarcoma [30]. Single case reports along with their review references bring the total of conjunctival rhabdomyosarcoma cases to 14 [28–35]. No sex predilection or specific age range has been identified. Embryonal, alveolar, and botryoid patterns have been reported. No intraocular invasion has been reported, but one case of subconjunctival extension as the presenting sign of an intraocular rhabdomyosarcoma has been reported.

The treatment of conjunctival rhabdomyosarcoma is no different than the presentation in other body sites; attempts at complete excision with follow-up chemotherapy and/or radiation therapy based on systemic staging work-up yield the greatest long-term survival [31]. Inability to completely excise the tumor increases the death rate with greater short-term findings of increased regional and systemic metastasis. One must weigh the morbidity of surgical resection against the side effects of radiation therapy especially around the eye and orbit which is increased in still developing sockets. Oculoplastic surgeons will be called upon for their expertise in the surgical management of these patients due to their periocular origin. Imaging studies are a must in guiding surgical decision-making. If the conjunctival lesion fits the profile of a suspected rhabdomyosarcoma, one should assume that it is arising from orbital or peribulbar tissue rather than conjunctiva alone just based on the infrequency of pure conjunctival rhabdomyosarcoma.

Leukemia/Lymphoma

Conjunctival involvement in pediatric leukemias and lymphomas as a presenting sign is rare. With leukemias, especially the acute forms, eye signs in general and conjunctival forms specifically are not unusual. Several large series have looked at the incidence of ocular abnormalities associated with pediatric leukemias [36–38]. A very recent series found 24% of all children diagnosed with acute myelogenous leukemia, and acute lymphoblastic leukemia had ocular signs [36]. Of this group with ocular signs, 12% had conjunctival signs of venous stasis, conjunctival hemorrhage, or conjunctival mass (Fig. 12.6). The venous stasis is thought to arise from leukemic hyperviscosity of these small vessels and is visible in the retina as well, while the conjunctival hemorrhages are thought to be from decreased platelet levels. Interestingly, in this series, low systemic platelet levels were significantly lower in children with ocular changes from their leukemia [36]. Only one third of the patients with eye signs had symptoms from their ocular changes.

Postmortem studies reveal that 27% of children with leukemia have ocular, orbital, and /or conjunctival changes [38]. Clinically, these present as either infiltration of tissues by leukemic cells or the manifestations of some systemic hemodynamic abnormality, usually hypercoagulation, with attendant physical signs. Proptosis, hypopyon, reduced visual acuity, and cranial nerve palsy can signal leukemic infiltration in the orbit, anterior chamber, optic nerve, and cavernous sinus, respectively. Conjunctival hemorrhages and tortuous vessels mark the presentation of hyperviscosity complicating leukemias [39]. Conjunctival mass formation from leukemia has been reported but carries no specific clinical features that allow accurate diagnosis of leukemic infiltration without biopsy [40]. Anterior orbital involvement can "spill" into the subconjunctival area and appear as an isolated conjunctival mass or hemorrhage.

There is a major change in the association of ocular findings in childhood leukemia and its association with increased mortality. Ridgway et al. and Ohkoshi and Tsiams both reported a greatly increased mortality risk with ocular findings in children with leukemia [37, 41]. The very recent publication by Bitirgen et al. found no increased risk of mortality in their large cohort of children followed long term with leukemia [36]. This may be due to advances in treatment that have led to increased survival rates in these acute pediatric leukemias.

With this increased survival, recurrences are predictably more commonly seen. A few case reports have been published describing eye findings as the first presentation of the recurrence [42, 43]. Three of the four cases in these two reports of eye findings heralding the recurrence of acute leukemia in previously treated children were initially diagnosed as acute iritis. These cases were initially treated with topical corticosteroids with a poor response to the treatment resulting in suspicion of a potential recurrence of the leukemia as a masquerade syndrome. These three cases underwent anterior chamber paracentesis and aqueous aspirates that showed leukemic recurrence. The fourth case presented as a hemorrhagic conjunctival mass that was biopsied showing leukemic cellular collections. These recurrences are a reminder of the protean features of recurrence in childhood leukemias and the importance of history taking regarding other systemic conditions with pediatric uveitis [43].



Fig. 12.6 Conjunctival extension of AML in a 3-month-old child

Pediatric ocular lymphoproliferative disorders continue to be rare with most large series of pediatric conjunctival lesions reporting no lymphomatous processes [3]. Several case reports of a single pediatric patient have been published identifying unilateral or bilateral conjunctival lymphomas of the anaplastic large cell, follicular, MALT, and extranodal marginal B-cell variants [44–48]. Several case reports have been published of benign reactive lymphoid hyperplasia with both unilateral and bilateral presentations [49, 50]. The clinical features are similar in appearance to adults with a salmon pink-colored, smooth, noninflamed, solid-appearing conjunctival lesion presenting on the bulbar conjunctiva or fornices (Fig. 12.7).

It is much more common for ocular adnexal lymphomas in any age group to arise in the orbit presenting with proptosis, but if the lymphoma is in the anterior orbit, a conjunctival

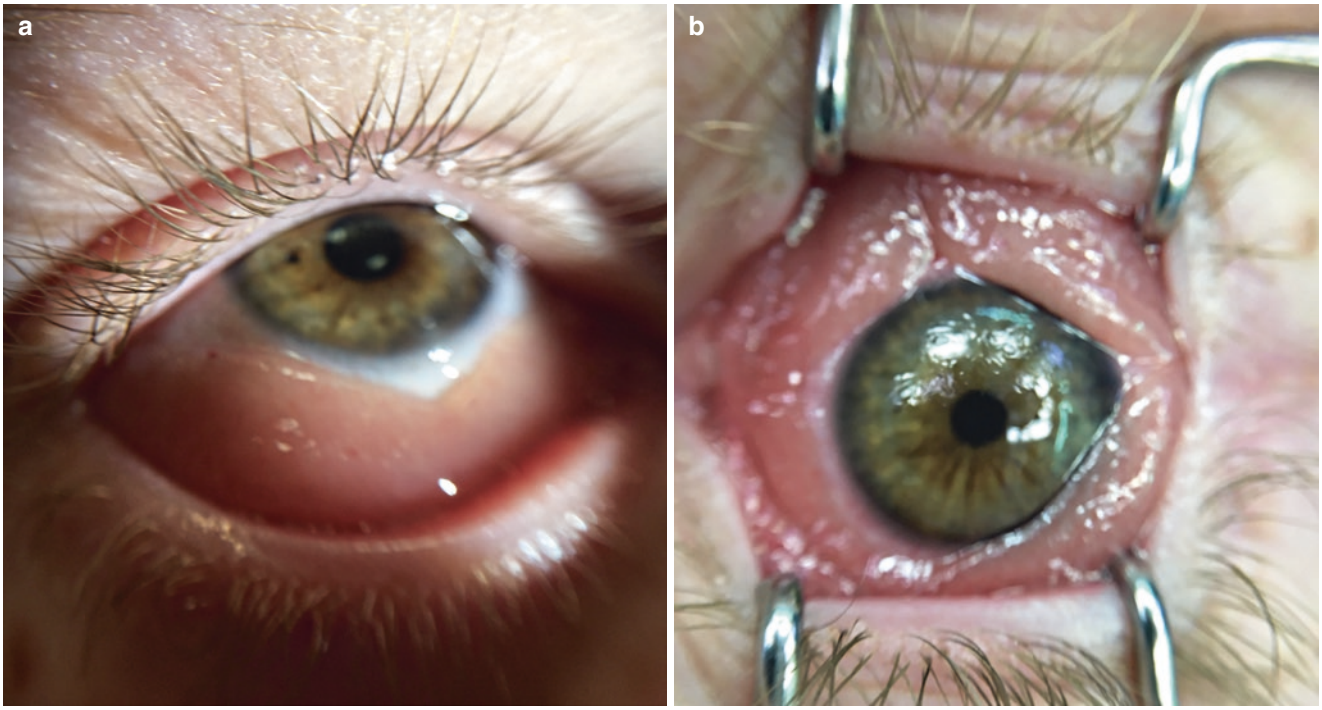


Fig. 12.7 (**a**, **b**) Conjunctival MALT lymphoma in a 6-year-old child

portion may be the visible component announcing the presence of this condition. With purely conjunctival onset, no other clinical findings such as proptosis, ptosis, motility disorders, or globe dystopia would be expected which should draw one's attention from the conjunctival component and the investigation of additional areas of involvement. MR imaging should be strongly considered with conjunctival lesions suspicious for lymphoma due to their rarity as an isolated presenting position. Conjunctival biopsy, if large, or resection, if small, with histopathologic and histoimmunologic analysis will be able to identify the lesion and direct appropriate workup and eventual treatments. Oculoplastic surgeons may be the primary referral for this intervention or for orbital biopsy to obtain adequate tissue.

Burkitt's lymphoma has been reported as an entity that can present with conjunctival involvement [51]. Although typically presenting in the orbit or extending from paranasal sinuses to involve the orbit, associated cranial neuropathy, proptosis, optic neuropathy, African descent, and an immunocompromised status such as positive HIV status or immunosuppressants for organ transplantation should alert one to this diagnosis. A report of three non-African non-immunocompromised patients with Burkitt's lymphoma along with a literature review accumulating 16 cases found the average age of presentation was 12 years old with 50% having coexisting sinus involvement [52]. This reminds us that lymphoma is always a systemic disease likely not arising from a single abnormality but a variety of cofactors such as genetic abnormalities and mutations and various viral and bacterial agents creating a treatment environment that currently includes chemotherapeutic agents, radiation therapy, and even antibiotics [44, 53–58]. The care of this condition always resides in the hands of pediatric oncologists.

Langerhans Cell Histiocytosis

Formerly known as a triad of conditions, eosinophilic granuloma, histiocytosis X, and Letterer-Siwe disease, Langerhans cell histiocytosis comprises a set of clinical presentations related to the tissue infiltration of the Langerhans cell, a type of histiocyte. Localized and systemic forms of this condition have varying prognoses, with fulminant malignant histiocytosis being uniformly fatal [59]. Approximately 20% of cases demonstrate orbital involvement with infiltration of these histiocytes in the temporal or sphenoid bones presenting with lid edema and proptosis. The uveal tract, sclera, extraocular muscles, optic nerve, and conjunctiva have rarely shown involvement [60, 61].

The conjunctival presentation is usually in the disseminated form with multisystem disease [62]. Most cases have periorbital bone involvement that extends into the lid soft tissue with attendant lid edema, chemosis, episcleral vessel dilation, and the appearance of a subconjunctival soft tissue mass. Imaging studies quickly define this not as an isolated conjunctival lesion but part of a multifocal systemic disease. However, a single case of an isolated conjunctival histiocytic lesion in a newborn with pathology similar to that of

Langerhans cell histiocytosis has been reported, but without other systemic involvements, it is difficult to classify this as part of this condition [63]. It is unlikely that oculoplastic surgeons will be involved in the management of this condition, but they may present urgently with these periocular findings without a firm diagnosis warranting this inclusion.

Squamous Cell Carcinoma

All ophthalmologists are likely to be familiar with the adult forms of ocular surface squamous cell neoplasia ranging from dysplasia, carcinoma in situ, and squamous cell carcinoma (SCCA). Many reports have established that this condition has several cofactors that increase the risk of onset of this malignant disorder: chronic ultraviolet exposure, certain viral infestations, smoking, exposure to coal tar, and chronic immunosuppression [64–66]. Most children have not been exposed to the environmental factors long enough for these tumors to form which is likely to be the reason these are rare under 20 years of age, but as with most rare conditions, significant assessment of epidemiologic factors is difficult simply due to low numbers of cases.

Conjunctival SCCA has been reported in a child as young as 3 or 4 years of age [67, 68]. Two conditions are known to predispose children to the development of conjunctival SCCA: xeroderma pigmentosa and acquired human immunodeficiency syndrome (AIDS) [69, 70]. Xeroderma pigmentosum is a rare autosomal recessive disorder creating a defect in one of eight genes responsible for the repair of ultraviolet-damaged DNA in epithelial cells resulting in early-onset skin cancers (basal cell carcinoma, squamous cell carcinoma, and melanoma) [71]. When accompanied by progressive neurological abnormalities such as ataxia, deafness, and mental retardation, it is named De Sanctis-Cacchione syndrome [72].

The conjunctival and lid skin changes that occur with xeroderma pigmentosa include scarring, symblepharon formation, cicatricial ectropion with corneal exposure, xerosis, melanosis, and the development of lid and conjunctival SCCA [69, 72]. Basal cell carcinoma and melanoma have been reported on facial skin and the scalp but do not appear to arise in childhood [72]. It is projected that 50% of children will develop a periocular malignancy by 20 years of age [69]. Siblings with this syndrome have developed conjunctival malignancies (Fig. 12.8) [73].

Unlike the adult form of conjunctival SCCA, these lesions occur as localized, reddish masses in sun-exposed conjunctiva with telangiectatic vessels. Multiple areas can be involved and the limbus is not the most common site [69, 72]. Invasion into the orbit or globe may occur, as these are rapidly progressive lesions, if not identified early on and may require more aggressive treatments. Regarding AIDS, conjunctival squamous cell carcinoma arising at a young age was once regarded as a marker for this condition. With ever-advancing therapies for AIDS, conjunctival SCCA and other secondary malignancies have greatly declined where these therapies have been available [74].

Therapy for squamous cell carcinoma of the conjunctiva has changed dramatically over the last 15 years changing from wide margin "no-touch" resection with adjuvant cryotherapy to topical antitumor medications such as mitomycin C, 5-fluorouracil, and interferon alpha-2b (also given as subconjunctival injection). These are frequently the mainstay either alone with smaller lesions or coupled with surgical resection and topical medications to "sterilize" the surface of any remaining cancerous or not yet identifiable dysplastic cells. Much more experience exists with the adult forms to potentially make practitioners comfortable with pediatric use with these medi-



Fig. 12.8 Xeroderma pigmentosa. (**a**) Intraoperative photograph showing facial features typical of xeroderma pigmentosa in a 6-year-old patient. Note the epibulbar mass almost filling the interpalpebral space in the left eye and severe ulcerative changes of the right lower lid. (**b**) Intraoperative photograph of the 5-year-old brother of the patient in (**a**), showing facial skin changes typical of xeroderma pigmentosa. A translucent medial epibulbar mass is present in the right eye. Inferior corneal opacification is present in the left eye (From Hertle et al. [73]. Reprinted with permission from Slack Incorporated)

cations. Cidofovir, approved for human papilloma viral therapy topically or as an injection, has been used on conjunctival and eyelid SCCA but would appear to play no role in the treatment of pediatric conjunctival SCCA due to its different causation. Oculoplastic surgeons could be involved in the care of these patients if intraocular or intraorbital extension occurs, requiring anterior or complete exenteration for tumor control.

Pediatric Intraocular Malignancies

Faced with a child harboring an intraocular mass, the ophthalmologist is obligated to rapidly diagnose the condition such that effective treatment can be undertaken. The diagnosis may require secondary studies such as ultrasonography, CT and/or MR imaging, systemic evaluations by consulting physicians in ophthalmology or pediatrics, and eventual surgical procedures for tissue diagnosis or curative resection. Most ophthalmologists refer these patients to centers in proximity of their practice whom are experienced in the diagnosis and treatments of potentially malignant intraocular lesions.

After establishment of the diagnosis of an intraocular malignancy in a child, oculoplastic surgeons may be called upon to surgically manage this child by performing an enucleation. Many questions will come from the parents regarding the condition, the procedure, the expected healing, prosthesis fitting once healed, and, most importantly, will this save the child's life. This section reviews the malignant ocular tumors of childhood with emphasis on the oculoplastic surgeon's role in the care of these special individuals.

Retinoblastoma

Perhaps no other ophthalmic condition has had as much change in its management than retinoblastoma over the last 20 years. At the time of publication of the first edition of this text, systemic chemoreduction was just beginning to be embraced as a replacement for direct retinal tumor treatment alone or combined with external beam radiotherapy for both unilateral and bilateral retinoblastoma. The need for improved visual outcomes and survival rates along with reduced induction of secondary malignancies drove these therapeutic migrations. Now, intravenous chemoreduction is largely supplanted by intra-arterial delivery of chemotherapeutic agents, via interventional radiographic ophthalmic artery cannulation, giving better targeting of the tumor load and hopefully less systemic and ocular side effects [75–79]. These changes along with earlier detection of the condition have led to a 5-year survival rate of approximately 96.5% but continued the risk of retaining useful vision from new tumor damage, especially in heritable bilateral retinoblastoma cases [80]. More eyes and patients are surviving these treatments.

Where does that leave the oculoplastic/orbital surgeon in the management of retinoblastoma? For the most part, it has not changed very much at all over the last 20 years. The clinical presentation of retinoblastoma is certainly well known to ophthalmologists: leukocoria, strabismus, and ocular inflammation are the initial signs in over 80% of retinoblastomas (Fig. 12.9). Other presenting signs include heterochromia, hyphema, increased intraocular pressure, decreased vision, rubeosis iridis, and phthisis bulbi. Anterior chamber involvement with iris nodules or free-floating tumor is rare and traditionally difficult to treat short of enucleation. With indirect ophthalmoscopy, the presence of multiple pink or white retinal tumors in one or both eyes is highly suggestive of retinoblastoma. A large unilateral tumor with a white-pink mulberry implant-like appearance is the classic retinal lesion and is virtually diagnostic of retinoblastoma (Fig. 12.10).

The dilation and examination of parents and siblings are important because the presence of a retinocytoma or regressed, calcified lesion in the retina nearly completely establishes the possibility of genetic inheritance. When examining children, it is important to keep in mind the lengthy differential diagnosis of retinoblastoma to help direct ancillary investigations (Table 1).

Once the possibility of retinoblastoma is established, at this point, the patient should be referred to an ocular oncologist who will pursue a careful systemic work-up to rule out metastatic disease. Thin-section, 1.5 mm non-contrasted and contrasted computer tomography (CT) of the orbit and head is used to look for calcification within the intraocular lesion

Table 12.1 Differential diagnosis of retinoblastoma

Persistent hyperplastic primary vitreous
Retinopathy of prematurity
Congenital cataract
Coats' disease
Optic nerve coloboma
Nematode endophthalmitis
Retinal dysplasia
Congenital toxoplasmosis
Retinal astrocytoma
Retinal detachment
Norrie disease
Uveitis
Metastatic endophthalmitis
Congenital retinoschisis
Congenital retinal fold
Familial exudative retinopathy
Medulloepithelioma
Persistent tunica vasculosa lentis
Tapetoretinal degeneration
Myelinated nerve fibers

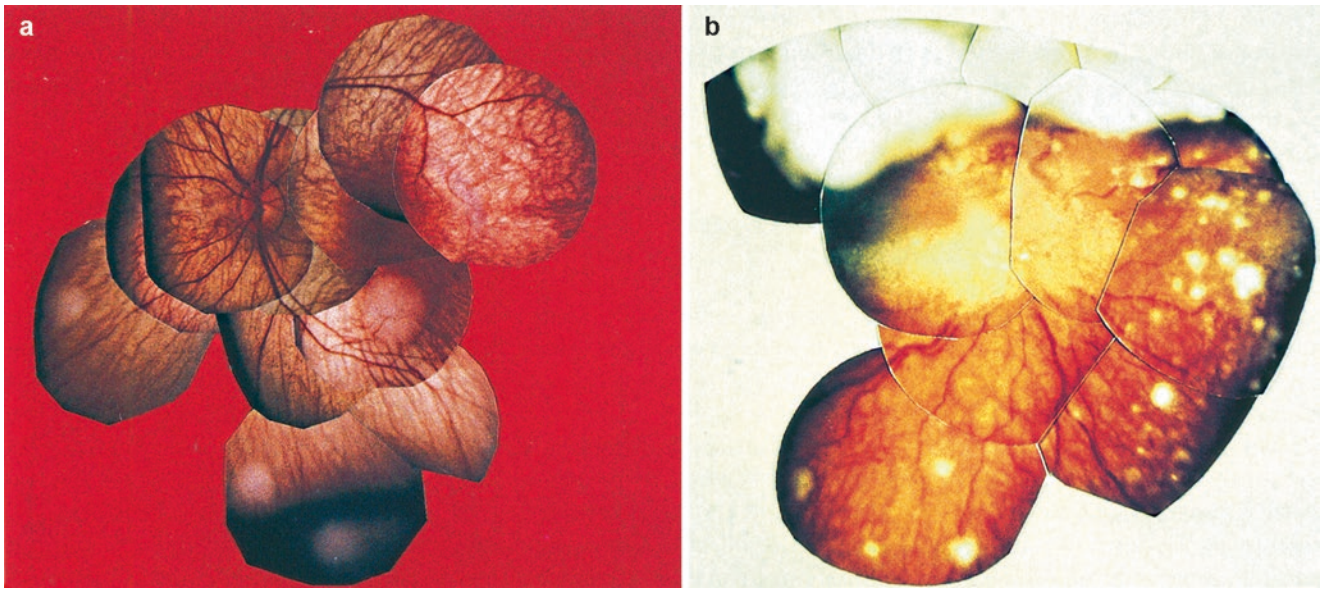


Fig. 12.9 Retinoblastomas. (**a**) Montage photograph of a child with hereditary retinoblastoma with multiple small tumor sites in one eye. (**b**) Montage photograph of child with a presumed somatic retinoblastoma with vitreous seeding and retinal implantation of retinoblastoma seeds. No tumors were in the opposite eye and long-term follow-up will be needed to determine if no other tumors will occur

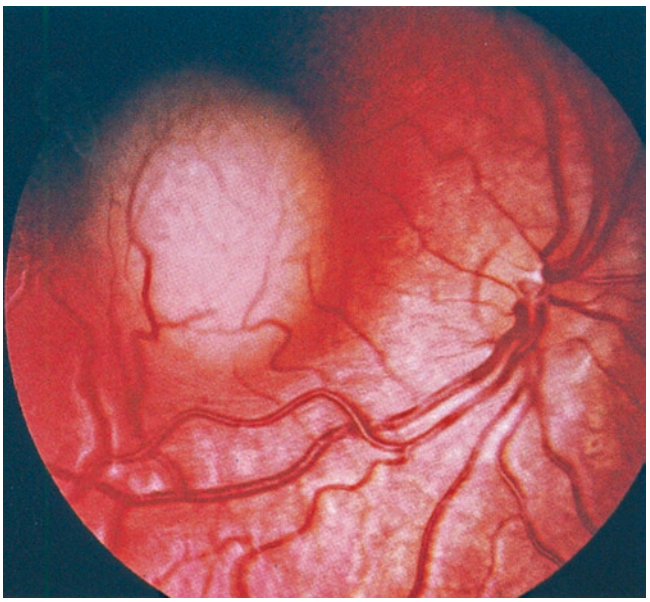


Fig. 12.10 Clinical appearance of retinoblastoma. Common clinical appearance of retinoblastoma with pinkish-white appearance, dilated feeder vessels, and specks of calcium visible in tumor



Fig. 12.11 CT of the orbits. Non-contrast CT of the orbits demonstrating intraocular with calcium consistent with retinoblastoma

and when found is virtually diagnostic of retinoblastoma (Fig. 12.11). Rare cases of calcification in *Toxocara* infection and intraocular abscess have been reported and require careful evaluation of the clinical aspects of the disease to differentiate their presentation from retinoblastoma [81, 82].

The non-contrast study shows calcifications better, while the contrasted study better identifies any secondary tumors. Any questionable findings should be pursued with magnetic resonance imaging, which is capable of detecting optic nerve extension better than other imaging techniques [83]. It is important to include the head during the imaging study to rule out the presence of a pinealoma or other midline intracranial primitive neuroectodermal tumors that can occur in children with germline mutations at the retinoblastoma locus (trilateral retinoblastoma).

Spiral CT scanning allows these imaging studies to be performed without anesthesia due to rapid scanning times [84]. Ultrasonography can also be used as a quick evaluation tool for the differentiation of retinoblastoma when high internal reflectivity and acoustic shadowing from calcifications are found [85]. Serology, to include a complete blood count, liver function tests, plasma carcinoembryonic antigen,

and ELISA for *Toxocara* (if clinically appropriate), is used to rule out metastatic disease or to rule in nematode endophthalmitis.

After a rapid review of these tests, the child is then examined under anesthesia at which time the following tasks are performed: a complete ocular examination with emphasis on a 360° scleral depressed retinal examination with retinal drawing to detect any tumor foci, performance of a technetium-99 injection for bone scan, lumbar puncture for cerebrospinal fluid cytology, two-site bone marrow biopsy, and possible treatment of selected tumors with targeted chemo- and/or radiation modalities. If intra-arterial delivery of chemotherapeutic agents has been ruled out, eyes more than 50% filled with tumor, eyes with anterior chamber extension, and eyes with glaucoma due to tumor invasion or neovascularization, or those tumors that have failed local treatment and/or radiation therapy, are typically enucleated.

No treatment has yet been found that eliminates the need for enucleation in some patients with retinoblastoma. The current chemoreduction therapies seem to delay the eventual need for enucleation in some patients, but, as yet, this does not seem to worsen their prognosis [86].

Additionally, a study comparing high-risk histopathologic features of eyes treated primarily with enucleation for retinoblastoma or following chemoreduction with a secondary enucleation for retinoblastoma found no significant difference in metastatic or survival rates [87].

Oculoplastics typically becomes involved in the treatment of retinoblastoma when either intraocular tumor load is no longer responsive to treatment or the eye is irreparably damaged with little hope for any useful vision due to this tumor load or side effects from the attempts to eradicate the tumor. Oculoplastic enucleation skills come into play to provide removal of the involved eye with an adequate specimen for the ophthalmic oncologist to determine if any high-risk pathology features (e.g., tumor through the lamina cribrosa of the optic nerve, tumor at the cut end of the optic nerve, extraocular extension through emissary canals, extensive choroidal invasion) are present and to replenish the orbital volume with an appropriate implant for best long-term orbital stability. Direct communication with the treating ophthalmologist for the patient being referred for enucleation is a must due to heritable retinoblastoma usually being bilateral, and, therefore, both eyes may be responding poorly to ongoing or past treatment. What the family thinks should be done might be different than what their treating physician considers of primary importance.

Once the decision for enucleation has been made, the surgeon must make a choice of an implant if one is to be primarily placed. Most surgeons would agree that primary placement is strongly indicated. Unsuspected extraocular extension can be dealt with by excision of contiguous orbital tissue but would warrant postoperative chemotherapy or radiation therapy as well. With radiotherapy waning in its usage with retinoblastoma, fewer implant problems after enucleation occur than in the past, but periocular chemotherapy with carboplatin and topotecan or past brachytherapy as treatments for intraocular retinoblastoma create a new set of potential issues for both postoperative healing, possible scleral thinning of the enucleated eye, and orbital tissue scarring that can complicate enucleation [88–91]. Despite this, a long-term follow-up (mean, 60 months) of 531 children with coated or wrapped hydroxyapatite implants with four or six extraocular muscles attached developed very few problems (0% extrusion, 1% implant infection, 3% implant exposure) [92]. Another study did not report this same success but did not limit their treatment to a single orbital implant. A 23-year study of 224 enucleations that utilized several different implants (acrylic, Allen, and scleral-wrapped hydroxyapatite) found a 4.6% exposure rate, a 2.7% extrusion rate, and a tripling of these events if the patient had undergone chemoreduction or external beam radiotherapy [93]. This relatively greater risk of implant complications was mirrored in a study of 135 children at St Jude's Research Hospital with 20.7% implant exposure, 11.9% socket contracture, 2.2% extrusion rate, and a 6.7% pyogenic granuloma formation rate [94]. Nearly 80% of the exposures resolved without treatment in this study, but chemotherapy and, especially, radiotherapy before or after the enucleation significantly raised the complication rate. Porous polyethylene orbital implants were used in 44 patients followed over a mean of 5 years after unilateral primary enucleation for retinoblastoma with no implant exposures, extrusions, or infections [95]. Another study looked at dermis fat grafts as a primary procedure in unilateral enucleations of retinoblastoma patients looking specifically at orbital volume compared to the nonoperated side over a median follow-up of 38.5 months [96]. Equal orbital volumes as measured on MRI scans were found, but patients who had undergone radiation or chemotherapy were excluded from the study leaving questions as how dermis fat would fare with concomitant chemotherapy or radiation therapy. One can conclude that any orbit with any implant will have some chance of healing post-enucleation with proximal perioperative need for chemotherapy and/or radiation therapy. Often, this therapy cannot wait an adequate time for orbital healing without increased risk for orbital recurrence or metastatic spread if high-risk pathology features are found. A case can be made for muscle attachment to a pervious implant that can be well covered by orbital and conjunctival tissue as the best approach to prevent implant complications.

Enucleation technique is well covered in this text in Chap. 42. Two points need to be emphasized in securing the removal of a globe with retinoblastoma. First, the length of optic nerve

segment is still an important consideration as tumor at the cut edge of the optic nerve is a very poor prognosticator for orbital recurrence and mortality [97]. Most studies suggest a length of 8 mm would be desirable. The pediatric orbit does not offer the posterior or periocular space that an adult has, making the approach to nerve transection more difficult. The temptation to try and gain more room to achieve a longer nerve segment is to push the globe more temporal or nasal to improve seeing the nerve. It is best to think of giving the enucleation scissors more room which means placing the globe on gentle anterior traction by securing clamps to the small stumps of the medial and lateral rectus muscles after they are disinserted from the globe. I personally do not like to pass sutures into the muscle insertions or sclera for fear of penetration or passage through a tumor laden emissary canal. Gentle forward traction yields 6 or 7 mm of anterior globe displacement and considerably improves the space for scissors. Blunt straight Stevens scissors or a slightly curved small Mayo scissors works well when inserted in the medial orbit straight posterior toward the optic canal.

Once successful transection of the optic nerve has been accomplished and any Tenon's has been separated freeing the globe, the second step is inspection of the sclera and the cut end of the optic nerve for any signs of gross tumor extension. If a short portion of the optic nerve is found (<5 mm), strong consideration should be given to obtaining several more millimeters of the intraorbital portion marking the true margin and placing this in a separate specimen cup. Careful inspection of the perioptic nerve sclera with all the short posterior ciliary vessels and nerves should be performed especially if intraocular tumor covers and hides the optic nerve on preoperative examination. Noting the exact position for the pathologist is important, but also resection of approximately 1 cm of surrounding orbital tissue should be performed to potentially reduce any orbital tumor load. Pathology is very important in deciding on staging but also high-risk features not only for postoperative adjunctive treatment decisions but also for long-term follow-up for local recurrence [98, 99]. Besides the implant, other considerations of tumor therapy also need to be followed (Table 2).

The research originally identifying the first tumor suppressor gene, RB1, to the 13q14.2 locus and the subsequent identification of what that gene produces, pRb, a chemical protein which functions as a regulator of gene expression, has shifted to studying ways to influence the loss of gene suppression utilizing the multitude of chemical pathways controlled by the pRb gene in oncogenesis [100]. The clinical importance of the retinoblastoma gene, RB1, rests not only with the importance in discovering its functions and how these may be manipulated into a treatment algorithm but also in its prediction of the aggressiveness of the patient's retinoblastoma and its predictive value for its transmission to future offspring [101–103]. Genetic counseling should not only be an important part of the care of all children with retinoblastoma but also their family. Determination of heritable versus somatic forms of retinoblastoma greatly affects their short-term prognosis (development of new tumors in the same eye or the other eye) and their long-term prognosis (risk of primitive neuroectodermal tumors and other nonocular malignant neoplasms). Examination of siblings and parents for signs of regressed retinoblastoma and the negative findings of intraocular pathology augment the counseling from genetics specialists and prepare the family for what is ongoing and what may be down the road. A regular ophthalmic follow-up schedule to monitor for new tumor growth or recurrence is essential.

Genetic testing will undoubtedly advance rapidly in the future, and these changes can be researched via the National Institute of Health Genetic Testing Registry (www.ncbi.nlm.nih.gov/gtr/).

Table 12.2 Post-enucleation follow-up points

Risk of genetic causation in unilateral presentation
Risk of second nonocular malignancies
Postradiation tumor risk
Follow-up examination schedule and metastatic evaluation
Genetic testing for the patient and siblings
Sibling examinations

Uveal Melanoma

Intraocular uveal melanoma is rare in children. A recent survey of the European Ophthalmic Oncology Group reported on the frequency of choroidal and ciliary body melanomas in children under 18 years of age reporting on the long-term prognosis of their collective 114 patients [104]. This represented less than 1% of their database cohort which mirrors other ocular oncologists reported incidence of uveal melanomas across all age groups [10]. Reports of uveal melanoma in children in the last 15 years have focused primarily on ciliary body and choroidal melanomas [9–11, 98]. Older series indicate initial clinical misdiagnosis with 20% of children having no suspicion of the presenting lesion being a melanoma but rather were diagnosed initially as glaucoma, vitreous hemorrhage, or Coats' disease [105].

Virtually all recent studies rely on the same methods for diagnosis as one would use for adults: dilated fundus exam, ocular ultrasonography, and a similar metastatic work-up including head, chest, and abdominal thin cut imaging studies looking for other potential malignancies. Faced with this diagnosis, several predisposing clinical conditions need to be

evaluated. First, ocular melanosis and oculodermal melanocytosis have a marked predisposition for uveal melanoma as discussed in the first section of this chapter. In one recent study, 11% of the study cohort was found to have oculo(dermal) melanocytosis [9]. In this same study, dysplastic nevus syndrome was diagnosed in 3% which is known to have increased uveal nevi and a lifetime 100% risk of early onset cutaneous melanoma [106, 107]. Neurofibromatosis has been reported in older literature to harbor an increased propensity over the general population of uveal melanomas, but this has largely been disproven [108]. Familial uveal melanoma syndrome is a very rare condition with the youngest reported onset at age 20 years [109].

The treatment for childhood uveal melanoma is the same as for adults with brachytherapy and enucleation being the primary considerations based on tumor size and location. The decision is reached after systemic work-up is negative for metastases. Children have better survival rates than adults: 10 year survival is 80% after treatment versus 64% in adults [9].

Other Intraocular Tumors

Metastatic lesions and other primary intraocular malignancies are exceedingly rare in children. Typically reported as single cases, these must be kept in mind if an intraocular mass does not have classic features of retinoblastoma or melanoma. The most common malignancy to show ocular involvement in children is leukemia [36, 37, 42]. As many as 9% of children with acute leukemia will have ocular involvement with the choroid being the most frequent site of involvement [41]. Clinically, a thickened, occasionally nodular appearance is seen in the choroid, while iris nodules, hypopyon, hyphema, and optic nerve head mass can be presenting signs as well. Diffuse histiocytosis can involve the choroid but not as frequent as orbital soft tissue or periorbital bone involvement [110]. Neuroblastoma usually displays orbital involvement with metastases but has been demonstrated at autopsy with choroidal invasion [111]. Other single case reports of mass-like choroidal metastases have been found in children with testicular carcinoma, fibrosarcoma, colon carcinoma, bronchial carcinoma, thyroid carcinoma, and soft tissue extraosseous sarcoma [112–114]. Some of these case reports were diagnosed by pathologic examination rather than by clinic appearance indicating that these would likely be very late findings in a disease course and not necessarily a presenting sign. Knowing this list gives one a starting place to look when the appearance of the intraocular condition fits no clear example of other primary intraocular malignancies in children.

Medulloepithelioma finishes the list of pediatric intraocular malignancies. Usually reported as individual case reports in the past, a recent retrospective study describes the clinical features, histopathology, treatments, and outcomes for 41 cases of ciliary body medulloepithelioma [114]. Thirty-five of the 41 cases were in children presenting at a mean age of 5 years. Unilateral in presentation, whitish in color, these are solid or cystic congenital rests of embryonic retina in the nonpigmented epithelium of the ciliary body. Once they have grown large enough to displace or erode through the iris, they are visible in the anterior chamber causing variable leukocoria, pupillary ectopia, glaucoma, and hyphema. Some cases have presented as extrascleral extension which is most commonly the time one finds metastatic disease. Not all medulloblastomas are malignant but all have that potential. Local resection has a high rate of recurrence leaving enucleation, plaque radiation, and external beam radiation as the remaining potential treatments [114].

References

1. Shields CL, Shields JA. Conjunctival tumors in children. Curr Opin Ophthalmol. 2007;18(5):351–60.
2. Cunha RP, Cunha MC, Shields JA. Epibulbar tumors in children; a survey of 282 biopsies. J Pediatr Ophthalmol Strabismus. 1987;24:249–54.
3. Zimmerman-Paiz MA, de la Riva GJC. Conjunctival tumors in children: histopathologic diagnosis in 165 cases. Arq Bras Oftalmol. 2015;78(6):337–9.
4. Dutton JJ, Anderson RL, Schelper RL, et al. Orbital malignant melanoma associated with ocular and oculodermal melanocytosis. Ophthalmology. 1984;91:497–507.
5. Gonder JR, Shields JA, Albert DM, et al. Uveal malignant melanoma associated with ocular and oculodermal melanocytosis. Ophthalmology. 1982;89:953–60.
6. Roldan M, Llanes F, Negrete O, et al. Malignant melanoma of the choroid associated with melanosis oculi in a child. Am J Ophthalmol. 1987;104:662–3.
7. Nick NA, Glew WB, Zimmerman LE. Malignant melanoma of the choroid in the nevus of Ota of a black patient. Arch Ophthalmol. 1982;100:1641–3.
8. Cowan TH, Balistocky M. The nevus of Ota or oculodermal melanocytosis: the ocular changes. Arch Ophthalmol. 1961;65:483–92.
9. Singh AD, Shields CL, Shields JA, Sato T. Uveal melanoma in young patients. Arch Ophthalmol. 2000;118:918–23.
10. Shields CL, Kaliki S, Arepalli S, et al. Uveal melanoma in children and teenagers. Saudi J Ophthalmol. 2013;27(3):197–201.
11. Kaliki S, Shields CL, Ganesh A, et al. Influence of age on young patients with uveal melanoma: a matched retrospective cohort study. Eur J Ophthalmol. 2013;43:208–16.
12. Shields CL, Kalika S, Livesey M, et al. Association of ocular and oculodermal melanocytosis with the rate of uveal melanoma metastasis analysis of 7872 consecutive eyes. JAMA Ophthalmol. 2013;131:993–1001.
13. DePotter P, Shields CL, Shields JA. Malignant melanoma of the conjunctiva. Int Ophthalmol Clin. 1993;33:25–30.

14. Jay B. Naevi and melanomata of the conjunctiva. Br J Ophthalmol. 1965;49:169–204.
15. McDonnell JM, Carpenter JD, Jacobs P, et al. Conjunctival melanocytic lesions in children. Ophthalmology. 1989;96:986–93.
16. Lavecq L, DePotter P, Jamart J. Conjunctival nevi clinical features and therapeutic outcomes. Ophthalmology. 2010;117(1):35–40.
17. Folberg R, McLean IW, Zimmerman LE. Conjunctival melanosis and melanoma. Ophthalmology. 1984;91:673–8.
18. Kim SK, Gombos DS, Esmaeli B. Management of conjunctival neoplasms. In: Esmadi B, editor. Ophthalmic oncology, MD Anderson Solid Tumor Oncology Series, vol. 6; 2010. p. 127–38.
19. Brownstein S, Faraji H, Jackson WB, et al. Conjunctival melanoma in children: clinicopathologic study of 2 cases. Arch Ophthalmol. 2004;124:1190–3.
20. Shields CL, Fasiuddin AF, Mashayekhi A, et al. Conjunctival nevi: clinical features and natural course in 410 consecutive cases. Arch Ophthalmol. 2004;122(2):167–75.
21. Maly A, Epstein D, Meir K, et al. Histological criteria for grading of atypia in melanocytic conjunctival lesions. Pathology. 2008;40(7):676–81.
22. Thiagalingam S, Johnson MM, Colby KA, et al. Juvenile conjunctival nevus: clinicopathologic analysis of 33 cases. Am J Surg Pathol. 2008;32(3):394–406.
23. Jakobiec FA, Colby K, Bajart AM, et al. Immunohistochemical studies of atypical conjunctival melanocytic nevi. Arch Ophthalmol. 2009;127(8):570–80.
24. Jakobiec FA, Bhat P, Colby KA. Immunohistochemical studies of conjunctival nevi and melanoma. Arch Ophthalmol. 2010;128(2):174–83.
25. Furusato E, Hidayat AA, Man YG, et al. WT1 and Ba12 expression in melanocytic lesions of the conjunctiva: an immunohistochemical study of 123 cases. Arch Ophthalmol. 2009;127(8):964–9.
26. Croxatto JO, Iribarron G, Ugrin L, et al. Malignant melanoma of the conjunctiva: report of a case. Ophthalmology. 1987;94(10):1281–5.
27. Shields CL, Shields JA, Honavar SG, et al. Clinical spectrum of primary ophthalmic rhabdomyosarcoma. Ophthalmology. 2001;108(12):3284–92.
28. Cameron JD, Wisk MR. Embryonal rhabdomyosarcoma of the conjunctiva: a clinicopathologic and immunohistochemical study. Arch Ophthalmol. 1986;104:1203–4.
29. Adamopoulou C, Rotberg L, Baker JD. Conjunctival papillomatous lesion. JAMA Ophthalmol. 2014;132(12):1481–2.
30. Castillo BV Jr, Kaufman L. Pediatric Tumors of the eye and orbit. Pediatr Clin N Am. 2003;50(1):149–72.
31. Shields CL, Shields JA, Hortivar SG, et al. Primary ophthalmic rhabdomyosarcoma in 33 patients. Trans Am Ophthalmol Soc. 2001;99:133–42.
32. Brichard B, DePotter P, Godfraind C, et al. Embryonal rhabdomyosarcoma presenting as conjunctival tumor. J Pediatr Hematol Oncol. 2003;25(8):651–2.
33. Joffe L, Shields JA, Pearah JD. Epibulbar rhabdomyosarcoma without proptosis. J Pediatr Ophthalmol. 1977;14(6):364–7.
34. Sekundo W, Roggenkemper P, Fischer HP. Primary conjunctival rhabdomyosarcoma: 2.5 years followup after combined chemotherapy and brachytherapy. Graefes Arch Clin Exp Ophthalmol. 1998;236(11):873–5.
35. Polito E, Pichierri P, Lofreddo A, et al. A case of primary botryoid conjunctival rhabdomyosarcoma. Graefes Arch Clin Exp Ophthalmol. 2006;244(4):517–9.
36. Bitirgen G, Bedviranli S, Caliskan CL, et al. Ophthalmic manifestations in recently diagnosed childhood leukemia. Eur J Ophthalmol. 2016;26(1):88–91.
37. Ohkhosi K, Tsiams WG. Prognostic importance of ophthalmic manifestations in childhood leukemias. Br J Ophthalmol. 1992;76:651–5.
38. Kincaid MC, Green WR. Ocular and orbital involvement in leukemia. Surv Ophthalmol. 1983;27:211–32.
39. Swartz M, Jampol LM. Comma-shaped venular segments of conjunctiva in chronic granulocytic leukemia. Can J Ophthalmol. 1975;10:458–61.
40. Taylor DSI, Day SH. Neuroophthalmic aspects of childhood leukemia. In: Neuroophthalmology focus. New York: Masson; 1982. p. 281–90.
41. Ridgway EW, Jaffe N, Walton DS. Leukemic ophthalmopathy in children. Cancer. 1976;38:1744–9.
42. Chocran IM, Morrison DG, Friedman DL, et al. Ophthalmic manifestations of relapsing acute childhood leukemia. J AAPOS. 2015;19(3):284–6.
43. Birnbaum AD, Tessler HH, Goldstein DA. A case of hypopyon uveitis nonresponsive to steroid therapy and a review of anterior chamber masquerade syndromes in childhood. J Pediatr Ophthalmol Strabismus. 2005;42(6):372–7.
44. Huh H, Armbrost S, Decker T, et al. MALT lymphoma of the conjunctiva in a 13 year old child – 5 year relapse-free follow up following antibiotic treatment. Klin Moubl Augenheilkd. 2016;233(1):79–84.
45. Kirwan C, Ngan BY, Halliday W, et al. Primary conjunctival anaplastic large cell lymphoma in a child. J AAPOS. 2013;17(4):437–9.
46. Wall PB, Traboulsi EI, Hsi ED, et al. Bilateral conjunctival lymphoma in a child. J AAPOS. 2015;19(2):183–5.
47. Ling X, Starck LC, Albano EA. Primary ocular adnexal lymphoma in pediatric patients: report of 2 cases and review of the literature. Pediatr Dev Pathol. 2003;6(5):458–63.
48. Kram DE, Brathwaite CD, Khatib ZA. Bilateral conjunctival extranodal marginal zone B-cell lymphoma. Pediatr Blood Cancer. 2010;55(7):1414–6.
49. Jastrzebski A, Burns BF, Jordan DR, et al. Bilateral benign reactive lymphoid hyperplasia of the conjunctiva in a pediatric patient. J Pediatric Ophthalmol Strabismus 2011;48 online:e69–71.
50. McLeod SD, Edward DP. Benign lymphoid hyperplasia of the conjunctiva in children. Arch Ophthalmol. 1999;47(6):832–5.
51. Weisenthal RW, Streeten BW, Dubensky AS, et al. Burkitt lymphoma presenting as subconjunctival mass. Ophthalmology. 1995;102:129–34.
52. Baker PS, Gold KG, Lane KA, et al. Orbital Burkitt lymphoma in immunocompetent patients: a report of 3 cases and review of the literature. Ophthal Plast Reconstr Surg. 2009;25(6):464–8.
53. Joshi W, Gagnon GA, Chadwick EG, et al. The spectrum of mucosa associated lesions in pediatric patients infected with HIV: a clinicopathologic study of six cases. Am J Clin Pathol. 1997;107:592–600.
54. Nadal D, Caduff R, Frey E, et al. Non-Hodgkins lymphoma in four children with the human HIV. Association with Epstein-Barr virus and treatment. Cancer. 1994;73(1):224–30.
55. Ohan CL, Smith JA, Shea DF, et al. Helicobacter pylori (H. Pylori) molecular signature in conjunctival mucosa-associated lymphoid tissue (MALT) lymphoma. Histol Histopathol. 2004;19:1219–26.
56. Chanudet E, Zhou Y, Bacon CM, et al. Chlamydia psittaci is variably associated with ocular adnexal MALT lymphoma in different geographic regions. J Pathol. 2006;209:344–51.
57. Verma V, Shan D, Siaving PC, et al. The role of infectious agents in the etiology of ocular adnexal neoplasia. Surv Ophthalmol. 2008;53:312–31.
58. Ponzoni M, Govi S, Licata G, et al. A reappraisal of the diagnostic and therapeutic management of uncommon histologies of primary ocular adnexal neoplasia. Oncologist. 2013;18(7):876–84.
59. Writing group of the Histiocyte Society. Histiocytosis syndromes in children. Lancet. 1987;1:208–9.

60. Lahav M, Albert DM. Unusual ocular involvement in acute disseminated histiocytosis X. Arch Ophthalmol. 1974;91:455–8.
61. Mittelman D, Apple DJ, Goldberg MF. Ocular involvement in Letterer-Siwe disease. Am J Ophthalmol. 1973;75:261–5.
62. Maceheron LJ, McNab AA, Elder J, et al. Ocular adnexal Langerhans histiocytosis. Clinical features and management. Orbit. 2006;25:169–77.
63. Monos T, Levy J, Lifshitz T, et al. Isolated congenital histiocytosis in the palpebral conjunctiva in a newborn. Am J Ophthalmol. 2005;139(4):728–30.
64. Shields JA, Shields CL. Eyelid, conjunctival and orbital tumors: an atlas and textbook. 3rd ed. Philadelphia: Lippincott Wolters Kluwers; 2012. p. 283–305.
65. Lee GA, Hirst LW. Ocular surface squamous neoplasia. Surv Ophthalmol. 1995;39(6):429–50.
66. Shields CL, Ramasubramanian A, Mellen PL, et al. Conjunctival squamous cell carcinoma arising in immunosuppressed patients (organ transplants, human immunodeficiency virus infections). Ophthalmology. 2011;118(11):2133–7.
67. Elsas FJ, Green WR. Epibulbar tumors in childhood. Am J Ophthalmol. 1975;79:1001–7.
68. Schulze-Schwering M, Chagalutea G, Molyneaux E. Treatment of cancer in a child with ocular xeroderma pigmentosa. J Pediatr Hematol Oncol. 2014;36(8):e540–2.
69. Goyal J, Rao V, Srinivasan R, et al. Oculocutaneous manifestations of xeroderma pigmentosa. Br J Ophthalmol. 1994;78:295–7.
70. Lewallen S, Shroyer KR, Keyser RP, et al. Aggressive conjunctival squamous cell carcinoma in 3 young Africans. Arch Ophthalmol. 1996;114:215–8.
71. Karass M, Naguib MM, Elawabdeh N, et al. Xeroderma pigmentosa: three new cases with an indepth review of the genetic and clinical characteristics of the disease. Fetal Pediatric Pathol. 2015;34(2):120–7.
72. Kraemer KH, Rapini RP, Beran M. Xeroderma pigmentosa: cutaneous, ocular and neurological abnormalities in 830 published cases. Arch Dermatol. 1987;123:241–50.
73. Hertle RW, Durso F, Meltzer JP, et al. Epibulbar squamous cell carcinomas in brothers with xeroderma pigmentosa. J Pediatr Ophthalmol Strabismus. 1991;28:350–3.
74. Karp CL, Scott IU, Chang TS, et al. Conjunctival intraepithelial neoplasia: a possible marker for human immunodeficiency virus infection? Arch Ophthalmol. 1996;114:257–61.
75. Shields CL, Lally SE, Leahy HM, et al. Targeted retinoblastoma management: when to use intravenous, intraarterial, periocular and intravitreal chemptherapy. Curr Opin Ophthalmol. 2014;25(5):374–85.
76. Abramson DH, Shields CL, Munier FL, et al. Treatment of retinoblastoma in 2015: agreement and disagreement. JAMA Ophthalmol. 2015;133(11):1341–7.
77. Shan CP, Shields CL, Shields JA. Chemotherapy for malignant ocular tumors. Dev Ophthalmol. 2016;55:337–43.
78. Wyse E, Handa JT, Friedman AD, et al. A review of the literature for intraarterial chemotherapy used to treat retinoblastoma. Pediatr Radiol. 2016;46(9):1223–33.
79. Ghasseni F, Khodabanda A. Risk definition and management strategies in retinoblastoma: common perspectives. Clin Ophthalmol. 2015;9:985–94.
80. Broaddus E, Tophan A, Singh AD. Survival with retinoblastoma in the USA: 1975-2004. Br J Ophthalmol. 2008;93:24–7.
81. Char DH, Hedges TR III, Norman D. Retinoblastoma: CT diagnosis. Ophthalmology. 1984;91:1347–50.
82. Shields JA, Shields CL, Eagle RC, et al. Calcified intraocular abscess simulating retinoblastoma. Am J Ophthalmol. 1992;114:227–9.
83. De Potter P, Shields CL, Shields JA, et al. The role of magnetic resonance imaging in children with intraocular tumors and simulating lesions. Ophthalmology. 1987;94:367–70.
84. O'Brien JM, Char DH, Tucker N, et al. Efficacy of unanesthetized spiral computed tomography scanning in initial evaluation of childhood leukocoria. Ophthalmology. 1995;102:1345–50.
85. Sterns G, Coleman D, Ellsworth R. The ultrasonographic characteristics of retinoblastoma. Am J Ophthalmol. 1974;78:606–11.
86. Yanuzzi NA, Francis JH, Marr BP, et al. Enucleation versus ophthalmic artery chemotherapy for advanced intraocular retinoblastoma: a retrospective analysis. JAMA Ophthalmol. 2015;133(9):1062–6.
87. Brennan KC, Qaddoumi I, Billups CA, et al. Comparison of high risk histopathological features in eyes with primary or secondary enucleation for retinoblastoma. Br J Ophthalmol. 2015;99(10):1366–71.
88. Kim JY, Park Y. Treatment of retinoblastoma: the role of external beam radiotherapy. Yonsei med J. 2015;56(6):1478–91.
89. Kiralti H, Kocabeyoglu S, Bilgic S. Severe pseudo-preseptal cellulitis following sub-Tenons carboplatin injection for intraocular retinoblastoma. J AAPOS. 2007;11(4):404–5.
90. Smith SJ, Smith BD, Mohnet BG. Ocular side effects following intravitreal injection therapy for retinoblastoma: a systematic review. Br J Ophthalmol. 2014;98(3):292–7.
91. Schmack I, Hubbard GB, Kang SJ, et al. Ischemic necrosis and atrophy of the optic nerve after periocular carboplatin injection for intraocular retinoblastoma. Am J Ophthalmol. 2006;142(2):310–5.
92. Shah SU, Shields CL, Lally SE, et al. Hydoxyapatite orbital implamt in children following enucleation: analysis of 531 sockets. Ophthal Plast Reconstr Surg. 2015;31(2):108–14.
93. Mouritis DC, Moll AC, Bosscha MI, et al. Orbital implants in retinoblastoma patients: 23 years experience and review of the literature. Acta Ophthalmol. 2016;94(2):165–74.
94. Shildkrot Y, Kirzhner M, Haik BG, et al. The effect of cancer therapies on pediatric ophthalmic sockets. Ophthalmology. 2011;97(12):1530–3.
95. Choi YJ, Park C, Jin HC, et al. Outcome of smooth surface tunnel porous polyethylene orbital implants (Medpor SST) in children with retinoblastoma. Br J Ophthalmol. 2013;97(12):1530–3.
96. Hauck MJ, Steele EA. Dermis fat graft implantation after unilateral enucleation for retinoblastoma in pediatric patients. Ophthal Plast Reconstr Surg. 2015;31(2):136–8.
97. Kim JW, Kathpolia V, Dunkel IJ, et al. Orbital recurrence of retinoblastoma following enucleation. Br J Ophthalmol. 2009;93(4):463–7.
98. Ye H, Du Y, Chen R, et al. The potential benefit of three versus six cycles of carboplatin, etoposide and vincristine in post-enucleation high risk patients with IRSS class 1 retinoblastoma. Curr Eye Res. 2016;9:1–6.
99. Sachdau UM, O'Brien JM. Understanding pRb: toward the necessary development of targeted treatments for retinoblastoma. J Clin Invest. 2012;122(2):425–34.
100. Mallipatna A, Marino M, Singh AD. Genetics of retinoblastoma. Asia Pac J Ophthalmol (Phila). 2012;5(4):260–4.
101. McEvoy JD, Dyer MA. Genetic and epigenetic discoveries in human retinoblastoma. Crit Rev Oncol. 2015;20(3–4):217–25.
102. Stone EM, Aldave AJ, Drack AV, et al. Recommendations for genetic testing of inherited eye diseases. Ophthalmology. 2012;119:2408–10.
103. Al-Jamel RT, Cassoux N, Desjardins L, et al. The pediatric choroidal and ciliary body melanoma study: a survey of the European Ophthalmic Oncology Group. Ophthalmology. 2016;123(4):898–907.
104. Barr GC, McLean IW, Zimmerman LE. Uveal melanoma in children and adolescents. Arch Ophthalmol. 1981;99:2133–6.
105. Rodriquez-Sains RS. Ocular findings in patients with dysplatic nevus syndrome. Ophthalmology. 1986;93:661–5.

106. Greene MH, Clark WH, Tucker MA, et al. High risk of malignant melanoma in melanoma-prone families with dysplastic nevi. Ann Intern med. 1985;102:458–65.
107. Honaver SG, Singh AD, Shields CL, et al. Iris melanoma in a patient with neurofibromatosis. Surv Ophthalmol. 2000;45(3):231–6.
108. Singh AD, Shields CL, DePotter P, et al. Familial uveal melanoma: clinical observations on 56 patients. Arch Ophthalmol. 1996;114:392–9.
109. Botham L, Blankenship SS. The eye in adrenal sympathicoblastoma (neuroblastoma): importance of ocular findings with the first pathologic report of metastatic tumor in choroid. Arch Ophthalmol. 1942;27:746–59.
110. Moore AT, Pritchard J, Taylor DSI. Histiocytosis X: an ophthalmological review. Br J Ophthalmol. 1985;69:7–14.
111. Ferry AP. The biologic behavior and pathologic features of carcinoma metastatic to the eye and orbit. Trans Am Ophthalmol Soc. 1973;71:373–88.
112. Rootman J, Carvounis EP, Dolman CL, et al. Congenital fibrosarcoma metastatic to the choroid. Am J Ophthalmol. 1979;87:632–6.
113. Kaliki S, Eagle RC Jr, Shields CL, et al. Ciliochoroidal metastasis as the intitial manifestation of an occult soft tissue extraosseous sarcoma in a 10 year old girl. J AAPOS. 2013;17(2):217–20.
114. Kaliki S, Shields CL, Eagle RC Jr, et al. Ciliary body medulloepithelioma: analysis of 41 cases. Ophthalmology. 2013;120(12):2552–9.

13 Oncologic Management for Liquid and Solid Tumors in Pediatric Oculoplastic Surgery

Naomi J. Balamuth, Tamara P. Miller, and Karuna Shekdar

Pediatric oncology represents a broad spectrum of disease, requiring a multidisciplinary approach. Here, we attempt to summarize the current approach to common pediatric malignancies with particular attention to those with ocular/orbital involvement.

Solid Tumors

Rhabdomyosarcoma

Epidemiology of Pediatric Rhabdomyosarcoma.

Pediatric rhabdomyosarcoma encompasses a heterogeneous group of tumors whose clinical behavior spans a broad spectrum. Rhabdomyosarcoma can arise anywhere in the body, though many arise in sites of skeletal muscle, including the orbit.

Rhabdomyosarcoma accounts for about half of the soft tissue sarcomas in children and adolescents and represents about 3% of childhood cancers. According to the SEER database, rhabdomyosarcoma occurred in 4.6 children/million between 1996 and 2003. The highest incidence is in the 1–4-year-old age group [1].

Clinical Presentation of Pediatric Rhabdomyosarcoma

Rhabdomyosarcomas can occur anywhere in the body. Low- and intermediate-risk tumors most often occur in locations with little skeletal muscle, like the orbit, pharynx, sinuses, vagina, and paratesticular tissues. Orbital tumors often present with proptosis or visual changes. The mass is usually painless and fixed to surrounding tissues. Regional lymph nodes may or may not be involved – a careful physical exam is essential (Figs. 13.1 and 13.2).

The majority of pediatric rhabdomyosarcomas occur spontaneously. A small fraction are associated with genetic syndromes, such as Li-Fraumeni syndrome [2], neurofibromatosis type 1 [3], Costello syndrome [4], Beckwith-Wiedemann syndrome [5], and Rubinstein-Taybi syndrome [6]. It is important to assess for any stigmata of these syndromes, as their diagnoses may carry implications for long-term screening.

Evaluation of Pediatric Rhabdomyosarcoma

With any suspicion of malignancy, a referral to a pediatric oncology center should be considered. Initial imaging and decisions about approach to biopsy/resection are critical, as violation of tissue planes may have implications for staging, treatment, and further local control.

The primary tumor should be imaged preoperatively with MRI, including evaluation of regional nodes. A metastatic evaluation will be guided by the histology/fusion status and presence or absence of nodal involvement. This may include chest CT for pulmonary metastases and a PET to detect distant bone, lymph node, or soft tissue disease.

Risk Group Classification of Pediatric Rhabdomyosarcoma

Rhabdomyosarcomas are designated with a group and a stage. The group and stage are used together to assign a risk group – low, intermediate, and high. Selection of a treatment protocol is based on the risk group designation.

The clinical group is determined by the extent of tumor when chemotherapy begins. Group I tumors have been fully resected, group II tumors have microscopic residual disease, group III tumors have macroscopic residual disease, and group IV tumors have metastases.

N.J. Balamuth (✉)
Children's Hospital of Philadelphia, Philadelphia, PA, USA
e-mail: BALAMUTH@email.chop.edu

T.P. Miller
Division of Oncology, Department of Pediatrics, The Children's Hospital of Philadelphia, Philadelphia, PA, USA

K. Shekdar
Perelman School of Medicine, University of Pennsylvania, Philadelphia, PA, USA

The Children's Hospital of Philadelphia, Philadelphia, PA, USA

© Springer International Publishing AG 2018

J.A. Katowitz, W.R. Katowitz (eds.), *Pediatric Oculoplastic Surgery*, https://doi.org/10.1007/978-3-319-60814-3_13

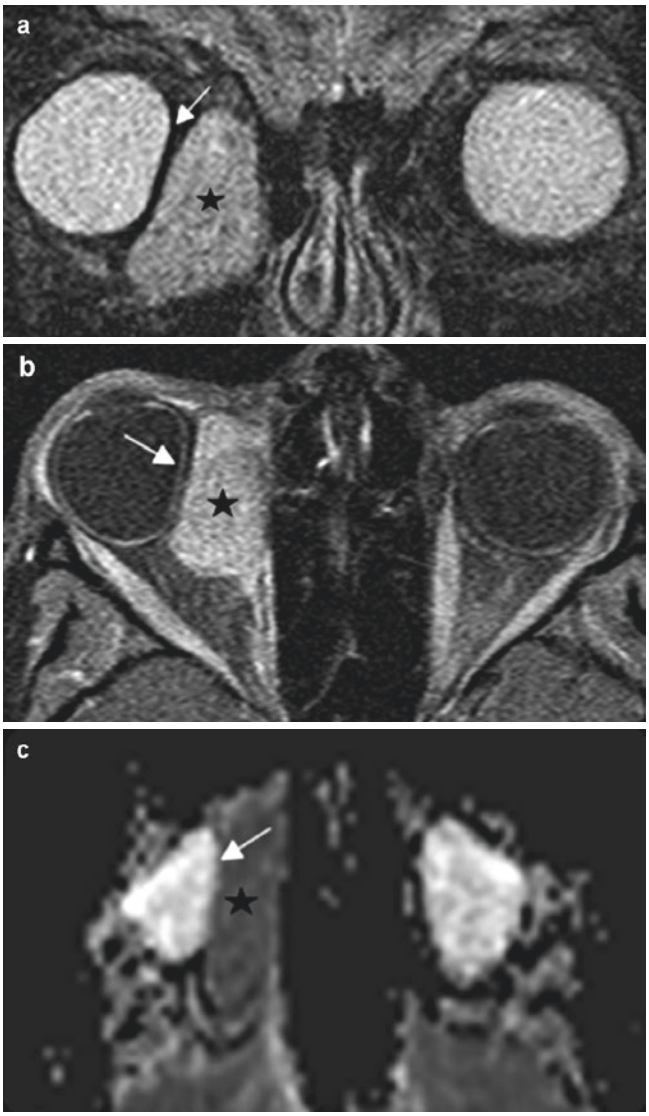


Fig. 13.1 Orbital rhabdomyosarcoma. Coronal T2-weighted with fat suppression (**a**) and axial post-contrast T1-weighted (**b**) and axial ADC map (**c**) images through the orbit showing an enhancing right orbital mass (*black**) with restricted diffusion within the medial extraconal space causing flattening of the globe (*white arrow*) and mass effect upon the medial rectus muscle. This orbital mass was consistent with a rhabdomyosarcoma

The stage for patients with rhabdomyosarcomas depends on the site of disease (orbit is favorable), size of the primary tumor (less than five centimeters is favorable), and the presence or absence of lymph node involvement.

Rhabdomyosarcoma can be divided into two histologic subtypes – embryonal and alveolar. Embryonal rhabdomyosarcoma tends to occur in the head/neck and genitourinary tract and is associated with a favorable prognosis. Alveolar rhabdomyosarcoma more commonly develops in the extremities and carries a less favorable prognosis.

More important than the histologic subtype is the presence (unfavorable) or absence (favorable) of a 1;13 or 2;13 translocation [7]. The genes rearranged by these translocations are PAX3 and PAX7, respectively. The fusion transcripts encode novel transcription factors, which are more potent than their wild-type counterparts. Assays for the presence of these fusion transcripts can be detected by RT-PCR.

Treatment of Pediatric Rhabdomyosarcoma

Enormous progress has been made over the past 50 years, improving both short- and long-term outcomes for patients with rhabdomyosarcoma. This has been a collaboration of surgical oncologists, medical oncologists, and radiation oncologists. Effective therapy combines both systemic multi-agent chemotherapy and local control, either surgery or radiation.

The current chemotherapy backbone includes vincristine, actinomycin D, and cyclophosphamide. A large cooperative group trial has allowed us to decrease the cumulative cyclophosphamide dose for low-risk patients, in hopes of preserving their fertility in the long term [8]. The addition of irinotecan to the backbone for patients with intermediate-risk disease has maintained their ~70% overall survival rate, while allowing for reduction in the cumulative cyclophosphamide dose. Various attempts at augmenting the intensity of therapy for high-risk patients have largely been futile to date, and the prognosis for this group remains grim [9].

Surgical and radiation oncology considerations in rhabdomyosarcoma are quite complex. Patients with a complete upfront excision (group I) fare best, although this is almost never feasible with an orbital tumor. Given the location, an initial, limited biopsy allows confirmation of the diagnosis and may allow the radiation oncologist to treat a much smaller field than had the entire orbit been contaminated.

Ewing Sarcoma

Epidemiology of Pediatric Ewing Sarcoma

Ewing sarcoma is an aggressive form of childhood cancer. The majority (~75%) arise from bone, with the remainder arising from soft tissues. While the long bones are most commonly affected, Ewing sarcoma can arise in the bones of the orbit as well (Fig. 13.3).

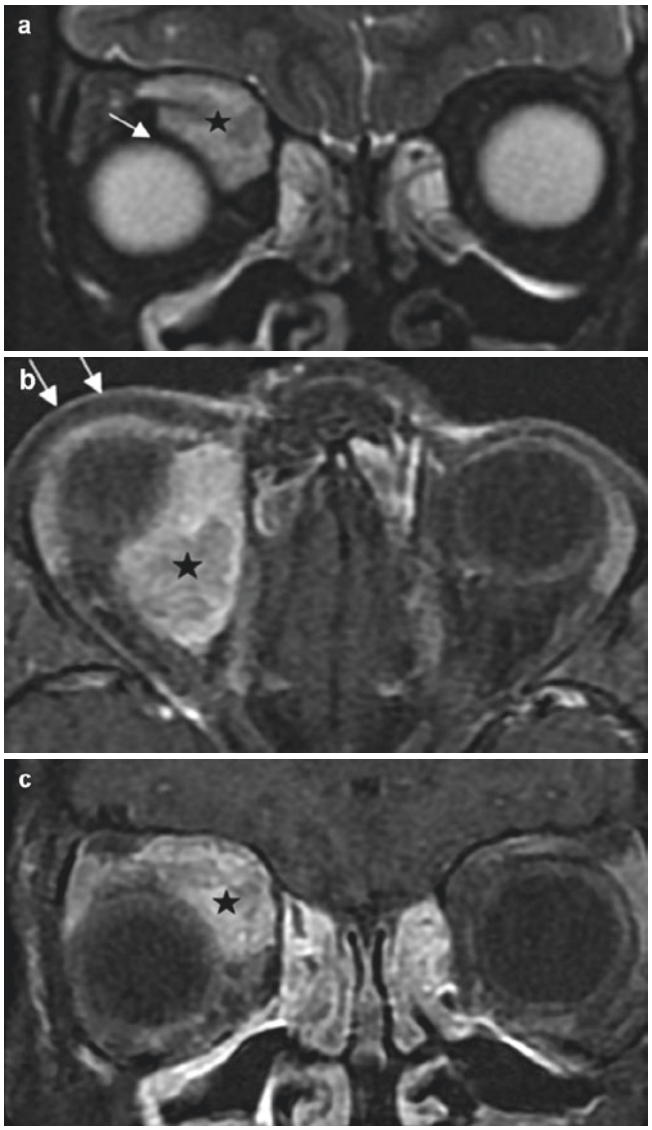


Fig. 13.2 Another orbital rhabdomyosarcoma. Coronal T2-weighted with fat suppression (**a**) and axial post-contrast T1-weighted (**b**) and axial post-contrast T1-weighted coronal (**c**) images through the orbits showing mass lesion (*black**) in the right superior medial orbit which is predominantly hyperintense on T2 and demonstrates avid enhancement. Inferior and lateral displacement (*single white arrow*) of the optic globe and proptosis (*double white arrow*) of the right globe. The imaging features are consistent with orbital rhabdomyosarcoma

Ewing sarcoma is the second most common primary bone tumor of childhood. Ewing sarcoma is more common in the Caucasian population and has a slight male predominance [10]. The majority of patients (~75%) present with localized disease. The lungs are the most common site of metastases, followed by bone and bone marrow.

Clinical Presentation of Pediatric Ewing Sarcoma

Symptoms at presentation depend on the location of the mass. Most patients present with pain or a palpable mass. Fever, weight loss, and night sweats may also be present. Careful assessment of the involved fields, including lymph nodes, is critical for ultimate planning of local control.

Evaluation of Pediatric Ewing Sarcoma

With any suspicion of malignancy, a referral to a pediatric oncology center should be considered. Initial imaging and decisions about approach to biopsy/resection are critical, as violation of tissue planes may have implications for staging, treatment, and further local control. Ewing sarcomas are often quite necrotic, so the surgeon must be careful to obtain adequate tissue for histologic and molecular testing.

Imaging of the primary tumor site, usually with MR, allows for a clear assessment of the extent of tumor involvement. Metastatic evaluation should include a non-contrast chest CT, whole-body PET scan, and bilateral bone marrow aspirates and biopsies.

Molecular Diagnosis of Pediatric Ewing Sarcoma

The majority of Ewing sarcomas carry a t(11;22) chromosomal translocation. This results in an EWS-FLI1 gene fusion, which activates a family of transcription factors involved in cellular proliferation and tumorigenesis. Identification of this translocation has become an integral part of the diagnosis of Ewing sarcoma [11], although it has not been convincingly linked to prognosis.

Risk Groups and Prognosis of Pediatric Ewing Sarcoma

The Children's Oncology Group defines three risk groups for Ewing sarcoma – patients with localized disease, patients with lung metastases only, and patients with bone and/or other metastases. Various groups have identified male sex, older age, larger tumor size, and histologic response as adverse prognostic signs, although these are not uniformly accepted.

Treatment of Pediatric Ewing Sarcoma

Cytotoxic chemotherapy has significantly improved prognosis for patients with localized Ewing sarcoma. Patients with metastases, unfortunately, continue to fare quite poorly. Effective therapy combines chemotherapy with primary tumor treatment. Primary tumor treatment involves surgical resection, radiation therapy, or a combination of both modalities.

Current chemotherapy for Ewing sarcoma uses a backbone of alternating cycles of vincristine, doxorubicin,

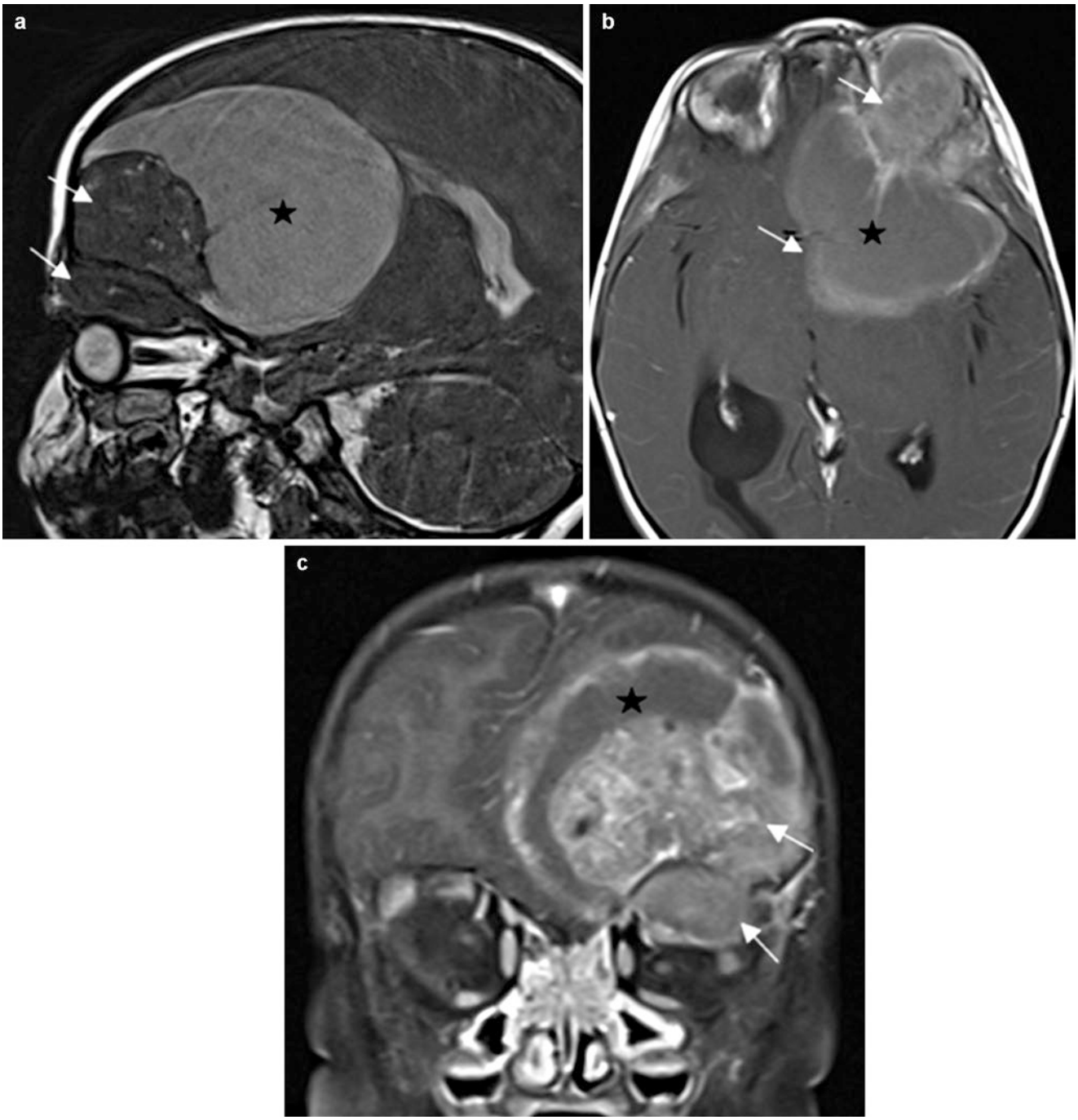


Fig. 13.3 Ewing sarcoma of the orbit sagittal T2 (**a**); post-contrast T1-weighted axial (**b**) and coronal (**c**) images through the orbit demonstrate a large mass with solid component (*white arrows*) and large cystic component (*black**), arising from the superior orbital wall with extension into the orbit and into the intracranial compartment in an extra-axial pattern into the left frontal region. Enhancement is seen within the solid portion of the mass and around the rim of the cystic portion. Diffusion restriction (not shown) was also noted in the solid portion of the mass. These findings indicate a malignant tumor such as a small blue cell tumor – Ewing sarcoma

and cyclophosphamide with ifosfamide and etoposide. A recent Children's Oncology Group study showed improved survival when chemotherapy cycles are delivered on an every 2-week cycle as compared to an every 3-week cycle [12].

Primary tumor treatment decisions are quite complex. Complete, en bloc surgical resection with negative margins is preferred. In some circumstances, this is not possible, or the ensuing disability is unacceptable. In those cases, or in those having undergone a surgical resection with positive margins, radiation therapy should be used, with consideration of proton radiotherapy, to spare surrounding tissues as much as possible.

Osteosarcoma

Epidemiology of Pediatric Osteosarcoma

Osteosarcoma is the most common primary tumor of the bone in childhood and represents about 5% of all childhood cancers. Osteosarcoma can occur in any bone in the body, and while orbital presentations are rare, they have been reported. The ability to cure osteosarcoma depends on the ability to achieve a complete resection, so orbital tumors present a particular challenge. The majority of patients present with localized disease. Lungs are the most common site of metastases, when they occur. There are also cases of osteosarcoma metastasizing to the orbital wall (Fig. 13.4).

Osteosarcoma has a bimodal age distribution. There is a peak in adolescence and a second peak in adults greater than 65 years old. Osteosarcoma is more common in the African-American population and has a slight male predominance [13]. Risk factors for the development of osteosarcoma include prior radiation, Li-Fraumeni syndrome, history of retinoblastoma, and Bloom syndrome.

Clinical Presentation of Pediatric Osteosarcoma

Osteosarcoma typically presents with pain and/or a palpable mass. Systemic symptoms such as fever, weight loss, and night sweats are usually absent. Physical examination often reveals a palpable mass. Nodal involvement is rare.

Evaluation of Pediatric Osteosarcoma

With any suspicion of malignancy, a referral to a pediatric oncology center should be considered. Initial imaging and decisions about approach to biopsy/resection are critical, as violation of tissue planes may have implications for staging, treatment, and further local control.

Imaging of the primary tumor site is best achieved with MR. Metastatic evaluation includes a CT chest, to assess for pulmonary disease. PET or bone scan is used to evaluate for bony metastases or skip lesions.

Risk Group and Prognosis of Pediatric Osteosarcoma

The most important prognostic factor in osteosarcoma is the ability to fully resect the primary tumor and metastatic sites. Other adverse prognostic factors include poor histologic response following chemotherapy, male sex, tumor in the axial skeleton, and tumors greater than 10 cm.

Treatment of Pediatric Osteosarcoma

Chemotherapy is critical to our ability to cure osteosarcoma, even in those with localized disease, supporting the presence of micrometastases not visible even with modern staging techniques. The long-standing backbone of chemotherapy includes cisplatin, doxorubicin, and methotrexate. This provides cure in about 75% of patients with localized disease. Efforts to intensify therapy have, to date, not yielded an improved outcome. For those with unresectable tumors or unresectable metastases, the prognosis is far worse.

As with all sarcomas, primary tumor treatment is a difficult decision. Osteosarcomas are not radiation sensitive, so we rely solely on surgery to achieve local control. Osteosarcomas can rarely be treated without some long-term disability. The goals

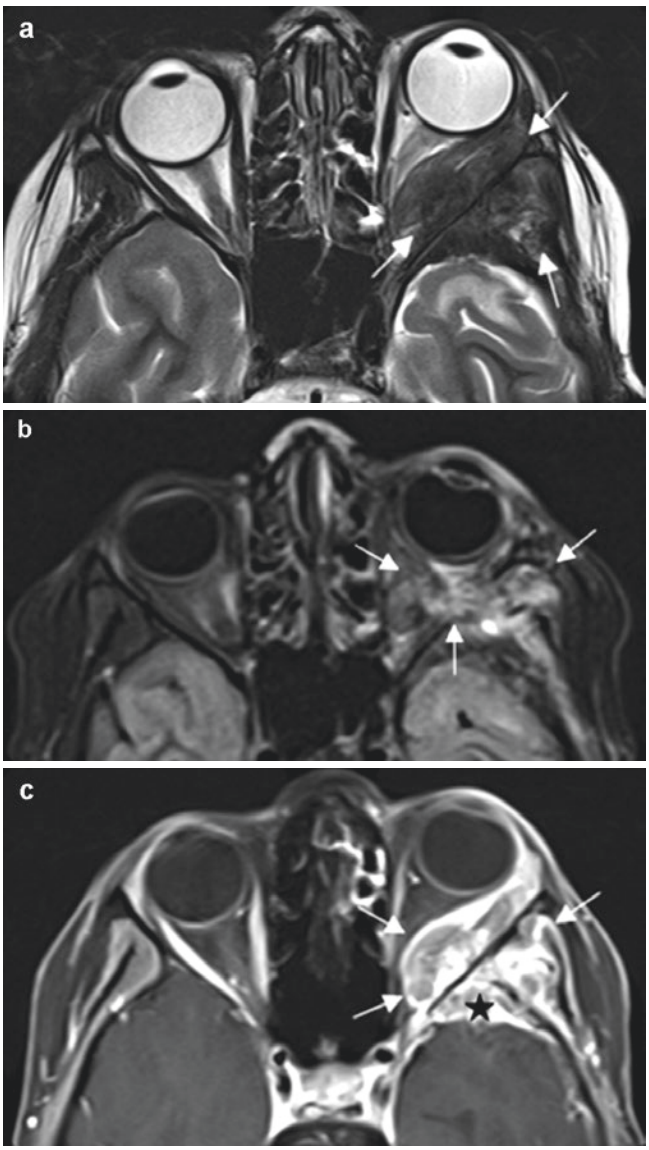


Fig. 13.4 MRI study images of a 13-year-old female patient with osteosarcoma metastasis involving the left lateral orbital wall. Axial T2-weighted (**a**), STIR (**b**), and post-contrast axial T1-weighted (**c**) images through the orbit demonstrate an expansile, destructive, enhancing mass (*white arrows*) involving the left lateral orbital wall and the greater wing of the sphenoid bone encroaching into the left retro-orbital space with displacement of the left optic globe anteriorly and medially and medial displacement of the left optic nerve sheath. Restricted diffusion (not shown) was noted within the mass. Also noted is contiguous extension into the left anterior temporal region (*black**)

of the patient must be seriously considered when proposing options for local control. Although limb salvage techniques have improved significantly over time, for a very active teenager committed to participation in sports, amputation may provide a more acceptable outcome.

Neuroblastoma

Epidemiology of Pediatric Neuroblastoma

Neuroblastoma represents an extraordinarily broad spectrum of disease, from spontaneously regressing tumors to high-risk, widely metastatic disease with a poor prognosis. Improved understanding of molecular and genetic features of these tumors has allowed for more detailed clinical classification.

Neuroblastoma can arise from any site along the sympathetic nervous chain. Metastases can involve the periorbital bones, leading to proptosis and periorbital ecchymoses. Tumors high in the thoracic region or in the neck can also cause a Horner's syndrome.

Neuroblastoma is the most common extracranial solid tumor of childhood, representing between 8% and 10% of childhood cancers. Neuroblastoma is largely a disease of infants and young children, although diagnosis of an adolescent or young adult is possible.

Clinical Presentation of Pediatric Neuroblastoma

Clinical presentation varies with the spectrum of disease. Low-risk tumors are often incidentally discovered, while children with high-risk disease are usually ill appearing at presentation. Fevers, bone pain, pallor, and fatigue are common for those with high-risk disease. Orbital metastases can present as "racoon eyes" (Figs. 13.5, 13.6, and 13.7). Genetic analysis of the tumor is critical for risk group assignment. The diagnostic biopsy should be generous, if possible, to ensure adequate specimen. Children presenting with orbital ecchymoses should undergo imaging in search of a primary tumor mass. In the absence of a primary tumor, the orbital lesion may need to be biopsied. There is no role for complete resection, only a diagnostic specimen.

Evaluation of Pediatric Neuroblastoma

The primary tumor should be imaged with cross-sectional imaging. Metastatic evaluation includes an MIBG scan and bilateral bone marrow aspirates and biopsies. A rare

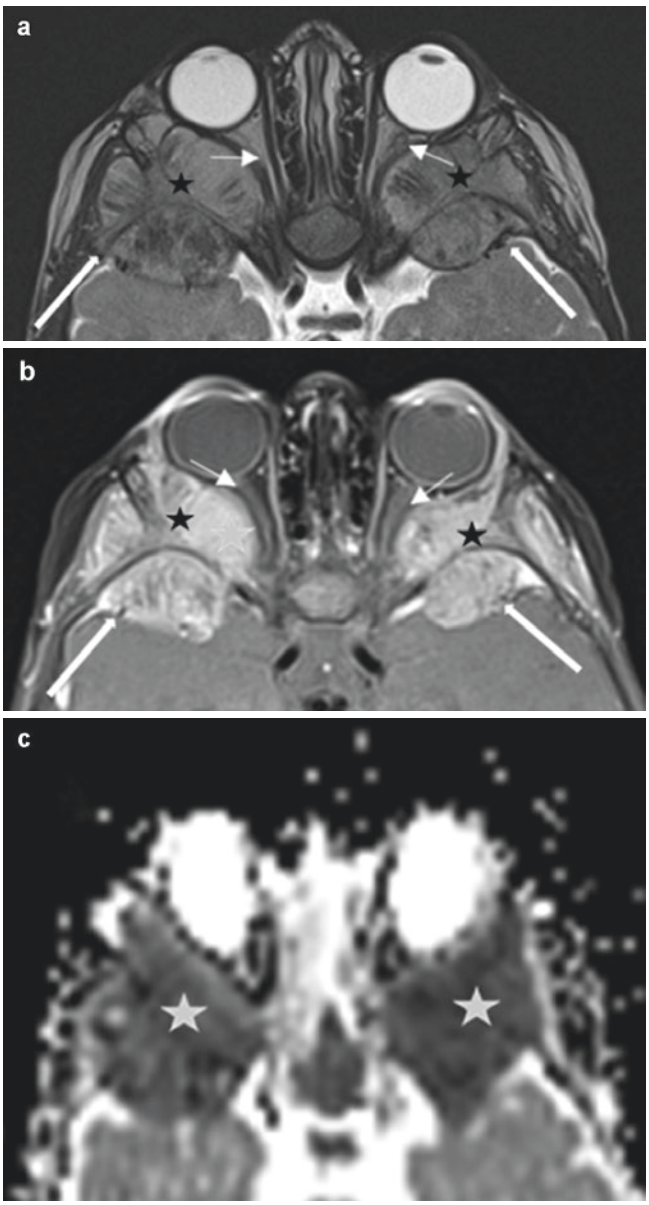


Fig. 13.5 One-year-old presenting with bilateral proptosis, fussiness, and bilateral temporal masses. Axial T2-weighted (**a**), axial post-contrast T1-weighted (**b**), and axial ADC map (**c**) through the orbits show mass lesions (*black**) with extensive periosteal reaction (*thick white arrows*) seen involving the bilateral temporal bones and lateral walls of the orbits with mass effect upon the bilateral optic nerve sheaths (*thin white arrows*). The bilateral masses demonstrate intracranial extension and mass effect upon the anterior portions of the temporal lobes. These mass lesions demonstrate restricted diffusion (*white**) and nearly homogeneous enhancement. Mild proptosis of the optic globes is evident. With the history of abdominal mass, these represent neuroblastoma metastases

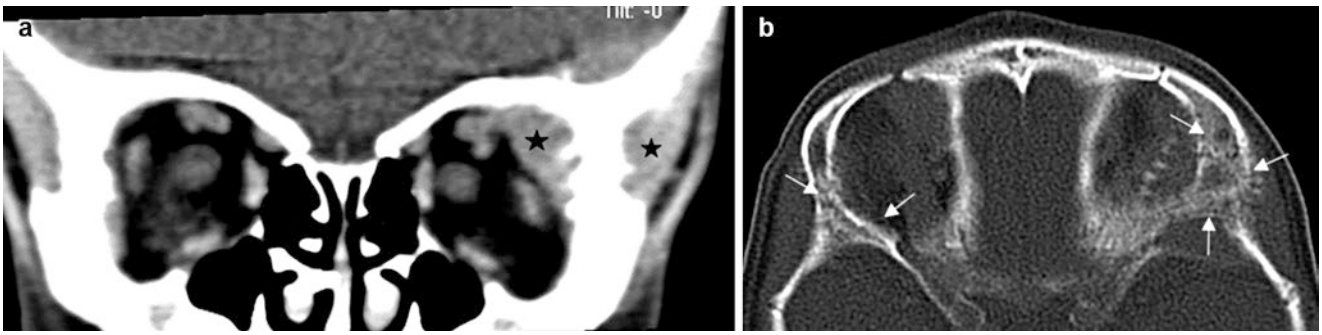


Fig. 13.6 Another metastatic neuroblastoma. Images from enhanced CT study of the orbit with coronal soft tissue (**a**) and axial bone (**b**) window images demonstrate mass lesion at the superolateral orbit (*black**) with spiculated periosteal involvement along the lateral orbital walls

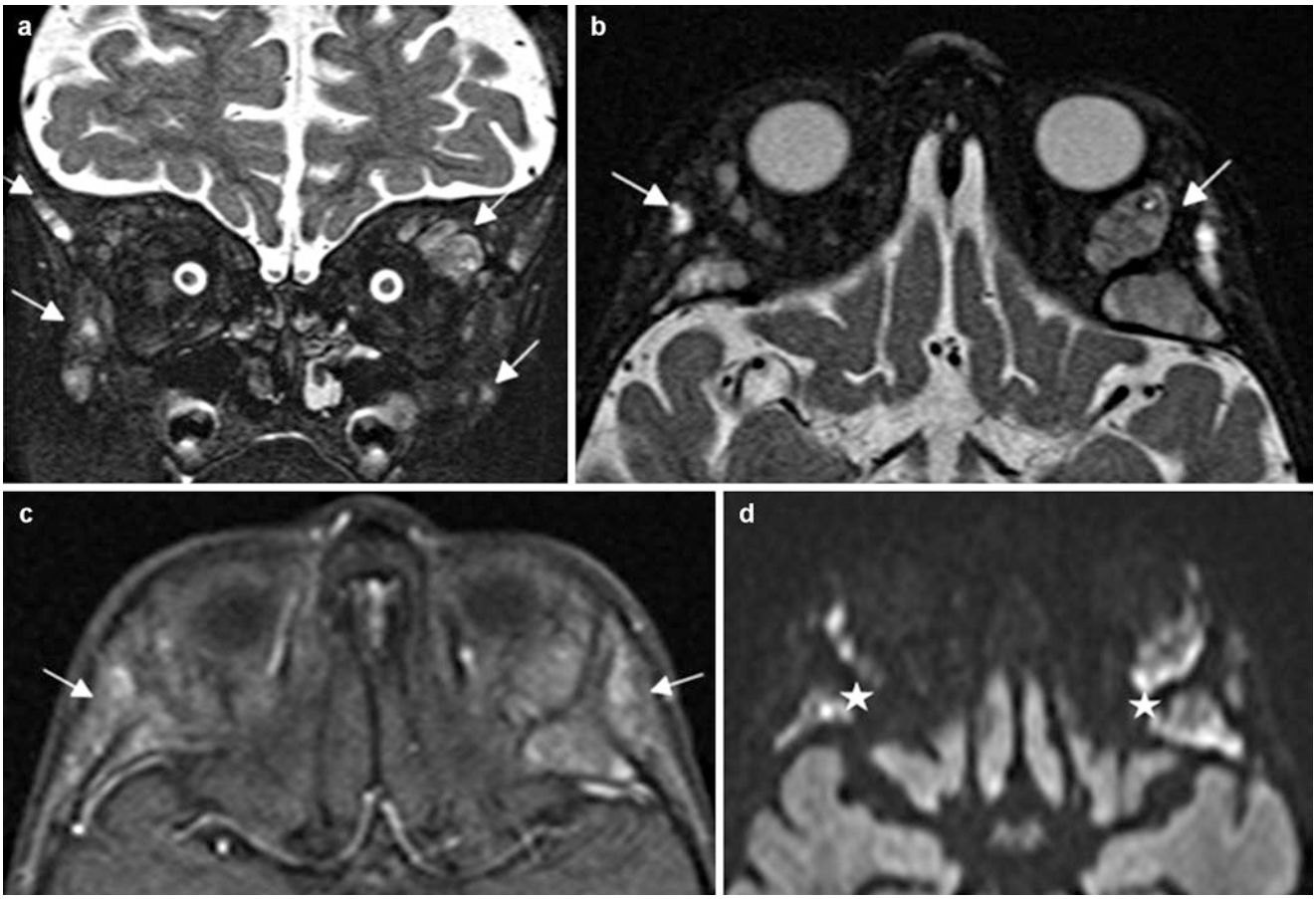


Fig. 13.7 MRI images of the orbit on the same patient as shown in Fig. 13.5. Coronal (**a**) and axial (**b**) T2-weighted with fat suppression and post-contrast axial T1-weighted (**c**) and axial diffusion (**d**) images through the orbit which show expansion of the left sphenoid bone and subperiosteal masses which involve both the lateral aspect of the bilateral, left greater than right orbits resulting in mass effect on the left ocular globe. This metastatic disease to the skull was consistent with the patient's known history of stage IV neuroblastoma

subset of neuroblastomas (~10%) is MIBG non-avid. In this case, a PET scan should be considered to definitively rule out metastases. Urinary catecholamines should also be evaluated.

Risk Group Classification of Pediatric Neuroblastoma

In an effort to standardize risk group classification, the International Neuroblastoma Risk Group (INRG) was developed. INRG establishes pretreatment risk grouping. Staging via INRG relies on presence of image-defined risk factors (i.e., extent of tumor infiltration, encasement of surrounding vessels, infiltration of adjacent organs, or intraspinal extension). L1 tumors lack image-defined risk factors, while L2 tumors do not. Stage M tumors have spread to other parts of the body. Stage MS includes tumors in children, < 18 months old, with a particular pattern of metastases – skin, liver, and/or bone marrow (<10% bone marrow involvement). In addition to the INRG classification, age of the patient, histology, level of differentiation, ploidy, and presence/absence of MYCN amplification are used to assign a risk group – very low, low, intermediate, or high.

Treatment of Pediatric Neuroblastoma

Low- and intermediate-risk tumors are treated with observation, surgery alone, or surgery plus chemotherapy. Treatment of high-risk neuroblastoma is multimodal and includes induction chemotherapy, surgical resection, stem cell transplant, radiation, and immunotherapy. With this intensive approach, long-term survival has reached ~50%. Disease evaluation prior to stem cell transplant determines the approach to "local" control. Patients with persistent sites of MIBG-avid disease, including the orbit, will have those sites irradiated posttransplant.

Liquid Malignancies

Leukemia

Epidemiology of Pediatric Leukemia

Pediatric acute leukemia is the most common malignancy of childhood. Leukemia is a malignancy of the hematopoietic stem cells. The two main types of pediatric acute leukemia are acute lymphoblastic leukemia (ALL) and acute myeloid leukemia (AML). ALL accounts for approximately 75–80% of acute leukemia in children, and AML accounts for most of the remaining 25–80% [14].

The incidence of ALL is approximately 30 cases per million in children younger than 20 years of age annually [15]. The peak incidence of ALL is between ages 3 and 5, but it can occur at all ages [15]. Boys are more likely to develop ALL than girls (55% of children with ALL are male), and Hispanic and white children are more likely to develop ALL than black children [15].

The incidence of AML is seven cases per million in children younger than 15 years annually [16, 17]. The incidence of AML has been reported at 11 cases per million at 2 years of age and 9 cases per million during adolescence. The lowest incidence is at 9 years of age [18]. There is no difference in incidence rates by sex or race. Hispanic children are more likely to develop AML than black children, who are slightly more likely to develop AML than white children [18].

There are multiple predisposition syndromes or genetic factors that predispose children to developing leukemia, although the majority of children have no known predisposing factors. Children with Down syndrome are at increased risk of developing either ALL or AML. Fanconi anemia, severe congenital anemia, Shwachman-Diamond syndrome, Diamond-Blackfan syndrome, neurofibromatosis type 1, Noonan syndrome, dyskeratosis congenita, familial platelet syndrome with predisposition to AML, congenital amegakaryocytic thrombocytopenia, ataxia-telangiectasia, Klinefelter's syndrome, Li-Fraumeni syndrome, and Bloom syndrome have all been associated with development of AML. There are multiple rare germline mutations that have been found in cases of familial ALL [15].

To date there are no well-defined environmental risk factors associated with development of leukemia; however, there are some reports that link development of AML to pesticides, petroleum products, and organic solvents [18]. However, children who have previously received radiation therapy, significant toxic radiation exposure, or prior chemotherapy are at higher risk of developing leukemia. Therapy-associated AML is attributed to certain chemotherapeutic agents and can initially present as myelodysplastic syndrome.

Presentation of Pediatric Leukemia

In acute leukemia, the bone marrow is replaced by neoplastic cells. However, the leukemic cells can also infiltrate other organs, especially the liver, spleen, lymph nodes, mediastinum, and testicles, or the central nervous system (CNS). Approximately 25% of children with ALL and 15% of children with AML have central nervous system (CNS) involvement [18, 19]. Leukemia can also affect the ophthalmologic system.

Children with leukemia may present with a wide range of symptoms. The most common symptoms are fever, fatigue, bleeding, bruising, bone pain, headaches, or infection. These symptoms are due to replacement of the bone marrow with leukemia cells and hyperviscosity in the blood. Children with high white blood cell counts may present with symptoms of leukostasis, particularly in the lungs or in the brain. Children with CNS involvement may present with nausea, vomiting, blurry vision, diplopia, lethargy, or seizures [20]. Leukemia can present with chloromas or masses of tumor cells. This is more likely to occur in AML than ALL. This can occur in the orbit or the CNS (Fig. 13.8).

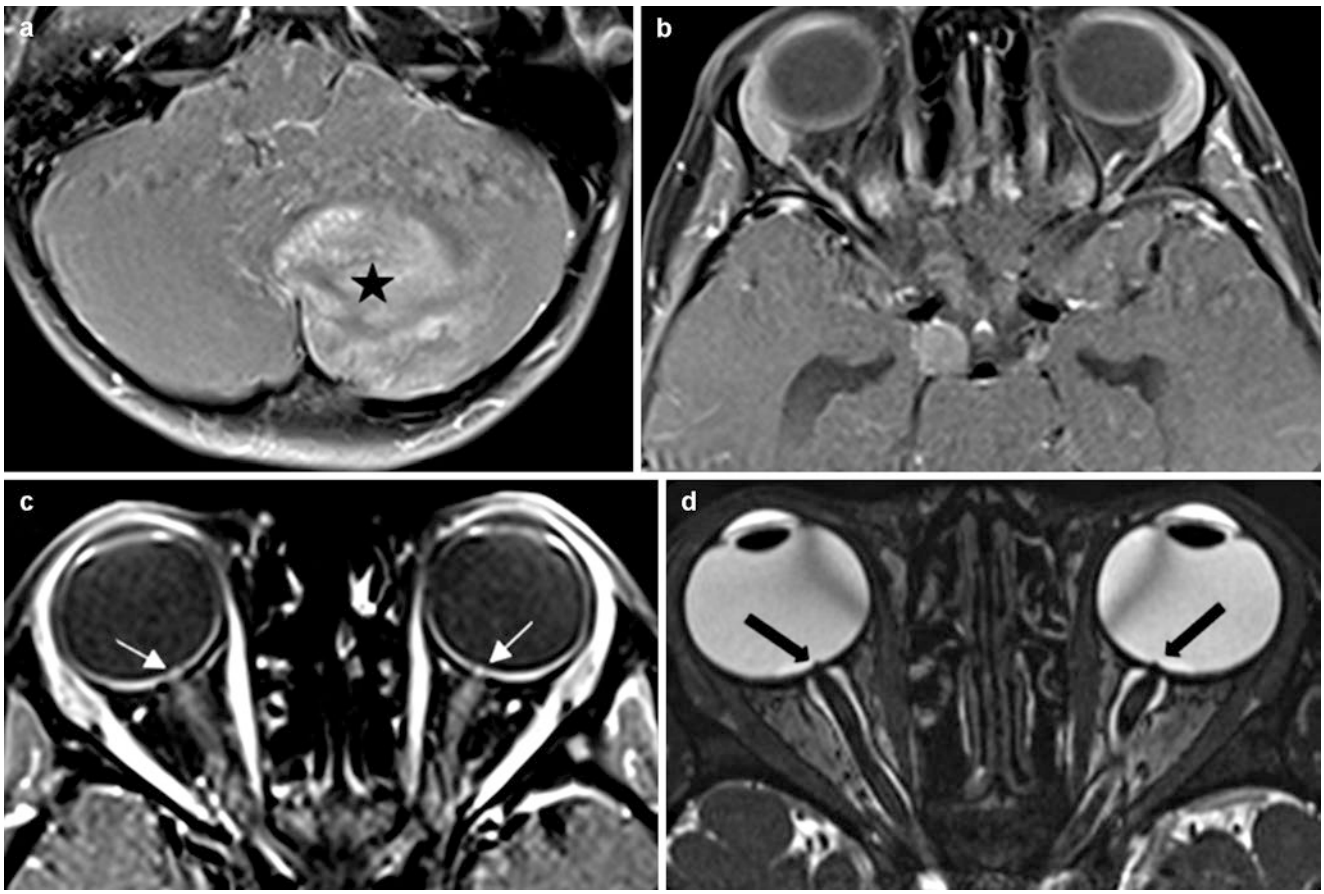


Fig. 13.8 Three-year-old patient with AML presenting with papilledema and ptosis. Axial post-contrast T1-weighted images through the cerebellum (**a**) and through the orbits and cavernous sinuses (**b**) show a mass lesion with patchy enhancement within the left cerebellar hemisphere (*black**) consistent with a chloroma and enhancing nodules (*black**) along the bilateral third cranial nerves representing metastatic nodules. Axial post-contrast T1-weighted image (**c**) showing enhancement (*white arrows*) and axial CISS image (**d**) through the orbits demonstrating protrusion of the optic disc (*black arrows*) indicating papilledema

Some studies report that approximately 9% of children with leukemia have involvement of the eye [21, 22]. Ophthalmologic involvement can be due to primary leukemic infiltration or secondary involvement [20]. The retina is the most common place of leukemic ocular involvement, and avascular ocular tissues are less likely to be involved [20]. Primary leukemia infiltration can occur through orbital infiltration, anterior segment uveal infiltration, or as ophthalmologic manifestations of CNS leukemic involvement [20]. CNS involvement can manifest as infiltration of the optic nerve, which may cause blurry vision or diplopia, or of other cranial nerves leading to cranial nerve palsies. Optic nerve involvement can be either due to direct infiltration of the nerve or due to swelling due to retrolaminar leukemia invasion or increased intracranial pressure [20] (Fig. 13.9). Leukemic CNS involvement leading to increased intracranial pressure can present as headaches, altered mental status, and blurry vision and can appear as papilledema. Some patients with ophthalmologic involvement may be asymptomatic. One report found that 17% of 82 children had ocular changes, but only 3.6% had symptoms [23]. Secondary involvement from leukemia may be due to the anemia, thrombocytopenia, or hyperviscosity found in leukemia. This may lead to ocular changes such as retinal or vitreous hemorrhage, vascular occlusions, or ophthalmologic infections [20] (Fig. 13.10).

Diagnosis of Pediatric Leukemia

Childhood leukemia is diagnosed by evaluation of the peripheral blood smear and the bone marrow. A bone marrow is performed when the peripheral blood smear raises suspicion for leukemia. All children with acute leukemia receive a lumbar puncture to determine if there is CNS involvement at the time of diagnosis. CNS leukemia is more common in ALL than in AML. Ophthalmologists recommend consideration of an ophthalmologic examination at the time of diagnosis of acute leukemia [20], but this is usually only obtained if the patient endorses symptoms.

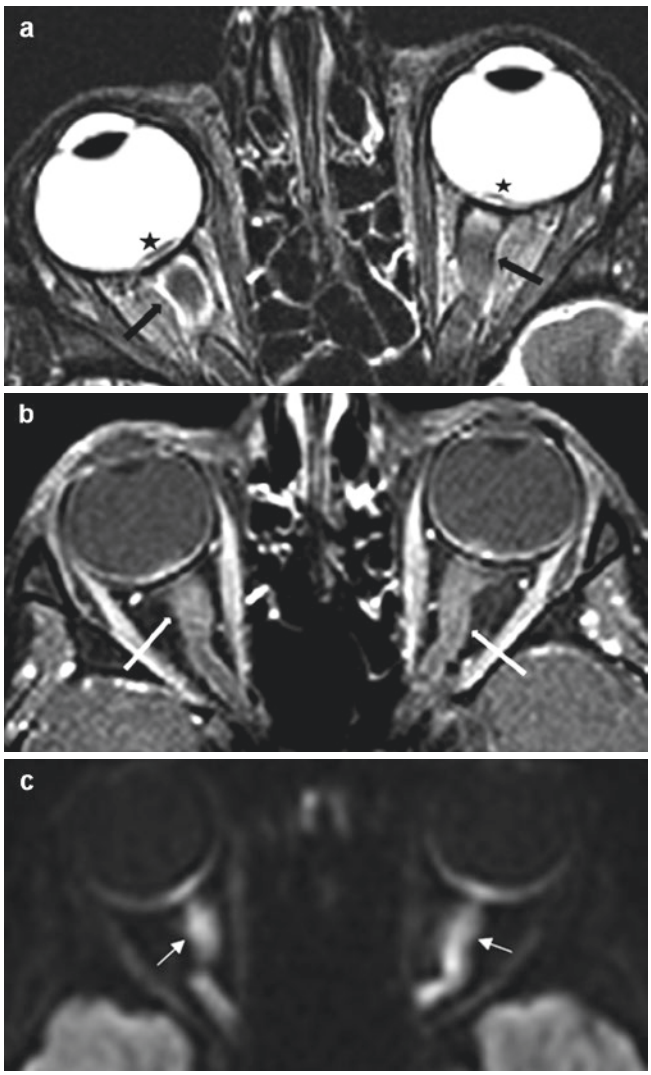


Fig. 13.9 Axial T2-weighted (**a**), axial post-contrast T1-weighted (**b**), and axial diffusion-weighted (**c**) images through the orbit of a patient with relapsed T-cell ALL showing thickening of the intraorbital segments of the bilateral optic nerves (*black arrows*) with restricted diffusion (*thin white arrows*) and post-contrast enhancement (*thick white arrows*) consistent with leukemic infiltration. Note the eversion of the optic discs consistent with papilledema (*black**)



Fig. 13.10 Coronal STIR (**a**) and post-contrast T1-weighted coronal (**b**) and axial (**c**) through the orbits demonstrate bright marrow signal abnormality and associated enhancement within the right lateral orbital wall extending along the lateral wall of the maxillary sinus (*white arrows*), consistent with leukemic infiltration

Treatment of Pediatric Leukemia

Treatment for childhood leukemia includes multi-agent chemotherapy. All children with leukemia receive intrathecal chemotherapy even if the initial, diagnostic lumbar puncture does not show evidence of CNS involvement. Prior to initiation of CNS-directed leukemia treatment, children with leukemia often relapsed in the CNS [15]. Therefore children are given prophylactic intrathecal therapy throughout the duration of their leukemia treatment.

Children with ALL receive approximately 6–8 months of intensive chemotherapy and then an additional 2–2.5 years of maintenance chemotherapy. Currently, the backbone of ALL treatment includes glucocorticoids, vincristine, asparaginase, anthracyclines, cyclophosphamide, methotrexate, cytarabine, mercaptopurine, thioguanine, and intrathecal chemotherapy. Intrathecal chemotherapy may include methotrexate, cytarabine, and hydrocortisone. Studies are ongoing through cooperative oncology group and industry clinical trials to find other

treatment options. Treatment for ALL begins with induction chemotherapy, which lasts 4–6 weeks. Induction chemotherapy will produce a remission for most children, but studies have shown that children need additional chemotherapy in order to prevent relapse. During the remaining intensive courses of chemotherapy, children receive weekly or more frequent intravenous chemotherapy and intermittent oral chemotherapy. In the maintenance phase, most children receive monthly intravenous chemotherapy and daily oral chemotherapy. Approximately 20% of children with CNS involvement of their ALL will receive CNS irradiation in additional to intrathecal chemotherapy to treatment their leukemia, but clinical trials are increasingly aiming to avoid cranial irradiation as primary ALL treatment due to the potential long-term side effects [15, 24].

Children with AML receive approximately 4–6 months of very intensive chemotherapy. Currently, the backbone of most pediatric AML chemotherapy includes cytarabine, anthracyclines, etoposide, and intrathecal chemotherapy. Intrathecal chemotherapy usually includes cytarabine and may include methotrexate and hydrocortisone. One subtype of AML, acute promyelocytic leukemia, is treated with a unique regimen that includes all-trans-retinoic acid and/or arsenic. As with ALL, cooperative oncology group and industry clinical trials are currently being performed to find other treatment options for all subtypes of AML. In each course of chemotherapy, children receive intensive chemotherapy in the first 2 weeks. The intensive chemotherapy causes the blood cell counts to fall. Once the blood counts have reached their nadir and then have recovered, the child can receive the next course of chemotherapy. Most children remain in the hospital for 4–6 weeks while awaiting count recovery, but some patients are discharged home during this time period [25, 26].

Some children with leukemia, based on their cytogenetics or response to therapy, or if they have relapsed disease, will require allogeneic bone marrow transplant to cure their leukemia. Approximately 5–10% of children with ALL receive an allogeneic bone marrow transplant during their initial therapy, and more than 50% of children with relapsed ALL receive an allogeneic bone marrow transplant [15]. In recent studies, 10–30% of children with AML received an allogeneic bone marrow transplant during their initial therapy [27]. All children with AML who relapse will require an allogeneic bone marrow transplant to be cured.

Children with leukemia may also receive targeted radiation due to clinical symptoms. Children with involvement of the ophthalmologic system need radiation to the involved sites in addition to treatment with systemic chemotherapy. Occasionally radiation is given alone for palliative, symptomatic relief if a patient has relapsed disease.

Prognosis of Pediatric Leukemia

The overall cure rate for ALL is 90% [15, 28]. Children with ALL are assigned a risk group based on their age, white blood cell count at presentation, immunophenotype, genetic mutations of the leukemia, and response to initial therapy. Treatment is intensified for children with higher-risk ALL. There are two distinct immunophenotypes based on cell surface and cytoplasmic expression of markers of lineage: precursor B-cell ALL accounts for 85%, and T-cell ALL accounts for 15% of childhood ALL [15]. T-cell ALL has had a lower survival rate than B-cell ALL historically, but advances in treatment options have improved survival in T-cell ALL significantly over time [15]. For B-cell ALL, age greater than 10, higher white blood cell count at presentation, and poor response to treatment are classified as high risk and require intensified treatment. Children less than 1 year of age have worse outcomes as well [15]. At the end of the first course of therapy, children undergo a bone marrow aspirate to assess their response to the first course of chemotherapy. Testing for submicroscopic ALL is performed to determine if there is minimal residual disease (MRD). MRD is used to determine risk group classification and treatment as well [15].

Approximately 15–20% of children with ALL experience disease relapse [15]. Shorter time intervals between initial diagnosis and relapse have worse prognoses. If a child relapses during therapy, the survival rate is only 20–30% [15]. If a child relapses after completing initial treatment, the survival rate is approximately 50% [15].

The overall cure rate for AML ranges from 50% to 70% [14, 17, 29]. Children with AML are currently classified as low risk or high risk based on cytogenetics, molecular mutations, and response to therapy. Children with AML have a bone marrow aspirate at the end of their induction chemotherapy to assess their response to therapy. If a child does not have a sufficient response to chemotherapy, he or she may need an allogeneic bone marrow transplant in addition to chemotherapy. Approximately 30–40% of children with AML will suffer disease relapse [30]. CNS relapse occurs in less than 5% of children with AML [14]. A recent study showed that girls had increased survival rates than boys, but the reason for this is not known [31].

Some reports have shown that ocular involvement leads to a worse prognosis for pediatric acute leukemia [32], but it is unclear how current treatment regimens affect this prognosis. If a child does relapse, it is possible that the relapse will occur in or include the ophthalmologic system even if he or she did not have ophthalmologic disease at initial presentation.

Lymphoma

Epidemiology of Pediatric Lymphoma

Lymphomas are the third most common pediatric cancer. Non-Hodgkin's lymphoma (NHL) accounts for approximately 60% and Hodgkin's lymphoma (HL) accounts for

approximately 40% of pediatric lymphoma [33]. Lymphomas are cancers of the lymph nodes and can be of B cell or T cell in origin. Involvement of the ophthalmologic system is rare in all types of pediatric lymphoma and is especially rare in HL [34].

The incidence of NHL is approximately 500 cases per year [33]. NHL is two times more common in white children than in black children and is 2–3 times more common in boys than in girls [33, 35]. There are geographic differences in the incidence of each type of NHL. The incidence of HL is approximately 380 children and 800 adolescents per year [35]. HL is the most common cancer in adolescence (ages 15–19) [35]. There is a male predominance in childhood, but there is no difference in adolescence. HL is more common in white children than black or Hispanic children [35].

NHL is more common in children with congenital and acquired immunodeficiencies, including ataxia-telangiectasia, Wiskott-Aldrich syndrome, and X-linked lymphoproliferative disease, and children who have previously undergone solid organ or bone marrow transplants [33]. The T-cell deficiencies in these patients are likely the cause of the development of NHL.

There are multiple types of NHL that are determined by the cell lineage and the maturity of the cell. The three most common types of NHL in children are Burkitt lymphoma, lymphoblastic lymphoma, and large cell lymphoma. Burkitt lymphoma is a B-cell lymphoma and has both sporadic and endemic variants. The endemic variant is common in equatorial Africa, accounting for approximately 50% of all pediatric malignancies [33]. Epstein-Barr virus (EBV) is almost always involved in the endemic variant of NHL, but is often not involved in the sporadic variant. Lymphoblastic lymphoma and large cell lymphoma can be T or B cell in origin. There are four main histologic variants of HL. These are nodular sclerosis, mixed cellularity, lymphocyte-predominant, and lymphocyte-depleted. EBV has been associated with development of HL [35].

Presentation of Pediatric Lymphoma

Children with lymphoma can present with a wide range of symptoms. Children can present with palpable lymphadenopathy, weight loss, night sweats, fevers, cough, shortness of breath, dyspnea, facial vomiting, and evidence of bowel obstruction. The specific symptoms are related to the location of the lymphoma. The enlarged lymph nodes can be rapidly or slow growing. Some patients will have multiple lymph node groups involved, while other patients will only have one area of lymphadenopathy. HL has contiguous nodal group involvement, while NHL does not.

While lymphoma is the most common cancer of the orbit in adulthood, pediatric lymphomas involving the ophthalmologic system are rare [36]. Having only been reported in case reports, the incidence is unknown [36]. One case report describes that one patient presented with a conjunctival mass, one patient presented with bilateral proptosis, and three patients presented with unilateral proptosis [36]. Another small case series reports that 20% of children with Burkitt lymphoma in Turkey had orbital involvement at initial presentation [37].

Diagnosis of Pediatric Lymphoma

Lymphoma is diagnosed through biopsy of an enlarged lymph node. This can be done through removal of the entire lymph node or with a core biopsy, depending on the location and size of the lymph node. If possible, removal of the entire lymph node can be beneficial to be able to evaluate the architecture of the lymph node histologically.

Treatment of Pediatric Lymphoma

The treatment for NHL is determined based on the type of NHL and the stage of the lymphoma. Staging is performed using the Murphy staging system for most types of NHL [38]. Treatment for Burkitt lymphoma and large cell lymphomas includes intensive, multi-agent chemotherapy and lasts 4–8 months. Currently the backbone of NHL treatment includes cyclophosphamide, cytarabine, doxorubicin, etoposide, methotrexate, prednisone, vincristine, and intrathecal chemotherapy. Studies are ongoing through cooperative oncology group and industry clinical trials to find other treatment options, including targeted agents for specific mutations. The treatment for lymphoblastic lymphoma resembles that for ALL including a maintenance chemotherapy phase and CNS prophylaxis.

Staging for HL is performed using the Ann Arbor system and the presence or absence of B symptoms. B symptoms, which include fever, weight loss of more than 10% of the patient's body weight over the preceding 6 months, and drenching night sweats, are prognostic. Children with B symptoms have a higher-stage HL and receive intensified treatment.

HL is sensitive to radiation and can be treated with radiation alone. However, the long-term morbidity from radiation is high, with high rates of cardiac and pulmonary disease and at least 10% of patients developing breast cancer by age 45 [35]. Therefore, current treatment protocols aim to use a combination of multi-agent chemotherapy and radiation while minimizing the use of radiation whenever possible [39]. The current backbone of HL treatment includes bleomycin, cyclophosphamide, doxorubicin, etoposide, prednisone, and vincristine. Treatment for HL is adjusted by sex in order to minimize gender-based side effects of chemotherapy. Further, therapy for HL is not only based on stage at initial presentation but also on response to the initial courses of chemotherapy. The necessity for radiation therapy for some patients is determined by the response to chemotherapy, and some patients can be cured without radiation [39].

Pediatric ophthalmic lymphoma is rare. As such there have been no well-described treatment modalities. One case report describes using chemotherapy alone in four of five patients and surgically removing the conjunctival mass in the fifth patient [36].

The standard of care for children with relapsed HL is high-dose chemotherapy and autologous bone marrow transplant; however, some children may be able to be treated with chemotherapy alone [40].

Prognosis of Pediatric Lymphoma

The prognosis of NHL depends on the type of lymphoma, but the cure rate ranges from 60% to 90% [35, 38]. Overall 10–30% of children with NHL will relapse [41]. The 5-year survival rate of HL approaches 98% [42]. Relapsed HL can be difficult to treat, but there is a high likelihood of cure with the exception of a small number of patients with refractory disease, 40 and is approximately 68% [39].

References

1. National Cancer Institute SEER Cancer Statitics Review 1975–2003, 2006.
2. Birch JM, Hartley AL, Blair V, et al. Cancer in the families of children with soft tissue sarcoma. Cancer. 1990;66:2239–48.
3. Sung L, Anderson JR, Arndt C, et al. Neurofibromatosis in children with Rhabdomyosarcoma: a report from the intergroup Rhabdomyosarcoma study IV. J Pediatr. 2004;144:666–8.
4. Gripp KW. Tumor predisposition in Costello syndrome. Am J Med Genet C Semin Med Genet. 2005;137C:72–7.
5. Smith AC, Squire JA, Thorner P, et al. Association of alveolar rhabdomyosarcoma with the Beckwith-Wiedemann syndrome. Pediatr Dev Pathol. 2001;4:550–8.
6. Miller RW, Rubinstein JH. Tumors in Rubinstein-Taybi syndrome. Am J Med Genet. 1995;56:112–5.
7. Skapek SX, Anderson J, Barr FG, et al. PAX-FOXO1 fusion status drives unfavorable outcome for children with rhabdomyosarcoma: a children's oncology group report. Pediatr Blood Cancer. 2013;60:1411–7.
8. Walterhouse DO, Pappo AS, Meza JL, et al. Shorter-duration therapy using vincristine, dactinomycin, and lower-dose cyclophosphamide with or without radiotherapy for patients with newly diagnosed low-risk rhabdomyosarcoma: a report from the soft tissue sarcoma Committee of the Children's oncology group. J Clin Oncol. 2014;32:3547–52.
9. Weigel BJ, Lyden E, Anderson JR, et al. Intensive Multiagent therapy, including dose-compressed cycles of Ifosfamide/Etoposide and vincristine/doxorubicin/cyclophosphamide, Irinotecan, and radiation, in patients with high-risk Rhabdomyosarcoma: a report from the Children's oncology group. J Clin Oncol. 2016;34:117–22.
10. Esiashvili N, Goodman M, Marcus RB Jr. Changes in incidence and survival of Ewing sarcoma patients over the past 3 decades: surveillance Epidemiology and end results data. J Pediatr Hematol Oncol. 2008;30:425–30.
11. Delattre O, Zucman J, Plougastel B, et al. Gene fusion with an ETS DNA-binding domain caused by chromosome translocation in human tumours. Nature. 1992;359:162–5.
12. Womer RB, West DC, Krailo MD, et al. Randomized controlled trial of interval-compressed chemotherapy for the treatment of localized Ewing sarcoma: a report from the Children's oncology group. J Clin Oncol. 2012;30:4148–54.
13. Mirabello L, Troisi RJ, Savage SA. Osteosarcoma incidence and survival rates from 1973 to 2004: data from the surveillance, Epidemiology, and end results program. Cancer. 2009;115:1531–43.
14. Rubnitz JE. How I treat pediatric acute myeloid leukemia. Blood. 2012;119:5980–8.
15. Hunger SP, Mullighan CG. Acute lymphoblastic leukemia in children. N Engl J Med. 2015;373:1541–52.
16. Zwaan CM, Kolb EA, Reinhardt D, et al. Collaborative efforts driving progress in pediatric acute myeloid leukemia. J Clin Oncol. 2015;33(27):2949–62.
17. Creutzig U, van den Heuvel-Eibrink MM, Gibson B, et al. Diagnosis and management of acute myeloid leukemia in children and adolescents: recommendations from an international expert panel. Blood. 2012;120:3187–205.
18. Rubnitz JE, Gibson B, Smith FO. Acute myeloid leukemia. Pediatr Clin N Am. 2008;55:21–51.
19. Pui CH, Campana D, Pei D, et al. Treating childhood acute lymphoblastic leukemia without cranial irradiation. N Engl J Med. 2009;360:2730–41.
20. Sharma T, Grewal J, Gupta S, et al. Ophthalmic manifestations of acute leukaemias: the ophthalmologist's role. Eye (Lond). 2004;18:663–72.
21. Kaikov Y. Optic nerve head infiltration in acute leukemia in children: an indication for emergency optic nerve radiation therapy. Med Pediatr Oncol. 1996;26:101–4.
22. Ridgway EW, Jaffe N, Walton DS. Leukemic ophthalmopathy in children. Cancer. 1976;38:1744–9.
23. Reddy SC, Menon BS. A prospective study of ocular manifestations in childhood acute leukaemia. Acta Ophthalmol Scand. 1998;76:700–3.
24. Vora A, Andreano A, Pui CH, et al. Influence of cranial radiotherapy on outcome in children with acute lymphoblastic leukemia treated with contemporary therapy. J Clin Oncol. 2016;34(9):919–26.
25. Getz KD, Miller TP, Seif AE, et al. A comparison of resource utilization following chemotherapy for acute myeloid leukemia in children discharged versus children that remain hospitalized during neutropenia. Cancer Med. 2015;4:1356–64.
26. Miller TP, Getz KD, Kavcic M, et al. A comparison of discharge strategies after chemotherapy completion in pediatric patients with acute myeloid leukemia: a report from the Children's oncology group. Leuk Lymphoma. 2016;57(7):1567–74.
27. Niewerth D, Creutzig U, Bierings MB, et al. A review on allogeneic stem cell transplantation for newly diagnosed pediatric acute myeloid leukemia. Blood. 2010;116:2205–14.
28. Pui CH, Yang JJ, Hunger SP, et al. Childhood acute lymphoblastic leukemia: progress through collaboration. J Clin Oncol. 2015;33(27):2938–48.
29. Arceci RJ, Sande J, Lange B, et al. Safety and efficacy of gemtuzumab ozogamicin in pediatric patients with advanced CD33+ acute myeloid leukemia. Blood. 2005;106:1183–8.
30. Kaspers GJ, Zimmermann M, Reinhardt D, et al. Improved outcome in pediatric relapsed acute myeloid leukemia: results of a randomized trial on liposomal daunorubicin by the international BFM study group. J Clin Oncol. 2013;31:599–607.
31. Hossain MJ, Xie L. Sex disparity in childhood and young adult Acute Myeloid Leukemia (AML) survival: evidence from US population data. Cancer Epidemiol. 2015;39:892–900.
32. Ohkoshi K, Tsiaras WG. Prognostic importance of ophthalmic manifestations in childhood leukaemia. Br J Ophthalmol. 1992;76:651–5.
33. Sandlund JT, Downing JR, Crist WM. Non-Hodgkin's lymphoma in childhood. N Engl J med. 1996;334:1238–48.
34. Gupta V, Kumar M, Gupta SK. Ptosis: a rare presentation of Hodgkin lymphoma. J Pediatr Hematol Oncol. 2014;36:163–5.

35. Ward E, DeSantis C, Robbins A, et al. Childhood and adolescent cancer statistics, 2014. CA Cancer J Clin. 2014;64:83–103.
36. Bakhshi S, Sidhu T. Pediatric orbital and ocular lymphomas. Pediatr Blood Cancer. 2008;50:940–1.
37. Cavdar AOGS, Yavuz G, Babacan E, Unal E, Uluoğlu O, Yücesan S, Magrath IT, Akar N. Burkitt's lymphoma between African and American types in Turkish children: clinical, viral (EBV), and molecular studies. Med Pediatr Oncol. 1993;21:36–42.
38. Cairo MS, Pinkerton R. Childhood, adolescent and young adult non-Hodgkin lymphoma: state of the science. Br J Haematol. 2016;173:507–30.
39. Donaldson SS. Finding the balance in pediatric Hodgkin's lymphoma. J Clin Oncol. 2012;30:3158–9.
40. Harker-Murray PD, Drachtman RA, Hodgson DC, et al. Stratification of treatment intensity in relapsed pediatric Hodgkin lymphoma. Pediatr Blood Cancer. 2014;61:579–86.
41. Shiramizu B, Mussolin L, Woessmann W, et al. Paediatric non-Hodgkin lymphoma – perspectives in translational biology. Br J Haematol. 2016;173:617–24.
42. Kelly KM. Hodgkin lymphoma in children and adolescents: improving the therapeutic index. Blood. 2015;126:2452–8.

14 Neuro-Ophthalmic Considerations in Pediatric Orbital and Oculoplastic Disease

Pavle Doroslovački, Grant T. Liu, and Robert A. Avery

Introduction

The pediatric oculoplastic surgeon frequently cares for patients whose clinical manifestations mimic or represent a neuro-ophthalmic condition. A familiarity with neuro-ophthalmic entities commonly seen by the oculoplastics subspecialist is critical, as proper recognition is essential to ensuring timely diagnosis, treatment, and, sometimes, the avoidance of unnecessary surgery. In a child with eyelid ptosis, conditions such a myasthenia gravis, Horner syndrome, and third nerve palsy must, among others, be considered as all can lead to significant morbidity if unrecognized or be indicative of a more sinister condition. Ocular motility deficits and ptosis with acute proptosis may be caused by cavernous sinus conditions (e.g., thrombosis or inflammation). On the other hand, subacute or chronic proptosis with or without vision loss can be seen in optic nerve gliomas, in which careful serial neuro-ophthalmic examinations often guide treatment decisions. In each of these cases, recognition of the possible neuro-ophthalmic implication is critical to implementing the appropriate diagnostic and therapeutic approach. The aim of this chapter is to familiarize the pediatric oculoplastic surgeon with the aforementioned disease entities, as well as several others that may be encountered in his or her practice.

Myasthenia Gravis

Myasthenia gravis is a disease characterized by fatigable muscle weakness due to impaired transmission at the neuromuscular junction in ocular and skeletal muscles. More than 90% of patients with myasthenia have ocular manifestations, primarily eyelid ptosis, and extraocular muscles weakness. The diagnosis of *ocular myasthenia gravis* is reserved for those patients whose weakness is limited to ocular motility and ptosis. Patients who manifest weakness beyond these structures (i.e., dysphagia, limb weakness) are labeled as *generalized myasthenia gravis*. Roughly half of patients present initially with either ocular or generalized forms of myasthenia. Of those presenting with purely ocular disease, no more than half progress to generalized myasthenia—typically within the first 2 years [1, 2]. Systemic muscle weakness may, on occasion, become so severe that respiratory function is compromised, constituting a *myasthenic crisis.*

An association of myasthenia with other autoimmune diseases, especially Graves disease, is well established, and familial cases are rare, but have been reported. While present in about 15% of adults with myasthenia, thymomas are rare in children, though thymic hyperplasia is a frequent finding on pathology after thymectomy. Although classically described as having two peaks of incidence, one in early adulthood and the other in the sixth or seventh decade of life, myasthenia gravis can present at any age [3]; below 18 years, it is termed *juvenile myasthenia gravis*. In children, ptosis has been reported to be present in around 95% of patients [4, 5]. Ptosis and ocular misalignment can induce amblyopia, with up to 25–50% of children requiring patching or other anti-amblyopic treatment, generally with good response [5, 6].

Myasthenia gravis is an autoimmune condition in which high-affinity IgG antibodies bind to postsynaptic nicotinic acetylcholine receptors (AChR) in the neuromuscular junction, leading to complement-mediated damage, blockage, and reuptake and degradation of the receptors [3, 7]. Extraocular muscles appear to be preferentially involved, possibly from an increased susceptibility to fatigue due to high firing rates, increased sensitivity to neuromuscular blockade, or unique antigens in their AChR complex [8]. Alternately, the preference for extraocular muscles may be a perceived effect, as only a mild degree of weakness, which would not be noted elsewhere, is needed to induce symptomatic diplopia. Certain drugs have been reported to induce myasthenia gravis [9, 10], while others, such as aminoglycosides, beta-blockers, and

P. Doroslovački (✉)
Department of Ophthalmology, MedStar Washington Hospital Center, Washington, DC, USA
e-mail: doroslov@gmail.com

G.T. Liu • R.A. Avery
Division of Ophthalmology, Children's Hospital of Philadelphia, Philadelphia, PA, USA

© Springer International Publishing AG 2018

J.A. Katowitz, W.R. Katowitz (eds.), *Pediatric Oculoplastic Surgery*, https://doi.org/10.1007/978-3-319-60814-3_14

fluoroquinolones, may exacerbate muscle weakness through an effect on neuromuscular transmission [11].

Symptoms from ocular myasthenia gravis include complaints related to ptosis and diplopia (Fig. 14.1). Patients with ocular myasthenia gravis will often report that their ptosis varies significantly throughout the day and between days and that it may change sides. Worsening ptosis in the evening or when tired, is a common complaint but is nonspecific. Diplopia is, likewise, variable over time and in pattern. Those with generalized involvement may additionally report muscle weakness, dysphagia, dysarthria, and dyspnea.

As mentioned previously, the most common clinical sign of myasthenia gravis is eyelid ptosis, which can be unilateral, bilateral, or alternating and is characteristically variable over time. *Fatigability*, which is strongly suggestive of myasthenia, may be elicited on examination, with a visible worsening of eyelid ptosis after sustained upgaze (e.g., for 30 seconds). *Curtaining*, or lowering of the contralateral eyelid when the more ptotic eyelid is mechanically elevated, is also suggestive, though not specific. The *Cogan lid twitch*, a brief, rapid overshoot of one or both eyelids with a slower recovery to resting position when recovering from downgaze, is also a characteristic, though not highly specific, finding [12]. A variant of the lid twitch, *lid hopping*, which consists of a hopping motion of the eyelids in attempted side gaze, can also be seen. Orbicularis oculi weakness is frequently present, and fatigue can sometimes be elicited with attempted sustained forceful eye closure, leading to gradual opening of the palpebral fissure despite efforts to keep the eye closed. Ocular motility deficits in myasthenia can follow any pattern and can deceptively mimic any ocular motor cranial nerve palsy. The eye movements may also exhibit fatigability after sustained gaze in a certain direction, and saccadic velocity may be decreased. Notably, the pupils are not involved clinically in myasthenia gravis.



Fig. 14.1 Juvenile myasthenia gravis. (**a**) Right eye ptosis and (**b**) adduction deficit and (**c**) left eye elevator deficit. The child had physiologic anisocoria

Simple bedside diagnostic tests for myasthenia gravis include the sleep test and ice test. In the former, patients are allowed to nap for 30 min; a visible improvement in their ptosis after resting is considered suggestive of myasthenia gravis [13]. The ice test involves the placement of an ice pack over the ptotic eyelid for 1 min, with an improvement in ptosis after the ice is removed indicative of likely myasthenia. Nonetheless, ice testing is not very practical in many children, who may not be able to cooperate with this test. Although the above testing maneuvers are simple and readily available, they are not definitive.

The diagnosis of myasthenia should be confirmed, with serum acetylcholine receptor antibody testing and, if possible, electromyography (EMG) with repetitive nerve stimulation testing, single-fiber electromyography, or edrophonium testing. Serum AChR binding antibody testing is essentially diagnostic of myasthenia gravis, as the test is highly specific. For adults, the antibody is present in about 90% of generalized myasthenia patients, but only in about 50–70% of those with ocular myasthenia [14–17]. In children, seronegativity appears to be even more frequent, with about 70% of generalized and 40% of ocular myasthenia patients being positive on antibody testing [2, 18, 19]. Testing for either AChR binding or modulating antibodies shows similar sensitivity in generalized myasthenia gravis (86%), and checking both titers increases the sensitivity slightly to around 90% [20]. AChR blocking antibodies appear to be present in just over half of generalized myasthenia patients, and titers may correlate with disease activity [20]. When performing serological testing for myasthenia, the binding antibody is usually the first-line test. If there is high clinical suspicion and the binding antibody is negative, modulating and blocking antibodies can be ordered subsequently in the attempt to increase diagnostic yield. In our experience, the sensitivity of antibody testing may also be augmented by repeating the serology several months after an initial negative test, when myasthenia gravis is still highly suspected in a patient. A minority of individuals with AChR antibody seronegative myasthenia have serum anti-muscle-specific kinase (anti-MuSK) antibodies. These patients, usually adults, generally have a predilection for oropharyngeal, cervical, and respiratory symptoms and more often require respiratory support

and plasma exchange for treatment [21–23]. Single-fiber EMG, which is very sensitive, and repetitive nerve stimulation EMG, though very helpful in diagnosing seronegative myasthenia in adults, are not practical in children because of the pain involved and inability to be performed under anesthesia. Pharmacologic testing with acetylcholinesterase inhibitors can also be used for the diagnosis of myasthenia, with a clear improvement in ptosis and/or ocular motility after administration being a positive result. Intravenous edrophonium or intramuscular neostigmine can be used in children, though the former requires placement of an IV cannula, and children must be monitored closely for side effects such as bradycardia and gastrointestinal upset. Pharmacologic testing appears to be about 90% sensitive in pediatric patients [2]. Pediatric patients with ocular myasthenia gravis do not need routine chest imaging to screen for a thymoma as this is exceptionally rare in children. In patients for whom thymectomy is planned, chest imaging with MRI is preferred due to the lack of ionizing radiation. In addition, if the clinical pattern of ptosis and ocular motor deficits is suggestive of focal cranial nerve involvement, the patient should undergo brain neuroimaging to exclude the possibility of an explanatory lesion before the diagnosis of myasthenia is made.

Oral acetylcholinesterase inhibitors, which increase the concentration of acetylcholine in the neuromuscular junction by slowing its enzymatic degradation, are the first-line treatment for myasthenia gravis. Most often, pyridostigmine is used. These agents work very well for systemic and oropharyngeal weakness, and reasonably well for ptosis, but are poor in improving ocular motility. The most common side effects are gastrointestinal upset, cramping, and diarrhea. Very often, chronic treatment with corticosteroids is required, but may lead to stunted growth. In cases of weakness resistant to acetylcholinesterase inhibitors and steroids, long-term immunosuppression with azathioprine or cyclosporine may be needed, despite many undesirable potential side effects. All myasthenic children under 8 years of age should be regularly screened for amblyopia and treated with patching or pharmacologic penalization if needed. There is limited, though growing evidence that thymectomy, via transsternal or thoracoscopic approaches [24], may increase the rate of spontaneous remission, decrease medication dependence, and reduce the risk of generalization in ocular myasthenics [6, 25]. In this regard, thymectomy should be strongly considered in all patients with either ocular or generalized myasthenia.

Congenital Myasthenic Syndromes

As in myasthenia gravis, the *congenital myasthenic syndromes* can also present with fatigable ocular and systemic weakness, usually presenting between birth and early childhood, but are not of an autoimmune or antibody-mediated etiology. This family of conditions is caused by genetic defects, most frequently in subunits of the nicotinic AChR, that lead to dysfunctional neurotransmission at the neuromuscular junction [26]. Available treatments include pyridostigmine, 3,4-diaminopyridine, quinidine, fluoxetine, and ephedrine, all exhibiting variable degrees of effectiveness [26]. These patients sometimes need ptosis surgery to prevent amblyopia and improve head position.

Horner Syndrome

Horner syndrome, consisting of the triad of unilateral upper and lower eyelid ptosis, pupillary miosis, and facial anhidrosis, should always be considered in the differential diagnosis of acquired or congenital pediatric ptosis, as it can be one of the early signs of a number of potentially threatening etiologies. The syndrome is caused by the disruption of the ipsilateral oculosympathetic pathway, which consists of three neurons. The first-order neuron starts in the hypothalamus and descends through the midbrain, pons, medulla, and spinal cord to synapse with the second-order neuron in the ciliospinal center of Budge at the C8-T2 spinal level. The axon of the second-order neuron then ascends along the paraspinal sympathetic chain and synapses with the third-order neuron in the superior cervical ganglion, which is located at the C3 spinal level just lateral and posterior to the palatine tonsil. The axons of the third-order neuron then follow the internal carotid artery up to the cavernous sinus where, after a brief course along the abducens (sixth) nerve, they join the ophthalmic branch of the trigeminal nerve to innervate the pupillary dilator muscle, ciliary body, Müller's (superior tarsalis) muscle, and inferior tarsalis muscle.

Disruption of any of the three neurons of the sympathetic pathway will cause a Horner syndrome, so an assessment of the entire sympathetic pathway must be performed. A lesion of the first-order neuron is infrequent in children, but when present is typically caused by brain tumors involving the hypothalamus or brainstem. More common are lesions involving the second-order neuron due to neuroblastoma or birth-related nerve root or brachial plexus injury. The third-order neuron can be disrupted in the setting of intraoral trauma, nasopharyngeal tumors, vascular anomalies, and carotid artery dissection, among others. Though uncommon in the pediatric population, about 7% of all craniocervical arterial dissections have been reported to occur in children or adolescents [27]. Although the most common reported etiology of Horner syndrome in childhood is idiopathic (~40%), one large series found that up to one-third of children with Horner syndrome of unknown etiology harbored an underlying mass lesion, with neuroblastoma accounting for 9% of total Horner cases [28]. In this regard, prompt and thorough evaluation of patients

with unilateral ptosis and miosis is critical to prevent delay in diagnosis and treatment of potentially life-threatening underlying etiologies. Neuroblastoma presenting with ocular signs appears to have a better prognosis overall, likely because the ophthalmic findings triggered earlier diagnosis and treatment of the malignancy [29].

Patients with Horner syndrome are frequently asymptomatic, although older children, adolescents, or parents may complain of a droopy eyelid or different colored irides. Rarely do patients or parents note asymmetric sweating. Patients and/or parents should be queried for history or symptoms associated with craniocervical arterial dissection such as minor neck trauma, sports injuries, new headaches, jaw pain, or dysgeusia. The examiner should also elicit any history of birth injury or craniocervical trauma.

The ptosis of Horner syndrome is usually mild, rarely more than 2 mm relative to the other eye, and a subtle inverse ptosis (from dysfunction of the inferior tarsalis muscle) may be seen, which is strongly suggestive of Horner syndrome (Fig. 14.2). The resultant narrowing of the palpebral fissure may result in pseudoenophthalmos. The miotic pupil is ipsilateral to the ptotic eyelid, and the degree of anisocoria between the two pupils increases in dim lighting, with the smaller pupil dilating poorly. A *dilation lag* may be seen on the affected side when lights are suddenly turned off, with the miotic pupil dilating to its dim-light size more slowly than the contralateral pupil. The absence of visible dilation lag does not rule out Horner syndrome. An iris on the affected side that is lighter than the contralateral side, termed *iris heterochromia*, is indicative of congenital or very long-standing Horner syndrome (Fig. 14.1). Asymmetric facial perspiration may result from first- and second-order lesions. Lower intraocular pressure on the affected side may be noted because of disrupted sympathetic input to the ciliary body, resulting in decreased aqueous humor production. In acquired cases, mild conjunctival hyperemia may occur on the affected side. As neuroblastoma can cause palpable lesions, children should be examined for cervical and axillary masses.



Fig. 14.2 Idiopathic left Horner syndrome in a child with ipsilateral ptosis, miosis, and lighter iris (heterochromia)

Pharmacologic testing for Horner syndrome can determine the need for imaging studies. The *cocaine test* is used to *confirm* whether or not Horner syndrome is present. Cocaine normally causes pupillary dilation by inhibiting the reuptake of synaptic norepinephrine from the sympathetic nerve terminal on the dilator pupillae muscle. Failure of the pupil to dilate with cocaine, thus, indicates the absence of norepinephrine in the sympathetic terminal due to disruption at any point in the ipsilateral sympathetic pathway. One drop of 10% cocaine solution is applied in each eye, and then this is repeated 5 min later. If anisocoria of ≥1.0 mm (with the affected side smaller) is present 30–60 min later, this is considered a positive cocaine test and indicative of true Horner syndrome on the side of the smaller pupil [30]. In our experience, cocaine can be safely administered to infants 3 months of age and older. Because of increasing difficulty in obtaining cocaine, *apraclonidine testing* has been proposed as an alternative confirmatory test [31, 32], although significant side effects, such as sedation, have been reported in younger children [33]. Being a weak α_1-adrenergic agonist, apraclonidine will not dilate a normal pupil, but will dilate a pupil with sympathetic denervation, as the α_1-adrenergic receptors on the dilator pupillae muscle become upregulated in the absence of oculosympathetic input. This denervation hypersensitivity takes several days to develop fully. Apraclonidine testing is performed by placing one drop of 0.5% or 1% apraclonidine in each eye and reassessing the patient after 30–60 min; a reversal of the anisocoria (with the previously miotic pupil becoming larger) is considered a positive test. Reversal of ptosis and any conjunctival hyperemia on the affected side may also be seen and support the presence of Horner syndrome. Apraclonidine testing may not be reliable if it is performed in the acute phase (e.g., 1 week) after the onset of Horner syndrome, as denervation hypersensitivity has not yet developed. Hydroxyamphetamine, which is used to distinguish between first-/second-order and third-order neuronal lesion, is no longer used at most centers because of its questionable reliability and limited availability. Most importantly, patients whose clinical presentation is very consistent with Horner syndrome should undergo a diagnostic workup despite the result of pharmacologic testing. Currently our practice is to confirm Horner syndrome with cocaine in children 2 years and younger and use apraclonidine for this purpose in those older than 2.

Children with pharmacologically confirmed or clinically evident Horner syndrome less than 1 year in duration should undergo imaging of the entire oculosympathetic pathway to exclude an explanatory lesion of consequence, unless the history and/or examination reveal a clear, definite etiology [34]. The optimal imaging studies are MRI with and without

contrast of the brain, neck, and upper chest, as well as MRA of the neck to rule out carotid dissection or malformation. MRA is superior to CTA in detecting arterial dissection due to the ability to visualize the mural thrombus in addition to showing the narrowed true lumen, which is the only finding on CTA [35]. Carotid ultrasound is not a reliable study to rule out arterial dissection, as the artery cannot be completely visualized and many cases would be missed [36]. Though urinary homovanillic acid (HVA) and vanillylmandelic acid (VMA) may be elevated in neuroblastoma, this is very rarely the case in patients with purely ocular findings [28]. Thus, testing HVA and VMA in this clinical context has limited utility. If available, children with suspected Horner syndrome would benefit from prompt referral to a pediatric neuro-ophthalmologist for confirmatory testing and further diagnostic evaluation.

Third Nerve Palsy

Third (oculomotor) nerve palsy is a possibility that should always be entertained in setting of ptosis, pupillary changes, and/or ocular motility abnormalities. The most common etiologies for third nerve palsy in children are distinctly different from what is seen in adults. Congenital third nerve palsy, thought to originate from an in utero insult to the nerve or midbrain nucleus, accounted for ~15% to 50% of cases in various series [37–42]. Trauma is the most common cause of acquired pediatric third nerve palsies, while other common etiologies include neoplasms and infection/inflammation (e.g., meningitis) [37–42]. Recurrent ophthalmoplegic cranial neuropathy (previously called ophthalmoplegic migraine) is a rare cause of recurrent painful ophthalmoplegia involving the third cranial nerve in the vast majority of cases and is now thought to be an inflammatory cranial mononeuropathy, as evidenced by gadolinium enhancement of the affected oculomotor nerve on MRI [43–45] (Fig. 14.3). This entity is a diagnosis of exclusion, which can only be invoked after other etiologies have been ruled out by appropriate neuroimaging and lumbar puncture; steroids may be helpful if administered promptly. Aneurysmal third nerve palsy is very rare in the pediatric population but has been reported even in prepubescent children [46, 47]. Diabetic microvascular oculomotor nerve palsy has been reported in children, but is extremely rare [48].

Clinically, oculomotor nerve palsy presents with variable degrees of eyelid ptosis, pupillary dilation, and impaired ocular supraduction, adduction, and infraduction. Ptosis may vary from absent to complete. Levator palpebrae function in the ptotic eyelid is decreased. The pupil may vary from normal (*pupil sparing*) to mid-dilated (usually 5–6 mm) with no response to light or attempted viewing of a near target. The affected eye tends to be hypotropic and exotropic in primary gaze, though hypotropia may be seen in upgaze with hypertropia in downgaze ("alternating hypertropia"). Complete ptosis with a dilated nonreactive pupil and absent supraduction, infraduction, and adduction is termed a *complete third nerve palsy*; any findings short of complete palsy constitute a *partial third nerve palsy*. Cases of congenital palsy often show signs of *aberrant regeneration*: elevation of the eyelid in attempted adduction or infraduction, or pupillary miosis on attempted adduction or infraduction, among others. If third nerve palsy is suspected, the pupils, eyelids, and ocular motility must all be carefully evaluated, with attention to the pattern of ocular misalignment.



Fig. 14.3 Axial T1-weighted MRI with gadolinium demonstrating enhancement of the third nerve (*arrow*) in a patient with an oculomotor palsy due to ophthalmoplegic migraine

Unless there is a clear, definite etiology backed by the patient's history or examination findings, all pediatric patients found to have a third nerve palsy should undergo detailed imaging of their brain and orbits (with attention to the path of the involved third nerve), preferably with MRI with and without contrast. Though remote, the possibility of an aneurysm should be ruled out with an MRA. If imaging does not show an explanatory lesion, LP should be performed to rule out a meningitic or inflammatory cause. In children who are 10 or older, a cerebral angiogram should be performed if MRI/MRA and LP are unrevealing, given the potentially devastating consequences of an undiagnosed aneurysm in a patient with a very long expected life span [47]. Amblyopia is very common in children with congenital or irreversible acquired oculomotor nerve palsies, often necessitating patching, multiple strabismus surgeries to achieve alignment in primary gaze, and surgical management of ptosis.

Congenital Fibrosis of the Extraocular Muscles (CFEOM)

The congenital fibrosis syndromes are characterized by bilateral nonprogressive ptosis and ophthalmoparesis, which are present at birth. The extraocular muscle hypoplasia and fibrosis are thought to be the result of congenital cranial dysinnervation [49, 50]. Eight distinct entities have been described to date, CFEOM1A, CFEOM1B, CFEOM2, CFEOM3A, CFEOM3B, CFEOM3C, Tukel syndrome, and CFEOM3 with polymicrogyria, based on phenotypic and genetic features [50]. CFEOM1 consists of bilateral severe ptosis, downward-pointing eyes, and bilateral supraduction deficits and has been associated with absence of the superior division of the oculomotor nerve [49, 50]. CFEOM1 is an autosomal dominant disorder which has been associated with mutations in the KIF21A gene for CFEOM1A and TUBB3 gene for CFEOM1B. On the other hand, CFEOM2 is autosomal recessive and presents with bilateral ptosis, exotropia, and supraduction, infraduction, and adduction deficits. It is caused by a mutation in the PHOX2A/ARIX gene, resulting in bilateral absence of the third and fourth cranial nerves [49, 50]. CFEOM3 is characterized by variable and asymmetric ptosis, variable exotropia, and variable impairment of horizontal and vertical eye movements. The disorder is inherited in an autosomal dominant fashion. CFEOM3A is linked to mutations in TUBB3 or TUBB2B, CFEOM3B is associated with KIF21A mutations, and CFEOM3C is associated with a chromosomal translocation [50]. CFEOM3 with polymicrogyria has been associated with pathologic variants in TUBB2B. Tukel syndrome is an autosomal recessive condition that is characterized by the association of variable ptosis and variable ophthalmoparesis in the third nerve distribution with oligodactyly and oligosyndactyly of the hands. Imaging in congenital fibrosis patients often reveals atrophy of the extraocular muscles [50]. Management generally involves treatment of amblyopia, correction of refractive error, as well as strabismus and ptosis surgery.

Chronic Progressive External Ophthalmoplegia (CPEO) and Kearns-Sayre Syndrome (KSS)

Gradually progressive bilateral ptosis, ophthalmoplegia, and orbicularis oculi weakness are hallmarks of CPEO, which can present at any age. It may begin asymmetrically, or unilaterally, but over time invariably progresses to bilateral, relatively symmetric involvement [51]. Diplopia is rare in CPEO because of the general propensity for symmetric bilateral involvement. Eye movements are often limited in all directions with low saccadic velocities. KSS comprises the association of CPEO appearing before age 20 and pigmentary retinopathy with at least one of the following: ataxia, heart block, or elevated cerebrospinal fluid protein level. Other reported abnormalities in KSS include hypoparathyroidism, diabetes, short stature, dementia, and sensorineural hearing loss [52]. Both CPEO and KSS fall into the category of mitochondrial myopathies and are associated with mitochondrial dysfunction, ragged red fibers on muscle biopsy, and large mitochondrial DNA deletions [51–53]. No effective pharmacological therapy is available, and these patients sometimes require ptosis and strabismus surgery for symptomatic relief [54]. Referral to cardiology and endocrinology is frequently necessary for evaluation and management of the systemic complications.

Myotonic Muscular Dystrophy (MMD)

MMD is a progressive, dominantly inherited condition, usually presenting in early adulthood, characterized by progressive weakness of the facial, neck, and distal more than proximal limb muscles. The disease can present in childhood or even the neonatal period, and ophthalmic manifestations can include "Christmas tree" cataracts, bilateral ptosis, and, occasionally, variable (often mild) degrees of ophthalmoplegia. Other features include frontal balding, "hatchet facies" due to temporalis muscle atrophy, testicular atrophy, diabetes, variable intellectual impairment, and cardiac anomalies. A hallmark of the condition is delayed muscle relaxation (myotonia), which manifests with difficulty in rapidly releasing a tightly grasped object or persistent contraction of the thenar muscles after percussion. Electromyography demonstrates characteristic persistent muscle fiber discharges after activation, producing a "dive-bomber" sound. MMD results from the expansion of an unstable trinucleotide repeat (CTG) in the DMPK gene on chromosome 19. Genetic testing can be performed, and greater than 34 repeats are considered abnormal [55]. The disease is inherited in an autosomal dominant fashion, with anticipation (increasing severity) noted in successive generations. Treatments include various ion channel blocking agents to help with the myotonia. Patients occasionally need bilateral surgical repair of their ptosis.

Cavernous Sinus Thrombosis

Septic thrombosis of the cavernous sinus is a potentially life-threatening complication of severe oral, facial, ear, and neck infections, caused by the hematogenous, occasionally direct, spread of bacteria via the valveless veins of the skull base. The most common offending agents are *Streptococci* and *Staphylococci* [56]. The clinical presentation tends to be

acute with pain, fever, proptosis, periocular edema, impaired ocular motility, conjunctival injection, and elevated intraocular pressure from impaired venous drainage. The abducens nerve is often the first to be involved, but there is often rapid progression to involve other cranial nerves, and complete ophthalmoplegia can be seen. Vision loss can develop from ocular ischemia due to impaired venous drainage or embolization. Bilateral cavernous sinus involvement can occur within a few days [56]. In one pediatric series, cerebral infarction developed in over half of patients, often after anticoagulation was initiated [57]. Cerebrospinal fluid analysis in over a third of patients is consistent with bacterial meningitis, and most have positive blood cultures [56]. Both contrast-enhanced CT and contrast-enhanced MRI appear to be very sensitive diagnostic tests, revealing widening and enhancement of the involved cavernous sinus with narrowing of the carotid artery [57, 58].

The mainstay of therapy for cavernous sinus thrombosis is the prompt initiation if appropriate intravenous antibiotics and surgical drainage of the infected site, if applicable. It is unclear if the addition of anticoagulation is of benefit [57, 58]. Unilateral versus bilateral involvement does not seem to influence outcomes [58]. Fortunately, with prompt and aggressive antimicrobial therapy, mortality rates are relatively low (8%), with about 70–75% of affected children retaining excellent neurological function [57, 58].

Optic Nerve Glioma

Primary optic nerve gliomas in childhood are almost always pilocytic astrocytomas that are an intrinsic optic nerve tumor. The majority of patients present before 10 years of age, and roughly half (10–70%) have neurofibromatosis type 1 (NF-1) [59–61]. About half of NF-1 patients with an optic pathway glioma develop vision loss due to the tumor [61], though the rate of vision loss from purely optic nerve gliomas is clearly lower. The clinical course of NF-1-associated optic nerve gliomas is highly variable, with many patients exhibiting long-term visual stability, despite the fact that most tumors show at least some gradual long-term growth, often with stabilization and occasionally regression [59–63]. Gliomas in patients without NF-1 tend to be more symptomatic and may exhibit more aggressive behavior with a greater incidence of growth and vision loss [59]. Most asymptomatic sporadic optic nerve gliomas in the population probably never present for clinical evaluation, though, so the above conclusion may be the result of selection bias specifically favoring symptomatic patients.

Clinically, patients often present with variable proptosis and a variable degree of vision loss. A relative afferent pupillary defect may be seen on the affected side, and the optic nerve head may be normal, swollen, or pale. A sensory strabismus or unilateral fine nystagmus seen in the affected eye may be noted. With large gliomas, the eye will often appear proptotic and inferiorly displaced with hypoglobus and hypotropia. On imaging, fusiform enlargement and enhancement of the optic nerve is best seen with MRI [64] (Fig. 14.4), while the presence of a *pseudo-CSF sign*, consisting of T2 bright material within the optic nerve sheath surrounding a hypointense optic nerve, is considered characteristic of NF-1 [65]. The diagnosis of optic nerve gliomas can almost always be made clinically with the aid of imaging; optic nerve biopsy is rarely needed. Optic nerve tortuosity on baseline MRI in NF-1 patients appears to be predictive of the subsequent development of optic pathway gliomas, but not necessarily of vision loss [66].

Optic nerve gliomas can be highly amblyogenic, underlining the importance of regular screening for amblyopia in these patients. Patching can significantly and rapidly improve visual acuity in some patients [67]. Given the variable and unpredictable course of optic nerve gliomas, the decision to treat should be based on clinically worsening vision (despite aggressive management of amblyopia) and/or radiographic evidence of tumor growth [68]. Traditional therapeutic regimens include chemotherapy with vincristine and carboplatin (first-line), with other chemotherapeutic agents available (see Chap. 15). Although previously reported to markedly improve vision in chiasmal gliomas [69], it has also been our experience that bevacizumab has been an effective treatment for children with isolated optic nerve gliomas. Tumor resection should only be considered in patients with severe disfiguring proptosis or a blind, painful eye. Optic nerve gliomas are discussed in much more detail in Chap. 15 (Neuro-oncologic Considerations) and Chap. 35 (Benign Pediatric Orbital Tumors).



Fig. 14.4 Axial T1-weighted MRI with gadolinium showing enlargement and enhancement of the right optic nerve (*arrow*), consistent with an optic nerve glioma

References

1. Bever CT, Aquino AV, Penn AS, Lovelace RE, Rowland LP. Prognosis of ocular myasthenia. Ann Neurol. 1983;14(5):516–9.
2. Afifi AK, Bell WE. Tests for juvenile myasthenia gravis: comparative diagnostic yield and prediction of outcome. J Child Neurol. 1993;8(4):403–11.
3. Drachman DB. Myasthenia gravis. N Engl J med. 1994; 330(25):1797–810.
4. Kim JH, Hwang JM, Hwang YS, Kim KJ, Chae J. Childhood ocular myasthenia gravis. Ophthalmology. 2003;110(7):1458–62.
5. Ortiz S, Borchert M. Long-term outcomes of pediatric ocular myasthenia gravis. Ophthalmology. 2008;115(7):1245–8.e1.
6. Pineles SL, Avery RA, Moss HE, et al. Visual and systemic outcomes in pediatric ocular myasthenia gravis. Am J Ophthalmol. 2010;150(4):453–9.e3.
7. Drachman DB, Adams RN, Josifek LF, Self SG. Functional activities of autoantibodies to acetylcholine receptors and the clinical severity of myasthenia gravis. N Engl J Med. 1982;307(13):769–75.
8. Kaminski HJ, Maas E, Spiegel P, Ruff RL. Why are eye muscles frequently involved in myasthenia gravis? Neurology. 1990;40(11):1663–9.
9. Liu GT, Bienfang DC. Penicillamine-induced ocular myasthenia gravis in rheumatoid arthritis. J Clin Neuroophthalmol. 1990;10(3):201–5.
10. Negevesky GJ, Kolsky MP, Laureno R, Yau TH. Reversible atorvastatin-associated external ophthalmoplegia, anti-acetylcholine receptor antibodies, and ataxia. Arch Ophthalmol. 2000;118(3):427–8.
11. Wittbrodt ET. Drugs and myasthenia gravis. An update. Arch Intern Med. 1997;157(4):399–408.
12. Cogan DG. Myasthenia gravis: a review of the disease and a description of lid twitch as a characteristic sign. Arch Ophthalmol. 1965;74:217–21.
13. Odel JG, Winterkorn JM, Behrens MM. The sleep test for myasthenia gravis. A safe alternative to Tensilon. J Clin Neuroophthalmol. 1991;11(4):288–92.
14. Lindstrom JM, Seybold ME, Lennon VA, Whittingham S, Duane DD. Antibody to acetylcholine receptor in myasthenia gravis. Prevalence, clinical correlates, and diagnostic value. Neurology. 1976;26(11):1054–9.
15. Vincent A, Newsom Davis J. Anti-acetylcholine receptor antibodies. J Neurol Neurosurg Psychiatry. 1980;43(7):590–600.
16. Soliven BC, Lange DJ, Penn AS, et al. Seronegative myasthenia gravis. Neurology. 1988;38(4):514–7.
17. Peeler CE, De Lott LB, Nagia L, Lemos J, Eggenberger ER, Cornblath WT. Clinical utility of acetylcholine receptor antibody testing in ocular myasthenia gravis. JAMA Neurol. 2015;72(10):1170–4.
18. Andrews PI, Massey JM, Sanders DB. Acetylcholine receptor antibodies in juvenile myasthenia gravis. Neurology. 1993;43(5):977–82.
19. Anlar B, Ozdirim E, Renda Y, et al. Myasthenia gravis in childhood. Acta Paediatr. 1996;85(7):838–42.
20. Howard FM, Lennon VA, Finley J, Matsumoto J, Elveback LR. Clinical correlations of antibodies that bind, block, or modulate human acetylcholine receptors in myasthenia gravis. Ann N Y Acad Sci. 1987;505:526–38.
21. Evoli A, Tonali PA, Padua L, et al. Clinical correlates with anti-MuSK antibodies in generalized seronegative myasthenia gravis. Brain. 2003;126(Pt 10):2304–11.
22. Guptill JT, Sanders DB, Evoli A. Anti-MuSK antibody myasthenia gravis: clinical findings and response to treatment in two large cohorts. Muscle Nerve. 2011;44(1):36–40.
23. Takahashi Y, Sugiyama M, Ueda Y, et al. Childhood-onset anti-MuSK antibody positive myasthenia gravis demonstrates a distinct clinical course. Brain Dev. 2012;34(9):784–6.
24. Parikh K, Vaidya A, Jain R. Preliminary results of VATS thymectomy for pediatric myasthenia gravis. Pediatr Surg Int. 2011;27(6):595–8.
25. Finnis MF, Jayawant S. Juvenile myasthenia gravis: a paediatric perspective. Autoimmune Dis. 2011;2011:404101.
26. Engel AG, Shen XM, Selcen D, Sine SM. Congenital myasthenic syndromes: pathogenesis, diagnosis, and treatment. Lancet Neurol. 2015;14(4):420–34.
27. Schievink WI, Mokri B, Piepgras DG. Spontaneous dissections of cervicocephalic arteries in childhood and adolescence. Neurology. 1994;44(9):1607–12.
28. Mahoney NR, Liu GT, Menacker SJ, Wilson MC, Hogarty MD, Maris JM. Pediatric Horner syndrome: etiologies and roles of imaging and urine studies to detect neuroblastoma and other responsible mass lesions. Am J Ophthalmol. 2006;142(4):651–9.
29. Musarella MA, Chan HS, Deboer G, Gallie BL. Ocular involvement in neuroblastoma: prognostic implications. Ophthalmology. 1984;91(8):936–40.
30. Kardon RH, Denison CE, Brown CK, Thompson HS. Critical evaluation of the cocaine test in the diagnosis of Horner's syndrome. Arch Ophthalmol. 1990;108(3):384–7.
31. Bacal DA, Levy SR. The use of apraclonidine in the diagnosis of Horner syndrome in pediatric patients. Arch Ophthalmol. 2004;122(2):276–9.
32. Chen PL, Hsiao CH, Chen JT, Lu DW, Chen WY. Efficacy of apraclonidine 0.5% in the diagnosis of Horner syndrome in pediatric patients under low or high illumination. Am J Ophthalmol. 2006;142(3):469–74.
33. Watts P, Satterfield D, Lim MK. Adverse effects of apraclonidine used in the diagnosis of Horner syndrome in infants. J AAPOS. 2007;11(3):282–3.
34. Kadom N, Rosman NP, Jubouri S, Trofimova A, Egloff AM, Zein WM. Neuroimaging experience in pediatric Horner syndrome. Pediatr Radiol. 2015;45(10):1535–43.
35. Shah GV, Quint DJ, Trobe JD. Magnetic resonance imaging of suspected cervicocranial arterial dissections. J Neuroophthalmol. 2004;24(4):315–8.
36. Arnold M, Baumgartner RW, Stapf C, et al. Ultrasound diagnosis of spontaneous carotid dissection with isolated Horner syndrome. Stroke. 2008;39(1):82–6.
37. Miller NR. Solitary oculomotor nerve palsy in childhood. Am J Ophthalmol. 1977;83(1):106–11.
38. Harley RD. Paralytic strabismus in children. Etiologic incidence and management of the third, fourth, and sixth nerve palsies. Ophthalmology. 1980;87(1):24–43.
39. Keith CG. Oculomotor nerve palsy in childhood. Aust N Z J Ophthalmol. 1987;15(3):181–4.
40. Ing EB, Sullivan TJ, Clarke MP, Buncic JR. Oculomotor nerve palsies in children. J Pediatr Ophthalmol Strabismus. 1992;29(6):331–6.
41. Kodsi SR, Younge BR. Acquired oculomotor, trochlear, and abducent cranial nerve palsies in pediatric patients. Am J Ophthalmol. 1992;114(5):568–74.
42. Schumacher-feero LA, Yoo KW, Solari FM, Biglan AW. Third cranial nerve palsy in children. Am J Ophthalmol. 1999;128(2):216–21.
43. Förderreuther S, Ruscheweyh R. From ophthalmoplegic migraine to cranial neuropathy. Curr Pain Headache rep. 2015;19(6):21.
44. Ambrosetto P, Nicolini F, Zoli M, Cirillo L, Feraco P, Bacci A. Ophthalmoplegic migraine: from questions to answers. Cephalalgia. 2014;34(11):914–9.
45. Gelfand AA, Gelfand JM, Prabakhar P, Goadsby PJ. Ophthalmoplegic "migraine" or recurrent ophthalmoplegic cranial neuropathy: new cases and a systematic review. J Child Neurol. 2012;27(6):759–66.
46. Yang YC, Laws DE, Chandna A. The rules of third nerve palsy in children. Eye (Lond). 1996;10(Pt 5):646–7.
47. Liu GT, Volpe NJ, Galetta SL. Eye movement disorders: third, fourth, and sixth nerve palsies and other causes of diplopia and

ocular misalignment. In: Liu GT, Volpe NJ, Galetta SL, editors. Neuro-ophthalmology: diagnosis and management. 2nd ed. Saunders Elsevier: New York; 2010.
48. Grunt JA, Destro RL, Hamtil LW, Baska RE. Ocular palsies in children with diabetes mellitus. Diabetes. 1976;25(5):459–62.
49. Heidary G, Engle EC, Hunter DG. Congenital fibrosis of the extraocular muscles. Semin Ophthalmol. 2008;23(1):3–8.
50. Whitman M, Hunter DG, Engle EC. Congenital fibrosis of the extraocular muscles. In: Pagon RA, Adam MP, Ardinger HH, Wallace SE, Amemiya A, Bean LJH, Bird TD, Fong CT, Mefford HC, Smith RJH, Stephens K, editors. GeneReviews® [Internet]. Seattle: University of Washington, Seattle; 1993–2016. http://www.ncbi.nlm.nih.gov/books/NBK1348/. Updated January 14, 2016. Accessed April 17, 2016.
51. Caballero PE, Candela MS, Alvarez CI, Tejerina AA. Chronic progressive external ophthalmoplegia: a report of 6 cases and a review of the literature. Neurologist. 2007;13(1):33–6.
52. Phadke M, Lokeshwar MR, Bhutada S, et al. Kearns Sayre syndrome – Case report with review of literature. Indian J Pediatr. 2012;79(5):650–4.
53. Mitsumoto H, Aprille JR, Wray SH, Nemni R, Bradley WG. Chronic Progressive External Ophthalmoplegia (CPEO): clinical, morphologic, and biochemical studies. Neurology. 1983;33(4):452–61.
54. Bau V, Zierz S. Update on chronic progressive external ophthalmoplegia. Strabismus. 2005;13(3):133–42.
55. Greenberg DA, Aminoff MJ, Simon RP. Motor disorders. In: Greenberg DA, Aminoff MJ, Simon RP, editors. Clinical neurology. 8th ed. New York: McGraw-Hill; 2012.
56. Dinubile MJ. Septic thrombosis of the cavernous sinuses. Arch Neurol. 1988;45(5):567–72.
57. Press CA, Lindsay A, Stence NV, Fenton LZ, Bernard TJ, Mirsky DM. Cavernous sinus thrombosis in children: imaging characteristics and clinical outcomes. Stroke. 2015;46(9):2657–60.
58. Smith DM, Vossough A, Vorona GA, Beslow LA, Ichord RN, Licht DJ. Pediatric cavernous sinus thrombosis: a case series and review of the literature. Neurology. 2015;85(9):763–9.
59. Wright JE, McNab AA, McDonald WI. Optic nerve glioma and the management of optic nerve tumours in the young. Br J Ophthalmol. 1989;73(12):967–74.
60. Listernick R, Charrow J, Greenwald M, Mets M. Natural history of optic pathway tumors in children with neurofibromatosis type 1: a longitudinal study. J Pediatr. 1994;125(1):63–6.
61. Balcer LJ, Liu GT, Heller G, et al. Visual loss in children with neurofibromatosis type 1 and optic pathway gliomas: relation to tumor location by magnetic resonance imaging. Am J Ophthalmol. 2001;131(4):442–5.
62. Alvord EC, Lofton S. Gliomas of the optic nerve or chiasm. Outcome by patients' age, tumor site, and treatment. J Neurosurg. 1988;68(1):85–98.
63. Dutton JJ. Gliomas of the anterior visual pathway. Surv Ophthalmol. 1994;38(5):427–52.
64. Haik BG, Saint Louis L, Bierly J, et al. Magnetic resonance imaging in the evaluation of optic nerve gliomas. Ophthalmology. 1987;94(6):709–17.
65. Brodsky MC. The "pseudo-CSF" signal of orbital optic glioma on magnetic resonance imaging: a signature of neurofibromatosis. Surv Ophthalmol. 1993;38(2):213–8.
66. Levin MH, Armstrong GT, Broad JH, et al. Risk of optic pathway glioma in children with neurofibromatosis type 1 and optic nerve tortuosity or nerve sheath thickening. Br J Ophthalmol. 2016;100(4):510–4.
67. Kushner BJ. Functional amblyopia associated with abnormalities of the optic nerve. Arch Ophthalmol. 1984;102(5):683–5.
68. Tow SL, Chandela S, Miller NR, Avellino AM. Long-term outcome in children with gliomas of the anterior visual pathway. Pediatr Neurol. 2003;28(4):262–70.
69. Avery RA, Hwang EI, Jakacki RI, Packer RJ. Marked recovery of vision in children with optic pathway gliomas treated with bevacizumab. JAMA Ophthalmol. 2014;132(1):111–4.

Neuro-Oncologic Considerations in Pediatric Oculoplastic Surgery

15

Peter de Blank, Michael D. Coffey, and Michael J. Fisher

Introduction

Primary orbital and periorbital tumors are rare in children and usually benign [1]. While some may threaten life, others may cause vision loss and disfigurement. For tumors that threaten only vision, treatment should balance the potential benefit of vision preservation against the potential late effects of surgery and other therapies. Clinical management of orbital tumors varies depending on tumor type and can present challenges to the oculoplastic surgeon. These tumors are best treated by a team of physicians with expertise in the orbital surgery, medical oncology, and radiation oncology as well as any underlying genetic predisposition.

Epidemiological information about orbital and periorbital tumors is scant and often derives from major referral centers whose data may be skewed by population bias based on the orbital tumors in which they specialize [2, 3]. A review of these reports demonstrates that the most common masses that arise in or near the orbit include benign cysts, inflammatory masses, and vascular lesions, accounting for 50–75% of patients seen [4]. Masses that are frequently managed with the input of a pediatric neuro-oncologist include benign or malignant tumors with intracranial extension, those that threaten to invade intracranially or that are commonly seen in genetic tumor predisposition syndromes (such as neurofibromatosis types 1 and 2).This chapter will review the most common primary orbital tumors, including optic pathway or optic nerve gliomas, optic nerve sheath meningiomas, orbital/periorbital plexiform neurofibromas (OPPN), and orbital rhabdomyosarcoma. It will review the epidemiology of these masses, their common clinical and radiographic presentations, their diagnosis and treatment considerations, as well as areas of future research. This chapter is not exhaustive, but is intended to provide an introduction to the concerns and considerations of the pediatric oncologist when considering orbital and periorbital masses.

P. de Blank (✉)
Division of Oncology, Cincinnati Children's Hospital Medical Center, Cincinnati, OH, USA

Department of Pediatrics, Cincinnati Children's Hospital Medical Center, Cincinnati, OH, USA
e-mail: peter.deblank@cchmc.org

M.D. Coffey
Radiology, University Hospitals Cleveland Medical Center, Cleveland, OH, USA

M.J. Fisher
Department of Pediatrics, Perelman School of Medicine at the University of Pennsylvania, Philadelphia, PA, USA

Neurofibromatosis Program, Neuro-Oncology Section, Center for Childhood Cancer Research, Philadelphia, PA, USA

Division of Oncology, The Children's Hospital of Philadelphia, Philadelphia, PA, USA

Optic Nerve Gliomas

Epidemiology

Optic nerve gliomas make up approximately 1.5–3% of all orbital tumors and are the most common tumor of the optic nerve [4]. They belong to a group of low-grade tumors called optic pathway gliomas (OPGs), which can arise anywhere along the optic pathway, including the optic nerve, chiasm, optic tract, or optic radiation, and represent 2–5% of pediatric gliomas [5]. Optic pathway gliomas are the most common brain tumor seen in children with neurofibromatosis type 1 (NF1), affecting as many as 15–20% of children with NF1 [6–8]. Although many NF1-associated OPGs are asymptomatic, vision loss can occur in up to 50% of affected children with NF1. In sporadic cases not associated with NF1, vision loss is a more common presentation [9, 10]. OPGs are frequently identified in children less than 6 years of age [8], although symptomatic OPGs may also develop in older children and adults [11].

Most OPGs involve the optic nerve and chiasm, but approximately 50% of tumors also affect more posterior structures including the optic tracts and radiations [10].

© Springer International Publishing AG 2018

J.A. Katowitz, W.R. Katowitz (eds.), *Pediatric Oculoplastic Surgery*, https://doi.org/10.1007/978-3-319-60814-3_15

Sporadic lesions are found more frequently in the chiasm and more frequently extend beyond the optic pathway [12]. Tumors that are limited to anterior structures (optic nerve, optic chiasm) have been associated with less aggressive behavior and better visual acuity outcomes [10, 13, 14]. However, recent reports suggest that tumor location and its effect on clinical outcome may be different for males and females. In a retrospective analysis of clinical data, optic pathway tumors restricted to the optic nerve were found equally in both males and females; however, females with NF1 and an optic nerve tumor required treatment three times more frequently than males with tumor restricted to optic nerve [15, 16].

Clinical Presentation

Asymptomatic ONGs may be identified during routine ophthalmologic screen (e.g., by noting optic pallor), which is standard practice for children with NF1, or by MR imaging for another indication. Although symptomatic ONGs commonly present with vision loss, young children rarely report decreased vision to parents or caregivers, and vision loss may be severe by the time the ONG is discovered [9, 17]. Proptosis is a frequent presentation to ophthalmic surgeons [18]. Other findings may include visual field loss, nystagmus, strabismus, amblyopia, and dyschromatopsia. Chiasm tumors may extend into the hypothalamus and cause precocious puberty, which may be the first manifestation of the glioma [17, 19].

Diagnostic Imaging

MRI is the gold standard for the diagnosis and surveillance of ONGs. Biopsy is not necessary for lesions with characteristic clinical and imaging features, especially in children with NF1. Biopsy may be considered when imaging is atypical and the diagnosis is in doubt; however, in most cases the risk of further vision loss from surgery outweighs the benefit [19].

On MRI, these tumors classically demonstrate sharply circumscribed fusiform thickening of the optic nerve. ONGs appear isointense on T1-weighted images and iso- to hyperintense on T2-weighted sequences (Fig. 15.1). Many tumors demonstrate gadolinium enhancement, but this is more commonly seen in sporadic rather than NF1-associated tumors [20]. Bilateral ONG is found almost exclusively in children with NF1. Tumor expansion may also cause kinking of the intraorbital segment of the optic nerve, and dilatation of the subarachnoid sleeve surrounding the optic nerve is common [21]. Optic nerve tortuosity is also common in children with NF1 [22]. Although tortuosity alone is not diagnostic of ONG, this finding may be associated with future development of ONG in children with NF1 [23].

Pathology

ONGs are histopathologically low-grade gliomas, typically pilocytic astrocytomas (WHO grade I), although other low-grade glioma histologies have been reported [24–26]. There is no histological difference between NF1-associated and sporadic versions [27]. By light microscopy, these tumors are composed of astrocytes that stain for glial fibrillary acidic protein (GFAP), often with characteristic Rosenthal fibers. Tumors which lack these characteristic findings may be classified as fibrillary (WHO grade II) tumors; however, tumor grade has not been correlated with tumor progression or behavior [28, 29].

Treatment Considerations

ONGs rarely threaten life but may threaten vision [30]. The goal of therapy, therefore, is to preserve vision. Surgery is rarely recommended since biopsy is usually unnecessary and surgical resection will sacrifice remaining vision. However, surgery may be useful for solitary optic nerve gliomas causing disfiguring and painful proptosis with blindness in the affected eye.

Early reports were concerned that solitary, progressive ONGs may progress into the chiasm or posterior structures and suggested consideration of surgical excision to prevent extension of the tumor [31]. However, more recent studies have demonstrated that tumor cells can be found in apparently normal tissue distant from the resected tumor mass, suggesting that surgical resection does not eliminate tumor risk [32]. To our knowledge, imaging progression of a solitary nerve glioma into the chiasm is extremely rare, and there is no evidence that surgical resection of a solitary ONG will prevent vision loss in the contralateral eye. Thus, performing surgery to prevent progression of the tumor to the chiasm is controversial and usually not recommended [33].

Children with NF1 and ONG that require treatment are most commonly treated with carboplatin-based chemotherapy regimens. Carboplatin and vincristine result in a 5-year progression-free survival of 69% in children with NF1 [34]. Visual acuity appears to improve in approximately one-third of children with NF1 treated with chemotherapy and remains stable in another one-third [14]. Treatment with radiation is associated with 10-year progression-free survival between 65% and 90% [35–38]. However, radiation is often avoided, especially in children with NF1, due to the associated risks of second malignancy, cerebrovascular disease, and endocrinopathies [36, 39, 40]. Chemotherapy options for children with sporadic ONG are broader, but

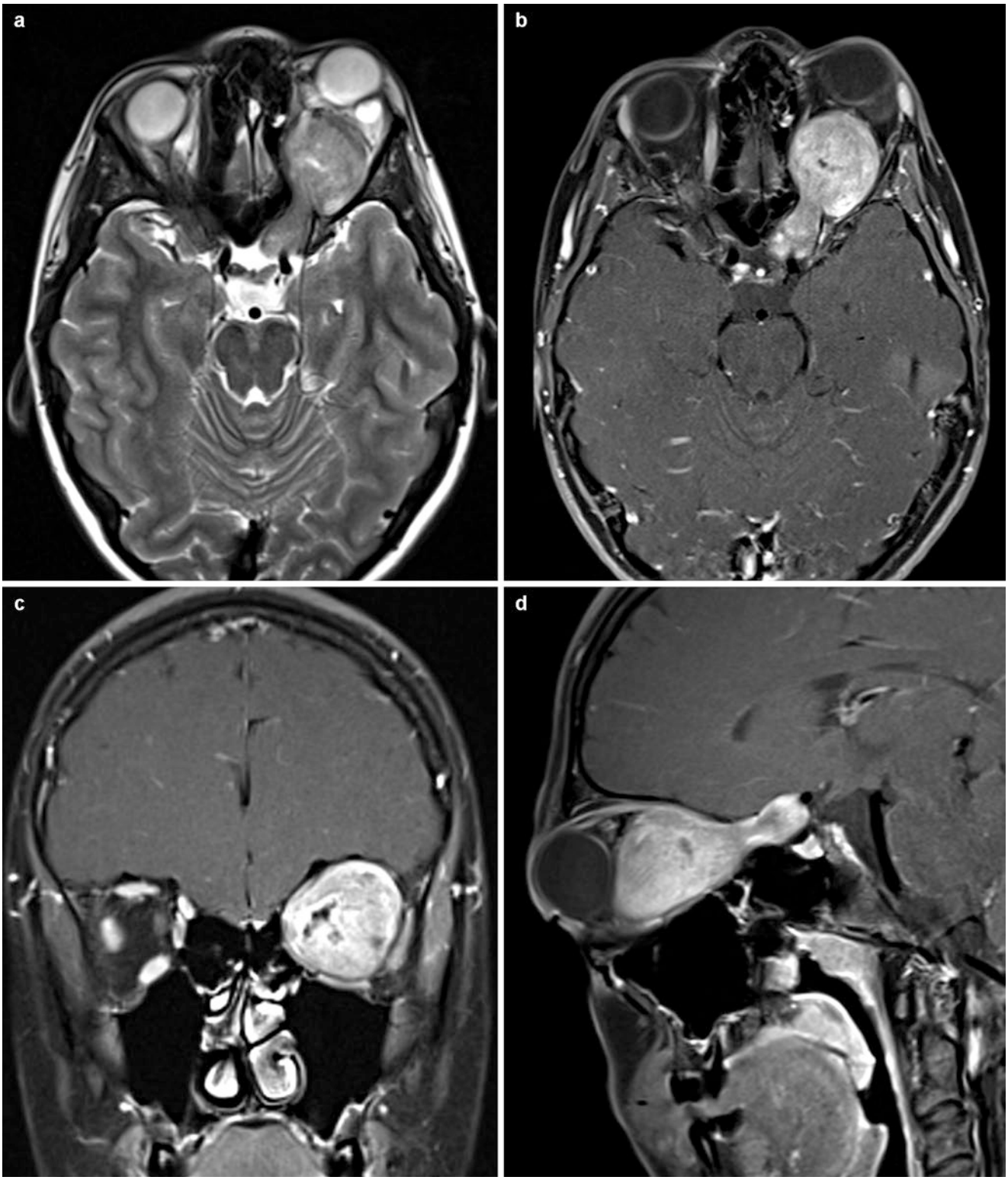


Fig. 15.1 A subject with left-sided optic nerve glioma with associated proptosis. The tumor appears mildly hyperintense on T2-weighted images (**a**) On fat-saturated, contrast-enhanced T1-weighted images in the axial (**b**), coronal (**c**), and sagittal (**d**) planes, the tumor appears brightly enhancing

not as effective. The most studied regimens are carboplatin and vincristine or thioguanine, procarbazine, lomustine, and vincristine (TPCV). In a randomized study in children with sporadic low-grade glioma, the 5-year event-free survival was 39% for carboplatin and vincristine and 52% for TPCV, although the difference was not statistically significant ($p = 0.10$) [30].

Future Directions

Historically, surgical resections for optic nerve gliomas required a combined intraorbital and intracranial approach that can result in significant morbidity and incomplete resection [32]. Recently, a globe-sparing approach by lateral orbitotomy was described in three children with sporadic optic nerve glioma [41]. In all three cases, the orbital and intraconal portions of the optic nerve and tumor were resected by lateral orbitotomy with excellent cosmetic results and normal retinal perfusion 8–40 months after the procedure. Residual tumor 2–3 mm posterior to the globe and in the prechiasmal optic nerve showed no evidence of progression on follow-up imaging. This less invasive approach to tumor debulking for disfiguring proptosis may limit complications and spare the orbit; however, further study is warranted with longitudinal follow-up to understand the implications of this novel method.

Optic Nerve Sheath Meningioma

Epidemiology

Optic nerve sheath meningioma (ONSM) is the most common primary tumor arising from the optic nerve sheath. It constitutes 2–5% of all primary orbital tumors and 2% of all meningiomas [2, 21]. ONSM is usually a disease of adulthood, and patients younger than 20 years account for only 4% of all primary ONSM [42]. The vast majority of primary pediatric cases arise from the intraorbital nerve sheath, with only 8% deriving from the intracanalicular region [42]. A female predominance is noted in both adult and pediatric ONSM [43].

Exposure to radiation is one of the most consistent risk factors associated with developing meningioma [21, 44]. Meningiomas frequently express hormone receptors (estrogen, progesterone, and/or androgen) and have been reported to change in size during pregnancy and menopause, leading many researchers to consider the relationship between endogenous and exogenous hormones and meningioma risk. However, studies examining exogenous (e.g., use of oral contraceptives or hormone replacement therapy) or endogenous (e.g., parity, age at menarche, menopausal status) hormones have not demonstrated a consistent risk of meningioma [44].

Clinical Presentation

The classic triad of optic atrophy, visual loss, and opticociliary shunt vessels is pathognomonic for ONSM but occurs as a triad in a minority of patients [42, 45]. The more common presentation includes painless, progressive visual acuity loss or visual field deficit over 1–5 years [45, 46]. In a review of primary pediatric ONSM, the most common clinical features included visual acuity loss (80%), visual field defects (48%), mild to moderate proptosis that was generally <5 mm (68%), optic disc atrophy (63%), optic disc edema (38%), and optociliary shunt vessels (28%) [43].

In children, ONSM is often associated with NF2. In a review of the literature, 5–7% of patients with NF2 also had ONSM, although these were not population-based studies and selection bias was unavoidable [47]. However, up to 10% of children with isolated meningioma eventually develop clinical stigmata of NF2 [48], and ONSM in a child should prompt evaluation for other stigmata of NF2.

Diagnostic Imaging

On CT imaging, ONSM may demonstrate areas of calcification. Although CT is useful for assessing configuration, bony changes, and calcification [1], MRI is superior for the assessment of soft-tissue involvement in the orbit and the evaluation of intracranial extension [43]. Fat-suppressed MR imaging with gadolinium contrast is the modality of choice for the evaluation of these tumors (Fig. 15.2). ONSMs are generally iso- or hypointense on T1-weighted images and hyperintense on T2-weighted images [49]. They are homogeneously enhancing masses that surround the optic nerve, which may be central or eccentrically positioned [1]. Meningiomas may cause an expansile mass or a thin sheet around the optic nerve, termed "en plaque meningioma" [1], which produces a "tram track" sign (when imaging along the length of the optic nerve) or "target sign" (on coronal imaging) [50]. Because of their hypercellular nature, meningiomas often show restricted diffusion with low apparent diffusion coefficient (ADC) values on diffusion-weighted imaging [51, 52].

Pathology

Two histologic patterns of meningioma are most common: a meningothelial pattern is characterized by sheets of polygon-shaped cells with interspersed vasculature trabeculae, and a transitional pattern demonstrates whorls of concentric spindle cells with occasional psammoma bodies [45, 46]. Among limited specimens in children, transitional and meningothelial were the most common histologic subtypes [43]. Meningiomas are graded as well-differentiated

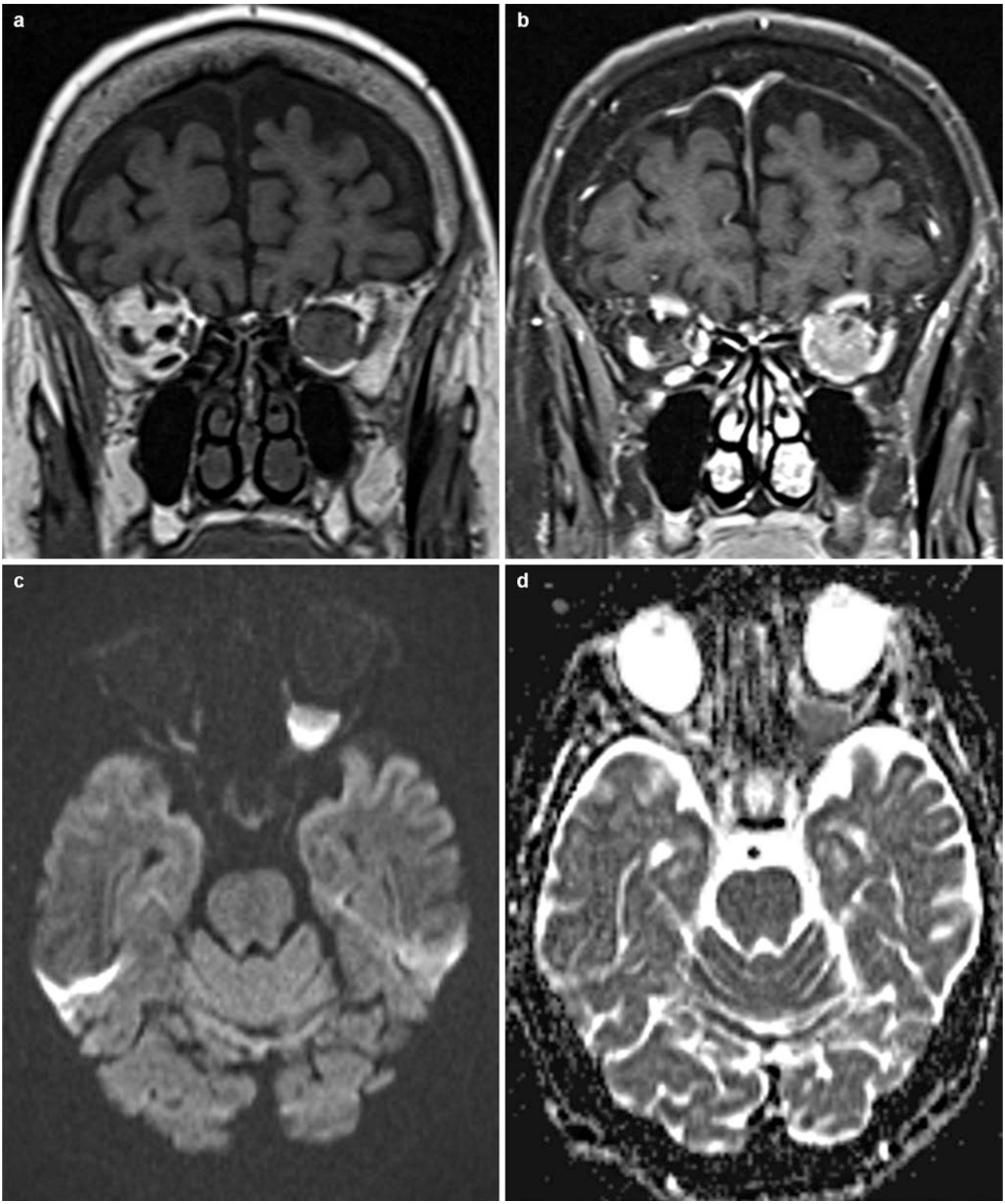


Fig. 15.2 Optic nerve sheath meningioma seen in coronal section within the left orbit on T1-weighted images (**a**) and T2-weighted images with fat saturation (**b**). Axial diffusion (**c**) and apparent diffusion coefficient (ADC) (**d**) images reveal restricted diffusion typical of these tumors

(WHO grade I), atypical (WHO grade II), or malignant (WHO grade III). In patients of all ages, WHO grade I histology is the most common in ONSM.

Treatment Considerations

Similar to ONGs, treatment for ONSM is commonly intended to preserve vision and is rarely required to preserve life. Pediatric ONSM is often considered more aggressive than its adult counterpart and is associated with higher rates of intracranial extension and recurrence [42, 45, 46, 53]. However, tumor-related mortality is no higher among children than adults, and in small cohorts, there has been no increased risk to vision in the contralateral eye among younger patients. There have been no reported deaths due to primary ONSM in children [43].

Vision loss in ONSM is thought to be caused by vascular compromise due to mass effect on the pia mater inducing ischemic changes that interfere with axonal transport [54]. Surgical resection is often impossible without significant risk of blindness in the affected eye [45, 46]. Fortunately, surgical biopsy is largely unnecessary, given the typical imaging features, examination findings, and clinical presentation of ONSM, although some have recommended biopsy in pediatric cases due to their relative rarity [43, 54]. Likewise, surgical fenestration of the dural sheath is rarely used because any observed improvements are frequently temporary due to continued tumor progression [54]. Surgical resection is therefore reserved for those patients who have already experienced significant compromise to their vision, those with disfiguring proptosis, or those with intracranial extension at risk for contralateral involvement [42].

Stereotactic fractionated radiotherapy is the therapy of choice for most adult patients and results in preservation or improvement in vision in approximately 80% of patients [54]. In a review of 64 subjects treated for ONSM and followed for at least 50 months, radiation alone preserved visual acuity, while other treatment modalities were associated with decreased visual acuity [55]. However, it is important to note that late complications of radiation can be substantial. Orbital radiation has been associated with local dermatologic changes, radiation retinopathy, central retinal artery occlusions, encephalopathy, and premature atherosclerosis, as well as secondary meningiomas [43]. Although conformal radiation is used routinely in adults, few cases in children have been documented, and the potential benefits of radiation in terms of stabilization of vision must be balanced against the risk of radiation-induced toxicities measured over the remaining life span of the patient.

Suspected pediatric primary ONSM should prompt investigation of concurrent NF2, and radiation should be avoided in individuals with NF2 whenever possible due to the increased risk of secondary malignant neoplasm or malignant transformation [56, 57]. If the ONSM is sporadic, vision is severely compromised and the tumor is limited to the orbit, then surgical resection can be curative. If vision is threatened but usable vision can be maintained, the risks and benefits of radiation therapy should be weighed for each case individually [43].

Future Directions

Children with NF2 treated with ionizing radiation have approximately 10 times the risk of developing a secondary neoplasm compared to children with NF2 treated conservatively [57]. However, there have been few studies to date investigating the late effects of radiation therapy in children with NF2-related ONSMs. Patients with NF2 are at increased risk for secondary tumors due to a defect in the NF2 tumor suppressor gene, and radiotherapy may present an increased burden to this population [47]. While visual loss will generally occur in untreated ONSM, it often is slow, is limited to the affected eye, and is not associated with mortality [58]. Further research in the late effects of treatment in children with NF2 is needed to help inform the clinical management of these tumors.

Orbital/Periorbital Plexiform Neurofibroma

Epidemiology

Plexiform neurofibromas (PN) are common benign tumors of peripheral nerves associated with NF1. These tumors often arise in the first decade of life and can involve any peripheral nerve although sensory nerve involvement of the orbit and periorbital region is common [21]. Plexiform neurofibromas that infiltrate the orbit, temporal region, and/or eyelids are called orbitotemporal plexiform neurofibromas (OPPN) and can cause significant disfigurement and interfere with vision [59]. Most of these tumors present within the first 2 years of life [59, 60]. Incidence of NF1-associated PN throughout the body ranges from 20% to more than 50% [61, 62]. The incidence of OPPN in NF1 is unknown but likely less than 10%.

Most PN are believed to be congenital and grow rapidly during early childhood [60], whereas PN found in adults may be more stable [63, 64]. Plexiform neurofibromas have an approximately 10% lifetime risk of transformation to malignant peripheral nerve sheath tumors over a lifetime, but the risk of malignant transformation specifically in OPPN is unknown.

Presentation

Most OPPN occur in the setting of NF1. Although OPPN are less common than ONG in children with NF1, their effects can be equally devastating to vision. Infiltration behind the orbit can cause proptosis, compression of the eye affecting globe length with resultant refractive error, as well as expansion of the eyelids and periorbital structures causing ptosis and obstruction of vision. These unilateral changes affecting the globe and visual axis put children at risk for amblyopia [59]. Etiologies of amblyopia can also include strabismus, occlusion, anisometropia, as well as the other etiologies described above.

OPPN often presents as a nodular periorbital mass, eventually progressing to mechanical blepharoptosis and eventually amblyopia. OPPN may extend into neighboring structures (forehead, midface) to cause further disfigurement and can invade the cavernous sinus. OPPN may also be associated with sphenoid wing dysplasia, thus allowing communication between the middle cranial fossa and the orbit with potential compression of the extraocular muscle and the optic nerve by the anterior temporal lobe [65].

Diagnostic Imaging

MR is frequently used to evaluate OPPN and assess its extension into soft tissues of the periorbital region. OPPN commonly appear as a nodular mass that infiltrates soft tissues (Fig. 15.3). The tumor is most often isointense on T1-weighted images and typically hyperintense on T2-weighted images. Areas of central low signal can frequently be seen on T2-weighted images. Tumors demonstrate variable contrast enhancement [1, 21]. OPPN may be difficult to distinguish from schwannomas, but OPPN are generally more infiltrative [1]. In addition, when there is clinical suspicion, PET imaging can help to detect sarcomatous transformation of PN [66, 67].

Pathology

Neurofibromas are benign nerve sheath tumors that form circumscribed tan-white masses when examined grossly. PN form large multinodular masses that are defined by their involvement of numerous nerve fascicles or multiple components of a nerve plexus. Microscopically, PN often show an admixture of areas resembling localized and diffuse-type neurofibromas [68]. Degenerative atypia, in the absence of hypercellularity, has been interpreted by some pathologists as "atypical neurofibroma," and there are concerns that such findings are a precursor for malignant transformation.

Treatment Considerations

Although guidelines for surveillance are not well established, children with OPPN should undergo comprehensive ophthalmologic evaluation regularly to test visual acuity, evaluate motility, and assess intraocular pressure and cycloplegic refraction [59]. Ophthalmologic examinations should occur biannually while children are young and at increased risk of continued tumor growth [59, 64].

Newly diagnosed OPPN should be observed, as many of these tumors will not progress. Unfortunately, there are no proven medical therapies to shrink or stop OPPN growth. Although some have attempted early surgical treatment to avoid further deformity and preserve vision [65, 69], surgical resection is typically not curative and usually consists of debulking procedures with reconstruction and ptosis repair [60].

The success of surgical resection is limited by the high risk of recurrence in subtotally resected tumors, particularly in young children [59, 70]. Debulking may be considered for visual decline, progressive disfigurement, or tumor progression toward a critical structure, but disease recurrence with functional and aesthetic relapse should be expected [63, 71]. In one sense, the term recurrence is really a misnomer as complete tumor resection is rare, and thus residual tumor can still continue to grow. Associated ophthalmic complications of OPPN, such as strabismus, amblyopia, and ptosis, should be treated nonsurgically whenever possible, but concerns for amblyopia as well as disfigurement may become important considerations for surgical intervention. Because recurrence is so common and OPPN management is multidisciplinary, children with OPPN should be referred to a specialist with experience in PN and supported by a multidisciplinary NF clinic.

Future Directions

Despite the impact that these tumors can have on vision and physical deformity in children with NF1, few guidelines exist regarding best clinical practices. Children with OPPN require coordinated, multidisciplinary care from ophthalmologists, surgeons, and oncologists well versed in NF1. The rise of new medications targeted at the molecular abnormalities within the tumor raises the possibility of effective therapies in the future [72]. In fact, a recent phase I study of the MEK inhibitor selumetinib has resulted in partial responses in over half of PN treated [73].

Consensus documents, similar to those available for ONG [8], are a necessary first step to directing clinical care and guiding future research for this tumor. A multidisciplinary task force, the OPPN Working Group, met in 2013 to discuss recommendations for care and challenges in clinical trial design for these complex tumors. Consensus recommendations from this group have been submitted for publication [74].

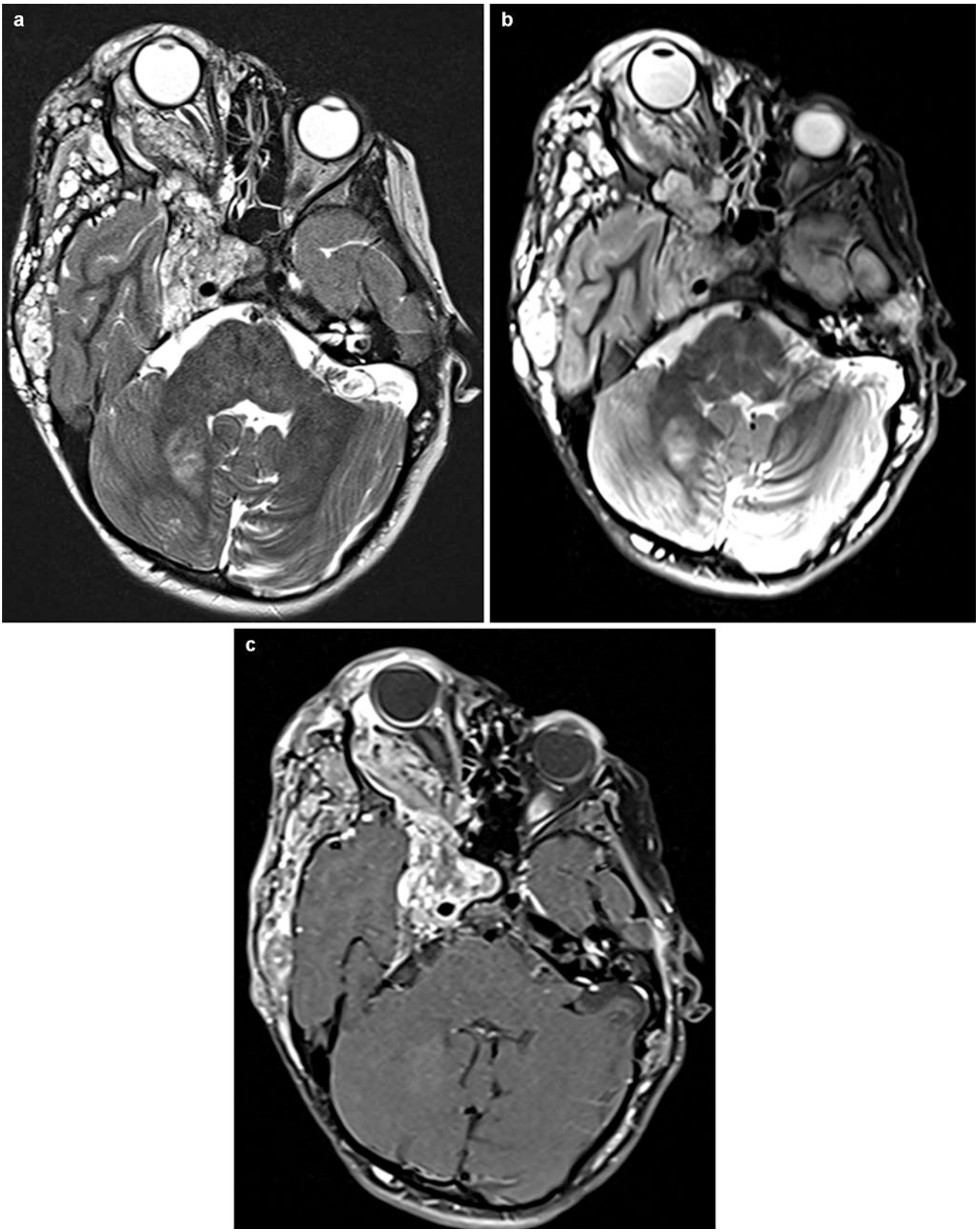


Fig. 15.3 A right-sided orbital/periorbital plexiform neurofibroma seen in axial section on T2-weighted image with fat saturation (**a**) and short tau inversion recovery (STIR) image (**b**) shows areas of high signal intensity. Post-contrast T1-weighted image (**c**) demonstrates enhancement

Orbital and Parameningeal Rhabdomyosarcoma

Epidemiology

Rhabdomyosarcoma is the most common primary orbital malignancy in children [2, 4, 75] and accounts for 5% of all childhood cancers [76]. This tumor occurs in the orbit in approximately 10% of all pediatric cases. Tumors in the orbit, conjunctiva, or eyelid are together called orbital rhabdomyosarcoma and have a more favorable prognosis than in many other locations [4]. However, tumors that invade the nasal cavity, paranasal sinuses, or nasopharynx are considered to be parameningeal, require more intensive therapy, and have a worse prognosis.

Approximately 350 new cases of rhabdomyosarcoma occur in the United States each year, of which roughly 35 are orbital. Rhabdomyosarcoma has a bimodal age distribution: although most tumors are diagnosed between 2–5 years of age, a second peak is seen in adolescence [77]. The mean age at diagnosis for orbital rhabdomyosarcoma is 8 years of age, and males are more frequently affected than females [75, 78].

Presentation

Although orbital rhabdomyosarcoma can rarely present insidiously, the most common presentation is rapid onset and progression of proptosis and displacement of the globe [75]. Among 33 consecutive cases of orbital rhabdomyosarcoma, the most common findings included proptosis (79%), paraxial globe displacement (79%), conjunctival congestion (61%), blepharoptosis (55%), dilated episcleral vessels (42%), and ocular motility restriction (42%) [78]. Changes in adjacent bone are frequently seen, and evaluation of intracranial extension and invasion of the paranasal sinuses at initial presentation are critical as these findings may alter management [79]. Tumors arising from parameningeal sites may produce nasal, aural, or sinus obstruction with or without mucopurulent or sanguineous discharge, but imaging is essential to define parameningeal involvement [80]. Distinguishing parameningeal rhabdomyosarcoma that invades the orbit from a true orbital rhabdomyosarcoma is crucial as this distinction will often influence therapy.

Diagnostic Imaging

Imaging is essential to the preoperative evaluation of orbital rhabdomyosarcoma to determine tumor location and size and is important in the postoperative phase to evaluate residual or recurrent disease. On CT imaging, rhabdomyosarcomas are frequently seen as a homogeneous orbital mass that is isodense compared to extraocular muscles and often shows contrast enhancement [1, 21, 81]. Although CT may be useful to demonstrate bony destruction [82], MR imaging is the standard of care to evaluate the primary site and the potential for parameningeal disease (Fig. 15.4). On T1-weighted sequences, rhabdomyosarcoma is typically iso- to hyperintense compared to muscle and hypointense compared to orbital fat. On T2-weighted sequences, hypointense, isointense, or hyperintense patterns can be seen. Moderate to marked enhancement with gadolinium is common [1, 21, 83]. PET imaging may also be a valuable adjunct for staging disease [21].

Pathology

Initially thought to derive from extraocular muscles, rhabdomyosarcoma actually develops from undifferentiated mesenchymal cells that have the capacity to differentiate into striated muscle [75]. The two common histologic subtypes (embryonal and alveolar) have distinct genetic features and prognoses. Embryonal histology is more frequent in orbital rhabdomyosarcoma (84% of cases) and portends better outcomes [84]. Histologically, embryonal rhabdomyosarcoma appears as elongated pleomorphic tumor cells with centrally located hyperchromatic nuclei surrounded by abundant eosinophilic cytoplasm [75]. Alveolar rhabdomyosarcoma has variable histology but most commonly presents as loosely adherent cells attached to a network of thin interstitial fibrovascular septa with many areas of freely floating cells in alveolar-like spaces [75]. Tumors with alveolar histology usually harbor a balanced chromosomal translocation between either PAX3 (from chromosome 2) or PAX7 (from chromosome 1) and FOXO1 (from chromosome 13) creating a fusion transcript PAX-FOXO1. Recent studies suggest that alveolar tumors that lack the PAX-FOXO1 fusion have outcomes similar to embryonal rhabdomyosarcoma [85, 86]. As a result, risk stratification and treatment allocation of rhabdomyosarcoma may rely on fusion status rather than histology in the future.

The diagnosis of rhabdomyosarcoma is usually made by direct open biopsy [80], and patients with suspicious lesions should be referred to a pediatric oncologist to complete a staging work-up before definitive surgery.

Treatment Considerations

Surgical biopsy is essential to establish a definitive diagnosis and histologic subtype in orbital rhabdomyosarcoma. Complete resection does not improve prognosis or significantly reduce treatment. Attempts at excision can threaten vision or range of motion and lead to microscopic

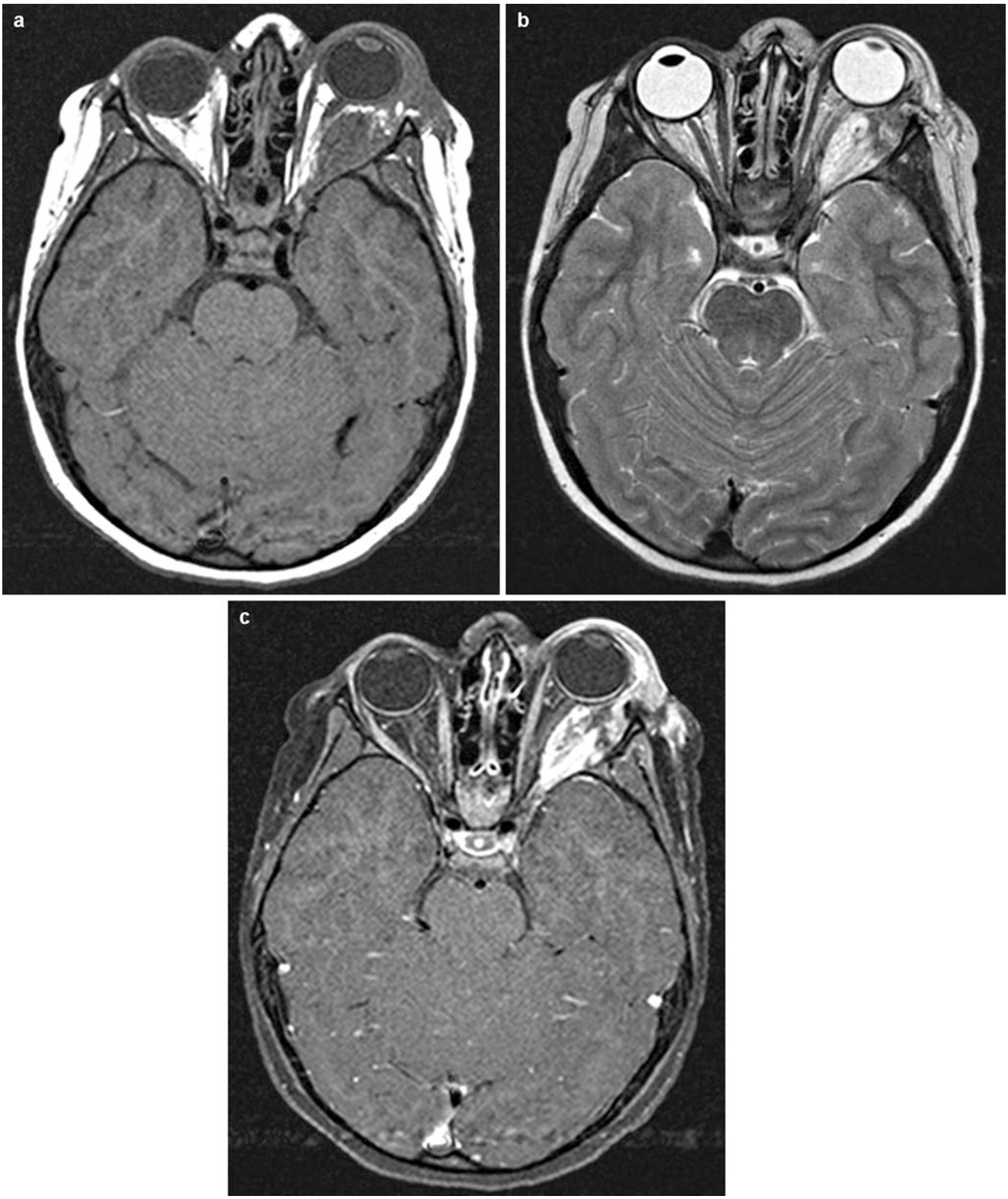


Fig. 15.4 A left-sided orbital rhabdomyosarcoma with parameningeal involvement seen in axial section on T1-weighted sequence (**a**) and T2-weighted sequence (**b**) Post-contrast T1-weighted image (**c**) demonstrates patchy enhancement

residual disease throughout the orbit that extends the field of radiation. Patients with residual orbital disease continue to have excellent outcomes after biopsy alone [87–89], and therefore nonexcisional therapy has become standard for low-risk rhabdomyosarcomas of the orbit in the Children's Oncology Group. After biopsy has been completed, patients are generally treated with a combination of chemotherapy and external beam radiation. Proton radiotherapy, when available, minimizes the radiation dose to normal tissues. Outcomes remain excellent for orbital rhabdomyosarcoma: 5-year overall survival is 95% for embryonal orbital rhabdomyosarcoma and 75% for alveolar orbital rhabdomyosarcoma [84].

Future Directions

Despite excellent progress in the treatment of rhabdomyosarcoma, many survivors of orbital rhabdomyosarcoma face significant late effects of their therapy. Radiation to the orbit can affect facial growth (through bony hypoplasia and facial asymmetry) and visual function (through cataracts, keratopathy, and retinopathy). In a review of survivors of childhood orbital rhabdomyosarcoma, the most common orbital late effects included cataract (82%), decreased visual acuity (70%), orbital hypoplasia (59%), dry eye (30%), chronic keratoconjunctivitis (27%), and retinopathy (6%) [90]. As a result, some European trials have attempted to limit or eliminate radiation to the orbit, at the cost of more intense chemotherapy and higher rates of recurrence [91]. In addition, newer methods for delivering radiation such as three-dimensional conformal techniques and proton beam radiation may limit normal structures in the treatment volume to reduce late effects of radiation [92].

Conclusion

Pediatric orbital and periorbital tumors are rare and require the multidisciplinary management of surgeons, ophthalmologists, and oncologists to guide care. While these tumors are typically benign, they can frequently cause both disfigurement and vision deficits. Many are associated with genetic predisposition syndromes, most notably neurofibromatosis types 1 and 2, and may require lifelong management. The care for these tumors must balance the goals of therapy against the potential harms of intervention. Because many benign orbital tumors may be chronic or recurrent, patients may require multiple therapies over the course of their lives. Judicious use of therapeutic interventions may spare patients unnecessary complications while maximizing their visual function.

References

1. Khan SN, Sepahdari AR. Orbital masses: CT and MRI of common vascular lesions, benign tumors, and malignancies. Saudi J Ophthalmol Off J Saudi J Ophthalmol Soc. 2012;26(4):373–83.
2. Shields JA, Shields CL, Scartozzi R. Survey of 1264 patients with orbital tumors and simulating lesions: The 2002 Montgomery Lecture, part 1. Ophthalmology. 2004;111(5):997–1008.
3. Kodsi SR, Shetlar DJ, Campbell RJ, Garrity JA, Bartley GB. A review of 340 orbital tumors in children during a 60-year period. Am J Ophthalmol. 1994;117(2):177–82.
4. Browning MB, Camitta BM. The surgeon's role in pediatric orbital malignancies: an oncologist's perspective. Ophthal Plast Reconstr Surg. 2003;19(5):340–4.
5. Dutton JJ. Gliomas of the anterior visual pathways. Surv Ophthalmol. 1994;38:427–52.
6. King A, Listernick R, Charrow J, Piersall L, Gutmann DH. Optic pathway gliomas in neurofibromatosis type 1: the effect of presenting symptoms on outcome. Am J Med Genet A. 2003;122A(2):95–9.
7. Listernick R, Charrow J, Greenwald M, Mets M. Natural history of optic pathway tumors in children with neurofibromatosis type 1: a longitudinal study. J Pediatr. 1994;125:63–6.
8. Listernick R, Louis DN, Packer RJ, Gutmann DH. Optic pathway gliomas in children with neurofibromatosis 1: consensus statement from the NF1 optic pathway glioma task force. Ann Neurol. 1997;41:143–9.
9. Listernick R, Ferner RE, Liu GT, Gutmann DH. Optic pathway gliomas in neurofibromatosis-1: controversies and recommendations. Ann Neurol. 2007;61(3):189–98.
10. Balcer LJ, Liu GT, Heller G, et al. Visual loss in children with neurofibromatosis type 1 and optic pathway gliomas: relation to tumor location by magnetic resonance imaging. Am J Ophthalmol. 2001;131:442–5.
11. Listernick R, Ferner RE, Piersall L, Sharif S, Gutmann DH, Charrow J. Late-onset optic pathway tumors in children with neurofibromatosis 1. Neurology. 2004;63(10):1944–6.
12. Cassiman C, Legius E, Spileers W, Casteels I. Ophthalmological assessment of children with neurofibromatosis type 1. Eur J Pediatr. 2013;172(10):1327–33.
13. Tow SL, Chandela S, Miller NR, Avellino AM. Long-term outcome in children with gliomas of the anterior visual pathway. Pediatr Neurol. 2003;28(4):262–70.
14. Fisher MJ, Loguidice M, Gutmann DH, et al. Visual outcomes in children with neurofibromatosis type 1-associated optic pathway glioma following chemotherapy: a multicenter retrospective analysis. Neuro-Oncology. 2012;14(6):790–7.
15. Diggs-Andrews KA, Brown JA, Gianino SM, Rubin JB, Wozniak DF, Gutmann DH. Sex is a major determinant of neuronal dysfunction in neurofibromatosis type 1. Ann Neurol. 2014;75(2):309–16.
16. Fisher MJ, Loguidice M, Gutmann DH, et al. Gender as a disease modifier in neurofibromatosis type 1 optic pathway glioma. Ann Neurol. 2014;75(5):799–800.
17. Hersh JH. Health supervision for children with neurofibromatosis. Pediatrics. 2008;121(3):633–42.
18. Shields JA, Shields CL. Pediatric ocular and periocular tumors. Pediatr Ann. 2001;30(8):491–501.
19. Leonard JR, Perry A, Rubin JB, King AA, Chicoine MR, Gutmann DH. The role of surgical biopsy in the diagnosis of glioma in individuals with neurofibromatosis-1. Neurology. 2006;67(8):1509–12.
20. Chateil JF, Soussotte C, Pedespan JM, Brun M, Le Manh C, Diard F. MRI and clinical differences between optic pathway tumours in children with and without neurofibromatosis. Brit J Radiol. 2001;74(877):24–31.
21. Purohit BS, Vargas MI, Ailianou A, et al. Orbital tumours and tumour-like lesions: exploring the armamentarium of multiparametric imaging. Insights Imaging. 2015;7(1):43–68.

22. Ji J, Shimony J, Gao F, McKinstry RC, Gutmann DH. Optic nerve tortuosity in children with neurofibromatosis type 1. Pediatr Radiol. 2013;43(10):1336–43.
23. Levin MH, Armstrong GT, Broad JH, et al. Risk of optic pathway glioma in children with neurofibromatosis type 1 and optic nerve tortuosity or nerve sheath thickening. Br J Ophthalmol. 2015;100(4):510–4.
24. Hoffman HJ, Soloniuk DS, Humphreys RP, et al. Management and outcome of low-grade astrocytomas of the midline in children: a retrospective review. Neurosurgery. 1993;33(6):964–71.
25. Laithier V, Grill J, Le Deley MC, et al. Progression-free survival in children with optic pathway tumors: dependence on age and the quality of the response to chemotherapy–results of the first French prospective study for the French Society of Pediatric Oncology. J Clin Oncol. 2003;21(24):4572–8.
26. Sutton LN, Molloy PT, Sernyak H, et al. Long-term outcome of hypothalamic/chiasmatic astrocytomas in children treated with conservative surgery. J Neurosurg. 1995;83:583–9.
27. Albers AC, Gutmann DH. Gliomas in patients with neurofibromatosis type 1. Expert Rev Neurother. 2009;9(4):535–9.
28. Rodriguez FJ, Perry A, Gutmann DH, et al. Gliomas in neurofibromatosis type 1: a clinicopathologic study of 100 patients. J Neuropathol Exp Neurol. 2008;67(3):240–9.
29. Cummings TJ, Provenzale JM, Hunter SB, et al. Gliomas of the optic nerve: histological, immunohistochemical (MIB-1 and p53), and MRI analysis. Acta Neuropathol. 2000;99(5):563–70.
30. Ater JL, Zhou T, Holmes E, et al. Randomized study of two chemotherapy regimens for treatment of low-grade glioma in young children: a report from the Children's Oncology Group. J Clin Oncol. 2012;30(21):2641–7.
31. Wright JE, McNab AA, McDonald WI. Optic nerve glioma and the management of optic nerve tumours in the young. Brit J Ophthalmol. 1989;73:967–74.
32. Spicer GJ, Kazim M, Glass LR, et al. Accuracy of MRI in defining tumor-free margin in optic nerve glioma surgery. Ophthal Plast Reconstr Surg. 2013;29(4):277–80.
33. Avery RA, Fisher MJ, Liu GT. Optic pathway gliomas [review]. J Neuroophthalmol. 2011;31(3):269–78.
34. Ater JL, Xia C, Mazewski CM, et al. Nonrandomized comparison of neurofibromatosis type 1 and non-neurofibromatosis type 1 children who received carboplatin and vincristine for progressive low-grade glioma: a report from the Children's Oncology Group. Cancer. 2016;122(12):1928–36.
35. Horwich A, Bloom HJG. Optic gliomas: radiation therapy and prognosis. Int J Radiat Oncol Biol Phys. 1985;11:1067–79.
36. Grabenbauer GG, Schuchardt U, Buchfelder M, et al. Radiation therapy of optico-hypothalamic gliomas (OHG)–radiographic response, vision and late toxicity. Radiother Oncol. 2000;54(3):239–45.
37. Jenkin D, Angyalfi S, Becker L, et al. Optic glioma in children: surveillance, resection, or irradiation? Int J Radiat Oncol Biol Phys. 1993;25:215–25.
38. Cappelli C, Grill J, Raquin M, et al. Long-term follow up of 69 patients treated for optic pathway tumours before the chemotherapy era. Arch Dis Child. 1998;79(4):334–8.
39. Sharif S, Ferner R, Birch JM, et al. Second primary tumors in neurofibromatosis 1 patients treated for optic glioma: substantial risks after radiotherapy. J Clin Oncol. 2006;24(16):2570–5.
40. Ullrich NJ, Robertson R, Kinnamon DD, et al. Moyamoya following cranial irradiation for primary brain tumors in children. Neurology. 2007;68(12):932–8.
41. Faisal YA, Katowitz WR, Fisher MJ, et al. Debulking optic nerve gliomas for disfiguring proptosis: a globe-Sparing approach by lateral orbitotomy alone. 42nd Annual Meeting North American Neuro-Ophthalmology Society. 2016.
42. Dutton JJ. Optic nerve sheath meningiomas. Surv Ophthalmol. 1992;37(3):167–83.
43. Harold Lee HB, Garrity JA, Cameron JD, Strianese D, Bonavolonta G, Patrinely JR. Primary optic nerve sheath meningioma in children. Surv Ophthalmol. 2008;53(6):543–58.
44. Barnholtz-Sloan JS, Kruchko C. Meningiomas: causes and risk factors. Neurosurg Focus. 2007;23(4):E2.
45. Berman D, Miller NR. New concepts in the management of optic nerve sheath meningiomas. Ann Acad med Singap. 2006;35(3):168–74.
46. Carrasco JR, Penne RB. Optic nerve sheath meningiomas and advanced treatment options. Curr Opin Ophthalmol. 2004;15(5):406–10.
47. Bosch MM, Wichmann WW, Boltshauser E, Landau K. Optic nerve sheath meningiomas in patients with neurofibromatosis type 2. Arch Ophthalmol. 2006;124(3):379–85.
48. Evans DG, Birch JM, Ramsden RT. Paediatric presentation of type 2 neurofibromatosis. Arch Dis Child. 1999;81(6):496–9.
49. Sheikh BY, Siqueira E, Dayel F. Meningioma in children: a report of nine cases and a review of the literature. Surg Neurol. 1996;45(4):328–35.
50. Mafee MF, Goodwin J, Dorodi S. Optic nerve sheath meningiomas. Role of MR imaging. Radiol Clin N Am. 1999;37(1):37–58, ix.
51. Sepahdari AR, Politi LS, Aakalu VK, Kim HJ, Razek AA. Diffusion-weighted imaging of orbital masses: multi-institutional data support a 2-ADC threshold model to categorize lesions as benign, malignant, or indeterminate. AJNR Am J Neuroradiol. 2014;35(1):170–5.
52. Fatima Z, Ichikawa T, Ishigame K, et al. Orbital masses: the usefulness of diffusion-weighted imaging in lesion categorization. Clin Neuroradiol. 2014;24(2):129–34.
53. Sibony PA, Krauss HR, Kennerdell JS, Maroon JC, Slamovits TL. Optic nerve sheath meningiomas. Clin Manifestations Ophthalmol. 1984;91(11):1313–26.
54. Eddleman CS, Liu JK. Optic nerve sheath meningioma: current diagnosis and treatment. Neurosurg Focus. 2007;23(5):E4.
55. Turbin RE, Thompson CR, Kennerdell JS, Cockerham KP, Kupersmith MJ. A long-term visual outcome comparison in patients with optic nerve sheath meningioma managed with observation, surgery, radiotherapy, or surgery and radiotherapy. Ophthalmology. 2002;109(5):890–9; discussion 899–900.
56. Baser ME, Evans DG, Jackler RK, Sujansky E, Rubenstein A. Neurofibromatosis 2, radiosurgery and malignant nervous system tumours. Br J Cancer. 2000;82(4):998.
57. Evans DG, Birch JM, Ramsden RT, Sharif S, Baser ME. Malignant transformation and new primary tumours after therapeutic radiation for benign disease: substantial risks in certain tumour prone syndromes. J Med Genet. 2006;43(4):289–94.
58. Turbin RE, Pokorny K. Diagnosis and treatment of orbital optic nerve sheath meningioma. Cancer Control J Moffitt Cancer Center. 2004;11(5):334–41.
59. Avery RA, Dombi E, Hutcheson KA, et al. Visual outcomes in children with neurofibromatosis type 1 and orbitotemporal plexiform neurofibromas. Am J Ophthalmol. 2013;155(6):1089–94. e1081.
60. Farris SR, Grove AS Jr. Orbital and eyelid manifestations of neurofibromatosis: a clinical study and literature review. Ophthal Plast Reconstr Surg. 1996;12(4):245–59.
61. Nguyen R, Dombi E, Widemann BC, et al. Growth dynamics of plexiform neurofibromas: a retrospective cohort study of 201 patients with neurofibromatosis 1. Orphanet J Rare dis. 2012;7:75.
62. Nguyen R, Kluwe L, Fuensterer C, Kentsch M, Friedrich RE, Mautner VF. Plexiform neurofibromas in children with neurofibromatosis type 1: frequency and associated clinical deficits. J Pediatr. 2011;159(4):652–5. e652.
63. Chaudhry IA, Morales J, Shamsi FA, et al. Orbitofacial neurofibromatosis: clinical characteristics and treatment outcome. Eye (Lond). 2012;26(4):583–92.
64. Oystreck DT, Morales J, Chaudhry I, et al. Visual loss in orbitofacial neurofibromatosis type 1. Ophthalmology. 2012;119(10):2168–73.

65. Erb MH, Uzcategui N, See RF, Burnstine MA. Orbitotemporal neurofibromatosis: classification and treatment. Orbit. 2007;26(4):223–8.
66. Ferner RE, Golding JF, Smith M, et al. [18F]2-fluoro-2-deoxy-D-glucose positron emission tomography (FDG PET) as a diagnostic tool for neurofibromatosis 1 (NF1) associated malignant peripheral nerve sheath tumours (MPNSTs): a long-term clinical study. Ann Oncol. 2008;19(2):390–4.
67. Ferner RE, Lucas JD, O'Doherty MJ, et al. Evaluation of (18)fluorodeoxyglucose positron emission tomography ((18)FDG PET) in the detection of malignant peripheral nerve sheath tumours arising from within plexiform neurofibromas in neurofibromatosis 1. J Neurol Neurosurg Psychiatry. 2000;68(3):353–7.
68. Rodriguez FJ, Folpe AL, Giannini C, Perry A. Pathology of peripheral nerve sheath tumors: diagnostic overview and update on selected diagnostic problems. Acta Neuropathol. 2012;123(3):295–319.
69. Jackson IT, Carbonnel A, Potparic Z, Shaw K. Orbitotemporal neurofibromatosis: classification and treatment. Plast Reconstr Surg. 1993;92(1):1–11.
70. Needle MN, Cnaan A, Dattilo J, et al. Prognostic signs in the surgical management of plexiform neurofibroma: the Children's Hospital of Philadelphia experience, 1974-1994. J Pediatr. 1997;131(5):678–82.
71. Jacquemin C, Bosley TM, Svedberg H. Orbit deformities in craniofacial neurofibromatosis type 1. AJNR Am J Neuroradiol. 2003;24(8):1678–82.
72. Blakeley JO, Plotkin SR. Therapeutic advances for the tumors associated with neurofibromatosis type 1, type 2, and schwannomatosis. Neuro-Oncology. 2016;18(5):624–38.
73. Widemann B, Leigh JM, Fisher MJ, et al. Phase I study of the MEK1/2 inhibitor selumetinib (AZD6244) hydrogen sulfate in children and young adults with neurofibromatosis type 1 (NF1) and inoperable plexiform neurofibromas (PNs). J Clin Oncol. 2014;32(suppl)(abstr 10018).
74. Avery RA, Katowitz JA, Fisher MJ, et al. Orbital/Peri-orbital plexiform Neurofibromas in children with Neurofibromatosis type 1: multi-disciplinary recommendations for care. Ophthalmology. 2017;124(1):123–32. doi:10.1016/j.ophtha.2016.09.020. Epub 2016 Nov 3.
75. Karcioglu ZA, Hadjistilianou D, Rozans M, DeFrancesco S. Orbital rhabdomyosarcoma. Cancer Control J Moffitt Cancer Center. 2004;11(5):328–33.
76. Crist W, Gehan EA, Ragab AH, et al. The third intergroup rhabdomyosarcoma study. J Clin Oncol. 1995;13(3):610–30.
77. Ognjanovic S, Linabery AM, Charbonneau B, Ross JA. Trends in childhood rhabdomyosarcoma incidence and survival in the United States, 1975-2005. Cancer. 2009;115(18):4218–26.
78. Shields CL, Shields JA, Honavar SG, Demirci H. Primary ophthalmic rhabdomyosarcoma in 33 patients. Trans am Ophthalmol Soc. 2001;99:133–42; discussion 142–133.
79. Sohaib SA, Moseley I, Wright JE. Orbital rhabdomyosarcoma–the radiological characteristics. Clin Radiol. 1998;53(5):357–62.
80. Hayes-Jordan A, Andrassy R. Rhabdomyosarcoma in children. Curr Opin Pediatr. 2009;21(3):373–8.
81. Zhu J, Zhang J, Tang G, et al. Computed tomography and magnetic resonance imaging observations of rhabdomyosarcoma in the head and neck. Oncol Lett. 2014;8(1):155–60.
82. Wende S, Aulich A, Nover A, et al. Computed tomography or orbital lesions. A cooperative study of 210 cases. Neuroradiology. 1977;13(3):123–34.
83. Yang WT, Kwan WH, Li CK, Metreweli C. Imaging of pediatric head and neck rhabdomyosarcomas with emphasis on magnetic resonance imaging and a review of the literature. Pediatr Hematol Oncol. 1997;14(3):243–57.
84. Kodet R, Newton WA Jr, Hamoudi AB, Asmar L, Wharam MD, Maurer HM. Orbital rhabdomyosarcomas and related tumors in childhood: relationship of morphology to prognosis–an Intergroup rhabdomyosarcoma study. Med Pediatr Oncol. 1997;29(1):51–60.
85. Missiaglia E, Williamson D, Chisholm J, et al. PAX3/FOXO1 fusion gene status is the key prognostic molecular marker in rhabdomyosarcoma and significantly improves current risk stratification. J Clin Oncol. 2012;30(14):1670–7.
86. Williamson D, Missiaglia E, de Reynies A, et al. Fusion gene-negative alveolar rhabdomyosarcoma is clinically and molecularly indistinguishable from embryonal rhabdomyosarcoma. J Clin Oncol. 2010;28(13):2151–8.
87. Sutow WW, Lindberg RD, Gehan EA, et al. Three-year relapse-free survival rates in childhood rhabdomyosarcoma of the head and neck: report from the Intergroup rhabdomyosarcoma study. Cancer. 1982;49(11):2217–21.
88. Heyn R, Ragab A, Raney RB Jr, et al. Late effects of therapy in orbital rhabdomyosarcoma in children. A report from the Intergroup rhabdomyosarcoma study. Cancer. 1986;57(9):1738–43.
89. Maurer HM, Beltangady M, Gehan EA, et al. The Intergroup rhabdomyosarcoma study-I. A final report. Cancer. 1988;61(2):209–20.
90. Raney RB, Anderson JR, Kollath J, et al. Late effects of therapy in 94 patients with localized rhabdomyosarcoma of the orbit: report from the Intergroup rhabdomyosarcoma study (IRS)-III, 1984-1991. Med Pediatr Oncol. 2000;34(6):413–20.
91. Koscielniak E, Harms D, Henze G, et al. Results of treatment for soft tissue sarcoma in childhood and adolescence: a final report of the German cooperative soft tissue sarcoma study CWS-86. J Clin Oncol. 1999;17(12):3706–19.
92. Yock T, Schneider R, Friedmann A, Adams J, Fullerton B, Tarbell N. Proton radiotherapy for orbital rhabdomyosarcoma: clinical outcome and a dosimetric comparison with photons. Int J Radiat Oncol Biol Phys. 2005;63(4):1161–8.

Molecular Pathology of Pediatric Oculoplastic Disorders

16

Vivian Lee, Tatyana Milman, and Ralph C. Eagle Jr

Diagnostic Tools Based on Protein Expression

Immunohistochemistry (IHC)

Developed as early as the 1940s [1], IHC has undergone numerous enhancements, becoming an indispensable tool in the pathologist's arsenal. It is widely used for the identification and diagnosis of specimens. IHC can also help characterize and stage tumors when used to detect cellular processes such as proliferation or cell death.

Method

The principal behind IHC is simple, which is to detect a unique attribute or set of attributes that can discriminate a specific tissue, disease, or pathology [2]. This is accomplished by raising antibodies that bind against specific antigens. Antigens are typically proteins expressed on the surface, cytoplasm, or nuclei of cells. Commonly, this method is used on sections of formalin-fixed paraffin-embedded (FFPE) tissue [3]. The specimen is identified or the diagnosis is determined by the IHC expression pattern. In practice, a battery of immunohistochemical stains directed against a number of potential tissue markers typically is employed. The final diagnosis is based on the tissue's pattern of positive and negative immunoreactivity to the panel of antibodies.

An antibody targeting a specific antigen is incubated with the specimen [2]. The antibody is conjugated to an enzyme, such as peroxidase, which catalyzes a reaction to produce a colored reaction product that can be detected with routine light microscopy. Alternatively, the antibody can be tagged with a fluorophore such as fluorescein that can fluoresce, requiring a special microscope to analyze (Fig. 16.1a). Different colored chromogens and fluorescent dyes are available. Selection of one over another may be clinically relevant, for example, the selection of a red chromagen instead of the more ubiquitous brown chromagen for the assessment of pigmented melanocytic lesions [4].

The antibody can be directly conjugated to the signaling molecule or a secondary antibody may be employed, referred to as direct and indirect antigen detection methods, respectively (Fig. 16.1b) [2]. The direct method involves a single staining step, where a labeled antibody binds directly to the antigen. The indirect method, on the other hand, involves two tiers of antibodies: an unlabeled primary antibody that binds to the specific antigen directly and a secondary antibody conjugated to an enzyme or fluorophore that couples with the primary antibody. The indirect method is often preferred because the signal is amplified by the coupling of several secondary antibodies to one primary antibody [5]. The direct method results in a less robust signal due to the 1:1 binding ratio between antibody and antigen but is simpler and more rapid. After IHC staining, a second counterstain such as hematoxylin or DAPI (4′,6-diamidino-2-phenylindole, dihydrochloride) often is performed to highlight or provide context for the IHC stain [2].

Applications

An extensive number of IHC markers are available [2]. A few common ones and their uses are listed in Table 16.1. Improvements in technique and buffers have led to better exposure of antigens and improved antibody-antigen coupling [2, 6, 7]. New IHC stains continue to be added as novel markers are discovered, some of which have reshaped our understanding of tumors [2, 5]. For example, neoplasms previously diagnosed as hemangiopericytoma on morphologic grounds have been reclassified by the World Health Organization (WHO) as solitary fibrous tumors (SFT),

V. Lee (✉)
University of Pennsylvania – Scheie Eye Institute, Philadelphia, PA, USA
e-mail: vivian.lee@uphs.upenn.edu

T. Milman • R.C. Eagle Jr
Department of Pathology, Wills Eye Hospital, Philadelphia, PA, USA

© Springer International Publishing AG 2018

J.A. Katowitz, W.R. Katowitz (eds.), *Pediatric Oculoplastic Surgery*, https://doi.org/10.1007/978-3-319-60814-3_16

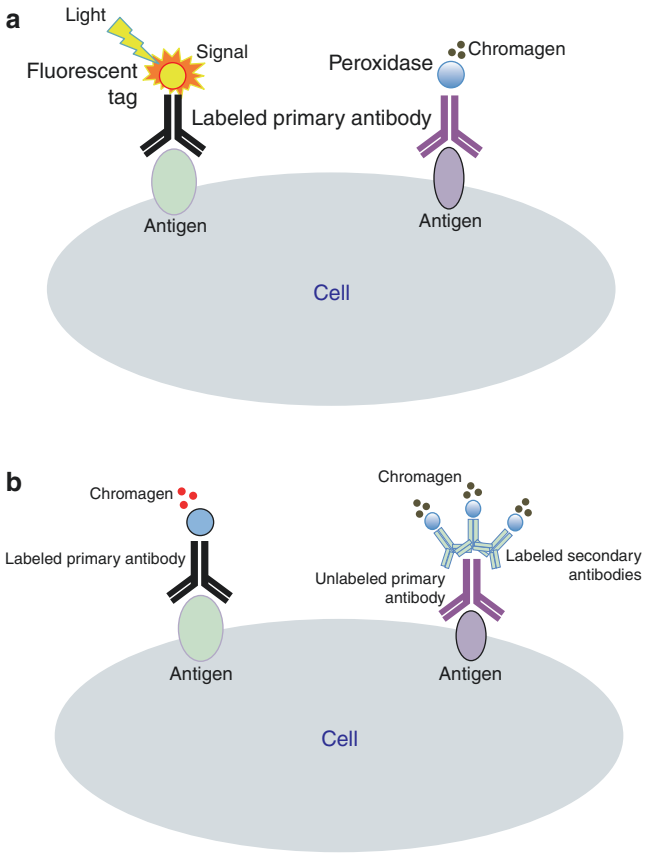


Fig. 16.1 (**a**) *IHC.* Schematic showing immunohistochemistry (IHC) methods. Antigen on the left is coupled with a fluorescently labeled primary antibody, which emits a signal when stimulated with light; antigen on the right is coupled with an enzymatically labeled primary antibody, which emits a colored (chromogen) signal when chemically activated. (**b**) *Direct and indirect IHC methods.* Graphic representation of direct and indirect antigen detection methods in immunohistochemistry (IHC). The direct method utilizes a labeled primary antibody to bind directly to an antigen, represented on the left, while the indirect method employs labeled secondary antibodies to bind with the unlabeled primary antibody-antigen complex, seen on the right. The direct method results in 1:1 signaling antibody-antigen complex. The signal in the indirect method is amplified since multiple secondary antibodies may bind to the primary antibody-antigen complex

Table 16.1 Common IHC stains and their targets [57]

Immunohistochemistry (IHC) markers	Target
S-100	Neural crest lineage
CD3, CD5	T-cells
CD20, CD79a	B-cells
SMA (smooth muscle actin)	Smooth muscle actin
DES (desmin)	Striated muscle (intermediate filament)
AE1/3 (pankeratin marker)	Cytokeratin marker
HMB45 (human melanoma black), melan A, MITF (microphthalmia transcription factor)	Melanocytes
NSE (Neuron specific enolase)	Neuroendocrine cells and tumors
Ki-67	Proliferating cells (G1, S, G2, and M cell cycle phases)

partially due to the discovery of the NAB2-STAT6 fusion gene [8, 9]. This fusion gene is easily detected by the nuclear expression of the carboxy terminal part of STAT6 on IHC staining [9]. The discovery of STAT6 and its expression in hemangiopericytomas have led a new understanding and reclassification of this tumor.

IHC can also predict a tumor's response to treatment, as illustrated by the expression of erythrocyte-type glucose transporter protein Glut-1 expression by capillary hemangiomas [10, 11]. Capillary hemangiomas are common vascular anomalies in the pediatric population that typically regress with age. In certain cases, however, early treatment is required to avoid long-term complications, such as amblyopia [12]. Beta-blockers have been successfully shown to cause regression of these lesions [13]. However, distinguishing capillary hemangioma from other vascular lesions, such as lymphatic or venous malformations or pyogenic granuloma, may be difficult based on clinical and morphological examination alone [10]. Positive expression of Glut-1 can help to confirm the histopathologic diagnosis of capillary hemangioma and, hence, its likely response to beta-blockers (Fig. 16.2) [10, 11].

Limitations

Despite its widespread use, IHC has some limitations. Enhancements to antibody-antigen signal may result in nonspecific binding and high background signals [2, 7]. Tumors, particularly of uncertain lineage, may also display atypical patterns of antigen expression [7]. The latter can mislead the pathologist, resulting in an erroneous diagnosis. Consequently, IHC stains must be carefully selected, and staining patterns must be rationally assessed to attain the correct diagnosis.

Flow Cytometry (FC)

FC has occupied many roles in research and medicine since devised in 1953 [14]. The introduction of fluorescence in 1968 [15] and multiple lasers in 1978 [16] expanded its domain in pathology. Currently, it is used most commonly in the diagnosis of blood-based disorders and cancers [17].

Method

Similar to IHC, FC characterizes a specimen by antigen-antibody interactions [17]. Instead of utilizing tissue sections, FC detects antigens or molecules suspended in liquid form. Typically, whole cells are subjected to FC, which is illustrated in Fig. 16.3. A sample is incubated initially with a panel of fluorescently labeled antibodies. Cells then travel in a cell-free buffer (sheath fluid), forming a single file of cells that pass through a laser. The signal, or emitted light, is measured at two angles, forward-scattered light (FSC) and side-scattered light (SSC), which helps characterize cell type.

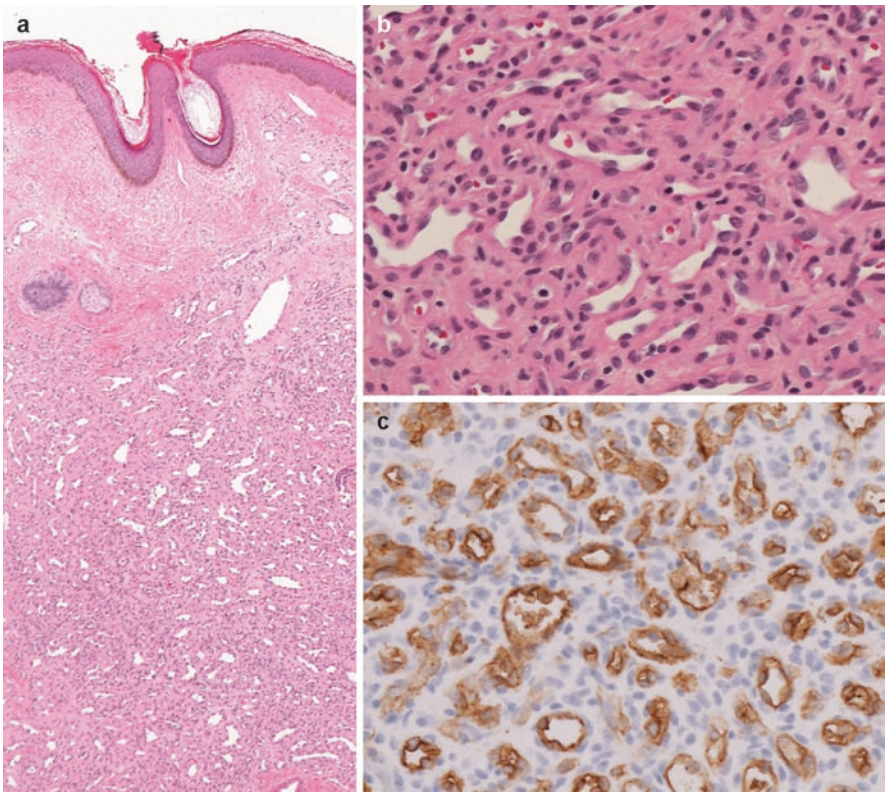


Fig. 16.2 *Glut-1 IHC.* Infantile hemangioma composed of benign proliferation of capillary-sized blood vessels lined by somewhat plump endothelial cells and with distinct lumen. No atypia or mitotic figures noted within the blood vessels or stroma. Low (**a**) and high (**b**) power magnifications shown. Immunohistochemistry (IHC) with Glut-1 highlights lesional endothelial cells (**c**) (Courtesy of Chrystalle Katte Carreon, MD; Department of Anatomic Pathology at The Children's Hospital of Philadelphia; Philadelphia, PA)

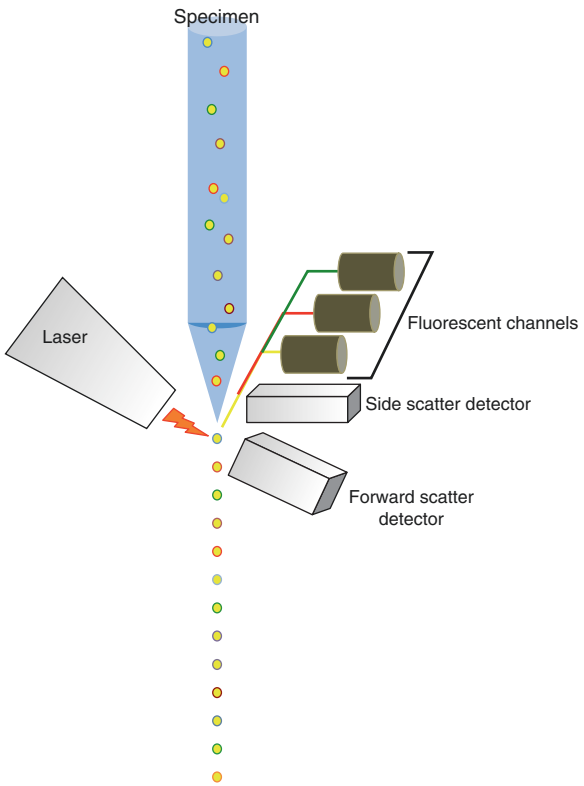


Fig. 16.3 *FC.* Illustration demonstrating flow cytometry (FC). Single-cell suspension incubated beforehand with a panel of fluorescently labeled antibodies travels through a sheath fluid. Individual cells pass through a laser, and forward and side-scattered lights are recorded. Fluorescent channels also record the fluorescent signals emitted from the antibodies attached to each cell

In addition, if a fluorescently labeled antibody is present, the laser or a series of lasers excites the fluorophore, which emits a signal that is detected by the fluorescence measuring station.

The data obtained is referred to as acquisition [17]. By adjusting the parameters, a desired antigen pattern can be selected and plotted graphically. Specific regions or traits can be aggregated by creating certain selection extractions, denoted as "gates." Improvements in computational methods now offer innovative gating strategies that assist in identifying rare, obscure populations [18].

Applications

Modern flow cytometers are able to analyze thousands of particles every second [17]. They usually have multiple lasers and fluorescence detectors, which allow for multiple antibody labeling and broader characterization. One of the most common applications of FC in pediatric ophthalmology is diagnosis of a lymphoproliferative neoplasm, such as acute myeloid leukemia (AML) [19]. AML can present with extramedullary involvement of the orbital tissues, known as myeloid sarcoma. The differential diagnosis includes tumors such as neuroblastoma or inflammatory conditions such as idiopathic orbital inflammatory syndrome (IOIS). FC can help distinguish AML from these other entities by its distinctive FC expression pattern (Fig. 16.4).

Cell sorting is another feature of FC. Fluorescence-activated cell sorting® (FACS) is a trademarked name that has been generalized to most FC cell sorters [20]. It allows a

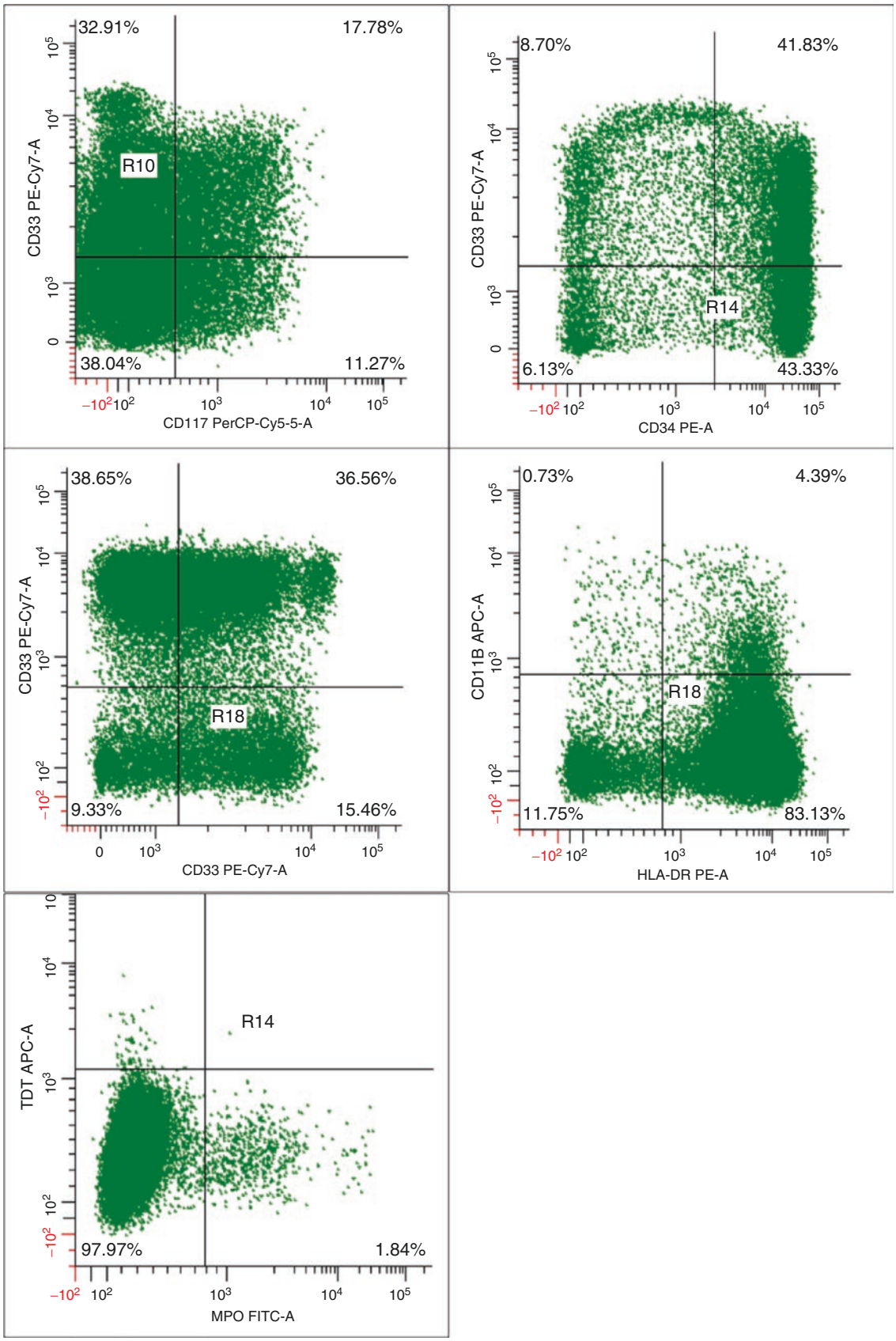


Fig. 16.4 Flow cytometric scatter plots of peripheral blood demonstrating immunophenotype typical of AML: CD13+, CD33(dim/var)+, CD34+, CD117(dim/var)+, HLA-DR+, MPO(small subset)+, and TdT- (Courtesy of Dale M. Frank, MD; Department of Pathology at the Hospital of the University of Pennsylvania; Philadelphia, PA)

heterogeneous mixture of cells to be sorted based on specific light scattering and fluorescent signals. The value of cell sorting recently has been underscored by the development of personalized treatments, such as peripheral blood stem cell transplants and T-cell-based gene therapy [17, 21, 22]. Some other instruments are able to capture digital images of individual cells. This allows the localization of fluorescent signals within or on the surface of cells, which can provide insight into spatial protein expression and cellular protein-protein interactions [23, 24].

Limitations

Despite the many advantages of FC, there are shortcomings. For solid tissue, FC requires disruption of the tissue to create single-cell preparations [17]. This precludes examination of the specimen's architecture, as well as the relative location of populations of cells in the tissue. Accordingly, surgical margins are nearly impossible to assess. While IHC employs sections of FFPE, fresh tissue is preferred for FC, limiting the use of fixed, frozen, and archival tissue [17]. Results are aggregated as well, which prohibits analysis of cell-cell interactions [17]. Lastly, analysis must be performed by an experienced FC pathologist due to the computational analysis that is necessary after acquisition [25].

Summary

Although the fundamental approaches to IHC and FC are analogous, both techniques have distinct advantages and disadvantages. IHC can be performed on FFPE sections, which is the customary method of preparing specimens. As a result, the submitting physician typically does not need to notify the pathologist in advance if IHC analysis is required. In addition, the pathologist has a multitude of antibodies at his or her disposal. As long as the tissue in the paraffin block is not exhausted, a variety of IHC stains can be performed. FC, on the other hand, is best performed on fresh tissue and requires a relatively large number of cells. As a result, proper sampling and handling of the specimen requires advanced notification by the submitting physician. However, the advantage of FC is the rapid and simultaneous assessment of a variety of antigens within a large population of cells.

Diagnostic Tools for Genetics and Genomics

Fluorescence in Situ Hybridization (FISH)

While the first two methods detect differences in cellular protein expression, FISH is a diagnostic tool that identifies and localizes genomic sequences [26]. The initial in situ hybridization experiments in 1969 utilized radioactivity to detect RNA-DNA hybridization [27]. Most recent modifications incorporate fluorescent probes, as well as probes that can hybridize to DNA, RNA, and RNA variants such as messenger RNA and microRNA [26, 28].

Method

As the name implies, FISH is based on the hybridization of a detectable probe to a desired genetic target [26]. Hybridization utilizes the precise coupling of nucleic acids: cytosine to guanine and adenine to thymine (or uracil in RNA). The probe usually is a cloned segment of DNA or RNA that is labeled with a fluorophore. Depending on the target, probes can vary in length. The sample and probes may need to be denatured to disrupt any hydrogen bonds between the bases, thereby priming the sample (Fig. 16.5). If the sequence of a probe matches the sample, hybrids form between the probe and its genetic target, while the rest washes away. A fluorescent signal is detected using a fluorescent microscope. Various specimen preparations can be assessed with FISH, including FFPE sections, frozen sections, and fine-needle aspirates.

Applications

FISH can be used for multiple purposes, including diagnosis, prognostication, and disease monitoring. A traditional application is metaphase chromosome analysis [26]. Previous techniques for karyotyping were cumbersome and time-consuming. With multifluor FISH, the process is made easier with the employment of probes that hybridize with entire chromosomes, painting each chromosome a unique fluorescent color. Deletions, duplications, and translocations are subsequently identified by their fluorescence pattern.

While this method is advantageous over prior ones, it still precludes detailed analysis of specific sequence rearrangements and alterations. Therefore, smaller probes that are specific to a particular locus are utilized for finer scrutiny of sequence variations [26]. For example, FISH can be used to detect clinically significant chromosomal translocations such as the Philadelphia chromosome (Ph) [29]. One of the first proofs for a genetic link to cancer, the Ph chromosome is characterized by a reciprocal translocation, resulting in the BCR-ABL fusion gene [30]. The BCR-ABL fusion gene is oncogenic and the causative basis for chronic myelogenous leukemia (CML). It is also used for prognosis in pediatric acute lymphoblastic leukemia (ALL), embodying an independent adverse risk factor [31]. Using FISH, the BCR-ABL fusion gene can be detected easily, and therefore, confirm diagnosis, assess prognosis, or monitor disease remission [29, 32].

Advancements in technique also have enabled pathologists to analyze interphase chromosomes as well as metaphase chromosomes [33]. This permits the analysis of many additional tumors with FISH, including rhabdomyosarcoma,

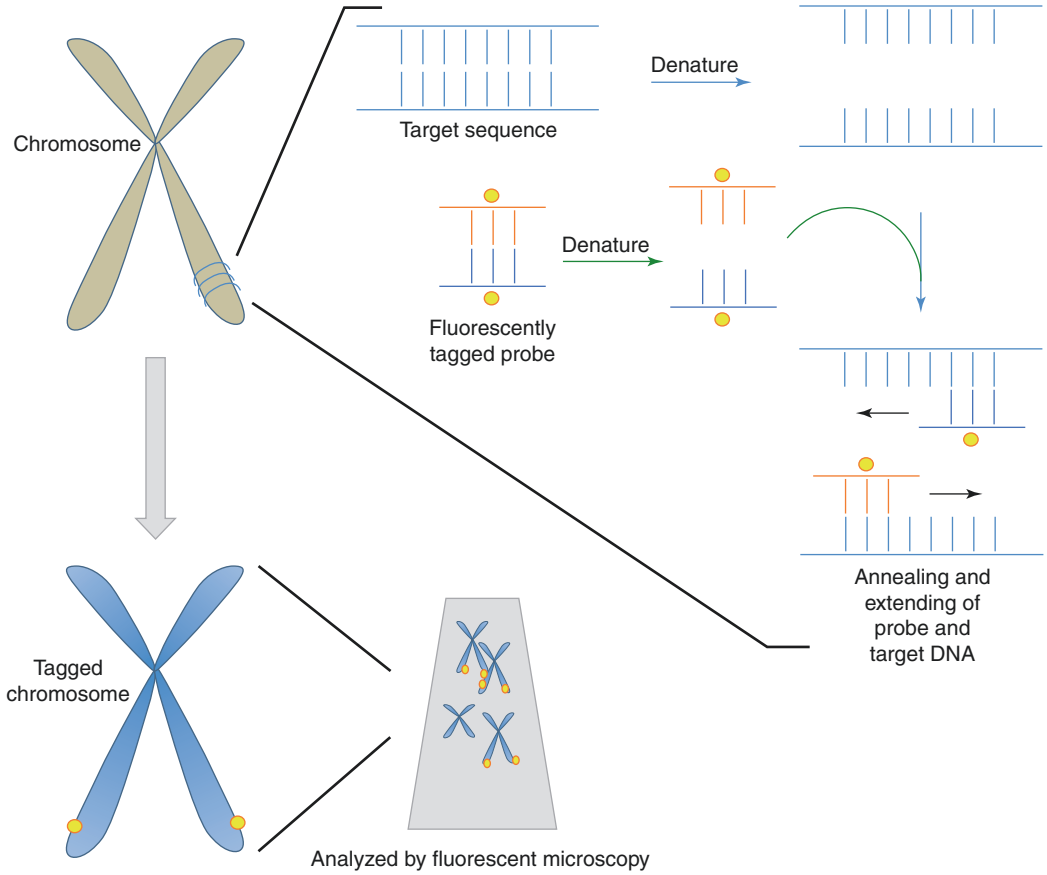


Fig. 16.5 *FISH.* Diagram exemplifying fluorescent in situ hybridization (FISH). Target sequence and fluorescently tagged probe undergo denaturing to separate strands. The probes are incubated with the sample. If the probe and sample express complimentary sequences, the probe anneals to the template and extends with the help of polymerases. Signals are then detected under fluorescent microscopy

the most common soft tissue sarcoma in children. Alveolar rhabdomyosarcoma (aRMS) is a rare subtype of rhabdomyosarcoma that behaves aggressively [34]. The *PAX3-FOXO1* fusion gene is a signature genetic marker found in aRMS, which can be detected by FISH [34, 35]. As illustrated in Fig. 16.6, the wild-type *FOXO1* gene appears as a single yellow point, formed by overlapping red and green signals. However, separate red and green signals disclose a translocation event in *FOXO1*, confirming the diagnosis of aRMS.

Limitations

As with all clinical tests, high sensitivity and specificity are essential to minimize false positive and negative results. Sensitivity of FISH depends on the resolution of the probe signal, while specificity relies on probe construction and accurate hybridization [26]. Resolution is limited by the ability to distinguish a distinct point, which is highly dependent on the conformation of the target. Chromosomes in metaphase are extremely compact, followed by interphase and then naked DNA. Resolution decreases with

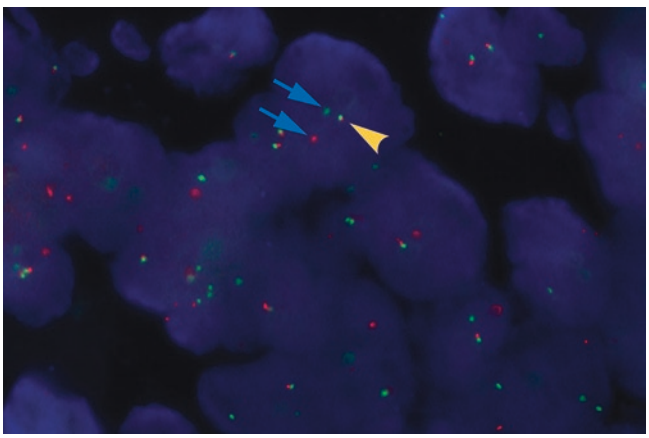


Fig. 16.6 *FOXO1 FISH.* Fluorescent in situ hybridization (FISH) study demonstrating widely separated *red* and *green signals* (*arrows*), consistent with translocation within *FOXO1* gene. The wild-type *FOXO1* gene lacks the translocation (overlapping *red* and *green signals* appear as *yellow signal*, *arrowhead*) (Courtesy of Paul J. L. Zhang, MD; Department of Pathology and Laboratory Medicine at the Hospital of the University of Pennsylvania, Immunohistochemistry Laboratory; Philadelphia, PA)

compaction, which can lead to errors in observations and interpretations [36]. Advancements in microscopy and automated analysis programs have overcome some obstacles to improve resolution significantly, even as far as single-molecule resolution [28].

While probe length may also contribute to sensitivity, where longer sequences are easier to detect than shorter sequences, probe construct greatly impacts specificity [26]. A long probe can partially anneal spuriously, leading to erroneous hybridization. A short strand of DNA or RNA can identify more specific targets, such as a translocation breakpoint [26, 36]. Dual-color break-apart probes, for example, are often employed in such cases. These probes are composed of different colored DNA segments on either side of a breakpoint [37]. If a breakpoint exists, two colors are observed, rather than a single-colored signal indicating no translocation breakpoint. These types of probes have greatly facilitated the visualization of a translocation breakpoint. However, potential diagnostic ambiguity may still arise, especially when the fusion partner is undetectable [37].

Polymerase Chain Reaction (PCR)

PCR is a relatively easy and inexpensive tool, used to detect a specific genetic sequence. Conceived by a chemist in 1983, PCR uses primers to straddle a target sequence and amplify it [38]. It is used commonly to diagnose and monitor diseases.

Method

The basis of PCR involves repeated cycles of heating and cooling reactions [38]. A sample is combined with polymerases and primers, which are short fragments composed of the complementary sequence to a target sequence. The PCR sample runs through various cycles of quick temperature changes. In cases of DNA samples, this causes the double strands to separate and allows the primers to anneal and extend with the assistance of DNA polymerases that are not denatured by high temperatures (Fig. 16.7). The latter are derived from thermophilic bacteria that live in hot springs. The result is the selective amplification of the DNA segment by several orders of magnitude. The PCR products are subsequently identified by a variety of methods, including gel electrophoresis. Other variations now include reverse transcriptase PCR (RT-PCR), which interrogates RNA sequences using reverse transcriptase and primers, and qualitative PCR (qPCR), which semiquantitates the gene of interest [39].

Applications

As with FISH, PCR routinely is used for the diagnosis of malignancies, such as lymphoproliferative and soft tissue neoplasms. In addition, PCR also is employed to detect infectious pathogens, including bacteria, viruses, and fungi [40, 41]. Many infectious pathogens are perceived as difficult to culture or slow-growing [42, 43]. PCR can overcome these obstacles if the pathogen's genetic sequence is known [40, 41]. Pathogenic strains with known sequence variations also can be discriminated from nonpathogenic strains. Moreover, due to the high sensitivity of this method, early detection is much more feasible compared to traditional culturing methods.

This application of PCR was helpful in identifying the cause of an outbreak of periorbital ulcers in neonates [44]. During a national shortage of erythromycin ophthalmic ointment, gentamicin ophthalmic ointment was used as an alternative for prophylaxis in neonates. Herpes simplex virus (HSV)-like periorbital lesions soon were observed, as seen in Fig. 16.8. PCR tests, however, excluded HSV as the cause. After careful investigation, gentamicin was deduced as the culprit. As a result, PCR prevented a large number of neonates from undergoing invasive systemic testing for HSV infection.

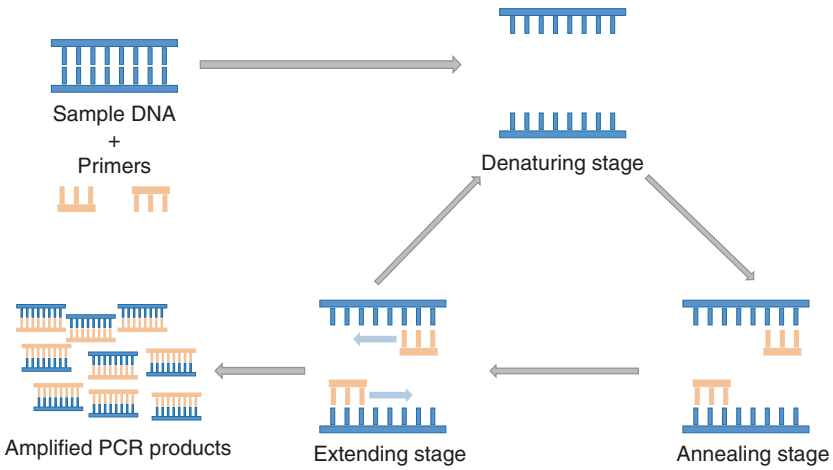


Fig. 16.7 *PCR.* Schema of polymerase chain reaction (PCR). A sample DNA with primers undergo cycles of rapid temperature changes. This causes the DNA to denature, allowing primers to anneal to their complimentary sequence and extend with polymerases. The cycle is repeated, which amplifies the targeted sequence



Fig. 16.8 Representative image illustrating periocular ulcerative lesions from gentamicin ophthalmic ointment. Negative PCR results excluded herpes simplex virus as an infectious cause of the dermatitis (Photograph courtesy of Stefanie L. Davidson, MD; Department of Ophthalmology at The Children's Hospital of Philadelphia; Philadelphia, PA. From Binenbaum et al. [44] with permission from Elsevier Limited)

Limitations

Despite the commonplace use of PCR in pathology, the technique does have drawbacks. Incorrect PCR products are a considerable challenge [39]. Small errors caused by contamination, spurious recombinations, and/or poor quality primers result in large errors because of the amplifying nature of PCR. DNA polymerases are also inherently prone to error, as they may cause nonspecific binding of primers [39]. Therefore, tremendous effort must be taken to avoid contamination, including a protected working space when preparing PCR samples, as well as careful primer design, construction, and verification. Improvements in buffers and polymerase solutions also have helped minimize errors while enhancing performance [39]. Finally, this method requires focused inquiries. Like FISH, primers must be selected beforehand, assuming that the sequence of interest is already known and validated.

Next-Generation Sequencing (NGS)

Another tool in the pathologist's arsenal for probing the genome is NGS. RNA and DNA sequencing were performed as early as the 1970s [45, 46]. Refinements led to the Sanger technique, which dominated the era of genomic sequencing until the introduction of NGS in the 1990s [47]. NGS is commonly used to sequence exomes, whole genomes, or RNA for pathologic mutations, variants, or biomarkers.

Method

As with FISH and PCR, NGS relies on the precise pairing of nucleic acids [47]. While the prior two methods rely on the coupling of short sequences to the target DNA/RNA, NGS relies on base-by-base pairing. DNA can be directly analyzed, while RNA must be converted to a complementary DNA (cDNA) library. In either case, the target sequence is enzymatically cut or mechanically sheared into very short segments [48]. Subsequent steps vary between the different commercially available platforms but essentially involve incubating the sample DNA or cDNA with tagged nucleotides. Using Illumina® sequencing as one example, this platform relies on fluorescently labeled nucleotides, like FISH [49]. The sample and primers are prepared on a slide or well and then amplified to form DNA colonies, referred to as DNA clusters. Individual nucleotides are incorporated one by one, and an image is captured after each cycle and analyzed. Because analysis is based on an image, very large arrays of DNA colonies can be captured and analyzed simultaneously. Another popular system is the Ion Torrent™ semiconductor sequencing, which utilizes semiconductor technology to detect a sequence [50]. In this method, a microwell containing the sample DNA template strand is mixed in with single nucleotides. As the nucleotides attach, hydrogen ions are released from the chemical reaction, which are then detected by a hypersensitive ion sensor. Depending on the number of released hydrogen ions, a specific electronic signal is generated, distinguishing the specific nucleotide.

With all of these platforms, enormous quantities of sequencing data are generated [51, 52]. The raw data that initially is acquired must be assembled into longer sequences, referred to as sequence assembly [52]. This may require editing of the raw reads, otherwise known as trimming, to eliminate artifacts downstream. The generated sequence is aligned to a reference genome, which is available from many databases online. Once the sequence is analysis ready, only then is the detailed process of actually analyzing the sequence initiated. This aspect of NGS has driven the demand for algorithms to analyze the data, leading to the bourgeoning field of bioinformatics. Other recent advancements in NGS enable the analysis of epigenetic changes, protein modifications, and infectious pathogen identification as well [47, 53].

Applications

Like the other two methods, NGS is used to identify known malignant gene markers. One of the most common applications in pediatric ophthalmology is genetic testing in retinoblastoma [54]. The most common pediatric intraocular malignant tumor, retinoblastoma, usually is caused by a mutation in the *Rb1* gene [54, 55]. The *Rb1* mutation may be germline or somatic, and the consequences thereof has tremendous implications for patient care. Therefore, all patients diagnosed with retinoblastoma, such as the patient in Fig. 16.9, undergo sequencing testing, which includes analysis of whole blood. In this case, a heterozygous nonsense germline mutation leading to premature termination codon of the *Rb1* gene was detected with whole blood NGS testing.

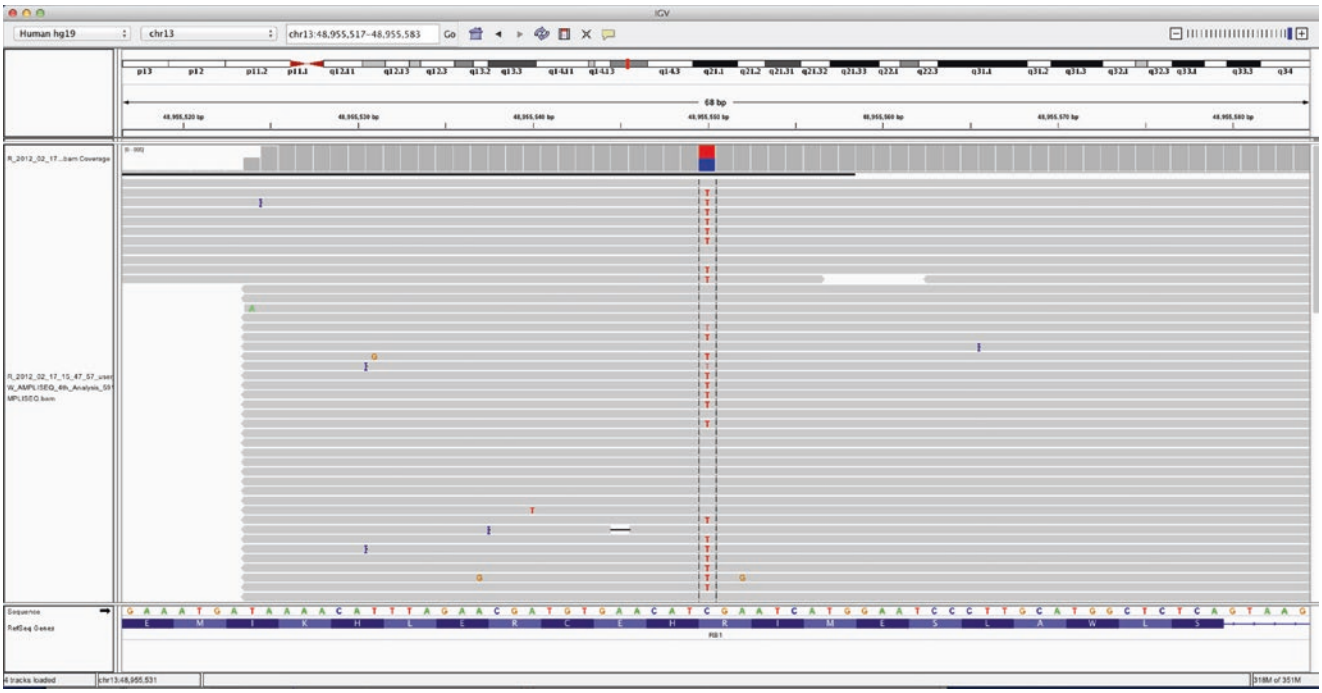


Fig. 16.9 *NGS.* Next-generation sequencing (NGS) identified a heterozygous nonsense mutation, c.1666C > T, p.Arg556X, in a patient diagnosed with simplex bilateral retinoblastoma. NGS reads shown were aligned to the "hg19" human reference sequence, using version 2.3 of IGV software (Integrative Genomics Viewer, aka "IGV," from Broad Institute) [58]. This pathogenic point mutation generates a premature termination codon in exon 17 of the RB1 gene (Courtesy of David Collins, PhD; Joan O'Brien, MD; and Harini V. Gudiseva; Scheie Eye Institute at the University of Pennsylvania; Philadelphia, PA)

Limitations

Because of the sensitivity of NGS, results are highly dependent on sample preparation [47–49, 53]. Execution of precise techniques and quality checks of the sample must be performed before NGS testing can be initiated. The sequences produced may reveal novel mutations or sequences that cannot be subsequently checked against a known control. Because de novo sequences can be uncovered, parallel quality check with Sanger sequencing may be required, which adds additional cost and time [47]. In addition, results are delayed compared to the other two methods due to the extensive computational analysis required [51].

Summary

The three diagnostic tools for genetics and genomics have many overlapping features. Nevertheless, each method has advantages and disadvantages. Because FISH is visualized, results can be quantified and localized in the cell. However, the method requires specific training, and there is risk for interpretation errors. PCR is a very simple and widely available tool. The straightforward prep and rapidity enhances its value. Nonetheless, because of its amplifying attributes, erroneous products from primer recombination, primer and sample recombination, and contamination are problematic. In addition, both of these methods require selection of specific primers and probes at the onset of the studies, which can narrow and discriminate the search from the beginning.

On the other hand, NGS is a method that does not require preselection of primers or probes. In fact, NGS can reveal de novo sequences that may disclose new findings. However, cost is still a limiting factor despite recent significant reductions. In-depth knowledge and experience are also required for sample preparation and data analysis. Specimens are usually prepared from fresh tissue, such as whole blood and fresh tumor. NGS results from FFPE specimens are not as robust given the protein-DNA interactions from the fixation process, but tremendous technological and computational advancements in this area are underway [56]. Lastly, a quick result is unfeasible because of the extensive computational analysis currently required.

Future Directions

As advancements are made in our understanding of the molecular pathways of ophthalmic disease, ocular pathology will continue to develop and evolve. The exciting new era of personalized medicine, in particular, has ushered in new

opportunities in diagnostic pathology. Discoveries at the research bench are rapidly being translated into clinical practice with the intimate assistance of pathology. The following chapter highlights this new frontier, which foretells exciting and promising treatments for patients.

References

1. Coons AH, Creech HJ, Jones RN. Immunological properties of an antibody containing a fluorescent group. Exp Biol Med. 1941;47(2):200–2.
2. Buchwalow IB, Böcker W. Immunohistochemistry: basics and methods. Berlin Heidelberg: Springer Science & Business Media; 2010. p. 153.
3. Humphrey PA, Dehner LP, Pfeifer JD. The Washington manual of surgical pathology. Philadelphia: Lippincott Williams & Wilkins; 2008. p. 804.
4. Brownstein S, Jiang K, Lam K, Burns B, Farmer J. Immunohistochemical analysis with a novel red chromagen of benign and malignant melanocytic lesions of the conjunctiva. Invest Ophthalmol Vis Sci. 2013;54(15):5894.
5. De Matos LL, Trufelli DC, de Matos MGL, da Silva Pinhal MA. Immunohistochemistry as an important tool in biomarkers detection and clinical practice. Biomark Insights. 2010;5:9–20.
6. Fritschy J-M. Is my antibody-staining specific? How to deal with pitfalls of immunohistochemistry. Eur J Neurosci. 2008; 28(12):2365–70.
7. Kakar S, Torbenson M, Jain D, Wu T-T, Yeh M, Ferrell LD. Immunohistochemical pitfalls in the diagnosis of hepatocellular adenomas and focal nodular hyperplasia: accurate understanding of diverse staining patterns is essential for diagnosis and risk assessment. Mod Pathol. 2015;28(1):159–60.
8. Fletcher CDM. The evolving classification of soft tissue tumours: an update based on the new WHO classification. Histopathology. 2006;48(1):3–12.
9. Doyle LA, Vivero M, Fletcher CD, Mertens F, Hornick JL. Nuclear expression of STAT6 distinguishes solitary fibrous tumor from histologic mimics. Mod Pathol: Off J United States Can Acad Pathol Inc. 2014;27(3):390–5.
10. Leon-Villapalos J, Wolfe K, Kangesu L. GLUT-1: an extra diagnostic tool to differentiate between haemangiomas and vascular malformations. Br J Plast Surg. 2005;58(3):348–52.
11. North PE, Waner M, Mizeracki A, Mihm MC. GLUT1: a newly discovered immunohistochemical marker for juvenile hemangiomas. Hum Pathol. 2000;31(1):11–22.
12. Schwartz SR, Kodsi SR, Blei F, Ceisler E, Steele M, Furlan L. Treatment of capillary hemangiomas causing refractive and occlusional amblyopia. J Aapos: Off Publ Am Assoc Pediatr Ophthalmol Strabismus Am Assoc Pediatr Ophthalmol Strabismus. 2007;11(6):577–83.
13. Léauté-Labrèze C, Dumas de la Roque E, Hubiche T, Boralevi F, Thambo J-B, Taïeb A. Propranolol for severe hemangiomas of infancy. N Engl J Med. 2008;358(24):2649–51.
14. Fulwyler MJ. Electronic separation of biological cells by volume. Science. 1965;150(3698):910–1.
15. Wolfgang D, Wolfgang G, Dittrich W. Flow-through chamber for photometers to measure and count particles in a dispersion medium [Internet]. DE1815352 (A1) Abstract of corresponding document: US3761187 (A), 1971 [cited 2016 Aug 16]. Available from: https://worldwide.espacenet.com/publicationDetails/biblio;jsessionid=p-rppGcNkkvwKkHjHvbNuyRE.espacenet_levelx_prod_3?FT=D&date=19710114&DB=&locale=en_EP&CC=DE&NR=1815352A1&KC=A1&ND=1
16. Salzman GC. Flow cytometry: the use of lasers for rapid analysis and separation of single biological cells. In: Leon Goldman MD, editor. The biomedical laser [Internet]. New York: Springer; 1981. [cited 2016 Aug 22]. p. 33–53. Available from: http://link.springer.com/chapter/10.1007/978-1-4612-5922-0_5.
17. Virgo PF, Gibbs GJ. Flow cytometry in clinical pathology. Ann Clin Biochem. 2012;49(1):17–28.
18. Kussick SJ, Kalnoski M, Braziel RM, Wood BL. Prominent clonal B-cell populations identified by flow Cytometry in histologically reactive lymphoid proliferations. Am J Clin Pathol. 2004;121(4):464–72.
19. Shields JA, Stopyra GA, Marr BP, et al. Bilateral orbital myeloid sarcoma as initial sign of acute myeloid leukemia: case report and review of the literature. Arch Ophthalmol. 2003;121(1):138.
20. Julius MH, Masuda T, Herzenberg LA. Demonstration that antigen-binding cells are precursors of antibody-producing cells after purification with a fluorescence-activated cell sorter. Proc Natl Acad Sci U S a. 1972;69(7):1934–8.
21. June CH, Maus MV, Plesa G, Johnson LA, Zhao Y, Levine BL, et al. Engineered T cells for cancer therapy. Cancer Immunol Immunother. 2014;63(9):969–75.
22. Riddell SR, Sommermeyer D, Berger C, Liu LS, Balakrishnan A, Salter A, et al. Adoptive therapy with chimeric antigen receptor modified T cells of defined subset composition. Cancer J: Sudbury Mass. 2014;20(2):141–4.
23. Han Y, Lo Y-H. Imaging cells in flow cytometer using spatial-temporal transformation. Sci Rep. 2015;5:13267.
24. Cheung MC, McKenna B, Wang SS, Wolf D, Ehrlich DJ. Image-based cell-resolved screening assays in flow: image-based cell screening assay. Cytometry a. 2015;87(6):541–8.
25. Jahan-Tigh RR, Ryan C, Obermoser G, Schwarzenberger K. Flow Cytometry. J Invest Dermatol. 2012;132(10):1–6.
26. O'Connor C. Fluorescence in Situ Hybridization (FISH). Nat Educ. 2008;1(1):171.
27. Gall JG, Pardue ML. Formation and detection of RNA-DNA hybrid molecules in cytological preparations*. Proc Natl Acad Sci U S A. 1969;63(2):378–83.
28. Cabili MN, Dunagin MC, McClanahan PD, Biaesch A, Padovan-Merhar O, Regev A, et al. Localization and abundance analysis of human lncRNAs at single-cell and single-molecule resolution. Genome Biol. 2015;16:20.
29. Yanagi M, Shinjo K, Takeshita A, Tobita T, Yano K, Kobayashi M, et al. Simple and reliably sensitive diagnosis and monitoring of Philadelphia chromosome-positive cells in chronic myeloid leukemia by interphase fluorescence in situ hybridization of peripheral blood cells. Leukemia. 1999;13(4):542–52.
30. Koretzky GA. The legacy of the Philadelphia chromosome. J Clin Invest. 2007;117(8):2030–2.
31. Uckun FM, Nachman JB, Sather HN, Sensel MG, Kraft P, Steinherz PG, et al. Clinical significance of Philadelphia chromosome positive pediatric acute lymphoblastic leukemia in the context of contemporary intensive therapies: a report from the Children's cancer group. Cancer. 1998;83(9):2030–9.
32. Raponi S, De Propris MS, Wai H, Intoppa S, Elia L, Diverio D, et al. An accurate and rapid flow cytometric diagnosis of BCR-ABL positive acute lymphoblastic leukemia. Haematologica. 2009;94(12):1767–70.
33. Trask BJ. Human cytogenetics: 46 chromosomes, 46 years and counting. Nat rev Genet. 2002;3(10):769–78.
34. Linardic CM. PAX3-FOXO1 fusion gene in rhabdomyosarcoma. Cancer Lett. 2008;270(1):10–8.
35. Pathology Handbook Review [Internet]. [cited 2016 Aug 19]. Available from: https://www.pathology.med.umich.edu/handbook/details.php?testID=4793
36. Hu L, Ru K, Zhang L, Huang Y, Zhu X, Liu H, et al. Fluorescence in situ hybridization (FISH): an increasingly demanded tool for

biomarker research and personalized medicine. Biomark Res. 2014;2:3.
37. Wolff DJ, Bagg A, Cooley LD, Dewald GW, Hirsch BA, Jacky PB, et al. Guidance for fluorescence in situ hybridization testing in hematologic disorders. J Mol Diagn: JMD. 2007;9(2):134–43.
38. Bartlett JS, Stirling D. A short history of the polymerase chain reaction. In: Bartlett JS, Stirling D, editors. PCR protocols [Internet]. Totowa: Humana Press; 2003. [cited 2016 Aug 19]. pp. 3–6. (Methods in Molecular Biology™). Available from: http://dx.doi.org/10.1385/1-59259-384-4%3A3.
39. Garibyan L, Avashia N. Polymerase chain reaction. J Invest Dermatol. 2013;133(3):1–4.
40. Cai HY, Caswell JL, Prescott JF. Nonculture molecular techniques for diagnosis of bacterial disease in animals a diagnostic Laboratory perspective. Vet Pathol: Online. 2014;51(2):341–50.
41. Yang S, Rothman RE. PCR-based diagnostics for infectious diseases: uses, limitations, and future applications in acute-care settings. Lancet Infect dis. 2004;4(6):337–48.
42. Browne HP, Forster SC, Anonye BO, Kumar N, Neville BA, Stares MD, et al. Culturing of "unculturable" human microbiota reveals novel taxa and extensive sporulation. Nature. 2016;533(7604):543–6.
43. Stewart EJ. Growing unculturable bacteria. J Bacteriol. 2012; 194(16):4151–60.
44. Binenbaum G, Bruno CJ, Forbes BJ, Snyder M, Mollen TJ, Schmidt B, et al. Periocular ulcerative dermatitis associated with gentamicin ointment prophylaxis in newborns. J Pediatr. 2010;156(2):320–1.
45. Padmanabhan R, Padmanabhan R, Wu R. Nucleotide sequence analysis of DNA. Biochem Biophys res Commun. 1972;48(5):1295–302.
46. Jou WM, Haegeman G, Ysebaert M, Fiers W. Nucleotide sequence of the gene coding for the bacteriophage MS2 coat protein. Nature. 1972;237(5350):82–8.
47. Goodwin S, McPherson JD, McCombie WR. Coming of age: ten years of next-generation sequencing technologies. Nat rev Genet. 2016;17(6):333–51.
48. Alberti A, Belser C, Engelen S, Bertrand L, Orvain C, Brinas L, et al. Comparison of library preparation methods reveals their impact on interpretation of metatranscriptomic data. BMC Genomics. 2014;15:912.
49. Bentley DR, Balasubramanian S, Swerdlow HP, Smith GP, Milton J, Brown CG, et al. Accurate whole human genome sequencing using reversible terminator chemistry. Nature. 2008;456(7218):53–9.
50. Rusk N. Torrents of sequence. Nat Methods. 2011;8(1):44.
51. Oliver GR, Hart SN, Klee EW. Bioinformatics for clinical next generation sequencing. Clin Chem. 2015;61(1):124–35.
52. Rodríguez-Ezpeleta N, Hackenberg M, Aransay AM. Bioinformatics for high throughput sequencing. New York: Springer Science & Business Media; 2011. p. 258.
53. De Magalhães JP, Finch CE, Janssens G. Next-generation sequencing in aging research: emerging applications, problems, pitfalls and possible solutions. Ageing res rev. 2010;9(3):315–23.
54. Li WL, Buckley J, Sanchez-Lara PA, Maglinte DT, Viduetsky L, Tatarinova TV, et al. A rapid and sensitive next-generation sequencing method to detect RB1 mutations improves care for retinoblastoma patients and their families. J Mol Diagn: JMD. 2016;18(4):480–93.
55. Rushlow DE, Mol BM, Kennett JY, Yee S, Pajovic S, Thériault BL, et al. Characterisation of retinoblastomas without RB1 mutations: genomic, gene expression, and clinical studies. Lancet Oncol. 2013;14(4):327–34.
56. Hedegaard J, Thorsen K, Lund MK, Hein A-MK, Hamilton-Dutoit SJ, Vang S, et al. Next-generation sequencing of RNA and DNA isolated from paired fresh-frozen and formalin-fixed paraffin-embedded samples of human cancer and normal tissue. PLoS One. 2014;9(5):e98187.
57. Eagle RC Jr. Immunohistochemistry in diagnostic ophthalmic pathology: a review: immunohistochemistry in diagnostic ophthalmic pathology. Clin Experiment Ophthalmol. 2008;36(7):675–88.
58. Robinson JT, Thorvaldsdóttir H, Winckler W, Guttman M, Lander ES, Getz G, et al. Integrative genomics viewer. Nat Biotechnol. 2011;29(1):24–6.

Genomic Applications for Pediatric Orbital Tumours

17

Timothy John Sullivan

Abbreviations

ERK	Extracellular signal-regulated protein kinase
mTOR	Mammalian target of rapamycin
MAPK	Mitogen-activated protein kinase
PTEN	Phosphatase and tensin homolog
PI3K	Phosphoinositide 3-kinase
PHTS	PTEN hamartoma tumour syndrome
Rb	Retinoblastoma
MEK	RAS-RAF-mitogen-activated protein kinase kinase

The previous chapter on molecular pathology of oculoplastic disorders has provided an insight into the important relationship between the orbital surgeon and pathologist, highlighting the pathological technics that underpin the management of pediatric orbital tumours. The importance of combining clinical and imaging information with the pathological assessment cannot be stressed too strongly. Pathological assessment has classically included morphological, immunohistochemical and flow cytometric and cytogenetic results. Both now and in the future, however, additional genetic, epigenetic, proteomic and metabolomic data will individualize targeted therapies for pediatric orbital tumours.

In order to fully understand this personalized approach to therapy, one needs to have a basic knowledge of the oncological process in order to have an understanding of potential therapeutic options. Firstly, one must understand the concepts of cell origin and cancer stem cells [1, 2]. For some well-differentiated tumours, the cell of origin might be obvious, but for many poorly differentiated lesions, a tumour's lineage may be unclear. In either case, the cell of origin undergoes various genetic changes usually mediated by oncogenes and tumour suppressor genes to develop a cell population of precursor tumour cells and eventually more evolved tumour cells. Some of these may acquire additional genetic or epigenetic changes which form a subpopulation of cancer stem cells (CSCs). These CSCs have the capability for self-renewal, can give rise to other tumour cells in a given population, demonstrate a greater resistance to chemotherapy and have an ability to repopulate after completion of chemotherapy.

There are certain hallmarks of cancer that influence all malignant tumours, and, again, these may provide targets for individualized treatments. While tumour cells are central to the process, however, they do not act alone. They develop amidst populations of recruited, ostensibly normal, bystander cells, tissue stroma, proteins and metabolites which form a heterotypic tumour microenvironment characterized by complex multidirectional interactions.

Hanahan and Weinberg have promulgated a concept of "hallmarks of cancer" that are common to tumour development [1, 3]. These hallmarks of cancer can enable us to better comprehend the development of tumours as we endeavour to develop specific treatments for eliminating the lesion, preventing recurrence and metastasis with minimal side effects (Table 17.1).

They also describe various normal cellular signalling pathways that are altered in cancer cells and can be portrayed as overlapping and interacting integrated circuits or pathways, supporting various functions including, but not limited to, motility, viability, cell stasis, differentiation and proliferation [4]. These include the Ras-Raf-MEK-ERK signalling pathway, hedgehog signalling pathway, canonical and noncanonical Wnt signalling and the P13K/AKT MTOR pathway [5–8]. Further PTEN and AKT can act as a powerful switch between oncogenes and tumour suppressor genes [9]. FGF also plays a role in influencing signalling pathways [10].

Additional factors influence the hallmarks of cancer, namely, genetic and epigenetic instability and tumour-induced or tumour-associated inflammation. Cancer cells may have increased susceptibility to local mutagens, and there may be reduced efficiency of tumour suppressors such

T.J. Sullivan
Department of Ophthalmology, School of Medicine, University of Queensland, Royal Brisbane and Women's Hospital, Lady Cilento Children's Hospital, Brisbane, QLD, Australia
e-mail: tjs001@bigpond.net.au

© Springer International Publishing AG 2018

J.A. Katowitz, W.R. Katowitz (eds.), *Pediatric Oculoplastic Surgery*, https://doi.org/10.1007/978-3-319-60814-3_17

Table 17.1 Hallmarks of cancer

1	Sustaining proliferative signalling	Conveyed by growth factors usually with tyrosine kinase domains
2	Evading growth suppressors	Often involves altering function of two major tumour suppressor genes encoding Rb and TP53 proteins
3	Resisting cell death	Apoptosis (extrinsic and intrinsic) downregulated by upstream and downstream effectors. Bcl-2 activity, loss of TP53
4	Enabling replicative immortality	Telomeric protection of the end of chromosomes confers immortality. TERT signalling of the Wnt pathway
5	Inducing angiogenesis	Upregulated VEGF-A and FGF stimulate angiogenesis. Thrombospondin-1 counteracts angiogenesis and is decreased in tumour formation
6	Activating invasion and metastasis	Decreased E-cadherin promotes invasion and metastasis. Tissue inhibitor of metalloproteinase 3 (TIMP-3) is also involved in this process (Choi) Epithelial mesenchymal transition leading to metastasis-driven cancer cells, extracellular matrix and tumour microenvironment
7	Deregulating cellular energy metabolism	Glucose metabolism is directed towards glycolysis. Energy is used for cell replication rather than standard metabolism. Mediated by activated oncogenes (RAS, MYC) and mutant tumour suppressors (TP53)
8	Evading immune destruction	Reduced immune surveillance seen in immunocompromised patients. Immunogenic cancer cells may secrete TGF-β to inactivate NK cells. Recruited Tregs may also be immunosuppressive

as TP53. Genetic mechanisms include alterations to DNA such as mutation, deletion, translocation, insertion, and aneuploidy [11]. Cell cycle can be influenced by a number of genes including Rb, p16INK4a, p15INK4b, 14–3-3, cyclin D2, cyclin E and p14ARF. Signal transduction is affected by ErbB2, RASSF1, LKB1/STK11 and APC. Apoptosis has many modifiers, but two genes involved include death-associated protein kinase gene (DAPK) and caspase-8lk. MGMT, MLH1, BRCA1, and FNACF all impact upon DNA repair. Telomerase activity via TERT and TERC impinges upon senescence [12]. The hedgehog pathway also influences these cancer signalling pathways [13].

Epigenetic mechanisms influence every stage of tumorigenesis and include those changes in gene function that are mitotically or meiotically heritable but are not associated with a change in DNA sequence [11]. Common epigenetic mechanisms include chromatin changes, histone modification, and DNA methylation [12]. Histone modifications are often covalent changes that result in switching the target gene off. There can also be microRNA changes. These small non-coding RNAs have an epigenetic role and can be oncogenic, tumour suppressor or context dependant. DNA contains the genetic code, but RNA acts as the messenger via transcription to express phenotype. Altered transcription leads to many human cancers and genetic disorders. The phenotypic expression of genes can be modified profoundly by epigenetic factors such as chromatin remodelling and histone modifications. Interestingly cancer cells usually have up to 10 genetic changes but between 100 and 1000 epigenetic modifications [11]. The epigenetic changes are important in tumour initiation and subsequent progression.

The interaction between tumour cells and the tumour microenvironment is critical. Tumour cells can elaborate tumour-associated antigens (TAA) which can assist in evasion of host immune responses. Various mesenchymal stem cells (MSCs), regulatory T cells (Tregs), macrophages and stromal fibroblasts interact and elaborate cytokines and other proteins facilitating tumour progression. Some of the normal immune cells, natural killers (NKs), dendritic cells and cytotoxic T lymphocytes are downregulated to allow tumour growth [14].

These complex genetic, epigenetic and proteomic changes in individual tumours are being assessed not just in the research laboratory but also in the clinical setting. Next generation sequencing has permitted this and will become increasingly available over the next decade. For this huge amount of data to be processed, the discipline of bioinformatics has burgeoned. This analysis allows testing signals be converted to data which is analysed for interpretation to allow therapeutic decisions [15]. Bioinformatics involve primary, secondary and tertiary analysis of data, which requires documentation and validation. Genomic analysis pipelines can allow comparison of an individual's genome to human reference sequences. NGS has been applied to a number of pediatric tumours that can occur in the orbit, most notably, rhabdomyosarcoma (RMS) [16, 17].

The types of cancer seen in the pediatric orbit are very different from those seen in adult practice, where carcinomas and lymphomas predominate. Rarely, carcinomas of the lacrimal gland arise in children, including adenoid cystic carcinoma. The pediatric population more commonly manifests tumours which present early and are possibly the result of disordered organogenesis. Tumours of uncertain origin occur and often fall into the undifferentiated or poorly differentiated sarcoma group, i.e. small round blue cell tumours [18]. With regard to rhabdomyosarcoma (RMS), it often occurs in areas largely devoid of skeletal muscle. RMS can be subdivided into alveolar, embryonal and pleomorphic types. Histogenically, it is presumed to derive from primitive mesenchymal cells. Mouse studies suggest that alveolar RMS may derive from myofibres, or late myoblasts. Embryonal RMS may arise from a differentiating myoblast [18].

ARMS usually carries specific chromosomal translocations that result in PAX3– or PAX7–FOXO1 fusion genes, with fusion positive lesions having a poorer prognosis.

ERMS commonly harbours loss of heterozygosity at 11p15.5 and gains of chromosomes 2, 8, and 12 in varying combinations3,4 [17]. Because of the relatively small number of genetic mutations in RMS, epigenetic factors are presumed to play a significant role. Recently, molecular cytogenetic alterations in RMS have been identified by array comparative genomic hybridization (aCGH). All RMS showed specific gains and losses. 12q13.12, 12q13.3 and 12q13.3-q14.1 were amplified. 1p21.1, 2q14.1, 5q13.2, 9p12, and 9q12 showed deletions. The mRNA levels of Gli1 and GEFT were elevated. Bioinformatic analysis showed that genes were enriched in functions such as immunoglobulin domain, induction of apoptosis, and defensin. This may allow the development of biomarkers and drug targets for RMS [17, 19]. Further whole-exome/whole-transcriptome sequencing, copy number (CN) and DNA methylome analyses have shed light on the genetic/epigenetic basis of RMS [16].

Looking at DNA methylation patterns, four distinct groups of RMS could be identified, which are in concordance with histological phenotype, mutation and copy number profiles and clinical course. A1and A2 subtypes correspond to alveolar histology with frequent PAX3/7 fusions and alterations in cell cycle regulators. E1 and E2 subtypes, or largely embryonal histology, are characterized by a high frequency of CN alterations and/or allelic imbalances, FGFR4/RAS/AKT pathway mutations and PTEN mutations/methylation. E2 was also characterized by p53 inactivation, which again correlated with poor outcome. The strong association with methylation status emphasizes the importance of epigenetic phenomena in RMS [16]. Another study identified differential transcriptional regulation of PAX3:FOXO1, suggesting that a histone deacetylase inhibitor might be able to convert fusion-positive lesions into a state similar to fusion-negative RMS, with a corresponding improved prognosis [20].

Ewing's sarcoma and PNET are similar primitive neuroectodermal tumours which show CD99 positivity on immunohistochemistry, with a characteristic genetic translocation t(11:22)(q24q12). These tumours can arise in bones with intramembranous ossification, possibly from cells with neuroepithelial or mesenchymal lineage, or possibly both. Beyond the genetic changes, Ewing's demonstrates epigenetic dysregulation. EWSR1-Fli1 is an oncogenic transcription factor with a myriad of downstream target genes that drive Ewing's sarcoma. Histones may also be altered and chromatin remodelling conformationally allows access to DNA for tumour progression [18]. Targeting EWS/FLI with a range of different agents is currently under investigation in clinical trials [21]. Localized disease has a reasonable prognosis with 65–75% 5-year survival rates, but up to a quarter of patients have metastatic disease at presentation, with a much poorer prognosis [21].

Histiocytic lesions are relatively common in pediatric orbital practice and include Langerhans' cell histiocytosis (LCH), predominately and less commonly juvenile xanthogranuloma (JXG), Rosai-Dorfman disease (RDD) and Erdheim-Chester disease (ECD) [22, 23]. LCH is known to be a clonal proliferation of myeloid derived cells. The non-LCH is thought to derive from monocytic or macrophage origin. These histiocytic lesions demonstrate BRAF V600E mutations resulting in activation of MAPK and or PI3K-AKT pathways. ARAF mutations are also seen in LCH and some JXG cases. RAF inhibitors have shown significant response in BRAF V600E histiocytoses, and MEK inhibitors have also been used with fewer results available [24, 25].

Neurofibromatosis 1 results from mutations or deletions of the neurofibromin gene, located at chromosome 17p11.2 [26]. Normally the gene product downregulates RAS protein. When neurofibromin is reduced, RAS GTP causes general cell growth and predispose to malignant change. While many of the ocular manifestations of NF1 are in the realm of the pediatric ophthalmologist, the orbital surgeon will encounter both plexiform neurofibromas and optic nerve or anterior visual pathway gliomas. Plexiform neurofibromas have been associated with progression to malignant peripheral nerve sheath tumours, accompanied by additional genetic and epigenetic events, including changes to TP53, Rb gene, PTEN and CDKN2A [27]. Plexiform neurofibromas can be enormously disfiguring and troublesome for affected individuals, with many lesions inoperable because of impingement on vital structures in the skull base. The RAF/MEK/ERK pathway is the key driver for sustained growth in these lesions [28, 29]. MEK inhibitors trametinib and selumetinib have shown promise in reducing lesion size [30] (Fig. 17.1). It is likely that long-term treatment will be required to prevent rebound enlargement.

Optic nerve gliomas, which are histologically low grade pilocytic astrocytomas, have abnormalities of the MAPK pathway. Next-generation sequencing has shown there are many MAPK genetic alterations, as well as BRAF fusions, methylation and transcription changes in these tumours [31]. While carboplatin and vincristine have been the chemotherapeutic agents of choice, targeted therapies are theoretically possible and with reduced side effects ultimately more desirable. Murine studies demonstrated MEK and Akt were hyperactivated in Nf1-deficient astrocytes in vitro and in Nf1 murine optic gliomas in vivo. MEK pharmacologic blockade also attenuated Nf1-deficient astrocytes as well as Nf1 optic glioma volume and proliferation [32]. This supports using pharmacologic inhibitors that target mTOR function in future human NF1 optic pathway glioma clinical trials.

Many vascular tumours are driven by the altered signalling pathways. Typical mutations are seen in the PTEN hamartoma-tumour syndrome. All of these patients have macrocephaly and about 50% have vascular anomalies [33].

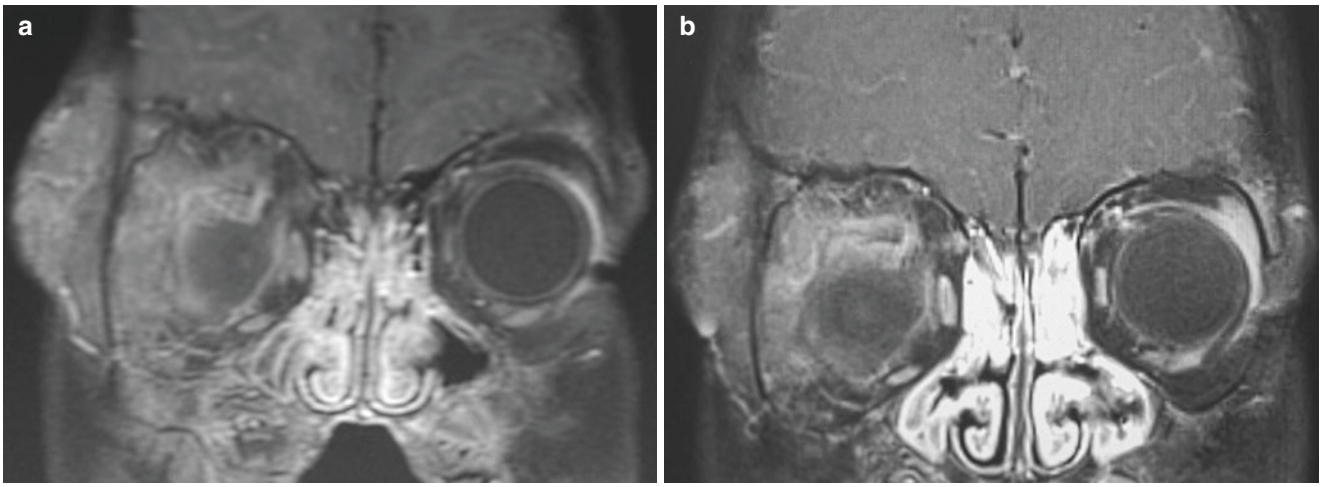


Fig. 17.1 (**a**) MRI of patient with orbital and periorbital plexiform neurofibroma prior to commencing the MEK inhibitor trametinib. (**b**) MRI of the same patient with orbital and periorbital plexiform neurofibroma after 19 months of taking the MEK inhibitor trametinib as part of a trial. This scan shows stability of the lesion, whereas all prior successive images showed progressive growth before commencing trametinib

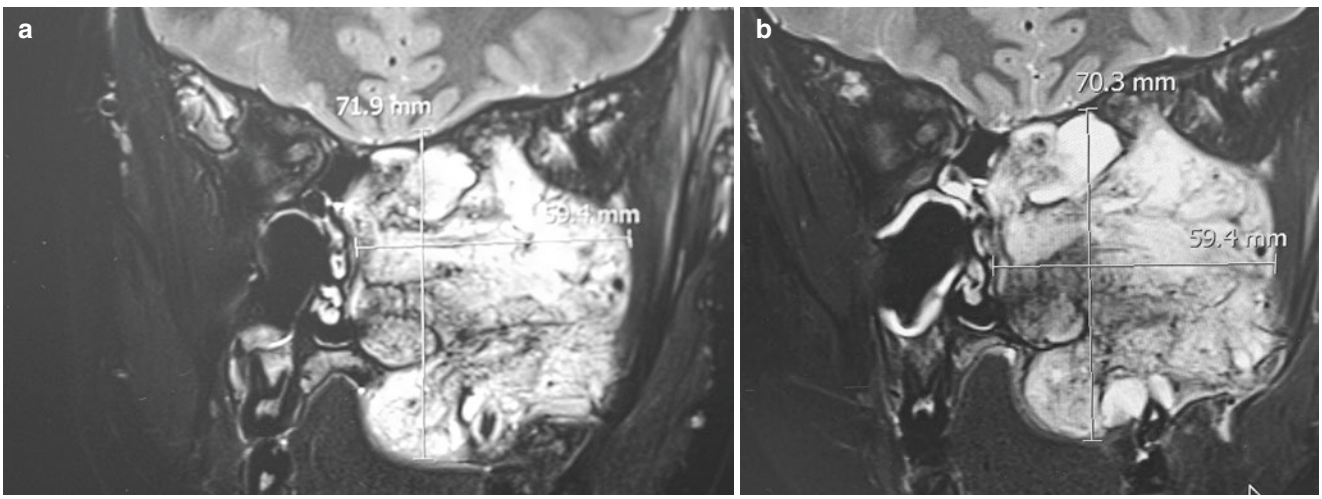


Fig. 17.2 (**a**) T1-weighted MRI, post contrast, of patient with a large pterygopalatine fossa and orbital PTEN vascular malformation prior to commencing the mTOR inhibitor sirolimus. (**b**) T1-weighted MRI, post contrast, of the same patient with a large pterygopalatine fossa and orbital PTEN vascular malformation 6 months after commencing the mTOR inhibitor Sirolimus, showing stability of the lesion. Previous successive scans demonstrated continued progressive enlargement

These have been shown to respond to treatment with mTOR inhibitors [34] (Fig. 17.2). Neuroblastoma, one of the more common pediatric orbital metastases, has also proved amenable to targeted therapy to improve outcomes [35].

This chapter has highlighted the genomic and epigenetic basis of pediatric orbital tumours, focusing on some of the more common lesions to illustrate how targeted and personalized care is accompanying the rapid advances in the laboratory [36]. What can be said at present, with some confidence, is that as a more complete understanding of the genetic and epigenetic aberrations, cancer pathways and proteomics develops, there will be a parallel improvement in available targeted therapies.

References

1. Hanahan D, Weinberg RA. Hallmarks of cancer: the next generation. Cell. 2011;144:646–74.
2. Visvader JE. Cells of origin in cancer. Nature. 2011;469:314–21.
3. Hanahan D, Weinberg RA. The hallmarks of cancer. Cell. 2000;100:57–70.
4. Hahn WC, Weinberg RA. A subway map of cancer pathways. Nat Rev Cancer. [online]. http://www.nature.com/nrc/poster/subpathways/index.html
5. Neuzillet C, Tijeras-Raballand A, de Mestier L, Cros J, Faivre S, Raymond E. MEK in cancer and cancer therapy. Pharmacol Ther. 2014;141:160–71.
6. Simoes AES, Rodrigues CMP, Borralho PM. The MEK5/ERK5 signalling pathway in cancer: a promising novel therapeutic target. Drug Discov Today. 2016;21:1654–63.

7. Asem MS, Buechler S, Burkhalter Wates R, Miller DL, Sharon Stack M. Wnt5a Signaling in Cancer. Cancers (Basel). 2016;8(9):79.
8. Mayer IA, Artega CL. The PI3K/AKT pathway as a target for cancer treatmen.T. Annu Rev Med. 2016;67:11–28.
9. Xie Y, Naizabekov S, Chen Z, Tokay T. Power of PTEN/AKT: molecular switch between tumor suppressors and oncogenes. Oncol Lett. 2016;12:375–8.
10. Katoh M, Nakagama H. FGF receptors: cancer biology and therapeutics. Med Res Rev. 2014;34:280–300.
11. Choi JD, Lee J-S. Interplay between epigenetics and genetics in cancer. Genomics Inform. 2013;11:164–73.
12. Shen H, Laird PW. Interplay between the cancer genome and epigenome. Cell. 2013;153:38–55.
13. Araujo SJ. The hedgehog Signalling pathway in cell migration and guidance: what we have learned from Drosophila melanogaster. Cancers (Basel). 2015;7:2012–22.
14. Liu M, Zhou MJ, Chen Z, Chen A. Understanding the epigenetic regulation of tumours and their microenvironments: opportunities and problems for epigenetic therapy. J Pathol. 2017;241:10–24.
15. Oliver GR, Hart SN, Klee EW. Bioinformatics for clinical next generation sequencing. Clin Chem. 2015;61:124–35.
16. Seki M, Nishimura R, Yoshida K, Shimamura T, Shiraishi Y, Sato Y. Integrated genetic and epigenetic analysis defines novel molecular subgroups in rhabdomyosarcoma. Nat Commun. 2015;6:7557.
17. Liu C, Li D, Jiang J, Hu J, Zhang W, Chen Y, Cui X, Qi Y, Zou H, Zhang W, Li F. Analysis of molecular cytogenetic alteration in rhabdomyosarcoma by array comparative genomic hybridization. PLoS One. 2014;9(4):e9492.
18. O'Sullivan M. Pediatric soft tissue tumor pathology: a happy morpho-molecular union. Semin Diagn Pathol. 2016;33:377–95.
19. Shern JF, Chen L, Chmielecki J, Wei JS, Patidar R, Rosenberg M, et al. Comprehensive genomic analysis of rhabdomyosarcoma reveals a landscape of alterations affecting a common genetic axis in fusion-positive and fusion-negative tumors. Cancer Discov. 2014;4:216–3.
20. Abraham J, Nuñez-Álvarez Y, Hettmer S, Carrió E, Chen HI, Nishijo K, et al. Lineage of origin in rhabdomyosarcoma informs pharmacological response. Genes Dev. 2014;28:1578–91.
21. Pishas KI, Lessnick SL. Recent advances in targeted therapy for Ewing sarcoma. F1000Research. 2016;5:2077.
22. Sullivan TJ. Histiocytic, hematopoietic, and lymphoproliferative disorders. Ch 27 244–249. In: Lambert SR, Lyons CJ, editors. Pediatric ophthalmology and strabismus. 5th ed. Philadelphia: Elsevier; 2017.
23. Maccheron LJ, McNab AA, Elder J, Selva D, Martin FJ, Clement CI, Sainani A, Sullivan TJ. Ocular adnexal Langerhan's cell histiocytosis: clinical features and management. Orbit. 2006;25:169–77.
24. Allen CE, Ladisch S, McClain KL. How I treat Langerhans cell Histiocytosis. Blood. 2015;126:26–35.
25. Durham BH, Diamond EL, Abdel-Wahab O. Histiocytic neoplasms in the era of personalized genomic medicine. Curr Opin Hematol. 2016;23:416–25.
26. Schnur RE. Type 1 neurofibromatosis: a geno-ocluo-dermatologic update. Curr Opin Ophthalmol. 2012;23:364–72.
27. Karajannis MA, Ferner RE. Neurofibromatosis-related tumors: emerging biology and therapies. Curr Opin Pediatr. 2015;27:26–33.
28. Rodriguez FJ, Raabe EH. mTOR: a new therapeutic target for pediatric low-grade glioma? CNS Oncol. 2014;3:89–91.
29. Gutmann DH. Eliminating barriers to personalized medicine: learning from neurofibromatosis type 1. Neurology. 2014;83:463–71.
30. Jessen WJ, Miller SJ, Jousma E, et al. MEK inhibition exhibits efficacy in human and mouse neurofibromatosis tumors. J Clin Invest. 2013;123:340–7.
31. Helfferich J, Nijmeijer R, Brouwer OF, et al. Neurofibromatosis type 1 associated giomas: a comparison with sporadic low grade gliomas. Crit Rev Oncol Hematol. 2016;104:30–41.
32. Kaul A, Toonen JA, Cimino P, et al. Akt- or MEK-mediated mTOR inhibition suppresses Nf1 optic glioma growth. Neuro-Oncology. 2015;17:843–53.
33. Tan WH. The spectrum of vascular anomalies in patients with PTEN mutations: implications for diagnosis and management. J Med Genet. 2007;44:594–602.
34. Schmid GL, Kässner F, Uhlig HH. Sirolimus treatment of severe PTEN hamartoma tumor syndrome: case report and in vitro studies. Pediatr Res. 2014;75:527–34.
35. Owens C, Irwin M. Neuroblastoma: the impact of biology and cooperation leading to personalized treatments. Crit Rev Clin Lab Sci. 2012;49:85–115.
36. Ahuja N, Sharma AR, Baylin SB. Epigenetic therapeutics: a new weapon in the war against cancer. Annu Rev Med. 2016;67:73–89.

Aesthetic Considerations in Pediatric Oculoplastic Surgery

18

Jill A. Foster and Femida Kherani

Introduction

While the functional aspects of preserving and optimizing developing visual function take precedence over beauty, respect and consideration for symmetry and cosmesis play an important role in planning and execution of pediatric plastic surgery. Even when our more complex and developed intellectual guidance system may identify that making judgments of value based on appearance is superficial and misleading, our primitive brain still seeks out symmetry and prefers faces with expected facial contours as signs of health and reproductive success [1]. Even neonates have the ability to distinguish beauty [2] and prefer to look at congruent faces [3]. While children of any age prefer images perceived as beautiful, social awareness of appearance and rejection of differences sharpens around the age of 5 or 6 and becomes the most intolerant in the early teens and then relents again with maturity.

It is also important to recognize that concerns about "abnormal" appearance play a major role in a child's sense of self and well-being. Even mild facial and ocular deformities are frequently the source of emotional stress for children in particular. This has been observed even in visually impaired children who cannot see themselves in a mirror but interpret the reactions of others. In addition, in the age of social media, there is greater emphasis on appearance as projected by social media. Efforts to improve a child's appearance have major benefits in psychosocial development and well-being. Self-consciousness about appearance alters interactions with family and peers, and consequently, this becomes a functional problem (not just cosmetic). When improved by intervention, confidence in appearance can help these children to better develop into productive and fulfilled adult members of society.

Certain tenants of beauty may be applied as generalizations for any physician involved in reconstruction or modification of the pediatric facial structures. Symmetry, "average" facial contours and "average" relationships of the facial units, and smooth, evenly colored skin that reflects light in the expected patterns are all key components of facial beauty. Using these goals as parameters for reconstructive design and surgical planning is a key tool for the creation of an aesthetically satisfactory result.

The unique features of growth and development both help and hinder reconstructive and surgical planning in the pediatric patient. In some cases, growth or iatrogenic facilitation of asymmetrical growth may be used as a tool to further the goal of symmetry. In other cases, asymmetric growth or failure of growth of mal-developed tissues may accentuate aberrations as the child matures. The surgical symmetry that was achieved at a younger age may dissipate and require further intervention. While pediatric incisions with simple primary closure may benefit with relative obscurity as the child ages, the cosmetic results of skin grafts are particularly challenging in children. These features of pediatric surgery also affect reconstructive and surgical decisions.

Cosmetic Considerations in Congenital Ptosis Repair

While achieving a clear visual axis is the primary goal of intervention for congenital ptosis, the goals of symmetry and "average" contours are also desired outcomes of intervention. The chapter on ptosis repair, Chap. 22, describes the preoperative evaluation and surgical techniques that are chosen to modify the lid position. There are, however, some additional techniques or variations of technique that may be employed to achieve the goals of symmetry and natural

J.A. Foster (✉)
Department of Ophthalmology, Nationwide Children's Hospital, Plastic Surgery Ohio, Ohio State University, Columbus, OH, USA
e-mail: fosterj@jillfoster.com

F. Kherani
Department of Surgery, University of Calgary, Calgary, Canada

Department of Ophthalmology, University of British Columbia, Vancouver, BC, Canada

© Springer International Publishing AG 2018

J.A. Katowitz, W.R. Katowitz (eds.), *Pediatric Oculoplastic Surgery*, https://doi.org/10.1007/978-3-319-60814-3_18

appearance. Particularly in the older child where retention of extra skin or orbicularis may not be as useful as it was in the younger-aged child, blepharoplasty may be performed at the time of the ptosis repair.

Choosing to remove the skin or skin and orbicularis from the eyelid at the time of ptosis repair to improve the eyelid fold is an example of adapting surgical technique to improve aesthetic outcome. This is particularly important in congenital ptosis because the maldevelopment of the eyelid muscle often requires muscle resection and therefore a shortening of the middle lamella. This shortening often results in a relative overlap of the anterior lamella, creating pediatric dermatochalasis with an overhanging eyelid fold following ptosis repair. The surgeon must face a conundrum in deciding if and how much of the eyelid fold to remove. The same eyelids that have poor levator function and require significant resection to elevate the lids (potentially creating more overhang of the skin) are the same eyes that are most likely to be prone to ocular surface exposure. Frontalis suspension surgery may also result in compounding the amount of tissue in the eyelid fold. When exposure presents significant concerns because of history of previous corneal ulcer, history of corneal insensitivity, history of previous surface exposure issues, history of decreased ocular motility, decreased Bell's response, or history of poor cognition and diminished responsiveness, the skin is typically left in place. Future intervention is always an option once adequate protection of the cornea has been established. In younger children who are not at significant risk for ocular surface exposure and where the overlapping lid fold will interfere with vision, blepharoplasty techniques are used to take away the excess skin. In older children where preservation of the skin for possible future adjustments is not necessary, conservative skin resection may also be performed at the time of levator resection or even in conjunction with a frontalis suspension (Fig. 18.1).

At the time of the procedure, the ptosis repair is performed first, and then with the eyelid in the new position, the upper skin is draped over the newly positioned eyelid, marking the overlap of the tissue along the eyelid crease with a skin marking pen. This redundant tissue is considered for possible resection. When the excess tissue has been removed, lid crease reformation is also performed to reestablish the connections between the levator muscle and the newly created lid crease. Even in cases of poor levator function, the scar from the lid crease reformation sutures helps to create the illusion of an eyelid crease.

Efforts to match the eyelid crease are also important aesthetic considerations in pediatric ptosis repair. The eyelid crease is formed by anterior attachments of the levator aponeurosis to the underside of the skin. In poor function ptosis or complete aponeurotic disinsertion, the eyelid crease may be indistinct or abnormally high on the involved lids. If one side has a more normal eyelid crease, this height may be used as the benchmark, and the lid incision is matched and marked on the contralateral eyelid. If both lid creases are indistinct, then preoperative measurements are used to set the height of the crease and the location of the incisions. Calipers are useful for locating and marking the planned incisions. If the crease is indistinct or requires modification, then techniques for eyelid crease reformation are used prior to and during closure. The hallmark of these techniques is creation of a purposeful scar attachment that will mimic the natural attachments between the skin and the levator aponeurosis to create the eyelid crease. Placing polyglactin 910 braided suture between the levator complex and the underside of the skin with a buried suture (buried interrupted 6.0 Vicryl {Ethicon, Cincinnati, OH} on a P-1 needle) is one effective lid crease reformation technique. The lid crease may also be magnified during skin closure by placing sutures from the skin to the levator aponeurosis and then to the skin on the other side of the incision. This also creates an adhesion between the skin and the levator complex. Either technique may be used individually, or both techniques may be used on the same eyelid when a very distinct lid crease is desired.

Asymmetric ptosis with poor levator function seen in concert with a contralateral relatively well functioning levator muscle represents one of the more convoluted surgical decision-making processes in congenital ptosis. The conservative choice will be to operate to raise only on the abnormal eyelid and accept compromise, recognizing that there is no mechanical way to get the two eyelids to move similarly. A more controversial but potentially better cosmetic choice would be to recommend that the frontalis suspension procedure be done on the poorly functioning lid and also be performed on the relatively normal eyelid along with extirpation of the levator muscle on the less ptotic side [4]. Crowell Beard described this technique in 1965. In patients with poor levator function and especially when there is amblyopia on the ptotic side, activation of frontalis drive on the more ptotic side may be difficult to achieve when the relatively normal eye and eyelid are working well without effort. In essence, using the bilateral technique, the surgeon is removing the better functioning levator muscle in a quest for improved symmetry and to require the use of the frontalis muscle to lift either eyelid. This requires discussion and consideration by the parents and the surgeon. A variation of this procedure termed the "Chicken Beard" was described by Alston Callahan [5] where the frontalis suspension is performed bilaterally but the levator muscle on the less ptotic eyelid remains intact.

Recognition that true unilateral congenital ptosis is a rare condition and that more commonly there is some alteration of function in the eyelid that appears to be more normal is also a useful concept in managing congenital ptosis. Sometimes better symmetry may be achieved by performing bilateral surgery, combining frontalis suspension on the more ptotic lid and conjunctival Mueller's muscle resection ptosis repair on the lid that appears to be the less ptotic lid. This could be nicknamed the "Chicken Katowitz."



Fig. 18.1 This patient had an initial ptosis repair at 5 months of age with a frontalis suspension procedure on the left upper eyelid. (**a**) Preoperative and (**b**) postoperative appearance of the eyelid. The skin was left intact at the time of her initial procedure, but when she returned at 5 years of age (**c**), it was elected to replace her silicone cable to re-elevate the eyelid, and at that time, the overlapping tissue in the lid fold was removed and lid crease reformation was performed to increase the symmetry between the two eyelids (**d**)

In some adolescents or even adults, mild ptosis that never mandated repair for visual distortion may present for relatively cosmetic repair or a repair focused mainly on appearance rather than preventing visual distortion. Recognition that this is still congenital ptosis with all the inherent differences in lid elasticity and muscle function (despite the patient's age and mild malposition) is important because the techniques and premises for repair remain those of congenital ptosis. Relatively decreased eyelid excursion and increased palpebral fissure in downgaze are clues to the congenital nature of the problem in the previously undiagnosed adolescent or young adult. Failure to recognize these differences may result in undercorrection of the ptosis if the repair is performed as if this were an acquired ptosis. Another consideration in initial ptosis repair in the older or adolescent child is toleration of lagophthalmos and nighttime exposure. Increased age at the time of initial congenital ptosis repair may also be a risk factor for postoperative problems with exposure. The older children and adolescents need a longer adaptation period with increased lubrication when adjusting to postoperative lagophthalmos.

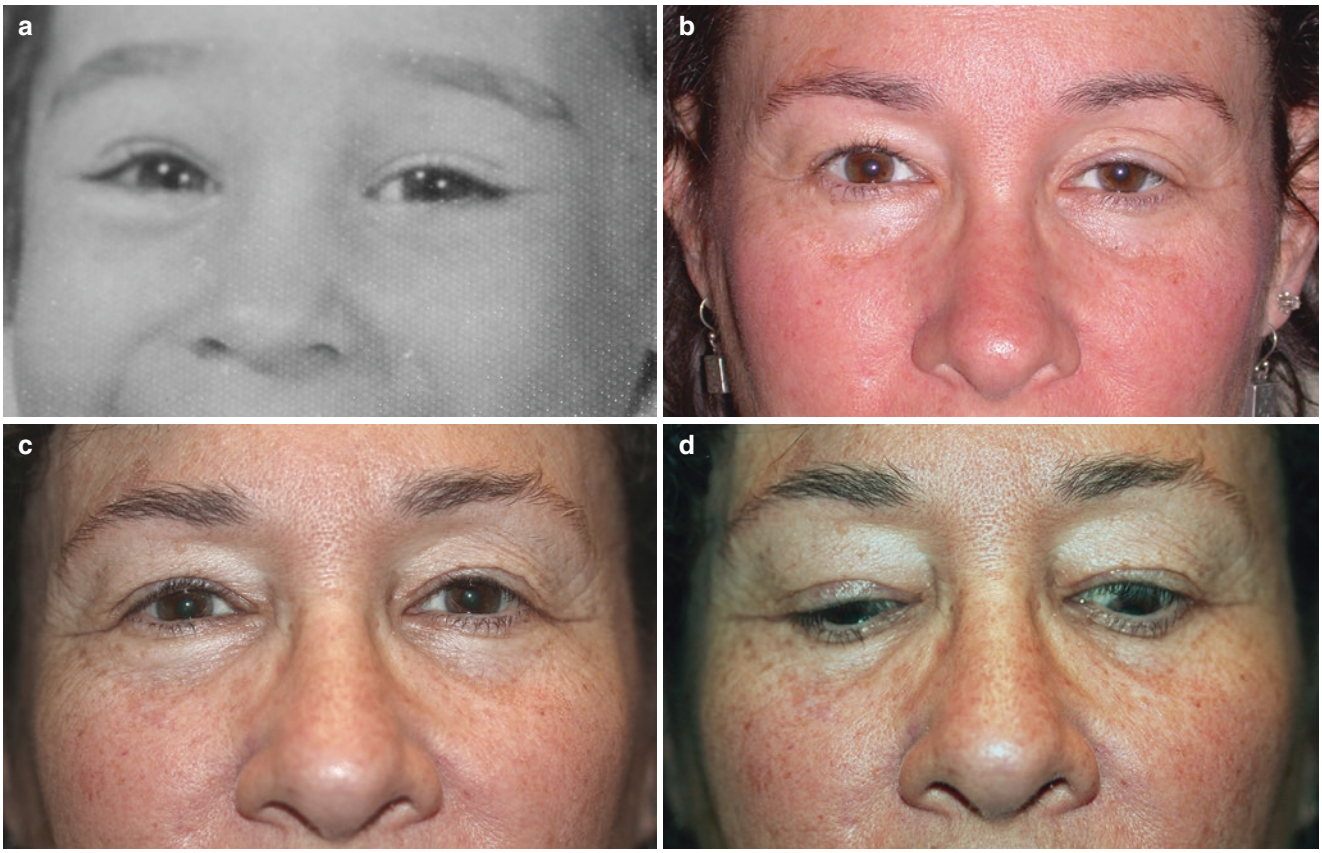


Fig. 18.2 Features of congenital ptosis seen in an adult requesting surgery for ptosis of the left upper eyelid. (**a**) The patient's photo as a child. (**b**) The patient presents as an adult requesting surgery for the droopy left upper eyelid. Note the lid crease and fold are also less distinct on the left. Lid crease reformation was performed in association with the external levator resection to improve the postoperative contour of the eyelid. Seven years later, her lid position and crease are stable (**c**). Note the decreased lid excursion of the ptotic lid in downgaze typical of congenital ptosis (**d**)

Eyelid crease symmetry remains an important consideration when operating on the otherwise mature patient with congenital ptosis. The same indistinct lid crease is seen and lid crease formation is indicated (Fig. 18.2).

In Marcus Gunn jaw wink ptosis, in addition to the ptosis, there is also a synkinetic abnormal elevation of the upper eyelid that occurs with activation of other facial musculature, typically the muscles of mastication. This abnormal eyelid movement and sometimes frank retraction of the eyelid with oral movement can be an aesthetically detracting feature of this variant of congenital ptosis. Correction of the ptosis and tightening of the levator muscle alone will not correct the overshoot of the eyelid that occurs with eating and speaking. The magnitude of the "wink" is helpful in deciding the technique of ptosis repair. The greater the magnitude of the overshoot, the more important it is to decrease the impact of the levator muscle on eyelid position. For example, in a very mild overshoot, ptosis repair alone may be considered. More commonly, a frontalis suspension procedure is used to elevate the eyelid, and the levator aponeurosis is disinserted from the anterior surface of the tarsus to diminish the synkinetic movement. If the overshoot is more profound, the levator complex can be released and then partially removed to help prevent reattachment and recurrence of the noticeable overshoot.

Cosmetic Considerations in Infantile Hemangiomas

Infantile hemangiomas present a significant cosmetic concern when they develop on the visible skin of the face or eyelid. Ophthalmic intervention is performed for mechanical ptosis, anisometropic amblyopia, or significant disruption of globe position. The full discussion of management of infantile hemangiomas is covered in Chap. 23. Beyond the medical aspects of vision protection, the color change or physical distortion in shape from the hemangioma is also cosmetically disturbing. When interventions have a relatively low incidence or severity of side effects, treating the lesion for cosmetic purposes may be reasonable. Early intervention may also diminish some of the long-term skin changes. The physician weighs the potential side effects associated with treatment against the social and aesthetic gains of a more normal appearance. In this disorder, the physician and family also consider that as the infant matures, the infantile hemangioma is likely to show spontaneous involution.

Topical or systemic beta-blockers (propranolol and timolol) have been used to successfully diminish the color and the bulk of the infantile hemangiomas. When successful, and in the absence of systemic side effects, propranolol is an excellent

first-line treatment for infantile hemangioma. Other treatment modalities are also considered when there is limited response, side effects occur, or if systemic conditions such as cardiac disorders or asthma preclude the use of propranolol. Surface laser is successful in diminishing what may be the most striking feature of the hemangioma, the color change in the skin [6, 7]. Laser (pulsed dye laser) can be used to superficially close the abnormal vascular lesions resulting in a much more normal appearance and also potentially diminishing some of the long-term impact of the lesion on the developing skin (Fig. 18.3). This technique is very helpful in decreasing the superficial component of the hemangioma, but the deeper mass remains



Fig. 18.3 In this figure, we see a patient whose infantile hemangioma was only moderately responsive to oral propranolol. Frontalis suspension was performed to elevate the eyelid margin and laser was performed to decrease the impact of the hemangioma. (**a**) The patient shortly after presentation. Propranolol and laser treatment are initiated as well as patching for amblyopia (**b**). A frontalis suspension procedure for the mechanical ptosis is performed at the time of additional laser treatment. Note the purpuric effects of the laser in (**c**). (**d**) The patient at age 5 after the treatments described above

unaffected. In beta-blocker unresponsive hemangiomas or in hemangiomas treated prior to propranolol therapy, systemic and intralesional steroids are and were employed. From an aesthetic perspective, skin changes from the lesion and also as side effects of the intralesional steroids may result in areas where the skin becomes atrophic or shows a loss of elasticity after regression (cigarette paper skin). Resection of these abnormal areas may improve the aesthetic outcome (Fig. 18.4). After involution, areas of irregularity or fibrosis may also persist in the location of the previous hemangioma. Appearance-based resection of the altered skin or residual mass is usually undertaken when the lesion is felt to have involuted.



Fig. 18.4 In the pre-beta-blocker era, vision-threatening hemangiomas were treated with systemic and intralesional steroids. Systemic side effects and also local effects could occur. This patient had an occlusive infantile hemangioma (**a**). Systemic steroids diminished the capillary hemangioma and the eyelid opened but also resulted in Cushingoid changes (**b**). Intralesional steroid-induced atrophy and involutional changes were apparent in the skin of the eyelid, brow, and forehead (**c**). Partial resection of the atrophic areas improves the appearance (**d**)

Cosmetic Considerations in Congenital Microphthalmos and Surgically Induced Anophthalmos in Children

The ongoing treatment of the child with microphthalmos has long-term goals of successful retention of a symmetrically sized ocular prosthesis and induction/maintenance of the normal eyelid and facial growth and development. Many factors influence the success of intervention: the initial degree of maldevelopment, the age of onset of treatment, the enthusiasm and endurance of the patient's family, and the availability of a skilled ocularist. In surgically induced loss of the eye during childhood, the starting point is usually one of more normal proportions, but removal of an eye in childhood also has similar concerns with respect to orbital volume replacement to try to create growth and symmetry of the affected side.

The treatment options and interventions for microphthalmos are covered in Chap. 40. These techniques are employed to try to compensate for the retarded growth of the soft tissues on the affected eyelids and replace the soft tissues that are missing in the orbit. Bone growth is often diminished as well. Successful treatment must start with increasing the horizontal and vertical aperture of the eyelids. In mild cases of microphthalmos, the skilled ocularist is sometimes able to improve the cosmetic appearance with an ocular prosthesis alone without requiring any surgical intervention. When the eye is small and the palpebral aperture is tiny, expansive materials such as hydrogel may be employed to increase the opening of the lids, and then increasing size rigid conformers fabricated by the ocularist help to expand the surface area of the socket and create mechanical pressure on the enlarging eyelids. Eyelid growth must be induced rather than surgically fabricated. As the eyelid aperture and socket surface area and the concavity of the space behind the eyelids are increased, the size of the conformer that can fit through the eyelids and fill the space may no longer create pressure on the eyelids. At this point, adding orbital volume to the soft tissue behind the conformer may create resistance to allow the prosthesis to push forward and stretch the eyelids. The earlier in development these techniques are utilized, the easier it is to take advantage of the plasticity of growth. Tissue expanders of various types have been used to successfully increase orbital volume and are sometimes ultimately replaced with living tissue such as dermis fat grafts. Dermis fat grafts in the younger child may act as the ultimate tissue expander by continuing to grow after implantation [8].

During the initial phases of rigid conformer expansion, because the conformer is changed so frequently, the ocularist may choose to use clear conformers or temporary conformers to expand the soft tissue. These conformers are typically clear and do not look like an eye. The pink tissue of the socket or the white of the microphthalmic eye is visible through the clear plastic. The clear plastic is also used if there is some hope that light perception may be present in the malformed eye. Even minor amounts of vision are protected. Ultimately around 1–2 years of age, the growth may slow enough that a longer-lasting prosthesis colored to match an eye may be used. Sometimes a microphthalmic eye may have enough intact corneal sensation that it is difficult to use a prosthesis because of discomfort. For these patients, a conjunctival flap or buccal mucous membrane grafts to cover the cornea may be necessary to make it comfortable to wear an ocular prosthesis.

In severe microphthalmos, creating the conjunctival cul-de-sac to maintain the prosthesis may also be challenging. Socket expansion can improve surface area and space, but surgical interventions may be necessary to create socket shape. Reformation of the cul-de-sacs is performed with suture to create adhesions, and mucous membrane grafting is added when necessary to increase the surface area of the socket. As with the eyelids, induction of natural growth to create the socket is always better and more predictable than surgical enlargement. Contraction and fibrosis may sometimes limit surgical goals.

Orbital volume discrepancies are always a feature of the microphthalmic socket but may also be features of enucleation and orbital trauma. Dermis fat grafting is a fundamental technique in volume augmentation for both the anophthalmic socket and also in orbits with a functioning eyeball in place. In the anophthalmic socket, dermis fat graft can be wrapped around the microphthalmic eye, or the corneal epithelium may be removed and the dermis fat placed over the surface of the existing globe. In the sighted eye, orbital implantation is most practically placed into the inferior cul-de-sac and below the existing eye. While dermis fat is an excellent choice for the younger child, in the older child, the size predictability of a synthetic implant may be beneficial. Synthetic options for orbital volume augmentation include solid silicone, nylon, porous polyethylene, rigid metallic implants, ePTFE, and autogenous bone. While the orbital volume augmentation may improve enophthalmos, hollowing of the superior sulcus improves less predictably with the increased inferior/posterior volume. Asymmetry in the upper eyelid fold with mild enophthalmos is a hallmark of even a very-well-repaired orbital fracture. In the adolescent with appearance-related concerns because of eyelid asymmetry, direct filling of the eyelid fold may be accomplished with soft tissue fillers or a "worm" of dermis fat placed into the eyelid and attached to the existing orbital fat [9].

Surgical Treatment of Proptosis in Children

While the incidence of Graves' disease is low in children, thyroid eye disease remains a feature of the autoimmune disease in children as well as adults. Children with thyroid eye disease have in general a milder version of the disease, but while they are less likely to develop optic neuropathy and strabismic myopathy, they are more likely than adults to manifest eyelid retraction and proptosis [10]. Proptosis and eyelid retraction that don't resolve are ultimately managed with orbital decompression and lid surgery. The surgical principles and techniques employed are similar to the techniques used in adults. Some unique considerations for orbital decompression in chil-

dren are avoiding the developing dental roots in the maxilla and avoiding the use of metallic implants that may ultimately become incorporated in the developing bone. Decompression for proptosis may facilitate improvement in the eyelid position and ultimately make correction of eyelid retraction more natural than trying to correct the appearance of an increased palpebral fissure by only adjusting the eyelid position.

Cosmetic Considerations in Eyelid and Periocular Lesion Removal

Conjunctival Nevus

While typically benign, a darkly pigmented conjunctival nevus can be a significant cosmetic detractant and removal may be considered. For changes in pigment, color, growth in size, or development of irregular margins, lesions should be removed for biopsy. For the cosmetic removal of a conjunctival lesion, one weighs the potential appearance of the conjunctival scar after removal over the unsightliness of the pigment. For lesions that are not in the interpalpebral zone and are partially covered by the eyelid, the small amount of pinkness that usually is left behind after conjunctival removal is less noticeable than the pigmented lesion. Lesions near the limbus or in the interpalpebral zone are less predictable with respect to cosmetic outcome and should be approached with more caution when describing the benefits of removal.

Congenital Kissing Nevus

The congenital kissing nevus manifests during fetal development when the eyelids are fused, resulting in abnormal areas of nevus that run along the adjacent upper and lower eyelid margins. This lesion often results in a significantly abnormal appearance to the eyelids and is often removed for its appearance alone. However, as a congenital nevus, it is also carefully monitored because there is some malignant potential of the lesion. The surgeon usually aims for removal of as much of the nevus as possible while leaving that portion of the lesion that would require removal of the eyelashes or deep enough to remove the eyelid. This results in a small line of residual nevus along the eyelid margin (Fig. 18.5).

Lipodermoid

Lipodermoids are one manifestation of Goldenhar syndrome. The growths are thick and pink and lumpy on the ocular surface. Usually, the lipodermoids appear to originate in the conjunctiva cul-de-sacs and then variably spread onto the palpebral surface. Sometimes the mechanical disruption of the blink necessitates their debulking, and sometimes the removal is primarily cosmetic. Unfortunately, it is very difficult to completely eradicate a lipodermoid, so debulking is performed with the intent to preserve as much of the normal tissue as possible while diminishing the redness and irregularity of the conjunctival surface. Removal of the existing lipodermoid does not always seem to preclude additional lipodermoid tissue redeveloping in that area, especially in growing children.

Limbal Dermoid

Limbal dermoids are another feature of Goldenhar syndrome and may cause significant visual as well as cosmetic concerns. Intervention for vision alteration is less

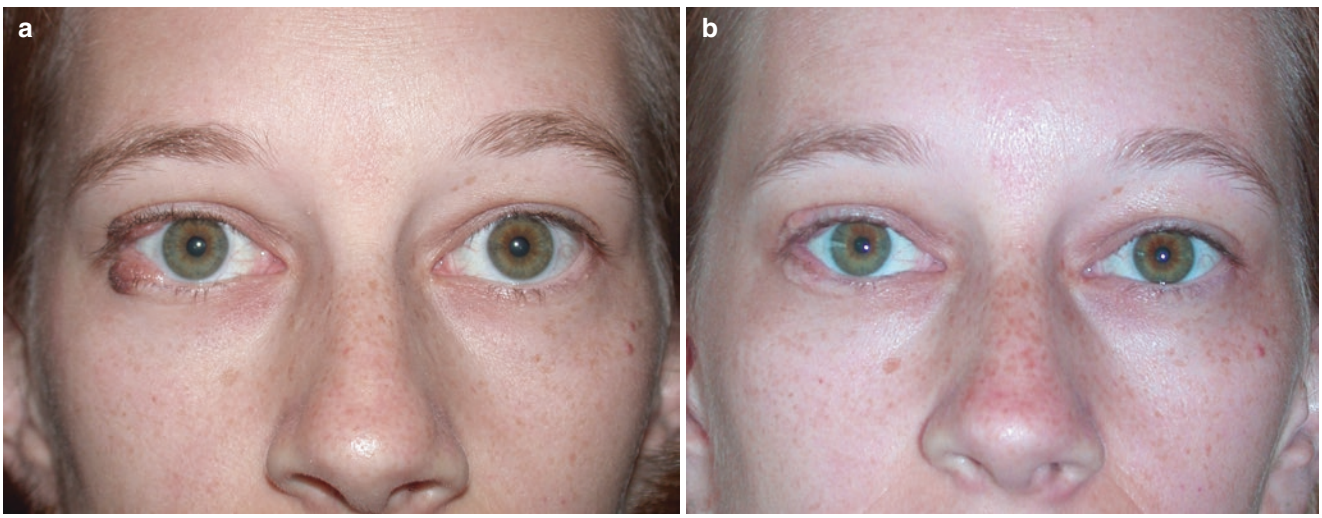


Fig. 18.5 (**a**) Preoperative and (**b**) postoperative appearance of a congenital kissing nevus that has been debulked to remove tumor and replace the missing skin with skin graft. The nevus is left intact along the eyelid margins to preserve the eyelashes and also because the cosmetic effect of the darker pigment is not as abnormal looking along the margin

controversial but both cosmetic and visual rehabilitation with limbal dermoids are challenging. The abnormal tissue typically extends full thickness through the eye wall, so lamellar dissection is used to thin the lesion and the surface is recovered. The thickness of the lesion may be improved, but removal is unlikely to result in a clear cornea or a completely natural appearance of the result. If the cosmetic goal is modest improvement, that may be achieved [11].

Periocular Soft Tissue Volume Augmentation in Children

Soft tissue fillers are a key treatment option for adult cosmetic facial rejuvenation and may have applications in pediatric cosmetic, appearance, and function-related concerns. The challenges of obtaining reimbursement for the soft tissue fillers, even when used for functional issues, have somewhat limited the development of applications in the pediatric age group. Areas of potential use and development include volume augmentation for the hollow superior sulcus, improvement of lower eyelid retraction, soft tissue expansion of the deficit in the lower eyelid in Treacher Collins syndrome [12] (Fig. 18.6), scar modification, volume augmentation to alleviate the hypoplastic maxilla, and tissue expansion for the preoperative cleft lip.

While autogenous fillers are always advantageous because of the paucity of an immune response and decreased risks of infection, hyaluronic acid fillers have a composition that matches the naturally occurring hyaluronic acid in the human body and have a voluminous and now multiyear history as a soft tissue replacement device in the human body. A harvest site is not necessary, and there is an unlimited supply available. The procedure is easier for patients as minimal anesthetic is required and may be performed in the office for older children.

Periocular soft tissue fillers can also be used to soften the appearance of scars. Typically, a depressed or contracted scar can be filled with a low viscosity filler such as Belotero (Merz, Greensboro, NC) or Restylane (Galderma, Fort Worth, TX). Use of dermal fillers in pediatric patients is considered off-label by the FDA, but with informed consent and thoughtful application, hyaluronic acid dermal fillers have been used by the authors in pediatric patients with positive outcomes. Furthermore, some fillers are proposed to stimulate collagen production and consequently could contribute to long-term improvement of scar due to dermal remodeling. In addition, dermal fillers can be used to improve symmetry in facial contours particularly in defects after trauma (Fig. 18.7).



Fig. 18.6 (**a**) This patient with Treacher Collins syndrome had significant lower eyelid and midface hypoplasia typical of the condition. (**b**) Initial treatment was performed with hyaluronic acid soft tissue filler to augment the lower eyelids.



Fig. 18.6 (continued) (**c**) Additional soft tissue filler was injected into the midface coincident with another unrelated surgical procedure. (**d**) The patient is seen at one year following the injection



Fig. 18.7 Sequential interventions to improve the appearance of a posttraumatic scar. The appearance of the forehead scar after a motor vehicle accident is improved with the use of soft tissue fillers. (**a**) The patient 6 months after the injury. (**b**) The dark foreign material has been excised from the wound, but the flash-less photo



Fig. 18.7 (continued) (**c**) shows the indentation that remains after the surgery. Poly-L-lactic acid, a bio-inductive filler agent, is injected into the lateral forehead to even out the surface of the tissue (**d**)

Camouflage and Makeup

Makeup can be used to camouflage facial defects and improve appearance [13]. Facial cosmetics improve appearance and can result in elevated levels of self-confidence. Makeup techniques use optical principles to improve symmetry. The use of light shades reflects more light and consequently emphasizes the facial feature and dark shades can de-emphasize features. In addition, makeup with a shiny finish can make the area appear larger and a matte finish can make it appear smaller. Increasing contrast around the eyes can emphasize the eyes and increase attractiveness. Light and dark powders can be used to contour and hide defects by complimenting other features. Scars can also be masked using a full-coverage foundation and concealer. Dermablend (Dermablend Corrective Cosmetics, Chicago, IL) is a good example of full-coverage foundation that can be helpful in masking scars and even depigmenting conditions such as vitiligo. Beauty balms (BB) and color correctors (CC) have an added advantage of minimizing pore appearance and make skin appear more homogenous in pigment and texture.

Eyebrows are a central focal point on the face. Eyebrows frame the eyes, the windows to the soul. Eyebrows shape faces and are integral in communication. Eyebrow makeup or tattoos can be useful to reform brows and improve contour and symmetry. Eyebrows can be planned using the golden ratio rule (1.618) of divine proportions. This mathematical ratio is used in art and architecture and found naturally in our solar system [14]. Brows can be reformed by tattoo techniques which include eyebrow embroidery/feathering or the powder fill technique. In addition to the eyebrow, blepharopigmentation can also be used for creating the illusion of a darker lash line and can be helpful in cases where eyelashes are absent or sparse. Blepharopigmentation has a very rare risk of fanning and eyelid margin necrosis [15]. Sparse eyelashes can also be treated with topical bimatoprost (Latisse) which can improve the appearance of the lash line by increasing the eyelash volume and length. Topical bimatoprost 0.03% has been shown to be effective in the treatment of eyebrow hypotrichosis in adult patients and can be considered for use in the pediatric patients [16, 17].

Cosmetic Concerns in the Management of Scar Formation

Scars are a natural part of the healing process. In some circumstances, aesthetically unappealing scarring can occur which may require intervention. Scars may be treated with topical agents, steroid therapy, lasers, and surgical revision. Scars may be minimized by planning primary surgery along the relaxed skin tension lines and avoiding excessive wound tension. Patient factors contribute to scarring – such underlying medical condition (connective tissue disease, diabetes,

smoking, UV exposure, and history of previous keloid formation).

Topical silicone sheets can be used as an initial treatment to improve scar appearance. If a scar is depressed, autologous fat or dermal fillers can also be used to improve the area of atrophy. For keloid and hypertrophic scars, traditional therapeutic modalities that have been effective include intralesional corticosteroids, laser therapy, and cryotherapy [18].

Topical application of vitamin A may improve the appearance of a scar; however, topical C may potentially cause a contact dermatitis [19, 20]. *Centella asiatica* (found in Skin Medica Scar Recovery Gel, Allergan, Irvine, CA) has been shown to aid wound healing [21].

Z-plasty is a surgical technique that can be used for scar revision. Z-plasty allows alteration of the scar length and vector with a transposition flap. By transposing and rotating two triangular flaps, the original scar is altered in length and direction. This technique is especially useful in cicatrized scar in a concavity, such as the medial canthus (see Chap. 4). The central arm of the Z-plasty should be aligned with the scar. The angles of the two side incisions can be placed at 60 degrees from the central incision. The central arm will rotate and thereby decrease the tension of the original wound. The wound is then closed at the corners with subcutaneous sutures to reduce tension. The Z-plasty can also be used to help close an elliptical defect with the O-Z plasty. This allows closure of the circular defect with the advantage of the transposition flap. The V-Y plasty is another option for revision of a contracted scar. The V is converted to a Y to release tension in the axis of the scar.

References

1. Rhodes G, Yoshikawa S, Palermo R, Simmons LW, Peters M, Lee K, Halberstadt J, Crawford JR. Perceived health contributes to the attractiveness of facial symmetry, averageness, and sexual dimorphism. Perception. 2007;36(8):1244–52.
2. Griffey JA, Little AC. Infant's visual preferences for facial traits associated with adult attractiveness judgements: data from eye-tracking. Infant Behav Dev. 2014;37(3):268–75.
3. Cassia VM, Valenza E, Simion F, Leo I. Congruency as a nonspecific perceptual property contributing to newborns' face preference. Child Dev. 2008;79(4):807–20.
4. Beard CA. New treatment for severe unilateral congenital ptosis and for ptosis with jaw-winking. Am J Ophthalmol. 1965;59:252–8.
5. Callahan A. Correction of unilateral blepharoptosis with bilateral eyelid suspension. Am J Ophthalmol. 1972;74:321–6.
6. Chinnadurai S, Sathe NA, Surawicz T. Laser treatment of infantile hemangioma: a systematic review. Lasers Surg Med. 2016;48(3):221–33.
7. Reddy KK, Blei F, Brauer JA, et al. Retrospective study of the treatment of infantile hemangiomas using a combination of propranolol and pulsed dye laser. Dermatol Surg. 2013;39(6):923–33.
8. Heher KL, Katowitz JA, Low JE. Unilateral dermis-fat graft implantation in the pediatric orbit. Ophthal Plast Reconstr Surg. 1998;14(2):81–8.
9. Czyz CN, Foster JA, Wulc AE. Superior sulcus volumetric rejuvenation utilizing dermis fat grafting. Aesthet Surg J. 2015;35(7):892–8.
10. Ben Simon GJ, Katz G, Zloto O, Leiba H, Hadas B, Huna-Baron R. Age differences in clinical manifestation and prognosis of thyroid eye disease. Graefes Arch Clin Exp Ophthalmol. 2015;253(12):2301–8.
11. Pirouzian A, Holz H, Merrill K, Sudesh R, Karlen KJ. Surgical management of pediatric limbal dermoids with sutureless amniotic membrane transplantation and augmentation. J Pediatr Ophthalmol Strabismus. 2012;49(2):114–9.
12. Goldberg RA, Lee S, Jayasundera T, Tsirbas A, Douglas RS, McCann JD. Treatment of lower eyelid retraction by expansion of the lower eyelid with hyaluronic acid gel. Ophthal Plast Reconstr Surg. 2007;23(5):343–8.
13. Hurwitz JJ, Eplett CJ, Sharpe J. Nonsurgical aesthetic alterations of the eyelids in pathological conditions. Can J Ophthalmol. 1990;25(4):197–201.
14. Swift A, Remington K. BeautiPHIcation™: a global approach to facial beauty. Clin Plast Surg. 2011;38(3):347–77.
15. Goldberg RA, Shorr N. Complications of blepharopigmentation. Ophthalmic Surg. 1989;20(6):420–3.
16. Beer KR, Julius H, Dunn M, Wilson F. Treatment of eyebrow hypotrichosis using bimatoprost: a randomized, double-blind, vehicle-controlled pilot study. Dermatol Surg. 2013;39(7):1079–87.
17. Carruthers J, Beer K, Carruthers A, et al. Bimatoprost 0.03% for the treatment of eyebrow hypotrichosis. Dermatol Surg. 2016;42(5):608–17.
18. English RS, Shenefelt PD. Keloids and hypertrophic scars. Dermatol Surg. 1999;25:631–8.
19. Baumann LS, Spencer JS. The effects of topical vitamin E on the cosmetic appearance of scars. Dermatol Surg. 1999;25:311–5.
20. Thiele JJ, Hsieh SN, Ekanayake-Mudiyanselage S, Vitamin E. Critical review of its current use in cosmetic and clinical dermatology. Dermatol Surg. 2005;31:805–13.
21. Widgerow A, Chait L, Stals R, et al. New innovations in scar management. Aesthet Plast Surg. 2000;24:227.

Psychosocial Issues in Pediatric Oculoplastic Conditions

19

Leanne Magee

Roughly 7 million people in the USA report having a visual disability. Little is known about the psychosocial functioning, quality of life, and appearance concerns among children, adolescents, and young adults in the USA with visual impairment. The limited research regarding psychosocial functioning in adults with ptosis and other disfiguring eye conditions suggests that distressed patients may experience high levels of anxiety, depression, social anxiety, social avoidance, and self-consciousness [1] and are likely to be negatively rated by others [2–5]. Children with severe visual impairment secondary to oculoplastic conditions are at risk for specific psychosocial problems, including social inhibition, social anxiety, negative self-appraisal, depression, and lower quality of life [1, 6]. Though adolescents with visual impairment were not found to differ from controls in the frequency of depression or in relationships with their parents and siblings, they did report more feelings of loneliness and difficulties making friends and are more likely to be victims of bullying than their sighted peers [7–10].

For many patients, medical and surgical interventions for congenital or acquired visual deficits and appearance differences can improve ophthalmologic functioning and facial appearance and in turn positively impact psychosocial functioning. However, coping with ongoing medical and surgical interventions may represent a significant source of stress for patients and families. As such, attending to the psychosocial needs of patients throughout the course of their development and medical treatment is key to maximizing outcomes.

L. Magee, PhD
Division of Plastic and Reconstructive Surgery,
Department of Child and Adolescent Psychiatry and Behavioral Sciences, The Children's Hospital of Philadelphia,
Philadelphia, PA, USA
e-mail: mageel@email.chop.edu

Psychosocial Risk Assessment

Children with congenital and acquired medical conditions, including those affecting the structure and function of the eye, experience unique risks related to social, emotional, and developmental functioning. Many families affected by pediatric disease and illness demonstrate effective coping and adjustment in the face of such challenges, but all patients and families are likely to experience varying levels of distress throughout all stages of diagnosis and treatment and as such are likely to benefit from targeted support. Routine evaluation of psychosocial risk among patients and families is critical to promptly identifying those in need of support and intervention matched to the assessed level of need [11].

The Pediatric Psychosocial Preventative Health Model [12] is a useful tool when considering varying levels of risk and matched interventions among families coping with pediatric health conditions. The PPPHM proposes a model for screening all families and children entering treatment, with higher levels of care recommended for those with highest levels of psychosocial risk. It assumes that most families in the pediatric healthcare setting are competent and exhibit adaptive functioning but recognizes that some families may experience expected distress related to diagnosis or specific aspects of treatment, while other families may exhibit preexisting difficulties that are increased with diagnosis and treatment such that they may experience significant distress and functional impairments.

Based on a public health framework, the PPPHM outlines three levels of risk with associated interventions. At the base level is the largest group, *Universal* families, who are experiencing expected levels of concern and distress about the child's condition but who are demonstrating resiliency and effective coping and adjustment [12]. Families at the Universal level benefit from the provision of general support and educational resources geared toward helping families identify the resources available to them to enhance coping and compliance. This can include psychoeducation about

© Springer International Publishing AG 2018

J.A. Katowitz, W.R. Katowitz (eds.), *Pediatric Oculoplastic Surgery*, https://doi.org/10.1007/978-3-319-60814-3_19

treatment, case management services, collaboration with schools, general supportive counseling, brief medical play, or referral to local and national condition-specific support networks.

At the next level are *Targeted* families, who experience continued or worsened vulnerability secondary to preexisting concerns in conjunction with the stressors of medical treatment [12]. Such families benefit from recommendations for psychosocial interventions to address their specific symptoms, as well as ongoing monitoring to determine whether they have continued or increasing support needs. For example, a family at the Targeted level may benefit from a brief course of supportive therapy to address a child's adjustment to diagnosis and treatment, compliance with medical treatments (e.g., eye drops, patching), and specific interventions to address procedural anxiety or fears of upcoming surgeries.

At the top level is the smallest group representing the highest level of risk and greatest need for psychosocial care, *Clinical* families. These patients and families exhibit multiple preexisting, chronic, and complex difficulties requiring intensive intervention with a behavioral health specialist such as a psychologist or a psychiatrist [12]. Such families are likely to experience escalating difficulties requiring crisis intervention, legal supports or consultation with child welfare agencies, psychiatric medication, or interventions designed to assure the safety of the patient and family members. Clinical families require the highest level of support and monitoring, even when the acute risk has passed.

Families can move from level to level within the PPPHM, either as a result of effective intervention or related to aspects of the child's medical condition and its treatment. Ongoing assessment of a family's level of risk allows for the tailoring of preventive, evidence-based, and cost-effective psychosocial care designed to enhance patient outcomes and quality of life. Psychosocial risk screening can be completed by many members of the patient's care team, especially when using validated parent-report measures such as the Psychosocial Assessment Tool (PAT) [13, 14]. Though initially designed for use with pediatric cancer populations, the PAT has since been studied and adapted to a wide range of pediatric health populations, including those with specific diseases like craniofacial conditions, and translated into multiple languages. This brief, parent-reported screener of psychosocial risk includes subscales assessing family structure and resources, family problems, social support, stress reactions, child problems, sibling problems, family functioning, and belief systems. Scores are designed to alert clinical staff to the family's current risk status and need for intervention at the Universal, Clinical, or Targeted level. Though the PAT and other screeners can be administered by most clinical staff, collaboration between ophthalmic surgeons and specially trained psychosocial providers can allow for the most effective and efficient evaluation and intervention. Ongoing assessment will help treatment teams best meet their patients' changing needs and help optimize patient outcomes and enhance quality of life in the face of congenital and acquired oculoplastic conditions.

Quality of Life

Quality of life (QOL) is broadly characterized as a multidimensional, subjective evaluation of the positive and negative aspects of one's life [15]. Health-related quality of life (HRQOL) focuses more specifically on perceived physical and mental health over time [16] and is comprised of physical, emotional, social, and cognitive factors as well as aspects of medical conditions and treatment, financial impact of health conditions, and community resources, policies, and practices that affect health and healthcare. As with the ongoing screening for psychosocial risk, it is important to assess HRQOL regularly to best understand the impact of medical conditions and their treatment on the individual's broader experience and to demonstrate the efficacy and clinical benefit of treatments.

The research exploring QOL among patients with oculoplastic conditions and treatments is limited, and even more so among pediatric patients. Adults with strabismus rated the condition as having a negative impact on multiple aspects of their lives, including employment, personal relationships, and self-image [17], and demonstrated that they are often perceived negatively by others due to their appearance difference [3, 4]. Postoperatively, adult strabismus patients reported improvements in perceptions of themselves and their personality traits and beliefs that they'd be perceived more positively by others [18]. Similarly, adult patients with blepharoptosis experienced postoperative improvements in vision and their abilities to perform fine manual work, reading, and watching television [19] as well as improvements in self-image [20]. In addition, photographs of adult patients with blepharoptosis and dermatochalasis were rated more negatively before surgical treatment [2]. However, a recent review of the literature found sparse evidence for improvements in quality of life among adults who received surgical treatment of common oculoplastic conditions such as thyroid eye disease, ptosis, and nasolacrimal duct obstruction compared to the hundreds of studies examining other ophthalmologic conditions such as cataracts [21].

Together, findings suggest that surgical intervention for some ophthalmologic conditions affecting vision and appearance may contribute to improvements in vision and function as well as perceptions of the self and social perceptions by others. However, the studies exploring these issues among adults and especially children are very limited, and the use of reliable and valid assessment tools is

limited. Increasingly, ophthalmologic surgeons recognize the importance of creating and refining psychometrically sound assessment tools to accurately and efficiently assess the quality of life and ophthalmologic functioning of adult and pediatric patients.

The LV Prasad-Functional Vision Questionnaire (LVP-FVQ) [22] and the Cardiff Visual Ability Questionnaire for Children (CVAQC) [23] assess visual functioning, and the Children's Visual Function Questionnaire (CVFQ) [24] assesses visual function and quality of life, but all three rely on parent proxy report. Focus groups of young patients with visual impairment and their parents indicate that they have similar concerns about psychosocial and school functioning [25]. However, children's perceptions of quality of life and the impact of health on functioning can often vary compared to parent and medical provider views of functioning [26–29]. This suggests that it is important to ask children directly about their experiences for the most comprehensive understanding of quality of life.

The Pediatric Quality of Life Inventory [30] assesses child self-report and parent proxy report of the child's generic physical, mental, social, and role functioning. It's been validated and used in healthy children as well as children with health issues, but fails to adequately assess the impact of living with a visual impairment and is not sensitive to changes in vision and appearance over time.

Recently, work has been done to create reliable and valid measures of child-centered vision-related quality of life. The Impact of Vision Impairment for Children (IVI_C) [31] is a vision-specific QOL scale designed with input from focus group discussions of children with visual impairment and validated among children and adolescents with and without visual impairment. It has been found to be a reliable and valid measure of quality of life among children aged 8–18 with vision impairment who are otherwise in good health [32]. Similarly, the Vision-related Quality of Life of Children and Young People (VQoL_CYP) instrument [33] was created using data from qualitative interviews of 10–15-year-olds with visual impairment or blindness, which was analyzed and evaluated to identify themes critical to a child-centered understanding of the impact of visual impairment on quality of life. The resulting 47-item measure assesses domains such as social relations, acceptance, and participation; independence and autonomy; psychological and emotional well-being; future aspirations and fears; functioning at home, school, and leisure; and treatment of eye conditions.

Additional research on children and adults in various stages of development and treatment, with a wide variety of oculoplastic conditions, using validated measures that examine child-reported experiences are needed to reliably demonstrate the clinical benefit of oculoplastic procedures on quality of life.

Body Image and Appearance Concerns

Body image, defined as perceptions and attitudes toward one's own physical appearance, is the largest contributor to self-esteem and self-concept among children and adolescents. Body image and appearance satisfaction can be conceptualized as having three main components: (1) an individual's objective appearance, (2) subjective evaluation of appearance (by self and others), and (3) the importance placed on appearance for self-worth. Adolescence is a key time in body image development, because of the normative, developmental challenges that influence and are influenced by body image, such as pubertal development, identity formation, and emergence of sexuality [34].

Positive body image is associated with high self-esteem, self-confidence in social situations, and healthy psychosocial functioning. Negative body image is a known risk factor for depression, social anxiety, and eating disorders, and it is consistently associated with lower quality of life and self-esteem. Body image has been widely studied in clinical (e.g., eating disorder patients) and nonclinical populations.

Individuals with visible differences commonly experience negative perceptions of the self and difficulties with social interaction, which can in turn contribute to negative emotions and thought processes, poor self-esteem and body image, and changes in behavior [35]. The objective characteristics of appearance difference, including the type, extent, and severity of disfigurement, are not predictive of body image and psychosocial adjustment [36, 37]. Psychological and body image functioning is best predicted by an individual's perceptions of how noticeable their difference is to others [38]. However, highly visible appearance differences, such as those affecting the eyes and face, are likely to be more noticeable to others and therefore have a greater influence on social interactions, perceptions by others, and therefore body image.

Body image among children with oculoplastic conditions and associated visual impairments has received little research attention. For patients with oculoplastic conditions, the objective appearance of the eye and/or face may be atypical, and depending on the severity of vision loss, they may be reliant on feedback from others and tactile sensations for subjective information about their appearance and societal appearance ideals. As such, they may have unique body image perceptions which can influence broader aspects of psychosocial functioning such as social, emotional, behavioral, and academic/occupational functioning in addition to factors related to medical and surgical decision-making.

The results of the few studies that have been conducted to date on body image in patients with visual impairment are mixed. These studies conducted often utilize small samples and varying methodologies (i.e., inclusion of patients with low vision versus severe impairment, lack of validated

measures, case studies, etc.), making interpretation and generalization of the results difficult. One study of German adolescents found that those with visual impairment had significantly less satisfaction with their bodies than controls [39]. To the contrary, other studies have found that those with visual impairment have higher body satisfaction than those without impairment [40, 41], and still others found no significant differences in self-esteem or self-concept between those with and without visual impairment [6, 42]. Another study on the body image of congenitally blind children found that children who believed they were judged by their parents as too thin had lower self-esteem, indicating that parents' (and potentially others') perceptions of appearance may play a role in the visually impaired child's body image and self-esteem [41].

Visible appearance differences, teasing or bullying, and multiple surgical changes in appearance throughout childhood and adolescence can contribute to difficulties with body image and in turn have a significant impact on broader psychosocial functioning, quality of life, and medical outcomes. Body image and appearance concerns may be a useful risk factor to target when developing interventions to prevent or improve psychosocial problems among youth with craniofacial and oculoplastic conditions. It is also important to consider whether the pediatric patient seeking medical and surgical treatment of an ophthalmologic condition affecting the structure, function, or appearance of the eye may also be managing broader medical conditions, such as congenital craniofacial anomalies, cancer, or traumatic injury, as this may contribute to a greater risk of distress and psychosocial impairment.

Psychosocial Support

As detailed above, it is natural for children and families to experience fears, worries, and anxieties about diagnosis, surgery, and other medical procedures to improve the function and appearance of the eye. Beyond treatment considerations, patients with functional and appearance differences associated with eye conditions also experience functional impairments that can influence emotional and behavioral functioning with family members and peers and in educational and occupational settings. These concerns can be eased by encouraging patients and families to develop effective coping skills by working with psychosocial support staff, such as a psychologist, social worker, or child life specialist or other specifically trained members of the treatment team.

A pediatric psychologist specializes in providing assessment, intervention, and consultation services to children who need support adjusting to a medical diagnosis, adhering to treatment recommendations, or making decisions about medical and surgical interventions. Pediatric psychologists can also provide support related to the trauma of an illness or procedure and help treat patients who are experiencing mental health issues such as anxiety and depression, social skills difficulties, or issues in family functioning associated with their medical condition and its treatment. For children with oculoplastic conditions affecting vision, a pediatric psychologist can also collaborate with school and other community members to ensure that the child receives appropriate levels of accommodation and support to maximize independent functioning.

A social worker's role is to offer support, information, and education to patients and families so they are appropriately connected to the hospital and community resources they need. Social workers can also answer questions about insurance, school access, employment and legal rights, and child advocacy and protection. A certified child life specialist can prepare children and their families for medical experiences by explaining what will happen, and why, in terms a child can understand. Child life specialists can provide age-appropriate recreational, developmentally supportive, and therapeutic play to help children develop coping skills, facilitate expression of feelings, and support them through all stages of their healthcare experience. They can orient children to the hospital before an admission, use toys to demonstrate common medical interventions, and provide play experiences to help distract and support patients and their families during their medical care.

Pediatric psychologists, social workers, child life specialists, and other specially trained clinicians can meet with families to ensure that they understand the nature of their child's condition and recommendations for treatment, as well as the risks and benefits of surgery and the alternatives to surgery when available. Psychosocial clinicians can work with children to ensure they have an age-appropriate understanding of their condition and its treatment. Children cope better with surgery and recovery when they know what to expect before, during, and after the day of surgery. Psychosocial clinicians can also help families to identify questions or concerns they may want to share with the medical team and discuss ways that the family can best prepare their child for surgery and recovery. Lastly, psychosocial support staff can address any comorbid mental health concerns that may be affecting the patient or family's functioning at home, at school, or with their medical team.

Among patients and families who are considering elective surgical procedures, the decision-making process can be complex. Early in diagnosis and treatment, particularly for congenital conditions affecting the structure and function of the eye and the surrounding soft tissue structures, such as the eyelids, the surgeon will outline the treatment plan with recommendations for what procedures are necessary at what time. As children get older, and functioning is maximized, they may be eligible for surgical procedures that normalize

or enhance their appearance. When possible, decisions about elective procedures should be made collaboratively, with input from the surgeon, parents, and child.

Though many older children and adolescents want to be involved in the decision-making process, it is common for patients who have undergone many surgeries to feel "burnout" and to decline surgeries that could have great benefit for them. Adolescents in particular are likely to make decisions based on the short term without thinking about long-term benefits because they don't want to miss more school or have to spend more time in the hospital. A pediatric psychologist can work with patients and their treatment team to facilitate communication about how a surgery might help them now and in the future, addressing the patient's fears and concerns, and help patients and families weigh the short- and long-term risks and benefits of pursuing or deferring elective procedures.

Psychologists can also help families to navigate issues related to appearance and identity through the lifespan, including responding to questions and comments about appearance differences, telling others about surgical procedures, or coping with teasing and bullying. One strategy that can be helpful is to script a response to commonly asked questions so that patients and their families can be prepared to manage challenges with confidence. Many patients with appearance differences have found that an effective response has three components: (1) acknowledging the appearance difference, (2) providing a brief but honest explanation, and (3) guiding the conversation onto other topics.

As young oculoplastic patients grow, they are likely to encounter all of the normal issues that children and adolescents face – making friends, interactions at school, teasing and bullying, body image, dating, emerging independence, and more. Childhood and adolescence can be challenging for all children, and having an appearance difference, particularly when compounded with visual impairment, and having to deal with medical and surgical procedures certainly add unique stressors to an already difficult time of life. Ensuring that the medical team is attending to the patient's and family's shifting psychosocial needs throughout the course of evaluation and treatment will contribute to optimizing outcomes and, ultimately, to enhance both the patient's quality of life and potential to become a more productive member of society.

References

1. Clarke A, Rumsey N, Collin JRO, Wyn-Williams M. Psychosocial distress associated with disfiguring eye conditions. Eye. 2003;17(1):35–40.
2. Bullock JD, Warwar RE, Bienenfield DG, Marciniszym SL, Markert RJ. Psychosocial implications of blepharoptosis and dermatochalasis. Tram Ophth Soc. 2001;99:65–72.
3. Coats DK, Paysse EA, Towler AJ, Dipboye RL. Impact of large angle horizontal strabismus on ability to obtain employment. Ophthalmology. 2000;107(2):402–5.
4. Olitsky SE, Sudesh S, Graziano A, Hamblen J, Brooks SE, Shaha SH. The negative psychosocial impact of strabismus in adults. J AAPOS. 1999;3(4):209–11.
5. Warwar RE, Bullock JD, Markert RJ, Marciniszyn SL, Bienenfeld DG. Social implications of blepharoptosis and dermatochalasis. Ophthal Plast Reconstr Surg. 2001;17(4):234–40.
6. Bolat N, Dogangun B, Yavuz M, Demir T, Kayaalp L. Depression and anxiety levels and self-concept characteristics of adolescents with congenital complete visual impairment. Turk Psikiyatri Dergisi Turk Psikiyatri Derg. 2011;22(2):77–82.
7. Horwood J, Waylen A, Herrick D, Williams C, Wolke D. Common visual defects and peer victimization in children. Invest Ophthalmol Vis Sci. 2005;46(4):1177–81.
8. Huurre TM, Aro HM. Psychosocial development among adolescents with visual impairment. Eur Child Adolesc Psychiatry. 1998 Jun;7(2):73–8.
9. Pinquart M, Pfeiffer JP. Psychological well-being in visually impaired and unimpaired individuals: a meta-analysis. BJVI. 2011;29(1):27–45.
10. Pinquart M, Pfeiffer JP. Perceived social support in adolescents with and without visual impairment. Res Dev Dis. 2013;34(11):4125–33.
11. Kazak AE, Schneider S, DiDonato S, Pai ALH. Family psychosocial risk screening guided by the Pediatric Psychosocial Preventative Health Model (PPPHM) using the Psychosocial Assessment Tool (PAT). Acta Oncol. 2015;54(5):574–80.
12. Kazak A. Pediatric Psychosocial Preventative Health Model (PPPHM): research, practice and collaboration in pediatric family systems medicine. Fam Syst Health. 2006;24:381–95.
13. Kazak AE, Prusak A, Mcsherry M, Simms S, Beele D, Rourke M, et al. The Psychosocial Assessment Tool (PAT) ©: pilot data on a brief screening instrument for identifying high risk families in pediatric oncology. Fam Syst Health. 2001;19(3):303–17.
14. Pai ALH, Patino-Fernandez AM, McHerry M, Beele D, Alderfer M, Reilly A, et al. The psychosocial assessment tool (PAT 2.0): psychometric properties of a screener for psychosocial distress in families of children newly diagnosed with cancer. J Pediatr Psychol. 2008;33:50–62.
15. The WHOQOL Group. The World Health Organization Quality of Life Assessment (WHOQOL): development and general psychometric properties. Soc Sci Med. 1998;46:1569–85.
16. Centers for Disease Control and Prevention: Health-Related Quality of Life (HRQOL) [Internet]. Atlanta: Centers for Disease Control and Prevention; 2016 [updated 2016 May 27; Cited 2016 August 8] Available from: http://www.cdc.gov/hrqol/index.htm.
17. Satterfield D, Keltner JL, Morrison TL. Psychosocial aspects of strabismus study. Arch Ophthalmol. 1993;111(8):1100–5.
18. Burke JP, Leach CM, Davis H. Psychosocial implications of strabismus surgery in adults. J Pediatr Ophthalmol Strabismus. 1997;34(3):159–64.
19. Battu VK, Meyer DR, Wobig JL. Improvement in subjective visual function and quality of life outcome measures after blepharoptosis surgery. Am J Ophthalmol. 1996;121:677–86.
20. Federici TJ, Meyer DR, Lininger LL. Correlation of the vision-related functional impairment associated with blepharoptosis and the impact of blepharoptosis surgery. Ophthalmology. 1999;106:1705–12.
21. Ridyard E, Inkster C. Measuring quality of life in oculoplastic patients. Int J Ophthalmol. 2014;7(1):133–8.
22. Gothwal VK, Lovie-Kitchin JE, Nutheti R. The development of the LV Prasad-functional vision questionnaire: a measure of functional vision performance of visually impaired children. Invest Ophthalmol Vis Sci. 2003;44(9):4131–9.

23. Khadka J, Ryan B, Margrain TH, Court H, Woodhouse JM. Development of the 25-item Cardiff Visual Ability Questionnaire for Children (CVAQC). Br J Ophthalmol. 2010;94(6):730–5.
24. Felius J, Stager DR Sr, Berry PM, Fawcett SL, Stager DR Jr, Salamao SR, et al. Development of an instrument to assess vision-related quality of life in young children. Am J Ophthalmol. 2004;138(3):362–72.
25. Decarlo DK, Mcgwin G, Bixler ML, Wallander J, Owsley C. Impact of pediatric vision impairment on daily life: results of focus groups. Optom Vis Sci. 2012;89(9):1409–16.
26. Cremeens J, Eiser C, Blades M. Factors influencing agreement between child self-report and parent proxy-reports on the Pediatric Quality of Life Inventory 4.0 (PedsQL) generic core scales. Health Qual Life Outcomes. 2006;4:58.
27. Eiser C, Morse R. Quality-of-life measures in chronic diseases of childhood. Health Technol Assess. 2001;5(4):1–157.
28. Eiser C, Morse R. The measurement of quality of life in children: past and future perspectives. J Dev Behav Pediatr. 2001;22(4):248–56.
29. Janse AJ, Sinnema G, Uiterwaal CSPM, Kimpen JLL, Gemke RJBJ. Quality of life in chronic illness: perceptions of parents and pediatricians. Arch Dis Child. 2005;90:486–91.
30. Varni JW, Seid M, Kurtin PS. PedsQL_4.0: Reliability and validity of the pediatric quality of life Inventory_version 4.0 generic core scales in healthy and patient populations. Med Care. 2001;39(8):800–12.
31. Cochrane G, Lamoreux E, Keeffe J. Defining the content for a new quality of life questionnaire for students with low vision (the Impact of Vision Impairment on Children: IVI_C). Ophthalmic Epidemiol. 2008;15(2):114–20.
32. Cochrane GM, Marella M, Keeffe JE, Lamoureux EL. The impact of vision impairment for children (IVI_C): validation of a vision-specific pediatric quality-of-life questionnaire using rasch analysis. Invest Ophthalmol Vis Sci. 2011;52(3):1632–40.
33. Rahi JS, Tadic V, Keeley S, Lewando-Hundt G. Capturing children and young people's perspectives to identify the content for a novel vision-related quality of life instrument. Ophthalmology. 2011;118(5):819–24.
34. Cash TF. Body image and plastic surgery. In: Sarwer DB, Pruzinsky T, Cash TF, Goldwyn RM, Persing JA, Whitaker LA, editors. Psychological aspects of reconstructive and cosmetic plastic surgery: clinical, empirical and ethical perspectives. Philadelphia: Lippincott, Williams and Wilkins; 2006. p. 37–59.
35. Rumsey N, Harcourt D. Body image and disfigurement: issues and interventions. Body Image. 2004;1(1):83–97.
36. Rumsey N. Body image & congenital conditions with visible differences. In: Cash TF, Pruzinsky T, et al., editors. Body image: a handbook of theory, research, and clinical practice. New York: Guilford; 2002. p. 226–33.
37. Rumsey N. Optimizing body image in disfiguring congenital conditions. In: Cash TF, Pruzinsky T, editors. Body image: a handbook of theory, research, and clinical practice. New York: Guilford; 2002. p. 431–9.
38. Harris D. Types, causes and physical treatment of visible differences. In: Lansdown R, Rumsey N, Bradbury E, Carr T, Partridge J, editors. Visibly different: coping with disfigurement. Oxford: Butterworth-Heinemann; 1997. p. 79–90.
39. Pinquart M, Pfeiffer JP. Body image in adolescents with and without visual impairment. Br J Vis Impair. 2012;30(3):122–31.
40. Pierce JW, Wardle J. Body size, parental appraisal, and self-esteem in blind children. J Child Psychol Psychiatr. 1996;37(2):205–12.
41. Shapiro DR, Moffett A, Lieberman L, Dummer GM. Domain-specific ratings of importance and global self-worth of children with visual impairments. J Vis Impair Blind. 2008;102(4):232–44.
42. Dias L, Hyman L, Manny RE, Fern K. Evaluating the self-esteem of myopic children over a three-year period. Optom Vis Sci. 2005;82(4):338–47.

Clinical Research Strategies in Oculoplastic Surgery

20

Gil Binenbaum

Organizing Your Study

A simple way to plan a research study is to outline the following elements, before collecting any data. Each element is discussed subsequently in detail:

1. Question
2. Design
3. Subjects
   - Inclusion criteria
   - Exclusion criteria
4. Data
   - Coding scheme for each variable
   - Medical records data
     - EMR derived data that does not require manipulation
     - EMR derived data that requires coding
     - Manually abstracted data from paper medical records or EMR
   - Image analysis, if applicable
     - Clinical photographs
     - Radiographic imaging
   - Prospectively collected data
     - Clinical measurements
     - Questionnaires
5. Analysis
   - Define each group/variable clearly
   - Study groups
     - Exposed/unexposed, cases/controls, etc.
   - Outcomes – define each variable
     - Primary – directly answer the study question
     - Secondary

G. Binenbaum, MD, MSCE
Shafritz Endowed Chair of Pediatric Ophthalmology Research, The Children's Hospital of Philadelphia, Perelman School of Medicine at the University of Pennsylvania, Philadelphia, PA, USA
e-mail: binenbaum@email.chop.edu; ERBRING@email.chop.edu

The Research Question

The most important element of a research project or literature review is the question you want to answer. The research question determines everything else about the study: the study design, the subjects, the data you need to collect, the type of analysis, and the relevance of potential confounding or bias in the results. Try to be as specific as possible about the question.

A common mnemonic for formulating a good research question is PICO:

P: Patient or Problem – Identify the patient or clinical problem (e.g., infants less than a year of age with nasolacrimal duct obstruction).

I: Intervention – "Intervention" is a broad term that could refer to an exposure or risk factor (e.g., prematurity, herpes simplex conjunctivitis), a diagnostic test (e.g., 5-min dye disappearance test), or a medical or surgical treatment (e.g., levator resection, endoscopic dacryocystorhinostomy).

C: Comparison – What is the alternative intervention (e.g., observation, placebo, balloon dacryoplasty) or comparison group (e.g., children who have not had herpes simplex conjunctivitis), if there is one?

O: Outcome – What is the clinical outcome of interest (e.g., resolution of epiphora, surgical complications, diagnosed with child abuse)?

When undertaking a research project, always start with clearly defining your question. Do not start with the data. In other words, rather than deciding to do a project on "ptosis" on the 200 children you have operated upon in the past 5 years and figuring out what reportable "story" you can find after collecting the data, ask a specific question, such as "In children with asymmetric bilateral congenital ptosis, which results in better eyelid height symmetry, performing the same procedure (frontalis sling) on both eyes or performing different procedures (frontalis sling and levator resection) on each eye?" The question comes first, not the data. However, the questions that can be answered depend upon the data this is available, and sometimes it is wise to adjust the research

© Springer International Publishing AG 2018

J.A. Katowitz, W.R. Katowitz (eds.), *Pediatric Oculoplastic Surgery*, https://doi.org/10.1007/978-3-319-60814-3_20

question according to the data this is most easily collected, particularly when dealing with EMR.

Before settling on the study question, perform a literature review to identify what has already been done, what gaps remain, and what your study can add. See "Critically Appraising a Paper" below.

Study Designs

Generally speaking, clinical research studies evaluate an association between an exposure (risk factor, type of treatment, test result, etc.) and a disease (outcome, complication, etc.). "Exposure" is a general term for a risk factor and could mean a specific sign or symptom, surgical procedure or technique, medication, test result, or behavior, like smoking. "Disease" is a general term for an outcome and could refer to a surgical outcome or complication, disorder, or medical event. Conceptualizing studies in this manner is helpful for understanding types of study design (Fig. 20.1). The choice of study design depends upon the research question, as well as characteristics of the disease or treatment being studied, availability of data, and the resources you have available to carry out the research.

Descriptive studies include case reports and series. These types of studies do not have a comparison group and therefore are primarily hypothesis-generating studies. They do not provide evidence of an association. Comparative or analytical studies compare two or more groups of patients and include cohort studies, case-control studies, and randomized clinical trials. Because there are comparison groups, the presence or absence and strength of an association can be described. A randomized controlled trial is also an experimental study and offers the highest degree of evidence of a therapeutic effect. Descriptions of each study type appear below.

Case Reports and Case Series

A case report or series describes the clinical findings or course of a single or multiple patients, respectively. These studies are very helpful for describing a unique case, novel syndrome, or therapeutic approach and to generate hypotheses to be evaluated with an analytical study. However, without a comparison group, the existence of or strength of an association between the risk factor (medication, clinical symptom or sign, surgical procedure, etc.) and the outcome (disease, surgical outcome, complication, etc.) cannot be determined. With a single case report, it is not possible to know if the findings are generalizable to other patients, as the patient may be unique. A case series is useful for reporting the clinical characteristics of a disease or group of patients who undergo a certain procedure, but without a comparison group, it is not possible to know if the characteristics are unique to that disease or if that procedure is truly associated with a higher success rate in comparison to other procedures. **Key point**: *Much of the surgical literature consists of case series, so keep in mind these fundamental issues, which limit the conclusions that can be drawn from the results of case series.*

Cohort Study

A cohort study is a study in which patients with and without a risk factor (exposed and unexposed) or who receive two alternative treatments are compared to see if the groups differ with respect to one or more outcomes. So in Fig. 20.1, the direction of investigation is from the left side of the diagram toward the right (from exposure to disease). The groups are defined by the presence of the risk factor. This type of study is helpful for looking at any number of outcomes that result from a single risk factor; for example, eyelid height symmetry and surgical complications (the outcomes) can be compared between

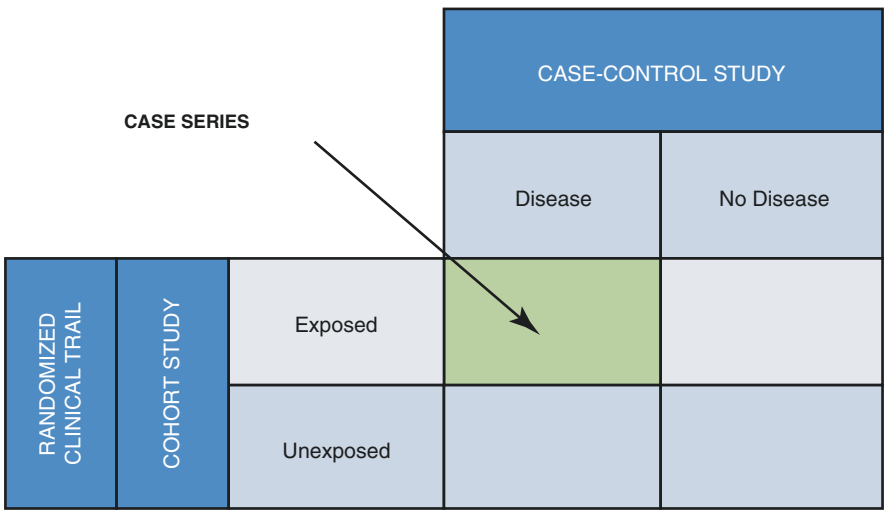


Fig. 20.1 Types of study designs

patients undergoing levator resection versus Fasanella-Servat procedure (the exposure or risk factor groups). The presence and strength of an association can be described, and it is possible to control for confounding variables (see confounding below) but only those factors of which you are aware and for which you collected data. When conducted prospectively, these studies take time and can be expensive to complete. Note that the comparison group in a cohort study may be referred to as a "control group," but this terminology is *not* the same as "controls" in a case-control study.

Case-Control Study

A case-control study is the reverse of a cohort study. The study groups are defined by the outcome (diseased or not diseased), not by the exposure. The groups are then compared for the presence of one or more risk factors. For example, patients with thyroid eye disease can be grouped into those who did (the cases) or did not (the controls) develop an optic neuropathy, and then the two groups can be compared to see if one group had more smokers in it than the other group. In Fig. 20.1, the direction of investigation is from the top row toward the bottom (from disease to exposure). As with a cohort study, the presence and strength of associations can be described, but they are vulnerable to specific types of bias and must be designed carefully, a discussion of which is beyond the scope of this chapter. But a case-control study is very helpful for evaluating multiple risk factors, particularly for rare diseases or outcomes, which would be inefficient to study with a cohort study. Note that the "controls" in a case-control study are the subjects who do not have the outcome. A common mistake by authors is describing their study as a case-control study because of the presence of a "control group" of patients who did not receive the medication being studied, even though they are comparing outcomes between two groups that have been defined by which treatment was received (the "medication" group and the "control" group). Such studies are in fact cohort studies, and the "controls" are study subjects who do not have the *exposure*. In a case-control study, "controls" refer to the study subjects who do not have the *disease*.

Randomized Controlled (Clinical) Trial (RCT)

An RCT or an experimental study is similar to a cohort study, as the groups are defined according to whether the subjects have a specific risk factor or received a specific treatment, but the assignment to each group is determined by the investigator, who, in the case of an RCT, randomly assigns each subject to a treatment group. The power of the study design lays in the randomization process, which is the only way to potentially control for not only known confounders but also for unknown confounding factors (see below). **Key point**: *An RCT is logistically complicated to execute but provides the strongest evidence of an association and causality.*

Prospective Versus Retrospective

The terms prospective and retrospective refer to the manner in which the data were collected, not to the type of study. For example, a cohort study can be conducted prospectively or retrospectively. Prospective data collection involves collecting data forward in time, as the events are occurring, which allows the investigators to take measures to maximize the reliability and completeness of the data. Retrospective data collection involves collecting data backward in time, after the events have already occurred, which has the advantage of efficiency. **Key point**: *Retrospective data collection in and of itself is* ***not*** *a study limitation*. This error is very commonly made by peer reviewers and authors. Data collected retrospectively are subject to various types of bias resulting from inconsistent and missing measurements, but even when such bias is present in a study, it may be irrelevant with regard to the strength of the study conclusions, depending upon the study question (see Bias below).

Blinding (Masking)

A blinded study is one in which the subjects and/or investigator are not aware of the group assignment of the subjects. In ophthalmology, we prefer to use the term "masked," for obvious reasons. Masking group assignment helps to guard against bias resulting from changes in the behavior of the subjects that influence the study outcomes or bias in the manner in which outcome measurements are made by the study investigators. Randomization and masking are not the same thing. Randomization refers to the process by which subjects are assigned to a study group. Masking refers to whether the subjects or investigators know that assignment.

Levels of Evidence

When evaluating the strength of the evidence available to answer your question, the first step is to consider the study design. The following hierarchy represents the strength of evidence from lowest to highest.

Lowest

1. Anecdotal experience
2. Expert opinion/consensus

Non-comparative studies
3. Case report
4. Case series

Comparative studies
5. Case-control studies
6. Cohort studies
7. Randomized controlled (clinical) trial
8. Meta-analysis of randomized trials

Highest

Subjects

Clearly define the inclusion and exclusion criteria for eligibility for enrollment in the study, by formulating a clear study question. Match the study subjects to the question you are posing. Specify characteristics such as age, study period, diagnosis, treatment received, and minimal follow-up length. Consider the characteristics necessary to assign a subject to an exposure or outcome group, the availability of data in the medical record, sample size requirements, and potential confounders. One method for dealing with confounders is to restrict enrollment to subjects that do, or do not, possess the confounding factor. For example, if studying the worsening of thyroid eye disease by alcohol use, smoking could be a confounding factor, because smoking is associated with both alcohol use and worsening of thyroid eye disease, so studying only patients who do not smoke or studying only patients who do smoke, and excluding the other group, would remove the potential for smoking to be a confounding factor. However, restricting the study sample in this manner could make the results less generalizable to other groups of patients. In this example, an alternative approach would be to not exclude based upon smoking status but rather control for confounding analysis (see below).

Sample Size

The sample size requirement for your study depends upon your study question. It is driven by statistical considerations. The sample size will increase with increasing power desired to detect a difference between groups, decreasing difference in the outcome being measured between groups (20% difference in surgical complications versus 10% difference), increasingly stringent definition of statistical significance (0.1 versus 0.05 versus 0.01), and increasing variability in the factor being measured among the study subjects. A biostatistician can help you to perform an appropriate sample size calculation.

Key point: *Having a specific sample size requirement is very important for ensuring that you will be able to answer your study question with the study you are proposing to do*. Without one, you may find out later that your non-statistically significant result is not interpretable, because you did not have enough statistical power to answer the study question. Sometimes, you need to use a "convenience sample" of all available patients with a given disease or undergoing a specific procedure, because the clinical volume is simply limited. In such cases, the study question may need to be modified into a question that is answerable with the data available.

Data Collection

Decisions about which data to collect are driven first and foremost by your study question and analysis plan. Ensure data are collected for exposure/ treatment group assignment, primary outcome measures, secondary outcome measures, and potential confounding variables (see Confounding below). When defining these variables, think critically about what data are recorded consistently in the medical record and measured in a reliable fashion. For example, if postoperative lagophthalmos is an outcome of interest, but it is not measured clinically in a consistent manner, using millimeters of lagophthalmos as an outcome variable may not be practical, whereas corneal exposure (yes or no) may be a more reliable and still clinically meaningful measure of the degree of lagophthalmos. Generally, good study planning will ensure that all required data variables are collected without collecting data that is never used. Resist the urge to collect as many variables as possible "just in case" they are needed, as this approach is inefficient and often results in wasted effort.

Key point: *Categorize and code variables using numbers rather than letters, because numbers are analyzable*. For example, 1 = female, 2 = male; 1 = levator resection, 2 = frontalis sling with autologous fascia lata, etc. As you create your data spreadsheet, always simultaneously keep an additional spreadsheet to serve as a data dictionary, in which the first column contains the variable name, and the second column contains the coding scheme for the variable. One approach to organizing a data file in Microsoft Excel or Google Sheets that facilitates analysis by a biostatistician, who will be using a common statistical software package for the analysis, is to have one sheet organized by "subject," containing variables (one per column) that occur only once (demographics, baseline risk factors, etc.) for each subject, with one row per subject, and a second sheet organized by "visit," containing variables that are unique to each clinical evaluation, with one row per office visit. If only baseline and latest follow-up measures are being collected, rather than numerous visits, then a separate "visit" sheet may not be necessary.

Electronic Medical Record (EMR) Data

The use of EMR systems presents a tremendous opportunity to answer research questions faster, with much larger amounts of data and greater numbers of subjects. Identification of subjects can be accelerated by using billing codes and setting inclusion and exclusion criteria that are defined based upon readily accessible variables from the EMR. However, to use this approach, you must plan ahead and consistently code each visit with all relevant codes, so that subjects are not missed when you eventually undertake a research study. EMR exports can be used to generate large data spreadsheets or comma-separated-values files, which are importable into spreadsheets. These data can then can be manipulated and analyzed.

Generally, EMR-generated datasets will require varying amounts of "augmentation" through manual data collection, as well as manual interpretation and coding of the data into analyzable, number-based datasets. The quantity of manual "augmentation" can range from a lot, in which case EMR-generated files still offer a very efficient data abstraction mechanism; to a little, in which case EMR greatly accelerates the project and multiplies the sample size; to none, which is an ideal. How much "augmentation" is necessary depends upon how data are recorded by the clinicians in the medical record, how data are stored and provided by the EMR, and of course the study question itself. For example, a research question involving only refraction data may require no manual data collection or coding, if the data are stored in the EMR separately for each eye; the refractions are broken down by sphere, cylinder, and axis; and these fields are used consistently by the clinicians performing the refractions. Under these circumstances, a dataset can be generated, and relatively simple statistical programming can be done to manipulate the data as necessary to answer the study question, without any manual manipulation or augmentation of the dataset. In contrast, studies that require analysis of radiology imaging reports will require the investigator to manually read and code those reports, though the EMR can rapidly generate a file of the reports. Similarly, strabismus examination documentation varies widely among pediatric ophthalmologists, with varying abbreviations and combinations of words (exotropia or XT) mixed with magnitudes (35 prism diopters) and control descriptors (poorly controlled) in single or multiple fields in the EMR, requiring an investigator to manually recode the EMR-generated dataset of strabismus measurements into discrete separate fields and codes or requiring a biostatistician to write complex coding algorithms to manipulate the data into an analyzable form. An intermediate example is a study of the prevalence of retinal hemorrhages among otherwise healthy children [1]. Such an uncommon finding can efficiently be studied using EMR data, because an EMR dataset can rapidly be searched by sorting a spreadsheet by fundus examination fields (disc, macula, vessels, periphery), permitting rapid identification of the very few children with this rare retinal finding.

Key point: *The ability to eventually access large amounts of data rapidly for research purposes depends upon you adopting a consistent, standardized way of recording data in the EMR in your daily clinical practice*. In EMR-based research, trade-offs can be made between increasing the efficiency of the study (i.e., less manual data collection and coding) and not taking into account some variables that were not consistently coded or recorded in the medical record. The importance of such limitations in the EMR naturally depends upon the study question, but such limitations can be minimized by standardizing your daily documentation. Think about how you or your colleagues code your visits for billing, record physical examination findings, and document assessments and plans. You can standardize your practices and facilitate EMR research by entering data as numbers or standard codes as much as possible; using predesigned or custom-designed data fields; working with your EMR provider to see how data can be recorded in discrete variables rather than in free text fields, which require excessive manipulation for research use; using diagnostic billing codes in a complete, consistent, and thorough way; and generally anticipating that you may eventually want to answer quality improvement or research questions in the future.

Data Analysis

As discussed above, a basic way to conceptualize the purpose of a clinical research study is the determination of the presence and strength of an association between an exposure and an outcome. For example, the exposure may be a specific surgical technique, compared to another technique, and the outcome may be a postoperative complication. Therefore, it is important to clearly define how groups are defined (exposed/unexposed, outcome present/outcome absent) for the analysis. These definitions and the analysis are determined by the study question, as are all aspects of the study design.

Key point: *A study can reveal a few possible types of associations:*

1. *No association* – the exposure and outcome are independent.
2. *Artifactual association* – there appears to be an association, but in fact it is a false association. An artifactual association can be due to one of two types:
   (a) *Chance* – random variation
   (b) *Bias* – systematic variation in the way the study was conducted

3. *Indirect association (confounding)* – there appears to be an association but in fact there is a confounding third variable that is responsible
4. *Causal association* – the exposure and outcome are in fact directly associated

Whatever the study result, it is important to always consider whether chance*,* bias*, or* confounding *could be responsible for the findings in your own study or in a paper you are reading.*

Chance and the P Value

By simple random chance, an association may be found when in fact there is no association. Chance can be addressed by biostatistics and statistical testing. A biostatistician will choose the correct statistical test, based upon the type (e.g., continuous, categorical, etc.) and distribution (e.g., normal) of data. A P value reports the chance that the observed association is due to random variation. By convention, statistical significance (the maximum percentage chance of a finding being due to random error that is acceptable) has been set at 5% ($P < 0.05$). However, this threshold is an arbitrary level. $P = 0.06$ is nearly identical to $P = 0.04$, particularly as this figure is also highly dependent upon the sample size (with a larger study, the same difference in surgical success rates will have a smaller P value). Similarly, $P = 0.001$ is quite a bit more significant than $P = 0.04$, as there is a 1 in 1000 (or 0.1%) chance the difference between groups is due to random variation, in comparison to a 1 in 25 (or 4%) chance that the difference is due to random variation. Therefore, always report the actual P value in your papers (e.g., report $P = 0.001$, $P = 0.07$, or $P = 0.35$; never report "$P < 0.05$" or "$P > 0.05$"), and when interpreting results, do not try to make much of a distinction between associations testing as $P = 0.04$ versus $P = 0.06$. More importantly, statistical significance does not necessarily imply clinical significance. For example, with a large enough number of subjects, a difference in vertical fissure length of 0.25 mm between treatment groups may be statistically significant but arguably is not clinically significant. In addition, a P value does not communicate the magnitude of an association like a risk ratio or odds ratio with confidence interval, which are more informative and useful measures of an association. Producers and consumers of the medical literature often place too much weight upon the singular importance of the P value.

Bias

Bias is a systematic error in the way the study was conducted that affects the measured association between the exposure and the outcome. **Key point**: *While chance and confounding can be measured and adjusted for in the analysis, bias is hard to measure, usually impossible to adjust for in the analysis, and must be addressed prophylactically in the study plan and conduct. Statistical analysis cannot repair bias.* A critical bias in study design can make the study results impossible to interpret. There are two broad categories of bias, selection bias and information bias. In both cases, differences arise with regard to both exposures and outcomes in a way that creates a false association or hides a true association, to a varying degree.

Selection bias refers to how subjects were chosen for and assigned to groups in the study. Selection bias arises when differences in the way the subjects are selected for exposure status (in a cohort study) or disease status (in a case-control study) are related to the other axis of interest (disease or exposure, respectively). Referral bias is one type of selection bias. For example, a pediatric oculoplastic surgeon working at a busy academic children's hospital undertakes a large case series to determine the prevalence of third nerve palsy among children presenting with acquired ptosis from any cause. She finds that the prevalence is surprisingly high, nearly 25%, but because she practices at a tertiary referral center, where such cases are likely to be funneled, the study sample is likely biased toward a higher prevalence. Note that it is not possible to know how skewed is this result without undertaking another study. Bias cannot be adjusted for in the analysis. In this hypothetical example, a large multicenter group of private practice and academic pediatric ophthalmologists undertake a similar series and find that only 2% of children with acquired ptosis have third nerve palsy, which is likely a less-biased estimate of the prevalence.

Information bias arises from differences in the way exposure or disease measures are made in the study groups. Information bias is also called misclassification bias. One type is recall bias, which occurs when cases and controls report prior exposures differently; for example, parents of children with congenital ptosis (cases) may report having had sushi during pregnancy at a greater rate than parents of children without ptosis (controls), because the former are seeking some explanation for their child's congenital abnormality, even though an equivalent proportion of parents ate sushi in both groups and maternal sushi consumption and congenital ptosis are unrelated. Another type of information bias is interviewer bias, which arises when there is a difference in the soliciting or interpreting of data between the two study groups; for example, an interviewer may question the mothers of children with congenital ptosis more intently to remember if they ever had sushi during the first trimester. Interviewer bias is more generally a type of ascertainment bias, in which the outcome or risk factor of interest is more likely to be identified in one group or another. For example, an ophthalmologist who believes strongly in a medication thought to enhance amblyopia treatment may more strongly encourage a child in the treatment group to try harder on visual acuity testing than a child in the control group. Again, these sorts of biases cannot be adjusted for in the analysis and may invalidate the results of the studies.

Preventing Bias

The keys to preventing bias in your study are to carefully design, plan, and conduct the study, thinking hard about and anticipating potential sources of bias. Recognizing bias can be a bit tricky, but with time, this very useful and logical skill can become second nature. One example of bias prevention is rigorously ensuring that data collection is the same for all subjects, by using close-ended questions, interviewer training, written protocols, checking of multiple data sources, and minimizing loss to follow-up.

Evaluating Bias

Key point: *When evaluating your own study or another study, it is critical to ask not only (1) "What possible biases may have influenced the study results?" but also (2) "What is the direction of the likely effect of the bias on the study results?" and (3) "How great might the distortion be?"* The latter two questions are critical for determining the relevance of the bias to the study results. Just because a bias exists does not mean it will meaningfully impact the validity of the study. For example, let us assume that a recall bias exists in the sushi and congenital ptosis study described above, because parents of children who have congenital ptosis are more likely to recall having had sushi than parents of children without a congenital abnormality. The likely *direction* of the effect that this bias would have on the study results would be to magnify an apparent association. Therefore, if the investigators find that there was no association between maternal prenatal sushi consumption and congenital ptosis, the recall bias, which would *make it more likely to find an effect*, does not change the study conclusion that there is no association (unless, of course, eating sushi has a *protective* effect against the development of congenital ptosis!). Similarly, in the example of selection bias, in which an academic pediatric oculoplastic surgeon found that 25% of children presenting with acquired ptosis had third nerve palsy, there was a significant referral bias, resulting in a large overestimation of the prevalence of disease in the population. However, had she determined that the prevalence was less than 0.5%, then the referral bias would not change the conclusion that the prevalence is lower than previously thought, because referral bias likely would have *raised* the observed prevalence.

Confounding

Confounding occurs when there is a mixing of the effect being studied with a third factor, which is related to both the exposure and the disease. For example, a study finds that alcohol use is associated with coronary artery disease, among middle-age adults. However, if alcohol use is associated with smoking, and smoking is associated with coronary artery disease, then the association between alcohol and coronary artery disease may be confounded by smoking. Remember that for confounding to exist, the third factor has to be related both to the exposure and to the disease or outcome. If the confounding factor is distributed different between the exposed and unexposed groups, then confounding can occur. Finally, confounding can make a false association appear true, or it can hide a true association.

Dealing with Confounding

Confounding can be addressed in the study design or in the data analysis.

Study Design

Restriction One approach is to simply restrict the study to subjects who all do or all do not have the confounding characteristic. For example, in the example above, if only patients who smoke or only patients who do not smoke are studied, then there is no possibility of confounding of the relationship between alcohol and heart disease by smoking, because there will not be a different prevalence of smoking among the two exposed groups (alcohol and no alcohol). If your study question is well crafted and specific, then restriction may be a good approach. However, restriction can limit generalizability and does not allow investigation of any possible interaction between the exposure and the confounder with regard to the outcome. For example, perhaps smoking has an even stronger association with heart disease among people who drink alcohol than among people who do not.

Randomization Randomizing the assignment of subjects to exposed/treatment and unexposed/alternative treatment groups is the best way to balance confounders between the groups. If a confounder is present equally in the two groups, it will not affect the association between the exposure and the outcome. Most importantly, randomization can balance not only *known* confounders but also *unknown* confounders, factors you are not aware of that are responsible for the effect you observe in the study. Note that even with randomization, it is still important to adjust for known confounders in the analysis (see multivariate analysis below), because although randomization provides the best balanced allocation of confounders between groups, an imbalance in the distribution of confounders among groups can still exist, just by chance.

Measuring Confounders

Key point: *It is fundamentally important that you think about, identify, and collect data on potential confounders, so that confounding can be explored and controlled for in the analysis.*

Analysis

The two primary analytical methods of dealing with confounding are stratifying and multivariable analysis.

Stratification In stratification, the study sample is broken up into groups based upon the potential confounder and each strata is analyzed individually. In the example above, the sample would be broken up into smokers and nonsmokers. Stratification reduces or prevents confounding, because it limits the variability of the confounding variable within the strata. It is like restriction (using the confounding variable as an inclusion or exclusion criteria for enrollment in the study) except at the analysis stage. Stratification has the advantages of allowing the investigator and reader to clearly see the relationships between exposure, outcome, and confounder, and is easy to carry out, but stratification becomes impractical when more than one or two confounding variables are being considered, because separate strata are required for every combination of confounding variables (e.g., 3 "yes/no" confounders requires $3 \times 3 = 9$ strata, and if some variables have more than two choices, then even more strata are needed).

A basic approach to stratification is to calculate an odds ratio (a measure of the strength of the association between exposure and outcome, see below) for the entire study sample. This measure is called an unadjusted or crude odds ratio. Individual odds ratios are then calculated separately for each strata. If the crude and strata-specific odds ratios are similar, then there is no confounding, and the crude odds ratio can be reported in the results. However, if the crude and strata odds ratios are different (e.g., greater than 10% different), then confounding is present, and the strata odds ratios should be reported. For example, if the alcohol-heart disease association OR = 2.25 for the entire sample, but when broken into smokers and nonsmokers the OR = 1.0 within each stratum, then confounding exists. Effect modification refers to a synergistic effect between the confounder and the exposure, in which the stratum-specific odds ratios differ from one another; this topic is beyond the scope of the chapter but would be considered by your biostatistician.

Multivariable analysis Multivariable analysis refers to the use of mathematical models to account for multiple confounders at once. Multivariable regression modeling can provide an independent measure of association of each exposure/confounder with the outcome after adjusting (controlling) for all the other exposures/confounders (variables) in the model. There are different types of regression models for different types of data. For example, when the outcome is a continuous variable, then linear regression is used. When the outcome is a dichotomous or binary (yes/no) outcome, such as disease/no disease or surgical success/failure, then logistic regression is used. Logistic regression is particularly useful, because the coefficients of the variables in the model can easily be converted into individual odds ratios (with confidence intervals) that have been adjusted for confounding. And the equation total represents the risk (i.e., 0–100%) of the outcome (surgical success/failure) occurring, so such an equation can be used for predictive modeling. One pitfall of using multivariable models is "over-adjusting." Statistical power is diluted with the addition of each new confounding variable and needs to be addressed by ensuring there is a sufficiently large number of subjects in the study. A rule of thumb is that ten subjects with the outcome event (e.g., surgical success, surgical complication, development of disease, etc.) are required for each variable added to the model.

Key point: *Multivariable analysis cannot correct problems with data collection*. Confounders cannot be controlled for without data on the confounders, the collection of which requires planning. And multivariable analysis cannot correct for information bias in the data collection procedures (see Bias, above).

Multivariable analysis is complicated and requires special software and a biostatistician. First univariable and stratified analyses are performed to explore associations. Then candidate variables are selected and categorized/coded, being sure to include statistically significant predictors from the univariable analyses, biologically important predictors, and potential confounders. Finally, an iterative process is undertaken to arrive at the most robust but parsimonious model. One of many possible approaches is to start with many variables and take out variables that are no longer significant one by one, in a step-by-step process. More complicated modeling may consider nonlinear terms and interaction terms (synergistic effects between the variables).

Odds Ratios

An odds ratio (OR) is a measure of association between the exposure and the outcome. Odds are the probability of event occurring divided by the probability of an event not occurring, as opposed to "risk," which is simply the probability of an event occurring. So the OR is the ratio of the odds of the disease among the exposed, divided by the odds of the disease among the unexposed. It is reported as a unit-less ratio (e.g., 1.5, 0.4, etc.). Note that an OR = 3 does not really mean that the exposed group is 3 times as likely to get the disease as the unexposed group, which is what a *risk* ratio of 3 means. The meaning of an *odds* ratio is less intuitive. However, it is easy to calculate an OR, and logistic regression models provide odds ratios adjusted for confounders, so odds ratios are a very useful measure of the strength of an association, and the higher the OR, the stronger the association. Just keep in mind that as the risk of an outcome increases (e.g., 2% risk of surgical complication versus 10% risk), and as the *risk ratio* or *odds ratio* gets farther from 1.0, the OR

becomes greatly magnified relative to the risk ratio (e.g., study data demonstrating a risk ratio of 1.3 might produce an OR of 1.4, while data showing a risk ratio of 3.5 may produce an odds ratio of 6.8).

Key point: *An OR = 1 means that there is no association between the exposure and the disease.*

Confidence Intervals

The OR is just one-point estimate of the association between exposure and outcome. It is a product of your study data, which are based upon a the sample of patients you have included in your study. Due to random variability between patients, another sample of the same number of subjects might produce a different OR. Therefore, reporting of a study measure (odds ratio, prevalence of disease, risk of complications, etc.) should be accompanied by a **confidence interval (CI)**. A CI roughly could be considered to represent a range of values in which the true OR (or disease prevalence, or complication rate) for the entire population of patients exists. This is not precisely the definition of a CI, but it is a practical and meaningful way to think about the CI. Typically, a 95% CI is reported, which matches the 5% (P = 0.05) significance level routinely used in clinical research. The CI around an OR is a more useful measure of statistical significance than a P value, because it gives some representation of the magnitude of effect. If the CI includes "1," then the P value will be greater than 0.05, and the association between exposure and outcome would be considered not statistically significant by that standard. Again, 0.05 is an arbitrary cutoff level (see "Chance and P values" above). If the observed OR = 3.2, and the 95% CI = 0.98–18.2, then technically this is not a statistically significant association, but the CI just barely includes 1.0, and the P value is likely to be very close to 0.05, so an association certainly may truly exist.

Key point: *The width of a confidence interval depends upon the sample size of the study.* As the sample size increases, the width of the CI decreases. The only way to have a completely precise measure of an association in a population would be to include the entire population of patients in the study.

Causation Versus Association

Association is only one step in establishing causation. For surgical procedures, it may indeed be obvious that a particular technique has caused a particular outcome. However, for less obvious connections, one should consider multiple factors when deciding on the likelihood of causation, including time sequence, specificity of the relationship, consistency or reproducibility, biological plausibility, coherence with existing information, quantitative magnitude of the association (e.g., OR), dose-response relationship, and of course the strength of the study design with regard to bias and confounding.

Writing a Clinical Research Paper

Effectively sharing your results is a fundamental step in producing helpful, generalizable clinical knowledge. This goal is achieved through abstracts, poster presentations, oral presentations, and peer-reviewed publications. To some, writing a paper is an onerous task. What follows below are paragraph-by-paragraph instructions for writing a research paper for publication.

Introduction

Do not write the word "introduction." Just start the paper. The introduction should be two and a half paragraphs.

Paragraph 1

Some general background on the disease and the research topic. For example, Congenital ptosis is prevalent among …. Surgical approaches to congenital ptosis vary ….

Paragraph 2

More specific background information from the literature and/or context of the research study. Highlight gaps in knowledge that your study are going to try to answer. Occasionally, there is more complicated background for a study, so an additional paragraph can be added; however, short and sweet is better. For example, levator resection has shown mixed results in children …. It is not clear whether ….

Paragraph 3

The third paragraph is a *half* paragraph long. Begin the paragraph with "We sought to [*insert objectives of the study*]." The primary objective is your study question rephrased into that format. The second sentence can present additional detail about the primary objective or could present a hypothesis: "We hypothesized that …." An additional sentence can present secondary objectives: "We also determined the [*insert secondary outcomes/objectives*]" or "We closely examined…"

Methods

Key point: *The methods and results sections are the most important parts of the paper.*

The methods section should be very factual and describe the study plan. Do not put study results in the methods section. The number of subjects goes in the results not the methods. The information presented in the methods section is your study plan, as laid out in your study plan outline and IRB protocol before you started the study.

Paragraph 1

Simply state the study design, study location/hospitals, study period, and IRB/HIPAA compliance: "We conducted a retrospective cohort study at the Hospital of America between August 1, 2005, and September 1, 2010 (the dates could also go in paragraph two when describing the subjects) … (add in detail as needed)." The study was approved by the IRB of the Hospital of America and conducted in compliance with the Health Insurance Portability and Accountability Act.

Paragraph 2

Describe the subjects: "Subjects were children undergoing ptosis prior to age 3 years …." "Inclusion criteria were …. [*list*]. Exclusion criteria were ... [*list*]." You can have additional explanation for reasons for these criteria if pertinent to justify your decisions as a way to avoid bias in the study design. Specify if masking was used and who was masked. Specify, "Subjects were identified by … [reviewing billing records, a clinical database, etc.]." Specify if patients/families were consented or if consent was waived by the IRB.

Paragraph 3

Describe data collected/data collection: "Data were abstracted from the medical record (or describe how collected)." Describe details of study measures, tests, etc. Describe the randomization protocol if application. Remember "data" is a plural word: the data "are," not the data "is."

Analysis

Have a subtitle in the methods section entitled "Analysis."

Paragraph 1

Specify how the study groups were defined, so it is clear who the exposed and unexposed subjects were or the cases and controls. Describe any matching used.

Paragraph 2

"The primary outcome was …. [define and explain how measured if necessary]." State the secondary outcomes as well. If there are multiple parts to the analysis, list them systematically in a logical way that goes from primary to secondary outcomes. You will present your results in the same exact order. "Descriptive statistics were calculated with means (SD), median (range) …." "[*Describe statistical test and methods for comparisons between groups for primary and secondary outcomes*.]" Ask your biostatistician for help describing the specific statistical tests, modeling methods, etc., which were performed. Justify these methods only if you made an unconventional choice or to clarify to the reviewers and readers why this approach is appropriate for the specific study question(s). Conclude with "All analysis was completed with [*name of statistical software program*].

Results

Paragraph 1

Describe the subjects ("X children met the inclusion criteria" ...). State how many subjects, their ages and sexes (if relevant), and other descriptive statistics. If applicable you can specify how many were excluded for various reasons. State how many had follow-up and the length of follow-up (mean, median, range, etc.). In a randomized trial or large cohort study, you should map out in a chart how many subjects were eligible, enrolled, excluded, and randomized to each group. If appropriate, be sure to specify the number of eyes in addition to the number of subjects.

Paragraphs 2, 3, etc.

Each successive Results section paragraph is for a new outcome/objective of the study. Follow as precisely as possible the order in which the outcomes were described in the Methods section. In this manner, the Methods and Results sequences are logical and cohesive.

Key point: *Just state the results – do not include any interpretation or judgment of the results in the Results section.* Just report the numbers: "2 (4%) children had complications"; do *not* write "Very few children had complications" in the Results section.

Tables

Often, creating empty tables as part of the study planning process will help you narrow your research question, ensure complete data collection, design an appropriate analysis plan, and, once you have populated the tables with data, help guide your thoughts for the Methods and Results sections. Tables are created for demographics/baseline characteristics,

primary outcomes, and secondary outcomes. Figures (bar charts, scatter plots, etc.) can be helpful for communicating results clearly and efficiently. Work with your statistician to produce clear, interpretable tables and figures.

Discussion

Paragraph 1

Start with a descriptive (not number-detailed) summary of the study findings: "We found that a minority of children had true strabismus following a diagnosis of pseudostrabismus...." Then continue the paragraph by going into more detail about those results, maybe comparing those results to prior reported findings, or addressing some special circumstances about the study.

Paragraph 2 (and 3 if necessary)

Discuss the study findings further, providing context from the literature and/or clinical practice. Highlight implications for practice.

Paragraph 4

Strengths and limitations. This paragraph is the most important part of the Discussion section of the paper. Compose it as follows: "Strengths of our study included … (list the strengths)." Then follow with, "However, there are important limitations to consider, including … (list the limitations only as general areas in this sentence, as you are about to use the rest of the paragraph to go into detail about each limitation)." **Key point**: *Try to identify and list as many potential limitations as possible.* Always try to think up as many limitations and holes in your study as possible, trying to make it sound as terrible as you can imagine. Think closely about sources of bias and confounding. Do not try to hide any limitations; authors who act like their study is perfect are demonstrating their ignorance, as all studies have limitations. It does not make the study or the paper weak to list limitations; to the contrary, doing so makes the paper stronger by demonstrating that you "know what you are talking about." In addition, if you have planned your study well, then you will usually have some justification or qualification for each limitation. State the limitation and follow with a sentence like "However, this potential bias would make it less likely to find an association, so it does not change the study conclusions." The implication is that the bias is not significant for this study question or these study conclusions. For example, "We found a very low incidence of retinal hemorrhages in our study. We did not exclude patients with diabetes. However, excluding patients who could have had retinal hemorrhages from diabetes would only have decreased our incidence estimate for retinal hemorrhages, and therefore the study conclusions would not change."

Paragraph 5

Concluding paragraph. Do not write a title "Conclusions." Just have an untitled final paragraph. Make general statements, summarizing and reiterating the study findings. Write a sentence or two about future studies, possibly addressing hypotheses raised by the study results or addressing gaps identified in the study design due to bias or confounding. Depending upon the subject matter, make some kind of wider (but not pompous) conclusion or statement about implications for clinical or surgical practice.

Reading a Paper

When reviewing a publication, follow the same outline for designing a study yourself, as discussed above. Consider the study question(s), study design, level of evidence, subject inclusion and exclusion criteria, types of data, reliability of data collection and outcome assessment, appropriateness of the analysis, sources of selection bias and information bias, and handling of potential confounders. It is critical to evaluate each of these features of the study to decide whether the results are valid and generalizable to your own practice. In practice, patient population, experience, and skill can vary greatly between surgeons, creating an important limitation to generalizability from surgical research studies. Keep this point in mind.

Finding the Take-Home Message

Key point: *The take-home message in a paper is in the Methods and Results sections. The Discussion section is often the worst place to look for the take-home message.* The discussion section is the least useful section for evaluating a study because the authors are heavily invested in their own study; they are often the least equipped and least objective of evaluators of their own research. If you find a thorough and extensive discussion of the limitations and implications of potential biases in the study, then you can be somewhat reassured of the competency of the authors. However, the best way to evaluate a study is to perform your own critical assessment of the methods and close examination of the study results.

Final Tips

- The study question is the most important aspect of a study. Every decision about design, analysis, and interpretation depends upon the study question.
- Do not skimp on creating a study outline. If you miss a crucial step, you could miss an opportunity to make an important contribution to clinical practice or at worst waste time and resources on a study that produces uninterpretable results.
- Plan ahead by considering potential bias and confounding; you can only adjust for confounders in the analysis if you have collected the data.
- Use your EMR system to your advantage. Anticipate that you may want to do research in the future. Invest a little time devising a scheme for documentation that will facilitate research later. Use discrete data entry fields in a disciplined fashion. Do not write text comments in fields intended for measurements/numbers. And minimize writing measurements/numbers in fields intended for text or in your narrative assessment and plan, because such data would need to be manually extracted.
- **Key point**: *When planning a study, if possible, collaborate with a biostatistician from the very beginning*. His or her expertise will help to force you to focus your study question, think about exactly how to define the subjects, identify what data you need, code and convert the data into something analyzable, and perhaps most importantly avoid bias in the study design. Once you provide the biostatisticians with the data, they can manipulate the data further and perform the analysis.

Reference

1. Binenbaum G, Christian C, Guttmann K, Huang J, Ying GS, Forbes BJ. Evaluation of temporal association between vaccinations and retinal Hemorrhage. JAMA Ophthalmol. 2015;133(11):1261–5.

Part II

Eyelids

Developmental Eyelid Abnormalities

21

Karen E. Revere, Jill A. Foster, William R. Katowitz, and James A. Katowitz

Embryologic Formation of the Eyelids

The major period of development for the face and skull takes place between the 4th to 8th weeks of gestation. To understand the pathogenesis of congenital eyelid deformities, a brief review of relevant embryology is helpful. A more complete review is presented in Chap. 2.

Nearly all of the facial tissues are derived from ectodermal neural crest cells, originating from the lateral margins of the embryonic neural folds during weeks 4–8 of gestation. The pharyngeal arches begin to form during week 4, and arch 1 is the major contributor to the face. Disruption in development of the five major facial prominences, originating from pharyngeal arch 1, can lead to a range of craniofacial anomalies. Eyelid development occurs somewhat separately from facial development and is more closely related to the development of the eye. Eyelid formation is identified in the 6-week fetus when ectoderm migrates over the developing lens vesicle. The rudimentary eyelids are identified as circumferential folds surrounding the optic vesicle (Fig. 21.1). Proliferation of mesenchyme creates elevations of tissue called processes that will contribute to the developing eyelids (Fig. 21.2).

The development of the eyelid occurs in 5 stages, beginning at week 6 of gestation [1]. *Stage 1* is characterized by the development of eyelid folds, which occurs with the migration of ectoderm over the developing lens vesicle. The eyelids fuse over the globe during *stage 2* and remain fused from week 8 to month 5 of gestation. During week 8 to month 7 of gestation, *stage 3*, formation of specialized eyelid structures occurs. The ectoderm on the inner surfaces of the folds will become conjunctiva, and the lacrimal gland will form from an invagination of the conjunctiva. The fusion of the folds contributes to differentiation and

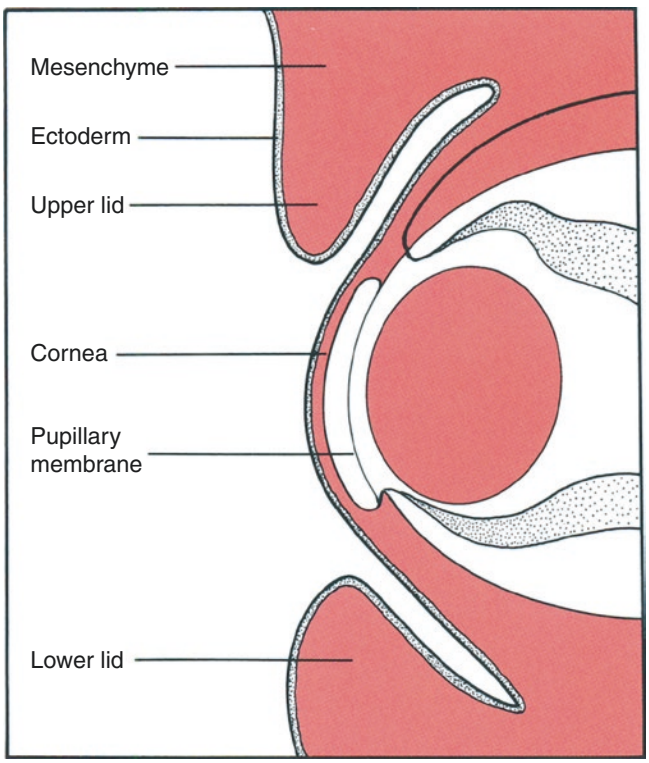


Fig. 21.1 Schematic representation of eyelid formation in the 7th week of gestation

K.E. Revere (✉)
Oculoplastics and Orbital Surgery, Ophthalmology, The Children's Hospital of Philadelphia, Philadelphia, PA, USA

Department of Ophthalmology, The Children's Hospital of Philadelphia and the Scheie Eye Institute, Philadelphia, PA, USA

Clinical Ophthalmology, The Perelman School of Medicine at the University of Pennsylvania, Philadelphia, PA, USA
e-mail: reverek@email.chop.edu

J.A. Foster
Ophthalmology, The Ohio State University, Oculoplastics, Nationwide Children's Hospital, Plastic Surgery Ohio, Columbus, OH, USA

J.A. Katowitz, MD, FACS • W.R. Katowitz, MD
The Children's Hospital of Philadelphia and The Edwin and Fannie Gray Hall Center for Human Appearance, University of Pennsylvania, Philadelphia, PA, USA
e-mail: katowitz@email.chop.edu; katowitzw@email.chop.edu

© Springer International Publishing AG 2018

J.A. Katowitz, W.R. Katowitz (eds.), *Pediatric Oculoplastic Surgery*, https://doi.org/10.1007/978-3-319-60814-3_21

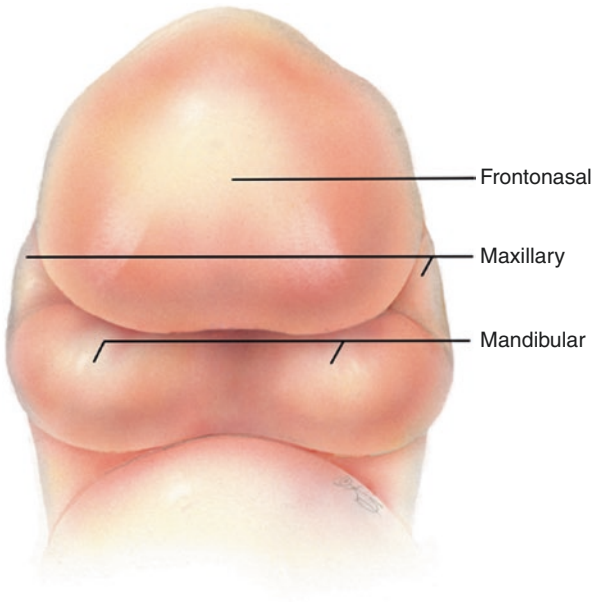


Fig. 21.2 Representation of the five main facial processes

development of marginal eyelid structures. Meibomian glands form as the result of ectodermal cords of tissue that invaginate along the eyelid margin and meet the mesenchyme. When the mesenchyme meets the ectodermal cords, the condensed mesenchyme forms the tarsal plates. The cilia and glands of Zeiss and Moll also develop as a result of invagination of ectoderm along the fused margins of the eyelid folds. Orbicularis oculi muscle develops from local mesenchymal tissue.

During *stage 4*, between 5 to 7 months of gestation, the eyelids start to separate. Eyelid separation begins as an intermittent process, with persistent fine epithelial strands connecting the lid margins until just prior to birth. The separation of the eyelids may occur by a process of apoptosis [2]. Maturation of the meibomian glands with resultant oily secretion and keratinization of the margin epithelium may also play a role in separation of the eyelids [3, 4]. *Stage 5* is characterized by structural differentiation and maturation of the eyelids, which is usually complete between month 7 of gestation and birth.

When the orderly sequence of migration and differentiation is disrupted, characteristic patterns of congenital malformation may occur. For example, when the eyelid folds fail to advance and cover the developing globe, complete or partial forms of cryptophthalmos occur [5]. If the eyelid folds fuse, but then fail to separate, forms of ankyloblepharon occur [6]. Colobomas occur when the eyelid folds are interrupted and adjacent tissues are unable to interact to influence growth, maturation, and differentiation. Proposed mechanisms for these disturbances in eyelid development include failure of fusion of the eyelid folds, amniotic bands, alterations in vitamin A metabolism [7], and abnormal migration of neural crest cells.

Stages of Eyelid Development

Stage 1: Migration of ectoderm over developing lens vesicle to form the eyelid folds
Stage 2: Fusion of the eyelids over the globe
Stage 3: Formation of specialized eyelid structures (meibomian glands, pilosebaceous units, etc.)
Stage 4: Separation of the eyelids
Stage 5: Further structural differentiation and maturation of the eyelids

Anatomy of the Eyelid: Surgical Considerations

When eyelid development proceeds in an orderly fashion, the outcome results in upper and lower eyelids that provide protection, lubrication, and a smooth surface over the eye. The anatomy of the eyelid should be studied in a layered and 3-dimensional fashion to understand the position and interactions of each eyelid component (Fig. 21.3) [8]. In the upper eyelid, the surface epithelium extends from the mucocutaneous junction to the eyebrow. The skin thickens as it approaches the brow. The smooth transition of the skin from the eyelid margin to the eyebrow is interrupted by the eyelid crease. In the non-Asian eyelid, the eyelid crease is formed by anterior fibrous extensions of the levator aponeurosis just above the superior border of tarsus. The position of the eyelid crease provides an external clue to the underlying level of the levator muscle insertion. Anterior to the levator complex is the preaponeurotic fat and the overlying orbital septum which inserts onto the levator aponeurosis and extends superiorly to fuse with periosteum at the arcus marginalis. In the non-Asian eyelid, this insertion of septum onto levator muscle usually occurs 3–10 mm above the superior tarsal border. In the Asian eyelid, the insertion of septum is usually below the superior tarsal border, resulting in a lower eyelid crease and allowing preaponeurotic fat to occupy a lower position in the eyelid.

Beneath the skin and subcutaneous tissue is the orbicularis oculi muscle, which acts as a circumferential sphincter for the eyelids. The orbicularis muscle is innervated by branches of the seventh cranial nerve and functions to depress the eyebrow and close the eyelids. The orbicularis muscle is divided into pretarsal, preseptal, and orbital components. In the medial canthal region, the fibrous attachments of the lower eyelid preseptal and pretarsal orbicularis muscle divide and wrap around the lacrimal sac. Thus, the coordinated action of the eyelid blink plays a vital role in lacrimal outflow (see Chap. 26). In the lateral canthal region, the fibrous attachments of the orbicularis muscle condense to become a part of the lateral canthal

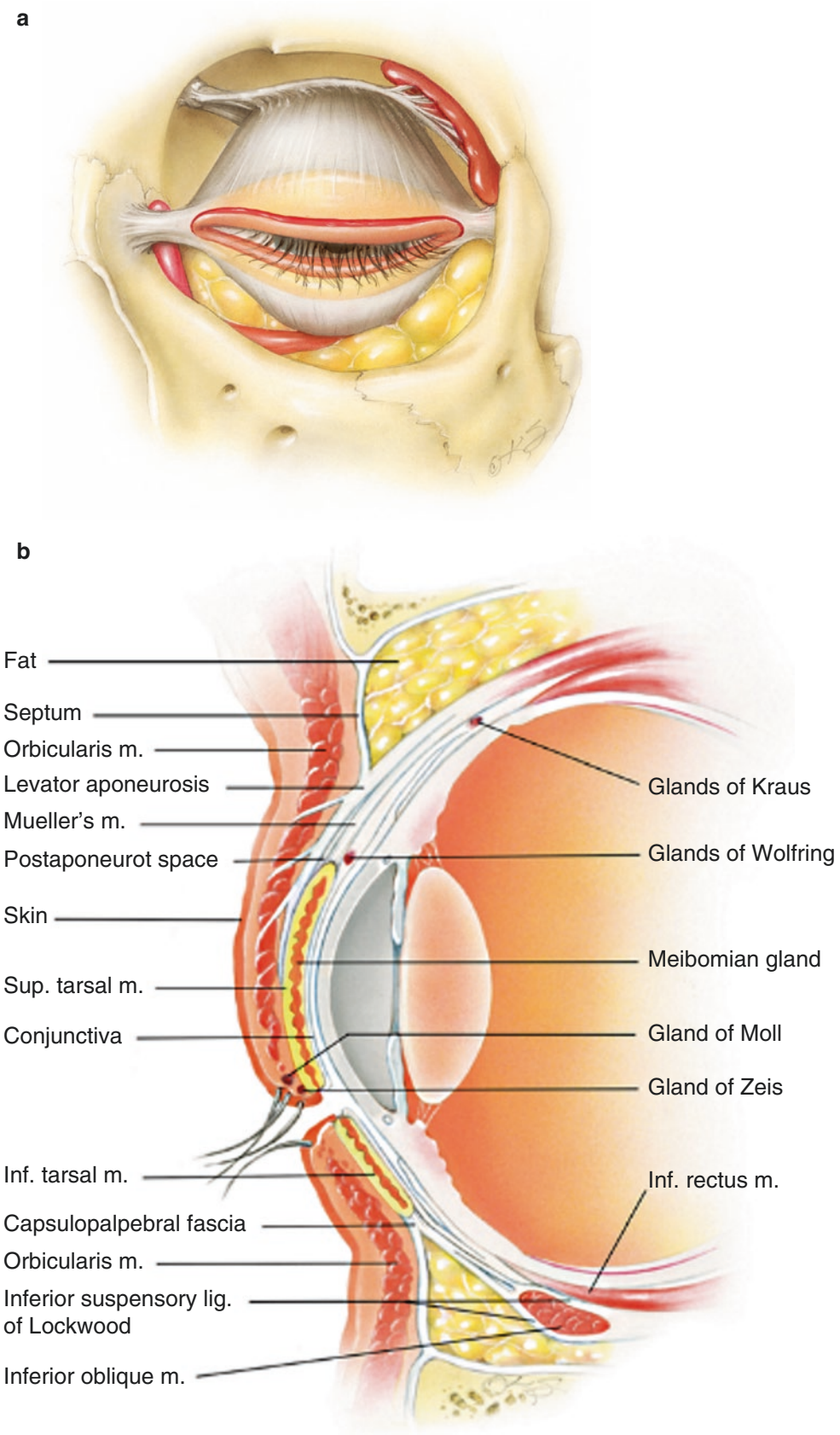


Fig. 21.3 Diagrammatic representation of the eyelid anatomy. (**a**) anterior view, (**b**) sagittal view

tendon. The most distal edge of the orbicularis in the upper and lower eyelid margins forms the gray line, named the muscle of Riolan. The meibomian gland orifices are located posterior to the gray line along the mucocutaneous junction.

While the levator aponeurosis attaches on the anterior aspect of tarsus, Müller's superior tarsal muscle, a sympathetically innervated smooth muscle, inserts at the top of tarsus. In an adult, the upper eyelid tarsus is usually between 8 and 10 mm in height. The superior palpebral arcade vasculature runs horizontally between the tarsus and Müller's muscle. The palpebral conjunctiva, which lines the internal aspect of the eyelid, is posterior to Müller's muscle and tarsus. The primary retractor of the upper eyelid is the levator palpebrae superioris muscle, which is innervated by the superior division of the oculomotor nerve (cranial nerve III). The levator muscle originates on the lesser wing of the sphenoid bone, just above the annulus of Zinn. It then runs anteriorly through the orbit in close approximation with the superior rectus muscle. Fibrous tissue bands between the levator muscle and superior rectus muscle are responsible for alterations in eyelid position after superior rectus muscle surgery.

The orbital septum is the anterior extension of the periosteum of the orbit. The septum is adherent to periosteum at the arcus marginalis. The septum is a fibrous, multilayered structure that is surprisingly strong in children. It acts as a mechanical barrier to protect the orbit from trauma and infection. The preaponeurotic fat is found behind the orbital septum and is surrounded by a wispy fibrous capsule. In children, the preaponeurotic fat is lighter in color and more "sticky" than in adults. In children, trimming of the fat should be avoided unless the fat interferes with successful closure of an eyelid incision.

Whitnall's ligament stretches from the lateral to medial orbit and wraps around the levator muscle like a rubber band [9]. The fibrous tissue may function as a suspensory ligament, a check ligament for the levator muscle, and as a pulley to transform the horizontal force of the levator muscle into a vertical force on the eyelid. The levator complex has fibrous attachments that spread out nasally and temporally to form the medial and lateral horns. The lateral horn splits the lacrimal gland into orbital and palpebral lobes and inserts on the lateral orbital tubercle. The medial horn inserts into the posterior arm of the medial canthal tendon.

In contrast to the upper eyelid, the lower eyelid is shorter in vertical dimension and has a shorter distance of excursion. The structures in the lower eyelid are analogous to those of the upper eyelid. The lower eyelid retractors include the capsulopalpebral fascia and the sympathetically innervated inferior tarsal muscle [10]. The capsulopalpebral fascia is analogous to the levator complex in the upper eyelid. It originates from the inferior rectus muscle, wraps around the inferior oblique muscle, and then turns vertically into the eyelid at Lockwood's ligament (analogous to Whitnall's ligament). Smooth muscle fibers join the capsulopalpebral fascia on its posterior surface before its insertion onto the inferior tarsal surface. The tarsus has 4 mm of vertical height in the lower eyelid. Similar to the upper lid, the marginal arcade vessels run horizontally between the tarsus and inferior tarsal muscle. A less well-formed peripheral arcade vessel is sometimes present.

Cryptophthalmos

Cryptophthalmos, or "hidden eye," is a rare disorder, characterized by failure of the eyelids to fuse. Isolated cryptophthalmos can either occur sporadically or in an autosomal recessive pattern. Cryptophthalmos can also be associated with two related syndromes, both of which display autosomal recessive inheritance patterns. The first is Fraser syndrome, caused by mutations in FRAS1 and FREM2 genes, characterized by cryptophthalmos, syndactyly, genitourinary tract malformations, craniofacial dysmorphism, orofacial clefting, mental retardation, and musculoskeletal anomalies [11]. The second is Manitoba oculotrichoanal syndrome, caused by a mutation in the FREM1 gene and characterized by cryptophthalmos, triangular growths of hair on the face, a bifid or broad nasal tip, and gastrointestinal anomalies [12].

Cryptophthalmos is thought to occur as a result of inappropriate formation and migration of the eyelid folds, with ultimate adherence of the eyelids to the ocular surface. In 1969, Francoise proposed a scale, still used today, that divided cryptophthalmos into three general types: complete (total), incomplete (partial), or an abortive/congenital symblepharon variant [13]. Complete cryptophthalmos is the most common form. The initial classification has more recently been expanded to also characterize the congenital symblepharon variant into mild, moderate, and severe based on the degree of eyelid, conjunctiva, and corneal integrity [14].

Complete cryptophthalmos is characterized by the forehead skin that extends over the globe and onto the cheek without differentiating into upper and lower eyelids (Fig. 21.4). The intraocular structures are grossly disorganized. Incomplete cryptophthalmos is characterized by a skin fold that covers only the medial aspect of the interpalpebral fissure. There may be a coloboma in the upper eyelid, intraocular contents are usually disorganized, and the bony orbit may be contracted [14]. In both complete and incomplete forms, an ocular cyst may be present. In the congenital symblepharon variant, there are usually formed eyelids, but the skin from the upper eyelid is fused with the superior aspect of the cornea or globe, obliterating the superior conjunctival cul-de-sac (Fig. 21.5). In these patients, the cornea may be clear at birth and keratinize postnatally if not adequately lubricated. Alternatively, the cornea may be keratinized at birth due to poor eyelid coverage in utero, resulting in incomplete development of the corneal layers (which occurs at week 8 – month 5 gestation) and exposure of the superior cornea to corneo-toxic renal excretory contents within the amniotic fluid [1]. Adnexal components of the eyelids (i.e., tar-

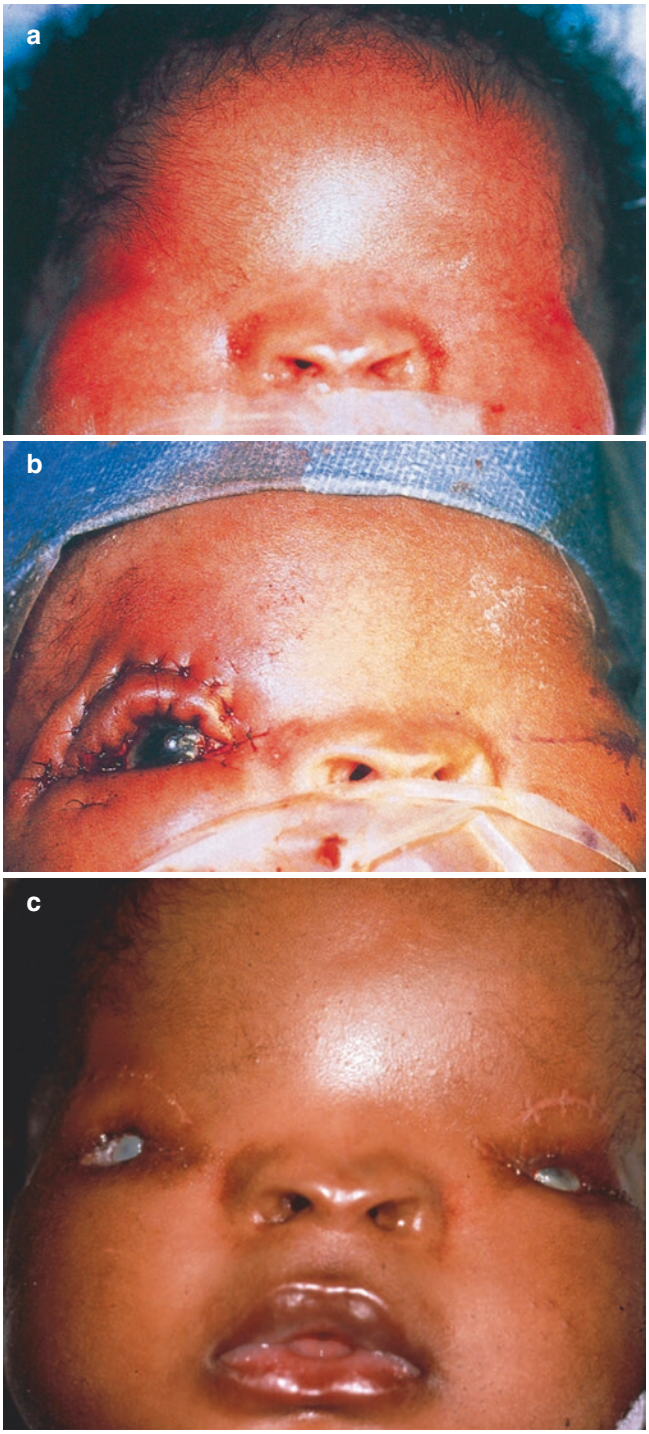


Fig. 21.4 Complete cryptophthalmos. (**a**) The surface epithelium passes smoothly from the forehead to the cheek. Brow cilia are present but distorted. There is continuity between the lateral eyebrow and the scalp hair. (**b**) With positive ERG findings, an attempt was made to create eyelids and open a pupillary axis. A total reconstruction of the anterior segment was done using a corneoscleral graft. There was no lens present. Oral mucous membrane was used to graft the inner surfaces of the skin that had been separated from the globe. (**c**) Surgery was successful in creating rudimentary eyelids and opening a palpebral fissure, but this did not result in useful vision



Fig. 21.5 Partial cryptophthalmos. (**a**) The partial cryptophthalmos in this patient shows surface epithelium confluent with the ocular surface on the medial aspect of the globe. Also note the absence of the medial eyebrow and the lateral displacement of the brow cilia. (**b**) The eyelid is reconstructed using the surface epithelium for the anterior lamella and a mucous membrane graft to replace the palpebral conjunctiva. Since the eye had no potential for visual function, the globe is covered by an ocular prosthesis

sus and meibomian glands) may be absent or rudimentary. It is not uncommon for this type of cryptophthalmos to be associated with nasal defects (including bifid and bulbous nose tip and elevation of the nasal ala), defects of the eyebrow, and a strip of hair extending downward from the scalp [14].

Prior to surgical intervention, the visual potential of the eye(s) should be determined. Underlying ophthalmic abnormalities, usually including corneal and anterior segment dysgenesis, are not always apparent. Ultrasonography can be useful in assessing the organization of intraocular contents. Electrophysiologic evaluation with electroretinogram (ERG)

and visual evoked potential (VEP) can be helpful in evaluating the visual potential of an affected eye. Eyelid sharing procedures for reconstruction are usually avoided when the eye may have useful vision. Computerized tomography (CT) can evaluate the bony orbital structures but should not be pursued unnecessarily in children given the exposure to radiation. A history of consanguineous parents can be ascertained, and, in children with other anomalous features (i.e., syndactyly), evaluation by a medical geneticist is warranted for screening of associated systemic conditions, such as Fraser or Manitoba oculotrichoanal syndrome.

Eyelid and ocular surface reconstruction must include consideration of the four major structural and functional components of the eyelids: mucus membrane for lubrication and a smooth posterior surface, tarsus for eyelid rigidity, eyelid retractor and protractor muscles for eyelid opening and closing, and skin to cover the external surface. All four functional components need to be present for adequate reconstruction, and many approaches have been described.

In partial cryptophthalmos, the surgeon may need grafts or flaps to replace the missing portions of the eyelid and conjunctiva. In the areas where the eyelid and globe are fused, caution should be taken because the surface epithelium is often continuous with the corneal surface, and this surgical plane is difficult to separate. If the eye is to be preserved, the surgeon needs to be prepared to graft the cornea when there is inadvertent penetration of the globe. The posterior lamella of the eyelid can be reconstructed, if necessary, with mucous membrane from the mouth or nose, cartilage from the ears or the nose, or allogeneic materials such as alloderm. The anterior lamella can be reconstructed with free skin grafts or local sliding or rotational skin flaps [13–15]. Since children have limited eyelid laxity, these reconstructive approaches are more successful if they can be deferred until an older age. However, if corneal exposure is a concern or visual rehabilitation is a priority, skin expanding techniques can be employed with the general plastic surgery team to make more available skin for reconstruction. Eyebrows can be remodeled using hair transplant techniques or tattooing.

Attempts at visual rehabilitation can be made in all forms of cryptophthalmos, although they are generally more successful in the incomplete and congenital symblepharon variants. The results of surgical reconstruction for complete cryptophthalmos have not been encouraging. Overall, visual potential is poor, and the rationale for surgical correction is usually to achieve better cosmesis with good lid support for possible future placement of an ocular prosthesis. None of the tissue substitutes for the posterior lamella contain the elements of normal tear secretion, and maintaining a clear corneal surface after eyelid reconstruction becomes a constant struggle. As in other forms of ocular dysgenesis with limited or absent visual function (i.e., microphthalmia), for more severe cases of partial cryptophthalmos, an oral mucous membrane graft over the cornea can be considered, allowing for an ocular prosthesis to be worn comfortably while also providing better overall cosmesis [16].

Clinical Anophthalmia and Microphthalmia

Congenital anophthalmia and microphthalmia (A/M) and coloboma are an interrelated group of congenital abnormalities that likely have an underlying genetic basis. Together, these disorders account for 15–20% of severe visual impairment in children worldwide [17, 18]. Microphthalmia and anophthalmia have an estimated prevalence of 1 per 7000 and 1 per 30,000 live births, respectively [19]. SOX2 and OTX2 gene mutations, which cause lens induction failure, account for up to 60% of bilateral cases of severe microphthalmos and clinical anophthalmos [19, 20] (see Chap. 39). Environmental factors such as gestationally acquired infections, maternal vitamin A deficiency, X-ray exposure, and thalidomide exposure may also play a role [14]. Lower socioeconomic class and consanquinity may also be risk factors for the development of microphthalmia [21].

Congenital anophthalmia is rare and refers to a complete absence of ocular tissue. It occurs when there is a failure in the optic vesicle to bud or early arrest of its development with subsequent degeneration. Failure of optic vesicle budding may be "primary," with involvement of ocular tissue only, or "secondary," with complete suppression of the forebrain. The latter condition is not compatible with life. Clinical anophthalmos is a more appropriate term, used to describe the clinical absence of a visible eye, although rudimentary eye structures are often present radiographically. In contrast, microphthalmia is defined by the presence of a small, often disorganized eye, with a corneal diameter less than 10 mm and an axial length less than 20 mm. It is thought to result from incomplete invagination of the optic vesicle into the optic cup or from defective closure of the embryonic fissure, sometimes leading to colobomatous microphthalmos with uveal coloboma or colobomatous cyst [22].

Clinical anophthalmia and microphthalmia may occur in isolation or in association with other systemic abnormalities related to errors in the development of the first and second branchial arches (which later contribute to most structures of the head and neck) during weeks 4–6 of embryogenesis. Conditions that result from abnormalities during this phase in gestational development are referred to as "oculo-auricular-vertebral spectrum" disorders [23]. Many patients with clinical anophthalmia or microphthalmia have associated systemic conditions that fit into this spectrum of disorders.

Clinical anophthalmia and microphthalmia can occur unilaterally or bilaterally. The smaller the eye or eye remnant, the more severely retarded the growth of the orbit and eyelids. Abnormalities of the eyelid occurring in association with microphthalmia include eyelid coloboma, decreased horizontal and vertical palpebral fissure length, decreased conjunctival surface area, and relative shortening of the posterior lamellae with or without congenital entropion [24]. Although the adnexal structures of the eyelids are present, they are commonly decreased in size and number compared to the normal eyelid. Changes in bone growth can result in a decreased midline to inner canthal distance, maxillary hypo-

plasia, a posteriorly displaced lateral orbital rim, decreased horizontal brow length, and a low supraorbital ridge.

Ocular pathology can include limbal dermoids, coloboma of the iris or retina, cataract, Duane's retraction syndrome, decreased corneal sensation (trigeminal nerve abnormality), and optic nerve hypoplasia [25]. In microphthalmia, glaucoma may occur in the setting of a short axial length and resultant chronic angle closure. Acute angle closure and pupillary block can also occur from a disproportionately large lens in a cramped anterior chamber [26]. In unilateral cases of microphthalmos, some of these associated ocular findings can also be present in the contralateral eye [27]. Over 50% of cases may be associated with systemic abnormalities, which can involve the central nervous system, face (cleft lip or palate, hemifacial microsomia, facial hypoplasia, micrognathia), skeletal system (anomalous limbs), ear (preauricular skin tags, deafness), heart (ventricular septal defects, tetralogy of Fallot, coarctation of the aorta), genitourinary system, and gastrointestinal system [25].

All neonates born with microphthalmia or anophthalmia should be promptly evaluated by the neonatal team or pediatrician to check for systemic manifestations of the "oculovertebral-auricular spectrum." If there are severe ocular abnormalities, evaluation by an ophthalmologist should occur within the first 2 weeks of life. In unilateral cases, it is important to examine both eyes, since the fellow eye can also be affected. In clinical anophthalmia, an ocular ultrasound can be helpful to look for eye structures. In microphthalmia, ultrasound can be useful in measuring baseline axial length in the clinic setting. Magnetic resonance imaging (MRI) or CT (if MRI not available) should be performed to evaluate the bony orbit outline and to check for intracranial abnormalities. Similar to cryptophthalmos, VEP and ERG can be useful for examination of visual potential. Genetic screening is useful and especially warranted if a clinical syndrome is suspected.

Initial management decisions in microphthalmia are generally guided by whether the eye has visual potential. In some cases, the answer is apparent when the ocular remnants are so rudimentary that there is no potential for useful vision. In other cases, however, it can be difficult to judge the visual potential of a microphthalmic eye. Since treatment with expanding conformers or orbital volume augmentation may disrupt the visual pathway, the decision about visual potential must be considered prior to therapeutic intervention. If good vision is possible, and even very rudimentary vision may be valuable in cases of bilateral microphthalmos, then some reconstructive steps of the orbit and eyelids may be modified or postponed to prevent amblyopia [24].

The normal eye of a child at birth is about 70% of its adult size. However, the face is much smaller at birth and only reaches 40% of its adult size by 3 months. Over the first 2 years of life, the face grows to about 70% of its adult dimensions [28]. In severe microphthalmia and anophthalmia, growth of the orbit, fornices, and eyelids is retarded as a result of reduced orbital volume and growth stimulation. Early intervention is important to avoid permanent structural abnormalities that may compromise use of an ocular prosthesis later in life. Expansion of the orbit and socket should be instituted as early as possible to stimulate growth. Initially, the physician should evaluate the size and shape of the socket. If the socket is sufficient to hold a conformer, the ocularist is consulted to begin soft tissue expansion with orbital conformers. The success of the conformer in altering eyelid shape and growth is best achieved when started at the youngest ages. Conformers are clear, which can facilitate visual development in the case of a positive VEP or ERG. Growth can be monitored by assessing clinical symmetry of the lids and brow and by following serial imaging measurements.

When the socket size is insufficient to hold a conformer, mucosal grafting with buccal mucosa or hard palate can be used to expand the socket surface area. In unilateral cases, the physician can monitor growth by comparing eyelid measurements to the contralateral (if normal) side or pediatric growth charts [29]. Despite placement in an anterior position, progressively increasing size conformers will gradually create space in the posterior socket in addition to stretching the eyelids. When the posterior space becomes large enough that it is difficult to pass the conformer through the palpebral fissure, orbital volume augmentation is performed. This typically occurs around 12 months of age. Synthetic materials or autogenous dermis and fat may be used (Fig. 21.6) [30]. The dermis portion of the dermis fat graft may also be used to enlarge the socket surface area. Conjunctiva will grow and cover the dermal surface when it is sewn over the edges of the dermis fat graft. Asymmetry in the vertical palpebral fissure may be improved by ptosis procedures, but augmentation of the horizontal palpebral fissure remains a surgical challenge. Releasing the lateral canthal tendon does not typically result in a cosmetically pleasing eyelid, limits future eyelid stretching due to scarring at the canthal angle, and should generally be avoided.

Hard palate mucosa is sometimes of value and may be harvested from the roof of the mouth to augment the socket surface area or to provide stability to the eyelids (see Chap. 4). The roof of the mouth is inspected, and the junction between the hard and soft palate is identified (Fig. 21.7). There is a color change in the mucosa as well as the difference in the palpable firmness of the palate structure. Harvesting is performed anterior to the junction. There is a central ridge across the arch of the hard palate where the mucosa is thin and firmly attached to the underlying periosteum. This area is avoided. The vascular supply to the palate enters through the incisive foramen just behind the two front teeth and through the palatine foramina, which are located laterally at the junction of the hard and soft palate. Graft harvesting in these areas is avoided. Just behind the incisive foramen, there are horizontal rugae in the mucosa. This rough area is usually not appropriate for grafting. The hard palate near the roots of the teeth heals very slowly, and this area is also avoided. The flattened area of hard palate between the alveolar ridge and the central arch is the appropriate area for graft harvesting.

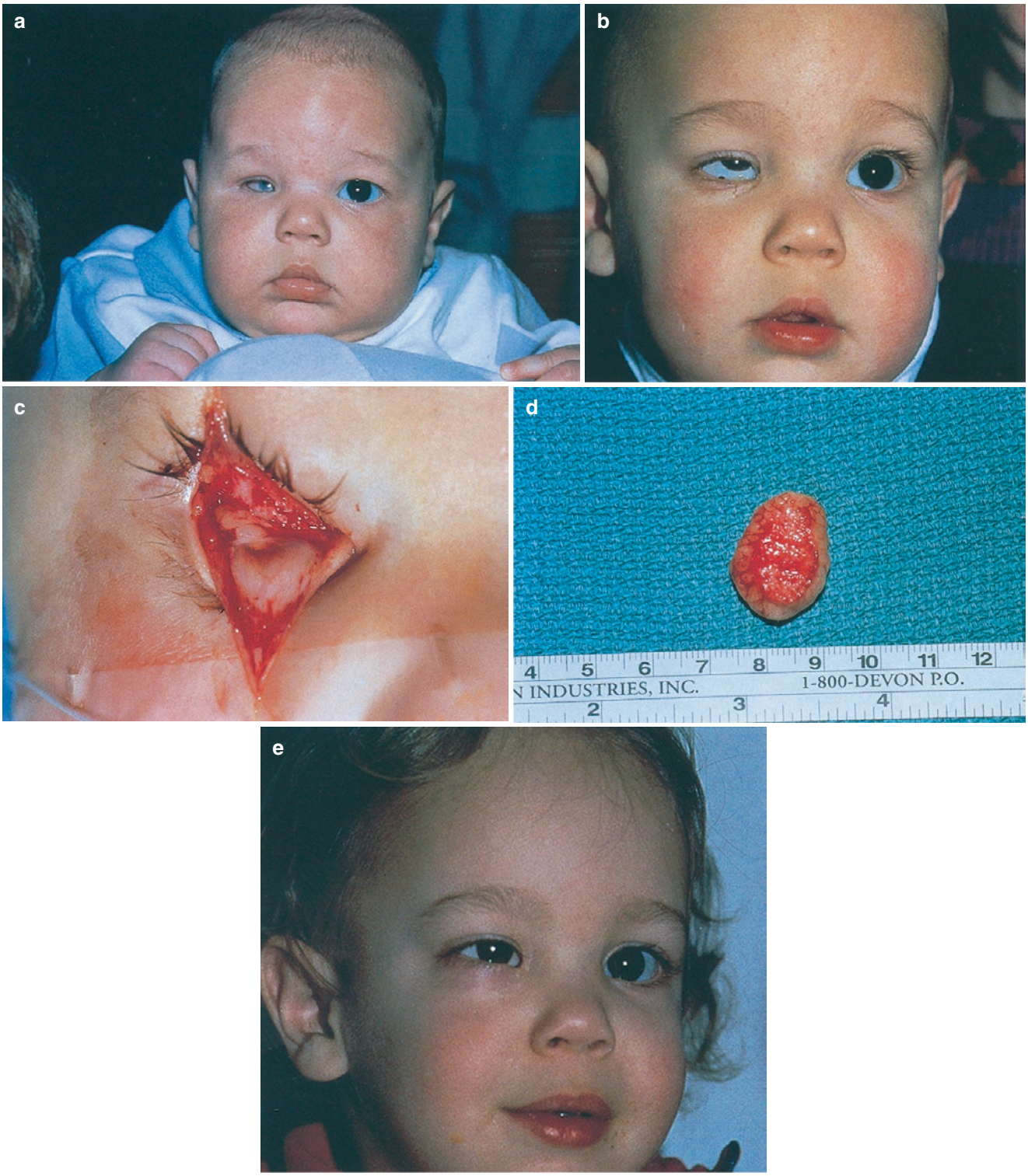


Fig. 21.6 Congenital microphthalmia. The condition was treated initially with progressively enlarging conformers followed by a dermis fat graft to augment the orbital volume. (**a**) Age 4 months at time of presentation. (**b**) Age 12 months, after treatment with increasing size conformers, the posterior socket has enlarged, creating room for volume augmentation. Because the socket size has outpaced the palpebral fissure opening, the current conformer can rotate within the socket. This is a signal to begin volume augmentation. (**c**) The conjunctiva is opened and blunt dissection used to create space for the dermis fat graft. (**d**) A dermis fat graft is harvested from the buttock. (**e**) Age 20 months with dermis fat graft and new prosthesis

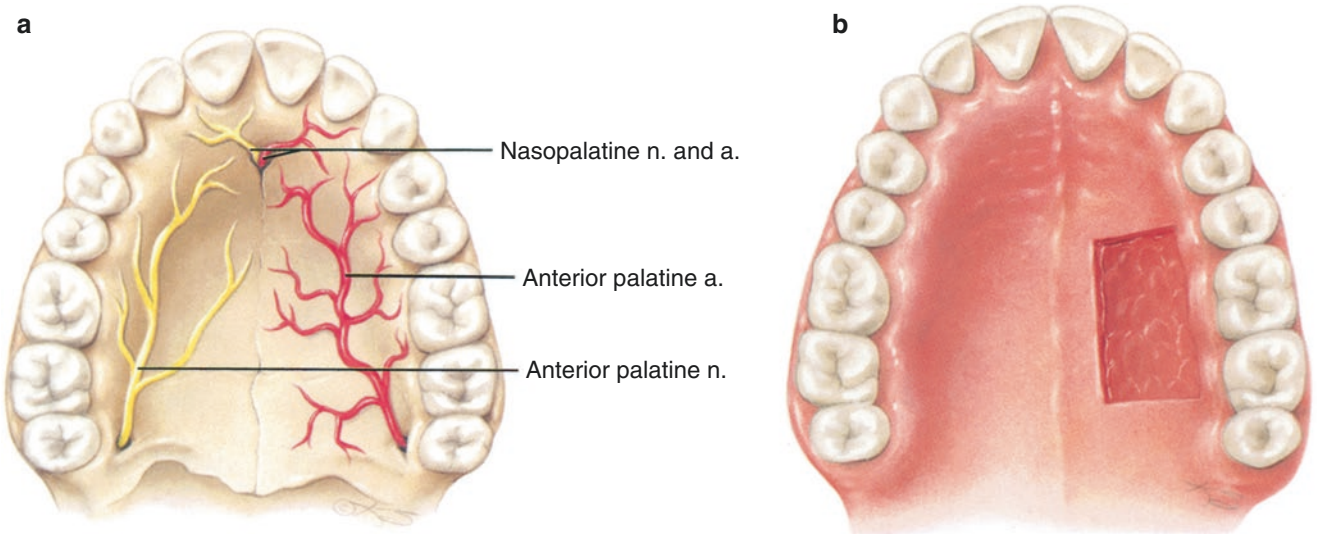


Fig. 21.7 Hard plate mucosal grafts. (**a**) Hard palate mucosal grafts should be harvested so as to avoid the gingiva, the palatine raphe, the nasopalatine foramen, and the greater palatine foramen through which pass corresponding nerves and vessels. (**b**) The graft site can be lightly cauterized for hemostasis as needed

The mucosa is infiltrated with local anesthesia and epinephrine. The local anesthesia will help with postoperative pain and the epinephrine for hemostasis. Marcaine 0.25% with 1/200,000 epinephrine is one choice of local anesthetic in children. About 1–2 ml of solution is injected. The hard palate will blanche with injection. The graft is marked, and then a No. 15 blade scalpel is used to incise the mucosa. Using the No. 15 blade scalpel, Westcott scissors, or dissection unit, the graft of mucosa is harvested leaving the underlying fat and periosteum intact. Cautery is used for hemostasis, and a strip of gelfoam soaked in thrombin is sewn over the areas of mucosal defect. Chromic gut or Vicryl suture (Ethicon) may be used. In the older child, a preformed palatal stent may be ordered from the dentist. The stent protects the healing palate from abrasion and decreases postoperative discomfort. The palate graft is then sewn into position in the socket or the eyelid using a resorbable suture such as 5-0 or 6-0 Vicryl. The hard palate mucosa is a versatile grafting material that simultaneously provides a mucosal surface as well as tissue rigidity. Since there is very little shrinkage of the hard palate mucosa, the graft is harvested to match the area of the defect. The first 3–6 weeks after surgery, the palate will sometimes shed white keratin material. This will stop after 3–4 weeks. The hard palate is a good surface replacement for the socket or the lower eyelid, but its use in the upper lid is limited because the irregular surface may cause corneal epithelial defects.

In cases of severe microphthalmia or anophthalmia, more aggressive orbit expansion must be undertaken. This has historically been done with frequent visits to the operating room using progressively larger acrylic socket expanders. More recently, hydrophilic expanders have successfully been used in the outpatient setting with good functional and cosmetic results [31]. These expanders, which are available in different sizes, can be placed in the socket with suture or glue tarsorrhaphy of the eyelids (see Chap. 39). Placement of a glue tarsorrhaphy, in particular, allows this to easily be done in the office. The average number of exchanges of hydrophilic implants is usually 2–3 times before age 2. Once the child is around 1 year of age, if sufficient space has been achieved, a dermis fat graft can be considered to promote continued orbital expansion.

It can be tempting to remove a non-seeing eye and place a dermis fat graft or an orbital implant at an early age. However, if possible, even a severely microphthalmic eye should be left in place since it will provide some stimulus to eyelid and orbital growth [32]. Static orbital implants are usually avoided, as they need to be changed in the operating room between 5 and 7 times before puberty and are associated with high incidences of wound dehiscence and implant extrusion [20]. Rarely, bone growth may be unresponsive to conformer expansion, and osteotomies and interpositional bone grafting can be considered (Fig. 21.8) [24].

In patients with microphthalmia and colobomatous cyst, gradual orbit expansion can be achieved by taking advantage of the natural expansion of the cyst from accumulation of fluid and/or glial tissue [26]. If enlargement of the cyst is too rapid, a needle decompression can be performed, although this should be cautiously done because there is often a direct connection between the cyst and the eye or brain. However, fluid usually will re-accumulate. Generally, by age 5, the orbit has reached 90% of its adult dimensions, and the eye and cyst can then be removed with placement of a more cosmetically acceptable ocular implant and prosthesis prior to the start of school [20]. Family members may need reassurance that this is the best approach since the appearance of microphthalmia with cyst can be discouraging. Prior to any surgical intervention, an MRI should be performed to assess the cyst size and whether there is any connection to the brain.

After initial successful socket expansion, the prosthesis and socket should be followed at least yearly for the first 5 years of life. As mentioned previously, microphthalmic

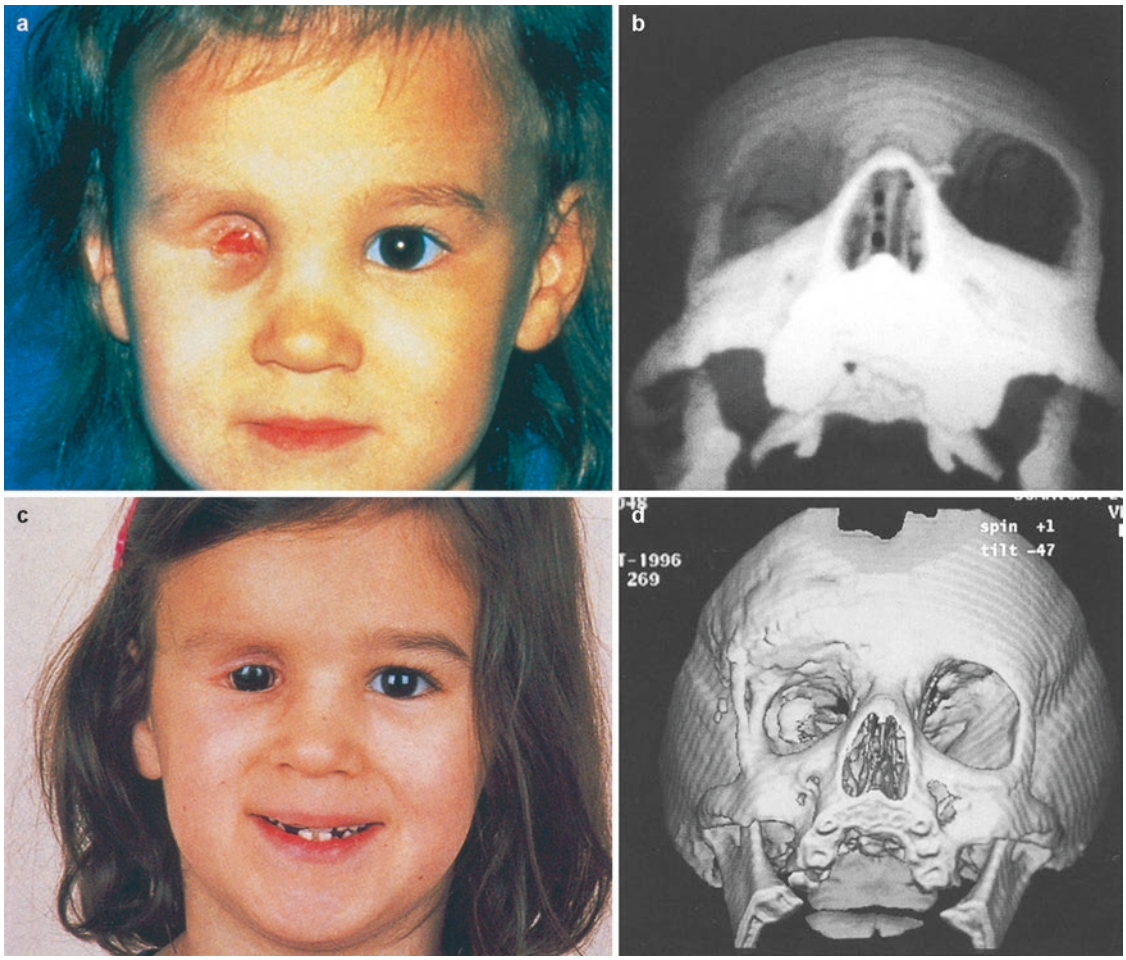


Fig. 21.8 Anophthalmia and hypoplasia. This patient had attempts at right socket expansion with bony and soft tissue hypoplasia. (**a**) At 3 years of age, this patient had a small socket unable to retain a prosthesis. (**b**) CT scan shows the relative bony hypoplasia on the right side. (**c**) The patient's appearance at 5 years of age following craniofacial expansion of the bony orbit. (**d**) The CT scan shows cranial bone grafts placed along the lateral orbital rim and the superior orbital rim to help improve facial symmetry

eyes are at risk for angle closure glaucoma, which may cause pain. Children with chorioretinal coloboma are at increased risk of retinal detachment, and precautions should be reviewed with parents. Polycarbonate glasses should be prescribed for refractive error and protection. Families and patients should be connected with vision support services soon after diagnosis to facilitate the best potential emotional and intellectual development of the child. A close relationship with an ocularist is essential.

Eyelid Colobomas

Eyelid coloboma describes an anatomic disruption or void along the eyelid margin with an overall prevalence of 0.7 per 10,000 births (Fig. 21.9) [19]. It can occur sporadically or be associated with other conditions such as Fraser syndrome (Fig. 21.4), Goldenhar syndrome (Fig. 21.10), and Treacher Collins syndrome where there may be a true notch or merely a drooping of the lateral lower lid often termed a pseudocoloboma (Fig. 21.11), CHARGE syndrome, Manitoba oculotrichoanal syndrome, and other rare variants. The exact prevalence of a sporadic coloboma is unknown



Fig. 21.9 Eyelid coloboma in the most common location between the junction of the middle and inner one-third of the upper eyelid

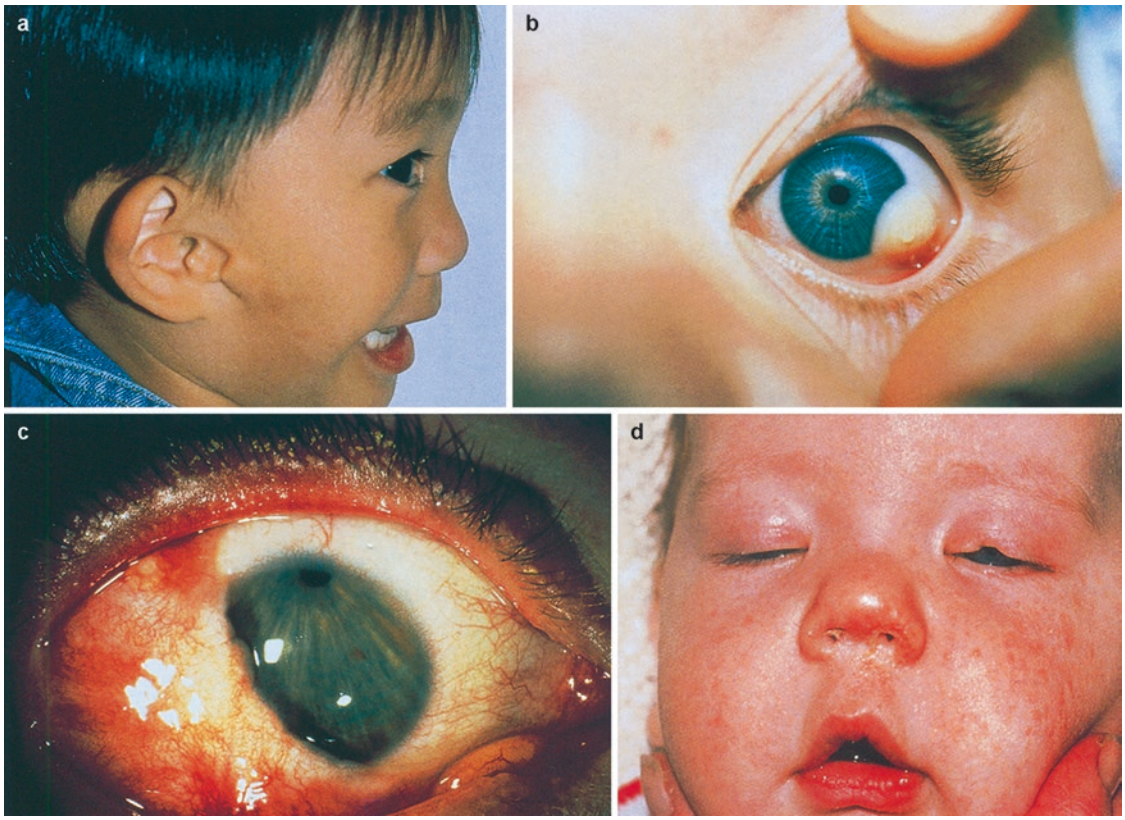


Fig. 21.10 Examples of the periocular manifestations of Goldenhar syndrome. (**a**) Preauricular skin tags; (**b**) limbal dermoid; (**c**) dermolipoma, corectopia; (**d**) upper eyelid coloboma



Fig. 21.11 Treacher Collins syndrome with an eyelid pseudocoloboma

[33]. In a true coloboma, there is an actual discontinuity in the eyelid margin. Pseudocolobomas occur in the eyelids when continuity in the superficial ectoderm of the eyelid margin is maintained but there is failure in development of the underlying mesenchymal tissues including orbicularis muscle and bone. Examples of this can be seen in the facial microsomias as well as in Treacher Collin Syndrome.

Embryologically, a coloboma may result from an error in ectodermal or mesodermal migration. Mechanical forces, such as amniotic bands, may also cause compressive tissue destruction of the developing eyelid. In the case of Goldenhar syndrome, the presence of a limbal dermoid may exert pressure on the eyelid, resulting in a focal failure of eyelid development. Abnormalities in the movement of fetal growth plates during embryogenesis can also explain variation in coloboma location. As such, colobomas may be seen in conjunction with other clefting phenomena or as part of a craniofacial syndrome. The system described by Tessier et al. [34] (see Chap. 38) can be helpful in characterizing colobomatous defects (Fig. 21.12). Colobomas vary in size and location but have some characteristic locations. In order of descending frequency, colobomas occur at the junction of the middle and inner one-third of the upper eyelid (Fig. 21.9), the central upper eyelid, the junction of the lateral and middle one-third of the lower eyelid, and at the junction of the middle and inner one-third of the lower eyelid [34].

While colobomas associated with Goldenhar syndrome, Fraser syndrome, or Treacher Collins syndrome are often bilateral, isolated simple colobomas are strictly unilateral, have no associated systemic signs, and do not usually present with significant corneal pathology. The size of the colobomatous lid defect may be overestimated in the clinical setting because of tissue elasticity and orbicularis muscle tone that pulls the colobomatous edges to either side.

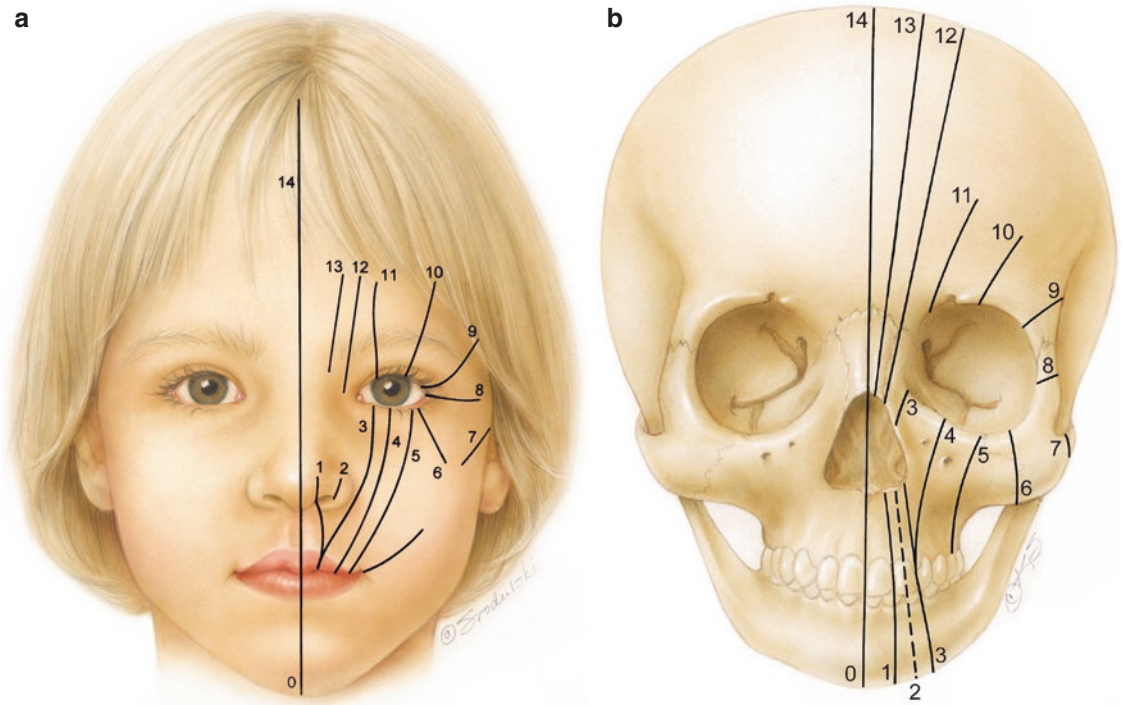


Fig. 21.12 Tessier clockface. The location of facial clefts can be described based on the geographic location of the cleft. This is derived from Tessier's numeric naming diagram. (**a**) Soft tissue defects. (**b**) Underlying bony defects

Associated ocular findings can include limbal dermoid in the case of Goldenhar syndrome, microphthalmos, iris coloboma, and osseous facial clefts. Facial abnormalities can include loss of ipsilateral eyebrow hair, a poorly formed supraorbital rim, cleft and lip palate, and a bifid nose. Additional clinical features of Goldenhar syndrome, Fraser syndrome, and Treacher Collins syndrome are described in Chap. 38 and elsewhere [33].

The pediatrician or neonatal team should be involved in the initial evaluation of a child with an eyelid coloboma to screen for syndromes. When applicable, referral to a geneticist for screening and counseling is warranted. A careful ophthalmologic exam should be performed, with special attention given to the condition of the cornea.

Appropriate management and protection of the ocular surface is crucial when dealing with eyelid coloboma. If the corneal epithelium is jeopardized, initial management should consist of ocular surface lubrication and, when necessary, occlusive dressing with plastic wrap. In the case of a small colobomatous defect (<25%) without evidence of keratopathy and a good Bell's phenomenon, watchful observation is often favored until 1–2 years of age prior to entering a preschool environment where considerations regarding appearance begin to emerge as a factor in psychosocial development [35]. Even large defects may be initially managed in this fashion if the cornea is adequately protected. However, lubrication with ointment and occlusion has the potential to create amblyopia, and this must be carefully monitored.

Location of Eyelid Colobomas (Most Common to Least Common)

1. Junction of the middle and inner one-third 1/3 of the upper eyelid
2. Central upper eyelid
3. Junction of the lateral and middle one-third 1/3 of the lower eyelid
4. Junction of the middle and inner one-third 1/3 of the lower eyelid

Repair of Upper Eyelid Colobomas

The technique used to repair a defect can be planned preoperatively based on its size. In an infant, small colobomas (<25% eyelid defect) can be closed primarily by excising the epithelial edges of the coloboma to create a wedge- or pentagon-shaped eyelid defect (Fig. 21.13). The edges of the tarsus are pulled together with interrupted 5-0 Vicryl sutures which are not tied until the eyelid margin has been repaired. Interrupted 6-0 or 7-0 Vicryl sutures are placed in three locations across the margin defect: lash line, gray line, and mucocutaneous junction. The distance from the entry site of the suture to the margin edge should be approximately 2 mm on either side, and the suture depth

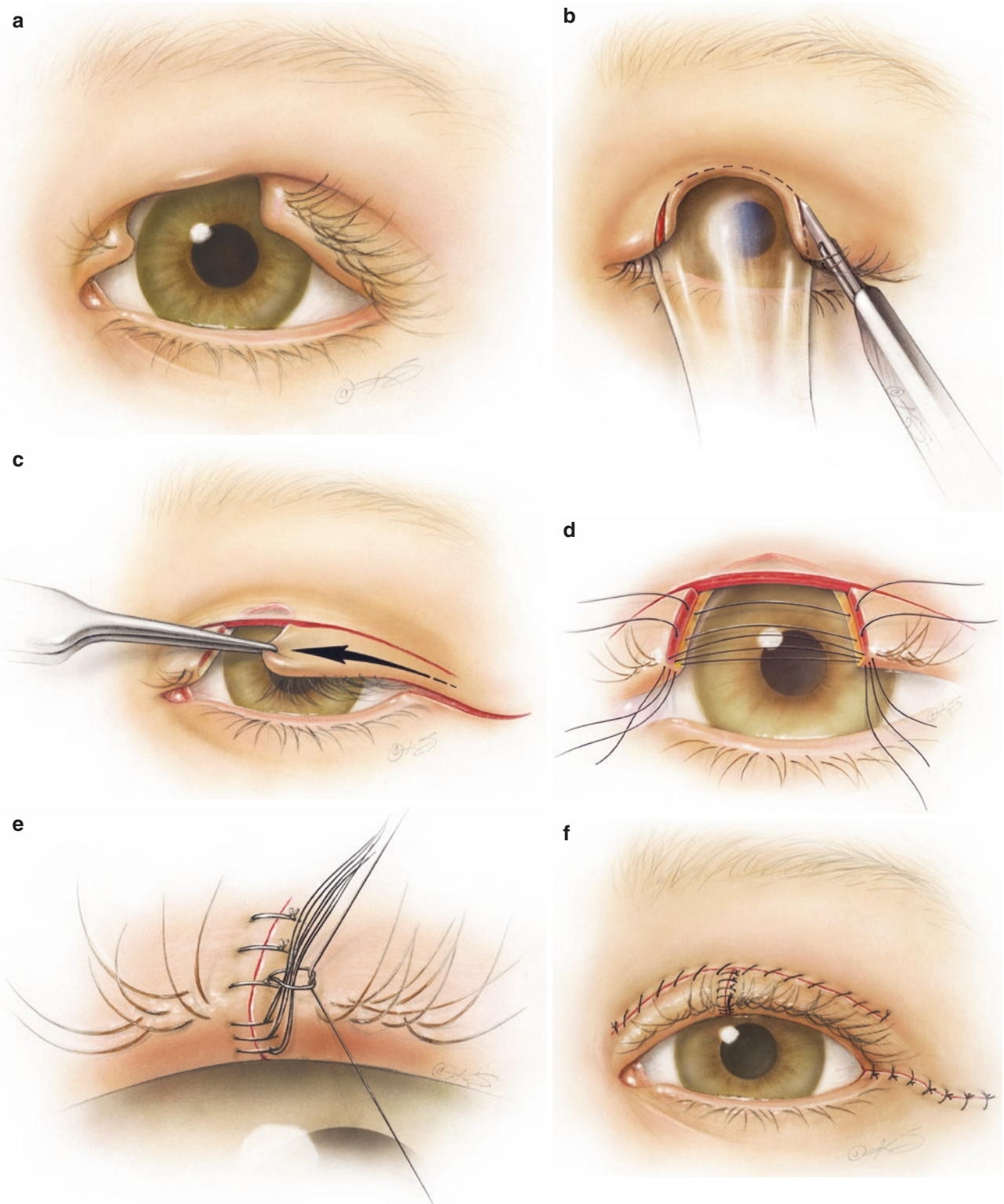


Fig. 21.13 Coloboma repair. (**a**) Upper eyelid coloboma. (**b**) The margins of the coloboma are trimmed to remove epithelium. (**c**) A lid crease incision and a lateral canthal incision allow approximation of the margins of the coloboma. (**d**) Interrupted 5-0 Vicryl sutures re-approximate the tarsus, and 6-0 or 7-0 Vicryl sutures are used to close the eyelid margin. All sutures are positioned before any are tied. (**e**) The ends of the margin sutures are pulled up and tied into one of the vertical skin sutures. (**f**) Skin closure completes the repair, using 6-0 plain gut suture



Fig. 21.14 Goldenhar syndrome. (**a**) Upper eyelid coloboma at age 1 week. (**b**) Preauricular appendages. (**c**) Two weeks postop at age 6 months following sliding flap repair with levator advancement. (**d**) Three months postop at age 9 months

should be about 2–3 mm. After the tarsal and margin sutures are tied, the orbicularis and skin are closed in one or two layers. 6-0 fast-absorbing gut sutures are preferable for skin closure, unless more tension on the wound requires 6-0 Vicryl for closure (Fig. 21.14).

For an eyelid defect >50% of the eyelid margin, tissue will need to be borrowed from other locations. Free tarsal or conjunctival grafts may be obtained from the upper lids; hard palate mucosa can be used in the lower lids; tarsus can be split in the upper eyelid to create a tarsal conjunctival flap; and skin grafts can be harvested from the retroauricular or supraclavicular areas, the upper eyelid, or from penis foreskin. Eyelid sharing procedures can be used in older children but may create amblyopia in younger children. However, when faced with uncontrolled corneal exposure and possible corneal ulceration, eyelid sharing techniques followed by aggressive amblyopia therapy may be necessary. In such instances, division of the transposed eyelid may be performed after 2 weeks rather than the recommended 4–6 weeks. In the upper eyelid, increased horizontal traction at the time of coloboma repair will sometimes create an upper eyelid ptosis. Advancement of the levator aponeurosis in the upper eyelid is sometimes performed in conjunction with coloboma repair to help prevent this problem.

In the older child or in a desperate situation, a Mustarde rotational transposition flap from the opposing eyelid can be used to close the defect and provide an anatomically matched

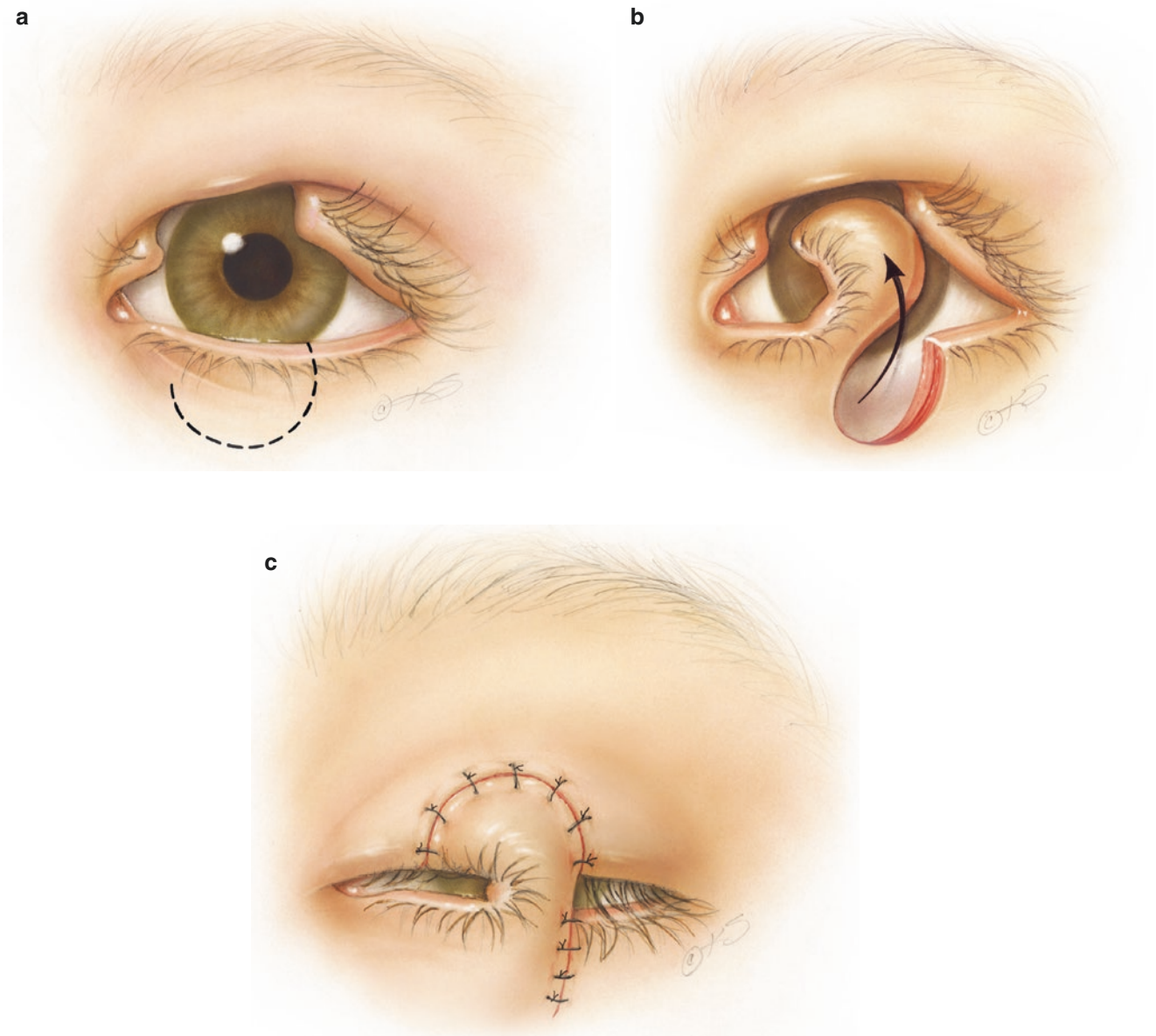


Fig. 21.15 Coloboma repair by the Mustarde rotating transposition flap technique from opposing lid. (**a**) Upper eyelid coloboma and marking of the pedicle flap in the lower eyelid. (**b**) The flap is rotated into the upper eyelid defect. (**c**) The flap is sewn into position and the lower lid defect pulled together. The flap is left in place for 4–6 weeks to allow for revascularization and then divided from the lower eyelid

eyelid margin (Fig. 21.15). This technique results in a cosmetically superior eyelid with an intact lash line, but the lashes are not certain to survive. Also, one must realize that the lashes of the lower eyelid are shorter and more dispersed than those of the upper eyelid. Nevertheless, with a broad base, the appearance of this upper eyelid reconstruction may be best in select cases. It is usually reserved for the older child or an infant with no potential for useful vision (Fig. 21.16). Again, with large skin needs, a team approach with plastic surgery can be employed where perioperative skin stretching is performed and used for subsequent eyelid reconstruction.

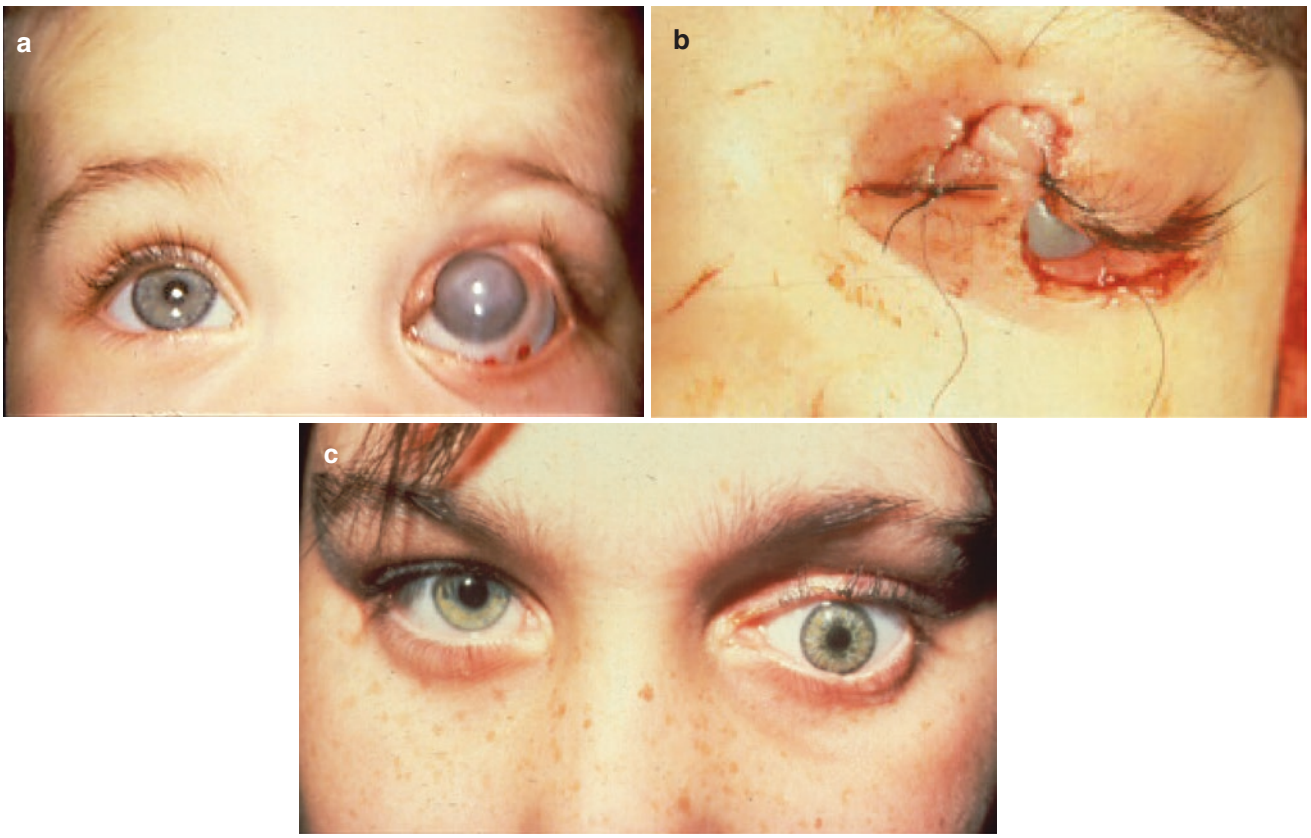


Fig. 21.16 Coloboma repair with lid-sharing Mustarde flap. (**a**) Upper eyelid coloboma in a 6-month-old with associated anterior segment dysgenesis, congenital glaucoma, and buphthalmos. (**b**) With no hope for functional vision, a Mustarde flap repair is performed at age 14 months. (**c**) The same patient at age 14 years with a cosmetic shell in place

Repair of Lower Eyelid Colobomas

As presented in box above, lower eyelid colobomas are less common than those occurring in the upper eyelid; and the least common are those involving the medial third of the lower lid. As discussed previously, the eyelid deformity most often found in the lower eyelid in Treacher Collins syndrome is more aptly termed a "pseudocoloboma," because there is continuity of the anterior lamella but discontinuity of the posterior lamella [24]. Occasionally, however, true colobomas with an eyelid notch and absence of cilia may also occur. Although the pseudocoloboma presents less danger to the ocular surface, successful cosmetic repair is challenging because the problem is not just the position of the lateral canthal tendon but also an absence of vertical and horizontal eyelid soft tissue. Repositioning of the lateral canthus and lower eyelid can be used with differing techniques based on the severity of the deformity. Rarely, simple repositioning of the lateral canthal tendon may be successful (Fig. 21.17). In more severe cases, hard palate or ear cartilage grafts have been used to support and lengthen the eyelid, and additional strength can be placed on the lateral canthal fixation with wire passed through drill holes in the lateral orbital rim. Ear cartilage is less desirable even when scored to gain more pliability. The hard palate graft is preferable or even use of other donor spacer materials such as alloderm.

For more extensive lower lid defect, particularly those associated with craniofacial clefting problems, a coordinated, multidisciplinary approach may be needed. Fig. 21.18 demonstrates such a complex repair. A decision was necessary regarding the primary need for reconstructive flaps in a child with partial cryptophthalmos, lower lid coloboma, microphthalmia, and clefting of both the lip and palate. Because the eye had no chance for useful vision, the concern for feeding issues due to the cleft lip and palate took preeminence in designing the flaps. Once these were outlined, it was possible to turn to solutions for the lower lid coloboma and the microphthalmic globe with an attached symblepharon. It was possible to design a rotating cheek flap for the lid repair and a protective conjunctival cover graft to permit use of a conformer shell and eventual cosmetic prosthetic shell, thus achieving both functional and appearance benefits.

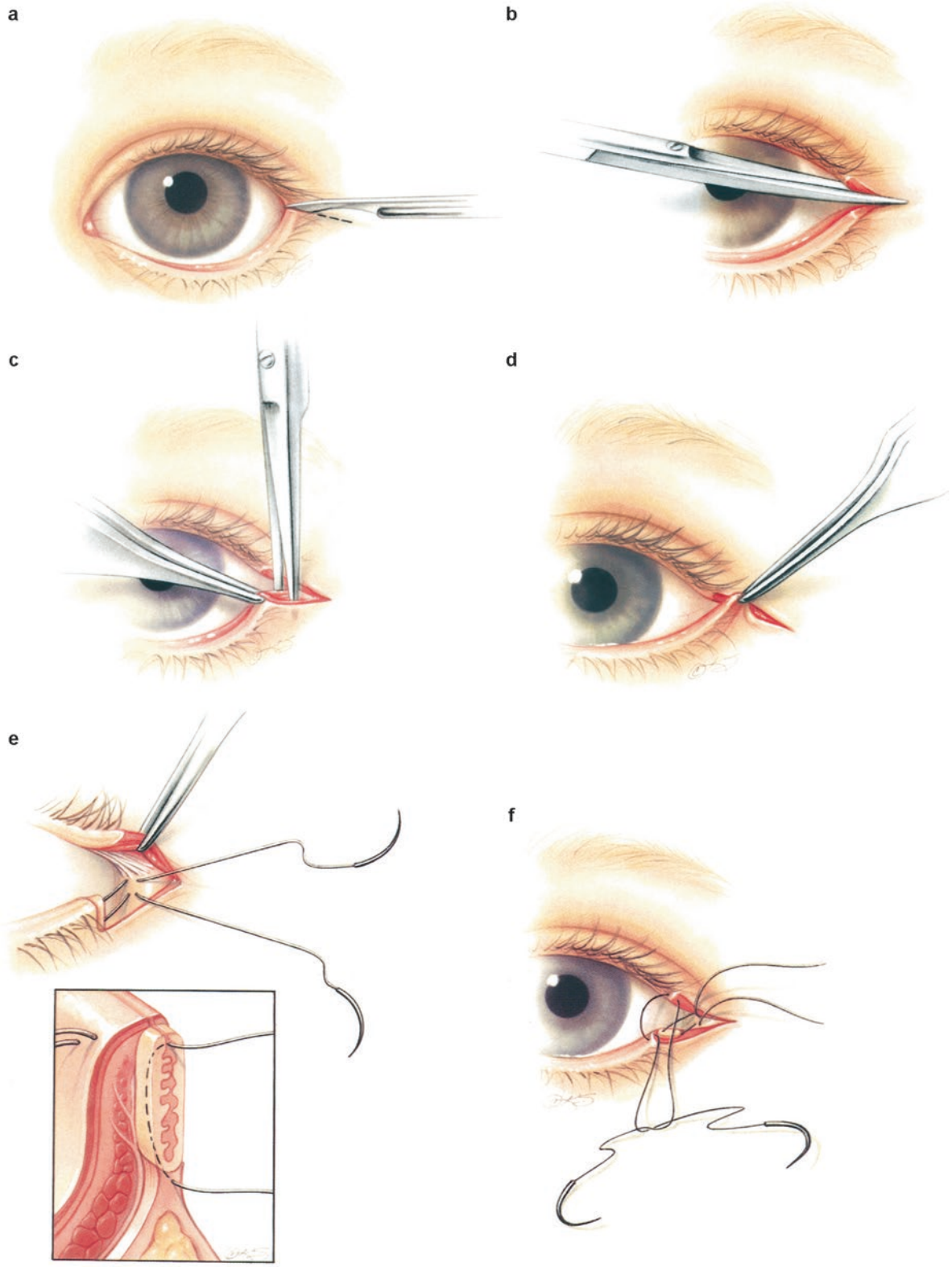


Fig. 21.17 Lateral canthoplasty. (**a**) Repair of the lower lid position begins with a lateral canthal skin incision. (**b**) The incision is completed to full thickness with a scissors. (**c**) The inferior limb of the lateral canthal tendon is released from its periosteal attachment. (**d**) The lid is pulled up into position to judge where the cut lid margin should be reattached to the lateral orbital rim. (**e**) The cut margin of the lower lid is secured with a double-armed 4-0 Vicryl suture that passes through the tarsal strip. Both ends of the suture are then passed through the lateral orbital rim periosteum. Alternatively, the suture may be passed through drill holes placed through the rim bone. (**f**) The lateral canthal angle is reformed with a suture passed from gray line to gray line in a buried fashion. This suture helps to keep a symmetric relationship between the edges of the lid margin. The skin is then closed with a resorbable suture



Fig. 21.18 Lower lid coloboma with partial cryptophthalmos and microphthalmia. (**a**) Microphthalmic globe and coloboma of probable amniotic band etiology with partial cryptophthalmos symblepharon in 1-year-old child. (**b**) Cleft lip and palate with flaps for repair outlined. (**c**) Mobilization of lip flaps for repair. (**d**) Dissection of Mustarde rotating cheek flap. (**e**) Cheek flap rotated into position. (**f**) Six months postoperative appearance. (**g**) 18 months postoperative appearance with successfully fitted ocular prosthesis

Transposition Flaps

Transposition flaps from the upper to lower eyelids can also be used in more severe cases to augment anterior lamella (Figs. 21.19 and 21.20). Repositioning of the lower eyelid is accomplished with resuspension of the lateral canthal tendon and augmentation of the anterior lamella with a skin and muscle transposition flap from the upper eyelid. The lateral canthal resuspension is performed as described above, but an additional incision is made through the skin and orbicularis in the subciliary region to release the soft tissue traction on the lower eyelid. The incision is made below the level of the tarsus to leave the marginal palpebral arcade intact. The skin, orbicularis, and, if necessary, orbital septum are opened to allow upward movement of the eyelid margin. The size of the defect is measured after the lateral canthal tendon is pulled into position. If possible, an equal-sized skin and orbicularis flap is created between the true eyelid crease and the eyebrow. To prevent downward traction on the brow, a total of 20 mm of upper eyelid skin should be left undisturbed. Care should be taken to avoid upper eyelid retraction in the by creation of an excessively large flap. The "flag" flap of skin and orbicularis is rotated into the lower eyelid defect and secured with 6-0 fast-absorbing gut. If no grafting is necessary to the posterior lamella, a similar technique can be used to create a free graft from the upper eyelid, with care taken to thin the graft as much as possible, as well as make small slit-like openings in the graft for serosanguinous drainage and increased graft viability.

In extremely severe cases of Treacher Collins syndrome, skin and muscle free flaps taken from elsewhere on the body can be interposed with the facial artery. This will provide an even larger volume of soft tissue than a free graft or transposition flap (Fig. 21.21). In some cases, bone grafts may also be necessary to augment malar and zygomatic hypoplasia and provide a buttress for the lower eyelid structures (see Chap. 8).

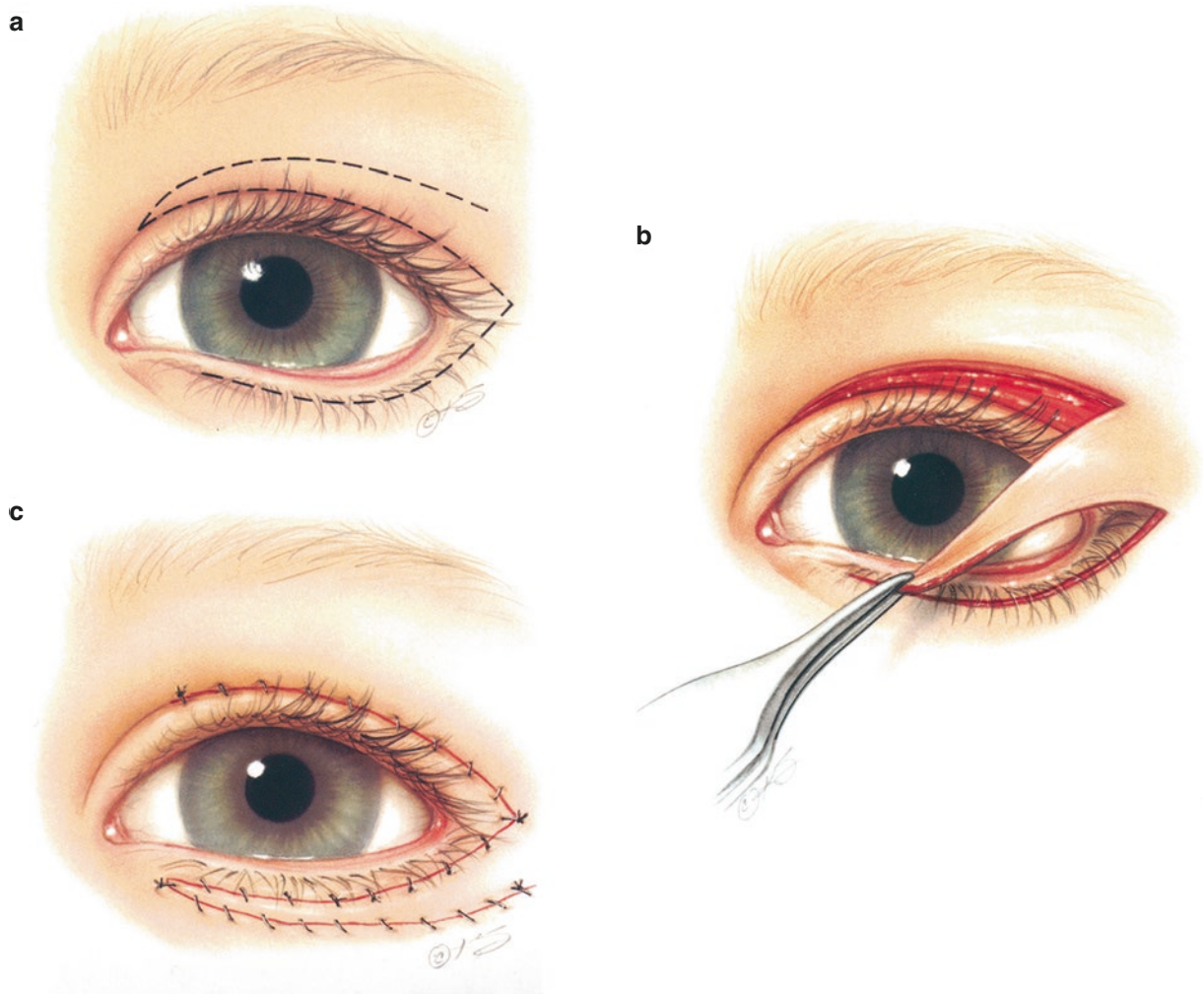


Fig. 21.19 Repair of lower eyelid pseudocoloboma with transposition flap technique. (**a**) The transposition flap is marked on the upper eyelid. The flap will be placed into the subciliary incision on the lower eyelid. (**b**) The transposition flap is rotated into position. (**c**) Sutured repair is completed



Fig. 21.20 Transposition flap surgery in Treacher Collins syndrome. (**a**) The upper eyelids have been marked to outline the tissue flaps. (**b**) The upper eyelid flap is draped laterally as the lower eyelid incision is made and the lateral canthal repositioning is performed. (**c**) Transposition flap placed into position. (**d**) Appearance of the eyelids 1 year later

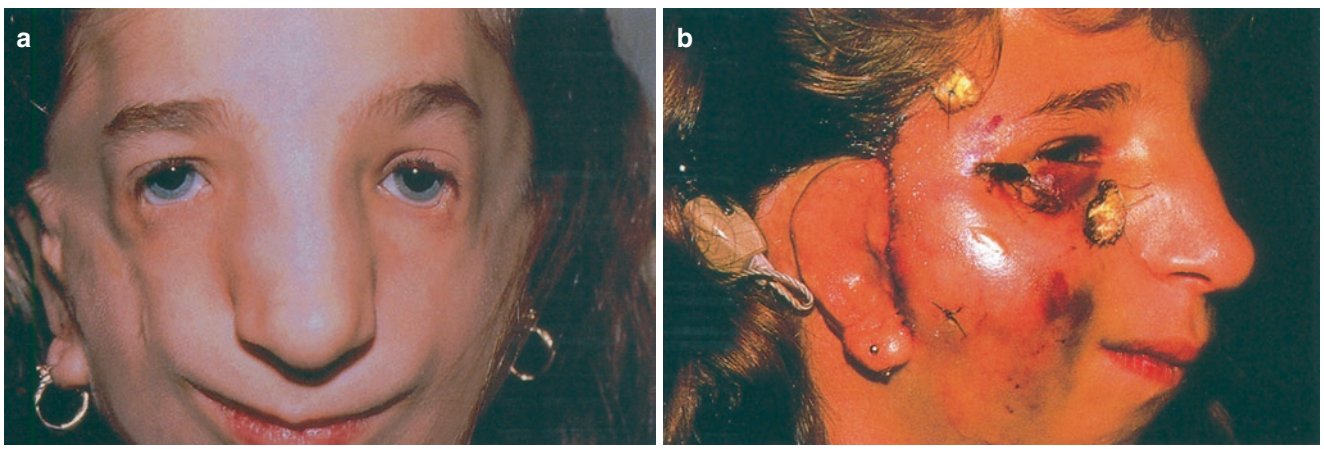


Fig. 21.21 Free flap for Treacher Collins syndrome defect. (**a**) This is a patient with Treacher Collins syndrome who already had transposition flaps from the upper eyelids into the lower eyelids but still had significant tissue deficit in the midface and lower eyelids. (**b**) A microvascular free flap was placed on the patient's right side



Fig. 21.21 (continued) (**c**) Graft harvesting location at the deltoid. (**d**) One month after the free flap, the filling in of soft tissue of the midface is apparent. (**e**) Six months postoperative, lateral view. (**f**) Six months postoperative, frontal view

Canthal Dystopias

Lateral canthal dystopias are frequently associated with Treacher Collin deformities as well as facial clefts. Repair of any inferiorly displaced lateral canthus associated with these deformities has really been covered in the previous discussion, including canthopexies and transposition flaps. In terms of medial canthal dystopias, however, while occurring less frequently, they are, for the most part, much more complex due to the proximity of the nasolacrimal outflow system which depends upon an anatomically sound medial canthal tendon surrounding the lacrimal sac for a functioning lacrimal pump. A transposition flap can also be used for the repair of this more difficult deformity (Fig. 21.22).



Fig. 21.22 Medial Canthal Dystopia with Left Upper Lid Colobomas. (**a**) A newborn with unusual skin tag on left upper lid with associated upper lid colobomas, medial canthal dystopia, iris coloboma, and absence of left nostril. (**b**) Close up view of (**a**). (**c**) Child now 9 months old; pathology report indicated that skin tag was actually an aberrant proboscis relating to absence of the left nostril and the presence of tearing. (**d**) Surgical plan to evaluate tear system, repair the canthal dystopia with a transposition flap as outlined with marking pen and upper lid colobomas with semi-circle flap. (**e**) Lower canaliculus found blocked before lacrimal sac; medial canthus then elevated and repositioned with 4-0 Vicryl canthopexy suture to match right side; flap transposed from upper to lower eyelid and upper lid coloboma resected; (**f**) Gray line marginal suture of 6-0 Vicryl placed after lateral cantholysis with additional 5-0 Vicryl sutures to secure tarsal wound. (**g**) Vertical upper lid incision required to remove small dermoid-like lesion at origin of aberrant proboscis previously removed and levator muscle resected as prophylactic step to reduce risk of occlusion amblyopia postop; upper lid reconstruction incisions closed with 6-0 Vicryl and plain gut. (**h**) Patient at 1 year postop being managed successfully with patching for amblyopia



Fig. 21.23 Ankyloblepharon. (**a**) Five-month-old with cleft lip and ankyloblepharon. (**b**) The lateral view shows the AFA disruption of eyelid separation

Ankyloblepharon

Ankyloblepharon describes a congenital eyelid condition that is characterized by completely or partially joined eyelids (Fig. 21.23) [3, 27]. A unique condition called ankyloblepharon filiforme adnatum (AFA) occurs when multiple strands of tissue connect the upper and lower eyelids [6, 36]. AFA has an incidence of 4.4 per 100,000 births [37]. Both conditions are of unknown etiology and occur sporadically. Because embryologic development up to the usual point of eyelid separation has occurred normally, eyelid and eye structures are normal. Secondary forms of ankyloblepharon can occur as a result of infection, ocular trauma, Stevens-Johnson syndrome/toxic epidermal necrolysis, and silicone tube intubation of the nasolacrimal system [38]. Iridogoniodysgenesis and the development of juvenile glaucoma can be associated with AFA. Systemically, AFA can be associated with cleft lip, cleft palate, hydrocephalous, meningomyelocele, imperforate anus, cardiac defects, and syndactyly. Several syndromes have also been associated with ankyloblepharon, including ankyloblepharon-ectodermal defects-cleft lip/palate syndrome, Edward's syndrome (trisomy 18), and CHANDS (curly hair, ankyloblepharon, and nail dysplasia syndrome).

A detailed ophthalmic exam should be performed. Genetic screening may be warranted. Given the risk of amblyopia in both forms of congenital ankyloblepharon, the eyelids should be surgically separated along the normal division, which is often easy to appreciate. This will provide a pattern of normal eyelid architecture that can be followed for the separation. A sharp scissors or a grooved director may be placed beneath the annealed eyelids to protect the ocular surface as a No. 15 blade scalpel is used to separate the tissue. Excess tissue is trimmed, and the conjunctiva is pulled over the internal eyelid margin to cover raw tissue and to protect the corneal surface. If separation of the eyelids is achieved in a timely manner, visual prognosis is excellent. Cosmetic appearance of the eyelids after separation is also usually very good.

Distichiasis and Trichiasis

Distichiasis may be either congenital or acquired and is characterized by cilia growing from the meibomian gland orifices. The congenital form is almost always associated with lymphedema distichiasis syndrome (LDS), an autosomal dominant condition (FOXC2 gene at 16q24.3) that is characterized by two parallel rows of cilia at the eyelid margin and lymphedema of the extremities [39]. LDS exhibits incomplete penetrance, with marked variability of expression, although distichiasis is almost always present. The lymphedema has a later onset (after age 10) and is generally not noticeable at the time of presentation. LDS may be associated with other congenital abnormalities, including ptosis, congenital heart defects, extradural spinal cysts, and cleft palate [39]. Isolated congenital distichiasis is extremely rare. The acquired form is more common and is seen most often in the setting of chronic inflammatory conditions, such as blepharitis, ocular cicatricial pemphigoid, Stevens-Johnson syndrome, and after chemical injury.

The eyelashes are a dermal appendage, and they differentiate in association with the glands of Zeis. These pilosebaceous units, and the meibomian glands, form by invagination of surface ectoderm along the eyelid margin [24]. Distichiasis results from a developmental error in which cilia form within or very close to meibomian gland orifices. The presence of cilia in this aberrant location may be asymptomatic or may cause irritation of the ocular surface from chronic lash-cornea touch. In the case of acquired distichiasis, chronic inflammation leads to metaplasia, which results in lash growth from meibomian gland orifices.

Clinically, distichiatic eyelashes can be seen emanating from meibomian gland orifices and usually traverse the entire length of the affected eyelid. Acquired distichiasis is more likely to be symptomatic than congenital.

Trichiasis is also an acquired lash abnormality in which the normal pilosebaceous units anterior to the meibomian glands become malpositioned. This can occur secondary to

chronic inflammation and cicatrization. Eyelashes rooted in the normal position grow toward the ocular surface and result in similar corneal and conjunctival irritation. Careful examination at the slit lamp allows for differentiation between trichiasis and distichiasis.

Given the association between congenital distichiasis and adolescent onset lymphedema, the pediatrician should be made aware of the clinical finding of distichiasis to coordinate routine follow-up through adolescence. Genetic testing may be helpful. For both distichiasis and trichiasis, regardless of etiology, treatment is based on the extent that the eyelashes come into contact with the ocular surface. If there is no lash touch to the cornea or conjunctiva, no treatment is necessary. When the lashes touch only the conjunctiva, lubricating ointment or drops may improve discharge or discomfort. If symptoms persist, definitive surgical intervention should be pursued. Corneal lash touch creates a higher risk of vision loss from corneal irregularity, ulceration, and scarring, and surgical treatment should be planned.

There are several surgical options for correction of distichiasis. More conservative approaches include electroepilation or cryotherapy (Fig. 21.24). However, these treatments can be associated with depigmentation and structural distortion at the lid margin (especially cryotherapy) and have a high rate of recurrence. Split thickness eyelid resection with removal of lash follicles offers a more permanent solution, but secondary trichiasis and entropion can occur. If treatment is initiated promptly, before permanent damage to the cornea occurs, prognosis is quite good. Families should be made aware that there can be recurrence of distichiatic or trichiatic lashes after surgical intervention and that repeat surgery may be required.

In an eyelid-splitting procedure (Figs. 21.25 and 21.26), a 15° super-sharp blade is used to incise the eyelid along the gray line of the eyelid margin. The abnormal lashes and the meibomian orifices remain along the posterior aspect of the incision, and the normal cilia are reflected anteriorly with the skin and orbicularis. A second incision is made posterior to the meibomian gland orifices and the aberrant lashes. This incision will run along the anterior aspect of the tarsus. The central strip of the eyelid margin is removed. Because the follicles may reside within the structure of the tarsus, the tarsal plate can be treated with cryotherapy using a double-freeze-thaw technique. The probe is oriented toward the cut surface of the tarsus and away from the eyelid surface epithelium. This will help to avoid skin pigmentary changes and scarring. This approach tends to have a high success rate with few complications related to eyelid malposition or skin pigmentation [40].

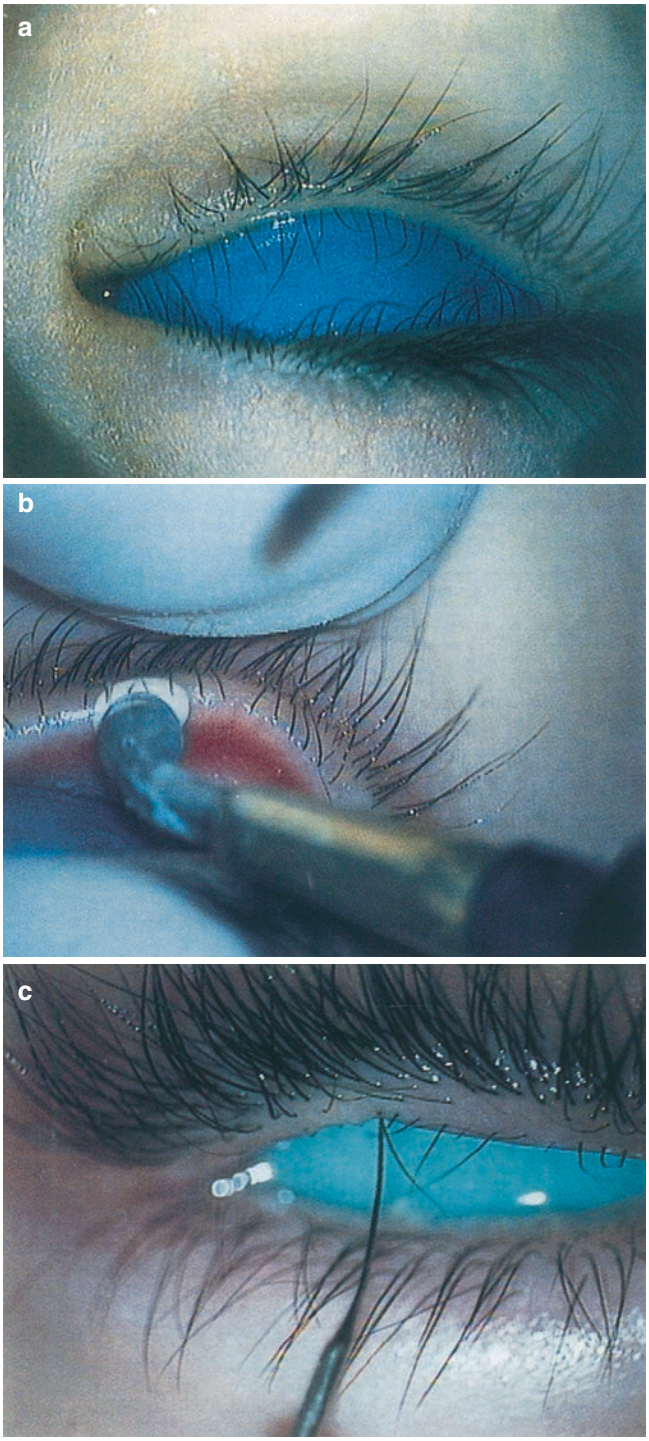


Fig. 21.24 Distichiasis. (**a**) Abnormal lash line from the meibomian orifices. (**b**) Cryotherapy is used to destroy the lash follicles. Two freeze-thaw cycles at 25 °C are utilized with care not to damage normal lash follicles. (**c**) Electroepilation may also be used to destroy the lash follicle base at 10–12 watts (not pictured here), and the lashes are then easily epilated

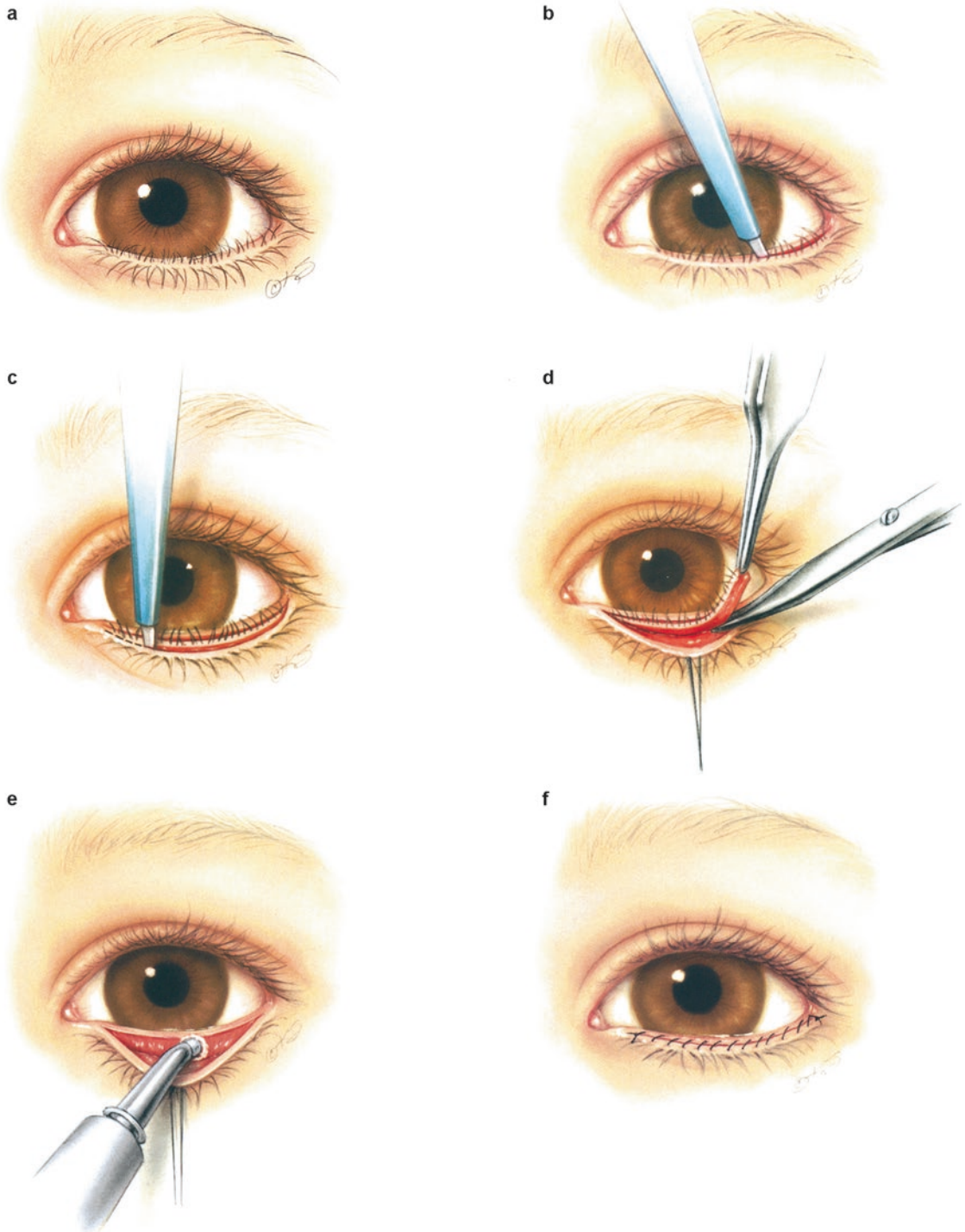


Fig. 21.25 (**a**) Lower eyelid districhiasis with an extra row of eyelashes emanating from the meibomian gland orifices. An incision is made with a supersharp blade along the posterior (**b**) and anterior (**c**) length of the districhiatic lashes. (**d**) The strip of extra lashes is fully excised. (**e**) Cryotherapy is applied to the base of the wound bed. (**f**) Ultimately, the wound is closed with a running dissolvable suture

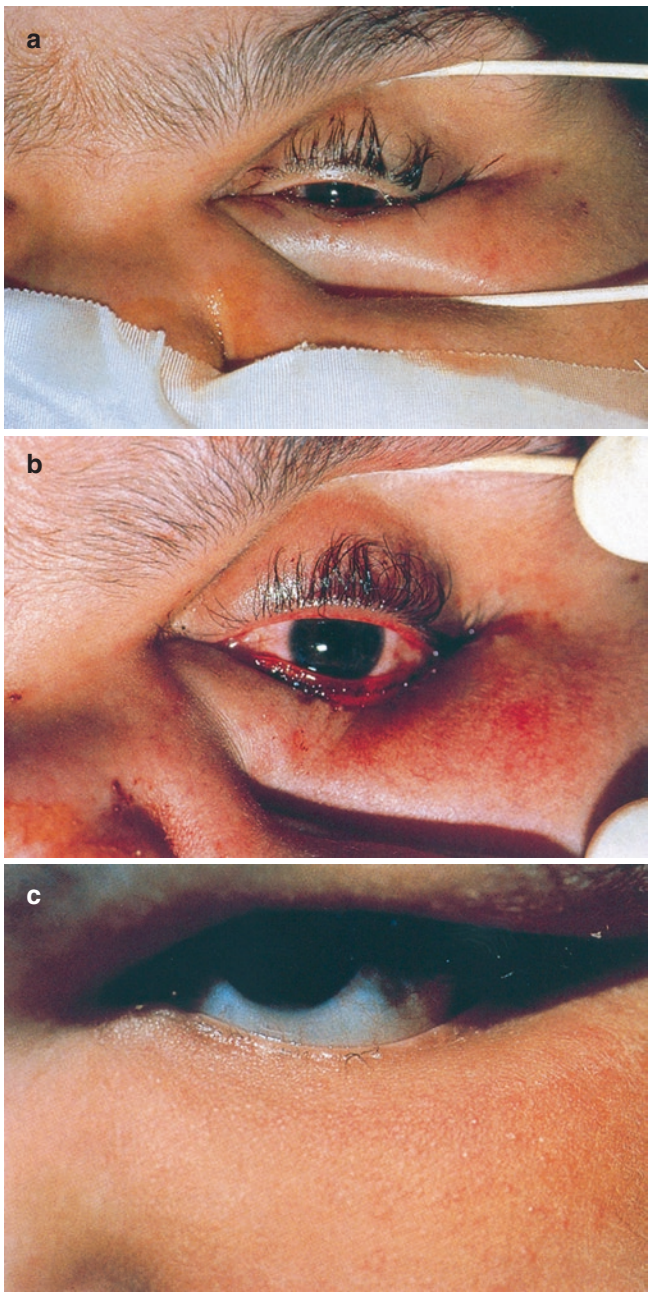


Fig. 21.26 Eyelid-splitting procedure for abnormal lashes. (**a**) Preoperative view of lower lid lash malposition. (**b**) Intraoperative view of the lid after lid splitting and cryotherapy to remove the lashes. (**c**) Postoperative photo with a small number of asymptomatic residual eyelashes

Epiblepharon and Entropion

Epiblepharon is a relatively common eyelid malposition, estimated to occur in up to 12.6% of Asian children aged 7–14 years old [41]. It usually affects the lower eyelid but can also be seen in the upper eyelid [41]. Although epiblepharon is mostly known as a pediatric condition, it is becoming more frequently reported in adults. Acquired epiblepharon has been described in thyroid eye disease and other conditions of proptosis [42]. It usually affects the lower eyelid and is characterized by a horizontal skin fold overriding the eyelid margin, causing inward rotation of the cilia (Fig. 21.27). Placement of gentle pressure on the eyelid fold usually momentarily re-establishes the normal position of the eyelid cilia. It may be caused by poor development of the eyelid retractors, failure of the eyelid retractors to gain access to the skin, hypertrophy of the orbicularis oculi muscle, or a pretarsal orbicularis muscle insertion too close to the eyelid margin with weak attachment to the underlying tarsus [43–45].

Epiblepharon is typically bilateral and generally affects the medial lower eyelids. Similar to other eyelid malpositions, ocular surface symptoms can range from none to severe, with foreign body sensation, discharge, photophobia, eye rubbing, epiphora, itching, frequent blinking, and eye redness. The severity of epiblepharon symptoms can be associated with the type and number of eyelashes [43]. Fine eyelashes, and very few lashes, are often less symptomatic than thick and plentiful lashes. This variability may account for some later presentations of symptomatic epiblepharon as eyelash quality changes with age. Decreased visual acuity from induced astigmatism can occur [45]. Khwarg and Lee proposed a grading scale for severity of lower eyelid epiblepharon based on height of the skin fold, area of corneal touch by cilia, and area of corneal erosion [46]. Others have proposed similar informal classification schema to help guide management in children with epiblepharon [43]. Epiblepharon of the lower lid can have a clinical appearance similar to entropion. However, in entropion the eyelid margin itself is rotated inward (Fig. 21.28), whereas in epiblepharon there is no margin rotation. If a semicircular epicanthal fold is also present, additional medial canthal tension can worsen epiblepharon [47].

Unless there are issues related to lash contact with the ocular surface or concerns about refractive amblyopia, epiblepharon can be managed conservatively with lubrication. Interestingly, even in the presence of corneal punctate erosions, some children do not complain [41]. As the nasal bridge grows, many cases of epiblepharon will resolve spontaneously [41, 48, 49]. The use of hyaluronic acid, injected into the suborbicularis space at the valley of the epiblepharon skin fold, has been described as an effective temporizing approach until self-correction occurs with age [48].

If surgical correction is pursued, similar approaches can be used for both epiblepharon and entropion. A non-incisional technique involves placement of eyelid-everting sutures, but this is associated with a high recurrence rate. The modified Hotz technique is an incisional procedure that involves resection of overriding the orbicularis and skin, with or without placement of anchoring sutures to the tarsal plate. This is a modification of the original surgical technique described by Hotz in 1879 for treatment of entropion and trichiasis

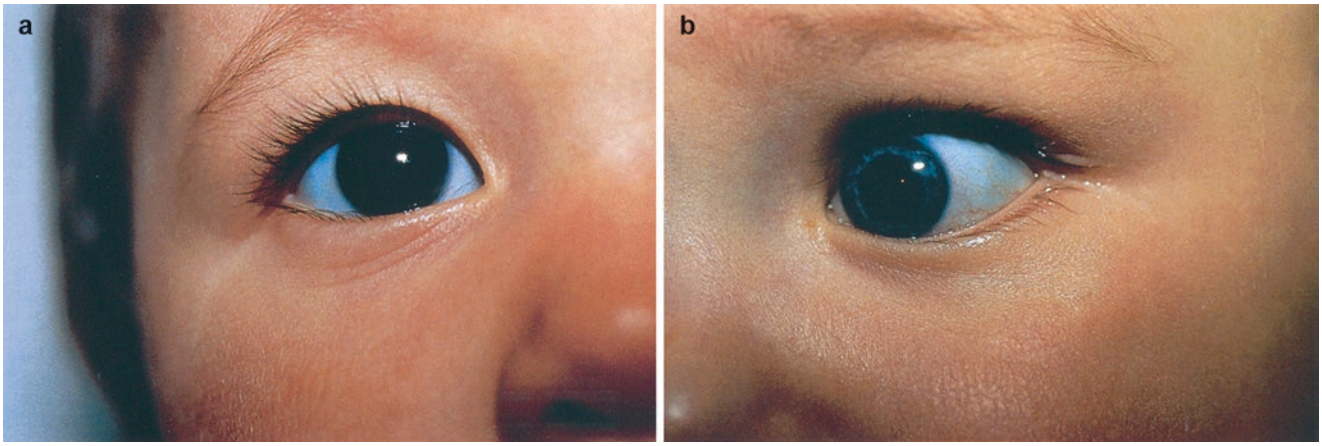


Fig. 21.27 Epiblepharon. (**a**) Appearance of the lid fold and lash rotation from an anterior view. (**b**) A lateral view



Fig. 21.28 Congenital entropion of bilateral lower lids

(Fig. 21.29). The nasal and temporal ends of the margin entropion are marked just below the inferior border of the tarsus in the lower eyelid. A horizontal ellipse is marked extending just beyond the medial and lateral extent of the margin entropion. The vertical height of the ellipse is approximately 2–2.5 mm. A No. 15 blade scalpel is used to incise the skin and orbicularis, which are removed using a curved iris scissors and fine-toothed forceps. The incision is closed with 6-0 Vicryl passed through the subcutaneous tissue of the lower aspect of the incision, through the lower eyelid retractors, through the interior edge of the tarsus, and out through the subcutaneous tissue skin (Fig. 21.30). The sutures are spaced approximately 2.5 mm apart. When the sutures are tied, the eyelid margin should be everted and slightly overcorrected. The skin is closed with 6-0 fast-absorbing gut. An effective transconjunctival approach has also been described with low recurrence rates and no external scar [50].

The modified Hotz procedure is very effective but is associated with an external eyelid scar. Postoperative eyelid ectropion and retraction can also occur. With definitive treatment, however, recurrence is rare. In addition to resolution of symptoms, parents are often pleased with the "bigger" eye appearance of children following surgery [43].

Unlike epiblepharon, primary congenital entropion is an abnormality that can occur unilaterally as well as bilaterally. Acquired entropion is more common in children and can be caused by trachoma, Stevens-Johnson syndrome, ocular cicatricial pemphigoid, herpes zoster or simplex, chemical injuries, or sporadic eyelid malposition. There are many theories, all based on small case series, about the mechanism of congenital entropion. Some think it is caused by inflammation of the eyelid structures at birth, producing contractures that result in entropion. Others think it is related to a partial absence of the tarsal plate or hypertrophy and overaction of the orbicularis, resulting in inversion of the tarsus [51]. Disinsertion of the lower eyelid retractors, traditionally thought to be a contributing factor of entropion in adults, has also been reported to cause congenital entropion [51]. In cases of acquired entropion, inflammation or infection can lead to conjunctival scarring and resultant cicatricial entropion.

Congenital entropion can be a difficult diagnosis to make. It is important to differentiate entropion, which is characterized by an inturning of the eyelid margin, from other causes of lash-corneal touch in infants, such as epiblepharon or distichiasis. In contrast to entropion, the eyelid margin is in an upright position in both epiblepharon and distichiasis. Unlike in some cases of epiblepharon, congenital entropion does not improve over time, and surgical correction is almost always required. Entropion is typically bilateral and most often involves the medial lower lids. Depending on the severity of lash contact with the ocular surface, symptoms may range from none to severe. If there is involvement of the cornea, an abrasion, ulceration, or scar may be present. Visual acuity will be affected, and deprivational amblyopia becomes a significant concern. If there is an underlying inflammatory or infectious etiology,

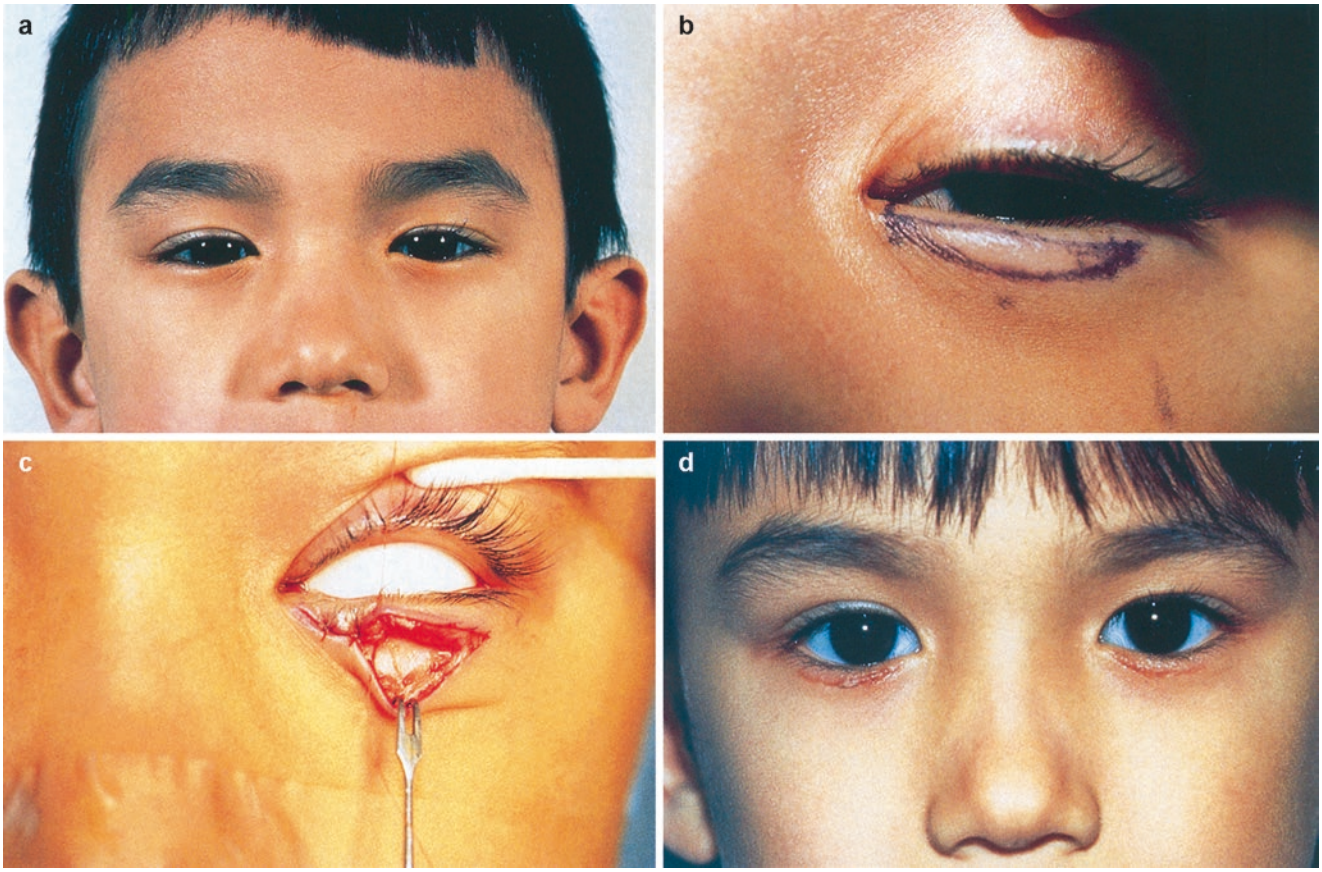


Fig. 21.29 Congenital entropion of the lower eyelids. (**a**) This 7-year-old has bilateral lower eyelid entropion with reactive upper lid ptosis from orbicularis spasm. (**b**) Marking the eclipse of the skin and orbicularis for excision. (**c**) Suture placement to reattach the lower eyelid retractors to the inferior border of the tarsus. (**d**) One year postoperative view after repositioning of the eyelashes. The palpebral fissure has also opened with relaxation of lower lid the orbicularis tone

other signs may be present, such as symblepharon. Tarsal kink syndrome is a rare form of entropion affecting the upper eyelid and resulting from a right angle inward rotation of the distal tarsal margin [52]. It can be congenital but more commonly is acquired and can cause severe corneal pathology.

In the case of acquired entropion in children, appropriate testing for Stevens-Johnson syndrome (skin biopsy), ocular cicatricial pemphigoid (conjunctival biopsy), and herpes zoster or simplex (conjunctival PCR studies) should be pursued. Although uncommon in the United States, trachoma is the most common infectious cause of blindness in the developing world [49]. Blindness results from repeated episodes of inflammation in the setting of *Chlamydia trachomatis* infection and subsequent conjunctival scarring, cicatricial entropion, and corneal ulceration and scarring. In the appropriate clinical setting, diagnosis should be made on a clinical basis. Laboratory detection of *C. trachomatis* is usually only done for research purposes [49].

Entropion does not resolve spontaneously [24]. Mild cases can be managed with ocular lubricants. The need for surgical intervention is based on the degree of cilia-induced corneal irritation. There are both non-incisional and incisional approaches. Non-incisional approaches involve placement of everting sutures to reattach the lower lid retractors to the tarsus [53]. The advantage of this technique is that it is minimally invasive, but there is a high recurrence rate. Incisional procedures also involve reattachment of the lower eyelid retractors to the tarsus but through a subciliary approach. This is a straightforward procedure with an excellent success rate but results in an external scar. A modified technique can be used with a smaller skin incision that just exposes the tarsus with placement of a rotating suture connecting the tarsal plate to subcutaneous tissue (Fig. 21.31) [24].

In the case of upper eyelid cicatricial entropion, a transverse blepharotomy with margin rotation (Wies procedure) can be performed [54]. A margin rotation technique can also be used. In the upper eyelid, the tarsus is modified with a horizontal V-shaped groove, which is pulled together to evert the eyelid margin (Figs. 21.32 and 21.33). An eyelid crease incision is made in the upper eyelid, and then the skin and orbicularis are reflected away from the anterior surface of the tarsus. The dissection plane does not extend as far down as the lash follicles.

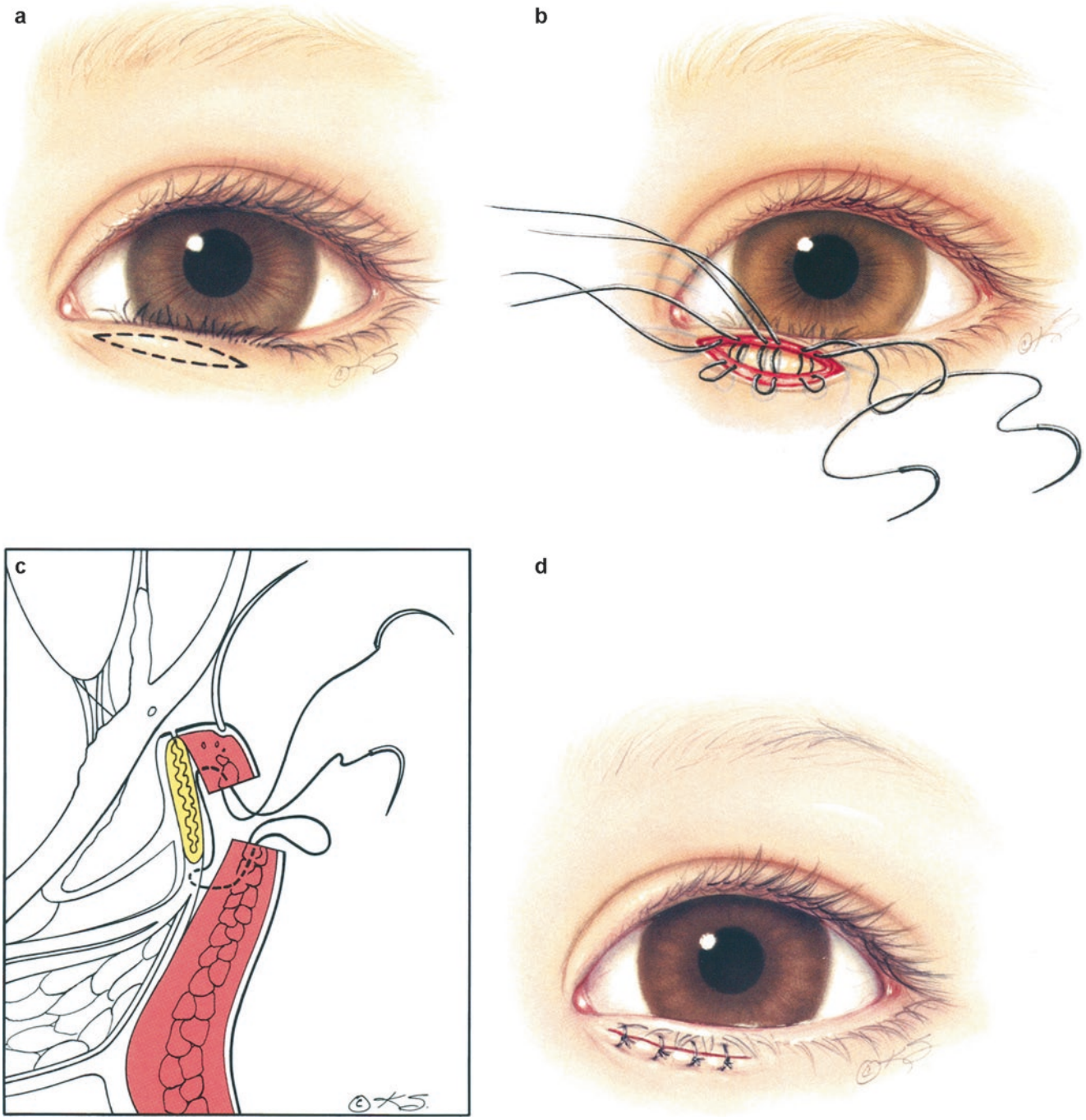


Fig. 21.30 Repair of congenital entropion of the lower eyelid. (**a**) The ellipse of the skin and orbicularis are marked for excision on the lid adjacent to the entropion. (**b**) Orbicularis and the lower eyelid retractors along the lower aspect of the incision are sewn to the tarsus and orbicularis along the superior edge of the ellipse using a double-armed suture. (**c**) Insert shows lateral view of suture placement to advance the lower lid retractors. (**d**) The skin is closed with absorbable suture

At the midpoint of the vertical height of the tarsus, a super-sharp blade is used to make two horizontal incisions that are beveled toward each other to create a V-shaped 1.5 mm-wide strip across the length of the tarsus. The base of the triangular strip of tarsus is on the anterior surface of the tarsus. The strip is removed, and then the edges are pulled together with 6-0 Vicryl mattress sutures. The skin is closed with a 6-0 nylon pullout stitch or 6-0 fast-absorbing gut suture.

With definitive incisional intervention, recurrence rates are quite low. Potential complications include scarring (more of an issue in unilateral cases), eyelid ectropion, and retraction, all possibly requiring future surgical intervention.

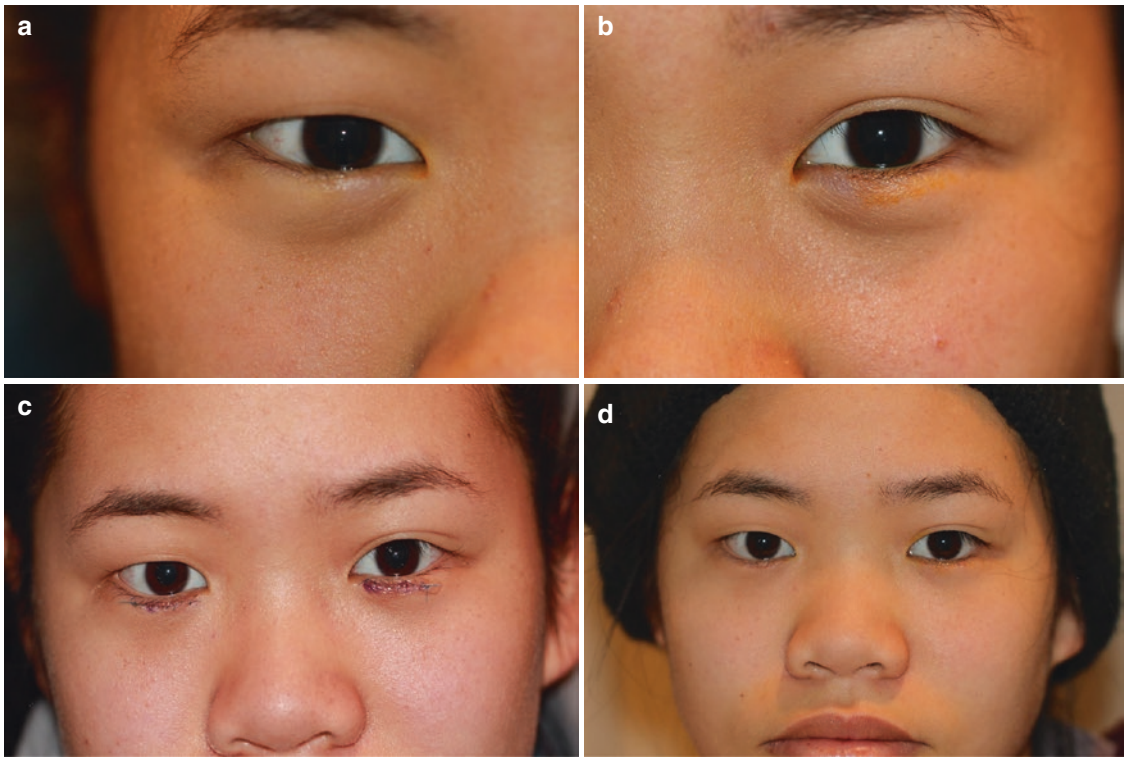


Fig. 21.31 Bilateral lower eyelid entropion. (**a**) Right eye. (**b**) Left eye. (**c**) One week after bilateral lower lid entropion repair with reinsertion of lower lid retractors onto the tarsus and excision of small strip of the skin and muscle. (**d**) One month postoperative with good eyelid position and minimal scar

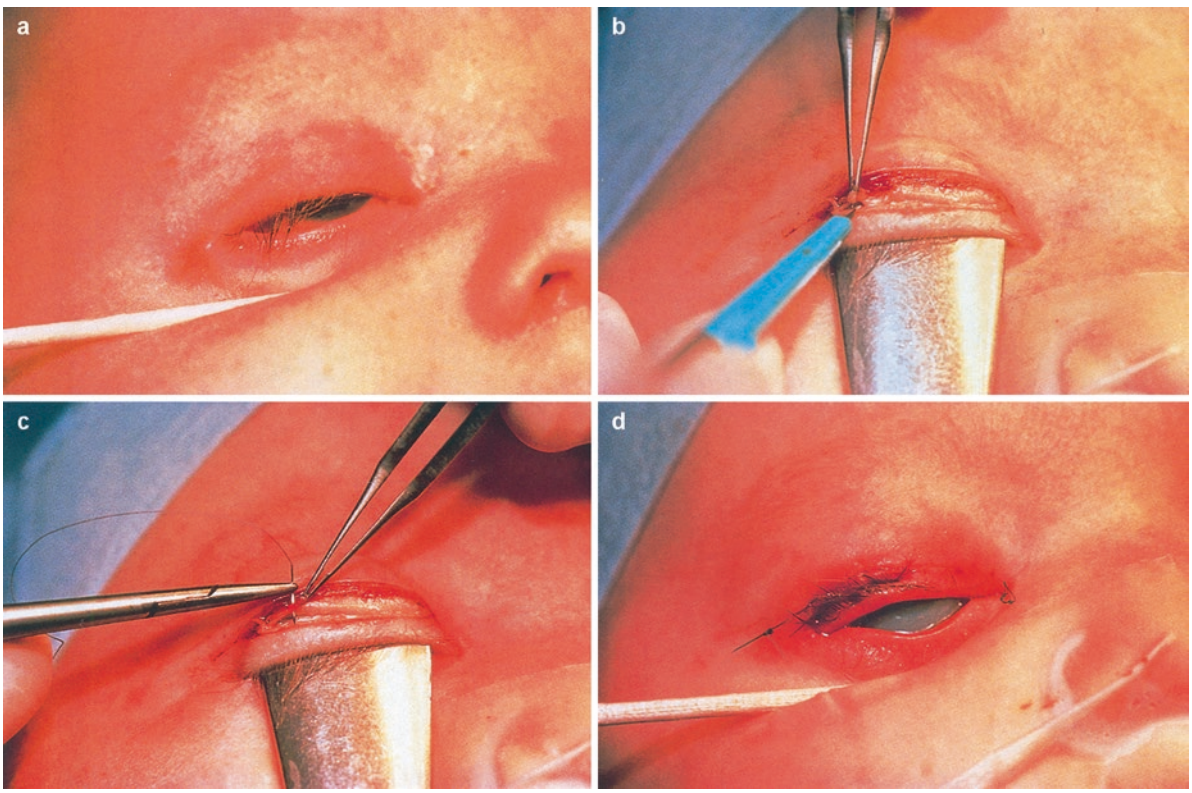


Fig. 21.32 Congenital upper eyelid entropion. (**a**) Upper eyelid with eyelash and eyelid margin malposition. (**b**) Super-sharp blade used to remove a horizontal triangular wedge of the tarsus across the entire length of the tarsus. (**c**) The edges of the wedge are approximated with a 6-0 Vicryl suture. (**d**) Immediate postoperative appearance with the desired overcorrection of the eyelid margin position. See also Fig. 21.33

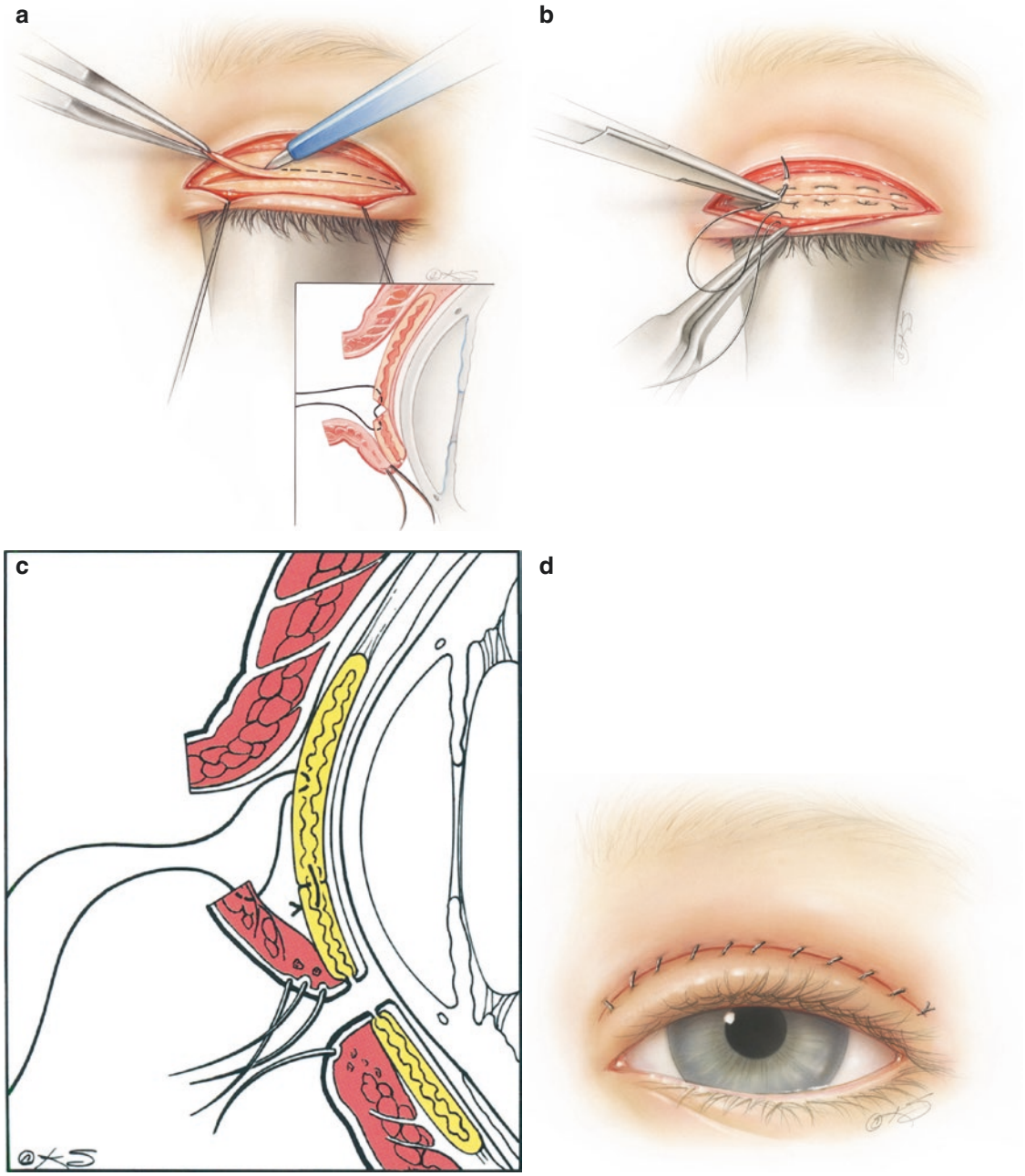


Fig. 21.33 Repair of congenital upper eyelid entropion. (**a**) The skin is incised to expose the underlying tarsus. A base anterior triangle of tarsus is removed across the extent of the entropion. The tarsus is sutured together to evert the lid margin. (**b**) The lash line is anchored to the tarsus to correct the eyelash ptosis. (**c**) Sagittal view of the lash positioning suture. (**d**) The skin is re-approximated to close the incision

Ectropion and Eversion

Ectropion can occur secondary to structural abnormalities of the eyelid or from inflammatory conditions that affect either the anterior or posterior lamella. The etiology of congenital ectropion is unknown but may occur more frequently after birth trauma. The incidence is higher in infants of African descent, as well as those who have trisomy 21 and colloidal skin diseases, such as ichthyosis [24]. Congenital eyelid ectropion is generally due to vertical shortening of the eyelid anterior lamella or elongation of the posterior lamella, lateral canthal tendon laxity (congenital absence of the lateral canthal tendon), or a combination of these problems. Other uncommon causes include: low orbicularis tone, lateral elongation of the eyelids, and failure of the orbital septum to fuse with the levator aponeurosis. In the newborn, congenital eyelid eversion can occur. This can be due to a chlamydial infection, and the presence of intracytoplasmic inclusion bodies will confirm the diagnosis which can be managed by an appropriate antibiotic. This inflammatory problem can cause

a more severe form of ectropion with complete eversion of the eyelid. Once everted, orbicularis spasm may act as a sphincter that leads to a cycle of conjunctival compression and secondary edema, preventing easy re-inversion of the eyelid. Ichthyosis also can be associated with eyelid retraction and ectropion as a result of chronic cicatrization of the anterior lamella (Fig. 21.34).

Congenital ectropion is typically bilateral and can involve the upper or lower eyelids. In cases of congenital eyelid eversion, the entire length of tarsus is completely everted. The everted tarsoconjunctival part of the lid, especially in cases of upper lid eversion, tends to protect the cornea, and ocular surface dryness is uncommon. Specific clinical exam findings (lid laxity, horizontal and vertical length of affected eyelid, or the presence of skin lesions) can provide clues about the underlying abnormality and help in treatment planning.

Management decisions should be guided by corneal and conjunctival health. Initial conservative options include ocular surface lubricants or taping of the eyelids [24]. Another possible temporizing solution is injection of hyaluronic acid into the suborbicularis plane of the upper eyelid [55]. While these options may be appropriate in certain clinical scenarios, none of them are long-term solutions. Taping the eyelids, in particular, can be amblyogenic. In severe cases, definitive surgical correction is often necessary. There are three overarching goals of surgery: (1) correct horizontal lid laxity (tightening of the lateral canthal tendon), (2) address the vertical deficiency of the anterior lamella (skin grafting), and (3) release of cicatrix [56].

Non-inflammatory congenital ectropion of the upper eyelid can be addressed with a technique similar to that used in floppy eyelid syndrome whereby a portion a lateral tarsus is excised (Fig. 21.35). The eyelid is everted over a bone plate or malleable retractor using a 4-0 silk margin suture to hold the eyelid. A triangular segment of tarsus, conjunctiva, and Muller's muscle is removed. The base of the triangle is oriented toward the eyelid margin. Buried interrupted 6-0 or 5-0 Vicryl suture is used to repair the defect. The tissue removal helps to correct the imbalance between anterior and posterior lamellae, but a skin graft to the anterior surface may also be necessary to correct a vertical deficiency.

Congenital ectropion may also be a feature of Down syndrome (Fig. 21.36). The defect may involve only a portion of the eyelid or the whole complex. Repair is undertaken for corneal surface exposure or modification of appearance. In some cases horizontal resuspension of the lower eyelid with a lateral canthopexy technique (Fig. 21.17) may correct the problem.

In patients with ichthyosis in whom skin grafting is necessary, there may be limited options for harvesting unaffected skin. An alternative approach in those patients with severe generalized disease may be to use a combination of inversion sutures, lateral canthal suspension, and aggressive lubrication (Fig. 21.34). Otherwise, if definitive surgical correction is pursued, recurrence rates for most cases of pediatric ectropion are very low. The one exception may be ichthyosis, in which there is a chronic pattern of skin change and cicatrization. Among these children, recurrent surgeries may be necessary. If corneal health can be maintained, visual potential is excellent.



Fig. 21.34 Ichthyosis contributing to lower eyelid retraction and ectropion. (**a**) At age 28 months, this child with ichthyosis has had a lateral tarsorrhaphy and lateral canthopexy on the right. The ectropion is more obvious on the left. (**b**) Six months later both lower eyelids have been repositioned to control the ectropion

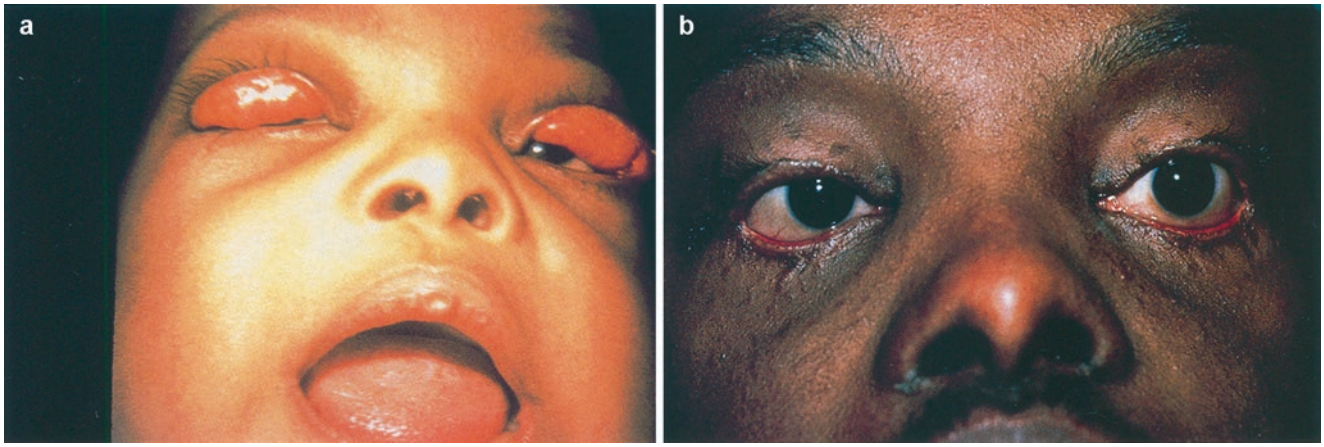


Fig. 21.35 Congenital ectropion of the upper lids. (**a**) Congenital ectropion of the upper lids. (**b**) The same patient 22 years following the initial repair

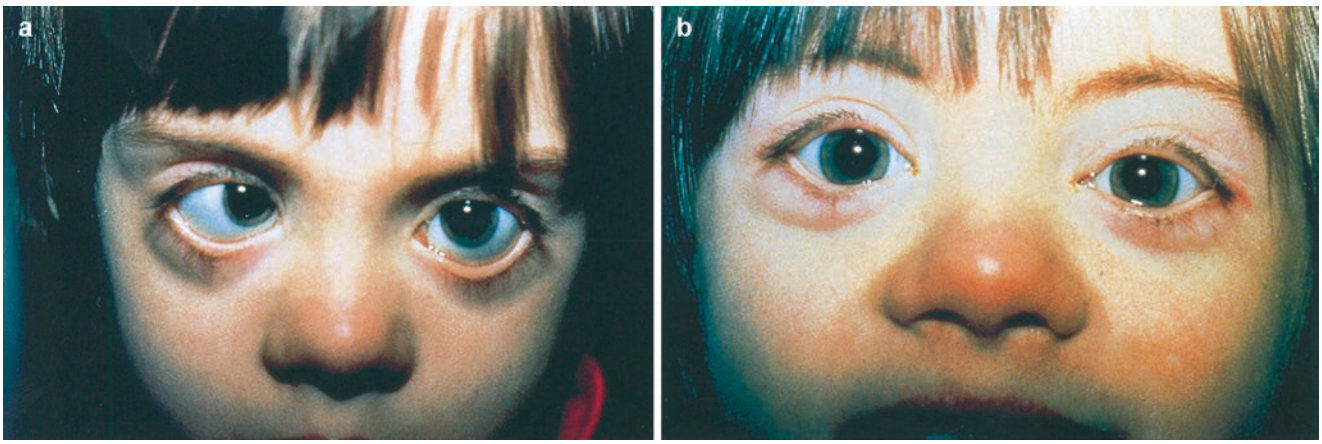


Fig. 21.36 Congenital ectropion of the lower lids in a patient with Down syndrome. (**a**) Preoperative appearance with lower eyelid ectropion and strabismus. (**b**) Postoperative photograph after strabismus surgery and lateral canthopexy

Congenital Eyelid Retraction

Isolated congenital eyelid retraction is rare, although stimulated infants may manifest superior scleral show that is not associated with systemic disease and that resolves with age (Fig. 21.37). More commonly, congenital eyelid retraction is associated with an underlying condition, such as orbital inflammation (i.e., thyroid eye disease (Fig. 21.38)), central nervous system disorder (i.e., facial nerve palsy, aberrant innervation of the oculomotor nerve, hydrocephalus, hydrocephalus, and dorsal midbrain syndrome), craniosynostosis (i.e., Crouzon or Pfeiffer's syndrome), anatomical variation (shallow orbits), pseudo-retraction from contralateral upper lid ptosis, or trauma/cicatrix [57]. Causes can be grouped into three major categories: myogenic, neurogenic, or mechanical [58]. The differential diagnosis of conditions causing eyelid retraction is extensive (Table 21.1) [58].

In children with eyelid retraction, the extent of superior or inferior scleral show should be documented. Close examination of the eyelids and cornea should be performed to evaluate for the presence of other eyelid abnormalities and any signs of ocular surface breakdown. The underlying etiology should be clearly understood before management is discussed. Neuro-ophthalmic evaluation should be considered.



Fig. 21.37 Congenital eyelid retraction

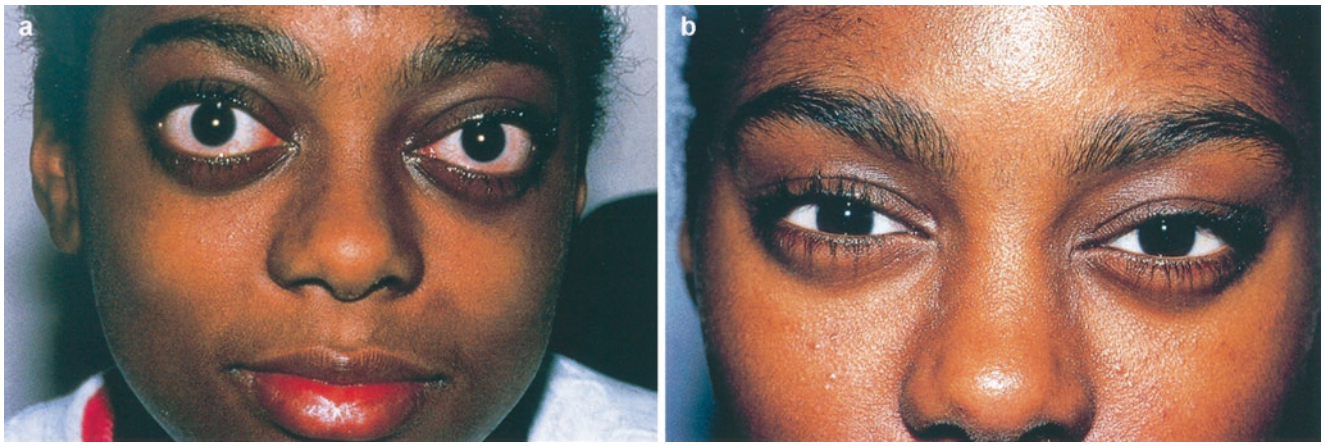


Fig. 21.38 Thyroid eye disease-related lower lid retraction. (**a**) This patient demonstrates lower lid retraction and exophthalmos from thyroid-associated ophthalmopathy. (**b**) The same patient after orbital fat decompression and recession of lower lid retractors

Table 21.1 Differential diagnosis of eyelid retraction in children

Neurogenic	Myogenic	Mechanical
Benign transient conjugate downward gaze in preterm infants "Eye-popping" reflex Dorsal midbrain syndrome Impending tentorial herniation Guillain-Barré syndrome Epilepsy Palatal myoclonus Marcus Gunn syndrome Congenital aberrant innervation of the oculomotor nerve Pseudoretraction from contralateral ptosis Orbital floor fracture with increased innervation to the superior rectus and levator muscles Dissociated vertical deviation Sympathomimetic eye drops Volitional	Congenital eyelid retraction Congenital hyperthyroidism/Grave's ophthalmopathy Congenital myotonia Myasthenia Gravis Postsurgical; inferior rectus recession (lower eyelid), superior rectus recession (upper eyelid), ptosis repair, enucleation	Tarsal kink syndrome Severe myopia Proptosis Craniosynostosis

In an infant with persistent scleral show or eyelid lagophthalmos, a full medical evaluation should be performed, including blood work for thyroid eye disease or other potential inflammatory conditions affecting the orbit, as well as orbital and brain imaging. In the case of craniosynostosis syndromes, genetic testing may be warranted.

Treatment of eyelid retraction is often guided by the degree of ocular surface exposure. In mild cases, ocular lubricants, patching, or cellophane moisture chambers can be used to keep the cornea well lubricated [24]. However, all of these approaches are potentially amblyogenic. If the cause of retraction is postsurgical or cicatrix related, eyelid finger massage can be an effective means of correction [39]. More permanent surgical options include: (1) temporary suture tarsorrhaphy, (2) permanent tarsorrhaphy, (3) levator aponeurosis recession, (4) Müller's muscle recession, or (5) autogenous or allogenic spacer placement [59].

In the child with mild unilateral eyelid retraction (less than 2 mm), there are cosmetic advantages to using a conjunctival incision to avoid a skin incision scar (Fig. 21.39). A 4-0 silk suture is placed in the central upper eyelid, and the eyelid is everted over a Desmarres retractor. An incision is made in the conjunctiva along the superior border of tarsus, and the plane between conjunctiva and Müller's muscle is dissected superiorly. The edge of the conjunctiva is tagged with 6-0 gut suture and retracted away from the underlying Müller's muscle. Müller's muscle can be released from its tarsal attachments either separately or in conjunction with the levator aponeurosis. Removal of Müller's muscle alone will result in a 1.5 to 2 mm drop in the upper eyelid position. If further eyelid recession is desired, levator aponeurosis can also be recessed. The amount of eyelid drop per mm of recession of the levator aponeurosis is unpredictable, but it usually takes 2–3 mm of recession to get a 1 mm drop in the upper

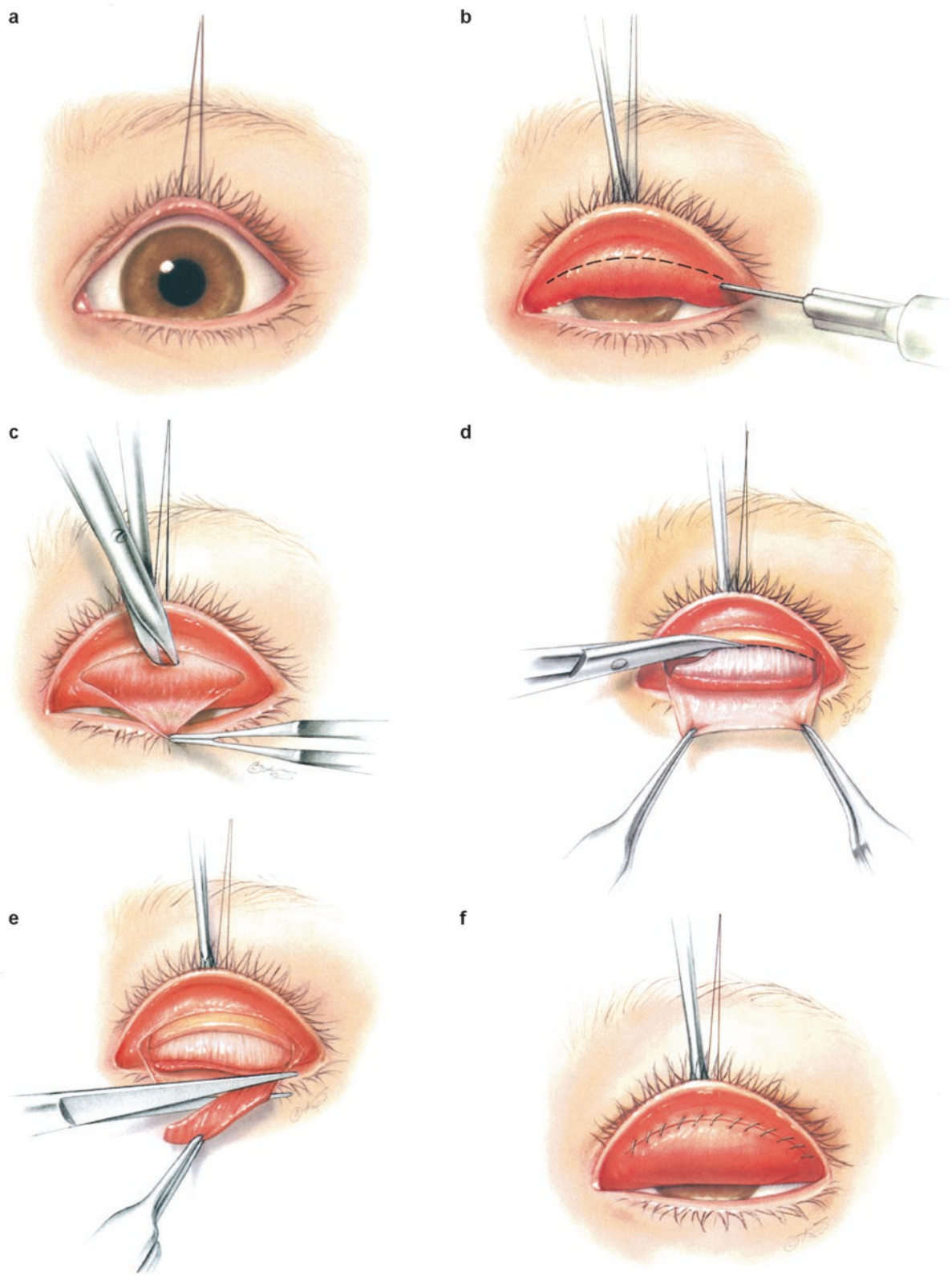


Fig. 21.39 (**a**) A 4-0 silk suture is placed in the upper eyelid for traction. (**b**) The conjunctiva is separated hydrostatically from Müller's muscle by injecting a solution of 0.25% bupivacaine with epinephrine 1:200,000. (**c**) The conjunctiva is retracted, and Müller's muscle is separated from its superior tarsal attachment. (**d**) Müller's muscle is excised. (**e**) Excess conjunctiva can be excised to prevent prolapse postoperatively. (**f**) The conjunctiva is reattached to the superior tarsal border with a 6-0 plain catgut suture

eyelid margin. When the retractors of the eyelid have been repositioned, the conjunctiva is sewn back into place using buried 6-0 gut suture.

In the patient with bilateral or more severe eyelid retraction, a skin incision approach will allow greater exposure of the levator and aponeurosis muscle (Fig. 21.40). An eyelid crease incision and skin and orbicularis are elevated. Aided by the elevation of orbicularis, a scissors is used to create a snip incision through the orbicularis. The skin and orbicularis of the upper portion of the incision are reflected superiorly using cautery or scissors. The underlying septum and preaponeurotic fat are identified, and the septum is opened to allow the fat to be peeled free from the underlying levator aponeurosis and muscle. A scissors is used to separate the levator aponeurosis from the tarsus, and then the plane between the levator and Müller's muscle is opened

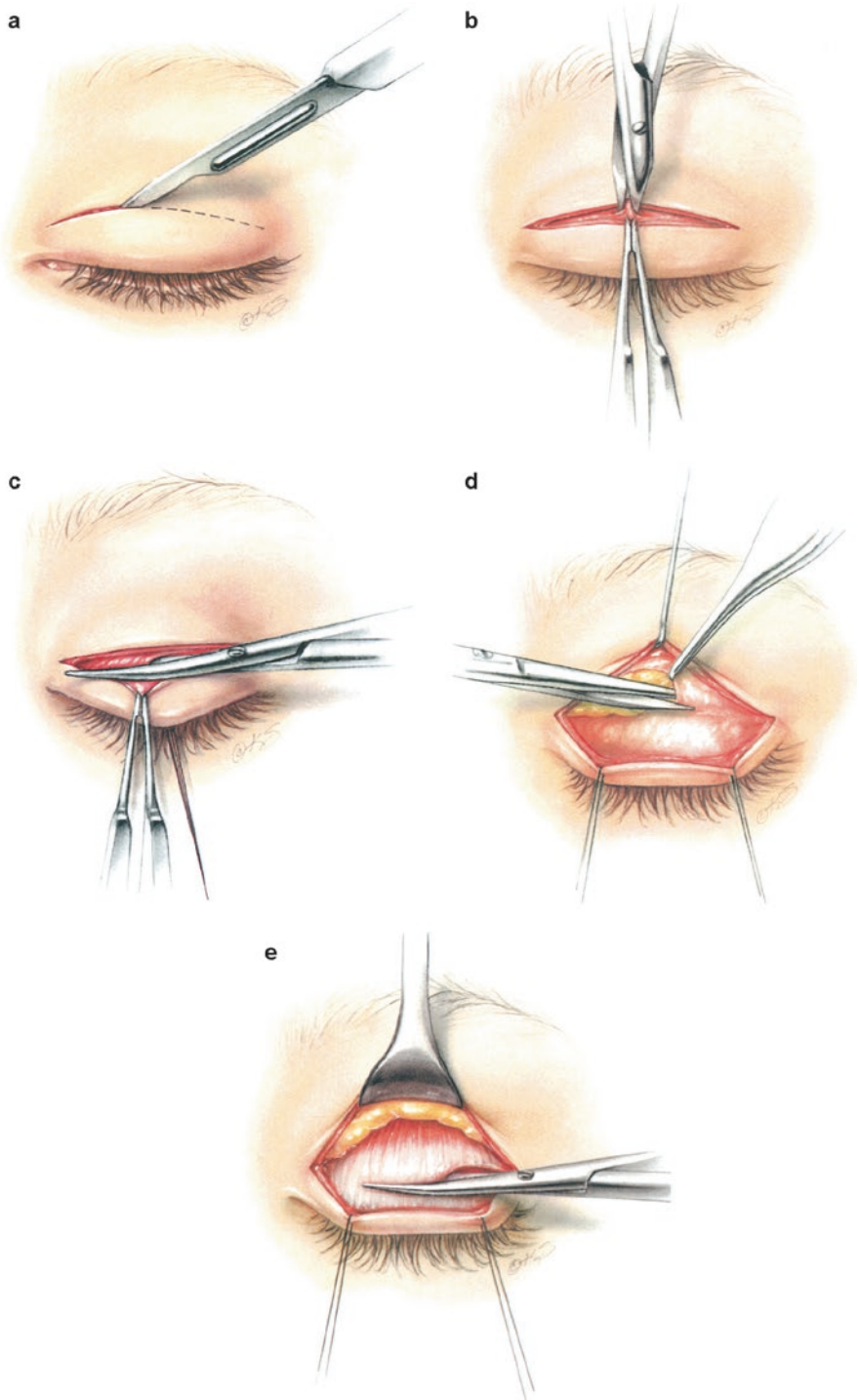


Fig. 21.40 External levator recession for repair of upper eyelid retraction. (**a**) To begin the upper eyelid retractor recession, an eyelid crease incision is made. (**b**) The skin and orbicularis are elevated as a cutdown incision is made to the level of the septum. (**c**) The skin and orbicularis are opened through the length of the eyelid crease incision. (**d**) The orbital septum is opened and incised. (**e**) The levator aponeurosis is separated from its tarsal attachments. The inferior edge of the aponeurosis is recessed and sutured down to the underlying Müller's muscle. In severe cases Müller's muscle can be excised and the aponeurosis recessed and sutured to the conjunctiva at a higher position

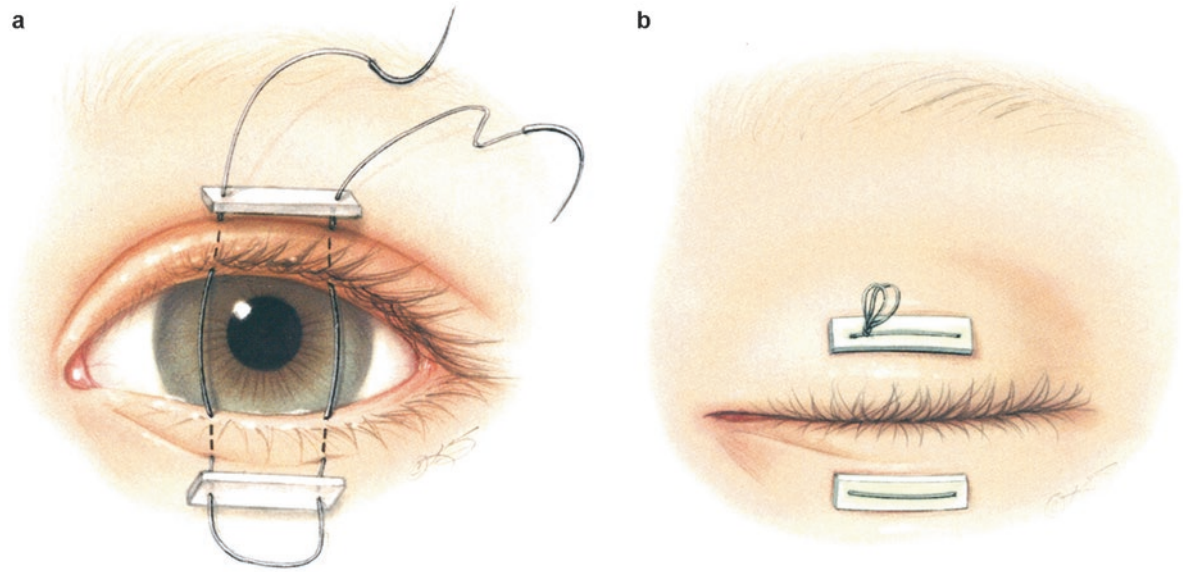


Fig. 21.41 Suture tarsorrhaphy. (**a**) The eyelids are pulled together with a horizontal mattress suture. The eyelid creases and the gray lines are used as entry and exit sites for the suture. Soft silastic or rubber bolsters can be used to protect the skin. (**b**) The suture may be tied in a slip knot so that it may be opened for corneal viewing

superiorly using sharp and blunt dissection to interrupt the intervening connective tissue. The levator muscle is recessed 2–3 mm for every 1 mm of upper eyelid retraction. The leading edge of the recessed levator muscle may be sewn down to the underlying Müller's muscle or, less frequently, may be separated from the tarsus by an interpositional spacer graft.

In cases of eyelid retraction that present with corneal ulceration, it may be necessary to consider a tarsorrhaphy as an immediate treatment option to protect the vision. Three types of tarsorrhaphy may be used: a simple suture tarsorrhaphy as either a mattress suture with or without a bolster (Fig. 21.41), a serpentine suture (Fig. 21.42), or a reversible margin annealing tarsorrhaphy (Fig. 21.43). A permanent tarsorrhaphy with a segment of upper eyelid tarsus transposed into the lower eyelid can also be done. In children, the latter is rarely appropriate. The serpentine stitch is passed from gray line to gray line in a running fashion. The free ends of the suture along the medial and lateral canthal ends can be steri-stripped to the skin or loosely tied as a loop on each end permitting an ability to open or pull this closed for either viewing the cornea or for protection. This will usually hold for several weeks. When a tarsorrhaphy is needed for a more extended period of time, but will be reversed in the future, the eyelid margins may be denuded of epithelium and sewn together to create a reversible attachment between the upper and lower eyelids (Fig. 21.43). The epithelium along the margin may be removed with a scissors or a super-sharp blade. The anterior lamellae are sewn together with 6-0 Vicryl suture. A horizontal mattress 6-0 Prolene suture with or without bolsters can additionally be placed for extra support.

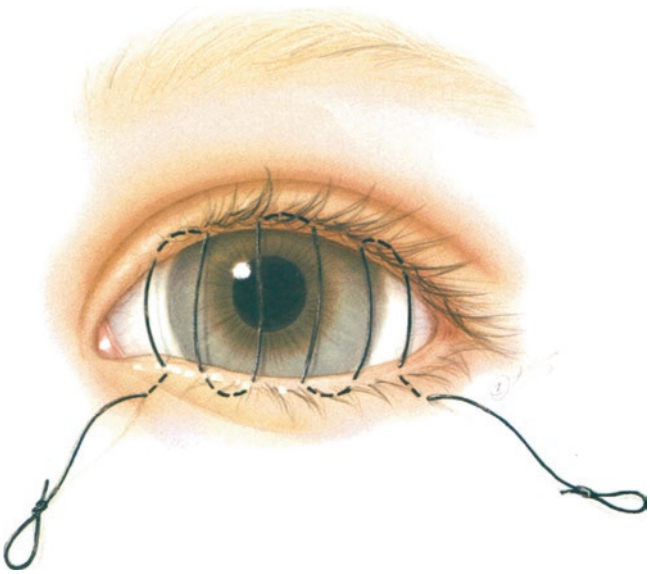


Fig. 21.42 Serpentine tarsorrhaphy. The suture is passed through the gray line in a serpentine fashion. When the suture is pulled taut, it will bring the eyelid margins together. It can also be loosened later to permit subsequent examination and then pulled taut once again for protection of the cornea

In patients with shallow orbits and eyelid retraction due to exophthalmos, corneal exposure may develop (Fig. 21.44). Exposure can initially be treated with surface lubrication and occlusive dressings, but a clear visual axis must be accomplished to prevent amblyopia. Surgical intervention includes release of eyelid retractors, tarsorrhaphy, spacer grafts to the mid and posterior lamella, and skin grafts to the

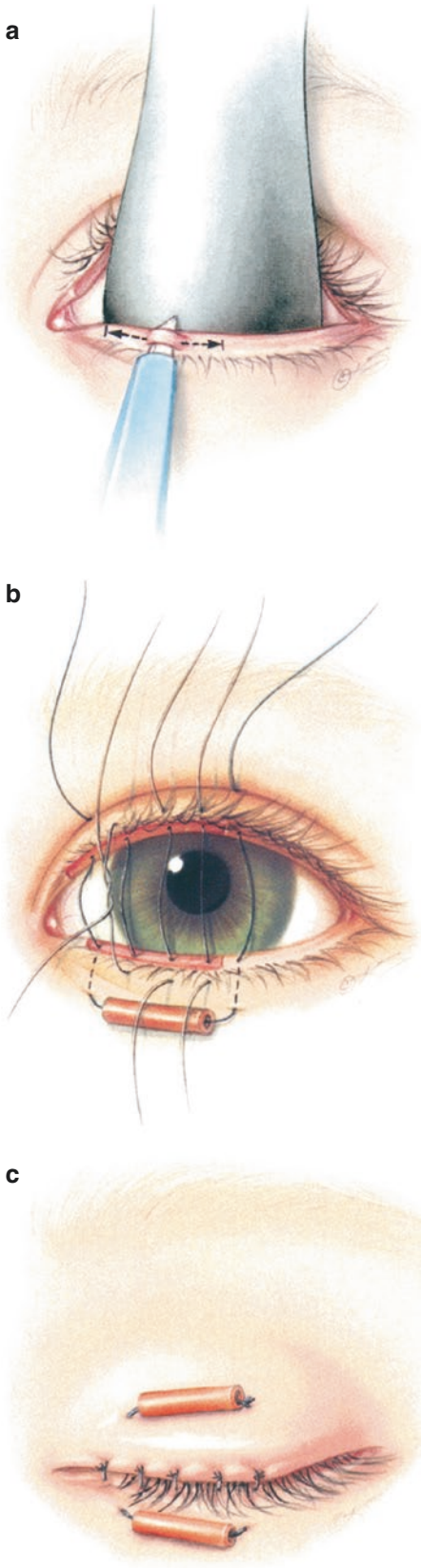


Fig. 21.43 Margin annealing tarsorrhaphy. (**a**) Lid margin denuded with sharp blade. (**b**) Margins sutured together with a 5-0 or 6-0 Vicryl suture. A 6-0 Prolene suture over Bolster can be used for more support. (**c**) Lids sutured together with Bolsters in place

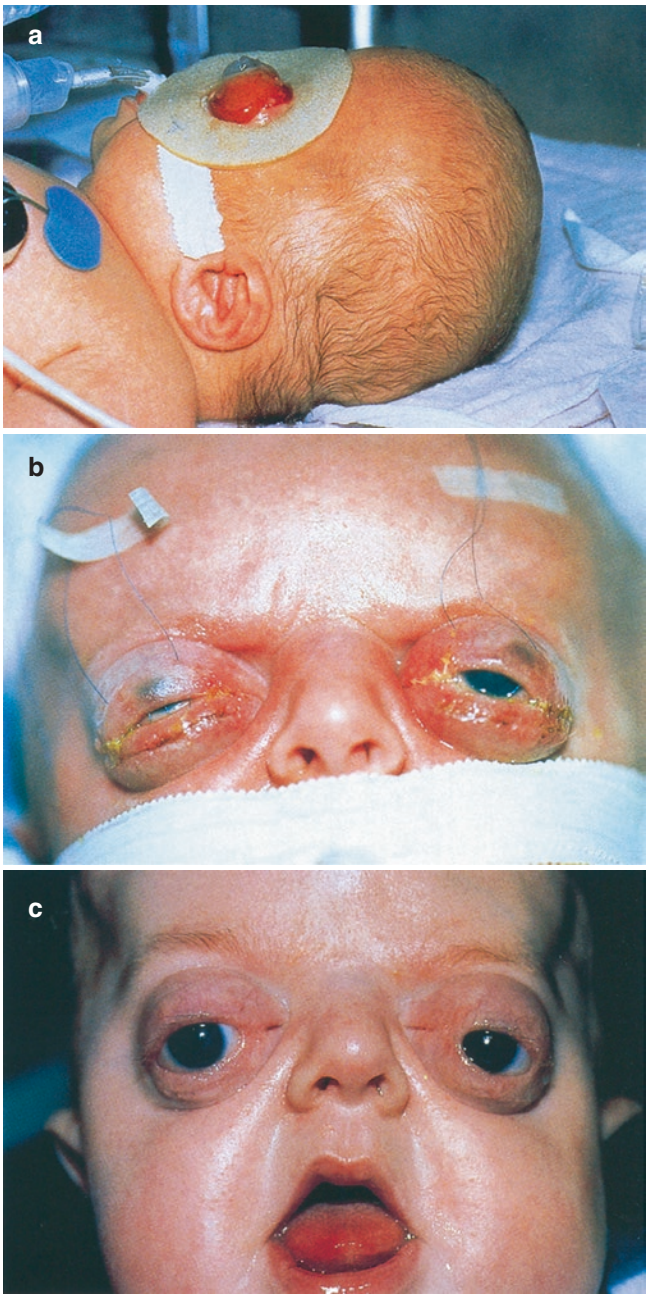


Fig. 21.44 Corneal exposure with eyelid retraction. (**a**) This patient's presentation at the time of birth with Pfeiffer's syndrome and severe exophthalmos. Plastic wrap corneal covers are in place. (**b**) Permanent medial and lateral tarsorrhaphies are placed, and central suture tarsorrhaphies are also present. (**c**) Postoperative appearance after eyelid surgery and cranial advancement of the supraorbital bar. The retractors of both the upper and lower eyelids were recessed and donor cartilage grafts placed in the lower eyelids

anterior lamella. Only rarely, and in very severe cases of proptosis and retraction, is bony orbital advancement necessary.

Some of the described techniques do not always produce reliable results. Recently, full-thickness or modified full-thickness blepharotomy has come into favor as a means to treat upper eyelid retraction. This technique is effective and

associated with more predictable changes in lid height [60, 61]. As with other aforementioned conditions, if the cornea is protected aggressively early in disease presentation, excellent visual potential can be maintained. Families should be counseled regarding the cosmetic implications of permanent tarsorrhaphy techniques in cases of severe eyelid retraction. If cosmesis or ocular surface dryness becomes concerns, additional surgeries may be necessary.

Euryblepharon and Centurion Syndrome

Euryblepharon and Centurion syndrome are uncommon congenital abnormalities, both resulting in lower lid ectropion. Euryblepharon describes a congenital widening of the horizontal palpebral fissure. It is commonly associated with varying degrees of lower lid ectropion, occurring because the horizontal length of the upper lid is longer than that of the opposing lower lid. Inferior displacement of the lateral canthal tendon often creates the appearance of lateral canthal dystopia. Centurion syndrome describes an eyelid malposition resulting from anterior displacement of the medial canthal tendon and a prominent nasal bridge. A relative weakness of the posterior limb of the medial canthal tendon and lack of posterior anchoring of the eyelid may also contribute. A retrodisplacement of the involved globe may also be present in certain patients [62]. In both conditions, there may be varying degrees of punctal ectropion.

Euryblepharon can be either bilateral or unilateral. It may be asymptomatic or associated with exposure keratopathy from impaired blink, poor eyelid closure, and lagophthalmos (Fig. 21.45). Patients with Centurion syndrome usually present with symptomatic tearing, which results from distraction of the medial eyelids and puncta from the globe [62]. This can be present at birth or develop later in childhood. Nasolacrimal duct probing and irrigation is usually normal, but lacrimal scintigraphy may reveal a functional obstruction of the nasolacrimal sac.

In mild cases of euryblepharon and Centurion syndrome, no treatment is necessary. For ocular surface dryness, lubricating drops or ointments can be used. When there is more severe corneal exposure or concerns related to cosmesis, lower eyelid repositioning can be performed. In euryblepharon syndrome, lateral lid laxity can be addressed with a lateral tarsal strip procedure. Vertical eyelid shortening, if present, may need to be treated with anterior and/or posterior lamellar grafts (Fig. 21.46). Centurion syndrome can be addressed by performing a medial cantholysis procedure, which allows for relaxation of the medial canthus and better apposition of the eyelids/puncta to the globe [62]. The subsequent position of the medial canthus should be evaluated intraoperatively after medial tendon release, and, if necessary, a posterior plication suture can be placed. If punctal ectropion is significant, a medial spindle procedure can be performed. In patients with



Fig. 21.45 Euryblepharon

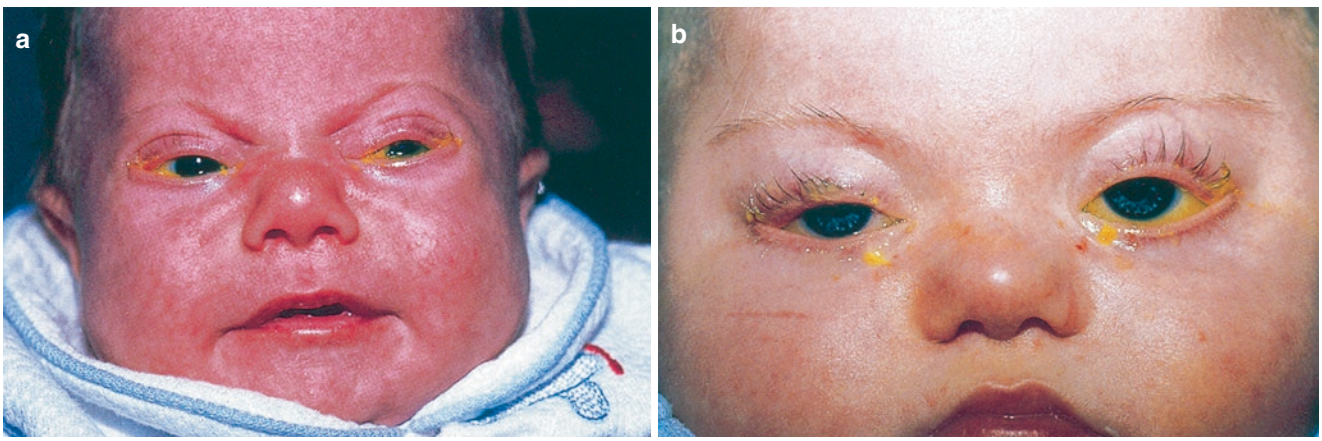


Fig. 21.46 Euryblepharon requiring skin graft procedure. (**a**) Three-month-old patient with Down syndrome and euryblepharon. (**b**) The lower eyelids were initially corrected with lateral canthal plication

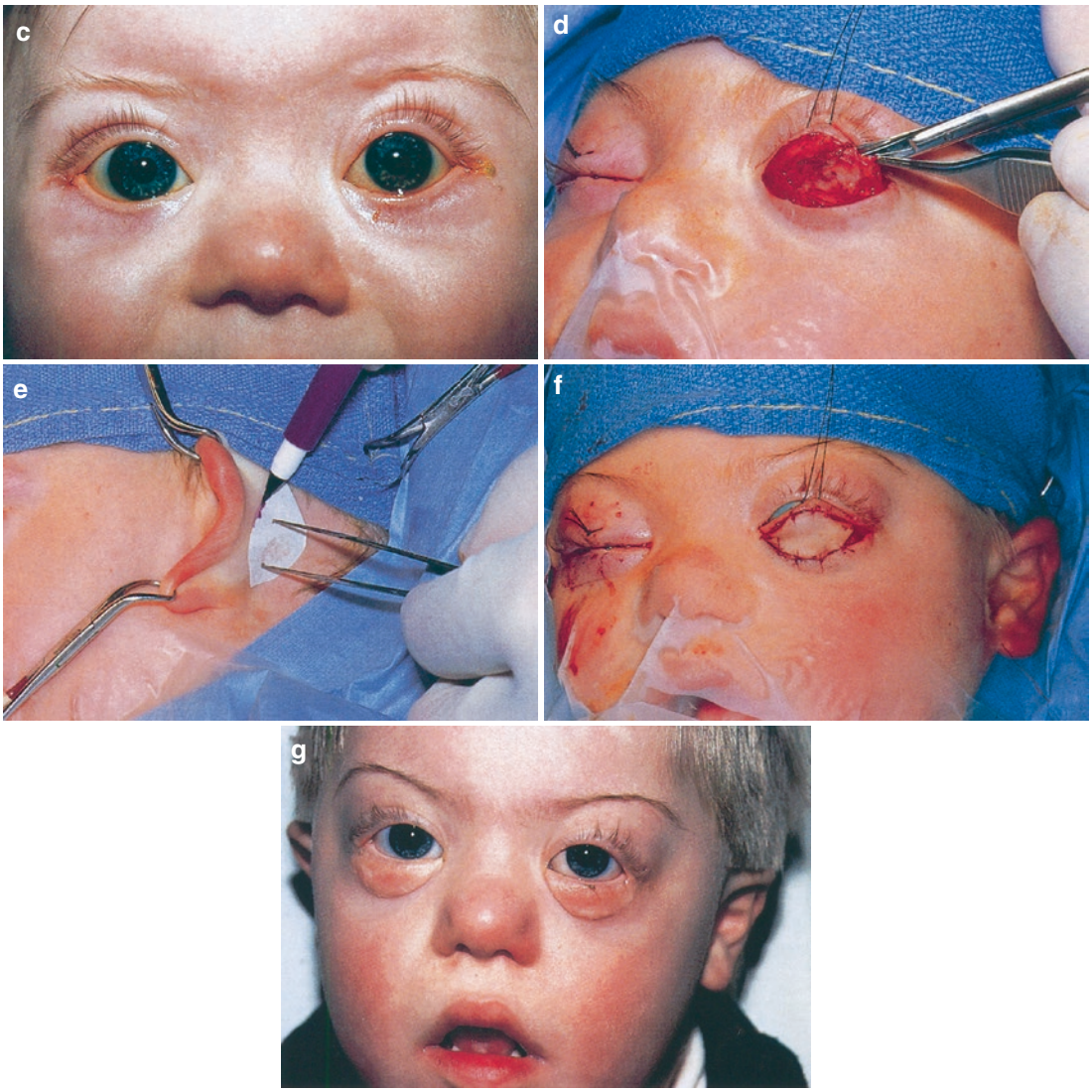


Fig. 21.46 (continued) (**c**) Over a period of 6 months, the lower eyelids returned to a position of retraction. (**d**) A skin graft procedure was undertaken because of a relative lack of anterior lamellae. The subciliary incision is opened and dissected to take traction off the lower eyelid. (**e**) An appropriately sized skin graft is harvested from the posterior auricular area. (**f**) The skin graft is sutured into position with a Frost retraction suture in place to keep upward traction on the eyelid. (**g**) This patient's appearance 9 months after the skin graft procedure

concomitant nasolacrimal duct obstruction, an external DCR can be performed simultaneously. Prognosis can be excellent in both conditions if eyelid malpositioning surgery is performed as necessary to protect the ocular surface.

Epicanthal Folds

Epicanthal folds are redundant folds of tissue in the medial canthal region. This may be a normal facial finding, an isolated facial developmental anomaly, or seen in conjunction with syndromes such as Down syndrome of blepharophimosis, ptosis, and epicanthus inversus syndrome (BPES).

Epicanthal folds are classified based on the origin and termination of the fold (Figs. 21.47 and 21.48) and are classified based on the origin and termination of the fold. Epicanthal folds fit into four general categories: supraciliaris (fold from eyebrow to over lacrimal sac fossa), epicanthus tarsalis (fold from upper eyelid to medial canthus), palpebralis (fold from upper eyelid to the lower eyelid, and inversus (fold from lower eyelid to medial canthus). Epicanthus tarsalis is anatomically normal in Asians. Epicanthus inversus is most common in BPES. Epicanthal folds are generally asymptomatic and nonamblyogenic. However, if prominent, they can be visually significant in certain directions of gaze. In BPES they can be prominent, especially when associated with telecanthus.

Since they are rarely vision threatening, epicanthal folds are surgically addressed if they are a cosmetic concern to patients and/or families. Mild folds often improve with age as the nasal bridge develops. If surgery is performed, there are a variety of flap designs that can be used to eliminate the fold and minimize scar formation, including a Y to V plasty (Fig. 21.49) or Mustarde 4 flap (jumping man) (Fig. 21.50). The Y-V plasty works well for smaller folds and the Mustarde



Fig. 21.47 Different types of epicanthal folds. (**a**) Supraciliaris, (**b**) tarsalis, (**c**) palpebralis, and (**d**) inversus

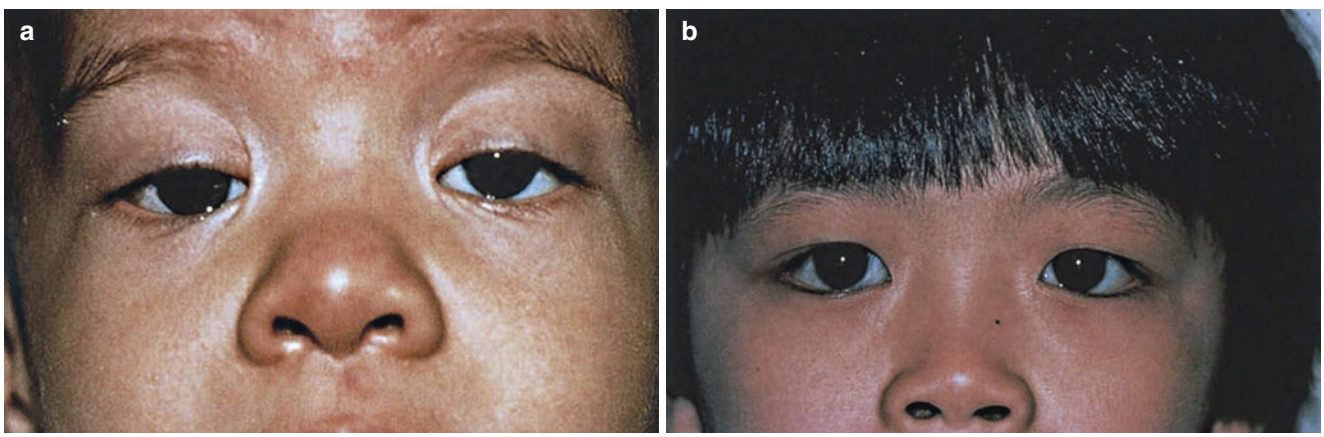


Fig. 21.48 Epicanthal folds. Different types of epicanthal folds. (**a**) Supraciliaris, (**b**) tarsalis

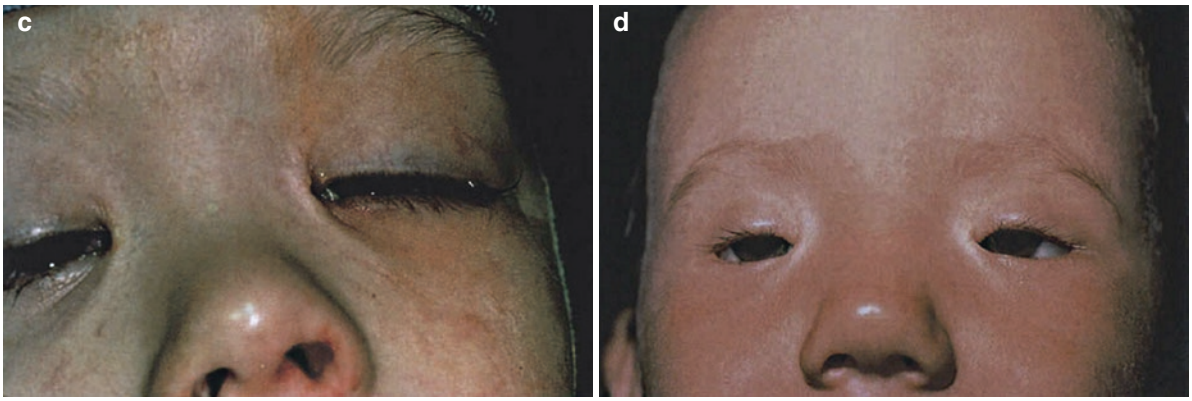


Fig. 21.48 (continued) (**c**) palpebralis, and (**d**) inversus

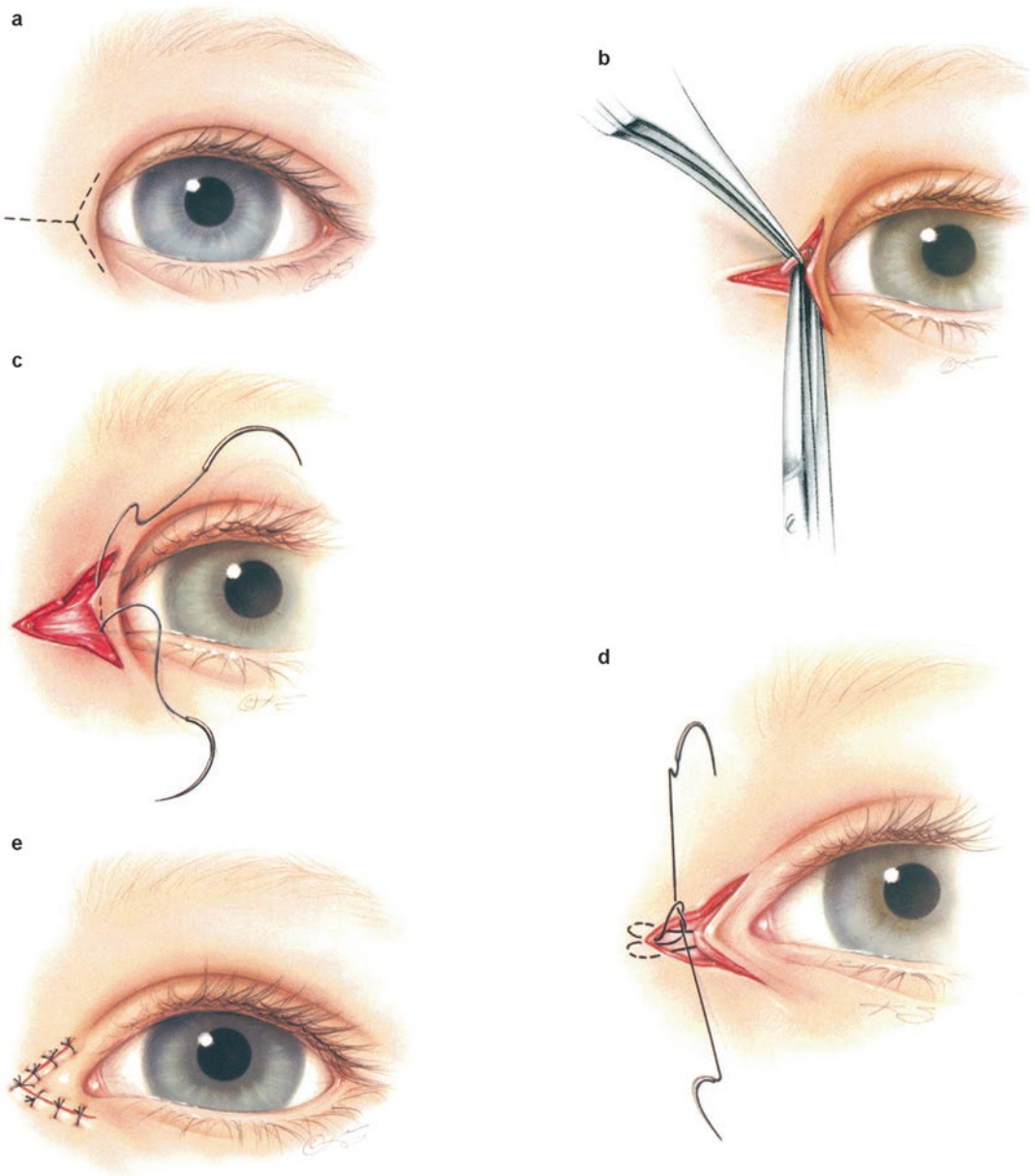


Fig. 21.49 Epicanthal fold repair: Y-V plasty. (**a**) The skin incision is marked with the arms of the Y placed across the epicanthal folds. (**b**) The fibrous tissue underlying the epicanthal fold is excised. (**c**) The canthal tendon is secured under the flap with a 4-0 Vicryl mattress suture on a P-2 needle (Ethicon). (**d**) The canthal tendon and skin flap are secured to periosteum and pulled medially. (**e**) The skin incision is closed

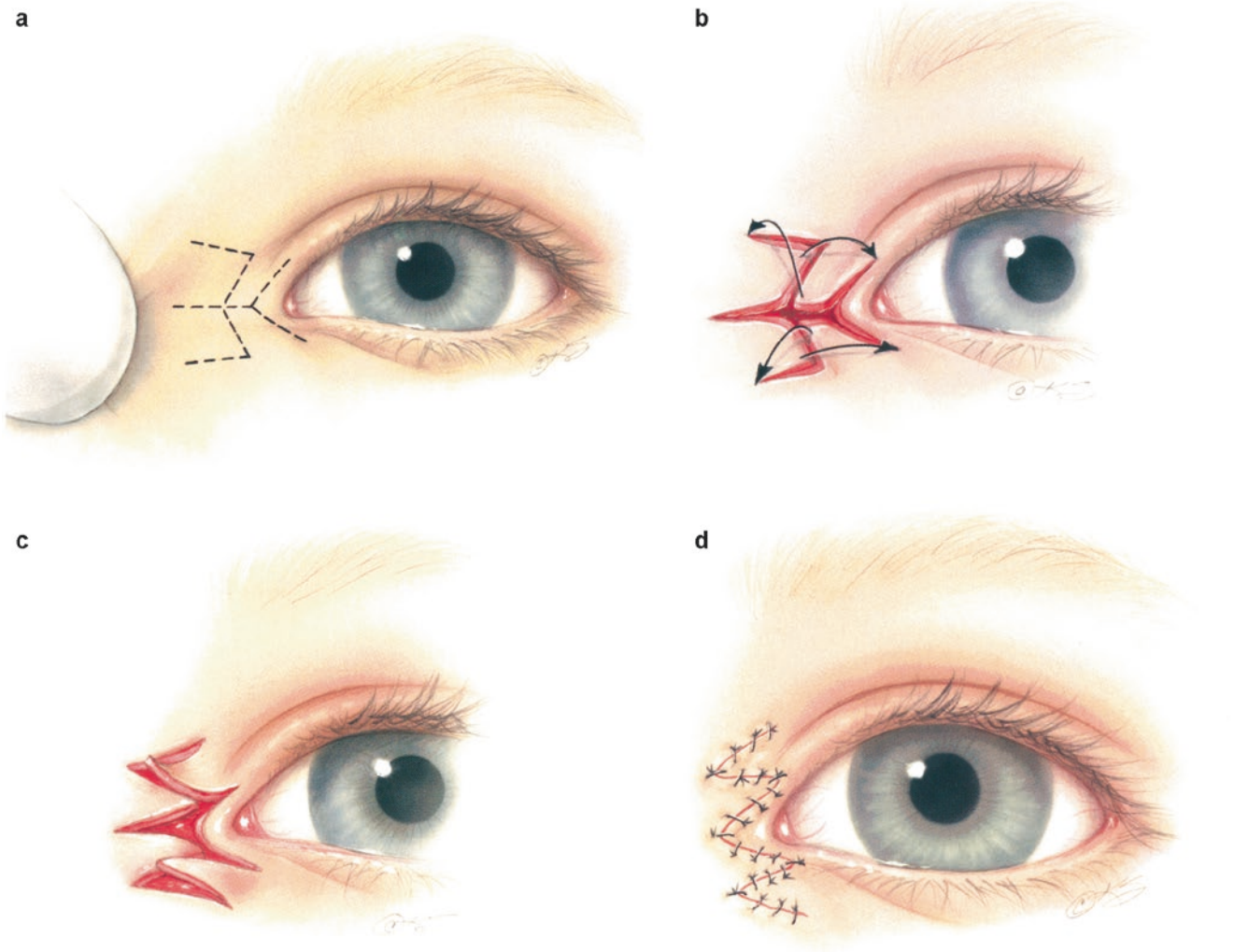


Fig. 21.50 Epicanthal fold repair: Mustarde "jumping man" technique. (**a**) The skin is marked with the "jumping man" figure. (**b**) The skin flaps are incised, and the fibrous tissue beneath the fold has been removed. The rotational pattern of the skin flaps is indicated. (**c**) The skin flaps are repositioned. (**d**) The flaps are anchored and sewn into place

for large epicanthal folds. The skin incisions are made and undermined to create small skin flaps. Beneath the epicanthal fold, there is often a fibrous band found in the subcutaneous tissue that should be carefully excised. The medial canthal tendon can be plicated or advanced with a 4-0 Vicryl suture. The skin flaps are then trimmed, re-aligned, and secured into place with a dissolving skin suture.

Blepharophimosis, Ptosis, and Epicanthus Inversus Syndrome (BPES)

BPES is defined by the presence of: (1) ptosis, (2) epicanthus inversus, (3) blepharophimosis, and (4) telecanthus (Fig. 21.51). It can be caused by an autosomal dominant mutation in the FOXL2 gene. Additional periocular anomalies associated with this condition include hypertelorism, hypoplasia of the superior orbital rims, lower eyelid ectropion, and a poorly developed nasal bridge. Type I BPES is associated with the above eyelid characteristics, as well as premature ovarian failure. Type II BPES is associated with only the eyelid findings. The exact prevalence of BPES is unknown [63]. The pediatrician should be involved in cases of BPES. Genetic testing should be pursued, as well as gynecologic surveillance of type I.

The timing and sequence of surgical correction for the ptosis and epicanthal folds has been debated. Some argue for a one-stage surgery where both are addressed early at the same time, while others feel that a two-stage surgery is best. Recently, one group described a large cohort of Asian children in whom a two-staged approach is performed (medial canthoplasty/canthopexy followed by external levator resection 6–12 months later). This approach was used with good cosmetic and functional results [64]. Our surgical approach at The Children's Hospital of Philadelphia for patients with BPES has been to perform a Y-V medial canthopexy/canthoplasty at the same time as the initial ptosis surgery (usually a frontalis suspension with silastic sling). Depending on the

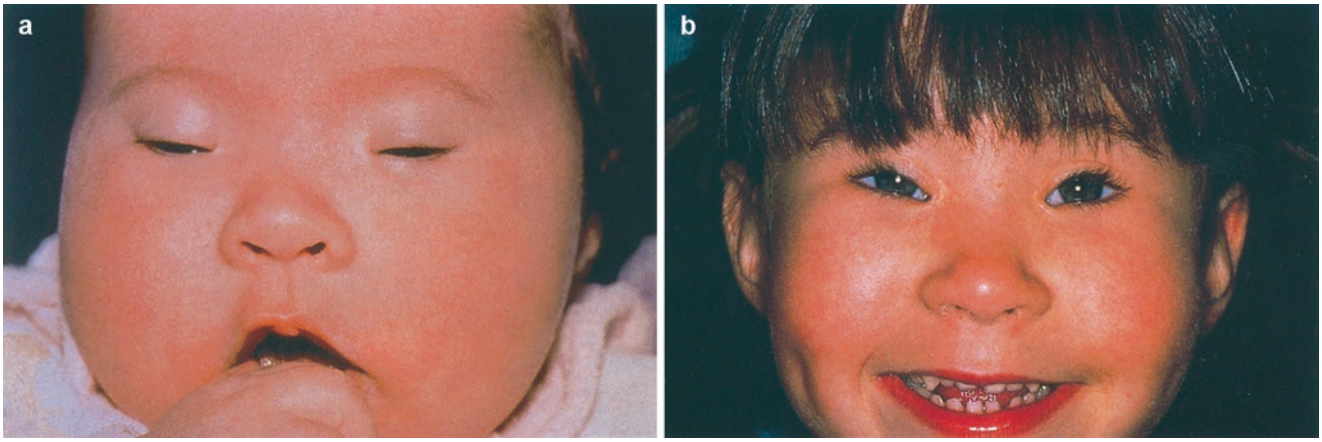


Fig. 21.51 BPES. (**a**) Two-month-old patient with ptosis, blepharophimosis, and epicanthal folds. (**b**) The same child at age 6 years after transnasal wiring, epicanthal fold repair, and frontalis suspension procedures



Fig. 21.52 Medial canthal tendon plication with Y-V flaps and simultaneous ptosis repair with silicone rod material in a patient with BPES. (**a**) Preoperative appearance at age 3 years. (**b**) Six months after surgery

severity of ptosis and whether amblyopia is a concern, this is usually done around 1 year of age as the child begins to stand and walk. If telecanthus continues to be a concern, we then plan to perform transnasal wiring between ages 3 and 4 years followed by further frontalis suspension with autogenous fascia lata between ages 4 and 5 years if further ptosis repair is needed for either functional or appearance concerns.

Telecanthus

When telecanthus accompanies epicanthal folds, repositioning of the medial canthus can be performed at the same procedure as the fold excision. Medial canthal tendon plication alone through a Y-V plasty incision may be effective to correct mild telecanthus (Figs. 21.49 and 21.52). The Y-V incisions, however, can also be used for transnasal wiring (Fig. 21.53). The Mustarde "jumping man" flap as described earlier is an alternative approach for transnasal wiring and especially with larger epicanthal folds (Fig. 21.50).

A preoperative CT scan is helpful to verify the level of the cribriform plate, which may be higher or lower than expected in some craniofacial syndromes. To remain extracranial, the transnasal wires need to be passed below the level of the cribriform plate. The skin flaps are chosen and created in bilateral medial canthal regions. If a Y to V plasty is being used, the design of the skin flaps is based on measurements that are done once general anesthesia has been initiated (Fig. 21.54). The intercanthal distance (IC) should be about half the interpupillary distance (PD). The interpupillary distance and the intercanthal distance are measured and recorded. The amount of intercanthal tightening necessary per side is then calculated to move each medial canthus one-half of the desired new intercanthal distance.

Once the medial canthal flaps are drawn, the areas are infiltrated with 0.5% Marcaine with epinephrine 1:200,000 and the

nose packed with oxymetazoline-soaked cottonoids. Care should be taken to keep the superior limb of the Y incision to be separate from the lid crease incision in order to avoid the potential for a postoperative epicanthal scar. Incisions are then made, and the medial canthal tendon, lacrimal sac, and periosteum are reflected laterally to expose the posterior lacrimal crest. Using a Freer elevator or mosquito hemostat, a small bony opening is made at the level of the anterior lacrimal sac fossa on both sides. The opening can be enlarged by removing the bone from the anterior lacrimal crest with a Kerrison punch or Sonopet drill (Stryker Instruments, 4100 E. Milham Ave., Kalamazoo, MI 49001, USA). This assists the movement of the canthal tendons medially as well as reducing any minor element of associated hypertelorism. Using a small free canthopexy needle, one end of a #30 gauge wire is passed through the canthal tendon beneath the apex of the medial canthal flap. A canthopexy awl is passed across the anterior ethmoidal space, from the opposite side through both bony openings in the lacrimal sac fossa. As the awl is being passed through the anterior ethmoidal space, a metal bone plate retractor should be used to protect the eye as the awl emerges out of the contralateral nasolacrimal sac fossa. Both free wire ends are then passed through the eye of awl, which is pulled back out the contralateral sac fossa opening. Again, a free canthopexy needle is used to pass one contralateral end of the wire through the canthal tendon beneath the apex of the opposite medial canthal flap. Both ends of the wire are then twisted until the appropriate medial canthal position is achieved. Excess wire is cut with a wire cutter, and the short ends of the wire are buried deep into the bony opening away from the eye and soft tissue of the medial canthal area.

The posterior placement of the transnasal wire is essential for appropriate positioning of the inner canthi. Because of the proximity of the lacrimal outflow system, there can be a tendency to anteriorly displace the transnasal wire. This can distort the inner canthal angle and result in the eyelids pulling away from the globe. When there is concern that the patient's anatomy may jeopardize the integrity of the lacrimal outflow system, prophylactic intubation of the system with silicone tubing may be performed. When hypertelorism accompanies telecanthus and extensive medial bone removal is planned by the craniofacial surgeons, prophylactic intubation can be considered.

As an aside, for unilateral telecanthus secondary to trauma, two drill holes on the opposite side of the nose must be made, and the wire is passed through the single osteotomy beneath the anterior lacrimal crest and then through the

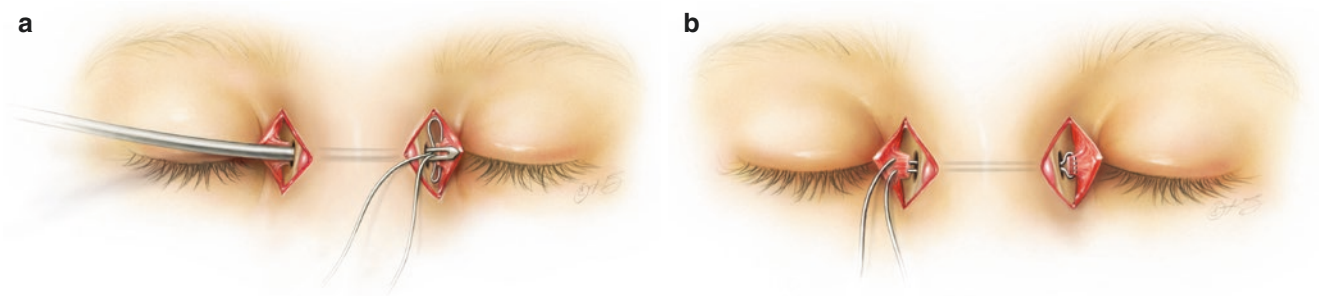


Fig. 21.53 Transnasal wiring. (**a**) The awl is in position to guide the medial canthal suture across the deep nasal pass. (**b**) The contralateral side is imbricated, and tightening of the suture will pull both tendons toward midline

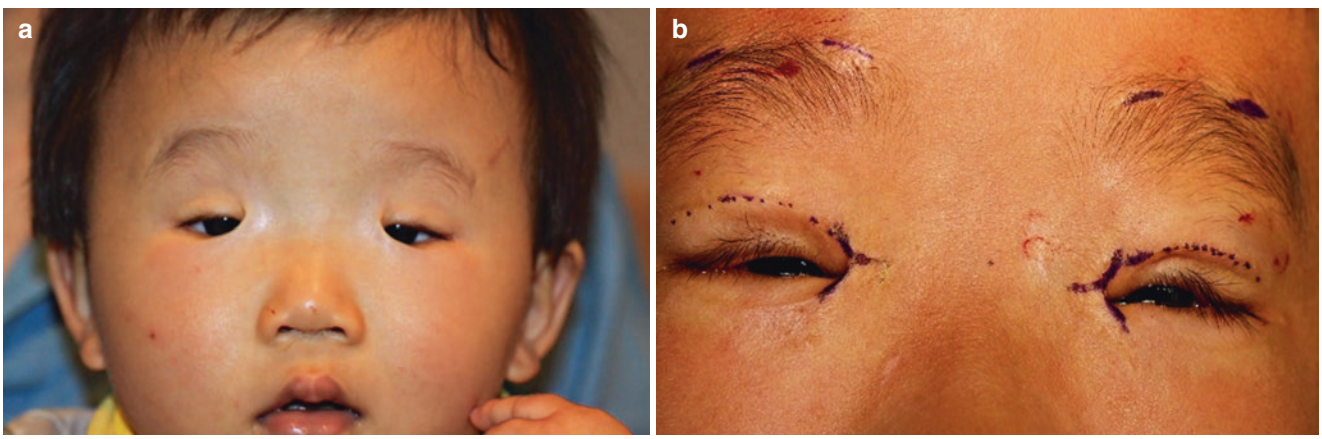


Fig. 21.54 Telecanthus and epicanthal fold repair with Y to V plasty with large free needle for transnasal wiring and use of the Sonopet drill. (**a**) BPES patient at age 1 year. (**b**) Preoperative Y-V-shaped medial canthal markings at age 6 years

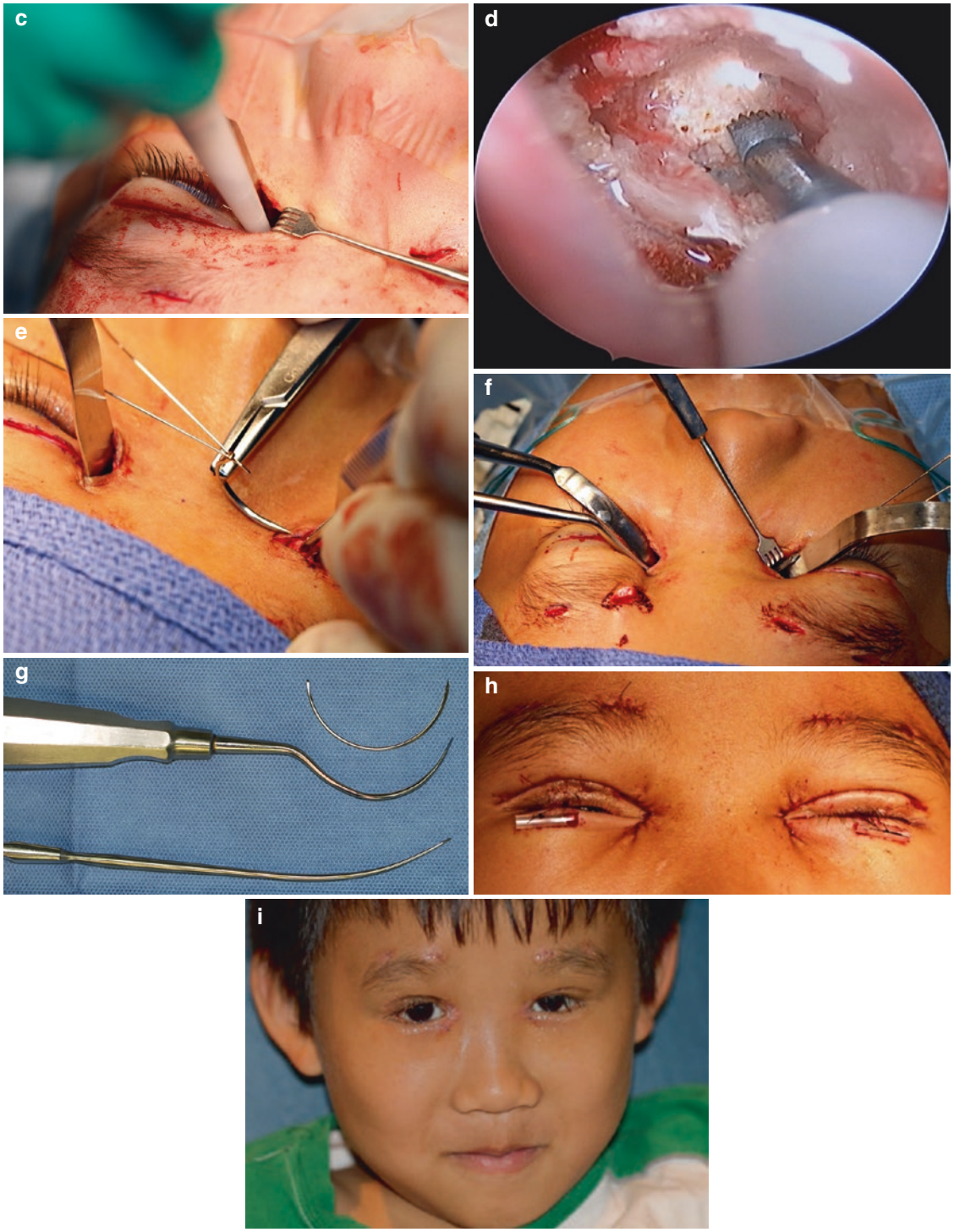


Fig. 21.54 (continued) (**c**) After incisions are made, a Sonopet drill is used here to create a bony rhinostomy on both sides for the transnasal wire to pass through. A Kerrison punch can be used as an alternative method. (**d**) Example of the Sonopet drill tip as it is used for an endoscopic DCR surgery. (**e**) A #30 wire is passed through the medial canthal tendon under the apex of the flap with a small canthopexy needle. (**f**) Both ends of the wire are then passed through a canthopexy awl or, as in this case, through the eye of a large curved needle (Richard-Allen Aspen Surgical Products, ½ inch cutting, #209102) which is then passed transnasally (using the eye of the needle opposite the sharp point and with a malleable retractor protecting the contralateral globe). The wire ends are retrieved on the opposite side, and, again, one end is passed through the medial canthal tendon and flap using a small free canthopexy needle (Richard-Allen Aspen Surgical Products, ½ inch cutting, #209102). (**g**) Different awl types and the free canthopexy needle (Richard-Allen Aspen Surgical Products, ½ inch cutting, #209102). (**h**) The wire ends are then twisted, thereby pulling the canthi to the desired location and the wounds closed. In this case, silastic frontalis suspension surgery was also performed at the same time and the eyes protected for the first few postoperative days with temporary lateral tarsorrhaphies. (**i**) One month postoperative, with slightly more brow recruitment on the right side; reduced telecanthus and improved scleral show visible medially on both sides



Fig. 21.55 Blepharophimosis. (**a**) Preoperative appearance at age 1 year. (**b**) Postoperative appearance at age 14 years, following telecanthus, and epicanthal fold repair with Mustarde jumping man flaps and transnasal wiring at age 4, followed by bilateral autogenous fascia lata suspensions at age 5 years

drill holes with a small canthopexy needle. The wires are then twisted over the intervening bone above the normal opposing lacrimal sac fossa. The cut ends can be placed inside one of the holes so they are less palpable under the skin surface (see Chap. 42). In some cases of BPES where there is only mild or moderate telecanthus, as mentioned previously, medial canthal tendon plication alone may improve the telecanthus (Fig. 21.48). Tendon plication is performed by bluntly dissecting out the fibers of the medial canthal tendon as they pass from the eyelid to the medial orbital wall. A mattress suture with 4-0 Vicryl on a P-2 needle can then be used to crimp the tendon like a ribbon. After the canthal plication suture is tied, the skin flaps are trimmed and sewn into position with a 6-0 Vicryl suture at the apex point and 8-0 Vicryl or 6-0 plain sutures at the skin edges (Figs. 21.54 and 21.55).

References

1. Sevel D. A reappraisal of the development of the eyelids. Eye (Lond). 1988;2(Pt 2):123–9.
2. Harris MJ, McLeod MJ. Eyelid growth and fusion in fetal mice. A scanning electron microscope study. Anat Embryol. 1982;164(2):207–20.
3. Duerksen K, Barlow WE, Stasior OG. Fused eyelids in premature infants. Ophthal Plast Reconstr Surg. 1994;10(4):234–40.
4. Doxanas MT, Anderson RL. Clinical orbital anatomy. Baltimore, MD: Williams and Wilkins; 1984. xi, 232p
5. Thomas IT, Frias JL, Felix V, Sanchez de Leon L, Hernandez RA, Jones MC. Isolated and syndromic cryptophthalmos. Am J Med Genet. 1986;25(1):85–98.
6. Rosenman Y, Ronen S, Eidelman AI, Schimmel MS. Ankyloblepharon filiforme adnatum: congenital eyelid-band syndromes. Am J Dis Child. 1980;134(8):751–3.
7. Warkany J, Schraffenberger E. Congenital malformations induced in rats by maternal vitamin a deficiency; defects of the eye. Arch Ophthalmol. 1946;35:150–69.
8. Dutton JJ. Atlas of clinical and surgical orbital anatomy. Philadelphia: Elsevier/Saunders; 2011. p. 1. online resource (xiii, 262 p).
9. Codere F, Tucker NA, Renaldi B. The anatomy of Whitnall ligament. Ophthalmology. 1995;102(12):2016–9.
10. Hawes MJ, Dortzbach RK. The microscopic anatomy of the lower eyelid retractors. Arch Ophthalmol. 1982;100(8):1313–8.
11. Slavotinek AM, Tifft CJ. Fraser syndrome and cryptophthalmos: review of the diagnostic criteria and evidence for phenotypic modules in complex malformation syndromes. J Med Genet. 2002;39(9):623–33.
12. Slavotinek AM, Baranzini SE, Schanze D, Labelle-Dumais C, Short KM, Chao R, Yahyavi M, Bijlsma EK, Chu C, Musone S, Wheatley A, Kwok PY, Marles S, Fryns JP, Maga AM, Hassan MG, Gould DB, Madireddy L, Li C, Cox TC, Smyth I, Chudley AE, Zenker M. Manitoba-oculo-tricho-anal (MOTA) syndrome is caused by mutations in FREM1. J Med Genet. 2011;48(6):375–82.
13. Ferri M, Harvey JT. Surgical correction for complete cryptophthalmos: case report and review of the literature. Can J Ophthalmol. 1999;34(4):233–6.
14. Subramanian N, Iyer G, Srinivasan B. Cryptophthalmos: reconstructive techniques--expanded classification of congenital symblepharon variant. Ophthal Plast Reconstr Surg. 2013;29(4):243–8.
15. Tran AQ, Lee BW, Alameddine RM, Korn BS, Kikkawa DO. Reconstruction of unilateral incomplete Cryptophthalmos in Fraser syndrome. Ophthal Plast Reconstr Surg. 2015;33:S73–5.
16. Heher KL, Katowitz JA. Oral mucous membrane grafts for corneal protection to permit prosthetic shell wear. Ophthal Plast Reconstr Surg. 1997;13(1):40–7.
17. Gilbert C, Foster A. Childhood blindness in the context of VISION 2020--the right to sight. Bull World Health Organ. 2001;79(3):227–32.
18. Hornby SJ, Gilbert CE, Rahi JK, Sil AK, Xiao Y, Dandona L, Foster A. Regional variation in blindness in children due to microphthalmos, anophthalmos and coloboma. Ophthalmic Epidemiol. 2000;7(2):127–38.
19. Williamson KA, FitzPatrick DR. The genetic architecture of microphthalmia, anophthalmia and coloboma. Eur J Med Genet. 2014;57(8):369–80.
20. Verma AS, Fitzpatrick DR. Anophthalmia and microphthalmia. Orphanet J Rare Dis. 2007;2:47.
21. Shah SP, Taylor AE, Sowden JC, Ragge NK, Russell-Eggitt I, Rahi JS, Gilbert CE, Surveillance G. Of eye anomalies special interest, Anophthalmos, microphthalmos, and typical coloboma in the United Kingdom: a prospective study of incidence and risk. Invest Ophthalmol Vis Sci. 2011;52(1):558–64.

22. Moore KL, Persaud TVN, Torchia MG. The developing human clinically oriented embryology. Philadelphia, PA: Elsevier; 2016. p. 1 online resource
23. Hennekam RCM, Allanson JE, Krantz ID, Gorlin RJ. STAT!Ref (Online service), Gorlin's syndromes of the head and neck, in Oxford monographs on medical genetics 58. 2010, Oxford University Press: Oxford, New York. p. 1 online resource (lxi, 1452 p).
24. Katowitz JA. Pediatric oculoplastic surgery. New York: Springer; 2002. xix, 694 p.
25. Tucker S, Jones B, Collin R. Systemic anomalies in 77 patients with congenital anophthalmos or microphthalmos. Eye (Lond). 1996;10(Pt 3):310–4.
26. Demirci H, Singh AD, Shields JA, Shields CL, Eagle RC. Bilateral microphthalmos and orbital cyst. Eye (Lond). 2003;17(2):273–6.
27. Chang L, Blain D, Bertuzzi S, Brooks BP. Uveal coloboma: clinical and basic science update. Curr Opin Ophthalmol. 2006;17(5):447–70.
28. Farkas LG, Posnick JC, Hreczko TM, Pron GE. Growth patterns in the orbital region: a morphometric study. Cleft Palate Craniofac J. 1992;29(4):315–8.
29. Goodman RM, Gorlin RJ. The malformed infant and child : an illustrated guide. New York: Oxford University Press; 1983. ix, 460 p.
30. Heher KL, Katowitz JA, Low JE. Unilateral dermis-fat graft implantation in the pediatric orbit. Ophthal Plast Reconstr Surg. 1998;14(2):81–8.
31. Gundlach KK, Guthoff RF, Hingst VH, Schittkowski MP, Bier UC. Expansion of the socket and orbit for congenital clinical anophthalmia. Plast Reconstr Surg. 2005;116(5):1214–22.
32. Ragge NK, Subak-Sharpe ID, Collin JR. A practical guide to the management of anophthalmia and microphthalmia. Eye (Lond). 2007;21(10):1290–300.
33. Tawfik HA, Abdulhafez MH, Fouad YA. Congenital upper eyelid coloboma: embryologic, nomenclatorial, nosologic, etiologic, pathogenetic, epidemiologic, clinical, and management perspectives. Ophthal Plast Reconstr Surg. 2015;31(1):1–12.
34. Tessier P. Anatomical classification facial, cranio-facial and laterofacial clefts. J Maxillofac Surg. 1976;4(2):69–92.
35. Mustardé JC. Plastic surgery in infancy and childhood. Edinburgh: Livingstone; 1971. xv, 581 p.
36. Akkermans CH, Stern LM. Ankyloblepharon filiforme adnatum. Br J Ophthalmol. 1979;63(2):129–31.
37. Cizmeci MN, Kanburoglu MK, Akelma AZ, Tatli MM. A stitched eye in the newborn: ankyloblepharon filiforme adnatum. J Pediatr. 2013;162(1):211–2.
38. Aslankurt M, Yasar I, Ozdemir M, Aslan L, Aksoy A. A case of secondary ankyloblepharon following bicanalicular silicone tube implantation. Ophthal Plast Reconstr Surg. 2012;28(5):382.
39. Dellinger MT, Thome K, Bernas MJ, Erickson RP, Witte MH. Novel FOXC2 missense mutation identified in patient with lymphedema-distichiasis syndrome and review. Lymphology. 2008;41(3):98–102.
40. O'Donnell BA, Collin JR. Distichiasis: management with cryotherapy to the posterior lamella. Br J Ophthalmol. 1993;77(5):289–92.
41. Kim JS, Jin SW, Hur MC, Kwon YH, Ryu WY, Jeong WJ, Ahn HB. The clinical characteristics and surgical outcomes of epiblepharon in Korean children: a 9-year experience. AM J Ophthalmol. 2014;2014:156501.
42. Chang EL, Hayes J, Hatton M, Rubin PA. Acquired lower eyelid epiblepharon in patients with thyroid eye disease. Ophthal Plast Reconstr Surg. 2005;21(3):192–6.
43. Sundar G, Young SM, Tara S, Tan AM, Amrith S. Epiblepharon in east Asian patients: the Singapore experience. Ophthalmology. 2010;117(1):184–9.
44. Levitt JM. Epiblepharon and congenital entropion. Am J Ophthalmol. 1957;44(1):112–3.
45. Preechawai P, Amrith S, Wong I, Sundar G. Refractive changes in epiblepharon. Am J Ophthalmol. 2007;143(5):835–9.
46. Khwarg SI, Lee YJ. Epiblepharon of the lower eyelid: classification and association with astigmatism. Korean J Ophthalmol. 1997;11(2):111–7.
47. Oh J, Lee K. Medial lower lid epiblepharon repair solely by skin-redraping medial epicanthoplasty. Br J Ophthalmol. 2014;98(10):1437–41.
48. Naik MN, Ali MJ, Das S, Honavar SG. Nonsurgical management of epiblepharon using hyaluronic acid gel. Ophthal Plast Reconstr Surg. 2010;26(3):215–7.
49. Taylor HR, Burton MJ, Haddad D, West S, Wright H. Trachoma. Lancet. 2014;384(9960):2142–52.
50. Wladis EJ. Transconjunctival epiblepharon repair. Ophthal Plast Reconstr Surg. 2014;30(3):271–2.
51. Tse DT, Anderson RL, Fratkin JD. Aponeurosis disinsertion in congenital entropion. Arch Ophthalmol. 1983;101(3):436–40.
52. Price NC, Collin JR. Congenital horizontal tarsal kink: a simple surgical correction. Br J Ophthalmol. 1987;71(3):204–6.
53. Quickert MH, Wilkes TD, Dryden RM. Nonincisional correction of epiblepharon and congenital entropion. Arch Ophthalmol. 1983;101(5):778–81.
54. Bleyen I, Dolman PJ. The Wies procedure for management of trichiasis or cicatricial entropion of either upper or lower eyelids. Br J Ophthalmol. 2009;93(12):1612–5.
55. Litwin AS, Kalantzis G, Drimtzias E, Hamada S, Chang B, Malhotra R. Nonsurgical treatment of congenital ichthyosis cicatricial ectropion and eyelid retraction using Restylane hyaluronic acid. Br J Dermatol. 2015;173(2):601–3.
56. Vallabhanath P, Carter SR. Ectropion and entropion. Curr Opin Ophthalmol. 2000;11(5):345–51.
57. Stout AU, Borchert M. Etiology of eyelid retraction in children: a retrospective study. J Pediatr Ophthalmol Strabismus. 1993;30(2):96–9.
58. Bartley GB. The differential diagnosis and classification of eyelid retraction. Ophthalmology. 1996;103(1):168–76.
59. Katowitz WR, Katowitz JA. Congenital and developmental eyelid abnormalities. Plast Reconstr Surg. 2009;124(1 Suppl):93e–105e.
60. Stewart KJ, Griepentrog GJ, Lucarelli MJ. Modified full-thickness anterior blepharotomy for upper eyelid retraction in children. J AAPOS. 2013;17(2):223–4.
61. Demirci H, Hassan AS, Reck SD, Frueh BR, Elner VM. Graded full-thickness anterior blepharotomy for correction of upper eyelid retraction not associated with thyroid eye disease. Ophthal Plast Reconstr Surg. 2007;23(1):39–45.
62. Sullivan TJ, Welham RA, Collin JR. Centurion syndrome. Idiopathic anterior displacement of the medial canthus. Ophthalmology. 1993;100(3):328–33.
63. Verdin H, De Baere E, Pagon RA, et al. Blepharophimosis, ptosis, and epicanthus inversus, in GeneReviews(R). Seattle (WA): University of Washington; 1993.
64. Song X, Jia R, Zhu H, Zhou Y, Sun Y, Lin M, Fu Y, Li J, Li Z, Lu L, Shen Y, Ge S, Fan X. A modified staged surgical intervention for blepharophimosis-ptosis-epicanthus inversus syndrome: 125 cases with encouraging results. Ann Plast Surg. 2015;74(4):410–7.

Pediatric Ptosis

22

William R. Katowitz and James A. Katowitz

Introduction

The word ptosis is translated into "fall" or "falling" and is derived from the Greek word πτῶσις. While ptosis is used to describe other descended anatomical structures, such as uterine or breast ptosis, the word blepharoptosis is specific to the eyelid. By convention, the *blepharo-* is dropped in most ophthalmic literature. The incidence of ptosis in children has been reported as 7.9 per 100,000 patients (birth prevalence of 1 in 842 births) as measured over a 40-year period in Olmsted County, Minnesota. In this study, 75% of these cases were simple congenital ptosis with 55% male and 45% female [1].

Surgical Anatomy of the Upper Lid

The skin of the eyelid is extremely thin, measuring about 0.6 mm in thickness. Superior to the eyelid crease, the skin and underlying preseptal orbicularis combine to form an anterior lamella that is loose and freely mobile over the underlying orbital septum and preaponeurotic fat. In contrast, the skin and pretarsal orbicularis muscle inferior to the crease are more securely attached to the underlying tarsus. In non-Asians the lid crease is usually located near the upper border of the tarsus and is created by insertions of the levator aponeurosis fibers into the fascicular bundles of the pretarsal orbicularis (Fig. 22.1). As the eyelid is elevated, this skin/muscle/tarsal complex is able to slide beneath the looser preseptal anterior lamella, enhancing the lid fold as it overhangs the lid crease.

The pretarsal and preseptal portions of the orbicularis muscle are innervated by the seventh cranial nerve and are responsible for eyelid closure. The frontalis muscle originates from the galea aponeurotica and inserts into the deep skin of the brow. The frontalis muscle serves as a secondary elevator of the lid, transmitting its force through the skin and orbicularis. The orbital septum is located posterior to the orbicularis muscle. It originates from the superior orbital rim and, in non-Asians, inserts into the levator aponeurosis 3–5 mm above the upper border of the tarsus (Fig. 22.1a). In the Asian eyelid, the insertion is often lower on the tarsus (Fig. 22.1b). The lid crease is thus frequently obscured by a lower overhanging lid fold or even eliminated by the interruption of the anterior attachments of the levator aponeurosis to the overlying pretarsal orbicularis and skin. Jeong et al. compared nine Korean eyelid cadavers to five Caucasian and found three causes for a lower or absent eyelid crease in the Asian eyelid. First, the orbital septum in Asian eyelid fuses to the levator aponeurosis at variable distances below the superior tarsal border. Second, preaponeurotic fat pad protrusion and a thick subcutaneous fat layer in Asian eyelids prevent levator fibers from extending toward the skin near the superior tarsal border, and finally the primary insertion of the levator aponeurosis into the orbicularis muscle and into the upper eyelid skin occurs closer to the eyelid margin in Asians [2]. Immediately posterior to the orbital septum lies the preaponeurotic fat pad. This is an important surgical landmark, because the levator aponeurosis is located just beneath the preaponeurotic fat.

The tarsus provides structural stability for the upper eyelid and consists of a semilunar, malleable, fibrous plate measuring about 1 mm in thickness, 22–25 mm in length, and 9–10 mm in height. The posterior surface of the tarsus is covered with conjunctiva, which is firmly adherent, forming the inner palpebral surface of the eyelid. Above the tarsal plate, the conjunctiva is bound tightly to the underlying Müller's muscle for the first 8–10 mm and then becomes more loosely attached superiorly.

Müller's muscle is a smooth muscle, innervated by the sympathetic chain. It originates from the posterior layer of the levator palpebrae superioris, inferior to Whitnall's liga-

W.R. Katowitz, MD • J.A. Katowitz, MD, FACS (✉)
The Children's Hospital of Philadelphia and The Edwin and Fannie Gray Hall Center for Human Appearance, University of Pennsylvania, Philadelphia, PA, USA
e-mail: katowitz@email.chop.edu; katowitzw@email.chop.edu

© Springer International Publishing AG 2018

J.A. Katowitz, W.R. Katowitz (eds.), *Pediatric Oculoplastic Surgery*, https://doi.org/10.1007/978-3-319-60814-3_22

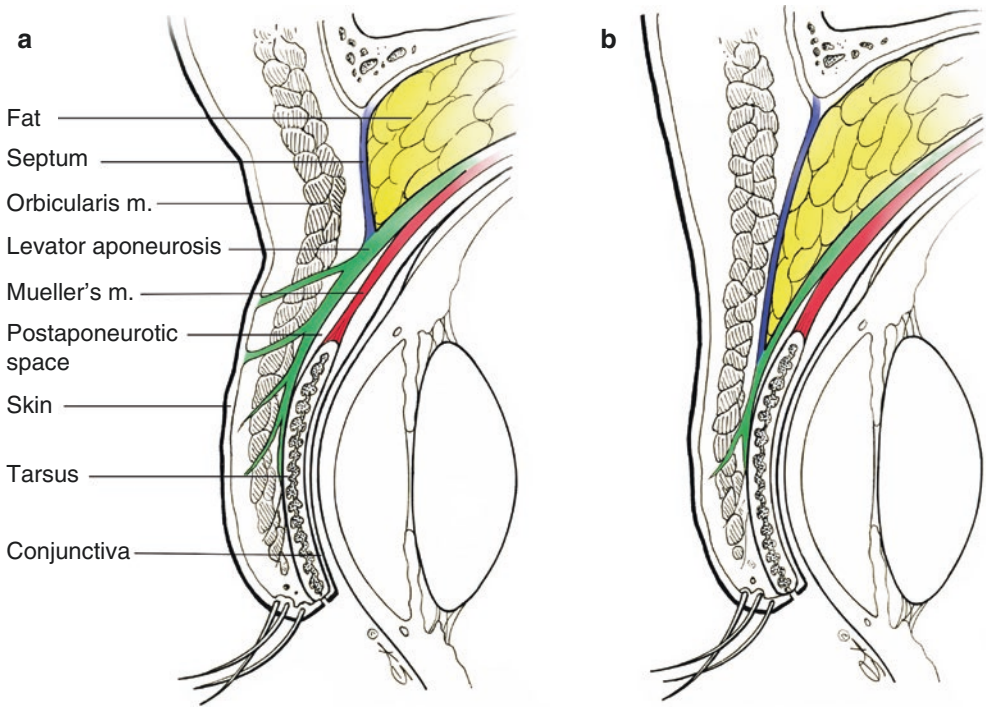


Fig. 22.1 Eyelid anatomy in cross section. (**a**) Non-Asian eyelid with the orbital septum (*blue*) inserting on the levator aponeurosis (*green*). Müller's muscle (*red*) originates from the levator muscle but lies below the levator aponeurosis. (**b**) Asian variation. The orbital septum (*blue*) fuses onto the levator (*green*) below the superior tarsal border or onto the tarsus [4]. Müller's muscle (*red*) still lies below the levator aponeurosis in a post-aponeurotic space

ment, and inserts into the upper border of the tarsal plate. The levator muscle, a striated muscle, is innervated by the third cranial nerve. It originates from the periorbita just above the annulus of Zinn and gradually fans out as it courses forward over the underlying superior rectus muscle. The levator's anterior muscular sheath becomes quite thickened and ends abruptly as a fascial band called Whitnall's superior transverse ligament. Whitnall's ligament appears to provide suspensory support for the levator, redirecting vector forces from horizontal in the orbit to vertical in the lid. It may also act as a check ligament to prevent posterior movement of the levator muscle [3].

Just inferior to Whitnall's ligament, the levator muscle divides into an anterior portion that becomes the levator aponeurosis and a posterior portion that is continuous with Müller's muscle. The levator aponeurosis is often stated to continue downward 14–20 mm before reaching its insertion. In our experience with children, however, the length of the tendon is much shorter, usually measuring 10–15 mm. As described earlier, the most superior fibers of the aponeurosis insert into the interfascicular septae of the pretarsal orbicularis muscle. Although a consensus has been reached regarding this portion of the aponeurotic insertion, debate continues over the importance of the termination site of the remaining fibers on the anterior surface of the tarsus. Classical teaching is that the majority of terminal fibers insert directly onto the inferior two-thirds of the anterior surface of the tarsus and that levator muscle contraction pulls on the tarsus in this fashion [5, 6]. In fact, probably only a small percentage of the fibers adhere tightly in this location, with only some of the most distal fibers attaching firmly as a thicker bundle across the lower 3–4 mm of the tarsus [5, 6].



Fig. 22.2 Upper lid section of an embryo. A section through the upper lid of a 105–mm embryo demonstrating the attachment of the levator aponeurosis to the orbicularis oculi. *MM* Müller's muscle, *SO* septum orbital, *LPS* levator palpebrae superioris, *TP* tarsal plate (From Werb [66]. Reprinted with permission from Taylor & Francis)

A number of anatomical dissections have documented that most of the aponeurotic terminal fibers insert into the fascial septae of the pretarsal orbicularis [3, 7, 8]. The levator aponeurosis thus appears to exert its major force of retraction to the anterior lamella, rather than directly to the tarsus. This concept is supported by Fig. 22.2, which demonstrates the developing attachment of the aponeurosis to the orbicularis muscle in a 105–mm embryo [7]. The relationship between

the insertions of the levator aponeurosis and Müller's muscle and the role they play in elevating the eyelid when the levator muscle contracts form the basis for continuing debate. These issues are discussed more extensively in the surgical treatment section of this chapter.

Pathophysiologic Classification

An attempt to understand the etiology of the ptosis in every patient is essential for assuring successful management. Although there are alternative methods for classifying pediatric ptosis, it is useful to divide types of ptosis into groups based on pathophysiologic mechanisms. Such categorization assists the surgeon in selecting the most appropriate surgical procedure. The four main pathophysiologic categories are myogenic, aponeurotic, neurogenic, and mechanical. Trauma is not considered a separate entity in our classification system, because most traumatic causes of ptosis fall into one of the four main categories. In addition to being able to distinguish between the various mechanisms, one must also be able to differentiate true ptosis from pseudoptosis, where the droop is due to other factors external to the lid, such as enophthalmos or microphthalmos.

Myogenic Ptosis

This type of ptosis is caused by an abnormality in the embryonic development of the levator palpebrae muscle. As a result, the levator muscle is usually dystrophic, with fibrotic or fatty tissue replacing healthy muscle fibers. The fibrotic nature of the muscle abnormality is exemplified by the resultant decrease in eyelid excursions. The eyelid not only demonstrates poor elevation in upgaze but also lags behind the motion of the globe on downgaze. Whereas healthy muscle is able to relax, allowing the eyelid to be lowered, the fibrotic tissue remains taut. As a result, many patients also demonstrate some degree of lagophthalmos, which also is frequently present when the patient is asleep. In some cases the orbital septum also appears to restrict motion of the lid, and when incised during surgery, an increased excursion of the lid can be demonstrated manually or voluntarily if the patient is not under general anesthesia.

The myogenic mechanism is responsible for the majority of congenital ptosis cases. The term "simple congenital ptosis" is sometimes used to refer to this particular type of congenital ptosis (Fig. 22.3). Myogenic ptosis is usually stationary and can occur unilaterally or bilaterally. An associated superior rectus weakness is reported in 5% of cases and may also be observed as a double-elevator palsy [9]. Usually no family history is present, but this type of ptosis can be transmitted as an autosomal-dominant trait. Light and electron microscopic studies have confirmed the dystrophic appearance of the levator muscle in congenital cases [8, 10].

Myogenic ptosis can be classified as mild (≤2 mm), moderate (3 mm), or severe (≥4 mm); most importantly, the degree of ptosis correlates inversely with the amount of levator function present – the greater the ptosis, the poorer the action of the levator. One of the more severe forms of myogenic ptosis is associated with blepharophimosis and for convenience is often categorized as the congenital eyelid syndrome or, more specifically, the blepharophimosis syndrome (BPES) (Fig. 22.4). This syndrome consists of blepharophimosis, epicanthus inversus, telecanthus, and ptosis. Lateral lower lid ectropion is sometimes also seen with this condition. The blepharophimosis eyelid syndrome is often found to be associated with mutations on the FOXL2 gene,

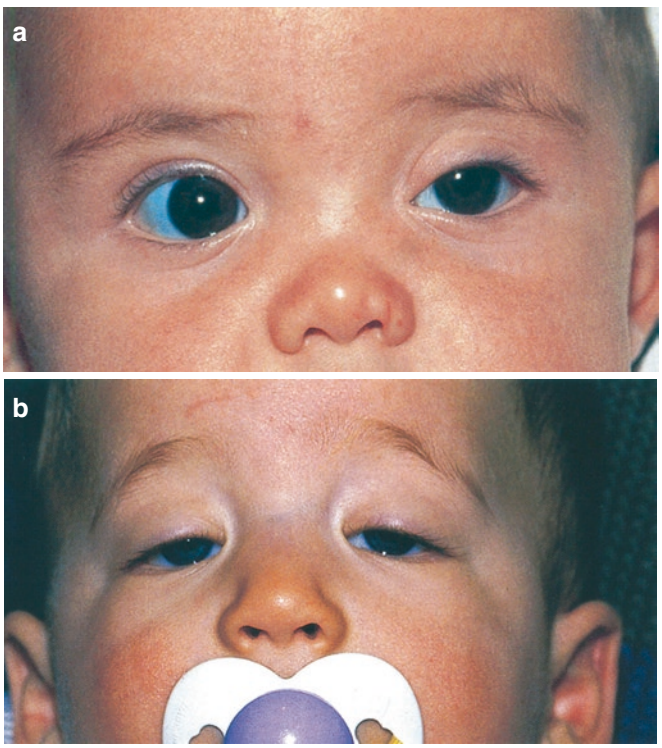


Fig. 22.3 Simple congenital ptosis. (**a**) Unilateral; (**b**) bilateral



Fig. 22.4 Congenital eyelid or blepharophimosis syndrome (BPES): blepharophimosis, epicanthus inversus, telecanthus and ptosis

and thus genetic testing is always recommended to patients and their parents with suspected BPES. Type I BPES is associated with premature ovarian failure. All female patients with FOXL2 gene mutation should have a consultation with an endocrinologist and an ultrasound of the ovaries upon reaching puberty.

Another myogenic condition is the congenital orbital fibrosis syndrome involving the extraocular muscles in addition to the levator muscle (Fig. 22.5). This is an extremely rare disorder that may be sporadic or familial. Although bilateral cases are more common in the literature, our experience has been greatest with unilateral cases with the involved eye rotated down and in [11]. The severe degree of ptosis is accompanied by enophthalmos. The child may attempt to compensate for the associated ptosis and restricted globe with adoption of a strange head position and use of the brows. If there is a strong family history, it is referred to as CFEOM1. CFEOM2 is an autosomal recessive disorder caused by mutation in the ARIX gene (602753) on chromosome 11q13 and is characterized by bilateral ptosis with eyes fixed in an exotropic position. CFEOM3 can be unilateral. CFEOM4, also known as Tukel syndrome, maps to 21q.CFEOM5 and is caused by mutation in the COL25A1 gene (610004) on chromosome 4q25 [12].



Fig. 22.5 Congenital orbital fibrosis syndrome

Although we use the term "myogenic" predominantly to describe a type of ptosis characterized by dysembryogenesis of the levator muscle, there are other dystrophic types of ptosis that present later in life. These include muscular dystrophy and chronic progressive external ophthalmoplegia and are relatively uncommon forms of pediatric ptosis. Chronic progressive external ophthalmoplegia (CPEO) is a mitochondrial disease. It results in a bilateral, severe, progressive ptosis with poor levator function. In addition, it can be associated with heart block, retinal pigment degeneration, and foveal atrophy (Kearns Sayre syndrome). Figure 22.6 depicts a patient with Kearns-Sayre who suffers from ptosis and poor vision. Figure 22.7 is another patient with CPEO. Mitochondrial diseases result from failures of the mitochondria, specialized compartments present in every cell of the body except red blood cells. Mitochondria are responsible for creating more than 90% of the energy needed by the body to sustain life and support growth. When they fail, less and less energy is generated within the cell. Cell injury and even cell death follow. If this process is repeated throughout the body, whole systems begin to fail, and the life of the person in whom this is happening is severely compro-

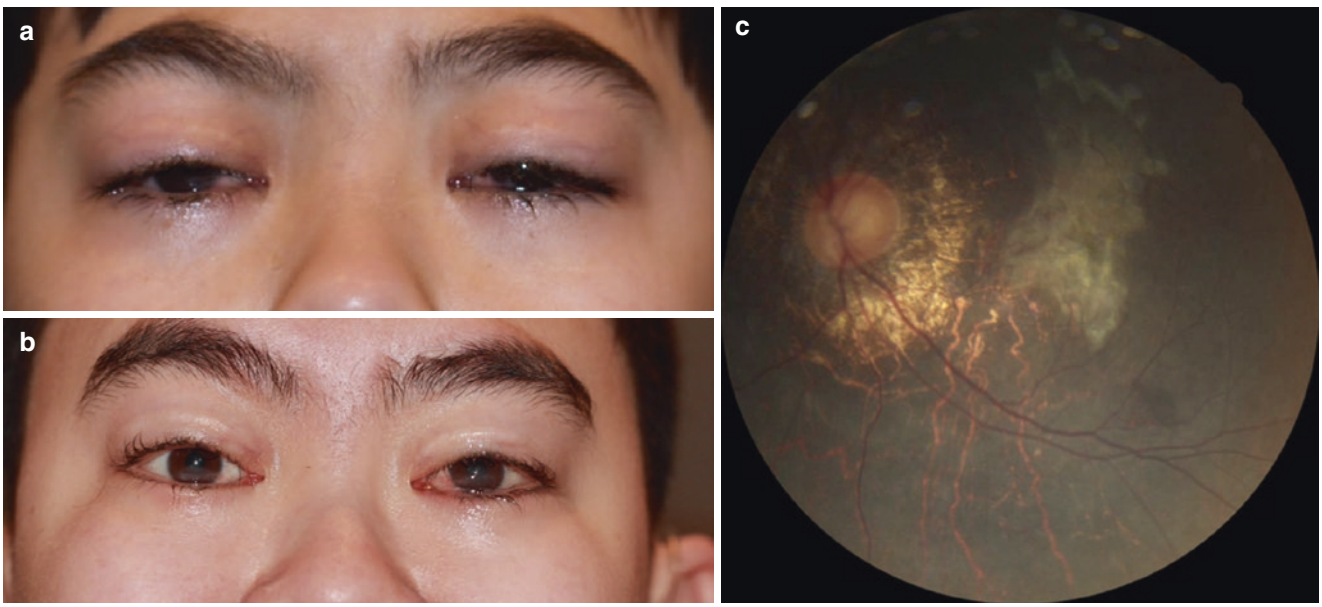


Fig. 22.6 Patient with CPEO and heart block (Kearns Sayre). (**a**) Preoperative photo showing bilateral ptosis. (**b**) Postoperative photo 6 years after bilateral autogenous fascia lata slings. (**c**) Fundus photograph of the right eye showing pigmentary retinopathy.

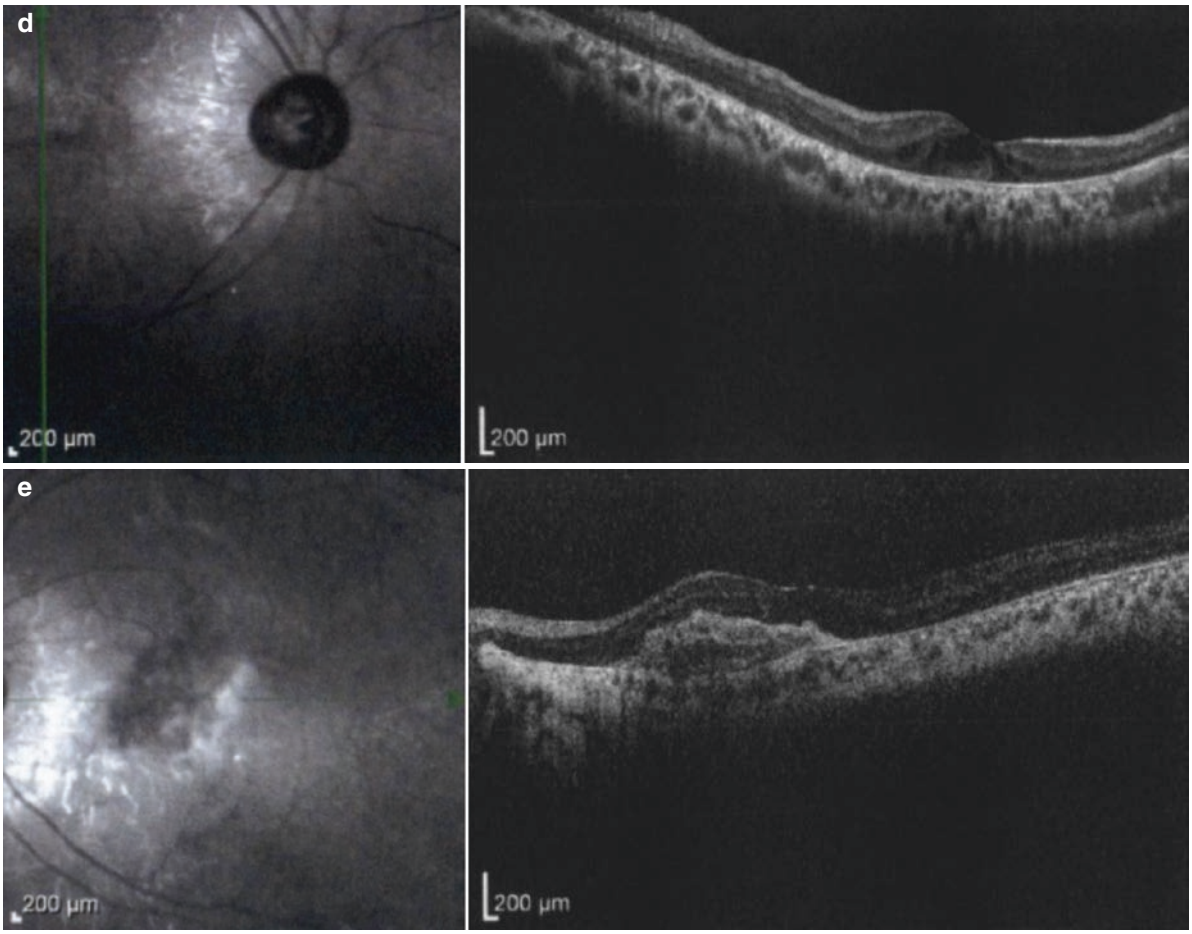


Fig. 22.6 (continued) (**d**) OCT, right and (**e**) OCT, left eye showing serious outer retinal atrophy with preservation of retinal pigment epithelium and photoreceptor cells in the macula only and virtually complete atrophy of these outer retinal layers beyond the very central macula

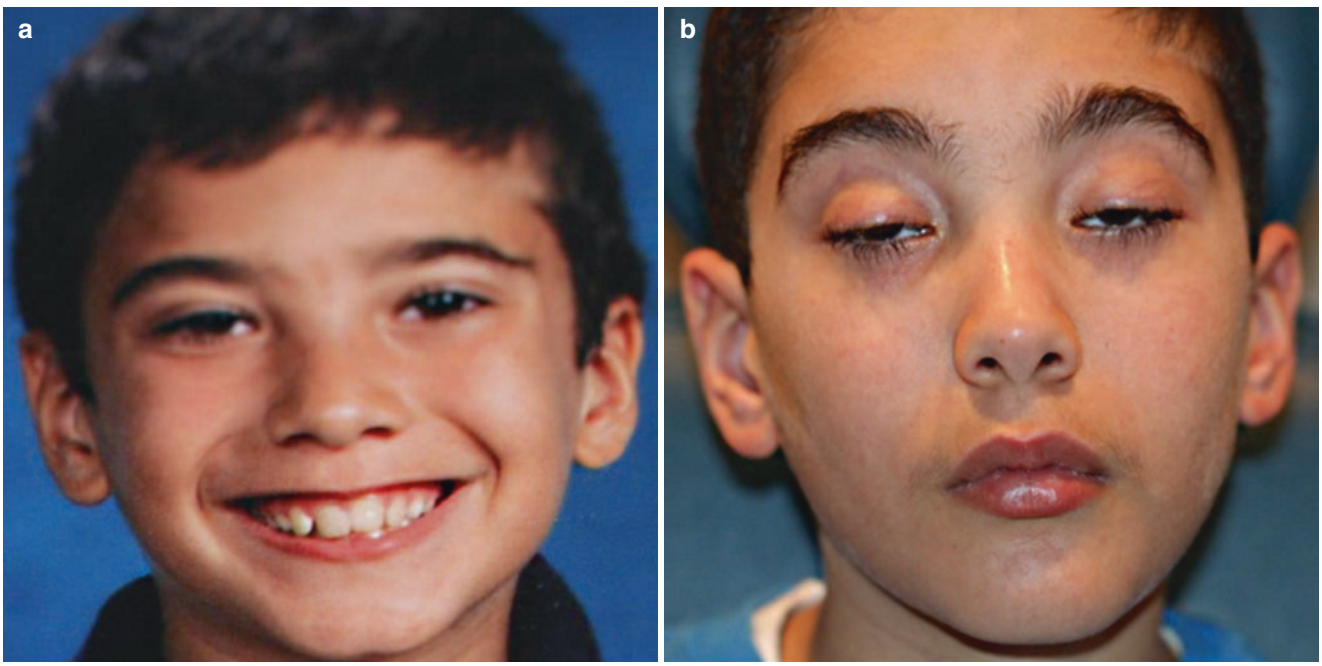


Fig. 22.7 Patient with severe ptosis due to CPEO. (**a**) Photo at age 9 years showing normal eyelid levels with no ptosis or motility limitation. (**b**) Photo of the same patient 2 years later at age 11 after rapid onset of this mitochondrial disorder with severe ptosis and head tilt.

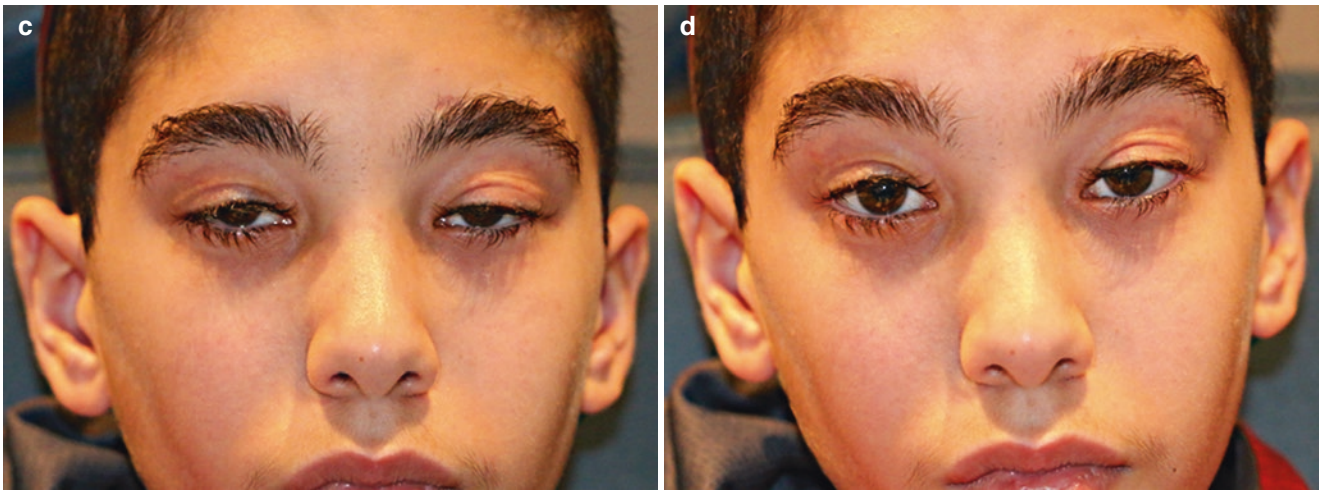


Fig. 22.7 (continued) (**c**) 6 months post-op bilateral silicone frontalis slings, purposely under-corrected with brows relaxed, but no head. (**d**) Same day at 4 months post-op with use of frontalis muscles for brow elevation

mised. Diseases of the mitochondria appear to cause the most damage to cells of the brain, heart, liver, skeletal muscles, kidney, and the endocrine and respiratory systems.

Myotonic dystrophy is a multisystem disease associated with weakness of peripheral muscles. It is a trinucleotide repeat, autosomal-dominant disease characterized by an inability to relax (myotonia) and muscle wasting (muscular dystrophy). Myotonic dystrophy type 1 is caused by mutations in the DMPK gene (chromosome 19), while type 2 results from mutations in the CNBP gene (chromosome 3). The specific functions of these genes are unclear. Oculopharyngeal muscular dystrophy is an inheritable form of ptosis that usually does not appear until the fifth decade of life. It presents with a progressive ptosis, weakness of the extraocular muscles, dysphagia, and proximal limb weakness. It can be autosomal dominant or recessive. Genetic testing for GCG trinucleotide expansions in the PABPN1 gene is recommended if this dystrophy is suspected.

Finally, thyroid eye disease, while usually associated with proptosis, eyelid retraction, and, less commonly in children, strabismus, can rarely present as a myogenic ptosis due to inflammatory infiltration of the eyelid retractors. Figure 22.8 depicts a 17-year-old patient with thyroid eye disease and acquired myogenic ptosis.

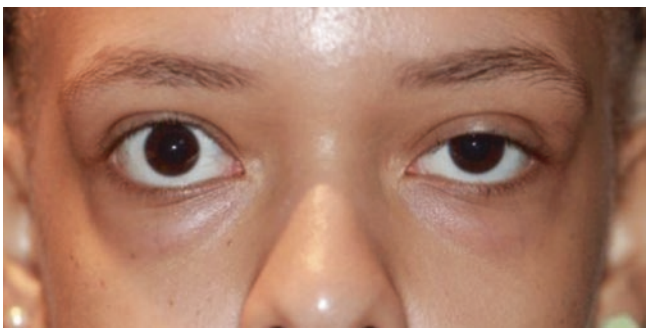


Fig. 22.8 A 17-year-old patient with left upper lid ptosis due to thyroid eye disease



Fig. 22.9 Aponeurotic ptosis. Ptosis of the left upper lid with higher lid crease on the affected side

Aponeurotic Ptosis

Aponeurotic ptosis, in contrast to the myogenic form, is thought to be caused by a defect in the tendon that may lead to ineffective transmission of the force generated by the contracting levator muscle. Since the levator muscle itself is healthy, this type of ptosis is characterized by normal levator function. The amount of ptosis can be variable, but a dehiscence or disinsertion of the aponeurosis is usually accompanied by a higher than normal lid crease (Fig. 22.9). Although this type of mechanism is most commonly associated with involutional ptosis in elderly patients, it can also be observed in children who either have a developmental defect or have suffered trauma such as forceps injury during birth.

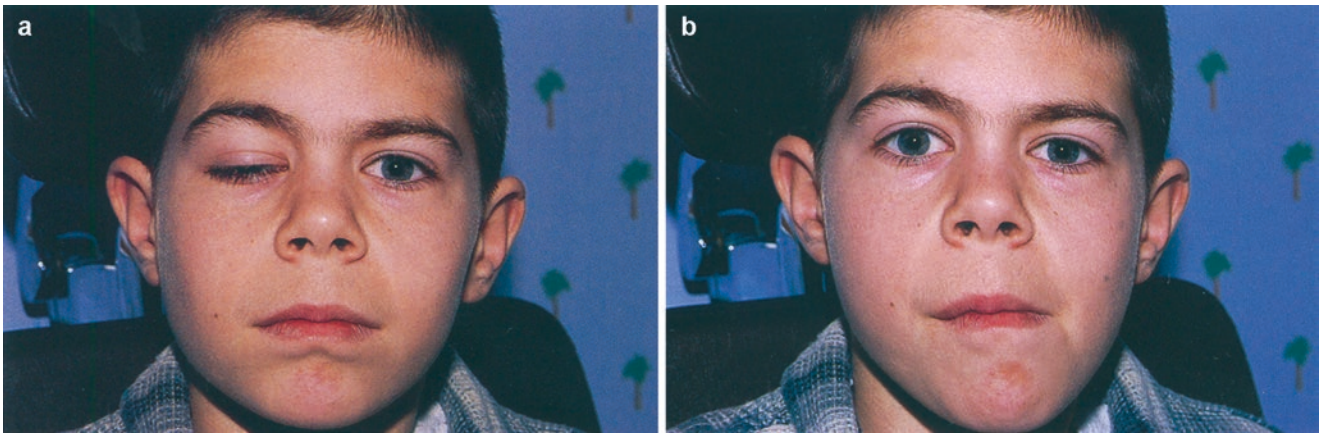


Fig. 22.10. Marcus Gunn jaw-winking ptosis. (**a**) Ptosis of the right upper lid; (**b**) elevation of the right upper lid when the mandible moves to the opposite side

Neurogenic Ptosis

Defects in innervation occurring during embryonic development can lead to neurogenic types of ptosis. Abnormal or synkinetic connections can occur between the third and fifth cranial nerves, producing a Marcus Gunn jaw-winking type of ptosis. An isolated defect of the third cranial nerve can lead to a congenital third-nerve palsy or paresis. Abnormalities involving parasympathetic innervation produce a congenital Horner syndrome. The latter two entities can also be acquired during childhood, usually secondary to trauma or tumor.

Marcus Gunn jaw-winking ptosis is fairly common, accounting for approximately 2–13% of congenital ptosis cases [13–15]. This type of ptosis is characterized by elevations of the lid coinciding with sucking or chewing movements (Fig. 22.10). The lid usually elevates when the internal and external pterygoid muscles move the jaw from side to side. Maximum elevation seems to occur most frequently when the jaw opens and the mandible moves to the side opposite the ptosis. Marcus Gunn ptosis occurs almost always unilaterally, more frequently on the left, and is usually sporadic without an inherited pattern. Some authors have reported that the condition improves with age [15, 16], but, more than likely, improvement results from learned behavior and better control of the lid's fluctuating position. Surgical intervention may also be a reason that this synkinetic phenomenon is seen infrequently in the adult population. We have personal experience with one patient who has had persistent jaw winking into her middle-aged years.

Congenital third-nerve palsies are rare. A complete third-nerve palsy is characterized by complete ptosis, a dilated nonreactive pupil, absent elevation, depression, and adduction of the eye on the involved side (Fig. 22.11). The palsy can also be partial, with varying degrees of dysfunction of the lid, pupil, and rectus muscles. Congenital third-nerve palsies are rarely associated with aberrant regeneration. In such instances, the ptotic lid may be seen to elevate on attempted elevation, depression, or adduction of the globe (Fig. 22.12). In contrast, acquired third-nerve palsies are more frequently associated with aberrant regeneration.

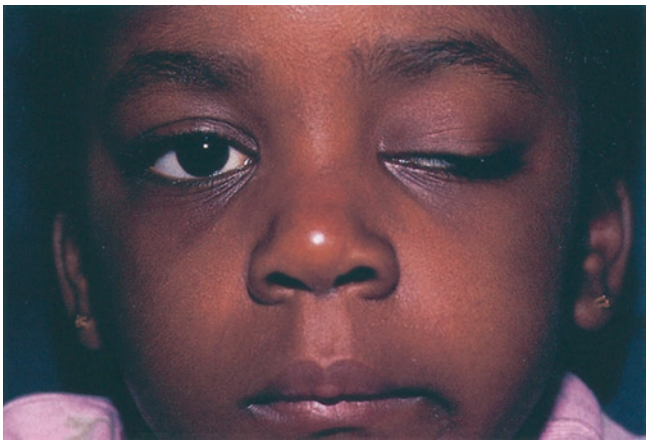


Fig. 22.11 Congenital third-nerve palsy. Complete ptosis associated with depression and abduction of the globe

Congenital Horner syndrome is caused by a disruption in parasympathetic innervation producing the classic triad of ptosis, miosis, and anhydrosis. One to 3 mm of ptosis of the upper lid is present, along with 1–2 mm of inverse ptosis of the lower lid. In addition to a small pupil that fails to dilate, a decrease in pigmentation of the iris on the involved side can also occur (Fig. 22.13). Heterochromia is more characteristic of the congenital form of Horner syndrome and thus can be useful in differentiating congenital cases from those that are acquired. The differentiation between cases is very important, in that any Horner syndrome acquired in childhood must be carefully evaluated for a potential tumor affecting the sympathetic pathway (Fig. 22.14). Rarely, neurogenic ptosis can be associated with an ophthalmoplegic migraine.

Although not truly a neurogenic cause, myasthenia gravis can also lead to ptosis in the pediatric age group. Myasthenia gravis may manifest by an increasing degree of

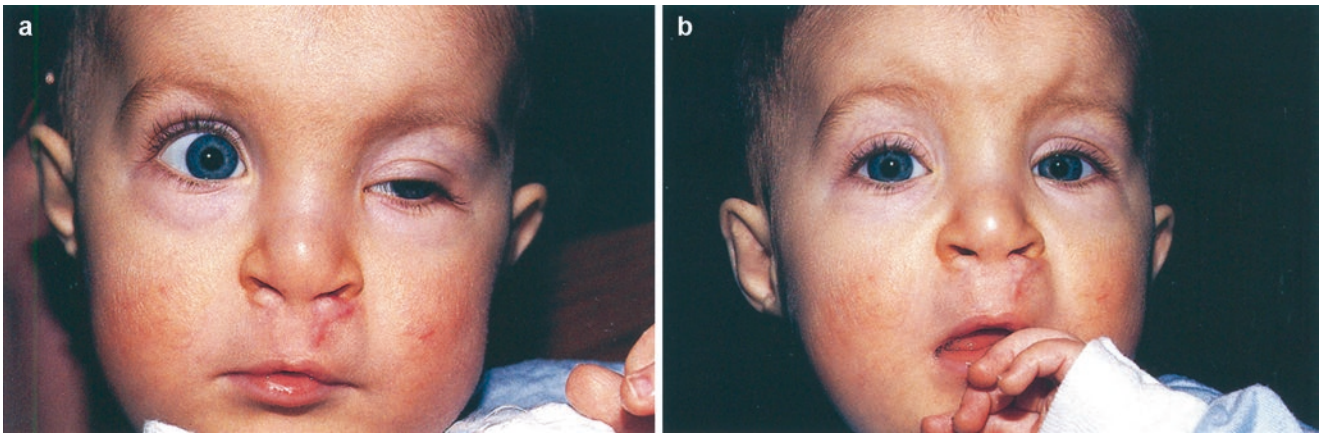


Fig. 22.12 Bilateral congenital third-nerve palsies with aberrant regeneration. (**a**) *Left gaze*: right upper lid is retracted and left upper lid is ptotic. (**b**) *Right gaze*: right and left upper lids assume a normal position

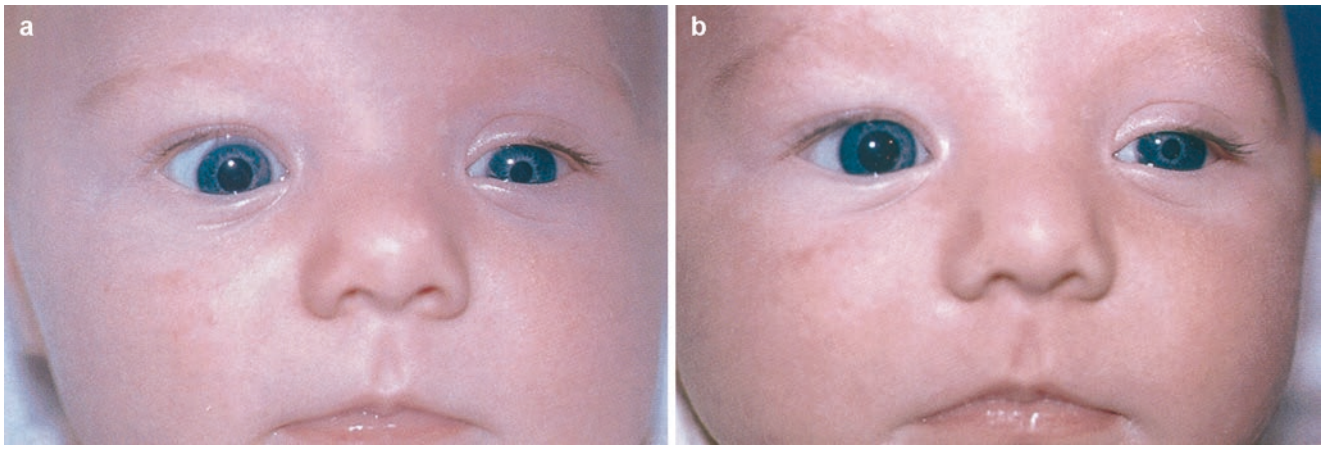


Fig. 22.13 Congenital Horner syndrome. (**a**) Ptosis and miosis in an infant with congenital idiopathic left Horner syndrome. (**b**) After instillation of 10% cocaine into both eyes at 0 and 5 min. When checked 45 min later, the right pupil was dilated, but the left pupil was not (Courtesy of David Kozart)

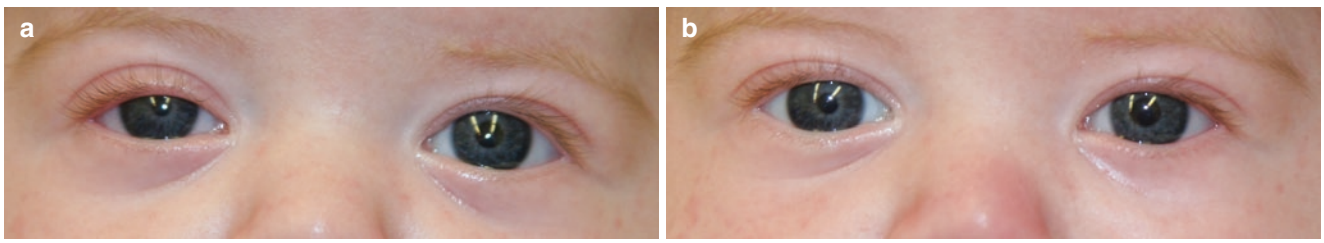


Fig. 22.14 Acquired Horner Syndrome due to a right-sided neck venolymphatic malformation. (**a**) Right-sided ptosis and miosis. (**b**) 2.5% phenylephrine testing: 5 min after one drop in the right eye shows improvement of the ptosis

ptosis as the day progresses; however, simple congenital ptosis associated with fatigue of the frontalis muscle due to prolonged use can also present in this fashion. Associated disturbances of extraocular muscle function are common in myasthenia and are helpful in differentiating these two conditions. Weakness of the orbicularis muscle on forced closure is also a useful sign in children. The Cogan lid twitch is one in-office examination test that can help in the diagnosis of myasthenia gravis. The Cogan lid twitch is elicited by having the patient look in downgaze, followed with upgaze. As the affected eye saccades up, the upper lid overshoots. Another in-office test readily available to the clinician is the ice test. An ice pack is applied to the affected upper eyelid for 5 min. A positive test is the improvement of ptosis by

greater than 2 mm or more. This temporary improvement in ptosis is due to the cold decreasing the acetylcholinesterase breakdown of acetylcholine at the neuromuscular junction. More acetylcholine collects in the junction and therefore increases the muscle contraction.

The serum anti-ACh receptor antibody titer is an assay that measures three different anti-ACh receptor antibodies found in myasthenia. These are the binding antibodies, blocking antibodies, and modulating antibodies. Binding antibodies are present in 85–90% of systemic MG patients and 50% of ocular MG patients. When binding antibodies are negative, blocking and modulating antibodies are then tested.

The challenge to this test, however, is that 10–15% of patients with systemic MG will test negative, as will 30–50% of patients with ocular MG. If the suspicion for MG remains high despite normal Ach receptor testing, MuSk assays can be tested [17].

Finally, if laboratory testing remains negative, the Tensilon test plays a very important role in diagnosing myasthenia in pediatric patients. The Tensilon test is most reliably performed by a neuro-ophthalmologist, but this may not always be practical. For patients weighing less than 30 kg, an intravenous dose of 0.15 mg/kg of edrophonium chloride is recommended. Twenty percent of the dose is initially injected, and the eyelid position is reevaluated at 1 min. If the eyelid position is unchanged, then an additional 40% of the dose is injected. This can be repeated once more if no effect is observed. Atropine (0.4 mg) for intravenous injection should be readily available to treat any significant cholinergic side effects. As an alternative test to intravenous administration of edrophonium, neostigmine methylsulfate can be given intramuscularly (the Prostigmin test). The recommended dose is 0.04 mg/kg, not exceeding a total dose of 1.5 mg (the adult dose). The neostigmine is injected along with atropine, and after 30–45 min, the eyelid position is reassessed. The obvious advantage of this method of testing is that by the time the Prostigmin has taken effect, the child is more likely to have stopped crying and is more easily observed. Regardless of the method of testing, however, if the ptosis is temporarily reversed, a diagnosis of myasthenia is confirmed, and treatment under the direction of a neurologist is then essential. Antibody tests and single-fiber electromyography can also be helpful in ruling out a diagnosis of myasthenia gravis.

Mechanical Ptosis

Mechanical ptosis is most commonly caused by the inability of the levator muscle to function properly due to the weight of a tumor mass, foreign body, or soft tissue swelling (Fig. 22.15). Although the levator muscle and aponeurosis are usually normal, these structures may become infiltrated by the disease process. Infantile hemangiomas and plexiform neurofibromas, which are commonly responsible for mechanical ptosis in children, are notorious for infiltrating the levator muscle complex and making simple excision difficult. Cicatricial processes secondary to trauma can also mechanically restrict the eyelid in a ptotic position even with an otherwise normally functioning levator.

Traumatic Ptosis

Traumatic ptosis can be considered congenital if the injury is presumed to have occurred in utero, secondary to amniocentesis, for example, or from injury during the birthing process. Congenital ptosis that is presumed to be traumatic in origin must be differentiated from the true myogenic form.

While traumatic ptosis can be due to any of the four pathophysiologic mechanisms described above, it may be difficult to identify the exact cause immediately following injury (Fig. 22.16). In some instances, such as a forceps or scissors injury occurring during birth, the cause may be immediately evident and early repair of the laceration is appropriate. For most cases of traumatic ptosis, however, the etiology is less clear. For this reason, it is important that such



Fig. 22.15 Left upper lid infantile hemangioma causing mechanical ptosis



Fig. 22.16 Traumatic ptosis. Acute onset of ptosis in a 3-year-old whose head was run over by the wheel of a car

patients be observed for at least 6–12 months prior to surgical repair, unless the threat of amblyopia mandates earlier intervention. With time, the amount of ptosis may improve sufficiently, or at least the etiology may become more apparent so that the appropriate surgical procedure can be selected.

In cases of penetrating trauma, a clue may be present as to the exact cause of the ptosis. If orbital fat is exposed in the wound, the underlying levator muscle is very likely to have been lacerated. Figure 22.17 depicts such a case. The presence of orbital fat warrants immediate exploration of the wound and repair of the lacerated levator muscle if necessary. While accidental trauma is most common, iatrogenic cases of ptosis can occur secondary to orbital, vascular, strabismic, or craniofacial surgical procedures. In general, if the threat of amblyopia can be successfully managed with occlusion therapy, surgical intervention should be delayed for the recommended 6–12 months, because many of these cases will spontaneously improve.



Fig. 22.17 Left traumatic ptosis due to an upper eyelid laceration with fat prolapse



Fig. 22.18 Right microphthalmos causing a pseudoptosis of the right upper lid

Many cases of apparent ptosis are not due to an actual abnormality in the eyelid but rather to other orbital, adnexal, or ocular problems. Identifying the true etiology is critical to assure proper correction of the problem. Pseudoptosis must be differentiated from true ptosis and can occur secondary to a number of conditions, including microphthalmos, anophthalmos, enophthalmos, phthisis bulbi, hypertropia, as well as eyelid inflammations, or infections (Figs. 22.18 and 22.19).

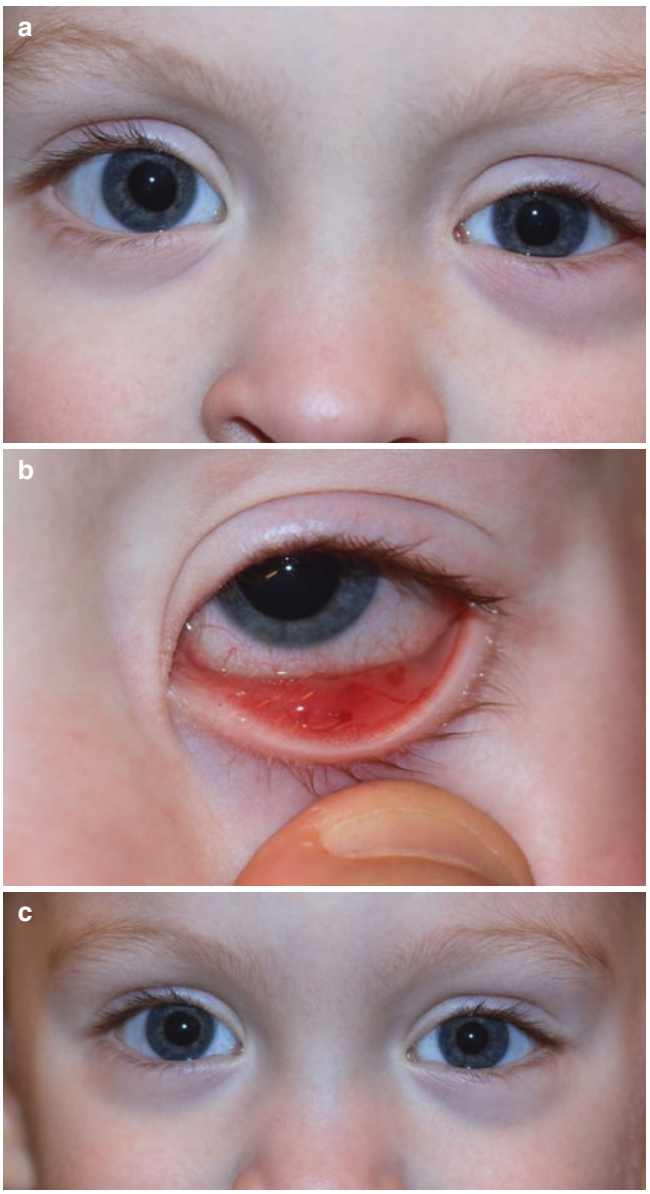


Fig. 22.19 (**a**) Acute onset left ptosis. (**b**) Membranous conjunctivitis is cause of droop. (**c**) Resolution of left ptosis is seen 3 weeks after topical steroid drops

Common Causes of Pseudoptosis

1. Contralateral eyelid retraction
2. Facial asymmetry (e.g., plagiocephaly)
3. Contralateral proptosis
4. Enophthalmos
5. Eyelid inflammation (e.g., conjunctivitis with or without membranes or pseudomembranes)
6. Microphthalmos, anophthalmos, or nanophthalmos
7. Phthisis bulbi
8. Anisometropia (with smaller eye being more hyperopic or less myopic)
9. Vertical strabismus

Clinical Evaluation

One of the more challenging aspects of managing congenital ptosis is obtaining adequate data upon which to base the surgical plan. Unlike most patients, children cannot be expected to fully cooperate, and thus accurate measurements cannot always be obtained. For this reason, taking a thorough history and observing the patient, often at a distance during play, are essential components of the evaluation. Obviously, if any measurements are obtainable, they are a welcome addition to the clinical assessment.

History

The ptosis evaluation should begin with a thorough history. Was the ptosis present at birth or acquired shortly thereafter? Has it improved, been stable, or worsened over time? Acquiring the details of the child's delivery is important in assessing the possibility of traumatic injury during the birthing process. Any illness or hospitalization should also be noted to rule out diseases, disorders, or syndromes that can be related to the presence of ptosis. A review of developmental milestones should also be obtained. Prior surgical interventions must be documented, particularly craniofacial procedures or other ophthalmic procedures. A family history may uncover an inherited type of ptosis.

A careful history can be extremely useful in revealing the clinical characteristics of a child's ptosis. The parents can frequently describe the degree of the ptosis and whether it appears to interfere with the child's vision. In today's age of smartphones, it is best to ask if the parents have any pictures to document severity and age of onset. They may notice the effort to elevate the lid with arching of the brows or the adoption of a chin-up head position. The variability of the ptosis should also be addressed. Is the ptosis constant, or does the lid level change over the course of the day? Is there evidence to support a synkinetic mechanism? Parents may note fluctuations in lid position while feeding their child. Although very rare, myasthenia gravis can cause congenital ptosis, and, as mentioned earlier, a variability in the degree of ptosis that markedly worsens toward the end of the day should alert the physician to this possibility. On the other hand, many parents will report an increase in the degree of the droop as the day progresses in cases of myogenic ptosis. This is particularly common in cases of severe myogenic ptosis and is related to fatigue of the brow from an attempt to elevate the lid. This same mechanism is also responsible for the increased droopiness present during illness and sleepiness.

Observation

As discussed earlier, observation becomes one of the strongest tools for examining young patients. As one obtains the history from the parents, one can also gather important clinical information by simply watching the child from a nonthreatening distance. If the child is distracted or disinterested, playful interactions can also be effective in capturing his/her attention. Such characteristics such as the degree of the ptosis, the use of the frontalis muscle, the adoption of a chin-up head position, the variability of the lid position, and the presence of strabismus can all be assessed without touching or frightening the patient.

Physical Examination

All examinations of pediatric patients with ptosis must include a careful assessment of visual function. Certainly one of the most potentially devastating sequela of a ptotic lid is amblyopia. Although more formal measurements of visual potential using pattern recognition cards, HOTV, Allen cards, and Snellen letters are ideal, they are not always obtainable in children (see Chap. 10). The clinician must frequently rely on clinical observations such as whether a fixation preference is present. The 10-prism diopter test can be very helpful in detecting moderate to severe amblyopia in the eye on the side of the ptosis. The best visual assessment for preverbal and nonverbal patients is Teller visual acuity measurement, which can be obtained as early as 3 months of age. This form of preferential gaze testing is very effective in identifying the presence of amblyopia and is covered in detail in Chap. 10.

Examination of the size and reactivity of the pupils is important from the standpoint that pupillary involvement can indicate an innervational etiology for the ptosis (i.e., third-nerve palsy or Horner syndrome). Similarly, a motility examination must be performed to identify any accompanying superior rectus weakness or any other type of strabismus.

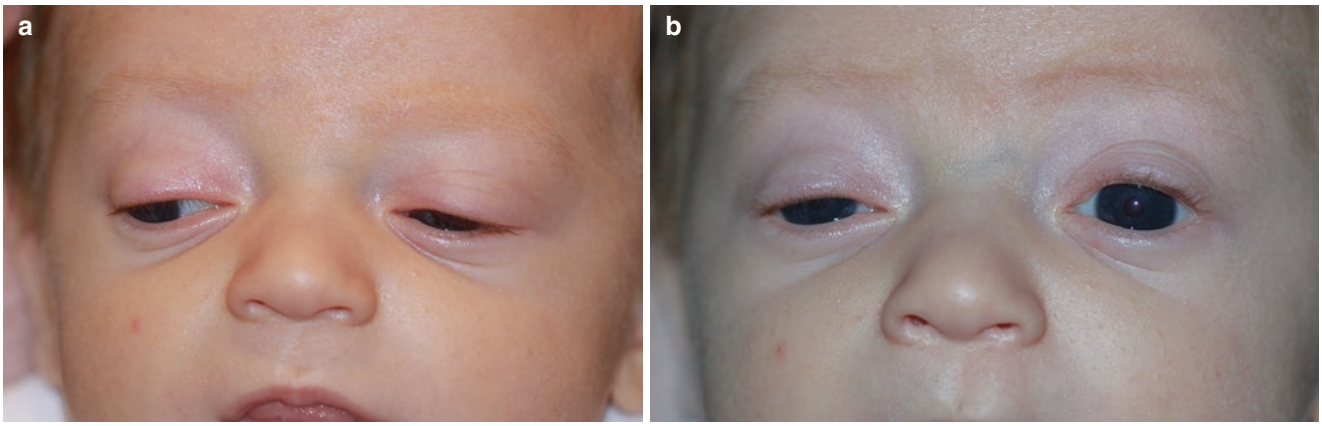


Fig. 22.20 Eye-popping reflex. (**a**) A newborn with right ptosis that is not appreciable. (**b**) Photo taken immediately after turning out the room lights exhibits the infant's eye-popping reflex and uncovers the right congenital ptosis

A normal Bell's phenomenon should be documented, if possible. The ability to elevate the globe, at least to some degree, is crucial both for protection of the globe and for proper tear film exchange over the cornea. The degree of lagophthalmos and exposure as well as the quality of tear film exchange following ptosis surgery are central concerns and are significantly influenced by the ability of the globe to elevate upon forced closure of the eyelids. A poor Bell's phenomenon can alert the clinician to more strongly consider the use of a temporary suture tarsorrhaphy or lower lid traction suture for corneal protection during the first few days following ptosis repair.

Often newborns, when seen in the office, are sleeping. Even after arousal, infants may remain somnolent. A great examination tool is to elicit the eye-popping reflex. This is where a newborn will open his or her eyes when the room lights are dimmed or turned off [18]. Figure 22.20 depicts a newborn with ptosis before and after turning off the room lights.

As for the external examination, one should attempt as many routine preoperative ptosis measurements as reasonably possible. In young children, only estimates performed at a distance may be obtainable, but even these can be of real practical value. The margin reflex distance (MRD_1) is most useful in that it measures the distance of the upper lid margin from an apical light reflex at the center of the cornea. This measurement is the most accurate method for assessing the degree of ptosis in that it is solely indicative of upper lid position and is not influenced by the position of the lower lid. In contrast, measurement of the vertical fissure height (VFH), the distance from the upper lid margin to the lower lid margin, is always affected by the lower lid position. The MRD_1 can easily be estimated by recognizing that the vertical dimension of the cornea is approximately 10 mm, and the apex of the cornea, therefore, centers a scale of 0 to +5 mm at the superior limbus and 0 to −5 mm at the inferior limbus. The normal MRD_1 in children is approximately +4.0 mm,

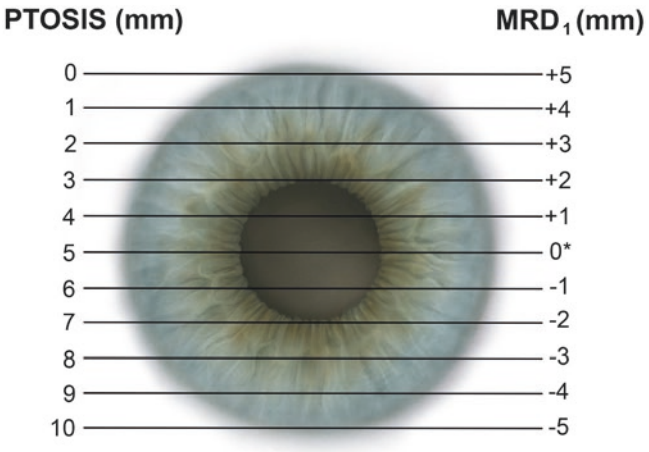


Fig. 22.21 Schematic comparing ptosis (in mm) to MRD_1

Table 22.1 Classification of ptosis based on millimeters of eyelid droop compared to MRD_1

Amount of ptosis	Millimeters of droop (from normal level)	MRD_1
Mild	≤2 mm	3
Moderate	3 mm	2
Severe	≥4 mm	≤1

but some people have an MRD closer to 3 at rest. If the ptosis splits the visual axis, the MRD_1 is 0, and if the lid goes below the center, then negative numbers apply (Fig. 22.21). MRD_2 refers to the position of the lower lid margin in relation to the apical light reflex. In practical terms for ptosis, the MRD_1 is really the most valuable measurement (Table 22.1).

When measuring either the MRD_1 or VFH, the effect of brow arching should be documented. Additionally, in some cases of what seems to be unilateral ptosis, the opposite eyelid may appear to be in a normal position while it is actually ptotic. This opposite eyelid appears "normal" as a result of the action of the frontalis muscle, which is elevating both upper lids. If the fron-

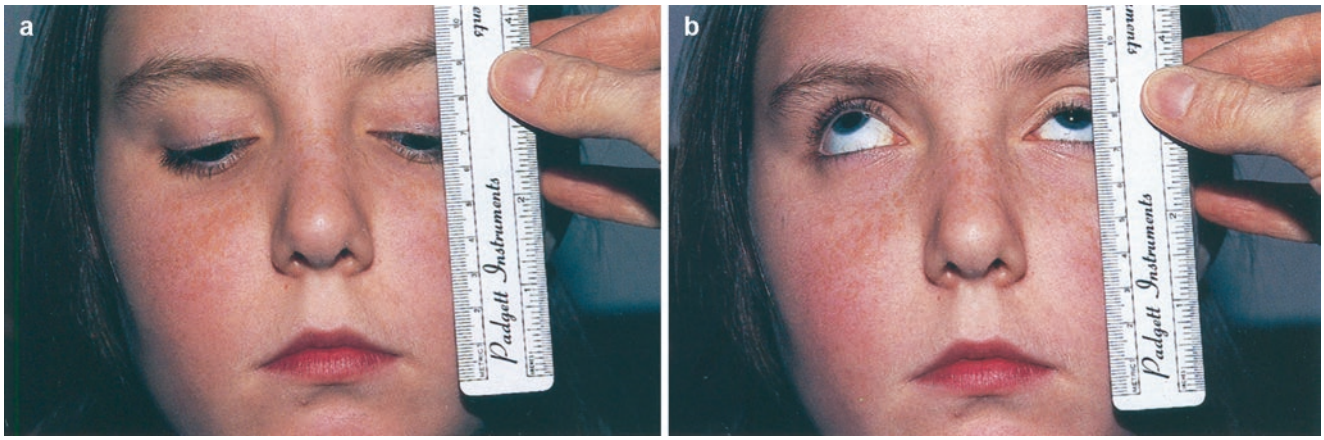


Fig. 22.22 Assessment of levator function. Levator function is assessed by measuring the levator excursion, which is the distance in millimeters that the eyelid margin moves from (**a**) downgaze to (**b**) upgaze

talis muscle is relaxed, then the ptosis of the "normal" side will be unmasked. This variation of Hering's law also has application in regard to levator function. A child may appear to have unilateral ptosis, when, in fact, overstimulation of the affected levator muscle is accompanied by overstimulation of the levator on the opposite side. If not recognized, this can also mask a true ptosis on the less affected side. Failure to identify the bilateral nature of such problems prior to surgery may lead to a less than desirable cosmetic result or even concerns from the patient's family that a "new" ptosis was caused by the surgery.

In addition to the MRD_1 and VFH, the position of the lid crease should be assessed. The distance of the crease from the central aspect of the lid margin is measured in millimeters as the lid is positioned in downgaze. This measurement is most important in cases of unilateral ptosis, since the surgically created lid crease should match the crease on the opposite side.

Although all of the previously described measurements are important, the most essential measurement is the amount of levator function present (Fig. 22.22). This measurement will most significantly influence the decision as to which surgical procedure is most appropriate. If possible, the frontalis muscle should first be immobilized by fixing the brow with a thumb. The position of the lid margin in extreme downgaze is then noted on a ruler held next to the eyelid, and the patient is then asked to look up to the ceiling. The distance that the lid margin travels in millimeters is termed the levator excursion and is indicative of the degree of levator function present. When examining young infants, one may obtain the same information by fixing the brow and moving a toy in an arc that leads the infant's eyes from downgaze to upgaze. The amount of levator function can be classified as poor if it is 4 mm or less, fair if 5–7 mm, good if 8–12 mm, and excellent if 13 mm or more [19] (Table 22.2).

In addition to obtaining the above measurements, the ptotic eyelid should be assessed for its response to phenylephrine and for the presence or absence of synkinetic movements, lid lag, or lagophthalmos. Five minutes following the instillation of a single drop of 2.5% phenylephrine to the eye on the ptotic side, the MRD_1 should be remeasured. Phenylephrine 10% should be avoided in all patients due to the risk (though remote) of systemic complications [20]. The degree to which the lid position responds to the phenylephrine is an essential factor in the determination of the proper surgical procedure. If the eyelid responds well, then an internal approach procedure involving shortening of Müller's muscle may be considered for the ptosis repair. Phenylephrine can also increase the VFH, not only by lifting the upper lid but also by contraction of the smooth muscle in the lower lid, causing a change in the MRD_2. This further emphasizes the importance of MRD_1 over VFH in planning for repair.

Table 22.2 Classification of levator function

Levator function	Eyelid excursion
Excellent	≥13 mm or greater
Good	8–12
Fair	5–7 mm
Poor	≤4 mm or less

The response of the opposite eyelid to unilateral instillation of phenylephrine to the more affected side is also important (Fig. 22.23). As discussed earlier, Hering's law may be responsible for masking a ptosis of the opposite eyelid. If the ptotic eyelid responds to phenylephrine and elevates out of the visual axis, the need for levator muscle contraction will then become less, and, as a result of Hering's law, the reduction of levator stimulation will occur on both sides. In such instances, the opposite eyelid, if ptotic to any degree, may have appeared normal before phenylephrine elevated the eyelid on the more severely affected side. This "normal" side will now drop to a lower and sometimes truly ptotic position. This information is important not only to alert parents to the

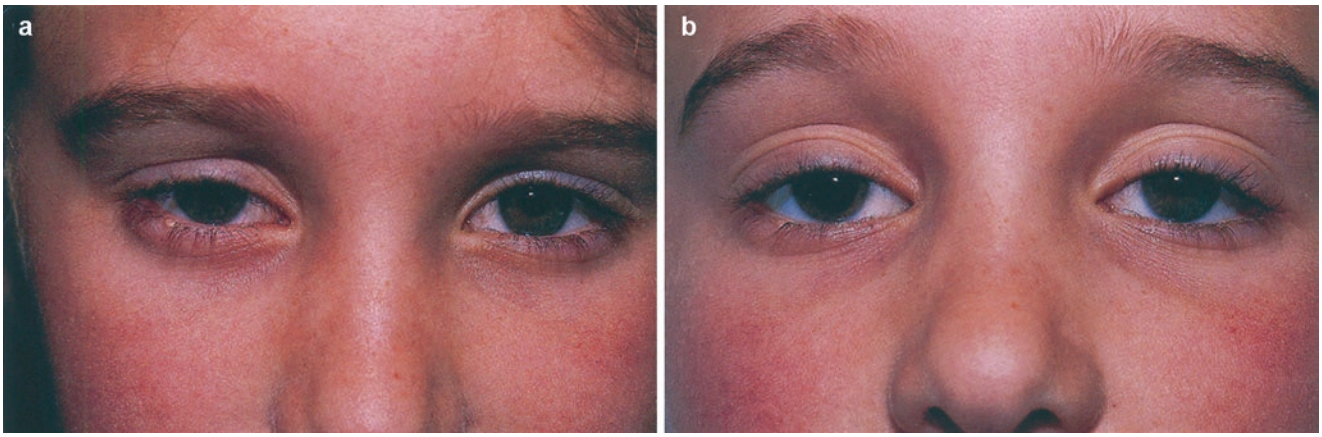


Fig. 22.23 Phenylephrine test. (**a**) Prior to instillation of phenylephrine, the right upper lid is ptotic while the left is in a normal position. (**b**) Following the instillation of phenylephrine, the right upper lid level becomes higher. In this example the left lid also becomes lower as there is less need for the levator muscle to contract of both sides (Hering's law), thus unmasking a latent ptosis

possibility of such a phenomenon occurring postoperatively but also to raise the possibility of the need for bilateral surgery. By using the phenylephrine test to demonstrate the bilateral nature of their child's problem, parents can thus be better informed and more prepared to participate in any decision regarding unilateral versus bilateral repair.

The synkinetic movements associated with the Marcus Gunn type of ptosis can usually be elicited by giving the infant a bottle, food, or a pacifier. As the infant sucks or chews, variations in the eyelid position are assessed. If synkinetic movements are present, the surgical plan must specifically consider this issue.

The presence of lid lag or lagophthalmos is most helpful in clarifying the etiology of the ptosis. If the ptotic eyelid becomes the higher lid upon excursion from upgaze to downgaze, then lid lag is present. The presence of this finding is particularly characteristic of the myogenic type of congenital ptosis and is due to the fibrotic nature of the levator muscle. Similarly, in the absence of a history of trauma, the presence of lagophthalmos upon gentle eyelid closure also implies a myogenic mechanism. In such instances the cornea will usually be exposed while the child sleeps even prior to surgical intervention. In some cases of congenital ptosis, in addition to the fibrotic nature of the muscle, a vertical shortening of eyelid skin may also contribute to lagophthalmos. Many of these patients also have abnormalities of the orbital septum that become apparent only at the time of surgery.

Since all of these measurements and assessments are potentially difficult in children, we document the position of the eyelids with digital photography. Even when lack of cooperation limits the thoroughness of the external examination, usually at least a few photographs can still be taken. These photographs are frequently useful in supplementing the recorded clinical information, which may have been difficult to obtain during the office examination. In this fashion an appropriate surgical procedure can more confidently be selected. Even when accurate measurements are obtainable, a photograph is always helpful in providing additional information and serving as an available reminder during the operative procedure. In addition, for the proof of medical necessity, clinical photographic documentation of clinically significant ptosis is required by many insurance companies.

Once the external examination is completed, an upright slit-lamp evaluation should be performed on those patients old enough to cooperate. If necessary a hand-held slit-lamp can be used. The quality of the tear film should be assessed, and the cornea should be examined for signs of exposure. Frequently, however, a standard slit-lamp evaluation is impractical, thus forcing one to modify the examination technique. Similar to the technique adopted for a dye disappearance test, fluorescein is instilled in both eyes, and the cobalt blue filter light of the slit lamp is used from a nonthreatening distance of 3–4 ft. to allow at least some assessment of both the tear film and corneal surface. In older children, both a measurement of the tear breakup time (TBUT) and a baseline tear secretion test (BTST) with topical anesthetic can be performed to evaluate basic tear function. Normal corneal sensitivity should also be documented if possible. Normal TBUT is >10 s, and a normal BTST should be >10 mm of wetting the filter paper strip.

Cycloplegic retinoscopy is mandatory for all pediatric patients with ptosis. A significant incidence of with-the-rule astigmatism occurs secondary to the weight of the ptotic lid against the globe [21]. If a sizable refractive error is uncovered, spectacle correction may be required [22]. Most importantly, a significant refractive error should alert the clinician to the possibility of amblyopia, which demands carefully monitoring. The current practice patterns for the treatment of refractive errors in children can be found on the American Academy of Ophthalmology website [23]. Occlusion therapy

should be initiated for any patient demonstrating signs of amblyopia. In addition, for infants and very young children with unilateral ptosis, we often recommend patching the normal eye for 0.5–1 h a day as an "insurance policy" against the development of amblyopia, even for those patients who appear to have equal vision in both eyes. A dilated funduscopic examination should also always be performed to complete the evaluation.

Surgical Treatment of Congenital Ptosis

Although most experienced clinicians would agree that surgery is indicated for a 4-month-old infant with severe ptosis and visual deprivation, controversy still exists as to when elective surgery should be performed in young patients without amblyopia. Traditionally, most textbooks have recommended that surgery be delayed until around the age of 5 years, just prior to the child's entering school. It has been argued that better measurements can be obtained when the child is older and that eyelid anatomy is better defined, thereby allowing the surgeon to achieve more satisfactory results [24–26].

Our approach has been different, however, and, while possibly appearing more radical, has consistently yielded satisfying surgical results from an appearance standpoint as well as good visual outcomes. In general, we recommend that most elective ptosis repairs be performed at approximately 1 year of age unless there is a major threat of visual deprivation (i.e., severe ptosis) requiring earlier intervention. We prefer to defer surgery until the infant is at least 3–6 months old to avoid any added risk of general anesthesia (see Chap. 5). We feel that more than adequate clinical information can be obtained even in the youngest of patients, and we have not found any limitations associated with operating on smaller anatomic structures. We also believe that by operating when patients are very young, we can reduce the emotional trauma often experienced by older children when they must come to the hospital for surgery. This approach is also beneficial for parents, since younger children are easier to manage postoperatively, particularly when applying lubricating drops or ointments for corneal exposure. Most importantly, however, we have found that young children are able to proceed more normally with visual, motor, and social development once their ptosis has been corrected.

Ptosis can interfere with motor development by forcing infants with severe eyelid droop to adopt a chin-up head position to clear the visual axis on the affected side. Although this head position is probably protective in regard to amblyopia, it has the potential to detrimentally affect the learning process of walking as well as putting stress on the cervical spine. In addition, a child's psychosocial development as he or she interacts with family and friends is significantly influenced by his/her appearance. Children are now exposed at early ages to group interactions at both nursery schools and day care centers, and young children are often very observant and vocal about anything abnormal in another child's facial appearance. A ptotic eyelid may draw comments that have a negative impact on the social interactions for both the child and his or her family. It is not uncommon for parents to inform us regarding negative comments such as their child being call a "pirate" at school by other children. This can lead to a child feeling alienated or actually being ostracized. By promoting early surgical intervention, we are able to relieve the parents and other family members of unwarranted social pressures and also influence a child's developing sense of self in a positive fashion. While writing this chapter and reviewing the literature for our first edition of this book in 2001, we discovered that Matthews in 1969 had recommended a similar approach for early ptosis repair based on a large pediatric ptosis series [27].

Even given the advantages stated above, we certainly would not promote earlier intervention if the results were not at least as satisfactory as those achieved with surgery delayed to prekindergarten age. Fortunately, excellent outcomes have been well documented in our experience. We are always careful, however, to discuss all the risks and benefits regarding timing and the choice of surgical procedure with the parents (or responsible guardian) and to inform them that ptosis repair is an elective procedure, unless there is a documented risk of significant amblyopia that requires early repair.

Choice of Operation

Once the decision to operate has been made, the surgeon must then select the procedure that will achieve the best result with the least risk of complications. Surgical procedures can be divided into two mechanistic categories: (1) use of anatomic structures *within the eyelid* that participate in the lifting force of the levator muscle and (2) use of structures *outside of the eyelid* that can assist in lid elevation. The first category can be further divided topographically into internal (posterior) and external (anterior) approaches. While the internal approach can be used for levator surgery, our preference is to use this for procedures involving some form of Müllerectomy. We prefer the external approach for aponeurotic advancement and/or levator resection. The second category is really limited to frontalis suspensions. Frontalis suspensions (or slings) can be performed with synthetic materials or with autogenous or preserved fascia lata. The advantages and disadvantages of these materials will be discussed later in this chapter. Although superior rectus surgery has been advocated in the past, such procedures are no longer recommended due to severe corneal exposure problems

Table 22.3 Selection of ptosis repair based on response to phenylephrine

Response to phenylephrine	Surgical procedure
Good (MRD_1 = 4–5)	Putterman Müllerectomy or modified Fasanella-Servat
Moderate (MRD_1 = 3)	Graded modified Fasanella-Servat or Werb procedure (i.e., graded Müllerectomy with tarsectomy)
Poor ($MRD_1 \leq 2$)	Levator surgery or frontalis suspension

Note: The degree of pre-op levator function is not critical in procedure selection if response is good-moderate

related to the inability of the upper lid to move over the corneal surface with ocular movements.

A systematic approach to the selection of surgical procedures for pediatric ptosis repair is essential for assuring the best possible results. We have developed specific guidelines based on over 50 years of clinical experience to assist in the selection process, but it is important to recognize that every case of pediatric ptosis is unique in character.

Although, traditionally, most surgeons have relied predominantly on levator function to guide their selection of surgical procedures, we have incorporated the results of the phenylephrine test into our decision-making. If the response to 2.5% phenylephrine achieves the desired postoperative MRD_1, then regardless of the degree of ptosis or the amount of levator function, an internal approach consisting of a Müllerectomy with or without tarsectomy is strongly considered. If the response is inadequate, then either an external approach procedure or a frontalis suspension must be selected, based on the amount of levator function present (Table 22.3). In cases of high-risk ptosis, such as third-nerve palsies, CPEO, double elevator palsy, or CFEOM, a minimal (or functional only) improvement in ptosis may be desirable due to the risk of corneal exposure. This may be performed by the undercorrection with a sling or some form of Müllerectomy.

Myogenic Ptosis

The process of selecting the most appropriate surgical procedure for cases of myogenic ptosis begins with the assessment of the patient's response to topical phenylephrine. We routinely use 2.5% phenylephrine for most patients. Although a higher concentration of phenylephrine 10% does actually stimulate Müller's muscle to a greater degree, the difference in response to the two drops does not appear to be enough to affect the surgical decision, and the 2.5% concentration greatly reduces the risk of systemic involvement [28]. In general, the height of the lid 5 min following the instillation of 2.5% phenylephrine can be duplicated with resection of the sympathetic muscle of Müller through an internal approach. Contrary to popular belief, Müllerectomies need not be limited to only those patients with 2 mm of ptosis or less [29, 30]. The response to phenylephrine is, in fact, often unrelated to the amount of levator function present. In some cases where only a fair amount of levator function is present (5–7 mm), the ptotic lid's response to phenylephrine may still be excellent, and a Müller muscle resection rather than a levator resection will result in a satisfactory correction with less potential for complications.

We believe that Müllerectomies are able to achieve a significant amount of eyelid elevation due primarily to the anatomical relationship between Müller's muscle and the levator complex as proposed by Werb [7]. Müller's muscle, through its attachment to the upper border of the tarsus, appears to be the structure most responsible for transmission of the lifting force generated by the contracting levator muscle. In a resting state when the sympathetic nervous system predominates, stimulation of Müller's muscle controls eyelid position by modifying the effect of levator contraction as it is transmitted to the eyelid. As such, fluctuations in sympathetic tone to Müller's muscle, as when one is tired or excited, alter the eyelid level, causing either ptosis or lid retraction, respectively. Similarly, Horner syndrome, which is caused by the interruption of sympathetic innervation to Müller's muscle, is associated with 1–2 mm of ptosis even with a completely normal levator complex. The striated levator muscle is unable to maintain the normal resting position of the eyelid without a normally functioning Müller's muscle. Although we feel that the importance of the role of Müller's muscle in eyelid elevation is too frequently underemphasized, at the same time we certainly recognize the major role played by the levator muscle. The effect of Müller's muscle in voluntary elevation of the lid is entirely dependent on a functioning levator muscle. This is well demonstrated by the situation of a complete third-nerve palsy, which leads to total ptosis regardless of whether Müller's muscle is maximally stimulated.

Due to the anatomical relationships described above, the instillation of phenylephrine stimulates a normal Müller's muscle to contract, which in turn leads to elevation of the eyelid. This response to phenylephrine can be duplicated by surgically shortening Müller's muscle; in essence, the end result is a higher "resting state" upper lid position. Even when poor to fair levator function is present, if the lid responds adequately to phenylephrine, while lid excursions may remain reduced, the upper lid position will nevertheless improve due to "strengthening" of the forces that are transmitted to the tarsus. One of the major advantages of Müller's muscle surgery is the virtual absence of lagophthalmos postoperatively. While this is of greatest importance for the involutional patient with dry eyes, it is still an advantage in the pediatric age group, although the greatest asset of this internal approach is its high degree of predictability with minimal risk. There is some limitation to this technique, however, in the occasional overhang of excess skin that can obscure the lid fold postoperatively. Of course, a blepharoplasty can be

combined with the internal approach if this is recognized as a concern preoperatively.

Müller's Muscle Surgery

Heinrich Müller first described the sympathetic muscle between the levator and the tarsus in 1858. In 1961, the Fasanella-Servat procedure was first described [31]. This involved an internal approach to the upper eyelid retractors. Beard in 1970 described a modified Fasanella involving the removal of tarsus conjunctiva and Müller's muscle [32], and Putterman in 1972 published the procedure with the removal of Müller's muscle and conjunctiva alone.

A number of variations of Müllerectomy procedures have been described over time, but we have predominantly relied on three of these: the Putterman and Werb procedures and a variation of the Fasanella-Servat procedure [7, 33] (see the Surgical Techniques section in this chapter). Putterman's procedure consists of a Müller's muscle-conjunctiva resection alone. He states that this is most useful for minimal degrees of congenital ptosis, and we concur, reserving this mainly for those patients with a good response to phenylephrine and only 2–3 mm of ptosis. We have less consistently achieved the desired result in those patients with more severe ptosis, and we attribute this to the fact that Putterman's procedure involves only a shortening of Müller's muscle without the advancement gained by a tarsectomy.

Both the Werb and the modified Fasanella-Servat procedures combine a Müllerectomy with an advancement of the muscle secondary to the tarsectomy and thus may achieve a greater amount of eyelid elevation. Although the anatomic purist must certainly dislike the idea of tampering with the tarsus, nevertheless both of these procedures have allowed us to more consistently achieve superior results for many patients and particularly those with larger degrees of ptosis who respond adequately to topical phenylephrine. Despite concerns regarding tarsectomy, many respected surgeons, such as Beard and Gavaris, still advocate its use in certain situations [34].

All three Müllerectomy procedures can be graded according to the patient's response to the phenylephrine test (Table 22.3). For those patients who achieve a MRD_1 that is either higher or lower than desired, both the amount of Müllerectomy and advancement can be adjusted. As to which procedure is used for a given patient, again we reserve Putterman's procedure for the mildest degrees of ptosis and the Werb procedure and modified Fasanella-Servat for those with more significant ptosis. In recent years, we have favored our variation of the Fasanella-Servat over Werb's procedure as it is simpler and less time consuming.

In 2012, we presented a consecutive series of 105 cases of modified tarso-conjunctival-Müllerectomies in 96 subjects. The average patient age was 5.82 years with an average follow-up of 6 months. A functional success was defined as a postoperative MRD_1 of 3 mm or greater, while a cosmetic success achieved a relative symmetry to the fellow eyelid of 1 mm or less as well. In this series, we achieved a functional success of 97% (102/105 cases) and cosmetic success in 93% (97/105 cases). The average MRD_1 improvement was 1.9 mm [35]. Figure 22.24 depicts a good example of a patient before a tarso-conjunctival Müllerectomy, after a drop of phenylephrine 2.5% and after surgery. Note the similarity in appearance of the eyelid after the phenylephrine test after surgery. Figures 22.24 and 22.25 are examples of the modified Fasanella. Figure 22.26 is of a patient who underwent a conjunctival Müllerectomy without a tarsectomy (Putterman approach).

More recently, a modification to the Müllerectomy was published which included an additional tarsectomy to augment the undercorrection of the preoperative phenylephrine test. This procedure could, perhaps, best be termed the Putterman Plus (Fig. 22.27). In this treatment algorithm, 9 mm of conjunctiva and Müller muscle are resected plus a

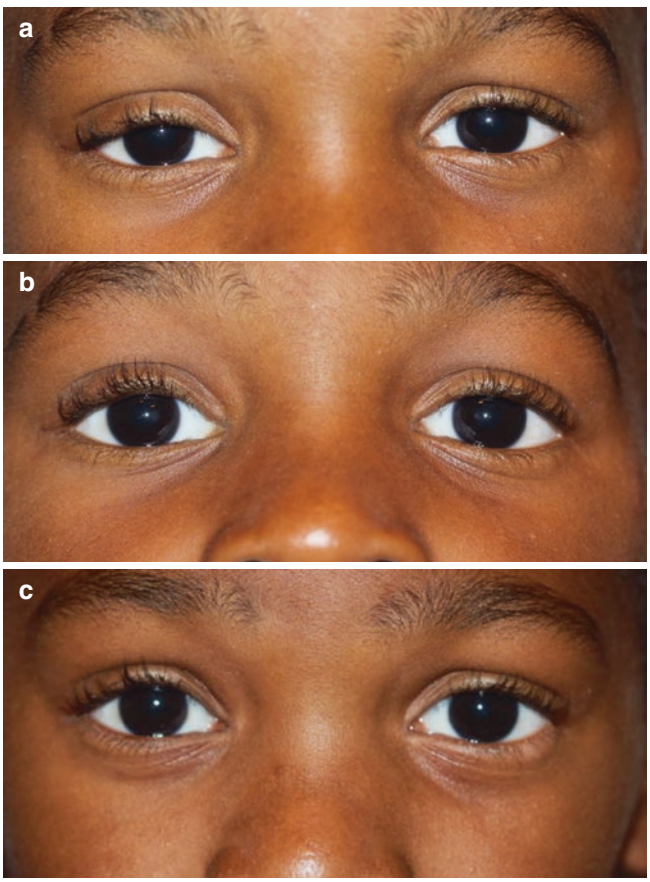


Fig. 22.24 Modified Fasanella-Servat procedure. (**a**) Preoperative photo of right ptosis. (**b**) Good response 5 min after the instillation of phenylephrine 2.5%. (**c**) Six months after surgery



Fig. 22.25 Modified Fasanella-Servat. (**a**) Preoperative photo. (**b**) Six months after surgery

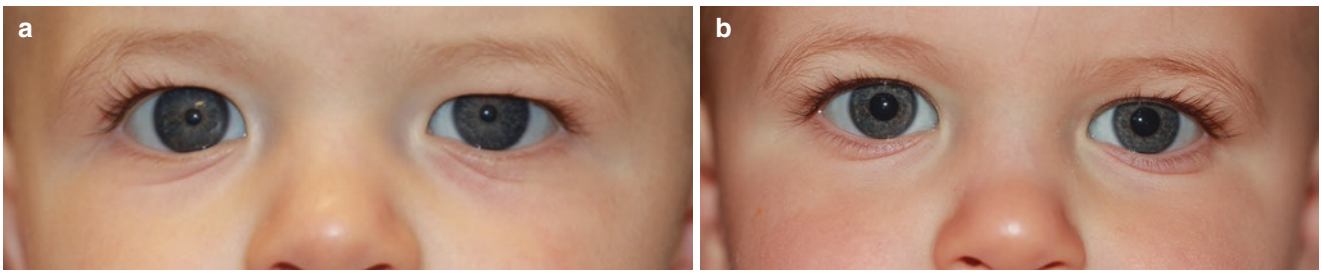


Fig. 22.26 Conjunctival-Müllerectomy (Putterman procedure). (**a**) Preoperative photo. (**b**) Six months postoperative photo

portion of tarsus with 1 mm of tarsus removed for every 1 mm of undercorrection on the phenylephrine test. Perry et al. reported 117 eyelids (68 patients) with a postoperative symmetry in 58 of 67 patients (87%) and no overcorrections [36]. This technique is exemplified in Fig. 22.28, which depicts a 9-year-old patient with Cornelia de Lange, who was a poor surgical candidate due to developmental delay. A conjunctival Müllerectomy was performed giving this patient a functional improvement in eyelid height with less chin-up position noted on follow-up.

The Werb procedure, however, is similar in concept and has an added advantage of being convertible to a full levator resection if considerations during the surgery warrant an alternative procedure. Gavaris describes a similar procedure in concept and has also achieved excellent results with this internal technique [34].

Regardless of which procedure is used, when there is an adequate preoperative response to phenylephrine, we have found the internal approach to be the most accurate in consistently achieving the desired postoperative result in the pediatric age group. The need for a general anesthetic is always a central issue in pediatric ptosis surgery, since this precludes intraoperative adjustments based on voluntary lid function. While most would agree that external levator procedures produce more accurate results when patients are able to cooperate intraoperatively, surgery on Müller's muscle is far less dependent on volitional eyelid movement. The amount of resection and/or advancement of Müller's muscle is predetermined during the preoperative evaluation. Unlike external levator procedures, which rely more heavily on the patient's cooperation during the examination to obtain more accurate measurements, the internal approach procedures can be based simply on the change of lid position observed following the instillation of phenylephrine. For both these reasons, in our experience, an adequate response to phenylephrine translates into a more predictable correction of ptosis and especially in the pediatric age group where accurate preoperative measurements are more difficult to achieve.

As mentioned earlier, one of the most valuable aspects of the internal approach is its ability to avoid problems associated with corneal exposure due to lagophthalmos. While both levator muscle surgery and frontalis suspension are associated with a significant degree of postoperative lagophthalmos,

Müllerectomies rarely affect eyelid closure. Particularly in those clinical situations where problems with corneal exposure are anticipated, a Müllerectomy can be performed much more safely and with very little risk of producing any degree of lagophthalmos. Accordingly, the postoperative care is much less demanding for parents because frequent application of lubricants is usually not necessary.

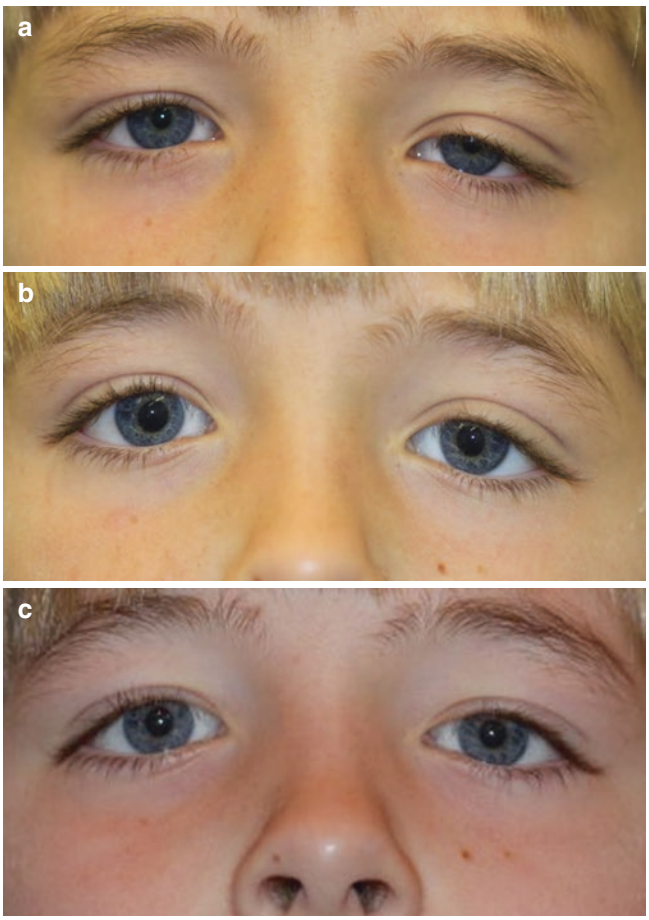


Fig. 22.27 Putterman-Plus procedure. (**a**) Preoperative photo. (**b**) Five minutes after the instillation of phenylephrine 2.5%. Notice the 1.5 mm of undercorrection of ptosis on the left side. (**c**) Six months after surgery with a conjunctival-Müllerectomy (9 mm) with a 2 mm tarsectomy

Although the internal approach does offer significant advantages, one limitation is its inability to correct marked asymmetries of the lid crease and lid fold. As an example, while a unilateral lid ptosis associated with fair levator function and poor crease formation may respond well to phenylephrine with improvement of the MRD_1, the lid crease may remain unformed, causing excess skin to hang over the lashes. If in this situation one performs a Müllerectomy procedure alone, the final result will not achieve satisfactory symmetry. Although Werb's internal approach procedure is capable of creating a lid crease and fold, in such instances, an external approach more readily permits adjustment of the aponeurosis and its relationship to the skin. If one is confronted with a situation where any degree of lagophthalmos poses a threat, one may opt to combine an internal approach with a skin or skin/muscle excision as is performed during cosmetic blepharoplasty surgery [37].

While Müllerectomy procedures offer many advantages, not all patients respond well to phenylephrine; and thus alternative procedures must then be used. In such instances, the type of surgery to be performed must be based predominantly on the amount of levator function present. While ptosis characterized by fair to excellent levator function can usually be satisfactorily corrected with some type of levator procedure, those cases with poor function will usually do much better with frontalis suspension.

Levator Surgery

Surgery involving the levator complex can be divided into two types: levator aponeurosis advancement and levator muscle resection. It is not the degree of eyelid ptosis, but the amount of levator function present, that determines which of these

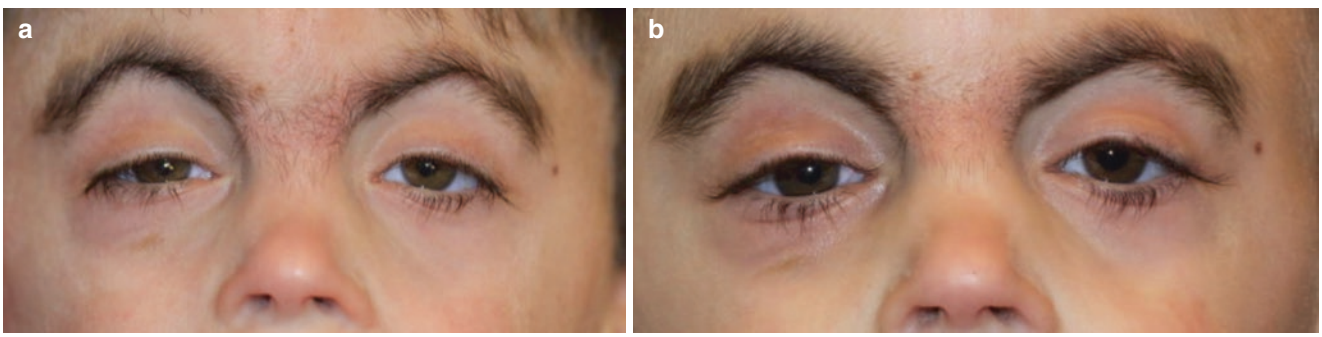


Fig. 22.28 Conjunctival-Müllerectomy for high-risk ptosis. (**a**) Preoperative photo of a 9-year-old male with Cornelia de Lange syndrome and developmental delay. (**b**) Postoperative photos taken 6 months after a bilateral conjunctival-Müllerectomy in which 9 mm of muscle and 1 mm of tarsus was excised on each side

procedures should be performed (Table 22.4). Levator aponeurosis advancement can be performed on those patients who demonstrate good to excellent levator function. Ptosis associated with good levator excursion (8–12 mm) can frequently be repaired with an aponeurosis advancement or resection. If excellent levator function is present (>13 mm), an aponeurotic advancement alone will usually suffice. Ptosis associated with excellent levator function is usually aponeurotic rather than myogenic and thus is discussed more extensively under the aponeurotic ptosis section. For those patients with poor to fair levator function (4–7 mm), a levator muscle resection is more often necessary to achieve adequate elevation of the ptotic lid (Figs. 22.29 and 22.30). Both the advancement and resection procedures can be further graded at the time of surgery to correlate with the degree of levator function.

Although large resections are certainly required for those cases with worse levator function, we have not found that the amount of levator function present can be easily correlated with formulaic precision to a resection of a predetermined length. While one surgeon's measurements may remain consistent, the amount of stretch placed on the cut levator muscle will be variable in the hands of different individuals, making it difficult to extrapolate millimeters of ptosis to millimeters of levator resection required. Furthermore, the degree of dystrophy, if severe, often yields a thin, easily stretched muscle that is difficult to measure both accurately and consistently. In many instances, even if sutures are placed at a predetermined location, the muscle is so flimsy that sutures do not hold with any certainty. Additionally, most formulas do not take into account whether the levator aponeurotic horns have been cut. When the horns have been cut, the resistance to stretch is dramatically changed, thus further affecting the accuracy of measuring a predetermined length of muscle resection.

Following Berke's concepts, we determine the amount of the resection to be performed by setting the position of the lid level at the time of surgery [38]. We base this decision not only on the strength of the levator muscle but also on the status of the levator aponeurotic horns. As a general rule, it is

Table 22.4 Selection of ptosis repair based on levator function

Levator function	Procedure
Excellent (≥13 mm)	Aponeurotic advancement
Good (8–12 mm)	Aponeurotic advancement or moderate levator resection (14–17 mm)
Fair (5–7 mm)	Large levator resection (18–22 mm)
Poor (≤4 mm)	Frontalis suspension preferred Maximal/supramaximal levator resection (as alternative)

Source: After Beard [34]

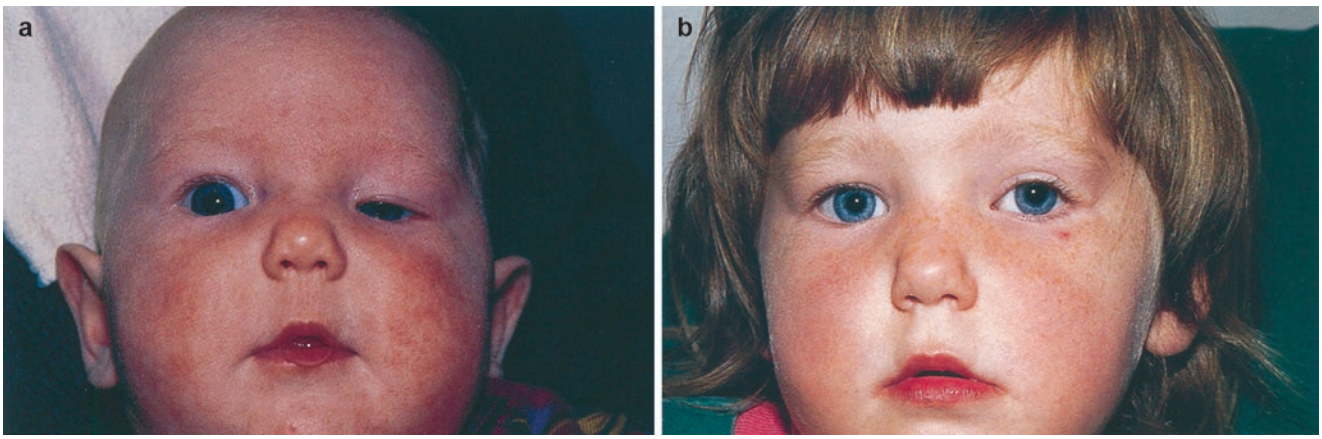


Fig. 22.29 Levator resection. (**a**) Preoperative. (**b**) Three years postoperative

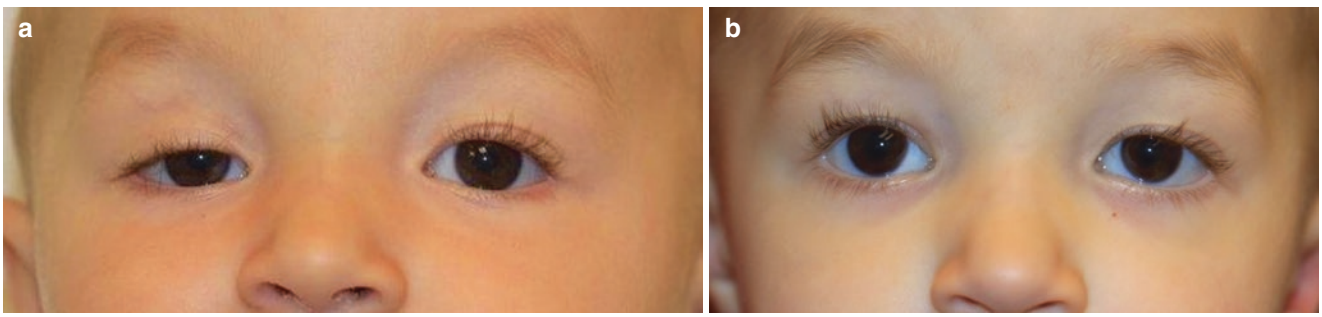


Fig. 22.30 Levator resection. (**a**) Preoperative. (**b**) One year postoperative

best to overcorrect myogenic ptosis "on the table," as opposed to the recommended undercorrection for acquired ptosis. The resting point of the lid margin, when the eye is held in primary position, should be related to the degree of levator function present preoperatively (Table 22.5). The poorer the levator function, the greater the overcorrection as the lid will drop postoperatively. If levator function is poor, then an overcorrection of 2 mm is advisable. If levator function is fair, then about 1 mm of overcorrection is ideal. For those cases of ptosis demonstrating good levator function, the lid should cover the cornea 2–3 mm and for excellent 3–4 mm. It should be emphasized that these settings are for congenital ptosis of the myogenic type and not for other causes of pediatric ptosis.

Contrary to what has been traditionally emphasized for maximal resections, we avoid cutting the aponeurotic horns whenever possible. We feel that these fibrous supports provide additional elasticity to the levator complex following a resection, acting much like elastic check ligaments. Although it is true that when the horns are cut one can mobilize the entire levator and pull it down so that more than 30 mm of muscle can be resected, too often this leads to a less than satisfactory final eyelid position with increased lid lag and lagophthalmos. If, indeed, one is forced to cut the horns to achieve an acceptable eyelid level, then the lid should be placed in an overcorrected position that is somewhat greater than that calculated by levator function alone.

By far the most challenging situations are those where the levator function is poor. Whereas in the past we usually elected to attempt a levator resection as a first procedure, over the last few years, we have been performing frontalis suspensions with increasing frequency. In general, we continue to perform levator resections on those patients whose ptosis falls into the category of poor to fair levator function and demonstrate at least 4 mm of eyelid excursion. If the amount of lid elevation with a large levator resection is not satisfactory, a "supramaximal" effect may be achieved by combining the resection with excision of a portion of the tarsus. Although some surgeons advocate extending the resection to Whitnall's ligament, achieving an actual suspension of the eyelid to the ligament [39], we feel that this maneuver is problematic due to the extreme degree of lagophthalmos that often occurs postoperatively. As an alternative we prefer to perform a tarsectomy with placement of the sutures through the levator muscle just anterior to Whitnall's ligament.

Table 22.5 Amount of levator surgery for congenital myogenic ptosis based on levator function and intraoperative eyelid level (under general anesthesia)

Levator function	Lid position on cornea
>10 mm of function	3–4 mm below the limbus; the eyelid should rise 2–3 mm postoperatively
8–9 mm of function	3 mm below the limbus; the eyelid should rise 1–2 mm postoperatively
6–7 mm of function	2 mm below the limbus; the eyelid should remain at the intraoperative level
5–6 mm of function	1 mm below the limbus; the eyelid should remain at that level or drop 1–2 mm postoperatively
0–4 mm of function	Frontalis suspension preferred

Source: Data from Berke [64] and Rathbun [65]

While we generally eschew any specific formulas of correlating millimeters of resection to millimeters of ptosis, for those who feel more comfortable with this approach, we can offer some guidelines. There are, however, a multiplicity of factors that the surgeon must process in deciding how much muscle to resect: (1) the degree of levator excursion; (2) the appearance of the muscle in terms of degree of dystrophy, thickness, or fibrosis; (3) whether the horns have been cut and how much this has affected the rebound elasticity of the levator complex when it is pulled down and released; (4) whether any tarsus has been resected; and (5) the position of the lid margin relative to the limbus when sutures are placed and temporarily tied with slip knots. The guidelines we suggest for millimeters of resection to millimeters of ptosis range from 3:1 for a relatively healthy-appearing muscle to 5:1 for a very thin, dystrophic muscle. Again our preference is to avoid cutting the horns and to set the lid relative to the limbus based on preoperative levator function as suggested by Berke. If we are unable to do a Müllerectomy based on the preoperative phenylephrine response, then the next most physiologic procedure is levator complex surgery based on Berke's principals.

Frontalis Suspension

Where our approach has changed most dramatically is in those cases where minimal to no levator function is present. Whereas we used to believe the old precept that the results of levator complex procedures are often more natural in appearance than frontalis suspensions for severe ptosis with poor levator function, we have been more and more satisfied with our frontalis suspension results. Many have argued in the past that a levator resection is more physiologically natural and can allow one to achieve better symmetry with the uninvolved side in unilateral cases. In practice, however, we have found little true difference in the aesthetic results between the two procedures. Furthermore, there is often as much or more lid lag and lagophthalmos following maximal levator resections, and, more importantly, undercorrections are much more common. While the rationale has been that if the eyelid remains ptotic following levator surgery, a frontalis suspension can always be performed as a secondary procedure, we now more frequently consider initial frontalis suspension. Even for those cases where we do choose to attempt a levator resection, we are always prepared to convert to a frontalis suspension on the table if we are not satisfied with the lid level achieved.

There is, then, little doubt in our minds that patients with 0–4 mm of levator function are more likely to achieve superior results following frontalis suspension. In those cases where the ptosis is bilateral, the decision to perform frontalis suspensions is probably easier for parents to accept. For those cases of unilateral ptosis, if there are parental reservations regarding the use of fascia lata or synthetic materials, one can always attempt a levator resection and then convert to a frontalis suspension on the table if satisfactory elevation of the eyelid cannot be achieved with levator surgery.

Over the years, frontalis suspension procedures have been performed using a variety of materials, with Supramid and silicone being among the most commonly selected alloplastic materials [40, 41]. If the child is old enough, one can use autogenous tissues as an alternative to alloplastic material. While temporalis fascia or ulnar flexor tendon can both be used [42, 43], our preference is to use tensor tendon fascia lata.

In general, we have followed Crawford's recommendations for harvesting fascia lata [44]. In normal children of 4–5 years of age, the femur has grown sufficiently to allow harvesting of tendon fascia lata. In younger children, it is usually difficult to obtain a sufficiently long strip of fascia as well as the tissue often being more fragile, and, therefore, preserved tissue has more often been recommended as an alternative. It is critical to harvest along the lateral leg and avoid the superior portion of the lateral fascia lata where the fibers run in a more oblique fashion [45]. Preserved fascia is commercially harvested from cadavers and then irradiated and washed in NaOH which appears sufficient to limit the chance for transmission of infectious material [46].

The ready availability of preserved fascia initially coincided with our increased frequency of performing frontalis suspension procedures (Tutoplast 0.2 or 0.3 mm width, IOP). Preserved fascia has offered a possible solution for severe ptosis in children under 5 years of age, whereas in the past, either the suspension surgery was delayed or a less effective alternative procedure was performed. The use of preserved fascia lata for older children also did enable one to shorten the time of surgical procedure and avoid creating an additional scar, which may be troublesome to some parents. Additionally, the leg incision and dissection of the tendon contribute most to postoperative discomfort, and thus a speedier and more pleasant recovery can be expected with the use of preserved tissue. The difficulty with using preserved fascia lata, however, has been a significant rate of recurrence due most likely to breakdown and resorption of the tissue**.**

Synthetic Materials Versus Preserved Fascia Lata

Ultimately, since publication of the first edition of this text, we have, over the past decade, converted to using silicone slings almost exclusively for children under the age of 4 with poor levator function (less than 4 mm) and with a poor response to phenylephrine 2.5%. We have performed over 500 cases with the Seiff frontalis sling set (BD Visitec) (see Fig. 22.31) and over 200 cases with the thinner silicone sling produced by FCI Ophthalmics (see Fig. 22.32). Both of these techniques will be covered later in this chapter.

We do acknowledge that debate continues as to whether autogenous fascia is superior to preserved material in regard to lasting results. Although Crawford reported a 90–97% short-term success rate with banked fascia lata and two other series reported a recurrence rate of approximately 8% associated with the use of donor fascia, the long-term results are more variable [43, 47]. Wilson and Johnson reported a recurrence rate of 43% after 7 years of follow-up using lyophilized fascia [48]. Other authors using irradiated fascia report a recurrence rate of 21% [49].

Another issue exists regarding suspension procedures as to whether a unilateral or bilateral sling should be performed in cases of unilateral ptosis [50]. Crowell Beard in his landmark text on ptosis felt that the normal levator should always be excised and bilateral slings done in order to provide optimum

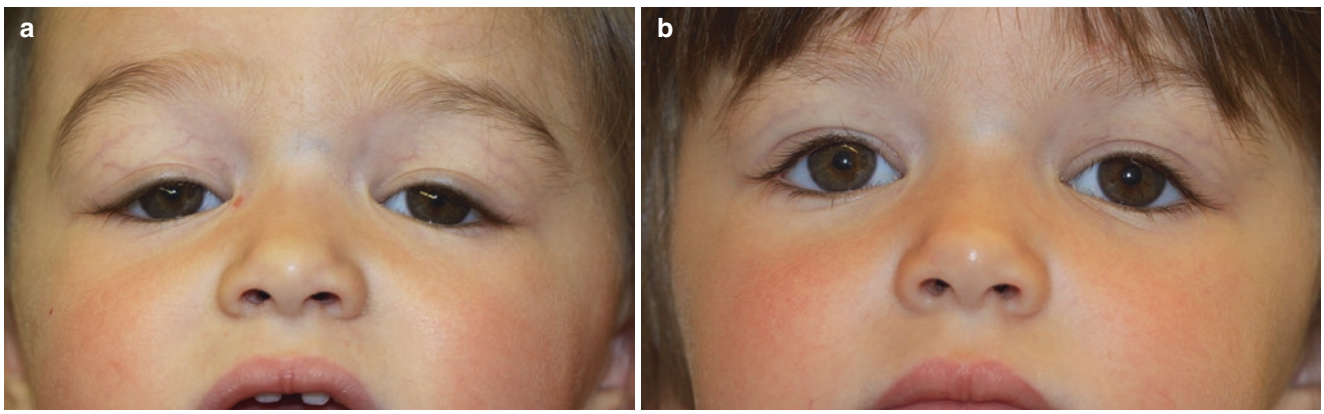


Fig. 22.31 Bilateral silicone sling frontalis suspension (BD Visitec) with a single-rhomboid technique. (**a**) Preoperative photo. (**b**) Six months postoperative

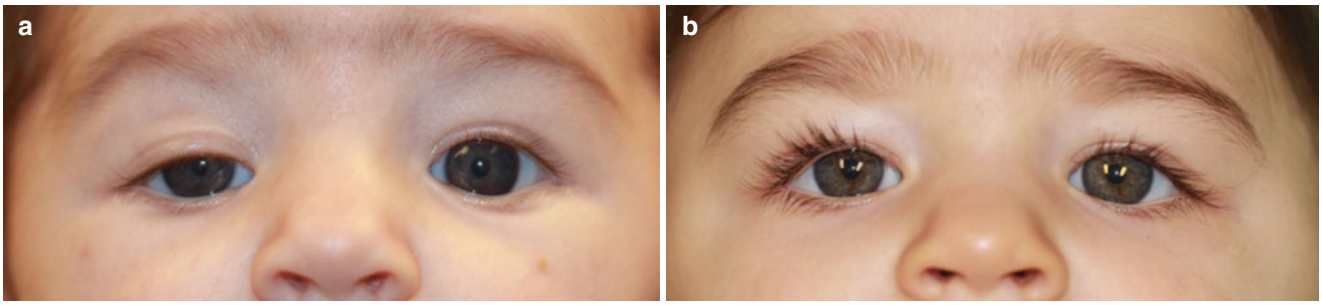


Fig. 22.32 Unilateral silicone sling frontalis suspension (FCI Ophthalmics) with a double-triangle technique. (**a**) Preoperative photo. (**b**) Six months postoperative

symmetry [34]. Others have agreed that bilateral slings should be done but without excising the normal levator. Some have recommended an alternative, detaching the levator from the tarsus and then suturing it to the superior orbital rim in order to avoid a synkinetic jaw wink as in the case of a Marcus Gunn ptosis [50]. Both eyelids are then suspended to the frontalis muscle. On the other hand, there are also those surgeons as well as parents, who feel that a healthy levator muscle should never be touched. In general, we are more in agreement with the latter thought process and prefer to perform unilateral slings for unilateral ptosis. Although we are satisfied with the results, we are always careful to involve the parents in the surgical decision, providing them with the pros and cons of both approaches. In our experience, however, most parents opt for unilateral surgery and are rarely disappointed with the results. Unilateral frontalis suspension, on the other hand, is not a perfect solution in all cases. A recent report, for example, raised concerns regarding persistent amblyopia in unilateral frontalis suspension. This is a particular problem when there is significant amblyopia on the ptotic side. With less desire to use the brows for elevation of the affected unilateral ptotic side, there appeared to be greater postoperative droop and, therefore, increased concerns regarding normal visual development [51]. There are options for this, however. One can switch to bilateral frontalis suspension with levator extirpation of the normal levator to force the child to use the frontalis muscle for further elevation. An alternative is to weaken the normal muscle unilaterally by recessing the normal levator muscle [52]. This essentially has a similar effect by causing the child to want to elevate the brow on the previously normal side. As long as there is bilateral elevation of the brows, then the amblyopic side will assume a more symmetrical lid position.

In regard to selecting the proper eyelid position intraoperatively for a frontalis suspension procedure, we generally recommend that the eyelid be raised to the desired postoperative height (usually an MRD_1 of 4–5 mm). The lid margin should rest at the level of the superior limbus, because the lid will drop at least 2 mm postoperatively. Care must be taken while raising the eyelid to avoid pulling the lid margin away from the globe. We believe that the "ideal" lid level is at a position where the child need not rely to any significant degree on using the frontalis muscle. If the child must use the frontalis to achieve good elevation of the eyelid, headaches or fatigue with a subsequent droop will often occur. This becomes not only a cosmetic concern, but also a potential functional problem. If the lid becomes ptotic whenever the brow is relaxed, amblyopia can still remain a significant threat. This approach, of course, does not apply to those cases of neurological or mitochondrial causes of ptosis where corneal exposure issues mandate a planned undercorrection.

Myogenic Ptosis with Associated Superior Rectus Muscle Weakness

These patients are approached in a similar fashion to those with isolated myogenic or simple congenital ptosis, but special attention must be directed at minimizing postoperative lagophthalmos. Any limitation of upgaze increases the risk of corneal exposure. Due to this potential complication, a Müllerectomy is the preferred surgical procedure whenever practical. As described earlier, one of the main advantages of this procedure is the absence of postoperative lagophthalmos. For those with an inadequate response to the phenylephrine test, one could consider a Putterman Plus as described earlier, or one must resort to either a levator resection or frontalis suspension. Unfortunately, those patients with ptosis associated with superior rectus muscle weakness tend to have severe ptosis with very limited levator function, and thus if one performs levator muscle surgery, a large resection is usually necessary. Since a large levator resection is inevitably associated with a significant amount of lagophthalmos, we, in general, prefer to perform a frontalis suspension procedure in this situation. If the threat of corneal exposure is particularly serious, we elect to use a synthetic material to suspend the eyelid to the brow; we can then easily reverse the procedure if significant corneal exposure should subsequently develop. If this technique of suspension proves successful without exposure problems, autogenous fascia lata can then be substituted at a

later date. Alternatively, if one should choose to use tendon fascia lata for the initial repair, then a slight undercorrection may be done to yield a postoperative lid level, which clears the visual axis by 1–2 mm, relying more on voluntary frontalis contraction for additional lift.

Blepharophimosis

The bilateral ptosis associated with blepharophimosis (the congenital eyelid syndrome) is usually severe and associated with poor levator function. These patients rarely respond to 2.5% phenylephrine, and levator resections tend to achieve less satisfactory results than frontalis suspensions. Although some surgeons advocate postponing correction of the accompanying epicanthal abnormalities, our approach to these patients is to perform bilateral frontalis suspension with silicone material when the child is around 1 year of age and to repair the epicanthal folds and telecanthus conservatively during the same surgery if at all feasible (Fig. 22.33) (see also Chap. 21). The purpose is to apply horizontal as well as vertical stretch to the lid fissure openings while also giving at least a functional improvement as well as some appearance benefit from lid crease formation. Transnasal wiring can be considered later around age 4 years if necessary and a more permanent frontalis suspension whenever the leg is long enough to harvest fascia lata, usually between 4–5 years of age.

Congenital Orbital Fibrosis Syndrome

Surgical correction of the ptosis in this disorder is particularly challenging due to the associated globe restriction. Unfortunately, these patients, in general, do not respond to phenylephrine, thus eliminating the option of an internal procedure with its inherent decreased risk of lagophthalmos. All alternative surgeries to elevate the upper eyelid are fraught with the risk of severe and intractable corneal exposure. The surgeon is therefore faced with the dilemma of either pursuing a solution that attempts to preserve vision or one that sacrifices vision in exchange for a more normal appearance. A balance must be found between function and appearance.

While each patient must be treated on an individual basis, our approach to these patients, in general, has been to acknowledge the very limited potential for normal visual function and to concentrate more on normal psychosocial development. Amblyopia management in this disorder is particularly challenging due to the restricted position of the globe and the constant need for corneal lubrication. Even with a concerted effort to promote normal visual development, more often than not, dense amblyopia ensues. Furthermore, the decision to pursue the promotion of normal visual function greatly limits the possibilities of achieving a near normal appearance. Our choice, when this is a unilateral problem, thus has been to primarily promote normal psychosocial development rather than visual function. We seek to achieve the most normal appearance possible, while also eliminating both the need to constantly lubricate the eye and to frequently visit the doctor's office.

Once one commits to enhancing the child's appearance, the issue of providing corneal protection must first be addressed before the ptotic eyelid can be safely elevated. Although conjunctival flaps have usually been used for the purpose of covering the cornea, we prefer to cover the corneal surface with an oral mucous membrane graft [53] (Fig. 22.34). Once the cornea is well protected, the eyelid can then be raised to an optimum level that could not otherwise be safely achieved. Successful ptosis repair in such cases often requires either maximal or supramaximal levator resection, full thickness lid excision (including skin, levator, and tarsus), or frontalis suspension (Figs. 22.29 and 22.30).



Fig. 22.33 Blepharophimosis. (**a**) Preoperative at age 5 years. (**b**) Nine years postoperative fascia lata frontalis suspension, telecanthus, and epicanthal fold repair with transnasal wiring

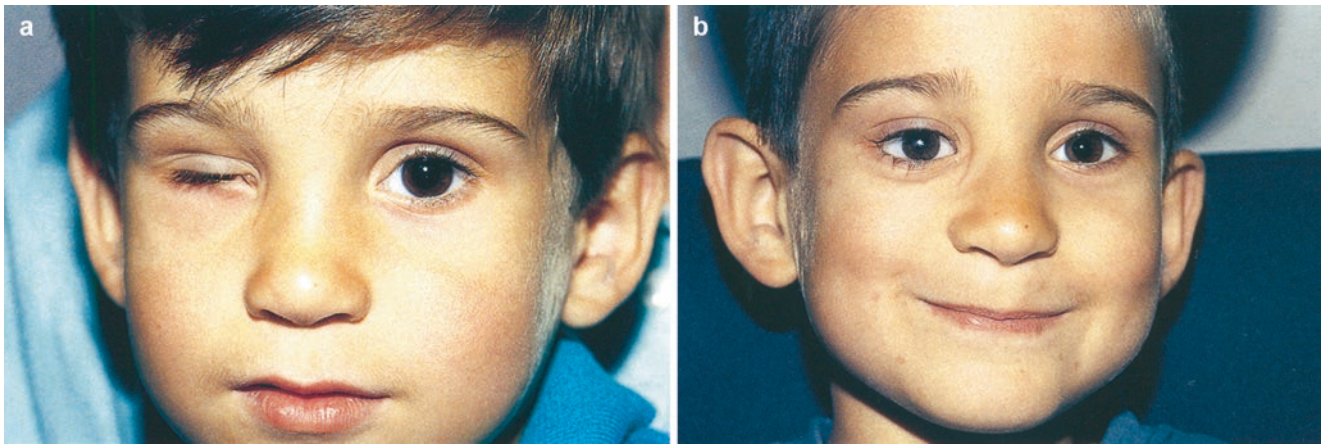


Fig. 22.34 Congenital orbital fibrosis syndrome. (**a**) Preoperative. (**b**) Three years postoperative, where a mucus membrane graft from the lower lip has been used as a corneal cover to permit prosthetic shell wear and to allow elevation of the upper lid without complications of exposure

The final step involves the fitting of a prosthesis that can be worn comfortably over the protected cornea (see Chap. 39).

While our approach has allowed us to achieve very satisfying results, we are the first to recognize the difficulty in choosing an approach that intentionally excludes promoting normal visual development in the affected eye. Any decision that will inevitably result in amblyopia is obviously not taken lightly, and for this reason both the parents and other consultants are purposefully involved in the often very extensive discussions. In most cases, however, significant amblyopia is already present at the time that the decision must be made, therefore making the sacrifice somewhat more acceptable. In addition, this approach does at least preserve the globe as a "spare tire," since the affected eye does maintain some degree of vision should the opposite normal eye ever be lost. Most importantly, this approach enables the child to look and feel normal, often for the first time in his or her life. In our experience, the benefits to both the child and family have far exceeded the risks.

Aponeurotic Ptosis

Aponeurotic ptosis is usually associated with excellent levator function and thus can be repaired with either a Müllerectomy procedure or a levator aponeurosis advancement. A Müllerectomy with or without tarsectomy may be performed for those patients demonstrating an adequate response to 2.5% phenylephrine. The quality of the response is judged not only on the upper eyelid position but also on the appearance of the lid crease and fold. If the symmetry is less than ideal, then an aponeurosis advancement procedure is usually preferred. In cases of true pediatric aponeurosis disinsertion, the edge of the disinserted aponeurosis should be easily visualized at the time of surgery. Unlike the myogenic form of ptosis where an overcorrection is desirable "on the table," the aponeurosis should be attached to the upper tarsal border without regard for position of the eyelid relative to the superior corneal limbus. Indeed, the eyelid should move very little and actually remain mostly closed upon reattachment of the aponeurosis to the tarsus.

Neurogenic Ptosis

Marcus Gunn Jaw-Winking Ptosis

The surgical approach to Marcus Gunn jaw-winking ptosis depends on the degree to which synkinetic excursions are present. For those patients with less than 2 mm of excursions, the approach is similar to that for myogenic ptosis. A Müllerectomy procedure may be preferred over a levator resection, since it is probably less likely to cause exacerbation of the synkinetic movement. Assessment of the eyelid dynamics following the instillation of phenylephrine is helpful in determining the most appropriate procedure. In the past, if, indeed, greater than 2 mm of synkinetic excursion was present, and satisfactory correction of the ptosis was felt to mandate an extirpation of the levator muscle in combination with a frontalis suspension. Extirpation of the levator muscle is most easily performed by going above Whitnall's transverse ligament and to avoid transecting the aponeurotic horns. Significant mobilization of the superior levator muscle complex can be achieved and resected. This approach preserves the normal anatomic connections of the aponeurosis and Müller's muscle to the tarsus. The results following frontalis suspensions in this fashion for this particular problem are very satisfying. While bilateral surgery gives the optimum cosmetic result, in our experience most parents have preferred unilateral surgery for this problem when given an informed choice and have been pleased with the results. Figure 22.35 is an example of a patient treated successfully with a unilateral levator resection alone without an extirpation.

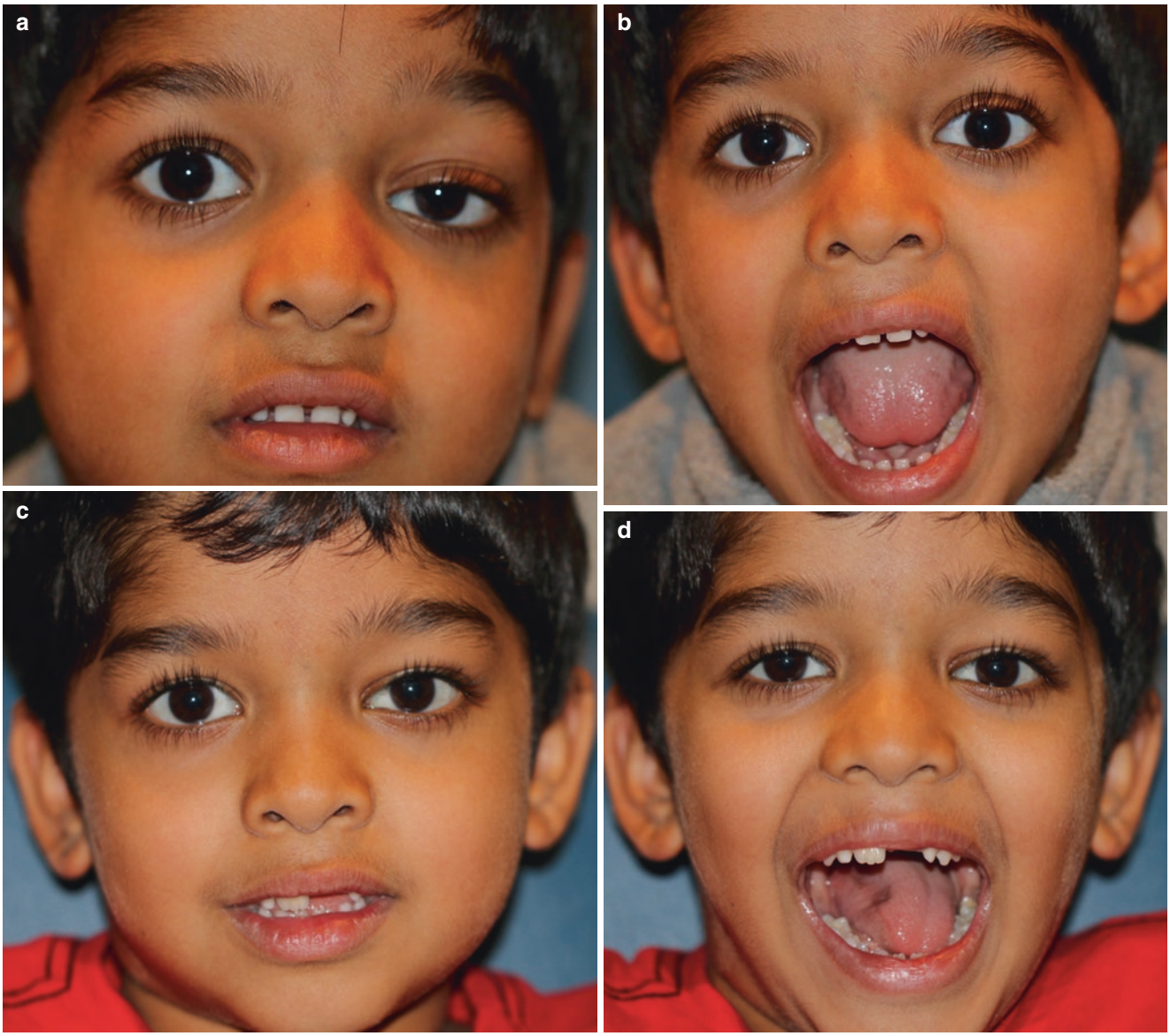


Fig. 22.35 Marcus Gunn jaw wink treated with a unilateral levator resection. (**a**) Preoperative photo of left ptosis. (**b**) Preoperative photo of jaw wink lid retraction when mouth opened widely. (**c**) Postoperative photo taken 9 months after a left levator resection without a levator extirpation. (**d**) Postoperative photo of the patient's jaw wink minimal elevation 9 months after surgery

Third-Nerve Palsy

Patients with third-nerve palsies who have ptosis accompanied by motility deficits are treated in a similar fashion as patients with myogenic ptosis associated with superior rectus weakness. These patients are at high risk for developing exposure problems, and thus some type of Müllerectomy is usually preferable, depending on the response to phenylephrine. A levator resection or frontalis suspension can be performed on those patients with an inadequate response to phenylephrine, but both of these procedures must be approached conservatively. A suspension procedure using synthetic material should be considered if the risk of exposure is particularly high, and a reversal of the procedure may be required. Reversibility is an important issue not only for patients with complete motility deficits but also for those patients with acute third-nerve palsies who require only a temporizing measure to improve visual functions, while nerve function hopefully returns over the pursuing 6–12 months.

Patients who develop aberrant regeneration of the third nerve may demonstrate significant synkinetic eyelid excursions and must be treated like patients with a Marcus Gunn jaw wink. These patients require frontalis suspensions usually following levator muscle extirpation, which is more frequently needed in contrast to the Marcus Gunn type of synkinesis.

Horner Syndrome

The ptosis of Horner syndrome is best corrected with some form of Müllerectomy. Since the abnormality in this syndrome involves disruption of the innervation to Müller's muscle, the lack of contractile force can be partially compensated for by shortening the length of the muscle. The amount of Müller's muscle resection and the decision as to whether to include excision of the tarsus are based on the response to the phenylephrine test.

Mechanical Ptosis

Surgery for mechanical ptosis is designed to address the specific cause of the lid malposition. If the ptosis is due to an infantile hemangioma, for example, surgery is less commonly required since treatment with a systemic beta-blocker such as propranolol will frequently improve the eyelid position (see Chaps. 6 and 23). Oral steroids or injections of steroid into the tumor, which were the mainstay of medical management in the past, are rarely needed today. Surgical debulking is required only when these tumors are unresponsive to medical modalities of treatment and amblyopia is a significant threat.

Figure 22.36 depicts a patient with deprivation amblyopia due to mechanical ptosis from an infantile hemangioma and poor responses to oral beta-blocker,

Lymphangiomas or the now preferred term venolymphatic malformations (VLM), on the other hand, do not respond readily to medical treatment and do not spontaneously regress with time. VLM, therefore, do require either sclerotherapy or surgical debulking when amblyopia is a significant concern. Unfortunately, surgery is often difficult, since microcystic VLMs, as well as most infantile hemangiomas, can be infiltrative in nature, making dissection of surgical planes very challenging. Hemorrhage will often complicate the procedure, and postoperative edema following VLM excision is frequently prolonged.

Plexiform neurofibromas also frequently require surgical debulking to correct a ptotic eyelid. Although most of these patients are improved following the surgery, neurofibromas are rarely completely excised. As a result, these tumors continue to grow, and additional procedures are frequently necessary. Furthermore, due to the infiltrative nature of these neural tumors, the tarsus, orbicularis, and skin as well as the levator muscle are frequently involved, leading to distortions of the eyelids that are difficult to correct. Since all too often the surgical results are less than optimal in these patients, advances in chemotherapy and possibly gene therapy may someday prove invaluable in controlling the growth of adnexal plexiform neurofibromas.

Traumatic Ptosis

To properly correct traumatic ptosis, one must first identify the mechanism responsible for creating the lid malposition. The surgical approach is then fashioned according to the specific type of ptosis present. By far the most important aspect of repairing traumatic ptosis is the timing of the procedure. Since many cases of acute ptosis following trauma will gradually improve with time, it is imperative to postpone surgery for at least 6 months to 1 year if the ptosis is possibly neurogenic in nature. In those instances where a temporary correction is required, a frontalis suspension should be performed using a silicone material. Such instances would include an acute traumatic ptosis affecting the visual axis in a child with potential for developing amblyopia or an acute ptosis involving an only eye with useful vision. By performing a frontalis sling with synthetic material, the surgery can be easily reversed should function of the lid return over time. Traumatic aponeurotic disinsertions do not require delay and can be corrected at any time.

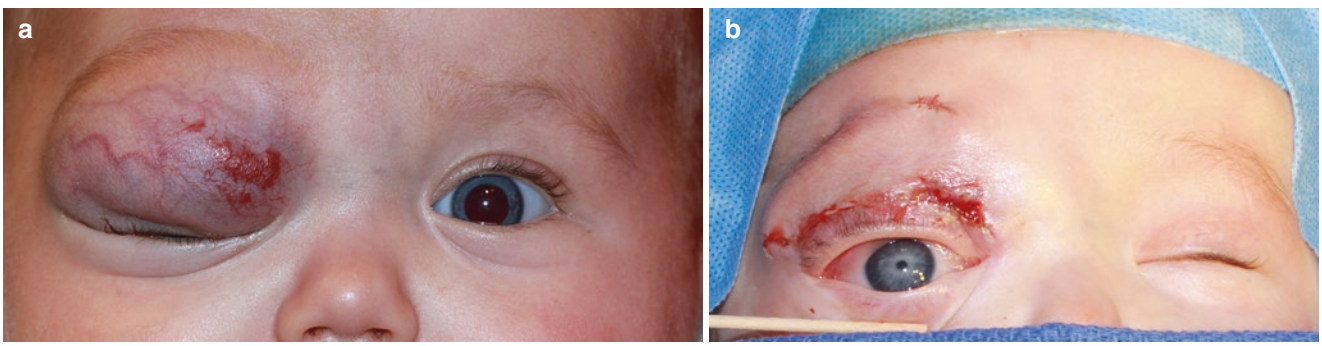


Fig. 22.36 Deprivation amblyopia due to severe mechanical ptosis in an infant who failed propranolol therapy for an orbital and eyelid infantile hemangioma. (**a**) Right eyelid and orbital infantile hemangioma. (**b**) Intraoperative photo after debulking tumor and the placement of a right upper eyelid silicone frontalis sling

Management of Asymmetric Bilateral Ptosis

Traditionally, when bilateral surgery has been necessary, it has been mandated that the same technique should always be used on each side regardless of the degree of levator function or the response to phenylephrine stimulation. This was the basis for Beard's original preference for Marcus Gunn ptosis requiring extirpation of the normal levator muscle as well as the abnormally innervated muscle followed by bilateral frontalis suspension. The so-called "chicken Beard" procedure was a later variation adopted by other surgeons where the normal levator muscle was spared, but bilateral suspensions were still done [54]. The degree of ptosis, however, is frequently asymmetric, and we have had excellent success with applying the most appropriate specific technique to each eyelid, based solely on the degree of levator function and/or the response of each individual lid to phenylephrine stimulation.

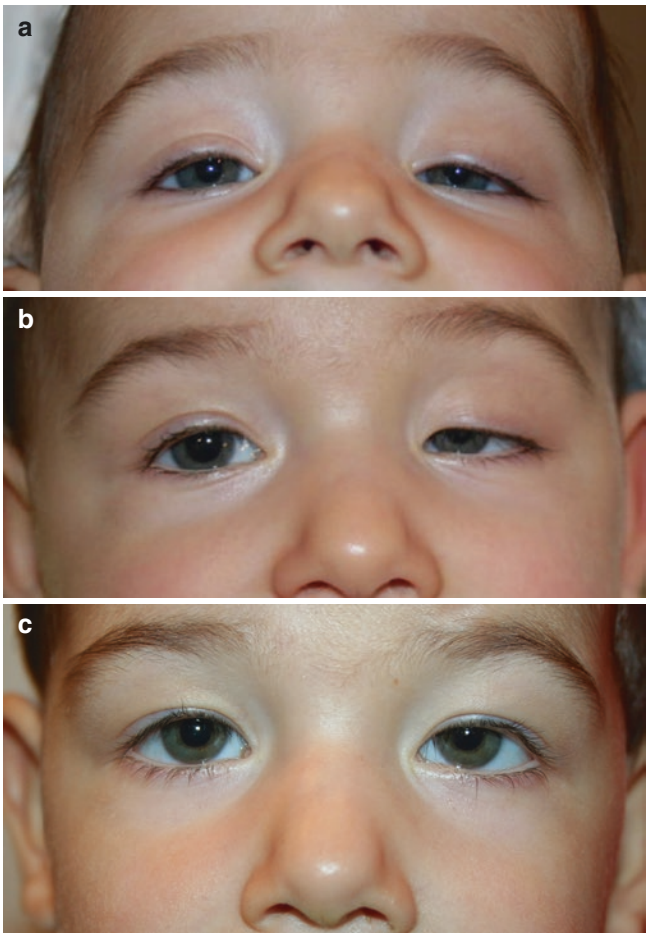


Fig. 22.37 (**a**) Bilateral ptosis patient with good levator function on the right side and poor left levator function on left. Note the chin-up position. (**b**) Right side 5 min response to 2.5% phenylephrine. Poor response on left with poor levator function. (**c**) Postoperative photo taken 8 months after a modified Fasanella procedure on the right side and a left frontalis suspension with a BD Visitec silicone sling. Good symmetry achieved despite use of two entirely different procedures

In many instances, we have performed a frontalis suspension on one side with a Müllerectomy or levator resection on the other side yielding acceptable outcomes from both a functional and appearance perspective (Fig. 22.37).

Simultaneous Versus Sequential Congenital Ptosis and Strabismus Repair

Strabismus is frequently seen in children with ptosis, occurring in 10–30% of patients [55, 56]. Conventional wisdom recommends a sequential approach for correction, with strabismus surgery being performed before ptosis surgery. The rationale for a staged approach is that correction of strabismus can affect eyelid position, requiring a fresh evaluation of ptosis after completion of strabismus surgery. There are disadvantages, however, to a staged approach, including multiple anesthesia events, inconvenience, and cost [57]. In our experience, we have found no difference in outcomes whether the procedures were staged or simultaneous.

We sought to compare the clinical outcomes of simultaneous versus sequential ptosis surgery and strabismus surgery in children. We conducted a retrospective cohort study of children requiring both ptosis surgery and strabismus surgery on the same eye over a 9-year period at The Children's Hospital of Philadelphia [58]. Simultaneous surgery occurred during a single general anesthesia episode. Sequential surgery occurred during two anesthesia episodes separated by at least 7 weeks. Procedures included external and internal ptosis repairs and vertical and horizontal strabismus surgeries. Outcomes were ptosis surgery success, defined as a marginal reflex distance (MRD1) of ≥2 mm, good lid contour, and good lid crease. Strabismus surgery's success was defined as ocular alignment within 10 PD of orthophoria for comitant strabismus or significant improvement in head position or ocular alignment for incomitant strabismus.

Our data did not demonstrate any advantage for sequential surgeries with regard to clinical outcomes, complications, or reoperations. Despite a theoretical risk of increased complications, particularly when internal repairs are paired with a strabismus procedure involving a superior muscle, no increased risk was seen. Performing ptosis and strabismus surgery together appears to be clinically effective, safe, and reduces anesthesia exposure during childhood [58].

Surgical Techniques

Putterman's Conjunctivo-Müllerectomy

1. Following sterile preparation, a 4–0 silk suture is passed through the upper eyelid skin and orbicularis to serve as a traction suture (often unnecessary). A medium-sized Desmarres retractor is used to evert the upper eyelid and

expose the conjunctiva. A caliper is then used to measure the amount of tissue to be resected based on the preoperative response to phenylephrine. This is usually 4.5 mm above the tarsal border when the response to phenylephrine has produced the desired elevation. This measurement can range from 2–5 mm depending on greater or lesser lid level response to phenylephrine. A t the appropriate location, 3 6–0 silk sutures can be passed through the conjunctiva to mark the distance (Fig. 22.38a), or several spots at this site can be marked with a cautery.

2. The conjunctiva and Müller's muscle are held on traction to separate Müller's muscle from the levator aponeurosis.
3. A Putterman clamp (Karl Ilg, St. Charles, IL) is positioned by placing one blade at the level of the marking suture and the other at the upper tarsal border. As the Desmarres retractor is removed, the clamp is closed with the blades, engaging conjunctiva and Müller's muscle. The clamp handle is then locked (Fig. 22.38b).

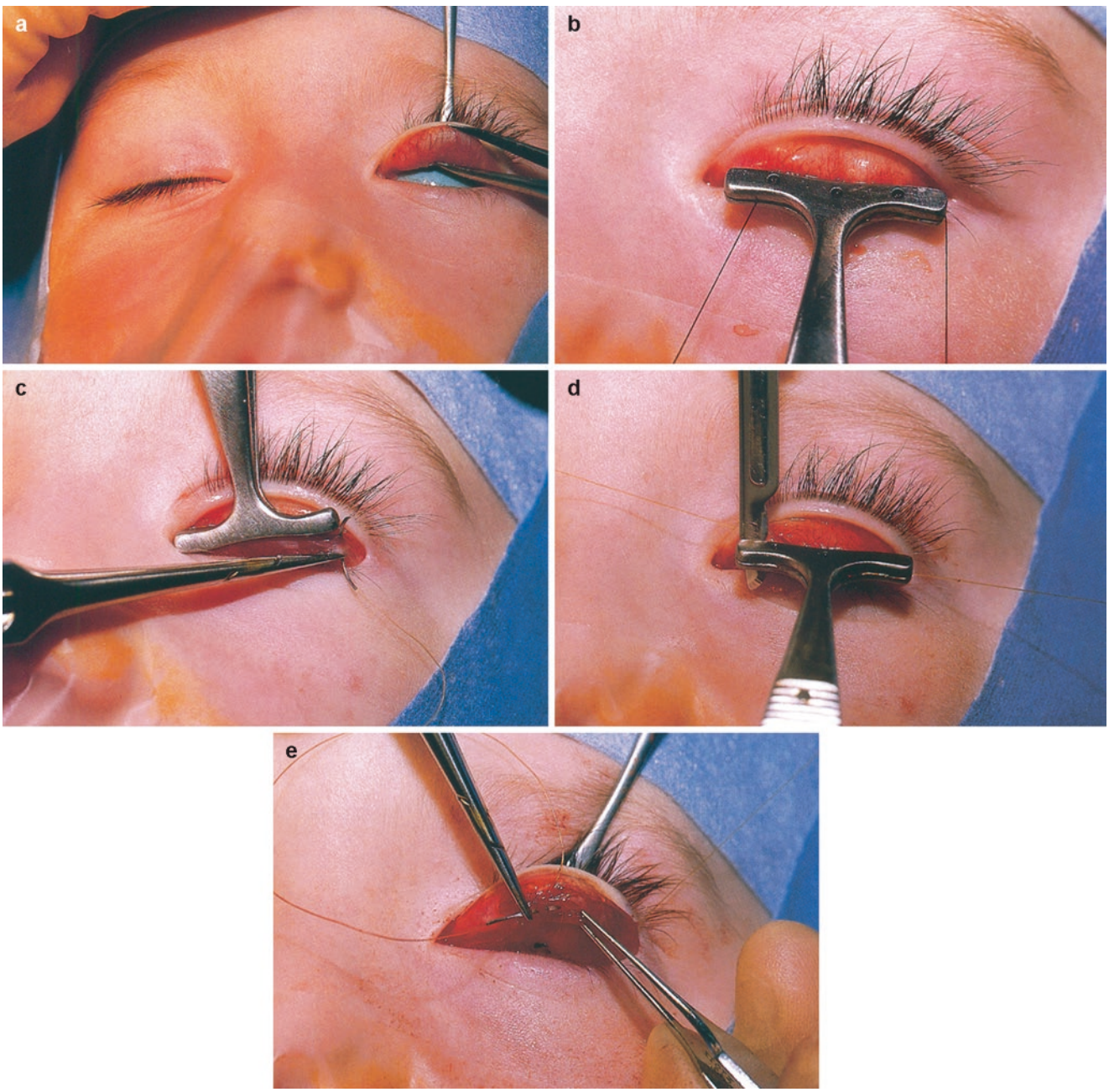


Fig. 22.38 Putterman conjunctivo-Müllerectomy

4. The upper eyelid skin and clamp are then pulled in opposite directions. These should move freely apart from each other; any encountered resistance signifies inadvertent incorporation of the levator aponeurosis in the clamp. The clamp must be reapplied until the proper orientation is achieved.
5. The clamp is then held straight up, and a 6–0 double-armed plain gut suture (usually with a G-1 needle) is run 1.5 mm below the clamp along the clamp's entire length. The sutures are placed 2–3 mm apart, incorporating the upper margin of the tarsus, Müller's muscle, and the conjunctiva (Fig. 22.38c).
6. The tissues held in the clamp are excised using a No. 15 blade. Care must be taken to avoid cutting the sutures (Fig. 22.38d).
7. The 5–0 suture is then run continuously to close the incision. Upon reaching the opposite end of the incision, each arm of the suture is passed through the conjunctiva and Müller's muscle. The suture can then be tied, with the knot buried under the conjunctiva in the upper temporal cul-de-sac (Fig. 22.38e) or anteriorized to the lateral eyelid skin crease.

Werb Procedure

1. Following sterile preparation, the lid is everted, and a No. 15 blade is used to create a full-thickness tarsal incision 1 mm below the upper border of the tarsus, along its full length. The incision enters the surgical plane between the anterior surface of Müller's muscle and the posterior surface of the levator aponeurosis (Fig. 22.39a). Two 4–0 silk sutures are placed through the tarsal segment at both ends to serve as traction sutures to aid the dissection (Fig. 22.39b).
2. Gentle traction is applied to separate the loose attachments to the anterior surface of Müller's muscle. This maneuver exposes the "white line," which is the aponeurosis folded over upon itself.
3. Next, the conjunctiva is bluntly dissected off the posterior aspect of Müller's muscle and incised 3 mm superior to the tarsal segment along its full length.
4. Three equidistant mattress-type sutures of 4–0 Prolene or silk (Werb's choice) or 4–0 chromic are passed first through the cut edge of conjunctiva and then through Müller's muscle at the level corresponding to the desired amount of resection. The portion of Müller's muscle inferior to the sutures is resected (Fig. 22.39c).
5. The sutures are then passed above the anterior surface of the tarsus and through the anterior lamella to exit above the lash margin (Fig. 22.39d, e). The sutures are tied over bolsters if nonabsorbable sutures are used (Fig. 22.39f). The level at which the suture passes over the tarsus to exit the skin will correspond to the new insertion of Müller's muscle. Figure 22.39g, h shows a schematic cross section of Werb repair. A lid crease can actually be created at the level where these sutures are tied. If absorbable sutures are used, these can be tied without bolsters in the lid crease.

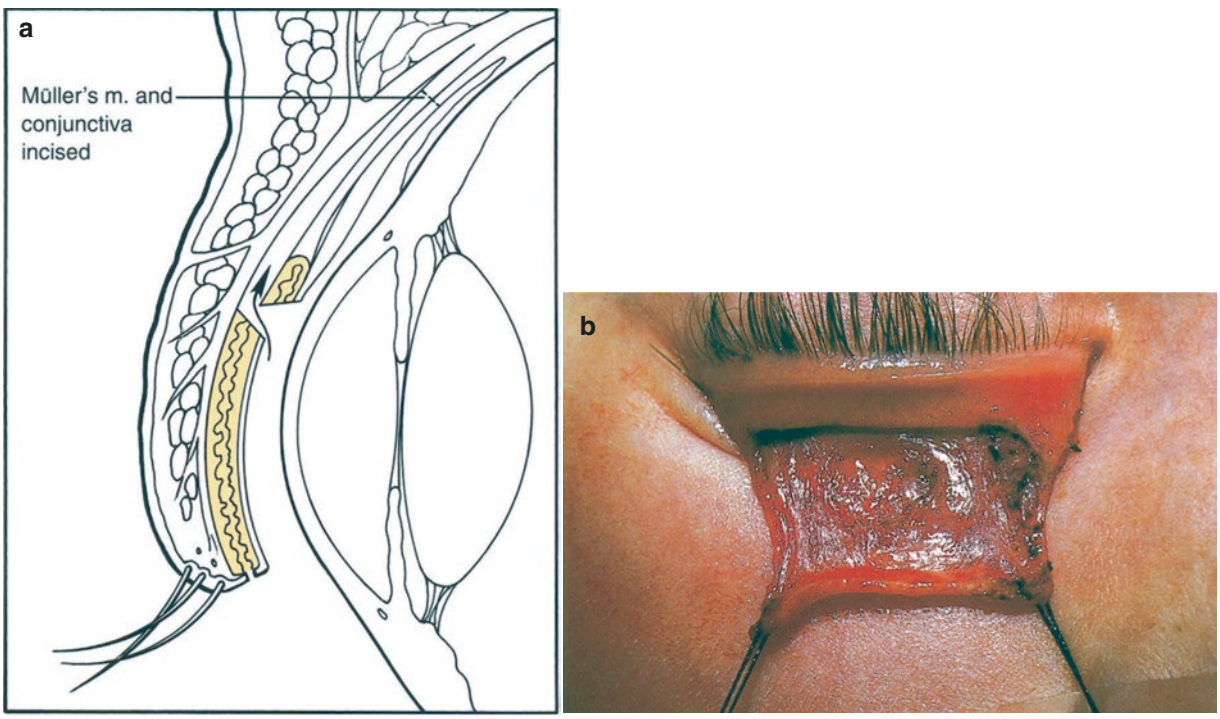


Fig. 22.39 Werb procedure

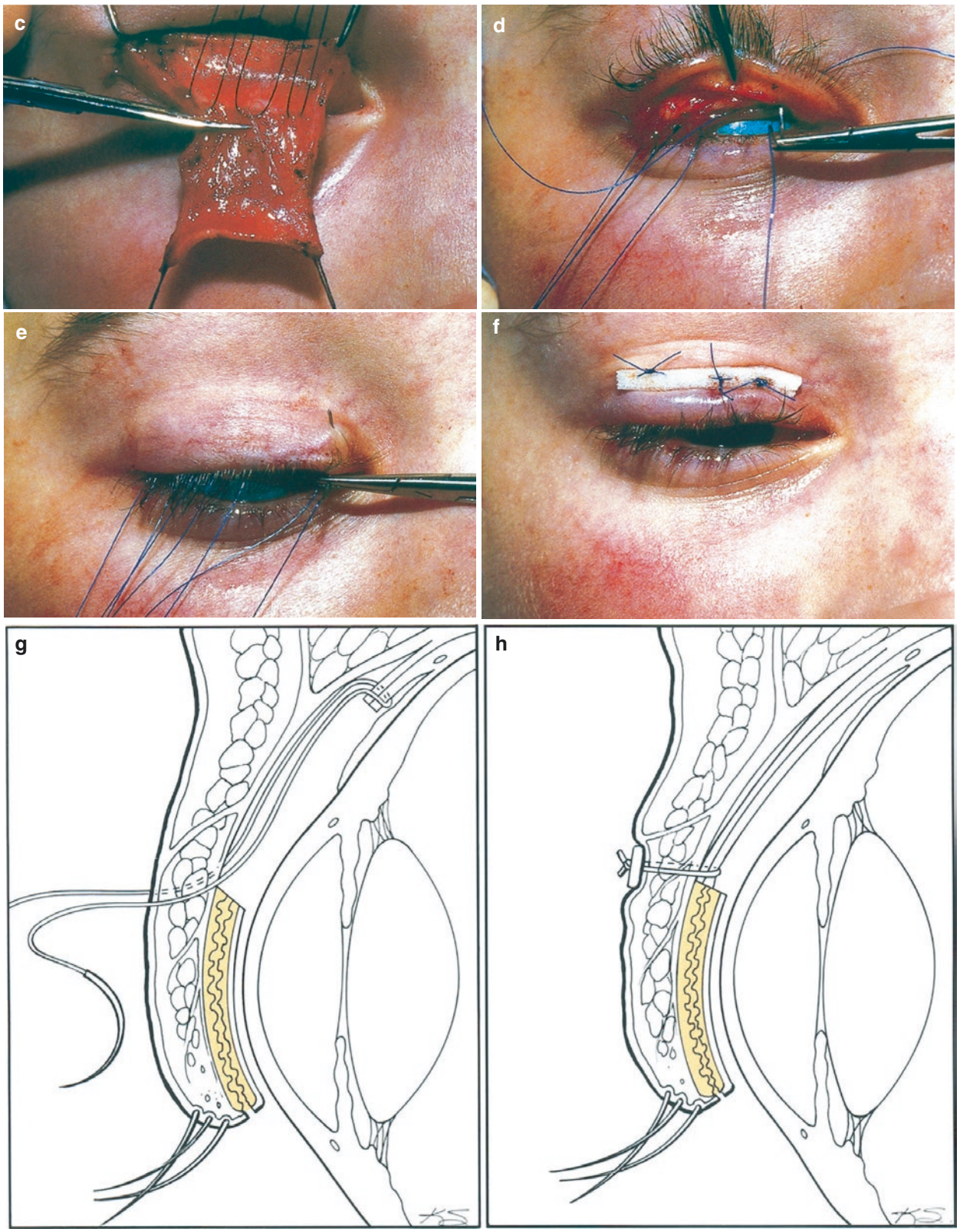


Fig. 22.39 (continued) Werb procedure

Modified Fasanella-Servat Procedure

1. Following sterile preparation, the upper eyelid is everted, and two curved hemostats are placed at the upper tarsal border. They are adjusted so that the tips meet centrally, and they are positioned no closer than 4 mm from the lower tarsal border. The hemostats incorporate tarsus, Müller's muscle, and conjunctiva (Fig. 22.40a).
2. 4–0 silk traction sutures are passed full thickness through the tissue approximately 3 mm below the clamps at both the nasal and temporal ends (Fig. 22.40b). These sutures are tied and used for traction.

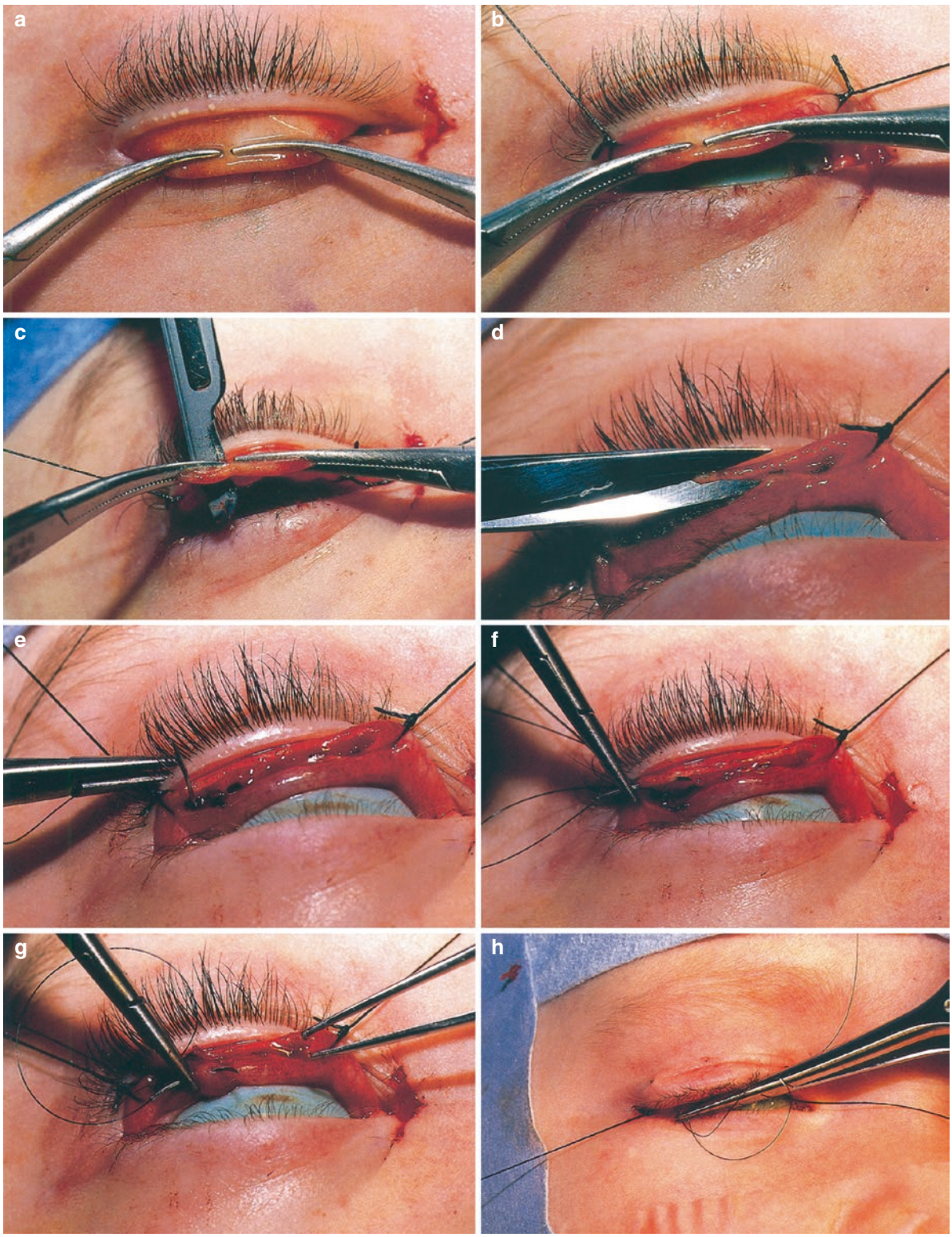


Fig. 22.40 Modified Fasanella-Servat procedure



Fig. 22.40 (continued) Modified Fasanella-Servat procedure

3. Traditionally a No. 15 blade has been used to excise the tissue held in the clamp by cutting between the clamp and the traction sutures, avoiding a peak of tarsus (Fig. 22.40c). An alternative is to remove the clamps and then to excise the crushed tissue with sharp scissors. This may permit a more controlled excision and also allow the surgeon to adjust the excision of tissue further medially or laterally, depending on the need for any contour correction (Fig. 22.40d).
4. A 5–0 nylon suture on a P-3 needle (Ethicon, Somerville, NJ) is passed through one end of the lid crease and out through the apex of the incision. The suture is run in a serpentine fashion, reattaching conjunctiva and Müller's muscle to the cut edge of the tarsus (Fig. 22.40e–g). Care should be taken to avoid incorporating the levator aponeurosis while suturing. The folded over aponeurosis will appear as a "white line." The amount of Müller's muscle advancement to the internal tarsal edge can be adjusted, depending on the preoperative response to phenylephrine and on the need for adjusting contour of the lid as well.
5. Upon reaching the opposite end of the incision, the suture is passed through the apex of the incision and out through the lid crease (Fig. 22.40h). The suture will be buried beneath the conjunctival surface much as in subcuticular placement and therefore will not irritate the cornea when pulled tight and tied (Fig. 22.40i).
6. The traction sutures are removed, and the lid is returned to its normal position. A plastic or metal lid plate is used to smooth the incision line by pressing directly on the skin surface with an index finger to flatten the tissues against the plate (Fig. 22.40j).
7. The 5–0 nylon suture is tied fairly snugly over the skin, creating a slight indentation. The suture is usually removed 1 week following surgery, but can be removed earlier, allowing adjustment of the lid level by manual traction if there is an overcorrection (Fig. 22.40k).

Levator Aponeurosis Advancement

1. A skin marker is used to draw an incision at the position of the desired lid crease. The lid is infiltrated subcutaneously with 0.5–1 mL of 0.25% bupivacaine with epinephrine 1:200,000.
2. Following sterile preparation, a No. 15 blade is used to make the skin incision along the previously placed mark. The orbicularis muscle is incised centrally with a snip and carefully cut along the full length of the incision. Care must be taken to avoid cutting the underlying levator aponeurosis, which is particularly vulnerable if the lid is put on traction.

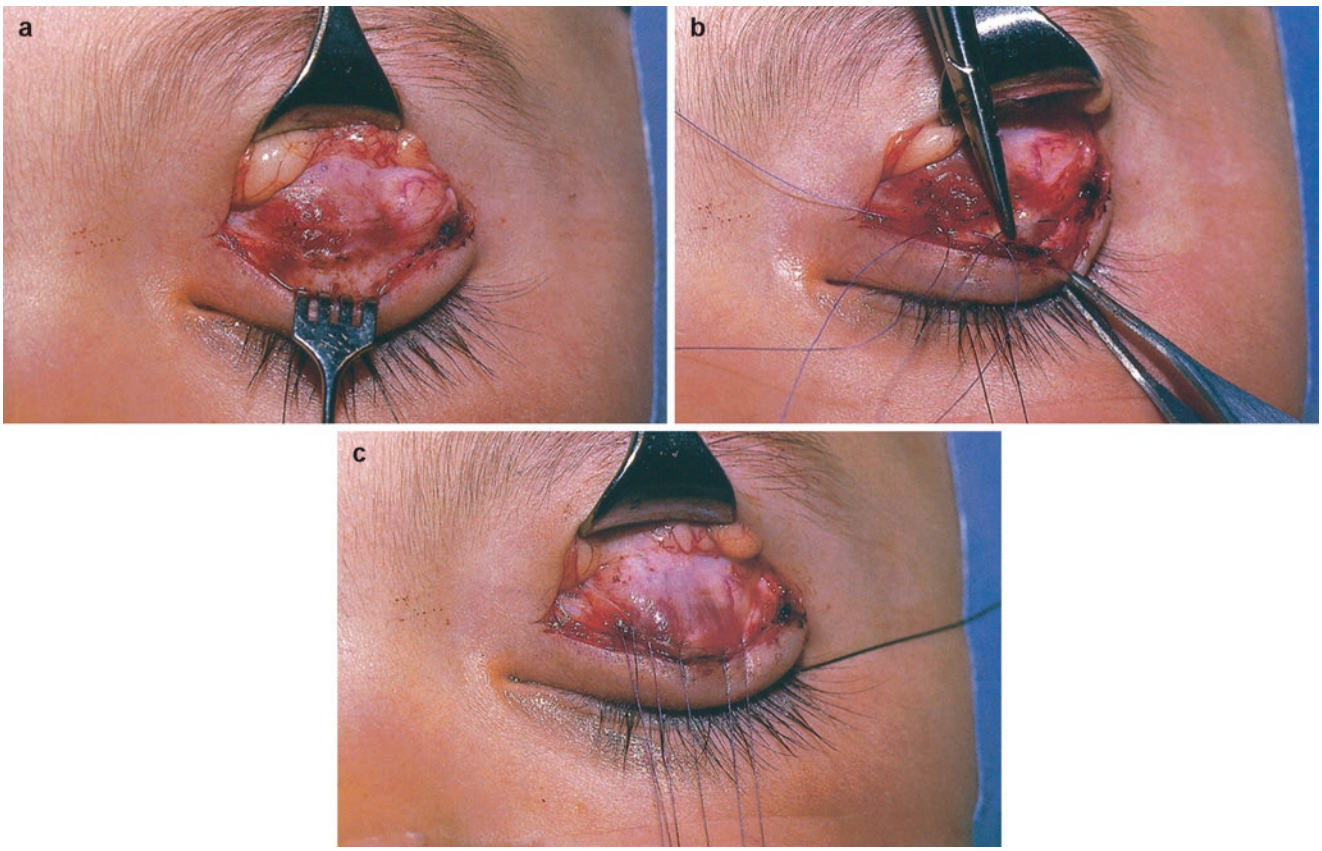


Fig. 22.41 Levator aponeurosis advancement

3. A skin-muscle flap is dissected superiorly until the septum and underlying preaponeurotic fat are identified. Gentle pressure on the globe will push fat and septum forward. The septum is then buttonholed in the superior aspect of the wound, and the incision is extended horizontally. Just posterior to the exposed preaponeurotic fat lies the levator aponeurosis. The edge of a dehisced levator aponeurosis may be identified as a white band (Fig. 22.41a).
4. The pretarsal orbicularis covering the superior aspect of the tarsus should be elevated, exposing bare tarsus. Three 6–0 double-armed polyglactin sutures with S-24 needles (Ethicon) are passed through partial-thickness tarsus 2–3 mm below the superior margin. The first suture should be placed in a position aligned halfway between the center of the pupil and the limbus. The remaining sutures are placed nasal and temporal to the first. The sutures are passed through the free edge of the levator in direct vertical alignment (Fig. 22.41b, c).
5. The sutures are temporarily tied with a bow knot, and the lid height and contour are assessed. The placement of the sutures through the aponeurosis is then adjusted to achieve the desired correction. Additional sutures can be placed if needed to adjust height and contour of the lid. The sutures can then be permanently tied. One end of each suture is passed through the subcutaneous tissue of the inferior edge of the skin incision and tied to the knot in the levator muscle to recreate the lid crease and fold. (We feel that this technique most closely recreates the natural appearance of the firm adherence of the pretarsal skin and orbicularis to the tarsus. A natural lid fold is thus created as the preseptal skin moves freely over the pretarsal skin and crease as the levator muscle contracts.)
6. The skin incision is closed with a running 6–0 fast-absorbing catgut suture.

Levator Resection

1. A skin marker is used to draw an incision at the position of the desired lid crease. The lid is infiltrated subcutaneously with 0.5–1 mL of 0.25% bupivacaine with epinephrine 1:200,000.
2. Following sterile preparation, a No. 15 blade is used to make the skin incision along the previously placed mark. The orbicularis muscle is incised centrally with a snip and cut along the full length of the incision.
3. A full-thickness buttonhole incision is made with closed scissors blades just above the superior temporal aspect of the tarsus. The closed scissors blades are passed along the palpebral aspect of the conjunctiva and pushed back through another buttonhole incision at the superomedial edge of the tarsus (Fig. 22.42a, b).

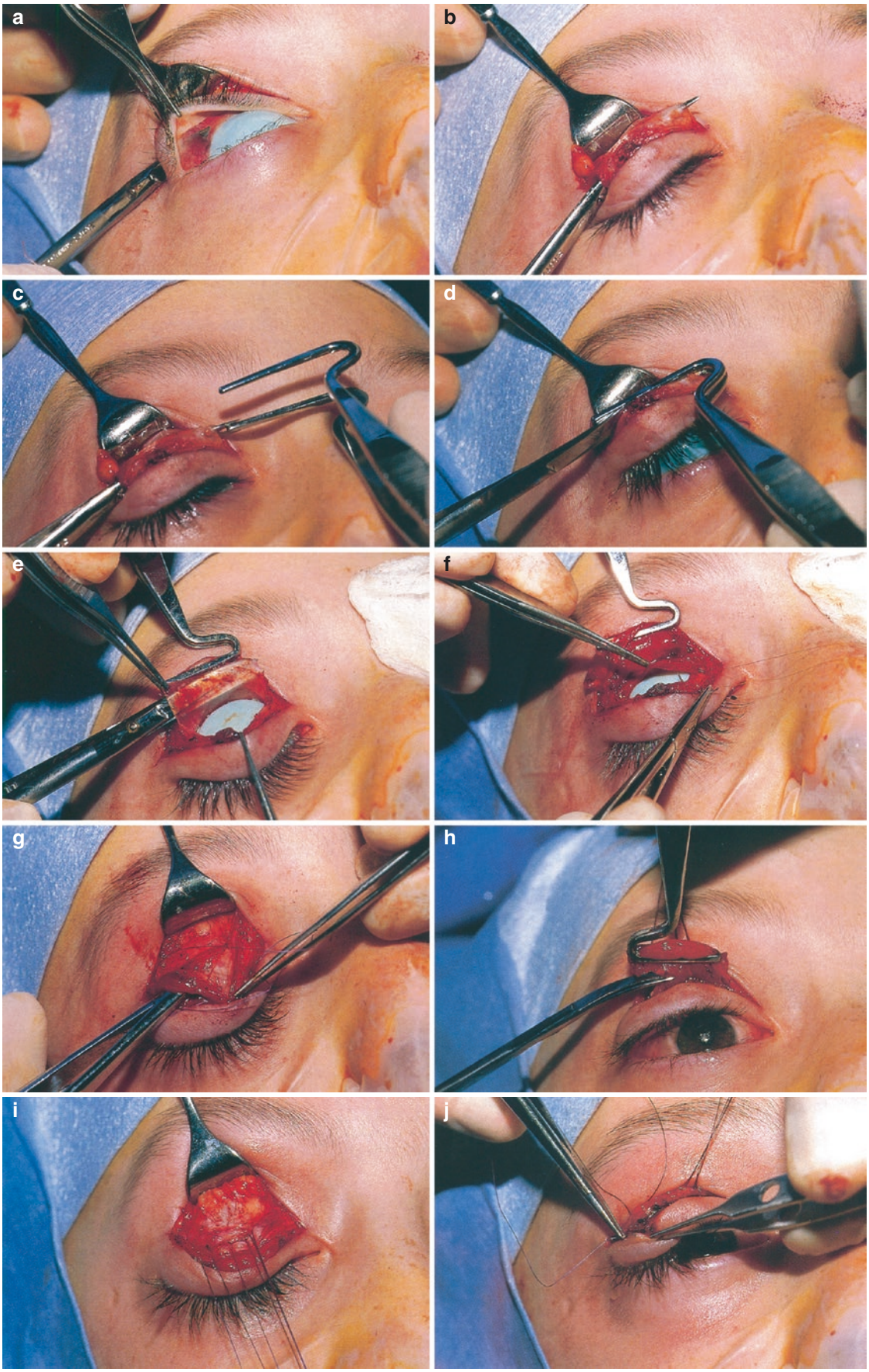


Fig. 22.42 Levator resection

4. The lower blade of the Berke ptosis clamp (Storz, St. Louis, MO) is grasped between the two blades of the scissors. As the scissors are withdrawn, the ptosis clamp is pulled across the tissue, with one arm of the clamp above and one arm below. The ptosis clamp is closed, incorporating conjunctiva, Müller's muscle, and levator aponeurosis (Fig. 22.42c).
5. A No. 15 blade or scissors is used to cut the tissue between the clamp and the superior border of the tarsus (Fig. 22.42d). In performing a "supramaximal" resection, the clamp can be adjusted to incorporate 2–3 mm of tarsus, so that the cut is through the tarsus and adherent palpebral conjunctiva. An alternative is to use sharp scissors to resect the tarsus after clamping and cutting the incorporated tissues.
6. The orbital septum is buttonholed in a location overlying the preaponeurotic fat. The septum is opened nasally and temporally, and the preaponeurotic fat is gently retracted. In some cases of myogenic ptosis, the septum is somewhat fibrotic or appears to be multicompartmental; when released, the lid will sometimes move more freely when manually manipulated to mimic levator excursion.
7. The tissue in the clamp is everted to reveal the underlying conjunctiva. Scissors are used to dissect the plane between conjunctiva and Müller's muscle. It is best to enter the conjunctiva 10–12 mm above the tarsus where there is a surgical plane for dissection. Spreading with the scissors will peel the more adherent portion of the conjunctiva away; 4–5 mm of conjunctiva is resected to minimize the chance of postoperative prolapse (Fig. 22.42e). We have found no adverse effect on tear film either objectively or subjectively from this resection of conjunctiva [36].
8. The conjunctiva must be carefully dissected free of Müller's muscle into the cul-de-sac, and this is most easily accomplished using a wet cotton-tip applicator. Blunt dissection must be continued deep into the superior fornix to lyse the loose connections between the levator and superior rectus muscles to reduce the chance of a postoperative hypotropia.
9. The conjunctiva is reattached to the upper tarsal border with approximately 4 interrupted 6–0 plain catgut sutures. The suture bites should be made partial thickness through the tarsal edge to avoid corneal contact with the suture (Fig. 22.42f).
10. Three double-armed 5–0 polyglactin sutures are passed through partial-thickness tarsus at a point 2–3 mm below the upper tarsal border. Each arm is passed superiorly through the levator muscle held in the clamp. The sutures are temporarily tied with a bow knot, the clamp is removed, and the lid height and contour are assessed. The placement of the sutures through the levator muscle is adjusted to achieve the desired correction. If the lid level is still insufficient, the sutures can be placed lower on the anterior tarsal surface, but not more than one-third the vertical distance from the superior tarsal border, or eversion may occur. When the lid height and contour are satisfactory, the sutures can then be permanently tied, and the excess Müller's and levator muscles are excised (Fig. 22.42g–i).
11. One end of each suture is passed through the subcutaneous tissue of the inferior edge of the skin incision and tied to the knot in the levator muscle to recreate the lid crease and fold (Fig. 22.42j). As mentioned earlier regarding aponeurosis advancement, this is accomplished by the pretarsal skin and orbicularis being held more snugly to the tarsus, with the preseptal skin lying more loosely over the orbital septum and preaponeurotic fat.
12. The skin incision is closed with a running 6–0 fast-absorbing catgut suture. This can be supplemented with 7–0 poly glycolic interrupted sutures as needed for wound security, particularly if there is a tendency for orbital fat prolapse (Dexon, Davis and Geek, Manati, PR).

    For any patient at risk of significant exposure following any ptosis repair and especially if unable to be easily followed postoperatively on a frequent basis, the use of a temporary tarsorrhaphy is recommended. Traditionally, a Frost type of protective suture can be passed through the gray line of the lower lid, for traction has been recommended. The suture is then secured to the forehead, drawing the lower lid up over the cornea. For the first 24–48 h following surgery, the suture can remain in place to provide adequate corneal protection, and the cornea can then be observed periodically, retaping the suture for longer periods, as needed.
13. Our preference is to place a nonabsorbable suture (5–0 black nylon) through the gray line of the upper lid brought out as a mattress suture tarsorrhaphy beneath the lash line of the lower lid. This can be tied with or without a bolster directly on the skin. This can be done as a temporary lateral tarsorrhaphy alone, or in severe problems, with little or no motility, as both a lateral and medial temporary support (Fig. 22.45i or Fig. 22.46i). This will protect the cornea and allow for a safer adjustment to exposure of the cornea postoperatively. It can be removed in 3–7 days or with a 5–0 chromic suture, allowed to dissolve over a 2–3 week period. Because exposure keratopathy can be devastating, most of the postoperative care of ptosis patients is directed toward limiting this spectrum of problems (see the postsurgical management section in this chapter).

Frontalis Suspension: Single Rhomboid Technique with Silicone (Sleeve Technique) (Fig. 22.43)

1. A skin marker is used to draw an incision at the position of the desired lid crease and two stab incisions located just above the brow aligned with the lateral and medial canthi. Care should be taken to avoid the supraorbital nerve and vessels. If a synthetic temporizing material is used and creation of a lid crease is unnecessary, two stab

incisions can be made at the medial and lateral end of the crease or just above the lashes. The lid and brow area are infiltrated subcutaneously with 2–3 mL of 0.25% bupivacaine with epinephrine 1:200,000.

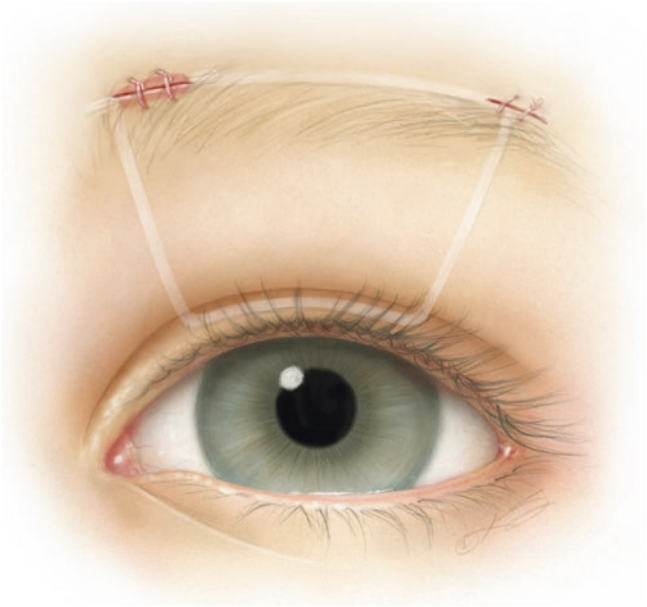


Fig. 22.43 Frontalis suspension drawing of single-rhomboid technique. A silicone sleeve is placed in the medial suprabrow incision

2. Following sterile preparation, a No. 15 blade is used to make the incisions along the previously placed marks. The orbicularis muscle is incised centrally with a snip and cut along the full length of the incision.
3. While purposefully avoiding dissection inferiorly over the tarsus, the needle of the Seiff frontalis silicone set (BD Visitec) is passed from as far temporally as possible, in the pretarsal space just superior to the lashes and avoiding the lash follicles. The needle is carefully passed to emerge from the incision at the nasal-most aspect of the lid. The contour is checked. If the lid is squared off, then small incisions can be made to decrease the length of passage across the tarsus (Fig. 22.44a). If the lid is peaked from too narrow a purchase, then either a new pass or suturing of the material directly to the tarsus with 6–0 Prolene, Vicryl, or silk can be done. An alternative is to convert to a double-triangle technique with this material (see below).
4. A metal plate is placed under the lid to protect against globe perforation. The sling needle is then passed from the medial aspect of the lid incision to the medial brow incision (Fig. 22.44b).
5. A similar maneuver is performed temporally (Fig. 22.44c).
6. The needle is passed from the temporal brow incision, arching superiorly into the frontalis muscle, before exiting through the nasal incision. Both ends of the silicone

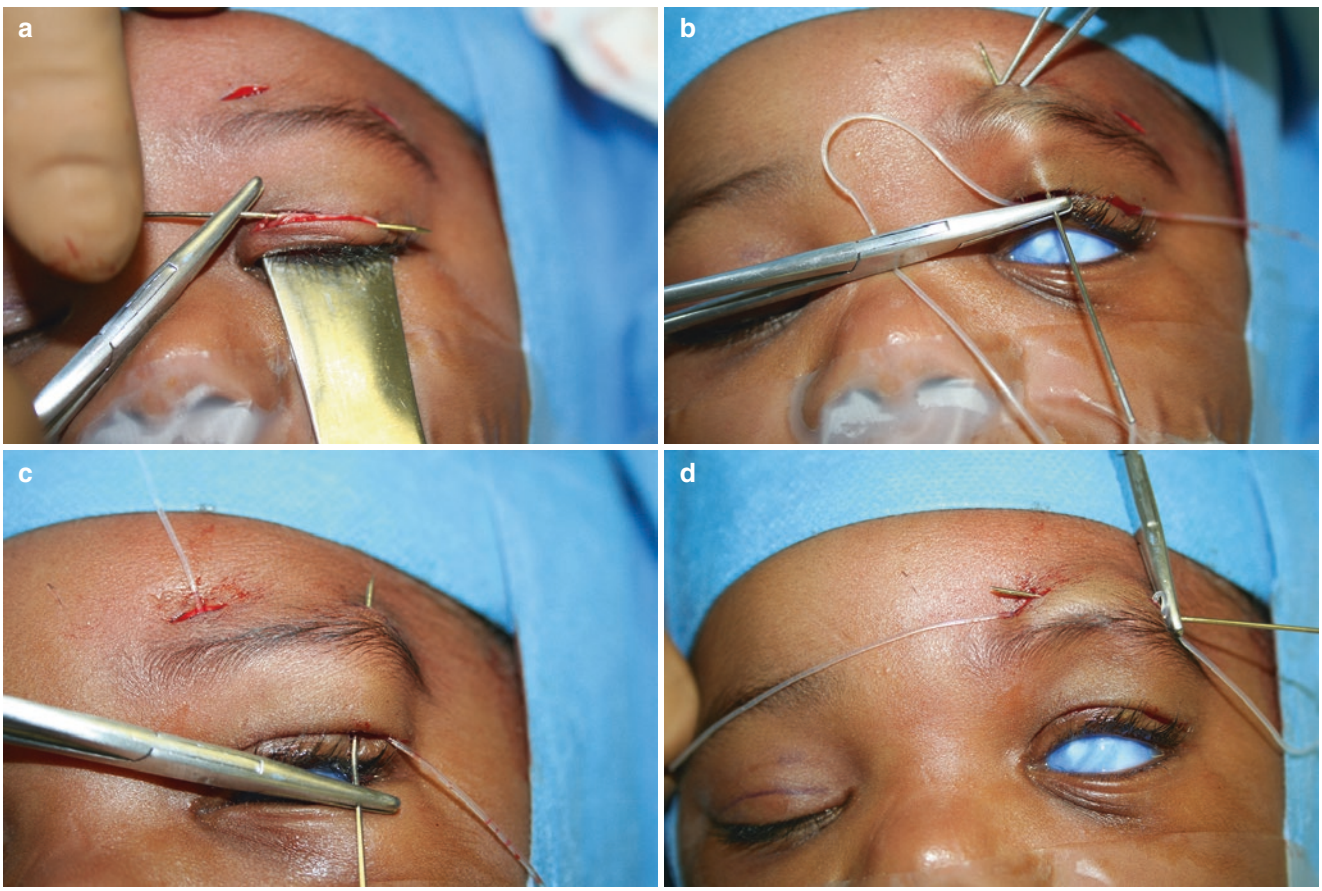


Fig. 22.44 Frontalis suspension steps for placement of single-rhomboid technique with silicone (BD Visitec)



Fig. 22.44 (continued) Frontalis suspension steps for placement of single-rhomboid technique with silicone (BD Visitec)

can now be pulled to determine the maximum lift before the lid margin lifts off the cornea and to estimate if there is excess skin superiorly (Fig. 22.44d).

7. The appropriate amount of skin is excised, and the lid incision is closed with a running 6–0 fast-absorbing catgut suture or a 6–0 plan gut suture on a TG140-s needle. It is best to be conservative with skin excision in order to allow for a more normal-appearing lid fold and crease. It is helpful to secure the pretarsal skin and orbicularis to the tarsus as is done in levator resection procedures.
8. Each end of the silicone is passed through the provided sleeve. Care is made to not nick the sling material with the needle tip as this will result in sling breakage. After adjusting the eyelid height, a 5–0 clear nylon suture is passed over the central sleeve to prevent silicone sling slippage (Fig. 22.44e–g).
9. The brow stab incisions are closed with single vertical mattress 5–0 Vicryl suture and three 6–0 vicryl sutures through the skin.
10. A temporary suture tarsorrhaphy as discussed above is recommended (Fig. 22.44g, h).

Frontalis Suspension: Double-Triangle Technique with Tied Silicone Knot Technique (Fig. 22.45)

1. A skin marker is used to draw an incision at the position of the desired lid crease and two stab incisions located just above the brow aligned with the lateral and medial canthi. Care should be taken to avoid the supraorbital nerve and vessels. If a synthetic temporizing material is used and creation of a lid crease is unnecessary, two stab incisions can be made at the medial and lateral end of the crease or just above the lashes. The lid and brow area are infiltrated subcutaneously with 2–3 mL of 0.25% bupivacaine with epinephrine 1:200,000.
2. Following sterile preparation, a No. 15 blade is used to make the incisions along the previously placed marks. The orbicularis muscle is incised centrally with a snip and cut along the full length of the incision (Fig. 22.46a). A small ellipse of skin is removed (Fig. 22.46b).
3. A silicone sling set (FCI Ophthalmics) is brought on to the surgical field. The surgeon may either use the needle that is suaged onto the silicone or cut off the needle and use a fine, spatulated Keith needle to pass the silicone (Fig. 22.46c). Care is made to pass the sling needle from the central eyelid to the medial crease incision. The needle should pass in the suborbicularis and pretarsal space.
4. Care is made to pass the sling needle from the central eyelid to the medial crease incision. The needle should pass in the suborbicularis and pretarsal space (Fig. 22.46e). The needle then passed under the skin and orbicularis to the medial suprabrow stab wound. Care is made to avoid the superior orbital notch. In addition, care should be made to allow the needle to emanate freely through the brow wound without including the dermis of the incision.

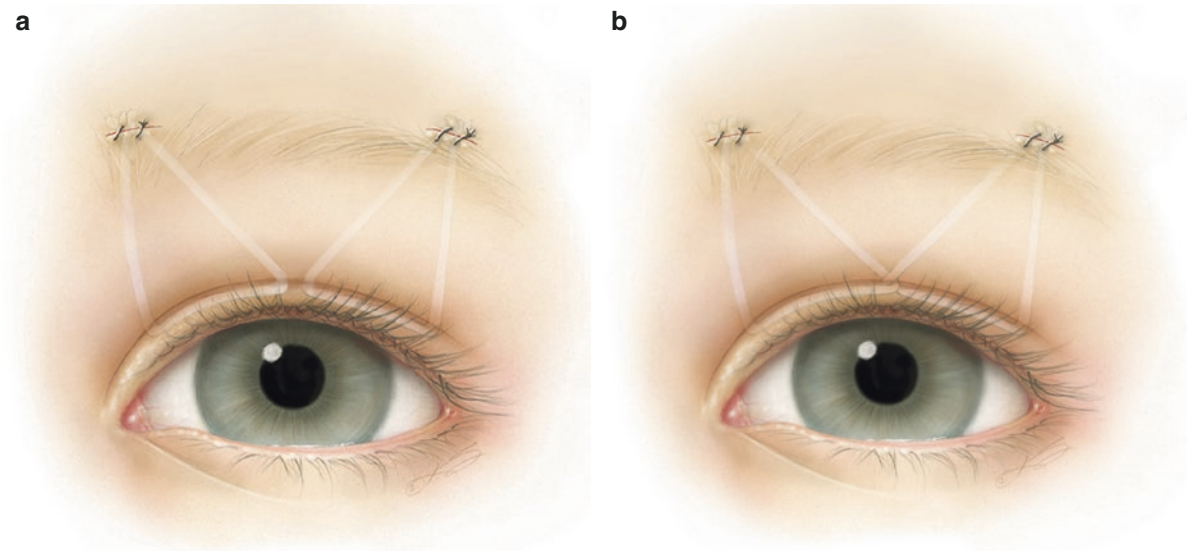


Fig. 22.45 Frontalis suspension: drawing demonstrating double-triangle technique. (**a**) Uncrossed technique with two slings. (**b**) Crossed technique, where the two slings are overlapped centrally

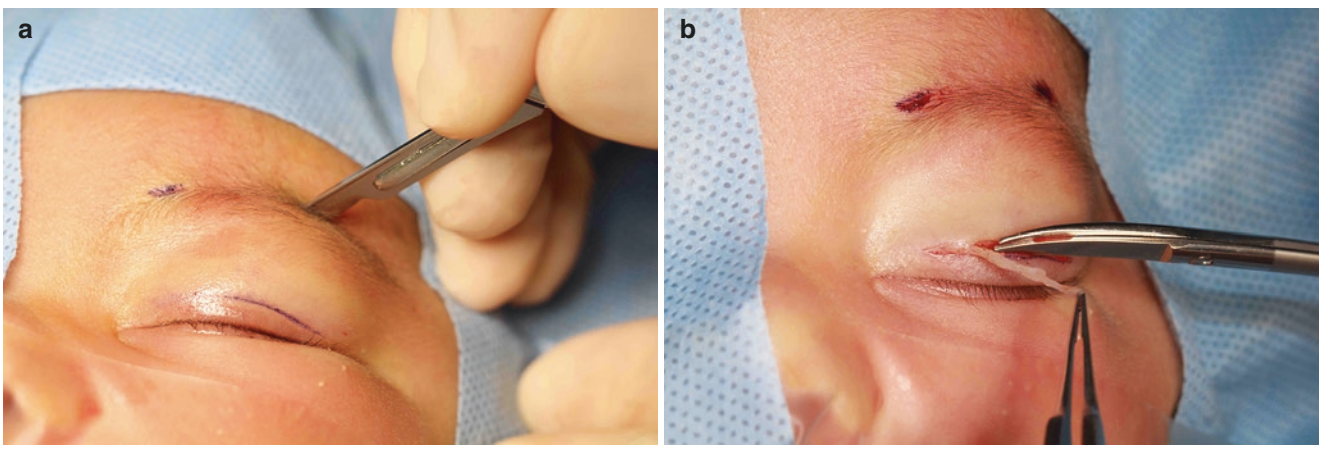


Fig. 22.46 Frontalis suspension surgical steps for double-triangle technique with silicone (FCI Ophthalmics)

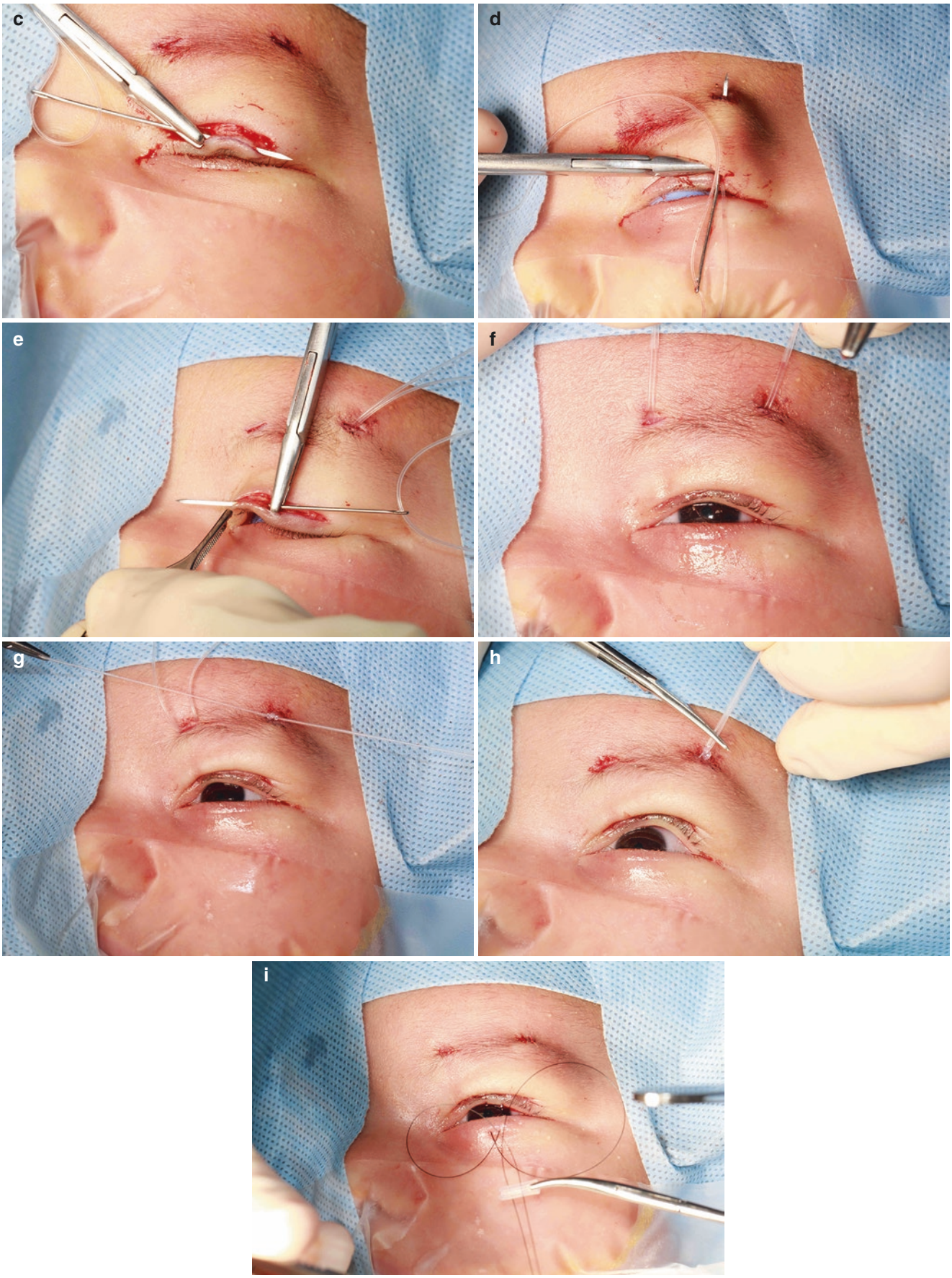


Fig. 22.46 (continued) Frontalis suspension surgical steps for double-triangle technique with silicone (FCI Ophthalmics)

5. A similar maneuver is performed temporally.
6. The appropriate amount of skin is excised (Fig. 22.46b), and the lid incision is closed with a running 6–0 fast-absorbing catgut suture or a 6–0 plan gut suture on a TG140-s needle. It is best to be conservative with skin excision in order to allow for a more normal-appearing lid fold and crease. It is helpful to secure the pretarsal skin and orbicularis to the tarsus as is done in levator resection procedures.
7. The scleral shell is removed. Each sling is tied onto itself in a 2–1-1 fashion after setting the desired eyelid height. Excess sling is cut, and the silicone knots are allowed to retract into the brow wounds (Fig. 22.46f–h). This maneuver is possible because the silicone is in the form of a thinner tube easily tied as described in contrast to the Visitec material requiring a sleeve because it is a slightly thicker rod rather than a tube.
8. The brow stab incisions are closed with single vertical mattress 5–0 Vicryl suture and three 6–0 Vicryl sutures through the skin.
9. A temporary suture is placed over a bolster (Fig. 22.46i).

Frontalis Suspension: Crawford Double-Rhomboid Technique (Pentagon)

This procedure (Fig. 22.47) is similar to the double-triangle technique except for the following variations: (1) Two slings are used rather than one. (2) These overlap one another centrally over the tarsus and then are tied individually as triangles at the nasal and temporal brow incisions. (3) The long ends of the fascial strips can then be passed to a central incision above the brow and tied.

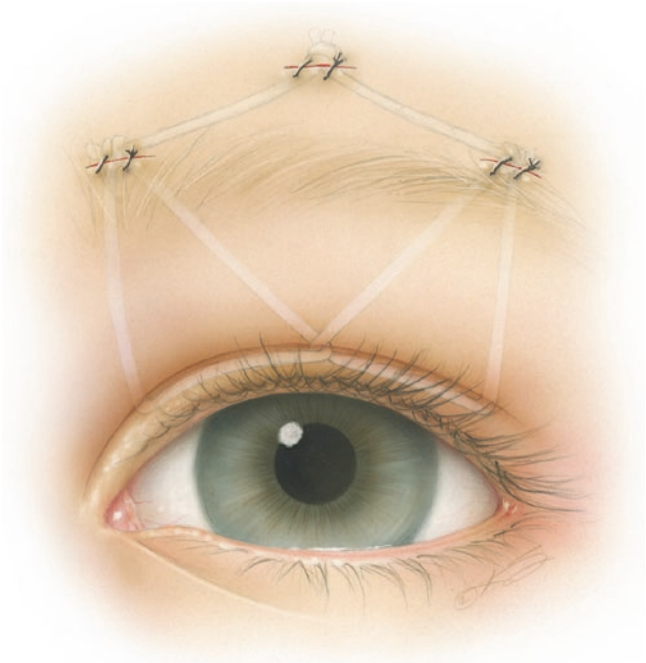


Fig. 22.47 Frontalis suspension: Crawford double-triangle technique with central brow incision for fascia lata suspension

Harvesting Autogenous Fascia Lata (Fig. 22.48)

1. The patient is positioned on the table with the donor leg flexed. A small roll is placed to elevate the trunk. The outer thigh from the knee to hip is prepped and draped.
2. The lateral condyle is located, and an incision is made vertically approximately 2 cm above, extending for a length of 2–3 cm. The incision extends along the tendon that runs from the anterior superior iliac spine to the lateral condyle of the femur (see Chap. 4).
3. The incision is made through the skin and fat to expose the underlying fascia. The fascia is easily identified by its glistening white appearance (Fig. 22.48a). Blunt dissection is performed to lyse all adhesions to the subcutaneous tissue, and this should be extended as far superiorly as possible. A long Metzenbaum-type scissors is useful for this purpose.
4. Incisions in the fascia are made to create a 10-mm-wide strip of fascia. The parallel incisions should be aligned in the direction of the fascial fibers. Blunt dissection is now performed below the fascia, passing the long scissors to separate fascia from muscle. The strip should be cut as long as the incision will allow under direct observation.
5. The end of the 10-mm strip is threaded into a Crawford fascia lata stripper (Storz). The instrument can be palpated through the skin and guided along the tendon. The stripper is pushed superiorly toward the anterior superior iliac crest, while the end of the fascia lata strip is grasped with a hemostat clamp. When approximately 20 cm have been obtained, the fascia is cut (Fig. 22.48b, c).
6. The adherent fat and connective tissue are cleaned from the strip using scissors. The harvested fascia can then be divided in half along its length to produce two 5-mm strips. This is facilitated by using a cutting board. The fascia is smoothed flat on the board, and a scalpel is used to divide the strip vertically at one end, using forceps for traction. The strip is separated while cutting with a scissors or scalpel (Fig. 22.48d).
7. The donor site on the leg is then closed as follows: Subcutaneous tissue is closed with a combination of interrupted vertical and horizontal mattress 4–0 and 5–0 Vicryl. The skin is closed with a running 5–0 subcuticular Monocryl suture (Ethicon, USA). The leg wound is washed, and Dermabond (Ethicon, USA) is applied to the leg wound (Fig. 22.48e).

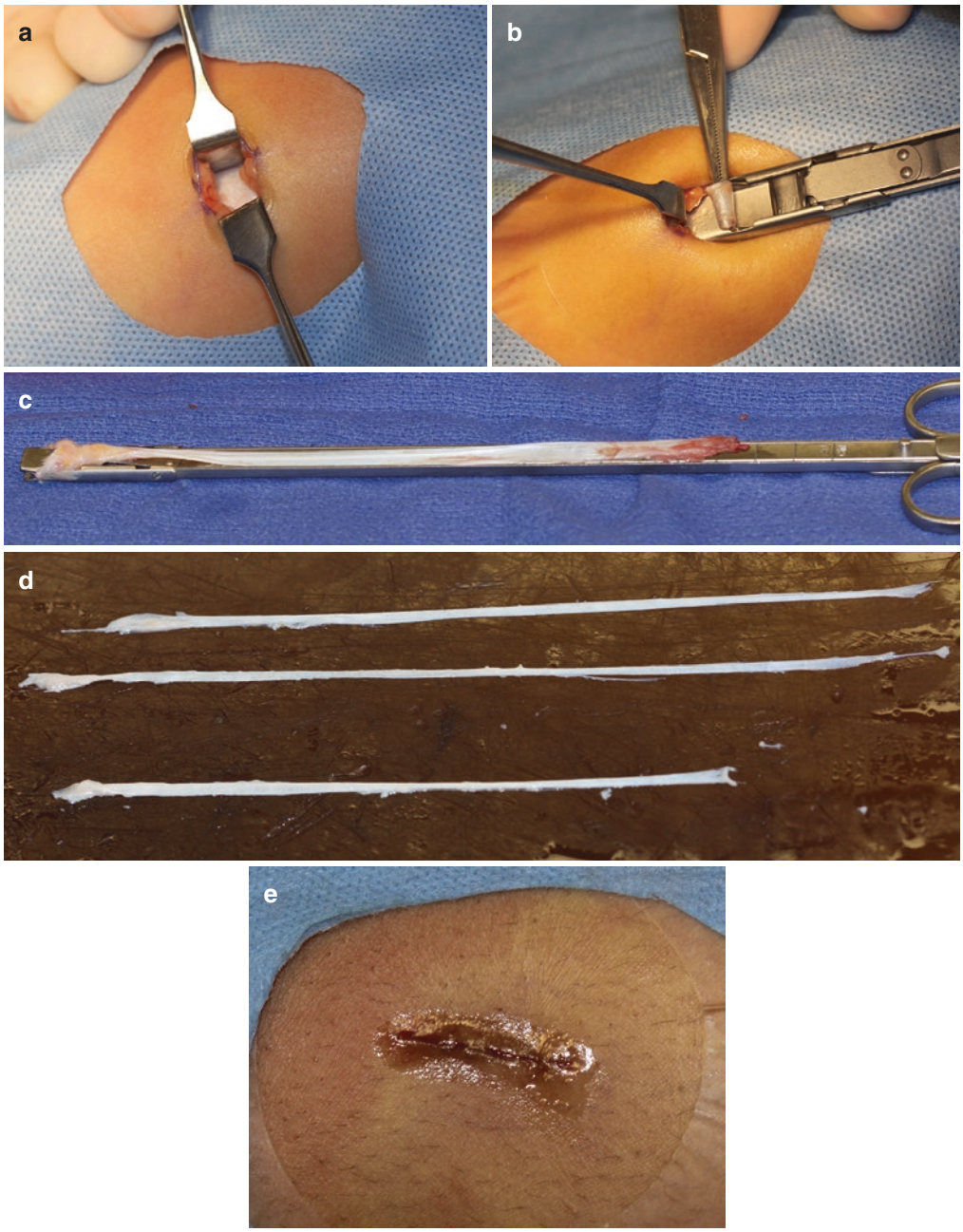


Fig. 22.48 Harvesting autogenous fascia lata. (**a**) A lateral leg incision is made 15 mm in length approximately 1 cm proximal to the lateral epicondyle of the femur. Care is made to dissect to the fascia lata. (**b**) Two longitudinal incisions are made in the fascia lata 1cmm apart, and a flap of fascia is raised and fed into the fascia lata stripper. A hernia retractor is used to raise the proximal end of the incision. (**c**) Harvested fascia lata. (**d**) The graft is cut longitudinally in to strips of equal width. (**e**) The wound is closed with vertical mattress Vicryl sutures and a running subcuticular Monocryl suture. The skin is closed with cyanoacrylate glue

Autogenous Fascia Lata Sling (Fig. 22.49)

1. As depicted in Fig. 22.46a, an eyelid crease incision and a lateral and medial suprabrow incision are made with a #15 blade.
2. With the use of a Wright needle, a single strip of fascia lata is passed under the pretarsal orbicularis approximately 3–4 mm above the eyelid margin (Fig. 22.49a). Care must be taken to evert the eyelid to confirm the tarsus has not been violated, thus exposing the sling to the corneal surface.
3. The Wright needle with fascia is passed from the eyelid crease incision below the orbicularis to the medial suprabrow incision. Care must be taken to not puncture the supraorbital notch (Fig. 22.49b). The central end of the fascia lata strip is passed in the same manner (Fig. 22.49c).
4. This is repeated in the same manner with a temporal fascia lata strip (Fig. 22.49d, e).



Fig. 22.49 Autogenous fascia lata sling. (**a**) After an eyelid incision and suprabrow stab incisions, the fascia lata sling is passed from the central eyelid to the medial eyelid with the use of a Wright fascia needle (**b**). This is passed in the suborbicularis and pretarsal plane. (**c**) The fascia is advanced to the suprabrow stab wound. (**d**) A lateral fascia strip is placed in the eyelids. (**e**) The fascia is pulled into place in the eyelid. (**f**) After both strips have been passed, the eyelid is inspected for good contour and elevation. (**g**) The eyelid crease incision is closed, and the fascia lata strips are tied and buried into the suprabrow incisions. (**h**) A lateral tarsorrhaphy has been placed to allow for good corneal coverage in the immediate postoperative period



Fig. 22.50 Bilateral autogenous fascia lata sling repair. (**a**) Preoperative photo. (**b**) Postoperative photo taken 4 days after surgery. Bilateral lateral suture tarsorrhaphies are in place. (**c**) Postoperative photo taken 1 year after surgery. (**d**) Lagophthalmos 1 year after surgery. This patient is no longer requiring eye lubrication. Despite her lagophthalmos she does not have dry eye due to her intact Bell's phenomenon. (**e**) Eyelid lag on downgaze seen 1 year after surgery. (**f**) Fascia lata donor site scar 1 year after surgery

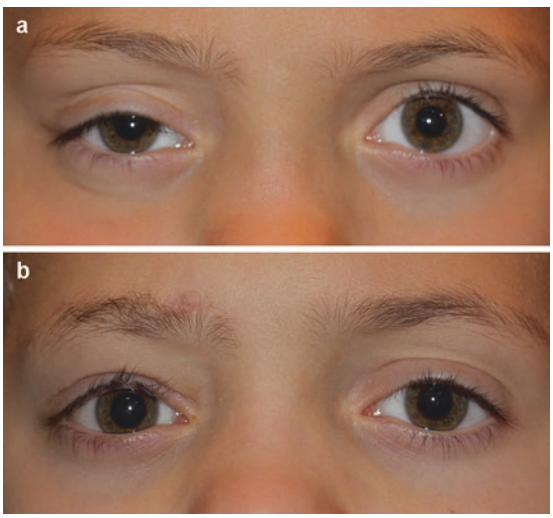


Fig. 22.51 Unilateral fascia lata sling repair. (**a**) Preoperative photo of marked right upper lid ptosis. (**b**) Postoperative photo taken 1 year after surgery. Note the left eyelid has lowered due to Hering's law

5. The eyelid crease is closed with a 6–0 plain gut suture (not pictured).
6. The fascia lata strips are tied in a 1–1-1 fashion to elevate the eyelid to a desired height (Fig. 22.49f). A 5–0 clear nylon suture is passed through the fascia lata knots.
7. After confirming good eyelid height and lid contour (Fig. 22.49g), a temporary lateral suture tarsorrhaphy is placed (Fig. 22.49h).

Figures 22.50 and 22.51 depict two patients who underwent autogenous fascia lata ptosis repairs.

Surgical Approaches for the Asian Eyelid

The anatomic differences in the eyelid of a patient of Asian descent have already been discussed. When planning ptosis surgery, one must be sensitive to the patient and the parents'

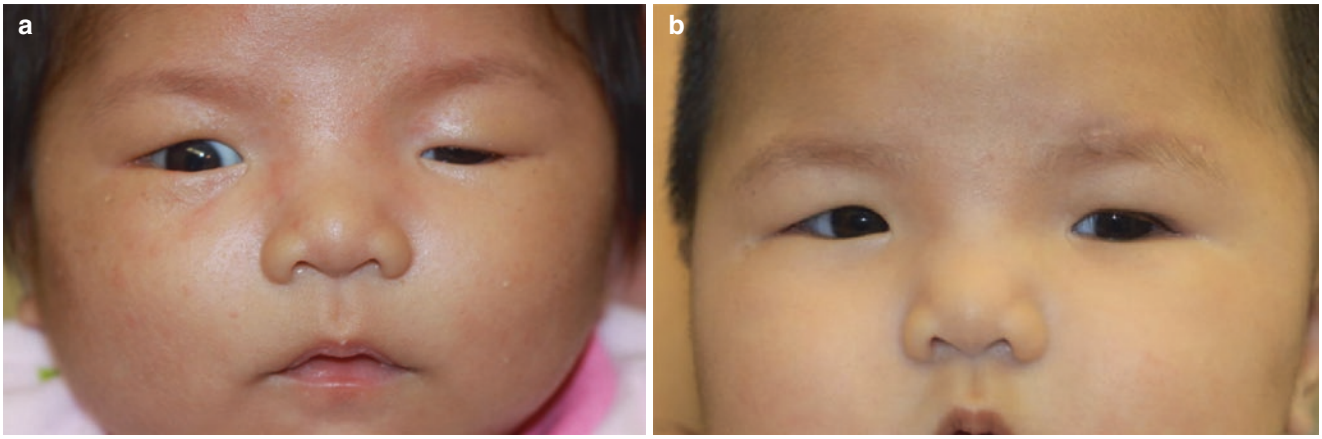


Fig. 22.52 Maintaining the appearance of the eyelid in an Asian patient with unilateral ptosis. (**a**) Preoperative photo taken at age 4 months. (**b**) Postoperative photo taken 5 months after a unilateral left silicone frontalis sling repair. Two supraciliary stab incisions were made just above the lash line. This patient had a left third-nerve palsy and subsequently underwent strabismus repair

wishes to either preserve the eyelid without a visible crease or to intentionally create a crease. While the "Westernization" of the eyelid with the formation of a crease is a desirable outcome to some people, the surgeon must always be sensitive to this and never assume a patient should desire this outcome. This is less of an issue with posterior approaches to the eyelid, such as the modified Fasanella or the Putterman procedure where the anterior anatomy of the eyelid has not been manipulated surgically. In any anterior approach, an eyelid crease incision will likely result in some form of visible skin fold. This can be accentuated during eyelid skin closure with 6–0 or 7–0 Vicryl sutures from the eyelid skin crease and orbicularis to the levator aponeurosis.

When the goal is to preserve the existing eyelid appearance with no visible crease, this can readily be accomplished during frontalis sling procedure by creating stab incisions just above the lash line in two or three places (depending on the sling configuration: rhomboid or double triangle). The sling can be passed into each stab wound in the suborbicularis and pretarsal plane and then up to the eyebrow. Figure 22.52 depicts a patient treated in such a manner.

To preserve a missing crease in levator resection, the incision must be made just above the lash line. Kim et al. published a small series using this technique with good cosmetic results [4]. In cases of blepharophimosis, maintaining the non-crease appearance is not always possible in order to achieve a good functional outcome. This is because the orbital septum and orbicularis require a degree of debulking to achieve an optimal lift.

Even with good surgical technique to preserve the non-crease appearance of the eyelid, a postoperative single or even double crease can occur [4]. As long as good surgical planning with patient and parental consent is obtained, the decision to maintain or alter the appearance of the eyelid has a reasonable chance for the desired outcome. It is especially important, however, in unilateral cases for parents (and patient when age appropriate) to understand the risk for an unwanted single or double crease in cases where the incision is placed just above the lash line.

Postsurgical Management

Most of the postoperative care of ptosis patients is directed toward limiting the spectrum of problems related to corneal exposure. Whereas those patients who undergo a Müllerectomy procedure are at very little risk of corneal exposure, other patients require aggressive lubrication regimens to assure a safe recovery. A mild antibiotic ointment prescribed four times a day is usually sufficient following Müllerectomy procedures. These patients are then seen in follow-up 5–7 days later for assessment of the eyelid position and removal of the suture if a modified Fasanella-Servat procedure has been performed.

The parents of patients undergoing either a levator resection or frontalis sling, on the other hand, require more detailed lubrication instructions. An application of an ointment every 2 h during the day and night is recommended for the first 24 h if no tarsorrhaphy has been placed. An antibiotic ointment that is relatively nontoxic to the corneal surface is applied four times daily, while an artificial tear ointment is used for the remaining applications. These patients are then evaluated in 24–48 h following the procedure. For patients who have had a protective suture tarsorrhaphy, application of lubricating ointment can be used every 4 hours with the suture in place. For these patients, if there is no evidence of any significant corneal exposure problem at the first postoperative visit, the suture tarsorrhaphy is usually removed at that time, but then lubrication is increased to every 2 hours during the day and 3–4 hours at night. These patients are then seen again for corneal evaluation in 4–5 days or prn any concerns. In general, the applications can then be reduced to every 3–4 h for the next 48 h. Gradual tapering of ointment over the next 2 weeks is usually done. Following this period, artificial tears

can usually be substituted for the ointment during the day, and gradually all forms of lubrication can be withdrawn. In the event that parents find it more difficult to apply the ointment, it is often helpful to melt the ointment into a more liquid form by running the tube under hot water for a short period of time. Parents frequently find that this technique assures more adequate coverage of the corneal surface.

Regardless of the type of lubrication regimen used, some degree of superficial punctate staining will often occur during the first few postoperative days. With gradual tapering of lubrication, however, the cornea usually becomes tolerant of the increased exposure.

For patients old enough to safely tolerate use of a plastic kitchen wrap patch without risk of suffocation, a less demanding regimen can be followed during the nighttime. The antibiotic ointment is first applied liberally to the cornea. A square of plastic kitchen wrap (or rectangle for bilateral procedures) is fashioned to cover the orbital rims, and the edges of the patch are secured to the skin with 1-inch strips of plastic tape so that an airtight seal is created. Upon removal after awakening in the morning, topical ointment application is resumed. In any situations, such as reduced ocular motility, where prolonged exposure is of greater concern, a temporary tarsorrhaphy should always be utilized to better permit the cornea to adjust to exposure.

All patients who have undergone a frontalis suspension, whether fascia lata or a synthetic material, are also placed on an oral antibiotic. We generally use a cephalosporin intravenously during the procedure and then orally for 7–10 days postoperatively.

Complications of Congenital Ptosis Surgery

One of the most challenging aspects of congenital ptosis surgery is its association with a relatively high incidence of postoperative problems. While problems are relatively common, they are usually not very serious. Certainly, one of the most common "complications" of congenital ptosis surgery is some degree of mild corneal exposure due to lagophthalmos. The result of less than perfect symmetry between the two eyelids is also a frequent concern for parents. This may be only due to postoperative edema and inflammation and is most often exemplified by an undercorrection of the lid position. Given that many cases of congenital ptosis are characterized by poor levator function, the surgeon (and parents) must be willing to accept the limitations of the repair regardless of which ptosis procedure is performed. In addition it is essential that the surgeon carefully discusses the risks and limitations of ptosis surgery, including possible complications, to the child's parents or guardian.

Although undercorrections are bound to occur, they can be minimized by properly selecting individual procedures and making appropriate modifications. As previously discussed, when performing any type of Müllerectomy, one must gauge the amount of surgery based on the patient's response to 2.5% phenylephrine. A less than desired response requires a larger Müllerectomy and/or a greater advancement of the muscle's insertion. In regard to levator resection procedures, as a general rule, it is best to overcorrect congenital ptosis "on the table," setting the lid in accordance to the amount of levator function present. Undercorrection following frontalis suspension may occur if the lid is not pulled up high enough at the time of surgery. It is therefore important to essentially raise the lid almost as high as possible.

Overcorrections in pediatric ptosis surgery occur rather infrequently. An overcorrection in the form of central peaking of the lid can be seen following Müllerectomy procedures, particularly if the levator aponeurosis is inadvertently sutured into the closure or if too much tarsus is excised on a modified Fasanella. Special care must therefore be taken to avoid incorporating the aponeurosis in the Müller muscle resection. A main advantage of the modified Fasanella-Servat procedure is the ability to manipulate the lid position in the early postoperative period. The 5–0 nylon suture can be removed in the first 4–5 postoperative days, and gentle traction can be applied to the lid margin wherever there is any area of overcorrection or asymmetry. If there is significant overcorrection in older children, a simple block of the area with local anesthesia allows the wound to be opened and the tissue released accordingly.

Overcorrections can also occur following levator advancement or resection. As with adults, postoperative massage can be performed for mild to moderate problems on those children who will tolerate it. Severe overcorrections accompanying levator resections and especially frontalis suspensions require immediate adjustment, because corneal exposure and subsequent ulceration can occur. If only a mild overcorrection exists, one can elect to observe the patient to see if the lid level will drop any further postoperatively. If a moderate overcorrection is present beyond the first 1–2 weeks postoperatively, one may elect to perform a Beard tarsotomy-type procedure. Beard recommends everting the eyelid and incising the tarsus along its full horizontal length 1 mm below the upper tarsal border. The tissues are separated using a 2:1 ratio of millimeters of separation to millimeters of desired droop [59]. As an alternative to the Beard tarsotomy, a levator recession can also be performed.

In addition to both under- and overcorrections, ptosis surgery can also lead to other types of eyelid malpositions. Because the tarsus plays a very important structural role in maintaining the position of the eyelid margin, any surgical procedure that involves the tarsal plate may affect the eyelid margin. A Fasanella-Servat procedure may, therefore, cause an entropion if too much tarsus is removed (Fig. 22.53). The overlying tension of the pretarsal orbicularis will overcome the ability of the altered tarsus to keep the eyelid margin properly positioned against the globe. To avoid this complication, at least 4 mm of tarsus should always remain following

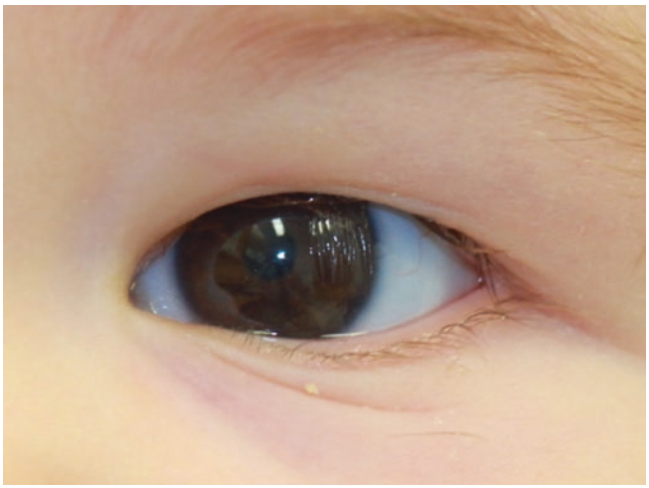


Fig. 22.53 Postoperative entropion status post a modified Fasanella



Fig. 22.54 Lateral lash ectropion status post a silicone sling placement

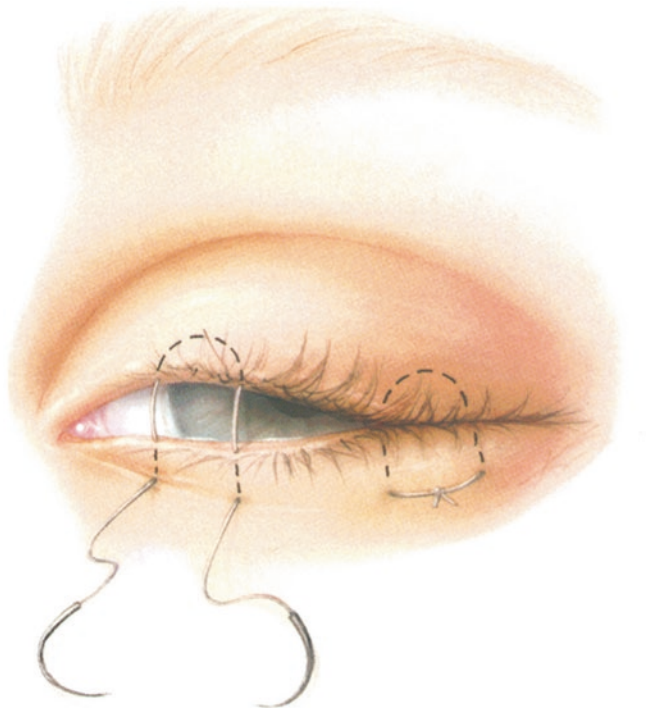


Fig. 22.55 Intermarginal gray line sutures keep the ocular surface protected but do not limit visualization of the globe unless tied with a slip-knot. This intermarginal suture technique can be done in any combination of central, lateral, and/or medial as dictated by the clinical situation

a tarsectomy. If an entropion results from inadequate tarsal support, then a free tarsal graft from the opposite lid may be necessary to correct the margin malposition.

Tarsal eversion can also occur, resulting in an ectropion of the eyelid margin. This is usually the result of sutures placed too far inferiorly on the anterior surface of the tarsus during levator muscle surgery. In regard to frontalis suspension, as mentioned previously, care must be taken upon lifting the lid to avoid pulling the tarsus away from the globe. This can sometimes even cause a "popping" sound as the lid lifts off the eye. With poor apposition, the upper lid inadequately spreads the tear film while blinking, and severe corneal exposure can occur. Unfortunately, this problem does not tend to sufficiently improve on its own, and revision of the surgical procedure is often required.

Occasionally, rather than a true ectropion, an isolated upward rotation of the lash line occurs following lid crease formation during levator muscle surgery. This usually results from overtightening of the sutures or a vertical shortage of skin from the lashes to the upper tarsal border. This can also occur when a frontal sling is placed too close to the eyelid margin (Fig. 22.54). Although corneal exposure is not a threat in this situation, the result is less than satisfactory cosmetically. If the deformity persists, it can usually be corrected by undermining the pretarsal skin and replacing the sutures to allow relaxation of the vertical tension on the eyelid margin.

Another complication concerning lashes is actual loss of cilia due to damage to the hair follicles. This can occur while exposing the anterior tarsal surface, if the skin and orbicularis are dissected too aggressively down to the lash follicles. Satisfactory correction of this complication is not possible without wedge resection of the colobomatous area.

By far the most serious complications encountered following ptosis repair are lagophthalmos with subsequent exposure keratopathy. In its mildest form, exposure is seen as superficial punctate staining of the cornea. With more severe exposure, however, a nonhealing corneal abrasion can occur that can progress to a corneal ulcer. A surgeon must always have a low threshold to place a temporary tarsorrhaphy in the setting of a corneal abrasion and even a corneal ulcer. Sometimes, both lateral and medial tarsorrhaphy are required (Fig. 22.55).

Frequently, patients with congenital ptosis will have some degree of lagophthalmos prior to surgery, and thus the surgeon must recognize that any type of surgical intervention may potentially worsen this problem. The risk of increasing the degree of lagophthalmos is, however, directly related to the surgical technique. As previously discussed, a main advantage of Müllerectomy surgery is the lower frequency of postoperative lagophthalmos. Extensive levator resections, on the other hand, quite commonly produce lid lag and lagophthalmos, and this is especially pronounced with a Whitnall's sling (Fig. 22.56). Lid lag and lagophthalmos are also almost always present at least to some degree



Fig. 22.56 Lagophthalmos and corneal abrasion. Lagophthalmos with resultant corneal abrasion following extensive levator resection with a Whitnall-type sling

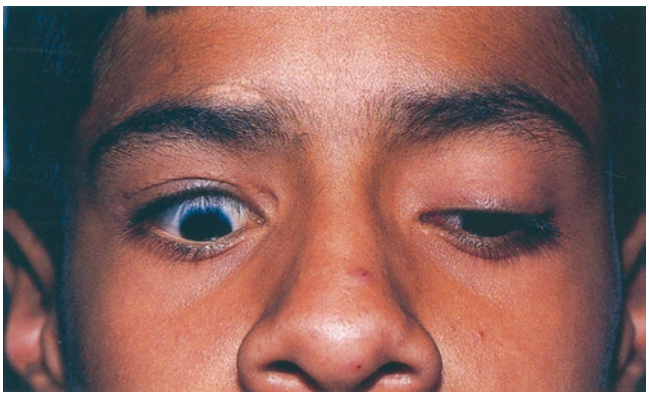


Fig. 22.57 Lid lag of the right upper eyelid following frontalis sling surgery

immediately following frontalis suspensions (Figs. 22.50e and 22.57). It is somewhat paradoxical, however, that the lid level will usually relax over time, more so following suspension procedures rather than following extensive levator resections. This does not manifest as a recurrence of ptosis but as an actual improvement of closure during sleep.

The ability to tolerate lagophthalmos is dependent on the presence of adequate tear flow and a good Bell's phenomenon. Preoperative evaluations that document decreased tear production or limited superior rectus function mandate a planned undercorrection to minimize the effects of lagophthalmos. In general, we prefer frontalis suspensions for those patients at risk for exposure, since extensive levator resections appear to be associated with persistent lagophthalmos. Regardless of the suspension material, the sling should be adjusted to achieve a tension that sets the lid at the "ideal level." If significant lagophthalmos is still a concern, temporary tarsorrhaphies can be used as described earlier (Fig. 22.55).

Although corneal abrasions have been considered a frequent complication of the original Fasanella-Servat procedure [33, 60], the modified procedure described here has successfully avoided this problem. Obviously, for those patients who do develop corneal abrasions, careful postoperative monitoring is essential. If the abrasion is small, frequent applications of lubrication in combination with daily follow-up visits may prove successful. In older patients, a thin plastic wrap commonly used in the home kitchen can be cut into a square and taped over the eyelids to create an inexpensive (and readily available) moisture chamber. In young children, however, where there is a potential threat of suffocation from the plastic wrap, this technique should not be utilized. For larger abrasions, a reverse traction suture may need to be placed in the lower lid margin. The addition of a nonsteroidal anti-inflammatory drop (Voltaren, Novartis Pharmaceuticals, East Hanover, NJ) used four times a day has been a useful adjunct for rapidly healing corneal abrasions and also reducing discomfort from associated inflammation. In selected cases, if there is good tear flow, a therapeutic bandage lens can also be a very effective means of controlling symptoms by providing a scaffold on which the epithelium can heal and by reducing pain. If the abrasion is resistant to treatment or if an actual ulceration occurs, a temporary tarsorrhaphy should be performed in conjunction with a reversal of the ptosis procedure if required.

Conjunctival prolapse is an infrequent complication that can occur in association with a levator resection. The prolapsing of conjunctiva is the result of dissection in the upper cul-de-sac in an attempt to lyse the loose connections between the levator and the superior rectus muscles. This maneuver must be performed to avoid a resultant hypotropia when the levator muscle is resected. Unfortunately, the dissection also lyses the suspensory connections of the levator muscle to the upper cul-de-sac, resulting in some redundancy of the conjunctiva. In general, prolapsing of the conjunctiva can be avoided by excising 4–5 mm of conjunctiva along with the resection of Müller's muscle and the levator. If prolapsing of the conjunctiva is noted intraoperatively, several mattress sutures of 5–0 chromic brought up from the cul-de-sac through the levator muscle and tied on its anterior surface can control this problem. If one wishes to achieve a deep crease, these sutures can be brought through each skin edge and tied. This same technique can also be used if conjunctival prolapsing occurs postoperatively and persists. In addition to taking care to avoid problems with prolapsing, one must also try to limit the amount of dissection of the conjunctiva in the temporal aspect of the lid. The lacrimal gland ductules are located in this region of the superior fornix and are prone to injury.

A suture granuloma can occur as a complication of a frontalis suspension when this procedure is performed with synthetic material (Fig. 22.58). This represents a reaction to a "foreign body" and occurs in approximately up to 13% of cases when Supramid is utilized [2, 61]. This is also more common in our experience with Ptose-up and other similar materials [46]. Infections, though uncommon, can be difficult to manage and often require sling removal with a delay in reoperation (Fig. 22.59). Unfortunately, satisfactory treatment of this problem almost always requires removal of



Fig. 22.58 Bilateral granulomas 2° to Supramid suture



Fig. 22.59 Eyelid granulomas due to chronic MRSA cellulitis in a patient status post a left frontalis ptosis repair with Supramid suture



Fig. 22.60 Unnatural central peaking of the eyelid margin. Unnatural central peaking of the eyelid margin following levator resection. Prolapse of the lacrimal gland obliterates the lid crease on the right side



Fig. 22.61 Asymmetry of the eyelid fold. Postoperative asymmetry of the eyelid fold following levator resection without skin excision performed on the right upper lid

the synthetic material initiating the granulomatous reaction. Antibiotic coverage is then used, while the infection and/or inflammation subsides, usually over 2–3 months. With the availability of preserved fascia, however, the procedure can now be revised sooner with far less risk of recurrence of the granulomatous reaction. Although autogenous fascia probably reduces this risk even further, chronic inflammation can still occur secondary to suture material used to support the knot or to close the skin.

In addition to the many complications that can endanger the function of the globe, a number of other problems can compromise the cosmetic result. One of the most challenging aspects of ptosis surgery is the ability to achieve a natural-appearing eyelid contour. A frontalis suspension always has the potential to result in a squared-off eyelid contour, while both Müllerectomy procedures and levator muscle surgery can lead to unnatural peaking of the lid margin (Fig. 22.60). If the surgeon is cognizant of the contour abnormality at the time of surgery, the contour can usually be reshaped by adding or adjusting sutures or by pulling on the lid with an appropriate pair of forceps at the point where the lid is highest. If the lacrimal gland is noted to be prolapsed during surgery, this can be repaired by passing a 5–0 chromic or polyglactin mattress suture through the superior edge of the gland and securing it to the periorbita of the lacrimal gland fossa. For contour abnormalities discovered after surgery, massage and simple observation over time may lead to adequate relaxation of the contour abnormality. Surgical revision of the problem may ultimately be required, however. Such intervention should be considered early if the abnormality is more than a mild problem, since the results of early correction appear to be superior to delayed repair [62].

Even though the repair of unilateral ptosis may result in an eyelid level that is symmetric with the opposite lid, the presence of asymmetry between the eyelid crease and fold may compromise final cosmesis (Fig. 22.61). Frequently this asymmetry in appearance is more noticeable than a difference in eyelid height. As discussed earlier, both Putterman's procedure and the modified Fasanella-Servat procedure do not sufficiently address correction of the lid crease and fold. Although Werb's procedure can adjust these to some degree, external levator procedures as well as our method of frontalis suspension are more appropriate for modifying these abnormalities. To achieve symmetry of the lid crease and fold, the surgeon must pay careful attention to the placement of the skin incision and must perform a graded excision of the eyelid skin. The height of the lid crease on the opposite healthy side should be measured with calipers and the skin incision marked at the

equivalent distance or even 1 mm lower to compensate for an upward migration of the crease postoperatively. As discussed earlier, we usually recommend reforming the crease with attachment of the subcutaneous tissue directly to the levator muscle through the use of the same sutures that attach the levator to the tarsus. This creates a long-lasting, natural-appearing crease and permits the lid fold to fall over the lid crease.

The lid fold is as important as the lid crease in achieving a satisfying cosmetic result. In those cases of severe ptosis with poor levator function, the eyelid skin tends to become stretched due to the low position of the lid. Understandably, if the eyelid is subsequently elevated to an appropriate level, redundancy of the eyelid skin will be present. Excision of excess skin must be performed very carefully to avoid postoperative hooding of the lashes. Likewise, care must be taken to avoid an overzealous excision of skin, which may lead to shallowing or even absence of a lid fold in addition to possible lagophthalmos postoperatively. In children it is probably better to remove little or no skin whenever possible. Additionally, overzealous removal of orbicularis must be avoided to prevent the creation of a deep unnatural crease. Careful assessment of the lid fold on the opposite side in unilateral cases is a critical step during the preoperative evaluation. Even when all of these steps are carefully followed, it is important to recognize that the final appearance of the lid fold will ultimately be determined by the postoperative eyelid level.

The final complication to be discussed is that of recurrent ptosis. Although all types of surgical procedures for ptosis repair are associated with some frequency of recurrent ptosis over time, certain types of frontalis suspension are associated with the highest. Frontalis suspensions using synthetic material have failure rates as high as 29–40% [39, 46]. Crawford reported a 5% rate of recurrence when autogenous fascia was used [31]. As mentioned previously, while rates as high as 43% have been reported with lyophilized fascia, more recently a series using irradiated donor tissue found a recurrence rate of 21% [47, 48].

Speculation continues as to why certain sling procedures eventually fail. In regard to Supramid or silicone slings, failure may be due to the fact that the diameter of the loop of synthetic material remains fixed as the child grows, and thus may start to cut through the soft tissues of the lid, leading to an increasing degree of ptosis over time [39]. Fascia lata, on the other hand, is broader and thus is less likely to cheese wire. Fascia lata may also become a more permanent part of the lid as it becomes incorporated into the lid tissues over time [63]. In addition to long-term failures, synthetic suspensions can also lead to an acute, rapid recurrence of ptosis. This usually occurs in the setting of trauma due to rupture of the suture; however, untying of the suture material is also possible. Acute recurrence of ptosis can also occur with the use of preserved fascia lata. This is most likely due to rejection of the donor tissue with subsequent absorption in the first few months following the repair.

The management of this type of recurrent ptosis, whether gradual or acute, requires a repeat suspension procedure. In the unusual case, where the suspension procedure was chosen only as a temporizing measure, levator function should be carefully reevaluated, and, if warranted, a levator resection procedure should be performed. Usually, however, a repeat suspension procedure, using either autogenous or donor fascia lata, will be the most plausible choice. Use of a double-rhomboid technique may be preferable for this type of recurrent ptosis. As far as the Müllerectomy-type procedures are concerned, unless there is still a vigorous response to phenylephrine, a levator resection will probably prove most suitable, as long as there is adequate levator function. In the situation where levator surgery fails, a repeat resection may be attempted, but more often than not, a frontalis suspension will achieve a superior result.

References

1. Griepentrog GJ, Diehl NN, Mohney BG. Incidence and demographics of childhood ptosis. Ophthalmology. 2011;118(6):1180–3.
2. Jeong S, Lemke BN, Dortzbach RK, Park YG, Kang HK. The Asian upper eyelid: an anatomical study with comparison to the Caucasian eyelid. Arch Ophthalmol. 1999;117(7):907–12.
3. Dutton JJ. The eyelids and anterior orbit. In: Atlas of clinical and surgical orbital anatomy. Philadelphia: WB Saunders; 1994. p. 113–38.
4. Kim MK, Rathbun JE, Aguilar GL, Seiff SR. Ptosis surgery in the Asian eyelid. Ophthal Plast Reconstr Surg. 1989;5(2):118–26.
5. Anderson RL, Beard C. The levator aponeurosis: attachments and their clinical significance. Arch Ophthalmol. 1977;95:1437–41.
6. Collin JR, Beard C, Wood I. Experimental and clinical data of the insertion of the levator palpebrae superioris muscle. Am J Ophthalmol. 1978;85:792–801.
7. Werb A. The upper lid: structure and restructure. Orbit. 1992; 11:63–73.
8. Kuwabara T, Cogan DG, Johnson CC. Structure of the muscles of the upper eyelid. Arch Ophthalmol. 1975;93:1189–97.
9. Callahan M, Beard C. Classification of ptosis. In: Ptosis. 4th ed. Birmingham, AL: Aesculapius; 1990. p. 52–87.
10. Berke RN, Wadsworth JAC. Histology of levator muscle in congenital and acquired ptosis. Arch Ophthalmol. 1995;53:413–28.
11. Hertle RW, Katowitz JA, Young TL, Quinn GE, Farber MG. Congenital unilateral fibrosis, blepharoptosis, and enophthalmos syndrome. Ophthalmology. 1992;99:347–55.
12. Fibrosis of Extraocular Muscles, Congenital, 1; CFEOM1. Online Mendelian Inheritance in Man®, An Online Catalog of Human Genes and Genetic Disorders. Updated 30 November 2016. http://www.omim.org/entry/135700. Accessed 1 Dec 2016.
13. Pratt SG, Beyer CK, Johnson CC. The Marcus Gunn phenomenon: a review of 71 cases. Ophthalmology. 1984;90:27–30.
14. Spaeth EB. The Marcus Gunn phenomenon: discussion, presentation of four instances and consideration of its surgical correction. Am J Ophthalmol. 1947;30:143–58.
15. Iliff CE. The optimum time for surgery in the Marcus Gunn phenomenon. Trans am Acad Ophthalmol Otolaryngol. 1970;74:1005–10.
16. Duke Elder S. Normal and abnormal development: congenital deformities. In: System of ophthalmology, vol. 3. St. Louis: Mosby; 1963. p. 900–5.
17. Myasthenia Gravis. American Academy of Ophthalmology. EyeWiki. http://eyewiki.aao.org/Myasthenia_Gravis. Accessed 1 Dec 2016.
18. Perez RB. The eye-popping reflex of infants. J Pediatr. 1972; 81(1):87–9.

19. Callahan M, Beard C. Surgery for levator maldevelopment ptosis. In: Ptosis. 4th ed. Birmingham: Aesculapius; 1990. p. 113–67.
20. Wilensky JT, Woodward HJ. Acute systemic hypertension after conjunctival instillation of phenylephrine hydrochloride. Am J Ophthalmol. 1973;76(1):156–7.
21. Harrad RA, Graham CM, Collin JRO. Amblyopia and strabimus in congenital ptosis. Eye. 1988;2:625–7.
22. Summers CG, Christiansen SP, Kemper AR, et al. Pediatric eye evaluations. San Francisco: American Academy of Ophthalmology; 2012. p. 19.
23. Pediatric Eye Evaluations PPP – 2012. AAO Pediatric Ophthalmology/Strabismus PPP Panel, Hoskins Center for Quality Eye Care, Comprehensive Ophthalmology, Pediatric Ophth/Strabismus. http://www.aao.org/preferred-practice-pattern/pediatric-eye-evaluations-ppp--september-2012. Accessed 1 Dec 2016.
24. Fox SA. Ptosis. In: Ophthalmic plastic surgery. 3d ed. New York: Grune & Stratton; 1963. p. 294–345.
25. Waller RR. Evaluation and management of the ptosis patient. In: McCord CW, editor. Oculoplastic surgery. New York: Raven; 1981. p. 15–69.
26. Iliff CE. Problems in ptosis surgery. In: Rycroft PV, editor. Corneoplastic surgery. Oxford, UK: Pergamon; 1969. p. 5–8.
27. Matthews D. Congenital ptosis. In: Rycroft PV, editor. Corneoplastic surgery. Oxford, UK: Pergamon; 1969. p. 15–29.
28. Glatt HJ, Fett DR, Putterman AM. Comparison of 2.5% and 10% phenyephrine in the elevation of upper eyelids with ptosis. Ophthalmic Surg. 1990;21:173–6.
29. Wiggs EO. The Fasanella-Servat operation. Ophthalmic Surg. 1978;9:48–57.
30. Hornblass A. Tarsectomy-muellerectomy (Fasanella-Servat procedure). In: Levine MR, editor. Manual of oculoplastic surgery. 2d ed. Boston: Butterworth-Heinemann; 1996. p. 105–7.
31. Fasanella RM, Servat J. Levator resection for minimal ptosis: another simplified operation. Arch Ophthalmol. 1961;65:493–6.
32. Beard C. Blepharoptosis repair by modified Fasanella-Servat operation. Am J Ophthalmol. 1970;69(5):850–7.
33. Putterman AM, Urist MJ. Müller's muscle—conjunctiva resection: a technique for treatment of blepharoptosis. Arch Ophthalmol. 1975;93:619–23.
34. Beard C. Newer ptosis procedures. In: Ptosis. 2d ed. St. Louis: Mosby; 1976. p. 189–212.
35. Katowitz W. Congenital ptosis: management guidelines in Muller surgery, World Congress of Pediatric Ophthalmology and Strabismus, 2012. Milan, Italy.
36. Perry JD, Kadakia A, Foster JA. A new algorithm for ptosis repair using conjunctival Müllerectomy with or without tarsectomy. Ophthal Plast Reconstr Surg. 2002;18(6):426–9.
37. Katowitz JA, Ellis FD, Wright KW, Wilson MW, Haik B. Myths and realities in oculoplastic surgery: Proceedings from the 52nd annual symposium of the new orleans academy of ophthalmology, New Orleans, LA, USA February 14-16, 2003. In: Balkan RJ, Ellis GS, Eusis HS, editors. At The Crossings: Pediatric Ophthalmology and Strabismus. 2004;283–9.
38. Berke RN. Blepharoptosis—congenital and traumatic—types of operation indicated for congenital and acquired ptosis. In: Troutman RC, Converse JM, Smith B, editors. Plastic and reconstructive surgery of the eye and adnexa. Washington, DC: Butterworths; 1962. p. 125–9.
39. Holds JB, McLeish WM, Anderson RL. Whitnall's sling with superior tarsectomy for the correction of severe unilateral blepharoptosis. Arch Ophthalmol. 1993;111:1285–91.
40. Katowitz JA. Frontalis suspension in congenital ptosis using 4–0 cable type polyfilament suture. Arch Ophthalmol. 1979;97:1659–63.
41. Tillett CW, Tillett GM. Silicone sling in the correction of ptosis. Am J Ophthalmol. 1966;62:521–3.
42. Morax S. Neuromuscular anomalies. In: Van der Meulen JC, Gruss JS, editors. Color atlas and text of ocular plastic surgery. London: Mosby-Wolfe; 1996. p. 83–101.
43. Broughton WL, Matthews JG, Harris DJ. Congenital ptosis: results of treatment using lyophilized fascia lata for frontalis suspensions. Opthalmology. 1982;89:1261–6.
44. Crawford JS. Repair of ptosis using frontalis muscle and fascia lata: a 20-year review. Ophthalmic Surg. 1977;8:31–40.
45. Jordan DR, Anderson RL. Obtaining fascia lata. Arch Ophthalmol. 1987;105(8):1139–40.
46. Bedrossian EH. HIV and banked fascia lata. Ophthal Plast Reconstr Surg. 1991;7:284–8.
47. Wagner RS, Mauriello JA, Nelson LB, Calhoun JH, Flanagan JC, Harley RD. Treatment of congenital ptosis with frontalis suspension: a comparison of suspensory materials. Ophthalmology. 1984;91:245–8.
48. Wilson ME, Johnson RW. Congenital ptosis: long-term results of treatment using lyophilized fascia lata for frontalis suspensions. Ophthalmology. 1991;98:1234–7.
49. Esmaeli B, Chung H, Pashby RC. Long-term results of frontalis suspension using irradiated banked fascia lata (Toronto Hospital of Sick Children, personal communication).
50. Dryden RM, Fleming JC, Quickert MH. Levator transposition and frontalis sling procedure in severe unilateral ptosis and the paradoxically innervated levator. Arch Ophthalmol. 1982;100:462–4.
51. Dortzbach RK, editor. Ophthalmic plastic surgery: prevention and management of complications. 1st ed. New York: Raven Press; 1994. p. 68–70. Chapter 4.
52. Pfeiffer, MJ. Brow suspension in complicated unilateral ptosis: Frontalis muscle stimulation via contralateral levator recession. In: Guthoff RF, Katowitz JA, editors. Essentials in ophthalmology. 2010. Vol. 3. p. 117–23.
53. Heher KL, Katowitz JA. Oral mucous membrane grafts for corneal protection to permit prosthetic shell wear. Ophthal Plast Reconstr Surg. 1997;13:40–7.
54. O'Donnell B, Codère F, Dortzbach R, Lucarelli M, Kersten R, Rosser P. Clinical controversy: congenital unilateral and jaw-winking ptosis. Orbit. 2006;25(1):11–7.
55. Anderson RL, Baumgartner SA. Strabismus in ptosis. Arch Ophthalmol. 1980;98:1062–7.
56. Griepentrog GJ, Mohney BG. Strabismus in childhood eyelid ptosis. Am J Ophthalmol. 2014;158:208–10.
57. McCracken MS, del Prado JD, Granet DB, Levi L, Kikkawa DO. Combined eyelid and strabismus surgery: examining conventional surgical wisdom. J Pediatr Ophthalmol Strabismus. 2008;45:220–4.
58. Revere KE, Binenbaum GB, Li J, Katowitz JA, Katowitz WR. Simultaneous versus sequential ptosis and strabismus surgery in children. Paper presentation. ESOPRS. 2015.
59. Callahan M, Beard C. Surgery for levator maldevelopment ptosis. In: Ptosis. 4th ed. Birmingham: Aesculapius; 1990. p. 113–67.
60. Rathbun JE. Eyelid surgery. Boston: Little, Brown; 1990. p. 201–57.
61. Butt DK, Jayaprakash Patil A, Abou-Rayyah YM. Modified Supramid brow suspension in paediatric ptosis. Orbit. 2014;33(4):252–5.
62. Shore JW, Bergin DJ, Garrett SN. Results of blepharoptosis surgery with early postoperative adjustment. Ophthalmology. 1990;97:1502–11.
63. Orlando F, Weiss JS, Beyer-Machule CK, Albert DM, Shapiro A. Histiopathologic condition of fascia lata implant 42 years after ptosis repair. Arch Ophthalmol. 1985;103:1518–9.
64. Berke RN. Ophthalmic plastic surgery: a manual. San Francisco: American Academy of Ophthalmology and Otolaryngology; 1964. p. 137.
65. Rathbun JE. Anterior approach to correction of levator maldevelopment ptosis. In: Levine M, editor. Manual of oculoplastic surgery. Boston: Butterworth–Heinemann; 1996. p. 79.
66. Werb A. The upper lid-structure and restructure. Mustarde lecture. Orbit. 1992;11(2):61–122.

Benign Pediatric Eyelid Tumors

23

William R. Katowitz, Christiana Eva Munroe, and James A. Katowitz

Benign tumors of the eyelid can be classified by their pathologic characteristics, but since a diagnostic biopsy is rarely needed, they are more logically discussed by their clinical presentation as follows below.

Vascular Lesions

The most common vascular lesions on the eyelid in children are seen either at birth or soon afterward and are pink, red, or purple in appearance. They are infantile hemangioma, nevus simplex, and nevus flammeus. Capillary hemangioma has classically been the term used to describe those lesions that are seen at birth or within a few weeks of life with a strawberry color or with a deeper component. These lesions are now called infantile hemangiomas in order to differentiate them from other acquired infantile hemangiomas that are acquired after infancy.

Infantile Hemangioma

The diagnosis and treatment of infantile hemangioma is covered in detail in the Dermatology sections of Chap. 6 and 7. An oculoplastic surgeon's approach to these lesions is first to confirm the diagnosis and to rule out PHACE syndrome. Infantile hemangiomas are usually not visible at birth. While some of these lesions are congenital, the history of a visible eyelid lesion at birth should raise a suspicion that the diagnosis may instead be that of a nevus simplex ("angel's kiss") or nevus flammeus ("port-wine stain"). Large lesions of the face (over 20 square centimeters) should raise one's suspicion for other possible abnormalities of the heart, eye, and brain. The PHACE syndrome includes *p*osterior fossa abnormalities, *h*emangioma, *a*rterial abnormalities, *c*ardiac defects, and *e*ye anomalies.

Infantile hemangiomas are the most common eyelid and orbital tumors of infancy. They are estimated to occur in 5% of infants [1]. They are composed of a network of abnormal capillaries with variable degrees of proliferation of the vessel endothelium. Mitotic figures may be seen within the lesion. Red blood cells and blood flow are present in the vascular channels of the lesion. They are the one pediatric vascular malformation that is truly proliferative. Infantile hemangiomas possess the histochemical marker GLUT-1 and involve proliferation of endothelial-like cells that contain these markers [2].

The clinical appearance of an infantile hemangioma depends on the size, depth, and growth stage of the lesion (Fig. 23.1). A thin and superficial infantile hemangioma will appear as an erythematous patch in the skin. The lesion will blanch with compression, and the epithelium may be smooth or it may be elevated with an intact but irregular surface. When the hemangioma involves the deeper eyelid tissues, it will take on a blood red to purple to blue appearance. In the case of a deep eyelid or an orbital mass, the color of the eyelid tissues may be normal, but the volume of the lesion disrupts the architecture of the eyelid. When a superficial component of the lesion is present, the infantile hemangioma becomes easier to differentiate from other space-occupying lesions that enlarge the eyelid. Recognition of the deeper lesions depends on clinical behavior, radiologic imaging, and, when necessary, biopsy. Magnetic resonance imaging (MRI) can help by using blood flow characteristics to assist in differentiating arterial and venous malformations from infantile hemangiomas. An alternative study is Doppler ultrasound where an infantile hemangioma displays high flow as compared to venous and lymphatic malformations which have low flow to no flow.

W.R. Katowitz, MD • J.A. Katowitz, MD, FACS (✉)
The Children's Hospital of Philadelphia and The Edwin and Fannie Gray Hall Center for Human Appearance, University of Pennsylvania, Philadelphia, PA, USA
e-mail: katowitzw@email.chop.edu; katowitz@email.chop.edu

C.E. Munroe
Oculoplastic and Orbital Surgery, The Children's Hospital of Philadelphia, Philadelphia, PA, USA

© Springer International Publishing AG 2018

J.A. Katowitz, W.R. Katowitz (eds.), *Pediatric Oculoplastic Surgery*, https://doi.org/10.1007/978-3-319-60814-3_23

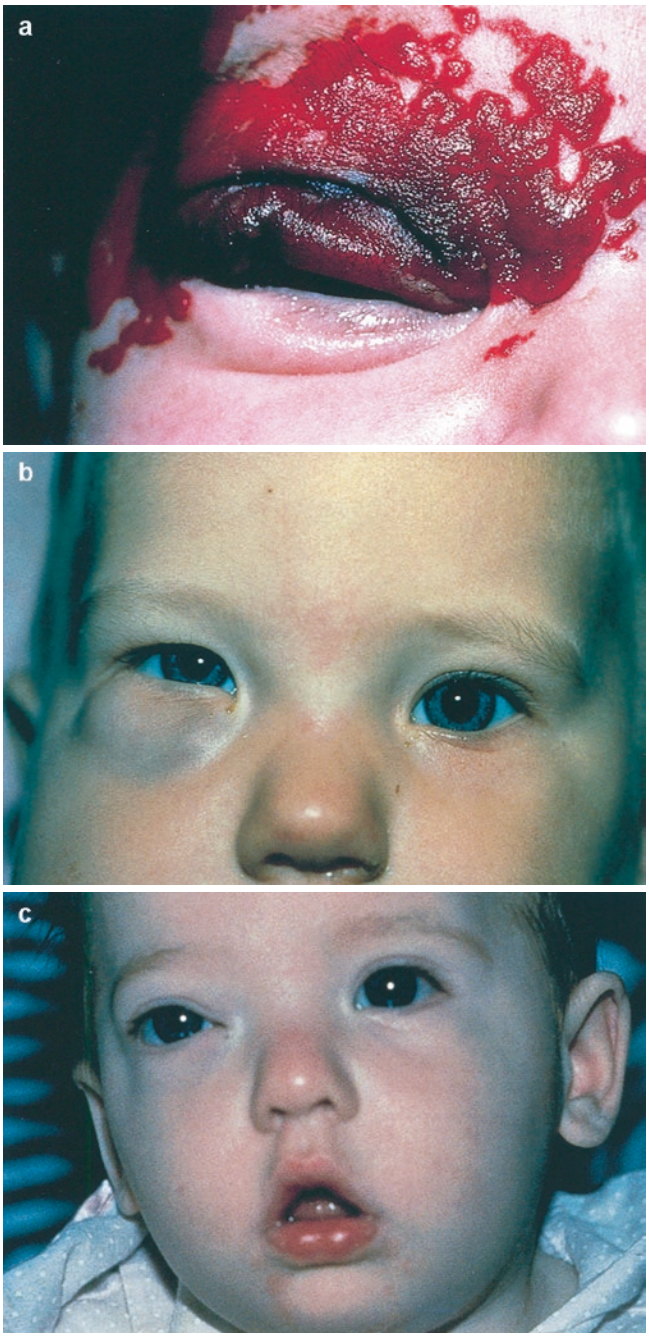


Fig. 23.1 Infantile hemangioma. (**a**) Superficial infantile hemangioma with the bright red appearance typical of epithelial involvement by the hemangioma. (**b**) Intermediate infantile hemangioma with the purplish-blue discoloration typical of a subdermal infantile hemangioma. (**c**) This patient has a right-sided deep eyelid and orbital infantile hemangioma, demonstrating a mass effect with no alteration of the skin texture or color

The eyelid infantile hemangioma has some other characteristic features. In the rapidly enlarging superficial skin lesion, the epithelium may become necrotic or ulcerated if the lesion outgrows the local blood supply. Treatment of the lesion may also precipitate devascularization and result in tissue necrosis with ulceration of the skin. The soft tissue mass of the infantile hemangioma lesion is spongy and easily compressible. The lesion blanches with compression. The classic clinical history of an infantile hemangioma predicts that the lesion will initially enlarge over the first 3–6 months of life, followed by spontaneous involution until the age of 9 years. Roughly half of all hemangiomas are no longer clinically visible by age 5 years and the rest by age 9 [3]. When the involution process begins, the previously red lesion may take on a grayish or beige hue, and as involution progresses, patches of normally colored epithelium interdigitate with the purple-gray and red tissue. The epithelium may return to a normal appearance, but larger lesions may cause permanent disruption in the dermal elastic tissue, resulting in thinning of the skin sometimes referred to as a "cigarette paper" appearance (Fig. 23.2).

Infantile hemangiomas may be present at birth or typically begin in the first few months of life. The lesion is more common in females than males. Without treatment, most lesions will involute, leaving behind little or no evidence of their prior presence. However, a subset of infantile hemangiomas can show dramatic growth over the first 10 months of age that may cause distortions of cosmetic and functional significance (Fig. 23.3). These lesions will also spontaneously involute by 9 years of age, but may require early intervention to prevent permanent sequelae from disruption of function. For the ophthalmologist, this will include monitoring and treatment for deprivational or anisometropic amblyopia. Preliminary evaluation of the pediatric patient with an eyelid infantile hemangioma should include tests of visual function and retinoscopy. Amblyopia may be caused by the eyelid position blocking the visual axis or from astigmatism due to eyelid or orbital pressure effects on the globe. In addition to compression effects on the globe, intraorbital growth can also produce secondary expansion of the bony orbital walls.

The nature and extent of an anterior eyelid lesion may be clinically apparent, but in patients where this is not the case, an MRI is a valuable imaging technique for identification and assessment of the extent of an infantile hemangioma. When the goal of the imaging is to help differentiate between an infantile hemangioma and a lymphangioma (venolymphatic malformation), MRI is helpful (Fig. 23.4). MRI better demonstrates the more heterogenous soft tissue structures of the lymphangioma as compared to CT imaging. The MRI scan may also be used to identify blood collections that can produce a "chocolate cyst" that can be found in lymphangioma and is not typical of an infantile hemangioma (see Fig. 23.11). On MRI, an infantile hemangioma will usually show characteristic flow voids or darker areas in the soft tissue structure where higher flow vascular structures are present (Fig. 23.4c). B-scan ultrasound of the infantile hemangioma will show irregular contours, and the



Fig. 23.2 Texture and pigmentation changes. (**a**) At age 14, this patient has soft tissue changes in the left upper eyelid and temporal skin that are characteristic of the "cigarette paper" texture that may occur when the infantile hemangioma involutes. (**b**) An oblique view of the texture and pigmentation changes

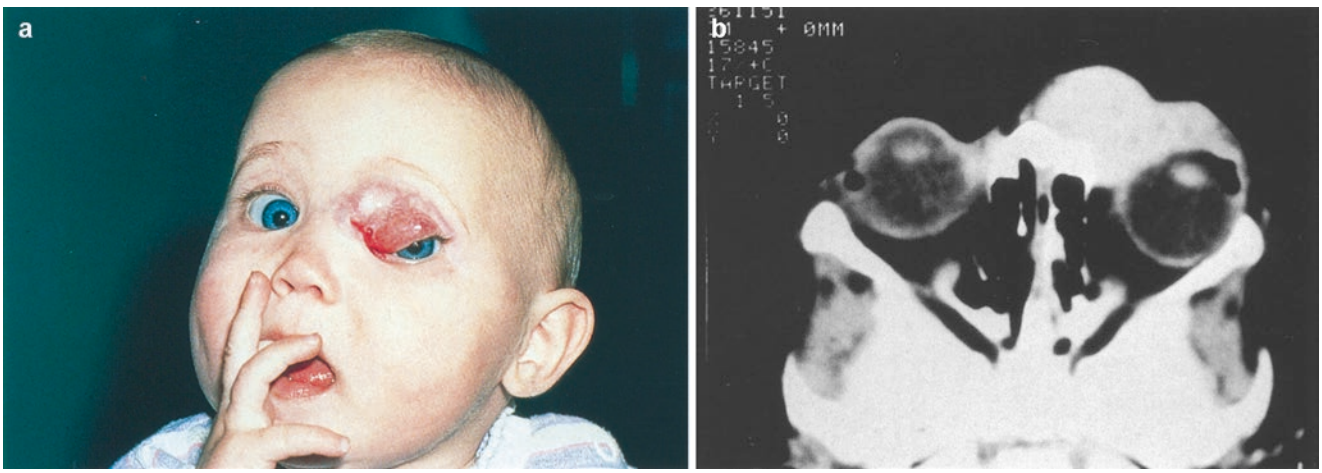


Fig. 23.3 Infantile hemangioma: CT scan. (**a**) Infantile hemangioma of the left upper eyelid and left medial canthal region. (**b**) CT scan of the same patient with intravenous contrast. Notice the smoothly irregular contour and borders of the hemangioma. On CT, the infantile hemangioma enhances markedly with intravascular contrast material

A-scan will show variable internal reflectivity in the high to medium range (Fig. 23.5).

Management of Infantile Hemangiomas

There are numerous treatment options for functionally or cosmetically disruptive infantile hemangiomas [4]. Although the majority of these lesions can be managed conservatively with observation, there is a subset in which the hemangioma may grow rapidly or become very large. In the periocular region, this is particularly problematic because of the resultant effects on the visual system. In one series of 50 patients with infantile hemangiomas of the eyelid followed over 5 years, the complication rate was 80% (60% with amblyopia) [5]. This potentially preventable loss of vision demands careful observation and early intervention. Amblyopia may occur as the result either of changes in refractive error or obscuration of the visual axis [6].

Correction of any significant refractive error and occlusion therapy are medical options for the treatment of early or mild amblyopia. More severe or progressive problems warrant treatment options that focus on techniques to decrease the size of the mass. One study shows that the treatment of anisometropic amblyopia is equally successful with either ocular intervention (spectacle correction/occlusion) or medical intervention (corticosteroids/surgery), but that corticosteroids/surgeries were more successful in the treatment of occlusion amblyopia [7]. Although it is difficult to know in the early phases which infantile hemangiomas will involute without sequelae and which will create functional deficits, the treatment options are less invasive and have fewer risks

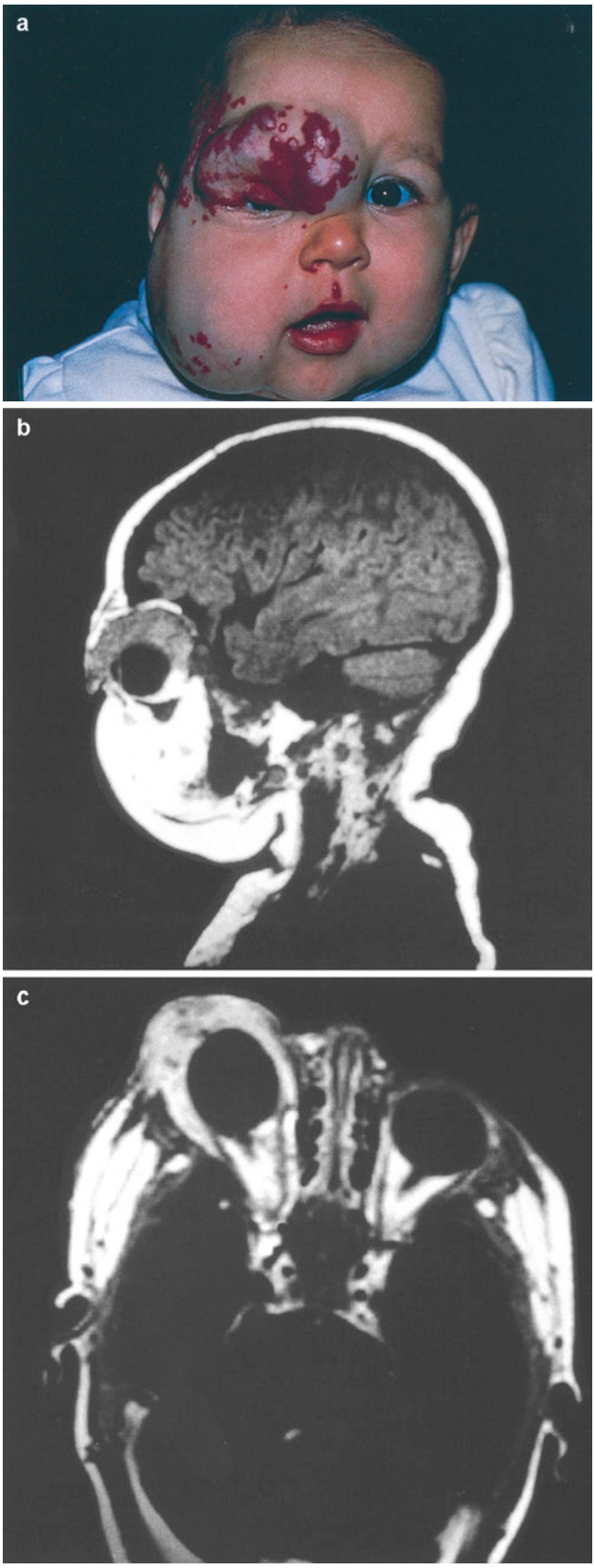


Fig. 23.4 Infantile hemangioma: MRI. (**a**) Infantile hemangioma of the face, upper eyelid, and brow. (**b**) Sagittal view MRI demonstrating the eyelid and orbital involvement by the infantile hemangioma. (**c**) Axial MRI scan with gadolinium shows the diffuse increase in signal intensity and the flow voids from vessels in the eyelid

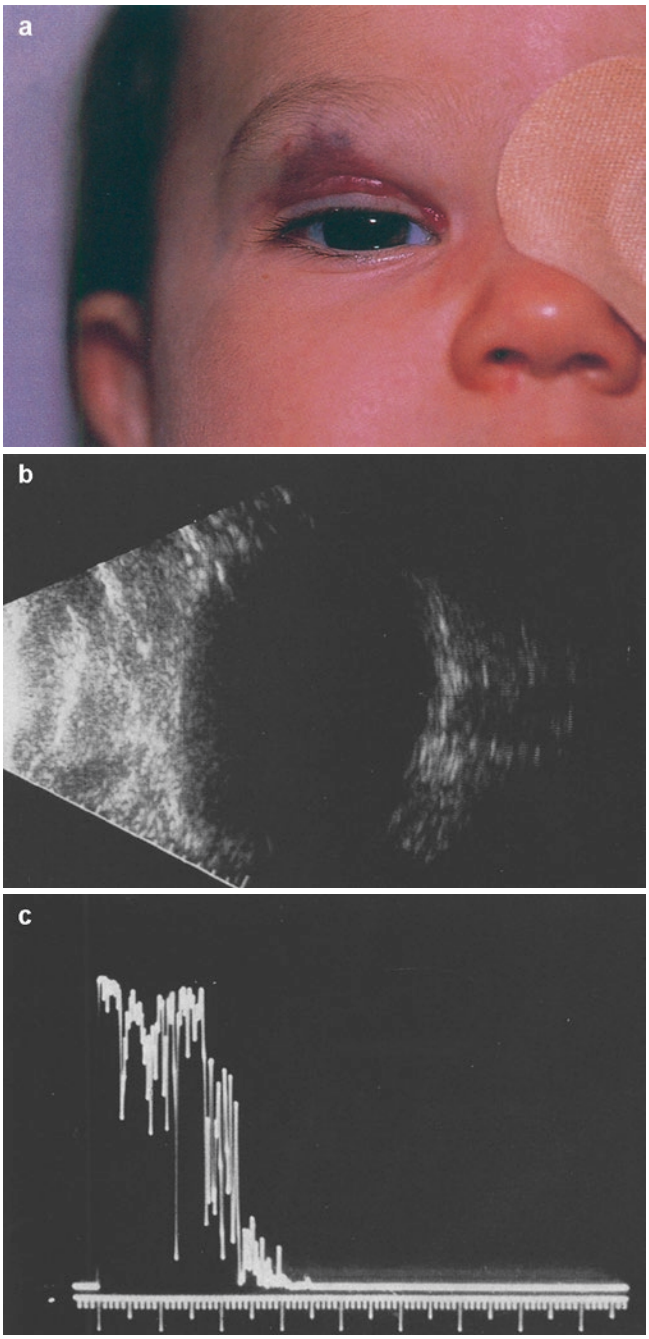


Fig. 23.5 Infantile hemangioma: ultrasound. (**a**) Clinical appearance of an upper eyelid hemangioma. (**b**) B-scan ultrasound of the lesion shows the irregular thickening of the eyelid anterior to the globe. (**c**) The A-scan ultrasound of the infantile hemangioma shows high internal reflectivity

when the lesion is smaller. For this reason, consideration may be given to more aggressive intervention even for smaller lesions that involve the eyelids.

In 2008 Leaute-Labreze et al. published the first series of patients successfully treated with oral beta blockers for infantile hemangioma [8]. This accidental discovery paved the way for the widespread use of oral and topical beta blockers as a first-line therapy for the treatment of infantile hemangiomas. In a large clinical trial of 460 patients, the beta-blocker propranolol was shown to be an effective

treatment at a dose of 3 mg per kilogram per day for 6 months. The known side effects of this beta blocker – hypoglycemia, hypotension, bradycardia, and bronchospasm – were infrequent [9]. This medication is best monitored safely under an inpatient protocol for infants younger than 2 months. For patients over the age of 2 months, outpatient propranolol induction can be acceptably monitored. A meta-analysis of 61 publications involving 5130 participants demonstrated that propranolol was more effective and safer than other therapies in treating infantile hemangioma [10] (Box 23.1).

Currently, the CHOP protocol follows the FDA guideline that children of 45 weeks gestation or older are candidates for outpatient propranolol therapy if they have a normal EKG. Blood pressure and heart rate are monitored for 1–2 h during an initial partial dose administration and again the following week when the full dose is administered. Propranolol appears to have fewer adverse side effects and may even be more effective than steroids in suppressing hemangiomas and causing them to involute more rapidly.

Box 23.1: Inpatient Admission Protocol

Admit to appropriate unit or ward. Optional: peripheral IV placement at the discretion of the on-service attending.

Baseline vital signs including temperature, HR, BP, with cardiorespiratory and oximeter monitor placement. In ICU, vital signs are monitored continuously. On inpatient ward, baseline vital signs are taken and then q2h vital signs × 2 following initial dose and subsequent dose escalations, then standard q4h vital signs.

Day 1

- Initiation of beta-blocker (propranolol) therapy as ORAL dose:
  <1 month of age: 0.5 mg/kg/day divided q8h × 3 doses
  ≥1 month of age: 1 mg/kg/day divided q8h × 3 doses
- Blood glucose measurement: OPTIONAL unless patient symptomatic. If elected, can be performed 1 h following each of first 2 doses at each dose range
- For critical values, hold dose, repeat measurement, and contact front-line physician if abnormal values persist or if patient is symptomatic:
  – Bradycardia: HR <80 bpm
  – Hypotension: <70 mm Hg (systolic) in infants [<5th percentile] or <30 mm Hg (diastolic) in infants
  – Hypoglycemia: <70 mg/dL [normal 60–105 mg/dL]

Day 2

- Beta-blocker (propranolol) therapy as ORAL dose at:
  <1 month of age: 1 mg/kg/day divided q8h × 3 doses
  ≥1 month of age: 2 mg/kg/day divided q8h × 3 doses
- Blood glucose measurement: OPTIONAL unless patient symptomatic. If elected, can be performed 1 h following each of first 2 doses at each dose range
- For critical values, hold dose, repeat measurement, and contact front-line physician if abnormal values persist or if patient is symptomatic:
  – Bradycardia: HR <80 bpm
  – Hypotension: <70 mm Hg (systolic) in infants [<5th percentile] or <30 mm Hg (diastolic) in infants
  – Hypoglycemia: <70 mg/dL [normal 60–105 mg/dL]

Day 3 (ONLY needed for those <1 month of age who initiated dosing at 0.5 mg/kg/day divided q8h)

- Initiation of beta-blocker (propranolol) therapy as ORAL dose at 2 mg/kg/day divided q8h x 3 doses
- Blood glucose measurement: OPTIONAL unless patient symptomatic. If elected, can be performed 1 h following each of first 2 doses at each dose range
- For critical values, hold dose, repeat measurement, and contact front-line physician if abnormal values persist or if patient is symptomatic:
  – Bradycardia: HR <80 bpm
  – Hypotension: <70 mm Hg (systolic) in infants [<5th percentile] or <30 mm Hg (diastolic) in infants
  – Hypoglycemia: <70 mg/dL [normal 60–105 mg/dL]

If symptomatic concerns arise, doses lower than 2 mg/kg/day may be used.

If suboptimal or partial results are obtained for complicated problems, doses may be escalated to 3–5 mg/kg/day in 0.5 or 1 mg/kg increments at the clinician's discretion as tolerated by the patient.

Post-admission Monitoring Visits

Once the target dose has been achieved, ambulatory heart rate and blood pressure monitoring is recommended monthly either at their primary care clinician's office or at the prescribing physician's office.

At follow-up visits once a month, dose adjustments may need to be made to accommodate the infant's

interval weight gain or if warranted due to clinical changes in the hemangioma.

Closer follow-up may be necessary if systemic corticosteroids are being tapered while still on beta-blocker therapy.

Anticipation is that beta-blocker therapy may be necessary for approximately 6–12 months, or until the child is 12–18 months of age due to the proliferative nature of infantile hemangiomas but can be adjusted to individual patient needs. Topical timolol may be added during the taper of beta-blocker or following discontinuation to help prevent recrudescence.

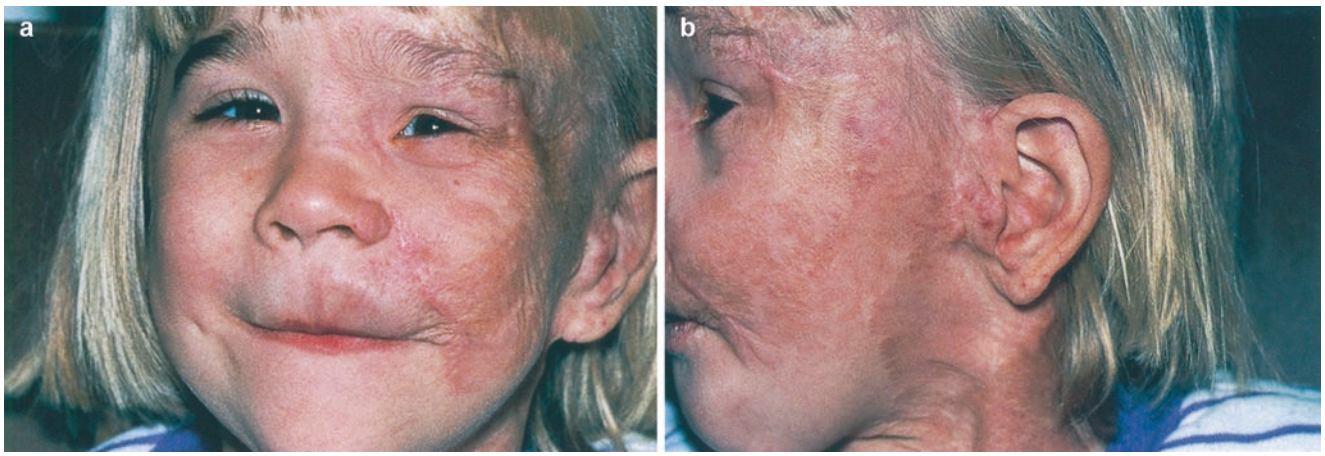


Fig. 23.6 Infantile hemangioma: radiation therapy. (**a**) Skin changes demonstrating scarring and atrophy following radiation therapy for infantile hemangioma of the left periocular region, cheek and neck. (**b**) Sagittal view of the soft tissue changes. This was treated with tissue expansion and sequential excision of the scar

Because propranolol is so effective in the treatment of infantile hemangiomas, systemic steroids are reserved for cases of patient who do not respond to propranolol or as a temporizing therapy for severe cases before beta-blocker induction can be attempted. Some physicians prefer both propranolol and systemic steroids for severe cases of hemangioma that require aggressive treatment.

Isolated lesions or predominantly smaller, flat hemangiomas can be treated with topical beta blocker effectively. The dose of 0.5% timolol gel-forming solution is typically used [11]. In a CHOP study, we found that 0.25% timolol gel-forming solution to be equally effective. This dosage can be used for small infants 4 months or younger [12]. In the past, treatment options that have been employed to decrease the mass of eyelid infantile hemangioma included intralesional corticosteroids, systemic corticosteroids, topical corticosteroids, superficial laser ablation, CO2 laser debulking, surgical debulking, systemic α-interferon, and radiotherapy. Radiation therapy is generally avoided because of the potential for significant scarring and atrophy (Fig. 23.6). Intralesional steroid injections were once popular but were a concern for potential central retinal artery occlusion (Fig. 23.7). In life-threatening cases, the use of α-interferon was reported as a therapeutic option [13–15]. There may be serious systemic side effects, however, including fever, neutropenia, hemodynamic changes at the onset of use, anorexia, and neurologic toxicity [16–18]. All of these modalities are now considered second-line therapies for patients who either fail beta-blocker therapy or in whom the treatment is contraindicated, such as in PHACES.

Vision-threatening hemangiomas of the eyelids may also be debulked surgically. Surgical intervention may be challenging because of the growth pattern of the infantile hemangioma. In some circumstances, imaging and clinical examination identify an anteriorly placed and well-circumscribed hemangioma. This pattern of growth is amenable to surgical excision. Eyelid lesions that are deep to the epithelium but anteriorly placed in the orbit and well circumscribed are also ideal for surgical removal. More commonly, however, the hemangioma will interdigitate with and become indistinguishable from the normal structures of the eyelid. This affects the surgeon's ability to distinguish the normal planes and surgical landmarks. When the lesion involves the epithelium, it will also be difficult to

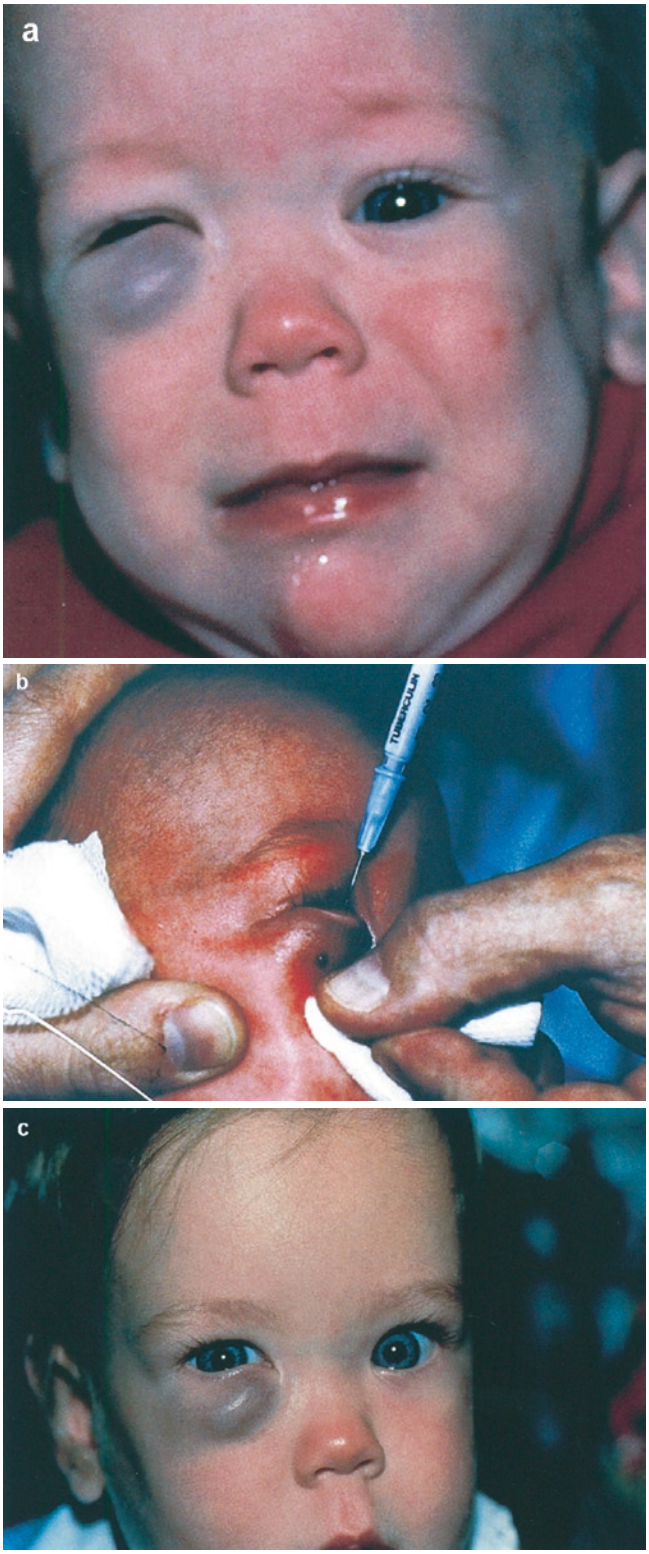


Fig. 23.7 Infantile hemangioma: corticosteroid treatment. (**a**) A lower eyelid infantile hemangioma extending up into the pupillary axis. (**b**) Intralesional injection of corticosteroid into the infantile hemangioma. (**c**) After injection, the infantile hemangioma is gradually shrinking out of the line of the visual axis

dissect a plane and not disrupt the circulation to the skin. Recognizing these limitations, it may still be valuable to surgically alter the eyelids in order to create a functional visual axis by decreasing the mechanical mass effect of the tumor (Fig. 23.8). The surgical CO2 laser has been beneficial to use as a tool to simultaneously vaporize and cauterize the tissue. The insulated point tip cautery can also be effective for removing an eyelid lesion. Consideration should be given to preoperative blood type and cross match if there is any concern for significant intraoperative blood loss. Postoperatively, these patients often have prolonged edema and may develop areas of tissue necrosis from alteration in the vascular supply to the lesion. These problems do not preclude a good cosmetic result as the child matures and the infantile hemangioma continues to involute.

Additional surgical options may be necessary when the child has completed the spontaneous involution or treatment process and is left with significant residual changes in the soft tissue. Smaller lesions or excess skin may be excised, but larger areas may require skin grafts or tissue expansion to replace the abnormal tissue with normal expanded skin from a nearby region (see Chap. 7).

Vascular Malformations

Vascular malformations of the eyelid and periorbital tissue may be venous, lymphatic, or arterial in nature. The term lymphangioma has typically been used to describe a mass that contains lymphatic and often venous channels. This term has since been replaced by venolymphatic malformation by the International Society of the Study of Vascular Anomalies (ISSVA) and updated to be lymphatic-venous malformation (LVM) [19]. Lymphatic-venous malformations that are visible on the eyelid typically extend into the orbit and are covered in greater detail in Chap. 35.

When there is a soft tissue component in the eyelids, LVM and other vascular malformations present with painless, compressible enlargement of the eyelid that may be accompanied by displacement of the globe (Fig. 23.9). Ocular motility may be impaired and the mass may demonstrate a Valsalva increase with crying or straining. There may be red or blue discoloration of the eyelid (Fig. 23.10). Some clinical features that help to distinguish the LVM from other periorbital lesions of childhood include a tendency for the lesion to increase in size with respiratory infections and the potential for sudden hemorrhage into a cystic space, which can result in an acute painful proptosis (Fig. 23.11). The presence of beaded cystic structures in the conjunctiva or on the roof of the mouth is also a feature that points toward the diagnosis of LVM. When the LVM involves the epithelium, the mass



Fig. 23.8 Infantile hemangioma: CO2 laser debulking. (**a**) Infantile hemangioma of the left upper eyelid. (**b**) The same patient following intralesional injection of corticosteroid. The palpebral fissure is improved, but the upper eyelid still covers the central visual axis. (**c**) The lesion is debulked using the CO2 laser for hemostasis. (**d**) The patient's immediate postoperative appearance. (**e**) One month following debulking surgery, the surrounding tissue necrosis and ulceration of the devascularized lid skin are seen. (**f**) At 5 years of age, there is still some thickening of the upper eyelid, but the skin is well healed, and the superficial components of the infantile hemangioma have undergone involution. (**g**) At 8 years of age, the mass effect of the hemangioma has resolved, but there are some residual skin changes and a ptosis of the upper eyelid. (**h**) The patient at 11 years of age following ptosis repair and removal of a small amount of skin in the upper eyelid to create a more symmetrical lid crease



Fig. 23.9 Lymphangioma of the left upper eyelid

has the appearance of dilated lymphatic channels characterized by a beaded cystic architecture. Deeper lesions may take on a purple or blue hue, especially when the potential spaces fill with blood. A growth spurt at the time of puberty may also occur. This probably represents an enlargement of the spaces rather than a true proliferation of cells. These lesions can also extend along the under surface of the skin into the forehead.

CT imaging will delineate the size and location of the vascular malformations, but MRI is more useful to help to differentiate between infantile hemangioma and lymphangioma. On CT an LVM may show less enhancement with contrast than the typical infantile hemangioma. MRI better documents the internal structure of the LVM, which is typically more heterogenous than an infantile hemangioma, and may show areas of hemorrhage that are hyperintense on T_1-weighted images. The margins of the lesions are typically irregular and do not follow the usual compartmental planes of the orbit. In addition, cystic

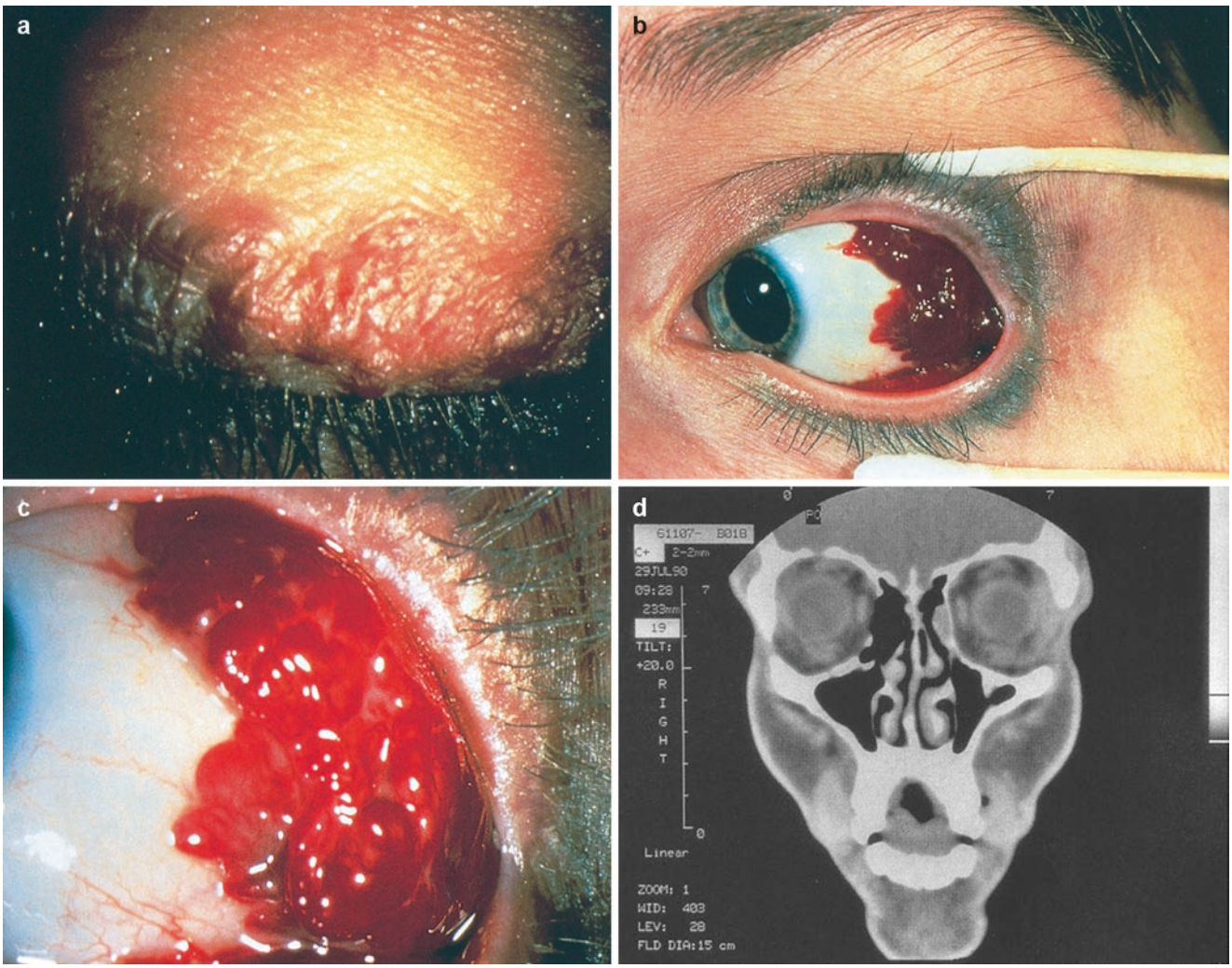


Fig. 23.10 Lymphangioma of the eyelid, conjunctiva, and superficial left orbit. (**a**) The upper eyelid margin. (**b**) The eyelids are separated to expose the lesion in the temporal conjunctiva. (**c**) A close-up of the conjunctiva shows the blood-filled cystic structures. In other patients, the conjunctival lesions may be filled with clear fluid rather than blood, but the texture is similar. (**d**) A coronal CT scan of this patient shows the soft tissue infiltration in the left lateral eyelids and orbit.



Fig. 23.10 (continued) (**e**) The axial CT scan shows a soft tissue thickening in the left lateral lid and conjunctiva. The soft tissue changes in this eyelid lymphangioma are quite homogenous. Orbital or larger lymphangiomas tend to have less distinct borders and may be more heterogeneous with cystic spaces

spaces of an LVM help to differentiate macrocystic LVM, which are cysts larger than 10 mm from microcystic (<10 mm). This treatment of these lesions is covered in Chap. 35.

Eyelid and Periocular Dermoid Cysts

The dermoid cyst is believed to originate when a portion of the embryologic ectoderm becomes inadvertently buried along the suture lines of moving fetal growth plates. The clinical presentation of the lesion [20] is divided into 2 groups that have different characteristics: anterior lesions and posterior lesions. The anterior cysts occur along the frontozygomatic, frontolacrimal, and frontoethmoidal sutures. The deeper dermoids develop along the lines of the sphenozygomatic and sphenoethmoidal sutures. The more anterior lesions become obvious at a younger age than the deeper orbital lesions.(Refer to Chap. 35 for a more detailed discussion of the orbital dermoid.)

The typical anterior dermoid cyst presents as a smooth, rounded, firm, non-tender mass (Fig. 23.12). The mass is not



Fig. 23.11 Superonasal cyst: MRI. (**a–c**) This 12-year-old woman presented with an acute onset of left periocular pain and proptosis. She had no previous history of any ophthalmic problems. The clinical photos demonstrate the downward displacement of her left globe and the proptosis.

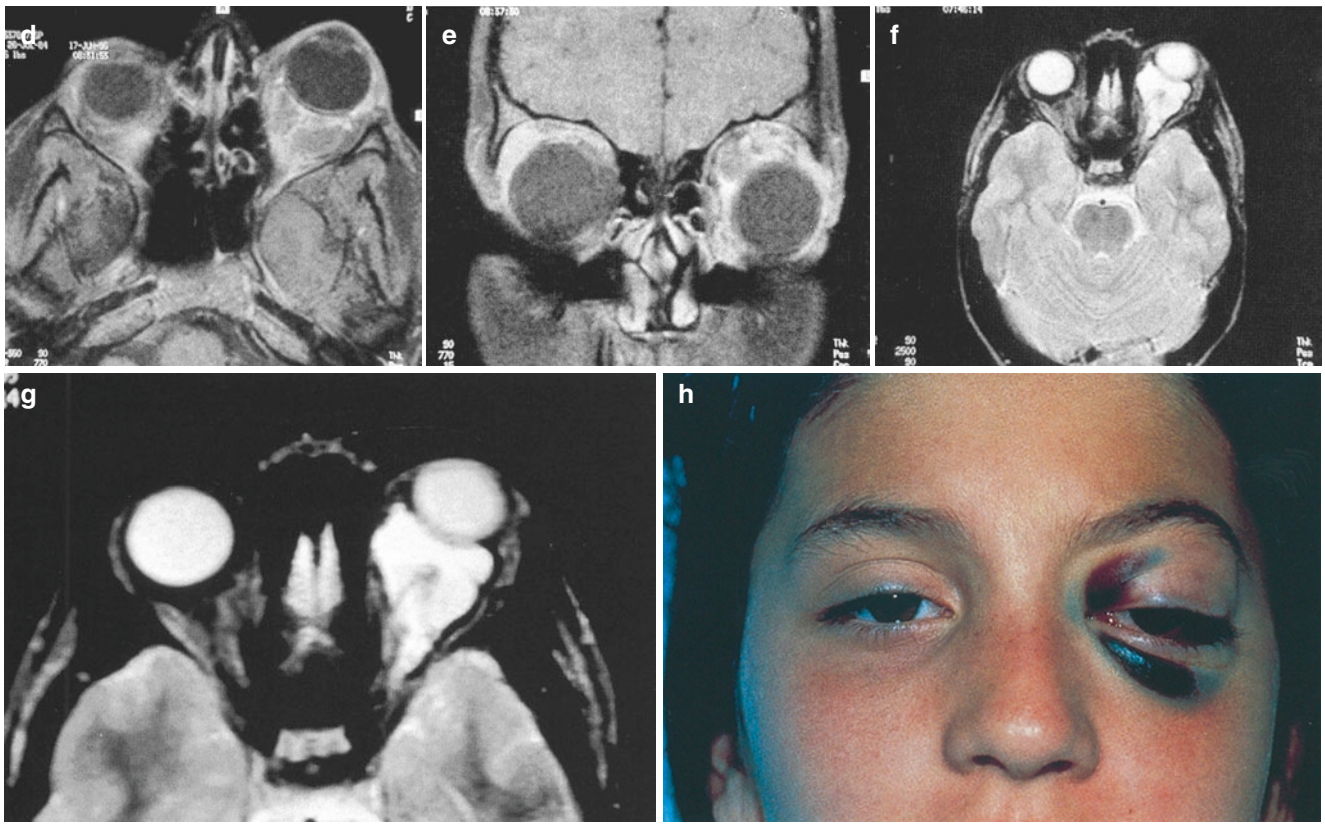


Fig. 23.11 (continued) (**d**) The axial MRI scan shows the presence of some irregular soft tissue and a large cystic structure in the retrobulbar space. (**e**) The coronal MRI shows the superonasal cystic structure with heterogenous soft tissue and the resultant downward displacement of the globe. (**f**) The T_2-weighted MRI shows the high-intensity material within the cyst. (**g**) The patient is in a prone position, and careful inspection of the cyst shows a layering of the red blood cells and plasma within the hemorrhagic "chocolate cyst." (**h**) Twenty-four hours later, the acute hemorrhage is visible with anterior dissection of the blood into the lids and conjunctiva

attached to the skin and is often adherent to the periosteum along the suture line. These cysts enlarge very slowly unless the cyst wall becomes disrupted. Exposure of the contents of the cyst to the immune system results in an acute inflammatory reaction with edema, erythema, and pain. The most common location for the cysts is the lateral brow, followed by the superonasal medial canthal region. On occasion, these cysts can fistulize to the skin and present as an isolated skin lesion which spontaneously drains a keratin-rich exudate.

The dermoid cyst has a characteristic appearance on CT scan. The CT shows an oval, smooth lesion with well-demarcated borders that may have some rim enhancement and lower central absorption with intravenous (IV) contrast. The surrounding bone may show molding or pressure changes. For anterior lateral dermoid cysts, CT is necessary only for an atypical lesion or a lesion that appears fixed and may possibly extend into the orbit. The CT will help in assessing the posterior extent of the cyst. Anterior medial lesions may be scanned to help differentiate the dermoid cyst from encephalocele, infantile hemangioma, or a lacrimal mass (Fig. 23.13). In general, while it is reasonable to image most lesions suspected to be dermoids, the classic firm, but non-fixed, lesion of the temporal brow need not be imaged. In any other location, however, imaging is indicated to rule out bony extension into a neighboring cavity. In the case of superomedial lesions, dermoids may be compressed by advancing bones and become dumbbelled into the nasal space as well as the external orbit. This can also occur temporally. In cases of a temporal lesion that is palpable and firm, but not moveable, imaging should always be ordered to rule out extension into the orbit or skull base.

The treatment for dermoid cysts is surgical excision. This is an elective procedure, but may be considered around 12 months of age for the anterior lesions and at the time of diagnosis for posterior lesions. Anterior lesions should be removed before the child becomes sufficiently mobile so as to be at risk for traumatic rupture of the dermoid cyst. The resultant inflammatory response can cause tissue fibrosis and scarring. When the lesion is removed, care is taken not to spill the cyst contents in the operative site for the same reason. A lid crease incision may be used to remove even very large dermoid cysts (Fig. 23.14). The eyelid crease incision creates the most cosmetically acceptable scar and provides access to superonasal as well as temporal dermoid cysts. If necessary, a sub- or suprabrow incision may be considered (Fig. 23.15). Often as a child grows, the brow cilia will thicken and obscure the scar, but this is not a reliable feature of brow incisions.

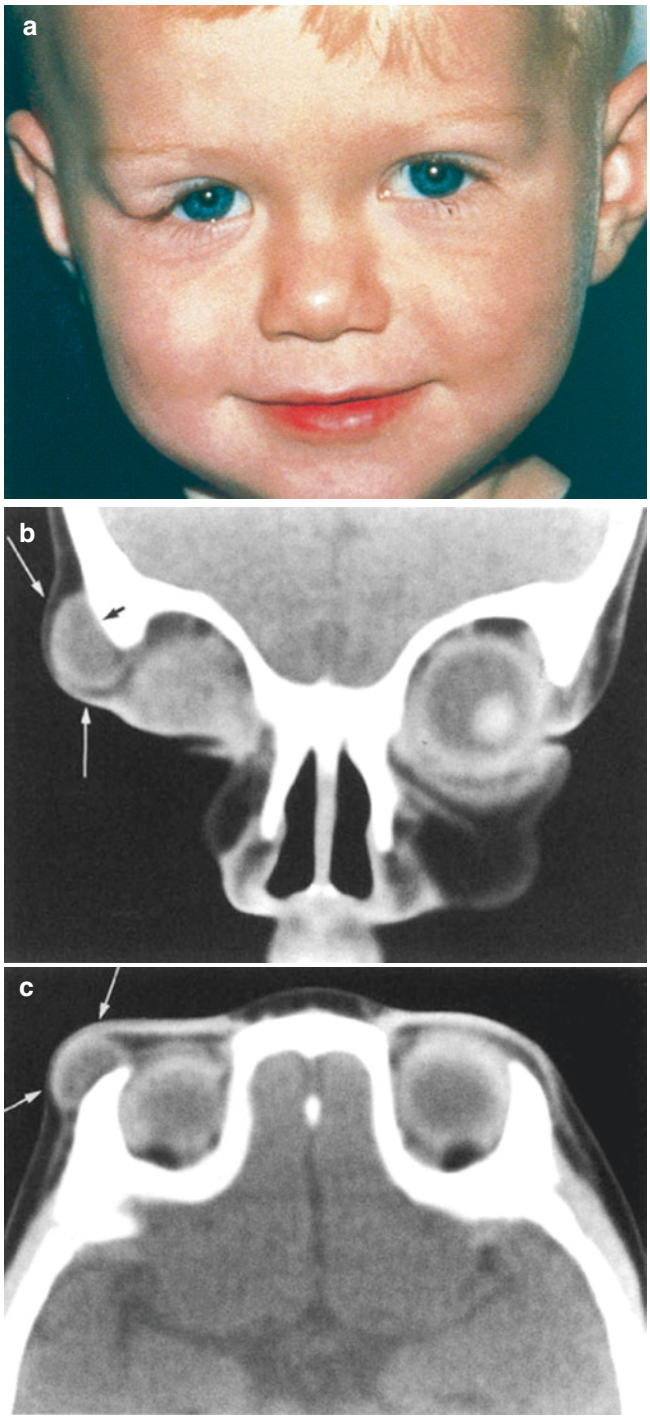


Fig. 23.12 Dermoid Cyst. (**a**) Clinical appearance of a dermoid cyst located in the supero-lateral eyelid. (**b**) The axial CT demonstrates a small, well-defined, subcutaneous mass (*arrows*). The dermoid causes slight flattening of the bone on which it lies. (**c**) The coronal CT shows the dermoid (*arrows*) with a denser capsule. The black arrow indicates the flattened bone, which is in contact with the dermoid cyst

When the skin has been opened, soft tissue blunt dissection, in concert with digital palpation, is used to identify the location of the dermoid cyst. The yellow color of the cyst contents will also help to distinguish it from the surrounding tissue. The cyst will usually be encapsulated by layers of wispy but tough fibrous tissue that may be carefully grasped to manipulate the cyst to expose the tissue attachments for surgical interruption. As a safer alternative, a retinal hammerhead-type cryoprobe may be applied to the capsule of the cyst and makes for easier traction and dissection. Release of the surrounding capsular attachments usually requires sharp dissection with a scissors, and the cyst will typically have an area of periosteal attachment that will also need to be sharply interrupted. A periosteal elevator may be helpful when the attachments are posterior to the cyst and difficult to directly visualize. The underlying bone may be thinned with an indentation that matches the cyst. At times the cyst will extend through an orbital wall into the orbit creating a "dumbbell" cyst. In cases of large dermoid cysts, grafting of bone, fat, or hydroxyapatite cement may be used to camouflage the postoperative indentation at the point of soft tissue loss. This is rarely necessary because the overlying tissue almost always obscures the indentation. The cyst is usually excised with the capsule intact, and the wound is closed in layers. The deeper tissues may be closed with 4–0 Vicryl sutures and the skin incision with a running subcuticular pull-out stitch of 5–0 nylon or polypropylene or a simple interrupted dissolving gut suture. If an inadvertent spill of the cyst contents occurs, or if iatrogenic decompression is necessary for visualization, the cryoprobe can be used to seal the ruptured area while dissection continues and the wound is profusely irrigated with saline prior to closure. The use of steroids to prevent inflammation may also be appropriate.

The epidermoid cyst (Fig. 23.15) is clinically similar to the dermoid cyst, but is distinguished by its pathology. The pathologic tissue is limited to epithelial components. Surgical removal is similarly accomplished through the eyelid crease or a brow incision.

Neurofibromatosis and Plexiform Neurofibromas

The term neurofibromatosis has been applied to disorders involving a combination of lesions derived from neural crest mesenchyme. One manifestation of this disorder, the plexiform neurofibroma, commonly involves the tissues of the eyelids, periorbital, and orbital. There are at least 2 distinct genetic forms of neurofibromatosis [21]. Type 1 (NF-1), also known as von Recklinghausen's disease or peripheral neurofibromatosis, is associated with a mutation in the long arm of chromosome 17 (see Chaps. 14 and 15). It is this category of neurofibromatosis that is associated with plexiform neurofibromas of the eyelid. Type 2 (NF-2) [22] is also known as central neurofibromatosis and is associated with a mutation in the long arm of chromosome 22. NF-2 is diagnosed by the presence of bilateral acoustic neuromas and can be associated with other central nervous system tumors, including meningiomas and schwannomas. Posterior subcapsular cataracts may develop in NF-2. The plexiform neurofibroma is a feature of NF-1 [23]. Seven diagnostic

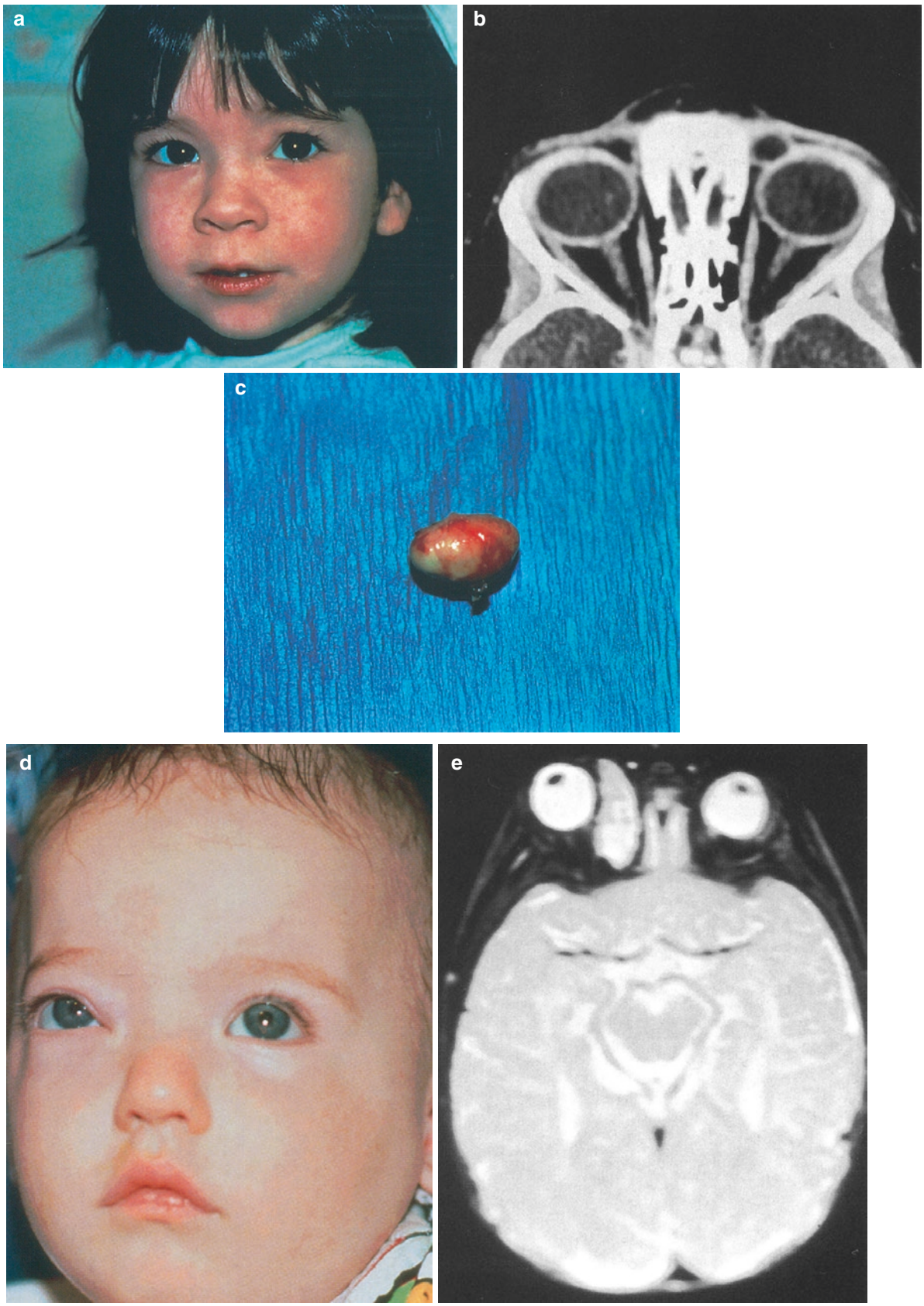


Fig. 23.13 Medial upper lid masses. (**a**) Clinical photograph of a left medial cystic structure. (**b**) Axial CT scan demonstrating a rounded and well-circumscribed mass at the frontonasal suture line consistent with a dermoid cyst. (**c**) Appearance of the same dermoid cyst after removal, a round, yellowish mass with surrounding fibrous tissue. (**d**) Another child also presents with a right medial upper lid mass. (**e**) An MRI scan shows an elliptical lesion in the medial orbit with a slightly heterogenous soft tissue nature. In this case the findings are compatible with an infantile hemangioma rather than a dermoid cyst

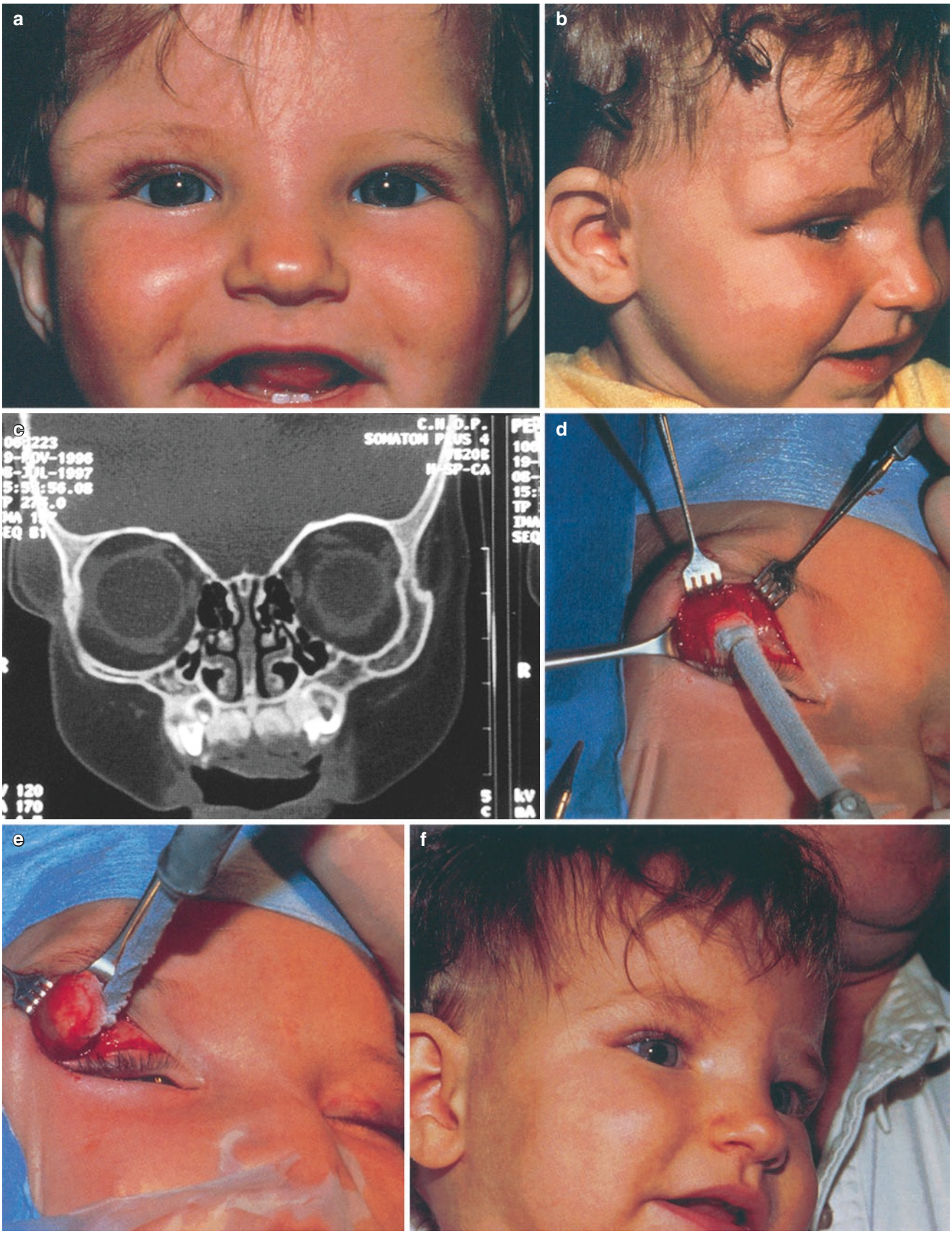


Fig. 23.14 Dermoid cyst: CT scan and removal. (**a**) Anterior view of a large superolateral dermoid cyst. (**b**) Oblique view of the same patient to better appreciate the size of the lesion. (**c**) The CT scan demonstrates the rounded cystic mass located at the frontozygomatic suture. (**d**) The surgical incision is made in the upper eyelid crease, and retraction of the lesion is accomplished with the cryoprobe. (**e**) Removal of the lesion. (**f**) Postoperative result: scar is hidden in lid

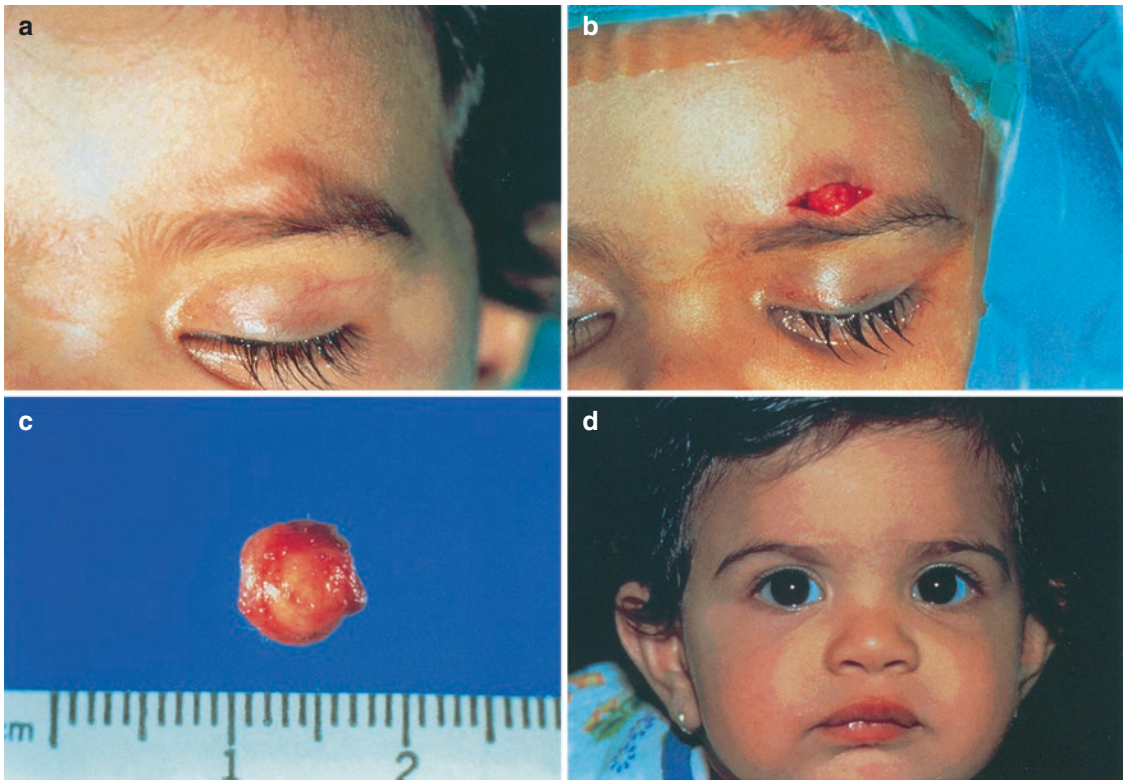


Fig. 23.15 Epidermoid cyst. (**a**) This epidermoid cyst is located just superior to the left brow. (**b**) A supraciliary incision was used to approach and expose this lesion. (**c**) The excised lesion is clinically indistinguishable from a dermoid, but has only epithelial components. (**d**) The appearance of the incision 2 weeks after surgery

criteria exist for NF-1, two of which need to be present to make the diagnosis: (1) presence of 6 or more cafe au lait spots; (2) occurrence of NF-1 in a first-degree relative; (3) intertriginous freckling; (4) 1 plexiform neurofibroma or 2 or more neurofibromas of any type; (5) a bony defect, such as sphenoid wing dysplasia or thinning of long bone cortex; (6) optic nerve glioma; and (7) 2 or more Lisch nodules on the iris. The plexiform neurofibroma typically presents as a characteristic S-shaped deformity of the upper eyelid (Fig. 23.16) seen in infancy or childhood. The lid may have a smooth compressible fullness or may take on the smoothly undulating nodular texture often described as a "bag of worms." Less commonly, neurofibromas can present as a solitary lesion rather than diffuse (Fig. 23.17). The plexiform neurofibroma may involve the orbital structures as well as the lid and surrounding soft tissues. Plexiform neurofibromas involving the eyelid, orbital, periorbital, and facial structures (termed OPPN) can result in significant visual loss in children. Equally important, OPPNs can cause significant alteration in physical appearance secondary to proptosis, ptosis, and facial disfigurement, leading to social embarrassment and decreased self-esteem (Fig. 23.18).

The pathologic features of the plexiform neurofibroma are characterized by a combined proliferation of Schwann cells, axons, and endoneurial cells surrounded by a perineural sheath [24]. This perineural sheath differentiates the plexiform neurofibroma from the diffuse and solitary types of neurofibroma. Although diffuse and solitary neurofibromas may also involve the eyelids, they are less common and have only a variable association with neurofibromatosis.

Both CT and MRI are helpful tools for evaluating the plexiform neurofibroma. On CT scan, the plexiform neurofibroma may appear as an infiltrative soft tissue mass with ill-defined borders. The lesion will demonstrate heterogeneous enhancement with IV contrast. The CT scan will also help to identify changes in surrounding bone. Adjacent bony structures may display thinning or erosion, and attention should be directed to the anatomy of the sphenoid wing to look for absence or hypoplasia. The sphenoid bone may be hypoplastic, defective, or absent. This malformation allows transmission of cerebrospinal fluid pulsations to the orbit and eyelids. Depending on the alteration in orbital volume, the eye may be either proptotic or enophthalmic. MRI imaging is better for demonstrating the full extent of the soft tissue infiltration (Fig. 23.19). This may include posterior spread into the pterygopalatine fossa and the superior orbital fissure. The plexiform neurofibroma will demonstrate increased signal intensity with infusion of gadolinium. The increased intensity will be heterogenous with the brain. The sphenoid wing defect may permit herniation of the temporal lobe into the orbit causing pulsatile exophthalmos. Surgical repair with bone grafting and titanium mesh may be needed to repair this defect (see Chap. 40).

Involvement of the lid by neurofibromas may lead to problems with mechanical ptosis, occlusion amblyopia, astigmatic anisometropic amblyopia, or significant cosmetic deformity.

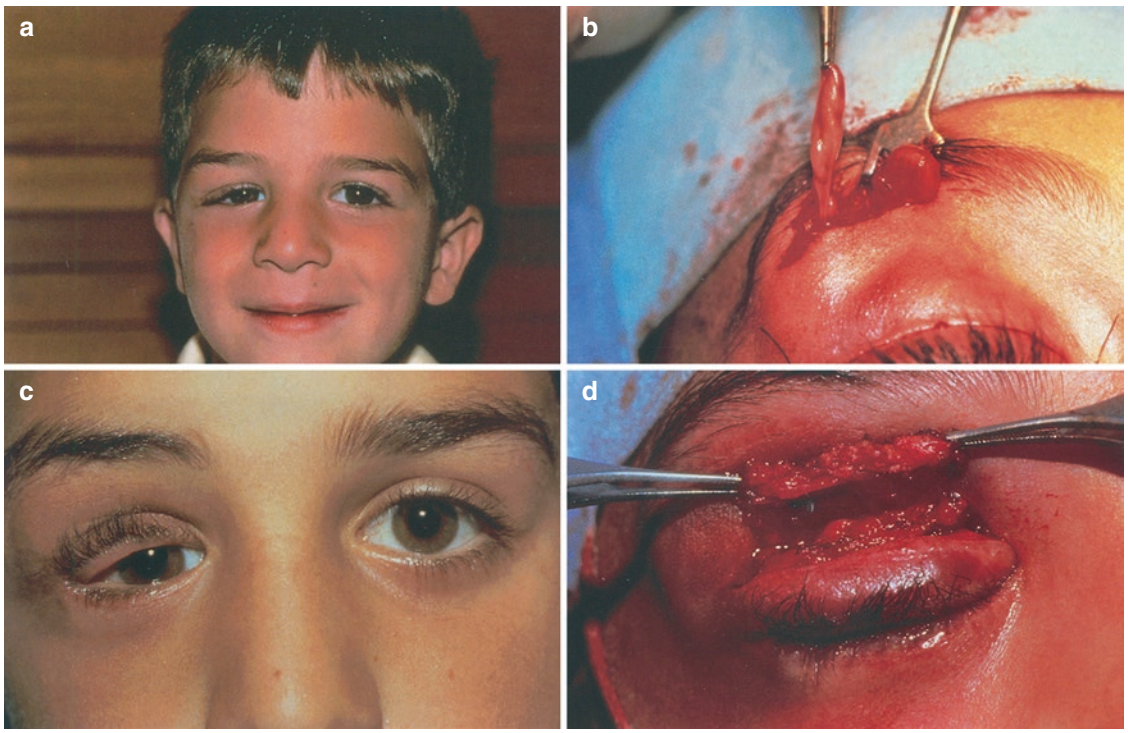


Fig. 23.16 Plexiform neurofibroma. (**a**) This patient was initially seen for the complaint of ptosis of the right upper eyelid. Although there were no systemic signs of neurofibromatosis, the fullness of the lid and the S-curve shape were clues to the presence of the plexiform neurofibroma. (**b**) Plexiform neurofibroma was removed at the time of surgery. (**c**) Five years later the plexiform neurofibroma has enlarged to involve both the upper and lower eyelids. (**d**) At the time of the patient's second eyelid surgery, the thickening of the levator complex by the neurofibroma is demonstrated

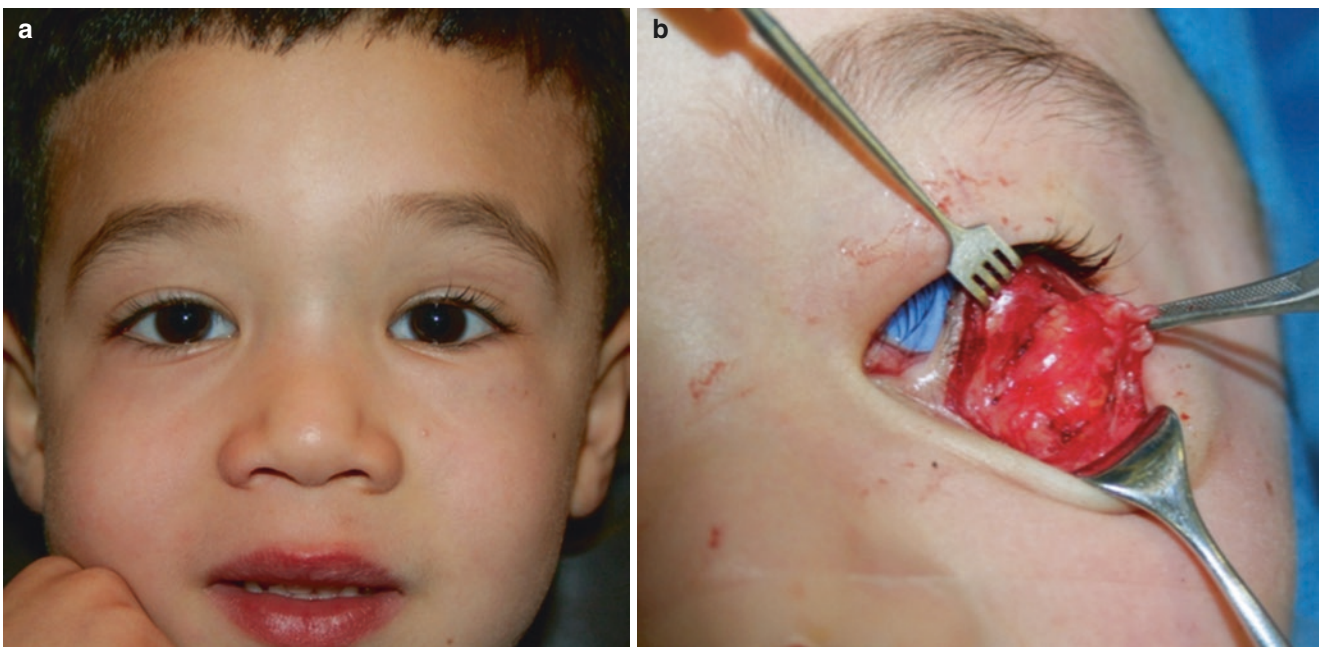


Fig. 23.17 Solitary neurofibroma. (**a**) A 4-year-old with a palpable mass in the left lower lid. (**b**) Solitary lesion exposed via a subciliary incision.



Fig. 23.17 (continued) (**c**) Six months postop excision of lesion

For these reasons, surgical debulking of lid neurofibromas may be indicated. Because of the infiltrative nature of the plexiform neurofibroma, complete excision is rarely possible. Surgical planning should include provisions for blood loss because of the vascular nature of the tumor. If extensive resection is planned, consideration must be given to control of blood loss and planning for safe replacement. The CO2 laser can be a useful tool that will simultaneously cut and cauterize the lesion. Because the practical goal of the surgery is debulking, these lesions tend to grow and "recur" over time. In actual fact, these are not true recurrences but rather new involvement of other nerves in the same region. Multiple procedures may be necessary over the lifetime of the patient. The time course will be variable, depending on the growth rate of the plexiform neurofibromas. Surgical efforts are further complicated by the infiltration of tumor into the tarsus itself. The lid margin can be 2 or even 3 times normal thickness. This is most common in the lateral half of the eyelid. Reconstructive efforts to thin the lid and/or to resect excess length can be attempted, but these are often less than satisfactory and difficulties with severe lagophthalmos and exposure are often encountered. A subcategory of patients with orbitotemporal neurofibromatosis will show dramatic tumor growth and resultant

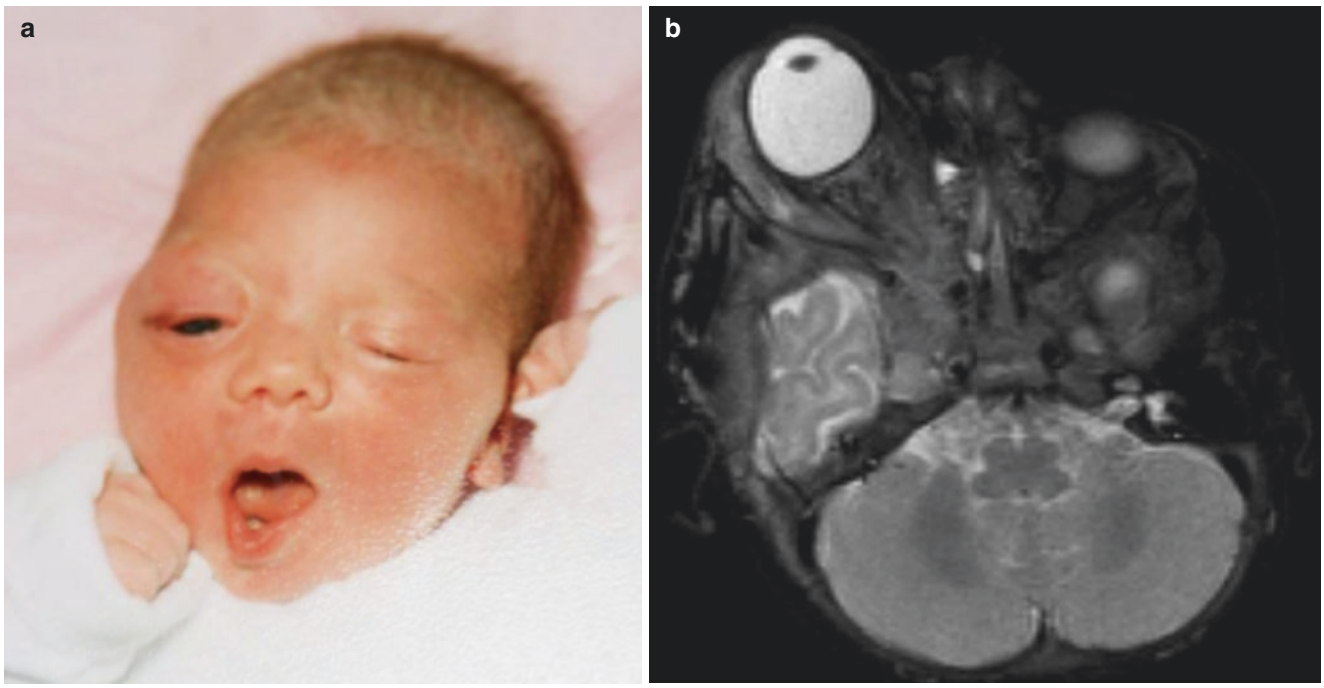


Fig. 23.18 Neonatal OPPN. (**a**) Newborn with OPPN. (**b**) Buphthalmic globe; moderate periorbital soft tissue changes; optic pathway glioma.



Fig. 23.18 (continued) (**c**) Post-enucleation for uncontrolled glaucoma; ocular implant in place; at age 3 years marked increase in periorbital and orbital tumor growth. (**d**) Increased orbital tumor growth with severe enlargement of bony orbit. (**e**) Severe proptosis with major appearance issues for family and child. (**f**) Lid crease approach to orbit for tumor excision; one third of lid to be resected with debulking and canthal reconstruction. (**g**) Levator muscle with orbital tumors excised.



Fig. 23.18 (continued) (**h**) Postop debulking with prosthesis in place. (**i**) Two months postop: lids symmetrical; higher brow indicates larger orbit; plexiform tumors still in cheek. (**j**) Two years postop lid reconstruction. Significant improvement in child's social acceptance and behavioral interactions. (**k**) Five years postop lid reconstruction continuing psychosocial benefit although there are still limitations to surgical correction from tumors acting as a tissue expander enlarging the cheek, nasal ala, lips, and bony orbit

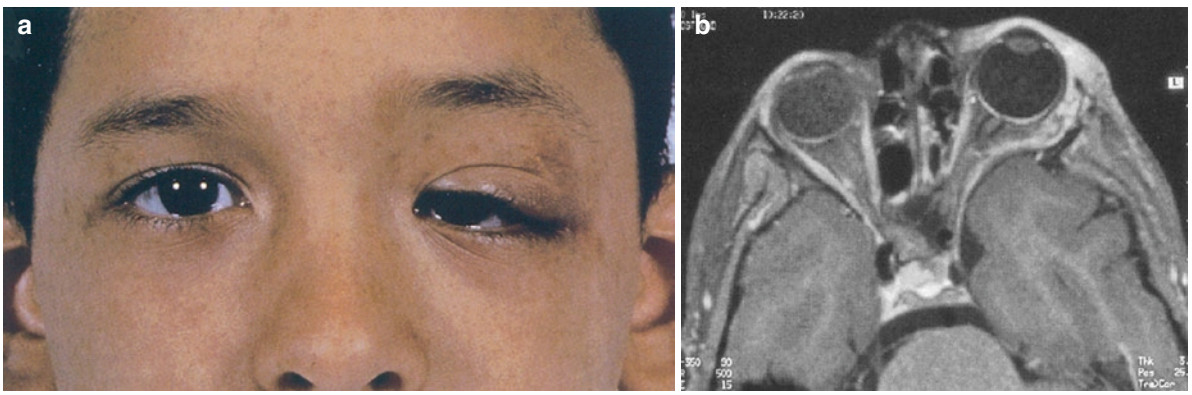


Fig. 23.19 Plexiform neurofibroma. (**a**) An 8-year-old patient with a history of neurofibromatosis type 1. He has a plexiform neurofibroma in the left upper eyelid that has been previously surgically debulked. (**b**) The axial MRI scan demonstrates the heterogeneous thickening of the soft tissue of the eyelid and lateral orbit. Because of the absence of the sphenoid wing, the difference in the temporal lobe position in the brain is also noted

functional and cosmetic impairment. The plexiform neurofibromas in these cases will disrupt soft tissue and stimulate orbital bone growth. Surgical debulking is often unable to keep pace with tumor growth (Fig. 23.20). New protocols are now assessing the efficacy of chemotherapeutic and immunomodulating agents in controlling the growth of plexiform neurofibromas (see Chap. 15).

Timing of Surgical Intervention

This section reflects concepts as previously presented by one of the authors (JAK) based on the efforts of a multidisciplinary group working on OPPN [25].

Because the rate and extent of growth of plexiform tumors in NF1 is unpredictable, there is no predictable



Fig. 23.20 Neurofibroma over a 12-year period. (**a**) The patient was initially seen at 1 year of age with plexiform neurofibroma causing ptosis and distortion of his right upper lid. (**b**) Four months later (age 18 months), debulking and lid repair temporarily corrected his ptosis, but the neurofibroma has continued to enlarge. (**c**) One year later (age $2^{1}/_{2}$), the lesion continues to enlarge, and the ptosis is becoming worse. (**d**) At 3 years of age, the orbital and eyelid neurofibromas are quite large, and even with patching his amblyopia is becoming problematic.



Fig. 23.20 (continued) (**e**) A CT scan at this time shows the soft tissue changes and the expansion of the orbital bone. (**f**) Debulking of the lesion is again performed at age 3. Significant ptosis is still present. (**g**) One and a half years later, at age $4^1/_2$, the lesion has again shown significant regrowth. (**h**) A coronal CT shows the lateral orbit neurofibroma and the marked enlargement of the orbital volume. Additional debulking surgery was performed. (**i**) At age $5^1/_2$, there is significant downward descent of the right globe, and the upper lid is thickened with limited mobility. The distortion of the brow position and cilia is noted. Additional debulking surgery is performed. (**j**) At age 6, there is persistent lymphedema of the conjunctiva and massive infiltration of the lid and orbital tissues with neurofibroma. Amblyopia patching continues, but the poor vision in the right eye limits compliance. (**k**) One and a half years later (age $7^1/_2$), the growth of the plexiform neurofibroma continues. The amblyopia therapy has failed to produce useful vision in the right eye. The downward descent of the right eye and the enlargement of the orbital volume have progressed. (**l**) A three-dimensional CT scan of the orbits shows the alteration created in the bone by the soft tissue expansion of the plexiform neurofibroma.



Fig. 23.20 (continued) (**m**) One year later at age $8^1/_2$ in the face of continued growth of the lesion, the decision is made to do a resection of the involved tissue, including the right eye, which did not move and had poor visual function. (**n**) Through a bi-coronal flap, plexiform neurofibromas were debulked. The eye was enucleated and volume replaced with a dermis fat graft. (**o**) The patient at age 9 after excision of the lesion and the globe. He is now wearing an ocular prosthesis. Ptosis still is present. (**p**) The patient at age $9^1/_2$. The prosthesis has remained stable. The lower face has shown some increase in size of the lesions of the right cheek. (**q**) Two years later (age $11^1/_2$), the soft tissue of the lids and orbits has remained relatively stable. (**r**) Patient at age $12^1/_2$. (**s**) Patient at age 16. Right fronto-temporal cranial bone deformity developing. Further reconstruction planned to repair right medial ptosis, elevate the right lower lid and soft tissues of the face to reduce the appearance of orbital dystopia, and fill in the depression between the zygoma and the cranial bone deformity

guideline regarding the optimal time for surgical intervention.

Adnexal tumors and the associated orbital deformities often continue progressing despite excision and repair. These are not true recurrences, but rather tumor growth from remaining periorbital and orbital tumors. This progression is more rapid in childhood and puberty but can still occur later in life. While exceedingly rare, the rapid growth of OPPN can indicate the possibility of a malignant peripheral nerve sheath tumor, in which surgical and medical therapy may be indicated. Parents or other caregivers may be extremely motivated for surgical excision of these tumors, but must be cautioned regarding the reality that multiple procedures are usually required for long-term OPPN tumor management.

Surgical Management Concerns: Are Multiple Procedures Really Worth the Effort?

In a 20-year study done at the NF1 Clinic at The Children's Hospital of Philadelphia, 131 patients had 302 procedures for head and neck tumors [26]. While the overall freedom from progression was 56%, tumors involving the head, neck, and face had double the probability of recurrence as compared to tumors excised from the extremities. The conclusion drawn from this study was that patients less than 10 years of age with lesions of head, neck, and face were unlikely to have long-term benefits from surgery since OPPN recurrence was so common. Development of an effective medical therapy was the recommended goal.

There are, however, a number of concerns with these recommendations. While medical therapy is certainly a major goal and would ideally be the preferred treatment, at this point more than 20 years later, we are still searching for an effective medical treatment for OPPN. Furthermore, avoiding surgery does not take into account either the functional or the psychosocial appearance concerns of these younger patients [25]. Unfortunately, there is only minimal data supporting either a functional or psychosocial benefit from surgical repair and especially with recurrent cases of OPPN so that multiple surgical excisions are not uniformly accepted as the preferred approach.

Functional Concerns

Amblyopia protection is the most common functional concern which can be due to multiple causes. With OPPN, this is most commonly due to occlusion by a ptotic lid (< age 8 years), but anisometropia from pressure of orbital or lid tumors on the eye as well as associated strabismus is also frequently a problem in this regard. Corneal exposure issues from proptosis and epiphora from lid malpositions are also common functional problems associated with OPPN, in particular.

Appearance Concerns

The progressive growth of these tumors creates periorbital soft tissue complications including ptosis, lid contour and asymmetry of the eyelids, canthal abnormalities, and skin changes [25]. Facial descent from the weight of OPPNs can also produce cheek and oral commissure deformities. Plexiform tumors in addition to gliomas within the orbit can produce proptosis leading to significant alterations in appearance. The psychosocial impact with a progressive deformity such as that caused by OPPN on a child's self-image and ultimate ability to be a productive and happy member of society is very much dependent on our ability through medical and surgical efforts to improve appearance.

Indications and Timing of Surgical Intervention

Both the timing and degree of surgical intervention are controversial subjects. Early surgery before age 10 years may be necessary due to functional concerns regarding amblyopia and the effects of expansion on both the periorbital soft tissues and the bony orbit. Early surgery is also important in attempting to maximize the child's cosmetic outcome and minimize psychosocial concerns from the deformities of OPPN growth as it affects not only the child but also the entire family constellation. A number of helpful recommendations are summarized below from the recent review of current concepts in the management of OPPN already cited [25].

Current Recommendations: Soft Tissues

Most congenital nasolacrimal problems associated with OPPN can be treated early. Intubation of the nasolacrimal system may offer protection from inadvertent damage during more extensive orbital surgery. Debulking of OPPN tumors invading the cheek early is somewhat controversial due to the potential of damage to the facial nerve. Tissue expansion with inflatable balloons can provide tissue for advancement to replace even large areas with skin deformities. While exenteration for a severe unilateral problem is mentioned in the literature, this should be avoided if at all possible. Facial transplantation for severe bilateral OPPN while possible should still be considered only as a last resort. Figure 23.20 demonstrates the necessity for early and continued surgical intervention for a newborn presenting with OPPN. The benefits from both a functional and psychological perspective have proven significant for both this child and for their family.

Current Recommendations: Bone

When there is visible pulsating exophthalmos, sphenoid bone defect repair can be of benefit, especially when there is progressive proptosis. Calvarial bone grafts with titanium mesh are useful in order to repair the sphenoid defect and minimize bone resorption. This should be considered on a case by case basis and is an even more critical issue when associated with a seeing eye.

Nevi

The nevus develops as a benign proliferation of the epidermal melanocytes. In children these may be congenital or acquired. Congenital nevi [27] are present at the time of birth and have a more variable size, color, and clinical nature than an acquired nevus. Many lesions are tan colored with darker spots of focal pigmentation. The eyelid skin may be thickened and somewhat irregular with an undulating or velvety surface. Because the eyelid margins are fused during fetal development, a "kissing" nevus may form on adjacent areas of the upper and lower lids when normal developmental changes split the two eyelids (Fig. 23.21). These types of congenital nevi tend to have melanocytic cells that show deeper layers of penetration on histologic evaluation, and the congenital nevus is thought to have a higher biologic potential to be a precursor of malignant melanoma. For cosmesis, amblyopia due to lid malposition, and because of concern for the development of malignant melanoma, surgical removal of the lesion may be contemplated. Prior to or at the time of removal, suspiciously pigmented tissue or areas of abnormal eyelid architecture are biopsied. In pigmented lesions where malignancy is a concern, it may be prudent to biopsy the lesion for permanent sections and diagnosis prior to excision. Pigmented lesions are better diagnosed on permanent tissue processing rather than frozen sections. The surgeon will want to know the depth of the tissue involved on the biopsy and will do a larger resection of surrounding tissue for a cutaneous malignancy, particularly melanoma. Fortunately, melanoma is rare in young children. Because of size, it is sometimes difficult to remove the nevus completely with one procedure. Staged removal with grafts and flaps is often necessary (Fig. 23.22).

Acquired nevi begin to appear at 6 months of age and continue to appear throughout life. In children, they are flat, pigmented spots that become more noticeable at 1–2 mm in diameter. As an adult, these nevi are monitored for pathologic changes, but this is rarely a concern with acquired nevi in children.

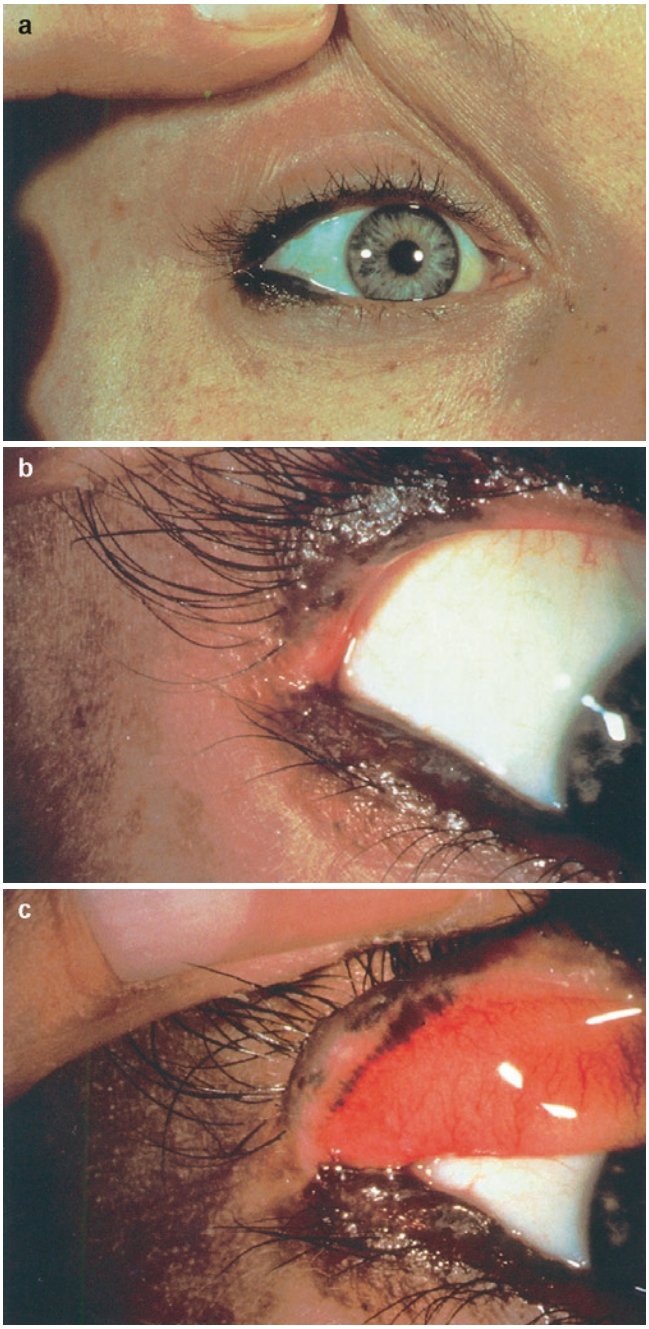


Fig. 23.21 Congenital nevus. (**a**) This patient has a congenital nevus involving the upper and lower eyelids. The lesion is named a "kissing" nevus because it occurs where the two eyelids were embryologically fused. (**b**) The close-up view shows the dark pigmentation with a slightly elevated lid margin. The lashes are intact and grow through the lesion. There is no ulceration of the epithelium, and the patient reports no alteration in the growth rate of the lesion. (**c**) Eversion of the lid shows the pigmenting involvement of the palpebral conjunctiva. Recall that the conjunctiva has its embryologic origin from invaginated epithelium

Congenital oculodermal melanocytosis (nevus of Ota) is also a congenital eyelid lesion (Fig. 23.23). The skin, sclera, and conjunctiva have a bluish-gray pigmentation, and the uveal tract may also show increased pigmentation [28, 29]. This condition is more common in Asians than Caucasians who also demonstrate an increased risk for uveal melanoma [30, 31].

Pilomatrixoma

The pilomatrixoma [32] (calcifying epithelioma of Malherbe) is a benign proliferation of hair matrix cells. This tumor is often called pilomatricoma in the dermatology literature. There is a predilection for appearance on the face

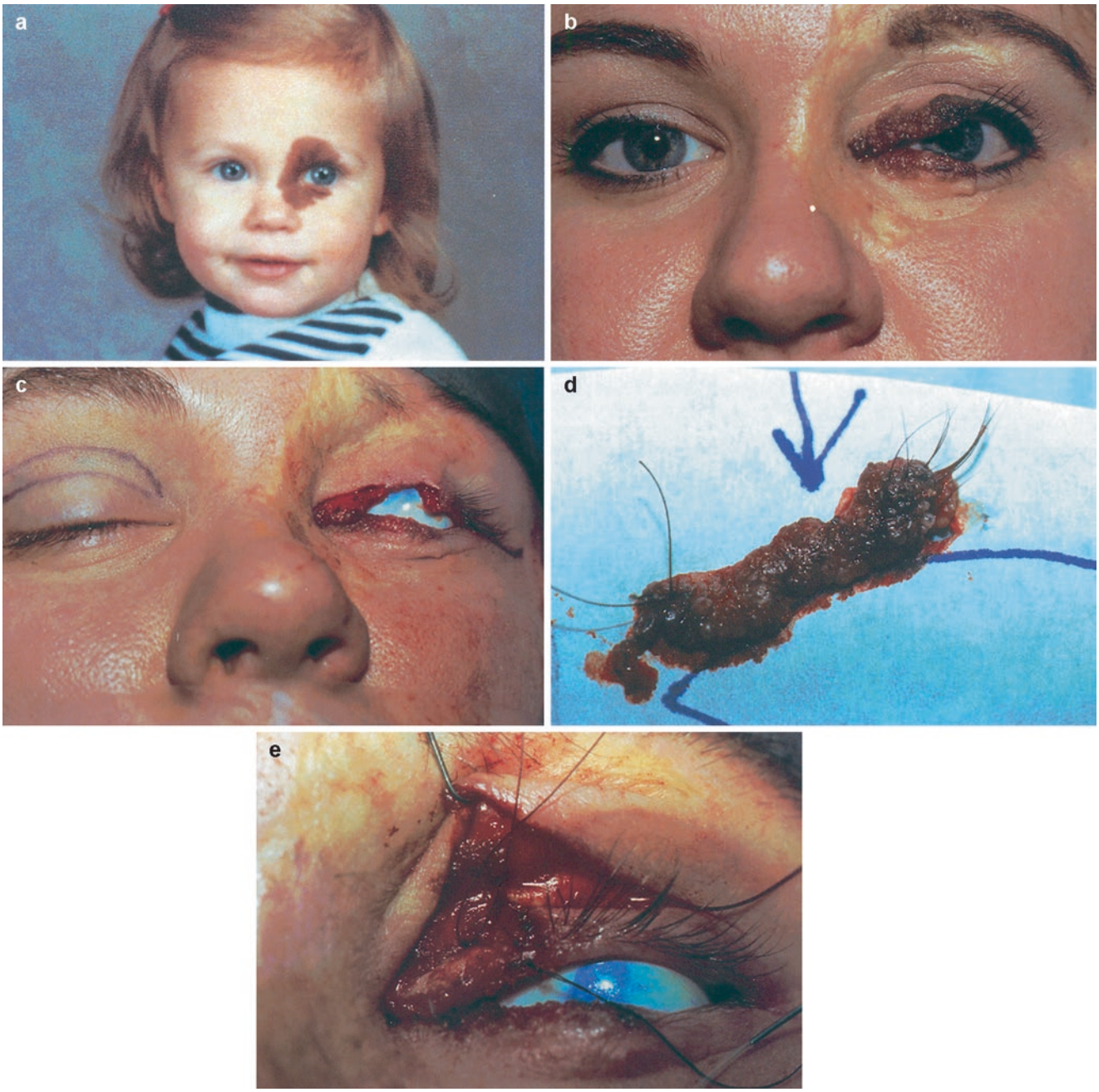


Fig. 23.22 Congenital nevus. (**a**) At the age of 4, this patient had extensive involvement of the lids by a congenital nevus. (**b**) The patient had excision and skin grafting procedures, but nevus remained at the lid margins. (**c**) The lid margin nevus was resected because of suspicious areas of black pigmentation. (**d**) The specimen from the upper lid is positioned for pathology. The lesion was read as benign. (**e**) The upper lid is repaired with a free tarsoconjunctival graft with a skin flap from the upper lid. The lower lid margin is left open to heal after the lid margin nevus was contoured using a Colorado cautery.

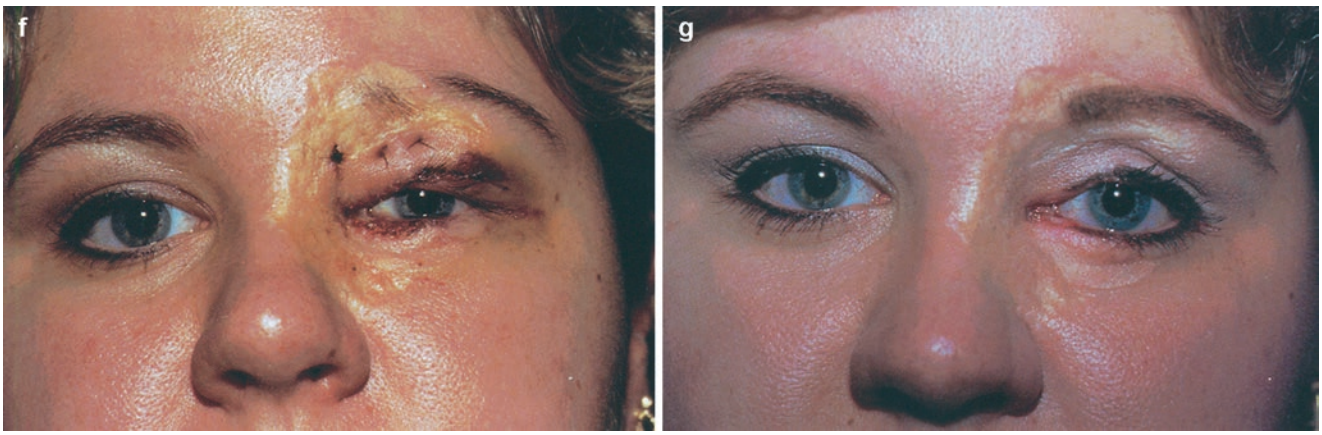


Fig. 23.22 (continued) (**f**) One week later the flap is healed into position and the lower lid is granulating. (**g**) The patient's postoperative appearance 4 months after surgery



Fig. 23.23 Oculodermal melanocytosis. (**a**) This patient has oculodermal melanocytosis. (**b**) The magnified view shows the pigmentary and texture changes in the eyelid skin. (**c**) The bluish-gray coloration of the conjunctiva and sclera are demonstrated

in the eyelids and eyebrow area. The lesions may occur at any age, but tend to occur in children, and have the clinical appearance of a solid subcutaneous nodule covered with intact epithelium. The overlying skin may have a pink to purple discoloration (Fig. 23.24). The lesion may be mistaken for a chalazion in the eyelid or a dermoid when located in the brow. These lesions are often adherent to the overlying skin. They should always be excised and the specimen sent for histopathologic evaluation due to the possible but rare occurrence of malignant transformation [33].

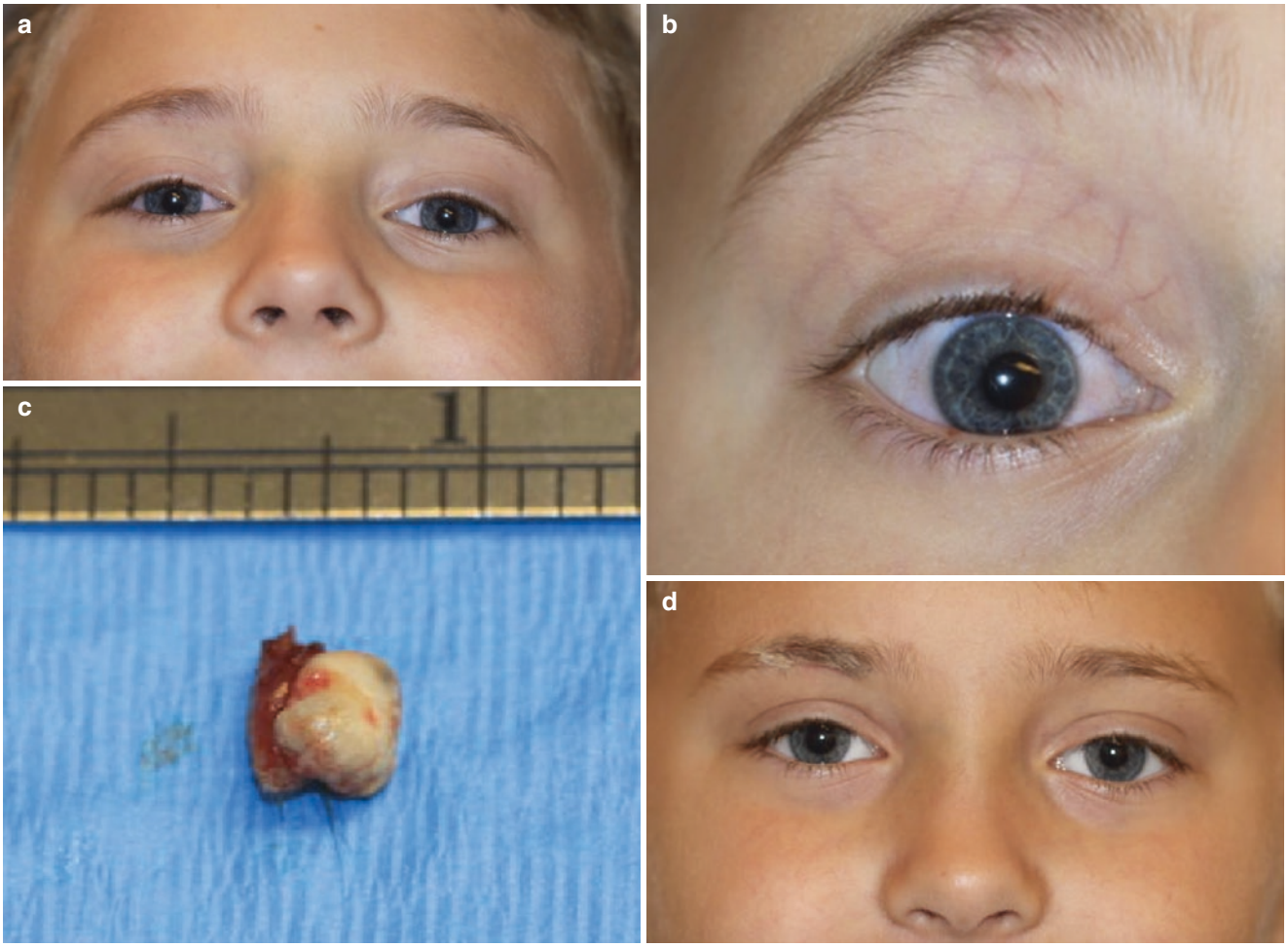


Fig. 23.24 Pilomatrixoma. (**a**) An 8-year-old male with a firm nodule below the right brow. (**b**) The lesion is firm but not fixed to the orbital rim. (**c**) Surgical specimen of this lesion, which was removed via sub brow incision. (**d**) Postoperative photo taken 1 month after surgery. The wound was closed with a subcuticular 5-0 Monocryl suture and Dermabond

Juvenile Xanthogranuloma

Juvenile xanthogranuloma falls into a group of disorders characterized by abnormal proliferation of histiocytes of the non-Langerhans type. This benign lesion occurs in the skin of infants and children, having the appearance of yellow or red smooth rounded papules or nodules (Fig. 23.25). The lesions are usually small and may be singular or multiple. The same lesion may also appear on the iris where it is classically described as an etiologic factor in atraumatic hyphema. The juvenile xanthogranulomas may also extend posteriorly into the orbit [30].

Smaller lesions may be excised for biopsy and diagnosis. Left undisturbed, the skin lesions usually resolve spontaneously. Larger lesions may respond to corticosteroid [34] and cryotherapy or require surgical excision (Fig. 23.26).

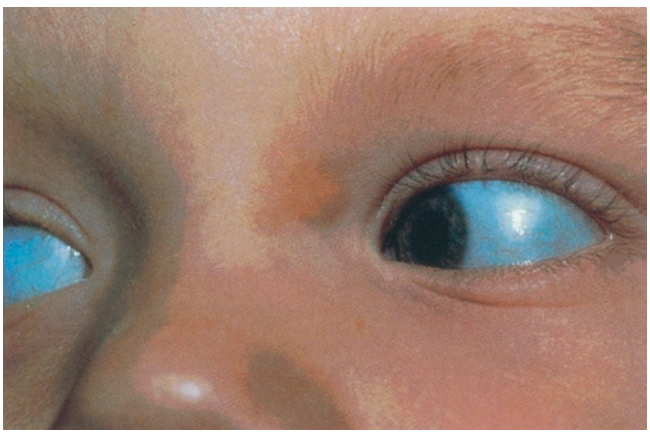


Fig. 23.25 Medial canthal skin lesion of juvenile xanthogranuloma

Chalazion

The chalazion is a common inflammatory lesion of the pediatric eyelid (Fig. 23.27). The problem originates in the oil glands of the lid margin when obstruction to outflow causes sludging and retention of the normal oil secretions. The glands of Moll and Zeiss at the eyelid margin, as well as the larger meibomian glands, may become infected acutely. This is usually referred to as a hordeolum noted at the lid margin. Chronic inflammation of the meibomian glands is characteristic for the diagnosis of chalazion. To the lay person, all of these lesions are referred to as styes. To the practitioner, it is



Fig. 23.26 Juvenile xanthogranuloma over a 16-year period. (**a**) This 5-month-old patient presented with a rapidly enlarging lesion of the left eyelids and medial canthus. The lesion caused ptosis and lower eyelid malposition resulting in obscuration of the visual axis. (**b**) The magnified view shows the yellowish color of the nodules and the irregular surface areas. The biopsy was determined to be juvenile xanthogranuloma. (**c**) The lesions showed minimal response to steroids. The patient was taken to the operating room where localized cryotherapy was attempted. After regression was observed postoperatively, in the area of cryotherapy-treated tissue, the entire lesion was treated with a double freeze-thaw technique. The tissue was monitored with a thermocouple at – 25 °C. (**d**) One year after surgery, patching for amblyopia is continued. (**e**) At 3 years of age, surface scarring and erythema remain, but are diminishing. (**f**) At 5 years of age, the surface skin changes are slowly improving, but the patient now presents with a palpable mass in the inferior orbit.

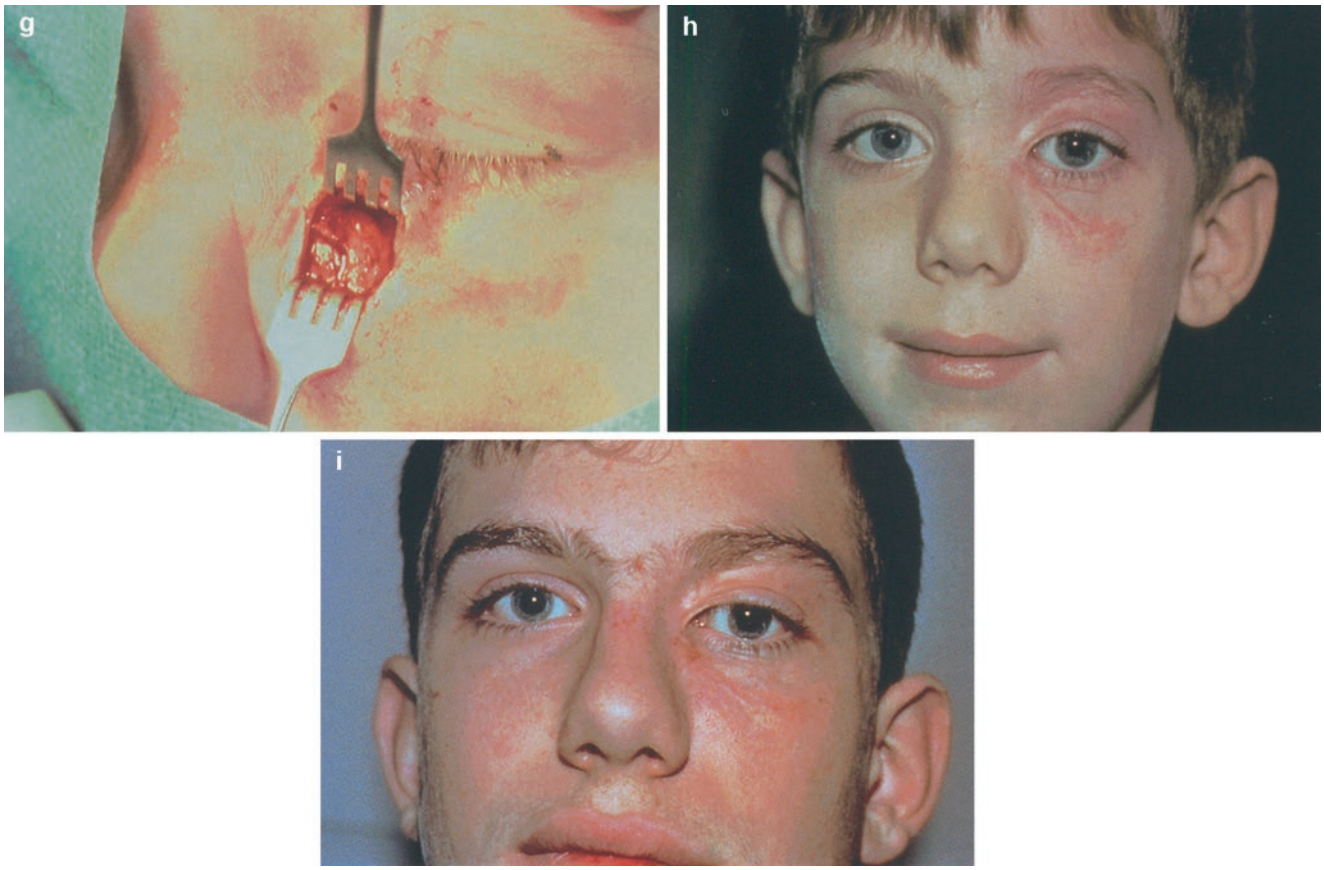


Fig. 23.26 (continued) (**g**) The orbital mass is surgically resected and represents an isolated orbital juvenile xanthogranuloma. (**h**) The patient at 9 years of age. (**i**) The patient at 16 years of age; visual acuity is 20/20 in each eye. A z-plasty repair is planned for the epicanthal fold

helpful to initially diagnose an acutely infected eyelid gland, or hordeolum, as these lesions are typically amenable to aggressive warm compresses and topical ophthalmic antibiotics for lesions that have broken through the skin (external hordeolum).

For a lesion to evolve into a chalazion, the lining walls of the meibomian glands break; the overlying soft tissue is exposed to the oil secretions which the body perceives to be foreign material. An inflammatory reaction then ensues that creates a warm, tender, erythematous, and indurated nodule in the eyelid. Chalazia are also best initially treated with compresses and may drain spontaneously and resolve. When the inflammatory component resolves, however, if an encysted nodule of secretions remains in the eyelid, then incision and drainage or corticosteroid injection may be advised for treatment. Both options will require sedation or general anesthesia in the pediatric age group. Triamcinolone 10 mg/mL can be injected directly into the cyst and into the surrounding inflammatory process. Usually 0.1 to 0.2 mL total are injected. For diffuse thickening and an accompanying inflammatory reaction, this treatment option will be appropriate. Temporary hypopigmentation has been reported after corticosteroid injection into the eyelid which is of greater concern for more darkly pigmented patients.

For most residual encysted chalazia, incision and drainage are necessary. To drain the lesion (Fig. 23.28), local anesthetic and epinephrine are injected for hemostasis and postoperative pain control. A chalazion clamp is placed on the lid, and the lid is everted to expose the palpebral conjunctiva and tarsus. The location of the cyst can usually be identified by erythema or a gelatinous appearance below the tarsus, but is sometimes elusive. Palpation of the eyelid with a cotton swab under the lid and a finger on the surface epithelium will sometimes allow the surgeon to palpate the nodule to ascertain its location. A scalpel blade is used to make an incision in the conjunctiva and tarsus and into the cyst. Extrusion of liquid and gelatinous oily material will occur when the cyst wall is opened. A chalazion curette is used to remove the contents of the cyst, and then the cyst wall is excised using a toothed forceps and small, sharp scissors. Occasionally, cysts can occur in the glands of Zeiss or Moll and be located in the anterior lamella of the lid margin. In this case the incision and drainage may be done from an anterior approach. For recurrent lesions, or marked inflammation in the surrounding tissues, the steroid injection maybe combined with the incision and drainage. The steroid is placed after drainage of the cyst. Sarcoid nodules and pseudorheumatoid nodules (granuloma annulare) may be mistaken for chalazia (Fig. 23.29). Atypical



Fig. 23.27 Chalazion. (**a**) Young child with multiple eyelid chalazia. (**b**) Young child with multiple large chalazia that have progressed to eyelid abscesses. (**c**) Chronic lower eyelid chalazion in an Asian child. (**d**) Scarring in the upper eyelid of a child with a chalazion treated conservatively with observation alone. Scarring due to chalazia can be more severe in patients of Asian descent due to the proximity of the orbital septum and fat in relation to the tarsus

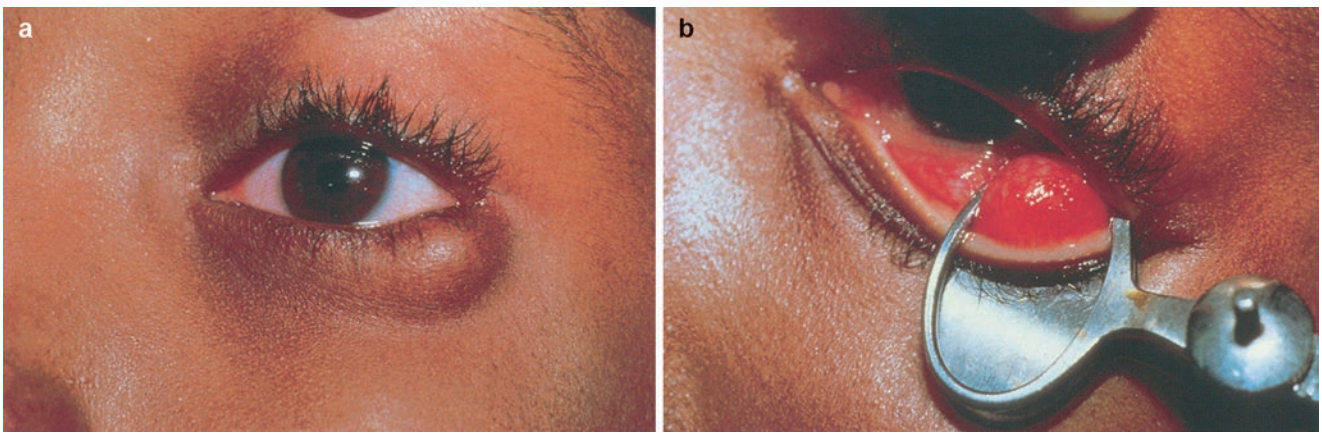


Fig. 23.28 Surgical drainage of a chalazion. (**a**) An acute chalazion in the left lower eyelid. (**b**) After general and local anesthesia, a chalazion clamp is placed on the everted lower eyelid.

lesions and recurrent chalazion in the same location should be biopsied at the time of excision.

For patients who suffer from chalazia, prevention is critical as it is quite easy to develop additional lesions. It is estimated that there are 140 meibomian glands of the eyelids (40 upper and 30 lower); thus a patient who has suffered from one lesion may be prone to have more. The overall health of the meibomian gland margin must be well maintained. Any blepharitis or meibomian gland dysfunction must be managed. Typically, a regimen of daily eyelid scrubs with some

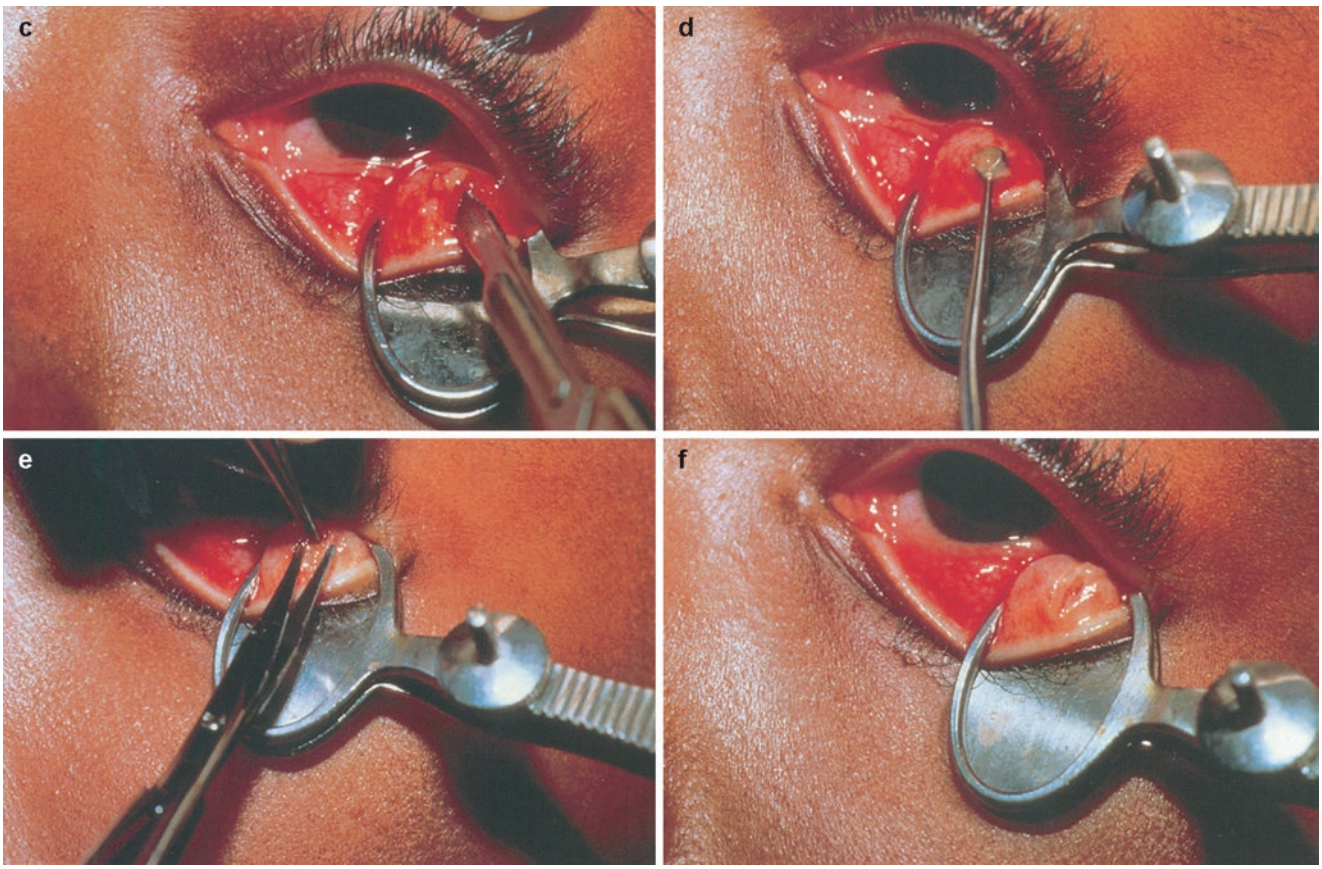


Fig. 23.28 (continued) (**c**) A scalpel is used to make a vertical incision in the palpebral conjunctiva and tarsus. (**d**) A chalazion curette is used to remove the contents of the cyst. (**e**) Scissors are used to remove the lining walls of the cyst. (**f**) The incision remains open at the end of the procedure for drainage

form of unscented non-irritating soap is indicated. If there is significant eyelid margin disease, a topical ophthalmic steroid ointment may be necessary to decrease the eyelid inflammation. For patients who suffer from multiple bouts of chalazia, some form of systemic anti-inflammatory medication may be considered. There are antibiotics as well as natural remedies, which exhibit anti-metalloproteinase. Omega-3 dietary supplements have been shown to improve meibomian secretions [35]. These vitamins are readily available as gummy bears and are now popular at many supermarkets. Flaxseed oil taken in a dose of 1000 mg a day may also be effective; however, this is only available in liquid form, and a full teaspoon is not as palatable. Fish oil contains docosahexaenoic acid (DHA) and eicosapentaenoic acid (EPA), which are thought to be more effective in preventing inflammation than the alpha-linolenic acid (ALA) that is found in flaxseed oil.

Granuloma Annulare

Granuloma annulare is a benign inflammatory abnormality of the skin and subcutaneous tissue characterized clinically by dermal papules and annular plaques. There are different forms of the disease: localized, generalized, subcutaneous, perforating, and arcuate dermal erythema. The subcutaneous form is most common in children and presents as firm painless nodules [36]. They can occur on the eyelid and most typically are found on the fingers. On histology they can resemble rheumatoid arthritis and have been called "pseudorheumatoid" nodules [37]. These lesions can be self-limited and resolve spontaneously, though there is a risk for recurrence. In the past, treatment included intralesional steroids, topical steroids, isotretinoin observation, and surgical excision [36]. Figure 23.29 depicts a patient with granuloma annulare of the eyelid treated with surgical excision.

Rosai–Dorfman

Rosai–Dorfman disease (RDD) is a non-malignant histiocytic proliferation that presents with painless cervical lymphadenopathy in over 80% of patients. It was previously known as sinus histiocystosis. In this disease macrophages proliferate extensively in the lymph node sinus (hence the moniker sinus histiocytosis). On histopathology emperipolesis is

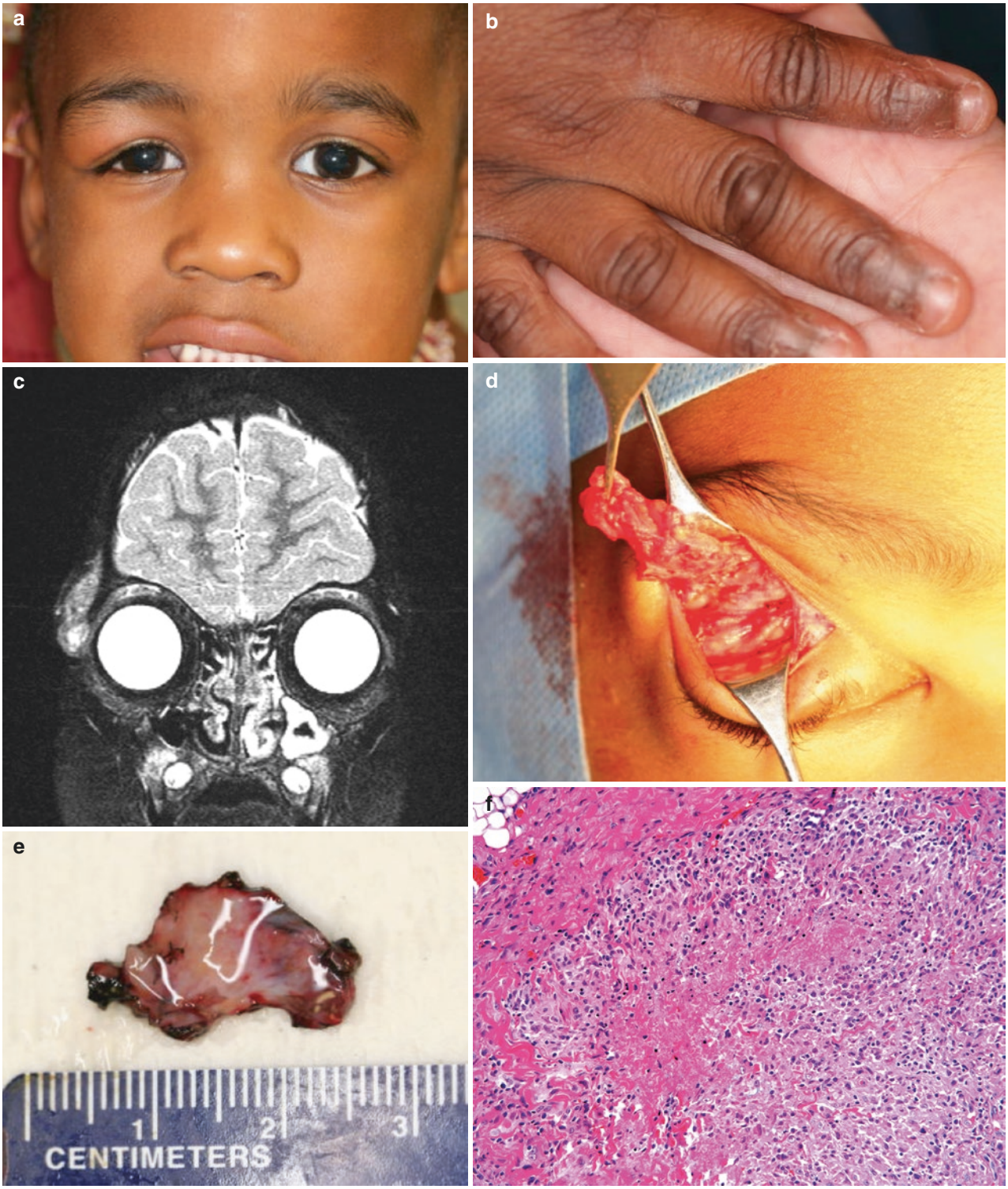


Fig. 23.29 Granuloma annulare of the eyelid. (**a**) A 3-year-old boy with painless mass of the right eyelid and sub brow. (**b**) Firm, subcutaneous nodules are present on both hands at the proximal and distal interphalangeal joints. (**c**) T_2-weighted MRI. There is a soft tissue mass involving the right lateral periorbital soft tissues which extends into the right upper eyelid and extends laterally along the temporalis muscle and the periosteum of the right frontal bone and zygoma. The lesion is hypointense on T1 and slightly heterogeneous on T2 and demonstrates avid homogeneous contrast enhancement. (**d**) Intraoperative photo showing an eyelid crease excision with a large subcutaneous mass that extends to the brow. (**e**) Post-excision picture of the specimen. (**f**) H&E stained section shows fibroadipose tissue containing numerous granulomas in a somewhat geographic distribution and of multiple different sizes. The granulomas are characterized by peripheral palisading of histiocytes around a central area of eosinophilic material which appears to be degenerating collagen. There is no significant neutrophil infiltration or necrosis. There are scattered lymphocytes noted around the periphery of the granulomas. Special stains for fungal organisms and acid fast bacilli are negative.

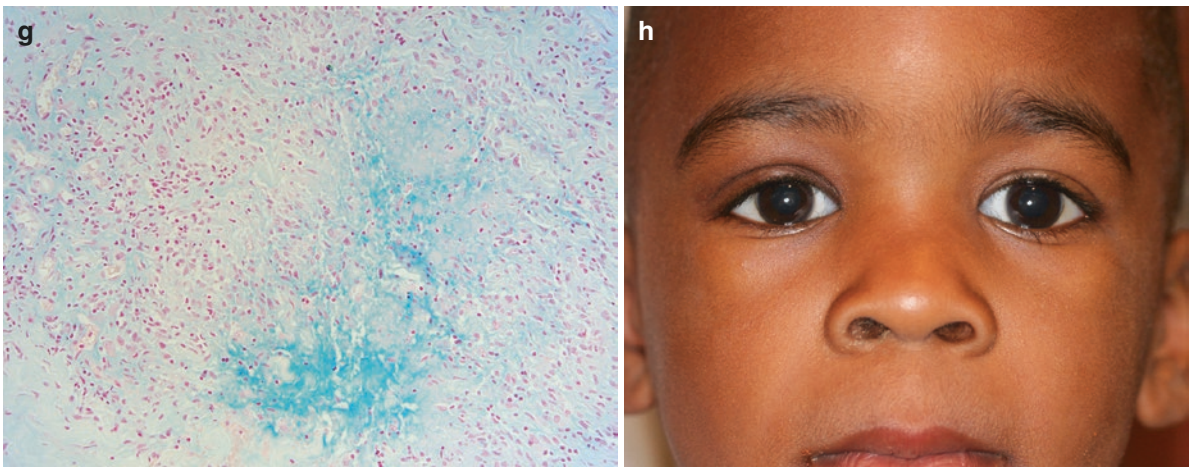


Fig. 23.29 (continued) (**g**) Alcian blue staining is positive indicating the presence of mucin. (**h**) Postoperative photo taken 3 months after surgery

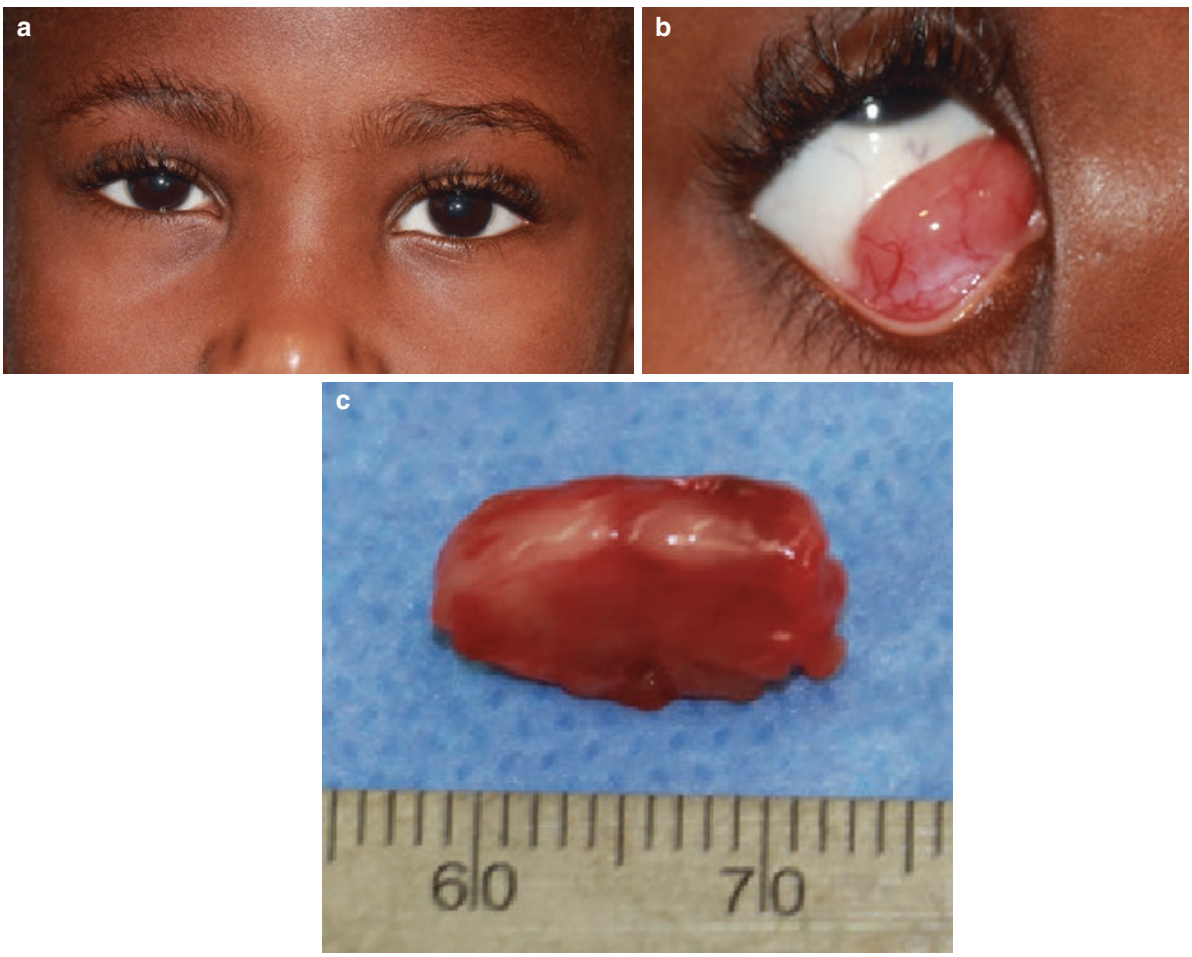


Fig. 23.30 Rosai-Dorfman disease of the eyelid and conjunctiva. (**a**) 5 year-old with 2 week history of a right sided mass visible medially. (**b**) The mass involves the palpebral conjunctiva. (**c**) Gross eyelid specimen photographed immediately after biopsy. Histopathology showed a mass partially lined by conjunctiva and composed of a mixed inflammatory infiltrate, plasma cell-rich and including large, pale histiocytes with emperipolesis. The lymphocytes are mixed B and T cells highlighted by CD3 and CD20. The pale histiocytes were strongly positive for S-100 and CD163. CD1a is negative, excluding the possibility of Langerhan's cell histiocytosis

noted where intact lymphocytes are found phagocytized within large histiocytes. The histiocytes are strongly positive for S-100 and CD163 and CD68. CD1a is negative, excluding Langerhan's cell histiocytosis (LCH). Eyelid lesions are extremely rare with the largest series of 8 patients who had orbital involvement [38]. Figure 23.30 depicts a child with a rapidly growing mass of the palpebral conjunctiva. The mass was excised and diagnosed as RDD.

References

1. Luu M, Frieden I. Haemangioma: clinical course, complications and management. Br J Dermatol. 2013;169:20–30.
2. Chen TS, Eichenfield LF, Fallon FS. Infantile hemangiomas: an update on pathogenesis and therapy. Pediatrics. 2013;131(1):99–108.
3. Bauland CG, Lüning TH, Smit JM, et al. Untreated hemangiomas: growth pattern and residual lesions. Plast Reconstr Surg. 2011;127(4):1643–8.
4. Bilyk JR, Adamis AP, Milliken JB. Treatment options for periorbital hemangiomas of infancy. Int Ophthalmol Clin. 1992;32:95–109.
5. Haik BG, Jakobiec FA, Ellsworth RM, Jones IS. Infantile hemangioma of the lids and orbit: an analysis of the clinical features and therapeutic results in 101 cases. Ophthalmology. 1979;86:760–89.
6. Robb RM. Refractive errors associated with hemangiomas of the eyelids and orbit in infancy. Am J Ophthalmol. 1977;83:52–8.
7. Motwani MV, Simon JW, Pickering D, Catalano RA, Jenkins PL. Steroid injection versus conservative treatment of anisometropic amblyopia in juvenile adnexal hemangioma. J Pediatr Ophthalmol Strabismus. 1995;2:26–8.
8. Léauté-Labrèze C, Dumas de la Roque E, Hubiche T, Boralevi F, Thambo JB, Taïeb A. Propranolol for severe hemangiomas of infancy. N Engl J Med. 2008;358(24):2649–51.
9. Léauté-Labrèze C, Hoeger P, Mazereeuw-Hautier J, Guibaud L, et al. A randomized, controlled trial of oral propranolol in infantile hemangioma. N Engl J Med. 2015;372(8):735–46.
10. Liu X, Qu X, Zheng J, Zhang L. Effectiveness and safety of oral propranolol versus other treatments for infantile hemangiomas: a meta-analysis. PLoS One. 2015;16:10.
11. Guo S, Ni N. Topical treatment for capillary hemangioma of the eyelid using beta-blocker solution. Arch Ophthalmol. 2010;128(2):255–6.
12. Chambers CB, Katowitz WR, Katowitz JA, Binenbaum G. A controlled study of topical 0.25% timolol maleate gel for the treatment of cutaneous infantile capillary hemangiomas. Ophthal Plast Reconstr Surg. 2012;28(2):103–6.
13. Ezekowitz RAB, Bulliken JB, Folhman J. Interferon alpha-2A therapy for life-threatening hemangiomas of infancy. N Engl J Med. 1992;326:1456–63.
14. Loughnan MS, Elder J, Kemp A. Treatment of massive orbital-infantile hemangioma with interferon alpha-2b: short-term results. Arch Ophthalmol. 1992;110:1366–7.
15. Hastings MM, Milot J, Barsoum D, et al. Recombinant interferon alpha-2b in the treatment of vision-treating infantile hemangiomas in childhood. J Am Assoc Pediatr Ophthalmol Strabismus. 1997;1:226–30.
16. Vesikari T, Nuutila A, Cantell K. Neurologic sequelae following interferon therapy of juvenile laryngeal papilloma. Acta Paediatr Scand. 1988;77:619–22.
17. Chang E, Boyd A, Nelson CC, et al. Successful treatment of infantile hemangiomas with interferon α-2b. J Pediatr Hematol Oncol. 1997;19:237–44.
18. Barlow CF, Priebe CJ, Mulliken JB, et al. Adverse effect of interferon alpha-2a in the treatment of hemangiomas of infancy on the early development of the central nervous system: a preliminary report. J Pediatr. 1997;132(3 Pt 1):527–30.
19. Wassef M, Blei F, Adams D, Alomari A, et al. Vascular anomalies classification: recommendations from the International Society for the Study of vascular anomalies. Pediatrics. 2015;136(1):e203–14.
20. Sherman RP, Rootman J, Lapointe JS. Orbital dermoids: clinical presentation and management. Br J Ophthalmol. 1984;68:642–52.
21. Mulvihill JJ. Neurofibromatosis 1 (Recklinghausen disease) and neurofibromatosis 2 (bilateral acoustic neurofibromatosis): an update. Ann Intern Med. 1990;113:39–52.
22. Perry DM, Eldridge R, Kaiser-Kupfer MI, et al. Neurofibromatosis 2 (NF2): clinical characteristics of 63 affected individuals and clinical evidence for heterogeneity. Am J Med Genet. 1994;52:450–61.
23. vom Deimling A, Krone W, Menon AG. Neurofibromatosis type 1: pathology, clinical features, and molecular genetics. Brain Pathol. 1995;5:153–62.
24. Spencer WH, et al., editors. Ophthalmic pathology: an atlas and textbook, vol. 3. Philadelphia: WB Saunders; 1986.
25. Avery RA, Katowitz JA, Fisher MJ, Heidary G, Dombi E, Packer R, Widemann BC, (on behalf of the OPPN Working Group). Orbital/Peri-orbital plexiform neurofibromas in children with neurofibromatosis type 1: multi-disciplinary recommendations for care. Ophthalmology, 2017;124:123–32.
26. Needle MN, Cnaan A, Dattilo J, et al. Prognostic signs in the surgical management of plexiform neurofibroma: the Children's Hospital of Philadelphia experience, 1974-1994. J Pediatr. 1997;131:678–82.
27. Kopf AW, Bart RS, Hennessy P. Congenital nevocytic nevi and malignant melanoma. J Am Acad Dermatol. 1979;1:123–30.
28. Kopf AW, Weidman AI. Nevus of Ota. Arch Dermatol. 1962;85:195–208.
29. Gupta GP, Gaugwar DN. Naevus of Ota. Br J Ophthalmol. 1965;49:364–8.
30. Yanoff M, Zimmerman LE. Histogenesis of malignant melanomas of the uvea, III: the relationship of congenital ocular and melanocytosis and neurofibromatosis to uveal melanomas. Arch Ophthalmol. 1967;77:331–6.
31. Velasquez N, Jones IS. Ocular and oculodermal melanocytosis associated with uveal melanoma. Ophthalmology. 1983;91:1472–6.
32. Vi C, Kimball GP, Craft JL, et al. Calcifying epithelioma: a clinicopathological analysis of 67 cases with ultrastructural studies of two cases. Int Ophthalmol Clin. 1982;22:63–86.
33. Sia PI, Figueira E, Allende A, Selva D. Malignant hair follicle tumors of the periorbital region: a review of literature and suggestion of a management guideline. Orbit. 2016;35(3):144–56.
34. Shields CL, Shields JA, Buchanon HW. Solitary orbital involvement with juvenile xanthogranuloma. Arch Ophthalmol. 1990;108:1587–9.
35. Macsai MS. The role of omega-3 dietary supplementation in blepharitis and meibomian gland dysfunction (an AOS thesis). Trans Am Ophthalmol Soc. 2008;106:336–56.
36. Felner EI, Steinberg JB, Weinberg AG. Subcutaneous granuloma annulare: a review of 47 cases. Pediatrics. 1997;100(6):965–7.
37. Pournaras J, Gibson AA. "Pseudorheumatoid" nodules in children. J Bone Joint Surg Br. 1971;53(4):724–8.
38. Tan JJ, Narang S, Purewal B, et al. Extranodal Rosai-Dorfman Disease of the Orbit: Clinical Features of 8 Cases. Ophthal Plast Reconstr Surg. 2016;32(6):458–61.

Malignant Pediatric Eyelid Tumors

24

Lama Khatib, Peter D. Fries, and William R. Katowitz

With the increasing diagnosis of malignant skin lesions in the adult population, the most common eyelid malignancies are the following: basal cell carcinoma, sebaceous carcinoma, and malignant melanoma. However due to the rarity of periocular skin malignancies in children, it is difficult to estimate their true frequency. The largest series thus far that examined lid lesions in children comes from the ocular pathology department at the Wilmer Institute. A total of 398 histopathologic specimens collected between 1923 and 1974 were evaluated, and only three of the 398 specimens or 0.75% were found to be malignant: one basal cell carcinoma, one squamous cell carcinoma, and one metastatic embryonal cell carcinoma [1]. Literature reviews involving systemic conditions that have an increased risk of pediatric skin malignancies report significantly higher statistics within that specifically predisposed population of children. A literature review of xeroderma pigmentosa in 1987 found a 97% chance of developing skin malignancies, with nearly half of the basal cell carcinomas and squamous cell carcinomas arising on the face, head, and neck occurring under age 20 [2]. The frequency of eyelid involvement is not specified in the report, but if even 5% of the cancers were on the eyelid, 18 cases of pediatric eyelid tumors would have occurred just in this condition alone. Given these conservative numbers compared to the volume of skin cancers diagnosed in the USA alone, it can be estimated that less than 1/10,000 skin cancers occur on the eyelids of children [3].

In this chapter, we will discuss isolated eyelid malignancies from a pediatric perspective as well as systemic conditions associated with the development of malignant eyelid and other cutaneous systemic malignancies in children.

Basal Cell Carcinoma

Despite numerous publications or small case series discussing pediatric basal cell carcinoma, no major reports or review articles exist specifically outlining the incidence, presentation, treatment, or recurrence of these as periocular lesions [4, 5]. Most do agree that these lesions are rare, may masquerade as benign-appearing lesions, and require excision with free surgical margins for the best chance of cure [4–7].

The presentation of basal cell carcinoma is often subtle, appearing similar to intradermal nevi or cutaneous granulomas without the typical adult changes, such as ulceration, loss of adnexal skin structures, or poor healing characteristics (Fig. 24.1). Most of these lesions are present for months

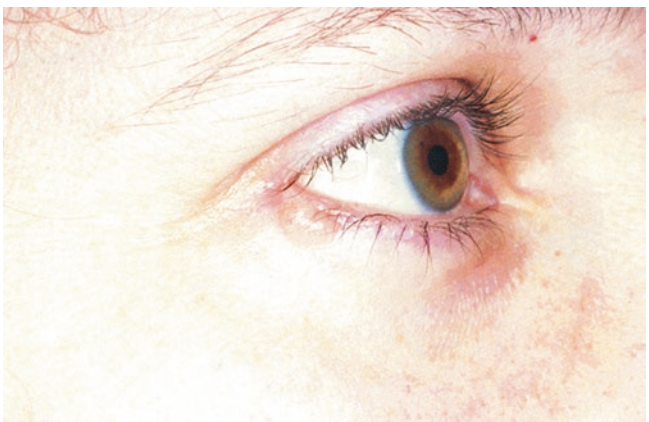


Fig. 24.1 Basal cell carcinoma. A 17-year-old female with a lateral canthal basal cell carcinoma

L. Khatib (✉)
Oculoplastic and Orbital Surgery, The Children's Hospital of Philadelphia, Philadelphia, PA, USA
e-mail: lamahkhatib@gmail.com

P.D. Fries, MD
Eye Surgeons Associates, PC, Bettendorf, IA, USA

W.R. Katowitz, MD
The Children's Hospital of Philadelphia and The Edwin and Fannie Gray Hall Center for Human Appearance, University of Pennsylvania, Philadelphia, PA, USA
e-mail: katowitzw@email.chop.edu

© Springer International Publishing AG 2018

J.A. Katowitz, W.R. Katowitz (eds.), *Pediatric Oculoplastic Surgery*, https://doi.org/10.1007/978-3-319-60814-3_24



Fig. 24.2 Xeroderma pigmentosa. (**a**) Intraoperative photograph showing facial features typical of xeroderma pigmentosa in a 6-year-old patient. Note the epibulbar mass almost filling the interpalpebral space in the left eye and severe ulcerative changes of the right lower lid. (**b**) Intraoperative photograph of the 5-year-old brother of the patient in (**a**), showing facial skin changes typical of xeroderma pigmentosa. A translucent medial epibulbar mass is present in the right eye. Inferior corneal opacification is present in the left eye (From Hertle et al. [12], reprinted with permission from Slack Incorporated)

with little rapid change prior to excision. Predisposing factors such as a family history of basal cell carcinoma or squamous cell carcinoma, especially when occurring at a young age, can alert the examiner to the potential association of several non-ophthalmic syndromes associated with an increased risk of basal cell carcinoma formation. However it has also been suggested that children living in areas of more intense UV radiation such as the southwest of the USA may be at increased risk of developing this malignancy de novo [8].

Histopathologic confirmation of a suspicious lesion can be challenging in the pediatric age group. For very young children, biopsy with frozen section evaluation under general anesthesia with immediate full excision with frozen section control of the tumor margins represents the best option for suspicious lesions. Older children will allow conventional biopsy techniques in the clinic setting with later surgical excision using frozen section control of the surgical margins in an operative setting. Tissue-preserving surgical excision is important due to the limitations in pediatric lid elasticity for repairing large defects. Continuous medical follow-up is warranted to maintain surveillance for other cutaneous malignancies associated with syndromes such as basal cell nevus syndrome [9].

Non-ophthalmic Conditions Associated with Pediatric Basal Cell Carcinoma

Basal cell nevus syndrome
Xeroderma pigmentosa
Linear nevus sebaceous syndrome
Epidermodysplasia verruciformis
Radiation dermatitis

Squamous Cell Carcinoma

Squamous cell carcinoma of the eyelids is much less common in children and occurs in the setting of predisposing systemic conditions and external influences. No reports exist defining this entity in the pediatric population except for occasional reports of younger patients as part of larger series discussing squamous cell carcinomas occurring in the general population in conjunction with other medical conditions. From those occasional cases, these lesions appear similar to adult squamous cell carcinoma on presentation but are most very likely associated with xeroderma pigmentosa (Fig. 24.2) [10–12]. One report estimates that for patients less than 20 years old with xeroderma pigmentosa, the risk of developing either basal cell or squamous cell carcinoma is 4800 times higher than the general population [13]. Doxanas et al. reported the largest series of squamous cell carcinoma of the eyelids yet had no patient under age 19 in that study [14].

Sebaceous Cell Carcinoma

Sebaceous cell carcinoma arises from the sebaceous glands of the eyelid (most commonly from the meibomian glands and less occasionally from the glands of Zeis), brow, and caruncle. It occurs more commonly in the upper eyelid due to more numerous glands as opposed to basal and squamous cell. Predominating in an elderly female population, it often masquerades as more benign-appearing entities such as

Table 24.1 Sebaceous carcinoma following radiation therapy, bilateral retinoblastoma, or both

Case no.	Study	Age (yrs)	Radiation	Dose	Reason
12	Lemos et al. [17]	12	Yes	2100cgy	Retinoblastoma
14	Boniuk and Zimmerman [16]	13	Yes	Unknown	Retinoblastoma
17	Current study	12	Yes	8900 cgy	Retinoblastoma

Summarized from Howrey RP et al. [18] (Reprinted with permission from John Wiley and Sons)

blepharitis, conjunctivitis, or chronic, recurring chalazia. In adults it accounts for approximately 1–5% of all eyelid malignancies but is rare elsewhere in the body [15]. Several cases involving the eyelid have been reported in children.

Three children, two patients aged 12 years, another aged 13 years, and among other reported adults developed sebaceous carcinoma of the eyelid years after high-dose radiotherapy for bilateral retinoblastoma [16–18] (Table 24.1). Knapp reported a 3½-year-old boy with an eyelid sebaceous cell carcinoma, but exact conclusions as to the accuracy of the histopathology are not definitive from his descriptions [19]. Ni et al. included a 16-year-old female in their series of 156 sebaceous carcinomas of the periocular region [20] but provided no specific information about the potential origins or associations of the lesion. Schlernitzauer and Font reported the development of sebaceous cell carcinoma in the eyelid of a boy treated with radiation therapy for a facial cavernous hemangioma [21]. Mirzamani et al. reported a 15-year-old male with a left cutaneous periorbital/temporal lesion [22].

Little information can be garnered from these clinical series to help specify incidence, treatment, or clinical course for pediatric sebaceous cell carcinoma. The significance of 15 cases after radiation seems to suggest that radiation and/or chemotherapy increases the likelihood for cutaneous malignancy in children. Whether retinoblastoma survivors treated with radiation therapy represent a group at particular risk remains suspect, with only these three cases reported. Prompt diagnosis followed by surgical excision seems to be the appropriate treatment, just as for adult cases.

Cutaneous Melanoma

Cutaneous melanoma is rapidly increasing in prevalence and incidence over the past 50 years, with nearly 200,000 new cases diagnosed annually [23]. It is unusual to occur as a primary malignancy of the eyelid in children. However it is typically diagnosed in association with large periocular congenital pigmented nevi or following periorbital irradiation for retinoblastoma [24, 25]. Rarely do these lesions arise de novo on the eyelid of children. Multiple series reporting a total of 48 melanomas of the eyelids did not have any children among the cohorts studied [26–29].

In adults, eyelid melanomas first appear as pigmented lesions with a change in color and size except when on the eyelid margin, where little pigmentation may occur and a more papillary appearance can predominate. Guidelines pertaining to the surgical resection of melanomas are set by the National institute of Health and the American Academy of Dermatology Task force on Melanoma. Virtually all lesions are treated with excisional biopsy followed by a variable margin of wide surgical excision (1–2 cm or more of normal surrounding skin) depending on the depth of invasion seen on the excisional biopsy (in situ, <1 mm, 1–2 mm, >2 mm) [30]. All patients subsequently require long-term surveillance for regional and systemic metastasis. Most patients are able to detect a clinical change, suggesting local recurrence of a previously resected melanoma, while systemic testing and physician examination typically helps detect metastasis [30]. Frozen section control and Mohs excision have proven to be inadequate for assessing complete excision in pigmented skin lesions, hence wide surgical excision after pathologic confirmation of the tumor characteristics and depth of invasion is recommended.

Premalignant Lesions

The relative risk for developing eyelid cancer in the pediatric population is increased in individuals identified with any of these conditions: congenital giant hairy nevi, xeroderma pigmentosa, and the linear nevus sebaceous syndrome. Pilomatrixoma (also called pilomatricoma) is an upper eyelid or lower eyebrow lesion that has the potential to transform into a carcinoma and is discussed in Chap. 23.

Congenital Giant Hairy Nevi

Congenital giant hairy nevi or congenital nevomelanocytic nevus (CNN) are heavily pigmented melanocytic nevi with raised surfaces, irregular borders, and heavy concentrations of hair that are visible at birth (Fig. 24.3). Approximately 20% involve the head and neck, of which over half have eyelid involvement [31]. Debate remains over the exact risk for malignant transformation to malignant melanoma; reports vary from 4.6 to 41% [32]. The larger numbers reported may be attributable to most of these series being reported from tertiary care centers that see more malignant transformations than benign lesions. A study at the University of Pennsylvania



Fig. 24.3 Congenital giant hairy nevus. (**a**) A 13-year-old male with a right facial congenital giant hairy nevus. Note the extension around the lateral canthus and involvement of the upper eyelid. (**b**) Close-up of the same patient showing a small conjunctival nevus adjacent to the marginal lower lid nevus

reported a 5.7% cumulative 5 year risk of developing melanoma in a large or giant CNN [33].

This transformation rate, along with a high mortality rate early after discovery of the malignant degeneration, has led to the recommendation for the prophylactic removal of these nevi to avoid future malignant transformation [24]. Due to their large size, full-thickness skin involvement, and proximity to eyelid margins, complete excision is functionally and cosmetically challenging. Laser therapy offers a better alternative since argon and Q-switched ruby lasers can target melanin. However this technique leaves potential nests of nevus cells for future malignant transformation. Additionally, loss of pigment following laser makes the clinical detection of change in color and potential malignant transformation in the nevi difficult.

The full-thickness excision of these lesions can be challenging. Besides simple excision with primary closure, full-thickness grafting, rotational flaps with or without tissue expansion, and microvascular free tissue transfer of muscle or composite tissue have been utilized in pediatric facial reconstructions. Each nevus requires a unique approach balancing surgical removal and reconstruction against the size and location of the nevus along with the risk of malignant transformation (see Chap. 13, Fig. 13.20).

Xeroderma Pigmentosum

Xeroderma pigmentosum (XP) is an autosomal recessive genetic disease that affects the enzyme system responsible for DNA repair after damage from ultraviolet radiation. It is characterized by cutaneous, ocular, and neurologic abnormalities (Fig. 24.2) [2]. The earliest manifestations appear between the ages of 1 and 2 years, as sun sensitivity with easy sunburning and freckling. Over time, malignant transformation to cutaneous basal cell carcinoma, squamous cell carcinoma, and malignant melanoma occurs with the latter two malignancies being the most common cause of death in XP patients. Incidence of the disease is low in the USA (1/250000) however it is more commonly seen in patients of Japanese and Middle Eastern descent [34]. A total of 97% of all skin malignancies develop in sun exposed areas, mainly the face, head, or neck regions; the median age for first diagnosis of one of these malignancies is 8 years old [2]. Progressive mental deterioration, deafness, delayed growth, and hyporeflexia are neurologic abnormalities reported in 25% of patients [35]. Any ocular tissue exposed to light can exhibit changes, resulting in eyelid and conjunctival malignancies, with resultant ectropion, exposure keratopathy, corneal neovascularization and loss of vision [10–12].

The most common genetic defect lies in the reduction or elimination of nucleotide excision repair (NER) enzymes. This biochemical defect in fibroblasts results in abnormal DNA repair after UV-induced damage and sets the stage for eventual malignant transformation with continued light exposure [36]. The exact incidence of cutaneous and conjunctival malignancies in this condition is not well established, but Kraemer et al. found 88 patients with neoplasms among the 830 reported cases studied, for an incidence of 10.6% [2]. For lid malignancies alone, his literature review could not pinpoint an exact frequency or histopathologic verification, but it appears that squamous cell carcinoma was the most common, followed by basal cell carcinoma and then malignant melanoma. Again, this syndrome should be considered quite strongly in a child diagnosed with any cutaneous eyelid malignancy.

Basal Cell Nevus Syndrome

Basal cell nevus syndrome also known as Nevoid basal cell carcinoma, Gorlin syndrome, and Gorlin-Goltz syndrome, is a rare autosomal dominant disorder caused by a mutation in the PTCH gene (Patched) gene found on chromosome 9 with

variable penetrance. It is characterized by the development of multiple basal cell carcinomas in the first and second decades of life. Other typical manifestations are jaw cysts (keratocystic odontogenic tumor, found in 75%), bifid ribs, mental retardation, cardiac fibromas, ovarian cysts/fibromas and testicular disorders. Facial features include frontal/temporo-parietal bossing, and mandibular prognathism. About 30% of affected individuals manifest ocular abnormalities [9, 37, 38]. Prominence of the supraorbital ridges, hypertelorism, canthal dystopia, strabismus, congenital cataract, congenital glaucoma, and colobomas of the choroid and optic nerve, and microphthalmia have been seen in patients with this syndrome [37, 38].

Basal cell carcinoma seen in basal cell nevus syndrome occur all over the body namely areas not exposed to the sun such as palms and soles of feet, whereas those in xeroderma pigmentosa occur almost exclusively in sun-exposed areas. Eyelid involvement is frequent in this condition, occurring in about 22% of cases. The upper lid is involved almost 3 times more than the lower lid, as opposed to the general non affected population where the lower eyelid is more frequently involved [39]. Lesions arise at a median age of 13 and bear a resemblance to trichoepitheliomas, except that they are widespread, centrally ulcerated, and large. The trichoepitheliomas seen in Brooke's tumor concentrate in the nasolabial fold, are small, and do not ulcerate. These basal cell carcinomas are also highly aggressive with 25% of affected individuals requiring exenteration secondary to invasive malignancy in the orbit [40]. Other malignancies in this syndrome are rare, except for cerebellar medulloblastomas, which have been reported in some cases.

Linear Nevus Sebaceous Syndrome

The linear nevus sebaceous syndrome, also known as Schimmelpenning syndrome, is a neurocutaneous condition characterized by one or more sebaceous nevi, usually appearing on the face or scalp. Central nervous system, ocular, skeletal, and cardiovascular anomalies are associated findings [41, 42]. Most cases manifest with a congenital nevus with minimal pigmentation. On histology, epidermal papillomatous hyperplasia is noted with overdevelopment of the sebaceous glands (Fig. 24.4). Clinically, the lesions appear as large, well-defined, yellow to orange in color, with a waxy, pebbly, papillomatous surface that frequently becomes more prominent around puberty [43]. Enlargement after this pubertal change is often associated with development of a secondary tumor, such as basal cell carcinoma or squamous cell carcinoma, and occurs in about 35% of patients [45].

This lesion was first described in in 1895 by Jadassohn as the cutaneous manifestation of a phakomatose syndrome characterized by the triad of linear nevus sebaceous, seizures, and mental retardation [43, 46, 47]. The ocular findings are myriad and occur in approximately 68% of patients



Fig. 24.4 Linear nevus sebaceous. A 10-year-old male with a linear nevus sebaceous involving the medial right upper lid with extension into the medial forehead

[43, 44, 47, 48]. These include upper lid colobomas, ptosis, ectropion, epibulbar choristomas, lipodermoids, corneal leukoma, iris and choroidal colobomas, strabismus, and microphthalmos, as well as numerous other single-case associations. Most malignant degenerations occur within the nevus itself and are typically basal cell carcinomas with rare reports of sebaceous cell carcinoma and squamous cell carcinoma [45]. An estimated malignant transformation rate of 35% warrants complete surgical excision for lesions associated with the linear nevus sebaceous syndrome.

Eyelid Malignancies Associated with Systemic Conditions

Three lid lesions seen in the pediatric age group have a high correlation with being associated with potentially lethal systemic conditions: Kaposi's sarcoma (in patients affected with AIDS), histiocytic lid lesions (Langerhans cell histiocytosis), and leukemic/lymphomatous lid infiltrations (acute myeloblastic leukemia/lymphoma).

Kaposi's Sarcoma

Kaposi sarcoma (KS) is a tumor commonly seen in acquired immunodeficiency syndrome (AIDS) occurring in approximately 50% of affected patients [49]. It presents with cutaneous lesions with or without internal organ involvement and is caused by an infection with Human Herpes Virus 8 (also known as KS-associated Herpes Virus KSHV). The viral cause for this tumor was established in 1994 [50]. Lesions in KS are reddish violaceous lesions that take the forms of macules, nodules, or patches that may be confluent. KS is not a true sarcoma (mesenchymal origin) as the name implies, histologic sections of

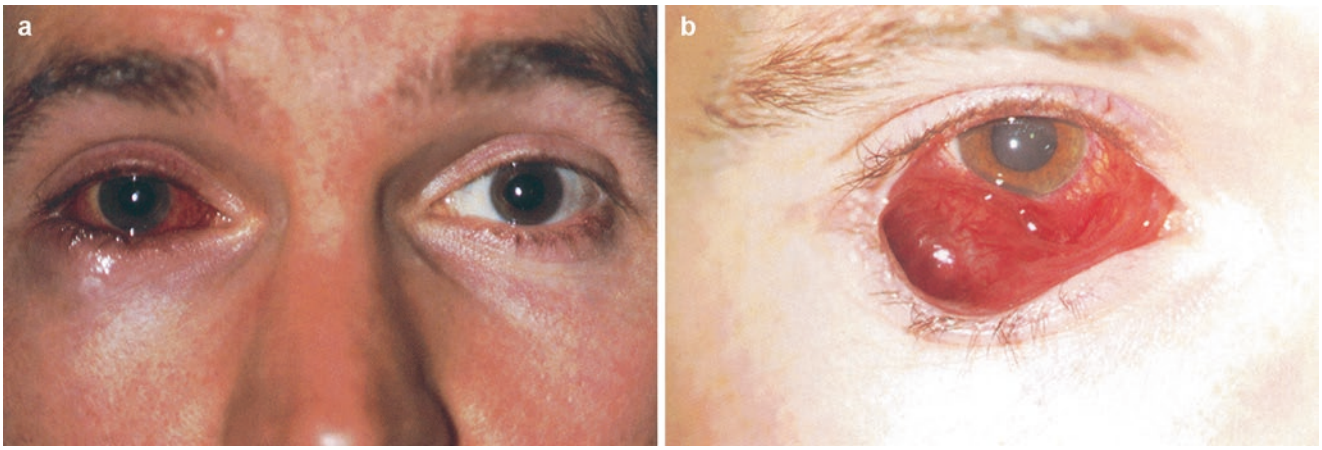


Fig. 24.5 Kaposi sarcoma. (**a**) A 17-year-old male with conjunctival and eyelid Kaposi sarcoma. (**b**) Close-up of the exposed conjunctival portion of Kaposi sarcoma. The palpebral portion is not visible in this photograph

the tumor reveal elongated spindle cells that form slits containing red blood cells [51]. Uncommon prior to 1982, when only 30 identifiable cases of ocular involvement could be identified, its association with AIDS has led to an epidemic of these cutaneous and visceral lesions [49]. KS infrequently results in significant morbidity or mortality.

While common in the adult population with AIDS, in children KS is a much less common cutaneous lesion but is much more aggressive in its course [41, 42]. KS is the presenting sign in 20% of adults with AIDS but is rarely so in children [49, 52, 53]. Head and neck involvement occurs in about 70% of affected adults, with about one-quarter of them having eyelid or conjunctival involvement; no such statistics are available for the pediatric age group but KS is estimated to occur 10 times less frequently [52, 53]. Little morbidity occurs from the eyelid component but its presence in the pediatric population suggests the possible rapid progression of AIDS-related complications or immunosuppression (Fig. 24.5) [52, 53].

Treating the cause of the immune dysfunction can slow or stop the progression of KS. Local treatment for KS lesions includes cryotherapy, intralesional chemotherapy with vinblastine, and radiation therapy [54]. Surgical excision is not recommended as tumor may re-appear in wound edges. All treatments result in temporary resolution of the treated lesions; radiation of eyelid/conjunctival lesions with 600–800 cGy in a single session lasts the longest, averaging a 34-week remission in the treated lesion [55, 56]. In children, the cosmetic benefits of radiation treatment and its rapid response compared with the potential local skin necrosis, scarring, repeated treatments, and other side effects of laser, cryotherapy, or intralesional injections make single-dose radiation treatment a preferred therapy for periocular KS lesions.

Langerhans Cell Histiocytosis

Langerhans cell histiocytosis is a rare disease, also previously known as eosinophilic granuloma, Hand-Schuller-Christian disease, and Letterer-Siwe disease. The last two were previously grouped under the term histiocytosis X to indicate its propensity for systemic involvement [57]. Langerhans cells are abnormal cells that arise from bone marrow and undergo clonal proliferation, causing skeletal disease, and multisystem disease as they can migrate to skin and lymph nodes. Ophthalmic involvement typically arises in orbital tissues with lytic bony inflammatory lesions and soft tissue extension, but can include ptosis, severe proptosis, globe luxation, papilledema, cavernous sinus syndrome, and even intraocular involvement [58]. It usually affcets children younger than 12 years old and is more common among caucasians. More aggressive forms occur in patients younger than 3 years old, with rapid progression, and involvement of bone marrow, vital organs, mucous membranes, and skin. A more insidious form of the disease occurs in patients aged around 12 years [59].



Fig. 24.6 Langerhans histiocytosis. Histiocytic lid lesion in a 15-year-old male with disseminated Langerhans histiocytosis syndrome

The skin lesions are typically yellow-red, raised, multiple, and widespread with occasional central ulceration

(Fig. 24.6). Biopsy of these lesions shows typical granulomatous inflammation with large histiocytes. The high likelihood of widespread disease in an ill child with cutaneous lesions and histopathologic findings warrants immediate pediatric referral.

Unusual Malignant Eyelid Lesions

Merkel Cell Tumors

Merkel cell tumors are carcinomatous growths arising from Merkel cells. The latter are a subgroup of clear oval neuroendocrine cells present in the basal layer of the epidermis. They are mainly but scarcely located in the outer root layer of the cilia hair follicles in the middle of the eyelid where most Merkel cell carcinoma is detected [60]. Prolonged sun exposure or a defective immune system increases the risk for Merkel cell carcinoma. Typically found in elderly individuals, they present as rapidly growing, painless red-blue nodules with frequent surface telangiectasias. Most arise in exposed areas of the head and neck and 20% arise on the eyelids or eyebrow [61]. From a pediatric perspective, only a single case has been reported, in a 15-year-old female, which arose on the eyelid and presented with metastasis [62]. Its clinical similarity to solitary hemangiomas can be misleading, hence a high index of suspicion is advised when encountering rapidly enlarging lesions arising de novo. Wide surgical excision is the preferred treatment.

Primary Mesenchymal Chondrosarcoma

Primary mesenchymal chondrosarcoma is a tumor arising in skeletal bones, but has been reported to have extra-skeletal orbital or periorbital presentation [63]. Presenting in young females, it is an aggressively growing lesion that requires exenteration but can metastasize later with a predilection for the lung. An unusual presentation has been reported however in a 15-year-old female, as a discrete, painless, rapidly growing nodule in the nasal left lower eyelid [64]. Biopsy revealed the diagnosis, since no clinical features allowed for its identification. Wide surgical excision was used for treatment. (Literature unchanged, no new reports).

Rhabdomyosarcoma

Rhabdomyosarcoma is the most common type of soft tissue sarcoma in children. It can present as an isolated eyelid mass that rapidly grows and may masquerade as an infantile hemangioma in younger children or infants [65]. High suspicion and prompt diagnosis is necessary before orbital invasion occurs. Incisional biopsy is required to make the exact diagnosis, and treatment consists of radiation and chemotherapy [66, 67]. Rhabdomyosarcoma is discussed in greater detail in Chap. 36.

Primary Mucinous Carcinomas

Primary mucinous carcinomas are adenocarcinomas of the eyelid cutaneous sweat glands. They occur more commonly in the elderly, however several cases have been reported in children as well [68, 69]. Presenting as slow-growing, lobulated, marginal eyelid lesions, gradual visual or eyelid symptoms lead to eventual biopsy and ultimate diagnosis. Prognosis is good with wide local excision with rare regional or systemic metastasis. Recent reports have suggested Mohs surgery for the excision of these lesions on the eyelid to reduce morbidity [70].

References

1. Doxanas MT, Green W, Arentsen JJ, Elsas FJ. Lid lesions of childhood: a histopathologic survey at the Wilmer Institute (1923–1974). J Pediatr Ophthalmol. 1976;13:7–13.
2. Kraemer KH, Lee MM, Scotto J. Xeroderma pigmentosa: cutaneous, ocular and neurologic abnormalities in 830 published cases. Arch Dermatol. 1987;123:241–50.
3. Boring CB, Squires TS, Tong T, Montgomery S. Cancer statistics, 1994. CA Cancer J Clin. 1994;44:7–26.
4. Henriksson C, Eldh J, Hersle K, Suurkula M. Basal cell carcinoma in children. Scand J Plast Reconstr Surg. 1981;15:157–8.
5. Milstone EB, Helwig EG. Basal cell carcinoma in children. Arch Dermatol. 1973;108:523–7.
6. McLean IW, Burnier MM, Zimmerman LE, Jakobiec FA. Tumors of the eye and ocular adnexa, 3d series. Washington, DC: AFIP; 1994. p. 19.
7. Shields JA, Shields CL. Ocular tumors of childhood. Pediatr Clin N am. 1993;40:805–26.
8. LeSueur B, Silvis N, Hansen R. Basal cell carcinoma in children: report of 3 cases. Arch Dermatol. 2000;136(3):370–2.
9. Anderson DE, Taylor WB, Falls HF, Davidson RT. The nevoid basal cell syndrome. Am J Hum Genet. 1967;19:12–22.
10. Goyal JL, Rao VA, Srninivasan R, Agrawal K. Oculocutaneous manifestations in xeroderma pigmentosa. Br J Ophthalmol. 1994;78:295–7.
11. Calugaru M, Barsu M. Exuberant epibulbar tumor penetrating into the orbit in xeroderma pigmentosa. Oftalmologia. 1992;36:375–81.
12. Hertle RW, Durso F, Metzler JP, Varsa EW. Epibulbar squamous cell carcinomas in brothers with xeroderma pigmentosa. J Pediatr Ophthalmol Strabismus. 1991;28:350–3.
13. Kraemer KH, Lee MM, Scotto J. DNA repair protects against cutaneous and internal neoplasia: evidence from xeroderma pigmentosa. Carcinogenesis. 1984;5:511–4.
14. Doxanas MT, Iliff WJ, Iliff NT, Green WR. Squamous cell carcinoma of the eyelids. Ophthalmology. 1987;94:538–41.
15. Kass LG, Hornblass A. Sebaceous carcinoma of the ocular adnexa. Surv Ophthalmol. 1989;33:477–90.
16. Boniuk M, Zimmerman LE. Sebaceous carcinoma of the eyelid, eyebrow, caruncle and orbit. TAAOO. 1968;72:619–41.
17. Lemos LB, Santa Cruz DJ, Baba N. Sebaceous carcinoma of the eyelid following radiation therapy. Am J Pathol. 1978;2:305–11.
18. Howrey RP, Lipham WJ, Schultz WH, Buckley EG, Dutton JJ, Klintworth GK, Rosoff PM. Sebaceous gland carcinoma: a subtle

second malignancy following radiation therapy in patients with bilateral retinoblastoma. Cancer. 1998;83(4):767–71.
19. Knapp H. On hypertrophy and degeneration of the meibomian glands. Trans Am Ophthal Soc. 1903;10:57–63.
20. Ni C, Searl SS, Kuo PK, et al. Sebaceous cell carcinomas of the ocular adnexa. Int Ophthalmol Clin. 1982;22:23–61.
21. Schlernitzauer DA, Font RL. Sebaceous gland carcinoma of the eyelid following radiation therapy for cavernous hemangioma of the face. Arch Ophthalmol. 1976;94:1523–5.
22. Mirzamani N, Sundram UN. A case of sebaceous carcinoma diagnosed in an adolescent male. J Cutan Pathol. 2011;38(5):435–8.
23. Azoury SC, Lange JR. Epidemiology, risk factors, prevention and early detection of melanoma. Surg Clin NA. 2014;94(5):945–62.
24. Trozak DJ, Rowland WD, Hu F. Metastatic malignant melanoma in prepubertal children. Pediatrics. 1975;55:191–204.
25. Traboulsi E, Zimmerman LE, Manz HJ. Cutaneous malignant melanoma in survivors of heritable retinoblastoma. Arch Ophthalmol. 1988;106:1059–61.
26. Garner A, Koornneef L, Levene A, Collin JR. Malignant melanoma of the eyelid skin: histopathology and behavior. Br J Ophthalmol. 1985;69:180–6.
27. Harris TJ, Hinckley DM. Melanoma of the head and neck in Queensland. Head Neck Surg. 1983;5:197–203.
28. Mortada A. Incidence of melanomata of ocular adnexa in U.A.R. (Egypt). Bull Ophthalmol Soc Egypt. 1969;62:321–8.
29. Naidoff MA, Bernadino VB, Clark WH Jr. Melanocytic lesions of the eyelid skin. Am J Ophthalmol. 1976;82:371–7.
30. Urist MM. Surgical management of primary cutaneous melanoma. CA Cancer J Clin. 1996;46:217–24.
31. Egan CL, Oliveria SA, Elenitsas R, et al. Cutaneous melanoma risk and phenotypic changes in large congenital nevi: a follow-up study of 46 patients. J Am Acad Dermatol. 1998;39(6):923–32.
32. Margo CE, Habal MB. Large congenital melanocytic nevus: light and electron microscopic findings. Ophthalmology. 1987;94:960–6.
33. Egan CL, Oliveria SA, Elenitsas R, et al. Cutaneous melanoma risk and phenotypic changes in large congenital nevi: a follow-up study of 46 patients. J Am Acad Dermatol. 1998;39(6):923–32.
34. Lehmann AR, McGibbon D, Stefanini M. Xeroderma pigmentosum. Orphanet J Rare Dis. 2011;6:70.
35. Kraemer KH, DiGiovanna JJ. Xeroderma Pigmentosum. 2003 Jun 20 [updated 2016 Sep 29]. In: Pagon RA, Adam MP, Ardinger HH, et al., editors. GeneReviews® [internet]. Seattle: University of Washington, Seattle; 1993–2016. Available from: https://www.ncbi.nlm.nih.gov/books/NBK1397/.
36. Day RS. Zeroderma pigmentosa variants have decreased repair of ultraviolet-damaged DNA. Nature. 1975;253:748–9.
37. Fehman S, Apt L, Roth A. The basal cell nevus syndrome. Am J Ophthalmol. 1974;78:222–6.
38. Kimonis V, Goldstein A, Pastakia B, Yang M, Kase R, DiGiovanna J, Bale A, Bale S. Clinical manifestations in 105 persons with nevoid basal cell carcinoma syndrome. Am J Med Genet. 1997;69(3):299–308.
39. Zackheim HS, Loud AV, Howell AB. Nevoid basal cell carcinoma syndrome: some histologic observations on the cutaneous lesions. Arch Dermatol. 1966;93:317–23.
40. Hammani H, Faggioni R, Streiff EB, Daiker B. Le syndrome d'epitheliomatose naevobasaocellulaire multiple. Ophthamologica. 1976;172:382–99.
41. Menascu S, Donner EJ. Linear nevus sebaceous syndrome: case reports and review of the literature. Pediatr Neurol. 2008;38(3):207–10.
42. Eisen DB, Michael DJ. Sebaceous lesions and their associated syndromes: part II. J Am Acad Dermatol. 2009;61(4):563–78.
43. Wilkes SR, Campbell RJ, Walker RR. Ocular malformations associated with the ipsilateral facial nevus of Jadassohn. Am J Ophthalmol. 1981;92:344–9.
44. Diven DG, Solomon AR, McNelly MC, Font RL. Nevus sebaceous associated with major ophthalmic abnormalities. Arch Dermatol. 1987;123:383–98.
45. Wilson-Jones E, Heyl T. Naevus sebaceus: a report of 140 cases with special regard to the development of secondary malignant tumors. Br J Dermatol. 1970;82:99–112.
46. Jadassohn J. Bemerkungen zur Histologie der systematisirten Naevi und ueber 'Talgdruesen-naevi'. Arch Dermatol Syph. 1895;33:355.
47. Katz B, Wiley CA, Lee VW. Optic nerve hypoplasia and the syndrome of nevus sebaceous of Jadassohn. Ophthalmology. 1987;94:1570–6.
48. Insler MI, Davim L. Ocular findings in linear sebaceous nevus syndrome. Br J Ophthalmol. 1987;71:268–72.
49. Zalla MJ. Kaposi's sarcoma: an update. Dermatol Surg. 1996;22:274–87.
50. Chang Y, Cesarman E, Pessin MS, Lee F, Culpepper J, Knowles DM, Moore PS. Identification of herpes virus-like DNA sequences in AIDS-associated Kaposi's sarcoma. Science. 1994;266(5192):1865–9.
51. Rosai J. Rosai and Ackerman's surgical pathology. 10th ed. Mosby, Amsterdam, Netherlands. 2011.
52. Nance KV, Smith ML, Joshi VV. Cutaneous manifestations of acquired immunodeficiency syndrome in children. Int J Dermatol. 1991;30:531–9.
53. Connor E, Boccon-Gibod L, Joshi V, et al. Cutaneous AIDS-associated Kaposi's sarcoma in pediatric patients. Arch Dermatol. 1990;126:791–3.
54. Webster GF. Local therapy for mucocutaneous Kaposi's sarcoma in patients with acquired immunodeficiency syndrome. Dermatol Surg. 1995;21:205–8.
55. Dugel PU, Gill PS, Frangieh GT, Rao N. Treatment of ocular adnexal Kaposi's sarcoma in the acquired immunodeficiency syndrome. Ophthalmology. 1992;99:1127–32.
56. Ghabriel R, Quivey JM, Dunn JP, Char DH. Radiation therapy of AIDS-related Kaposi's sarcoma of the eyelids and conjunctiva. Arch Ophthalmol. 1992;110:1423–6.
57. Favara BE, Jaffe R. Pathology of Langerhans cell histiocytosis. Hematol Oncol Clin North Am. 1987;1:75–92.
58. Moore AT, Pritchard J, Taylor DSL. Histiocytosis X: an ophthalmological review. Br J Ophthalmol. 1985;69:7–13.
59. Favara BE, McCarthy RL, Milerau GW. Histocytosis X. Hum Pathol. 1983;14:663–9.
60. May CA, Olsterland I. Merkel cell distribution in the human eyelid. Eur J Histochem. 2013;57(4):e33.
61. Warner TFCS, Uno H, Hafez R, et al. Merkel cells and Merkel cell tumors: ultrastructure, immunocytochemistry and review of the literature. Cancer. 1983;52:238–45.
62. Gherardi G, Marveggio C, Sdglich F. Parotid metastasis of Merkel cell carcinoma in a young patient with ectodermal dysplasia: diagnosis by fine needle aspiration cytology and immunocytochemistry. Acta Cytol. 1990;34:831–6.
63. Guccion J, Font RL, Enzinger FM, et al. Extraskeletal mesenchymal chondrosarcoma. Arch Pathol. 1973;95:336–40.
64. Rohrbach JM, Steuhl KP, Pressler H, et al. Primary extraskeletal mesenchymal chondrosarcoma of the lid. Graefes Arch Clin Exp Ophthalmol. 1991;229:172–7.
65. Knowles DM, Jakobiec FA, Potter GD, Jones IS. Ophthalmic striated muscle neoplasms: a clinico-pathologic review. Surv Ophthalmol. 1976;21:219–61.
66. Lee YC, Hsu YH, Yang SH, Huang TL. Congenital eyelid rhabdomyosarcoma. Ophthal Plast Reconstr Surg. 2016;32(5):e104–6.
67. Sharifi M. Embryonal rhabdomyosarcoma of upper lid in 15-year-old patient. Case Rep Ophthalmol Med. 2014;2014:157053. doi:10.1155/2014/157053. Epub 2014 Feb 9.
68. Rodriquez MM, Lubowitz RM, Shannon GM. Mucinous (adenocystic) carcinoma of the eyelid. Arch Ophthalmol. 1973;89:493–196.
69. Wright SD, Font RL. Mucinous sweat gland adenocarcinoma of the eyelid: a clinicopathologic study of 21 cases with histochemical and electron microscopic observations. Cancer. 1979;44:1757–71.
70. Chavez A, et al. Primary cutaneous mucinous carcinoma of the eyelid treated with Mohs surgery. JAAD Case Report. 2019;1(2):85–7.

Pediatric Eyelid and Adnexal Trauma

25

Jordan E. Hollsten, Scott M. Goldstein, Donald A. Hollsten, and James A. Katowitz

The image of a child hit in the eye by a rock, a ball, or the fist of an acquaintance is often pictured when eyelid and periocular trauma is mentioned. Fortunately, the eyeball is covered by the lids, surrounded by the orbital rim, and cushioned by the orbital fat. As a result, the eyelid and adnexa absorb the brunt of the injury. In a review of 5671 patients with ocular trauma reporting to a hospital, 3.0% had severe enough trauma to induce lid laceration [1].

As early as the perinatal period, humans are subject to trauma. Amniotic bands, a poorly understood intrauterine disorder, can lead to a variety of ophthalmic as well as systemic malformations. Facial clefting syndromes have been associated with bands and present a complex challenge to the oculoplastic surgeon (See Chap. 39). Birth trauma, especially in forceps deliveries, can lead to contusions, lacerations, hematomas, crush injuries, and fractures.

Types of Trauma and Injuries

The majority of lid and adnexal injuries in children are accidental in nature. The mechanism of accidental trauma in children can be divided into a few broad categories: blunt trauma, sharp trauma, projectile trauma, and burns. The forms of trauma especially in children can be multiple and often rather bizarre (Fig. 25.1). When evaluating patients with trauma, one should elicit the exact nature of the underlying event including how the trauma happened, what was involved, when it occurred, and what type of function the patient had before the injury. Unfortunately, some pediatric traumas are unwitnessed, and thus the concern for retained foreign bodies must remain high. Injuries occur in a variety of settings. A 1997 study found that 30% of ocular traumas occurred during domestic activity, 24% during play time or sporting activity, and 17% at school [2]. This was furthered by a 2008 Columbian study, showing 44.4% of injuries occurred at home. Between 40% and 63.3% were without adult supervision when the event occurred [3].



Fig. 25.1 Types of trauma. An example of the often unusual types of trauma that can be encountered in the pediatric patient population. A screen door handle impaled this 9 year old as he chased his brother into the house

J.E. Hollsten
Ophthalmology, Plastic and Reconstructive Surgery, University of Texas Health Science Center at San Antonio, San Antonio, TX, USA

S.M. Goldstein
Oculoplastic Service, Wills Eye Hospital, Ophthalmology, Jefferson Medical College, Perelman School of Medicine, University of Pennsylvania, Philadelphia, PA, USA

Oculo-Facial Plastic Surgery, Tri-County Eye Physicians and Surgeons, Southampton, PA, USA

D.A. Hollsten (✉)
Ophthalmology, Plastic and Reconstructive Surgery, University of Texas Health Science Center at San Antonio, San Antonio, TX, USA
e-mail: dahollsten@sbcglobal.net

J.A. Katowitz, MD, FACS
The Children's Hospital of Philadelphia and The Edwin and Fannie Gray Hall Center for Human Appearance, University of Pennsylvania, Philadelphia, PA, USA
e-mail: katowitz@email.chop.edu

© Springer International Publishing AG 2018

J.A. Katowitz, W.R. Katowitz (eds.), *Pediatric Oculoplastic Surgery*, https://doi.org/10.1007/978-3-319-60814-3_25

Blows to the ocular area from falling or absorbing a blow, as well as the impact of projectiles like rocks and toys, account for a substantial portion of injuries. In a 1990 study, accidental blows or falls were associated with 37% of ocular trauma, while 27% of injuries occurred during play time and sports activity. Other causes of eye injuries included motor vehicle accidents (11%) and burns (9%) [4]. In another review of 238 children, a Norwegian group found the most common source of injuries were projectiles (22%), toys like balls and arrows (18%), sticks/pencils (10%), and falls (10%) [5].

Trauma to the eyelids and adnexal injury can cause contusions, crush injuries, abrasions, lacerations, puncture wounds, avulsions, or burns. It is not unusual for some combination of these tissue responses to be present. For example, a single dog bite can lead to a puncture wound, a hematoma, a laceration, and an abrasion. In the United States, 44,000 facial injuries occur annually from dog bites, and the majority of the victims are children [6]. Furthermore, dog bites are commonly a source of canalicular laceration in the children, most of whom are boys under 10 years of age [7].

Blunt trauma to the lids and ocular adnexa most commonly result in contusions and hematomas. Because of the fascial planes in the periocular area associated with the loose connections in the subcutaneous tissue, hematomas in the eyelids often remain localized and can expand to an impressive size (Fig. 25.2). It is always important to evaluate the orbit and globe for more serious injuries when large hematomas are present in the lid (Fig. 25.3).

The shearing force and compressive nature of blunt trauma can often cause avulsions. These types of lacerations are usually irregular, deep, and often have pieces of tissue that bridge the defect. Furthermore, lacerations from crush injuries can be more extensive in the deeper tissue planes in association with extensive edema and contusion. A review of 222 patients with ocular injuries by LaRoche et al. found that 3% also had lid lacerations [8].

When evaluating a lid laceration, it is important to inspect for damage to the lacrimal drainage system which can modify the treatment plan. Sharp trauma from knives, for example, will lead to smooth, well-defined lacerations (Fig. 25.4). Also, the amount of surrounding edema and hematoma is much less when compared to a laceration induced by a blunt, crushing injury. Puncture wounds are another form of sharp injury. Again, these wounds can often look very superficial and harmless since there is usually little edema or bleeding. The presence of a retained foreign body or deep tissue damage needs to be considered in any puncture wound (Fig. 25.5). Careful exploration and irrigation of these wounds are required. When a patient is examined a few hours after an injury, a wound has had time to stick together due to fibrin and clotting. Thus it is critical when examining a patient to apply a wet compress over the wound and mildly



Fig. 25.3 Lid hematoma in a 4-year-old child. The pressure of the hematoma is causing superior displacement of her globe



Fig. 25.2 Lid hematomas secondary to blunt trauma. Lid hematomas from blunt trauma can remain localized and expand in size; they can also obscure significant injury to the globe



Fig. 25.4 A seemingly minor eyelid laceration with ptosis. Surgical exploration confirmed involvement of the levator muscle in the laceration

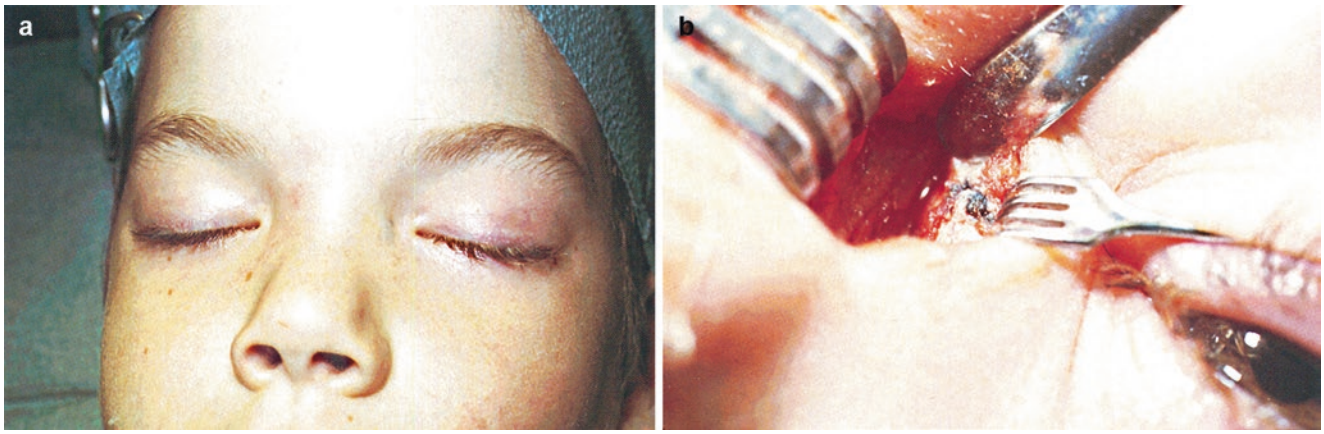


Fig. 25.5 Foreign body in lacrimal sac. (**a**) Eight-year-old patient with hemophilia and no history of trauma developed epiphora over preceding year. (**b**) Exploration of lacrimal sac reveals graphite foreign body. Family later recalls puncture wound from a pencil several years before. Appropriate hematologic factors were given preoperatively and successfully controlled hemorrhage during surgery

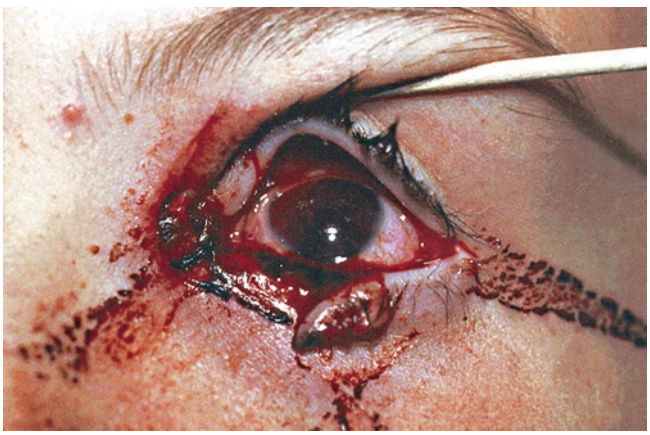


Fig. 25.6 Example of blunt trauma (rock) causing both a lid laceration and rupture of the globe

manipulate the tissue. Sometimes an eyelid that appears apposed is actually covering a large laceration. If this is not tolerated, a sedated exam in the emergency room or under general anesthesia is warranted. Before any manipulated of the ocular adnexa, however, a penetrating or perforating ocular injury must be ruled out. A low threshold must be held to examine a patient under anesthesia to rule out an ocular injury.

Projectiles are a common source of eyelid and ocular injury. Rocks, slingshots, arrows, bungee cords, toys, and balls are some of the many objects that can cause trauma when hurled. The impact of the object can cause lacerations, hematomas, and severe injury to the globe. This illustrates that a full eye exam is imperative in every trauma patient (Fig. 25.6).

Air guns that shoot pellets and BBs are another dangerous source of eyelid and ocular projectile trauma. A study done at Johns Hopkins University revealed that 91% of air gun shooters were male as were 89% of the victims. On average, the victims were 13 years old. An interesting point of this study was that 45% of the victims were the intended target, while 26% of those injured were hurt because of a ricochet [9]. Almost all of the injuries were caused by an acquaintance.

Explosion injuries in children are almost always from fireworks. An article published in a 1996 study found that 29% of firework injuries were noted to involve the eye and 18% involved other areas of the face. Almost all the injuries occurred in a 3-week period around the July 4 US Independence Day celebration. The victims averaged 8.5 years in age and about three quarters were male. The most common type of injury was a burn (72%), and firecrackers were the most common type of firework device involved (42%) [10].

Evaluation

Since pediatric trauma is often unusual, an accurate history is imperative. If the injury was due to a fall, the height of the fall and the impact surface should be determined. If the child was struck with an object, the type of object (wood, metal, rock, glass, etc.) and an estimate of the speed of the object (thrown, shot, etc.) should be determined. Knowledge of the mechanism and severity of trauma will help to guide the physician in the initial diagnosis and management of the damage. If the object causing the trauma is available, it should be inspected. A pencil, for example, should be examined to rule out the loss of its tip or any fragments. This would necessitate orbital imaging.

The level of consciousness of the child immediately following and subsequent to the injury should be determined if at all possible. A patient must be cleared by the emergency room or primary trauma team to be examined. Even the ophthalmologist should remember the value of assessing for

airway, breathing, and circulation (the trauma A-B-C's) before examining the eyes and eyelids. It is also important to obtain the immunization status of the child and a past medical history including current medications being used and any known allergies.

As with any form of ophthalmic trauma, the first concern after insuring the integrity of the airway, respiratory, and circulatory systems is the status of the visual system. When the patient's age and type of trauma allow the practitioner to obtain a visual acuity, it should always be documented. A near vision card is usually quite satisfactory for this purpose. In younger children, the ability to fixate on an object with the opposite eye covered is an excellent indication of an intact visual system.

The pupillary response to light stimulation also provides invaluable information. When the visual acuity cannot be obtained, the pupil response may be the only evidence of an intact visual system. The presence of an afferent pupillary defect (Marcus Gunn pupil) may be the only evidence of optic nerve damage in the presence of severe trauma.

Once the integrity of the vision has been established, attention turns to the visible trauma. In many cases, all of the damage from the trauma is readily visible. Four major concerns should be addressed during this secondary survey. First, are there any retained foreign bodies? The mechanism of trauma will help guide this concern, but it is safest to assume the presence of retained foreign bodies with any projectile-type injury until determined otherwise. Second, is there any missing tissue? Although it is very unusual for even the most severe trauma to result in significant loss of tissue, first appearances can be very deceiving (Fig. 25.7). With large lacerations, tissue will contract and give the appearance of a gap secondary to tissue loss. In most instances, however, all tissue is present and can be repositioned. Third, what is the status of the lacrimal system? With many types of lid trauma, the lacrimal system can be damaged, if not directly, then as a result of the force of the trauma. A 2008 article demonstrated that 66% of eyelid lacerations involved the canalicular system [11].

Structurally, the lid medial to the punctum is the weakest and, therefore, the most likely to tear with blunt force [12]. Involvement of the lacrimal drainage channels should be assumed with any avulsion or laceration extending into this area. The canaliculi lie between the anterior and posterior arm of the medial canthal tendon (Fig. 25.8). The canaliculi and both arms of the tendon are usually damaged as a unit. Finally, what damage could be present that is not readily visible? A high level of suspicion is helpful. Is there traumatic optic neuropathy? Is there a fracture? Is the globe damaged? Could there be intracranial damage? A detailed, systematic approach should allow the practitioner to determine all of the above.

Ancillary testing is an important part of the diagnostic process. Any suspicion of fractures or metallic foreign bodies should be further evaluated by the use of narrow-cut computer tomography (CT) scans (see Chaps. 32 and 42). Magnetic resonance imaging is far superior to CT scans in the evaluation of soft tissue, however, has not place in the setting of trauma before the presence of a retained metallic foreign body has been ruled out the presence of deep hemorrhage is readily seen and not distorted by bone. Retained foreign bodies often appear as a low-intensity signal or relative void in the soft tissue on MRI scans, both confirming their presence and providing guidance for removal [13, 14]. High-resolution Doppler ultrasound may also have a roll in the diagnosis and localization of retained foreign bodies, particularly when there is a high level of suspicion and the answer is not evident using the conventional methods of imaging [15].

A final note concerning the evaluation of lid and adnexal trauma in the pediatric patient population is necessary. It is an unfortunate reality that children can be the victims of

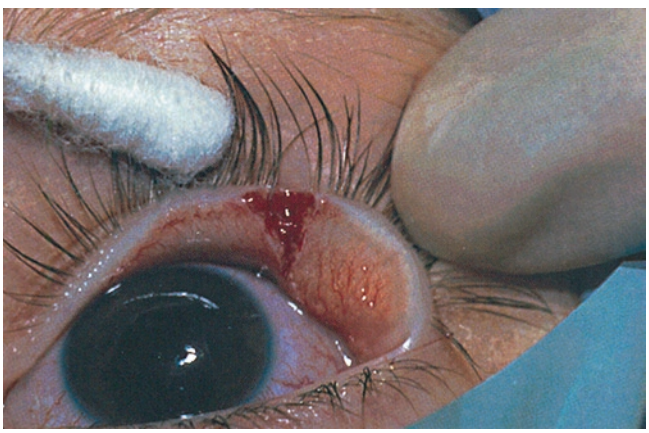


Fig. 25.7 A lid margin laceration that was difficult to see until the lid was everted

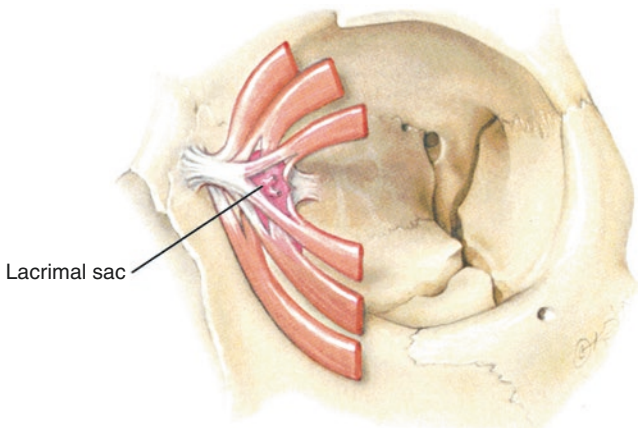


Fig. 25.8 Medial canthal anatomy. Artistic rendition of the medial canthal anatomy. Note the lacrimal drainage channels lying between the anterior and posterior arms of the medial canthal tendon. The anterior arm attaches to the anterior lacrimal crest. The posterior arm attaches to the posterior lacrimal crest

abuse or non-accidental trauma (NAT or Suspected Child Abuse and Neglect, SCAN). While the vast majority of children evaluated for trauma in this area are not the unfortunate recipients of accidental trauma, the possibility of NAT (or SCAN) cannot be ignored. Child abuse is a serious problem with grave ramifications for the child and caregiver. It is important, therefore, to look specifically for signs that may help to identify victims of abuse. A dilated fundus exam can be performed, looking for retinal hemorrhages to assist in the diagnosis. If the history does not fit the physical findings or if the trauma is repetitive, NAT (or SCAN) must be considered and appropriate social agencies consulted.

Management

The first priority in lid and adnexal management is the overall health of the patient. Facial trauma is often associated with other, possibly more severe trauma. Life-threatening injuries must be managed first. Injuries to the visual system should be managed next.

Most often, management of pediatric lid trauma will require the use of general anesthesia. While repair is urgent, a surgeon can safely wait until the patient has not eaten for 6–8 h, allowing the stomach to empty so that general anesthesia can be more safely employed. This will give the practitioner time to administer tetanus toxoid and consult with other physicians, if necessary. During this time, the injured areas can be coated with an antibiotic ointment and covered with sterile gauze. An exception to this is the presence of an open globe. Repair should be performed as soon as possible in this situation. While not desirable, delayed repair of lid trauma can be safely performed. Lid lacerations can be closed primarily as late as 1–2 days after injury because of the excellent blood supply present in facial soft tissue [16]. Copious irrigation of the wounds during surgery helps to reduce the incidence of postoperative infections. If the wound is from a dog bite or appears infected, antibiotics are started too.

Repair of wounds that do not involve the lid margin are usually straightforward but can be misleading and may involve more damage than is apparent at first glance. This is especially true with penetrating injuries, which can involve the levator complex in the upper lid or even involve the globe. The presence of visible preaponeurotic fat indicates penetration of the orbital septum and possible levator damage. After the wound is cleaned, deep layers are approximated with care taken to insure that appropriate anatomic relationships are maintained. Only the eyelid retractors and conjunctiva should be sutured and never the orbital septum as direct closure of the latter can result in lagophthalmos. For brow and non-marginal lid lacerations, the authors prefer to use a 4-0, 5-0, or 6-0 polyglycolic acid (Vicryl) suture to repair the deep layers (Fig. 25.9). The thinnest suture that supports the wound tension should be utilized. The skin is closed with a 6-0 plain or fast-absorbing gut. For linear sub- or supra-brow lacerations, skin closure with a 5-0 nylon or Prolene suture is also an effective option if the child will tolerate suture removal 5–7 days later. These sutures can be secured as a looped knot at each end to help facilitate suture removal. An application of a cyanoacrylate glue for additional skin closure support can also be an added step that may be useful in many pediatric situations to maintain good closure. The deep sutures provides the structural integrity to the wound during healing while the gut or running subcuticular suture approximates the skin edges if more security for wound tension is required. The use of absorbable sutures on the skin is a particular advantage in the pediatric population. The trauma and difficulty of suture removal is eliminated, and the final scar at the site of the injury is usually quite acceptable.

Trauma involving the lid margin is more involved. Proper closure of the margin is imperative to avoid notching, rotation, or lash deformities. Also, the degree of injury

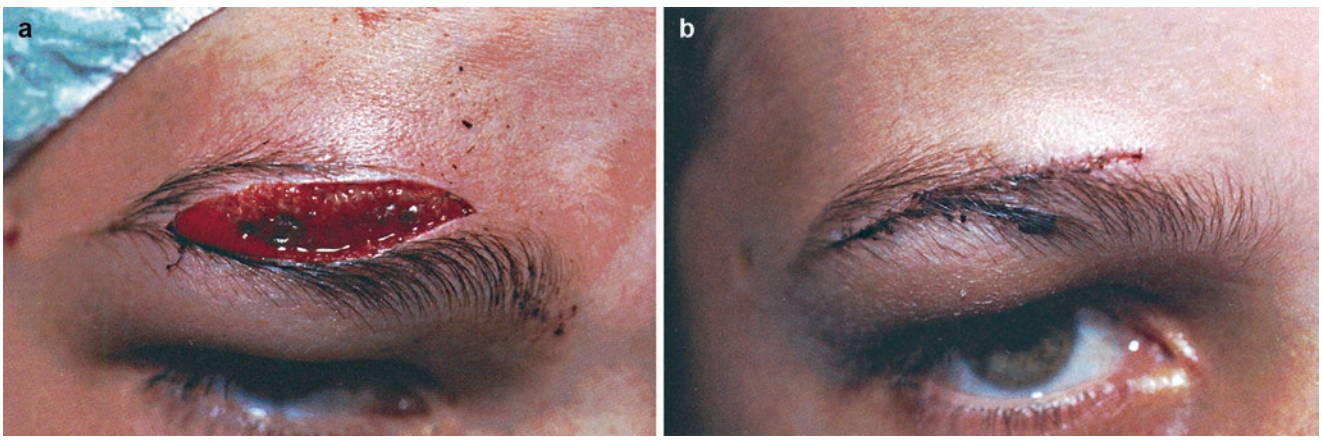


Fig. 25.9 Deep brow laceration. (**a**) Laceration before surgical closure with retracted tissues. (**b**) Laceration 1 week after multilayer closure

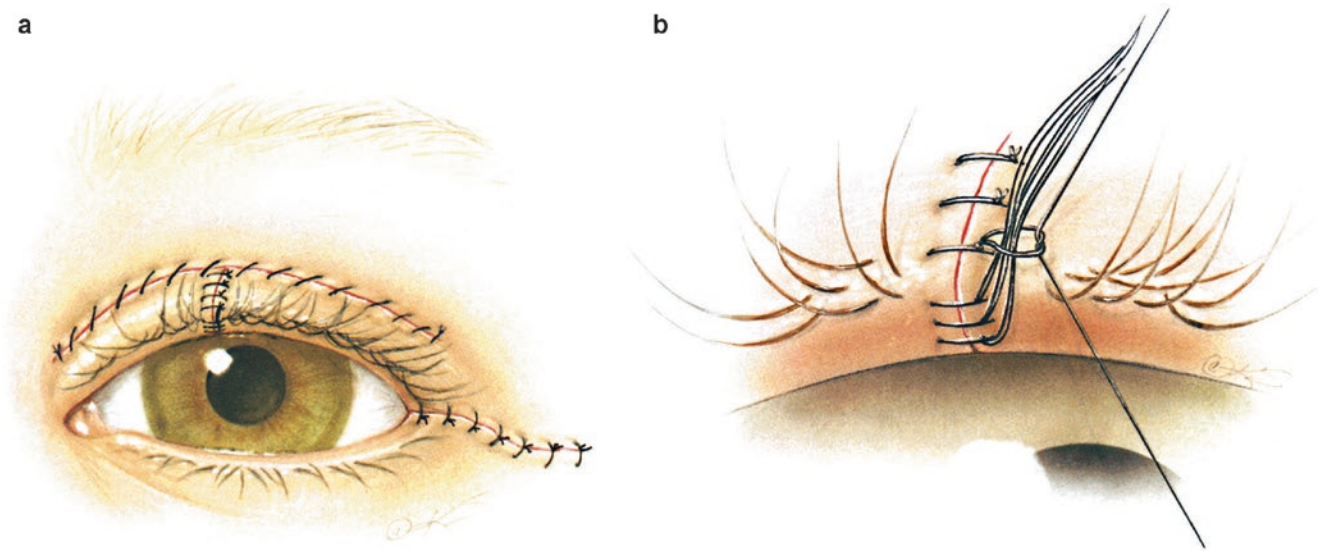


Fig. 25.10 Artistic rendition of a lid margin defect. (**a**) Three preplaced sutures in margin and tarsal edges ready for closure. (**b**) Marginal sutures tied into first skin suture to avoid corneal irritations

may not be suspected at the time of exam. The key to a good result is accurate approximation of the gray line of the lid margin [17]. If this suture is properly placed, the remainder of the repair will fall into place (Fig. 25.10). Typically, three marginal sutures are placed. The first passes through the gray line. Using a 6-0 chromic gut or Vicryl suture, the needle is introduced into the lid approximately 1 mm from the edge of the wound. It arcs more widely before exiting into the wound 2–3 mm below the lid margin. It is then introduced into the soft tissue on the other side of the wound at the same depth, mirroring the track of the suture on the first side. The suture is brought together and used to place traction on the lid margin. The wound edges and lid margins are examined. If the alignment is not satisfactory, the suture is withdrawn and repositioned. If the alignment is correct, then additional 6-0 sutures are placed through the lash line at the anterior edge of the lid margin and the mucocutaneous junction on the posterior edge of the lid margin (Fig. 25.11). Alignment is checked with each suture placement. An alternative option for younger patients is to place a vertical mattress suture through the gray line with a 5-0 Vicryl on a P-2 needle with the knot buried in the margin and then a single vertical mattress 6-0 Vicryl anterior to this in the lash line with the knot buried in the same fashion. This has the advantage of not having to remove sutures and removes the risk of the child grabbing at the eyelid sutures and ripping them out.

Keeping the lid margin on traction after the lid margin sutures have been placed, the tarsal plate is re-approximated. The tarsal plate in the lower lid usually closes satisfactorily with two interrupted partial thickness sutures of 6-0 Vicryl suture. The authors prefer an S-29 needle for ease of passage. A larger P-1 needle can also be used but is

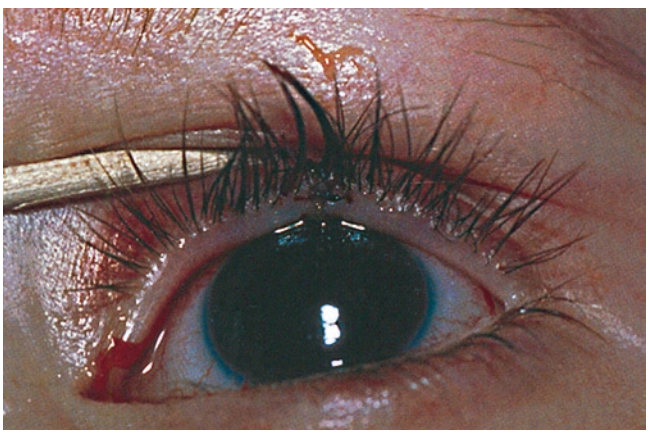


Fig. 25.11 An alternate method of lid margin closure in the pediatric population. The lid margin laceration shown in Fig. 25.7 is closed with 6-0 Vicryl sutures, burying the knots

a cutting needle, not spatulated like the S-29. The P-1 needle does have the advantage of being slightly bigger. The tarsal plate in the upper lid usually requires three sutures to approximate the edges properly. The soft tissue is then closed with a muscle layer of 6-0 Vicryl and skin closure of 6-0 fast-absorbing gut or 6-0 plain gut. The tails of the marginal sutures are left long and draped onto the skin away from the globe. They are secured in that position with a final suture, usually 6-0 in size as well. The redundant tails of the lid margin sutures are then cut. In this fashion, the marginal suture ends are tied away from the cornea, minimizing the chance of irritation or abrasion from the sutures. An alternative, in children, is to close the lid margin with 6-0 Vicryl and bury the knots. Either technique will eliminate the need for post-op suture removal (Fig. 25.11).

Canalicular Lacerations

Repair of any associated damage to the lacrimal system is performed at the same time as soft tissue repair. Although there has been debate about the need to repair a single canalicular laceration, it is preferable to do so. Experimental data indicates that some individuals can develop epiphora with single canalicular obstruction [18]. Also, the quantity of tear flow through the upper and lower lid systems varies among individuals, making it hazardous to assume that an intact lower lid canaliculus will be adequate to handle all tear flow [19]. Finally, the goal of any trauma reconstruction should be to restore normal function as much as possible. The use of silicone stenting has an increased success when left in place at least 90 days.

The first major decision before repairing a canalicular laceration is whether to suture the canaliculus for repair or simply repair the margin and surrounding tissues. Kersten and Kulwin demonstrated that direct anastomosis of the canalicular epithelium was not necessary in a series of 59 patients that had 100% patency on probing and irrigation post-stent removal [20]. This was also confirmed by an animal model by Conlon et al. [21].

The first step in repairing the torn or lacerated canaliculus is the placement of silicone stent to act as a surgical stent and scaffolding during the healing process. The Crawford bicanalicular system (Jedmed, Atlanta, GA) has proven to be relatively safe and easy to use but has been replaced mostly by the development of monocanalicular silicone stents such as the Monoka and the mini-Monoka (FCI Ophthalmics, P.O. Box 465, Marshfield Hills, MA 02051). Silicone intubation is accomplished after the wounds have been cleaned and irrigated but before other soft tissue closure. Oxymetazoline and local anesthesia containing epinephrine (1:200,000) can be applied with cottonoids into the inferior meatus. This will constrict the nasal mucosa and ease retrieval of the tubes from the nose. The local anesthesia with epinephrine is injected into the area of damage in the medial canthus to assist with hemostasis. The use of 0.5% bupivacaine will also provide some postoperative pain relief.

The more common clinical picture usually involves damage to only one canaliculus. With a bicanalicular system, the undamaged system is intubated first. This gives the surgeon a guide for the direction and depth of the lacrimal drainage system. The punctal side of the damaged canaliculus is then intubated, bringing the probe and tube into the area of damage. Once again, the more common techniques at present involve mostly monocanalicular stenting which can be done individually for both canaliculi, if needed. The advantage of the monocanalicular stents is their ease of removal in the office without general anesthesia and the avoidance of canalicular slitting which is seen fairly commonly with bicanalicular stents (Fig. 25.12).

Sometimes using the operating microscope or magnifying loupes to enhance the view, the white colored epithelial tissue of the canaliculus is sought. Many tricks have been described to assist the surgeon with this endeavor, including use of fluorescein and other colored liquids, as well as air bubbles, to highlight the location of the medial edge of the torn canaliculus [22]. Such techniques, however, are rarely necessary. Knowledge of the anatomic path of the canaliculus, meticulous hemostasis, and the magnification provided by the microscope will almost always allow the medial canalicular tissue to be directly visualized. The key is looking along the edge of the caruncle superiorly for a superior canaliculus and inferiorly for the inferior canaliculus, knowing the canaliculi travel on a 30 degree trajectory and come together just medial to the caruncle posteriorly. A search is sometimes necessary, but with patience, the white epithelium of the canaliculus can usually be found.

The most common problem preventing ready identification of the medial edge of the canaliculus is a failure to appreciate the posterior course of the canaliculus as it passes medially toward the sac. This results in a futile search for the torn edge in tissue located too anteriorly, thereby missing the deeper location of the torn medial end.

If the physician is unable to locate the medial edge, one should move the search deeper into the wound and if

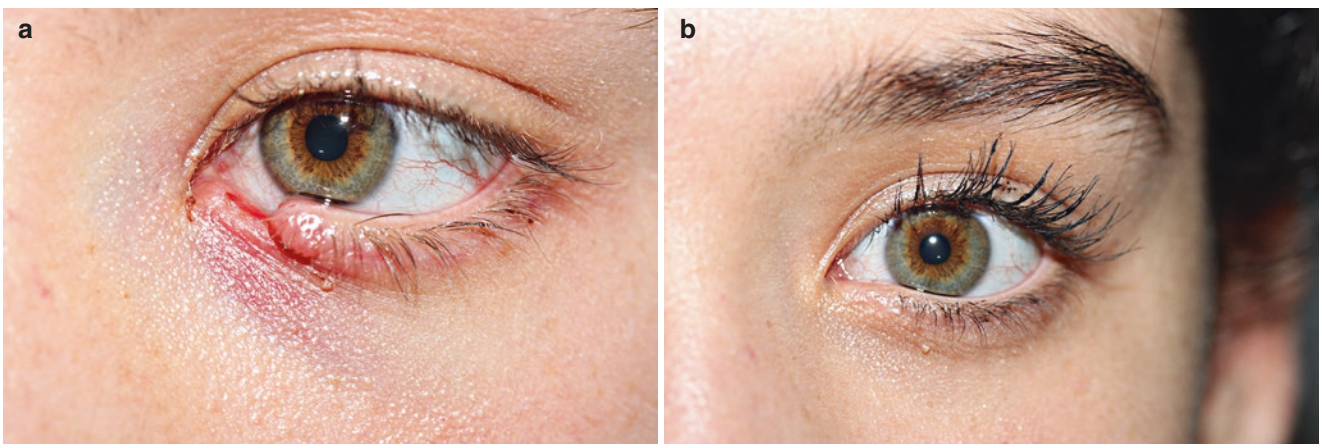


Fig. 25.12 (**a**) Full-thickness laceration of the lower eyelid with canalicular involvement. The injury was accrued due to the shearing force of blunt trauma. (**b**) Postoperative appearance 2 months after the repair with a monocanalicular stent

necessary, try the injection techniques suggested above. In the past, use of a pigtail probe was also suggested but because of the design it has generally been discouraged for inexperienced surgeons. It can damage the common canaliculus (internal punctum) and thereby create a much more severe upper system problem. This is most certainly true when the original Worst probe was used due to the small hook on the end used to pull a suture through the common canaliculus [23]. A newer pigtail probe with a French eyelet, however, has more recently been designed and can be used with great success (Storz #E4251C). It is available in both adult and pediatric sizes. Gentle manipulation may then allow passage of the probe through the opposite canaliculus to reveal a very deeply placed cut at the medial end of the canaliculus. The surgeon must never force the pigtail probe as this risks the creation of a false passage. One must be aware that 10–20% of humans have no common canaliculus; thus, the pigtail probe will not pass easily into the fellow eyelid and should be immediately abandoned. Generally, this technique is reserve for very medial eyelid lacerations or avulsions. A great technique developed at the Children's Hospital of Philadelphia by Forbes et al. involves the use of the full size Monoka stent [24] (Fig. 25.13). The Prolene thread guide from the Monaka stent is advanced into the punctum of the

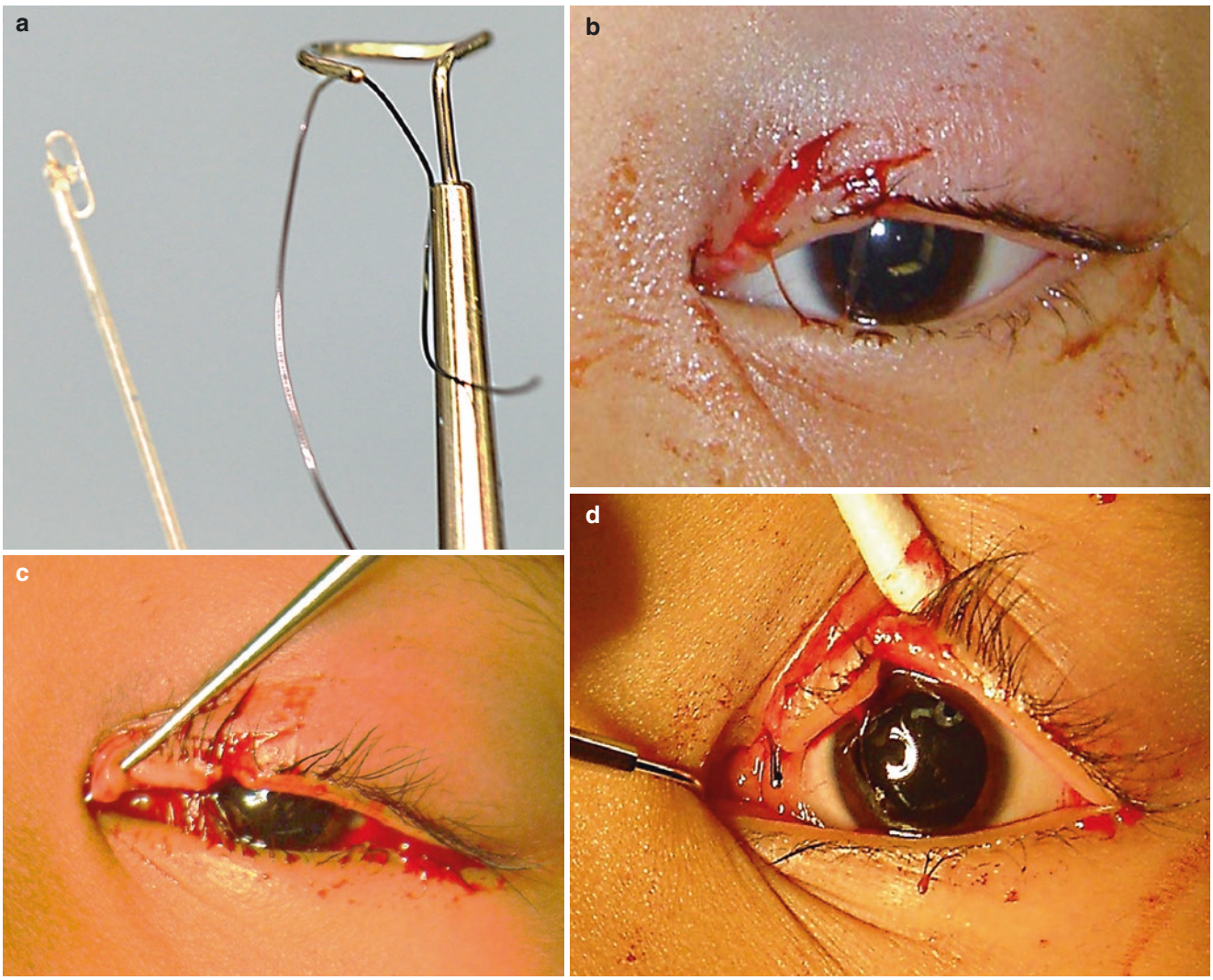


Fig. 25.13 Canalicular avulsion repair with a pigtail probe. (**a**) The new pigtail probe: note the French eyelet. This is the smaller pediatric size with the cut end of the thinner suture from the Monaka stent passed through the tiny hole, which then permits the attached silastic stent (seen to the left of the pigtail probe in this photo) to be pulled through the lacerated canaliculus and out of the opposite punctum. (**b**) Left upper eyelid laceration. Note the medial canthus appears intact. (**c**) Upper canalicular laceration: a lacrimal dilator is extended from the punctum to the torn distal canaliculus. Note: with lateral traction, the upper eyelid medial canalicular involving laceration is revealed. (**d**) The pigtail probe is passed into the intact, lower eyelid punctum and rotated to emerge out of the torn upper proximal canaliculus.

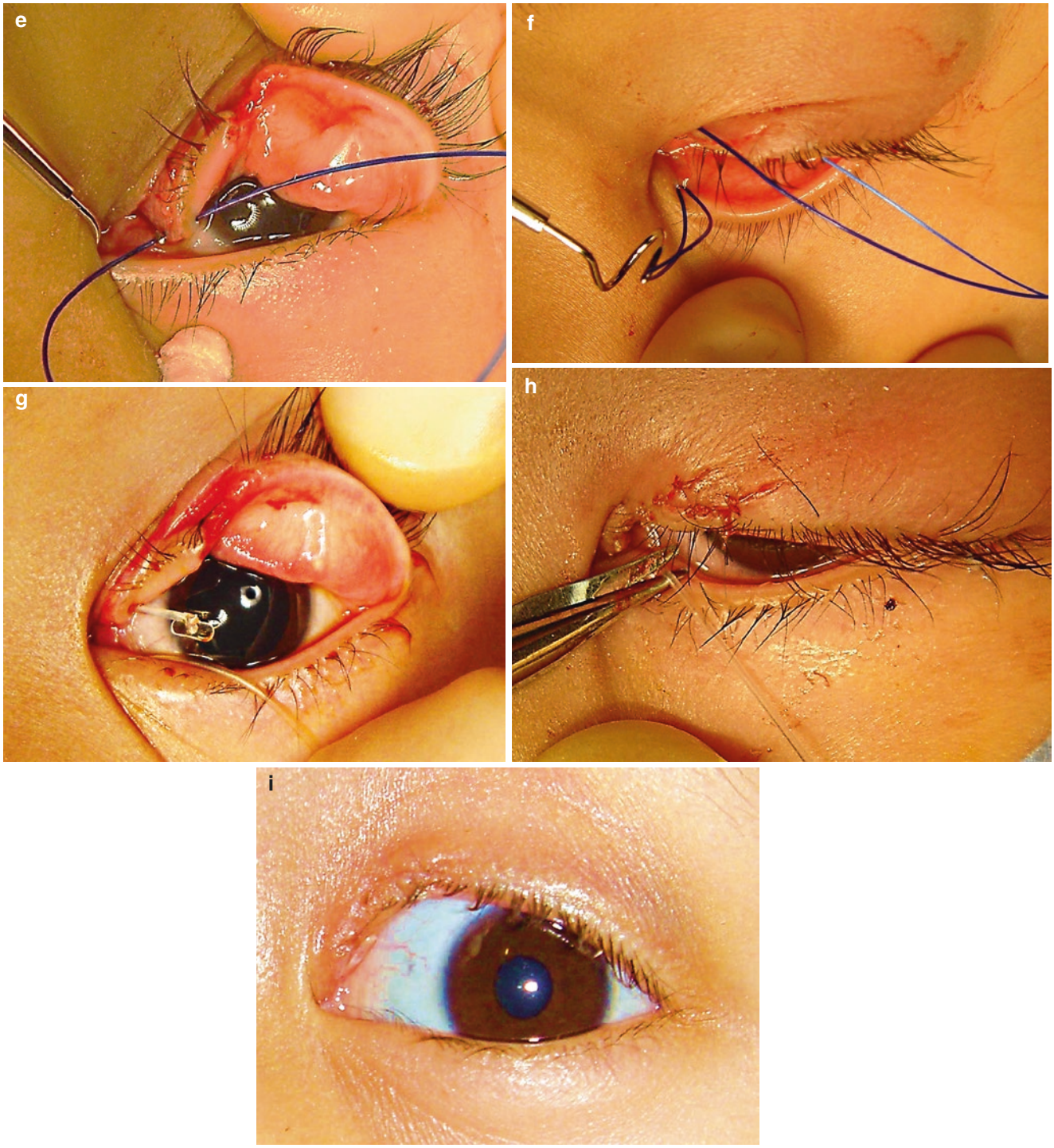


Fig. 25.13 (continued) (**e**) The thinner Prolene thread guide of the monocanalicular stent is advanced through the upper eyelid punctum, out the distal, torn canaliculus and into the eyelet of the pigtail probe. (**f**) The pigtail is rotated backward pulling the Prolene thread guide of the Monoka out of the intact, lower eyelid. (**g**) The stent is pulled until the collarette of the stent is ready to be seated. (**h**) After the central and medial lacerations are repaired and the stent is seated in the upper punctum, excess stent is cut flush at the level of the lower eyelid punctum. (**i**) Postoperative picture

injured canaliculus and out the torn canaliculus. The pigtail probe is inserted into the opposite normal punctum and canaliculus and carefully rotated through the common canaliculus to emerge from the torn medial end. The Prolene suture is then threaded into the French eyelet of the pigtail probe, and the probe is rotated back out of the normal apposing canaliculus and punctum. This then permits pulling the silastic stent though the entire canalicular system and out of the intact punctum. This technique is a modification of the cerclage technique for which the pigtail probe was originally designed. The punctal plug end of the stent can then be properly seated into the punctum.

Once the medial edge of the torn canaliculus has been found, a probe with silicone tubing attached is passed through it into the sac and advanced into the nose. If a mini-Monoka is used, this stent is shortened so it passes into the lacrimal sac. If bicanalicular intubation is used, the opposite canaliculus (if normal) is intubated first. If only one canaliculus has been damaged, the mini-Monoka device designed specifically for single canalicular laceration is an alternative method of repair (FCI Ophthalmics, P.O. Box 465, Marshfield Hills, MA 02051) (Fig. 25.14).

Repair of the wound can now proceed. The authors use the following techniques to repair the canaliculus (Fig. 25.15). The first suture placed is a 6-0 Vicryl with an S-14 or S-24 needle. It is passed through the tissue immediately posterior to the torn canaliculus on either side of the laceration. This tissue represents the posterior arm of the medial canthal tendon and is the structure that must be repaired to restore both normal contour of the lid and normal contact of the eyelid against the globe. This suture is not yet tied. The canalicular epithelium is then approximated with 7-0 or 8-0 polyglycolic acid (if desired) or not sutured at all. The suture is placed so the knot will be on the outside of the canaliculus. If a surgeon prefers to anastomose the canalicular epithelium directly, then ideally, three interrupted sutures located 120° apart around the circumference of the canaliculus are placed. In reality, the depth and details of the damage may, at times, only allow for the placement of two sutures around the circumference. The 8-0 sutures are not tied until the 6-0 suture has been tied, re-approximating the tissue and allowing the 8-0 sutures to be tied with minimal tension, preventing breakage.

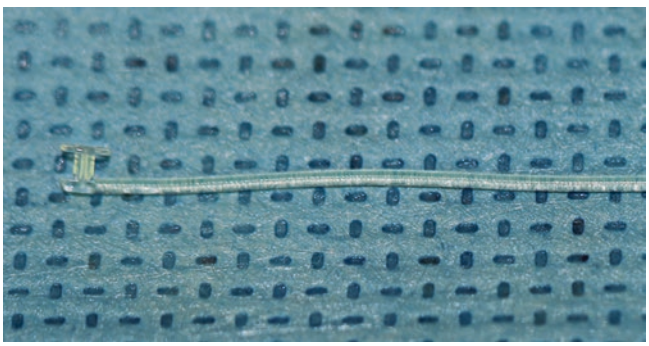


Fig. 25.14 The mini-Monaka device is a silastic rod rather than a tube, like the Monaka stent. The long rod length can be cut to fit within the lacrimal sac while bridging the repaired canalicular laceration. The mini-Monaka is securely anchored at the punctum by the plug so that knots or sutures are unnecessary to hold it in place. It is most useful for treating only a single canalicular laceration involving the proximal 2/3 of the lacerated canaliculus

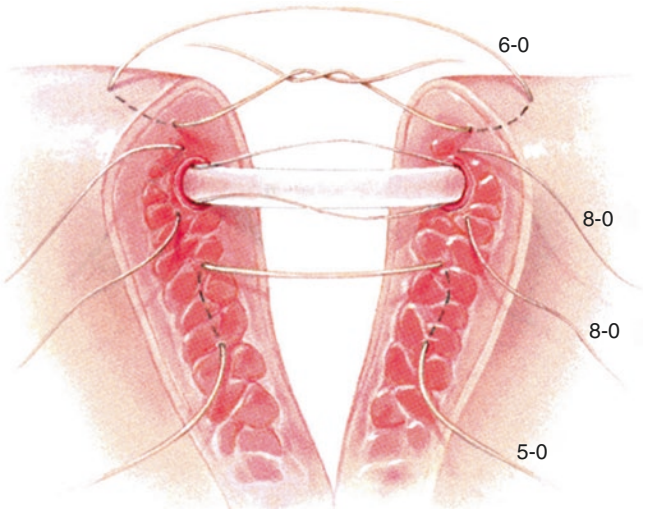


Fig. 25.15 Repair of canalicular laceration:The lacerated canaliculus intubated with a silastic stent. A 6-0 Vicryl suture is placed in the gray line to approximate the edges of the wound but then left loose. 5-0 Vicryl suture can then be placed between the deep orbicularis tissues attached to the posterior limb of the medial canthal tendon which inserts on the posterior lacrimal crest. 8-0 Vicryl sutures are placed to join the cut ends of the canaliculus. The deep suture is tied first followed by the canalicular sutures and the marginal suture last if utilized. The skin is closed with interrupted absorbable sutures of 6-0 or 7-0 Vicryl

Once again, it must be stressed that direct closure of the canaliculus is not necessary and is purely depends on the surgeon's preference. At CHOP, we have not directly closed the canalicular epithelium since 2006 and in the last 10 years, have only had one patient require additional surgery. This patient had a bicanalicular injury due to an air gun piston injury at an auto shop [24].

The anterior arm of the medial canthal tendon is repaired to insure a normal external appearance of the medial canthal angle. The remainder of the wound is then closed in the usual fashion, with absorbable sutures used on the skin. If the silicone intubation is bicanalicular, then the ends are either tied with a square knot and cut or secured with a retinal sponge as described in Chap. 27. If a mini-Monoka intubation was used, then the end of the silicone rod is cut to retract into the lacrimal sac or into the nostril if a Ritleng probe pulled monocanalicular stent was used. A suggested 90-day period or more results in improved anatomic patency, which is in turn associated with a significantly lower rate of epiphora [25].

Adnexal lacerations can be much more extensive than the lids alone (Fig. 25.16). The principles of careful layered closure are critical. The levator complex can be repaired with absorbable sutures if detached in extensive lacerations. It is important to rule out potential further damage to the globe beneath the lids.

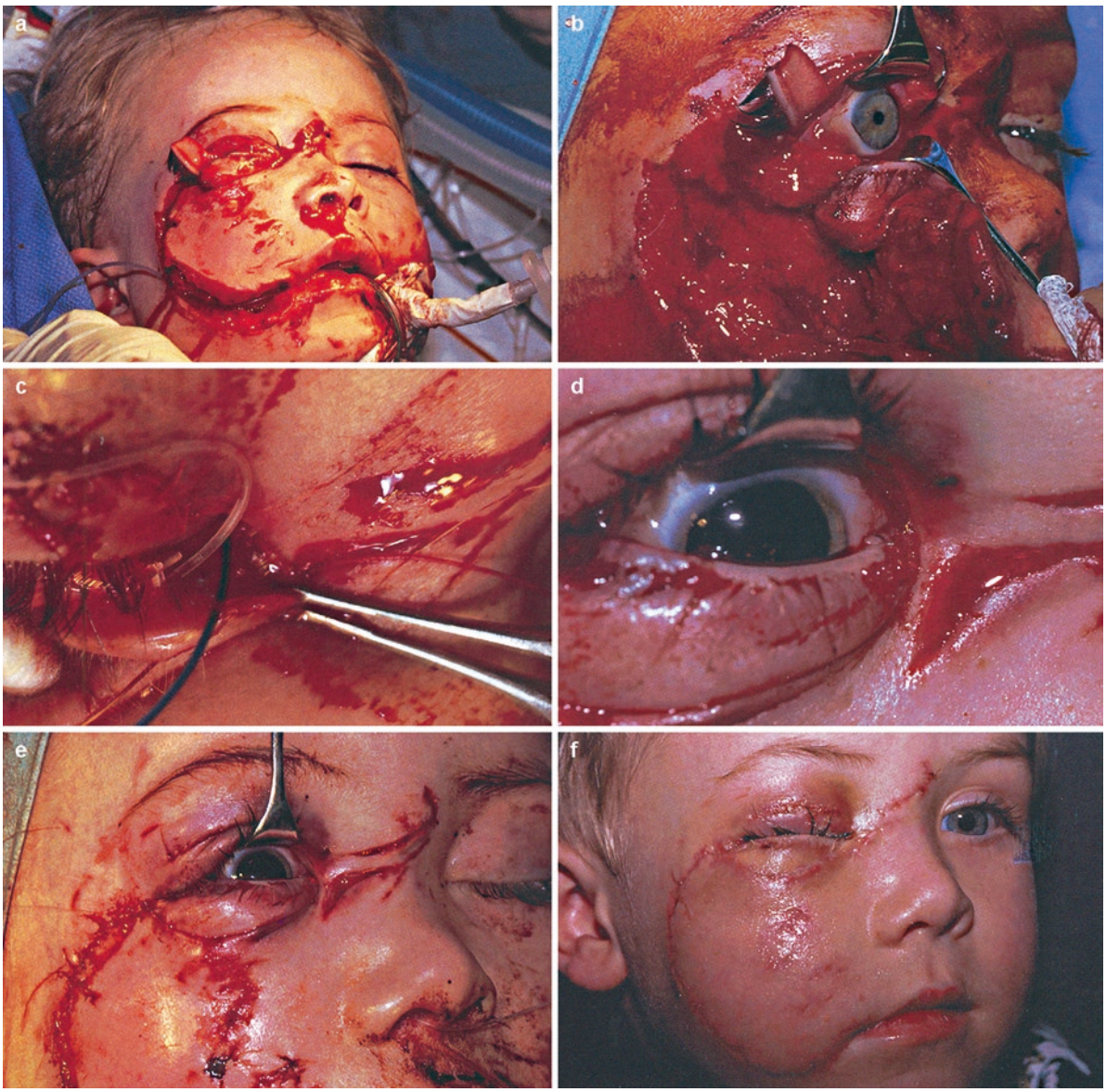


Fig. 25.16 Severe dog bite injury. (**a**) Dog bite lacerating eyelids, lower canaliculus, cheek, and interior of nose. (**b**) Cheek flap retracted; Stenson's duct intact; upper lid laceration lateral to punctum and canaliculus. (**c**) Lower canalicular laceration; monocanalicular stent with 4-mm collarette seen in center of photo. (**d**) Upper lid laceration repaired; monocanalicular stent in place. (**e**) Lateral canthal angle repaired with 4-0 Vicryl sutures to periosteum in area of the lateral orbital tubercle; 5-0 Vicryl is used to create a sharp lateral canthal angle. (**f**) 2-week postoperative; edema and traumatic ptosis persist

Other Forms of Lid Trauma

While most referrals to the ophthalmic plastic surgeon will be lid lacerations, other forms of lid trauma deserve mention.

Lid Hemorrhage

Blunt trauma can result in the collection of large amounts of blood in the lid soft tissue. Though the presentation can be dramatic, treatment should be conservative. Cold compresses can be applied if tolerated by the patient. This helps control further hemorrhage and assists with pain management. Resolution takes place over a few weeks depending on the extent of the hematoma. An exception is a large loculated hematoma which may benefit from drainage with an 18 gauge needle followed by a pressure dressing to reduce chances of reaccumulation of fluid.

Abrasions

Blunt trauma with any shearing motion can remove the epithelium and a variable depth of dermis. This leaves an area of exposed subcutaneous tissue allowing hemorrhage and exudation to ensue. A crust will cover the area if no treatment is

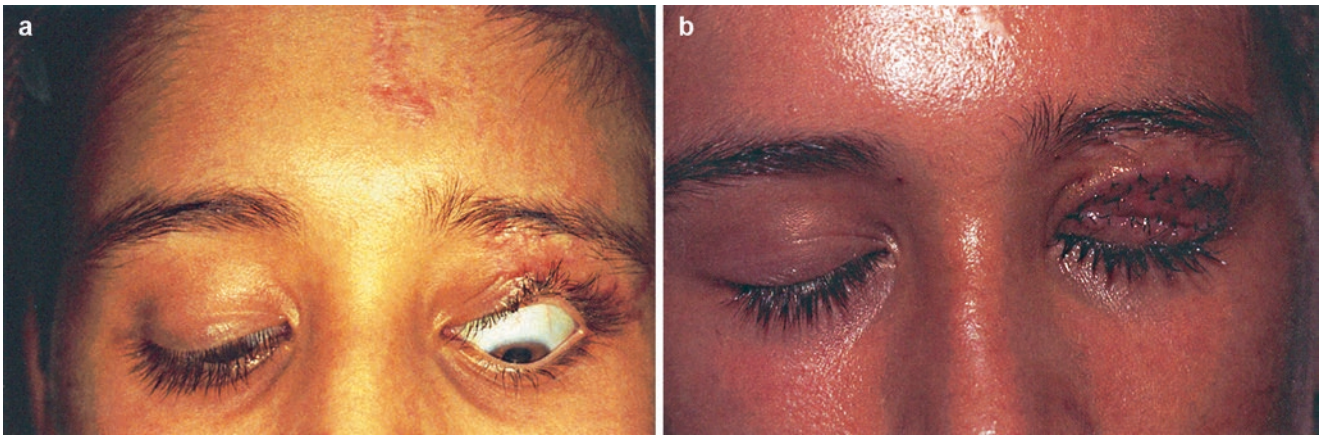


Fig. 25.17 Cicatricial retraction. (**a**) Cicatricial retraction and lagophthalmos in the upper lid of young male 3 months after motor vehicle accident. (**b**) Appearance of the lid 1 week after full-thickness retroauricular skin graft placed in lid after surgical release and excision of cicatrix

provided. Therapy should involve daily cleansing of the wound to remove any crusts. The wounds can be coated with an antibiotic ointment or even a bland petrolatum product like Aquaphor to keep the area moist and to help prevent infection.

Large, deep abrasions can cause cicatricial retraction of the lid margin or cicatricial ectropion. Meticulous wound care during the healing phase will help prevent or minimize this complication. Should it develop, lubrication should be used to keep the ocular surface moist. All cicatrix evolve, reaching their tightest contraction about 6–8 weeks after injury. Over the next 4–6 months, the scar will mature, stretching and becoming more flexible. Any surgical correction of the lid malposition should be delayed, if possible, until after the scar has matured and the lid position has stabilized. Often, conservative management will result in a normally positioned and functioning lid. If treatment is required, the cicatrix should be released and the gap created filled with a full-thickness skin graft (Fig. 25.17). Retroauricular skin is an excellent donor site for eyelid grafting.

Puncture Wounds and Penetrating Injuries

Most puncture wounds and penetrating injuries appear benign on first inspection. It is important that these wounds be carefully examined and cleaned. Thorough irrigation with sterile water or saline will significantly decrease the bacterial load from the instrument of injury. Imaging studies are also useful in localizing retained foreign bodies. Plain film X-ray and CT scans are helpful in locating metallic objects lodged in the soft tissue or globe. MRI can be helpful in locating vegetative matter (Fig. 25.18). If the entry wound is relatively small, the wound can be left to heal on its own. Antibiotic therapy is often utilized to minimize the incidence of post-injury infection. Finally, a tetanus shot should also be administered.

Burns

Burns involving the eyelids of the pediatric patient present a particularly challenging clinical situation to the ophthalmic plastic surgeon. A complete discussion of periocular burn management is beyond the scope of this chapter, but several points can be made.

Management of periocular burns is divided into acute and chronic phases. The acute phase starts with the burn injury. It involves heavy lubrication and aggressive use of suture tarsorrhaphies to protect the cornea from damage secondary to exposure and infection. If the ocular surface is de-epithelialized despite maximum lubrication and appropriate use of the tarsorrhaphy, a conjunctival flap will protect the surface of the eye. An alternative is the use of an amniotic membrane to maintain the ocular surface health [26]. The chronic phase, usually starting about 30 days after injury, is directed toward reconstruction of the lids if it is necessary. Split-thickness grafts are the usual therapy, but lid sharing procedures and mucous membrane grafting may be required [27].

The risk of amblyopia should be considered with any form of occlusive therapy, including heavy lubrication. If only one eye is injured, the other eye can be therapeutically patched. Lubrication therapy can be manipulated to create 2–3 h a day when the ocular surface is mostly free of ointments. Surgical reconstruction of the lids may be performed earlier than usual so that use of the suture tarsorrhaphy can be minimized or eliminated.

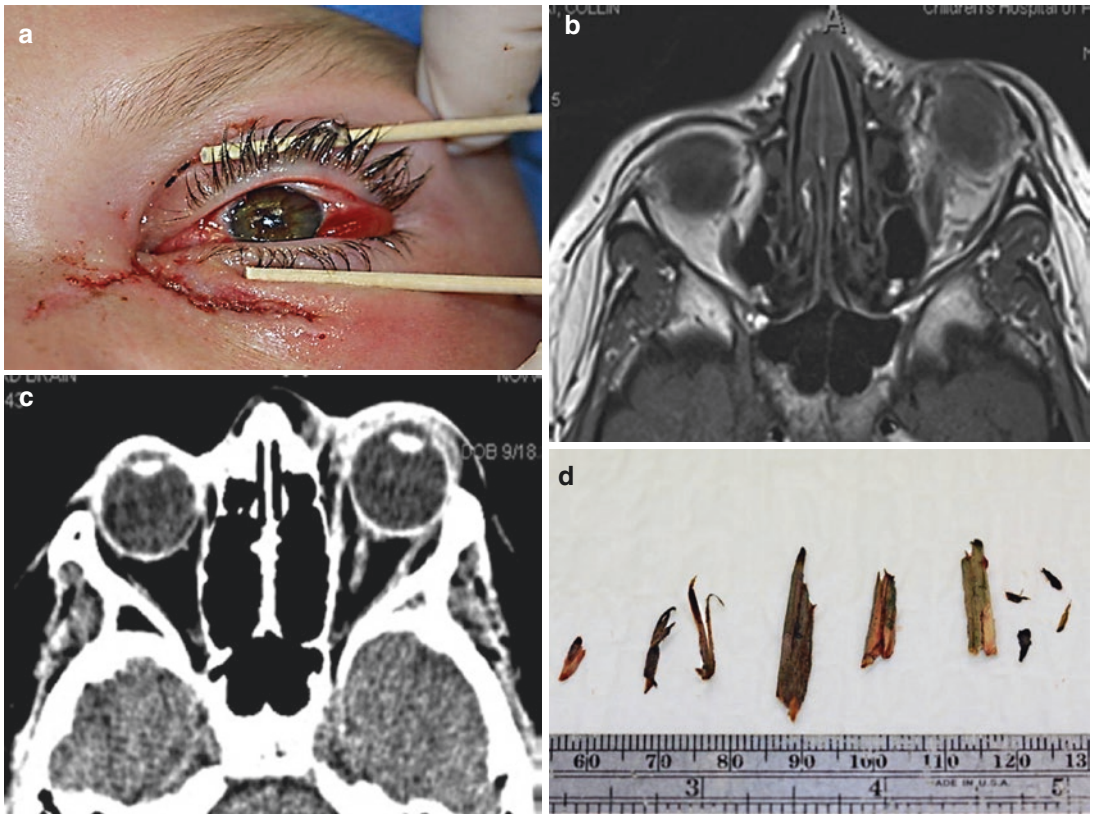


Fig. 25.18 (**a**) 13-year-old status post-laceration repair in the emergency room. He was discharged home but presented 4 days later with increased orbital pain and cellulitis. He was noted to have fallen off his bike into bushes and sustained and left lower eyelid injury. (**b**) CT scan performed in the emergency room showed no foreign bodies. (**c**) MRI obtained 4 days after injury shows intraconal foreign bodies suspected to be organic matter. (**d**) Foreign bodies removed from the orbit of the same patient

Conclusion

The repair of lid and adnexal trauma in the pediatric age group requires an appreciation of the needs of the maturing visual system as well as the requisite diagnostic and surgical skills to achieve a successful functional and cosmetic outcome.

References

1. MacEwen CJ. Eye injuries: a prospective survey of 5671 cases. Br J Ophthalmol. 1989;73(11):888–94.
2. Umeh BE, Umeh OC. Causes and visual outcome of childhood eye injuries in Nigeria. Eye. 1997;11:485–95.
3. Serrano JC, Chalela P, Arias JD. Epidemiology of childhood ocular trauma in a northeastern Colombian Region. Arch Ophthalmol. 2003;121(10):1439–45.
4. Stahlman E, Elman M, Daub E, Baker S. Causes of pediatric eye injuries: a population based study. Arch Ophthalmol. 1990;108:603.
5. Takvam JA, Midelfart A. Survey of eye injuries in Norwegian children. Acta Ophthalmol. 1993;71:500–50.
6. Gonnering RS. Ocular adnexal injury and complications in orbital dog bites. Ophthalmic Plast Reconstr Surg. 1987;3:231–5.
7. Murchison AP, Bilyk JR. Pediatric canalicular lacerations: epidemiology and variables affecting repair success. J Pediatr Ophthalmol Strabismus. 2014;51(4):242–8.
8. LaRoche GR, McIntyre L, Schertzer RM. Epidemiology of severe eye injuries in childhood. Ophthalmology. 1988;95:1603–7.
9. Schein OD, Enger C, Tielsch JM. The context and consequences of ocular injuries from airguns. Am J Ophthalmol. 1994;17:501–6.
10. Smith GA, Knapp JF, Barnett TM, Shields BJ. The rockets' red glare, the bombs bursting in air: fireworks-related injuries to children. Pediatrics. 1996;98:1–9.
11. Naik MN, Kelapure A, Rath S, et al. Management of Canalicular Lacerations: epidemiological aspects and experience with Mini-Monoka monocanalicular stent. Am J Ophthalmol. 2008;145(2):375–80.
12. Wulc A, Arterberry J. The pathogenesis of canalicular laceration. Ophthalmology. 1991;98:1243–9.
13. Green B, Kraft S, et al. Intraorbital wood: detection by magnetic resonance imaging. Ophthalmology. 1990;97:608–11.
14. Nagae LM, Katowitz WR, Bilaniuk LT, Anninger WV, Pollock AN. Radiological detection of intraorbital wooden foreign bodies. Pediatr Emerg Care. 2011;27(9):895–6.
15. Glasier CM, Brodsky MC, Leitheser RE Jr, et al. High resolution ultrasound with Doppler: a diagnostic adjunct in orbita and ocular lesions in children. Pediatr Radiol. 1992;22(3):174–8.
16. Hanselmayer H. Prognosis of injured canaliculi in relation to elapsed time until primary operation. Ophthalmologica. 1973;166(3):175–9.
17. Nesi F. Lid lacerations. In: Levine M, editor. Manual of oculoplastic surgery. 2nd ed. Boston: Butterworth-Heinemann; 1996. p. 29–32.

18. Lindberg J, Moore C. Symptoms of canalicular obstruction. Ophthalmology. 1988;95:1077–9.
19. White W, Glover A, et al. Relative canalicular flow as assessed by dacryoscintigraphy. Ophthalmology. 1989;96:167.
20. Kersten RC, Kulwin DR. "One-stitch" canalicular repair. A simplified approach for repair of canalicular laceration. Ophthalmology. 1996;103(5):785–9.
21. Conlon MR, Smith KD, Cadera W, Shum D, Allen LH. An animal model studying reconstruction techniques and histopathological changes in repair of canalicular lacerations. Can J Ophthalmol. 1994;29(1):3–8.
22. Reifler D. Management of canalicular laceration. Surv Ophthalmol. 1991;36:113–32.
23. Jordan D, Nerad J, Tse D. The pigtail probe revisited. Ophthalmology. 1990;97:512–9.
24. Forbes BJ, Katowitz WR, Binenbaum G. Pediatric canalicular tear repairs – revisiting the pigtail probe. J AAPOS. 2008;12(5):518–20.
25. Wu SY, Chen RJ, Tsai YJ, et al. Analysis of bicanalicular nasal intubation in the repair of canalicular lacerations. Jp J Ophthal. 2010;54(1):24–31.
26. Fish R, Davidson R. Management of ocular thermal and chemical injuries, including amniotic membrane therapy. Curr Opin Ophthalmol. 2010;21(4):317–21.
27. Hollsten D, White W. Management of periorbital burns. Semin Ophthalmol. 1994;9(3):152–164.22.

Part III

The Nasolacrimal System

Evaluation of Tearing in Children

26

Maryam Nazemzadeh and Yasmin S. Chambers

Tearing in children is a common problem seen in the practice of both pediatricians and ophthalmologists. Although most pediatric tearing complaints are related to an impatency in the nasolacrimal duct [1], many other conditions involving the nasolacrimal system, as well as the lid and eye, can cause tearing. This chapter will discuss the anatomic and physiologic mechanisms for normal tear outflow as well as how tearing symptoms may be appropriately and effectively evaluated in the pediatric age group.

To fully appreciate tear outflow in a child, one must first appreciate the anatomy of the lacrimal drainage system as well as the mechanism by which tears are pumped away from the surface of the eye. Following this, a detailed discussion of the critical steps regarding history, physical exam, as well as ancillary tests useful in the evaluation of lacrimal outflow will be reviewed.

Anatomy of the Lacrimal Drainage System

The lacrimal drainage system (Fig. 26.1) begins with tiny openings called the lacrimal punctum (pl: puncta) at the inner aspect of each eyelid. The puncta sit on a mound known as the lacrimal papillae. Each punctum lies approximately 6 mm lateral to the inner canthus, and when the lids are closed, the puncta are in direct contact with the globe. When the lids are opened, however, the arc of the upper lid pulls the upper punctum approximately 0.5 mm nasal to the lower punctum. In their normal position, they face inward, lying in the groove between the plica semilunaris and the globe [2]. The openings to the puncta are 0.2–0.3 mm in diameter but can be dilated to a larger diameter because their walls are surrounded by elastic tissue.

From the puncta, tears travel into the canaliculi. The first part of each canaliculus is an approximately 2-mm vertical portion with an internal diameter of roughly 1 mm. At the base of the vertical section of canaliculus, there is a saccular dilation to 1.5–2 mm. This is termed the ampulla and signifies where the vertical canaliculus becomes horizontal.

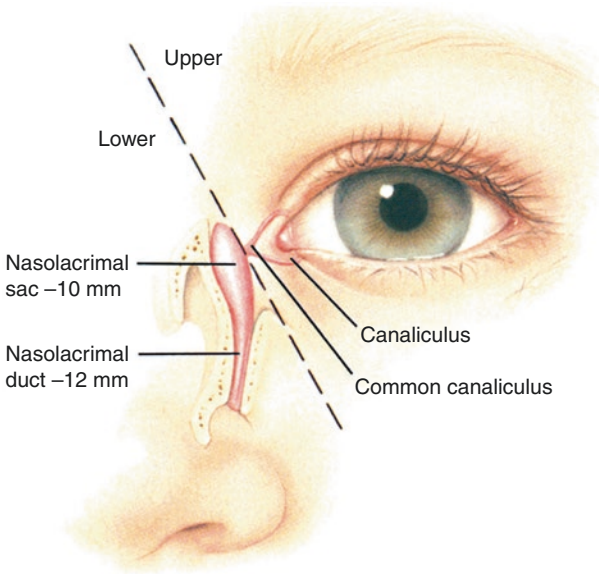


Fig. 26.1 Anatomy of lacrimal outflow system. Canaliculi are approximately 10 mm in length. A 2-mm vertical portion widens from punctum into an ampulla where it joints the horizontal canaliculus to enter the sac at the common canaliculus. These structures constitute the upper system. The sac and nasolacrimal duct constitute the lower system

M. Nazemzadeh (✉)
Oculofacial Plastic and Reconstructive Surgery, Rostami Oculofacial Plastic Consultants, Sanctuary Cosmetic Center, Reston, VA, USA
e-mail: marnaz17@gmail.com

Y.S. Chambers
Ophthalmology, The Everett Clinic, Seattle, WA, USA

© Springer International Publishing AG 2018

J.A. Katowitz, W.R. Katowitz (eds.), *Pediatric Oculoplastic Surgery*, https://doi.org/10.1007/978-3-319-60814-3_26

The horizontal canaliculus is approximately 8 mm in length and arcs with the eyelid curve toward the medial canthus. The diameter of the horizontal canaliculus narrows to slightly less than 1 mm, although the elastic tissue that surrounds both the vertical and horizontal canaliculi allows for their dilation to several times their normal width.

The upper and lower canaliculi join in approximately 90% of people to form a common canaliculus or internal punctum. This joining occurs at an angle of roughly 25°. The common canaliculus continues for another 3–5 mm before emptying into the lacrimal sac. Just prior to joining the sac, there is frequently a small dilation in the common canaliculus, called the sinus of Maier. There are numerous infoldings that create a valve-like structure, known as the valve of Rosenmuller, at the opening of the common canaliculus into the lacrimal sac; this valve prevents reflux of sac contents back into the canaliculi to exit onto the surface of the eye.

The common canaliculus empties into the lacrimal sac at the junction of the upper third and lower third of the sac. This occurs just posterior to the medial canthal tendon. Because the bulk of the sac lies below the medial canthal tendon, inflammatory and infectious sac processes commonly manifest as swellings below this structure. As will be discussed later in this chapter, this intimate relationship between the lacrimal sac and the medial canthal tendon is also important for the proper functioning of the lacrimal pump.

The sac can be arbitrarily divided into two parts: a fundus and a body. The fundus of the sac is that portion lying above the common canalicular opening and is 3–5 mm in length. The body is the remaining distal portion down to the entrance to the duct and is approximately 10 mm in length. The sac lies in the lacrimal fossa, a bony depression formed by the frontal process of the maxillary bone anteriorly and the lacrimal bone posteriorly. The fossa and sac are positioned anterior to the orbital septum and, thus, are preorbital not orbital structures.

Like the canaliculi and the nasolacrimal duct, the lacrimal sac is lined by pseudostratified ciliated columnar epithelium (e.g., respiratory epithelium) [3, 4]. The lacrimal sac is also richly invested with goblet cells whose mucous secretion may become important in nasolacrimal system obstructions.

The nasolacrimal system continues from the sac as a duct within the lateral wall of the nose. The interosseous portion of the duct is approximately 12 mm long and is directed inferiorly and slightly lateral and posterior. There are numerous constrictions within the duct that may often be felt on duct probing, but the most important infolding clinically is at the duct's most distal end, termed the valve of Hasner. This fold of tissue is often the last part of the system to canalize [5]. The duct enters the nose under the inferior turbinate and within the inferior meatus. The meatal portion of the duct may be up to 5 mm long. There is some variation in exactly where within the inferior meatus the duct enters. Generally, the ostium for the duct is located anteriorly within the meatus, approximately 2.5 cm posterior to the naris.

It is convenient to divide the lacrimal system into two parts: an upper (proximal) system and a lower (distal) system. The upper system extends from the puncta through to including the common canaliculus. The lower system represents the sac through to the ostium of the duct in the inferior meatus. This anatomic division is useful in selecting management strategies for specific nasolacrimal drainage problems.

In children there can be variation in both the structures and relative measurements simply due to the system's immaturity. These variations may contribute to the development of an obstruction or may become important if probing or more invasive lacrimal surgery is performed. During the first year of life, the distance from the punctum of either canaliculus to the floor of the nose is approximately 20 mm, whereas in adults this distance can range from 30 to 40 mm. In addition, the inferior meatus in children is flat and allows little space between the floor of the nose, the lateral nasal wall, and the inferior turbinate (Fig. 26.2). With age, this space increases. The lacrimal sac area is also less developed in children than in adults, a factor that can be important during dacryocystorhinostomy. The lacrimal crests are flat and poorly developed in small children, and the sac fossa is often shallow. Also, the relative compactness of the nose in some children sometimes leaves the ethmoidal air cells in an anterior location [6].

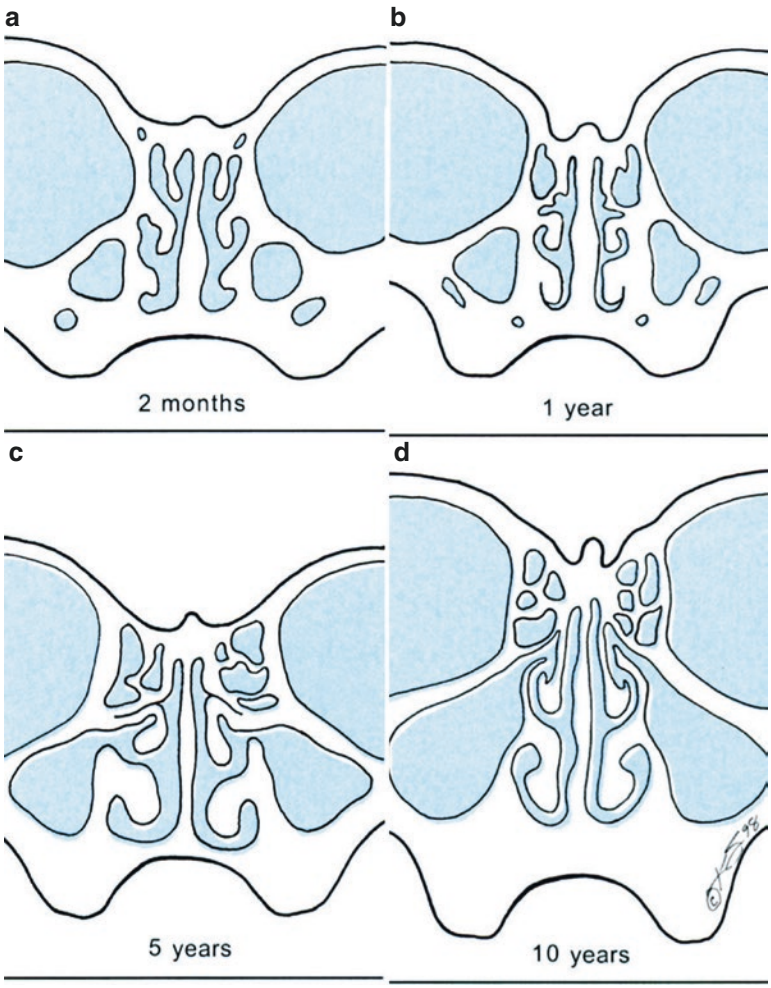


Fig. 26.2 Nasal fossa and sinuses. Coronal sections through nasal fossa and sinuses demonstrating sizes and relationships through various ages: (**a**) 2 months, (**b**) 1 year, (**c**) 5 years, and (**d**) 10 years (After Bernstein [19])

The Lacrimal Drainage Pump

Proper drainage of tears requires not only a patent nasolacrimal system but also a functioning tear pump (Fig. 26.3). A functioning tear pump requires a good working relationship between the lids, medial canthal tendon, and the sac. The process of tear drainage, then, is one that is dependent on the opening and closing of the lids.

With lid closure, the superficial and deep heads of the pretarsal orbicularis muscle contract. These heads of the orbicularis surround the puncta and canaliculi. Contracture, therefore, closes the puncta and compresses and shortens the canaliculi in a horizontal manner. With lid closure, the deep head of the preseptal orbicularis also contracts. This part of the preseptal orbicularis is intimately related to the lacrimal sac fascia, and its contraction pulls on the sac, thereby expanding it. This expansion creates "negative pressure" or a drawing force within the sac, which pulls in tears from the compressed and shortened canaliculi. As the eyelid opens, the orbicularis relaxes. The natural elastic properties of the lacrimal sac cause it to collapse, and this forces the tears within the sac into the duct and down into the nose. As the orbicularis relaxes, the canaliculi return to their normal position and the puncta open. Capillary attraction then draws tears into the puncta and canaliculi, and the cycle repeats itself with the next blinking movement of the eyelids.

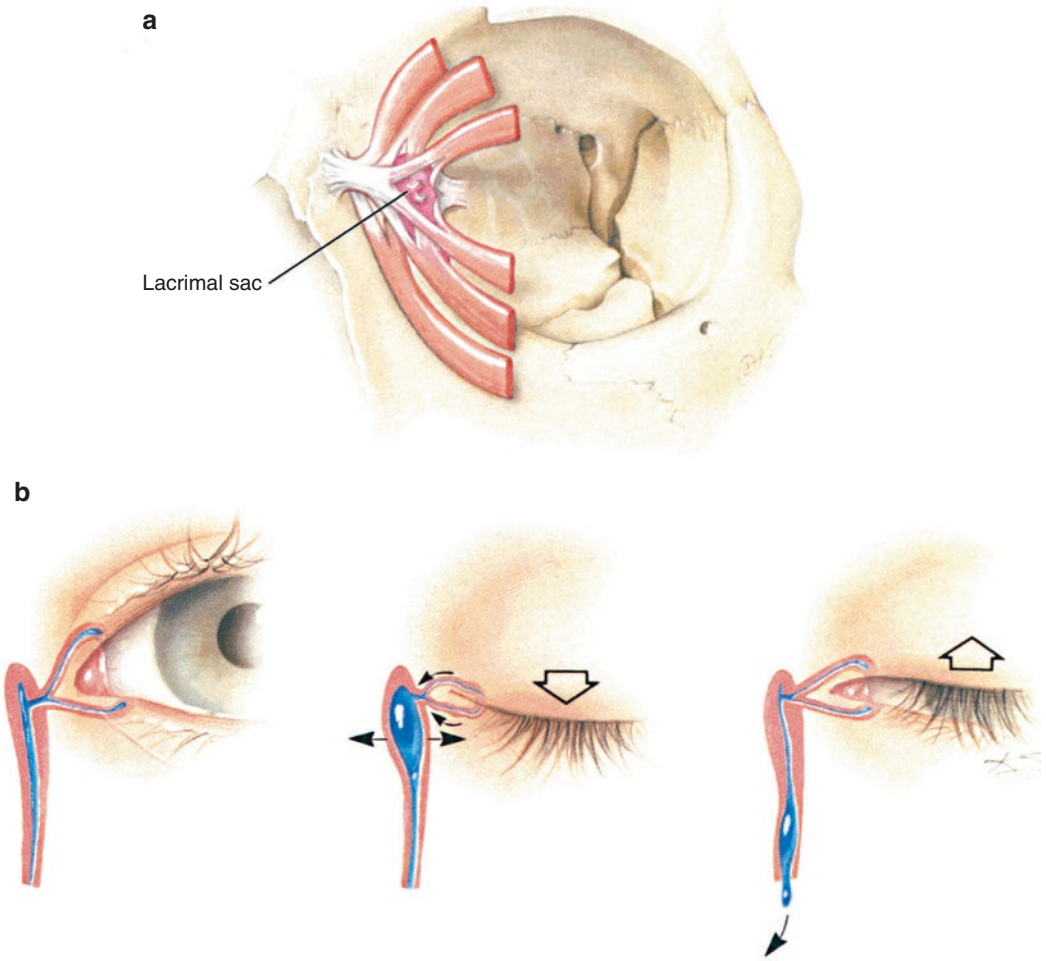


Fig. 26.3 Lacrimal pump. (**a**) Anatomic relationships of medial canthal tendon and lacrimal sac. (**b**) Stages of lacrimal pump cycle with blinking

History

A thorough history is an essential part of any medical evaluation, and this is especially true when evaluating tearing in the pediatric patient. The exam is limited by virtue of the patient's age and level of cooperation. Thus, in-office tests that are practical for adults, such as diagnostic irrigation and nasal evaluation, are not practical for most children. Nonetheless, a detailed history can provide a great deal of diagnostic information.

Obviously, the pediatric patient is not usually able to provide this detailed history, and the physician must turn to the child's caretaker. It is important to obtain the history from the child's primary caretaker—the person who is with the child when the tearing occurs and who can describe the symptoms. If the child is brought to the physician by someone other than the primary caretaker (a member of the extended family or a parent whose daily contact is limited, etc.), then efforts should be made to discuss the child's symptoms with the person in closest contact with the child.

Children with a nasolacrimal system abnormality tend to have frequent symptoms. Tearing is the most associated symptom of a nasolacrimal system abnormality; however mattering of the eyelashes, mucoid or mucopurulent discharge, redness, and changes of the skin around the eyelids (due to stagnant tears and breakdown of superficial skin) are other frequently encountered problems. A child may exhibit one or more of these symptoms, and the physician should try to identify how the child manifests the problem and what is the daily chronology of events.

It is important to ascertain the frequency with which the symptoms are noted. Are the symptoms constant or intermittent? Have they increased or decreased in frequency? Are there any aggravating or relieving factors? For example, does the tearing occur only when the patient is outside in the cold or wind? Does a patient with crusting have epiphora only

when in harsh environmental conditions? Likewise, is tearing noted or exacerbated only when the child has an upper respiratory infection? The answers to such questions can help to tell if the condition is improving on its own (as what happens in most instances of congenital nasolacrimal duct obstruction) and distinguish between patients with a complete obstruction and those with a stenosis that only intermittently obstructs. This also helps raise suspicions that the tearing is caused by allergy and not a true obstruction (as in a child who is fine except when outside in the spring or fall and who complains of itching or frequently rubs his/her eye).

The laterality of the symptoms should also be noted and correlated with any obvious facial abnormalities. Although up to two-thirds of congenitally impatent systems are unilateral [1, 7], a child with a facial or nose deformity and tearing on the same side may well have more than an imperforate duct ostium.

At what age did the symptoms first appear? A child's tear production begins after the first few weeks of life [5, 8]; thus, truly congenitally impatent systems should manifest symptoms early. If the child was asymptomatic at first and developed symptoms after the first few months of life, then the problem is unlikely to be an impatent valve of Hasner. It is also useful to know if the child was full term and, if not, what his/her age adjusted for gestational dates is. With recent advances in neonatology, premature children have higher rates of survival. A child born at 30 weeks gestation who presents to your office with tearing 2 months after birth is really only 38 weeks gestational adjusted age. Since the nasolacrimal system is known to open at or shortly after birth in term infants [8], this child's tearing is not to be unexpected and would allow for a longer trial of conservative management.

The occurrence of a precipitating event should be questioned. A child born with a bluish gray mass under the medial canthus or who developed a red, tense swelling in the canthal region will require different actions and may yield different clinical courses than a 2-month-old with crusting. Likewise, the history of trauma is essential because the possibility of canalicular or bony canal involvement portends different prognoses and therapeutic strategies.

Finally, in every evaluation of pediatric epiphora, it is essential to inquire about problems such as blepharospasm, eye rubbing, avoidance of light, or nystagmoid eye movements. A child with infantile glaucoma may present with similar symptoms, and misdiagnosis may lead to a visually devastating outcome. Therefore, it is important to perform a complete ophthalmologic evaluation on all children who present with tearing.

A thorough history must also include questioning about other medical conditions as well as past medical and surgical events. Children with craniofacial abnormalities such as a cleft palate, Goldenhar or Crouzon syndrome, and other conditions manifesting a hypoplastic maxilla, such as Treacher Collins syndrome, hemifacial microsomia, various facial clefts, and trisomy 21, have been reported to have associated nasolacrimal duct obstruction (Fig. 26.4) [9, 10]. In addition, various skin conditions, such as Stevens-Johnson syndrome, herpes simplex, and varicella, may lead to punctal or canalicular scarring and thus cause tearing (Fig. 26.5) [9]. In addition, any history of nasal or sinus surgery or radiation treatments to the midface area is important. Although rare, there are also reports of nasolacrimal duct obstruction due to altered mucous secretion in cystic fibrosis and from abnormal bone growth from fibrous dysplasia [9]. The contributions of such conditions to tearing in afflicted patients should not be overlooked.

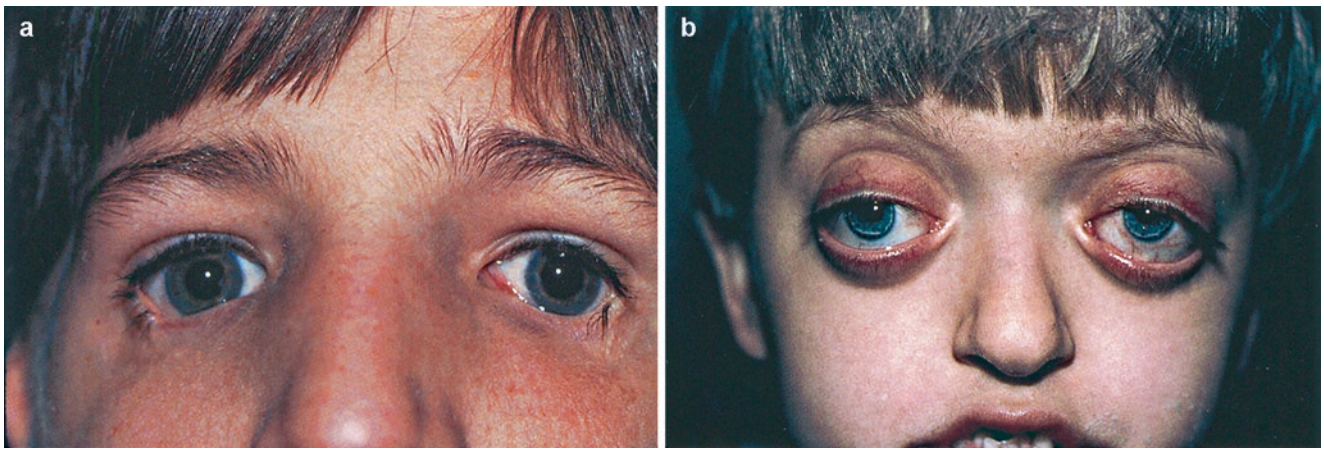


Fig. 26.4 Epiphora. Epiphora related to syndromic lid malpositions causing corneal exposure: (**a**) Treacher Collins syndrome and (**b**) craniofacial dysostosis (Crouzon syndrome with shallow orbits)



Fig. 26.5 Stevens-Johnson syndrome. Lid and lash malposition secondary to Stevens-Johnson syndrome. Punctal scarring can also contribute to overflow if there is still adequate tear production



Fig. 26.6 "Wet eye." "Wet eye" with associated redness and crusting secondary to outflow obstruction

Examination

Examination of the child begins as soon as the physician enters the exam room. Observation of the patient from a distance can yield quite a bit of information and can be done while you are questioning the parent/caretaker about the child's symptoms. During this time the child may be sitting on the parent's lap or playing in the room and may not feel as threatened by your presence as when your full attention is turned toward him/her. With simple observation, one can determine if there is an increased tear meniscus in one of both eyes, if there is crusting of the lashes, or if there is redness/swelling on the lids or medial canthal region (Fig. 26.6). Are the lids red and macerated as would occur from a chronic blepharoconjunctivitis? Is there an obvious lid malposition (i.e., ectropion, entropion, or epiblepharon)? Are the lids obviously lax or malpositioned? Do the corneal diameters appear enlarged? Is the child excessively blinking or bothered by light? Also, it is important to note any obvious facial abnormalities that may be related to nasal bone pathology.

As you observe the child from a distance and take the history from the parent, try to establish a rapport with the child, show an interest in what he/she is playing with, engage the child's attention, and enlist the parents help in turning the child's attention and trust toward you. Realize that no matter how affable you are and how well the exam seems to be going as you sit talking with the parents, once you physically approach and touch the child, he or she may become completely uncooperative. Thus, a fast, directed exam is essential.

Palpation of the lacrimal sac area is probably the most useful physical exam maneuver. As you apply firm pressure over the medial canthus, check for reflux from the puncta. Recovery of material implies a patent upper system with the block being distal to the sac. This test is fairly sensitive, but not very specific, and thus failure to note any reflux does not rule out a lower system abnormality.

If there is any swelling in the medial canthal region, note whether it is above or below the medial canthal tendon. Swellings below the medial canthal tendon generally signify a dacryocystitis. Conversely, swelling above the tendon may be neoplastic in nature or may reflect anterior ethmoidal mucoceles or nasofrontal encephaloceles, thus warranting further investigation [11].

In older, more cooperative children, it may even be possible to perform a slit-lamp biomicroscope exam. Pay close attention to the position and obvious patency of the puncta. Observe the lids, conjunctiva, and cornea for any pathology that may contribute to tearing. If possible, check the ocular surface for fluorescein staining to rule out any surface drying that could produce reflex tearing.

Finally, all examinations should include a comprehensive ocular evaluation. Vision should be checked, ocular motility noted, the pupils evaluated, and the anterior segment examined. A dilated fundus exam with cycloplegic retinoscopy should be performed as well. It is important that other, more serious causes of tearing, such as infantile glaucoma, be ruled out. If there is any question about the possibility of glaucoma, an examination under anesthesia should be considered to check the intraocular pressure, perform gonioscopy, and examine the eyes more closely. In addition, you may be the first to diagnose infantile glaucoma as well as other conditions such as anisometropia, strabismus, and so on that could affect visual development and require treatment.

In-Office Testing

While various in-office tests can be used to evaluate tear outflow in adults, poor patient cooperation in children limits the amount of in-office testing. Saccharin taste tests [12] and Jones dye tests, while useful in adults, have virtually no role in pediatric evaluation. In addition, while diagnostic tear system irrigations are possible in adults, such diagnostic irriga-

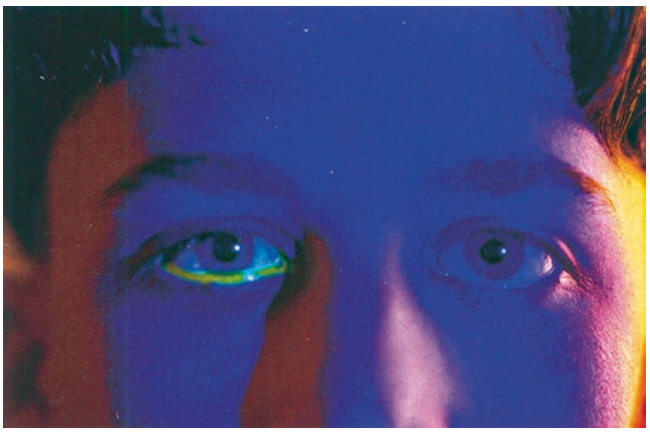


Fig. 26.7 Fluorescein dye disappearance test. Positive fluorescein dye disappearance test with increased tear meniscus on right side indicating outflow obstruction. Left side is normal and dye has disappeared within 5 min of instillation

tions (different from in-office probing, as discussed in Chap. 27) are usually not possible in children. Nonetheless, there is a remarkably useful qualitative test of tear outflow that can be performed on virtually every patient, including the youngest infants and the most uncooperative toddlers, namely, the dye disappearance test (DDT).

The dye disappearance test [13] is performed by wetting a fluorescein strip with topical anesthetic and then instilling the dye into the inferior fornix of each eye. Excess dye is wiped from the lids and cheek. After 5 min the tear meniscus is examined using the cobalt blue light of the slit lamp. In patients with normal tear outflow, the meniscus should be relatively unstained at 5 min. Impeded outflow, however, will be evident as retained fluorescein dye and can be graded in severity from trace to 3+ (Fig. 26.7). In performing this test, it is helpful if an assistant and not the examining physician places the drop in the child's eye. If the physician instills the drop, the child's trust of the doctor may be destroyed, and when the doctor returns to evaluate the test, the child may become uncooperative. In addition, the cobalt blue light should be directed at the child from a distance of a few feet. This reduces the perceived threat and can even be turned into a game for the child by prompting him to "look at the light." A negative dye disappearance test is a good indicator of a patent nasolacrimal system. A positive test, however, only indicates poor outflow and does not specifically localize the problem.

Role of Imaging in Congenital Nasolacrimal Duct Obstruction

Both computed topography (CT) and magnetic resonance imaging (MRI) can have a role in the diagnosis of nasolacrimal duct obstruction. Specifically, in cases where swelling exists above the level of the medial canthal tendon, imaging is necessary to evaluate for possible neoplasms, encephaloceles, or ethmoidal mucoceles. Although pediatric hospitals utilize pediatric CT scanners with low-dose ionizing radiation, the exposure to radiation continues to be a widely accepted concern. Recent studies demonstrate significant associations between the estimated radiation doses provided by CT scans to bone marrow and brain and subsequent incidence of leukemia and brain tumors. Cumulative ionizing radiation doses from two to three head CT scans could almost triple the risk of brain tumors, and five to ten head CT scans could triple the risk of leukemia. Therefore the use of a CT scan in the pediatric population requires justification, and other diagnostic means which do not involve ionizing radiation should be considered if appropriate [15].

Magnetic resonance imaging, however, does not emit ionizing radiation and is an excellent diagnostic tool in certain circumstances. In cases of suspected neoplasm, encephalocele, dacryocystocele (refractory to conservative measures), and mucocele, an MRI can give useful information for both diagnosis and surgical planning. The downside of MRI in the pediatric population is the need for a general anesthetic as well as less bony visualization as compared to CT imaging.

Ancillary Tests of Nasolacrimal System Outflow

Dacryocystography (DCG)

DCG is a radiologic test that is helpful in assessing the site and degree of nasolacrimal obstruction. It is quite useful in detailing fistulae, mucoceles, neoplasms, and stones in the lacrimal outflow system. DCG provides a qualitative but not quantitative measure of tear outflow.

Prior to the test, baseline anterior-posterior and lateral films of the orbit are taken. A nonviscous water- or oil-based radiopaque dye is then injected into each lower canaliculus via a lacrimal cannula. Serial anterior-posterior and oblique films are then taken at 15 and 30 min postinjection. Increased resolution of the system has been made possible by advances in radiologic technology: macrodacryocystography (MDCG) and digital subtraction MDCG [14]. These techniques allow for larger image size and less bone interference, making visualization of the entire outflow tract possible (Fig. 26.8).

This test has many limitations, particularly in the pediatric population. In children, it requires a general anesthetic. Since the child is asleep, supine, and not blinking, the test under these conditions is nonphysiologic. In addition, the dye is injected into the canaliculus with a force that may be greater than the patient's own lacrimal pump. Thus, functional blocks may be falsely opened by the dye's injection. DCG also exposes the patient to a fair amount of radiation.

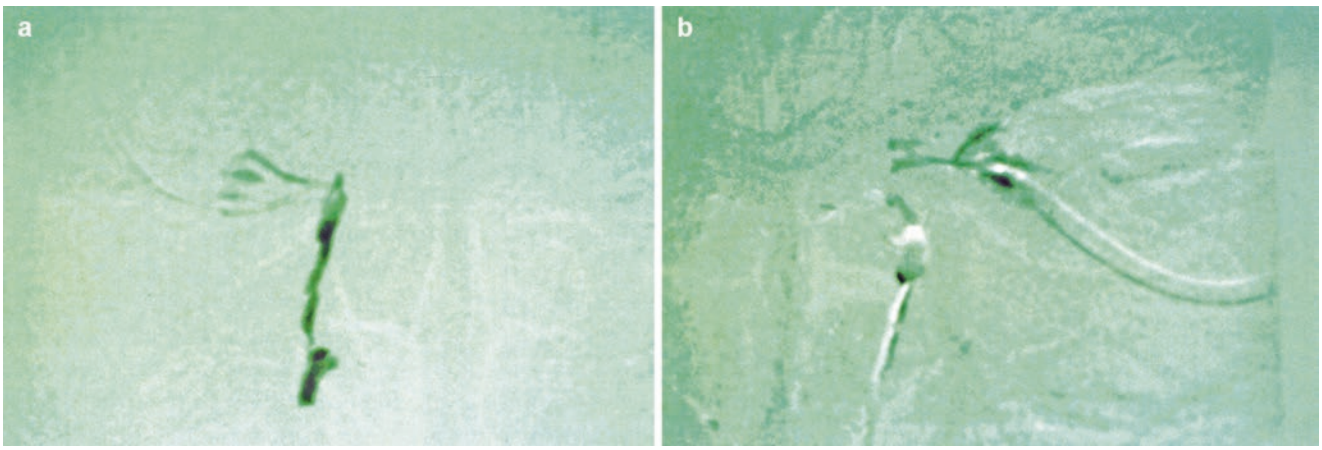


Fig. 26.8 Dacryocystogram. (**a**) Normal dacryocystogram and (**b**) abnormal dacryocystogram with stone in sac

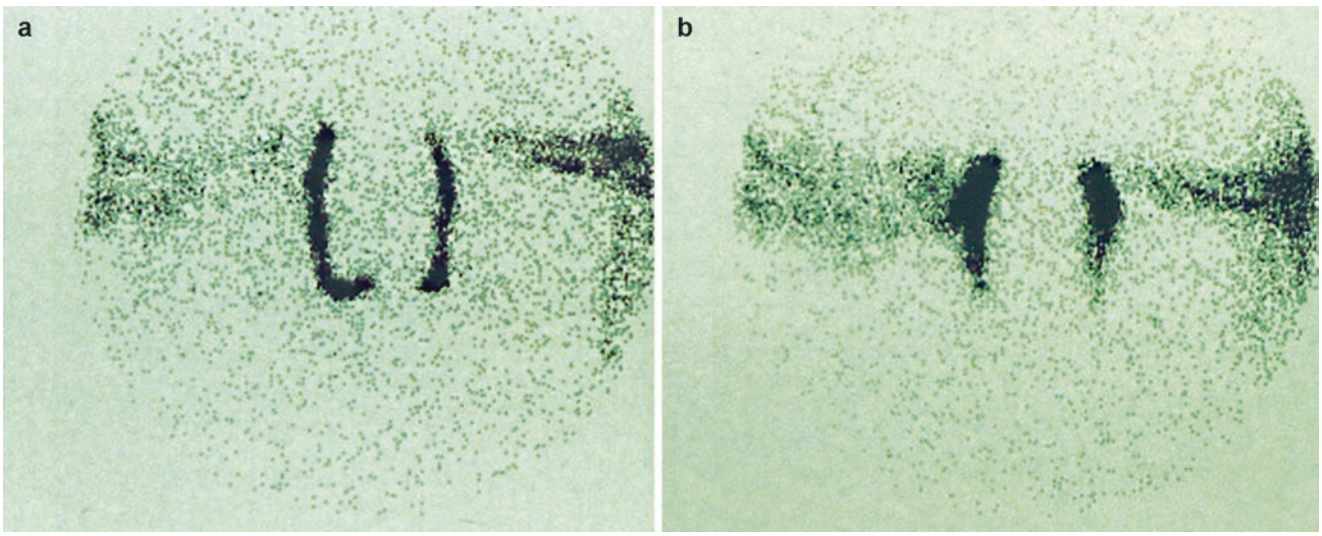


Fig. 26.9 Lacrimal scintigram. (**a**) Normal lacrimal scintigram and (**b**) abnormal lacrimal scintigram

The dose of radiation to the lens of the eye during DCG is estimated to be 3000 mrad as compared to 370 mrad from an anterior-posterior skull x-ray [16]. Many of the conditions most readily imaged by DCG (e.g., neoplasms and stones) rarely affect children. For these reasons DCG has a limited role in the evaluation of pediatric tearing problems.

Dacryoscintigraphy (Lacrimal Scintigraphy)

Dacryoscintigraphy (DSG) is another imaging test that gives a qualitative assessment of lacrimal outflow. Developed by Rossomondo et al. in 1972 [17], it has been useful in the evaluation of pediatric tearing problems [16]. It can often be done with the patient awake, obviating the need for anesthesia. In addition, it exposes the patient to much less radiation than either DCG or plain skull x-ray. Estimates are that patients with normal tear outflow will have their lens exposed to 4–14 mrad of radiation during DSG, while patients with a complete obstruction will be exposed to 40 mrad [16].

Before performing the test, patients are premedicated with oral potassium perchlorate (6 mg/kg) to block thyroidal uptake of the radioactive tracer. A gamma camera that has been fitted with a pinhole collimator and a 1-mm insert is used for image acquisition. Patients are positioned in front of the camera such that both the lateral canthi and the tip of the nose are within the camera's view. Ten microliters containing 100 μCi of technetium-99 m pertechnetate is then instilled into each eye. Sequential analogue images are then taken four times per minute for 20 min. Flow into the sac is generally seen within 1 min and flow into the duct within 2–3 min (Fig. 26.9) [17, 18].

To help differentiate delayed clearance because of an anatomic block due to a functional problem, the patient can be asked to perform different maneuvers during the DSG. Forceful blinking during the test can increase the

effectiveness of the lacrimal pump and help to overcome any functional abnormality. Likewise, forceful sniffing during the test creates a low-pressure gradient within the nose and can help to overcome an anatomic block [16].

Even children as young as 2 years can be studied without anesthesia, usually by having their parents hold them into the camera [16]. Infants, on the other hand, often must be sedated for a DSG. Sedation, however, alters blinking and thus affects transit time. Manual blinking of the lids has been tried in such situations [16], but this can affect the validity of the test. Nonetheless, in selected children the DSG can provide useful information, particularly when the history and physical exam suggest an atypical situation.

Summary

The evaluation of nasolacrimal obstruction in pediatric patients requires good history taking and physical exam skills. The history should be thorough and should be taken from the person who has the most contact with the child and who actually sees the symptoms occur. The age of onset, laterality, frequency, past treatments, and the specific nature of symptoms are all important historical facts. In addition, the patient's past medical and surgical history, family history, and any other physical anomalies should be considered. The exam should begin with simple observation of the patient, most easily done while the physician is taking the history. Any epiphora, crusting, redness, swelling, and obvious lid, facial, or nose abnormalities should be noted. A dye disappearance test is an excellent qualitative test of tear outflow and is easily performed in even the smallest of children. A complete ophthalmologic exam is also necessary to rule out other causes of tearing, the most significant being infantile glaucoma, as well as to assure an otherwise normal ocular state. Imaging modalities such as CT scans and MRIs may be indicated in certain cases, although CT scans necessitate justification due to the exposure of ionizing radiation. Ancillary tests such as dacryocystography and dacryoscintigraphy are useful for selected patients whose history and exam findings are atypical. In-office diagnostic irrigation, taste tests, and Jones dye tests are not practical in the pediatric population.

References

1. Nelson L, Calhoun J, Menduke H. Medical management of congenital nasolacrimal duct obstruction. Ophthalmology. 1985;92:1187.
2. Katowitz J, Kropp T. Congenital abnormalities of the lacrimal drainage system. In: Hornblass A, editor. Oculoplastic, orbital and reconstructive surgery. Baltimore: William 8c Wilkins; 1990.
3. Divine R, Anderson R, Bumsted R. Bilateral congenital lacrimal sac mucoceles with nasal extension and drainage. Arch Ophthalmol. 1983;101:246.
4. Weinstein G, Biglan A, Patterson J. Congenital lacrimal sac mucoceles. Am J Ophthalmol. 1982;94:106.
5. Guerry D, Kendig E. Congenital impatency of the nasolacrimal duct. Arch Ophthalmol. 1948;193:39.
6. Nowinski T, Flanagan J, Mauriello J. Pediatric dacryocystorhinostomy. Arch Ophthalmol. 1985;103:1226.
7. Veirs E. Disorders of the nasolacrimal apparatus in infants and children. J Pediatr Ophthalmol. 1966;3:32.
8. Cassidy T. Developmental anatomy of the nasolacrimal duct. Arch Ophthalmol. 1952;47:141.
9. Welham R, Hughes S. Lacrimal surgery in children. Am J Ophthalmol. 1985;99:27.
10. Caputo A, Smith N, Cinotti A, Angiuoli D. Definitive treatment of congenital lacrimal sac fistula. Arch Ophthalmol. 1978;96:1443.
11. Katowitz J, Low J. Lacrimal drainage surgery. In: Tasman W, Jaeger E, editors. Duane's clinical ophthalmology. Philadelphia: Lippincott; 1993.
12. Hornblass A. A simple taste test for lacrimal obstruction. Arch Ophthalmol. 1973;90:435.
13. MacEwen C, Young J. The fluorosceine dye disappearance test (FDT): an evaluation of its use in infants. J Pediatr Ophthalmol Strabismus. 1991;28:302.
14. Galloway J, Kavic T, Raflo G. Digital subtraction MDCG: a new method of lacrimal imaging. Ophthalmology. 1984;91:956.
15. Pearce MS, Salotti JA, Little MP, McHugh K, Lee C, Kim KP, et al. Radiation exposure from CT scans in children and subsequent risk of leukemia and brain tumors: a retrospective cohort study. Lancet. 2012;380:499–505.
16. Heyman S, Katowitz J, Smoger B. Dacryoscintigraphy in children. Ophthalmic Surg. 1985;16:703.
17. Rossomondo R, Carlton W, Trueblood J. A new method of evaluating lacrimal drainage. Arch Ophthalmol. 1972;88:523.
18. Chavis R, Welham R, Maisey M. Quantitative lacrimal scintillography. Arch Ophthalmol. 1978;96:2066.
19. Bernstein L. Pediatric sinus problems. Otolaryngol Clin North Am. 1971;4:128.

Initial Management of Pediatric Lower System Problems: Probing and Silicone Stents and Balloons

27

William R. Katowitz, Maryam Nazemzadeh, and James A. Katowitz

Congenital Abnormalities

Congenital nasolacrimal duct obstruction (CNLDO) is one of the most common eye abnormalities and occurs in roughly 20% of infants [1, 2]. A range of symptoms from an increased tear lake, tearing, discharge, and even a medial canthal mass are present due to either a persistent membrane at the valve of Hasner or some other structural abnormality to the tear system that disrupts proper tear outflow. The very word obstruction is misleading. While most congenital forms are due to a distal membrane, some forms of lacrimal duct stenosis may also be present, thus impeding tear outflow [3].

Tearing and or discharge in the first 12 months of life should be suspicious for congenital nasolacrimal duct obstruction. This warrants a full ophthalmologic work-up including a dilation and refraction. Any newborn with a medial eyelid mass just below the medial canthal tendon should raise a suspicion for an amniotic fluid-filled lacrimal sac (amniotocele) or mucus-filled lacrimal sac (lacrimal mucocele). This is often associated with an intranasal cyst and can be the cause of a nasal airway obstruction [4]. The presence of a small skin fistula in the lower medial eyelid is also a cause of tearing and discharge symptoms. This is a nasolacrimal fistula (anlage duct) that most typically connects to the common canaliculus [5]. Finally, structural abnormalities due to craniofacial and clefting syndromes can cause lower tear system outflow obstructions that will require surgical correction. This chapter addresses the initial approach to lower tear system abnormalities in children.

Dacryostenosis

Dacryostenosis may be defined as a partial or complete block of the nasolacrimal duct. The most common cause of this problem is the failure of canalization of the duct at its mucosal entrance beneath the inferior meatus of the nose at the location of the valve of Hasner. It was Cassady who sectioned 15 full-term still born babies and found that 73.33% of his subjects had this membrane [3]. Complete osseous obstruction also can occur, especially in association with anomalous passages, but relative narrowing causing decreased tear outflow is also a common occurrence [5, 6]. Abnormalities within the nasal passages, such as deviation of the nasal septum or impaction of the inferior turbinate on the membranous portion of the duct, may also contribute to the obstruction [7, 8].

Dacryostenosis in the first year of life should be managed conservatively whenever possible [9, 10]. This is because the spontaneous rate of resolution is very high in children under the age of 12 months with varied reported rates from 80% to 94.7% [7, 11–13]. A recent randomized control study by the Pediatric Eye Disease Investigator Group (PEDIG) found in children with symptoms enrolled between the ages of 6 and 10 months the rate of resolutions 6 months after enrollment was 66% (77/117 eyes) [14]. The traditional approach has been to combine massage of the nasolacrimal sac and duct (Crigler massage) with topical instillation of an antibiotic [7, 11]. Many physicians prefer the drop form because there is some thought that ointment bases dissolve more slowly and may not enter the system as effectively or may even contribute to the obstruction. However, the ointment form is particularly useful in conjunction with massage. Parents must be

W.R. Katowitz, MD • J.A. Katowitz, MD, FACS
The Children's Hospital of Philadelphia and The Edwin and Fannie Gray Hall Center for Human Appearance, University of Pennsylvania, Philadelphia, PA, USA
e-mail: katowitzw@email.chop.edu; katowitz@email.chop.edu

M. Nazemzadeh (✉)
Oculofacial Plastic and Reconstructive Surgery, Rostami Oculofacial Plastic Consultants, Sanctuary Cosmetic Center, Reston, VA, USA
e-mail: marnaz17@gmail.com

© Springer International Publishing AG 2018

J.A. Katowitz, W.R. Katowitz (eds.), *Pediatric Oculoplastic Surgery*, https://doi.org/10.1007/978-3-319-60814-3_27

carefully instructed as to how to perform lacrimal sac massage properly. It is helpful to lubricate one forefinger with antibiotic ointment and place it over the medial canthal area along the inferior lacrimal crest. The responsible person should be shown how to slide the fingertip in an inferior direction, placing moderate pressure over the sac and duct, using the antibiotic ointment as a lubricant to minimize skin irritation (Fig. 27.1). This motion can be demonstrated on the person's own face as well as on the child's affected side or sides. The demonstration on the child is important since parents often underestimate the stability of their child's nasal bones and therefore do not massage firmly enough to be effective. There has been controversy as to whether massage really does affect the tear column. However, Foster and Katowitz have previously demonstrated that the Crigler method of massage actually does in fact force fluid down the obstructed nasolacrimal ducts (Fig. 27.2) [15]. If crusting and discharge are present, the antibiotic ointment can be applied several times daily to the conjunctival cul-de-sac. The authors usually prefer either erythromycin or a polymyxin B-bacitracin combination and have not seen any complications of long-term use (6–9 months) using these topical antibiotics as described [16, 17]. It should be noted that patients may develop an allergy to any of these topical antibiotics. Polymyxin and especially neomycin are more likely to cause allergies most commonly observed with a child who is rubbing his/her eyes. The skin will usually appear red and indurated and small pustules may even form. In such instances the medication should be stopped immediately.

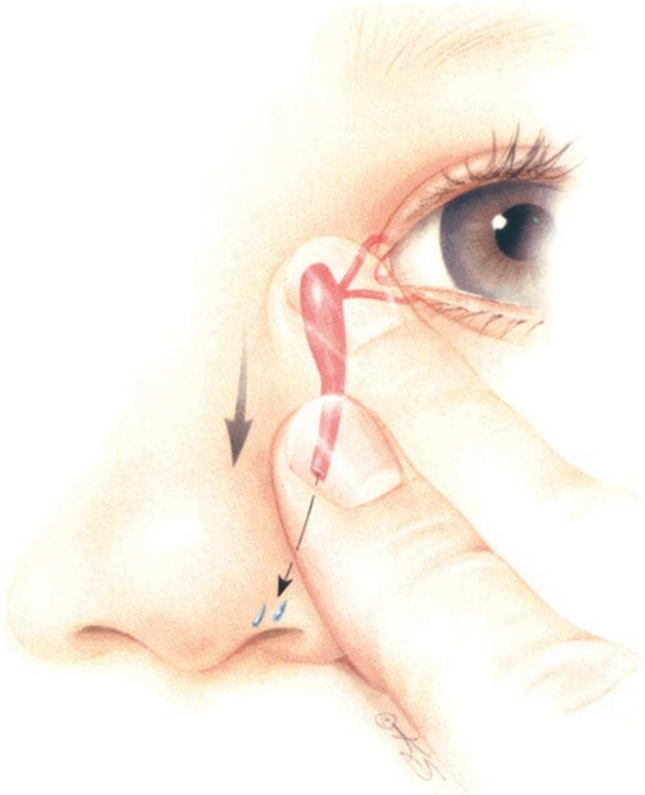


Fig. 27.1 Crigler method of massage

Conservative or Surgical Management for Dacryostenosis: Why and When

There has been long-standing controversy regarding the correct timing for initial probing of a child with nasolacrimal duct obstruction [18–21]. The authors recommend that conservative measures be instituted and if this proves unsuccessful then initial probing be done when the patient is approximately 1 year of age. This recommendation is based on a large study by Katowitz and Welsh [21] (Fig. 27.3). In this study of 572 eyes, the success rate with initial probing was 96.4% in patients younger than 13 months. In patients older than 13 months, however, the mean success rate was 54.7%. When broken down into smaller age categories, a stepwise progression in success rates was observed from 76.4% for patients between 13 and 18 months to 33.4% for patients older than

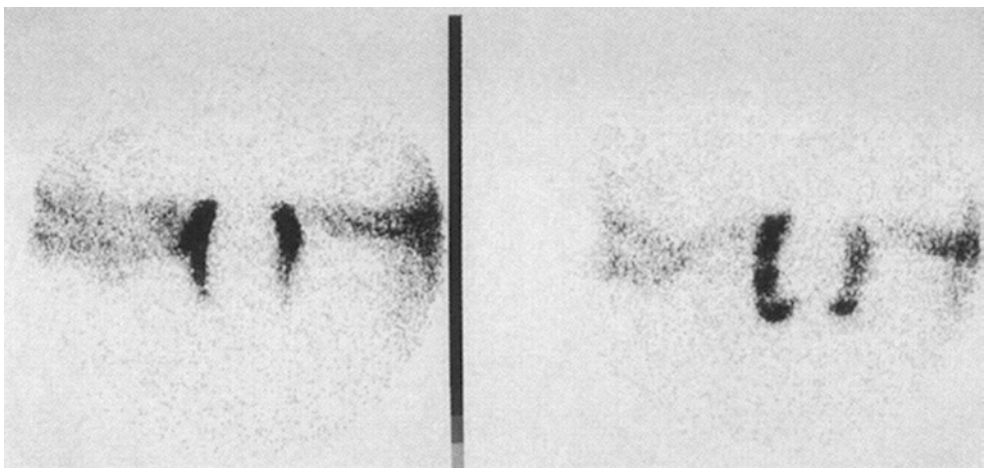


Fig. 27.2 Obstruction of nasolacrimal ducts. Lacrimal scintigraphy demonstrating obstruction of nasolacrimal ducts. Movement of tear columns following digital massage by the Crigler method

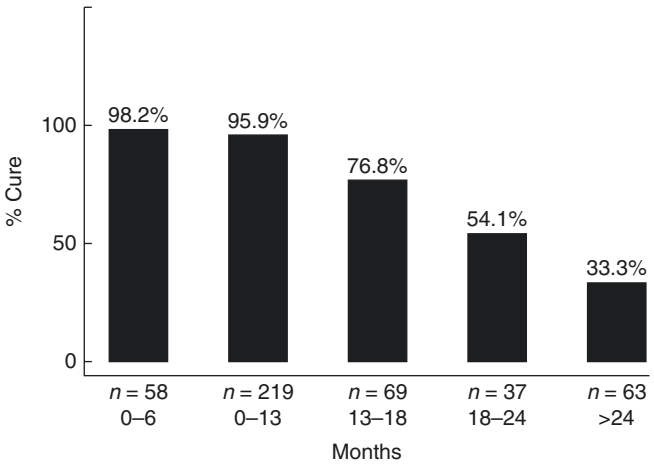


Fig. 27.3 Percentage of cure with initial probing (From: Welsh and Katowitz [56]. Reprinted with permission from Wolters Kluwer Health)

24 months. In addition, the number and complexity of subsequent procedures appeared to increase along with the age at which the initial probing was performed.

In contrast to the declining success rate with age seen in our population group, Robb [22] reported a 92% success rate, in 303 eyes, after probing for congenital nasolacrimal duct obstruction in patients over 1 year of age. There was, in fact, a 92.6% success rate (25 of 29 patients) reported in this series in children probed over 36 months of age. Kushner [23], in contrast, reported an overall success rate of 70% in patients undergoing probing and irrigation between the ages of 18 and 48 months. He categorized obstructions as *simple* (involving the valve of Hasner) or *complicated* (involving a narrow duct or mechanical valve-like obstruction in the canaliculus). In children with a simple membrane at the valve of Hasner, 100% had resolution of epiphora following probing and irrigation, regardless of age. In the complicated group, however, the results were only 36% success following probing and irrigation.

Honavar reported a success rate with probing of 73% with one attempt and 80% with repeat probing in 60 eyes of children older than 24 months [24]. Furthermore, he identified factors predictive of probing failure to include age greater than 36 months, bilateral involvement, failed conservative therapy, failed earlier probing, dilated lacrimal sac, and a tight bony canal. In Honavar's series, outcomes could further be divided into those children with membranous obstruction faring better with 91% success with probing, as compared to those with tight bony obstruction having only 42% success. Similar to the age-dependent findings of Katowitz and Welsh, Honavar noted a stepwise progression in success rates, with 97% success in the age group of 24–36 months, 75% in the age group of 37–48 months, and 42.9% in children beyond 48 months [24]. It would appear that the lower success rates in older children observed in our study and those of Kushner and Honavar may be explained by the suggestion of Paul and Shepard [25] that this may well represent a self-selection process where spontaneous resolution does not occur because a more complex type of obstruction has been present since birth [23].

It is important to consider the actual gestational age of the child. An infant who was born prematurely should be given a period of postnatal time to respond to conservative therapy that is equivalent to that for a full-term infant. Probing should always be the first step regardless of age. Additional steps at the time of the initial procedure should be undertaken only if the clinical situation warrants further intervention.

A major point of controversy regarding congenital dacryostenosis is whether to probe infants in the office or under a general anesthetic in a hospital setting [7, 11, 17, 21, 25, 26]. This controversy primarily applies to initial probing procedures. All children who have had failed in-office probings should have the second procedure repeated under general anesthesia. In deciding whether a general anesthetic should be used for the initial or routine type of probing, the most obvious concern is the associated risk with general anesthesia, particularly during the first 6 months of life. Obviously, the pediatric experience of the anesthesiologist and the hospital operating room staff is a critical factor in opting for a general anesthetic. Parents should be full participants in any decision regarding the choice of office surgery or the use of a general anesthetic. In patients with straightforward nasolacrimal duct obstruction, the chances for spontaneous resolution are excellent. In a child with apparent routine dacryostenosis, we recommend conservative measures until the child is 12 months of age, at which point a general anesthetic should be used for probing to evaluate and possibly treat the nasolacrimal duct obstruction. This permits a more thorough diagnostic evaluation as well as greater therapeutic options.

Irrigation of the infant nasolacrimal system in the office can be difficult and is not recommended, but probing of the duct alone can be accomplished more easily [5, 7, 9, 17]. Some surgeons prefer the lower canaliculus for office probing, but it is usually best to avoid the risks of damaging this channel. Therefore, if possible, we recommend initial probing of the upper canaliculus. The distinction between therapeutic and diagnostic probing is once again important. Office probing in an infant is primarily therapeutic, particularly for dacryocystitis or for an amniotocele in a newborn. Since there is less control over the child in the office, there is less time to safely feel for veils or strictures at various points along the lacrimal drainage system that may influence therapeutic measures. In addition, additional steps that might be needed for more complicated forms of obstruction, such as turbinate infracture,

balloon dilation, or silicone intubation, cannot be done in an office probing.

An infant's nasolacrimal system must be probed very gently because the punctum is so delicate. Wide dilators may tear the punctum. The Jones punctal dilator (OP7002, V. Mueller, Chicago, IL) or a dull safety pin that will not dilate past a #1 Bowman probe size should be used [17]. Because Bowman probe sizes vary depending on the manufacturer, the physician should be familiar with the actual width of the probe in use [18]. During an in-office probing, the child need not be completely mummified. The head can be held firmly, and the surgeon can sit at the child's head or side, performing the probing from this position. Jones and Wobig [5, 27, 28] prefer to use a #0 or smaller probe in an infant and to leave the probe in place for 5 min after confirming its presence in the inferior meatus of the nose. They believe that this practice allows the mucosa to retract around the probe, which facilitates a successful result.

We consider office probing in patients older than 3–4 months unnecessarily traumatic to the child, the parents, and the surgeon. As long as there is availability for excellent pediatric anesthesia, we prefer a general anesthetic after this age. General anesthesia allows the surgeon to perform a complete diagnostic and therapeutic probing as well as an examination of the inferior nose. It also provides the opportunity for retinoscopy and a complete examination of the fundus if necessary due to difficulties with the child in the outpatient examination. A number of respected surgeons, however, prefer office probing in patients as old as 8 months [18]. Since 90% of these obstructions will clear by 1 year of age, our preference is to follow conservative management until this time and then to do a diagnostic and therapeutic probing under general anesthesia [10]. This also permits infracture of the inferior turbinate and/or silicone intubation to be done at the time of initial probing as indicated [5, 7, 8, 21].

Management of Dacryoceles (Mucoceles/Amniotoceles)

While it usually is not necessary to perform probing before 1 year of age, one exception is a congenital dacryocele, often described as a mucocele or amniotocele [29, 30]. These terms refer to a sterile accumulation of mucus or possibly amniotic fluid, which may become trapped in the lacrimal sac. It is presumed that this can occur due to a combined effect of nasolacrimal duct obstruction at the valve of Hasner and a one-way valve effect at the junction of the common canaliculus (at the valve of Rosenmuller) and the lacrimal sac. The sac becomes dilated and is seen as a bluish mass inferior to the medial canthal tendon (Fig. 27.4). This swelling is frequently misdiagnosed as a hemangioma, because of its similar discoloration. For a congenital dacryocele without signs of infection, the initial approach is to massage the lacrimal sac in an attempt to open the obstruction. Massaging too vigorously, however, can rupture the dilated lacrimal sac and produce a cellulitis. This will require systemic antibiotic therapy and management similar to that required for an acute dacryocystitis. If gentle massage is not effective in opening the obstruction, however, then gentle office probing, as described above, may be indicated. Schnall and Christian [31] also advocate an initial trial of medical management, consisting of massage and warm compresses with topical antibiotic drops for noninfected dacryoceles and intravenous antibiotics for infected cases. If the dacryocele does not resolve within a 1- to 2-week period, they recommend probing the nasolacrimal system. In their study, 76% (16 of 21 dacryoceles) resolved with medical management.

All physicians should be aware of the high association of intranasal cysts with dacryoceles, amniotoceles, and frank dacryocystitis. These can also develop at the meatal end of the nasolacrimal duct (Fig. 27.5) in association with dacryoceles. These cysts may be more common than previously recognized before the advent of nasal endoscopy. Payesse et al. reported

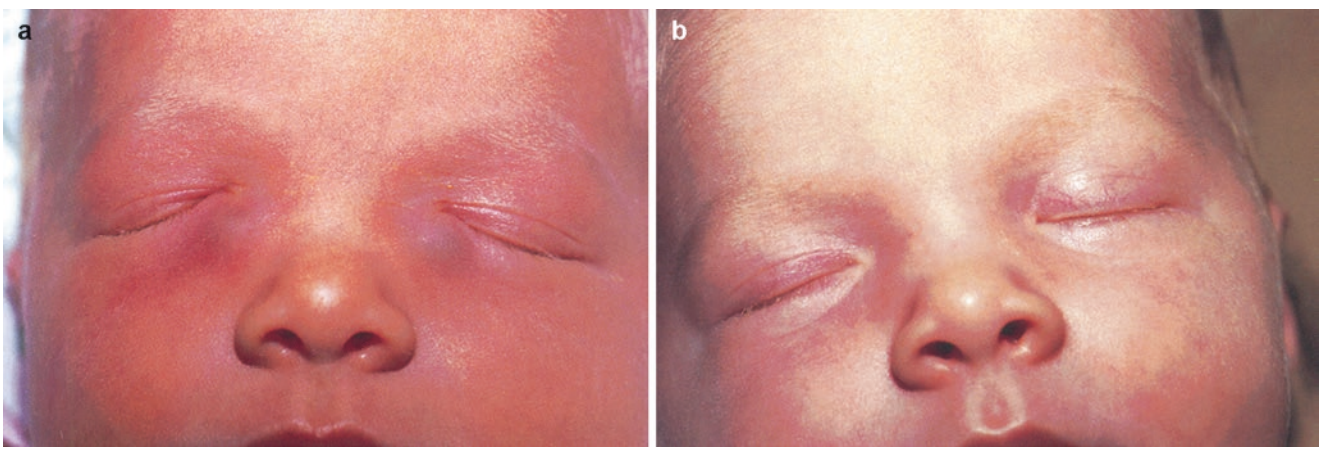


Fig. 27.4 Dacryocele. (**a**) Dacryocele (amniotocele) seen as bluish mass below the medial canthal tendon on both sides. (**b**) The same patient 2 weeks after bilateral office probing

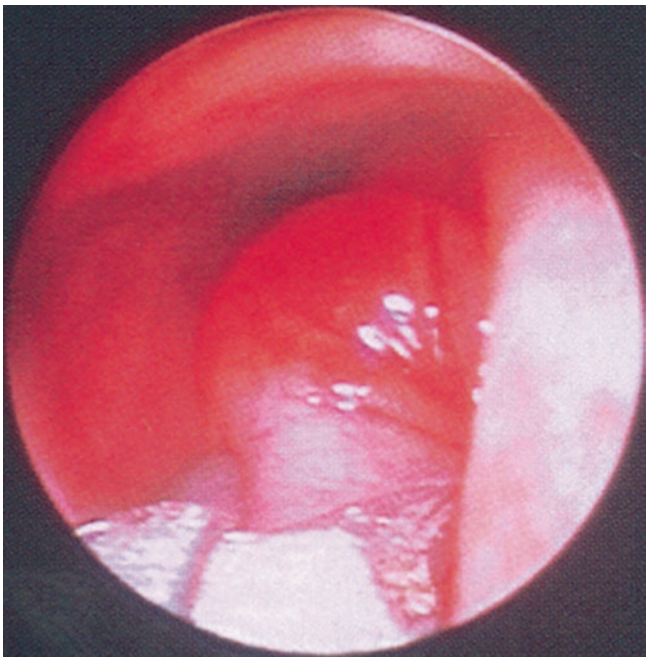


Fig. 27.5 Nasolacrimal duct cyst viewed through endoscope

concurrent intranasal mucoceles in 23 of 30 dacryoceles (77%). In addition, 60% developed dacryocystitis or preseptal cellulitis [32]. Levin et al. found an intranasal cyst in 23/24 patients with either dacryoceles or dacryocystitis [4]. For this reason bilateral dacryoceles should never be probed in the office because the risk of nasal airway obstruction mandates a more controlled procedure under general anesthesia [13]. For unilateral office probings that fail, one should presume that an intranasal cyst is present, and the patient should be scheduled in a timely manner for surgical ablation, if necessary. Some patients with a unilateral cyst may actually have an asymptomatic cyst on the contralateral system. We have found this in a few of our congenital dacryocele patients who were treated in the operating room. Figure 27.6 depicts a 2-month-old with a right-sided dacryocele who was found to have bilateral intranasal cysts below the inferior turbinates. The technique we prefer for removing these cysts involves the introduction of a microdebrider device (2.9-mm trip-cut/shaver, Medtronic) with an inferior turbinate infracture, if necessary. Simple marsupialization of these cysts may not adequately debride them, and recurrence can more easily occur unless a significant portion of the cyst wall is removed.

Neonatal Dacryocystitis

Acute dacryocystitis of the newborn, in our experience, represents another indication for office or bedside probing of the nasolacrimal duct in patients younger than 12 months (Fig. 27.7) [5, 7, 33]. This is a medical emergency, however, in an infant and requires hospitalization with IV antibiotic therapy and careful monitoring to avoid rapid progression into orbital cellulitis or systemic bacteremia. In acute dacryocystitis, there are other signs of inflammation, and there may also be associated fever and an elevated white blood cell count. During the period of acute inflammation, the lacrimal sac can be tapped with a tuberculin needle and syringe (Fig. 27.8) [33]. This will create a tiny opening that will not fistulize, as might occur with a scalpel incision. It also allows smears to be taken immediately for early diagnosis, as well as material for culture and sensitivity so that specific systemic antibiotics can eventually be utilized. Decompression of the sac is quickly achieved and this gives immediate relief of discomfort. Furthermore, with the needle in position, the syringe can be changed to instill 0.5 mL of a bactericidal antibiotic solution. A broad-spectrum antibiotic is also given intravenously until a more specific antibiotic can be identified by the cultures and sensitivities obtained from the tap. After several days, when the acute inflammation subsides, bedside or office probing is valuable in most cases because it usually opens the duct and allows tear drainage so that repeat dacryocystitis does not occur. Probing must be done very gently, using a very small probing instrument, such as a No. 000 or 0000 Bowman probe (or 0.5-mm- or 0.6-mm-diameter FCI probe). It is usually dangerous to probe the nasolacrimal duct in the setting of acute inflammation because false passages may be created. However, if dacryocystitis recurs after such probing, an evaluation under general anesthesia will be required, and a dacryocystorhinostomy (DCR) may even be necessary to avoid repeated infection [34]. Once again the risk of an associated intranasal cyst is high, thus a low suspicion for an endonasal examination and treatment is paramount.

More recently, we have addressed dacryocystitis surgically with an endonasal endoscopic approach. If there is in fact an intranasal cyst, this is debrided. If, however, there is a bony obstruction under the inferior turbinate, an endonasal endoscopic dacryocystorhinostomy is performed. This technique is addressed in Chap. 28.

Probing and Irrigation Under General Anesthesia

When probing under general anesthesia is planned, a laryngeal masked airway (LMA) can be used as an alternative to intubation because it allows free access to the nose for retrieval of dye and irrigation of fluids (Figs. 27.9 and 27.10) (see Chap. 5) [35]. It also maintains the airway, even if it becomes necessary to perform silicone intubation of the nasolacrimal system. An intravenous drip should be established before the surgeon performs the actual probing and irrigation. The risk of laryngospasm is always a concern, especially when only using a face mask. We prefer the LMA when there is an experienced pediatric anesthesia team monitoring the patient. Laryngospasm is a life-threatening airway emergency that can be avoided by taking care to inject a

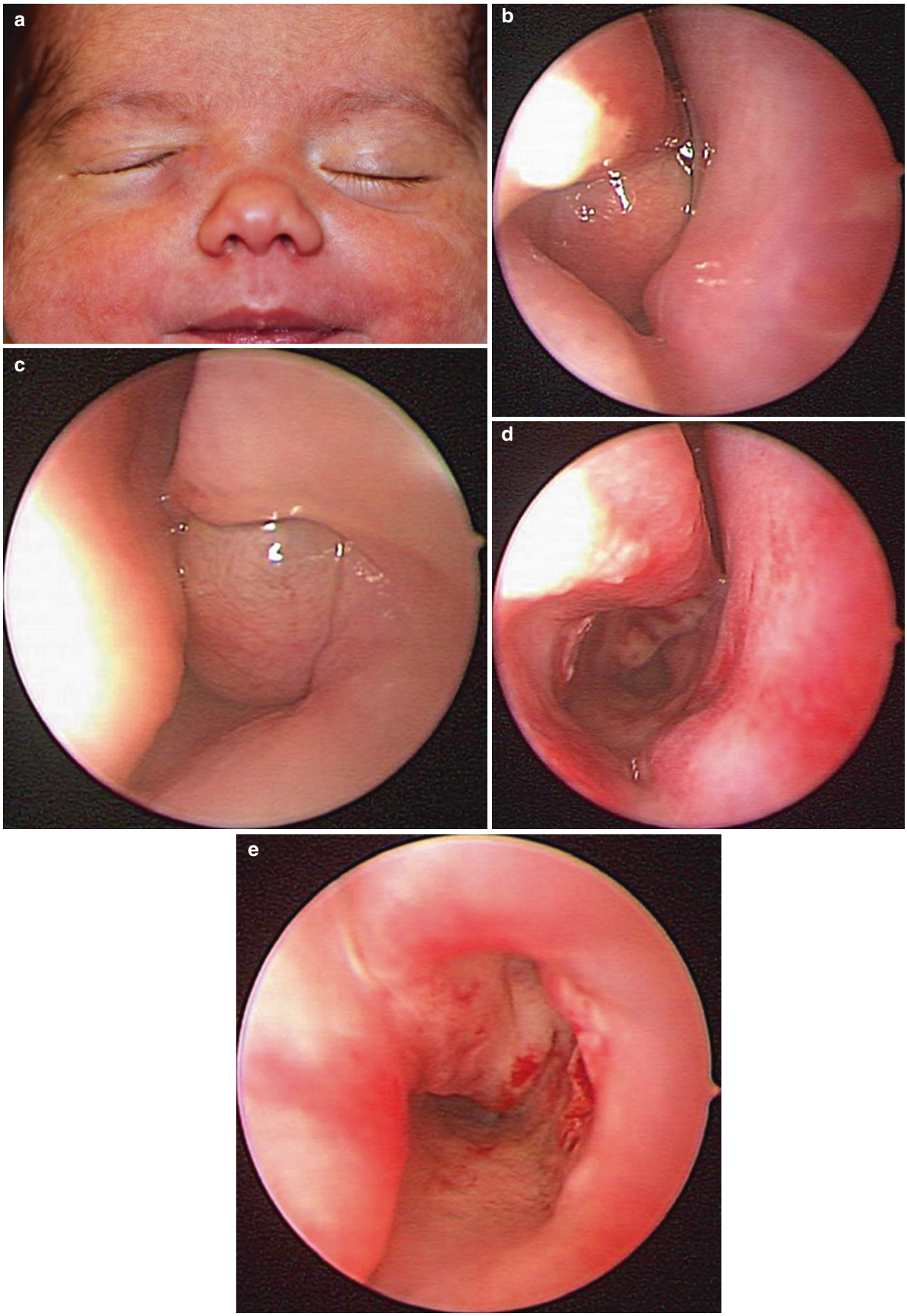


Fig. 27.6 Intranasal Cysts. (**a**) A 2-month-old child with a right-sided dacryocele. (**b**) and (**c**) Right and left intranasal cysts below the inferior turbinates. (**d**) and (**e**) Cyst walls removed with a microdebrider

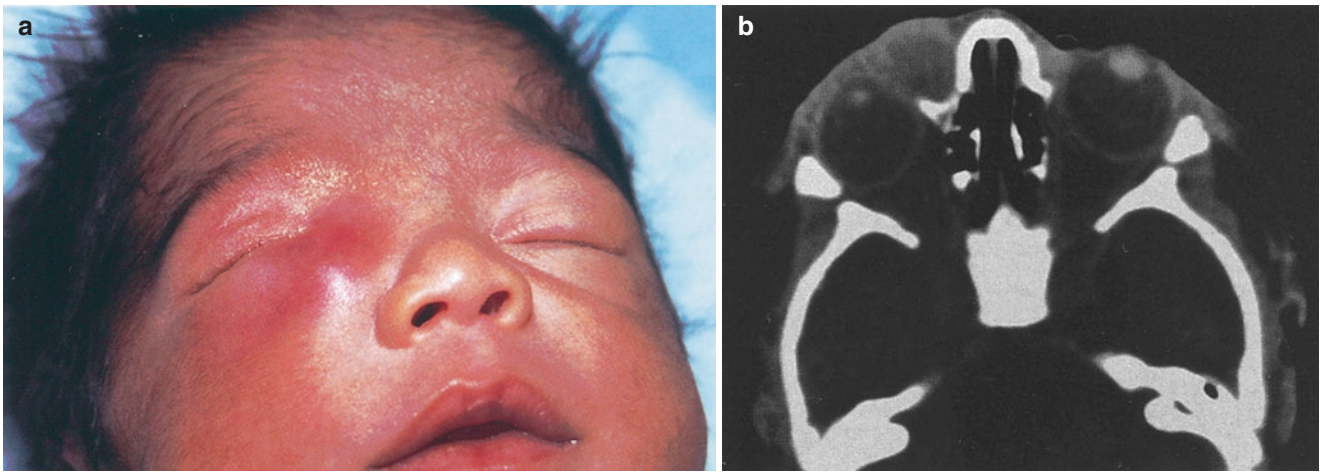


Fig. 27.7 Neonatal dacryocystitis. (**a**) Neonatal dacryocystitis. (**b**) CT scan showing dilated nasolacrimal sac; referral was for an incorrectly diagnosed orbital mass

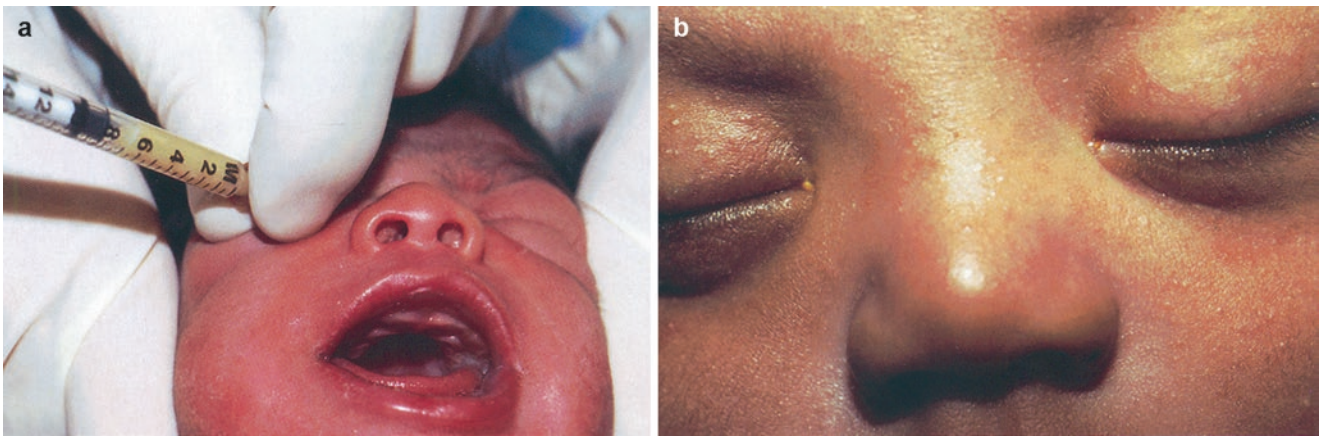


Fig. 27.8 Neonatal dacryocystitis. (**a**) Tuberculin syringe tap of the lacrimal sac for neonatal dacryocystitis; note 0.8 mL purulent material withdrawn from lacrimal sac. (**b**) The same patient 1 week post-office probing with #000 Bowman probe

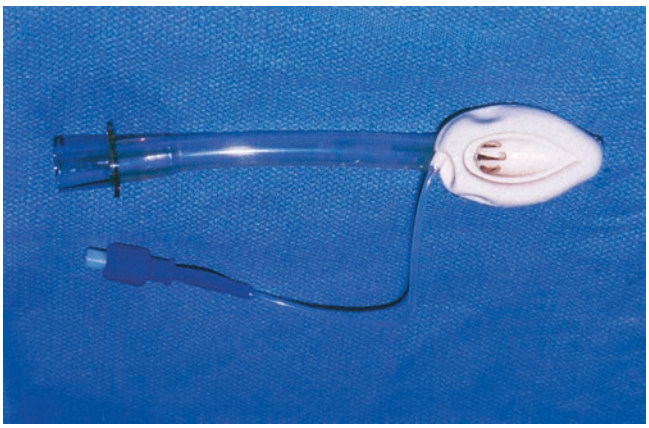


Fig. 27.9 Laryngeal mask

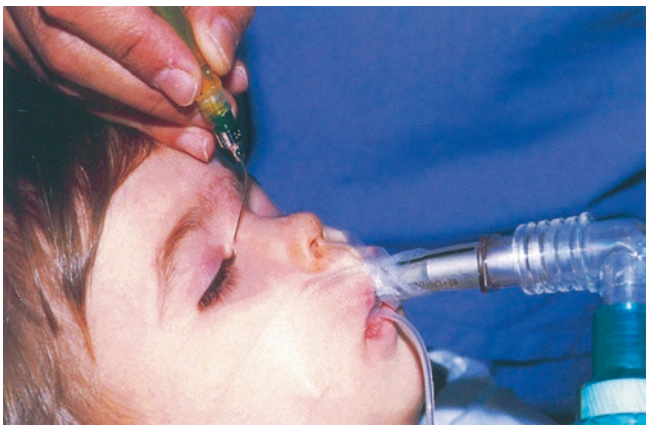


Fig. 27.10 Laryngeal mask in position. Laryngeal mask allows better access to the nose and increased safety as compared to a routine face mask

minimal volume of fluorescein on irrigation (0.5 ml or less) and taking care to minimize bleeding in the nose. It is helpful to spray oxymetazoline 0.05% (Afrin, Schering, Liberty Corners, NJ) into each operative nostril to control hemostasis. If there is any concern about maintaining the child's airway, then endotracheal intubation should always be done.

When the child is asleep, careful examination of the puncta and canaliculi should first be performed. Any lacrimal fistula should be noted. If both puncta are present on an operative side, only the upper punctum need be dilated. Great care must be made to minimally dilate the punctum so as not to tear the surrounding orbicularis fibers. This will increase the risk of a monocanalicular stent loss or bicanalicular punctal slitting. An experienced lacrimal surgeon can sometimes probe the punctum without dilating it, but the probe should never be forced, as there is always the risk of creating a false passage.

To probe and irrigate the outflow system, a lacrimal cannula (blunt 23-gauge needle) attached to a 2-mL Luer lock syringe containing several milliliters of a diluted fluorescein solution should be used. The surgeon should feel for veils and strictures in each canaliculus, as well as at the internal common canaliculus, before attempting to probe the nasolacrimal duct. The surgeon can attempt to use hydrostatic pressure irrigation while occluding the opposite punctum, as the initial effort to open the lower (distal) portion of the nasolacrimal system, but in our experience, this is rarely an effective method of clearing the obstruction. If there is regurgitation from the inferior punctum with an associated lower obstruction, then this indicates patency of the inferior canaliculus without the need for an additional step to check this part of the outflow system.

The lacrimal cannula can be used as a probe because its diameter is between a #0 and a #00 Bowman probe. The best cannula tip is smooth with the port on the side. The cannula is shaped into a slight curve and is passed gently into the nasolacrimal duct via the upper canaliculus (Fig. 27.11). The lower canaliculus should be manipulated as little as possible. This is mainly because if the upper is patent, it is unnecessary to stress this channel with probing the lacrimal duct since the lower eyelid must be elevated an additional 45°, thus increasing the risk of upper system injury. Furthermore, as will be described later, in the case of monocanalicular stenting, the upper punctum should be treated since its anatomic location is usually more medial than the lower. Thus, the collarette of this type of stent has less chance of irritating the cornea.

If any resistance is encountered because the cannula is too large, the surgeon should withdraw the instrument immediately and use a smaller Bowman probe. The probing instrument is slipped down into the nasolacrimal duct until it meets resistance, which most commonly occurs at the lower end. Regardless of whether the irrigation cannula or a Bowman probe is used, the instrument should slide easily into the duct. Forcing the instrument inferiorly may create a false passage. The surgeon then should turn the curve of the cannula medially and, with a gentle but firm push, enter the nose beneath the inferior turbinate. When the cannula is passed through the duct, any scraping sensation, rather than a smooth, sliding sensation, usually indicates a false passage. In such instances, the instrument should be withdrawn. The surgeon should then make another gentle attempt to find the normal channel. If passage into the nose is not achieved because of a presumed false passage, one can either perform an endonasal examination to identify the patency of the valve of Hasner or consider proceeding immediately to a DCR. Many times, however, it is best to reschedule this for a later date following another attempt at gentle probing first which is sometimes successful after inflammation encountered during the first unsuccessful probing has settled.

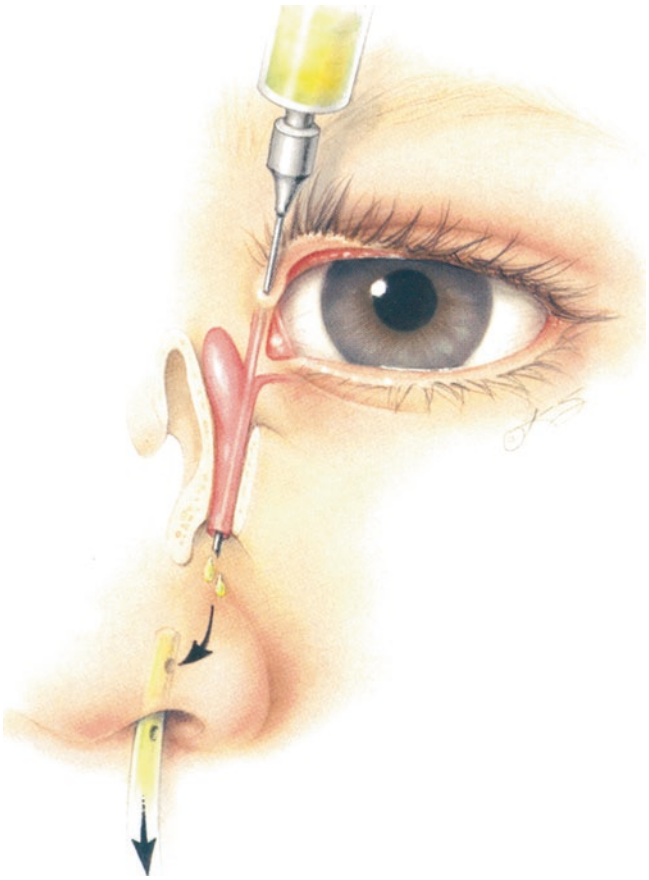


Fig. 27.11 Probing and irrigation of the nasolacrimal system. The cannula is slipped down to the point of obstruction and pushed through gently but firmly. Dye is injected from the syringe, and the patency of the system is confirmed by suctioning the dye from the inferior meatus with a soft pediatric-size plastic suction catheter

Location of the probe in the inferior meatus can be confirmed by metal-to-metal contact with a large second probe placed through the nostril under the inferior turbinate. Direct visualization of the probe can also be instructive, particularly in complicated cases. This can be accomplished by using an endoscope. It is helpful to shrink the nasal mucosa with a 4% cocaine solution or with oxymetazoline 0.05%

(Afrin, Schering, Liberty Corners, NJ). During irrigation, dye is then collected from the inferior meatus of the nose with a soft, plastic pediatric-size suction catheter (No. 10 French Argyle oxygen catheter, Dow Corning, New York) [27]. Fluorescein dye is preferred for any system that has a high probability of requiring silicone intubation. In the past, methylene blue was a useful and readily available dye but has the main drawback of staining tissue and instruments. Unless a patient has a known fluorescein allergy, this dye is always preferred over methylene blue which stains the tissues unnecessarily. After these steps are completed, an intranasal examination should always be performed. If the inferior turbinate seems to be impacted over the nasolacrimal duct, it can be infractured medially toward the septum with a Freer elevator (Fig. 27.12). After probing and irrigation with dye is completed, an antibiotic-steroid solution is then irrigated through the upper canaliculus of each nasolacrimal system. The suction catheter is placed in the nasal passage prior to irrigation to minimize the threat of laryngospasm caused by the collection of irrigating fluid in the posterior pharynx. On occasion, there will still be regurgitation of this solution from the opposite canaliculus. It is then useful to occlude the opposite punctum with a cotton-tipped applicator and then to inject more solution through the duct, again collecting this with the suction catheter.

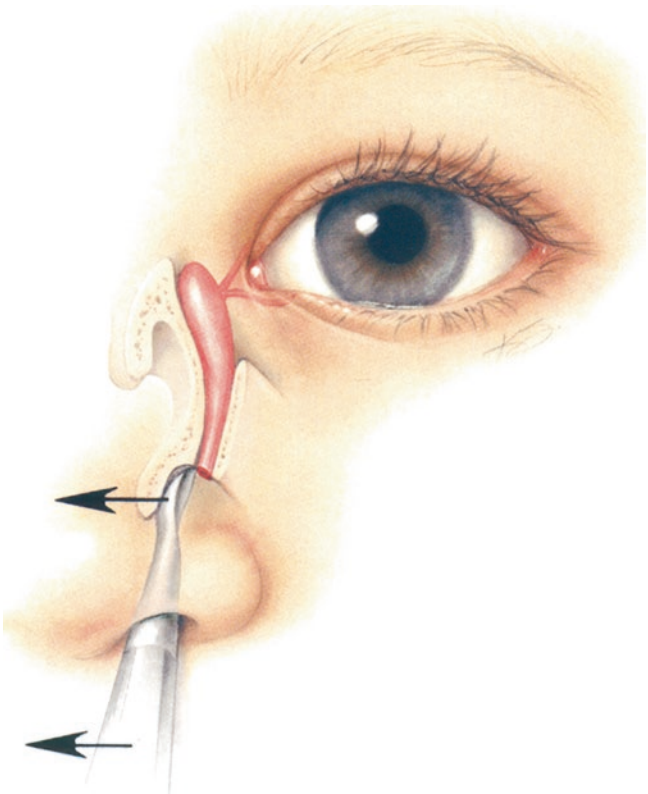


Fig. 27.12 Infracture of the inferior turbinate. A periosteal elevator is slipped into the inferior meatus and advanced along the length of the under surface of the inferior turbinate. The patient's head is stabilized, and the turbinate is pushed medially by distributing force along the entire length of the turbinate rather than just at one point. This step minimizes trauma while creating a larger space for the exit of tears from the valve of Hasner at the distal end of the nasolacrimal duct. The instillation of oxymetazoline (Afrin) into the inferior meatus before this maneuver reduces intraoperative and postoperative bleeding

Parents are instructed to use an antibiotic-steroid drop four times daily for the next week. The patient is seen in the office 2–3 weeks postoperatively. If one attempt at simple irrigation and probing is not successful, then the irrigation and probing can be repeated, including infracture of the inferior turbinate if this was not previously performed. Unless there is very rapid outflow on this repeat attempt with little resistance during irrigation, we usually proceed immediately to balloon dilation or silicone intubation of the nasolacrimal system.

Treatment for a Failed Probing

The patient who has persistent symptoms after an initial probing and irrigation procedure will likely require additional intervention to permanently cure their tearing. Ideally, this would be accomplished by only one more procedure under general anesthesia. The classic approach to a failed probing has been to simply repeat the same procedure [36, 37]. The main criticism to this approach, however, is the fact that it is not really introducing a new treatment method. An alternative to repeat probing is to surgically widen the nasolacrimal duct with either a balloon or probe with or without the placement of a stent that intubates the entire nasolacrimal outflow system. A more recent surgical approach that is becoming a readily adopted practice is to treat the nasolacrimal duct with a balloon or a stent as a primary procedure immediately after probing. The purpose is to avoid the risk of a reoperation [38, 39]. In this approach, a surgeon would consider probing a potential failure either because (1) there was an element of stenosis that would require stenting or (2) even with a simple membranous obstruction, the surgeon prefers to stent the system to prevent any membrane reepithelialization. Some authors prefer to use a canalicular endoscope to diagnose and treat CNLDO [41]. However, it is the opinion of the authors that while this is a helpful diagnostic tool, it is more invasive and ultimately unnecessary given the high success of stent placement and/or balloon dacryoplasty without this additional technique.

Balloon Dilation of the Nasolacrimal Duct

Becker et al. [40] and Hutcheson et al. [42] published their results using an inflatable balloon catheter as an alternative to silicone intubation in children who have failed previous lacrimal system probing or who presented at an older age of onset. The LacriCATH balloon lacrimal catheter (Atrium Medical Products, Birmingham, AL) is very similar to a

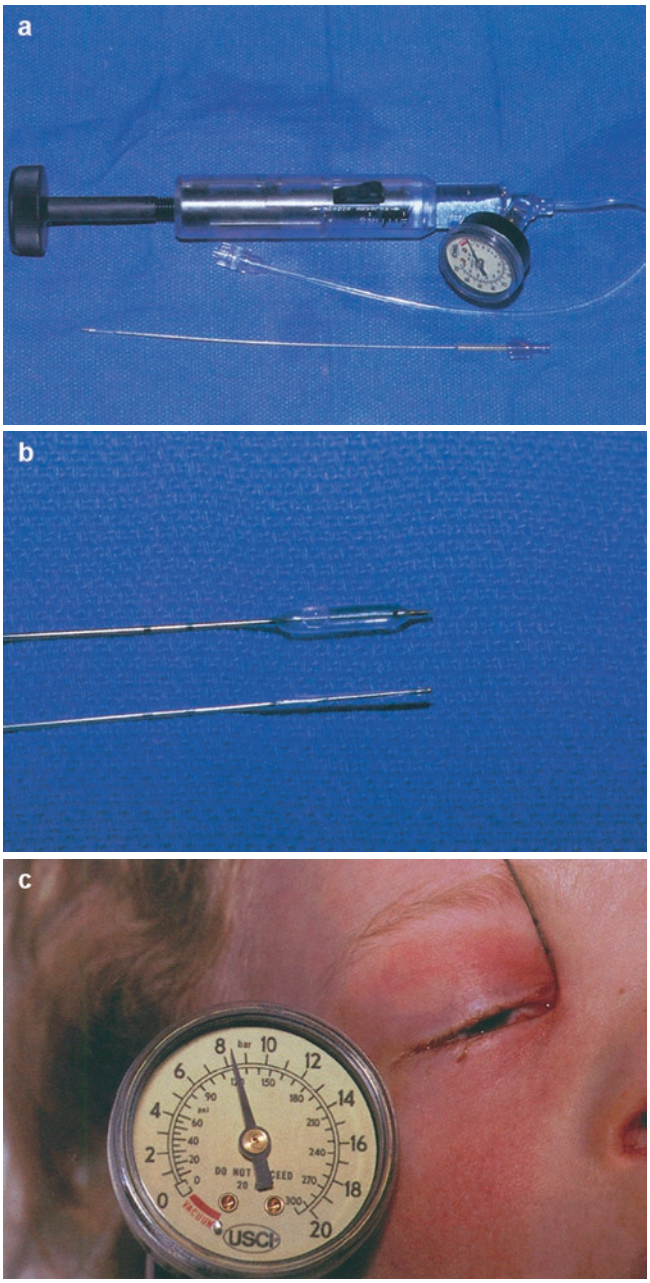


Fig. 27.13 Balloon catheter. (**a**) Balloon catheter inflation apparatus with adjacent uninflated catheter. (**b**) A 2-mm balloon catheter inflated with saline, adjacent to uninflated catheter. (**c**) Gauge showing balloon catheter being inflated to 8 atm after being placed in the nasolacrimal duct

classic balloon angioplasty device. It consists of a small polyurethane inflatable balloon on a semiflexible guide wire, which is inserted through the upper canaliculus through the nasolacrimal duct. The LacriCATH is then inflated to a pressure of 8 atm for 90 s. This is then repeated, without moving the catheter, for an additional 60 s. This device presumably dilates the nasolacrimal duct while it is inflated, thus enhancing the patency of the lower nasolacrimal system (Fig. 27.13).

Previous studies of lacrimal balloon dilation with similar instruments have yielded success rates ranging from 56% to 97%. The variability in results may be due to the differences in perioperative management. For example, Becker et al. used postoperative oral steroids, whereas Hutcheson et al. did not. The use of this method as a primary procedure in effect is the same as an initial probing, which has a very high success rate. The use of this technique may have more proven value for failed DCR surgery, but our initial experience with this technique for failed probing or problematic cases has been approximately 90% which is comparable to our results with bicanalicular intubation, with slight improvement of results with the use of silicone intubation. Further controlled studies are needed to determine the efficacy and role of lacrimal duct balloon dilation with and without silicone intubation.

Silicone Intubation of the Nasolacrimal Duct

In the presence of nasolacrimal bony or mucosal stenosis, a simple probing and irrigation procedure is often not adequate to permanently cure the tearing child. Silicone stent placement is a minimally invasive procedure that can achieve lasting nasolacrimal patency once removed. The mechanism by which this stent is successful in treatment has not been proven. It is possible the stent prevents membrane reepithelialization or scar tissue formation due to intraductal inflammation. Alternatively, we suggest that a stent, if placed in a young growing child, may stimulate ductal bony growth. This has yet to be proven but can be postulated that younger children with a rapidly growing head may have better ductal growth stimulation with stent intubation [38, 39].

Intubation Materials

Silicone tubing #5941 with an external diameter of 0.025 mm is preferred for both pediatric and adult use, as was originally described by Quickert and Dryden [43]. The tubing can be stretched over a #0 tapered probe (Quickert 4220, Storz, St. Louis, MO). It can also be glued in place with silicone bonding glue before autoclaving if desired. Currently, a variety of packaged intubation sets (e.g., the Crawford probing set, 28–0185; retrieval hook, 28–0186, Jedmed Instrument, St. Louis, MO; or Ritleng system, FCI,

Paris, France) are also available. They are more expensive but avoid the need to prepare the probes with tubing. The important features to consider in choosing a packaged set for nasolacrimal intubation are that the metal probe is malleable enough to minimize the trauma to the duct and the nasal structures and that the tubing is bonded sufficiently to the probes so that it will not slip off when pulled through the nasolacrimal system. For bicanalicular intubation, if a metal probe is used, the authors prefer the Crawford intubation set. Detachment of the silicone from the probe occurs most frequently when the junction of the tubing and the probe is pulled slowly through the punctum into the nasolacrimal system during retrieval from within the inferior meatus. Usually, detachment can be prevented by dilation of the punctum before insertion of the probe, application of an ointment for lubrication at the metal and silicone interface, and pulling the tubing rapidly through the system.

In 1988, Long introduced the monocanalicular stent [44]. This was further modified by Fayet and marks a significantly simplified technique for stent insertion with great ease in stent removal [45].

Monocanalicular Stents

The original monocanalicular stent (FCI Ophthalmics) is available in a pulled from with the use of a probe inserter (Monoka, FCI Ophthalmics), as a pulled rod (Mono-Crawford, FCI Ophthalmics) or simply as a pushed stent with no intranasal retrieval (Masterka, FCI Ophthalmics). The indications for the use of all of these stents are not identical. The Monoka and Mono-Crawford can treat all ductal stenosis, while the pushed Masterka is ideal for mucosal obstructions and mild stenosis only. The overall efficacy of the Monoka stent has been reported in several large series previously. Fayet reported a 90.6% success rate in 1028 cases [45], and Engel had a 96% success rate in 803 cases [38]. In our series of 638 consecutive cases, we had a success rate of 92.8% [39].

Pulled Monoka and Mono-Crawford Insertion

The monocanalicular stent (Monoka or Mono-Crawford, FCI Ophthalmics) is a punctal plug that is connected to a silicone tube. While the stent has a lumen, it is occluded by the plug end and thus only functions as a structural rod and not as a drain. The stent is available with multiple-sized plugs with an endplate called a collarette that sits external to the punctum (Fig. 27.14). In pediatric patients, the 3-mm size is used for all first operations, and a 4 mm is reserved for cases of reoperation or where the punctum is noted to be too large and the stent will not seat well with a propensity to fall out spontaneously. The Monoka stent is inserted with the use of a Ritleng probe (Fig. 27.15). This instrument must be carefully inspected before each use. If the end of the probe is best, the instrument should be discarded immediately and not be used again. This is because the lumen end of the probe can be bent and care should be made to prevent this occurrence. If the instrument tip is bent, do not attempt to straighten it. This will then place a risk of the instrument breaking in the nasolacrimal system upon reuse [46, 47]. Care must be taken to avoid hemorrhage with the Ritleng hook that is used to retrieve the Monoka from the nose.

Once general anesthesia has been induced, it is always best to start with a probing and irrigation procedure as prescribed. A Ritleng probe is then inserted into the punctum (make sure the

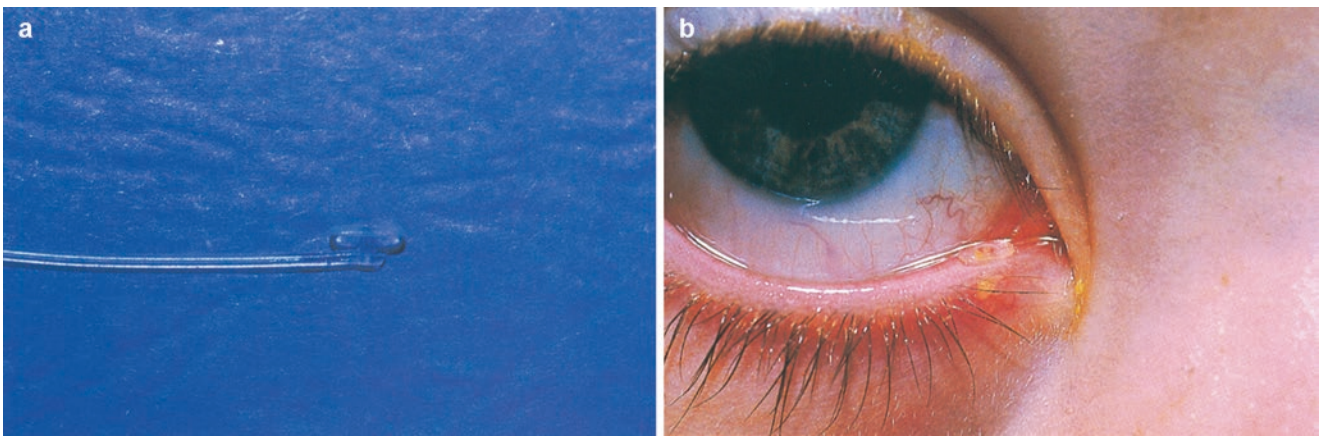


Fig. 27.14 Monocanalicular stent. (**a**) Monoka monocanalicular silicone tubing. It is available with either a 3- or 4-mm punctal plug. (**b**) Monoka monocanalicular tubing in proper position with the punctal plug positioned flush with the lid margin

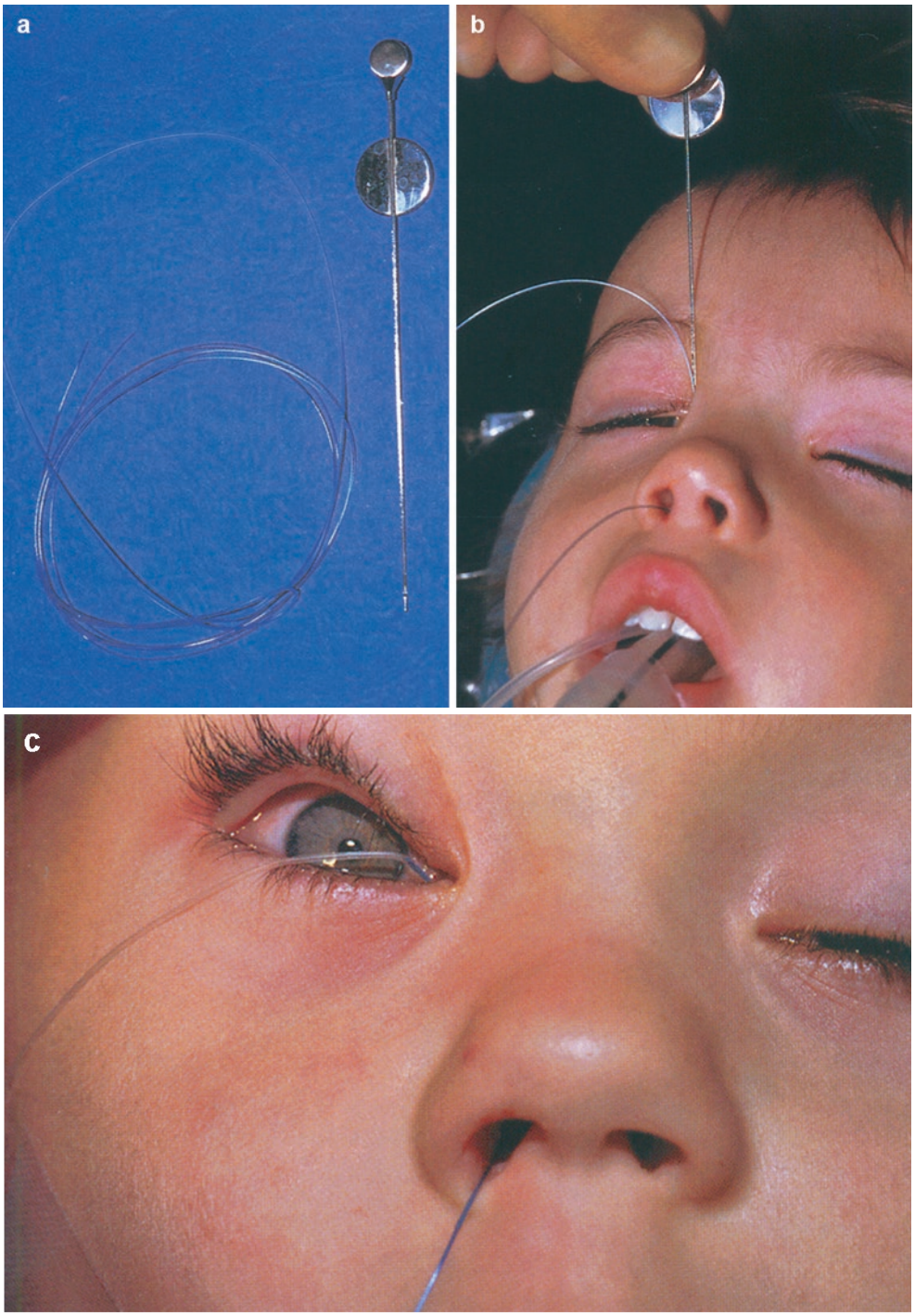


Fig. 27.15 Ritleng intubation. (**a**) Ritleng intubation set consisting of grooved metallic introducing probe and silicone tubing with attached Prolene leader. (**b**) Example of how the Prolene leader is slid out of the grooved probe (once the probe is fed into the nasolacrimal system). This may come out spontaneously as shown here but more frequently requires a crochet-type hook to pull the Prolene suture from the nostril. (**c**) Ritleng Prolene/silicone tubing, after metallic probe was removed, prior to feeding the silicone portion into the nasolacrimal system

stylet of the Ritleng probe is inside the lumen of the probe before insertion). As mentioned earlier, care must be made to avoid over dilating the lacrimal punctum. With the eyelid everted, the Ritleng probe is inserted into the punctum. With lateral traction, the Ritleng probe is angled toward the medial canthal tendon and cautiously advanced into the canaliculus and through the common canaliculus (if present) into the lacrimal sac. A hard stop should be palpated when the probe is passed through the canalicular system and into the lacrimal sac. This corresponds to the medial sac wall just lateral to the lacrimal bone (lacrimal sac fossa). With care the Ritleng probe is elevated to the medial brow and advanced into the nasolacrimal duct. This maneuver should never be forced as a false passage can easily be created, and the Ritleng probe can also be damaged [47]. When the Ritleng probe is advanced beyond the valve of Hasner, a second hard stop should be palpated, and care must be taken to avoid puncturing through the nasal floor. This can easily occur and be confused as representing a bony ductal obstruction. A size # 0 or 1 Bowman probe should be advanced into the nose under the inferior turbinate to confirm

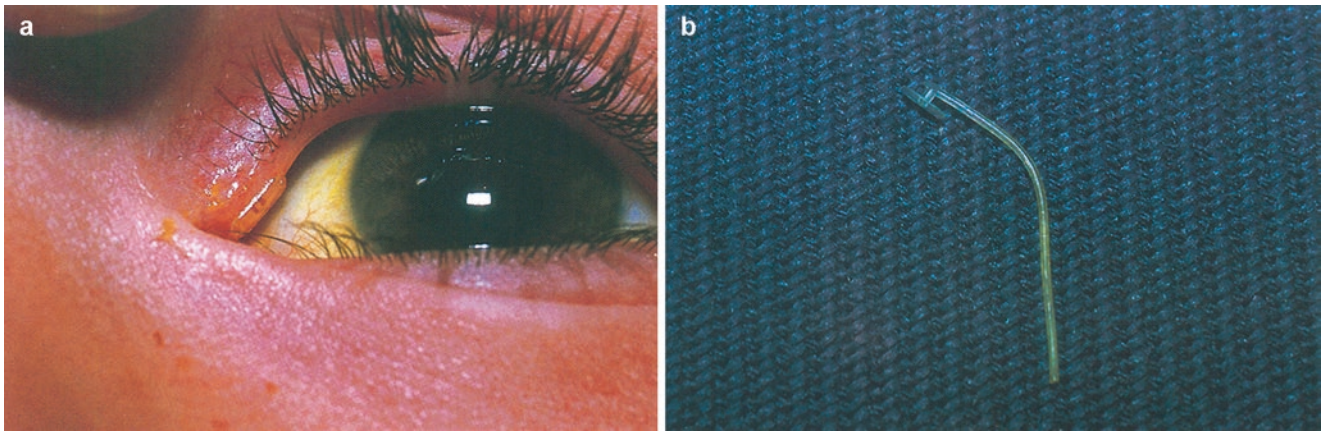


Fig. 27.16 Monoka monocanalicular tubing. (**a**) Monoka stent properly inserted in the left upper punctum. (**b**) Monoka monocanalicular tube that was removed from the left upper canalicular system after being placed 6 months earlier. The tubing has taken the contour of the canaliculus/nasolacrimal duct anatomy

the proper location of the Ritleng probe in the nose. This maneuver referred to as metal-to-metal contact is critical to this procedure and if not confirmed can give the surgeon the false impression that the probe is in the correct position. There can be anatomic variations where the ductal end is covered by the mucosa or even bone, thus preventing the Ritleng from entering the nose. In these instances, a Monoka stent will simply be prevented from entering the nasal space. If metal-to-metal contact is not achieved, then a nasal endoscope should be used to properly diagnose the cause of the distal obstruction. If not available, then the case should be aborted without stent insertion and rebooked for a time when a proper endoscopic evaluation can be done.

After metal-to-metal contact is made confirming a good position of the Ritleng probe, the surgeon can then insert a Monoka stent. It is helpful to rotate the Ritleng probe so that the gutter is visible anteriorly. This allows for the distal port of the probe to face forward so the stent can enter the nose anteriorly (occasionally the stent thread will actually emerge from the nasal vestibule upon insertion if the Ritleng probe is rotated to face anteriorly). The self-threading monocanalicular stent (Monoka) has a Prolene suture guide that is suaged onto the silicone stent. This suture is advanced into the Ritleng probe after the stylet has been removed. We find that the best surgical instrument for insertion is a Castroviejo needle holder. The suture can be advanced in several mm increments until there is a hard stop. One should avoid letting any resistance bend the Prolene as it will then be difficult to advance the suture. If this happens, it is best to withdraw the suture and cut it above the bend. At this point the needle holder is again used to lightly grasp (taking care to not crush) the Prolene and advance the suture in 2–3-mm increments until it appears that there is sufficient length to pull it from the nose. This is best accomplished with the Ritleng hook. The hook is passed under the inferior turbinate until there is metal-to-metal contact. The hook is turned to catch the Ritleng probe. The probe is slowly withdrawn until it passes out of the hook which then presumably can now pull the suture as a loop out of the nose. This may take several attempts. If this still fails, another alternative method is to use a small alligator forceps or the Castroviejo needle holder to grasp the metal probe end and slowly withdraw the probe until the suture can be grasped and pulled out of the nose. The Prolene suture actually thins (at about 30 cm). The thinner suture can then be pulled into the gutter of the Ritleng probe which is completely withdrawn from the system allowing the silicone stent to now be pulled into the duct and out the nose. Once the punctal plug of the stent sits flush to the punctum, it can be seated with only mild traction assisted by the thin needle of the punctal plug inserter that can be placed in the hole of the collarette. Then, with the stent on mild traction, the silicone tube is cut at the nasal opening. Care must be made to not pull too tightly as the silicone will then retract too far into the duct and no longer bridge through the valve of Hasner. The plug should sit securely in the punctum (Fig. 27.16).

Once the stent has been inserted and hemostasis has been confirmed, anesthesia can be withdrawn, and the patient is transported out of the operating room. The stent can then be left in place for a period of postoperative observation. In our practice, we see patients 3 weeks after surgery to confirm the stent is in place, and we remove the stent in the office in 3 months. Stent removal can be achieved with a non-toothed Adson forceps. The DDT (dye disappearance test) is used both pre- and post-op and may remain positive with the stent in place, although in most instances it is negative at the 3-month post-stent removal visit.

The Mono-Crawford device is inserted with the Crawford-type rod that is suaged to the stent and without a Ritleng. The stent is removed with a Crawford hook, and the stent is seated and cut in the same manner as the Monoka.

Pushed Monocanalicular Stents

The Masterka stent is a more recent model of the monocanalicular stent and uses a "pushed" versus a more classic "pulled technique". The Masterka stent's anchoring plug collarette for punctal fixation is similar to the original Monoka stent; however, the metallic guide is located inside the silicone tube. It is available in three different sizes (30, 35, and 40 mm), and the size is determined by the surgeon at the time of the procedure. Initial dilation and probing of the punctum and nasolacrimal duct are performed as previously described. Next, the Masterka sizer is placed through the punctum and then through the nasolacrimal duct down to the nasolacrimal floor. The length of the stent can be read directly from the markings along the sizer. It is important to note that the length of the stent should always be longer than the distance between the punctum and nasolacrimal duct obstruction, preferably reaching nasolacrimal floor. Once the length of the Masterka is determined, the sizer is removed, and the Masterka stent with its guide wire is placed into the nasolacrimal duct. The guide is removed slowly much like winding a watch while remaining in the vertical axis of the nasolacrimal duct. During this process, the fixation plug is secured from coming out of the punctum with pressure from the inserter or with a Castroviejo needle holder loosely surrounding the metal guide holding the plug in the punctum while the guide is carefully withdrawn. The plug collarette can then be seated into the punctum with a punctal inserter as done for the Monoka insertion (Fig. 27.17).

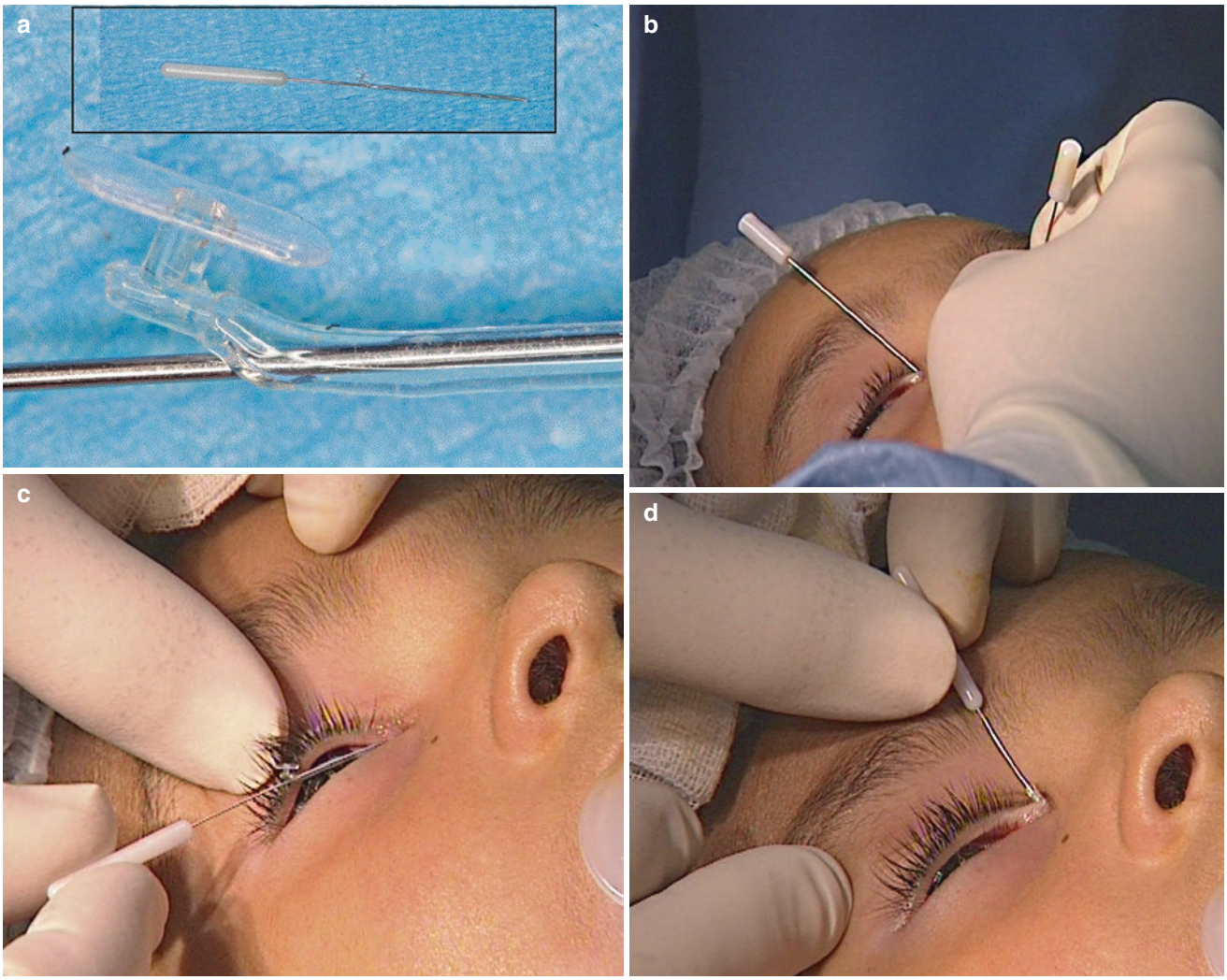


Fig. 27.17 Masterka monocanalicular stent (Courtesy of FCI Ophthalmics and Bruno Fayet). (**a**) Probe inside Masterka stent showing punctal plug collarette. (**b**) Guide probe in the nasolacrimal duct with markings at 30, 35, and 40 mm; second probe checking position of guide on the floor of the nose. (**c**) After measuring appropriate length of stent with the guide probe, Masterka stent is inserted using the "pushed" technique. (**d**) Masterka is fully inserted.

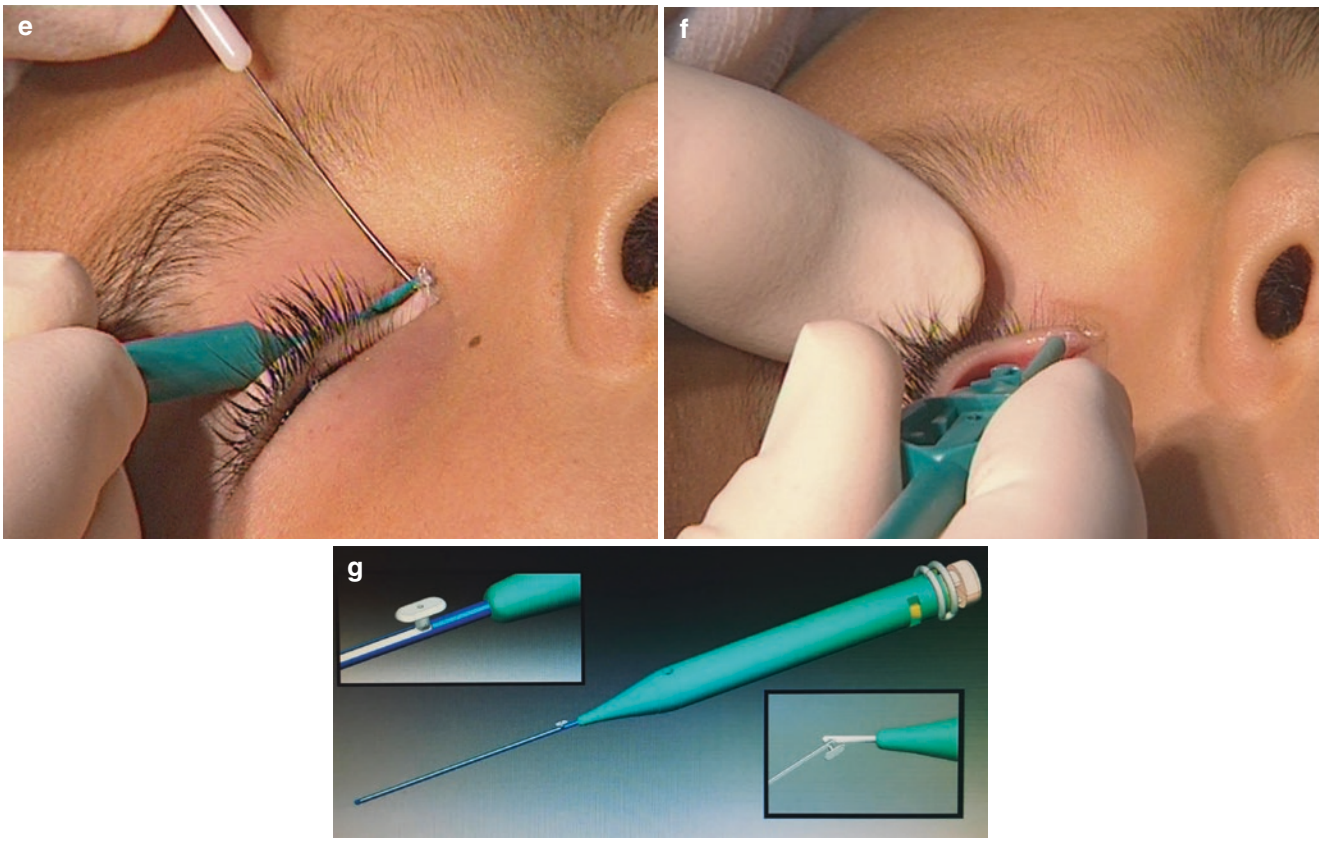


Fig. 27.17 (continued) (**e**) Guide probe is twisted for removal. (**f**) Stent in the punctum secured with plug inserter. (**g**) The new FCI Lacrijet system can insert a Masterka stent into nasolacrimal duct within a metal guide; the stent remains place as the guide is retracted by twisting the handle; the stent is then secured with the punctal inserter as in (**f**)

The primary indication of the Masterka stent is for the use of simple mucosal nasolacrimal duct obstructions, repair of canalicular trauma or canalicular agenesis, and DCR procedures in certain instances. Further indications are currently being studied. The primary advantage of this "pushed" technique versus the classic "pulled" technique is that it does not require intranasal retrieval, which causes less trauma to the nasal mucosa and nasolacrimal duct. This in turn causes less bleeding and decreases the potential for complications such as laryngospasm. In certain instances, general anesthesia with intubation can be avoided, and the use of a face mask airway can be employed instead [48, 49]. While a lower success rate has been a concern in children under 2 years of age with complex forms of NLDO, we have, nevertheless, found the Masterka stent to be useful in a younger subset of patients with more complex forms of congenital NLDO [50].

A new instrument for MasterKa insertion, the FCI Lacrijet, is now being tested with great promise. This instrument has the MasterKa stent inside a metallic probe which can be withdrawn while the stent remains within the nasolacrimal duct. This may completely eliminate the potential bunching up of the Masterka stent in more complex forms of NLDO.

Bicanalicular Stents

Before the advent of the monocanalicular stent, the bicanalicular stent was the only option for silicone intubation. Bicanalicular stents are available from different manufacturers. The Crawford bicanalicular stent (FCI Ophthalmics) has a malleable rod with a small bulb on the end that allows for intranasal retrieval with a Crawford hook. The Guibor stent (Visitec) and the O'Donoghue (BD Visitec) bicanalicular stents are mainly used in dacryocystorhinostomy surgery. While the use of bicanalicular stents has declined given the popularity of monocanalicular stents, it still has some use in DCR and Canaliculo-DCR procedures. It also is useful for bicanalicular lacerations, not only as a stent but also for the support it can provide in stabilizing any associated medial canthal avulsion.

Bicanalicular Stent Insertion

Passage and retrieval of the metal probes attached to these bicanalicular stents can be difficult. Intubation of the nasolacrimal system requires the surgeon to negotiate several right-angle turns, particularly when entering through the

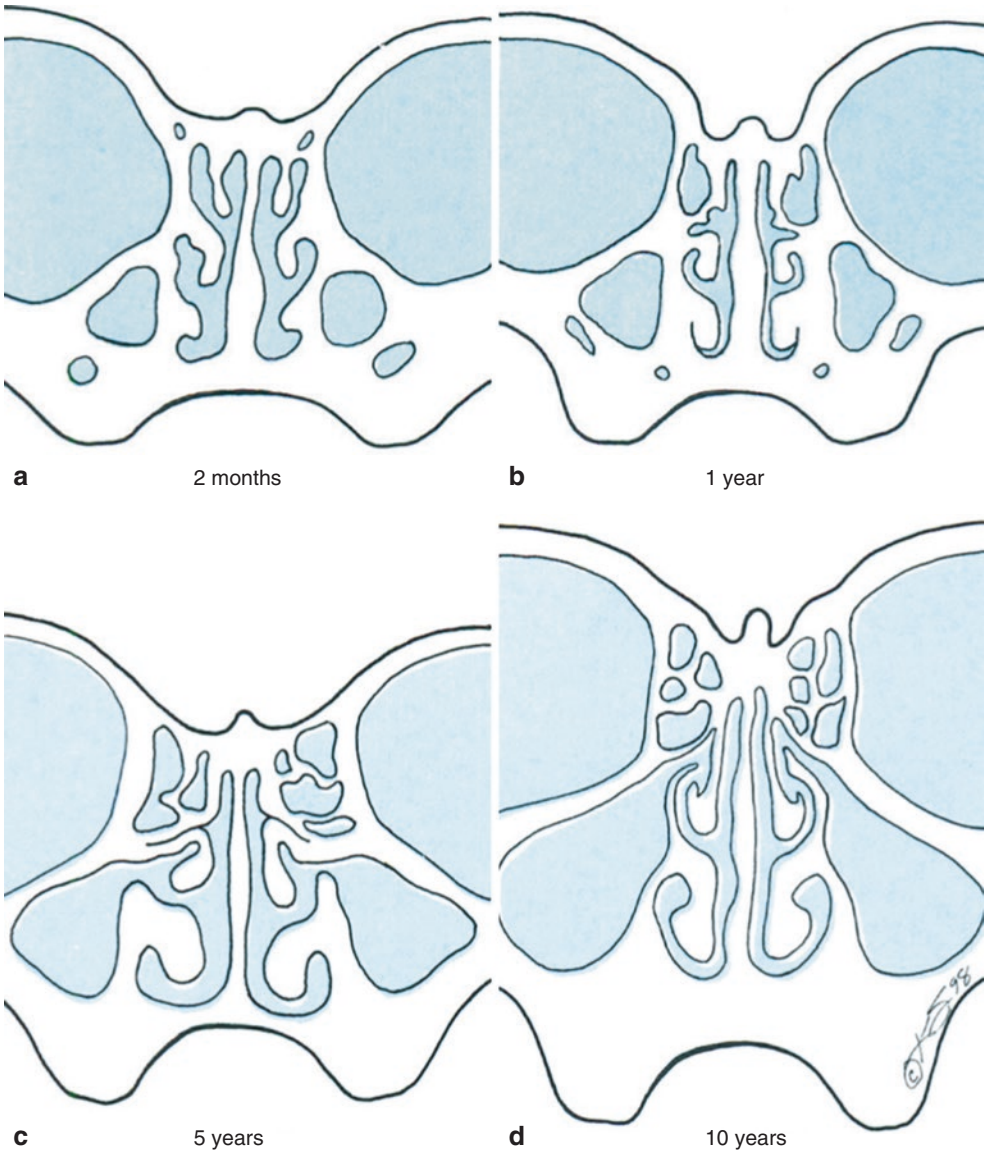


Fig. 27.18 Coronal sections. Coronal sections through the nasal fossa and sinuses showing their sizes and relationships through various ages: (**a**) 2 months, (**b**) 1 year, (**c**) 5 years, and (**d**) 10 years (Adapted from Bernstein [57])

lower canaliculus. Furthermore, as the probe emerges near the floor of the nose, it can be difficult to withdraw, especially in a young child. This problem occurs because the inferior meatus in a child is compact, with little space existing between the floor of the nose, the lateral nasal wall, and the inferior turbinate (Fig. 27.18) [51]. Silicone intubation of the nasolacrimal duct can be particularly traumatic if the probes are not malleable. By the age of 3 years, more space has developed, but it is still less than half of that present in the adult. For this reason, it can be difficult to reach in and withdraw the metal probe and tubing from inside the nose without causing trauma to the nasolacrimal duct. Enlarging this space by shrinking the nasal mucosa with 4% cocaine or 0.05% oxymetazoline (Afrin), and infracturing the turbinate toward the nasal septum, as previously described, allows visualization of the probe and facilitates probe removal. Many methods have been devised in an attempt to improve the original grooved director retrieval method of Quickert and Dryden. A curved hemostat often can be used successfully in a large child, particularly when the turbinate is infractured. However, the malleable Crawford-type probes offer an advantage in that they can be retrieved, even in a small infant, by the use of an ingenious hook that can grasp the olive tip at the end of the metal probe (Fig. 27.19) [43, 52]. On occasion, the Crawford probe olive tip may be too large to pass through the common canaliculus. The lacrimal cannula may pass through, but even with careful dilation, there may be persistent resistance to the olive tip of the Crawford tube. One should never force an instrument through a "soft stop" created by stenosis in the common canalicular area. The soft tissues of the medial canthus will be seen to move medially in contrast to the "hard stop" when a probe or cannula hits the bony medial wall of the lacrimal sac fossa.

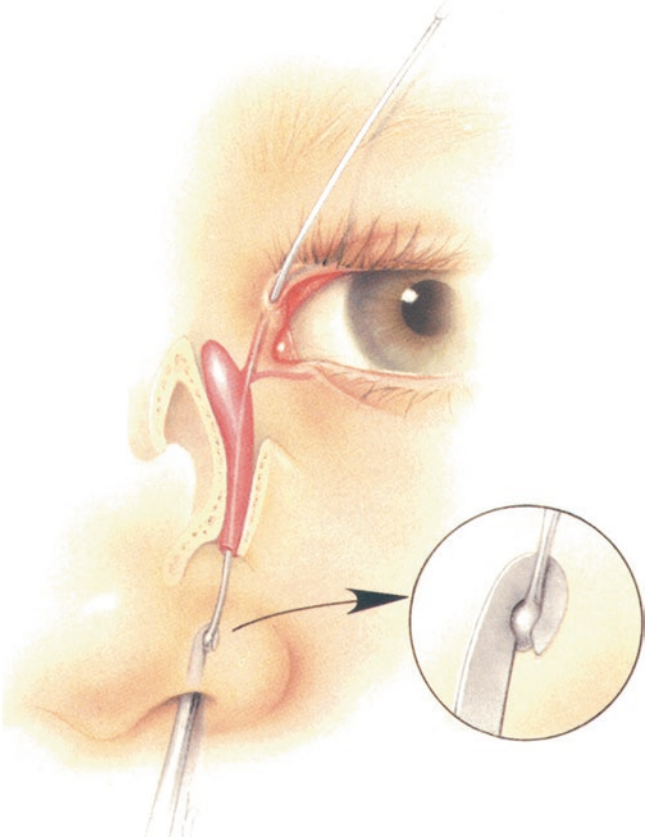


Fig. 27.19 Crawford bicanalicular-type probe insertion. Initial Crawford probe insertion and removal with a crochet-type hook. For the bicanalicular-type stent, a second probe is inserted in the opposite punctum and then retrieved with the crochet hook

Fixation of Bicanalicular Stents

The method of fixation of the cut end of the silicone tubing inside the nose has been controversial [53]. Our preferred method has been to secure the silicone tubing in place by passing each probe through a small piece of retinal sponge and then to tie square knots securing the loop in the appropriate position (Fig. 27.20). The size of the loop is an important factor. There should be 2–3 mm of lateral motion of the loop at the medial canthus when it is pulled with a muscle hook after the sponge is positioned properly beneath the inferior turbinate. The ends should be cut so that they are not visible externally. The sponge fits snugly beneath the inferior turbinate. This technique, when properly done, has virtually eliminated the complication of the child dislodging the tubing material. It does have the major disadvantage of usually requiring a second anesthetic for removal of the sponge and tubing.

The Ritleng intubation system described earlier for pulled monocanalicular stent insertion has been adapted for bicanalicular insertion as well. The Ritleng intubation system introduces a Prolene thread guide into a grooved metallic probe that opens into the inferior meatus. The Prolene is then retrieved via the nostril. The silicone tubing comes attached to the Prolene guide on each side so that when the Prolene is pulled out of the nostril, the silicone tubing follows (Fig. 27.16). A loop is then present at the medial canthus, and both ends of the tubing can then be tied in a single square knot similar to the method described by Quickert. Pe et al. [54] used the Ritleng intubation method in 24 eyes with congenital nasolacrimal duct obstruction with a 97% success rate, similar to that of traditional methods of silicone intubation. The Prolene guides spontaneously exited the nostril in 70% of the cases. The ends can also be passed through a silicone cuff as described for DCR surgery in Chap. 28.

Postoperative Management

Silicone intubation of the nasolacrimal system can be done as an outpatient day surgery procedure if experienced pediatric anesthesia and hospital staff are available. The patient is routinely given an antibiotic ointment to be used twice daily and then decreased to bedtime use alone after several days. Patients are seen 2–3 weeks postoperatively and then 3–4 months later if there are no unusual problems. Timing of stent removal will be discussed later in the chapter.

Complications

Parents should be cautioned about postoperative bleeding from the nose. Frank hemorrhage is uncommon but can be serious in the young child because of the small total body blood volume. Oxymetazoline nasal spray, cold compresses, and elevation of the head in bed will usually suffice. If significant hemorrhage persists, however, nasal packing or even cautery may be necessary, requiring possible hospitalization and assistance from an otorhinolaryngologist. Fortunately, this complication is extremely rare.

Cheese wiring, or slitting, of the canaliculi and puncta (Fig. 27.21) can occur with bicanalicular stenting not only if the loop is too tight initially but also because of the rapid growth of young children. The loop has a fixed length, so slitting of the canaliculi may occur as the face grows larger. A slit of up to one-half of the canalicular length does not seem to cause any problems in the otherwise normal canaliculus and will often seal spontaneously, but it is a complication that should be avoided if possible. The loop should be tied loosely enough to allow for some growth, but not so loosely that it will prove irritating to the cornea on adduction of the globe. A granuloma of the punctum or canaliculus (Fig. 27.22) can also occur following silicone intubation. This problem can be corrected by simple excision of the granuloma with gentle cautery of the base.

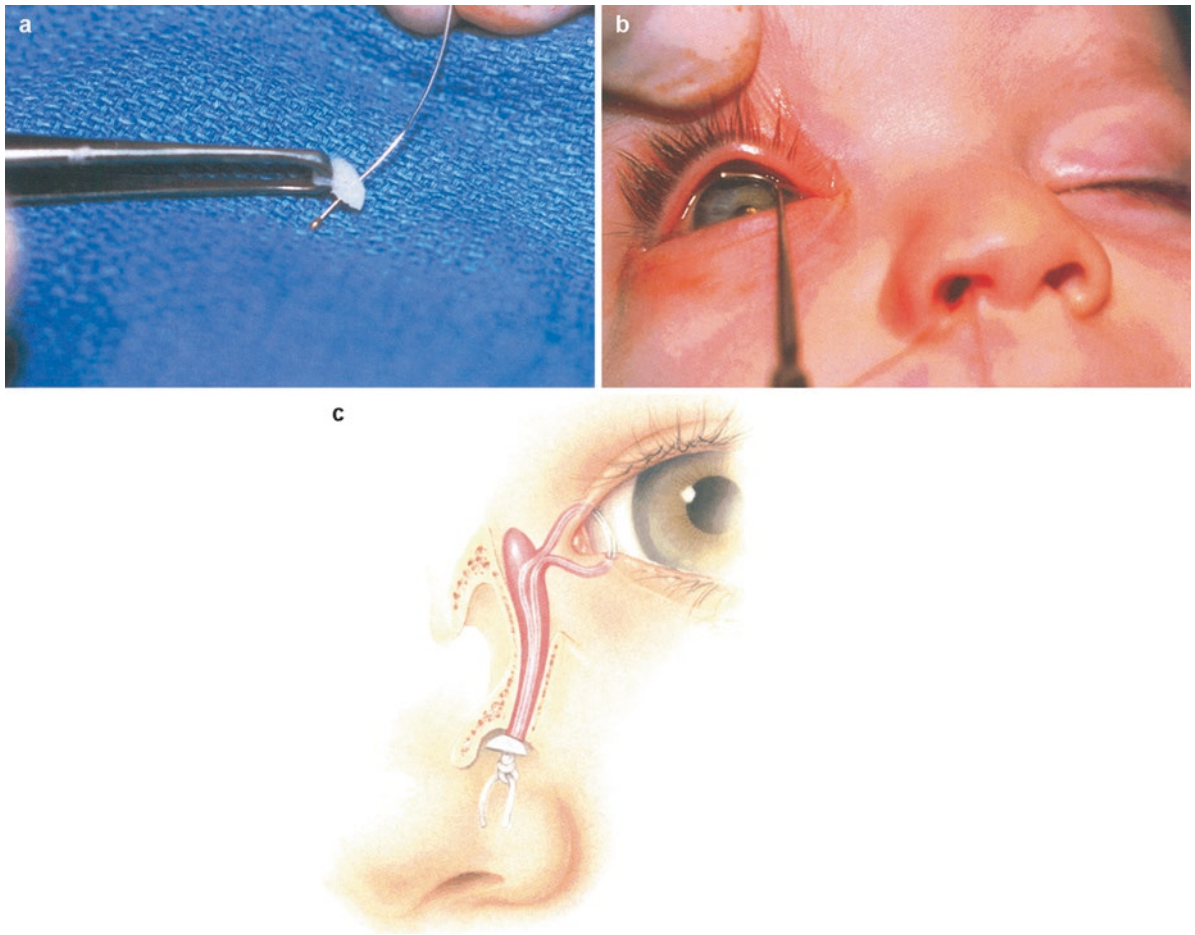


Fig. 27.20 Fixation of tubing. (**a**) Probes passed through piece of retinal sponge and then tied with multiple square knots after adjusting loop in inner canthus. (**b**) Loop should be able to move easily from the punctum to medial corneal limbus. (**c**) Schematic drawing demonstrating proper position of silicone tubing in nasolacrimal drainage system

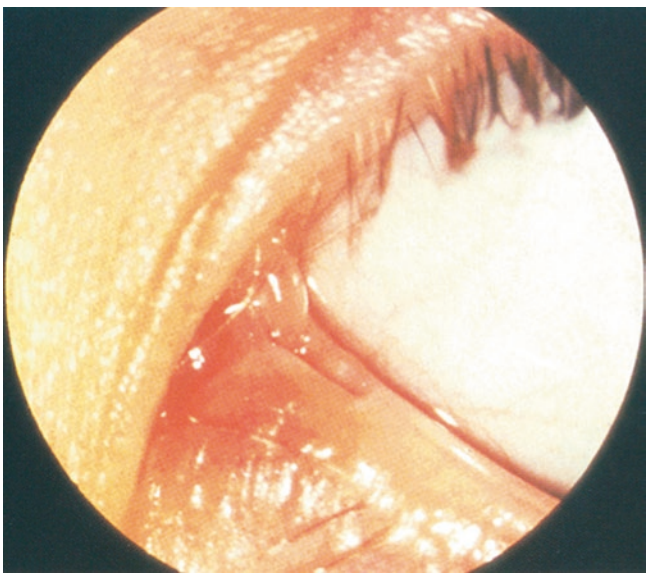


Fig. 27.21 Cheese wiring. Slitting of the lower canaliculus secondary to the tubing loop being tied to tightly. It also can occur if the tubing loop is left in place for too long in a rapidly growing child (From Katowitz and Low [34]. Reprinted with permission from Wolters Kluwer Health)



Fig. 27.22 Pyogenic granuloma. Granuloma of the punctum secondary to the placement of silicone tubing



Fig. 27.23 Extruding bicanalicular stent. Loop of tubing secured too loosely, enabling the child to pull the knotted silicone ends into the lacrimal sac. This is less likely with the sponge fixation technique or use of a larger silicone cuff with the knots tied below this (From Katowitz and Low [34]. Reprinted with permission from Wolters Kluwer Health)

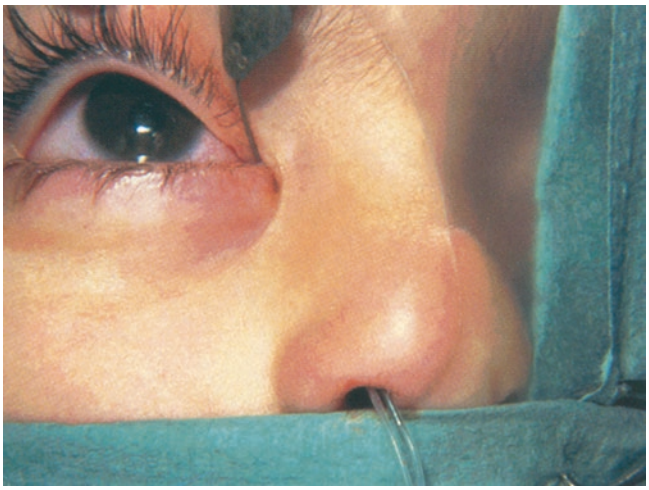


Fig. 27.24 Removal of prolapsed stent. To protect the common internal punctal opening, the loop of tubing can be cut and a thin Bowman probe inserted into lumen of silicone tubing from the upper canaliculus. The probe is then passed through the nasolacrimal duct and the tubing retrieved from the floor of the nose (From Katowitz and Low [34]. Reprinted with permission from Wolters Kluwer Health)

Complications related to monocanalicular intubation include pyogenic granuloma, corneal or conjunctival abrasion, intracanalicular migration of the tubing, and exteriorization and loss of the tubing. Monocanalicular intubation does, however, reduce the risk of canalicular slitting. Because it requires no intranasal fixation and may be removed from the punctum with a blunt forceps in the office (Fig. 27.16), it may provide a useful alternative by avoiding a second anesthetic required when a retinal sponge/multiple knot fixation has been used. Indeed, our experience with this technique has been positive and has largely replaced our previous practice of bicanalicular intubation.

Perhaps the most frequent complication is the displacement of the silicone tubing up the duct and into the lacrimal sac. The use of square knots alone for fixation in the pediatric age group allows the potential problem to develop if the child rubs or grasps the loop at the medial canthus and pulls the tubing and knots up into the nasolacrimal duct and sac. This problem will be seen as a long loop of the tubing visible at the medial canthus and extending toward the cornea or actually lying on the cornea (Fig. 27.23). This complication can be remedied by cutting the tubing and pulling the knots through the common internal punctum and upper canaliculus but only if a simple square knot has been tied so that the knot is not large enough to damage the common canaliculus [55]. The ends of the tubing can be sutured to the lateral nasal wall, but this can also pull free. When multiple knots have been tied, we prefer to cut the loop at the medial canthal angle and place a #0000 probe into the lumen of the silicone tubing that emerges from the upper punctum (Fig. 27.24). This probe, attached to the tubing (in effect, a reversal of the usual intubation method), can be passed down through the lacrimal drainage system, as in the original nasolacrimal duct probing technique, and identified in the inferior meatus. The tubing can be retrieved with either a myringotomy alligator forceps or the Crawford hook. If necessary, the system can then be reintubated [55].

Table 27.1 Success rate of bicanalicular silicone intubation according to age

Age (months)	Number of eyes	Success rate (%)
6–13	4/4	100
13–18	21/23	91.3
18–24	53/62	85.5
24 +	82/103	79.6

From: Welsh and Katowitz [56]. Reprinted with permission from Wolters Kluwer Health

Table 27.2 Success rate of bicanalicular silicone intubation related to the amount of time silicone remained in position

Age (months)	3 months	3–6 months	>6 months
6–13	0	2/2 (100%)	2/2 (100%)
13–18	4/6 (66.7%)	8/8 (100%)	9/9 (100%)
18–24	5/9 (55.6%)	28/32 (87.5%)	20/21 (95.2%)
24 +	5/10 (50.0%)	42/60 (70.0%)	35/43 (81.4%)

From: Welsh and Katowitz [56]. Reprinted with permission from Wolters Kluwer Health

Removal of Silicone Tubing

The appropriate timing of tubing removal lacks unanimity among lacrimal surgeons. In Tables 27.1 and 27.2 from Welsh and Katowitz [56], various age groups are analyzed as to the success rate of bicanalicular silicone intubation related

to the amount of time the silicone remained in place [56]. In the 13- to 18-month age group, the overall success rate of silicone intubation was 66.7% if the tubes were left in place 3 months, compared to a success rate of 100% if the silicone tubing remained in place greater than 3 months. In the 18- to 24-month age group, success was significantly greater (95.2%) if the tubes were left in place greater than 6 months, compared to only 55.6% success if left in position 3 months. A similar disparity was noted in the 24+ month age group, where a success rate of 81.4% was noted if tubes were in place greater than 6 months, compared to a success rate of only 50% if the tubes were left in place for 3 months [57]. Based on this study and subsequent experience, we now leave silicone tubing in position for 3 months for simple mucosal nasolacrimal duct obstructions. In children younger than 2 years old with complex (bony obstruction or severe scarring) obstructions, the stent is left in place for 6 months. For children older than 2 years of age with complex obstructions, stents are typically left in place for 1 year [44, 54, 56, 58, 59]. This period appears to allow the duct and its mucosal lining to respond to the stent effect of the silicone tubing. Response to a stent is probably related to the more rapid growth, observed in the young child. This is similar in concept to the response of a microphthalmic orbit with tiny lid fissures to the use of increasingly larger conformers. The use of the dye disappearance test is a useful indicator for tube removal. If there is normal outflow, even with the silicone material in place, then early removal is probably acceptable.

In the young child with bicanalicular stents, removal of silicone tubing fixed with a retinal sponge usually requires general anesthesia using a laryngeal mask. Occasionally, in a very cooperative child, removal can be done as an office procedure, similar to removal of tubing in an adult. Visualization of the interior meatus through a nasal speculum is aided by the use of 4% cocaine or oxymetazoline nasal spray to shrink the nasal mucosa. In an older child, blowing the nose in the office and suctioning in the operating room also may be helpful in placing the tubing in an anterior location for removal. It is important to first locate and secure the ends of the silicone tubing with a needle holder or myringotomy forceps; only then should the loop be cut with a blunt-tipped scissors in the medial canthal area after a topical anesthetic is instilled. The tubing can then be pulled from the anterior meatus. A fiber-optic head lamp or indirect ophthalmoscope may be useful, but a thin endoscope sometimes proves invaluable for locating the ends. The use of this instrument, however, usually requires cooperation from the child or a general anesthetic. On occasion, the Crawford hook that is designed to retrieve the metal probe attached to the silicone tubing can be used to retrieve the tubing. Given the success rates with balloon catheters and monocanalicular stents, these techniques have supplanted bicanalicular intubations for the most part and thus avoided the problems of fixation and the potential need for a general anesthetic for removal.

In children with monocanalicular stents, there is less need to use sedatives or general anesthesia. The child can be held in the caregiver's arms and his/her head can be stabilized by an assistant. With the use of a forceps or Castroviejo needle holder, the fixation plug or head of the stent can be removed with ease. If this cannot be performed in the office due to lack of cooperation, then the use of sedation or even a general anesthetic is indicated. If this is indeed required, then a repeat probing and irrigation can be performed to ensure that the system is truly patent.

Failure of Silicone Intubation

If silicone intubation and balloon dacryoplasty have failed, then a DCR will usually be required. A DCR may also be necessary if an acute dacryocystitis cannot be controlled by simple probing and intravenous antibiotics. Several studies have demonstrated a high success rate of DCR in the pediatric age group, equaling that of the adult population. A concern in DCR surgery at a young age, however, has been the potential for disruption of nasal bone growth. The surgery does not disturb any growth plates, and we have not seen any documented effect of facial asymmetry after bilateral DCRs even when performed as young as 6 weeks of age. The details of this procedure are described in Chap. 28.

Other Abnormalities of the Lacrimal Sac

Early probing for mucoceles (amniotoceles) and for neonatal dacryocystitis was discussed earlier. These entities usually are seen at birth or in the immediate postpartum period [28, 57]. Another congenital abnormality of the sac is the anlage or supernumerary duct, which may also originate from the common canaliculus. Surgical management of these supernumerary channels is discussed in Chap. 29.

Neoplasms of the lacrimal sac are extremely rare in children but can, if present, produce a true functional block. Clinical signs of such tumors are swelling above the medial canthal tendon and/or blood-tinged tears. Dacryocystography may be helpful in diagnosing such masses. A frozen section biopsy is mandatory. Malignancy of the sac is one of the few indications for dacryocystectomy. The nasopharynx should not be opened if there is any question of lacrimal sac malignancy because of the potential risk for local spread of a malignant tumor. Immediate oncologic consultation is mandatory.

Major Congenital Craniofacial Deformities

Any of the lacrimal abnormalities described above can occur singly or in combination with craniofacial anomalies. Repair of each entity is identical to that described for routine

lacrimal problems, but the timing of repair is different [60]. Deformities such as telecanthus, epicanthal folds, orbital volume problems, and many canthal deformities can be managed during the initial craniofacial reconstruction. Nasolacrimal problems, however, except for simple dacryostenosis or acute dacryocystitis, are best treated after major bone shifts or onlay bone grafts in the midface region have been completed. Unfortunately, good results are too easily undone by subsequent surgery, and repeat lacrimal procedures are particularly difficult and have significantly less potential for success.

Acquired Lacrimal Problems

Acquired problems of the nasolacrimal system can occur from infection, stones, medications, trauma, or other sources of inflammation [61]. In children, acquired problems of the lower system are not common, except for trauma, and most traumatic problems that do occur involve the upper system (canaliculi). The lower system may be involved in Le Fort fractures as discussed in Chap. 42.

In summary, our approach to most lower system obstructions is to follow conservative management consisting of massage of the nasolacrimal sac and duct for approximately 1 year. Topical antibiotics can be used as needed for any associated conjunctivitis. After 1 year of age, the logical sequence in our experience is to do a diagnostic and therapeutic probing under general anesthesia. This may be combined with an infracture of the inferior turbinate, balloon dacryoplasty, or silicone intubation at the time of initial probing depending on the complexity of the obstruction. Silicone intubation should be avoided in children less than 6 months in most instances and in cases of acute dacryocystitis. If probing and balloon dacryoplasty plus a silicone should prove unsuccessful, then a DCR is the next step. Bypass tubes are by definition not necessary for lower system blocks but may in unusual circumstances be the end-stage procedure if repeated manipulations or inflammation creates canalicular stenosis.

References

1. MacEwen CJ, Young JD. Epiphora during the first year of life. Eye (Lond). 1991;5(Pt5):596–600.
2. Moscato EE, Kelly JP. Weis sA. Developmental anatomy of the nasolacrimal duct: implications for congenital obstruction. Ophthalmology. 2010;117:2430–4.
3. Cassady JV. Developmental anatomy of nasolacrimal duct. AMA Arch Ophthalmol. 1952;47(2):141–58.
4. Levin AV, Wygnanski-Jaffe T, Forte V, Buckwalter JA, Buncic JR. Nasal endoscopy in the treatment of congenital lacrimal sac mucoceles. Int J Pediatr Otorhinolaryngol. 2003;67(3):255–61.
5. Jones LT, Wobig JL. Newer concepts of tear duct and eyelid anatomy and treatment. Trans Am Acad Ophthalmol Otolaryngol. 1977;82:603.
6. Busse H, Miller KM, Kroll P. Radiologic and histological findings of the lacrimal passages of newborns. Arch Ophthalmol. 1980;98:528.
7. Peterson RA, Robb RM. The natural course of congenital obstruction of the nasolacrimal duct. J Pediatr Ophthalmol Strabismus. 1978;15:246.
8. Kushner BJ. Congenital nasolacrimal system obstruction. Arch Ophthalmol. 1982;100:597.
9. Jones LT. Anatomic approach to problems of the eyelids and lacrimal apparatus. Arch Ophthalmol. 1961;66:111.
10. Sutula FC. Management of tearing in children. In: Focal points 1989: clinical modules for ophthalmologists VII, module II. San Francisco: American Academy of Ophthalmology. p. 1989.
11. Nelson LB, Calhoun JH, Menduke FI. Medical management of congenital nasolacrimal duct obstruction. Ophthalmology. 1985; 92:1187.
12. Price HW. Dacryostenosis. J Pediatr. 1947;30(3):302–5.
13. Paul TO. Medical management of congenital nasolacrimal duct obstruction. J Pediatr Ophthalmol Strabismus. 1985;22:68–70.
14. Pediatric Eye Disease Investigator Group. Resolution of congenital nasolacrimal duct obstruction with nonsurgical management. Arch Ophthalmol. 2012;130(6):730–4.
15. Foster JA, Katowitz JA, Heyman S. Results of dacryoscintigraphy in passage of congenitally blocked nasolacrimal duct. Ophthal Plast Reconstr Surg. 1996;12:27–32.
16. Veirs ER. Disorders of the nasolacrimal apparatus in infants and children. J Pediatr Ophthalmol. 1966;3:32.
17. Crigler LW. The treatment on congenital dacryocystitis. JAMA. 1923;81:23.
18. Kushner BJ. Congenital nasolacrimal system obstruction. Arch Ophthalmol. 1982;100:597–600.
19. El-Mansoury J, Calhoun JH, Nelson LB, Harley RD. Results of late probing for congenital nasolacrimal duct obstruction. Ophthalmology. 1982;93:106.
20. Robb RM. Probing and irrigation for congenital nasolacrimal duct obstruction. Arch Ophthalmol. 1986;104:378.
21. Katowitz JA, Welsh MG. Timing of initial probing and irrigation in congenital nasolacrimal duct obstruction. Ophthalmology. 1987;95:698.
22. Robb RM. Success rates of nasolacrimal duct probing at time intervals after 1 year of age. Ophthalmology. 1998;105:1307.
23. Kushner BJ. The management of nasolacrimal duct obstruction in children between 18 months and 4 years old. J AAPOS. 1998; 2:57.
24. Honavar SG, Prakash VE. Outcome of probing for congenital nasolacrimal duct obstruction in older children. Presented at the AAO 1998 annual meeting, New Orleans.
25. Paul TO, Shepherd R. Congenital nasolacrimal duct obstruction: natural history and the timing of optimal intervention. J Pediatr Ophthalmol Strabismus. 1994;31:362–7.
26. Guerry D, Kendy EL. Congenital inpatency of the nasolacrimal duct. Arch Ophthalmol. 1948;39:193.
27. Wobig J. Astra symposium, Colorado Springs, November; 1981.
28. Jones LT, Wobig JL. Surgery of the eyelids and lacrimal system. Aesculapius: Birmingham; 1976.
29. Weinstein GS, Biglan AW. Congenital lacrimal sac mucoceles. Am J Ophthalmol. 1982;94:106.
30. Devine RD, Anderson RL, Burnstead RM. Bilateral congenital lacrimal sac mucoceles with nasal extension and drainage. Arch Ophthalmol. 1983;101:246.
31. Schnall BM, Christian CJ. Conservative treatment of congenital dacryocele. J Pediatr Ophthalmol Strabismus. 1996;33:219–21.
32. Payesse E, Coats D, Bernstein J, Go C, de Jong A. Management and complications of congenital dacryocele with concurrent intranasal mucocele. J AAPOS. 2000;4(1):46–53.
33. Smith B, Tenzel RR, Buffam FV, Boynton JR. Acute dacryocystic retention. Arch Ophthalmol. 1976;94:1903.

34. Katowitz JA, Low J. Lacrimal drainage surgery. In: Tasman W, editor. Duane's clinical ophthalmology, vol. 5. Philadelphia: Lippincott-Raven; 1995. Chapter 79.
35. Leach AB, Alexander CA. The laryngeal mask: an overview. Eur J Anesthesiol. 1991;4(Suppl):19.
36. Singh Bhinder G, Singh Bhinder H. Repeated probing results in the treatment of congenital nasolacrimal duct obstruction. Eur J Ophthalmol. 2004;14(3):185–92.
37. Elibol et al. ESOPRS/BOPSS meeting; 2006.
38. Engel JM, Hichie-Schmidt C, Khammar A, Ostfeld BM, Vyas A, Ticho BH. Monocanalicular silastic intubation for the initial correction of congenital nasolacrimal duct obstruction. J AAPOS. 2007;11:183–6.
39. Munroe C, Khatib L, Shaffer J, Binenbaum G, Katowitz WR. Silicone stent length and loss: outcomes of 638 consecutive pediatric cases with monocanalicular intubation for pediatric nasolacrimal duct obstruction. Meeting abstract. Fall ASOPRS, Las Vegas; 2015.
40. Becker BB, Berry ED, Koller H. Balloon catheter dilation for treatment of congenital nasolacrimal duct obstruction. Am J Ophthalmol. 1996;4121304.
41. Heichel J, Bredehorn-Mayr T, Struck HG. Congenital nasolacrimal duct obstruction from an ophthalmologist's point of view : causes, diagnosis and staged therapeutic concept. HNO. 2016;64(8):619–20.
42. Hutcheson KA, Drack AV, Lambert SR. Balloon dilation for treatment of resistant nasolacrimal duct obstruction. J AAPOS. 1997;1:241.
43. Quickert MH, Dryden RM. Probes for intubation in lacrimal drainage. Trans Am Acad Ophthalmol Otolaryngol. 1970;74:431.
44. Long JA. A method of monocanalicular silicone intubation. Ophthalmic Surg. 1988;19(3):204–5.
45. Bernard JA, Fayet B, Pouliquen Y. New models of the punctum plug and inserter. Bull Soc Ophtalmol Fr. 1989;89(10):1131–2.
46. Fayet BE, Katowitz WR, Racy E, Ruban JM, Katowitz JA. An update to monocanalicular stent surgery. Int J Ophthalmol. 2016;9(5):797–8.
47. Thuro BA, Kelkhoff AJ, Pemberton JD. Investigating the role of metal fatigue in a case of ritleng probe fracture: its causes and prevention. Ophthal Plast Reconstr Surg. 29(1):e20–1.
48. Fayet B, Katowitz WR, Racy E, Ruban JM, Katowitz JA. Pushed monocanalicular intubation; an alternative stenting system for the management of congenital nasolacrimal duct obstructions. J AAPOS. 2012;16(5):468–72.
49. Fayet B, Racy E, Ruban JM, Katowitz JA. Pushed monocanalicular intubation. Pitfalls, deleterious side effects, and complications. J Fr Ophthalmol. 2011;34(9):597–607.
50. Khatib L, Nazemzadeh M, Revere K, Katowitz, WR and Katowitz JA. Use of the Masterka for complex nasolacrimal duct obstruction in children. JAAPOS. 2017;5(21):380–3.
51. Leone CR, Van Gemert JV. The success rate of silicone intubation in congenital lacrimal obstruction. Ophthalm Surg. 1990;21:90.
52. Shore JW, McCord CD. Modified Crawford hook. Am J Ophthalmol. 1982;94:255.
53. Lauring L. Silicone intubation of the lacrimal system: pitfalls, problems and complications. Ann Ophthalmol. 1976;8:489.
54. Pe MR, Langford JD, Linber JV, et al. Ritleng intubation system for treatment of congenital nasolacrimal duct obstruction. Arch Ophthalmol. 1998;116:387.
55. Patel B, Anderson R. Transcanalicular removal of Silicone nasolacrimal tubes. Ophthal Plast Reconstr Surg. 1997;13:74–5.
56. Welsh MG, Katowitz JA. Timing of silicone tubing removal after intubation for congenital nasolacrimal duct obstruction. Ophthal Plast Reconstr Surg. 1989;5:43–8.
57. Bernstein L. Pediatric sinus problems. Otolaryngol Clin N Am. 1971;4:128.
58. Werb A. Surgery of epiphora. Int Ophthalmol Clin. 1964;4:377.
59. Durso F, Hand SL Jr, Ellis FD, Helveston EM. Silicone intubation in children with nasolacrimal obstruction. J Pediatr Ophthalmol Strabismus. 1980;17:389.
60. Whitaker L, Katowitz JA. Facial anomalies involving the nasolacrimal apparatus. In: Tessier P, Callahan A, Mustarde J, Salyer K, editors. Symposium on plastic surgery in the orbital region. St. Louis: Mosby; 1974.
61. Jones LT. The cure of epiphora due to canalicular disorders, trauma, and surgical failures on the lacrimal passages. Trans Am Acad Ophthalmol Otolaryngol. 1962;66:506.

Management of Pediatric Lower System Problems: Dacryocystorhinostomy

28

William R. Katowitz, Yasmin S. Chambers, and Maryam Nazemzadeh

Introduction

The first known dacryocystorhinostomy (DCR) procedure may have been performed by the Andalusian oculist and author named Al-Ghafiqi who wrote a book dated in the mid-twelfth century describing a procedure that resembles a DCR [1]. The modern-day external DCR is often credited to Woolhouse from the eighteenth-century England [2]. Dacryocystorhinostomy is most often a secondary surgery to patients who have previously undergone less invasive procedures such as probing and irrigation with or without a balloon or stent. The primary goal of the surgery is a redirection of the outflow of the canaliculi directly into the nose via a surgical rhinostomy (osteotomy).

Some believe that pediatric DCR is less successful than in adults because of a less clearly defined anatomy, rapidly growing facial bone centers, and a tendency to develop scar tissue more easily. Many studies show, however, this to be untrue with the success rate for pediatric DCR actually similar to that seen in adults (88–96%) [3–5].

The etiologic causes of nasolacrimal obstruction that may require a dacryocystorhinostomy in children include (1) congenital, (2) traumatic, (3) infectious, (4) secondary to tumor, or (5) associated with cranial facial abnormalities (i.e., clefting syndromes, craniosynostoses) [3, 6]. In our approach, the steps prior to performing a DCR would include a single probing, possible infracture of the inferior turbinate, balloon dilation, and/or silicone stent intubation. This assumes the absence of a true bony obstruction of the duct, which would preclude the above steps. In addition, although it is unusual to require a DCR in children less than 1 year of age, it can be successful in children as young as 2 weeks of age in our experience at the Children's Hospital of Philadelphia. Surgery at a very young age is usually necessary only in cases of severe dacryocystitis associated with agenesis of the intraosseous portion of the nasolacrimal duct. The presence of an intranasal cyst in an infant that is often associated with a congenital dacryocele, amniotocele, or dacryocystocele may also require some variation of a DCR surgical approach that is usually performed endonasally with an endoscope.

Anatomical Considerations

There are some anatomical differences between the pediatric patient and the adult patient. The lacrimal sac fossa, which is made up of equal parts of the lacrimal bone and the nasal process of the maxilla, is poorly defined with a minimally developed anterior lacrimal crest, and this may result in some difficulty in selecting the proper site for the osteotomy. It is helpful to recall that the anterior lacrimal crest is contiguous with the inferior orbital rim.

The superior portion of the anterior lacrimal crest can be identified by the insertion of the medial canthal tendon. When the lacrimal sac fossa is identified, the osteotomy can be positioned appropriately. In children, it is usually easier to initiate the osteotomy through the very thin lacrimal bone of the posterior portion of the lacrimal sac fossa than it is through the relatively thicker nasal process of the maxilla.

Paranasal sinuses are generally less developed in younger patients (see Chap. 2). The ethmoid air cells are generally present at birth but continue to expand until puberty. The maxillary sinus is actually the first sinus to develop. It measures approximately 7 × 4 × 4 mm in a term infant and grows

W.R. Katowitz, MD
The Children's Hospital of Philadelphia and The Edwin and Fannie Gray Hall Center for Human Appearance, University of Pennsylvania, Philadelphia, PA, USA
e-mail: katowitzw@email.chop.edu

Y.S. Chambers (✉)
Ophthalmology, The Everett Clinic, Seattle, WA, USA
e-mail: yaschambers@gmail.com

M. Nazemzadeh
Oculofacial Plastic and Reconstructive Surgery, Rostami Oculo-facial Plastic Consultants, Sanctuary Cosmetic Center, Reston, VA, USA

© Springer International Publishing AG 2018

J.A. Katowitz, W.R. Katowitz (eds.), *Pediatric Oculoplastic Surgery*, https://doi.org/10.1007/978-3-319-60814-3_28

2 mm vertically and 3 mm posteriorly per year before it reaches its adult size of approximately 34 × 33 × 23 mm with a volume of approximately 14.75 mL [7]. In older children, the ethmoid air cells may extend anteriorly into the area of the osteotomy. This may then require a partial ethmoidectomy to allow successful fistulization of the lacrimal sac with the nasal mucosa. It is important that the osteotomy does not extend above the superior border of the medial canthal tendon because of the proximity of the cribriform plate and the risks of cerebrospinal fluid leaks.

It is also important for the pediatric lacrimal surgeon to be familiar with the intranasal anatomy, especially if an endoscopic approach to dacryocystorhinostomy is to be utilized. The lacrimal sac fossa is related to the anterior portion of the middle meatus of the nose. The lacrimal bone is located anterior to the superior attachment of the middle turbinate. This attachment is somewhat variable. The middle turbinate also has direct connection with the cribriform plates, so care needs to be taken when manipulating the middle turbinate to avoid a cerebrospinal fluid leak. The lacrimal bone is approximately 0.5 cm anterior to the bulla ethmoidalis. The lacrimal bone is 0.91 ± 0.2 cm from the inferior turbinate [8]. The osseous canal of the nasolacrimal duct is formed by the lacrimal, maxillary, and ethmoid bones. This is somewhat variable because the maxilla usually contributes to the anterior lateral and posterior walls of the duct [9]. Superiorly, the medial wall is formed by the lacrimal bone and inferiorly by the concha of the inferior turbinate (ethmoid bone). The nasolacrimal duct ostium is located high under the inferior turbinate approximately 10–15 mm from its tip, depending on the age of the patient, and thus empties into the inferior meatus.

When an endonasal approach is made for DCR surgery, an adequate intranasal space is created to prevent adhesions to the common canaliculus (CC), as well as scarring to the rhinostomy. To accomplish this, the anatomic landmark of the operculum of the middle turbinate (OMT) is useful, because the maxilla-lacrimal suture (MLS) sits 1–2 mm behind the OMT (Fig. 28.1) [10]. The incision of the nasal mucosa thus should begin directly adjacent to the OMT and extend inferiorly to the mucosa just above the inferior turbinate. The cleavage of this mucoperiosteal flap simultaneously raises the uncinate process (UP), which is a wing- or boomerang-shaped piece of bone that forms the first layer of the middle meatus. In all cases, it should expose the MLS. This reliable marker prevents the excessive denudation of the lacrimal bulge anteriorly, and it also prevents the breakage of the lamina papyracea because the cleavage will uniformly begin anteriorly against the maxilla [10].

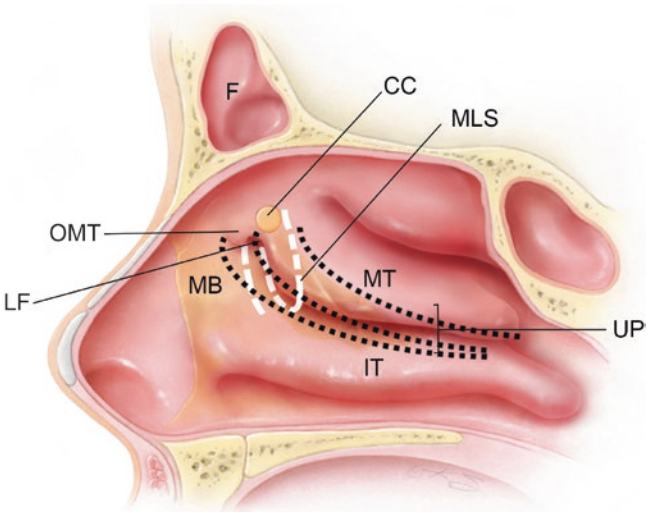


Fig. 28.1 Endonasal view-schematic rendition of the anatomy of the lacrimal fossa (LF) of the right side. The white dotted line represents the projection of the first ethmoidal cell, according to Blaylock et al. [11], onto the upper part of the inferior turbinate. The *black dotted lines* represent three common retrolacrimal, lacrimal, and maxillary projections. *CC* common canaliculus, *FS* frontal sinus, *IT* inferior turbinate, *MB* maxillary bone, *MlS* maxillo-lacrimal suture-junction between the MB and the lacrimal bone, *MS* maxillary sinus, *MT* middle turbinate, *OMT* opercule of the middle turbinate, *UP* uncinate process (Adapted from Fayet [10])

Preoperative Evaluation

Preoperative evaluation should include a thorough history of the nature of the epiphora, including antibiotics used for prior infections, prior probing procedures, or stenting treatments (silicone stent or balloon catheter). Additionally, any history of seasonal allergies, previous episodes of conjunctivitis, upper respiratory or sinus infections, or prior trauma should be explored. Further medical history should be gathered concerning bleeding diathesis, related congenital syndromes, anesthetic problems, or cardiac anomalies requiring perioperative antibiotic treatment.

In addition to the standard ocular exam, which includes screening for anatomical abnormalities, strabismus, or amblyopia, the in-office evaluation should include a dye disappearance test to grade the degree of obstruction and uncover any previously unnoticed drainage problems on the uninvolved side. Slit lamp examination is used to confirm the presence of the eyelid punctum and to rule out the presence of a fistula. If a patient is old enough to tolerate it, an in-office probing and irrigation can be performed. This can be accomplished with a standard 23-gauge lacrimal cannula or, more ideally, with a disposable 25-gauge lacrimal cannula (Storz, USA). Imaging studies of the orbits and face may be

ordered if there is a concern regarding a history of prior trauma or the presence of a craniofacial syndrome.

Finally, a well-informed family is crucial to a positive outcome. Fully discussing pre- and postoperative expectations, including antibiotic treatment, bloody drainage, care and monitoring of silicone tubing, and suture removal, can allay the fears of most families. In the unlikely event that intraoperative findings necessitate a different surgical plan (such as upper system blockage requiring a Pyrex tube), prior discussion with the child's family will best prepare them for the most appropriate treatment.

External Versus Endoscopic Approach to Dacryocystorhinostomy

The decision on the surgical approach chosen for dacryocystorhinostomy depends on a number of factors, including the age of the patient, the intranasal anatomy, and the availability of specialized equipment. The main disadvantage of the external DCR is the cutaneous scar, but for the occasional lacrimal surgeon, the external DCR is technically less demanding: Hemorrhage can be controlled more easily, and a relatively larger osteotomy can be created, which may be especially important in pediatric patients because of the increased rate of bone growth and possible closure of the osteotomy [12, 13]. When performing a DCR through an external incision, it is easier to obtain pathological specimens of the lacrimal sac, although this is rarely critical in children. In addition, direct anastomosis of the anterior and posterior lacrimal flaps is readily accomplished with an external approach. This is not typically attempted in an endonasal approach.

The main advantage of endoscopic dacryocystorhinostomy is the absence of a small facial scar. However, endoscopic dacryocystorhinostomy in children is especially demanding because of the small intranasal space. Because of this, pediatric sinuscopes (0° 2.8-mm diameter) are frequently utilized, which presents further difficulties in the visualization of the intranasal area. Microendoscopes have also been designed for transcanalicular lacrimal surgery [14]. Another major advantage of the endoscopic approach is that it removes a major intra- and postoperative source of bleeding – the orbicularis muscle.

With the advent of an ultrasonic bone aspirator as well as nasal mucosal microdebriders, the endoscopic endonasal approach to DCR surgery has become an elegant procedure with similar surgical results when compared to the external approach. Fayet et al. published his results of a very large series of endoscopic DCR. This series was in adult patients with an average age of 66 with a success rate of 94% in 300 cases [10]. Jung et al. reported their success in 1083 consecutive cases of 92.7% in patients with an average age of 57 [15]. In both of these series, the surgical rhinostomy was created with Kerrison rongeurs. In our series of endoscopic endonasal DCR performed with an ultrasonic bone aspirator (Stryker, USA) in 71 consecutive pediatric cases (47 subjects) including those with Down syndrome, we had a success rate of 62/71 cases (87.3%). This rate improves to 58/62 (93.5%) when patients with Down syndrome are removed [16]. A literature review enDCR publications in pediatric patients identified 14 studies, 393 procedures overall. The overall success rate for all of these publications was 87% [17].

Stent Nomenclature

Silicone stents are repeating polymers of siloxane. Nasolacrimal stents are often actually manufactured as tubes; however, in nasolacrimal stent design, tears do not pass through the tube lumen. Thus, the term tube is misleading and the word stent is more representative. Silastic is a silicone tubing trademarked in 1948 by Dow Corning. Most stents used today in nasolacrimal surgery are now made with silicone that is not actually Silastic but instead generic silicone tubing. We are thus dropping the term Silastic tubing as it is now dated and misleading: Stents are tubes, but tears do not pass through them. Stents are made of silicone but usually not Silastic silicone.

External Dacryocystorhinostomy in Children

It is especially important that blood loss be minimized in the pediatric age group. A 20–40-mL blood loss in a 1-year-old child is a much higher percentage of total blood volume than it would in an adult. Although dacryocystorhinostomy in adults is often performed using local anesthesia with sedation, it is generally not possible to use local anesthesia alone in young children. General endotracheal anesthesia is preferred, especially in the very young child. It is helpful to have an anesthesia team that is experienced in pediatric techniques (Chap. 5). If possible, mild hypotensive anesthesia will help to minimize blood loss. Preoperative nasal packing with neurosurgical cottonoids saturated with 1 ml of epinephrine 1:1000 solution (1 mg/cc or 0.1%) mixed with 1 ml of 0.05% oxymetazoline is also helpful in limiting blood loss in children. It is critical to alert the anesthesiologist that epinephrine is being applied into the nose and to monitor for tachycardia. No more than 1 ml of epinephrine 1:1000 should

be used intranasally for packing in a bilateral case. In addition, if there are no medical contraindications, 1–2 mL of 0.25% bupivacaine or 0.5% Xylocaine with 1:200,000 epinephrine can be infiltrated in the medial canthal area prior to surgical prepping of the patient. This provides vasoconstriction, which also helps minimize operative blood loss. The simple application of two cotton tips (Q-tips) per surgical side dipped in epinephrine 1:1000 and pressed intranasally at the level of the middle turbinate should suffice.

Alternatively, the middle meatus on the appropriate side is packed with neurosurgical cottonoids saturated with 0.05% oxymetazoline. One may mix the oxymetazoline with an equal amount of 4% cocaine if this is acceptable to the anesthesiologist. Cocaine administered in this manner may produce toxic hypertensive or tachyarrhythmic side effects, and one should be familiar with appropriate dosing in young children [18].

After general anesthesia and injection of vasoconstricting agents, adequate time is allowed for them to exert their effect (approximately 5 minutes). During this time, the patient is prepped and draped in sterile manner for upper facial surgery. The location of the incision is somewhat variable in children, depending on the presence or absence of an epicanthal fold. If an epicanthal fold is present, the incision can be placed somewhat medial to the epicanthal fold if it is not to be repaired at the same time. More often the DCR can be performed through planned Y to V or Z-plasty incisions (see Chap. 21). Additionally, a certain number of patients will also have associated craniofacial anomalies, which will be operated upon at the same time. This situation may require a somewhat different external incision, for example, using a Y to V incision in the presence of telecanthus or altering the incision to excise a lacrimal anlage if present [19]. For the most part, however, a straight, vertical incision is usually preferred in the medial canthal area instead of a curved incision, which may tend to bowstring (Fig. 28.2).

Alternatively, a medial lower lid crease is also a useful site for an incision, which provides an excellent cosmetic outcome. After incising the skin, bleeding vessels are gently cauterized, and further dissection is carried out in a blunt fashion using a Freer elevator to dissect through the orbicularis muscle. Dissection is carried down to the periosteum of the anterior lacrimal crest. Lacrimal rakes (Storz, St. Louis, MO) are helpful in retracting the medial edge of the incision to allow blunt dissection to proceed posteriorly. Alternatively, a medium size muscle hook can be used for retraction. Depending on the location of the angular vessels, they are usually retracted out of the operative field either medially or laterally, depending on their relationship to the incision. If cut, they can be cauterized, although traction beneath the rakes is frequently sufficient for adequate hemostasis. After reflecting the orbicularis muscle off the anterior lacrimal crest, it is necessary to reflect the inferior portion of the anterior limb of the medial canthal tendon superiorly. The sharper

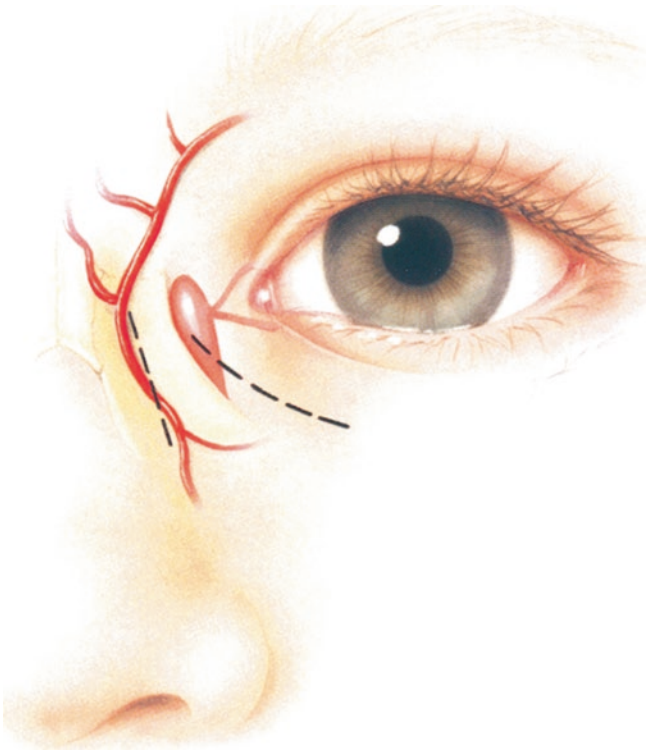


Fig. 28.2 Incisions for external dacryocystorhinostomy. The *dotted lines* indicate the two incisions used in an external dacryocystorhinostomy in children: the lid crease and the medial canthal incisions. If epicanthal fold surgery is being performed at the same time, the DCR may be performed through Y-V or Mustarde Z-plasty flaps

end of the Freer elevator or scalpel is then used to incise the periosteum of the anterior lacrimal crest in a vertical fashion extending from the edge of the medial canthal tendon interiorly along the anterior lacrimal crest. The periosteum and lacrimal sac are then easily reflected laterally, revealing the shallow lacrimal sac fossa, which comprises the frontal process of the maxilla and the very thin lacrimal bone (Fig. 28.3).

After the lacrimal sac is retracted laterally, the osteotomy can be initiated in a number of ways. In the very small child, a 2.3-mm-diameter-tip otodrill (Xomed-Treace, Jacksonville, FL) is useful in initiating the osteotomy without violating the nasal mucosa. In most young children, the lacrimal sac fossa can frequently be infractured through the thin lacrimal bone by using the blunt end of a hemostat (Fig. 28.4). In older children with thicker bone, an Arruga trephine that is 10 mm in diameter (Dixie, London, UK) can also be used to initiate the osteotomy (Fig. 28.5). There are two types of trephines: One has a sharp central point and coarser teeth to engage the bone and is used to create the initial cut. The other has finer teeth and can be gently worked down to the nasal mucosa and then rocked back and forth to remove a cylinder of the bone to expose the intact nasal mucosa beneath. The advantage of the trephine over other methods is the controlled exposure of the nasal mucosa as well as creating an adequate opening for the use of rongeurs.

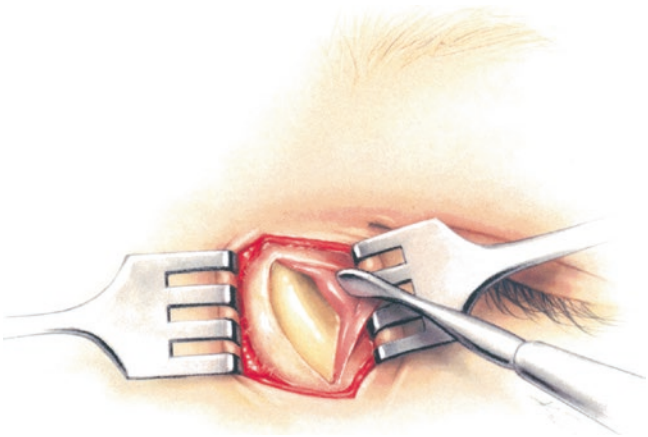


Fig. 28.3 Incision of the periosteum on the anterior lacrimal crest. The periosteum on the anterior lacrimal crest is incised with either the sharper end of the Freer elevator or a #1.5 Bard-Parker scalpel blade. The periosteum is reflected revealing the lacrimal sac fossa

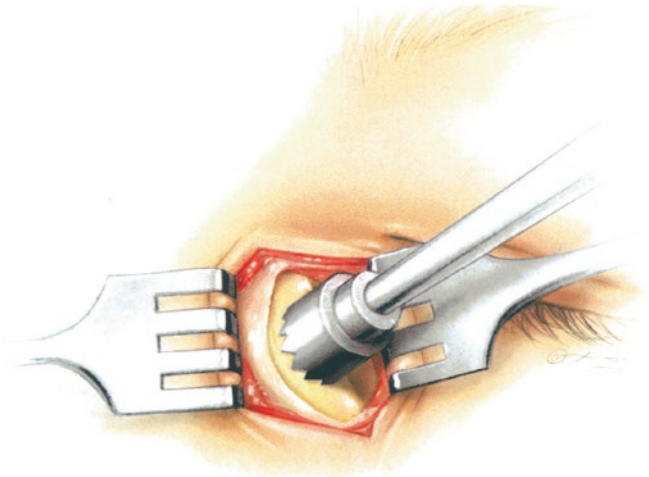


Fig. 28.5 Arruga trephine. An Arruga trephine may also be used to initiate the osteotomy in older children

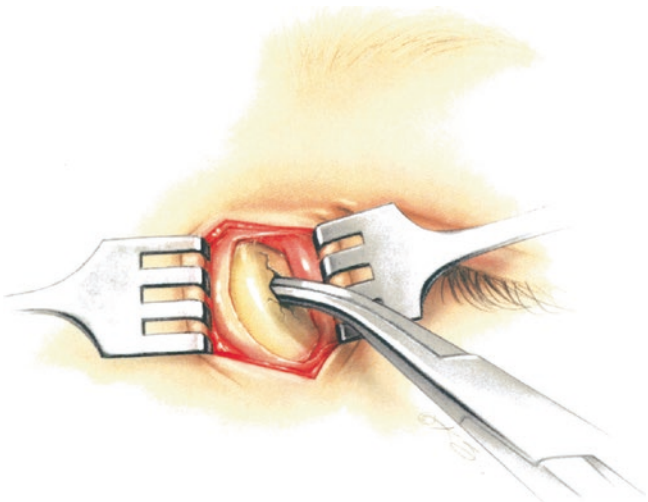


Fig. 28.4 Infracturing. A hemostat can be used to infracture the thin nasal bone in posterior/inferior lacrimal sac fossa. After the infracturing, spreading of the hemostat may enlarge the initial osteotomy. Care is taken to avoid damaging the underlying nasal mucosa

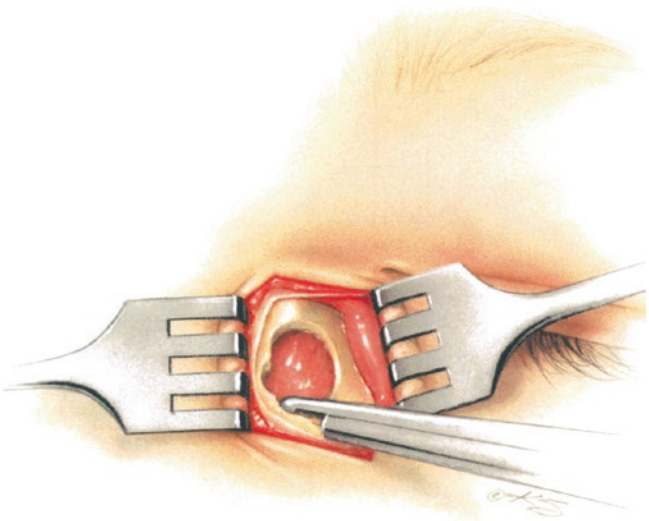


Fig. 28.6 Enlargement of ostium. The osteotomy is enlarged with neurosurgical microrongeurs

Ultimately, the easiest approach in all patients for external DCR is to outfracture the anterior ethmoid just posterior to the posterior lacrimal crest. A Rollet Rugine (John Weiss International, Milton Keynes, UK) can be used or a mosquito hemostat. This will allow enough space for a small-sized Kerrison rongeur to be used to create the initial rhinostomy. Care should be made to remove the bone from a posterior to anterior fashion, thus allowing better visualization and identification of the skull base.

The osteotomy is then enlarged to approximately 15 mm in diameter by removing most of the anterior lacrimal crest, the lacrimal sac fossa, and the posterior lacrimal crest with Kerrison rongeurs (Figs. 28.6 and 28.7) (Storz). A large osteotomy is important since there is a potential for closure with growth of the facial bones, and with a small rhinostomy, the lacrimal and mucosal flaps can more easily come into contact with the common canaliculus and cause scarring and a persistent lacrimal sac. It is important to place the osteotomy inferiorly so that should there ever be a need for a Pyrex tube bypass operation it could be adequately placed in the medial canthus. This involves the removal of the anterior portion of the nasal process of the maxilla at the juncture of the inferior orbital rim. In addition, if cotton tips are used, they should be retracted during the formation of the rhinostomy. The advantage of cotton tips (Q-tips) is that the wooden sticks can be readvanced to tent the nasal mucosa during the bony work to better identify the nasal mucosa and associated nasal space. Although care should also be taken to avoid tearing the nasal mucosa, this will sometimes occur. It is helpful to tilt the trephine so that the entrance into the nose occurs at the inferior edge. In this fashion the nasal mucosa can hinge

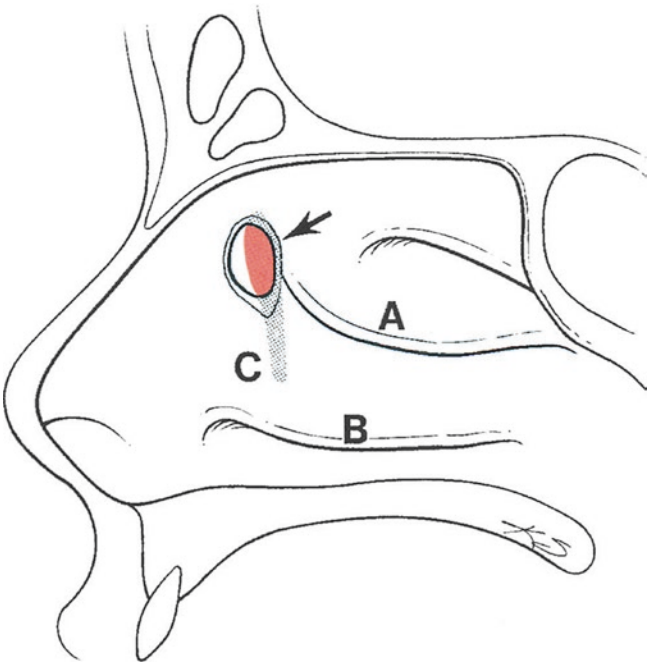


Fig. 28.7 Sagittal view of the DCR ostium (*arrow*). (*A*) Middle turbinate, (*B*) inferior turbinate, and (*C*) nasolacrimal duct

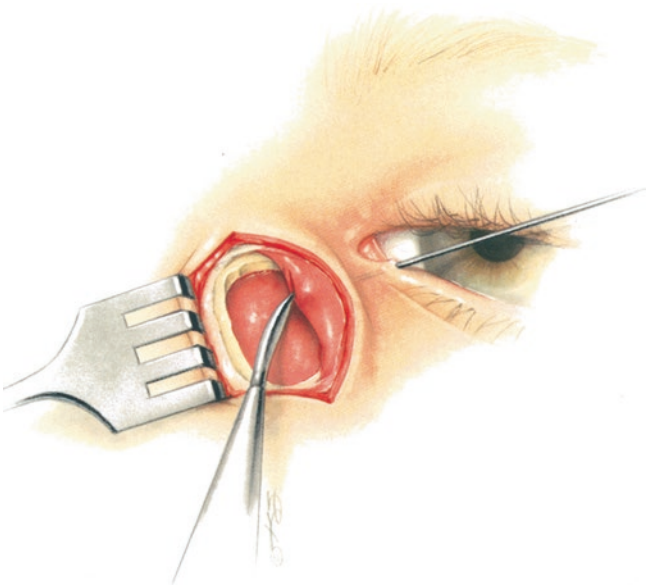


Fig. 28.8 Creating mucosal flaps. A vertical incision is made in the lacrimal sac to create anterior and posterior nasal mucosal flaps. Because of its angulation, a #66 Beaver blade is useful in this portion of the procedure. It can also be used to create a vertical incision in the nasal mucosa to create anterior and posterior mucosal flaps

superiorly when the flaps are cut. If the nasal mucosa remained intact throughout the creation of the osteotomy, it is injected with a small amount of 0.5% Xylocaine with 1:200,000 epinephrine to provide further vasoconstriction of the mucosal flap. It is frequently helpful at this point to pack the wound with neurosurgical cottonoids saturated with 1:200,000 epinephrine or liquid thrombin if there are no contraindications.

After allowing adequate time for vasoconstriction and hemostasis, the packing is removed, and a curved hemostat is used intranasally to tent the nasal mucosa outward (or the cotton tips can be advanced). Using a #11 blade, a large anterior mucosal flap is created (Fig. 28.8). This can also be made with the Colorado needle on a monopolar cautery unit. At this point, if there is any significant hemorrhage, a neurosurgical cottonoid or Gelfoam saturated with thrombin can be passed intranasally to tamponade the mucosa around the osteotomy. Because of rapid facial and bone growth, we favor silicone intubation in children to prevent closure of the osteotomy. At this point in the operation, a lacrimal probe (Storz) with attached silicone tube is passed through the lower canaliculus and used to tent the lacrimal sac outward. The #11 blade is used to create a vertical incision in the lacrimal sac from its fundus to the neck, creating both anterior and posterior mucosal flaps. An alternative is to use the Werb right-angle scissors to cut the junction of the nasolacrimal sac to the duct. One blade of the scissors is introduced into the sac, and the incision is carried superiorly to the fundus of the sac to create as large of an anterior flap as possible. At this point, a portion of the posterior lacrimal sac is excised for pathological examination. If the surgeon prefers, this posterior lacrimal flap can be anastomosed to the posterior nasal mucosal flap with a 5–0 or 6–0 Vicryl suture. The lacrimal probe with the attached silicone stent is then pulled out through the incision, and the other end of the tube with its attached probe is passed through the upper canaliculus into the lacrimal sac and brought out through the incision (Fig. 28.9). A silicone cuff that is packaged with the Guibor probe (Xorned-Treace, Jacksonville, FL) is cut to approximately 7–10 mm (depending on the size of the child's intranasal anatomy) and passed over the probes and silicone stents (Fig. 28.10). The probes are then removed, and a hemostat is placed up the nose and used to pull the tubes through the osteotomy out through the nares. Multiple surgical knots are then tied so that the cuff is secured. The excess silicone stent is then cut off just inside the nostril and removed. It is not necessary to suture the ends of the tube in the nose, because they are easily visible in the middle meatus, even in a small child.

An alternative to bicanalicular stenting is to use a monocanalicular stent (FCI ophthalmics) which has the advantage of being easier to remove and has been shown to be effective in DCR surgery (Fig. 28.11) [20].

The anterior flaps of nasal mucosa and lacrimal sac mucosa are then sutured meticulously with two to three interrupted sutures of 4–0 chromic or Vicryl material

(Ethicon) (Fig. 28.12). A P-2 needle is preferred due to its small size and radius of curvature. Suturing of the posterior flaps is optional. Then 4–0 chromic or Vicryl sutures are used to attach the periosteum medial to the lacrimal sac to the periosteum at the anterior lacrimal crest area. Alternatively, if the nasal mucosa is torn in creation of the osteotomy and a poor anterior mucosal flap is created, a larger anterior flap of lacrimal sac mucosa can be sutured to the periosteum at the anterior edge of the osteotomy. However, it is helpful to try to anastomose the lacrimal sac mucosa to at least a remnant of nasal mucosa intranasally. The silicone stent must be adjusted prior to securing its position with multiple knots. There should be no tension at the puncta by the loop in the medial canthus. It should rest midway between the puncta and the corneal limbus. The skin is then usually closed with a running 5–0 subcuticular nylon suture (Fig. 28.12c). If interrupted 6–0 or 5–0 fast-absorbing gut sutures (Ethicon) are used, then deeper support is usually necessary with 5–0 or 6–0 Vicryl mattress sutures to keep the wound in good apposition.

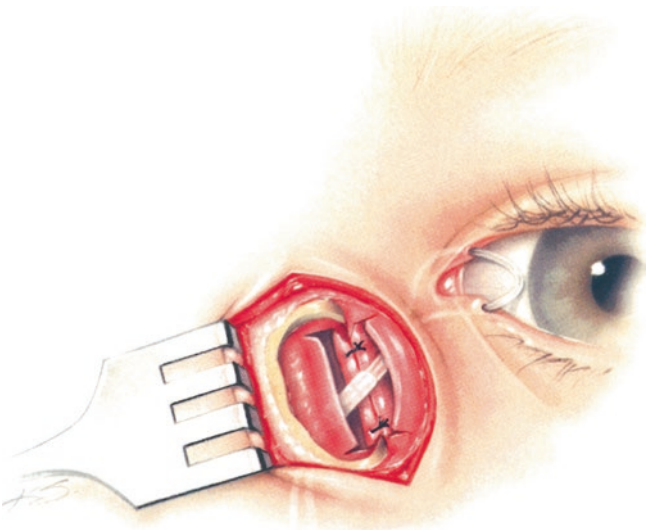


Fig. 28.9 Silicone stents. Silicone stents are passed through the puncta, sac, and DCR osteotomy and brought out through the wound

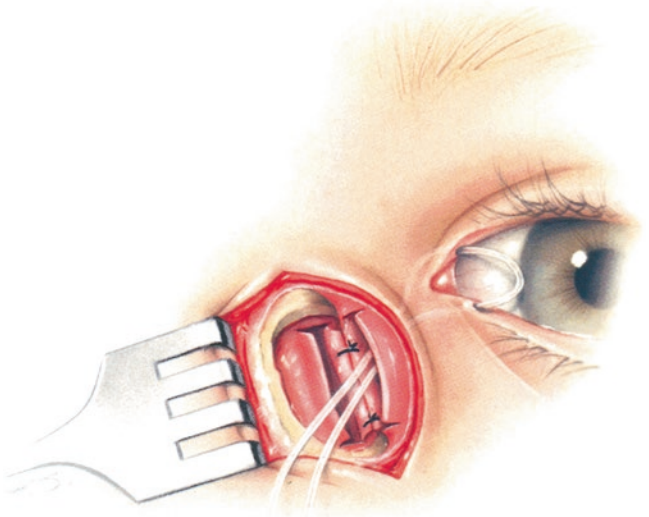


Fig. 28.10 Fixation of the silicone stent. Each probe with tubing attached is passed through a length of larger bore silicone, which creates a noose effect for securing the loop of tubing. The loop should be loose enough to pull halfway to the corneal limbus without tension. The probes are then removed, and multiple knots are tied at the appropriate tension. The excess silicone ends are cut, and the knot and cuff are allowed to retract into the nose

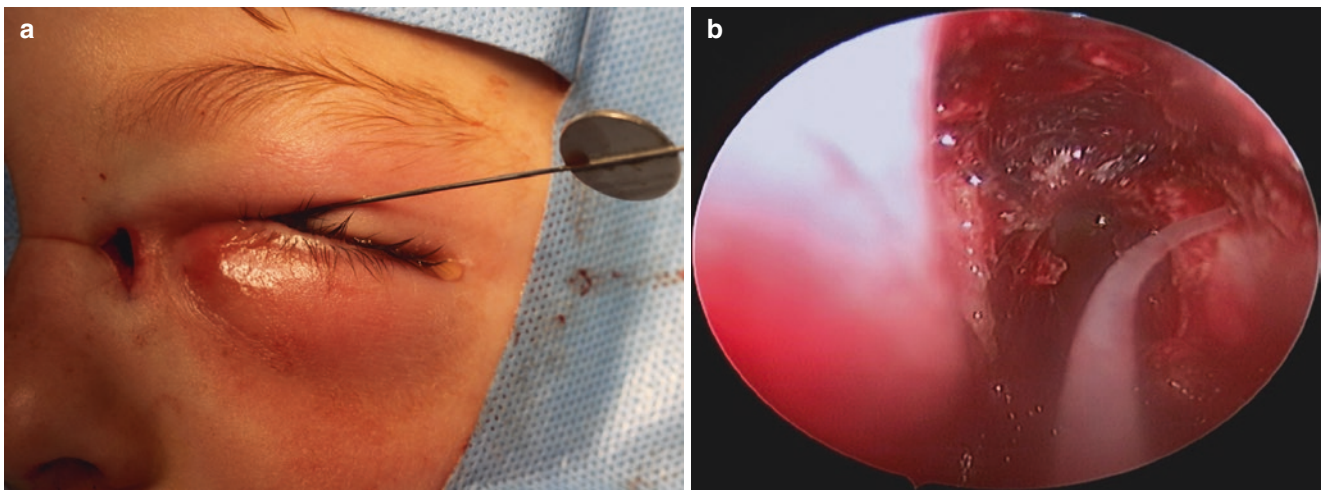


Fig. 28.11 Use of the self-threading monocanalicular stent (Monoka, FCI Ophthalmics) in external DCR surgery. (**a**) A Ritleng probe is passed from the punctum through the common canaliculus. A Monoka stent can then be advanced into the Ritleng probe (see Chap. 27 for this technique). (**b**) Intranasal endoscopic view of a Monoka stent emanating from the common canaliculus after an external DCR

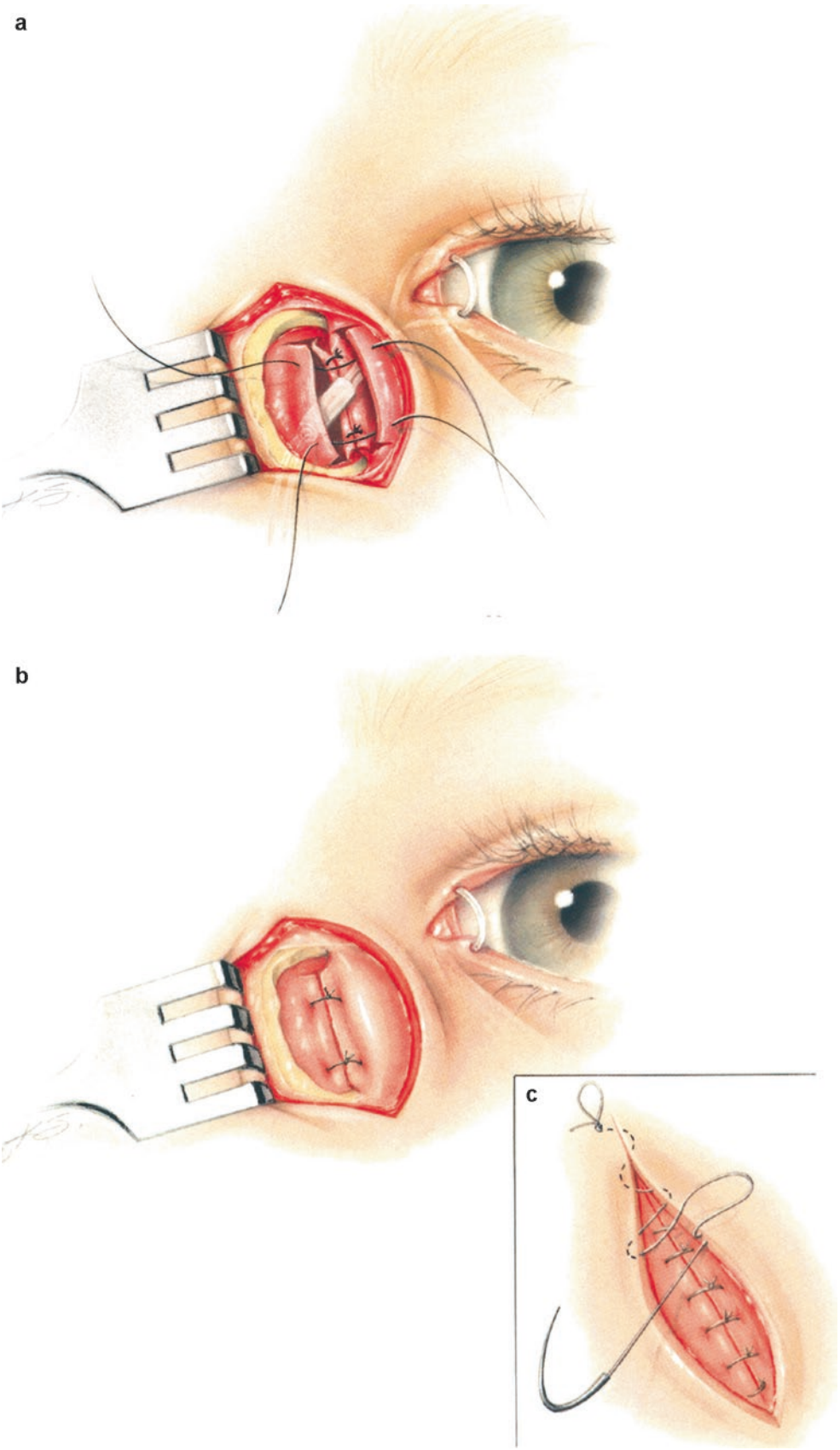


Fig. 28.12 Suturing of the mucosal flaps and the periosteum. (**a**) Both posterior nasal and lacrimal sac mucosal flaps are sutured with interrupted 4–0 chromic or Vicryl sutures. (**b**) The anterior flaps are sutured above the silicone stent. (**c**) Inset shows a running 5–0 nylon subcuticular suture closure of the DCR incision site

Postoperative Care for External Dacryocystorhinostomy

Immediately postoperatively, an antibiotic steroid ophthalmic ointment (Tobradex, Alcon Laboratories) is placed in the eye and along the incision. For the first day or two postoperatively, if the child is cooperative, cold compresses are placed to the operative area as much as possible. Adequate analgesia, antiemetics, and sleeping with the head elevated are commonly used techniques to minimize postoperative bleeding. Postoperative nasal decongestants are not routinely used, and the parents are cautioned that they may see bloody tears or some nasal oozing. Parents are instructed to call should significant nasal hemorrhage occur. The Tobradex ointment is used three to four times a day for 5–7 days. Oral antibiotics are administered for 5 days postoperatively. The patient is seen for a postoperative visit 5–7 days following the surgery. At that time, if a nylon suture was used, it is removed. The patient is then checked 3–4 weeks later, and the parents are instructed to observe the tube to be sure that cheese wiring of the canaliculus does not occur. The tube is generally removed at 8–12 weeks postoperatively. This is usually easily done in the office by restraining the child and grasping the tube in the middle meatus with a small mosquito hemostat and cutting it at the medial canthus with a blunt-tipped scissors. Alternatively, the ends may be pulled from the nose and one strand of the tubing cut above the knot, thus avoiding accidental injury to the eye. General anesthesia or laryngeal mask anesthesia is rarely necessary.

Endonasal Dacryocystorhinostomy

Endonasal approaches to dacryocystorhinostomy date back to the late nineteenth century when Caldwell [21] described a nasal approach to lacrimal duct obstruction. Intranasal dacryocystorhinostomy was utilized mainly by otolaryngologists, although it never obtained the popularity of external dacryocystorhinostomy until recently. It was revived in the late 1980s [22] and popularized by Gennering and others in the ophthalmic community in the early 1990s. With the introduction of the rigid endoscope, endoscopic dacryocystorhinostomy (eDCR) became a viable option to achieve this successful fistulization of the common canaliculus into the nasal space [23, 24]. Endoscopic dacryocystorhinostomy (enDCR) may be utilized in children with the use of a laser [25, 26]. The major difficulty is the size of the nasal passages, which usually mandates a smaller diameter sinuscope.

It is helpful to have both pediatric (0° and 30° 2.8-mm diameter) and adult (0° and 30° 4-mm diameter) sinuscopes (Karl Stortz, Tuttlinsen, Germany) available, although, as mentioned above, in small children a pediatric sinuscope is much more useful and easier to manipulate because of its small size. The larger size scope has the main benefit of a better view of the surgical field because it is a wider scope. When possible, the 4-mm diameter scope is used.

The main decision in surgical planning for edDCR in children is how the surgical rhinostomy will be accomplished. The common instrument set of an external DCR is usually sufficient to accomplish enDCR surgery with the exception of the need for endoscopes. Kerrison rongeurs are readily available and perfectly efficient in enDCR surgery for the creation of a surgical rhinostomy in pediatric patients. The largest reviews to date of enDCR have used the Kerrison rongeur [10, 17]. The main challenge to this instrument is the tight intranasal space in pediatric patients. This requires the use of smaller Kerrison rongeurs. We use a Kerrison rotating rongeur (Jedmed, St. Louis, MO). This instrument has the added advantage of a shaft that rotates into eight different "biting" positions allowing the surgeon to maintain a comfortable hand position. The largest drawback to the Kerrison rongeur is the inability to debride the superior most portion of the surgical rhinostomy both safely and comfortable. Because this is continuous with the skull base, this bone must be removed with care.

An alternative instrument is a microdrill. Typically the diamond burr drill tip is employed to accomplish this. The microdrill has the added benefit of being able to dissect bone up to the skull base with ease and has the added benefit of being very rapid in its dissecting speed. We currently use the Straightshot M4 microdebrider (Medtronic, Mansfield, MA) with a diamond burr tip. There are many other drill systems available. We prefer this system because it has interchangeable dissecting tips, and we will also use the same hand piece with a tri-cut blade. The greatest drawback to the microdrill, however, is the risk for iatrogenic injury. This high-powered instrument, if used aggressively, can easily dissect into unwanted surgical territory. There is a risk for intraorbital dissection where both orbital fat and extraocular muscles can easily become ensnared by the drill time. More typically, if the surgeon is not careful, the nasal septum can be accidentally injured, and finally, the injury of greatest concern is the potential violation of the skull base.

A major breakthrough for enDCR surgery in pediatric patients that has allowed for the safe formation of a surgical rhinostomy is the advent of the ultrasonic bone aspirator (UBA). One such device is the Sonopet® (Stryker Corporation, Kalamazoo, MI, USA) which was first introduced in Japan in 1974 as a neurosurgical device. This instrument has been approved for surgery in the USA by the FDA since 2002. The device consists of a console (Fig. 28.13a), a hand piece (Fig. 28.13b, c), and a tip (Fig. 28.13d, e). The console is the main control box with switches for ultrasonic power regula-



Fig. 28.13 The Sonopet® ultrasound bone aspirator. (**a**) Main unit that allows one to control the instrument ultrasound power, suction, and irrigation. (**b**) The straight hand piece, (**c**) the angled hand piece, (**d**) the Spetzler claw, and (**e**) the Payner 360° tip (Courtesy of Stryker, USA)

tion, suction, and irrigation. We use the angled hand piece, which is best suited for pediatric patients. Several bone-cutting tips are available, but of most utility in lacrimal surgery are the Spetzler claw (Fig. 28.13d) and the Payner 360 (Fig. 28.13e). An enDCR with the use of an ultrasonic bone aspirator is shown in Fig. 28.15.

The UBA uses ultrasonic vibration to emulsify the bone with minimal heat production or damage to surrounding soft tissue [27]. The hand piece motor is a piezoelectric unit, consisting of a stack of ceramic crystals. When these crystals become electrically charged, they expand and contract causing the longitudinal motion of the device tip with oscillation

occurring at 25,000 times per second (25 kHz). In addition a torsional motion is produced by helical weakness/reliefs in the shaft of the tip, and this redirects the ultrasonic pulse from a purely longitudinal one to a torsional. The benefit of this type of oscillation is that soft tissue containing elastin will readily absorb these vibrations, whereas bone and other firm tissues containing collagen will break apart. The anatomical significance of this is a smooth and controlled osteotomy sparing any damage to the lacrimal sac mucosa and common canaliculus and hence a lower incidence of iatrogenic soft tissue injury and less postoperative complications. Minimal manual pressure is needed to allow for tip movement as opposed to the more traditional instruments. The simultaneous irrigation reduces heat and keeps a clear field, while suction ensures that debris and liquid are quickly removed from the field. When used for bone-cutting properties, we used the manufacturer-recommended console settings: ultrasonic power at 100%, suction at 50%, and irrigation at 20 ml/min. These settings can be easily changed based on the situation and the surgeon's preference.

A major drawback to this device is its cost. The entire unit is currently over $100,000, and at our institution it is shared with the neurosurgery and otolaryngology services. In addition, the surgical tips are over $500 for each case. These costs are simply impractical for a small practice and surgical center. It is our hope that, over time, however, these costs will decline to permit more general use of this device.

Finally, some surgeons prefer to use lasers to create a surgical rhinostomy. This can be accomplished with a CO_2 or KTP laser [25]. Because of the increased expense and no evidence that it results in a higher success rate [28, 29], KTP laser or CO_2 laser is used with less frequency for endoscopic dacryocystorhinostomy (enDCR) in children. One of the keys to surgical success is the creation of a large osteotomy to allow optimum exposure of the common canaliculus. A major drawback with the use of lasers alone is the creation of only a small osteotomy. Some surgeons will use a laser and then place a balloon (Atrion Medical Products, Arab, Alabama) either intranasal or intraduct to enlarge this osteotomy [30].

For pediatric endoscopic dacryocystorhinostomy, general as well as local anesthetic and vasoconstrictive agents are used in similar fashion to that for an external dacryocystorhinostomy. The 19-gauge fiber-optic light pipe (Trek Medical Products, Mukwonago, WI) is also helpful to identify the lacrimal sac fossa intranasally. The 19-gauge fiber-optic light pipe is passed through the upper or lower canaliculus in a very gentle fashion.

The light pipe does present a risk for causing burn injury. For this reason, the lowest effective intensity setting is preferred when using the light pipe. With the operating room lights dimmed, the sinuscope is used to visualize the light spot intranasally, thus identifying the location of the proposed osteotomy (Fig. 28.14). This is usually inferior and slightly anterior to the anterior insertion of the middle turbinate on the lateral wall of the nose. Using a long 27-gauge needle, this area of the nasal mucosa is then injected with 0.5% Xylocaine with 1:200,000 epinephrine. The nasal mucosa overlying the light spot is incised with a 3.8-MHz radiosurgical unit with a curved F1 broad-needle electrode (Ellman, Hewlett, NY) using the fully rectified wave, cut, and coagulation mode. Alternatively, a monopolar cautery unit with a Colorado needle tip can be used. A Freer elevator

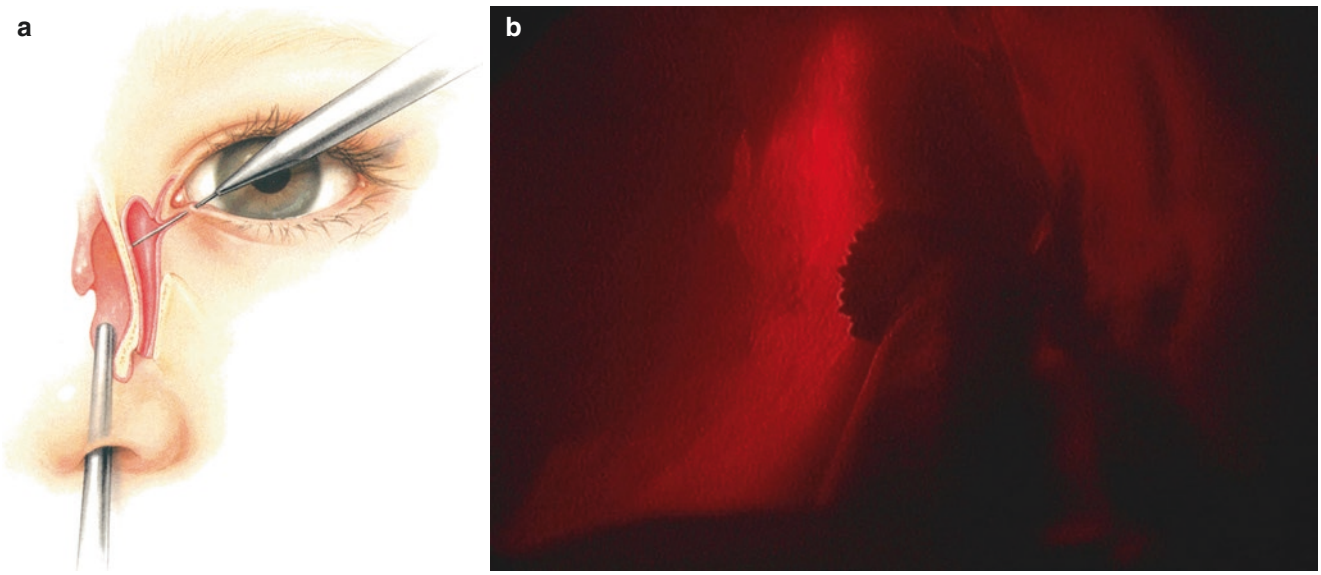


Fig. 28.14 Vitrectomy light pipe. (**a**) The 19-gauge vitrectomy light pipe in the lacrimal sac, transilluminating the appropriate site for the osteotomy that is visualized using the nasal endoscope. (**b**) The lacrimal sac fossa is transilluminated and visible in the intranasal space via an endonasal endoscopic view. A Sonopet® instrument will be used to create a bony rhinostomy to expose the lacrimal sac

is then used to create a mucosal flap and raise the uncinate process. This flap can then be removed with either Kerrison rongeurs or with a tricot microdebrider (2.9-mm tricot tip, Medtronic, Mansfield, MA). Hemostasis must be maintained, and if necessary cautery should be used. Alternatively, ½′ by 3′ cottonoids dipped in oxymetazoline 0.5% solution can be used.

A bony osteotomy is then created. Once again, this can be accomplished with either a Kerrison rongeur, an otodrill with a 2–3-mm tip (Xomed-Treace), or the ultrasonic bone aspirator (Sonopet®, Stryker).

It is usually possible to avoid tearing the lacrimal sac during the creation of the osteotomy. If the anterior tip of the middle turbinate is interfering with creation of the osteotomy, it can be injected with 0.5% Xylocaine with 1:100,000 epinephrine and then resected using intranasal turbinate scissors (Storz). If adequate vasoconstriction is obtained at the beginning of the procedure, further cautery is rarely necessary. One must be careful to avoid infracturing the middle turbinate too aggressively because of its insertion near the cribriform plate. Aggressive manipulation may cause a fracture in the cribriform plate, resulting in postoperative cerebrospinal fluid (CSF) leaks, as the dura invaginates into the superior aspect of the middle turbinate [31].

After the osteotomy is created, the light pipe is used to tent out the lacrimal sac, and a vertical incision is performed to create both anterior and posterior mucosal flaps (Fig. 28.15). Using Takahashi forceps (Storz), the posterior lacrimal sac can be removed for biopsy (if necessary). A Kerrison rongeur can be used to remove the anterior and posterior lacrimal sac flaps. The light pipe is removed, and a stent is placed advanced from the eyelid punctum through the common canaliculus. We currently have used the Monoka or Masterka stent in enDCR surgery (FCI Ophthalmics) with great success, though there are now many silicone stent products currently. The main advantage of a monocanalicular stent is the ease of in-office removal without the need for an intranasal maneuver to

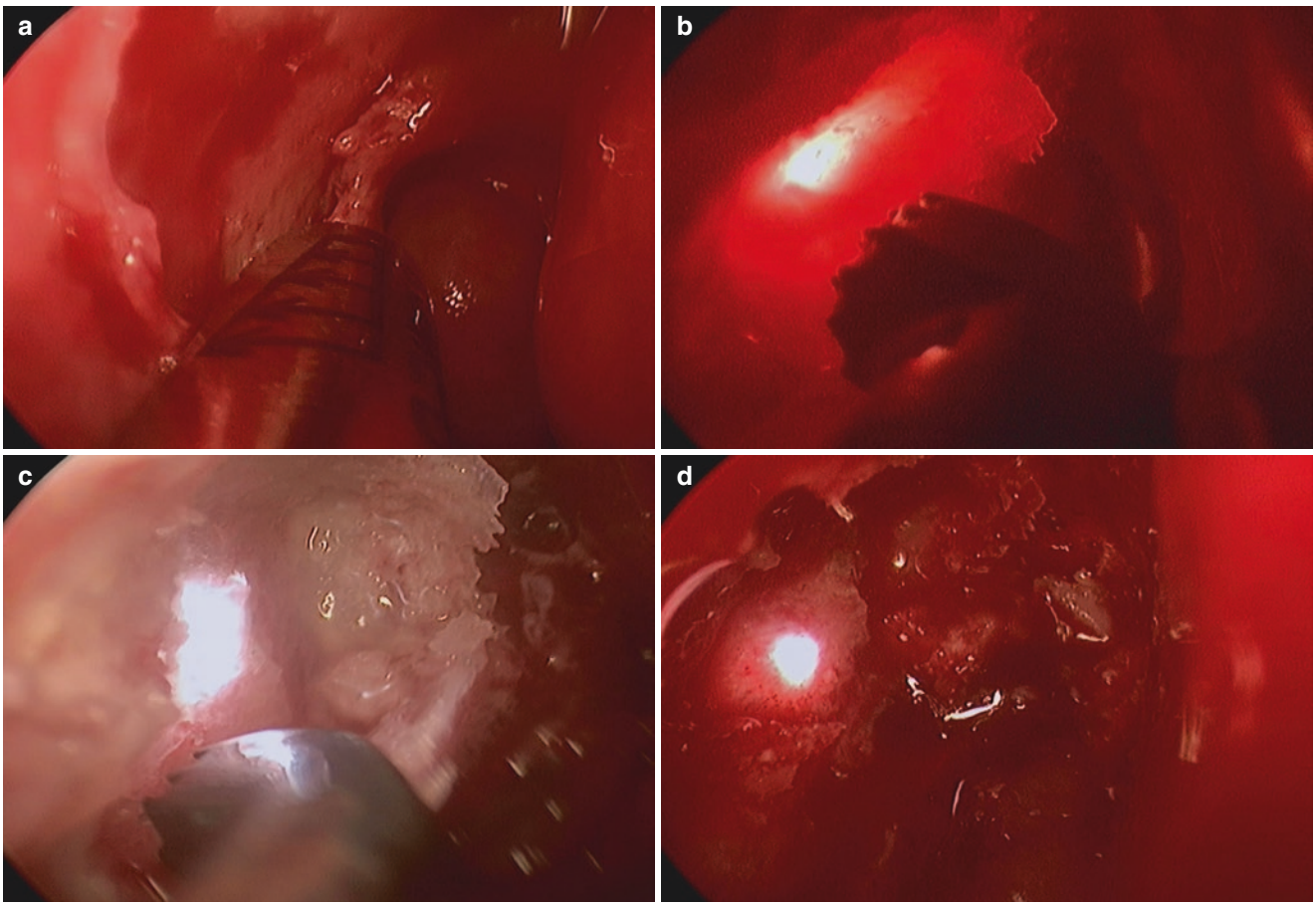


Fig. 28.15 enDCR with the Sonopet® ultrasound bone aspirator. (**a**) A nasal mucosal incision is made corresponding to the transillumination of the lacrimal sac fossa (not pictured). A mucosal flap is elevated with a Freer elevator (not pictured). With the use of a microdebrider (Medtronic, Minneapolis, MD), a nasal flap is removed (this could also be accomplished with Kerrison rongeurs). (**b**) The lacrimal sac fossa is transilluminated at the level of the common canaliculus. The endoscope light is turned off for better localization. (**c**) Creation of bony rhinostomy with the ultrasonic bone aspirator. The lacrimal sac is exposed with bone removal. (**d**) After the creation of a bony rhinostomy, the light pipe is visible within the lacrimal sac. The light pipe (or a lacrimal probe) is used to tent the sac medially, and with the use of a sickle blade, and vertical incision is made in the lacrimal sac (not pictured).

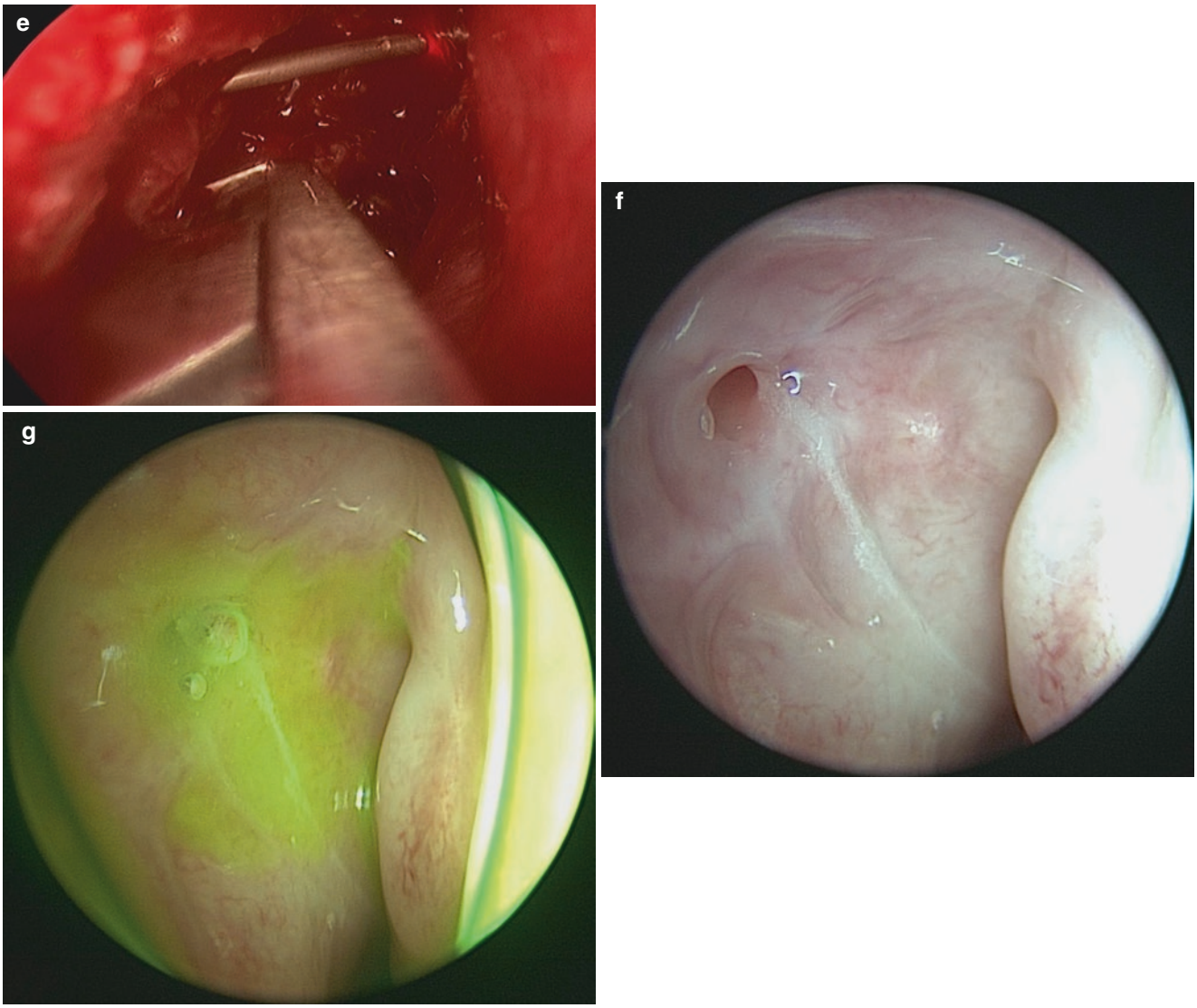


Fig. 28.15 (continued) (**e**) To prevent unwanted adhesions of the medial lacrimal mucosa to the common canaliculus, and to prevent the closure of the lacrimal flaps, the anterior and posterior flaps can be debrided with a Kerrison rongeur. This is much safer than to attempt sac wall debulking with a microdebrider, which could injure the orbital fat, extraocular muscles, and the eye itself. The system can then be intubated with a mono- or bicanalicular stent (not pictured). (**f**) Postoperative picture showing the common canaliculus visible along the lateral nasal wall 6 months after surgery (status post 2 months of stent intubation). (**g**) Free flow of fluorescein is noted

remove the stents. Also, there is no canalicular slitting that can occur with the use of a bicanalicular silicone stent.

Postoperative Care

In general, postoperative care for an endoscopic DCR is similar to that for external dacryocystorhinostomy. There is frequently less bruising, however, and cold compresses are not necessary following endoscopic dacryocystorhinostomy. Although frequent endoscopic cleansing of the osteotomy site is recommended in adults, this is not possible in young children. Because of the relatively higher dose effects in small children, intranasal steroids are not routinely used.

Complications

The most worrisome complication of pediatric dacryocystorhinostomy, especially in the very small child or infant, is extensive hemorrhage. Transfusion is rarely necessary, but it is important to discuss this possibility preoperatively with the patient's parents or legal guardian. Judicious use of preoperative and intraoperative vasoconstrictive agents helps to prevent significant hemorrhage. Bipolar and Bovie cautery can also be used intraoperatively to minimize hemorrhage. Usually a dacryocystorhinostomy can easily be performed with less than 10–15 mL of blood loss. The skin incision for external dacryocystorhinostomy is kept as short as possible in children and is rarely longer than 15 mm in length.



Fig. 28.16 Punctal granuloma associated with a Monoka stent. The stent was removed and the granuloma improved with topical steroid/antibiotic drops

The skin incision in a child usually heals well and within a year postoperatively is barely visible. However, care must be taken in patients with epicanthal folds to avoid exacerbating the epicanthal fold by improper placement of the incision. In some instances if epicanthal fold repair is required, unilateral or bilateral DCRs can be done through either Y-V or Mustarde-type Z-plasty flaps.

The two main complications of bicanalicular silicone intubation are slitting of the lower canaliculi and punctal granuloma (Fig. 28.16) [29]. If there is early cheese wiring of canaliculus, then the silicone stent must be removed early. In general, 4–5 mm of cheese wiring of the canaliculus either heals quickly or still permits normal tear outflow in children following removal of the silicone stent. This is similar to the situation seen in adults when the canaliculus is opened to scrape it out in cases of chronic canaliculitis secondary to actinomycetes. Nevertheless, because of the potential for more extreme slitting in children, it is important for both the parents and the physician to keep close watch of a bicanalicular stent postoperatively. Granulomas can generally be excised at the time of tube removal and rarely recur following removal of the stent. A short course of a topical antibiotic steroid is also useful. Gentle cautery may be needed, however, for a recurrent granuloma.

Dacryocystorhinostomy Failure

While dacryocystorhinostomy failure is really an unfavorable result rather than a true complication, some thoughts regarding management should be discussed. The most common cause is closure of the bony ostium or mucosal flaps by scarring. Excision of the scar or destruction with laser can be done endoscopically. The KTP laser fiber-optic delivery cable fits easily into the pediatric canaliculus. The KTP laser is useful for creating an opening, but care must be taken to avoid damage to the septum during its use. After the punctum and canaliculus are dilated, the KTP fiber-optic delivery cable is introduced into the superior canaliculus and advanced into the lacrimal sac up to the ostium and the soft tissue blockage site (Fig. 28.17). The light will be visible through the scarred mucosa and permits visualization while creating the opening (Fig. 28.18). Once a new opening has been created (Fig. 28.19), the system can then be intubated with silicone material as previously described, or the new opening can be further dilated with a 5-mm balloon catheter or 2–3-mm size if there is any resistance to the larger size in the canaliculus or common opening.

When using the balloon catheter, it is passed through the upper nasolacrimal system until the tip of the balloon protrudes through the previously obstructed ostium and into the nose (Fig. 28.20a). The balloon is inflated with saline to 9 atm for 90 s, which is then repeated for another 60 s (Fig. 28.20b). The balloon is deflated and removed, and the Crawford silicone stenting is used to intubate the newly created opening (Fig. 28.21). If desirable, a larger diameter silicone stent (Stentube–Atrion Medical Products) can be used. Only anecdotal reports have confirmed our adjunctive use of the balloon catheter with the KTP laser for treatment of failed dacryocystorhinostomies. Whether there is any efficacy in adding balloon dilatation to KTP laser and silicone intubation still needs to be determined in the long-term patency of the dacryocystorhinostomy.

Interestingly, the balloon catheter has also been suggested as the sole primary treatment of failed incisional dacryocystorhinostomy. Usage in this manner assumes a previously created larger osteotomy, where the secondary obstruction is assumed to be soft tissue in nature. The procedure involves first dilating the puncta, canaliculi, and obstructed ostium into the nose with a Bowman probe of appropriate size that will permit a 2- or 3-mm balloon. The wider 5-mm balloon is usually too broad for pediatric use. The balloon catheter is next passed through the upper nasolacrimal system until the tip of the balloon protrudes through the previously obstructed ostium and into the nose. As described previously, the balloon is inflated with saline to 9 atm for 90 s, which is then repeated for only 60 s. Silicone tubing is then used to maintain patency in cases of complete obstruction. As with the use of the balloon catheter for primary dacryocystorhinostomy, there is scant peer-reviewed literature describing the experience or outcome using the balloon catheter as a primary treatment for failed dacryocystorhinostomies. Further

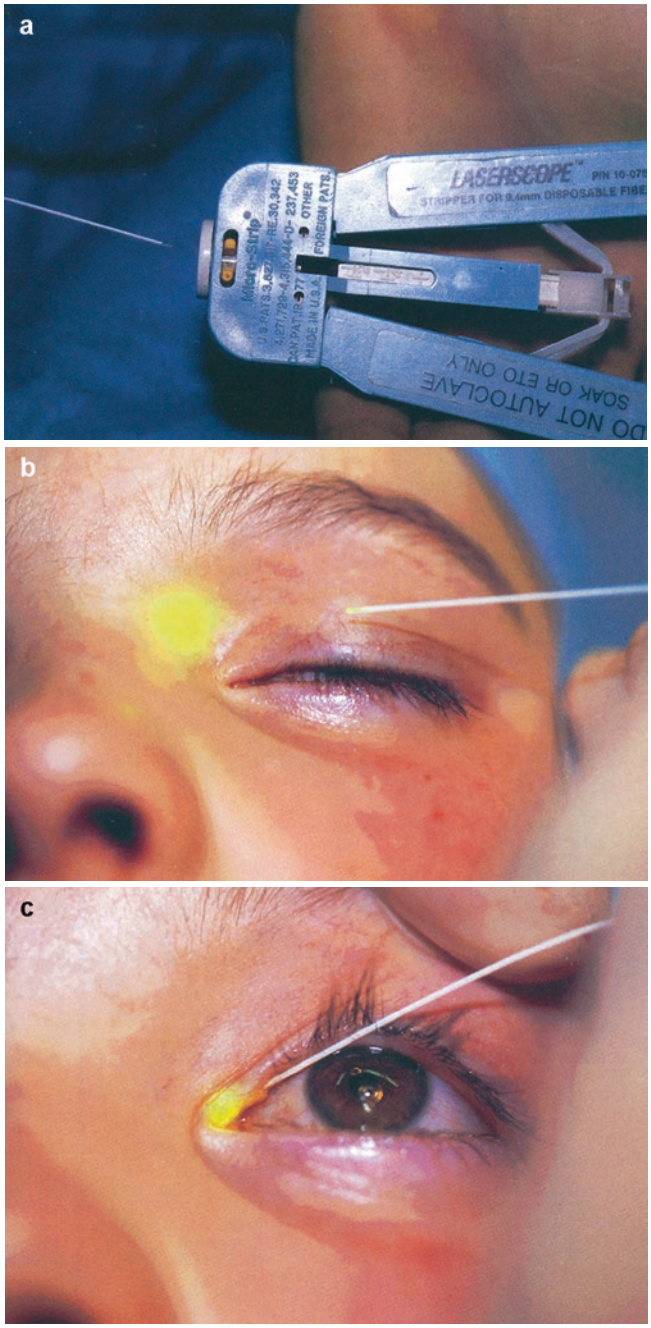


Fig. 28.17 KTP laser. (**a**) The KTP laser fiber-optic delivery cable is scored and stripped prior to use. (**b**) Green light demonstrates aiming beam from end of fiber-optic cable. (**c**) The laser cable is next introduced into the upper canaliculus and passed through the lacrimal sac until the point of obstruction is reached

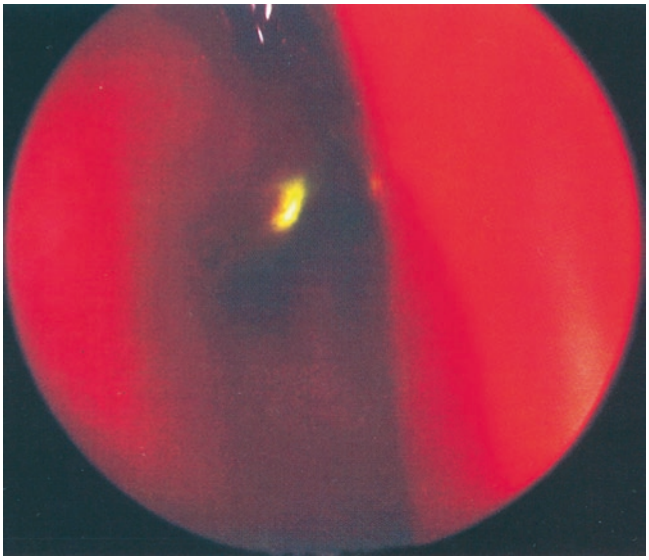


Fig. 28.18 Occluded DCR nasal opening and KTP laser. Endoscopic view of the occluded DCR nasal opening on the lateral nasal wall (*left*) with the KTP laser beam visible behind the scarred mucosa

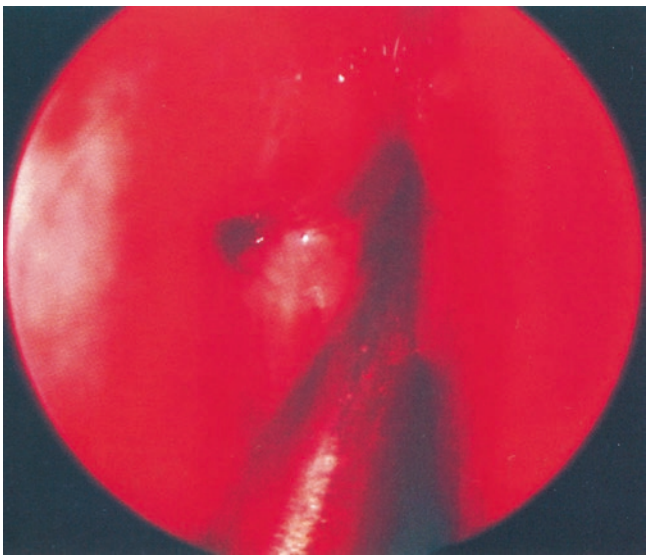


Fig. 28.19 DCR nasal opening after patency is reestablished with the KTP laser

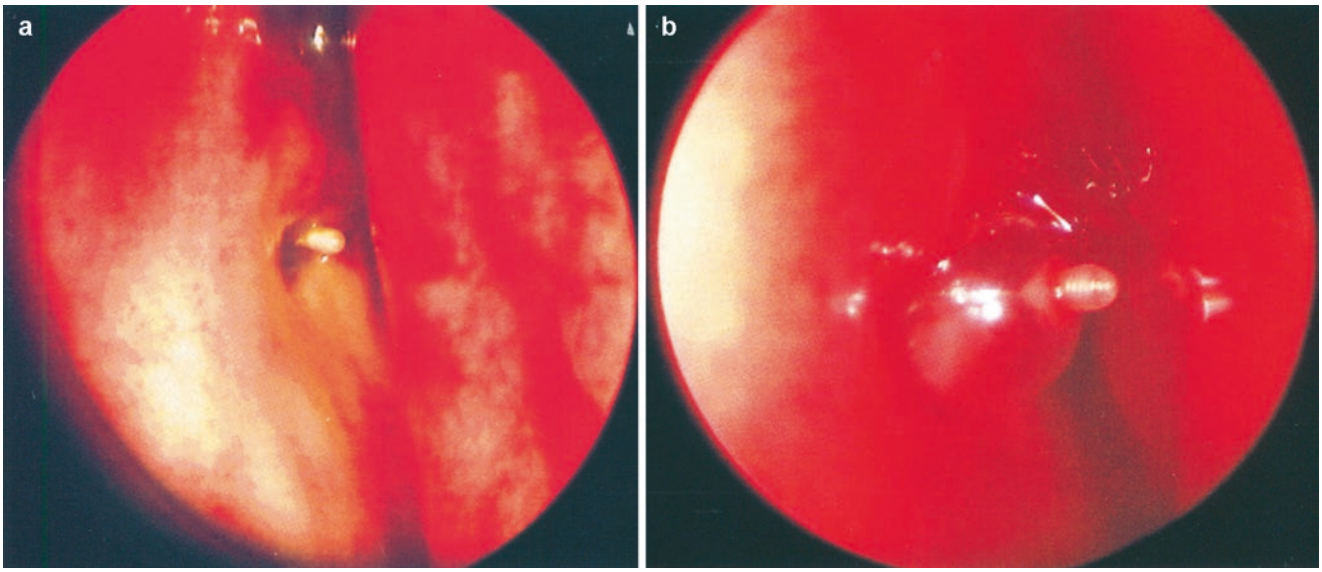


Fig. 28.20 Balloon catheter. (**a**) A 5-inm balloon catheter is introduced to the level of the earlier obstruction, with the tip just visible inside the nose. (**b**) The balloon is inflated, further lysing any soft tissue adhesions, thus enlarging the DCR lumen

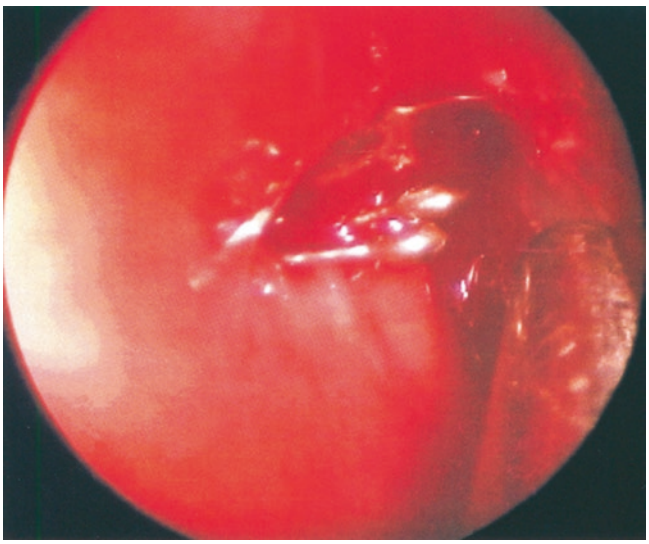


Fig. 28.21 Crawford tubes. The Crawford tubes being introduced through the newly established DCR opening. The attached silicone tubing will remain in place 8–12 weeks to help ensure long-term patency of the DCR

studies are needed to conclusively demonstrate the value of this interesting concept.

Intranasal scarring occurs after all DCR surgeries. Ideally, this does not involve the common canaliculus or cause a cicatricial closure of the surgical rhinostomy. One technique to prevent this is the direct application or intramucosal injection of mitomycin C. This is particularly useful following a failed DCR with scarring of the flaps or bony ostium. The anti-metabolite is a cell-cycle nonspecific alkylating agent, which inhibits DNA, RNA, and protein synthesis, and has antiproliferative or antifibroblastic activity [32]. A large review of 562 subjects who underwent randomized control studies found MMC to have a better success rate in external DCR [33]. MMC was also shown to be effective in enDCR cases [32]. Dolmetsch et al. published a large series of 71 consecutive cases of enDCR in patients 16 years and younger. In their technique neurosurgical cottonoid soaked in mitomycin C at 0.5 mg/ml was placed at the osteotomy site for 5 min. They reported a 94.4% success rate [34]. At the Children's Hospital of Philadelphia, we typically reserve the use of MMC for cases of severe intranasal scarring in failed cases or patients with known autoimmune diseases such as juvenile rheumatoid arthritis.

A useful surgical instrument for scarring within the canaliculus or at the level of the common canaliculus is the Sisler trephine (Beaver-Visitec, Waltham, MA). The advantage of this single-use disposable trephine is that it is more readily available and cheaper than the KTP laser. For obstructions within the canaliculus, the trephine is advanced to the obstruction, the stylet is retracted, and the obstructive tissue is lysed. The canaliculus is then intubated. For obstructions at the level of the common canaliculus (Fig. 28.22), the device is inserted into the upper or lower canaliculus and advanced to the scarred common canaliculus. The stylet is removed, and the scar is lysed. The system is then best intubated with a mono- or bicanalicular stent. The stent is left in place for at least 3 months.

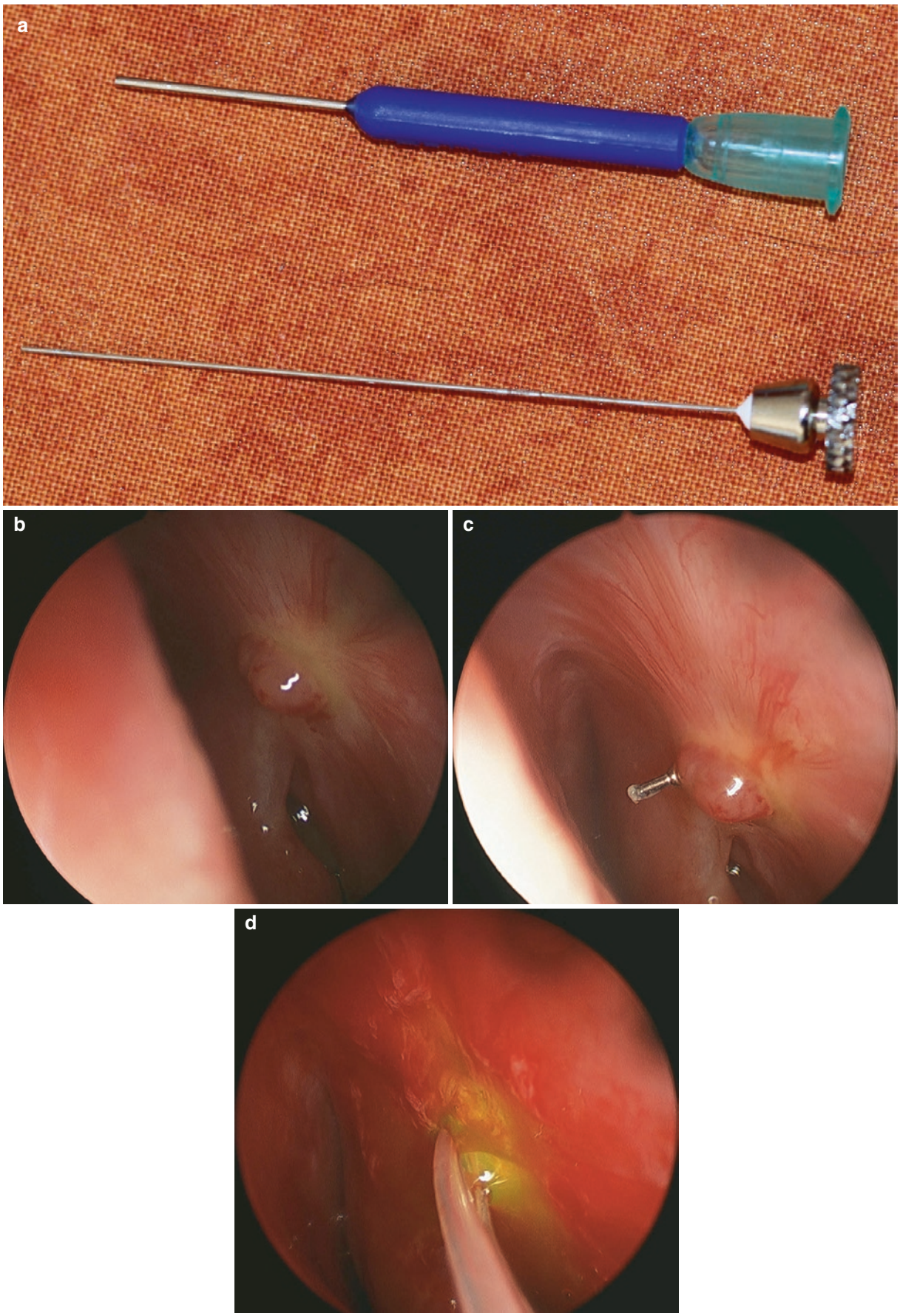


Fig. 28.22 Sisler trephine. (**a**) Trephine and stylet. (**b**) Scar over the common canaliculus status post enDCR. (**c**) Scar lysis with the Sisler trephine. (**d**) Bicanalicular stent intubation after scar lysis. There is good flow of fluorescein through the common canaliculus into the nasal space

References

1. Giasin O, Yeo DC, Aguirre A. Just how old is the modern dacrocystorhinostomy? Br J Ophthalmol. 2014;98(8):1134–5.
2. Chandler PA. Dacryocystorhinostomy. Trans Am Ophthalmol Soc. 1936;34:240–63.
3. Welharn RAN, Hughes SM. Lacrimal surgery in children. Am J Ophthalmol. 1985;9:27–34.
4. Nowinski TS, Flanagan JD, Mauriello J. Pediatric dacryocystorhinostomy. Arch Ophthalmol. 1985;103:1226–8.
5. Barnes EA, Abou-Rayyah Y, Rose GE. Pediatric dacryocystorhinostomy for nasolacrimal duct obstruction. Ophthalmology. 2001;108(9):1562–4.
6. Elder MJ. Pediatric dacryocystorhinostomy. Aust N Z J Ophthalmol. 1992;8:333–6.
7. Ritter FM. The paranasal sinuses: anatomy and surgical technique. 2d ed. St. Louis: Mosby; 1978.
8. Rebeiz EE, et al. Anatomic guidelines for dacryocystorhinostomy. Presented to the eastern section of the Triological society. Philadelphia; 1991.
9. Whitnall SE. The nasolacrimal canal: the extent to which it is influenced by the maxilla and the influences on its caliber. Ophthalmoscope. 1912;10:557–8.
10. Fayet B, Katowitz WR, Racy E, Ruban JM, Katowitz JA. Endoscopic dacryocystorhinostomy: the keys to surgical success. Ophthal Plast Reconstr Surg. 2014;30(1):69–71.
11. Blaylock WK, Moore CA, Linberg JV. Anterior ethmoid anatomy facilitates dacryocystorhinostomy. Arch Ophthalmol. 1990;108:1774–7.
12. Welham RAN, Wulc AE. Management of unsuccessful lacrimal surgery. Br J Ophthalmol. 1987;71:152.
13. McLachlan DL, Shannon GM, Flanagan JC. Results of dacryocystorhinostomy: analysis of the reoperations. Ophthalmic Surg. 1980;11:427–130.
14. Emmerick KH, Ungerechts R, Meyer Rusenberg HW. Possibilities and limits of minimal invasive lacrimal surgery. Orbit. 2000;19(2):67–71.
15. Jung SK, Kim YC, Cho WK, Paik JS, Yang SW. Surgical outcomes of endoscopic dacryocystorhinostomy: analysis of 1083 consecutive cases. Can J Ophthalmol. 2015;50(6):466–70.
16. Katowitz W. Pediatric enDCR with an ultrasonic bone aspirator. World Ophthalmology Congress, February 8, 2016.
17. Gioacchini FM, Alicandri-Ciufelli M, Kaleci S, Re M. The outcomes of endoscopic dacryocystorhinostomy in children: a systematic review. Int J Pediatr Otorhinolaryngol. 2015;79(7):947–52.
18. Meyers EF. Cocaine toxicity during dacryocystorhinostomy. Arch Ophthalmol. 1980;98:842–3.
19. Birchansky LD, Nerad JA, Kersten RC, Kulwin DR. Management of congenital lacrimal sac fistula. Arch Ophthalmol. 1990;108:388–90.
20. Detorakis ET, Mavrikakis I, Ioannakis K, Pallikaris IG. Monocanalicular intubation in external dacryocystorhinostomy. Ophthal Plast Reconstr Surg. 2011;27(6):439–41.
21. Caldwell GW. Two new operations for obstruction of the nasal duct with preservation of the canaliculi. Am J Ophthalmol. 1893;10:189.
22. Stedman GM. Transnasal dacryocystorhinostomy. Otolaryngol Clin N Am. 1985;18:107.
23. Kennedy DW. Functional endoscopic sinus surgery. Technique Arch Otolaryngol. 1985;111:643–9.
24. Woog JJ, Kennedy R, Custer PL, Kaltreider SA, Meyer DR, Camara JG. Endonasal dacryocystorhinostomy: a report by the American Academy of Ophthalmology. Ophthalmology. 2001;108:2369–77.
25. Massaro BM, Gonnering RS, Harris GJ. Endonasal laser dacryocystorhinostomy. A new approach to nasolacrimal duct obstruction. Arch Ophthalmol. 1990;108:1172–6.
26. Kong YT, Kim TI, Kong BW. A report of 131 cases of endoscopic laser lacrimal surgery. Ophthalmology. 1994;101:1793–800.
27. Pribitkin EA, Lavasani LS, Shindle C, Greywoode JD. Sonic rhinoplasty: sculpting the nasal dorsum with the ultrasonic bone aspirator. Laryngoscope. 2010;120:1504–7.
28. Gennering RS, Lyon DB, Fischer JC. Endoscopic laser assisted lacrimal surgery. Am J Ophthalmol. 1991;111:152–7.
29. Katowitz JA, Kropp TM. Congenital abnormalities of the lacrimal drainage system. In: Hornblass A, editor. Oculoplastic, orbital, and reconstructive surgery, vol. 2, orbit and lacrimal system. Baltimore: Williams & Wilkins; 1990.
30. Emmerich KH, Ungerechts R, Meyer-Rüsenberg HW. Transcanalicular microendoscopic laser DCR: technique and results. Klin Monatsbl Augenheilkd. 2012;229(1):39–41.
31. Fayet B, Racy E, Assouline M. Cerebrospinal fluid leakage after endonasal Dacryocystorhinostomy. J Fr Ophtalmol. 2007;30(2):129–34.
32. Kamal S, Ali MJ, Naik MN. Circumostial injection of mitomycin C (COS-MMC) in external and endoscopic dacryocystorhinostomy: efficacy, safety profile, and outcomes. Ophthal Plast Reconstr Surg. 2014;30(2):187–90.
33. Feng YF, Yu JG, Shi JL, et al. A meta-analysis of primary external dacryocystorhinostomy with and without mitomycin C. Ophthalmic Epidemiol. 2012;19:364–70.
34. Dolmetsch AM, Gallon MA, Holds JB. Nonlaser endoscopic endonasal dacryocystorhinostomy with adjunctive mitomycin C in children. Ophthal Plast Reconstr Surg. 2008;24(5):390–3.

Management of Pediatric Upper System Problems: Punctal and Canalicular Surgery

29

Sarah M. Jacobs, Christopher B. Chambers, William R. Katowitz, and James A. Katowitz

Congenital Abnormalities

The lacrimal drainage system develops from the ectodermal tissue present in the cleft between the nasal (lateral) and maxillary processes during embryologic development. During the sixth week of embryonic life, an outbudding from this solid ectodermal cord of cells occurs. The outbudding bifurcates in the medial canthal area and projects into the upper and lower lids to eventually form the canalicular portions of the lacrimal drainage system [1]. These outgrowths reach the lid margin at 12 weeks of gestation. Each canaliculus has a long, horizontal portion as well as a vertical component consisting of an ampulla and punctal opening. The punctum opens at the top of a small elevation on the lid margin termed the papilla. The papillae and puncta are formed during the seventh month of gestation, at which time the drainage system becomes fully patent.

While the most common congenital nasolacrimal problems involve impeded tear drainage through the lower system (nasolacrimal duct obstruction or dacryostenosis), upper system problems can also occur, including abnormalities of the puncta, canaliculi, or external fistulae/anlage ducts.

S.M. Jacobs • C.B. Chambers (✉)
Department of Opthalmology, University of Washington, Seattle, WA, USA
e-mail: cbc108@uw.edu

W.R. Katowitz, MD • J.A. Katowitz, MD, FACS
The Children's Hospital of Philadelphia and The Edwin and Fannie Gray Hall Center for Human Appearance, University of Pennsylvania, Philadelphia, PA, USA
e-mail: katowitzw@email.chop.edu; katowitz@email.chop.edu

Congenital Supernumerary (Anlage) Ducts

A congenital lacrimal fistula is a congenital connection between the lacrimal drainage system and the external skin surface, allowing drainage from the ocular surface to exit through the skin rather than flowing down the ductwork into the nose. While a fistula may arise from any point along the upper or lower nasolacrimal drainage system, most originate from the lacrimal sac as supernumerary or anlage channels (Fig. 29.1 [2–5]). Parents or children may report clear tears or mucous discharge from a small opening near the medial canthus.

Supernumerary Duct Repair (Figs. 29.2 and 29.3)

1. With a lacrimal cannula, irrigate a small amount of diluted methylene blue into the duct to outline the mucosal lining down to the lacrimal sac.
2. Place an appropriately sized probe into the supernumerary duct.

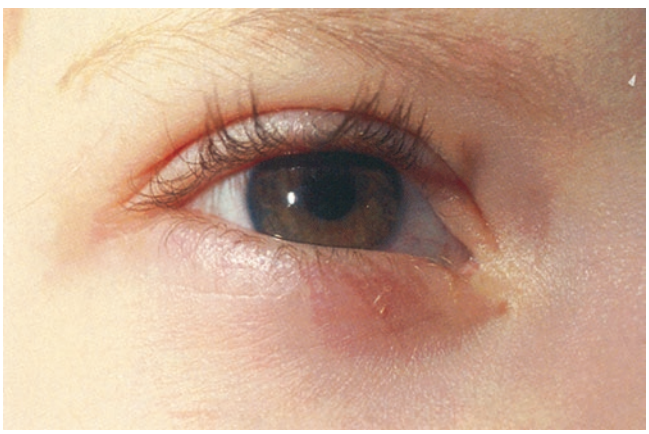


Fig. 29.1 A supernumerary duct with associated absence of punctum and canaliculus

© Springer International Publishing AG 2018

J.A. Katowitz, W.R. Katowitz (eds.), *Pediatric Oculoplastic Surgery*, https://doi.org/10.1007/978-3-319-60814-3_29

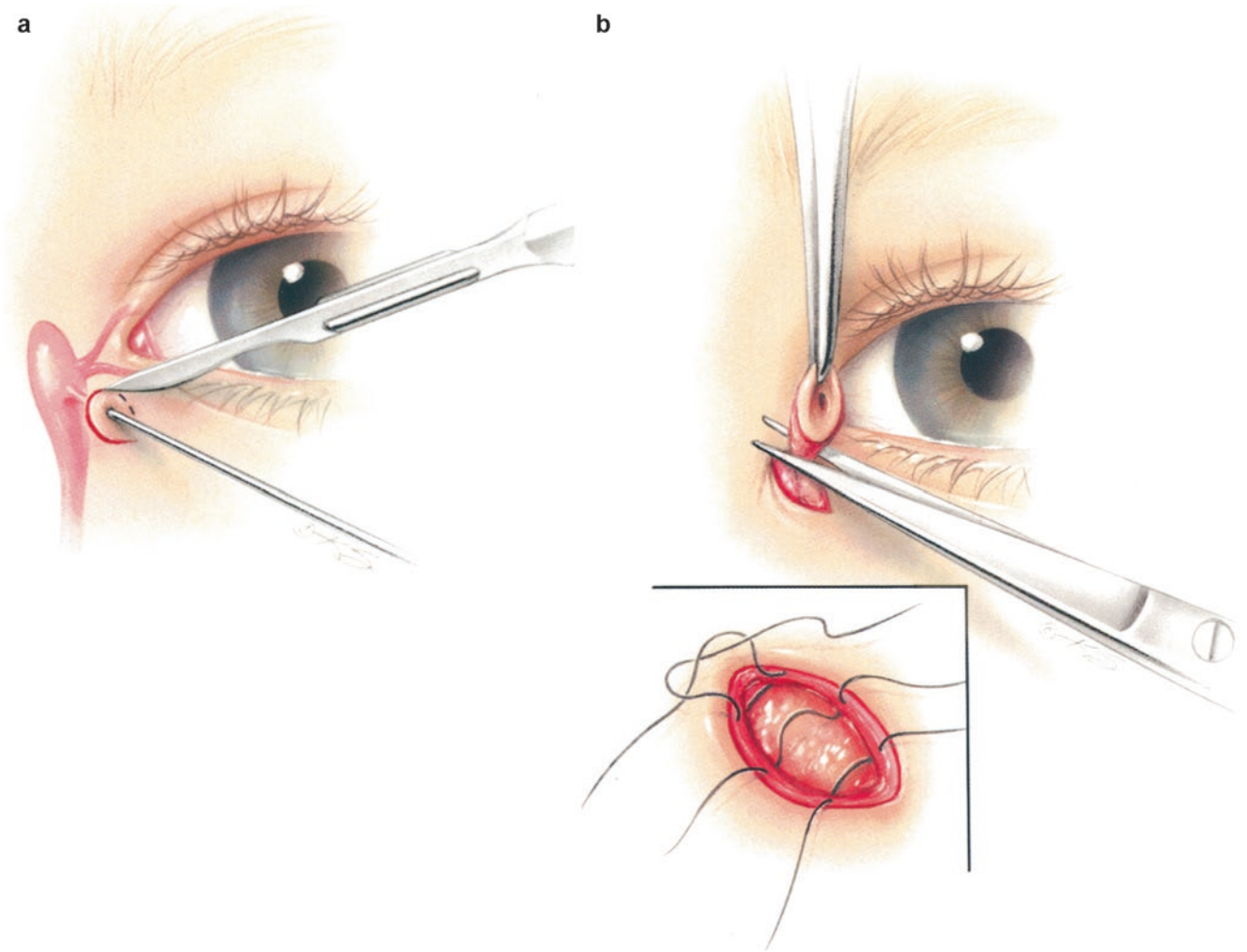


Fig. 29.2 Illustrations of surgical steps in repair of a supernumerary duct. (**a**) After diluted methylene blue is injected into the duct with the lacrimal cannula, an ellipse is cut through the skin and muscle. Using a probe as a guide, careful dissection is completed to the junction of the duct and the sac. (**b**) The supernumerary duct is ligated at its junction with the sac with 5-0 absorbable suture and cut. The subcutaneous tissue and skin are closed with appropriate interrupted sutures as shown in the inset

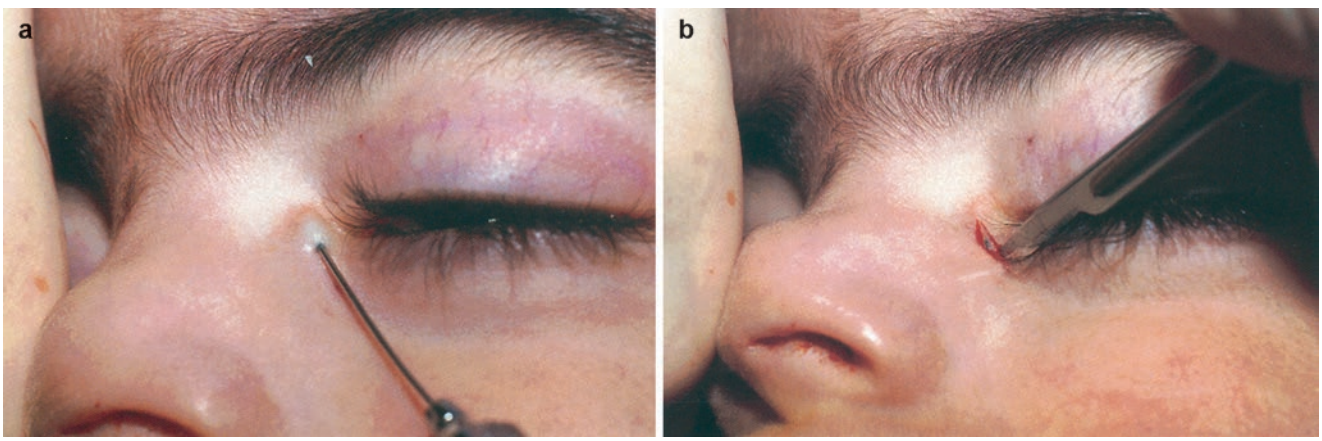


Fig. 29.3 Clinical example of corresponding surgical steps in repair of supernumerary duct. (**a**) Diluted methylene blue is injected into the duct with the lacrimal cannula. (**b**) An ellipse is cut through the skin and muscle.

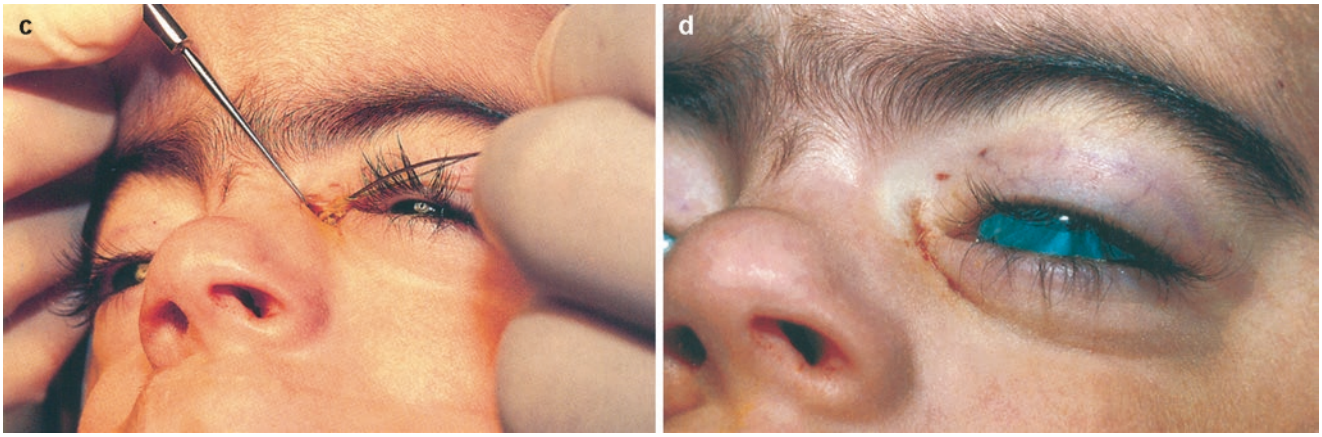


Fig. 29.3 (continued) (**c**) Using a probe as a guide, careful dissection is completed to the junction of the duct and the sac. The supernumerary duct is ligated at its junction with the sac with 5-0 absorbable suture and cut. (**d**) The subcutaneous tissue and skin are closed with appropriate interrupted sutures

3. Cut a conservative ellipse of the skin around the probe, following the duct lumen down to the lacrimal sac.
4. Use an absorbable suture to ligate the base of the duct at its junction with the sac.
5. Perform a layered closure of the muscle and skin.

This simple excision and closure will be sufficient to prevent fistula reformation if there is no blockage to tear flow more distally in the nasolacrimal duct. In the authors' experience, simple probing and irrigation combined with excision and ligation of the fistula have proven successful in the majority of cases [4]. However, if there is a lower system obstruction that appears unresponsive to simple probing, silicone stent intubation of the nasolacrimal duct or a dacryocystorhinostomy (DCR) will be required to eliminate this problem.

Abnormalities of the Puncta and Canaliculi

There is a wide spectrum of obstructive abnormalities of the puncta and canaliculi, ranging from simple congenital veils to complete canalicular atresia [2, 3]. These abnormalities can sometimes be associated with other systemic findings in certain genetic disorders. For example, Levy-Hollister syndrome, otherwise known as the lacrimo-auriculo-dento-digital (LADD) syndrome, involves an underdeveloped or absent punctum and/or nasolacrimal duct obstruction leading to chronic epiphora and occasionally dacryocystitis. The lacrimal abnormalities of LADD are accompanied by syndromic features including low-set cup-shaped ears, mild to severe hearing loss, underdeveloped peg-shaped front teeth, xerostomia due to hypoplastic salivary glands, and hand deformities such as small, absent, or duplicated thumbs. Ectrodactyly-ectodermal dysplasia-clefting (EEC) syndrome, which is characterized by cleft lip/cleft palate and absent or anomalous digits, is also associated with punctal or canalicular abnormalities [6–10]. Congenital anomalies of the upper lacrimal system in conjunction with abnormal digits, limbs, or ears should prompt an evaluation by a pediatric genetic specialist.

Punctal Agenesis

The mildest form of punctal agenesis presents as a congenital veil, which is an epithelial membrane covering the punctal opening of an otherwise-normal canaliculus. Surgery of the punctum should always be as conservative as possible. For simple punctal veils, a gentle puncture followed by dilation and irrigation often will suffice (Fig. 29.4). In contrast to simple veils, severe punctal agenesis may include a greater degree of atresia involving the vertical and horizontal canaliculus as well.

Canalicular Atresia

Canalicular atresia or agenesis is a congenital narrowing or the absence of any portion of the canaliculus. It can be categorized as (1) proximal (adjacent to the punctum), (2) mid-canalicular, or (3) distal (adjacent to or involving the common internal punctum). For greater degrees of canalicular atresia, more significant surgical steps are required.

The use of dacryocystography may be helpful in exploring for the presence or absence of canaliculi. However, this test always requires a general anesthetic in the pediatric age group and should therefore be coordinated with the surgical correction when possible. If dacryocystography is not readily available, an alternative approach is the use of dilute methylene blue to determine the pathway of fluid flow within the lacrimal system:

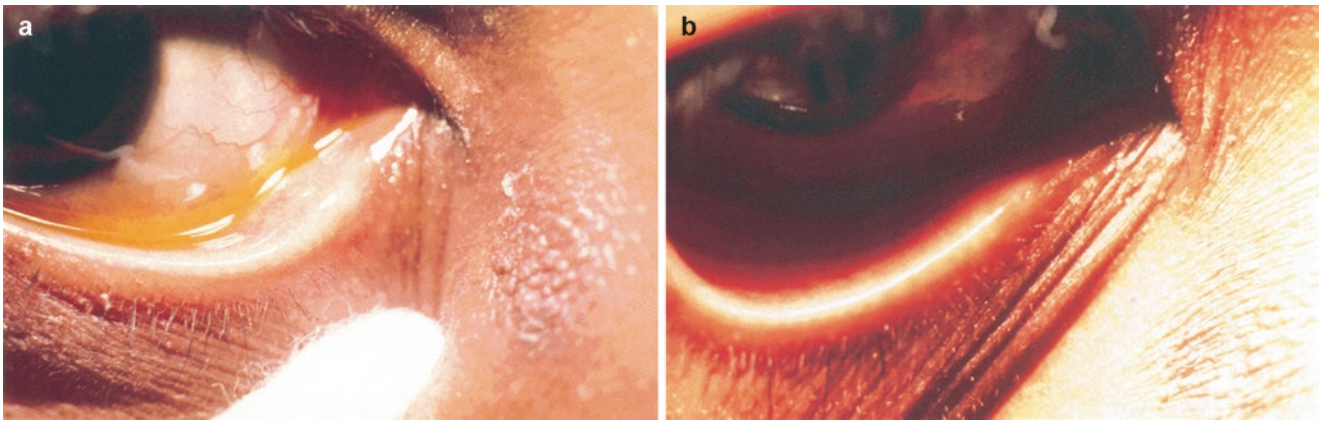


Fig. 29.4 Punctum. (**a**) Congenital veil of punctum in the right eye. (**b**) One year after simple puncture and dilation of the opened punctum without the use of any stent

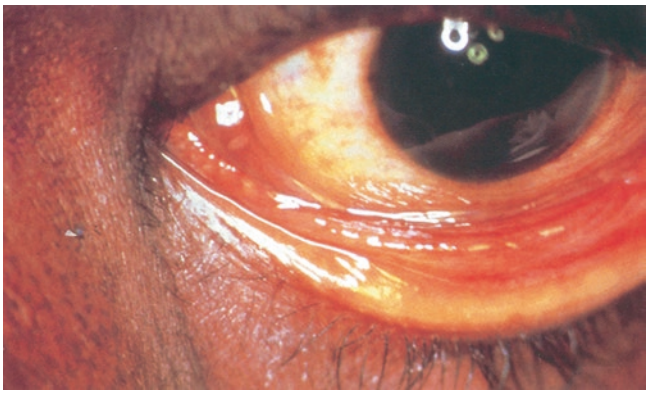


Fig. 29.5 Congenital absence of both puncta on the left side

- If one normal punctum and canaliculus is present, then methylene blue is irrigated into the sac through that punctum, and then the palpebral conjunctiva of the upper and lower lids are examined for retrograde flow of dye into the abnormal canaliculus.
- If both puncta are absent but there *is* evidence of a lacrimal papilla, then consideration can be given to a percutaneous injection of dilute methylene blue solution into the lacrimal sac (Figs. 29.5 and 29.6). After injection, the surgeon applies pressure over the lacrimal sac area, then the conjunctival surface of the lid margin can be examined for retrograde flow of methylene blue. Of note, if there is *no definite lacrimal papilla*, the percutaneous injection of methylene blue is not recommended. Even with the presence of a papilla, there is a very low success rate (10%).
- If the dye is not seen on external exam after irrigation or injection, an incision can be made in the lid margin at the lateral edge of the lacrimal papilla. If the dye is noted in the cutdown area, then a mucosal lined canaliculus is presumed to be present nearby.
- If the dye can be suctioned from the nose after injection or irrigation into the upper system, this indicates that the sac and duct are at least partially patent. In this case, a silicone stent tube can be placed through the nasolacrimal system for persistent dacryostenosis. Alternatively, if there is significant obstruction in the lower system, then a DCR is required.

A Single Canaliculus is Patent

Under typical conditions, a normal patent superior canaliculus will drain ~15% of tears, while a normal inferior canaliculus drains the other ~85%. When one canaliculus is impeded, drainage through the remaining canaliculus may increase to meet the demand. Thus, even with one absent punctum or canaliculus, it is possible for a patient to be asymptomatic and require no intervention.

If a patient with a single patent canaliculus does have epiphora, it may be due to insufficient drainage through the upper *or* the lower nasolacrimal system (dacryostenosis). To assess for a lower system blockage, probing and irrigation should be done through the patent canaliculus. If lower obstruction is identified, then a monocanalicular silicone stent can be placed, such as the Monoka (FCI, Mansfield Hills, MA) (Fig. 29.7).

There are multiple methods to restore or establish bicanalicular flow in a patient with only one patent canaliculus. One method involves retrograde probing through a DCR incision [11]. After opening the lacrimal sac, an attempt is made to visualize a common internal punctum. A blunt right-angle (Werb) probe or an angled #00 Bowman probe can be passed from the sac toward the lid in an effort to identify the length of any patent canaliculus. A sharp Werb probe can then be used to puncture up through the lid margin from the inside, creating a pseudo-punctum on the lid margin connecting to the patent canaliculus. An alternative is to puncture the lid margin externally and then introduce an 18- or 19-gauge Teflon intravenous catheter to create a new channel from the lid margin into the sac. The new passage can then be threaded with Silastic tubing to create a new common internal punctum [12–15].

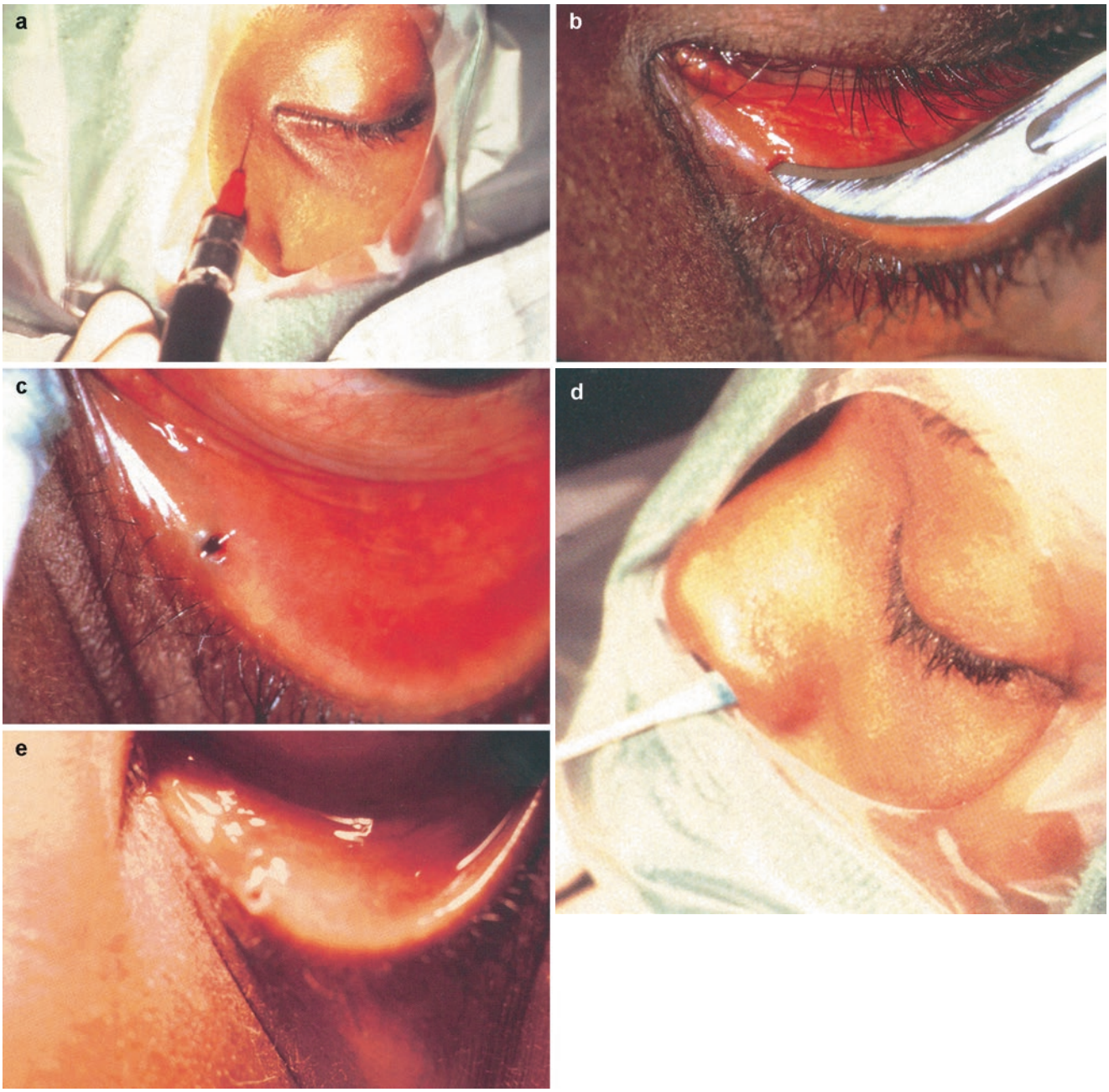


Fig. 29.6 Repair of punctal and partial canalicular agenesis. (**a**) Methylene blue injected through the medial canthal tendon to the area of presumed lacrimal sac in same patient. (**b**) If pressure placed on the sac does not show dye on the lid margin, a cutdown is done over the lacrimal papilla or approximately 8 mm lateral to the canthal angle to search for possible patent canaliculus. (**c**) Probing of the cutdown shows a canaliculus that is patent to the lacrimal sac, as evidenced by methylene blue being seen in the cutdown site when pressure is placed on the sac. (**d**) The lower system is open as shown by the methylene blue collected from the nose. When the lower system is open, only Silastic intubation of the system through the nasolacrimal duct is required. (**e**) After Silastic tubing was in place for 3 months, the punctum remains patent at 1-year follow-up (From Katowitz and Low [5]; with permission)

Neither Canaliculus Is Patent

If both puncta are absent, then surgical exploration of the internal common puncta within the lacrimal sac opening in the setting of DCR may permit retrograde probing to deliberately create a false passage out to the eyelid margin [11, 13, 14]. In our experience, success requires a sufficient length of preexisting patent canaliculus. Unless the naturally patent segment extends to midcanaliculus (within 4 mm of punctum), such false passages will not usually remain patent. As a general rule, if there is an absence of normal puncta and canaliculi in both the upper and lower lid, then a conjunctivodacryocystorhinostomy (CJDCR) will be necessary (see Chap. 30).

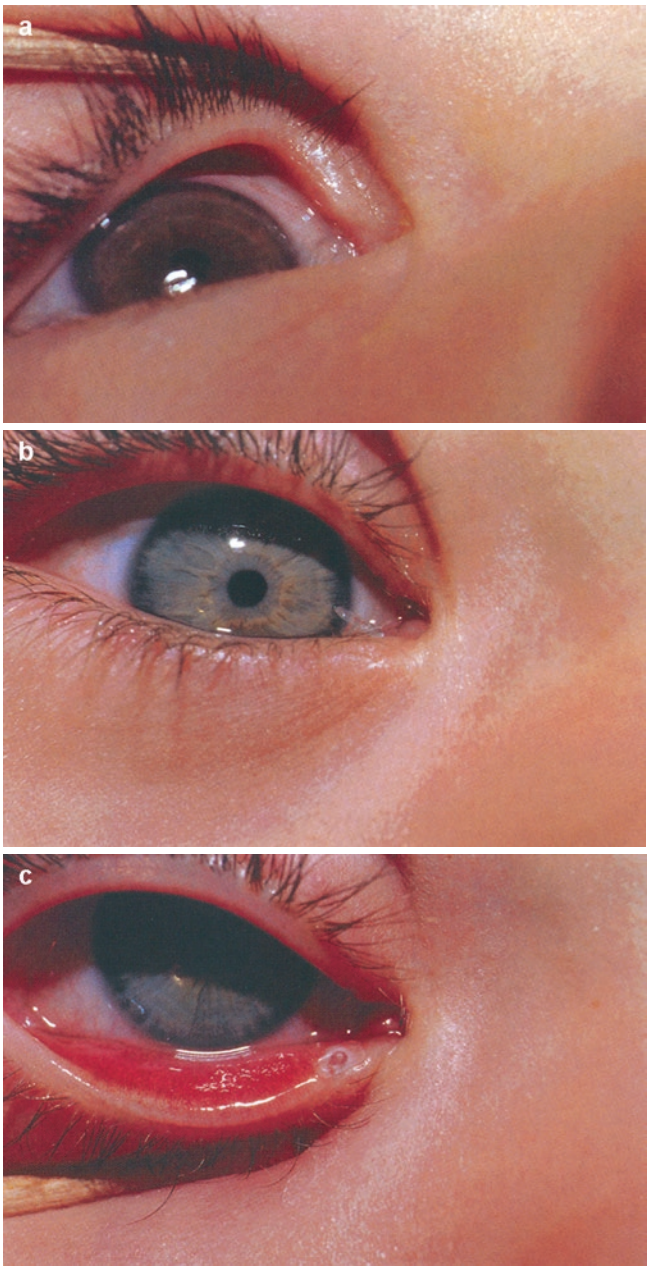


Fig. 29.7 Agenesis of the upper punctum. (**a**) Absent upper punctum with normal inferior punctum and canaliculus. (**b**) After simple probing of nasolacrimal duct unsuccessful in the same patient, a monocular stent is inserted (Monoka, FCI Ophthalmics, Marshfield Hills, MA). (**c**) Normal position of Monoka stent with 4-mm collar

Distal or Common Canalicular Agenesis

Blockages in the distal canalicular system require a bypass procedure, consisting of either a CJDCR (see Chap. 30) or a canaliculodacryocystorhinostomy (CLDCR). The CJDCR creates a new passage from the ocular surface near the caruncle, directly through a lacrimal fossa osteotomy into the nose, and then holds the passage patent with a glass tube (Jones tube) through which drainage can flow. In contrast, CLDCR involves excision of the blocked distal canaliculus followed by microsurgical anastomosis of the patent canalicular segment directly to the nasolacrimal sac, in an effort to retain usage of the canalicular drainage pathway [16].

Hurwitz has differentiated two distinct situations amenable to CLDCR [17, 18]:

- Common canaliculus-DCR: This procedure is performed when the patient has obstruction at the level of the common canaliculus. A DCR ostium is created. The canaliculus is probed via the punctum to reach the point of blockage at the common canaliculus. Through an open cutdown, the scar tissue obstructing the common canaliculus is excised. Bicanalicular silicone stent tubes are threaded through the puncta, across the cut common canaliculus, through the lacrimal sac and into the nose via the DCR ostium (Fig. 29.8). The distal end of the canaliculus is anastomosed to anterior and posterior flaps of the lacrimal sac with sutures.
- Canaliculo-DCR: This procedure is performed when the patient has obstruction at the level of one or both distal canaliculi, near the junction with the common canaliculus. A probe is advanced via the punctum until it reaches a soft stop at the point of canalicular obstruction. If the blockage is at least 8 mm from the punctum, the CLDCR can proceed. (A dacryocystogram may be useful to identify the exact site of obstruction, but measurement of the distance from the punctum to a soft stop is a good indicator). A DCR ostium is created. The canalicular blockage is excised through an open cutdown. A silicone stent tube is threaded through the system and into the nose via the DCR ostium, then the cut canaliculus is anastomosed to the lacrimal sac.

In either of these procedures, the usage of a canalicular trephine is an alternative to open cutdown for excision of the canalicular blockage. A trephine (Sisler trephine available from Beaver-Visitec International, Waltham, MA) is introduced through the punctum and advanced to the soft stop. The stylet is withdrawn, and then a rotary twisting movement is used to cut through the scar tissue as the trephine is advanced through the blockage and into the sac, similar to advancing a probe. Stents are then placed without the need for anastomotic sutures. Success rates above 80% have been reported [19].

Hurwitz reports a 75% success rate for common canaliculus-DCR surgery and a 50–60% rate for the CLDCR. This technique may be effective in cases of limited distal blocks in the canaliculi, and it gives a more physiologic result than CJDCR. However, CLDCR has fallen out of favor over the past 20 years due to its technical difficulty and its inability to correct extensive blocks in the canalicular system despite earlier optimistic reports [8]. As

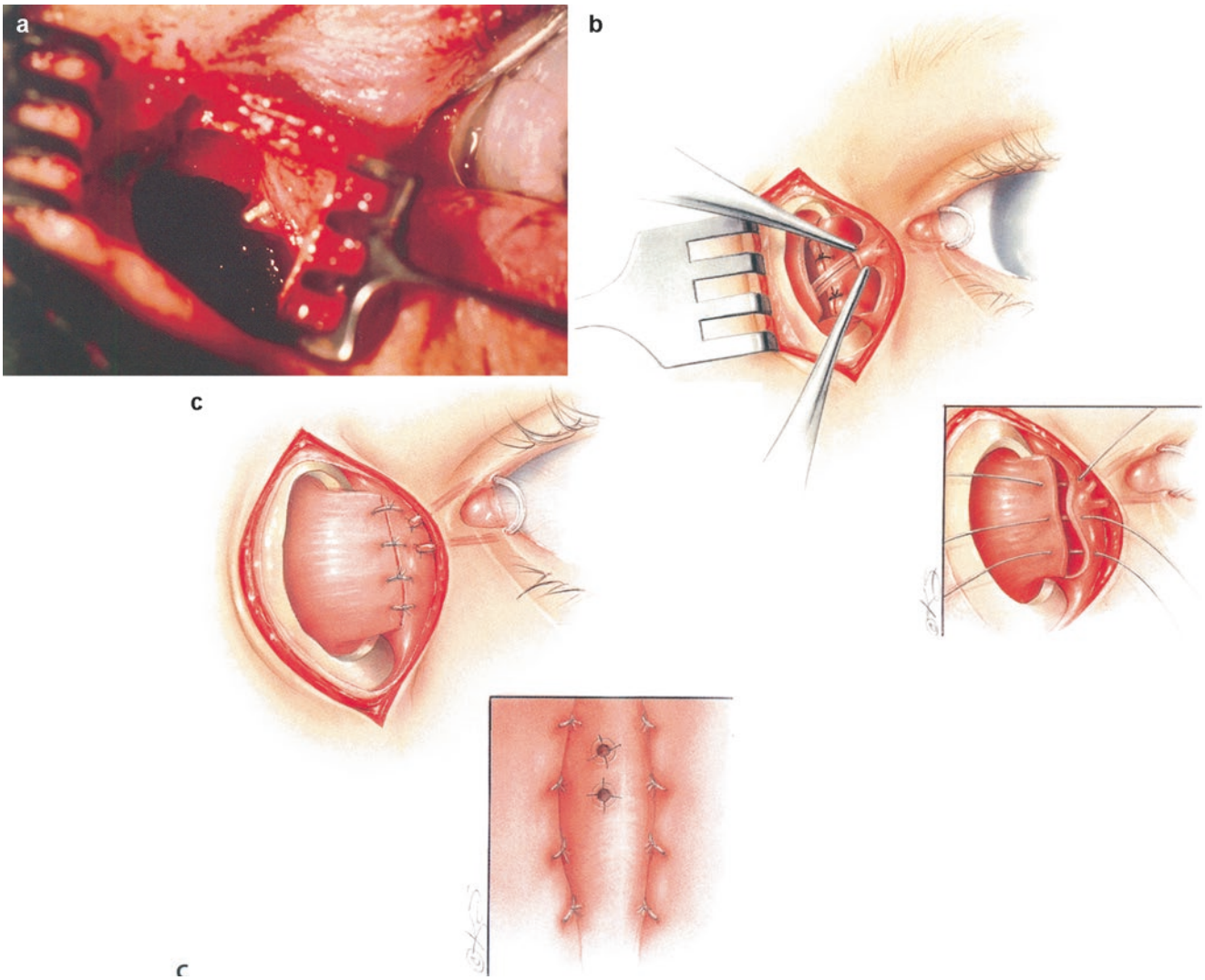


Fig. 29.8 Canalicular obstruction and canaliculodacryocystorhinostomy (CLDCR). (**a**) Probe exiting common internal punctum following excision of obstruction. (**b**) Common canaliculus-DCR where an anastomosis of the common opening is made from a patent area of the canaliculus and lacrimal sac to nasal mucosa through the DCR ostium. The lacrimal sac incision has been made just medial to the obstructed common canaliculus. The flap of lacrimal sac is then folded back and sutured to join a small posterior flap of nasal mucosa. Scar tissue over the common opening has been cut away as shown in (**a**), and Silastic tubes have been inserted. The inset shows mobilization of a large nasal mucosal flap sutured to the smaller anterior flap developed from the common opening and adjacent lacrimal sac. (**c**) If the obstruction has involved both distal canaliculi, resection of the obstruction, therefore, removes any common opening. After inserting Silastic tubing, each cut end of the patent canaliculus can then be sutured separately to openings created in the lacrimal sac wall using 8-0 sutures as shown in the inset

such, CLDCR is far less common than CJDCR for controlling epiphora due to canalicular causes [5, 13, 14, 17].

Common Canalicular Stenosis

Common canalicular stenosis is congenital or acquired narrowing of the common canaliculus, with a broad range of severity. It is distinct from true agenesis as there is a lumen present and because it can arise at any time in a previously patent system. The simplest form may involve a congenitally tight valve of Rosenmuller at the junction between canaliculus and lacrimal sac. This tight valve may prevent even the passage of a Crawford probe, thus making intubation with Silastic difficult. Sometimes, one can pass a probe through one canaliculus, but the opposite one will demonstrate resistance with a soft stop. Whether this represents an actual separate entrance of the canaliculus into the sac or a better angle allowing easier passage through the valve of Rosenmuller at the common internal punctum cannot be demonstrated without either direct endoscopic visualization, canalicular dacryocystography, or by opening the sac

for exploration during a DCR. In most instances, however, with gentle perseverance, one can often pass a thin probe (#0000 Bowman or 0.5-mm FCI) through each canaliculus into the sac. Careful dilation with succeedingly larger probes may then permit passage of a Ritleng probe (FCI, Paris, France) so that silicone stent intubation can be completed with this system (see Chap. 18). Care must be taken not to force the probe or catheter through the common internal punctum if it is tight. Carefully increasing the Bowman probe size and lubricating the catheter or probe tip with ointment helps permit safe passage into the nasolacrimal duct.

Acquired Proximal Canalicular or Punctal Stenosis

In the pediatric population, punctal and canalicular stenosis usually occurs from viral infections, such as herpes and varicella zoster, or secondary to trauma [24]. Stenoses due to toxic effects from topical medications or from neoplasms are exceedingly rare among pediatric patients [25]. Reaction to environmental allergens can also create an intermittent canalicular obstruction secondary to inflammation and edema during acute episodes [24, 25]. Wide dilation may suffice for acquired punctal and vertical canalicular stenosis, but more frequently some form of punctoplasty may be required. While several punctoplasty methods have been advocated, we recommend that the punctum and canalicular portion of the lacrimal pump mechanism should be preserved. The 2-snip procedure works well to provide a sufficient opening while preserving enough capillary action to allow normal function of the lacrimal pump mechanism (Fig. 29.9). Alternatively, a 3-snip procedure may be performed, but this can result in ineffective pump function [5].

Canaliculitis

Localized painful swelling of one canaliculus can occur as a cause or an effect of lacrimal obstruction. While it is frequently related to stones of a fungal etiology, the most common cause of canaliculitis is *Actinomyces israelii*, a filamentous gram-positive rod [26]. A seeping, pouting punctum with overlying redness and tenderness is classically described. The lacrimal sac itself is spared. Usually *Actinomyces* is sensitive to penicillin G, but smears and cultures will help in the selection of more specific topical and systemic antibiotics [27]. Despite antibiotic therapy, a surgical procedure is often required. Simple irrigation and probing of the canaliculus usually is ineffective. A small curette can be used to break up concretions, but it may cause further scarring if it is forced

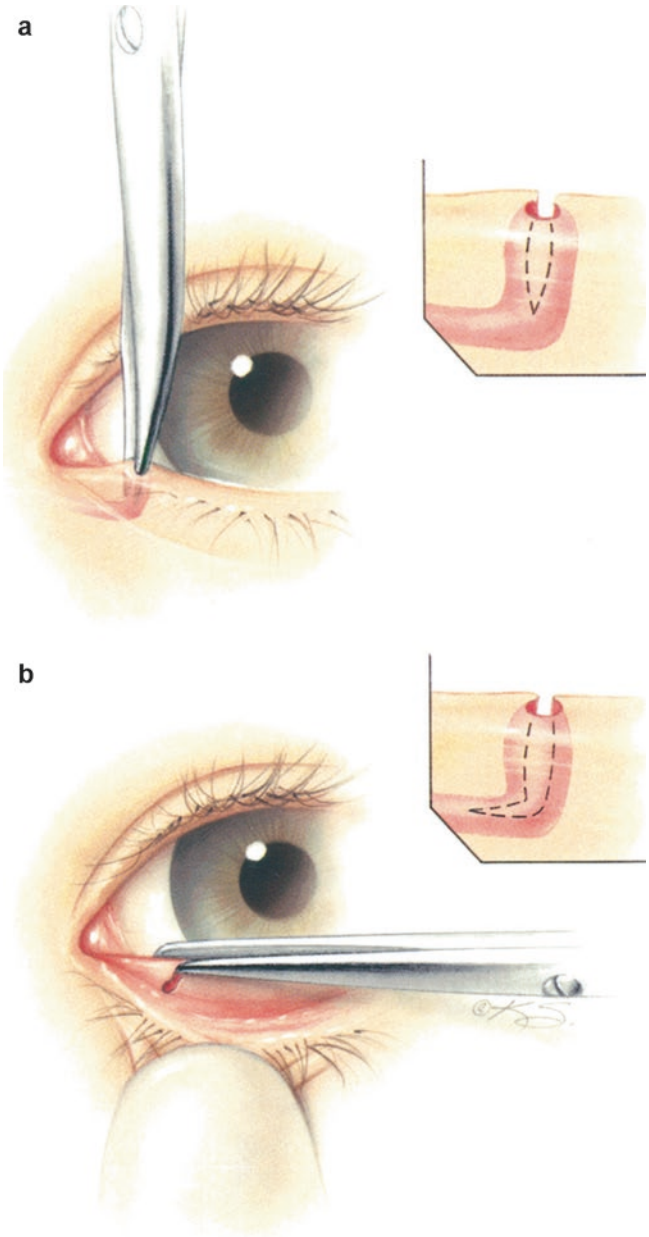


Fig. 29.9 The 2-snip procedure. (**a**) A vertical cut is made to the base of the ampulla. (**b**) The scissors is passed horizontally into the canaliculus, and a 3- to 4-mm cut is made

through the punctum. Another approach is either to unroof the canaliculus by slitting it from the punctum to the area of concretions or to dissect horizontally over the affected area of the canaliculus. The surgeon places a probe in the punctum and canaliculus and carefully cuts down onto the metal. A careful curetting of stones, if present, can then be done through the incision. A specimen should be sent for bacterial and fungal staining, cultures, and sensitivities. Silicone stent tubing can be used as a stent after this type of procedure, with the canaliculus and overlying tissues closed with interrupted 7-0

absorbable sutures. Often, however, spontaneous closure will be effective without a stent. If Silastic material is used, it should remain in place for several months as long as there is no significant irritation or recurrent infection [26, 27]. The dye disappearance test can be a useful guide regarding tube removal: When normal dye disappearance is demonstrated, then the tube can usually be safely removed.

Dacryolith stones in the lacrimal sac are very rare in the pediatric population and usually are not of fungal etiology. Stones occur most frequently in older women but, when present in children, can also produce intermittent obstruction. Irrigation and probing may indicate patency, even when epiphora is present. Lacrimal sac stones can act like a ball valve and further confuse clinical evaluation because of intermittent epiphora. Dacryocystography is the most helpful tool in diagnosing this problem but typically requires general anesthesia in young children. A DCR may be needed to resolve the issue.

Eyelid Abnormalities as a Cause of Epiphora

Eyelid Malpositions

Newborns may present with complete eversion of the upper lids, which may be secondary to nontrachomatous chlamydial infection (see Chap. 21). The tarsal kink syndrome may also result in upper lid ectropion requiring surgical correction [20–23]. Typically, conservative therapy with topical lubrication and temporary patching solves the problem. Occasionally a tarsorrhaphy may be necessary.

Some newborns, especially those with Down syndrome, may have deficiency of the anterior lamella. Correction may necessitate a skin graft and possibly more extensive lid retraction repair. Eversion of the upper lids may also be the result of horizontal redundancy and may require a wedge resection or a tarsal strip repair.

Although not as common a problem in the pediatric age group as in older patients, lid laxity and punctal eversion can occur. In pediatric patients, this eversion responds to vertical cautery on the conjunctival side of the lid; thermal tightening of the cauterized tissue pulls the lid back into proper position. An alternative treatment involves excision of an ellipse of conjunctiva and tarsus, followed by reapproximation of the wound edges with several buried interrupted absorbable sutures. This procedure should rotate the punctum into a normal position. True medial canthal ectropion requires more extensive repair, such as the lazy-T procedure advocated by Smith, or actual plication of the medial canthal tendon [28]. These lid procedures are reviewed in Chap. 12. One should be aware that in children, punctal and lid eversion problems are more commonly secondary to trauma or following surgery for developmental abnormalities rather than due to true laxity [28, 29].

Eyelid Margin Abnormalities

A variety of mechanical problems of the lid margin and its fascial support can produce epiphora or tearing, due to inability of the normal blink-dependent tear pump mechanism to move secretions across the ocular surface and into the punctal drains.

Irritation from Eyelashes

Congenital entropion, distichiasis, or trichiasis can stimulate reflex tearing and cause epiphora, despite the presence of a patent nasolacrimal drainage system. Appropriate steps should be taken to identify and correct these problems.

Trichiasis due to entropion or epiblepharon can be surgically corrected. Standard procedures such as rotation of the lid margin for entropion, or excision of excess skin and orbicularis muscle for epiblepharon, can eliminate these causes of epiphora (see Chap. 21).

Trichiasis in an otherwise well-positioned eyelid may be secondary to chronic blepharitis or other causes of inflammation. Any topical medications or facial skin care products which may be provoking inflammation should be stopped. The misdirected lashes can be managed by cryosurgery, electrolysis, or a variety of lid margin procedures to ablate the follicles.

Traumatic or Iatrogenic Causes of Epiphora

Trauma can occur at any site in the nasolacrimal drainage system. The more common forms of trauma can range from chemical or thermal burns to avulsions and lacerations (see Chap. 25).

Thermal, Chemical, or Radiation Therapy Burns

Energy from many different sources can cause a burn. For example, stenosis can be caused by radiation therapy for treatment of orbital rhabdomyosarcoma [21]. Regardless of the energy source, the treatment is much the same. As compared to cases of congenital stenosis, stenting is more likely to be required when the stenosis is caused by burns. This is due to increased scar formation with burn injuries. Also for that reason, the tubing must be left in for much longer than the usual period to prevent cicatricial closure of the lumen. If tolerated, maintaining stents in place for 6+ months is advisable.

Surgical Injury

Children born with craniofacial syndromes such as Crouzon or Apert often undergo orbital advancement procedures with

transnasal wiring, which can damage the canalicular system. This then requires Silastic intubation of the nasolacrimal drainage system or, if more severe, CJDCR.

Lacerations

Lacerations of the punctum or the lacrimal sac alone are rare and can be repaired primarily. The most common form of laceration to the nasolacrimal drainage system involves the canaliculus. The guiding principle in the repair of the canaliculus is to reestablish patency of the damaged system with minimal risk to normal portions of the system. These principles are covered thoroughly in Chap. 25 of this volume. The use of the original pigtail probe in canalicular repair is contraindicated because it can too easily damage the sac and common internal punctum. A newer version, however, with a rounded suture eye has some advantages in certain situations (see Chap. 25). Bicanalicular Silastic intubation has proven effective, but newer monocanalicular devices have had promising results [29]. For canalicular lacerations, we prefer to leave the stent in place for a minimum of 3 months.

References

1. Kaplan LJ. Embryology of the bifunctional lacrimal system. Adv Ophthalmic Plast Reconstr Surg. 1984;3:109.
2. Welham RAN, Bergin DJ. Congenital lacrimal fistulas. Arch Ophthalmol. 1985;103:545.
3. Tsibidas P, Roussos J. Supernumerary lacrimal canaliculi. Ann Ophthalmol. 1979;11:265.
4. Caputo A, Smith R, Conotti A, et al. Definitive treatment of congenital lacrimal sac fistula. Arch Ophthalmol. 1978;96:1443.
5. Katowitz JA, Low J. Lacrimal drainage surgery. In: Tasman W, editor. Duane's clinical ophthalmology, vol. 5. Philadelphia: Lippincott-Raven; 1995. Chapter 79.
6. Hollister DW, Klein SH, Dejager HJ, Lachman RS, Rimoin DL. The lacrimo-auriculo-dento-digital syndrome. J Pediatr. 1973;83:438–44.
7. Levy WJ. Mesoectodermal dysplasia: a new combination of anomalies. Am J Ophthalmol. 1967;63:978–82.
8. Heinz GW, Bateman JB, Barrett DJ, Thangavel M, Crandall BF. Ocular manifestations of the lacrimo-auriculo-dento-digital syndrome. Am J Ophthalmol. 1993;115:243–8.
9. Bixler D, Spivack J, Bennett J, Christian JC. The ectrodactyly-ectodermal-dysplasia-clefting (EEC) syndrome. Clin Genet. 1971;3:43–51.
10. Rodine EDS, Richieri-Costa A. EEC syndrome: report on 20 new patients, clinical and genetic considerations. Am J Med Genet. 1990;37:42–53.
11. Katowitz JA. Silicone tubing in canalicular obstruction. Arch Ophthalmol. 1974;91:459.
12. Moch B, Seiff SR, Arroyo J. Congenital absence of the lacrimal puncta. Ophthalmic Surg. 1995;26:53–6.
13. Lyons CJ, Rosser PM, Welham RA. The management of punctal agenesis. Ophthalmology. 1993;100:1851–5.
14. Wearne MJ, Beigi B, Davis G, Rose GE. Retrograde intubation dacryocystorhinostomy for proximal and midcanalicular obstruction. Ophthalmology. 1999;106:2325–9.
15. Cahill KV, Burns JA. Management of epiphora in the presence of congenital punctal and canalicular atresia. Ophthal Plast Reconstr Surg. 1991;7:167–72.
16. Jones BR, Corrigan MJ. Obstruction of the lacrimal canaliculi. In: Proceedings of the second international Comeal-plastic conference. Pergamon: London/Oxford; 1967/1969.
17. Doucet TW, Hurwitz JJ. Canaliculo-dacryocystorhinostomy in the management of unsuccessful lacrimal surgery. Arch Ophthalmol. 1982;100:619.
18. Hurwitz JJ, ed. Canaliculodacryocystorhinostomy. In: The lacrimal system. Philadelphia: Lippincott-Raven; 1996: 297–302.
19. Zadeng Z, Singh M, Singh U. Role of lacrimal canalicular trephination and mini-Monoka stent in the management of idiopathic distal canalicular obstructions. Asia Pac J Ophthalmol. 2014;3(1):27–31.
20. Dryden RM, Doxanas MT. Eyelid malpositions: ectropion and entropion. In: McCord Jr C, editor. Oculoplastic surgery. New York: Raven; 1982. Chapter 11.
21. Callahan M, Callahan A. Ophthalmic plastic surgery. Aesculapius: Birmingham; 1981.
22. McCarthy RW. Lamellar tarsoplasty: a new technique for correction of horizontal tarsal kink. Ophthalmic Surg. 1984;15:859–60.
23. Biglan AW, Buerger GF. Congenital horizontal tarsal kink. Am J Ophthalmol. 1980;89:522–4.
24. Bouzas A. Canalicular inflammation in ophthalmic cases of herpes zoster and simplex. Am J Ophthalmol. 1965;60:713.
25. Spaeth GL. Nasolacrimal duct obstruction caused by topical epinephrine. Arch Ophthalmol. 1967;77:35.
26. Ellis PP, Bausor SC, Fuler JM. Streptothrix canaliculitis. Am J Ophthalmol. 1960;52:36.
27. Blanksma LJ, Slijper J. Actinomycotic dacryocystitis. Ophthalmologica. 1978;176:145.
28. Smith B. The "lazy-T" correction of ectropion of the lower punctum. Arch Ophthalmol. 1976;94:1149–50.
29. Ruban JM, Guigon B, Boyrivent V. Analyse de l'efficacite de la sonde d'intubation mono-canaliculo-nasale grande collerette dans le traitement du larmoiement par obstruction congenitale des voies lacrymales d'excretion du nourrisson. J Fr Ophthalmol. 1995;18:377–83.

Management of Pediatric Upper System Problems: Conjunctivodacryocystorhinostomy

30

Scott M. Goldstein and James A. Katowitz

The upper portion of the lacrimal drain, from the puncta to the common canaliculus, is narrow compared to the lower half of the system and susceptible to injury or malformation. Once damaged and scarred, it is quite difficult to reestablish flow through the remainder of the lacrimal system. The conjunctivodacryocystorhinostomy (CJDCR) procedure, as originally described by Jones, involves the use of a Pyrex tube to create a fistula from the conjunctiva to the nasal mucosa as a means to bypass the lacrimal drain all together [1]. For adults, this procedure is considered the standard method of treatment for epiphora due to significant obstruction of the canaliculi or internal common punctum. In contrast, most oculoplastic surgeons are hesitant to perform CJDCRs for pediatric patients with similar problems, because this procedure is associated with a fairly high frequency of complications [2–9]. As a result, some have advocated not performing this surgery on children younger than 10 years [7]. In the last few decades, many CJDCRs have been completed on patients 16 years old and younger at the Children's Hospital of Philadelphia and in most instances have been able to achieve successful resolution of epiphora with placement of a bypass tube [10]. Approximately one-quarter of these procedures have been performed on children less than 5 years of age, and while we have generally been pleased with the results, the need for frequent revisions, often requiring general anesthesia, makes proper patient selection essential. In addition to thoroughly exhausting the possibility of more physiologic nasolacrimal reconstructive procedures, the patient's signs and symptoms must be severe enough to warrant intervention. The decision to perform a CJDCR must be accompanied by a full family commitment to devote significant time and effort toward assuring a successful surgical outcome. Postoperative complications or difficulties will likely occur, and both the physician and family must be prepared to cope with these as they arise. Although we recognize that the CJDCR is not the ideal solution, when given no other options, this procedure can provide significant relief to children who have been frustrated by chronic discharge and epiphora.

Indications

Canalicular obstruction in the pediatric age group can be due to a number of etiologies. In comparison to adults, congenital malformations are responsible for a much larger proportion of cases. Such congenital malformations can range from complete atresia of the puncta and canaliculi to isolated segmental obstructions of the upper nasolacrimal drainage system (Fig. 30.1). Frequently, the canalicular malformations are a part of more global abnormalities associated with various craniofacial syndromes. In our experience, approximately 50% of pediatric CJDCRs have been performed on patients with significant craniofacial abnormalities [7] (Fig. 30.2). In addition to congenital involvement of the canalicular system, these craniofacial patients can also develop obstructions secondary to surgical procedures, such as orbital advancement, telecanthus, or hypertelorism repair. Nonsurgical trauma is another common cause of upper system obstruction in children, particularly since this age group tends to be accident-prone. Damage to the canaliculi from radiation treatment or from chronic bacterial or viral infection can also occur but is far less common in the pediatric population.

Once an upper system block is identified, the most important step in determining whether a patient is a candidate for

S.M. Goldstein, MD (✉)
Oculoplastic Service, Wills Eye Hospital, Department of Ophthalmology, Jefferson Medical College and Perelman School of Medicine, University of Pennsylvania, Philadelphia, PA, USA

Oculo-facial Plastic Surgeon, Tri-County Eye Physicians and Divisions, Vantage EyeCare, Philadelphia, PA, USA
e-mail: goldstein@tricountyeye.com

J.A. Katowitz, MD, FACS
The Children's Hospital of Philadelphia and The Edwin and Fannie Gray Hall Center for Human Appearance, University of Pennsylvania, Philadelphia, PA, USA
e-mail: katowitz@email.chop.edu

© Springer International Publishing AG 2018

J.A. Katowitz, W.R. Katowitz (eds.), *Pediatric Oculoplastic Surgery*, https://doi.org/10.1007/978-3-319-60814-3_30

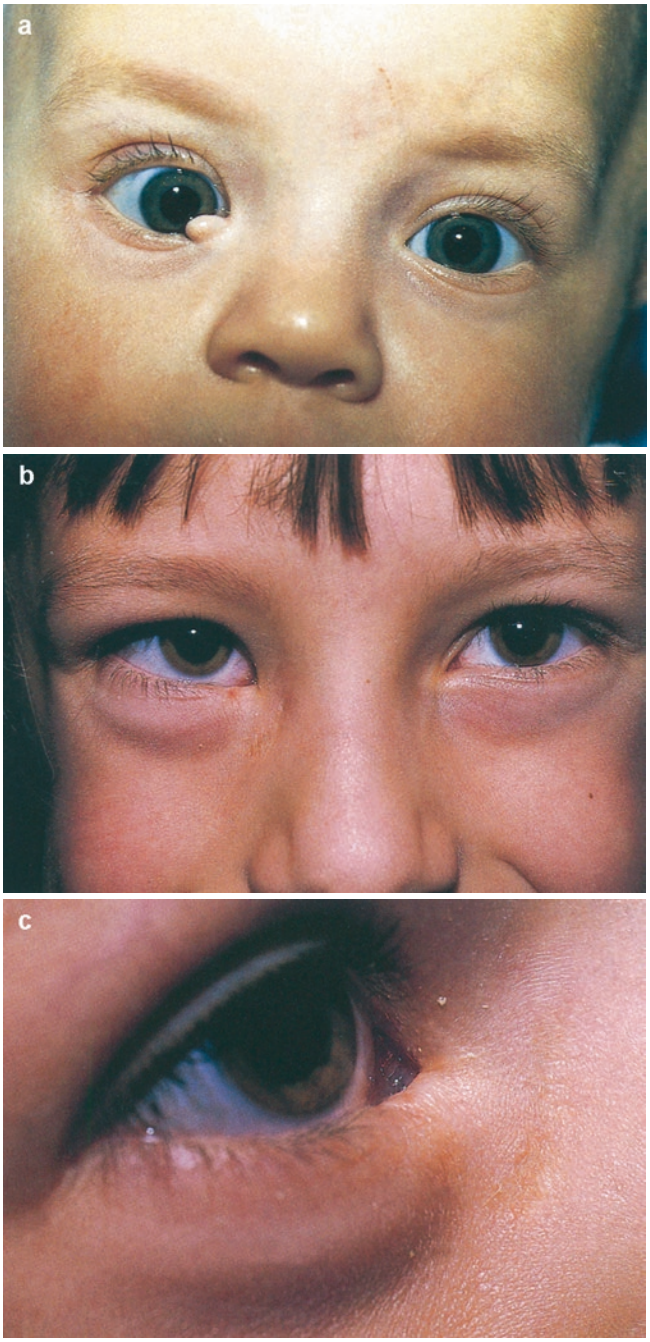


Fig. 30.1 Canaliculus repair with CJDCR. (**a**) Absence of lower canaliculus with the presence of a secondary canaliculus within cartilaginous appendage. Complete stenosis of the distal third of the upper canaliculus. (**b**, **c**) Four years following CJDCR with patent bypass tube in good position

CJDCR surgery is to fully delineate the extent of the obstruction. Since bypass surgery requires long-term attention, alternative procedures should be thoroughly explored. Both the length and the location of the obstruction can influence the choice of surgical technique.

In general, the smaller the obstruction, the greater the chance the native lacrimal system can be reconstructed and opened. If a distal canalicular obstruction is limited to the entrance into the lacrimal sac, Silastic intubation in combination with a dacryocystorhinostomy (DCR) should first be attempted [11]. In addition, distal canalicular trephination with bicanalicular stenting with DCR can improve success [12]. Intuitively, the likelihood of achieving a successful result with these procedures is far greater if the probe can be easily passed through the obstruction without creating a false passage. For those situations where the blockage is more severe, some surgeons have advocated performing a DCR with Silastic intubation in combination with a CJDCR, so that in the event that the DCR and Silastic intubation fail, a bypass permanent tube is already in place [13, 14]. If the bypass tube can be temporarily occluded without recurrence of tearing, then the Pyrex tube can be subsequently removed. Unfortunately, with younger children, limited cooperation makes this far less practical, and we do not routinely follow this suggestion.

As an alternative to a DCR with Silastic intubation, some surgeons have advocated open excision of the segment of blocked canaliculus with reanastomosis directly to the lacrimal sac (Fig. 30.3). This technique is termed a canaliculodacryocystorhinostomy (CLDCR). Although CLDCRs are associated with a significant failure rate, this technique can be particularly useful for those obstructions limited to the common canaliculus [15, 16]. In the appropriate patient, a DCR can be performed in combination with excision of the blockage, suturing of the canalicular flaps to the lacrimal sac, and insertion of Silastic tubing as a stent.

A CJDCR, therefore, can be contemplated in any patient with canalicular obstruction that has either failed a DCR with Silastic intubation or a canaliculodacryocystorhinostomy or has such extensive blockage that an alternative procedure cannot be performed. A patient falling into any of these categories must then be assessed for severity of symptoms. In general, when the epiphora is mild or occurring intermittently in a young child, we recommend delaying surgery and reevaluating the patient at a future date. This is partly due to the fact that the rapid growth of the face in the first 5 years of life may often require revisions of



Fig. 30.2 Craniofacial deformity and repair. (**a**) Example of craniofacial deformity demonstrating Tessier clefts 4 and 7 present on the right side with macrostomia. (**b**) Partial cryptophthalmos. (**c**) Following coloboma repair with Mustarde rotating cheek flap and cleft lip repair. (**d**) Open-approach CJDCR. (**e**) Ten days following surgery with spectacle camouflage. (**f**) Seven years following placement of bypass tube

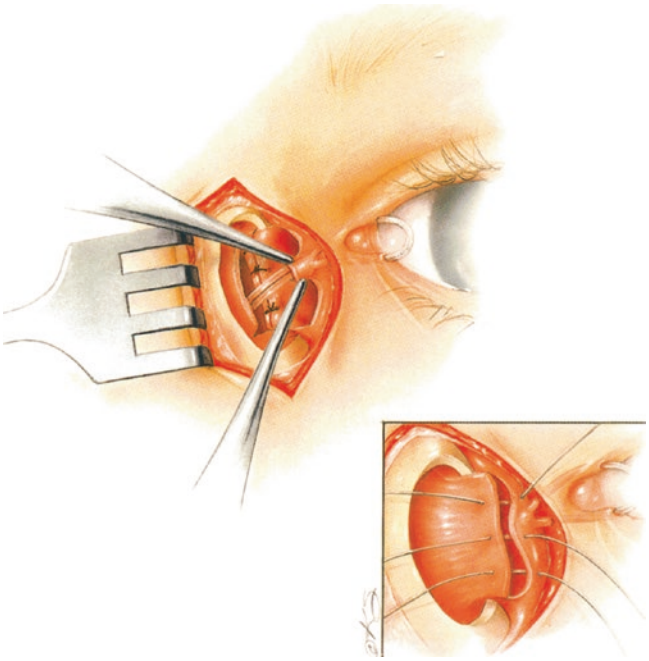


Fig. 30.3 Common canaliculodacryocystorhinostomy (CLDCR). Anastomosis of patent area of common canaliculus to nasal mucosa

the static small tube as it is outgrown. A CJDCR also becomes a much more attractive solution for epiphora once a patient is old enough to tolerate in-office manipulations of the bypass tube as well. For those younger patients with constant epiphora or recurrent bouts of infection, the benefits from a CJDCR may prove substantial enough to warrant earlier intervention.

Children with craniofacial syndromes are managed in a slightly different manner in that the threshold for performing a bypass procedure may be somewhat lower. Such patients will undoubtedly require multiple procedures under general anesthesia, and thus the opportunity to revise or adjust a bypass tube more readily exists. Additionally, these patients and their families are usually more accepting of the reality that multiple surgical attempts may be required to manage difficult upper system obstructions.

By far the most important consideration in deciding to perform a CJDCR is whether a fully informed family is prepared to devote the time and effort necessary to assure a successful outcome. They must understand from the beginning that their child may have to undergo multiple procedures requiring general anesthesia. In addition to revisions or adjustments that will be performed in the hospital or office, the parents or guardians will have to devote time to the care of their child's bypass tube on a regular basis. Daily maintenance of the tube is required throughout a lifetime. Frequent physician follow-up visits are necessary even in the most ideal situation, with a minimum of two visits a year. Once the family has been well informed and has fully accepted the challenge, a CJDCR can be the solution to a very persistent and aggravating problem.

Surgical Technique

Lester Jones first introduced his surgical technique in 1962, and since that time the placement of a Pyrex tube has become the standard and most popular method of performing a CJDCR [1]. Although surgeons have experimented with several different bypass materials, none have functioned as well as the Jones tube. Silicone, polyethylene, polypropylene, and polytetrafluorethylene have all been tried as substitute materials for bypass tubes, but the excellent capillarity of Pyrex cannot be reproduced with any of these alternative materials [17, 18]. Additionally, accumulation of protein deposits in the lumen with other synthetic materials has tended to be greater than with glass. Venous and mucous membrane grafts have also been used but once again demonstrate inferior capillarity function [19, 20]. Unfortunately, these grafts are not sturdy and undergo gradual stenosis, which further limits tear flow. A more recently described approach using a tubed pedicle of nasal mucosa in adults may show some promise but may be more challenging to accomplish in pediatric patients with smaller amounts of tissue available, especially at younger ages [21].

The Jones Pyrex tube has thus withstood the test of time. The Jones Pyrex tube (Gunther Weiss, Portland, OR) is available in a variety of lengths, shapes, and angles, allowing the surgeon to more successfully fit a tube in both younger and older children (Fig. 30.4). In addition to size and shape, other modifications like frosted tubes, tubes coated in porous polyethylene, and distal soft silicone flanges have been brought to market as means to minimize



Fig. 30.4 Jones tube set

migration [22–24]. These are however better suited for adult patients and are more prone to complications. Jones tubes can also be manufactured with a suture eye in the collar, which is a useful modification for the pediatric age group since these tubes often need to be exchanged over time. Securing the tube in place with a nonabsorbable suture makes postoperative management easier, because loss of the tube is less likely to occur with sneezing or nose blowing as well. For those tubes without a hole in the collar, the tube can still be secured by tying a suture beneath the collar around the outside diameter. Another system of Pyrex bypass tubes is also available. The Cox tube set (Eye Foundation Hospital, Birmingham, AL) is similar to that of the Jones tubes but includes a trocar, a stylet for insertion, and a measuring instrument to determine the appropriate length of tube needed (Fig. 30.5). Cox tubes come in a variety of lengths and angles; they vary slightly from the Jones tube in that they have a wider lumen and usually a larger collar or flange (Fig. 30.6).

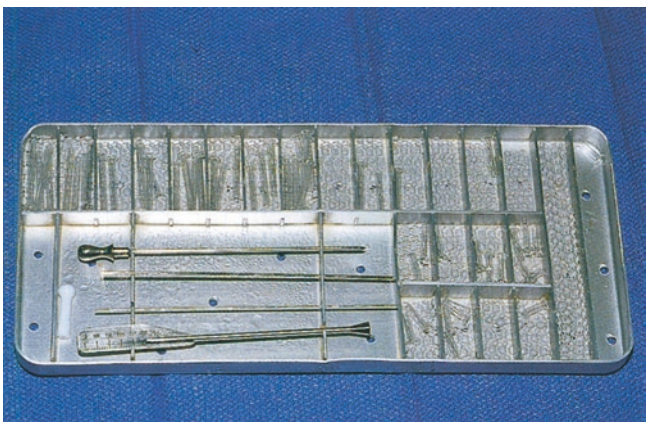


Fig. 30.5 Cox tube set

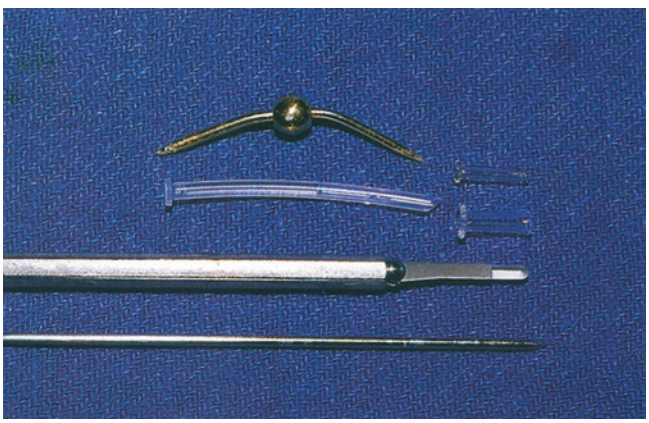


Fig. 30.6 Apparatus. From top to bottom, left to right: gold dilator, polyethylene tube, Jones tube, Cox tube, Beaver blade, and trocar

Procedure

A DCR is essential for the best placement and function of the bypass tube. If the tube is placed without creating mucosal flaps, there may be a small potential for future dacryocystitis unless the canalicular system is completely scarred over and no tears can find their way into the lacrimal sac. If a DCR has been done in a prior surgical effort, the glass tube can be inserted by a closed approach. When there has been no previous DCR, an open approach for bypass tube placement is typically performed. Nasal endoscopy is an invaluable adjunct to CJDCR surgery and should be utilized at various points in the procedure, when available. It is of particular value in estimating tube position and length in the nose. If a nasal endoscope is not available, direct inspection of the nasal cavity with a speculum and headlamp can be substituted.

Closed Approach

This technique is used when a DCR has been done previously. The steps involved are as follows:

1. A small portion of the caruncle may be excised if necessary to accommodate the flange of the tube (Fig. 30.7a).
2. A sharp trocar, an 18 g needle, or a 14–18 g IV angiocatheter is passed at a 45° angle in an inferior and somewhat anterior direction (Fig. 30.7b). If the path is blocked by the middle turbinate, fiber-optic endoscopic assistance can be helpful in performing a partial anterior middle turbinectomy [25]. If a deviated septum inhibits proper placement of the tube, a septoplasty may be required.
3. A #69 Beaver blade can be passed from the caruncle into the nose adjacent to the trocar (Fig. 30.7c). This is satisfactory for placement of the wider Cox tubes, but it is preferable for the thinner Jones tubes to pass the thin guide probe from the Cox set through the trocar opening. If an angiocatheter is used in place of the trocar, the catheter is left in place, and the guidewire can be passed down its lumen. In either instance, this permits placement of a 1.5 mm Henderson trephine passed down the probe to widen the pathway sufficiently for a snug fit around the Jones Pyrex tube [26].
4. The measuring instrument belonging to the Cox set may be used to determine the appropriate length of tube needed, but we often prefer an alternative technique. After the trocar is advanced to the nasal septum, it is then clamped at the level of the caruncle (Fig. 30.7d). The length distal to the clamp is measured. This length minus 3 mm is the

length of the tube that will sit in a position 3 mm from the septum (Fig. 30.7e). With this length as a guide, an endoscope is then used to estimate the width of the meatus. The ideal tube length is such that the tube projects 2–3 mm into the meatus from the lateral wall of the nose. As an aside, the angiocatheter can also be clamped in a similar fashion to estimate length prior to its removal.

5. After the thin steel probe is passed through the channel made with the trocar and the trephine is used to widen the opening, the appropriate length Pyrex tube is inserted over the probe after a single 6–0 clear nylon suture has been passed through the hole in the tube collar (or slipped around the neck of the tube) and tied tightly. The tube is then pushed into the proper position using the silicone

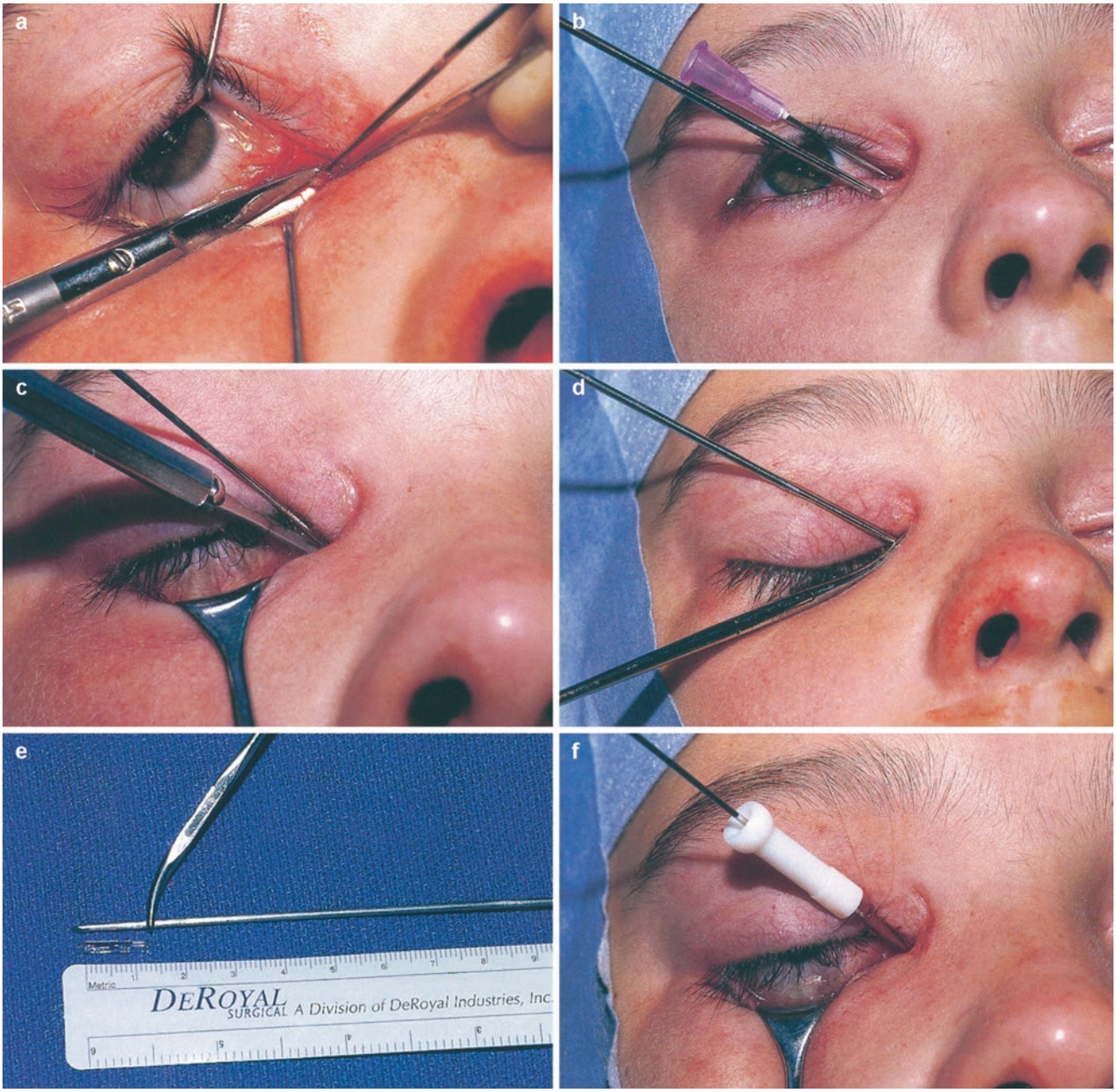


Fig. 30.7 Closed-approach conjunctivodacryocystorhinostomy (**a**) removal of anterior portion of caruncle, (**b**) 18g needle passed on desired angle from caruncle into the nose, (**c**) Trochar placement following the original path of the needle which is further incised with a #69 beaver blade as needed, (**d**) clamp the trochar at the caruncle after confriming intranasal position to measure the length of the Jones tube needed, (**e**) measure and confirm Pyrex tube length, (**f**) insertion of Tube over the trochar with the help of the inserter,

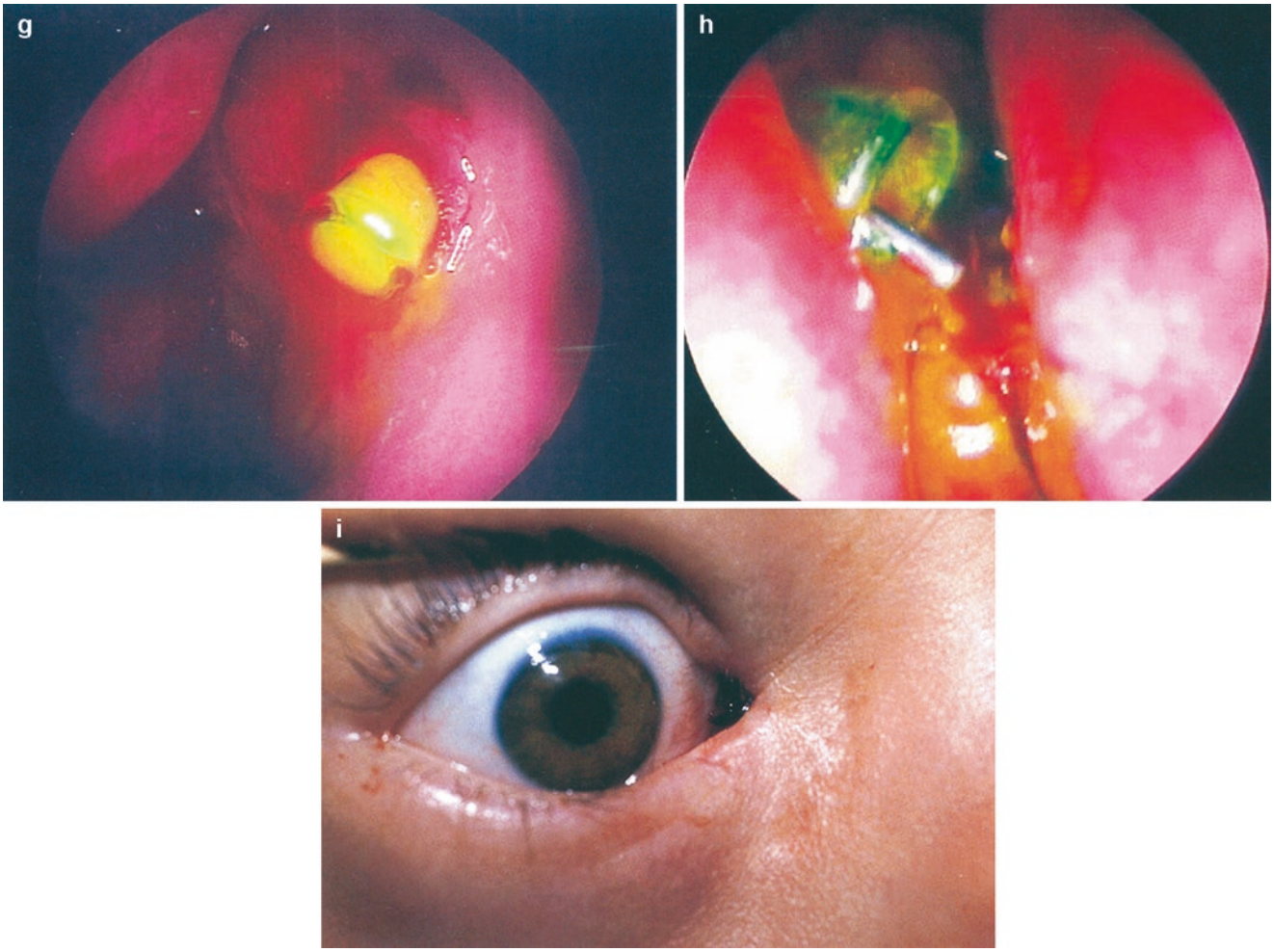


Fig. 30.7 (continued) (**g**, **h**) examples of endoscopic view of well positioned Jones tube, (**i**) view of properly positioned tube in caruncle

insertion cuff (Fig. 30.7f). If the thin Cox probe is unavailable, a Bowman probe can be substituted.

6. As stated in step 4, the tube should project 2–3 mm into the nose, but not touch the turbinate or septum. Figure 30.7g demonstrates ideal positioning in a wide middle meatus. Figure 30.7h reveals a tube that is positioned with the inferior end of the tube barely emerging from the opening in the lateral nasal wall. Further advancement of the tube is limited, however, by the short distance to the septum. In this particular situation where the meatus is narrow, such a compromise may be required but the risk of tube displacement is greater. In some instances, a nasal septoplasty may be required to provide adequate room for the bypass tube.
7. The needle attached to a 6–0 nylon or absorbable suture is then passed behind the lid margin, deep into the posterior palpebral tissues at the medial canthus, tied, and cut so that the tube is well secured in an appropriate position (Fig. 30.7i).

Open Approach

If a DCR has not been previously performed, the steps for a routine DCR (see Chap. 29) are followed to the point of suturing the lacrimal and nasal mucosal flaps. Steps 1–6 of the closed approach for tube insertion are then performed (Fig. 30.8). The anterior flaps of the lacrimal sac and nasal mucosa are sutured together above the bypass tube, and the

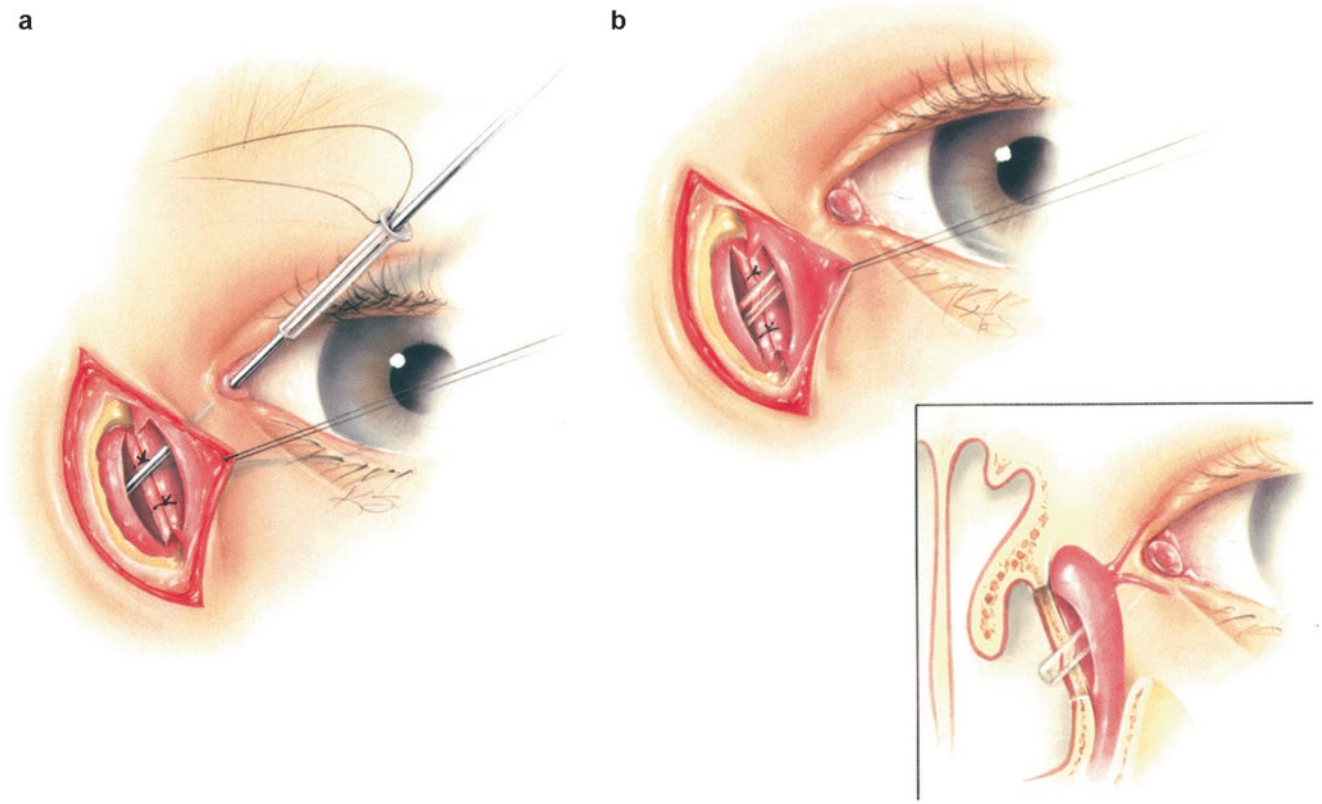


Fig. 30.8 Open-approach conjunctivodacryocystorhinostomy. (**a**) Pyrex tube inserted over probe. (**b**) Tube collar secured flaps sutured; *inset* shows tube in proper position in the meatus

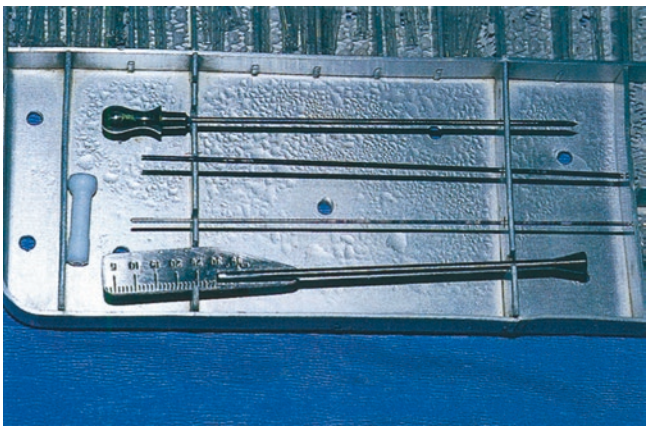


Fig. 30.9 Cox tube set. Top to bottom, left to right: trocar, silicone inserter, two stylets, and measuring instrument

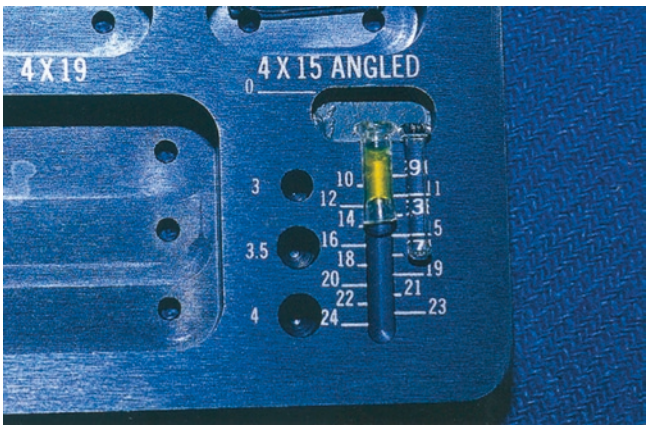


Fig. 30.10 Jones tube set gauge for measuring flange size and length

remaining steps of the DCR procedure are then completed. It is generally not necessary to suture the posterior flaps when a bypass tube is inserted.

We find the trocar, thin guide probe, and silicone insertion cuff from the Cox system to be useful for placement of both the original Jones tubes and the wider Cox tubes (Fig. 30.9). The measuring gauge on the Jones set is also helpful because it allows us to confirm both the size of the flange and the length of the selected tube (Fig. 30.10). In regard to the actual selection of a particular type of tube, we find, in general, that the Cox tubes with larger flanges often work best as an initial tube for patients with craniofacial abnormalities. The heavier Cox tube has, in our hands, replaced the use of a polyethylene tube as an initial tube as originally described by Lester Jones (Fig. 30.6). As the healing process creates cicatrization and the tube fits more snugly, it can then be replaced with a thinner Jones tube if needed. The thinner Jones tubes with smaller flanges (3.5 mm) are usually the best ultimate choice as they are less visible and appear to function most satisfactorily in our experience (Fig. 30.11).

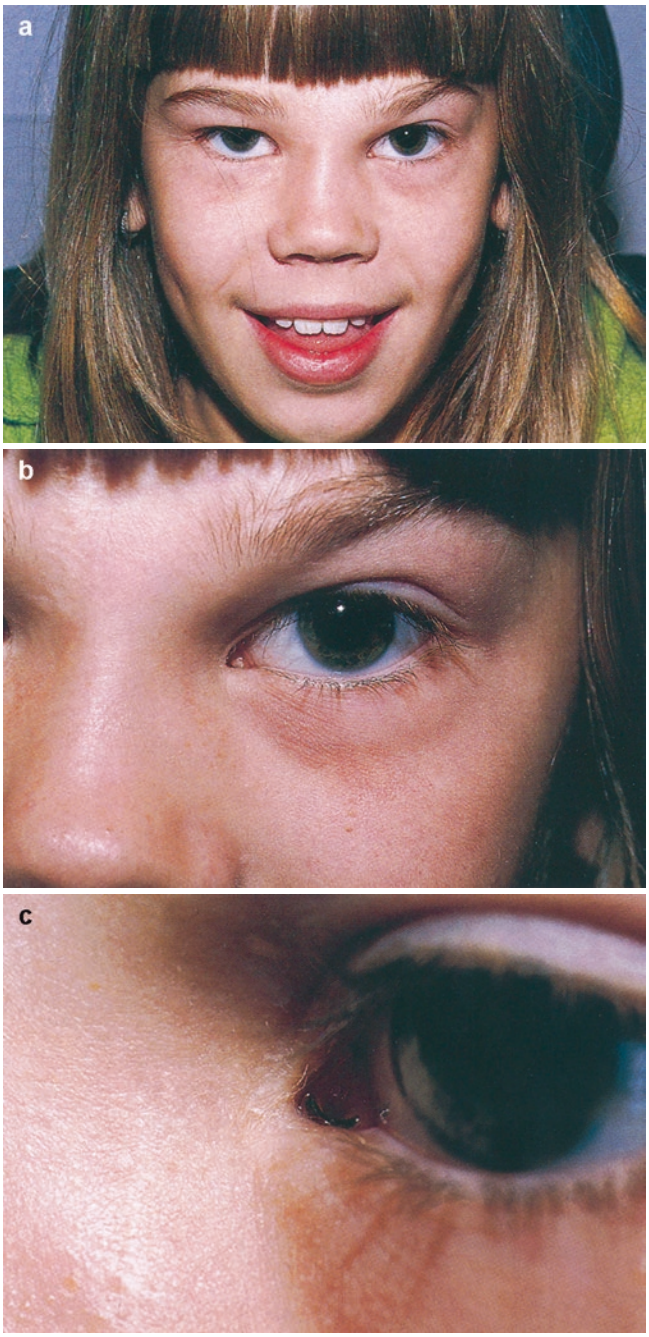


Fig. 30.11 Well-positioned Jones tube in (**a**) and (**b**), with lower lid being manually retracted in (**c**) to better view Pyrex tube

Alternative Minimally Invasive Approach

The standard CDCR approach described above has proved to work well in children where facial growth is expected to alter the path and size of the Jones tube, especially in younger children. Nonetheless, a minimally invasive approach without DCR has been described by several groups in older children and adults [7, 27]. In these approaches a sharp instrument such as Westcott scissors, a 14 g angiocatheter, or a 14 g needle is passed through the caruncle and the thin lacrimal bone to enter the nasal cavity, often under endoscopic or endonasal guidance. These approaches avoid a skin incision and skip opening the lacrimal system. These techniques simply puncture the lacrimal bone to enter the nasal cavity where a more snug opening now exists for Jones tube placement. Once the path is created, it can be dilated with the Jones or Cox dilators, and the Jones tube can be placed over a guidewire or probe. This "poke through" approach tends to be much faster, limits anesthesia time, and has a high success rate of 86–100%. However, it can make tube exchange much more difficult.

Postoperative Management

Postoperative management of the Pyrex tube is difficult in the pediatric age group but is not impossible. Following surgery, a topical antibiotic drop is used four times per day for 2 weeks. If a permanent suture was used to close the skin incision, this suture can be removed 5–7 days after surgery, although in most cases of young children, this step is avoided. The remainder of the postoperative care is directed primarily at maintaining patency of the tube and preventing dislocation.

While periodic syringing is easily performed at home or in the office on adult patients, children may require an examination under anesthesia if mucus obstruction of the tube occurs. For this reason, any steps that may help reduce the frequency of blockage should be undertaken. A simple trick, which is well tolerated by even the youngest of patients, is the use of a contact lens wetting solution once daily to help reduce mucus formation. Older children can be instructed to suck in air through the tube by quick inspiration while closing the soft palate and pinching both nostrils. For those occasions when the tube becomes obstructed, 10% acetylcysteine drops can be given several times daily. This can often be obtained from a compounding pharmacy although it is also available as a bronchial spray. The mucolytic action of the agent will sometimes clear the tube. Since it is not harmful to the globe or adnexa, we recommend a trial of 10% acetylcysteine prior to subjecting a child to general anesthesia.

Prevention of tube dislocation is far more challenging. Very little can be done to instruct the youngest children, but older children can be directed to close their eyes or hold a finger or tissue over the medial canthal region when they sneeze or blow their nose. Although the tube is more secure when sutured, it still can all too easily become dislodged. In those instances of partial tube extrusion, firm pressure with a cotton-tipped applicator applied over the tube flange may lead to successful repositioning. For those cases of significant tube migration, a revision procedure under general anesthesia is necessary. In the event that a tube completely extrudes, one may be able to replace it in the office in older children. If this is to be attempted, however, it must be done as soon as



Fig. 30.12 Partially extruded Cox tube



Fig. 30.13 Pyogenic granuloma occluding tube

possible after the tube is lost while the channel remains patent. The use of the gold Jones dilators can certainly be helpful when replacing a tube in an office setting (Fig. 30.6). While some of the older children can tolerate these manipulations, most pediatric patients will require general anesthesia.

Complications

As exemplified by the need for fairly aggressive postoperative management, the CJDCR, even in the most ideal situation, is associated with a significant failure rate. In our experience with pediatric CJDCRs, on the average, a patient requires roughly 1.5 procedures to obtain a successful surgical outcome [10]. These patients thus require frequent follow-up visits. While many of these visits will be on an "as needed" basis, routine assessments must be carried out every 6 months in an attempt to diagnose and manage any complication at an earlier stage.

Bypass tube extrusion and migration are the most common reasons for CJDCR failures (Fig. 30.12) [20]. Roughly 40–57% of all tubes placed will migrate, become dislodged, or require some adjustment [9, 24, 28]. This significant rate of tube malposition occurs even in a setting where almost all tubes are secured with a permanent suture. As stated earlier, most children will require general anesthesia for bypass tube adjustments; fortunately, however, in most cases surgical revision will lead to successful tube repositioning.

Following extrusion and migration, the next most common cause of failure is tube obstruction. This can be caused by mucus buildup in the lumen of the tube or by occlusion of the tube at the collar due to either conjunctival overgrowth or formation of a pyogenic granuloma (Fig. 30.13). More recently, it has been recognized that the tubes can become coated in a biofilm that can create chronic issues as well [24]. Older children can generally tolerate probing and irrigation of the tube in the office for rinsing and clearing mucus obstruction; otherwise, once again, surgery under general anesthesia is required.

Less common complications related to pediatric CJDCR surgery include nasal obstruction secondary to scarring, infections, restriction of globe motility [29], and skin fistula formation. The incidence of nasal scarring can certainly be reduced through the use of an endoscope while positioning the tube during surgery. If the tube is properly situated away from the middle turbinate and nasal septum, the likelihood of causing a subsequent nasal obstruction becomes much less. In the event that either a dacryocystitis or preseptal cellulitis occurs, the tube should be removed, which can usually be done in the office, and systemic antibiotics should be prescribed. Once the acute infection has resolved, replacement with a new tube can be considered. Restriction of globe motility can occur if the tube migrates and pushes against the globe. Proper repositioning can be achieved with surgery. Skin fistula formation also requires surgery because the fistulous track must be completely excised.

Although one would theorize that breakage of the glass bypass tube related to trauma would be another potential complication in this accident-prone age group, we have fortunately never seen this occur in any patient who has had a CJDCR, even in those participating in contact sports. Furthermore, in our experience, keloid formation, atypical face pain, scleral erosion, eyelid ulceration, or eyelid inflammation, as have been reported in adults, have not appeared to be significant problems for pediatric patients [30].

References

1. Jones LT. The care of epiphora due to canalicular disorders, trauma and surgical failures on the lacrimal passages. Trans Am Acad Ophthalmol Otolaryngol. 1962;66:506–24.
2. Burger D. Conjunctivo-dacryocystorhinostomy: curse or cure? Trans Ophthal Soc NZ. 1984;36:59.
3. Welham RA, Guthoff R. The Lester Jones tube: 15 year follow-up. Graefes Arch Clin Exp Ophthalmol. 1985;223:106.
4. Lamping K, Levine MR. Jones tubes: how good are they. Arch Ophthalmol. 1983;101:260–1.
5. Nissen JN, Sorenson T. Conjunctivorhinostomy: a study of 21 cases. Acta Ophthalmol. 1987;65:30.
6. Rosen N, Ashkenazi I, Rosner M. Patient dissatisfaction after functionally successful conjunctivodacryocystorhinostomy with Jones tube. Am J Ophthalmol. 1994;117:636–42.
7. Ali MJ, Honavar SG, Naik M. Endoscopically guided minimally invasive bypass tube intubation without DCR: evaluation of drainage and objective outcomes assessment. Minim Invasive Ther Allied Technol. 2013;22(2):104–9.
8. Komínek P, Cervenka S, Matousek P, Pniak T, Zeleník K. Conjunctivocystorhinostomy with Jones tube – is it the surgery for children? Graefes Arch Clin Exp Ophthalmol. 2010;248(9):1339–43.
9. Nemet AY, Fung A, Martin PA, Benger R, Kourt G, Danks JJ, Tong JC. Lacrimal drainage obstruction and dacryocystorhinostomy in children. Eye (Lond). 2008;22(7):918–24.
10. Heher KL, Katowitz JA, Johnson MA. Pediatric conjunctivodacryocystorhinostomy. Plastic and reconstructive surgery 1998 annual meeting, New Orleans, November; 1998.
11. Werb A. The surgery of canalicular obstructions. In: Rycroft PV, editor. Corneo-plastic surgery. Oxford, UK: Pergamon; 1969. p. 87–99.
12. Paik JS, Cho WK, Yang SW. Bicanalicular double silicone stenting in endoscopic dacryocystorhinostomy with lacrimal trephination in distal or common canalicular obstruction. Eur Arch Otorhinolaryngol. 2012;269(6):1605–11.
13. Steinsapir KD, Glatt HJ, Putterman AM. A 16-year study of conjunctival dacryocystorhinostomy. Am J Ophthalmol. 1990;109:387–93.
14. Putterman AM, Epstein G. Combined Jones tube–canalicular intubation and conjunctival dacryocystorhinostomy. Am J Ophthalmol. 1981;91:513–21.
15. Hurwitz JJ, Rutherford S. Computerized survey of lacrimal surgery patients. Ophthalmology. 1986;93:14.
16. Hurwitz JJ, Archer KF. Canaliculodacryocystorhinostomy. In: Linberg JV, editor. Lacrimal surgery. New York: Churchill Livingstone; 1988. p. 263–80.
17. Reinicke RD, Carroll JM. Silicone lacrimal tubing implantation. Trans Am Acad Ophthalmol Otolaryngol. 1969;73:85.
18. Hurwitz JJ. Teflon tubes for stenting and bypassing the lacrimal drainage pathways. Ophthalmic Surg. 1989;20:855–9.
19. Leone CR. Conjunctivodacryocystorhinostomy with buccal mucosal graft. Arch Ophthalmol. 1995;113:113–5.
20. Huang TT, Sasaki K, Nozaki M. Reconstruction of the lacrimal excretory system. Plast Reconstr Surg. 1992;90:399–404.
21. Lee JW. Nasolacrimal duct reconstruction with nasal mucoperiosteal flap. Ann Plast Surg. 2007;59(2):143–8.
22. Steele EA, Dailey RA. Conjunctivodacryocystorhinostomy with the frosted jones pyrex tube. Ophthal Plast Reconstr Surg. 2009;25(1):42–3.
23. Bagdonaite L, Pearson AR. Twelve-year experience of Lester Jones tubes-results and comparison of 3 different tube types. Ophthal Plast Reconstr Surg. 2015;31(5):352–6.
24. Steele EA. Conjunctivodacryocystorhinostomy with Jones tube: a history and update. Curr Opin Ophthalmol. 2016;27(5):439–42.
25. Fang CH, Patel P, Huang G, Langer PD, Eloy JA. Selective partial middle turbinectomy to minimize postoperative obstruction following Lester Jones tube placement. Am J Otolaryngol. 2015;36(3):330–3.
26. Henderson PN. A modified trephining technique for the insertion of Jones tube. Arch Ophthalmol. 1985;103(10):1582–5.
27. De voto MH, Bernardini FP, de Conciliis C. Minimally invasive conjunctivodacryocystorhinostomy with Jones tube. Ophthal Plast Reconstr Surg. 2006;22(4):253–5.
28. Sekhar GC, Dortzbach RK, Gonnering RS, Lemke BN. Problems associated with conjunctivodacryocystorhinostomy. Am J Ophthalmol. 1991;112:502–6.
29. Shin DH, Kim YD, Lee CH, Johnson ON 3rd, Woo KI. Restrictive strabismus and diplopia 2 years after conjunctivodacryocystorhinostomy with Medpor-Coated Tear Drain. Ophthal Plast Reconstr Surg. 2015;31(6):e159–62.
30. Bartley GB, Gustafson RO. Complications of malpositioned Jones tubes. Am J Ophthalmol. 1990;109:66–9.

Part IV

The Orbit

Classification and Evaluation of Orbital Disorders in Children

31

William R. Katowitz and Peter D. Fries

The suspicion of orbital disease in a child produces anxiety and concern in the patient, the family, and the treating physician. Thorough examination of an orbital problem, especially if the child is uncomfortable, is a particular challenge. The physician must be tolerant, gentle, and a careful observer. Avoiding close contact with the child at the first encounter is often appropriate. A substantial amount of information can be derived simply by allowing the child to play and interact within the office environment. One can usually identify with relative ease such problems as strabismus, motility deficits, lid and conjunctival injection, and proptosis and achieve a reasonable estimate of the degree of discomfort a child may be experiencing. It is critical to examine the patient's entire head as craniosynostosis, and plagiocephaly may cause facial and orbital asymmetry and thus relative proptosis. As the child becomes less frightened, the physician may then be able to perform a more thorough examination. On occasion, a detailed examination is possible only after several encounters with the child, once he or she has developed a level of improved comfort and confidence. In some instances, if the clinical suspicion of disease is high and the examination is difficult, immediate noninvasive imaging may be required.

Neuro-ophthalmic Localization of Disease

While an entire chapter has been devoted to ophthalmologic examination of the pediatric patient (see Chap. 10), certain highlights are worth considering in regard to orbital disease. The value of noninvasive imaging for the gross localization and pathologic identification of orbital lesions is indisputable. However, a detailed orbital examination can define the functional deficit produced by the lesion and may provide subtle evidence of microscopic invasion into surrounding normal tissues. Without this information, any treatment plan and, in particular, any surgical planning will be imprecise and may even be incorrect. Additionally, the most sensitive measure of progression or remission of disease is often clinical and not radiographic.

The localization of orbital disease involves two general questions: (1) Is the process confined to the orbit or has it originated or extended outside the orbital space? (2) Which of the orbital spaces is occupied by the lesion?

Extraorbital problems are frequently intracranial lesions that may invade the orbit. These are typically located in the optic chiasm, cavernous sinus, optic canal, or orbital apex. Homonymous hemianoptic defects characterize lesions posterior to the optic chiasm. Chiasmal lesions are identified by bitemporal visual field defects along with the absence of proptosis or ocular motility deficits. A junctional lesion (located at the juncture of the optic nerve and the chiasm) produces an ipsilateral central scotoma and a contralateral temporal hemianopsia, initially above the horizontal midline. A more anteriorly located lesion involving the optic nerve will produce a visual field defect that is unilateral and does not respect the vertical midline. Instead, scotomas are likely to be horizontal or produce general field suppression, especially if the lesion is circumferential to the optic nerve. While it may be difficult or impossible to obtain an automated or Goldmann visual field in a child, simple confrontation fields can be performed. Hand puppets or brightly colored objects held in each hand and gradually introduced into the peripheral field while holding the child's attention centrally will often yield useful localization information.

Lesions that impinge upon or invade the cavernous sinus may produce both motor and sensory defects. It is not possible to distinguish lesions that invade the cavernous sinus from those that produce pressure effects on the region. Cavernous sinus lesions feature impairment of cranial nerves III, IV, $V_{1,2}$, and VI. The abducens nerve is particularly

W.R. Katowitz, MD (✉)
The Children's Hospital of Philadelphia and The Edwin and Fannie Gray Hall Center for Human Appearance, University of Pennsylvania, Philadelphia, PA, USA
e-mail: katowitzw@email.chop.edu

P.D. Fries, MD
Eye Surgeons Associates, PC, Bettendorf, IA, USA

© Springer International Publishing AG 2018

J.A. Katowitz, W.R. Katowitz (eds.), *Pediatric Oculoplastic Surgery*, https://doi.org/10.1007/978-3-319-60814-3_31

sensitive to pressure effects and is likely to be the first to be involved. Pure cavernous sinus lesions do not produce optic neuropathy or proptosis. The effect of a mass lesion on the venous drainage of the orbit may not be apparent if it occurs slowly. If venous outflow obstruction occurs rapidly, conjunctival venous engorgement, proptosis, elevation of intraocular pressure, and dilation of the retinal veins may be identified in addition to a limitation of ocular rotation. Limitation of ocular motility may be the result of either a nerve palsy, as noted above, or the general congestion of the orbital tissues due to outflow obstruction. Involvement of cranial nerves III, IV, VI, and V_1, while sparing the maxillary division of the trigeminal nerve, is indicative of a superior orbital fissure process.

The optic canal contains the optic nerve, ophthalmic artery, and sympathetic nerves. Tumors that enlarge within the bony confines of the optic canal can result in rapid loss of acuity and peripheral visual field. Sympathetic involvement in these types of lesions is unusual, as additional sympathetic orbital innervation follows other pathways into the orbit.

Within the orbital confines, it may be possible to determine whether a lesion is invasive, resulting in a fibrous process, or whether it is encapsulated. Encapsulated orbital lesions frequently produce proptosis and optic neuropathy but more rarely result in motility or sensory deficits. If the process is invasive, however, and does not respect the planes of the orbit or produce fibrotic impairment of motility, then sensory dysfunction will more often precede the development of optic neuropathy. Serial orthoptic evaluations are often the most sensitive measure of disease progression in such cases. Distinguishing neuropathic motility impairment from that resulting from invasion of the extraocular muscle or surrounding Tenon's space may be difficult. Two features of fibrotic myopathy distinguish it from neurogenic causes. Forced duction testing, if it can be performed, will reveal restriction of duction in cases of fibrosis. In other cases, an unusual pattern of muscle involvement will suggest that the disease is myogenic rather than neurogenic. As an example, impairment of inferior rectus function that spares the pupil or medial rectus suggests a lesion affecting the extraocular muscle and not the oculomotor nerve.

History

Historical details of importance can be myriad, but certain items have proven value. The age of the patient at the time of first identification of a lesion can suggest whether it is congenital or acquired. Acquired neoplasias rarely occur within the first 6 months of life and are more likely to be identified after the first year. In contrast, congenital lesions are, by definition, present at birth, but they may grow slowly and therefore only become apparent later in life. An example is the dermoid cyst when it arises from the sphenozygomatic suture. Such lesions may go unnoticed until the third to fourth decade of life when the intraorbital component may grow large enough to produce proptosis. Any history of birth trauma should be recorded since an orbital hemorrhage may be apparent soon after birth or produce a reparative granuloma in response to non-resorbed blood months or years later. Other seemingly insignificant or minor traumas should be detailed regardless of how remote the event. We have seen a number of foreign body granulomas that are first noted years after a seemingly innocuous injury.

The duration and pace of evolution of a lesion are important factors in defining the growth pattern of the tumor. Generally, lesions that grow very slowly are benign. Lesions with an intermediate growth pattern are more likely to represent a neoplasm. Very rapid growth can be malignant or benign, as is seen from an orbital cellulitis or ruptured dermoid cyst. Associated pain generally indicates inflammation, rapid tumor expansion, or neural invasion. Prior surgery, whether orbital, strabismic, eyelid, or in other more remote sites, may produce a granuloma or reveal the primary site of metastatic disease. Travel abroad may result in inadvertent infection with unusual bacterial, viral, or parasitic organisms. The child's caretaker should be asked about the presence of pigmented or other cutaneous lesions and, if known, the existence of any familial inherited genetic condition (i.e., neurofibromatosis).

The general health of the child should be evaluated and include a complete review of systems, growth and nutritional patterns, concurrent disease, and medication history. A review of old photographs is often helpful but frequently overlooked. It is extremely helpful to review old pictures of the patient. With the current technology, many parents have a family library of photos on their smartphones or tabloid devices. When possible, a family should be encouraged to bring in old photographs as well as previously obtained imaging on a CD-ROM disk. Sometimes, lesions present for far longer than that described by even concerned parents are easily identified in a chronological review of serial childhood photographs.

Physical Examination

A thorough orbital examination in a child is often more difficult than in the adult. Many of the examinations are invasive and frightening to the infant. It is therefore advisable to carefully observe the child while obtaining the history from the parents. We find it critical to start with photography. A fixation device such as a toy or even a video or game displayed on a smartphone or tabloid can be used to gain and hold a patient's attention. Ideally, a photograph with a worm's-eye view (taken from the chin up) is obtained to document the relative orbital position (Fig. 31.1). Alternatively, a bird's eye view photograph (taken from above the head) can be used. We prefer an SLR camera with a 50 or 100 mm macro lens for clinical photography.

Gross measures of globe position, head posture, lid shape and dynamics, extraocular motility, tear outflow, and conjunctival disease can be assessed without disturbing the child. After a general measure of the condition is obtained, the evaluation can then become as detailed as the child will allow. Measurements of optic nerve function, including visual acuity, color vision, pupillary reactions, cycloplegic refraction, and, if possible, visual field testing, are important. External examination should also include measurements of globe position. Axial measurements are made with either a Hertel or Luedde exophthalmometer. Extra-axial displacement is judged and interpalpebral and interpupillary distances are measured. It is helpful to hold a ruler across the brow to document measurements. The examiner can then zoom on the screen of the SLR camera to confirm adnexal data, such as the interpalpebral, interpupillary, and horizontal fissure lengths (Fig. 31.2). The resistance to retropulsion is graded but remains a highly subjective test of questionable clinical value.

Attention is then addressed to the eyelids. They are judged for asymmetries in color (e.g., hemorrhage may indicate lymphangioma or neuroblastoma), shape (e.g., an S-shaped curve may indicate neurofibroma or dacryoadenitis), temperature (e.g., warmth may suggest infection), palpable or pulsatile mass, function, and position. Cranial nerves III, IV, and VI are assessed by orthoptic measurement. Restrictive

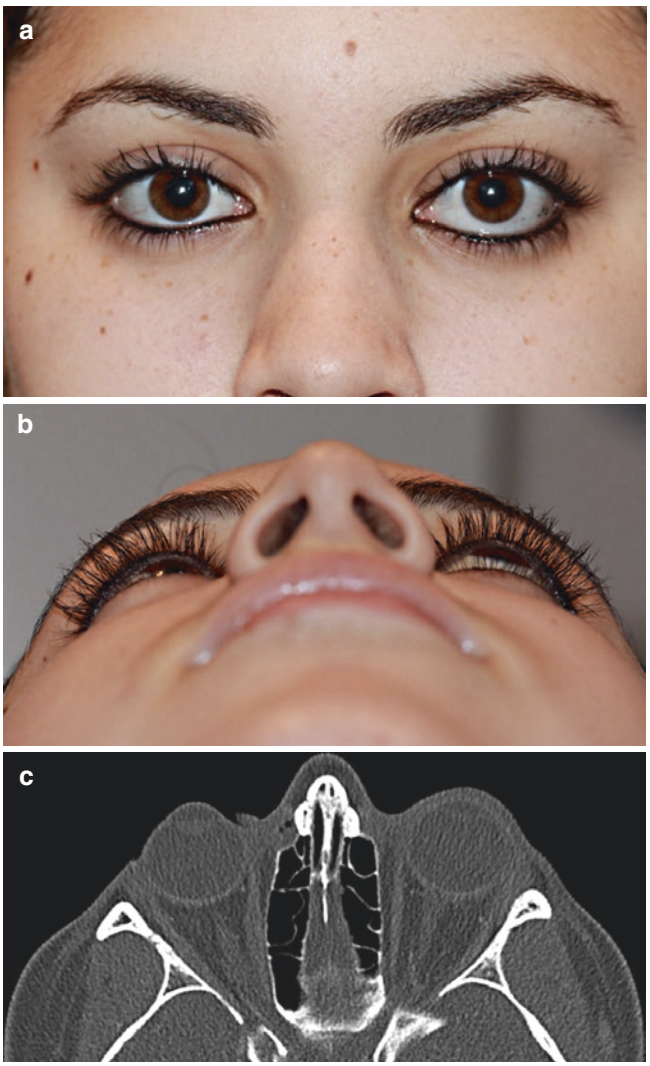


Fig. 31.1 Relative left proptosis due to left axial myopia (pseudoproptosis). (**a**) A teenager with a prominent left eye relative to the right side. (**b**) Worm's-eye view showing relative left proptosis. (**c**) Axial CT showing a large left eye, which had an axial length of 27 mm (the right was 24 mm). This patient had a refraction of −0.25D on the right and −8.00D on the left

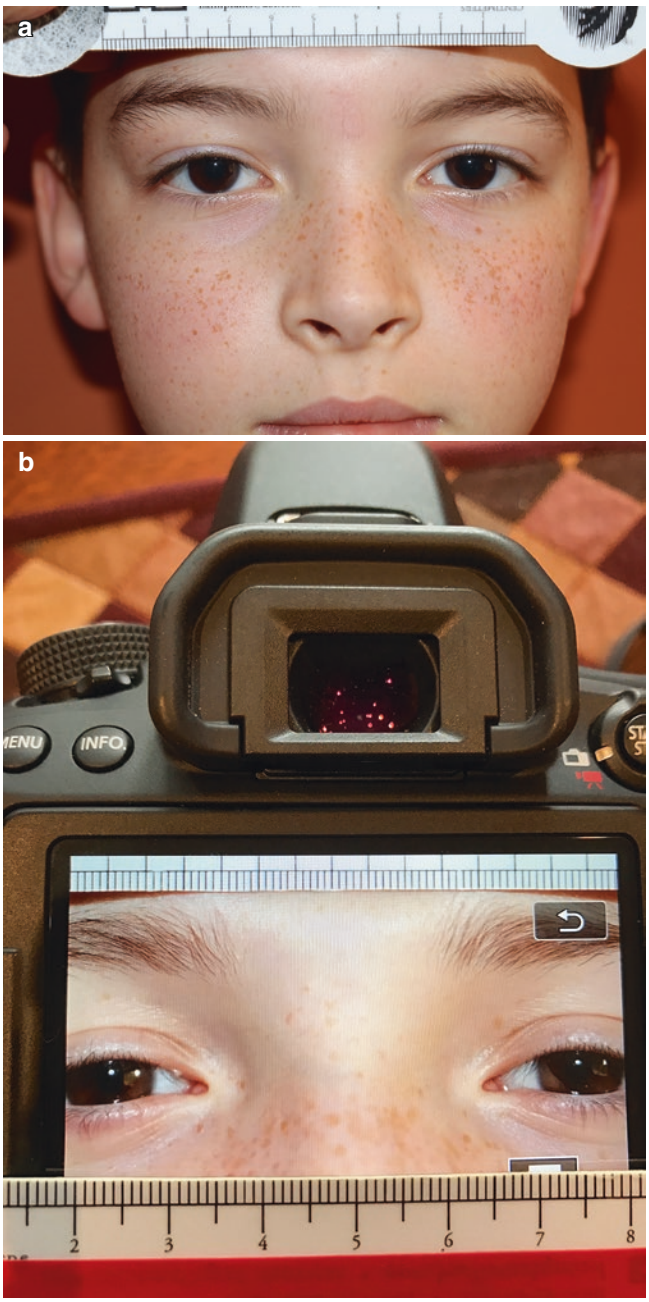


Fig. 31.2 Use of an SLR camera and ruler. (**a**) Clinical photograph with a ruler held against the patient's brow. (**b**) By magnifying the viewer on the camera to scale with a matching ruler, eyelid measurements can be made on the photograph of the patient

strabismus may be identified by forced duction tests if the child can cooperate. Sensation in all three distributions of the trigeminal nerve, including the corneal and nasal tip branches of the nasociliary nerve, is tested for bilateral symmetry.

The corneas are inspected for the presence of lesions consistent with systemic disease (i.e., amyloid). The conjunctiva is inspected for chemosis and vascular engorgement or tortuosity, which may be signs of venous outflow obstruction from orbital congestion due to mass effect or arteriovenous fistulization. The conjunctiva may also contain follicles (sarcoid) or nodules (lymphoid, amyloid, or metastatic disease). The anterior chamber may contain pathologic cells. These may be inflammatory, as seen in orbital inflammatory disease, or malignant, as occasionally seen in leukemia. The iris should be examined for Lisch nodules, which are considered pathognomonic for neurofibromatosis.

The retina can provide information regarding both vascular as well as neural diseases. Vascular and perivascular anomalies include vasculitis, inflammatory infiltrates, Roth spots, flame hemorrhages associated with systemic hypercoagulable states that occur in certain processes, infectious infiltrates, and hamartomas (i.e., tuberous sclerosis). Nerve fiber layer infarction may be associated with ischemia of the posterior pole that on occasion is the consequence of a rapidly growing, most often inflammatory, lesion. Nerve fiber layer loss is associated with chronic papilledema and more insidious optic nerve pallor. Careful examination of the region of the nerve fiber layer loss can identify the location of a focal lesion.

The choroid is the most frequent site of metastatic lesions in the eye. Choroidal folds, in general, herald an orbital process. When congenital choroidal folds do occur, they are most often bilateral. Unilateral folds usually result from posterior scleritis or pressure on the globe by a tumor. The optic disc provides information regarding the health of the optic nerve fibers and vascular supply as well as the pressure within the subarachnoid space. The identification of optic nerve edema in a child requires additional studies to rule out raised intracranial pressure or other causes of edema from infectious to pseudopapilledema from optic nerve head drusen. Optic nerve ultrasound and optical coherence tomography (OCT) are now readily available technologies though their application in the uncooperative patient can be limited.

Neuroimaging

The most revolutionary advance in the treatment of orbital disease was the development of high-resolution, noninvasive imaging techniques. The need for a diagnostic biopsy is currently a relatively rare event due to the characteristic appearance of most orbital lesions. Today the greatest difficulty occurs more from the relatively uniform availability of both computed tomography (CT) and magnetic resonance (MR) imaging technology (see Chap. 32). If the incorrect imaging modality is selected or if inappropriate images are ordered, then inaccurate assessment of the disease process may result. We suggest the following guidelines for appropriate selection of neuroimaging modalities from the perspective of the orbital surgeon.

The first principle is that MR is superior to CT in resolving soft tissue detail, while CT provides better bone resolution. CT is faster and cheaper than MR but produces ionizing radiation, which is generally of low exposure, depending on the extent of the study requested. The recent development of spiral CT imaging has resulted in further savings in imaging time (approximately 40 s for an orbital examination), which routinely eliminates the need for sedation and virtually never requires the general anesthesia or anesthetic monitoring that is occasionally required for MR imaging in the pediatric age group. Spiral CT image acquisition also permits the same volumetric analysis and multiplanar imaging capabilities heretofore available only with magnetic resonance imaging (MRI). This is a low-dose CT protocol now used in children to reduce the overall delivery of radiation during CT studies; nevertheless, one should consider an alternative to CT imaging when possible [1–3].

CT imaging is done in the setting of trauma to rule out retained metallic foreign bodies and to better evaluate for changes to the bony anatomy. We use CT almost exclusively to rule out orbital fractures, as a preoperative assessment for bony orbital decompression and for the assessment of the sinuses and orbits for infection and nasolacrimal obstructions. CT imaging will typically be faster and cheaper to the patient and institution and, in our experience, is more readily available to schedule. MR, on the other hand, is far superior in evaluating any soft tissue lesion within the orbit and is, in fact, necessary when CT can be misleading (see Chaps. 35 and 36). MR has the added advantage of diffusion weighted imaging, which will show that restricted diffusion is lesion suspicious for malignancy [4]. Both CT and MR imaging are covered in great detail in Chap. 32.

Orbital ultrasound imaging was developing at approximately the same time as CT imaging. It is generally more readily available, generates neither a high-field magnetic effect nor ionizing radiation, provides real-time diagnostic information, and is particularly suited to the diagnosis of cystic lesions. Its greatest limitations are the lack of deep orbital imaging (quality images of only the anterior one-half of the orbit are provided by the standard 10-MHz probe), the lack of image resolution relative to CT or MR, and the relative inability to determine anatomical relationships to other orbital structures in a static image for surgical planning. These shortcomings have limited the use of orbital ultrasound in our experience except for the rapid screening of an orbit for the presence of an orbital mass. The 30° test for enlargement of the optic nerve sheath is a useful parameter in detecting optic nerve thickening and sheath expansion. Color Doppler flow ultrasonography is a technique that can add information

about vascular lesions and potentially avoid further imaging. A high-flow lesion in an infant with an expanding eyelid mass, for example, would suggest an infantile hemangioma, whereas low or no flow might suggest a veno-lymphatic malformation [5]. We still err on obtaining orbital imaging (usually MR) if there is any suspicion of a growing orbital mass.

Angiographic interventional neuroradiology can be both diagnostic and, in some cases, therapeutic but is now almost never utilized with the advent of MRA and MRV imaging (see Chap. 32).

Predominantly venous lesions can also be outlined with injection techniques and in some cases treated by percutaneous embolization. However, in those cases, the sclerosing agents that are introduced may result in fulminant inflammatory responses. One must be prepared in such cases to operate on an emergency basis if optic neuropathy results from massive postinjection inflammation congestion (see Chap. 35).

Optical coherence tomography is a noninvasive imaging modality that can be used to evaluate the optic nerve and macula. This technology is under intense investigation as a monitoring modality for optic nerve disease as it relates to optic pathway gliomas [6], as well as in patients with suspected raised intracranial pressure due to tumors or craniosynostosis [7].

Classification

Many authors have sorted pediatric orbital disorders utilizing a variety of organizational schemes. Pathological series, usually generated at teaching institutions, typically include many examples of rare and unusual orbital tumors, since these are the lesions referred from the outlying community of practitioners due to diagnostic or experienced limitations. Often missing are entities that the comprehensive or pediatric ophthalmologist is most familiar with and most comfortable treating, such as orbital dermoids and orbital cellulitis. Similarly, clinically based series will have a heavy propensity toward these types of orbital processes and will lack a broad expanse and depth of unusual lesions. Additionally, some series may be heavily weighted toward referral of certain lesions to an institution or individual because of personal reputation or interest, thus skewing the series data. Such variability has, no doubt, led to the confusion and debate in the literature about the frequency and incidence of pediatric orbital diseases.

Table 31.1 attempts to rectify and balance these shortcomings by compiling the six largest series of pediatric orbital lesions into one large compendium. These series

Table 31.1 Orbital tumors in children

	Iliff and Green Wilmer 1978 *n* = 174	Crawford Toronto 1983 *n* = 572	Shields et al. Wills 1986 *n* = 250	Rootman Univ of B.C. 1988 *n* = 241	Kodsi Mayo Clinic 1994 *n* = 340	Katowitz CHOP 1996 *n* = 243
		Benign orbital tumors				
Cystic lesions						
Dermoid	52	6	115	*27*	*65*	71
Lipodermoid	0	0	0	*7*	0	4
Microphthalmia with cyst	5	0	3	3	2	1
Sweat gland cyst	0	0	0	1	0	2
Mucocele	0	5	1	2	4	0
Implantation cyst	0	0	0	2	0	0
Simple epithelial cyst	1	0	12	1	5	6
Cephalocele	1	2	0	0	3	0
Lacrimal duct cyst	2	0	0	0	1	0
Infectious/inflammatory lesions						
Orbital cellulitis or abscess	0	226	0	17	0	2
Dacryoadenitis	0	1	5	0	0	0
Reactive lymphoid hyperplasia	0	0	5	0	0	0
Idiopathic orb. Inflammation	9	5	41	14	20	13
Thyroid orbitopathy	0	107	0	24	0	0
Scleritis	0	0	0	1	0	0
For. body granuloma	0	0	0	0	7	0
Noninflam, lacrimal abnormal	5	0	0	0	0	0
Neurogenic lesions						
Optic nerve glioma	9	17	5	13	47	2
Meningioma	5	0	1	2	9	3
Plexiform neurofibr.	11	14	2	9	16	33
Teratoma	3	1	0	0	2	3
Neurilemoma	0	0	1	0	1	0
Paraganglioma	0	0	0	0	1	0

(continued)

Table 31.1 (continued)

	Iliff and Green Wilmer 1978 *n* = 174	Crawford Toronto 1983 *n* = 572	Shields et al. Wills 1986 *n* = 250	Rootman Univ of B.C. 1988 *n* = 241	Kodsi Mayo Clinic 1994 *n* = 340	Katowitz CHOP 1996 *n* = 243
Vascular lesions						
Capillary hemangioma	14	0	10	23	40	14
Lymphangioma	10	4	4	14	12	7
Cavernous hemangioma	0	13	2	0	1	0
Varix	0	0	0	12	0	1
AV shunt	3	3	1	5	4	0
Vascular malform.	0	3	0	0	4	2
Angiofibroma	0	3	0	0	1	0
Hemangiopericytoma	0	0	0	0	1	0
Secondary hemorrhage	1	5	0	0	1	0
Trauma						
Fracture	0	0	0	16	0	0
Foreign body	0	0	0	2	0	5
Orbital hemorrhage	0	25	0	0	0	0
Degenerative						
Post-RT atrophy	0	0	0	5	0	0
Fat prolapsed	1	0	0	1	0	0
Amyloidosis	1	0	0	0	0	0
Histiocytic lesions						
Langerhans histiocytosis	1	2	1	0	8	3
Juv. xanthogranuloma	0	0	0	0	0	2
Fibrous histiocytosis	0	0	0	2	0	0
Bony lesions						
Fibrous dysplasia	2	4	0	7	13	5
Aneurysmal bone cyst	0	0	0	2	1	0
Osteoma	0	1	0	2	2	0
Orbital asymmetry	0	48	0	8	0	0
Ossifying granuloma	2	0	2	1	1	2
Osteopetrosis	0	1	0	0	0	0
Hyperostosis	0	1	0	0	0	0
Fat-containing lesions	4	0	16	0	4	19
Pseudoproptosis	0	0	0	1	0	0
		Malignant orbital tumors				
Rhabdomyosarcoma	15	14	10	5	26	27
Leukemia/lymphoma	2	23	1	1	5	5
Soft tissue sarcomas[a]	6	9	2	5	9	5
Secondary retinoblastoma	6	1	9	0	14	1
Histiocytosis X	0	18	0	3	4	3
Neuroblastoma	1	9	0	1	3	0
Adenoid cystic carcinoma of lacrimal glands	0	0	1	2	0	0
Malignant teratoma	1	0	0	0	1	0
Nasopharyngeal carcinoma	0	1	0	1	0	0
Esthesioneuroblastoma	0	0	0	0	1	1
Malignant schwannoma	0	0	0	0	0	1
Orbital melanoma	0	0	0	0	1	0
Medulloblastoma metastatic to optic nerve	0	0	0	1	0	0
Metastatic astrocytoma	1	0	0	0	0	0

Sources: Iliff and Green [8], Crawford [9], Shields and Bakewell [10], Rootman [11], Kodst and Shetlar [12], Katowitz [13]

[a]Includes undifferentiated sarcoma (10), Ewing's sarcoma (5), sarcomas secondarily invading the orbit (5), fibrosarcoma (5), alveolar soft part sarcoma (4), chondrosarcoma (2), osteosarcoma (2), lymphosarcoma (1), myxosarcoma (1), and chondromyosarcoma (1)

represent the largest number of patients and should yield a greater dilution of the previously mentioned factors. Even with the obvious limitations mentioned above, it is our hope that this may offer a broader and less biased representation of pediatric orbital tumors. The categories combine both pathological headings and clinical headings in an attempt to include as many entities as close as possible to their author's original classification. A perusal of this long table yields a wealth of information and comparative data for those who see and treat pediatric orbital conditions. A review of this table may provide a more complete categorization of pediatric orbital disorders for use in both clinical and diagnostic settings. In the succeeding chapters, reference will be made to this table in estimating the occurrence and incidence of specific pediatric orbital disorders.

References

1. Linton OW, Mettler FA. National conference on dose reduction in CT, with an emphasis on pediatric patients. AJR Am J Roentgenol. 2003;181:321–9.
2. European guidelines on quality criteria for computed tomography. EUR 16262. http://www.drs.dk/guidelines/ct/quality/index.htm. Accessed 21 Apr 2008.
3. Kalra MK, Maher MM, Toth TL, et al. Strategies for CT radiation dose optimization. Radiology. 2004;230:619–28.
4. Lope LA, Hutcheson KA, Khademian ZP. Magnetic resonance imaging in the analysis of pediatric orbital tumors: utility of diffusion-weighted imaging. J AAPOS. 2010;14(3):257–62.
5. Parentin F, Borzaghini L, Perissutti P. The role of ultrasonography in the diagnosis of orbital lymphangiomas. Ophthalmologica. 2001;215(3):238–40.
6. Avery RA, Hwang EI, Ishikawa H, Acosta MT, Hutcheson KA, Santos D, Zand DJ, Kilburn LB, Rosenbaum KN, Rood BR, Schuman JS, Packer RJ. Handheld optical coherence tomography during sedation in young children with optic pathway gliomas. JAMA Ophthalmol. 2014;132(3):265–71.
7. Swanson J, Xu W, Aleman T, Mitchell B, Wes A, Chen SS, Bender L, Heuer G, Katowitz W, Bartlett S, Taylor J. Optical coherence tomography can detect intracranial hypertension in young children with Craniosynostosis. Plast Reconstr Surg. 2015;136(4 Suppl):39.
8. Iliff WJ, Green WR. Orbital tumors in children. In: Jakobiec FA, editor. Ocular and adnexal tumors. Birmingham: Aesculapius Publishing Company; 1978. p. 669–84.
9. Crawford JS. Diseases of the orbit. In: Crawford JS, Morin JD, editors. The eye in childhood. New York: Grune & Stratton; 1983. p. 361–94.
10. Shields JA, Bakewell B, Augsburger JJ, et al. Space occupying orbital masses in children: a review of 250 consecutive biopsies. Ophthalmology. 1986;93:379–84.
11. Rootman J. Frequency and differential diagnosis of orbital disease. In: Rootman J, editor. Diseases of the orbit. Philadelphia: J.B. Lippincott Co.; 1988. p. 124.
12. Kodst SR, Shetlar DJ, Campbell RJ, et al. A review *of* 340 orbital tumors in children during a 60-year period. Am J Ophthalmol. 1994;117:177–82.
13. Katowitz JA. Unpublished data from the Children's Hospital of Philadelphia; 1996.

Imaging of the Pediatric Orbit

32

Larissa T. Bilaniuk, Ann P. Murchison, and Jurij R. Bilyk

Orbital and visual pathway abnormalities that occur in the pediatric age group cover a wide spectrum, and most are distinct or differ in frequency from adult orbital lesions [1]. Also, because in the very young, the orbit is a growing, changing structure, it can reflect by its size and shape the loss of native intraorbital tissue or the growth of intraorbital lesions. Thus, imaging modalities such as computed tomography (CT) and magnetic resonance imaging (MRI) play important roles, not only in detection, delineation, and characterization of the various entities but also in monitoring the evolution of processes and their effect on the orbit and the rest of the facial structures. Imaging is particularly important and useful in the very young child, when clinical evaluation of visual function is difficult and may not be precise. However, in order to obtain technically good images, sedation is usually required, which entails a dedicated sedation team who not only administers the sedation but also monitors patients during and after the studies.

While CT and MRI are both important modalities for imaging the orbit, each technique has its advantages and disadvantages [2]. CT is the optimal technique for demonstration of bone detail and the presence of calcification and is the procedure of choice for initial evaluation of orbital trauma and infections, as well as for patients with contraindications for MRI. Soft tissue and bone three-dimensional CT reconstructions are valuable in the evaluation and management of patients with orbital asymmetries and craniofacial anomalies. Spiral (helical) CT permits rapid acquisition of images (3–5 s for 12–20 images) with decreased radiation exposure [3]. Multidetector array technology has also improved the speed and resolution of CT images. In simple terms, older CT relied on a two-dimensional ("single-row") detector array opposite a fan-beam X-ray source. Multidetector CT adds additional detector arrays in the Z-axis ("multiple rows"), providing a three-dimensional scanning ability [4]. This allows for excellent coronal and parasagittal reconstructions from rapidly obtained axial images, eliminating the need for patient repositioning, an important advantage when imaging children. However, this may come at a cost of higher radiation exposure in certain situations, especially when newer 64-detector arrays are used.

Although CT is a more established technique and more widely used for routine evaluation of the orbit, MRI, because of the recently introduced faster scanning techniques and availability of thin sections with high resolution and contrast enhancement with fat suppression [5], has become a serious competitor for CT. Familiarity and experience with both modalities are required for correct judgment of when and how to use each technique. CT and MRI typically play complementary rather than competitive roles in the evaluation of the orbit. MRI, with its multiplanar capability, sensitivity to flow, and superior soft tissue discrimination (especially at the skull base and in the central nervous system), is the procedure of choice for evaluation of optic nerve, vascular abnormalities, and lesions with extraorbital extension [6, 7]. The fact that MRI does not involve ionizing radiation is of particular importance in the evaluation of children, especially those that require serial studies as, for example, children with visual pathway gliomas.

The Basics of Orbital CT and MRI

CT and MRI are complex technologies that are constantly evolving. It is both impossible and really unnecessary to provide the ophthalmic and orbital specialist with an in-depth discussion of the myriad techniques used by our

L.T. Bilaniuk, MD, FACR (✉)
Department of Radiology, Children's Hospital of Philadelphia, 3401 Civic Center Boulevard, Philadelphia, PA 19104-4399, USA
e-mail: bilaniuk@email.chop.edu

A.P. Murchison, MD, MPH
Director, Wills Eye Emergency Department, Wills Eye Hospital, 840 Walnut St., Philadelphia, PA 19107, USA

J.R. Bilyk, MD
Skull Base Division, Wills Eye Hospital, Neuro-Ophthalmology Service, 840 Walnut St., Suite 930, Philadelphia, PA 19107, USA

© Springer International Publishing AG 2018

J.A. Katowitz, W.R. Katowitz (eds.), *Pediatric Oculoplastic Surgery*, https://doi.org/10.1007/978-3-319-60814-3_32

neuroradiologic colleagues in their daily imaging routines. In this section, however, we shall attempt to present a practical summary of the basic techniques in CT and MRI that while admittedly oversimplified may at least be helpful in appreciating how these techniques work to provide useful diagnostic imaging.

Computed Tomography

CT requires an X-ray source that passes through the patient to a fanned detector array on the opposite side. Early technology required a stepwise accumulation of data in slices, which were then stacked into axial images. Any coronal or sagittal reconstruction would result in "step artifacts," which affected anatomic detail. Because coronal images are essential in interpreting orbital scans, the patient had to be repositioned on the gantry, with their neck hyperextended. Needless to say, this technique was difficult in uncooperative patients or in those with cervical spine pathology, not even considering the even greater difficulty in attempting this for the pediatric patient. The introduction of slip ring technology allowed for helical or spiral CT imaging, where the X-ray source and detector array wound themselves in a spiral, while the patient gantry moved in the opposite direction. This not only markedly reduced imaging time but also improved out-of-plane (coronal, sagittal) reconstructions. However, initial helical scanners still relied on a single detector array along an arc of the scanner's ring. More recently, multidetector CT (see previous section) utilizes a spiral technique but adds multiple rows of detectors, providing an additional axis for imaging. This not only precludes the need for patient repositioning but provides rapid imaging with no loss of resolution for coronal and sagittal views.

An orbital CT must always include, at a bare minimum, axial and coronal views with bone and soft tissue windows. Axial scans alone are inadequate and may miss pathology. The clinician should always review both soft tissue and bone windows – each window maximizes the detail for particular anatomy. Intravenous contrast is also helpful and often critical but is not necessary in all cases as, for example, in a trauma patient suspected of having an orbital fracture, where this will provide little information of diagnostic benefit.

CT angiography (CTA) is a powerful tool for evaluating neurovascular anatomy but comes at the cost of significant radiation exposure and contrast load. Furthermore, CT and CTA provide much less soft tissue information than MRI and MR angiography (MRA). It is important to remember that pediatric pathology differs significantly than that observed in an adult and relatively common diagnoses in adults may be rare in children. As an example, an oculomotor palsy in an adult immediately raises the specter of an expanding posterior communicating artery aneurysm, and the clinician will appropriately order an urgent and readily available CT and CTA. However, a young child presenting with this clinical picture is far more likely to harbor a brain tumor causing compression on the oculomotor nerve. Therefore, in a pediatric oculomotor palsy, it would be prudent to spare the child unnecessary and significant radiation exposure from a CT/CTA and obtain far more soft tissue information with an MRI/MRA.

Magnetic Resonance Imaging

One major and unique advantage of CT in the orbit is that orbital fat acts as a "negative contrast" – it disappears on CT images, revealing the native anatomy and any pathology in good detail. This advantage disappears at the orbital apex, however, where the local anatomy is crowded and the relative increase in the bone component washes out soft tissue detail. It is also problematic in the central nervous system, where the anatomy on CT is fairly homogenous. MRI depicts bony anatomy less well than CT but provides better information about bone marrow and shows markedly better soft tissue detail than CT. This is especially useful in the skull base (e.g., cavernous sinus, orbital fissures) and brain. MRI also provides excellent soft tissue information in the orbit, *provided that correct orbital MRI techniques are used*. Orbital MRI technique differs significantly from brain MRI protocols. One major issue for the clinician to remember is that orbital fat is hyperintense (bright) on T1-weighted images. If gadolinium is infused, abnormal processes will enhance (become hyperintense) and potentially disappear into the normal fat signal. Therefore, one critical tenet of orbital MRI is to always suppress fat when infusing gadolinium. In other words, all orbital studies should be ordered "with gadolinium and fat suppression" and not simply "with gadolinium."

Signal intensities on various MRI weighting provide a relatively complex algorithm for specific orbital pathologies. Remember that vitreous and CSF (which are mostly water) are "dark" on T1 weighting and "bright" on T2 weighting. As an oversimplification, this pattern also holds for many orbital tumors *before gadolinium infusion* (after gadolinium infusion, most pathology enhances – i.e., becomes hyperintense). There are exceptions to this rule that are worth memorizing, because they provide the clinician with valuable clues as to etiology (Table 32.1). Processes that are hyperintense on *precontrast* T1 weighting are inspissated material and thick mucus (e.g., mucoceles), fat (e.g., dermoid cysts, lipoma, liposarcoma), melanin (e.g., melanotic melanoma), subacute blood (e.g., subacute subperiosteal hematoma, blood cyst), and heavy metal (scavenged by certain fungi).

The most useful views for the clinician on MRI of the orbit are precontrast T1 weighted and T2 weighted (often with fat suppression) and postcontrast T1 weighted with fat suppression. Three additional MRI techniques are worth mentioning, as they have practical implications for the orbital surgeon and neuro-ophthalmologist.

1. When imaging a patient suspected of having demyelinating disease, T2-weighted fluid-attenuated inversion recovery (FLAIR) images are invaluable. The first signs of demyelination typically occur periventricularly, and in T2 weighting, the bright CSF makes this area difficult to interpret. FLAIR technique suppresses the signal from CSF and highlights areas of demyelination (Fig. 32.1).
2. Diffusion-weighted imaging (DWI) and apparent diffusion coefficient (ADC) are routinely performed for brain, orbit, face, and neck MRI, and in spite of greater anatomic distortion and decreased resolution in the head and neck, these techniques help to more specifically characterize lesions. Briefly, DWI measures Brownian motion of water. In processes composed of tightly packed, small cells with a high nuclear-to-cytoplasmic ratio (e.g., lymphoma, retinoblastoma), diffusion is restricted, and a characteristic signal intensity is noted on DWI and ADC. Several studies have shown potential utility in distinguishing between orbital processes using this technique [8–12]. In addition, DWI is helpful in distinguishing abscess from other inflammatory processes; thick purulent material restricts on diffusion sequence.
3. Three-dimensional constructive interference in steady state (3D CISS) is a fully refocused steady-state gradient-echo, T2 MRI sequence that is particularly useful for the evaluation of any structure surrounded by CSF, particularly the cranial nerves (Fig. 32.2) [13, 14]. Cavernous sinus imaging is also enhanced by this technique. 3D CISS is also of particular interest to skull base surgeons, since CSF rhinorrhea can be identified with these MR sequences [15]. Because of the physics of MRI, any image plane can be easily obtained, and for certain cranial nerves, oblique coronal and oblique sagittal views may be ideal. One major limitation of 3D CISS is its long acquisition time.

Table 32.1 Orbital pathologies that are hyperintense on precontrast T1-weighted MRI

Lesions containing lipid	Dermoid/epidermoid cysts, lipomas, liposarcomas
Lesions containing mucus[a]	Dermoid/epidermoid cysts, mucoceles
Subacute blood	Hematic cysts, subperiosteal hematomas, blood cysts within lymphangiomas
Lesions containing melanin	Melanoma

[a]Hyperintensity increases as the protein content in mucus increases (becomes more viscous)

MRA approaches or equals the resolution of CTA in many academic centers but is a time-consuming technique. One advantage of MRA over CTA is that it may be performed (with less than ideal resolution) without contrast material; this is an important issue in patients who cannot tolerate contrast material because of medical comorbidities. Finally, MR venography (MRV) is exceedingly useful in evaluating patients for central venous sinus thrombosis.

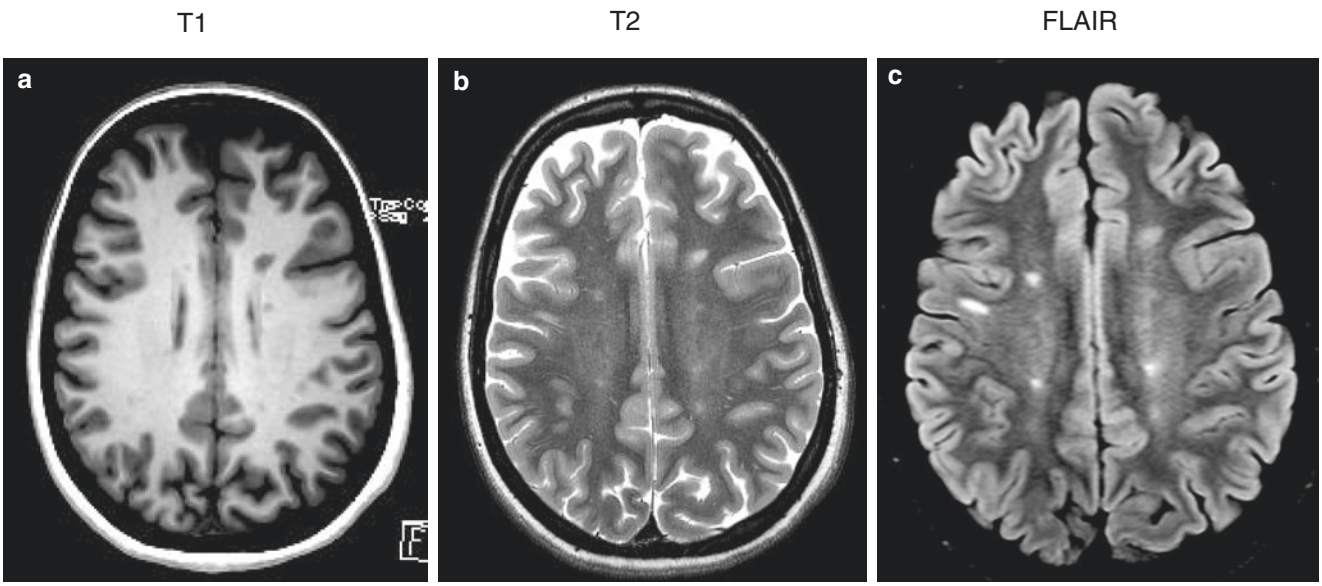


Fig. 32.1 T2 FLAIR of demyelination. (**a**) Axial, precontrast T1 MRI shows the largest lesion in the left frontal white matter. CSF is dark on T1. (**b**) On T2-weighted MRI, areas of increased signal suggestive of demyelination are noted. Note that CSF is hyperintense. (**c**) On T2 FLAIR imaging, the CSF is suppressed, and the areas of demyelination are obvious as increased intensity signal

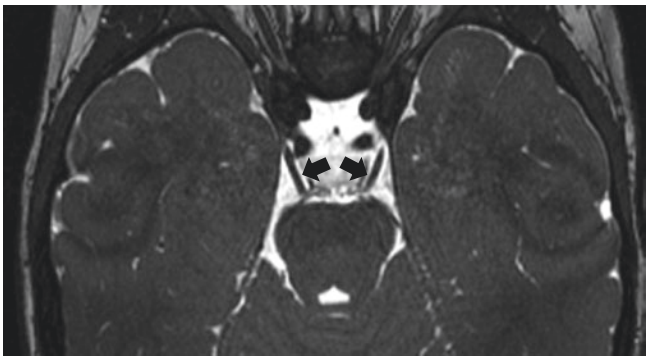


Fig. 32.2 3D–CISS images of the oculomotor nerves. Axial, T2-weighted 3D–CISS MRI demonstrates the oculomotor nerves (*arrows*) traveling through the CSF-filled cistern

Any patient presenting with bilateral disc swelling suspicious for papilledema should undergo MRV as part of their work-up.

Pediatric Concerns with CT and MRI

Radiation exposure is inevitable with CT, and this is a major concern, especially in young patients who have a higher risk of cancer per dose of radiation as compared to adults. MRI is the modality of choice for evaluation of orbital and intracranial soft tissues and the visual pathway, but gadolinium use has risks in patients with renal disease and other morbidities. Because MRI requires exposure to a strong magnetic field, its use in patients with certain types of defibrillators and pacemakers or in patients harboring metallic foreign bodies may be contraindicated. MRI is also contraindicated as the initial imaging modality in evaluating trauma because of the possibility of an occult retained metallic foreign body.

With increased dependence on imaging techniques for the evaluation and management of orbital disease, it is important that clinicians also be familiar with the adverse effects of these modalities and ways to prevent them. In this section, we discuss the various pitfalls of using intravenous contrast agents for CT and MRI, with special emphasis on contrast-induced nephropathy and nephrogenic systemic fibrosis. We also discuss the risks of radiation exposure from CT and recommendations to minimize the radiation dose.

Contrast Agents

One of the major impacts of renal function in the evaluation of orbital pathology is the use of intravenous contrast agents for CT and MRI. The safety of intravenous contrast agents is highly dependent on renal function. Intravenous contrast (IVC) is the most common cause of iatrogenic acute kidney injury [16]. Contrast-induced nephrotoxicity (CIN) is uncommon in patients with normal kidney function, with an incidence of 1–2%. However, the incidence rises dramatically to as high as 25% in patients with chronic kidney disease [16]. CIN typically occurs within 3 days of contrast infusions with a peak serum creatinine at 3–5 days, usually returning to baseline in 7–10 days. Prevention of CIN mainly involves adequate precontrast hydration, either with intravenous isotonic saline or with unrestricted oral fluid intake [17]. Nonionic iodinated contrast material appears to be safer for the kidneys than ionic iodinated contrast material, at least when measured by creatinine clearance. As an aside, CIN from appropriately dosed gadolinium infusion is either nonexistent or exceedingly rare.

With regard to CT contrast agents, several issues must be stressed. First, because of the potential for seizure and vasculopathic complications with iodinated contrast, nonionic contrast agents are used in the vast majority of central nervous system imaging with CT, including the orbit [18]. Fatal reactions are rare, ranging between 1 in 20,000 and 40,000 examinations utilizing contrast material; of note, fatality rates are similar between high-osmolar ionic contrast and low-osmolar nonionic preparations. However, transient ischemic attacks and cerebrovascular infarctions during cerebral angiography occur much more frequently, at a rate of 1.6% in high-risk patients. Second, the seemingly age-old custom of inquiring about shellfish allergies as a possible harbinger of contrast allergy is unfounded as no reliable link has been identified. However, any history of a previous contrast-related reaction is important, as this increases the risk of subsequent reaction fivefold. Atopy (including asthma) also increases the risk of allergic reaction.

Intravenous corticosteroids have been recommended as a "premedication" for at-risk patients. It is important to note, however, that there is no unequivocal proof of short-term corticosteroid efficacy in preventing contrast-induced anaphylactoid reactions. Furthermore, adequate suppression of basophils and histamine production is typically delayed for 4–6 h after corticosteroid infusion, and such a delay may be untenable in emergency situations. One common algorithm in at-risk patients is an oral dosing of corticosteroids beginning at least 6 h prior to contrast infusion, with or without oral antihistamines. Low-osmolarity nonionic agents appear to have a lower incidence of allergic reaction. An excellent summary for management of a variety of contrast-induced reactions is available for download from the American College of Radiology (ACR) Manual on Contrast Media, version 9, 2013 [19].

Nephrogenic systemic fibrosis (NSF) is a scleroderma-like syndrome related to the infusion of gadolinium during MRI [20]. It is most frequently associated with renal failure,

may be progressive, and may affect multiple organ systems. NSF is admittedly rare, and its incidence depends on the specific type of gadolinium compound used. As an example, gadodiamide has an NSF incidence of 1:2913 (0.03%), while gadopentetate dimeglumine has a much lower incidence of only 1:44,224 (0.002%) [20–22]. The overall incidence of NFS appears to be decreasing in the United States, likely because of the avoidance of higher-risk gadolinium preparations, more effective patient screening, and avoidance of use of gadolinium in high-risk patients, as well as more discriminant use of other MRI contrast materials.

NSF typically occurs in patients with the clinical triad of gadolinium infusion for MRI, renal failure (either chronic or acute), and a "pro-inflammatory state" (recent major surgery, endovascular injury, sepsis, malignancy, thrombosis, etc.) [23, 24]. In patients with significant renal failure, the incidence of NSF is estimated at about 4%, with 45% of affected patients suffering from severe disability and with a mortality of up to 31% [23, 24]. Of note, no effective therapy exists for treatment of NSF, and there is no evidence that pretreatment of patients with corticosteroids or pre−/post-gadolinium dialysis has any effect on the incidence and severity of NFS. Skin changes in NSF begin days to months after gadolinium infusion, with an average of 11.5–14 days [23–25].

Although NSF is rare, the severity and potential mortality of the syndrome requires cautious use of gadolinium in patients at higher risk for NSF [22, 23]. The US Food and Drug Administration (FDA) has published recommendations regarding gadolinium use, which are summarized in Table 32.2 [26].

The American College of Radiology has recently noted in its Manual on Contrast Media (version 10.2) that dose-dependent gadolinium deposition has been noted within brain tissue in patients who underwent serial contrast-enhanced MRIs [19]. Deposition mainly occurred in the dentate nucleus and globus pallidus, but histopathologic examinations have also revealed gadolinium in the frontal lobe white matter and in the prefrontal cortex [27, 28]. Importantly, the deposition can occur in patients with an intact blood–brain barrier and no evidence of hepatic or renal disease and has been documented in children undergoing serial MRI with contrast. Thus far, the clinical significance of these findings is unknown, and no adverse effects have been noted, but the FDA is actively investigating this phenomenon. In the meantime, clinicians should be aware of this issue. Gadolinium infusion during MRI frequently provides critical imaging information and often needs to be used in initial, routine MRI [27]. However, in cases where serial MRI is indicated in a child (e.g., monitoring for glioma progression), the utility of a non-contrast MRI should be discussed with the neuroradiologist. Some experts also recommend the use of higher stability, macrocyclic gadolinium preparations, which have lower deposition rates [27, 28].

Table 32.2 FDA recommendation regarding gadolinium use in MRI

Do *not* use gadolinium in: Patients with a GFR of <30 ml/min/1.73m^3 Acute renal failure from hepatorenal syndrome Perioperative liver transplantation Unless diagnosis is essential with contrast-enhanced MRI
Use gadolinium *with caution* in: Patients with a GFR of <60 ml/min/1.73m^3
All patients undergoing contrast-enhanced MRI should be screened for kidney disease by history or laboratory evaluation: Screen all patients for acute kidney injury or other causes of decreased renal function Obtain GFR in all patients at risk for chronically reduced renal function (age >60 years, hypertension, diabetes mellitus, etc.)

Data obtained from Krefting [26]

Radiation Exposure in CT

A significant amount of data has been published since 2001 on the subject of radiation exposure from computed tomography (CT) [29–32], resulting in a broad spectrum of interpretation by the media and in the literature [33, 34]. This, in turn, has led to appropriate concern among patients and the parents of young patients as to the potential cancer risk from CT. This section reviews the available data and summarizes the conclusions and recommendation of our radiology colleagues. Of note, most of the concerns regarding radiation effects of CT pertain to children (especially young children) as compared to adults [34].

First, it is critical to remember that CT is an extremely powerful diagnostic tool that is readily available and is appropriate to use when clinically justified, even in children [35]. As a blanket statement, the risk of potential future cancer from a single CT is far less than the diagnostic benefit, especially in emergency situations [36, 37]. CT requires the use of a certain amount of ionizing radiation – there is simply no way around the basic physics of the technology. However, the radiation dosage of a diagnostic CT can be adjusted to lower levels without compromising diagnostic quality – the ALARA concept (as low as reasonably achievable).

Until recently, the actual risk of future cancer from low-level radiation exposure was not definitively quantified by any large study [36]. The majority of published conclusions relied on extrapolation from atomic bomb victims where there was whole-body exposure or from mathematical models [34, 38]. However, since 2012, two major studies have been published which quantify CT radiation risk and have reached some sobering conclusions [39, 40].

The study of ionizing radiation effects on the body is complex and beyond the scope of this chapter. Briefly, however, radiation affects specific tissues in different ways. As an example, studies on atomic bomb survivors concluded that the lung is more sensitive to the carcinogenic effects of radiation exposure than the liver, skeletal muscle, or skin [29, 37]. Furthermore, the dose of radiation from a CT study that

strikes the body ("entrance dose") is not equivalent to the absorbed radiation by the body [39]. It is difficult to accurately quantify the risk of future malignancy from low-dose radiation exposure because low-dose radiation is a weak carcinogen [36, 39]. However, it is important to note that three expert panels, including the National Academy of Sciences, have concluded that there is a potential cancer risk even with low-level exposure and that this risk rises with increasing exposure [37]. In addition, the concept of "radiation effect" is critical in understanding the radiation risk from CT. Put simply, two types of radiation effects exist [34]. Deterministic effects are well known to the orbitologist and are typified by high-dose radiation to the orbit (or any anatomic structure) over a short period of time, usually for the treatment of malignancy, resulting in myriad side effects (e.g., keratopathy, retinopathy, optic neuropathy, etc.). Stochastic effects are secondary to low doses of ionizing radiation absorbed over a long period of time, as seen in serial imaging, be it CT, mammography, etc. Although the side effects from such stochastic radiation are not immediately obvious, they do accumulate over time and are definitely more of an issue in the pediatric, as compared to the adult population.

The risk of radiation exposure is significantly different in children than in adults for multiple reasons [37]. First, children are more sensitive to the effects of radiation exposure than adults because of active tissue growth and development, with an estimated tenfold overall increased neoplastic potential [30]. Second, because of their age and statistically longer life span, children have more time in the ensuing decades to manifest any ill effects of radiation exposure; put simply, it is far more likely to see a radiation effect that takes 40 years to manifest in someone who is 10 years old than in someone who is 50 years old although, until recently, the magnitude of this risk from low-level exposure was difficult to accurately quantify. Third, unless the baseline radiation exposure parameters are adjusted for children, an equivalent dose has a higher effect on the smaller cross-sectional anatomic area of a child than of an adult; even with such adjustment, the final radiation dose effect to a child may be up to 50% higher than in an adult [41, 42]. Fourth and perhaps most pertinent to the reader, the pediatric brain is especially sensitive to radiation effects [39], and at least a portion of the brain is unavoidably imaged during an orbital study. Finally, the ubiquity of CT in medicine and expanding indications for CT has led to ever-increasing utilization.

The use of diagnostic CT in the United States has risen by more than 20-fold, from 2 million studies annually in 1980 to almost 80 million in 2009 [31, 32]. Seven million CT studies are performed on children annually in the United States, and this number increases an average of 10% per year. Of note, the majority of brain CTs performed in children is for head trauma [30, 40, 43–45]. CT also accounts for a disproportionately high amount of total radiation exposure in medicine. A study from one academic radiology department published by Mettler and colleagues in 2000 concluded that although CT accounted for only 11% of procedures using ionizing radiation, 67% of all ionizing radiation was attributable to this modality [45].

Perhaps most importantly, CT of one organ system can be performed using a variety of techniques with a wide range of radiation exposure. This concept is extremely important to keep in mind for pediatric CT. As noted in a review by Brody and Frush, increasing the dose of radiation in an effort to improve image (and presumably diagnostic) quality has its limits, and after a certain threshold, additional radiation simply has no effect on improved diagnostic accuracy [37]. Therefore, lower doses of ionizing radiation in pediatric CT are preferable and do not necessarily compromise the quality of the study. The ALARA concept has markedly reduced radiation exposure in children from CT studies, by 50–90% since about 2001, and these techniques continue to undergo refinement [30, 37, 40, 46].

The results of two recent large studies on radiation exposure from CT in children are worth summarizing in detail. Pearce and colleagues analyzed a national health-care database in the United Kingdom and identified just over 175,000 pediatric patients that met the inclusion criteria of the study [39]. Of note, of 283,919 CT scans performed, the majority (64%) were of the head, an area of particular importance to the reader. The authors of the study estimated that the average total dose from one brain CT in a child ranged between 28 and 44 mGy depending on age and gender (Table 32.3) [39]. The rates of leukemia and brain tumors in patients undergoing CT were analyzed based on dose. A significantly increased risk of both maladies was found in patients who received certain threshold cumulative radiation doses. Specifically, the relative risk (RR) of leukemia in patients with a cumulative dose of at least 30 mGy (mean 51.13 mGy) was 3.18 compared to those children who received less than 5 mGy. With regard to brain tumors, the RR was 3.32 in patients with a cumulative dose of 50 mGy (mean 104.16 mGy). The authors estimated that for children younger than 15 years, these threshold cumulative doses amounted to five to ten head CTs

Table 32.3 Estimated radiation doses from one brain CT utilizing estimated standard CT dosages after 2001

	Males		Females	
Age at brain CT (years)	Brain dose (mGy)	Red bone marrow dose (mGy)	Brain dose (mGy)	Red bone marrow dose (mGy)
0	28	8	28	8
5	28	9	28	9
10	35	6	35	6
15	43	4	44	6
20	35	2	42	2

Data from Pearce et al. [39]

for a 50 mGy bone marrow dose and two to three head CTs for a 60 mGy brain dose. Put another way, the authors concluded that one head CT before the age of 10 years would result in one excess case of leukemia and one excess brain tumor per 10,000 patients. Of note, multiple studies have concluded that younger children, especially those <5 years of age, are particularly sensitive to ionizing radiation [39, 40]. Admirably, Pearce et al. also pointed out that, first, pediatric leukemia and brain tumors are relatively rare events and that tripling this risk from CT radiation exposure still makes these entities rare events and, second, the increased lifetime cancer risk from CT is "very small" compared with the natural occurrence of malignancy in the general population which may make the benefits of CT more important "providing it is clinically justified." Herein lies the crux of the discussion: while CT is a powerful and lifesaving technology, with a now-proven underlying cancer risk, it therefore should be used only when appropriate and then very judiciously.

In the second large study, Mathews and colleagues compared 680,211 pediatric patients who underwent CT with 10,939,680 who did not [40]. Mathews et al.'s study echoed the findings of Pearce et al. regarding subsequent leukemia development, providing independent confirmation of the previous study's findings; a cumulative dose of 30 mGy resulted in a relative risk of 3.18. Brain CT was associated with an excess incidence rate for brain cancer of 2.97/100,000 person-years. Put another way, the authors estimated 1 excess brain malignancy per 4000 brain CTs. As already noted, the authors also confirmed that children <5 years of age had the highest relative risk. However, even older children and adolescents showed an increased cancer risk following CT. Serial CT also increased the risk, presumably due to increased cumulative radiation dosages. Of particular interest to the reader, facial CT was associated with only a borderline increased RR of subsequent malignancy (IRR = 1.14). Since an orbital study is essentially a subseries of a standard maxillofacial protocol, it is reasonable to extrapolate this facial CT finding for orbital scans. In other words, based on the findings of Mathews et al., an orbital series should have a lower risk for subsequent brain or hematopoietic tumor development than a standard brain CT. However, this statement must be tempered by the varying protocols used at different health-care facilities, some of which may extend a standard orbital series more cephalad, thereby exposing more of the brain to radiation, as well as the fact that in many (if not most) orbital injury cases, the head is scanned along with the orbits as a precaution.

Mathews and colleagues also brought up some important limitations to their study (which do not change, however, the prevailing opinion among radiologists that even low-dose radiation exposure increases cancer risk, albeit by a very small amount). First, as already noted, the authors point out that CT dosing protocols, especially for pediatric scans, have undergone a profound change since 2001 and that the current cancer risk from CT radiation may be smaller than calculated from older data. Second, the possibility of reverse causation may explain some of the increased brain tumor risk seen from head CT. In other words, symptomatology may have prompted initial brain imaging, which failed to diagnose an early, small lesion that went on to grow until the diagnosis was made several years later; thus, the undiagnosed tumor prompted the initial CT, and therefore the CT did not cause the tumor. Of note, the authors still found an increased solid and hematopoietic cancer risk following CT exposure, even when all brain tumors were excluded from analysis.

What, then, is the role of CT in pediatric orbital disease? First, as already stated, it is important to recognize that CT remains a valid and powerful tool in the pediatric population. In cases of head and orbital trauma, CT remains the imaging modality of choice because of its ready availability, rapid acquisition time, excellent resolution of bony and soft tissue orbital anatomy, and reasonable resolution of brain anatomy, especially in cases of acute intracranial hemorrhage. That said, it is also important to remember that a pediatric brain CT carries an increased risk of brain malignancy when compared to facial (i.e., orbital) CT based on the results of Mathews et al.'s study and a brain CT should not be a knee-jerk response to every case of pediatric orbital trauma.

The authors recommend the following guidelines for the judicious and appropriate use of orbital CT, much of it gleaned from the recommendations of the American College of Radiology:

1. *The right scan for the right pathology*. In general, CT is excellent for imaging bone and therefore is useful in the evaluation of trauma and orbital infection (which is often secondary to adjacent paranasal sinus disease). CT is also helpful in the diagnosis of metallic and wooden foreign bodies [47]. Unless indicated, avoid including a brain CT with the orbital study. Consider MRI in nonurgent orbital pathology.
2. *Avoid plain X-rays*. There are few indications for "screening" plain films of the face (see Table 32.4). On occasion, a plain X-ray is necessary to rule out occult metal prior to MRI. Otherwise, plain films should be avoided; they simply do not provide adequate detail of orbital or periocular pathology and still expose the patient to radiation.
3. *Order the right scan the first time*. An axial imaging study of the brain is *not* equivalent to a dedicated orbital and facial study with axial and coronal views. Sometimes both the central nervous system and the orbit require imaging, but very often, imaging of the orbit suffices. In one study, the estimated effective dose from a head CT in a 5-year-old child was 4mSV, equal to about 200 chest X-rays [37]. On occasion, the clinical findings may

Table 32.4 Orbital imaging options in a child presenting with exophthalmos and their relative radiation risk

Radiologic procedure	Rating	Comments	Relative radiation level
MRI head and/or orbit without/with contrast	8	See sections on nephrogenic systemic fibrosis and gadolinium deposition in brain	0
MRI head and/or orbit without contrast	7	Lack of contrast limits the detail of normal anatomy and pathology	0
MRA head and neck without/with contrast	4	See sections on nephrogenic systemic fibrosis and gadolinium deposition in brain	0
CT head and/or orbit with contrast	6	See sections on radiation exposure and contrast-induced nephrotoxicity	☢☢☢☢
CT head and/or orbit without contrast	5	Lack of contrast limits the detail of normal anatomy and pathology	☢☢☢☢
CTA head and neck	2	CTA results in significant radiation exposure. Use MRA when possible	☢☢☢☢☢
Plain X-ray of orbit	1	Although radiation exposure is low, plain X-ray of the orbit has very low diagnostic value. Usually limited to ruling out occult metallic foreign body prior to MRI in suspected cases	☢

Rating scale: *1, 2, 3* usually not appropriate; *4, 5, 6* may be appropriate; *7, 8, 9* usually appropriate

obviate the need for CT. As an admittedly controversial example, one could argue that routine CT imaging in a pediatric white-eyed blowout fracture (WEBOF) is of little use because of the pathognomonic clinical features and predictable intraoperative findings; that said, at present, preoperative CT imaging of a suspected WEBOF remains the standard of care.

4. *Communicate*. Discuss with the radiologist or emergency room physician the *specific* area of concern, stressing the need for axial and coronal views limited to the orbit, unless brain imaging is indicated.
5. *Insist on seeing the actual scan* (and not simply the report) if the patient is being referred from another institution. In more routine cases, a delay of several days while the mislaid compact disc of the scan is being mailed is of little consequence. However, in an urgent situation (WEBOF, orbital abscess, etc.), absence of the actual images may force the physician to repeat the study, resulting in more radiation exposure for the child. If possible, make every attempt to obtain a digital copy of the original scan in a timely fashion to avoid reimaging.
6. *Make sure that your imaging facility has specific pediatric protocols* with decreased radiation exposure using the ALARA concept. All facilities accredited by the American College of Radiology must have pediatric protocols in place [37].
7. When possible, maximize diagnostic accuracy by having *the study interpreted by a pediatric radiologist or neuroradiologist*. Discuss any specific clinical suspicions (WEBOF, occult wooden foreign body, etc.) with the radiologist *prior* to the study to maximize CT technique.
8. *When possible, use single-pass technology*. Newer multidetector CTs, such as CTA, are extremely useful in certain clinical situations but are usually unnecessary in typical trauma or infection cases [46].
9. *Consider other imaging modalities* (MRI, ultrasound), especially if serial imaging is needed. When possible, use MR angiography rather than CT angiography in children.
10. *Discuss with the patient's parents the rationale for the use of CT* in their particular clinical situation, the necessity of ionizing radiation in CT, and the fact that radiation dosages will be age and size adjusted. In one study, a majority of parents were unaware that CT exposed their child to ionizing radiation [48]. As importantly, this study also found that providing information about radiation exposure in CT did not change the parents' decision to proceed with imaging.

Table 32.4 from the American College of Radiology provides an excellent summary of various orbital imaging options and their relative radiation risk for a child presenting with exophthalmos [49]. Note that MRA carries a safer rating than CTA and does not require ionizing radiation. It is also important to note that a plain X-ray of the orbit carries the worst rating because it provides essentially no clinical information despite exposure to (albeit low) doses of ionizing radiation.

Developmental Anomalies

Imaging modalities play a major role in the evaluation of a child with a developmental ocular or orbital lesion [2]. While there often is external evidence of an abnormality, the full extent of the malformation can be appreciated only on multiplanar images. Various orbital deformities, bony defects, or calcifications/ossifications are best shown with CT, but the morphology of soft tissue derangements is best demonstrated with MR, including associated intracranial abnormalities.

Abnormal Globe

Imaging is helpful in delineating and characterizing globe abnormalities, which include anophthalmia (Fig. 32.3), microphthalmia (Figs. 32.4 and 32.5), macrophthalmia (Fig. 32.6), colobomas (Figs. 32.7 and 32.8), buphthalmos, and staphylomas. In ophthalmology, colobomas refer to defects in ocular structures that result from incomplete closure of the fetal (embryonic) fissure. Colobomas are common developmental malformations and usually are bilateral [50]. In cases of coloboma, the optic nerve head may be small and slit-like (Fig. 32.7), or there may be a large,

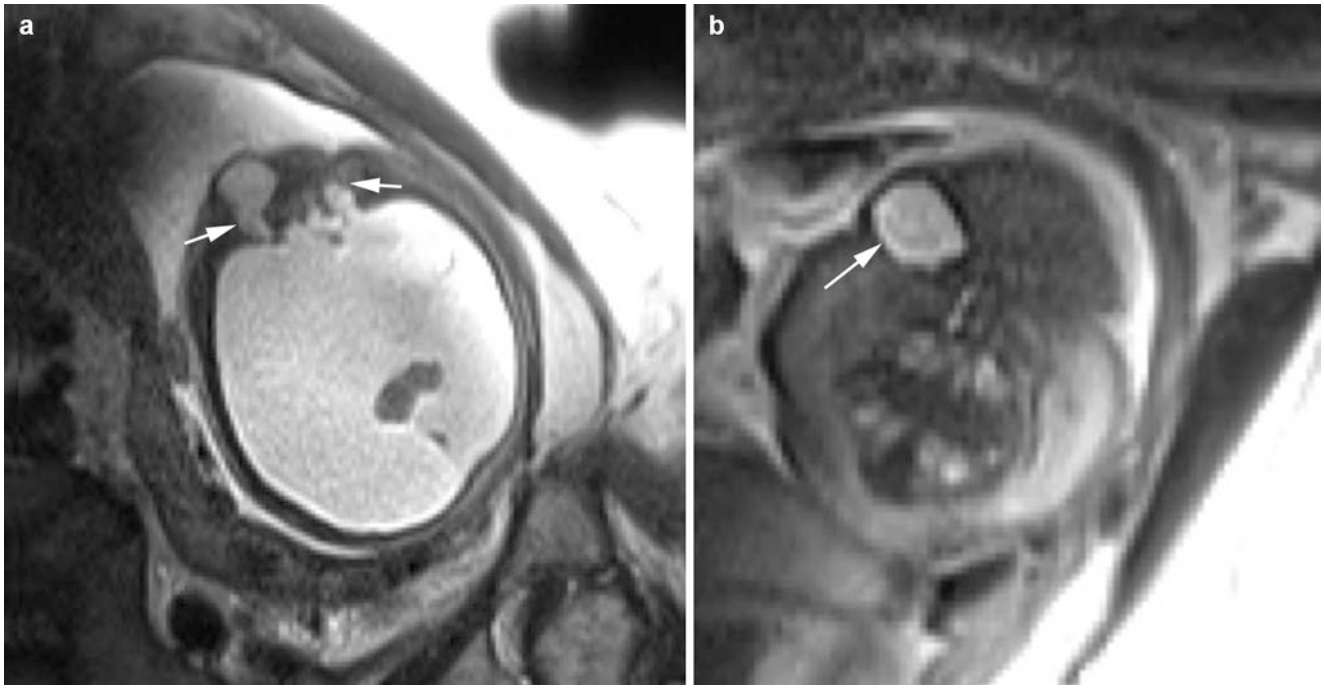


Fig. 32.3 Fetal MRI of anophthalmia. (**a**) A T2 image (fetal axial) of a 26-week gestation fetus with hydrancephaly. Note that the cranium is filled with CSF. The right globe is essentially an extension of the CSF communicating via a widened nerve sheath (*left arrow*) with absence of the optic nerve. There is no lens. A small cystic projection is present in the left orbit with no visible globe (*right arrow*). (**b**) Fetal coronal T2 image shows the abnormal right globe (*arrow*), with left anophthalmia

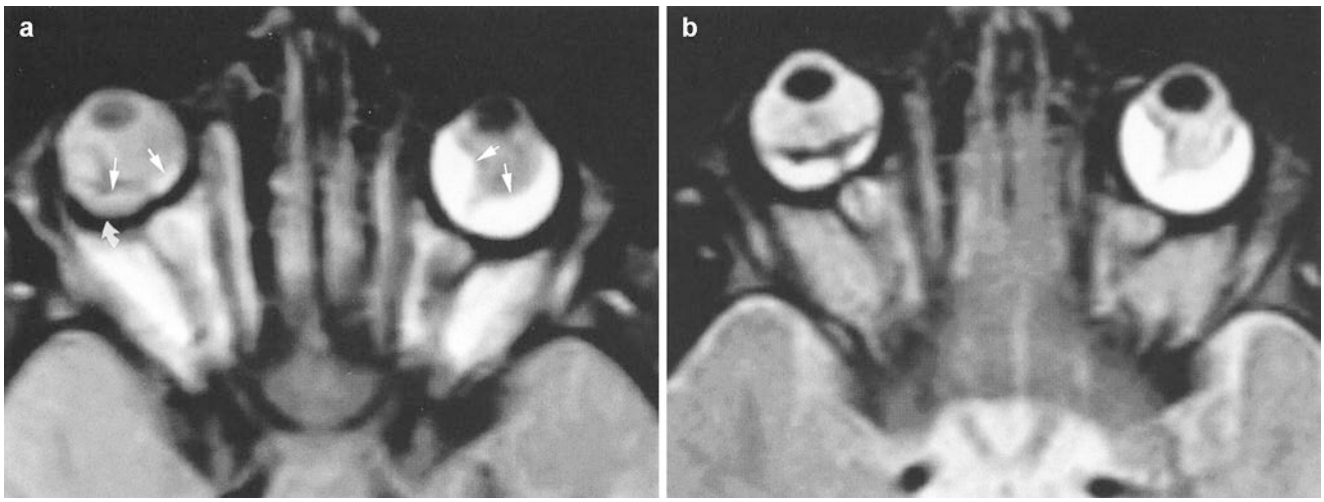


Fig. 32.4 Bilateral microphthalmia with chronic retinal detachment in a $3^{1}/_{2}$-year-old autistic child. (**a**) Axial proton density-weighted MR image reveals bilaterally small globes with retinal detachment (*straight arrows*). The *curved arrow* points to isointense subretinal fluid. (**b**) Axial T2-weighted image reveals marked hypointensity along the detached retina due to calcification. The calcification was identified on computed tomography (not shown here). Note that the isointense subretinal fluid in the right eye on proton density has become hyperintense on T2 imaging

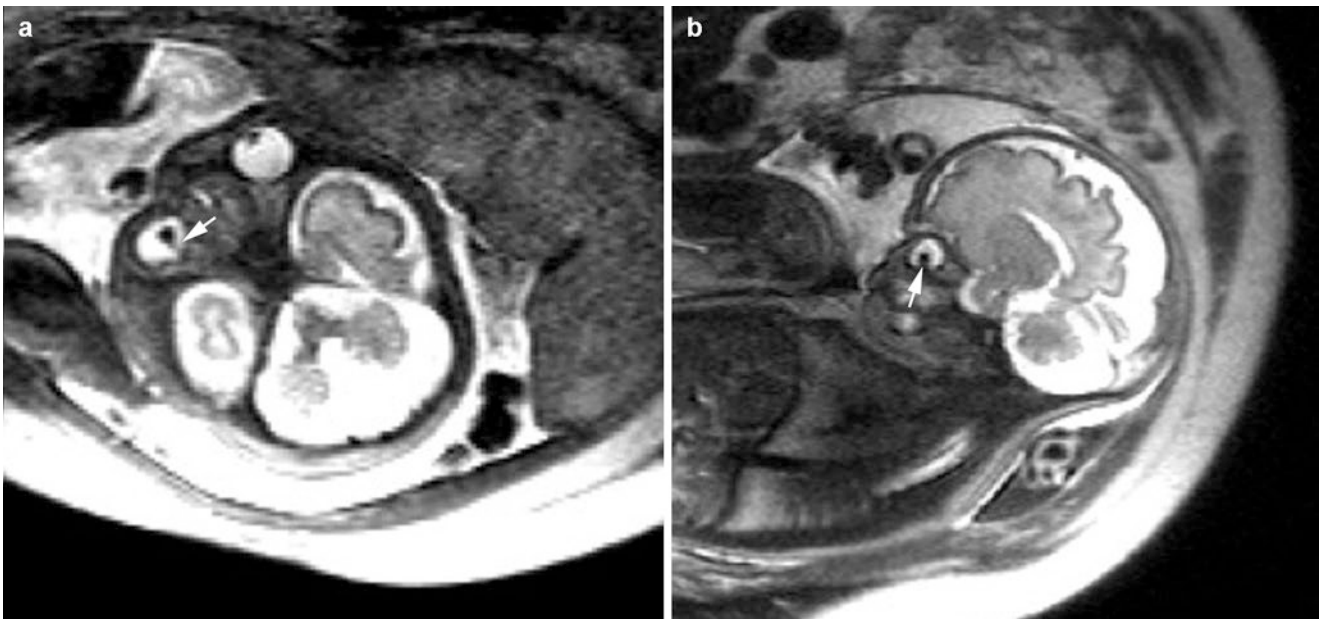


Fig. 32.5 Fetal MRI of microphthalmos in a 25-week gestation fetus with a hypoplastic right heart and left cleft palate. (**a**) Fetal axial T2 image shows right microphthalmia with a small posterior coloboma and a deformed, malpositioned lens. A thin stalk (*arrow*) projecting from the lens to the coloboma most likely represents persistent hyperplastic primary vitreous. (**b**) Sagittal fetal T2 image again demonstrated the deformed, small globe with a distorted lens

funnel-shaped staphylomatous excavation with the optic disc at the apex of the defect. The latter type of coloboma is also referred to as morning glory syndrome. Large colobomas are easily detected (Fig. 32.8), but even small defects in the optic nerve heads can be shown on images (Fig. 32.7) when a high-resolution, thin-section T2 sequence is utilized or with a particularly specific sequence such as HASTE (half-Fourier acquisition single-shot turbo spin echo) which shows excellent contrast between fluid-filled and soft tissue structures (Fig. 32.9). Microphthalmos with cyst represents a severe colobomatous malformation when the inner layer of retina proliferates and herniates through the enclosed fetal fissure to form one or more cysts, which may be small (Fig. 32.10) or very large (Fig. 32.11).

Buphthalmos

Buphthalmos, or an enlarged eye ("ox eye"), is most commonly seen in primary congenital or early-onset infantile glaucoma; there is also an association with neurofibromatosis type 1, due to secondary glaucoma from neurofibromas. In addition, intraocular pathology, including tumor, can also lead to globe enlargement. In primary congenital glaucoma, there is resistance to normal outflow of aqueous humor due to an abnormally developed trabecular meshwork. This results in increased intraocular pressure, which causes enlargement of the globe and thinning of the sclera [51]. CT or MR demonstrates not only the macrophthalmia with an enlarged anterior chamber and flattened lens but also its effect on the bony orbit, which may have up to 15% increased volume (Fig. 32.6).

Optic Nerve Hypoplasia

Minimal symmetrical hypoplasia of the optic nerves may be difficult to detect clinically as well as on images. However, if the optic hypoplasia is unilateral, making comparison to the normal side possible, or if the hypoplasia is moderate to severe, then it can be detected on images. In such cases, it is important to obtain thin, contiguous sections and to look at the nerves in more than one plane to avoid making an error due to volume averaging. Optic nerve hypoplasia may be an isolated anomaly or may be associated with other abnormalities, as in the case of septo-optic dysplasia (Fig. 32.12) [52]. Coronal T2-weighted MRI is usually the best technique for evaluation of optic nerve size.

Cryptophthalmos

In cryptophthalmos, there is failure of development of lid folds, and as a result, the eyes are hidden by continuous overlying skin (Fig. 32.13) [53, 54]. The underlying globes typically are abnormal, having large anterior colobomas with absence of lenses or abnormal anterior chambers (Fig. 32.13). Cryptophthalmos is part of a syndrome that includes anomalies of extremities with craniofacial and urogenital abnormalities.

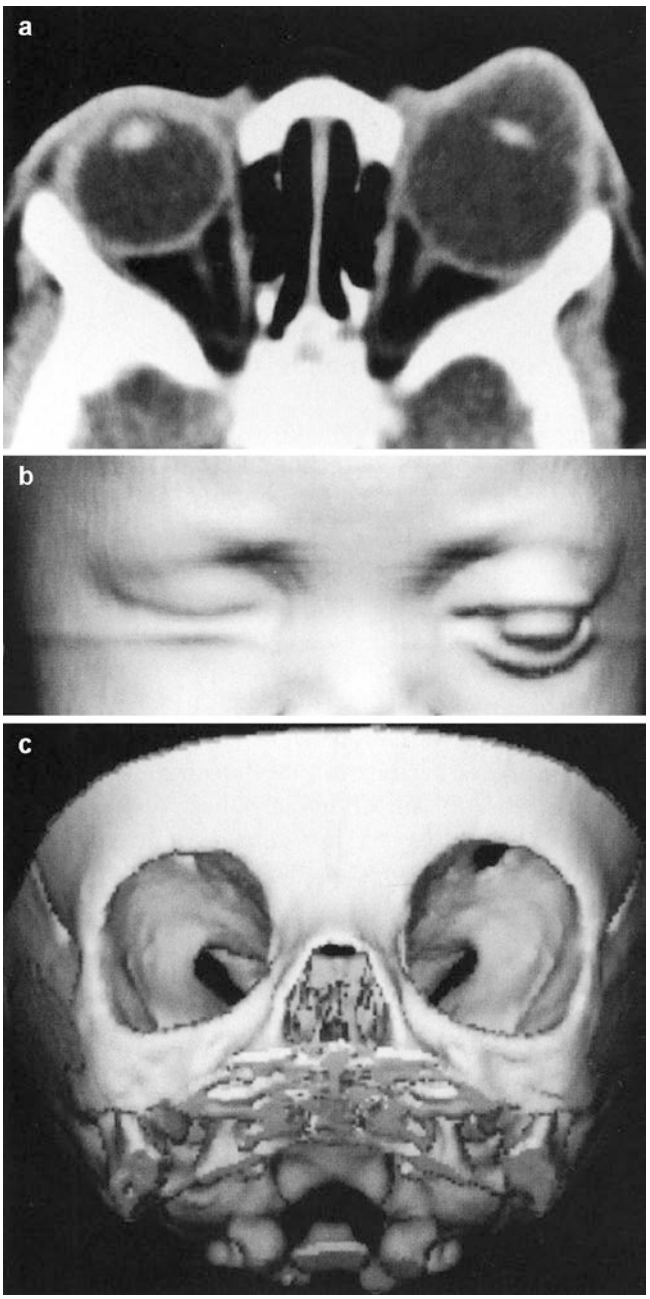


Fig. 32.6 Congenital glaucoma in a 3-month-old child. (**a**) Axial CT reveals a markedly enlarged left globe with expanded anterior chamber. (**b**) A three-dimensional CT soft tissue reconstruction shows well the enlarged left globe. (**c**) Three-dimensional CT bone reconstruction of the orbits reveals marked asymmetry, with an enlarged left orbit

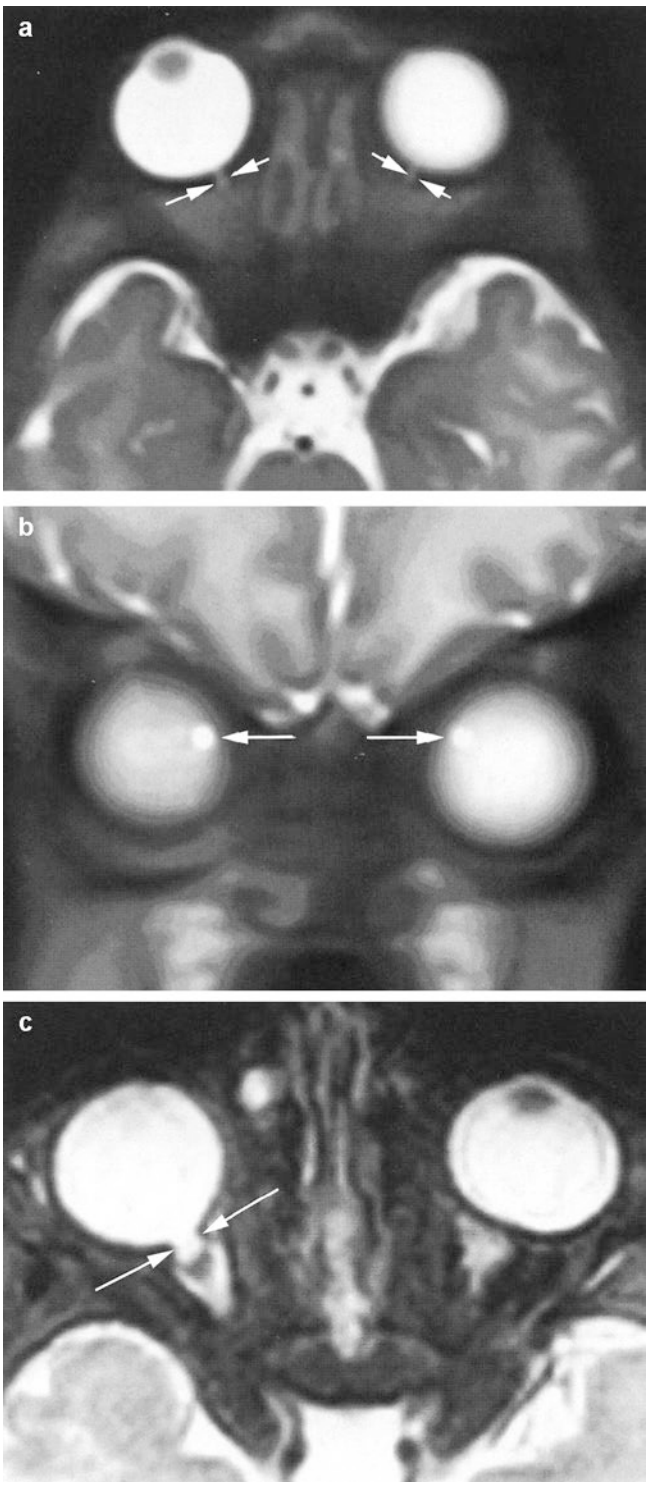


Fig. 32.7 Bilateral optic nerve head colobomas in two infants. (**a**) Axial T2-weighted HASTE image shows slit-like defects (*arrows*) in the optic nerve head regions. (**b**) Coronal HASTE image obtained through the posterior portions of the globes reveals the colobomas (*arrows*). HASTE imaging is sensitive to the presence of fluid, and even though it does not reveal in detail other portions of the orbit, it is useful whenever there is a question of a fluid-containing abnormality, such as a cleft, cyst, or fistula. Each image takes 1.2 s, and, therefore, HASTE imaging often can be performed without sedation. (**c**) Axial conventional T2-weighted MR scan in another infant shows a coloboma (*arrows*) with an abnormally widened right optic nerve adjacent to the coloboma.

Dermoid and Epidermoid Cysts

Dermoid and epidermoid cysts are the most frequent developmental cysts to occur in the orbit and represent choristomas, which are malformations of tissue that normally are not found at a given anatomic site. These cysts result from sequestration of ectoderm in the wall of the orbit or within the lids by

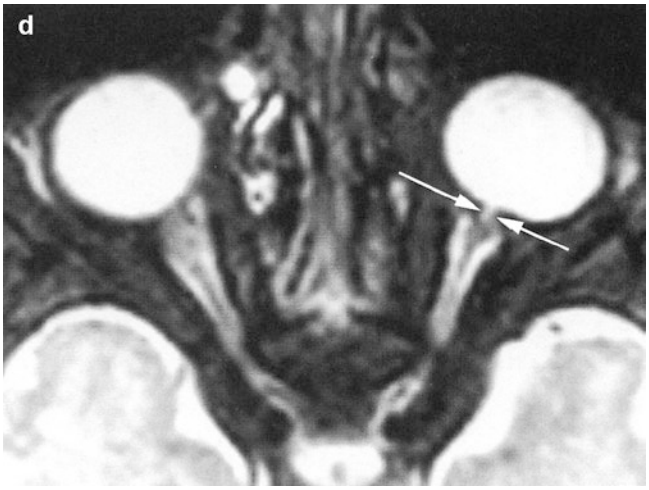


Fig. 32.7 (continued) (**d**) Axial T2 scan slightly inferior to that shown in (**c**) reveals a smaller coloboma (*arrows*) on the left. The left optic nerve is also abnormally widened just posterior to the coloboma. *HASTE* half-Fourier acquisition single-shot turbo spin echo

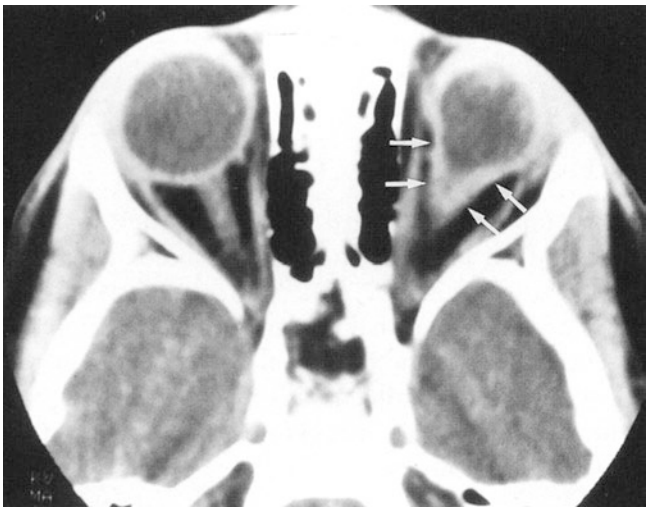


Fig. 32.8 Left morning glory coloboma in a 2-year-old girl. Axial CT scan reveals left microphthalmia and a large posterior coloboma (*arrows*), having a configuration reminiscent of the morning glory flower

advancing midfacial and frontal waves of neural crest during embryogenesis and typically occur either superolaterally (frontozygomatic suture) or superomedially (frontoethmoidal suture). Dermoid cysts, which are more common than epidermoid cysts, are lined by keratinizing squamous epithelium and contain dermal appendages (sebaceous glands, hair follicles) and keratinaceous debris and fatty substances. Epidermoid cysts are lined by epidermis without adnexal structures and contain desquamated keratin. The slow enlargement of the cysts causes pressure erosion of the adjacent bone, resulting in flattening (Fig. 32.14), thinning, and scalloping of the bone (Fig. 32.15). Occasionally such a cyst may break through the bone and displace dura mater. These developmental cysts have well-defined margins unless they have ruptured and caused an inflammatory reaction (Fig. 32.16). Also, the cysts may be associated with tracts that extend into adjacent structures (e.g., temporalis fossa, cranial vault, paranasal sinuses).

The density on CT or the intensity on MRI of dermoid or epidermoid cysts ranges from that of cerebrospinal fluid to that of fat, and the lesions may be heterogeneous due to mixture of fat and other desquamated debris (Fig. 32.17) [55]. The heterogeneity of the signal coupled with pockets of hyperintensity on precontrast T1-weighted images helps to distinguish dermoid/epidermoid cysts from other orbital pathologies. Only a few orbital processes manifest this hyperintensity on precontrast T1-weighted images, and these exceptions are worth remembering, as they narrow the differential diagnosis (Table 32.4). Occasionally, there may be calcification in the capsule of a dermoid/epidermoid cyst. As just noted, identification of the lipid/protein content leads to the correct diagnosis, but most cysts tend to be isointense to extraocular muscle, and the diagnosis is often based on location and morphology. Only the cyst capsule shows enhancement with contrast. On DWI, most cysts show restricted diffusion – an important sign that reinforces the diagnosis of dermoid/epidermoid cyst (Fig. 32.18).

A developmental cyst should be differentiated from dacryocystocele (Fig. 32.19), which forms due to obstruction at the intranasal opening of nasolacrimal duct (valve of Hasner) and may be seen in a newborn. In such a case, one can identify a markedly dilated nasolacrimal duct (Fig. 32.19b); furthermore, the inferomedial location of a dacryocystocele is an uncommon site for dermoid/epidermoid cyst formation.

Orbital Teratoma

Orbital teratomas are choristomas (tissue at the wrong anatomic location) that are composed of tissue from all three germ cell layers – ectoderm, mesoderm, and endoderm – and are usually benign. These congenital tumors typically contain disorganized tissues but, rarely, may have fetal features. It is speculated that lack of normal response of tissue to inducers results in teratoma formation [56, 57]. Orbital teratomas generally present at birth with marked proptosis and then continue to grow rapidly [58]; they can also be demonstrated on fetal MRI. CT and MR demonstrate the teratomas as large multicystic masses that cause prominent expansion of the bony orbit (Fig. 32.20) [2]. Imaging studies are important in delineating teratomas and identifying their vascularity, determining whether there is an intracranial component and differentiating the teratomas from microphthalmos with a cyst, dermoid cyst, meningoencephalocele, and hemangioma or venolymphatic malformations located deep within the orbit.

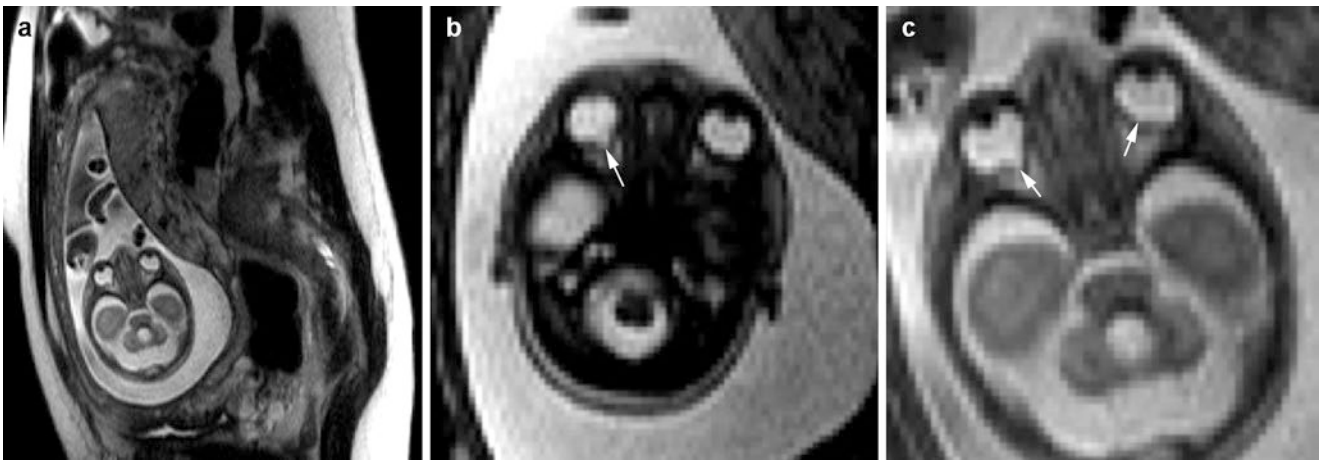


Fig. 32.9 Fetal HASTE MRI of bilateral colobomas in a 22-week gestation fetus. (**a**) Sagittal maternal and axial fetal image. (**b**) On close-up, the axial T2 HASTE image reveals a large right coloboma (*arrow*). (**c**) In this image, a subtle left coloboma is also evident (*right arrow*)

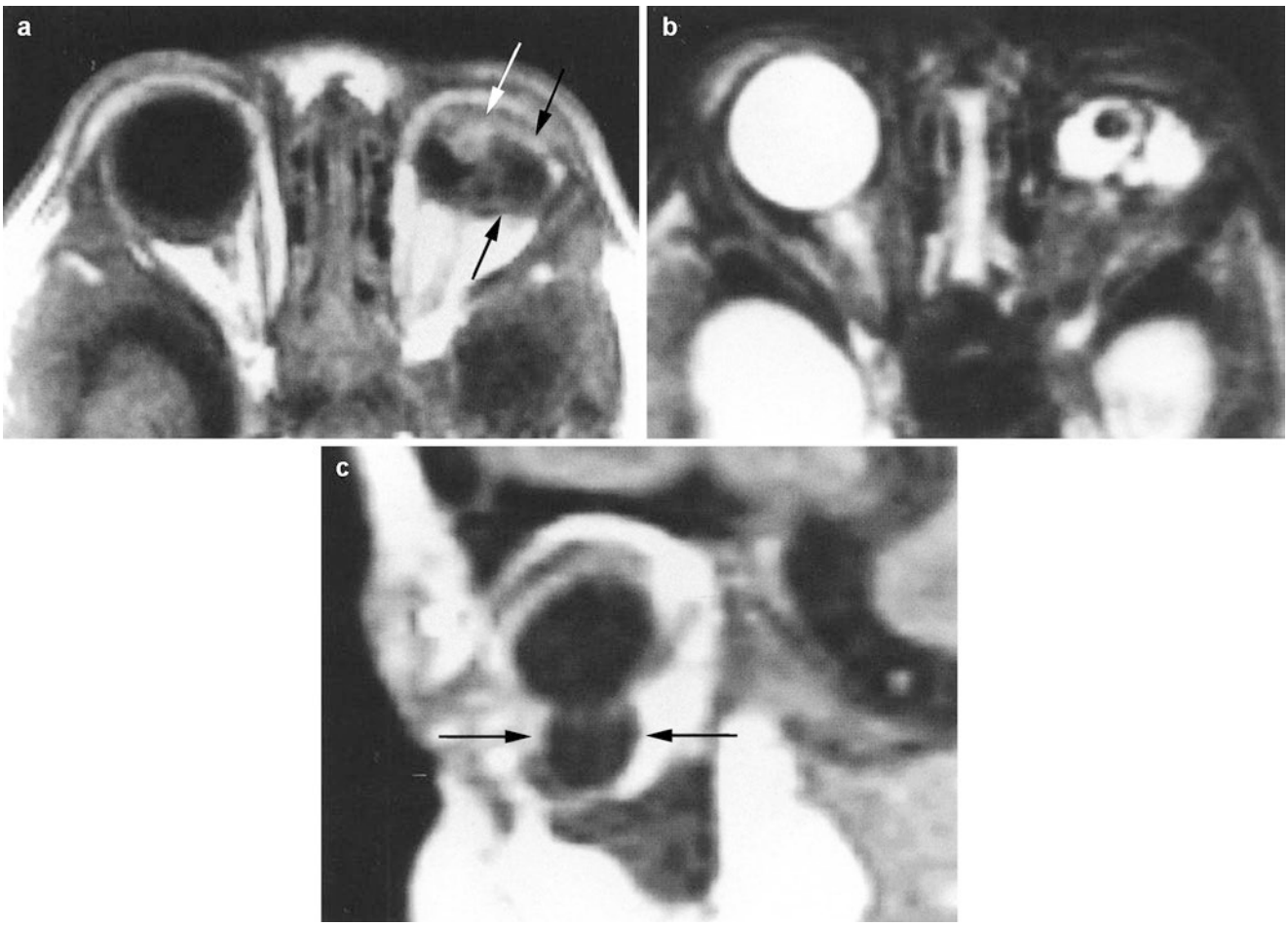


Fig. 32.10 Microphthalmia with two cysts in a 3-week-old boy. (**a**) Axial T1-weighted MR shows a very small globe with deformed lens (*white arrow*) and an irregular cyst (*black arrows*) lateral to the globe. (**b**) Axial T2-weighted image better differentiates the small globe from the laterally located cyst. Note that the lens has become very hypointense. (**c**) Sagittal MRI reveals another cyst (*arrows*) inferior to the abnormal globe

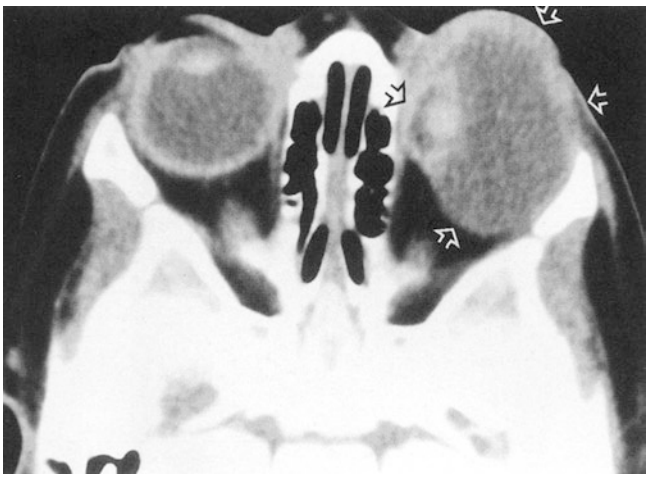


Fig. 32.11 Left microphthalmos with a large cyst. Axial CT shows a very large cyst (*white arrows*) that expands the bony orbit and a very small malformed globe (*black arrow*) with an irregular denser lens (Courtesy of Richard Boyer, MD, Primary Children's Medical Center, Salt Lake City, Utah)

Glial–Neural Hamartomas

Glial–neural hamartomas occur rarely in the orbit and, therefore, often are difficult to diagnose. However, they should be considered as a possible diagnosis when an orbital mass is discovered at birth or shortly thereafter and lacks the characteristics of the more frequent pediatric orbital tumors, such as a capillary hemangioma, lymphangioma, dermoid, or teratoma. The glial–neural hamartomas may be well defined or infiltrative (Figs. 32.21 and 32.22) [59]. The presence of other congenital abnormalities (Fig. 32.22d) such as an abnormal globe, optic nerve, or extraocular muscles may be helpful in reaching the correct diagnosis by indicating maldevelopment as an etiology. However, if orbital structures appear normally formed and the glial–neural hamartoma is poorly defined (Fig. 32.21), then such a glial–neural malformation may be difficult to differentiate from fibromatosis or a rhabdomyosarcoma.

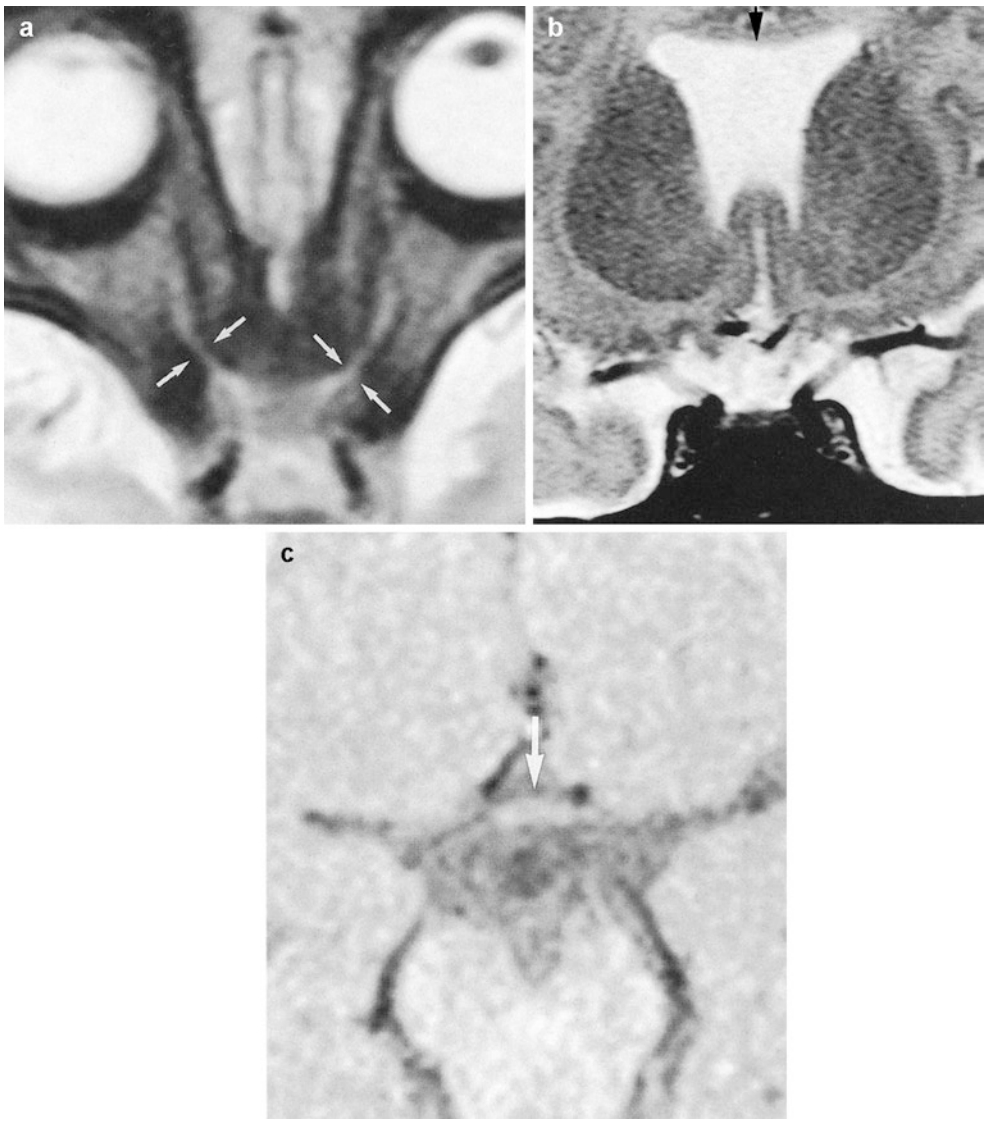


Fig. 32.12 Septo-optic dysplasia in a 2-month-old girl. (**a**) Axial T2-weighted MRI shows markedly narrowed optic canals (*arrows*) reflecting optic nerve hypoplasia. (**b**) Coronal T2-weighted image shows the typical absence of septum pellucidum (*arrow* points to where the septum pellucidum should be located). Normally this section should show the chiasm in the suprasellar region; it is not identified in this case because it is so hypoplastic. (**c**) Axial T1-weighted image at level of suprasellar cistern shows a very thin chiasm (*arrow*)



Fig. 32.13 Cryptophthalmos in a newborn boy with Fraser syndrome. (**a**) A clinical photograph of a different patient with cryptophthalmia reveals complete absence of lids. (**b**) Coronal CT shows the abnormal globes, disorganized anterior segments with calcifications (*arrows*), as well as a midline facial abnormality with abnormally wide nasal cavities and a cleft palate. (**c**) A 2-mm-thick axial CT section reveals continuous skin over the globes, which are abnormal and have expanded, partially calcified (*arrows*) anterior cysts (colobomas) instead of anterior chambers. The lenses are absent. (**d**) Axial T1-weighted MRI shows continuous skin with some underlying subcutaneous fat (*arrows*) over each globe. Again demonstrated are the abnormal globes with expanded anterior cysts and absence of lenses. The calcifications that were noted on computed tomography are not visualized on MRI. (**e**) Axial T2-weighted MRI shows markedly abnormal globes. A thin septum (*arrows*) can be identified separating the anterior cysts from the globes. The cysts have slightly greater intensity than the globes

Abnormalities of Extraocular Muscles

Strabismus (ocular misalignment) occurs frequently in children and involves various clinical patterns. Although the most common type of strabismus is congenital, other conditions may mimic it, and these may be related to neurologic disease, which should be promptly diagnosed and treated [60]. In this regard, imaging plays an important role for it can demonstrate cranial base and intracranial lesions responsible for cranial nerve palsies that result in paralytic strabismus. MRI can reveal and characterize cavernous sinus lesions, such as cranial nerve schwannoma (Fig. 32.23),

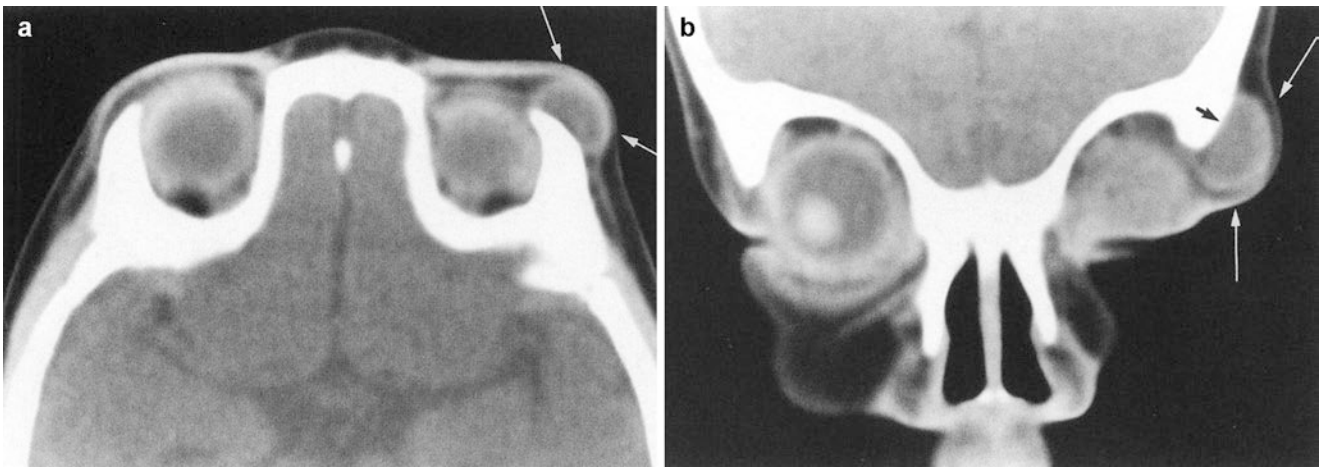


Fig. 32.14 Paraorbital, preseptal dermoid cyst in an infant boy. (**a**) Axial CT shows a small, well-defined, subcutaneous mass (*arrows*) with a denser capsule. The dermoid causes slight flattening of the bone on which it lies. (**b**) Coronal CT shows the dermoid (*arrows*) with a denser capsule. The *black arrow* indicates the flattened bone, which is in contact with the dermoid cyst

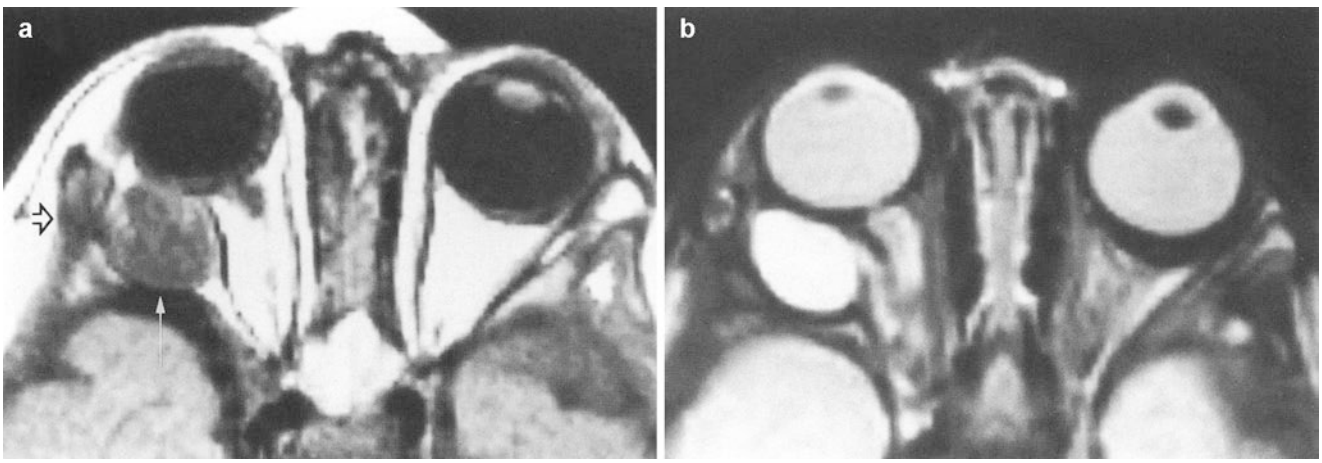


Fig. 32.15 An inclusion cyst in a 2-week-old girl either representing a dermoid or an epidermoid cyst. (**a**) Axial T1-weighted MRI shows an oval-shaped extraconal mass (*white arrow*), which displaces the globe and is associated with thickening and deformity of the lateral orbital wall (*open arrow*). (**b**) Axial T2-weighted MR shows the hyperintense oval-shaped mass and the scalloping of the lateral orbital wall. The signal characteristics in this case indicate that the cyst contains little fat or viscous mucus

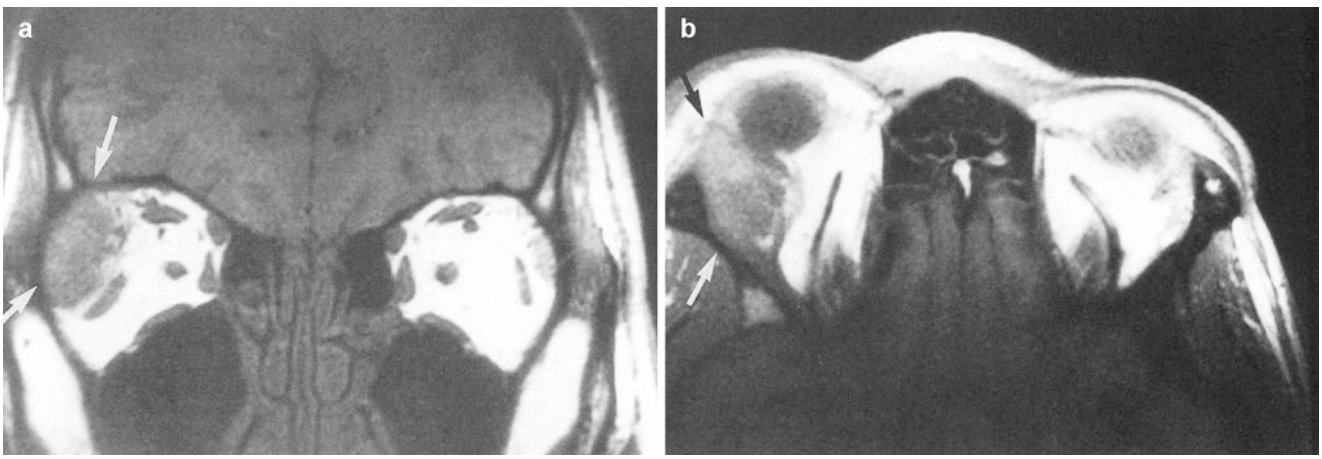


Fig. 32.16 Ruptured dermoid cyst. (**a**) Coronal T1-weighted MRI shows a right extraconal mass (*arrows*) that has an irregular margin due to inflammatory reaction. (**b**) Axial T1-weighted image shows a slightly heterogeneous oval extraconal mass (*arrow*) with an irregular margin. The region of slightly increased intensity within the mass is consistent with lipid.

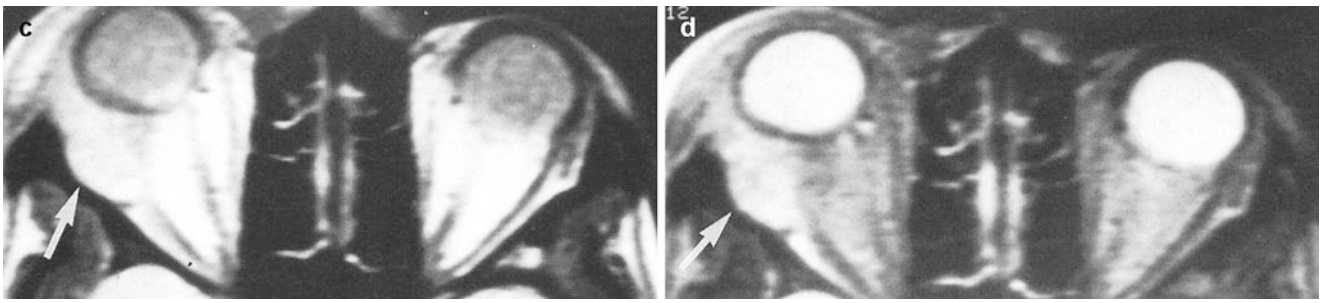


Fig. 32.16 (continued) (**c**, **d**) Proton density and T2 images reveal the dermoid to be of heterogeneous increased intensity and show well the focal bone scalloping (*arrow*)

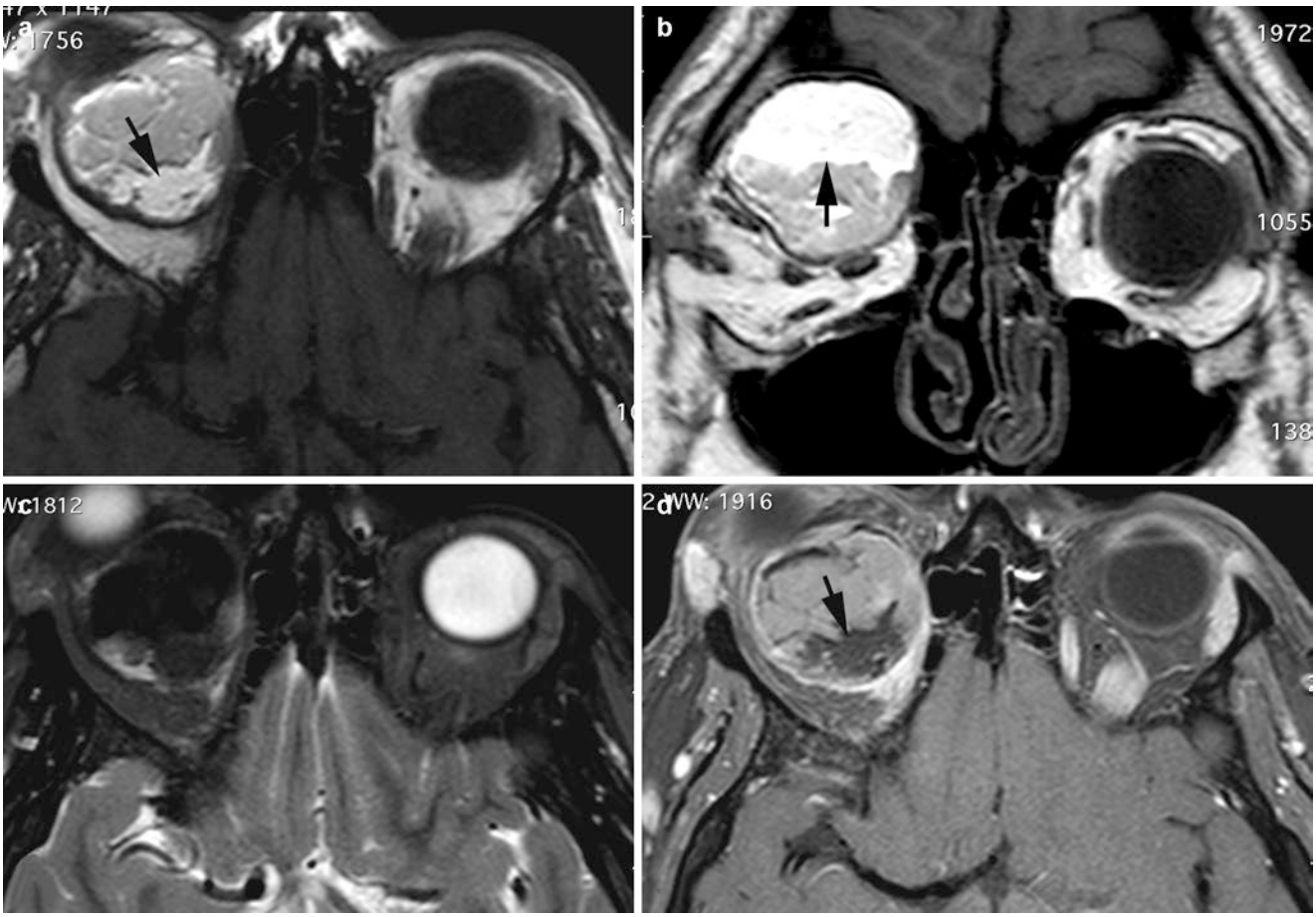


Fig. 32.17 Large epidermoid cyst of the right orbit. (**a**) Axial, precontrast T1-weighted MRI shows a spherical, well-defined mass. Note the heterogeneity in signal. The hyperintense signal posteriorly (*arrow*) represents the lipid component of the cyst. (**b**) Coronal, precontrast T1-weighted image also shows the lipid component (*arrow*). (**c**) Axial T2-weighted image. (**d**) Postcontrast, T1-weighted MRI with fat suppression reveals enhancement anteriorly. The fat signal in the posterior portion of the cyst is suppressed (*arrow*). Note that the intralesional fat mirrors the signal intensity and behavior of the normal intraconal orbital fat

inflammation (Fig. 32.24), or aneurysm (Fig. 32.25). In addition, brain parenchymal traumatic, infectious, inflammatory, demyelinating, ischemic, and neoplastic lesions responsible for cranial nerve palsies are well demonstrated by MRI even when they are very small and located within the brainstem [61].

The excellent morphologic detail of the orbital structures provided by CT and MRI can also be helpful in the more complicated cases of ocular misalignment and fixation. Differential diagnosis can be provided between extraocular muscle absence (Fig. 32.26) [62], malfunction, and actual restriction due to fibrosis (Fig. 32.27) or fibrotic mass

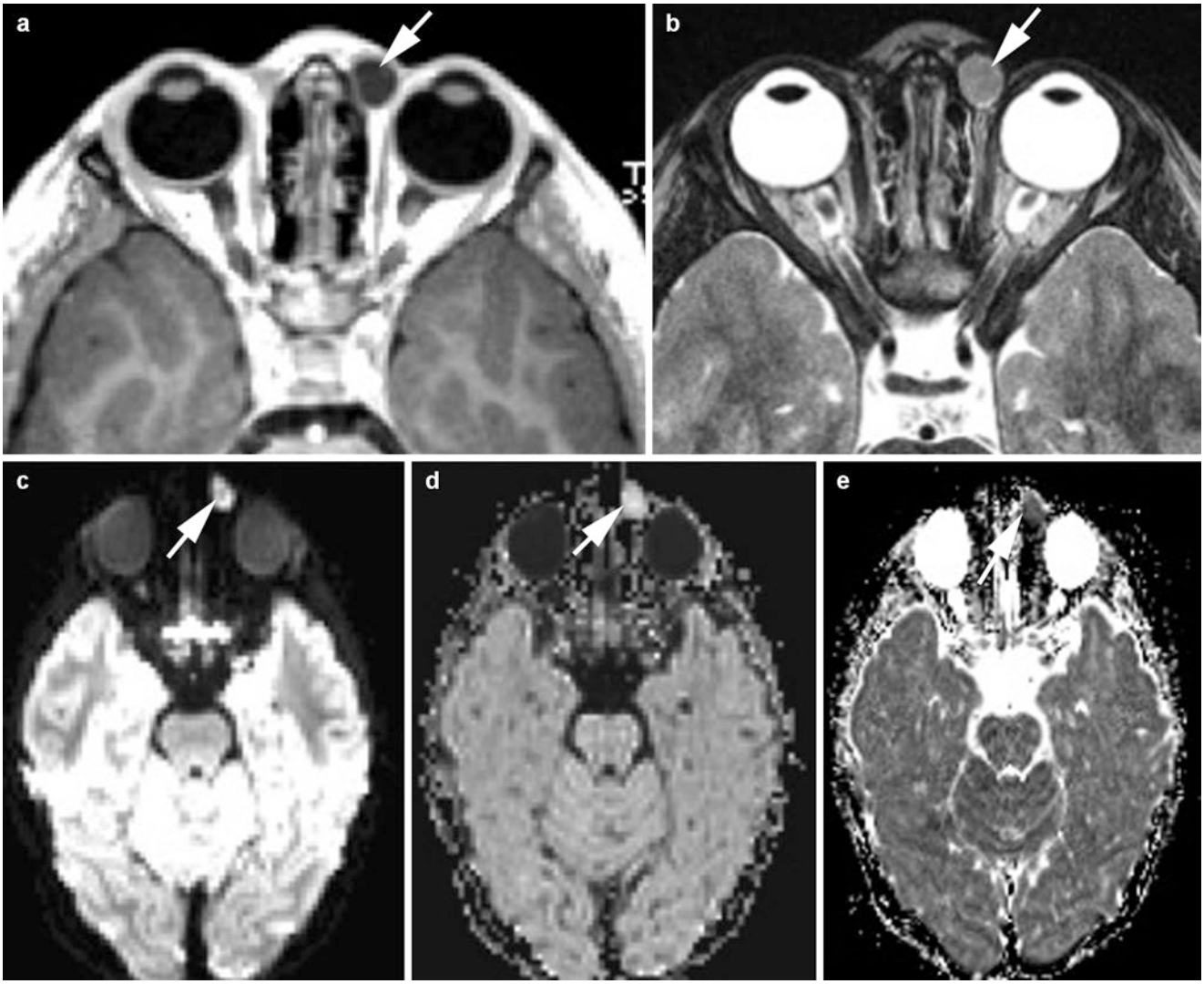


Fig. 32.18 DWI of a dermoid cyst. (**a**) Axial, precontrast T1-weighted MRI of a dermoid cyst (*arrow*) near the left frontoethmoidal suture. Note that in this case, the lesion is hypointense but brighter than vitreous. This is likely because of the lack of intralesional lipid; the cyst is mostly made up of mucus. (**b**) On axial T2 weighting, the cyst (*arrow*) is hypointense to vitreous, but not completely dark. (**c**) Axial DWI shows the bright signal of restricted diffusion (*arrow*), again likely due to thick mucus within the lesion. (**d**) Axial diffusion tensor imaging. (**e**) Axial ADC. The pattern seen on images (**c–e**) (*arrows*) is consistent with restricted diffusion due to the viscous contents of the dermoid cyst

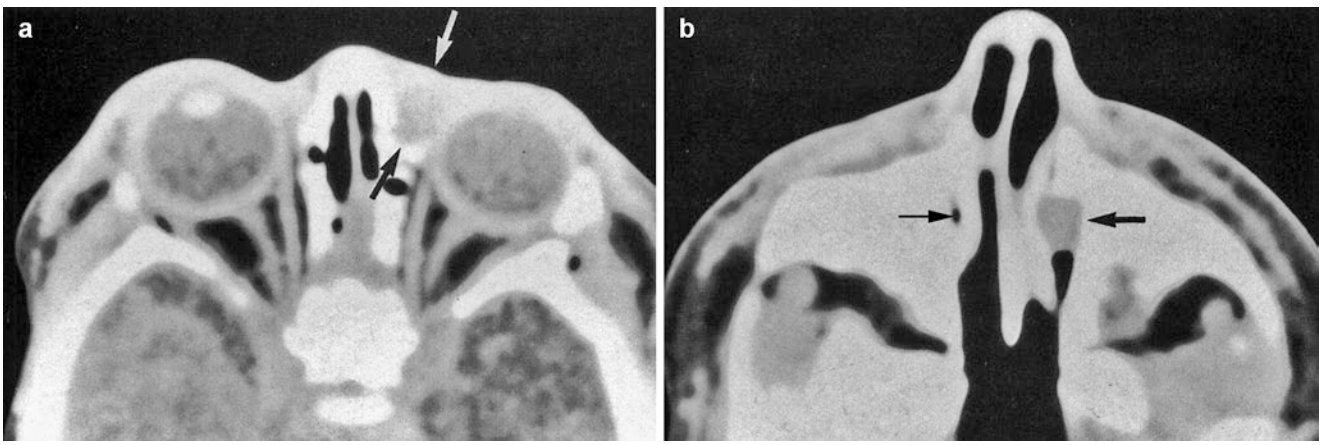


Fig. 32.19 Dacryocystocele due to obstruction of nasolacrimal duct in a newborn boy. (**a**) Axial CT shows a cystic mass (*arrows*) medial to the left globe. (**b**) Axial CT of nasal cavity reveals a dilated nasolacrimal duct (*wider arrow*). The *black*, *narrow arrow* indicates the normal duct

(Fig. 32.28). If there are complications after strabismus surgery (e.g., slipped muscle, excessive scarring) (Fig. 32.29), imaging can be utilized to assess the problem and to plan further management.

Traumatic Orbital Lesions

The type and frequency of orbital traumatic lesions that occur in children depend on the age of the child. Young children (<4 years) manifest atypical orbital fractures from blunt trauma for two reasons. First, the cranial-to-maxillofacial ratio in infants is very high (8:1) and progressively decreases to 2.5:1 in adulthood [63–65]. Younger children also lack pneumatized frontal sinuses, which act to distribute forces applied to the forehead. Young children therefore are especially prone to orbital roof fractures, which may result in intracranial and orbital subperiosteal hemorrhages, as well as cerebrospinal fluid leakage into the orbit (Fig. 32.30) [63, 64, 66–68]. Because of the flexibility of the young cranial bones and the background pulsatility of the brain, a "growing fracture" of the orbital roof may result. Older children and teenagers have a spectrum of traumatic lesions similar to that of adults, including blowout, tripod, and midface fractures [68]. One important exception to this adult pattern is the propensity of older children and teenagers to sustain greenstick fractures of the orbital floor and medial wall (Fig. 32.31), also known as the "white-eyed blowout fractures" [69–71].

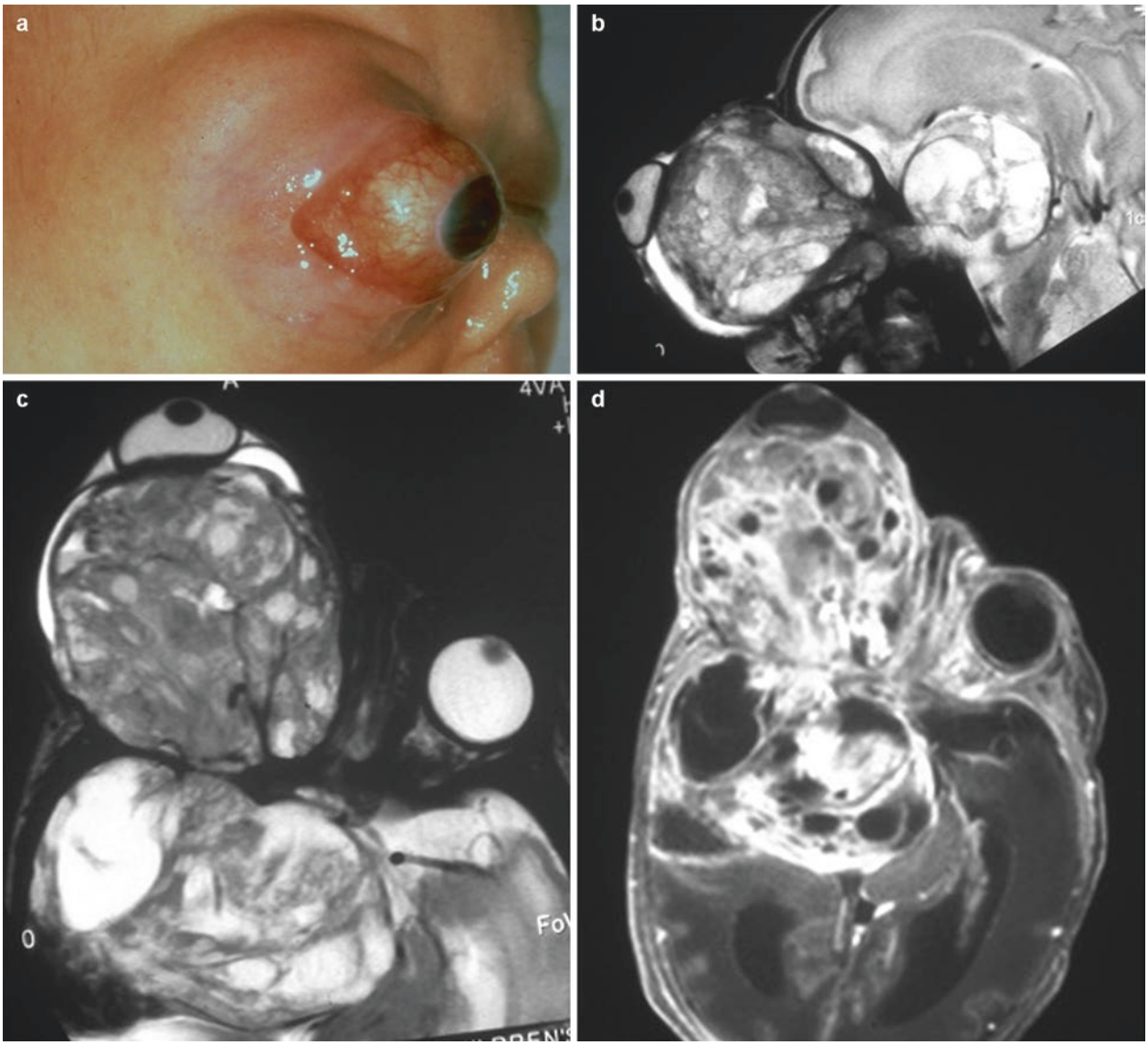


Fig. 32.20 Cranio-orbital teratoma. (**a**) Clinical photograph of a newborn with marked right exophthalmos. (**b**) Sagittal T2-weighted MRI reveals a heterogeneous mass filling the right orbit and extending through the skull base intracranially. (**c**) Axial T2-weighted MRI. (**d**) Axial, postcontrast T1-weighted image with fat suppression. Note the marked distortion of the right globe and the native intracranial anatomy. The teratoma parasitized the brain's blood supply, resulting in a large stroke and death

Imaging in such cases may appear deceptively normal, since the trapdoor nature of the fracture snaps back into normal position immediately after the injury [70, 71]. However, patients with WEBOF often present with severe restrictive external ophthalmoplegia and vasovagal symptoms misdiagnosed as concussion because of tight and ischemic entrapment of the extraocular muscle (EOM) adjacent to the fracture. WEBOF represent an ophthalmic emergency; delay in release of the entrapped muscle may result in permanent ischemic injury and strabismus. WEBOFs are best diagnosed on coronal views, with careful attention to the course and contour of the adjacent EOM (Fig. 32.32). Sagittal images can also be helpful in delineation of the inferior and superior rectus muscles.

Penetrating orbital injury is more common in children than adults and is particularly frequent in younger children, who often tend to fall while playing or running with sharp objects or toys. Evaluation of very young children who have sustained penetrating orbital injury may be difficult due to lack of cooperation as well as lack of exact history and information as to type of trauma and type of penetrating object. The presence of a foreign body may not be externally obvious. Furthermore, a detailed history is often difficult to obtain. There may be both superficial and deep components of a foreign body, and organic (wooden) FBs may be present. Therefore, it is important to evaluate the entire orbit as well as the adjacent structures, the paranasal sinuses, and brain.

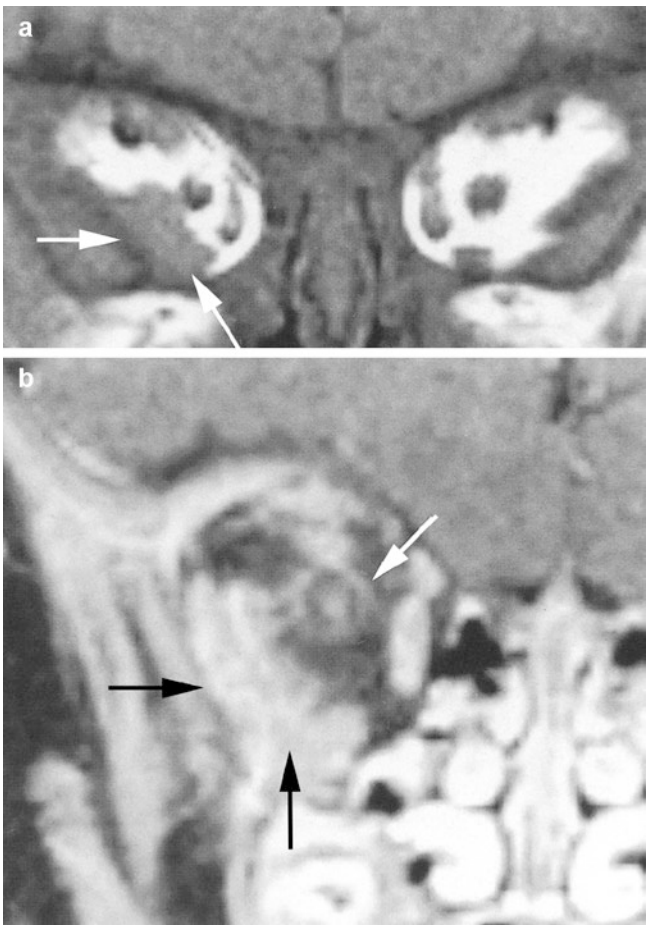


Fig. 32.21 A glial neural hamartoma that presented with a tonic pupil in a 4-month-old child. (**a**) Coronal T1-weighted MRI reveals an irregular mass (*arrows*) in the inferotemporal quadrant of the right orbit. (**b**) Coronal MRI following contrast infusion and fat suppression reveals enhancement of the mass (*black arrows*) that is isointense to the rectus muscles. Abnormal enhancement (*white arrow*) is also noted around the optic nerve–sheath complex and within intraconal fat

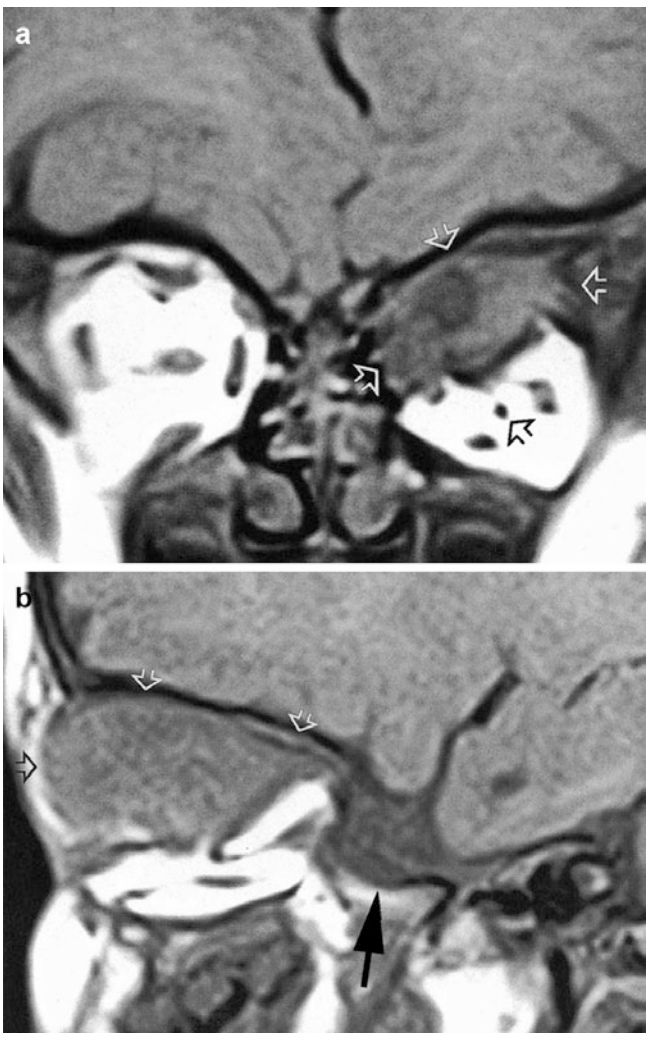
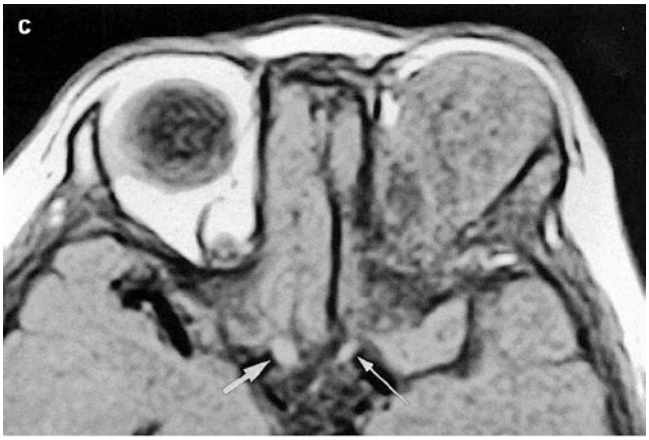


Fig. 32.22 Anophthalmos with neuroglial malformation. A degenerated optic vesicle resulting in anophthalmos with neuroglial malformation in the extraconal portion of the left orbit in an 8-month-old born without a left eye along with partial agenesis of the corpus callosum and an abnormal left cerebral hemisphere. (**a**) Coronal T1-weighted MRI shows a large superior extraconal mass (*white arrows*) displacing the orbital contents. The rectus muscles and optic nerve–sheath complex are markedly hypoplastic. (**b**) Sagittal T1-weighted MRI shows the mass (*white arrows*) occupying more than one-half of the orbit. The *black arrow* points to an abnormally enlarged subarachnoid space, posterior to the orbit and anterior to the temporal lobe.



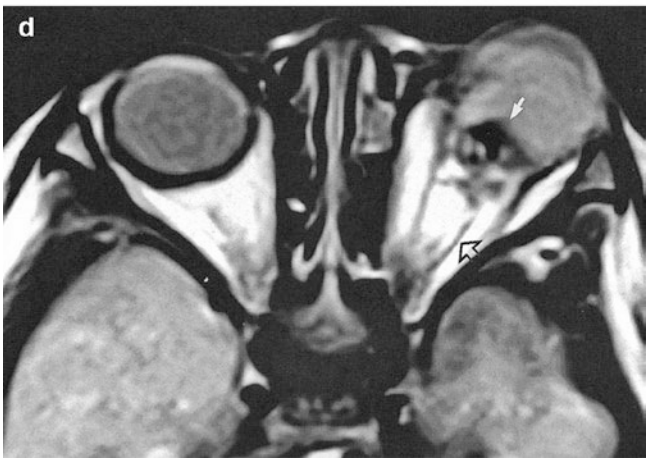
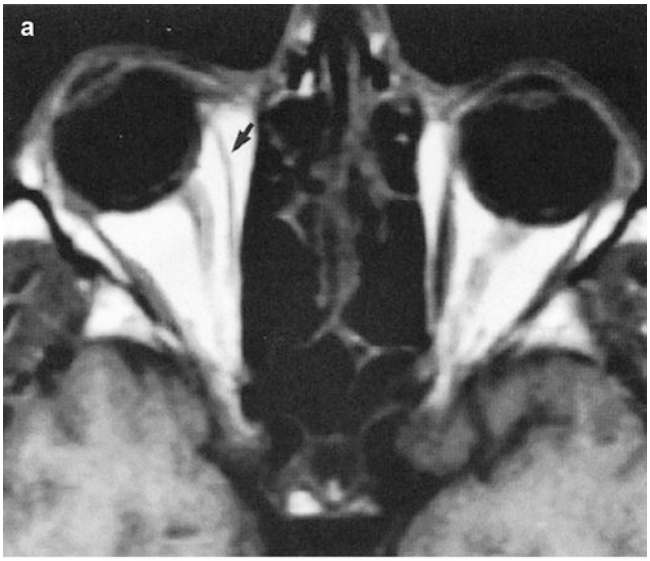


Fig. 32.22 (continued) (**c**) Axial T1-weighted MRI through the superior orbits shows the extensive, slightly heterogeneous mass on the left. The intracranial left optic nerve (*thin arrow*) is atrophic compared to the right optic nerve (*thick arrow*). (**d**) Axial proton density MRI obtained through the inferior orbits shows the normal globe on the right and the most anterior–inferior portion of the mass on the left, which mimics a globe. Note that the signal intensity of the mass is similar to brain tissue and is higher than that of the normal globe. There is an irregular region of hypointensity (*white arrow*) just posterior to the mass, which is consistent with markedly atrophic abnormal left globe (secondary anophthalmos). The medial and lateral rectus muscles extend to this region. A very thin optic nerve–sheath complex (*black arrow*) can also be identified extending from the irregular tissue



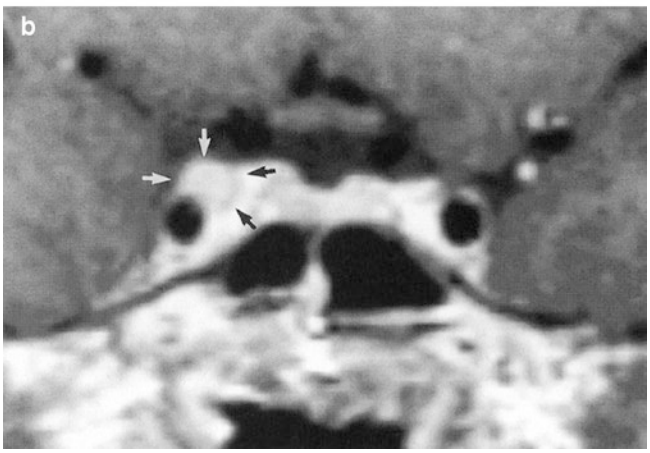


Fig. 32.23 Oculomotor schwannoma. Right oculomotor schwannoma resulting in atrophy of extraocular muscles and right exotropia. (**a**) Axial T1-weighted MRI reveals deviation of the right globe laterally and a markedly thin right medial rectus muscle (*arrow*). (**b**) Contrast-enhanced coronal MRI of the cavernous sinuses reveals a small mass (*arrows*) of the right oculomotor nerve abutting the carotid siphon (seen as a flow void)

CT is the initial modality of choice for evaluation of orbital–facial trauma, not only because it is the best technique for demonstration of fractures (Figs. 32.31 and 32.32) and acute hemorrhages but also because of the possibility of the presence of a metallic body (Fig. 32.33) or organic foreign body. Because some metallic foreign bodies may be ferromagnetic, an MRI as an initial imaging study is contraindicated in orbital trauma [72]. However, once the presence of a ferromagnetic foreign body has been excluded, MRI can be very helpful in demonstrating the course of penetration, the fractures (Fig. 32.34), retained foreign bodies (Figs. 32.33 and 32.35), and the extent of soft tissue injury, such as vascular injury. Multiplanar MR is useful in showing the relationship of foreign bodies to optic nerve (Fig. 32.36c, d) and vessels as well as posttraumatic soft tissue and bony distortion. The use of contrast material in follow-up studies helps to show the degree of inflammatory reaction caused by the foreign material (Fig. 32.36) [73].

If left behind in the orbit, organic material or material that can corrode will cause progressive infectious and inflammatory changes. It is important to remember that the density or intensity of wooden foreign bodies on CT and MRI varies with the degree of hydration of the wood. Dry wood is hypodense on CT (Figs. 32.37 and 32.38) or hypointense on MR (Fig. 32.36) and thus can be easily overlooked or mistaken for air. On MRI, a foreign body consisting of dehydrated wood (Fig. 32.36) or of graphite (Fig. 32.35) can

appear similar to cortical bone or air. On CT, it is important to view the images utilizing a wide window in order to better appreciate the structure and internal heterogeneity of foreign bodies and to differentiate them from air (Fig. 32.37) [74]. Another helpful technique is to measure the Hounsfield unit of known air (e.g., in the paranasal sinuses) and compare it to the area of concern; true orbital emphysema should have a nearly identical Hounsfield reading, while a wooden FB masquerading as air would provide a significantly different number (Fig. 32.38) [47].

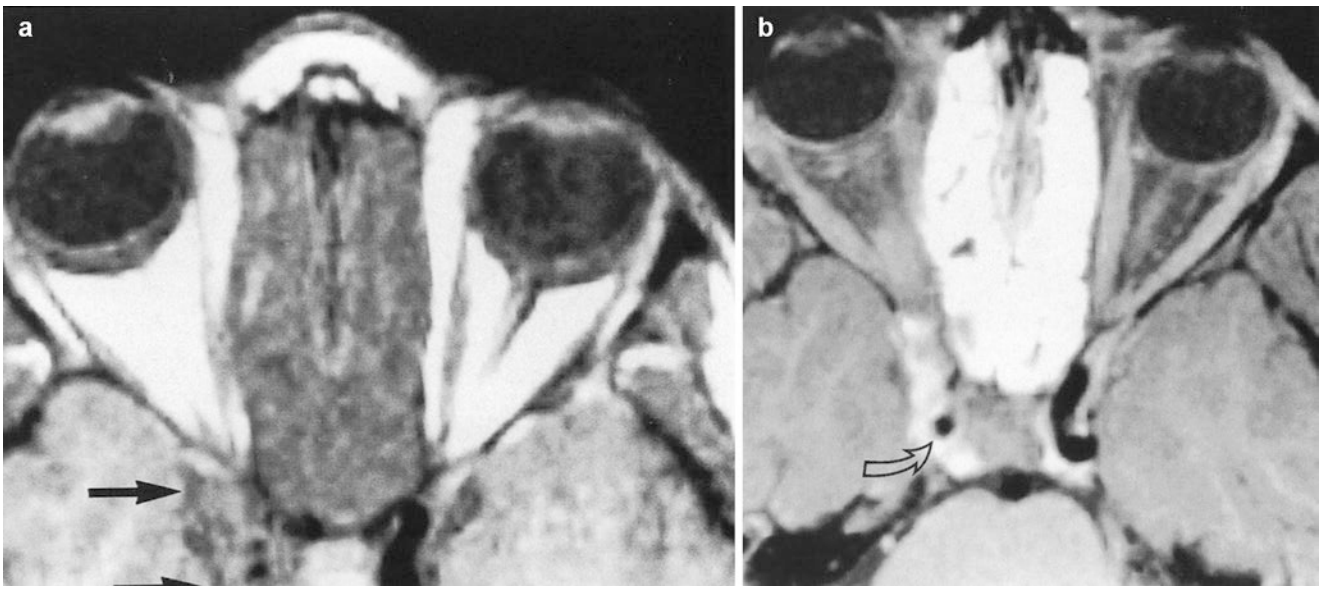


Fig. 32.24 Inflammation in the right cavernous sinus. (**a**) Axial T1-weighted MRI shows slight expansion of the right cavernous sinus (*arrows*) and marked narrowing of the intracavernous carotid artery. Also note the extensive opacification of the ethmoid and sphenoid sinuses due to paranasal sinus disease. (**b**) Axial T1-weighted MRI after gadolinium enhancement and fat suppression shows enhancement in the enlarged cavernous sinus and the narrowed carotid artery (*arrow*). Note the lack of definition of the anatomic structures at the apex of the right orbit in contrast to the normal left orbit

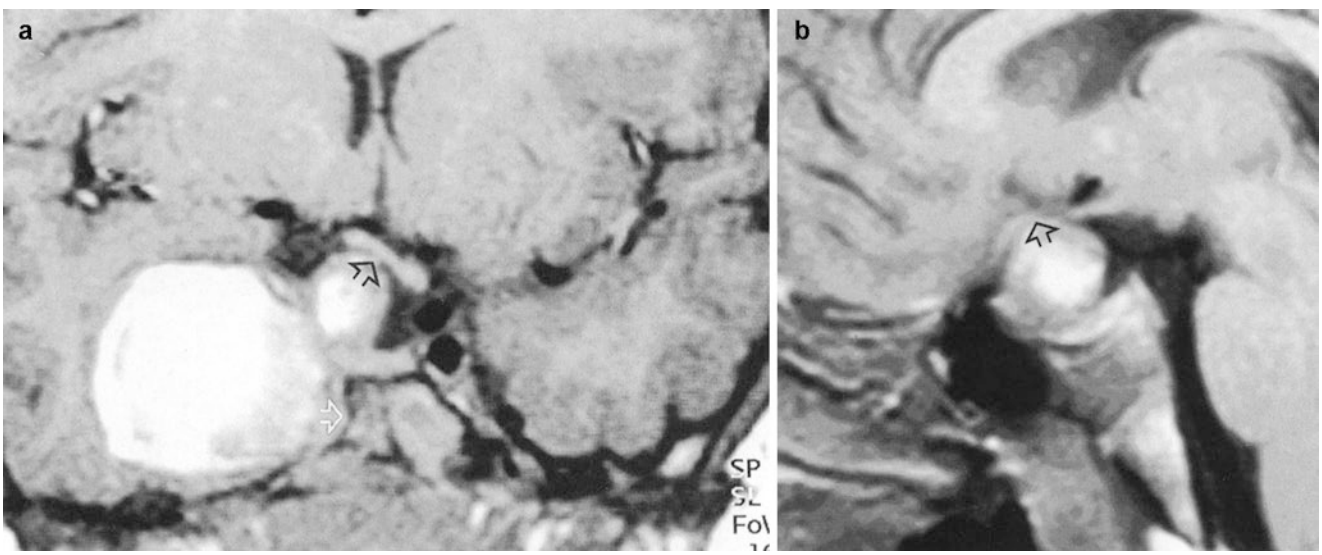


Fig. 32.25 Giant clotted aneurysm eroding the right orbital apex and displacing the optic nerve and chiasm. (**a**) Coronal T1-weighted MRI shows a multilobulated aneurysm with the medial lobule markedly displacing the chiasm (*black arrow*) and causing pressure erosion of the sphenoid bone (*white arrow*). (**b**) Parasagittal T1-weighted MRI shows the medial lobule of the aneurysm projecting into the sella turcica and elevating the chiasm (*arrow*).

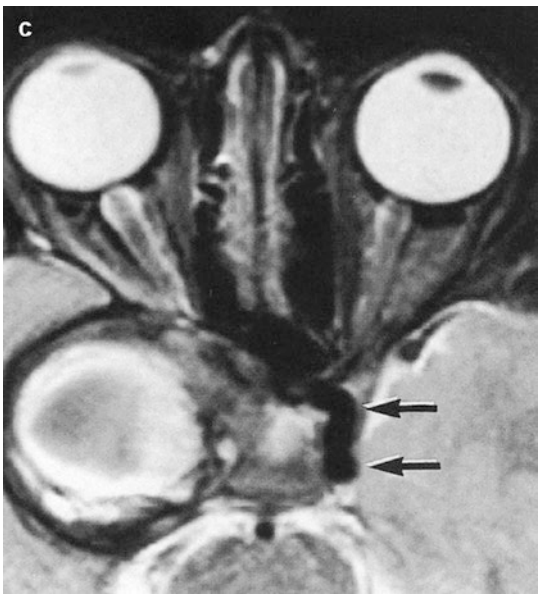


Fig. 32.25 (continued) (**c**) On axial T2-weighted MRI, the large, round aneurysm with a hypointense wall, hyperintense inner rim, and central hypointensity erodes the apex of the right orbit. The right carotid artery is not identified; the left (*arrows*) is obvious

Infections and Inflammatory Lesions

Infections

Infection is the most frequent indication for emergency imaging of the pediatric orbit. Pediatric orbital infections are common and are most often related to sinusitis; in younger children, orbital cellulitis is almost exclusive from adjacent ethmoid sinusitis, since the other paranasal sinuses are still rudimentary (Fig. 32.39). The infections range in extent and severity, being limited to the preseptal region or involving the deeper orbital structures or even the intracranial space [75]. Imaging is critical in aiding the clinician in determining the type and extent of the infection at the time of diagnosis and also in monitoring the response to therapy. CT with contrast enhancement is the initial procedure of choice, as it is readily available in most hospitals and quickly provides the necessary information about the orbital soft tissues, the integrity of bony walls, and the condition of the paranasal sinuses. The use of contrast material is necessary to distinguish a diffuse inflammatory process from an abscess. Contrast material is also necessary to detect and delineate

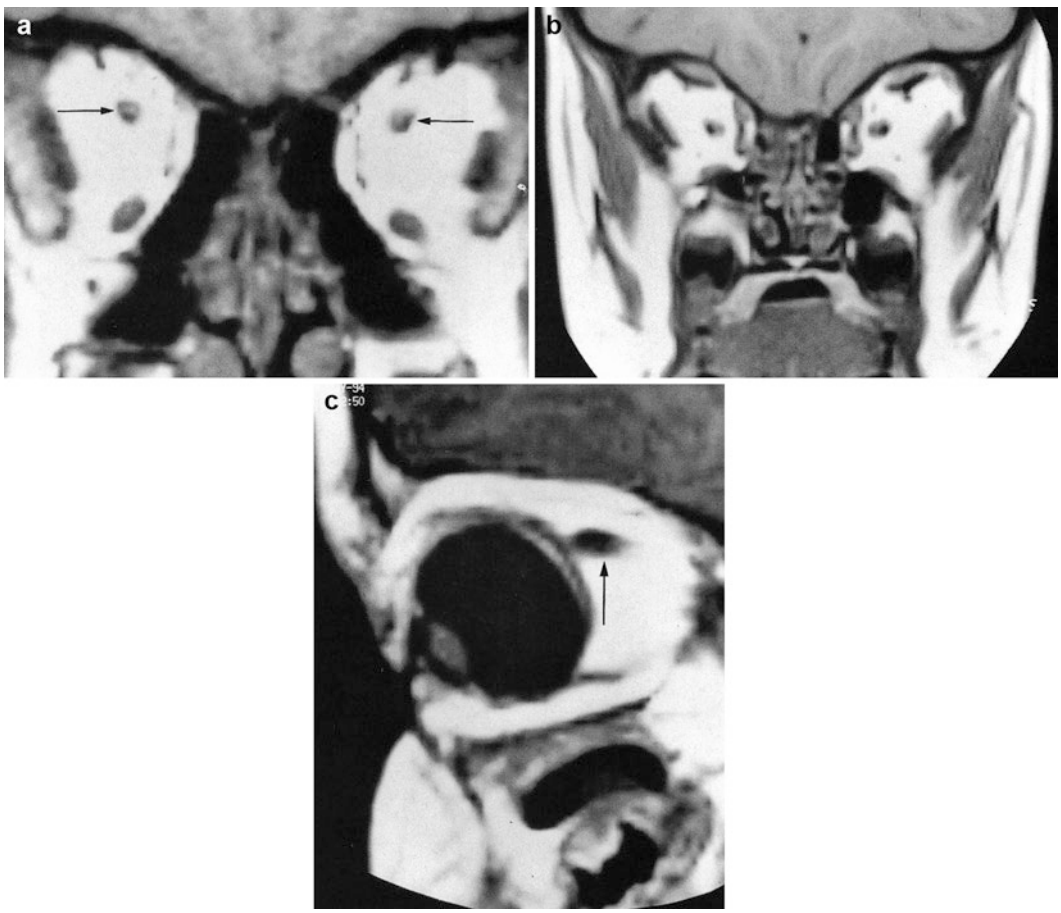


Fig. 32.26 Bilateral double elevator palsy. (**a**) Coronal T1-weighted MRI shows bilateral absence of the superior recti and atrophic superior oblique and medial rectus muscles. The location of the optic nerves (*arrows*) in the upper portions of the orbits is due to the resultant hypotropia. Compare this to a normal coronal of orbits shown in (**b**). (**c**) Parasagittal T1 MRI shows the globe in a hypotropic position, with absence of the superior rectus muscle. The *arrow* points to the optic nerve

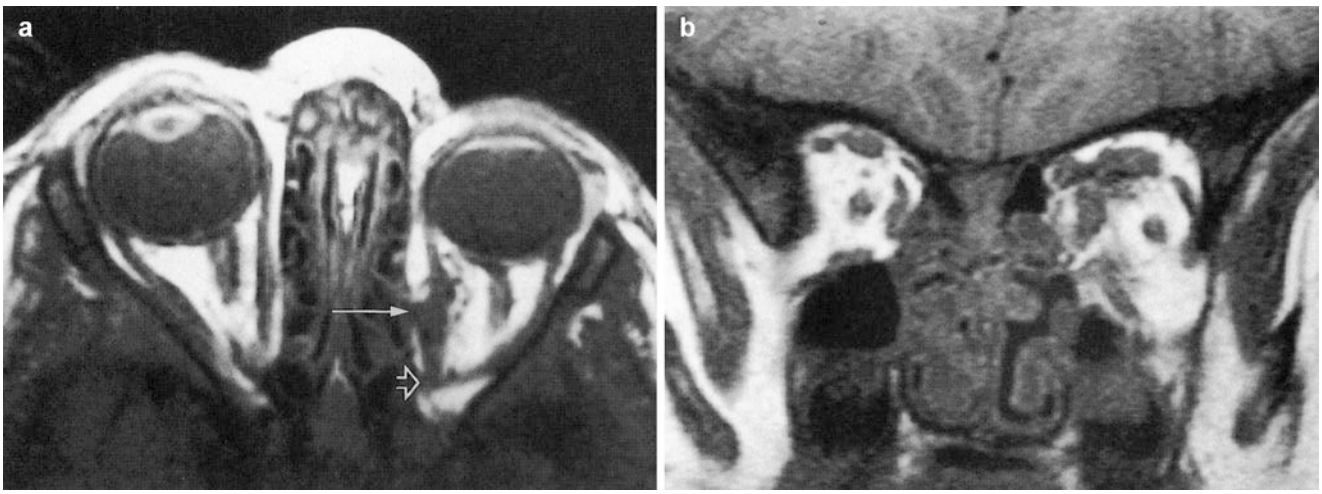


Fig. 32.27 Congenital orbital fibrosis in an 11-month-old girl with enophthalmos since birth. (**a**) Axial T1-weighted MRI shows a thickened and irregular left medial rectus muscle (*arrow*). The left lateral rectus crosses the apex of the orbit to meet the short medial rectus muscle (*open arrow*). The lateral wall of the left orbit is shorter than that of the normal orbit on the right. (**b**) Coronal T1-weighted MRI reveals the fibrotic process causing obliteration of the margins and thickening of the extraocular muscles in the left orbit. There is abnormal widening of the superior extraconal space. The left orbit is enlarged and the left maxillary sinus is hypoplastic

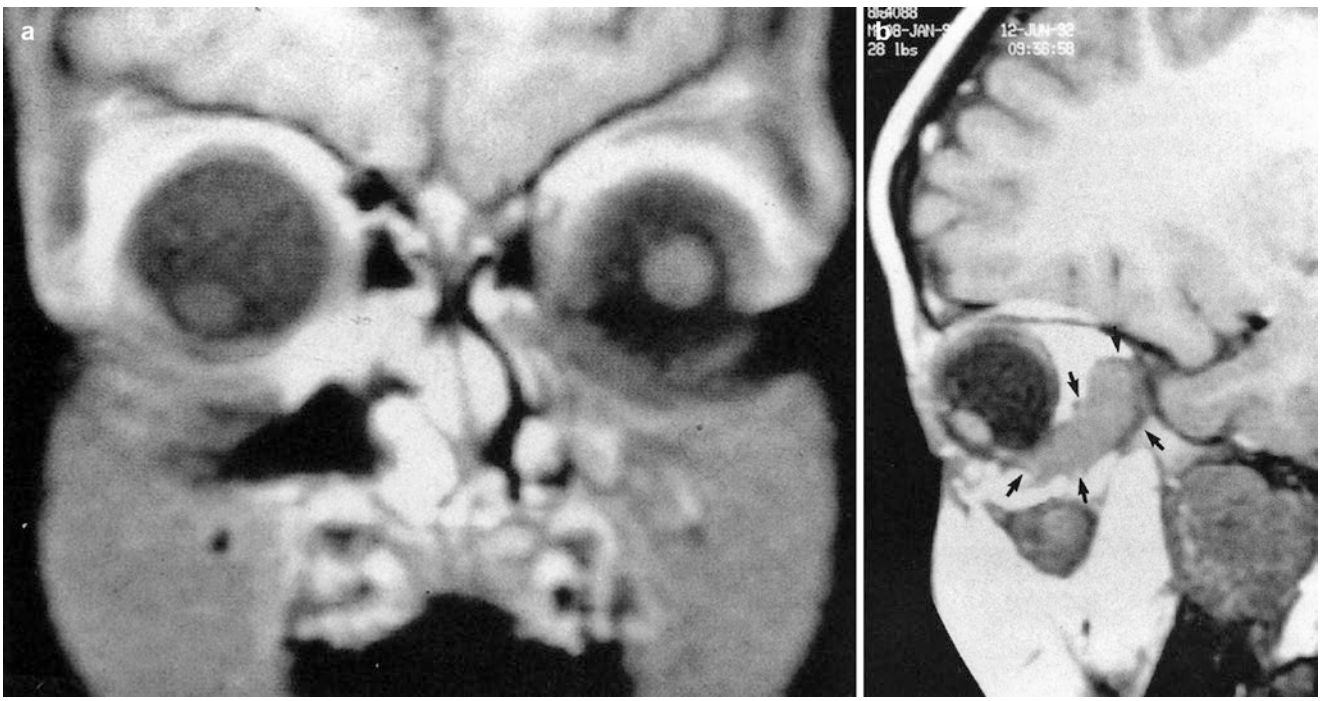


Fig. 32.28 A 5-month-old child with right hypotropia due to fibrosing mass of the inferior rectus muscle. (**a**) Coronal T1-weighted MRI shows marked asymmetry in the position of the lenses. The right eye is fixed in downward gaze position. (**b**) Sagittal T1-weighted MRI reveals a soft tissue mass (*arrows*) along the course of the inferior rectus

intracranial complications such as epidural or subdural empyemas (Fig. 32.40).

While MRI does not provide information about the thin cortical bone, the inflammatory process can be identified with various MRI sequences (Fig. 32.41), and the landmarks of the sinuses and the margins of an abscess can be very well demonstrated on contrast-enhanced, fat-suppressed MRI images (Fig. 32.41c). An orbital abscess located in a more atypical position inferiorly rather than medially in the orbit or a subfrontal epidural empyema may be difficult to demonstrate on pure axial CT scan; in such cases, multidetector CT is invaluable since, as already mentioned, detailed coronal and parasagittal images can be obtained from rapid axial imaging. If CT does not provide specific information

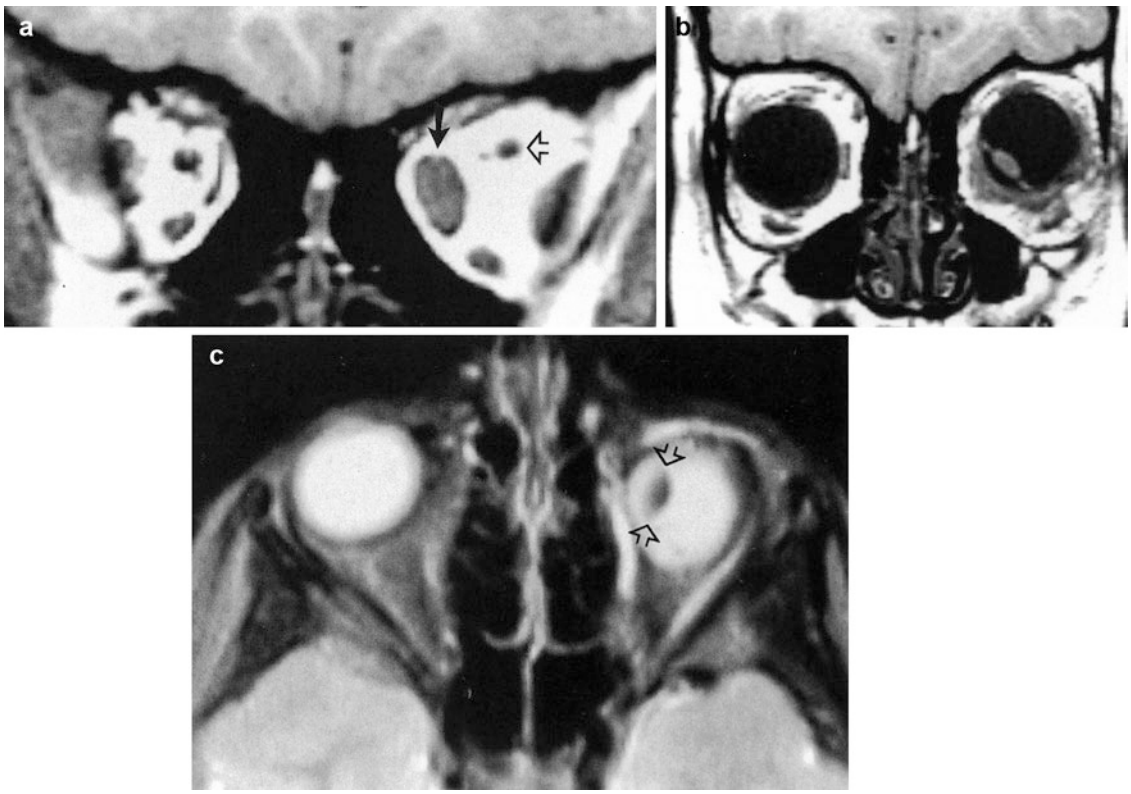


Fig. 32.29 Severe ocular malalignment with marked thickening of the left medial rectus muscle. The patient had multiple previous surgical procedures for strabismus. (**a**) Coronal T1-weighted MRI shows marked thickening of the right medial rectus muscle (*arrow*). The optic nerve/sheath complex (*open arrow*) is elevated (compare to the right side). (**b**) Coronal T1-weighted image shows the left globe turned inferomedially (note the grossly abnormal position of the lens). The globe is also surrounded by irregular fibrotic tissue. (**c**) Axial T2-weighted MRI shows the abnormal position of the globe with the lens (*arrows*) directed medially

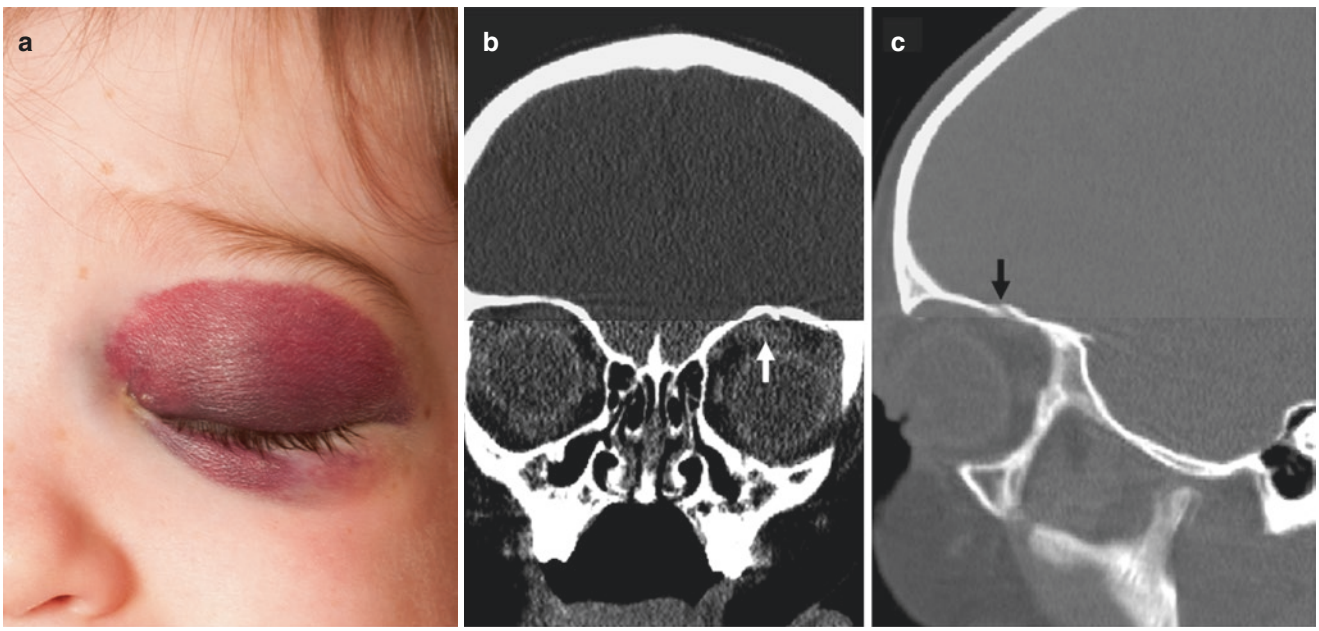


Fig. 32.30 Orbital roof fracture with resultant subperiosteal hematoma. (**a**) Clinical photograph of a 2-year-old child following blunt trauma. (**b**) CT, coronal soft tissue window shows a small subperiosteal hematoma (*arrow*). (**c**) CT, parasagittal bone window reveals a small fracture (*arrow*) in the orbital roof.

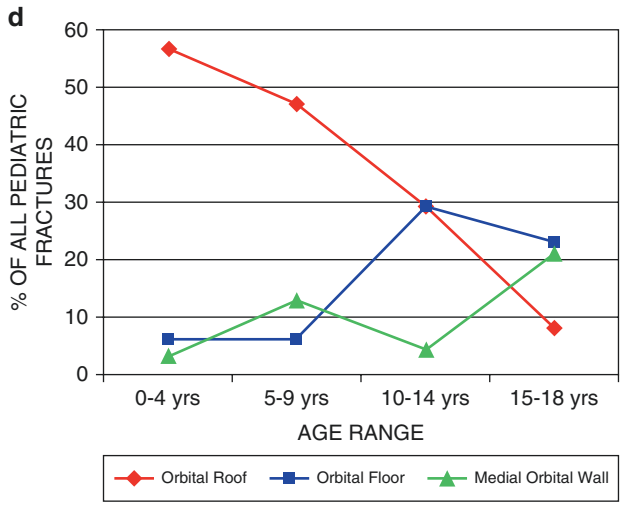


Fig. 32.30 (continued) (**d**) Graphic representation of specific fracture incidence as a percentage of all pediatric orbital and midfacial fractures across multiple age groups (Data compiled from Ref. [64])

with significant proptosis and/or a question of intracranial complication, then MRI with contrast enhancement should be performed (Fig. 32.42). MRI can also reveal involvement of diploic bone by osteomyelitis or infarction better than CT [76]. In case of a retained foreign body that is not ferromagnetic, MRI with contrast enhancement can provide valuable information as to position of the foreign body and the extent of inflammatory reaction (Figs. 32.35 and 32.36). MRI can be helpful in delineating infectious inflammation from noninfectious inflammation, especially in cases of abscess formation: purulence restricts diffusion (Figs. 32.43 and 32.44). Both contrast-enhanced CT and MRI will show superior ophthalmic vein (SOV) thrombosis/thrombophlebitis, an ominous finding in orbital cellulitis that is associated with septic cavernous sinus thrombosis (Fig. 32.45). Precontrast T1-weighted MRI often shows an increased signal in SOV thrombosis.

Allergic mycotic sinusitis, usually due to aspergillus, can be seen in teenagers who are immunocompetent, especially if they have a history of allergic rhinitis and nasal polyposis. Generally, the complaints are fairly nonspecific and chronic and include long-standing nasal obstruction. However, the imaging findings of sino-orbital aspergillosis are so dramatic that frequently they are misinterpreted as an aggressive tumor by those unfamiliar with the entity. The contents of the sinuses produce marked expansion and remodeling of the sinuses and not infrequently remodel or thin bone to break out beyond the sinuses into the orbit (Fig. 32.46) or intracranially. MRI plays a major role in the diagnosis of allergic sinonasal polyposis by characterizing the contents of the sinuses, which have complex signal intensities. On T1-weighted images, the material within the sinuses shows heterogeneity ranging from low to high intensity. On T2-weighted images, a large portion of the contents will show marked hypointensity (Fig. 32.46). This is due to a combination of factors: decreased amounts of free water and the presence of macromolecular proteins in retained mucus, paramagnetic ions (the fungus may scavenge heavy metals), and mycetomas [77–79]. On CT, the chronic allergic fungal sinusitis appears as extensive bony expansion and destruction with the contents showing increased attenuation. The bony changes actually are not due to destruction but



Fig. 32.31 Medial WEBOF in a young teenager. (**a**) Note the severe horizontal gaze restriction of the right eye.

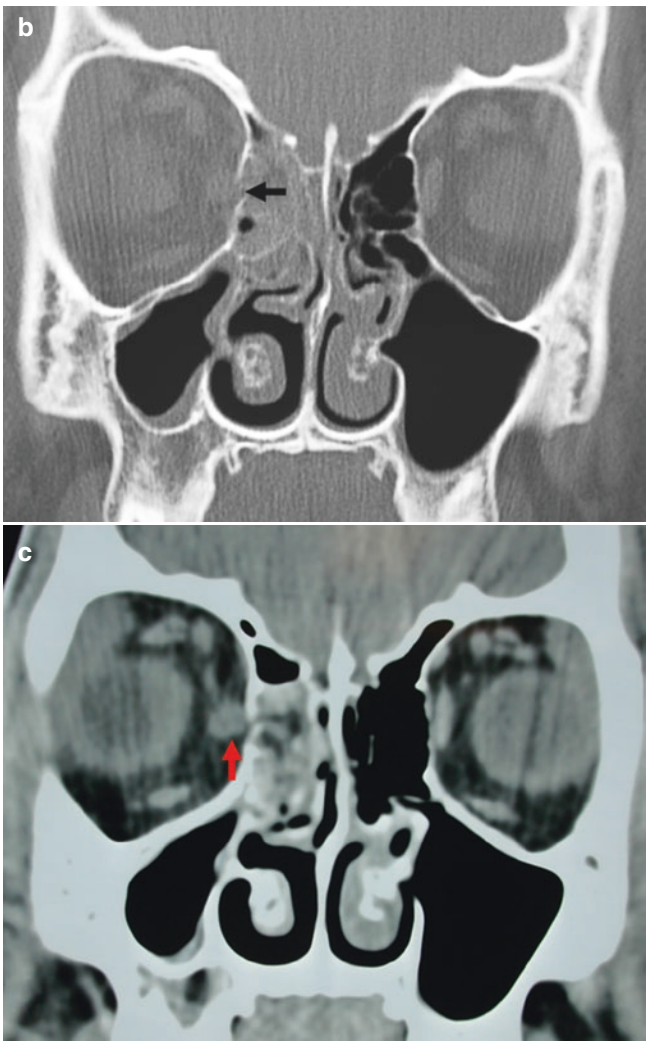


Fig. 32.31 (continued) (**b**) On coronal bone window CT, a narrow fracture in the right lamina papyracea is noted (*arrow*). (**c**) Coronal soft tissue window CT shows a marked distortion of the right medial rectus muscle (*arrow*) compared to the left, consistent with entrapment of the muscle within the confines of the fracture



Fig. 32.32 WEBOF and the "missing muscle sign." A teenager was struck in the left orbit with a baseball. He immediately complained of nausea, was diagnosed with a concussion, and underwent head CT. After subsequent transfer, an orbital CT was performed. (**a**, **b**) Coronal soft tissue windows on CT of the orbits. Note that the left inferior rectus appears to be missing but has actually herniated into the maxillary sinus (*arrows*) along with some surrounding radiolucent fat. A narrow fracture is present. (**c**) On more posterior cuts, the inferior rectus (between the *arrows*) is incarcerated within the trapdoor fracture, with resultant ischemia

to marked thinning and deossification secondary to pressure erosion (Fig. 32.47). CT images may also reveal areas of calcification within the affected paranasal sinuses, which is a relatively specific sign of sino-orbital aspergillosis. Contrast enhancement may be seen both on CT and MR on periphery of the expansile lesions.

Idiopathic Orbital Inflammation (Orbital Pseudotumor)

Idiopathic orbital inflammation (IOI) is most common during middle age but can be encountered in older children, usually after age 10 [80]. The etiology is unclear, but IOI appears to be a T cell-mediated response to intraorbital soft tissue antigens [81, 82]. The process may be acute or chronic, and the spectrum of sites involved ranges from small foci of infiltration or single muscle involvement to diffuse, extensive infiltration of all of the orbital contents and even structures along the skull base (Fig. 32.48). On occasion, IOI may spill

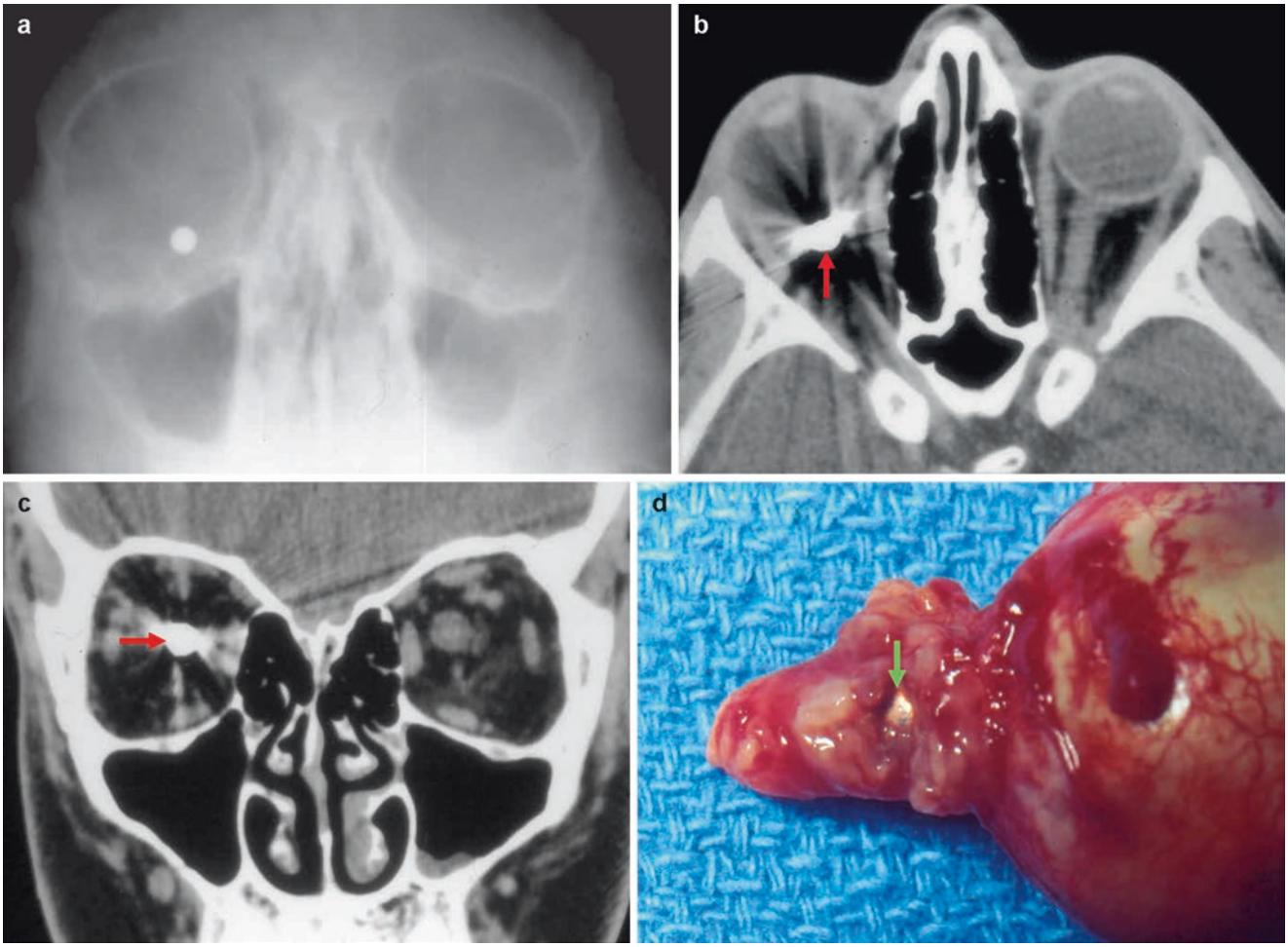


Fig. 32.33 Metallic orbital foreign body. (**a**) Scout film of a boy accidently shot with a BB gun. Note the spherical foreign body located in the right orbit. No accurate anatomic data can be obtained from the plain film. (**b**, **c**) Axial and coronal CT soft tissue windows localize the BB (*arrows*) to the area of the optic nerve. Note the scatter artifact caused by the metal within the BB. (**d**) The patient underwent subsequent enucleation because of a posterior globe rupture. Both the rupture and the BB imbedded in the optic nerve (*arrow*) are obvious in the gross pathology specimen

over to involve the posterior sclera and choroid (Fig. 32.49). Children tend to get the myositis type of IOI and may manifest bilateral involvement (Fig. 32.50). Both CT and MRI are excellent at imaging the extent of orbital involvement, but MRI is better at demonstrating the extraorbital extent into the cavernous sinus or through the inferior orbital fissure. One of the more frustrating aspects of pediatric IOI is its differentiation from orbital cellulitis. Orbital cellulitis is the most common cause of exophthalmos in the pediatric age group, and IOI presents with very similar signs and symptoms, including explosive onset of pain and eyelid swelling/erythema. Correct interpretation of imaging is often the linchpin for diagnosis. In most cases, IOI is imaged initially with CT because of the possibility of underlying cellulitis and sinusitis. As already mentioned, the vast majority of pediatric orbital cellulitis is secondary to adjacent sinusitis. The presence of clear sinuses but inflammatory findings on imaging is highly suggestive (but not definitively diagnostic) of IOI; as already mentioned, the possibility of an occult and infected foreign body must be entertained in such cases, even without a known history of trauma. The clinician should also remember that, in a minority of cases, rhabdomyosarcoma may also present with inflammatory signs.

Other forms of inflammation, most notably sarcoidosis and sino-orbital granulomatosis with polyangiitis (Wegener granulomatosis), typically follow a more indolent course. Both of these entities may erode adjacent bone, however mimicking malignancy or sino-orbital aspergillosis.

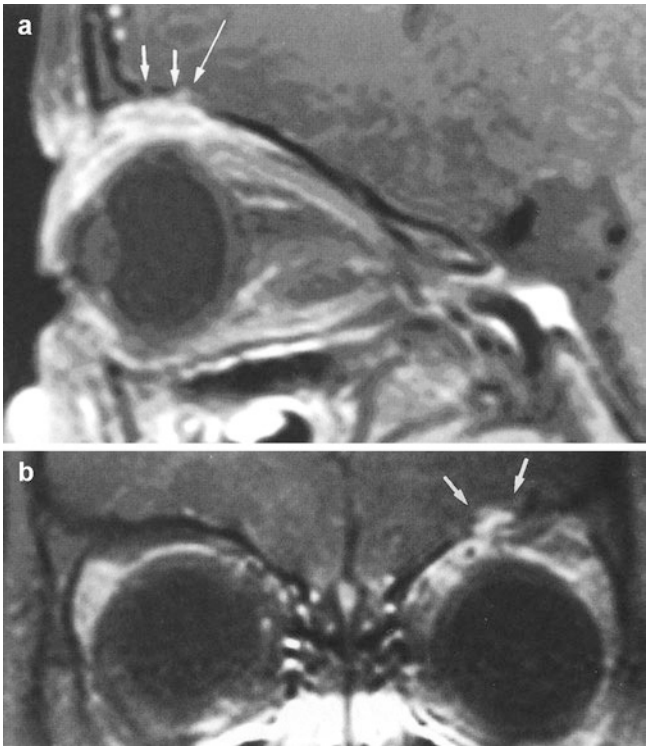


Fig. 32.34 Fracture of the orbital roof in a young child. The findings on initial CT were indeterminate (reconstructed coronal images were suboptimal), but metallic foreign body was ruled out; therefore, an MRI was performed to better elucidate the extent of the skull base injury. (**a**) Sagittal postcontrast fat saturation T1-weighted MRI with fat saturation reveals two interruptions (*arrows*) in the cortex of the orbital roof. In addition, a small amount of hyperintense tissue (*long arrow*) can be seen projecting superiorly at the site of fracture. (**b**) Coronal T1-weighted postcontrast, fat saturation image again reveals a fracture in the roof of the orbit with enhancing tissue (*arrows*) projecting through the fracture. Contrast material is typically not utilized in evaluation of acute trauma. However, in this case because some time had elapsed after the initial injury, contrast material was infused because the presence of a posttraumatic, enhancing inflammatory/hemorrhagic reaction was anticipated

Optic Neuritis

A portion or the entire optic nerve, and sometimes even the chiasm, can be involved by an inflammatory process. Although demyelinating disease is rare in the pediatric age group, optic nerve inflammation may be a manifestation of multiple sclerosis; therefore, the brain should be imaged in addition to the orbits (Fig. 32.51). Both CT and MRI can demonstrate optic neuritis, but MRI is much more sensitive in detection of optic nerve swelling and inflammation, particularly in the intracanalicular and intracranial portions, and is the imaging modality of choice in such cases. MRI is also the procedure of choice for evaluation of the brain for

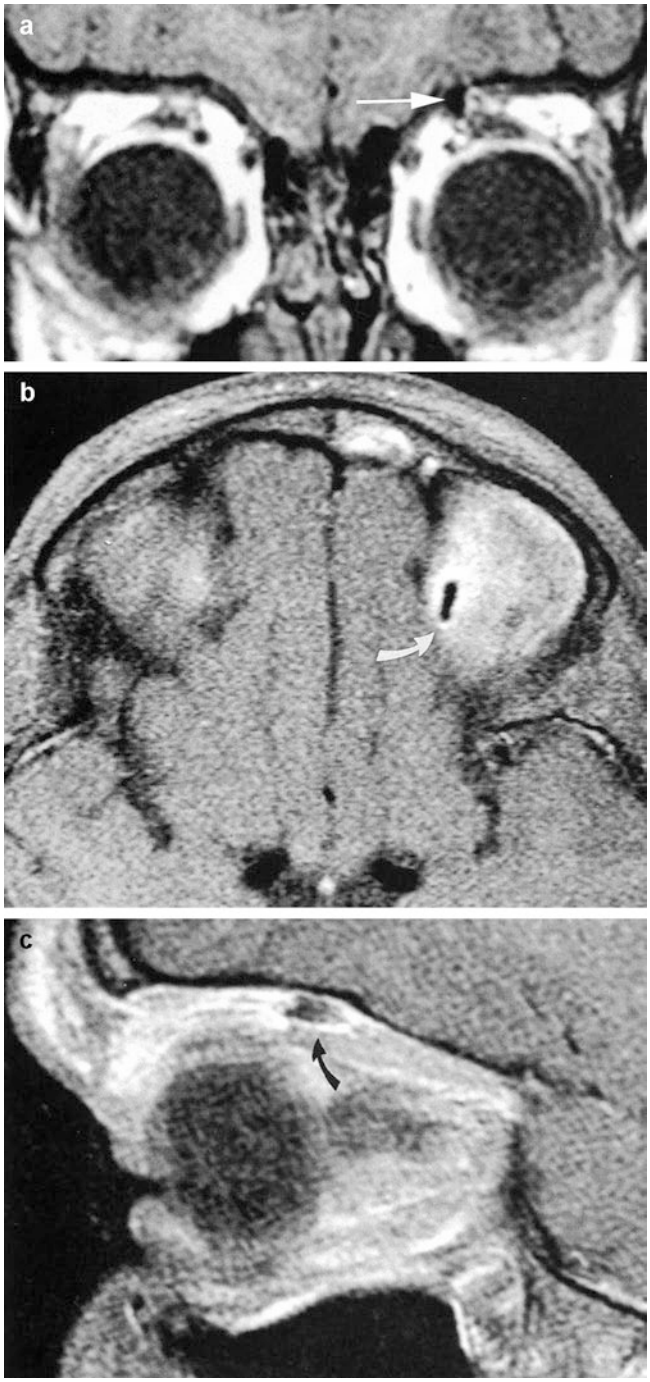


Fig. 32.35 Retained foreign body (graphite from a pencil) in the superior extraconic space of the left orbit. (**a**) Coronal T1-weighted MRI shows a hypointense foreign body (*arrow*). The cortex of the orbital roof appears interrupted at the site of the foreign body. (**b**) Axial section through the superior portion of the orbits, after gadolinium infusion and fat suppression, reveals the foreign body (*arrow*) surrounded by enhancement. There is also abnormal enhancement of the soft tissues of the left orbit due to inflammation. (**c**) Sagittal section with gadolinium and fat suppression reveals the foreign body (*arrow*) in the superior extraconal portion of the orbit. This section is not in the plane of the discontinuity in the roof of the orbit

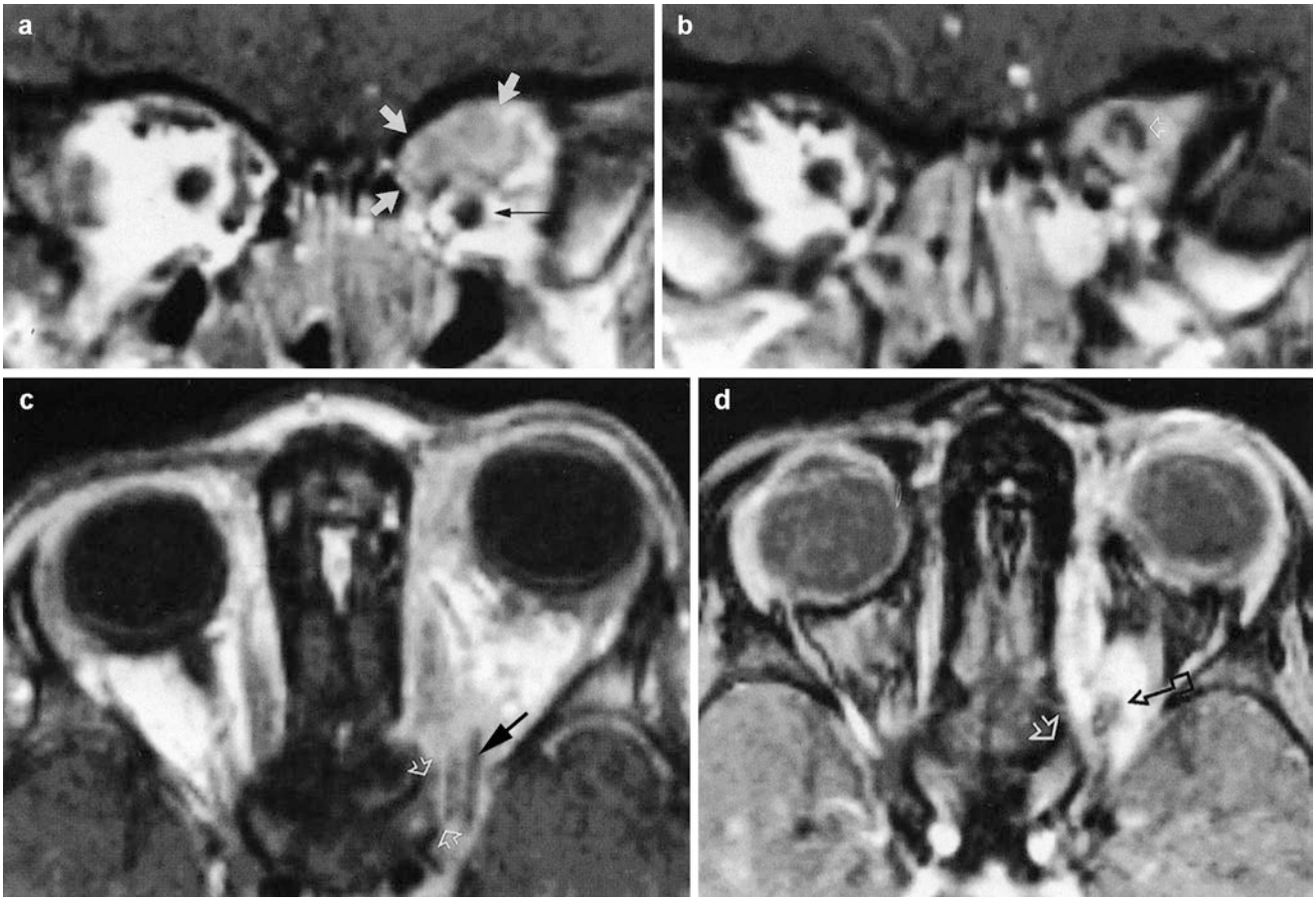


Fig. 32.36 Organic foreign body in posterior orbit. Penetrating orbital injury resulting in a reactive inflammatory mass around a retained foreign body. The patient had fallen onto stubble in a field. A foreign body was noted on images at the orbital apex, and because of its location, no surgical removal was attempted. The patient has been followed with serial MRI. Because of the organic nature of the foreign body, there has been recurrent and increasing inflammatory reaction around it. (**a**) Coronal T1-weighted image from a study performed 1 month after injury shows a mass in the superior aspect of the left orbit (*white arrows*) displacing the left optic nerve–sheath complex (*black arrow*). There is slight contrast enhancement of the mass. (**b**) A coronal section posterior to (**a**) again shows an inflammatory mass. At this level, a horseshoe-shaped foreign body (*arrow*) can be identified within the inflammatory mass, which obliterates all the anatomic landmarks within the posterior orbit. (**c**) Axial T1-weighted MRI shows the posttraumatic inflammatory/fibrotic mass at the left orbital apex and also the foreign body (*black arrow*), which crosses from the apex of the orbit into the anterior portion of the cavernous sinus. Note the proximity of the foreign body to the intraorbital opening of the optic canal (*open arrows*). (**d**) An axial, postcontrast MRI with fat saturation shows the extent of the posttraumatic inflammatory process, which involves the medial aspect and apex of the left orbit and which once again shows prominent contrast enhancement. A portion of the foreign body (*black arrow*) can be seen within the inflammatory mass. Note the proximity of the mass and foreign body to the optic nerve (*white arrow*)

multiple sclerosis, acute demyelinating encephalomyelitis, cerebral vasculitis, central nervous system sarcoidosis, and a host of other inflammatory or vasculitic entities. Because demyelination occurs preferentially in the periventricular regions, T2-weighted images with FLAIR technique (which suppresses the hyperintense signal of CSF in the ventricles) should be performed.

On imaging, the inflamed optic nerve appears enlarged, shows increased intensity on T2, and enhances after intravenous contrast material enhancement. Often the entire optic nerve–sheath complex will appear enlarged, somewhat indistinct, and irregular or "shaggy" after contrast enhancement (Figs. 32.51 and 32.52). If there is involvement of the optic nerve head (papillitis), this can also be shown on MR (Fig. 32.52).

Optic nerve inflammation may also be due to a variety of infectious (e.g., Lyme disease) and noninfectious etiologies (Fig. 32.53). One particular entity to keep in mind is optic nerve sarcoid (Fig. 32.54), which may present in a patient with a known history of systemic sarcoidosis or as an isolated finding that may or may not progress to systemic involvement. In isolated cases, the serum angiotensin-converting enzyme level may be normal [83, 84].

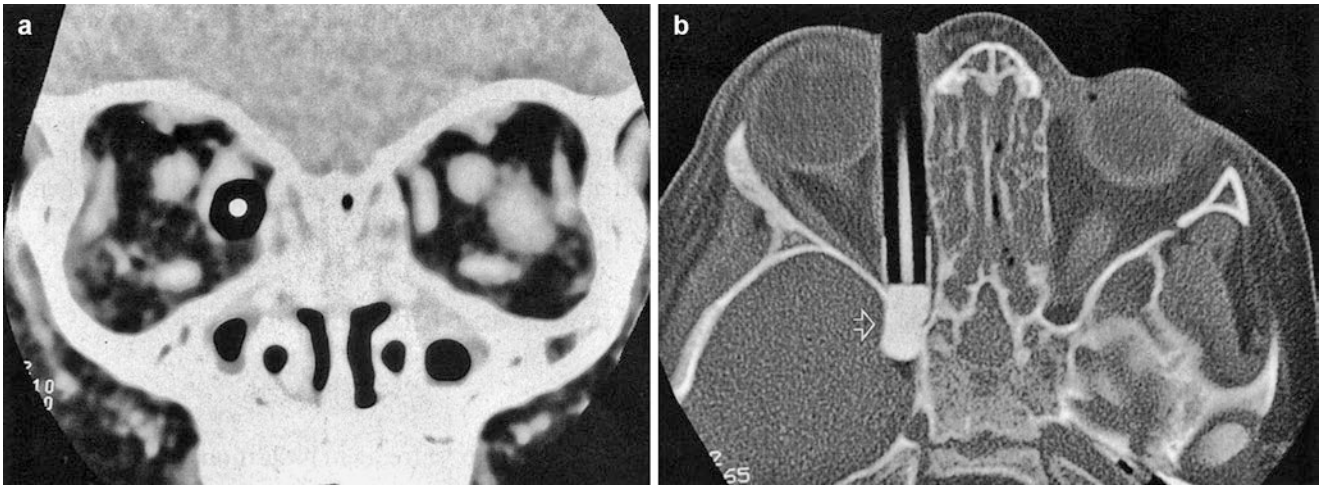


Fig. 32.37 Wooden foreign body (pencil) in the right orbit. (**a**) Coronal CT scan reveals a foreign body in the medial extraconal space of the right orbit. The characteristics of this foreign body are typical of a pencil. The dry wood is markedly hypointense, similar to that of air, and the center is hyperintense due to the graphite center. The pencil displaces and distorts the right medial rectus muscle. (**b**) Axial CT scan. Once again, the radiopaque graphite core is surrounded by radiolucent wood. The eraser (*arrow*), which is hyperdense, has passed through the superior orbital fissure and projects into the region of the anterior cavernous sinus. Because the eraser is soft, it has molded to the medial bony structures



Fig. 32.38 Wooden foreign body on CT. Depending on the hydration, intraorbital wooden foreign bodies are notorious for being misdiagnosed as air on CT. Expanding the window (e.g., using a bone rather than soft tissue window) may show a subtle difference between the foreign body and known air (e.g., in a paranasal sinus). A more accurate method is to simply measure the Hounsfield units (HUs) in the area of intraorbital concern and compare this to known air. This patient was initially diagnosed as having intraorbital emphysema on axial CT (note elongated very low density in the orbit) and started on corticosteroids for presumed inflammation. The orbital consultant noted that the orbital lesion (*red rectangle*, −303HU) differed markedly from known air in the ethmoid sinus (*green rectangle*, −1006HU). A stick surrounded by abscess was identified during orbitotomy and removed (Courtesy of Peter A. D. Rubin, MD)

Vascular Lesions

Vascular lesions occur frequently in the head and neck region of children and represent an important and substantial component of pediatric orbital abnormalities [85, 86]. Proper management of orbital vascular lesions, which include different entities with distinct pathophysiology and hemodynamics, depends on correct determination of the type of lesion. In this regard, imaging plays an important role, as it provides information not only on the location and extent of the lesion but also on the nature of the lesion [6]. However, variability and disagreements in the classification of vascular lesions have led to confusion and caused difficulty both in diagnosis and treatment. A significant degree of controversy existed in the past as to what various vascular lesions represent, what their origin is, and how they should be named [87]. Much of the confusing nomenclature stems from ignorance of pathophysiology. More recently, a systematic approach has been codified by the International Society for the Study of Vascular Anomalies (ISSVA) [87–89]. Briefly, vascular lesions are classified in three tiers. First, lesions are either tumors (active endothelial cell proliferation) or malformations (endothelial cell dysmorphogenesis or normal turnover). Second, lesions exhibit either low flow (venous malformations, lymphatic malformations, lymphaticovenous malformations) or high flow patterns (arteriovenous malformations, congenital arteriovenous fistulas) [89]. Finally, lesions are broadly classified as arterial, venous, capillary, lymphatic, or of mixed type. Unfortunately, there has been adherence to the old nomenclature, partly due to lack of awareness and partly due to reluctance to change established terminology. Mulliken states that the term *hemangioma* has been used as a generic term to refer to numerous vascular lesions, both congenital and acquired, that have had different etiologies and natural histories [90]. Because the suffix

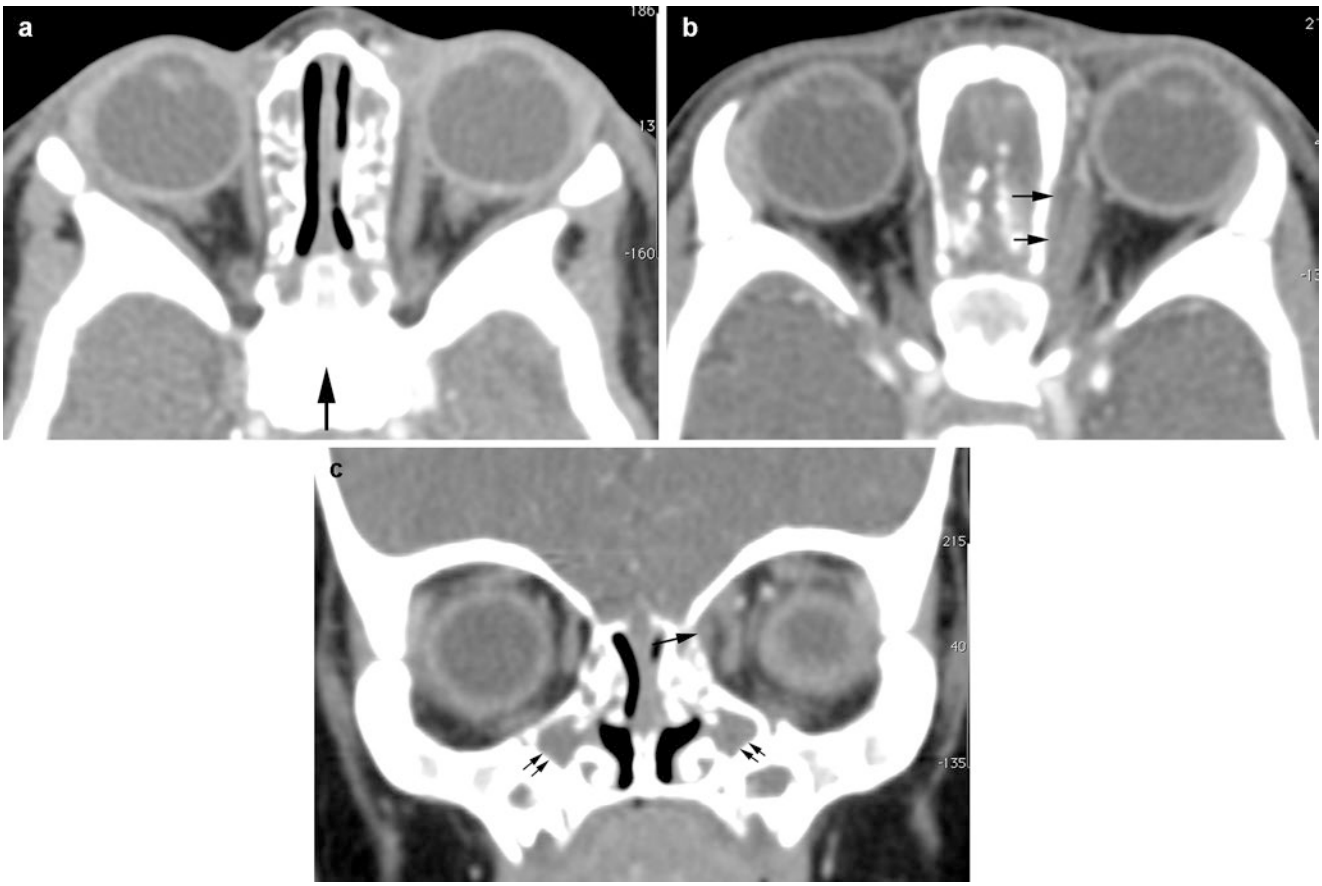


Fig. 32.39 Early subperiosteal orbital abscess vs inflammatory phlegmon. A 2-year-old girl was transferred for progressive proptosis, erythema, and fever. She was diagnosed with a small left subperiosteal collection from adjacent ethmoidal sinusitis and responded rapidly to intravenous antibiotic therapy. The pneumatization pattern of the sinuses as well as the relatively large size of the globes compared to the orbital volume provides important clues as to the patient's age. (**a**) Axial soft tissue window of a postcontrast CT shows opacification of both ethmoid sinuses. Note that the sphenoid sinus has not yet pneumatized (*arrow*) and will not be fully developed until her teenage years. (**b**) Axial CT, postcontrast, soft tissue axial view reveals a small, medial subperiosteal collection (*arrows*) consistent with either abscess or inflammatory phlegmon. A landmark study by Harris concluded that in children younger than 9 years old, most subperiosteal collections are either sterile or mono-organismal with aerobic pathogens and respond to intravenous antibiotics alone in 93% of cases. (**c**) Because the CT was performed using multidetector technology, repositioning for coronal views was unnecessary. This postcontrast, coronal soft tissue window also shows the medial subperiosteal collection (*single arrow*) and the rudimentary maxillary sinuses (*double arrows*)

-oma indicates the presence of a neoplasm, Mulliken argues that terms ending in *-oma* should not be used for vascular malformations [90]. Mulliken and Glowacki recommend that the term *hemangioma* should be reserved for a true vascular neoplasm that contains proliferating endothelial cells with increased mitotic activity [91]. *Capillary hemangioma* (*hemangioma of infancy*) would meet these criteria during its proliferating phase, but *cavernous hemangioma* and *lymphangioma* would not, since they are likely vascular malformations. Unlike the capillary hemangiomas, which eventually involute, vascular malformations do not, and generally they grow proportionally with the child [90, 91]. Although present at birth, vascular malformations may not become manifest until later in life, during childhood or young adulthood.

Modern imaging techniques play an important role in the management of orbital vascular lesions, influencing the type of therapy instituted and the approach used if surgery is performed (see Chap. 35). Information provided by imaging is particularly important in the case of lesions located deep in the orbit because their vascular nature is not evident to the examining clinician. Finally, modern imaging techniques are contributing to the correct characterization of orbital vascular lesions and are providing further basis for correct nomenclature.

The majority of orbital vascular lesions undergo imaging with conventional CT or MRI. The use of CT and MR angiography (CTA and MRA, respectively) as well as MR venography (MRV) has been reported in the past but has limitations. Because of the relatively small size of orbital lesions com-



Fig. 32.40 Methicillin-resistant *Staphylococcus aureus* (MRSA) infection of the orbit. (**a**, **b**) Axial CT images (soft tissue windows) of a 6-month-old child with rapidly progressive right proptosis. On the right, there is an infiltrative process in the inferior and lateral orbit that extends to the orbital apex and the superior and inferior orbital fissures. Note that the pterygopalatine fossa is involved on the right (*white arrows*). Compare the opacified affected side with the radiolucent, fat-filled uninvolved side (*black arrows*). (**c**, **d**) Coronal soft tissue windows reveal opacification of the ethmoid sinuses and the rudimentary maxillary sinus (*arrows*). MRSA infection can spread rapidly along the skull base and result in intracranial infection. Cellulitis from an odontogenic source should also be considered in cases of rapid progression. (**e**, **f**) A 5-year-old girl presented with lateral facial edema and lid swelling. Note the subperiosteal collection (*arrows*) located laterally in the right orbit. The paranasal sinuses are clear. Also note the soft tissue edema overlying the temporalis. A lateral subperiosteal abscess is highly atypical and raises the possibility of atypical organisms (MRSA, mycobacteria) or fluid and blood from an adjacent sphenoid wing infarction occasionally seen in patients with sickle cell disease [76]. Because an accurate history may be unobtainable from a child, an occult penetrating injury or foreign body should also be considered in such cases. In this case, urgent drainage revealed MRSA

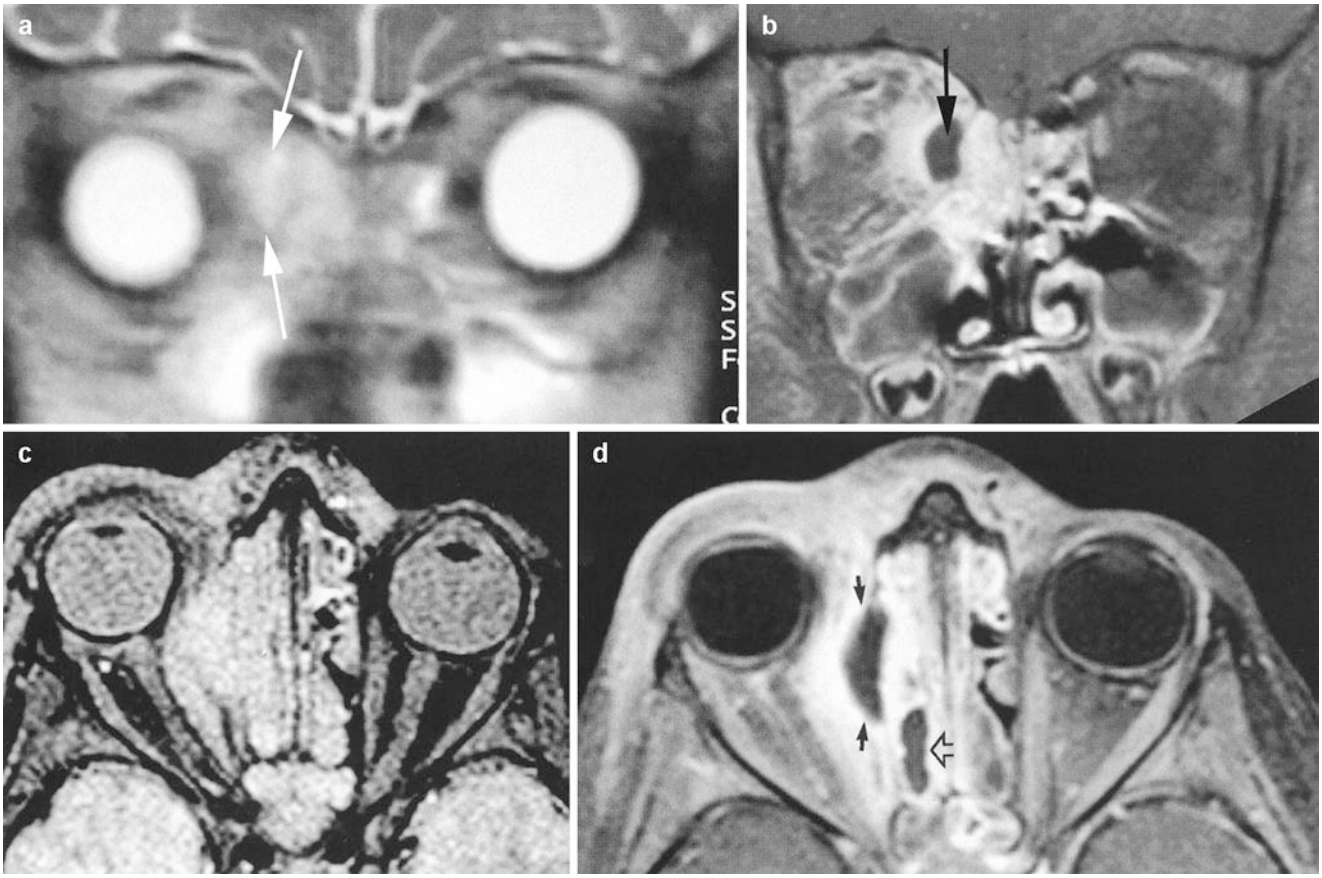


Fig. 32.41 Orbital cellulitis and subperiosteal abscess due to sinusitis in a 5-year-old boy. (**a**) Coronal T2-weighted MRI HASTE image, which takes only 1.2 s per section, reveals a hyperintense mass (*arrows*) with secondary compression and displacement of the right globe. This type of fast imaging permits rapid, initial screening to check for location of pathology, an important technique in young, uncooperative children. (**b**) Coronal T1MRI with contrast enhancement and fat saturation reveals a large subperiosteal abscess (*arrow*) along the medial wall of the right orbit. In addition, there is abnormal enhancement throughout the right orbit, which results in loss of definition of individual structures and indicates diffuse inflammation. Compare to the normal orbit on the left. (**c**) An axial inversion recovery MRI scan shows the extensive inflammatory process in the medial aspect of the right orbit extending to the optic nerve/sheath complex; however, this sequence does not provide anatomic detail of the medial wall of the orbit and does not distinguish abscess from diffuse inflammation. (**d**) Axial T1-weighted postcontrast image with fat suppression provides the best information. It reveals the exact site of the subperiosteal abscess (*small arrows*). Evidence of cellulitis is indicated by the increased enhancement in the medial aspect of the orbit. Another collection of pus is noted in the posterior right ethmoid sinus (*open arrow*)

pared to those elsewhere in the body, resolution of the vascular flow may be difficult. The use of dynamic MRA using TRICKS (time-resolved imaging of contrast kinetics) for orbital lesions has been reported in a small series with an 85% accuracy in identifying vascular entities [92]. More recently, assessing ADC values on DWI was found to be effective in distinguishing thrombosed and non-thrombosed venous malformations from other solid orbital tumors in a small series of patients [93]. However, in some cases, conventional arteriography is still necessary to assess flow patterns accurately.

Capillary Hemangiomas (Hemangioma of Infancy)

The capillary hemangioma represents the most common orbital vascular tumor of infants and is more common in females. It is often present at birth or becomes manifest shortly thereafter. Fetal imaging has revealed that capillary hemangiomas may be detected prior to birth. Hemangiomas often involve the eyelids, but they can also be located in the superficial and/or deep orbital components (Figs. 32.55, 32.56, and 32.57); clinical differentiation from other mass



Fig. 32.42 Subperiosteal abscess with intracranial extension. (**a**) Axial CT image of a patient with visual loss and proptosis. Note the slight tenting of the right globe. There is edema of the right medial extraconal fat and marked thickening of the right medial rectus muscle. (**b**) Coronal CT shows opacification of the right paranasal sinuses and a diffuse process displacing the medial rectus, superior rectus, and superior oblique muscle (*arrow*). The brain appears normal. Note that this is an unenhanced scan; contrast material helps to delineate subperiosteal orbital abscesses. (**c**) Because of the optic neuropathy, the patient was taken to the operating room urgently for drainage. Postoperatively, he developed meningeal signs. On coronal, postcontrast T1-weighted MRI with fat suppression, an epidural abscess is noted along the right frontal lobe (*arrow*). (**d**) Dural enhancement (*arrows*) consistent with meningitis is also seen. The patient responded to intravenous antibiotics

lesions is especially difficult in more deeply located tumors. In such cases, imaging plays an important role in the diagnosis. The extent and location of orbital hemangiomas varies, ranging from the frequent superomedial orbital location to total infiltration of the orbital contents and at times to intracranial extent. Also, hemangiomas may extensively involve the face, scalp, and neck (Fig. 32.58). Grossly, hemangiomas consist of multiple lobules separated by septa that contain vessels. Larger vessels which supply and drain the tumor can be identified on the periphery of the tumor.

Histologically, the tumors consist of numerous capillaries with extensively proliferating endothelial cells.

Capillary hemangiomas typically go through a growth spurt during the first year of life, usually during the first 6 months. They then begin to involute, largely disappearing within the next few years, but usually become complete by the sixth or seventh year of life. Generally, the more rapid the growth spurt, the more rapid the involution. During the involution phase, lobules of the tumor diminish in size, fatty tissue between them increases, and the vascularity of the lesion

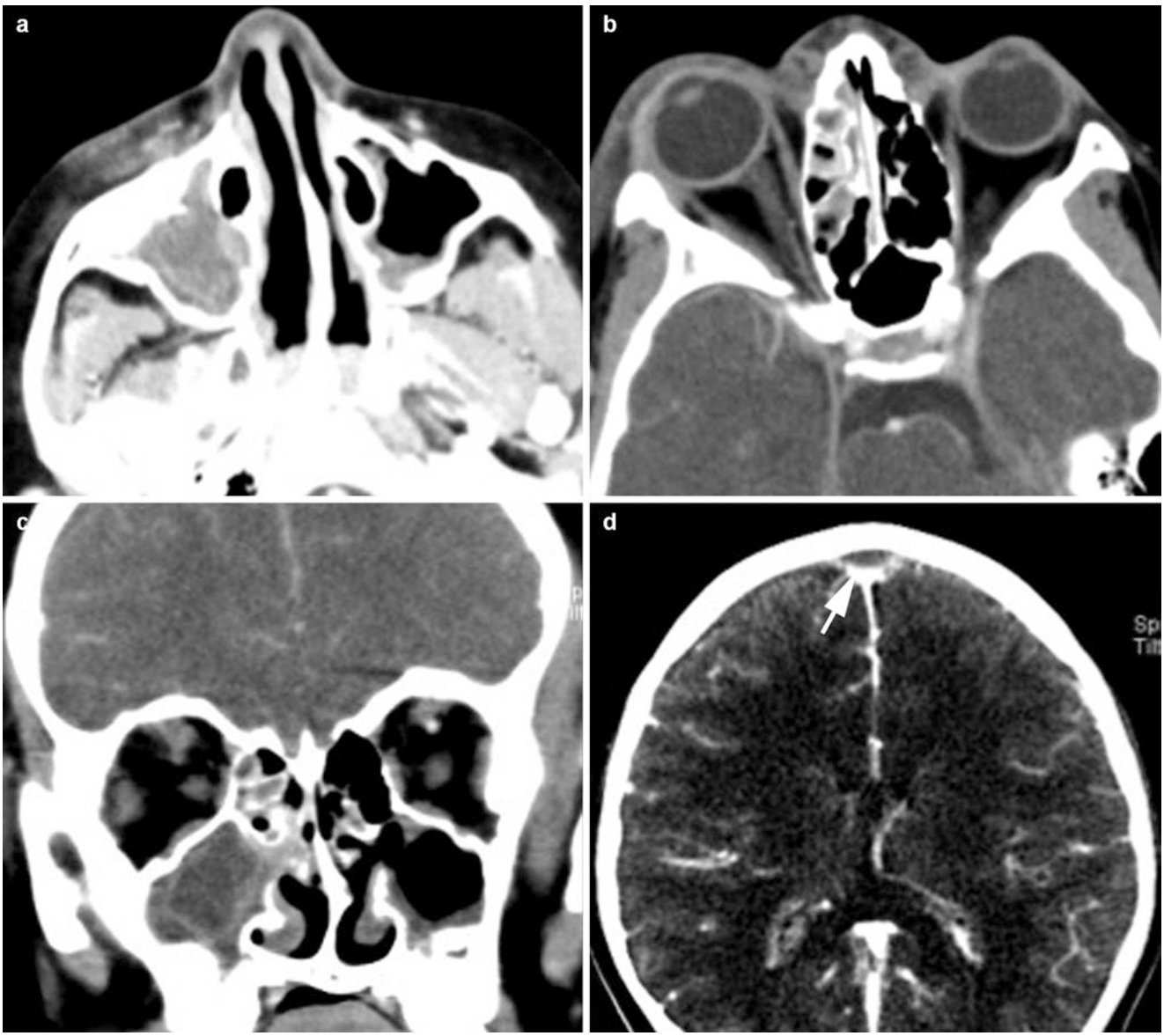


Fig. 32.43 Restricted diffusion from a subdural empyema. An 8-year-old boy presented with preseptal cellulitis, severe headache, and neck pain. Two contrast-enhanced axial soft tissue CTs (**a**, **b**) show swelling of the right cheek, preseptal cellulitis, and opacification of the right maxillary and ethmoid sinuses. (**c**) Contrast-enhanced coronal CT shows the right paranasal disease without intracranial abscess. (**d**) Axial contrast-enhanced CT obtained through the brain shows a small epidural abscess slightly displacing the sagittal venous sinus (*arrow*). Also seen is a very subtle thin low-density collection along the right frontal lobe. This type of extent is consistent with subdural collection.

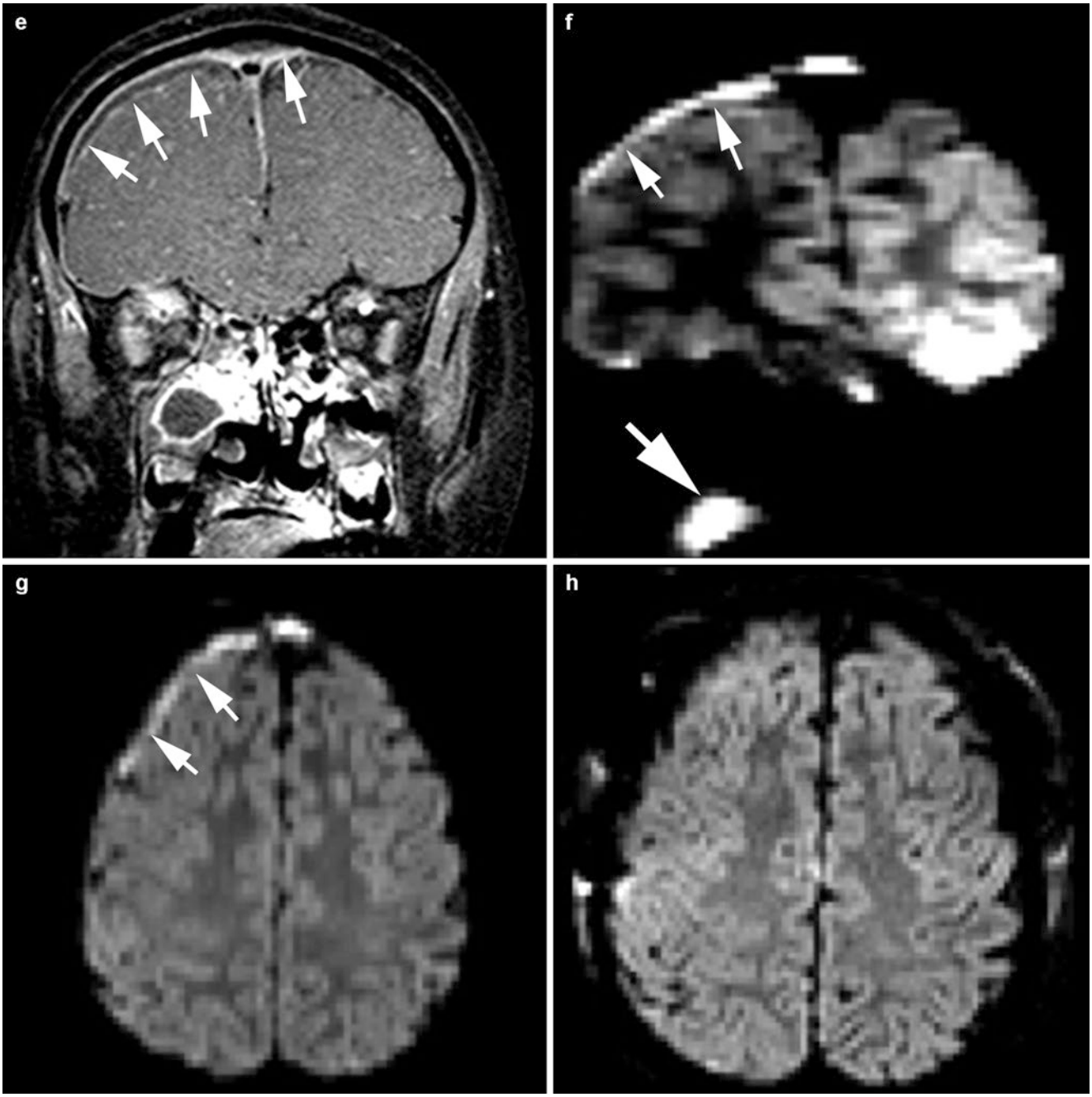


Fig. 32.43 (continued) (**e**) On coronal, postcontrast MRI with fat suppression, the subdural collection is evident (*arrows*). (**f**) On coronally imaged DWI, restriction is noted in the area of the collection (*small arrows*), highly suggestive of a subdural empyema. Also note restricted diffusion in the midline at site of the small epidural empyema and in the right infected maxillary sinus (*large arrow*). (**g**) Axial DWI demonstrated restricted diffusion within the collection. The patient was taken to the operating room urgently for drainage of the paranasal sinuses and the intracranial collection. Both a subdural and epidural empyema was found. (**h**) Postoperative axial DWI shows resolution of the restricted diffusion with no evidence of stroke. The patient recovered fully without neurologic deficits. The finding of a subdural empyema very frequently represents a neurosurgical emergency. If clinical findings raise the possibility of intracranial involvement by infection, MRI with DWI should be performed



Fig. 32.44 DWI and ADC of a subperiosteal abscess. (**a**) On postcontrast, T1-weighted coronal MRI with fat suppression, the subperiosteal abscess is hypointense (*arrow*) compared to enhancement of the adjacent inflamed periosteum. Also note the paranasal sinus congestion. There is also extensive contrast enhancement of the remaining orbital tissues indicating cellulitis. Thin dural enhancement is present along the right orbital roof and the frontal lobe. (**b**) On T2-weighted imaging, the abscess is hyperintense compared to intraconal fat. (**c**) On axial DWI, note the bright signal within the abscess cavity consistent with restricted diffusion (*arrow*). (**d**) On axial ADC, the signal becomes dark, again consistent with restricted diffusion. Compare the DWI and ADC signals within the abscess to those of the vitreous, which is essentially water with free diffusion

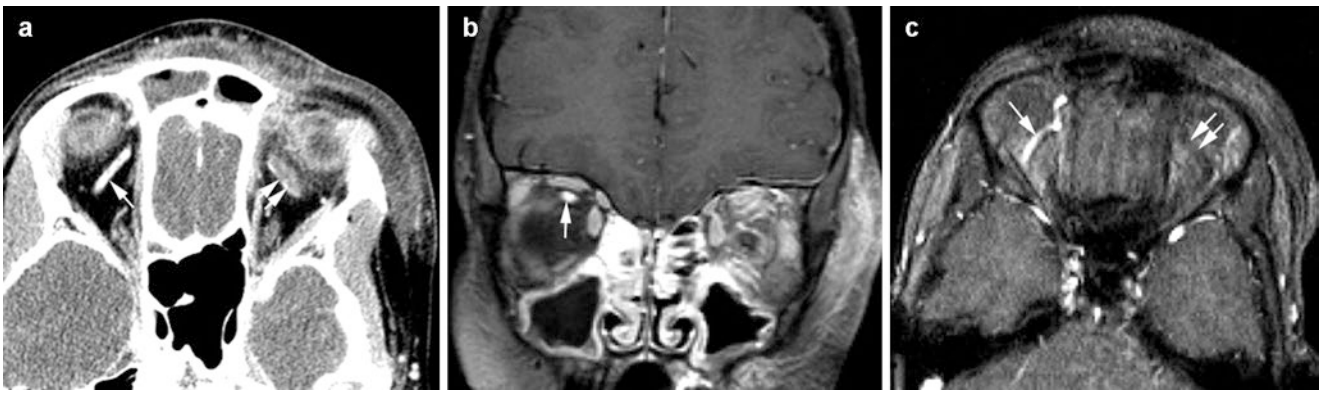


Fig. 32.45 Left orbital cellulitis with superior ophthalmic vein thrombophlebitis. (**a**) Contrast-enhanced axial CT shows normal enhancement in the right SOV (*single arrows*). Note the lack of contrast on the involved side (*double arrow*). (**b**) Coronal, postcontrast T1-weighted MRI with diffuse paranasal sinus disease and infiltration of the left intraconal space. The right SOV enhances normally (*arrow*). The thrombosed left SOV remains unenhanced. (**c**) Note the asymmetry between the normal right SOV (*single arrow*) and the thrombosed left SOV (*double arrow*) on MRV

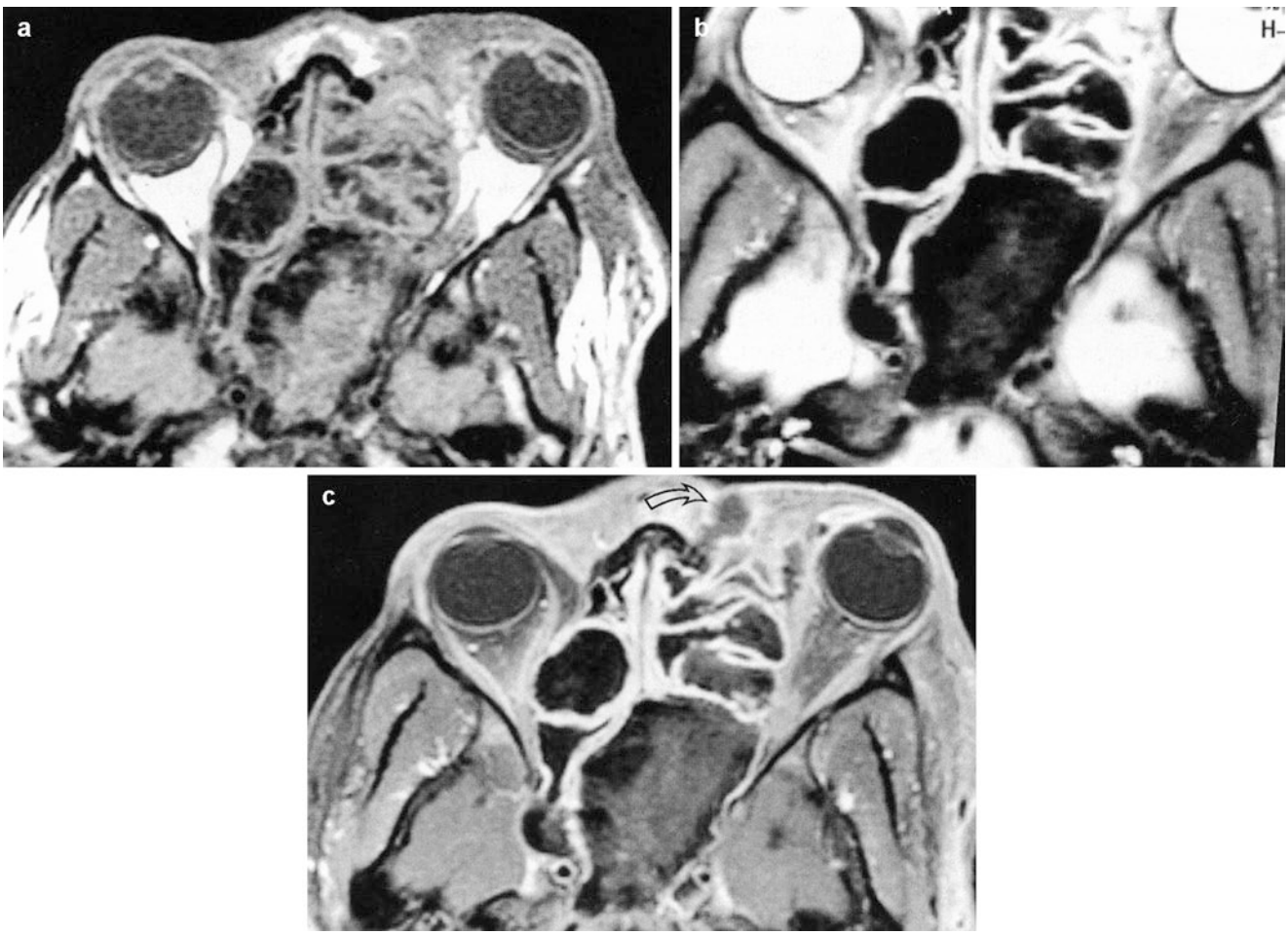


Fig. 32.46 Chronic aspergillosis of the paranasal sinuses. (**a**) Axial T1-weighted MRI shows marked expansion, greater on the left, of the ethmoid and sphenoid sinuses. As a result, there is encroachment into both orbits resulting in hypertelorism and proptosis, especially on the left. The content of the paranasal sinuses ranges in signal intensity from hypo- to isointense. Note that the regions of hypointensity seen within the sinuses are not air but are due to markedly desiccated material that produces hardly any signal. There is a fine reticular pattern within the hypointense material, helping to differentiate it from air. (**b**) T2-weighted axial MR shows that the contents of the sinuses have decreased in intensity in comparison to T1. There is evidence of increased signal in the mucosa lining the abnormal expanded sinus air cells. (**c**) Axial, postcontrast MRI with fat suppression again shows the markedly expanded hypointense ethmoid and sphenoid sinuses and enhancement of the sinus mucosa. There is breakout of the process (*arrow*) into the anterior soft tissues

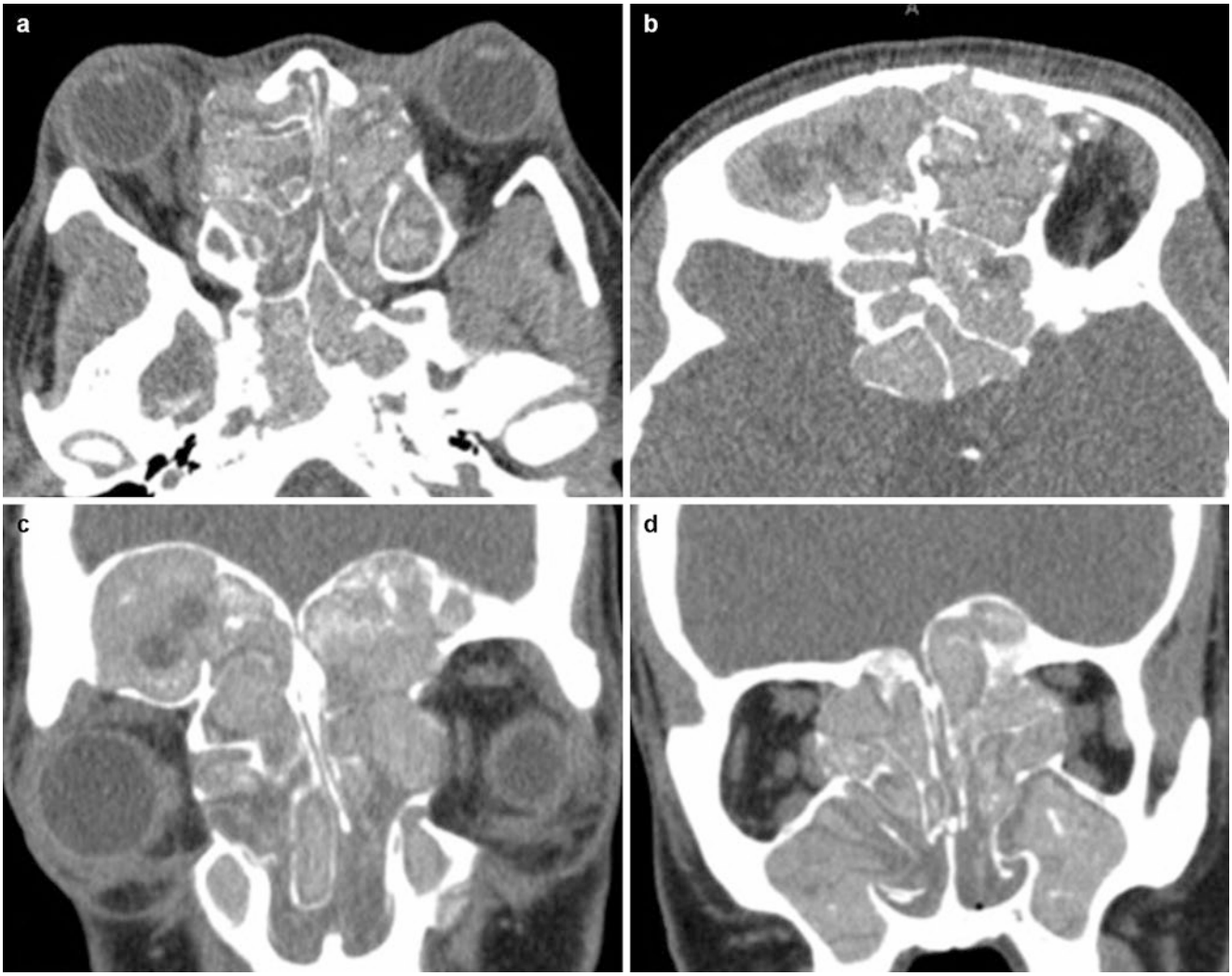


Fig. 32.47 Chronic sino-orbital aspergillosis on CT. (**a**, **b**) Axial soft tissue windows show a marked expansion and opacification of the paranasal sinuses, resulting in hypertelorism (note the position of the globes) due to expansion of the central face by the process. (**c**, **d**) Coronal soft tissue views. The opacification within the sinuses is heterogeneous, corresponding to the fungal mass and retained mucus. Also note the scattered calcification within the sinuses; this is typical and highly specific for sinonasal aspergillosis. The bones of the skull base have been remodeled between the sinuses, orbits, and anterior cranial fossa

decreases. Eventually, the lesion disappears completely. However, if the hemangioma was very large to begin with, focal bony orbital expansion with fatty tissue, containing mild fibrosis and vessels, may remain.

Imaging plays an important role in detecting capillary hemangiomas, particularly when the lesions are deep and thus their nature is not obvious to the clinician [89]. Imaging is especially helpful in differentiating a capillary hemangioma, with its lobules and flow voids, from other pathologies such as rhabdomyosarcoma (which is solid), metastatic neuroblastoma (which is solid, permeating bone, and forming bony spicules), and venolymphatic malformations (which often consist of cysts of varying size). Both CT and MRI show an irregularly marginated mass that enhances prominently after intravenous injection of contrast material. However, MRI is the best technique for characterization of hemangiomas. Capillary hemangiomas have slightly higher intensity than muscle on T1-weighted images and become hyperintense to fat and muscles on T2-weighted images. On both T1- and T2-weighted images, the characteristic heterogeneity caused by the interlobular vessels and septa is seen. To demonstrate and delineate the lesion best, it is necessary to have a contrast-enhanced T1 image where the fat is suppressed and a T2-weighted image that is also fat suppressed. Suppression of signal from fat leads to much greater conspicuity of the capillary hemangiomas. In addition to helping to predict the correct histology of the lesion, MRI not only delineates the mass precisely and shows its effect and relationship to adjacent structures but can also be utilized to monitor the response to therapy. Finally, serial MRI avoids

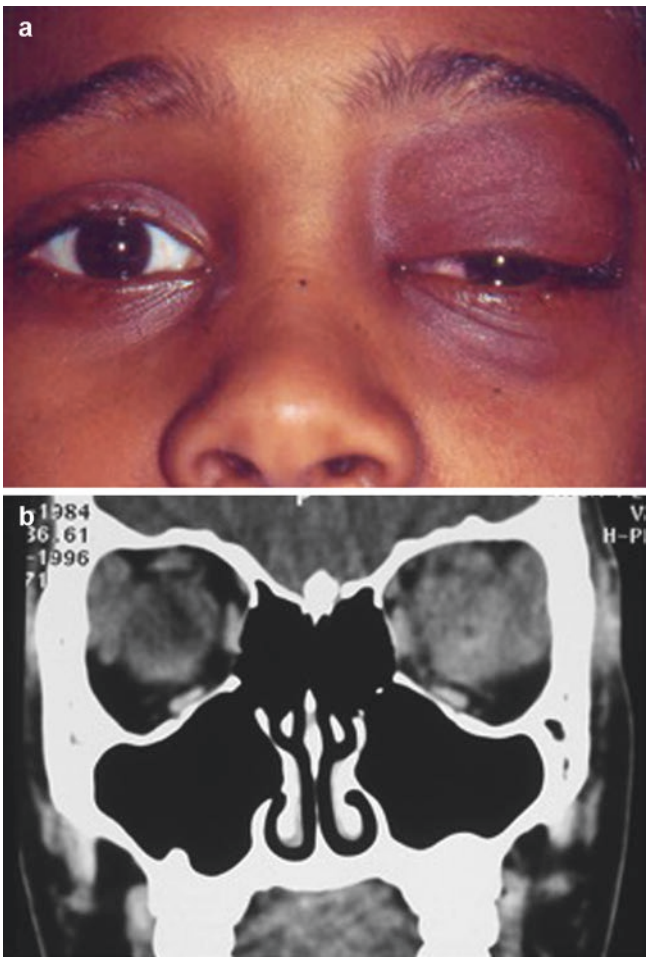


Fig. 32.48 Pediatric IOI. This 13-year-old child presented with pain of sudden onset, proptosis, external ophthalmoplegia, and low-grade fever. (**a**) Note the "boggy," somewhat pink edema of the left eyelids. (**b**) An urgent CT was obtained. On this coronal soft tissue window, the paranasal sinuses are completely clear. A poorly defined opacification is present within the left intraconal space surrounding the optic nerve. There was no evidence of foreign body. The patient's signs and symptoms cleared completely within 48 h of initialing corticosteroids

any cumulative radiation effects of serial CT, an important consideration in the very young children who harbor capillary hemangioma.

Orbital Lymphaticovenous Malformations

The long-used term lymphangioma causes confusion because this lesion does not represent a true vascular neoplasm but rather a vascular malformation. Lymphangioma has been recently subsumed into the broader category of *orbital lymphaticovenous malformation* (OLM). OLM has been classified as no flow (type 1), venous flow (type 2), and arterial flow (type 3) by the Orbital Society [94] and as venous dominant or lymphatic dominant by the ISSVA [89, 95]. Venous-dominant lesions maintain communication with normal circulation and expand with a Valsalva maneuver, while lymphatic dominant lesions do not.

Many OLMs are combined malformations, having characteristics of both venous and lymphatic components. They occur frequently in the head and neck region, including the orbit, becoming evident at birth or during early childhood. They often present abruptly due to intralesional hemorrhage ("chocolate cyst"), which can cause lid and forehead mass, proptosis, and, when massive and intraconal, even optic nerve compression and decreased motility. The hemorrhage is thought to be due to minor trauma, stagnation of blood, or spontaneous due to the fragile nature of the neovascular tufts. The lesions may also enlarge when a patient develops head and neck or respiratory infections, possibly due to hyperplasia of the lymphatic component of the malformation.

As already noted, clinical evaluation of patients with lymphatic dominant OLM will fail to reveal change in size of the lesions with Valsalva maneuver or with change in head position; one of the criteria for differentiation of these lesions from orbital varices is the lack of communication with systemic circulation. Valsalva maneuver can be used both clinically and radiographically to distinguish OLM from a venous malformation (varix). Multidetector CT technique can easily image a patient's orbits in one breath hold, revealing dilation of the lesion [89, 96]. Dynamic CTA with a Valsalva maneuver during the venous phase may also be helpful in identifying both arterial and venous components of each lesion but should be used sparingly in young children because of increased radiation exposure compared to routine CT [89].

OLMs lack a capsule and often cross anatomic compartments; thus, they can have both intra- and extraconal components. Histopathologically, the lesions are composed of thin-walled, endothelial-lined channels, some containing serous fluid and/or blood. There is great variability between the lesions and within a given lesion as to size of the channels, ranging from very large cysts to spongelike microcystic spaces [89]. The lesions often contain new and old blood products, lymphocytic aggregates, bundles of smooth muscle fibers, and loose connective tissue septa [97]. The presence of hemosiderin, cholesterol clefts, lipid-laden macrophages, and foreign body reaction indicates previous hemorrhages.

The gross pathologic heterogeneity of OLMs is reflected in both CT and MR images, but particularly on MRI, which is better than CT in delineation and characterization of OLMs. MRI can detect the presence of old blood products and shows with greater detail the various components of the lesion [89]. The OLMs sometimes appear to consist of a single large cyst containing blood (also referred to as cystic hygroma) (Fig. 32.59) or to be composed of tiny serpiginous channels/cysts that infiltrate tissues and show partial contrast enhancement (Figs. 32.60, 32.61, and 32.62) [89]. The sites of most prominent contrast enhancement correspond to venous channels within the lesion and the sites from which hemorrhages

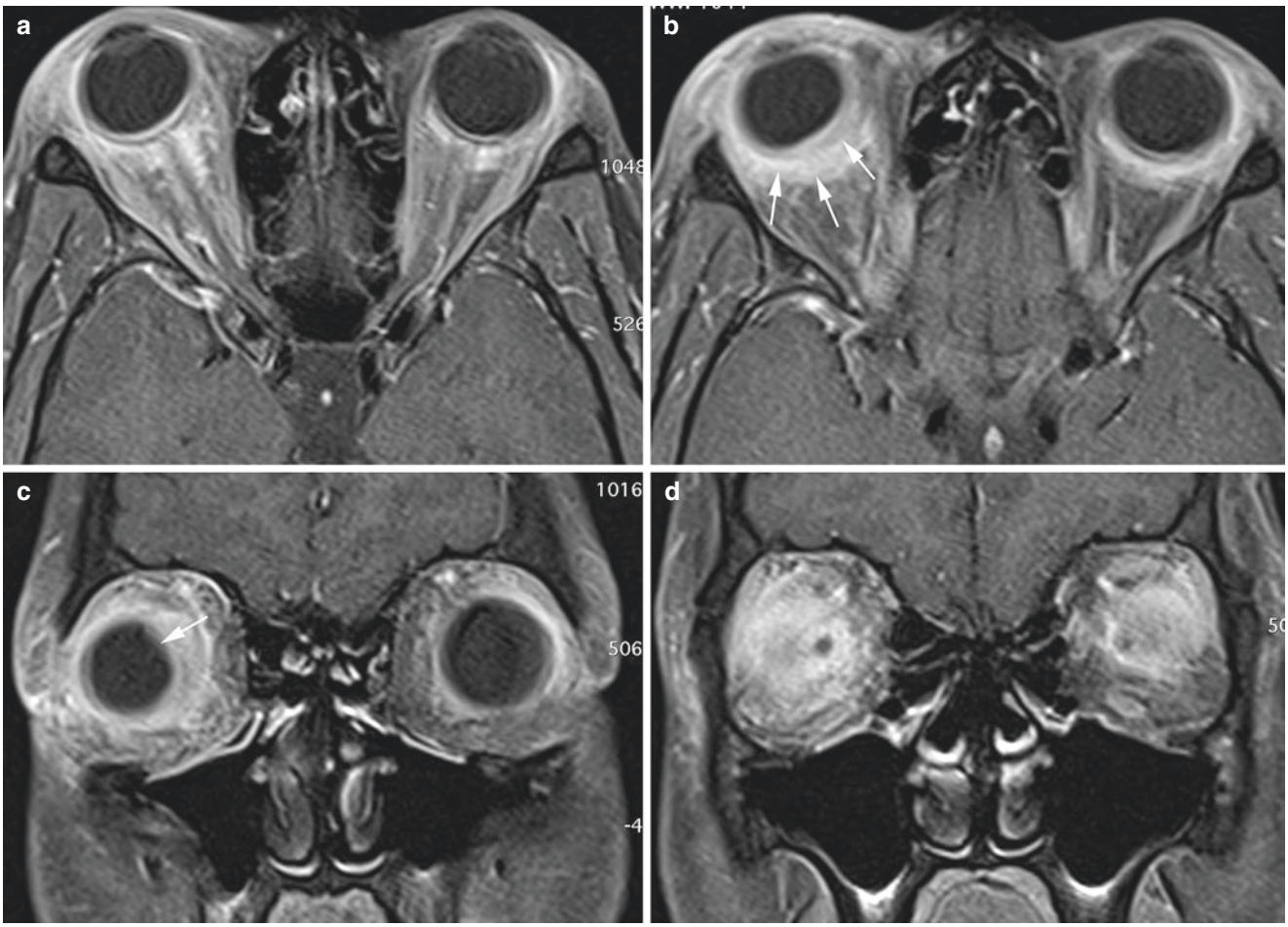


Fig. 32.49 IOI and posterior scleritis. This teenager noted recurrent bout of acute eyelid swelling and redness associated with pain. He underwent multiple courses of oral and intravenous antibiotic therapy for suspected orbital cellulitis. During his last event, the patient noted blurred vision in the right eye. Examination showed choroidal and retinal folds across the macula. An MRI was performed. Postcontrast T1-weighted images with fat suppression are shown. (**a**) Axial image shows enhancement around the right optic nerve spilling into the surrounding fat of the intraconal space. Choroidal thickening is also present. (**b**) Note enhancement involving the posterior sclera (*arrows*). Also note the distortion of the posterior curvature of the globe. (**c**) Coronal view shows enhancement around the sclera, with distortion of the globe (*arrow*). (**d**) Coronal view posterior to the globe shows diffuse enhancement of the intraconal fat surrounding the optic nerve. The patient's signs and symptoms resolved with 72 h of corticosteroid therapy



Fig. 32.50 Recurrent IOI (myositis). Sequential CT and MRI of a child with bilateral myositis who manifested signs and symptoms only on the left side in August 2007. Note the diffuse enlargement of the extraocular muscles bilaterally. Repeat imaging demonstrates significant resolution of extraocular muscle inflammation 1 month after oral corticosteroid treatment was instituted. In February 2008, she had a recurrence of her symptoms on the left side only (note the enlargement of the medial, lateral, and superior rectus muscles on MRI) and was treated successfully with methotrexate and infliximab

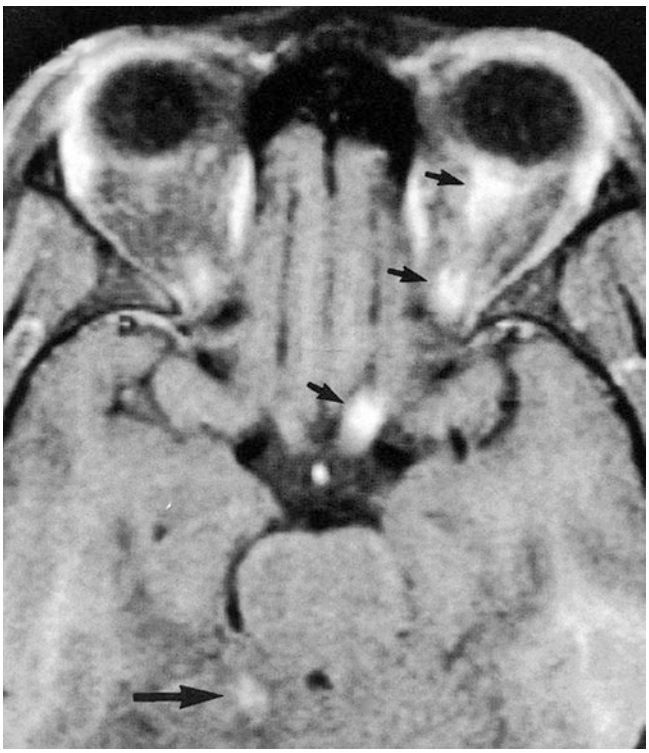


Fig. 32.51 Optic neuritis in an 11-year-old girl with multiple sclerosis. Postcontrast axial T1-weighted MRI with fat suppression shows enlargement and enhancement of the left optic nerve (*short arrows*). There is also an enhancing plaque (*long arrow*) in the right cerebellum consistent with demyelinating disease

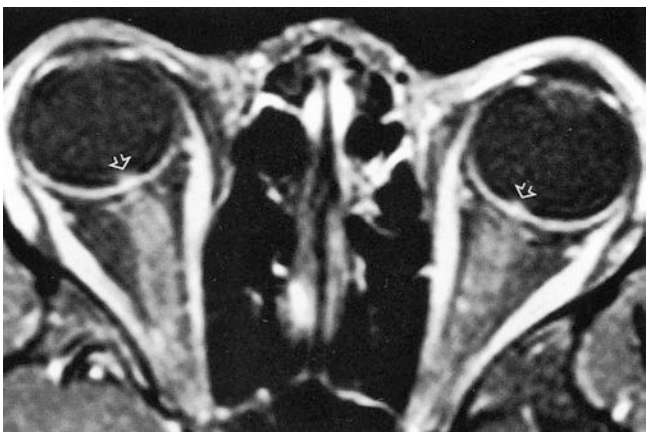


Fig. 32.52 Bilateral optic neuritis and papillitis. Axial T1-weighted, postcontrast MRI with fat suppression demonstrates elevation and enhancement of the optic discs (*arrows*). The optic nerve/sheath complexes are enlarged and show enhancement

originate [97]. Such hemorrhages may cause acute prominent proptosis (Fig. 32.60). MRI provides critical information for management of patients, particularly if decompressive surgery, needle drainage, or sclerotherapy is contemplated, by showing the site of the hemorrhagic component and its effect on the adjacent structures, such as the optic nerve.

Neoplasms

Retinoblastoma

Retinoblastoma, which arises from neuroectodermal cells, is the most common intraocular malignancy of childhood, with an incidence between 1 in 15,000 and 1 in 30,000 live births [98]. The tumor accounts for 1% of early childhood deaths and 5% of childhood blindness in the United States. Although the tumor is congenital, it is usually not recognized at birth [99]; the average age at the time of diagnosis is 13 months in the United States [100] and may be much later in some parts of the world [101]. While both ophthalmoscopic and B-scan ultrasonographic examinations are invaluable in the diagnosis of retinoblastoma, patients may need to be evaluated with CT or MRI to determine the number of tumors and whether there is retrobulbar/optic nerve or intracranial spread [102]. Neuroimaging is also helpful in ruling out the possibility of the "trilateral retinoblastoma," which affects both eyes and the pineal gland (pineoblastoma). CT is particularly helpful in patients in whom the diagnosis of retinoblastoma is unclear because of its sensitivity in demonstrating the characteristic DNA–calcium complexes within the tumor (Fig. 32.63) [99]. However, MRI is superior to CT in extraocular localization of lesions (particularly within the optic nerve) and in differentiation of tumor from retinal fluid (Fig. 32.64). MRI also supersedes CT in the differentiation of various intraocular lesions that cause leukocoria and in detection and delineation of optic nerve involvement, extraocular spread, and intracranial metastases [102].

Retinoblastoma appears on CT as a calcified intraocular mass that shows contrast enhancement (Fig. 32.63). The calcifications may be small or large and may be single or multiple. On MRI, the tumor is slightly to moderately hyperintense to vitreous on T1 weighting and becomes prominently hypointense on T2 weighting (Fig. 32.64). Unless the tumor is densely calcified, the calcifications may not be detected on MRI. Retinoblastoma detection by MRI is improved when gadolinium and fat suppression are utilized. The tumor shows moderate to marked enhancement with contrast. Because the lesion is highly cellular, retinoblastoma also restricts diffusion on DWI (Fig. 32.65). DWI may be helpful in following patients with retinoblastoma following therapy (Fig. 32.66).

Optic Nerve Glioma

Gliomas of the visual pathway have been the subject of great interest as well as much controversy because of their variability in growth and extent and because of their unpredictable behavior [103–108]. There has even been disagreement as to their nature – whether they represent true tumors or

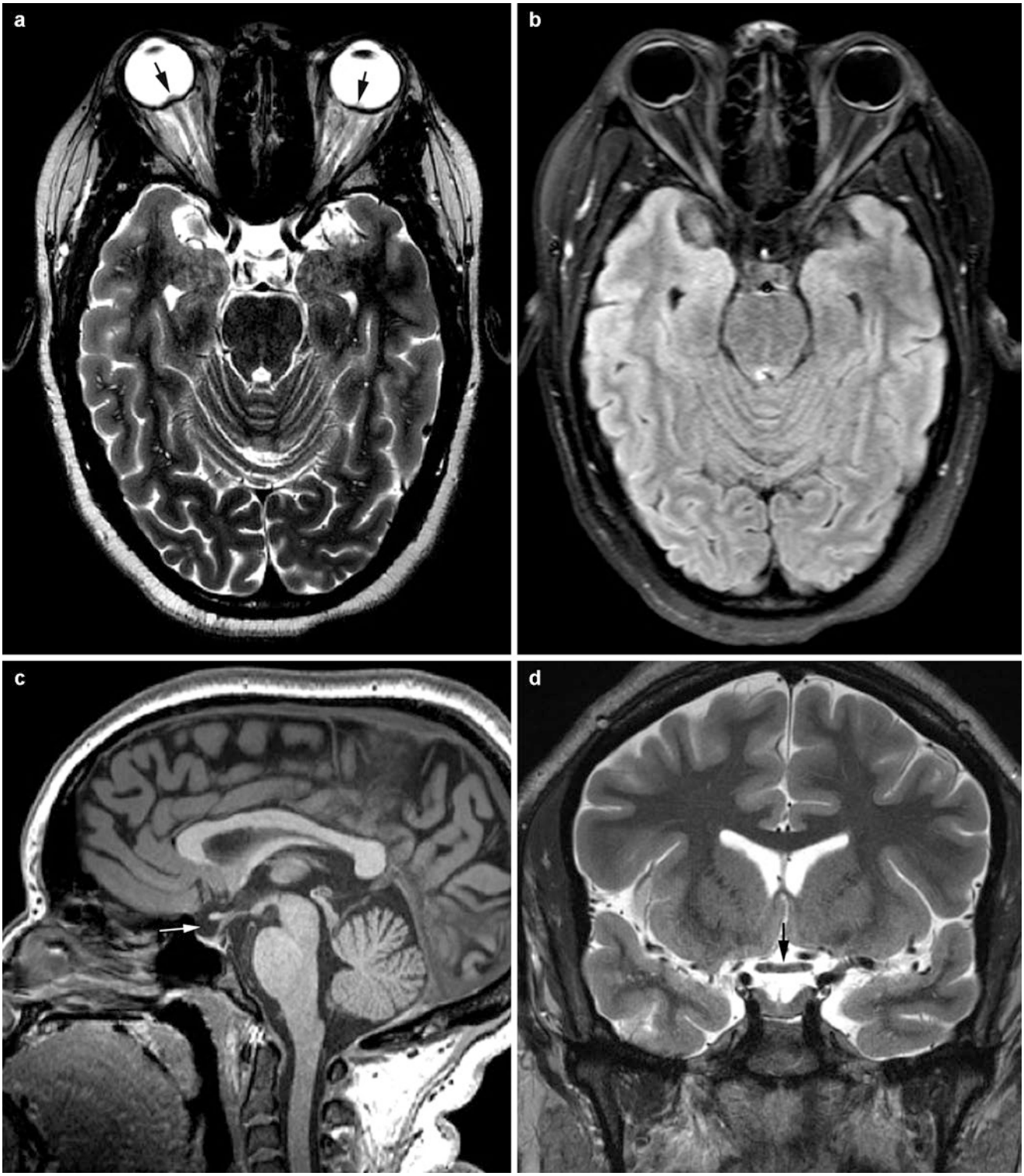


Fig. 32.53 DWI of ischemic papillitis. (**a**, **b**) Axial T2-weighted and FLAIR MRI of a 17-year-old girl with idiopathic intracranial hypertension (pseudotumor cerebri). Note the elevated optic nerve heads (*arrows*). The ventricles and sulci are prominent. Posterior globe flattening is also obvious on the FLAIR image. (**c**) A sagittal T1-weighted image shows a partially empty sella (*arrow*). (**d**) On coronal T2 weighting, the optic chiasm is obvious (*arrow*) surrounded by the bright signal of CSF. In a patient of this age, the pituitary gland should be robust and bulge slightly against the chiasm. In this case, CSF signal is seen between the pituitary gland and the chiasm because of the partially empty sella.



Fig. 32.53 (continued) (**e**) On axial, postcontrast T1-weighted MRI with fat suppression, enhancement of the optic nerve heads and nerve sheaths is present. (**f**) On axial DWI, restricted diffusion is present in the optic nerve heads (*arrows*), consistent with ischemic papillitis



Fig. 32.54 Optic nerve sarcoid. A 15-year-old boy presented with progressive, painless visual loss in the right eye over months. Poor vision and pale right optic nerve were present on clinical exam. An MRI was performed. (**a**) Axial, T1-weighted postcontrast image with fat suppression shows diffuse enhancement of the optic nerve/sheath complex along the entire intraorbital, intracanalicular, and prechiasmal course of the right optic nerve (*arrows*). The chiasm is normal. (**b**) Coronal image shows enhancement across the entire area of the optic nerve and surrounding sheath (*arrow*). Systemic work-up was unremarkable. An optic nerve biopsy showed granulomatous inflammation consistent with sarcoidosis. The patient was treated with methotrexate. Two years later, he developed pulmonary symptoms with an elevated serum angiotensin-converting enzyme

hamartomas, although recent reports lend support to the former [109–112]. Optic pathway glioma is the most frequent tumor of the optic nerve in children and usually presents during the early part of the first decade with progressive, nonpulsatile exophthalmos and limitation of eye movement. There is a slight female predominance. Most of the tumors are pilocytic astrocytomas. There is a high association between the optic gliomas and neurofibromatosis type 1 (NF-1), with some series reporting >50% association [113]. The exact incidence is not known because of incompleteness of some published reports; the reported incidence of optic gliomas in NF-1 patients generally ranges from 15% to 21%.

The evaluation and management of visual pathway gliomas is difficult because of their erratic growth pattern, need for long-term follow-up, and, at times, lack of correlation between symptomatology and morphology of the tumor. Until the advent of the modern imaging with CT and MRI, but particularly MRI, the actual extent of the gliomas as well as the associated brain changes seen in NF-l [114] could not be appreciated. Therefore, the experience accumulated in the

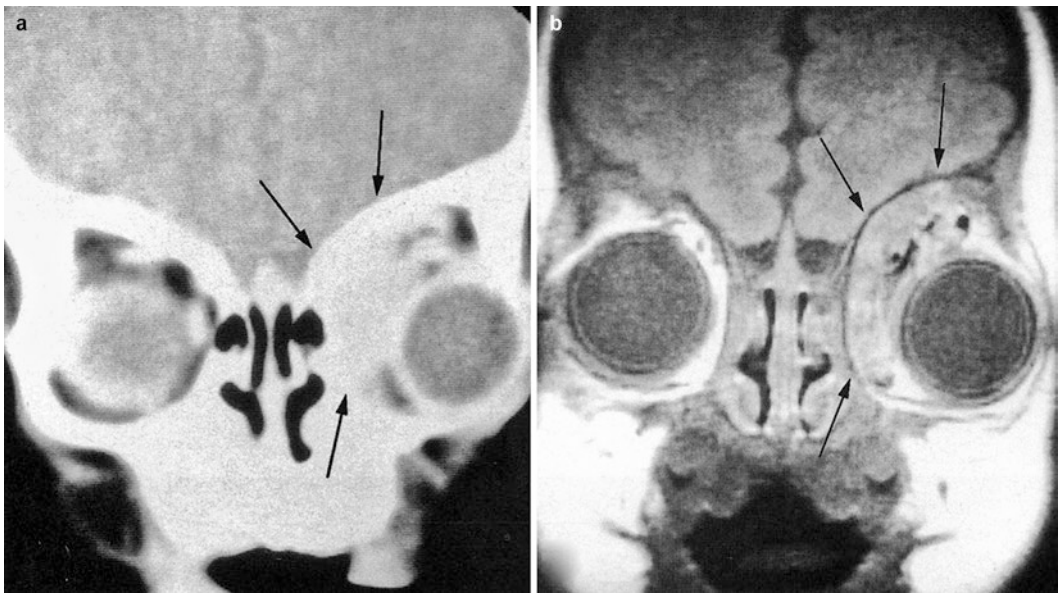


Fig. 32.55 Capillary hemangioma. Capillary hemangioma in the left orbit that presented with rapid development of proptosis in an infant. (**a**) Coronal contrast-enhanced CT reveals a large contrast-enhancing mass (*arrows*) in the superomedial aspect of the left orbit. The mass displaces the globe inferolaterally. (**b**) Coronal T1-weighted MRI better reveals the internal architecture of the capillary hemangioma (*arrows*). It is heterogeneous due to multiple lobules and hypointense round or curvilinear vessels. Also well demonstrated is the expansion of the left orbit, which is much larger than the normal right orbit

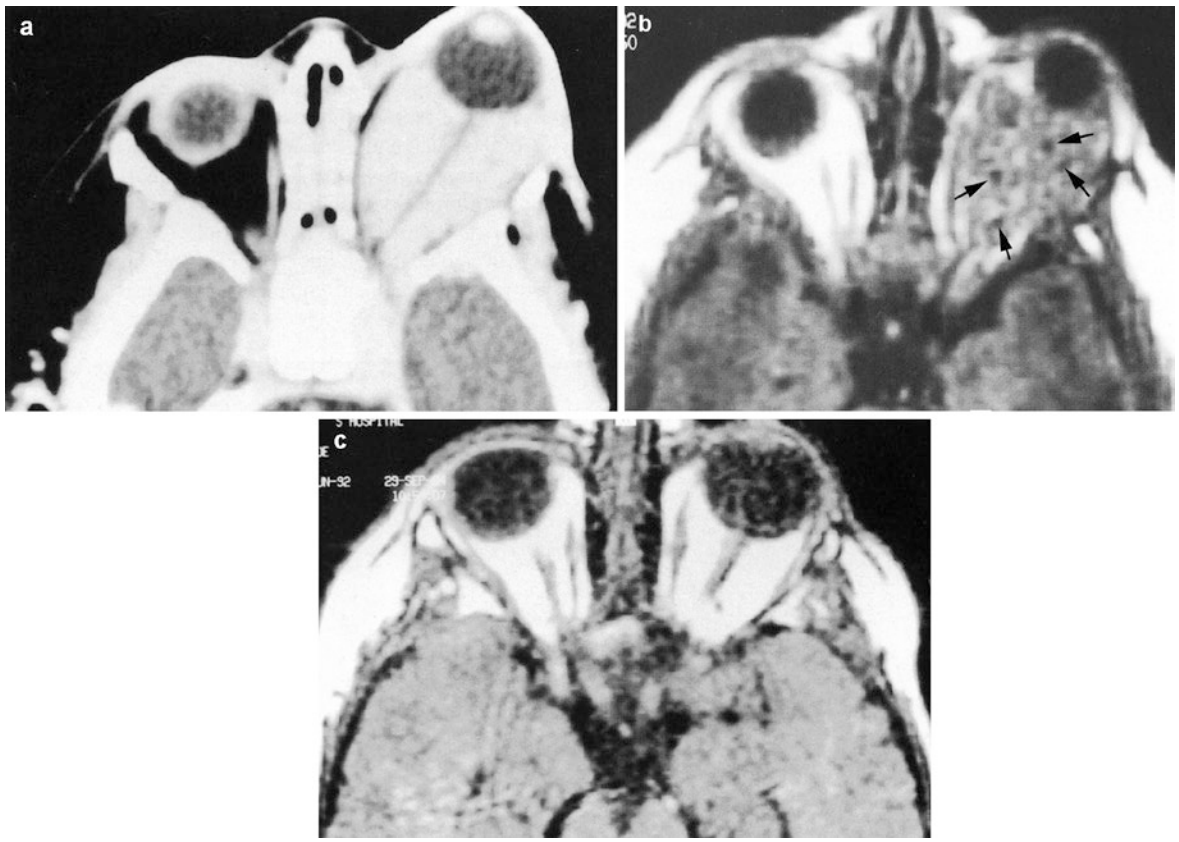


Fig. 32.56 Capillary hemangioma. Large, diffuse capillary hemangioma which presented with rapidly developing proptosis. (**a**) Axial CT after contrast enhancement reveals a contrast-enhancing mass filling and expanding the left orbit with stretching of the left optic nerve. (**b**) T1-weighted MRI reveals multiple lobules and signal voids (*arrows*) within this mass, typical of a capillary hemangioma. (**c**) A follow-up scan, 2 years after initial diagnosis, reveals complete resolution of the capillary hemangioma. This hemangioma was initially misdiagnosed as another tumor, and a biopsy was performed elsewhere by a lateral approach. The pathologic findings raised a question of neurofibroma, and an orbital exenteration was contemplated. After referral, however, the specificity of MRI findings led to correct diagnosis and management with oral steroids

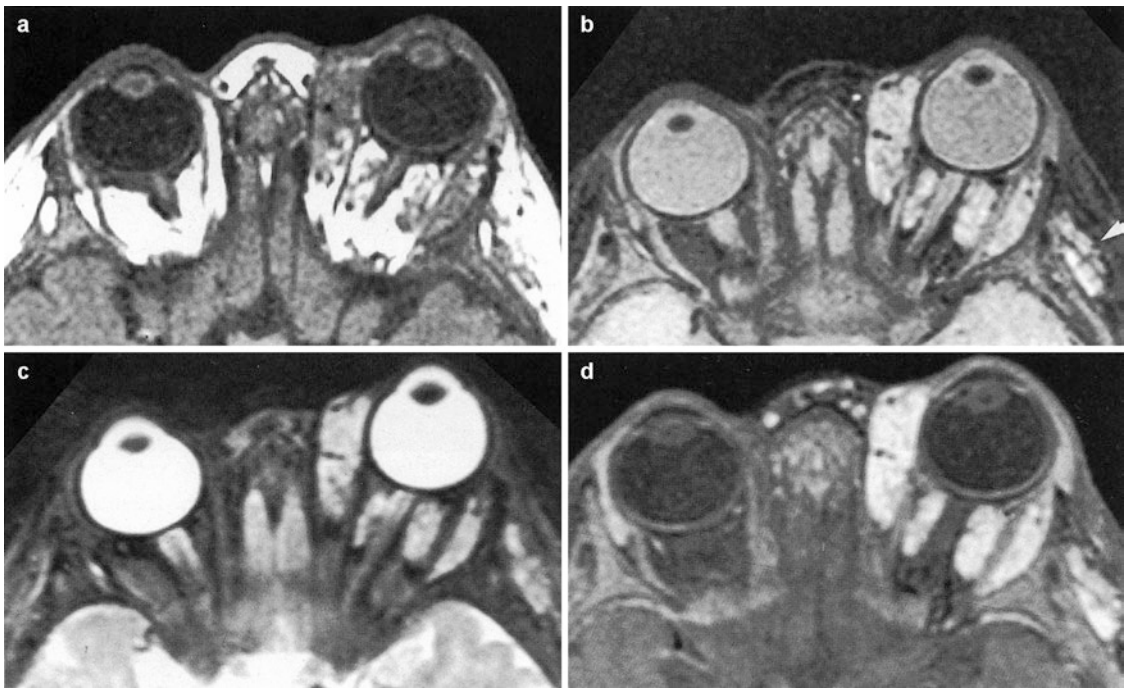


Fig. 32.57 Capillary hemangioma. Large capillary hemangioma of the left orbit demonstrated with various MRI sequences. (**a**) Axial T1 MRI shows a poorly defined heterogeneous mass involving both the extraconal and intraconal components of the left orbit. Dot-like flow voids within the mass indicate vessels. (**b**) An axial T2 STIR image of the orbit reveals the internal architecture of the capillary hemangioma, showing multiple internal lobulation as well as flow voids. With this sequence, orbital fat is hypointense, and the fluid-containing structures show moderate intensity but less than the lesion. In addition to the intraorbital component, there is also a small lobule (*arrow*) in the temporalis fossa. Note how the hemangioma encases the medial and lateral rectus muscles and the optic nerve/sheath complex. (**c**) Axial T2-weighted image reveals moderately increased intensity within the hemangioma. Again, multiple lobules and vessels are demonstrated within the lesion. (**d**) Axial, postcontrast T1-weighted image with fat suppression reveals prominent enhancement of the hemangioma

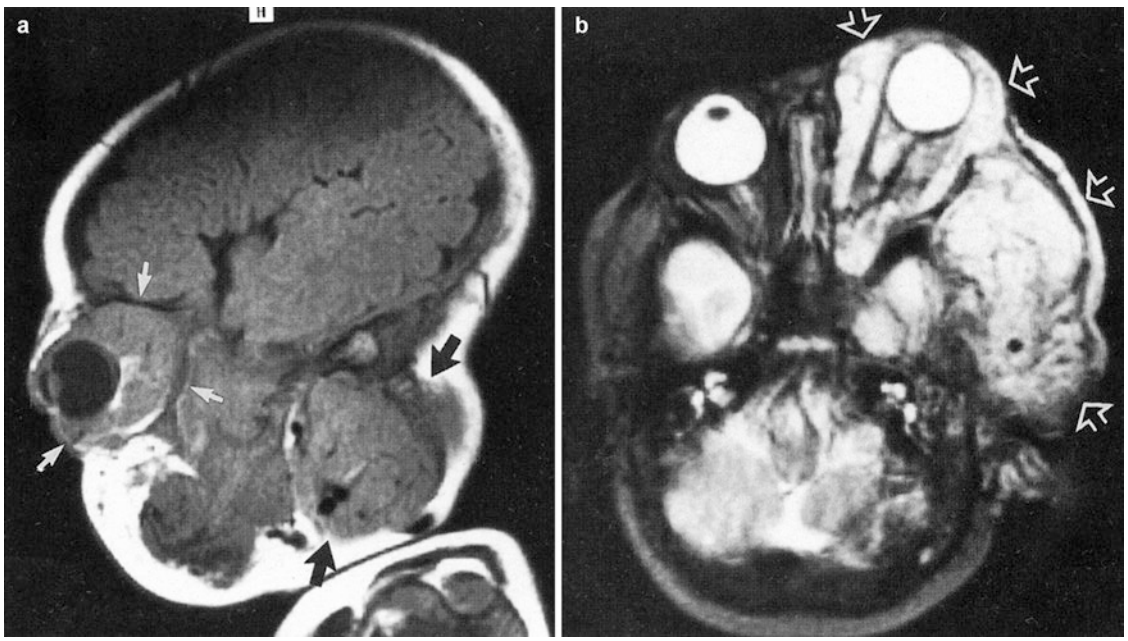


Fig. 32.58 Extensive orbital and neck capillary hemangioma in a 2-month-old girl. (**a**) Sagittal T1-weighted MRI shows marked expansion of the left orbit and encasement of the globe by a capillary hemangioma (*white arrows*). Several large vessels, seen as signal voids, are present in the neck portion of the hemangioma (*black arrows*). Also note fine linear hypointensities separating lobules within the orbital and neck portions of the hemangioma. (**b**) Axial T2-weighted MRI shows increased intensity with fine linear hypointensities in the large hemangioma (*arrows*)

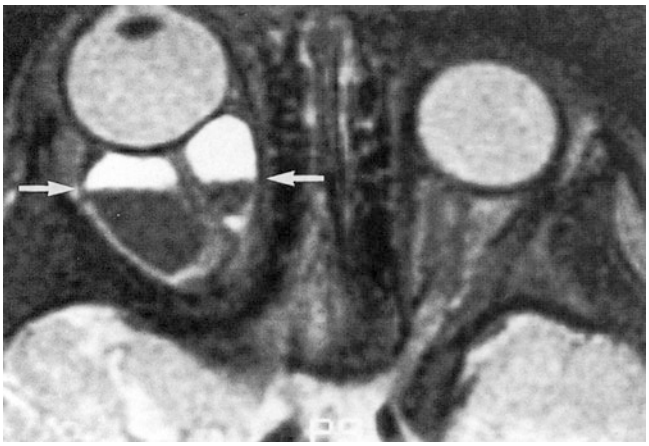


Fig. 32.59 Hemorrhagic cystic hygroma. Hemorrhagic cystic hygroma of the right orbit in a 2-year-old girl with two episodes of acute painless proptosis. Axial T2-weighted MR of a large cystic intraconal lesion conforming to the bony orbit and containing a fluid–fluid level (*arrow*) within it. The dependent, very dark (hypointense) content of the cyst is due to deoxyhemoglobin, while the hyperintense portion consists of methemoglobin (Courtesy of Dr. Neil R. Miller, Baltimore, MD)

literature is usually variable and inconsistent, not only because the series reported reflect different eras of radiologic imaging but also because the clinical data are frequently incomplete. Optic pathway gliomas are considered to be rare orbital tumors, but at pediatric hospitals with large ophthalmology and oncology departments and dedicated neurofibromatosis clinics, such tumors are encountered frequently. Some visual pathway gliomas are even discovered on routine screening of NF-1 patients, before the tumors have manifested clinically.

MRI with contrast material enhancement is the modality of choice for evaluation of the visual pathway gliomas. It is more sensitive and precise than CT in delineation of intracranial components of visual pathway gliomas and NF-1-related changes, and it is more accurate in demonstrating the architecture of intraorbital gliomas. The variability in morphology and pathologic features of optic nerve gliomas is reflected on CT but is far superior on MR images. Enlargement of the optic nerve–sheath complex may be tubular (Fig. 32.67), fusiform (Figs. 32.68 and 32.69), or focal

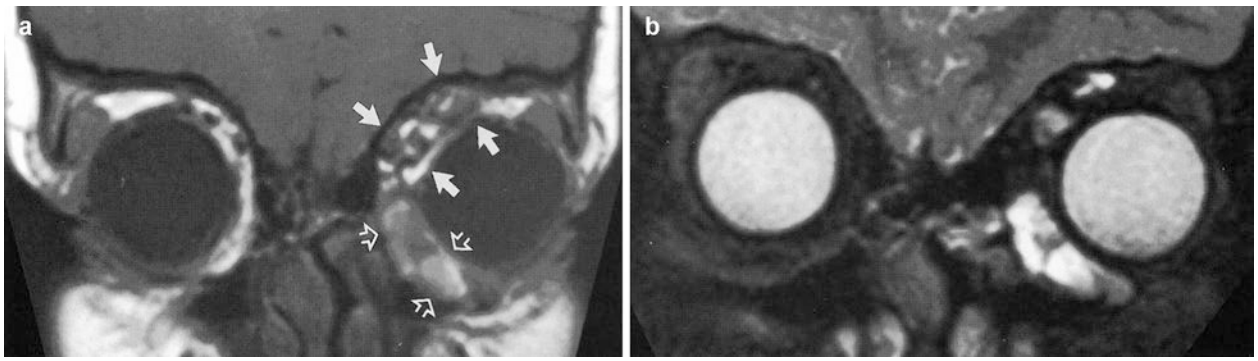


Fig. 32.60 OLM (lymphangioma) in a 7-year-old girl. (**a**) Coronal, precontrast T1-weighted MRI reveals a multilobulated, heterogeneous mass (*arrows*) in the left orbit. *Open arrows* indicate those regions that are of higher intensity due to hemorrhage (blood in methemoglobin stage). (**b**) T2-weighted coronal image shows well the typical multilobulated and heterogeneous pattern within an OLM

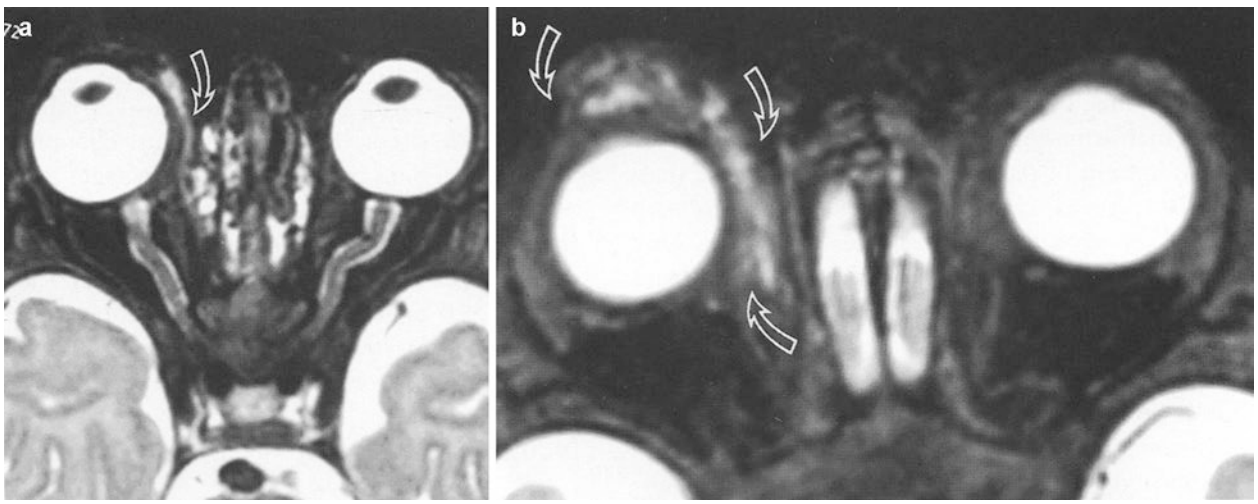


Fig. 32.61 OLM (lymphangioma) of the right orbit in a 7-month-old boy. (**a**) Axial T2-weighted MRI at the level of the globes reveals a small portion of the OLM as a linear increased intensity (*arrow*). Note the excellent delineation of the optic nerves and the subarachnoid space containing CSF around them. (**b**) Axial T2-weighted MRI obtained at a slightly higher level reveals the rest of the heterogeneous, finely multilobulated lesion (*arrows*)

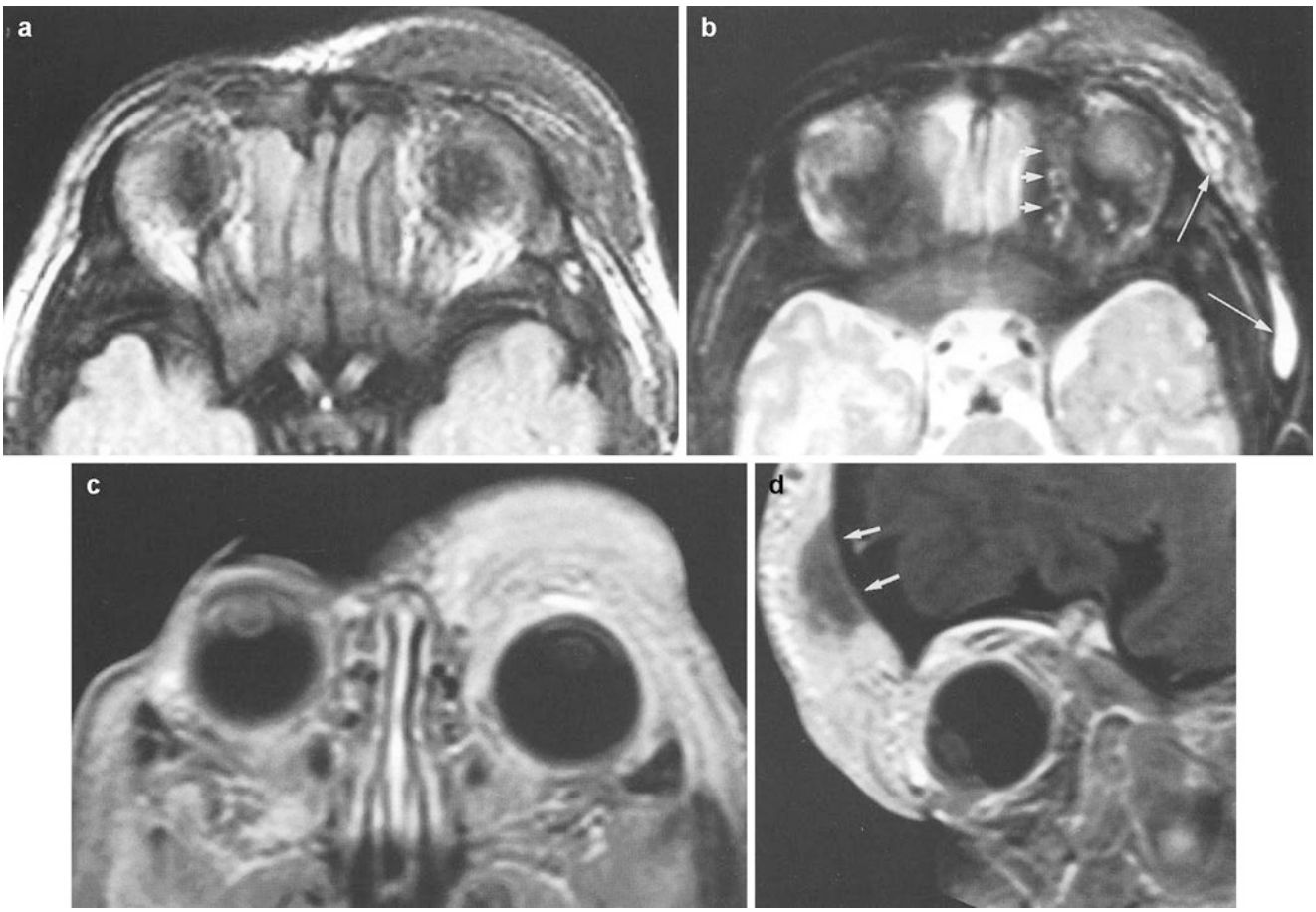


Fig. 32.62 Capillary OLM (lymphangioma) in a newborn. The patient was born with left facial and scalp mass which was thought to be related to trauma during birth. However, no change was noted over a period of 2 weeks, and CT was interpreted as showing old hematoma. MRI was performed to further characterize the mass. (**a**) Axial inversion recovery MRI shows a large mass with a linear serpiginous pattern within it anterior to the left orbit. (**b**) Axial T2-weighted image shows that the mass has an intraorbital component (*arrows*) along with focal collections of fluid (*long arrows*). (**c**) Axial, postcontrast MRI with fat suppression reveals fairly homogeneous enhancement of the mass, but containing a fine linear/serpiginous pattern. (**d**) Sagittal, postcontrast MRI with fat suppression shows a fine beadlike pattern within the mass along with a large collection of hypointense fluid (*arrow*) in the portion of the OLM on the forehead. The amount of contrast enhancement suggests either a large venous component to the venolymphatic malformation or an infectious/inflammatory component not typically seen in a lymphatic malformation

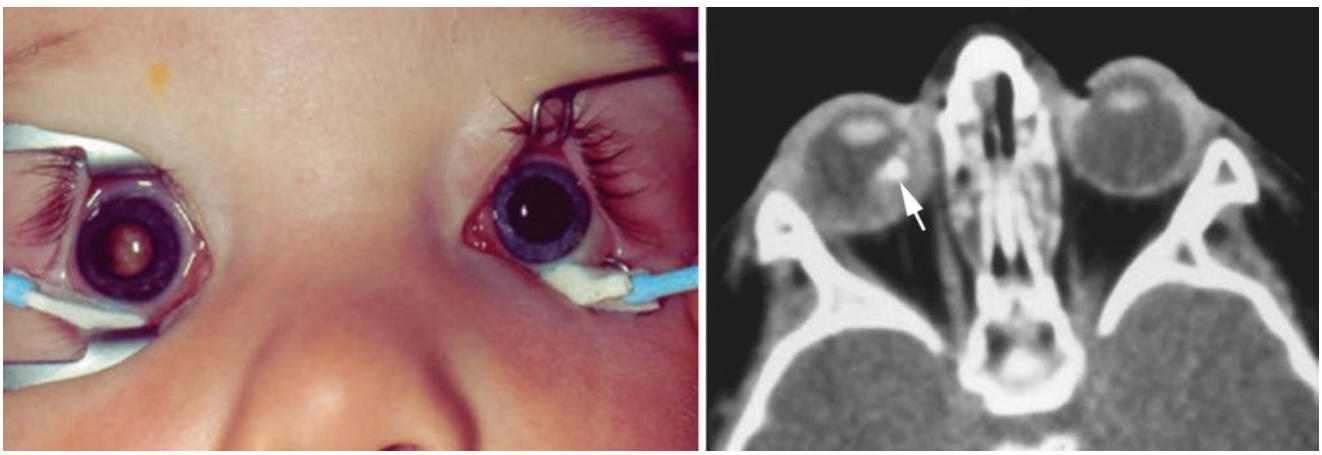


Fig. 32.63 A 2-year-old child was noted to have right leukocoria. A large retinoblastoma was diagnosed on examination under anesthesia with B-scan ultrasonography. A CT was performed to rule out extrascleral extension or optic nerve involvement, revealing intralesional calcification (*arrow*) on this axial, soft tissue window, consistent with the diagnosis. There is probable associated retinal detachment

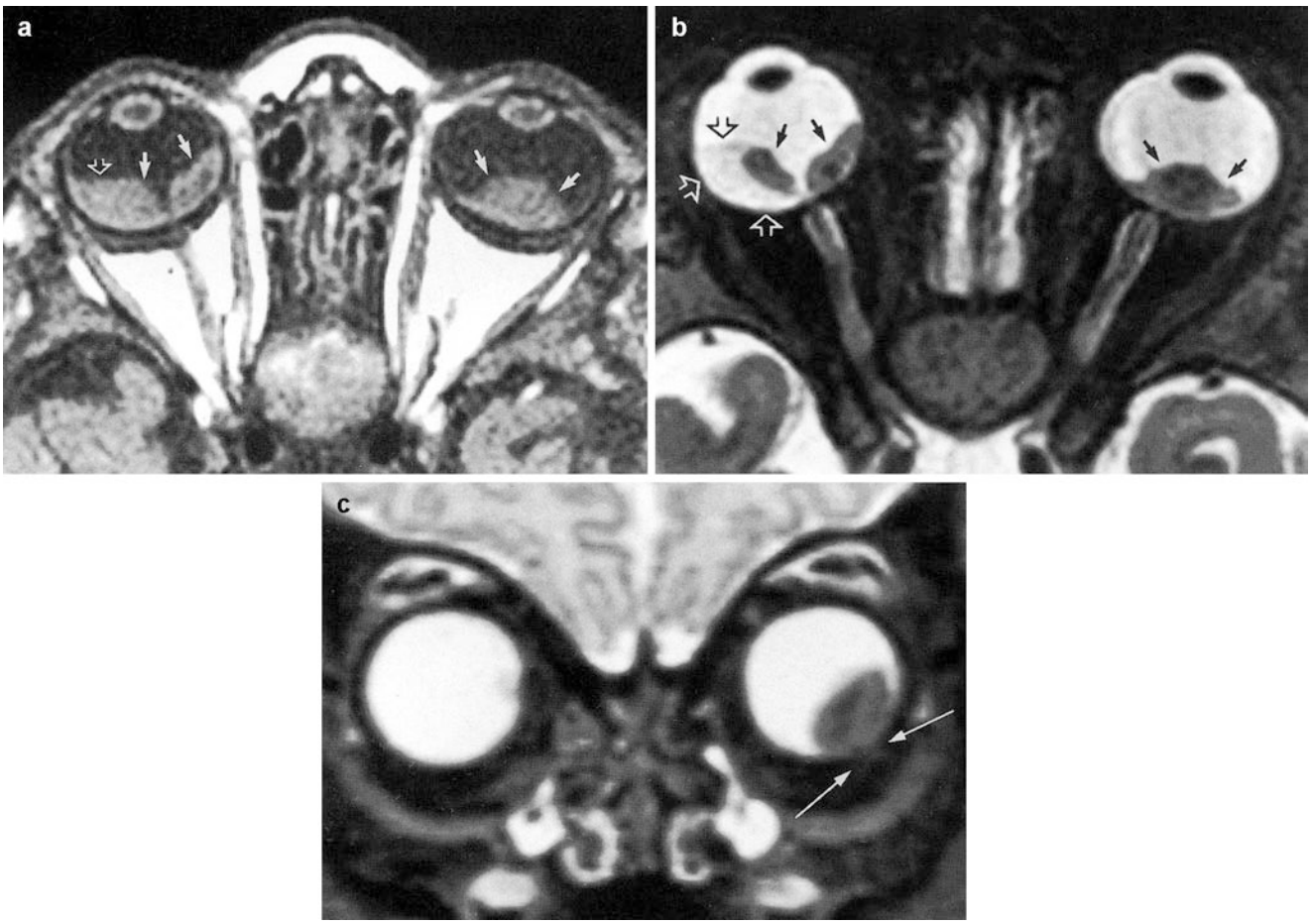


Fig. 32.64 Bilateral retinoblastoma with retinal detachment on the right. (**a**) Axial T1-weighted MRI shows bilateral ocular masses (*arrows*). The *solid arrows* point to the retinoblastoma, and the *open arrow* indicates subretinal fluid in the right globe, which on this sequence is indistinguishable from tumor. (**b**) Axial T2-weighted MRI reveals the bilateral retinoblastomas (*solid arrows*) to be markedly hypointense and easily separates subretinal fluid (*open arrows*), which is hyperintense, from the retinoblastoma in the right globe. (**c**) Coronal T2-weighted MRI reveals that the large retinoblastoma on the left has extended extrasclerally (*arrows*)

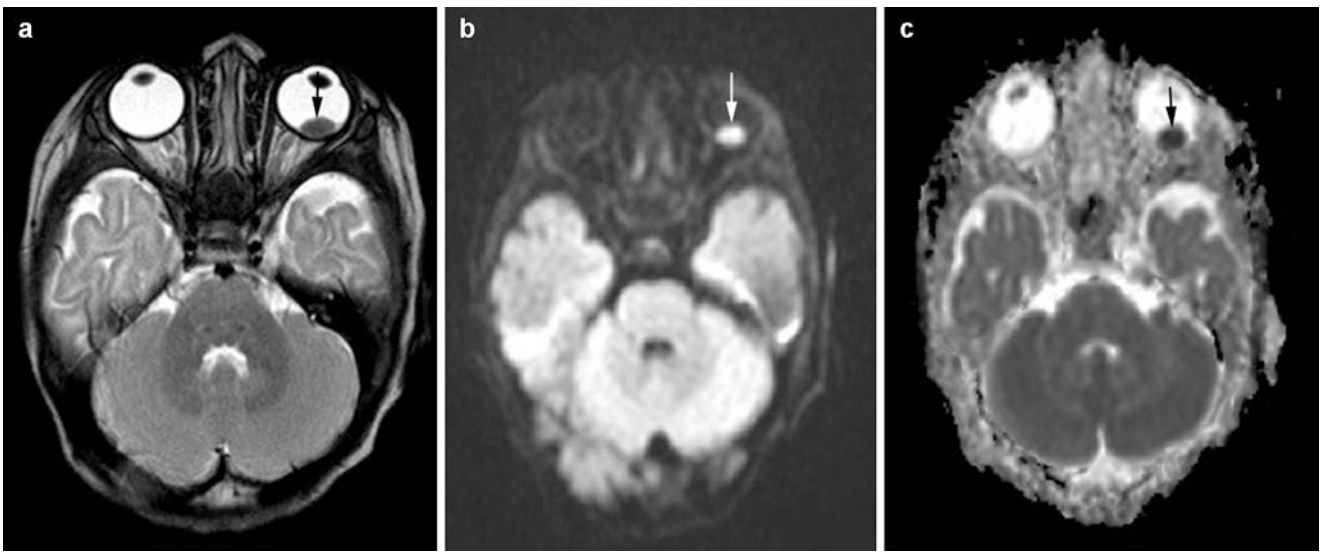


Fig. 32.65 A 9-week-old girl with a left retinoblastoma with restricted diffusion. (**a**) On T2-weighted MRI, a hypointense signal is seen within the lesion (*arrow*). (**b**) Restricted diffusion on DWI is seen as a bright signal (*arrow*). (**c**) Note the decreased signal on ADC (*arrow*). This low signal on ADC is helpful in confirming true restricted diffusion on DWI. If a high signal is noted on both DWI and ADC, then diffusion is not restricted, but rather "T2 shine-through" is present

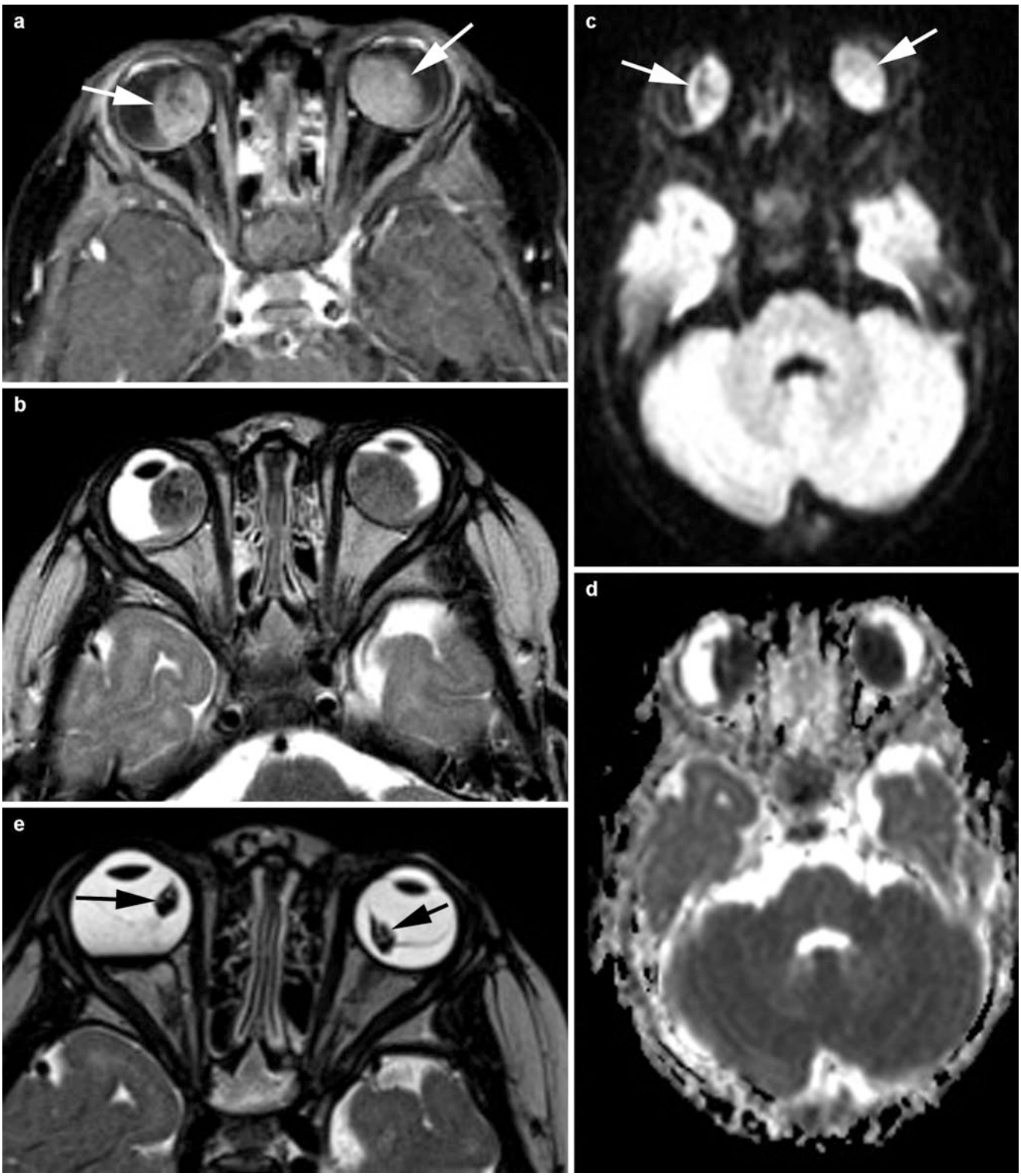


Fig. 32.66 Bilateral retinoblastoma following intra-arterial chemotherapy in a 1-year-old child. (**a**) Axial, postcontrast T1-weighted MRI with fat suppression demonstrates bilateral enhancing lesions (*arrows*). (**b**) On T2 weighting, the retinoblastomas are hypointense to vitreous. (**c**) Axial DWI shows the bright signal (*arrows*) of restricted diffusion consistent with a tightly packed, highly cellular tumor. (**d**) Axial ADC confirms restricted diffusion. Note that the signal is hypointense, the opposite of that seen in DWI. Compare the DWI and ADC signals of the retinoblastomas to those of the adjacent vitreous, which does not restrict diffusion. (**e**) Axial T2-weighted image shows focal, markedly hypointense signals (*arrows*) that did not show restricted diffusion on DWI and ADC. This residuum is consistent with dystrophic calcification at the site of the previous lesions and is often seen in long-term follow-up imaging of posttreatment retinoblastoma. There are bilateral retinal detachments

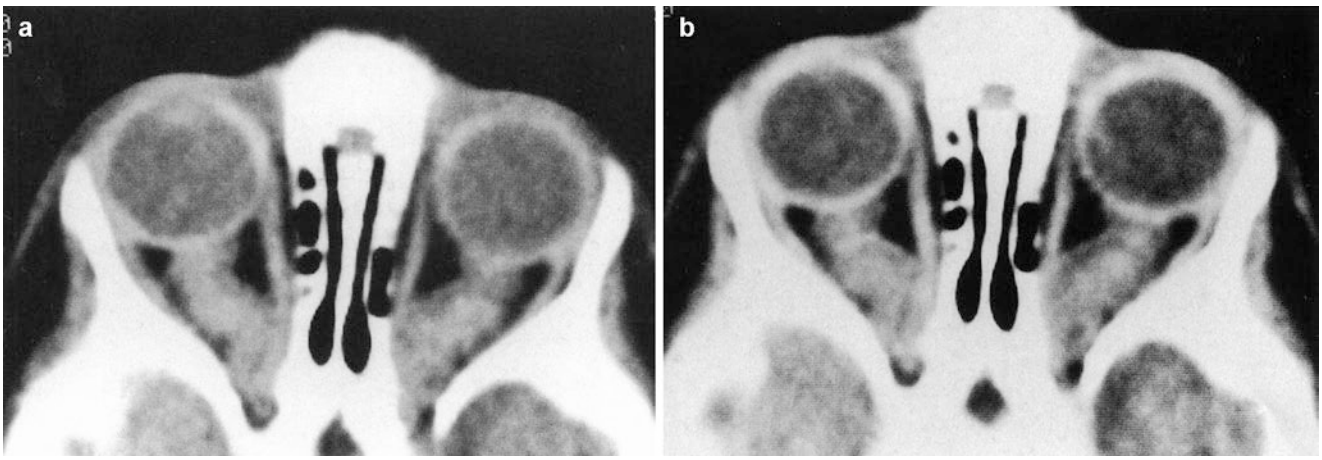


Fig. 32.67 Bilateral optic nerve gliomas in a 2-year-old patient with neurofibromatosis type 1. (**a**) Axial non-enhanced CT shows tubular enlargement of both optic nerve/sheath complexes, which are also slightly heterogeneous and tortuous. (**b**) Following injection of contrast material, there is minimal enhancement of the central portions of the large optic nerve/sheath complex

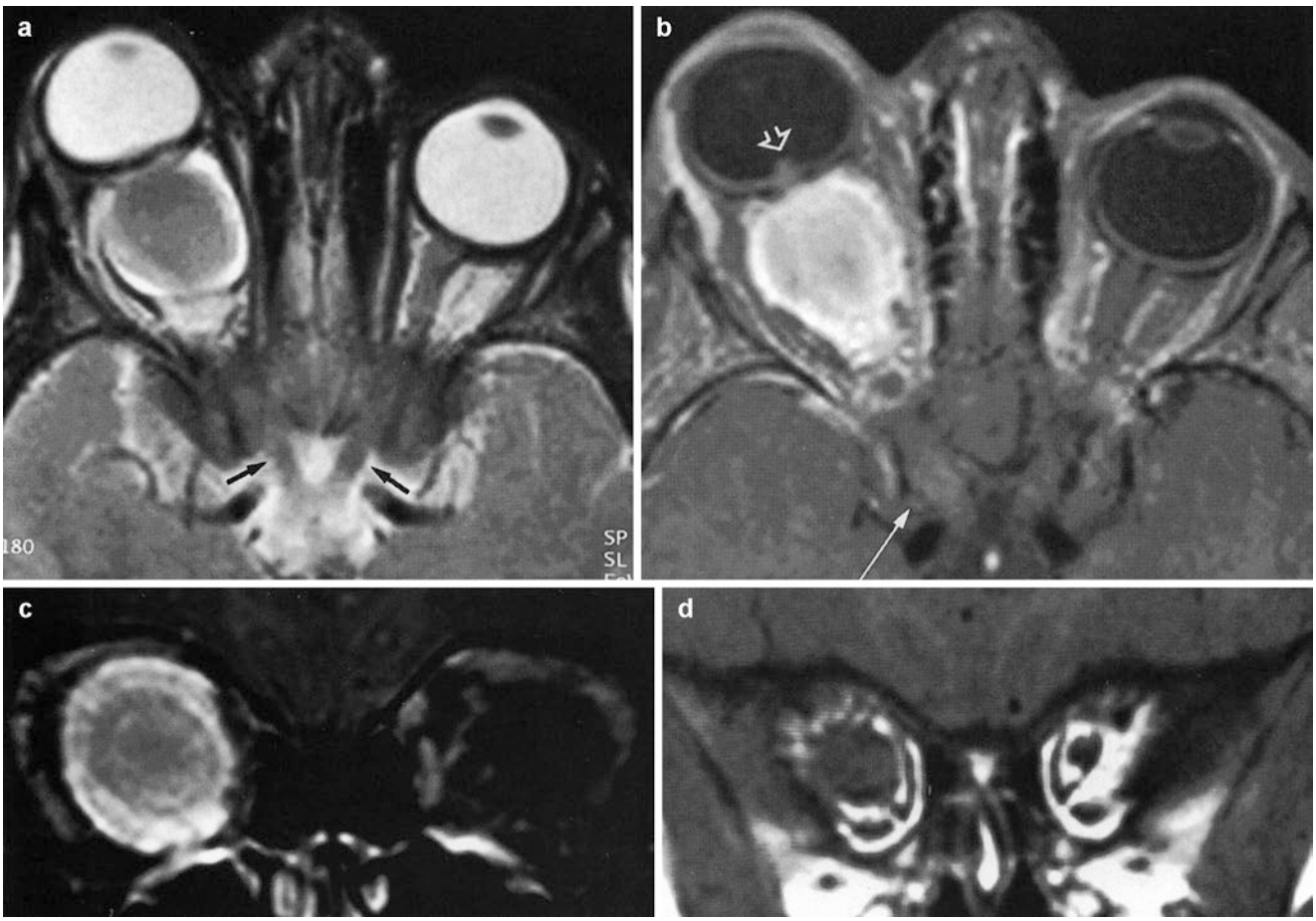


Fig. 32.68 Right optic glioma in a 2-year-old girl. (**a**) Axial T2-weighted MRI shows the right optic glioma to be hypointense centrally and only bright in the periphery. The tumor causes prominent distortion of the globe. The intracranial optic nerves (*arrows*) and the chiasm appear normal in size. (**b**) Axial T1-weighted MRI after gadolinium infusion and fat suppression shows multiple layers of varying intensity within the large optic glioma, with periphery being the brightest. Also note that a portion of the glioma bulges at the optic nerve head (*open arrow*). The intracanalicular portion of the optic nerve enhances only minimally but is enlarged (*arrow*). (**c**) Coronal, postcontrast T1-weighted MRI with fat suppression reveals a large, contrast-enhancing mass with concentric layers of differing intensity, greatest along the periphery. (**d**) Coronal T1-weighted MRI obtained through the posterior one-third of the orbit shows the optic glioma with fairly homogenous signal intensity.

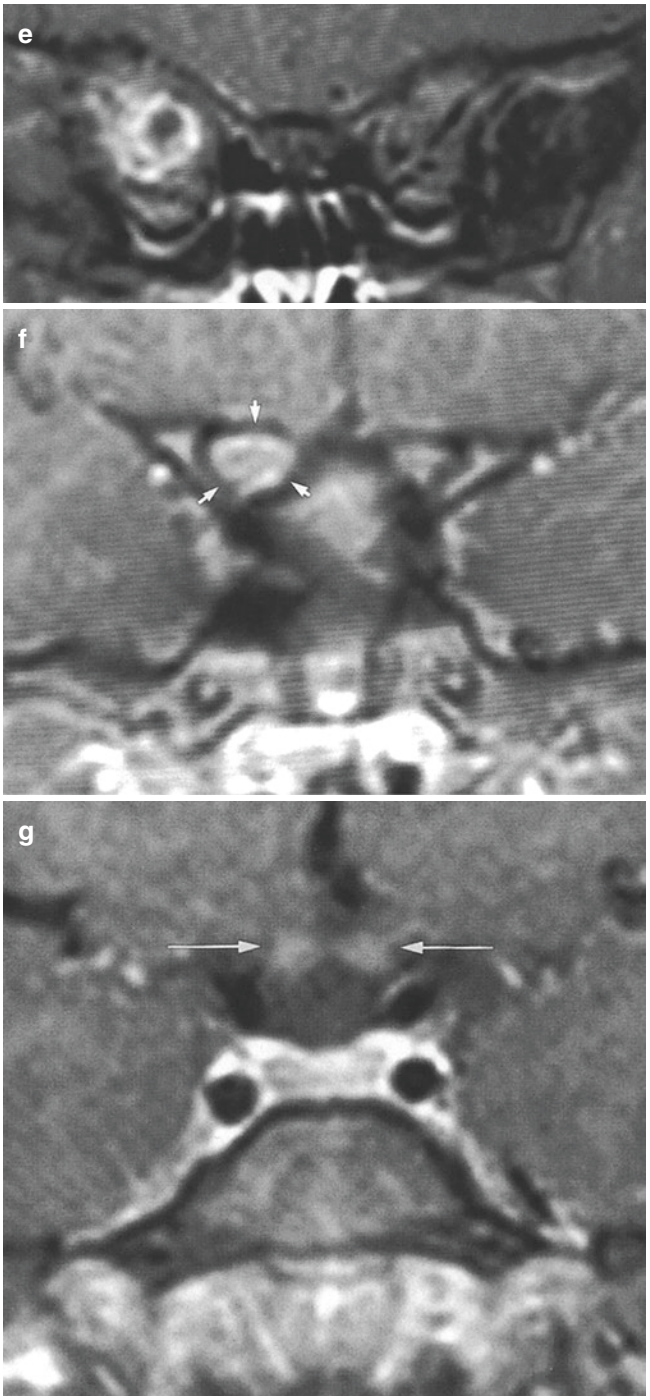


Fig. 32.68 (continued) (**e**) Coronal image, obtained at a similar level as shown in (**d**), but after contrast enhancement and fat suppression, once again shows greatest enhancement in the periphery with a hypointense central portion. (**f**) Coronal, postcontrast MRI with fat suppression reveals an enhancing, enlarged intracanalicular portion of the optic glioma (*arrows*). Note again that the periphery enhances more than the center. (**g**) Coronal, postcontrast T1-weighted MRI with fat suppression reveals no abnormality in the intracranial optic nerves (*arrows*) as they join to form the chiasm. Some consider the peripheral enhancement and signal to be arachnoidal hyperplasia associated with glioma

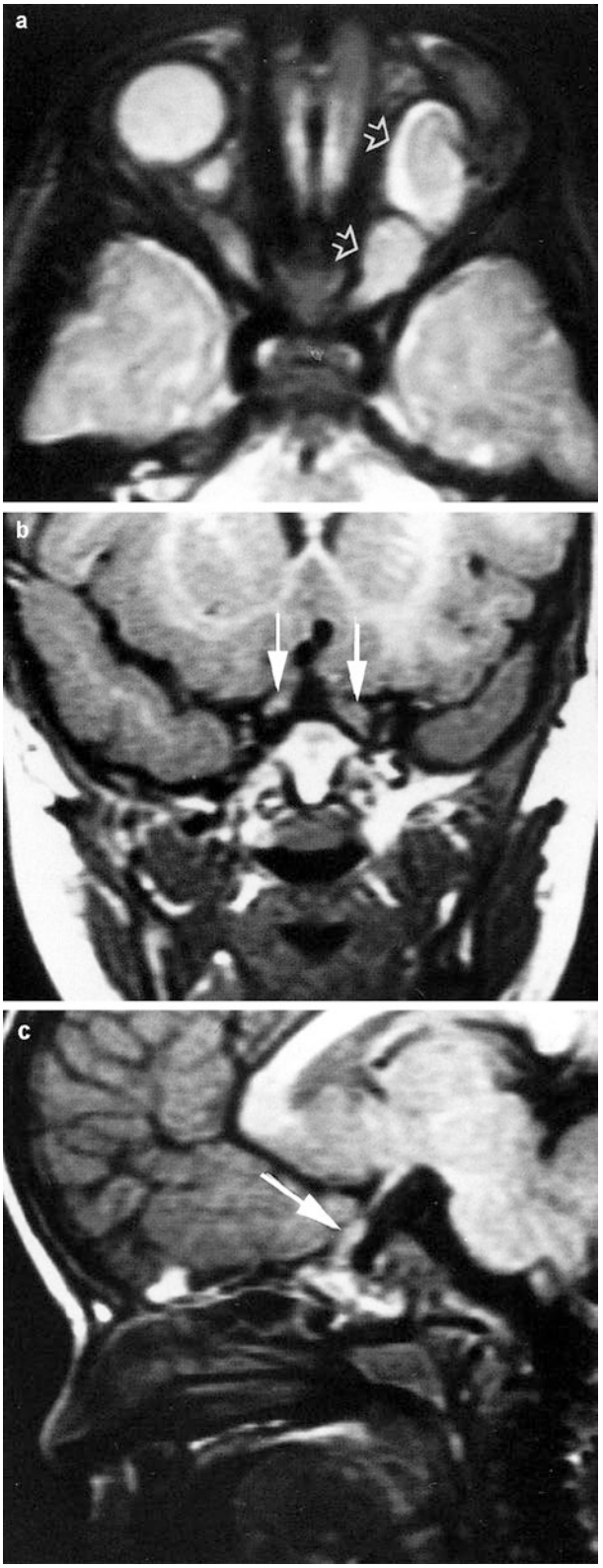


Fig. 32.69 Large glioma of the left optic nerve in a 1-year-old boy. (**a**) Axial T2-weighted MRI reveals a large heterogeneous glioma (*arrows*), which produces fusiform enlargement of the left optic nerve. (**b**) Coronal T1 scan shows asymmetry in size of intracanalicular optic nerves (*arrows*), with the left one being abnormally enlarged. (**c**) Sagittal T1 scan shows slight enlargement of the intracranial component of the left optic nerve (*arrow*)

(Fig. 32.70), and in each case when the tumor is large, kinking of the optic nerve–sheath complex results. The size and extent of the intraorbital optic gliomas do not correlate with the degree of intracranial involvement. Large intraorbital tumors may have no (Fig. 32.68) or little (Fig. 32.69) intracranial extent, whereas small optic nerve gliomas may have extensive intracranial components (Figs. 32.70 and 32.71). MRI is much more sensitive than CT in detecting abnormalities of the intracranial visual pathways (Fig. 32.72) [115].

The growth pattern of optic gliomas occurring in patients with NF-1 has been reported to be different from those that affect patients without NF-1 [113]. Patients without NF-1 more often have unilateral, large, fusiform optic nerve tumors (Fig. 32.68). In contrast, patients with NF-1 tend to have tumors that are bilateral, with intracranial involvement, and the optic nerve/sheath complex shows tubular (Fig. 32.67) or lobulated enlargement with elongation and kinking. These optic nerve gliomas tend to have a heterogeneous appearance

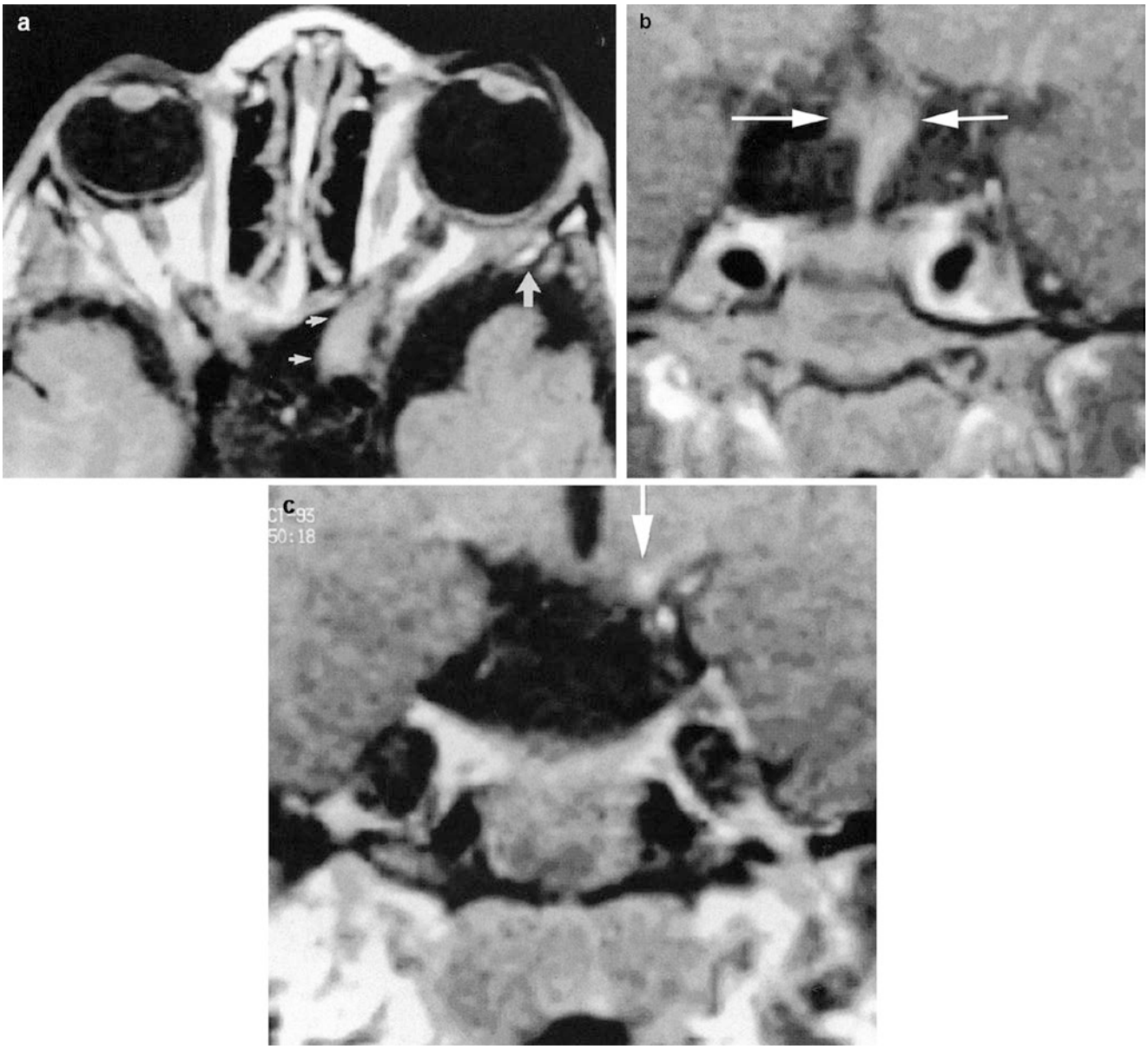


Fig. 32.70 Visual pathway glioma in a 3-year-old patient with neurofibromatosis. (**a**) Axial T1-weighted image shows glioma in the intracanalicular and intracranial portions of the left optic nerve (*small arrows*). In addition, the left globe is enlarged, consistent with buphthalmos. There is a defect in the left sphenoid wing (the so-called Orphan Annie sign). The *thick arrow* indicates the lateral margin of the defect. Note that there is enlargement of the subarachnoid space at the site of the sphenoid dysplasia. (**b**) Coronal, postcontrast image reveals slight enlargement and distortion of the chiasm (*arrows*). The abnormal chiasm does not enhance. (**c**) A coronal section posterior to that of the chiasm shows abnormal enhancement in the left optic tract (*arrow*). This type of "skip enhancement" is not uncommon in optic pathway glioma and hints at a possible multifocal pathogenesis

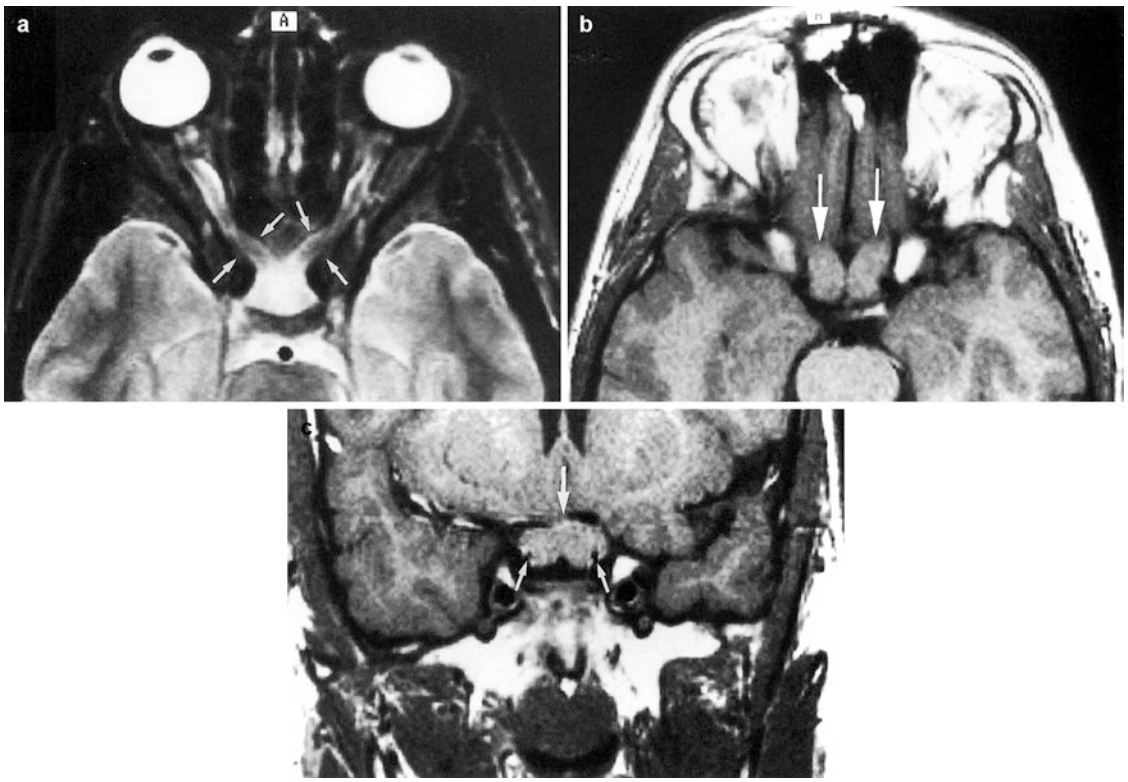


Fig. 32.71 Enlarged optic nerves and chiasm. (a) Axial T2-weighted MRI shows enlargement of the subarachnoid space of the intracanalicular portions of the optic nerves (*arrows*), seen as hyperintense CSF surrounding the optic nerves. (**b**) Axial T1 MRI shows markedly enlarged intracranial portions of the optic nerves (*arrows*). (**c**) A coronal T1 image reveals a markedly enlarged chiasm (*thick arrow*). The ophthalmic arteries (*small arrows*) are encased by the tumor bilaterally

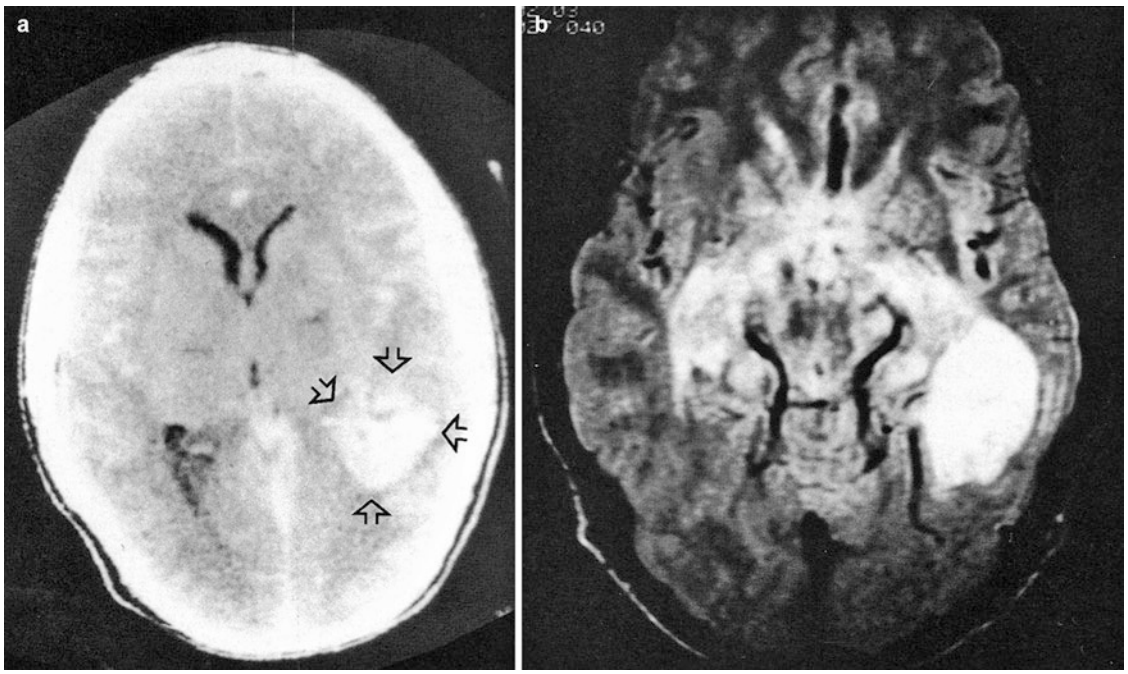


Fig. 32.72 Extensive visual pathway glioma. (**a**) CT at the level of the basal ganglia reveals a contrast-enhancing mass (*arrows*) that compresses the atrium of the left lateral ventricle. Lower sections did not show any enhancement in the chiasm or optic tracts. (**b**) An axial T2 MRI, performed just inferior to the level shown in (**a**), reveals abnormal increased signal in the region of chiasm, optic tracts, and medial temporal lobes and in a large mass in the left posterior temporal lobe. Postcontrast MRI (not shown) showed enhancement only in the large temporal mass but not in the remainder of the visual pathways

on CT, on T1- and T2-weighted MRI, and also after contrast administration. The glioma may extend extraneurally into the subarachnoid space, encircling the nerve, but not involving the dura. Also, the tumor may be associated with arachnoid hyperplasia, accumulation of mucinous material, or cysts, and this accounts for the heterogeneity of the MRI signal.

MRI is useful not only in the initial diagnosis and delineation of the visual pathway gliomas but also in follow-up, which requires years to decades. Because a child will require multiple serial studies, an additional advantage of MRI is that it does not involve the ionizing radiation of CT.

Plexiform Neurofibroma

Plexiform neurofibromas are the most frequent orbital manifestation of neurofibromatosis (Fig. 32.73) [116]. The tumors are diffusely infiltrating and highly vascular, producing enlargement and irregularity of extraocular muscles, lacrimal glands, and the optic nerve/sheath complex (Figs. 32.73 and 32.74). They may coexist with optic nerve glioma (Fig. 32.73). When the neurofibroma is large, it induces secondary enlargement of the bony orbit (Fig. 32.73), and when it extends beyond the orbit, it widens the fissures along the apex. In addition to neurofibroma, sphenoid wing dysplasia



Fig. 32.73 Plexiform neurofibroma of the orbit and the left temporalis fossa. (**a**) T1-weighted, precontrast axial MRI shows marked expansion of the left orbit by an infiltrative, lobulated process that fills the anterior and lateral portions of the orbit. The neurofibroma also extends posteriorly into the cavernous sinus. There is prominent sphenoid wing dysplasia (*larger arrow*) compared to the normal greater wing of the sphenoid bone (*smaller arrows*) on the right; the widened subarachnoid space and temporal lobe extend anteriorly into the area of the sphenoid wing dysplasia. There is tortuosity and enlargement of the right optic nerve, indicating optic glioma. (**b**) An axial T2-weighted image reveals individual lobules of the plexiform neurofibroma, each having slightly increased intensity on the periphery and lower intensity in the center. This is the fairly typical pattern of plexiform neurofibroma. Some of the larger lobules are indicated by *arrows*. (**c**) Axial, postcontrast MRI again shows an enhancing, infiltrative plexiform neurofibroma in the temporalis fossa and orbit. Note that the more characteristic lobules of plexiform neurofibroma show central contrast enhancement with peripheral low intensity (*arrows*). Contrast enhancement and fat suppression clearly reveal the dysplasia in the left sphenoid wing, compared to the normal sphenoid wing on the right. (**d**) Sagittal, postcontrast MRI with fat suppression shows a serpiginous lobular pattern to the neurofibroma located above the globe. This corresponds to the "worm-like" or "cord-like" feeling upon palpation of plexiform neurofibromas. Again, note the large defect in the posterior portion of the orbit due to the sphenoid wing dysplasia

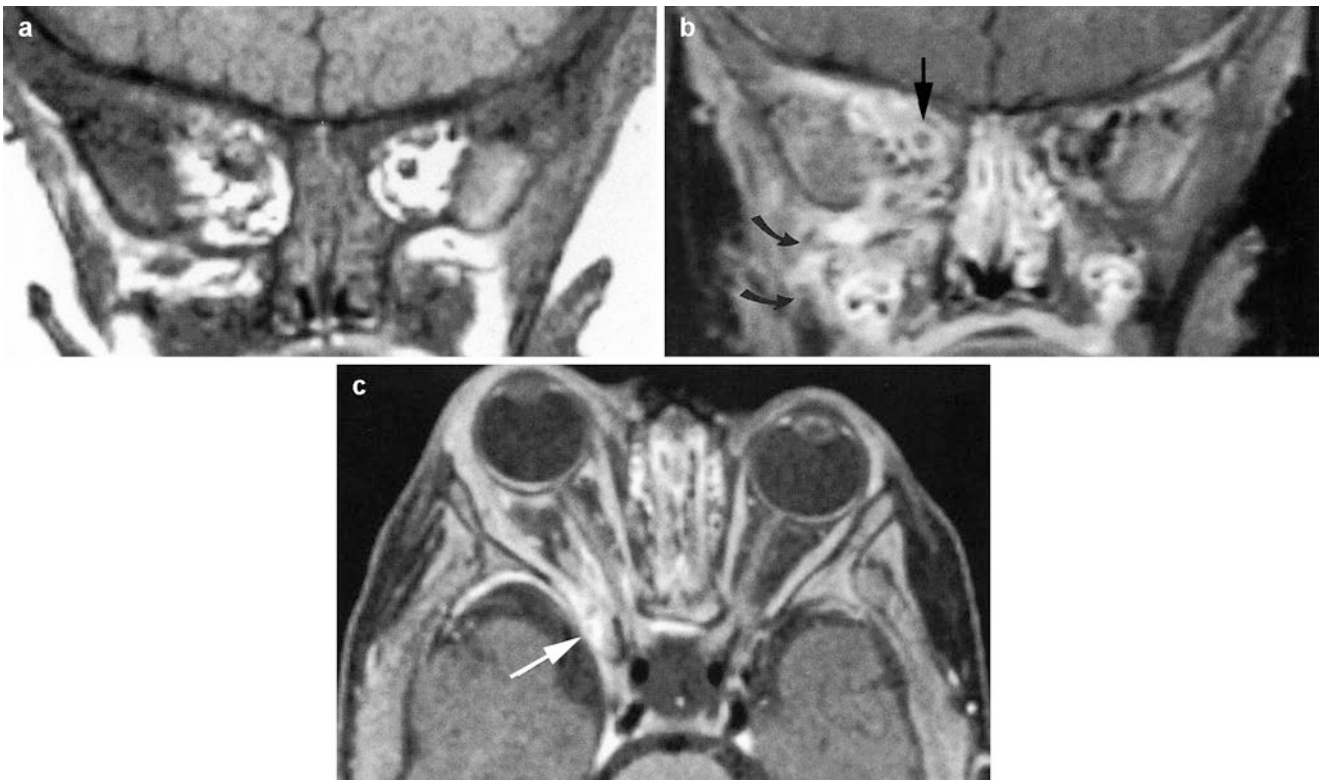


Fig. 32.74 Plexiform neurofibroma of the right orbit in a 10-month-old child. On CT (not shown here), the optic nerve–sheath complex was enlarged and mimicked an optic glioma. Only MRI was able to distinguish the optic nerve from the adjacent plexiform neurofibroma. (**a**) Coronal T1-weighted MRI shows an enlarged orbit with a poorly defined mass that obliterates anatomic landmarks such as the superior rectus muscle and the optic nerve/sheath complex. Compare to the normal orbit on the left. (**b**) Coronal image (slightly more posterior than (**a**)) obtained postcontrast with fat suppression reveals the enhancing plexiform neurofibroma infiltrating the right orbit, encircling the optic nerve/sheath complex (*straight arrow*) and extending through the inferior orbital fissure to infiltrate the facial structures (*curved arrows*). (**c**) Axial, postcontrast MRI with fat suppression shows the infiltrative nature of the plexiform neurofibroma in the right orbit. It is enhancing and encircling the optic nerve/sheath complex and extends through the superior orbital fissure into the anterior cavernous sinus (*arrow*)

may be another manifestation of NF-1 (Fig. 32.73). A very large defect or absence of the greater wing of the sphenoid bone in NF-1 may produce pulsatile exophthalmos due to brain tissue abutting orbital soft tissue, sometimes called the "Orphan Annie sign."

Because the plexiform neurofibromas lack a capsule and are infiltrative, they appear on images as serpiginous, cord-like masses that course through orbital fat and produce enlargement and irregularity of orbital structures (Figs. 32.73 and 32.74). Frequently, plexiform neurofibroma extends through the superior orbital fissure and produces enlargement of the cavernous sinus (Fig. 32.74). On CT, neurofibromas are of lower attenuation than muscle, and they show prominent contrast enhancement. On T1-weighted MRI, the tumors are of slightly greater intensity than muscle, while on T2-weighted images, they are prominently hyperintense. Frequently, the lesions are heterogeneous on T2 images, containing central hypointensity, which probably represents the fibrous component of the tumor [117]. The peripheral, markedly hyperintense portion of the neurofibroma consists of a myxoid matrix. Thus, on T2 MRI, the finding of a lesion that contains lobules with central hypointensity and peripheral hyperintensity (Fig. 32.73b) is pathognomonic of plexiform neurofibroma.

Neurofibromatosis type 2 is associated with central nervous system meningiomas and schwannomas, especially of the vestibular nerve. Small schwannomas of the cranial nerves may be difficult to visualize, leading to diagnostic dilemmas in children presenting with cranial nerve palsies and "normal" neuroimaging. As already noted, T2 3D–CISS MRI is particularly useful in imaging of cranial nerves and associated abnormalities in the cisternal spaces and the cavernous sinus [118]; this MRI sequence should be considered in patients presenting with cranial neuropathies and "normal" imaging with more conventional sequences (Fig. 32.75).

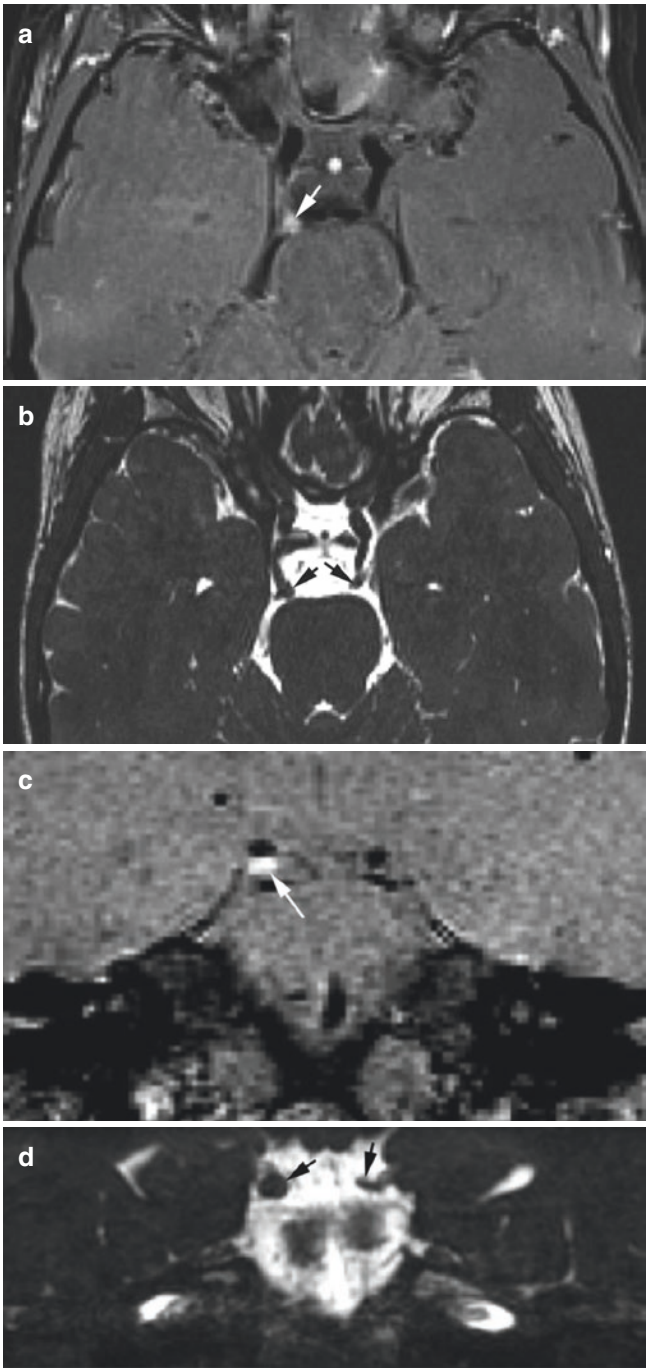


Fig. 32.75 3D–CISS imaging of a presumed oculomotor nerve schwannoma. An 8-year-old child presented with a right oculomotor nerve palsy. (**a**) Axial, 2-mm-thick T1-weighted, postcontrast MRI shows enhancement of the right cranial nerve (*arrow*) as it enters the interpeduncular cistern. (**b**) Axial, 0.5-mm-thick T2 3D–CISS image demonstrates an enlarged and slightly nodular right oculomotor nerve (*arrow*) compared to the normal left nerve (*arrow*). (**c**) Coronal, postcontrast T1-weighted MRI again demonstrates enhancement of the right oculomotor nerve (*arrow*). (**d**) Coronal 3D–CISS shows the asymmetry in the diameters of the two oculomotor nerves (*arrows*)

Meningioma

Meningiomas can involve orbital tissues by extending from an intracranial site or can originate in the orbit from the optic nerve sheath [119, 120], from periosteum, or from ectopic arachnoidal rests within the orbit. In adults, the most common type of orbital meningioma is one that extends into orbit from adjacent structures (usually the greater sphenoid wing) [121]. Compared to adults, meningiomas are infrequent in children and, when they occur in the orbit, more frequently arise from arachnoidal rests or are of optic nerve–sheath origin more commonly than involving the orbit by extension. Unlike adult meningiomas, which exhibit a significant female preponderance, in pediatric patients, there is an equal sex distribution. Pediatric meningiomas usually occur in teenagers and can have an association with neurofibromatosis. Those arising from rests on the periosteum are associated with focal paranasal sinus enlargement (Figs. 32.76 and 32.77), similar to the blistering seen with planum sphenoidale meningiomas. Such orbital meningiomas typically lie along one of the walls of the orbit, where they produce bony changes. Pediatric perineural (optic nerve sheath) meningiomas have characteristics similar to those seen in adults. On CT, meningiomas are hyperdense to fat and show prominent enhancement. Optic nerve–sheath meningiomas may show nests of calcification on CT. On MRI, meningiomas are either iso- or hypointense to muscle on T1 weighting and are hypo-, iso-, or hyperintense on T2 weighting. They tend to enhance dramatically with gadolinium.

Rhabdomyosarcoma

Rhabdomyosarcoma is the most common primary malignant orbital tumor and also the most common mesenchymal tumor of childhood [122]. It can arise at various sites in the orbit, or it can originate in the paranasal sinuses and then extend into the orbit. Rhabdomyosarcoma is an aggressive tumor that causes rapid evolution of unilateral proptosis and ptosis. Correct prompt diagnosis and therapy, which includes chemotherapy and radiotherapy, yield excellent results [50, 123] (see Chap. 36). It is therefore important to suspect the presence of rhabdomyosarcoma in any child with a rapid appearance of proptosis and also to differentiate the rhabdomyosarcoma from such lesions as hemangioma, OLM, neuroblastoma, and orbital infection/inflammation, which may also present with acute proptosis (Fig. 32.78). In this regard, imaging (particularly MRI) plays a critical role [6].

Rhabdomyosarcomas appear on CT and MR as relatively homogeneous, well-defined masses (Figs. 32.79 and 32.80). They may or may not be associated with bone changes. It is important to note that even though orbital rhabdomyosarcomas are aggressive, there may be no bone destruction at presentation [124] or there may be only bone scalloping (pressure erosion of bone), thus mimicking a more slowly growing tumor. The diagnosis may be particularly difficult when the rhabdomyosarcoma has not produced any bony changes and is associated with inflammatory reaction around it. Bony destruction is more often seen with paranasal rhabdomyosarcomas.

Evaluation of a child suspected of having an orbital rhabdomyosarcoma should include multiplanar imaging without

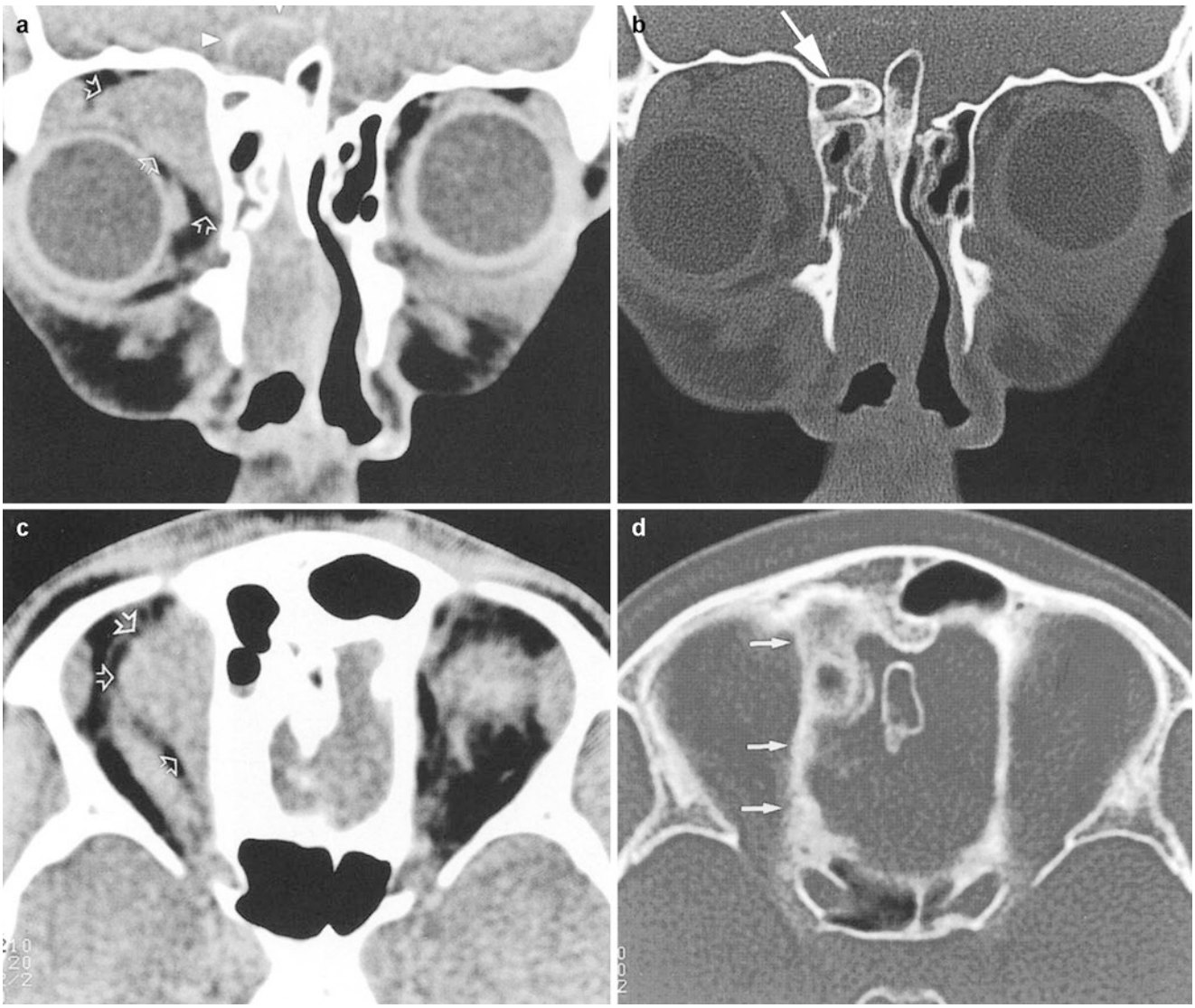


Fig. 32.76 Orbital and cranial base meningioma in a 6-year-old girl. (**a**) Coronal, non-enhanced, soft tissue CT shows the mass in the superomedial aspect of the right orbit (*open arrows*). A mass of lower intensity with peripheral calcification (*arrowheads*) is noted intracranially abutting the crista galli. Another component of the meningioma is present in the upper right nasal cavity. (**b**) Bone window reveals the asymmetry between the two orbits and also fine sclerotic changes in the bones of the right ethmoid and crista galli and an extra air cell (*arrow*) above the right ethmoid sinus. (**c**) Axial soft tissue CT of the superior orbits shows the soft tissue mass (*arrows*) flattened against the medial wall of the right orbit. (**d**) Axial CT and bone window, at the same level as (**c**), show permeative sclerotic changes (*arrows*) in the superomedial wall of the right orbit.

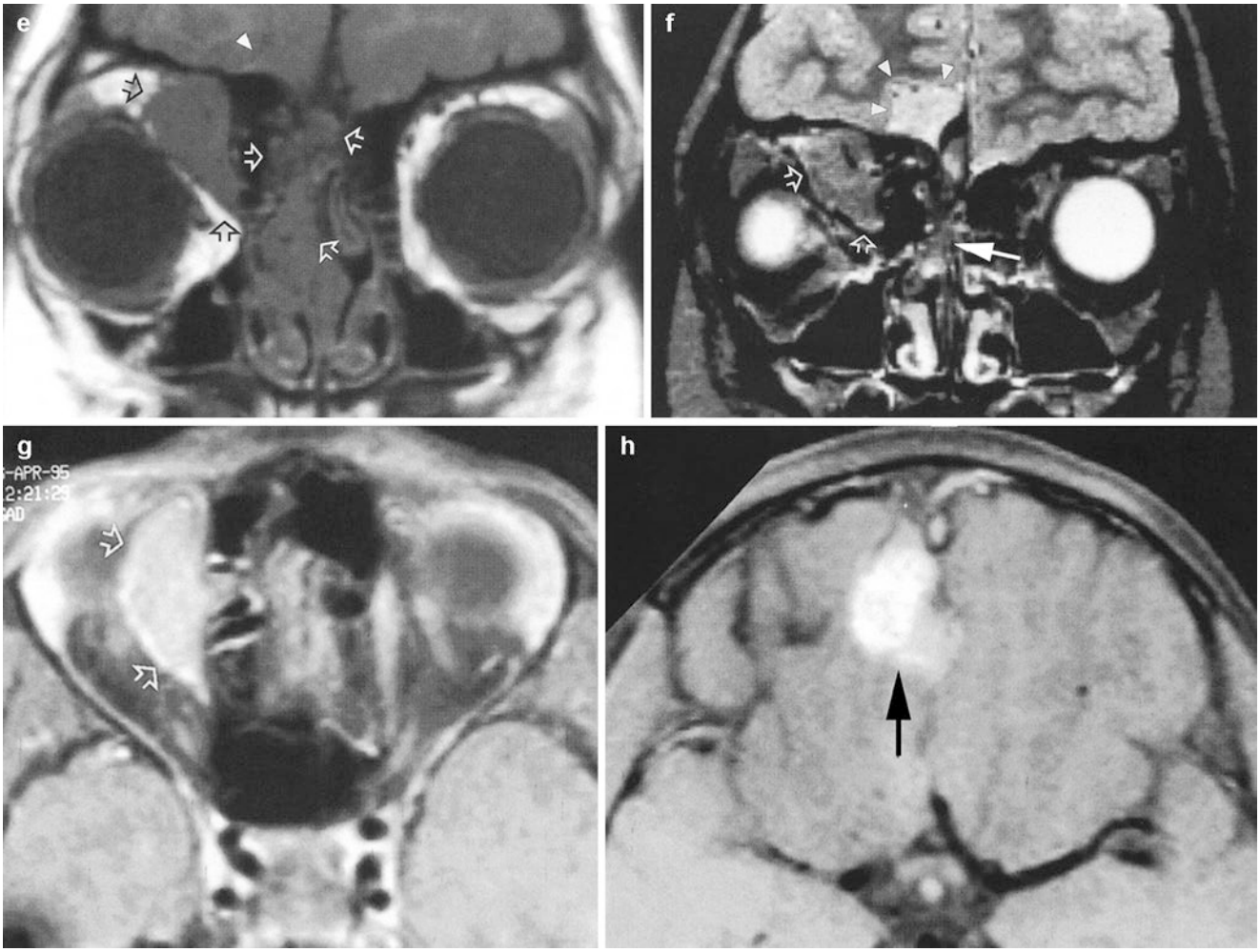


Fig. 32.76 (continued) (**e**) Coronal, precontrast T1-weighted MRI shows the intraorbital mass (*black arrows*) and the irregular intranasal mass (*white arrows*). The faint linear hypointensity (*arrowhead*) corresponds to the calcification on periphery of the intracranial component of the meningioma shown in (**a**). (**f**) Coronal T2-weighted MRI (slightly more posterior than that shown in (**e**)) demonstrates that the components of meningioma have different intensity, with increased intensity in the intracranial component (*arrowheads*) and decreased intensity in the intraorbital (*open white arrow*) and intranasal components (*arrow*). The intranasal portion of the tumor is smaller on this image than on (**e**) because it is a more posterior section. (**g**) Axial, postcontrast MRI with fat suppression shows robust enhancement of the mass (*arrows*) lying along the medial wall of the right orbit. (**h**) Axial, postcontrast MRI reveals the intracranial portion of the meningioma (*arrow*) with slightly heterogeneous enhancement but more intense than the intraorbital component

and with contrast enhancement of the orbit as well as of the brain to demonstrate intracranial extension of tumor that may be subclinical at the time of presentation [124, 125]. Extraorbital spread into the calvarium or paranasal sinuses spread is a poor prognostic sign associated with a high recurrence rate.

CT provides the best bony detail (Fig. 32.78), while MRI is more accurate in the delineation of the rhabdomyosarcomas. On CT, the tumor appears as mass that is isodense to slightly hyperdense to extraocular muscle and generally shows uniform contrast enhancement. On MRI, the rhabdomyosarcomas are close to the intensity of muscle on T1 weighting, show slightly heterogeneous contrast enhancement (Figs. 32.79 and 32.80), and are variable in signal intensity on proton density and T2-weighted images. The tumors have been reported to be slightly hyperintense on T2-weighted images [125] (Fig. 32.80) but often can be hypointense (Fig. 32.79e). The greater ability of MRI to show the internal architecture of lesions permits differentiation of rhabdomyosarcoma, which is a fairly homogeneous solid tumor, from hemangioma and OLM, which have characteristic internal structure. MRI also provides diffusion-weighted imaging (DWI) of rhabdomyosarcoma, often showing restriction due to the tightly packed, cellular nature

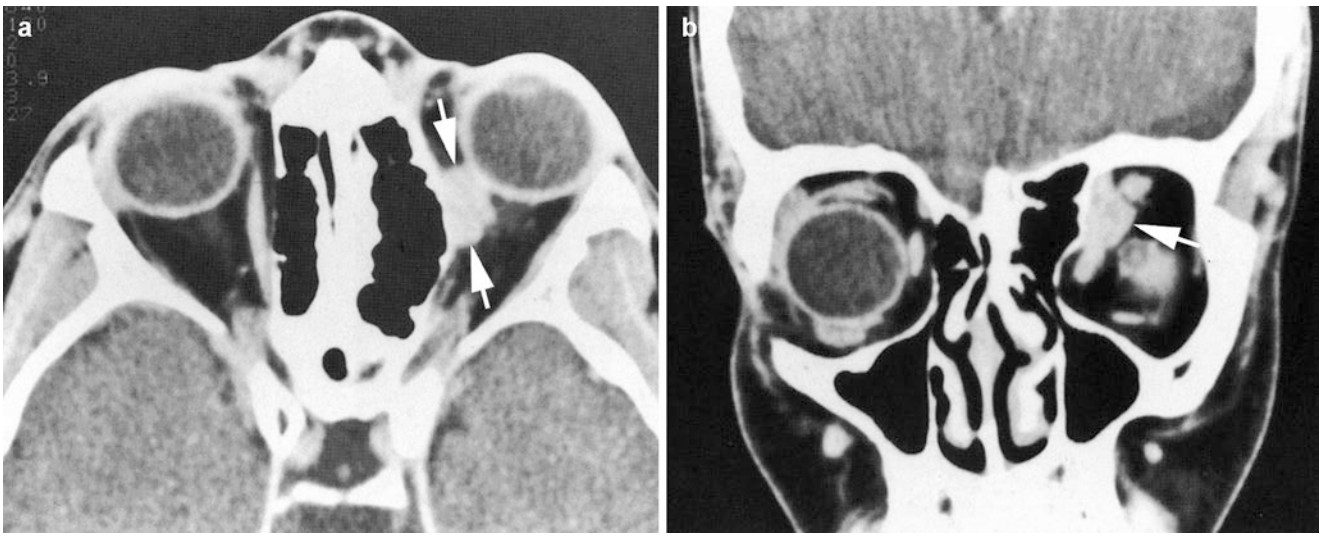


Fig. 32.77 Ectopic orbital meningioma in a 14-year-old boy with neurofibromatosis. (**a**) Axial CT, soft tissue window, shows a contrast-enhancing soft tissue mass (*arrows*) that lies along an enlarged left ethmoid sinus and displaces the globe anteriolaterally. The enlargement and lateral bulging of the ethmoid sinus is consistent with the so-called blistering due to a meningioma. (**b**) A contrast-enhanced coronal CT again reveals the abnormally enlarged left ethmoid sinus. The meningioma (*arrow*) is based on the medial wall of the orbit at site of ethmoidal enlargement and lies between the superior and medial rectus muscles



Fig. 32.78 Progressive exophthalmos in an 8-year-old boy. This child was referred after failing to respond to corticosteroids for suspected inflammatory myositis (IOI) of the medial rectus muscle. Axial (*top*) and coronal (*bottom*) soft tissue windows are shown. The initial reading at an outside hospital was myositis of the medial rectus muscle. However, note that on careful examination, the medial rectus (*arrows*) is distinctly separate from the abutting orbital mass. The mass distorts the normal muscle contour. Also note that the orbital walls are intact and there is no evidence of sinus or intracranial invasion. Urgent biopsy revealed embryonal rhabdomyosarcoma and chemotherapy was curative. Note that orbital rhabdomyosarcoma rarely arises from extraocular muscles; it is a tumor of the pleuripotential mesenchymal cells within the orbit. Confinement to the orbit is a significant prognostic sign; local extension into the calvarium or the sinuses decreases survival

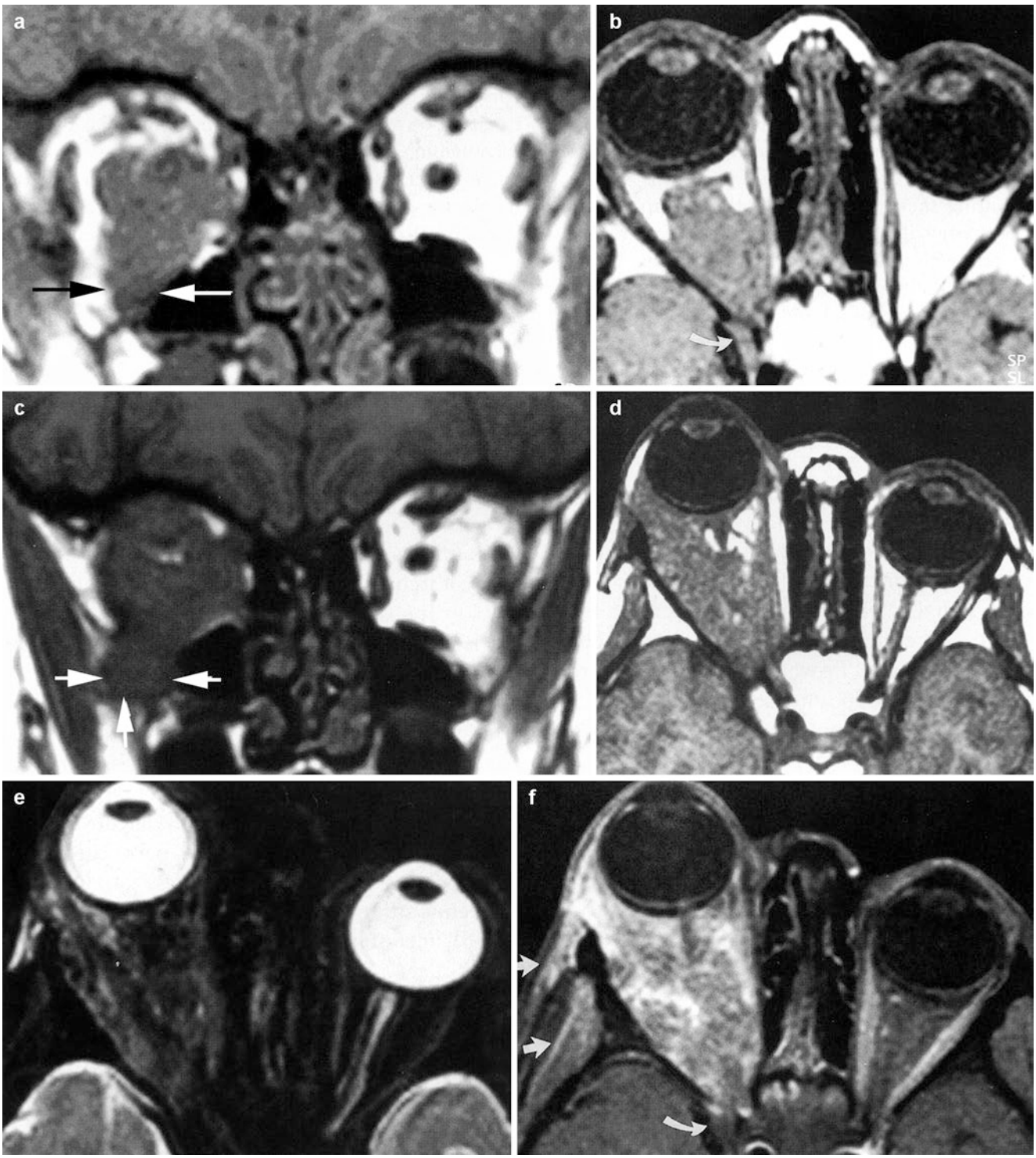


Fig. 32.79 Rapidly progressive rhabdomyosarcoma of the right orbit in a 3-year-old girl. (**a**) Coronal, precontrast T1-weighted MRI shows a solid-appearing irregular mass that causes obliteration of the landmarks of the optic nerve/sheath complex and inferior rectus muscle. The mass widens and extends into the inferior orbital fissure region (*arrows*). (**b**) Axial, precontrast T1-weighted MR shows the mass filling the posterior orbit, widening the superior orbital fissure, and extending into the cavernous sinus (*arrow*). (**c**) Five months later, a coronal, precontrast T1-weighted MR shows significant increase in the mass, which now fills most of the orbit and shows a greater inferior extent (*arrows*). The tumor grew despite chemo- and radiation therapy given at the time of diagnosis. (**d**) Axial, precontrast T1-weighted MRI, also 5 months after initial diagnosis, shows again the marked progression of the mass causing prominent proptosis. (**e**) Axial T2-weighted image shows the typical low signal of a rhabdomyosarcoma. Note the normal optic nerve–sheath complex on the left, with the hyperintense subarachnoid space outlining the optic nerve. While often the rhabdomyosarcomas can show low T2 signal, their signal can be variable, ranging from low T2 to high T2 signal. (**f**) Axial T1-weighted MR after gadolinium and fat suppression shows the heterogeneous, contrast-enhancing mass filling the orbit and extending beyond it laterally (*straight arrows*) and posteriorly into the cavernous sinus (*curved arrow*).

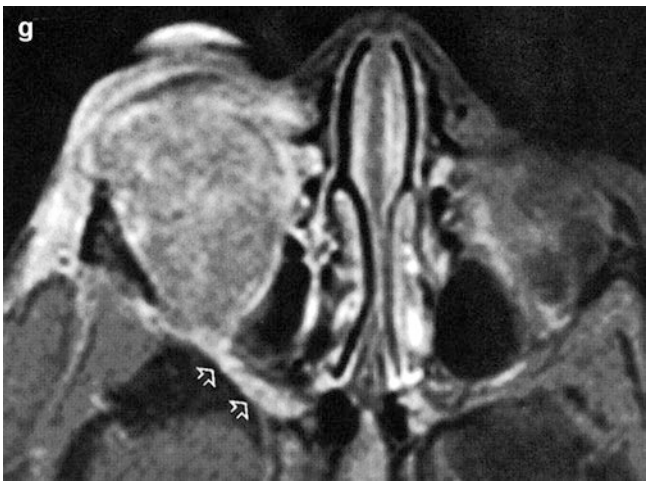


Fig. 32.79 (continued) (**g**) A lower axial section performed at the same time as the image in (**f**) shows well the large mass and extent into the pterygomaxillary fossa (*arrows*)

of the lesions but sometimes also showing only moderate restriction depending on edema, necrosis, and other factors (Fig. 32.81). Differentiation from orbital developmental orbital masses, such as glial–neural hamartomas and Langerhans cell histiocytosis, may be difficult at times.

Metastatic Tumors

Metastatic tumors to the pediatric orbit are uncommon, in contradistinction to adults. Neuroblastoma is the most common tumor to metastasize to the orbit in infants and young children and is only second to rhabdomyosarcoma as the most frequent pediatric malignant orbital tumor. It has a propensity to hemorrhage and thus may present with sudden onset of proptosis. Therefore, the rapid appearance of proptosis and ecchymosis in an infant or young child should raise suspicion of metastatic neuroblastoma. Bilateral

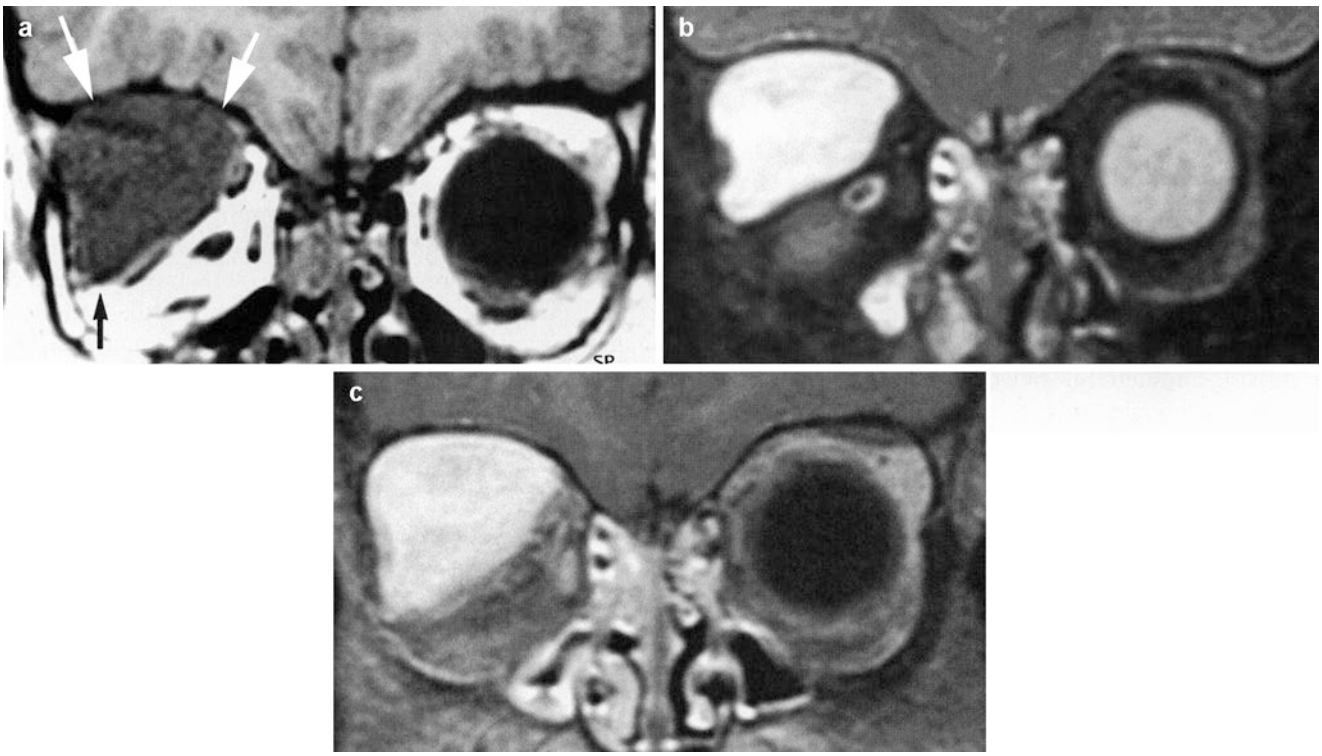


Fig. 32.80 Large rhabdomyosarcoma of the right orbit presenting with rapidly developing proptosis in a 2-year-old boy. (**a**) Coronal, precontrast T1-weighted MRI reveals a large extraconal mass (*arrows*) that displaces the normal orbital anatomy inferomedially. The mass appears solid and homogeneous. (**b**) Coronal T2-weighted image reveals increased intensity in the mass with very minimal heterogeneity and a solid appearance. (**c**) Coronal, postcontrast T1-weighted image with fat suppression reveals prominent, fairly homogeneous enhancement of the mass



Fig. 32.81 Diffusion-weighted imaging of rhabdomyosarcoma. (**a**) Axial CT, soft tissue window. Note the erosion of the lamina papyracea as the sinonasal alveolar rhabdomyosarcoma invades the orbit. (**b**) Coronal CT, soft tissue window. (**c**) T1-weighted, precontrast MRI shows a homogenous, solid mass isointense to muscle. (**d**) On coronal, T1-weighted precontrast MRI, the mass can be distinguished from inspissated mucus within the maxillary sinus (*arrows*). The protein content of the mucus makes it appear hyperintense to the lesion. (**e**) T2-weighted axial image. (**f**) On DWI, the lesion shows only minimal restriction. Rhabdomyosarcoma may restrict diffusion significantly, consistent with a tightly packed tumor containing small cells with a high nuclear-to-cytoplasmic ratio. Not all rhabdomyosarcoma will follow this pattern, but when present, it helps to distinguish this lesion from other causes of acute proptosis, most notably capillary hemangioma, OLM, and IOI, all of which should show much lower restriction on DWI

metastasis may present with a classic "raccoon" appearance externally. Typically, the tumor causes a permeative, lytic–sclerotic pattern in the bones, often with bone spicules, and extends beyond as a soft tissue mass. The bony changes and the soft tissue masses can be well demonstrated both with CT and MRI (Fig. 32.82). However, MRI is more sensitive to any retained blood products that may be present within the tumor. The differential diagnosis on the basis of the imaging appearance (diffuse permeative bony pattern and soft tissue masses) includes granulocytic sarcoma (leukemic infiltration) [126], metastatic retinoblastoma (Fig. 32.83), metastatic Ewing sarcoma, and extensive histiocytosis.

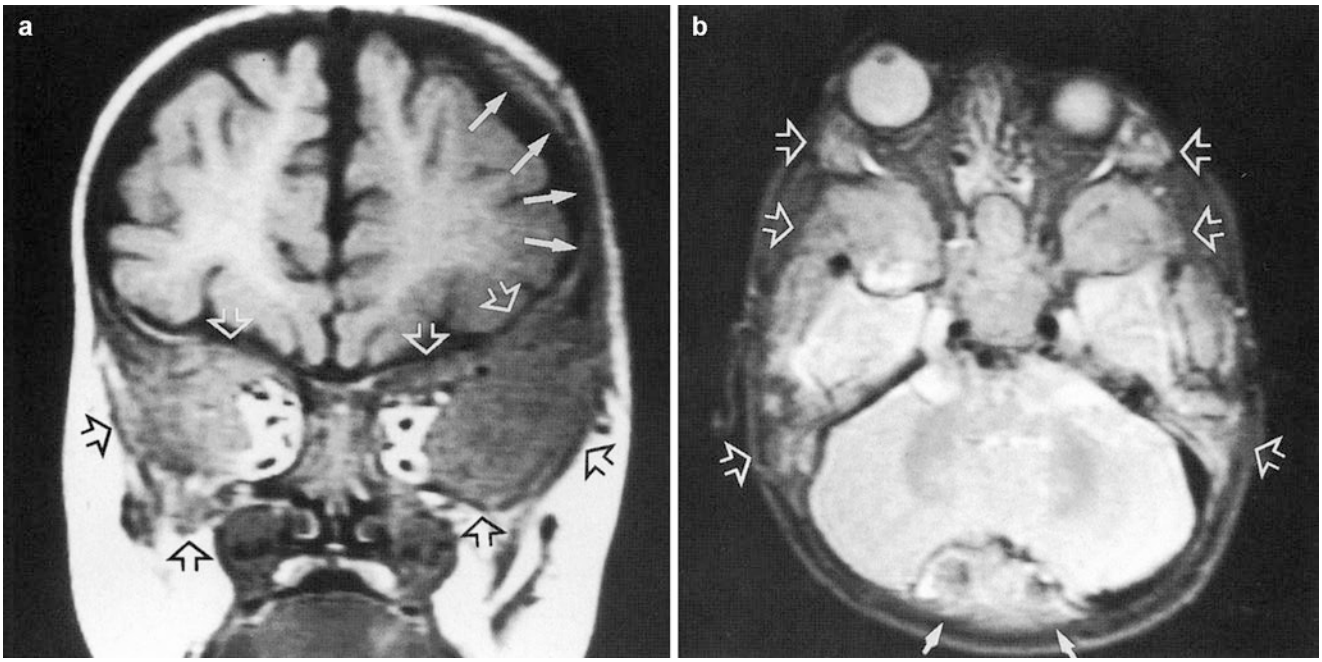


Fig. 32.82 Extensive metastatic neuroblastoma in both orbits and the calvarium. (**a**) Coronal T1-weighted MR shows extensive infiltration and expansion of the orbital walls (*open arrows*) as well as involvement of the left calvarium (*solid arrows*). (**b**) Axial T2-weighted MRI shows extensive involvement of the cranial base by the tumor (*open arrows*), which is moderately hypointense. There is also a typical deposition of neuroblastoma at the torcular Herophili (*solid arrows*)

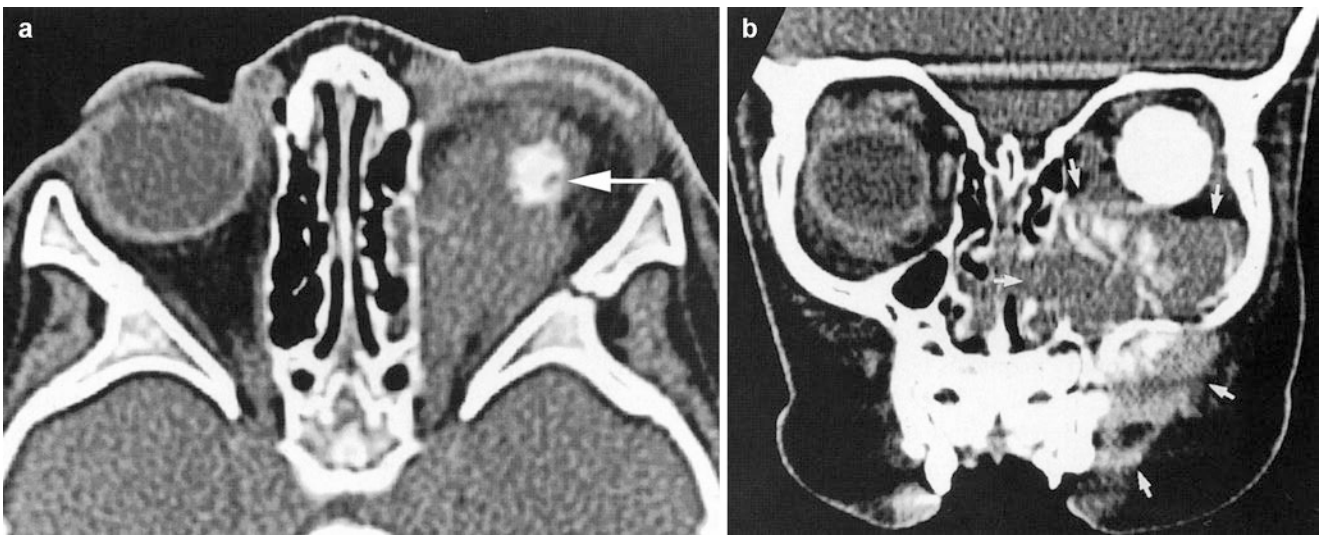


Fig. 32.83 Recurrent retinoblastoma in a 2-year-old boy who had had previously enucleation for retinoblastoma. (**a**) Axial CT scan shows nearly complete infiltration of the left orbit and slight extent into the adjacent ethmoid sinus. The most inferior portion of the prosthesis (*arrow*) is included in this section. (**b**) Coronal CT scan reveals a destructive mass in the left face (*arrows*) that involves the inferior portion of the left orbit and the left maxillary sinus. The mass expands the inferior orbit elevating the hydroxyapatite orbital implant

It is important to remember that neuroblastoma may also result in a variety of neuro-ophthalmologic findings from intracranial, lung apex, or neck involvement. A young child presenting with an acquired Horner syndrome should be suspected of harboring a neuroblastoma and undergo appropriate work-up and imaging of the sympathetic chain (Fig. 32.84).



Fig. 32.84 Acquired Horner syndrome from metastatic neuroblastoma. A 3-year-old girl presented with a left droopy lid of 2 months' duration. Note the anisocoria. CT imaging was performed (*bottom*). Note the left apical lung mass (*larger arrows*) causing the Horner syndrome. A large mass was also noted in the abdomen (*small arrows*). Further work-up confirmed neuroblastoma with left lung metastasis (Courtesy of James Katowitz, MD)

Miscellaneous

Langerhans Cell Histiocytosis

Langerhans cell histiocytosis (LCH) is now the accepted, all-encompassing term for the disease spectrum that previously was divided into eosinophilic granuloma, Hand–Schüller–Christian disease, and Letterer–Siwe disease. The pathogenesis of LCH is still under debate, with some arguing that it represents a reactive, inflammatory process, while others posit that it is a genuinely neoplastic, malignant process. A more recent interpretation favors a neoplastic etiology, although this is somewhat tempered by terms such as "inflammatory myeloid neoplasia." The BRAF V600E mutation typically occurs in the aggressive, multisystem variant of LCH and is absent in the localized form [127, 128]. The extent and severity of disease appear to be related to the stage at which the myeloid dendritic cell precursor of the Langerhans cell is affected by extracellular signal-related kinase (ERK) hyperactivation [127, 128]. LCH generally presents with a rapidly progressive, painful swelling. In the orbit, it most often involves the superolateral quadrant, producing a soft tissue mass with sharply marginated bone destruction. Generally on CT, the mass appears homogeneous and shows homogeneous enhancement. However, wider window photography of the CT images may reveal a peripherally denser rim compared to the mass (Fig. 32.85a). This peripheral rim is also shown on MR, and the central components show heterogeneity with regions of slight hyperintensity on T1-weighted images (Fig. 32.85b) and of hypointensity on T2-weighted images, perhaps reflecting fibrosis and/or hemorrhage. Differential diagnosis includes rhabdomyosarcoma. The histiocytosis may also be extensive, producing infiltrative soft tissue masses with bony destruction (Fig. 32.86).

Fibrous Dysplasia

Fibrous dysplasia is probably a developmental mesodermal disorder, and the lesion represents both arrested and altered maturation of the bone. In this disease, normal bone becomes replaced with immature, woven bone within a fibrous stroma. The monostotic type of fibrous dysplasia, which occurs with regular frequency in the orbit and along the skull base, is limited to one site but involves more than one bone, crossing sutures. The bone expansion due to fibrous dysplasia results in displacement and compression of adjacent soft tissue structures such as the optic nerve. The bony changes, consisting of bony widening and ground-glass pattern, are best demonstrated with CT (Fig. 32.87a), and three-dimensional CT is helpful in demonstrating the orbital and facial asymmetry that can result from this disease. Optic neuropathy

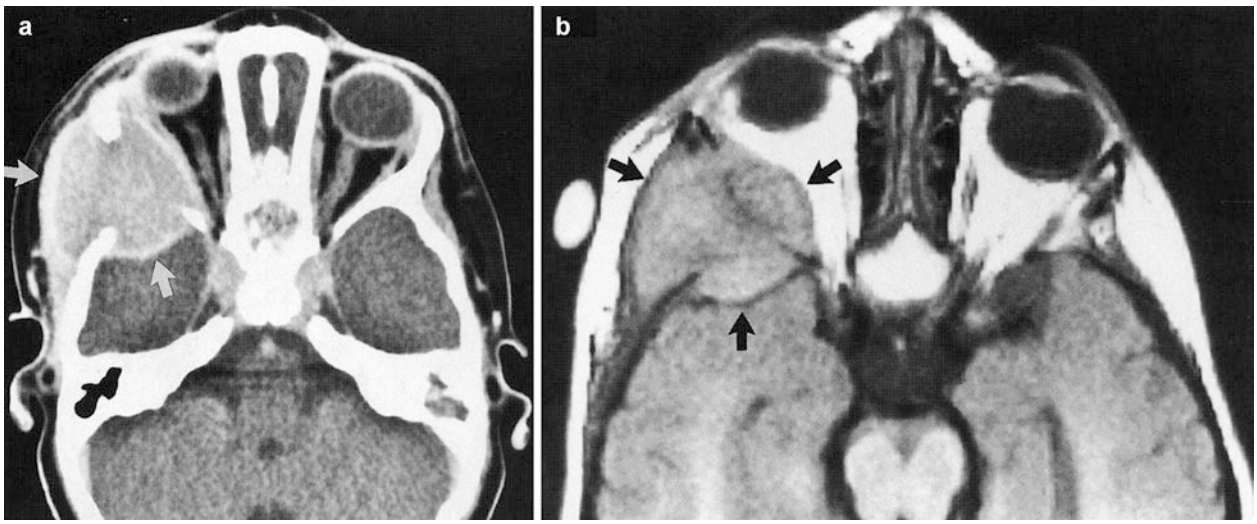


Fig. 32.85 Localized Langerhans cell histiocytosis of the right lateral orbit in a 1-year-old girl. (**a**) Axial contrast-enhanced CT shows destruction of the lateral wall of the right orbit by an enhancing, well-defined mass (*arrows*) with a denser peripheral rim. (**b**) Axial, precontrast T1-weighted MRI also shows the well-delineated mass (*arrows*) that destroys the bone and expands into the lateral aspect of the orbit and posteriorly into the middle cranial fossa

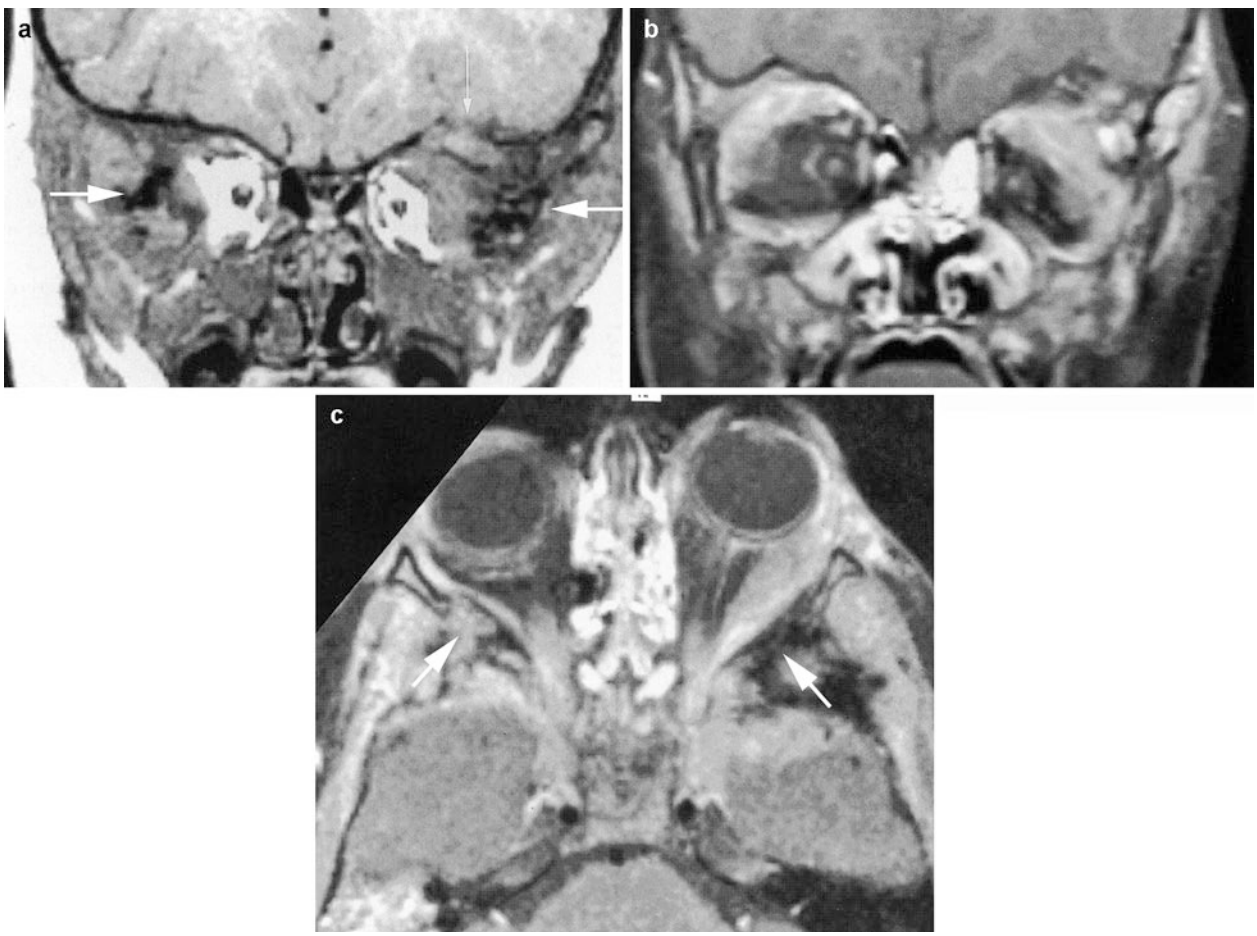


Fig. 32.86 Extensive histiocytosis involving both orbits in a 3½-year-old female. (**a**) Coronal T1-weighted MRI shows extensive distortion of the superolateral orbital bones (*arrows*) by soft tissue infiltrative masses that extend beyond the bone into the orbits (more so on the left) and into the temporalis fossae and facial structures. (**b**) Coronal T1-weighted, postcontrast MRI with fat suppression shows enhancement of the infiltrative histiocytosis. Note how the extraosseous masses encroach on the orbital fat, which is hypointense. (**c**) Axial T1-weighted, postcontrast MRI with fat suppression shows extensive abnormality of the bones of the cranial base, including the orbits, with distorted and irregular bones and enhancing soft tissue masses extending beyond the bony margins (*arrows*)

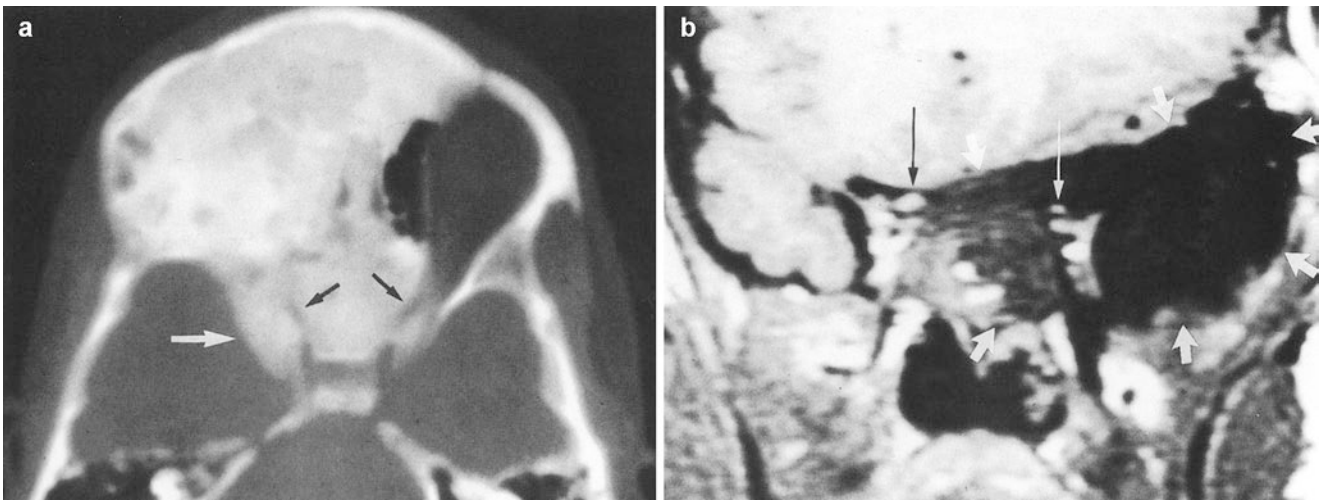


Fig. 32.87 Orbital fibrous dysplasia. (**a**) Axial, bone window CT reveals prominent thickening of the bone involving the right orbital roof along with the ethmoid and sphenoid sinuses; note the typical ground glass appearance that is most apparent on bone window. Only a small portion of the left ethmoid sinus is spared. Note the prominent thickening of the right anterior clinoid process (*white arrow*). There is narrowing of both optic canals (*black arrows*). (**b**) Coronal T1 MRI obtained on another patient shows fibrous dysplasia of the left orbit and sphenoid bones (*thick arrows*). There is prominent narrowing of the left optic canal (*narrow white arrow*). Compare to the normal canal and normal size of the optic nerve on the right (*black arrow*). On MRI, the signal of the bone involved by fibrous dysplasia may mimic the signal (actually the lack of signal) of air. Note that the very hypointense signal of the lesser and greater wings of the sphenoid is similar to that of the air-filled nasopharynx seen in the midline

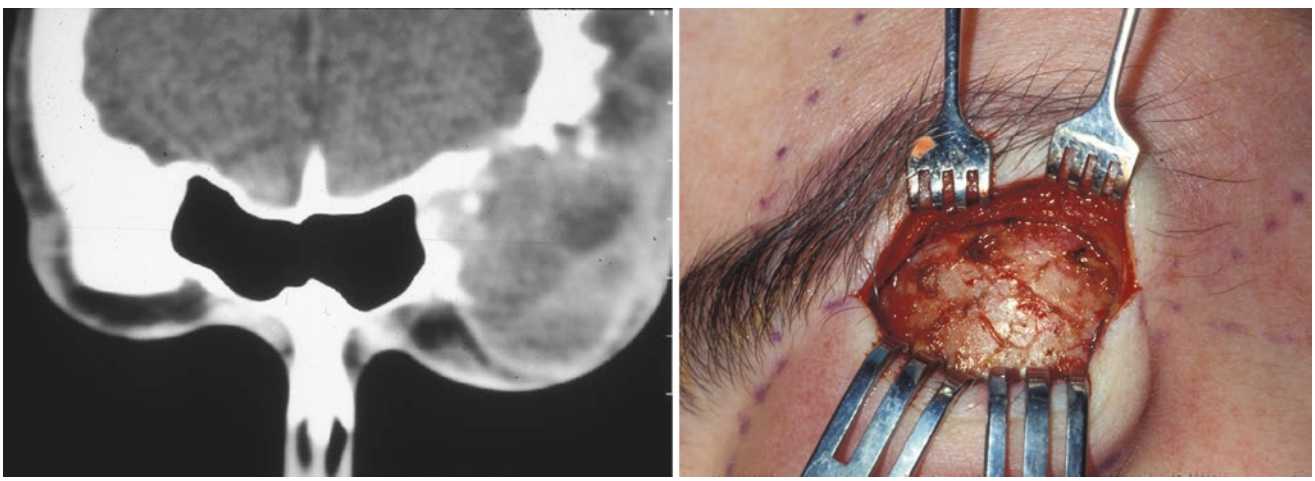


Fig. 32.88 Aneurysmal bone cyst causing compressive optic neuropathy in a teenager with McCune–Albright syndrome. Coronal CT (*top*) of a patient presenting with acute proptosis and swelling in a patient with McCune–Albright syndrome. Note the multiloculated and destructive changes in the left frontal bone and superior orbital rim secondary to a rapidly expanding aneurysmal bone cyst. Intraoperative photograph (*bottom*) prior to drainage

may occur due to narrowing of the optic canal. The lesions of fibrous dysplasia may be so hypointense on MRI that they may not be distinguishable from adjacent air-filled structures; therefore, small foci of fibrous dysplasia may be missed on MRI. However, this is not an issue when the process is extensive and when MRI's multiplanar capability and superior soft tissue discrimination permit visualization of the nerves (Fig. 32.87b) and vessels within canals and fissures narrowed by fibrous dysplasia. Polyostotic fibrous dysplasia is a feature of McCune–Albright syndrome. Acute orbital exacerbations from rapidly expanding aneurysmal bone cysts may be seen on areas of fibrous dysplasia (Fig. 32.88).

References

1. Hopper KD, Sherman JL, Boal DK. Abnormalities of the orbit and its contents in children: CT and MR imaging findings. AJR Am J Roentgenol. 1991;156(6):1219–24.
2. Bilaniuk LT, Farber M. Imaging of developmental anomalies of the eye and the orbit. AJNR Am J Neuroradiol. 1992;13(2):793–803.
3. Coleman LT, Zimmerman RA. Pediatric craniospinal spiral CT: current applications and future potential. Semin Ultrasound CT MR. 1994;15(2):148–55.
4. Boone JM. Multidetector CT: opportunities, challenges, and concerns associated with scanners with 64 or more detector rows. Radiology. 2006;241(2):334–7.
5. Tien RD, Chu PK, Hesselink JR, Szumowski J. Intra- and paraorbital lesions: value of fat-suppression MR imaging with paramagnetic contrast enhancement. AJNR Am J Neuroradiol. 1991;12(2):245–53.
6. Bilaniuk LT, Zimmerman RA, Newton RH. Magnetic resonance imaging: orbital pathology. In: Newton TBL, editor. Radiology of the eye and orbit. New York: Raven Press; 1990.
7. Bilaniuk LT, Rapoport RJ. Magnetic resonance imaging of the orbit. Top Magn Reson Imaging. 1994;6(3):167–81.
8. Kapur R, Sepahdari AR, Mafee MF, et al. MR imaging of orbital inflammatory syndrome, orbital cellulitis, and orbital lymphoid lesions: the role of diffusion-weighted imaging. AJNR Am J Neuroradiol. 2009;30(1):64–70.
9. Razek AA, Elkhamary S, Mousa A. Differentiation between benign and malignant orbital tumors at 3-T diffusion MR-imaging. Neuroradiology. 2011;53(7):517–22.
10. Politi LS, Forghani R, Godi C, et al. Ocular adnexal lymphoma: diffusion-weighted mr imaging for differential diagnosis and therapeutic monitoring. Radiology. 2010;256(2):565–74.
11. Prat MC, Surapaneni K, Chalian H, DeLaPaz RL, Kazim M. Ocular adnexal lymphoma: monitoring response to therapy with diffusion-weighted imaging. Ophthal Plast Reconstr Surg. 2013;29(6):424–7.
12. Sepahdari AR, Aakalu VK, Setabutr P, Shiehmorteza M, Naheedy JH, Mafee MF. Indeterminate orbital masses: restricted diffusion at MR imaging with echo-planar diffusion-weighted imaging predicts malignancy. Radiology. 2010;256(2):554–64.
13. Chavhan GB, Babyn PS, Jankharia BG, Cheng HL, Shroff MM. Steady-state MR imaging sequences: physics, classification, and clinical applications. Radiographics. 2008;28(4):1147–60.
14. Hingwala D, Chatterjee S, Kesavadas C, Thomas B, Kapilamoorthy TR. Applications of 3D CISS sequence for problem solving in neuroimaging. Indian J Radiol Imaging. 2011;21(2):90–7.
15. Algin O, Hakyemez B, Gokalp G, Ozcan T, Korfali E, Parlak M. The contribution of 3D-CISS and contrast-enhanced MR cisternography in detecting cerebrospinal fluid leak in patients with rhinorrhoea. Br J Radiol. 2010;83(987):225–32.
16. Pattharanitima P, Tasanarong A. Pharmacological strategies to prevent contrast-induced acute kidney injury. Biomed Res Int. 2014;2014:236930.
17. Akyuz S, Karaca M, Kemaloglu Oz T, et al. Efficacy of oral hydration in the prevention of contrast-induced acute kidney injury in patients undergoing coronary angiography or intervention. Nephron Clin Pract. 2014;128(1–2):95–100.
18. Grossman RI, Yousem DM. Neuroradiology: the requisites. 2nd ed. Philadelphia: Mosby; 2003.
19. Media ACoRCoDaC. ACR manual on contrast media. 2013; version 10.2: http://www.acr.org/~/media/37D84428BF1D4E1B9A3A2918DA9E27A3.pdf. Accessed Sept 2016.
20. Wertman R, Altun E, Martin DR, et al. Risk of nephrogenic systemic fibrosis: evaluation of gadolinium chelate contrast agents at four American universities. Radiology. 2008;248(3):799–806.
21. Yang L, Krefting I, Gorovets A, et al. Nephrogenic systemic fibrosis and class labeling of gadolinium-based contrast agents by the Food and Drug Administration. Radiology. 2012;265(1):248–53.
22. Thomsen HS, European Society of Urogenital R. ESUR guideline: gadolinium-based contrast media and nephrogenic systemic fibrosis. Eur Radiol. 2007;17(10):2692–6.
23. Schlaudecker JD, Bernheisel CR. Gadolinium-associated nephrogenic systemic fibrosis. Am Fam Physician. 2009;80(7):711–4.
24. Marckmann P, Skov L, Rossen K, Thomsen HS. Clinical manifestation of gadodiamide-related nephrogenic systemic fibrosis. Clin Nephrol. 2008;69(3):161–8.
25. Garovic VD, Helgen KE. Images in clinical medicine. Nephrogenic fibrosing dermopathy. N Engl J Med. 2007;357(2):e2.
26. Krefting I. Gadolinium-Based Contrast Agents (GBCAs) and the NSF risk: regulatory update: U.S. FDA. 2011.; http://www.fda.gov/downloads/advisorycommittees/committeesmeetingmaterials/drugs/peripheralandcentralnervoussystemdrugsadvisorycommittee/ucm241072.
27. Roberts DR, Chatterjee AR, Yazdani M, et al. Pediatric patients demonstrate progressive T1-weighted hyperintensity in the dentate nucleus following multiple doses of gadolinium-based contrast agent. AJNR Am J Neuroradiol. 2016;37(8):1427–31.
28. Hu HH, Pokorney A, Towbin RB, Miller JH. Increased signal intensities in the dentate nucleus and globus pallidus on unenhanced T1-weighted images: evidence in children undergoing multiple gadolinium MRI exams. Pediatr Radiol. 2016;46:1590–98.
29. Brenner DJ, Hall EJ. Computed tomography – an increasing source of radiation exposure. N Engl J Med. 2007;357(22):2277–84.
30. Shah NB, Platt SL. ALARA: is there a cause for alarm? Reducing radiation risks from computed tomography scanning in children. Curr Opin Pediatr. 2008;20(3):243–7.
31. Brenner DJ, Hricak H. Radiation exposure from medical imaging: time to regulate? JAMA. 2010;304(2):208–9.
32. Hall EJ, Brenner DJ. Cancer risks from diagnostic radiology. Br J Radiol. 2008;81(965):362–78.
33. Tubiana M, Feinendegen LE, Yang C, Kaminski JM. The linear no-threshold relationship is inconsistent with radiation biologic and experimental data. Radiology. 2009;251(1):13–22.
34. Chen JX, Kachniarz B, Gilani S, Shin JJ. Risk of malignancy associated with head and neck CT in children: a systematic review. Otolaryngol Head Neck Surg. 2014;151(4):554–66.
35. Pearce MS. Patterns in paediatric CT use: an international and epidemiological perspective. J Med Imaging Radiat Oncol. 2011;55(2):107–9.
36. Amis ES Jr, Butler PF, Applegate KE, et al. American College of Radiology white paper on radiation dose in medicine. J Am Coll Radiol. 2007;4(5):272–84.
37. Brody AS, Frush DP, Huda W, Brent RL. Radiation risk to children from computed tomography. Pediatrics. 2007;120(3):677–82.
38. Brenner D, Elliston C, Hall E, Berdon W. Estimated risks of radiation-induced fatal cancer from pediatric CT. AJR Am J Roentgenol. 2001;176(2):289–96.
39. Pearce MS, Salotti JA, Little MP, et al. Radiation exposure from CT scans in childhood and subsequent risk of leukaemia and brain tumours: a retrospective cohort study. Lancet. 2012;380(9840):499–505.
40. Mathews JD, Forsythe AV, Brady Z, et al. Cancer risk in 680,000 people exposed to computed tomography scans in childhood or adolescence: data linkage study of 11 million Australians. BMJ. 2013;346:f2360.
41. Meulepas JM, Ronckers CM, Smets AM, et al. Leukemia and brain tumors among children after radiation exposure from CT scans: design and methodological opportunities of the Dutch Pediatric CT Study. Eur J Epidemiol. 2014;29(4):293–301.

42. Ware DE, Huda W, Mergo PJ, Litwiller AL. Radiation effective doses to patients undergoing abdominal CT examinations. Radiology. 1999;210(3):645–50.
43. Frush DP, Applegate K. Computed tomography and radiation: understanding the issues. J Am Coll Radiol. 2004;1(2):113–9.
44. Linton OW, Mettler FA Jr. National conference on dose reduction in CT, with an emphasis on pediatric patients. AJR Am J Roentgenol. 2003;181(2):321–9.
45. Mettler FA Jr, Wiest PW, Locken JA, Kelsey CA. CT scanning: patterns of use and dose. J Radiol Prot. 2000;20(4):353–9.
46. Frush DP. Pediatric dose reduction in computed tomography. Health Phys. 2008;95(5):518–27.
47. Shelsta HN, Bilyk JR, Rubin PA, Penne RB, Carrasco JR. Wooden intraorbital foreign body injuries: clinical characteristics and outcomes of 23 patients. Ophthal Plast Reconstr Surg. 2010;26(4):238–44.
48. Larson DB, Rader SB, Forman HP, Fenton LZ. Informing parents about CT radiation exposure in children: it's OK to tell them. AJR Am J Roentgenol. 2007;189(2):271–5.
49. Committee ACoRA. ACR appropriateness criteria. Orbits, vision and visual loss; 2012. https://acsearch.Acr.Org/docs/69486/narrative. Accessed Sept 2016.
50. Pagon RA. Ocular coloboma. Surv Ophthalmol. 1981;25(4):223–36.
51. Anderson DR. The development of the trabecular meshwork and its abnormality in primary infantile glaucoma. Trans Am Ophthalmol Soc. 1981;79:458–85.
52. Barkovich AJ, Fram EK, Norman D. Septo-optic dysplasia: MR imaging. Radiology. 1989;171(1):189–92.
53. Francois J. Malformative syndrome with cryptophthalmia. Int Ophthalmol Clin. 1968;8(4):817–37.
54. Levine RS, Powers T, Rosenberg HK, Siegel CA, Bilaniuk LT. The cryptophthalmos syndrome. AJR Am J Roentgenol. 1984;143(2):375–6.
55. Nugent RA, Lapointe JS, Rootman J, Robertson WD, Graeb DA. Orbital dermoids: features on CT. Radiology. 1987;165(2):475–8.
56. Krafka J. Teratoma: an explanation of its cause based on the organizer theory of embryology. Arch Path. 1936;21:756.
57. Alkemade PP. Congenital teratoma of the orbit. Ophthalmologica. 1976;173(3–4):274–85.
58. Levin ML, Leone CR Jr, Kincaid MC. Congenital orbital teratomas. Am J Ophthalmol. 1986;102(4):476–81.
59. Brooks-Kayal AR, Liu GT, Menacker SJ, Heher KL, Katowitz JA, Bilaniuk LT. Tonic pupil and orbital glial-neural hamartoma in infancy. Am J Ophthalmol. 1995;119(6):809–11.
60. Braffman BH, Zimmerman RA, Rabischong P. Cranial nerves III, IV and VI: a clinical approach to the evaluation of their dysfunction. In: Harnsberger R, editor. Seminars in ultrasound, CT and MR. Philadelphia: Grune & Statton; 1987. p. 185–213.
61. Blake PY, Mark AS, Kattah J, Kolsky M. MR of oculomotor nerve palsy. AJNR Am J Neuroradiol. 1995;16(8):1665–72.
62. Rosner RS. Double elevator paralysis. Am J Ophthalmol. 1963;55:87–93.
63. Hatton MP, Watkins LM, Rubin PA. Orbital fractures in children. Ophthal Plast Reconstr Surg. 2001;17(3):174–9.
64. McGraw BL, Cole RR. Pediatric maxillofacial trauma. Age-related variations in injury. Arch Otolaryngol Head Neck Surg. 1990;116(1):41–5.
65. Maisel H. Postnatal growth and anatomy of the face. In: Mathog RH, editor. Maxillofacial trauma. Baltimore: Willimas & Wilkins; 1984.
66. Koltai PJ, Amjad I, Meyer D, Feustel PJ. Orbital fractures in children. Arch Otolaryngol Head Neck Surg. 1995;121(12):1375–9.
67. Chapman VM, Fenton LZ, Gao D, Strain JD. Facial fractures in children: unique patterns of injury observed by computed tomography. J Comput Assist Tomogr. 2009;33(1):70–2.
68. Hink EM, Wei LA, Durairaj VD. Clinical features and treatment of pediatric orbit fractures. Ophthal Plast Reconstr Surg. 2014;30(2):124–31.
69. Jordan DR, Allen LH, White J, Harvey J, Pashby R, Esmaeli B. Intervention within days for some orbital floor fractures: the white-eyed blowout. Ophthal Plast Reconstr Surg. 1998;14(6):379–90.
70. Parbhu KC, Galler KE, Li C, Mawn LA. Underestimation of soft tissue entrapment by computed tomography in orbital floor fractures in the pediatric population. Ophthalmology. 2008;115(9):1620–5.
71. Lane K, Penne RB, Bilyk JR. Evaluation and management of pediatric orbital fractures in a primary care setting. Orbit. 2007;26(3):183–91.
72. Kelly WM, Paglen PG, Pearson JA, San Diego AG, Soloman MA. Ferromagnetism of intraocular foreign body causes unilateral blindness after MR study. AJNR Am J Neuroradiol. 1986;7(2):243–5.
73. Bilaniuk LT, Zimmerman RA. Facial trauma. New York: Churchill Livingstone; 1984.
74. Dalley RW. Intraorbital wood foreign bodies on CT: use of wide bone window settings to distinguish wood from air. AJR Am J Roentgenol. 1995;164(2):434–5.
75. Zimmerman RA, Bilaniuk LT. CT of orbital infection and its cerebral complications. AJR Am J Roentgenol. 1980;134(1):45–50.
76. Rebsamen SL, Bilaniuk LT, Granet D, et al. Orbital wall infarction in sickle cell disease: MR evaluation. AJNR Am J Neuroradiol. 1993;14(3):777–9.
77. Zinreich SJ, Kennedy DW, Malat J, et al. Fungal sinusitis: diagnosis with CT and MR imaging. Radiology. 1988;169(2):439–44.
78. Som PM, Dillon WP, Curtin HD, Fullerton GD, Lidov M. Hypointense paranasal sinus foci: differential diagnosis with MR imaging and relation to CT findings. Radiology. 1990;176(3):777–81.
79. Som PM, Dillon WP, Fullerton GD, Zimmerman RA, Rajagopalan B, Marom Z. Chronically obstructed sinonasal secretions: observations on T1 and T2 shortening. Radiology. 1989;172(2):515–20.
80. Spindle J, Tang SX, Davies B, et al. Pediatric idiopathic orbital inflammation: clinical features of 30 cases. Ophthal Plast Reconstr Surg. 2016;32(4):270–4.
81. Wilner HI, Cohn EM, Kling G, Jampel RS. Computer assisted tomography in experimentally induced orbital pseudotumor. J Comput Assist Tomogr. 1978;2(4):431–5.
82. Wladis EJ, Iglesias BV, Gosselin EJ. Characterization of the molecular biologic milieu of idiopathic orbital inflammation. Ophthal Plast Reconstr Surg. 2011;27(4):251–4.
83. Frohman LP, Guirgis M, Turbin RE, Bielory L. Sarcoidosis of the anterior visual pathway: 24 new cases. J Neuroophthalmol. 2003;23(3):190–7.
84. Srinivasan A, Kleinberg TT, Murchison AP, Bilyk JR. Laboratory investigations for diagnosis of autoimmune and inflammatory periocular disease: part II. Ophthal Plast Reconstr Surg. 2016;
85. Bonavolonta G, Strianese D, Grassi P, et al. An analysis of 2,480 space-occupying lesions of the orbit from 1976 to 2011. Ophthal Plast Reconstr Surg. 2013;29(2):79–86.
86. Shields JA, Shields CL, Scartozzi R. Survey of 1264 patients with orbital tumors and simulating lesions: the 2002 Montgomery lecture, part 1. Ophthalmology. 2004;111(5):997–1008.
87. Nassiri N, Rootman J, Rootman DB, Goldberg RA. Orbital lymphaticovenous malformations: current and future treatments. Surv Ophthalmol. 2015;60(5):383–405.
88. Lowe LH, Marchant TC, Rivard DC, Scherbel AJ. Vascular malformations: classification and terminology the radiologist needs to know. Semin Roentgenol. 2012;47(2):106–17.
89. Rootman J, Heran MK, Graeb DA. Vascular malformations of the orbit: classification and the role of imaging in diagnosis and treatment strategies*. Ophthal Plast Reconstr Surg. 2014;30(2):91–104.
90. Mulliken JB. Classification of vascular birthmarks. Philadelphia: WB Saunders; 1988.

91. Mulliken JB, Glowacki J. Hemangiomas and vascular malformations in infants and children: a classification based on endothelial characteristics. Plast Reconstr Surg. 1982;69(3):412–22.
92. Ramey NA, Lucarelli MJ, Gentry LR, Burkat CN. Clinical usefulness of orbital and facial time-resolved imaging of contrast kinetics (TRICKS) magnetic resonance angiography. Ophthal Plast Reconstr Surg. 2012;28(5):361–8.
93. Kalin-Hajdu E CJ, Grumbine FL, Hirabayashi KE, Glastonbury CM, Vagefi MR, Kersten RC. Diffusion weighted imaging as a method of diagnosing distensible orbital venous malformations. Paper presented at: ASOPRS2016; Chicago.
94. Harris GJ. Orbital vascular malformations: a consensus statement on terminology and its clinical implications. Orbital Society. Am J Ophthalmol. 1999;127(4):453–5.
95. Heran MK, Rootman J, Sangha BS, Yeo JM. Dynamic arterial and valsalva-augmented venous phase multidetector CT for orbital vascular lesions: a pictorial review*. Ophthal Plast Reconstr Surg. 2014;30(2):180–5.
96. Rubin PA, Bilyk JR, Dunya IM, Weber AL. Spiral CT of an orbital venous malformation. AJNR Am J Neuroradiol. 1995;16(6):1255–7.
97. Graeb DA, Rootman J, Robertson WD, Lapointe JS, Nugent RA, Hay EJ. Orbital lymphangiomas: clinical, radiologic, and pathologic characteristics. Radiology. 1990;175(2):417–21.
98. Pendergrass TW, Davis S. Incidence of retinoblastoma in the United States. Arch Ophthalmol. 1980;98(7):1204–10.
99. Zimmerman RA, Bilaniuk LT. Computed tomography in the evaluation of patients with bilateral retinoblastomas. J Comput Tomogr. 1979;3(4):251–7.
100. Ellsworth RM. The practical management of retinoblastoma. Trans Am Ophthalmol Soc. 1969;67:462–534.
101. Lennox EL, Draper GJ, Sanders BM. Retinoblastoma: a study of natural history and prognosis of 268 cases. Br Med J. 1975;3(5986):731–4.
102. Mafee M. Magnetic resonance imaging: ocular pathology. New York: Raven; 1990.
103. Packer RJ, Savino PJ, Bilaniuk LT, et al. Chiasmatic gliomas of childhood. A reappraisal of natural history and effectiveness of cranial irradiation. Childs Brain. 1983;10(6):393–403.
104. Packer RJ, Sutton LN, Bilaniuk LT, et al. Treatment of chiasmatic/hypothalamic gliomas of childhood with chemotherapy: an update. Ann Neurol. 1988;23(1):79–85.
105. Alvord EC Jr, Lofton S. Gliomas of the optic nerve or chiasm. Outcome by patients' age, tumor site, and treatment. J Neurosurg. 1988;68(1):85–98.
106. Wright JE, McNab AA, McDonald WI. Optic nerve glioma and the management of optic nerve tumours in the young. Br J Ophthalmol. 1989;73(12):967–74.
107. Jenkin D, Angyalfi S, Becker L, et al. Optic glioma in children: surveillance, resection, or irradiation? Int J Radiat Oncol Biol Phys. 1993;25(2):215–25.
108. Dutton JJ. Gliomas of the anterior visual pathway. Surv Ophthalmol. 1994;38(5):427–52.
109. Hoyt WF, Baghdassarian SA. Optic glioma of childhood. Natural history and rationale for conservative management. Br J Ophthalmol. 1969;53(12):793–8.
110. Walrath JD, Engelbert M, Kazim M. Magnetic resonance imaging evidence of optic nerve glioma progression into and beyond the optic chiasm. Ophthal Plast Reconstr Surg. 2008;24(6):473–5.
111. Miller NR. Optic pathway gliomas are tumors! Ophthal Plast Reconstr Surg. 2008;24(6):433.
112. Glass LR, Canoll P, Lignelli A, Ligon AH, Kazim M. Optic nerve glioma: case series with review of clinical, radiologic, molecular, and histopathologic characteristics. Ophthal Plast Reconstr Surg. 2014;30(5):372–6.
113. Stern J, Jakobiec FA, Housepian EM. The architecture of optic nerve gliomas with and without neurofibromatosis. Arch Ophthalmol. 1980;98(3):505–11.
114. DiPaolo DP, Zimmerman RA, Rorke LB, Zackai EH, Bilaniuk LT, Yachnis AT. Neurofibromatosis type 1: pathologic substrate of high-signal-intensity foci in the brain. Radiology. 1995;195(3):721–4.
115. Bilaniuk LT, Zimmerman RA, Savino PJ. Visual pathways. Neuroimaging Clin N Am. 1993:371–83.
116. Zimmerman RA, Bilaniuk LT, Metzger RA, Grossman RI, Schut L, Bruce DA. Computed tomography of orbitalfacial neurofibromatosis. Radiology. 1983;146(1):113–6.
117. Burk DL Jr, Brunberg JA, Kanal E, Latchaw RE, Wolf GL. Spinal and paraspinal neurofibromatosis: surface coil MR imaging at 1.5 T1. Radiology. 1987;162(3):797–801.
118. Held P, Nitz W, Seitz J, et al. Comparison of 2D and 3D MRI of the optic and oculomotor nerve anatomy. Clin Imaging. 2000;24(6):337–43.
119. Dutton JJ. Optic nerve sheath meningiomas. Surv Ophthalmol. 1992;37(3):167–83.
120. Lindblom B, Truwit CL, Hoyt WF. Optic nerve sheath meningioma. Definition of intraorbital, intracanalicular, and intracranial components with magnetic resonance imaging. Ophthalmology. 1992;99(4):560–6.
121. Newman SA, Jane JA. Meningiomas of the optic nerve, orbit, and anterior visual pathways. In: Al-Mefty O, editor. Meningiomas. New York: Raven; 1991. p. 461–94.
122. Lane KA, Bilyk JR, Jakobiec FA. Mesenchymal, fibroosseous, and cartilaginous orbital tumors. In: Albert DM, Miller JW, Azar DT, Blodi BA, editors. Albert and Jakobiec's principles and practice of ophthalmology. 3rd ed. Philadelphia: Saunders; 2008.
123. Jereb B, Haik BG, Ong R, Ghavimi F. Parameningeal rhabdomyosarcoma (including the orbit): results of orbital irradiation. Int J Radiat Oncol Biol Phys. 1985;11(12):2057–65.
124. Zimmerman RA, Bilaniuk LT, Littman P, Raney RB Jr. Computed tomography of pediatric craniofacial sarcoma. J Comput Tomogr. 1978;2(2):113–21.
125. Yousem DM, Lexa FJ, Bilaniuk LT, Zimmerman RI. Rhabdomyosarcomas in the head and neck: MR imaging evaluation. Radiology. 1990;177(3):683–6.
126. Banna M, Aur R, Akkad S. Orbital granulocytic sarcoma. AJNR Am J Neuroradiol. 1991;12(2):255–8.
127. Berres ML, Merad M, Allen CE. Progress in understanding the pathogenesis of Langerhans cell histiocytosis: back to Histiocytosis X? Br J Haematol. 2015;169(1):3–13.
128. Zinn DJ, Chakraborty R, Allen CE. Langerhans cell Histiocytosis: emerging insights and clinical implications. Oncology (Williston Park). 2016;30(2):122–32. 139

Pediatric Orbital and Periocular Infections

33

Scott M. Goldstein, Jill A. Foster, and James A. Katowitz

Orbital and periorbital infections are the most common causes of acute orbital inflammation in children. Despite the widespread availability of neuroimaging and advances in antibiotic therapy, these conditions may still result in significant morbidity and mortality. The conditions of orbital cellulitis and preseptal cellulitis may present with similar patterns of eyelid edema and erythema but are two distinct anatomic disease processes with different etiologies. Both conditions have a peak incidence in childhood, but preseptal cellulitis tends to occur in younger children, particularly toddlers [1–5].

Preseptal Cellulitis

Preseptal cellulitis is an infectious process limited to the skin and subcutaneous tissues anterior to the orbital septum. The orbital septum provides a biologic barrier to the advance of infection from the preseptal area into the orbit. Preseptal cellulitis (Fig. 33.1) is the most common type of periocular infection [6] and typically is a less severe process than orbital cellulitis. Preseptal cellulitis, however, can sometimes be associated with sepsis and bacterial meningitis and should not be considered a benign process [7]. Predisposing factors to the development of preseptal cellulitis include local trauma, skin infection like hordeolums, and upper respiratory infection in young children [8]. Less commonly, conjunctivitis, chalazion, and dacryocystitis are implicated as the etiology of the preseptal infection. Complications attributed to preseptal cellulitis include orbital extension of the disease (2.5–17%) [2, 8, 9], skin abscess requiring surgical intervention (8%) [2], eyelid necrosis (1–2%) [10], and intracranial spread of the disease process (2–3%) [2].

Patients with preseptal cellulitis typically present with a short history of eyelid edema and erythema. The eyelid may be warm and tender to palpation. Predisposing factors, such as an insect bite, skin abrasion, hordeolum, chalazion, dacryocystitis, conjunctivitis, or traumatic foreign body, may be identified during the physical exam. Preseptal cellulitis may cause ocular signs such as chemosis and conjunctival erythema. However, proptosis, pupillary changes, and limited motility are signs of orbital involvement and are not included in the constellation of signs of preseptal disease. Fever and elevated white blood cell count are inconsistent features too. The differential diagnosis for preseptal cellulitis includes periocular allergic reactions, bug bites, angioneurotic edema, trauma, renal disease, thyroid eye disease, and early orbital cellulitis without orbital signs.

Preseptal cellulitis is typically treated with antibiotics. In addition, surgical drainage of collections of purulent material is required if an abscess is present. Antibiotic choice is governed by the suspected infective agent(s) and the age of the patient. Neonates and infants are hospitalized for intravenous antibiotics and monitoring. There are varied opinions on the age when outpatient treatment for preseptal cellulitis becomes appropriate. In children, and particularly infants, the immune system is less effective in defending against infection by encapsulated bacteria [11]. An infant's homeostatic mechanisms are also more fragile than those of a child or adult. We do not promote a dog-

S.M. Goldstein (✉)
Oculoplastic Surgery Service, Wills Eye Hospital, Department of Ophthalmology, Jefferson Medical College and Perelman School of Medicine, University of Pennsylvania, Philadelphia, PA, USA

Oculo-facial Plastic Surgeon, Tri-County Eye Physicians and Divisions, Vantage EyeCare, Philadelphia, PA, USA
e-mail: scottygmd@gmail.com; goldstein@tricountyeye.com

J.A. Foster
Associate Clinical Professor of Ophthalmology, Havener Eye Center at The Ohio State University and Oculoplastic Service, Nationwide Children's Hospital, Columbus, OH, USA

Ophthalmic Surgeons and Consultants of Ohio, Columbus, OH, USA

J.A. Katowitz, MD, FACS
The Children's Hospital of Philadelphia and The Edwin and Fannie Gray Hall Center for Human Appearance, University of Pennsylvania, Philadelphia, PA, USA
e-mail: katowitz@email.chop.edu

© Springer International Publishing AG 2018

J.A. Katowitz, W.R. Katowitz (eds.), *Pediatric Oculoplastic Surgery*, https://doi.org/10.1007/978-3-319-60814-3_33

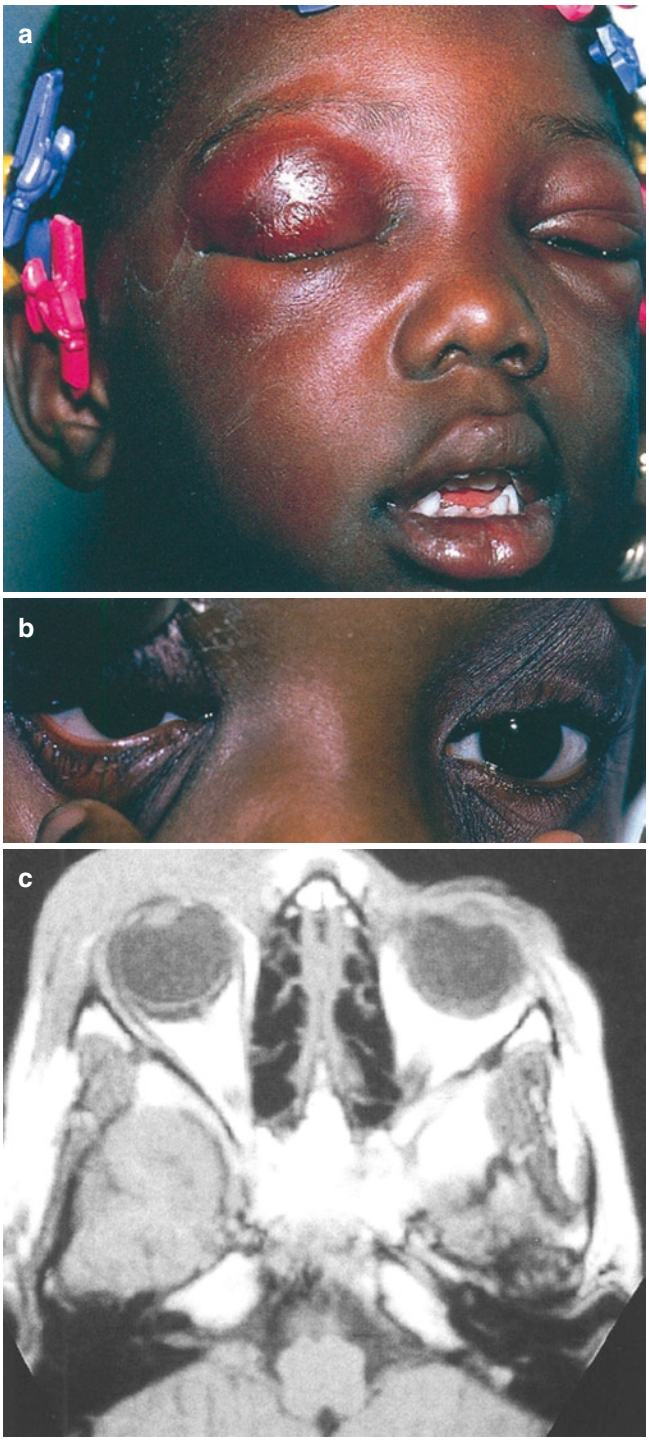


Fig. 33.1 Preseptal cellulitis. (**a**) Clinical appearance of a posttraumatic preseptal cellulitis in a 7-year-old child who scraped her eyelid on the corner of a bed frame. (**b**) Ocular exam on this patient shows absence of conjunctival inflammation, absence of proptosis, and normal motility. (**c**) The MRI scan of this patient shows thickening of the preseptal soft tissue, absence of sinus disease, and no evidence of a foreign body

matic absolute age cutoff for outpatient versus inpatient management of preseptal cellulitis. Rather, we recommend utilization of clinical judgment with a degree of caution. Under the age of 1 year, it is often accepted that a preseptal cellulitis should be managed and monitored on an inpatient basis particularly if the child appears systemically ill or cannot be closely monitored. Between the age of 1 and 5 years, milder cases can be managed with outpatient treatment utilizing appropriate oral antibiotics and close follow-up. Sicker toddlers should be admitted for IV antibiotics. After age 5, it is acceptable to treat stable patients on an oral regimen.

The most common pathogens found in children with preseptal cellulitis are *Staphylococcus aureus* and *Streptococcus* species [7, 8, 12, 13]. Furthermore, methicillin-resistant *S. aureus* has become a more prominent factor in the past 10 years [14]. Other bacteria, like *Streptococcus pneumoniae* and *Haemophilus influenzae*, used to be more prevalent; however, the introduction of the pneumococcal and H. flu vaccines has dramatically reduced the incidence of these infections over the past quarter century [15–18]. Cultures may be obtained by collecting purulent material at the site of the infection, while blood cultures should be obtained in children who are febrile. Culturing the conjunctiva or aspiration of the leading edge of the cellulitis is less rewarding in the yield of positive cultures. Initial selection of antibiotics may be guided by the Gram stain and then modified according to the results of the culture and sensitivities. Specific antibiotic regimens become rapidly outdated, but a suggested regimen is provided below. When available, consultation with a pediatric infectious disease specialist is recommended. When there is a superficial component to the infection, the periorbital skin may also be treated with a topical antibiotic. The preseptal cellulitis should be reevaluated 24–36 h into treatment, at which time improvement should be apparent. Failure to improve or worsening of the disease should initiate a reconsideration of imaging to rule out an abscess, foreign body, or postseptal disease. Antibiotic choices should also be reviewed when culture results are available or be reconsidered with the prevalence of antibiotic resistance that exists today. For routine imaging of a preseptal cellulitis, computed tomography scan (CT) better delineates the bone structure of the orbit, but in cases of a suspected nonmetallic foreign body, magnetic resonance imaging scan (MRI) may be more sensitive.

Surgery is indicated if an abscess or foreign body is identified. These should be drained or removed. The original site of the trauma may be used for surgical access, or an adjacent surgical landmark may be appropriate. Incisions placed in the lid crease in the upper eyelid, the subciliary area in the lower lid, or the lateral canthal angle will leave a cosmetically acceptable scar. After removal of the foreign body and drainage of the purulent material, the area is copiously irrigated with saline or antibiotic solution. The area of the wound or incision may be left open with a drain to prevent reaccumulation of the abscess.

Necrotizing fasciitis (Fig. 33.2) is a more acute and severe infection caused by aerobic or anaerobic microorganisms that is characterized by its rapid spread along and through the soft tissue, causing necrosis of the fascia, overlying skin, and subcutaneous soft tissue. This condition may occur in the eyelids and orbit [19, 20]. Mortality rates for this type of infection range from 30 to 76%. Patients develop systemic toxicity with sepsis, organ failure, respiratory failure, and death. The diagnosis should be considered in any soft tissue infection presenting with signs of systematic toxicity and

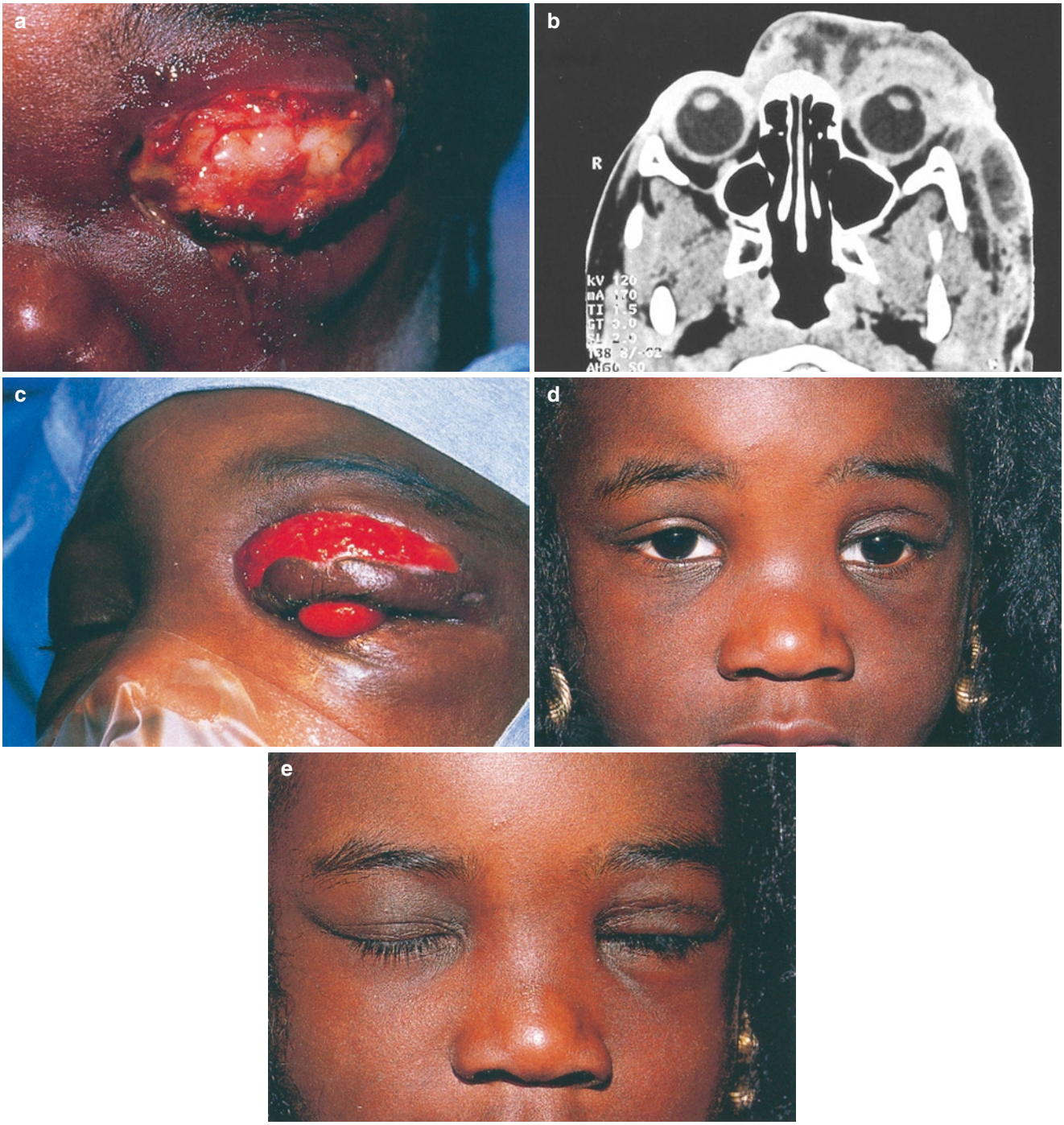


Fig. 33.2 Necrotizing fasciitis. (**a**) This 4-year-old presented with a history of soft tissue trauma to the upper lid with rapidly progressing necrosis of the tissues over the next 2 days. (**b**) The CT scan shows marked soft tissue edema and subcutaneous gas. (**c**) Granulation tissue forming 2 weeks following surgical debridement. Note prolapsed upper cul-de-sac. (**d**) Postoperative appearance 5 months following excision of prolapsed tissue and repair by multiple mattress sutures of 5–0 chromic catgut. No skin grafting was necessary, only spontaneous granulation. (**e**) Downgaze with minimal lid lag

marked edema, because the prognosis is closely linked with early recognition. In children, *Streptococcus* and polymicrobial culture results are reported [20]. Therapy includes broad-spectrum antibiotics (penicillin, aminoglycoside, and metronidazole), early and aggressive surgical debridement, systemic support, and hyperbaric oxygen.

Antibiotic Treatment for Preseptal Cellulitis

Inpatient

Vancomycin 10–15 mg/kg IV Q 8 hours and clindamycin 15–25 mg/kg/day divided Q 8 h.

Outpatient

Trimethoprim/sulfamethoxazole 10 mg/kg/day TMP divided q12 h.

Clindamycin 10–25 mg/kg/day divided Q8 h.

Orbital Cellulitis

Orbital cellulitis is differentiated from preseptal cellulitis by the presence and signs of the postseptal infectious disease process. Orbital cellulitis most commonly arises from spread of contiguous sinus disease but can also arise from traumatic violation of the orbit with implantation of infectious material, trans-septal spread of preseptal cellulitis, or metastatic hematogenous spread of infection to the orbit. The infection may also begin as a dental abscess that spreads to the orbit. Since the orbital process most often arises from spread of infection from the paranasal sinuses, it is helpful to have an ENT consultation involved early with these patients as sinus surgery is an integral part of successful management when surgery is required [21]. Chronic sinusitis is identified as the cause of orbital infection in 75–85% of cases [22]. Conversely, orbital involvement occurs in only 0.5–3% of patients with acute sinusitis [23]. In children, the infected sinus cavities most often seen in association with orbital cellulitis are the ethmoid air cells.

The sinuses and orbit have several anatomic relationships that predispose to the communication of infection and inflammatory processes. Natural dehiscences are often present in the orbital walls, especially the lamina papyracea over the ethmoid sinuses [24]. Bony dehiscences are also reported in the walls of the sphenoid sinus [25]. These disruptions in the sphenoid bone put the optic nerve at risk for septic optic neuritis. The thin wall of the lamina papyracea may also erode in the face of infection, allowing direct communication of the purulent material within the sinus to the subperiosteal space of the orbit. Vascular flow of the valveless orbital veins will allow blood flow to occur from the sinuses to the orbit, another avenue for communication of the infection. The anterior and posterior ethmoidal foramina are additional natural conduits between the sinuses and orbit. All of these features of orbital and sinus anatomy create an avenue for transmission of sinus infection to the orbit.

Definitions of the clinical characteristics of orbital complications of sinusitis were described in a classification system developed by Hubert [26], Smith and Spencer [27], and, more recently, Chandler et al. [6] in the twentieth century. Although the classification system (below) should not be overemphasized as a stepwise progression of the disease process, the description of the clinical characteristics remains a valuable way of defining the severity and location of the infectious process. Orbital imaging is also helpful in staging orbital cellulitis [28]. Nonetheless, it is the clinical exam, disease severity, and progression that are the paramount factors in determining treatment.

Class I (inflammatory edema, Fig. 33.3) is defined by the clinical characteristics of eyelid edema and erythema. This may occur because of congestion of the venous drainage system or transmission of inflammatory mediators from the infected sinuses into the periorbital soft tissue. This stage is sometimes called a preseptal cellulitis, but it is preferable not

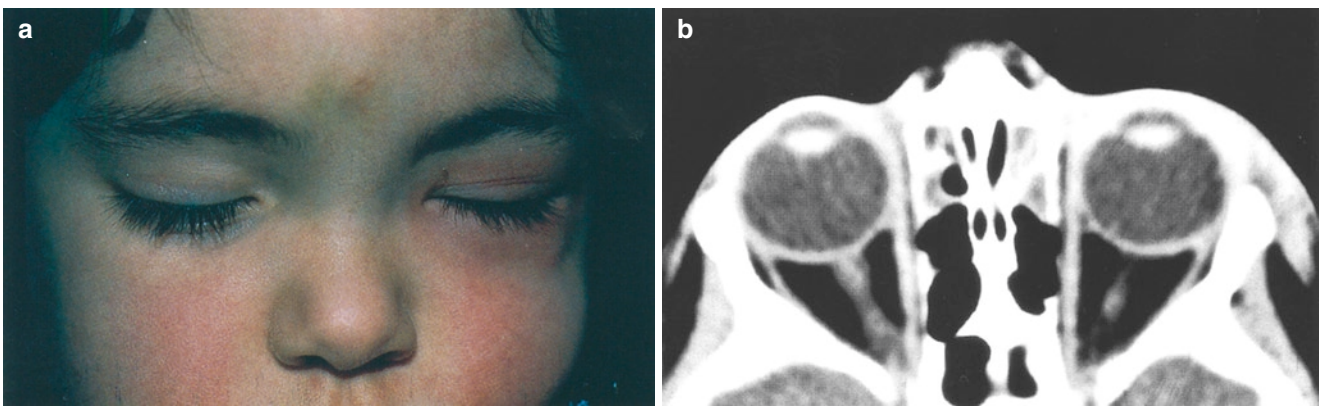


Fig. 33.3 Sinusitis with preseptal inflammation. (**a**) This patient has edema and erythema of the left periocular region. (**b**) The CT scan demonstrates soft tissue edema of the eyelids, opacification of the ethmoid air cells, and normal orbital contents

to use the same term that is used for a preseptal infectious process. In orbital cellulitis, this is an inflammatory response to the sinusitis. Orbital signs of decreased motility, proptosis, or alteration of the pupillary response are absent in the patients who fit the description of class I.

Class II (orbital cellulitis, Fig. 33.4) is differentiated from class I by the presence of eyelid findings and signs of orbital involvement, such as proptosis, restriction of extraocular movements, pupillary defects, and alteration in vision. The diagnosis is confirmed with radiologic evidence of postseptal soft tissue changes. These changes are diffuse soft tissue thickening within the contents of the orbit. Localized collections of infectious material are described in the other classes.

An additional class could be added to the Chandler classes to describe the clinical process of a subperiosteal effusion (Fig. 33.5). This effusion typically develops between the periosteum of the medial orbital and the underlying ethmoid sinuses. The effusion is an inflammatory elevation of the medial periosteum with sterile fluid found between the periosteum and the medial orbital bony wall. By imaging, it is difficult to assess whether this collection is an inflammatory process or whether it will be purulent material [29]. A collection of purulent subperiosteal material is the next classic step in the Chandler classification system (class III subperiosteal abscess, Fig. 33.6). An effusion may resolve when the sinusitis is medically treated, but a subperiosteal abscess is more likely to be resistant to antibiotic treatment and require surgical intervention. Many papers have been written trying to determine what size subperiosteal abscess can be managed medically versus which larger ones require surgery [30–32].

These subsets of patients with subperiosteal fluid collections are challenging to the clinician because the two groups will be similar by clinical appearance and radiologic imaging but will differ in the necessity for surgical drainage. The signs and symptoms of the subperiosteal fluid collections are often similar to class I or class II. At times a subperiosteal

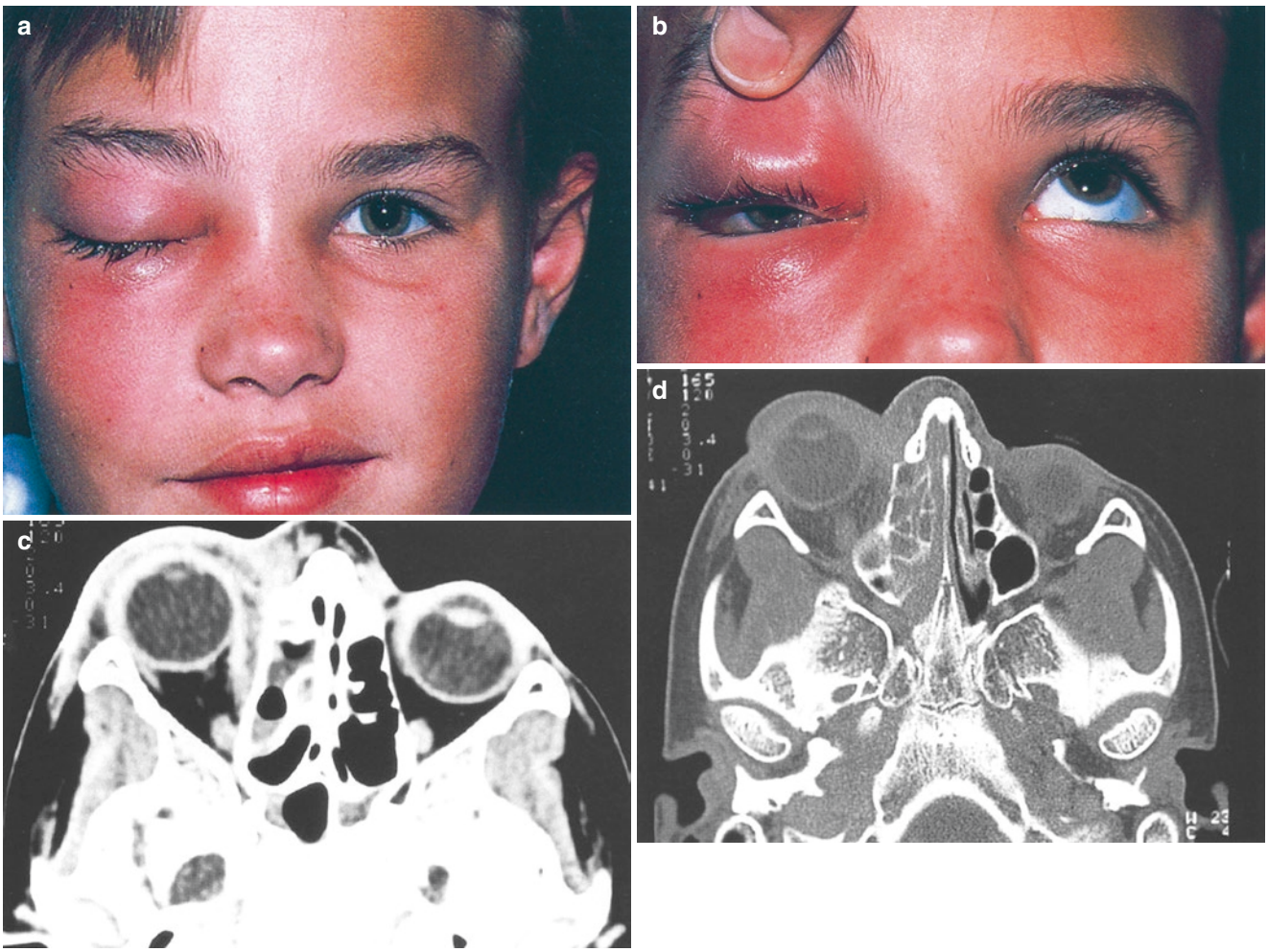


Fig. 33.4 Orbital cellulitis. (**a**) External photograph shows edema and erythema of the right periocular region. (**b**) This patient's attempted upgaze with limitation of motility. (**c**) CT scan shows the soft tissue thickening of the orbital tissue. (**d**) The CT bone windows better demonstrate the extent of the sinus opacification

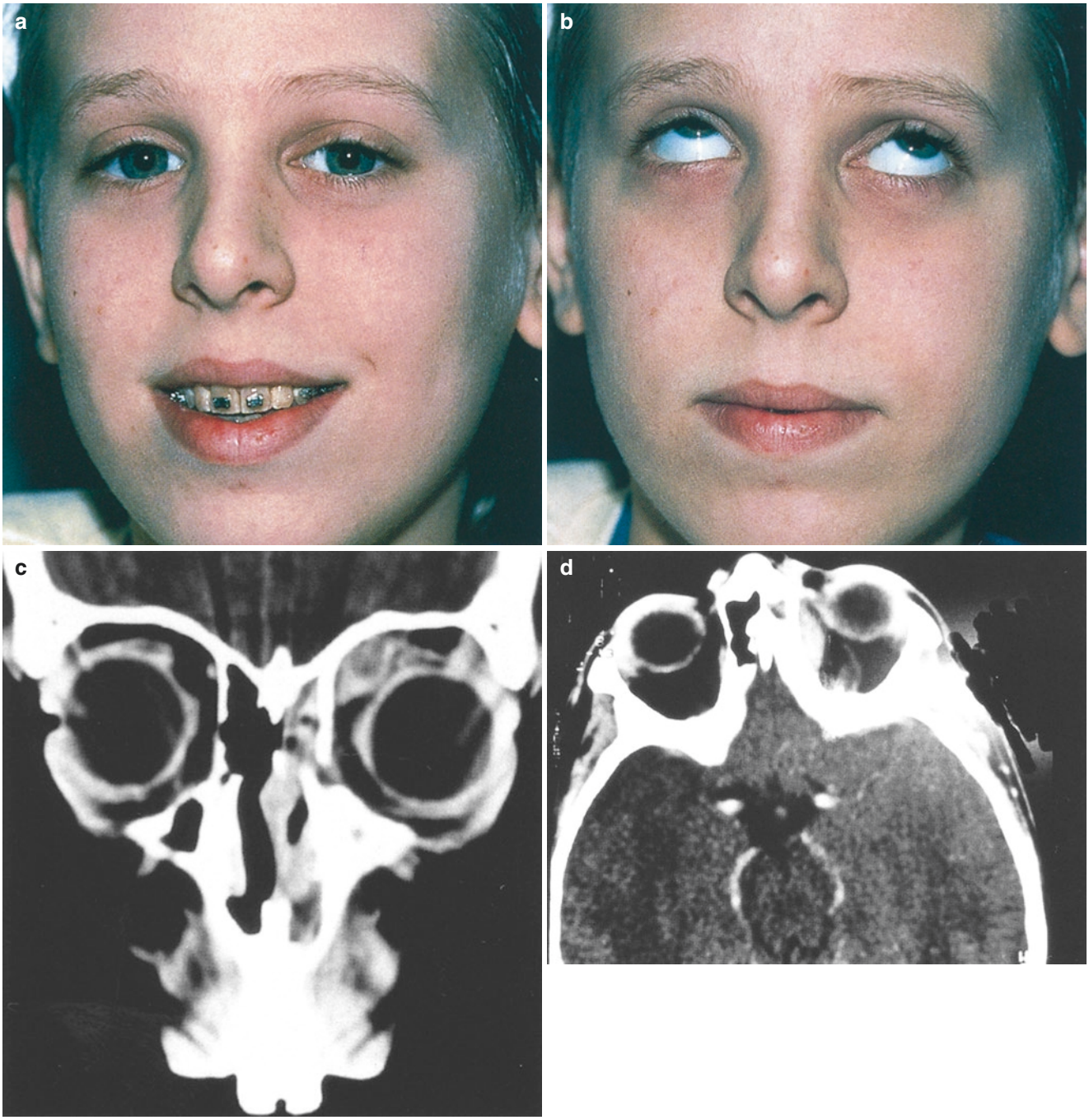


Fig. 33.5 Subperiosteal effusion. (**a**) This 11-year-old patient presented with a complaint of double vision. (**b**) The alteration in motility is seen in upgaze. (**c**) The coronal CT scan demonstrates his left-sided sinusitis and subperiosteal fluid collection. (**d**) Axial CT shows the medial subperiosteal fluid collection. Surgical drainage showed a clear effusion under the periosteum of the medial orbital wall

effusion or subperiosteal abscess will cause a nonaxial proptosis, whereas typically the proptosis caused by diffuse orbital cellulitis will move the globe anteriorly. In the case of a subperiosteal effusion or abscess, the globe is deviated away from the location of the fluid collection. The presence of a subperiosteal fluid collection is recognized only after imaging studies and then becomes a management issue. In a stable patient with good vision and no afferent pupillary defect, it is usually appropriate to initiate a trial of antibiotics rather than moving directly to surgical drainage [33]. Antibiotics alone may clear the sinusitis and an inflammatory effusion may respond without surgical intervention. Patients with decreased vision, afferent pupillary defects, or other deteriorating clinical signs should have urgent drainage



Fig. 33.6 Subperiosteal abscess in orbital cellulitis. (**a**) Photograph in primary gaze demonstrating edema, erythema, and proptosis. (**b**) Photograph in upgaze demonstrating limitation of ocular motility in the left eye. (**c**) CT scan of this patient with ethmoidal sinusitis, a medial subperiosteal abscess, and orbital cellulitis

[30]. At the time of surgery, the subperiosteal fluid may be cultured and smeared to determine whether it is an effusion or purulent fluid.

When the periosteum loses its integrity, or when there is inoculation of the infectious material directly into the orbit, an orbital abscess or collection of purulent material within the soft tissues of the orbit may occur (class IV, orbital abscess, Fig. 33.7). This direct continuity between the purulent material and the orbital tissue puts the orbital structures at higher risk for complications. The septic material and the inflammatory response arc toxic to the orbital tissues. The abscess must be drained, and it is not unusual for successful resolution of an intraorbital abscess to require more than one drainage attempt. However, as noted earlier, combined drainage of sinus infection and the orbital abscess has a lower incidence of reaccumulation of the infection [32]. In the case of an intraconal abscess, it may be necessary to temporarily disinsert an extraocular muscle to access the abscess for drainage. As with any abscess, a pathway for postoperative drainage should be maintained. Sterile rubber bands or Penrose drains may be used for this purpose in the case of an intraorbital abscess.

When the infectious and inflammatory processes follow the venous system posteriorly, a cavernous sinus thrombosis may result (class V). When the infection begins as a unilateral problem, the spread of lid edema and skin discoloration to both sides is a clue to possible extension to the cavernous sinus. Another warning sign is identified when cranial nerve palsies become bilateral or when the motility deficit is identified as a paresis rather than orbital restriction. The physician should be alerted to this when abnormal findings in the extraocular motility are out of proportion with the degree of orbital edema and proptosis. Mental status changes or signs of meningeal irritation will often accompany the cavernous sinus thrombosis. An MRI will be used to diagnose the presence of cavernous sinus thrombosis. *T*2- and proton-weighted images with gadolinium will show high signal luminal narrowing or absence of flow. When a cavernous sinus thrombosis is confirmed, there are relatively few management changes that can be made if the patient has already been adequately treated with antibiotics and all abscesses drained. Heparin therapy has been described, but has not been shown to be helpful in properly controlled studies, and may be precarious in a patient who will need further acute surgical intervention. Ultimately, early suspicion and recognition, with aggressive multidisciplinary treatment, are the keys to managing this rare but devastating complication [34].

Regardless of age, the signs and symptoms of orbital cellulitis mandate hospital admission and intravenous antibiotics as well as dictate the potential need for surgery. The child is admitted and stabilized while intravenous antibiotics are started. As mentioned earlier, antibiotic choices quickly become outdated as the bacteriology of these infections evolve, but suggestions for preliminary choices relevant in 2016 are described below.

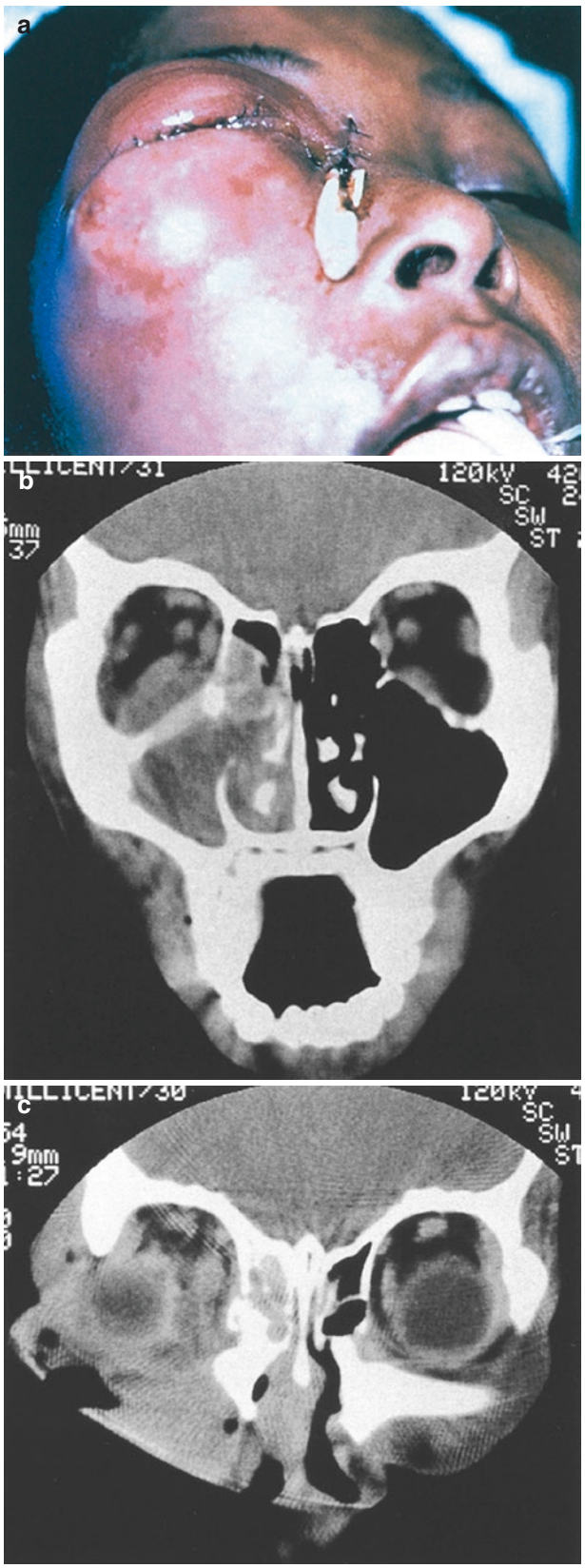


Fig. 33.7 Orbital abscess. (**a**) Intraoperative photo of right orbital abscess. (**b**) CT scan of this patient when the infection was confined to a subperiosteal abscess. (**c**) CT scan 4 days later when the infection has spread to the orbital tissues

Antibiotic choices may be modified according to suspected or cultured bacterial agents. Blood cultures are taken before the antibiotics are started, and other focal lesions, such as conjunctivitis, should be cultured. Screening cultures of normal conjunctiva or the nasopharynx are rarely useful. The organisms responsible for orbital infections are often difficult to determine because of the polymicrobial nature of sinusitis and the abundance of normal bacterial flora on mucosal and skin surfaces. Cultures should be carefully interpreted. Previous antibiotic therapy may also cloud the culture results. In children with orbital cellulitis, the most common organisms isolated by sinus aspirate cultures are *S. aureus*, *Streptococcus* species, and anaerobic species [7, 8, 13, 35]. Particularly in younger children, bacteremia may also be present in cases of orbital cellulitis [23]. Children younger than age 4 have impaired humoral immunity to bacteria with polysaccharide capsules such as *H. influenzae* [7], and bacteremia with these organisms is used to be seen more commonly in this age group. Thankfully, vaccination for *H. influenzae* had a dramatic reduction in these infections.

Once the antibiotics are initiated, the patient is sent for radiologic imaging. Except in certain instances, a CT scan will be requested. That noted, repetition of imaging is unnecessary after the initial scan noting the extent of the infection and treatment is started. Imaging can lag behind the clinical exam, and repeat CT scan, specifically, will expose children to ionizing radiation, which is not entirely innocuous. If cavernous sinus thrombosis, fungal infection, or a vegetative foreign body are anticipated, an MRI scan may be more helpful. In general, the CT scan will adequately image the orbital and sinus processes and better delineate the integrity of the bone.

The results of the imaging are correlated with the patient's signs and symptoms and progress on antibiotic therapy. When the scan of the patient with orbital cellulitis shows sinusitis and/or localized abscess in the orbit in conjunction with a new afferent pupillary defect and significant decreased vision, surgical intervention is indicated. In the child with normal vision and no afferent pupillary defect, close observation is reasonable while medical therapy is initiated. The presence of sinusitis or a subperiosteal elevation in this situation is a softer indication for surgical intervention. Judgment will be used in the face of the patient's total clinical picture over a 24- to 36-h period of observation or immediate intervention with surgery. When medical management is chosen, if there is any deterioration in the clinical signs, or if the patient fails to improve in 24–48 h, surgery is again clearly indicated. The presence of an orbital abscess that is not confined by the periosteum is another immediate indication for surgical intervention.

Early and aggressive use of intravenous antibiotics is often very successful in treating the majority of infections [36]. Children 9 years old and younger usually respond to

antibiotics alone, even if there is a small subperiosteal abscess, as these collections tend to represent simple aerobic bacterial collections [31, 36]. Broad-spectrum coverage is particularly important in teenagers as they typically have polymicrobial infections more similar to adults. Often, patients will show a clinical response in 12–24 h. Again, as long as the patient is clinically stable, there is no significant compromise to visual function and there is no large atypical abscess, the antibiotics should be given an opportunity to work. In addition, steroid therapy can be helpful at reducing inflammation and morbidity once the infection responds to the antibiotics [37]. Steroids are often started after a C-reactive protein level falls below 4 mg/dl [38]. Interestingly, Harris recently looked at the evolution of pathogens causing subperiosteal abscess over the previous 40 years [39]. He noted a change in some of the species of *Staphylococcus* and *Streptococcus*, but generally the same patterns of infection exist. Children under 9 years of age tended to have simple aerobic infections, while older children still had polymicrobial infections. The response rate to antibiotics remained about the same as well. One important difference in the past 10 years, however, has been the increased incidence of methicillin-resistant *Staphylococcus aureus* (MRSA) infection. Thus, as the article notes, the clinical exam supersedes age in determining any need for surgery. Moreover, despite the clinical changes in bacteria from vaccines and antibiotics over time, therapeutic management still remains about the same over the years.

The purpose of surgery when necessary is to drain localized collections of bacteria and purulent material in the orbit and sinus as well as open normal drainage of the sinus into the nasal cavity. In children, this most commonly means an approach to the ethmoid sinuses and medial orbit. The medial orbit can be approached through a lid crease, medial canthal, or transcaruncular incision that also provides access to the ethmoid sinuses (Fig. 33.8). In the older child, endoscopic sinus surgery (FESS) techniques are preferred for sinus drainage. When the maxillary sinus is involved, trans-nasal FESS or a Caldwell–Luc approach may be used for sinus drainage and the inferior orbit drained through a subcillary or lid crease incision in the lower eyelid. In the older child where the frontal sinuses are developed, a superior orbital process is also possible (Fig. 33.9). This may be drained through a lid crease or sub-brow incision. Irrespective of the location of the drainage, an open postoperative drainage site must remain patent to prevent reaccumulation of the abscess. Sterile rubber bands, Penrose drains, or suction drainage may be incorporated.

Other conditions may simulate orbital infectious processes in children, most notably orbital inflammatory disease (see Chap. 34). Orbital inflammatory disease may present with a

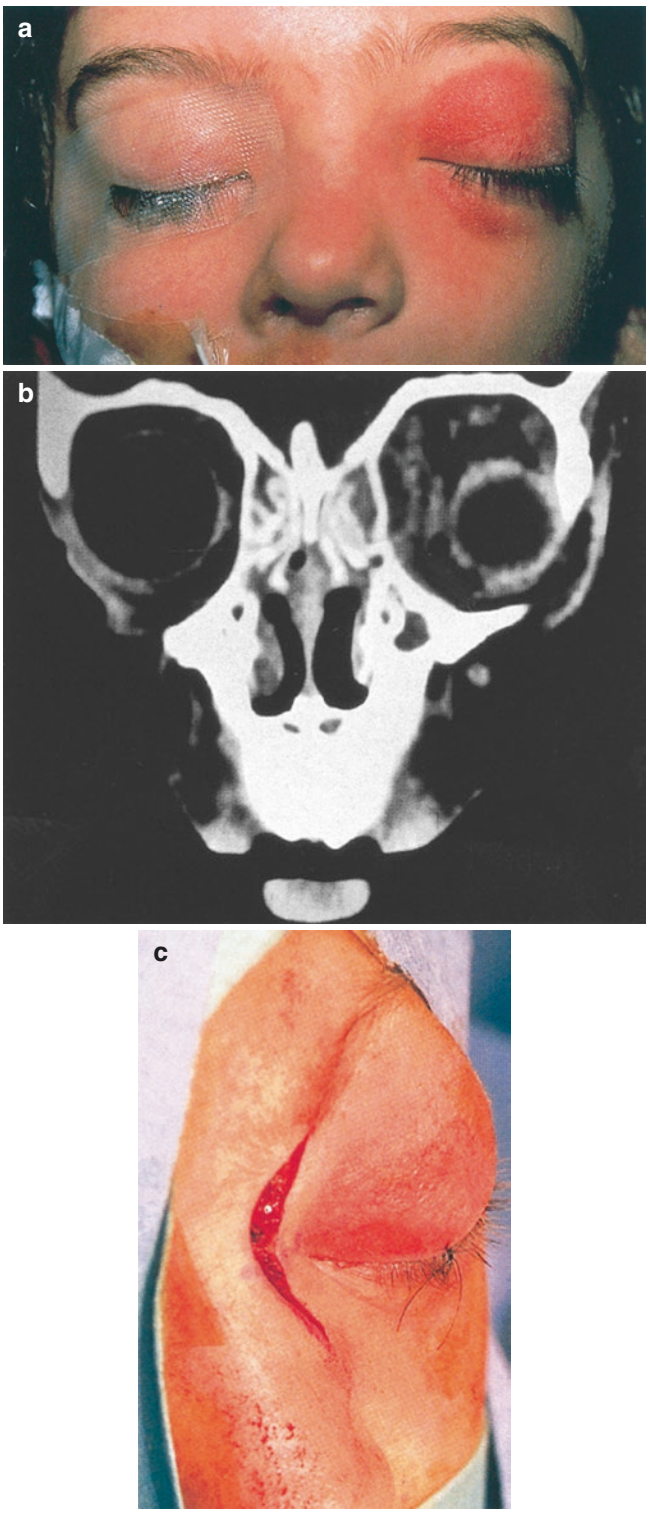


Fig. 33.8 Drainage of ethmoid sinuses and medial orbit. (**a**) A 10-year-old patient with orbital cellulitis, ethmoid sinusitis, and a medial subperiosteal abscess. (**b**) Coronal CT scan demonstrating the radiologic findings; note the medial periosteal elevation over the ethmoid sinuses. (**c**) The abscess is drained through a Lynch incision and an endonasal approach

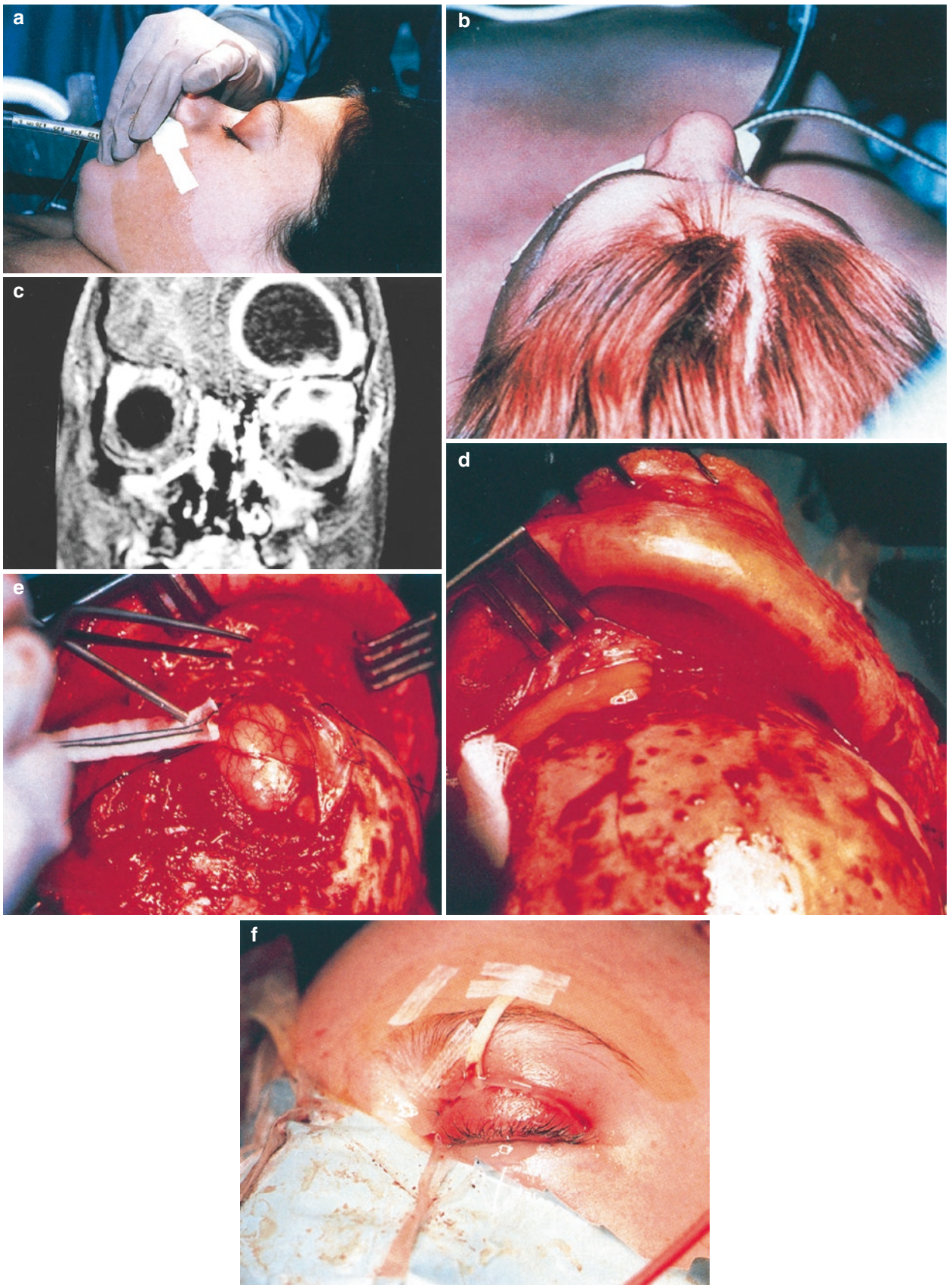


Fig. 33.9 Intraorbital and intracranial abscess. (**a**) This 11-year-old presented with eyelid edema 1 week after being hit in the left eye area with a baseball. (**b**) Proptosis is noted on the patient's left side. (**c**) The MRI scan shows an intraorbital and intracranial collection of fluid. Fractures in the ethmoid and frontal sinuses provided a route for the sinus pathogens to cause an abscess in the superior orbit and in the frontal cortex. (**d**) Drainage of the superior orbital abscess. (**e**) Location of the intracranial abscess. (**f**) External drains in place for the superior orbital abscess



Fig. 33.10 Orbital inflammatory disease. (**a**) Clinical appearance demonstrating pinker hue of periorbital inflammation. (**b**) Early conjunctival chemosis. (**c**) Proptosis. (**d**) Limited mobility on gaze right

similar picture of swelling of the lids, proptosis, erythema of the periocular skin, motility limitations, chemosis, and visual disturbance (Fig. 33.10). Like orbital cellulitis, orbital inflammatory processes are most often unilateral but may be bilateral. There are some subtle differences in the clinical appearance. The color of the periocular inflammation in orbital cellulitis has a redder hue compared to the pinker hue of orbital inflammatory disease. An accompanying iritis may be seen in orbital inflammatory disease but would be atypical of orbital cellulitis. Conjunctival chemosis occurs earlier in orbital inflammatory disease than in orbital cellulitis. Radiologic imaging will help the physician to distinguish orbital cellulitis from orbital inflammatory disease (see Chaps. 32 and 34). The presence of contiguous sinus disease will be a significant feature pointing more to an infectious process. Thickening of the extraocular muscles, enlargement of the lacrimal gland, or a "shaggy" appearance of the orbital fat in the absence of sinus disease will be more typical of an inflammatory process. The clinical picture of the two processes may still be very similar and will sometimes warrant starting IV antibiotics when infection cannot be ruled out. When there are no radiologic indications of infection, and when the condition does not respond to 24 h of IV antibiotics, corticosteroids replace or are added to the antibiotic treatment regimen.

Because of its acute progression and the erythema and thickening of the eyelid skin, rhabdomyosarcoma may also simulate orbital cellulitis. Unlike orbital cellulitis, pain is an unusual feature of rhabdomyosarcoma and may help to distinguish between the two processes. Radiologic imaging will identify bone destruction and invasion with disruption of the architecture of the surrounding structures by the rhabdomyosarcoma. This would be atypical of orbital cellulitis. Biopsy of the sinus or orbital tissue will confirm the diagnosis.

Other conditions that may mimic bacterial orbital cellulitis include carotid cavernous fistula, Wegener's granulomatosis, herpes simplex cellulitis (Fig. 33.11), ruptured dermoid cyst (Fig. 33.12), necrotic retinoblastoma [40], orbital trauma, sickle cell disease with bone infarction (Fig. 33.13), and thyroid eye disease. Imaging, clinical course, and the absence of response to antibiotics are diagnostic features that will provide information to lead the physician to these alternative diagnostic choices.

Despite prompt antibiotic therapy and surgical intervention, orbital infections may lead to serious complications. Intracranial complications such as cavernous sinus thrombosis, subdural abscess, epidural abscess, brain abscess, meningitis, and death have been reported [22, 24, 41]. Decrease or loss of vision may also occur. Mechanisms for this loss of vision include septic optic neuritis, compressive injury to the optic nerve, and thromboembolic lesions to the nerve, retina, or choroid. Permanent orbital scarring may lead to

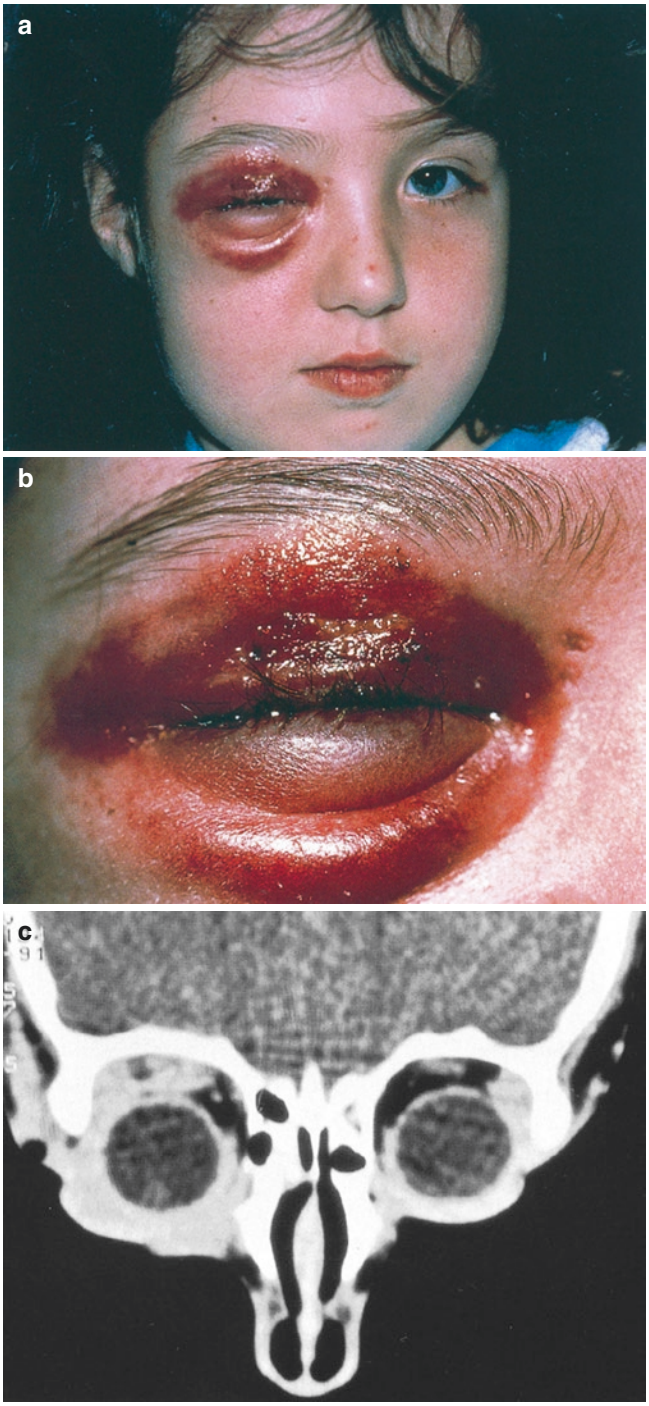


Fig. 33.11 Herpes simplex cellulitis. (**a**) This 12-year-old patient had a mild case of chicken pox and developed a right orbital cellulitis. The process did not respond to intravenous antibiotics, and the tissue culture was positive for herpes simplex I virus. (**b**) The close-up of the eyelid shows the unusual deep red nature of the eyelid erythema. (**c**) The CT scan shows diffuse soft tissue thickening in the orbit with clear sinuses

disruptions in extraocular movement. Scarring of the lids, conjunctiva, and cornea may also occur from the infection or as a result of proptosis and exposure.

Chandler Classification of Orbital Complications in Acute Sinusitis

I. Inflammatory edema
II. Orbital cellulitis
III. Subperiosteal abscess
IV. Orbital abscess
V. Cavernous sinus thrombosis

Antibiotic Treatment for Orbital Cellulitis

Inpatient

Ampicillin/sulbactum 300–600 mg/kg/day divided Q 8 h and clindamycin 15–25 mg/kg/day divided Q 8 h.

Ampicillin/sulbactum 300–600 mg/kg/day divided Q 8 h and vancomycin 10–15 mg/kg IV Q 8 h.

Fungal Infections of the Orbit

Mucormycosis

Mucormycosis is a fungal infection caused by organisms from the genera *Mucor*, *Rhizopus*, and *Absidia.* These are ubiquitous organisms found in air, soil, vegetable matter, bread mold, and fecal material. It is rare for mucormycosis to occur in a normal host [42]. The condition is most commonly seen in diabetic patients with ketoacidosis or in an immunocompromised host.

Mucormycosis affects the orbit by secondary spread from fungal sinusitis. The disease process begins with invasion of the mucosa of the nose, pharynx, or sinuses. Spread occurs by progression along the arterial vascular walls. This leads to occlusion of the vessel and downstream infarction. This vascular thrombosis is responsible for one of the difficulties of treating mucormycosis. The vascular occlusion limits delivery of intravenous antifungal medications to the location of the infection. The infarction also spreads the tissue damage and necrosis beyond the extent of the actual infection.

The typical patient with mucormycosis presents with a history of an underlying medical condition and unilateral orbital inflammation exhibiting cranial nerve palsies that are

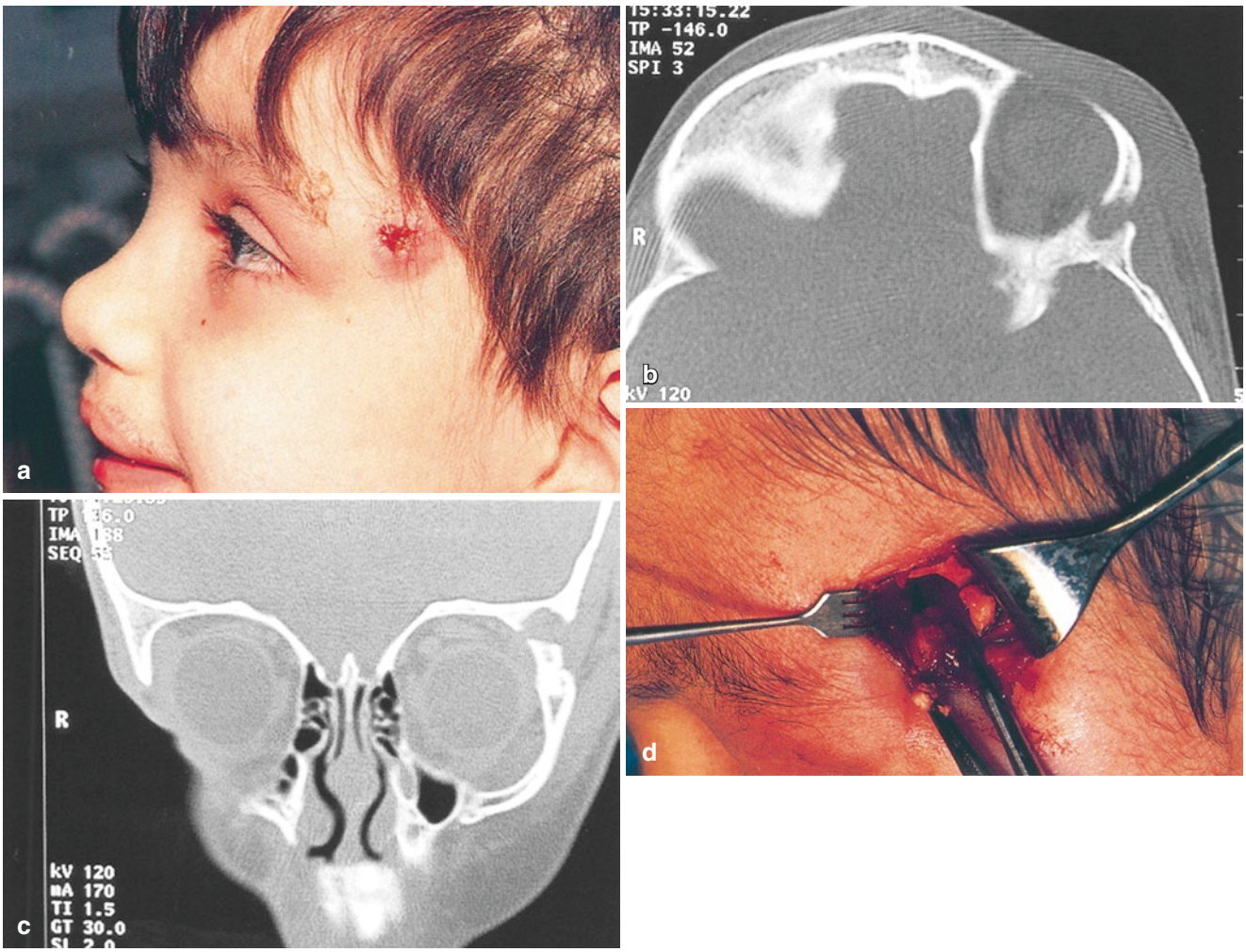


Fig. 33.12 Dermoid misdiagnosed as recurrent orbital cellulitis. (**a**) This 8-year-old had a recurrent episode of orbital cellulitis and purulent draining through a temporal skin fistula following removal of a "sebaceous cyst." (**b**) The axial CT shows soft tissue edema and a natural dehiscence in the bone of the lateral orbital rim. (**c**) The presence of an orbital soft tissue lesion in the area of the bone dehiscence is noted on the coronal CT scan. (**d**) Surgical excision of the "dumbbell" dermoid cyst extending from the orbit to the temporalis fossa

out of proportion with the degree of inflammation. The patient may have severely limited ocular movements, corneal anesthesia, visual loss, and pain. Clues that this represents fungal infection rather than bacterial are the early visual loss and the ophthalmoplegia out of proportion to the level of orbital inflammatory signs. Early visual loss can be caused by central retinal artery occlusion or vascular compromise of the choroidal or ciliary circulation. The nasal and hard palate mucosa may also provide clues to the diagnosis of mucormycosis. A dark, crusted eschar in either location raises the physician's suspicion of a fungal infection, although these signs only occur late in the infection. The diagnosis is confirmed by biopsy of the affected tissue. Large branching nonseptate hyphae will be seen on the hematoxylin and eosin staining.

Orbital and sinus imaging with a CT scan will show sinusitis and orbital soft tissue edema. The CT scan in mucormycosis will sometimes be misleading with a relatively normal appearance, but an MRI scan may be more sensitive in delineating the extent of the sinus mucosal disease.

Treatment for mucormycosis includes surgical debridement of infected and necrotic tissue, systemic amphotericin, amphotericin irrigation, and hyperbaric oxygen. The underlying medical condition that lowered the patient's resistance should be controlled and corrected. For patient in diabetic ketoacidosis, an insulin drip and aggressive approach



Fig. 33.13 Sickle cell orbital bone infarction simulating orbital cellulitis. (**a**) This 10-year-old patient presented with eyelid edema, eyelid erythema, and pain on ocular movement. (**b**) The conjunctiva of the left eye is chemotic with what appeared to be subconjunctival abscess. (**c**) The axial CT scan showed thickening of the lateral orbital soft tissue and clear sinuses. (**d**) Coronal images show the localized collection of fluid in the superotemporal orbit. Intravenous antibiotics were initiated, but the patient had no clinical response. (**e**) A bone scan was ordered, which identified the bone infarction in the greater wing of the sphenoid

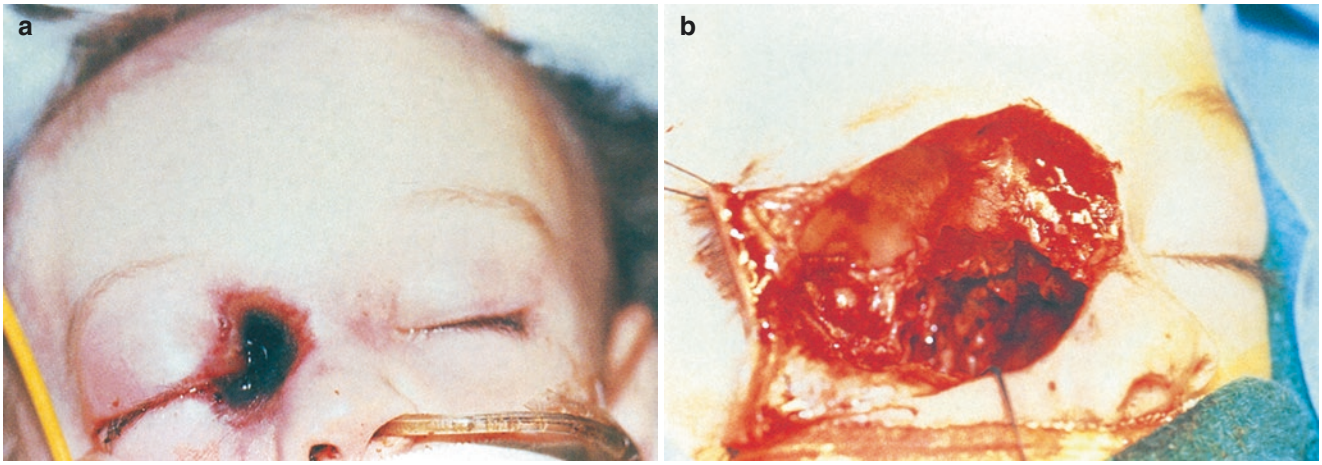


Fig. 33.14 Mucormycosis. (**a**) A 14-month-old child with necrotic medial central soft tissue and lethargy was found to be in diabetic ketoacidosis. Biopsy of the necrotic tissue was positive for fungus. (**b**) Surgical debridement of the affected tissue included exenteration of the orbit

to correcting the metabolic acidosis can be lifesaving. Intravenous amphotericin B in doses up to 1 mg/kg/day can be administered up to a total dose of 2–4 g. Unfortunately, because of the vascular occlusion that is a hallmark of mucormycosis, the necessary surgical resection may be quite large (Fig. 33.14). Aggressive surgical debridement may include exenteration. Again because of limited delivery of intravenous amphotericin to the affected tissues, local irrigation has also been used with some success. The irrigation solution is composed of a 0.25-mg/mL solution of amphotericin B in sterile water. Irrigation of the affected area is performed two times per day [43].

Aspergillosis

Aspergillosis is a fungus of the ascomycetes class. Like *Mucor*, *Aspergillus* is a ubiquitous organism. It can be found colonizing the respiratory and gastrointestinal tracts. In the orbit, aspergillosis can present in at least two clinical scenarios [44]: invasive and infectious. Invasive aspergillosis presents in the immunocompromised host as a sinusitis with rapid progression into the orbit and cranium. Again, like mucormycosis, a necrotizing vasculitis with tissue necrosis is present. This form of the disease is treated with debridement and intravenous amphotericin B. Alternatively, the disease can present in a healthy host. In these cases, a chronic infection of the sinuses occurs with sinus symptoms. There is chronic erosion through anatomic barriers and into the orbit producing orbital signs. The most common signs and symptoms in the orbit are cellulitis, proptosis, ptosis, diplopia, and pain. This form of the disease is also treated with surgical debridement, restoration of normal sinus drainage, and antifungal therapy. Treatment for the immunocompetent host, a more conservative approach to surgical debridement, may still be successful [42].

The diagnosis is confirmed by tissue biopsy showing septate fungal elements on hematoxylin and eosin staining. Multiple biopsies should be taken because of tissue necrosis and better sensitivity to confirm the diagnosis.

References

1. Jackson K, Baker SR. Clinical implications of orbital cellulitis. Laryngoscope. 1986;96:568–74.
2. Jackson K, Baker SR. Periorbital cellulitis. Acad Neck Surg. 1987;9:227–34.
3. Botting AM, McIntosh D, Mahadevan M. Paediatric pre- and post-septal peri-orbital infections are different diseases. A retrospective review of 262 cases. Int J Pediatr Otorhinolaryngol. 2008 Mar;72:377–83.
4. Gonçalves R, Menezes C, Machado R, Ribeiro I, Lemos JA. Periorbital cellulitis in children: analysis of outcome of intravenous antibiotic therapy. Orbit. 2016 Aug;35:175–80.
5. Mathew AV, Craig E, Al-Mahmoud R, Batty R, Raghavan A, Mordekar SR, Chan J, Connolly DJ. Paediatric post-septal and preseptal cellulitis: 10 years' experience at a tertiary-level children's hospital. Br J Radiol. 2014;87:1033.
6. Chandler JR, Lanjenbrunner PJ, Stevens ER. The pathogenesis of orbital complications in acute sinusitis. Laryngoscope. 1970;80:1414–28.
7. Weiss A, Friendly D, Eglin K, et al. Bacterial periorbital and orbital cellulitis in childhood. Ophthalmology. 1983;90:195–203.
8. Israele V, Nelson JD. Periorbital and orbital cellulitis. Pediatr Infect Dis J. 1987;6:404–110.
9. Newell FW, Leveille AS. Management and complications of bacterial periorbital and orbital cellulitis. Metab Pediatr Syst Ophthalmol. 1982;6:209–14.
10. Scott PM, Bloome MH. Lid necrosis secondary to streptococcal periorbital cellulitis. Ann Ophthalmol. 1981;13:461–5.
11. Robbins JB, Schneerson R, Arguman M, Handzel ZT. Haemophilus influenzae type B: disease and immunity in humans. Ann Intern Med. 1973;78:259–69.

12. Gellady AM, Schulman SJ, Ayoub EM. Periorbital and orbital cellulitis in children. Pediatrics. 1978;61:272–7.
13. Rubinstein JB, Handler SD. Orbital and periorbital cellulitis in children. Head Neck Surg. 1982;5:15–21.
14. Pandian DG, Babu RK, Chaitra A, Anjali A, Rao VA, Srinivasan R. Nine years' review on preseptal and orbital cellulitis and emergence of community-acquired methicillin-resistant Staphylococus aureus in a tertiary hospital in India. Indian J Ophthalmol. 2011;59:431–5.
15. Peña MT, Preciado D, Orestes M, Choi S. Orbital complications of acute sinusitis: changes in the post-pneumococcal vaccine era. JAMA Otolaryngol Head Neck Surg. 2013 Mar;139(3):223–7.
16. Rimon A, Hoffer V, Prais D, Harel L, Amir J. Periorbital cellulitis in the era of Haemophilus influenzae type B vaccine: predisposing factors and etiologic agents in hospitalized children. J Pediatr Ophthalmol Strabismus. 2008;45:300–4.
17. Ambati BK, Ambati J, Azar N, Stratton L, Schmidt EV. Periorbital and orbital cellulitis before and after the advent of Haemophilus influenzae type B vaccination. Ophthalmology. 2000;107:1450–3.
18. Sharma A, Liu ES, Le TD, Adatia FA, Buncic JR, Blaser S, Richardson S. Pediatric orbital cellulitis in the Haemophilus influenzae vaccine era. J AAPOS. 2015;19(3):206–10.
19. Shayegani A, MacFarlane D, Kazim M, Grossman ME. Streptococcal gangrene of the eyelids and orbit. Am J Ophthalmol. 1995;120:784–92.
20. Moss RL, Musemeche CA, Kosloske AM. Necrotizing fasciitis in children: prompt recognition and aggressive therapy improve survival. J Pediatr Surg. 1996;31:1142–6.
21. Dewan MA, Meyer DR, Wladis EJ. Orbital cellulitis with subperiosteal abscess: demographics and management outcomes. Ophthal Plast Reconstr Surg. 2011;27:330–2.
22. Schramm VL, Curtin HD, Kennerdell JS. Evaluation of orbital cellulitis and results of treatment. Laryngoscope. 1982;92:732–8.
23. Gans H, Sekula J, Wlodyka J. Treatment of acute orbital complications. Arch Otolaryngol. 1974;100:329–32.
24. Williamson-Nobel FA. Diseases of the orbit and its contents secondary to pathological conditions of the nose and paranasal sinuses. Ann R Coll Surg. 1954;15:46–64.
25. Stammberger H. Functional endoscopic sinus surgery. Philadelphia: Decker; 1991. p. 68.
26. Hubert L. Orbital infections due to nasal sinusitis. NY State J Med. 1937;37:1559–64.
27. Smith AT, Spencer ST. Orbital complications resulting from lesions of the sinuses. Ann Otol Rhinol Laryngol. 1948;57:5–27.
28. Le TD, Liu ES, Adatia FA, Buncic JR, Blaser S. The effect of adding orbital computed tomography findings to the Chandler criteria for classifying pediatric orbital cellulitis in predicting which patients will require surgical intervention. J AAPOS. 2014;18(3):271–7.
29. Handler EC, Davey IC, Hill JC, Lauryssen L. The acute orbit: differentiation of orbital cellulitis from periosteal abscess by computerized tomography. Neuroradiology. 1991;33:15–8.
30. Le TD, Liu ES, Adatia FA, Buncic JR, Blaser S. The effect of adding orbital computed tomography findings to the Chandler criteria for classifying pediatric orbital cellulitis in predicting which patients will require surgical intervention. J AAPOS. 2014;18:271–7.
31. Emmett Hurley P, Harris GJ. Subperiosteal abscess of the orbit: duration of intravenous antibiotic therapy in nonsurgical cases. Ophthal Plast Reconstr Surg. 2012;28(1):22–6.
32. Erickson BP, Lee WW. Orbital cellulitis and subperiosteal abscess: a 5-year outcomes analysis. Orbit. 2015;34:115–20.
33. Rubin SE, Rubin LG, Zito J, Goldstein MN, Eng C. Medical management of orbital subperiosteal abscess in children. J Pediatr Ophthalmol Strabismus 1989;26:21–26.
34. Frank GS, Smith JM, Davies BW, Mirsky DM, Hink EM, Durairaj VD. Ophthalmic manifestations and outcomes after cavernous sinus thrombosis in children. JAAPOS. 2015;19(4):358–62.
35. McKinley SH, Yen MT, Miller AM, Yen KG. Microbiology of pediatric orbital cellulitis. Am J Ophthalmol. 2007;144:497–501.
36. Harris GJ. Subperiosteal abscess of the orbit. Age as a factor in the bacteriology and response to treatment. Ophthalmology. 1994;101:585–95.
37. Pushker N, Tejwani LK, Bajaj MS, Khurana S, Velpandian T, Chandra M. Role of oral corticosteroids in orbital cellulitis. Am J Ophthalmol. 2013;156:178–83.
38. Davies BW, Smith JM, Hink EM, Durairaj VD. C-reactive protein as a marker for initiating steroid treatment in children with orbital cellulitis. Ophthal Plast Reconstr Surg. 2015;31:364–8.
39. Liao JC, Harris GJ. Subperiosteal abscess of the orbit: evolving pathogens and the therapeutic protocol. Ophthalmology. 2015;122:639–47.
40. Shields JA, Shields CL, Survarnamanii C, et al. Retinoblastoma manifesting as orbital cellulitis. Am J Ophthmol. 1991;112:442–9.
41. Walters EC, Waller H, Hiles DA, Michaels RH. Acute orbital cellulitis. Arch Ophthalmol. 1976;94:785–8.
42. Baum JL. Rhinorbital mucormycosis occurring in an otherwise apparently healthy individual. Am J Ophthalmol. 1967;63:335–9.
43. Harris GJ, Will BR. Orbital aspergillosis: conservative debridement and local amphotericin irrigation. Ophthalmic Plast Reconstr Surg. 1989;5:207–11.
44. Green WR, Font RL, Zimmerman LE. Aspergillosis of the orbit: report of ten cases and review of the literature. Arch Ophthalmol. 1969;82:302–13.

Pediatric Orbital Inflammatory Disorders

34

Katherine A. Lane, Melissa A. Lerman, and Jurij R. Bilyk

Introduction

Orbital inflammatory disease describes a spectrum of processes, ranging from specific to nonspecific, which can occur in all age groups (Table 34.1). Although much of our information about orbital inflammation is gleaned from adult cohorts, orbital inflammation affects the pediatric population as well. There is a growing understanding of the importance of considering this population as a separate subgroup in orbital inflammatory disorders, as the clinical presentation, clinical course, and therapeutic choices may differ in young patients.

This chapter will review our current understanding of pediatric orbital inflammatory disease and treatment.

Idiopathic Orbital Inflammation

Idiopathic orbital inflammation [4–6] (IOI) is a term used to describe a syndrome of nonspecific inflammation of orbital tissue with no identifiable local or systemic cause. This condition was first described by Birch-Hirschfeld in 1905, who coined the term "pseudotumor" [7]. Numerous other names have been proposed for this group of disorders, including idiopathic inflammatory syndrome, inflammatory orbital pseudotumor, and nonspecific orbital inflammatory syndrome [8–10]. IOI is currently a diagnosis in transition, as improving diagnostic capabilities have chipped away at what was once "idiopathic" or "nonspecific". Sarcoidosis, granulomatosis with polyangiitis (GPA, Wegener granulomatosis), thyroid eye disease (TED), IgG4-related inflammation (IgG4-RD), Sjögren syndrome, systemic lupus erythematosus, and histiocytic syndromes (Erdheim-Chester and Rosai-Dorfman diseases) are no longer included under the umbrella term "nonspecific"; they are now classified as specific orbital inflammations with their own immunologic or histopathologic markers. Table 34.1 summarizes a common classification scheme of IOI, the more common types of specific orbital inflammations, and other disease entities which may mimic IOI and should therefore be considered in the differential diagnosis.

Although IOI is grouped among the more common orbital disorders in adults, it is postulated to be rare in the pediatric population. Early studies demonstrated that patients under the age of 18–20 years comprise between 6.6% and 16% of all IOI patients [11–13].

Etiology

Our understanding of the etiology of IOI has benefited from recent advances in immunologic and histopathologic abilities to identify and measure cytokines and antibodies. The classic signs and symptoms of IOI presumably represent the clinical manifestation of one or more autoimmune and cell-mediated processes, the triggers for which are a source of current scrutiny. A "pathologic construct" proposed by Dr. Gerald Harris has correlated specific cells present in surgical specimens with particular clinical symptoms [5]. For example, macrophages activated by pro-inflammatory cytokines cause lysis of cells, escalating a cascade of inflammation and causing tissue

K.A. Lane, MD (✉)
Ophthalmic Consultants of Vermont,
South Burlington, VT, USA
e-mail: katealane@gmail.com

M.A. Lerman, MD
Division of Rheumatology, The Children's Hospital of Philadelphia, Philadelphia, PA, USA

J.R. Bilyk
Professor of Ophthalmology, Skull Base Division, Neuro-Ophthalmology Service, Wills Eye Hospital, Philadelphia, PA, USA

© Springer International Publishing AG 2018

J.A. Katowitz, W.R. Katowitz (eds.), *Pediatric Oculoplastic Surgery*, https://doi.org/10.1007/978-3-319-60814-3_34

Table 34.1 Noninfectious orbital inflammation

A. Nonspecific orbital inflammation
Idiopathic orbital inflammation (based on anatomic location of inflammation) [1–3]
Myositis (inflammation of an extraocular muscle)
Dacryoadenitis (inflammation of the lacrimal gland)
Peribulbar (posterior scleritis, Tenonitis)
Orbital fat
Orbital apex
Cavernous sinus (presumed Tolosa-Hunt syndrome)[a]
Sclerosing[a]
B. Specific orbital inflammation
Sarcoidosis
ANCA-associated vasculitis:
Granulomatosis with polyangiitis (Wegener granulomatosis)
Eosinophilic granulomatosis with polyangiitis (Churg-Strauss syndrome)
Thyroid eye disease
Sjögren syndrome (typically as a dacryoadenitis)
IgG4-related orbitopathy (including IgG4-related dacryoadenitis)
Orbital xanthogranulomatosis with adult-onset asthma[b]
Histiocytic disorders:
Langerhans cell histiocytosis
Unifocal (eosinophilic granuloma)
Multifocal unisystem (Hand-Schüller-Christian variant)
Multifocal multisystem (Letterer-Siwe disease)
Sinus histiocytosis with massive lymphadenopathy (Rosai-Dorfman disease)
Polyostotic sclerosing histiocytosis (Erdheim-Chester disease)
Medication-related (e.g. bisphosphonates, implimumab)
Rare:
Inflammatory bowel disease (ulcerative colitis, Crohn disease)
Systemic lupus erythematosus
Polyarteritis nodosa
C. Orbital disorders that may mimic noninfectious orbital inflammation
Orbital infections:
Bacterial cellulitis, abscess, mucopyocele
Fungal (especially sino-orbital aspergillosis
Viral (especially dacryoadenitis associated with Epstein-Barr virus)
Occult orbital foreign bodies (especially wood)
Ruptured dermoid cyst
Rhabdomyosarcoma
Leukemic infiltrate/granulocytic sarcoma
Metastasis (in children, especially neuroblastoma)
Lymphangioma/venolymphatic malformation (especially with acute intralesional hemorrhage
Lymphocytic lesions (reactive and malignant)

A. Classification schema for idiopathic orbital inflammation (IOI). B. Specific orbital inflammation (listed as estimation from most to least common). C. Other disorders that may mimic orbital inflammation
[a]Not considered as part of IOI spectrum by some experts
[b]Usually a disorder of adults

injury and fibrosis which can result in the clinical symptoms of orbital pain, swelling, and impaired function [5].

More recently, Wladis and colleagues have demonstrated that gamma interferon and interleukin-12 levels are markedly elevated in IOI when compared to normal, noninflamed tissue profiles and that IOI may be a T-cell-mediated phenomenon [14]. The results of further studies should not only contribute to our understanding of the pathology of IOI, but also may identify targets for treatment with specific biologic agents.

Presentation

The classic presentation of IOI includes the abrupt onset, often over the course of hours, of periorbital pain accompanied by eyelid edema, erythema, and chemosis (Fig. 34.1). Other common features include proptosis, diplopia, and visual changes. When supported by positive findings on appropriate imaging studies and in the absence of any other identifiable cause, this clinical presentation is considered by some to be diagnostic.

In contrast to adults, pediatric patients are more likely to present with bilateral disease [13, 15–17] (Fig. 34.2) and ptosis [18]. Constitutional signs and symptoms, such as headache, fever, and malaise, may also be more common in children [15, 18–20], and children are more likely to have recurrent disease [1, 15]. Although pain is reported in over 75% [1] of adult patients with IOI, two recent cohort studies suggest that periorbital pain may not be a meaningful indicator of IOI in children, reported in only 17% and 57% of cases, similar to other inflammatory processes [18, 19].

Many of the signs and symptoms of pediatric IOI mimic those of infection. Since orbital infection is the most common cause of acute proptosis in children and has the potential for rapid progression, it is of paramount importance to rule out an infectious etiology (especially orbital spread of adjacent paranasal sinusitis) in all patients with suspected IOI (Fig. 34.1d).

The initial symptoms and signs of IOI in children are summarized in Table 34.2.

Orbital Imaging

Dedicated orbital imaging is an essential part of the diagnostic protocol for any orbital process. Imaging may be by either CT or MRI, although both modalities are associated with drawbacks particular to the pediatric population.

The preferred orbital imaging modality for the evaluation of suspected pediatric IOI remains orbital computed tomography (CT). CT is easily available, images surrounding bone in detail, and provides adequate soft tissue information. When possible, intravenous contrast should be used. Pediatric CT protocols are essential to minimize radiation exposure. Orbital inflammatory lesions have a common radiologic characteristic of an irregular margin adjacent to the focus of the inflammation, despite a variable location of involvement in the orbit, aptly described by Jakobiec as "crabgrass in the orbit", especially when the process involves the intraconal fat [2, 8]. The involved tissues usually enhance

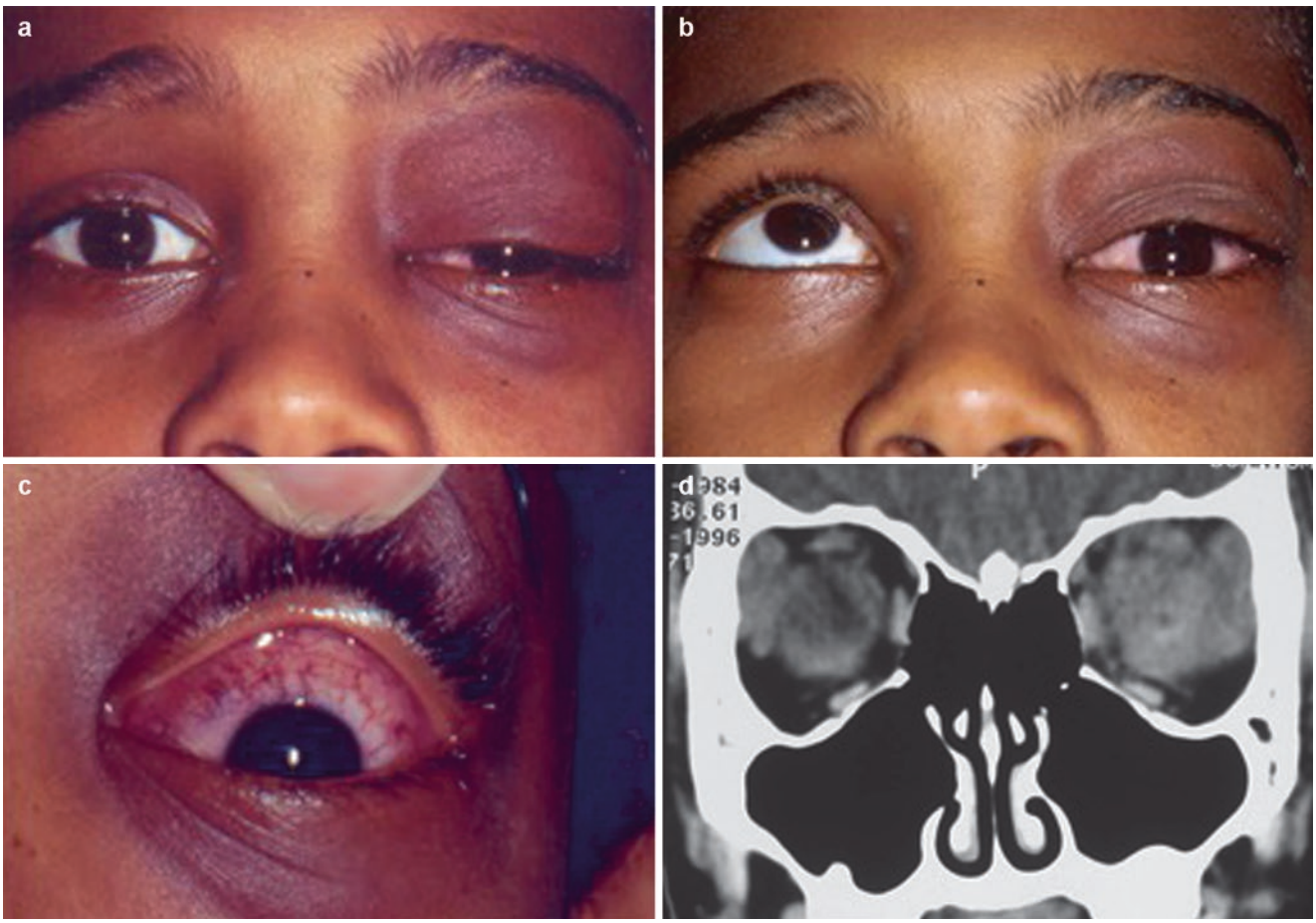


Fig. 34.1 IOI. A 13-year-old boy presented with acute onset of left periorbital pain, swelling, and diplopia. (**a**, **b**) External appearance with limitation of upgaze. Note that the swelling is boggy but not tense and pink rather than the typical red of bacterial infection. (**c**) Conjunctival chemosis and injection. (**d**) On coronal CT, soft tissue window, a poorly circumscribed intraconal opacification is present surrounding the optic nerve. Note that the paranasal sinuses are clear

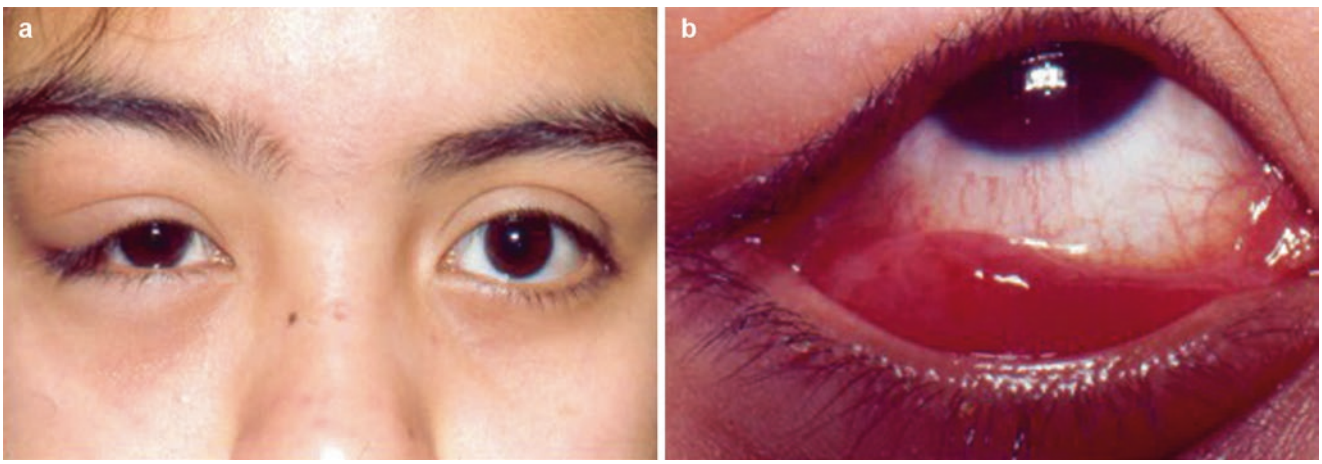


Fig. 34.2 IOI. An 11-year-old girl presented with sudden onset of right upper eyelid edema, neck swelling, and low-grade fever. She had a mildly elevated white count with eosinophilia. (**a**) External appearance. Note the lack of eyelid erythema. (**b**) Conjunctival thickening suggestive of the classic "salmon patch" seen in periocular lymphoproliferative disease.

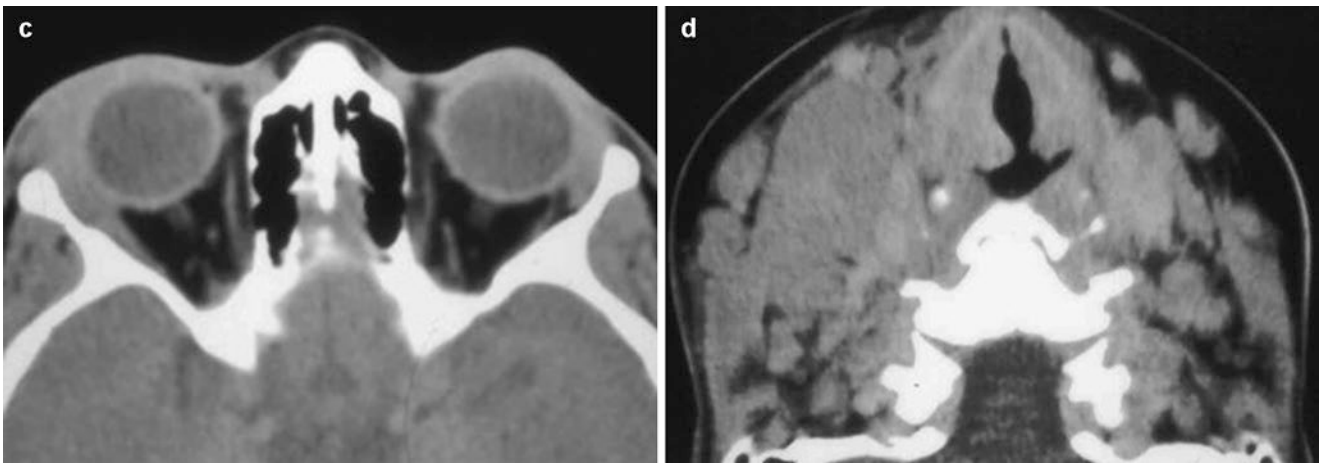


Fig. 34.2 (continued) (**c**) Axial CT, soft tissue window. Note the diffuse enlargement of the right lacrimal gland with spillover into the adjacent eyelid tissue. The ethmoidal sinuses are clear. (**d**) Axial CT, soft tissue window, of the lower face/upper neck shows enlargement of the parotid gland and cervical submandibular lymph nodes. Tissue biopsy revealed nonspecific inflammation consistent with IOI. All symptoms resolved within 48 h of intravenous corticosteroid infusion

Table 34.2 Most common initial symptoms and signs of idiopathic orbital inflammation in pediatric patients [12, 18–20]

Signs and Symptoms	Percentage
Lid swelling	16.7–93
Proptosis	23–80
Extraocular motility disorders	37–70
Pain	17–69
Conjunctival injection and/or chemosis	20–55
Globe displacement	13–45
Palpable mass	3–58
Ptosis	25–57
Iritis, photophobia	3–24
Pain on eye movements	21–50
Lid erythema, warmth	10–21
Pupillary involvement	21
Vision loss	8–10

with contrast media. Bone destruction or hypertrophy is not seen in IOI and would suggest malignancy or infection. Adjacent paranasal sinus opacification is not often seen, even though IOI may follow an upper respiratory infection (Figs. 34.1d and 34.2c); the presence of sinus opacification raises the possibility of an infectious etiology. Multi-scan CT techniques permit superb views in all planes from a rapid (<60 s) scan in the supine position.

Improved magnetic resonance imaging (MRI) technology has led to more rapid scanning times, albeit considerably longer than typical multi-scan CT, making MRI feasible for pediatric patients and avoiding any radiation exposure; younger children may still require sedation to minimize motion artifacts during longer MRI sequences. While MRI does often reveal more detailed information about involved soft tissue, it does not usually provide much more information about IOI lesions when compared to CT, provides less information about bone changes, and is usually more expensive. B-scan ultrasonography can be used for evaluating anterior orbital lesions, but provides no information about surrounding bones, does not image the posterior one-third of the orbit, and is usually more difficult to interpret than CT and MRI.

Evaluation

The evaluation of patients suspected of having IOI is summarized in Table 34.3. The work-up should include a review of systems and a physical exam, as there may be systemic symptoms caused by the orbital inflammation or by a preceding upper respiratory infection; the symptoms may also herald the diagnosis of an underlying systemic autoimmune disease. Headache, vomiting, sore throat, anorexia, abdominal pain, lethargy, and weight loss have been noted in some cases. IOI alone should not cause a significant fever, although a low-grade fever may be present in some cases. Baseline laboratory studies for patients with IOI may include a complete blood cell count (CBC) with differential (cytopenias are seen in inflammation and malignancy), erythrocyte sedimentation rate (ESR), C-reactive protein (CRP), comprehensive metabolic panel (CMP), urinalysis (possible urine protein/creatinine and urine calcium/creatinine ratios), antinuclear antibody (ANA) (if positive, should be followed by evaluation for specific antibodies), rheumatoid factor (RF), angiotensin converting enzyme, anti-neutrophil cytoplasmic antibody (ANCA) [21], thyroid function studies (TSH, free T3, free T4, thyroid-stimulating immunoglobulin), EBV serologies, placement of PPD, fecal calprotectin, serum total immunoglobulin G, and/or Lyme serology in patients living in or having traveled to endemic areas. The eosinophil count may be elevated in some cases of pediatric IOI. While these studies cannot "rule in" IOI, they may be helpful in ruling out other entities. Of note, not all patients require an extended work-up, especially if the clinical and radiographic presentation is classic for IOI.

Table 34.3 Evaluation of patients with suspected orbital inflammatory disorders

Ophthalmic exam (including dilated funduscopic exam), physical exam, review of systems, medical history	
Complete blood count (CBC) with differential, C-reactive protein (CRP), erythrocyte sedimentation rate (ESR), comprehensive metabolic panel (CMP), urinalysis	
Orbital imaging (CT or MRI)	
Additional tests may be selected if the orbital inflammation is subacute, chronic, or recurrent and a specific etiology is suspected:	
Disorder	*Test*
Sarcoidosis	Serum angiotensin converting enzyme (ACE), lysozyme Chest X-ray or CT Urine calcium/creatinine ratio (Gallium scan)[a]
Thyroid eye disease	T3, T4 Thyroid-stimulating hormone Thyroid-stimulating immunoglobulin, thyroid peroxidase
Granulomatosis with polyangiitis Eosinophilic granulomatosis (Churg-Strauss syndrome)	Anti-neutrophil cytoplasmic antibody (ANCA) If positive 1. Anti-proteinase (pr3) 2. Anti-myeloperoxidase (MPO)
IgG4-related disease	Serum IgG4, serum IgG, IgG4/IgG ratio
Epstein-Barr virus (usually dacryoadenitis)	Epstein-Barr nuclear antigen (EBNA) Viral capsid antigen (VCA)-IgG and IgM
Systemic lupus erythematosus, Sjögren syndrome	Antinuclear antibody (ANA) titer, if positive: ANA profile (dsDNA, RNP, Smith, SS-A, SS-B) Urine protein/urine creatinine ratio +/− anti-phospholipid antibodies

[a]Recent studies have questioned the utility of gallium scanning in patients with suspected sarcoidosis

The Question of Tissue Biopsy

The role of orbital biopsy in the diagnosis of IOI has been debated at length in the literature [5, 6, 16, 22]. Briefly, some experts posit that an orbital biopsy should be attempted in all patients before beginning steroid treatment of presumed IOI, provided the tissue in question is easily accessible, arguing that "inflammation" is not a diagnosis but may be a sign of a potentially dangerous underlying tissue process [6]. Others counter that a corticosteroid trial is part of a diagnostic and therapeutic protocol in patients who present in a manner typical for IOI and who have corroborating imaging studies, and that orbital exploration may expose the typical IOI patient to unnecessary surgical risk [1, 5, 15]. These experts reserve orbital biopsy for patients with an atypical presentation, for those who do not experience an immediate and sustained response to corticosteroids, and for those whose symptoms recur.

Philosophic differences aside, clinical practice typically marries axioms of both camps. Most agree that in the case of orbital myositis or an inflammatory lesion of the orbital apex, the risks of iatrogenic injury should be weighed against the benefits of histologic confirmation [23]. Similarly, advocates of biopsy argue that there is an unacceptably high incidence of malignancy in lacrimal gland masses [8, 24] and that any easily accessible involved tissue should be biopsied. In addition, any atypical presentations (subacute onset of symptoms, recurrence of symptoms on or after steroid taper, bone erosion on imaging) or a history of local or distant malignancy should prompt a biopsy.

In the pediatric population, where the specter of malignancy includes metastatic neuroblastoma, rhabdomyosarcoma, and leukemic lesions, among others (see Chap. 36), which may present in a manner similar to IOI, few would argue with the importance of tissue biopsy of accessible tissue, especially the lacrimal gland.

When performed, histologic evaluation should include consideration for malignancy, granulomas (e.g. sarcoidosis), inflammatory bowel disease and tuberculosis, vasculitis (e.g., ANCA-associated vasculitis, polyarteritis nodosa)), atypical infection (fungus, mycobacteria), and IgG4 staining. If tissue biopsy (especially of the lacrimal gland) for suspected IOI is performed, consideration should be given to debulking with or without intralesional corticosteroid injection. A recent study concluded that this may decrease recurrence of IOI [25]. If possible, systemic corticosteroid treatment should be withheld until biopsy has been performed to minimize any masking of serious pathology by corticosteroid therapy.

Treatment

Treatment of IOI is usually initiated based on characteristic clinical and orbital imaging findings. A bacterial infection must be excluded if there is one or more of the following findings: pyrexia, increased white blood cell count (WBC) with neutrophilia and left shift, or CT- or MRI-documented sinusitis. One should also consider the possibility of infection or inflammation from an occult, organic foreign body in children, who frequently do not admit to a history of previous trauma. If infectious orbital cellulitis or dacryoadenitis is a possibility, it is best to obtain blood cultures and treat with broad-spectrum systemic antibiotics for 48 h (see Chap. 33, Orbital Infections) before initiating corticosteroids; of note, there is no clear evidence that corticosteroids, when used in conjunction with systemic antibiotics, worsen the course of pediatric orbital cellulitis [26].

Corticosteroids

If there is no concern for an infectious etiology, the mainstay of treatment for IOI is corticosteroids (CS). Corticosteroids inhibit the explosive inflammatory cascade of IOI at almost every level by suppressing levels of pro-inflammatory cytokines. While parenteral steroids may be used in select cases, the most common route of administration is oral. A starting dose of 1.0–1.5 mg/kg/day of prednisone is usually tapered over the following weeks to months depending on how rapidly the inflammation resolves [11]. A definite improvement should be evident within 48 h of adequate prednisone therapy, and some consider this rapid response to be diagnostic of IOI (Fig. 34.3) [27]. Others counter that patients with other inflammatory, infectious, or neoplastic entities may also demonstrate improvement on systemic CS and, therefore, a "steroid response" cannot be diagnostic of IOI [6, 22, 28]. In addition, caution should be taken in patients who have an initially good response but who cannot be easily tapered off CS therapy or if recurrence occurs after successful taper. Such cases are considered "atypical" and should prompt a review of the case, consideration of tissue biopsy, and/or further systemic work-up.



Fig. 34.3 IOI. The patient showed in Fig. 34.1 before (*top*) and 24 h after (*bottom*) initiation of oral corticosteroid therapy. Note near-complete resolution of the patient's external signs. The patient also noted complete resolution of pain and diplopia

The use of CS over weeks to months is not without significant drawbacks. Children treated with CS may experience increased appetite, weight gain, gastritis, headache, poor sleep, and mood lability (that can in rare cases cause psychosis) [29]. Additionally, elevated blood and intraocular pressure and elevated blood sugar may be seen, although these complications are less common in the pediatric population [29, 30]. Some of the short-term side effects, especially on mood and sleep, may be mitigated by administration of CS in the morning to mimic the endogenous cortisol burst. The classic "Cushingoid appearance" (moon facies, buffalo hump, central obesity) is due to the redistribution of fat reserves, coupled with an increased appetite. This, as well as cutaneous striae, can develop quickly in some children and may have long-term effects on self-image, especially in teenagers. Corticosteroids also have an effect on linear growth by inhibiting the synthesis of type I procollagen, which is essential for bone growth [31]. This phenomenon is especially prevalent with prolonged treatment regimens (>6 months) [29]. Fortunately, CS also inhibit closure of epiphyseal plates [29, 31]. Long-term studies of children treated with oral CS for capillary hemangioma [29] or inhaled CS [30] for asthma demonstrate that there is often a rebound in growth after CS taper, allowing children to rejoin previous growth curves and attain normal adult height.

Due to the potential of side effects related to systemic CS treatment, some clinicians suggest local intra-orbital injections of triamcinolone acetonide in cases of inflammatory masses or dacryoadenitis [32, 33]. It should be noted that this is an off-label use of the medication and carries the rare but inherent risk of intravascular embolization of particulate matter [34] and that, in children, this likely necessitates sedation, all of which limit effective access to this treatment modality. The use of other, non-particulate CS agents (e.g., dexamethasone) is not well reported.

Radiation

Radiation is an effective treatment for IOI, especially in patients who are CS responsive but intolerant of CS-related side effects [27, 35]. Low doses of external beam irradiation (2000 cGy total in 200 cGy fractions) have an efficacy equivalent to CS medications in the treatment of IOI [36, 37]. Despite a recent study showing significant associations between estimated radiation doses from CT scans and the subsequent incidence of leukemia and brain tumors [38], documented complications related to orbital irradiation within this treatment dose range (i.e., cataract formation, retinal microvascular changes, keratoconjunctivitis sicca, induction of secondary carcinomas) are extremely rare [37]. However, the specter of children previously treated with external beam radiation at

higher doses (5000–6000 cGy) for retinoblastoma [39] and rhabdomyosarcoma [40] looms large. In these patients, there is a marked increase in the incidence of secondary tumors within the radiation field. Additionally, the degree of bony hypoplasia and soft tissue deformities has been shown to be inversely proportional to the patient's age at treatment and is much less severe if treated after the age of 3–4 years [41].

Other Treatment Options

Increasingly there is literature to support the use of immunomodulatory (IMT) agents in other systemic inflammatory conditions (see section "Pharmacotherapy" below), and these agents may be employed in the treatment of IOI; the guidance of a pediatric rheumatologist or oncologist is advisable.

Classification of IOI

IOI can be classified into six groups based on anatomic location and clinical presentation: anterior, diffuse, diffuse sclerosing, apical, myositic, and lacrimal [8]. Anterior, myositic, and lacrimal are the most common presentations and also usually have the best response to CS therapy.

Anterior

The anterior presentation may be either acute or subacute (Fig. 34.4). Pain is usually a significant complaint. Tissue involvement usually extends no further posteriorly than the posterior aspect of the globe. Lid edema and erythema, exophthalmos, mildly decreased extraocular muscle movements, decreased visual acuity, chemosis, and diffuse bulbar conjunctival injection may be present. The most severe cases may be accompanied by iridocyclitis, especially if there are recurrent or bilateral episodes [11, 12, 42, 43]. Posterior scleritis with exudative retinal detachment may also occur (Fig. 34.5). There is usually a prompt improvement with CS therapy, although steroid-sparing agents or biologic therapy with tumor necrosis factor-alpha inhibitors (e.g., infliximab) may be necessary for long-term control.

Diffuse

Diffuse IOI is much less frequent than anterior IOI. It is more likely to be subacute, remitting and progressive and to result in residual scarring. It usually causes lid edema, exophthalmos, decreased extraocular muscle movements, decreased visual acuity, chemosis, and bulbar conjunctival injection. It responds to CS therapy, but maintenance therapy may be required if it is recurrent.

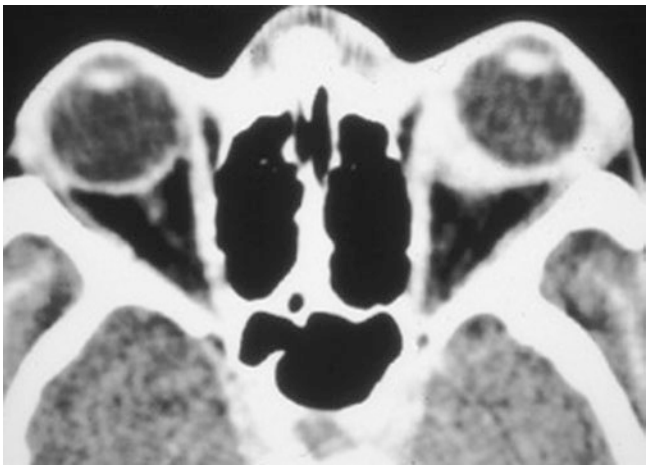


Fig. 34.4 Anterior IOI. Axial CT (soft tissue window) demonstrates marked thickening of Tenon capsule secondary to inflammation ("tenonitis")

Sclerosing

Sclerosing IOI differs from diffuse IOI in several respects [8, 44]. It is more likely to present insidiously with less pain and inflammation, to be less responsive to CS therapy, and to result in fibrosis, which can cause permanent damage to the extraocular muscles, the levator muscle, and the optic nerve. Initially the fibrosis may involve only a portion of the orbit but can progress to involve the entire orbit (Fig. 34.6). Early aggressive therapy with CS, cyclophosphamide, and external radiation therapy offers the best prognosis for arresting this category of IOI [8, 44]. Medical and radiation management is typically frustratingly ineffective. Histopathologically, fibrosis overwhelms the inflammatory component, and, not surprisingly, therapy geared toward inflammation does not work. Sequential orbital debulking may provide temporary relief, and in extreme cases of progressive disease and pain, orbital exenteration may be necessary. Some experts have justifiably questioned whether sclerosing IOI is in fact a subtype of IOI or a completely separate entity of progressive idiopathic orbital fibrosis [45, 46].

Apical

Apical presentation is usually subacute and often recurs. Pain is often severe. Decreased vision and decreased extraocular muscle movements are likely. Exophthalmos, lid edema, chemosis, and bulbar conjunctival injection are usually mild (Fig. 34.7). Optic neuritis, apical tumors, and Tolosa-Hunt syndrome must be considered in the differential diagnosis. In rare cases, optic neuropathy may occur and progress rapidly to permanent visual loss [47].

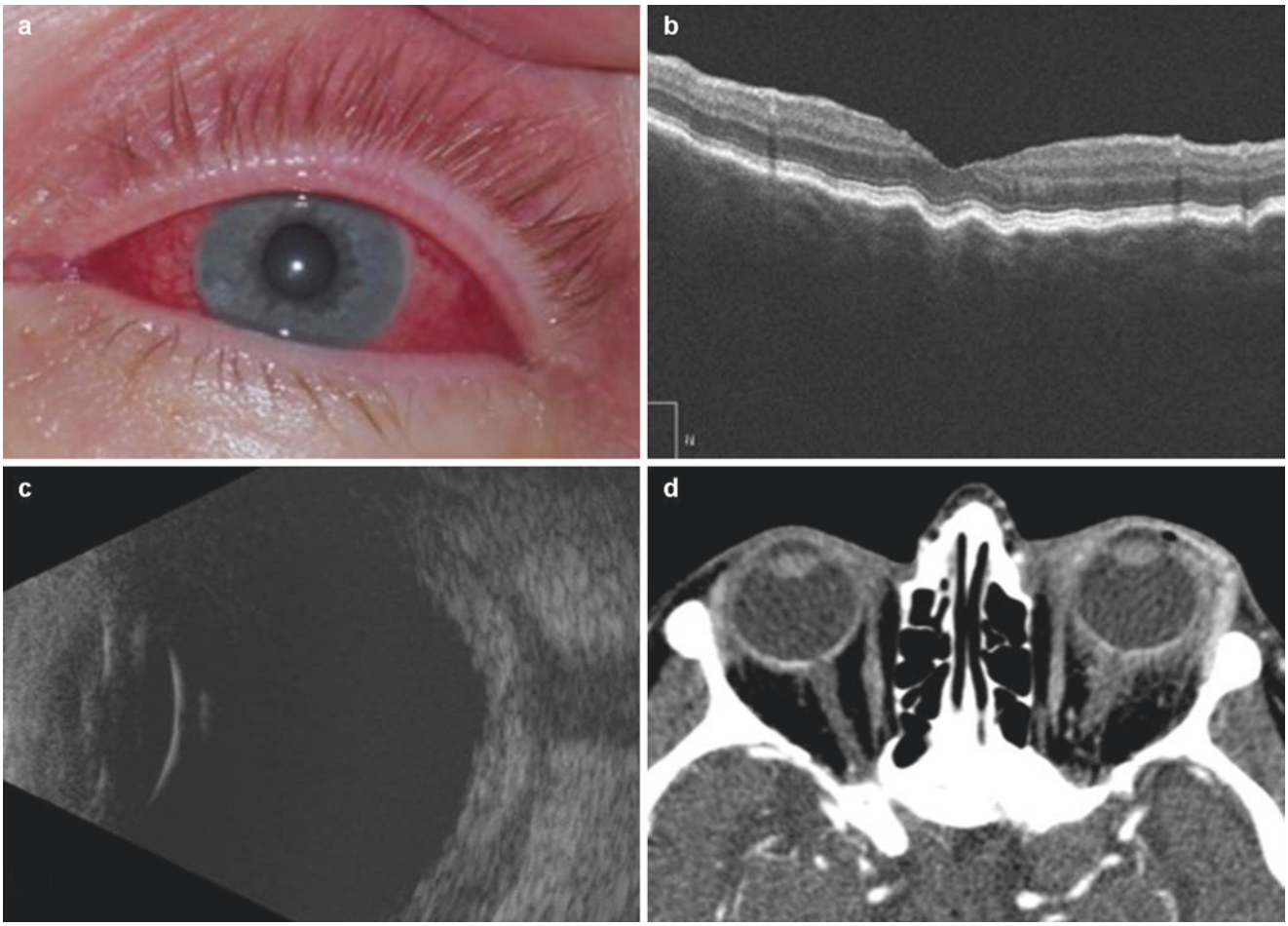


Fig. 34.5 Posterior scleritis. (**a**) Sudden onset of left eye pain, blurred vision, and diffuse, violaceous conjunctival and episcleral injection. (**b**) Optical coherence tomography of the macula shows diffuse chorioretinal folds. (**c**) B-scan ultrasonography demonstrates marked choroidal thickening with a characteristic "T-sign". (**d**) Axial CT (soft tissue window) shows diffuse thickening of the left sclera with inflammatory spillover into the bulbar conjunctiva

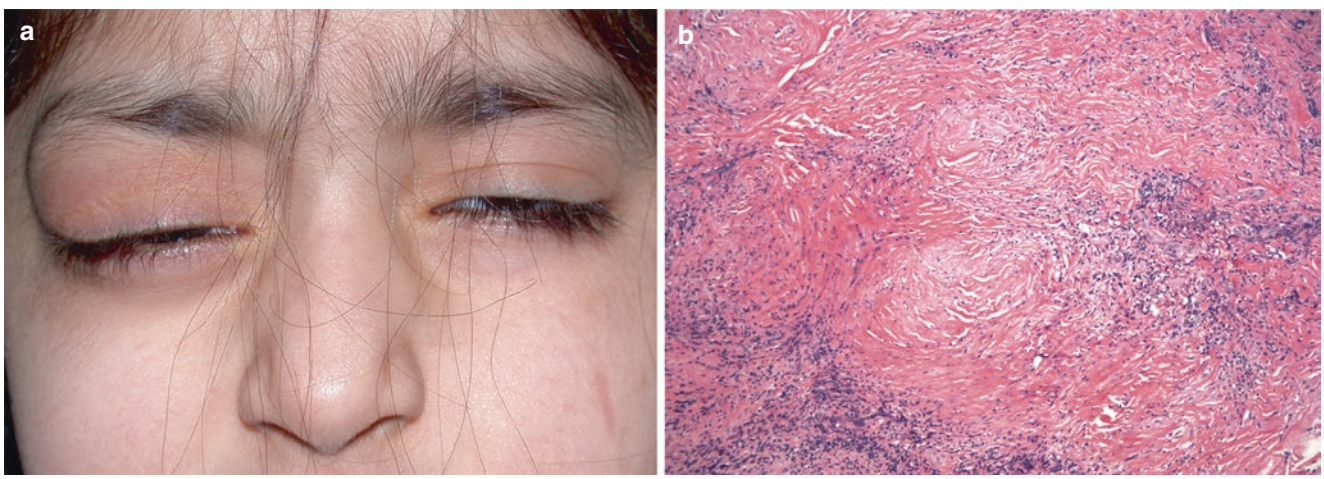


Fig. 34.6 A 6-year-old girl presented with non-painful, progressive proptosis over several months. (**a**) External ophthalmoplegia with a distinct lack of eyelid erythema was present on exam. (**b**) Eventual orbital biopsy revealed fibrosis with mild inflammation.



Fig. 34.6 (continued) (**c**, **d**) Axial and coronal CT images demonstrate a large superolateral mass. In this case, the surrounding bone showed no change. In some cases of sclerosing pseudotumor, erosion of orbital walls may be present with extension of the process into the adjacent paranasal sinuses. (**e**, **f**) The lesion on T1-weighted, pre-contrast MRI (axial and coronal). The adjacent sinus congestion was unrelated to the fibrosing orbital process

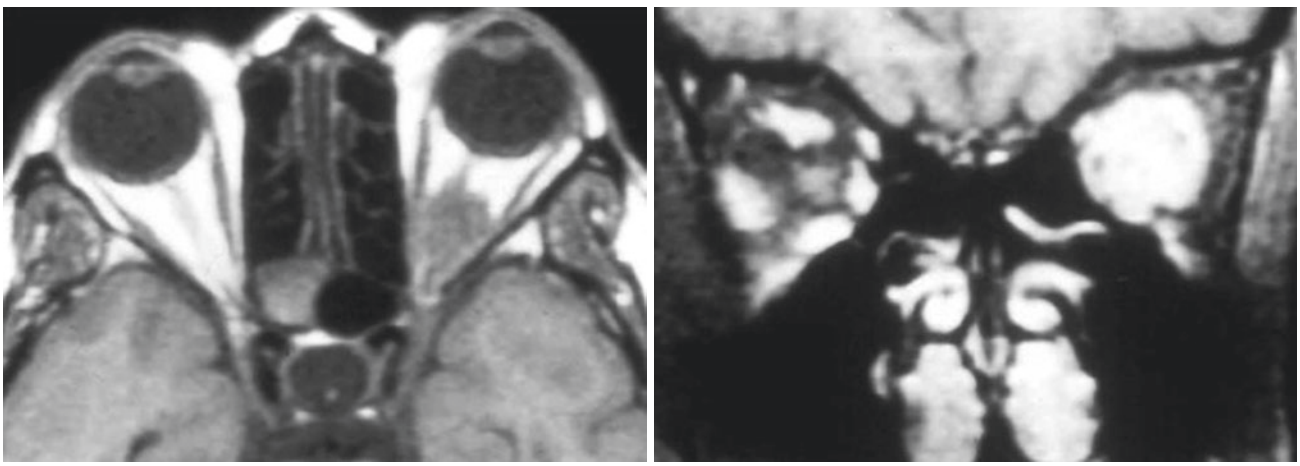


Fig. 34.7 Orbital apical IOI. Axial, pre-contrast (*left*) and coronal, post-contrast T1-weighted MR images of an apical inflammatory process that presented with pain, external ophthalmoplegia, and mild optic neuropathy. Intravenous corticosteroids resulted in prompt resolution of symptoms

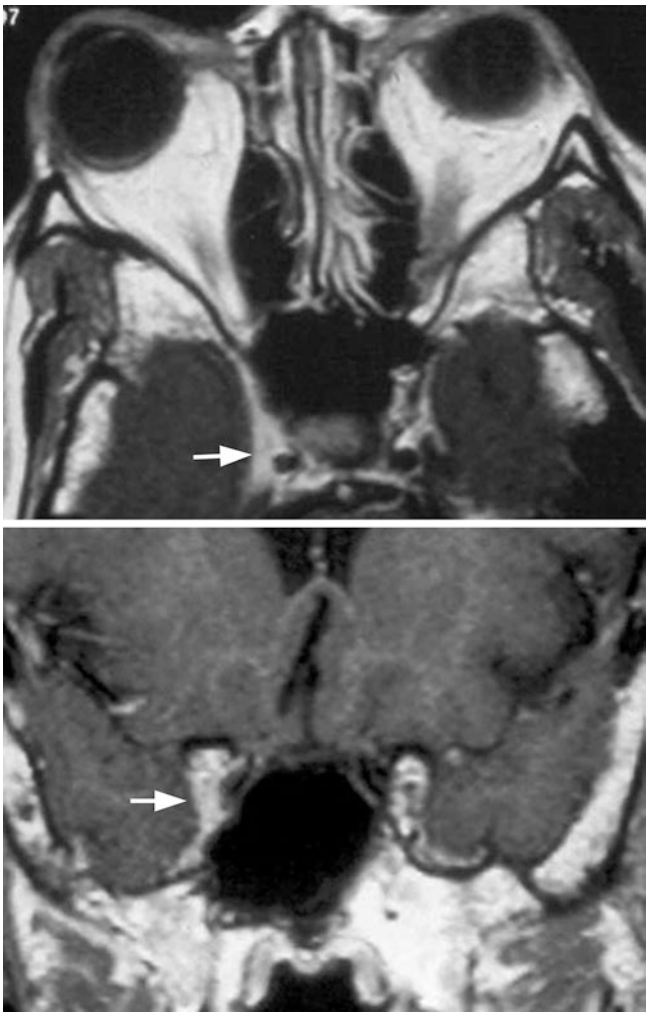


Fig. 34.8 Presumed Tolosa-Hunt syndrome. Axial (*top*) and coronal (*bottom*) post-contrast T1-weighted MR images of a patient presenting with pain and external ophthalmoplegia but no eyelid signs. Note the enlargement and enhancement of the right cavernous sinus (*arrows*)

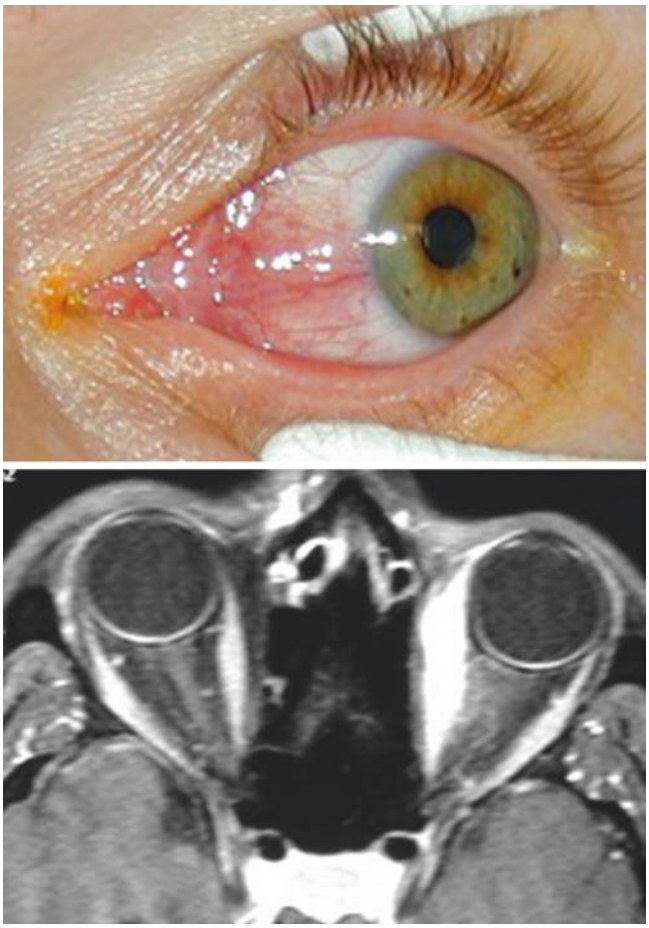


Fig. 34.9 Myositis. Injection is noted over the insertion of the left medial rectus muscle (*top*) in this patient with sudden onset of pain. Axial post-contrast T1-weighted MRI with fat suppression shows diffuse enlargement and enhancement of the left medial rectus muscle. Note that the tendon is relatively spared, a finding suggestive of thyroid eye disease. Recent studies have questioned the validity of using tendinous involvement or sparing as a reliable sign of specific pathologies

Tolosa-Hunt syndrome is also described as an idiopathic inflammatory condition, but is centered intracranially – posterior to the orbital apex in the cavernous sinus or posterior to the superior orbital fissure (Fig. 34.8) [48]. Of note, some experts do not classify Tolosa-Hunt syndrome as a subtype of IOI, but as a separate entity of granulomatous inflammation of the cavernous sinus and carotid siphon. Tolosa-Hunt syndrome typically presents with severe pain and external ophthalmoplegia secondary to cranial neuropathy within the cavernous sinus. Pain responds rapidly to appropriate CS doses, but the cranial neuropathy may linger for weeks to months. Tolosa-Hunt syndrome also has a propensity for recurrence and for contralateral cavernous sinus involvement. It is generally a presumptive diagnosis, since biopsy of the cavernous sinus is not without significant risk; other diagnoses which may show some response to CS therapy should be considered, including metastasis, lymphoma, meningioma, and even aneurysm.

Orbital Myositis

Orbital myositis is usually acute. Diplopia is a common presenting symptom. There is usually pain on eye movement, especially when the affected muscle(s) contracts or stretches. Lid edema, chemosis, and bulbar conjunctival injection are frequent (Fig. 34.9). Visual acuity is usually not impaired. Response to CS is usually rapid and dramatic [8, 10, 11, 49]. One or more rectus or oblique muscles can be affected (Fig. 34.7) [50, 51]. The muscle enlargement typically involves the entire muscle including the tendon, which helps to differentiate it from the tendon-sparing muscle enlargement of TED [49]. However, the validity of this teaching has been questioned recently by Moembaerts [52]. The margins of the muscle may appear distinct without the irregular margins seen on CT scans of other forms of IOI. Recurrences can occur months or years later involving the same or different muscles in the same or the other orbit. The differential

diagnosis includes TED, arteriovenous fistulas (e.g., direct or indirect carotid cavernous fistulas), superior ophthalmic vein thrombosis, and tumors involving extraocular muscles.

Lacrimal Gland (Dacryoadenitis)

Lacrimal gland involvement may be acute or subacute. Pain is not usually as severe as in the other forms of IOI. Tender, palpable enlargement of the lacrimal gland is usually present. The lid is usually more swollen temporally with an S-shaped contour deformity. Chemosis and bulbar conjunctival injection are often present, especially temporally. Vision is not usually affected. Exophthalmos is typically minimal, although the globe may be displaced inferiorly and medially (Fig. 34.10). The differential diagnosis includes viral and bacterial dacryoadenitis and tumors, as well as specific orbital inflammations (e.g., sarcoidosis, Sjögren syndrome). It is important to remember that a variety of disorders, including primary epithelial malignancies and lymphoproliferative disease, may present in an identical fashion. As already noted, because of the surgical accessibility of the lacrimal gland, some experts recommend biopsy in all cases of suspected dacryoadenitis.

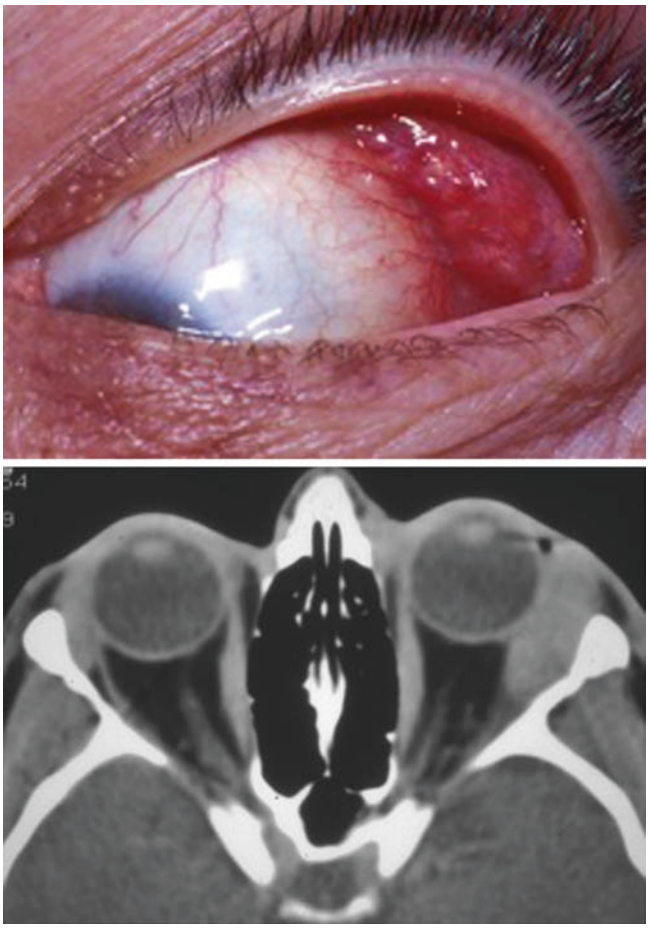


Fig. 34.10 Dacryoadenitis. Acute onset of pain and swelling in the area of the left lacrimal gland. Note the enlargement and inflammation of the palpebral lobe of the gland (*top*). On axial CT (soft tissue window), a diffuse enlargement of the orbital lobe is also noted. The process is molding to the globe and not distorting it. The adjacent bone is intact. In some cases, spillover of inflammation onto the intraconal fat or adjacent extraocular muscles may also be seen. Note that other processes, including primary lacrimal gland epithelial malignancies and lymphoma, may present in an identical fashion and may show response, albeit temporary, to corticosteroid therapy

Specific Orbital Inflammation

Sarcoidosis

Sarcoidosis is a chronic multisystem disease with the pathologic hallmark of non-caseating granulomas [53, 54] affecting the lungs, heart, skin, lymph nodes, joints, and orbit. Uveitis, dermatitis, and arthritis are the triad of early-onset childhood sarcoidosis (Blaus disease) in children younger than 5 years old, but disease in older children may parallel that in adults (pediatric -onset adult sarcoidosis) [55]. There is no specific finding or laboratory test which can conclusively diagnose sarcoidosis. The diagnosis relies, instead, on the combination of clinical history, the histologic evidence of non-caseating granulomas, and the exclusion of other possible causes [54]. Angiotensin converting enzyme [56] is produced by granuloma cells and may be elevated in up to 66% of patients diagnosed with sarcoidosis [57]; of note, the ACE level parallels the burden of disease and may be normal in localized forms of sarcoidosis. Because of the activation of macrophages, elevated 1,25-dihydroxy-vitamin D3, and/or hypercalcemia may be signs of sarcoidosis. In the United States, the disease affects blacks more frequently than whites (although there is a high incidence in patients of northern European heritage) [58]; in adults it is more common in women than in men, but this may not be the case in children.

Ophthalmic manifestations occur in up to 20% of patients with sarcoidosis, most commonly seen as uveitis, retinal vasculitis, and asymptomatic conjunctivitis, and may herald the discovery of systemic disease in 30–50% of patients [59]. However, sarcoidal findings may also be isolated, especially early in the course of the disease. Within the orbit, sarcoidosis can unilaterally or bilaterally involve the lacrimal gland, the extraocular muscles, and other soft tissues (Fig. 34.11) [60, 61]. Sarcoidal infiltration of the optic nerve and central nervous system may also occur (Fig. 34.12). The most common complaint in a large series of biopsy-proven sarcoidosis was that of a slowly progressive mass (88.5%), followed by proptosis (42%), discomfort as opposed to pain (30.8%), ptosis (27%), and restricted extraocular motility (23%) [62].

Radiologically, orbital involvement can manifest as a discrete mass or as a diffuse infiltrative process. In the lacrimal gland, a well-defined homogenous enlargement and bilateral involvement are common; extraocular muscles may be

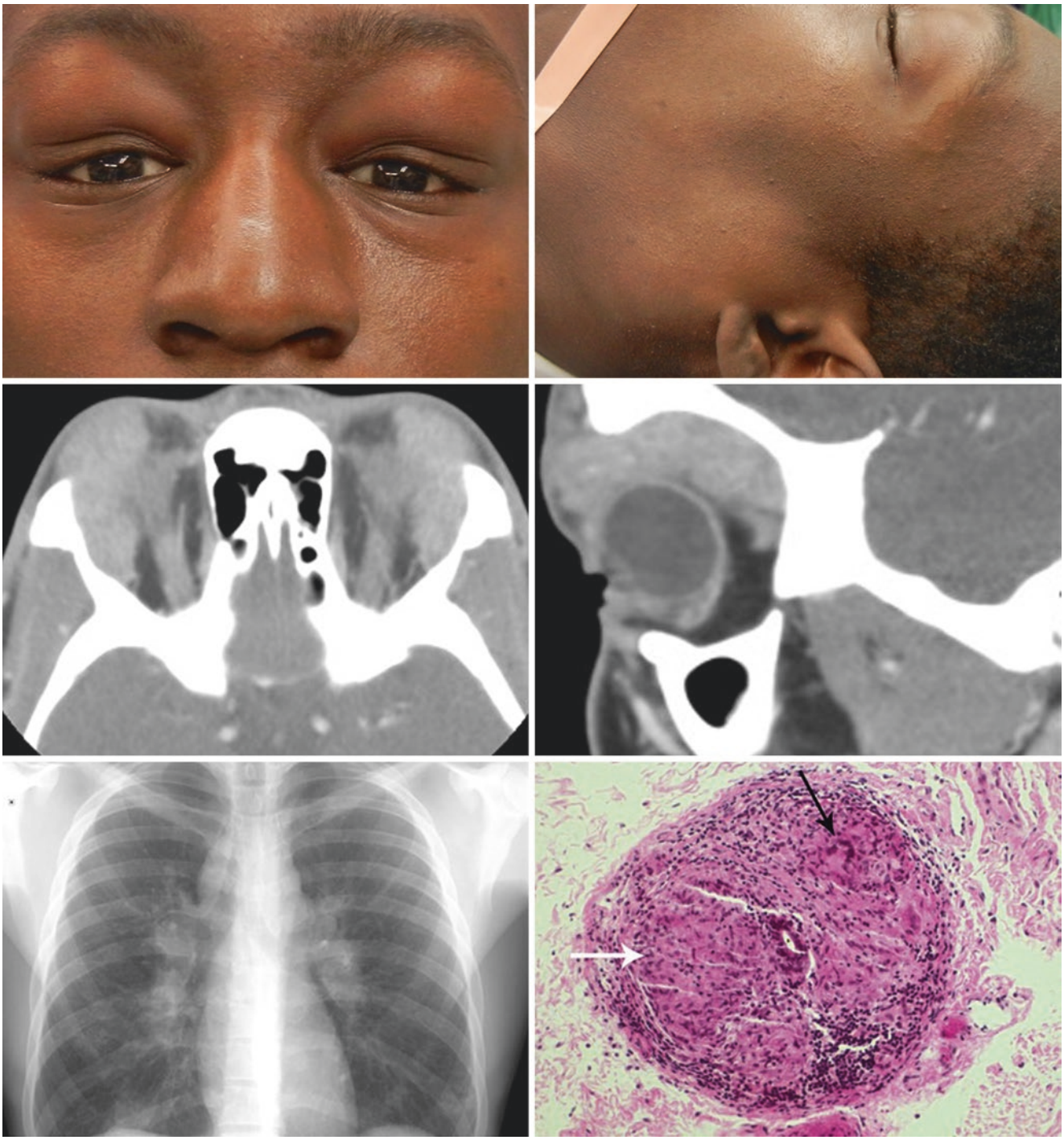


Fig. 34.11 Sarcoidosis. A 17-year-old patient presented with painless swelling of the upper eyelids. Top: On clinical exam, firm nodules were palpated across both upper lids; bilateral parotid enlargement was also noted. Middle: CT images (axial and parasagittal soft tissue windows) demonstrate nodular enlargement of both lacrimal glands extending into surrounding orbital soft tissue. Bottom left: Hilar adenopathy was identified on subsequent chest X-ray. Bottom right: Biopsy of the lacrimal gland revealed non-caseating granulomatous inflammation (*white arrow, granuloma; black arrow, Langerhans giant cell*). The patient's ACE level was elevated

involved, often in conjunction with adjacent orbital or lacrimal gland involvement [62].

Orbital inflammation in the setting of known systemic sarcoidosis should never be confused with IOI; however, there is some confusion in the ophthalmic literature regarding the diagnosis of solitary orbital sarcoid. This entity was reviewed by Mombaerts and colleagues, who presented a series of 7 patients and reviewed 30 more in the literature.

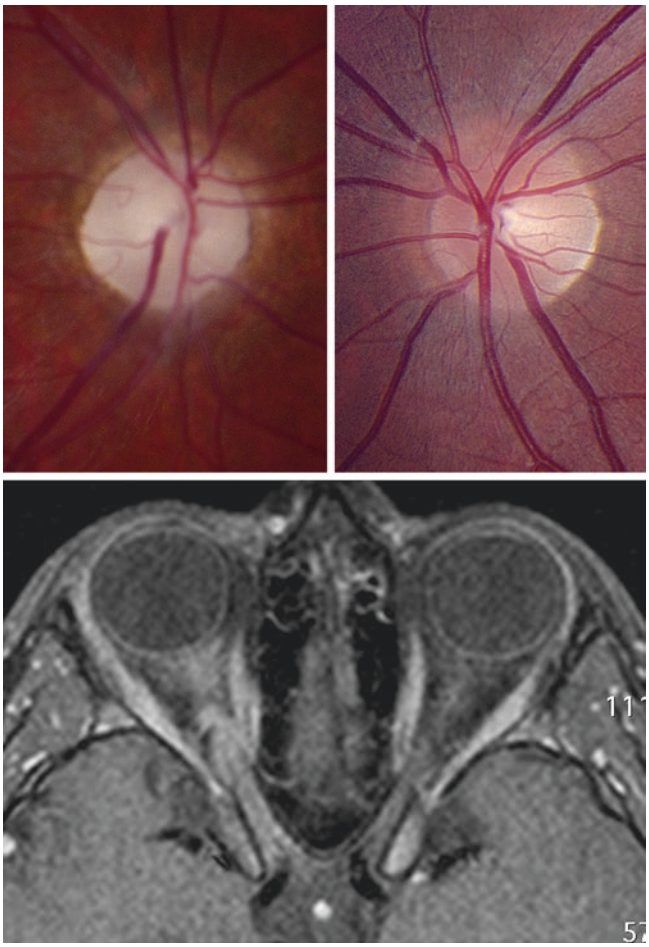


Fig. 34.12 Optic nerve sarcoid. A 15-year-old boy presented with progressive right visual loss over 18 months. Clinical exam revealed no light perception in the right eye with a pale optic nerve; the left optic nerve appeared normal (*top*). On MRI, diffuse enhancement of the optic nerve almost reaching the chiasm was observed (*bottom*, T1-weighted post-contrast with fat suppression). Systemic work-up, including ACE and chest CT, was normal. Optic nerve biopsy showed non-caseating granulomatous inflammation. Eighteen months later, the patient developed pulmonary symptoms. Further work-up revealed systemic sarcoidosis

All patients presented with unilateral signs of inflammation or mass effect and demonstrated non-caseating granulomas on biopsy [63]. None were found to have systemic sarcoidosis. These cases may represent "idiopathic granulomatous orbital inflammation" [62, 63], although thorough investigation must first rule out other potential causes. Specific immunologic and microbiologic workups include tests for GPA, serologic and skin tests for fungal infections, and culture/staining for mycobacteria. The distinction between solitary orbital sarcoid and idiopathic orbital granulomatous inflammation may be academic, as both are diagnoses of exclusion and are treated in a similar manner [62].

As with most inflammatory diseases, corticosteroids (CS) are the mainstay of initial treatment for both systemic and limited sarcoidosis, but other immunotherapeutics (IMT) should be started concomitantly with the goal of weaning patients off CS within the first 2–6 months (see section "Pharmacotherapy" below). Currently, the most frequently used agents for this are methotrexate and tumor necrosis factor-alpha inhibitors [59]. Patients are kept in remission for a prolonged period of time before medications are weaned. Sarcoidosis can go into lifelong remission, although relapses occur in over 50% of patients.

Occasionally patients present with lacrimal gland sarcoidosis but do not require systemic treatment for other system involvement. In these cases, some experts suggest local injections of long-acting CS [33]. The efficacy of this therapy has not been proven in a large series of patients, and there are risks associated with periocular injections of CS (see discussion above) [34, 64–66].

Granulomatosis with Polyangiitis

Granulomatosis with polyangiitis (GPA) is a necrotizing granulomatous vasculitis, usually affecting small vessels. It classically presents with constitutional symptoms and affects the respiratory tract, the sinuses, and the kidneys, although it can affect any organ system [67, 68]. It rarely occurs before adolescence. In a recently published pediatric cohort, the large majority of patients had sino-nasal and/or ear involvement along with constitutional symptoms and respiratory involvement [69]. Subglottic stenosis is not an uncommon complicating feature of pediatric disease. If untreated, the systemic variant of GPA may have a mortality of >90%. The disease may burn out in 1–2 years but may persist for longer. Although no single finding or laboratory test is diagnostic, the majority of patients with systemic GPA will have positivity for anti-neutrophil cytoplasmic antibodies (ANCA). A child or adolescent is said to have GPA by EULAR/PRINTO/PRES 2008 criteria if at least two of the following criteria are present: (1) granulomatous inflammation on biopsy, (2) upper airway involvement, (3) laryngo-tracheo-bronchial stenosis, (4) pulmonary involvement, (5) ANCA positivity, or (6) renal involvement [70].

Ocular involvement occurs in 52–61% of patients at some point during the disease course [71], with fewer than 10% involving adnexal structures and 7–30% involving the orbit. The frequency may be lower in the pediatric population [21, 72]. Cases of GPA involving the orbit are typically part of a more limited form of the disease (also known as sino-orbital GPA) affecting the ear, nose, throat and upper airway, but sparing the kidneys [73, 74], and it is important for physicians to appreciate that few cases with disease limited to the orbit progress to systemic disease (Fig. 34.13) [75]. This "limited" form may have a chronic remitting coarse, in contrast to the fulminant "systemic" form which progresses quickly to multisystem damage and renal failure [71, 75].

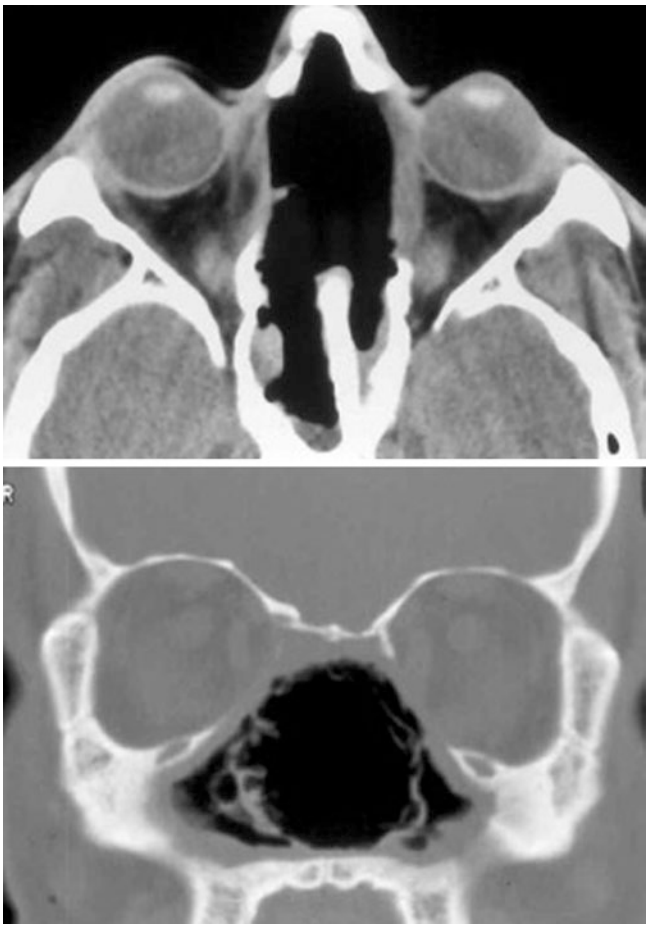


Fig. 34.13 GPA. CT axial soft tissue window (*top*) and coronal bone window (*bottom*) of a patient with limited (sino-orbital) GPA. Note the widespread bone destruction in the paranasal sinuses and medial orbits. Scarring was also present along the medial rectus muscles, resulting in a large angle cicatricial esotropia

Ophthalmic involvement can result from contiguous extension of respiratory system involvement in the nose and sinuses or from discrete ocular lesions. Nasal and sinus involvement can spread to the nasolacrimal duct and lacrimal sac leading to epiphora and/or dacryocystitis. Bone destruction on imaging is the rule. GPA can also lead to orbital inflammation, mimicking IOI. Discrete focal lesions not caused by contiguous spread can affect the extraocular muscles, retina, uvea, conjunctiva, lids, cornea, and sclera [72]. Ocular or facial pain was a presenting symptom in 75% of patients in one large series [73]. A third of patients with orbital GPA had associated ocular inflammation, which is less common in IOI [75]. Also in contrast to IOI, GPA often exhibits bilateral disease [73, 75].

Radiologically, GPA can show bone destruction, a highly atypical feature for IOI (Fig. 34.13). Additionally, GPA lesions appear hyperintense on T2-weighted MRI, in contrast to many other orbital lesions, both neoplastic and inflammatory [76]. This discrepancy is thought to be due to the abundance of fibrocollagenous tissue present in the granulomatous lesions. It is important to note, however, that chronic inflammation, as seen in long-standing IOI, may also appear hyperintense on T2 images [77].

Serum ANCA is a sensitive, although not specific, indicator of ANCA-associated vasculitis (AAV) [78]. Immunofluorescence for cytoplasmic-ANCA (c-ANCA) (as opposed to perinuclear ANCA), along with antigen-specific anti-proteinase 3 (Pr3) positivity (as opposed to myeloperoxidase positivity), increases sensitivity and specificity for GPA. The antigen-specific anti-proteinase 3 Ab, often a c-ANCA pattern, is positive in 96% of patients with active generalized disease [79, 80]. It is positive in a lower percentage of patients with limited (sino-orbital) disease [81]. False-positive results of proteinase antibodies are rare in contrast to the rate seen with ANCA testing. Because atypical ANCAs can occur in inflammatory bowel disease, another granulomatous disease, it can sometimes be difficult to distinguish the two diseases. In certain patients, ANCA titers can parallel disease activity. In those in whom this is the case, ANCA titers can be useful in monitoring the response to medical therapy and may help determine relative quiescence when surgical intervention (e.g., dacryocystorhinostomy) might be safest [78].

A biopsy is recommended when feasible in all cases of GPA to confirm the diagnosis, even when c-ANCA is positive [82]. Occasionally, orbital biopsies in patients with GPA show minimal inflammation. Nasal biopsies are more likely than orbital biopsies to show the pathologic triad of vasculitis, granulomatous inflammation with giant cells, and tissue necrosis. For this reason, biopsies are often taken from multiple sites.

Children with orbital inflammation resulting from GPA should be under the care of a pediatric rheumatologist. Other than diagnostic biopsies, reconstructive orbital or lacrimal surgery should be deferred until the clinical course and/or serologic testing suggest inactivity, which can often be induced by high-dose CS; a variety of treatments are used to maintain remission (see Therapeutic discussion). While azathioprine was frequently used in the past [83], currently, rituximab is becoming the treatment of choice [84–87], especially for orbital disease [88]. Many practitioners also use trimethoprim and sulfamethoxazole (co-trimoxazole) as a disease suppressant [89, 90].

The most common therapeutic oculoplastic procedures required in orbital GPA are for nasolacrimal duct obstruction. Dacryocystorhinostomy is usually the most effective surgical treatment but can be complicated by nasocutaneous fistulas if attempted, while the disease is still active [91]. Dacryocystectomy is an alternative treatment for recurrent or chronic dacryocystitis without epiphora.

Orbital inflammation may occur in other vasculitides. Its involvement in systemic lupus erythematosus will be discussed later. There have been a very few reported cases orbital involvement in eosinophilic granulomatosis with polyangiitis (Churg-Strauss disease) (Fig. 34.14), polyarteritis nodosa, Behçet disease [72], Cogan syndrome, and Takayasu arteritis.

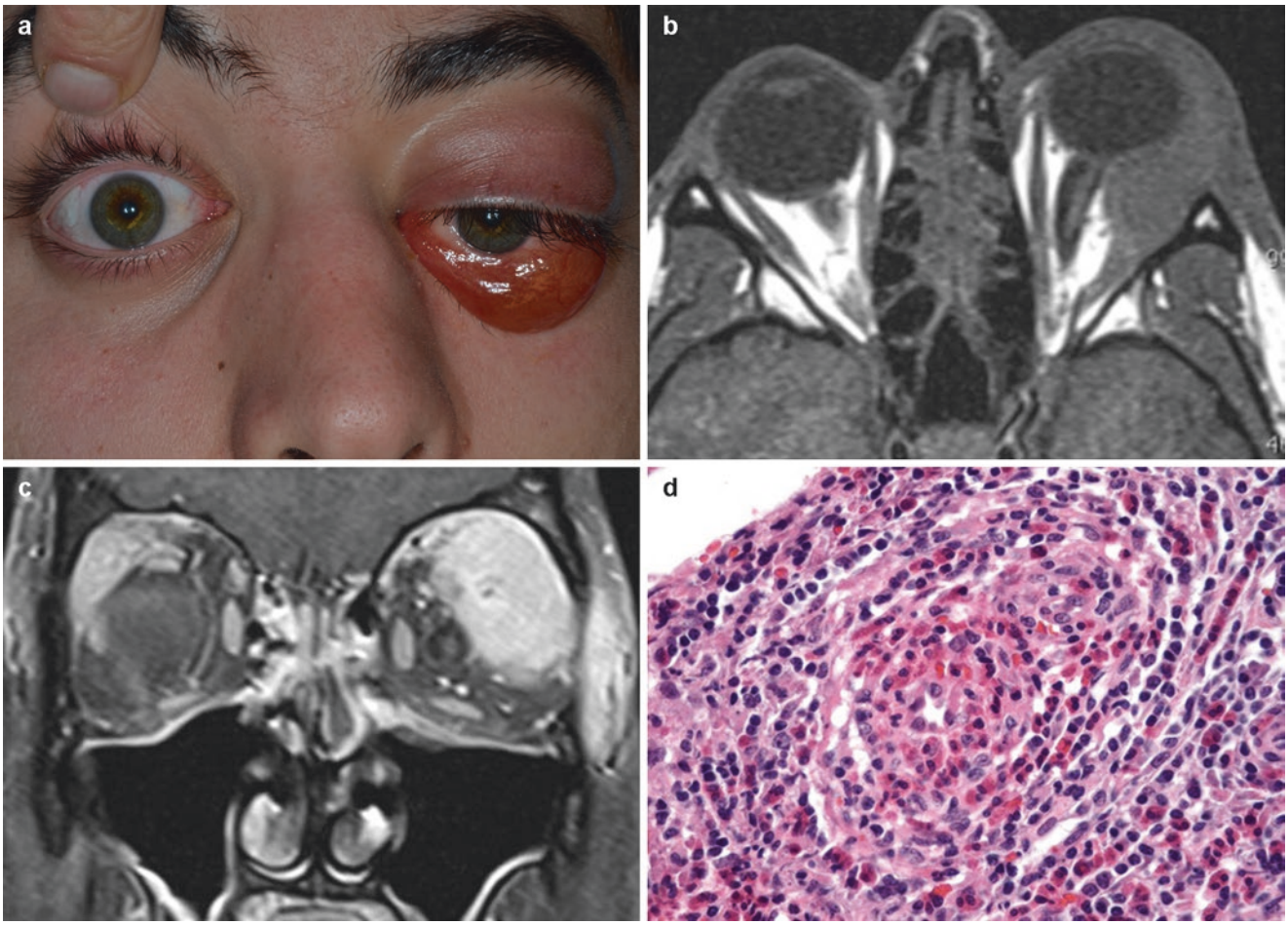


Fig. 34.14 Eosinophilic granulomatosis with polyangiitis (Churg-Strauss syndrome). A 19-year-old male presented with a 3-week history of left exophthalmos and diplopia. One year prior, he had developed an abducens nerve palsy from a central venous sinus thrombosis of unknown etiology. (**a**) External appearance. (**b**) Axial pre-contrast T1-weighted MRI demonstrates a mass in the area of the left lacrimal gland molding to the globe. (**c**) Coronal post-contrast T1-weighted MRI shows diffuse enhancement of the lesion. (**d**) Biopsy revealed eosinophilic granulomatosis. The mass resolved rapidly and completely with systemic corticosteroids with no evidence of local or systemic recurrence

Orbital and ocular adnexal involvement has not been reported in the third AAV – microscopic polyangiitis.

Thyroid Eye Disease

TED is an immune-mediated orbital inflammatory disease most commonly associated with autoimmune hyperthyroidism or Graves disease, although it can also occur in patients who are hypothyroid or euthyroid. A review of the literature suggests that between 1% and 63% of children with Graves disease exhibit signs of ophthalmopathy; however, in children this tends to be mild (Fig. 34.15) [92, 93]. Common presenting signs mimic those seen in adults with TED, including exophthalmos, upper eyelid retraction, acquired epiblepharon, corneal erosion, and lagophthalmos [92, 94]. When present, the proptosis in the pediatric populations occurs almost exclusively from expansion of the orbital fat compartment, with only mild enlargement of the extraocular muscles [92].



Fig. 34.15 TED. A 14-year-old girl presented complaining of left upper eyelid ptosis. On exam, right upper eyelid retraction was noted. Initial serologic testing showed no evidence of thyroid dysfunction. Four months later, elevation of thyroid-stimulating immunoglobulin was noted, and 8 months after presentation, she was serologically hyperthyroid. No periocular progression has occurred over a 2-year follow-up

Children with TED, like adults, typically experience progressive ophthalmopathy for 1–2 years and then remain stable [95]. Similar to associations seen in the adult population, exposure to secondhand smoke in children with Graves disease may lead to a higher prevalence of orbital disease [96].

The management of TED in the pediatric age group mirrors that of adults with mild orbital disease: achieving a euthyroid state may resolve eyelid retraction and stare; conservative therapy with lubrication for ocular irritation [92, 94]; surgical intervention, while rarely required, for corneal exposure or appearance issues. Fortunately, vision-threatening corneal ulcerations, optic nerve damage, and diplopia have never been reported in this age group [92].

IgG4-Related Disease

Immunoglobulin G4-related disease (IgG4-RD) is an increasingly recognized syndrome that can appear with multiple organ involvement, typically with tumorlike swelling and a lymphoplasmacytic infiltrate rich in IgG4-positive plasma cells; serum IgG4 concentrations are not always elevated. The disease was first recognized in the pancreas but now is understood to have the potential to involve virtually every organ system, including the orbit (IgG4-ROD). In 2012, a consensus statement (the "Boston Consensus") defined the histologic parameters for IgG4-RD diagnosis (see Table 34.4). In order to exclude lymphoma misdiagnosed as IgG4-RD, most experts recommend staining for immunoglobulin light chain κ or λ restriction.

There are a limited number of case reports of pediatric IgG4-RD in the literature, mostly involving the abdominal and thoracic cavities. Interestingly, the differential diagnosis of lymphadenopathy includes IgG4-RD, and benign/reactive lymphadenopathy is common in children and rarely worked-up. Although speculative, the incidence of pediatric IgG4-RD may in fact be higher than reported, and an increasing awareness of this disease spectrum may be reflected in the literature in the future.

The number of papers describing ocular and orbital involvement (IgG4-ROD) has also steadily increased over the last few years [98]. Sites of involvement include the lacrimal gland, the lacrimal sac, extraocular muscles, orbital adipose tissue, the eyelids, and conjunctival tissues [99]. Lesions are often infiltrative in nature and are characteristically T2 hypointense and gadolinium enhancing on MRI [100]. As opposed to IOI, IgG4-ROD is often painless, presenting with eyelid swelling and/or diplopia (Fig. 34.16) [99, 101]; bilateral involvement is common [101]. In hindsight, many cases of "idiopathic" sclerosing orbital inflammation may indeed have been undiagnosed IgG4-ROD [102].

In one meta-analysis, the mean age of onset of "definite" and "probable" cases of IgG4-ROD is 55.5 years (standard deviation = 12.9 years) [99]. There have been fewer than two dozen cases of the disease in pediatric patients reported in the literature [103–105].

Treatments for patients with IgG4-ROD most often include induction with systemic CS, along with radiotherapy, conven-

Table 34.4 Histologic parameters for IgG4-RD diagnosis [97]. Note that certain parameters change depending on the anatomic site of involvement. Furthermore, corticosteroid therapy at time of histopathologic review may affect results

1. Dense lymphoplasmacytic infiltrate
2. Fibrosis, which must be storiform in at least a region
3. Obliterative phlebitis. The fibrosis of lacrimal glands is less likely to be storiform and more likely to be collagenous)
4. Immunohistochemically there must be >50 IgG4+ plasma cells (PC)[a]; IgG4+ PCs should comprise >40% of all IgG+ PCs in 3 hpf

[a]This differs from the Boston Consensus, which requires >200 IgG4+ cells/hpf in the lacrimal gland

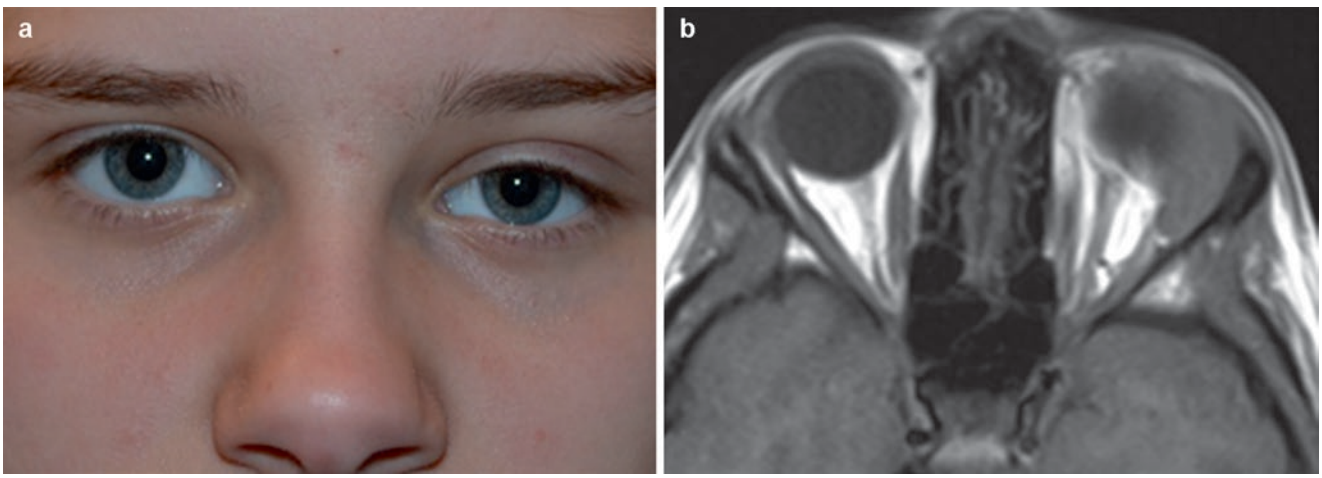


Fig. 34.16 IgG4-related orbitopathy. A 14-year-old girl presented with painless lid swelling of several months' duration with only a partial response to prednisone. (**a**) Eyelid swelling without erythema. Note the S-shape of the left upper eyelid suggestive of a lacrimal gland process. (**b**) Axial, pre-contrast T1-weighted MRI shows an isointense lesion molding to the globe.

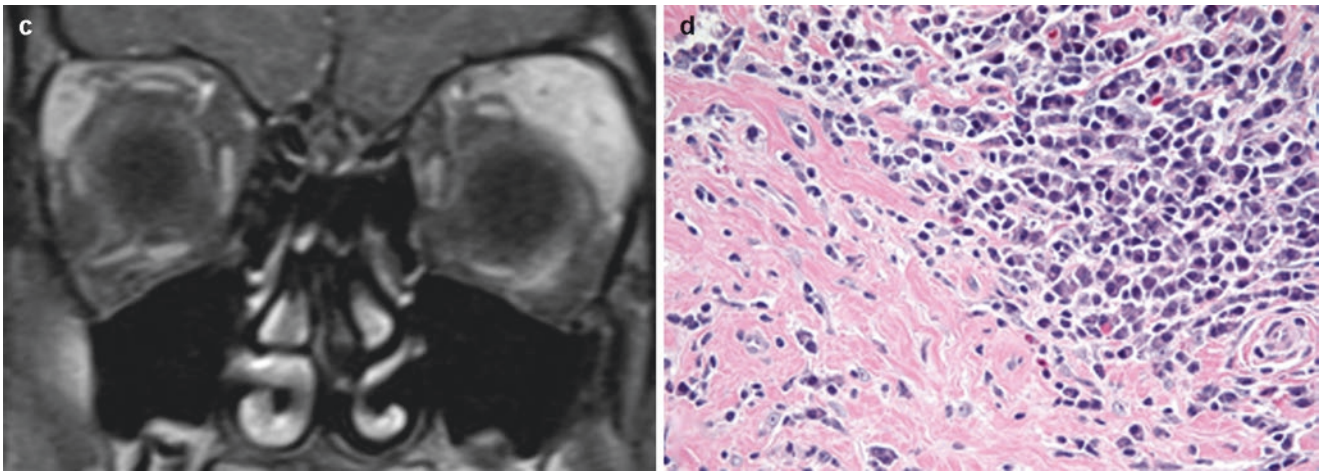


Fig. 34.6 (continued) (**c**) Coronal, post-contrast T1-weighted MRI with diffuse enhancement of the mass. (**d**) Histopathology showed areas of lymphoplasmacytic infiltrate transitioning into dense fibrosis. Increased IgG4 staining of plasma cells was confirmed on immunohistochemistry

tional IMT, and/or rituximab [99, 101], to maintain disease remission. IMT have been efficacious for some in maintaining long-term response to steroid-sparing treatment. However, a recent analysis of adults with IgG4-related pancreatitis demonstrated no statistical difference in time to relapse between those treated with CS alone (and weaned) vs. those treated with initial CS and maintained on IMT [106]. Conversely, treatment with rituximab (see section "Pharmacotherapy") has resulted in more durable remission in IgG4-RD. Some practitioners are using rituximab alone, without CS, as an induction agent. When relapses occur, patients may respond to repeat treatment. This treatment paradigm may radically decrease steroid toxicity, although it does come with its own set of adverse effects and may be more costly, at least in the short term.

Systemic Lupus Erythematosus

Systemic lupus erythematosus (SLE) is an immune complex-mediated disease that can result in multisystem inflammation that may affect any organ including the joints, skin, lungs, kidneys, heart, and central nervous system [107]. The onset is most common in females (8:1) between the ages of 9 and 15 years. Serum antinuclear antibody (ANA) levels are almost universally elevated in this syndrome if treatment has not been initiated. The ANA may also be elevated in other autoimmune disease as well as in 10–20% of healthy individuals. When the ANA is positive and concern is high for autoimmune disease, one must evaluate the more specific antibodies-an ANA "profile". In the ANA profile, anti-double-stranded DNA and anti-Smith are most specific for SLE, whereas, for example, SS-A/anti-Ro and SS-B/anti-La associate with Sjögren syndrome.

As many as 20% of patients with SLE can show ocular involvement with retinal vasculitis [108]. Anterior orbital inflammation is occasionally seen [109, 110]. These manifestations respond to the systemic treatment that is used to treat the SLE. Orbital inflammation is most often seen when the disease is active systemically, and symptoms may wax and wane. Treatment usually consists of induction treatment with CS (intravenous or oral) with addition of a combination of the following agents for induction and maintenance of disease control: cyclophosphamide, rituximab, methotrexate, mycophenolate mofetil, and/or azathioprine. Hydroxychloroquine is a crucial component of any long-term maintenance treatment plan but requires 6–12 months of use to become effective. SLE is a lifelong disease, with periods of remission and relapse. It can be fatal, and exacerbations warrant aggressive therapy by a rheumatologist.

Sjögren Syndrome

Sjögren syndrome (SS) is a clinical entity characterized primarily by keratoconjunctivitis sicca and xerostomia [111]. The existent American-European Consensus Group criteria for diagnosis of SS are shown in Table 34.5.

These criteria may not capture those with earlier stages of disease, wherein inflammation is present but has not yet caused damage. The American College of Rheumatology has proposed the SICCA criteria that may help to identify patients with early disease, and newer guidelines are under development [113]. Case definition requires at least two out of the following three:

1. Positive serum anti-SSA and/or anti-SSB or (positive rheumatoid factor and ANA ≥1:320)
2. Ocular staining score ≥3
3. The presence of focal lymphocytic sialadenitis with focus score ≥1 focus/4 mm^2 in labial salivary gland biopsies

Pediatric SS likely has been underdiagnosed because sicca symptoms are not yet present; there are to date no accepted pediatric-specific guidelines [114]. SS can be primary or secondary – coexisting with another autoimmune

Table 34.5 Revised international classification criteria for Sjögren syndrome (AESG) [112]

I.	Ocular symptoms – a positive response to at least one of the following questions: 1. Have you had daily, persistent, troublesome dry eyes for more than 3 months? 2. Do you have a recurrent sensation of sand or gravel in the eyes? 3. Do you use tear substitutes more than three times a day?
II.	Oral symptoms – a positive response to at least one of the following questions: 1. Have you had a daily feeling of dry mouth for more than 3 months? 2. Have you had recurrently or persistently swollen salivary glands as an adult? 3. Do you frequently drink liquids to aid in swallowing dry food?
III.	Ocular signs – that is, objective evidence of ocular involvement defined as a positive result for at least one of the following two tests: 1. Schirmer I test, performed without anesthesia (<5 mm in 5 min) 2. Rose bengal score or other ocular dye score (>4 according to van Bijsterveld's scoring system)
IV.	Histopathology: In minor salivary glands (obtained through normal-appearing mucosa), focal lymphocytic sialadenitis, evaluated by an expert histopathologist, with a focus score >1, defined as a number of lymphocytic foci (which are adjacent to normal-appearing mucous acini and contain more than 50 lymphocytes) per 4 mm2 of glandular tissue
V.	Salivary gland involvement – objective evidence of salivary gland involvement defined by a positive result for at least one of the following diagnostic tests: 1. Unstimulated whole salivary flow (<1.5 ml in 15 min) 2. Parotid sialography showing the presence of diffuse sialectasis (punctate, cavitary, or destructive pattern), without evidence of obstruction in the major ducts 3. Salivary scintigraphy showing delayed uptake, reduced concentration, and/or delayed excretion of tracer
VI.	Autoantibodies – presence in the serum of the following autoantibodies: 1. Antibodies to Ro(SSA) or La(SSB) antigens or both

disease, such as SLE, mixed connective tissue disease, dermatomyositis, vasculitis, systemic sclerosis, autoimmune liver disease, and hemolytic anemia. Even when primary, clinical manifestations of SS are not restricted to the exocrine glands and may include fatigue, rashes, arthritis, interstitial lung disease, nephritis, and neurologic involvement.

SS is manifested by lymphocytic infiltration and sclerosis of the lacrimal and salivary glands, resulting in decreased production of tears and saliva [115]. Tear lysozyme levels are diminished, whereas they are increased in sarcoidosis [116]. When there is active inflammatory involvement of the lacrimal and salivary glands, these structures may be enlarged and tender. Systemic CS and IMT, such as methotrexate, mycophenolate mofetil, and/or rituximab, may be of value during this active phase. Hydroxychloroquine should be initiated to help prevent future disease flares. Once the lacrimal and salivary glands are damaged, treatment is best aimed at managing dry eye complications and dry mouth. SS increases the risk of lacrimal gland lymphoma, typically of the indolent extranodal marginal zone variety [117].

Crohn Disease

Crohn disease is an idiopathic chronic disease characterized by segmental, granulomatous inflammation of gastrointestinal mucosa. It typically presents in the second to fourth decade of life although it presents in younger children as well. Typical symptoms include diarrhea, fever, weight loss, anemia, and/or gastrointestinal bleeding, although it can follow a more indolent course and, especially in children, arthritis and poor growth may precede GI symptoms. Gastrointestinal complications include abscesses, fistulas, strictures, and perforations. Endoscopy, radiologic imaging, and biopsy are used to evaluate these problems.

Crohn disease is complicated by ocular involvement in 4–10% of cases [118]. This can manifest as keratoconjunctivitis, peripheral corneal ulcers, blepharitis, episcleritis, scleritis, iridocyclitis, and macular edema. Unilateral or bilateral orbital inflammation occurs more rarely [119, 120]. Crohn disease can present as optic neuritis, myositis, diffuse IOI, or dacryoadenitis [121]. Ocular inflammation can be, although more rarely, manifested in ulcerative colitis as well. The orbital inflammation is treated similarly to IOI and responds to the same classes of agents used to treat systemic disease. In addition to CS, there is a growing use of tumor necrosis factor inhibitors to treat Crohn disease, and infliximab and adalimumab have been shown to be useful for disease-associated orbital inflammation [88, 122]. Treatment plans should be made in consultation with the patient's gastroenterologist.

Histiocytic Disorders

Histiocytes are cells of the mononuclear phagocytic system cells – dendritic cells (DC) and macrophages. Histiocytic disorders are classified into three types by the Histiocyte Society – Class 1 or dendritic cell (DC) disorders, Class 2 or macrophage disorders, and Class 3 or malignant histiocytic diseases. The DC disorders include Langerhans cell histiocytosis (LCH, previously histiocytosis X), juvenile xanthogranuloma (JXG), and Erdheim-Chester disease (ECD) [123]. Hemophagocytic lymphohistiocytosis (HLH, primary and secondary forms) and Rosai-Dorfman disease (RDD or sinus histiocytosis with massive lymphadenopathy) are macrophage histiocytoses. LCH, ECD, and RDD can, in isolation, affect the orbit.

Langerhans Cell Histiocytosis (LCH)

LCs are antigen-presenting dendritic cells in the skin and mucosa. They are characterized by "racquet-shaped" cytoplasmic granules (Birbeck bodies or LC granules) seen by electron microscopy and by positivity for S100 and CD1a on immunohistochemistry. In LCH, LCs associate with mature eosinophils, lymphocytes, and multinucleated giant cells to

form granulomas and give rise to a new name for this disease complex: Langerhans cell granulomatosis (LCG) [124]. Historically, LCH was divided into three categories: localized bone involvement (eosinophilic granuloma), multifocal bone disease (Hand-Schuller-Christian disease), and a fulminant systemic disorder (Letterer-Siwe disease) [124]. Eosinophilic granuloma represents unifocal LCG, typically occurring in adults. The Hand-Schuller-Christian variant is multifocal LCG. Letterer-Siwe disease is felt to have represented an associated group of disorders that were not necessarily LCG. Mortality that was associated with the Letterer-Siwe category does not appear to have been due to LCG.

LCH occurs most commonly in the young pediatric age group, often 1–3 years of age, with a 2:1 male predominance. Ophthalmic manifestations may be seen in up to 30% of patients [125]. The prognosis of this syndrome is worse when it presents in young children (under the age of 3 years), when it is multifocal, and when it shows clinical signs of rapid progression. In these cases, treatment may include low-dose local radiation, cytotoxic agents, and systemic CS.

Unifocal LCH (also known as eosinophilic granuloma) in the orbit most commonly involves the superotemporal orbital rim in adolescents and young adults [125]. This results in a subacute, solitary lytic bone lesion with adjacent bone sclerosis (Fig. 34.17). Patients may show cutaneous discoloration from the diffusion of blood degradation products. These isolated lesions are almost always cured by limited surgical debridement. It is not unusual to find the lytic lesion to be filled with a dark fluid with no appreciable solid tissue within the lesion. Curettage of the lytic cavity generally provides an adequate specimen for pathological evaluation. Postoperatively, observation alone is advisable. Of note, the involved orbital bone not infrequently remodels into its native configuration after simple curettage [126].

Multifocal LCG can involve the orbital bones, causing lytic bone lesions, adjacent fibrosis, bone sclerosis, shallow orbits, exophthalmos, and diabetes insipidus. This can be associated with multiple lytic bone lesions scattered over the cranial vault.

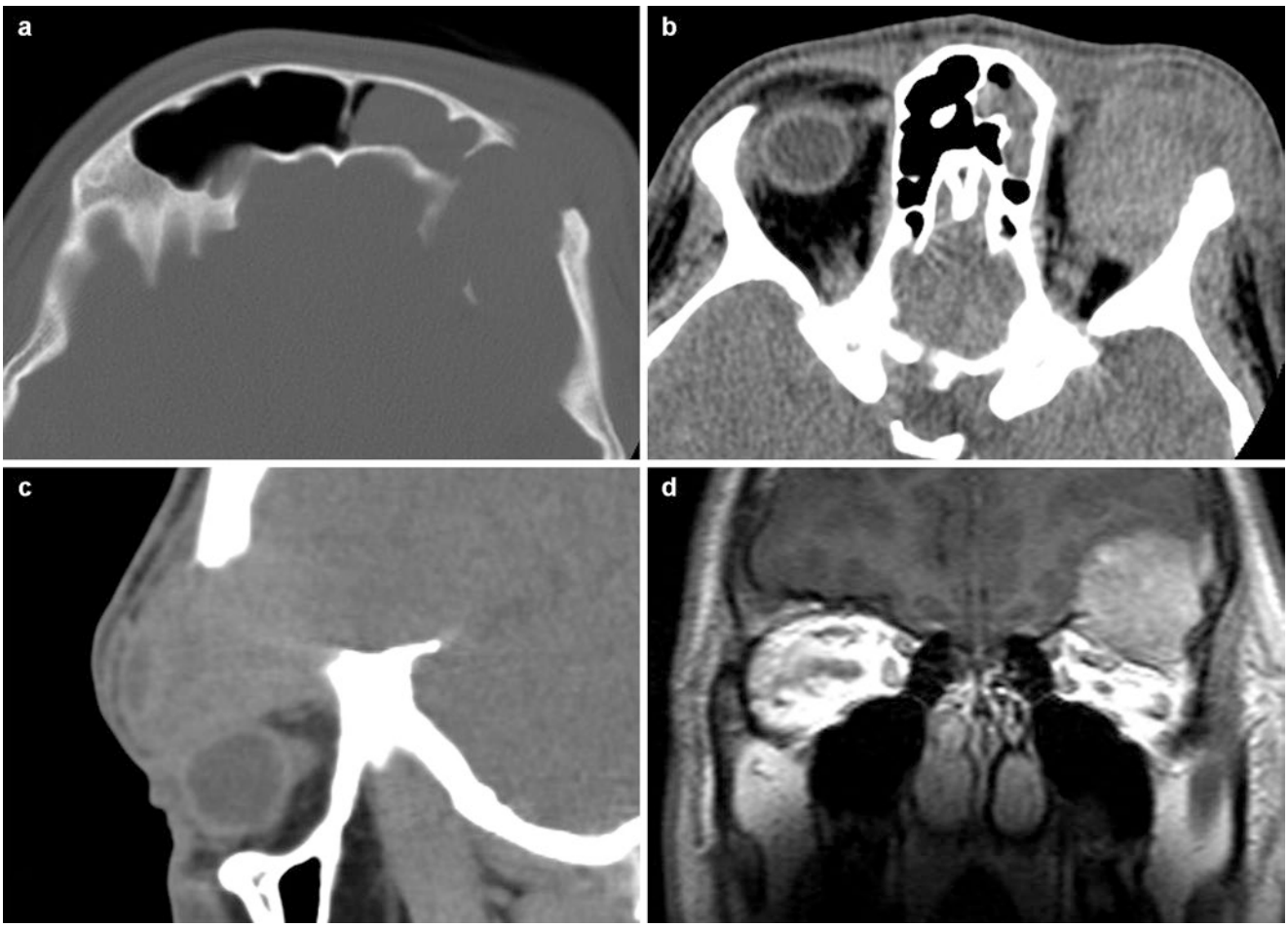


Fig. 34.17 Unifocal LCH (eosinophilic granuloma). (**a**) On axial CT (bone window), significant destruction of the left bony skull base is evident. (**b**) Axial CT (soft tissue window) demonstrates a large soft tissue mass centered around the superolateral orbit, the most common location of orbital eosinophilic granuloma. Note the destruction of the lateral orbital rim. (**c**) Parasagittal CT (soft tissue window) shows the orbital mass eroding through the skull base into the anterior cranial fossa. (**d**) On post-contrast coronal MRI, the mass enhances diffusely with contrast. Adjacent bone erosion is the rule in eosinophilic granuloma, and this finding often raises the possibility of malignancy

Radiation, systemic CS, and cytotoxic agents are used to treat multifocal disease, but are rarely necessary for cases of localized disease.

Rosai-Dorfman Disease (RDD) [127]

This Class 2 histiocytosis is not uncommonly restricted to the head and neck and can affect the orbit. Patients often have large painless lymphadenopathy, constitutional symptoms along with systemic inflammation, including elevated ESR and cytopenias. In RDD, macrophages proliferate extensively in the lymph node sinus (hence the moniker "sinus histiocytosis"). Their most characteristic histologic feature is emperipolesis – macrophages wrap themselves around other cells. They are identified on immunohistochemistry by their S100 and CD68 positivity with the absence for CD1a staining. RDD has an older average age of onset (20 years) than does LCH. It may affect males more frequently than females, but this discrepancy is also lower than in LCH. Lesional resection is used for localized disease. RDD may spontaneously regress, but many patients have an indolent course. The most promising nonsurgical treatments have included B-cell depletion, methotrexate, and cyclosporine, although low-dose radiation has been used for recalcitrant invasive head and neck lesions. The prognosis for those in whom the orbit or eyelid are affected seems better than for those with intraocular involvement.

Ruptured Orbital Dermoids

Orbital dermoid cysts that rupture can produce an inflammatory reaction due to the release of epithelial elements into the orbital tissues. These can also become infected. A rupture can occur spontaneously, as the result of trauma, or as a result of incomplete surgical excision. Systemic antibiotics may be helpful if there are clinical signs of infection. The definitive treatment is complete debridement. This can be difficult, since the epithelial elements may spread along multiple tissue planes.

Foreign Bodies

Orbital foreign bodies (FBs) can produce inflammatory and infectious reactions. Metallic, glass, and plastic FBs can often remain in the orbit without causing problems. Removal is advisable if there are complications resulting from pressure against the optic nerve or globe or if extraocular movements are affected. Organic FBs such as wood and cotton are prone to cause recurrent inflammation and infection (Fig. 34.18) [128], sometimes with devastating visual sequelae, and should be promptly removed.

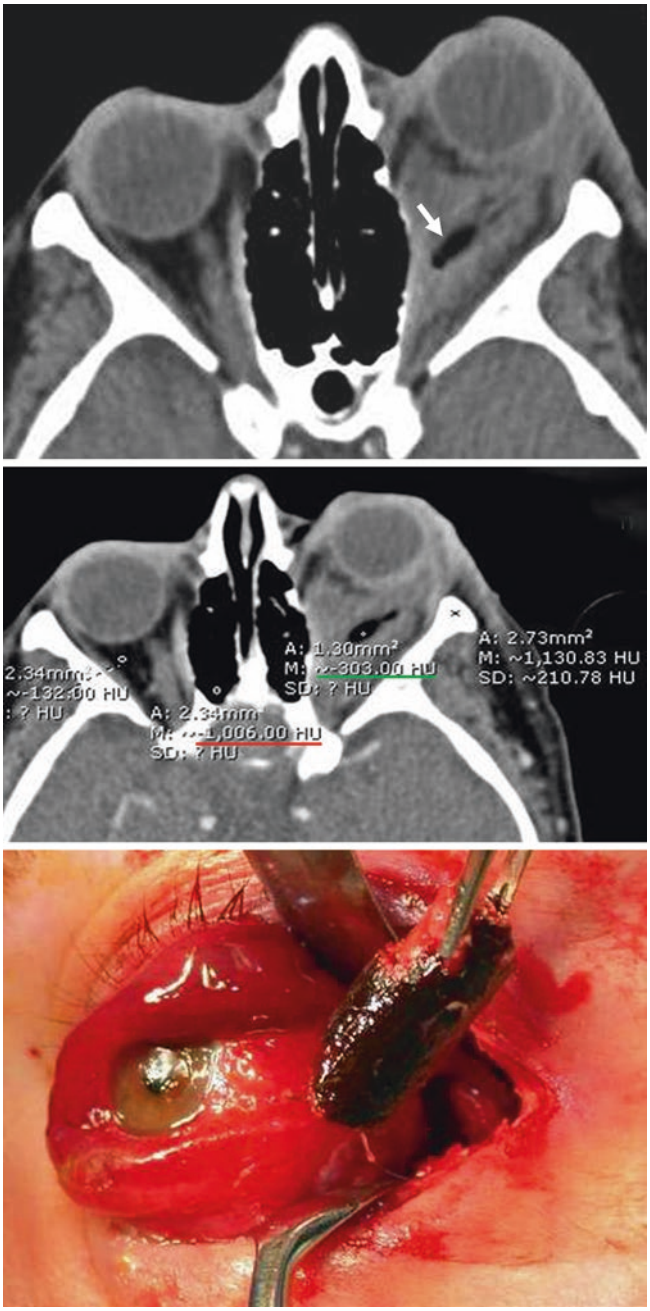


Fig. 34.18 Occult wooden foreign body. Top: Axial CT (soft tissue window) of a patient who lacerated her eyelid from a tree branch 6 days prior. The CT was read as left orbital hemorrhage with air. She was placed on intravenous antibiotics and corticosteroids but progressed clinically with increased orbital inflammation and hand motion vision on the left. Middle: An orbital specialist was consulted, and the CT was reassessed. On axial bone window, multiple measurements were performed of CT densities. Note that air in the ethmoid sinus (*red line*) has a markedly different value (−1000.6 HU) compared to the presumed air (*green line*) in the left orbit (−303 HU). This large disparity of values raised the suspicion that the intra-orbital "air" was actually a wooden foreign body. Bottom: The patient was taken to the operating room urgently and a large wooden foreign body removed. Her orbital inflammatory signs abated rapidly, and vision slowly improved to 20/200. HU, Hounsfield unit (Case courtesy of Peter A. D. Rubin, MD)

Occasionally children may have orbital FBs resulting from unwitnessed trauma. Periocular injuries of questionable origin need to be carefully explored at the time of primary repair and may require preoperative orbital imaging. An organic FB is often not visible or mimics air on CT scans, especially if the foreign material is small [129]. Once organic foreign material has been present and caused an inflammatory reaction, the penumbra of inflammation may be radiographically visible even if the FB is not. MRI provides additional information in cases of organic FBs and is often used in concert with CT [128, 129].

Pharmacotherapy

In about one quarter of adult [1] patients treated with corticosteroids (CS) alone for orbital inflammatory disorders have persistent inflammation (CS resistant) or disease recurrence upon steroid wean or discontinuation (CS dependent). As long-term exposure to CS carries numerous toxicities (see discussion in section "Idiopathic Orbital Inflammation" above), alternate steroid-sparing immunomodulatory treatment (IMT) options should be used in these situations. Rather than using radiotherapy, many practitioners now reach directly for IMT, including conventional as well as biologic agents. Most experts in inflammatory disease divide treatment into two phases: induction and maintenance. In some cases, the induction may be with CS alone. Most practitioners will not wait for CS resistance or dependency but rather will preemptively choose an IMT agent(s) to replace CS in the maintenance phase.

Conventional Immunomodulatory Agents

Methotrexate

Low-dose weekly methotrexate (MTX) is the first-line disease-modifying antirheumatic drug (DMARD) for rheumatoid arthritis, juvenile idiopathic arthritis, and many other rheumatic diseases, including those that involve the eye. Possibly because of practitioner comfort with this agent, it has been used as a second-line agent to treat IOI. MTX is a folate analogue that acts at multiple places to interfere with purine and pyrimidine biosynthesis, limiting cell division in malignancy and immune responsiveness. It may dampen inflammation by acting to increase levels of adenosine, thereby interfering with neutrophil adherence [107, 130, 131]. MTX is administered at 0.5–1 mg/kg/week, orally, or subcutaneously. The subcutaneous form has increased bioavailability – with fewer GI side effects – although, especially in children, there may be more psychiatric side effects associated with needle usage. Oral doses seem to be maximally absorbed at 15 mg, with a plateau in absorption thereafter; doses up to 25 mg can be administered subcutaneously with good absorption [132]. Most often, low-dose MTX is well tolerated and quite safe, even for prolonged use in children. Risks of MTX include infection and cytopenias (both rare), fatigue, nausea/vomiting, and transaminitis (which resolves with dose decrease). Fatigue and gastrointestinal side effects are most common the day following administration and are lessened with daily folate administration (1 mg daily). Women of reproductive age should also be counseled that MTX is a teratogen. It is primarily cleared by the kidneys and should be used with caution in those with decreased renal function. It is contraindicated with alcohol use. Toxicity labs (CBC and CMP) should be obtained at baseline, 1 month after initiation, and every 3–4 months thereafter according to the American College of Rheumatology guidelines. As MTX may not be effective for 8–12 weeks, an inability to dramatically wean CS in the first 2–3 months of MTX therapy should not be considered a failure.

Methotrexate is commonly used as a maintenance therapy for inflammatory diseases, including those with systemic and/or orbitally restricted inflammation [133, 134]. Despite its frequent use, there is only one case series of MTX use for orbital inflammatory disease. In 2001, Smith reported that 9 of 14 adults with noninfectious orbital inflammatory disease benefited from MTX, although 4 of those who did not respond actually discontinued treatment prior to study completion [135]. Of all treated patients, six were able to stop MTX (median 10–25 months) without symptom recurrence. While the goal of MTX use is to spare CS exposure, only 5/6 patients initially on CS were able to completely stop CS. It is the practice of one of the authors (MAL) to treat for 1–2 years of quiescence, off CS, before attempting to discontinue methotrexate for inflammatory disease.

Mycophenolate Mofetil (MMF, CellCept®)

This prodrug of mycophenolic acid blocks guanine synthesis by reversibly inhibiting inosine monophosphate dehydrogenase. It particularly affects dividing lymphocytes. As does MTX, MMF interferes with inflammation by multiple mechanisms, including inhibition of monocyte adhesion. MMF is administered orally with twice daily dosing, 600 mg/m^2/dose (up to a maximum of 1500 mg twice daily). The side effect profile includes cytopenia, increased risk of infection, and teratogenicity. MMF carries a relatively high risk of diarrhea, especially at initiation, which can result in discontinuation of therapy. The authors have found that a slow up-titration over 1–1.5 months limits diarrhea and increases patient acceptance. MMF requires dose reduction with decreased renal function. Toxicity labs should be obtained regularly as the dose is increased and then every 3–4 months.

In a large single-center cohort of ocular inflammatory diseases, of 84 mostly adult patients treated with MMF, 5 had IOI. The authors of the study did not specifically delineate the outcomes in IOI patients, but 82% of patients overall achieved steroid-sparing control of inflammation within a median time of 3.5 months [136]. In another single-center adult study of IOI, MMF resulted in complete resolution of the 4/5 adult patients who were able to tolerate it. Some patients had been CS dependent, with multiple courses of disease reactivation, and one had failed radiation. Each had resolution of inflammation (median follow-up 8.5 months) and either discontinuation or dramatic reduction of CS doses [137]. While many of the reports of treatment come from the adult literature, one case series reported on ten children with inflammatory lesions of the orbit treated by rheumatologists at the Great Ormond Street Hospital for Children [138]. Two children with IOI were treated with methotrexate, after induction treatment with CS; one reactivated with CS wean and was successfully switched to MMF. Most of the other children had exposure to multiple IMT therapies, but the sequence of use is not described. Independent reports have described children with IgG4-RD who have achieved successful CS discontinuation on MMF (n = 3) [104, 105, 139] but also one child who failed MTX and MMF and required cyclophosphamide. MMF is no longer considered a treatment of choice for GPA [83].

Azathioprine

This prodrug of 6-mercaptopurine (6-MP) integrates into DNA and inhibits de novo purine synthesis. Azathioprine (AZA) impacts both lymphocytes and monocytes, although it is most effective in lymphocytes because these cells lack salvage pathways. AZA may also exert is immunomodulatory effects through other, poorly understood, mechanisms. AZA is administered once daily at 0.5–2.5 mg/kg/day (maximum 150 mg/day). It is important to assess individual's levels of thiopurine methyltransferase, the enzyme that inactivates 6-MP; deficiencies can make AZA toxic, whereas high serum levels may require increases in the dose. The most common side effect is nausea and/or diarrhea, which, as with MMF, can be limited by a slow up-titration. As an immunosuppressant, there is an increased risk of infection. Other potential side effects include bone marrow suppression (most often affecting lymphocytes), transaminitis, and interstitial pneumonitis. It is renally cleared. AZA crosses the placenta, but the fetal liver cannot metabolize AZA. Toxicity labs should be obtained regularly, while the dose is increased, and then every 3–4 months. In systemic GPA with renal involvement, AZA is well demonstrated to be an effective maintenance agent, preferable to MMF [83]. AZA was a useful adjunctive agent to CS for induction in two children with IgG4-RD, although it was inadequate monotherapy in one and long-term outcome in not known in the second [140, 141].

Cyclosporine

This is not an antimetabolite but is a member of the calcineurin inhibitor class of drugs (along with tacrolimus). By binding to calcineurin, cyclosporine (CsA) limits translocation of nuclear factor of activated T cells (NFAT) to the nucleus and reduces interleukin-2 (IL-2) production and T-cell activation. It also inhibits the production of other cytokines while increasing the production of transforming growth factor-β1, an inhibitory growth factor. Absorption of CsA is variable. CsA carries numerous side effects, including renal and liver toxicity, GI intolerance (oral ulcers, nausea, and vomiting), hypertension, gingival hyperplasia, and paresthesias. Dosage ranges from 3 to 5 mg/kg/day. In addition to regular CBC and complete metabolic panel motoring with initiation and then with maintenance, particularly close attention should be paid to creatinine levels. Blood pressure should be assessed weekly at initiation and then at least monthly. Drug troughs should be maintained at 125–175 μg/ml. CsA metabolism can be greatly affected by other drugs (e.g., NSAIDs) and foods (e.g., grapefruit). Calcineurin inhibitors are not reached for frequently as first-line CS-sparing agents, but they have been used in recalcitrant cases of diseases with ocular and orbital inflammation.

Cyclophosphamide

Before the availability of safer conventional and biologic IMT, patients with resistant disease were frequently treated with the cytotoxic alkylating agent cyclophosphamide (CYC). CYC induces lymphopenia and results in a higher risk of infection than the other agents discussed above. It induces considerable short-term side effects, including nausea and vomiting during and immediately after administration, alopecia, and interstitial cystitis (which can be prevented by co-administration with mesna, a "chemoprotectant" that reduces the undesired side effects of certain chemotherapy drugs.) Its longer-term risks include development of bladder cancer, decreased fertility, and premature ovarian failure. The fertility issue is particularly concerning in pediatric medicine; although the risk is lower for prepubertal children than for adolescents. Cumulative doses of <7 g carry lower risks of impacting fertility. Sperm banking should be considered for postpubertal males before administration. CYC can be administered orally or intravenously. Pulse intravenous dosing (every 2 weeks to every month) is increasingly felt to be as effective as daily dosing and to cause fewer toxicities [142]. Doses should be adjusted based upon renal function and 10–14 day lymphocyte and neutrophil nadirs. Nonetheless, CYC continues to be used in some induction regimens, in particular for GPA and SLE [142]. Even in these diseases, CYC-sparing induction regimens are becoming more standard, as they are shown to be similarly effective to CYC [84, 143]. CYC may be used a rescue medication when other regimens fail.

Biologic Agents

Tumor Necrosis Factor-Alpha Inhibitors

The cytokine tumor necrosis factor (TNF) plays a pleiotropic role in inflammatory responses. In the late 1990s, drugs engineered to directly target TNF were approved by the Federal Drug Administration (FDA) and came to market. The first was infliximab (IFX) a chimeric human-murine antibody that binds with high affinity to TNFα (anti-TNFα). It is comprised of human Fc and murine variable regions. Because this makes it immunogenic in humans, it is often co-administered with methotrexate. Etanercept, a soluble TNF receptor that binds TNFα, was approved soon thereafter. The third agent to come to market was adalimumab (ADA), a fully humanized monoclonal antibody to TNFα. Newer agents, with longer half-lives, as well as biosimilars are continually being developed but will not be addressed further in this text.

IFX is administered intravenously. After loading doses at week 0, 2, and 6, IFX is administered every 4–8 weeks. Dosing ranges from 3 to 20 mg/kg (with higher doses often used in pediatric inflammatory eye disease). ADA is administered subcutaneously at doses of 20 mg (for <30 kg) and 40 mg (≥30 kg) every 2 weeks (although weekly use is beneficial in some cases). As TNFα is crucial in granuloma clearance, individuals must be tested for latent tuberculosis before initiation; an increased level of suspicion should be maintained for invasive fungal infections in endemic areas (e.g., histoplasmosis). Patients should have CBC and CMP assessed 1 month after initiation and then every 3–6 months thereafter. There are few subjective side effects from anti-TNFα agents (no fatigue or nausea) save for discomfort from the injections and a risk of local reactions for subcutaneously injected agents. There is a risk of transfusion reaction with IFX [144, 145], although this may be limited by administration with methotrexate to limit development of human anti-chimeric antibodies. The FDA issued a black box warning in 2009 [146] that individuals receiving IFX may have an increased risk of future malignancy. Subsequent studies have not supported this nor have they demonstrated a significantly increased risk of serious infections; as such, anti-TNFα drugs appear to be relatively safe medications [147–152].

Because of their beneficial effects, as a class, anti-TNFα drugs have transformed the landscape of treatment for rheumatoid arthritis, juvenile idiopathic arthritis, psoriasis, ankylosing spondylitis, Crohn disease, Behçet disease, sarcoidosis, and inflammatory eye disease (idiopathic and systemic disease associated). However, only the monoclonal antibody anti-TNFα has been efficacious for uveitis [153, 154]. Garrity reported the largest series of individuals treated with anti-TNFα (all infliximab) for orbital inflammation [88]. All but one of the seven adults had an underlying systemic diagnosis, including Crohn disease, psoriasis, and Behçet disease, and all had recalcitrant disease. Two had been CS dependent, and the other five had failed regimens of CS along with irradiation, CsA, MTX, 6-MP, AZA, and/or CYC. Six of seven improved ($n = 3$) or achieved quiescence ($n = 3$). Multiple other authors have reported cases in which individuals with IOI or CD-associated orbital inflammation had good response to infliximab, after failing other CS-sparing agents [122, 155–158].

Rituximab

Rituximab (RTX), a chimeric humanized monoclonal antibody to CD20, is a cell surface marker expressed on all B cells save pro-B and plasma cells. While RTX results in B-cell depletion through antibody-mediated and complement-mediated cytotoxicity, it is also postulated to work by additional mechanisms. B-cell depletion (as monitored by the number of $CD19^+$ cells) is detectable in the first 1–2 months after treatment; B cells repopulate within 6–9 months. Rituximab was initially used to treat lymphoma at 375 mg/m^2 weekly for four doses. It has been used to great benefit in rheumatic diseases, including rheumatoid arthritis (resistant to anti-TNFα), GPA, IgG4-RD, and SLE. In pediatrics, alternate dosing of 500 mg/m^2 (maximum 1000 mg/dose) at week 0 and 2 is also used. The risks of RTX include infusion reactions, increased risk of infection, and progressive multifocal leukoencephalopathy (PML) secondary to viral reactivation. As prolonged hypogammaglobulinemia has developed in some patients, immunoglobulins should be assessed before treatment and then after B-cell repletion.

RTX has been particularly well studied in AAV. While CYC was the induction treatment of choice for in AAV, two different large randomized controlled trials demonstrated that RTX could effectively replace CYC to induce remission [85, 159, 160]. Two other randomized controlled studies demonstrated that RTX was as effective as AZA, if not more so, to maintain remission in AAV [84, 161]. RTX was efficacious in controlling disease and decreasing CS treatment in five adults with GPA-associated orbital disease that had been resistant to IMT, including CYC [162]. However, one study that retrospectively evaluated outcomes of treatment with RTX (+/−CYC) in 37 patients with ophthalmic GPA, of which 17 had orbital disease, suggested that induction with CYC might still provide decreased risk of relapse over RTX treatment alone [87]. Similarly, RTX has been used, often with CS-sparing success, to treat IOI [163–165]. In a novel therapeutic approach, three adult patients with IOI tolerated and were successfully treated with intralesional low-dose RTX [166]. While RTX had been reported as effective for IgG4-ROD in numerous case reports, in 2015, Carruthers published beneficial results in a 30 patient prospective pilot study, in which 8 patients had ocular involvement [56]. Almost all patients showed some beneficial response, and 77% achieved the primary outcome (improved responder index, the absence of disease

flares in the first 6 months, and no need for CS in months 2–6). RTX is an important agent to consider in GPA-associated orbital inflammation, IgG4-ROD, and recalcitrant IOI. Additionally there are preliminary reports suggesting efficacy of RTX in the treatment of patients with active thyroid eye disease [167].

Conclusion

Pediatric orbital inflammatory disease, both nonspecific and specific, mirrors that seen in adult populations in many ways. There are, however, disparities in presentation, differential diagnosis, and age-specific considerations in treatment regimens and toxicities. It should also be noted that orbital inflammatory disease is a subject that will continue to adjust to improved diagnostic capabilities and treatment algorithms.

References

1. Yuen SJ, Rubin PA. Idiopathic orbital inflammation: distributions, clinical features and treatment outcome. Arch Ophthalmol. 2003;121:491–9.
2. Flanders AE, Mafee MF, Rao VM, et al. The characteristics of orbital pseudotumor and other orbital inflammatory processes. J Comput Assist Tomogr. 1989;13:40–7.
3. Weber AL, JF, Sabates NR. Pseudotumor of the orbit. Neuroimaging Clin North Am. 1996;6:73–91.
4. Jakobiec F, Ones IS. Orbital Inflammation. Philadelphia: Lippincott-Raven; 1995.
5. Harris G. Idiopathic orbital inflammation: a pathologic construct and treatment strategy. Ophthal Plast Reconstr Surg. 2006;22(2):79–86.
6. Rose G. A personal view: probability in medicine, levels of (un) certainty and the diagnosis of orbital disease (with particular reference to orbital 'pseudotumor'). Arch Ophthalmol. 2007;125:1171–2.
7. Birch-Hirschfield A. Zur diagnostik und pathologie der orbital tumoren. Ber Dtsch Ophthal Ges. 1905;32:127–35.
8. Rootman J, Chang W, Jones D. Distribution and differential diagnosis of orbital disease. 2nd ed. Philadelphia: Lippincott Williams & Wilkens; 2003.
9. Chavis RM. Inflammatory Orbital Pseudotumor. Arch Ophthalmol. 1978;96(10):1817.
10. Kennerdell JS, Dresner SC. The nonspecific orbital inflammatory syndromes. Surv Ophthalmol. 1984;29(2):93–103.
11. Mottow LS. Idiopathic inflammatory orbital Pseudotumor in childhood I: clinical characteristics. Arch Ophthalmol. 1978;96(8):1410.
12. Mottow-Lippa L, Jakobiec FA, Smith M. Idiopathic inflammatory orbital Pseudotumor in childhood II: results of diagnostic tests and biopsies. Ophthalmology. 1981;88(6):565–74.
13. Blodi FC, Gas JD. Inflammatory pseudotumour of the orbit. Br J Ophthalmol. 1968;52:79–93.
14. Wladis EJ, Iglesias BV, Gosselin EJ. Characterization of the molecular biologic milieu of idiopathic orbital inflammation. OPRS. 2011;27(4):251–4.
15. Mottow L, JF, Smith M. Idiopathic inflammatory orbital pseudotumor in early childhood: clinical characteristics. Arch Ophthalmol.
16. Mombaerts I, Goldschmeding R, Sclingemann RO, Koornneef L. What is orbital pseudotumor? A clinical pathological review. Surv Ophthalmol. 1996;41:66–78.
17. Berger JW, Rubin PA, Jakobiec FA. Pediatric orbital pseudotumor: case report and review of the literature. Arch Ophthalmol. 1996;36(1):161–77.
18. Yan J, Qiu H, Wu Z, et al. Idiopathic orbital inflammatory pseudotumor in Chinese children. Orbit. 2006;25:1–4.
19. Spindle J, Tang SX, Davies B, et al. Pediatric idiopathic orbital inflammation: clinical features of 30 cases. OPRS. 2015;32(4):270–4.
20. Belanger C, Zhang KS, Reddy A, et al. Inflammatory disorders of the orbit in childhood: a case series. Am J Ophthalmol. 2010;150:460–3.
21. Cabral DA, Uribe AG, Benseler S, O'Neil KM, Hashkes PJ, Higgins G, et al. Classification, presentation, and initial treatment of Wegener's granulomatosis in childhood. Arthritis Rheum. 2009;60(11):3413–24.
22. Mombaerts I, Rose GE, Garrity JA. Orbital inflammation: biopsy first. Surv Ophthalmol. 2016;61(5):664–9.
23. Rootman J, MM, White V, et al. The classification and management of acute orbital pseudotumors. Ophthalmology. 1982;89:1040–8.
24. Shields JR, SC, Scartozzi R. Survery of 1,264 patients with orbital tumors and simulating lesions: the 2002 Montgomery lecture, part I. Ophthalmology. 2004;111:997–1008.
25. Mombaerts I, Cameron JD, Chanlalit W, Garrity JA. Surgical debulking for idiopathic dacryoadenitis: a diagnosis and a cure. Ophthalmology. 2014;121(2):603–9.
26. Yen MT, Yen KG. Effect of corticosteroids in the acute management of pediatric orbital cellulitis with subperiosteal abscess. Ophthal Plast Reconstr Surg. 2005;21(5):363–6; discussion 6–7.
27. Leone CR, Lloyd WC. Treatment protocol for orbital inflammatory disease. Ophthalmology. 1985;92(10):1325–31.
28. MombaertsI SR, Goldeschmeding R, et al. Are systemic corticosteroids useful in the management of orbital pseudotumors? Ophthalmology. 1996;103:521–8.
29. Boon LM, MD, Mulliken, JB. Complications of systemic corticosteroid therapy for problematic hemangioma. Plast Reconstr Surg. 1999;104:1616–23.
30. Leone FT, FJ, Szefler SJ, West SL. Systematic review of the evidence regarding potential complications of inhaled corticosteroid use in asthma: collaboration of American College of Chest Physicians, American Academy of allergy, asthma, and immunology. Chest. 2003;124:2329–40.
31. Hughes I. Steroids and growth (editorial). Br Med J (Clin Res Ed). 1987;295:683.
32. Goldberg R, McCann JD, Shorr N. Idiopathic orbital inflammatory disease. Arch Ophthalmol. 2004:1092–3.
33. Krohel GB, Carr EM, Webb RM. Intralesional corticosteroids for inflammatory lesions of the orbit. Am J Ophthalmol. 1986;101(1):121–3.
34. Thomas EL, Laborde RP. Retinal and Choroidal vascular occlusion following Intralesional corticosteroid injection of a Chalazion. Ophthalmology. 1986;93(3):405–7.
35. Sergott RC. Radiotherapy for idiopathic inflammatory orbital Pseudotumor. Arch Ophthalmol. 1981;99(5):853.
36. Smitt MC, DS. Radiation therapy for benign disease of the orbit. Semin Radiat Oncol. 1999;9:179–89.
37. Gordon KB, CD, Sagerman RH. Late effects of radiation on the eye and ocular adnexa. Int J Radiat Oncol Biol Phys 1995;31:1123–39.
38. Pearce MS, Salotti JA, Little MP, McHugh K, Lee C, Kim KP, et al. Radiation exposure from CT scans in childhood and subsequent risk of leukaemia and brain tumours: a retrospective cohort study. Lancet. 2012;380(9840):499–505.
39. Ju DM, Moss M, Crikelair GF. Effect of radiation on the development of facial structures in retinoblastoma cases. Am J Surg. 1963;106:807–15.

40. Lawrence W, SE, Maurer HM. Late effects of therapy in orbital rhabdomyosarcoma in children: a report from the intergroup rhabdomyosarcoma study (IRS). Cancer. 1986;1738–43.
41. Fiorillo A, MR, Vassallo P, et al. Radiation late effects in children treated for orbital rhabdomyosarcoma. Radiother Oncol. 1999;53:143–8.
42. Bloom JN, GE, Byrne BJ. Orbital pseudotumor in the differential diagnosis of pediatric uveitis. J Pediatr Ophthalmol Strabismus. 1992;29:59–63.
43. Hertle RW, GD, Goyal AK, et al. Orbital pseudotumor in the differential diagnosis of pediatric uveitis (letter). J Pediatr Ophthalmol Strabismus. 1993;30:61.
44. Rootman J, McCarthy M, White V, Harris G, Kennerdell J. Idiopathic Sclerosing inflammation of the orbit. Ophthalmology. 1994;101(3):570–84.
45. Rootman J, McCarthy M, White V, Harris G, Kennerdell J. Idiopathic sclerosing inflammation of the orbit. A distinct clinicopathologic entity. Ophthalmology. 1994;101(3):570–84.
46. Hsuan JD, Selva D, McNab AA, Sullivan TJ, Saeed P, O'Donnell BA. Idiopathic sclerosing orbital inflammation. Arch Ophthalmol. 2006;124(9):1244–50.
47. Eftekhari K, Chikwava KR, Katowitz WR. Idiopathic orbital inflammation leading to unilateral blindness over a 2-day presentation in a child. Ophthal Plast Reconstr Surg. 2011;27(2):e46–7.
48. Hunt WE, Meagher JN, LeFever HE, Zeman W. Painful ophthalmoplegia: its relation to indolent inflammation of the cavernous sinus. Neurology. 1961;11(1):56.
49. Moorman CM, Elston JS. Acute orbital myositis. Eye. 1995;9(1):96–101.
50. Wan WL, Cano MR, Green RL. Orbital myositis involving the oblique muscles. Ophthalmology. 1988;95(11):1522–8.
51. Patrinely JR, Osborn AG, Anderson RL, Whiting AS. Computed tomographic features of Nonthyroid Extraocular muscle enlargement. Ophthalmology. 1989;96(7):1038–47.
52. Mombaerts I, Tousseyn T, Van Limbergen E, Demaerel P. Clinically recognizing enlarged extraocular muscles from lymphoid origin. Ophthalmology. 2015;122(1):217–8.
53. Siltzbach L, editor. Sarcoidosis. New York: McGraw-Hll; 1980.
54. Daniele R. Sarcoidosis: diagnosis and management. Hosp Pract. 1983;18:113–6, 9–22.
55. Shetty AK, Gedalia A. Childhood sarcoidosis: a rare but fascinating disorder. Pediatr Rheumatol Online J. 2008;6:16.
56. Carruthers MN, Topazian MD, Khosroshahi A, Witzig TE, Wallace ZS, Hart PA, et al. Rituximab for IgG4-related disease: a prospective, open-label trial. Ann Rheum Dis. 2015;74(6):1171–7.
57. Johns CJ, MT. The clinical management of sarcoidosis: a 50 year experience at the Johns Hopkins Hospital. Medicine. 1999;78:65–111.
58. Bresnitz EA, Strom BL. Epidemiology of sarcoidosis. Epidemiol Rev. 1983;5:124–56.
59. Pasadhika S, Rosenbaum JT. Ocular Sarcoidosis. Clin Chest Med. 2015;36(4):669–83.
60. Obenauf CD, Shaw HE, Sydnor CF, Klintworth GK. Sarcoidosis and its ophthalmic manifestations. Am J Ophthalmol. 1978;86(5):648–55.
61. Karma A. Ophthalmic changes in sarcoidosis. Acta Ophthalmol Suppl. 1979;141:1–94.
62. Prabhakaran C, SP, Esmali B, et al. Orbital and adnexal sarcoidosis. Arch Ophthalmol. 2007;125:1657–62.
63. Mombaerts I, SR, Goldscheding R, et al. Idiopathic granulomatous orbital inflammation. Ophthalmology. 1996;103:2135–41.
64. Shorr N, Seiff SR. Central retinal artery occlusion associated with periocular corticosteroid injection for juvenile hemangioma. Ophthalmic Surg. 1986;17(4):229–31.
65. Sutula FC, Glover AT. Eyelid necrosis following intralesional corticosteroid injection for capillary hemangioma. Ophthalmic Surg. 1987;18(2):103–5.
66. Droste PJ, Ellis FD, Sondhi N, Helveston EM. Linear subcutaneous fat atrophy after corticosteroid injection of Periocular Hemangiomas. Am J Ophthalmol. 1988;105(1):65–9.
67. Straatsma BR. Ocular manifestations of Wegener's Granulomatosis. Am J Ophthalmol. 1957;44(6):789–99.
68. Bullen CL, Liesegang TJ, McDonald TJ, DeRemee RA. Ocular complications of Wegener's Granulomatosis. Ophthalmology. 1983;90(3):279–90.
69. Bohm M, Gonzalez Fernandez MI, Ozen S, Pistorio A, Dolezalova P, Brogan P, et al. Clinical features of childhood granulomatosis with polyangiitis (wegener's granulomatosis). Pediatr Rheumatol Online J. 2014;12:18.
70. Ozen S, Pistorio A, Iusan SM, Bakkaloglu A, Herlin T, Brik R, et al. EULAR/PRINTO/PRES criteria for Henoch-Schonlein purpura, childhood polyarteritis nodosa, childhood Wegener granulomatosis and childhood Takayasu arteritis: Ankara 2008. Part II: final classification criteria. Ann Rheum Dis. 2010;69(5):798–806.
71. Reinhold-Keller E, BN, Latza U, et al. An interdisciplinary approach to the care of patients with Wegener's Granulomatosis. Long term outcome in 155 patients. Arthritis Rheum. 2000;43:1021–32.
72. Rothschild PR, Pagnoux C, Seror R, Brezin AP, Delair E, Guillevin L. Ophthalmologic manifestations of systemic necrotizing vasculitides at diagnosis: a retrospective study of 1286 patients and review of the literature. Semin Arthritis Rheum. 2013;42(5):507–14.
73. Perry SR, RJ, White VA. The clinical and pathologic constellation of Wegener granulomatosis of the orbit. Ophthalmology. 1991;104:1683–94.
74. Isa H, Lightman S, Luthert PJ, Rose GE, Verity DH, Taylor SR. Histopathological features predictive of a clinical diagnosis of ophthalmic granulomatosis with polyangiitis (GPA). Int J Clin Exp Pathol. 2012;5(7):684–9.
75. Tan LT, Davagnanam I, Isa H, Taylor SR, Rose GE, Verity DH, et al. Clinical and imaging features predictive of orbital granulomatosis with polyangiitis and the risk of systemic involvement. Ophthalmology. 2014;121(6):1304–9.
76. Courcoutsakis NA, CC, Sneller MC, et al. Orbital involvement in Wegener granulomatosis: MR findings in 12 patients. Neuroradiology. 1997;21:452–8.
77. Atlas SW, GR, Savino PJ, et al. Surface-coil MR of orbital pseudotumor. Am J Neuroradiol. 1987;8:141–6.
78. Radice A, Bianchi L, Sinico RA. Anti-neutrophil cytoplasmic autoantibodies: methodological aspects and clinical significance in systemic vasculitis. Autoimmun Rev. 2013;12(4):487–95.
79. Pulido JS. Ocular manifestations of patients with circulating Antineutrophil cytoplasmic antibodies. Arch Ophthalmol. 1990;108(6):845.
80. Kalina PH, Garrity JA, Herman DC, DeRemee RA, Specks U. Role of testing for Anticytoplasmic autoantibodies in the differential diagnosis of Scleritis and orbital Pseudotumor. Mayo Clin Proc. 1990;65(8):1110–7.
81. Woo TF, Wilcsek G, et al. Australasian orbital and adnexal Wegener's granulomatosis. Ophthalmology. 2001;108:1535–43.
82. Kalina PH, Lie JT, Campbell RJ, Garrity JA. Diagnostic value and limitations of orbital biopsy in Wegener's Granulomatosis. Ophthalmology. 1992;99(1):120–4.
83. Hiemstra TF, Walsh M, Mahr A, Savage CO, de Groot K, Harper L, et al. Mycophenolate mofetil vs azathioprine for remission maintenance in antineutrophil cytoplasmic antibody-associated vasculitis: a randomized controlled trial. JAMA. 2010;304(21):2381–8.
84. Specks U, Merkel PA, Seo P, Spiera R, Langford CA, Hoffman GS, et al. Efficacy of remission-induction regimens for ANCA-associated vasculitis. N Engl J Med. 2013;369(5):417–27.

85. Stone JH, Merkel PA, Spiera R, Seo P, Langford CA, Hoffman GS, et al. Rituximab versus cyclophosphamide for ANCA-associated vasculitis. N Engl J Med. 2010;363(3):221–32.
86. Calich AL, Puechal X, Pugnet G, London J, Terrier B, Charles P, et al. Rituximab for induction and maintenance therapy in granulomatosis with polyangiitis (Wegener's). Results of a single-center cohort study on 66 patients. J Autoimmun. 2014;50:135–41.
87. Joshi L, Tanna A, McAdoo SP, Medjeral-Thomas N, Taylor SR, Sandhu G, et al. Long-term outcomes of rituximab therapy in ocular Granulomatosis with Polyangiitis: impact on localized and Nonlocalized disease. Ophthalmology. 2015;122(6):1262–8.
88. Garrity JA, Coleman AW, Matteson EL, Eggenberger ER, Waitzman DM. Treatment of recalcitrant idiopathic orbital inflammation (chronic orbital myositis) with infliximab. Am J Ophthalmol. 2004;138(6):925–30.
89. Zycinska K, Wardyn KA, Zielonka TM, Krupa R, Lukas W. Co-trimoxazole and prevention of relapses of PR3-ANCA positive vasculitis with pulmonary involvement. Eur J Med Res. 2009;14(Suppl 4):265–7.
90. Stegeman CA, Tervaert JW, de Jong PE, Kallenberg CG. Trimethoprim-sulfamethoxazole (co-trimoxazole) for the prevention of relapses of Wegener's granulomatosis. Dutch Co-Trimoxazole Wegener Study Group. N Engl J Med. 1996;335(1):16–20.
91. Hardwig PW, Bartley GB, Garrity JA. Surgical Management of Nasolacrimal Duct Obstruction in patients with Wegener's Granulomatosis. Ophthalmology. 1992;99(1):133–9.
92. Goldstein SM, KW, Moshang T, Katowitz JA. Pediatric thyroid-associated orbitopathy: the Children's Hospital of Philadelphia experience and literature review. . Thyroid. 2008;18(9):997–9.
93. Chan W, WG, Fan DS, et al. Ophthalmopathy in childhood Graves' disease. Br J Ophthalmol. 2002;86:740–2.
94. Lim NC, AS, Sundar G. Pediatric thyroid eye disease- the Singapore experience. Orbit. 2013;33 96–103.
95. Uretsky SH, Kennerdell JS, Gutai JP. Graves' Ophthalmopathy in childhood and adolescence. Arch Ophthalmol. 1980;98(11):1963–4.
96. Krassas GE, WW. Smoking and autoimmune thyroid disease: the plot thickens. Eur J Endocrinol. 2006;154:777–80.
97. Deshpande V, Zen Y, Chan JK, Yi EE, Sato Y, Yoshino T, et al. Consensus statement on the pathology of IgG4-related disease. Mod Pathol. 2012;25(9):1181–92.
98. McNab AA, MP. IgG4-related ophthalmic disease. Part II: clinical aspects. OPRS. 2015;31(3):167–78.
99. Andrew N, KD, Selva D. IgG4-related orbital disease: a meta-analysis and review. Acta Ophthalmol. 2013;91(8):694–700.
100. Toyoda K, OH, Kutomi K, et al. MR imaging of IgG4-related disease in the head and neck and brain. AJNR Am J Neuroradiol. 2012;33:2136–9.
101. Plaza JA, GJ, Dogan A, et al. Orbital inflammation with IgG4-positive plasma cells: manifestation of IgG4 systemic disease. Arch Ophthalmol. 2011;129(4):421–8.
102. Ferry JA, Klepeis V, Sohani AR, Harris NL, Preffer FI, Stone JH, et al. IgG4-related orbital disease and its mimics in a western population. Am J Surg Pathol. 2015;39(12):1688–700.
103. Notz G, IA, Bilyk JR. IgG4-related dacryoadenitis in a 13 year-old girl. OPrS. 2014;30(6):e161–3.
104. Karim F, Loeffen J, Bramer W, Westenberg L, Verdijk R, van Hagen M, et al. IgG4-related disease: a systematic review of this unrecognized disease in pediatrics. Pediatr Rheumatol Online J. 2016;14(1):18.
105. Griepentrog GJ, Vickers RW, Karesh JW, Azari AA, Albert DM, Bukat CN. A clinicopathologic case study of two patients with pediatric orbital IgG4-related disease. Orbit. 2013;32(6):389–91.
106. Hart PA, Topazian MD, Witzig TE, Clain JE, Gleeson FC, Klebig RR, et al. Treatment of relapsing autoimmune pancreatitis with immunomodulators and rituximab: the Mayo Clinic experience. Gut. 2013;62(11):1607–15.
107. Cassidy J, Petty RE. Textbook of pediatric rheumatology. Philadelphia: WB Saunders; 2001.
108. Gold DH, Morris DA, Henkind P. Ocular findings in systemic lupus erythematosus. Br J Ophthalmol. 1972;56(11):800–4.
109. Brenner EH, Shock JP. Proptosis secondary to systemic lupus Erythematosus. Arch Ophthalmol. 1974;91(1):81–2.
110. Amirlak I, Narchi H. Isolated orbital pseudotumor as the presenting sign of systemic lupus erythematosus. J Pediatr Ophthalmol Strabismus. 2008;45(1):51–4.
111. Shearn MA. Sjogren's syndrome. Med Clin North Am. 1977;61(2):271–82.
112. Vitali C, Bombardieri S, Jonsson R, Moutsopoulos HM, Alexander EL, Carsons SE, et al. Classification criteria for Sjogren's syndrome: a revised version of the European criteria proposed by the American-European consensus group. Ann Rheum Dis. 2002;61(6):554–8.
113. Shiboski SC, Shiboski CH, Criswell L, Baer A, Challacombe S, Lanfranchi H, et al. American College of Rheumatology classification criteria for Sjogren's syndrome: a data-driven, expert consensus approach in the Sjogren's international collaborative clinical alliance cohort. Arthritis Care Res (Hoboken). 2012;64(4):475–87.
114. Bartunkova J, Sediva A, Vencovsky J, Tesar V. Primary Sjogren's syndrome in children and adolescents: proposal for diagnostic criteria. Clin Exp Rheumatol. 1999;17(3):381–6.
115. Srinivasan A, Kleinberg TT, Murchison AP, Bilyk JR. Laboratory investigations for diagnosis of autoimmune and inflammatory Periocular disease: part I. Ophthal Plast Reconstr Surg. 2016;32(5):321–8.
116. deLuise VP, Tabbara KF. Quantitation of tear lysozyme levels in dry-eye disorders. Arch Ophthalmol. 1983;101(4):634–5.
117. Voulgarelis M, Moutsopoulos HM. Mucosa-associated lymphoid tissue lymphoma in Sjogren's syndrome: risks, management, and prognosis. Rheum Dis Clin North Am. 2008;34(4):921–33, viii.
118. Tan JH, Chu HP, Das L, Arkachaisri T. Orbital pseudotumour as a presentation of paediatric ulcerative colitis. Singapore Med J. 2014;55(10):e169–71.
119. Young RSK, Hodes BL, Cruse RP, Koch KL, Garovoy MR. Orbital pseudotumor and Crohn disease. J Pediatr. 1981;99(2):250–2.
120. Squires RH, Zwiener RJ, Kennedy RH. Orbital myositis and Crohn's disease. J Pediatr Gastroenterol Nutr. 1992;15(4):448–51.
121. Katsanos A, Asproudis I, Katsanos KH, Dastiridou AI, Aspiotis M, Tsianos EV. Orbital and optic nerve complications of inflammatory bowel disease. J Crohns Colitis. 2013;7(9):683–93.
122. Verma S, Kroeker KI, Fedorak RN. Adalimumab for orbital myositis in a patient with Crohn's disease who discontinued infliximab: a case report and review of the literature. BMC Gastroenterol. 2013;13:59.
123. Favara BE, Feller AC, Pauli M, Jaffe ES, Weiss LM, Arico M, et al. Contemporary classification of histiocytic disorders. The WHO Committee on Histiocytic/reticulum cell proliferations. Reclassification working Group of the Histiocyte Society. Med Pediatr Oncol. 1997;29(3):157–66.
124. Lieberman PH, Jones CR, Steinman RM, Erlandson RA, Smith J, Gee T, et al. Langerhans cell (Eosinophilic) Granulomatosis. Am J Surg Pathol. 1996;20(5):519–52.
125. Herwig MC, Wojno T, Zhang Q, Grossniklaus HE. Langerhans cell histiocytosis of the orbit: five clinicopathologic cases and review of the literature. Surv Ophthalmol. 2013;58(4):330–40.
126. Glover AT, Grove AS Jr. Eosinophilic granuloma of the orbit with spontaneous healing. Ophthalmology. 1987;94(8):1008–12.
127. McClellan SF, Ainbinder DJ. Orbital Rosai-Dorfman disease: a literature review. Orbit. 2013;32(5):341–6.
128. Shelsta HN, BJ, Rubin PA, Penne RB, Carrasco JR. Wooden intraorbital foreign body injuries: clinical characteristics and outcomes in 23 patients. OPRS. 2010;26(4):238–44.

129. Green BF, Kraft SP, Carter KD, Buncic JR, Nerad JA, Armstrong D. Intraorbital wood. Ophthalmology. 1990;97(5):608–11.
130. Cronstein BN, Eberle MA, Gruber HE, Levin RI. Methotrexate inhibits neutrophil function by stimulating adenosine release from connective tissue cells. Proc Natl Acad Sci U S A. 1991;88(6):2441–5.
131. Chan ES, Cronstein BN. Methotrexate--how does it really work? Nat Rev Rheumatol. 2010;6(3):175–8.
132. Schiff MH, Jaffe JS, Freundlich B. Head-to-head, randomised, crossover study of oral versus subcutaneous methotrexate in patients with rheumatoid arthritis: drug-exposure limitations of oral methotrexate at doses >/=15 mg may be overcome with subcutaneous administration. Ann Rheum Dis. 2014;73(8):1549–51.
133. Cremers JP, Drent M, Bast A, Shigemitsu H, Baughman RP, Valeyre D, et al. Multinational evidence-based world Association of Sarcoidosis and Other Granulomatous Disorders recommendations for the use of methotrexate in sarcoidosis: integrating systematic literature research and expert opinion of sarcoidologists worldwide. Curr Opin Pulm Med. 2013;19(5):545–61.
134. Pagnoux C, Mahr A, Hamidou MA, Boffa JJ, Ruivard M, Ducroix JP, et al. Azathioprine or methotrexate maintenance for ANCA-associated vasculitis. N Engl J Med. 2008;359(26):2790–803.
135. Smith JR, Rosenbaum JT. A role for methotrexate in the management of non-infectious orbital inflammatory disease. Br J Ophthalmol. 2001;85(10):1220–4.
136. Thorne JE, Jabs DA, Qazi FA, Nguyen QD, Kempen JH, Dunn JP. Mycophenolate mofetil therapy for inflammatory eye disease. Ophthalmology. 2005;112(8):1472–7.
137. Hatton MP, Rubin PA, Foster CS. Successful treatment of idiopathic orbital inflammation with mycophenolate mofetil. Am J Ophthalmol. 2005;140(5):916–8.
138. Boulter EL, Eleftheriou D, Sebire NJ, Edelsten C, Brogan PA. Inflammatory lesions of the orbit: a single paediatric rheumatology centre experience. Rheumatology (Oxford). 2012;51(6):1070–5.
139. Kalapesi FB, Garrott HM, Moldovan C, Williams M, Ramanan A, Herbert HM. IgG4 orbital inflammation in a 5-year-old child presenting as an orbital mass. Orbit. 2013;32(2):137–40.
140. Guerriero S, Di Leo E, Piscitelli D, Ciraci L, Vacca A, Sborgia C, et al. Orbital pseudotumor in a child: diagnostic implications and treatment strategies. Clin Exp Med. 2011;11(1):61–3.
141. Jariwala MP, Agarwal M, Mulay K, Sawhney S. IgG4-related orbital inflammation presenting as unilateral pseudotumor. Indian J Pediatr. 2014;81(10):1108–10.
142. de Groot K, Harper L, Jayne DR, Flores Suarez LF, Gregorini G, Gross WL, et al. Pulse versus daily oral cyclophosphamide for induction of remission in antineutrophil cytoplasmic antibody-associated vasculitis: a randomized trial. Ann Intern Med. 2009;150(10):670–80.
143. Appel GB, Contreras G, Dooley MA, Ginzler EM, Isenberg D, Jayne D, et al. Mycophenolate mofetil versus cyclophosphamide for induction treatment of lupus nephritis. J Am Soc Nephrol. 2009;20(5):1103–12.
144. Tambralli A, Beukelman T, Weiser P, Atkinson TP, Cron RQ, Stoll ML. High doses of infliximab in the management of juvenile idiopathic arthritis. J Rheumatol. 2013;40(10):1749–55.
145. Aeschlimann FA, Hofer KD, Cannizzaro Schneider E, Schroeder S, Lauener R, Saurenmann RK. Infliximab in pediatric rheumatology patients: a retrospective analysis of infusion reactions and severe adverse events during 2246 infusions over 12 years. J Rheumatol. 2014;41(7):1409–15.
146. Diak P, Siegel J, La Grenade L, Choi L, Lemery S, McMahon A. Tumor necrosis factor alpha blockers and malignancy in children: forty-eight cases reported to the Food and Drug Administration. Arthritis Rheum. 2010;62(8):2517–24.
147. Costenbader KH, Glass R, Cui J, Shadick N. Risk of serious infections and malignancies with anti-TNF antibody therapy in rheumatoid arthritis. JAMA. 2006;296(18):2201; author reply 3-4.
148. Askling J, van Vollenhoven RF, Granath F, Raaschou P, Fored CM, Baecklund E, et al. Cancer risk in patients with rheumatoid arthritis treated with anti-tumor necrosis factor alpha therapies: does the risk change with the time since start of treatment? Arthritis Rheum. 2009;60(11):3180–9.
149. Beukelman T, Haynes K, Curtis JR, Xie F, Chen L, Bemrich-Stolz CJ, et al. Rates of malignancy associated with juvenile idiopathic arthritis and its treatment. Arthritis Rheum. 2012;64(4):1263–71.
150. Simard JF, Neovius M, Hagelberg S, Askling J. Juvenile idiopathic arthritis and risk of cancer: a nationwide cohort study. Arthritis Rheum. 2010;62(12):3776–82.
151. Schneeweiss S, Korzenik J, Solomon DH, Canning C, Lee J, Bressler B. Infliximab and other immunomodulating drugs in patients with inflammatory bowel disease and the risk of serious bacterial infections. Aliment Pharmacol Ther. 2009;30(3):253–64.
152. Beukelman T, Xie F, Chen L, Baddley JW, Delzell E, Grijalva CG, et al. Rates of hospitalized bacterial infection associated with juvenile idiopathic arthritis and its treatment. Arthritis Rheum. 2012;64(8):2773–80.
153. Smith JA, Thompson DJ, Whitcup SM, Suhler E, Clarke G, Smith S, et al. A randomized, placebo-controlled, double-masked clinical trial of etanercept for the treatment of uveitis associated with juvenile idiopathic arthritis. Arthritis Rheum. 2005;53(1):18–23.
154. Lerman MA, Rabinovich CE. The future is now: biologics for non-infectious pediatric anterior uveitis. Paediatr Drugs. 2015;17(4):283–301.
155. Miquel T, Abad S, Badelon I, Vignal C, Warzocha U, Larroche C, et al. Successful treatment of idiopathic orbital inflammation with infliximab: an alternative to conventional steroid-sparing agents. Ophthal Plast Reconstr Surg. 2008;24(5):415–7.
156. Osborne SF, Sims JL, Rosser PM. Short-term use of infliximab in a case of recalcitrant idiopathic orbital inflammatory disease. Clin Experiment Ophthalmol. 2009;37(9):897–900.
157. Prendiville C, O'Doherty M, Moriarty P, Cassidy L. The use of infliximab in ocular inflammation. Br J Ophthalmol. 2008;92(6):823–5.
158. Adams AB, Kazim M, Lehman TJ. Treatment of orbital myositis with adalimumab (Humira). J Rheumatol. 2005;32(7):1374–5.
159. Jones RB, Tervaert JW, Hauser T, Luqmani R, Morgan MD, Peh CA, et al. Rituximab versus cyclophosphamide in ANCA-associated renal vasculitis. N Engl J Med. 2010;363(3):211–20.
160. Guerry MJ, Brogan P, Bruce IN, D'Cruz DP, Harper L, Luqmani R, et al. Recommendations for the use of rituximab in anti-neutrophil cytoplasm antibody-associated vasculitis. Rheumatology (Oxford). 2012;51(4):634–43.
161. Guillevin L, Pagnoux C, Karras A, Khouatra C, Aumaitre O, Cohen P, et al. Rituximab versus azathioprine for maintenance in ANCA-associated vasculitis. N Engl J Med. 2014;371(19):1771–80.
162. Pelegrin L, Jakob E, Schmidt-Bacher A, Schwenger V, Becker M, Max R, et al. Experiences with rituximab for the treatment of autoimmune diseases with ocular involvement. J Rheumatol. 2014;41(1):84–90.
163. Schafranski MD. Idiopathic orbital inflammatory disease successfully treated with rituximab. Clin Rheumatol. 2009;28(2):225–6.
164. Kurz PA, Suhler EB, Choi D, Rosenbaum JT. Rituximab for treatment of ocular inflammatory disease: a series of four cases. Br J Ophthalmol. 2009;93(4):546–8.
165. Suhler EB, Lim LL, Beardsley RM, Giles TR, Pasadhika S, Lee ST, et al. Rituximab therapy for refractory orbital inflammation: results of a phase 1/2, dose-ranging, randomized clinical trial. JAMA Ophthalmol. 2014;132(5):572–8.
166. Savino G, Battendieri R, Siniscalco A, Mandara E, Mule A, Petrone G, et al. Intraorbital injection of rituximab in idiopathic orbital inflammatory syndrome: case reports. Rheumatol Int. 2015;35(1):183–8.
167. Silkiss RZ, Reier A, Coleman M, Lauer SA. Rituximab for thyroid eye disease. Ophthal Plast Reconstr Surg. 2010;26(5):310–4.

Benign Pediatric Orbital Tumors

35

William R. Katowitz, Peter D. Fries, and Michael Kazim

Introduction

Tumors of the orbit identified in the pediatric population are relatively rare lesions. Most are congenital hamartomas or choristomas. Of those that develop after birth, the majority are benign. Table 35.1 compiles the experience involving pediatric benign orbital tumors in recent retrospective studies. A total of 1820 lesions are reported in six separate series, representing the largest experience of pediatric orbital disease in print. Incidence varies among the series, but approximately 8–19% of these lesions were malignant (see Chap. 36). The largest group of benign pediatric orbital disorders among these series is infectious and inflammatory disorders, which are dealt with in separate chapters in this text. Structural, vascular, neurogenic, ossifying, and fibrous lesions arising in the pediatric orbit are reviewed in this chapter.

Many of the benign lesions have identifiable external characteristics that enable the examiner to diagnose the lesion based on historical and physical findings. One of the best examples is infantile hemangioma. The cutaneous features of this condition allow for immediate confirmation of its presence and are so rarely missing from the clinical features of the lesion that they are virtually required to confidently diagnose the condition (this lesion is also covered in Chap. 6). Similarly, plexiform neurofibromas have a tactile quality likened to a "bag of worms" that, when coupled with the cutaneous stigmata of neurofibromatosis, permits distinct clinical diagnosis without resorting to other ancillary diagnostic tests. Dermoid cysts have consistent anatomic locations and physical findings, allowing for their rapid identification with a high degree of accuracy. Although all cases are not classic and a differential diagnosis exists for all conditions, these particular entities account for nearly 60% of all pediatric orbital tumors, with the vast majority being diagnosed correctly based on clinical criteria alone. Any lesion of the orbit lacking the typical coloration of capillary hemangiomas, the cutaneous findings of neurofibromatosis, the consistent anatomic positioning of anterior orbital dermoids, or the external inflammation and physical findings of orbital cellulitis must be treated and evaluated in an expeditious manner because such a lesion has approximately a 50% chance of being malignant. In this chapter, we review the clinical findings, biological behavior, imaging features, and recommended treatment for benign tumors of the pediatric orbit.

W.R. Katowitz, MD (✉)
The Children's Hospital of Philadelphia and
The Edwin and Fannie Gray Hall Center for Human Appearance,
University of Pennsylvania, Philadelphia, PA, USA
e-mail: katowitzw@email.chop.edu

P.D. Fries, MD
Eye Surgeons Associates, PC, Bettendorf, IA, USA

M. Kazim
Ophthalmology & Surgery, Columbia University,
New York, NY, USA

© Springer International Publishing AG 2018

J.A. Katowitz, W.R. Katowitz (eds.), *Pediatric Oculoplastic Surgery*, https://doi.org/10.1007/978-3-319-60814-3_35

Table 35.1 Benign orbital tumors in children

	Iliff and Green [290] $n = 174$	Crawford [291] $n = 572$	Shields et al. [292] $n = 250$	Rootman [293] $n = 241$	Kodsi [294] $n = 340$	Katowitz [295] $n = 243$
Cystic lesions						
Dermoid	52	6	115	27	65	71
Lipodermoid	0	0	0	7	0	4
Microphthalmos with cyst	5	0	3	3	2	1
Sweat gland cyst	0	0	0	1	0	2
Mucocele	0	5	1	2	4	0
Implantation cyst	0	0	0	2	0	0
Simple epith cyst	1	0	12	1	5	6
Cephalocele	1	2	0	0	3	0
Lacrimal duct cyst	2	0	0	0	1	0
Infectious/inflammatory lesions						
Orbital cellulitis or abscess	0	226	0	17	0	2
Dacryoadenitis	0	1	5	0	0	0
Reactive lymphoid hyperplasia	0	0	5	0	0	0
Idiopathic orbital inflammation	9	5	41	14	20	13
Thyroid orbitopathy	0	107	0	24	0	0
Scleritis	0	0	0	1	0	0
Foreign body granuloma	0	0	0	0	7	0
Non-inflammatory lacrimal abnormality	5	0	0	0	0	0
Neurogenic lesions						
Optic nerve glioma	9	17	5	13	47	5
Meningioma	5	0	1	2	9	3
Plexiform neurofibroma	11	14	2	9	16	33
Teratoma	3	1	0	0	2	3
Neurilemmoma	0	0	1	0	1	0
Paraganglioma	0	0	0	0	1	0
Vascular lesions						
Capillary hemangioma	14	0	10	23	40	14
Lymphangioma	10	4	4	14	12	7
Cavernous hemangioma	0	13	2	0	1	0
Varix	0	0	0	12	0	1
AV shunt	3	3	1	5	4	0
Vascular malformation	0	3	0	0	4	2
Angiofibroma	0	3	0	0	1	0
Hemangiopericytoma	0	0	0	0	1	0
Secondary hemorrhage	1	5	0	0	1	0
Trauma						
Fracture	0	0	0	16	0	0
Foreign body	0	0	0	2	0	5
Orbital hemorrhage	0	25	0	0	0	0
Degenerative						
Post-radiation atrophy	0	0	0	5	0	0
Fat prolapse	1	0	0	1	0	0
Amyloidosis	1	0	0	0	0	0
Histiocytic lesions						
Langerhans histiocytosis	1	2	1	0	8	3
Juvenile xanthogranuloma	0	0	0	0	0	2

Table 35.1 (continued)

	Iliff and Green [290] $n = 174$	Crawford [291] $n = 572$	Shields et al. [292] $n = 250$	Rootman [293] $n = 241$	Kodsi [294] $n = 340$	Katowitz [295] $n = 243$
Fibrous histiocytoma	0	0	0	2	0	0
Bony lesions						
Fibrous dysplasia	2	4	0	7	13	5
Aneurysmal bone cyst	0	0	0	2	1	0
Osteoma	0	1	0	2	2	0
Orbital asymmetry	0	48	0	8	0	0
Ossifying granuloma	2	0	2	1	1	2
Osteopetrosis	0	1	0	0	0	0
Hyperostosis	0	1	0	0	0	0
Fat-containing lesions	4	0	16	0	4	19
Pseudoproptosis	0	0	0	1	0	0

Sources: Iliff and Green [290], Crawford [291], Shields et al. [292], Rootman [293], Kodsi et al. [294], and Katowitz [295]

Structural Orbital Lesions

Dermoid/Epidermoid Cysts

One of the most easily recognized congenital orbital lesions is the group of choristomas commonly referred to as dermoid cysts. Correct pathological terminology would further delineate these lesions as epidermoid cysts (only showing histologic evidence of epidermal components), dermoid cysts (adnexal structures as well as epidermal components), and lipodermoid cysts (where fat is a prominent feature of the choristoma). All of these lesions are choristomas, which is derived from the Greek word *choristos*. This means separated and the term is applied for normal tissue in an abnormal place. For ease in terminology, the more popular term dermoid cyst will be used in this chapter to refer to this entire group and will not specifically define the histopathological contents. Lipodermoid cysts have a typically subconjunctival location and are rare as a subcutaneous entity but have been included in this section due to their similar genesis.

Dermoid cysts account for 1–46% of all pediatric orbital lesions in the series revealed in Table 35.1, with most oculoplastic and orbital textbooks indicating that 40–50% of all orbital pediatric lesions are dermoids. These cystic tumors arise from epidermal rest cells pinched during embryogenesis by the underlying bony structures as they advance toward closure. Periorbital dermoids account for approximately 10% of head and neck dermoid cysts. Most occur near the frontozygomatic or frontonasal suture.

Dermoid cysts can be divided into superficial and deep varieties [1]. Superficial dermoids have a classic appearance as painless, firm, sometimes mobile subcutaneous masses usually lateral in the upper eyelid and anterior orbit (Fig. 35.1). Parents usually discover these lesions in the first year of their child's life as the child grows and loses periorbital facial fat, revealing their location, or by accidental palpation, usually during washing of the child's face. Rarely, superficial dermoids can present as an acute inflammatory lesion with periocular erythema, tenderness, and swelling due to rupture of the cyst with resultant subcutaneous inflammation from the extruding keratin. This presentation usually arises from direct trauma with resultant cyst rupture. Other sites of occurrence are medial in the upper lid near the frontonasal or frontolacrimal suture or in the temporalis fossa (Figs. 35.2 and 35.3). Most are 1–2 cm in size and grow in tandem with the child's maturation.

Deep orbital dermoids remain hidden for longer periods, presenting later in life with the slow onset of proptosis or globe dystopia. If significant combined orbit/temporalis fossa components are present (the so-called dumbbell-type dermoid) or if they are isolated to the temporalis fossa, swelling of the temple area can be the initial presentation [2]. Most deep dermoids are located laterally in the orbit near the sphenozygomatic suture and can involve the lateral rectus muscle, about the superior orbital fissure, or extend through this into the intracranial cavity (Fig. 35.4). Deep orbital dermoids are less common in the posterior medial orbit where they arise adjacent to the sphenoethmoidal suture. An additional presentation is that of a draining fistula from the lateral

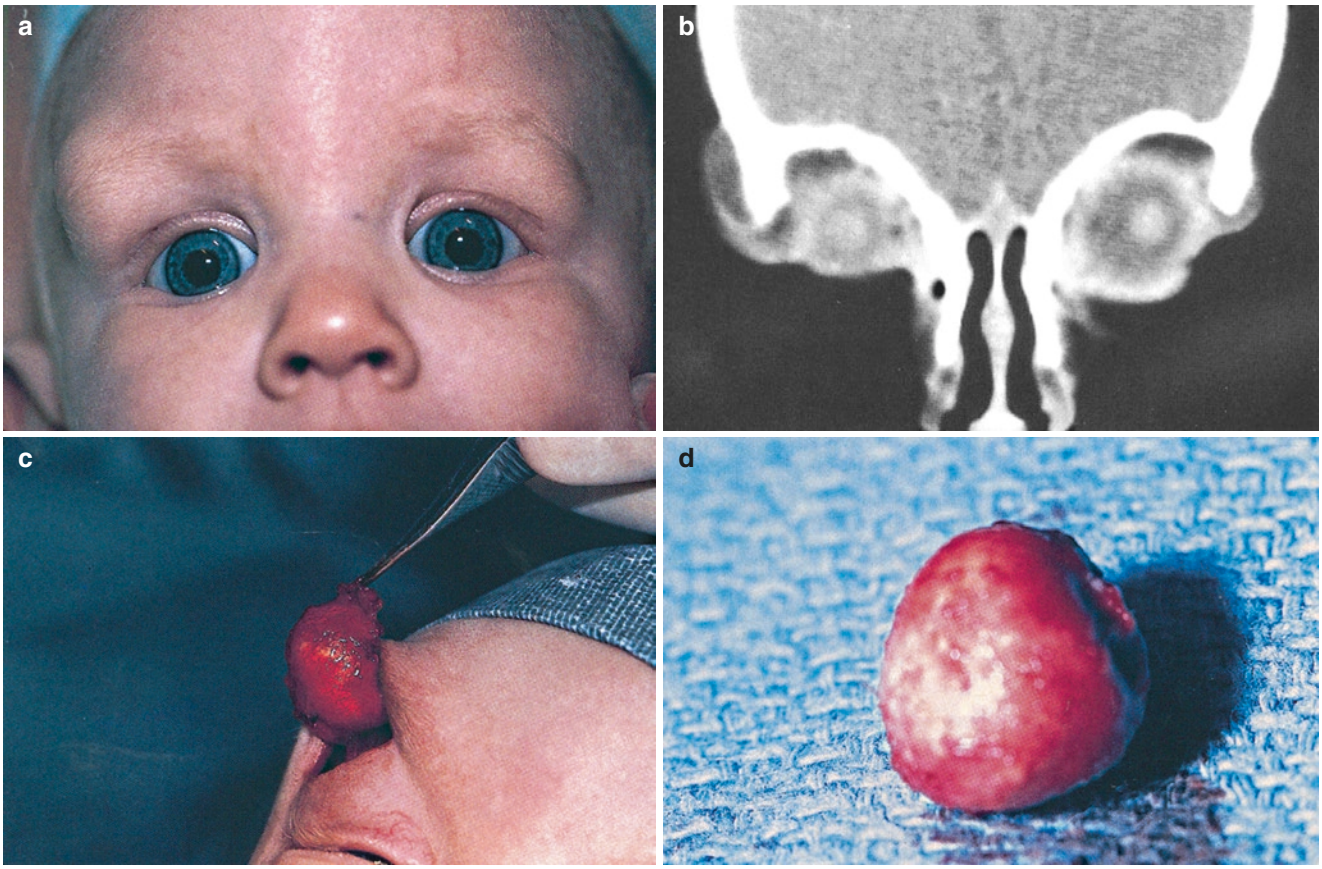


Fig. 35.1 Superficial dermoid. (**a**) A 1-year-old child with right superolateral superficial dermoid. (**b**) Coronal CT scan demonstrating radiolucent dermoid external to the lateral orbital rim. (**c**) Intraoperative demonstration of dermoid removal through an upper eyelid incision. (**d**) Intact cyst is inspected for any ruptures prior to submission for histopathologic evaluation

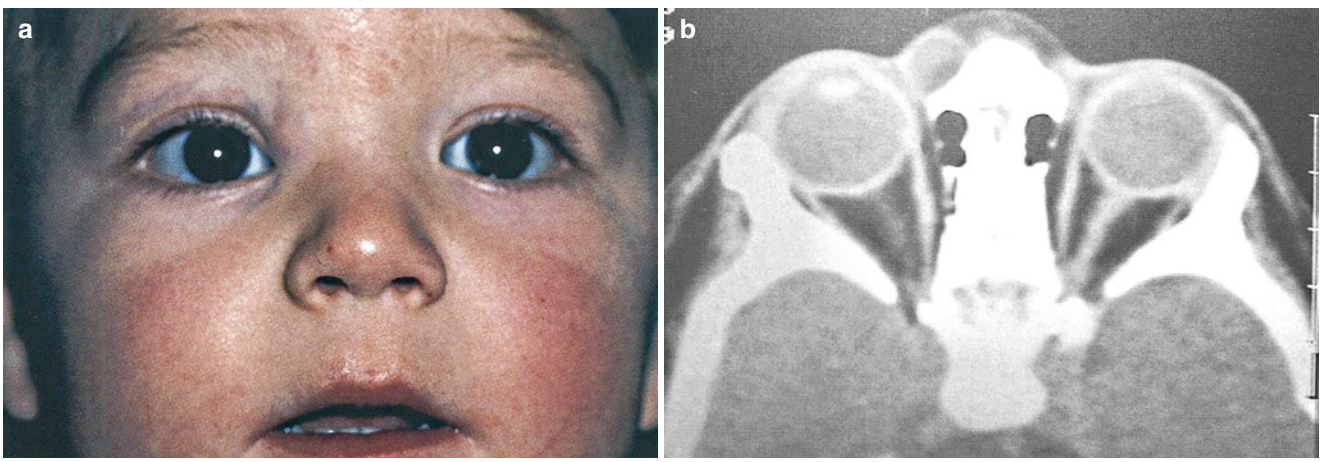


Fig. 35.2 Superficial dermoid. (**a**) A 2-year-old child with medial right superficial dermoid evident as a subtle swelling just superior to the medial canthal tendon. (**b**) Axial noncontrast CT scan shows the typical features of a dermoid with a well-defined cyst wall, homogenous cyst contents, and mild bony molding adjacent to the lesion.

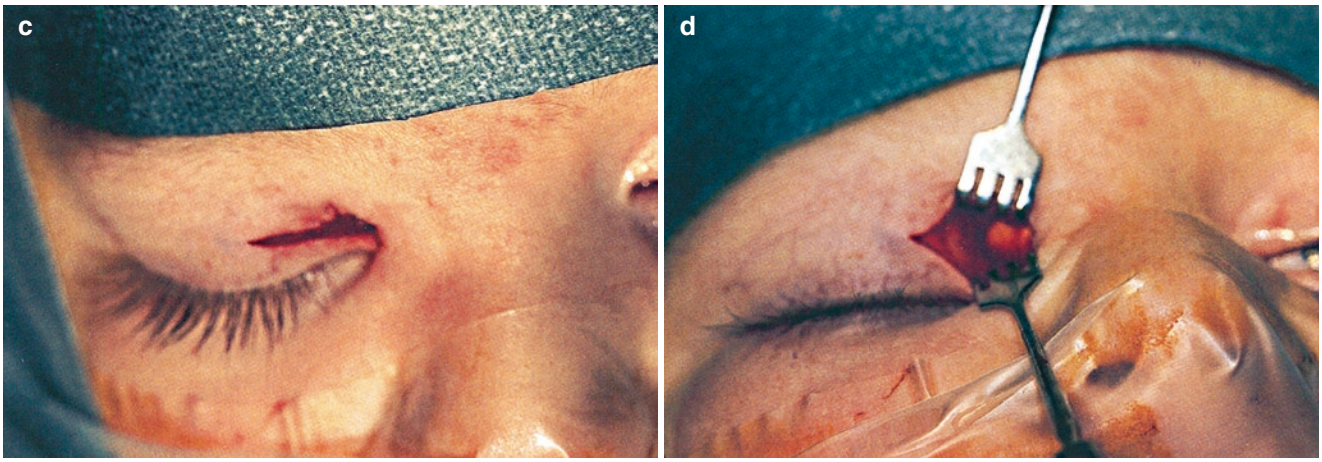


Fig. 35.2 (continued) (**c**) Intraoperative photograph showing medial lid crease incision placement. (**d**) With retractors in place stretching the skin medially, the dermoid can be visualized

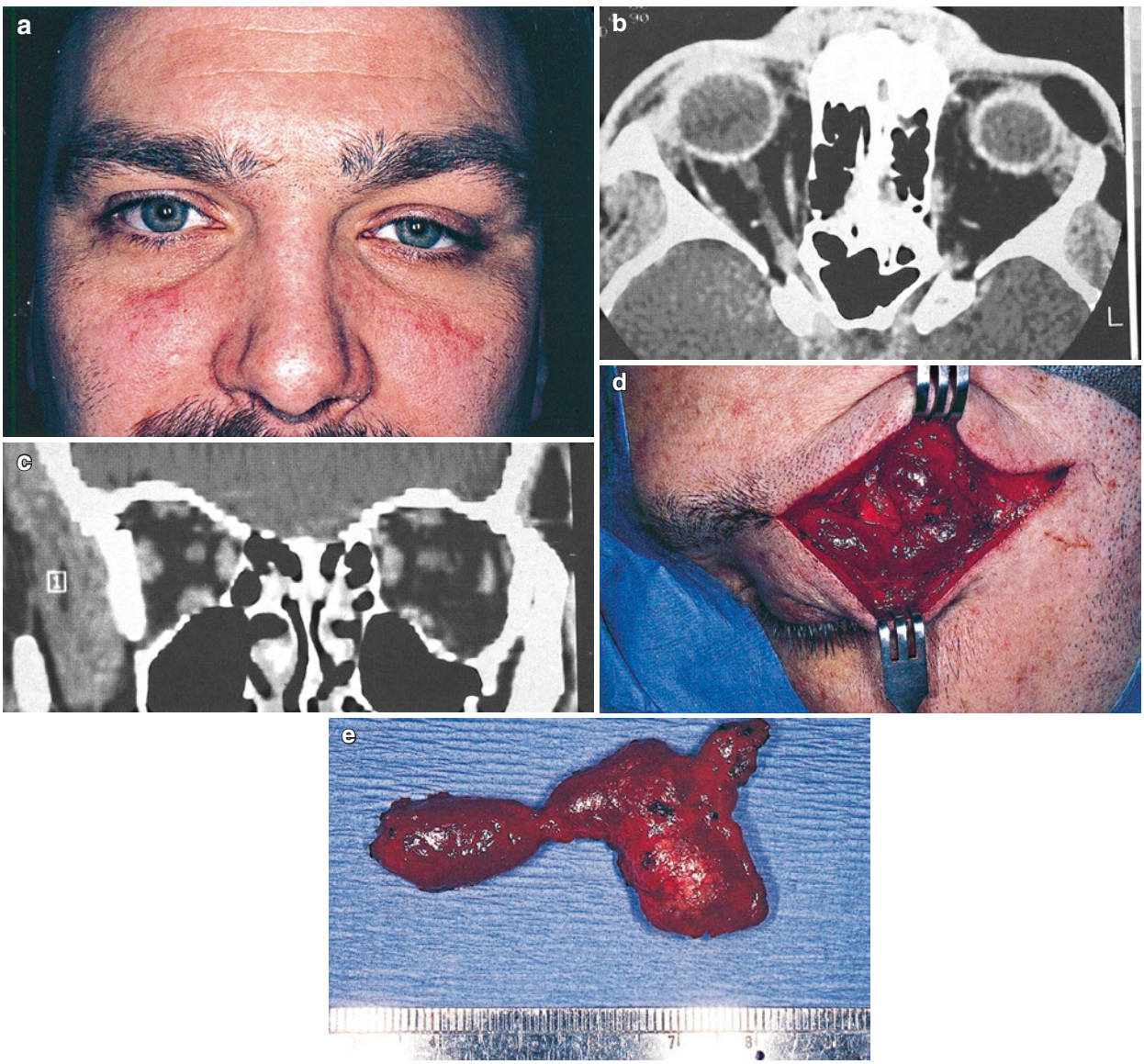


Fig. 35.3 Dermoid. (**a**) A 20-year-old male with swollen left upper eyelid for 3 years demonstrating a lateral, slightly mobile mass in the upper lid. Palpation of the lesion showed extension into the temporalis fossa prompting CT evaluation. (**b**) Axial noncontrast CT shows a cystic lesion in the anterior lateral left orbit adjacent to a second identical lesion in the temporalis fossa. (**c**) Coronal CT demonstrates the depth of the temporalis involvement. (**d**) Intraoperative photograph depicting the position and extent of this dermoid approached through a modified lateral orbitotomy incision. (**e**) Photograph showing the size of the lesion and its extensions

upper eyelid or the temple [3]. For deep orbital dermoids, physical examination usually reveals a smooth, rounded mass just palpable inside the anterior orbital rim or, more typically, no specific findings other than proptosis, globe dystopia, or, in the most advanced cases, optic neuropathy.

Imaging studies such as computed tomography (CT) or magnetic resonance imaging (MRI) are needed if the dermoid is fixed and nonmobile or presents with inflammatory signs or fistulization, or if proptosis, globe dystopia, temporalis fossa swelling, or optic neuropathy are present. Generally, imaging studies should be ordered for any lesion suspected of being a dermoid that is not in the superolateral quadrant of the orbit. This is due to the fact that orbital dermoids can dumbbell into adjacent structures. Fig. 35.5 depicts a temporal dermoid that extends into the orbit. Fig. 35.6 is of a dermoid that fistulized to the skin and was noted to extend into the skull base. Fig. 35.7 is of a medial dermoid that is an extension of a nasal dermoid. The goal for imaging studies is to confirm the clinical diagnosis and determine, in suspicious clinical cases, the presence or extent of a deep orbital component. Depending on the intraluminal tissue components of the cyst, imaging findings can be quite varied. Generally, well-circumscribed, superficial dermoids show a uniform appearance on CT evaluation representative of the intraluminal keratin, but they may also show radiolucent areas if fat is present (Fig. 35.8). It is rare to see calcium in these cysts, although giant orbital dermoids may show a rather characteristic finding of calcium in the cyst wall, which is rarely seen in orbital lesions other than an occasional mucocele [4]. MRI usually shows a uniform signal with phase-shift artifacts along the cyst borders but can show a dramatic multisignal appearance if fat is present due to its high signal intensity on T_1-weighted images (Fig. 35.4). Bony defects are rare in

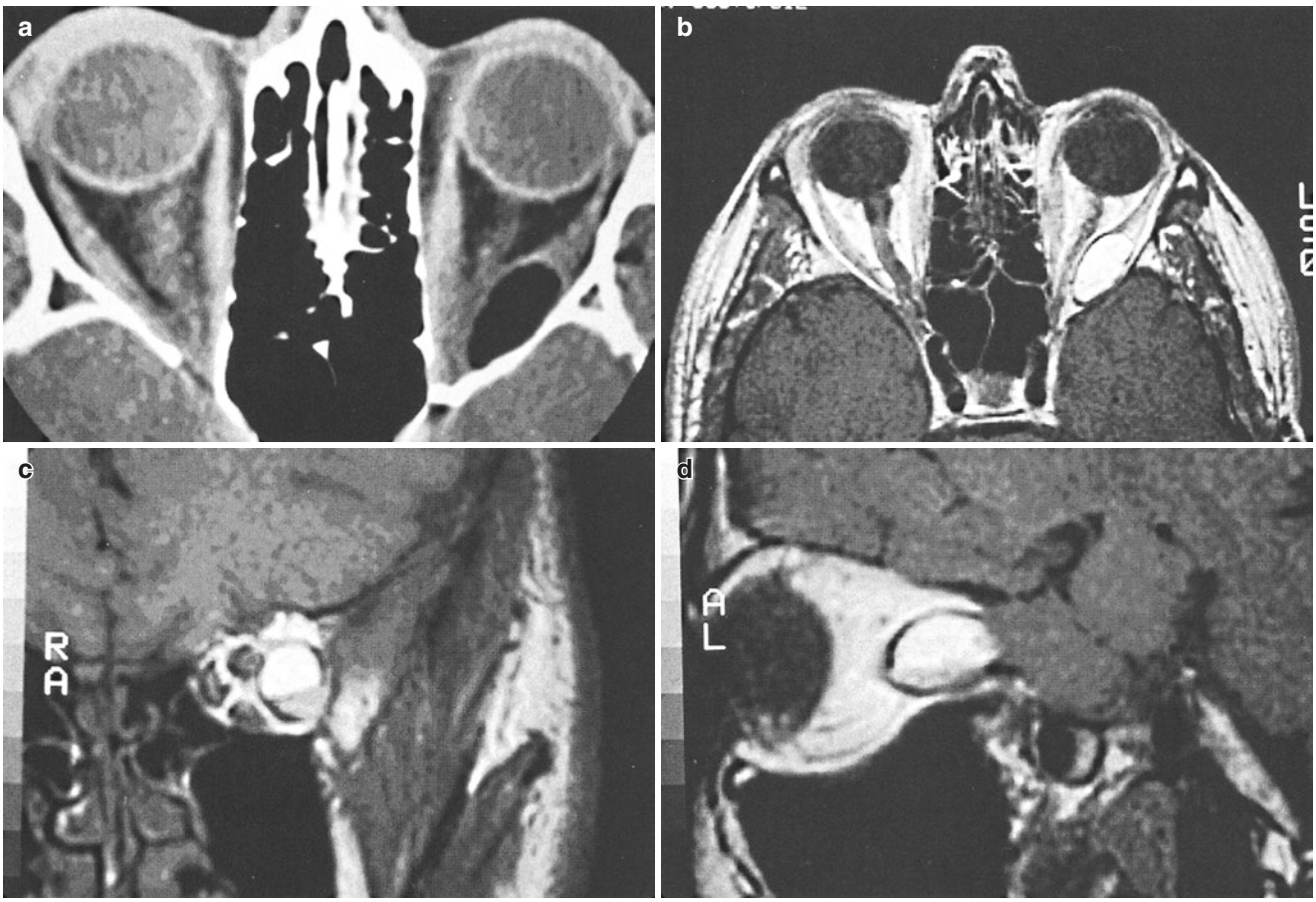


Fig. 35.4 Deep dermoid. (**a**) Axial CT scan showing a deep orbital dermoid occupying the posterior lateral orbit and obscuring the posterior half of the lateral rectus muscle. Mild bony molding is seen. The cyst contents are very radiolucent and are reminiscent of fat. (**b**) Axial MRI demonstrating the same lesion. Uniform signal intensity is seen with shift artifact along the anterior portion of the dermoid. (**c**) Coronal MRI reveals two signal intensities within the lesion; this finding appears to be unique to dermoids. The lateral rectus muscle can be seen along the superolateral border of the dermoid on this scan. (**d**) Sagittal MRI showing the two signal intensities in the dermoid

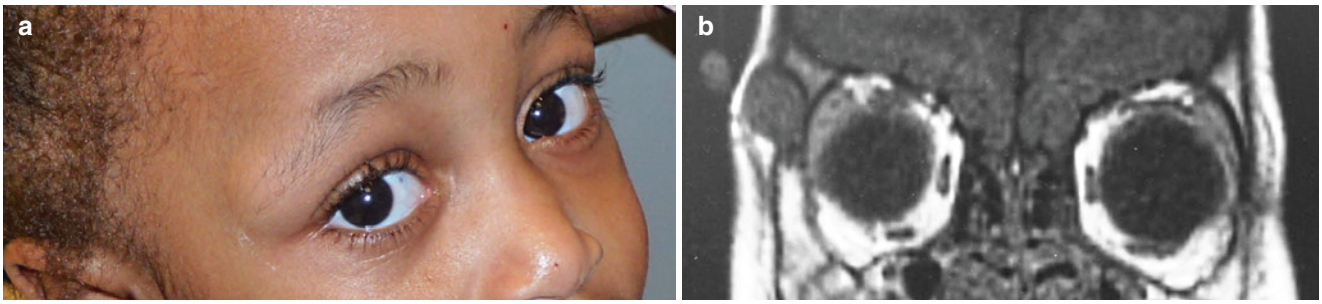


Fig. 35.5 (**a**) Large temporal dermoid. (**b**) T_1-weighted MRI showing extra- and intraorbital component of a large dermoid

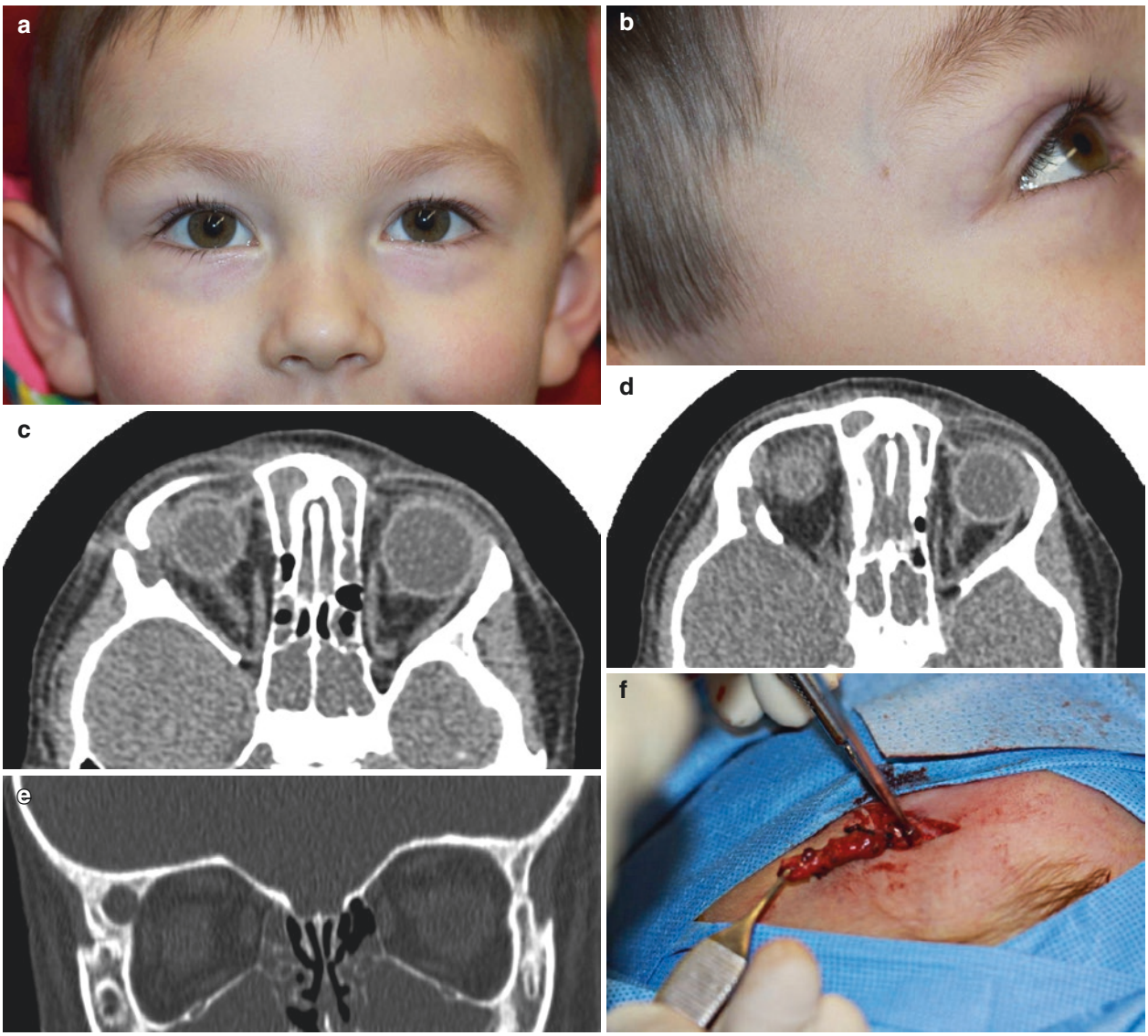


Fig. 35.6 Temporal dermoid with skin fistula and intraorbital and intracranial extension. (**a**) Superotemporal dermoid. (**b**) Skin fistula that was noted to drain a keratin rich substance. (**c**) Axial CT showing a temporal orbital wall defect. (**d**) Axial CT showing extension of this temporal orbit into the skull base. (**e**) Coronal CT showing the dermoid cyst within the zygoma of the lateral orbital wall. (**f**) Intraoperative photo of the temporal dermoid being excised along with the skin fistula

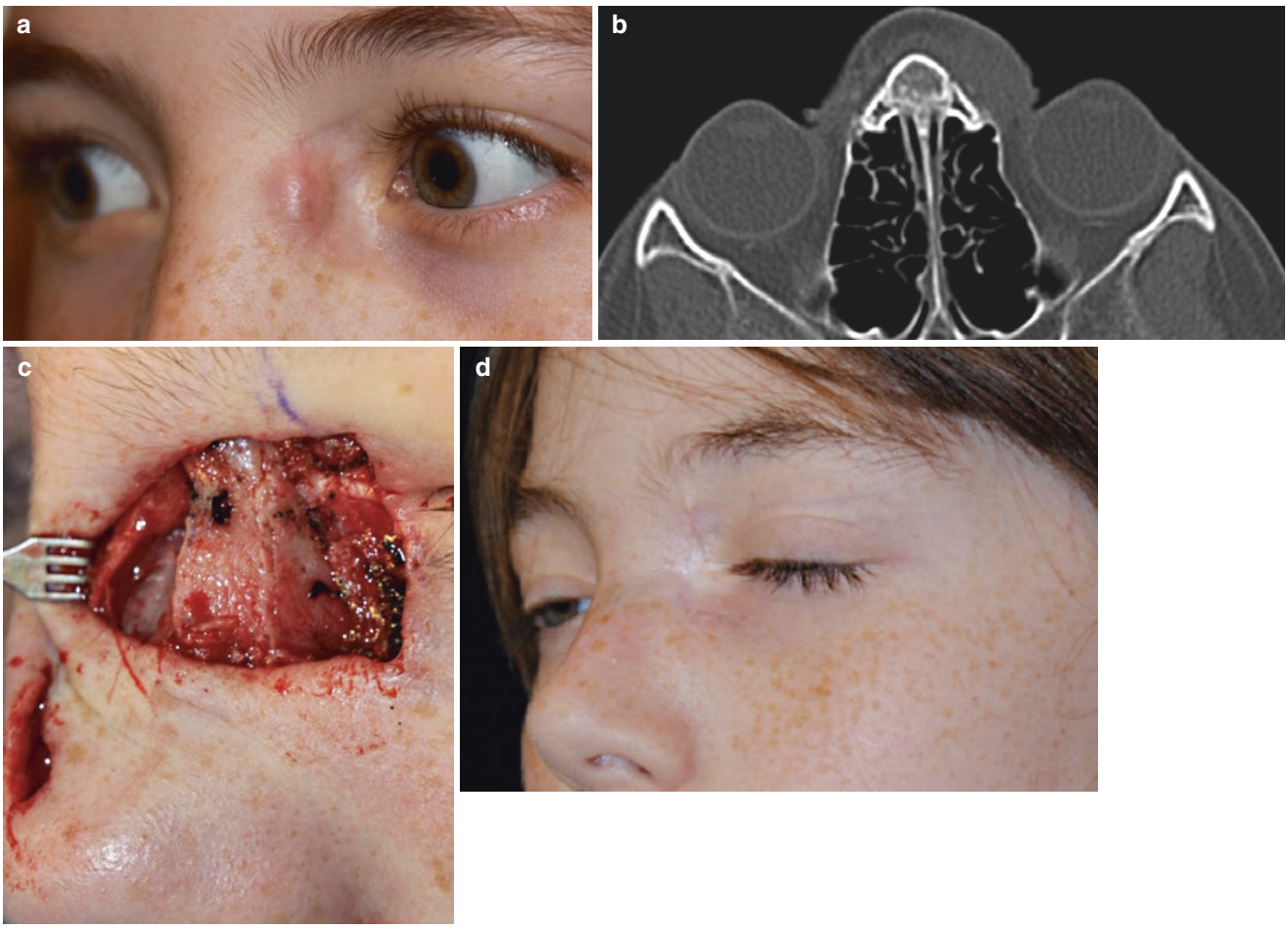


Fig. 35.7 Nasal bone dermoid with extension into the medial orbit (**a**) Medial skin fistula noted after removal of a medial dermoid. The patient had not been previously scanned, and a skin fistula formed months after excision. (**b**) Axial CT showing a dermoid cyst within the anterior nasal bones. (**c**) Intraoperative photo showing the tract through the nasal bones into the fistula. On the bottom right is a nasal skin fistula that had extended into the dermoid as well. (**d**) Postoperative photo taken 6 months after surgery

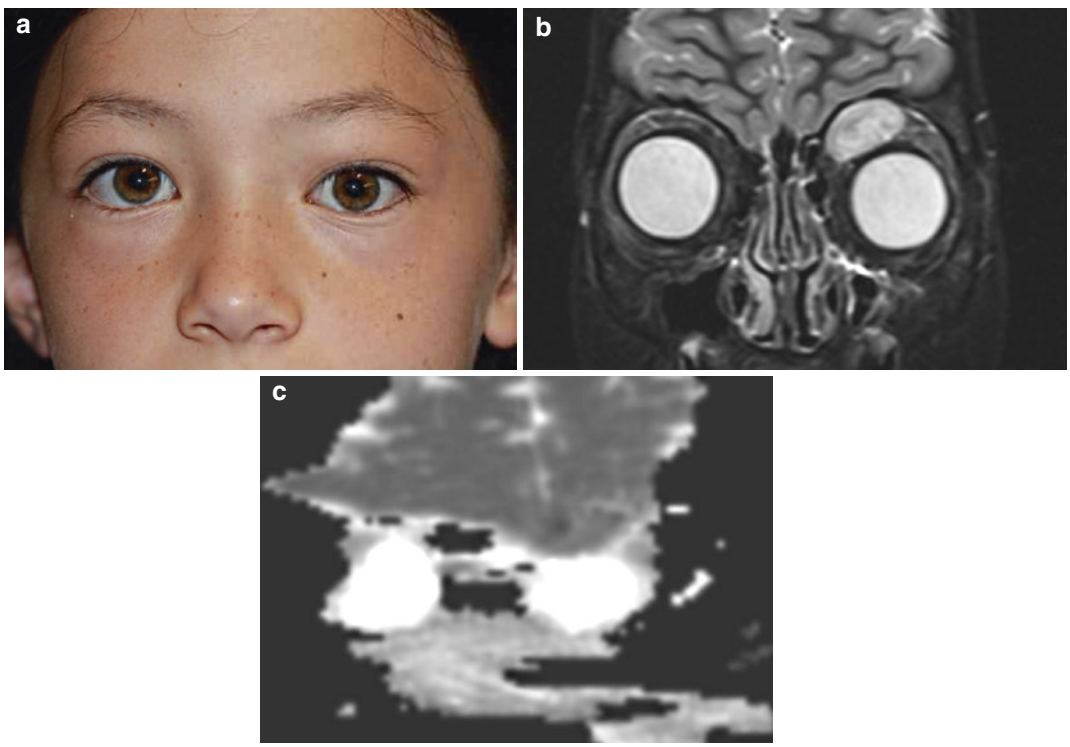


Fig. 35.8 Orbital dermoid simulating a malignancy. (**a**) Left hypoglobus due to an orbital mass. (**b**) T2-weighted MRI showing a large extraconal mass displacing the eye inferiorly. (**c**) Diffusion weighted imaging with a central area of restricted diffusion raising the concern for a malignant process. Pathology of the lesion confirms the diagnosis of a dermoid cyst

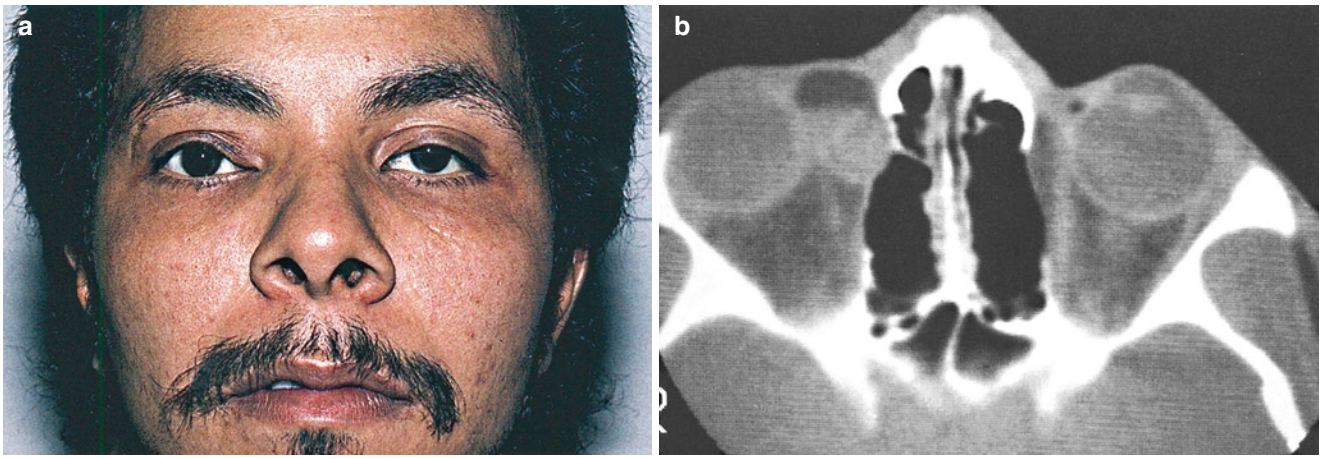


Fig. 35.9 Medial dermoid. (**a**) A 19-year-old male with right superomedial orbital lesion present for 5 years without growth. (**b**) Axial CT scan shows the medial dermoid with two different radiolucent areas. The anterior portion contained fat, while the posterior portion contained keratin on pathologic analysis after surgical removal

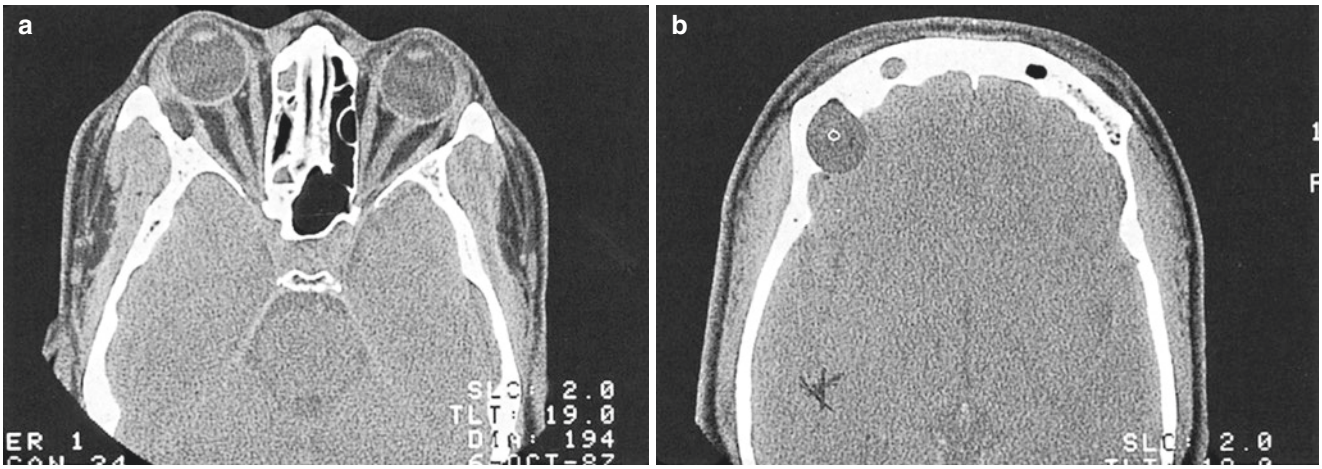


Fig. 35.10 Deep dermoid. (**a**) Axial CT scan showing a deep orbital dermoid with lateral orbital wall bony molding. (**b**) A slightly higher level on the CT scan reveals extensive molding of the frontal bone secondary to the dermoid

children except for occasional minor indentation molding; adults with deep dermoids can have impressive bony molding or erosion (Fig. 35.9). A full-thickness bony defect may occur with dumbbell dermoids as the intraorbital and temporalis fossa portions connect through the lateral orbital wall, and widening of orbital fissures may occur for those deep dermoids that extend intracranially (Fig. 35.6). Large intraorbital dermoids can be initially misdiagnosed as malignant lesions. This is especially true is dermoids with packed keratin, which can show diffusion restriction on diffusion-weighted imaging (DWI) on MRI. Fig. 35.10 is an example of such a lesion.

The treatment for orbital dermoids is surgical excision. The timing of the excision is based on the size of the lesion, the presence of lid or globe displacement, any inflammation, and, at times, parental wishes. Since these lesions grow with the child, most become increasingly obvious and may displace normal lid or orbital structures, including the globe itself. Removal should be performed so that accidental rupture does not occur from periocular trauma, which can spread the cyst contents subcutaneously and make complete extraction difficult. Dermoids left to enlarge for years can cause permanent bony or soft tissue malformation. In addition, delaying dermoid cyst excision can lead to skin fistulization (Fig. 35.6). Superficial dermoids of the lateral and medial orbit can easily be reached by a lid crease incision, which allows excellent visibility of the lesion with placement of the cutaneous scar in the natural medial or lateral upper lid crease [5, 6]. This has virtually replaced direct incision over the lesion for superficial dermoids.

Care must be taken to remove the dermoid intact without rupturing the capsule to avoid postoperative orbital granulomatous inflammation, which can smolder with retained dermoid components. The use of a cryoprobe can be of value in dermoid excision particularly if a small break occurs in the capsule (Fig. 35.11). The cryoprobe can be applied over the rent, sealing it and allowing for continued traction on the



Fig. 35.11 Use of a cryoprobe with a hammerhead handpiece for dermoid removal

dermoid to complete the dissection. Also, the surgeon must look for small extensions connected to bone when the dermoid is relatively immobile on clinical evaluation, as this may represent vestigial portions of the original epidermis pinched between bony structures and could lead to a subsequent inflammatory reaction or recurrence of the lesion if a portion of the dermoid remains unresected.

The surgical excision of deep orbital dermoids is typically undertaken in teenage years or in adulthood, since this is when most of these hidden orbital lesions are discovered. The decision to remove the dermoid depends on its size, its location, its relationship to surrounding structures, and how it affects the function of these structures. These same factors also help determine the approach used for removal of the dermoid; otolaryngologic or neurosurgical consultation and surgical support may be necessary for ethmoidal or deep orbital apex/orbital fissure involvement.

Dissection of the orbital portion is done first, attempting to completely shell out the lining of the dermoid as free of normal orbital tissues as possible. Within the confines of the orbital space, visualization of the base is attempted. If the lesion cannot be directly mobilized for removal of its base from its bony attachments, evacuation of the dermoid's contents allows room for mobilization and excision of the remaining portion. Care must be taken to avoid spillage of the dermoid contents into normal orbital tissues. For deep dermoids that extend into adjacent cavities, surgical removal may be approached through that cavity. This approach may also be used with dumbbell dermoids that occupy the orbit and temporalis fossa. Direct removal of the temporalis portion through a lateral orbitotomy incision can be assisted by removal of the lateral orbital rim and wall, allowing access to the orbital portion (Fig. 35.3). For superficial dermoids, complete removal of the cyst wall is necessary to prevent recurrence or orbital inflammation. Some lesions, especially those that extend intracranially through the orbital apex, may be impossible to remove due to potentially severe functional deficits, but, if evacuated and conservatively resected, may take years to reform. Some surgeons have advocated marsupialization of the dermoid but this could be technically challenging for deeply placed lesions and could offer a route for infection from an exogenous route.

Sclerotherapy with the aid of fluoroscopic needle guidance is an option for deep orbital lesions. Some cystic lesions are amenable to this treatment [7]. The major risk of dermoid cyst removal is recurrence. Intraorbital rupture, incomplete cyst removal or delayed removal may allow for islands of cyst epithelium to continue to produce keratin. This can cause chronic inflammation and cyst recurrence that can take decades to present (Fig. 35.12).

On histopathological examination, the lining of the cyst consists of typical keratinizing stratified squamous epithelium with variable adnexal structures. Cyst contents usually consist of keratin alone, but fat, hair, and sebaceous material may also be seen. An interesting finding noted by several authors involves the identification of small ruptures in the cyst wall with a surrounding limited granulomatous inflammatory reaction in a number of cases. None of these cases had coincident signs of orbital inflammation, indicating that a large rupture is probably necessary to produce clinically evident signs of inflammation. It is clear, then, that the dreaded complication of persistent orbital inflammation from incomplete cyst removal probably requires large amounts of residual debris and that small evacuated remnants are well tolerated, although they are highly likely to recur even decades after resection. Complete cyst removal, therefore, remains the goal in the surgical management of this lesion.

Dermolipomas

Dermolipomas represent an ectopia of skin and its adnexal structures within conjunctival tissues. Usually located temporally on the globe, argument exists as to whether dermolipomas represent a true orbital condition or, rather, a conjunctival choristoma. In any event, one cannot argue about the potential involvement of orbital structures, including the lacrimal gland, lacrimal ductules, or the lateral rectus muscle, by these congenital growths, making discussion of these unusual lesions important for the pediatric oculoplastic surgeon. Inspection under a slit lamp is critical. If hairs are visible the lesion is more likely a dermoid cyst. The lack of hair supports the diagnosis of dermolipoma.

Table 35.1 indicates the rarity of dermolipomas with only 11 cases reported in all six series used to compile the table. This may represent the author's preference for identifying these as conjunctival lesions or their individual propensity for avoiding surgical resection and, therefore, the relative absence of large numbers of these lesions in histopathologic studies. Most dermolipomas are discovered accidentally in

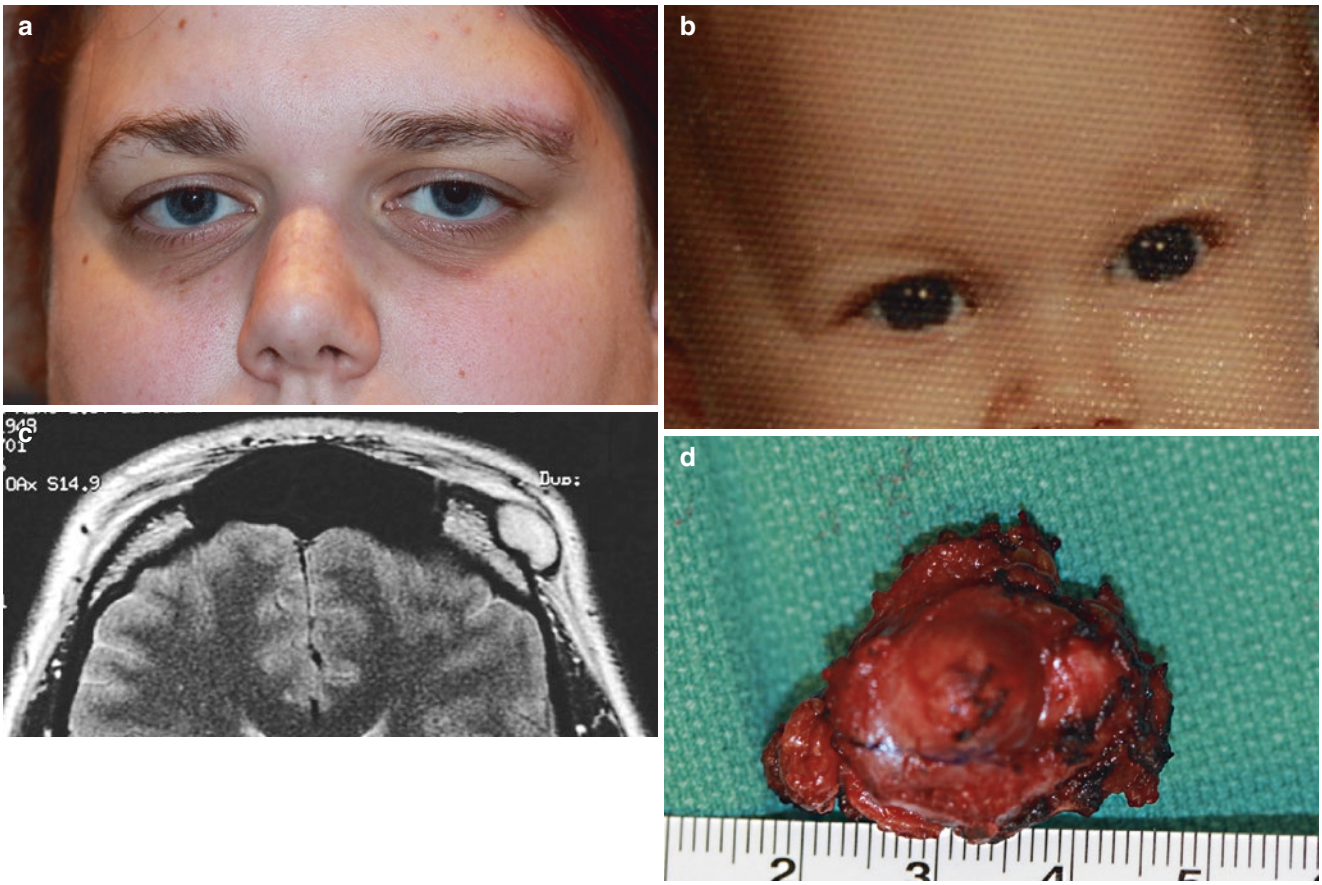


Fig. 35.12 Recurrent dermoid cyst. (**a**) Preoperative photo of a 22-year-old female who was referred for a forehead lesion. She was status post a biopsy via a superior brow incision. The initial specimen showed only chronic inflammation. (**b**) Infant photo of the same patient shows a superotemporal lesion that was removed at age 1. (**c**) Axial MRI with large cyst below the temporalis but above the frontal bone. (**d**) Photo of large specimen excised from the same supra-brow incision. Pathology showed a dermoid cyst with chronic inflammation

late childhood or in the early teenage years, usually as the result of lid manipulation or, as in our experience, during the search for a presumed foreign body. Sometimes seen on an emergency basis at the request of the child's primary care practitioner due to their sudden discovery, these yellowish-white, superotemporal epibulbar masses elicit alarmed reactions from the referring physician, patient, and parents who insist it is a new entity. Typically soft, moderately displaceable, and noninflamed, the surface is usually smooth but may have an irregular texture or hair-bearing areas (Fig. 35.13). Most are small and hidden completely by the lid, although some may be large enough to encroach upon the limbus. When bilobed, they may be more visible and thus more likely to be diagnosed at a younger age (Fig. 35.14). Their typical appearance and position should give the ophthalmologist every confidence in declaring their congenital origin. For lesions that have an anterior position, old photographs may show some of the lesion peeking out of the lateral canthal area, convincing parents and the patient of its long-time presence (Fig. 35.15).

Dermolipomas share the histopathologic features more typical of limbal dermoids than dermoid cysts [8]. The main differences between the histopathology of the dermolipoma and the orbital dermoid cyst are the presence of a stroma made of dense collagen bundles, a disproportionate amount of fat, and the usual absence of pilosebaceous units within the dermolipoma. Accordingly, dermolipomas are seen much more frequently in a number of congenital developmental disorders, usually involving the craniofacial complex: Goldenhar syndrome, Treacher Collins syndrome, linear nevus sebaceous syndrome, hemifacial microsomia, and in facial cleft 7 as described by Tessier [9]. Usually the other facial and cranial stigmata of these conditions will be obvious, but bilateral presentations of dermolipomas should prompt extreme suspicion for one of these conditions, if not already diagnosed.

Imaging studies are necessary only when surgical resection is anticipated, if globe restriction is found, or if the clinical appearance is not typical for a dermolipoma. CT evaluation demonstrates either a soft tissue-density mass or a cystic-appearing lesion with well-circumscribed borders and a radiolucent center usually identical to that of intraconal fat located temporally in the orbit (Fig. 35.16). Unusual posterior extension can help to explain motility

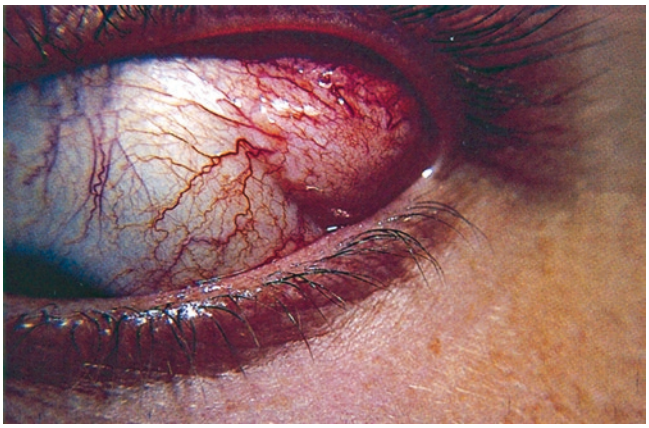


Fig. 35.13 Dermolipoma. Typical position, placement and appearance of dermolipoma

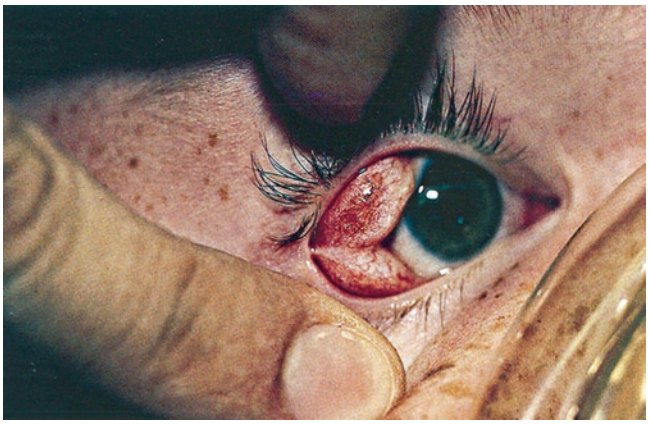


Fig. 35.14 Large bilobed dermolipoma. Surgical excision was advised secondary to recurrent dellen formation

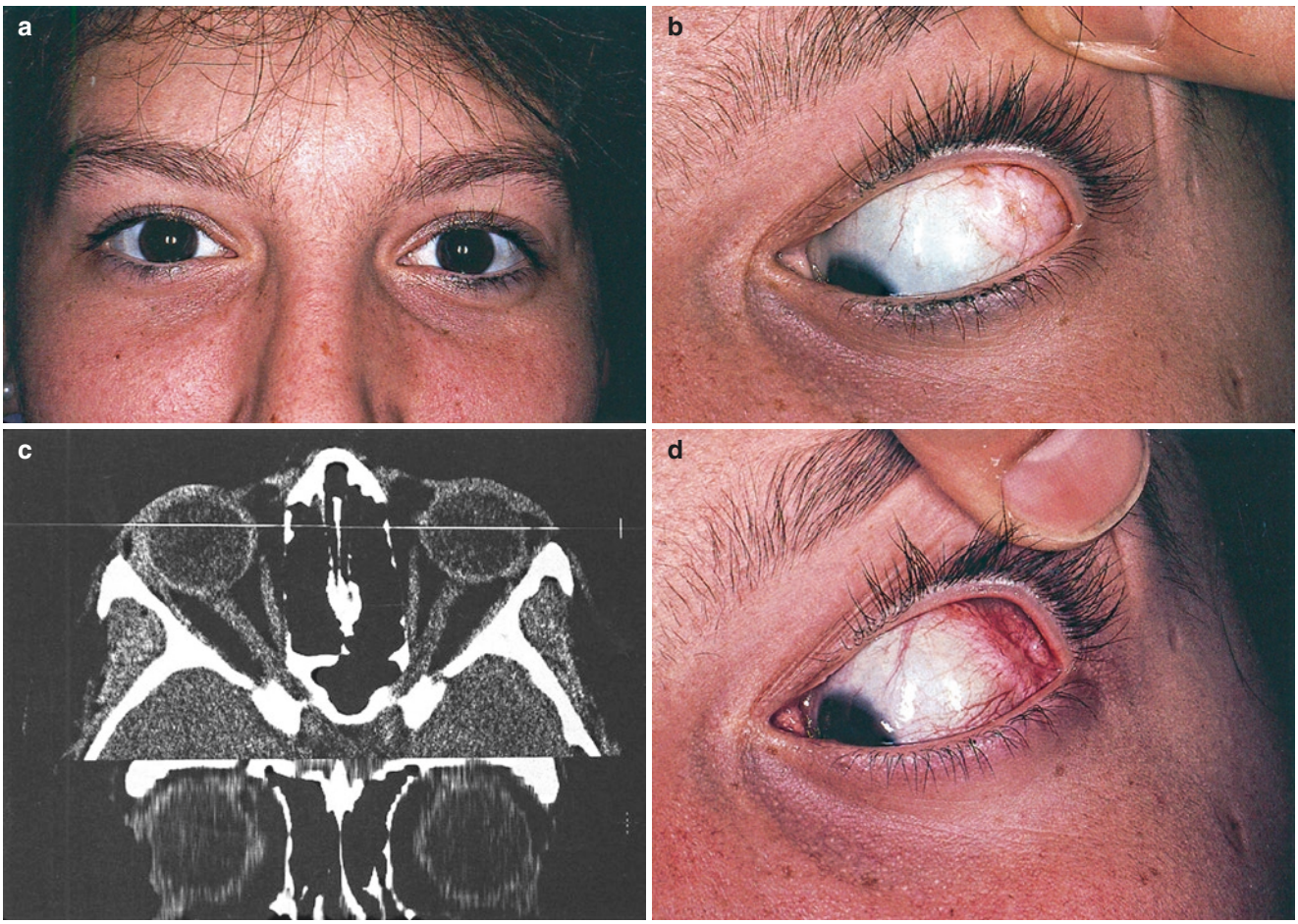


Fig. 35.15 Dermolipoma. (**a**) A 12-year-old with a 2-year history of intermittent foreign body sensation in the left eye. Careful evaluation of the left lateral canthus in this photograph shows the visible tip of the lesion. (**b**) Most of the lesion is visible with manual retraction of the upper lid. Several hairs emanate from the central anterior surface of the dermolipoma. (**c**) Axial CT with coronal reconstruction shows the lateral, juxtalacrimal location of the dermolipoma with its characteristic cystic appearance and radiolucent center that has the same density as orbital fat. Note on the axial scan that the right lateral orbit also demonstrates a small dermolipoma. (**d**) Six months after surgical resection. Surgical resection was performed because of persistent foreign body sensation



Fig. 35.16 Complex epibulbar dermoid associated with Goldenhar syndrome. A right medial exotropia is present. This required strabismus surgery due to an abnormally formed lateral rectus

restriction and caution the surgeon against deep orbital exploration due to involvement of the lateral rectus muscle (Fig. 35.17) [10]. Lacrimal gland dysfunction would be distinctly unusual, as would inflammatory signs.

Consideration of surgical resection should be tempered with the knowledge that more reports exist about the postoperative complications of dermolipoma resection than about the lesion itself [11]. The presence of large dermolipomas that cause lid vaulting from the surface of the globe and dellen formation, adnexal structures such as hair that cause persistent foreign body sensation, and the anterior protrusion of visible dermolipomas are valid indications for conservative resection of these lesions [12]. Complications generally result from attempts at complete resection. Intraoperatively, the boundaries of the lesion are difficult to define because the intraorbital fat may be separated by only an ill-defined fascial plane. The close proximity of the lacrimal ductules, the palpebral lobe of the lacrimal gland, the lateral rectus muscle, and the lateral horn of the levator palpebrae superioris further complicates complete resection. The surgical goal should be conservative resection of the symptomatic portion of the lipodermoid. In most cases this would involve resection of the visible epibulbar portion of the tumor up to but not into the fornix. This avoids the lacrimal ductules, the lateral rectus muscle, and the horn of the levator, while removing the most visible portion of the tumor along with any irritating adnexal structures. Complications such as blepharoptosis, diplopia, and keratitis sicca are more likely to be avoided. A frank discussion about these potential complications helps patients and their parents understand the potentially complicated surgical nature of dermolipoma resection and may make them more willing to accept a recommendation to forego surgical resection when only purely cosmetic indications exist.

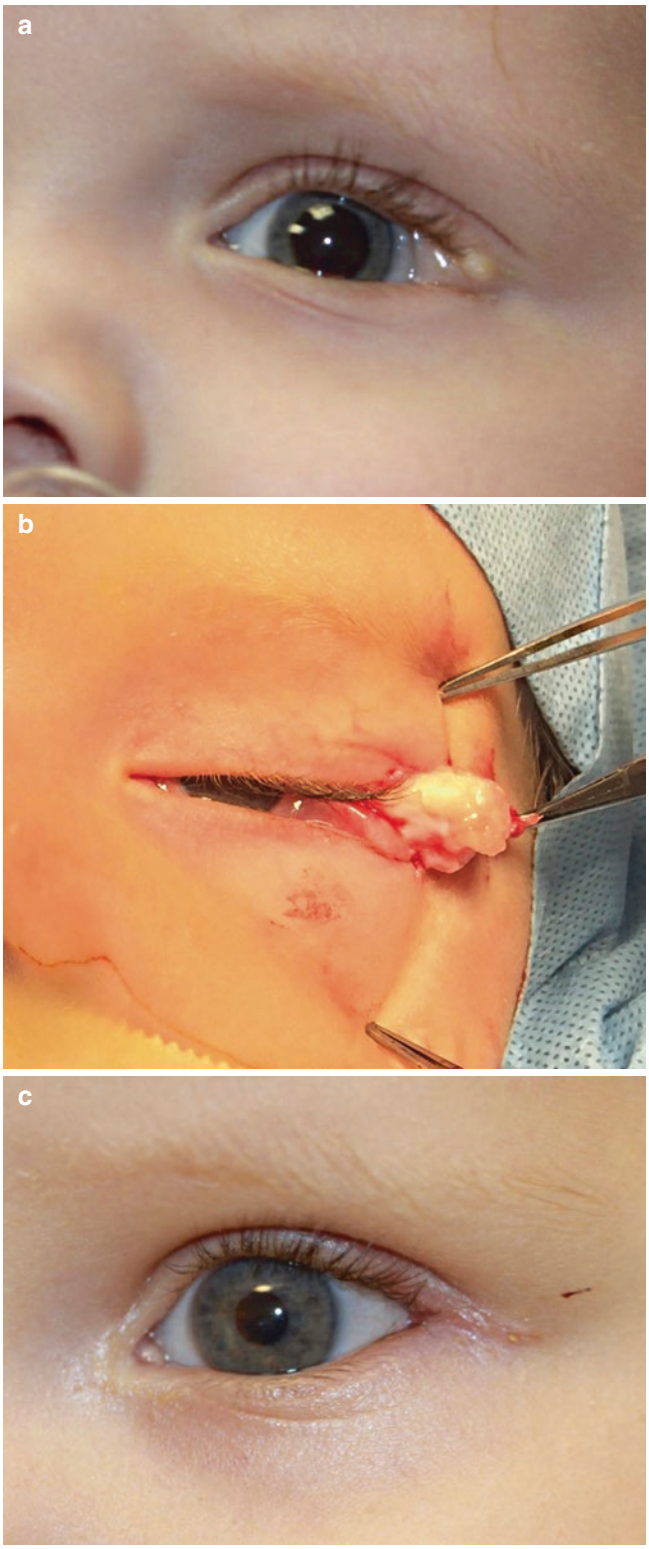


Fig. 35.17 Complex dermoid. (**a**) Large lateral canthal dermoid and associated eyelid coloboma. (**b**) Surgical debulking via a lateral canthal incision. (**c**) Postoperative photo taken 4 months after surgery

Phakomatous Choristoma

Phakomatous choristoma (Zimmerman's tumor) is a rare congenital tumor believed to represent ectopic ectodermal tissue of lenticular origin [13]. The clinical presentation is of a subcutaneous or preseptal orbital mass localized to the inferomedial aspect of the lower eyelid or orbit [14–17] (Fig. 35.18). The histological appearance is of ectopic lenticular epithelium that expresses lens-specific immunological markers for crystallin proteins and stains positive for immunohistochemical markers S-100 and vimentin, which are specific for filaments of lenticular tissue. A firm mass that may be adherent to the inferior orbital rim located in the inferior medial orbit (corresponding to the quadrant of the closure of the fetal fissure) [18–20].

Other Orbital Choristomas

Complex choristoma is the best term to describe a group of orbital lesions representing a variety of ectopic tissues found both superficially and deep within the orbit. Their presentation

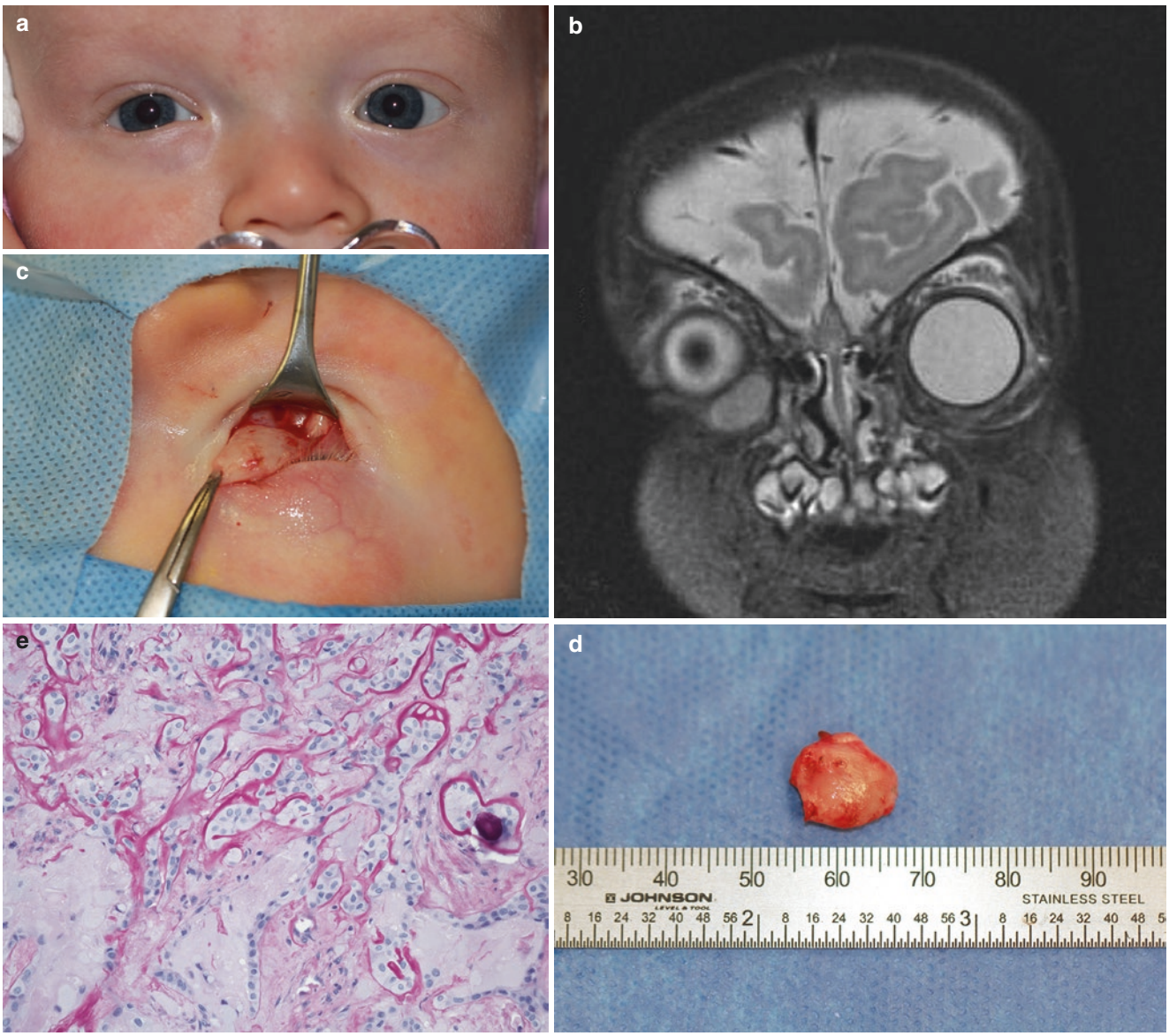


Fig. 35.18 Phakomatous choristoma. (**a**) Eyelid mass in a child on the right side that is adherent to the orbital rim. (**b**) T2 weighted MRI showing a large inferior orbital mass. (**c**) Intra-operative photo showing a transconjunctival lower eyelid incision with an inferior medial mass adherent to the orbital rim. (**d**) Photograph of the surgical specimen. (**e**) Histopathologic evaluation showed a well-demarcated mass composed of collagenized and myxoid stroma, with nests of epithelial cells interspersed throughout. Some epithelial cells displayed a cuboidal morphology and were arranged in glandular configurations with abundant, pale staining eosinophilic cytoplasm. Few epithelial cells were large and swollen, showing signs of early degeneration, similar to Wedl cells seen in posterior subcapsular cataracts. The stroma contained rare central psammoma-like calcifications

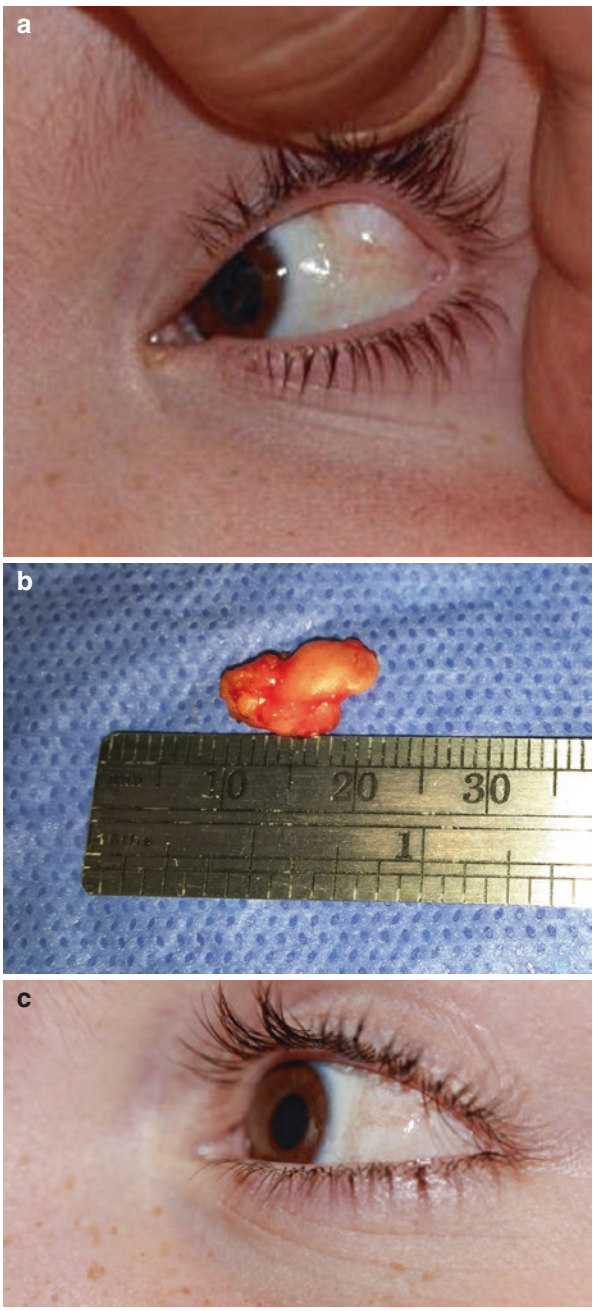


Fig. 35.19 Complex dermoid. (**a**) Large conjunctival lesion, dermoid. (**b**) A large tooth is visible within the lesion that was adherent to the sclera. (**c**) Postoperative photo taken 3 months after surgery

is often similar to a dermoid cyst. Located primarily in the lateral orbital compartment, they are most often discovered in late childhood due to the growth of the lesion announcing its presence. Some may be epibulbar in location, in which case a distinctly more vascular external appearance is seen, while others may occur deeper in the orbit [21, 22].

The most common ectopic tissue found in these orbital rests is lacrimal gland (Fig. 35.19), but brain, conjunctiva, and respiratory epithelium have also been reported [23–27]. These lesions are not extensions from contiguous structures but are isolated within the orbit, making their exact diagnosis difficult until surgically excised and pathologically evaluated. The existence of these tissues in the orbit results from erroneous migration of embryogenic tissues that settle with normal orbital tissues and later develop into their final histogenic form.

Microphthalmos with Cyst

This cystic orbital lesion represents the arrested closure of the fetal fissure at approximately 4 weeks of fetal life (8-mm stage), resulting in a persistent ocular defect. Neuroectodermal tissue that is attached to and contiguous with the globe fills with aqueous fluid, resulting in slow expansion of the cyst and globe displacement that is usually superior and medial. The cystic portion can be variable in size on clinical presentation and the degree of microphthalmos may also be mild or severe [28]. Generally, the larger the cyst at birth the more microphthalmic the globe. If no globe is present, the term congenital cystic eye applies. This earlier embryogenic failure of development of the primary optic vesicle may mimic microphthalmos with cyst and can also present with a large, multicystic orbital mass [29].

Depending on the degree of failure in the fetal fissure, the cyst may be small or large at birth. A large colobomatous defect resulting from poor fetal fissure closure manifests with a congenitally large cystic component obvious at birth. These are typically unilateral, cause proptosis with superior globe displacement, and can have a characteristic bluish coloration. Transillumination can rapidly help one distinguish this condition from orbital teratomas and encephaloceles. Late cases of cyst enlargement have been reported even after decades of quiescence, indicating that some additional breakdown in cyst/eye coupling allows expansion in the colobomatous cyst [30]. Bilateral cases have been reported, but are often asymmetric and have been associated with 13q deletion syndrome, ring deletion of chromosome 18 and with trisomy 18 [31, 32].

Imaging techniques, including CT scan and orbital ultrasonography, can confirm clinically evident lesions or diagnose indeterminate ones. The cystic component is echolucent ultrasonically, while the microphthalmic eye shows some echogenicity due to the vitreous. CT or MRI can demonstrate the globe/cyst relationship along with the attachments to the cyst wall (Fig. 35.20). The cyst contents appear very close in density to normal vitreous on MR imaging [33].

The treatment of microphthalmos depends on the size of the cyst and the resultant functional orbital dysmorphism along with considerations involving the function and displacement of the globe (see also Chap. 39). Expanding large cysts

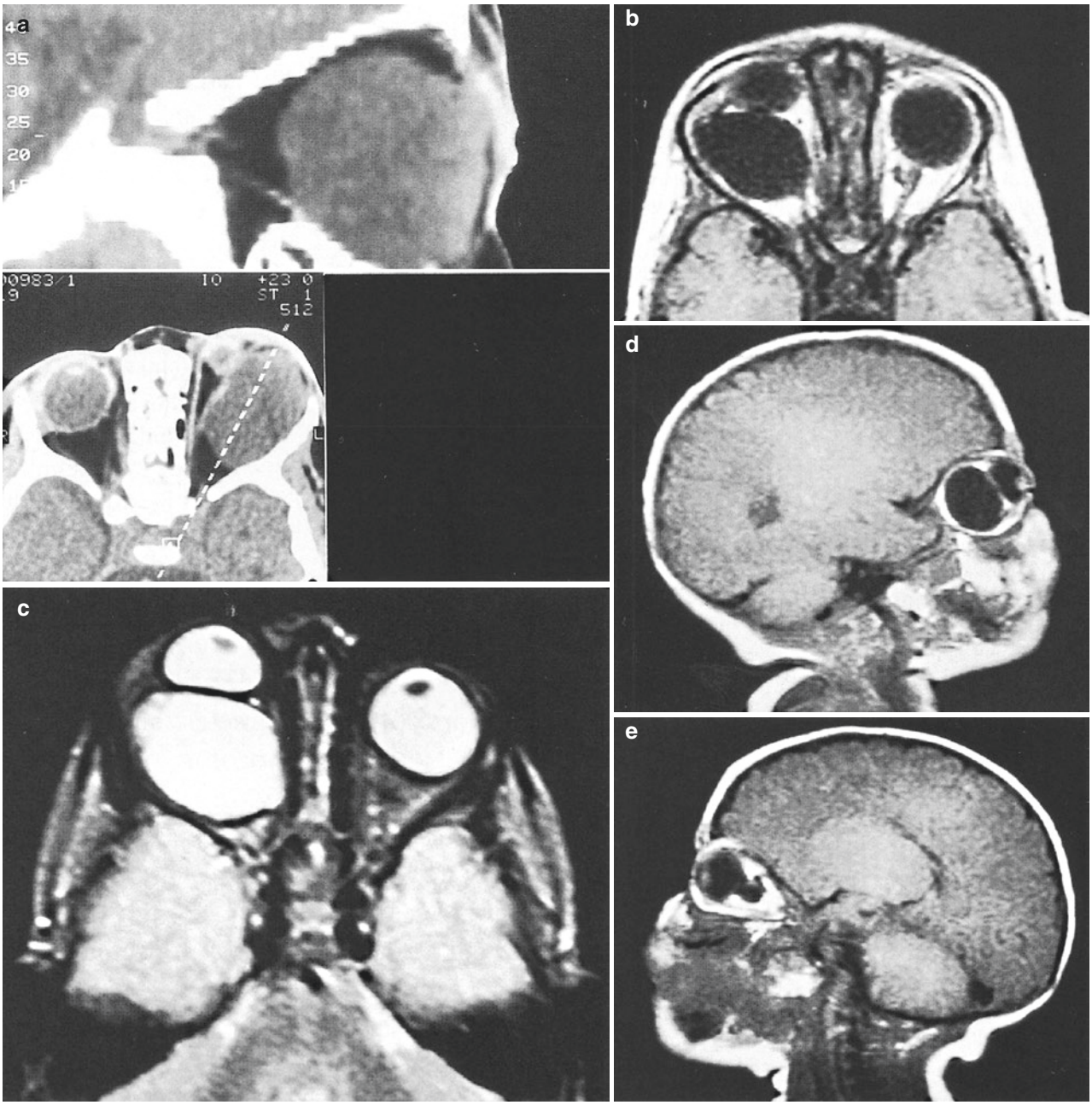


Fig. 35.20 Large cyst with microphthalmos. (**a**) Axial CT scan with coronal reconstruction demonstrating large cyst with microphthalmos. Cyst contents appear isointense with brain and vitreous. (**b**) MRI scan of 2-year-old male with bilateral microphthalmos with cyst. Axial T_1-weighted image demonstrates a large cyst in the right orbit posterior to a microphthalmic eye. Note the bony molding of the lateral orbital wall. The left orbit shows a nearly normal size globe with a small cyst. (**c**) Axial T_2-weighted image showing bright signal within the right orbital cyst isointense with the intravitreal signal. (**d**) Sagittal Tr-weighted image of the right orbit demonstrating the large cyst. (**e**) Sagittal T_2-weighted image demonstrating the smaller cyst attached to the globe in the left orbit

with nonfunctioning microphthalmic globes are best addressed by complete cyst excision and enucleation. For huge cysts, drainage intraoperatively may be necessary to even begin dissection. Preservation of as much orbital tissue as possible is necessary with large cysts, because little may be left for coverage of an orbital implant. Dermis-fat grafts can work well in this situation, even in very young children, because these sockets may already be well expanded due to the large cyst size, allowing for placement of large amounts of autogenous material (see Chaps. 36 and 39). Smaller cysts with cosmetically acceptable globes can undergo successful removal of the cyst alone [34] (Fig. 35.21). Large cysts with orbital expansion and proptosis are best treated with excision (Fig. 35.22). Even repeated needle aspiration of the cyst has been successful in permanently reducing cyst size [35]. Despite these surgical avenues, observation will be all that is necessary for the major-

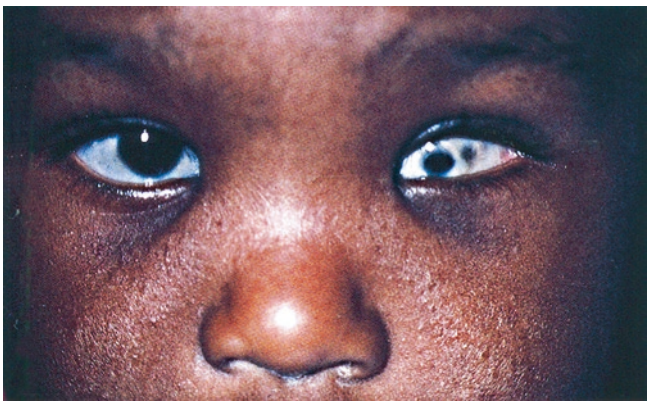


Fig. 35.21 After removal of a large colobomatous cyst. Postoperative photograph of the patient in Fig. 35.20 after removal of large left orbital colobomatous cyst with globe still intact. Cosmetic shell was fit over this globe

ity of these colobomatous cysts along with cosmetic shell management in concert with an ocularist.

Mucocele

Paranasal sinus obstruction with resultant entrapment of mucus, pressure increase with eventual erosion of surrounding bone, and spread into adjoining head and neck cavities such as the orbit defines the term mucocele. If found to be infected, the term mucopyocele applies. Mucoceles have traditionally been thought to result from stenosis of the sinus ostia. A history of nasal or facial fractures, chronic allergies, recurrent or chronic sinusitis, chronic polyposis, or past sinus or nasal surgery reveals potential routes through which sinus ostium damage or scarring may occur. Others believe that mucoceles form when sinus mucosa cysts gradually enlarge, causing secondary obstruction of the sinus ostium [36]. A definitive cause based on historical information is lacking in about 30% of patients presenting with orbital involvement from paranasal sinus mucoceles.

Mucoceles presenting with orbital involvement in the pediatric population are rare. In the compiled series tabulated in Table 35.1, only 12 cases were identified among a total of 1820 pediatric patients with orbital processes, for an incidence of less than 1%. None of the series gives detailed information as to the cause of mucoceles in affected children. However, two particular conditions have been associated with mucocele formation in children: allergic rhinitis and cystic fibrosis [37, 38]. In adults, it is estimated that 60% of all mucoceles arise from the frontal sinus, 30% from the ethmoids, and the final 10% from the maxillary sinus. Sphenoid mucoceles are rare [39, 40]. In children, most mucoceles arise from the ethmoid sinuses secondary to the delayed aeration and formation of the frontal sinus that begins only around 11 years of age.

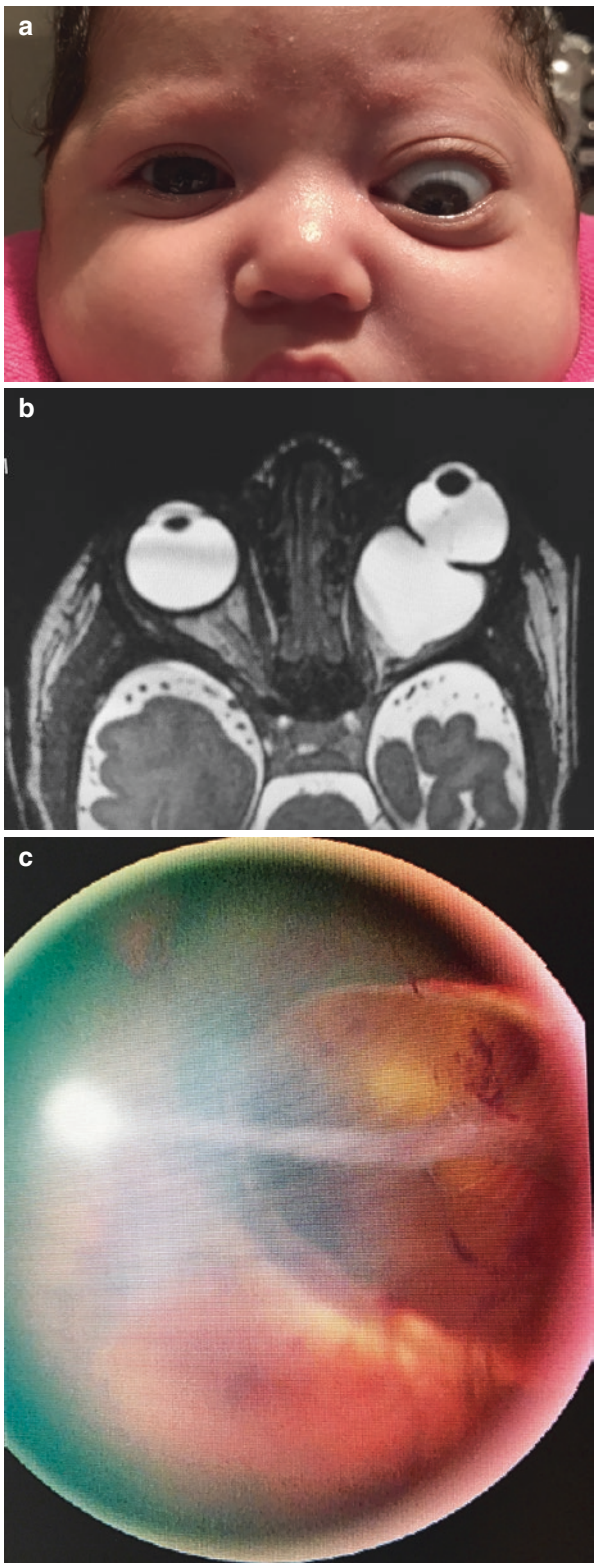


Fig. 35.22 Large colobomatous cyst with proptosis. (**a**) Clinical photo showing disfiguring proptosis. (**b**) Color fundus photo of chorioretinal coloboma and cyst cavity. (**c**) T_2-weighted axial MRI showing left eye with large cyst and orbital expansion

Clinical signs associated with orbital involvement of mucoceles include proptosis, inferior or lateral globe dystopia, upper eyelid swelling, telecanthus, diplopia secondary to gaze restriction, and decreased vision. Few patients have all these symptoms on presentation. The most common combination of symptoms is lid swelling and globe displacement. Palpation of a firm superonasal mass helps in the clinical diagnosis of mucoceles. Occasional episodes of more acute inflammation with pain, redness, and swelling, limitations of ocular motility, and displacement or proptosis of the globe may herald an infection or spontaneous leakage of the mucocele due to its continued expansion. Since the ethmoids are the most common location of pediatric mucoceles, lateral globe dystopia with associated hypertelorism and telecanthus is the most common presentation. Most cases are unilateral, but approximately 5% may involve both orbits.

Imaging studies easily delineate these lesions. CT scanning of the head and orbits remains the most valuable imaging modality due to its ability to localize focal areas of bony dehiscence, thereby providing delineation of the extent of the lesion as well as its morphology [41]. The identification of these bony dehiscences is important during the surgical correction of the mucocele to avoid penetrating into other cavities such as the intracranial space or orbit, resulting in potential recurrence, injury to the brain or eye, or spread of any infected material. The mucocele appears as a homogenous mass within the affected sinus that enlarges and expands the bony sinus margins rather than destroying them (Fig. 35.23b). Typically the contents are isodense with brain. With contrast enhancement, the cyst contents fail to enhance while the rim may enhance, especially if inflammatory episodes have occurred. Calcifications may be seen in the rim as well. The cyst may expand into the orbit or intracranial cavity if the bone erodes. The prolapsed cavity subsequently displaces intraorbital contents.

MR imaging may show these prolapses with more detail than CT [42]. Variations in the viscosity of the cyst contents along with breakdown and desiccation of solid components are the proposed explanations for the variable MR features, which are usually hypointense on T_1-weighted images and hyperintense on T_2-weighted images. Mucoceles have a fairly characteristic appearance, but congenital encephaloceles may present with similar clinical signs. CT should be able to show the bony avenue through which the sinus contents herniate into the cranium and orbit.

Mucoceles require surgical correction to avoid damage to nonsinus structures. Frontoethmoidal mucoceles have traditionally been treated by an external Lynch-type incision, yielding access to both the frontal and ethmoidal areas. This approach also lends itself to the identification and dissection of the periorbita from the epithelial lining of the cyst, isolating the orbital contents from potential injury when the cyst lining is peeled or obliterated [43]. In cases where previous inflammation or infection has occurred, the cyst lining may be adherent to and nondissectable from the periorbita. With most pediatric mucoceles involving the ethmoid sinuses, obliteration of the mucocele is less attractive due to continued facial growth in young children and the amount of surgery necessary to completely remove all ethmoidal cells involved. Reestablishment of drainage of the mucocele into the nasal cavity seems to be a worthwhile approach with ethmoidal involvement. A medial lid crease approach offers an external view through a cosmetically acceptable incision site

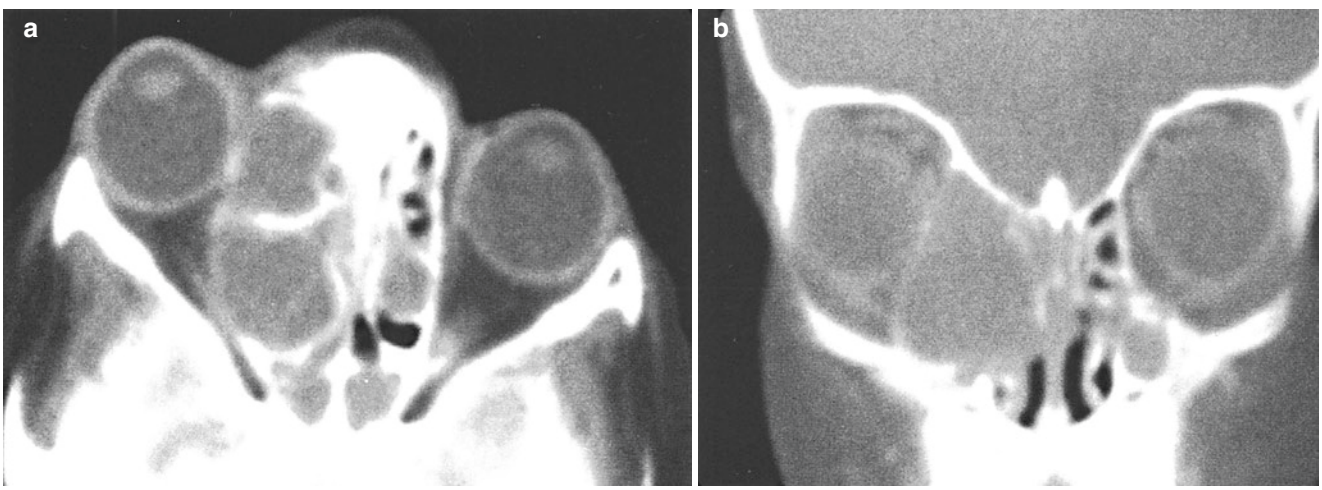


Fig. 35.23 Repair of mucocele, external approach. (**a**) Axial CT scan of a 6-year-old child with cystic fibrosis and a 4-month history of progressive swelling of the right upper eyelid. All the ethmoid air cells on the right are involved, while the middle ethmoidal air cells and the sphenoid sinus are involved on the left. (**b**) Coronal scan of the same patient showing the thinning and bowing of the medial orbital wall into the orbit, trapping the globe against the lateral orbital wall



Fig. 35.23 (continued) (**c**) The surgical repair of this mucocele was undertaken through a medial lid crease incision as depicted here. (**d**) Retraction of the surgical planes demonstrates the mucocele cyst contents eroding through the cyst wall in the superomedial orbit. (**e**) After evacuation of the cyst contents and removal of the anterior air cells, internal fistulization into the nasal cavity to recreate adequate drainage was stented with a catheter and left in place for 3 weeks. (**f**) A 7-day postoperative photograph depicts near equal globe position, well-healed incision site, and no signs of orbital inflammation

(Fig. 35.23c–f). Alternatively, intranasal approaches with endoscopic guidance have enjoyed increasing utilization among otolaryngologists and may be applicable in these cases as well (Fig. 35.24 and see Chap. 9).

Occasionally, lacrimal drainage mucoceles are large enough to cause proptosis [44]. A large intranasal component can be seen such as the patient in Fig. 35.25, who was treated with an intranasal cyst removal. This can result in cyst reduction without the need for an orbitotomy or external DCR.

The potential surgical complications include recurrence, orbital injury, including diplopia from a misplaced or damaged trochlea, intracranial transgression with cerebral spinal fluid (CSF) leak through unrecognized bony dehiscences, and extensive bleeding from attempts to extirpate all cyst lining epithelium [45]. The most grave complication to the eye from endonasal endoscopic surgery was an inadvertent enucleation, which was has been previously reported [46]. Otolaryngologic colleagues can provide invaluable assistance in planning and completing the surgical repair of mucoceles in the pediatric population.

Orbital Teratoma

Teratoma is the term used to describe a neoplastic growth of tissue containing all three germ cell layers. Endothelial,

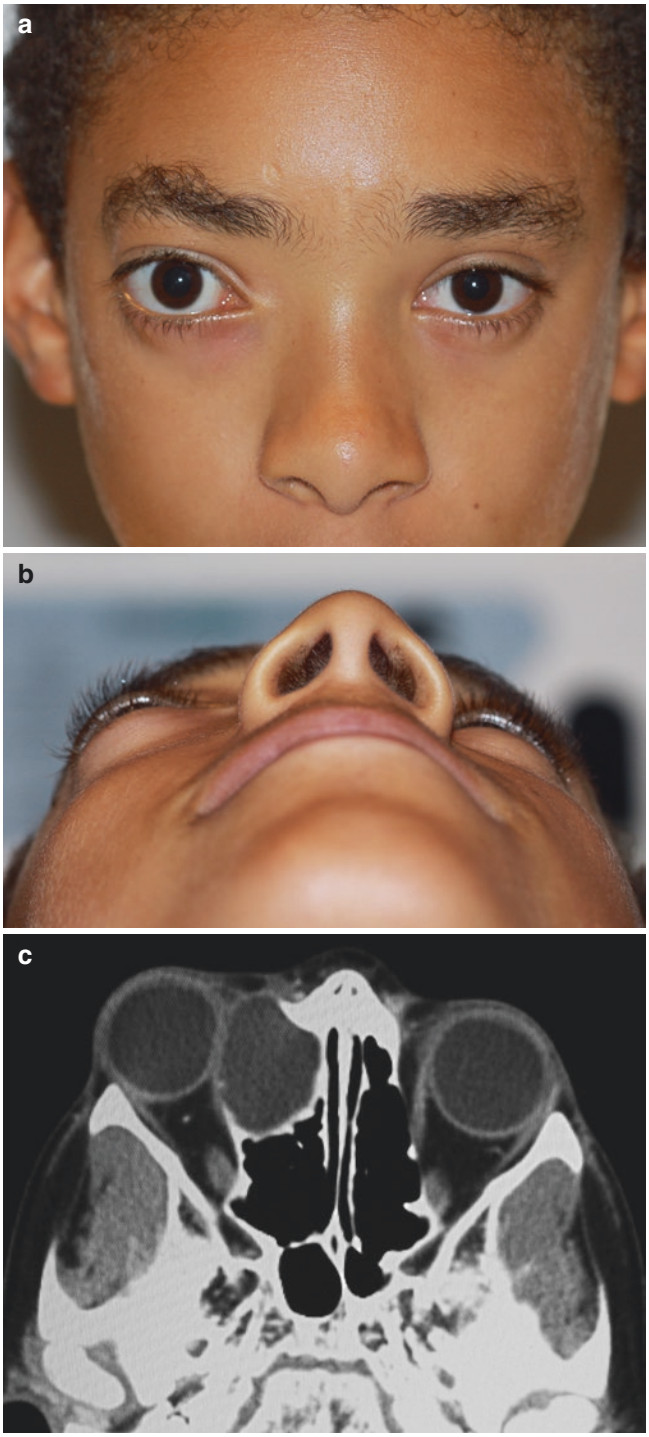


Fig. 35.24 Repair of mucocele, endonasal endoscopic approach. (**a**) External photograph of 13-year-old male with lateral displacement of the right eye. (**b**) Worm's eye view showing right proptosis. (**c**) Axial CT showing a large ethmoidal mucocele with right medial wall remodeling causing right-sided proptosis. This patient subsequently underwent an endonasal procedure for cyst reduction (not pictured)

epithelial, and mesothelial components can be found in these rare congenital tumors. These are believed to arise from primitive germ cells that may be ectopic or may have migrated during embryogenesis to the site of involvement. More common in sites other than the head and neck, only nine cases of orbital teratoma were recorded in the series tabulated in Table 35.1, for an incidence of less than 1%. Cervical, sacral, gonadal, and mediastinal locations account for over 70% of all teratoma presentations. Mamalis et al. reviewed the literature in 1985 and found approximately 60 cases primary to the orbit, including the two reported in their article [47]. Females outnumber males 2:1 with nearly all orbital teratomas present at birth.

Most orbital teratomas are small and appear similar to a well-circumscribed dermoid. Located adjacent to the globe instead of near the site of bony closures, some may be as large as 10 cm in diameter on presentation, creating a rather alarming appearance made even more grotesque if the face, sinuses, or cranium are also involved [48] (Fig. 35.26). Universally unilateral, most are located in the inferior orbit, displacing the globe superiorly and have a characteristic red-orange coloration when large and a yellowish-white appearance when small. The globe may be completely invisible, displaced under the upper eyelid, and so compressed that vision is lost. Rarely, they may extend into the intracranial space [49]. Smaller lesions that grow rapidly may show progressive signs of visual compromise such as decreasing motility, afferent pupillary defect, or an amaurotic pupil with continued globe displacement. Some cases with very small teratomas may show progressive proptosis with development of a palpable mass, mimicking other rapidly growing lesions of infancy, such as lymphangioma, capillary hemangioma, rhabdomyosarcoma, metastatic neuroblastoma, or leukemia.

Teratomas can be cystic or solid. CT evaluation demonstrates these internal features as well as the relationship to other vital orbital structures. Heterogeneity of the internal contents is frequent and calcifications are not uncommon in solid teratomas. The histopathology of teratomas shows evidence of all germ cell layer tissues in various stages of maturation. Intestinal structures, glandular elements, and secretory choroidal plexus are frequently found, accounting for cystic features within the teratoma and helping to explain its often rapid enlargement.

Treatment for these lesions is based on the size of the teratoma, presence of vision in the affected globe, and involvement of other orbital, sinus, or cranial structures. If vision is present, attempts can be made to separate the teratoma from the globe and optic nerve during orbitotomy. Successful preservation of vision is possible in some cases but is frequently not possible with large teratomas [50]. With no identifiable visual function and a deformed globe, limited exenteration of the globe and teratoma is undertaken in an attempt to preserve uninvolved orbital structures. Complete teratoma removal is important because of reports of malignant features in these tumors and the report of malignant transformation in an incompletely excised

lesion [51, 52]. For those children too ill to undergo surgery, decompression of the cystic component may offer adequate temporization to allow for later successful surgery [53]. Complicated teratomas involving other cranial structures often require more radical surgical efforts, usually combining craniotomy and sinus surgery, by a team of appropriate specialists [54]. Incompletely excised teratomas require surveillance for regrowth and malignant transformation. Serum α-fetoprotein and human chorionic gonadotropin levels can be useful in monitoring tumor response when chemotherapy is used to treat recurrent, malignant, or unresectable teratomas [55]. Social service support for the family is necessary to help with planning for the child's home care and to preserve parental/child bonding in these potentially devastating cases.

Orbital Cephalocele

Cephaloceles represent the failure of embryonic surface ectoderm to separate from neuroectoderm, resulting in continued intimacy of these developing tissues. A persistent connection between brain tissue, meninges, or the combination of these with orbital contents is broadly termed orbital

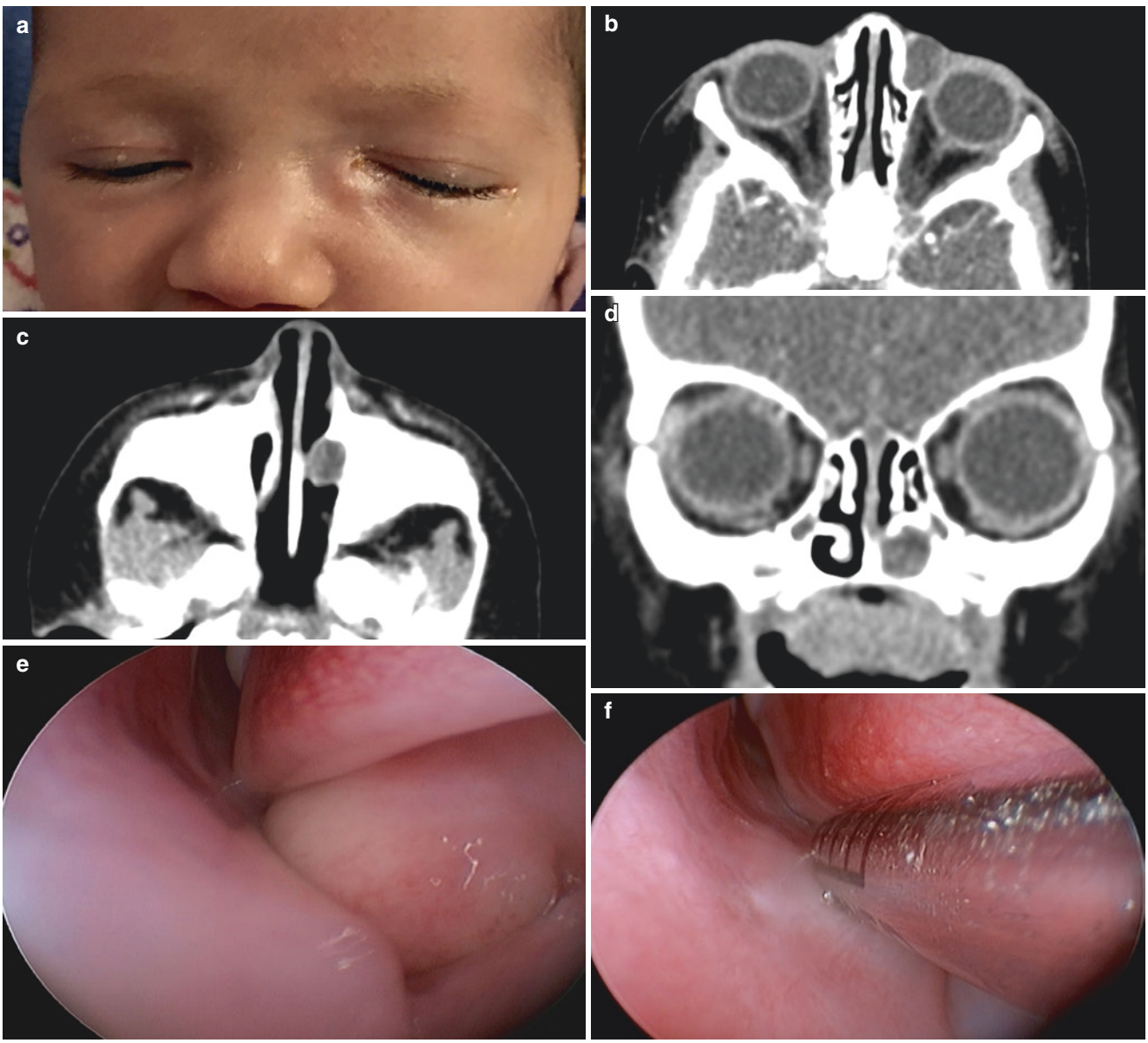


Fig. 35.25 Repair of mucocele, endonasal endoscopic approach. (**a**) External photograph of 3-week-old girl with large medial canthal cyst and lateral globe displacement. (**b**) Axial CT showing left lacrimal mucocele with globe displacement. (**c**) Axial CT showing an intranasal cyst extending through the valve of Hasner. (**d**) Coronal CT shows this cyst under the inferior turbinate, which is displaced upward. (**e**) Intranasal photograph of this cyst under the inferior turbinate (**f**) Excision of this cyst with a microdebrider (Medtronic, Mansfield, MA)

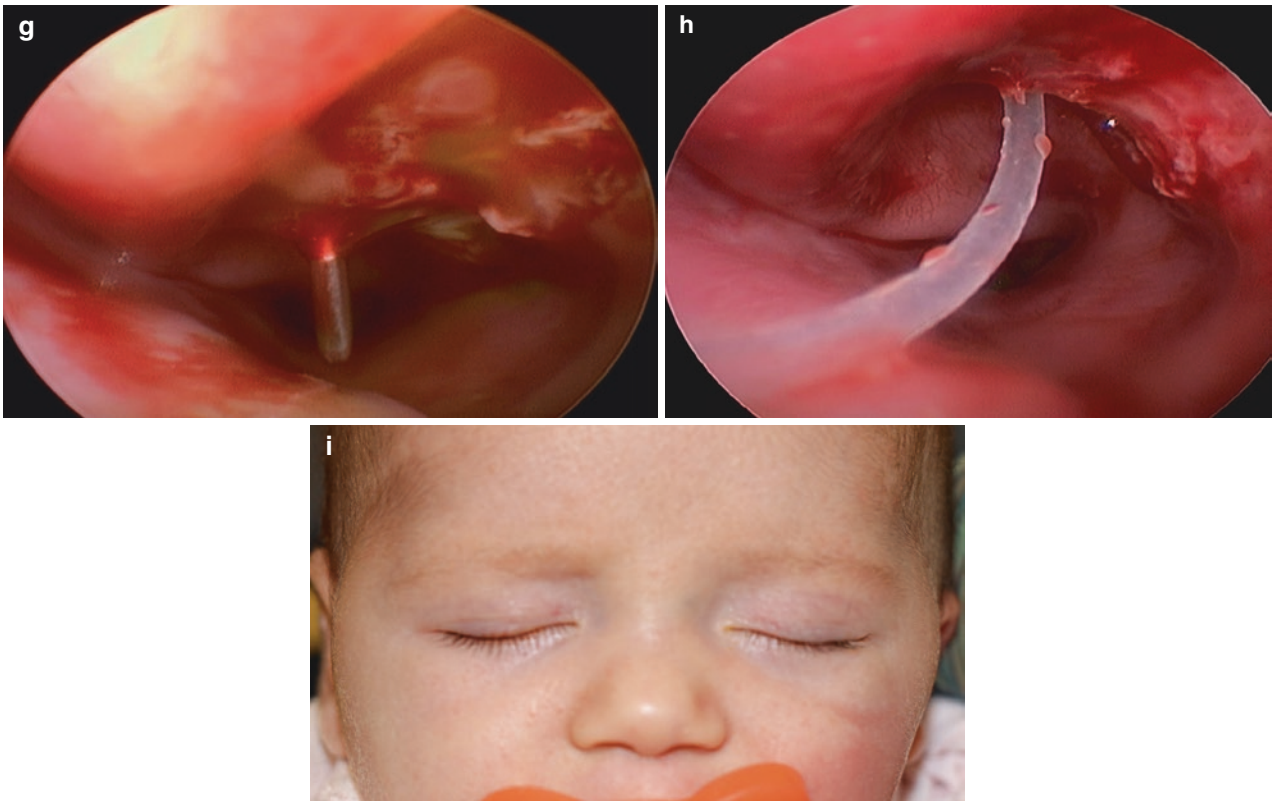


Fig. 35.25 (continued) (**g**) A 23 gauge lacrimal cannula is picture emanating from the inferior portion of the lacrimal duct into the nasal space. (**h**) A monocanalicular stent is intubated into the left lacrimal system. (**i**) Postoperative photograph taken 10 days after surgery showing complete resolution of the medial canthal cyst



Fig. 35.26 Large orbital teratoma. A 5-day-old infant with large right orbital teratoma presenting with classic orange-red color displacing globe superiorly in the orbit. Globe can be seen as darkish structure covered by thinned upper eyelid

cephalocele. More specifically, meningeal herniation is termed meningocele, while the presence of both brain and meninges is called meningoencephalocele. The term encephalocele would apply to the herniation of brain alone, which in the orbit is usually heterotopic tissue without true connection to the intracranial cavity. It is hard to imagine a situation other than heterotopia where the brain would herniate without meninges. This herniation occurs through a bony defect in the frontal skull base that may extend not only into the orbit but also into the ethmoid sinuses, the nasal cavity, or the opposite orbit depending on the size of the defect.

Orbital cephaloceles are rare. Only six cases are reported in Table 35.1 for an incidence of approximately 0.3% among all pediatric orbital tumors. An exact occurrence rate is unknown, but an increased frequency is seen in Southeast Asia [56]. The highest association is seen among children with congenital craniofacial clefts where bony defects in a variety of skull areas lead to the herniation of intracranial

contents [9] (Fig. 35.27). Anterior cephaloceles are usually visible from birth, while deeper lesions may not manifest until late childhood or early adulthood.

The location and size of the bony dehiscence and resultant tissue herniation through this dehiscence will determine the effect on the orbit and eye along with the clinical presentation. A sincipital cephalocele as depicted in Fig. 35.27 produces an inferior and lateral orbital dystopia. A more nasal herniation near the frontonasal suture will produce lateral globe dystopia, while a medial dehiscence more posteriorly near the frontoethmoidal suture will produce a clinical picture of later-onset proptosis and lateral globe dystopia. Far posterior dehiscences, such as is seen in neurofibromatosis with a missing greater wing of the sphenoid, may produce only proptosis. Centrally placed cephaloceles, termed basal cephaloceles, produce the classic features of a broad nasal root, hypertelorism, and telecanthus when large. These arise from dehiscences along the cribriform plate. These masses are usually soft and spongy and may enlarge with Valsalva maneuvers. Occasionally, a pulsatile quality may be visible. Some of these may not have a significant anterior component and may present later in life with ophthalmic signs resulting from encroachment of the cephalocele on the visual system. Morning glory disk, nasolacrimal obstruction, ocular motility abnormalities, monocular vision loss, and communication with the lower eyelid have been some of the findings resulting in the discovery of an associated cephalocele [57–60]. Rarely, a cephalocele may present as a mass below the medial canthus thus simulating a lacrimal mucocele or amniotocele. For this reason, orbital imaging should be considered, especially in the setting of an attempted probing and irrigation without successful lacrimal mucocele reduction. Fig. 35.28 depicts such a case of a medial canthal mass that was referred for a lacrimal mucocele; however, a large cephalocele was noted on imaging.

CT proves to be the most useful imaging study. The extent and outline of the bony abnormality is easily seen, as is the connection of the cephalocele contents to the brain (Fig. 35.29). Demonstrating the tissue herniation is very important to the CT diagnosis of cephaloceles and helps differentiate these from lesions that may have a similar clinical appearance, such as superficial and deep dermoids, small teratomas, or mucoceles. This is important especially with small meningoceles because of the surgical implications of exploring these lesions and finding intracranial connections.

The treatment of orbital cephaloceles requires support from neurosurgical colleagues and may require the help of a craniofacial surgery team. The size, location, and extent of the cephalocele determine the approach to the excision and repair of both the bony and soft tissue involvement. Small, anterior lesions with minimal bony dehiscence can be approached extracranially with excision of the herniating material, enlargement of the bony defect to facilitate meningeal closure, bony repair with autogenous or banked bone, and cutaneous closure. Most cases, however, will require a careful preoperative plan that usually entails intracranial separation of normal brain and meninges from the herniating component, watertight repair of the dural defect, and elimination of the osseous opening with later excision of the orbital portion through extracranial routes (Fig. 35.28). Very large



Fig. 35.27 Severe unilateral exorbitism. Severe unilateral exorbitism in a child with frontonasal dysplasia demonstrating a rounded protuberance over the left orbit in the frontal bone consistent with a cephalocele

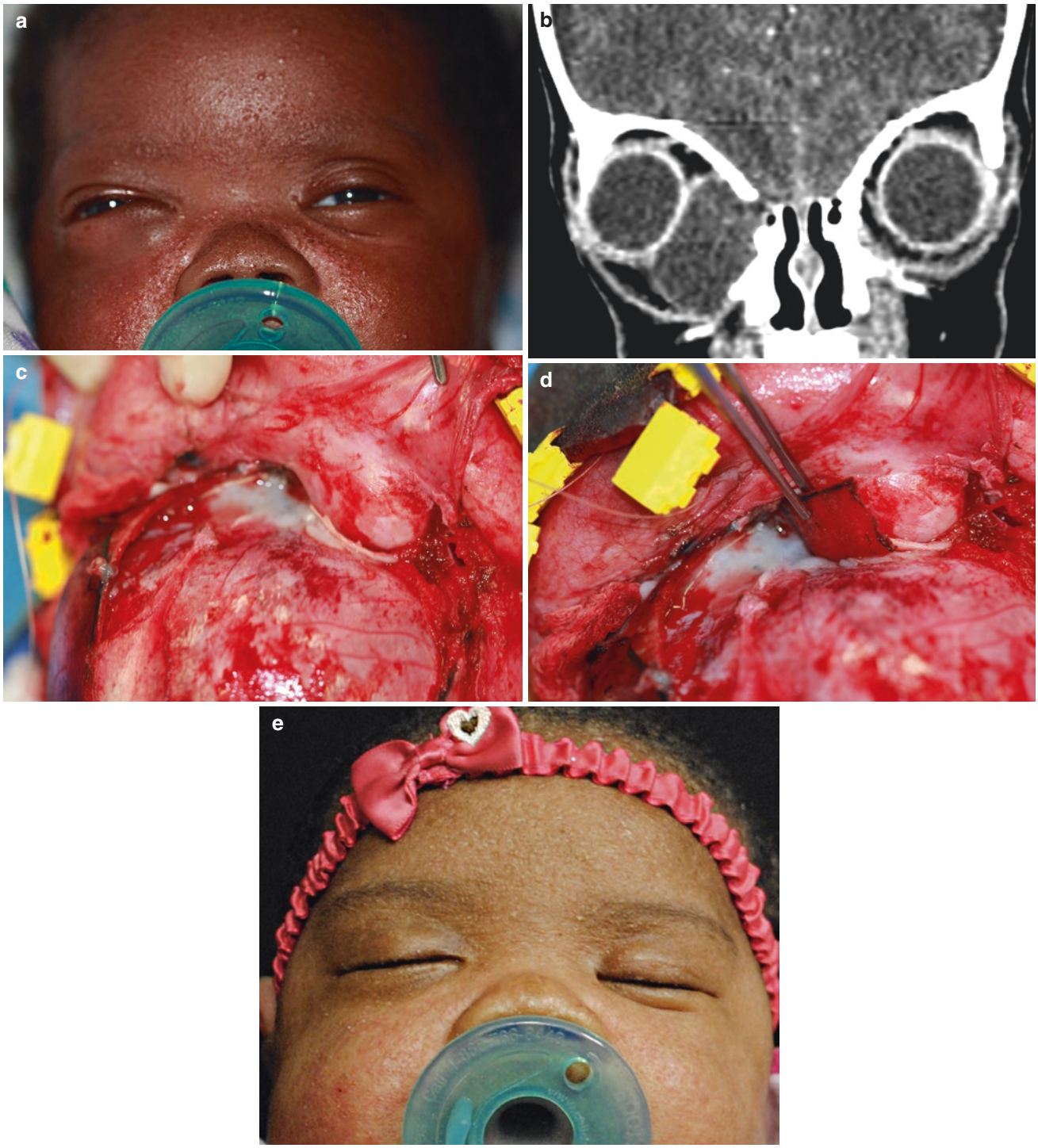


Fig. 35.28 Large fronto-orbital encephalocele mimicking a lacrimal mucocele. (**a**) 4 day-old child with bluish mass below the medial canthus. The mass was noted to be slightly lateral the lacrimal sac fossa and thus imaging was obtained. (**b**) Axial CT showing a skull base defect with a large fronto-orbital encephalocele. (**c**) Intraoperative photo showing the skull base defect. (**d**) A free cranial bone graft was used to repair the skull base defect. (**e**) Postoperative photo taken 2 months after surgical repair

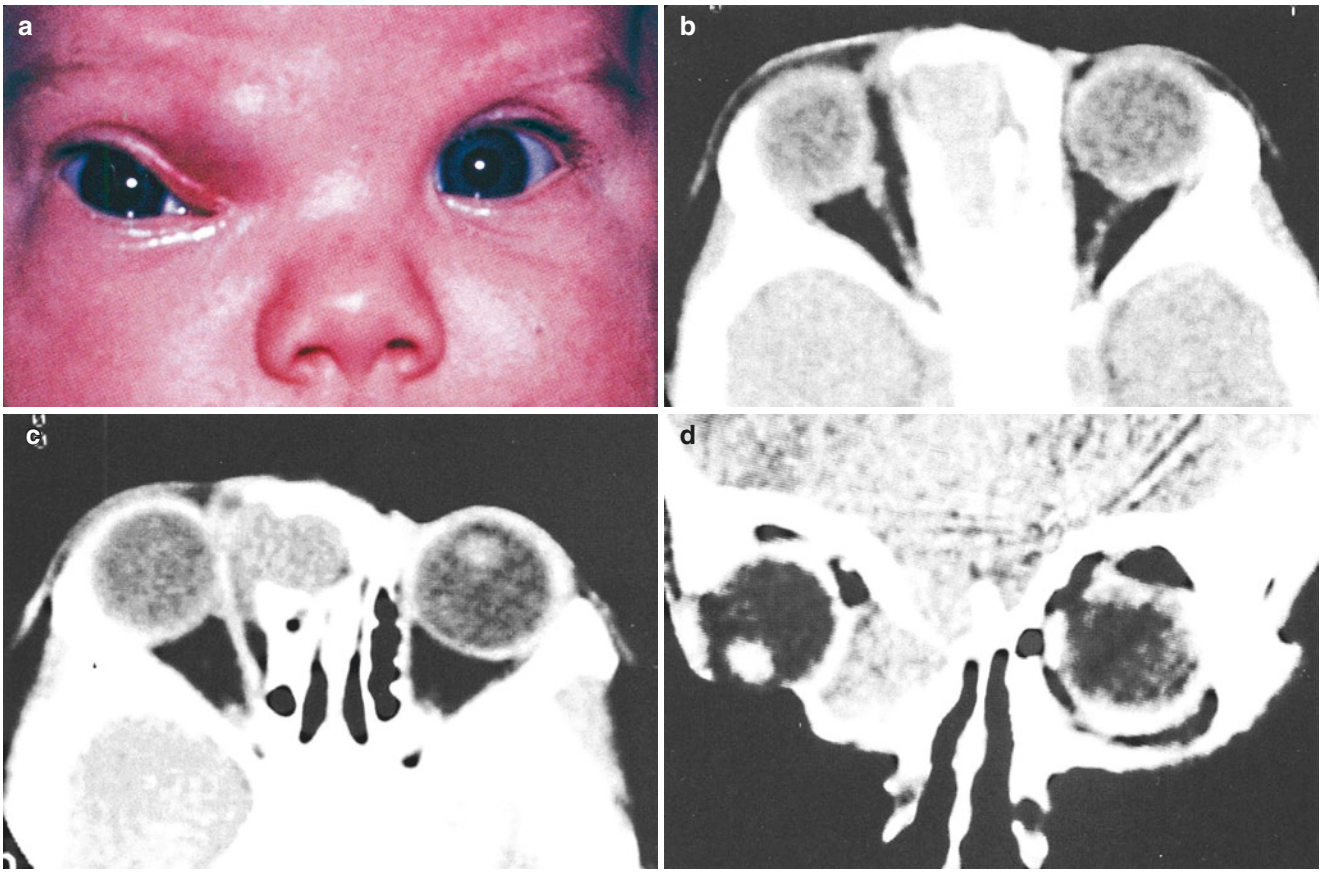


Fig. 35.29 Bony abnormalities. (**a**) A 1-year-old child with telecanthus, exorbitism, and a rounded right superomedial orbital mass that bulged further with crying. (**b**) Axial CT scan of the child demonstrating a cribriform plate bony defect that is occupied by a mass isodense with brain. Note the peripheral low-density rim around the mass reminiscent of the CSF space around the peripheral portion of the brain. (**c**) Slightly lower level axial scan demonstrating herniation of mass into the anteromedial right orbit. (**d**) Coronal CT scan of the same patient shows the meningoencephalocele herniating through the bony dehiscence into the medial right orbit

meningoencephaloceles require craniofacial support to tackle the formidable challenge of eliminating the defect itself but also repairing the secondary cranial and facial effects, resulting in a reduction of any exorbitism, telecanthus, or other associated abnormalities [61, 62]. Complete removal of the herniated portion is necessary to prevent recurrence.

Orbital Vascular Lesions

Traditionally, the classification of orbital vascular lesions has been based on topographic description. While this schema is well ensconced in the medical literature and offers a semblance of immediate appreciation of the lesion when examining a patient, it offers little understanding of the embryologic origins, pathophysiologic determinants, and hemodynamic considerations that ultimately help categorize and effect appropriate management strategies. Several practitioners have championed the cause of reclassification of orbital vascular lesions in an effort to level terminology and definitions in this often confusing set of orbital lesions.

Rootman deserves credit as one of the first individuals to utilize strict pathologic and hemodynamic features to reclassify these vascular lesions into three categories: malformations, shunts, and new growths [63, 64]. New growths are not present at birth, have endothelial proliferation, and are usually well circumscribed radiologically.

Infantile hemangioma, cavernous hemangioma, and single cell line neoplasms such as hemangiopericytoma and malignant angiosarcoma are examples of this category. Malformations are present at birth, grow parallel to the growth of the patient, have flat endothelial cells with dysplastic vessels, and are diffusely arranged in the orbit. Lymphangiomas (now called venolymphatic malformations) emphasize these clinical features. Shunts are an abnormal connection between the arterial and venous systems and can be congenital, acquired, or arise by malformation. Dural fistulas and arteriovenous malformations are representative of this class.

Stressing the importance of lesional hemodynamics as a classification tool, the Orbital Society has issued a consensus statement on the classification of orbital vascular lesions amplifying the importance of hemodynamics in the categorization of these processes [65]. Broken down into no flow, venous flow, and arterial flow malformations, no consideration is given to lesions that arise by new growth, leaving a large void for a universal classification scheme covering all orbital vascular lesions. The hemodynamics of the lesion do produce the majority of symptoms in the presentation and classification of the lesion, such as the rapid onset of proptosis, vascular congestion and swelling, orbital dysfunction and bruit associated with a high-flow carotid-cavernous sinus fistula versus the often low-flow dural fistula with its less obvious and often insidious onset of vascular dilation, increased intraocular pressure, mild proptosis, variable orbital dysfunction, and usual lack of an audible bruit. These hemodynamic features are what we recognize most in a clinical setting and utilize for diagnosis. As Rootman points out and as the Orbital Society classification demonstrates, the variability of vascular flow among lesions still creates difficulties in clinical diagnosis. One must consider not only hemodynamics and clinical presentation, but imaging studies to help determine the type of orbital lesion one is dealing with. While contrasted CT and MRI remain important first tools in accurate identification, one must consider more sophisticated imaging techniques such as Doppler ultrasonography, MR arteriography, and even invasive venography and arteriography when high-flow lesions are suspected. This may save the practitioners from emptying the "chocolate cyst" of a lymphangioma and discovering a congenital venous shunt that will challenge any practitioner's orbital surgical skills in the face of potential exsanguination in a 3-year-old.

The International Society for the Study of Vascular Anomalies (ISSVA) updated its own classifications for vascular anomalies in 2015 [66]. Due to additional lesions identified since its previous scheme from 1997 (Table 35.2), Rootman has simplified this table to apply to orbital lesions and incorporated the previously published Orbital Society classification Scheme [67]. This is summarized below:

Vascular malformations often show a confusing spectrum of signs and symptoms at presentation and on pathological evaluation. This is not surprising given the multitude of vascular elements that can manifest in a single lesion (venous, arterial, lymphatic, and capillary elements). As such, one often cannot diagnose an orbital vascular lesion or determine the correct surgical or nonsurgical treatment based only on its clinical and radiologic features. One must be prepared to include the considerations of hemodynamic flow, neoplasia, and additional imaging studies to help choose correct treatment strategies. These newer classification attempts are meant to emphasize the diversity and variable combinations of features representing orbital vascular lesions. This section retains the established clinical classification system for these vascular lesions while awaiting future studies refining treatment strategies that correlate to the terminology utilized in the newer systems.

Table 35.2 ISSVA Classifications for vascular anomalies

Vascular Tumors	Vasular Malformations:			
Benign	Simple	Combined	Of major named vessels	Associated with other abnormalities
	CM	Capillary-Venous	Refer to www.issva.org	Refer to www.issva.org
Locally aggressive or borderline	LM	Capillary-lymphatic		
Malignant	VM	Capillary-arterovenous		
	AVM	Lymphatic-venous		
	AV Fistula	Capillary-lymphatic-venous		
		Capillary-lymphatic-venous Capillary-lymphatic-arteriovenous Capillary-venous-arteriovenous Capillary-lymphatic-venous-arteriovenous		

Classification of Congenital Vascular Malformations (Phenotypes)

High Flow
- Arterial aneurysm
- Arteriovenous fistula
- Arteriovenous malformation

Low Flow
- Simple
  - Venous malformation*
    - Distensible
      - Nondistensible
        - Cavernous venous malformation
  - Lymphatic malformation
    - Macrocystic
    - Microcystic (diffuse/microscopic)
    - Mixed (macrocystic/microcystic)
- Combined[a]
  - Lymphaticovenous malformation
  - Venous dominant- lLymphatic dominant.

*Some or all of a VM may have distensible components on Valsalva maneuver.

[a]Combined malformations may be composed of any combination of distensible or nondistensible venous components and any subtype of LM (macrocystic/microcystic/mixed).

Infantile Hemangioma

While most commonly affecting the cutaneous portions of the eyelids and face, infantile hemangiomas with orbital involvement are not unusual. The surface features identifying this condition to almost all practitioners can be missing with isolated orbital infiltration, making its diagnosis challenging. With this chapter devoted to benign pediatric orbital tumors, it is difficult to discuss isolated orbital infantile hemangiomas alone due to the spectrum of presentation and involvement one sees clinically; thus, cutaneous and deep lesions are discussed together in this section (see also Chaps. 6, 7, and 23).

The exact incidence of infantile hemangioma varies widely in reported series. Table 35.1 compiles 101 cases of pediatric infantile hemangioma in the six series surveyed. These cases include superficial hemangiomas (anterior to the orbital septum), deep hemangiomas (posterior to the orbital septum), and combined hemangiomas (both anterior and posterior components). This represents an incidence of 5.6% among all pediatric orbital lesions, which is less frequent than other benign processes, such as orbital cellulitis, dermoid cysts, idiopathic orbital inflammation, and thyroid orbitopathy for the series surveyed. Among these individual series, the incidence ranged from 0% to 11.8%, but in no instance was it the most common benign pediatric orbital lesion. Haik et al. reported on their experience treating 101 cases of capillary hemangioma in children and found that 33% of these patients had skin lesions alone, 7% had only orbital involvement without any cutaneous manifestations, and the remaining 60% had a combination of both superficial and deep components [75]. Females outnumbered males 3:2 and 95% of patients presented under 6 months of age. A distinct predilection for the superior orbit and lid is a consistent feature.



Fig. 35.30 Superficial infantile hemangioma. Classic appearance of a superficial infantile hemangioma with nondermatomal, bright red coloration. This distribution can be described as segmental.

The clinical features of infantile hemangioma vary, depending on its subcutaneous depth. Superficial infantile hemangiomas start as small flat foci of dermal collections of abnormal capillaries characterized by endothelial cell proliferation into an organized network of basement-membrane-lined vascular channels that undergo rapid expansion over several weeks to months. Once well vascularized, their typical bright red coloration is apparent (Fig. 35.30). Generally, the faster these lesions enlarge, the faster they will involute. This is often clinically evident by the appearance of two signs: fine stellate areas of pale scarring in an area of previous vascularity or the onset of necrosis with skin breakdown. One should be concerned for a constellation of abnormalities called PHACE syndrome when examining a patient with a large plaque-like hemangioma of the face that is over 20 sq. cm^2 in size. This was first described by Frieden et al. as abnormal arteries, especially those of the central nervous system, coarctation of the aorta, cardiac defects, and unusual ophthalmologic abnormalities can also occur [68]. The ocular abnormalities include the morning glory disk anomaly and microphthalmia. These plaque-like hemangiomas are referred to as segmental hemangiomas, because they form over zones of facial development and not skin dermatomes. Fig. 35.31 depicts a series of patients diagnosed with PHACE after noting large facial hemangiomas. This subject is covered more extensively in Chap. 6.

The lesions are generally unilateral, painless, and compressible with a characteristic spongy feeling on palpation. Deeper subcutaneous involvement changes the color to a more purple tone, although the epidermis still may contain visible, red vascular channels (Fig. 35.32). Isolated eyelid involvement can occur but other facial, forehead, or mucosal lesions may be present (Fig. 35.31). Rarely, significant hematologic sequestering can occur within extensive capillary hemangiomas, especially with visceral lesions, resulting in a bleeding diathesis called the Kasabach–Merritt syndrome [69]. Infantile hemangiomas isolated within the orbit usually show no external features other than proptosis, although globe displacement and restricted ocular motility will also be clues to the presence of a significant orbital component (Fig. 35.33).

With the rapid onset of this condition, deep infantile hemangiomas can mimic the clinical presentation of rhabdomyosarcoma and metastatic neuroblastoma or, if present at birth, a teratoma. Children with metastatic neuroblastoma usually are ill and can have eyelid ecchymosis, which is unusual with infantile hemangiomas. With teratomas, growth can be rapid but usually produces nonaxial proptosis, whereas infantile hemangiomas within the orbit are relatively diffuse and produce mostly axial proptosis. Rhabdomyosarcomas are usually seen in slightly older children, helping to differentiate it from the early onset of infantile hemangioma. In addition, cutaneous color changes with infantile hemangioma and some enlargement with Valsalva maneuvers can help separate infantile hemangiomas from other orbital processes. Combined infantile hemangiomas (involvement on both sides of the orbital septum) merge these features and make up the largest percentage of infantile hemangiomas brought to the attention of the ophthalmologist. Although unusual, isolated conjunctival presentations have the same reddish coloration and enlargement seen with the superficial infantile hemangioma (Fig. 35.34). Some conjunctival involvement is seen in up to one-third of patients with either superficial or combined infantile hemangiomas [70].

Imaging studies have helped to differentiate the orbital components of this entity from other infiltrating orbital processes [71–73]. B-scan ultrasonography demonstrates an irregular mass that blends in with normal orbital structures. Variable internal reflectivity is seen and corresponds to the histology of the hemangioma: solid areas of endothelial proliferation yield low reflectivity, moderate echoes result from ectatic vascular channels, and high reflectivity originates from the fibrous septae in the tumor lobules. CT imaging reveals a diffuse, relatively homogeneous soft tissue mass that usually infiltrates throughout the orbit, although some may be well

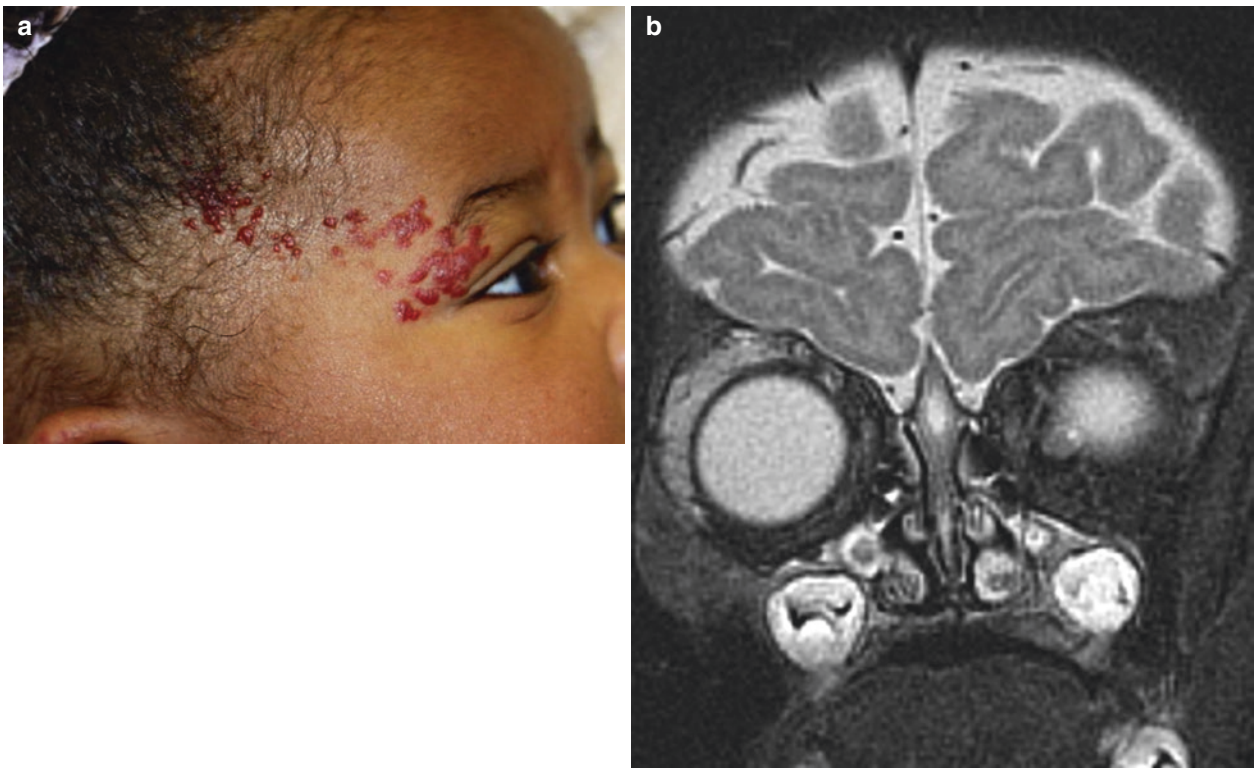


Fig. 35.31 PHACE. (**a**) Right forehead and eyelid segmental hemangioma. (**b**) T2-weighted MRI showing eyelid and intraobrital extension of the infantile hemangioma



Fig. 35.31 (continued) (**c**) Brain MRA showing vascular anomalies within the skull base. (**d**) 2 month-old girl with a large left segmental hemangioma and PHACE. (**e**) A 1 month-old girl with a large left facial hemangioma who was found to have PHACE

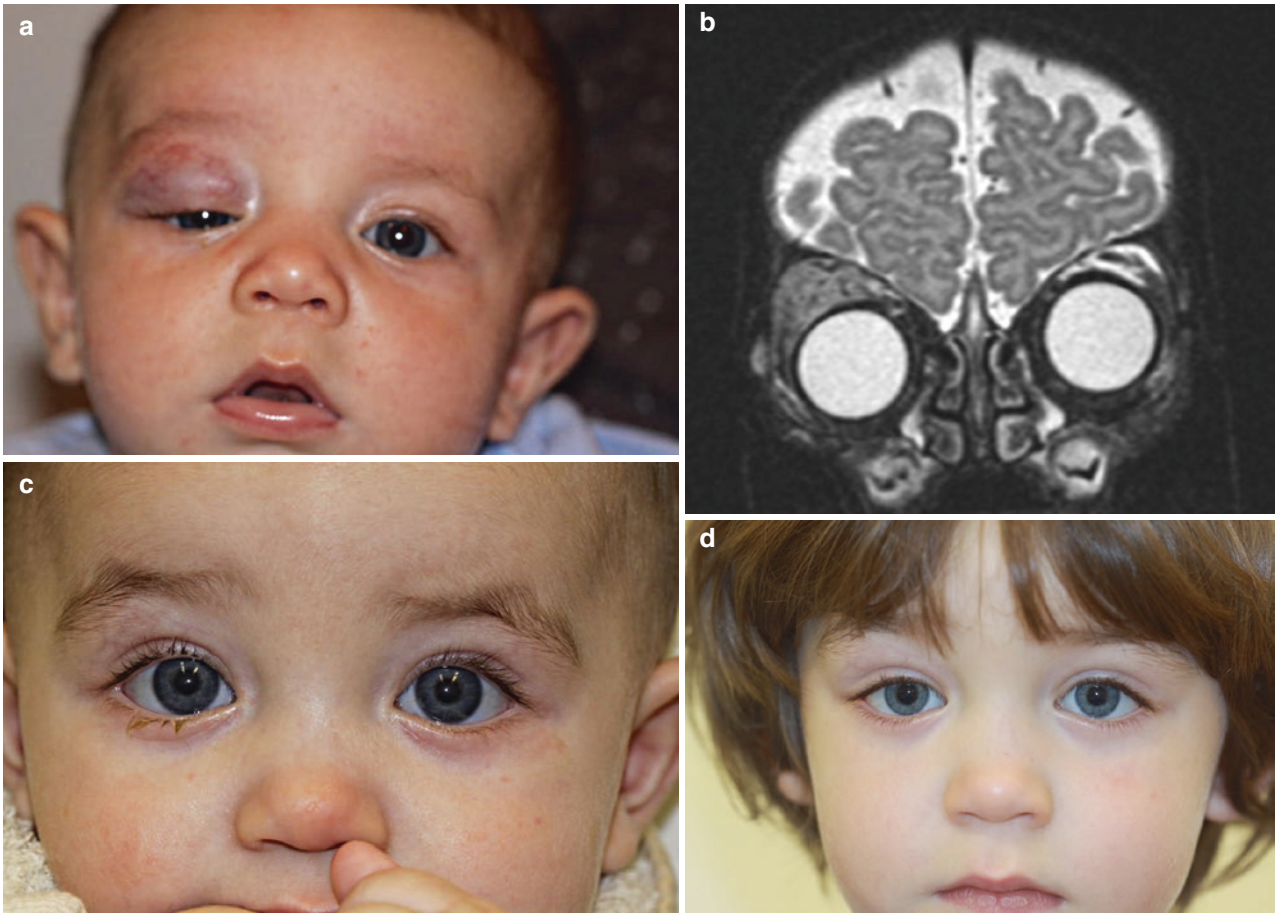


Fig. 35.32 Large orbital infantile hemangioma. (**a**) Severe ptosis due to anterior extension of an orbital infantile hemangioma. (**b**) T_2-weighted coronal MRI shows inferior globe displacement. (**c**) Clinical photo taken only 4 weeks after ongoing oral beta-blocker (Propranolol) therapy. (**d**) Clinical photo taken at age 2, 6 months after completion of beta-blocker therapy

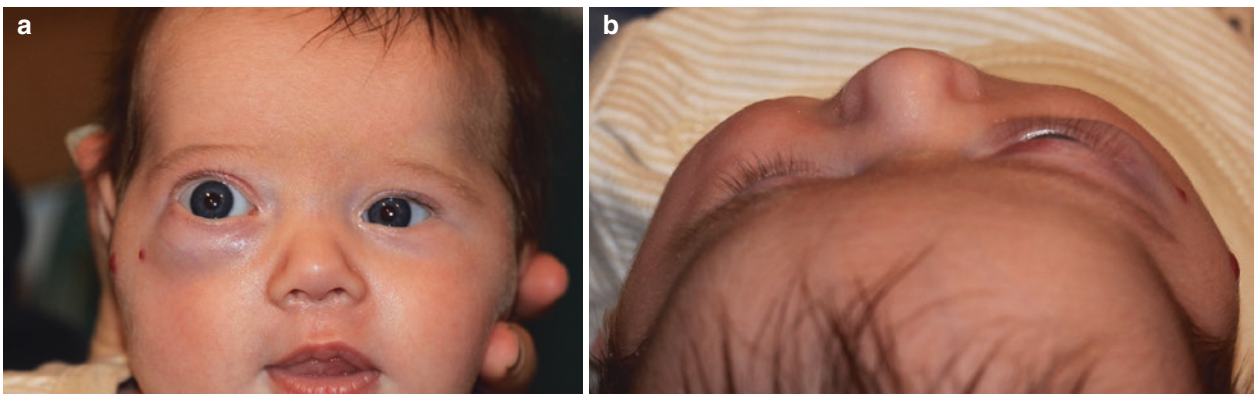


Fig. 35.33 Large orbital infantile hemangioma. (**a**) 2 month-old with a hypertropia and superior globe displacement due to an infantile hemangioma of the orbit. (**b**) Superior view showing the extent of right sided proptosis

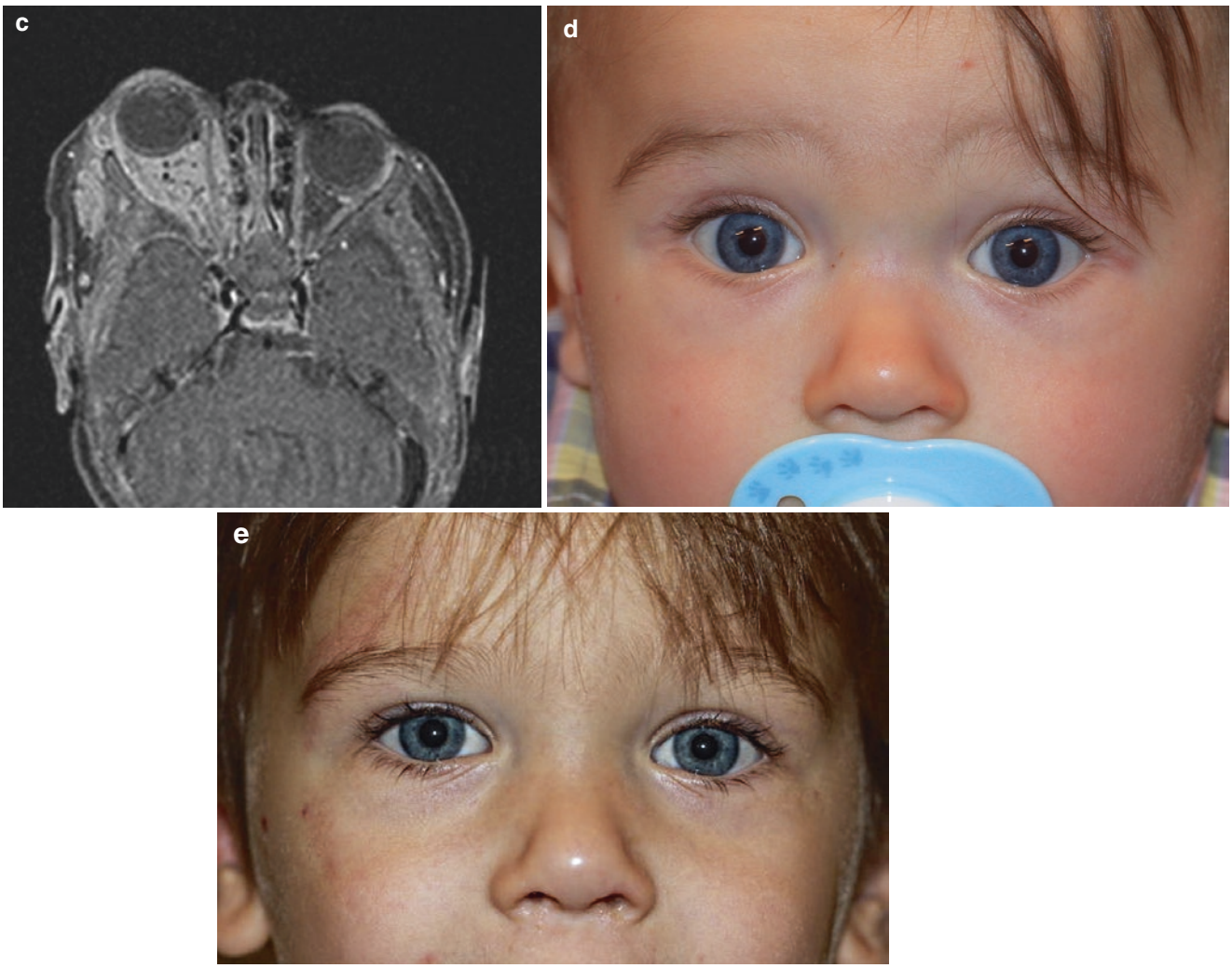


Fig. 35.33 (continued) (**c**) T1-weighted axial MRI showing a large right orbital infantile hemangioma. There is extension of the right orbital mass into the right Meckel's cave via the foramen rotundum. (**d**) 4 months after the induction of oral beta-blocker therapy with near-full resolution of globe displacement. (**e**) Clinical photo take at 30 months of age. This was 1 year after the completion of oral beta-blocker. This patient was treated with oral propranolol for a total of 18 months



Fig. 35.34 Isolated conjunctival infantile hemangioma. Since this lesion covered the inferior punctum it was treated successfully with topical timolol 1% gel forming solution ophthalmic eye drops

circumscribed. While this modality is readily available, it should be avoided as it can mislead the physician regarding the possibility of a malignancy. Rather, MRI is a far superior imaging modality for studying orbital vascular tumors. On MRI, high flow rate produces black, serpiginous areas termed "signal voids" on both T_1- and T_2-weighted images (Fig. 35.33c). Within the time frame of radio frequency stimulation of the imaged tissue and signal acquisition, the stimulated blood flows out of the vessel and is replaced by nonstimulated blood, which yields no signal and a resultant dark image. The infantile hemangioma is of intermediate signal strength on T_1-weighted images and appears isointense with brain. On T_2-weighted images, the hemangioma is relatively hyperintense but maintains a similar intensity to that of brain.

The effects of the infantile hemangioma on visual function and orbitofacial form are why this lesion maintains such high interest among ophthalmologists and primary care practitioners. Amblyopia occurs frequently and can affect as many as 64% of patients with periocular hemangiomas [74]. Astigmatism, anisometropia, strabismus, and sensory deprivation from occlusion can all play a role in amblyopia development due to the direct effects of the infantile hemangioma on the eye. Despite aggressive treatment for both the hemangioma and the amblyopia, Haik et al. found 63% of children (29/46) with periocular infantile hemangiomas have a visual acuity difference greater than two lines between the involved and uninvolved eyes after 5 years of follow-up [75]. They also found that 26% (12/46) had visual acuities of less than 20/200 in the affected eye. Boyd and Collin were able to demonstrate a reduction in the incidence of amblyopia from 80% to 53% when steroid injections were used to treat periocular infantile hemangiomas [74]. Strabismus is seen in approximately one-third of patients, with vertical deviations and esotropias most common [75, 76]. All patients with superficial infantile hemangiomas are left with cutaneous stigmata, including dilated capillaries, "cigarette paper" skin, variable pigmentation, and residual subcutaneous masses from the involuted hemangioma (Fig. 35.35). Proptosis from deep hemangiomas displays a regression pattern that parallels the amount of maximal proptosis: If more than 4 mm of proptosis was present originally, 40% of these patients will have greater than 2 mm or more of residual proptosis [75]. Significant orbital and ocular dystopia may remain from bony expansion or deformity despite tremendous involution of the soft tissue component of the hemangioma (Figs. 35.32 and 35.33).

Infantile hemangiomas show a universal trend toward spontaneous regression that is best termed involution. Although variable in degree, it is evident in virtually every case. The exact mechanism for the initial aggressive growth of these lesions and the resultant involution is not known. Mast cells are seen in high concentrations in proliferating hemangiomas; a 30-fold increase is detectable versus location-matched normal tissues [77]. As the hemangioma involutes, the concentration of mast cells declines and fibroblasts and macrophages can be seen to congregate near the remaining mast cells. Later stages of involution show the formation of cytoplasmic bridges between mast cells and active fibroblasts, intimating that the mast cells recruit and direct fibrosis within the involuting infantile hemangioma [78]. Despite lacking an exact mechanism, resolution of these hemangiomas occurs in 49% of patients by 5 years of age and in 72% by 7 years of age [79]. Margileth and Museles found a similar regression rate of 30% at 3 years of age, 60% by 4 years of age, and 76% at 7 years of age [80]. Fig. 35.36 shows the progression of involution over 7 years in a patient.



Fig. 35.35 Involuting infantile hemangioma in a 7-year-old boy. He was treated as an infant with oral steroids alone. Now at age 7 his hemangioma has involuted, however, ptosis persists. The vision on the right is poor due to deprivation amblyopia

The decision to treat periocular hemangiomas is dependent on the consideration of four factors: the location of the hemangioma, the extent of the hemangioma, the degree of amblyopia or the potential for amblyopia development, and the presence of significant systemic hemangiomas. If no signs of amblyopia, anisometropia, severe proptosis with exposure keratopathy, induced astigmatism greater than 1.5 diopters, or total pupillary occlusion are present, reevaluation every 1–3 months is recommended to ensure that no progressive changes occur to induce amblyopia or adversely affect visual development. Despite the lack of ophthalmic indications, treatment may be necessary for periocular infantile hemangiomas if the potential for maceration and erosion of the overlying epidermis exists, which may in turn lead to scarring or infection. Some systemic hemangiomas that require treatment cause obstruction or bleeding in the oral, nasal, or pharyngeal passages and pose breathing or feeding problems for the child.

A variety of treatments are available for infantile hemangiomas. However, oral beta-blockers has been the new goal standard of therapy since 2008 when it was first published as a treatment for severe infantile hemangiomas [81]. While corticosteroids can accelerate the involutional process and may be administered by the oral, injectable, or topical routes, this treatment is a second-line therapy now [82–87]. The systemic treatment of infantile hemangiomas is covered more extensively in Chap. 6, and eyelid involvement is discussed in greater detail in Chap. 23.

In the past, intralesional injection of the steroid has been a popular for infantile hemangioma. This, however, has carried the risk of a retinal vascular occlusion and with the advent of oral and topical beta-blockers has fallen out of favor [81, 88].

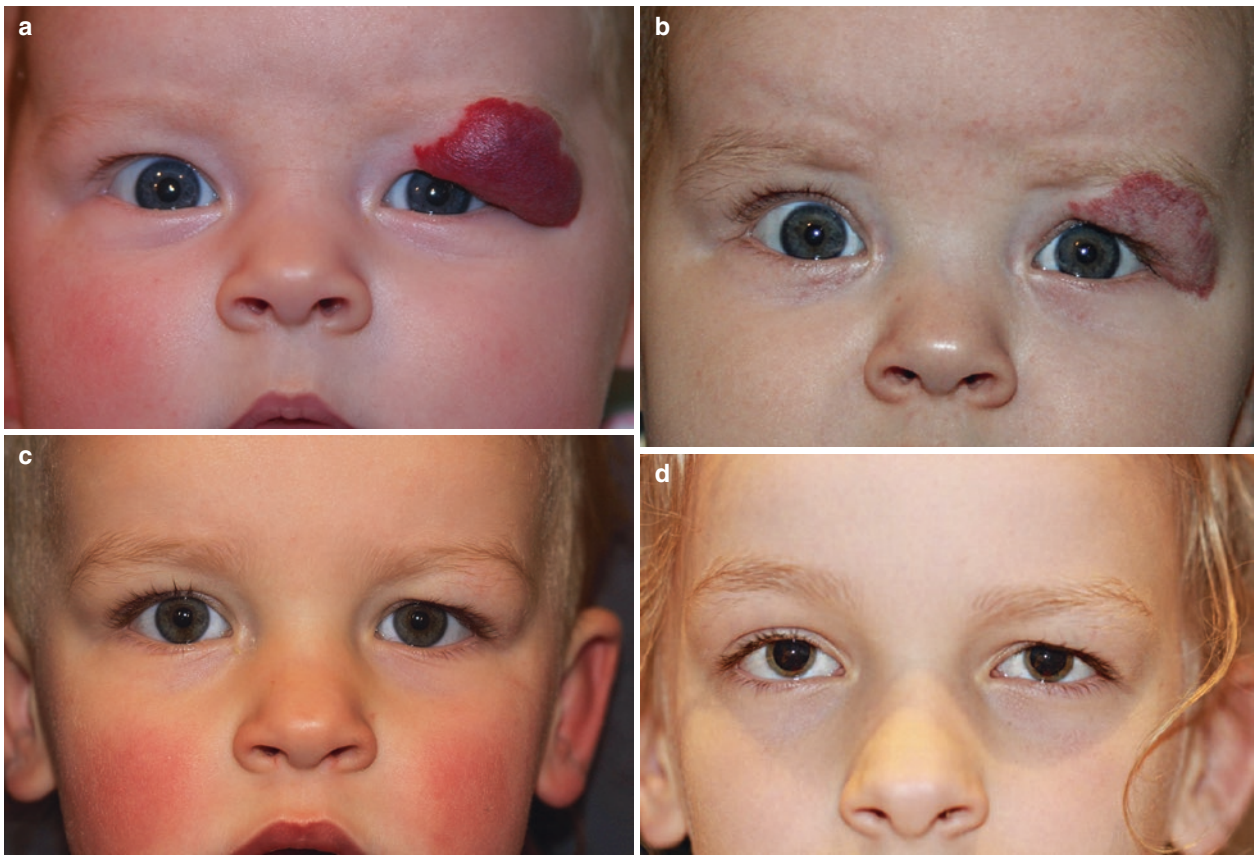


Fig. 35.36 The progression of periorbital infantile hemangioma. (**a**) Age 3 months. There is a large left upper eyelid hemangioma causing mechanical ptosis. (**b**) Age 12 months. After being treated with oral prednisone for 4 months the lesion is lighter in color and the ptosis has improved. (**c**) Age 3 years. The hemangioma has further involuted though there is persistent skin overhang. (**d**) Age 7 years. There is still significant skin overhang despite near-full involution of the left eyelid hemangioma

Even with a good response to oral beta-blocker, a superficial component to an infantile hemangioma may need additional treatment. Cutaneous hemangiomas have thus been successfully treated with a variety of other modalities. External beam radiation therapy, noncontact Nd:YAG laser, argon laser, continuous wave 577-nm tunable dye laser,carbon dioxide laser, and injections of interferon alfa-2b have been successful in treating infantile hemangiomas [75, 83–94]. This is discussed in further detail in Chap. 6. The noncontact Nd:YAG laser and the argon laser both use thermal injury to the blood vessel as a way to induce vessel closure and lesion involution. The argon laser is absorbed superficially while the noncontact Nd:YAG laser penetrates to a depth of 5–7 mm, yielding greater potential lesion shrinkage. Scarring results from the vessel closure and is somewhat unpredictable with either modality. The carbon dioxide laser coagulates blood vessels in a defocused mode and will create significant scarring if used for the visible surface features of an infantile hemangioma. It has usefulness during surgical resection of residual hemangiomas due to its combination cauterizing and cutting capabilities (see Fig. 35.39). The tunable dye laser operating at 577 nm is selectively absorbed by the beta peak of oxyhemoglobin. Isolated cautery of dermal capillaries can be achieved with short exposures (<10 ms), while adjusting the wavelength to 585 nm coupled with longer exposures can achieve deeper penetration while maintaining vascular selectivity [74].

The surgical excision of infantile hemangiomas is a viable alternative to nonsurgical treatments in hemangiomas that have failed to regress adequately, in those in which visual dysfunction still remains, and in cosmetically unacceptable lesions [95, 96]. Careful surgical excision attempting to debulk rather than completely excise the lesion coupled with clear surgical goals and adequate exposure of the operative area is essential prior to embarking on these sometimes challenging cases, especially if diffuse infiltration of the hemangioma is identified. Isolation and preservation of important normal orbital structures is essential. Preoperative orbital imaging is a necessity to help determine the extent of the lesion and plan the surgical approach (Figs. 35.37 and 35.38). The carbon dioxide laser can be a useful surgical adjunct in

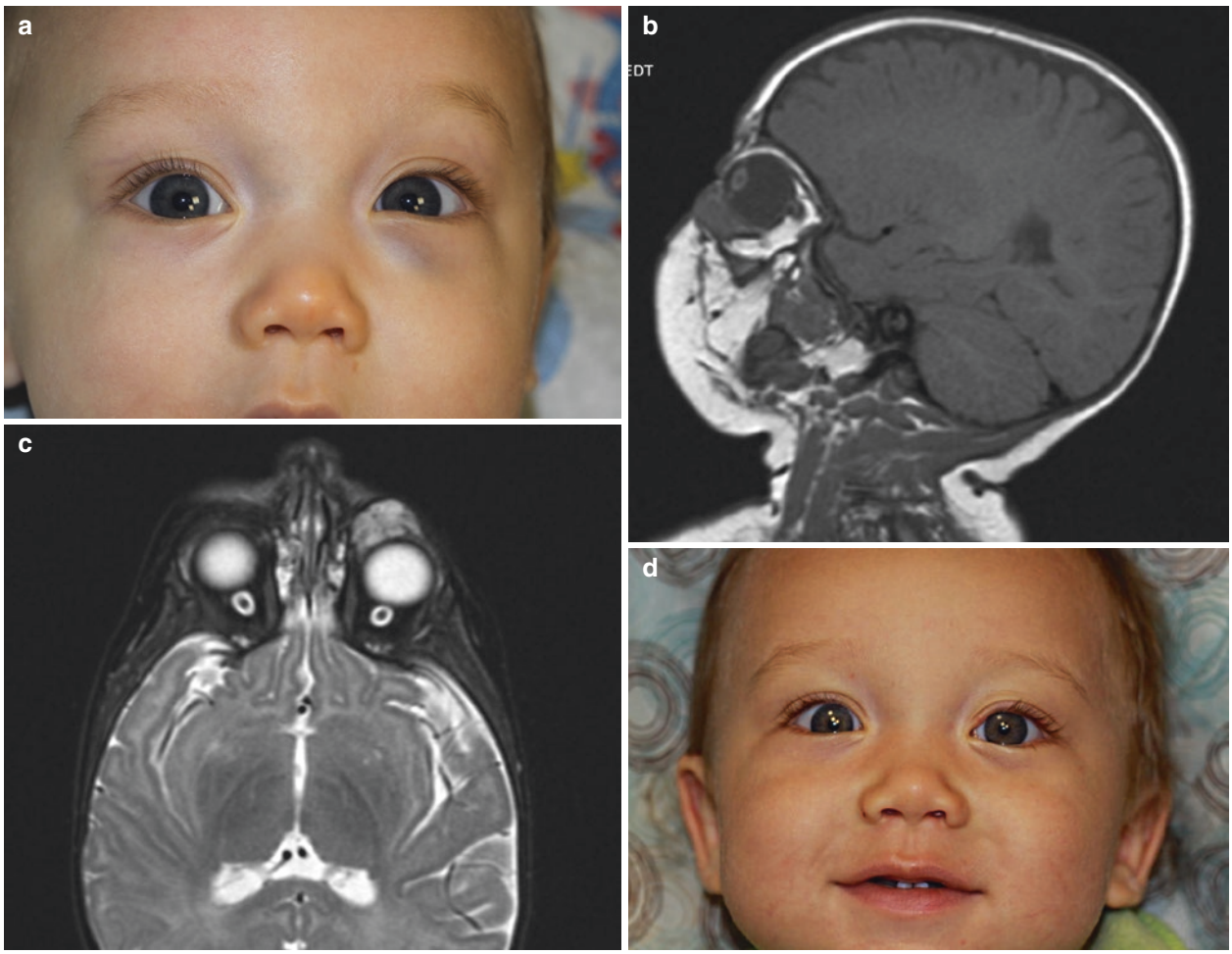


Fig. 35.37 Surgical debulking of an orbital infantile hemangioma. (**a**) Preoperative photo. There is a mild left hyperglobus and left hypertropia. (**b**) T_1-weight sagittal MRI showing an infantile hemangioma of the left orbit inferior to the eye and pushing it upward. (**c**) T_2-weighted axial MRI showing the anterior extent of the lesion. (**d**) Postoperative photo taken 4 months after surgical debulking. A transconjunctival approach was made just below the tarsus of the lower eyelid without the use of canthotomy or cantholysis

helping to limit blood loss, but must be used with care to avoid damaging normal structures (Fig. 35.39). Isolated, small hemangioma of the eyelid can be removed with relative ease (Fig. 35.40) if there is poor response to oral beta-blocker and there is a concern for occlusion amblyopia.

Venolymphatic Malformation (Lymphangioma)

Lymphangiomas are now classified by the International Society for the Study of Vascular Anomalies (ISSVA) as a malformation of venolymphatic origin. These malformations are one of the more frustrating orbital conditions requiring treatment to avoid visual compromise. They are a benign collection of thin-walled lymphatic and vascular channels isolated from the hemodynamics of the arterial and venous systems. Similar to infantile hemangiomas, these lesions can be classified into superficial, deep, and combined types. Signs and symptoms of its presence often are visible in the first 5 years of life.

In Table 35.1, 51 cases of lymphangiomas (VLM) involving the orbit were reported in the six series of pediatric orbital tumors for a frequency of 2.8%. Male and female frequency is equal, without predilection for either orbit. Bilateral cases are distinctly rare. Jones reported his experience with 62 lymphangiomas in 1959, which remains the largest reported series to date [97]. His observations regarding the involvement of periocular structures reflects the cumulative experience of other authors since his report: 25% of patients have only orbital involvement (deep lymphangioma), 32% demonstrate only conjunctival or lid involvement (superficial lymphangioma), and approximately 43% involve both anterior and posterior periocular structures (combined lymphangioma). The lesions persist

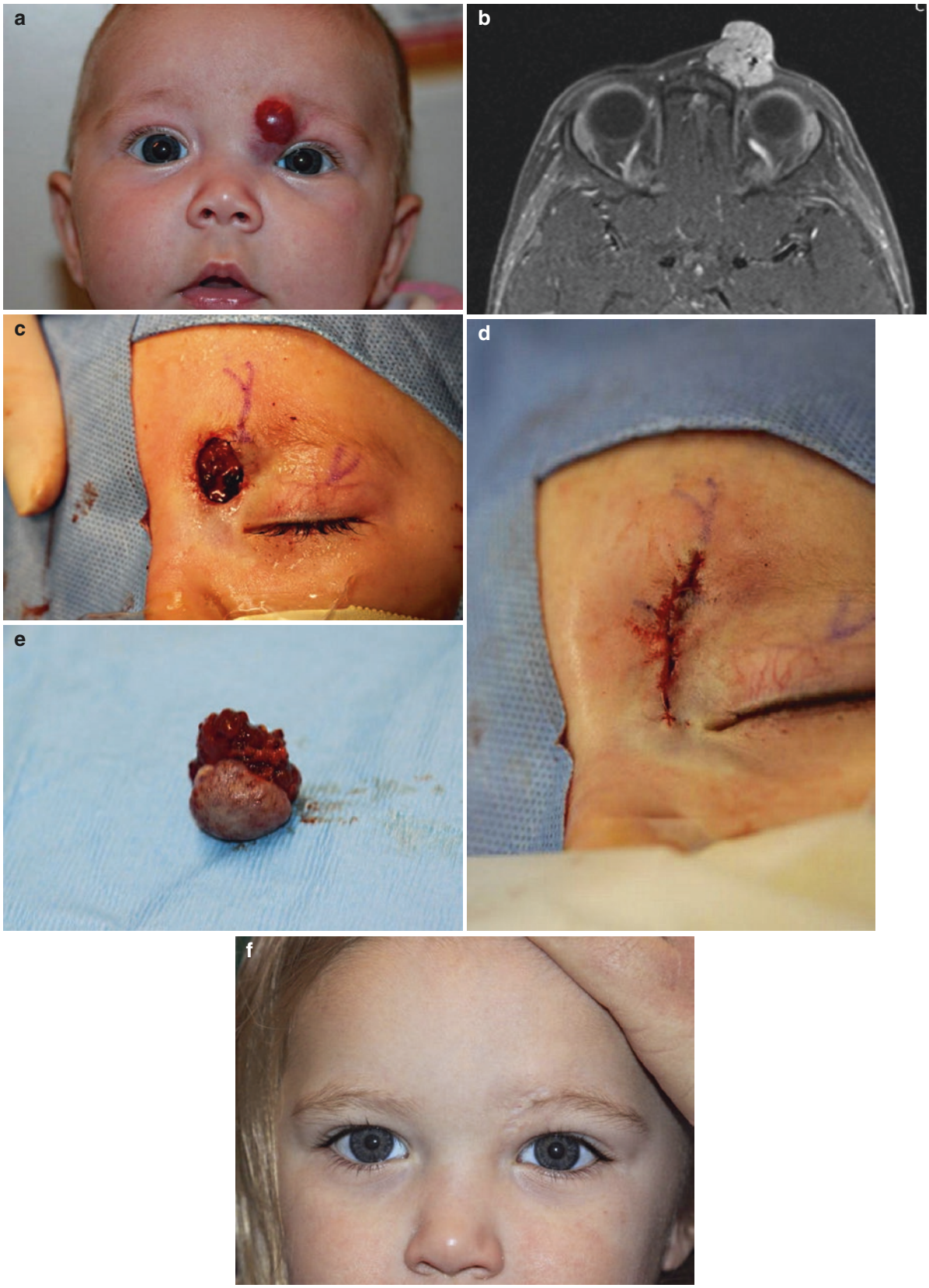


Fig. 35.38 Surgical debulking of a large infantile hemangioma. (**a**) Preoperative photo showing a large anterior lesion in the superomedial brow and eyelid. (**b**) T_1-weighted MRI showing the lesion as along the medial orbital rim, but anterior to the orbital septum. (**c**) Intraoperative photo taken after debulking of the lesion. An ellipse of skin was removed. (**d**) Intraoperative photo showing closure of the incision. (**e**) Photo of the infantile hemangioma lesion. (**f**) 1 year after surgery. A superomedial brow scar is visible. This case illustrates the risk of surgical excision of visible scar formation and supports the medical treatment approach first as a more ideal option

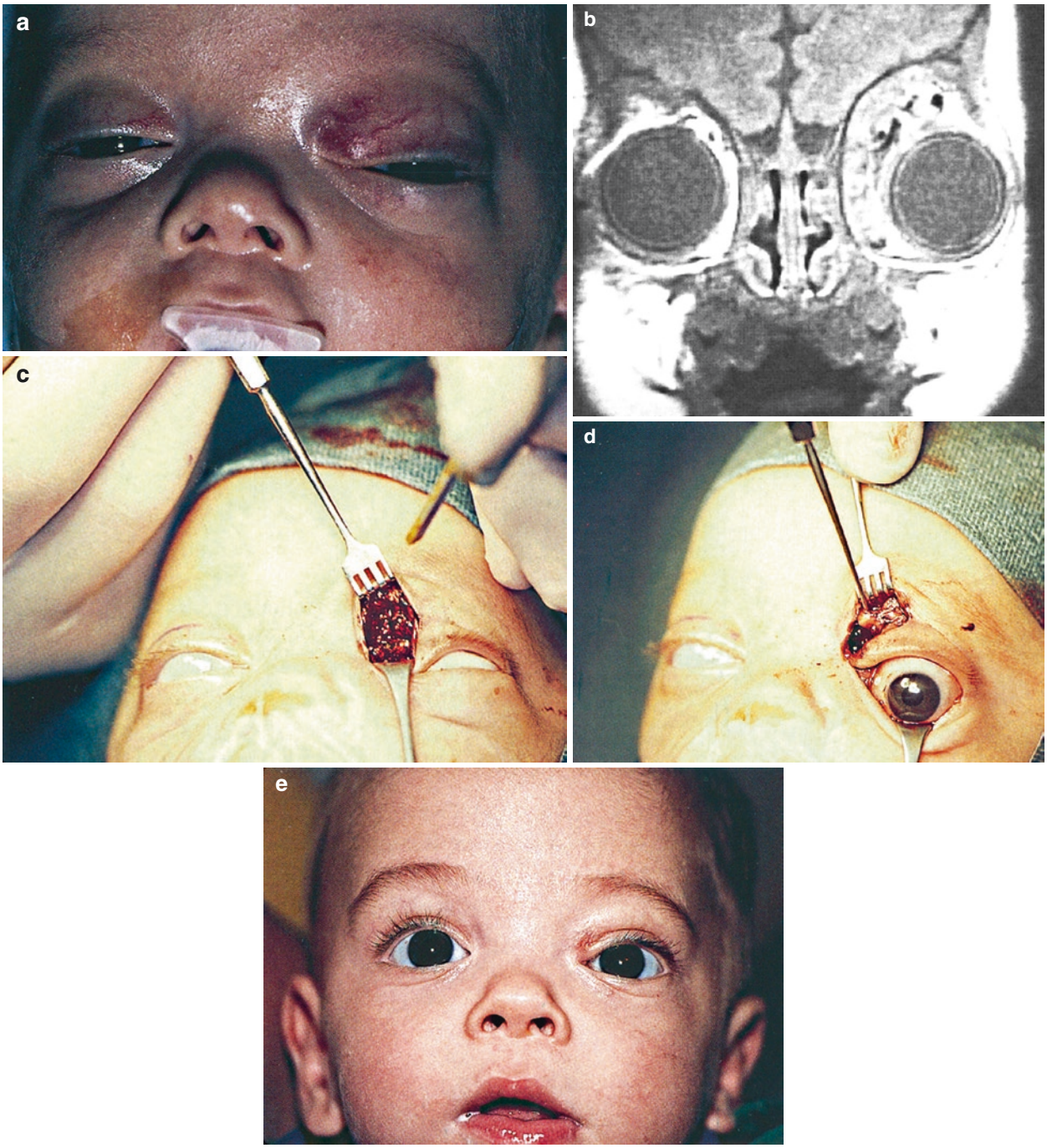


Fig. 35.39 Deep medial and superior capillary hemangioma. (**a**) An 8-month-old male with significant deep medial and superior capillary hemangioma producing proptosis, globe dystopia, and restricted extraocular motility with resultant amblyopia unresponsive to steroids. (**b**) Coronal MRI showing extent of the hemangioma. (**c**) Intraoperative excision through medial lid crease incision utilizing carbon dioxide laser for cauterization and de-bulking of the tumor. (**d**) Careful surgical dissection allows identification of normal orbital structures; the superior oblique tendon is isolated on a muscle hook and results in the globe depression seen in the photograph. (**e**) A 3-month postoperative photograph demonstrating marked reduction of proptosis and globe displacement

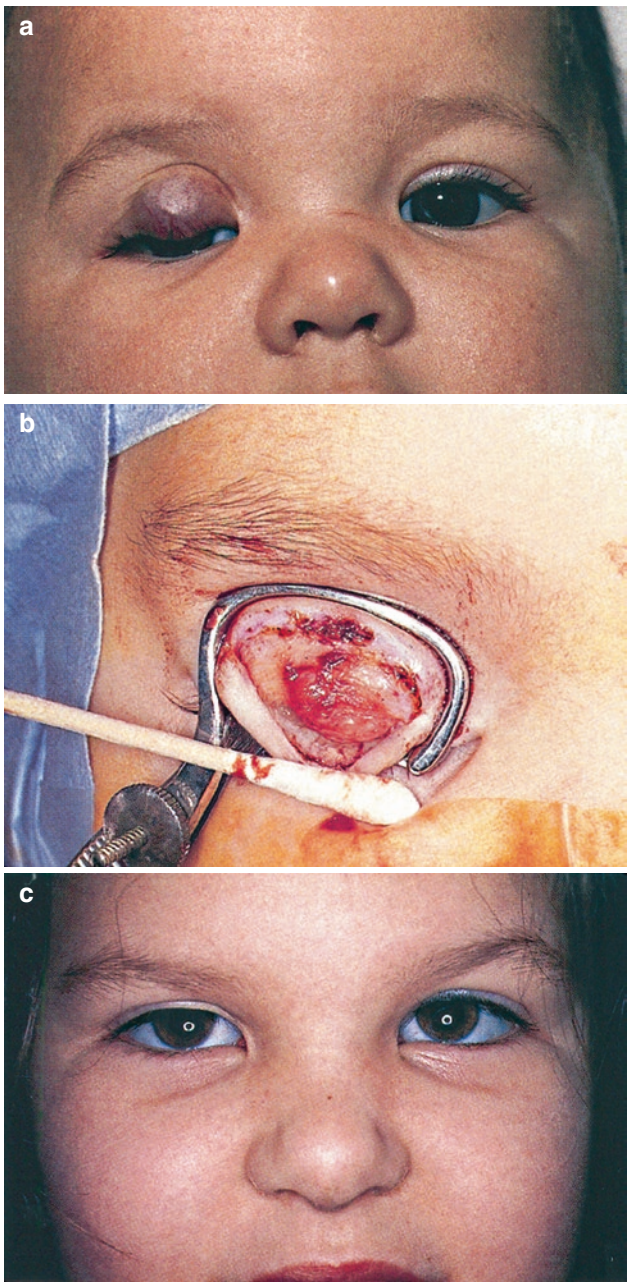


Fig. 35.40 Superficial hemangioma. (**a**) Isolated superficial hemangioma centered in the central upper lid with obstruction of visual axis and demonstrable amblyopia. Two previous intralesional steroid injections failed to produce significant involution. (**b**) Surgical excision demonstrates the isolated lesion. Repair of a central levator aponeurosis defect was necessary. (**c**) A 1-year postoperative photograph showing excellent lid position with slight residual ptosis but clearance of visual axis

for life and rarely show any growth or involution once the patient is past 18 years of age. Ten percent of patients may have involvement of other head and neck structures with a peculiar predilection for palatal mucosa when deep orbital involvement is present (Fig. 35.41).

The clinical signs and symptoms that announce the presence of orbital VLM are dependent on the location of the lesion within the orbit. Superficial lymphangiomas typically present earlier in life due to their visible component and anterior placement [98]. If conjunctival elements are present, small cystic or blood-filled dilated channels can be visible on the globe, in the fornix, or on the palpebral conjunctiva (Fig. 35.42). Subcutaneous VLM appear as soft, spongy masses frequently involving the anterior orbit. The periocular position causes globe displacement away from the lesion and may affect ocular motility. No specific cutaneous changes differentiate it from similarly appearing lesions, such as neurofibromas and infantile hemangiomas. Enlargement may occur during upper respiratory tract infection due to expansion of lymphoid tissue that is present in many orbital lymphangiomas [99].

Deep VLM are typically diagnosed later than their superficial counterparts due to the lack of any anterior stigmata. Periodic enlargement with mild trauma or upper respiratory infection can infer their presence. The most common presenting sign results from sudden hemorrhage into intralesional cystic spaces, producing the sudden onset of proptosis, pain, decreased vision, limited motility, and periocular ecchymosis [100]. These cystic enlargements, termed "chocolate cysts" because of the dark, thick material within the cyst found on surgical exploration, can produce tremendous amounts of proptosis, exposure keratitis, optic nerve compromise, and conjunctival edema or hemorrhage [101]. Emergent orbital decompression by ultrasonically guided percutaneous needle aspiration, open drainage, or orbital decompression may be necessary to prevent permanent visual loss (Figs. 35.43 and 35.44) [102].

MR imaging is particularly helpful in localizing the area of hemorrhage, ascertaining the extent of the lymphangioma, and helping to prepare a surgical approach [103, 104]. Clear distinction between lymphatic spaces, hemorrhagic components, and even the age of the hemorrhages can be ascertained using MRI. Acute hemorrhages have deoxygenated hemoglobin, yielding a low signal intensity on both T_1- and T_2-weighted images. Subacute hemorrhages have undergone red blood cell lysis with release of methemoglobin giving a medium signal intensity on T_1-weighted images and high

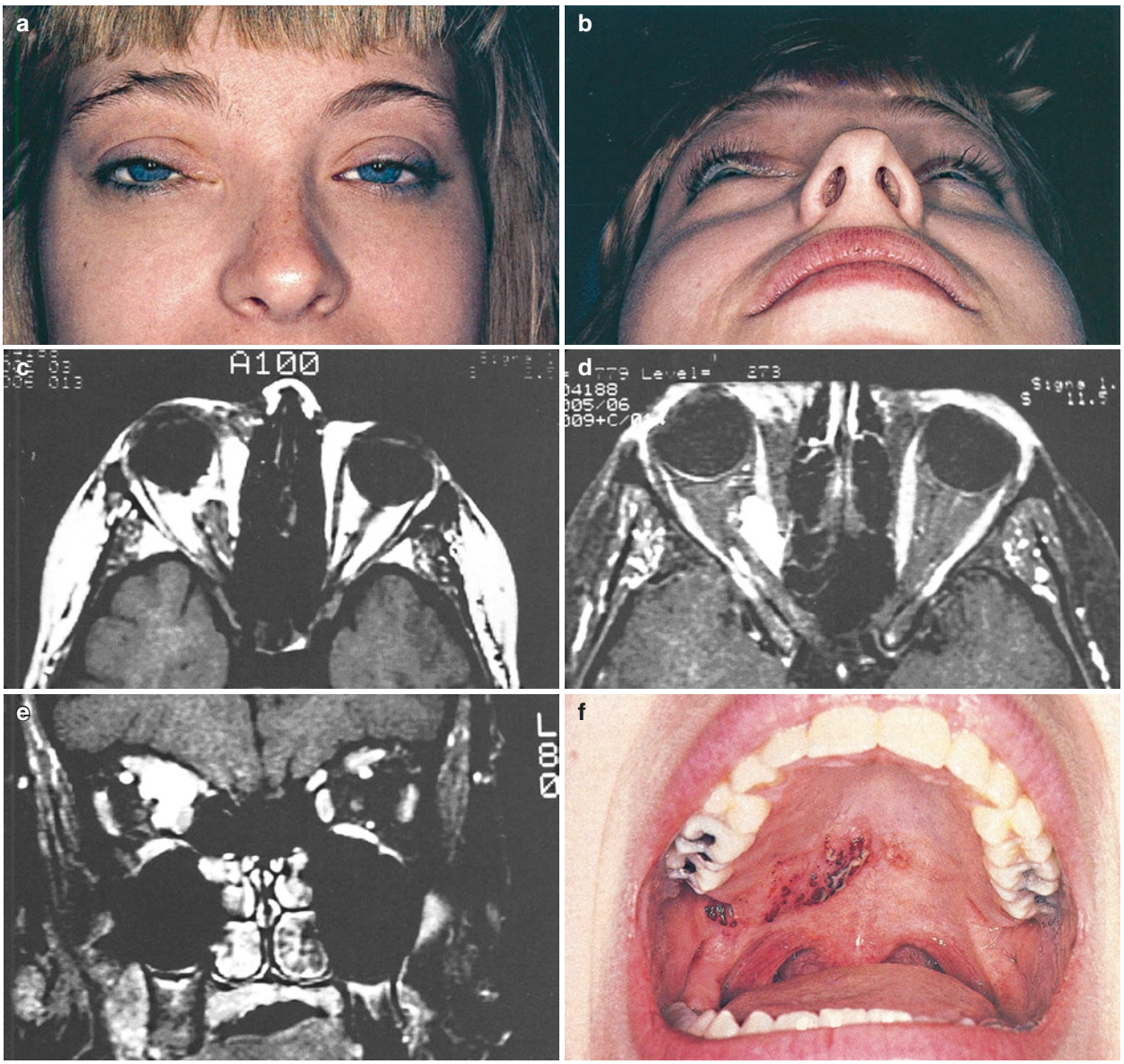


Fig. 35.41 Combined lymphangioma. (**a**) An 18-year-old female with right proptosis and globe displacement from a combined lymphangioma. Note lateral globe dystopia from medial canthal involvement. (**b**) Mild proptosis apparent on right. (**c**) T_1-weighted axial MRI demonstrating low signal intensity apical lymphangioma and medial canthal component. Serpiginous channels within the lesion are visible in the medial canthal area. (**d**) Contrast-enhanced T_2-weighted axial image shows a high signal intensity in both components indicative of chronic blood products (hemosiderin). Note the apical lesion outlining the optic nerve, which travels within the lesion. (**e**) Contrast-enhanced coronal T_2-weighted image shows high signal intensity of the lymphangioma and demonstration of its relationship to the extraocular muscles and optic nerve. (**f**) Intraoral photograph of this patient showing ipsilateral palatal mucosal lymphangioma that would bleed spontaneously

signal intensity on T_2-weighted images. Chronic cysts have had their blood components transform into more degenerated products such as ferritin and hemosiderin, which have high signal intensities as well. Some cysts can have repetitive hemorrhages and may show both acute and chronic components on imaging studies. The VLM itself, without hemorrhage, is a rather diffuse lesion, frequently extending both intraconally and extraconally, and demonstrates low signal intensity on T_1-weighted images and high signal intensity on T_2-weighted images. Gadolinium can show enhancement of the rim of well-circumscribed lesions, but fat suppression techniques provide the best image definition with enhanced



Fig. 35.42 Conjunctival involvement of a venolymphatic malformation

studies. Smaller hemorrhages not affecting visual or ocular function should be managed conservatively without surgical intervention, since much of the volume of the chocolate cyst will absorb over time. Imaging of orbital VLM is also covered in Chap. 32 [105]. The monoclonal antibody D2–40 is a highly sensitive and specific marker of lymphatic endothelium, which can now aid in identifying VLM and distinguish these tumors from hemangioma [106].

Treatment for VLM has evolved since the introduction of sclerotherapy. In the past, oral steroids were used as a temporizing agent with surgery being reserved for cases of vision loss and disfigurement. With the advances of sclerotherapy, however, surgery can be considered as a second-line treatment for failures to responds to sclerotherapy or for severe cases of vision loss requiring surgery decompression (Fig. 35.43). No oral medical therapy alone has been shown to be effective. Sildenafil has been

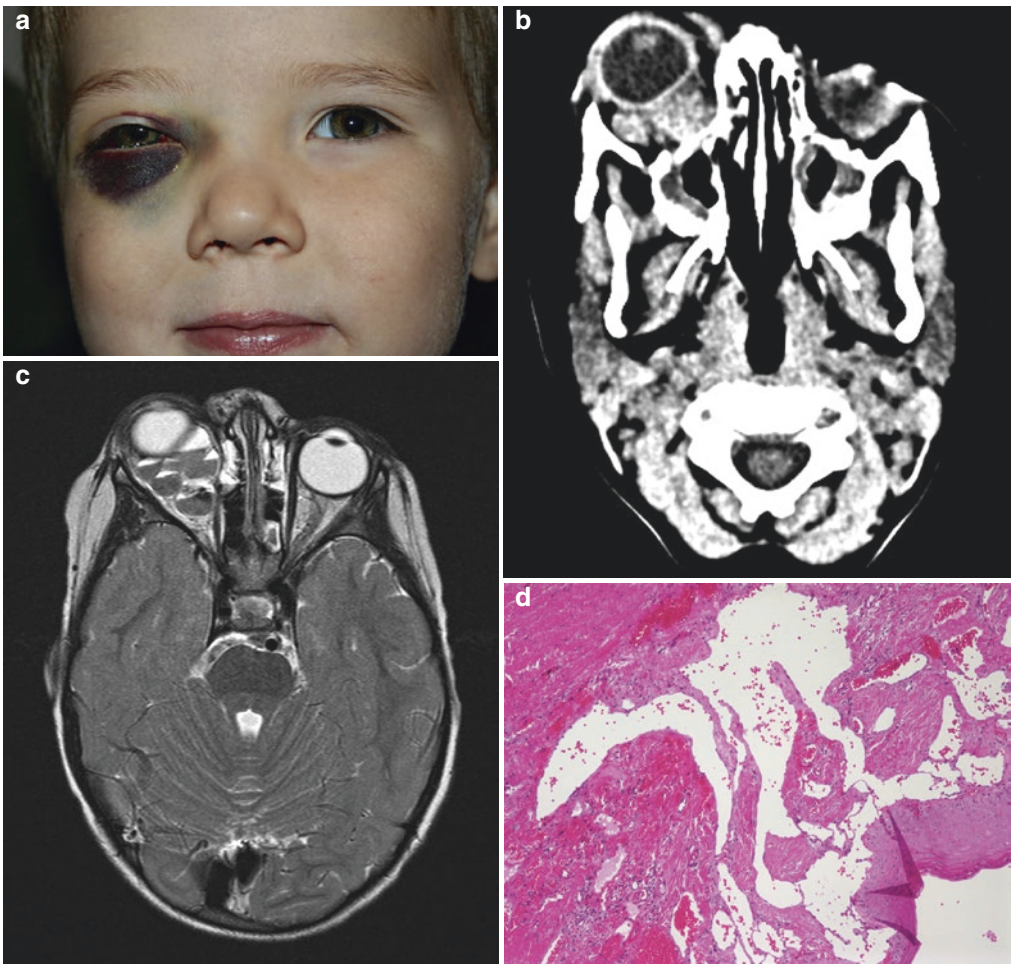


Fig. 35.43 Orbital venolymphatic malformation with vision loss. (**a**) 3 year-old with sudden onset proptosis, ecchymosis and edema. (**b**) Orbital CT performed at the emergency room where the patient presented showed an intraconal mass. (**c**) T_2-weighted MRI performed 1 week after onset of symptoms shows greater proptosis and large macrocysts within the extraconal and intraconal space. (**d**) Low-power micrograph of the surgical specimen demonstrating gaping vascular spaces in the superficial dermis separated by fibrous septae and lined by flattened endothelium. Scattered red cells are present within these spaces, consistent with previous hemorrhage (H&E, 100X)

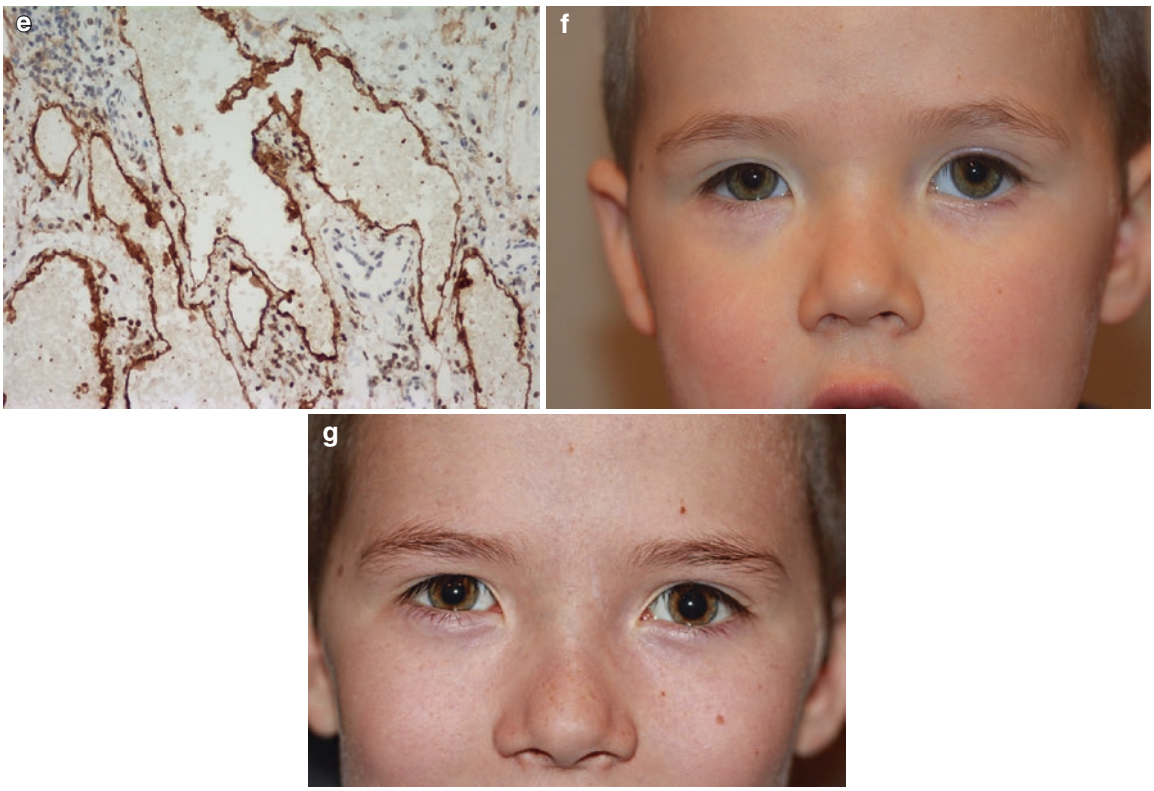


Fig. 35.43 (continued) (**e**) The monoclonal antibody D2–40 is a highly sensitive and specific marker of lymphatic endothelium, which can now aid in identifying VLM and distinguish these tumors from hemangioma [106]. (**f**) 3 months post-operative for a medial and lower eyelid transconjunctival orbitotomy with debulking of the VLM. (**g**) 7 years after surgery with no clinical evidence of recurrence



Fig. 35.44 Hemorrhage within a venolymphatic malformation. Severe proptosis and globe exposure due to extensive hemorrhage within an orbital lymphangioma

used with some success, but only in small a very small series [107].

Intraorbital sclerotherapy can be performed by the surgeon under direct visualization or percutaneously [108]. The ideal treatment is as a combined approach with an interventional radiologist under fluoroscopic guidance. Sclerosing agents that have been used are ethanol, doxycycline, sodium morrhuate, OK-432, sodium tetradecyl sulfate, and bleomycin under direct or fluoroscopic guidance [108–112]. Cahill et al. published their experience in treating 20 micro- and macrocystic orbital lymphatic malformations. 14 of the lesions were deep, 4 superficial, and 2 were combined. 14 of the 20 patients underwent percutaneous sclerotherapy with in an interventional radiology suite with the patient under deep intravenous sedation or general anesthesia. Access to macrocysts (>1 cm) was performed with ultrasound guidance and a coaxial 5F pigtail catheter system. The macrocysts were treated with dual-drug chemoablation, with injections of sodium tetradecyl sulfate 3%, followed by aspiration and then injection of ethanol 98% solution. After aspiration of the ethanol, macrocyst drainage catheters were placed with suction drainage for 3 days before catheter removal. The average number of treatments required to achieve complete cyst ablation in patients with lymphatic malformations was 1.7 and for venolymphatic malformations was 3.0 [112].

In our experience, as a combined procedure with interventional radiology, we have used the agent bleomycin for extraconal lesions and doxycycline for intraconal lesions. The avoidance of bleomycin in the intraconal space is due to concern for inflammation and the risk for optic neuropathy. Fig. 35.45 depicts a patient treated by our service. The patient had a severe recurrence 18 months after her first treatment but has been symptom-free after the second round of sclerotherapy.

Surgical approaches to orbital venolymphatic malformation are very challenging. Especially in cases where there is diffused microcystic disease (Fig. 35.46). In some cases orbital decompression can be effective in relieving associated headaches and corneal exposure (Fig. 35.47). Adequate preoperative imaging is paramount before surgery. Ideally, this is obtained within days before surgery as these lesions can expand and contract. Conservative supportive care is advised unless significant visual dysfunction, proptosis with

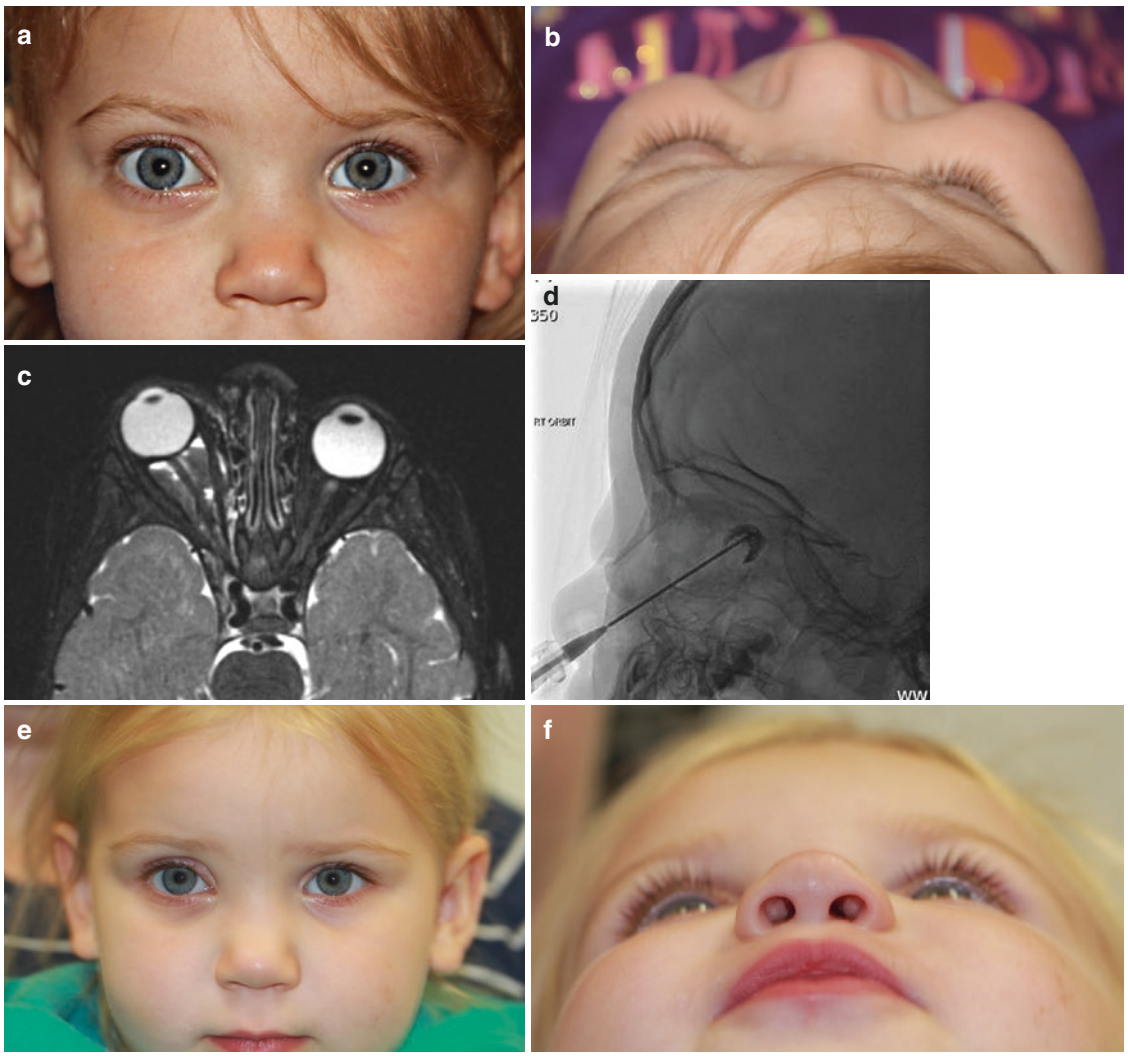


Fig. 35.45 Percutaneous sclerotherapy by interventional radiology for the treatment of orbital venolymphatic malformation. (**a**) 2 year-old girl with sudden painless proptosis. (**b**) Scalp view showing proptosis. (**c**) T_2-weighted axial MRI showing an intraconal mass with multiple cysts and fluid levels. (**d**) Fluoroscopy guided sclerotherapy with intralesion injection of bleomycin. (**e**) 3 months post-sclerotherapy. (**f**) 3 months post-sclerotherapy worm's eye view with reduction of proptosis

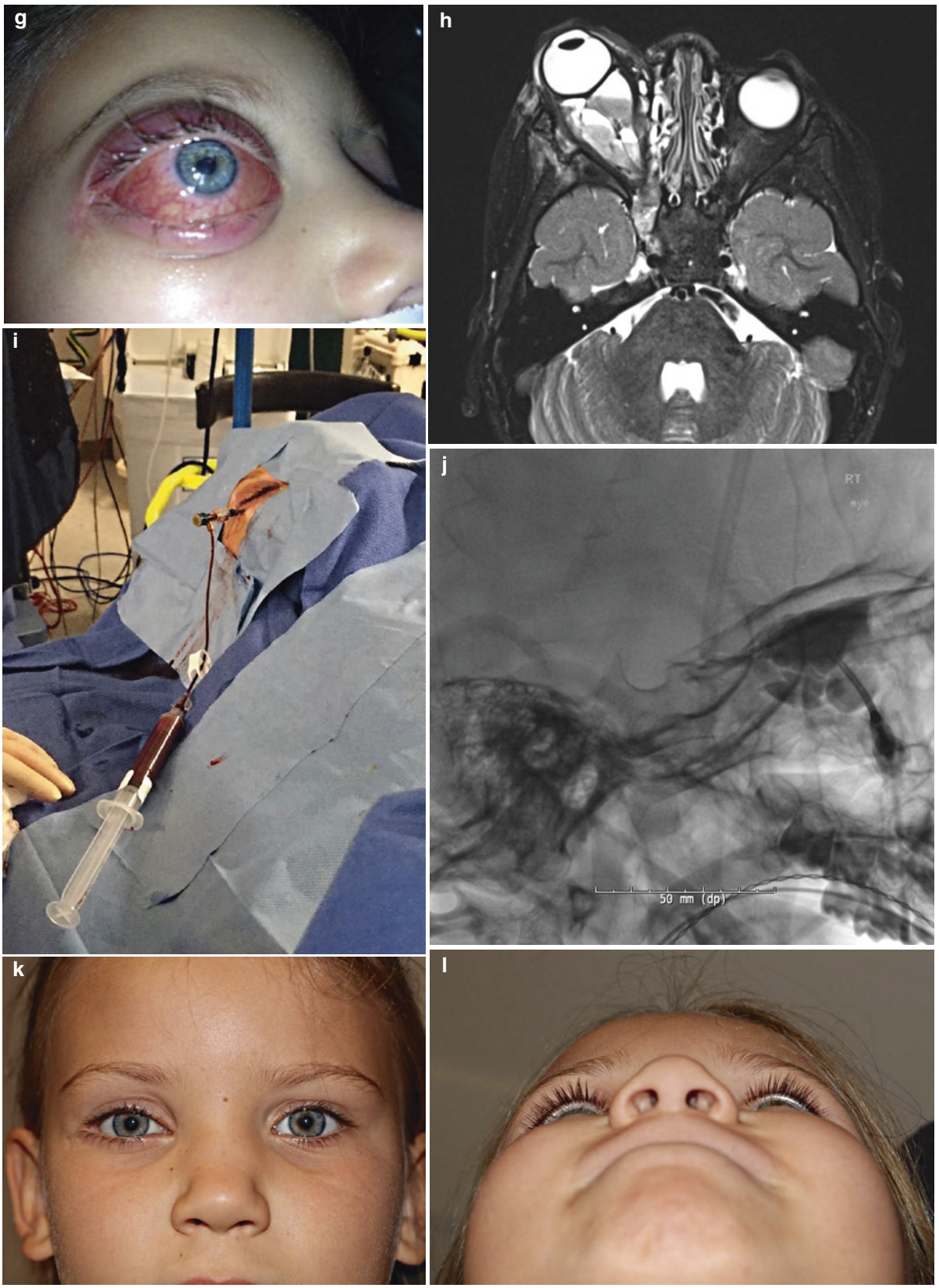


Fig. 35.45 (continued) (**g**) Age 4, 2 years after first treatment with severe proptosis, pain and vision loss (afferent pupillary defect). (**h**) T_2-weighted axial MRI showing an intraconal mass with multiple cysts and fluid levels noted to be larger than the previous study. (**i**) Intraoperative photo showing an intraorbital catheter needle draining 10 ml from the orbital VLM under ultrasound guidance. (**j**) Intraoperative fluoroscopy showing the injection of 4 U of bleomycin into a macrocyst of the orbital VLM. (**k**) Age 5, 1 year after the second sclerotherapy treatment with normal vision and resolution of proptosis. (**l**) Worm's eye view showing reduction of proptosis

exposure, pain, or optic nerve compromise is identified. Careful counseling of the parents and the patient is mandatory prior to any attempt to improve the cosmetic appearance of the affected individual. Realistic goals should be carefully outlined prior to surgery. The intraoperative use of carbon dioxide lasers, bipolar cautery, and possibly B-scan ultrasonography can help limit blood loss, improve resection of lymphatic components, and help locate small cystic structures in an often disorienting surgical field [104]. Some authors have advocated the used of tissue glues such as fibrin glue or cyanoacrylate [113, 114]. Since complete removal is not routinely achieved, surgical resection should be limited to avoid damage to normal orbital structures. Reoperations may be necessary, especially with diffuse VLM, because of recurrent cystic hemorrhages. In the most extreme of cases with severe disfigurement, intractable pain, and gross orbitofacial disproportion combined with compromised visual and ocular function may necessitate exenteration to end symptoms and improve the quality of life for the patient. It should be stressed, however, that with careful planning, sclerotherapy is often the most effective treatment modality in treating these lesions to preserve vision and restore cosmesis.

Orbital Varix

The incidence of varicosities involving the orbit in the pediatric population is low. In Table 35.1 we find only 13 varicosities in the orbits of children among a total of 1820



Fig. 35.46 The challenge or surgical intervention in the treatment of orbital venolymphatic malformation with adnexal involvement. (**a**) 1-year-old boy with mechanical ptosis due to a combined VLM with anterior extension. (**b**) Status post eyelid debulking and levator resection. (**c**) Age 4 with expansion of eyelid and orbital VLM. (**d**) 1-year status post orbital and eyelid debulking

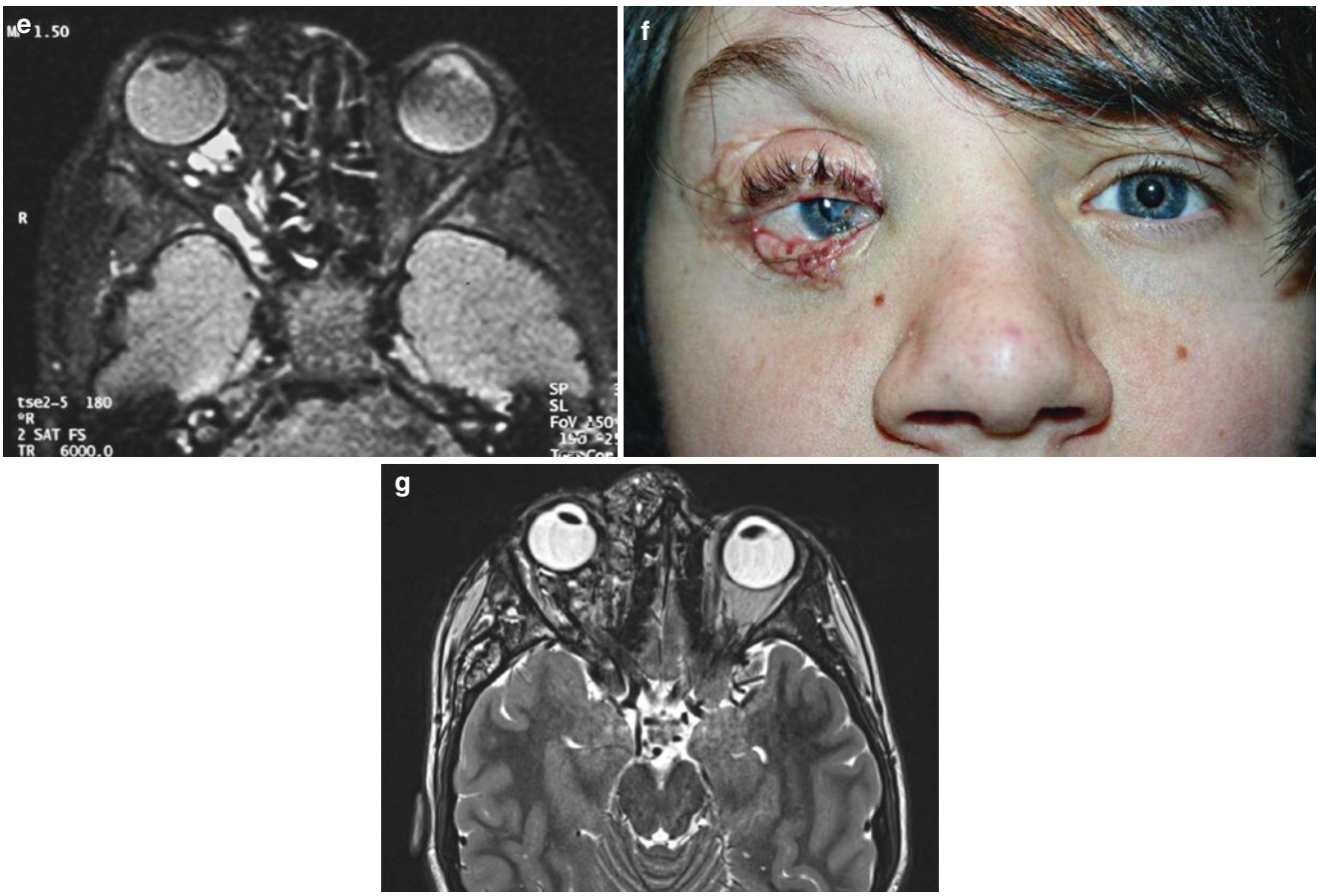


Fig. 35.46 (continued) (**e**) T_2-weighted axial MRI showing orbital VLM. (**f**) Age 16 with extensive conjunctival scarring. (**g**) Age 16 T_2-weighted axial MRI showing extensive intra- and extraconal microcystic VLM

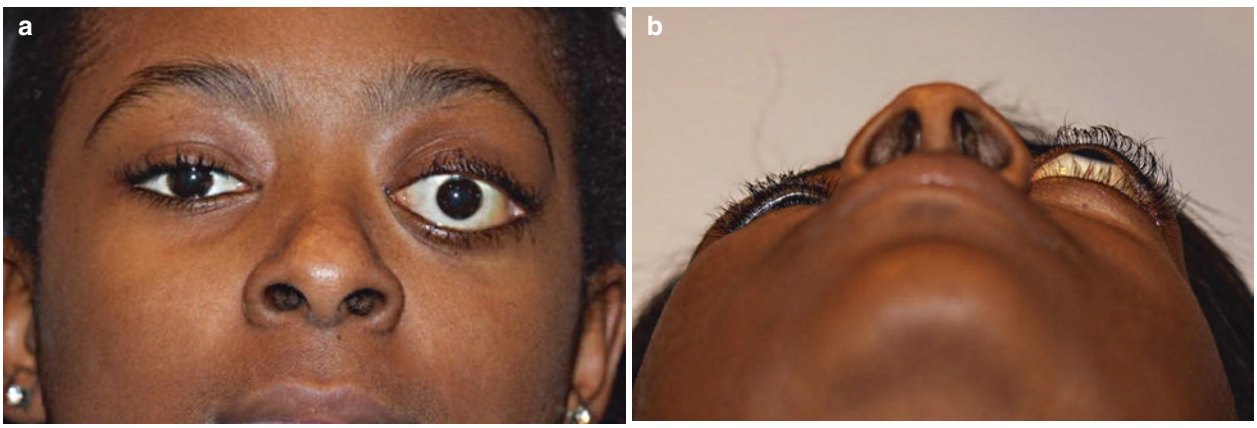


Fig. 35.47 The use of orbital decompression to reduce proptosis, improve cosmesis and resolve associated headaches. (**a**) A 17-year-old female with severe left sided proptosis due to an orbital venolymphatic malformation (VLM). (**b**) Worm's eye view showing extent of relative left sided proptosis

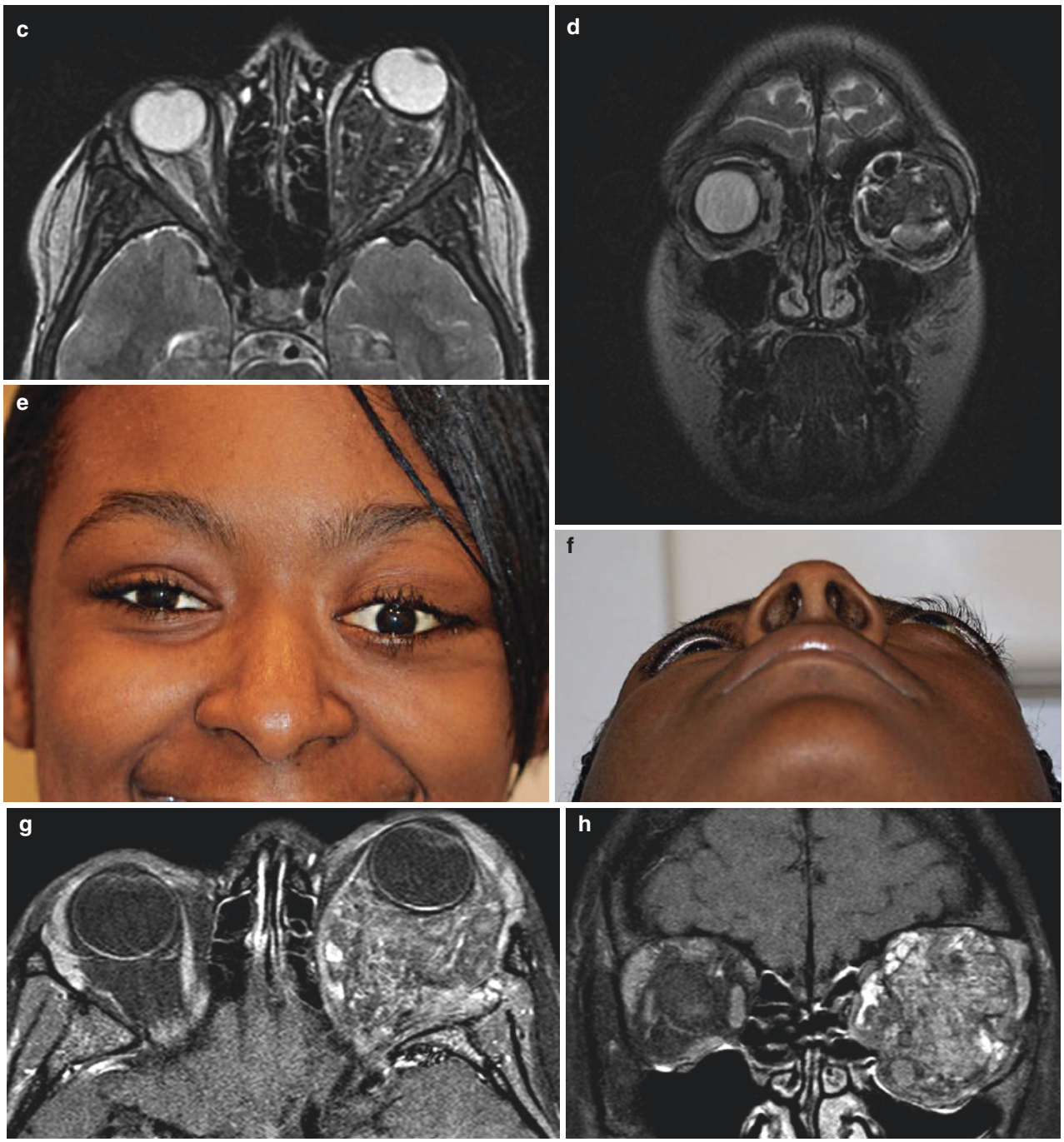


Fig. 35.47 (continued) (**c**) Axial T_s-weighted MRI showing a massive intraconal lesion that is predominantly microcystic. (**d**) Coronal T_2-weighted MRI showing inferior macrocystic component of the large orbital VLM. (**e**) Postoperative photo taken 1 year after a left 3-wall orbital decompression (lateral, medial and floor). (**f**) Worm's eye view taken1 year after a left three-wall orbital decompression showing reduction of left proptosis. (**g**) Postoperative Axial T_1-weighted MRI showing extent of orbital decompression with prolapse of the VLM through the bone windows. (**h**) Postoperative Coronal T_1-weighted MRI after 3-wall orbital decompression

lesions for an incidence of 0.7%. Of these, 12 were treated by one author who labeled them as distensible ($n = 4$) and nondistensible ($n = 8$) varicosities based on the presence of clinical evidence of connections to the systemic venous system [115]. A varix consists of either a segmental, irregular dilation in a vein (usually distensible) or a tangled mass of ectatic venous channels (usually nondistensible). If connected to the systemic venous system, distension occurs with Valsalva maneuvers, such as coughing, sneezing, bending, or straining. These distensions in the system can produce remarkable proptosis, strikingly visible venous enlargement, or pain (Fig. 35.48). Noticeable since

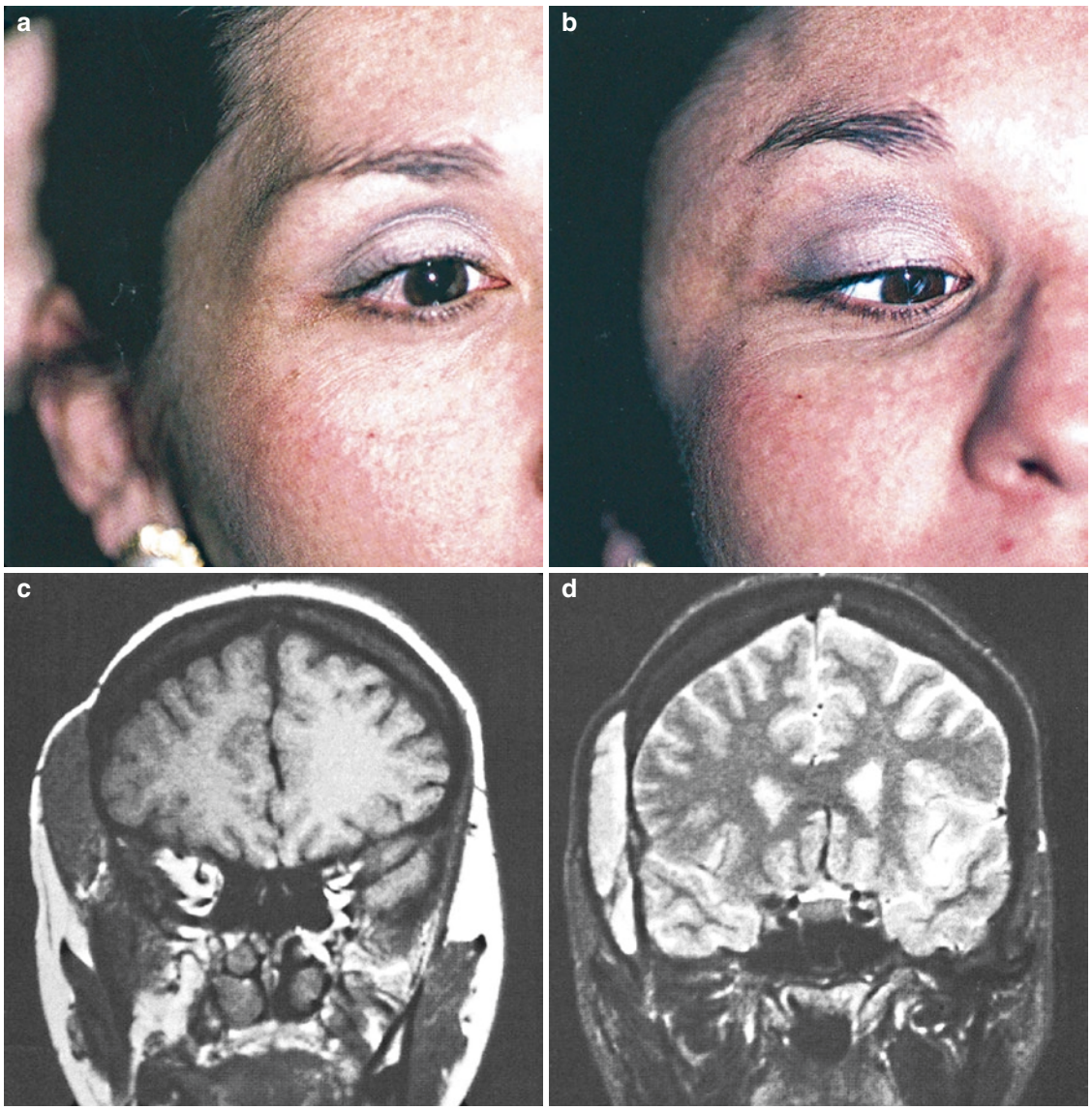


Fig. 35.48 Temple varix and Valsalva maneuver. (**a**) An 18-year-old female showing normal appearance to right periorbital area and temple without Valsalva. (**b**) Valsalva maneuver produces profound temple engorgement as well as mild proptosis and fullness of the superior lid sulcus. (**c**) Coronal T_1-weighted MRI showing a large temple varix with lateral intraorbital component. Note the low-intensity signal of the varix. (**d**) Coronal T_2-weighted MRI showing temporal varix and relatively high signal intensity usually isointense with brain

early childhood, periodic thrombosis and hemorrhage are rarely seen in the distensible variety. Thrombosis and hemorrhage do occur in the nondistensible varix and can produce more protracted orbital manifestations, including visual deficit and restricted ocular motility. Most interventions are performed to occlude or remove these vascular anomalies [116].

Other literature reports of pediatric orbital varicosities are rare [117, 118]. Wright's series of orbital vascular anomalies included 31 cases of a condition he termed congenital orbital varices. It actually accounted for the majority of all orbital vascular abnormalities among all ages seen at Moorfields Eye Hospital up to 1973; it was even more common than infantile hemangiomas in children or cavernous hemangiomas in adults. Wright determined that these were venous abnormalities based on periodic variable proptosis in some patients and demonstrable radiopacity produced after intravenous injection of contrast material through involved dilated subcutaneous veins. Some of the cases had cystic channels in the conjunctiva and hard palate reminiscent of lymphangiomas, along with sudden proptosis with intraorbital chocolate cysts, which has prompted other authors to question the categorization of the lesions presented by Wright [99]. Further evidence is the lack of lymphangiomas reported by Wright in his series. Rootman and Graeb suggested that there were similarities between

the nondistensible orbital varicosities he had seen clinically and the cases presented by Wright [115]. Despite questions as to the exact nature of all the lesions in Wright's series, it is clear that several of his cases involved distensible varicosities.

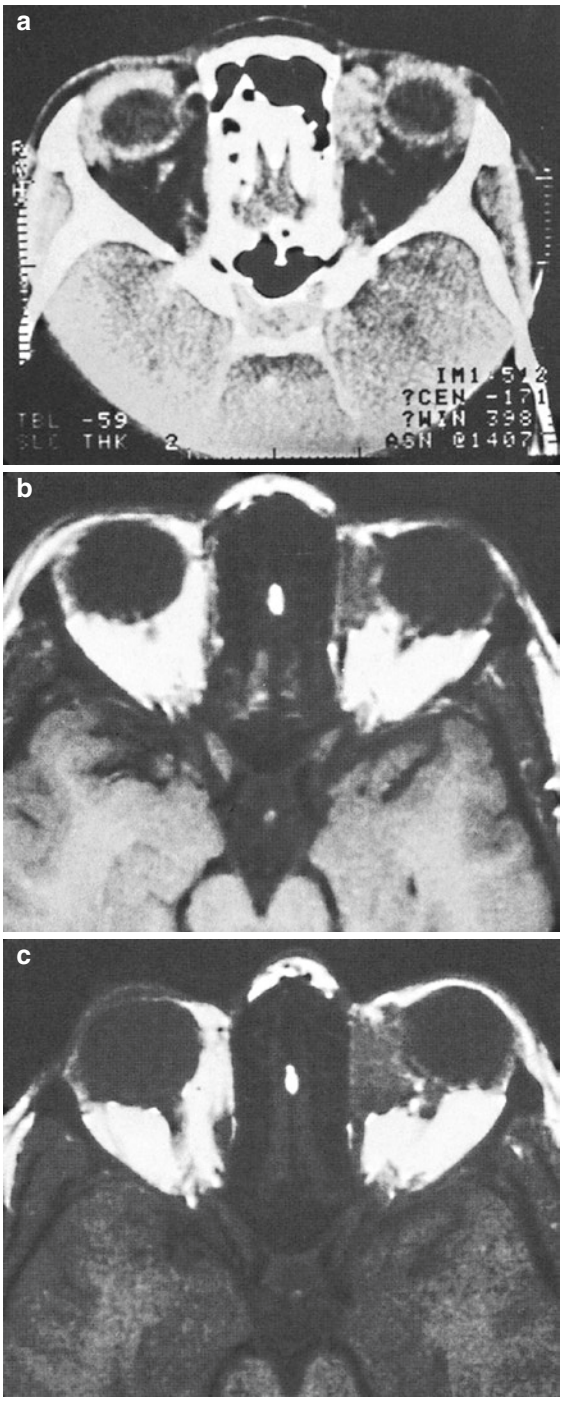


Fig. 35.49 Medial orbital varix. (**a**) Axial CT scan showing lobulated, irregular medial orbital varix displacing the globe laterally. (**b**) Axial T_1-weighted MRI depicting similar shape and position while patient is scanned in the supine position. (**c**) Repeat MRI with patient in a prone position showing distension and enlargement of the varix

Several imaging techniques are useful in evaluating the presence, identification, and extent of orbital varicosities. B-scan ultrasonography elegantly demonstrates the dilated vascular channels of orbital varicosities [119]. Color Doppler imaging supplies two-dimensional structural imaging and the ability to detect the speed and direction of blood flow within vessels, helping to ascertain the venous or arterial nature of a lesion [120]. The findings with color Doppler imaging correlate well with CT and MR findings. MR imaging in particular gives clear detail about the extent and content of varicosities. Its irregular border and localized nature, especially well seen on T_1-weighted images, help to differentiate it from other vascular abnormalities [121]. Its clinical distensibility can be replicated on MR imaging studies, furthering its differentiation (Fig. 35.49). CT can demonstrate phleboliths within the varix that are not seen with other orbital vascular abnormalities other than its rare occurrence with lymphangiomas (Fig. 35.50). Venography, once the standard for imaging orbital varices, has fallen out of favor with the success of noninvasive imaging techniques [122].

Recent advances in interventional radiology have offered an alternative to surgical treatment. Transcatheter embolization with coils, direct percutaneous injection of n-butyl cyanoacrylate glue, percutaneous injection of bleomycin, and transvenous endovascular sclerotherapy (via the inferior ophthalmic vein) using a microcatheter balloon and bleomycin have all been described [113, 123]. Surgical treatment has traditionally involved orbitotomy with isolation, evacuation, and ligation of the varix. Indications for surgical treatment are limited to progressive or sudden enlargement of the orbital varix with visual compromise or for cosmetic reasons [124–126]. Bleeding appears to be the main complication of surgical intervention with varices. Caution is the best approach to surgical intervention of orbital varices. If this must be undertaken then it is useful to request blood for possible transfusion from parents and family if at all possible. Careful ligation with surgical clips is necessary to avoid intraoperative and postoperative hemor-



Fig. 35.50 Orbital varix and phleboliths. CT scan showing superior orbital varix with numerous phleboliths

rhage. With thrombosed varices, extirpation of the clot and cautery may be all that is necessary. With increasing neuroradiologic invasive skills, the surgical treatment of these vascular lesions of the orbit is becoming increasingly limited to those who prove recalcitrant to interventional radiologic techniques.

Infantile Orbital Hemorrhage

A rare but dramatic lesion, infantile orbital hemorrhage, is a congenital cystic collection of blood within the orbit, producing proptosis and globe exposure [127]. Also termed congenital hematic cyst, its dramatic presence at birth brings frantic calls from the neonatologist requesting an emergency ophthalmic consultation to help differentiate this condition from other orbital processes presenting at birth such as microphthalmos with cyst, rhabdomyosarcoma, teratoma, and retinoblastoma with extraocular extension. With congenital hematic cysts, the eye is normal in shape with no observable or palpable mass. B-scan ultrasonography can demonstrate its cystic component quickly in the nursery. CT evaluation can pinpoint its intraorbital location and confirm its cystic nature (Fig. 35.51). While in the scanner, CT-directed needle aspiration can allow for decompression of the lesion. Char found this successful in four of his five cases [128]. His fifth case required surgical extirpation of the cyst and its lining. Two cases of spontaneous resolution are known to the authors. Interventional treatment for this condition should be based on signs of extreme proptosis with exposure keratopathy or visual compromise. The additional history of birth trauma, low Apgar scores, or hematologic abnormality in a child with congenital proptosis should prompt consideration of this condition.

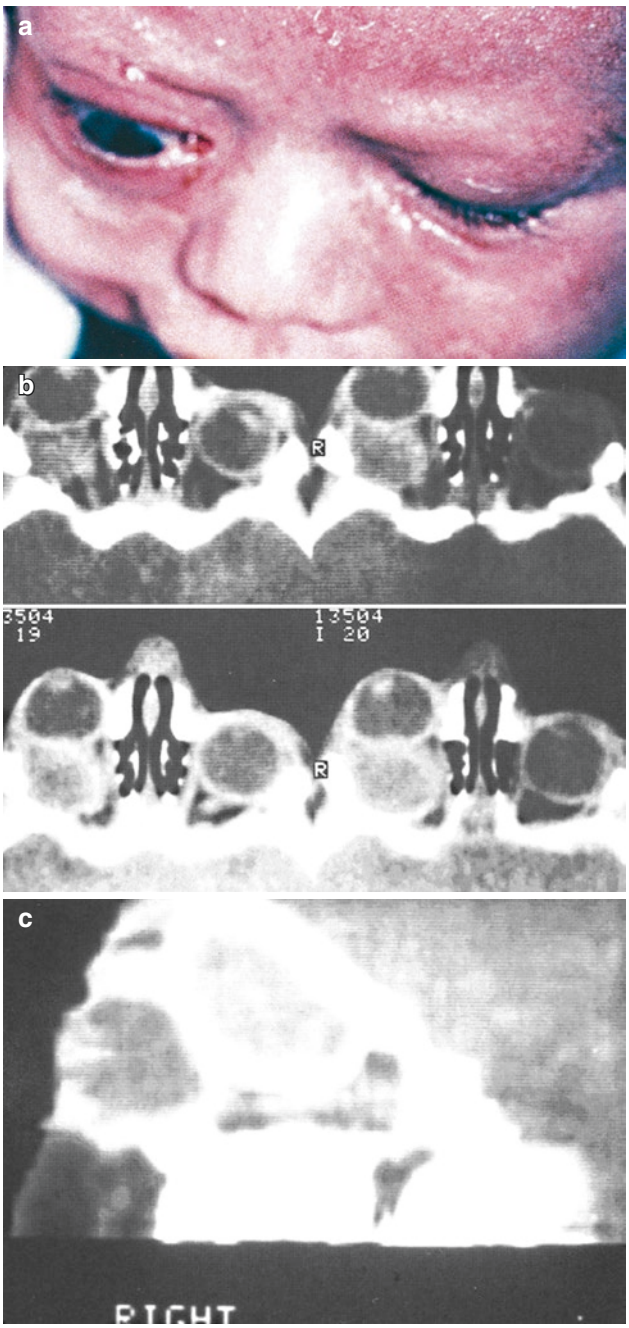


Fig. 35.51 Severe proptosis and orbital cyst. (**a**) A 2-day-old infant with severe right proptosis without microphthalmos, visible or palpable orbital mass, ecchymosis, or pulsations. (**b**) Sequentially more superior axial CT scans show large orbital cyst with enhancing rim. (**c**) Sagittal reformation demonstrates the extraconal location of this cyst. CT-directed needle aspiration evacuated the cyst without clinical recurrence

Cavernous Hemangioma

Cavernous hemangioma is a vascular lesion consisting of well-encapsulated, closely packed, large vascular channels lined by thin, flattened endothelial cells. It was thought to arise from infantile hemangiomas, but Iwamoto and Jakobiec showed the distinct histopathologic differences between these two lesions with electron microscopic analysis [129]. Table 35.1 records 16 cavernous hemangiomas from the 1820 pediatric orbital tumors. This is a much larger accounting than is available in the literature, where no series reports the incidence of cavernous hemangioma in children. The largest series by Harris and Jakobiec included 66 cases, of which one was an 18-year-old male [130]. The clinical features are similar to those in adults: axial proptosis of slow onset with later visual dysfunction as the lesion grows. No cutaneous abnormalities or enlargement with Valsalva maneuvers are seen. CT and MRI show a well-circumscribed mass without significant enhancement or the diffuse, lobulated appearance seen with infantile hemangiomas or lymphangiomas. Surgical removal is considered when visual dysfunction is present.

Neuronal Tumors

Optic Nerve Glioma

Optic nerve gliomas are discussed in great detail in Chaps. 14 and 15. Optic nerve gliomas make up approximately 1.5–3% of all orbital tumors and are the most common tumor of the optic nerve [114]. They belong to a group of low-grade tumors called optic pathway gliomas (OPG), which can arise anywhere along the optic pathway, including the optic nerve, chiasm, optic tract, or optic radiation, and represent 2–5% of pediatric gliomas [114]. Most optic nerve gliomas are solitary lesions. The tumor may be located solely within the orbit, bridge the orbito-cranial space, or reside within the intracranial space alone. Modern imaging permits noninvasive diagnosis and localization, which are keystones to management coupled with clinical visual abnormalities. With modern, high-resolution MR, imaging alone is often adequate for diagnosis, especially in patients with known NF-1. OPG biopsy carries the grave problem of severe vision loss, and thus should be reserved for cases of atypical presentation and appearance on MRI [131].

Gliomas are the most common intrinsic optic nerve tumors of childhood. Table 35.1 records 93 cases reported in the six compiled series for an incidence of 5.1% of all childhood orbital lesions. Male and female preponderance is equal when comparing all gliomas of the optic pathways. In a large retrospective study of the world's literature, Dutton reported a 2:1 female to male ratio when the glioma involved the optic nerve alone [114]. The mean age at presentation has varied widely in literature reports, with some indicating the mid-teens and others the middle of the first decade. Dutton's review firmly establishes the wide range for presentation of optic nerve gliomas, with 70% diagnosed in the first decade of life and 90% by age 20 [114]. The mean age of presentation in that review was 8.8 years. Symptomatic optic gliomas affecting vision, motility, or globe position tend to be diagnosed earlier and have a higher association with neurofibromatosis type 1 [132]. Ten percent of patients are older than 20 when diagnosed; the oldest individual was diagnosed at age 80 [133]. Of 63 cases reviewed at the AFIP, 48 were in whites and 9 were in blacks, with 9 cases not recording race, for an approximate ratio of 5.3 to 1 [134].

Gliomas arise from astrocytic glial cells found only in localized areas of the brain: the cerebellum, periventricular regions, and optic pathways, including the optic nerve [135]. The histopathology of these lesions shows a benign proliferation of these astrocytic cells within the substance of the optic nerve or in other intracranial primary sites of origin that can expand against or into the surrounding pia and arachnoid into the subdural space. Two growth patterns are seen: perineural and intraneural. The circumferential growth of proliferating astrocytes mixed with mucinous and microcystic degeneration seen in the perineural pattern widens the subarachnoid space, leaving the dura intact [136]. The optic nerve is compressed in the center of the glioma, yielding the classic features recognized on CT and MRI that are much more highly associated with neurofibromatosis type 1 [137]. The intraneural growth pattern enlarges the nerve with intraaxial astrocytic proliferation and little cystic degeneration while extending into and obliterating the subarachnoid space. This extension may provoke fibrovascular and meningothelial cell proliferation termed arachnoid hyperplasia, which may clinically simulate tumor extension and may histopathologically simulate optic nerve sheath meningioma, creating diagnostic difficulties, especially if isolated within the orbit [138, 139]. MRI T_2-weighted images can differentiate this process from true tumor enlargement [140]. Vascular proliferation and atypia are common, while mitotic figures are rare. Malignant transformation has been found in two cases of pediatric optic nerve gliomas but is an exceedingly rare occurrence [141, 142].

The association of neurofibromatosis type 1 (NF-1) with optic pathway gliomas is well established. Dutton's review found that 29% of patients reported in the literature with optic pathway gliomas have the stigmata of NF-1 [114]. A limiting factor in this determination is the lack of any mention of neurofibromatosis features among the patients in some of the case reports, which may underestimate the frequency of this association. MRI studies by Listernick found a 15% incidence of anterior visual pathway optic gliomas among unselected patients with NF-1 [143]. In a later study, screening MRI studies that failed to reveal any optic pathway lesions in the first year of life demonstrated optic nerve and chiasmal gliomas with follow-up imaging in four patients, indicating that a negative imaging study early in life may be unreliable for predicting future visual pathway involvement [144]. Due to variability such as this, a National Institutes of Health Consensus Conference recommended against routine neuroimaging studies screening for visual pathway lesions if the patient was asymptomatic [145].

The location of visual pathway involvement from gliomas is highly variable. The advent of neuroimaging studies, especially MRI, has greatly improved the ability to detect tumor extent, although microscopic extension still prevents complete and exact tumor localization. In data including the pre-CT era, only 25% of gliomas are confined to the optic nerve alone and demonstrate no chiasmal involvement [114]. For gliomas primarily within the chiasm, 47% involve at least one optic nerve, and 46% involve the adjacent hypothalamus or third ventricle. Packer et al. reported the largest series of MRI data on localization, with 50% of patients with NF-1 having chiasmal and one optic nerve involved, 42% with chiasmal, optic nerve, and optic tract involvement, and 8% with extension into the hypothalamus [146]. In this same study, patients without NF-1 demonstrated the following: 48% of the tumors were in the chiasm alone; 21% involved the chiasm, adjacent optic nerves, and optic tracts; 21% extended

into the hypothalamus; and only 3% demonstrated chiasm and optic nerve involvement. NF-1 patients appear to have more extensive and multifocal visual pathway involvement based on these comparisons but only 46% of NF-1 patients demonstrated visual symptoms or progressive neurological deficits versus 100% of patients without NF-1. It would seem that patients with NF-1 show slower or less neurological sequelae from their lesions despite more extensive and multifocal involvement. Interestingly, approximately 50% of NF-1 patients with optic pathway gliomas will develop non-optic pathway brain tumors within several years of the diagnosis of the glioma [147].

Lesions involving the optic nerve alone were previously believed to be more commonly identified in NF-1 patients. Housepian's review of 114 cases of optic glioma demonstrated optic nerve involvement alone in 80% of neurofibromatosis patients, whereas non-neurofibromatosis patients had isolated optic nerve involvement only 16% of the time [148]. Dutton's review of the literature of isolated optic nerve involvement shows nearly equal incidence among NF-1 and non-NF-1 patients with isolated optic nerve involvement when Housepian's data is excluded [114]. Also, in the review of these data, seven patients were found to have isolated bilateral optic gliomas. All had NF-1, supporting previous contentions of this association.

Documenting the progression of gliomas has been difficult. Clinical signs, psychovisual measurements, and radiological criteria are the three main parameters used for comparison. Fisher et al. recommend that vision be the main outcome in measure for NF1-OPG trials [149]. Because of the slow progression and long intervals of apparent dormancy common to visual pathway gliomas, long-term studies hold the most telling evidence of the true nature of these lesions. Rush et al. evaluated 85 cases of histologically verified gliomas of the optic nerve and chiasm that were followed for up to 43 years [150]. Of the 33 patients with optic nerve tumors, 85% survived a mean duration of 17 years; none died who had complete resection of the tumor with microscopically negative nerve margins. Of patients with chiasmal involvement, 56% died in a mean duration of 19 years; those with involvement of adjacent brain structures died significantly sooner. Alvord and Lofton compiled the data of 623 previously reported cases of optic nerve or chiasmal glioma and applied a mathematical model to derive more statistically significant results [151]. They found that while the behavior of the tumors varied, overall there was a general trend toward declining growth rate over time. Increasing age at the time of diagnosis correlated with a poorer long-term prognosis. Those younger than 20 years at the time of diagnosis had a 20-year survival rate of 65%, while the group diagnosed at older than 50 years had an 80% 10-year mortality rate. Mortality rates were higher among patients with chiasmal involvement at the time of diagnosis and higher still when involving the hypothalamus or third ventricle.

The clinical signs and symptoms of visual pathway gliomas depend on the size and location of the tumor. Intraorbital gliomas produce axial proptosis and visual loss and are reported as the presenting symptom in approximately 90% of cases (Fig. 35.52). Vision loss varies and is often severe and out of proportion to the proptosis. On occasion, the visual loss may be sudden in onset and can be due to cystic degeneration, necrosis, or hemorrhage in or around the optic nerve glioma [152, 153]. Seventy-five percent present with an afferent pupillary defect [154]. Visual field loss is common and over half present with identifiable optic atrophy. Nearly half the patients with intraorbital optic nerve gliomas have disk swelling, which is half as frequent when the tumor arises in the chiasm. Strabismus, oculomotor abnormalities, pain, headache, nystagmus, and endocrine signs (obesity, precocious puberty, diabetes insipidus) from hypothalamic involvement all can be presenting signs of optic gliomas. In young children, the vision loss may be manifest as amblyopia or strabismus. Profound proptosis may limit ocular rotations and produce corneal decompensation and

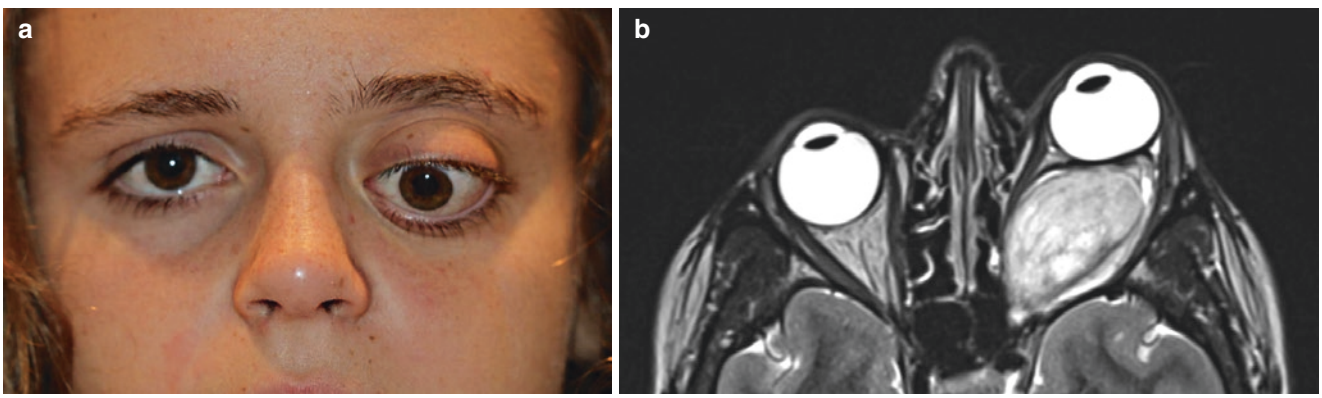


Fig. 35.52 Optic nerve glioma with proptosis. (**a**) Severe left sided proptosis. (**b**) T_2-weighed MRI showing large intraorbital optic nerve glioma

spontaneous prolapse of the globe. Although rare, intraocular extension of the glioma may occur [141]. Tumors involving the optic radiations will not produce proptosis; visual field defects will, however, be present. The increased risk of optic nerve gliomas in patients with neurofibromatosis mandates base-line neuro-ophthalmic examinations and radiologic investigation when indicated by the clinical findings.

Until the advent of MR imaging, computerized tomography was the standard diagnostic imaging modality for optic nerve gliomas [155]. Whether using MRI or CT scanning, images should be rendered in the axial and coronal planes both with and without contrast (see Chap. 32). On CT evaluation, optic nerve gliomas produce fusiform enlargement of the optic nerve usually isodense with brain. Most cases demonstrate involvement of most of the intraorbital section of optic nerve although discrete tumor localization can yield an appearance similar to a circumscribed orbital tumor. The optic nerve is usually not identifiable within the tumor and calcification is rarely present. The nerve and sheath are often kinked at nearly 90° in the anterior one-third of the orbit. Due to similar tissue characteristics on CT, gliomas of the optic canal, chiasm, and optic radiations are not well outlined. Limited contrast enhancement of the glioma coupled with its marginal tissue differentiation makes MRI a better imaging study when clinical signs of chiasmal or posterior visual pathway lesions are present [156]. Optic gliomas are hypo- or isointense on T_1-weighted images and hyperintense on T_2-weighted images. Fat suppression techniques and gadolinium contrast enhancement greatly improve the imaging capabilities of these lesions, especially on T_1-weighted scans [157] (Fig. 35.53). These features help in the follow-up and treatment planning of gliomas [137].

Standardized A-scan and two-dimensional B-scan echography can be of value in differentiating these tumors from other intraorbital lesions, especially in cases where neuroimaging studies fail to give definitive diagnoses. Widening of the optic nerve is a hallmark of glioma. A fusiform enlargement can be measured on standardized A-scan, with the anterior dimension usually 50% greater in diameter than a normal 2.5-mm optic nerve and the posterior nerve more than 100% greater in diameter [158]. Sharp, maximally reflective anterior and posterior spikes match the pathological findings of confinement within the dura. Internal reflectivity is low and regular, helping to distinguish gliomas from the higher reflectivity seen with meningiomas [159]. The mucinous and cystic components seen in older and longer standing gliomas are also an important differentiating feature, causing a more irregular reflectivity.

The treatment of visual pathway gliomas is guided by the location of the tumor and visual potential. Extensive investigations of surgical resection, radiation therapy, and chemotherapy have not yielded resounding success for the majority of patients in terms of visual preservation or improved life expectancy. The challenge with these tumors lies in the unpredictability of the clinical course of each lesion and the long-term evolution in each case coupled with the fact that many cases will advance extremely slowly or not at all.

Prior to determining any need for treatment, clinical and radiographic baselines need to be established. These include measurement of visual acuity, the presence and degree of any afferent pupillary defect, visual fields, proptosis, corneal integrity, optic disk swelling, or atrophy, and contrast-enhanced MRI of the head and orbits. Clinical evaluation alone of these ophthalmic parameters should be initially done quarterly to give some idea of the growth pattern of the glioma if the patient did not present with advancing clinical signs. The frequency of evaluation is adjusted, depending on clinical and radiographic findings. Pediatric consultation looking for the clinical features of neurofibro-

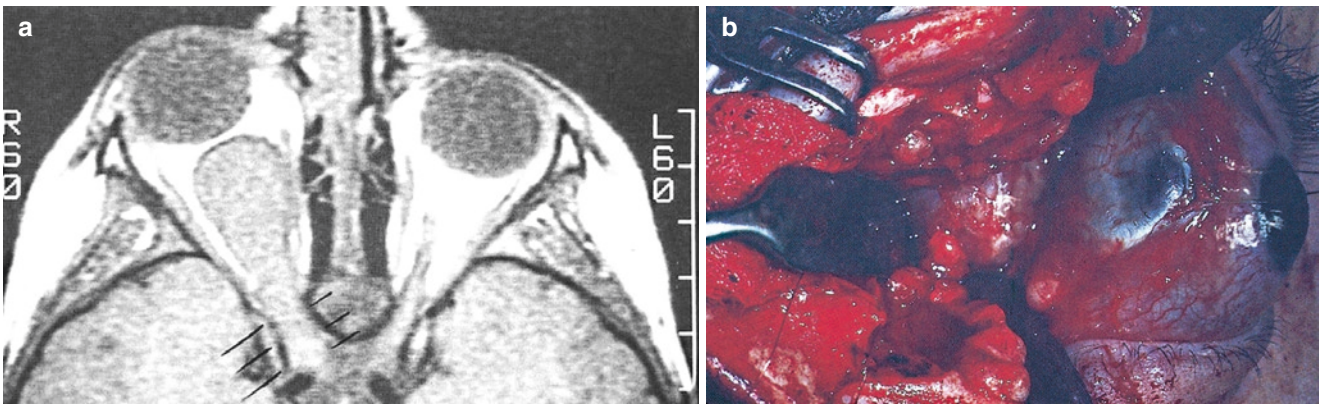


Fig. 35.53 Optic nerve glioma. (**a**) Contrast-enhanced MRI demonstrating large optic nerve glioma that involves the intracranial portion of the optic nerve. The posterior extent of the glioma is well visualized in this axial image. (**b**) View of the glioma in (A) through the lateral orbitotomy approach. Lateral rectus muscle is detached from the globe. The glioma can be seen as a fusiform enlargement directly behind and attached to the globe

matosis is important to help detect the presence of other systemic involvement by additional neuroglial and neurofibrous growths. Direct treatment of the glioma may be necessary if deterioration of the clinical picture or radiographic evidence of disease progression exists and further threatens neural and endocrine function. Obstructive hydrocephalus from third ventricle involvement or chiasmal involvement producing pituitary insufficiency will require supportive treatment even though direct treatment to the glioma may not coincidentally start.

Conservative therapy with periodic clinical and radiographic observations and measurements is the current line of therapy for all patients unless progressive changes induce clinical visual loss, extreme proptosis with corneal exposure, pain, progressive visual field loss, or other neural or endocrine malfunction. The treatment of these lesions with systemic chemotherapy is discussed in Chap. 15. Many studies have established the slow or nonexistent progression of gliomas, especially when limited to the intraorbital portion of the optic nerve. Hoyt and Bagdassarian firmly established how treatment may not lead to better visual outcome [160]. Both treated and untreated pediatric patients had nearly identical visual parameters with a mean follow-up of just under 10 years. Forty percent of patients in both groups retained visual acuity of 20/40 or better over the course of that follow-up. Recognizing the limited follow-up in this long-term disease, Imes and Hoyt were able to review 28 of the original 36 patients, all of whom had chiasmal involvement [161]. The median follow-up was 20 years, and nearly 80% of both groups showed no signs of visual deterioration. Obviously, the vast majority of patients will not require treatment of their optic nerve or chiasmal glioma. This is complicated somewhat by the fact that some patients will show progression radiographically despite clinically stable visual parameters and that some cases will spontaneously regress showing improved visual acuity even without treatment or any intervention [162–165].

As discussed in Chap. 15, performing surgery to prevent progression of the tumor to the chiasm is controversial and usually not recommended [165]. Extirpation of the intraorbital and intracanalicular optic nerve containing a glioma via an intracranial superior orbitotomy has been espoused as not only the best surgery for these patients but also the treatment of choice [151, 167–170]. This surgery is reserved for unilateral cases that radiographically invade the optic canal but spare the chiasm or when proptosis produces medically uncontrollable corneal decompensation or gross disfigurement. Tse et al. published a series of 11 patients treated with this approach. In this series there were no cases of tumor recurrence with a median follow-up of 56 months [170]. The challenge to this approach, however, is that microscopic tumor may still present on margin after resection. Sullivan et al. published a series of 13 patients with optic nerve gliomas. 12 of the 13 had a combined craniotomy-orbitotomy approach. Of these, 3 (27%) demonstrated evidence of microscopically positive margins on histopathologic examination [171]. In the past we have preferred a transcranial approach and resection of the optic nerve from the globe to just short of the chiasm to assure complete extirpation of the tumor. Should tumor be evident at the proximal end of the resected specimen at the time of histopathologic inspection, we have not attempted to resect the residual tumor within the chiasm, because surgical damage to the contralateral visual pathway may result. Additionally, there is no assurance that further resection into the chiasm will obtain a tumor-free margin. Supporting this approach is Alvord and Lofton's retrospective study finding no deaths and only a 14% recurrence rate in up to 20 years follow-up in children who had complete microscopic resection of their nonchiasmal optic nerve glioma compared with a 5% mortality rate and 71% progression rate in those with no treatment [151]. Surgery for chiasmal involvement fares worse with increased risk of recurrence, visual morbidity, and mortality, suggesting avoidance of chiasmal surgery for any gliomatous involvement [52, 164].

As an alternative to a transcranial approach with the goal of maximal debulking, we have begun the practice of orbital debulking alone. At the date of this publication, we have performed this surgery successfully on five patients with no evidence of tumor progression on follow-up (range 1–4 years) [172]. Fig. 35.54 depicts one of these patients. Each patient was approached via a lateral orbitotomy along with a resection of the optic nerve glioma leaving a 3 mm stump of nerve posterior to the sclera and resecting the tumor up to the annulus of the Zinn in the orbital apex. This approach of orbital debulking along has been described previously in the English literature [168].

Radiotherapy has undergone the greatest amount of evaluation as a treatment modality for anterior visual pathway gliomas involving the chiasm or hypothalamus. However, radiation is often avoided, especially in children with NF1, due to the associated risks of secondary malignancy, cerebrovascular disease, and endocrinopathies [173–176]. At issue is what percentage of patients will progress to significant visual morbidity, pituitary morbidity, or mortality without treatment, and does radiotherapy offer significant long-term reduction in morbidity and mortality. Multiple studies offer conflicting results regarding both aspects of the above issue. Imes and Hoyt argue strongly for no radiotherapeutic intervention, since the optic glioma-related mortality was 29% in their follow-up study when radiotherapy was given to treat chiasmal gliomas versus 7% mortality when no treatment was rendered [137]. These results represent one of the longest follow-up intervals in any study of visual

pathway gliomas (20-year mean follow-up). Its major limitation is that only 28 patients were involved and over half died in the follow-up period from secondary tumors not involving the visual pathways.

Alvord and Lofton found interesting data from their retrospective literature review [151]. With up to 20 years of follow-up, patients having optic gliomas limited to the intraorbital portion of the optic nerve who received greater than 4500 cGy of radiotherapy had no progression, recurrence, or deaths. If dosages less than this were administered, 51% progressed or recurred and 7% died. If no treatment was given, 71% progressed and 7% died. This compares to their evaluation of surgical resection of the intraorbital optic nerve without radiation or chemotherapy in which 14% had recurrences and none died. All recurrences occurred in patients who had microscopic tumor at the cut end of the resected nerve. These data, culled from 85 clinical studies, indicate equal success in controlling recurrence, progression, and mortality with either surgical resection with clear margins or radiotherapy of greater than 4500 cGy. In this same study looking at chiasmal gliomas without hydrocephalus (no clinically significant hypothalamic invasion), those treated with less than 4500 cGy of radiotherapy or in whom no treatment was given showed a 56% rate of progression or recurrence and a 35% mortality rate with up to 20 years of follow-up. If 4500 cGy or more of radiotherapy was given, the rate of progression or recurrence was 61%, while mortality was slightly lower at 32%. Thus, little difference is seen between low- and high-dose radiotherapy for chiasmal gliomas. If hydrocephalus occurs with chiasmal involvement, 74% recurred or progressed, with 57% dying, if left untreated; 90% recurred or progressed, with 60% dying, if treated with less than 4500 cGy; and 49% recurred or progressed, with 29% dying, when given greater than 4500 cGy of radiotherapy. This study would tend to support the use of 4500 cGy of radiotherapy for intraorbital optic nerve glioma and chiasmal glioma with hydrocephalus but not for chiasmal glioma without hydrocephalus. Flickinger et al. found similar benefits from high-dose radiotherapy for patients with chiasmal gliomas without hydrocephalus, unlike Alvord and Lofton [169]. Dutton also reviewed radiation therapy for visual pathway gliomas, focusing on results with at least 10 years of follow-up and found virtually no difference in radiation-treated patients compared with individuals who received no treatment [114].

A major detraction of the Alvord and Lofton study is the lack of a review of the long-term side effects from radiotherapy given at an early age from the papers that were used to produce their data. Neurological, endocrine, and vascular sequelae from both low- and high-dose radiotherapies are well documented in young children. Panhypopituitarism, growth hormone deficiency, precocious puberty, amenorrhea, diabetes insipidus, brain atrophy, and cerebrovascular occlusion from Moyamoya disease can occur in up to 55% of children given lateral port chiasmal radiotherapy even at doses as low as 2400 cGy [177–182]. We consider radiotherapy of the chiasm to be contraindicated prior to age 5 years secondary to the potential for pituitary damage with resultant growth delays, diabetes insipidus, and other hypopituitary effects. A large number of chiasmal gliomas will not be treatable given these restrictions, engendering interest in chemotherapy as an additional treatment alternative.

The number of studies assessing the usefulness and applicability of chemotherapy for visual pathway gliomas is increasing. This subject is covered more extensively in Chap. 15. Children with NF1 and ONG that require treatment are most commonly treated with carboplatin-based

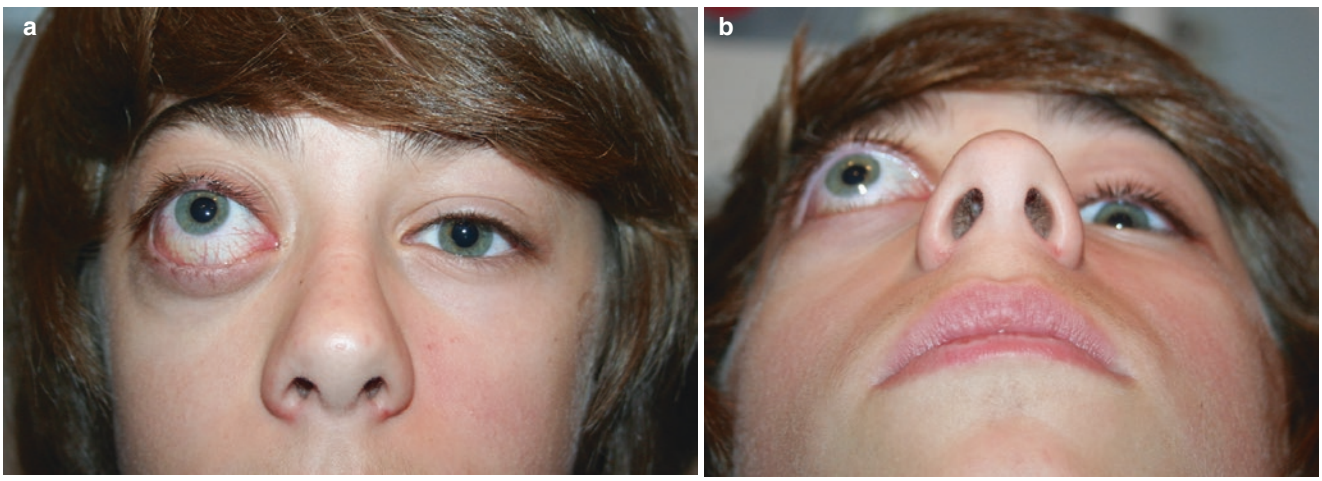


Fig. 35.54 Optic nerve glioma debulking surgery only without complete resection via a lateral orbitotomy approach. (**a**) Preoperative photo showing disfiguring proptosis. (**b**) Worm's eye view

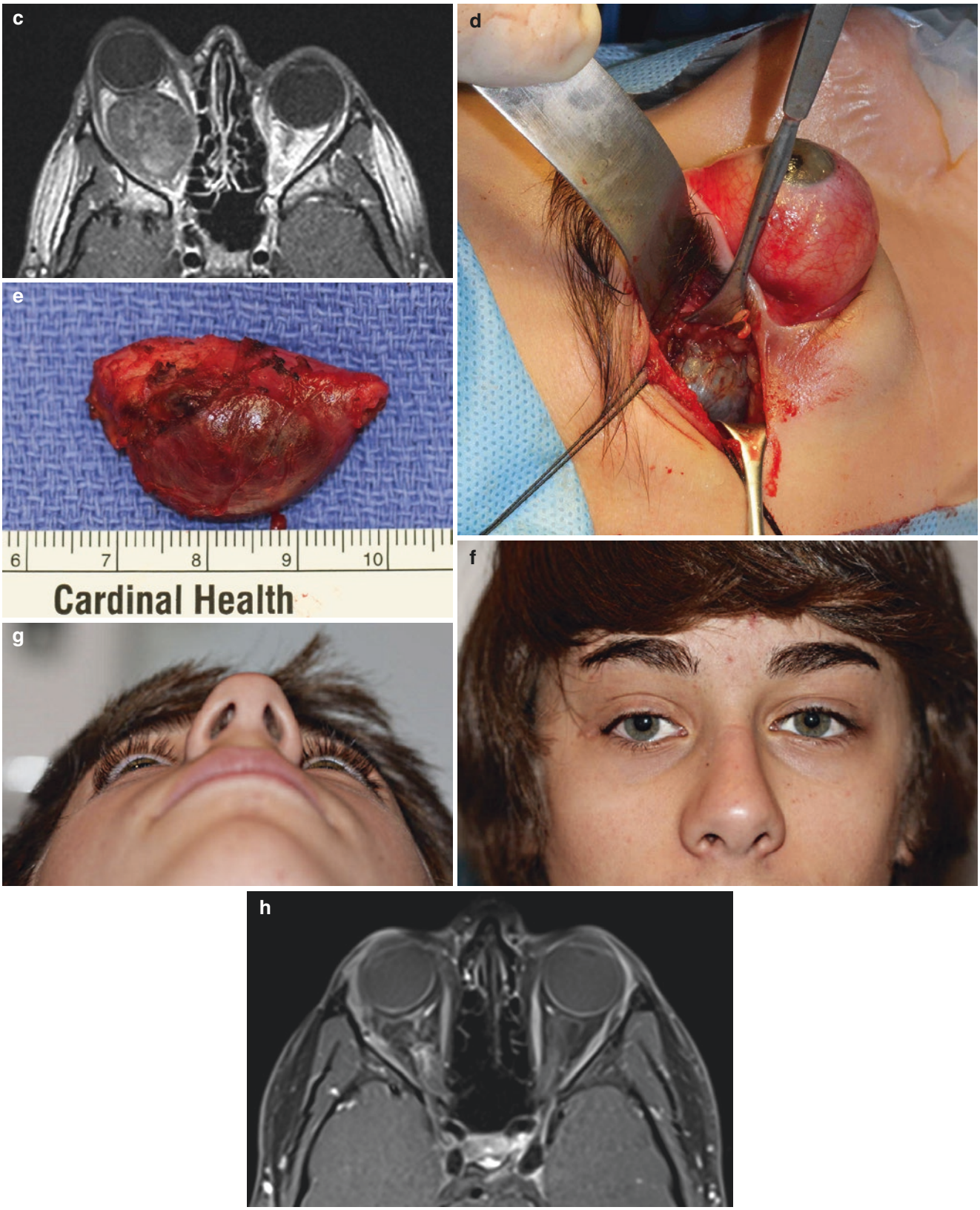


Fig. 35.54 (continued) (**c**) T_1-weighted MRI showing a large optic nerve glioma. (**d**) Intraoperative photo. A lateral orbitotomy was performed to expose the optic nerve lesion. (**e**) Optic nerve glioma specimen. (**f**) Postoperative photo. (**g**) Worm's eye view showing postoperative reduction of right proptosis. (**h**) Postoperative T_1-weighted axial MRI showing section of resected optic nerve glioma with only a small apical stump

chemotherapy regimens. Carboplatin and vincristine results in a 5-year progression-free survival of 69% in children with NF1 [183]. Chemotherapy options for children with sporadic ONG are broader, but not as effective. The most studied regimens are carboplatin and vincristine or thioguanine, procarbazine, lomustine, and vincristine (TPCV).

Given these data, several points can help guide treatment decisions for patients with visual pathway gliomas [184–187]. First, patients with neurofibromatosis type 1 fare better with less mortality and visual morbidity than non-NF-1 patients. Second, establishing ophthalmic and neuroimaging evaluations on a regular basis can identify clinically significant changes in visual and neurological functions, offering the potential for treatment opportunities prior to progressive irreversible functional loss. Third, the lack of clinical and radiological progression is a relative contraindication to any treatment. Fourth, transcranial surgical extirpation of the intraorbital and intracanalicular optic nerve with globe preservation may be avoided since the lateral orbitotomy approach with orbital debulking is an option for disfiguring proptosis. Fifth, MRI with contrast enhancement and fat suppression techniques offers the best mode of neuroimaging evaluation and subsequent radiographic follow-up for visual pathway gliomas.

Orbital Meningioma

Meningiomas are benign tumors thought to arise from the meningothelial cells found in the meninges. Larger collections of these cells, termed arachnoidal granulations, populate the dural sinuses and veins and are where most intracranial meningiomas arise. Smaller collections are found in the olfactory groove, sphenoid ridge, and tuberculum sellae. These arachnoidal villi can also proliferate into meningiomas and, due to their close proximity to the orbit, may secondarily invade the orbit or optic nerve. Among all age groups, these secondary orbital and optic nerve meningiomas account for approximately 90% of all meningeal tumors found in the socket, with primary optic nerve sheath meningiomas (ONSM) accounting for the other 10% [188]. The origin of primary ONSM is similar to that of other meningiomas; arachnoidal villi that penetrate into the dural optic nerve sheath are the most likely tissue from which ONSM arise [189]. Other authors have suggested that ectopic meningeal cells populate the orbit and are the source of these meningiomas, but histopathologic examination of the vast majority of cases shows connections to the optic nerve sheath [189].

ONSM account for approximately 1–2% of all meningiomas. Table 35.1 records 20 meningiomas of the optic nerve sheath, for an incidence of 1.1% among all orbital lesions in the pediatric population. Traditionally, ONSM arise in middle age, with a 3:1 female preponderance. It used to be thought that nearly half of the cases arose in children [191, 192]. In 1992, Dutton reviewed the 498 reported cases of ONSM in the world's literature and found only a 4% incidence of pediatric presentation [193]. Wright reported a similar incidence, with only 1 child in his series of 16 cases [194]. The youngest reported case occurred in a 2.5-year-old [195]. No preference is seen for either orbit in unilateral cases. Only 5% of cases are bilateral and tend to be diagnosed at a younger age [188]. In bilateral cases, the mean age for onset of vision loss in the first eye is 12 years old, with the second eye developing vision loss on average 18 years later, with a range of 2–27 years [193].

An unusual feature for bilateral cases is the high association of these meningiomas occurring within the optic canal (canalicular meningiomas) [196]. Dutton found a 65% incidence of canalicular meningiomas among those cases with bilateral presentation versus only a 5.7% incidence among all meningiomas primary to the optic nerve sheath [193]. Given the anatomic limitations of the optic canal space and the growth of the meningioma over time, it is easy to see why these lesions are discovered earlier than those that are intraorbital. Why the frequency of bilaterality and asymmetric visual loss appears so commonly among canalicular meningiomas is unclear, although Trobe et al. demonstrated biopsy-positive meningioma along the tuberculum sellae in a case of "bilateral canalicular meningiomas" [198].

Meningiomas of the optic nerve sheath are also seen more commonly among individuals with neurofibromatosis type l [189]. Up to 9% of patients with ONSM have NF-1 [186]. This frequency coupled with that of optic gliomas can make for considerable difficulty in differentiating optic nerve lesions in patients with NF-1. One large review notes that the association of ONSM with NF-1 is greater in the pediatric age group (35%) as compared to adults (9%). Also, there is a great incidence of intracranial extension (44%) as compared to adults (20%) [198].

The clinical presentation of optic nerve sheath meningioma in children is slightly different from that seen in adults. Visual decline is more pronounced and proptosis is greater in the childhood period. The most common symptoms and signs encountered in children with ONSM are proptosis, progressive visual loss, restricted ocular motility, progressive optic atrophy with optociliary shunts, visual field abnormalities, and an afferent pupillary defect (Fig. 35.55). The classic triad of visual loss, optic atrophy, and optociliary shunt vessels signaling ONSM in adults may not have had enough time to develop in childhood cases. A large degree of suspicion for ONSM should be reserved for the child who has mild visual loss, an afferent pupillary defect, mild proptosis, and optic disk swelling without optociliary shunt vessels. The proptosis is usually axial, is slowly progressive, and follows the degree of visual loss. Early in the course of the disease, visual loss may be mild. Strabismus or unexplained refractory amblyopia may be the earliest

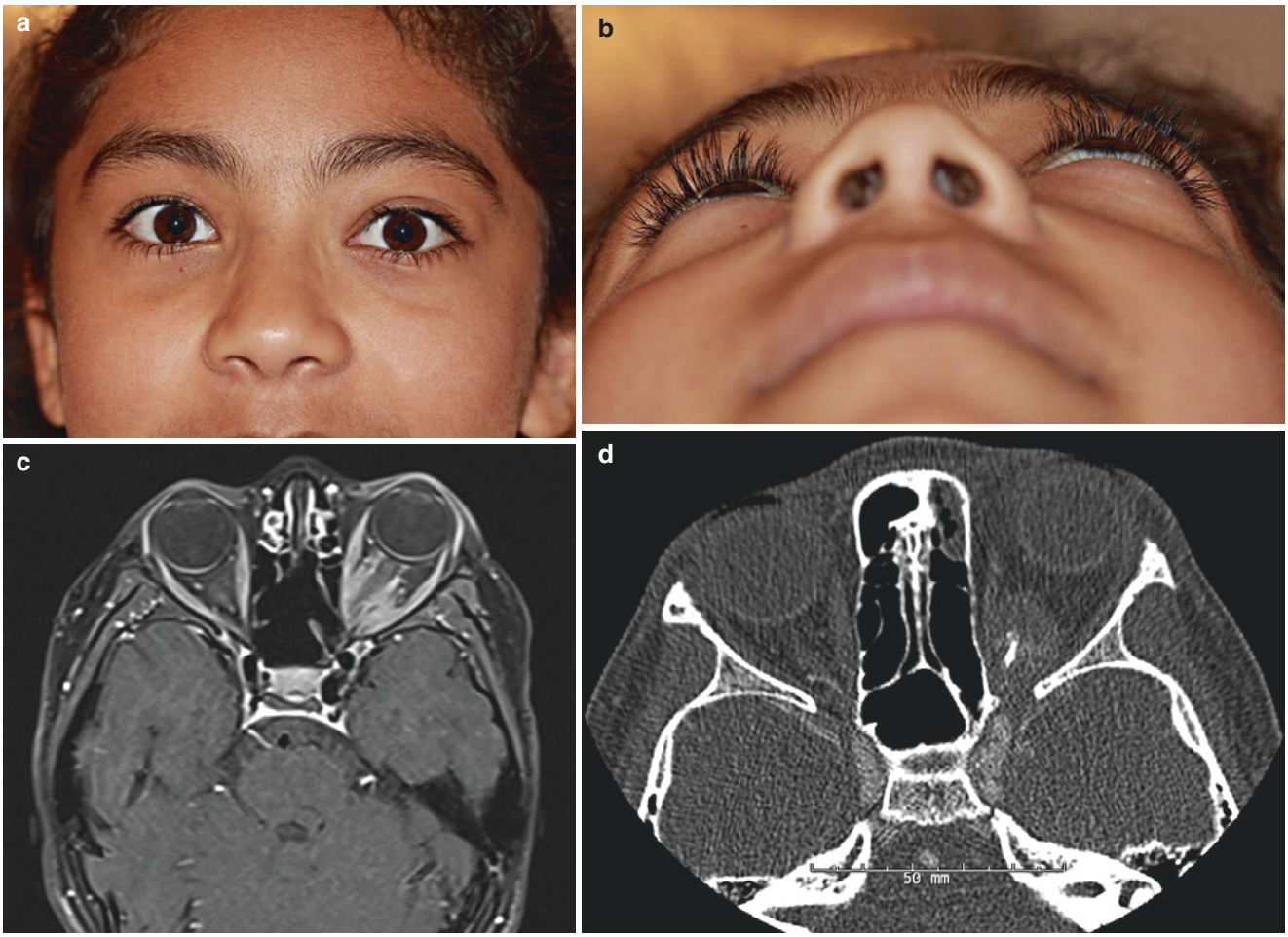


Fig. 35.55 Optic nerve meningioma. (**a**) 10 year-old female with left-sided proptosis. (**b**) Worm's eye view showing left sided proptosis. (**c**) T_1-weighted axial MRI of optic nerve meningioma in posterior half of left orbit. Optic nerve is seen to run through the center of the lesion; the "tram-track" sign. (**d**) Axial Ct showing calcification within the lesion

clinical signs. More profound visual loss can evolve over decades, with approximately 68% eventually declining to hand-motion vision or worse [199]. Gaze-evoked amaurosis and transient visual obscurations are reported in up to one-quarter of patients. Afferent pupillary defects arise coincident with visual loss. Restricted motility is thought to arise from the stiffening optic nerve with progressive tumor growth. This tumor growth surrounds and slowly compresses the optic nerve, resulting in optic atrophy with optociliary shunt vessels. If the meningioma is identified early, optic disk swelling may be seen that eventually progresses on to atrophy and optociliary shunt vessel formation [200].

Canalicular meningiomas do not produce proptosis, usually have more profound vision loss, and have a lower incidence of disk swelling due to the posterior location [178]. The visual field abnormalities reported with ONSM are typical for compressive optic nerve lesions: peripheral constriction, cecocentral scotomas, altitudinal defects, and enlarged blind spots can all occur [188, 194, 201].

Noninvasive imaging studies have paved the way in the management of ONSM by increasing the ability to noninvasively diagnose this lesion with a high degree of certainty. Thin-section axial and coronal CT scans yield features that enable differentiation from other optic nerve lesions [155]. Narrow, diffuse tubular enlargement of the optic nerve with moderate to high enhancement upon administration of intravenous contrast is the most common appearance on axial CT scanning. Kinking of the optic nerve and cystic degeneration, so commonly seen with optic nerve glioma, are not seen with optic nerve meningioma. Polar expansion of the tumor at its anterior extent usually just behind the globe or at its posterior extent in the orbital apex with bony remolding help identify ONSM. A more globular mass with a central lucency where the optic nerve passes through represents tumor growth outside the optic nerve sheath. This central lucency may be more visible with contrast enhancement on coronal CT images and is termed the tram-track sign. Irregular excrescences along the margin of tubular optic

nerve meningiomas indicate tumor erosion along the optic nerve sheath that is distinct to meningiomas [202]. Calcifications are common in long-standing meningiomas.

The morphologic MRI findings are much the same as CT. T_1-weighted MR images appear isointense with brain, while T_2-weighted images are slightly hyperintense [203]. Gadolinium enhancement improves the visualization of these lesions along with fat suppression techniques [204, 205]. In the optic canal and chiasmal areas, MR is the preferred imaging study to detect tumor extent. Echography shows obvious widening of the optic nerve, with an irregular acoustic signature and medium reflectivity. Internal calcifications along with a lack of subarachnoid fluid and a negative 30° test suggest a meningioma [158].

The natural course of ONSM is one of progressive enlargement with compression or invasion of the optic nerve and loss of visual function over years to decades. Sarkies plotted presentation vision against ultimate visual acuity in his study of 22 patients with ONSM followed for up to 11 years and found a visual decline of at least two Snellen lines in all patients, with over half the patients progressing to worse than 20/200 with or without treatment [201]. Imaging studies show tumor growth that parallels vision loss, leading some authors to suggest that measures of optic nerve function may be a more accurate way of following these lesions [206]. Extension can occur along with enlargement of these tumors. Intraocular extension is rare but has been reported in a 13-year-old child, presenting as a white subretinal mass emanating from the optic nerve head [207]. Posterior extension into the chiasm or the opposite optic nerve from intraorbital ONSM occurs over time in a minority of patients but does not invade the brain [208]. Increased intracranial pressure and pituitary dysfunction have not been associated with ONSM with chiasmal extension and its presence should make one consider an olfactory groove or sphenoidal ridge meningioma with secondary optic nerve spread, especially if initial imaging studies show this extent of involvement [188, 208]. Malignant transformation of intracranial meningiomas occurs in about 10–15% of cases but has yet to be described with primary ONSM [209].

In an extensive literature review, Dutton raised doubts about the current management of primary ONSM upon finding no deaths attributable to these tumors except from attempted surgical interventions [193]. With no reported cases of malignancy in pediatric patients, it would seem that the only threat from intracranial extension is to the opposite optic nerve via chiasmal invasion. This concept is of utmost importance in determining if any treatment other than observation should be considered in pediatric patients with primary optic nerve sheath meningiomas.

A variety of surgical manipulations of the optic nerve have been attempted to cure ONSM [191, 195, 199, 210]. Although there have been isolated reports of surgical removal of en plaque optic nerve tumors with preservation or improvement in vision, complete loss of vision is most common. Decompression of the nerve sheath has been advocated, but we avoid this approach because it has been associated with massive orbital extension requiring exenteration. Twenty-five percent of resected ONSM recur and up to 30% of surgical attempts lead to serious complications, including death. Clearly, surgical intervention with ONSM should be limited to attempts at complete removal of the lesion for intractable pain or severe proptosis if it is confined to the intraorbital portion of optic nerve on MR imaging. Few data exist to determine the success of surgical removal in terms of visual preservation or postoperative tumor recurrence when the tumor has extended into the chiasm and threatens or is affecting opposite optic nerve function. Resection is accomplished through a cranio-orbitotomy to permit complete removal of the tumor and optic nerve, including the canalicular portion, and thereby prevent intracranial spread. We favor the same surgical approach if resection is performed to treat profound proptosis.

Radiotherapy has been applied as an alternative treatment for ONSM alone or in combination with surgical resection in adult patients to halt the progression of visual loss [195, 211, 212]. Less than 15 cases have been reported, but nearly 75% have maintained or improved pretreatment vision over a 2- to 6-year follow-up. Total radiation dosage averaged 5500 cGy. Although an attractive option, radiation therapy in young children carries a number of significant risks as compared to adults, including secondary tumor induction in the field of radiation, delayed bony growth, and pituitary hypoplasia with treatment near the chiasm, which cause us to avoid its application in this condition.

Faced with a child harboring a primary ONSM, the choices of treatment appear to have greater consequence than observation alone. Sequential careful vision and visual field examinations along with thin-section contrasted CT or MRI allow for early detection of lesion progression. In the case of functionally or radiographically progressive tumor confined to the orbit, one might consider early surgical extirpation to attempt to prevent future intracranial extension, but the potential operative complications coupled with a 42% recurrence rate compared with an estimated 20% intracranial extension rate without surgical intervention makes that decision very difficult [193, 199, 210]. Surgical extirpation should be strongly considered with a blind eye coupled with intractable pain or disfiguring proptosis. Radiation therapy should be considered if the child is over approximately 14 years of age, but long-term results remain speculative. While chemotherapy combined with radiotherapy shows some promise in improving survival in patients with malignant intracranial meningiomas, its role in optic nerve sheath meningiomas has not been explored [213].

Primary intraosseous or ectopic meningioma of the skull is a rare tumor accounting for about 1% of meningioma [214]. These lesions can follow the meninges and extend through bony sutures into the orbit. This exemplified in Fig. 35.56.

Neurofibromas

Neurofibromatosis is an autosomally dominant inherited trait with nearly complete penetrance that affects approximately 1 in 3000 live births [215]. Genetic mapping studies have isolated defects on chromosome 17 in some patients with neurofibromatosis type 1 [216]. Such widely variable expressivity exists for this condition that uniform diagnostic criteria have been established to enable accurate labeling [217]. Two or more of the following criteria must be present to diagnose neurofibromatosis type 1:6 or more café au lait spots greater than 5 mm in diameter in prepubertal patients and greater than 15 mm in diameter in postpubertal patients, axillary or inguinal freckling, two or more neurofibromas of any type or one plexiform neurofibroma, optic glioma, two or more Lisch nodules, a distinctive osseous lesion such as sphenoid dysplasia or thinning of the long bone cortex with or without pseudoarthrosis, or a first-degree relative with NF-1 by these same criteria. Note that three of these major criteria directly involve the ocular and orbital regions, which is why the ophthalmologist is often called upon to help establish the diagnosis in suspicious cases.

The ophthalmic findings in NF-1 are well established and include Lisch nodules; choroidal hamartomas; prominent corneal nerves; congenital glaucoma; eyelid, conjunctival, and choroidal cafe au lait spots; isolated neurofibromas of the eyelids, orbit, conjunctiva, and cornea; plexiform neurofibromas of the eyelids and orbit; optic nerve glioma; optic nerve sheath meningioma; and absence of the greater wing of the sphenoid [218]. Optic nerve sheath meningioma and optic nerve glioma have already been discussed. Here we address the peripheral nerve tumors found in the pediatric population, some of which are highly associated with NF-1: plexiform neurofibroma, isolated neurofibroma, and diffuse neurofibromas.

Plexiform neurofibromas are the most common form of benign neurogenic orbital tumor seen in children. Table 35.1 lists 85 cases of plexiform neurofibroma among the 1820 total pediatric orbital cases for an incidence of 4.7%. The association with NF-1 is legendary, prompting some authors to suggest that its presence in the orbit is "pathognomonic" of neurofibromatosis. Any nerve may be affected, although there is a predilection for sensory nerves. These neurofibromas consist of diffuse intertwining bundles of Schwann cells, axons, and fibroblasts surrounded by a perineural sheath that grows without respect to tissue boundaries, insinuating itself anywhere in the lids and orbit. Frequently located laterally in the upper eyelid, the classic appearance of an "S-shaped" eyelid is achieved by the distortion of the lid margin due to this enlarging subcutaneous lesion that often has a prominent lacrimal component when producing this appearance. Not well encapsulated, these highly vascularized, tangled nerves proliferate and produce a feeling on palpation as if a "bag of worms" was within the soft tissue. Any area where the plexiform neurofibroma extends to just under the skin is frequently thickened, producing pigmentary changes and, at times, astonishing amounts of redundancy. The more grotesque features of NF-1 are due to this type of severe cutaneous change, which is termed elephantiasis neuromatosis. Malignant degeneration is rare.

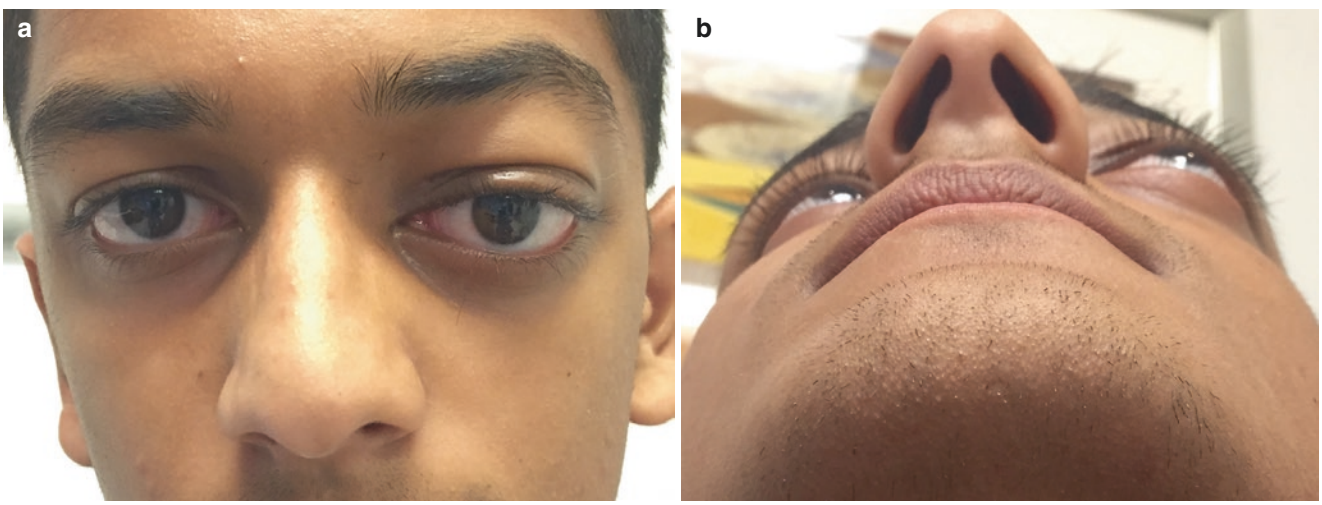


Fig. 35.56 Orbital roof meningioma. (**a**) 16-year-old with proptosis and disfigurement. (**b**) Worm's eye view showing proptosis

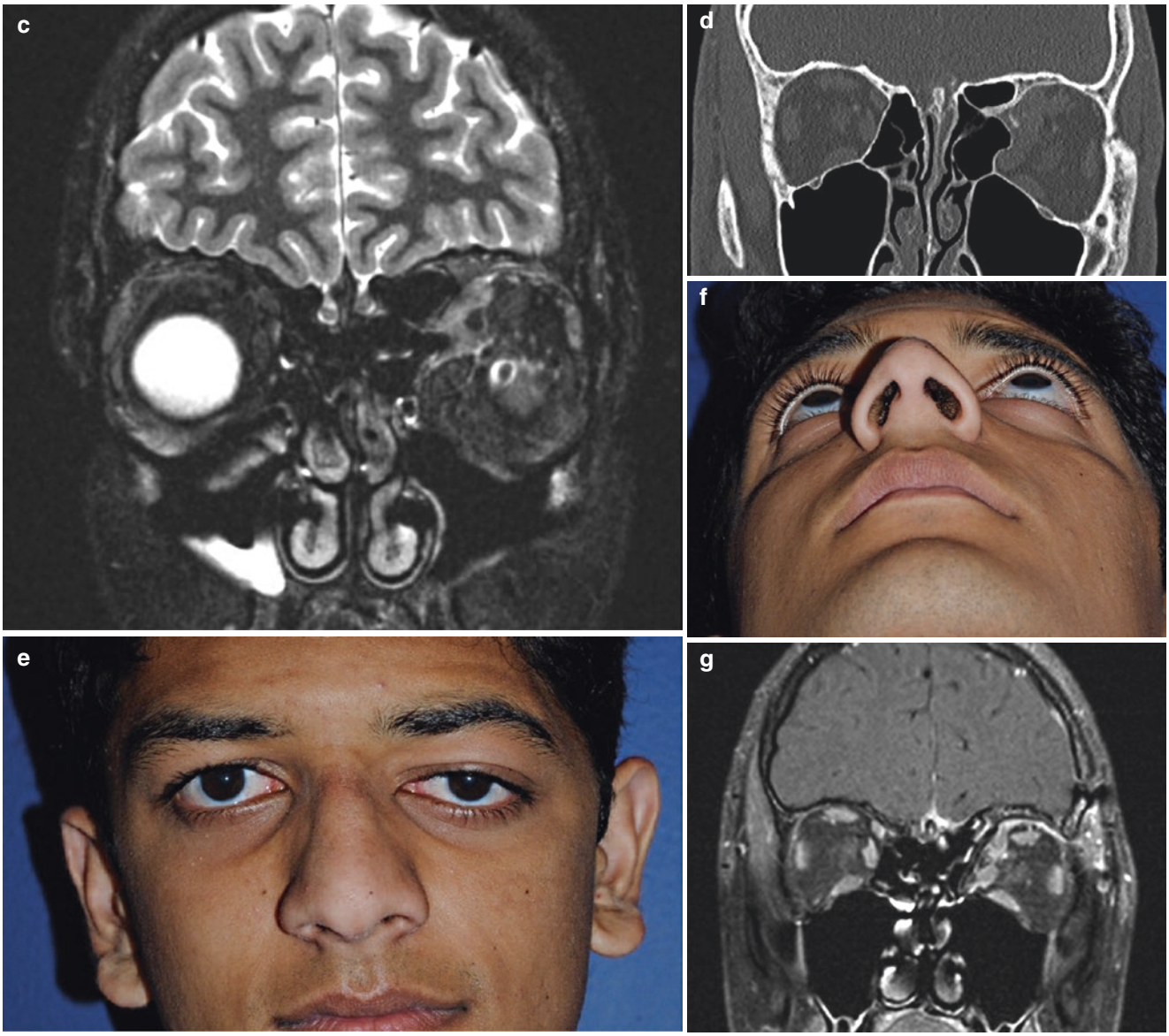


Fig. 35.56 (continued) (**c**) Axial CT showing an infiltrative lesion in the superior medial orbit. (**d**) *T1*-weighted coronal MRI shows extension of the lesion into the meninges of the skull base. The patient underwent an orbital biopsy via and eyelid crease incision. Pathology confirmed the diagnosis of meningioma. (**e**) 6 months status post bicoronal craniotomy followed by orbital bandeau then exenteration of the frontal sinuses bilaterally and the left lamina propecia and into the ethmoid sinuses for removal of the orbital tumor and then intradural removal of the planum sphenoidale meningioma. (**f**) Worm's eye view showing reduction of proptosis and globe displacement. (**g**) Postoperative *T1*-weighted coronal MRI enhancing extraconal lesion in the superomedial aspect of the left orbit and smaller intracranial epidural soft tissue component along the planum ethmoidale, posterior to the crista galli

When affecting the eyelid, the soft tissues are thickened and hypertrophied and often demonstrate the surface changes of cutaneous hypertrophy with hyperpigmentation (Fig. 35.57). Plexiform neurofibromas frequently present in the first decade of life and often in just the first few years [219]. Growth is variable, often occurring sporadically with long periods of apparent dormancy interrupted by alarming accelerations in size (Fig. 35.58). Other head and neck occurrences of plexiform neurofibromas are common with a peculiar proclivity for the sympathetic nerve chain that results in a preganglionic Horner syndrome [218]. Fortunately, sarcomatous degeneration of orbital plexiform neurofibromas is rare. Those that do

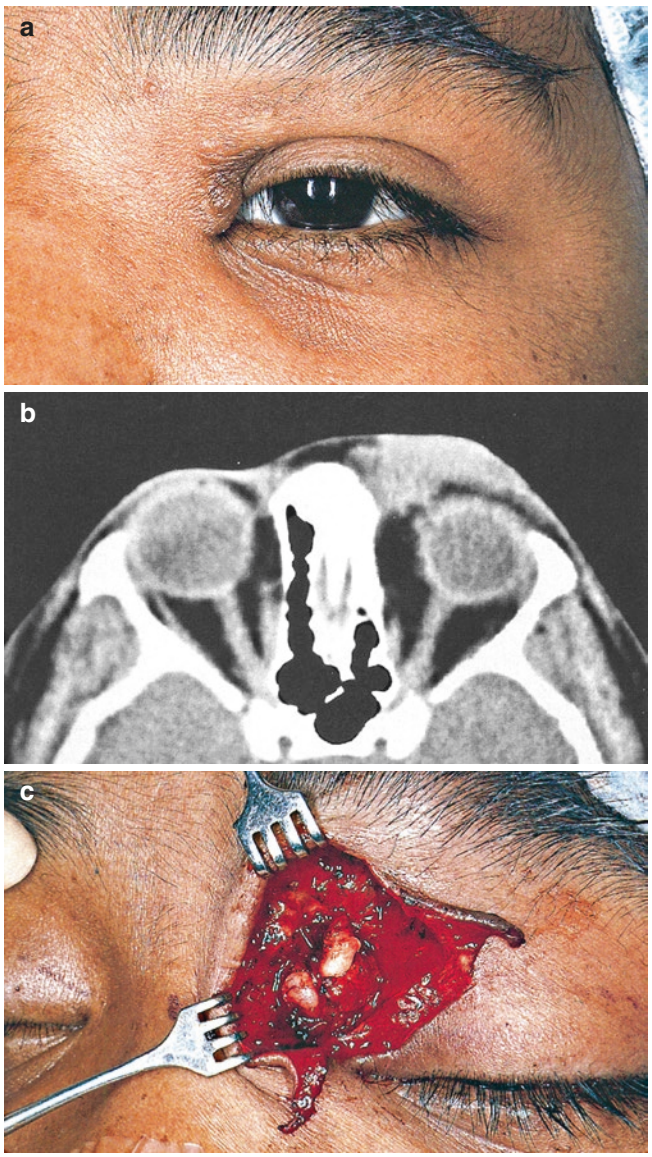


Fig. 35.57 Plexiform neurofibroma. (**a**) A 12-year-old female with medial upper eyelid plexiform neurofibroma. Note verrucous, pigmented cutaneous changes. (**b**) Axial noncontrast CT demonstrating diffuse extent of plexiform neurofibroma in medial lid with extension laterally in a preseptal plane without orbital invasion. (**c**) Intraoperative photograph demonstrates the multiple thickened, tortuous nerves creating the plexiform neurofibroma

undergo this transformation are typically paraspinal or abdominal and do so years after the discovery of the originally benign lesion [220]. Progressive and continuous recurrences of orbito-palpebral plexiform neurofibromas are the hallmark of this condition throughout childhood, requiring repetitive surgical debulking in an attempt to preserve both function and cosmesis in the involved tissues.

CT evaluation of these patients identifies a moderately enhancing soft tissue mass devoid of clearly defined borders insinuating itself in the orbit, eyelids, and intracranial compartments without respect to normal anatomic confines [221, 222]. Involvement of the extraocular muscles, intraconal sensory or motor nerves, or cavernous sinus produces nodular or multinodular enlargement of these structures. Absence of the sphenoid wing is the most typical bony orbital deformity, but long-standing soft tissue volume expansion may produce a more generalized enlargement of the bony orbital volume when compared to the contralateral orbit. Widening of normal orbital ostia, such as the superior orbital fissure or zygomaticotemporal foramen, yields important clues as to the potential extension of these lesions outside of the orbital space. This has a major bearing on any surgical planning. On MR imaging, plexiform neurofibromas tend to be isointense with vitreous on T_1-weighted images and hypointense compared to vitreous on T_2-weighted images but have the same gross features as seen on CT [223, 224].

The management of plexiform neurofibromas that involve the periocular and orbital regions has yet to settle on a single, successful regimen. Multiple series have been devoted to unique or broad-based treatment efforts, most having a surgical basis, that provide acceptable surgical debulking and modest cosmetic improvements [225–229]. The success of surgical resection is limited by the high risk of recurrence in subtotally resected tumors, particularly in young children. The concept of tumor recurrence is really a misnomer as there is no regrowth of tumor but rather only continued progression due to the growth of residual tumor tissue not completely excised. Debulking may be considered for visual decline, progressive disfigurement, or tumor progression toward a critical structure, but disease progression with functional and aesthetic relapse should be expected [230]. All measures currently fail to provide long-lasting control of these lesions because surgical excision is generally incomplete (due to the lack of neurofibroma encapsulation and involvement of normal anatomic structures), and it is bloody (due to the profound vascularity of these lesions). Patients are subject to significant postoperative edema, which is slow to resolve. As a result, multiple operative procedures are required over the life of the patient with decreasingly satisfactory results, as repeated surgeries produce increasingly distorted anatomy and greater challenges in preserving normal anatomic structures. Nevertheless, despite these limitations, the psychosocial benefit in gaining some measure of a more acceptable appearance cannot be minimized.

Because of the surgical limitations, efforts have been made in the past to search for medically based treatments that could halt or slow the progressive growth of these lesions. Clinically significant potential for control of pain, itching, tenderness, and even growth of neurofibromas was reported in two trials of ketotifen fumarate, a benzocycloheptathiophene compound that is a powerful mast cell stabilizer [231, 232]. Mast cells are found in large concen-

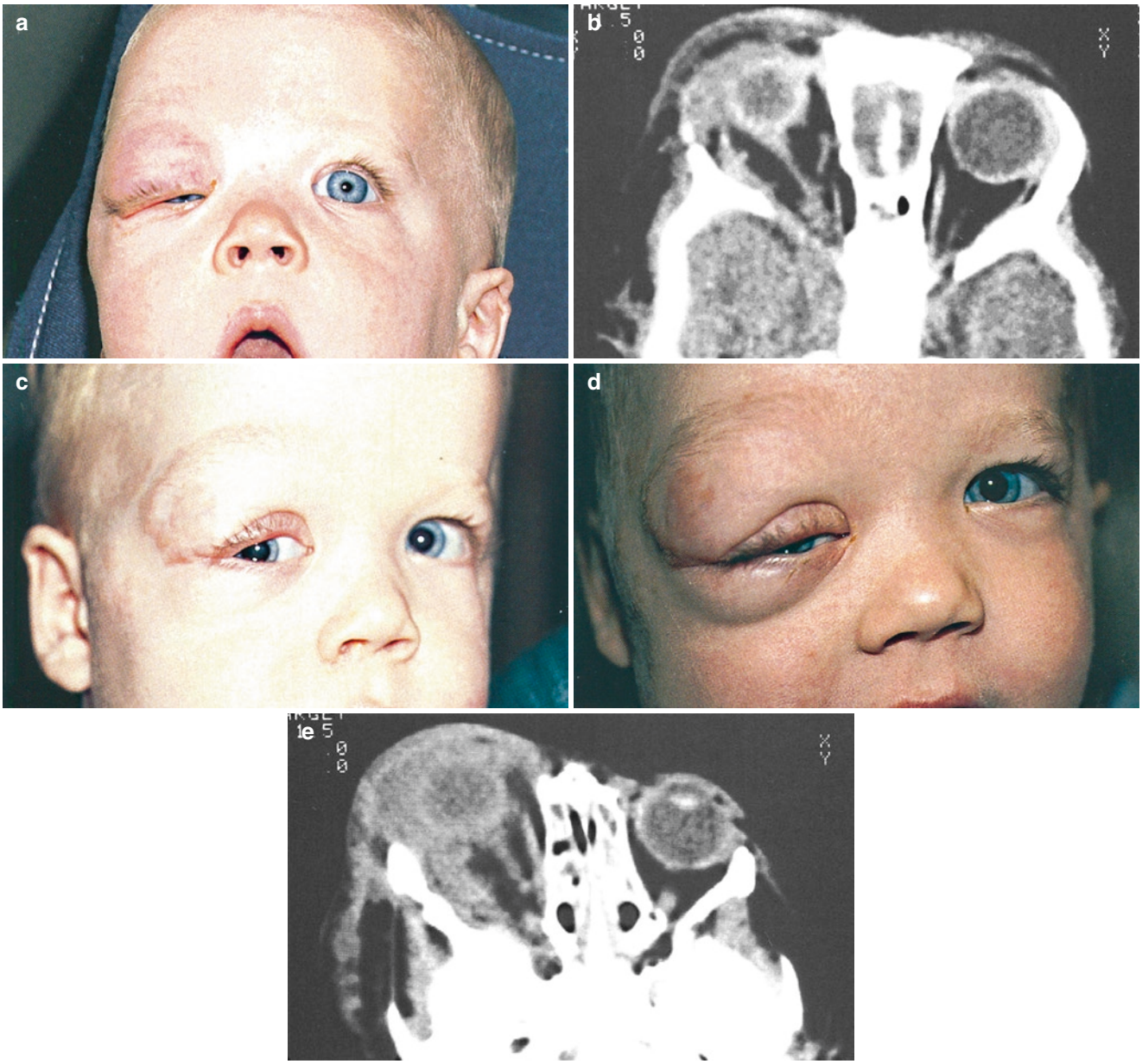


Fig. 35.58 Plexiform neurofibroma. (**a**) A 14-month-old male with 5-month history of progressive swelling and enlargement of the right upper eyelid with proptosis due to a plexiform neurofibroma. Note severe ptosis and S-shaped curve to the upper eyelid margin. (**b**) Noncontrast axial CT showing extent of anterior and lateral orbital involvement by the plexiform neurofibroma. Note the absence of the sphenoid bone in this superior orbital scan. (**c**) Three months after surgical debulking of plexiform neurofibroma through a transcutaneous upper eyelid incision with levator advancement. Residual bulk of tumor is most visible in the region superior to the lateral canthus and mid-eyelid. (**d**) A 1-year postoperative photograph demonstrating extensive progression of the plexiform neurofibroma with inferior globe displacement, proptosis, recurrent blepharoptosis, and lower eyelid involvement. (**e**) Noncontrast axial CT showing the anterior and lateral orbital involvement. Note the lateral and medial wall molding from the chronic intraorbital mass effect

trations in neurofibromas and may stimulate tumor angiogenesis, resulting in growth, severe itching, and pain. Particularly striking in one study was the decrease in growth rate or actual shrinkage of facial, paraspinous, peripheral, and abdominal neurofibromas in 90% of patients treated with 2–4 mg of ketotifen per day over an average 33-month period [231]. Unfortunately, this compound is not available in the United States, and no other studies have been reported.

Several novel studies have been launched or are in the planning stages at centers across the United States (see Chap. 15). A randomized phase II trial of 13-*cis*-retinoic acid, interferon alfa-2a, and etoposide was begun at the Children's Hospital of Philadelphia in 1995 [233]. These compounds

have shown effectiveness at retarding tumor angiogenesis and tumor growth and were used either alone or in combination in a nonblinded fashion without a control group in an attempt to reduce or reverse neurofibroma growth. The combination of interferon and *cis*-retinoic acid exhibited enough promise that a multicentered, double-blinded trial evaluating this combination in the treatment of plexiform neurofibroma has been established. Thalidomide is also a potent inhibitor of angiogenesis and has been proposed for evaluation among children with complicated or progressive neurofibromas; the Children's Hospital of Philadelphia, Washington Children's Hospital, and the Cleveland Clinic are collaborating in this evaluation [233].

The rise of new medications targeted at the molecular abnormalities within the tumor raise the possibility of effective therapies in the future [234]. In fact, a recent phase I study of the MEK inhibitor selumetinib has resulted in partial responses in over half of PN treated [235]. The phase II trial of pirfenidone in children and young adults with neurofibromatosis type 1 and progressive plexiform neurofibromas, however, was not shown to be effective [236].

Jackson et al. originally divided orbitofacial neurofibromatosis into three distinct groups, each with a different surgical approach [228]:

1. Group one: orbital soft tissue involvement with a seeing eye
2. Group two: orbital soft tissue and significant bony involvement with a seeing eye
3. Group three: orbital soft tissue and significant bony involvement with a poorly seeing or absent eye

We prefer a classification system that makes a distinction between tumors involving the eyelids alone and a broader category of periorbital soft tissues and the orbit alone, including both its soft contents and surrounding bony envelope as follows [237]:

This system has a better application for oculoplastic surgical planning:

1. Eyelid tumors alone
   - With seeing eye
   - Without seeing eye
2. Periorbital tumors (lids/brows/mid–lower face)
   - With seeing eye
   - Without seeing eye
3. Periorbital and orbital tumors with/without significant bony involvement
   - With seeing eye
   - Without seeing eye

The surgical excision of plexiform neurofibromas depends on the extent and degree of soft tissue involvement. Small neurofibromas can be managed with aggressive local debulking or resection through standard cutaneous approaches with attention toward preservation of normal structures [225]. Severe cases with unsightly proptosis, marked cutaneous manifestations, and a deformed orbit with a non-seeing eye may require more advanced resection techniques, including enucleation, orbital osteotomies to reduce the expanded orbital space, bone grafts for orbital osseous dysplasia, and combined orbitocraniotomy for any intracranial component [226]. Kennerdell and Maroon reinforced the usefulness of the carbon dioxide laser in orbital cases since it can both vaporize identifiable plexiform neurofibromas and provide excellent hemostasis, enhancing surgical effectiveness, especially in pediatric cases [230]. The carbon dioxide laser is used for photovaporization and not cutting in these cases of orbital surgery. An exact scheme outlining the surgical procedures for plexiform neurofibromas is unavailable due to the variety and uniqueness of every presentation. The above surgical references offer an excellent guide to help in surgical decision-making (see also Chap. 37).

Isolated neurofibromas are rarely identified in the orbit; Henderson estimated that they account for approximately 2% of all neurofibromas seen in the periocular region [238]. Generally affecting sensory nerves, slow enlargement producing gradual proptosis that is generally not appreciated until middle age is the most common presentation and may also include orbital pain, strabismus, and compressive optic neuropathy [239]. A few cases have been reported in children. While markedly adherent to the involved nerve, these tumors do not possess the substantial vascularity that exists in the plexiform variety, yielding a greater chance for surgical cure. A small percentage may be associated with neurofibromatosis type 1, but most cases are sporadic. It would not be unusual to find multiple isolated lesions within one orbit [239, 240].

CT reveals a homogenous and well-circumscribed soft tissue density that has uniform contrast enhancement. Longstanding lesions often demonstrate orbital wall expansion and remolding from the pressure effect of the proximate tumor. MRI demonstrates lesions hypointense on T_1-*weighted* images and hyperintense on T_2-weighted images. B-scan ultrasonography demonstrates a well-defined lesion of low internal reflectivity.

Treatment of these lesions is dictated by the severity of the mass effect that is produced and the associated symptoms of the patient. Resection is considered for lesions producing compressive optic neuropathy, pain, or disfigurement. The surgical approach is dictated by the location of the mass. Less vascular than the plexiform variety, solitary neurofibromas pose fewer surgical complications. Efforts should be made to identify the function of the involved nerve both prior to surgery and intraoperatively. Sensory nerve function loss is of lesser consequence than motor loss. In the latter case,

attempts should be made to preserve the function of the nerve by careful dissection of the tumor from the nerve with the assistance of the operating microscope. The presence of multiple tumors should be revealed on preoperative imaging studies but careful digital palpation of the orbit intraoperatively has been recommended due to some small lesions being found at surgery only after the largest lesion was removed [239].

Diffuse neurofibromas are rare, generally affecting the skin and sparing the orbit. A close association with NF-1 is seen in these patients where involvement of the orbit produces diffuse infiltration of the soft tissues with proptosis, lid deformity, restricted motility, and declining vision with progressive orbital disease. Clinical differentiation from plexiform neurofibroma can be difficult; diffuse neurofibromatosis seems to lack the "bag of worms" feeling on palpation. Radiologically, it has many of the same features as the plexiform variety. Surgical resection is typically subtotal and complicated by the significant tumor vascularity and lack of encapsulation. Resection should be avoided and, if necessary, limited in extent.

Schwannoma

Schwannomas, also called neurilemmomas, are benign proliferations of the Schwann cell envelope of peripheral nerves. Within the orbit, they may affect any of the sensory or motor nerves. Producing slowly progressive, painless proptosis, these lesions are much more commonly diagnosed in adults than children and are not typically associated with neurofibromatosis [241]. Table 35.1 reports only two of these lesions among the 1820 pediatric orbital cases; the literature also finds an incidence of less than 1% among all orbital lesions among patients of all ages [242]. These lesions may be located anywhere in the orbit. Extraorbital locations such as the eyelid have also been described [243]. Only a few orbital cases have been reported in children [244]. Besides proptosis, motility dysfunction and pain are the commonest presenting signs and symptoms, since these lesions do not affect nerve function until late in the course. Optic neuropathy is a late feature that depends on the proximity of the tumor and produces secondary compression of the optic nerve. Small apically located tumors may produce profound visual symptoms before there is evidence of proptosis, while a more anteriorly located mass will feature proptosis before optic neuropathy is documented. The mass effect of the tumor adjacent to the globe may also produce choroidal folds. Malignant degeneration of schwannomas is not as common as is seen with plexiform neurofibromas but has been reported in the pediatric population [245, 246]. Seen as a primary lesion, it may be difficult to differentiate from an isolated neurofibroma. Transformation from an incompletely resected benign schwannoma has been associated with rapid regrowth of the lesion [247]. Long-term survival has not been well studied in malignant cases but other body site statistics indicate that wide resection offers the best chance of cure [248].

CT scan reveals a homogeneous, well-circumscribed soft tissue density that may be either intra- or extraconal. It displaces surrounding structures, and long-standing lesions may produce remodeling or frank erosion of surrounding bone. Contrast dye may produce a small degree of enhancement. MR features a discrete, homogeneous soft tissue density that is hypointense on T_1 and hyperintense on T_2. There is little enhancement with the use of gadolinium. These features are similar to isolated neurofibromas, which is not surprising given the histopathologic features of each. B-scan ultrasonography may offer the best chance of differentiating these lesions: neurofibromas are reported to have low internal reflectivity with a rapid attenuation of echoes within the lesion that is felt to be highly characteristic [249].

Treatment is primary excision when mass effect (i.e., optic neuropathy, proptosis) is significant or if the pattern of tumor growth accelerates, suggesting malignant degeneration. The route for orbitotomy is determined by the site of the tumor. The mass may be removed whole, if small, or in a fragmented fashion if larger. In such cases, we find a carbon dioxide laser coupled to an operating neurosurgical microscope useful in the dissection and removal of the mass. Small volumes of residual tumor that surround important normal orbital structures are left unresected and generally remain stable without recurrence. Regular follow-up examinations are necessary due to potential malignant transformation. If histologic inspection reveals a malignant schwannoma, exenteration is recommended.

Ossifying Lesions

Osteoma

Osteomas are lesions of unknown etiology consisting of areas of increased ossification found within facial and skull membranous bone. Three histologic subtypes—ivory, mature, and fibrous—identify these unusual lesions in the pediatric age group, with only five cases seen among the 1820 pediatric orbital processes compiled in Table 35.1, representing less than 0.3% of tumors. Argument exists as to whether osteomas arise in the orbit or are secondarily present, having arisen from the sinuses, which are the most common primary site [250]. Most osteomas appear to arise from in or near the frontoethmoidal complex and usually become clinically apparent in the second decade of life or later. The clinical signs and symptoms of these slow-growing osteomas vary depending on the site from which they arise. Sinus obstruction with pain and recurrent sinusitis

occurs with involvement of the sinus ostia, while intracranial extension produces infection and meningitis-like symptoms. Intraorbital extension of an osteoma produces proptosis that is usually nonaxial and slowly progressive (Fig. 35.59a). Anterior osteomas secondarily involving the orbit may be palpable, while those that arise more posteriorly may show signs of neurovascular compromise. In a few cases, the proptosis may progress rapidly, resulting from an associated acute sinusitis or adjacent hemorrhage. In addition to acute sinusitis resulting in orbital cellulitis and meningitis, we have seen one case in which acute dacryocystitis resulted from obstruction of the nasolacrimal duct. Optic neuropathy can occur if cellulitis occurs acutely or if the lesion grows slowly to a critical size. Osteomas have been reported in conjunction with Gardner syndrome (intestinal polyposis), which also has been associated with "bear-track" retinal pigment epithelial hyperplasia [251].

CT scanning provides the best noninvasive imaging technique. The use of bone window density in the axial and coronal planes reveals the interface of normal bone and tumor. Osteomas will appear uniformly hyperintense but bone windows reveal internal nonhomogeneity (Fig. 35.59b). Histologically, osteoid predominates, but there may be a viable amount of fibrous tissue within the osteoma accounting for the areas of lucency identified on bone windows of the CT scan. Pathologists will variably describe the lesions as osteoma or fibrous osteoma, whereas we feel this reflects a spectrum of disease without clinical significance.

Excision is performed by whatever approach provides the most direct access. We have been able to approach lesions that extend between the frontal and maxillary sinuses through a bifrontal craniotomy [252]. However, smaller lesions may be excised through a more direct approach. Trans-sinus excision with central cavitation of the osteoma followed by collapse of its perimeter and removal with rongeurs has also proven successful. The lesions routinely cleave from the surrounding normal bone, which is easy to identify intraoperatively. Reconstruction of the bony orbital wall that was resected with the osteoma is required only if its absence will result in functional or cosmetic deformity. Examples are the orbital rim, the anterior third of the orbital roof, and the medial wall of the orbit. If the osteoma is completely excised, then, in our experience, recurrence is unlikely. Subtotal resections can be expected to regrow, but the generally slow growth pattern may make it clinically insignificant over time.

Osteoblastoma

A clinically and histologically distinct orbital ossifying lesion, the osteoblastoma occurs rarely in the pediatric orbit [253]. Originally termed osteoid osteomas, these lesions represent growing rests of osteolytic tissue with varying degrees of calcification. Reported most commonly in the vertebral column, they arise as isolated lesions often adjacent to but not intimate with surrounding bony structures, which is a different radiologic picture than that seen with osteomas, ossifying fibromas, and fibrous dysplasia. Primary orbital lesions and extensions from the sinuses may cause proptosis, periocular swelling, and redness. CT demonstrates a soft tissue mass with variable calcifications. Surgical removal is the recommended mode of treatment, although complete extirpation may be limited due to involved normal structures [254]. In orthopedic series, incomplete removal results in a

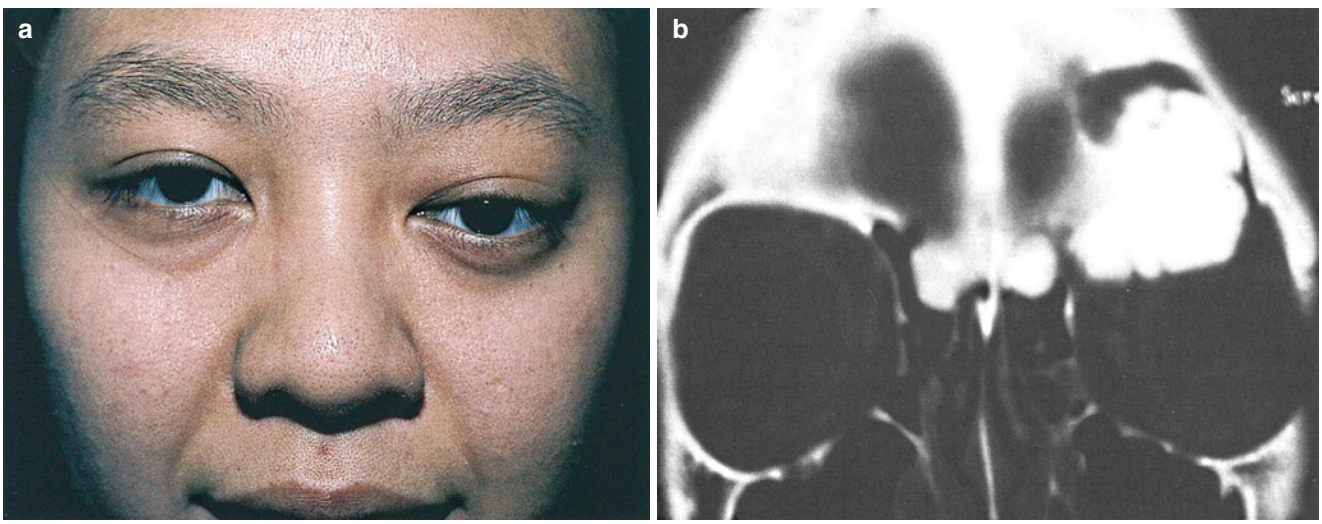


Fig. 35.59 Osteoma. (**a**) Teenager with inferior globe displacement secondary to orbital encroachment by an osteoma. (**b**) Coronal CT demonstrates calcified mass in the frontal sinus with orbital extension

10–15% recurrence rate, with 10% of those recurrences showing sarcomatous transformation [255]. No recurrences have been reported with en bloc resection.

Juvenile Ossifying Fibroma

Ossifying fibromas are a subset of facial and mandibular bone tumors that are typically slow growing and primarily occur in adults. When they arise in children, a much more aggressive clinical picture arises with bony erosion and invasion into surrounding tissues and organs. This distinct subgroup is termed juvenile ossifying fibroma. Its pathologic features of benign spindle cell stroma embedded with small, round (psammomatoid) ossicles have raised interest in changing the nomenclature to psammomatoid ossifying fibroma (POF) of the orbit [256].

Clinically, POF arise from the ethmoid sinuses or the superior orbital plate of the frontal bone, grow slowly, expanding into the orbit, and produce signs and symptoms by mass effect in similar fashion to osteomas. They are often not identified until the second decade of life, when a review of facial photographs often yields evidence of proptosis unrecognized by the patient or family members. Most cases present with proptosis, although optic nerve compression with papilledema and decreased vision may also occur. At the time of diagnosis, the lesions are typically large, averaging 5.3 cm in diameter [256].

CT scanning features a predominately osseous lesion with a greater relative soft tissue component [257]. On occasion, the radiographic picture can be confused with fibrous dysplasia. However, the distinction between normal and abnormal bones tends to be clearer in the case of ossifying fibroma. MRI features have been reported in one case and proved to be of little value due to the lack of bony demonstration [258]. Histologically, a well-vascularized fibrous stroma with psammomatoid islands distinguishes it from other fibro-ossifying orbital lesions.

Treatment is by surgical excision (Fig. 35.60). Indications for excision include disfiguring proptosis, exposure keratitis, and compressive optic neuropathy. Surgical excision is accomplished by the same means as described for osteoma. Similarly, the lesion is easy to distinguish from the surrounding normal bone intraoperatively. Complete surgical resection is rarely complicated by recurrence.

Aneurysmal Bone Cyst

Aneurysmal bone cysts are nonmalignant, cystic, expansile lesions of the bone typically found in the metaphyses of long bones in children. Their occurrence in the orbit is rare but well over a dozen cases have been reported [259, 260]. All the walls of the orbit have given rise to these erosive and lytic bony lesions and the sinuses have also been the primary site of origin with secondary orbital involvement [261]. Eighty-five percent occur in individuals under the age of 20 without sex predilection. The presenting ocular symptoms are most commonly painless proptosis with a lower rate of ptosis, frontal headache, diplopia, and loss of vision [262]. Radiographic evaluation is best performed with CT imaging and shows an intraosseous mass with lytic and erosive bone changes combined with variable, irregular intralesional calcifications. Minimal to no surrounding bony rim is seen and no invasion of other tissues occurs.

The histopathology of these lesions demonstrates grossly multicystic, nonendothelial lined spaces that are empty or filled with hemorrhagic debris. A whorled, vascular stroma with lamellar bone occurs and may have significant osteoid formation and a distinct rim of calcification. These changes are thought to arise from altered reparative processes within the affected bone. Aneurysmal bone cysts are seen to occur with other bony lesions and are reported to be associated with trauma, both of which obscure the true etiology of these lesions [263].

The treatment of aneurysmal bone cyst is based on the progression of orbital signs and symptoms, with surgical removal being the most commonly employed treatment. The usually distinct margins of this tumor coupled with a normally slow biological growth result in a low rate of recurrence. Due to the lytic nature of these lesions, bony repair of the resection site may be necessary if functional limitations are encountered or expected at the time of tumor resection. Orthopedic treatments have included intraoperative curettage combined with surgical resection, cryotherapy, and radiation therapy for recurrent lesions, but, to date, no orbital cases have been reported to recur [263].

Osteopetrosis

Osteopetrosis tarda is a rare congenital bone condition characterized by increased thickness and density of all bones, which may result in encroachment on the marrow cavity with loss of marrow production and narrowing of skull foramina with consequent neuronal disruption. These bony changes result in a structural weakening of the bones, with an increased susceptibility to fractures, leading to identification of the disease when a child is x-rayed for evaluation of other injuries. The more severely affected children are diagnosed during infancy, demonstrating failure to thrive, anemia, thrombocytopenia, hepatosplenomegaly (due to extramedullary hematopoiesis), and lymphadenopathy, all directly related to loss of marrow producing capacity. This severe form is inherited as an autosomal recessive condition; a

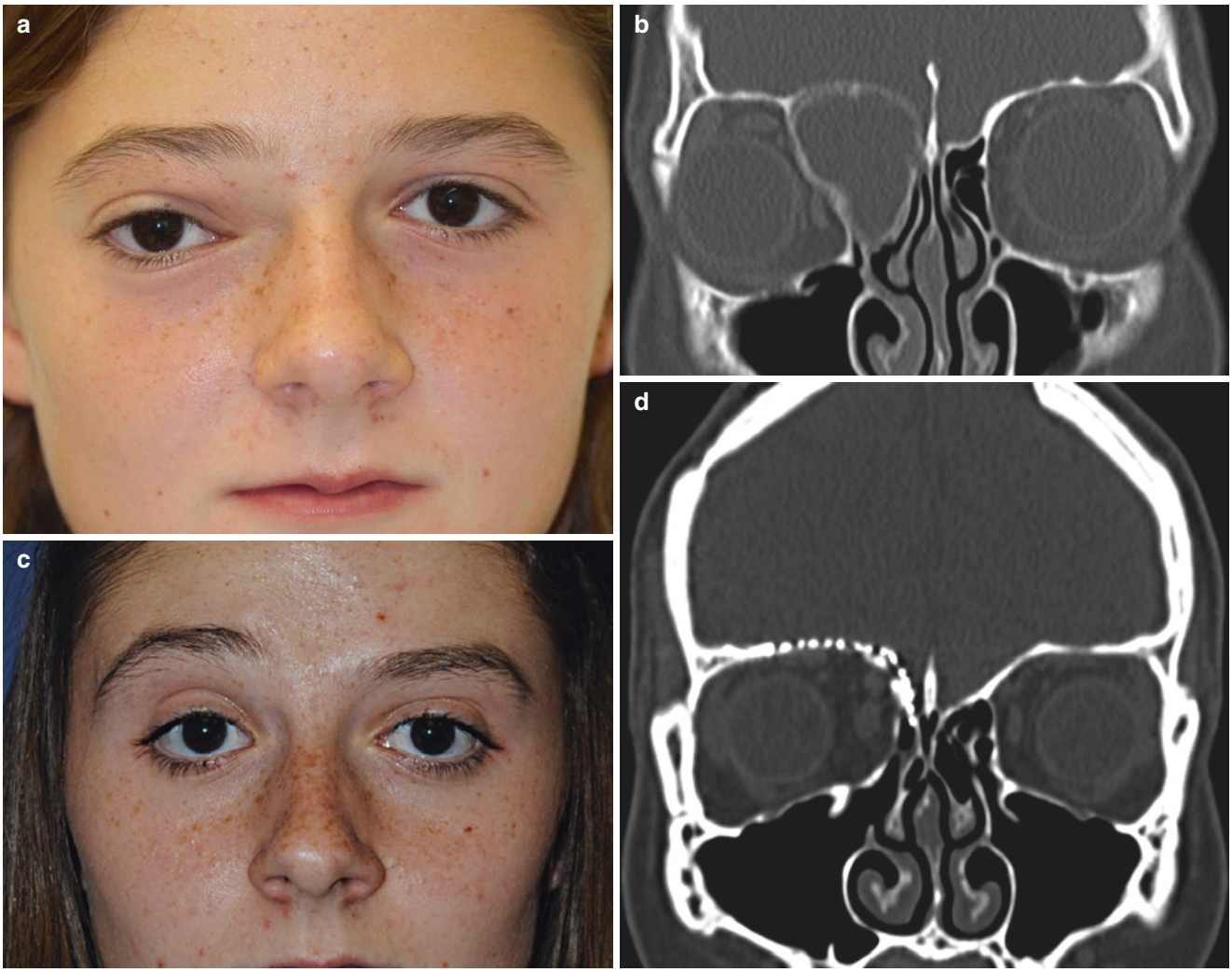


Fig. 35.60 Juvenile ossifying fibroma. (**a**) 15-year-old female with lateral globe displacement. (**b**) Expansile low attenuation lesion centered in the right frontal ethmoidal recess with extension into the anterior right ethmoid air cells, superior aspect right nasal cavity and medial right orbit. There is remodeling, and the osteogenesis and focal regions of thinning of the osseous rim surrounding this low-density lesion. An MRI was also obtained, and the most likely diagnosis was a mucocele. The patient underwent an unsuccessful functional endoscopic sinus procedure to decompress the lesion. Biopsy of the lesion showed a juvenile ossifying fibroma. (**c**) Postoperative photo 6 months after a craniotomy for tumor resection with resection of the anterior skull base, frontal sinus exoneration and removal of the medial orbital wall. The bony defect was repair with titanium mesh and cranial bone graft. (**d**) Postoperative CT 4 years postsurgical resection and reconstruction. The titanium mesh used to reconstruct the orbital roof is visible

milder autosomal dominant form is frequently diagnosed by coincidence from x-ray studies at a much later age in childhood and does not have the systemic and ocular complications associated with the autosomal recessive form.

The ophthalmic complication associated with this condition is compressive optic neuropathy with vision loss and optic atrophy. The skull base is frequently affected in the severe form of osteopetrosis, with resultant narrowing of the optic canals seen on imaging studies [264]. Severe bony involvement may produce proptosis, other orbital cranial nerve palsies, and bony nasolacrimal duct obstruction [265, 266]. The vision loss and optic atrophy may not always be due to optic nerve compression by a narrowing optic foramen; reports of abnormal electroretinogram findings with severe vision loss but with normal appearing retinas need to be taken into consideration and evaluated in these children [267].

In a child with evidence of poor vision and x-ray findings of optic canal narrowing, electrophysical studies should be performed to determine the nature of the vision loss. An abnormal visual evoked response (VER) suggests optic nerve compromise, and optic canal decompression may help to avoid additional vision loss and permanent optic atrophy [268]. Additionally, static or diurnal increased intracranial pressure occurs in some children and can cause optic nerve compromise and require neurosurgical shunting to preserve

vision. These children will also have an abnormal VER but will usually demonstrate optic nerve head swelling not seen in cases of visual dysfunction caused by optic canal narrowing. Lumbar puncture is necessary to help differentiate these two potential causes of progressive vision loss. Other clinical symptoms are addressed with bone marrow transplantation, which can reverse bone density changes as measured both clinically and by photon absorptiometric scans [269, 270].

Fibrous Orbital Tumors

Fibrous Dysplasia

Fibrous dysplasia is a disorder of bone maturation of unknown etiology characterized by the replacement of normal bone by a cellular fibrous stroma containing immature bony cells that are similar to what is observed histopathologically at the woven bone stage of normal osteogenesis. Most cases are identified in children, although the disease progression may be so slow that it escapes recognition until adult years [271]. The majority of cases show isolated, single-site (monostatic) involvement usually involving the cranial base, maxilla, or mandible; multiple-site (polyostotic) involvement is unusual. The polyostotic form of fibrous dysplasia may represent one manifestation of a clinical complex known as McCune-Albright syndrome, which also includes endocrine abnormalities, long-bone deformities, cutaneous pigmentation, and facial fibrous dysplasia [272]. The growth of the facial lesions can be sporadic and may be linked to growth hormone, since the rapid growth phase tends to conclude by the end of the second decade, although some lesions continue to expand into adulthood [253].

Ophthalmic complications have long been recognized in fibrous dysplasia due to the frequent involvement of cranial bones. Most pediatric cases of fibrous dysplasia will present with a variety of ocular symptoms: proptosis and globe displacement due to orbital encroachment by the dysplastic bone, vision loss secondary to optic nerve compression at the optic canal, diplopia from cranial nerve compression in the superior orbital fissure, and epiphora from closure of the bony nasolacrimal duct [273] (Fig. 35.61). The exact presentation depends on which skull bones are affected. Maxillary enlargement will produce superior globe displacement, cheek distension, and epiphora from nasolacrimal duct compromise. Sphenoid involvement produces axial proptosis and gradual vision loss from optic canal compression of the optic nerve. Sudden vision loss from hemorrhage into the cystic spaces of the dysplastic bone has caused permanent blindness [274]. Although rare, bilateral optic nerve compression and vision loss have occurred from sella turcica involvement [275]. Most cases are unilateral even when several contiguous cranial bones show involvement. Fibrous dysplasia of the frontal bone may present with inferior globe displacement, marked enlargement of the brow region, and scalp hypesthesia from supraorbital nerve compromise. Secondary orbital effects may also arise from fibrous dysplasia:

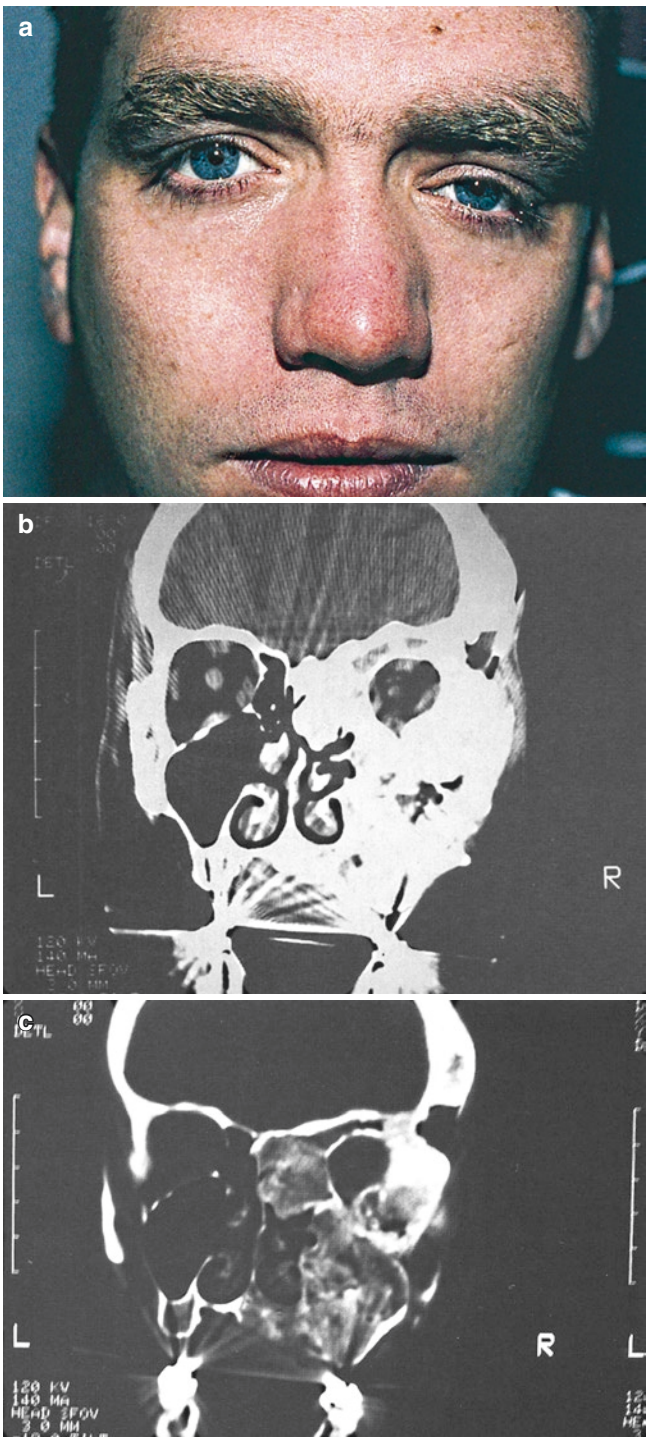


Fig. 35.61 Periorbital fibrous dysplasia. (**a**) Clinical photograph of teenager with left periorbital fibrous dysplasia. (**b**) Soft tissue window CT demonstrates large periorbital mass with calcification limiting orbital volume. (**c**) Bone window CT demonstrates moth-eaten appearance with fibrous lacunae typical for fibrous dysplasia

Ossifying fibromas and mucoceles may arise from or within the dysplastic lesion, and malignant transformation to osteosarcoma and fibrosarcoma within areas of fibrous dysplasia has been reported [276].

This variety of presenting symptoms and signs can mimic other orbital processes, making imaging studies an important diagnostic aid. Plain film radiography demonstrates a mixed picture of both lytic and sclerotic bony changes [277]. CT imaging yields the best information characterizing this bony process [278]. A peculiar mix of irregular lytic and sclerotic changes serves to identify this dysplastic process. Bony thickenings are intermixed with cystic areas, trabeculations, and areas of increased bone density. Once recognized, these features help differentiate this process from lesions that produce a similar but less striking imaging appearance: en plaque meningioma, some fibromas, and, rarely, bone cysts. Three-dimensional CT imaging has proven useful in the planning of craniofacial procedures for the treatment of fibrous dysplasia [279]. MRI can help in the planning of any surgical intervention by better imaging of intraorbital contents and the optic nerve in relation to the dysplastic fibrous process.

The treatment of fibrous dysplasia is dependent on the involvement of normal structures, their functional compromise, and the degree of facial disfigurement. Modern craniofacial techniques using intracranial and extracranial combined approaches for large en bloc resection and debulking of fibrous dysplasia with immediate reconstruction using split-thickness calvarial grafts have produced astounding cosmetic results [271]. At question for these heroic surgical procedures is whether functional improvement is achieved, especially in the case of optic nerve compromise, and whether the surgery delays or halts the unpredictable progression of the dysplastic process. Most studies evaluating functional vision loss in fibrous dysplasia have focused on optic nerve compromise from sphenoid bone involvement and the role of optic nerve decompression [280, 281]. The most recent study by Chen et al. found only two of nine patients who underwent "therapeutic" optic nerve canal decompression for functional vision loss who had any improvement in vision [280]. One of these patients required two procedures to achieve a "useful improvement" in vision from light perception to finger counting at 30 cm. Four other patients had intracranial optic nerve decompression for "prophylactic" indications without demonstrating any preoperative visual acuity changes. The indication for "prophylactic" surgery was based on radiologic evidence of optic canal involvement by the fibrous dysplasia and on a 1968 report of progressive visual compromise among patients who had plain film evidence of optic canal narrowing [282]. Unfortunately, the short-term follow-up of these patients does not indicate whether "prophylactic" decompression is helpful in preventing vision loss. This would appear to have potential merit, given the poor results of visual return in patients who have optic nerve decompression after sudden or progressive slow visual loss.

Longer-term studies are needed to prove the efficacy of this approach. In general, however, we would not advocate the routine use of prophylactic decompression of the optic canal in these cases. Current thinking is that optic canal decompression should be employed early in patients who demonstrate decreased vision and CT evidence of optic nerve compression in order to avoid continued progressive visual decline. Decreased visual evoked potentials, restricted visual fields with cecocentral scotoma, and declining red saturation testing coupled with any visual acuity compromise should trigger consideration of the procedure. Long-term follow-up despite short-term visual stability should be continued due to the progressive nature of fibrous dysplasia and the potential for future visual decline.

Acute visual loss in fibrous dysplasia is poorly understood. Several case reports shed some light on the differential diagnosis of this clinical situation that may guide the physician toward successful reversal of the visual decline. Sudden visual loss after minor head trauma resulted in light perception vision in a 14-year-old with sphenoethmoid fibrous dysplasia [283]. The ophthalmic artery was not visualized on angiography preoperatively and a hematoma was found in dysplastic tissue at the time of emergent optic canal decompression. Postoperatively, vision improved to count fingers and the ophthalmic artery filled on the postoperative angiogram. Sudden visual loss to count fingers in an adult male with fibrous dysplasia due to a cystic structure within the dysplastic tissue over the optic canal was successfully surgically decompressed with return of 20/25 visual acuity [284]. The cystic structure was found to be a mucocele, which was removed along with fibrous tissue at the time of surgery. Unilateral sphenoidal fibrous dysplasia was found in a patient who suffered acute visual loss that was completely reversed by emergent optic canal decompression [285]. A second episode of acute visual loss in the same eye was successfully reversed with high-dose intravenous steroid therapy without additional surgical intervention.

These cases demonstrate potential mechanisms of vision loss in patients with fibrous dysplasia. The source of visual loss in all cases involved acute compression of the optic nerve in the region of the optic canal due to mucocele, hematoma, and presumed inflammation. Careful, rapid imaging studies of the optic canal area are needed to decipher these potential causes. MRI may prove very useful in these circumstances because it may differentiate inflammatory changes, bloody collections, and inspissated mucous. These findings may dictate whether emergent surgical intervention will be of value. Immediate institution of megadosage intravenous steroids may delay or reverse permanent visual loss.

Fibrous Histiocytoma

Fibrous histiocytoma is a tumor consisting of a curious mixture of proliferating fibrous elements mixed with histiocyte-like cells in a collagen matrix with a variable component of lipid, capillaries, reticulin, lymphocytes, and macrophages. These features have engendered multiple names for these lesions in the past: xanthogranuloma, fibrous xanthoma, xanthofibroma, and dermatofibroma. The term fibrous histiocytoma now encompasses all these past entities.

Most fibrous histiocytomas occur in the extremities and abdomen. When found in the orbit, they account for less than 5% of all fibrous histiocytomas. These lesions exhibit slow, progressive expansion with resultant proptosis, diplopia, palpable mass, visual decline, and orbital pain [286]. The majority is seen in adulthood, but childhood diagnosis occurs in about 4% of orbital fibrous histiocytomas; one has been diagnosed at infancy [287]. Only two fibrous histiocytomas were found in a review of pediatric orbital series tabulated in Table 35.1. Equal sex predilection and orbital laterality is seen, but most lesions do show a preference for the superior orbit. Fibrous histiocytomas have been found as primary tumors in the lacrimal sac, on the eyelid, and on the epibulbar surface.

Three classifications of fibrous histiocytoma can be made based on clinical activity and histopathologic features: benign (63%), locally aggressive (26%), and malignant (11%) [286]. Benign lesions are well circumscribed and very slow growing, with minimal nuclear pleomorphism and rare mitotic figures on light microscopy. Long term, these show a 31% incidence of local recurrence after excision but have no associated long-term morbidity or mortality. Locally aggressive lesions demonstrate infiltration of local and nearby tissues. Histopathologically, poorly circumscribed margins with increased tumor cellularity, pleomorphism, and mitotic figures are seen. After excision, 57% recur, with 8% of patients dying within 10 years because of tumor extension.

Malignant fibrous histiocytomas are the least common type. Large-scale cellular pleomorphism and frequent mitotic figures are common in these lesions. Necrosis and hemorrhage are also common in the malignant variety and are not seen in the other types. Sixty-four percent of excised malignant lesions recurred. The 10-year survival was only 23%, based on aggressive local recurrence and spread into contiguous brain structures or through systemic metastases, typically to the lung. Another subvariety, angiomatoid malignant fibrous histiocytoma, seemingly has a pediatric preference, shows extensive vascular elements with hemorrhage, and has been reported in the orbit [288, 289]. Malignant transformation of benign fibrous histiocytoma has occurred after radiotherapy was used to prevent recurrence [286]. While most cases found to be malignant are primarily in the orbit, orbital metastasis from other body sites has occurred [289].

Neuroimaging studies help to anatomically define the presence of these tumors, but no specific features on CT or MRI are capable of differentiating this lesion from similar orbital processes such as cavernous hemangioma, hemangiopericytoma, neurilemmoma, and even dermoid cysts. MRI may be helpful in differentiating primary malignant fibrous histiocytoma if significant intratumor hemorrhage or necrosis is present.

Because of recurrences and the subsequent lack of responsiveness of these tumors to radiotherapy and other modalities, it is clear that the preferred treatment of benign and locally aggressive fibrous histiocytoma is complete surgical excision [286]. Sectioning of the tumor should be performed at the time of excision and frozen section analysis requested to determine if malignancy is present. If so, exenteration should then be performed. Recurrences of benign tumors can be observed and reoperated if functional limitations are seen. Recurrent locally aggressive lesions should undergo exenteration due to their potential for causing death from locally invasive disease and for their risk of malignant potential.

References

1. Grove AS Jr. Orbital disorders: diagnosis and management. In: McCord Jr CD, editor. Oculoplastic surgery. New York: Raven; 1981. p. 274.
2. Cullen JF. Orbital diploic dermoids. Br J Ophthalmol. 1974;58:105–6.
3. Pollard ZF, Calhoun J. Deep orbital dermoid with draining sinus. Am J Ophthalmol. 1975;79:310–3.
4. Grove AS Jr. Giant dermoid cysts of the orbit. Ophthalmology. 1979;86:1513–8.
5. Wolfley DE. The lid crease approach to the superomedial orbit. Ophthalmic Surg. 1985;16:652–6.
6. Kronish JW, Dortzbach RK. Upper eyelid crease surgical approach to dermoid and epidermoid cysts in children. Arch Ophthalmol. 1988;106:1625–7.
7. Golden RP, Shiels WE, Cahill KV, Rogers GL. Percutaneous drainage and ablation of orbital dermoid cysts. J AAPOS. 2007;11(5):438–42.
8. Spencer WH, Zimmerman LE. Congenital and developmental abnormalities of the conjunctiva. In: Spencer WH, editor. Ophthalmic pathology: an Allas and textbook. Philadelphia: Saunders; 1985. p. 123–4.
9. Fries PD, Katowitz JA. Congenital craniofacial anomalies of ophthalmic importance. Sum Ophthalmol. 1990;35:87–119.
10. Jakobiec FA, Stagner AM, Katowitz WR, Eagle RC Jr. A microanatomic abnormality of the lacrimal gland associated with Goldenhar syndrome. Surv Ophthalmol. 2016;61(5):654–63.
11. Beard C. Dermolipoma surgery, or, "an ounce of prevention is worth a pound of cure". Ophthal Plast Reconstr Surg. 1990;6:153–7.
12. Bond JB, Haik BG, Taveras JL, et al. Magnetic resonance imaging of orbital lymphangioma with and without gadolinium contrast enhancement. Ophthalmology. 1992;99:1318–24.
13. Zimmerman LE. Phakomatous choristoma of the eyelid. A tumor of lenticular anlage. Am J Ophthalmol. 1971;1:167–77.
14. Eustis HS, Karcioglu ZA, Dharma S, et al. Phakomatous choristoma: clinical, histopathologic, and ultrastructural findings in a 4 month-old boy. J Pediatr Ophthalmol Strabismus. 1990;27:208–11.

15. Seregard S. Phakomatous choristoma may be located in the eyelid or orbit or both. Acta Ophthalmol Scand. 1999;77(3):343–6.
16. Leatherbarrow B, Nerad JA, Carter KD, et al. Phakomatous choristoma of the orbit: a case report. Br J Ophthalmol. 1992;76:507–8.
17. Peres LC, da Silva AR, Belluci AD, Cruz AA. Phakomatous choristoma of the orbit. Orbit. 1998;17(1):47–53.
18. Ellis FJ, Eagle RC Jr, Shields JA, Shields CL, et al. Phakomatous Choristoma (Zimmerman's tumor). Immunohistochemical confirmation of lens-specific proteins. Ophthalmology. 1993;100(6):955–60.
19. Dithmar S, Schmack I, Volcker HE, Grossniklaus HE. Phakomatous choristoma of the eyelid. Graefes Arch Clin Exp Ophthalmol. 2004;242(1):40–3.
20. Shields JA, Kaden IH, Eagle RC, et al. Orbital dermoid cysts: clinicopathologic correlations, classification, and management. Ophthal Plast Reconstr Surg. 1997;13:265–76.
21. Pokorny KS, Hyman BM, Jakobiec FA, et al. Epibulbar choristomas containing lacrimal tissue: clinical distinction from dermoids and histologic evidence of an origin from the palpebral lobe. Ophthalmology. 1987;94:1249–61.
22. Green WR, Zimmerman LE. Ectopic lacrimal gland tissue: report of eight cases with orbital involvement. Arch Ophthalmol. 1967;78:318–25.
23. Newman NJ, Miller NR, Green WR. Ectopic brain in the orbit. Ophthalmology. 1986;93:268–72.
24. Newton C, Dutton JJ, Klintworth GK. A respiratory epithelial choristomatous cyst of the orbit. Ophthalmology. 1985;92:1754–7.
25. Call NB, Baylis HI. Cerebellar heterotopia in the orbit. Arch Ophthalmol. 1980;98:717–9.
26. James CRH, Lyness R, Wright JE. Respiratory epithelium lined cysts presenting in the orbit without associated mucocele formation. Br J Ophthalmol. 1986;70:387–90.
27. Jakobiec FA, Bonanno PA, Sigelman J. Conjunctival adnexal cysts and dermoid. Arch Ophthalmol. 1978;96:1404–9.
28. Lieb W, Rochels R, Gronemeyer U. Microphthalmos with colobomatous orbital cyst: clinical, histological, immunological and electronmicroscopic findings. Br J Ophthalmol. 1990;74:59–62.
29. Baghdassarian SA, Tabbara KF, Matts CS. Congenital cystic eye. Am J Ophthalmol. 1973;76:269–75.
30. Nowinski T, Shields JA, Augsburger JJ, et al. Exophthalmos secondary to massive intraocular gliosis in a patient with colobomatous cyst. Am J Ophthalmol. 1984;97:641–3.
31. Guterman C, Abbout E, Mets MB. Microphthalmos with cyst and Edwards' syndrome. Am J Ophthalmol. 1990;109:228–30.
32. Warburg M. An update on microphthalmos and coloboma: a brief survey of genetic disorders with microphthalmos and coloboma. Ophthalmic Paediatr Genet. 1991;12:57–63.
33. Weiss A, Greenwald M, Martinez C. Microphthalmos with cyst: clinical presentations and computed tomographic findings. J Pediatr Ophthalmol Strabismus. 1985;22:6–12.
34. Polito E, Leccisotti A. Colobomatous ocular cyst excision with globe preservation. Ophthal Plast Reconstr Surg. 1995;11:288–92.
35. Waring GO, Roth AM, Rodrigues MM. Clinicopathologic correlations of microphthalmos with cyst. Am J Ophthalmol. 1976;82:714–21.
36. Lund VJ. Anatomical considerations in the etiology of frontoethmoidal mucoceles. Rhinology. 1987;25:83–8.
37. de Juan E Jr, Green WR, Iliff NT. Allergic periorbital mucopyocele in children. Am J Ophthalmol. 1983;96:299–303.
38. Stool S, Kertesz E, Sibinga M, et al. Exophthalmos due to pyocele of the sinus in children with cystic fibrosis. Trans Am Acad Ophthalmol Otolaryngol. 1966;70:811–6.
39. Johnson LN, Heplen RS, Yee RD, et al. Sphenoid sinus mucocele (anterior clinoid variety) mimicking diabetic ophthalmoplegia and retrobulbar neuritis. Am J Ophthalmol. 1990;102:111–4.
40. Stanton MB. Sphenoid sinus mucocele. Am J Ophthalmol. 1970;70:991–4.
41. Vashist S, Goulatis RK, Dayol Y, et al. Radiological evaluation of mucocele of the paranasal sinuses. Br J Radiol. 1985;58:959–63.
42. Dillon WP, Som PM, Fullerton GD. Hypointense MR signal in chronically inspissated sinonasal secretions. Radiology. 1990;174:73–8.
43. Neel HB, McDonald TJ, Facer GW. Modified lynch procedure for chronic frontal sinus disease: rationale, technique and long-term results. Laryngoscope. 1987;97:1274–9.
44. Bernardini FP, Cetinkaya A, Capris P, Rossi A, Kaynak P, Katowitz JA. Orbital and periorbital extension of congenital dacryocystoceles: suggested mechanism and management. Ophthal Plast Reconstr Surg. 2016;32(5):e101–4.
45. Lund VJ, Rolfe ME. Ophthalmic considerations in frontoethmoidal mucoceles. J Laryngol Otol. 1989;103:667–9.
46. Chang JR, Grant MP, Merbs SL. Enucleation as endoscopic sinus surgery complication. JAMA Ophthalmol. 2015;133(7):850–2.
47. Mamalis N, Garland PE, Argyle JC, et al. Congenital orbital teratoma: a review and report of 2 cases. Surv Ophthalmol. 1985;30:41–6.
48. Hoyt WF, Joe S. Congenital teratoid cyst of the orbit. Arch Ophthalmol. 1962;68:196–201.
49. Gnecco JP, Messa Ó, Ayala-Gómez A, Castro-Núñez J. Immature orbital Teratoma with intracranial extension. J Craniofac Surg. 2016;27(6):1614–5.
50. Chang DF, Dallow RL, Walton DS. Congenital orbital teratoma: report of a case with visual preservation. J Pediatr Ophthalmol Strabismus. 1980;7:88–95.
51. Soares EJC, da Silva Lopes K, de Souza Andrade J, et al. Orbital malignant teratoma: a case report. Orbit. 1983;2:235–42.
52. Garden JW, McManis JC. Congenital orbito-intracranial teratoma with subsequent malignancy: case report. Br J Ophthalmol. 1986;70:111–3.
53. Nicholson DH, Green WR. Pediatric ocular tumors. New York: Masson; 1981. p. 215–7.
54. Weiss AH, Greenwald MJ, Margo CE. Primary and secondary orbital teratomas. J Pediatr Ophthalmol Strabismus. 1989;26:44–9.
55. Grosfeld JL, Billmire DF. Teratomas in infancy and childhood. Curr Probl Cancer. 1985;9:1–53.
56. Rapport RL II, Dunn RC Jr, Alhady F. Anterior encephalocele. J Neurosurg. 1981;54:213–9.
57. Koenig SB, Naidich TD, Lissner G. The morning glory syndrome associated with sphenoidal encephalocele. Ophthalmology. 1992;89:1368–73.
58. Rashid ER, Bergstrom TJ, Evans RM, et al. Anterior encephalocele presenting as nasolacrimal obstruction. Ann Ophthalmol. 1986;18:132–6.
59. Monica ML, Connolly ES, Kalil RF. Basal encephalocele presenting with monocular vision loss. J Clin Neuroophthalmol. 1984;4:9–13.
60. Jensen CH, Medgysi S. Meningocele communicating to the lower eyelid discovered during removal of xanthelasmata. Br J Plast Surg. 1986;39:257–9.
61. Lello GE, Sparrow OC, Gopal R. The surgical correction of fronto-ethmoidal meningoencephaloceles. J Craniomaxillofac Surg. 1989;17:293–8.
62. Koopman CF, Reynolds AF. Combined neurosurgical-otolaryngologic operative approach to a massive nasoepithelial encephalomeningocele. Otolaryngol Head Neck Surg. 1981;89:545–9.
63. Rootman J, Graeb DA. Vascular lesions. In: Rootman J, editor. Diseases of the orbit. A multidisciplinary approach. Philadelphia: Lippincott; 1988. p. 525–68.
64. Rootman J. Vascular tumors of the orbit: classification and management. In: Blood, sweat and tears: orbital disease and oculoplastics in the New Millenium. 43rd Annual Postgraduate Symposium in Ophthalmology, Ohio State University Medical Center, Columbus, OH, 10–11 March 2000.

65. Harris G for the Orbital Society. Orbital vascular malformations: a consensus statement on terminology and its clinical implications. Am J Ophthalmol. 1999;127:453–I55.
66. Wassef M, Blei F, Adams D, Alomari A, Baselga E, Berenstein A, Burrows P, Frieden IJ, Garzon MC, Lopez-Gutierrez JC, Lord DJ, Mitchel S, Powell J, Prendiville J, Vikkula M, ISSVA Board and Scientific Committee. Vascular anomalies classification: recommendations from the International Society for the Study of vascular anomalies. Pediatrics. 2015;136(1):e203–14.
67. Rootman J, Heran MK, Graeb DA. Vascular malformations of the orbit: classification and the role of imaging in diagnosis and treatment strategies. Ophthal Plast Reconstr Surg. 2014;30(2):91–104.
68. Frieden IJ, Reese V, Cohen D. PHACE syndrome. The association of posterior fossa brain malformations, hemangiomas, arterial anomalies, coarctation of the aorta and cardiac defects, and eye abnormalities. Arch Dermatol. 1996;132(3):307–11.
69. Neidhart JA, Roach R. Successful treatment of skeletal hemangioma and Kasabach-Merritt syndrome with aminocaproicacid. Am J med. 1982;73:434–8.
70. Haik BG, Karcioglu ZA, Gordon RA, et al. Capillary hemangioma (infantile periocular hemangioma). Surv Ophthalmol. 1994;38:399–426.
71. Bilaniuk LT, Rapoport RJ. Magnetic resonance imaging of the orbit. Top Magn Reson Imaging. 1994;6:167–81.
72. Sklar EL, Quencer RM, Byrne SF, et al. Correlative study of the computed tomographic, ultraonographic and pathologic characteristics of cavernous versus capillary hemangiomas of the orbit. J Clin Neuroophthalmol. 1986;6:14–21.
73. Torres C, Kelly JK, Watts FB Jr. Capillary hemangioma of the orbit: the role of computed tomography. Am Osteopath Assoc. 1987;87:687–91.
74. Boyd MJ, Collin JRO. Capillary hemangiomas: an approach to their management. Br J Ophthalmol. 1991;75:298–300.
75. Haik BJ, Jakobiec FA, Ellsworth RM, et al. Capillary hemangioma of the lids and orbit: an analysis of the clinical features and therapeutic results in 101 cases. Ophthalmology. 1979;86:760–89.
76. Stigmar G, Crawford JS, Ward CM, et al. Ophthalmic sequelae of infantile hemangiomas of the eyelids and orbit. Am J Ophthalmol. 1978;85:806–13.
77. Glowacki J, Mulliken JB. Mast cells in hemangiomas and vascular malformations. Pediatrics. 1982;70:48–51.
78. Dethlefsen SM, Mulliken JB, Glowacki J. An ultrastructural study of mast cell interactions in hemangiomas. Ultrastruct Pathol. 1986;10:175–83.
79. Bowers RE, Graham EA, Tomlinson KM. The natural history of the strawberry nevus. Arch Dermatol. 1960;82:59–72.
80. Margileth AM, Museles M. Cutaneous hemangiomas in children. JAMA. 1965;194:135–8.
81. Léauté-Labrèze C, Dumas de la Roque E, Hubiche T, Boralevi F, Thambo JB, Taïeb A. Propranolol for severe hemangiomas of infancy. N Engl J Med. 2008;358(24):2649–51.
82. Mazzola RF. Treatment of haemangiomas in children by intralesional injection of steroids. Chir Plast (Berl). 1978;4:161–7.
83. Kushner BJ. Intralesional corticosteroid injection for infantile adnexal hemangioma. Am J Ophthalmol. 1982;93:496–506.
84. Hiles DA, Pilchard WA. Corticosteroid control of neonatal hemangiomas of the orbit and ocular adnexa. Am J Ophthalmol. 1971;71:1003–8.
85. Fost NC, Esterly NB. Successful treatment of juvenile hemangiomas with prednisone. J Pediatr. 1968;72:351–7.
86. Cruz OA, Zarnegar SR, Myers SE. Treatment of periocular capillary hemangioma with topical clobetasol propionate. Ophthalmology. 1995;102:2012–5.
87. Elsas FJ, Lewis AR. Topical treatment of periocular capillary hemangioma. J Pediatr Ophthalmol Strabismus. 1994;31:153–6.
88. Shorr N, Seiff SR. Central retinal artery occlusion associated with periocular corticosteroid injection for juvenile hemangioma. Ophthalmic Surg. 1986;17:229–31.
89. Apfelberg DB, Maser MR, White DN, et al. Benefits of contact and non-contact YAG laser for periorbital hemangiomas. Ann Plast Surg. 1990;24:397–408.
90. Gladstone GJ, Beckman H. Argon laser treatment of an eyelid margin capillary hemangioma. Ophthalmic Surg. 1983;14:944–6.
91. Ashinoff R, Geronemus RG. Capillary hemangiomas and treatment with the flash lamp-pumped pulsed dye laser. Arch Dermatol. 1991;127:202–5.
92. Chopdar A. Carbon-dioxide laser treatment of eyelid lesions. Trans Ophthalmol Soc UK. 1985;104:176–80.
93. Loughnan MS, Elder J, Kemp A. Treatment of a massive orbital capillary hemangioma with interferon alfa-2b: short term results. Arch Ophthalmol. 1992;110:1366–7.
94. Garden JM, Bakus AD, Paller AS. Treatment of cutaneous hemangiomas by the flashlamp-pumped pulse dye laser: prospective analysis. J Pediatr. 1992;120:555–60.
95. Walker RS, Custer PL, Nerad JA. Surgical excision of periorbital capillary hemangiomas. Ophthalmology. 1994;101:1333–40.
96. Deans RM, Harris GJ, Kivlin JD. Surgical dissection of capillary hemangiomas: an alternative to intralesional corticosteroids. Arch Ophthalmol. 1992;110:1743–7.
97. Jones IS. Lymphangiomas of the ocular adnexa: an analysis of 62 cases. Trans Am Ophthalmol Soc. 1959;57:602–65.
98. Pang P, Jakobiec FA, Iwamoto T, et al. Small lymphangiomas of the eyelids. Ophthalmology. 1984;91:1278–84.
99. Iliff WJ, Green WR. Orbital lymphangiomas. Ophthalmology. 1979;86:914–29.
100. Dryden RM, Wulc AE, Day D. Eyelid ecchymosis and proptosis in lymphangioma. Am J Ophthalmol. 1985;100:486–7.
101. Eiferman RA, Gushard RH. Chocolate cysts of the orbit. Ann Ophthalmol. 1986;18:156–7.
102. Skalka HW, Callahan MA. Ultrasonically-aided percutaneous orbital aspiration. Ophthalmic Surg. 1979;10:41–3.
103. Kazim M, Kennerdell JS, Rothfus W, et al. Orbital lymphangioma: correlation of magnetic resonance images and intraoperative findings. Ophthalmology. 1992;99:1588–94.
104. Kennerdell JS, Maroon JC, Garrity JA, et al. Surgical management of orbital lymphangioma with the carbon dioxide laser. Am J Ophthalmol. 1986;102:308–14.
105. Wilson ME, Parker PL, Chavis RM. Conservative management of childhood orbital lymphangioma. Ophthalmology. 1989;96:484–189.
106. Fukunaga M. Expression of D2-40 in lymphatic endothelium of normal tissues and in vascular tumours. Histopathology. 2005;46(4):396–402.
107. Gandhi NG, Lin LK, O'Hara M. Sildenafil for pediatric orbital lymphangioma. JAMA Ophthalmol. 2013;131(9):1228–30.
108. Katowitz WR, Kazim M. Venous-lymphatic malformations (Lymphangioma) of the orbit: diagnostic and therapeutic challenges. In: Katowitz J, Guthoff R, editors. Essentials of ophthalmology, oculoplasticsand orbit. New York: Springer; 2007.
109. Schwarcz RM, Ben Simon GJ, Cook T, Goldberg RA. Sclerosing therapy as first line treatment for low flow vascular lesions of the orbit. Am J Ophthalmol. 2006;141(2):333–9.
110. Ogita S, Tsuto T, Deguchi E, Tokiwa K, Nagashima M, Iwai N. OK-432 therapy for unresectable lymphangiomas in children. J Pediatr Surg. 1991;26(3):263–8.
111. MacIntosh PW, Yoon MK, Fay A. Complications of intralesional bleomycin in the treatment of orbital lymphatic malformations. Semin Ophthalmol. 2014;29(5–6):450–5.
112. Hill RH, Shiels WE, Foster JA, Czyz CN, Stacey A, Everman KR, Cahill KV. Percutaneous drainage and ablation as first line therapy for macrocystic and microcystic orbital lymphatic malformations. Ophthal Plast Reconstr Surg. 2012;28(2):119–25.

113. Vadlamudi V, Gemmete JJ, Chaudhary N, Pandey AS, Kahana A. Transvenous sclerotherapy of a large symptomatic orbital venous varix using a microcatheter balloon and bleomycin. J Neurointerv Surg. 2016;8(8):e30.
114. Dutton JJ. Gliomas of the anterior visual pathways. Surv Ophthalmol. 1994;38:427–52.
115. Rootman J, Graeb DA. Venous anomalies. In: Rootman J, editor. Diseases of the orbit. Philadelphia: Lippincott; 1988. p. 553–7.
116. Bullock JD, Goldberg SH, Connelly PJ. Orbital varix thrombosis. Ophthalmology. 1990;97:251–6.
117. Ball WS, Towbin RB, Kaufman RA. Pediatric case of the day: orbital varix. Radiographics. 1987;7:1181–2.
118. Wright JE. Orbital vascular anomalies. Trans Am Acad Ophthalmol Otolaryngol. 1974;78:OP606–16.
119. Ossoinig KC. Echographic differentiation of vascular tumors in the orbit. In: Thijssen JM, Verbeek AM, editors. Ophthalmic echography. Dordrecht: Junk; 1981. p. 283.
120. Wildenhain PM, Lehar SC, Dastur KJ, et al. Orbital varix: color flow imaging correlated with CT and MR studies. J Comput Assist Tomogr. 1991;15:171–3.
121. Osborn RE, DeWitt JD, Lester PD, et al. Magnetic resonance imaging of an orbital varix with CT and ultrasound correlation. Comput Radiol. 1986;10:155–9.
122. Vignard J, Clay C, Bilaniak LT, et al. Venography of the orbit: an analytic report of 43 cases. Radiology. 1974;110:373–84.
123. Takechi A, Uozumi T, Kiya K, et al. Embolisation of orbital varix. Neuroradiology. 1994;36:487–9.
124. Ward PH. The treatment of orbital varicosities. Arch Otolaryngol Head Neck Surg. 1987;113:286–8.
125. Beyer R, Levine MR, Sternberg I. Orbital varices: a surgical approach. Ophthal Plast Reconstr Surg. 1985;1:205–10.
126. Rathbun JE, Hoyt WF, Beard C. Surgical management of orbitofrontal varix in Klippel–Trenaunay–Weber syndrome. Am J Ophthalmol. 1970;70:109–12.
127. Skalka HW, Callahan MA. "Congenital" hematic cyst of the orbit. Ann Ophthalmol. 1979;11:1103–7.
128. Char DH. Pediatric orbital tumors. In: Char DH, editor. Clinical ocular oncology. 2nd ed. Philadelphia: Lippincott–Raven; 1997. p. 289.
129. Iwamoto T, Jakobiec FA. Ultrastructural comparison of capillary and cavernous hemangiomas of the orbit. Arch Ophthalmol. 1979;97:1144–53.
130. Harris GJ, Jakobiec FA. Cavernous hemangioma of the orbit: an analysis of 66 cases. J Neurosurg. 1979;51:219–34.
131. Revere KE, Katowitz WR, Katowitz JA, Rorke-Adams L, Fisher MJ, Liu GT. Childhood optic nerve glioma: vision loss due to biopsy. Ophthal Plast Reconstr Surg. 2017;33(3S Suppl 1):S107–9.
132. Listernick R, Charrow J, Greenwald M, et al. Natural history of optic pathway tumors in children with neurofibromatosis type 1: a longitudinal study. J Pediatr. 1994;125:63–6.
133. Wulc AE, Bergin DJ, Barnes MD, et al. Orbital optic nerve glioma of adult life. Arch Ophthalmol. 1987;107:1013–6.
134. Yanoff M, Rl D, Zimmerman LE. Juvenile pilocytic astrocytoma ("glioma") of optic nerve: clinicopathologic study of 63 cases. In: Jakobiec FA, editor. Ocular and adnexal tumors. Birmingham: Aesculapius; 1978. p. 685–707.
135. Marquardt MD, Zimmerman LE. Histopathology of meningiomas and gliomas of the optic nerve. Hum Pathol. 1982;13:226–35.
136. Stern J, Jakobiec FA, Housepian EM. The architecture of optic nerve gliomas with and without neurofibromatosis. Arch Ophthalmol. 1980;98:505–11.
137. Imes RK, Hoyt WF. Magnetic resonance imaging signs of optic nerve gliomas in neurofibromatosis 1. Am J Ophthalmol. 1991;111:729–34.
138. Cooling RJ, Wright JF. Arachnoid hyperplasia in optic nerve glioma: confusion with orbital meningioma. Br J Ophthalmol. 1979;63:596–9.
139. Zimmerman LE. Arachnoid hyperplasia in optic nerve glioma. Br J Ophthalmol. 1980;64:638–9.
140. Seiff SR, Brodsky MC, MacDonald G, et al. Orbital optic glioma in neurofibromatosis: magnetic resonance diagnosis of perineural arachnoidal gliomatosis. Arch Ophthalmol. 1987;105:1689–92.
141. de Keizer RJW, de Wolff-Rouendaal D, Bots GTA, et al. Optic glioma with intraocular tumor and seeding in a child with neurofibromatosis. Am J Ophthalmol. 1989;108:717–25.
142. Wilson WB, Finkel RS, McCleary L, et al. Malignant evolution of childhood chiasmal pilocytic astrocytoma. Neurology. 1976;26:322–5.
143. Listernick R, Charrow J, Greenwald MJ, et al. Optic gliomas in children with neurofibromatosis type 1. J Pediatr. 1989;114:788–92.
144. Listernick R, Charrow J, Greenwald MJ. Emergency of optic pathway gliomas in children with neurofibromatosis type 1. After normal neuroimaging results. J Pediatr. 1992;121:584–7.
145. Neurofibromatosis Conference Statement. National Institutes of Health Consensus Development Conference. Arch Neurol. 1988;45:575–8.
146. Packer RJ, Bilaniuk LT, Cohen BH, et al. Intracranial visual pathway gliomas in children with neurofibromatosis. Neurofibromatosis. 1988;1:212–22.
147. Kuenzle C, Weissert M, Roulet E, et al. Followup of optic pathway gliomas in children with neurofibromatosis type 1. Neuropediatrics. 1994;25:295–300.
148. Housepian EM. Management and results of 114 cases of optic glioma (abstract). Neurosurgery. 1977;1:67–8.
149. Fisher MJ, Avery RA, Allen JC, Ardern-Holmes SL, Bilaniuk LT, Ferner RE, Gutmann DH, Listernick R, Martin S, Ullrich NJ, Liu GT, REiNS International Collaboration. Functional outcome measures for NF1-associated optic pathway glioma clinical trials. Neurology. 2013;81(21 Suppl 1):S15–24.
150. Rush JA, Younge BR, Campbell RJ, et al. Optic glioma: long-term followup of 85 histopathologically verified cases. Ophthalmology. 1982;89:1213–9.
151. Alvord EC Jr, Lofton S. Gliomas of optic nerve or chiasm: outcome by patient's age, tumor site and treatment. J Neurosurg. 1988;68:85–98.
152. McLeod AR. Acute blindness in childhood optic glioma caused by hematoma. J Pediatr Ophthalmol Strabismus. 1983;20:31–3.
153. Jordan DR, Anderson RL, White GL Jr, et al. Acute visual loss due to a calcified optic nerve glioma. Can J Ophthalmol. 1989;24:335–9.
154. Borit A, Richardson EP Jr. The biological and clinical behavior of pilocytic astrocytomas of the optic pathways. Brain. 1982;105:161–87.
155. Jakobiec FA, Depot MJ, Kennerdell JS, et al. Combined clinical and computed tomographic diagnosis of orbital glioma and meningioma. Ophthalmology. 1984;91:137–55.
156. Haik BG, Saint Louis L, Bierly J, et al. Magnetic resonance imaging in the evaluation of optic nerve gliomas. Ophthalmology. 1987;94:709–17.
157. Hendrix LE, Kneeland JB, Haughton VM, et al. MR imaging of optic nerve glioma: value of gadopentetate dimeglumine and fat-suppression technique. Am J Radiol. 1990;155:849–54.
158. Gans MS, Frazier Byrne S, Glaser JS. Standardized A-scan echography in optic nerve disease. Arch Ophthalmol. 1987;105:1232–6.
159. Ossoinig KC. A-scan echography and orbital disease. Mod Probl Ophthalmol. 1975;14:203–35.
160. Hoyt WJ, Baghdassarian SA. Optic gliomas of childhood: natural history and rationale for conservative management. Br J Ophthalmol. 1969;53:793–8.
161. Imes RK, Hoyt WE. Childhood chiasmal gliomas: update on the fate of patients in the 1969 San Francisco study. Br J Ophthalmol. 1986;70:179–82.

162. Venes JL, Latack J, Kandt RS. Postoperative regression of opticochiasmtic astrocytoma: a case for expectant therapy. Neurosurgery. 1984;15:421–3.
163. Brzowski AE, Bazan C, Mumma JV, et al. Spontaneous regression of optic glioma in a patient with neurofibromatosis. Neurology. 1992;42:679–81.
164. Glaser J, Hoyt WF, Corbett J. Visual morbidity with chiasmal glioma: long-term studies of visual fields in untreated and irradiated cases. Arch Ophthalmol. 1971;85:3–12.
165. Avery RA, Fisher MJ, Liu GT. Optic pathway gliomas [review]. J Neuroophthalmol. 2011;31(3):269–78.
166. Aarabi B, Long DM, Miller NR. Enlarging optic chiasmal glioma with stable visual acuity. Surg Neurol. 1978;10:175–7.
167. Levin LA, Jakobiec FA. Optic nerve tumors of childhood: a decision-analytical approach to their diagnosis. Int Ophthalmol Clin. 1992;32:223–40.
168. Wright JE, McNabb AA, McDonald WI. Optic nerve glioma and the management of optic nerve tumours in the young. Br J Ophthalmol. 1989;73:967–74.
169. Flickinger JC, Torres C, Deutsch M. Management of low-grade gliomas of the optic nerve and chiasm. Cancer. 1988;61:635–42.
170. Shriver EM, Ragheb J, Tse DT. Combined transcranial-orbital approach for resection of optic nerve gliomas: a clinical and anatomical study. Ophthal Plast Reconstr Surg. 2012;28(3):184–91.
171. Spicer GJ, Kazim M, Glass LR, Harris GJ, Miller NR, Rootman J, Sullivan TJ. Accuracy of MRI in defining tumor-free margin in optic nerve glioma surgery. Ophthal Plast Reconstr Surg. 2013;29(4):277–80.
172. Katowitz WR, Fisher MJ, Liu, G, Katowitz JA. Debulking optic nerve gliomas for disfiguring proptosis: a globe-sparing approach by lateral orbitotomy alone. ASOPRS 46th Annual Fall Scientific Symposium, ASOPRS 2015.
173. Grabenbauer GG, Schuchardt U, Buchfelder M, et al. Radiation therapy of optico-hypothalamic gliomas (OHG)--radiographic response, vision and late toxicity. Radiother Oncol: Journal of the European Society for Therapeutic Radiology and Oncology. 2000;54(3):239–45.
174. Sharif S, Ferner R, Birch JM, et al. Second primary tumors in neurofibromatosis 1 patients treated for optic glioma: substantial risks after radiotherapy. J Clin Oncol. 2006;24(16):2570–5.
175. Ullrich NJ, Robertson R, Kinnamon DD, et al. Moyamoya following cranial irradiation for primary brain tumors in children. Neurology. 2007;68(12):932–8.
176. Lloyd LA. Gliomas of the optic nerve and chiasm in childhood. Trans Am Ophthalmol Soc. 1973;71:488–535.
177. Kovalic JJ, Grigsby PW, Shephard MJ, et al. Radiation therapy for gliomas of the optic nerve and chiasm. Int J Radiat Oncol Biol Phys. 1990;18:927–32.
178. Rappaport R, Brauner R. Growth and endocrine disorders secondary to cranial irradiation. Pediatr Res. 1989;25:561–7.
179. Brauner R, Malandry F, Rappaport R. Growth and endocrine disorders in optic glioma. Eur J Pediatr. 1990;149:825–8.
180. Davis PC, Hoffman JC Jr, Pearl GS, et al. CT evaluation of effects of cranial radiation therapy in children. Ant J Neuro Radiol. 1986;7:639–44.
181. Okuno T, Prensky AL, Gado M. The Moyamoya syndrome associated with irradiation of optic glioma in children: report of 2 cases and review of the literature. Pediatr Neurol. 1985;1:311–6.
182. Ater JL, Xia C, Mazewski CM, et al. Nonrandomized comparison of neurofibromatosis type 1 and non-neurofibromatosis type 1 children who received carboplatin and vincristine for progressive low-grade glioma: a report from the Children's oncology group. Cancer. 2016;122(12):1928–36.
183. Needle MN, Phillips P MD, Sutton L, et al. A phase II pilot evaluation of the efficacy of etoposide for progressive optic pathway glioma in patient with neurofibromatosis 1. Children's Hospital of Philadelphia Treatment Protocol, Sept. 1995.
184. Janss AJ, Grundy R, Cnaan A, et al. Optic pathway and hypothalamic-chiasmatic gliomas in children younger than age 5 years with a 6-year followup. Cancer. 1995;75:1051–9.
185. Garvey M, Packer RJ. An integrated approach to the treatment of chiasmatic-hypothalamic gliomas. J Neuro-Oncol. 1996;28:167–83.
186. Rodriguez LA, Edwards MSB, Levin VA. Management of hypothalamic gliomas in children: an analysis of 33 cases. Neurosurgery. 1990;26:242–7.
187. Cunningham JM, Kimmel DW, Scheithauer BW, et al. Analysis of proliferation markers and p53 expression in gliomas of astrocytic origin: relationships and prognostic value. J Neurosurg. 1997;86:121–30.
188. Wilson WB. Meningiomas of the anterior visual system. Surv Ophthalmol. 1981;26:109–27.
189. Spencer WH. Primary neoplasms of the optic nerve and its sheath: clinical features and current concepts of pathogenetic mechanisms. Trans Am Ophthalmol Soc. 1972;70:490–528.
190. D'Alena PR. Primary orbital meningioma. Arch Ophthalmol. 1964;71:832–6.
191. Karp LA, Zimmerman LE, Borit A, et al. Primary intraorbital meningiomas. Arch Ophthalmol. 1974;91:24–8.
192. Hudson AC. Primary tumors of the optic nerve. R Ophthalmol Hosp Rep. 1912;18:317–439.
193. Dutton JJ. Optic nerve sheath meningiomas. Surv Ophthalmol. 1992;37:167–83.
194. Wright JE. Primary optic nerve sheath meningiomas: clinical presentation and management. Trans Am Acad Ophthalmol Otolaryngol. 1977;83:617–25.
195. Kennerdell JS, Maroon JC, Malton M, et al. The management of optic sheath meningiomas. Am J Ophthalmol. 1988;106:450–7.
196. Craig WM, Gogela LJ. Intraorbital meningiomas: a clinicopathologic study. Am J Ophthalmol. 1949;32:1663–80.
197. Vanikieti K, Preechawat P, Poonyathalang A. Pediatric primary optic nerve sheath meningioma. Int Med Case Rep J. 2015;8:159–63.
198. Trobe JD, Glaser JS, Post JD, et al. Bilateral optic canal meningiomas: a case report. Neurosurgery. 1978;3:68–74.
199. Wright JE, McNab AA, McDonald WI. Primary optic sheath meningioma. Br J Ophthalmol. 1989;73:960–6.
200. Imes RK, Schatz H, Hoyt WF, et al. Evolution of optociliary veins in optic nerve sheath meningioma. Arch Ophthalmol. 1985;103:59–60.
201. Sarkies NJC. Optic nerve sheath meningioma: diagnostic features and therapeutic alternatives. Eye. 1987;1:597–602.
202. Daniels DL, Williams AL, Syvertsen A, et al. CT recognition of optic nerve sheath meningioma: abnormal sheath visualization. AJNR. 1982;3:181–4.
203. Alper MG, Sherman JL. Gadolinium enhanced magnetic resonance imaging in the diagnosis of anterior visual pathway meningiomas. Trans Am Ophthalmol Soc. 1989;87:384–415.
204. Zimmerman CF, Schatz NJ, Glaser JS. Magnetic resonance imaging of optic nerve meningiomas: enhancement with gadolinium-DTPA. Ophthalmology. 1990;97:585–91.
205. Tien RD, Chu PK, Hesselink JR, et al. Intra- and paraorbital lesions: value of fat-suppression MR imaging with paramagnetic contrast enhancement. Am J Neuroradiol. 1991;12:245–53.
206. Henderson JW. Meningioma. In: Henderson JW, editor. Orbital tumors. 3d ed. New York: Raven; 1994. p. 377–81.
207. Cibis GW, Whittaker C, Wood WE. Intraocular extension of optic nerve mengingioma in a case of neurofibromatosis. Arch Ophthalmol. 1985;103:404–6.
208. Walsh FB. Meningiomas, primary within the orbit and optic canal. In: Glaser JS, Smith JL, editors. Neuro-ophthalmology. St. Louis: Mosby; 1975. p. 166–90.

209. Maier H, Ofner D, Hittmair A, et al. Classic, atypical and anaplastic meningioma: three histopathological subtypes of clinical relevance. J Neurosurg. 1992;77:616–23.
210. Alper MG. Management of primary optic nerve meningiomas. J Clin Neuroophthalmol. 1981;1:101–17.
211. Kupersmith MJ, Warren FA, Newell J, et al. Irradiation of meningiomas of the intracranial anterior visual pathway. Ann Neurol. 1987;21:131–7.
212. Smith JL, Vuksanovic MM, Yates BM, et al. Radiation therapy for primary optic nerve meningiomas. J Clin Neuroophthalmol. 1981;1:85–99.
213. Verma SK, Satyarthee G, Borkar SA, Singh M, Sharma BS. Orbital roof intradiploic meningioma in a 16-year-old girl. J Pediatr Neurosci. 2015;10(1):51–4.
214. Chamberlain MC. Adjuvant combined modality therapy for malignant meningiomas. J Neurosurg. 1996;84:733–6.
215. Riccardi VM. Neurofibromatosis: phenotype, natural history and pathogenesis. 2d ed. Baltimore: Johns Hopkins University Press; 1992.
216. Wallace MR, Marchuk DA, Anderson LB, et al. Type 1 neurofibromatosis gene: identification of a large transcript disrupted in three NF-1 patients. Science. 1990;249:181–6.
217. Farris SR, Grove AS Jr. Orbital and eyelid manifestations of neurofibromatosis: a clinical study and literature review. Ophthal Plast Reconstr Surg. 1996;12:245–59.
218. Huson S, Jones D, Beck L. Ophthalmic manifestations of neurofibromatosis. Br J Ophthalmol. 1987;71:235–8.
219. White AK, Smith RJH, Bigler CR, et al. Head and neck manifestations of neurofibromatosis. Laryngoscope. 1986;96:732–7.
220. Riccardi VM, Powell PP. Neurofibrosarcoma as a complication of von Recklinghausen neurofibromatosis. Neurofibromatosis. 1989;2:152–65.
221. Reed D, Robertson WD, Rootman J, et al. Plexiform neurofibromatosis of the orbit: CT evaluation. Am J Neuroradiol. 1986;7:259–63.
222. Linder B, Campos M, Schafer M. CT and MRI of orbital abnormalities in neurofibromatosis and selected craniofacial anomalies. Radiol Clin N am. 1987;25:787–802.
223. Bognanno JR, Edwards MK, Lee TA, et al. Cranial MR imaging in neurofibromatosis. Aw J Radiol. 1988;151:381–8.
224. Aoki S, Barkovich AJ, Nishimura K, et al. Neurofibromatosis types 1 and 2: cranial MR findings. Radiology. 1989;172:527–34.
225. Tenzel RR, Boynton JR, Miller GR, et al. Surgical treatment of eyelid neurofibromas. Arch Ophthalmol. 1977;95:479–83.
226. Jackson IT, Carbonnel A, Potparic Z, et al. Orbitotemporal neurofibromatosis: classification and treatment. Plast Reconstr Surg. 1993;92:1–11.
227. Morax S, Herdan ML, Hurbli T. The surgical management of orbito-palpebral neurofibromatosis. Ophthal Plast Reconstr Surg. 1988;4:203–13.
228. Jackson IT, Laws ER Jr, Martin RO. The surgical management of orbital neurofibromatosis. Plast Reconstr Surg. 1983;71:751–8.
229. Needle MN, Cnaan A, Dattilo J, Chatten J, Phillips PC, Shochat S, Sutton LN, Vaughan SN, Zackai EH, Zhao H, Molloy PT. Prognostic signs in the surgical management of plexiform neurofibroma: the Children's Hospital of Philadelphia experience, 1974–1994. J Pediatr. 1997;131(5):678–82.
230. Kennerdall JS, Maroon JC. Use of carbon dioxide laser in the management of orbital neurofibromatosis. Ophthalmol Surg. 1990;21:138–40.
231. Riccardi VM. Mast-cell stabilization to decrease neurofibroma growth: preliminary experience with ketotifen. Arch Dermatol. 1987;123:1011–7.
232. Riccardi VM. A controlled multiphase trial of ketotifen to minimize neurofibroma-associated pain and itching. Arch Dermatol. 1993;129:577–81.
233. Blakeley JO, Plotkin SR. Therapeutic advances for the tumors associated with neurofibromatosis type 1, type 2, and schwannomatosis. Neuro-Oncology. 2016;18(5):624–38.
234. Widemann B, Leigh JM, Fisher MJ, et al. Phase I study of the MEK1/2 inhibitor selumetinib (AZD6244) hydrogen sulfate in children and young adults with neurofibromatosis type 1 (NF1) and inoperable plexiform neurofibromas (PNs). J Clin Oncol. 2014;32(suppl):abstr 10018.
235. Widemann BC, Babovic-Vuksanovic D, Dombi E, Wolters PL, Goldman S, Martin S, Goodwin A, Goodspeed W, Kieran MW, Cohen B, Blaney SM, King A, Solomon J, Patronas N, Balis FM, Fox E, Steinberg SM, Packer RJ. Phase II trial of pirfenidone in children and young adults with neurofibromatosis type 1 and progressive plexiform neurofibromas. Pediatr Blood Cancer. 2014;61(9):1598–602. doi:10.1002/pbc.25041. Epub 2014 Apr 22
236. Avery RA, Katowitz JA, Fisher MJ, et al. Orbital/Peri-orbital plexiform Neurofibromas in children with Neurofibromatosis type 1: multi-disciplinary recommendations for care. Ophthalmology. 2016;124:123–32.
237. Molloy PT, Needle JN, Cnaan A, et al. A randomized phase II trial of cis-retanoic acid or interferon alpha 2a in the treatment of plexiform neurofibroma in patients with neurofibromatosis type 1. Cancer, (in press).
238. Henderson JW. Orbital tumors. Philadelphia: Saunders; 1973. p. 297.
239. Krohel GB, Rosenberg PN, Wright JE, et al. Localized orbital neurofibromas. Am J Ophthalmol. 1985;100:458–64.
240. Shields JA, Shields CL, Lieb WE, et al. Multiple orbital neurofibromas unassociated with von Recklinghausen's disease. Arch Ophthalmol. 1990;108:80–3.
241. Rootman J, Goldberg C, Robertson W. Primary orbital schwannomas. Br J Ophthalmol. 1982;66:194–204.
242. Henderson JW. Orbital tumors. 3d ed. New York: Raven; 1994. p. 229.
243. Shields JA, Kiralti H, Shields CL, et al. Schwannoma of the eyelid in a child. J Pediatr Ophthalmol Strabismus. 1994;31:332–3.
244. Schatz H. Benign orbital neurilemmoma: sarcomatous transformation in von Recklinghausen's disease. Arch Ophthalmol. 1971;86:268–73.
245. Das Gupta TK, Brasfield RD. Solitary malignant schwannoma. Ann Surg. 1970;171:419–128.
246. Ivekovic R, Skegro I, Mandic Z. Orbital schwannoma. Orbit. 1996;15:37–9.
247. Eviatar JA, Hornblass A, Herschorn B, et al. Malignant peripheral nerve sheath tumor of the orbit in a 15-month-old child: nine year survival after local excision. Ophthalmology. 1992;99:1595–9.
248. White HP. Survival in malignant schwannoma: an 18-year study. Cancer. 1971;27:720–31.
249. Coleman DJ, Jack RL, Franzen LA. Neurogenic tumors of the orbit. Arch Ophthalmol. 1972;88:380–4.
250. Grove AS Jr. Osteomas of the orbit. Ophthalmic Surg. 1978;9:23–39.
251. Whitson WE, Orcutt JC, Walkinshaw MD. Orbital osteoma in Gardner's syndrome. Am J Ophthalmol. 1986;101:236–40.
252. Sevel D, James HE, Burns R, et al. McCune-Albright syndrome (fibrous dysplasia) associated with an orbital tumor. Ann Ophthalmol. 1984;16:283–6.
253. Leone CR Jr, Lawton AW, Leone RT. Benign osteoblastoma of the orbit. Ophthalmology. 1988;95:1554–8.
254. Lowder CY, Berlin AJ, Cox WA, et al. Benign osteoblastoma of the orbit. Ophthalmology. 1986;93:1351–4.
255. Jackson RP. Recurrent osteoblastoma: a review. Clin Orthop. 1978;131:229–33.
256. Margo CE, Ragsdale BD, Perman KI, et al. Psammomatoid (juvenile) ossifying fibroma of the orbit. Ophthalmology. 1985;92:150–9.
257. Shields JA, Nelson LB, Brown JF, et al. Clinical, computed tomographic and histopathologic characteristics of juvenile

ossifying fibroma with orbital involvement. Am J Ophthalmol. 1983;96:650–3.
258. Fakadej A, Boynton JR. Juvenile ossifying fibroma of the orbit. Ophthal Plast Reconstr Surg. 1996;12:174–7.
259. Ronner HJ, Jones IS. Aneurysmal bone cyst of the orbit: a review. Ann Ophthalmol. 1983;15:626–9.
260. Powell J, Glaser J. Aneurysmal bone cysts of the orbit. Arch Ophthalmol. 1975;93:340–2.
261. Johnson TE, Bergin DJ, McCord CD. Aneurysmal bone cyst of the orbit. Ophthalmology. 1988;95:86–9.
262. Yee RD, Cogan DG, Thorp TR, et al. Optic nerve compression due to aneurysmal bone cyst. Arch Ophthalmol. 1977;95:2176–9.
263. Ruiter DJ, van Rijssel TG, van der Velde EA. Aneurysmal bone cysts: a clinicopathologic study of 105 cases. Cancer. 1977;39:2231–9.
264. Ellis P, Jackson WE. Osteopetrosis: a clinical study of optic nerve involvement. Am J Ophthalmol. 1962;53:943–53.
265. Aasved H. Osteopetrosis from the ophthalmological point of view: a report of 2 cases. Acta Ophthalmol. 1970;48:771–7.
266. Beighton P, Hamersma H. Ophthalmological complications in the sclerosing bone disorders. Ophthalm Paedtr Genet. 1985;6:129–34.
267. Hoyt CS, Billson FA. Visual loss in osteopetrosis. Am J Dis Child. 1979;133:955–8.
268. Al-Mefty O, Fox JL, Al-Rodhan N, et al. Optic nerve decompression in osteopetrosis. J Neurosurg. 1988;68:80–4.
269. Sorrell M, Kapoor N, Kirkpatrick D, et al. Marrow transplantation for juvenile osteopetrosis. Am J Med. 1981;70:1280–7.
270. Kaplan FS, August CS, Dalinka MK, et al. Bone densitometry observations of osteopetrosis in response to bone marrow transplantation. Clin Orthop. 1993;294:79–84.
271. Moore AT, Buncic JR, Munro IT. Fibrous dysplasia of the orbit in childhood: clinical features and management. Ophthalmology. 1985;92:12–20.
272. Harris WH, Dudley HR Jr, Barry RJ. The natural history of fibrous dysplasia: an orthopedic, pathological and roentgenographic study. J Bone Joint Surg. 1962;44:207–33.
273. Liakos GM, Walker CB, Carruth JAS. Ocular complications in craniofacial fibrous dysplasia. Br J Ophthalmol. 1979;63:611–6.
274. Ronner HJ, Trokel SJ, Hilal S. Acute blindness in a patient with fibrous dysplasia. Orbit. 1982;1:231–4.
275. Weyand RD, Craig WM, Rucker CW. Unusual lesions involving the optic chiasm. Proc Stf Mtg Mayo Clin. 1952;27:505–11.
276. Gross CW, Montgomery WW. Fibrous dysplasia and malignant degeneration. Arch Otolaryngol. 1967;85:653–7.
277. Fries JW. The roentgen features of fibrous dysplasia of the skull and facial bones: a critical analysis of thirty nine pathologically proven cases. Am J Roentgenol Radium Therapy, Nucl med. 1957;77:71–88.
278. Newton TH, Bilaniuk LT, editors. Radiology of the eye and orbit. New York: Raven; 1990. p. 5.70, 9.44.
279. Altman NR, Altman DH, Wolfe SA, et al. Three-dimensional CT reformation in children. Am J Roentgenol. 1986;146:1261–7.
280. Chen YR, Breidahl A, Chang CN. Optic nerve decompression in fibrous dysplasia: indications, efficacy and safety. Plast Reconstr Surg. 1997;99:22–30.
281. Papay F, Morales L, Flaharty P, et al. Optic nerve decompression in cranial base fibrous dysplasia. J Craniofac Surg. 1995;6:5–10.
282. Sassin JF, Rosenberg RN. Neurological complications of fibrous dysplasia of the skull. Arch Neurol. 1968;18:363–74.
283. Kurokawa Y, Sohma T, Tsuchita H, et al. Hemorrhage into fibrous dysplasia following minor head injury: effective decompression for the ophthalmic artery and optic nerve. Neurol Surg. 1989;32:421–6.
284. Weisman JS, Hepler RS, Vinters HV. Reversible visual loss caused by fibrous dysplasia. Am J Ophthalmol. 1990;110:244–9.
285. Arroyo JG, Lessell S, Montgomery WW. Steroid-induced visual recovery in fibrous dysplasia. J Clin Neuroophthalmol. 1991;11:259–61.
286. Font RL, Hidayat AA. Fibrous histiocytoma of the orbit: a clinicopathology study of 150 cases. Hum Pathol. 1982;13:199–209.
287. Biedner B, Rothkoff L. Orbital fibrous histiocytoma in an infant. Am J Ophthalmol. 1978;85:548–50.
288. Enzinger F. Angiomatoid malignant fibrous histiocytoma. Cancer. 1979;44:2147–55.
289. Caballero LR, Rodriguez AC, Sopelana AB. Angiomatoid malignant fibrous histiocytoma of the orbit. Am J Ophthalmol. 1981;92:13–5.
290. Iliff WJ, Green WR. Orbital tumors in children. In: Jakobiec FA, editor. Ocular and adnexal tumors. Birmingham: Aesculapius Publishing Company; 1978. p. 669–84.
291. Crawford JS. Diseases of the orbit. In: Crawford JS, Morin JD, editors. The eye in childhood. New York: Grune & Stratton; 1983. p. 361–94.
292. Shields JA, Bakewell B, Augsberger JJ, et al. Space occupying orbital masses in children. A review of 250 consecutive biopsies. Ophthalmology. 1986;93:379–84.
293. Rootman J. Frequency and differential diagnosis of orbital disease. In: Rootman J, editor. Diseases of the orbit. Philadelphia: J.B. Lippincott Co.; 1988. p. 124.
294. Kodsi SR, Shetlar DJ, Campbell RJ, et al. A review of 340 orbital tumors in children during a 60-year period. Am J Ophthalmol. 1994;117:177–82.
295. Katowitz JA. Unpublished data from the Children's Hospital of Philadelphia, 1996

Malignant Pediatric Orbital Tumors

36

William R. Katowitz and Peter D. Fries

Considerable challenge confronts the ophthalmologist when first encountering a child with proptosis. Besides the alarm and worry of the parents, one has to overcome an anxious, often withdrawn child who has been through one or several attempted or complete examinations. With persistence, time, and gentleness, the examination can be completed, yielding many clues as to the origin of the orbital condition.

Many thoughts crowd the mind of the examiner in this situation, foremost of which is often the potential for a malignant lesion. This can be evaluated by the presence of external features of the more common benign pediatric orbital lesions, such as the consistent position of epidermoids, the purple/red discoloration with infantile hemangiomas, and the characteristic head and face changes seen in specific craniofacial disorders associated with proptosis and the cutaneous abnormalities of neurofibromatosis (see Chap. 35). Lacking these more common signs, however, one has to seriously consider a malignant process in the presence of proptosis and begin the clinical and laboratory steps to accurately diagnose the condition.

Many series have been devoted to the clinical or pathological diagnosis of orbital conditions in the pediatric age group [1–7]. Table 36.1 lists the pediatric malignant orbital lesions as reported from these series. One cannot help but notice the variability among each type of lesion as to how common it appears in the individual series. One institution reported 23 cases of orbital involvement with leukemias and lymphomas, whereas others reported only one case. This disparity is due to the type of reporting institution (tertiary centers receiving more advanced or unusual cases), whether the series is clinically, surgically, or pathologically based, and the reputation of the individual or institution receiving the referral. One may also note the relative paucity of cases of orbital rhabdomyosarcoma (RMS). This reflects just how rare this malignant tumor is, though it should be at the top of any physician's differential of diagnoses that must be ruled out.

The incidence of a malignant orbital lesion as the cause of proptosis in a child or adolescent ranges from 7.9% to 18.8% (Table 36.1). The most common primary malignant orbital lesion in all US series is rhabdomyosarcoma, which accounts for 37.9% (97/256) of all pediatric malignant orbital lesions and 5.3% (97/1820) of all pediatric orbital lesions in the series listed in Table 36.1. Metastatic leukemia and lymphoma account for 14.5% of malignant orbital lesions, while orbital recurrences of retinoblastoma were found in 12.1% of the cases. A total of 28 individuals with Langerhans cell histiocytosis yielded a 10.9% occurrence rate among malignant lesions. A variety of primary and secondary non-rhabdomyosarcoma soft tissue sarcomas accounted for 14.1% of orbital malignancies. These are listed at the bottom of Table 36.1. Metastatic neuroblastoma was found in 5.5%, with most rare orbital entities each accounting for less than 1.5% of the total.

Using the information from these series, the clinical features of malignant orbital lesions combined with imaging studies can often lead the examiner toward an early and correct diagnosis even without a biopsy. However, unusual presentations, rapid progression with systemic features, or confusing clinical scenarios may require biopsy despite typical clinical features or imaging results. In certain disease states, biopsy may be required for staging or treatment decisions regardless of clinical or imaging results. In general, it is never wrong to err on a lesion biopsy, though lesions can be diagnosed with a high level of confidence with high-resolution MRI imaging (e.g., orbital venolymphatic malformation discussed in Chap. 35 and optic pathway glioma as discussed in Chaps. 14 and 35).

W.R. Katowitz, MD (✉)
The Children's Hospital of Philadelphia and
The Edwin and Fannie Gray Hall Center for Human Appearance,
University of Pennsylvania, Philadelphia, PA, USA
e-mail: katowitzw@email.chop.edu

P.D. Fries, MD
Eye Surgeons Associates, PC, Bettendorf, IA, USA

© Springer International Publishing AG 2018

J.A. Katowitz, W.R. Katowitz (eds.), *Pediatric Oculoplastic Surgery*, https://doi.org/10.1007/978-3-319-60814-3_36

Table 36.1 Malignant orbital tumors in children

	Iliff and Green [1] *n* = 174	Crawford [3] *n* = 572	Shields et al. [2] n = 250	Rootman [6] *n* = 241	Kodsi et al. [5] *n* = 340	Katowitz et al. [7] *n* = 243
Rhabdomyosarcoma	15	14	10	5	26	27
Leukemia/lymphoma	2	23	1	*1*	5	*5*
Langerhans Cell histiocytosis	0	18	0	3	4	3
Soft tissue sarcomas[a]	6	9	2	5	9	5
Neuroblastoma	1	9	0	1	3	0
Retinoblastoma	6	1	9	0	14	1
Adenoid cystic carcinoma of lacrimal gland	0	0	1	2	0	0
Nasopharyngeal carcinoma	0	1	0	1	0	0
Esthesioneuroblastoma	0	0	0	0	1	1
Malignant schwannoma	0	0	0	0	0	1
Orbital melanoma	0	0	0	0	1	0
Medulloblastoma metastatic to optic nerve	0	0	0	1	0	0
Malignant teratoma	1	0	0	0	1	0
Metastatic astrocytoma	1	0	0	0	0	0
Total malignant tumors/% all orbital lesions in series	32/18.4%	75/13.1%	23/9.2%	19/7.9%	64/18.8%	43/17.7%

[a]Includes chondrosarcoma (2), myxosarcoma (1), fibrosarcoma (5), Ewing sarcoma (5), lymphosarcoma (1), osteosarcoma (2), chondromyosarcoma (1), alveolar soft part sarcoma (4), undifferentiated sarcoma (10), and sarcomas secondarily invading the orbit (5)

Primary Orbital Malignancies

Rhabdomyosarcoma

Rhabdomyosarcoma (RMS) is the most common soft tissue malignancy occurring in children, accounting for nearly 5% of all childhood malignancies and 20% of soft tissue tumors [8]. As already outlined, it is also the most common primary orbital malignancy in children, representing approximately 40% of cases. There are approximately 250 cases of RMS diagnosed in the USA per year. Approximately 10%–15% of these occur in the orbit [9]. With these yearly estimates, there are most likely about 37 new cases of RMS that occur in the orbit in the USA per year. This lesion is so rare that in the Shields review of orbital tumors over a 30-year period, they report only 35 cases [10]. In our experience at the Children's Hospital of Philadelphia (CHOP), we see almost one new case of orbital RMS per year. This is helpful to keep in mind when reassuring families, but is in no way a comfort to the physician who must always remain vigilant when diagnosing orbital tumors. We once had a weekend on call at CHOP where we diagnosed two separate cases of orbital RMS in a single day!

Originally thought to arise from striated muscle, pluripotential mesenchymal cells appear to be the source of the malignant transformation in all types of childhood rhabdomyosarcoma [11, 12]. Seen even in the eighth decade, approximately 75% of primary orbital rhabdomyosarcomas, however, occur in the first decade of life with another 22% diagnosed in the second decade [11]. A bimodal age distribution has been identified based on tumor histology: embryonal and alveolar cell types occur in childhood, and the pleomorphic variety is more common in adulthood. Additionally, two peaks seem common in childhood, with ages 1 and 7 years on average accounting for the most common age presentations. Female slightly outweigh male preponderance 3:2. The average age at diagnosis is approximately 7 years, although the malignancy has been reported at birth and as late as 78 years of age [11, 13].

Rhabdomyosarcoma can involve the orbit as a primary tumor or through secondary invasion. In older reports, this differentiation was not often recognized because the histopathologic features of striated muscle cells gave the impression of a striated muscle tumor and kept researchers from recognizing that these tumors can arise from parameningeal sites and invade the orbit secondarily. The term parameningeal not only includes intracranial sites of origin but is used generally to include all non-orbital head and neck sites such as the retropharyngeal space, the sinuses, and the pterygoid fossa. Of the series mentioned, only Henderson acknowledges this difference in orbital presentation and found 17 cases of primary orbital RMS and 21 cases of secondary orbital involvement in his series [5]. Despite this difference in site of origin, diagnostic and treatment considerations with orbital involvement change little whether the tumor is of primary or secondary origin.

Classically, orbital rhabdomyosarcoma presents as a rapidly enlarging process with proptosis or globe dystopia, lid swelling, and inflammation in a previously healthy child (Fig. 36.1). Typically painless, the signs and symptoms

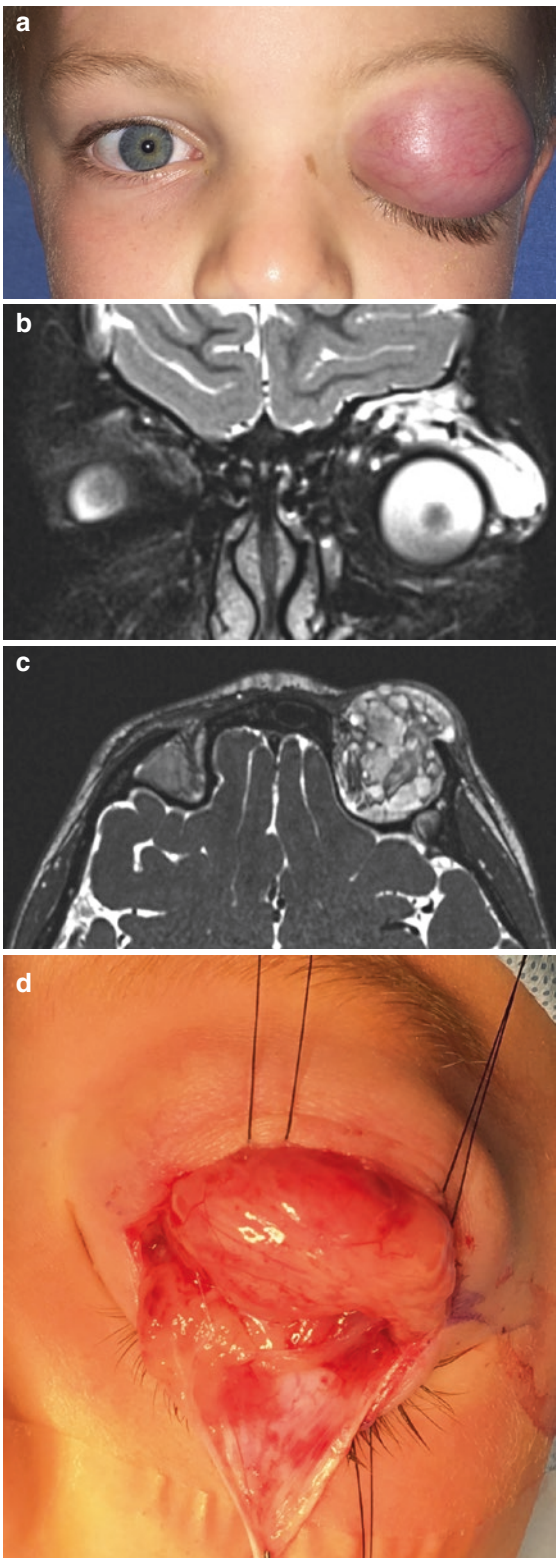


Fig. 36.1 Rhabdomyosarcoma. (**a**) Clinical photograph of a 5-year-old boy with a 2-week history of left eyelid swelling and proptosis. (**b**) T2-weighted coronal MRI showing an irregular mass in the upper eyelid. (**c**) T1-weighted axial MRI shows an irregular mass filling the superior orbit. (**d**) Intraoperative photograph of tumor in the left superior orbit. An eyelid crease incision was made. The orbital septum was incised and reflected downward. Pathology and cytogenetic studies were performed on this mass, which was embryonal rhabdomyosarcoma

worsen rapidly over a period of days, often mimicking a suspected traumatic injury, especially when edema and a rather consistent bluish or reddish/purple discoloration are present. Vision loss is an unusual feature early on except in secondary orbital RMS, where approximately 35% of patients present with vision worse than 20/200 secondary to apical involvement from these parameningeal tumors. Twenty-five percent of patients have a palpable orbital mass, and blepharoptosis is seen in about 20% of patients on presentation, which almost always accompanies the periorbital swelling. Less commonly, the primary site of presentation can occur in the eyelid, as seen in about 20% of cases where lid signs dominate the clinical presentation with a notable lack of proptosis and 7% of presentations can be subconjunctival with a visible, well-demarcated mass (the so-called botryoid type). Rarely, RMS can present as a slow, indolent process of intermittent swelling, tearing, or inflammation, delaying diagnosis and treatment [14]. Delays in diagnosis can also occur due to similar signs and symptoms shared by other pediatric orbital processes, including Langerhans cell histiocytosis, orbital cellulitis, metastatic neuroblastoma, ruptured dermoid cysts, granulocytic sarcoma, microcystic venolymphatic malformation, and idiopathic orbital inflammations. This differential diagnostic list should be kept in mind when faced with a child presenting with an acute, progressing orbital process.

Four major categories of histopathologic appearance are used to classify orbital rhabdomyosarcoma: embryonal, alveolar, pleomorphic, and botryoid. This classification was first proposed by Horn and Enterline [15]. Very few tumors demonstrate pure histologic patterns, so the predominant pattern is used to define the histologic category. The major feature one uses to diagnose RMS is the presence of rhabdomyoblasts, which are small, densely eosinophilic, round cells with hyperchromatic nuclei and small nucleoli. Increasing degrees of differentiation reveal larger cells with abundant eosinophilic cytoplasm containing fibrillary material that can resemble a spider web (called spider cells) or can be shaped like tadpoles, spindles, or racquets. Strap cells can sometimes be identified (Fig. 36.2). A strap cell is a description of a primitive cell with an elongated cytoplasm resembling a strap as it presumably is differentiating toward development as a muscle fiber. Cross striations help to identify the most differentiated cells, which look like muscle fibers and can be found in about 50–60% of embryonal cell-type and around 30% of alveolar cell-type lesions (Fig. 36.2). Immunoperoxidase staining for myoglobin, periodic acid-Schiff (PAS) stain for glycogen, and electron microscopy for thin or thick myofilaments or Z-lines can further distinguish borderline lesions with indistinct features. The desmin stain is particularly useful in that it is very specific for rhabdomyosarcoma. It stains a specific filament present in the cytoplasm of this tumor and helps to differentiate it from other small cell tumors [16].

The embryonal subtype is the predominant histopathologic pattern in about 65% of orbital rhabdomyosarcomas

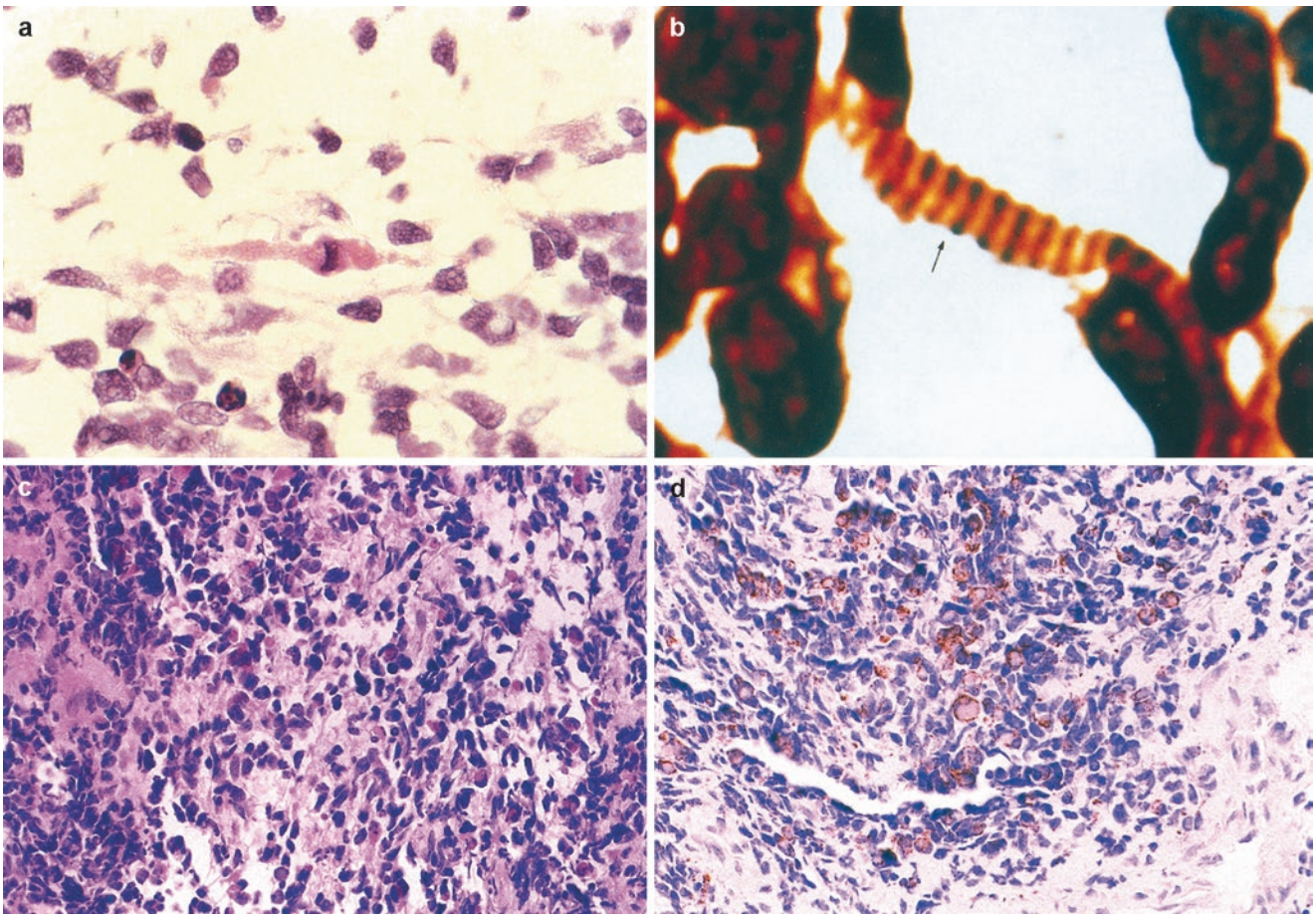


Fig. 36.2 Light microscopy of rhabdomyosarcoma of the orbit. (**a**) Strap cell (H and E stain, ×500) (Courtesy of Nasreen Sayed, MD). (**b**) Rhabdomyoblast with cross striations (small arrow) (Courtesy of Francis LaPiana, MD and AFIP). (**c**) Embryonal pattern of rhabdomyosarcoma with scant cytoplasm in cells (H and E stain). (**d**) Desmin stain of cells from same patient (×40) (Courtesy of Marta Guttenberg, MD)

and demonstrates a mixture of myxoid and compact pleomorphic cellularity with abundant mitotic figures. If presenting as a subconjunctival mass and revealing this histologic pattern, it is referred to as a botryoid, reflecting the terminology used for other mucosa-related RMS, and accounts for about 7% of all orbital presentations [17]. Alveolar RMS demonstrates poorly differentiated tumor cells reminiscent of lung alveoli. Viable tumor cells are arranged at the periphery adherent to the septa with degenerative cells appearing to float freely in the center. Better-differentiated rhabdomyoblasts are less common in this cell type but can be found within the septa. It has been suggested that this cell type is seen more commonly in the inferior orbit and constitutes approximately 30–35% of cases of orbital RMS [16].

Pleomorphic rhabdomyosarcoma is the least common histologic variant, occurring primarily in adults and accounting for only 1–2% of orbital presentations. Variably sized, loosely arranged, deeply eosinophilic cells with many types of rhabdomyoblasts account for the pleomorphic name. Cross striations are rare, but glycogen is frequently present.

Older reports suggested a correlation between cell type and prognosis in orbital rhabdomyosarcoma [16]. Other authors find no significant difference in survivability based on histologic type but rather on site of origin: orbital versus parameningeal [18–21]. Patients treated with wide surgical excision alone or with a variety of other ancillary treatments prior to 1972 demonstrated only a 22% survival rate [17]. Presentation of primary orbital disease treated with incisional biopsy, with or without debulking, radiation, and chemotherapy, utilizing past Intergroup Rhabdomyosarcoma Study (IRS) criteria carries a 91% rate of local control and an 82% 2-year disease-free interval [18, 19]. Parameningeal RMS treated with radiation and chemotherapy after biopsy demonstrated a 61% 6-year survival rate in one series from Memorial Sloan Kettering Cancer Center, but only a 33% 4-year survival rate reported from 12 cases at the Mayo Clinic [16, 20]. It seems that the only reason for the improvement in the rates of local recurrence and survival for patients reported in the older versus newer literature is the choice of treatment rendered: wide local excision prior to 1972 versus radiation and chemotherapy.

The new IRS-V study combines group, stage, and histologic subtype to allocate patients to three different therapeutic protocols according to risk of recurrence. Low-risk patients have an estimated 3-year rate of 88%, intermediate-risk patients have an estimated 3-year failure-free survival rate of 55 ± 76%, and high-risk patients have a 3-year failure-free survival rate of <30% [22].

When evaluating a child with a suspected orbital rhabdomyosarcoma, review of the differential diagnosis list helps in guiding the initial work-up. A careful history and physical examination revealing symptoms or signs of sinus disease, upper respiratory infection, trauma, previous dermoid cyst, or manifestations of orbital lymphangioma can help direct the examination. This should be performed within 24 h due to the potentially rapid progression of these tumors and the attendant proptosis, corneal exposure, and vision loss that can ensue.

Thin-section computerized tomographic (CT) evaluation of the orbit and sinuses with contrast enhancement yields orbital and extraorbital localization of the process along with details of the surrounding bone to reveal any extraorbital spread or bony destruction that helps guide biopsy, surgical management, and systemic work-up [16]. This study modality, while more readily available, cannot easily differentiate rhabdomyosarcoma from other benign lesions and can sometimes be misleading and raise the suspicion for RMS. Magnetic resonance imaging (MRI) has become the ideal imaging modality to differentiate RMS from other lesions. Diffusion-weighted imaging (DWI) and apparent diffusion coefficient (ADC) mapping are additional studies performed during MRI that can further differentiate a lesion. Figure 36.3 shows four cases with orbital lesions that were referred with imaging for a presumed diagnosis of RMS. With the use of DWI imaging, the lesions were better identified for the risk for malignancy. All four lesions were biopsied, but only one of the four was in fact RMS. The role of orbital imaging in RMS is covered in more detail in Chap. 32. RMS on MRI is usually homogenous, well circumscribed, and within orbital soft tissues, not arising from the extraocular muscles. They are isointense to muscle on T1-weighted images and hyperintense on T2-weighted imaging. Contrast enhancement is best seen with fat-suppressed T1-weighted imaging. Often there is restriction seen on DWI.

Evaluation by a pediatric oncologist to help stage the disease is important (see Chap. 13). Physical examination and ancillary studies for extraorbital spread, regional or distant lymphatic involvement, or possible metastasis to the lungs, bone marrow, or brain are important for staging the disease and for posttreatment metastatic evaluations. Table 36.2 lists the IRSG surgical-pathologic grouping system [22]. Table 36.3 is the IRSG staging system.

If imaging studies demonstrate features consistent with rhabdomyosarcoma, orbital biopsy should be performed. This should occur with minimal delay as previously discussed. The imaging study and its demonstration of the position of the orbital lesion will reveal the best approach for biopsy, which is usually through an anterior lid crease incision for superior orbital lesions or through a transconjunctival or subciliary incision for lower orbital presentations. Adequate tissue for biopsy should be sent to pathology fresh for both frozen and permanent sectioning from which DNA can be obtained for cytogenetic studies.

In the last two decades, multiple gene mutations have been identified in RMS tumors. This has helped to aid in the diagnosis of these lesions, but has also shown the limitation of histologic evaluation as some lesions can be identified histologically as one subtype, but may have the genetics of a different RMS subtype, thus altering the staging of the tumor. This very thing occurred in one patient we recently followed. The patient underwent an incisional biopsy with pathologic assessment most consistent with embryonal RMS. However, subsequent molecular genetic testing of the biopsy specimen was positive for the PAX3/PAX7-FKHR chimeric gene, indicating that the tumor was actually an alveolar RMS. The patient received a more intensive chemotherapy regimen and also received proton beam radiotherapy. After chemotherapy and proton irradiation, the patient's tumors shrank considerably, and she has remained in remission at over 3 years of follow-up. This patient is illustrative of the new tools available to the orbital specialist including both molecular genetic testing and proton beam irradiation for diagnosing and treating orbital RMS [23] (Fig. 36.4).

A controversy still exists regarding whether more aggressive tumor debulking is indicated for RMS tumors that occur in the orbit alone. While some literature supports the benefit of overall survival with RMS tumor debulking [24], some oncologists and radiation therapists prefer simple biopsy alone followed by chemotherapy and radiation without debulking in an effort to decrease the risk of ocular and periocular iatrogenic injury [25]. It is thus important to work closely with an oncologist, radiation oncologist (and ideally a tumor board), in developing a specific management plan for each patient.

Armed with the tumor diagnosis from the histopathology specimen and the disease stage from the oncology evaluation, therapeutic chemotherapy and radiation regimens can be decided on. Most primary orbital RMS would fall under a group II staging, assuming no distant metastatic sites were found. Several regimens of radiation therapy and chemotherapy have evolved from the different stages of the Intergroup Rhabdomyosarcoma Study. Combination chemotherapy utilizing vincristine, actinomycin-D, and cyclophosphamide (VAC) coupled with local radiotherapy with a dosage range of 4500–5500 cGy yielded markedly improved local tumor control and survival for patients with rhabdomyosarcoma with primary orbital disease over surgical excision alone [19, 26]. Although primary orbital RMS

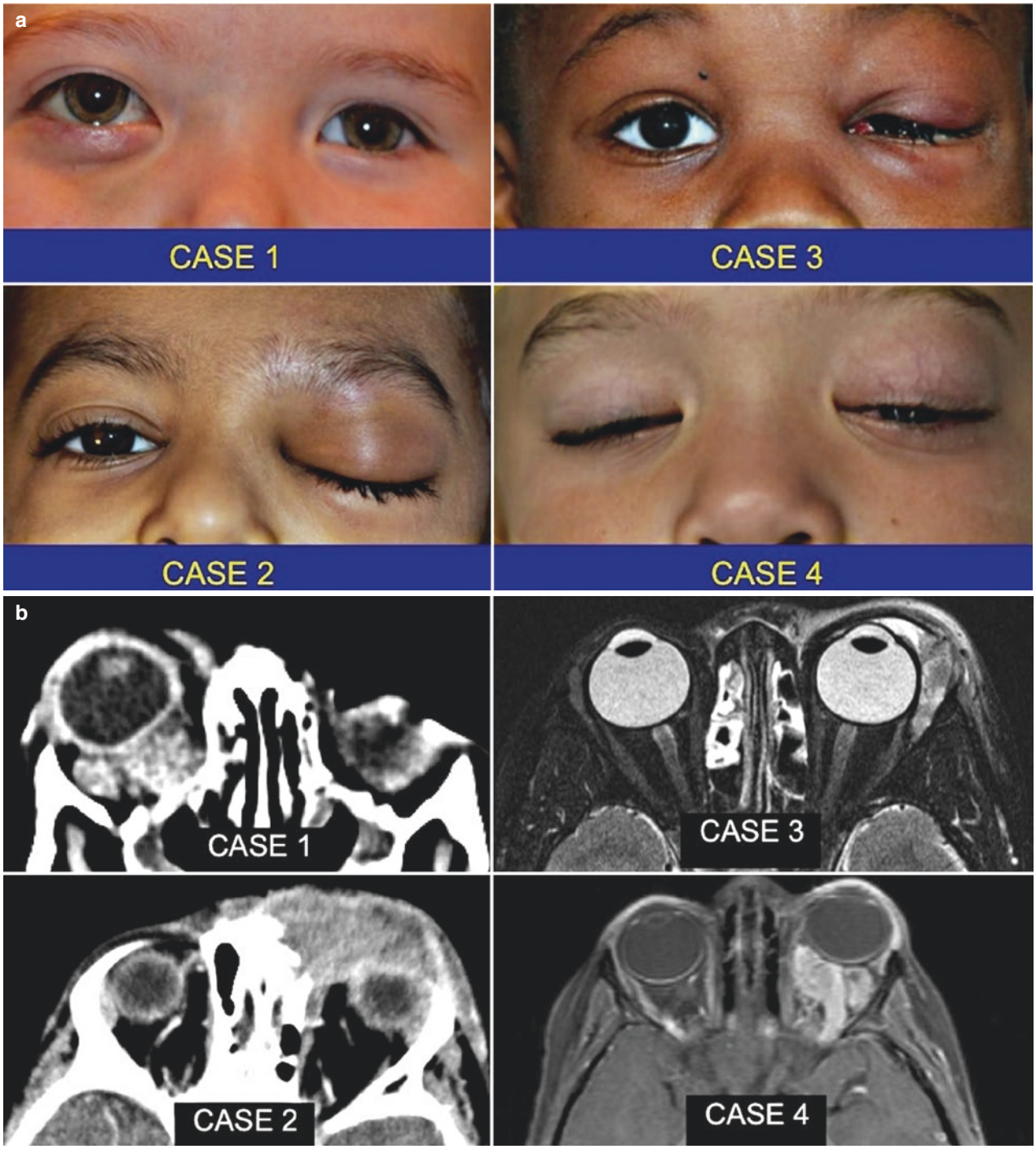


Fig. 36.3 Four cases of presumed rhabdomyosarcoma. (**a**) *Top left*, case 1: 4-year-old boy with a rapid onset of painless proptosis. *Bottom left*, case 2: 5-year-old boy with rapid onset of ptosis with mild discomfort. *Top right*, case 3: 9-year-old boy with history of *left upper* eyelid edema and erythema, which did not improve with oral antibiotics. *Bottom right*, case 4: 8-year-old girl with painless proptosis that has progressed over 10 days. (**b**) *Top left*, case 1: axial CT shows an intraconal heterogeneous mass. *Bottom left*, case 2: axial CT showing an infiltrative superior orbital mass with bony lysis. *Top right*, case 3: T2-weighted axial MRI showing an infiltrative mass in the superolateral orbit. *Bottom right*, case 4: T1-weighted axial MRI showing an intraconal heterogeneous orbital mass.

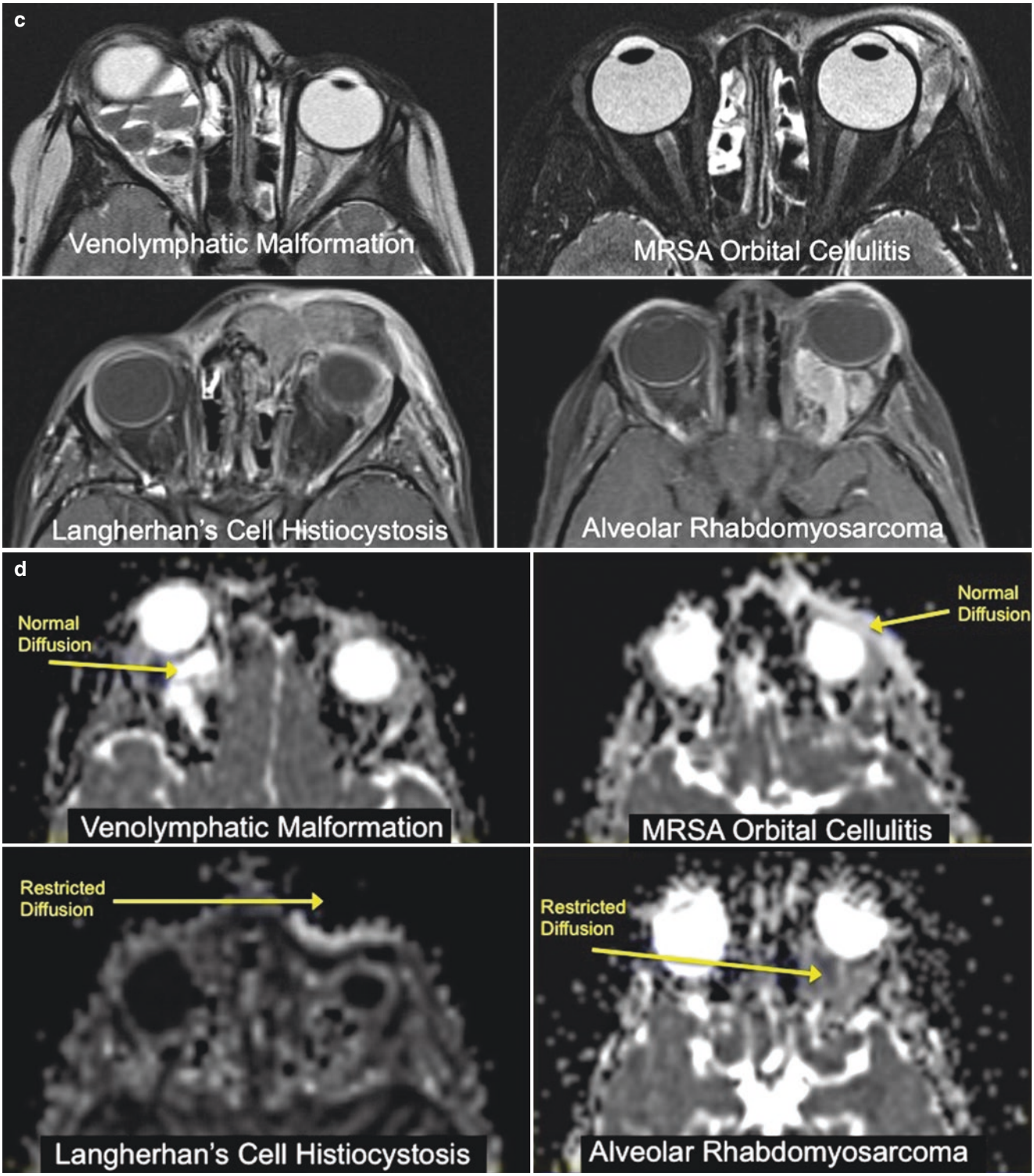


Fig. 36.3 (continued) (**c**) *Top left*, case 1: additional imaging was obtained showing an intraconal, orbital mass with macrocysts and fluid levels. Because the patient had vision loss with an afferent pupillary defect, the patient underwent orbital biopsy. Pathology diagnosed with lesion as venolymphatic malformation. *Bottom left*, case 2: additional imaging was obtained showing a heterogeneous mass in the superior orbit on T1-weighted axial MRI. Biopsy of the orbit confirmed the diagnosis as Langerhans cell histiocytosis. The lesion was curetted and treated directly with methylprednisolone. *Top right*, case 3: orbital biopsy showed a lesion with acute inflammation only. Specimen culture grew methicillin-resistant *Staphylococcus aureus* (MRSA). *Bottom right*, case 4: orbital biopsy of the lesion confirmed the diagnosis of alveolar rhabdomyosarcoma. (**d**) *Top left*, case 1: normal diffusion noted on apparent diffusion coefficient mapping (ADC) associated with diffusion-weighted imaging (DWI) suggesting the lesion hypocellular and likely benign as seen in orbital venolymphatic malformation. *Bottom left*, case 2: restriction is noted on the ADC image derived from DWI imaging raising the suspicion of a malignant lesion. *Top right*, case 3: normal diffusion on the ADC image in a patient with MRSA orbital cellulitis. *Bottom right*, case 4: restriction on the ADC mapping image in orbital rhabdomyosarcoma

Table 36.2 IRSG surgical-pathologic grouping system [22]

Group	Definition
I	Localized tumor, completely removed with pathologically clear margins and no regional lymph node involvement
II	Localized tumor, grossly removed with (a) microscopically involved margins; (b) involved, grossly resected regional lymph nodes; or (c) both
III	Localized tumor, with gross residual disease after grossly incomplete removal or biopsy only
IV	Distant metastases present at diagnosis

Table 36.3 IRSG staging system [133]

Stage	Sites of primary tumor	Tumor size (cm)	Regional lymph nodes	Distant metastases
1	Orbit, non-PM head/neck; GU non-bladder/prostate; biliary tract	Any size	N0, N1	M0
2	All other sites	≤5	N0	M0
3	Any site	≤5 >5	N1 N0 or N1	M0
4	Any site	Any size	N0 or N1	M1

PM Parameningeal, *GU* genitourinary, *N0* regional nodes not clinically involved by tumor, *N1* regional nodes clinically involved by tumor, *M0* no distant metastases, *M1* distant metastases at diagnosis [133]

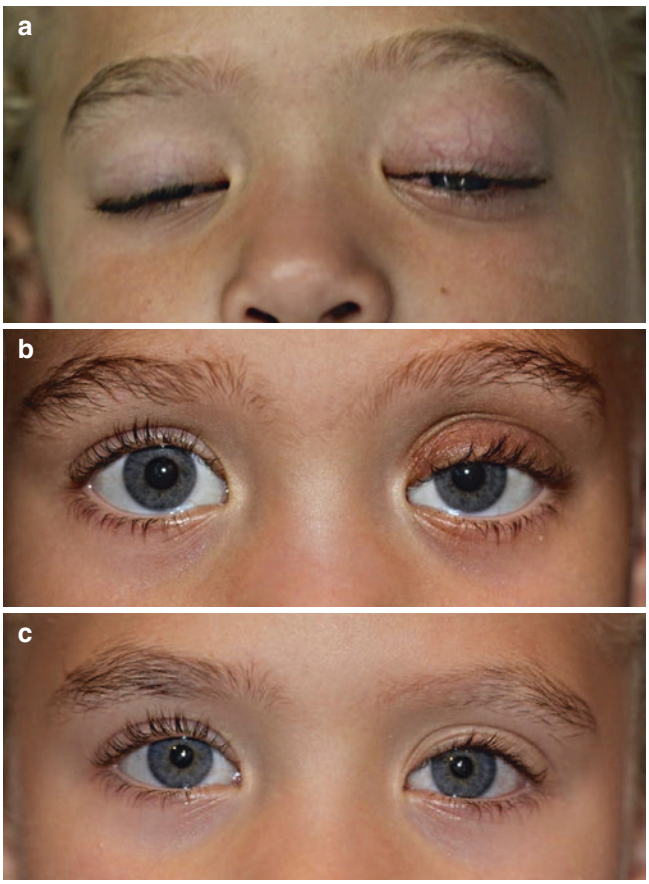


Fig. 36.4 Alveolar rhabdomyosarcoma. (**a**) An 8-year-old girl presents with painless proptosis that has progressed over 10 days. (**b**) 6-month status post-IRSG treatment protocol with chemotherapy and proton beam radiation. Ptosis with good levator function is noted on the left side. (**c**) 6-month status post-left modified Fasanella ptosis repair

Table 36.4 Histopathologic risk classification for rhabdomyosarcoma (RMS)

I. Superior prognosis
1. Botryoid RMS
2. Spindle cell RMS
II. Intermediate prognosis
1. Embryonal cell RMS
III. Poor prognosis
1. Alveolar RMS
2. Undifferentiated sarcoma
IV. Subtypes whose prognosis is not presently evaluable
1. RMS with rhabdoid features

treatment protocols for local control and survival are not related to cell type on histopathology, other extremity sites do have a variable prognosis based on histopathologic typing, as demonstrated in Table 36.4 [27]. These results have been the basis for changes in the treatment regimens in studies II and III of the IRS to improve survivability among the higher-risk cell types, especially alveolar and undifferentiated rhabdomyosarcoma [28, 29].

Significant morbidity can occur from these treatments in young children [30]. Cataracts are a nearly universal complication from the radiotherapy, with visual loss seen in nearly 80% of children treated with orbital rhabdomyosarcoma. Bony orbital hypoplasia results in about 50% of radiation-treated children, with resultant enophthalmos and ptosis, especially when treatment is required under 7 years of age. Keratitis sicca and conjunctival telangiectasia occur with dosages above 5000 cGy. The exact incidence of radiation optic neuropathy and retinopathy secondary radiation is difficult to evaluate due to the occurrence of dense cataracts, precluding adequate examination of the fundus to document these complications. As is seen in other childhood cancer survivors, those with RMS are now demonstrating secondary malignancies years after treatment [31]. Leukemias seem to be related to high doses of cyclophosphamide (>16.8 g/m^2). Solid tumors have a tendency to arise in the irradiated field and correlate with actinomycin-D dosage of over 9.6 mg/m^2, implicating it as a radiation inducer. In our experience, postradiation ptosis is a common occurrence and will necessitate a ptosis repair. This is ideally delayed for at least 3–6 months to observe if there is any improvement in eyelid height and levator function and to monitor for postradiation keratoconjunctivitis.

Rhabdomyosarcoma stands as a shining example of a cancer for which improved therapy has been fostered through large cooperative trials. Although the treatment of orbital RMS carries significant risks to the eye, survival is excellent, except in those children who present with distant disease. Challenges still exist in reducing the ocular side effects in this otherwise successful therapeutic protocol.

Ectomesenchymoma

This very rare soft tissue tumor is composed of both neuroectodermal and mesenchymal neoplastic elements. The embryologic origin of malignant ectomesenchymomas is the pluripotent migratory cells of neural crest, which give rise to all connective tissue of the globe and orbit [32]. It is often misdiagnosed initially as rhabdomyosarcoma. The presence of neuroectodermal elements helps the pathologist differentiate this lesion from rhabdomyosarcoma [33]. A 2002 review found only 60 reported cases of which only three occurred in the orbit. When the tumor's predominant element is rhabdomyosarcoma, the treatment is tailored closely to the IRSG protocol for RMS with a similar prognosis. Figure 36.5 depicts our experience with a patient with this rare tumor [32].

Soft Tissue Sarcomas

Mesenchymal components of the orbit or other parts of the body that undergo malignant transformation are termed malignant sarcomas. Striated muscle, smooth muscle, connective tissue septa, fat cells, and the cartilage of the trochlea are the mesenchymal soft tissues in the orbit. Primary malignant degeneration in the pediatric population involving orbital mesenchyme is highly unusual. Large clinical series reviewing pediatric soft tissue sarcomas are dominated by rhabdomyosarcoma and often do not include information concerning the orbit as a primary site of neoplasm [34]. Most non-ophthalmic publications report these sarcomas under the more general category of head and neck sarcomas [35].

Table 36.1 includes data from over 1800 cases of pediatric orbital tumors reviewed at six institutions [1–7]. Thirty-six cases of non-rhabdomyosarcoma (non-RMS) soft tissue sarcomas primary to the orbit were identified, accounting for 2.0% of all pediatric orbital lesions seen at these institutions. These included ten undifferentiated sarcomas, five fibrosarcomas, five cases of Ewing sarcoma, five sarcomas secondarily invading the orbit from adjacent areas, four cases of alveolar soft part sarcoma, two chondrosarcomas, two osteosarcomas, one myxosarcoma, one lymphosarcoma, and one chondromyosarcoma. Only alveolar soft part sarcoma has been subjected to large series analysis to define the clinical parameters of the lesion.

No specific symptoms, signs, or imaging features occur with any regularity enabling identification of these lesions prior to biopsy. Wide surgical resection seems to be the preferred treatment for localized lesions, although IRS treatment regimens have been utilized with some success [35].

Alveolar soft part sarcoma is a malignant soft tissue tumor presumably of myogenic origin, affecting peripheral tissues more than head and neck regions [36]. In the study by Enzinger and Weiss of 143 cases from the AFIP, 27.3% involved the head and neck, with most found in the orbit and tongue [37]. Font and coauthors reported 17 cases involving the orbit [36]. Of these tumors, 9 were in children, with a 2:1 female preponderance and two-thirds involving the right orbit. All developed rapidly over a period of 1–3 months with proptosis, swelling, and dilated conjunctival vessels

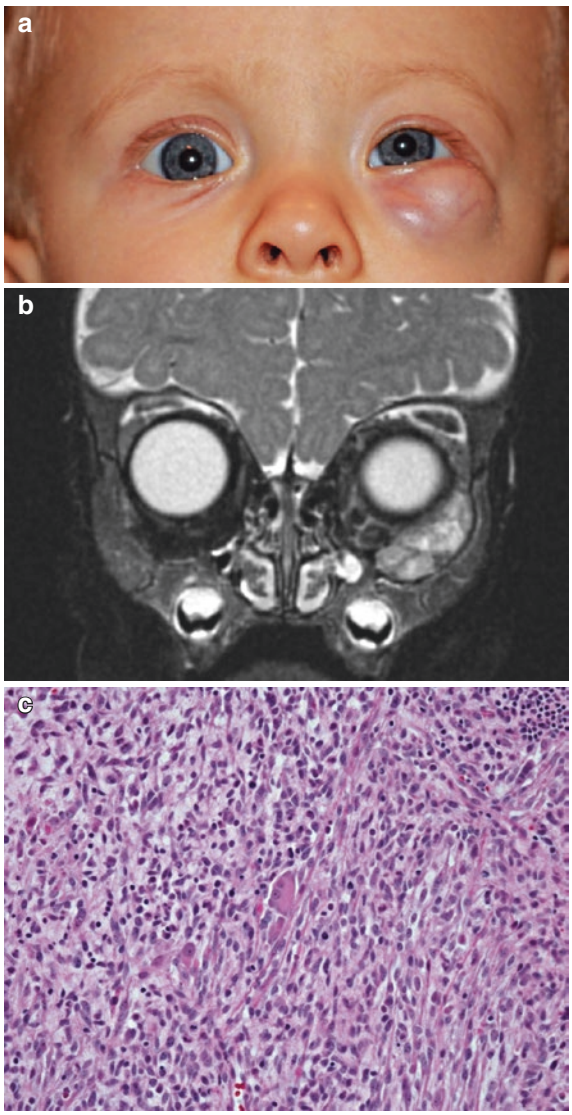


Fig. 36.5 Ectomesenchymoma. (**a**) A 9-month-old with a left orbital tumor that was initially treated for RMS with chemotherapy was referred due to worsening proptosis while on chemotherapy. (**b**) Coronal MRI with heterogeneously T2 hyperintense and avidly enhancing mass lesion in the extraconal fat of the left orbit at the inferior and medial aspects of the orbit. An incisional biopsy was performed via a lateral canthal and swinging lower eyelid incision. Histopathology showed a malignant ectomesenchymoma. (**c**) A mixture of undifferentiated primitive small blue cells and more differentiated spindle and strap cells with bright red cytoplasm, consistent with embryonal rhabdomyosarcoma. In addition, scattered maturing ganglion cells are present. Immunostains reveal that the spindled and undifferentiated cells are strongly and diffusely positive for desmin, with approximately 30% displaying nuclear positivity for myogenin. Immunohistochemistry for PAX5 is negative. The ganglion cells and neuritic cell processes stain with NSE, S-100, PGP9.5, and synaptophysin. GFAP is negative. The presence of these neuronal elements in an otherwise typical embryonal rhabdomyosarcoma is consistent with ectomesenchymoma

(Fig. 36.6). Imaging studies demonstrate a homogenous anterior orbital mass often displacing the globe and showing moderate enhancement with contrast administration. On biopsy, the tumor often appears well circumscribed and bleeds profusely secondary to the numerous vascular channels. It may appear to be encapsulated. Histologic analysis shows large polyhedral tumor cells lining fibrous trabeculations inside a pseudocapsule border, giving these tumors their characteristic alveolar appearance. PAS tissue preparations demonstrate positive-staining crystalline structures present in nearly all alveolar soft part sarcomas but not seen in any other tumors. Due to the large degree of tumor vascularity, distant metastases to the lung, bone, and brain are seen in about 33% of patients with extremity alveolar soft part sarcoma, whereas no reported cases with orbital presentation have had metastases on initial diagnosis. Surgical excision is the most common therapy because these tumors have demonstrated considerable radioresistance. Chemotherapy has been tried for metastatic disease with mixed results [38]. Long-term survival for these patients is poor, with universal fatality 20 years after diagnosis, although prolonged disease-free intervals are common [39].

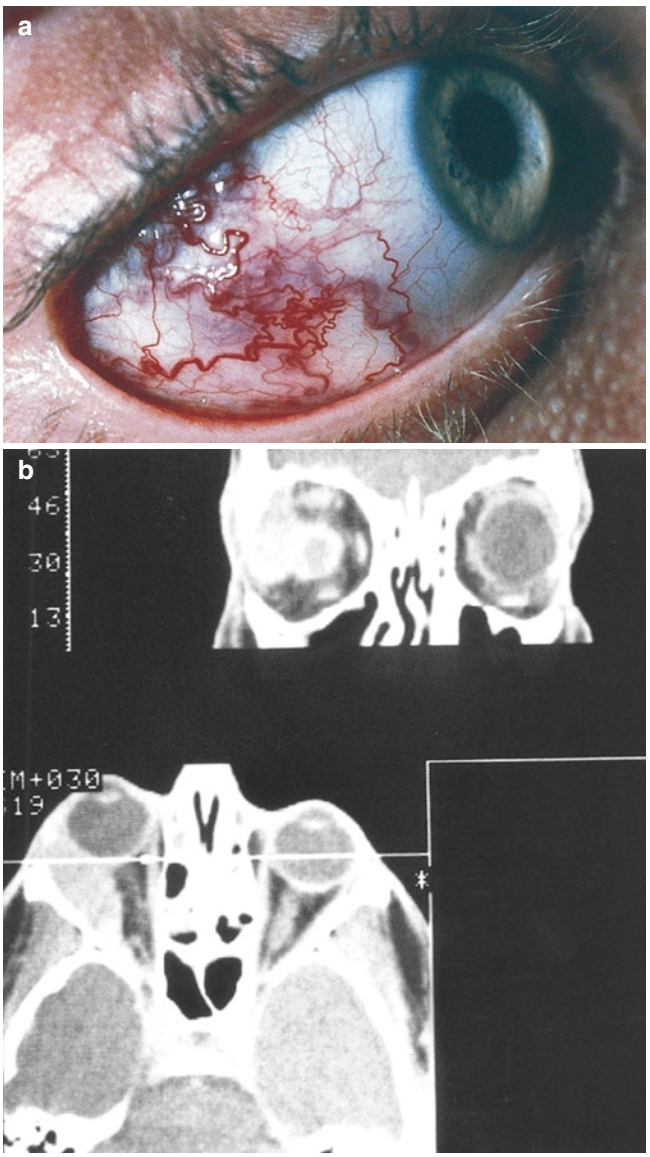


Fig. 36.6 Alveolar soft part sarcoma. (**a**) Clinical photograph demonstrating an alveolar soft part sarcoma arising from the lateral orbit. (**b**) Axial CT scan with coronal reconstruction showing the intraorbital placement and features of the lesion in the patient in (**a**)

Angiosarcoma is a rare soft tissue sarcoma more commonly seen in adults [40]. The orbit is an unusual site for head and neck involvement but Hufnagel and colleagues were able to add 14 cases from the literature to their case of primary orbital angiosarcoma [41]. Ten of the fifteen patients were children in this series, which is unusual compared with other sites involved by angiosarcoma. Most patients present with a short history of proptosis with a posterior orbital location and with proptosis, eyelid swelling, and ptosis if the more typical anterosuperior lesion is seen. CT demonstrates a circumscribed mass with enhancement on contrast administration that may infiltrate surrounding structures. Biopsy demonstrates the characteristic angiomatous pattern with irregular lumina and clefts forming sinusoids lined by anaplastic endothelial cells. Due to the abundance of vascularity within the tumor, hematogenous metastases are common and give this tumor a poor prognosis. Treatment usually involves radical excision such as exenteration, since it appears that local control is important for long-term outcome due to its poorly circumscribed nature. Despite adding radiation and chemotherapy, only 10% of pediatric patients are alive after 3 years [41].

Mesenchymal chondrosarcoma is another rare malignancy showing a tendency to arise in bone, as one would expect by the well-differentiated cartilage seen in these tumors. Extraskeletal sites are uncommon but show a predilection for meninges, extremities, and the orbit [42]. These tumors show a peak incidence in the second and third decades of life. Its occurrence in females seems more prominent, and it presents with slow proptosis, diplopia, headache, and pain. CT may show an irregular mass with scattered calcifications and opacities where cartilaginous and bony differentiation occurs. Radical excision is the treatment of choice for these highly malignant tumors with poor prognosis [43]. In the series of ten cases reported by Guccion et al., only one patient survived more than 5 years, a child treated by exenteration for the orbital chondrosarcoma [42].

An important tumor not reported from any institution in Table 36.1 is the endodermal sinus tumor (also called yolk sac tumor or infantile embryonal carcinoma), a malignant neoplasm arising from persistent yolk sac endoderm (germ cells destined to become reproductive glands). These germ cells usually migrate through the mesentery to the genital ridge to become an undifferentiated gonad. Migrating germ cells may alight in aberrant midline locations such as the orbit, where they usually disappear with continued fetal development. Their persistence gives rise to extragonadal germ cell tumors of which endodermal sinus tumor is one malignant variant. Its name arose from histologic similarities among germ cell

tumors involving the ovary and certain structures in rat placenta [44]. Typically seen around 1 year of age, proptosis is the main clinical feature in these rare pediatric orbital tumors. They are diagnosed earlier than other extranodal sinus tumors, presumably because of their orbital location, and so aggressive treatment, including surgical excision and triple drug chemotherapy, can result in long-term survival [45]. Clinical and histopathologic features may mimic RMS; immunoperoxidase staining localized to the cytoplasm of the tumor cells is positive for α-fetoprotein in this tumor, helping to differentiate it from RMS. It is suggested that loss of serum levels of α-fetoprotein can help monitor for tumor control as other extranodal sites register this potentially helpful change [46].

Perhaps the rarest of orbital tumors is the nonrenal malignant rhabdoid tumor. This is thought to be of primitive mesenchymal cell origin and typically arises in the kidney. When occurring in children in a nonrenal setting, this tumor is often lethal. One report of a congenital malignant rhabdoid tumor of the orbit has been reported [47]. Figure 36.7 is a similar case in a patient we biopsied.

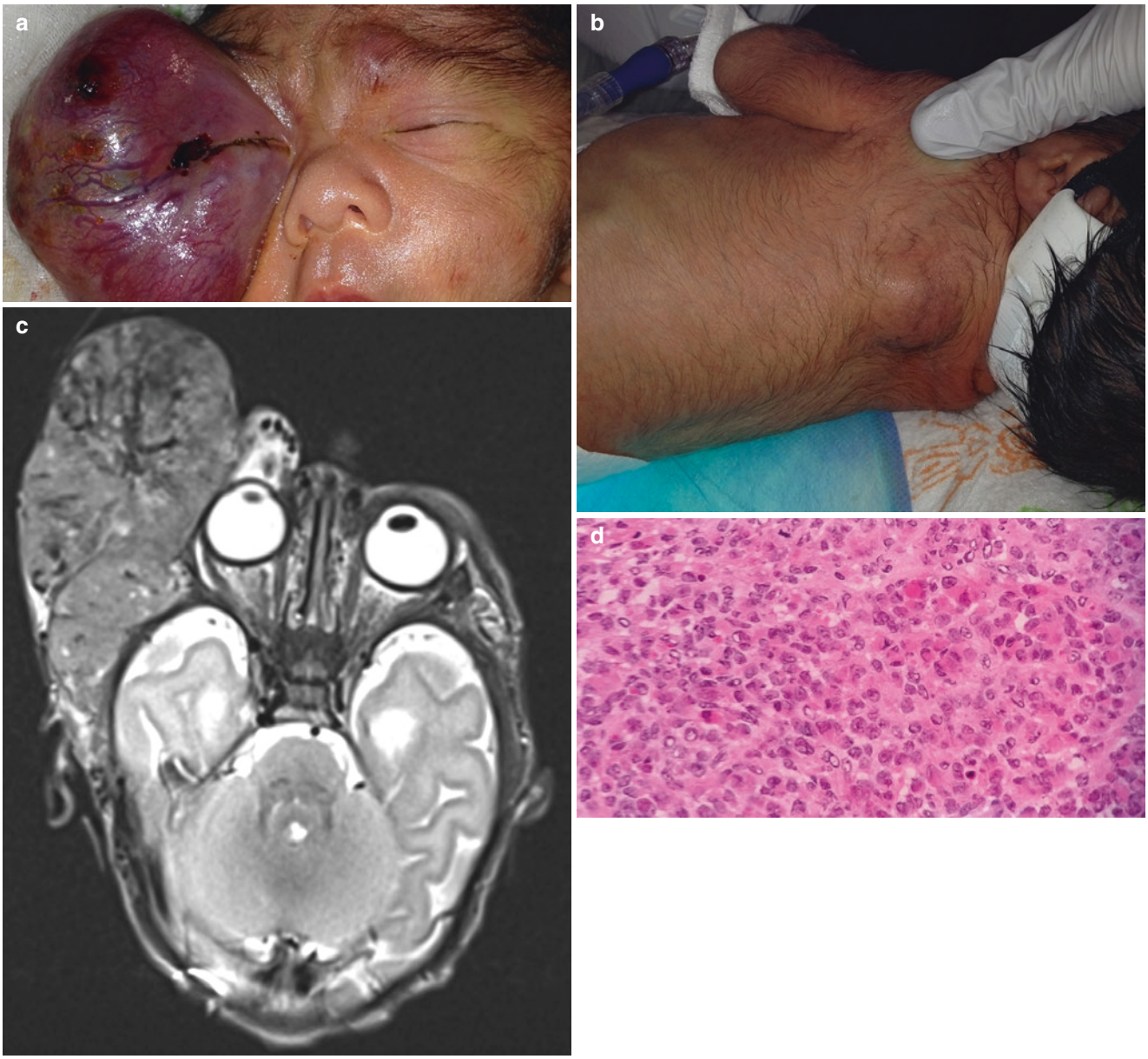


Fig. 36.7 Congenital malignant orbital rhabdoid tumor. (**a**) A 4-day-old girl was seen in the NICU for a large orbital tumor. (**b**) Multiple subcutaneous masses palpable on the trunk and extremities. (**c**) T2-weighted MRD showing a huge lobulated heterogeneous mass with extensive vascularity involving the right side of the face and neck with right intraorbital extension and mass effect on the adjacent structures. (**d**) Histopathology densely cellular proliferation of cohesive epithelioid and focally spindle-shaped neoplastic cells. The neoplastic cells have enlarged, frequently eccentrically located ovoid, vesicular nuclei with irregular nuclear contours, conspicuous nucleoli, and a moderate amount of clear to eosinophilic cytoplasm. The tumor grows in a solid sheet pattern. Mitoses and apoptoses are readily seen. These findings and loss of INI-1 immunohistochemical expression are in keeping with a diagnosis of malignant rhabdoid tumor

The diagnosis of most non-RMS soft tissue sarcomas will be made on biopsy. Additional pathologic studies, as discussed in this section, should be done to help differentiate these tumors from rhabdomyosarcoma. With such limited numbers of cases, treatment decisions regarding degree and aggressiveness of surgical intervention, presurgical versus postsurgical chemotherapy, and the role and timing of radiation therapy will depend on pediatric oncology consultation, institutional experience, and the results of case reports showing treatment success. IRSG-style studies may prove beneficial for these rare orbital tumors.

Adenoid Cystic Carcinoma

Typically a primary epithelial lacrimal gland tumor in adults, several cases of this neoplasm have been reported in children [48–52]. Adenoid cystic carcinoma received its name based on the histopathologic features of closely packed cell aggregates separated by large ovoid spaces likening its low-power microscopic appearance to Swiss cheese. In adults, it is the most common epithelial malignancy involving the lacrimal gland. In children, it is the most common epithelial malignancy of the lacrimal gland, though extremely rare in children. The onset of symptoms typically precedes diagnosis by about 1 year, with progressive symptoms of proptosis, globe displacement, and orbital pain being the reasons for patients seeking ophthalmic evaluation. No specific deviations from this presentation are seen in children with adenoid cystic carcinoma compared with adults [50].

There are no specific imaging features that allow one to diagnose adenoid cystic carcinoma directly. Bony invasion is seen in about 33% of cases, but two pediatric cases reported by Rootman and Dolman showed only expansion without invasion, prompting these authors to speculate that perhaps this occurs due to the more pliable nature of bone in children [48]. Five histologic patterns are seen in this tumor: cribriform (Swiss cheese), solid (basaloid), sclerosing, comedocarcinoma, and tubular (ductal). All or several of these patterns may be present in one tumor, but one usually predominates. Gamel and Font reported only a 21% 5-year survival rate among adult patients, demonstrating a basaloid pattern on histopathology, whereas nonsolid patterns had a 71% 5-year survival [53]. Perineural invasion is accredited with being both the source of pain with these tumors and the reason for local and distant recurrence. Direct extension into the intracranial cavity, along with lung metastases, results in a nearly 100% mortality rate 20 years after tumor diagnosis [54]. Treatment consists of initial frozen section biopsy to confirm preoperative suspicions, followed immediately by en bloc excision of the lacrimal gland, tumor, and surrounding orbital bones with or without orbital exenteration in an attempt to resect any potential residual disease. Radiotherapy has been advocated, but two series show no increased survival with its use, although some reserve this modality for local recurrences after radical surgery [53]. It is estimated that the 15-year survival rate is a dismal 22% [53]. More recently Tse et al. have treated this lesion with intra-arterial chemotherapy as a neoadjuvant approach before definitive tumor excision [54]. This has also shown a good initial success in a pediatric patient who eventually underwent a lid-sparing exenteration [52].

Metastatic Orbital Malignancies

Orbital metastases must be strongly considered when faced with a potentially malignant orbital process in children. In Table 36.1, 87 cases were identified, with 14 of these originating from neuroblastoma and 37 occurring from leukemic/lymphomatous disorders. Other sources include 28 cases of Langerhans cell histiocytosis, 5 cases of Ewing sarcoma, 1 metastatic osteosarcoma, 1 metastatic astrocytoma, and 1 metastasis to the optic nerve from a medulloblastoma. Metastases are the second leading cause of a malignant disorder in the orbit of a child, just behind rhabdomyosarcoma.

Leukemic/Lymphomatous Disorders

It is hard to estimate the exact frequency with which hematopoietic malignancies involve the orbit in children (see Chap. 13). At the Hospital for Sick Children in Toronto, 1609 cases of childhood leukemia and 727 cases of childhood lymphoma were diagnosed between 1919 and 1981 [55]. Thirty-six of the leukemia cases had "significant" ophthalmic involvement, which included choroidal and retinal infiltration, optic nerve infiltration, anterior segment infiltration with glaucoma, iritis, iris mass and/or hypopyon, and orbital infiltration. It is not clear how frequent each of these actually occurred, due to a lack of examination in asymptomatic patients, but the highest percentage was seen in children with acute myeloblastic leukemia (8%) versus those with the acute lymphoblastic varieties (3%). Only three of the 727 lymphoma cases had ocular involvement: all 3 cases involved orbital infiltration by non-Hodgkin lymphomas. None of the 482 cases of Hodgkin disease had orbital or ocular involvement according to this 1983 survey, although an orbital pediatric series at the same institution published in 1967 indicated that 3 cases of orbital proptosis in children with Hodgkin disease had been seen [56] (Fig. 36.8).

Necropsy studies confirm the rarity of orbital involvement in childhood leukemia. Robb et al. looked specifically at eye findings and found an 8% incidence of leukemic infiltration of the optic nerve, but many cases were at the nerve head rather than in the orbital portion of the optic nerve [57]. How

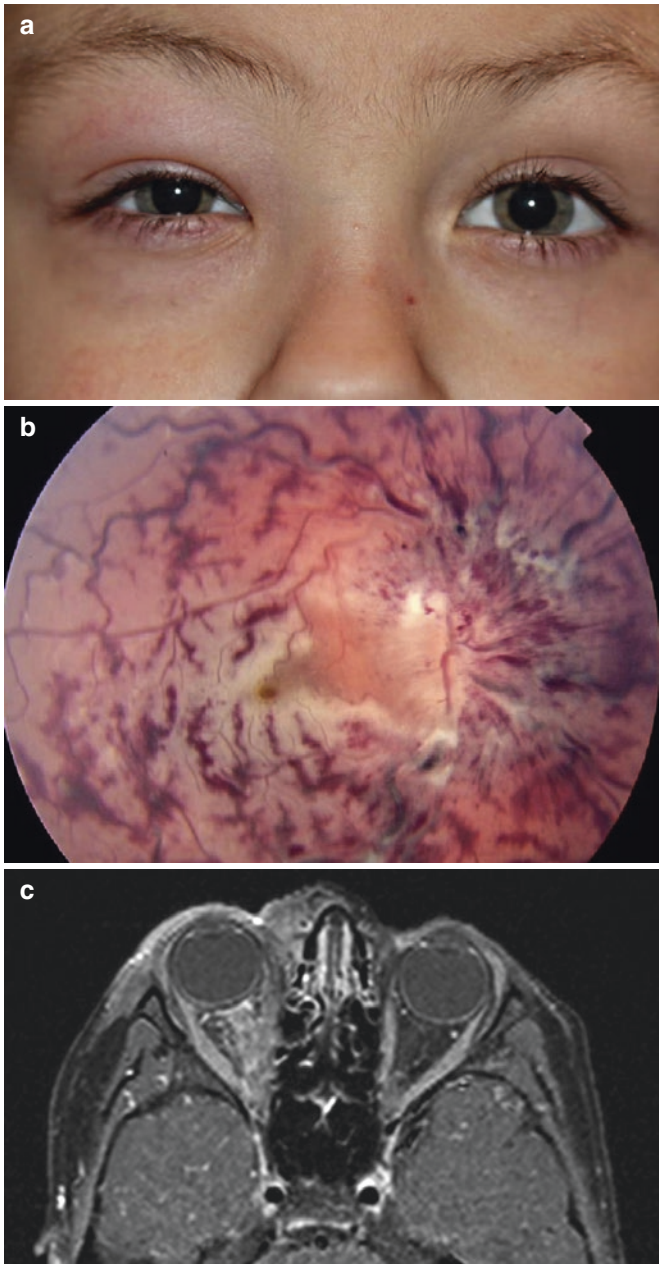


Fig. 36.8 Optic nerve and orbital AML. (**a**) 8-year-old with vision loss and eyelid swelling with proptosis. (**b**) Right fundus photograph showing optic nerve infiltration and retinal venous occlusion. (**c**) T1-weighted MRI: the right intraorbital optic nerve is diffusely enlarged, with predominantly peripheral enhancement, abutting the optic nerve head, with convex contour into the ocular globe. There is also an enhancing infiltrate of the medial rectus

many were clinically symptomatic or had visual disturbances is unknown. Ridgeway et al. reported only 6 cases of leukemic orbitopathy in their study of 657 children with leukemia; 5 of the 6 were cases of acute myelogenous leukemia with meningeal involvement [58]. In Japan, Ohkoshi and Tsiaris followed 28 children with leukemic ocular involvement for up to 84 months [59]. Three children demonstrated orbital infiltration manifesting as proptosis (as in Fig. 36.9). All three had central nervous system and bone marrow involvement of acute myelogenous leukemia at the time orbital signs were manifest, and all died within 15 months of diagnosis. The 5-year survival rate for the group of children in that study with any ocular metastasis was 21% versus the 5-year survival rate of 46% among those who showed no ocular involvement [59].

Acute myeloid leukemia (AML) shows a greater propensity for orbital involvement than other types of leukemia in childhood. This specific relationship uniting the orbital presentation of granulocytic sarcoma and the systemic appearance of AML is extremely important because of the orbital component's propensity to arise prior to the systemic manifestations of the leukemia, often by months [60]. If AML is diagnosed early, children can be treated successfully to prevent the eventual widespread dissemination of the tumor and affect a better long-term outlook. Originally termed chloroma, due to the greenish discoloration of the tumor within the orbits seen on autopsy, proptosis was the presenting sign in approximately 8% of children with AML [55] (Fig. 36.10). Zimmerman and Font reported 33 cases of chloroma and found that 75% presented under 10 years of age, with a median of 7 years old [60]. One-third of patients demonstrated no peripheral blood or bone marrow signs of AML for 4–15 months after biopsy of the orbital mass, whereas the other two-thirds of patients had evidence of AML within 2 months of orbital presenting signs.

Interpretation of the histopathology is important for early intervention. Composed of small, basophilic, round, undifferentiated cells, it can appear very similar to other small, round cell neoplasms, such as lymphoma, neuroblastoma, or rhabdomyosarcoma, on pathology evaluation. CT features are typically non-definitive, and, coupled with its clinical presentation of rapid-onset proptosis in an otherwise healthy child, AML may easily be confused with other pediatric orbital malignancies, inflammations, and infections [61]. Thus, MRI is a much superior modality in evaluating a child with suspected proptosis, especially in the setting of known leukemia.

Given the rarity of pediatric orbital lymphomas, a specimen showing small, basophilic, undifferentiated cells and lacking the cross striations typical for rhabdomyosarcoma on cellular histopathology should give rise to the strong consideration of granulocytic sarcoma, which can be ruled out by performing a Leder stain for esterase activity, which will be positive in granulocytic sarcoma but negative in the previously mentioned malignancies. Ultimately, cytogenetic and molecular analyses are employed to confirm the diagnosis, determine the plan for treatment, and define prognostic risk [62].

Treatment is directed toward the detectable disease with orbital radiotherapy given if no systemic component is found and chemotherapy utilized for generalized disease. Vigilance



Fig. 36.9 Leukemic intraocular involvement. (**a**) A 3-month-old child demonstrating bilateral proptosis from orbital involvement of acute myelogenous leukemia. (**b**) Child with anterior chamber "pseudohypopyon" from leukemic intraocular involvement. (**c**) Same child as in (**b**) showing a fine-needle aspiration of tumor cells from the anterior chamber

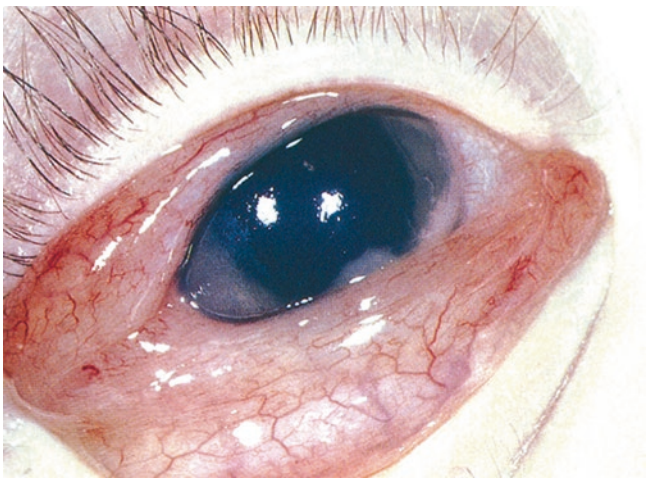


Fig. 36.10 Orbital granulocytic sarcoma. Clinical photograph demonstrating the external appearance of a patient with orbital granulocytic sarcoma

and frequent testing are necessary if no systemic component is found at the time of orbital presentation again since two-thirds of patients will have systemically detectable leukemia within 2 months.

Pediatric orbital lymphomas are rare, as previously outlined. Most cases are reported as part of a larger series from ophthalmologists, whereas non-ophthalmic series of head and neck tumors in children rarely include lymphomas of the orbit [63]. Most cases are B-cell lymphomas of the non-Hodgkin variety, although one recent report found an isolated T-cell lymphoma in the orbit of an 8-year-old child [64].

The largest experience of orbital lymphoma in children is found in the African region spanning 15° north and south of the equator, where an endemic Burkitt's lymphoma frequently secondarily invades the orbit from maxillary or sinus primary sites [65–67]. This African type occurs at an average age of 7 years and usually presents with a jaw or maxillary mass that progresses rapidly and can involve the orbit in approximately 15% of patients. In America, where Burkitt's lymphoma is not endemic, the presentation is somewhat different, with abdominal tumors predominating at an average age of onset around 12 years old. Unlike its African counterpart, previous infection with Epstein-Barr virus is usually not seen. This is verified by the expression of Epstein-Barr virus genome in the tumor cells of 96% of endemic cases versus only 10–20% of non-endemic cases [68]. Even so, both the endemic and non-endemic types express cell surface immunoglobulins characterized by a cytogenetic translocation between the *c-myc* oncogene located on the 24th band of the short arm of the 8th chromosome (8q24) and at one of a variety of immunoglobulin loci (14q32, heavy chains; 2p12, light chain kappa; 22q11, light chain lambda) [69]. This translocation leads to the deregulation of the *c-myc* oncogene, which is important for tumorigenesis [70].

With a rapid doubling time, these lymphomas often reach tremendous size, frequently invading adjacent structures and cavities. Meningeal infiltration is present in about 20% of cases with malignant pleocytosis, cranial nerve palsies, or epidural mass effects. Orbital signs include globe displacement with painless proptosis and chemosis. Imaging studies show an often large, homogenous mass extending into the orbit from the surrounding paranasal sinuses with bone destruction and occasional intracranial extension. Parameningeal rhabdomyosarcoma and granulocytic sarcoma can have similar features, and adequate biopsy with careful histopathologic evaluation is essential. A uniform background of large lymphocytes interspersed with large, pale-staining histiocytes or macrophages is known as the "starry-sky" appearance typical for Burkitt's lymphoma.

Since most patients have widely disseminated disease on diagnosis and since the tumor has a rapid doubling time, Burkitt's lymphoma is exquisitely responsive to chemotherapeutic agents [71]. Cyclophosphamide alone yielded good tumor remission, but is now often combined with vincristine, methotrexate, and corticosteroids. Large tumor loads may need debulking prior to initial chemotherapy, and prophylactic brain irradiation is added in patients with bone marrow involvement due to the high incidence of eventual meningeal involvement. Remission is possible in over 50% of patients, with minimal systemic tumor and low tumor volume correlating best with good prognosis.

Neuroblastoma

Well known as a metastatic process involving the orbit in childhood, neuroblastoma is a malignant tumor of primitive neuroblasts that derive from neural crest cells and are destined to become elements of the autonomic nervous system. Arising in the abdomen, thoracic, cervical, and pelvic regions as primary sites of origin, these highly malignant neural tumors present as a localized mass in the involved region. The average age at diagnosis is 2 years, with 90% of cases diagnosed before age 5 [72–74]. Of these tumors, 60–72% are found in the abdomen. Slightly more common in males, it is estimated that 8% of cases present with ophthalmic features, while approximately 20% of cases will eventually have some ophthalmic manifestations [72, 75]. There are approximately 600 new cases of neuroblastoma in the USA each year, with a prevalence of approximately 1 case per 7000 births [76].

The most common presentation of ocular involvement from neuroblastoma is characterized by the sudden onset and rapid progression of proptosis, ptosis, and the classic sign of periorbital swelling with ecchymosis (Fig. 36.11). Most cases metastatic to the orbit have their primary site of origin in the abdomen in either adrenal or paraspinal locations, and 40% of cases have a bilateral orbital presentation. Over several weeks, symptoms and signs worsen, mimicking inflammatory conditions of the orbit, trauma, or rapidly progressing neoplasias. The metastatic process shows a preference for the superolateral orbital bones and soft tissue, with the zygoma a distant second as an orbital metastatic site. The classic presentation of bilateral proptosis with periorbital ecchymosis is seen in only 50% of cases with orbital involvement and is often unilateral or non-ecchymotic early on (Fig. 36.12) [75]. The differential diagnosis of malignant orbital conditions similar in presentation includes leukemia, granulocytic sarcoma, rhabdomyosarcoma, Ewing



Fig. 36.11 Metastatic neuroblastoma. Patient with mild bilateral proptosis and lid ecchymosis from metastatic neuroblastoma

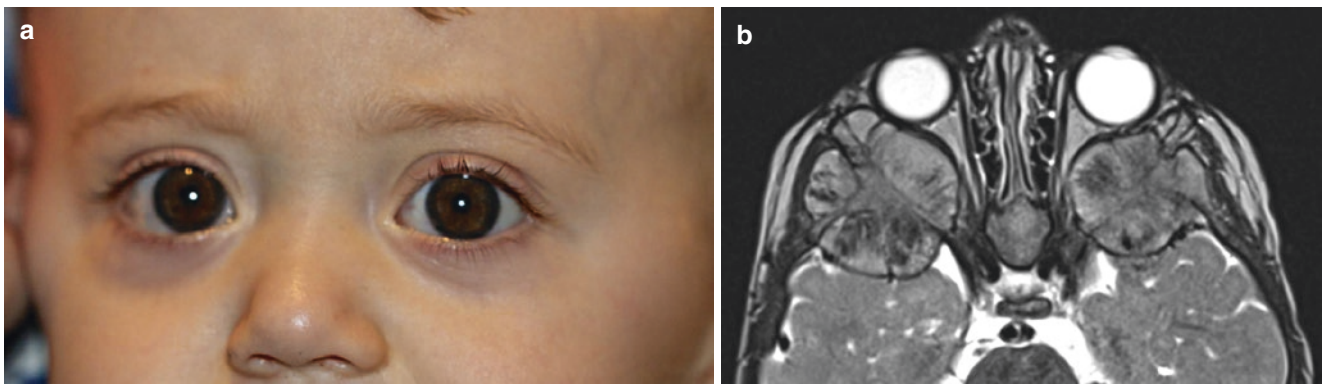


Fig. 36.12 Initial presentation of metastatic neuroblastoma. (**a**) 5-year-old who presents with severe head pain and with bilateral temporal masses. (**b**) T2-weighted MRI with isointense mass lesions with extensive periosteal reaction seen involving the bilateral temporal bones and lateral walls of the orbits with mass effect upon the bilateral perioptic spaces. The bilateral masses demonstrate intracranial extension and mass effect upon the anterior portions of the temporal lobes as well as bilateral adjacent dural enhancement.

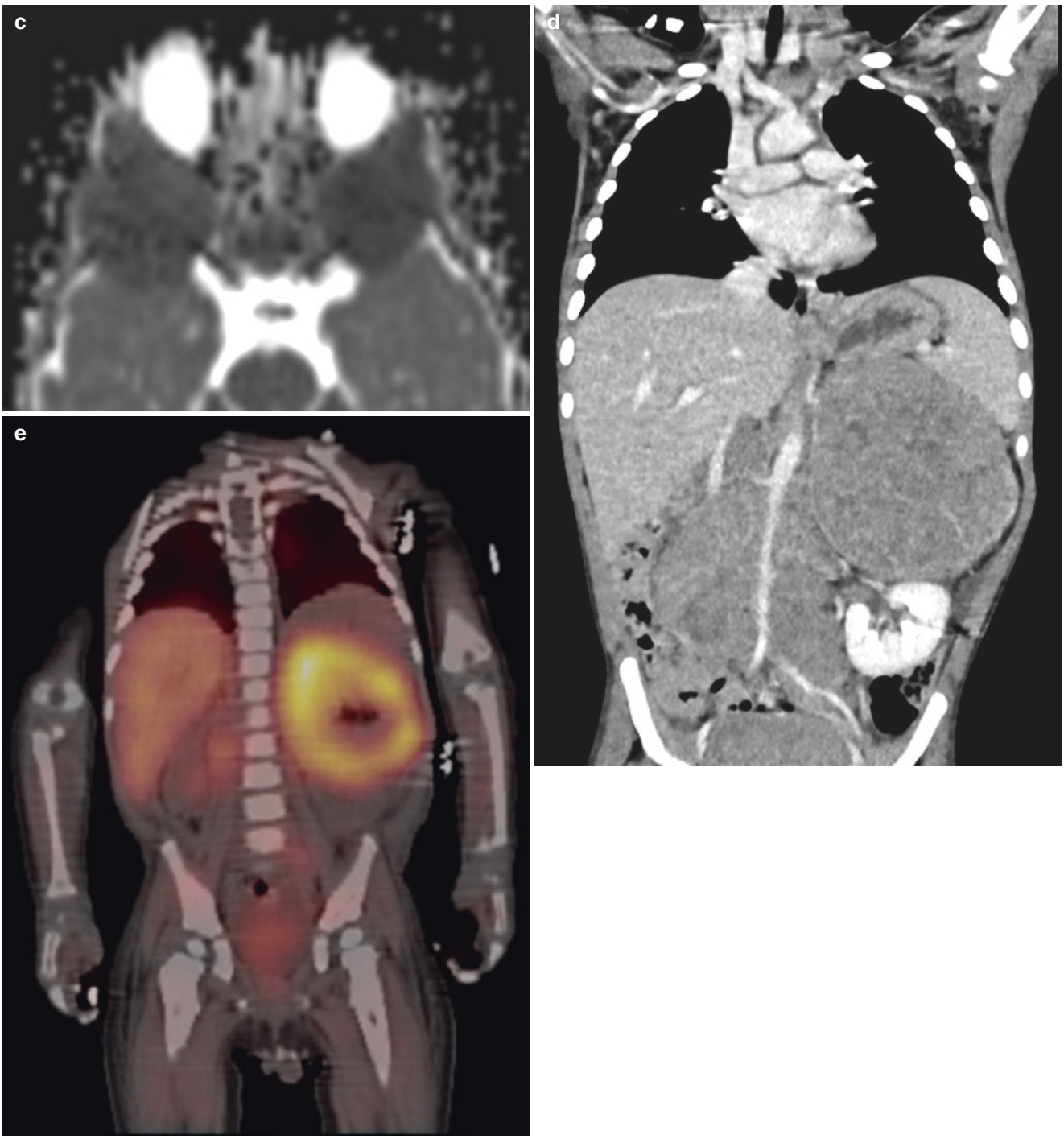


Fig. 36.12 (continued) (**c**) DWI Imaging with restricted diffusion. (**d**) Abdominal CT with large left-sided mass. (**e**) Single-photon emission computed tomography (SPECT) imaging showing abnormal uptake in the left abdomen corresponding to a large adrenal mass, which was proven to be neuroblastoma on biopsy

sarcoma, medulloblastoma, and Wilms' tumor, while benign conditions with rapid onset include orbital cellulitis, orbital abscess, and eosinophilic granuloma. CT examination shows bony destruction with extension of a mass into the lateral orbit, temporalis fossa, and middle cranial fossa that surrounds the metastatic site, typically involving the lateral sphenoid.

Several other presentations involve ocular findings. Congenital or acquired Horner syndrome may be the presentation in a child with a primary neuroblastoma involving the paracervical sympathetics or a mediastinal neuroblastoma in the lung apex that involves secondary sympathetic neurons as they travel around the mediastinal

vessels prior to ascending along the carotids into the head and neck [77, 78]. A neck mass may be palpable or jugular venous distension may be observable. Both should be carefully looked for in an infant with Horner syndrome. Less common is the finding of opsoclonus associated with neuroblastoma. Usually not an isolated finding, less than 3% of children with neuroblastoma will show opsoclonus, which is typically seen in conjunction with myoclonic motor activity and truncal ataxia [75, 79]. Unusual with this finding is that all these children will have localized disease (abdominal, paracervical, adrenal, and pelvic locations) and not metastases, prompting the suggestion that this type of presentation may be related to an autoimmune paraneoplastic process [80]. Direct metastasis to the eye is rare but has been seen in the iris, in the bilateral choroid, and as an anterior chamber hypopyon [80–83].

Additional testing needs to be performed in a child presenting with these signs or symptoms. Perhaps simplest and most important is a good physical examination. Most of the primary sites at which neuroblastoma will arise are easily accessible by both observation and palpation. These children on presentation are sick and are frequently examined in their parents' laps, whereas children who present with primary orbital malignancies, such as rhabdomyosarcoma, are usually playful and active. Observation for opsoclonus, neck mass, jugular venous distension, myoclonic activity, and abdominal distension may reveal the site of origin. The examining physician should attempt to palpate for an abdominal or neck mass.

For patients with proptosis, orbital MRI evaluation should be combined with neck, chest, abdominal, and pelvic MRI studies in children found to have signs of possible neuroblastoma, since these are very young children and often are scanned while sedated or anesthetized. Blood and urine samples may demonstrate cellular neuroendocrine products such as catecholamines and their metabolites (vanillylmandelic acid [VMA] or homovanillic acid [HVA]) in up to 75% of patients. However, a much smaller percentage of patients, estimated at around 30%, will produce these compounds when the tumor is poorly differentiated on histopathology [84]. Early involvement by pediatric oncologists will help to stage the disease and determine the correct course of treatment.

Good correlation between ocular presenting signs and the survival of the patient stresses the importance of recognizing the possibility of neuroblastoma in patients manifesting any of the abovementioned ocular signs. Musarella et al. reviewed 80 pediatric patients who presented with ocular signs heralding their neuroblastoma [75]. The 3-year survival rate directly correlated with the ocular presentation: proptosis, Horner syndrome, and opsoclonus, showing survival rates of 11, 78, and 100%, respectively. Those with proptosis have the worst prognosis since they have metastatic disease, while patients with Horner syndrome are announcing the location of their primary lesion and may not have metastases yet. Aggressive, rapid diagnosis and therapy are a necessity in this instance. As previously mentioned, opsoclonus probably reflects an autoimmune response and may signal a protective benefit correlating to the 100% 3-year survival rate with this ocular sign.

Suspicion of the disease followed by correct staging with MRI evaluation, serology for catecholamines, bone scan, and at least two-site bone marrow biopsy helps determine the correct treatment regimen or directs biopsy or surgical resection of the lesion if no metastases are found. Fine-needle aspiration biopsy offers good tissue diagnostic capabilities along with adequate samples for special stains and electron microscopy if light microscopy fails to elucidate the correct diagnosis [85]. The Children's Oncology Group Neuroblastoma Risk Stratification System is based on the International Risk Grouping system. For treatment purposes patients are assigned into low-, intermediate-, and high-risk categories (according to phase III treatment protocols) based upon the analysis of age at diagnosis, stage, histopathology, MYCN amplification status, and DNA index [86]. The MYCN gene amplification occurs in approximately 20% of primary neuroblastoma tumors and is strongly associated with metastatic disease and poor prognosis.

However, it can still be difficult to differentiate the blue-staining, small, round, poorly differentiated neoplastic cells from other similar histopathologic malignancies such as rhabdomyosarcoma, lymphoma, Ewing sarcoma, and Wilms' tumor [87]. Better-differentiated tumors can demonstrate neurite and rosette formation with central neural processes, allowing for light microscopic diagnosis. Unfortunately, metastatic sites, which are often where the tissue biopsy is obtained, often demonstrate absent neural differentiation, and ancillary histopathologic techniques become the primary means of diagnosis. Neuroblastoma is keratin negative and vimentin negative on immunohistochemical staining. Neuron-specific enolase is a useful marker, but is also positive in other central nervous system tumors, amine precursor uptake and decarboxylation (APUD) cell-derived neoplasms (e.g., Merkel cell tumors), melanomas, schwannomas, and rhabdomyosarcomas. Electron microscopy can show dense core granules, which are pathognomonic when present. Rapid catecholamine fluorescent techniques induce autofluorescence in neoplasms containing primary amines and can be useful in identifying neuroblastomas in undifferentiated specimens [75]. Molecular studies have shown an inconsistent deletion at chromosome lp and overexpression of the *N-myc* oncogene at locus 2p24, which is associated with advanced disease and a poorer prognosis [88, 89].

Several groups of patients have a vastly superior survival rate with neuroblastoma. Already mentioned is the 78% survival rate in children presenting with Horner syndrome and the 100% survival rate for children demonstrating

opsomyoclonus. Breslow and McCann found that children presenting with neuroblastoma under the age of 12 months had a 72% survival rate, compared with the 12% 2-year survival rate if presenting after 2 years of age [90]. Additional associations for higher survival rates were afforded when neuroblastoma was intrathoracic stage I, II, or IV-S after work-up and when the patient was older than age 6 at presentation [74, 91]. Shimada et al. used patient age, cytologic differentiation, mitosis-karyorrhexis index, nodularity, and extent of schwannian stromal components to classify patients into favorable and unfavorable survival groups [92].

The exact treatment of neuroblastoma differs from institution to institution. Cisplatin, cyclophosphamide, vincristine, Adriamycin, and etoposide are used in various combinations, with 60–70% of patients responding with complete or partial resolution of metastatic lesions in 4–6 months [93]. Primary tumor control with surgical excision for residual tumor may then be attempted either with or without adjunctive radiation therapy.

Langerhans Cell Histiocytosis

The Langerhans cell is an antigen-presenting dendritic histiocyte with minimal phagocytic capacity. As part of the mononuclear phagocytic system, it primarily acts as an immune mediator and potent antigen-presenting cell and can be found in several organs throughout the body, especially the skin, thymus, bronchial mucosa, and lymph nodes. Langerhans was the first to describe its unique cytoplasmic organelle, the Birbeck granule.

Histiocytosis refers to the group of diseases that result from the accumulation or proliferation of histiocytes in tissues, resulting in a variety of clinical conditions manifesting as inflammatory, destructive, or malignant foci [94]. This group of disorders has undergone many name changes over the last 15 years and is now simply termed Langerhans cell histiocytosis [95]. While in many instances this actually represents an orbital inflammatory disorder, it has traditionally been categorized as an orbital tumor and especially when it has systemic involvement (see Chap. 34). The original terminology used to describe the spectrum of this disease comprised three clinical entities of differing systemic involvement: eosinophilic granuloma, Hand-Schuller-Christian disease, and Letterer-Siwe disease. Most practitioners have since agreed that these three entities are a spectrum of a specific cellular derangement referred to as histiocytosis X. More recently, the Histiocyte Society suggested renaming the condition Langerhans cell histiocytosis, amplifying the cellular origin of the condition and unifying all previous names under this general heading [96].

Subsets of this condition that describe clinical groupings of similar signs and symptoms are still useful and have clinical relevance. Unifocal eosinophilic granuloma is equivalent to the previous condition termed eosinophilic granuloma. Multifocal eosinophilic granuloma replaces Hand-Schuller-Christian disease, and diffuse histiocytosis substitutes for diffuse histiocytosis X and Letterer-Siwe disease. Malignant histiocytosis refers to a highly lethal disease of rapidly progressive multisystem involvement from infiltrating anaplastic mononuclear cells [97]. Not specifically included in original descriptions of histiocytic disorders, it was added to one staging scheme because of Langerhans cell histiocytes being identified in the lesions despite its rapid onset and uniformly lethal outcome, which is different from the usual course of other forms of this condition [98].

The presentation of Langerhans cell histiocytosis (LCH) can begin as unifocal bony involvement (single-system LCH) or can start as or progress to widespread multi-organ disease (multisystem LCH) (Table 36.5). The underlying lesion is a granulomatous-histiocytic infiltration in the affected tissues often associated with accumulations of eosinophils and lymphocytes. Histologic variation is common as the lesion progresses through necrosis, xanthomatous change, and, ultimately, fibrosis, which occurs in the later stages of the disease. The tissues most often affected by this process are the medullary cavities of bone, skin, lymph nodes, lung, liver, spleen, gastrointestinal tract, and bone marrow. Which tissues are affected at presentation or in the course of the disease determines the stage and treatment for the patient.

It is estimated that the incidence of LCH in children is two to five cases per million per year in the USA [100]. Children account for over 70% of most patients. Approximately 60% present as stage 0 or I, and only about 20% progress on to higher stages. Roughly 40% present with

Table 36.5 Clinical classification of LCH [99]

Single-system LCH (SS-LCH)	*One organ/system involved (uni- or multifocal)* Bone: unifocal (single bone) or multifocal (>1 bone) Skin Lymph node (not the draining lymph node of another LCH lesion) Lungs Hypothalamic-pituitary/central nervous system Others (e.g., thyroid, thymus)
Multisystem LCH (MS-LCH)	*Two or more organs/systems involved* With or without involvement of "risk organs"
Indications for systemic therapy [99]	
SS-LCH with "CNS-risk" lesions SS-LCH with multifocal bone lesions (MFB) SS-LCH with "special site" lesions MS-LCH with/without involvement of "risk organs"	

multi-organ involvement. Ophthalmic involvement in these conditions is relatively rare but is important, because it may be the heralding sign of potential systemic involvement, allowing the ophthalmologist to begin an investigation that may prolong or improve a patient's life. Moore et al. reviewed their experience involving 76 children with LCH and found 18 (24%) that had involvement in the bones and soft tissues of the orbit [96]. Only three patients presented with proptosis or periorbital swelling as the initial sign of their disease. Additional ophthalmic involvement was primarily seen as neuro-ophthalmic manifestations, including papilledema, optic disk swelling, ptosis, and transient seventh cranial nerve palsy due to cranial base bony lesions affecting these nerve pathways. Other sites reported with direct ocular involvement include the uveal tract, retina, sclera, and meninges around the optic nerve [101–104].

Clinically, the features of unifocal involvement in the periorbital region start as the progressive onset of lid swelling, bony pain, and occasional globe displacement (Fig. 36.13a). Most patients have mild symptoms that begin a gradual progression over 1–6 months of increasing periocular inflammation and edema. Younger patients show a tendency to more rapid progression. The symptoms are frequently assumed to be those of orbital cellulitis, but oral antibiotics have no effect on the progression. Tenderness over the lesion, which is often centered over the superolateral orbit (frontal bone) or cheek area (zygoma), seems more pronounced in children who have a more rapid onset. Continued worsening prompts radiologic evaluation that demonstrates a lytic bone lesion on plain film radiography and a rather characteristic, sharply delineated radiolucency of expanding bone in early stages on orbital CT evaluation. In later stages,

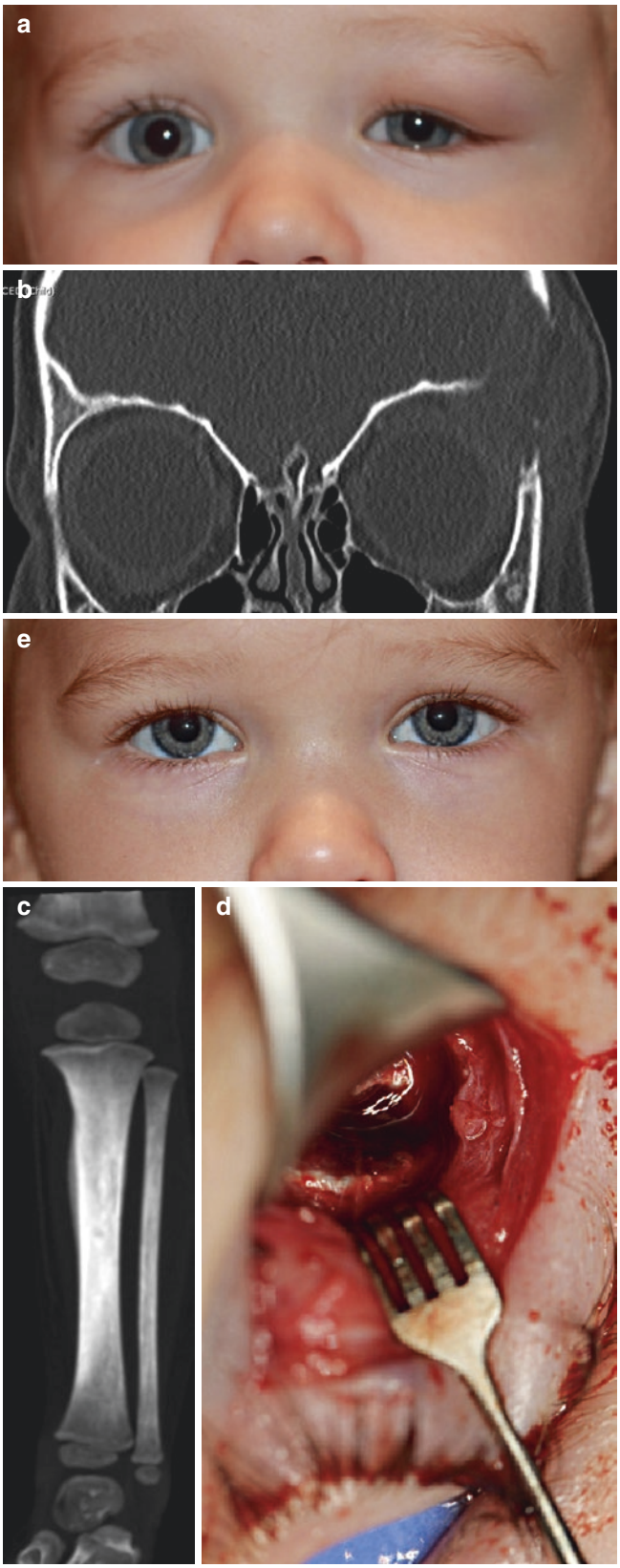


Fig. 36.13 Orbital LCH in a 2-year-old girl with multisystem disease (skeletal, lung, liver). (**a**) Left upper eyelid edema and mechanical ptosis with mild proptosis. (**b**) Lytic lesion in the frontal bone and lateral orbital wall that developed while on chemotherapy for multisystem disease. (**c**) Lytic lesion in the proximal to distal one-third of the tibial diaphysis with associated cortical thickening and periosteal reaction compatible with Langerhans cell histiocytosis. Because of her multisystem LCH, she was treated with systemic chemotherapy (vinblastine and prednisone). (**d**) Intraoperative photo. Left anterior orbitotomy via a left upper eyelid crease incision. A large orbital rim defect is seen with a deep necrotic mass visible. This was curetted and aspirated and methylprednisolone was irrigated into the bony defect. Histopathology found a mixed inflammatory infiltrate with neutrophils, lymphocytes, and scattered multinucleated giant cells. The atypical mononuclear cells stain positively with CD1a, S100, and langerin consistent with LCH. (**e**) 2-month postoperative photo showing well-healed eyelid crease incision and significant improvement of eyelid edema and ptosis

when the lesion breaks out of the thinning cortical bone, a moth-eaten erosive bony defect remains within, which is a soft tissue component encasing variable amounts of bony remnants (Fig. 36.13b). These findings often lead to biopsy, which shows histiocytic proliferation, eosinophilic infiltration, multinucleated giant cells, and varying degrees of necrosis [105]. Ultrastructural analysis demonstrates Birbeck granules, which are racquet-shaped microtubular structures involved in antigen processing. Immunohistochemical studies and DNA flow cytometry data show expression of la, T6, OKT6, and S100 glial protein but both diploid and aneuploid DNA content in the Langerhans cells [106, 107]. Recent studies demonstrate monoclonal populations of Langerhans cells in histiocytic lesions, indicating that somatic gene mutations may play a role in the etiology and pathogenesis of LCH [108]. Currently mutations that aberrantly activate RAF/MEK/ERK signaling in over two-thirds of patients with LCH may direct a target therapy strategy [95].

Faced with a single lesion, one has to look for additional systemic signs of more multisystem disease [109]. The skin should be carefully examined for involvement that may appear as a scaly papular eruption, a petechial purpuric lesion, xanthomatous lesions, or ulcerative nodules [110]. Abdominal examination for hepatosplenomegaly should be performed as well as inguinal, axillary, and cervical palpation for lymph node enlargement. Whole-body skeletal surveys inspect for multifocal bony involvement, helping to stage the condition for later treatment. CT of the head is important to specifically look at the pituitary fossa for bony erosion that is the source for diabetes insipidus due to the destruction of the pituitary by the inflammatory process. A complete blood count, liver function tests, and renal function tests reveal any organ dysfunction, which can be involved in diffuse histiocytosis. Dental examination with panoramic x-ray has also been advocated due to the frequent finding of mandibular lesions in multifocal eosinophilic granuloma [111]. Chest x-ray reveals not only rib and thoracic bony lesions but also the extent of any lung parenchymal involvement. Technetium-99 bone scan does not offer better lesional detection than skeletal survey [112].

Once staged, treatment can be decided upon based on the results of bone and organ system testing. Single-system LCH has been successfully treated with curettage, steroid injection, and possible low-dose radiotherapy and by observation [113–116]. At the time of biopsy, generous debulking of the lesion with preservation of the periorbita while avoiding intracranial contents and direct curettage of bone will cure over 90% of these periorbital lesions. Given the benign nature of the lesion and its rather typical CT findings, observation alone can be entertained without biopsy if the systemic work-up is completely negative. One must carefully follow these children for any signs of progression both in terms of local and systemic involvement with the help of pediatric consultation. Increasing erosion with periorbital inflammation, pain, or progressive proptosis with visual compromise deserves intervention with either intralesional steroid injection or low-dose radiotherapy (400–600 cGy). Practitioners have noted a tendency toward delayed bone maturation and hypoplastic bony development in irradiated bony areas that may leave a noticeable asymmetry later. Not known is whether this dose of radiotherapy has the potential to induce secondary malignancies as seen in other conditions such as retinoblastoma.

Multisystem LCH can be treated with either multifocal radiotherapy directly to the lesions or with systemic chemotherapy [115, 117]. Since direct injection of steroid successfully treats unifocal lesions, oral steroids would seem attractive for multifocal lesions. However, the relatively long healing course of these lesions with frequent relapses while on prednisone (3–66 months), the repeated radiographic examinations necessary to determine if the lesions are responding, and the long-term side effects of steroids make this a relatively poor option [88]. Nonetheless, it is chosen under some circumstances. Currently, vinblastine and prednisone remain the standard of care for children with multisystem LCH. The combination of cytarabine and cladribine is the current standard for second-line therapy of refractory cases with vital organ dysfunction [99].

Diffuse histiocytosis requires treatment with chemotherapy due to multi-organ involvement. Malignant histiocytosis is typically included with these Langerhans cell disorders, but recent evidence indicates that this is an anaplastic large cell lymphoma based on genomic and phenotypic analysis [118]. This seems to be a different entity than the relapsing diffuse histiocytosis or the progressive Langerhans cell histiocytosis characterized by prominent involvement of blood, bone marrow, viscera, and skin with a fulminant and potentially fatal course [119].

While direct ocular and orbital involvement with LCH is unusual, its presentation should prompt rapid evaluation due to the potential presence or progression to multisystem disease or malignant transformation. Greenberger studied the results of therapy in LCH by reviewing their success in the treatment of 127 pediatric patients with an average follow-up of 8 years [100]. The 5-year survival rate for unifocal and multifocal eosinophilic granuloma was approximately 93%, but none of the patients died of the manifestations of LCH itself. Deaths in the follow-up period were related to other causes, including appendicitis, trauma, and hepatocellular carcinoma. The latter patient had a unifocal lesion in the clavicle, which was curetted, and then received 12 months of chlorambucil and was disease-free for 14 years until the carcinoma arose. It is not known whether the chemotherapy had a role in the development of the hepatocellular carcinoma. Another survivor in this group went on to have a child who also developed eosinophilic granuloma. Of the 14 patients in this series

who presented with eosinophilic granuloma, 2 (14%) went on to develop other organ involvements. Two patients presented with orbital signs.

From these data, 6% showed signs of orbital or ocular involvement; 9% progressed to worse stages of the disease despite therapy in some cases, reminding us of the need for careful long-term follow-up. The overall long-term survival was 63%, which was skewed by the 43% survival seen among those patients who presented with disease prior to their second birthday. Treatment for this condition has significant morbidity and potential mortality as 4% developed second malignancies [98].

Ewing Sarcoma

Alluded to in the previous section discussing soft tissues sarcomas, Ewing sarcoma (ES) is a highly malignant, small, round cell tumor arising in or around bony structures in the extremity. Originally thought to be of primary bone origin, substantiative cytogenetic and immunocytochemical evidence now suggests that this tumor arises from neural cells of parasympathetic lineage [120]. ES tumors are part of the Ewing sarcoma family tumors (EWFT) to include classic ES of bone, extraosseous ES, peripheral primitive neuroectodermal tumor, and Askin tumor of the thoracic wall. Over half of these tumors arise in the extremities with the orbit involved primarily through metastases [121]. Only 4% arise primarily in the head and neck region, but primary orbital involvement has been reported along with contiguous spread from adjacent sinuses [122–124]. A definitive diagnosis can be achieved via cytogenetic studies searching for translocations in the locus of the ES gene on chromosome 22, which have been demonstrated in more than 85% of ESFT cases [125]. Typically seen in the second decade of life, the orbital presenting signs are of steady, quick-onset proptosis or globe displacement. CT evaluation shows an irregular pattern of bony destruction with an associated soft tissue mass. Systemic evaluation with whole-body skeletal survey is important to determine whether orbital involvement is primary or secondary. Histopathologic diagnosis is often difficult to establish with this frequently anaplastic tumor, because it can be similar to other small cell neoplasms such as osteogenic sarcoma and neuroblastoma (Fig. 36.14).

Treatment in the past has resulted in a 10% 5-year survival rate, but more recent use of multi-agent chemotherapy and local aggressive radiation therapy or surgical resection has improved survival to approximately 70% [126–128]. Cyclophosphamide, dactinomycin, vincristine, and doxorubicin are used as first-stage treatment in a 12-week induction cycle to control potential metastatic spread prior to addressing the primary tumor. This regimen may also shrink the primary tumor, making it more amenable to local resection rather than radiation therapy. Radiation in a dose of approximately 6000 cGy yields nearly a 90% control rate [127]. Primary tumors amenable to surgical resection yield a better tumor-free interval than radiation therapy for local control when surgical margins are free of tumor. Additional chemotherapy can be combined with radiation therapy for residual metastatic sites, but higher complications ensue due to enhancement of radiation effects with adjuvant chemotherapy. Additionally, about 20% of patients have demonstrated late-onset secondary tumors, most commonly osteogenic sarcoma, with combination therapies [128]. Careful follow-up must be maintained due to the high risk of late recurrence with this tumor.

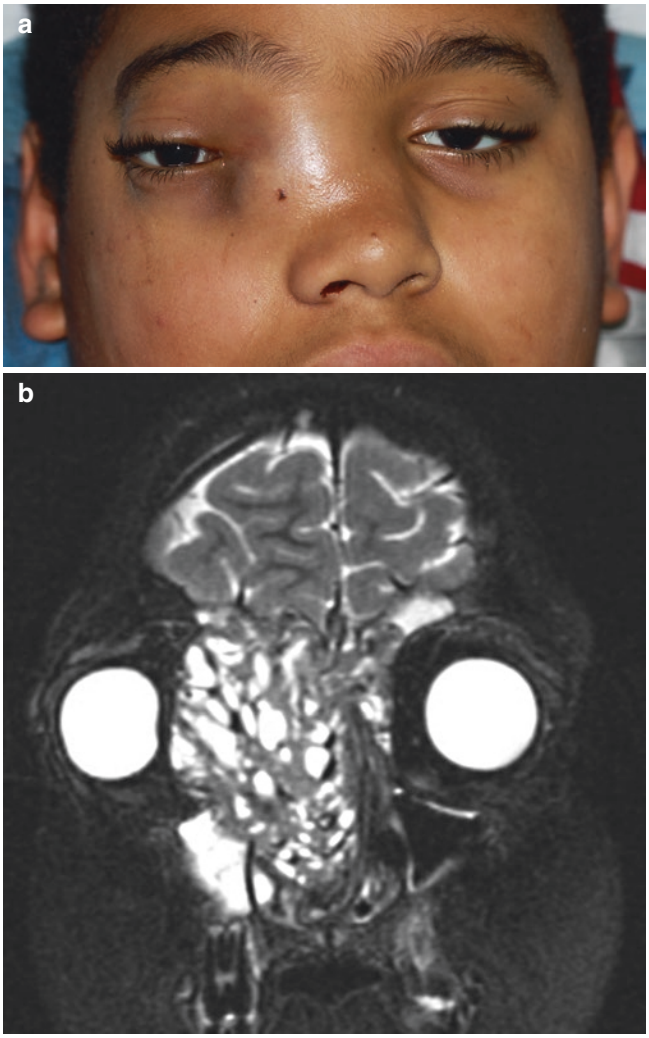


Fig. 36.14 Ewing Sarcoma in a 13-year-old male. (**a**) Right orbital displacement from large sinus mass. (**b**) T2-weighted MRI showing a large solid and cystic mass centered in upper part right nasal cavity and anterior ethmoid air cells, with extension into the anterior intracranial cavity abutting and indenting the anterior-inferior aspect of the right frontal lobe, with slight dural enhancement. There is also tumoral extension into the medial extraconal right orbit with marked mass effect resulting in lateral displacement of the right orbital contents, deformed contour of the right eye globe, proptosis, and resultant stretching of the right optic nerve and extraocular muscles

Peripheral Primitive Neuroectodermal Tumor

Primitive neuroectodermal tumors (PNET) is a group of malignant small cell tumors that arise from primitive neuroectodermal progenitor cells. When occurring outside the central nervous system, they are referred to as peripheral primitive neuroectodermal tumors (pPNET). Orbital PNETs are a subclass of pPNET. It is now recognized that these malignancies are a part of the Ewing sarcoma (ES) tumors. This is supported by evidence of the similarity in highly characteristic chromosomal translocations involving the long arms of chromosome 11 and 22, t(11;22)(q24;q12), which is demonstrated in more than 85% of ES family of tumor cases [129]. A major differentiation between PNET and ES is the large degree of neural differentiation found in PNET cells compared with the relative lack of neural differentiation features in ES [130]. A 2011 review found only 16 reported cases of pPNET of the orbit [132]. Most of these cases were treated with surgical debulking followed by chemotherapy with or without radiotherapy. This is an aggressive tumor with bony invasion. The risk for distant metastasis in orbital pPNET was noted to occur in 2 of the 16 cases reported in the literature [131]. We have experience in treating one patient with pPNET (Fig. 36.15). After a biopsy was performed, the patient underwent a successful lid-sparing exenteration with dermis fat graft placement.

Secondary Orbital Malignancies

Less common than primary or metastatic malignancies in the pediatric population, secondary malignancies accounted for 15.6% of all malignant pediatric orbital tumors as seen in Table 36.1. The majority of these tumors were secondary recurrences of retinoblastoma in anophthalmic sockets. Sinus-origin sarcomas, nasopharyngeal carcinoma, and esthesioneuroblastoma accounted for the few remaining cases. The large propensity of secondary retinoblastoma is different from other reports of pediatric orbital tumors where sinus carcinomas typically account for more than 50% of secondary tumors [132]. Rare cases of intracranial primary malignancies, such as glioblastomas, eyelid and conjunctival malignancies with intraorbital spread, and tumors of lacrimal sac origin eventually eroding into the orbit, can be found in textbooks. We discuss only retinoblastoma and esthesioneuroblastoma in this chapter due to their decided tendency to affect the pediatric population.

Retinoblastoma

Most cases of secondary retinoblastoma seen in the USA come from orbital recurrences after enucleation of eyes with high-risk tumors or from extraocular extension of the tumor in an untreated patient, usually from a Third World country [133]. While rare, it can be seen as a hematogenous metastasis from a primary intraocular retinoblastoma to the previously unaffected orbit [134]. With improvements in the recognition, diagnosis, and treatment of primary intraocular retinoblastoma, orbital extensions and recurrences are becoming increasingly unusual. As proof of this decreasing incidence, a recent study at the Harkness Eye Institute in New York found only 3 cases of orbital involvement among the 175 cases seen between 1980 and 1986 for an incidence of 1.7% compared with previous experience in their institution of a rate estimated at 10% [135, 136].

Orbital involvement from direct intraocular spread occurs by penetration of tumor cells through scleral emissary channels after intraocular choroidal invasion. Histopathologic features suggesting a high likelihood of orbital recurrence after enucleation include tumor cells present at the cut end of optic nerve, significant choroidal invasion, periemissarial tumor cells not extending to the scleral surface, and the presence of episcleral nodules of tumor [137]. Accidental penetration of an eye containing retinoblastoma at the time of enucleation or radiotherapeutic plaque application can also seed the orbit with tumor cells, increasing the risk of secondary orbital involvement.

The clinical presentation of orbital retinoblastoma is one of slowly increasing proptosis or orbital fullness with displacement of the orbital implant and prosthesis. Typically painless, gradual progression over weeks to months produces gross proptosis with lid swelling, a reddish-blue mass, and periocular ecchymosis (Fig. 36.16). A mass may be palpable in the socket but can be hard to detect because of the orbital implant. Prominent vasculature can be seen providing the reddish-blue coloration and lid ecchymosis. CT evaluation shows a moderately enhancing soft tissue mass, without calcification, filling the orbital cavity and often centered on the orbital implant (Fig. 36.16b). Diagnosis can be made by incisional biopsy or fine-needle aspiration biopsy. Repeat systemic evaluation should be carried out to detect other sites of metastases. Although controversial now as to which patient with primary intraocular retinoblastoma should receive some or all of the established metastatic tests, such as lumbar puncture, bone scan, two-site bone marrow aspiration and biopsy, neuroimaging of the head, blood chemistry profile, and physical examination for lymphatic spread, all practitioners would agree that all tests should be done in the case of an orbital retinoblastoma [138, 139].

Treatment of this orbital disease begins with maximal debulking of the orbital tissues if gross quantities of orbital tumor are present to prevent further local or distant tumor spread and to reduce tumor load in anticipation of aggressive chemotherapy and local radiotherapy. Exenteration does not seem to add any specific increase in tumor control, since



Fig. 36.15 Peripheral primitive neuroectodermal tumor (pPNET). (**a**) 14-month-old girl with rapid left proptosis. (**b**) T2-weighted MRI image. There is a rounded, heterogeneous intraconal lesion in the medial left orbit. The lesion deviates the optic nerve superolaterally and compresses and flattens the posterior medial surface of the left globe, with proptosis. The lesion shows marked restricted diffusion on DWI imaging raising the suspicion of a hypercellular lesion that is malignant. (**c**) Low-power micrograph of the exenteration specimen for this patient. The tumor invades the sclera but does not extend as far as the choroid. Papilledema is seen. (**d**) High-power histology of the specimen. Tumor cells basically consist of small round to oval and sometimes pleomorphic nuclei with moderately fine to coarse chromatin. The sheets of cells are irregularly separated by the fibrocollagenous tissue. There are a greater number of tumor cells expressing GFAP primarily in the deeper portions of the tumor. This is consistent with a pPNET. (**e**) 13-year post-eyelid-sparing exenteration with ocular prosthesis in place. (**f**) Left dermis fat graft still fills the orbit. (**g**) T2-weighted MRI taken 13 years after exenteration showing left orbital dermis fat graft and ocular prosthesis

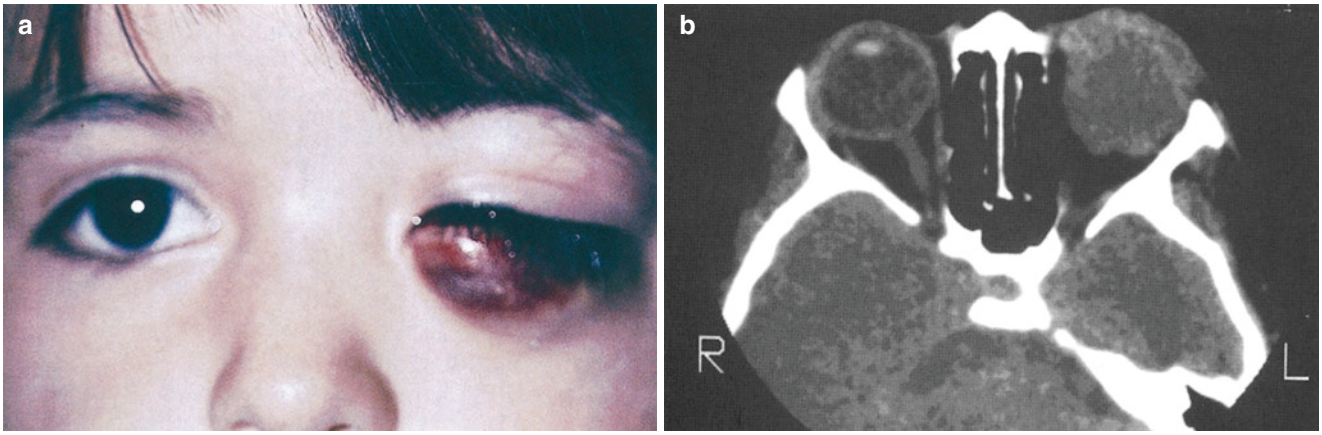


Fig. 36.16 Retinoblastoma. (**a**) A 5-year-old female with orbital recurrence of retinoblastoma. (**b**) Axial CT showing soft tissue mass without calcification surrounding and obscuring the orbital implant in the anophthalmic socket

surgical margins free of tumor are difficult to achieve in the socket. Chemotherapy using vincristine, cyclophosphamide, cisplatinum, etoposide, and intrathecal methotrexate in a variety of combinations offers an improved chance of increased survival compared to past rates as low as 10% [140, 141]. Radiotherapy is added as a primary treatment prior to or combined with chemotherapy for small intraorbital tumor recurrences or for residual orbital disease not responsive to surgical debulking and systemic chemotherapy. The decision to use radiation therapy is based on previous use in the orbital area to control the intraocular tumor, whether any radiotherapy was given post-enucleation in high-risk individuals, and the chance of developing additional complications in the radiation field, such as delayed bony growth or intracranial injury due to radiation induction from concomitant chemotherapy. Induction of late second tumor formation seen in genetic retinoblastoma survivors is less of an issue, since these tumors do not develop exclusively in the field of radiation. Aggressive management in these cases is necessary to prevent intracranial spread, hematogenous metastasis, and local lymphatic extension that increase both the morbidity of the treatment and the potential mortality from the disease.

Esthesioneuroblastoma

This tumor, previously termed olfactory neuroblastoma, arises from the neuroepithelial sensory cells of the olfactory mucosa and gradually grows to fill the upper nasal cavity, extend into the sinuses, and eventually expand into the orbit. Esthesioneuroblastoma is a member of the Ewing sarcoma and PNET family. The translocation commonly seen in Ewing sarcoma and PNETs (EWS/FLI1 genes) has been confirmed in esthesioneuroblastoma cell lines [142]. Signs and symptoms of orbital involvement represent a late stage of this previously highly malignant tumor. Over 250 cases of this tumor have been described. A bimodal incidence based on age is seen, with a peak around age 20 and a second peak around age 50 [143]. An interesting pathologic correlation shows a more undifferentiated tumor at the younger peak with less olfactory differentiation seen in the tumor [129].

The incidence of ophthalmic manifestations varies among studies. Rakes et al. found 53% of their patients with ophthalmic signs and symptoms on presentation versus Levine et al. who found only 12% of their patients experiencing any ophthalmic signs or symptoms during the course of their disease [143, 144]. The ophthalmic signs of the disease vary as well, depending on the anatomic location of the tumor and its area of extension. Those patients with a more posterior location develop posterior orbital involvement with cranial nerve palsies, rapid vision loss with papilledema and afferent pupillary defect, and periorbital pain and headaches from extension through the posterior ethmoid or sphenoid sinuses. More anterior tumor origination extends through the anterior ethmoids to involve the orbit, presenting with proptosis, lid swelling, ptosis, and tearing with an injected eye. These findings, although not specific for this tumor, usually prompt an imaging study of the head, which demonstrates a well-enhanced soft tissue mass high in the nasal cavity with bony destruction as it extends into the sinuses and/or orbit. The clinical diagnosis of esthesioneuroblastoma is suggested by the combination of these orbital and radiographic findings along with the ongoing history of a congested nasal passage with variable epistaxis. A mass may be visualized in the superior nasal recesses, allowing for biopsy and definitive confirmation.

The clinical staging of the disease imparts some predictability to the course of the tumor. Elkon et al. found a 5-year survival rate of 75% in group A patients (tumor limited to the nasal cavity), 68% in group B patients (tumor into one or more paranasal sinuses), and 28% in group C patients (tumor extent beyond the sinuses and nasal cavity)

[145]. With a combination of aggressive craniofacial resection, radiation therapy, and chemotherapy, Levine et al., in their limited population of 26 patients, achieved average 4-year survival rates of 100, 75, and 86% in patient groups A, B, and C, respectively [144]. Despite these advances, recurrences of tumor occur in over 50% of "cured" patients; many times these recurrences are 10–20 years after treatment. While helpful in managing the tumor load, radiation and chemotherapy may only stall this relentless malignancy. Radical surgical resection would seem to be the best management for the patient, but in stage B and C patients, significant morbidity or residual tumor may be unavoidable.

References

1. Iliff WJ, Green WR. Orbital tumors in children. In: Jakobiec FA, editor. Ocular and anexal tumors. Birmingham: Aesculapius; 1978. p. 669–84.
2. Shields JA, Bakewell B, Augsburger JJ, et al. Space occupying orbital masses in children: a review of 250 consecutive biopsies. Ophthalmology. 1986;93:379–84.
3. Crawford JS. Diseases of the orbit. In: Crawford JS, Morin JD, editors. The eye in childhood. New York: Grune & Stratton; 1983. p. 361–94.
4. Templeton AC. Orbital tumors in African children. Br J Ophthalmol. 1971;55:254–61.
5. Kodsi SR, Shetlar DJ, Campbell RJ, et al. A review of 340 orbital tumors in children during a 60-year period. Am J Ophthalmol. 1994;117:177–82.
6. Rootman J. Frequency and differential diagnosis of orbital disease. In: Rootman J, editor. Diseases of the orbit. Philadelphia: Lippincott; 1988. p. 124.
7. Katowitz JA, Johnson M, Heher K. Unpublished data from the Children's Hospital of Philadelphia; 1996.
8. Shields JA, Shields CL. Rhabdomyosarcoma: review for the ophthalmologist. Surv Ophthalmol. 2003;48(1):39–57.
9. Maurer HM, Beltangady M, Gehan EA, Crist W, Hammond D, Hays DM, Heyn R, Lawrence W, Newton W, Ortega J, et al. The Intergroup rhabdomyosarcoma study-I. A final report. Cancer. 1988;61(2):209–20.
10. Shields JA, Shields CL, Scartozzi R. Survey of 1264 patients with orbital tumors and simulating lesions: the 2002 Montgomery lecture, part 1. Ophthalmology. 2004;111(5):997–1008.
11. Kassek SH, Copenhaver R, Arean VH. Orbital rhabdomyosarcoma. Am J Ophthalmol. 1965;60:811–7.
12. Knowles DM II, Jakobiec JA, Potter GD, et al. The diagnosis and treatment of rhabdomyosarcoma of the orbit. In: Jakobiec FA, editor. Ocular and adnexal tumors. Birmingham: Aesculapius; 1978. p. 708–34.
13. Ellenbogen E, Lesky MA. Rhabdomyosarcoma of the orbit in the newborn. Am J Ophthalmol. 1975;80:1024–7.
14. McDonough RL, Leib ML. Atypical presentation of orbital rhabdomyosarcoma: a report of two cases. J Pediatr Ophthalmol Strabismus. 1995;32:262–5.
15. Horn RC, Enterline HT. Rhabdomyosarcoma: a clinicopathological study and classification of 39 cases. Cancer. 1958;2:181–99.
16. Porterfield JT, Zimmerman LE. Rhabdomyosarcoma of the orbit: a clinicopathologic study of 55 cases. Virchows Arch A. 1962;335:329–44.
17. Levy MR. Subconjunctival rhabdomyosarcoma. Am J Ophthalmol. 1968;65:452–4.
18. Henderson JW. Tumors of primitive mesoderm, smooth muscle and adipose tissue. In: Henderson JW, editor. Orbital tumors. 3d ed. New York: Raven; 1994. p. 202–8.
19. Abramson DH, Ellsworth RM, Tretter P, et al. The treatment of orbital rhabdomyosarcoma with irradiation and chemotherapy. Ophthalmology. 1979;86:1330–5.
20. Wharam M, Beltangady M, Hays D, et al. Localized orbital rhabdomyosarcoma: an interim study of the Intergroup rhabdomyosarcoma study committee. Ophthalmology. 1987;94:251–4.
21. Haik BG, Jered B, Smith ME, et al. Radiation and chemotherapy of parameningeal rhabdomyosarcoma involving the orbit. Ophthalmology. 1986;93:1001–9.
22. Raney RB, Maurer HM, Anderson JR, Andrassy RJ, Donaldson SS, Qualman SJ, Wharam MD, Wiener ES, Crist WM. The Intergroup rhabdomyosarcoma study group (IRSG): major lessons from the IRS-I through IRS-IV studies as background for the current IRS-V treatment protocols. Sarcoma. 2001;5(1):9–15.
23. Eftekhari K, Chambers CB, Goldstein SM, Katowitz WR, Katowitz JA. Alveolar rhabdomyosarcoma masquerading as embryonal subtype: the value of modern molecular diagnostic testing. Ophthal Plast Reconstr Surg. 2015;31(2):e43–5.
24. Blakely ML, Lobe TE, Anderson JR, Donaldson SS, Andrassy RJ, Parham DM, Wharam MD, Qualman SJ, Wiener ES, Grier HE, Crist WM. Does debulking improve survival rate in advanced-stage retroperitoneal embryonal rhabdomyosarcoma? J Pediatr Surg. 1999;34(5):736–41. discussion 741–2
25. Chen C, Shu HK, Goldwein JW, Womer RB, Maity A. Volumetric considerations in radiotherapy for pediatric parameningeal rhabdomyosarcomas. Int J Radiat Oncol Biol Phys. 2003;55(5):1294–9.
26. Hays D, Soule EH, Lawrence W, et al. Extremity lesions in the Intergroup rhabdomyosarcoma study (IRS-1): a preliminary report. Cancer. 1982;48:1–8.
27. Newton WA Jr, Gehan EA, Webber BL, et al. Classification of rhabdomyosarcomas and related sarcomas: pathologic aspects and proposal for a new classification—an Intergroup rhabdomyosarcoma study. Cancer. 1995;76:1073–85.
28. Heyn R, Beltangady M, Hays DM, et al. Results of intensive therapy in children with localized alveolar extremity rhabdomyosarcoma: a report from the Intergroup rhabdomyosarcoma study. J Clin Oncol. 1989;7:200–7.
29. Crist W, Behan EA, Newton WA Jr, et al. Intergroup rhabdomyosarcoma study III. Cancer. 1994;74:2579–88.
30. Heyn R, Ragab A, Raney RB Jr, et al. Late effects of therapy in orbital rhabdomyosarcoma in children: a report from the Intergroup rhabdomyosarcoma study. Cancer. 1986;57:1738–43.
31. Scaradavou A, Heller G, Sklar CA, et al. Second malignant neoplasms in long-term survivors of childhood rhabdomyosarcoma. Cancer. 1995;76:1860–7.
32. Paikos P, Papathanassiou M, Stefanaki K, Fotopoulou M, Grigorios S, Tzortzatou F. Malignant ectomesenchymoma of the orbit in a child: case report and review of the literature. Surv Ophthalmol. 2002;47(4):368–74.
33. Boue DR, Parham DM, Webber B. Clinicopathologic study of ectomesenchymomas from Intergroup rhabdomyosarcoma study groups III and IV. Pediatr dev Pathol. 2000;3:290–300.
34. Miser JS, Pizzo PA. Soft tissue sarcomas in childhood. Pediatr Clin N am. 1985;32:779–800.
35. Wiener ES. Head and neck rhabdomyosarcoma. Semin Pediatr Surg. 1994;3:203–6.
36. Font RL, Jurco S, Zimmerman LE. Alveolar soft part sarcoma of the orbit: a clinicopathologic analysis of seventeen cases and review of the literature. Hum Pathol. 1982;13:569–79.

37. Enzinger FM, Weiss SW. Malignant tumors of uncertain etiology. In: Enzinger FM, Weiss SW, editors. Soft tissue tumors. 2d ed. St. Louis: Mosby; 1988. p. 929–65.
38. Simmons WB, Haggerty HS, Ngan B, et al. Alveolar soft part sarcoma of the head and neck: a disease of children and young adults. Int J Pediatr Otorhinolaryngol. 1989;17:139–46.
39. Lieberman P, Foote F, Stewart F, et al. Alveolar soft part sarcoma. Jama. 1966;198:1047–58.
40. Morrison WH, Byers RM, Garden AS, et al. Cutaneous angiosarcoma of the head and neck. A therapeutic dilemma. Cancer. 1995;76:319–27.
41. Hufnagel T, Ma L, Kuo T-T. Orbital angiosarcoma with subconjunctival presentation: report of a case and literature review. Ophthalmology. 1987;94:72–8.
42. Guccion JG, Font RL, Enzinger FM, et al. Extraskeletal mesenchymal chondrosarcoma. Arch Pathol. 1973;95:336–45.
43. Sevel D. Mesenchymal chondrosarcoma of the orbit. Br J Ophthalmol. 1974;58:882–6.
44. Telium G. Endodermal sinus tumors of the ovary and testis: comparative morphogenesis of the so-called mesonephroma ovarii (Schiller) and extraembryonic (yolk-sac allantoic) structures of the rat placenta. Cancer. 1959;12:1092–103.
45. Margo CE, Folberg R, Zimmerman LE, et al. Endodermal sinus tumor (yolk sac tumor) of the orbit. Ophthalmology. 1983;90:1426–31.
46. Palmer PE, Safai H, Wolfe AJ. Alpha-1 antitrypsin and alphafetoprotein: protein markers in endodermal sinus (yolk sac) tumors. Am J Clin Pathol. 1976;65:575–81.
47. Stidham DB, Burgett RA, Davis MM, Plager DA. Congenital malignant rhabdoid tumor of the orbit. J AAPOS. 1999 Oct;3(5):318–20.
48. Rootman J, Dolman P. Adenoidcystic carcinoma. In: Rootinan J, editor. Diseases of the orbit: a multidisciplinary approach. Philadelphia: Lippincott; 1988. p. 886–95.
49. Dagher G, Anderson RL, Ossoinig KC, et al. Adenoid cystic carcinoma of the lacrimal gland in a child. Arch Ophthalmol. 1980;98:1098–101.
50. Wolter JR, Henderson JW. Adenoid cystic carcinoma in the orbit of a child. J Pediatr Ophthalmol. 1969;6:47–9.
51. Ley JA, Wolter JR. Adenoid cystic carcinoma: as seen in the orbit of a 12-year-old Vietnamese girl. J Pediatr Ophthalmol. 1969;6:162–5.
52. Eneh A, Parsa K, Wright KW, Strube YN. Pediatric adenoid cystic carcinoma of the lacrimal gland treated with intra-arterial cytoreductive chemotherapy. J AAPOS. 2015 Jun;19(3):272–4.
53. Gamel JW, Font RL. Adenoid cystic carcinoma of the lacrimal gland: the clinical significance of a basaloid histologic pattern. Hum Pathol. 1982;13:219–26.
54. Tse DT, Kossler AL, Benedetto PW. Long-term outcomes of neoadjuvant intra-arterial cytoreductive chemotherapy for lacrimal gland adenoid cystic carcinoma. Ophthalmology. 2013;120:1313–23.
55. Gallie BL, Musarella MA, Chan HSL. Ocular oncology. In: Crawford JS, Morin JD, editors. The eye in childhood. New York: Grune & C Stratton; 1983. p. 325.
56. Crawford JS, Morin JD, editors. The eye in childhood. Chicago: Yearbook Medical; 1967.
57. Robb RM, Ervin LD, Sallan SE. A pathological study of eye involvement in acute leukemia of childhood. Trans am Ophthalmol Soc. 1978;76:90–101.
58. Ridgeway EW, Jaffe N, Walton DS. Leukemic ophthalmology in children. Cancer. 1976;38:1744–9.
59. Ohkoshi K, Tsiaris WG. Prognostic importance of ophthalmic manifestations in childhood leukemia. Br J Ophthalmol. 1992;76:651–5.
60. Zimmerman LE, Font RL. Ophthalmologic manifestations of granulocytic sarcoma (myeloid sarcoma or chloroma). Am J Ophthalmol. 1975;80:975–90.
61. Pomeranz SJ, Hawkins HH, Towbin R, et al. Granulocytic sarcoma (chloroma): CT manifestations. Radiology. 1985;155:167–70.
62. Khaled S, Al Malki M, Marcucci G. Acute myeloid leukemia: biologic, prognostic, and therapeutic insights. Oncology (Williston Park). 2016;30(4):318–29.
63. Cunningham MJ, Myers EN, Bluestone CD. Malignant tumors of the head and neck in children: a twenty year review. Int J Pediatr Otorhinolaryngol. 1987;13:279–92.
64. Leidenix MJ, Mamalis N, Olson RJ, et al. Primary T-cell immunoblastic lymphoma of the orbit in a pediatric patient. Ophthalmology. 1993;100:998–1002.
65. Blakemore WS, Ehrenberg M, Fritz KJ, et al. Rapidly progressive proptosis secondary to Burkitt's lymphoma: origin in the ethmoidal sinuses. Arch Ophthalmol. 1983;101:1741–5.
66. Ziegler JL. Burkitt's lymphoma. N Engl J med. 1981;305:735–42.
67. Zak TA, Fisher JE, Afshani E. Infantile non-African Burkitt's lymphoma presenting as bilateral fulminant exophthalmos. J Pediatr Ophthalmol Strabismus. 1982;19:294–9.
68. Magrath I. The pathogenesis of Burkitt's lymphoma. Adv Cancer Res. 1990;55:133–270.
69. Dalla-Favera R, Bregni M, Erickson J, et al. Human *c-myc* oncogene is located on the region of chromosome 8 that is translocated in Burkitt lymphoma cells. Proc Natl Acad Sci U S A. 1982;79:7824–34.
70. Lombardi L, Newcomb E, Dalla-Favera R. Pathogenesis of Burkitt lymphoma: expression of an activated *c-myc* oncogene causes the tumorigenic conversion of EBV-infected human B lymphoblasts. Cell. 1987;49:161–83.
71. Ziegler JL. Treatment results of 54 American patients with Burkitt's lymphoma are similar to the African experience. N Engl J med. 1977;297:75–80.
72. Wilson LMK, Draper GJ. Neuroblastoma, its natural history and prognosis: a study of 487 cases. Br med J. 1971;3:301–7.
73. Evans AE, D'Angio GJ, Randolph J. A proposed staging for children with neuroblastoma: children's cancer study group. Cancer. 1971;27:374–8.
74. D'Angio GJ, Evans AE, Koop CE. Special pattern of widespread neuroblastoma with a favorable prognosis. Lancet. 1971;1:1046–9.
75. Musarella MA, Chan HSL, DeBoer G, et al. Ocular involvement in neuroblastoma: prognostic implications. Ophthalmology. 1984;91:936–40.
76. Gurney JG, Ross JA, Wall DA, et al. Infant cancer in the U.S. histology-specific incidence and trends, 1973 to 1992. J Pediatr Hematol Oncol. 1997;19:428–32.
77. Jaffe N, Cassady R, Petersen R, et al. Heterochromia and Horner's syndrome associates with cervical and mediastinal neuroblastoma. J Pediatr. 1975;87:75–7.
78. Beckerman BL, Seaver R. Congenital Horner's syndrome and thoracic neuroblastoma. J Pediatr Ophthalmol Strabismus. 1978;15:24–5.
79. Sandok BA, Kranz H. Opsoclonus as the initial manifestation of occult neuroblastoma. Arch Ophthalmol. 1971;86:235–6.
80. Altman AJ, Baehner RL. Favorable prognosis for survival in children with coincident opso-myoclonus and neuroblastoma. Cancer. 1976;37:846–52.
81. Cibis GW, Freeman A, Pang V, et al. Bilateral choroidal neonatal neuroblastoma. Am J Ophthalmol. 1990;109:445–9.
82. Alio J, Faci A, Garcia-Julian G, et al. Anterior chamber metastasis from neuroblastoma. J Pediatr Ophthalmol Strabismus. 1982;19:299–302.
83. Browns GT, Walls RP, Murphree AL, et al. Neonatal neuroblastoma metastatic to the iris. Cancer. 1983;52:929–31.
84. Reynolds C, German D, Weinberg A, et al. Catecholamine fluorescence and tissue culture morphology: techniques in the diagnosis of neuroblastoma. Am J Clin Pathol. 1981;75:275–84.

85. Silverman JF, Dabbs DJ, Ganick DJ, et al. Fine needle aspiration cytology of neuroblastoma, including peripheral neuroectodermal tumor, with immunocytochemical and ultra-structural confirmation. Acta Cytol. 1988;32:367–76.
86. Weinstein JL, Katzenstein HM, Cohn SL. Advances in the diagnosis and treatment of neuroblastoma. Oncologist. 2003;8(3):278–92.
87. Silverman JF, Joshi W. FNA biopsy of small round cell tumors of childhood: cytomorphologic features and the role of ancillary studies. Diagn Cytopathol. 1994;10:245–55.
88. Avet-Loiseau H, Venuat AM, Benard J, et al. Morphologic and molecular cytogenetics in neuroblastoma. Cancer. 1995;75:1694–9.
89. Bourhis J, Dominici C, McDowell H, et al. *N-myc* genomic content and DNA ploidy in stage IV neuroblastoma. J Clin Oncol. 1991;9:1371–5.
90. Breslow N, McCann B. Statistical estimation of prognosis for children with neuroblastoma. Cancer res. 1971;31:2098–103.
91. Blatt J, Gula MJ, Orlando SJ, et al. Indolent course of advanced neuroblastoma in children older than 6 years at diagnosis. Cancer. 1995;76:890–4.
92. Shimada H, Chatten J, Newton WA Jr, et al. Histopathologic prognostic factors in neuroblastoma tumor: definition of ganglioneuroblastoma and an age-linked classification of neuroblastoma. J Natl Cancer Inst. 1984;73:405–16.
93. Hartmann O, Pinkerton CR, Philip T, et al. Very-high-dose cisplatin and etoposide in children with untreated advanced neuroblastoma. J Clin Oncol. 1988;6:44–50.
94. Moore AT, Pritchard J, Taylor DSI. Histiocytosis X: an ophthalmological review. Br J Ophthalmol. 1985;69:7–14.
95. Aricò M. Langerhans cell histiocytosis in children: from the bench to bedside for an updated therapy. Br J Haematol. 2016 Jun;173(5):663–70.
96. Writing group of the Histiocyte Society. Histiocytosis syndromes in children. Lancet. 1987;1:208–9.
97. Zucker JM, Chillaux JM, Vanel D, et al. Malignant histiocytosis in childhood: clinical study and therapeutic results in 22 cases. Cancer. 1980;45:2821–8.
98. Greenberger JS, Crocker AC, Vawter G, et al. Results of treatment of 127 patients with systemic histiocytosis (Letterer–Siwe syndrome, Schuller–Christian syndrome and multifocal eosinophilic granuloma). Medicine. 1981;60:311–38.
99. Histiocyte Society Evaluation and Treatment Guidelines, 2009.; https://histiocytesociety.org/document.doc?id=290
100. Arceci RJ. Histiocytoses and disorders of the reticuloendothelial system. In: Blood, principles and practice of hematology. Philadelphia: Lippincott; 1995. p. 915–45.
101. Rupp RH, Holloman KR. Histiocytosis X affecting the uveal tract. Arch Ophthalmol. 1970;84:468–70.
102. Lahav M, Albert DM. Unusual ocular involvement in acute disseminated histiocytosis X. Arch Ophthalmol. 1974;91:455–8.
103. Mittelman D, Apple DJ, Goldberg MF. Ocular involvement in Letterer–Siwe disease. Am J Ophthalmol. 1973;75:261–5.
104. Epstein DL, Grant WM. Secondary open-angle glaucoma in histiocytosis X. Am J Ophthalmol. 1977;84:332–6.
105. Favara BE, Jaffe R. The histopathology of Langerhans cell histiocytosis. Br J Cancer Suppl. 1994;23:S17–23.
106. Goldberg NS, Bauer K, Rosen ST, et al. Histiocytosis X: flow cytometric DNA-content and immunohistochemical and ultrastructural analysis. Arch Dermatol. 1986;122:446–50.
107. Ornvold K, Carstensen H, Larsen JK, et al. Flow cytometric DNA analysis of lesions from 18 children with Langerhans cell histiocytosis (histiocytosis X). Am J Pathol. 1990;136:1301–9.
108. Yu RC, Chu C, Buluwela L, et al. Clonal proliferation of Langerhans cells in Langerhans cell histiocytosis. Lancet. 1994;343:767–9.
109. Histiocyte Society Writing Group. Histiocytosis syndromes in childhood, II: approach to the clinical and laboratory evaluation of children with Langerhans cell histiocytosis. Med Pediatr Oncol. 1989;17:492–501.
110. Winkelmann RK. The skin in histiocytosis X. Mayo Clin Proc. 1969;44:535–49.
111. Hartman KS. Histiocytosis X: a review of 114 cases with oral involvement. Oral Surg. 1980;49:38–49.
112. Parker BR, Pinckney L, Etcubanas E. Relative efficacy of radiographic and radionuclide bone surveys in the detection of the skeletal lesions of histiocytosis X. Radiology. 1980;134:377–82.
113. Kindy-Degnan NA, Laflamme P, Duprat G, et al. Intralesional steroid in the treatment of an orbital eosinophilic granuloma. Arch Ophthalmol. 1991;109:617–8.
114. Greis PE, Hankin FM. Eosinophilic granuloma: the management of solitary lesions of bone. Clin Orthop. 1990;257:204–9.
115. Cassady JR. Current role of radiation therapy in the management of histiocytosis X. Hematol Oncol Clin North Am. 1987;1:123–9.
116. Glover AT, Grove AS Jr. Eosinophilic granuloma of the orbit with spontaneous healing. Ophthalmology. 1987;94:1008–12.
117. Starling KA. Chemotherapy of histiocytosis X. Hematol Oncol Clin North Am. 1987;1:119–22.
118. Schmidt D. Monocyte/macrophage system and malignancies. Med Pediatr Oncol. 1994;23:444–51.
119. Cline MJ. Histiocytes and histiocytosis. Blood. 1994;84:2840–53.
120. Horowitz ME, Tsokos MG, Delaney TF. Ewing's sarcoma. Ca. 1992;42:300–20.
121. Wilkins RM, Pritchard DJ, Burgert EO Jr, et al. Ewing's sarcoma of bone: experience with 140 patients. Cancer. 1986;58:2551–5.
122. Howard DJ, Lund VJ. Primary Ewing's sarcoma of the ethmoid bone. J Laryngol Otol. 1985;99:1019–23.
123. Rootman J, Chan KW. Ewing's sarcoma. In: Rootman J, editor. Diseases of the orbit. Philadelphia: Lippincott; 1988. p. 382.
124. Woodruff G, Thorner P, Skarf B. Primary Ewing's sarcoma of the orbit presenting with vision loss. Br J Ophthalmol. 1988;72:786–92.
125. Alio JL, Sales-Sanz M, Vaz MA, Barrancos C, Reguero ME, Diamantopoulus J, Poveda P. Primary extraosseous Ewing sarcoma of the orbit. Ophthal Plast Reconstr Surg. 2013;29(3):91–3.
126. Razek A, Perez A, Tefft M, et al. Intergroup Ewing's sarcoma study, local control related to radiation dose, volume and site of primary lesion of Ewing's sarcoma. Cancer. 1980;46:516–23.
127. Rosen G, Capartos B, Nirenberg A, et al. Ewing's sarcoma, ten year experience with adjuvant chemotherapy. Cancer. 1981;47:2204–11.
128. Hayes FA, El T, Hustu HO, et al. The response of Ewing's sarcoma to sequential cyclophosphamide and adriamycin induction therapy. J Clin Oncol. 1983;1:45–55.
129. Johnson LN, Rohel GB, Yeon EB, et al. Sinus tumors invading the orbit. Ophthalmology. 1984;91:209–14.
130. Chokthaweesak W, Annunziata CC, Alsheikh O, Ng JD, Wilson DJ, Mansoor A, Kaimatchiev V, Weatherhead R, Rootman J, Mannor G, Leelapatranurak K, Korn BS, Kikkawa DO. Primitive neuroectodermal tumor of the orbit in adults: a case series. Ophthal Plast Reconstr Surg. 2011;27(3):173–9.
131. Alyahya GA, Heegaard S, Fledelius HC, et al. Primitive neuroectodermal tumor of the orbit in a 5-year-old girl with microphthalmia. Graefes Arch Clin Exp Ophthalmol. 2000;238:80–6.
132. Romero R, Castano A, Abelairas J, Peralta J, Garcia-Cabezas MA, Sanchez-Orgaz M, Arbizu A, Vallejo-Garcia J. Peripheral primitive neuroectodermal tumour of the orbit. Br J Ophthalmol. 2011;95(7):915–20.

133. Rootman J, Ellsworth RM, Hofbauer G, et al. Orbital extension of retinoblastoma: a clinicopathological study. Can J Ophthalmol. 1978;13:72–80.
134. Mohan K, Gupta A, Saini JS, et al. Retinoblastoma metastatic to the contralateral orbit. Br J Ophthalmol. 1990;74:311–2.
135. Grabowski EF, Abramson DH. Intraocular and extraocular retinoblastoma. Hematol Oncol Clin North Am. 1987;1:721–35.
136. Ellsworth R. Orbital retinoblastoma. Trans Am Ophthalmol Soc. 1974;72:79–88.
137. Magramm I, Abramson DH, Ellsworth RM. Optic nerve involvement in retinoblastoma. Ophthalmology. 1989;96:217–22.
138. Mohney BG, Robertson DM. Ancillary testing for metastasis in patients with newly diagnosed retinoblastoma. Am J Ophthalmol. 1994;118:707–11.
139. O'Brien JM, Harbour JW, Smith B, et al. Utility of initial metastatic tests and serial bone scans in patients with retinoblastoma. Invest Ophthalmol Vis Sei. 1995;36:S494–9.
140. Goble RR, McKenzie J, Kingston JE, et al. Orbital recurrence of retinoblastoma successfully treated by combined chemotherapy. Br J Ophthalmol. 1990;74:97–8.
141. Pratt CB, Crom DB, Howarth C. The use of chemotherapy for extraocular retinoblastoma. Med Pediatr Oncol. 1985;13:330–3.
142. Sorensen PH, Wu JK, Berean KW, et al. Olfactory neuroblastoma is a peripheral primitive neuroectodermal tumor related to Ewing sarcoma. Proc Natl Acad Sci U S A. 1996;93:1038–43.
143. Rakes SM, Yeatts RP, Campbell RJ. Ophthalmic manifestations of esthesioneuroblastoma. Ophthalmology. 1985;92:1749–53.
144. Levine PA, McLean WC, Cantrell RW. Esthesioneuroblastoma: the University of Virginia experience 1960–1985. Laryngoscope. 1986;96:742–6.
145. Elkon D, Hightower SI, Lim ML, et al. Esthesioneuroblastoma. Cancer. 1979;44:1087–94.

Surgical Approaches to the Pediatric Orbit

37

Michael Kazim, William R. Katowitz, and James A. Katowitz

Contained within a volume of only 40 mL, the density of critical structures within the orbit makes surgical intervention difficult. The complexity is increased by the obliquity of the arrangement of the nerves, blood vessels, and muscles within the pyramidal bony confines. This results in a continuous change in the distance between structures in the operative plane as one travels posteriorly in the orbit. Further complicating matters is the ubiquity of the orbital fat that envelopes the intra- and extraconal structures. Only in the sub-Tenon's and subperiosteal spaces are potential fat-free spaces appreciated. In all other orbital compartments, the surgeon's view of both normal and pathological structures is obscured by orbital fat.

These inherent structural difficulties require that the surgeon be well versed in orbital anatomy and noninvasive imaging. In-depth knowledge of each permits preoperative identification, localization, and planning of the operative approach to a lesion that will minimize surgical morbidity.

An anatomic approach to surgical planning identifies five surgical spaces (Fig. 37.1): subperiosteal, extraconal, intraconal, subarachnoid, and sub-Tenon's. Some lesions remain entirely within one of the orbital spaces. The surgical approach can then be directed specifically to that space. More commonly, however, lesions will bridge more than one surgical space and invade normal structures. In such cases, the approach chosen should minimize damage to normal structures. Lesions should also be localized with respect to the optic nerve. This is critical, since lesions should not be drawn across the optic nerve when resection is attempted. Finally, the location of the nearest wall of the orbit is important if the lesion is located in the posterior half of the orbit where a more anterior resection is precluded. In such cases, removal of one or more walls of the orbit may be required to provide access to the operative space. Additional clues to the relationship between a tumor and adjacent critical structures can be derived from a preoperative neuro-ophthalmic evaluation and can be used to further refine the surgical plan. Careful postoperative outcome assessment and long-term monitoring in certain cases may be required.

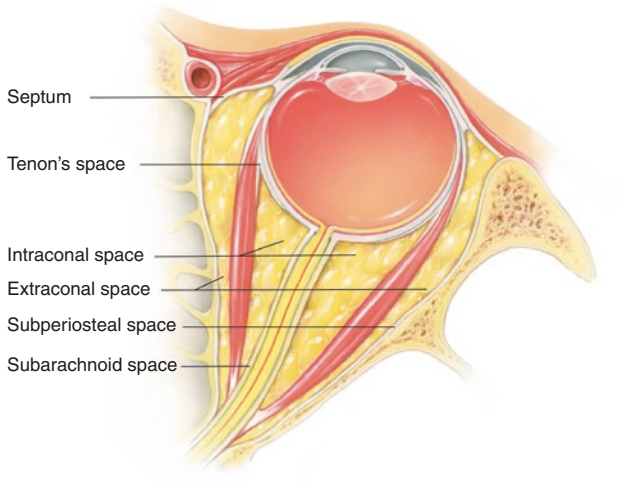


Fig. 37.1 Surgical orbital spaces

After a lesion is identified, characterized, and localized, a careful definition of the surgical goals must be considered. In general, interventions are either diagnostic or therapeutic. Diagnostic biopsies are reserved for lesions that are inadequately characterized clinically or radiographically, are invasive, and are potentially responsive to medical therapy.

M. Kazim, MD (✉)
Departments of Ophthalmology and Surgery,
Columbia University Medical Center, New York, NY, USA
e-mail: mk48@cumc.columbia.edu

W.R. Katowitz, MD • J.A. Katowitz, MD, FACS
The Children's Hospital of Philadelphia and
The Edwin and Fannie Gray Hall Center for Human Appearance,
University of Pennsylvania, Philadelphia, PA, USA
e-mail: katowitzw@email.chop.edu; katowitz@email.chop.edu

© Springer International Publishing AG 2018

J.A. Katowitz, W.R. Katowitz (eds.), *Pediatric Oculoplastic Surgery*, https://doi.org/10.1007/978-3-319-60814-3_37

Diagnostic biopsies must remove a representative portion of the lesion while preserving normal surrounding structures. The specimen may be inspected intraoperatively. Results of the frozen section histology may alter the surgical plan by limiting what was initially planned as a larger resection. Frozen section histopathology is, however, not as diagnostically reliable as permanent histopathology, and, consequently, it is rare that more extensive surgery be performed on the basis of frozen section pathology. Complete excision is reserved for lesions that are well-encapsulated or invasive lesions that are malignant or are likely to result in local recurrence and destruction of normal structures. In cases of an invasive lesion with slow growth, little risk of local destructive behavior, or metastasis, sequential debulking as clinically required is advisable.

Advances in orbital surgery in the past 25 years include noninvasive imaging, the operating microscope, the endoscope, and microdissection instruments. These tools have permitted access to lesions once considered inoperable as well as minimizing the invasiveness of surgery, all resulting in significantly less postoperative functional and cosmetic deformity. This chapter describes by operative approach the various orbital spaces, the typical lesions found in each space, and the surgical procedures that may be used to enter the described surgical space. It is not meant to provide a detailed atlas for orbital surgery but rather a topographic approach, describing with how to reach specific compartments within the pediatric orbit. More detailed information on the specifics of each orbital procedure is available in several cited texts [1–4].

Surgical Approaches to the Anterior Orbit

Anterior approaches to the orbit (Fig. 37.2) provide access to the anterior half of the orbital contents. Both extraconal and the extraperiosteal spaces are accessible via this approach. Typical lesions encountered in these spaces are dermoids of the nasofrontal and frontozygomatic sutures, hemangioma (capillary and cavernous), and lymphangioma. Although any of these incisions can provide access to the anterior orbit, the most commonly used are the lid crease, subciliary, and transconjunctival incisions. The choice of incision is dependent on the quadrant in which the lesion is located. Greater detail on medial, lateral, superior, and inferior orbitotomy will be presented in the section on approaches to the posterior orbit.

Upper Eyelid Skin Approach

It is generally possible to reach the anterior orbit through a lid crease incision in the upper lid (Fig. 37.3). If greater vertical or temporal exposure is required, the incision may be extended temporally in a lid fold. The lid crease is marked with a methylene blue pen, and the incision is infiltrated with 0.25% Marcaine (bupivacaine) with epinephrine 1:200,000. A silk traction suture is often helpful when placed in the lid margin. The incision is made through the skin. Judicious use of bipolar cautery along the skin edge minimizes wound shrinkage and scarring. Orbicularis muscle is divided and spread bluntly to enter the avascular preaponeurotic plane. In this plane, dissection superiorly will identify the translucent orbital septum. Care should be taken to avoid injury to the underlying levator aponeurosis. Opening the septum reveals the preaponeurotic or postseptal fat (Fig. 37.4). Temporally located is the lacrimal gland, which is paler and firmer than the central or nasal fat pads (Fig. 37.5). Within the substance of the nasal fat pad are the trochlea, the superior ophthalmic vein, and the transverse ligament of Whitnall, which serves as a suspensory support for the levator complex. Whitnall's ligament also divides the lacrimal gland into its orbital and palpebral portions (Fig. 37.6). All of these structures are

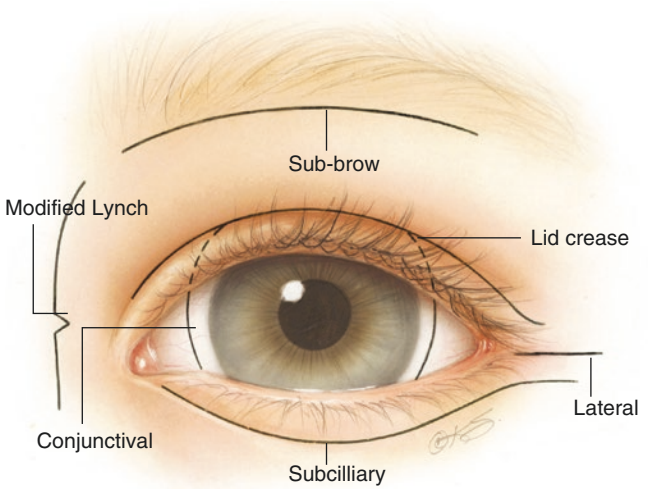


Fig. 37.2 Anterior orbitotomy incisions. (**a**) Sub-brow. (**b**) Modified lynch. (**c**) Conjunctival. (**d**) Lid crease. (**e**) Lateral. (**f**) Subciliary

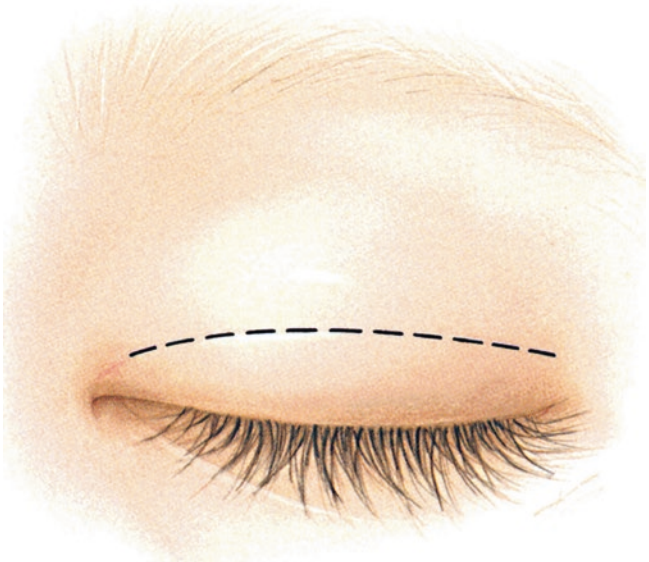


Fig. 37.3 Upper eyelid crease incision

obscured by the orbital fat, and care must be taken to avoid injury during dissection. Anterior orbital masses, particularly vascular tumors or malformations, can be reached by this approach (Fig. 37.7). Access to the deeper intraorbital and intraconal spaces is limited to the nasal compartment (Figs. 37.8 and 37.9). Access to the superior subperiosteal

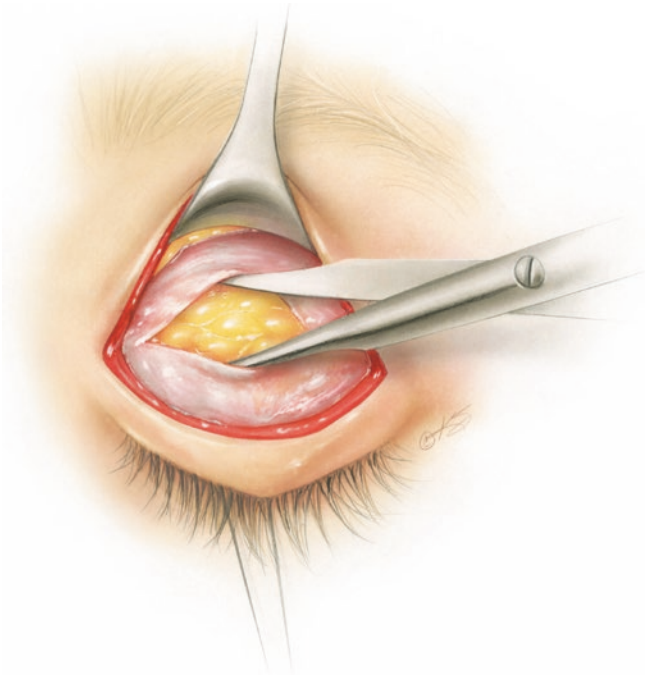


Fig. 37.4 Orbital septum. The lid crease incision has been made and the orbicularis muscle divided. The orbital septum is bluntly opened with curved scissors, revealing orbital fat

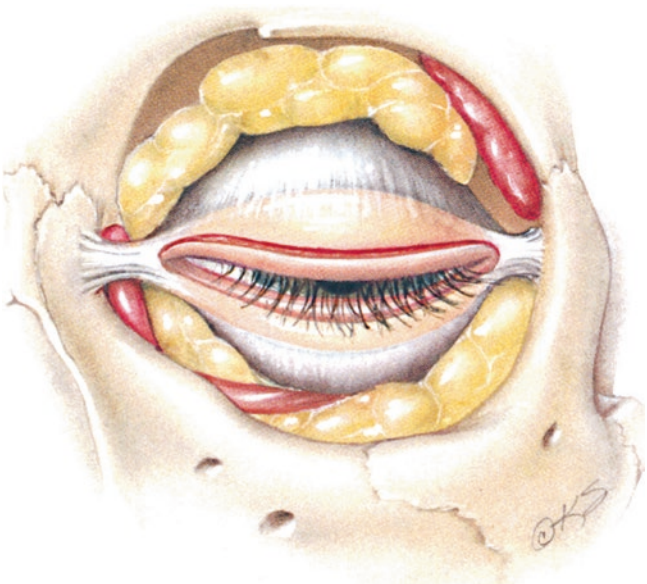


Fig. 37.5 Anterior orbital fat. There are two postseptal or preaponeurotic fat pads in the upper eyelid. The nasal and central fat pads are illustrated. The lacrimal gland is vulnerable to damage during dissection in the lateral superior orbit. In the lower eyelid there are three fat pads. The inferior oblique muscle divides the medial and central pads. The lateral fat pad covers the inferotemporal space, which affords the safest access into the intraconal compartment from the inferior approach

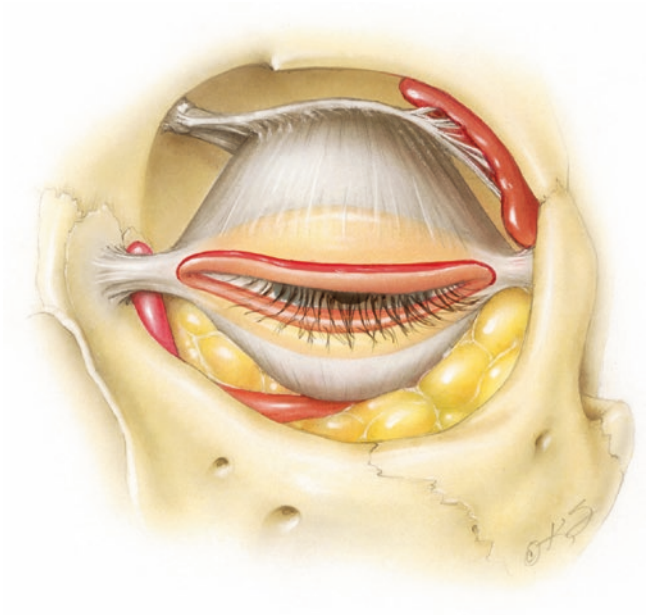


Fig. 37.6 Superior orbit with fat pads removed. The trochlea and superior oblique tendon are now visible as is the superior transverse ligament of Whitnall and the lacrimal gland

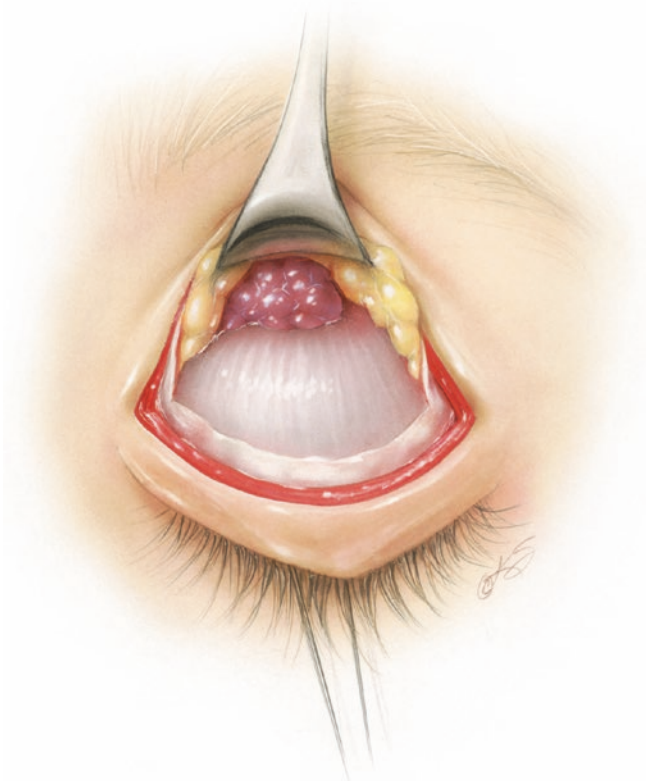


Fig. 37.7 Anterior orbital lesion. The orbital fat is reflected superiorly with a retractor exposing the levator aponeurosis and revealing a vascular lesion of the anterior superior orbit

space is made by extending the dissection superiorly toward the rim of the orbit. Ultimately, this dissection will carry beneath the brow fat pad. The orbital periosteum may be opened horizontally, and, with a periosteal elevator, blunt dissection in the subperiosteal plane may proceed posteriorly into the orbit (Fig. 37.10).

Subciliary Lower Eyelid Approach

A similar procedure can be performed through a subciliary incision in the lower eyelid. A myocutaneous flap is developed, revealing the orbital septum. Three fat pads exist in the lower eyelid: The temporal is the largest, the central is the

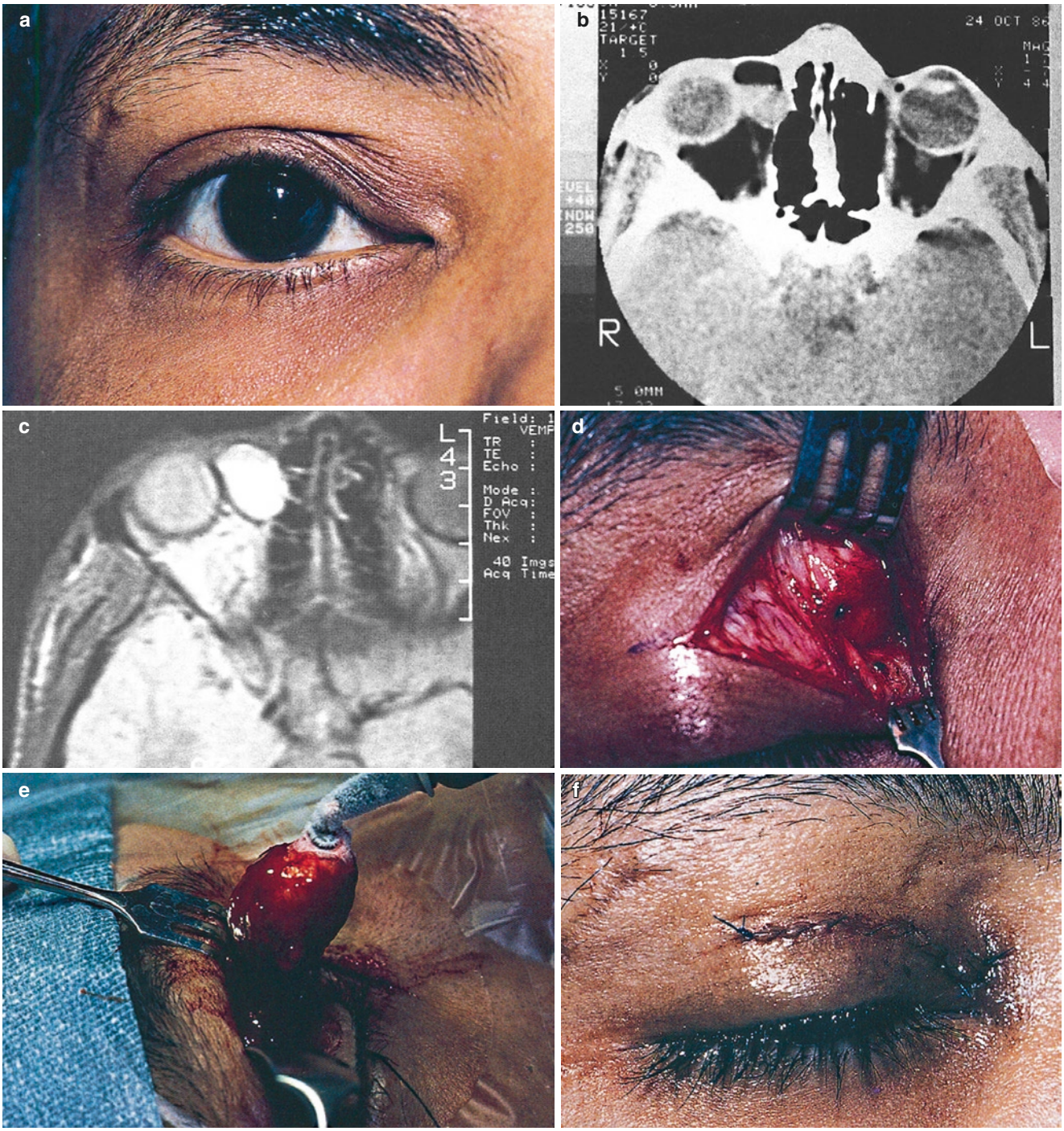


Fig. 37.8 Lid crease incision for orbital dermoid. (**a**) Medial ptosis secondary to orbital dermoid cyst. (**b**) CT scan of dermoid. (**c**) MRI scan of dermoid. (**d**) Exposure of tumor through lid crease incision. (**e**) Traction with cryoprobe. (**f**) Closure of skin incision with running 6–0 monofilament suture

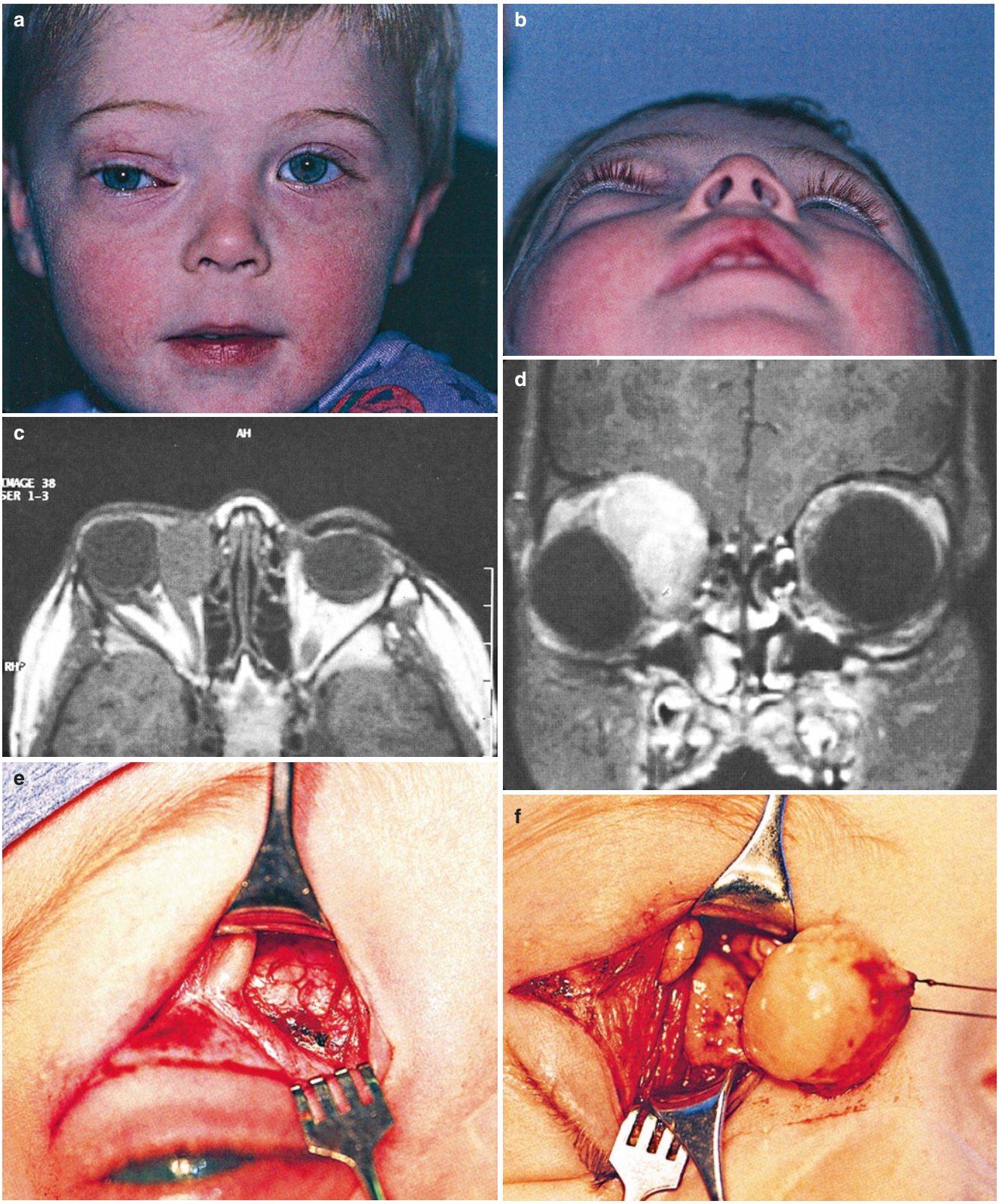


Fig. 37.9 Lid crease approach for excision of orbital rhabdomyosarcoma. (**a**) Mass pushing right globe down and out. (**b**) Right orbital proptosis secondary to tumor. (**c**) CT scan with axial view of orbital tumor demonstrating pressure on globe in same patient. (**d**) Coronal view of same patient. (**e**) Lid crease approach demonstrating mass in superonasal quadrant. (**f**) Traction suture elevating tumor; frozen section biopsy confirms rhabdomyosarcoma.

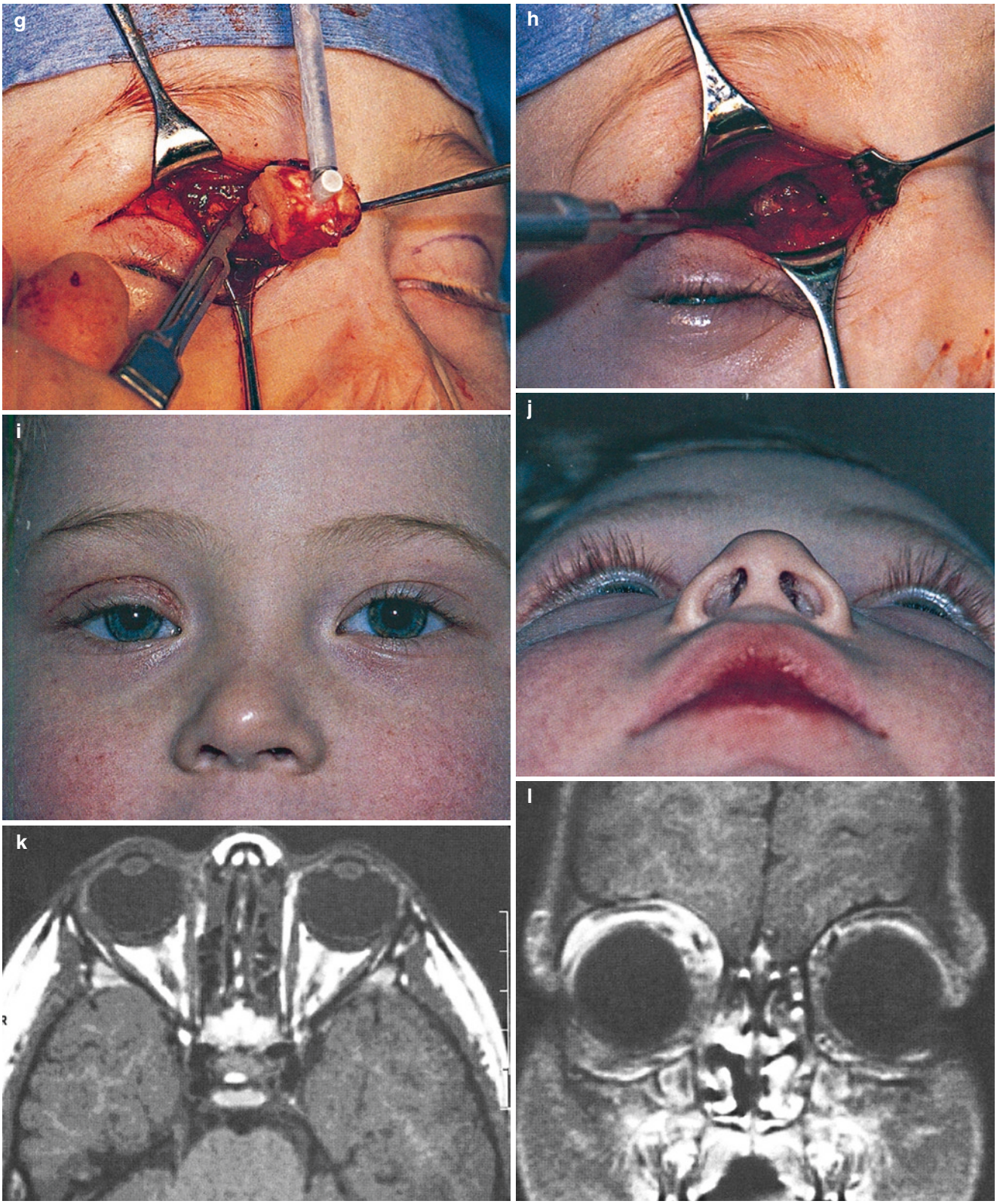


Fig. 37.9 (continued) (**g**) Further debulking of tumor assisted by use of cryoprobe. (**h**) Completion of debulking effort; significant tumor safely removed with care not to damage orbital structures. (**i**) Two-week post-op appearance. (**j**) Proptosis reduced at 2 weeks post-op. (**k**) Post-op CT axial scan at 2 weeks demonstrating reduction of tumor and improved position of globe. Chemotherapy regimen begun to be followed by course of orbital radiation. (**l**) Post-op coronal CT scan at 2 weeks

smallest and borders the belly of the inferior oblique on its medial side, and the nasal is lateral to the lacrimal sac and borders the inferior oblique muscle on its lateral side (Fig. 37.5). Dissection deep into the intraconal space is best accomplished through the inferotemporal space. Inferior dissection in the preseptal space reveals the inferior orbital rim. Horizontal division and reflection of the inferior orbital periosteum allow access to the floor and inferomedial wall of the orbit. This approach provides good visualization of orbital floor, rim, and medial wall fractures. Additional details regarding lower lid approaches to the orbit will be presented in the section on inferior orbitotomy.

Alternatively, the inferior subperiosteal space may be reached through a lower lid transconjunctival approach (Figs. 37.11, 37.12, and 37.13). This approach avoids altogether a scar associated with the skin incision and minimizes the risk of vertical eyelid retraction, which is occasionally encountered with the subciliary approach. In the subciliary approach, a lateral canthotomy and inferior cantholysis are performed to release the lower lid laterally from its attachments to the lateral orbital rim. A 4–0 silk lid margin suture is used to reflect the lid. The conjunctiva is incised horizontally approximately 5 mm inferior to the inferior tarsal border. Using monopolar cautery, the lower lid retractors are incised and blunt retraction used to expose the orbital periosteum, which is opened as described above (Fig. 37.14). This transconjunctival incision can be extended behind the caruncle to provide

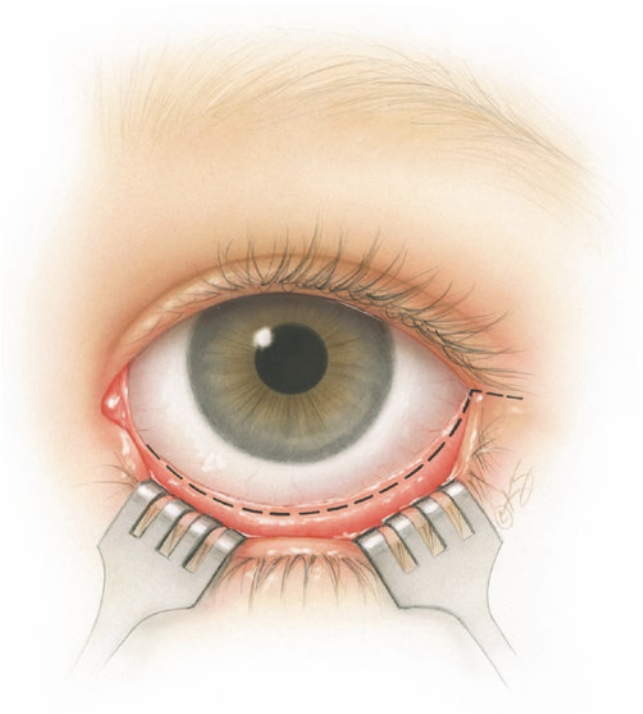


Fig. 37.11 Transconjunctival incision. The transconjunctival incision is marked by a *dotted line* 3 mm below the inferior border of the tarsus. It is an alternative to a subciliary incision for access to the inferior orbit. The incision can be carried laterally to divide the lateral canthal angle in order to provide greater exposure when required. It can also be extended medially as a transcaruncular approach for access to the medial intraconal, extraconal, or subperiosteal spaces

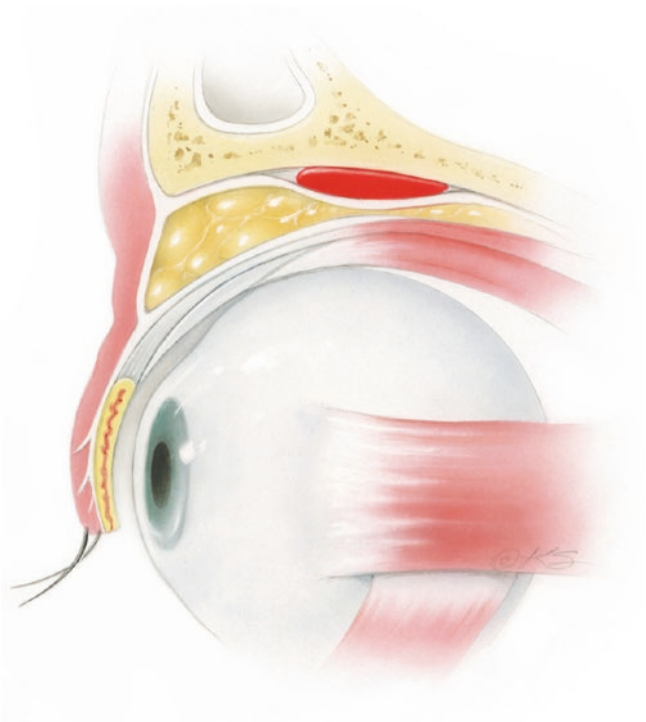


Fig. 37.10 Lid crease incision for access to lacrimal gland, subperiosteal space, and mid-orbit

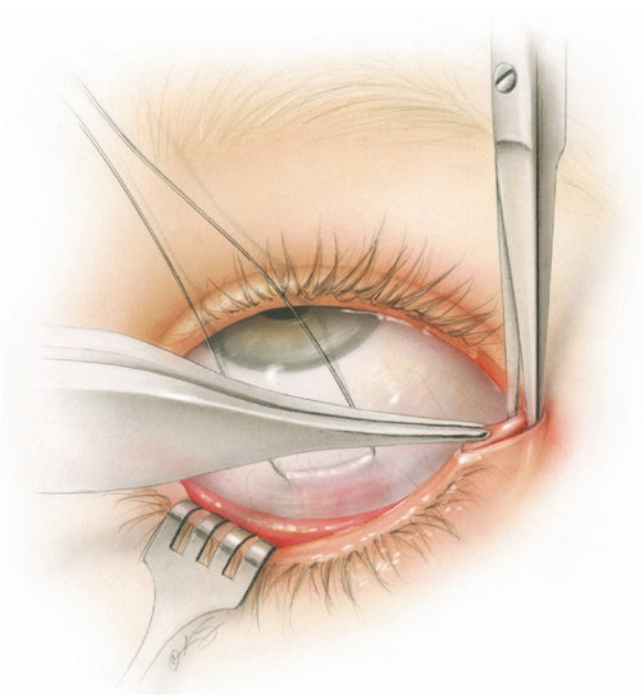


Fig. 37.12 Canthotomy and cantholysis. Further exposure is achieved by performing a canthotomy and cantholysis, which releases the inferior crus of the lateral canthal tendon

greater exposure of the medial orbital wall. Care must be taken not to damage the lacrimal sac with this dissection.

In the above cases, the periosteum is closed with interrupted absorbable sutures, as is the conjunctiva in the transconjunctival approach. The lid is reattached to the posterior lateral orbital periosteum with 4–0 absorbable sutures and the skin closed with absorbable suture material. The orbital septum and orbicularis muscle are not sutured closed, as this may contribute to postoperative lid retraction.

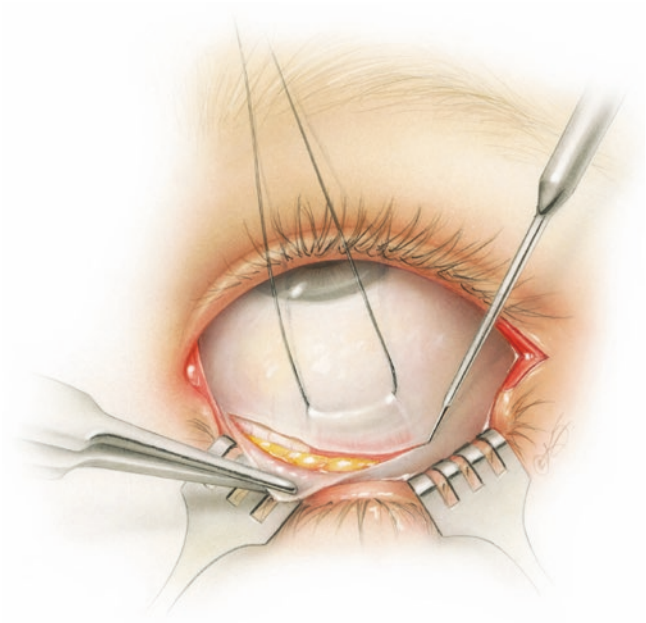


Fig. 37.13 Traction suture. A 4–0 silk traction suture is placed beneath the inferior rectus muscle to aid in rotating the globe and identifying the inferior rectus muscle intraoperatively. The conjunctival incision can be made with either blade scissors or a needle point electrocautery

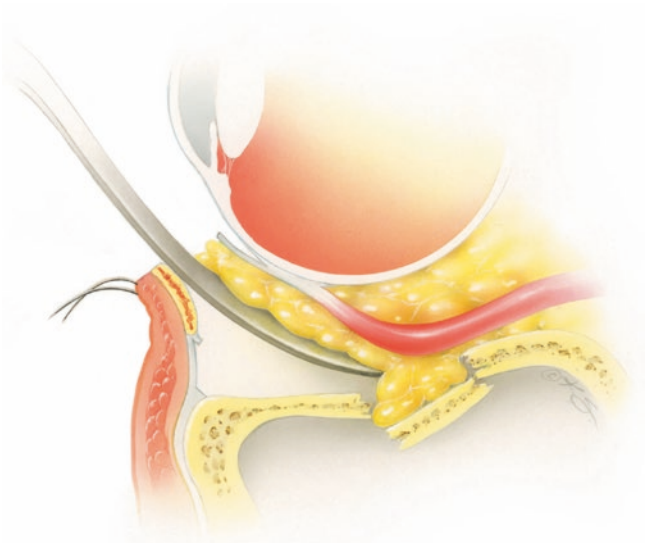


Fig. 37.14 Dissection of the subperiosteal plane. The dissection of the subperiosteal plane is facilitated by use of malleable retractors, which in this case demonstrates prolapsed fat through an orbital fracture

Bulbar Transconjunctival Orbitotomy

The bulbar transconjunctival approach (Figs. 37.15, 37.16, and 37.17) provides direct access to the intraconal, sub-Tenon's, and subarachnoid spaces. Posteriorly located lesions can be more easily reached surgically if the bulbar transconjunctival approach is combined with a lateral orbitotomy (described below). This allows the globe to be rotated temporally into the defect in the lateral wall of the orbit. Lesions in these spaces include cavernous hemangioma, lymphangioma, schwannoma, neurofibroma, metastatic disease, and optic nerve lesions.

Procedure

The operation may be performed either nasally or temporally. To reach the intraconal space, insufficient room exists to provide access via the inferior or superior transconjunctival routes.

A lid speculum is placed between the eyelids, and a 90° conjunctival peritomy is performed nasally. Relaxing incisions are made inferonasally and superonasally and the ends of the conjunctiva are marked for easy identification at the conclusion of the case (Fig. 37.15). The medial rectus muscle is isolated on a muscle hook, and a double-armed 6–0 Vicryl suture is passed in a double-locking fashion through the muscle belly approximately 2 mm posterior to the insertion of the muscle to the globe. The muscle is disinserted anterior to the suture and the ends of the suture secured with a seriphine. A 5–0 silk or Mersilene suture (Ethicon) is woven through the insertion of the medial rectus muscle and

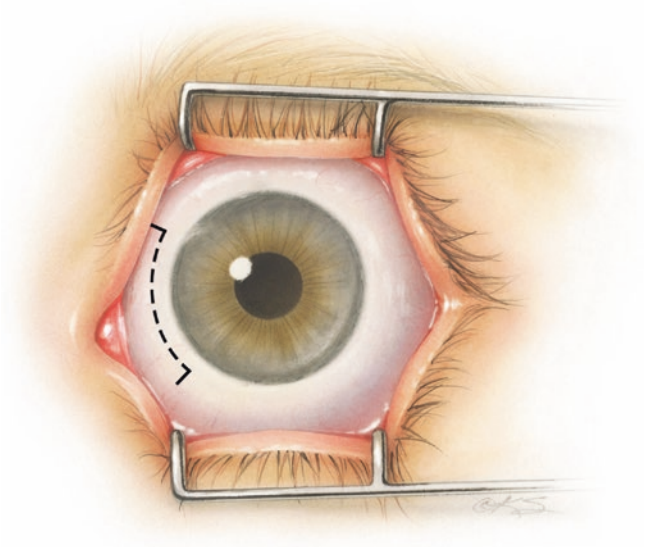


Fig. 37.15 Bulbar transconjunctival orbitotomy. A transconjunctival incision is made perilimbal for approximately 90° through both conjunctiva and Tenon's capsule. This can be extended behind the caruncle for greater exposure to the intraconal, extraconal, and subperiosteal spaces of the medial orbit

used to rotate the globe temporally (Fig. 37.16). The lid speculum is removed and the intraconal space entered bluntly with Q-tips and malleable retractors. A variety of self-retaining retractors have been devised for use in this region. We generally do not require their use, but we employ neurosurgical Greenberg retractors when stable retraction is desired.

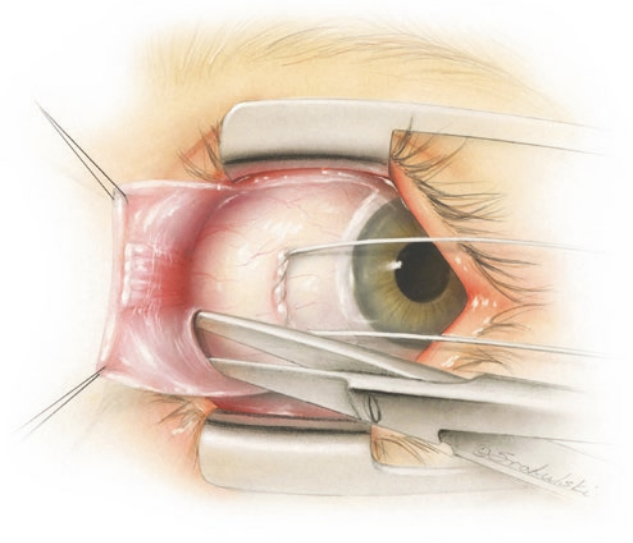


Fig. 37.16 Access to the medial intraconal space. The medial rectus muscle is disinserted from the globe, and a suture is placed in a continuous running fashion through the stump of the tendon. Curved scissors are used to open posterior Tenon's capsule. With the globe rotated laterally and the medial rectus muscle pulled medially, ready access is available to the medial intraconal space

If anteriorly located in the intraconal space, the tumor may be removed bluntly as classically described with the assistance of a cryoprobe to provide traction; however, we have come to prefer 4–0 silk traction sutures as they produce the same traction but do not obstruct visualization of the small surgical field as can occur when the cryoprobe is employed. We limit the use of sharp dissection to limit injury to surrounding structures. Magnification with a neurosurgical operating microscope is particularly helpful for dissecting less well-encapsulated lesions (i.e., lymphangioma) from the surrounding tissues. When required, a laser may be delivered through the microscope. As mentioned earlier, if more posterior exposure is required, a lateral orbitotomy may be performed to allow the globe to reflect laterally into the temporalis fossa. If access to the optic nerve is required, posterior Tenon's capsule must be opened with blunt-tipped Westcott scissors and the optic nerve isolated with long Q-tips. Nerve sheath fenestration and biopsies are performed nasally in this fashion (Fig. 37.17).

After the lesion has been removed and hemostasis secured with irrigation and bipolar cautery, the traction suture is removed, the original insertion of the medial rectus muscle is trimmed from the sclera, the medial rectus muscle is reattached to the globe, and the conjunctiva is closed with a fine absorbable suture.

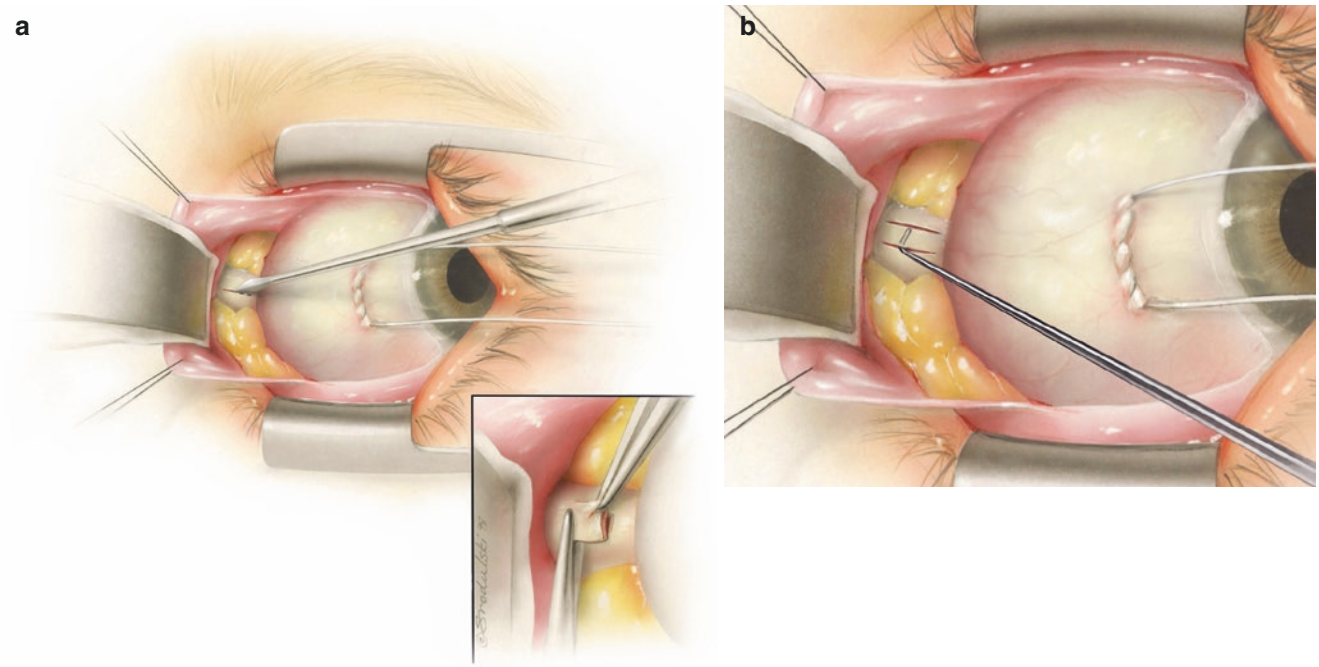


Fig. 37.17 Optic nerve sheath decompression. (**a**) Using malleable retractors and blunt dissection with cottonoids the optic nerve can be identified. For optic nerve sheath decompression, the sheath is opened with a myringotomy-type sickle or MVR blade. (**b**) A small muscle hook can then be used to break up any septations between the pia matter and the dura which then can permit better outflow of CSF fluid in order to decompress pressure on the optic nerve. The inset shows a complete window cut in the nerve sheath using neurosurgical micro-scissors and forceps and the aid of an operating microscope. The sickle blade can also be used to make two or three linear incisions

Surgical Approaches to the Posterior Orbit

To access deeper lesions in the orbit when an anterior approach is inadequate, reference to the nearest orbital wall is an important consideration. In such cases, the orbital wall may serve as a guide to reach more posterior portions of the orbital space of concern. One or more orbital walls may also require removal in order to provide sufficient access.

Medial Orbitotomy

The lateral nasal/Lynch approach to the orbit permits access to the medial wall of the orbit from the frontoethmoidal suture to the ethmoidal-maxillary suture and as far posterior as the sphenoid sinus if the ethmoid air cells are removed (Fig. 37.18). Both the subperiosteal and extraconal spaces may be entered through this approach. The most common lesion encountered in the subperiosteal space of the nasal orbit is a subperiosteal abscess. Less common are lesions arising from the ethmoid sinus (i.e., mucocele, osteomas, neuronal tumors, and hemangiopericytomas).

A more recently described approach to the medial orbit is via the transcaruncular incision. This transconjunctival approach provides equal access to the medial surgical space when compared to the Lynch incision without the cutaneous scar. The incision begins approximately 1 cm more posteriorly than the Lynch incision and thereby limits the surgical dissection required. The only clinical scenario, which may favor a Lynch approach, is an orbital abscess that requires postoperative drainage. In this case, percutaneous drainage through the conjunctival incision is impractical. Both procedures are described below.

An alternative approach to the medial orbit is trans-nasally via endoscopy (see Chap. 8). This can be combined with oculoplastic approaches to the inferior, lateral, and superior orbit as in orbital bone decompression for thyroid ophthalmopathy.

Procedure

Lynch Incision

A vertical curvilinear incision is marked along the thick skin of the lateral aspect of the nose and injected with 0.5% Lidocaine with epinephrine. A skin incision is made with a #15 blade, and the muscle is divided with a coagulating Bovie cautery. The periosteum is incised with a blade, and a periosteal elevator is used to bluntly develop the subperiosteal plane (Fig. 37.19) (see also Chap. 8). A subperiosteal abscess is easily drained in this fashion (Fig. 37.20). Care should be taken not to damage the medial canthal tendon or, if dissection is carried superiorly, the trochlea. If either tendon is reflected with its associated periosteum, simple closure of the periosteum at the conclusion of the case will restore normal function to both structures. Approximately 20 mm posterior to the orbital rim is the anterior ethmoid artery, followed 10 mm still further posterior by the posterior ethmoid artery. Both should be carefully cauterized or ligated with clips prior to division. The arteries also serve as important landmarks of the cribriform plate.

Ethmoidectomy is performed by entering the anterior ethmoid air cells with either a drill or more commonly a curved clamp. The air cells are then removed in sequence from an anterior to posterior direction with pituitary forceps. If required, the frontal sinus may also be entered. Unless the wall of the sinus has been destroyed by a tumor or mucocele,

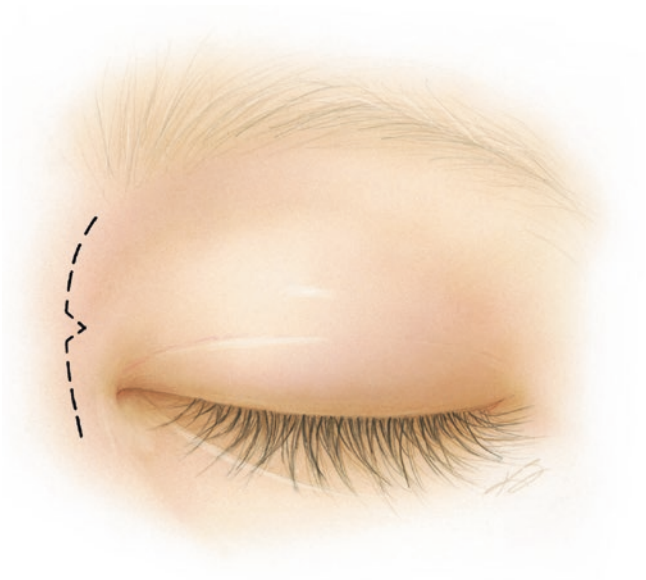


Fig. 37.18 Modified lynch incision. The central "V" reduces the chance of web formation in the medial canthal region

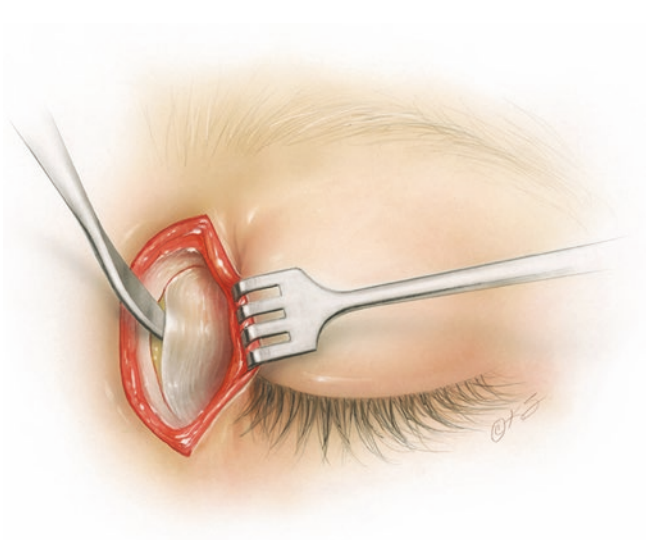


Fig. 37.19 Periosteal incision. The dissection is carried through the skin and orbicularis muscle, and the angular vessels are reflected or cauterized. The periosteum is incised and reflected with a periosteal elevator

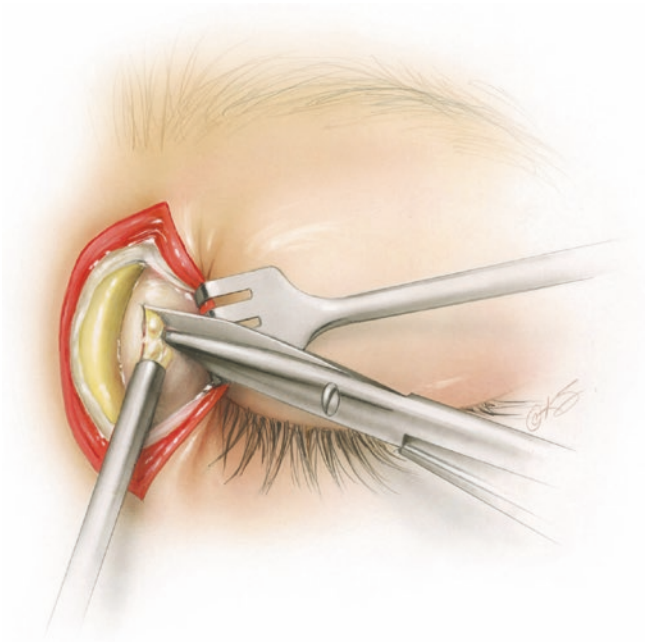


Fig. 37.20 Subperiosteal abscess opened and drained

a drill is generally required to penetrate the bone. In both cases drainage into the nose after sinus resection is advisable to prevent recurrent sinus infection. This is produced by introducing a clamp or rongeur through the sinus into the nasal antrum. To maintain patency of the opening, a drain is kept in place postoperatively for several days.

If access to the extraconal space is required through this incision, this can be achieved by incising the periosteum. To avoid injury to the medial rectus muscle, it is helpful to have a suture beneath the belly of the muscle. Traction on the muscle will produce a dimple in the orbital periosteum and help to identify the location of the muscle. The periosteal incision should be made in the horizontal plane either superior or inferior to the belly of the muscle. Dissection then proceeds bluntly with Q-tips and malleable retractors within the intra- and extraconal spaces.

At the completion of the surgery, the deep and superficial periosteal layers are closed with interrupted absorbable sutures. The skin is closed in two layers.

Transconjunctival (Retrocaruncular) Incision for a Medial Orbitotomy

To access the medial wall via the conjunctival, an incision is made either just posterior to the caruncle or by splitting the caruncle as initially described. With the caruncle on traction, a Westcott scissor is used to make a curvilinear incision of the conjunctival to the superior and inferior nasal quadrants. Again with the caruncle on traction, a curved Stephens scissor is used to bluntly dissect to the medial wall of the orbit in the avascular plane just posterior to the lacrimal sac to expose the periosteum just behind the posterior lacrimal crest. The periosteum is incised and reflected with a periosteal elevator (Fig. 37.21). The perforating anterior and posterior ethmoidal neurovascular bundles can be cauterized and divided as described above. Access from the subperiosteal space to the intraorbital extraconal and inferior or superior intraconal spaces are accessible upon dividing the periosteum longitudinally. After completion of the surgical procedure, closure is accomplished simply with 8–0 Vicryl sutures.

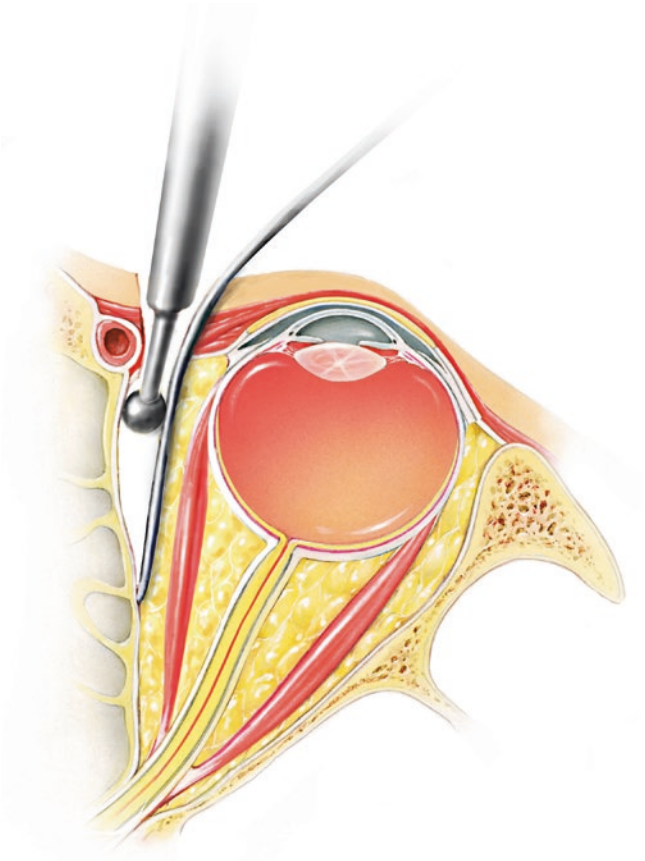


Fig. 37.21 Transconjunctival incision to access the medial orbital just posterior to the caruncle

Lateral Orbitotomy

The lateral orbitotomy (Figs. 37.22, 37.23, 37.24, 37.25, 37.26, and 37.27) is the classic approach to the orbit and was the prototypical surgical approach to the orbit for diagnostic orbital surgery in the pre CT scan era. Preoperative noninvasive imaging has vastly improved the diagnosis of proptosis obviating the need for diagnostic orbitotomies in majority of cases. When surgery is indicated, high-resolution imaging have also refined surgical planning such that currently the lateral orbitotomy approach is reserved for lesions in the temporalis fossa, lateral wall of the orbit (sphenoid or zygomatic bones), lateral extraconal space, or the intraorbital space lateral to the optic nerve. The procedure may be performed with or without removal of the lateral orbital wall, based on the exposure that is required. Lesions in this region include histiocytic lesions, dermoid cysts, lacrimal gland tumors, neuronal

tumors (neurofibromas and schwannomas), rhabdomyosarcoma, and fibrous histiocytoma. The optic nerve can be isolated from this approach. Although the optic nerve is further from the lateral wall than it is from the medial approach, some surgeons prefer the lateral approach when performing optic nerve sheath fenestration to treat benign intracranial hypertension. Alternatively, it is valuable as a second operative site for cases in which a medial fenestration has failed.

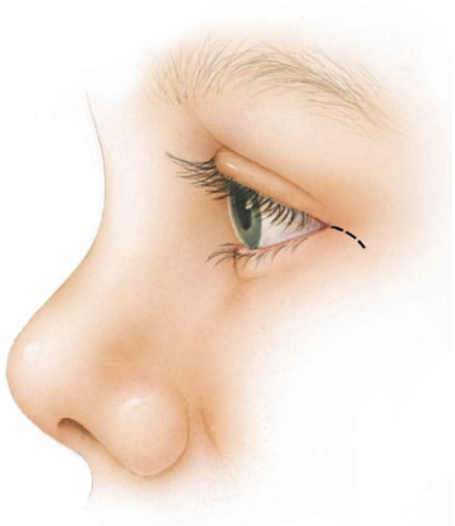


Fig. 37.22 Lateral orbitotomy. A skin incision is placed in the lateral canthal angle rhytid. Sometimes the skin incision for a lateral orbitotomy is placed 3 mm lateral to the lateral canthal angle to avoid disruption of the lateral canthal angle. If greater exposure is required, the lateral canthal angle as well as both the superior and inferior attachments of the tendon to the lateral orbital rim can be divided. Alternatively, for lesions in the lacrimal fossa, the incision can be extended from the superior lid crease, thereby avoiding the canthal angle

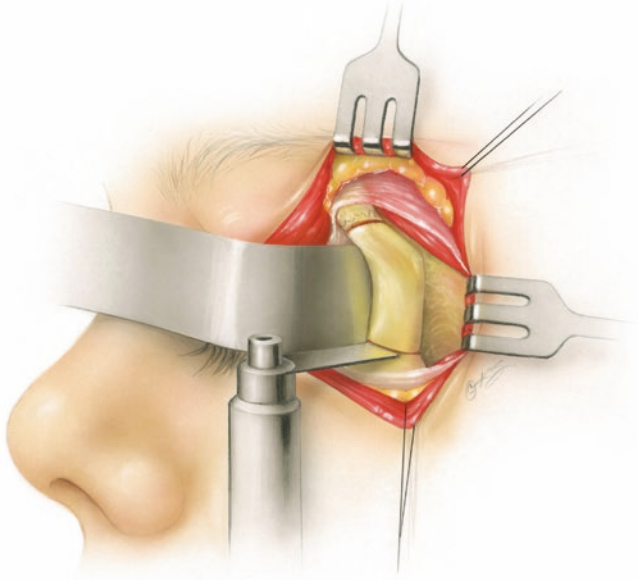


Fig. 37.24 Osteotomies. Malleable retractors are positioned to protect the soft tissues and an oscillating saw is used to make two osteotomies at the desired sites. A bone rongeur is used to remove the bone flap

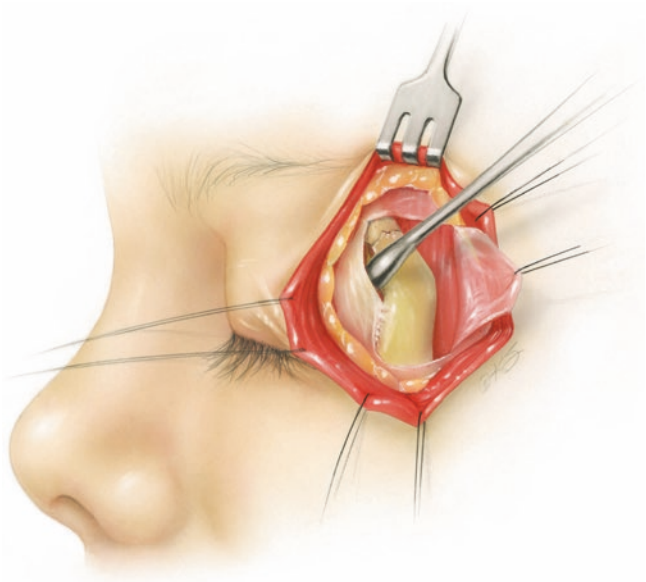


Fig. 37.23 Temporalis fascia and reflection of the periorbita. The skin is divided, and the avascular plane anterior to the temporalis fascia is exposed bluntly. The lateral orbital periosteum is divided and relaxing incisions made superiorly at the level of the frontozygomatic suture and inferiorly at the level of the orbital floor. The periosteum and the attached temporalis muscle are reflected laterally. The muscle is best disinserted using a cutting electrocautery. The periorbita is reflected with a periosteal elevator. Perforating zygomaticofacial vessels are cauterized

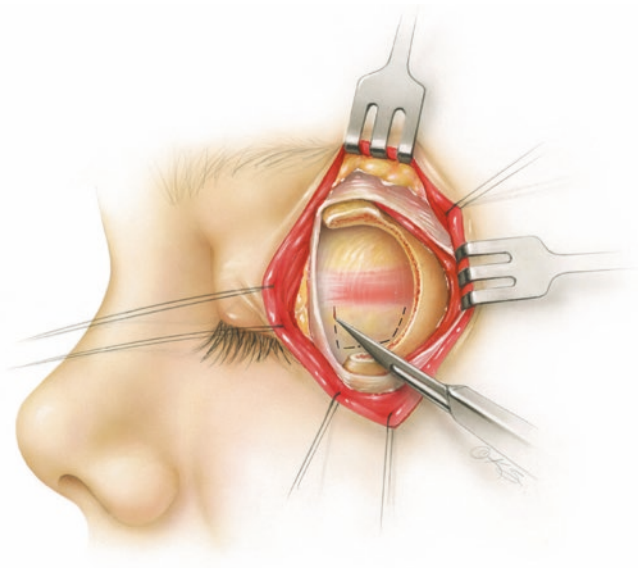


Fig. 37.25 Opening the periorbita. The periorbita is incised with a #15 blade. A traction suture placed earlier behind the lateral rectus muscle insertion helps to identify the muscle after the periorbita is opened. The traction suture aids with identification of the lateral rectus muscle. The incision can be made either above or below the muscle horizontally preserving Tenon's capsule if possible. An alternative is to create a superiorly based flap as demonstrated in this figure

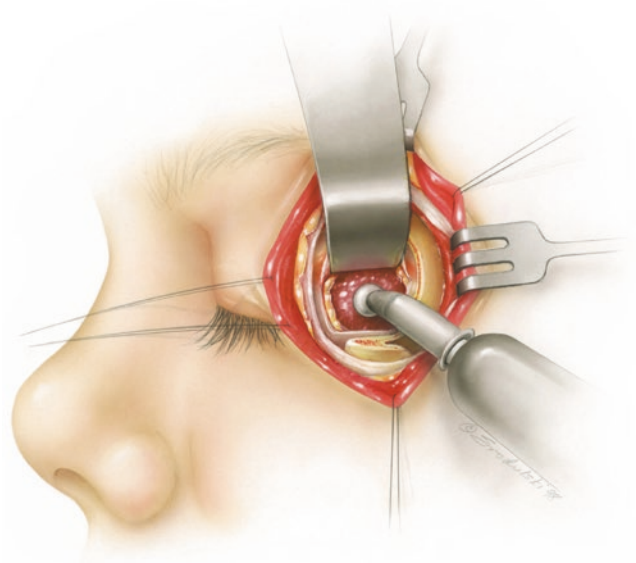


Fig. 37.26 Isolation of the lesion. The lateral rectus muscle is retracted and the lesion isolated with blunt dissection. Often a cryoprobe aids in gently extracting the lesion

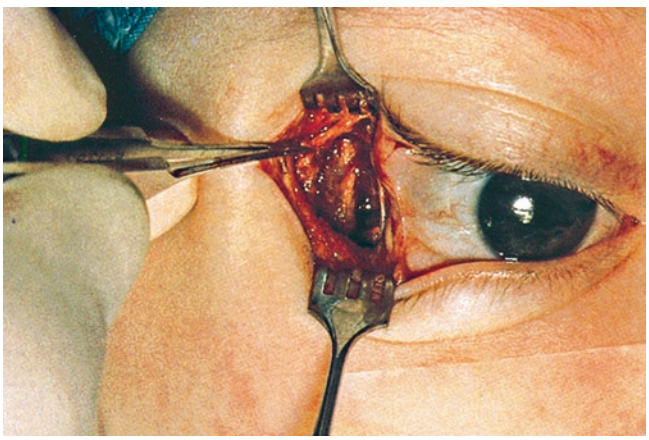


Fig. 37.27 Lateral orbitotomy in 8-week-old infant with proptosis. Biopsy of infiltrating mass of orbit and lateral orbital rim revealed acute myelogenous leukemia (AML) (Courtesy of Jill F. Foster, MD)

Procedure

There are many incisions described for the lateral approach. In an attempt to maximize exposure and cosmesis, we currently employ either the extended upper lid crease incision or the lateral canthotomy incision. The extended upper lid crease approach is generally inconspicuous and provides access to the lateral periosteum without the need to divide the lateral canthal tendon from the eyelids. This makes the ultimate wound closure more straightforward and avoids inadvertent canthal dystopia. The approach is limited as to its access to the inferior aspect of the lateral orbital rim. This translates into the need to extend further lateral into the temple the cutaneous incision in cases where the inferior osteotomy needs to be placed at the superior edge of the zygomatic arch or still further inferior. In those cases the skin incision can be reduced in length by utilizing the lateral canthal approach. Except for the skin and subcutaneous dissection, the procedures are identical.

The lateral canthal approach begins with a horizontal skin incision in a lid crease. The lateral canthal tendon is divided horizontally and then the superior and inferior crus are each released from the lateral periosteum (Fig. 37.22).

A 4–0 silk traction suture is passed beneath the belly of the lateral rectus muscle to facilitate identification during the orbital dissection. After the skin and subcutaneous tissue is opened, the temporalis fascia is exposed by blunt dissection from the superior to inferior extent of the lateral orbital rim. The lateral orbital periosteum is incised with Bovie cautery 2 mm lateral to the rim and with a Freer elevator reflected intraorbitally and laterally. The intraorbital dissection is most easily accomplished by beginning either above or below the lateral canthal tendon, since this is the region of most secure attachment. Reflection of the periorbita reveals the zygomaticofacial and zygomaticotemporal neurovascular bundles, which are cauterized with bipolar cautery prior to division. On occasion, if the lesion is anteriorly situated or easily dissected and mobilized, there will be sufficient exposure without bone removal. In other cases, the periosteum and attached temporalis muscle are reflected laterally (Fig. 37.23). With retractors in place, superior and inferior osteotomies are created with a sagittal saw (Fig. 37.24). The osteotomies are placed to provide access to the lesion but are generally limited superiorly by the inferior extent of the anterior cranial fossa, which should be noted on the preoperative CT scan and inferiorly by the zygomatic arch. Modifications of the osteotomies are occasionally necessary. In most cases the incisions can be aligned with the horizontal extension of the inferior and superior rims of the orbit laterally.

Drill holes may be placed at this time to be used at the conclusion of the case to secure the bone. Rongeurs are used to remove the bone flap. Greater posterior exposure can be achieved by removal of the anterior aspect of the sphenoid bone with bone rongeurs and drills. The bone in this location is thick and contains a vascular bone marrow space. Bone wax is helpful in controlling bleeding in this site but should be used judiciously to avoid granuloma or sterile abscess formation in reaction to excess retained paraffin.

When traction is applied to the lateral rectus muscle via the silk suture, the periorbita above it will dimple. The periorbita is then divided horizontally above or below the muscle with a #15 blade and curved scissors (Fig. 37.25). If, as described above, the lateral approach is to be combined with a medial transconjunctival approach, the lateral bone removal must be at least 30 mm in rostral–caudal height to accommodate the reflected globe, and the lateral canthal tendon must be divided with the lateral periorbita. Dissection within the intraconal space is most safely accomplished with Q-tips and malleable retractors. Gentle traction applied with a cryoprobe, or as we prefer, silk sutures placed in the substance of the lesion, may be useful such as when the

lesion is encapsulated like a cavernous hemangioma (Fig. 37.26). Infiltrating lesions in the mid-or posterior orbit can also be reached by a lateral orbitotomy for biopsy and possible debulking (Fig. 37.27). Sharp dissection is avoided to minimize damage to normal tissues. When required, bipolar cautery is preferred, but most bleeding may be controlled with gentle pressure and may be assisted with thrombin-soaked Gelfoam. After biopsy or removal of the lesion, it is important to assure that there is no active bleeding. We generally feel that the use of drains within the orbit provides little relief from the effects of a postoperative orbital hemorrhage and may increase the risk of infection. Consequently, we reserve the use of percutaneous drains for those cases where significant postoperative bleeding is a risk.

We advocate, where possible, closure of the periorbita with absorbable sutures, as this speeds the recovery of full lateral rectus function. The bone is replaced and secured with a nonabsorbable suture. Wires or microplates may be used but are not generally required. If previously divided, the lateral canthal angle is reconstructed and the periosteum closed in an interrupted fashion with a heavy-gauge absorbable suture. The subcutaneous tissue is closed with absorbable sutures and the skin with a subcuticular nylon suture. A firm pressure dressing is applied to the eye to prevent bleeding due to elevated blood pressure during extubation. It is then removed when the child is awake in the recovery to permit the monitoring of the condition of the eye.

Inferior Orbitotomy

The inferior orbitotomy provides access to the anterior–inferior intraconal as well as the subperiosteal space, including the floor of the orbit (roof of the maxillary sinus). The most common pathologies approached in this fashion are fractures of the orbital floor. Subperiosteal abscess is equally well approached in this fashion. Intraorbital lesions in the anterior two-thirds of the orbit, such as lymphangioma, hemangioma, rhabdomyosarcoma, and some tumors of neural origin, may be removed through this approach. More posteriorly located lesions that require more than biopsy are not as easily accessible without a combined surgical approach. Often a lateral orbitotomy will aid in those lesions lateral to the optic nerve. Those that are directly beneath the optic nerve, apically or medially located in the inferior orbit, may be more easily approached through the maxillary antrum.

Procedure

The incision can be made in one of three locations. Traditionally, the incision for an inferior orbitotomy was made directly over the orbital rim in a natural skin fold. While this incision does provide direct access to the orbital rim and overlying periosteum, it produces a less cosmetically acceptable scar. Alternatively, the incision may be made in the subciliary location approximately 2 mm inferior to the lid margin. As was discussed earlier in the section on anterior orbitotomy, a skin and muscle flap is dissected in the avascular plane beneath the orbicularis muscle. The orbital septum is identified and may be opened for lesions within the intraconal and extraconal spaces (Fig. 37.28). If a subperiosteal dissection is required, an incision is made inferior to the orbital rim directly through the periosteum with the Bovie cautery. In both of the above-described approaches, traction on the lid may be applied with a marginal silk suture. Generally we prefer the transconjunctival approach with or without canthotomy/inferior cantholysis, as it is the least apparent postoperatively and measurably reduces the risk of postoperative lid retraction or ectropion.

If a canthotomy is required for reasons of improved exposure, the lateral canthal angle is divided horizontally, followed by disinsertion of the inferior crus of the lateral canthal tendon to release it from the lateral orbital rim. Stephens scissors are used to bluntly dissect from lateral to nasal in the plane between the lower lid retractors and the orbicularis muscle. The conjunctiva and lower lid retractors are divided approximately 5 mm inferior to the inferior border of the tarsus horizontally with monopolar cautery. Dissection is carried inferiorly to open the orbital septum if required or directly to the orbital rim to divide the periosteum. Dissection in the intra-or extraconal spaces is performed as described above. The subperiosteal dissection for drainage of an abscess cavity is generally best approached through an external incision, since a drain to the skin will be required in addition to a nasal antrostomy.

In cases of an orbital floor fracture, it is important to clearly visualize the limits of the fracture. The posterior extent is most often difficult because it may reach as far posterior as the posterior wall of the maxillary sinus (adjacent to the palatine bone and within 1 cm of the optic canal). Failure to address this area of pathology is the most frequent cause of persistent postoperative diplopia. After the fracture has been repaired, the osteotomized bone is replaced and secured with miniplates or wires. The fracture itself may be repaired with autogenous bone or alloplastic material, including Silastic, Teflon, Supramid, or, as we prefer, Medpor. In general, the material is secured to the surrounding bone with screws through the plate or to the rim using the imbedded titanium plates found in the Titan version of the Medpor plate (Fig. 37.29). In the case of Medpor implant, we favor using the thinnest implant appropriate to the application and have in general used the barrier implant as we feel that it reduced the risk of adhesion of the adjacent rectus muscle to the porous surface of the implant. The periosteum is closed with interrupted absorbable sutures. We feel it is particularly important to cover any titanium implant with periosteum, as it is our experience that titanium exposed to surrounding soft tissues results in avid scar tissue formation. This in turn has been associated with eyelid retraction and diplopia, both of which are challenging to repair. The conjunctiva is closed with

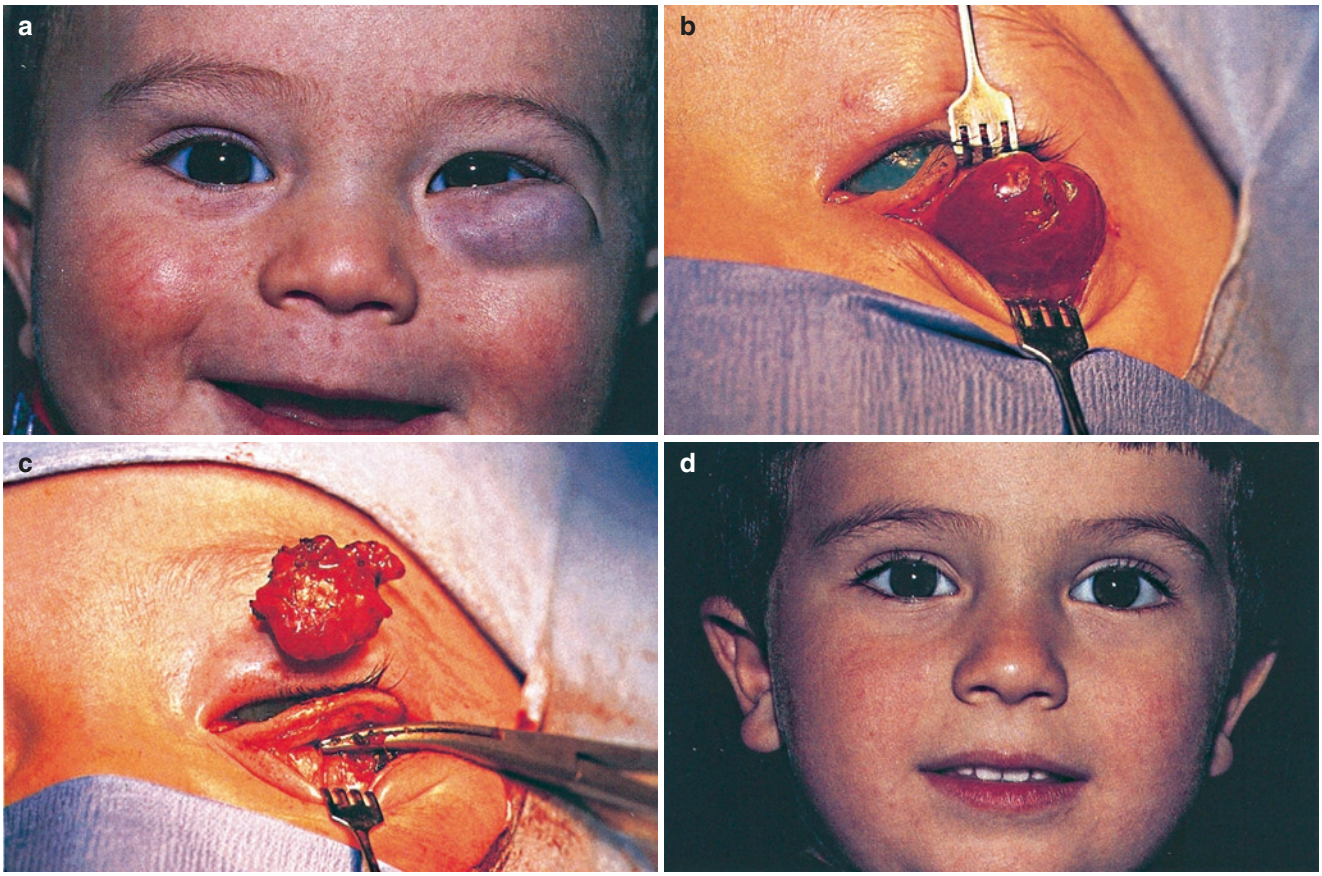


Fig. 37.28 Inferior orbitotomy. (**a**) Ten-month-old child with inferior orbital mass. (**b**) Subciliary incision revealing mass. (**c**) Large encapsulated type of capillary hemangioma removed. (**d**) Appearance of child 2½ years following surgery

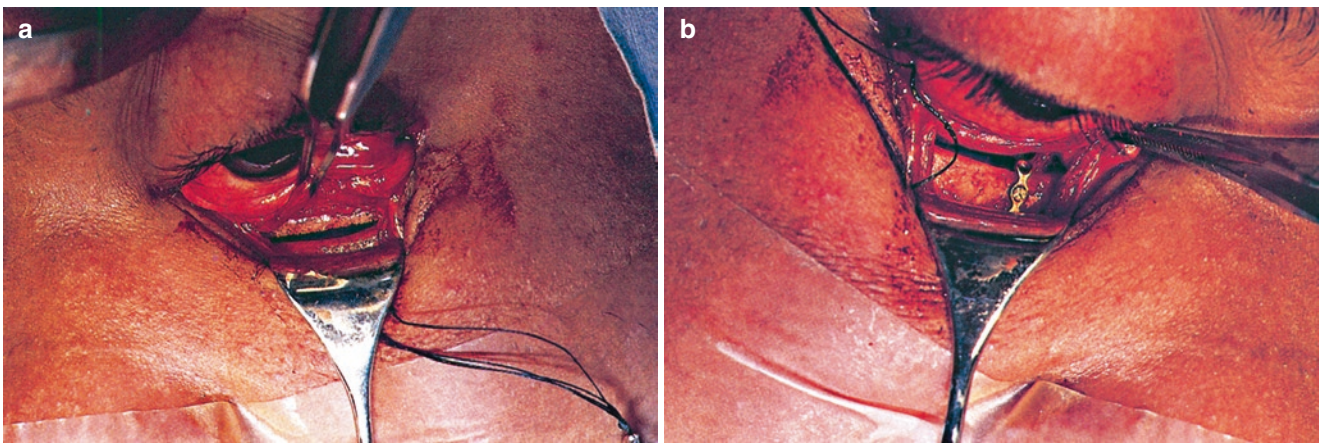


Fig. 37.29 Orbital floor fracture repair. (**a**) Medpor channeled implant (Porex) placed over floor fracture. (**b**) Miniplate inserted in channel bent over inferior orbital rim and secured with 4 mm screw

absorbable sutures. There is no need to reattach the lower lid retractors separately, since they are functionally attached to the conjunctiva and will heal spontaneously. The lateral aspect of the lower lid is reattached to the posterior aspect of the orbital rim periosteum. The silk traction suture is fixed to the brow for the first evening to suspend the lid margin and reduce postoperative lid retraction.

Superior Orbitotomy

The superior orbit is invaded by many of the same tumors that are identified in the inferior orbital space. Vascular lesions (hemangioma and lymphangioma) are common. The superior nasal orbit is a common location of rhabdomyosarcoma. Bony lesions include osteoma, fibrous dysplasia,

chondroma, and the uncommon malignant chondrosarcoma. Fractures of the orbital roof in children are more common than in the adult population. The variance in incidence is thought to be due to the lack of a developed frontal sinus in children, which when fully formed serves to dissipate the force of a blow. Congenital masses in the superior orbit include mucoceles and dermoid cysts. Lesions of the lacrimal gland in children generally are inflammatory, but we have seen one case of benign mixed lacrimal gland tumor in an 8-year-old. As is the case in the inferior orbit, the direct superior approach to the orbit permits biopsy and excision of more anteriorly located lesions. Those located posteriorly or coincidentally involving the intracranial space are generally most successfully approached by a combined cranio-orbital approach. The description of a cranio-orbitotomy is included in the craniofacial and neurosurgical chapter (see Chap. 40). This approach can also be used for decompression of the bony optic nerve canal.

Procedure

The superior orbital space may be approached through either the subperiosteal or intraorbital spaces. The subperiosteal space is entered through a sub-brow incision or preferably an upper lid crease incision, as it leaves an inconspicuous scar. We currently reserve the sub-brow approach for those cases in which postoperative drainage of an abscess is anticipated. A sub-brow incision is placed just below the brow hairs (Fig. 37.30). The incision is injected with epinephrine to promote hemostasis. The subcutaneous tissues are divided with electrocautery, including the periosteum. The same plane can be reached from lid crease incision and by carrying the preaponeurotic dissection superiorly above the orbital septum to the sub-brow tissue (Fig. 37.31).

The periosteal flap is reflected with an elevator. Care should be taken not to damage the frontal branch of the supraorbital nerve. The subperiosteal dissection can be carried posteriorly, or, if required, the periorbita may be divided to enter the orbital space (Fig. 37.32). If the periorbita is opened, it is advisable to place traction sutures on the lid margin and the superior rectus

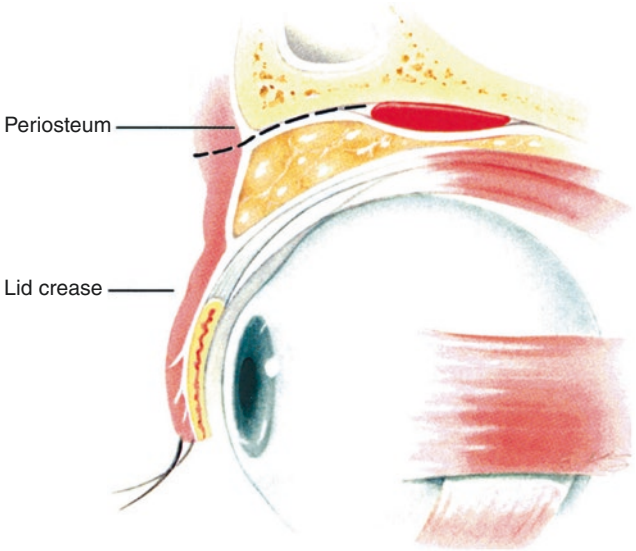


Fig. 37.31 Sagittal view of the sub-brow approach. The dotted line represents the subperiosteal dissection to a lesion in the anterior superior subperiosteal space

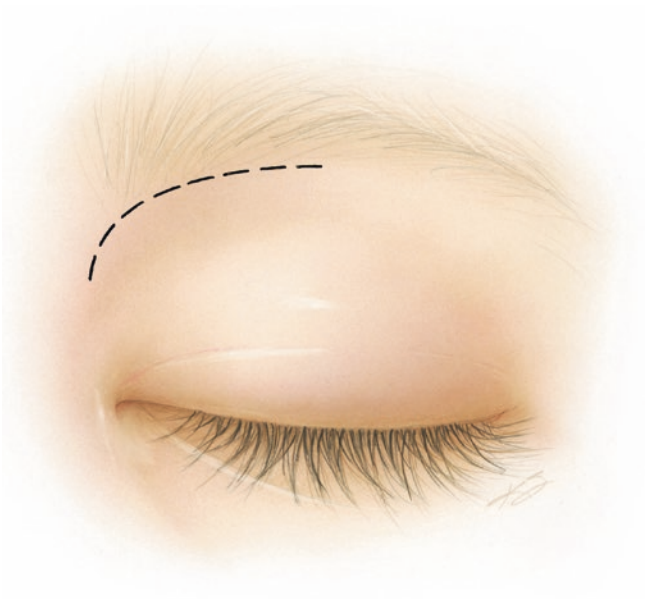


Fig. 37.30 Sub-brow incision for approach to the anterior superior nasal quadrant

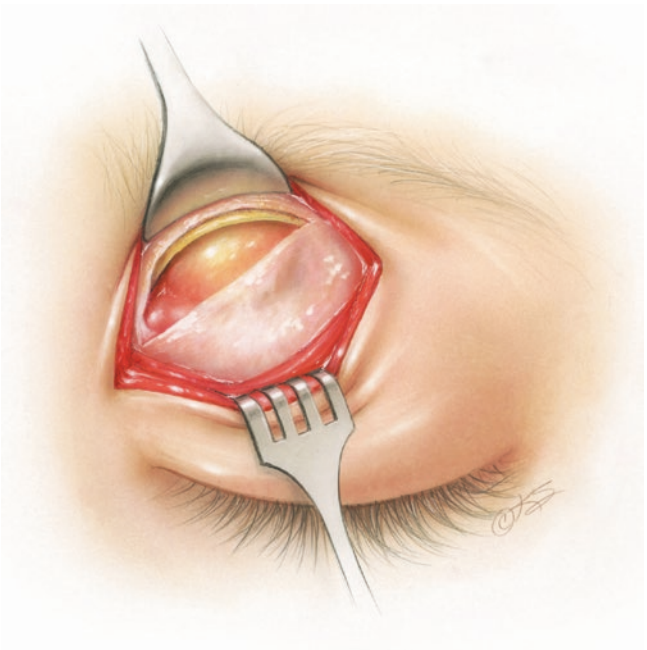


Fig. 37.32 Sub-brow incision. The skin is retracted and orbicularis muscle divided. The periosteum is opened and the septum reflected to reveal an orbital mass

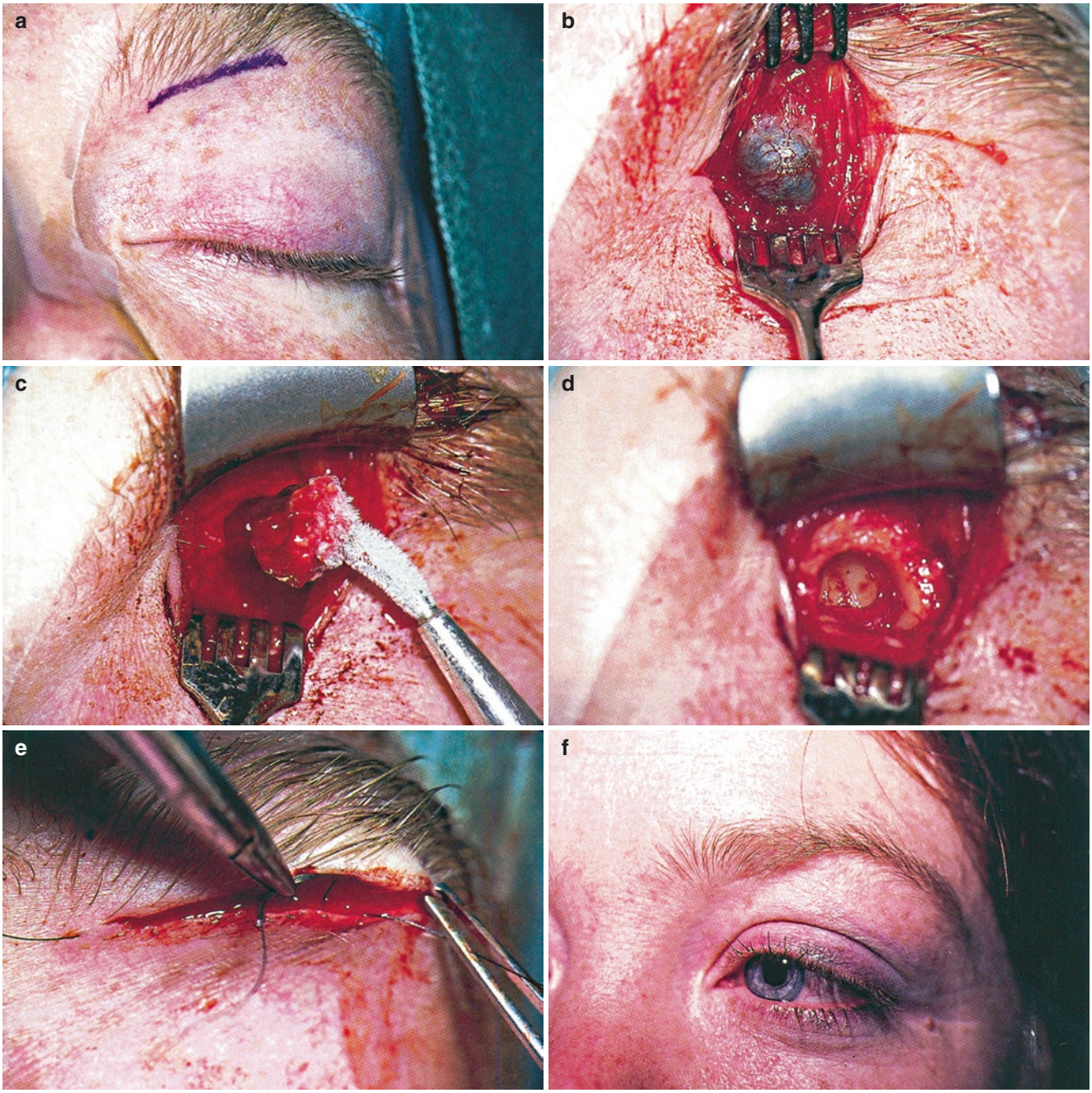


Fig. 37.33 Sub-brow incision. (**a**) Sub-brow incision marked with methylene blue. (**b**) Vascular lesion (cavernous hemangioma) exposed. (**c**) Lesion removed with careful dissection and traction by cryoprobe. (**d**) Bony cavity expanded secondary to gradually to vascular lesion. (**e**) Subcuticular closure with 5–0 nylon suture on P-3 needle (Ethicon). (**f**) Postoperative appearance at 6 months

muscle to avoid injury to the intraorbital structures. After biopsy or removal of the lesion, hemostasis is assured with the assistance of bipolar cautery. The periosteum is closed with an absorbable suture. Deep tissues are approximated in layers, and the skin is closed with nylon or absorbable interrupted sutures (Fig. 37.33).

Alternatively, the superior as well as the nasal orbit can be approached through a coronal incision as described in Chap. 40. Because of a potentially visible scar with male pattern baldness in later life, we generally avoid this incision in boys unless a cranio-orbital approach is indicated.

Transcranial Orbitotomy

The transcranial approach to the orbit is favored for lesions of the optic canal and optic nerve. In addition, lesions of the orbital apex inaccessible to the anterior approaches described in earlier sections are within reach if the lesion is located above the optic nerve (Fig. 37.34). This approach is most routinely valuable for resections of the optic nerve from chiasm to globe. There are unusual cases requiring orbitectomy that are also approached by the transcranial route.

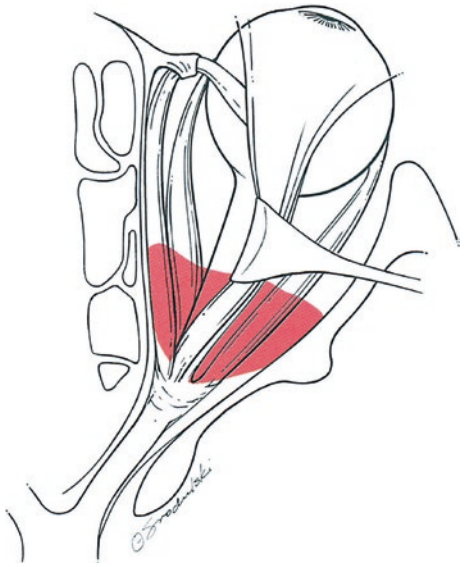


Fig. 37.34 Surgical space at the orbital apex accessible through a transcranial approach



Fig. 37.35 Transcranial orbitotomy. With the orbital roof removed, the thin periorbita is visible. Shown in shadow are the underlying orbital structures. The roof of the optic canal has also been removed with drills and rongeurs

Procedure

The neurosurgical details of the transcranial approach are described in Chap. 40. Certain details regarding the orbital dissection deserve detailed description. The superior orbital rim need not be routinely removed for cases involving only the posterior and mid-orbit. However, if access is required to the anterior orbit, especially if the globe is proptotic, then it will generally be necessary to remove the orbital rim. Failure to do so will make exposure to the posterior aspect of the globe, as is required for optic nerve resections, difficult. If a posterolateral approach is required, the lateral orbital wall may be removed en bloc as part of the orbital roof osteotomy.

Access to the intraconal space requires that the roof of the orbit be removed in the zone of interest. This is generally performed by using a fine chisel and then enlarging the bone incision with fine Kerrison rongeurs. The bone flap is removed and the orbital periosteum exposed (Fig. 37.35). The periosteum is thin, and the underlying levator muscle and frontal nerve are often visible. The periosteum is incised parallel to the levator muscle and either nasal or temporal to the muscle, depending on the location of the lesion in question.

If the optic nerve is to be resected, the periosteum is incised temporal to the muscle, and using blunt dissection, the levator muscle, superior rectus muscle, and orbital fat are reflected nasally with malleable retractors (Fig. 37.36).

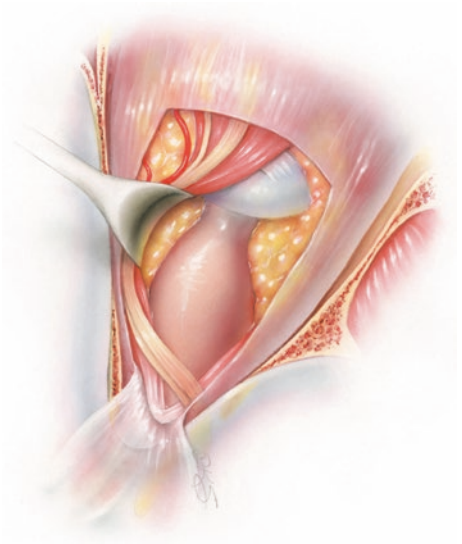


Fig. 37.36 Levator muscle/superior rectus complex. The periosteum is removed and carefully dissected from the underlying levator muscle and supraorbital nerve. The levator aponeurosis/superior rectus complex is reflected medially. Blunt dissection with malleable retractors and cottonoids ultimately reveals the optic nerve, here shown with a glioma

This dissection is aided by the use of cottonoids beneath the retractors. This approach avoids inadvertent injury to the oculomotor, trochlear, and frontal nerves as they traverse the orbit from lateral to nasal across the optic nerve. The orbital fat makes difficult the identification of both normal structures and the lesion that is to be biopsied or resected. To facilitate the dissection, we use malleable retractors and cottonoids to both dissect and reflect tissues. For optic nerve gliomas, intracranial resection is done first. The annulus of Zinn is carefully identified and then divided (Figs. 37.37 and 37.38). This permits removal of the tumor (Fig. 37.39).

After the biopsy or resection of the tumor has been addressed, reconstruction of the orbit follows. The periorbita is replaced with a sheet of DuraGen. The orbital rim is replaced and fixated with miniplates or wires. The anterior one-third of the orbital roof should be replaced or, if resected, reconstructed to prevent pulsatile proptosis. We generally favor split cranial bone for reconstruction. While titanium mesh is simple to use, it can be associated with scarring that results in levator muscle dysfunction. In addition, there is a greater rate of infection or extrusion with the mesh as compared to split bone grafts. The transcranial approach is sometimes required for bony lesions involving the orbital roof or posterior orbit (Fig. 37.40). As mentioned earlier, it can also be used for decompression of the bony optic nerve canal in unusual circumstances related to trauma, for example.

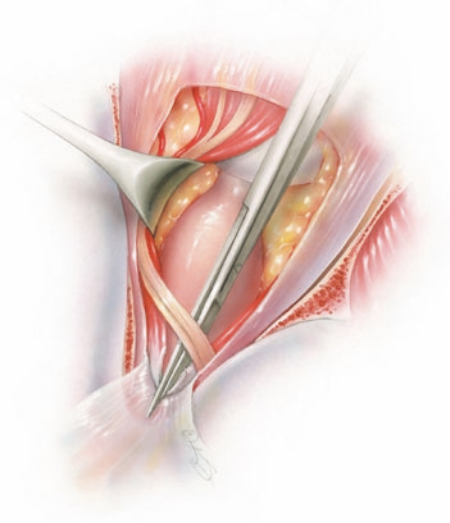


Fig. 37.38 Annulus of Zinn. The annulus of Zinn is divided with scissors

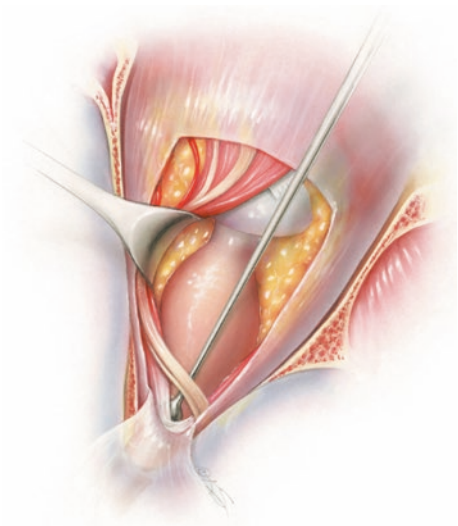


Fig. 37.37 Optic nerve, oculomotor nerves, and annulus of Zinn. Microdissectors carefully isolate the optic nerve, oculomotor nerves, and annulus of Zinn

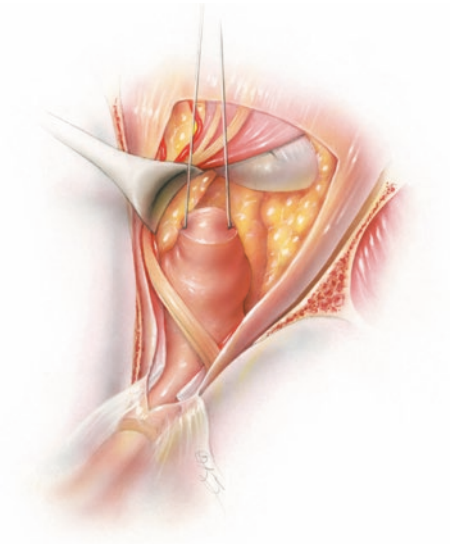


Fig. 37.39 Removal of optic nerve glioma. The optic nerve is severed from the posterior aspect of the globe and anterior to the chiasm. It is then slipped out of the optic canal. The annulus is generally repaired

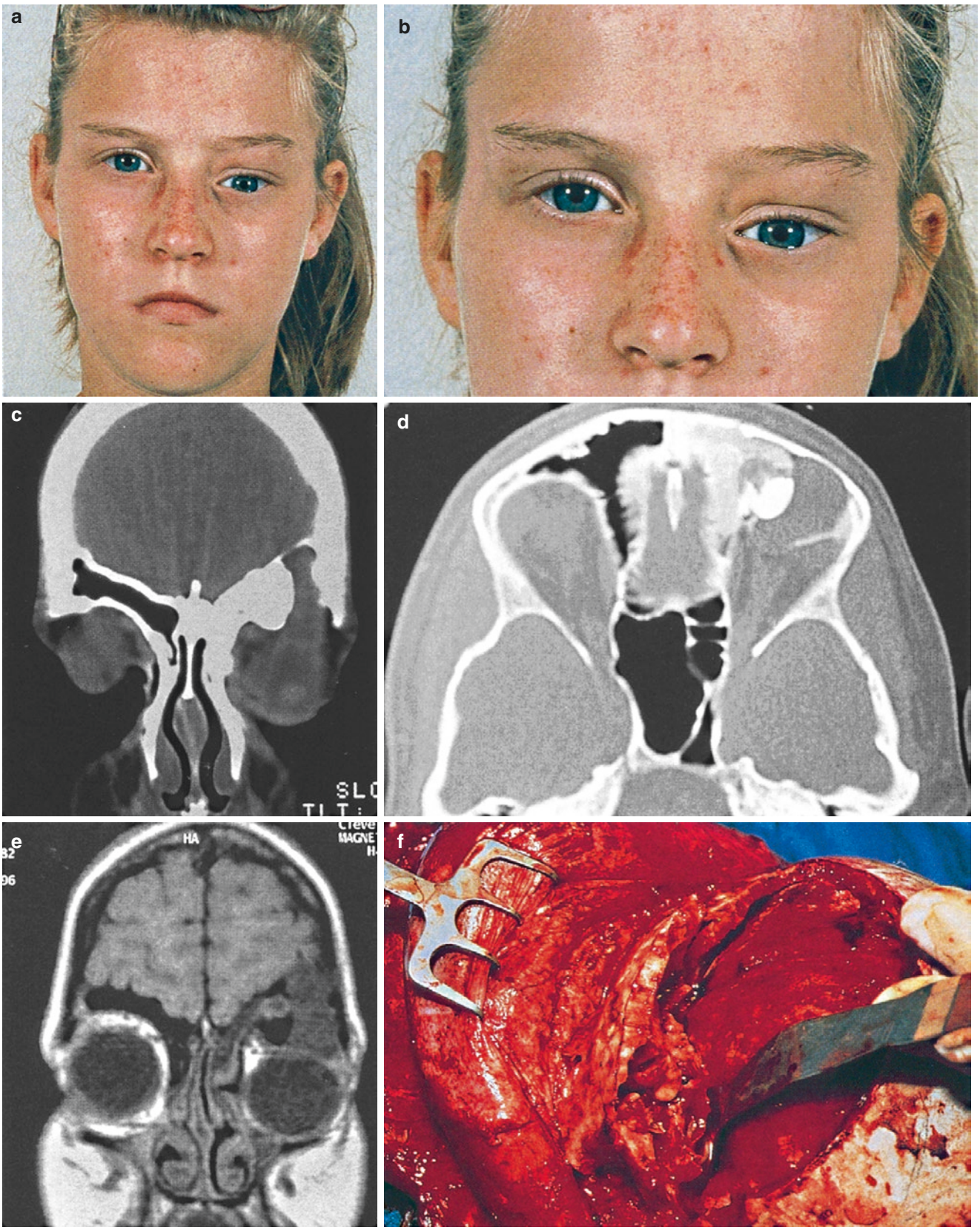


Fig. 37.40 Transcranial approach for osteoma of frontal bone (Courtesy of Jill F. Foster, MD and Francis Papay, MD). (**a**) Sixteen-year-old with left orbital dystopia. (**b**) Close-up view showing left orbit depressed by 4 mm. (**c**) Coronal CT view demonstrating homogenous bony mass measuring 2.5 × 5 cm involving the anteromedial aspect of the left orbit. (**d**) Axial view of lesion. (**e**) Coronal MRI view of orbit. (**f**) Transcranial approach after craniotomy; orbital roof and rim exposed.

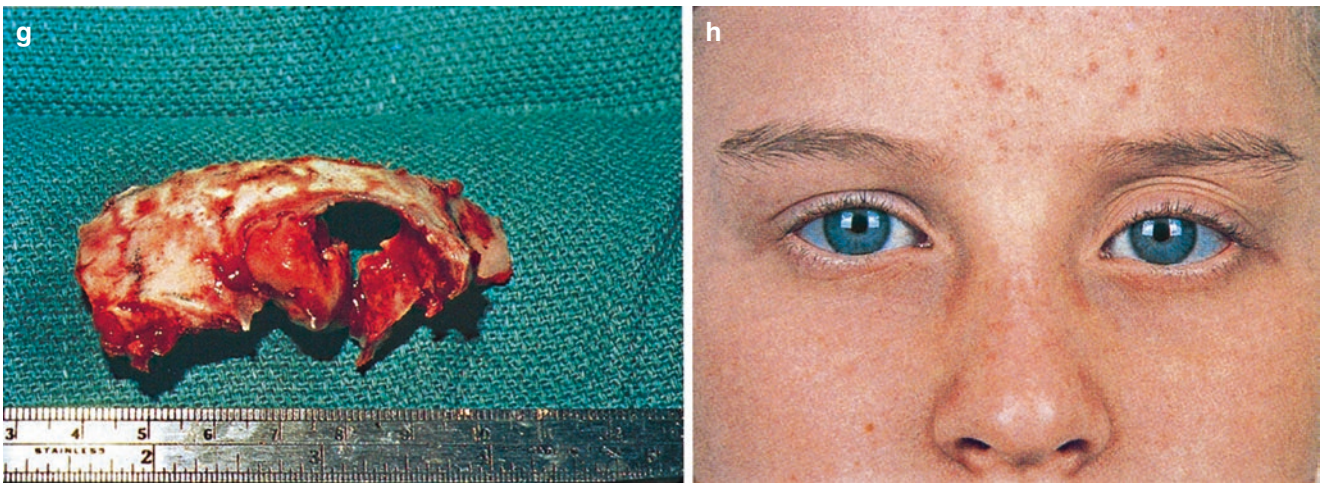


Fig. 37.40 (continued) (**g**) Resected area of bone. (**h**) Three-month postoperative appearance of patient

Orbital Fat Decompression

Orbital fat decompression was introduced as a surgical technique to treat adults suffering from Thyroid Eye Disease who are demonstrated by noninvasive imaging to have proptosis resulting predominantly from expansion of the orbital fat compartment. While an unusual cause of proptosis in children, Thyroid Eye Disease often spares the rectus muscles and selectively affects the orbital fat. We have seen numerous cases in which the proptosis results entirely from fat expansion. In such cases we have successfully employed orbital fat decompression to reduce proptosis (Fig. 37.41).

We believe that removal of orbital fat in such cases is safer than orbital bone decompression, because it has been shown to have a significantly lower rate of postoperative extraocular motility impairment, sinusitis, orbital cellulitis, cerebrospinal fluid leakage, and optic neuropathy. It is of particular value in the pediatric population because the paraorbital sinus pneumatization may be incomplete, and, as a result, surgical decompression into this space may not provide the generally anticipated results. Surgical on the growing otherwise normal sinus cavities may also result in long-lasting sinus abnormalities in this group.

Procedure

Orbital fat decompression may be accomplished through a variety of surgical approaches, all of which have been described in detail in this chapter. The two that have been most successfully utilized in children have been the transconjunctival lower lid and the upper lid crease incisions. Intraoperatively, the patients receive intravenous antibiotics and corticosteroids. These are continued for three postoperative doses of antibiotics and 2–3 days of corticosteroids, depending on the amount of postoperative swelling. Since fat is to be removed from the intra-and extraconal spaces, an appreciation for the location of the extraocular muscles must be maintained throughout the procedure. It may be of benefit to apply traction to the insertion of the muscle to locate them during deep dissection.

Debulking of the orbital fat is always performed through the lower lid, where, in general, the most abundant fat volume is accessible. When clinically apparent as prominence of the superonasal fat pad, or if more significant amounts of proptosis exist, then an upper lid approach is also indicated.

The lower lid incision is usually made transconjunctivally, but if the eyelid is tightly apposed to the globe, as is often the case when the proptosis is significant, a lateral canthotomy and inferior cantholysis provide greater access to the lateral orbital compartment. The conjunctival incision is made approximately 2–3 mm below the inferior border of the tarsal plate. Rake retractors are used to reflect the lid margin and tarsal plate anteriorly. A 4–0 silk suture is placed through the conjunctiva and adherent lower eyelid retractors to reflect them superiorly and to simplify identification of the underlying orbital septum. The septum is opened bluntly and the three fat pads identified.

The nasal fat pad is isolated first. Using primarily blunt dissection with Q-tips and then sharp dissection with Bovie cautery, the extraconal fat is advanced anteriorly with gentle traction. Malleable retractors are placed into the wound to shield the lacrimal sac, eyelid, and globe. As the intermuscular septations and surrounding scar tissue are divided with the Bovie cautery, more of the intraconal fat is easily advanced. Approximately 1–2 mL of fat can be removed from this quadrant. The central fat pad is addressed next. There is little fat volume in this space routinely, and only extraconal fat can be excised. Excessive removal of fat should be avoided because it may result in a hollowed out appearance of the cutaneous

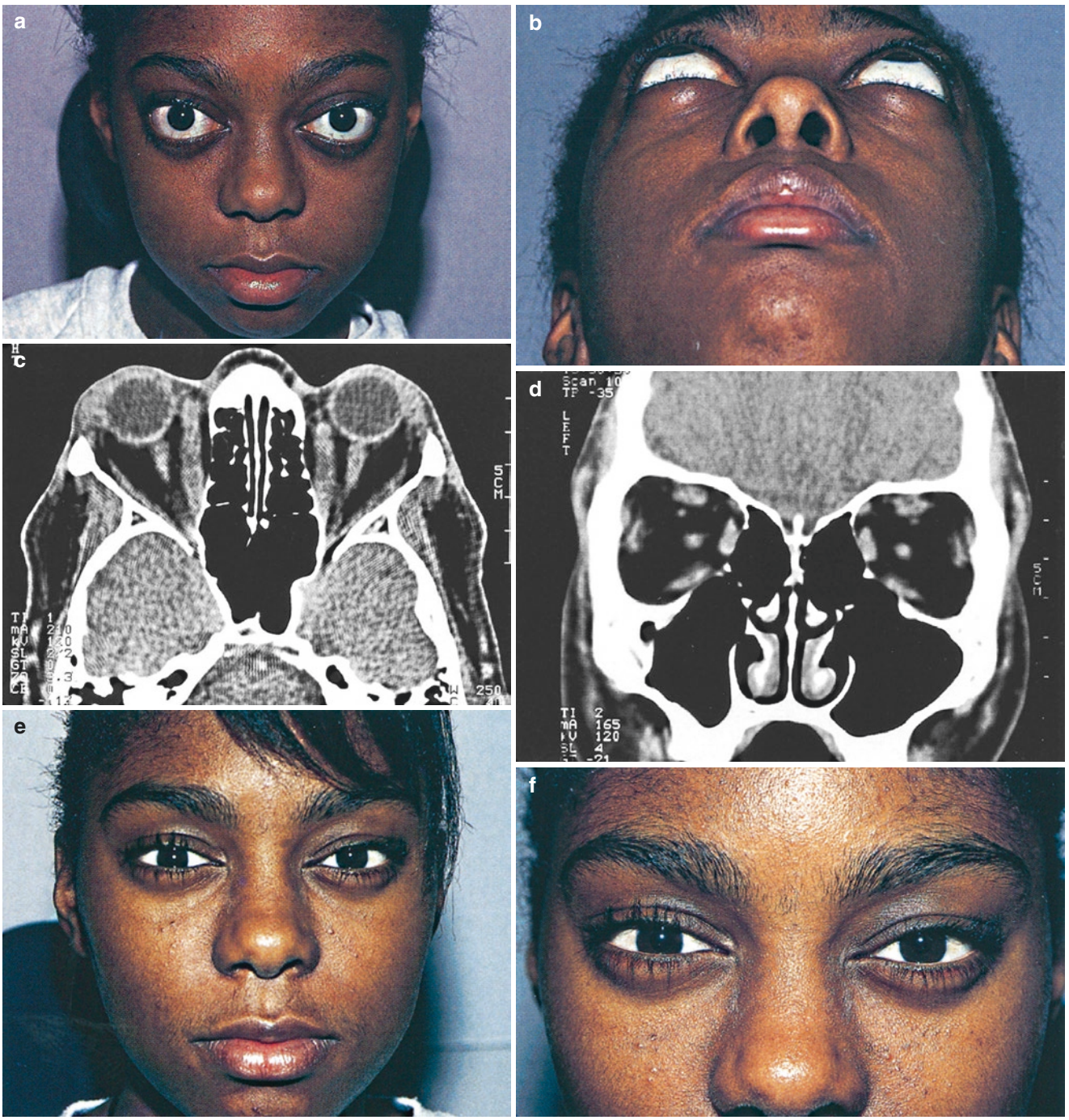


Fig. 37.41 Orbital fat decompression. (**a**) This 12-year-old patient presented with significant proptosis and lid retraction. Hertel exophthalmometer measurements were 24 mm OD and 25 mm OS over a base of 100. In addition to discomfort from exposure, her thyroid condition significantly affected her appearance. (**b**) Proptosis of both eyes from inferior view. (**c**) Axial CT view of patient showing enlarged medial rectus muscles. (**d**) Coronal view of CT scan showing minimal enlargement of other extraocular muscles with large areas of fat as the predominant cause of proptosis in this patient. (**e**) One year postoperative appearance following orbital fat decompression. Hertel measurements are now 17 and 19 over a base of 100. A medial superior upper lid incision and inferior lateral excision through a transconjunctival approach were used. Lower lid retractors were recessed at the same time in order to repair lid retraction. (**f**) Close-up view. The patient has had no diplopia and no lagophthalmos for 5 years of follow-up

lower eyelid contour. The inferior oblique muscle travels through this space and should be identified.

Finally, the inferotemporal space is debulked. The largest volume of fat can be retrieved from this quadrant. The anatomic boundaries to the removal of fat are the lateral orbital wall, the lateral rectus superiorly, the inferior rectus medially, and the globe superonasally. The intraconal fat is removed as described above with the aid of a malleable retractor protecting the globe and the lower eyelid. Approximately 2–3 mL of fat can be removed from this quadrant.

In each quadrant, as fat is removed with the Bovie cautery, care is taken to assure excellent hemostasis. Periodic irrigation with a saline solution limits heat buildup from cauterization. The conjunctiva is closed with 2 absorbable sutures. If a canthotomy/cantholysis has been performed, it is repaired with a 4–0 Vicryl suture.

If further fat volume is to be removed from the superior aspect of the orbit, we routinely confine the dissection to the superonasal quadrant. This region yields the greatest volume of fat and avoids provoking postoperative lid retraction, which occurs in Gravess patients due to excessive fibroblast activity producing adhesions of the levator aponeurosis to the orbital rim. The temporal third of the upper lid is occupied by the lacrimal gland and not productive of fat, given the routine approach. The nasal fat pad is accessed through a lid crease incision. A silk traction suture through the lid margin improves exposure. The orbital septum is opened bluntly and the orbital fat dissected with Q-tips from the surrounding tissues.

The trochlea, superior ophthalmic vein, and supratrochlear nerve occupy this quadrant. The trochlea is palpated and a malleable retractor placed superotemporally to it to avoid injury. The superior ophthalmic vein can often be gently dissected from the surrounding fat. If possible, efforts should be made to preserve the vein, since this will limit postoperative orbital congestion. The terminal branches of the supratrochlear nerve are often sacrificed as part of the fat resection. Sensation in the superonasal quadrant routinely returns within 6–9 months. Dissection of fat in this quadrant routinely yields 2 mL of fat. After hemostasis is assured, the skin is closed with absorbable or nylon suture.

The children are admitted for postoperative observation for orbital hemorrhage, and, if tolerated, ice packs are applied for 48 h after surgery. Skin sutures are removed at 5–7 days post-op. The full effect of the removal of orbital fat is generally appreciated at 3–4 months after surgery.

Orbital Bone Decompression

Pediatric patients who suffer from more profound proptosis may benefit from bony orbital decompression. This technique has been applied extensively in adults who suffer from stable phase thyroid eye disease or dysthyroid optic neuropathy, and the same concepts can be extended to pediatric patients when appropriate. The orbital surgeon must be aware of the chance for orbital (and head growth) and ideally delay surgery, when possible, until a child is into their teenage years.

The earliest modern day decompression was described by Dollinger in 1911 [5]. The orbital bones easily accessed by the orbital surgeon are the lateral, medial, and orbital floor. Where the orbital roof via a transfrontal approach was advocated by Nafzinger in 1931, it is time consuming with a greater risk of patient morbidity [6]. In the 1980s, a two-walled medial and floor decompression was popular though this approach carried a relatively high risk of postoperative diplopia [7]. The concept of a "balanced" decompression involving the lateral and medial walls was reported by some authors to have a lower incidence of postoperative diplopia [8]. Another approach published by Kikawa et al. describes a graded orbital decompression based on the severity of proptosis [9]. Using the categories defined by Kalmann, these authors performed lateral orbital wall decompression with orbital fat removal if exophthalmos was less than 22 mm, additional medial wall decompression if exophthalmos was between 22 and 25 mm, and three-wall decompression with removal of the orbital floor if exophthalmos was greater than 25 mm [10, 11].

Surgical planning and proper patient selection are critical for optimal surgical success. In patients with thyroid eye disease, orbital imaging and proper thyroid function monitoring are necessary to confirm stable phase thyroid eye disease. In patients with predominant orbital fat compartment expansion, an orbital fat decompression may be more optimal. Bony decompression may also be applied in cases of proptosis due to mass effect of orbital tumors or other malformations (see Fig. 35.47 or Fig. 37.46).

Procedure

A lateral orbital wall decompression is accomplished via a lateral canthotomy incision or a lateral fornix transconjunctival incision to access the lateral orbital wall. In the lateral canthal approach, the malar surface of the zygoma is exposed via a lateral canthotomy. If necessary an inferior cantholysis is used for better exposure. A bony window is made in the zygoma and sphenoid to allow for orbital tissue prolapse. Care must be made to remove bone up to the frontozygomatic suture to allow for lacrimal gland prolapse into the temporalis fossa. Bony decompression may be accomplished with the use of a powered saw to remove a portion of the malar surface of the zygoma followed by the use of Kerrison rongeurs (Fig. 37.42). An alternative is to use powered burr for bone removal. This allows for better scalloping of the lacrimal gland fossa. More recently, we have employed an ultrasonic bone aspirator with a 360° tip for bone removal which carries the added advantage of a smaller risk for soft tissue injury. With the approach, the surgeon has the opportunity to remove additional orbital fat if desired.

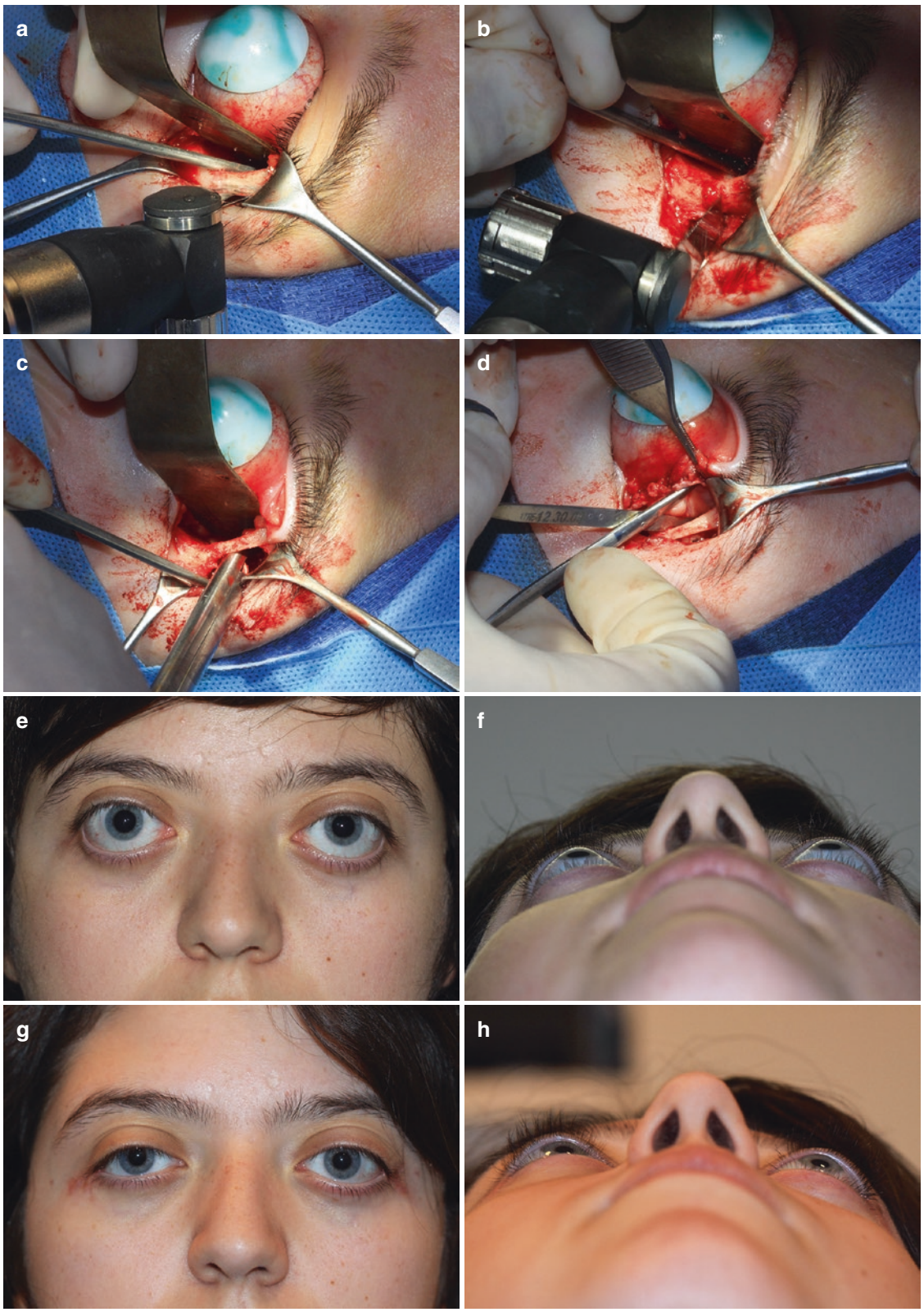


Fig. 37.42 Lateral orbital wall decompression via a large lateral orbital window. (**a**) After a lateral canthotomy, the malar surface of the zygoma is exposed, a periosteal flap is elevated, and a saw is used to create separate the zygoma 3 mm posterior to the rim. (**b**) A vertical bony incision is made in the zygoma. (**c**) After removal of a posterior flap of the zygoma, Kerrison rongeurs are used to create a lateral orbital window in the zygoma and sphenoid. (**d**) The periosteum is opened to allow for orbital prolapse. (**e**) Teenager with thyroid-associated proptosis. (**f**) Worm's eye view. (**g**) Postoperative photo taken 6 months after surgery. (**h**) Worm's eye view with reduction of proptosis

The orbital floor may be approached with a subconjunctival incision 1 mm below the level of the tarsus (Fig. 37.43). This allows for the separation of the orbital septum from the overlying orbicularis muscle. Care must be made to preserve the inferior orbital nerve bundle and the inferomedial orbital strut. Aggressive inferomedial orbital wall removal (involving the orbital strut) can result in postoperative hypoglobus and induct silent sinus syndrome [13]. The orbital floor bones can easily be infractured with a curved hemostat and further debulked with Kerrison rongeurs. Alternatively, the lower eyelid may be swung via an inferior cantholysis with the same conjunctival incision 1 mm below the tarsus. This allows for better exposure of the orbital floor with less retraction required for exposure.

The medial orbital wall is readily accessed via a transconjunctival incision just posterior to the caruncle. Care is made to dissect at a 45° angle to the posterior lacrimal crest. A periosteal incision is made with monopolar cautery, and the periosteum is retracted medial. It is helpful to identify the anterior and posterior ethmoidal arteries, as this will alert the surgeon to the proximity of the optic nerve. As per the *24–12-6* rule, the posterior ethmoidal artery is 6 mm anterior to the optic nerve canal in an average adult [14]. The bones of the medial orbital wall can be removed with simple bony out-fracture and debulking with endonasal forceps. Care, once again, must be made to preserve the inferomedial orbital strut to prevent globe prolapse and an induced silent sinus syndrome.

Orbital navigation is an available intraoperative technology that will aid the surgeon in locating the orbital anatomy. This is especially helpful for medial wall decompression and in identifying the cranial floor in lateral wall decompression (Stryker, Kalamazoo, MI, and Medtronic, Minneapolis, MN). Figures 37.44, 37.45, and 37.46 show examples of patients with stable thyroid eye disease, disfiguring proptosis that underwent a balanced orbital decompression customized to that particular patient.

As with orbital fat decompression, patients are admitted to the hospital for vision monitoring and pain control. Due to postoperative edema, the full benefit of bony orbital decompression may take 3–6 months to be appreciated.

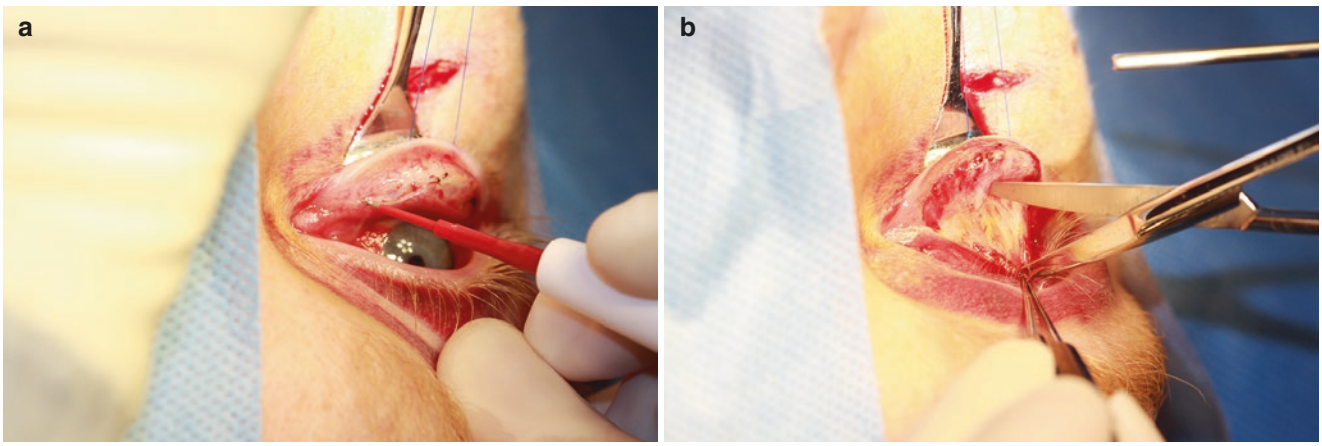


Fig. 37.43 Approach to the orbital floor. (**a**) The lower eyelid is everted over a Desmarres retractor. (**b**) Vertical dissection is performed to separate the orbital septum from the overlying orbicularis muscle

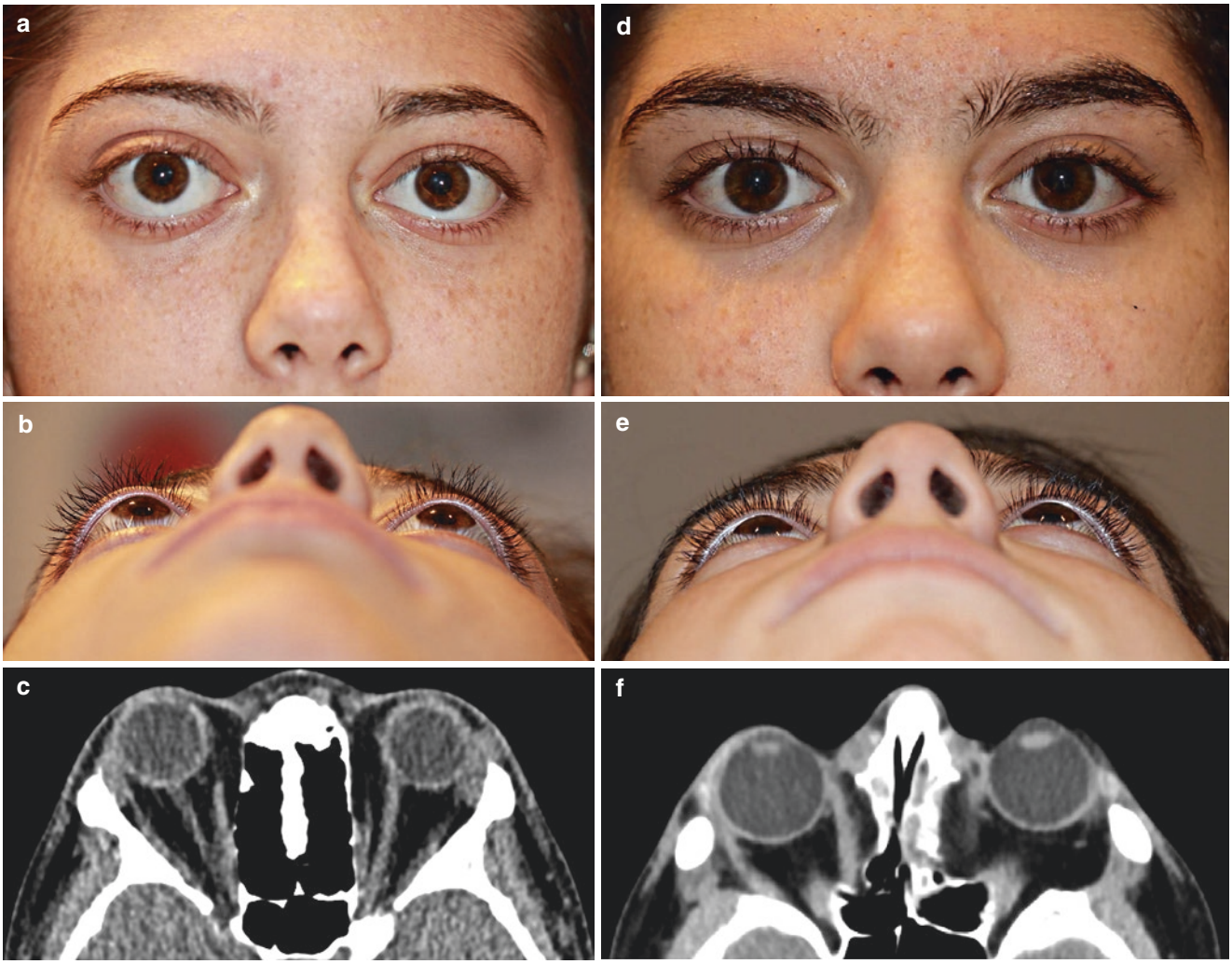


Fig. 37.44 Bilateral orbital decompression for symmetric proptosis with the ultrasonic bone aspirator. (**a**) A 16-year-old female with bilateral proptosis due to thyroid eye disease. (**b**) Worm's eye view showing bilateral proptosis. (**c**) Preoperative axial CT showing shallow orbit, proptosis, orbital fat expansion, and mild muscle enlargement. (**d**) Postoperative photo taken 1 year after bilateral two-wall orbital decompression (lateral and medial) and inferolateral orbital fat pad decompression. (**e**) Worm's eye view showing a bilateral reduction in proptosis. (**f**) Postoperative axial CT taken 1 year after a bilateral lateral and medai wall decompression. Note the significant bilateral reduction in axial proptosis

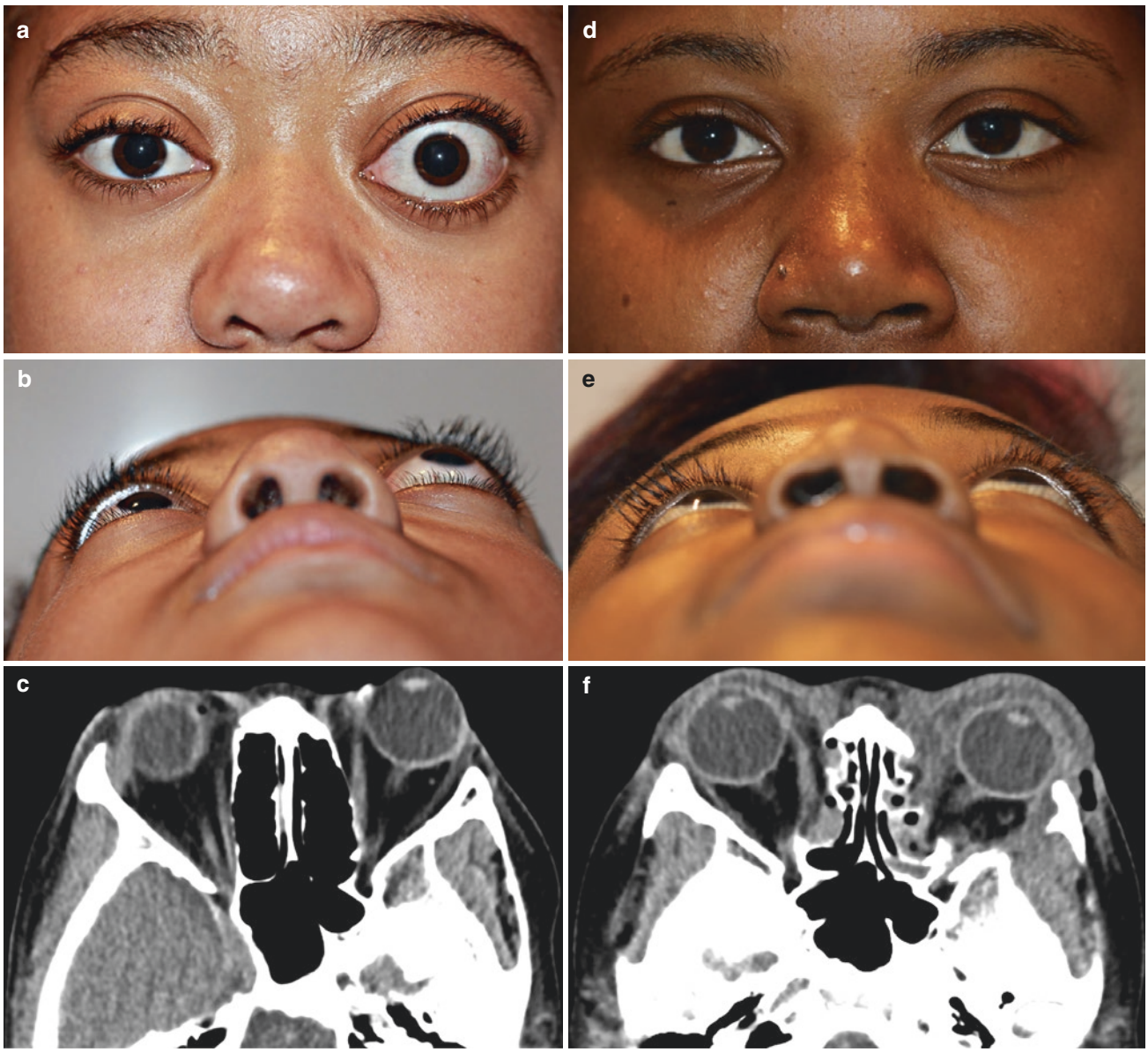


Fig. 37.45 Bilateral balanced decompression for asymmetric proptosis due to thyroid eye disease. (**a**) A 12-year-old female with asymmetric proptosis due to thyroid eye disease. (**b**) Worm's eye view showing asymmetric proptosis. (**c**) Axial CT of the orbits showing proptosis. (**d**) Postoperative photo taken 2 years after a right medial and a left medial and lateral decompression surgery showing an improvement in symmetry proptosis reduction. (**e**) Post operative worm's eye view photo taken 2 years after decompression surgery good posterior medial decompression was accomplished. (**f**) Postoperative CT taken 1 day after bilateral balanced orbital decompression. The Sonopet ultrasonic bone aspirator was used on the left lateral orbital wall. With the use of image guidance (Stryker, Kalamazoo, MI)

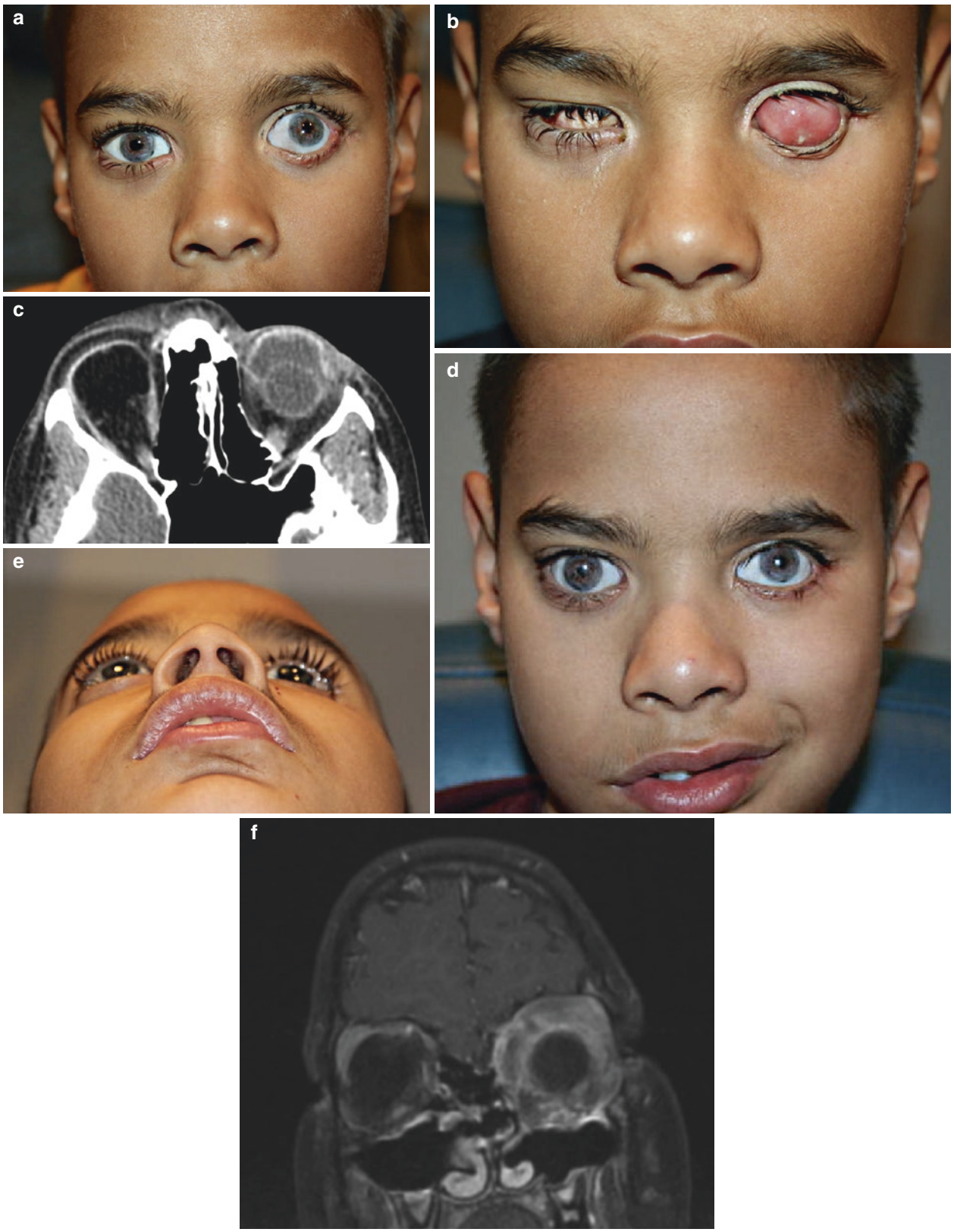


Fig. 37.46 Orbital decompression for non-thyroid-associated proptosis. (**a**) A 10-year-old male who has an expanding left anterior staphyloma is unable to retain his left prosthesis. He also wears a right prosthesis and is status post a right dermis fat graft after removal of a microphthalmic eye. (**b**) With the prosthesis removed, the left anterior staphyloma is visible in the orbit. This patient has light perception vision on the left side and can still appreciate light with his prosthesis in place. (**c**) Axial CT showing an anterior staphyloma. (**d**) Postoperative photo taken 1 year after a left orbital floor and medial wall decompression. (**e**) Worm's eye view showing a reduction in relative proptosis. (**f**) Postoperative T_1-weighted MRI showing a medial wall and orbital floor decompression

References

1. Rootman J, Stewart B, Goldberg RA. Orbital surgery: a conceptual approach. Philadelphia: Lippincott-Raven; 1995.
2. Lemke BN, Della Rocca RC. Surgery of the eyelids and orbit: an anatomical approach. Appleton & Lange: Norwalk; 1990.
3. Henderson JW, Campbell RJ, Farrow GM, Garrity JA. Orbital tumors. 3d ed. New York: Raven Press; 1994.
4. Dutton JJ. Atlas of clinical and surgical orbital anatomy. Philadelphia: WB Saunders; 1994.
5. Dollinger J. Die drickentlastlung der augenhokle durch entfurnung der ausseren orbitalwand bei hochgradiegen exophthalmos und konsekutwer hornhauterkronkung. Dtsch med Wochenschr. 1911;37:1888–90.
6. Naffziger HC. Progressive exophthalmos following thyroidectomy; it's pathology and treatment. Ann Surg. 1931;94(4):582–6.
7. Bailey KL, Tower RN, Dailey RA. Customized, single-incision, three-wall orbital decompression. Ophthal Plast Reconstr Surg. 2005;21(1):1–9.
8. Goldberg RA. The evolving paradigm of orbital decompression surgery. Arch Ophthalmol. 1998;116(1):95–6.
9. Kikkawa DO, Pornpanich K, Cruz RC Jr, Levi L, Granet DB. Graded orbital decompression based on severity of proptosis. Ophthalmology. 2002;109(7):1219–24.
10. Kalmann R, Mourits MP, van der Pol JP, Koornneef L. Coronal approach for rehabilitative orbital decompression in Graves' ophthalmopathy. Br J Ophthalmol. 1997;81(1):41–5.
11. Fichter N, Guthoff RF, Schittkowski MP. Orbital decompression in thyroid eye disease. ISRN Ophthalmol. 2012:1–12.
12. Goldberg RA, Perry JD, Hortaleza V, Tong JT. Strabismus after balanced medial plus lateral wall versus lateral wall only orbital decompression for dysthyroid orbitopathy. Ophthal Plast Reconstr Surg. 2000;16(4):271–7.
13. Rose GE, Lund VJ. Clinical features and treatment of late enophthalmos after orbital decompression: a condition suggesting cause for idiopathic "imploding antrum" (silent sinus) syndrome. Ophthalmology. 2003;110(4):819–26.
14. Rontal E, Rontal M, Guilford FT. Surgical anatomy of the orbit. Ann Otol Rhinol Laryngol. 1979;88(3 Pt 1):382–6.

Congenital Craniofacial Deformities: Ophthalmologic Considerations

38

Karen E. Revere, Brian J. Forbes, William R. Katowitz, and James A. Katowitz

Congenital craniofacial disorders frequently affect the eye and ocular adnexa, presenting diagnostic and therapeutic challenges to the ophthalmologist. Appropriate management of these patients requires recognition of the major craniofacial syndromes and their ophthalmic features. An understanding of the embryogenic basis of these deformities is also essential. The following chapter is a review of the major congenital craniofacial disorders, with particular emphasis on aspects of ophthalmic and oculoplastic significance. These disorders are conveniently separated into two broad clinical categories: the craniosynostoses and clefting disorders. Both the craniosynostoses and clefting disorders may occur in isolation or as part of a well-recognized syndrome. The major clinical characteristics of each type of disorder are reviewed, again emphasizing their more common ophthalmic features. The proper timing of surgical intervention is discussed, as well. Specific craniofacial surgical procedures are more fully discussed in Chap. 40.

K.E. Revere (✉)
Oculoplastics and Orbital Surgery, Ophthalmology, The Children's Hospital of Philadelphia, Philadelphia, PA, USA

Department of Ophthalmology, The Children's Hospital of Philadelphia and the Scheie Eye Institute, Philadelphia, PA, USA

Clinical Ophthalmology, The Perelman School of Medicine at the University of Pennsylvania, Philadelphia, PA, USA
e-mail: reverek@email.chop.edu

B.J. Forbes
Ophthalmology, University of Pennsylvania/Children's Hospital of Philadelphia, Philadelphia, PA, USA
e-mail: forbesb@email.chop.edu

W.R. Katowitz, MD • J.A. Katowitz, MD, FACS
The Children's Hospital of Philadelphia and The Edwin and Fannie Gray Hall Center for Human Appearance, University of Pennsylvania, Philadelphia, PA, USA
e-mail: katowitzw@email.chop.edu; katowitz@email.chop.edu

Embryology Review

A familiarity with the embryology of the human skull and face is essential to understand the developmental aberrations that occur in many of the congenital craniofacial disorders (see Chap. 2). Many of these deformities can be delineated from specific stages of normal embryonic development. The human facial architecture is established very early in gestation, with recognizable human features present by the end of the eighth week of gestation. Not surprisingly, most major aberrations in the development of the face occur during this early period. Rudimentary facial development occurs in the third to fourth week of gestation with invasion of adjacent mesenchyme by dorsal neural crest cells. This produces five distinct facial processes: a central frontonasal process, two paired maxillary processes, and two paired mandibular processes (Fig. 38.1). The mandibular processes arise from the first branchial arch, and the maxillary processes form as buds off the superior lateral portion of the mandibular processes. The ectodermal furrows between these processes are eventually filled in by proliferating mesenchyme and neural crest tissues. Persistence of these ectodermal cells results in failure of fusion of facial processes and is one of the primary etiologies of the clefting phenomena ("true" facial clefts).

During the fifth week of gestation, the two mandibular processes may begin to fuse centrally, the furrow between them filling with migrating neural crest cells (Fig. 38.2). The first branchial groove, below the mandibular processes, also fills with mesenchyme centrally; the patent lateral portion will form the external auditory meatus. Six swellings arise, three cephalad and three caudal to the lateral aspect of the first branchial groove and will eventually give rise to the

© Springer International Publishing AG 2018

J.A. Katowitz, W.R. Katowitz (eds.), *Pediatric Oculoplastic Surgery*, https://doi.org/10.1007/978-3-319-60814-3_38

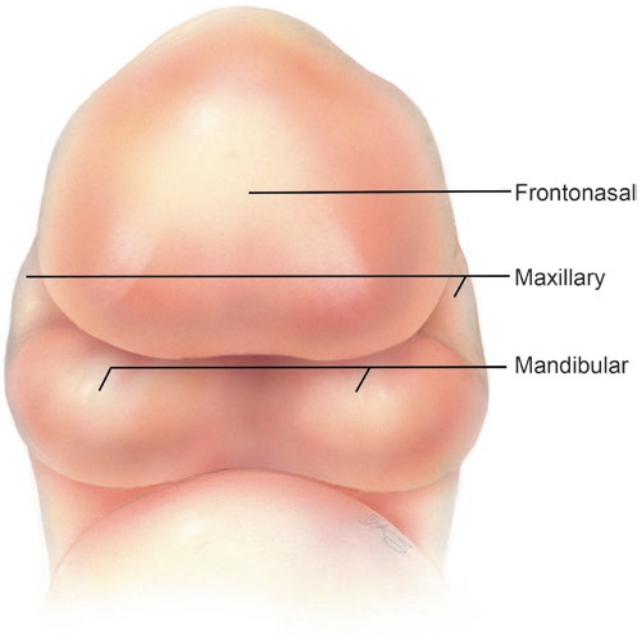


Fig. 38.1 Five main facial prominences. *F* frontal, *Mx* maxillary, *Mn* mandibular

external ear. Ear anomalies can arise from this time forward. The maxillary processes continue to enlarge, flanking the recently perforated stomodeum to form the primitive oral cavity. The most prominent event in the fifth week is the enlargement of the medial and lateral nasal swellings, accompanied by the invagination of the intervening nasal placodes into olfactory grooves. The eyes appear as elevations on the lateral face as the optic vesicle reaches the overlying ectoderm, forming a two-layered optic cup.

In the sixth week, fusion of the medial nasal processes produces a central mass of tissue, which will ultimately give rise to the soft tissue of the nose, the central upper lip, and the premaxilla. The lateral nasal processes will become the nasal alae. The mandibular processes have completed fusion by the end of week 6. The maxillary processes continue to enlarge and approach the nasal processes. The furrow between the maxillary and nasal processes deepens, forming the naso-optic groove (Fig. 38.3). This groove will incorporate neuroectodermal cells, forming the canal that will become the nasolacrimal duct. Persistence of the naso-optic groove produces oculo-oral clefts.

Relative growth of tissues including decreased rate of growth of the frontonasal process accompanied by increased expansion of the lateral head gives the appearance

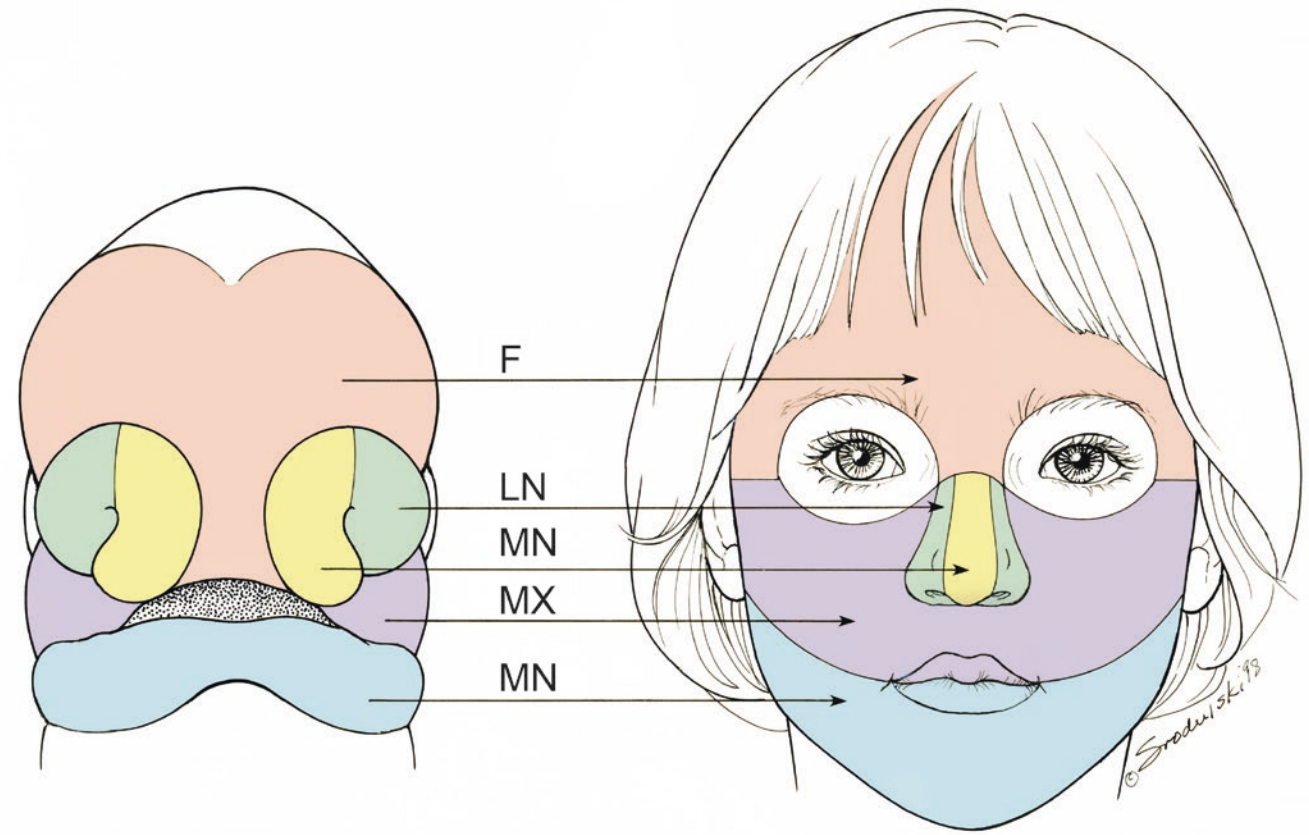


Fig. 38.2 Derivatives from neural crest cells in the adult face

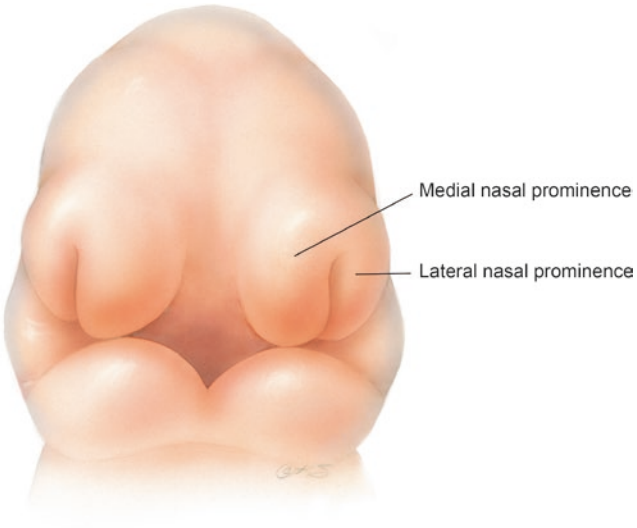


Fig. 38.3 The developing face: sixth week. Frontal view of the sixth-week embryo shows fusion of the maxillary processes to the lateral nasal groove forming the nasolacrimal furrow. The rudimentary eyes are seen laterally positioned (Adapted from Converse et al. [134])



Fig. 38.4 The developing face: seventh week. Maxillary and mandibular fusions are complete. Frontal rotation of the orbits continues. Note the prominent nasofrontal overhang (Adapted from Converse et al. [134])

of medial migration of the eyes during the seventh week of gestation (Fig. 38.4). Abnormalities in this differential growth rate may result in hypertelorism. Lower facial fissures and furrows have nearly all closed by this

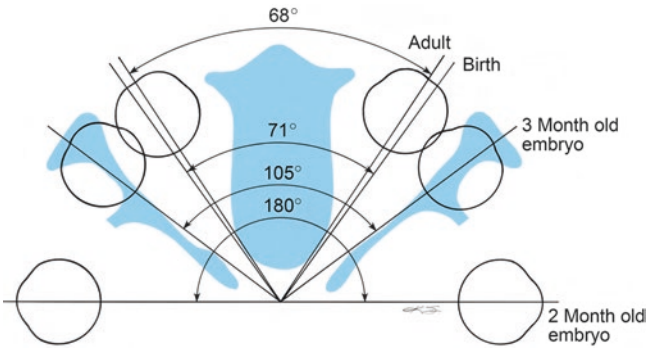


Fig. 38.5 Separation of the globes at different stages of gestation. (Modified from Fries and Katowitz [48], with permission)

time, and the maxillary processes have fused at the midline. The frontonasal process lengthens vertically as it collapses horizontally, forming a transverse furrow at the bridge of the nose. The eyelids appear as ridge-like elevations and begin the enlargement process that leads to fusion.

By the eighth week of gestation, the face has taken on a human appearance. The nares are oriented anteriorly. The eyes are still relatively widely spaced and will continue their medial migration until approximately 4 months gestation. The angle of exorbitism will slowly decrease during gestation and will continue to narrow even after birth and into adulthood (Fig. 38.5). The eyelids fuse at weeks 9–10 and reopen at weeks 25–26. The nasal bridge develops between 8 and 12 weeks, with reorientation of the nares from anterior to caudal. Elongation and growth will proceed from this point forward, but the major architecture of the face is in place by the end of this early fetal period.

An appreciation of the development of the bony skull is also critical to understanding congenital craniofacial deformities. The developing skull has two major components: the cranial base and calvarium. The calvarium arises from neural crest mesoectodermal cells, which condense on the cartilaginous precursors of the crista galli, lesser wings of the sphenoid, and petrous ridges. Beginning in weeks 5–6, these sites give rise to the dura mater which rapidly grows to surround the enlarging brain [1] (Fig. 38.6). These dural sheets meet and determine the sites of the cranial sutures, which are kept open to allow for intracranial expansion (Fig. 38.7). The bone of the cranium arises from osteoblastic centers at dural sutural condensations. Premature fusion, or synostosis, occurs when this process of intentional patency fails, resulting in the head deformities characteristic of the craniosynostoses (Figs. 38.8 and 38.9).

The second major component of the developing cranium is the cranial base. Neural crest mesoectoderm gives rise to basal cartilages that flank and eventually surround the notochord. The alisphenoid, orbitosphenoid, and prechordal cartilages develop into the sphenoid, zygomatic, temporal, and ethmoid bones (Fig. 38.6). Premature fusion of the cranial base sutures can result in reduced midfacial growth and shallow orbits, particularly with sphenozygomatic and sphenoethmoidal synostosis. The prechordal cartilage also gives rise to the nasal septum. Growth of the nasal septum and ethmoid sinuses allows for the collapse of the wide interorbital distance of the embryonic face.

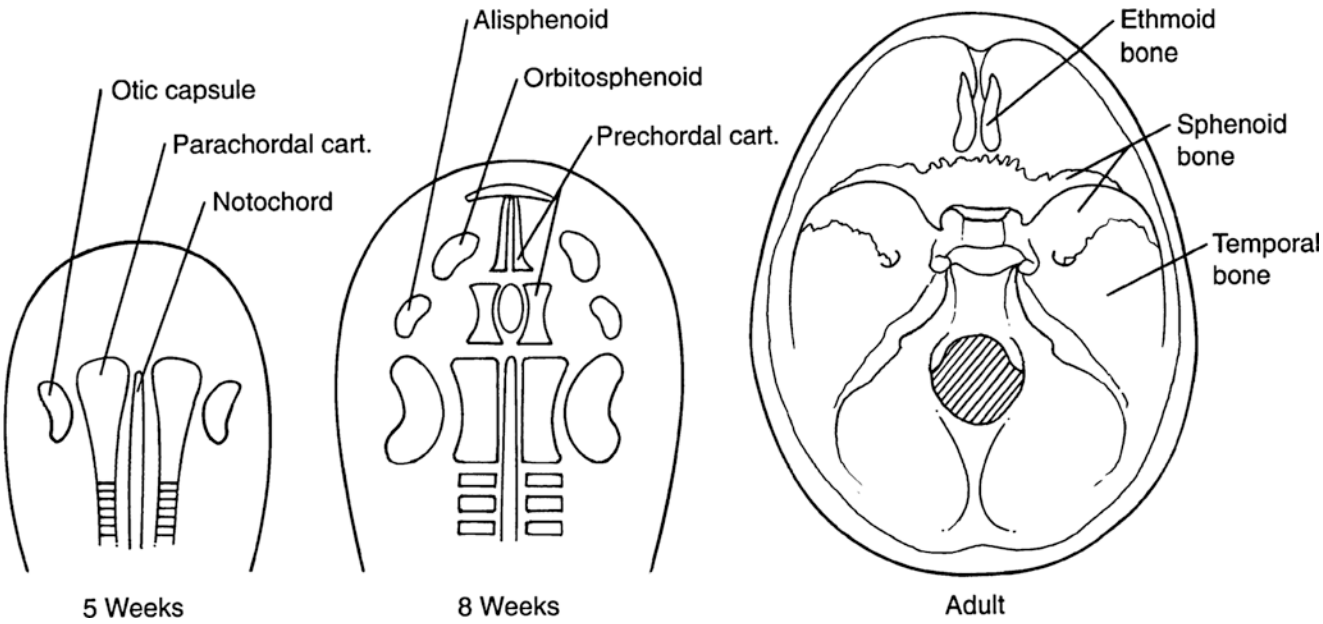


Fig. 38.6 Cranial base cartilage. Schematic representation of the cranial base cartilage at 5 and 8 weeks of gestation. The complete adult cranial base is shown at right (Adapted from Friede [135])

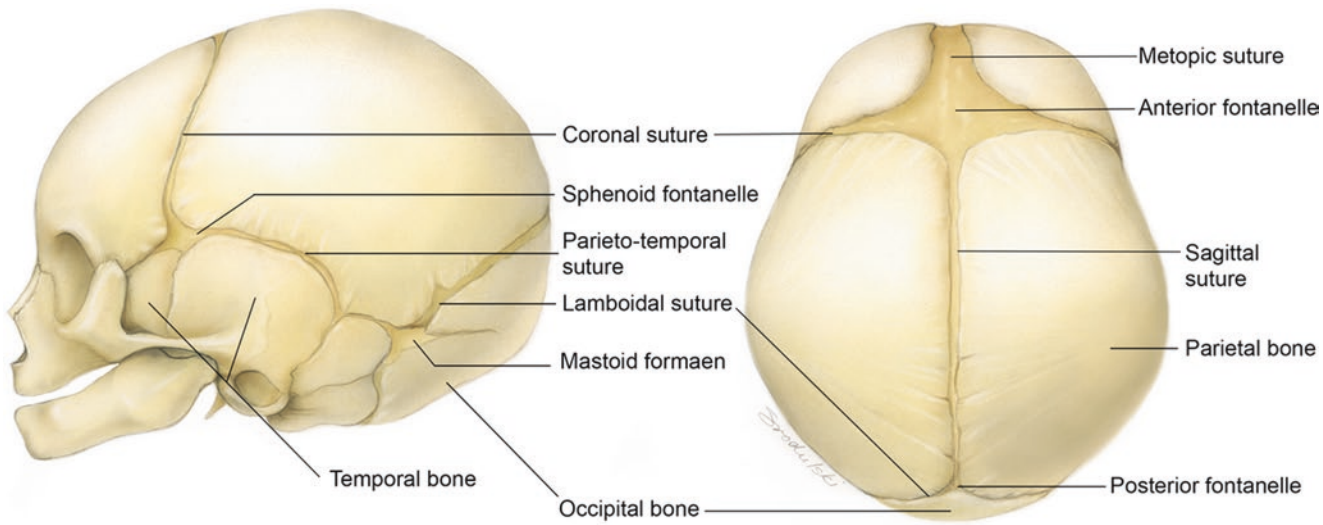
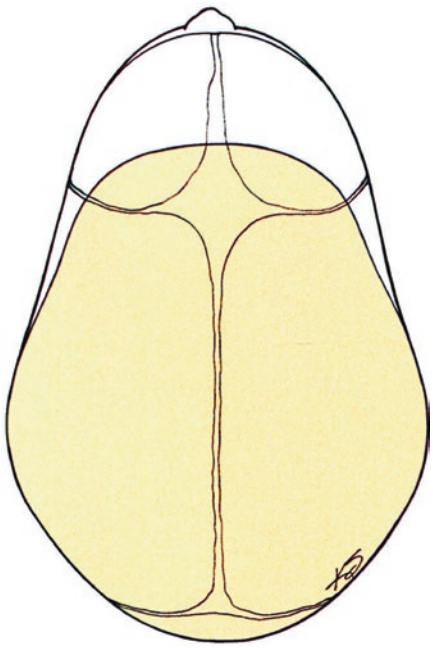


Fig. 38.7 Normal sutures and fontanelles of the fetal skull

Fig. 38.8 Scaphoid skull. An example of Virchow's law, closure of the sagittal suture produces a boat-like (scaphoid) skull shape. Normal skull appears as shaded area of drawing



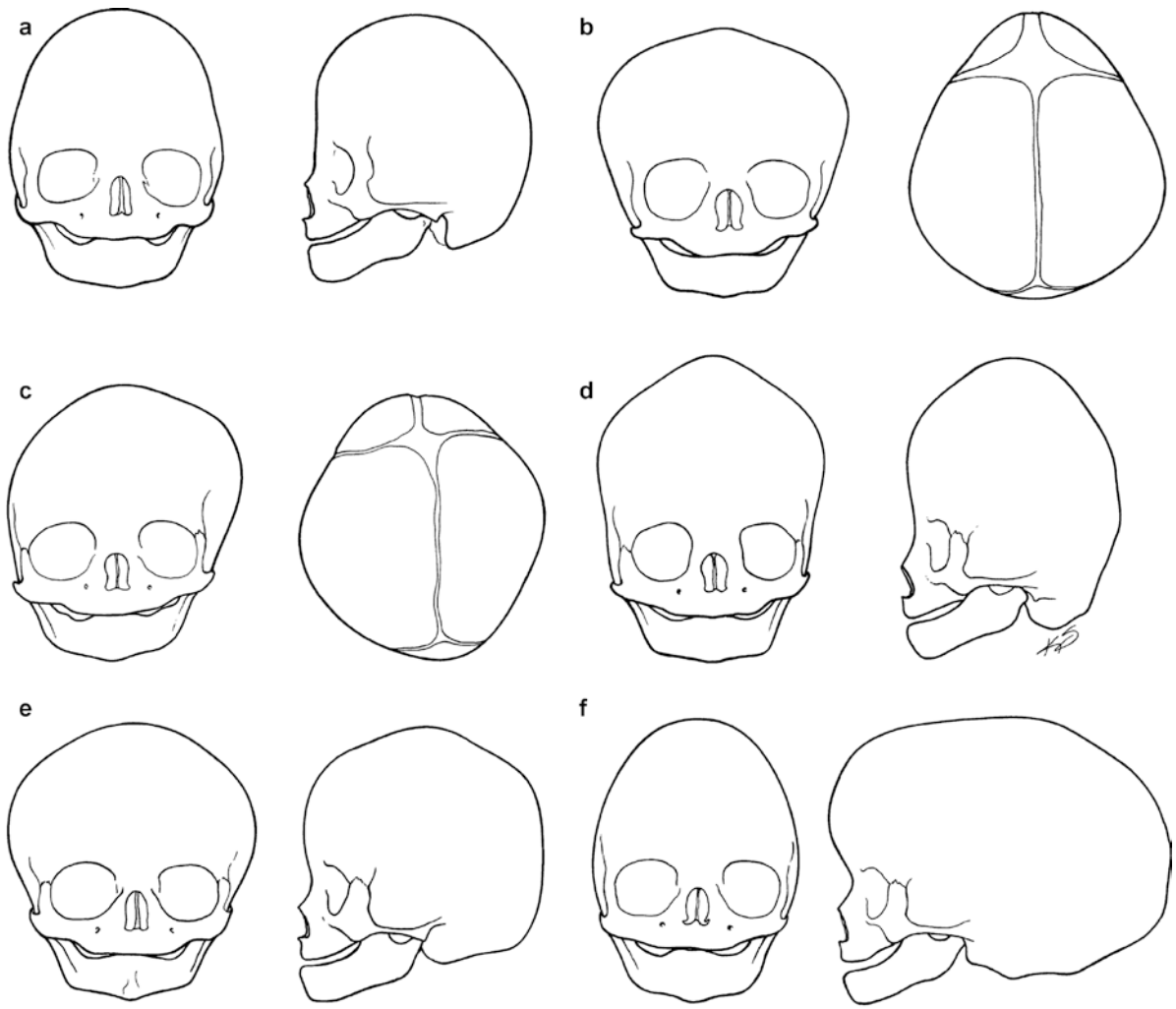


Fig. 38.9 Common calvarial abnormalities resulting from craniosynostosis: (**a**) oxycephaly, (**b**) trigonocephaly, (**c**) plagiocephaly, (**d**) acrocephaly, (**e**) brachycephaly, (**f**) scaphocephaly

Craniosynostoses

The craniosynostoses are an etiologically and pathogenetically heterogeneous group of disorders that share the common feature of premature closure of one or more of the cranial sutures (Fig. 38.7). This premature closure results in inhibition of growth in a direction perpendicular to the involved suture, with growth proceeding normally parallel to the involved suture (Virchow's law) [2] (Fig. 38.8).

Specific terms have been coined to describe the typical skull deformities associated with various synostoses (Fig. 38.9). The term *oxycephaly* was originally used as a synonym for any craniosynostosis and was thus applied to all deformities of the skull [3]. However, this term is now used to refer to multiple synostoses, usually including at least coronal and sagittal sutures. This produces compensatory upward growth of the cranium, resulting in a "tower" skull. *Brachycephaly* refers to the cranial deformity arising from bilateral coronal synostosis. This produces a shortened calvarium from front to back, with exaggerated upward growth, allowed by a patent sagittal suture. When delayed closure of the anterior fontanelle causes a pointing of the top of the skull, the term *acrobrachycephaly* is applied. *Plagiocephaly* is a term coined by Virchow to describe the bony abnormality resulting from the unilateral premature closure of the coronal suture, producing a variety of asymmetric deformities, depending on the location and extent of synostosis. Table 38.1 outlines specific cranial deformations and their respective synostotic sutures (see also Chap. 40).

Approximately 15% of patients with craniosynostosis are diagnosed with an identifiable craniosynostosis syndrome. The craniosynostosis syndromes are genetic disorders with specific inheritance patterns. For many of the dysmorphic syndromes, it is possible to find families that display a particular phenotype in either an autosomal-dominant, autosomal-recessive, or X-linked manner [4]. Non-syndromic craniosynostosis may also display a familial component, with similar suture involvement in several members of the same family [5]. With the advancement of gene mapping and cloning techniques, investigation of both the simple and complex human craniofacial dysmorphologies has expanded rapidly. Progress in molecular biology has localized the genetic defect in many families with craniosynostosis syndromes. Crouzon, Apert, and Pfeiffer syndromes have been genetically linked by mutations of the fibroblast growth factor receptor 2 gene (FGFR2) on the long arm of chromosome 10, specifically 10q25–q26 [6–12]. Even non-syndromic forms of craniosynostosis have been linked to mutations in the FGFR gene [13]. Fibroblast growth factor receptor 8, which plays an important role in outgrowth and patterning of the face, central nervous system, and extremities also maps to human chromosome 10q25–26, suggesting that some forms of acrocephalosyndactyly may involve mutations in this gene, as well [6].

Crouzon Syndrome

Crouzon syndrome accounts for approximately 4.8% of all cases of craniosynostosis, making it the most common of the craniosynostosis syndromes. The birth prevalence has been calculated to be 16.5 per 1,000,000 [14, 15]. Crouzon syndrome is inherited in an autosomal-dominant fashion. As mentioned, the defect has been mapped to several mutations of the FGFR2 gene and has thus far displayed significant genetic homogeneity [11, 16]. FGFR2 is a member of the tyrosine kinase receptor family and has a high affinity for peptides that signal the transduction pathways for embryogenesis, cellular differentiation and polarity, and mitogenesis of the developing face and skull [9, 17, 18]. In Crouzon syndrome, the FGFR2-mediated effect on the ERK-MAPK regulatory pathway may play an important role in the development of the craniosynostosis phenotype [19].

Suture involvement in Crouzon syndrome is variable; coronal and sagittal synostosis are most common, followed by lambdoidal synostosis [20]. This pattern leads to the typical features of a shortened calvarium, steep forehead, and

Table 38.1 Skull deformities arising from craniosynostosis

Deformity	Suture	Characteristics
Oxycephaly	Multiple synostoses including coronal and sagittal	"Tower skull" (turricephaly alternative term) Compensatory upward movement of the cranium
Brachycephaly	Bilateral coronal suture	Shortened calvarium front to back Upward growth allowed by patent sagittal suture
Acrobrachycephaly	Bilateral coronal with patient anterior fontanelle	Pointed top of the skull Delayed closure of the anterior fontanelle
Plagiocephaly	Unilateral coronal	Asymmetric deformity Variable depending on extent and location
Scaphocephaly	Interparietal sagittal	Elongated, narrow skull resembling the hull of a ship
Trigonocephaly	Metopic	Triangular frontal area Keel-shaped forehead
Triphyllocephaly	Lambdoidal and coronal	"Cloverleaf skull" (Kleeblattschadel) Trilobar skull with cerebral eventration through open sagittal suture and anterior fontanelle



Fig. 38.10 Patient with Crouzon syndrome. Characteristic features include brachycephaly, exorbitism, hypoplastic maxilla, low-set ears, and strabismus

flattened occiput. Acrobrachycephaly and oxycephaly are characteristic, though triphyllocephaly, or cloverleaf skull, may also occur. Midface retrusion and shallow, widespread orbits are caused by hypoplasia of the frontal, ethmoid, sphenoid, and maxillary bones. This results in the classic Crouzon phenotype of hypertelorism and exophthalmos (Fig. 38.10) [21, 22].

Of the non-craniofacial manifestations of Crouzon disease, stylohyoid ligament calcification (50%), cervical spine abnormalities (40%), and elbow abnormalities (18%) are most common. Though not associated with syndactyly, minor hand deformities are present in 10%. Other musculoskeletal and visceral anomalies are also seen [23].

Vision loss can occur for a range of reasons in Crouzon syndrome. As mentioned previously, the most common ocular findings are hypertelorism and proptosis, which, if severe, can lead to exposure keratopathy and even globe subluxation [24–26]. Other reported anterior segment findings in Crouzon patients are numerous and have included megalocornea, microcornea, keratoconus, aniridia, anisocoria, blue sclera, cataract, corectopia, ectopia lentis, glaucoma, iris coloboma, nystagmus, and optic nerve hypoplasia [27].

Optic nerve involvement, either optic atrophy or papilledema, is also a common finding, present in up to 80% of patients in a 1958 study by Bertelson [28] though more recent reports have shown a lower percentage of optic nerve involvement [22]. The etiology of optic nerve disease is not well understood. Crouzon patients with optic atrophy often have near-normal optic canal dimensions [22]. As with all the craniosynostoses, optic nerve swelling must raise suspicion for elevated intracranial pressure and headache, which may occur in up to 60% of Crouzon patients [29].

Strabismus is commonly found in Crouzon syndrome, occurring in up to 92% of those affected and can lead to amblyopia, which is the most common cause of visual impairment in these patients [15, 25, 26, 30]. Various alignment patterns have been described, including esotropia, exotropia, and hypertropia. Absent or abnormally inserting extraocular muscles, common in the craniofacial syndromes, contribute to specific strabismus patterns [31]. Absent or abnormal superior oblique muscles and excyclorotation of the orbits can result in relative overaction of the inferior oblique muscles or pseudo inferior oblique overaction, causing the common V-pattern exotropia [32]. Recently, with the use of computed topography or magnetic resonance imaging, the rectus extraocular muscles have been found to insert on the globe more laterally in Crouzon patients, which contributes to the common V-pattern exotropia. For example, if the superior rectus inserts more laterally, when it is engaged, it pulls the eye upward and outward instead of just upward [33]. Refractive errors, including significant compound astigmatism and anisometropia, are very common in this group of patients [15, 25].

While other behavioral issues related to social perceptions may develop in children with Crouzon syndrome, mental retardation is uncommon. A recent study found most children to have IQ measurements similar to a normative database [34]. Cases of impaired mental functioning may be related to damage from prior episodes of raised intracranial pressure. Seizures and structural abnormalities of the brain, such as agenesis of the corpus callosum, hypoplasia of the septum pellucidum, ventriculomegaly, and encephalomalacia, are also reported and may contribute [12].

Apert Syndrome

Apert syndrome (acrocephalosyndactyly) comprises approximately 4.5% of all cases of craniosynostosis. It has a distinct phenotype, characterized by craniosynostosis, exorbitism, midface hypoplasia, and severe, symmetric syndactyly of the hands and feet [35]. Birth prevalence, fairly uniform over different populations, has been estimated to be between 1 per 65,000 births, with an increased incidence in advanced paternal age [36–38]. Though the syndrome is inherited in an autosomal-dominant fashion, most cases present as de novo mutations (likely related to the decreased reproductive behavior in this group of patients), with the mutation rate calculated to be 7.8×10^{-6} per gene per generation [36]. In 1995, two adjacent mutations were identified in the FGFR2 gene on the long arm of chromosome 10 [10, 39]. More recently, two additional de novo mutations have been identified on the same gene [40]. As in some of the other craniosynostoses, a paternal age effect has been seen with Apert



Fig. 38.11 Patient with Apert syndrome. Characteristic features include brachycephaly with frontal overhang, "parrot-beak" nose, ptosis, strabismus, and midface retrusion. Note the high, arched palate



Fig. 38.12 Syndactyly in Apert syndrome. Hand of a child with Apert syndrome showing proximal syndactyly of digits 2 and 3, 4 and 5, and near-total fusion of digits 3 and 4

syndrome. The term "selfish spermatogonial selection" has been used to describe this association. This is characterized by the dysregulation of spermatogonial cell behavior through *RAS*-mediated pathways allowing for clonal expansion of mutant sperm in the older male population [41].

Typical features of Apert syndrome include oxycephaly, a flattened occiput, a severely hypoplastic midface, a prominent "parrot-beak" nose, hypertelorism, proptosis, strabismus, and low-set ears (Fig. 38.11). The Apert calvaria at birth is characterized by coronal synostosis and a widely gaping midline defect. The midfrontal region of the brain may not be covered with bone during early infancy, which often produces a prominent frontal pseudoencephalocele [42]. As the child matures, coalescence of bony islands closes this midline defect. The temporal bones are obliquely situated in all patients with Apert syndrome, and triphyllocephaly or cloverleaf skull is found in approximately 4% of patients [42].

Another defining feature of Apert syndrome is true megalocephaly with postmortem brain weights dramatically above the 95th percentile regardless of age [42]. Central nervous system abnormalities, including defects of the corpus callosum and limbic structures, misshapen brain, and gyral anomalies, can occur in up to 12% of patients [43, 44]. Ventriculomegaly is reported to occur in about 60% of patients, though frank increased intracranial pressure is less common. Compared to Crouzon syndrome, intelligence is more likely to be subnormal [34, 43].

The ophthalmic manifestations of Apert syndrome closely parallel those of Crouzon syndrome, although hypertelorism and proptosis are often less prominent. Elevated intracranial pressure can occur in up to 83% of patients, with secondary papilledema and/or optic nerve pallor [45]. Extraocular muscle anomalies have been described, which contribute to strabismus and amblyopia [32, 46]. Refractive error, including astigmatism, is also common [47]. Less common ophthalmic findings include keratoconus, ectopia lentis, congenital glaucoma, and oculocutaneous albinism [47–49].

The associated orthopedic findings make Apert syndrome unique among the craniosynostoses. Syndactyly of the hands typically presents as a mid-digital mass involving the second, third, and fourth digits with variable proximal interdigital syndactyly (Fig. 38.12). The first and fifth digits are variably involved. A foot deformity in Apert syndrome is very characteristic and predictable, with progressive synostosis on what is presumably an unsegmented cartilaginous mass. Medial deviation of the great toe, fusion of the two phalanx digits, and progressive fusion of the midfoot and hindfoot in a supinated position are all characteristic [50]. Other orthopedic manifestations can be present and contribute to progressive loss of joint motion [51–53].

A range of other problems can occur in Apert syndrome. Oropharyngeal manifestations are frequently severe and can include a characteristic trapezoidal-shaped mouth with a Byzantine-arch-shaped palate (Fig. 38.11). Cleft soft palate and bifid uvula have been reported in 30–75% [54, 55]. Midface hypoplasia is also common and can lead to difficulty with intubation during general anesthesia, as well as generalized breathing issues and obstructive sleep apnea [56]. Dental anomalies include delayed tooth eruption, ectopic tooth eruption, severe bite malocclusion, and crowding of teeth. Cardiovascular and genitourinary anomalies occur in around 10% of those affected [57]. Apert patients also often develop severe acne in adolescence, which is thought to occur from abnormally sensitive androgen receptors [58] (Fig. 38.13).

Pfeiffer Syndrome

Pfeiffer syndrome is generally inherited in an autosomal-dominant fashion, although it can less commonly occur sporadically. It is thought to occur in about 1 in 70,000 live births [59]. Similar to other acrocephalosyndactyly syndromes, Pfeiffer syndrome is caused by mutations in the FGFR gene family, specifically FGFR2 gene on chromosome 10 and FGFR1 gene on chromosome 8 [60]. These mutations are thought to cause premature ossification of the cranial sutures secondary to dysregulation of osteoblast and chondrocyte differentiation [61–63]. Interestingly, identical genotypic mutations of FGFR 2 have been identified in Crouzon syndrome, which is quite phenotypically distinct from Pfeiffer syndrome, suggesting that there may be other factors involved in phenotypic presentation of these conditions [63]. Alternatively, Pfeiffer and Apert syndromes are clinically similar, but genetically very distinct. There is also some phenotypic overlap with Muenke syndrome, although Muenke is caused by FGFR3 mutations.

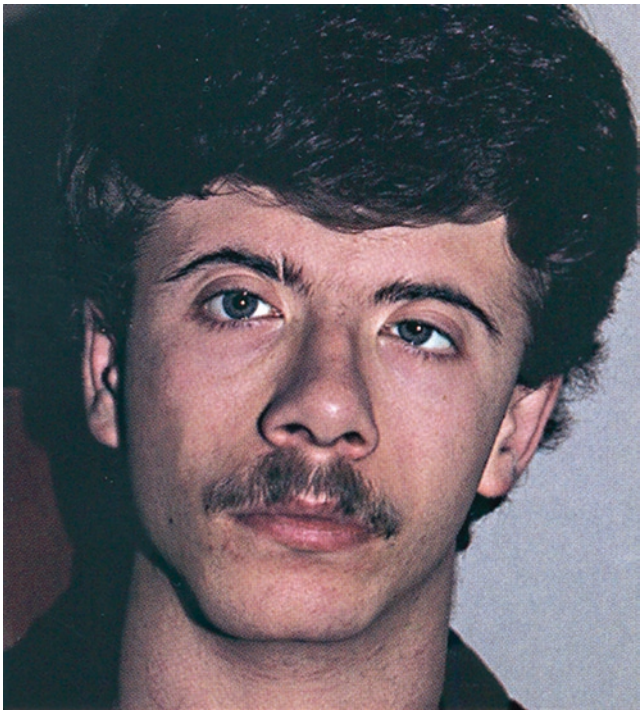


Fig. 38.13 Patient with Saethre–Chotzen syndrome. Characteristic features include low-set hairline, ptosis, strabismus, mild facial asymmetry, and low-set ears

Patients with Pfeiffer syndrome have premature fusion of the coronal and lambdoid sutures and occasionally the sagittal sutures. In more severe phenotypes, a cloverleaf skull can develop. Hydrocephaly, seizures, and, less commonly, mental retardation/developmental delay may accompany synostosis. The characteristic facial appearance is a very wide head with flat occiput, high forehead, small nose with a low nasal bridge, and hypertelorism [64]. Midface hypoplasia is common with associated maxillary hypoplasia, highly arched palate, malocclusion, and crowded teeth. These features may contribute to breathing difficulties and increase risks with general anesthesia. Patients have broad and deviated thumbs and first toes, often with partial syndactyly on the hands and feet (Fig. 38.14).

Ocular findings in Pfeiffer syndrome can be similar to Crouzon syndrome, with moderate-severe proptosis, hypertelorism, and lateral canthal dystopia. Papilledema can occur with raised intracranial pressure. More recently, it has

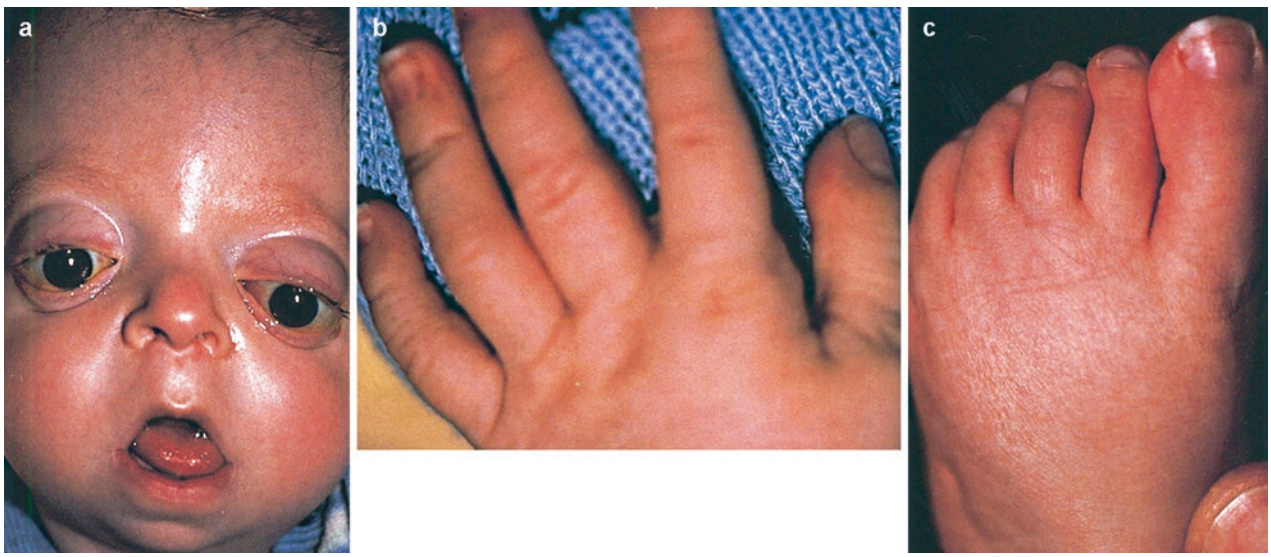


Fig. 38.14 Patient with Pfeiffer syndrome. (**a**) Clinical photograph demonstrating exophthalmos, hypertelorism, small mandible, "parrot-beaked" nose, recessed supraorbital ridges, and increased forehead height. (**b**) Enlarged thumb of same patient. (**c**) Broad, long great toe

become apparent that FGFR mutations in Pfeiffer syndrome may also play a role in anterior segment development, with one patient recently found to have microcornea, limbal sclerotization, corectopia, and glaucoma. Thus, close anterior segment examinations are also important with regular intraocular pressure monitoring [65].

Based on phenotype severity, Pfeiffer syndrome has been divided into three clinical subtypes. Type 1 or "classic" Pfeiffer syndrome is characterized by individuals with relatively mild manifestations including brachycephaly, midface hypoplasia, and finger and toe abnormalities. It is usually associated with normal neurologic development and with either FGFR1 or 2 mutations. Type 2 consists of a "cloverleaf skull," extreme proptosis, skeletal abnormalities, and developmental delay. Type 3 is similar to type 2, but without the cloverleaf skull. Both types 2 and 3 have an increased risk of death due to severe neurological and respiratory impairment. These types are more often associated with FGFR2 mutations. There can be significant clinical overlap between clinical subtypes, making characterization difficult [64].

Saethre–Chotzen Syndrome

Saethre–Chotzen syndrome (acrocephalosyndactyly, type III) is a heterogeneous, autosomal-dominant disorder characterized by craniosynostosis, facial dysmorphism, and mild limb abnormalities (Fig. 38.13) [66]. In 1997, it was found to be associated with mutations in the *TWIST1* gene on chromosome 7p21–22 [67]. The *TWIST1* gene functions in mesenchymal signaling during embryogenesis. Mutations in the *TWIST1* gene are thought to lead to genomic haploinsufficiency, which causes uncontrolled receptor signaling and changes cranial skeletal development, ultimately leading to premature cranial suture closure [68, 69]. With the ability of genotypic diagnosis, many patients previously diagnosed with Saethre–Chotzen have actually been re-characterized as having a Muenke craniosynostosis from an FGFR3 mutation (see next section for a more detailed discussion of Muenke syndrome) [70, 71]. Since its discovery, over 100 TWIST1 mutations have been identified. Not surprisingly, as a result of the variety of TWIST1 mutations, there is significant variability in the Saethre–Chotzen phenotype [72].

Because of its heterogenous phenotype, Saethre–Chotzen is particularly challenging to diagnose clinically. As illustrated above, genetic testing is an important tool for definitive diagnosis. Classic features include a low frontal hairline, prominent crus helicis (ear anomaly), and syndactyly of the index and middle fingers. Brachydactyly and clinodactyly can also occur. While bilateral coronal craniosynostosis is the most common suture anomaly, not all patients with Saethre–Chotzen have craniosynostosis [66, 73, 74]. Recently, a unique pattern of craniosynostosis has been described in these patients involving fusion of the metopic, bicoronal, and anterior sagittal sutures, which has been termed "peace sign synostosis" [75]. Unlike in Apert, Crouzon, and Pfeiffer syndromes, midface hypoplasia is rare in Saethre–Chotzen [74, 75].

Similar to Apert syndrome, a highly arched palate, cleft palate, and dental anomalies can occur. A depressed nasal bridge can be found. Intelligence is frequently normal, although some degree of cognitive limitation, schizophrenia, and/or seizure disorder have been described [76]. The ears are small and low set, and hearing may be diminished [74, 77, 78].

Ophthalmic features in Saethre–Chotzen syndrome differ from the other craniosynostoses. Upper eyelid ptosis is much more common, occurring in up to 90% of patients. There may also be downward slanting of the palpebral fissures [74]. Proptosis and hypertelorism are not prominent features. Lacrimal duct stenosis and tearing can occur [79]. Strabismus is common and present in over half of patients. Other variable features include refractive error (usually myopia and/or astigmatism) and optic atrophy [74].

Muenke Syndrome

Muenke syndrome was first described in 1996. Since then, many patients who were thought to have Saethre–Chotzen syndrome have been re-characterized as having Muenke syndrome by genetic testing [80]. It is inherited in an autosomal-dominant fashion and is characterized by a mutation in the FGFR3 gene [81]. Of all patients with genetically confirmed craniosynostosis, 25–30% are thought to have Muenke syndrome [82]. With an incidence of 1 in 30,000 live births, it now constitutes the most common craniosynostosis syndrome.

The Muenke phenotype is heterogenous, with some patients having no clinical features, some having only craniosynostosis, and others having presentations that overlap with other craniosynostosis syndromes (i.e., Crouzon, Saethre–Chotzen, or Pfeiffer). It is characterized by uni- or bilateral coronal synostosis, broad toes, and carpal and calcaneal fusions [83]. The characteristic facial features include a flat forehead, elevated or depressed eyebrows, anterior displacement of the ears, and deviation of the nasal root. Bilateral coronal synostosis usually results in brachycephaly, but turribrachycephaly ("tower shaped" skull) or a cloverleaf skull can also be observed. Macrocephaly without craniosynostosis can occur. Again, there may be no synostosis at all.

Other variable features, similar to those seen in the craniosynostoses that also evolve from FGFR mutations include intracranial anomalies, midface hypoplasia, a highly arched palate, cleft lip/palate, sensorineural hearing loss, skeletal

abnormalities, brachydactyly (short fingers/toes), broad thumbs/toes, and syndactyly. Patients may be developmentally normal or may have mental retardation, developmental delay, or epilepsy. Up to 30% of affected individuals may have some degree of developmental delay [71, 81].

Ophthalmic manifestations are highly variable. Affected individuals can have hypertelorism, telecanthus, lateral canthal dystopia, and ptosis. Proptosis, unlike in Crouzon and Pfeiffer syndromes, is rare. Strabismus is the most common ocular finding in Muenke syndrome. Anisometropia can also occur. As such, amblyopia is not uncommon. Similar to the other craniosynostoses, optic nerve damage can occur from occult-raised intracranial pressure [84].

Carpenter Syndrome

Carpenter syndrome is a rare, autosomal-recessive condition with an incidence of 1 per 1 million live births [85]. It is characterized by brachycephaly and a classic cloverleaf-shaped skull, but distinguishable from some of the other craniosynostosis syndromes based on the presence of syndactyly, polydactyly, and an autosomal-recessive inheritance pattern. It has been mapped to a mutation in the *Ras*-like in rat brain 23 (RAB23) gene on chromosome six. This gene plays an important role in sonic hedgehog signaling pathways during embryogenesis [86].

Craniofacial abnormalities in Carpenter syndrome include shallow supraorbital ridges, micrognathia, midface hypoplasia, external ear malformations, depressed nasal bridge, and an upturned nose. In order of decreasing frequency, the sagittal, metopic, coronal, and lambdoid sutures are most commonly affected [87]. Most patients have some degree of intellectual disability [86]. Furthermore, over half of those affected will have some form of central nervous system abnormality. Increased intracranial pressure can occur with secondary hydrocephalus. Congenital heart disease, hypogenitalism, obesity, and umbilical hernia are associated [88].

The ocular findings of Carpenter syndrome are less well defined due to the rarity of the disease, though hypertelorism with relative telecanthus and epicanthal folds have been described in most cases [89].

Clefting Syndromes

The second major group of craniofacial abnormalities falls under the umbrella of clefting syndromes. The clefting syndromes encompass a wide variety of disorders from complex malformations involving the whole head to more subtle defects in apposition of junctional facial structures. Clefts



Fig. 38.15 Facial clefting. Patient illustrating a midline facial cleft affecting the lip and nostril, possibly due to failure of the maxillary process to fuse

may arise as part of a recognizable syndrome (e.g., Treacher–Collins) or in non-syndromic forms. The origin of facial clefting is not well understood, and there may be different factors involved depending on the cleft type. Two major mechanisms have been proposed. The first is that a failure of fusion occurs between the embryologic facial processes, resulting in true or primary clefts. This type of clefting is restricted to the following borders: lateronasomaxillary clefting (naso-ocular clefts), medionasomaxillary clefting (cleft lip), intermaxillary clefting (cleft palate), and maxillomandibular clefting (macrostomia) [3] (Fig. 38.15). The failure of fusion is thought to arise from deficient epithelial cell degeneration with inappropriate persistence of epithelium between the borders of the facial processes. The second major proposed mechanism relates to a failure of mesodermal migration to fill the facial processes, resulting in structural collapse and epithelial dehiscence. Other theories of cleft formation have included failure of neural crest cell migration, failure of neural crest cell degeneration, and/or failure of ossification (producing "pseudo-clefts" not associated with true facial sutures) [90–93].

Facial clefting may arise as the result of a single gene defect, either as part of a syndrome (e.g., Treacher–Collins, velo-cardio-facial syndrome) or as an isolated phenotypic effect (X-linked cleft palate with ankyloglossia, autosomal-dominant orofacial clefting) [94]. Both trisomy 13 and 18 are associated with clefting [95]. Cleft lip, cleft palate, and atypical facial clefting have been reported to be associated with maternal use of cocaine [96], antiepileptic drugs [97], and benzodiazepines [98]. Clefting has been induced in animal models with administration Dilantin, corticosteroids, 6-aminonicotinamide, and retinoids, which cause a first and second branchial arch syndrome in rats [99].

Regional Classification of Clefts Affecting the Orbital Adnexa

Paul Tessier's classification of the craniofacial clefts, introduced in 1976, remains the most widely accepted and universally recognized means of describing the location of facial clefting. It is a topographic, not a pathogenetic, classification scheme. As seen in Fig. 38.16, Tessier's system divides the face vertically through the midline, assigning the number 0 to the lower facial midline and the number 14 to the upper facial midline. Each major cleft is assigned a number, progressing in a clockwise manner about the orbit on the right side of the face and in a counterclockwise manner on the left [100]. Each cleft may involve both soft tissue and underlying bony skeleton.

To better clarify the ophthalmic consequences of the clefting syndromes, Fries and Katowitz grouped the orbital clefts into four regional categories progressing from medial to lateral, as outlined in Table 38.2 and Fig. 38.17 [48].

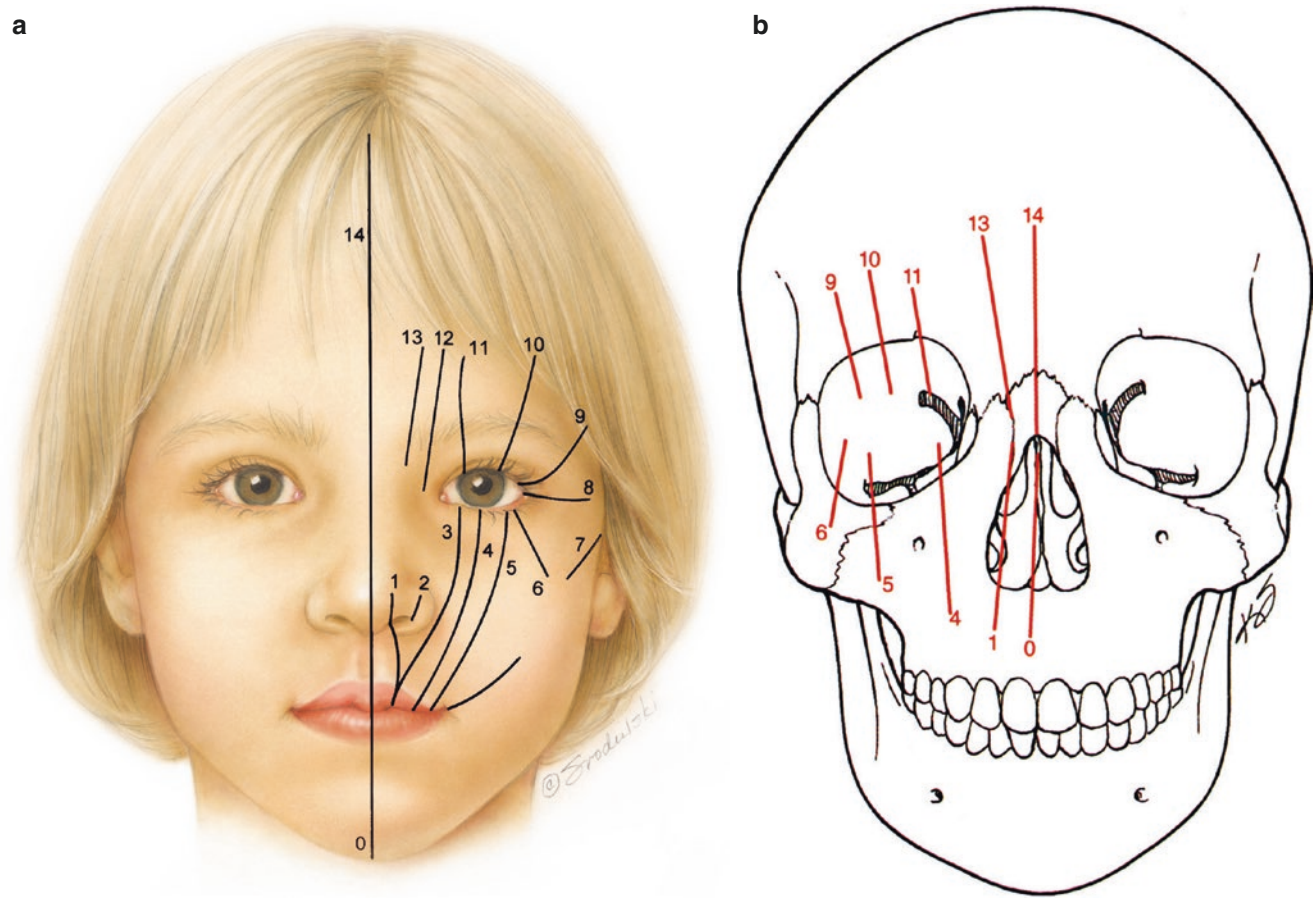


Fig. 38.16 Tessier's clockface system. Numbers progress clockwise for the left eye and counterclockwise for the right eye. (**a**) Soft-tissue clefts. (**b**) Bony clefts (Adapted from Tessier [100])

Table 38.2 Regional classification of orbital adnexa in the clefting disorders

Region	Presentation	Tessier clefts
Area 1		
Median facial clefts	Hypertelorism	0, 1, 13, 14
Area 2		
Medial canthal and nasolacrimal clefts	Median canthal dystopia	2, 3,4
	Nasolacrimal disorders	11, 12, 13
Area 3		
Central eyelid clefts	Colobomatous defects	4, 5, 6, 9, 10, 11
Area 4		
Lateral canthal clefts	Lateral canthal dystopia	6, 7,8

Source: From Fries and Katowitz [48], with Permission

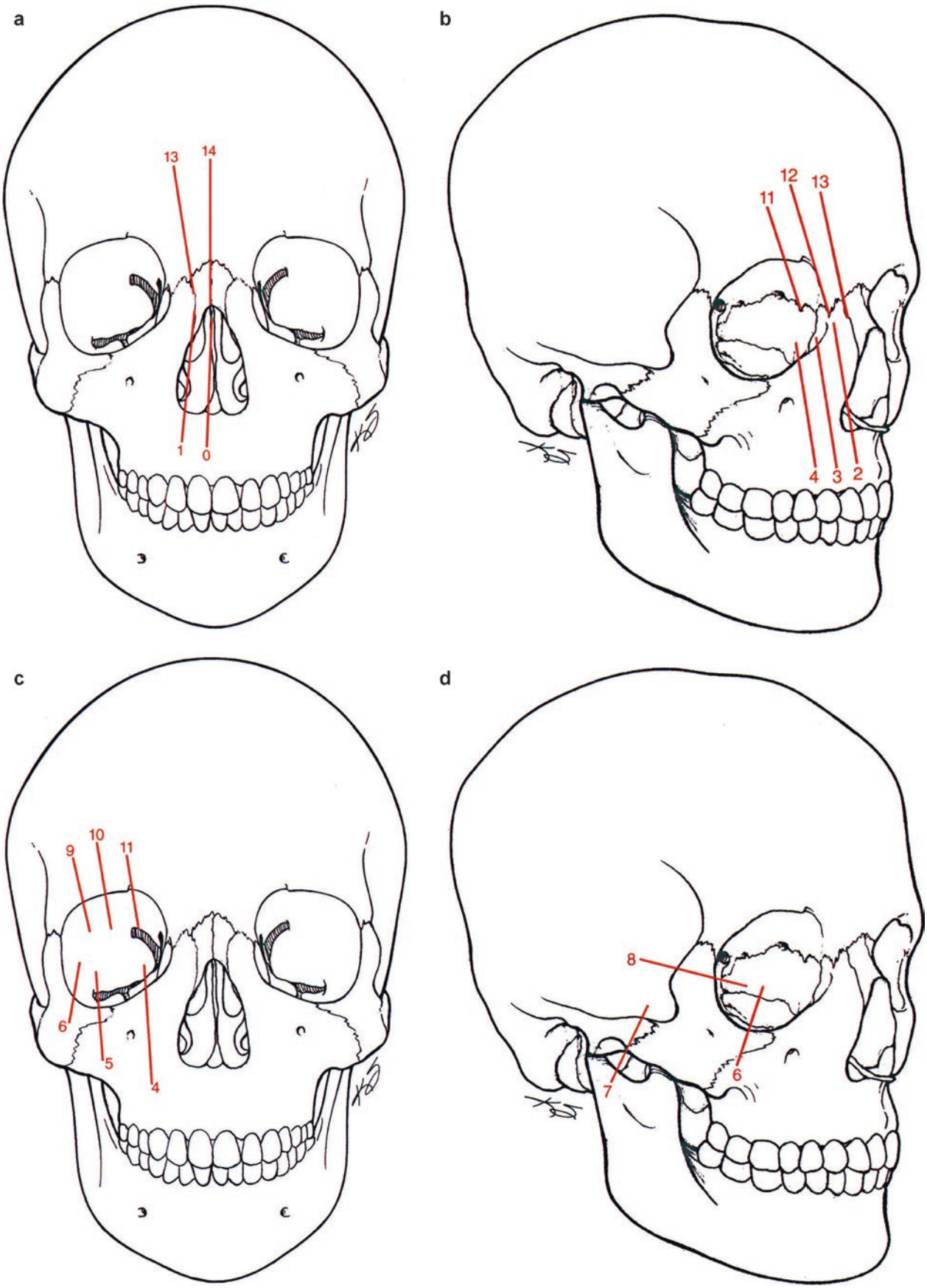


Fig. 38.17 Regional classification of the facial clefts. (**a**) Area I: median cleft positions. (**b**) Area II: medial canthal and nasolacrimal cleft positions. Note relation to punctum and infraorbital foramen for cleft number 4. (**c**) Area III: eyelid cleft positions. (**d**) Area IV: lateral canthal and facial cleft positions (Adapted from Fries and Katowitz [48])



Fig. 38.18 Regional classification: Area l. Midline facial Tessier numbers 0–14 demonstrating cleft hypertelorism, frontal encephalocele, and bifid nose

Area I: Median Facial Clefts

Midline facial clefts vary in severity (Fig. 38.18). The primary manifestation of this group of clefts (0, 1, 13, 14) is orbital hypertelorism. Hypertelorism associated with midline clefts, labeled by Tessier as the 0–14 clefting syndrome, is more commonly known as median craniofacial dysraphia or the median facial cleft syndrome [101]. Features of this syndrome include hypertelorism; midline facial cleft involving the nose, lip, and sometimes the palate; broadened nasal root; lack of formation of the nasal tip; bifid anterior cranium; and widow's peak. Fourteen clefts involving the upper midface but sparing the lower face can sometimes produce the syndrome of frontal encephalocele or giant pneumatization of the frontal sinus. This cleft allows herniation of the frontal lobes through the area of the frontal sinus and is characterized by a widened forehead, hypertelorism, and widely spaced eyebrows. Paramedian clefts (numbers 1 and 13) generally occur unilaterally and produce asymmetric hypertelorism through lateral displacement of the orbit on the affected side.

Area II: Medial Canthal and Nasolacrimal Clefts

The naso-ocular clefts (Tessier numbers 2, 3, 11, and 12) may produce varying degrees of hypertelorism, generally of lesser severity than the midline clefts (Fig. 38.19). Telecanthus, medial canthal dystopia, and nasolacrimal abnormalities are



Fig. 38.19 Regional classification: Area II. Medial canthal/nasolacrimal patient with micrognathia, telecanthus, absent nostril, and nasolacrimal system on the right



Fig. 38.20 Patient with Tessier cleft number IV. Cleft involves the left maxilla, lid, and oral cavity, possibly secondary to pressure necrosis a swallowed amniotic band

characteristic. The lower face clefts (Tessier cleft numbers 2, 3, and 4) are more common than the upper face clefts (numbers 10, 11, and 12), which generally only occur paired with their lower face counterparts (e.g., the 4–10, 3–11, or 2–12 cleft pairs).

Cleft number 2 is the most medially located, producing hypertelorism, medial maxillary bone involvement (often with distal nasolacrimal duct obstruction), and a moderate degree of canthal dystopia. Cleft number 3 lies along the embryonic lateral nasal groove and presents with nasal alar colobomas, more severe medial canthal dystopia, nasolacrimal disturbance, and variable ocular involvement. Nasolacrimal disturbance is often severe, involving both the upper and lower systems. A 3–11 cleft pair adds the features of medial 1/3 upper eyelid coloboma and a dysplastic forehead with inferior eyebrow displacement.

Cleft number 4 may produce features of both regional area 2 (medial canthal/nasolacrimal group) and regional area 3 (lid group) (Fig. 38.20). Severe clefting results in lower



Fig. 38.21. Regional classification: Area III. Tessier clefts 10, 11 affecting the upper lid and superior orbital rim



Fig. 38.22 Regional classification: Area IV. Lateral clefts Tessier 6, 7, 8. Note auricular deformities

eyelid abnormalities, medial canthal dystopia, and canalicular disruption. Milder clefting often spares the medial canthus and lacrimal system, producing only a medial lower eyelid coloboma.

Area III: Eyelid Clefts

The eyelids are primarily affected by Tessier cleft numbers 4, 5, and 6 inferiorly and numbers 9, 10, and 11 superiorly (Fig. 38.21). These clefts may be associated with the clinical description of partial cryptophthalmos. Cleft number 5, which runs from just medial to the corner of the mouth to between the middle and lateral third of the lower lid, is usually seen in association with an upper cleft number 9 [102]. The number 5 cleft produces a deep V-shaped coloboma, with the lower eyelid being pulled into the cleft line. The corner of the mouth is likewise displaced superiorly toward the cleft. The globe is frequently microphthalmic or anophthalmic, and the orbital contents may prolapse into the maxillary sinus through an absent orbital floor.

Area IV: Lateral Canthal Clefts

Cleft 6 may be grouped with both the lid regional group and the lateral canthal group (Fig. 38.22). Cleft 6 does not have an oral component and involves the lateral part of the lower lid and underlying malar eminence. The bony defect results in lateral canthal dystopia and hypoplasia of the lateral lid structures, producing the pseudocoloboma characteristic of Treacher–Collins syndrome.

Cleft number 7 crosses the zygomatic arch as it runs from the corner of the mouth across the lower cheek, inferior and lateral to the orbit (Fig. 38.22). Auricular tags, ear deformities, mandibular and maxillary hypoplasia, parotid, tongue, and soft palate hypoplasia can be present in severe forms [103]. Maxillary and zygomatic deformity results in lateral canthal dystopia, and the trigeminal and facial nerves may be affected.

Cleft 8 runs from the frontozygomatic suture to the lateral canthal angle, usually causing a true lateral canthal coloboma with fusion of the lid defect to the underlying conjunctiva (Fig. 38.22). The 6, 7, and 8 clefts are often associated with a spectrum of findings that can be classified into syndromes.

Clefting Syndromes

A significant number of the recognizable clefting syndromes involve clefts 6, 7, and 8, which together, with other distinguishing abnormalities, are represented in the syndromes of Goldenhar, Treacher–Collins, and hemifacial microsomia. Also discussed here is the phenomenon of amniotic band disruption, which is thought to be a purely mechanical cause of clefting.

Treacher–Collins Syndrome

In 1949, Franceschetti and Klein suggested a classification scheme for Treacher–Collins syndrome separating affected patients into five categories (see Table 38.3). In some parts of the world, it is even referred to as Franceschetti–Klein syndrome. Tessier was the first to recognize that the condition was associated with facial clefting, specifically complete or incomplete number 6, 7, and 8 clefts [100]. Treacher–Collins syndrome (mandibulofacial dysostosis) is an autosomal

Table 38.3 Classification of Treacher–Collins syndrome

Form	Clinical characteristics	Tessier clefts
Complete	Nearly all typical features	6: Orbital: eyelid pseudocoloboma, bony hypoplasia of the zygomaticomaxillary suture 7: Temporal, zygomatic, and maxillary bony hypoplasia, macrostomia, ± soft palate, tongue abnormality 8: Fronto-zygomatic suture: zygomatic hypoplasia, oblique palpebral fissures
Incomplete	Less severe and extensive	6: As above
Abortive	Lower lid pseudocoloboma Zygoma hypoplasia	Variable
Unilateral	Limited to one side of the face	Unilateral, varying severity
Atypical	Incomplete form with atypical features	Variable

Source: Adapted from Franceschetti and Kline [68]



Fig. 38.23 Treacher–Collins syndrome. Photograph of a patient with features typical of Treacher–Collins syndrome

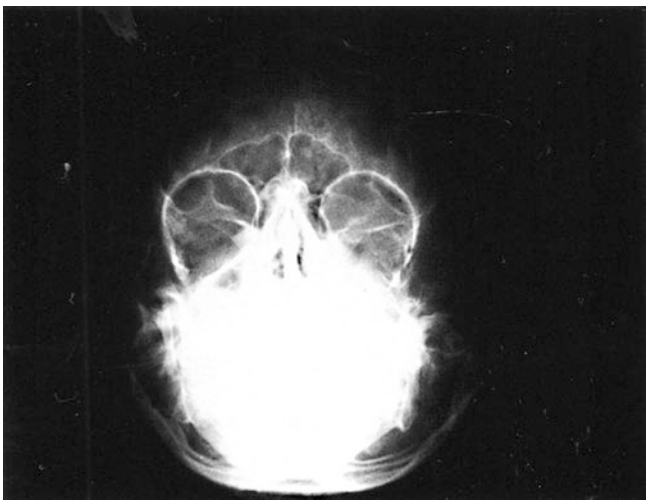


Fig. 38.24 Treacher–Collins syndrome. Same patient as in Fig. 38.23, demonstrating bony defects

dominant clefting syndrome with variable penetrance and expression. Its incidence is about 1 in 50,000 live births [104]. The gene responsible for Treacher–Collins syndrome has been localized to the long arm of chromosome 5 (5q32–33.2.) [105–108]. While other genetic mutations have been implicated, TCOF1 mutations occur in over 93% of cases. Mutations can occur in an inherited fashion or de novo. The TCOF1 gene product, Treacle, is thought to be involved in neural crest cell signaling during embryogenesis of the head and neck, specifically of the first and second branchial clefts [109]. Loss-of-function mutations in TCOF1 lead to neuroepithelial and neural crest apoptosis that produces the Treacher–Collins phenotype [110].

The major features of Treacher–Collins syndrome are external ear malformations, conductive hearing loss, hypoplastic zygoma, lateral canthal dystopia with an antimongoloid slant of the palpebral fissures, pseudocoloboma or true coloboma (usually of the lateral lower eyelid), flattening of the nasofrontal angle, micrognathia with macrostomia, abnormal dentition, and malocclusion [111]. The flattened nasofrontal angle, together with macrostomia and receding chin, produces the characteristic bird- or fishlike facies of the Treacher–Collins patient (Fig. 38.23). Additional reported abnormalities include cleft palate and sinus (Fig. 38.24), orbital hypoplasia, strabismus, cataract, distichiasis, high myopia, dermolipoma, and lens subluxation [112–115].

The most salient ophthalmic findings in Treacher–Collins syndrome are the significant lid and adnexal abnormalities present in the majority of patients [116]. Subnormal horizontal palpebral fissure length and lateral canthal dystopia with inferomedial displacement of the lateral canthus (producing pseudocoloboma) is most commonly encountered. Medial displacement of the lateral canthus with forced eyelid closure and resultant shortening of the horizontal fissure (fissure narrowing sign) has been described [75]. With normal interorbital distances, these patients do not commonly have hypertelorism. Other eye findings include partial thickness eyelid coloboma of the nasal half to two-thirds of the lower lids, absence of the inferior lacrimal puncta, lacrimal duct atresia, distichiasis, hypoplasia of lashes over the medial two-thirds of the lower eyelid, and orbital hypoplasia. Refractive errors usually include anisometropia and regular astigmatism, which generally occurs without any consistent orientation of the axis relative to the lower lid defect [116, 117]. Microphthalmos, strabismus, cataract, high myopia, dermolipoma, and lens subluxation may also occur.

Oculo-Auriculo-Vertebral Spectrum

Goldenhar first described a syndrome in 1952 that consisted of epibulbar dermoids, preauricular appendages, and mandibular hypoplasia. Gorlin and colleagues later expanded this to the "oculo-auriculo-vertebral spectrum" [104]. Oculo-auriculo-vertebral (OAV) spectrum can present with a high degree of phenotypic variation. The mildest form may be characterized by unilateral microtia and/or pre-auricular skin tags, which are commonly referred to as hemifacial microsomia. At the other end of the spectrum is Goldenhar syndrome, which is thought of as a more severe expression involving microtia with mandibular hypoplasia, cervical spine anomalies, and/or epibulbar dermoids.

The genetics of OAV spectrum are not well understood. While most cases are sporadic, a genetic predisposition has been proposed based on growing evidence in the literature [118]. Several chromosomal abnormalities have been identified in different cohorts of patients including deletions of 5p15, 12p13.33 (WNT5B gene), 14q23.1, and 22q [119]. Environmental factors have also been proposed in the development of Goldenhar syndrome including maternal diabetes during pregnancy, thalidomide, vasoactive drugs, and smoking. Vascular disruption, in particular, is thought to play a possible role due to increased prevalence in twin conceptions [120]. Similar to Treacher–Collins syndrome, it is thought to be a disorder of craniofacial morphogenesis involving the first and second branchial arches. However, it is much more common, affecting 1 in 3500 live births [121]. The Goldenhar subset accounts for 4–10% of OAV spectrum. One proposed mechanism of Goldenhar syndrome is thought to be related to disturbances in the behavior and migration of cranial neural crest cells [122].

Hemifacial microsomia typically affects the right side of the face, although it can occur bilaterally with one side more severely affected (Fig. 38.25). The mandibular deformity is thought to be a defining feature. Some cases are relatively mild with only minimal trouble with mouth opening on the affected side and normal radiographic jaw appearance. Other cases are much more severe with mandibular and/or temporal bone hypoplasia. This may be accompanied by varying degrees of hypoplasia of the muscles of mastication on the affected side. There are varying degrees of ear deformities (or microtia). In addition to external ear deformities, there are often middle and inner ear abnormalities with associated hearing loss (although complete deafness is uncommon). Approximately 15% of cases may have associated vertebral anomalies, including fused or absent vertebrae. Rarely, there is a facial nerve palsy on the affected side, which may be correlated with the severity of ear abnormalities. Palate and dental anomalies are also common.

The typical features of Goldenhar syndrome include corneoscleral dermoids, orbital dermoids or lipodermoids, upper lid colobomas, unilateral mandibular aplasia or hypoplasia, auricular malformations, preauricular skin tags, and vertebral anomalies [77] (Figs. 38.26 and 38.27). The orbit may be variably affected and is frequently smaller on the affected side. Other features that can be seen in Goldenhar syndrome are similar to those described above as part of the OAV spectrum.



Fig. 38.25 Hemifacial microsomia. Photograph of a patient with hemifacial microsomia affecting the left side of the face



Fig. 38.26 Goldenhar syndrome. Photograph of a patient with Goldenhar syndrome, illustrating epibulbar dermoid, pre-auricular skin tags, microtia, and macrostomia

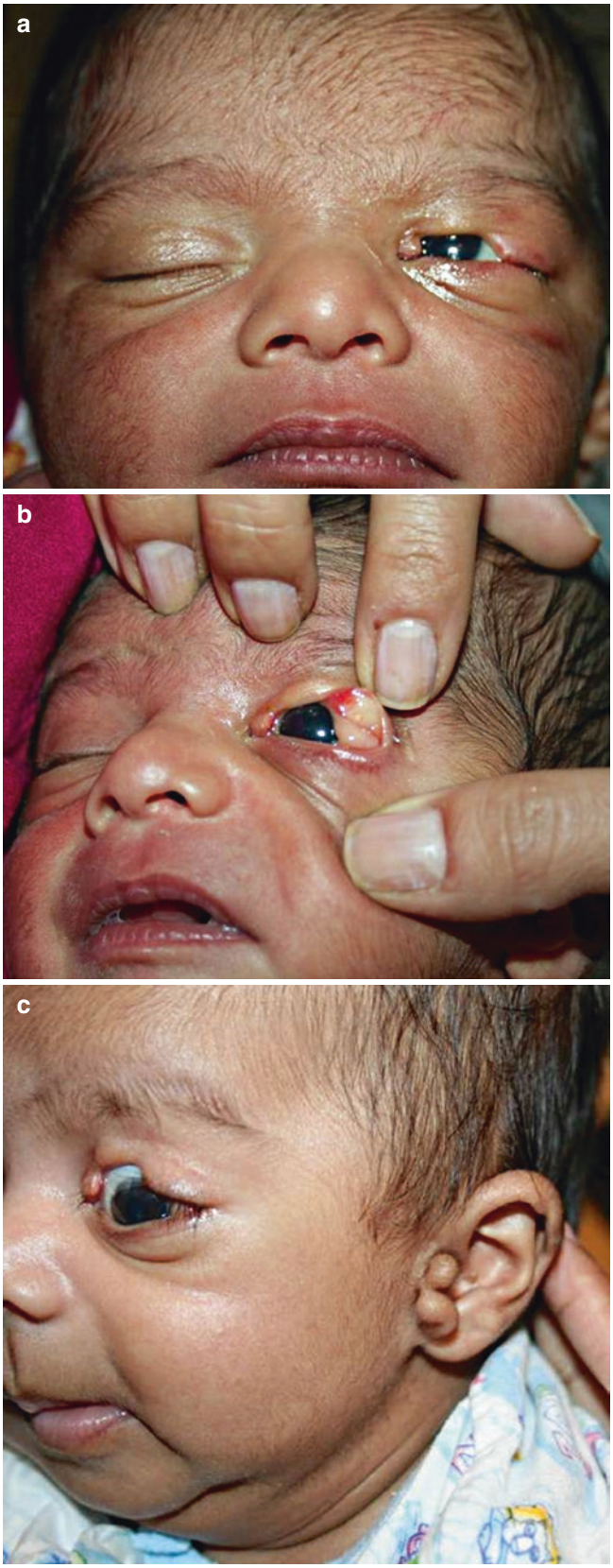


Fig. 38.27 Goldenhar syndrome. Photograph of a patient with Goldenhar syndrome, illustrating an (**a**) upper eyelid coloboma, (**b**) epibulbar dermolipoma, and (**c**) pre-auricular skin tags

Ocular findings are common in Goldenhar syndrome. In fact, many authors require the presence of a periocular dermoid to establish the diagnosis. Upper eyelid colobomas, mostly temporal in location, occur in 12–20% of cases. Mansour's large series displayed a 12% incidence of ptosis and an 11% incidence of nasolacrimal abnormalities, primarily nasolacrimal duct obstruction and lacrimal fistulas [123]. Horizontal palpebral fissure shortening, lid skin tags, and iris coloboma can occur less frequently. Various forms of strabismus, including Duane retraction syndrome, have been reported in up to 10–19% of patients [123–125].

Amniotic Band Syndrome

Highly variable clefts may result from mechanical restriction or constriction of the developing fetus by amniotic bands. Malformations from amniotic band syndrome do not follow a specific pattern of disruption and are often quite severe. Bands anchored to the corner of the mouth as a result of fetal swallowing of amniotic fluid may stretch across the face and disrupt formed tissues or prevent normal facial development. As demonstrated in Fig. 38.28, limb constriction deformities and amputations can occur with a predilection for distal, central digits of the upper extremity. Foulkes' review of 71 cases revealed abnormal gestational history in 60%, concurrent diagnoses in 50%, club feet in nearly one-third of patients, and an average of three involved limbs. The average patient required three reconstructive procedures [126]. Evidence from associated internal organ dysgenesis suggests damage occurring relatively early in gestation, probably prior to 26 days [127].

Ophthalmic abnormalities can include a combination of bony orbital clefts, lid colobomas that are often contiguous with facial clefts, ptosis, ectropion, and lacrimal outflow obstruction [128]. The globe may be directly affected: corneal leukomas and gross disturbance of the globe have been described. Unilateral chorioretinal defects or lacunae have also been reported [129, 130].

Management

Team Approach

The unique and complex abnormalities encountered in the craniofacial patient are best managed by a team of specialists. Coordinated efforts are made to tailor the nature and timing of intervention to the overall well-being of the individual patient. The craniofacial team includes members from many other services, including genetics, plastic surgery, neurosurgery, oral surgery, orthodontics/dentistry,



Fig. 38.28 Amniotic band syndrome. (**a**) Amniotic bands around ankles. (**b**) Amputation of digits from amniotic bands. (**c**) Adult with similar loss of digits and bands remnants visible. (**d**, **e**) Clefting defects resulting from band anchored in the mouth or nose, creating orbital, facial, and cranial defects

ophthalmology, otolaryngology, anesthesia, psychiatry, psychology, dietary, and social work. We have an interdisciplinary approach for following these patients in which multiple visits with different services are planned for a single day. At the end of the day, members from the different teams meet as a group to discuss management goals and surgical plans for each patient. See Chap. 40 for a more extensive discussion of the surgical approaches to these patients.

Ophthalmic Examination and Surgical Considerations

Baseline Exam (Craniofacial Sheet)

A complete baseline eye examination is performed prior to any craniofacial surgery, and information is recorded on a preprinted examination sheet (Fig. 38.29). The craniofacial examination sheet outlines the essential information necessary to evaluate the ocular and adnexal status of the craniofacial patient. Our goal is to perform a systematic evaluation for every patient at every visit. For example, a patient with epiphora that appears to be related to a lower lid deformity arising from a number 3 cleft may also have actual nasolacrimal system abnormalities that could be overlooked without a systematic evaluation of all structures.

Vision and Alignment

Amblyopia is responsible for the majority of vision loss in patients with craniofacial disorders. Amblyopia may arise for many reasons, including corneal opacification, protective tar-

Fig. 38.29 Craniofacial eye examination sheet

Name: _____ Date: _____
Medical Record Number: _____
Age: _____ DOB: _____
Referring MD: _____
Allergies: _____
Current Medications: _____

Past Medical/Surgical Diagnoses:
1. _____
2. _____
3. _____
4. _____

History (onset, progression, surgery):

Vision Testing:
Visual acuity: OD _____ OS _____
Technique used: _____
Worth 4 dot: OD _____ OS _____
Color vision: OD _____ OS _____
Visual field: OD _____ OS _____
Nystagmus present: OD _____ OS _____
Describe: _____

Alignment:
Technique used: _____
Right
_____ _____ _____
_____ _____
_____ _____ _____

Left
_____ _____ _____
_____ _____
_____ _____ _____

Anterior and Posterior Segment Examination:
IOP: OD _____ OS _____
Refraction: OD _____ OS _____
Pupils:
SLE:
Lids/lashes:
Conjunctiva/sclera:
Cornea:
Anterior chamber:

Fig. 38.29 (continued)

Iris:
Lens:
Anterior vitreous
DFE:
Optic nerve:
Macula:
Vessels:
Periphery:

Oculoplastic Exam:
Ptosis: MRD1: OD _____ OS _____
Post phenylephrine 2.5%: OD _____ OS _____
Levator Function: OD _____ OS _____
Lid Crease Height: OD_____ OS_____
Bell's Phenomenon: OD _____ OS _____
MRD2: OD _____ OS _____
Lash ptosis: OD _____ OS _____
Lid contour: OD _____ OS _____
Lagophthalmos: OD _____ OS _____
Coloboma upper/lower: OD _____ OS _____
Epicanthal folds: Type: OD _____ OS _____
Canthal dystopias medial/lateral: OD _____ OS _____
Horizontal Fissure Length: OD _____ OS _____
Intercanthal Distance: OD _____ OS _____
Interpupillary Distance: OD _____ OS _____
Epiphora: OD _____ OS _____
DDT 5 minutes: OD _____ OS _____
Proptosis: OD _____ OS _____
Vertical Globe Position (+/-): OD _____ OS _____
Retropulsion: OD _____ OS_____

Imaging:
CT scan:
MRI scan:

Impression:

Craniosynostosis- Type:

Clefting Syndrome- (Tessier Number):

Specific Oculoplastic Diagnoses:
1. _____
2. _____
3. _____
4. _____

medial canthal dystopia, telecanthus, clefting, or gross anomaly of the nose to suggest a bony abnormality involving the nasolacrimal duct and increase suspicion of nasolacrimal disruption.

A dye disappearance test is a relatively easy manner to assess the lacrimal outflow system, particularly in young children. Standard nasolacrimal and tearing tests, such as the basal secretion test, Schirmer test, and Jones tests, may be possible in older children (see Chap. 26).

Exophthalmos

Accurate measurement of the degree of exophthalmos is important, particularly in those syndromes where proptosis is an accompanying feature. Craniofacial surgery may cause postoperative swelling and a resultant increase in proptosis. Conversely, clinically obvious postoperative enophthalmos may occur and was noted in 37.7% of 61 patients following orbital osteotomies and transposition for craniofacial malformations [132]. Hertel or Luedde

sorrhaphy, ptosis, strabismus, anisometropia, or prolonged use of occlusive bandages. As such, vision examination with cycloplegic refraction and prompt initiation of amblyopia treatment is important in this patient population. The difficult task of assessing visual acuity in preverbal children may be compounded by the coexistence of physical and cognitive difficulties associated with craniofacial disorders. See Chap. 10 for a more detailed discussion of the ophthalmic examination in children, as well as the appropriate management of amblyopia.

Evaluation of motility and ocular alignment is crucial in the craniofacial syndromes because extraocular muscle abnormalities are frequently present. Absent muscles or abnormal extraocular muscle insertions, orbital deformity, cranial nerve disruption, and craniofacial surgery may all contribute to the presence of motility disturbance and strabismus. This patient population is also at high risk for developing elevated intracranial pressure, which can manifest with abduction deficits and subtle esotropias. Evaluation of binocular function and stereopsis should be performed initially, followed by evaluation of tropias, phorias, and limitations of movement (see Chaps. 10 and 11).

Globe

The pupils are carefully inspected for symmetry, shape, and reaction to light. The detection of a relative afferent pupillary defect or poorly reactive pupil may signal the presence of optic nerve disease (i.e., in the case of elevated intracranial pressure). Corneal dermoids or lipodermoids are usually visible on gross inspection. If possible, a more detailed examination of the cornea should be performed with a portable or stationary slit lamp. Otherwise, cobalt blue illumination of fluorescein on the corneal surface, even from a distance, can reveal irregularities resulting from corneal exposure. This part of the examination is especially important because the cornea is susceptible to exposure from proptosis, eyelid colobomas, eyelid malposition (i.e., ectropion/entropion), as well from postoperative lagophthalmos or too much exposure from ptosis repair. Other threats to the corneal integrity include trichiasis, distichiasis, and lid retraction. Although cataracts are not common in the craniosynostoses, the lens is assessed with careful attention to the red reflex or by direct examination with a slit lamp. A dilated fundoscopic examination should be performed in all patients, noting any optic nerve, vascular, or retinal abnormalities. Particular attention should be paid to the optic nerve in this population, especially given the increased prevalence of raised intracranial pressure and possible papilledema [131]. For children who are difficult to examine, an exam under anesthesia can be considered and combined with surgeries that may be planned by other services.

Eyelids

The lids and canthal regions are frequently abnormal in craniofacial disorders. Craniofacial surgery will also often alter the soft tissue relationship of the lids and canthi, necessitating accurate pre- and postoperative measurements. The soft tissue distance between the medial canthi (intercanthal distance) and the interpupillary distance are measured, taking note of the presence of telecanthus. Normal intercanthal distance is usually less than 20 mm in infants, less than 24 in older children, and less than 30 mm in adults [34]. The measurement of interpupillary distance may require adjustment if there is concurrent strabismus. An intercanthal to interpupillary distance ratio greater than 50% is indicative of telecanthus. Although primary telecanthus may occur in Blepharophimosis and Waardenburg syndromes, the presence of hypertelorism often parallels telecanthus in many craniofacial syndromes.

The medial and lateral canthi are inspected, and any upward or downward displacement is noted. The lateral canthus is normally positioned at a level 1–2 mm above the level of the medial canthus. Medial canthal dystopia with a downward dislocation of the medial canthus is often noted in disorders involving the nasomaxillary skeleton. Lateral canthal dystopia with downward displacement of the lateral canthus (anti-mongoloid slant) is associated with the malar hypoplasia of Treacher–Collins syndrome; other 6, 7, 8 clefting syndromes; as well as with a variety of craniofacial dysostosis syndromes. Upward dislocation (mongoloid slant) of the lateral canthus may occasionally be seen with plagiocephaly or sphenofrontal dysplasia [3].

The horizontal and vertical palpebral fissures are measured and recorded. Ptosis is evaluated by noting margin reflex distance, levator function, and lid level response to 2.5% phenylephrine in infants and 10% phenylephrine in older children. The eyelids are inspected carefully for colobomas, retraction, lagophthalmos, entropion, ectropion, trichiasis, distichiasis, and epicanthal folds.

Nasolacrimal System

Lacrimal secretory function (tear production) is not often affected in the craniofacial syndromes. Nasolacrimal outflow abnormalities, however, are common and may arise as a result of coexisting facial deformity (congenital) or from surgical intervention (acquired). Failure of distal canalization of the nasolacrimal system (an imperforate valve of Hasner) is probably no more common in the craniofacial newborn than in the population at large (1–6%) [117].

Other distinct anatomic abnormalities of the tear drainage system occur with higher frequency. Abnormalities of the lacrimal system are particularly frequent as part of clefting disorders and may include lateral displacement of the puncta, elongation of the canaliculi, absence of the puncta, absence of the lacrimal duct or sac, and bony abnormalities, including the lacrimal fossa. Minor abnormalities of structure are of little significance if they do not result in obstruction of the lacrimal outflow system. Evaluation of epiphora should begin with a careful history of the nature of the tearing problem and any associated history of infection. The presence, position, and patency of the puncta should be noted, as well as underlying bony abnormality, such as

exophthalmometry may be misleading in craniofacial syndromes due to anatomic variations of the lateral orbital rim position. Adjustments may be made in an attempt to approximate accurate measurements. Patient cooperation may be increased with the Luedde device, particularly in young children, since it is a smaller measuring device that is much less threatening than Hertel-type devices (Fig. 38.30).



Fig. 38.30 Luedde measuring device for proptosis

Ophthalmic and Oculoplastic Surgical Considerations

See Chap. 40 for a more detailed discussion of general craniofacial considerations for surgical correction in craniosynostoses. The ophthalmologist plays a crucial role in the monitoring of ocular structures, particularly the optic nerve and cornea, which may impact the timing of major intervention. Any ophthalmic or oculoplastic procedures required should be coordinated with other members of the craniofacial team to minimize anesthesia exposure and reoperations. There are, of course, situations where independent surgical repair is appropriate.

Corneal Exposure

Exophthalmos in Crouzon and Apert syndromes can be severe. If full lid closure is prevented by severe proptosis and corneal exposure threatens the integrity of the globe, orbital advancement may be required within the first few weeks of life (Figs. 38.31, 38.32, 38.33, 38.34, 38.35, and 38.36). Usually, however, frequent moist chamber occlusive dressings, temporary suture tarsorrhaphy, or large lateral tarsorrhaphy is a sufficient temporizing measure and allows delay

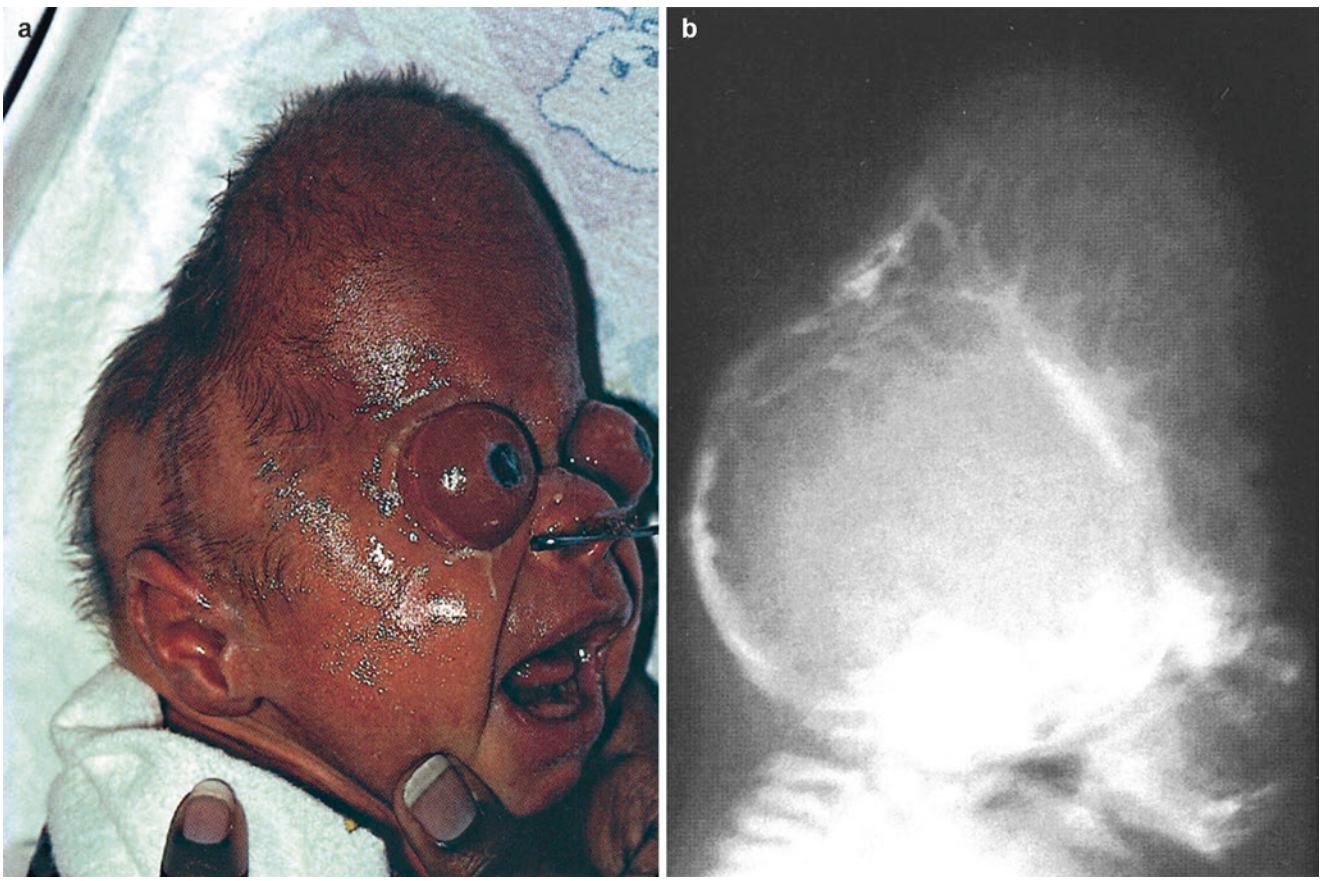


Fig. 38.31 Cloverleaf synostosis (Kleeblattschädel or triphyllocephaly). (**a**) A patient with all sutures except metopic fused. (**b**) Plain film of same patient demonstrates trilobar skull with pressure mottling of the skull where brain can find exit only through open metopic suture



Fig. 38.32 Severe corneal exposure. Temporary protection of severe corneal exposure with lubricating eye ointment and plastic wrap

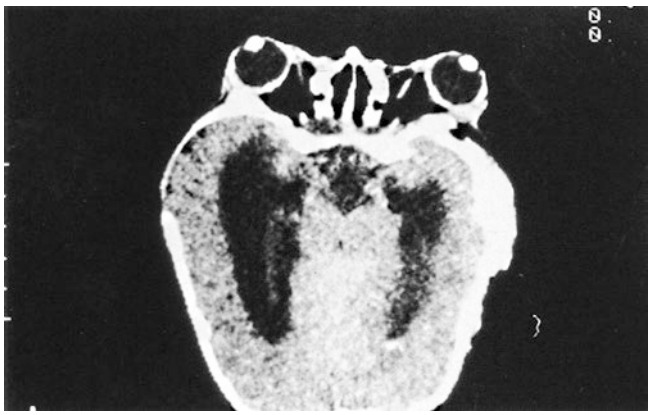


Fig. 38.33 Severe exorbitism. CT scan of the patient in Fig. 38.31 demonstrating severe exorbitism with absent lateral orbital walls; note effects of hydrocephalus on ventricles

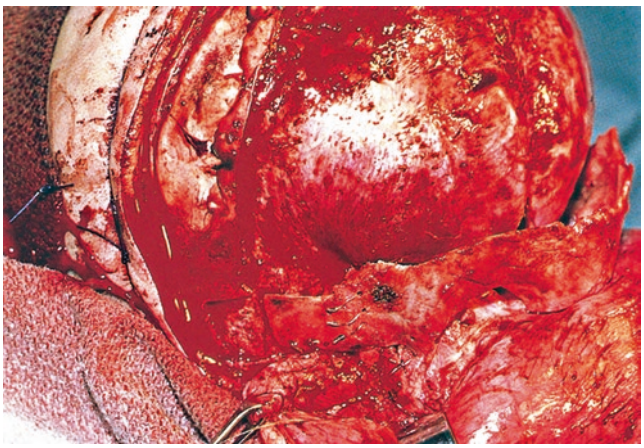


Fig. 38.34 Craniofacial advancement of orbits combined with release of sutures

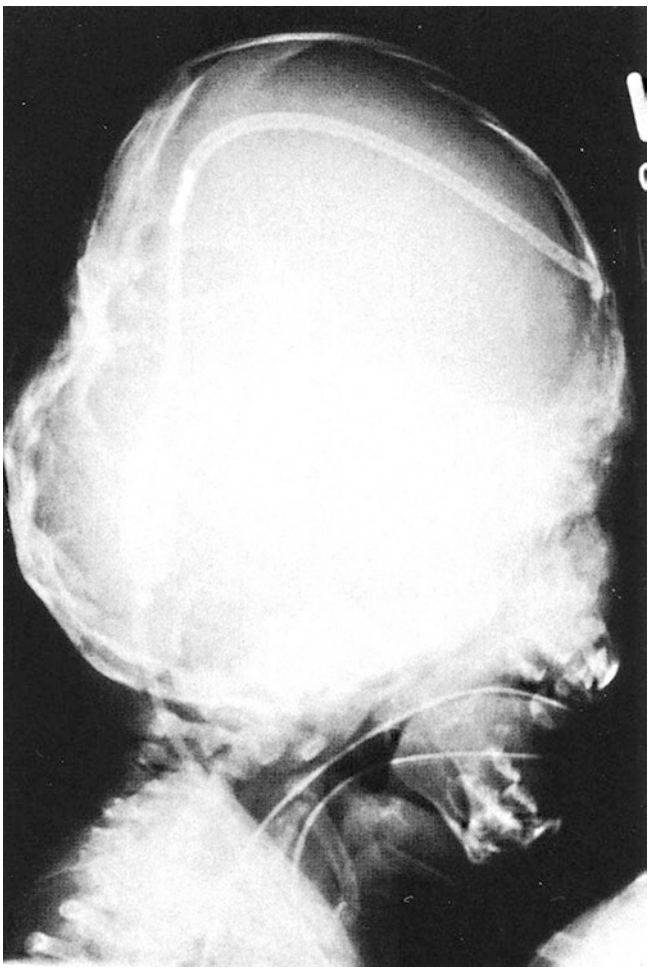


Fig. 38.35 Neurosurgical shunt for hydrocephalus. CT scan of the patient in Fig. 38.31 after orbital advancement and placement of a neurosurgical shunt for hydrocephalus

of major craniofacial surgery. In severe cases, tarsorrhaphies to protect the corneas may even require disinsertion of the upper and lower lid retractors. These procedures must be weighed against the potential risk of amblyopia during the critical period of vision development in younger children.



Fig. 38.36 Total tarsorrhaphies. Postoperative protection of the corneas by total tarsorrhaphies. Incision and release of upper and lower lid retractors is required

Large lid colobomas that prevent adequate coverage of the cornea may also result in severe exposure. Repair of colobomas is usually delayed until at least 6 months of age if the integrity of the cornea is not threatened (see Chap. 21). Sliding or rotational flaps, rather than lid-sharing techniques, are preferred in the pediatric population to prevent deprivational amblyopia. Similarly, the use of occlusive bandages is minimized. In some instances, earlier team repair is required. Colobomas may also be associated with other corneal or adnexal deformities, such as partial cryptophthalmos (Figs. 38.37, 38.38, 38.9, and 38.40). Repair may require mucous membrane grafting. In some instances, where amblyopia is severe, a cosmetic scleral shell may be a useful adjunct in improving appearance if corneal scarring has occurred.

Canthal Deformities

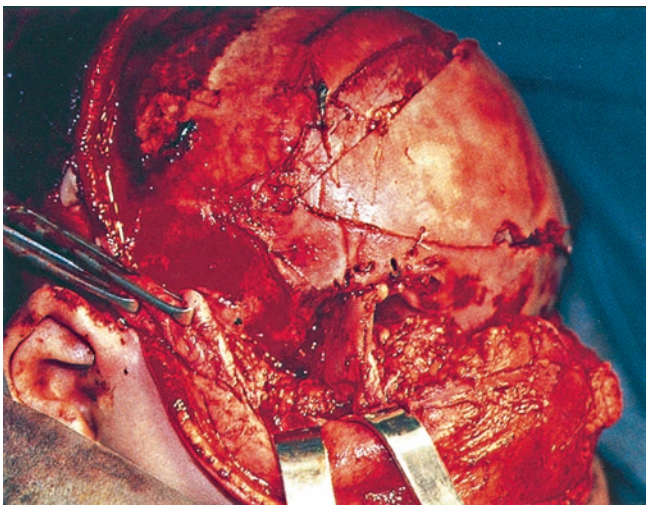
Canthal dystopias are often repaired as part of the initial craniofacial surgery. Medial canthopexy to address medial canthal dystopia and transnasal wiring for the correction of telecanthus are easily achieved at this time. The complex nature of some lateral canthal dystopias may require multiple interventions with augmentation of bony structures prior to definitive canthopexy. Craniofacial surgery itself may produce canthal abnormalities, which can later be repaired by the oculoplastic surgeon.

Nasolacrimal Anomalies

In the absence of dacryocystitis or dacryocystocele, congenital epiphora in the craniofacial patient without major deformities of the midface is managed in the typical conservative fashion. The correction of epiphora arising from deformities in the midface and medial eyelids is best deferred until bony reconstruction of the midface is com-



Fig. 38.37 Tessier 10, 11 cleft. (**a**) Patient with Tessier 10, 11 cleft. (**b**) Lateral view demonstrates fusion of the medial lid to the cornea as in partial cryptophthalmos



plete by the craniofacial service. If definitive craniofacial correction is delayed until the teenage years, minor nasolacrimal procedures such as probing and irrigation with or without silastic intubation may be performed earlier. Importantly, a previously functioning dacryocystorhinostomy, canaliculodacryocystorhinostomy, or conjunctivorhinostomy can often be rendered dysfunctional by craniofacial repair, which is why we prefer to wait until craniofacial surgery has been completed. Adaptation of standard surgical technique may be required in the face of underlying anatomic abnormalities, but a high rate of success can be achieved [133]. Use of bypass Pyrex tube procedures are ultimately more frequently required, and the need for secondary procedures is higher due to the severity of structural abnormality (see Chaps. 28 and 30).

Fig. 38.38 Cranial bone used to create lateral orbital wall

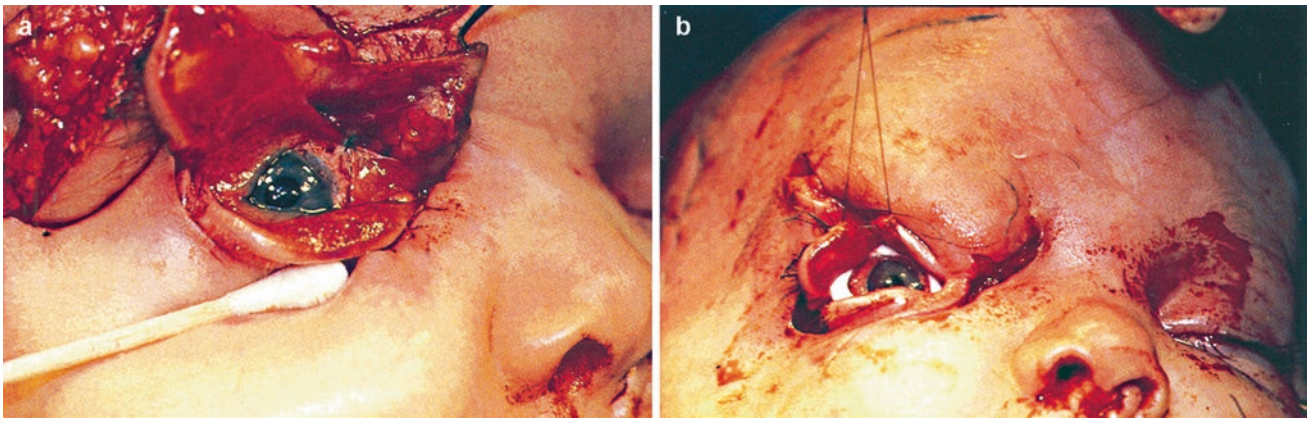


Fig. 38.39 Lid coloboma repair. (**a**) The lid is dissected from the cornea and the conjunctiva is mobilized to create a cul-de-sac. (**b**) The lid coloboma is repaired. A Teflon symblepharon ring conformer is custom-fashioned



Fig. 38.40 The patient in Fig. 38.39, 6 years later. (**a**) Wearing a cosmetic scleral shell. (**b**) Note camouflage effect of spectacles

Ptosis

The timing of ptosis repair should be coordinated to allow a minimum number of procedures and increase the likelihood of the definitive repair. Unless deprivational amblyopia is a concern, this often translates into deferring ptosis repair until all craniofacial procedures that may affect the position of the eyelids are complete. A temporizing frontalis suspension using a synthetic material may be necessary in young children to prevent amblyopia (see Chap. 22).

Strabismus

Surgical management of the various motility disorders encountered in the craniofacial population follows the same basic tenets as all strabismus surgery (see Chap. 11). Primary strabismus is often not adversely affected by dissection of the periorbita during craniofacial procedures, allowing for correction of ocular misalignment prior to orbital procedures, if necessary. The strabismus surgeon needs to be prepared to encounter unusual configuration of the extraocular muscles, including anomalous insertions, as well as hypoplastic or absent extraocular muscles. Preoperative CT, MRI, or ultrasound may help to identify anatomic variations prior to surgery.

Summary

Congenital craniofacial disorders present unusual and complex management situations for both the primary ophthalmologist and the oculoplastic surgeon. Proper evaluation of these patients requires recognition of specific syndromes and their accompanying ophthalmic features. Repair of ocular and adnexal deformities must be coordinated with other members of the craniofacial team. Preservation of vision is the primary goal, often requiring early and aggressive intervention. During major craniofacial repairs, a number of soft tissue concerns can be addressed, including eyelid contour deformities, telecanthus, and canthal dystopias. More frequently, however, specific ocular and adnexal concerns are handled independently of major craniofacial repair, including ptosis repair and strabismus surgery. Nasolacrimal problems can be handled simultaneously when simple probing and irrigation or Silastic intubation is indicated. More involved nasolacrimal surgeries (dacryocystorhinostomy or bypass procedures) are best delayed until major midface skeletal reconstruction is complete.

References

1. Smith DW, Tondury G. Origin of the calvaria and its sutures. Am J Dis Child. 1978;132:662–6.
2. Virchow R. Uber den crestinismus, namentlick in franken, and uber pathologische Schadelformen. Verb Phys Med Ges Warsburg. 1851;2:230–51.
3. van der Meulen JCH, et al. Classification of craniofacial malformations. In: Strieker M, et al., editors. Craniofacial malformations. New York: Churchill Livingstone; 1990.
4. Moore GE. Molecular genetic approaches to the study of human craniofacial dysmorphologies. Int Rev Cytol. 1995;158:215–77.
5. Le Merrer M, Ledinot V, Renier D, et al. Genetic counseling in craniostenosis: results of a prospective study performed with a group of studies on craniofacial malformations. J Genet Hum. 1988;36:295–306.
6. White RA, Dowler LL, Angeloni SV, et al. Assignment of FGF8 to human chromosome 10q25–q26: mutations in FGF8 may be responsible for some types of acrocephalosyndactyly linked to this region. Genomics. 1995;30:109–11.
7. Preston RA, Post JC, Keats BJ, et al. A gene for Crouzon craniofacial dysostosis maps to the long arm of chromosome 10. Nat Genet. 1994;7:149–53.
8. Reardon W, Winter RM, Rutland P, et al. Mutations in the fibroblast growth factor receptor 2 gene cause Crouzon syndrome. Nat Genet. 1994;8:98–103.
9. Jabs EW, Li X, Scott AF, et al. Jackson-Weiss and Crouzon syndromes are allelic with mutations in fibroblast growth factor 2. Nat Genet. 1994;8:275–9.
10. Wilkie AO, Slaney SF, Oldridge M, et al. Apert syndrome results from localized mutations of FGFR2 and is allelic with Crouzon syndrome. Nat Genet. 1995;9:165–72.
11. Kan SH, Elanko N, Johnson D, et al. Genomic screening of fibroblast growth-factor receptor 2 reveals a wide spectrum of mutations in patients with syndromic craniosynostosis. Am J Hum Genet. 2002;70:472–86.
12. Fernandes MB, Maximino LP, Perosa GB, Abramides DV, Passos-Bueno MR, Yacubian-Fernandes A. Apert and Crouzon syndromes-cognitive development, brain abnormalities, and molecular aspects. Am J Med Genet A. 2016;170:1532–7.
13. Heuzé Y, Holmes G, Peter I, Richtsmeier JT, Jabs EW. Closing the gap: Genetic and Genomic Continuum from Syndromic to Nonsyndromic Craniosynostoses. Curr Genet Med Rep. 2014;2(3):135–45.
14. Cohen MM Jr, Kreiborg S. Birth prevalence studies of Crouzon syndrome: comparison of direct and indirect methods. Clin Genet. 1992;41:12–5.
15. Gray TL, Casey T, Selva D, Anderson PJ, David DJ. Ophthalmic sequelae of Crouzon syndrome. Ophthalmology. 2005;112(6):1129–34.
16. Ma HW, Lajeunie E, Le Merrer M, et al. No evidence of genetic heterogeneity in Crouzon craniofacial dysostosis. Hum Genet. 1995;96:731–5.
17. Li X, Young NM, Tropp S, Hu D, Xu Y, Hallgrímsson B, Marcucio RS. Quantification of shape and cell polarity reveals a novel mechanism underlying malformations resulting from related FGF mutations during facial morphogenesis. Hum Mol Genet. 2013;22(25):5160–72.
18. Stanier P, Pauws E. Development of the lip and palate: FGF signalling. Front Oral Biol. 2012;16:71–80. Albertson RC, Yelick PC. Fgf8 haploinsufficiency results in distinct craniofacial defects in adult zebrafish. Dev Biol. 2007;306(2):505–15.
19. Pfaff MJ, Xue K, Li L, Horowitz MC, Steinbacher DM, Eswarakumar JV. FGFR2c-mediated ERK-MAPK activity regulates coronal suture development. Dev Biol. 2016;28:242–50.
20. Kolar JC, Munro IR, Farkas LG. Patterns of dysmorphology in Crouzon syndrome: an anthropometric study. Cleft Palate J. 1988;25:235–44.
21. Atkinson FRB. Hereditary cranio-facial dysostosis or Crouzon's disease. Med Press. 1937;195:118.
22. Kreiborg S. Crouzon syndrome: a clinical and roentgencephalometric study. Scand J Plast Reconstr Surg (Suppl). 1981;18:28.

23. Proudman TW, Moore MH, Abbott AH, David DJ. Non-craniofacial manifestations of Crouzon's disease. J Craniofac Surg. 1994;5:218–22.
24. Miller MT. Ocular abnormalities in craniofacial malformations. Int Ophthalmol Clin. 1984;24:143.
25. Hertle RW, et al. Visual loss in patients with craniofacial synostosis. J Pediatr Ophthalmol Strabismus. 1991;28:344–9.
26. Kreiborg S, Cohen MM Jr. Ocular manifestations of Apert and Crouzon syndromes: qualitative and quantitative findings. J Craniofac Surg. 2010;21:1354–7.
27. Perlman JM, Zaidman GW. Bilateral keratoconus in Crouzon's syndrome. Cornea. 1994;13:80–1.
28. Bertelson TI. The premature synostosis of the cranial sutures. Arch Opthalmol (Copenhagen). 1958;5(suppl):47–66.
29. Abu-Sittah GS, Jeelani O, Dunaway D, Hayward R. Raised intracranial pressure in Crouzon syndrome: incidence, causes, and management. J Neurosurg Pediatr. 2016;17(4):469–75.
30. Coats DK, Paysse EA, Stager DR. Surgical management of V-pattern strabismus and oblique dysfunction in craniofacial dysostosis. J AAPOS. 2000;4:338–42.
31. Caputo AR, Lingua RW. Aberrant muscular insertions in Crouzon's disease. J Pediatr Ophthalmol Strabismus. 1980;17:239–41.
32. Diamond GR, Whitaker LA. Ocular motility in craniofacial reconstruction. Plast Reconstr Surg. 1984;73:31–5.
33. Weiss AH, Phillips J, Kelly JP. Crouzon syndrome: relationship of rectus muscle pulley location to pattern strabismus. Invest Ophthalmol Vis Sci. 2014;55(1):310–7.
34. Maliepaard M, Mathijssen IM, Oosterlaan J, Okkerse JM. Intellectual, behavioral, and emotional functioning in children with syndromic craniosynostosis. Pediatrics. 2014;133(6):e1608–15.
35. Cohen MM Jr, Kreiborg S. A clinical study of the craniofacial features in apert syndrome. Int J Oral Maxillofac Surg. 1996;25:45–53.
36. Cohen MM Jr, Kreiborg S, Lammer EJ, et al. Birth prevalence study of the Apert syndrome. Am J Med Genet. 1992;42:655–9.
37. Breik O, Mahindu A, Moore MH, Molloy CJ, Santoreneos S, David DJ. Central nervous system and cervical spine abnormalities in Apert syndrome. Childs Nerv Syst. 2016;32:833–38.
38. Glaser RL, Broman KW, Schulman RL, Eskenazi B, Wyrobek AJ, Jabs EW. The paternal-age effect in Apert syndrome is due, in part, to the increased frequency of mutations in sperm. Am J Hum Genet. 2003;73:939–47.
39. Park WJ, Theda C, Maestri NE, et al. Analysis of phenotypic features and FGFR2 mutations in Apert syndrome. Am J Hum Genet. 1995;57:321–8.
40. Oldridge M, Zackai EH, McDonald-McGinn DM, et al. De novo alu-element insertions in FGFR2 identify a distinct pathological basis for Apert syndrome. Am J Hum Genet. 1999;64:446–61.
41. Goriely A, Wilkie AO. Paternal age effect mutations and selfish spermatogonial selection: causes and consequences for human disease. Am J Hum Genet. 2012;90:175–200.
42. Cohen MM, Kreigorg S. Unusual cranial aspects of Apert syndrome. J Craniofac Genet Dev Biol. 1994;14:48–56.
43. Murovic JA, Posnick JC, Drake JM, et al. Hydrocephalus in the Apert syndrome: a retrospective review. Pediatr Neurosurg. 1993;19:151–5.
44. Cohen MM Jr, Kreiborg S. Visceral anomalies in Apert syndrome. Am J Med Genet. 1993;45:758–60.
45. Marucci DD, Dunaway DJ, Jones BM, Hayward RD. Raised intracranial pressure in Apert syndrome. Plast Reconstr Surg. 2008;122(4):1162–8.
46. Cuttone JM, Brazis PT, Miller MT, et al. Absence of the superior rectus muscle in Apert's syndrome. J Pediatr Ophthalmol Strabismus. 1979;16:349–54.
47. Khong JJ, Anderson P, Gray TL, Hammerton M, Selva D, David D. Ophthalmic findings in apert syndrome prior to craniofacial surgery. Am J Ophthalmol. 2006;142(2):328–30.
48. Fries PD, Katowitz JA. Congenital craniofacial anomalies of ophthalmic importance. Surv Ophthalmol. 1990;35:87–119.
49. Buncic JR. Ocular aspects of Apert syndrome. Clin Plast Surg. 1991;18:315–9.
50. Mah J, Kasser J, Upton J. The foot in Apert syndrome. Clin Plast Surg. 1991;18:391–7.
51. Wood VE, Sauser DD, O'Hara RC. The shoulder and elbow in Apert's syndrome. J Pediatr Orthop. 1995;15:648–51.
52. Kasser J, Upton J. The shoulder, elbow and forearm in Apert syndrome. Clin Plast Surg. 1991;18:381–9.
53. Cohen MM, Kreiborg S. Skeletal abnormalities in the Apert syndrome. Am J Med Genet. 1993;47:624–32.
54. Kreiborg S, Cohen MM Jr. The oral manifestations of Aperts syndrome. J Craniofac Genet Dev Biol. 1992;12:41–8.
55. Buchanan RC. Acrocephalosyndactyly or Apert's syndrome. Br J Plast Surg. 1968;21:406–18.
56. Antón-Pacheco JL, Luna Paredes C, Martínez Gimeno A, García Hernández G, Martín de la Vega R, Romance García A. The role of bronchoscopy in the management of patients with severe craniofacial syndromes. J Pediatr Surg. 2012;47(8):1512–5.
57. Cohen MM Jr, Kreiborg S. An updated pediatric perspective on Apert syndrome. Am J Dis Child. 1993;147:989–93.
58. Krafchik B. Acne in Apert syndrome. Clin Plast Surg. 1991;18:407.
59. Moore MH, Cantrell SB, Trott JA, et al. Pfeiffer syndrome: a clinical review. Cleft Palate Craniofac J. 1995;32:62–70.
60. Schell U, Hehr A, Feldman GJ, et al. Mutations in FGFR1 and FGFR2 cause familial and sporadic Pfeiffer's syndrome. Hum Mol Genet. 1995;4:323–8.
61. Eswarakumar VP, Horowitz MC, Locklin R, et al. A gain-of-function mutation of Fgfr2c demonstrates the roles of this receptor variant in osteogenesis. Proc Natl Acad Sci U S A. 2004;101:12555–60.
62. Yin L, Du X, Li C, et al. A Pro253Arg mutation in fibroblast growth factor receptor 2 (FGFR2) causes skeleton malformation mimicking human Apert syndrome by affecting both chondrogenesis and osteogenesis. Bone. 2008;42:631–43.
63. Agochukwu NB, Solomon BD, Muenke M. Impact of genetics on the diagnosis and clinical management of syndromic craniosynostoses. Childs Nerv Syst. 2012;28:1447–63.
64. Vogels A, Fryns JP. Pfeiffer syndrome. J Rare Dis. 2006;1:19.
65. Barry GP, Ny BM, Zackai EH, Grunwald L, Forbes BJ. A case report of a patient with Pfeiffer syndrome, an FGRF 2 mutation (Trp290Cys) and unique ocular anterior segment findings. Ophthalmic Genet. 2010;31(4):193–5.
66. Pantke OA, et al. The Saethre–Chotzen syndrome. Birth Defects. 1975;11:190–225.
67. el Ghouzzi V, Le Merrer M, Perrin-Schmitt F, Lajeunie E, Bent P, Renier D, Bourgeois P, Bolcato-Bellemin AL, Munnich A, Bonaventure J. Mutations of the TWIST gene in the Saethre-Chotzen syndrome. Nat Genet. 1997;15(1):42–6.
68. Connerney J, Andreeva V, Leshem Y, Muentener C, Mercado MA, Spicer DB. Twist 1 dimer regulates cranial suture patterning and fusion. Dev Dyn. 2006;235:1345–57.
69. Connerney J, Andreeva V, Leshem Y, et al. Twist1 homodimers enhance FGF responsiveness of the cranial sutures and promote suture closure. Dev Biol. 2008;318:323–34.
70. de Heer IM, de Klein A, van den Ouweland AM, et al. Clinical and genetic analysis of patients with Saethre-Chotzen syndrome. Plast Reconstr Surg. 2005;115:1894–902.
71. Kress W, Schropp C, Lieb G, et al. Saethre-Chotzen syndrome caused by *TWIST1* gene mutations: functional differentiation from Muenke coronal synostosis syndrome. Eur J Hum Genet. 2006;14:39–48.
72. Cunningham ML, Seto ML, Ratisoontorn C, Heike CL, Hing AV. Syndromic craniosynostosis: from history to hydrogen bonds. Orthod Craniofac Res. 2007;10:67–81.
73. Evans CA, Christiansen RL. Cephalic malformations in Saethre–Chotzen syndrome. Radiology. 1976;121:399–403.

74. Foo R, Guo Y, McDonald-McGinn DM, Zackai EH, Whitaker LA, Bartlett SP. The natural history of patients treated for TWIST1-confirmed Saethre-Chotzen syndrome. Plast Reconstr Surg. 2009 Dec;124(6):2085–95.
75. Tahiri Y, Bastidas N, McDonald-McGinn DM, Birgfeld C, Zackai EH, Taylor J, Bartlett SP. New pattern of sutural Synostosis associated with TWIST Gene mutation and Saethre-Chotzen syndrome: peace sign Synostosis. J Craniofac Surg. 2015;26(5):1564–7.
76. Gallagher ER, Ratisoontorn C, Cunningham ML. Saethre-Chotzen syndrome. In: Pagon RA, Adam MP, Ardinger HH, Wallace SE, Amemiya A, Bean LJH, Bird TD, Fong CT, Mefford HC, Smith RJH, Stephens K, editors. GeneReviews® [Internet]. Seattle: University of Washington, Seattle; 1993–2016. 2003 May 16 [updated 2012 Jun 14].
77. Paznekas WA, Cunningham ML, Howard TD, et al. Genetic heterogeneity of Saethre-Chotzen syndrome, due to *TWIST* and *FGFR* mutations. Am J Hum Genet. 1998;62:1370–80.
78. Johnson D, Horsley SW, Moloney DM, et al. A comprehensive screen for *TWIST* mutations in patients with craniosynostosis identifies a new microdeletion syndrome of chromosome band 7p21.1. Am J Hum Genet. 1998;63:1282–93.
79. Anderson PJ, Hall CM, Evans RD, Hayward RD, Harkness WJ, Jones BM. The cervical spine in Saethre-Chotzen syndrome. Cleft Palate Craniofac J. 1997;34:79–82.
80. Bellus GA, Gaudenz K, Zackai EH, Clarke LA, Szabo J, Francomano CA, Muenke M. Identical mutations in three different fibroblast growth factor receptor genes in autosomal dominant craniosynostosis syndromes. Nat Genet. 1996;14:174–6.
81. Muenke M, Gripp KW, McDonald-McGinn DM, Gaudenz K, et al. A unique point mutation in the fibroblast growth factor receptor 3 gene (*FGFR3*) defines a new craniosynostosis syndrome. Am J Hum Genet. 1997;60:555–64.
82. Wilkie AO, Byren JC, Hurst JA, Jayamohan J, et al. Prevalence and complications of single gene and chromosomal disorders in craniosynostosis. Pediatrics. 2010;126:e391–400.
83. Kruszka P, Addissie YA, Yarnell CM, Hadley DW, et al. Muenke syndrome: an international multicenter natural history study. Am J Med Genet A. 2016;170(4):918–29.
84. Jadico SK, Huebner A, McDonald-McGinn DM, Zackai EH, Young TL. Ocular phenotype correlations in patients with TWIST versus FGFR3 genetic mutations. J AAPOS. 2006;10:435–44.
85. Kadakia S, Helman SN, Healy NJ, Saman M, Wood-Smith D. Carpenter syndrome: a review for the craniofacial surgeon. J Craniofac Surg. 2014;25(5):1653–7.
86. Jenkins D, Seelow D, Jehee FS, et al. RAB23 mutations in Carpenter syndrome imply an unexpected role for hedgehog signaling in cranial-suture development and obesity. Am J Hum Genet. 2007;80:1162–70.
87. DerKaloustian VM, Sinno AA, Nassar SI. Acrocephalopolysyndactyly type II (Carpenter's syndrome). Am J Dis Child. 1972;124:716–8.
88. Taravath S, Tonsgard JH. Cerebral malformations in Carpenter syndrome. Pediatr Neurol. 1993;9:230–4.
89. Eaton AP, Sommer A, Kontres SB, et al. Carpenter's syndrome: acrocephalopolysyndactyly type II. Birth Defects. 1974;10:249–60.
90. Vermeij-Keers CHR, Poelmann RE. The neural crest: a study of cell degeneration and the improbability of cell migration in mouse embryos. Neth J Zool. 1980;30:74–81.
91. Patten BM. The normal development of the facial region. In: Pruzansky S, editor. Congenital anomalies of the face and associated structures. Springfield: Charles C. Thomas; 1961. p. 48.
92. Johnston MC. The neural crest abnormalities of the face and brain. Birth Defects. 1975;11:416–40.
93. Weston JA. A radioautographic analysis of the migration and localization of trunk neural crest cells in the chick. Dev Biol. 1963;6:279–310.
94. Davies AF, Stephens RJ, Olavesen MG, et al. Evidence of a locus for orofacial clefting on human chromosome 6p24 and STS content map of the region. Hum Mol Genet. 1995;4:121–8.
95. Snijders RJ, Sebire NJ, Psara N, et al. Prevalence of facial cleft at different stages of pregnancy. Ultrasound Obstet Gynecol. 1995;6:327–9.
96. Fries MH, Kuller JA, Norton ME, et al. Facial features of infants exposed prenatally to cocaine. Teratology. 1993;48:413–20.
97. Lindhout D, Omtzigt JG. Teratogenic effects of antiepileptic drugs: implications for the management of epilepsy in women of childbearing age. Epilepsia. 1994;35(Suppl 4):S19–28.
98. McElhatton PR. The effects of benzodiazepine use during pregnancy and lactation. Reprod Toxicol. 1994;8:461–75.
99. Granstrom G, Kullaa-Mikkonen A. Experimental craniofacial malformations induced by retinoids and resembling branchial arch syndromes. Scand J Plast Reconstr Surg Hand Surg. 1990;24:3–12.
100. Tessier P. Anatomical classification of facial, craniofacial and laterofacial clefts. J Maxillofac Surg. 1976;4:69–94.
101. Kawamoto HK Jr. Incidence, pathology and classification of orbital clefts and the pathology of orbital hypertelorism. In: Converse JM, et al., editors. Symposium on diagnosis and treatment of craniofacial anomalies. St Louis: Mosby; 1979. p. 164.
102. Mann I. A theory of the embryology of oxycephaly. Trans Ophthalmol Soc UK. 1935;55:279–300.
103. Kawamoto HK Jr. The kaleidoscopic world of rare craniofacial clefts: order out of chaos (Tessier classification). Clin Plast Surg. 1976;3:529–72.
104. Gorlin RJ, Cohen MM Jr, Hennekam RCM. Syndromes of the head and neck. New York: Oxford University Press; 2001.
105. Dixon MJ, Read AP, et al. The gene for Treacher Collins syndrome maps to the long arm of chromosome 5. Am J Hum Genet. 1991;49:17–22.
106. Dixon MJ, Dixon J, Raskova D, et al. Genetic and physical mapping of the Treacher Collins syndrome locus: refinement of the localization to chromosome 5q32–33.2. Hum Mol Genet. 1992;1:249–53.
107. Loftus SK, Edwards SJ, Scherpbier-Heddema T, et al. A combined genetic and radiation hybrid map surrounding the Treacher Collins syndrome locus on chromosome 5q. Hum Mol Genet. 1993;2:1785–92.
108. Jabs EW, Li X, Lovett M, et al. Genetic and physical mapping of the Treacher Collins syndrome locus with respect to loci in the chromosome 5q3 region. Genomics. 1993;18:7–13.
109. Theveneau E, Mayor R. Neural crest migration: interplay between chemorepellents, chemoattractants, contact inhibition, epithelial-mesenchymal transition, and collective cell migration. Wiley Interdiscip Rev Dev Biol. 2012;1:435–45.
110. Dixon J, Brakebusch C, Fässler R, Dixon MJ. Increased levels of apoptosis in the prefusion neural folds underlie the craniofacial disorder. Treacher Collins syndrome. Hum Mol Genet. 2000;9(10):1473–80.
111. Rogers BO. Berry–Treacher–Collins syndrome: a review of 200 cases. Br J Plast Surg. 1979;17:109–13.
112. Tay MT, Quah BL. Mandibulofacial dysostosis: the eye signs of a case study. Singap Med J. 1991;32:365–7.
113. Whitaker LA, Katowitz JA, Randall P. The nasolacrimal apparatus in congenital facial anomalies. J Maxillofac Surg. 1974;2:59–63.
114. Hurwitz P. Mandibulofacial dysostosis. Arch Ophthalmol. 1954;51:69–74.
115. Franceschetti A, Klein D. The mandibulofacial dysostosis: a new hereditary syndrome. Acta Ophthalmol. 1949;27:144–9.
116. Hertle RW, Ziylan S, Katowitz JA. Ophthalmic features and visual prognosis in the Treacher Collins syndrome. Br J Ophthalmol. 1993;77:642–5.
117. Wang FM, Millman AL, Sidoti PA, Goldberg RB. Ocular findings in Treacher Collins syndrome. Am J Ophthalmol. 1990;110:280–6.

118. Vendramini-Pittoli S, Kokitsu-Nakata NM. Oculoauriculovertebral spectrum: report of nine familial cases with evidence of autosomal dominant inheritance and review of the literature. Clin Dysmorphol. 2009;18:67–7.
119. Beleza-Meireles A, Clayton-Smith J, Saraiva JM, Tassabehji M. Congenital malformations Oculo-auriculo-vertebral spectrum: a review of the literature and genetic update. J Med Genet. 2014;51:635–45.
120. Werler MM, Sheehan JE, Hayes C, Mitchell AA, Mulliken JB. Vasoactive exposures, vascular events, and hemifacial microsomia. Birth Defects Res (Part A). 2004;70:389–95.
121. Mastroiacovo P, Corchia C, Botto LD, Lanni R, Zampino G, Fusco D. Epidemiology and genetics of microtia-anotia: a registry based study on over one million births. J Med Genet. 1995;32:453–7.
122. Minoux M, Rijli FM. Molecular mechanisms of cranial neural crest cell migration and patterning in craniofacial development. Development. 2010;137:2605–21.
123. Mansour AM, Wang F, Henkind P, et al. Ocular findings in facio-auriculovertebral sequence (Goldenhar–Gorlin sequence). Am J Ophthalmol. 1985;100:555.
124. Baum JL, Feingold M. Ocular aspects of Goldenhar's syndrome. Am J Ophthalmol. 1973;75:250–4.
125. Feingold M, Gellis SS. Ocular abnormalities associated with the first and second arch syndromes. Surv Ophthalmol. 1968;14:30–42.
126. Foulkes GD, Reinker K. Congenital constriction band syndrome: a seventy-year experience. J Pediatr Orthop. 1994;14:242–8.
127. Bamforth JS. Amniotic band sequence: Streeter's hypothesis reexamined. Am J Med Genet. 1992;44:280–7.
128. Miller MT, Deutsch TA, Cronin C, Keys CL. Amniotic bands as a cause of ocular abnormalities. Int Ophthal Clin. 1987;104:270–9.
129. Hashemi K, Traboulsi E, Chavis R, et al. Chorioretinal lacuna in the amniotic band syndrome. J Pediatr Ophthalmol Strabismus. 1991;28:238–9.
130. Hollsten DA, Katowitz JA. The ophthalmic manifestations and treatment of the amniotic band syndrome. Ophthal Plast Reconstr Surg. 1990;6:1–15.
131. Liasis A, Nischal KK, Walters B, et al. Monitoring visual function in children with syndromic craniosynostosis: a comparison of 3 methods. Arch Ophthalmol. 2006;124:1119–26.
132. Motoki DS, Altobelli DE, Mulliken JB. Enophthalmos following transposition for craniofacial malformations. Plast Reconstr Surg. 1993;91:416–28.
133. Hicks C, Pitts J, Rose GE. Lacrimal surgery in patients with congenital cranial and facial anomalies. Eye. 1994;8:583–91.
134. Converse JM, McCarthy JG, Wood-Smith D, editors. Symposium on diagnosis and treatment of craniofacial anomalies. St. Louis: Mosby; 1979. p. 17.
135. Friede H. Normal development and growth of the human neurocranium and cranial base. Scand J Plast Reconstr Surg. 1981;15:163–9.

Management of the Microphthalmic Orbit

39

Karen E. Revere, James A. Katowitz,
Maryam Nazemzadeh, and William R. Katowitz

This chapter reviews current concepts in the management of congenital anophthalmia and microphthalmia. When discussing this subject, there can be some confusion as to proper definitions. This is because the term microphthalmia is often applied to a spectrum of disorders ranging from the absence of any visible globe to those where there may be only a minimal decrease in the size of the eye and orbit. Even more subtle findings may be included in this clinical category, such as a shortened conjunctival cul-de-sac with deficient conjunctival lining and/or small eyelid fissures with retarded lash growth. Strictly speaking, microphthalmia refers to a small, disorganized eye. Some ocular structure is usually visible on clinical examination. This is in contrast with nanophthalmia, which refers to a small but well-organized and functional eye. The terms microphthalmia and anophthalmia are synonymous with microphthalmos and anophthalmos, and both appear as interchangeable in published literature describing these congenital abnormalities. In the genetics literature, anophthalmia and microphthalmia are abbreviated as A/M for convenience, and we will use this combined term as well when we are referring to both entities together.

K.E. Revere (✉)
Oculoplastics and Orbital Surgery, Ophthalmology, The Children's Hospital of Philadelphia, Philadelphia, PA, USA
e-mail: Karen.revere@gmail.com

J.A. Katowitz, MD, FACS • W.R. Katowitz, MD
The Children's Hospital of Philadelphia and The Edwin and Fannie Gray Hall Center for Human Appearance, University of Pennsylvania, Philadelphia, PA, USA
e-mail: katowitz@email.chop.edu; katowitzw@email.chop.edu

M. Nazemzadeh
Oculofacial Plastic and Reconstructive Surgery, Rostami Oculofacial Plastic Consultants, Sanctuary Cosmetic Center, Reston, VA, USA

The term anophthalmia refers to an absence of ocular tissue and can be further divided into "true" anophthalmia and "clinical" anophthalmia. "True" anophthalmia is a rare condition and often incompatible with life. It is defined as the complete absence of ocular tissue within the orbit and is usually associated with other severe intracranial abnormalities. The term "clinical" anophthalmia is actually more accurate for describing the majority of situations where there is no visible eye clinically. While there may be no visible small globe, there is almost always some rudimentary ocular structure, however, that can be observed on computer tomography (CT) or magnetic resonance imaging (MRI) (Fig. 39.1).

Appropriate management of A/M is primarily determined by the type and severity of the eyelid and conjunctival and orbital deformities. One child may have no clinically apparent globe and, like a patient with a true anophthalmic socket, require prolonged and complicated socket management. In contrast, another child may only have a small globe and require minimal therapy with assistance of an ocularist to produce a prosthesis for an acceptable cosmetic appearance. Each child's situation must be carefully assessed to formulate a customized and appropriate treatment plan. Because of such wide variations in clinical phenotype, it is difficult to have set protocol with a uniform timetable as to the specific management steps necessary for rehabilitating each child [1]. The guiding principle is to follow a conservative approach especially in the early years of childhood and to avoid surgery (if possible), particularly to the lids and conjunctival cul-de-sacs. Conservative efforts for orbital volume enhancement are also preferred. After sufficient orbit and socket expansion is achieved with successful fitting of an ocular prosthetic, however, soft tissue surgical corrections may then be needed for ptosis, entropion, ptosis, or lid retraction, to name a few more common problems that often require later correction.

© Springer International Publishing AG 2018

J.A. Katowitz, W.R. Katowitz (eds.), *Pediatric Oculoplastic Surgery*, https://doi.org/10.1007/978-3-319-60814-3_39

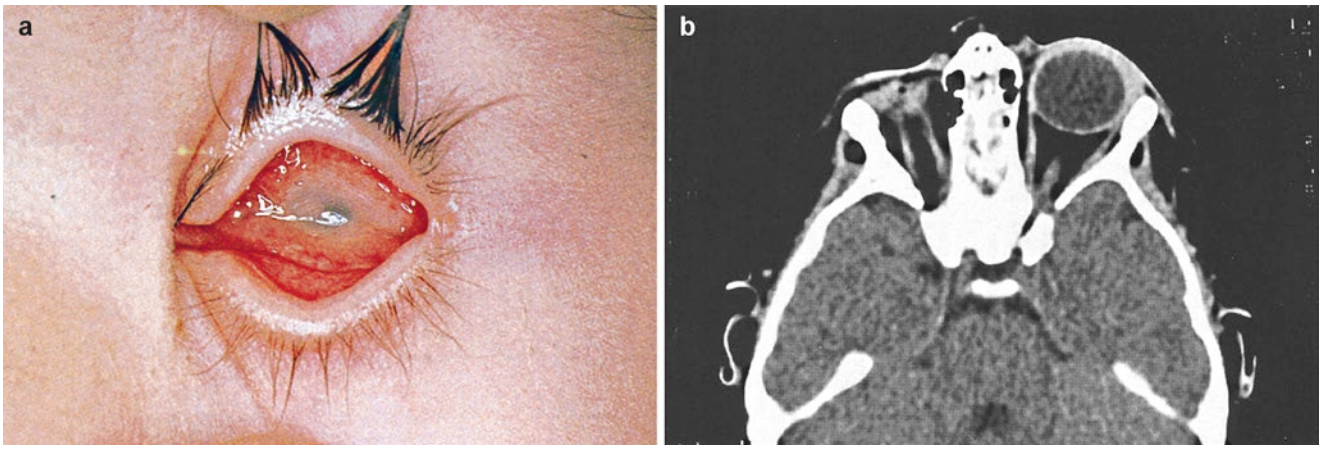


Fig. 39.1 Clinical anophthalmia. (**a**) Example of clinical anophthalmia in which no globe or ocular remnant can be seen on external examination. (**b**) Imaging, however, reveals a small ocular remnant with rectus muscles attached, demonstrating that this is not true anophthalmia, but rather a severe form of microphthalmia

In the subsequent sections, we will discuss our approach for managing these difficult clinical situations by reviewing the following: etiology, incidence, evaluation, treatment, and family resources.

Etiology

Most cases of congenital A/M are sporadic mutations, although environmental insults may also play an etiologic role. Environmental factors such as gestationally acquired infections (rubella, cytomegalovirus), maternal vitamin A deficiency, maternal LSD use, X-ray exposure, thalidomide exposure, and mechanical trauma to the fetus have been reported to play a role causing A/M [2–8]. Lower socioeconomic class and consanguinity may also be risk factors for the development of microphthalmia [9].

Congenital anophthalmia is rare and refers to a complete absence of ocular tissue. It occurs when there is a failure of the optic vesicle to bud or early arrest of its development with subsequent degeneration. Failure of optic vesicle budding may be "primary," with involvement of ocular tissue only, or "secondary," with complete suppression of the forebrain. This latter condition is usually not compatible with life. Clinical anophthalmia, as discussed earlier, is a more appropriate term for describing the clinical absence of a visible eye since rudimentary eye structures are usually present radiographically. In contrast, microphthalmia is defined by the presence of a small, often disorganized eye, with a corneal diameter less than 10 mm and an axial length less than 20 mm. It is thought to result from incomplete invagination of the optic vesicle into the optic cup or from defective closure of the embryonic fissure, sometimes leading to colobomatous microphthalmia with uveal coloboma or colobomatous cyst [10].

Clinical anophthalmia and microphthalmia may occur in isolation or in association with other systemic abnormalities related to errors in the development of the first and second branchial arches (which later contribute to most structures of the head and neck) during weeks 4–6 of embryogenesis. Conditions that result from abnormalities during this phase in gestational development are referred to as "oculo-auricular-vertebral spectrum" disorders [11]. Many patients with clinical anophthalmia or microphthalmia have associated systemic conditions that fit into this spectrum of disorders. Clinical anophthalmia and microphthalmia can occur unilaterally or bilaterally. The smaller the eye or eye remnant, the more severely retarded the growth of the orbit and eyelids. Abnormalities of the eyelid occurring in association with microphthalmia include eyelid coloboma, decreased horizontal and vertical palpebral fissure length, and decreased conjunctival surface area with relative shortening of the posterior lamellae with or without congenital entropion [12]. Although the adnexal structures of the eyelids are present, they are commonly decreased in size and number compared to the normal eyelid.

Changes in bone growth can result in a decreased midline to inner canthal distance, maxillary hypoplasia, a posteriorly displaced lateral orbital rim, decreased horizontal brow length, and a low supraorbital ridge.

Associated ocular pathology can include limbal dermoids, coloboma of the iris and/or retina, cataract, Duane's retraction syndrome, decreased corneal sensation (trigeminal nerve abnormality), and optic nerve hypoplasia [13]. In microphthalmia, glaucoma may also occur in the setting of a short axial length and resultant chronic angle closure. Acute angle closure and pupillary block can also occur from a disproportionately large lens in a cramped anterior chamber [14]. In unilateral microphthalmia, some of these associated ocular findings can also be present in the contralateral eye [15]. Over 50% of cases may be associated with systemic abnormalities, which frequently can involve the central nervous system, face (cleft lip or palate, hemifacial microsomia, facial hypoplasia,

micrognathia), skeletal system (anomalous limbs), ear (preauricular skin tags, deafness), heart (ventricular septal defects, tetralogy of Fallot, coarctation of the aorta), genitourinary system, and gastrointestinal system [13]. The relationship of congenital A/M to a variety of syndromes and anomalies makes it important for affected patients to undergo an initial genetic evaluation at the time of diagnosis.

Incidence

Congenital microphthalmia and anophthalmia are interrelated congenital abnormalities that likely have an underlying genetic basis. The true incidence and prevalence of congenital anophthalmia can only be surmised, even with current epidemiological data from specific localities, and is estimated to be about 0.2–0.6 per 10,000 births [16]. Together, these disorders account for 15–20% of severe visual impairment in children worldwide [17]. Microphthalmia and anophthalmia have an estimated prevalence of 1 per 7000 and 1 per 30,000 live births, respectively [18]. SOX2 and OTX2 gene mutations, which cause lens induction failure, account for up 60% of bilateral cases of severe microphthalmia and clinical anophthalmia [18, 19]. There are reports of pedigrees demonstrating autosomal-dominant, autosomal-recessive, and recessive X-linked inheritance with anophthalmia [20–24].

Evaluation

The evaluation of the microphthalmic patient requires a comprehensive and multispecialty approach. The discovery of a small or absent eye with an associated orbital socket deformity is certainly a disturbing and unexpected finding to both family and the neonatal medical staff. Similar to all new patient evaluations, a complete medical history must be obtained, including both pre-and postnatal history, current and past medications, allergies, and family history, with particular attention to any genetic disorders. Some microphthalmic patients will have had extensive medical evaluation, including genetic and ophthalmic consultation, soon after birth. In many cases, however, an extensive ophthalmic evaluation is deferred.

All neonates born with microphthalmia should be promptly evaluated by the neonatal team or pediatrician to check for systemic manifestations of the "oculo-vertebral-auricular spectrum." If there are severe ocular abnormalities, evaluation by an ophthalmologist should occur within the first 1–2 weeks of life. In unilateral cases, it is important to examine both eyes, since the fellow eye can also be affected. In clinical anophthalmia, an ocular ultrasound can be helpful to look for eye structures. In microphthalmia, ultrasound can be useful in measuring baseline axial length. Magnetic resonance imaging (MRI) or CT should also be performed to evaluate the bony orbit and check for intracranial abnormalities. Similar to cryptophthalmos, VEP and ERG can be useful for evaluation of visual potential. Genetic screening may be warranted if a clinical syndrome is suspected.

Since facial maturation is significantly influenced by orbital growth, clinical anophthalmia and microphthalmia can cause varying consequences to overall facial development (Fig. 39.2). In a Caucasian population in Canada, Farkas et al. determined age-related orbital growth patterns in 1594 healthy children 1–18 years of age. Measuring both the intercanthal and biocular (outer lateral canthus to outer lateral canthus) distances, this study demonstrated that approximately 90% of orbital growth occurs by the age of 5 years [25]. It is therefore critical to develop an appropriate and early treatment plan for all pediatric patients with an

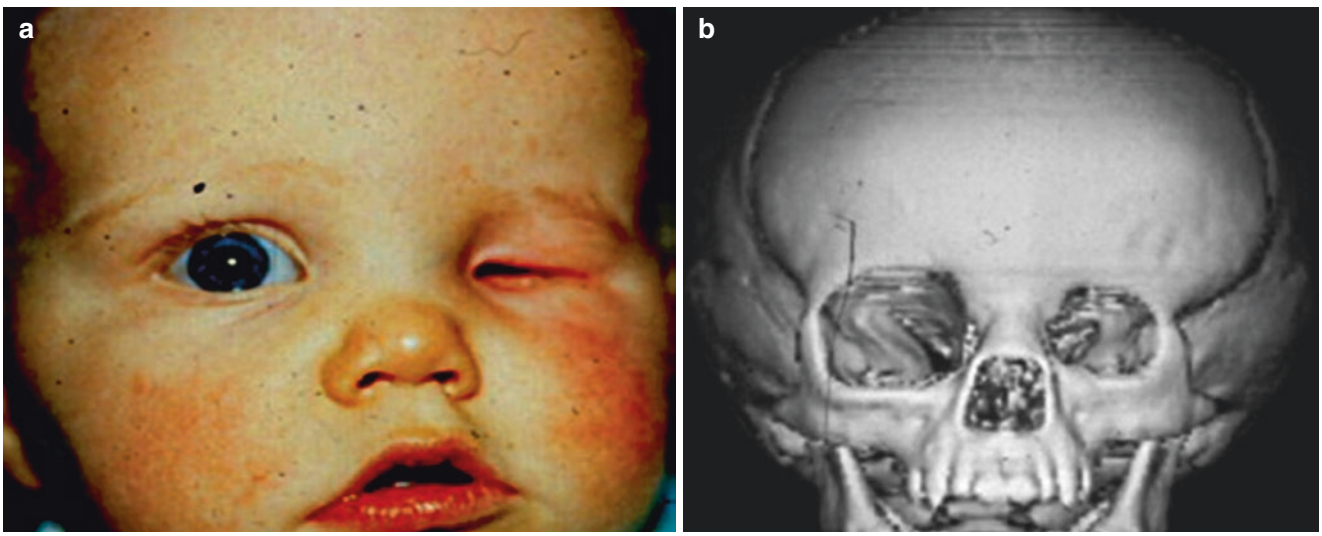


Fig. 39.2 (**a**) 8-month-old child with left microphthalmia with shortened horizontal lid length and anterior lamella of the upper lid as well as a smaller conjunctival socket. (**b**) The lower brow on the left side is indicative of a smaller orbit with significant orbital asymmetry

anophthalmic or microphthalmic socket. Patients should be seen at birth or as soon as an abnormality is recognized. If there is delay in management, asymmetries in orbital and facial skeletal development may be permanent.

Initial management decisions in microphthalmia are generally guided by whether the eye has visual potential. In some cases, the answer is clearly apparent when the ocular remnants are so rudimentary that there is no potential for useful vision. In other cases, however, it can be difficult to judge the visual potential of a microphthalmic eye. Since treatment with expanding conformers or orbital volume augmentation may disrupt the visual pathway, the decision about visual potential must be considered prior to therapeutic intervention. If some vision is possible, particularly in a bilateral problem, even if only very rudimentary, then some reconstructive steps of the orbit and eyelids may be considered. When there is potential for good vision, whether unilateral or bilateral, surgical intervention may be modified or deferred to prevent amblyopia [12].

While preservation of vision may not be a concern in cases of severe microphthalmia and clinical anophthalmia, these clinical situations still present difficult challenges for achieving cosmetically acceptable eyelids and orbital symmetry. This is related to the reduction in normal eyelid fissure length, as well as inadequate conjunctival lining and orbital space, which limits the size and shape of the fornices. These abnormalities often complicate artificial eye placement, as well as the timely progression of incremental prosthetic fittings. Unilateral deformities present the greatest difficulties because the contralateral normal side is much larger in both external and internal dimensions. From an appearance standpoint, the unilateral cases usually demonstrate a degree of asymmetry that is extremely difficult, or even impossible, to overcome [26].

The initial examination is often a difficult experience for the family because their attention is usually directed toward finding reasons for the microphthalmia and in maintaining hope for some physical sign indicating vision. From the perspective of the treating physician, it is important to be patient and to develop good rapport with the family so that an appropriate treatment plan can be quickly initiated. It is often difficult for parents, and even physicians unfamiliar with these syndromes, to fully appreciate the long-term cosmetic ramifications if such problems are not aggressively treated at an early age. Most patients must undergo a lengthy, time-consuming rehabilitative process. It is important to constantly assess the family's resolve as well as the child's physical, mental, and emotional development as the treatment plan is pursued.

Ophthalmic Evaluation

The ophthalmic examination should initially focus on establishing whether there is visual potential. In unilateral cases, specific concerns are first directed toward the microphthalmic socket, but it is important to perform a complete dilated exam on the contralateral, unaffected side as well. As described elsewhere in this book (Chap. 10), an age-appropriate vision test should be performed. Even an observation of intact fixing and following behavior can be helpful in determining a plan for socket and orbit expansion.

ERG or VEP testing may be helpful in objectively assessing whether there is visual potential in young, preverbal children. As mentioned previously, vision assessment is a critical first step toward planning any cosmetic rehabilitation and providing the parents or guardians with objective evidence as to their child's potential visual status. Covering an eye that might have significant visual potential with mucus membrane and/or an opaque shell would obviously produce unacceptable amblyopia. In both unilateral and bilateral cases of microphthalmia, parents or guardians are often reluctant to proceed with such a treatment plan directed mainly toward appearance without definitive evidence that the microphthalmic eye has little or no visual potential. The use of electrophysiologic testing is often invaluable in demonstrating the absence of vision to family members reluctant to accept this reality.

Oculoplastic Evaluation

Once vision is assessed, the remainder of the evaluation should consist of determining the extent of the adnexal deformities, including the eyelid length and position, lash position, condition of the conjunctival cul-de-sacs, lacrimal system patency, and overall development of the head and neck. Absence of a globe, not only retards growth of the socket and overlying soft tissues, but also affects the growth of the maxilla, maxillary sinus, and mandible [27]. When facial asymmetry is present, it is often observed as a decrease in the projection of the malar eminence and mandibular length on the affected side, as well as a decrease in the size of the anterior orbit (Fig. 39.3). Highlighting the presence of these facial deformities to parents is helpful in emphasizing the urgency of treatment for the microphthalmic socket.

The oculoplastic examination should proceed with the measurement of eyelid characteristics. This includes horizontal fissure length (measured in millimeters from medial to lateral canthus), position of the eyelash margin, level and contour of both upper and lower eyelids, position of the brow, levator function, and clinical presence of puncta. The distance between the lid fissure and the brow may be reduced, creating a compressed appearance of the midface [28]. If the position of the brow is low, this is a visible clue that the orbit may be smaller on that side. This pattern of hypoplasia is common in microphthalmia and anophthalmia, but less dramatic retardation can also result from a normal eye that is removed in early infancy without adequate volume replacement for the enucleated globe.

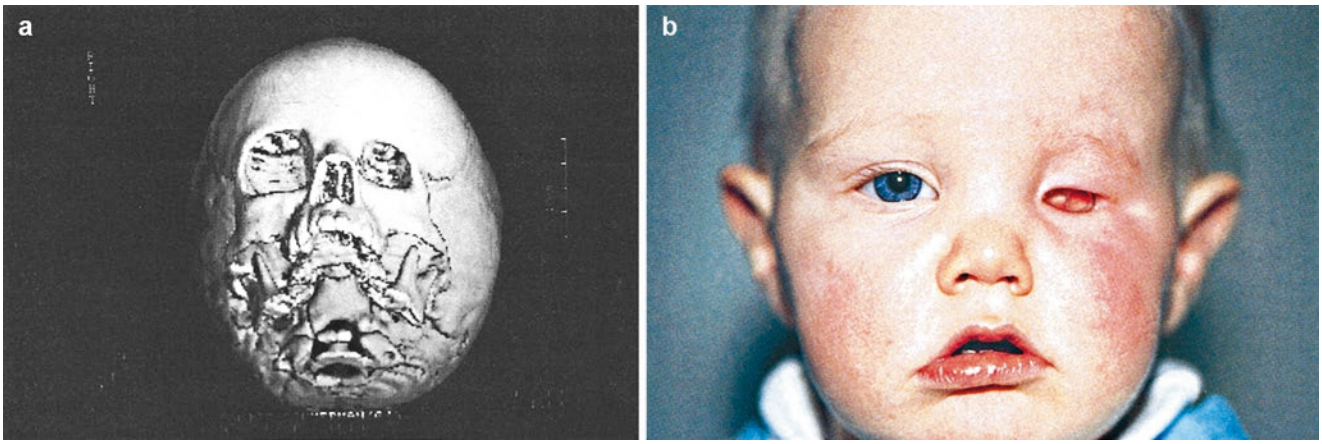


Fig. 39.3 Microphthalmia and facial maturation. (**a**) 3-D CT reconstruction demonstrating hypoplasia of the entire left side of the face secondary to severe microphthalmia. Note the retrusion of the zygoma and malar eminence; growth of the mandible is also frequently retarded. (**b**) Facial maturation on the left side has been significantly influenced by the clinical anophthalmia. The patient's forehead, maxilla, mandible, and zygoma have developed less on the left as compared to the normal right side

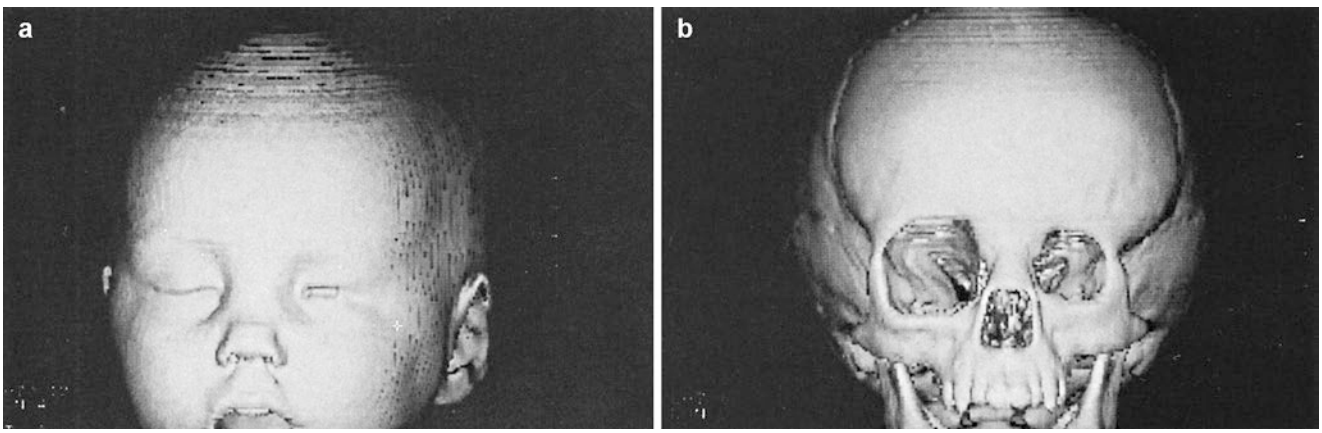


Fig. 39.4 Microphthalmia and orbital hypoplasia. (**a**) Soft tissue 3-D reconstruction from CT data of a patient with left-sided microphthalmia. (**b**) Corresponding bony 3-D reconstruction demonstrating hypoplasia of the left orbit

Upper and lower conjunctival cul-de-sacs should be examined and may be diminished in size due to congenital hypoplasia rather than any secondary process of contraction. Utilizing topical anesthetic, a muscle hook can be inserted into the cul-de-sacs to gauge depth and development. Depending on the severity of microphthalmia, care must be taken to avoid traumatizing any corneal surface present. Regardless of the visual potential or globe size, the microphthalmic patient is at risk for external infections and potential corneal infection or even endophthalmitis if examined or treated aggressively without regard for these possibilities.

Additional examination, particularly when a globe is present, includes globe size, motility, presence and condition of the corneal surface, and status of the intraocular contents. A dye disappearance test is useful in determining tear outflow. Photographic documentation is helpful. Imaging modalities, such as ocular ultrasound, MRI, and CT, can also be utilized both for the initial evaluation and long-term follow-up.

Imaging Techniques

The primary imaging modalities for evaluating patients with anophthalmia or microphthalmia include CT and MRI. In the past, computerized tomography has been the preferred imaging modality for assessing the microphthalmic orbit. The advantage of CT is its excellent bone imaging, which permits rapid identification of orbital and facial landmarks. Three-dimensional (3-D) reconstructions can also be generated from CT data, which can be helpful in surgical planning (Fig. 39.4). Over the past several years, however, we have been relying more on magnetic resonance imaging as a primary imaging technique for A/M patients. MRI can be used to visualize the orbital soft tissue contents in exquisite detail, but it can also provide an accurate assessment of the anterior-posterior dimensions as well as the size and shape of the anterior orbital entrance [29]. It has been our observation that there has been little or no difference between CT and MRI as far as clinical decisions are concerned. The major

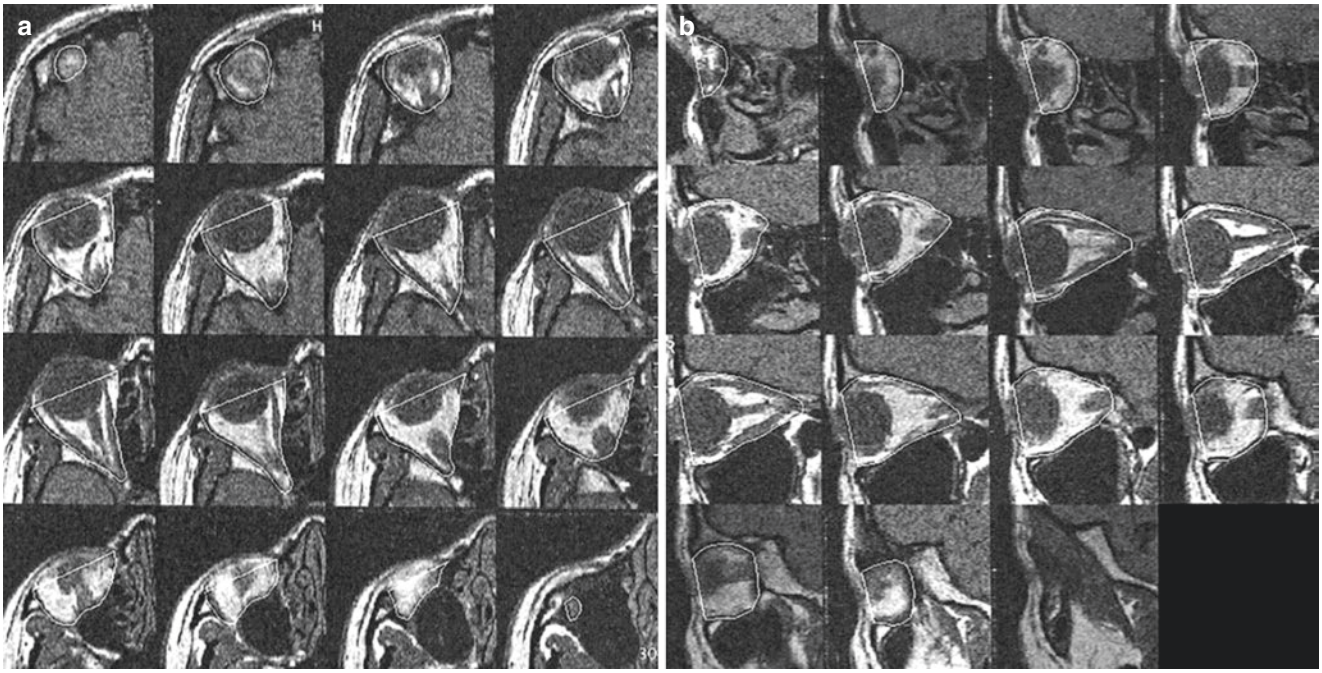


Fig. 39.5 MRI used to follow orbital growth. MRI can be used to serially follow orbital growth without radiation exposure. The bony orbit appears as a black line. Volumetric estimates can be calculated similar to that for CT. (**a**) Axial sections of orbit outlined in white. (**b**) Sagittal sections outlined

advantage of MRI, however, is its ability to permit multiple imaging sessions and long-term follow-up without radiation exposure. However, MRI examinations are often longer and usually require a general anesthetic in young children.

MRI, like CT, can yield volumetric analysis of the bony orbit (Fig. 39.5). Regardless of the imaging modality, review of the literature indicates an unfortunate lack of standardization. This is a major problem because there appears to be little understanding of how subjective selection of anatomic endpoints can markedly affect orbital volumetric results. We have recently endeavored to catalog normal orbital volumes for healthy children across different ages (unpublished). This would help to standardize normal parameters and help provide age-specific goals for orbital expansion in congenital microphthalmia. For this reason, comparison of various studies is difficult and perhaps misleading. In the clinical management of the microphthalmic orbit, it may be more important to accurately measure the orbital entrance and depth rather than overall volume.

While an initial MRI or CT is helpful to definitively establish the baseline orbital volume and orbital contents in cases of A/M, we find that regimented yearly imaging is not always necessary. A good response to socket expansion can be evaluated by the external position of the eyebrow and often does not require frequent imaging. If the brows are symmetric in both height and length, then socket expansion is occurring as we would like and imaging is not necessary as further confirmation. However, each child is unique, and there are some cases (especially those that are more refractory to socket expansion) where more frequent imaging may be helpful for clinical decision making.

Another technique that may hold future promise is 3-D ultrasound. There have recently been efforts to standardize fetal ocular growth using ultrasonography in normal fetuses [30].

Current clinical research with this technique should enhance the prenatal recognition of patients with ocular, orbital and facial deformities [31, 32]. This may prove to be of particular value for prenatal analysis regarding possible fetal surgical repair in the future [33] (see Chap. 3). More recently, fetal MRI has been used to measure fetal ocular development at different stages of gestation [34]. This has helped to develop the realm of fetal imaging further. Now, fetal MRI is also being used to diagnose microphthalmia prenatally [35, 36] (Fig. 39.6). Early diagnosis has led to improved parent understanding, reduced anxiety, and more efficient channeling of affected children to the appropriate subspecialists, such as pediatric ophthalmology and oculoplastic surgery.

Current Therapies

The goals of treatment for microphthalmia are threefold: (1) enlarge the bony orbit; (2) expand the conjunctival space and fornices; and (3) increase both horizontal and vertical fissure

length [37]. The guiding principle is conservative therapy and avoidance of surgery, if possible, which can cause cicatricial changes and may inhibit further efforts to expand the soft tissues and ultimately limit the placement of a well-fitting prosthetic shell.

Initial efforts should be directed toward expansion of the lid fissures, because severe phimosis of the eyelids effectively limits access to the orbit. This expansion process has been traditionally managed by an ocularist using progressively larger, acrylic conformers to stretch the lids and conjunctival lining, both vertically and horizontally. Interestingly, even though this process is directed toward anterior soft tissue expansion, it does also provide significant stimulus for bony orbital growth in many cases. Historically, the oculoplastic surgeon has been dependent on the ocularist for initial management in order to achieve as optimum a result as possible.

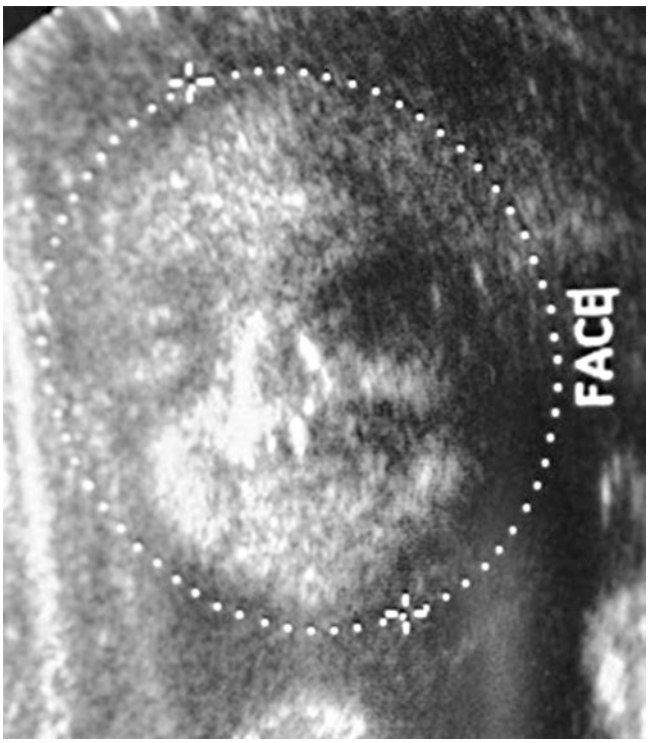


Fig. 39.6 Prenatal ultrasound with black circle demonstrating left anophthalmia

The Role of the Ocularist

As indicated above, the ocularist is a critical member of the multidisciplinary team ideally assembled for management of the A/M patient. Eyelid and conjunctival expansion are really the most important initial steps in rehabilitation of the A/M orbit. Progressive conformer expansion by an experienced ocularist has been the mainstay of soft tissue expansion but can also stimulate bony orbital growth (Figs. 39.7 and 39.8) [38]. In the majority of cases, the ocularist has been able to expand the eyelids and stimulate orbital growth sufficiently to assist in the development of facial symmetry. This, however, is a lengthy process somewhat dependent on economic and demographic considerations. In addition, it requires commitment on the part of the family to consistently follow instructions including the frequent office visits required to achieve the desired results. It is absolutely essential that all medical and ancillary personnel treating these children understand the importance and urgency of ensuring early and consistent intervention, whether by the ocularist or by use of one of the newer expansion techniques available to the oculoplastic surgeon which will be discussed later in this chapter.

Early and aggressive surgical intervention, however, should be avoided if at all possible. It is critical to avoid doing a lateral canthotomy as the subsequent scarring interferes with the ability to stimulate expansion of the lateral cul-de-sac and canthus (Fig. 39.9).

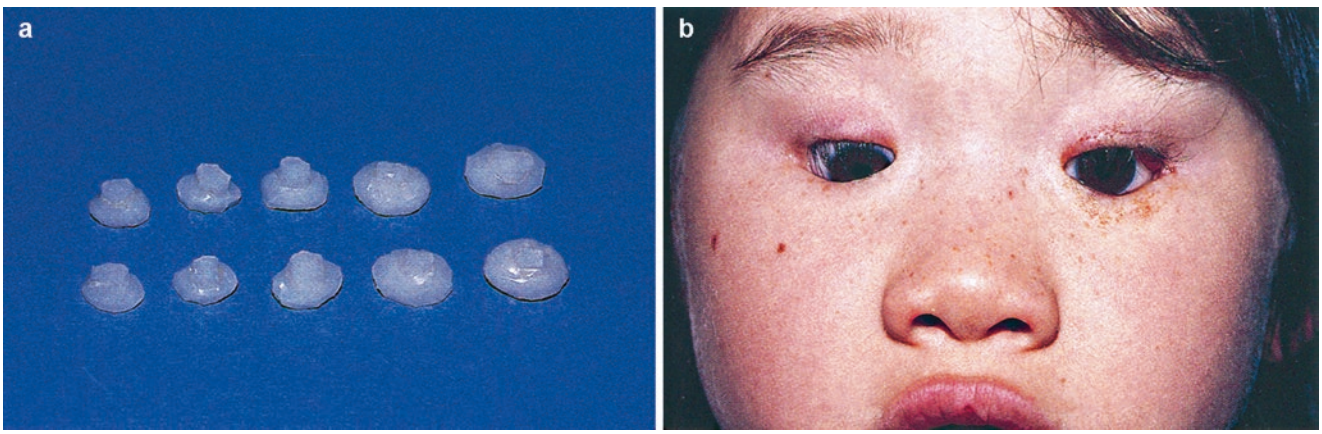


Fig. 39.7 Progressive conformer expansion. (**a**) Progressive increasing conformer sizes over a 1-year period. (**b**) Progressive conformer expansion permitting cosmetic shells in severe bilateral microphthalmia. Anterior-posterior depth is satisfactory, but stimulating horizontal growth has not been as successful

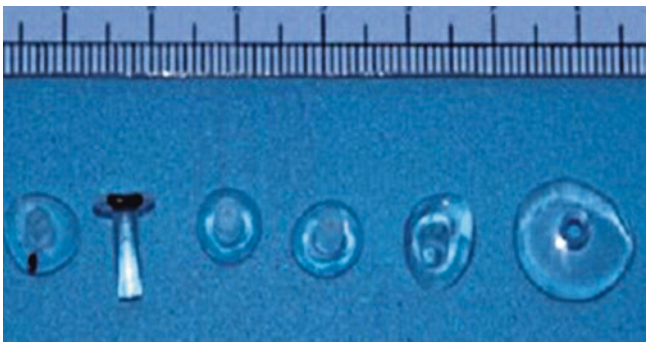


Fig. 39.8 Another type of clear conformers with stems for ease of insertion and removal

We advocate an initial oculoplastic evaluation as soon after birth as medically possible. Progressive conformer expansion maximizes a child's opportunity for a good cosmetic outcome (Fig. 39.10). Conformer expansion will often stimulate adequate growth of lids and orbit such that surgical intervention can be avoided. Early expansion may also rapidly yield a large enough socket to accommodate a painted prosthetic shell, which helps to reduce psychological trauma for the family. A cosmetically acceptable prosthetic shell is a good initial goal, because families frequently encounter inappropriate and unkind words from relatives, neighbors, or complete strangers regarding their child's appearance. The response can be variable, however, with some orbits being more resistant to conformer expansion (Fig. 39.10). Historically, many lids and orbits have responded well to the traditional ocularist's approach with progressive conformer shell exchange. In a microphthalmic child with a visible cornea, however, this is not always achievable (Fig. 39.11). More frequently, this is too uncomfortable and an alternative is to protect the cornea with a mucus membrane cover graft, which will permit full-time wearing of a conformer shell (Fig. 39.12). This surgical technique will be discussed in detail later in this chapter.

Managing subtle facial and socket asymmetry in unilateral microphthalmic patients can sometimes be improved by using prescription eyeglasses. Plus and minus lenses, prisms, and cylinders can be prescribed to mask size and position differences between a patient's normal orbit and socket as compared to the microphthalmic side. Plus lenses can magnify an otherwise small socket (Fig. 39.13). Likewise, the use of prisms within a patient's eyeglasses can appear to move the image of a dystopic orbit/socket either up or down, depending on the strength and position of the prism. These techniques do not replace early aggressive conformer expansion or surgical intervention when required, but can be useful in situations of subtle asymmetries after adequate socket and lid expansion.

Frequent communication with the ocularist is necessary to monitor the treatment plan and to gauge progress. There may be cases in which the ocularist is unable to keep pace

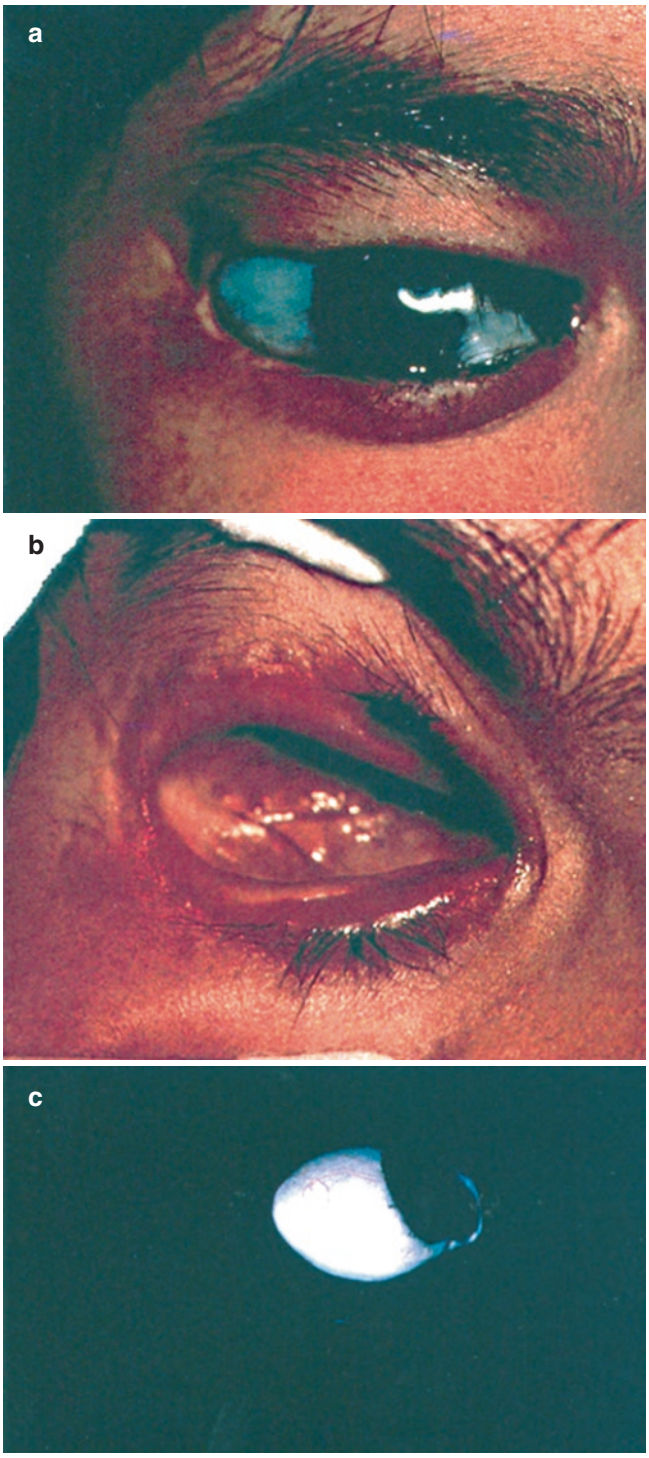


Fig. 39.9 Negative effects of early socket surgery. (**a**) Lateral canthal surgery has resulted in poor depth in the lateral cul-de-sac in a patient referred to CHOP for evaluation and repair. (**b**) Lateral canthal edges had been opened early in life and deepened with a skin graft. Note the position of the lashes, which have remained compact because the lid margin has not been stimulated sufficiently to grow horizontally. Lashes cover only two-thirds of the lid length, which further compromises the appearance. (**c**) Because of limited conjunctival space and shortened lateral fornix, a large boat-like prosthesis, which is too heavy, does not permit an optimum fit and significantly inhibits motility

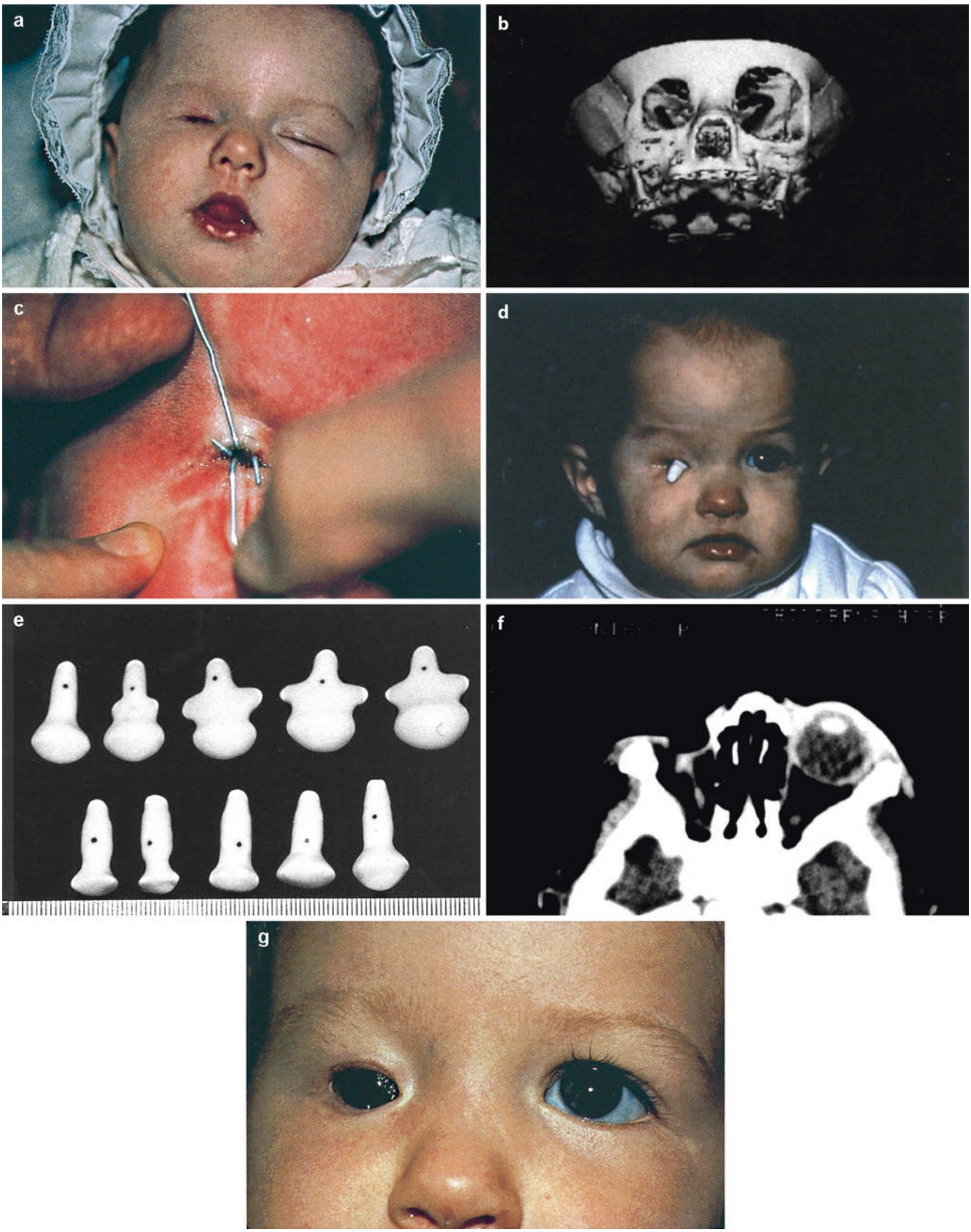


Fig. 39.10 Microphthalmia correction with prosthesis. (**a**) Severe right-sided microphthalmia (clinical anophthalmia). (**b**) 3-D reconstruction demonstrating a small right orbit. (**c**) Fissures are so small that only bent paper clips could permit observation of the socket. (**d**) Stem-type conformer expansion after several months. (**e**) Increasing sizes of conformers over an 18-month period; note the volume being obtained in A-P depth. (**f**) Axial CT demonstrating better A-P depth than horizontal length. (**g**) Patient with prosthesis at age 3. Note persisting hypoplasia as demonstrated by smaller right brow as well as decreased lid fissure length

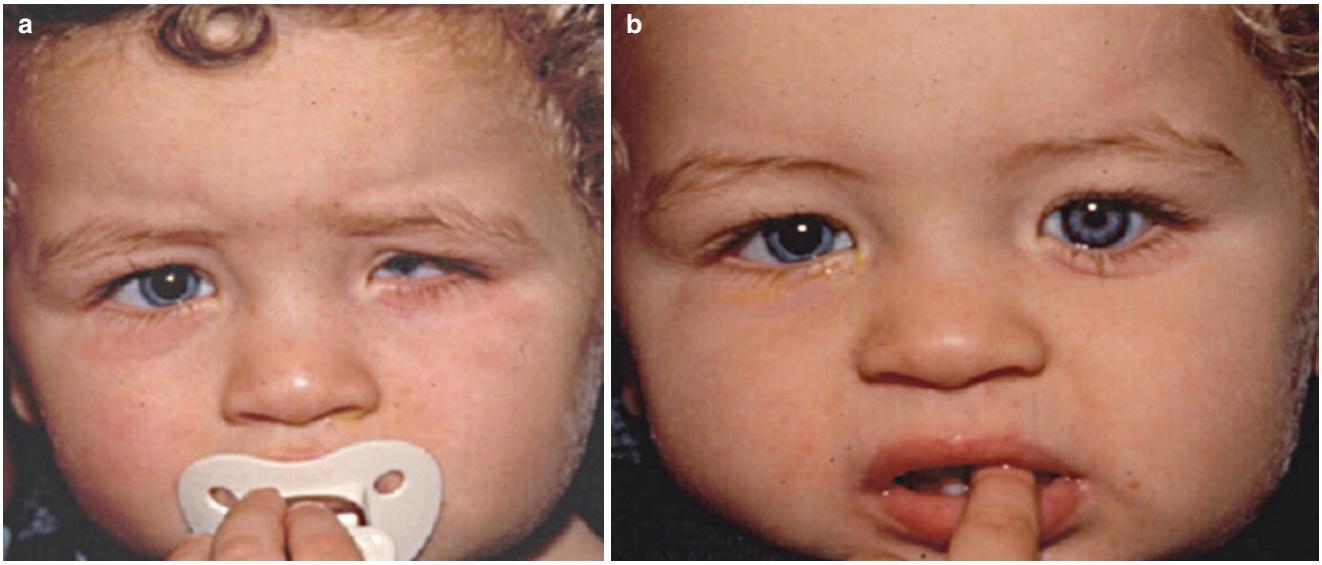


Fig. 39.11 18-month-old with milder form of left microphthalmia. (**a**) Clear conformer in place over a small cornea. (**b**) Periodic exchange of a vaulted prosthetic shell offered good cosmetic outcome without corneal irritation or need for mucous membrane grafting

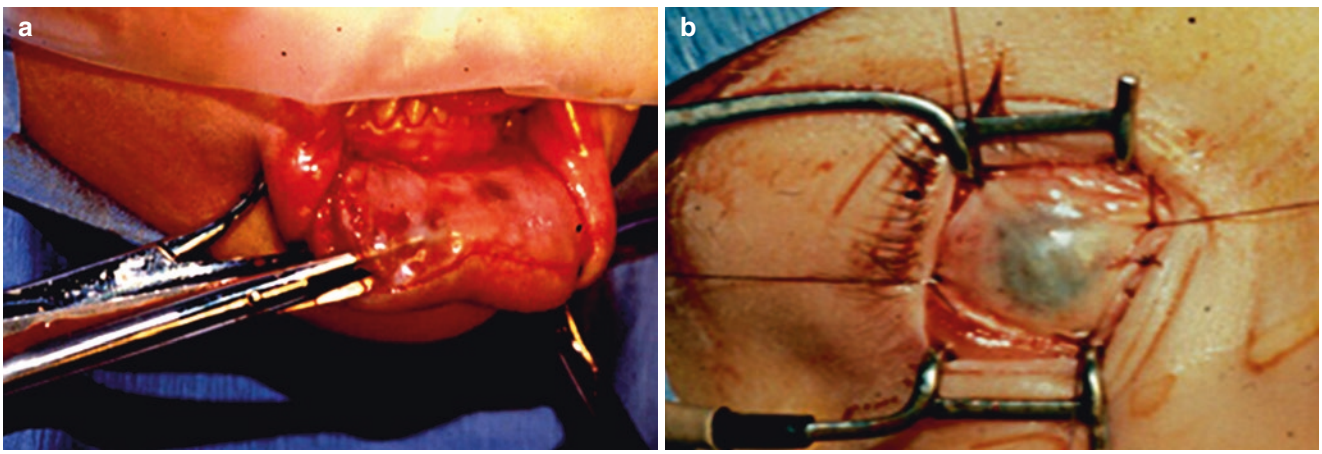


Fig. 39.12 Intraoperative photos of (**a**) harvesting lower lip oral mucus membrane graft and (**b**) securing this a protective cover graft over the cornea

with overall orbital and facial size on the contralateral (normal) side. Aside from poor patient or family compliance, the ocularist may face additional challenges, including poor initial conformer retention because of a severely anophthalmic socket, lack of the response of the lids to stretching efforts, or poor response of the bony orbit to initial conformer expansion.

Expansion of the Eyelids and Socket

Lengthening of the eyelid fissures, both horizontally and vertically, is a major goal for the ocularist. Progressive expansion of the eyelids is necessary to achieve symmetry of the periorbital structures and to accommodate a properly sized prosthesis. With continued eyelid expansion, there will be a concomitant increase in the conjunctival surface area of the socket. The enlargement of both the eyelids and socket will allow the fitting of well-retained prostheses. It is important for the ophthalmologist to examine these children and to communicate frequently with the ocularist during the period of active expansion.

The period of time for active expansion is not clearly delineated. The pediatric skull is thought to achieve 90% of its adult dimension by about the age of 5 years old [25]. However, we feel that efforts to expand the orbit may be attempted up until 6–7 years of age. This information is especially valuable in managing patients who present to your clinic later in life, having never experienced previous attempts at socket expansion.

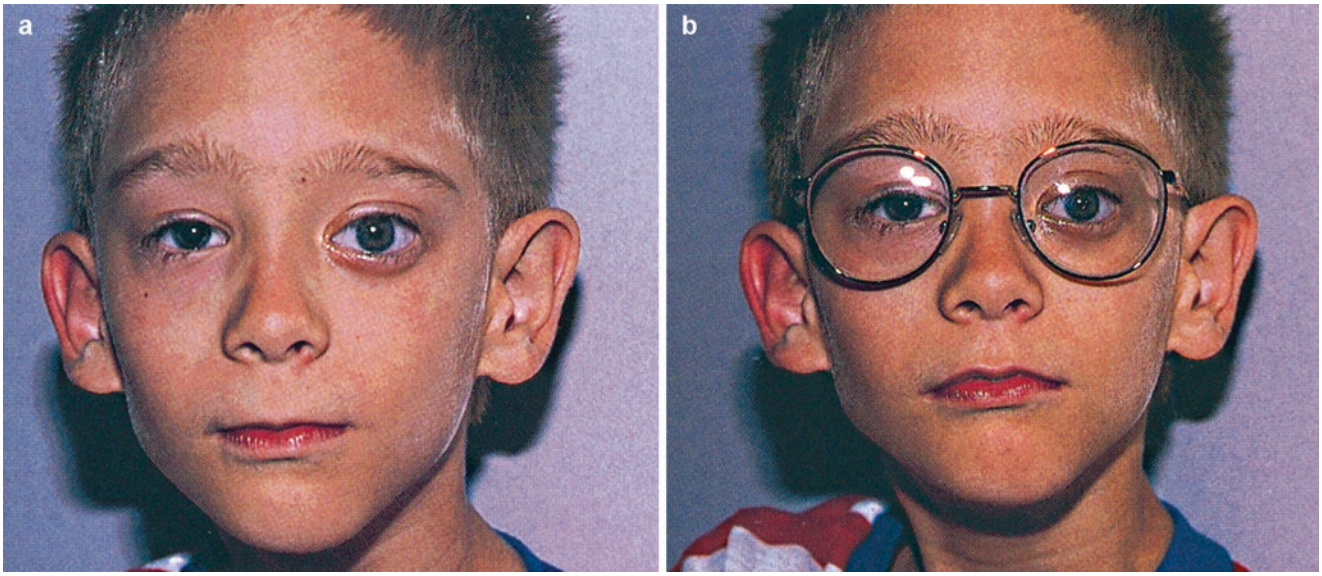


Fig. 39.13 Dermis fat graft. (**a**) Patient with a more prominent prosthetic appearance of the left orbit secondary to overgrowth of a dermis fat graft. (**b**) Use of a −5.00 diopter lens on the left side of the spectacles reduces the image size and results in a more cosmetically pleasing appearance by approaching symmetry. This may defer the need for surgical debulking of the dermis fat graft. Vertical and horizontal orbital dystopia can also be masked to some degree with the addition of prisms to a patient's spectacles

However, in patients with more severe forms of microphthalmia, expansion may not proceed as expected because of initial difficulty in retaining a conformer. This may occur for two reasons. First, there may be a severe deficiency of the conjunctiva lining, as evidenced by poorly formed cul-de-sacs. Second, some children with more mild forms of microphthalmia with a visible globe and cornea, as mentioned earlier, may not be able to tolerate a conformer or prosthetic (despite the slightly vaulted curvature of these structures). In such cases, mucus membrane grafting can be used to reconstruct as a protective corneal cover. Contrary to what many families believe, placement of a mucus membrane graft (if thin enough) over the surface of the eye does not completely eliminate the ability of a child to see light and even color. An ocular prosthesis can additionally be fashioned to have a clear central opening so that vision can be preserved at the same time that cosmetic rehabilitation is achieved.

Deficient conjunctival surface area/or a shortened cul-de-sac is a more difficult problem to solve and can portend failure of expansion. If this difficulty becomes apparent early in the expansion process, overall success will be limited. The majority of problems occur with a blunting of the lateral cul-de-sac, thereby limiting both the retention of an adequate sized ocular prosthesis. It is critical to maintain a stimulus to the medial and lateral canthi to ensure maximum horizontal expansion. The grafting of mucus membrane is a method we have found to improve deficiencies in the conjunctival lining and cul-de-sacs in some of these challenging situations [39].

Surgical Expansion of the Socket

As mentioned above, one way to increase the conjunctival surface area in the microphthalmic socket is by using grafts. There are many available graft sources, including autologous, homologous, and alloplastic options. Mucus membrane from the mouth, hard palate, conjunctiva or tarsus from the contralateral eye, allogenic hard palate grafts (i.e., Alloderm), or amniotic membrane can all be used with varying advantages and disadvantages for each material [40]. Usually parents are less inclined to pursue grafting options that involve surgery and conjunctival excision from the contralateral (normal) eye. However, sometimes there are unique cases where a contralateral ptosis exists for which a Muller's muscle conjunctival resection or Fasanella-Servat procedure is performed. In these situations, excised conjunctiva and/or tarsus can be saved and used for forniceal reconstruction in the microphthalmic socket.

In mild cases of contraction, sometimes adjusting the ocular prosthesis alone or correcting an entropion with standard surgical techniques such as anterior lamellar repositioning procedures can achieve somewhat reasonable results [41]. However, if contraction is severe, augmentation of the posterior lamella is often required. In these cases, our preferred donor tissue is mucus membrane from the mouth. Others have also found this method of rehabilitation to the A/M socket to be ideal, as well [42]. The ideal donor sites of the oral mucus membrane are either the lower lip (Fig. 39.13) or buccal surface of the cheek. Additionally, hard palate mucosa

may be harvested from the roof of the mouth to augment the socket surface area or to provide stability to the eyelids as discussed earlier. We use these grafts both to reconstruct the fornices and stabilize the eyelids, as well as to cover the cornea in cases where there is a rudimentary ocular surface that is becoming irritated with ocular prosthesis use.

Prior to obtaining an oral mucus membrane graft, local anesthetic (0.5% bupivacaine 1:200,000) with epinephrine is injected in sufficient quantity so as to balloon the tissue. Towel clamps assist in retracting either the lower lip or cheek to allow more room for harvesting the graft (Fig. 39.12). Outlining the size of the proposed graft is helpful in maintaining orientation. Usual donor graft size is approximately 15 × 15 mm. The full-thickness graft is obtained by both blunt and sharp dissection. Care must be taken to avoid even a pinpoint perforation as this will expand when sutured over the cornea with the potential for retraction and exposure of the underlying cornea. The harvested graft is thinned of residual dermal elements, wrapped in a gauze pad, and soaked in a 10% povidone-iodine solution. It is very important to thin the graft as much as possible; otherwise it is more likely to contract on the ocular surface and decenter, making ocular prosthesis position suboptimal. Furthermore, if it contracts too much and pulls off part of the corneal surface, ocular surface irritation with prosthesis use may become an issue. Additionally, in those patients with preserved light perception or hand motion vision, a thinner graft over the cornea will likely not occlude their limited visual abilities. Typically, the donor site is left unsutured and allowed to granulate [43]. This is usually well tolerated by children and does not require a postoperative oral analgesia wash or antibiotic wash. We generally only advise that patients avoid high-acid content citrus foods until the area has re-epithelialized.

In difficult situations where there is serious contraction, the conjunctival cul-de-sacs can be incised, and a mucus membrane graft can be sutured or held in place with a properly sized clear conformer. This conformer-mucus membrane graft combination is then inserted so that the raw mucous membrane edges fill the cul-de-sac and palpebral defects (Fig. 39.14). In most cases, a simple serpentine tarsorrhaphy with 5–0 nylon suture will suffice to hold the conformer or a central mattress suture tarsorrhaphy with bolsters.

In some very refractory cases or in highly uncooperative patients who may easily displace the conformer manually, the conformer can be sutured in position after forniceal deepening and lining this area with graft material. This is achieved by drilling holes into a standard clear conformer using a straight drill tip in the operating room. Nonabsorbable mattress sutures of 5–0 Prolene are then threaded to through these holes. The conformer is properly positioned, and the sutures are passed through the orbital rim periosteum in all four quadrants and externalized through the skin where they can be secured without bolsters. This serves to firmly anchor the conformer to the orbital rims (Fig. 39.15).

Amniotic membrane is another consideration for lid and socket reconstruction. This is a relatively new option and is gaining popularity in the oculoplastics community for socket reconstruction [44, 45]. Its use has been extensively described in other subspecialty areas of ophthalmology, including for pterygium removal, ocular burns treatment, and ocular surface inflammation (i.e., Stevens-Johnson syndrome) filtration procedures, and in combination with procedures for limbal stem cell transplantation. It is relatively available, has no patient morbidity (no painful oral lesion), and does not manifest significant contractural changes during the healing process because it has innate antifibroblastic properties [46]. One group recently compared amniotic membrane and mucus membrane grafting in patients with contracted, anophthalmic sockets [47]. They found similar results in forniceal depth and socket expansion at 3 months between the two groups but found there to be significantly more contraction in the mucus membrane group at 1 year, suggesting that perhaps amniotic

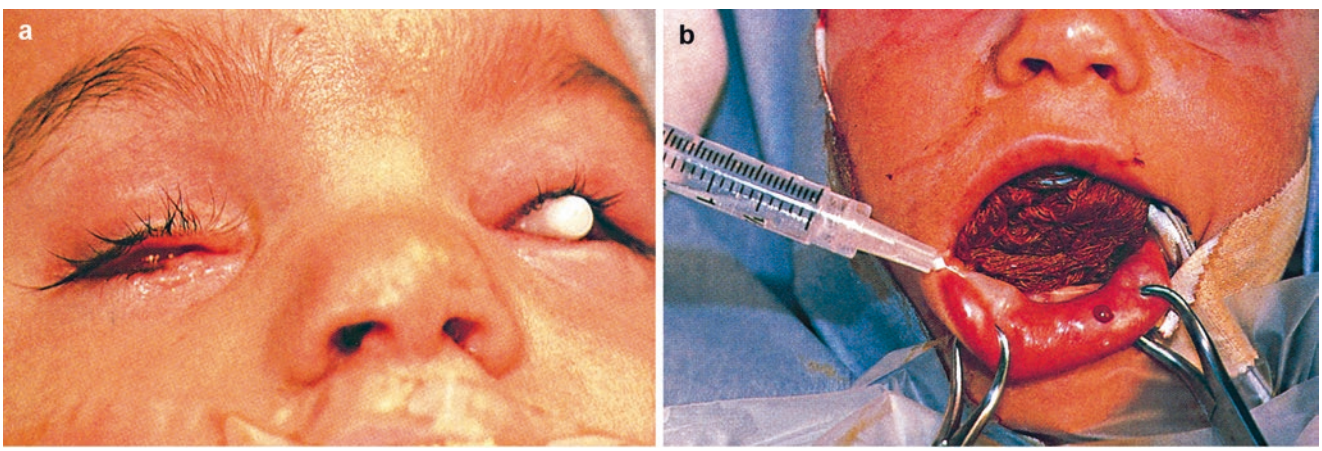


Fig. 39.14 Cul-du-sac reconstruction with mucous membrane graft. (**a**) Patient unable to retain conformer on right side due to a shallow lateral cul-de-sac. (**b**) The lower lip is infiltrated with 0.5% bupivacaine with 1:200,000 epinephrine.

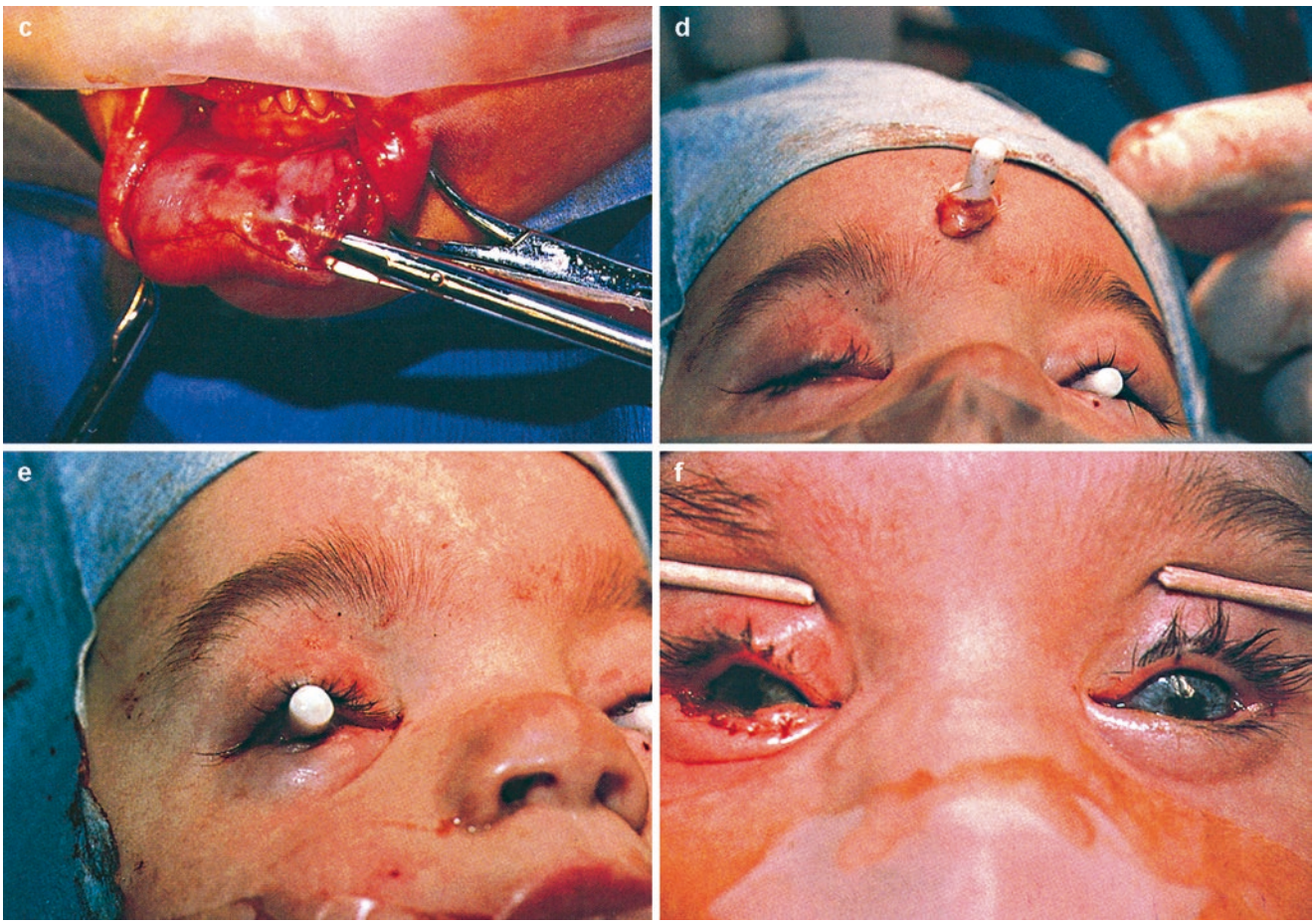


Fig. 39.14 (continued) (**c**) The oral mucous membrane graft is undermined with sharp scissors; care is taken not to create a buttonhole. (**d**) The graft can be thinned and sewn over a conformer which can be used as a guide for placement. (**e**) Stent can either be left in place or, after the graft edges are secured to the lid, removed for insertion of a cosmetic prosthesis. (**f**) Cosmetic shell placed into socket. A 5–0 nylon serpentine suture tarsorrhaphy can be utilized to ensure retention of the shell and left in place for up to 3 weeks

membrane grafting may be superior to mucus membrane grafting. None of their study patients had microphthalmia, which is an obvious limiting factor in the application of their conclusion to the A/M population. However, as more research is performed, amniotic membrane grafting may become a more relevant therapy for use in the A/M sockets.

We have used amniotic membrane in two forms for our patients with A/M who needed forniceal deepening procedures. We have found success with free amniotic membrane grafts but prefer the cryopreserved variety (instead of the dehydrated version) because of increased antifibroblastic properties. We have also used Prokera rings (Prokera), which is a ring over which amniotic membrane is draped and secured (Fig. 39.16). These have been used more commonly for recalcitrant corneal abrasion and ulceration management but have worked well in the context of A/M socket reconstruction. The advantage of the ring is that the ring itself provides additional support in the fornices during the healing process, which we feel increases the chances of grafting success and forniceal expansion.

The Prokera ring has been particularly useful for complex reconstructive situations where there has been virtually no conjunctival cul-de-sacs as in the problem presented in Fig. 39.17. This was an unusual congenital anomaly with a large upper lid coloboma, a microphthalmic eye and a large dermoid cyst in the inferior cul-de-sac pushing down the lower lid. As the globe was threatened by exposure with a poor prognosis for vision, a decision was made to utilize the dermoid tissue as a protective cover for the cornea. There was also a hypoplastic malar area on the right side and a cleft lip and palate which fit with a #4 Tessier cleft, possibly from an amniotic band etiology. A series of staged procedures was needed to reach a point where an attempt at creating conjunctival cul-de-sacs might be feasible.

In addition to being useful in clinical anophthalmia, where additional lining is necessary to promote socket and lid expansion, mucus membrane grafting can be helpful in less severe cases of microphthalmia where an eye is clinically visible. In cases where there is a small globe and cornea, attempts can be made to place a deeply vaulted pros-

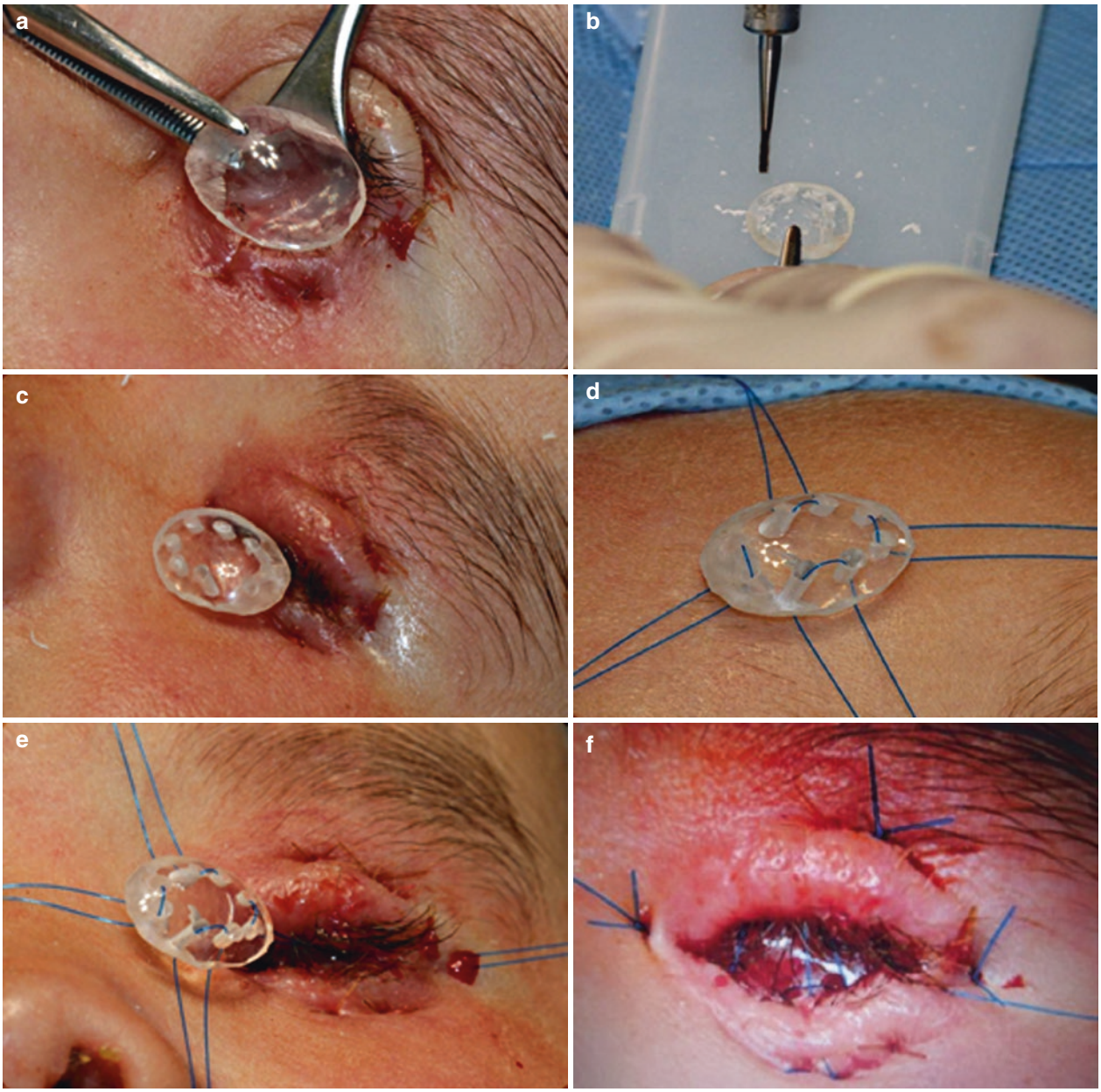


Fig. 39.15 (**a**) A clear conformer is fitted to the affected socket. (**b**, **c**) Holes are manually drilled into the conformer. (**d**) 5–0 Prolene sutures are threaded through the conformer, and (**e**, **f**) the sutures are passed along arcus marginalis and secured to skin

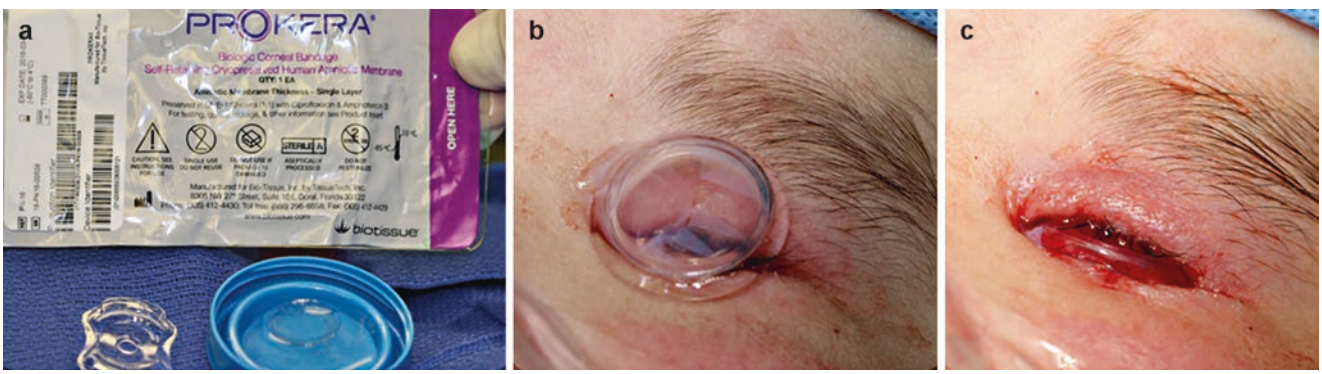


Fig. 39.16 (**a**) Prokera ring in blue cap and (**b**) before placement into the socket. (**c**) Appearance of the ring as it is being slipped into the socket

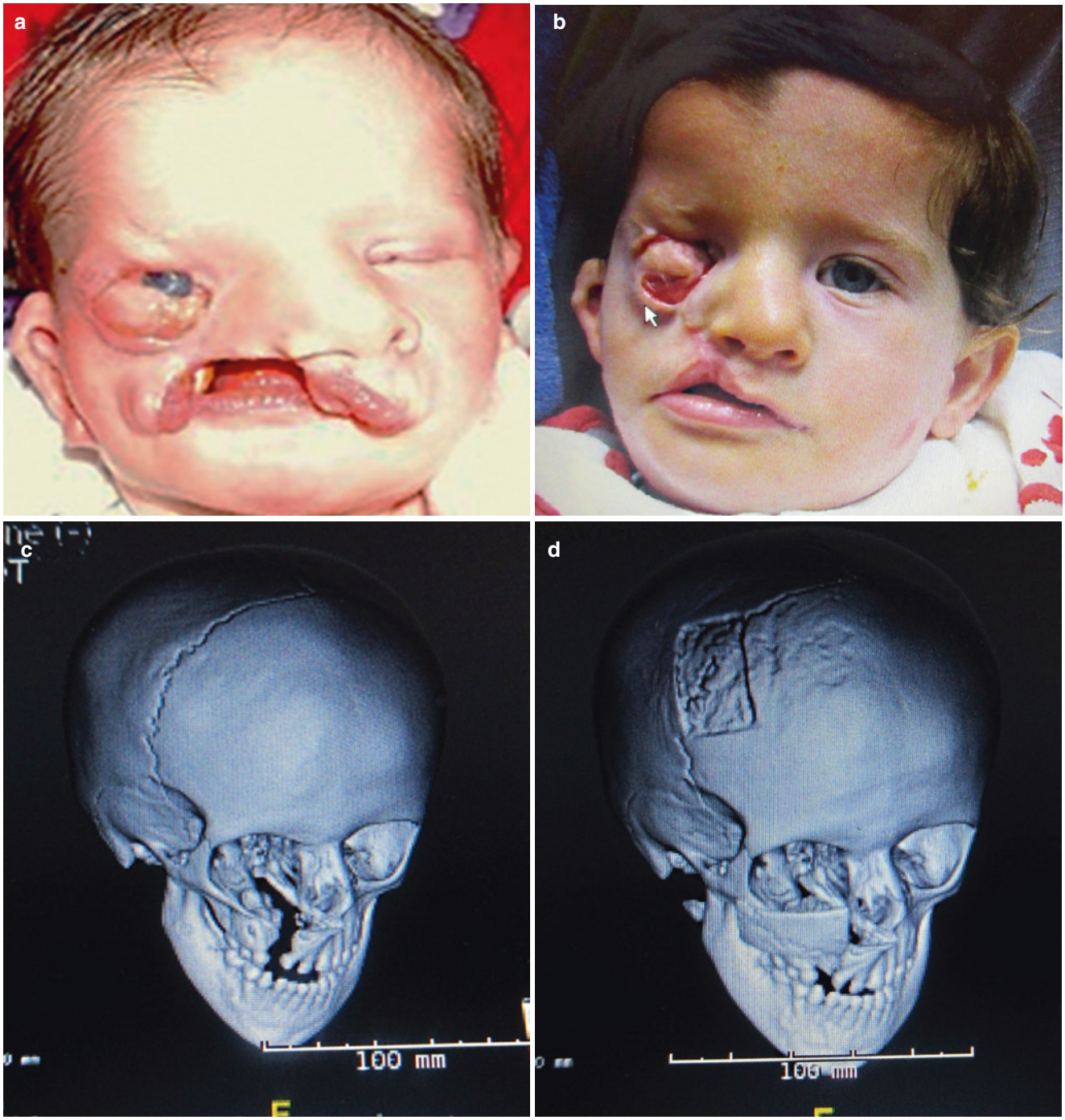


Fig. 39.17 (**a**) Newborn male infant with a large right upper lid coloboma and medial lower lid coloboma, microphthalmic eye, large dermoid cyst in the inferior cul-de-sac pushing down lower lid, cleft lip, and palate. (**b**) Patient at age 20 months, 18 months post dermoid cyst moved to protect globe and 5 months post cleft lip and palate repair. (**c**) 3-D CT reconstruction at age 6 years showing malar bony cleft. (**d**) CT scan showing post-op cranial and iliac bone grafts to repair malar bone cleft at age 7 years.



Fig. 39.17 (continued) (**e**) 5 months following bone grafts and fat injections to malar area and pre-op placement of cheek tissue expander. (**f**) 4 months post gradual expansion via distant scalp port of tissue expander; expander now ready for removal; rotating flap marked with methylene blue as well as area for scar tissue excision. (**g**) Removal of implant and creation of rotating cheek flap for lower lid reconstruction. (**h**) Deflated tissue expander after removal from malar area. (**i**) 6 months post-op cheek flap rotation with removal of vertical scar. (**j**) Repair of right upper lid coloboma 2 months later now at age 8 years.



Fig. 39.17 (continued) (**k**) Further revision of upper lid coloboma, debulking of dermoid and insertion of Prokera ring after deepening the cul-de-sacs. (**l**) Prokera ring in position for planned removal after at least 6 months. (**m**) One month post removal of Prokera ring with clear conformer in good position. (**n**) Patient with right prosthesis at 1 year post-op Prokera ring; right lateral canthopexy/plasty planned for better lid fissure symmetry with left side

thetic shell over the small cornea. However, sometimes patients cannot tolerate this solution and experience bothersome ocular surface irritation. In such situations, oral mucus membrane can be used to cover the cornea, and a prosthetic eye can then be more comfortably worn without ocular surface irritation [43]. This also promotes full-time prosthetic wear, which improves expansion results because of increased wearing time. While this is usually reserved for patients without functional vision in the affected eye, many parents are under the misconception that a mucus membrane graft will completely eliminate all vision. To the contrary, mucus membrane grafting to the cornea does not

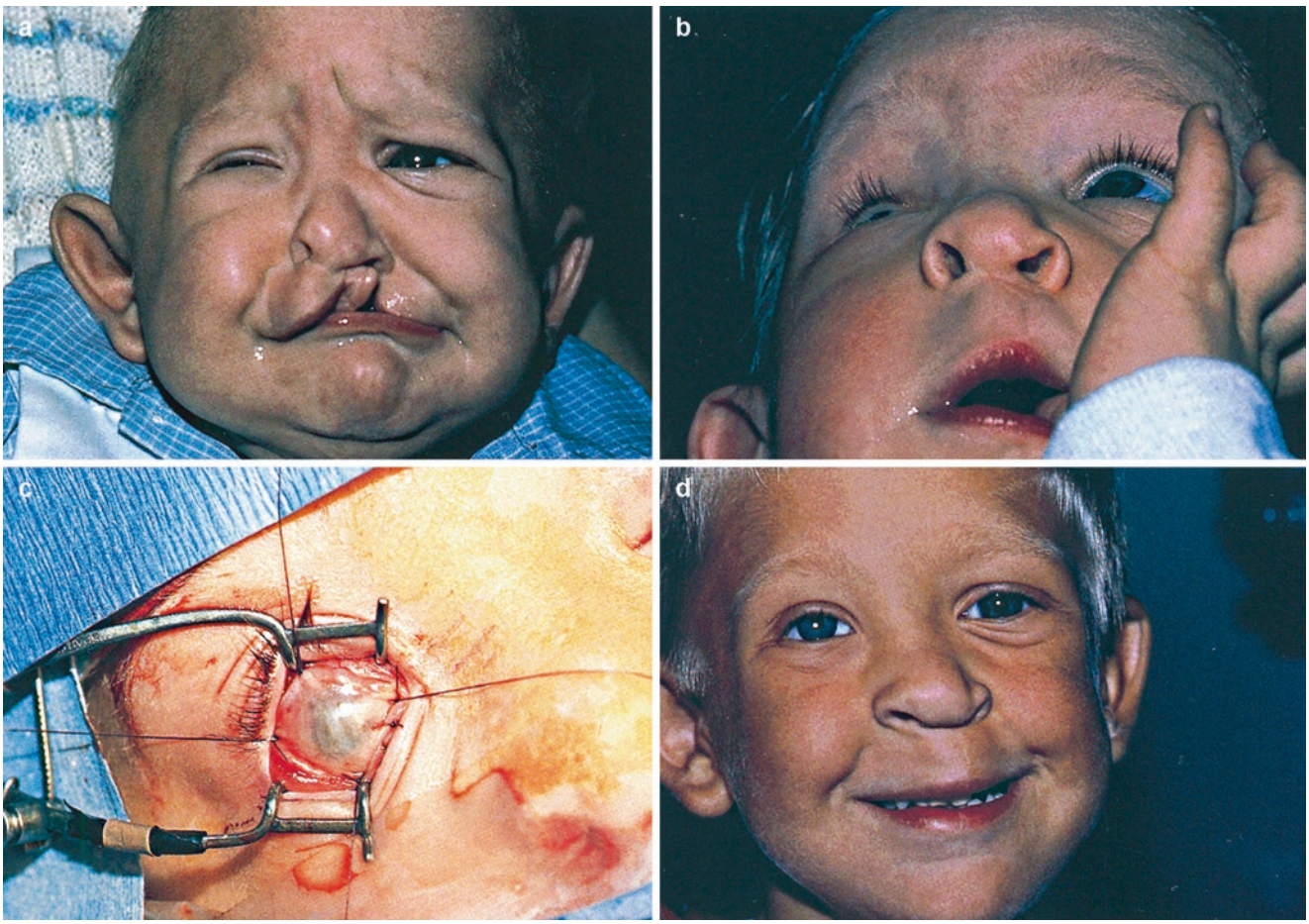


Fig. 39.18 Mucous membrane graft as corneal protective cover. (**a**) Patient with microphthalmic right eye with poor visual potential and a cleft palate. (**b**) Same patient after cleft repair but unable to tolerate cosmetic shell; note retrusion of the globe and lids on the right side. (**c**) Mucous membrane graft used as a corneal protector over globe. (**d**) Successful full-time wear of cosmetic shell permitting more rapid and pleasing symmetry of the lid fissures, lashes, and orbital volume

eliminate light perception, color perception, or even motion perception. This is important to explain in situations where cosmesis and lid growth would be considerably improved with prosthetic use. The results of this approach are illustrated in Fig. 39.18.

Bony Orbital Expansion

While the lids are expanded via anteriorly directed pressure, the conjunctiva and fornices are expanded via posterior and radially directed pressure. And, therein lies the inherent challenge of optimal socket and lid expansion for the microphthalmic patient. What one gains in posterior pressure is often lost in anterior pressure and vice versa. Conformers must be progressively enlarged, but not enlarged so much that they cause pain or result in contraction of the cul-de-sacs. Alternatively, if they are too small, they will not provide appropriate expansion. At the same time that the conformer is stretching horizontally and vertically, it has to be bulky enough to exert sufficient posterior pressure to the conjunctiva and orbital contents, but not so bulky that it cannot be retained. An additional issue with some cases of isolated conformer expansion is that the soft tissues tend to mold to the shape of the conformer, which can result in a dumbbell, spherical, or acorn-shaped conjunctival fornix that does not accommodate an optimum ocular prosthesis.

There is a subset of patients who have microphthalmia with colobomatous cyst (Fig. 39.19). In these patients, gradual orbit expansion can be achieved by taking advantage of the increased orbital volume of the cyst from accumulation of fluid and/or glial tissue [14]. In many cases, no additional socket expanding efforts are necessary. However, if enlargement of the cyst is too rapid, it can cause excess growth of the bony orbit and lead to facial asymmetry. In such situations, while a needle decompression of the cyst can be performed, this should be considered with caution because there

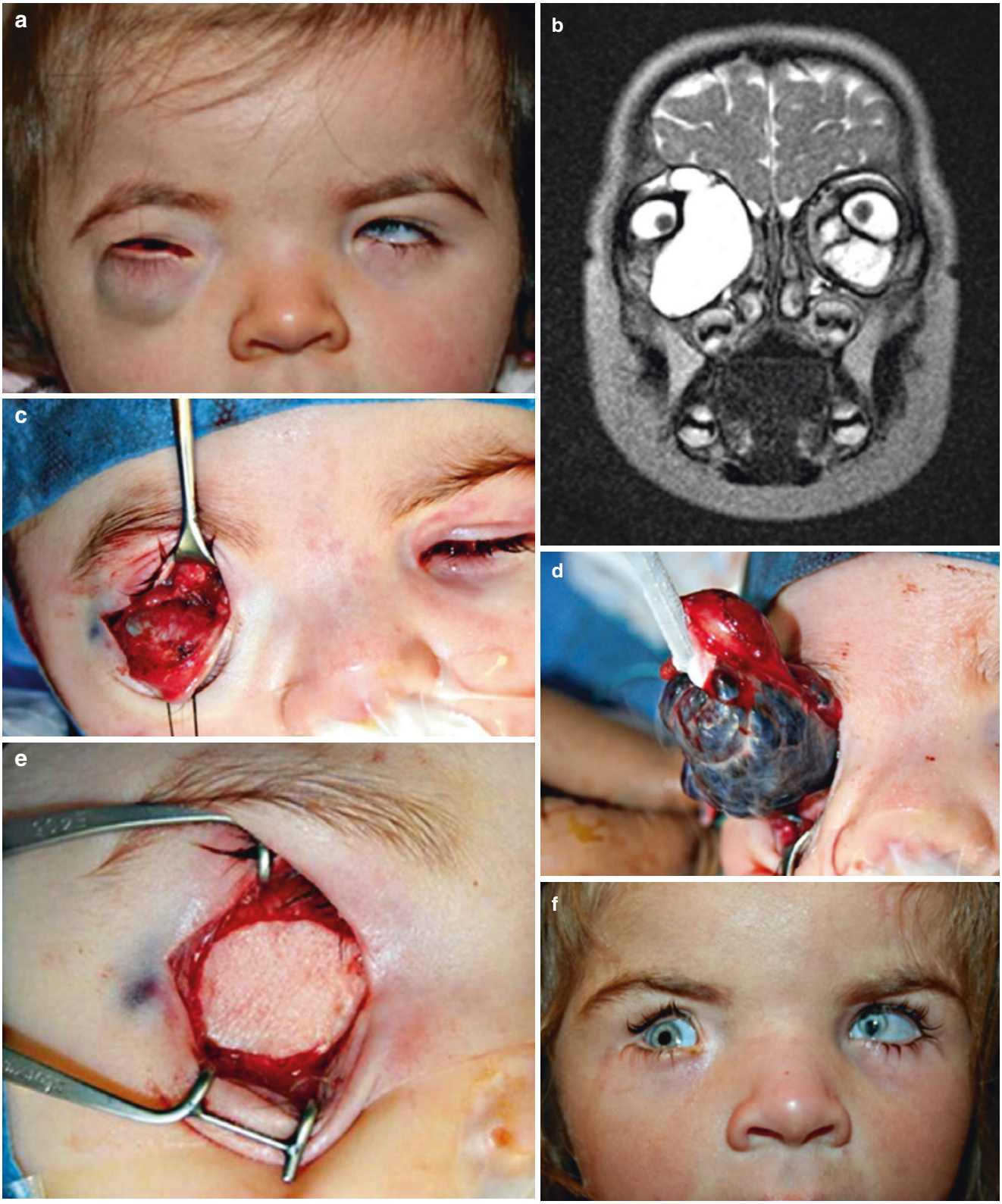


Fig. 39.19 2-year-old with right microphthalmia and colobomatous cyst. (**a**) Eye and cyst have been left in place to facilitate orbital expansion. (**b**) MRI showing large size of cyst and early signs of overexpansion of the orbit promoting (**c**) right enucleation and cyst excision with (**d**) use of the cryotherapy probe to fully excise the lesion intact. (**e**) Subsequent placement of a dermis fat graft in the right socket. (**f**) Postoperative appearance 2 years later showing acceptable facial symmetry

is often a direct connection between the cyst and the eye or brain. Additionally, needle decompression is not an effective definitive therapy because fluid will usually re-accumulate. Generally, when the orbit has reached 90% of its adult dimensions by around 5 years of age, the eye and cyst can then be removed and an ocular implant and prosthesis can be placed prior to the start of school [19]. Earlier removal, however, may be considered if the orbital asymmetry is becoming pronounced. Family members may need reassurance that delaying is usually the best approach since the appearance of microphthalmia with cyst can be discouraging. Prior to excision, an MRI should be performed to assess the cyst size and whether there is any connection to the brain.

For the purpose of clarity in this chapter, a sequential approach is being presented where eyelid expansion occurs before bony orbital expansion. However, the reality is that both should ideally be occurring simultaneously. This, of course, has been the goal of the ocularist and, for the most part, has been achieved with gradually enlarging conformer size. The disadvantages, however, have been the length of time with multiple office visits to accomplish this and the unfortunate fact that there are those cases that just will not respond to this type of conservative management. There have been numerous efforts to find alternative solutions for managing these complex A/M cases, and some are reviewed below for historical perspective.

Orbital Sphere Implantation

One older approach for orbital expansion has utilized placement of solid orbital spheres into the orbit, with or without enucleation or evisceration depending on the size of the small globe or any ocular remnant. However, the smaller bony orbit usually limits the size of implant that one is able to place, resulting in uniformly disappointing outcomes. An alternative is to place progressively larger orbital implants, but the downside to this approach is frequent trips to the operating room with general anesthesia [48]. If an implant is placed that is too large, there is also a risk of extrusion, which can then lead to devastating cicatricial changes that may limit future socket expansion.

Inflatable Orbital Implants

As a result of the problems with implanting solid spheres, early experimentation with alternative methods led to the development of inflatable balloon tissue expanders, implanted via either a bicoronal flap or surgical orbitotomy. Early animal studies involved placement of expandable implants with distant injection ports, seated beneath the scalp. These could be routinely inflated to promote orbital expansion in parallel with skull growth (Fig. 39.20). This technique was eventually approved for use in humans (Fig. 39.21). Rodallec reported 30 cases of pediatric anophthalmia and microphthalmia fitted with an intraconal tissue expander [49]. In microphthalmic cases, Rodallec eviscerated the existing small globe and utilized the scleral coat as a buffer for implant placement, attempting to maintain the expander in an axial and intraconal position. A similar technique was utilized by Grossman et al. in five patients with unilateral congenital microphthalmia [50]. A spherical inflation device (micromodel 3608–10; PMT Corporation, Chanhassen, MN) was placed intraconally behind scleral flaps after evisceration (Fig. 39.22). The inflation tubing was then passed through a 3 mm osteotomy at the

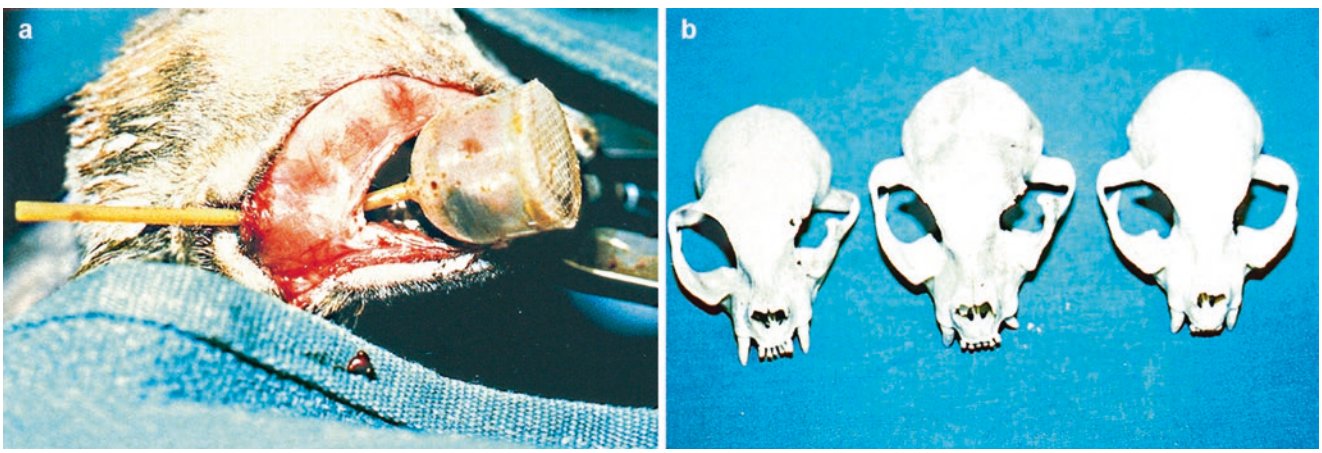


Fig. 39.20 Enucleation and tissue expansion in a kitten. (**a**) Subperiosteal tissue expander placed in a kitten animal model following enucleation. (**b**) Kitten skull on the left demonstrates the effects of enucleation of the left eye without placement of any implant. Center skull demonstrates effect of subperiosteal expander of the left orbit. The right skull is a control, without enucleation or tissue expansion (Courtesy of Scott Bartlett, MD)

sphenozygomatic suture to allow the inflation tubing to pass from the orbit through a subtemporalis tunnel. This was connected to a microinjection port placed through a scalp incision to rest above the ear. An acrylic conformer was placed in the conjunctival cul-de-sac after suturing the scleral flaps over the balloon. After 3 months, the balloon was inflated with 0.5 ml of saline each month until a volume of 22 mm was obtained. The balloon was then removed and a 20–22 mm solid orbital implant inserted. An ocular prosthesis was then fabricated. In all cases the horizontal lid length was within 5% of the normal contralateral side, and there was improved orbital symmetry, as well.

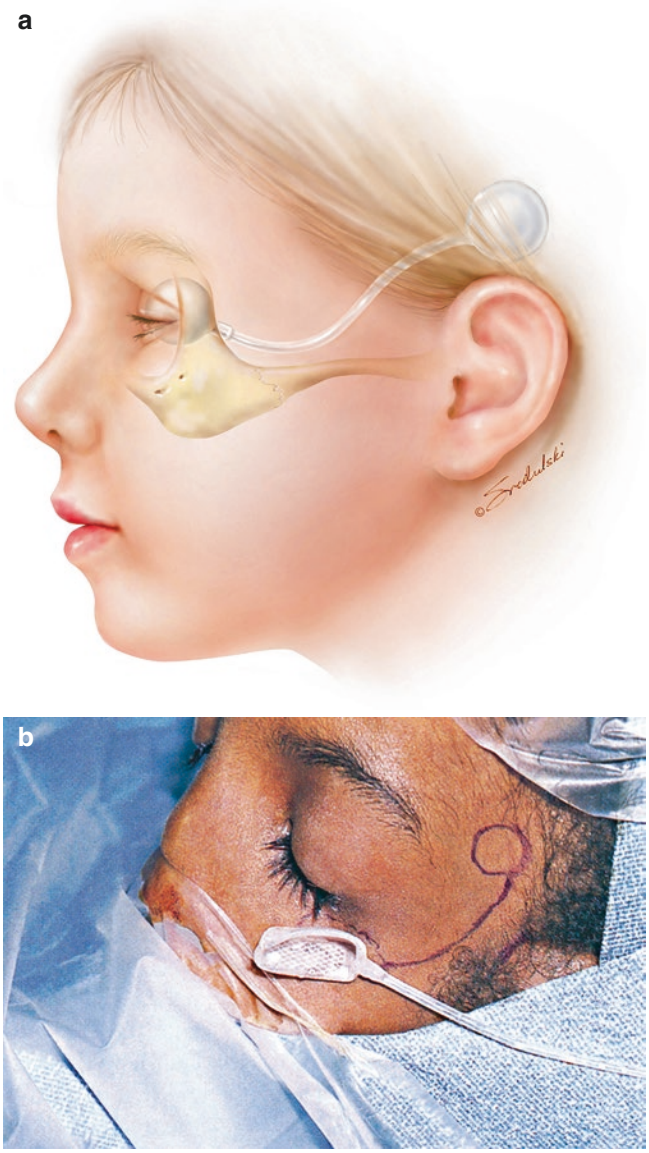


Fig. 39.21 (**a**) Schematic of inflatable posterior orbital expander with buried port under scalp. (**b**) Common type of tissue expander requiring a buried injection port

It should be noted, however, that in those cases where there was a microphthalmic globe large enough to eviscerate, the soft tissues might well have responded to more conventional serial conformer expansion, although growth of the orbit might not have been stimulated as effectively. Additionally, this approach does require a relatively invasive initial procedure, with multiple return trips to the operating for saline injection under anesthesia, which is less than ideal for the pediatric population. Recent evidence suggests that exposure to multiple general anesthesia events in young animals and children (especially if under the age of 3) may diminish learning ability and memory skills and potentially lead to long-term behavioral issues [51, 52] (see Chap. 5). While further research is needed (and the anesthesia and pediatric communities have not formally embraced these findings), it should heighten our concerns regarding the potential negative effects of multiple general anesthesia episodes in young children.

In an effort to reduce the surgical complexity and potential morbidity demanded by distant injection ports, we attempted orbital tissue expansion at the Children's Hospital of Philadelphia (CHOP) with an inflatable device placed anteriorly in the conjunctival space and with an anterior port accessible for saline injections without the need for a general anesthetic. Orbital tissue expansion was achieved in six children (ten orbits) with clinical anophthalmia after failing to achieve adequate results with aggressive serial conformer socket expansion. The tissue expander was designed to fit in the cul-de-sac with an anterior self-sealing stem. The device was inflated biweekly with saline using the exposed port readily accessible between the eyelid fissures (Fig. 39.23). In most cases, it was difficult to objectively quantify the effectiveness of tissue expansion because of concurrent surgical intervention for associated craniofacial anomalies. Yet, in several orbits there appeared to be some positive changes attributable to the tissue expanders (Fig. 39.24). Horizontal fissure length was also improved. Patient difficulties with the orbital tissue expanders were similar to those reported by Rodallec [49].

Inflation pressures in some of these designs have been found to reach 150–200 mmHg, which can be uncomfortable for both the patient and parents. To minimize inflation pressure spikes, one group developed a pulsatile orbital expander that transmits steady carotid pulsations to the orbit [53]. However, ultimately these devices all carry inherent risks of tissue ischemia, infection, and extrusion especially when placed posteriorly in the orbit and with a distant buried port (Fig. 39.25) [54]. Although inflatable expanders can be effective, they have not been commonly accepted for use in the management of A/M by the majority of oculoplastic surgeons.



Fig. 39.22 Intraconal orbital tissue expander with distant injection port. (**a**) Balloon implant being inserted into intraconal space behind flaps of sclera after evisceration of microphthalmic globe contents. (**b**) Inflation tubing being passed through opening in lateral orbital wall and under temporalis muscle to join microinjection port which will lie subcutaneously above the ear. (**c**) Three-month postoperative intraconal placement of tissue ex pander in left microphthalmic orbit. (**d**) One year after incremental 0.5 ml monthly injections to reach 22 mm diameter. (**e**) CT scans demonstrating pre-expansion of intraconal tissue expander (*top*) and post-op effects after gradual expansion of balloon (*bottom*). (**f**) Appearance after post-expansion and fitting of prosthetic shell. (**g**) Preoperative appearance of left microphthalmic orbit before tissue expansion (From: Gossman et al. [50] Reprinted with permission)

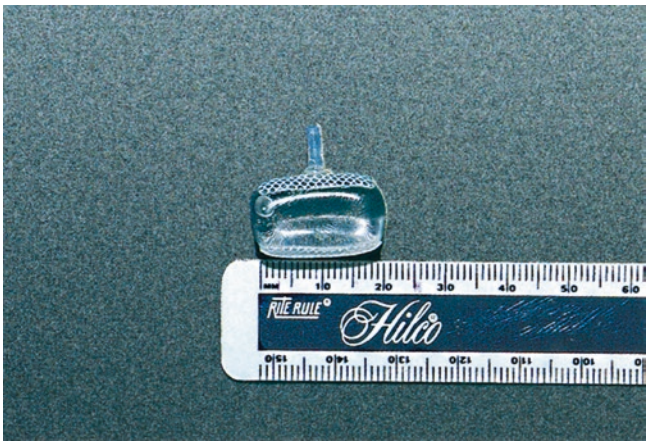


Fig. 39.23 Custom-designed orbital expander with visible port (CUI, Carpinteria, CA) that can be filled with saline through the lid fissures

Osmotic Orbital Expanders

In an effort to further simplify orbital expansion, reduce anesthesia episodes in very young children, and minimize parent struggles related to the management approach, a technique of progressively larger osmotic socket expanders has more recently and extensively been utilized. The osmotic hydrogel expanders, in particular, have become one of the most promising innovations in tissue expansion for anophthalmia and microphthalmia. As first reported by Wiese, Vogel, and Guthoff et al. [54, 55], these expanders are similar in concept to the HEMA enlargers reported earlier by Downes, Lavin, and Collin [56]. The hydrogel material consists of a hydrophilic modified copolymer of methyl methacrylate and vinyl pyrrolidone (MMA-VP). The material, which is similar to that found in soft contact lenses and some intraocular lenses,

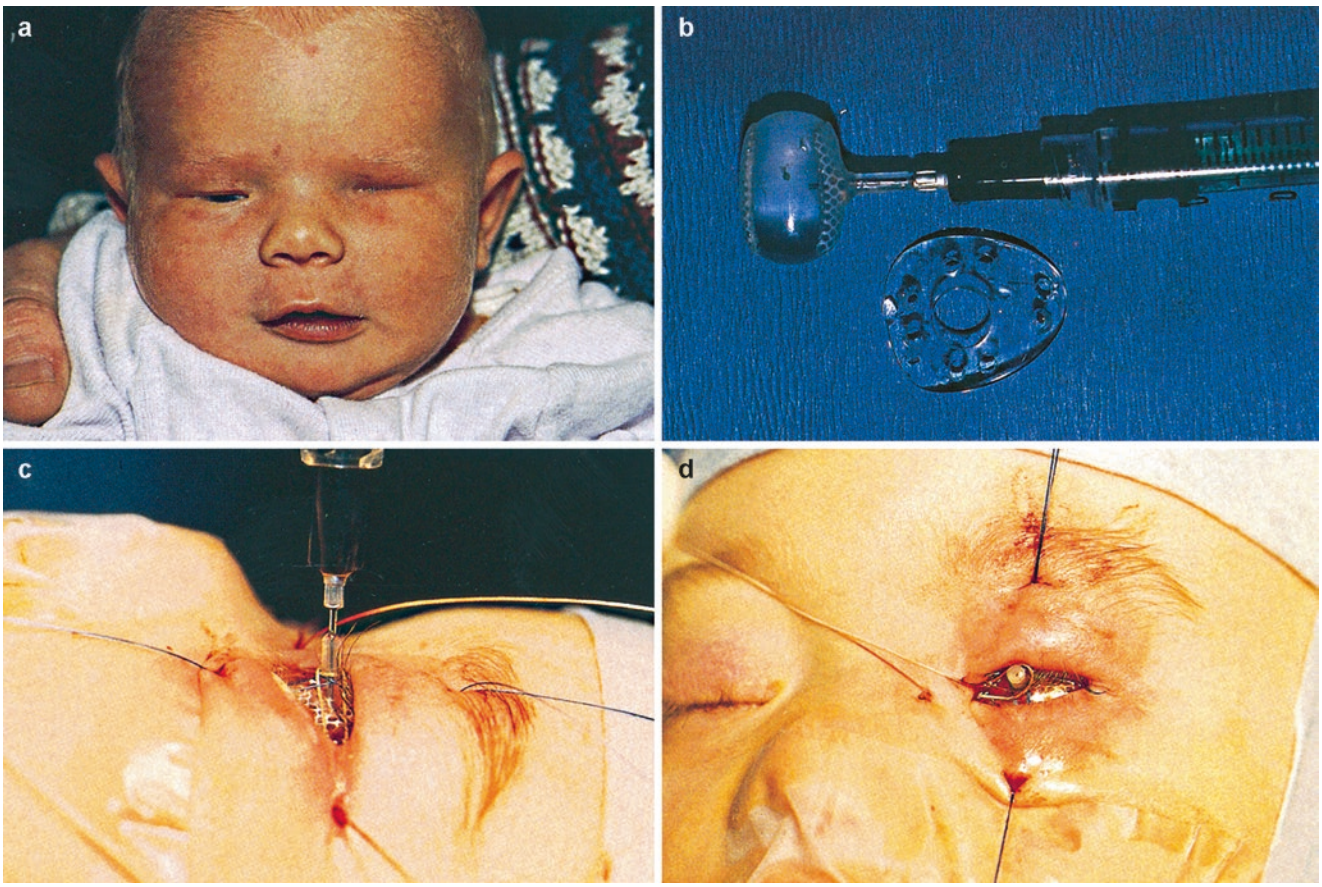


Fig. 39.24 Use of custom saline-filled anterior expander in severe microphthalmia. (**a**) Patient with severe left microphthalmia at age 6 months. (**b**) Custom expander inflated with saline; conformer holds expander in place. (**c**) Expander placed into the cul-de-sac minimally inflated. Conformer with drill holes for sutures and a central hole for the port is inserted. (**d**) Overlying conformer sutured to superior and inferior orbital rim periosteum with 5–0 monofilament sutures.



Fig. 39.24 (continued) (**e**) Patient at 2 months postoperative after expander has been filled with biweekly saline injections. (**f**) Frontal view of patient at 2 months postoperative. (**g**) Patient 3 years post-expander; 2 years post dermis fat graft and cosmetic shell. (**h**) Slight asymmetry is camouflaged by spectacles with a + 2.00 diopter lens on the left. (**i**) Patient 7 years post dermis fat graft with prosthetic shell. (**j**) View of socket and graft without shell

has a much greater capacity for swelling (10–12X as compared to the 1.19 of HEMA) and has had application for socket expansion for children with congenital A/M.

Use of hydrogel expanders has now been described extensively in the literature [57]. The technique reported by Schittkowski et al. followed the original methods of Weise et al. placing a hydrogel sphere intraconally and either an acrylic conformer or a hydrogel hemisphere anteriorly in the conjunctival space with the lids securing the implant during expansion by a tarsorrhaphy [55, 58]. Their technique the utilized several exchanges for larger hydrogel spheres requiring a general anesthetic.



Fig. 39.25 Example of inflatable device extrusion. (**a**) Inflatable device extruding from left socket. (**b**) Injection port visible on left side of head. (**c**) Explantation of device from the scalp and (**d**) from the socket. (**e**) After explantation of the inflatable device, a 2 ML hydrogel sphere expander is being inserted into the socket. (**f**) Serpentine suture tarsorrhaphy for securing hydrogel sphere during expansion phase

CHOP Method of Hydrogel Expansion

Given our positive experience of obtaining reasonable expansion of both the bony orbit and the lids and conjunctival space with our anteriorly placed inflatable expander, we thought that it might be unnecessary to place the hydrogel spheres posteriorly. We initially use a hemisphere in most cases where the lid fissures are tiny and then progress to spheres when there is sufficient space. In many instances, however, the child may have been managed by an ocularist using progressive conformer expansion and have sufficient space to start with a hydrogel sphere. Some of these referrals from the ocularist are because of a poor response to bony orbital expansion, and the hydrogel method has been a welcome addition to our options for managing these problems.

Hydrogel expanders come either as a sphere (for orbital expansion) or as a hemisphere (for conjunctival expansion). They are quite small, depending on the size, in their dehydrated form, but significantly expand when they are hydrated [59, 60]. They are inserted in their dry state and gradually expand over several days to their fully inflated sizes, a roughly tenfold increase in volume (Fig. 39.26). For example, in its dry state, a 5 ml hydrogel sphere is 9 mm in diameter but increases to 22 mm when fully hydrated.

Figure 39.27 gives a visual image of expansion of a small hydrogel sphere over a 24 hour period. The swelling is produced by osmotic forces from tear and fluid production within the socket can lead to dramatic soft tissue changes within 24 h. By 48 h, they have reached nearly their full volume, and this can be maintained for 2–3 months. The hydrogel expander exerts a constant pressure of about 20–25 mmHg, which appears to be better tolerated than the high-pressure spikes associated with inflatable balloon implants.

The beauty of osmotic hydrogel expansion is that it can eliminate the need for serial trips to the operating room. While the most common approach is still to utilize a general anesthetic for hydrogel exchange and suture tarsorrhaphy (in order to prevent the hydrogel from falling out before it is fully expanded), we have found that this same process can be achieved in the clinic setting without general anesthesia by using a glue tarsorrhaphy instead of a suture tarsorrhaphy for lid closure. Placement of a glue tarsorrhaphy, in particular, allows this to easily be done in the office. We also feel that the use of glue minimizes the risk of damage to the eyelids. If the force of the hydrogel is stronger than the orbit can accommodate, it will simply force open the glue tarsorrhaphy and the expander can extrude without damage to the lids. We use superglue on the lid margins applied in the office immediately after insertion of a hydrogel expander into the socket (Fig. 39.28). The temporary glue tarsorrhaphy prevents the hydrogel from falling out before it is expanded (which usually happens over the next 2–3 days). In select cases when the parents are willing, we have recently started to attempt hydration of the hydrogel spheres with artificial tears, placing tape to occlude the lids, and asked for the child to be brought back in 1–2 hours. In some of these cases, the hydrogel has expanded enough so that we then do not even need to perform a glue tarsorrhaphy (Fig. 39.29).

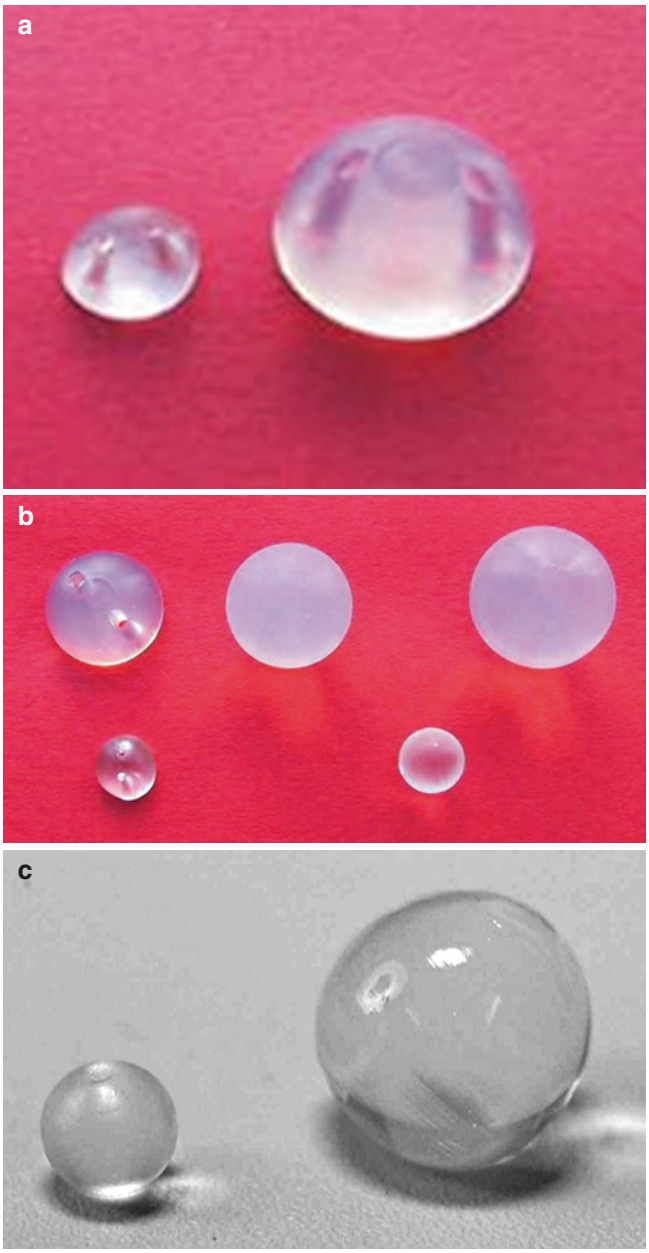


Fig. 39.26 Hydrogel implants. (**a**) Hemispheres, pre- and post-hydration. (**b**, **c**) Spheres, pre- and post- hydration

We have now adopted this approach for many of our moderate–severe microphthalmia patients and have been very pleased with the results. We usually start with a hydrogel hemisphere (FCI Ophthalmics), which are available in 0.4,

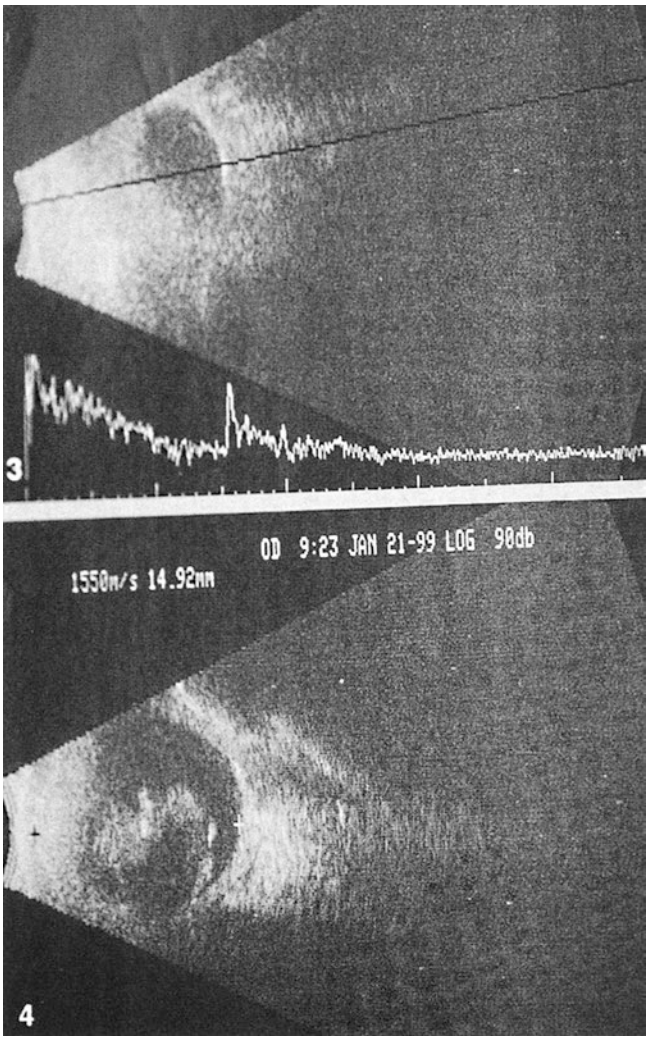


Fig. 39.27 Ultrasound of hydrogel implant after 24 h (*top*) and after 48 h demonstrating increase of expander diameter from 7.5 to 14.9 mm (*bottom*) (From Bacskulin et al. [55]; with permission from Springer)

0.9, 1.5, and 2.0 ML volumes. These hemispheres swell more rapidly than previous formulations and take about 1–2 days to acquire their final size. After hemisphere expansion, we transition to hydrogel spheres, which are available in 1, 2, 3, 4, and 5 ML volumes. These can take up to 4 days to reach their full volume. See Table 39.1 for a size correlation between dehydrated and hydrated volumes of hydrogel hemispheres and spheres.

Depending on the size of the implant, there is often rapid expansion (1–2 h) after hydrogel placement (Fig. 39.29), and the orbit shows significant changes as early as 1 month (Fig. 39.30). Horizontal fissure length appears to increase more rapidly than that seen with conventional serial conformer expansion. We have found that we can follow the size and position of the brow in these patients as a guide for when to perform hydrogel exchange. We exchange the hydrogels in the office by placing proparacaine drops into the socket and using a Freer elevator to remove the fully inflated hydrogel. The average number of exchanges of hydrophilic implants is usually 3–4 times before age 2. This depends somewhat on how early we are able to start this process. If hydrogel expansion is initiated within the first weeks postnatal, we may reach a sufficient size space for a dermis fat graft (DFG) even by age 1 year. The dermis fat graft with its ability to grow will promote continued orbital expansion (see subsequent discussion).

In some cases, there is inadequate socket expansion with isolated anteriorly placed hydrogels because of lack of posterior stimulation for growth or because of poor patient cooperation (manually picking apart the hydrogel). In these situations, we have performed a small surgical procedure in order to implant a hydrogel into the intraconal space. Usually we use a small, centrally placed incision in the conjunctiva, to avoid the risk of erosion after the hydrogel

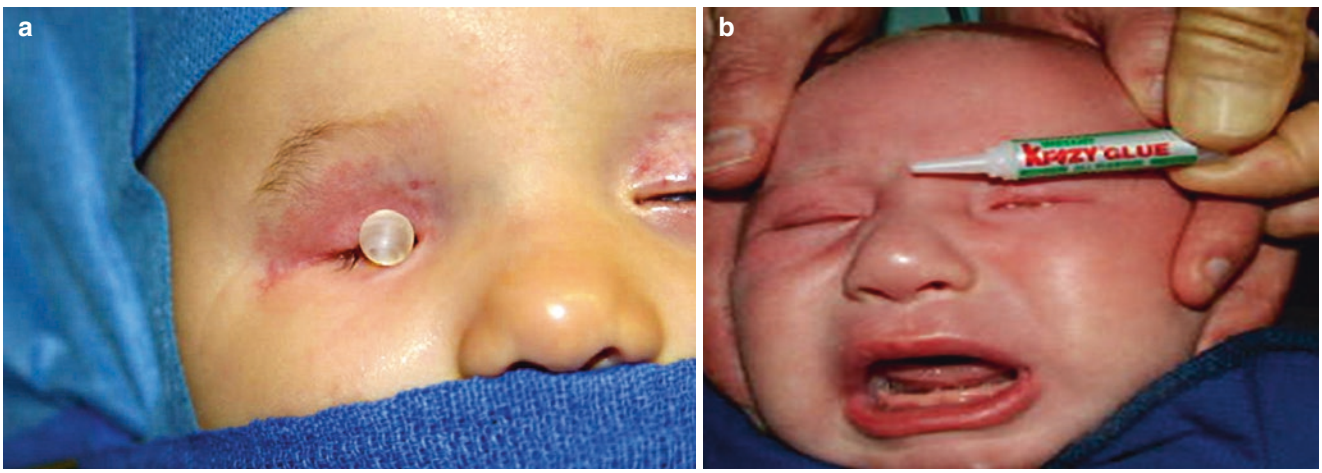


Fig. 39.28 (**a**) Five ML spherical hydrogel expander before placement into the right socket and (**b**) with a glue tarsorrhaphy to maintain the hydrogel in place until it increases in size

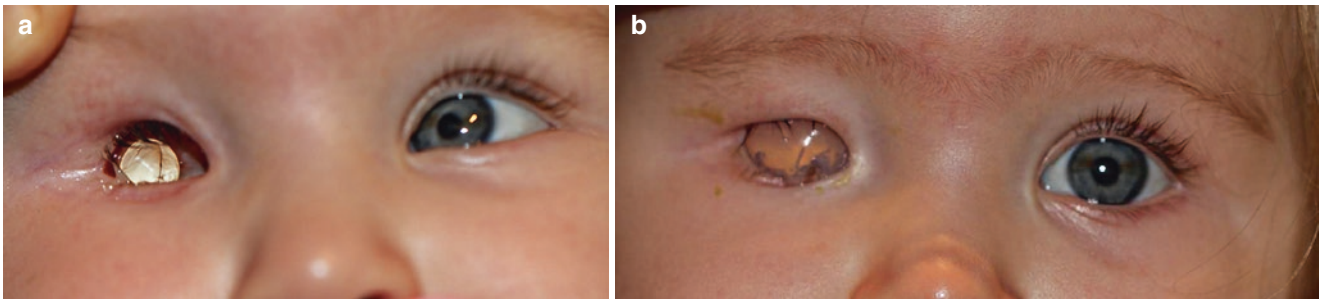


Fig. 39.29 (**a**) Immediate placement of hydrogel implant and (**b**) implant size after several hours

Table 39.1 Size correlations between dehydrated and hydrated hydrogel hemispheres and spheres

Hydrogel hemisphere (ML)	Before swelling		After swelling		Swelling time
	Volume (ML)	Diameter (mm)	Volume (ML)	Diameter (mm)	
0.4	0.06	6	0.4	11.2	1 day
0.9	0.13	8	0.9	14	1 day
1.5	0.20	9	1.5	18	1 day
2.0	0.28	10	2.0	20	2 days
1	0.12	6	1	12.4	1 day
2	0.30	8	2	15.5	2 days
3	0.30	8	3	18.0	3 days
4	0.43	9	4	19.7	4 days
5	0.4	9	5	21.8	4 days

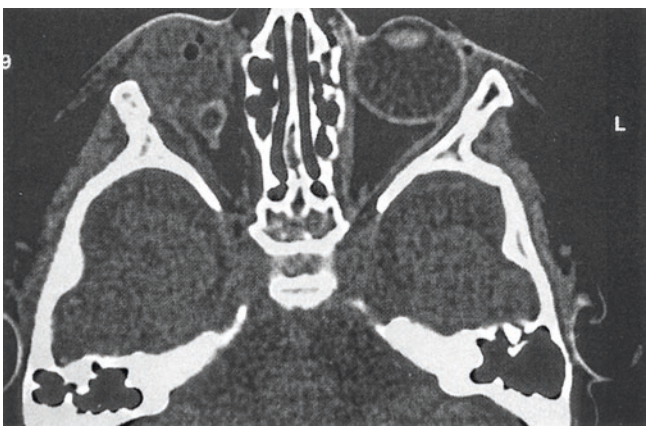


Fig. 39.30 CT scan demonstrating fully hydrated hydrogel expander in socket after 1 month (From Bacskulin et al. [55]; with permission from Springer)

expands. The surgical procedure is particularly simple and effective for socket expansion, especially when done very early in life (Fig. 39.31). We will replace these intraconal hydrogels over time until there has been enough socket expansion for placement of a dermis fat graft or sphere. However, for some patients, we have left the hydrogels in for years without any problems with extrusion or unwanted expansion.

Dermis Fat Graft as an Orbital Implant

At the Children's Hospital of Philadelphia), we have had extensive experience with the use of dermis fat grafts (DFG) for pediatric A/M socket rehabilitation. Our experience with the use of a DFG for this type of problem began with an unusual case involving a microphthalmic child with corneal cyst (Fig. 39.32) [61]. Complicating the presentation were associated cysts in the orbit and the possibility of prolapsed intracranial contents through a large sphenoid wing defect. Planning an enucleation and tumor excision at the age of 6 weeks, inserting a standard ocular implant was considered problematic, not only because of the small size required for this very young age, but also because of the large sphenoid wing defect present in this orbit. Implantation of a 12 mm DFG provided sufficient volume replacement without the potential risks of a migrating foreign body implant. After more than 18 years of follow-up, this DFG has grown to over 25 mm (Fig. 39.33).

The advantage of dermis fat implant in children is that it is a living, autogenous graft with an ability to grow in tandem with the child's overall body growth. Unlike the problem of fat atrophy in adults, it is rare to see this in children. In fact, when implanted in children under age 3, with overall body fat weight gain, the DFG can mirror this, producing more volume than necessary with resultant proptosis of the prosthesis [62]. In these cases, fat graft debulking of the graft is a simple procedure although it does, however, require a general anesthetic.

Dermis fat grafts are used with varying frequency throughout the entire spectrum of anophthalmic and microphthalmic rehabilitation [63, 64]. In microphthalmic patients, it is necessary to make an initial decision as to the status and/or viability of the existing globe or globe remnant. Some children will present with a severely disfigured or very small, almost imperceptible globe. In these

cases, we generally can secure the DFG without excising this tissue. With a small globe, we prefer enucleation with primary DFG implantation. In cases where there has been a previous enucleation with implant placement, the implant is usually removed at the time of DFG placement. Our technique for dermis fat graft implantation at all times includes the suturing of any identifiable extraocular muscles to the DFG in an attempt to improve future prosthetic motility as well as to encourage overall orbit, soft tissue, and socket expansion.

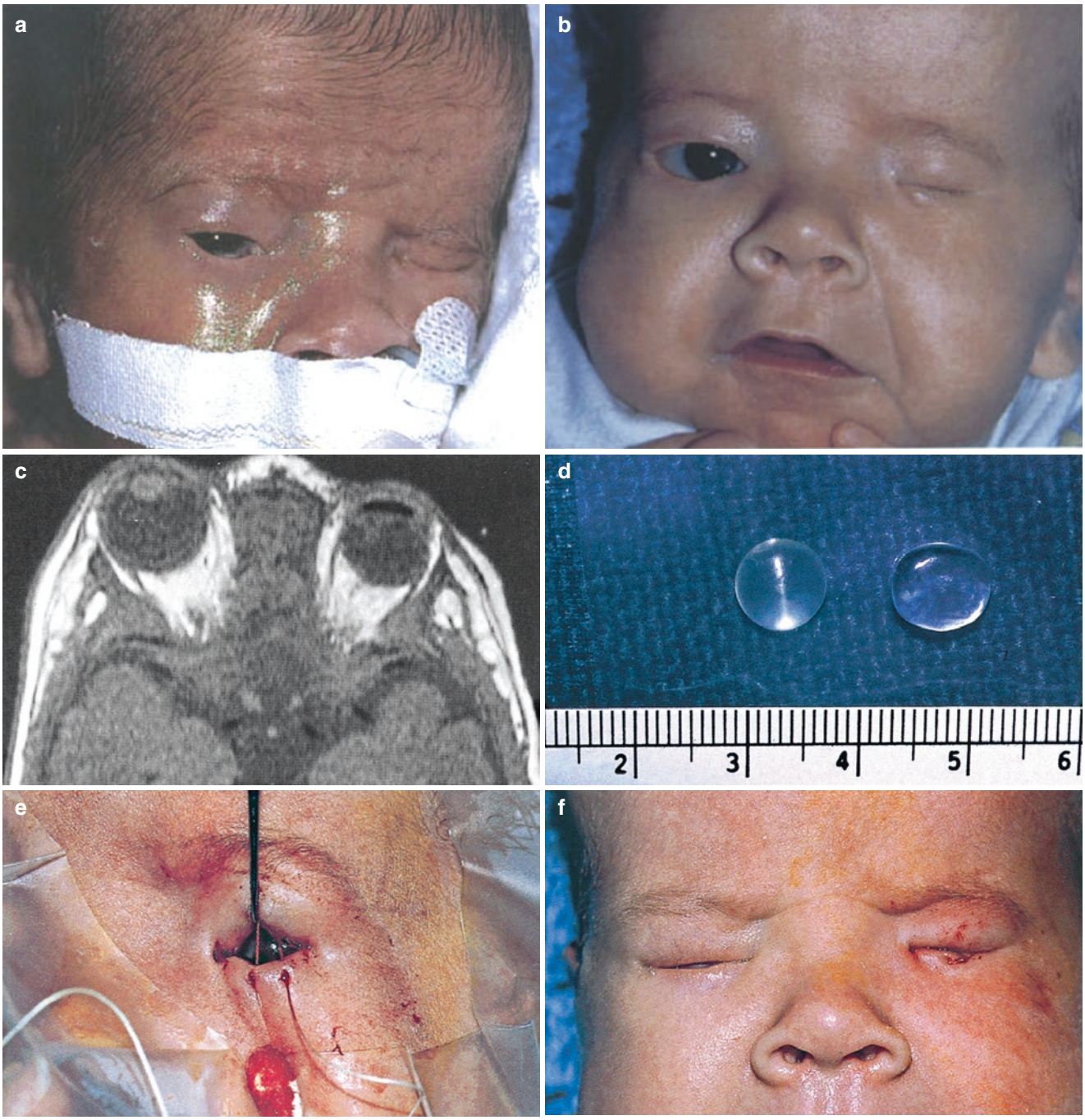


Fig. 39.31 Early use of hydrogel implant in management of a premature infant. (**a**) Infant at birth with unilateral microphthalmia (27-week gestation). Note that the right eye has fetal appearance. (**b**) Infant after 11 weeks of tiny conformer socket expansion. (**c**) MRI scan with small conformer at 40-week gestation (13 weeks after birth). (**d**) Hydrogel expander matching hard conformer diameter. (**e**) Hydrogel conformer placed in socket. (**f**) Temporary tarsorrhaphy through gray line of upper lid and secured through lower lid gray line, tied without bolster in subciliary position. Horizontal lid fissure length 14 mm on right side and 9 mm on left.

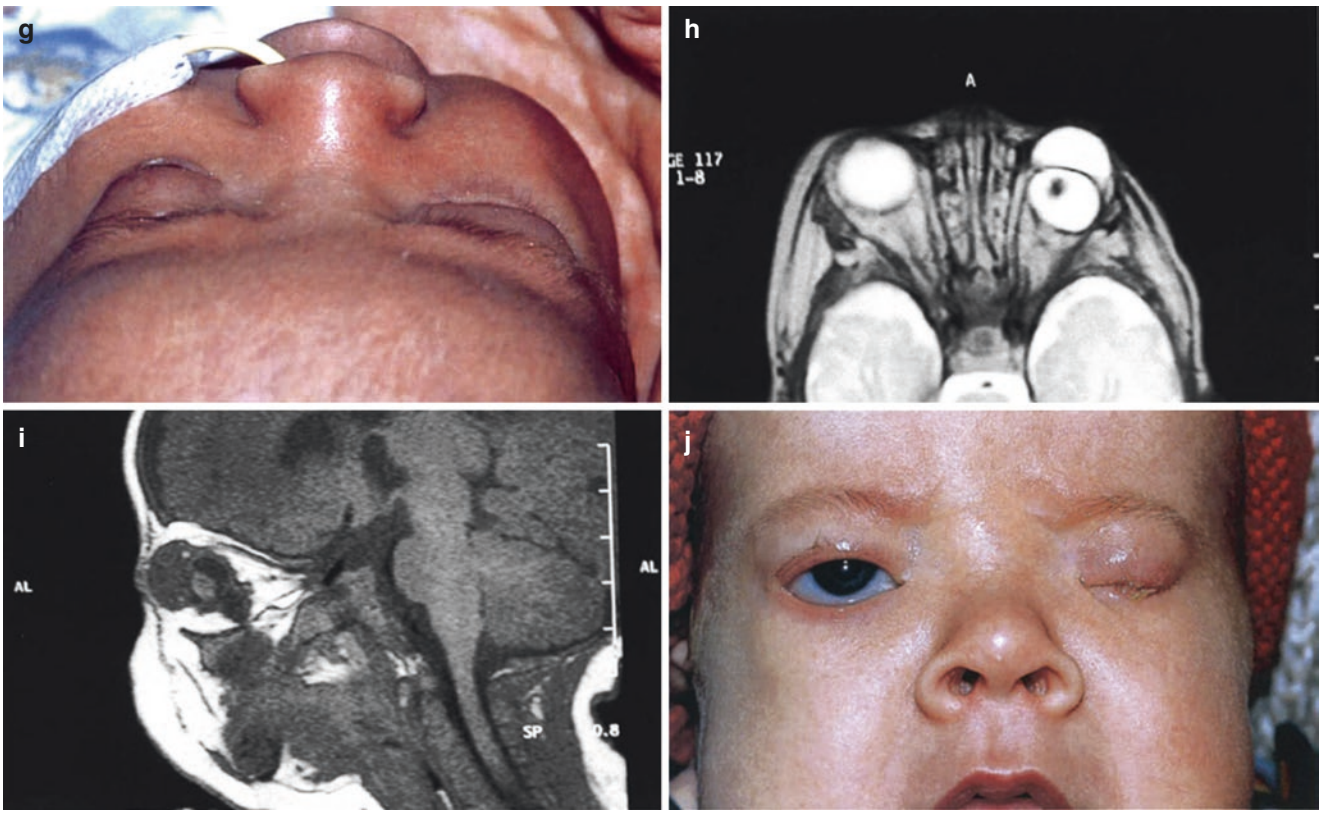


Fig. 39.31 (continued) (**g**) Three days post-op hydrogel conformer; note fullness on left side. Horizontal fissure length on left increased to 11 mm. (**h**) MRI T2 axial scan 3 days post-op demonstrates hydration of hydrogel conformer; note increased diameter as compared to scan in (C). (**i**) Sagittal T1 view on day 3 shows vertical dimensions of implant. (**j**) Post-expansion appearance

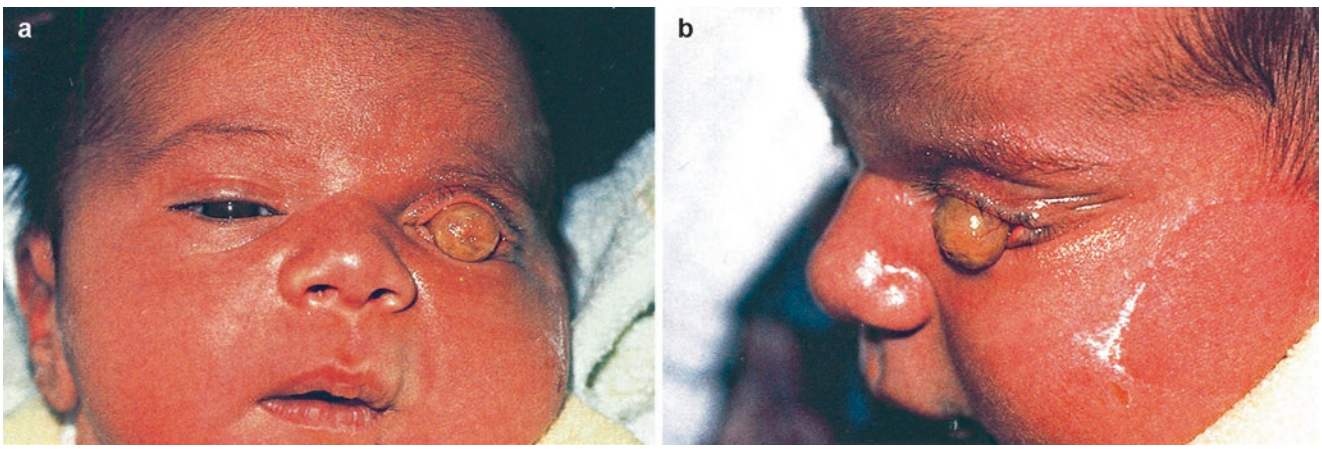


Fig. 39.32 Use of dermis fat graft as orbital implant in 6-week-old infant. (**a**) A 6-week-old infant with microphthalmia and corneal cyst. (**b**) Lateral view of same patient.

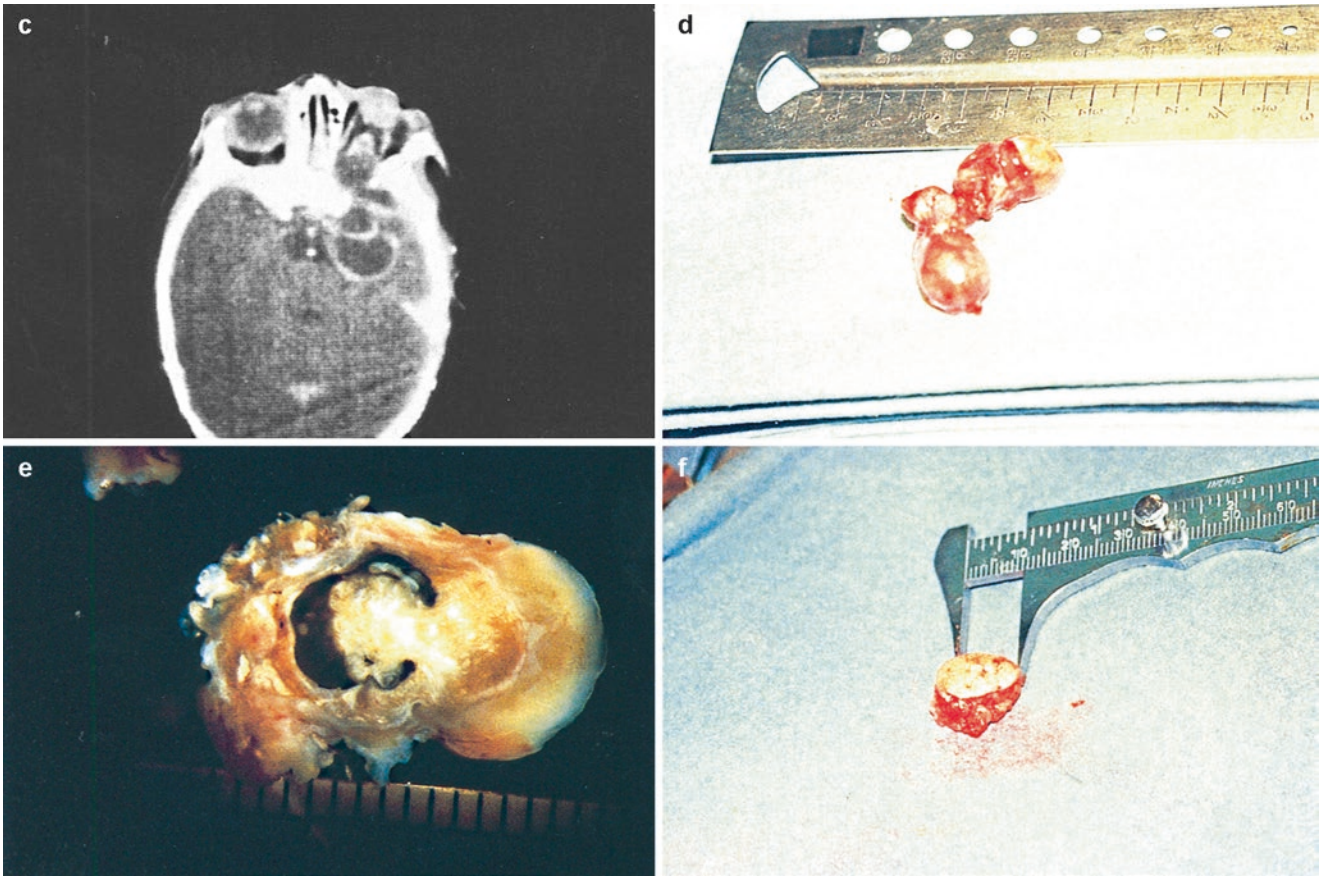


Fig. 39.32 (continued) (**c**) CT scan demonstrating microphthalmia with cysts of orbit noted as extradural through sphenoid wing defect. (**d**) Enucleated globe with attached teratomas of the orbit; cysts contained respiratory and GI epithelium. (**e**) Cross section of globe. (**f**) 12 mm dermis fat graft from buttock

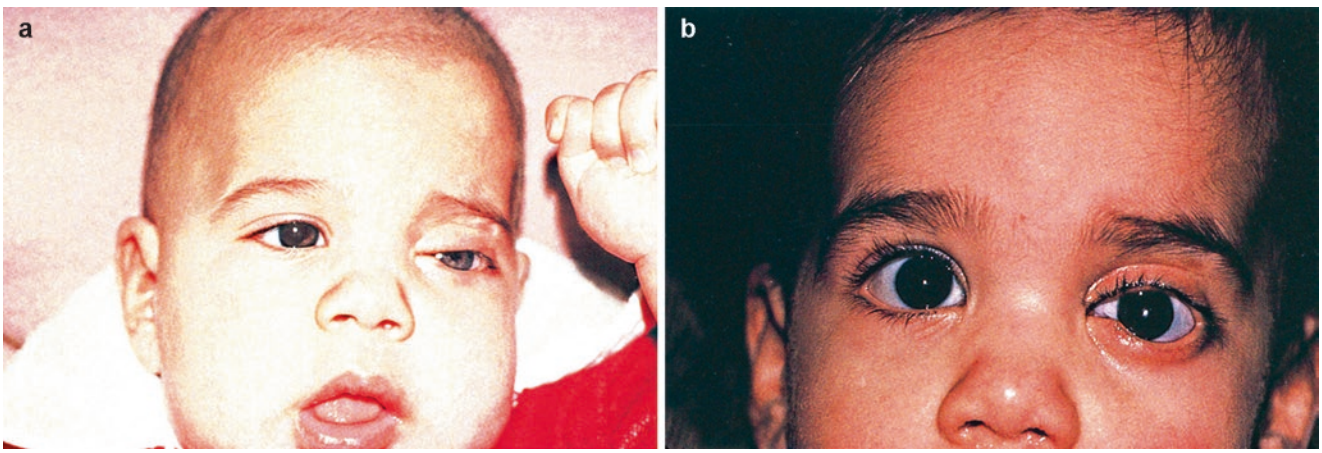


Fig. 39.33 Same patient from Fig. 39.32 who received dermis fat grafting to the left socket as a child. (**a**) 3-month post-op. (**b**) 3-year postoperative.



Fig. 39.33 (continued) (**c**) Note the growth of the graft at 3 years prior to repair of lower lid deformity. (**d**) Patient at age 12 years. (**e**) Patient at age 16 years. (**f**) CT scan at age 16 years; dermis fat graft now 25 mm with overlying prosthetic shell

We generally use dermis fat grafting only *after* we have obtained sufficient expansion of the orbit and lids. The technique of dermis fat implantation has been used successfully to fill the increased anterior-posterior volume achieved by prosthetic or hydrogel enlargement of the orbit [37]. Use of a DFG can also help to ensure expansion of the orbit (Fig. 39.34). Expansion of the lid fissures is also aided in the horizontal and vertical planes by permitting use of a thinner shell over the DFG, which can better transmit stretching forces in these directions. Sufficient depth of the cul-de-sacs is, of course, critical to retain the shell, but the forces in lid expansion are best distributed horizontally and vertically with a thinner prosthesis. The curve of a prosthetic may also play a role by pushing the lids forward thus applying another force vector for expansion.

Although numerous donor sites are available, we prefer obtaining the DFG from the buttock in children (Fig. 39.35). The area of the DFG is outlined in an elliptical shape, and small puncture sites are made around the entire graft site. A dermabrader is preferred for removing the epithelial skin layer from the donor site. Dermis is identified once the surface epithelium is removed and pinpoint bleeding becomes visible. A #15 scalpel blade connects the previously made stab incisions outlining the donor site. Sharp cutting scissors are used to excise the dermis and fat as one structure, keeping the fat component larger and wider than the dermis. The majority of dermis fat grafts harvested range in diameter from 12 to 20 mm, depending on the age of the child and the orbital volume requirements. Closure of the donor site is completed with deep and subcuticular 3–0 and 4–0 vicryl sutures. The skin is then closed with a running 4–0 clear monocryl suture in a subcuticular manner. The donor area is covered with skin glue (Dermabond) and a semiocclusive dressing (Tegaderm with Telfa pad).

If DFG implantation is preceded by enucleation, a standardized technique can be utilized. In cases without a globe,

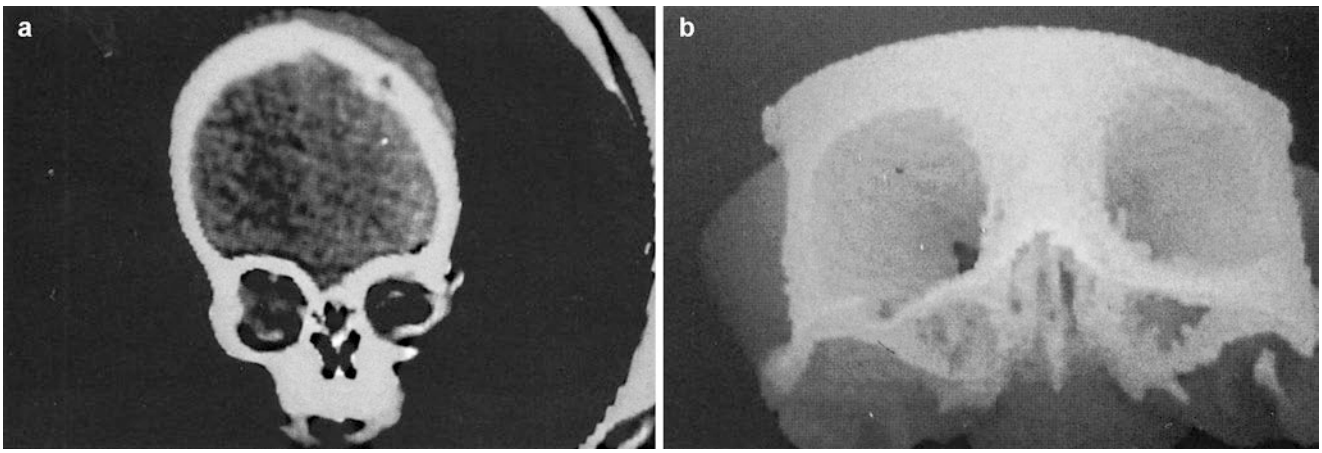


Fig. 39.34 Changes in orbital volume in the microthalmic orbit before and after dermis fat grafting. (**a**) Early-generation CT scan of the patient in Fig. 39.31 at 2 months, with left-sided microphthalmia; note the orbital asymmetry. (**b**) 3-D CT reconstruction of the same patient at age 6 years; less orbital asymmetry following the combination of dermis fat graft as an orbital implant and overlying cosmetic shell. Growth of the dermis fat graft allows the use of a thin prosthetic shell, which can transmit stretching forces more evenly to the eyelids

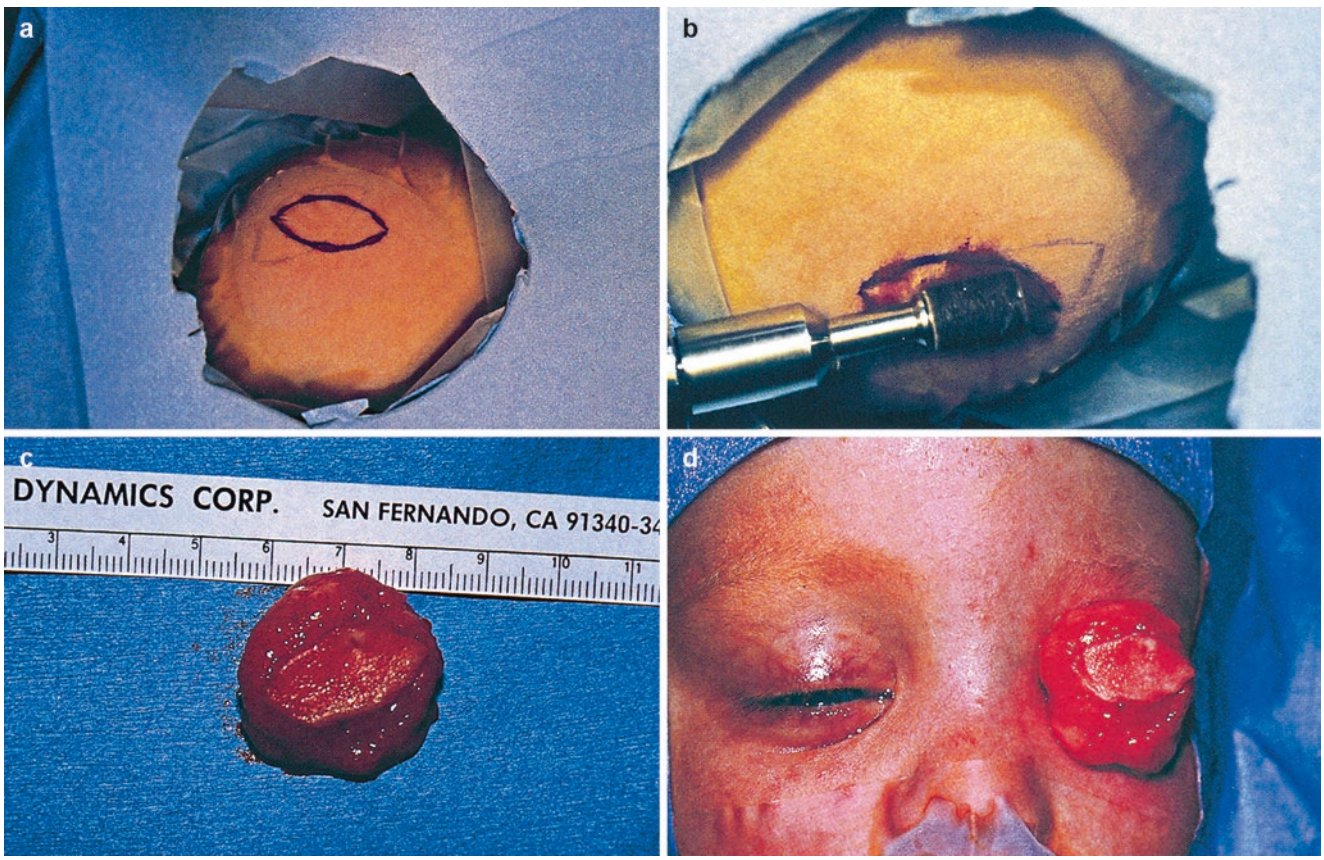


Fig. 39.35 Dermis fat graft as orbital implant. (**a**) Dermis fat donor site outlined on buttock. (**b**) Multiple superficial stab incisions are used to outline the graft edges; a dermabrader is used to remove epithelium down to the dermis. (**c**) The fat component of the dermis fat graft is larger in all dimensions than the skin component. (**d**) Graft is placed over left orbit.

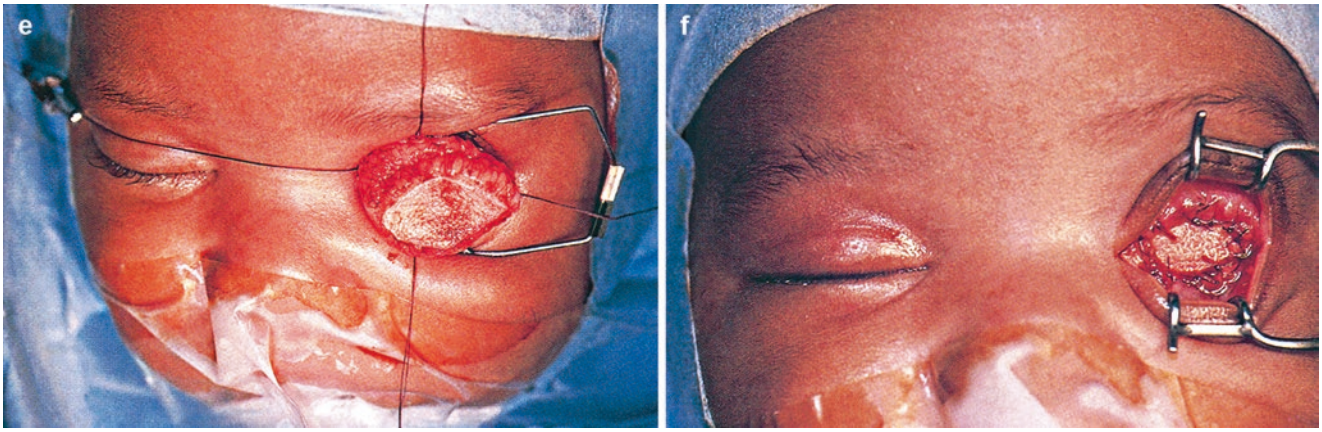


Fig. 39.35 (continued) (**e**) Rectus muscles isolated and sutured to graft and conjunctiva and excess fat is trimmed. (**f**) Multiple interrupted 5–0 polyglactin sutures are used to prevent fat prolapse

the conjunctiva-Tenon's layer is opened horizontally. A potential space is created by blunt dissection. If extraocular muscles are present or identifiable, they are individually tagged with 5–0 double-armed vicryl sutures. Ideally, a sufficient volume of dermis fat is placed into the socket, without causing excessive pressure or inability to close the eyelids over a conformer. The sutures are attached to the graft, simulating the normal position of the rectus muscles. The conjunctiva-Tenon's layer is then re-approximated to the dermis edge with additional 5–0 vicryl, interrupted sutures. It is important to close the conjunctiva and Tenon's layer carefully, so as to prevent any fat prolapse. A conformer is placed at the conclusion of the procedure, so that the cul-de-sacs are maintained without undue pressure, which might weaken the wound [62].

As outlined earlier, in pediatric patients, we generally favor autogenous orbital implantation, but there are circumstances in which a non-autogenous orbital implant may have value as an additional source of volume. A variety of orbital implants are available that can be utilized to augment orbital volume and further stimulate expansion in this patient population. In addition to dermis fat, examples of material used for orbital volume augmentation include glass, silicone, hydroxyapatite, polymer-coated hydroxyapatite, and porous polyethylene [65–67]. There has been extensive experience with spherical intraconal implants. Placement of a sphere in the orbit has been shown to promote orbital bone growth, particularly when combined with a prosthetic shell. In selected cases we have utilized a technique where a silicone or ceramic sphere is placed in the orbit behind a DFG or other intraconal implant. The addition of a silicone sphere in these patients can aid attempts to increase soft tissue expansion. More recently, we have also started to augment orbital volume by using hydrogel expander placement behind dermis fat grafts. The addition of a silicone or hydrogel sphere behind a previously placed DFG can further enhance orbital volume, thereby increasing the stimulus for bony orbital growth. We have found this technique especially useful in the occasional case in which a DFG has provided lining but where more volume is still missing. Once again the increase in volume permits use of a thinner prosthetic shell, which can better distribute forces horizontally and vertically to the lids and fornices. With the positive long-term experience of intraconal hydrogel sphere implantation, we now prefer this for additional volume. The advantage of such a secondary implant is the benefit of only a small incision needed centrally through a previously placed DFG or the posterior conjunctival socket wall for a dehydrated hydrogel sphere. This is easily inserted through the small incision which is sutured with several interrupted 4–0 or 5–0 vicryl sutures which will hold with minimal risk of extrusion as the hydrogel swells to its full size. See Figs. 39.36 and 39.37 for examples of the full sequence of hydrogel expansion followed by dermis fat grafting.

We recently performed a retrospective review of 50 patients (51 eyes) with A/M who underwent insertion of osmotic hydrogel expanders. Expanders were maintained in the anterior socket with a cyanoacrylate glue tarsorrhaphy. Procedures were done without local or general anesthesia in an outpatient setting. All cases but one were unilateral (the bilateral case received hydrogel expanders in both eyes.) Orbital growth was compared by end sphere volume, which ranged from 2 to 4 mL and also estimated by measurements taken from pre- and postoperative CT and MR scans. Horizontal fissure lengths were sequentially recorded at initial and follow-up visits. Follow-up scans were grouped into the following time points after placement: 3–6 months, 6–12 months, 1–2 years, 2–5 years, and 5–10 years. Based on imaging measurements, pre-implanted volumes of the microphthalmic eye were estimated to be an average of 3.6 mL, as compared to 5.7 mL for post-expansion orbital volume. Horizontal fissure lengths

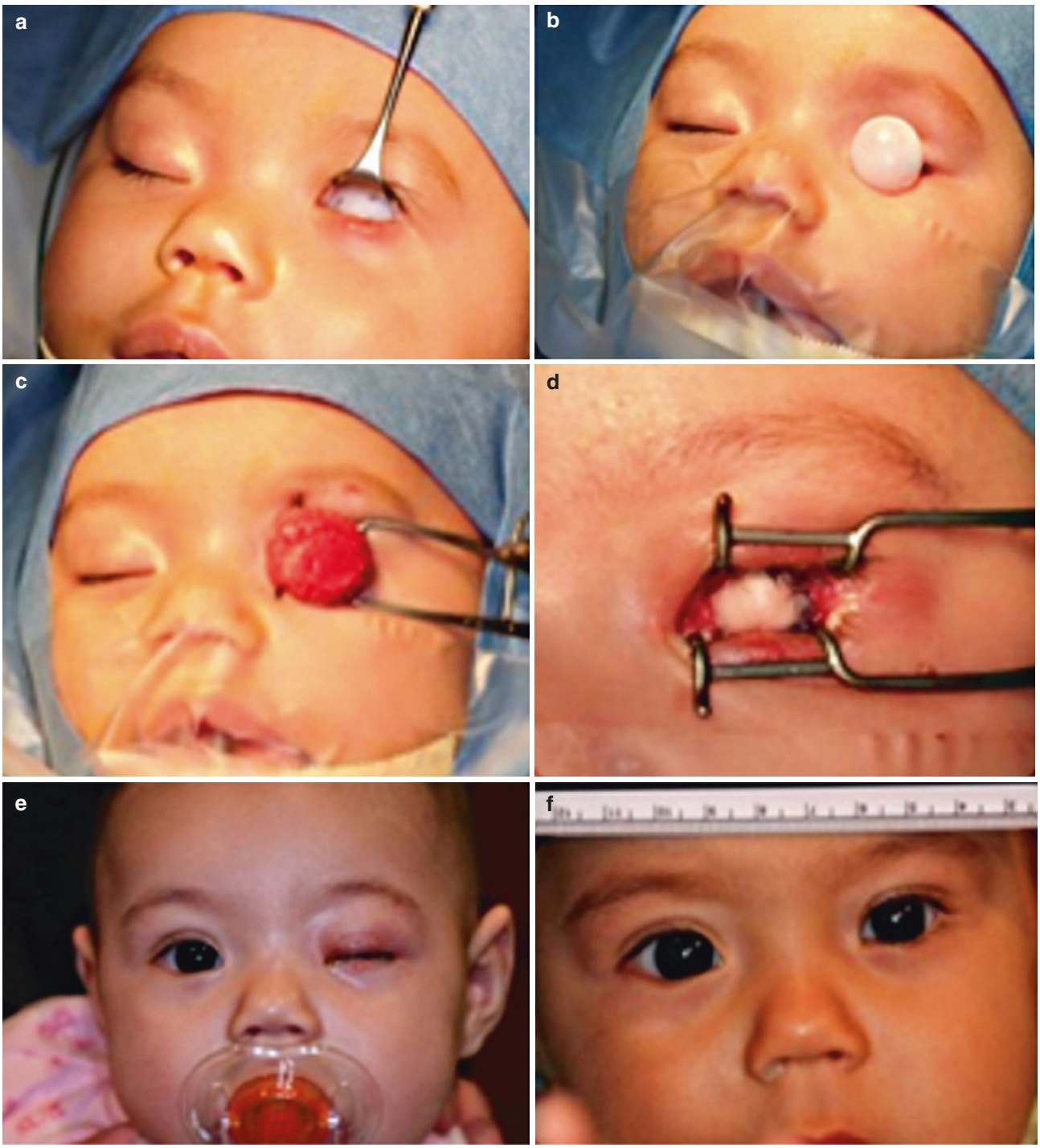


Fig. 39.36 (**a**) Girl with unilateral left microphthalmia who had (**b**) progressive hydrogel expansion. (**c**–**e**) Ultimately, she had dermis fat grafting to the left socket with a nicely fitted ocular prosthetic at 18 months (**f**).



Fig. 39.36 (continued) (**g**) She continued to demonstrate orbital expansion with age and ultimately had a very successful outcome here at age 5 and (**h**) at 12 years with obvious psychosocial benefit with good symmetry and a well-fitting cosmetic prosthesis



Fig. 39.37 (**a**) Newborn with bilateral clinical anophthalmia who had progressive socket enlargement with increasing hydrogel hemispheres and spheres (**b**) placed with (**c**) glue tarsorrhaphies and



Fig. 39.37 (continued) (**d**) good orbital expansion. (**e**) Bilateral hydrogel expanders in place. (**f**) She ultimately had dermis fat grafting bilaterally and (**g**) was able to tolerate prosthetic shells with a nice cosmetic outcome

demonstrated similar growth patterns. No complications were noted with these outpatient procedures.

The conclusion of the study supported the premise that insertion of osmotic hydrogel expanders in the anterior socket of anophthalmic and microphthalmic patients is an efficacious, safe, and noninvasive technique for orbital and eyelid expansion. It confirmed that the procedure can be done easily in the office with minimal concern for complications. It further supported the concept that anterior placement of hydrogel expanders stimulates orbital and horizontal palpebral fissure growth allowing for improved symmetry and favorable esthetic results in less time than traditional serial conformer expansion [68].

Socket Management After Orbital Volume Expansion

Another area of difficulty encountered by the ocularist treating microphthalmia is what to do when adequate space in the orbit is achieved, but the size and weight of the prosthetic shell has become unwieldy. In most cases, aggressive, conformer expansion will adequately stimulate eyelid fissure lengths, socket size, and orbital volume but, unfortunately, in some patients expansion, may proceed more in an anterior-posterior direction and not adequately stimulate proper horizontal and vertical eyelid fissure growth. As expansion proceeds in an anterior-posterior direction, the

prosthetic conformer or prosthetic eye will necessarily have to be made larger. This increase in size, however, usually is more spherical or pear shaped to fill up the developing orbital space. This cycle, if continued, may result in adequate anterior-posterior depth but less than satisfactory horizontal eyelid fissure expansion. The prosthesis usually becomes heavier and more difficult to retain within the socket, and the pressure effects are not sufficient in the horizontal and vertical directions. In such cases, augmenting the orbital volume with an implant may allow a thinner prosthetic shell to be utilized for better horizontal and vertical fissure growth.

Adnexal Problems in A/M

While the major focus in managing anophthalmia and microphthalmia is directed toward expansion of the lids, conjunctival space, and bony orbit, there are major issues involving the periorbital tissues that often require surgical intervention. As discussed above, they most commonly have to do with lid position, as entropion and ptosis are frequent issues in the more serious forms of A/M. Summarized below are both developmental and secondary adnexal problems that occur with A/M and, in particular, when associated with craniofacial disorders (see also Chaps. 25 and 40).

Lid problems
Ptosis
Entropion
Lash ptosis
Lid retraction
Colobomas
Canthal abnormalities
Epicanthal folds
Telecanthus
Microphthalmia with cyst
Cryptophthalmos
Partial
Complete
Nasolacrimal problems with tearing
Punctal atresia or absence
Canalicular atresia
Dacryoceles
Intranasal cysts
Single (absent) nostril
Isolated
Fronto-nasal dysplasia

Lid problems dominate as adnexal issues with A/M because a tight conformer will often produce an entropion. This may disappear as the lids expand over time, but it is not uncommon to persist and require surgical repair. The techniques for repair of these adnexal issues are by and large standard techniques, but we will highlight a few more complex adnexal challenges here (see Chap. 25). We discussed microphthalmia with cyst earlier, but Fig. 39.38 demonstrates

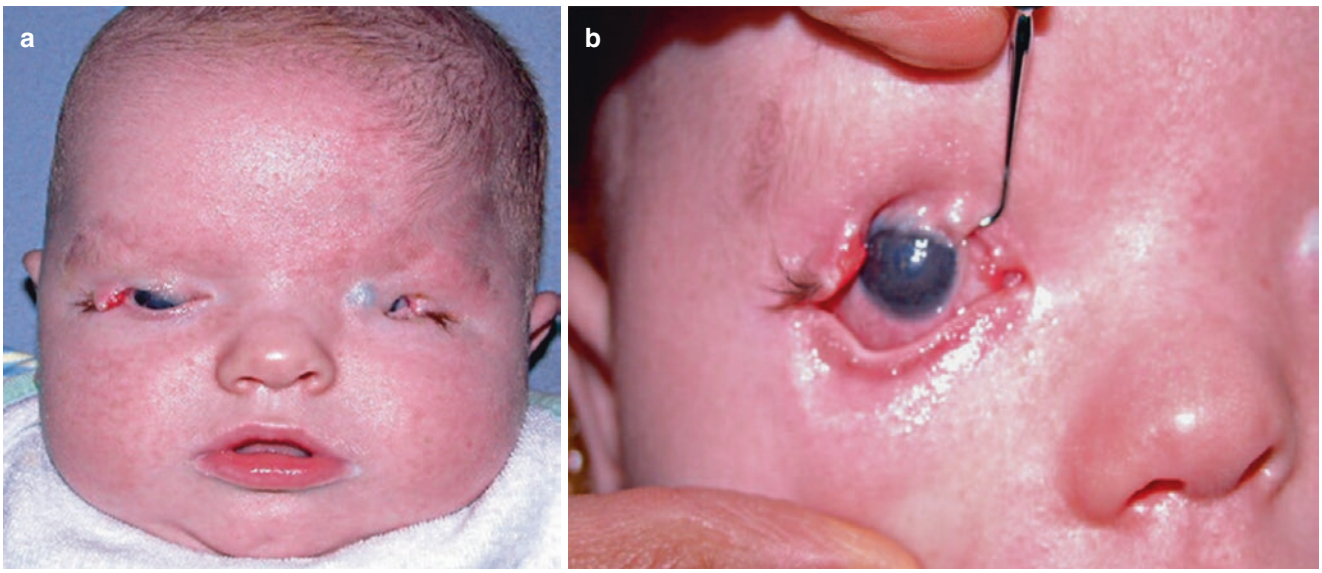


Fig. 39.38 Right partial cryptophthalmos and left microphthalmia with cyst. (**a**) Coloboma of right upper lid with symblepharon attached to superior cornea. (**b**) Absent superior cul-sac.



Fig. 39.38 (continued) (**c**) Repair of left upper lid coloboma repaired with sliding flap; cyst in medial orbit retained as an orbital expander for the microphthalmic orbit. (**d**) Repair of right upper lid coloboma by sliding flap, partial cryptophthalmos symblepharon repaired with lamellar keratectomy and conjunctivoplasty. (**e**) Left upper lid coloboma repair dehisced, medial cul-de-sac shallow, preparation made for Cutler-Beard transposition flap from lower lid. (**f**) Flap in place with oral mucus membrane graft supported by anchored conformer to deepen medial cul-de-sac. (**g**) 6 months post-op separation of transposition flap. (**h**) 6 years post-op ptosis and telecanthus repairs now at age 11 years; VA = 20/25 on right side; wearing cosmetic prosthesis successfully on left side.



Fig. 39.39 Microphthalmia with fronto-nasal dysplasia and tearing with an absent right nostril. (**a**) Associated cleft lip and palate; no encephalocele present but has optic nerve colobomas. (**b**) Serial conformer expansion begun at age 6 months. (**c**) 6 months post-op DFG on left at age 2 years, significant tearing an increasing problem on the right side. (**d**) 6 years post DFG and 4 years post-op right dacryocystectomy with functioning pyrex tube placed through septum to left nostril. Relative symmetry of horizontal fissure length: 25 mm OD and 22 mm OS

how there can be multiple adnexal issues that present together at birth and require careful planning to achieve the best outcome from both a functional and appearance perspective.

Another example of difficult surgical planning for adnexal problems is demonstrated in Fig. 39.39.

As discussed earlier, there is a close association of A/M to craniofacial disorders, and these patients usually require craniofacial surgical correction based on other factors than the concurrent presence of anophthalmia or microphthalmia. The need for craniofacial surgery due to failure to adequately expand the lids, conjunctival space, and bony orbit is fortunately rare.

Craniofacial Surgery

As stated above, craniofacial reconstruction of the anophthalmic and microphthalmic orbit is generally reserved for those patients who have failed to achieve adequate expansion or facial symmetry despite aggressive conformer therapy. Craniofacial surgery can reposition and repair skeletal defects, but will generally not increase the soft tissue volume unless combined with vascularized flaps, as is sometimes used for anophthalmic sockets postradiation. In certain cases, craniofacial reconstruction can be combined at a later date with both eyelid surgery and orbital volume augmentation,

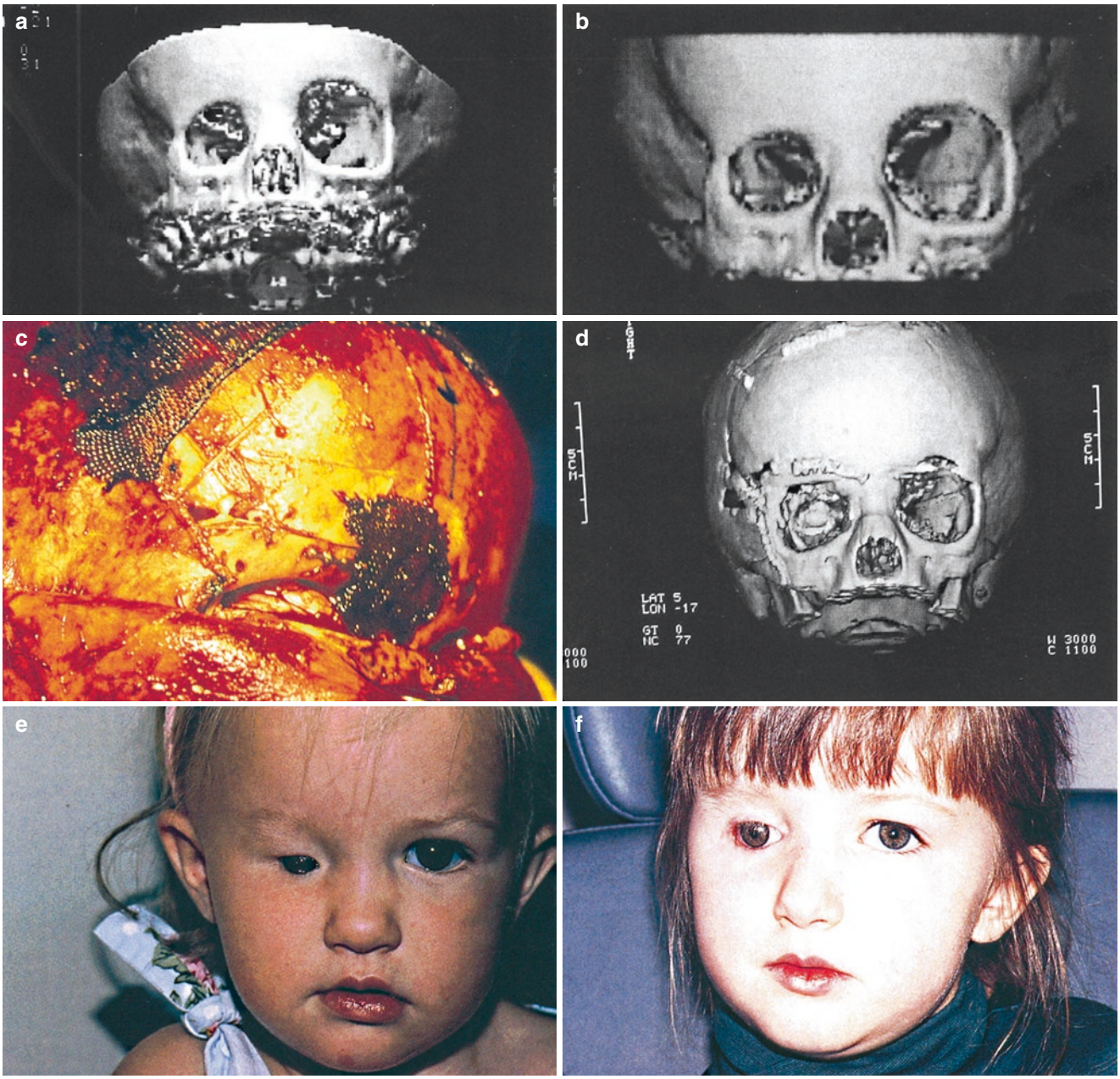


Fig. 39.40 Bony orbital expansion. (**a**) 3-D reconstruction of microphthalmic right orbit, patient at age 6 months. (**b**) Same patient 2 years later with only limited bony orbital response to conformer expansion and dermis fat grafting. (**c**) Craniofacial procedure to expand bony orbit. (**d**) 3-D reconstruction showing enlarged orbital space. (**e**) Preoperative craniofacial procedure. (**f**) 1-year postoperative appearance; socket expansion is improved, though orbits are still somewhat asymmetric

so as to improve facial symmetry and allow the fitting of a properly sized prosthesis. In cases with severe bony asymmetry, where one side is normal and the other hypoplastic, early surgical expansion of the orbit may be the best option [69]. In most instances of severe microphthalmia, we have been conservative and have tried progressive conformer or hydrogel expansion, but the bone may not respond well to noninvasive expansion. As demonstrated by the patient in Fig. 39.40, nonsurgical soft tissue expansion produced minimal bony orbit expansion. Following craniofacial

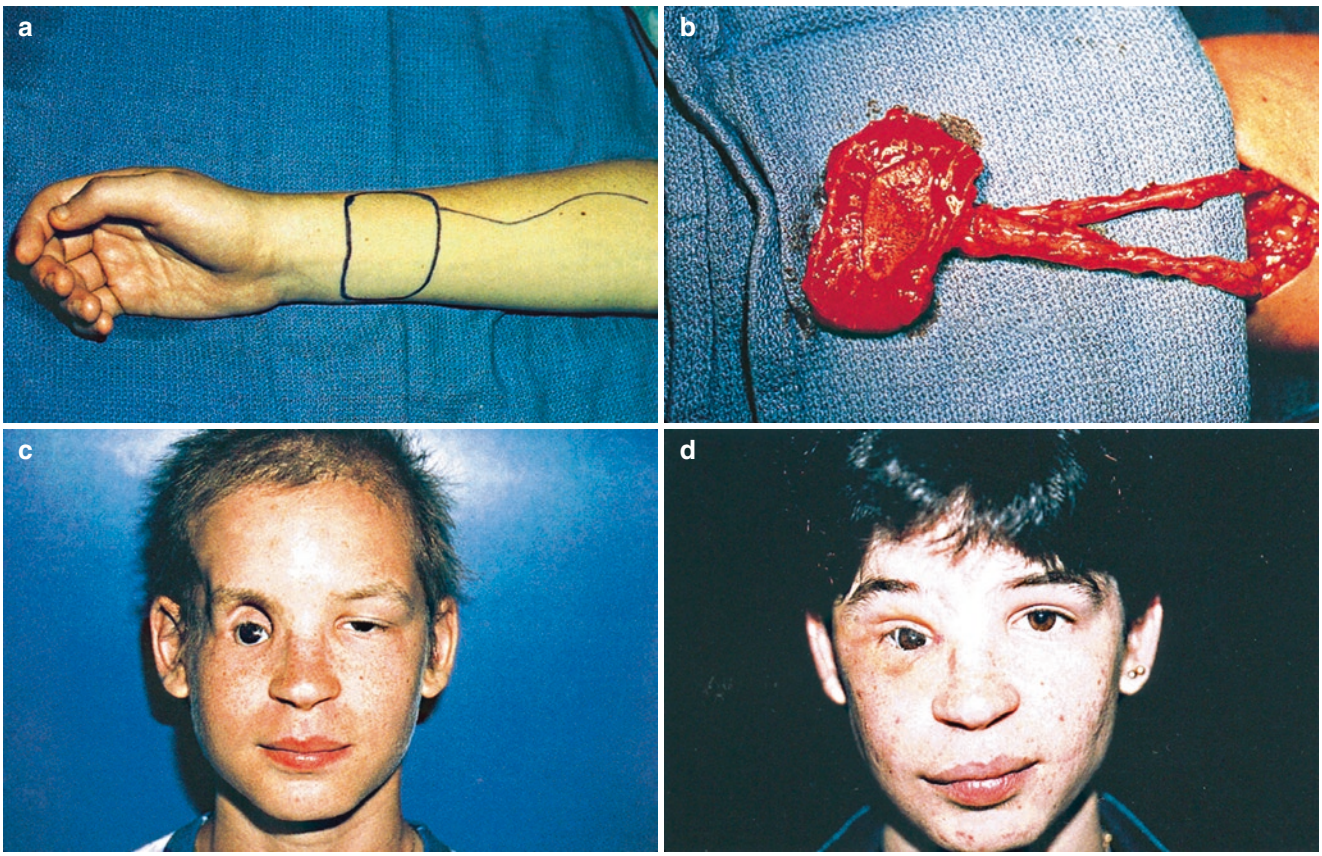


Fig. 39.41 Microvascular free flap. (**a**) Radial forearm flap outlined with methylene blue. (**b**) Graft harvested, demonstrating isolated artery and vein anastomosis with temporal vessels. (**c**) Patient with longstanding problem retaining prosthetic shell. Note severe atrophy of periorbital soft tissues and temporalis muscle secondary to radiation following enucleation for retinoblastoma. (**d**) 2-year postoperative radial forearm free flap (Courtesy of Scott Bartlett, MD)

reconstruction with orbital expansion, there was more room for an ocular prosthesis.

Radiation and the Microphthalmic Socket

Retardation of orbit and socket growth can be severe following enucleation and radiation [70, 71]. This was previously seen with problematic retinoblastoma cases (Fig. 39.41), although with evolving management options for retinoblastoma, radiation is becoming a less common treatment. While dermis fat grafts can be successfully used as a primary enucleation implant for many retinoblastoma or other cancer cases, they may not take well where there has been significant radiation atrophy and retarded orbital growth. In these instances use of a microvascular free flap may be required, and a radial forearm flap is particularly useful for these very difficult microphthalmic sockets [72]. Another approach that has been described with success is use of an expanded superficial temporalis fascial flap to provide revascularization to the socket and support further grafting efforts with mucous membrane [73].

Family Resources

As previously discussed, the family's interactions and the developmental progress of the child are critical to the overall treatment plan. Monitoring the child's eyelid, orbital, and facial development is of prime importance during the majority of patient visits. Yet the treating physician also needs to be cognizant of the family dynamics and the child's physical and educational requirements. Every child and family should be directed to an appropriate medical social worker to assist in resource planning. This would include the coordination of medical benefits for medical and ocularist services and referrals to appropriate community agencies. Children with severe visual impairment also need to be directed to a multidisciplinary early intervention program.

Several families have formed an international support group and information database for those interested in anophthalmia and microphthalmia. ICAN, the International Children's Anophthalmia Network (1–800-580-ICAN), provides a valuable resource for both physicians and families, not only by advocating ongoing research into the etiology of these conditions, but also by directing families to the

proper resources for children with similar ocular disorders and allowing them to share their personal experience with each other.

References

1. Handler L, Heher K, Katowitz J. Congenital and acquired anophthalmia. Curr Opin Ophthalmol. 1994;5:84–90.
2. Marchac D, Cophignon J, Achard E, Duformental C. Orbital expansion for anophthalmia and micro-orbitism. Plast Reconstr Surg. 1977;59:486–91.
3. Frenkel LD, Keys MP, Hefferen SJ, Rola-Pleszczynski M, Bellanti JA. Unusual eye abnormalities associated with congenital cytomegalovirus infection. Pediatrics. 1980;66:763–6.
4. Pabst W. Thalidomide and congenital abnormalities of the eye. Ber Dtsch Ophthalmol Ges. 1964;65:209–15.
5. Margolis S, Martin L. Anophthalmia in an infant of parents using LSD. Ann Ophthalmol. 1980;12:1379–81.
6. Sarma V. Maternal vitamin A deficiency and fetal microcephaly and anophthalmia. Obstet Gynecol. 1959;13:299–301.
7. Achelis E. Anophthalmos als folge eines interruption versuches. Med Klin. 1950;45:1214–5.
8. Subramanian N, Iyer G, Srinivasan B. Cryptophthalmos: reconstructive techniques–expanded classification of congenital symblepharon variant. Ophthal Plast Reconstr Surg. 2013;29(4):243–8.
9. Shah SP, Taylor AE, Sowden JC, Ragge NK, Russell-Eggitt I, Rahi JS, Gilbert CE, G. Surveillance of Eye Anomalies Special Interest. Anophthalmos, microphthalmos, and typical coloboma in the United Kingdom: a prospective study of incidence and risk. Invest Ophthalmol Vis Sci. 2011;52(1):558–64.
10. Moore KL, Persaud TVN, Torchia MG. The developing human clinically oriented embryology. Philadelphia: Elsevier; 2016. p. 1. online resource.
11. Hennekam RCM, Allanson JE, Krantz ID, Gorlin RJ, STAT!Ref (Online service). Gorlin's syndromes of the head and neck, Oxford monographs on medical genetics, 58. Oxford/New York: Oxford University Press; 2010. p. 1. online resource (lxi, 1452 p.)
12. Katowitz JA. Pediatric oculoplastic surgery. New York: Springer. xix; 2002. 694 p.
13. Tucker S, Jones B, Collin R. Systemic anomalies in 77 patients with congenital anophthalmos or microphthalmos. Eye (Lond). 1996;10(Pt 3):310–4.
14. Demirci H, Singh AD, Shields JA, Shields CL, Eagle RC. Bilateral microphthalmos and orbital cyst. Eye (Lond). 2003;17(2):273–6.
15. Chang L, Blain D, Bertuzzi S, Brooks BP. Uveal coloboma: clinical and basic science update. Curr Opin Ophthalmol. 2006;17(5):447–70.
16. Bardakjian TM, Steinberg L, Schneider A. The genetics of anophthalmia/microphthalmia. J Ophthal Prosthetics. 1997;2:15–22.
17. Gilbert C, Foster A. Childhood blindness in the context of VISION 2020–the right to sight. Bull World Health Organ. 2001;79(3):227–32.
18. Williamson KA, FitzPatrick DR. The genetic architecture of microphthalmia, anophthalmia and coloboma. Eur J Med Genet. 2014;57(8):369–80.
19. Verma AS, Fitzpatrick DR. Anophthalmia and microphthalmia. Orphanet J Rare Dis. 2007;2:47.
20. Leonard A. Hereditary anophthalmia in the progeny of an X-irradiated female rat. Jikken Dobutsu. 1977;26:255–7.
21. Russell-Eggitt I, Fielder AR, Levene MI, Young ID. Microphthalmos in a family. J Med Genet. 1984;21:301.
22. Sensi A, Incorvaia C, Sebastiani A, Calzolari E. Clinical anophthalmos in a family. Clin Genet. 1987;32:156–9.
23. Kohn G, El-Shawwa R, El Rayyes E. Isolated "clinical anophthalmia" in an extensively affected Arab kindred. Clin Genet. 1988;33:321–4.
24. Pearce WG, Nigam S, Rootman J. Primary anophthalmos histiological and genetic features. Can J Ophthalmol. 1974;9:141–5.
25. Farkas LG, Posnick JC, Hreczko TM, Pron GE. Growth patterns in the orbital region: a morphometric study. Cleft Palate Craniofac J. 1992;29:315–8.
26. Posnick JC, Farkas LG. The application of anthropometric surface measurements in craniomaxillofacial surgery. In: Farkas LG, editor. Anthropometry of the head and face. 2d ed. New York: Raven Press; 1994. p. 125–37.
27. Kennedy RE. The effect of early enucleation on the orbit in animals and humans. Adv Ophthalmic Plast Reconstr Surg. 1992;9:1–39.
28. Merritt JH, Trawnik WR. Prosthetic and surgical management of congenital anophthalmia. J Ophthal Prosth. 1997;2:1–14.
29. DeMarco JK, Bilaniuk LT. Magnetic resonance imaging: technical aspects. In: Newton TH, Bilaniuk LT, editors. Radiology of the eye and orbit: modern radiology, vol. 4. New York: Raven; 1990. p. 1.1–1.14.
30. Feldman N, Melcer Y, Levinsohn-Tavor O, Orenstein A, Svirsky R, Herman A, Maymon R. Prenatal ultrasound charts of orbital total axial length measurement (TAL): a valuable data for correct fetal eye malformation assessment. Prenat Diagn. 2015;35(6):558–63.
31. Busa T, Legendre M, Bauge M, Quarello E, Bretelle F, Bilan F, Sigaudy S, Gilbert-Dussardier B, Philip N. Prenatal findings in children with early postnatal diagnosis of CHARGE syndrome. Prenat Diagn. 2016;36(6):561–7.
32. Leung E, Diaz-Barbosa M, Alabiad C, Hodapp E, Tse D, Murray TG, Castaner JC, Martin D, Berrocal AM. Prenatal ultrasonographic detection of ophthalmic diseases. J Pediatr Ophthalmol Strabismus. 2012 May 22;49 Online:e26–e29.
33. Lee A, Deutinger J, Bernaschek G. Three dimensional ultrasound: abnormalities of the fetal face in surface and volume rendering mode. Br J Obstet Gynecol. 1995;102:302–6.
34. Brémond-Gignac DS, Benali K, Deplus S, Cussenot O, Ferkdadji L, Elmaleh M, Lassau JP. In utero eyeball development study by magnetic resonance imaging. Surg Radiol Anat. 1997;19(5):319–22.
35. Dar SA, Johal SC, Marino MJ, Singh AD. Prenatal diagnosis of colobomatous microphthalmos. J Pediatr Ophthalmol Strabismus. 2015;52 Online:e22–e25.
36. Fernández-Mayoralas DM, Recio-Rodríguez M, Fernández-Perrone AL, Jiménez-de-la-Peña M, Muñoz-Jareño N, Fernández-Jaén A. In utero diagnosis of PHACE syndrome by fetal magnetic resonance imaging (MRI). J Child Neurol. 2014;29(1):118–21.
37. Katowitz JA, Heher K, Handler L. Use of dermis-fat graft as an orbital implant in congenital microphthalmia. J Ophthal Prosthetics. 1997;2:23–9.
38. Dootz GL. The ocularists' management of congenital microphthalmos and anophthalmos. In: Bosniak SL, editor. Advances in ophthalmic plastic and reconstructive surgery. New York: Pergamon; 1991. p. 41–56.
39. Molgat YM, Hurwitz JJ, Webb MCF. Buccal mucous membrane-fat graft in the management of the contracted socket. Ophthalmic Plast Reconstr Surg. 1993;9:267–72.
40. Sullivan SA, Dailey RA. Graft contraction: a comparison of acellular dermis versus hard palate mucosa in lower eyelid surgery. Ophthal Past Reconstr Surg. 2003;19:14–24.
41. Hashikawa K, Terashi H, Tahara S. Therapeutic strategy for the triad of acquired anophthalmic orbit. Plast Reconstr Surg. 2007;119:2182–91.
42. Kim CY, Woo YJ, Lee SY, Yoon JS. Postoperative outcomes of anophthalmic socket reconstruction using an autologous buccal mucosa graft. J Craniofac Surg. 2014;25(4):1171–4.
43. Heher K, Katowitz J. Oral mucous membrane grafts for corneal protection to permit prosthetic shell wear. Ophthalmic Plast Reconstr Surg. 1997;13(l):40–7.

44. Bajaj MS, Pushker N, Singh KK, Chandra M, Ghose S. Evaluation of aniotic membrane grafting in the reconstruction of contracted socket. Ophthal Plast Reconstr Surg. 2006;22(2):116–20.
45. Poonythalang A, Preechawat P, Pomsathit J, Mahaisaviriya P. Reconstruction of contracted eye socket with amniotic membrane graft. Ophthal Plast Reconstr Surg. 2005;21(5):359–62.
46. Dua HS. Amniotic membrane transplantation. Br J Ophthalmol. 1999;83:748–52.
47. Kumar S, Sugandhi P, Arora R, Pandey PK. Amniotic membrane transplantation versus mucous membrane grafting in anophthalmic contracted socket. Orbit. 2006;25:195–203.
48. Tucker SM, Sapp N, Collin R. Orbital expansion of the congenitally anophthalmic socket. Br J Ophthalmol. 1995;79:667–71.
49. Rodallec A. Orbit and eyelid expansion: introrbital expander prosthesis. In: vanderMullen JC, Gruss JS, editors. Ocular plastic surgery. London: Mosby-Wolfe; 1996. p. 55–9.
50. Gossman MD, Monay J, Roberts DM. Expansion of the human microphthalmic orbit. Ophthalmology. 1999;106(10):2005–9.
51. Rappaport BA, Suresh S, Hertz S, Evers AS, Orser BA. Anesthetic neurotoxicity – clinical implications of animal models. N Engl J Med. 2015;372:796–7.
52. Flick RP, Katusic SK, Colligan RC, Wilder RT, Voigt RG, Olson MD, Sprung J, Weaver AL, Schroeder DR, Warner DO. Cognitive and behavioral outcomes after early exposure to anesthesia and surgery. Pediatrics. 2011;128:1053–61.
53. Wagner A, Schneider C, Lagogiannis G, et al. Pulsatile expansion therapy for orbital enlargement. Int J Oral Maxillofac Surg. 2000;29:91–5.
54. Weise KG, Vogel M, Guthoff R, Gundlach K. Treatment of congenital anophthalmos with self-inflating polymer expanders: a new method. J Craniomaxillofac Surg. 1999;27:72–6.
55. Bacskulin A, Vogel M, Gundlach K, Hingst V, Guthoff R. New osmotically active hydrogel expander for enlargement of the contracted anophthalmic socket. Graefes Arch Clin Exp Ophthalmol. 2000;238:24–7.
56. Downes R, Lavin M, Collin R. Hydrophilic expanders for the congenital anophthalmic socket. Plast Reconstr Surg. 1992;9:57–61.
57. Schittkowski M, Gundlach KK, Guthoff R. Treatment of congenital clinical anophthalmos with high hydrophilic hydrogel expanders (abstract; in German). Ophthalmologe. 2003;100:525–34.
58. Schittkowski MP, Katowitz JA, Gundlach KKH, Guthoff RF. Self-inflating hydrogel expanders for the treatment of congenital anophthalmos. Essentials in ophthalmology: oculoplastics and orbit. London: Springer; 2005.
59. Wiese KG. Osmotically induced tissue expansion with hydrogels: a new dimension in tissue expansion? A preliminary report. J Craniomaxillofac Surg. 1993;21:309–13.
60. Wiese KG, Heinemann DEH, Ostermeier D, et al. Biomaterial properties and biocompatibility in cell culture of a novel self-inflating hydrogel tissue expander. J Biomed Mater Res. 2001;54:179–88.
61. Katowitz JA, Bruce D, Whitaker LA. Orbital teratomas associated with microphthalmic corneal cysts. In: Marchac D, editor. J Craniofacial surgery. Berlin: Springer; 1987. p. 467–70.
62. Heher K, Low J, Katowitz J. Unilateral dermis-fat implantation in the pediatric orbit. Ophth Plastic and Reconstr Surg. 1998;14(2):81–8.
63. Mitchell KT, Hoolsten DA, White WL, et al. The autogenous dermis-fat orbital implant in children. J Am Assoc Pediatr Ophthalmol Strab. 2001;5:367–9.
64. Chen D, Heher K. Management of the anophthalmic socket in pediatric patients. Curr Opin Ophthalmol. 2004;15:449–53.
65. Perry AC. Advances in enucleation. Ophthalmol Clin N Am. 1991;4:173–82.
66. Shields JA, Shields CL, De Potter P. Hydroxyapatite orbital implant after enucleation experience with 200 cases. Mayo Clin Proc. 1993;68:1191–5.
67. Kirzhner M, Shildkrot Y, Haik BG, Qaddoumi I, Rodriguez-Galindo C, Wilson MW. Pediatric anophthalmic sockets and orbital implants: outcomes with polymer-coated implants. Ophthalmology. 2013;120(6):1300–4.
68. Nazemzadeh M; Katowitz WR; Sulewski M Jr, Katowitz, JA. Hydrogel expansion and glue Tarsorrhaphy for congenital Anophthalmia and Microphthalmia, Poster Presentation, Annual Meeting European Society of Oculoplastic and Reconstructive Surgery, Budapest, Hungary, 2014.
69. Kiskadden WS, McDowell AJ, Keiser T. Results of early treatment of congenital anophthalmos. Plast Reconstr Surg. 1949;4:426–33.
70. Nasser QJ, Gombos DS, Williams MD, Guadagnolo BA, Morrison WH, Garden AS, Beadle BM, Canseco E, Esmaeli B. Management of radiation induced severe anophthalmic socket contracture in patients with uveal melanoma. Ophthal Plast Reconstr Surg. 2012;28(3):208–12.
71. Shildkrot Y, Kirzhner M, Haik BG, et al. The effect of cancer therapies on pediatric anophthalmic sockets. Ophthalmology. 2011;118:2480–6.
72. Li D, Jie Y, Liu H, Liu J, Zhu Z, Mao C. Reconstruction of anophthalmic orbits and contracted eye sockets with microvascular radial forearm free flaps. Ophthal Plast Reconstr Surg. 2008;24(2):94–7.
73. Foster JA, Castro E, Papay FA. Reconstruction of the irradiated contracted socket with an expanded superficial temporalis fascial flap. Am J Ophthalmol. 1999;127(5):621–2.

Oculoplastic Considerations in Pediatric Craniofacial Surgery

40

Sanjay Naran, Michael F. Spadola, Phillip B. Storm, and Scott P. Bartlett

It has been almost half a century since the pioneering work of Paul Tessier of Paris opened the door to a vast new arena in the treatment of deformities of the upper facial skeleton [1–3]. Working first in the anatomic laboratory and then cautiously in patients with severe cranio-orbital deformities, Tessier first presented his dramatic results in 1967. Prior to that time, limited access approaches to the orbit and periorbital structures put restrictions on the results that could be obtained in the treatment of disorders in this area [4]. By extensive exposure through transcoronal and periorbital incisions, Tessier established three basic principles that remain the foundation for cranio-orbital work today:

1. Safe exposure to the orbit can be obtained by a combined extracranial and transcranial approach.
2. Bony segments can be osteotomized and completely removed, manipulated, and replaced without extensive secondary resorption or remodeling of the bone.
3. Major orbital shifts can be performed without unacceptable risks of ocular or neural injury.

Although initially applied to the treatment of congenital anomalies of the facial skeleton, these techniques have now been applied to a variety of deformities, including not only those secondary to development and growth but also tumors [5], trauma [6], and metabolic disease [7]. More recently, these techniques have also proven efficacious in aesthetic enhancement of the facial skeleton [8].

In this chapter, we briefly review the general techniques of cranio-orbital surgery and outline the specific use of these techniques in the management of complicated craniofacial disorders. In keeping with the goals of this text, we primarily confine our discussion to those deformities whose primary component is the orbit.

Classification of Craniofacial Deformities

By definition, craniofacial anomalies are a diverse group of congenital, developmental, or acquired anomalies of the cranial, orbital, or facial skeleton. Although the skeletal anomaly is frequently the basis for classification and management, equally important are associated soft tissue deficiencies, excesses, or displacements, which are the most outwardly visible manifestations of the disease.

The classification of congenital craniofacial anomalies can be bewildering. Gorlin and coworkers [9] have identified over 190 congenital syndromes of the head and neck. Rather than try to place these diverse syndromes into a complicated classification scheme, it is more practical to utilize a modified American Cleft Palate-Craniofacial Association (ACPA) classification [10] as a guide. This classification system allows us to consider the syndromes and deformities in large diagnostic groups and therefore to establish principles for their management. A modified ACPA classification system includes:

1. Rare craniofacial clefts using the Tessier classification system
2. Craniosynostosis:
   (a) Syndromic
   (b) Nonsyndromic
3. Atrophy and hypoplasia

S. Naran
Division of Plastic Surgery, Children's Hospital of Philadelphia, Philadelphia, PA, USA

University of Pennsylvania, Philadelphia, PA, USA

M.F. Spadola
The Children's Hospital of Philadelphia, Philadelphia, PA, USA

P.B. Storm
Division of Neurosurgery, Children's Hospital of Philadelphia, Philadelphia, PA, USA

University of Pennsylvania Perelman School of Medicine, Philadelphia, PA, USA

S.P. Bartlett (✉)
Division of Plastic and Reconstructive Surgery, Children's Hospital of Philadelphia, Philadelphia, PA, USA
e-mail: scott.bartlett@uphs.upenn.edu

© Springer International Publishing AG 2018

J.A. Katowitz, W.R. Katowitz (eds.), *Pediatric Oculoplastic Surgery*, https://doi.org/10.1007/978-3-319-60814-3_40

4. Neoplasia, hypertrophy, and hyperplasia
5. Unclassified craniofacial deformities

A sixth categorization useful to this discussion would include miscellaneous craniofacial conditions, such as trauma, metabolic disorders, and the like.

Approaching the Craniofacial Deformity: The Craniofacial Team

Congenital as well as acquired craniofacial deformities may involve a variety of organ systems and associated anomalies [9]. As such, a multidisciplinary team approach to both the evaluation and management of these conditions is paramount. Centers of excellence should be regionalized to allow a concentrated experience that is periodically reviewed to assure that the types of surgery being performed are appropriate, the timing of that surgery is optimal, and the complications are minimized. Such groups will also stimulate appropriate clinical and experimental research into the management of these deformities.

The craniofacial team frequently includes, but is not restricted to, the following:

1. Craniofacial surgeon
2. Neurosurgeon
3. Oculoplastic surgeon
4. Pediatric ophthalmologist
5. Otolaryngologist
6. Geneticist
7. Pediatrician
8. Physical anthropologist
9. Orthodontist and pedodontist
10. Psychologist
11. Radiologist
12. Speech therapist
13. Anesthesiologist
14. Nurse (patient care coordinator)

It is our practice that patients with significant craniofacial deformities see the team on a regular basis for monitoring and decision-making regarding the timing of intervention. As techniques have evolved and become more standardized, and as patients with congenital diagnoses progress through their care, it is not absolutely necessary that they see all members of the craniofacial team.

Once a new patient with a deformity has been identified and examined by the members of the craniofacial team and all associated anomalies have been noted, further diagnostic studies may be indicated. Although simple x-rays were utilized extensively during the early years of craniofacial surgery, they have been largely supplanted by more sophisticated imaging techniques such as two- and three-dimensional computed tomography (CT) scans and magnetic resonance imaging (MRI) [11, 12]. Cephalometrographic and panoramic x-rays, however, still provide useful information in the treatment planning of lower face deformities. Also of value are frequent life-size photographs for use in the operating room and to assist in evaluating the results of therapy. A life-size photograph, in which a grid has been superimposed, frequently gives exact measurement to the degree of deformity (e.g., orbital dystopia) and therefore guides the necessary treatment.

Once these initial evaluations have been made, the craniofacial team meets as a group to plan the surgical and nonsurgical therapy. Following specific interventions, follow-up is mandated and further treatment suggested. Due to the vagaries of growth in both the normal infant and the craniofacially deformed, the timing of intervention may vary significantly. Although specific guidelines for timing have been outlined and are mentioned below, it is generally accepted that surgical intervention when indicated is based on both functional and psychological needs [13]. The latter are frequently as important as the former. Timely intervention to improve appearance and, therefore, self-esteem is essentially functional and should be given equal weight in the consideration of the treatment of these deformities.

Surgical Planning and General Operative Techniques

Once an operative plan has been established and all preoperative evaluations have been concluded, the operation can commence. Preparation for surgery includes not only the usual blood and urine analysis but also familiarization of the parents and the patient with the operating room complex, the intensive care unit (ICU), and the aftercare areas. At this time, details of

bandages, dressings, monitoring lines, expectations, and the like can be reviewed.

Once the patient is anesthetized, it is essential that proper monitoring be provided. Because the major facial osteotomies often involve significant blood loss, large-bore IVs in addition to arterial lines are mandated. A temperature monitor is also essential in the very young patient. Decompression of the central nervous system spaces by means of a lumbar drain may be required at the discretion of the neurosurgeon. Blood transfusion is typically required and, since these procedures are elective or semi-elective, time is usually available for donor-directed blood. Use of blood-conserving measures such as cell-saver and preoperative dosing with erythropoietin may be efficacious in reducing the need for donor-directed blood transfusion [14–16]. For the larger procedures, we set aside fresh frozen plasma and platelets and perform specific bleeding studies preoperatively. Because the operative field frequently includes the eyes and paranasal sinuses, antibiotic prophylaxis is mandated, usually in the form of a second-generation cephalosporin.

During the operation, constant dialogue between the surgeon and anesthesiologist is necessary. Blood losses are replaced early to insure that one does not get behind in transfusion requirements in the small patient. Manipulations of the head and neck during surgery pose a special problem in the pediatric patient and care of the endotracheal tube must be taken. Fixation of the tube with waterproof tape or dental wiring is appropriate.

Once the operation is satisfactorily completed, the wounds are closed. We utilize drains for all transcranial procedures. The drain is usually removed in 48–72 h. In cases complicated by a dural tear or a small spinal fluid leaks, a drain may continue to draw spinal fluid away or may potentiate any inadvertent communication of the cranial base by drawing in microorganisms from the upper nasal passages, so the drain may be placed to gravity in those cases. A head dressing is usually placed for 1–2 days postoperatively, and the patient is awakened and transferred to the ICU.

Patients with complicated transcranial procedures usually spend 1 day in the ICU for close neurological monitoring. Precise fluid and electrolyte replacement should be performed with frequent checking of bleeding parameters and blood counts [17]. Heavy sedation is to be avoided so that the neural examination is reliable. Once patients have stabilized in the ICU, they can frequently be transferred to the floor for several additional days of monitoring prior to discharge. Most children can be discharged on the fourth or fifth postoperative day, provided that swelling is resolving and there is no sign or symptom of infection. Perioperative antibiotics should be continued for 48–72 h unless specific indications dictate otherwise. It is our practice to check hematocrit as well as electrolytes for 2–3 days postoperatively to be certain that no signs of bleeding or inappropriate antidiuretic hormone (ADH) levels develop. Following discharge, the patient is usually assessed in the clinic within the first 1–2 weeks and at greater intervals thereafter, depending on need.

The specific approaches to the craniofacial skeleton [18] depend on the area to be treated. In general, incisions should be placed in inconspicuous locations and closed in an atraumatic fashion.

For the upper face and orbit, incisions include the standard bicoronal approach with or without a transconjunctival or subciliary incision, if the lower orbit is in need of treatment. The coronal incision is an ear-to-ear incision carried down to the subgaleal plane (Fig. 40.1a). To prevent bleeding from the wound edge, it is frequently desirable to infiltrate the entire upper face, in particular the area of the superior orbital rims, with a dilute solution of epinephrine (1/400,000) and Kenalog and to place blocking sutures on either side of the wound. Alternatively, Raney clips can be utilized after the incision is made. The use of the Colorado cautery is also helpful in minimizing blood loss. The incisions should be broken up into a series of zigzag cuts or a sinusoidal curve to minimize scar visibility under hair. In the young patients with little hair, a complete head shave is frequently performed, while in the older patient shaving a strip of hair with adequate cleansing of the skin and hair preoperatively is all that is required.

Once the coronal incision is made, the coronal flap is turned forward. At the superior orbital rim region, the subperiosteal plane is entered and further dissection performed. The dissection is carried over the rim into the orbit, and in this plane a complete superior orbital degloving is performed (Fig. 40.1b). The lateral canthal attachment and the lateral canthal soft tissue mass should be identified and a suture placed for fixation at the termination of the procedure. Both temporal muscles are dissected in a subtemporal plane out of their respective temporal fossae. At this point in

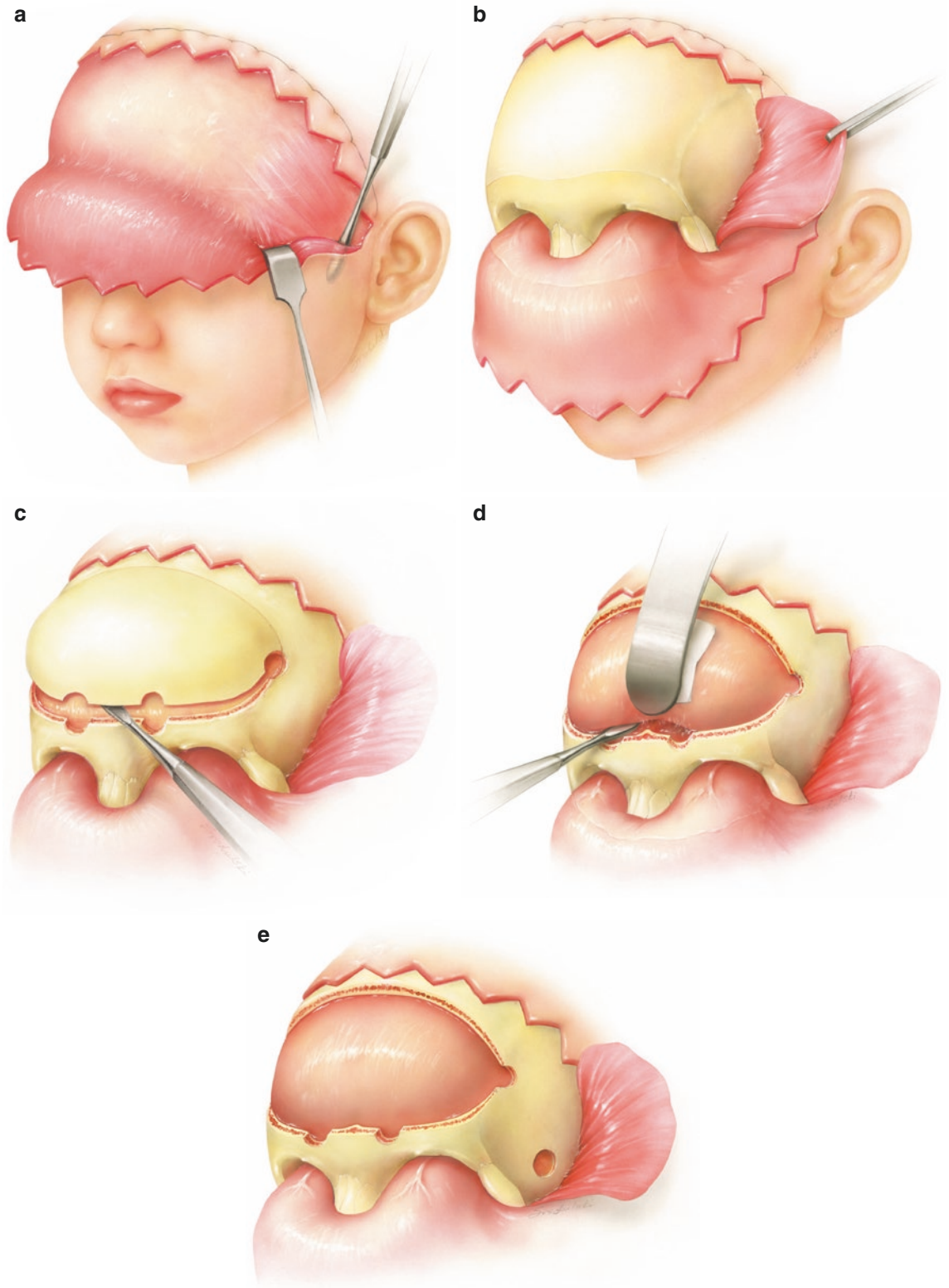


Fig. 40.1 Preparation for transcranial orbital osteotomy. (**a**) The coronal incision to the upper face involves a stair-step incision preceded by blocking suture placement to minimize blood loss. The plane of dissection is above the temporalis muscle and between the galea and periosteum. (**b**) At the level of the supraorbital rims, the plane of dissection goes from subgaleal to subperiosteal at which point the upper orbits may be degloved, providing wide exposure to this region. In preparation for a craniotomy, the temporalis muscle is reflected out of its temporal fossa. (**c**, **d**) Following burr hole placement, the frontal bone flap is removed. The frontal lobes are reflected from the anterior cranial fossa in an extradural plane, providing access to the orbital roof, nasoethmoid region, and medial and lateral orbital walls. (**e**) A burr hole in the temporal region provides access for clearing of the middle cranial fossa to facilitate transcranial orbital osteotomy

the operation, the neurosurgeon performs a unilateral or bifrontal craniotomy with a clearing of the anterior cranial fossa and middle fossa to allow the brain to be safely retracted and the orbital osteotomies completed (Fig. 40.1c, d). Great care must be taken in the midline to avoid tearing of the dura in the cribriform area. Frequently, access to the middle cranial fossa requires a temporal burr hole to facilitate dissection (Figure 40.1e).

If exposure to the inferior orbit is required, either a transconjunctival approach with a lateral canthotomy or a subciliary incision can be made. These incisions, described elsewhere in this text (see Chap. 38), are carried down to the inferior orbital rim where the periosteum is incised and a subperiosteal orbital floor dissection is completed. The dissection will link laterally with the dissection from above. Medially, care must be taken to avoid injury to the medial canthal tendon and nasolacrimal system. Most often, surgery of the medial orbit can be accomplished by osteotomy of the canthal bearing segment of the bone and appropriate repositioning. If this cannot be performed, the medial canthal tendon should be disinserted from its attachment for later reattachment with a transnasal suspension wire. However, this should be avoided, if at all possible, due to the intricate detail and aesthetics of this region. In such circumstances, although we do not routinely prophylactically intubate the nasal lacrimal system, this can be considered.

Once the surgical procedures are completed, the wound is closed. The lateral canthus is resuspended through small drill holes in the lateral orbital rim. The temporalis muscle is resuspended with a combination of sutures to small drill holes in the bone or to wires or plates. Closure of the subciliary wound can be performed with a single running nonabsorbable suture or fine interrupted dissolving sutures. The coronal incision is typically closed with a deep suture to the galea and a fast-absorbing plain gut suture to the skin.

During procedures on the superior orbit, it is almost always necessary to cut and remove the bone. As mentioned previously, the bone can be safely removed en bloc and then manipulated ex vivo. Manipulation of the bone is frequently done by a partial osteotomy and bending with reinforcement with wires or small microplates [19, 20] (Fig. 40.2). In those instances in which the bone must be removed for pathological conditions, bone grafts are necessary. In the young patient, the bone can frequently be partially osteotomized and bent, while in the older patients, this may not be possible and a complete osteotomy is required. Following replacement, the manipulated bones or

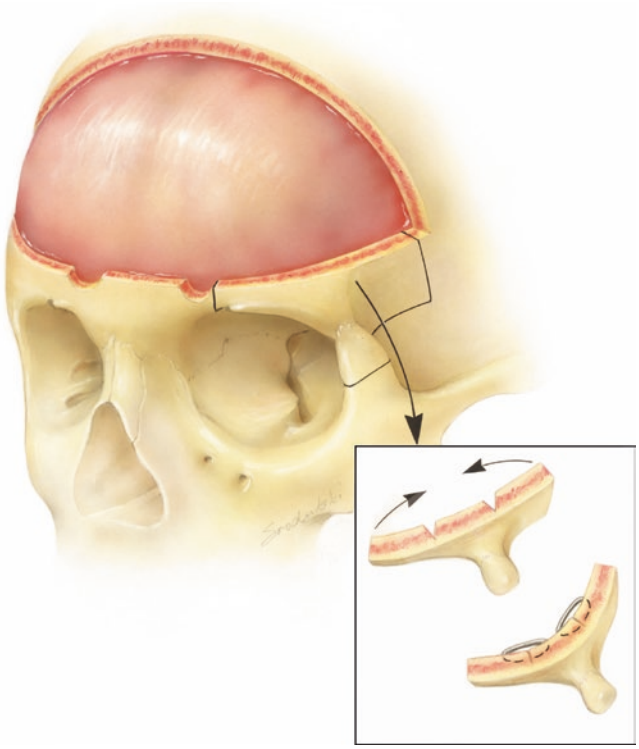


Fig. 40.2 Bone bending. The osteotomized segment can be manipulated ex vivo by creating small kerf cuts on the inner surface (see inset). This allows forceful bending held in position by wires or suture as illustrated also in the inset. In the very young patient, bony bending can frequently be performed without partial osteotomy using specialized bone bending forceps

bone grafts are fixed in position. Most often, this takes the form of wire suture with micro- and miniplates reserved for those situations where structural stability dictates otherwise. In the infant patient, such wires and plates may passively translocate to an intracranial position with growth [21]. We have seen no instances of problems from these [22], but in children below the age of 8–10, we prefer resorbable suture and absorbable plates and screws. In older patients, titanium plates and screws can be used without these considerations.

If bone grafts are required, they can come from several sources. In the patient less than 1 year of age, strips of bone can be taken from the posterior aspect of the frontal bone flap. Infants of this age generally always regenerate this bone gap from the underlying dura. In the older child and adult, when this does not occur, alternative bone sources must be used. Cranial bone can be taken, harvested as strips from the posterior outer calvarial surface using a combination of burrs and osteotomes (Fig. 40.3a–d). Alternatively, the frontal

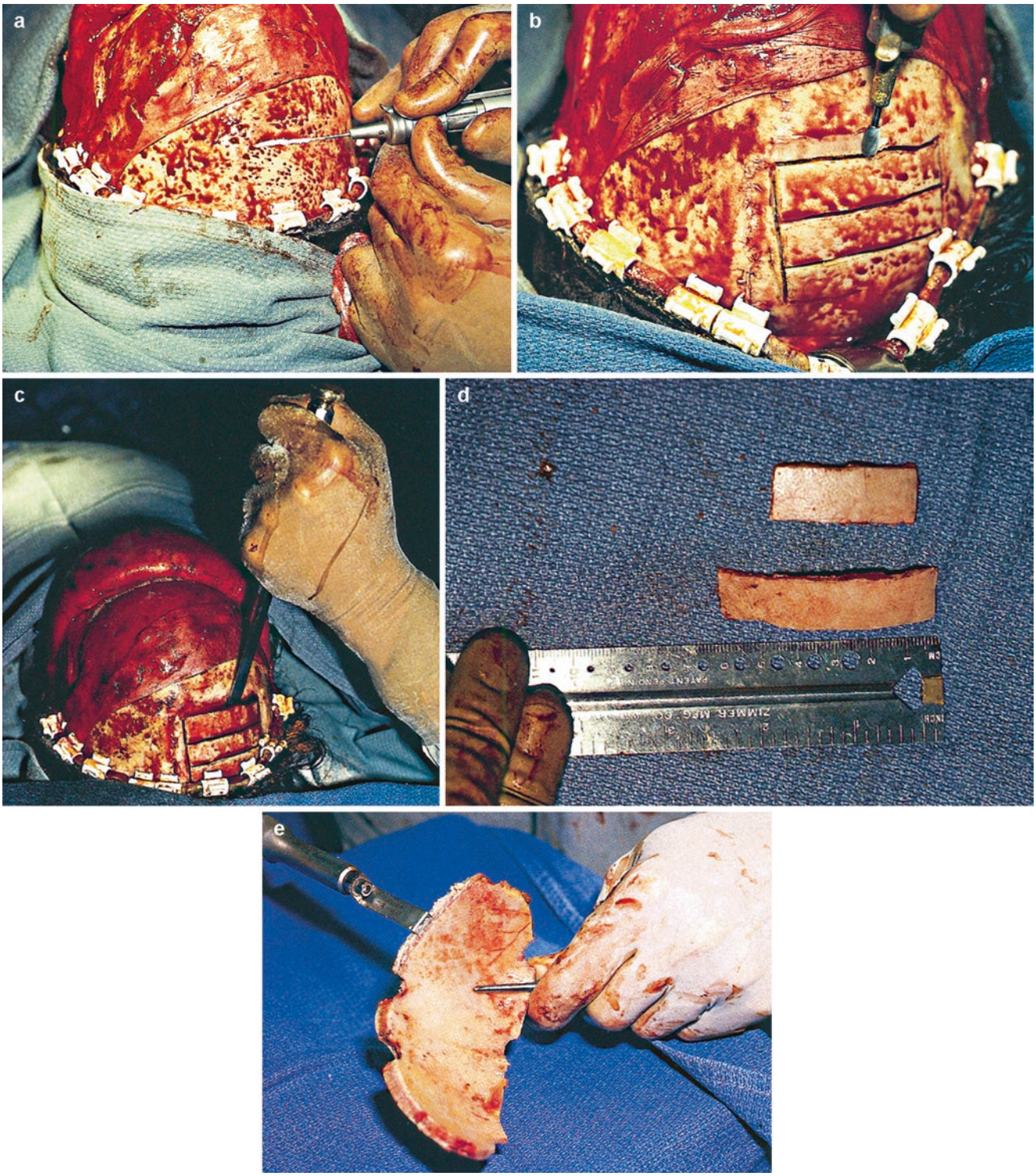


Fig. 40.3 Bone harvesting. (**a**) The initial stage in cranial bone harvest for the outer cortical surface involves cutting a series of parallel channels through the cortical bone into the diploic space. (**b**, **c**) After the initial channels are cut, a contouring burr (**b**) is used to bevel the edge of the bone to allow insertion of a straight osteotome (**c**). (**d**)The osteotome and mallet can then be used to harvest uniform strips of outer cortical bone. (**e**) An alternative method when a craniotomy has been completed is to use the oscillating saw and osteotomes to split inner from outer cortex. This allows the bone flap to be replaced without any visible deformity and provides a large source of bone

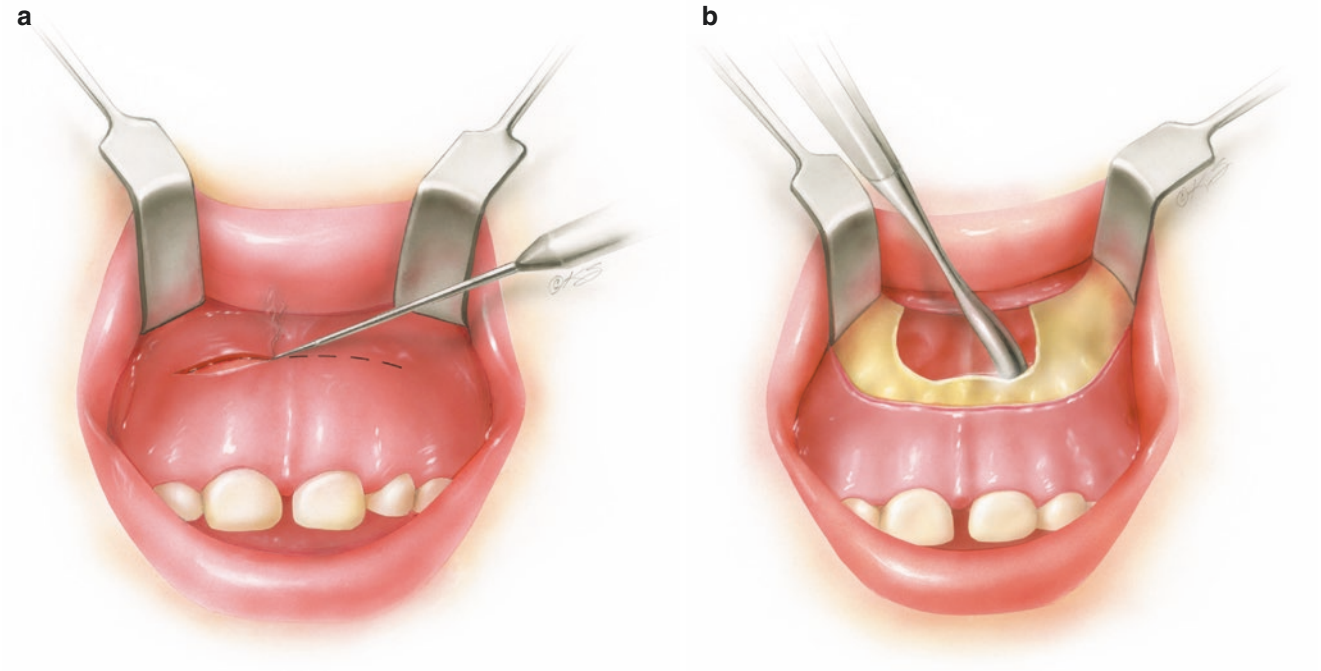


Fig. 40.4 Midface exposure. In addition to transpalpebral incisions, midface exposure is facilitated by the gingival buccal incision. After first incising the mucosa (**a**) a subperiosteal dissection can be used to expose the alveolus, the nose, and the lower malar midface structures (**b**)

bone flap can be split with the bone taken from the inner surface to preserve the integrity and contour of the outer cortex (Fig. 40.3e). Bone grafts from the cranial region are preferred, because they have an improved survival when used in the craniofacial region, involve no additional operative sites, and are associated with little morbidity if done properly [23, 24]. However, when additional bone is needed, rib or iliac bone can be utilized.

Bone substitutes are a controversial area. Although a great deal of effort is now underway to develop good bone substitutes and bioceramics, at present autogenous bone remains the material of choice [24]. Alloplastic materials in general should be avoided. The increased risk of infection when operating near the paranasal sinuses, the long-term effects of alloplasts, and their lack growth potential all argue against their use.

There are other approaches to the craniofacial skeleton. The ophthalmologist is not likely to be involved in these cases but should be familiar with them. The midface is frequently approached by a combination of intraoral upper buccal sulcus incisions with or without midfacial degloving (Fig. 40.4) and the standard lower lid incision. The lower face or mandible can be approached with a combination of intraoral lower buccal sulcus incisions and strategically placed cervical incisions.

The Management of Specific Craniofacial Disorders

Rare Craniofacial Clefts

Although the rare craniofacial clefts were initially classified into centric and acentric [10], the experience of Tessier [25, 26] dictated a separate approach. Based on his clinical experience, the orbit is used as a center of reference along with the midline, and clefts radiating around the orbit are numbered based on their position (Fig. 40.5). A horizontal line drawn through the mid-axis of the orbit separates facial clefts below from orbital clefts above. Typically, a cleft that involves both the face and cranium is a craniofacial cleft. These clefts are numbered from 1 to 14, and it is usual for

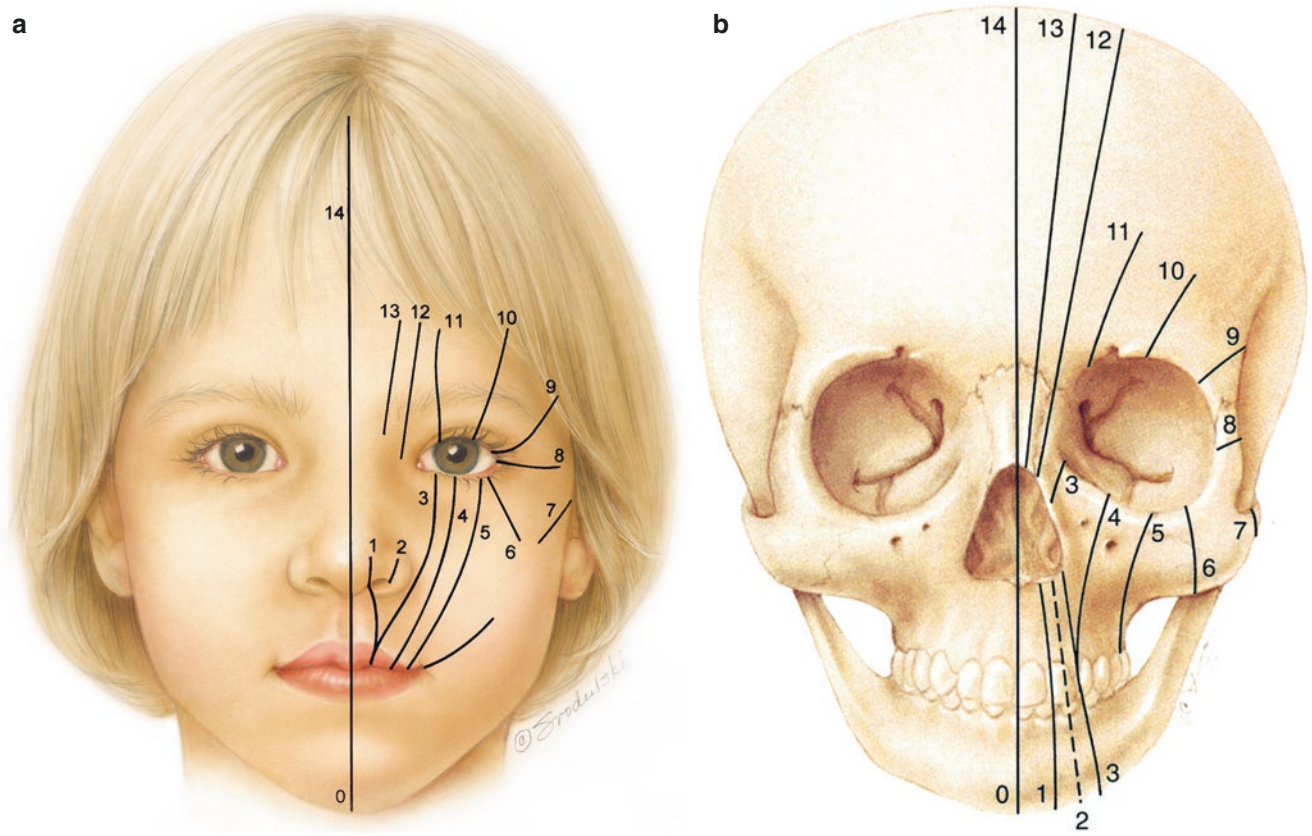


Fig. 40.5 The Tessier classification of rare craniofacial clefts. As mentioned in the text, a horizontal line drawn through the mid-axis of the orbits separates facial clefts below from orbital clefts above with a numbering system beginning in the midline and progressing counterclockwise around the orbit like the spokes of a wheel. (**a**) Soft tissue cleft positions. (**b**) Bony cleft positions

combination clefts to add to a total of 14 (i.e., cranial cleft 10 is usually associated with facial cleft 4). It should be stressed that the clefts may present as true through and through clefts of both bone and soft tissues or may be represented merely by furrows in each. Additionally, clefts in the medial region may be associated with either tissue deficiency or tissue excess [26]. Facial clefts are not usually associated with genetic transmission, with the exception of the Treacher Collins syndrome (mandibulofacial dysostosis), which can be considered a true clefting phenomenon.

The principles in the management of these clefts are not dissimilar to those of the management of the more common cleft of the lip and palate. The bony deformity is addressed by appropriate osteotomy and repositioning of segments, with or without the addition of bone grafts, while the soft tissue is managed by a combination of mucosal flaps for lining and skin flaps for skin closure [25–29]. In each of the latter cases, this is accomplished by the use of local rotation flaps, Z-plasties, or the like (Fig. 40.6). These maneuvers reposition malpositioned structures such as the lips, eyelids, and brows to their normal position. The median and paramedian clefts may be associated with hypertelorism and are discussed separately. It is beyond the scope of this discussion to give examples of each type of Tessier cleft, but specific examples are included in Fig. 40.7. Although surgery for these disorders is frequently done in infancy and early childhood, disruption of the growth matrix by the clefting process and by surgery necessitates frequent review of the condition with adjunctive procedures undertaken as required.

As one might imagine, any clefting phenomenon that involves the orbit may lead to a significant disruption of the ocular adnexa. Clefts in or near the medial canthus may lead to medial canthal dystopia in either a horizontal or vertical dimension. Also, lateral canthal abnormalities of position may be seen. Since the nasolacrimal system occupies a key position in the medial facial region, disruption of this structure by clefts of this region is common. For these severe

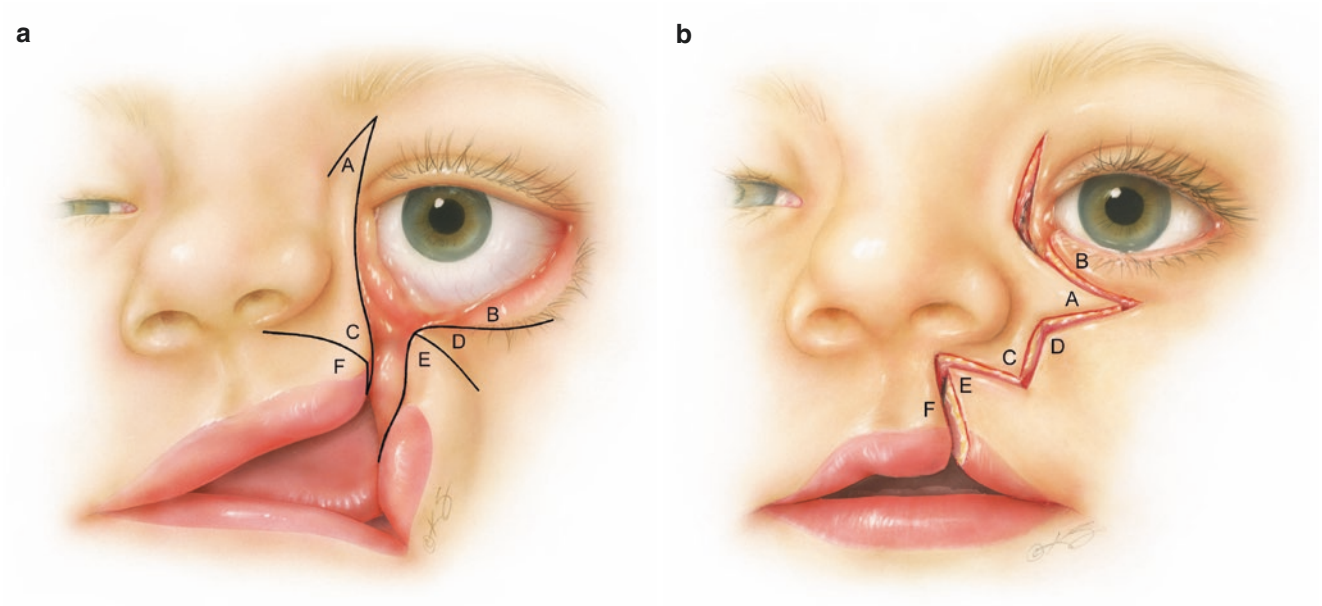


Fig. 40.6 Repair of Tessier #4 cleft. (**a**) Multiple Z-plasties are designed to increase vertical length and to fill the defect with skin–muscle flaps. In this instance, three Z-plasties are utilized. (**b**) Flap A is really a transposition-type flap, which also raises the medial canthal angle. The alar base is rotated down with flaps B and C transposed. Flaps D and E complete the third Z-plasty, assisting in lip reconstruction. The cleft lip is repaired much like an eyelid coloboma by excising the edges and carefully matching the appropriate anatomic landmarks on each side



Fig. 40.7 Examples of rare craniofacial clefts. (**a**) Tessier No. 0 cleft; (**b**) bilateral Tessier No. 3–11 clefts; (**c**) left-sided Tessier No. 3–11 or 4–10 cleft; (**d**) left-sided Tessier No. 4 or 5 cleft and right-sided Tessier No. 7 cleft

canthal dystopias, refixation by separation of the canthal tendon from bone and wiring may be in order. Alternatively, segmental osteotomy of the medial orbital wall with the canthal attachment intact may be undertaken. The nasolacrimal system can be addressed by any of the current techniques available, including intubation and stenting or complete reconstruction. This topic is covered elsewhere (see Chaps. 26, 27, 28, 29, and 30).

Treacher Collins Syndrome

Treacher Collins syndrome, or mandibulofacial dysostosis [30, 31], is justifiably classified as a syndrome involving clefts 6, 7, and 8 of the Tessier system. This condition affects 1 in 50,000 live births is inherited as an autosomal-dominant disorder with variable penetrance often involving genetic mutations in, but not limited to *TCOF1*, *POLR1D*, and *POLR1C* [32, 33]. Manifestations of this disorder involve both the bone and soft tissue. Bony deformities (Fig. 40.8) are characterized by poorly developed or deficient inferior and lateral orbital rims, frequently with a bony cleft and absent or hypoplastic zygomas. The maxilla and mandible typically are vertically deficient posteriorly with a resultant anterior deficiency and open bite deformity. In concert with this bony deficiency, the ocular adnexa are characterized by downward sloping of the palpebral fissure and inferior displacement of the lateral canthus with colobomata and pseudocolobomata of the lids and malar midface soft tissue deficiency (Fig. 40.9). Patients typically have ear deformities, varying from complete microtia to a minimally deformed pinna [34].

Principles in the management of this condition involve both the bony and soft tissue deformity. Although, conceptually, Treacher Collins syndrome seems easy to manage, the soft tissue deficiencies make the results of therapy disappointing in many circumstances. For the bony deficiency, bone grafts to the lateral orbit and malar midface area via a transcoronal extracranial approach are appropriate [35] (Fig. 40.10). The soft tissue deficiency, however, contributes to a high rate of resorption for these bone grafts, and they frequently need to be repeated. Vascularized cranial bone grafts have been utilized with some improved success [36], but the extra time and effort

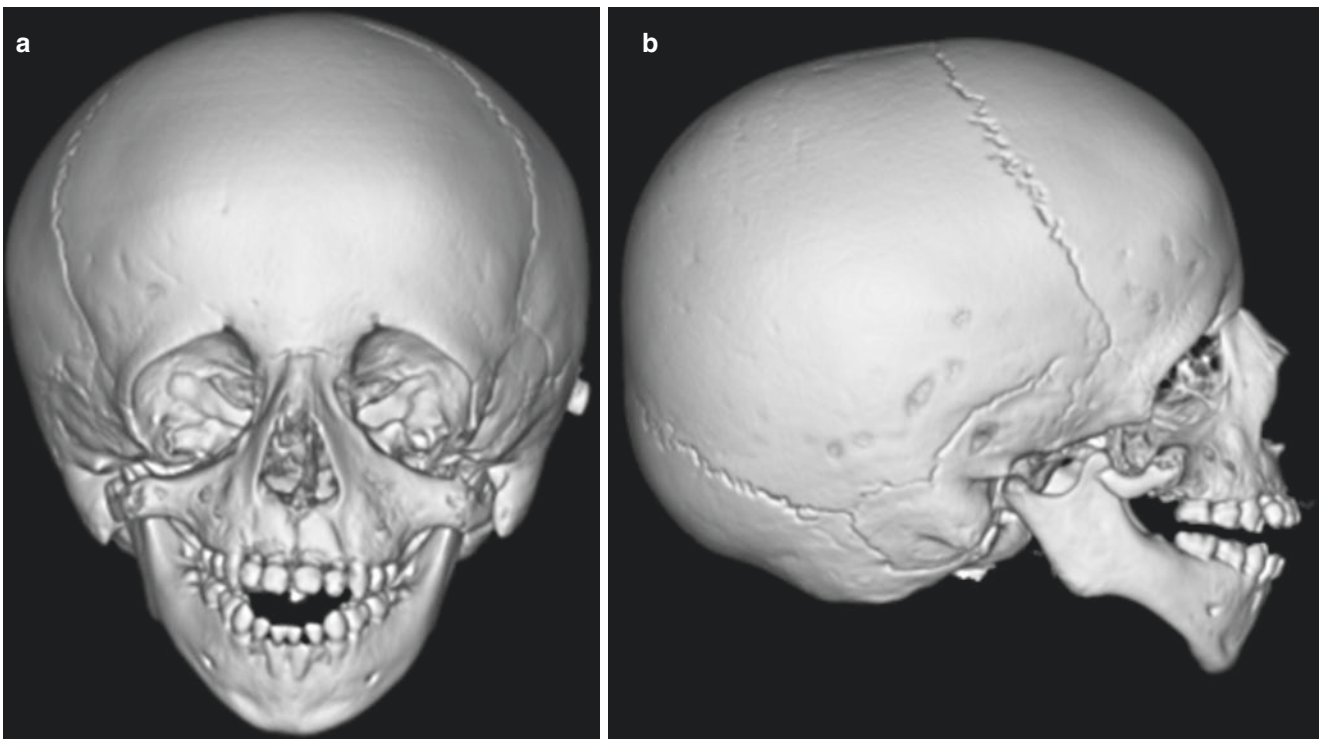


Fig. 40.8 Treacher Collins syndrome. (**a**) Schematic representation of the bony deformity of mandibulofacial dysostosis (Treacher Collins syndrome). Note the absent zygomatic arch and malar eminence, absence of the lateral orbital wall, hypoplastic posterior mandible, and anterior open bite deformity. (**b**) Three-dimensional image of patient with Treacher Collins syndrome showing anatomy similar to that of Fig. 40.8a

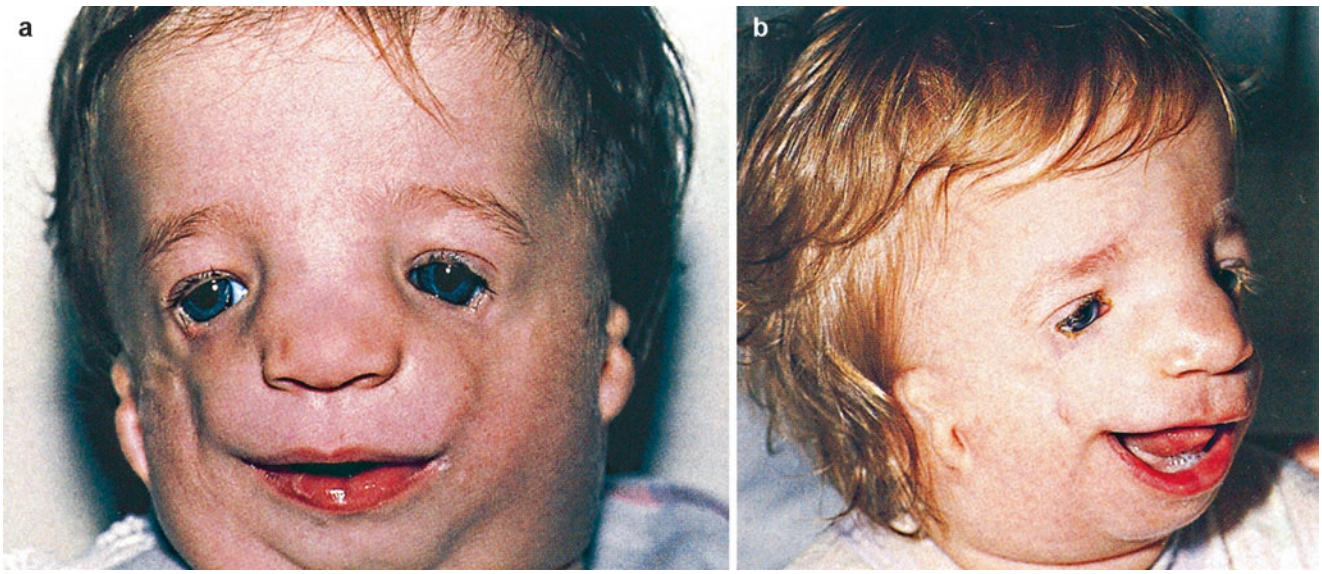


Fig. 40.9 The typical appearance of the patient with Treacher Collins syndrome. (**a**) Lateral facial clefts or soft tissue deficiency that overlies hypoplastic malar bones. Also shown are the downsloping palpebral fissures with pseudo-colobomata of the lower eyelids; (**b**) a diminutive mandible and microtia are also present

involved in their harvest and their limitations of position make them infrequently the first choice. Our experience dictates that initial bone grafting may best be followed in adolescence by repeat bone grafting or by the use of synthetics (e.g., silicone elastomer, polytetrafluorethylene) to augment the malar region once basal bone continuity is established.

The soft tissue deficiencies and malpositions demand special expertise. These techniques are described elsewhere in this text and consist of lateral canthopexy, Z-plasty of the coloboma, cheek flap advancement, and upper lid to lower lid pennant switch or transposition flaps [37]. They are frequently performed as secondary procedures by the oculoplastic surgeon once the initial bony correction has been completed (see Chap. 21).

The lower face deformities also demand attention. A combination of maxillary and midface osteotomies to level and advance the occlusion is required in the most severe cases. In the less mildly affected patient, a combination of orthodontic correction and advancement genioplasty may be all that are required. The technique of distraction osteogenesis of the mandible [38], in which the mandible is cut and gradually elongated as new bone forms, has proven application to the child of intermediate age with a moderate to severe deformity (Fig. 40.11) [39].

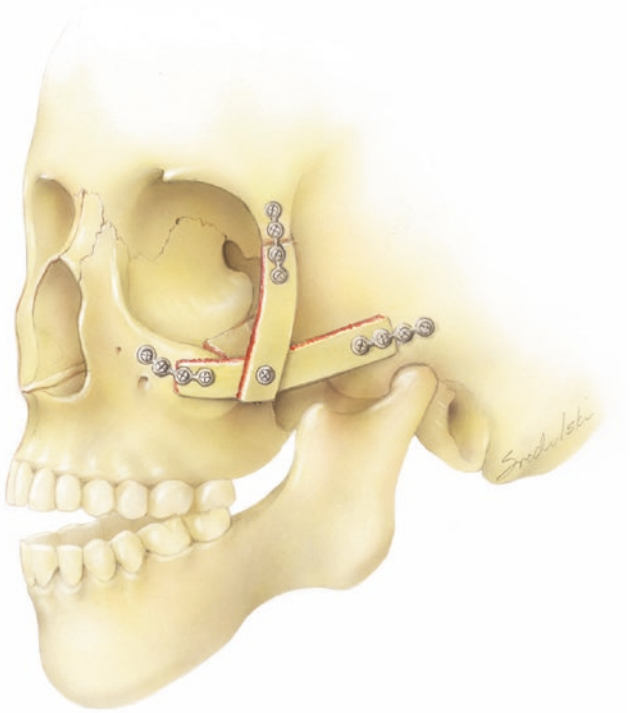


Fig. 40.10 Schematic of bony reconstruction of the malar orbitozygomatic complex in Treacher Collins syndrome. Bone grafts are placed to recapitulate the normal zygomatic eminence, arch, and lateral orbital walls

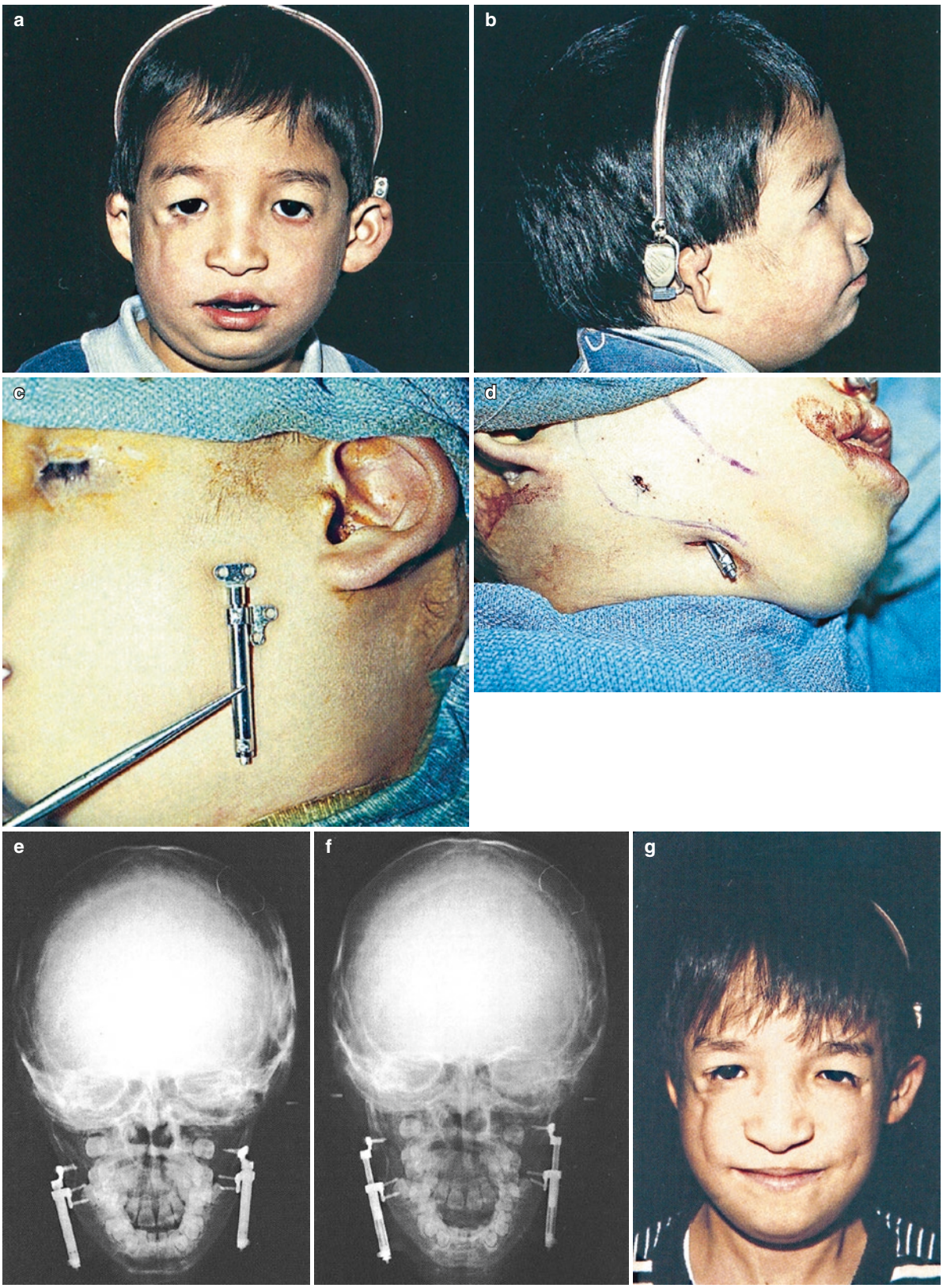


Fig. 40.11 Distraction osteogenesis. Management of the hypoplastic mandible in Treacher Collins syndrome by distraction osteogenesis. (**a**, **b**) Preoperative views. (**c**) Intraoperative view demonstrating distractor prior to placement. (**d**) Following distractor placement through a transoral approach. The distractor activator exits through the skin inframandibular position. (**e**) A-P cephalogram of the skull before distraction is initiated. (**f**) Following activation of the distractor, lengthening of the posterior mandible is observed. (**g**) Postoperative view of the patient showing significant elongation of the posterior mandible

Craniosynostosis

Craniosynostosis occurs when one or more cranial vault or cranial base sutures undergo premature fusion [40, 41]. The function of a suture is to allow passive expansion of the skull and face during growth of the brain, eye, facial muscles, teeth, and sinuses. These seams allow passive growth to go unimpeded. In general, once growth is complete, sutures may fuse and become nonfunctional [42]. This occurs at a variable time in life for each suture, the earliest suture to fuse being the metopic suture, which fuses at approximately age 7 months. If these sutures close prematurely, brain, orbital, or midface growth is prevented. Virchow first noted that skull deformities are caused not only by an inhibition of growth at right angles to the prematurely closed suture but by compensatory growth in the cranium where sutures remain patient [40].

The craniosynostoses are broken down into two broad categories, the syndromic and nonsyndromic groups. Syndromic synostoses are those in which one or more cranial vault and base closures are associated with other dysmorphic features. The most common syndromic synostoses include Apert syndrome, Crouzon syndrome, Pfeiffer syndrome, and Saethre–Chotzen syndrome.

In addition to the syndromic synostoses, there is a large group of nonsyndromic premature suture closures. These are classified based on the resultant skull shape after the premature suture closure occurs.

The first attempts at correction of these deformities were made over 100 years ago when linear craniectomies or removal of the synostosed suture was performed [43, 44]. Although this allowed room for subsequent brain growth, the sutures frequently resynostosed and deformity recurred. Additionally, such simple synostectomies did not improve an already established facial deformity [4]. In 1967 Paul Tessier described his technique for a transcranial approach to the orbit, midface, and vault by osteotomy and repositioning in the treatment of these deformities [1, 2]. A wide variety of technical refinements occurred over the subsequent decades. The most frequent reason for referral to the craniofacial team is dysmorphic craniofacial appearance in an infant or young child. The need for surgery and the timing of surgery for craniofacial dysostosis is based in part on optimizing the cosmetic goals of the proposed surgery and in part on concern that premature closure of the cranial sutures may constrict brain growth [45]. The volume of the brain nearly triples in the first year of life [46], and brain growth continues until about 8 years of age when the sutures normally begin to close. If multiple sutures are closed before brain growth is complete, the result may be mental retardation, headaches, papilledema, and optic atrophy. Ideally, cranial decompressive surgery is done very early in life, when the facial bones are soft and the cosmetic goals of surgery cannot yet be fully achieved. It is the task of the neurosurgeon on the craniofacial team to assess the need for early surgery, even if this commits the child to multiple procedures.

Patients with single-suture craniosynostosis are generally believed not to suffer brain constriction, regardless of the severity of the deformity, except in a minority of patients. Thus, timing of surgery for isolated sagittal, lambdoid, metopic, and unilateral coronal synostosis is usually determined by cosmetic goals alone. This concept has been challenged. Patients with single-suture synostosis have been studied using invasive intracranial pressure (ICP) monitoring, and ICP was found to be elevated in 8% of children with unilateral coronal synostosis, 25% of children with sagittal synostosis, and 33% of patients with metopic synostosis [47]. This may reflect the difficulty in determining which sutures are functionally closed, since cases of presumed unisutural craniosynostosis may actually have multiple closed sutures. In most cases, sagittal and coronal synostoses are surgically treated before 1 year of age anyway, and elevated ICP is rarely a concern. Syndromic craniofacial dysostosis such as Crouzon syndrome and Apert syndrome are often associated with premature closure of multiple sutures, and there is concern that brain constriction may occur without early surgery. Even in the absence of overt signs and symptoms of intracranial hypertension, the theoretical possibility exists that foreshortening of the anterior cranium may cause underdevelopment of the frontal lobes resulting in neuropsychological problems. Apert syndrome and to a lesser extent Crouzon syndrome are associated with mental deficiency, but it is unclear to what extent this is due to brain constriction or multifactorial genetic factors.

Surprisingly, few data are available to relate ICP to craniofacial syndromes, but the number of patients experiencing elevated ICP may be greater than initially presumed [48]. Marchac and colleagues reported that 20% of children with craniosynostosis have elevated ICP as determined by monitoring [49]. They recommend that frontal suture release be carried out for brachycephaly at age 2–4 months, with formal orbitofrontal advancement at a later stage.

For most other craniofacial syndromes, including plagiocephaly, surgery can be delayed until age 6–12 months [50]. The cloverleaf deformity (Kleeblattschädel) is a special case. This clinical picture of trilobar skull triphyllocephaly arises from either Crouzon or Apert syndromes and implies pancraniosynostosis with severe brain constriction. Surgery is undertaken in early infancy and consists of removal of most of the cranial vault in one or two stages [51, 53]. When this is done early enough, the bone will reform with functional sutures, and the children may have normal neurocognitive development. Orbitofrontal advancement is usually required at a later stage. In severe cases, venous obstruction may lead to intracranial hypertension and hydrocephalus and hindbrain herniation [52, 53].

Children with complex multisutural craniofacial syndromes must be monitored for delayed intracranial hypertension, even if early decompressive surgery has been performed [54]. Raised ICP is considered in patients with bulging fontanelle,

progressive frontal bone protrusion or turricephaly, headaches, irritability, and vomiting. Examination for papilledema has been considered the most reliable screening test, and it appears to be quite sensitive in children older than 8 years but relatively insensitive in younger children [49]. Patients with suspected intracranial hypertension should be evaluated with CT scan with bone windows or MRI scans of the head to look for hydrocephalus and shunted if appropriate. Patients with persistent headaches and normal-sized ventricles are candidates for cranial expansion if papilledema is present or scans reveal obliteration of basal cisterns. Patients without papilledema and in whom sutures are closed radiographically may be appropriate for invasive ICP monitoring with a fiber-optic device. The normal limit of resting ICP is poorly defined, but some authors have used 15 mmHg as a cutoff [55].

Children with severe hydrocephalus may acquire secondary craniosynostosis. With a functioning shunt, the head may have no stimulus for growth for several months until the brain expands to fill the calvarium, and the sutures may close because there is no driving force to keep them patent. These patients may show signs or symptoms of increased ICP with functioning shunts and small ventricles and tend to have frequent shunt malfunction. They may present with frequent headaches or with isolated papilledema and visual loss [56], underscoring the importance of routine ophthalmological care of these patients. The diagnosis is made by either skull films or 3-D CT scanning of the cranium to evaluate patency of the sutures and to look for the "copper-beaten" appearance of the skull. The surgical correction usually requires a major reconstruction of the cranial vault [57], including bifrontal expansion and orbital advancement or posterior vault distraction [58].

Patients with craniofacial syndromes may have accompanying brain malformations as well. It is important to identify the likelihood of developmental delay, so that the family may be counseled and reasonable choices can be presented regarding the appropriateness of cosmetic surgery. Patients with isolated sagittal, lambdoidal, and unilateral coronal synostosis are presumed to have normal developmental potential, and brain imaging is not required in most cases. Craniofacial syndromes may be divided into "nonsyndromic forms", in which premature closure of a cranial suture is the sole manifestation of the condition, and "syndromic forms", in which craniosynostosis is part of a more widespread complex, often with a defined inheritance pattern.

Nonsyndromic Synostoses

Approximately 85% of patients with craniosynostosis are nonsyndromic [59]. Premature closing of the sagittal suture (Fig. 40.12) is one of the most common forms of nonsyndromic synostosis. It is more common in male infants and is easily diagnosed by observing the classic scaphocephalic appearance of the head with frontal bossing. The orbits are not involved. There is no associated mental retardation, and raised intracranial pressure is infrequent (<25%), even in untreated cases. The diagnosis is established by clinical examination, and radiographic evaluation is not necessary in routine cases. A variety of surgical procedures have been described, all of which are successful in treating the deformity if carried out in the first 6 months of life [64]. The older child requires a total calvarial reconstruction, which is a formidable procedure [57].

Lambdoid synostosis is quite rare and results in unilateral or bilateral flattening of the occiput accompanied by a palpable ridge over the lambdoid suture. A far more common cause of occipital flattening and cranial asymmetry is positional molding, or positional plagiocephaly. Infants are often encouraged to sleep on their backs, and if the child has a degree of torticollis, the infant will acquire a parallelogram configuration to the skull when viewed from above, with anterior displacement of the ear on the side of the flat occiput (Fig. 40.13). In severe cases, the frontal region will bulge on the opposite side. Increased intracranial pressure and developmental delay do not accompany either isolated lambdoid synostosis or positional molding, and treatment is directed at the deformity. In most cases, the condition spontaneously improves or responds to physical therapy for torticollis and positional devices that encourage the child to sleep on the opposite side. In more severe cases, a custom-fitted molding helmet may be utilized, but its utility is limited to the first 12 months of life. A CT scan with 3-D bone reconstructions may demonstrate cases of true lambdoid synostosis. Surgery is considered for children with marked deformity that has not improved sufficiently with conservative measures by 10 months to a year of age.

Unilateral coronal synostosis (Fig. 40.14) is second only to sagittal synostosis as a form of single-suture closure. The appearance is characteristic (Fig. 40.15), with forehead flattening and supraorbital retrusion on the affected side. The orbit may also be elevated with a widened palpebral fissure while the ipsilateral cheek is flattened. The anterior–posterior (AP) skull radiograph or 3-D CT reconstruction will demonstrate the "harlequin" eye, corresponding to the clinically evident elevation of the superolateral orbital wall (Fig. 40.15c). Occasionally, it may be difficult to distinguish unilateral coronal synostosis from positional molding in early infancy. A period of observation may be helpful, since molding will often spontaneously improve, whereas true synostosis will not. Radiographic evaluation is helpful in doubtful cases. Raised intracranial pressure, hydrocephalus, and developmental delay are unusual in cases of unilateral coronal synostosis.

A procedure has been described that can be accomplished in early infancy in which the lateral orbital roof is greenstick fractured and the frontal bone is advanced [65]. At our institution, however, most patients undergo formal craniofacial reconstruction at 6–12 months of age when the orbit has sufficiently ossified to permit a rigid reconstruction. The procedure consists of bicoronal scalp incision and a unilateral frontal craniotomy on the affected side (Fig. 40.16a). In severe cases in which the opposite frontal area has severe compensatory bossing, a bilateral frontal craniotomy is preferred with or without bilateral osteotomy of the supraorbital bar [66]. Osteotomies of the orbital roof and frontozygomatic

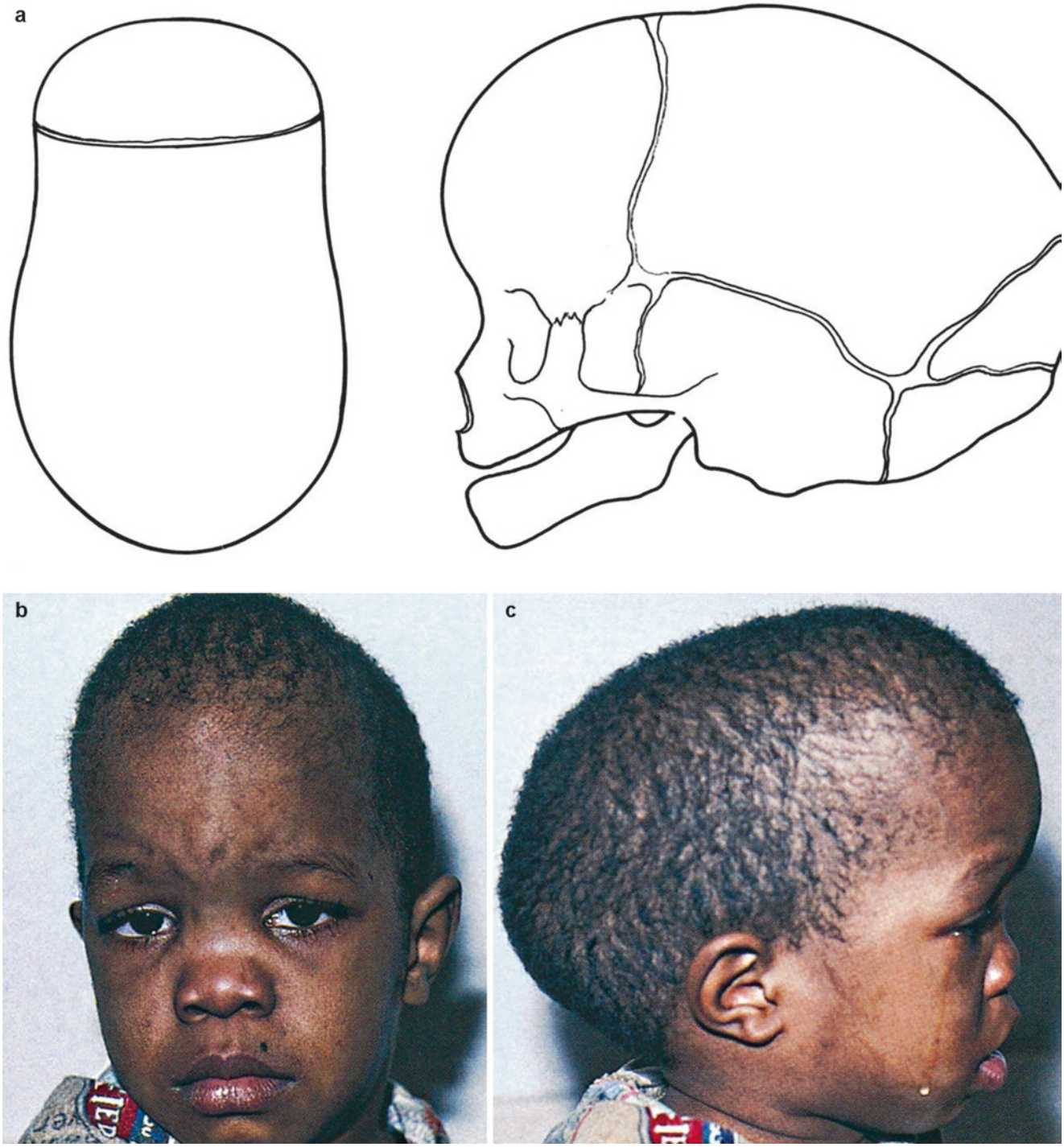


Fig. 40.12 Sagittal craniosynostosis. (**a**, **b**) Premature closure of the sagittal suture disallows transverse growth and results in compensatory anterior–posterior growth leading to the typical scaphocephalic head shape. (**c**) A-P and lateral photograph of a child with established scaphocephaly

process are carried out, and the lateral orbital bar is advanced and rigidly secured with wire and microplates. The frontal bone is then also advanced and secured (Fig. 40.16b). The cosmetic result is usually satisfactory, with good to excellent results after 3 years expected in 89% of cases [66] (Fig. 40.17).

Premature closure of the metopic suture (Fig. 40.18) results in keel-like narrowing of the frontal area (trigonocephaly), a pinched-in appearance of the lateral orbital and temporal regions, and often hypotelorism. Imaging studies will demonstrate the keel (Fig. 40.19) and aid in assessing the degree of true bony hypotelorism, which may be difficult to evaluate by simply observing the child, especially if there are accompanying epicanthal folds. Although increased intracranial pressure is uncommon, developmental delay

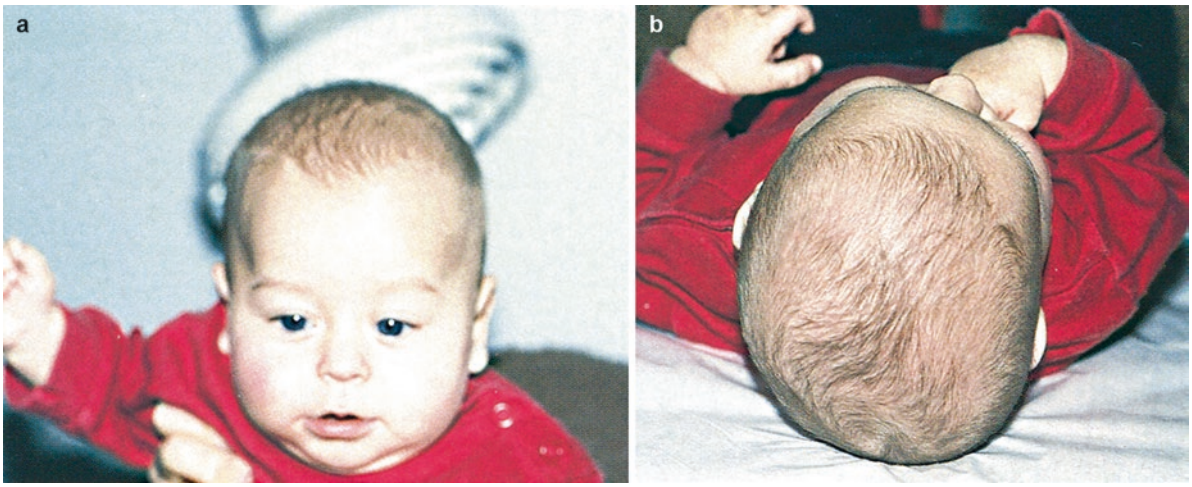


Fig. 40.13 Positional plagiocephaly. (**a**) Flattening of the right frontotemporal and left occipitoparietal region with compensatory expansion of the skull in the right occipital and left frontal position. (**b**) Superior view; from above; this does not represent a true craniosynostosis, but deformational change

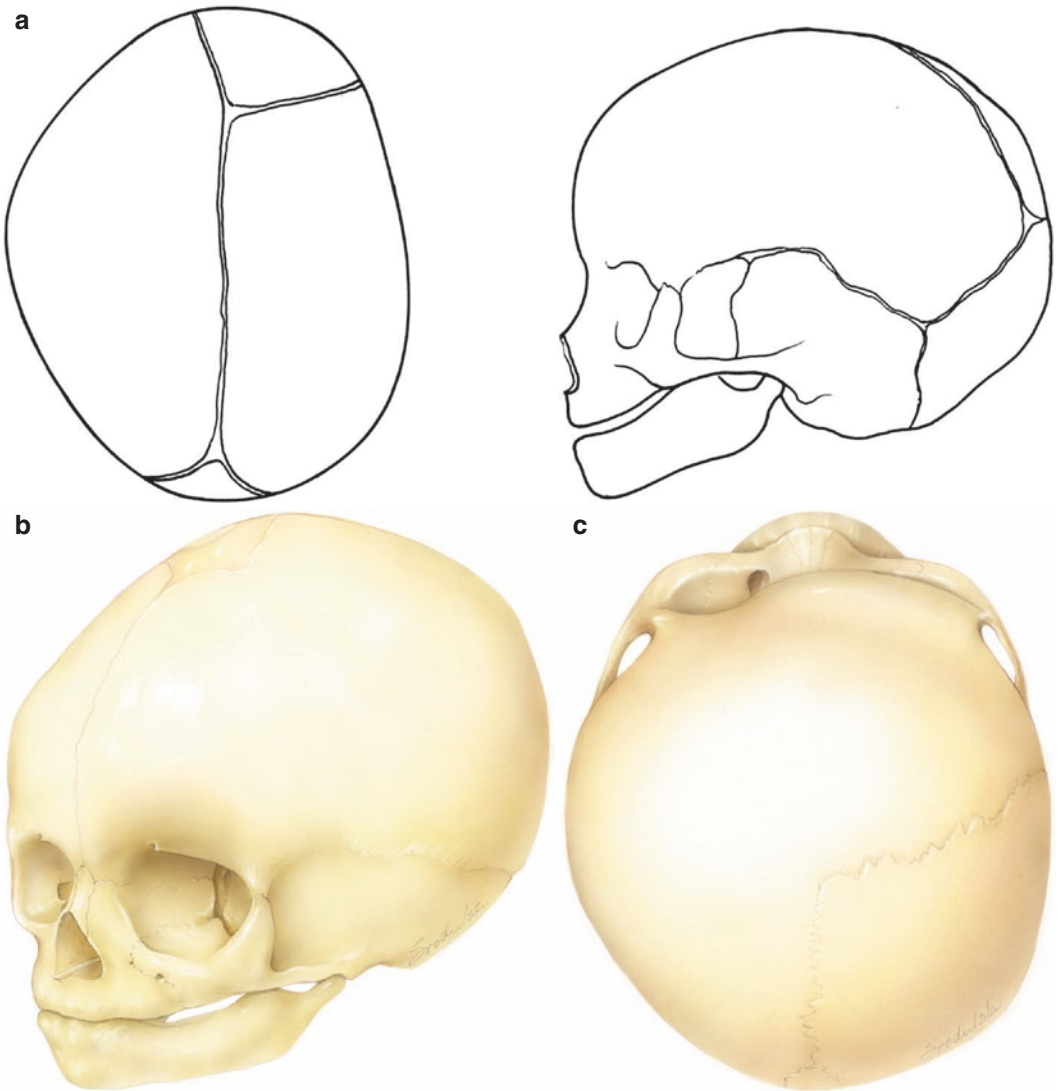


Fig. 40.14 Unicoronal synostosis. (**a**, **b**) The deformity of unicoronal synostosis resulting in ipsilateral frontotemporal orbital retrusion often associated with a compensatory transverse bulge on the ipsilateral side. (**c**) Note that, in early cases, symmetry of the malar region is frequently preserved as seen from above

may occur with trigonocephaly, due to coexisting midline brain anomalies, such as holoprosencephaly. In the absence of significant hypotelorism, surgery consists of bifrontal craniotomy, bilateral out-fracturing of the frontal bones leaving the midline bone affixed to the midline dura, and drilling of the midline keel of a bone [67]. The operation may be performed easily between 6 weeks and 6 months of age. When significant hypotelorism is noted or if there is significant retrusion of the lateral orbits, surgery is delayed until 6 months of age or older, so that midline osteotomies of the cranial base can be accomplished and the orbits can be moved laterally and anteriorly with interposition bone grafts to widen both the forehead and supraorbital bar [68, 69] (Fig. 40.20).

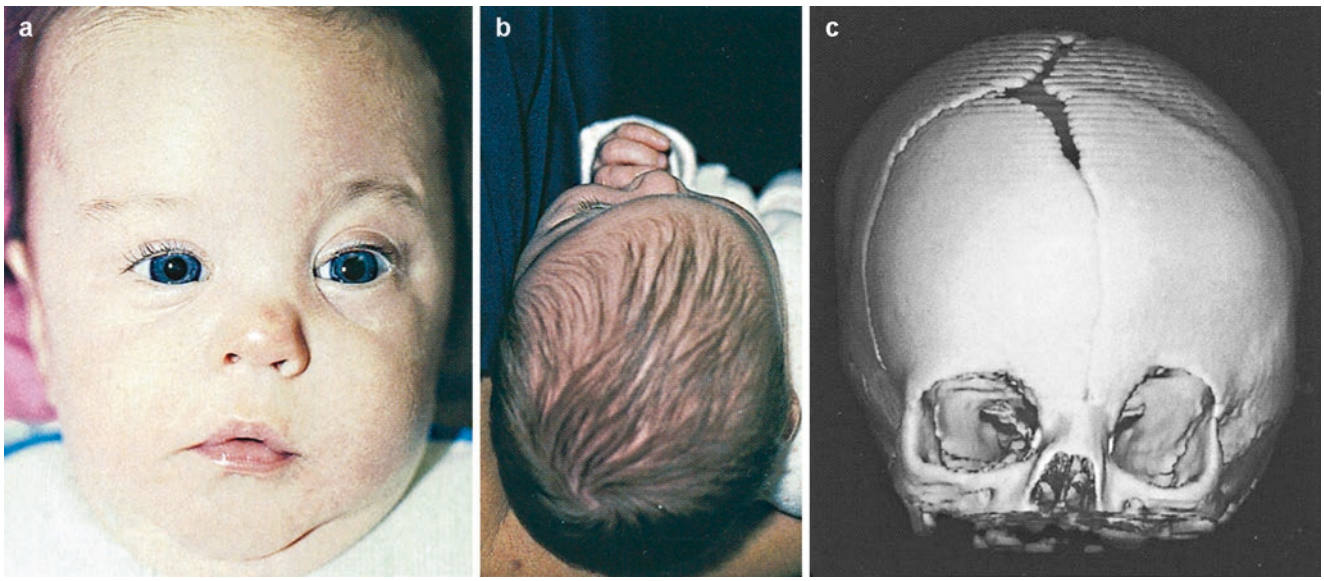


Fig. 40.15 Unicoronal synostosis. (**a**, **b**) Left unicoronal synostosis seen in frontal projection and from above. Note the upward, outward slant, and widening of the palpebral fissures, deviation of the nasal root to the affected side, and absence of retrusion of the subjacent zygoma. (**c**) Three-dimensional image of a right unicoronal synostosis showing a fused coronal suture and the typical harlequin deformity to the orbit, which corresponds to those findings observed clinically

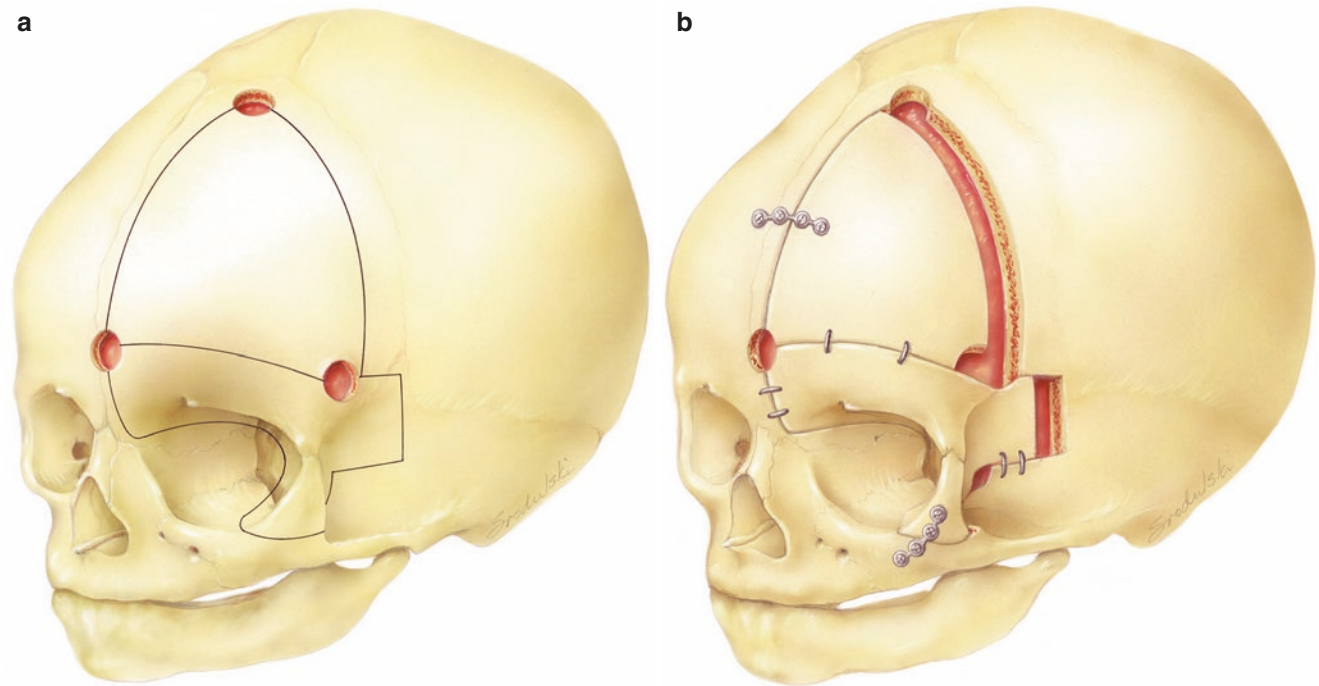


Fig. 40.16 Craniotomy and unilateral osteotomy. (**a**) Burr holes and lines of incision for craniotomy and unilateral osteotomy of the orbits. (**b**) Following ex vivo bending and manipulating, the osteotomized orbital segment is replaced in an anteriorly advanced position and fixated to stable basal bone. Replacement of the craniotomy following forceful bending completes the bony repair. In the infant, the small, bony gaps left posteriorly are filled with bone scraping harvested from the inner table of the frontal bone and will reossify

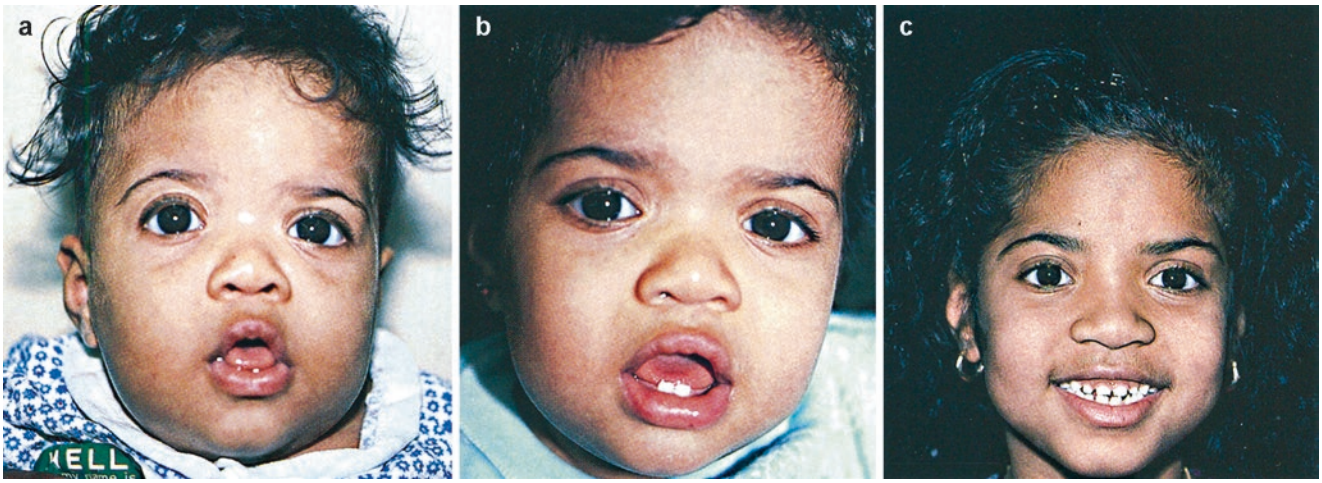


Fig. 40.17 Unicoronal synostosis, correction, and follow-up. (**a**) Preoperative frontal view showing patient with right unicoronal synostosis. Note the widened palpebral fissure with the superiorly and laterally displaced orbital roof and rim with temporal hollowing. The forehead on the affected side is flattened and blends into the orbital deformity. (**b**) Following unilateral fronto-orbital advancement and repositioning, the patient is seen 6 months postoperatively. Note improved symmetry in forehead, orbit, and palpebral fissure dimensions. (**c**) Same patient as shown in (**a**) and (**b**) seen 6 years postoperatively. In this case, normalization of the craniofacial skeleton in infancy has led to improved fronto-orbital growth on the affected side so that symmetry is maintained

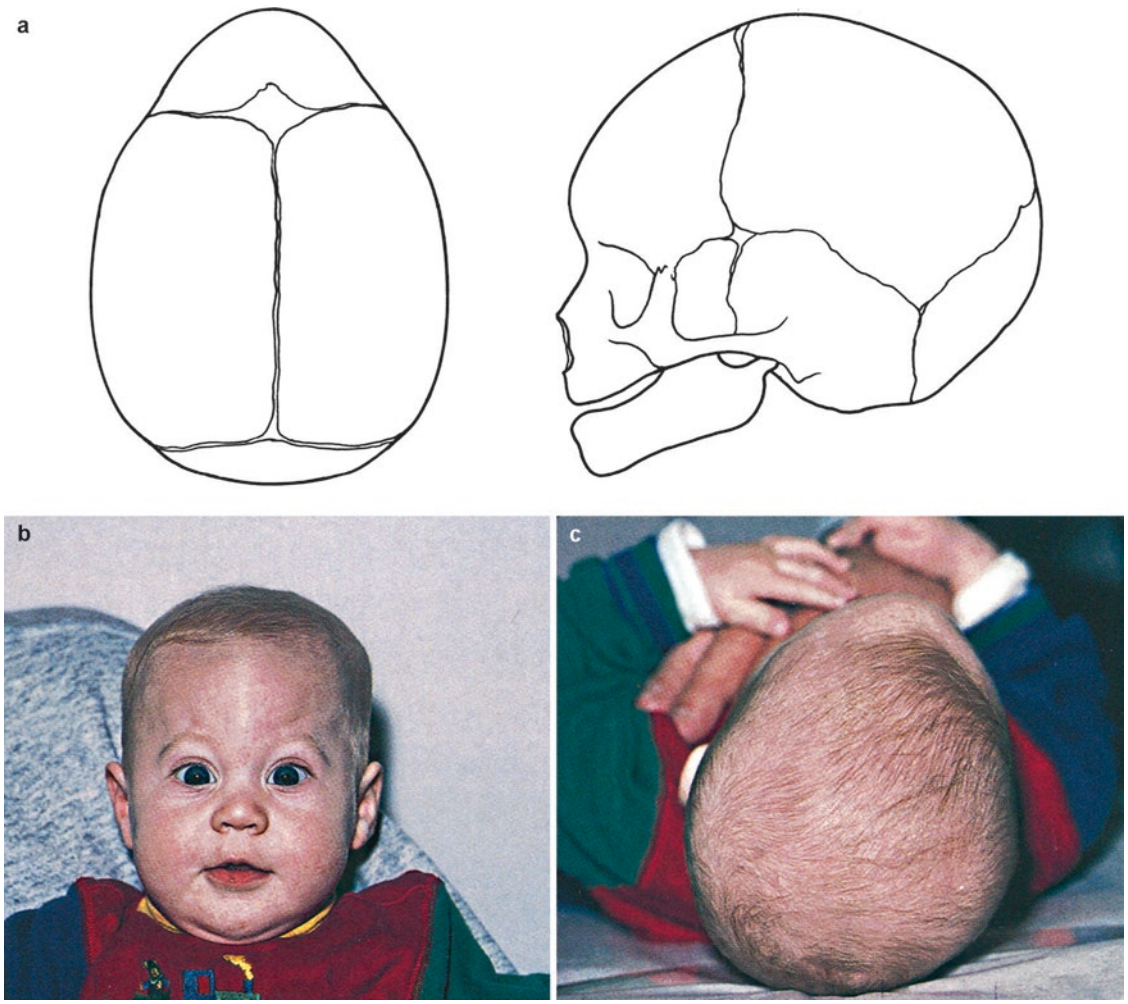


Fig. 40.18 Trigonocephaly. (**a**) Schematic representation of the typical deformity of trigonocephaly. Note the keel-shaped midline, frontal prominence, and the compensatory lateral retrusion of the supraorbital rim and temporal region. (**b**, **c**) A-P and vertex view of a patient affected with trigonocephaly, demonstrating the soft tissue findings of premature fusion of the metopic suture

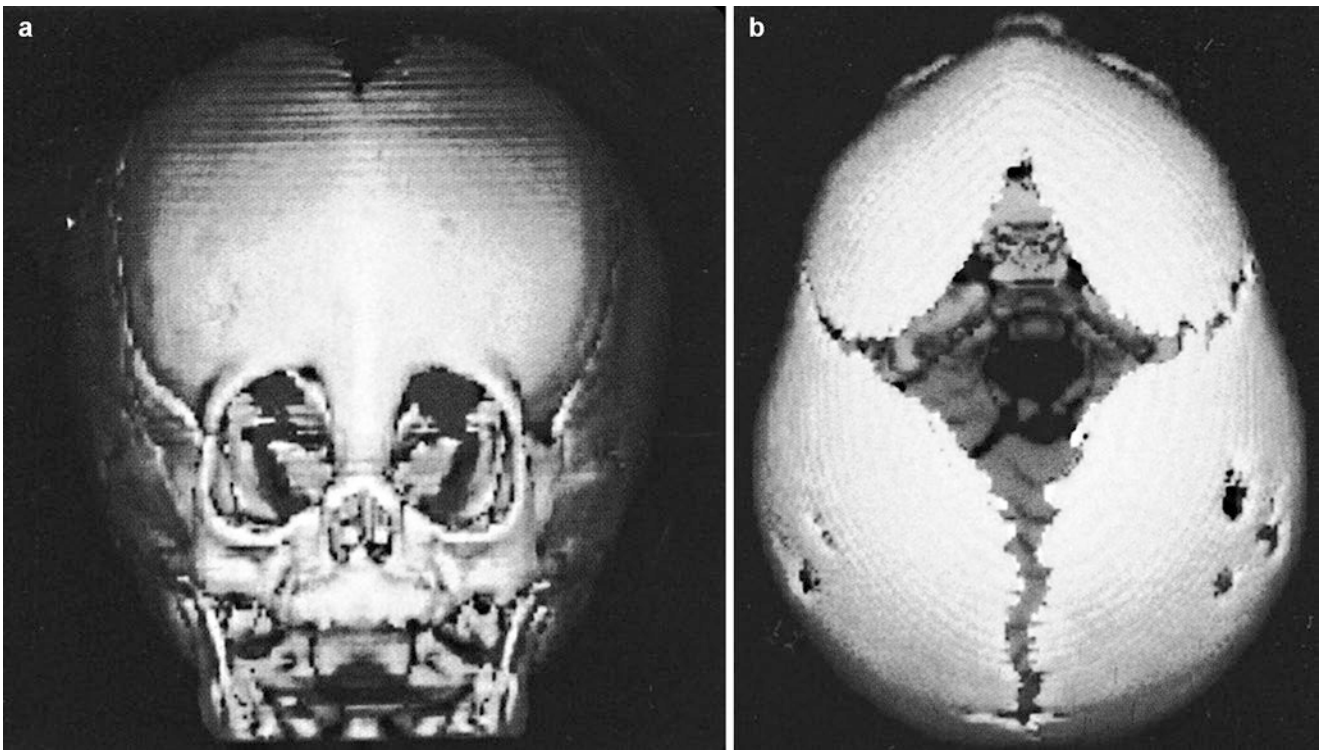


Fig. 40.19 Trigonocephalic deformity. (**a**) A-P view of a three-dimensional CT of the trigonocephalic deformity. Especially evident in (**a**) is the hypertelorism that can be seen in severe forms of this synostosis. (**b**) Vertex view

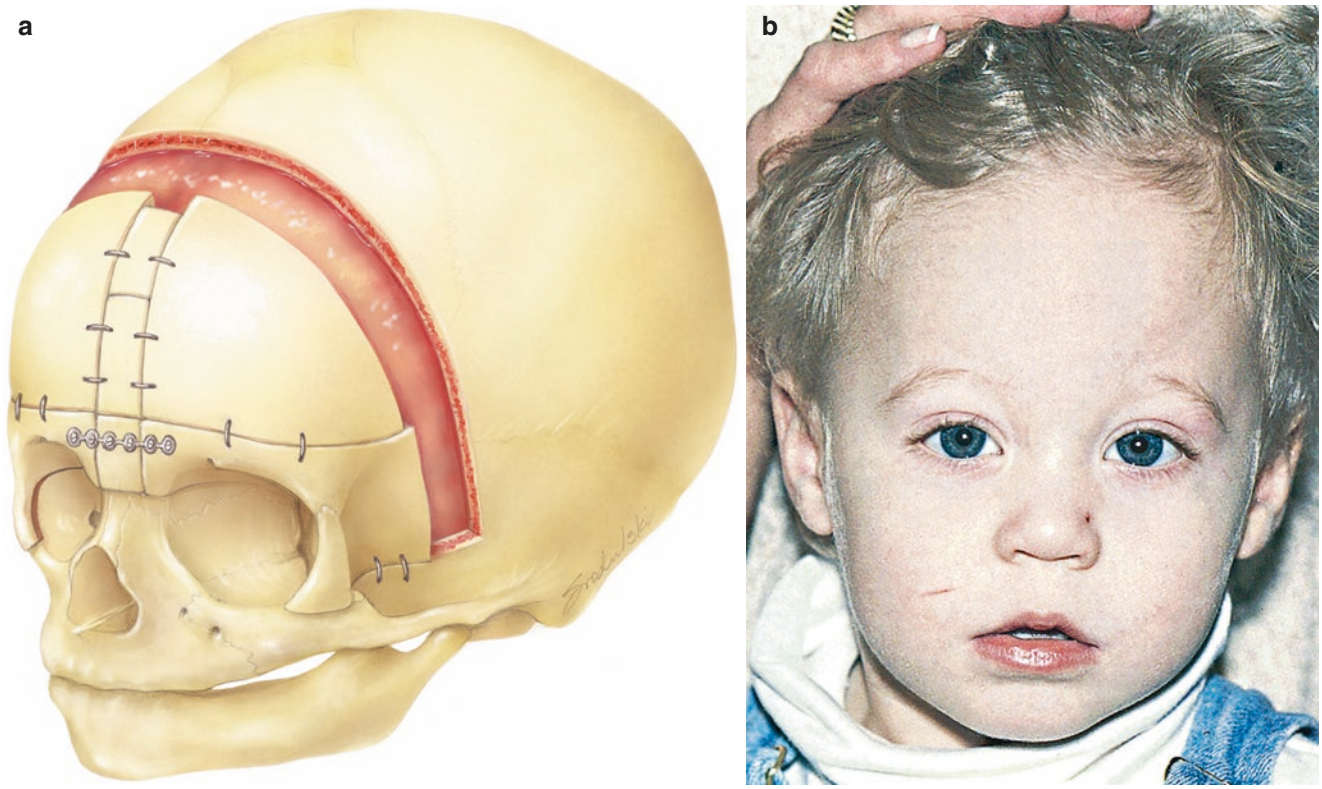


Fig. 40.20 Correction of trigonocephalic deformity. (**a**) Correction of the trigonocephalic deformity involves fronto-orbital transverse expansion with interpositional bone grafts in the supraorbital bar and forehead regions. In cases in which the orbit is retruded, advancement of the lateral orbital rim is also appropriate. (**b**) A-P photograph of the patient shown in Fig. 40.18b demonstrating improved fronto-orbital configuration following surgery

Premature closure of multiple cranial sutures is frequent in syndromic forms of craniosynostosis. Occasionally, sporadic cases of multiple suture synostoses occur in the absence of other abnormalities. Simultaneous closure of both coronal and lambdoid sutures will result in brachyturricephaly (Fig. 40.21). Increased intracranial pressure may result, and failure of expected head growth, a "copper-beaten" appearance of the skull on radiographs (Fig. 40.22), or overt symptoms of intracranial hypertension, such as persistent vomiting or papilledema, suggest the need for urgent surgery. In early infancy, a "floating forehead" operation is performed, in which both coronal sutures are opened, and a wide osteotomy is performed along the frontal base so that the entire frontal bone is permitted to spontaneously advance with brain growth [70]. In the older child, a total calvarial reconstruction with simultaneous advancement of the supraorbital bar will be required [71]. The patient is placed in the prone position with the neck extended. A large bifrontal craniotomy and bilateral occipital craniotomies are performed, leaving a T-shaped tripod of the bone over the posterior sagittal sinus and on the sides. The turricephaly is corrected by removing the bone from the legs of the tripod and gently lowering the vertical height of the cranium as the brain is permitted to move forward and backward with barrel stave out-fracturing of the basicranial ring and bifrontal advancement of the supraorbital bar. The craniotomy flaps are then recontoured and rigidly secured to the remaining bone.

Syndromic Synostoses

Premature closure of cranial sutures occurs in numerous genetic syndromes [9, 41]. For the most part, these involve

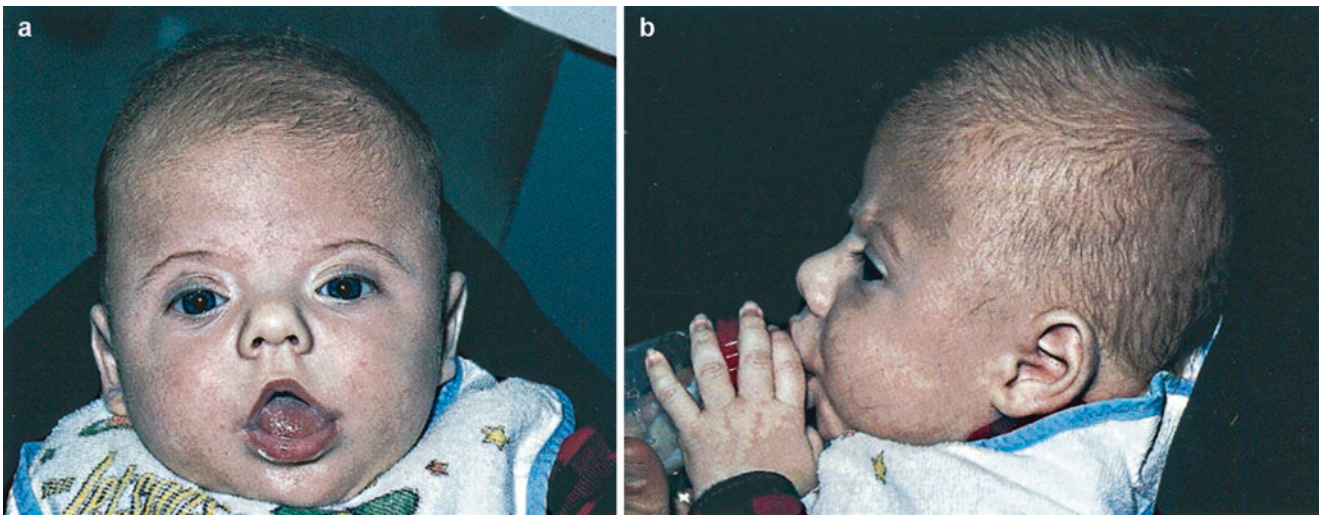


Fig. 40.21 Premature closure of sutures. (**a**) Appearance of a patient with premature closure of both coronal and lambdoid sutures. Note the turribrachycephaly deformity with a foreshortened anterior–posterior dimension to the skull and an increased vertical height. In this case, exorbitism is not prominent but may be seen in more severe cases. (**b**) Lateral view

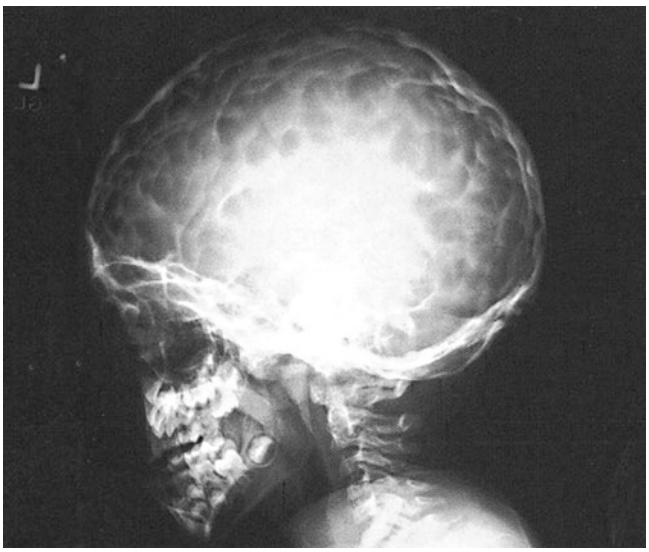


Fig. 40.22 Erosion of the inner cortex. Untreated increased intracranial pressure will lead to erosion of the inner cortex of the skull by the pulsating brain. This may lead to the so-called "beaten silver" or "thumbprinting" appearance and demands semi-urgent treatment

bilateral closure of the coronal sutures, with simultaneous closure of the frontoethmoidal and frontosphenoidal sutures, resulting in a foreshortened anterior cranial base, brachycephaly with bilateral orbital retrusion, and midface hypoplasia. When severe, there is also associated exorbitism (Fig. 40.8). Rarely, all of the cranial sutures are affected, and the skull assumes a trilobar configuration (Kleeblattschädel or cloverleaf skull). The most common of these is Crouzon syndrome [9] (Fig. 40.23), which is inherited as an autosomal-dominant trait typically involving FGFR tyrosine kinase activity but is frequently sporadic [59]. It is characterized by bilateral coronal synostosis, shallow orbits, exorbitism, and midface deficiency. Intelligence is often normal if early surgery is performed, and hydrocephalus is infrequent. Cases in which increased intracranial pressure is suspected are managed with a floating forehead procedure performed in the first few weeks of life [60]. In most cases, surgery is delayed until 6–10 months of age, at which time bifrontal craniotomy and bilateral advancement of the supraorbital bar can be accomplished at the same time (Fig. 40.24). Often, repeat bifrontal and supraorbital advancements are required in later childhood or adolescence to achieve an optimal cosmetic result [45]. The final stage is midface advancement by a LeFort III osteotomy [72], which does not require craniotomy (Fig. 40.25). The operation requires completion of secondary dentition and consists of horizontal sectioning of the

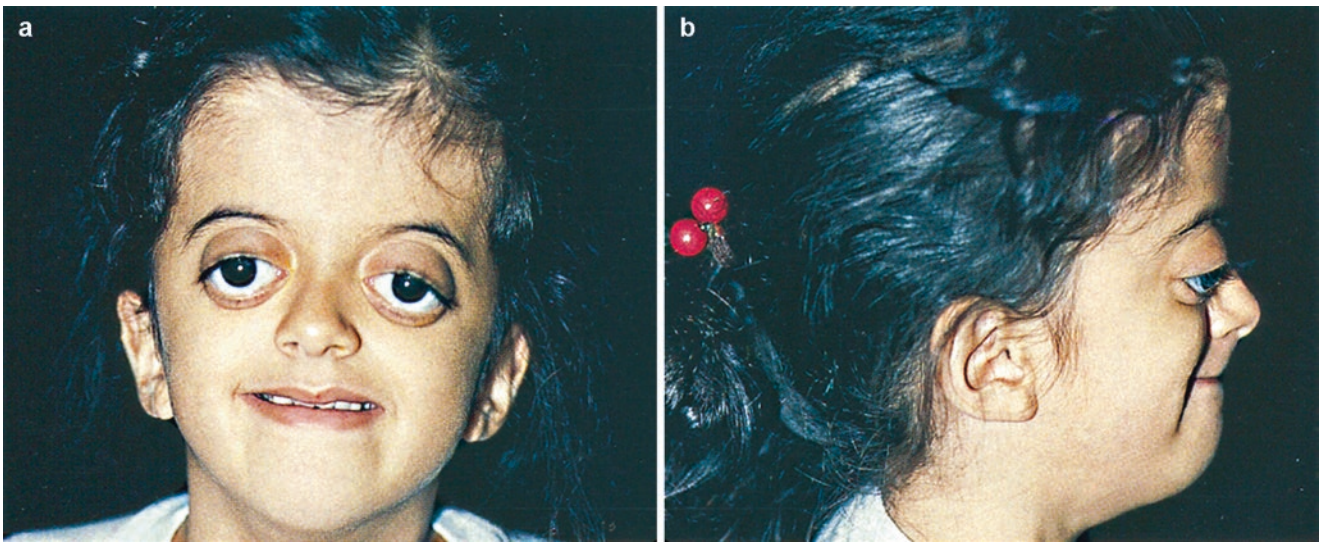


Fig. 40.23 Crouzon disease. (**a**) The most common syndromic synostosis is Crouzon disease. This patient evidences the classical findings of turribrachycephaly with supraorbital retrusion, a small, beak-like nose and prominent exorbitism. Also visible is the developing midface hypoplasia. (**b**) Lateral view

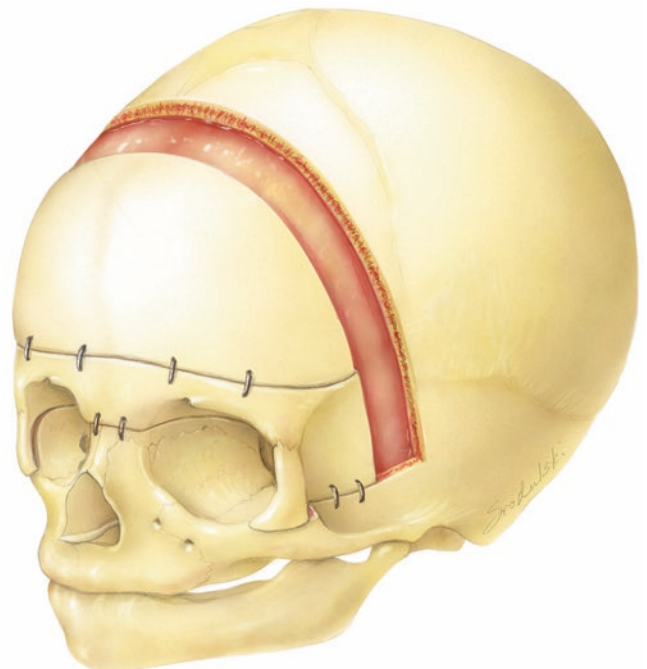


Fig. 40.24 Fronto-orbital advancement to treat syndromic synostosis. Treatment of the forehead and orbits in infancy for syndromic synostosis takes the form of fronto-orbital advancement. In this case, the entire supraorbital bar is advanced as a single piece. The forehead segment may be either advanced concurrently or cut into segments that are rotated 90 or 180° and switched right to left to result in an improved forehead contour

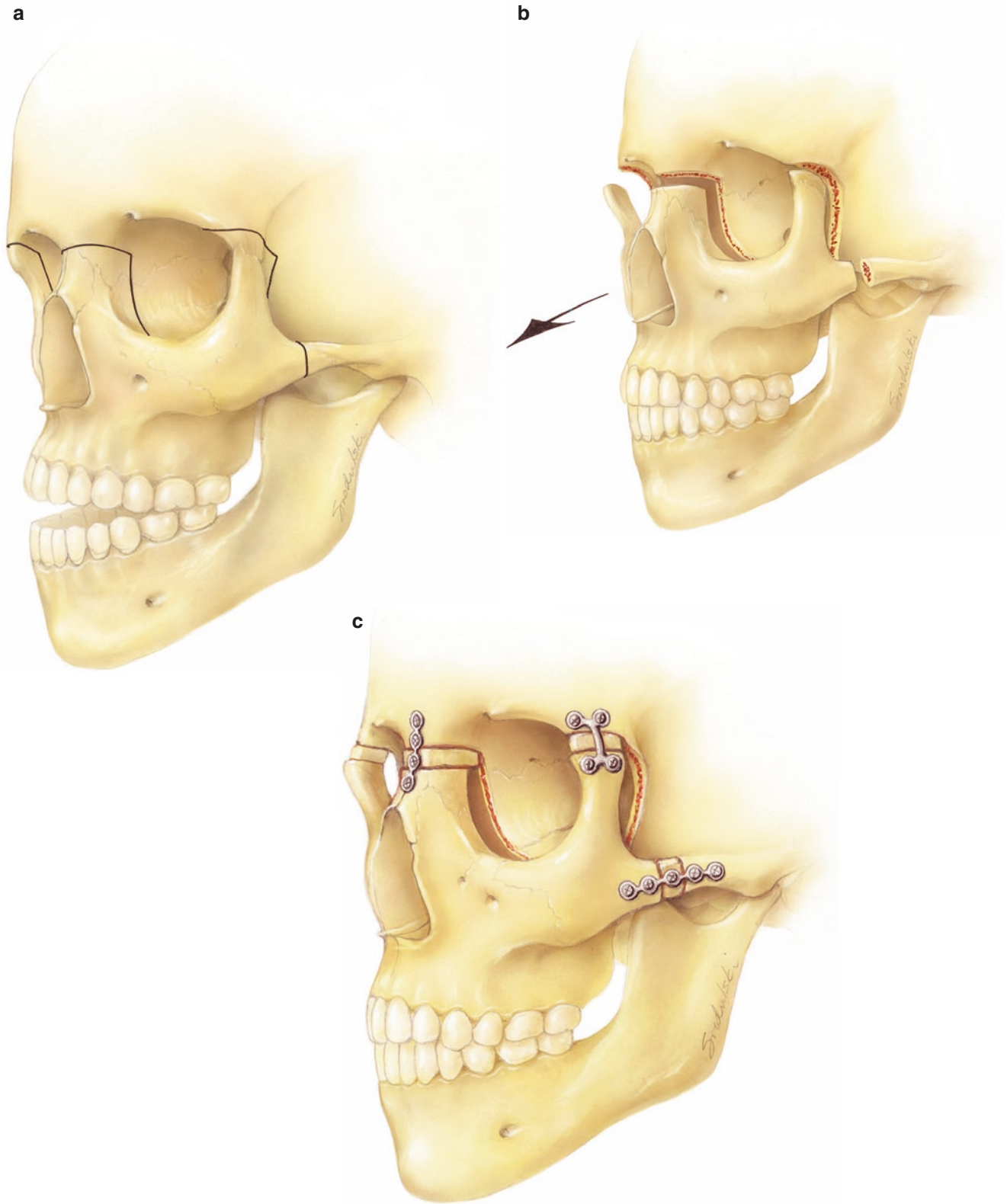


Fig. 40.25 Subcranial LeFort III advancement. In severe syndromic synostosis, midface hypoplasia is typically managed by a subcranial LeFort III advancement. Although minor differences in technique and osteotomy sites have been described, the typical lines of incision are shown in (**a**). (**b**) The midface has been disimpacted and moved forward, keying into the lower mandibular occlusion for stabilization and accurate position. (**c**) Following advancement, interposition bone grafts and plates stabilize the fixation. In the older child, intermaxillary fixation with dental arch bars and wires is also utilized

root of the nose into the orbital wall and continuation of the osteotomy along the medial wall behind the lacrimal sac to the inner third of the orbital floor. The lateral wall of the orbit is split in the sagittal plane, and osteotomy is continued to the orbital floor. Osteotomy is then extended through the malar bone, and the maxilla is advanced and fixed with wires, plates, and interposition bone grafts [2, 3].

Other relatively common syndromes have similar craniofacial deformities, accompanied by various other features. Apert syndrome [9], (autosomal dominant) (Fig. 40.26) which has been linked to alterations in FGFR tyrosine kinase activity [60], is a more severe form, often with more obvious exorbitism, strabismus, ocular hypertelorism, high-arched palate, and syndactyly of the hands and feet. Mental retardation is common, and it is unclear how much of this is genetically determined or to what extent it is preventable with early cranial decompressive surgery. Hydrocephalus is common. Carpenter syndrome [9] (autosomal recessive) consists of similar craniofacial features, accompanied by mental deficiency, preaxial polysyndactyly of the feet and hands, displacement of the patellae, genua valga, short stature, obesity, and cardiac anomalies. Multiple mutations in *Rab23* have been shown to be involved in the development of Carpenter syndrome [61]. Pfeiffer syndrome [9] (autosomal dominant) includes ocular hypertelorism, down-slanting palpebral fissure, midface hypoplasia, broad thumbs and great toes, and variable cutaneous syndactyly. Saethre–Chotzen syndrome (autosomal dominant), in addition to craniosynostosis, includes a low-set frontal hairline, ptosis of the eyelids, deviated nasal septum, and variable syndactyly of fingers and toes. Management of these and other syndromic synostoses parallels that as outlined for Crouzon syndrome, but the midface growth potential in Saethre–Chotzen syndrome is greater, and these patients may not require midface surgery (see Chap. 38). Loss-of-function mutations in the *TWIST1* transcription factor gene have been associated with the development of Saethre–Chotzen syndrome [62, 63].

As mentioned, the timing of these various types of intervention remains controversial. Suffice it to say, for the mild nonsyndromic synostosis, surgery in infancy is to be preferred [64, 65, 68]. At this age, the bones are malleable and more easily shaped, craniotomy gaps created frequently fill in with bone spontaneously, and correction of the brain growth restriction performed at this stage is associated with improved neurocognitive outcomes, albeit at the cost of a higher rate of major secondary revision. Surgery performed at a later age is associated with improved long-term maintenance of the aesthetic correction, but at the determent

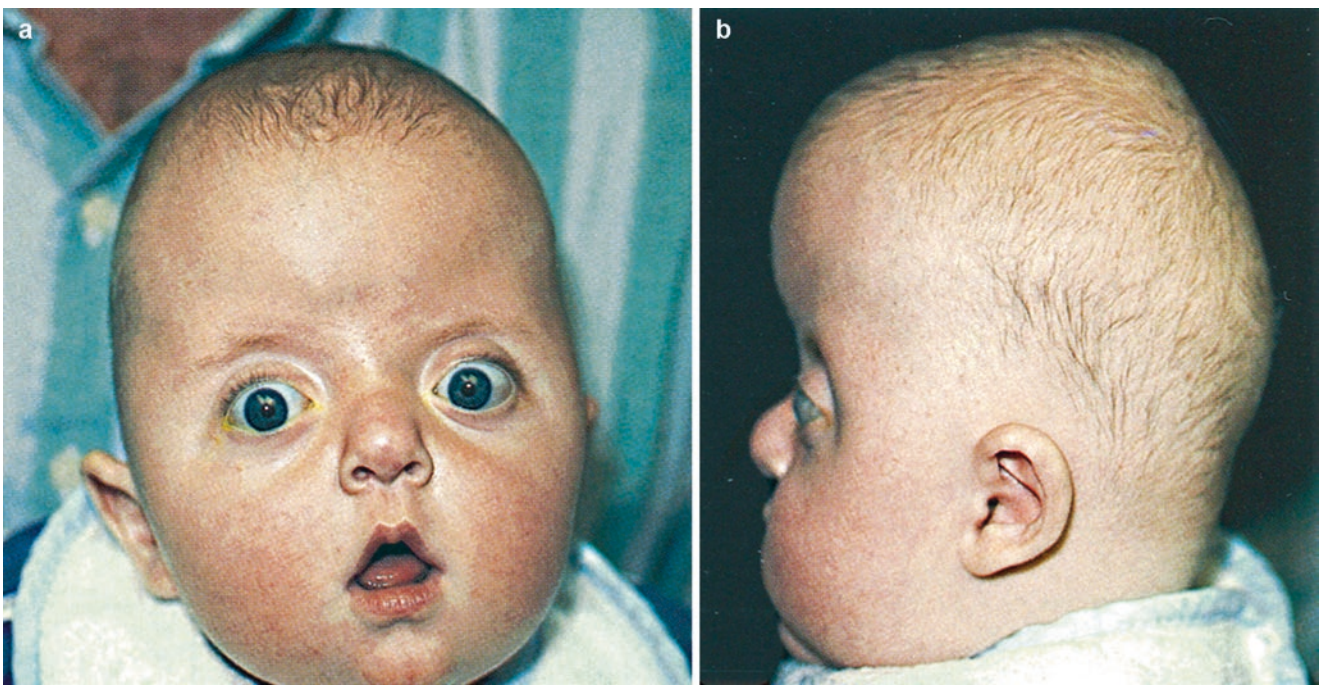


Fig. 40.26 Apert syndrome. (**a**) Typical appearance of an infant with Apert syndrome. Note the turribrachycephaly with a foreshortened anterior–posterior dimension to the skull and exorbitism. Also seen is the diminutive nose. Not shown is the syndactyly of the hands and feet characteristic of this disease. (**b**) Lateral view

of neurocognitive development [71, 72]. The syndromic synostoses frequently have an associated midface or cranial base growth disturbance that disallows such predictable outcomes. Surgery in this group may require several repeat surgical procedures over the growth period of the individual [66]. In general, procedures for the severe synostoses are done when functional needs dictate this, but if psychological (appearance-related) needs are evident, then surgical interventions are individualized to optimize appearance.

Virtually all syndromic synostoses have associated ocular–adnexal abnormalities, either as part of the primary condition or as a result of the correction of the bony deformity [73]. These include strabismus, nasolacrimal obstruction, canthal dystopia, and ptosis.

Orbital Hypertelorism

Orbital hypertelorism (OHT) is a condition in which the entire orbit is laterally displaced with an increase in the interorbital distance [74]. OHT is not a diagnosis in itself but is a component of other disorders. The most common etiologies of hypertelorism include craniosynostosis, midline and paramedian clefts, frontonasal dysplasia, encephaloceles, and other tumors or metabolic conditions [75] (Fig. 40.27). In some of the midline disorders, the brain may be affected, and appropriate diagnostic studies, as well as input from geneticists and neurosurgeons, are appropriate. The normal interorbital distance from dacryon to dacryon is 25 mm in the adult female and 28 mm in the adult male. The associated soft tissues add between 4 and 6 mm of distance, so when measuring from inner canthus to inner canthus, to get an estimate of orbital hypertelorism, this number must be subtracted. Based on the diagnosis of the primary condition, orbital hypertelorism may be associated with a number of adnexal abnormalities, which include, but are not limited to, strabismus, nasolacrimal dysplasia, canthal dystopias and clefts, or deficiencies of the soft tissue.

The management of orbital hypertelorism is based on the severity. For the milder cases, medial wall osteotomy and repositioning of the canthal bearing segment are to be preferred [18, 75] (Fig. 40.28). For the more severe deformities, a 360° orbital osteotomy with translocation medially of the entire orbit and its contents is the accepted approach (Fig. 40.29). When there is also a midline clefting-type phenomenon with abnormalities of the midface and occlusion, a facial bipartition procedure may be advised [76] (Fig. 40.30). At the time of surgery, it may be necessary to detach the medial and lateral canthal tendons. These are reinserted following osteotomy and repositioning, at which time nasal reconstruction in the form of onlay bone grafts is generally performed. The midline tissue excesses or deficiencies are either rearranged or excised. In general, once the basal skeleton is corrected, attention should be directed to adnexal problems. However, since most osteotomies involving the maxilla may damage unerupted teeth if performed early (before age 5 years), adnexal surgery may be performed earlier in life as required, with the understanding that repeat surgery on these structures may be needed once these osteotomies are completed.



Fig. 40.27 Orbital hypertelorism. (**a**) Example of orbital hypertelorism associated with frontal nasal dysplasia. (**b**) Orbital hypertelorism associated with midline cleft

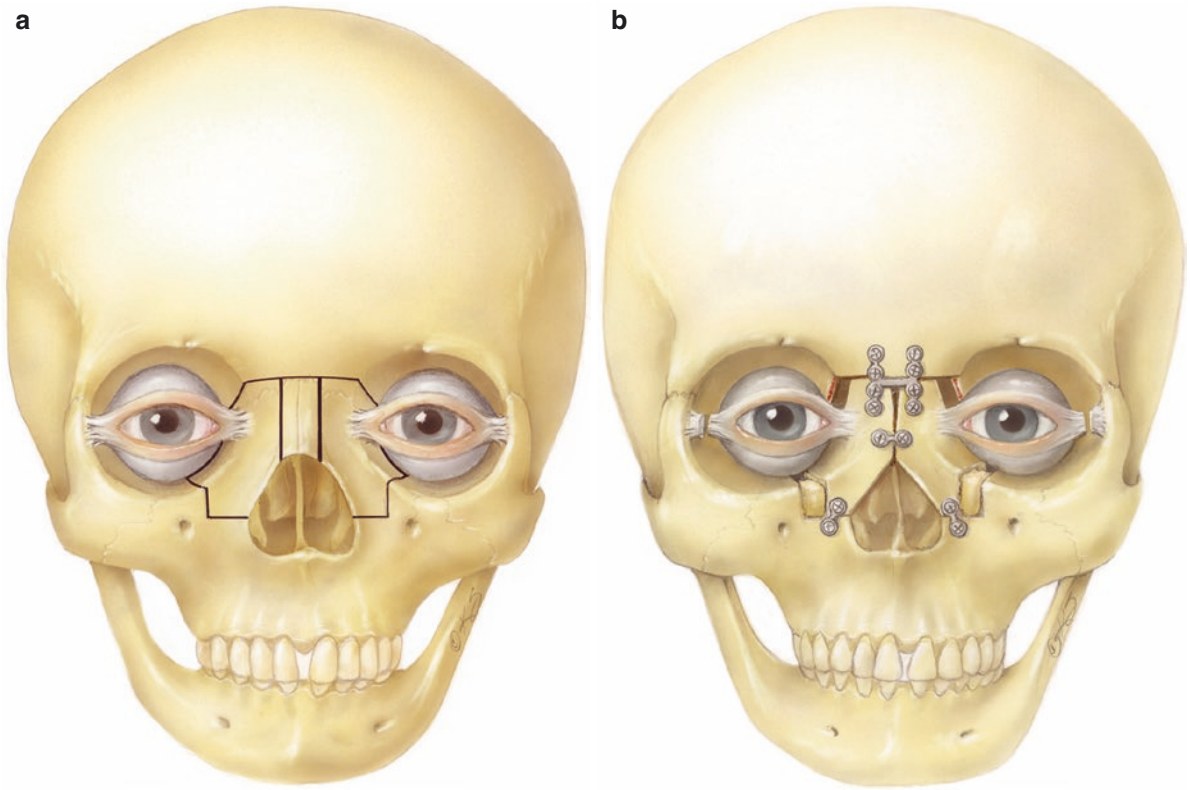


Fig. 40.28 Subcranial correction for mild orbital hypertelorism. (**a**) For the milder orbital hypertelorism, a subcranial correction can be performed. This involves medial wall orbital osteotomies. (**b**) Resection of midline bone and medial translocation with fixation and interposition bone grafts is then completed

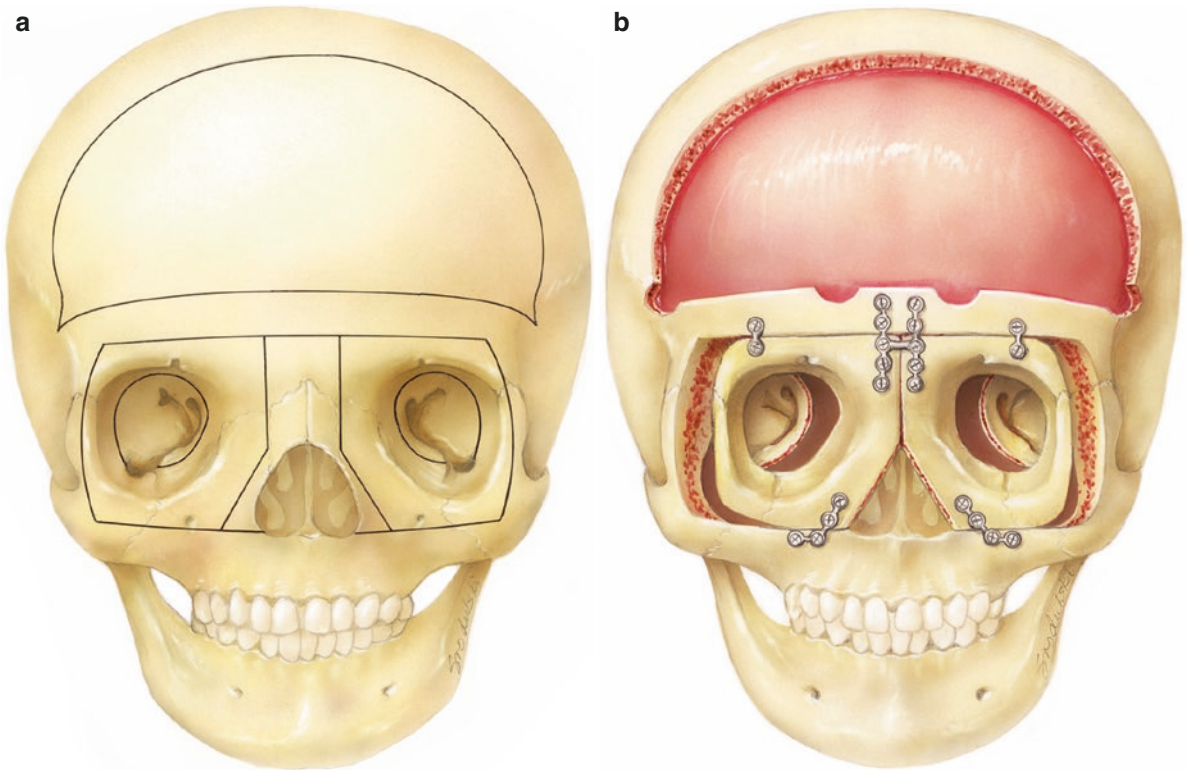


Fig. 40.29 Transcranial orbital osteotomy. (**a**) For more severe cases of orbital hypertelorism, a transcranial 360° orbital osteotomy is performed in concert with resection of the dysplastic midline bone. (**b**) This is followed by medial translocation, fixation, and bone grafting

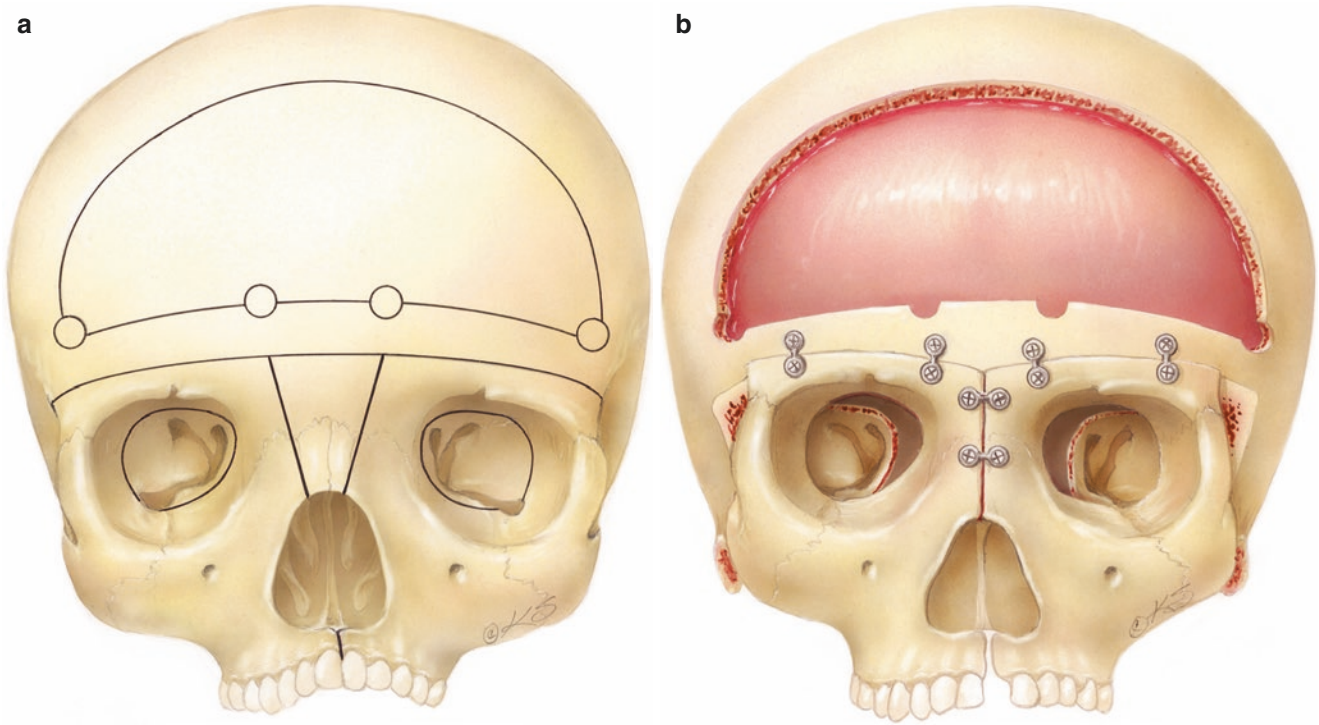


Fig. 40.30 Facial bipartition. (**a**) In cases of hypertelorism associated with a midline clefting phenomenon which extends to involve the maxillary occlusion, a facial bipartition is performed. (**b**) This involves complete mobilization of each hemifacial skeleton with midline translocation and fixation

Atrophy and Hypoplasia

Atrophy and hypoplasia comprise the next major diagnostic group. It includes a number of different entities, such as Binder nasomaxillary hypoplasia, Romberg disease, microphthalmia, radiation atrophy, and the like.

Romberg disease [77], or progressive hemifacial atrophy, is a rare condition in which a child born with a normal facial configuration develops progressive atrophy of the skin, subcutaneous tissues, muscles, and, in severe cases, bone (Fig. 40.31). It is unilateral in the vast majority of cases and has no known cause. Suspected etiologies include viral illness, autoimmune disorders, and disorders of the sympathetic nervous system [78]. The disease usually begins in childhood with a period of slowly progressive atrophy lasting as long as 8–12 years, followed by stabilization without further atrophy. It is commonly believed that during the atrophying process, no intervention should be undertaken lest the reconstructive materials (i.e., flap transfer or fat grafting) become part of the atrophic process. In the majority of cases, the most significant deformity is outside of the orbit itself, although the atrophying condition may involve the lid and adnexal structures. Colobomas of the lid and uveal system have been described, as has enophthalmos [79].

The treatment of established atrophy generally follows basic craniofacial surgical principles. Bony defects are first augmented with appropriate bone grafts, which may include the correction of enophthalmos. The treatment of the atrophic soft tissue is usually by subcutaneous placement of the tissue, utilizing de-epithelialized cutaneous microvascular free flaps, or fat grafting [80, 81]. Lid deficiencies and malpositions may be managed with small dermis grafts, canthopexies, repositioning, or the like. An example of a child with Romberg disease and lid involvement is shown in Fig. 40.31.

The late effects of radiation therapy present many manifestations similar to Romberg disease. Radiation in infancy and childhood to the orbit and periorbital structures may be accompanied by profound hypoplasia as normal growth in the surrounding tissues occurs (Fig. 40.32a, b). If radiation therapy is combined with orbital enucleation for the treatment of malignancy, severe orbital hypoplasia will develop. As in Romberg disease, the treatment of the radiation deformity is with the transfer of well-vascularized nonirradiated flap tissue to the orbit and periorbital structures [82] (Fig. 40.32c–d). In severe cases, in which the lids and adnexa are badly scarred and nonreconstructible, prosthetic replacement is the treatment of choice. The recently introduced osseo-integrated implants, used in dental rehabilitation, have



Fig. 40.31 Romberg disease. (**a**) A severe case of Romberg disease or hemifacial atrophy. (**b**) Note the severe atrophy of the left facial tissues, including both soft tissue and bone. Note as well the involvement of the lower lid, which is also affected by the atrophying process. (**c**) The contralateral side of the face is completely unaffected

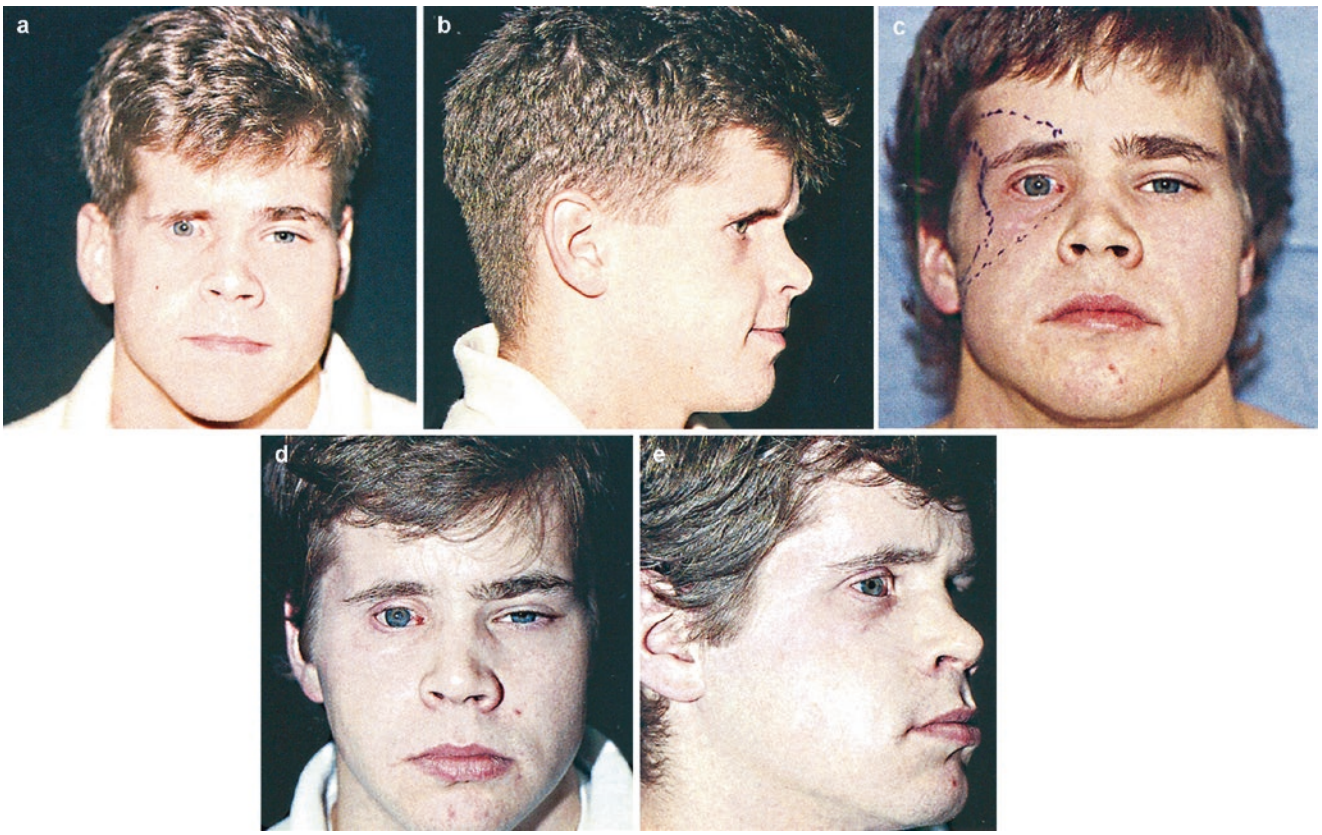


Fig. 40.32 Flap transfer. (**a**, **b**) Late effects of orbital irradiation for the treatment of orbital tumors can produce a condition similar to Romberg's disease. Note hypoplasia of the right orbit, temple, and midface in concert with underdevelopment of the globe, lid, and adnexal structures. (**c**) Preoperative markings for placement of a vascularized tissue transfer in the periorbital region. In this case, a scapular free flap anastomosed to the temporal vessels was chosen. (**d**, **e**) Appearance 6 months following flap transfer with improved contour in the lower forehead, temple, and malar regions. The lid and adnexal structures will be addressed separately

now been applied to the upper facial skeleton and may provide a firm bony anchor for attachment of more lifelike orbital prostheses.

Microphthalmos is another hypoplastic condition of uncertain etiology. Although it may be seen in both rare craniofacial clefts, severe cases of hemifacial atrophy, and associations with various genetic trisomies, duplications, and deletions, it is equally common as an isolated entity [83]. As will be detailed elsewhere in this textbook (Chap. 39), the treatment of microphthalmos usually involves stretching or expansion of available soft tissues. Progressive enlargement of orbital conformers, dermis grafts, and the like are appropriate. Bony tissue expansion by the placement of intraorbital expanders with progressive inflation has been shown to be efficacious in experimental studies and early clinical trials are encouraging [84].

In the older child with established microphthalmos, the soft tissue expansion is frequently hindered by the small bony orbit. In these cases, a transcranial bony orbital expansion to allow further soft tissue expansion may be appropriate [85]. This will involve a frontal craniotomy with osteotomy of the superior and lateral orbit with transverse and vertical expansion, as shown in Fig. 40.33. Subsequent to the bony expansion, further soft tissue expansion and augmentation can be considered. An example of a patient treated by this method is shown in Fig. 40.34.

Hypertrophy, Hyperplasia, and Neoplasia

This category includes a number of conditions that may cause enlargement of the facial skeleton and associated structures. Conditions such as fibrous dysplasia, neurofibromatosis, and benign hemihypertrophy fall into this group. Although tumors are rare, examples include Langerhans cell histiocytoses, rhabdomyosarcoma, retinoblastoma, optic nerve gliomas, and germ cell tumors.

Fibrous dysplasia of bone is a condition of unknown etiology in which there is a bony fibrous proliferation [86]. The bony involvement may occur any place in the facial skeleton and is usually a single focus. However, polyostotic disease may be present, frequently with endocrine involvement, and café au lait macules, and is termed McCune–Albright syndrome [87, 88]. Fibrous dysplasia most commonly occurs through an activating mutation in GNAS, a G-protein involved in the cAMP pathway, during early development [88, 89]. In the orbital region, fibrous dysplasia may result in orbital dystopia or proptosis. Diagnosis is established by plain radiographs and 3-D CT scans. If the disease is limited in extent, wide complete resection with autogenous bone reconstruction is the treatment of choice. With more extensive disease, especially when it involves the cranial base, reduction of the dysplastic process by contouring and partial resection may be all that can be performed [90]. This must be

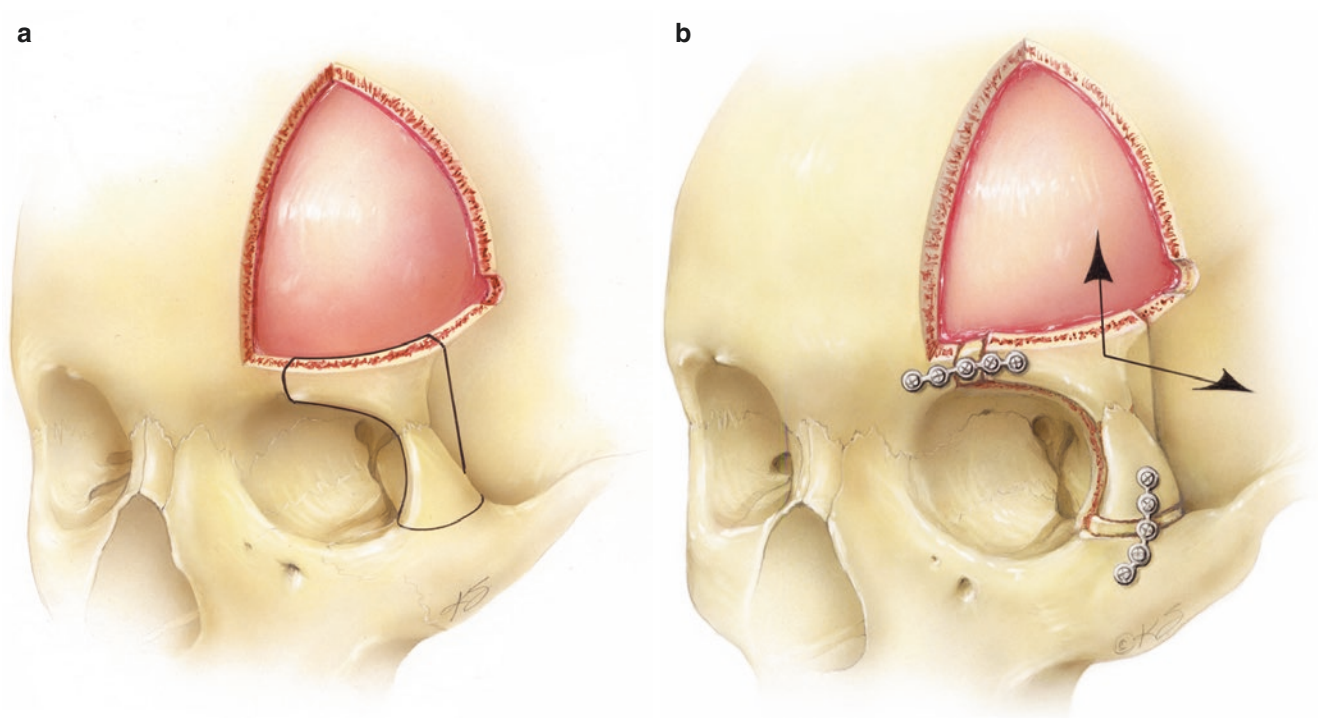


Fig. 40.33 Bony orbital expansion. (**a**) The technique of bony orbital expansion for microphthalmia. (**b**) In this case, the supraorbital segment has been expanded superiorly and laterally and fixated with plates and interposition bone grafts

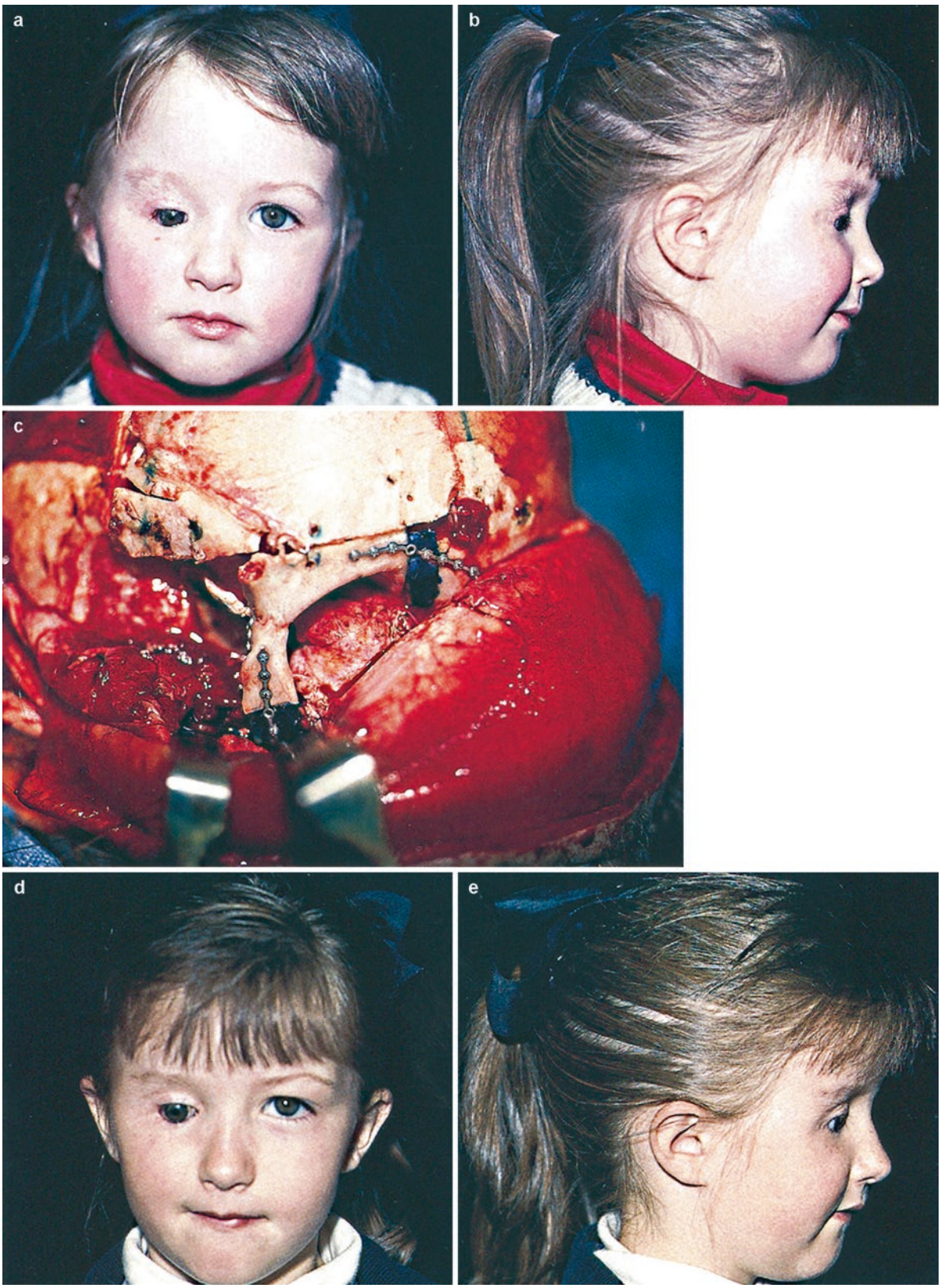


Fig. 40.34 Osteotomy, expansion, and fixation. (**a**, **b**) Preoperative appearance of a patient with a right microphthalmos. Bony restriction of this socket disallowed further lid expansion by conformer therapy. (**c**) Intraoperative photograph demonstrating the osteotomy of the superior and lateral orbit with superior and transverse expansion and fixation. Interposition bone grafts are shown in blue. (**d**, **e**) Patient seen postoperatively. Further soft tissue expansion will be necessary to realize the bony orbital gain

undertaken with the understanding that the subsequent course of the disease is unpredictable, regrowth may occur, and additional contouring or partial resection may be necessary. In those cases in which the disease process involves the orbital apex, frequent ophthalmologic examination is mandated. This process can cause progressive visual deterioration, and in these cases optic canal decompression or partial resection may be required. Examples of orbital involvement with this disease are represented in Figs. 40.35 and 40.36.

In addition to bony tumors such as fibrous dysplasia, numerous soft tissue orbital and periorbital tumors may be seen [5]. If oncologically indicated, soft tissue resection may be appropriate. Although the smaller and more anteriorly situated tumors can be approached through the lids or conjunctiva, larger, posteriorly situated tumors may require a different approach. We have found that a combined intracranial–extracranial approach to the posterior orbit in the treatment of selected tumors may be advisable and carry the least morbidity (Chap. 39). In these procedures, a frontal craniotomy and clearing of the anterior and middle cranial fossa are followed by extensive osteotomy of the orbital roof and lateral wall (Fig. 40.37). At this point, tumor resection can be performed, followed by replacement of osteotomized segments, bone graft replacement of resected bone, and resuspension of soft tissues. For those tumors in the infratemporal space, access may be gained extracranially with partial orbital osteotomy. As with all tumor resections, secondary lid and adnexal dysfunction may be seen. Treatment of these deformities is outlined elsewhere in this text (Chap. 25).

Miscellaneous Conditions

Included in this section are a variety of miscellaneous conditions, such as orbital and upper facial trauma, encephaloceles, and isolated orbital dystopias. Severe facial trauma in children frequently results in extensive facial fractures of the cranial base and orbit [91] (Fig. 40.38). Due to the small facial mass relative to the cranium, these upper facial fractures are seen more commonly in young children. Frequently, the severe injuries involve disruption of the cranial base, frontal bone, and orbital roof and walls. When displacement is significant and when neural injury or dural tears are suspected, the standard transcranial approach with or without lid access incisions is employed. For a lesser degree of trauma, extracranial access only may be required. A frontal craniotomy will allow exposure of the cranial base and orbital roof and repair of any neural or dural injuries, as well as reduction and stabilization of fracture segments. In the young child, simple wire fixation is preferred, while in the older child, the use of plate and screw fixation is appropriate (see Chap. 42). Severe orbital and cranial bone trauma may lead to secondary orbital deformities as the traumatized tissue fails to grow and develop normally in concert with the opposite side. Secondary posttraumatic correction, therefore, may be indicated at a later date, taking the form of orbital and midfacial osteotomy and reposition and bone graft augmentation of the upper face, midface, and orbit.

Encephaloceles are neural tube defects in which gliotic brain protrudes through an opening in the dura, bone, and occasionally skin to present as a mass. Most encephaloceles are sporadic, but some may be associated with certain genetic syndromes, such as Meckel–Gruber syndrome [92]. When the encephalocele is in the occipital region, the patient is often microcephalic and mental retardation is common. Patients with nasoethmoidal and nasofrontal encephaloceles, in contrast, are often of normal intelligence. The condition is usually evident at birth as a skin-covered mass in the region of the nasion, and frequently there is accompanying hypertelorism, presumably because the protruding brain prevents the orbits from moving together during embryogenesis. Pure ethmoidal (basal) encephaloceles may be occult and discovered only when patients present with cerebrospinal fluid leakage and recurrent meningitis or as nasal or pharyngeal masses. In some instances, only a small pit in the midline of the nose suggests the possibility of a small sinus tract or dermoid cyst, which may have an intracranial extension. For this reason, any patient with hypertelorism, a midline craniofacial mass or pore, or cleft should undergo a magnetic resonance scan of the brain and basicranium prior to any surgical procedure. Surgery for nasofrontal encephalocele is usually best performed in infancy or early childhood. Surgery for hypertelorism is best delayed, and staged procedures may be necessary.

Isolated orbital dystopias in which there is vertical or horizontal displacement of the globe are unusual [93]. These may be seen as a component of a rare craniofacial cleft, hemifacial microsomia, or as an isolated entity. Treatment of these entities follows principles outlined previously. Through a transcranial approach, a 4-wall orbital osteotomy is completed, and the entire orbit and its contents, including both medial and lateral canthal tendon, are repositioned in a horizontal or vertical dimension with fixation and bone graft placement (Fig. 40.39). Surgery is usually delayed until after age 5 or 6 years when damage to maxillary tooth buds can be minimized.

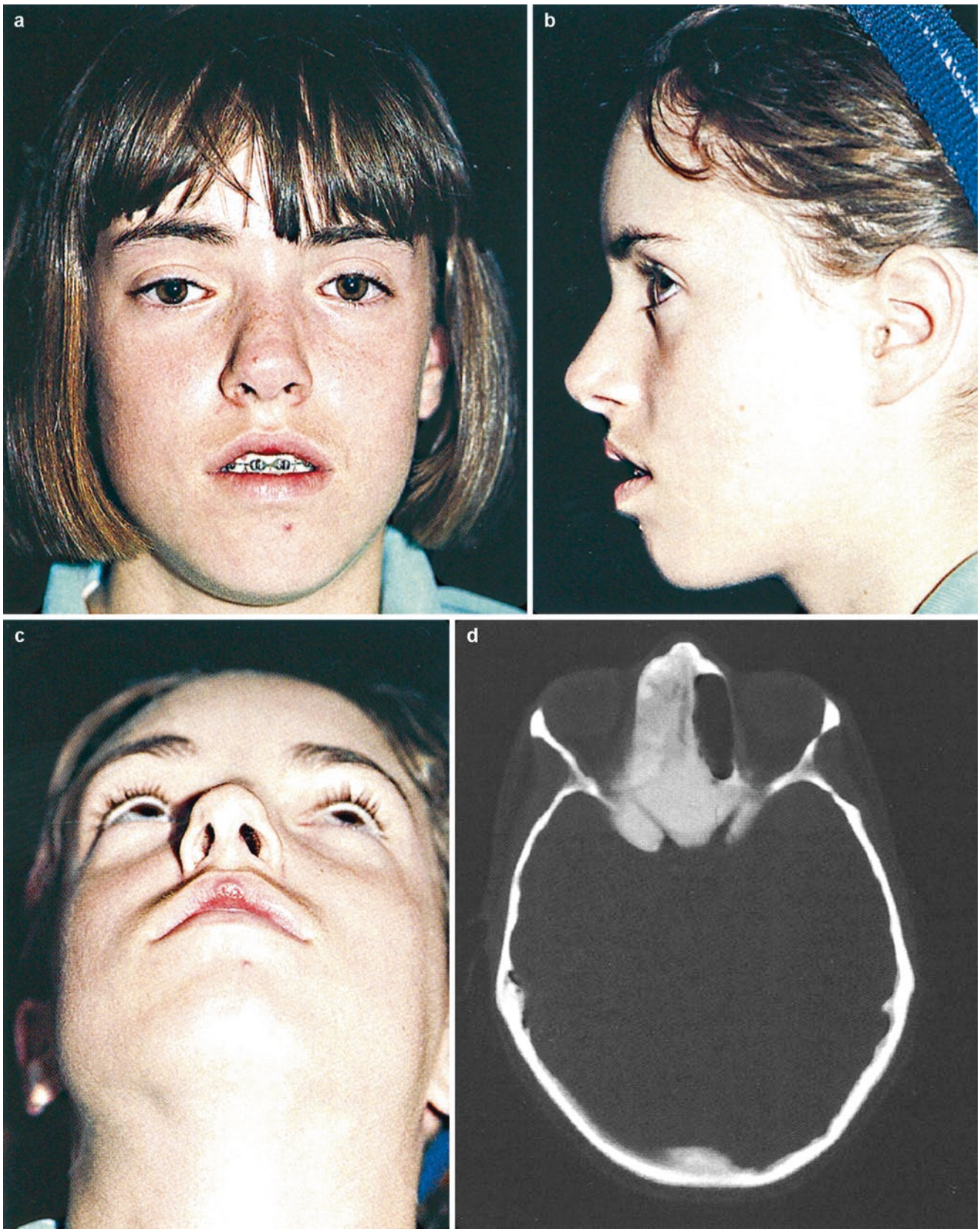


Fig. 40.35 (**a**–**d**) Orbital involvement of fibrous dysplasia of the nasoethmoid region. In this case, minimal orbital findings are seen, since most growth of the disease process has occurred in the nasoethmoid region. Special attention must be given to the orbital apex to prevent progressive optic nerve pressure-related atrophy

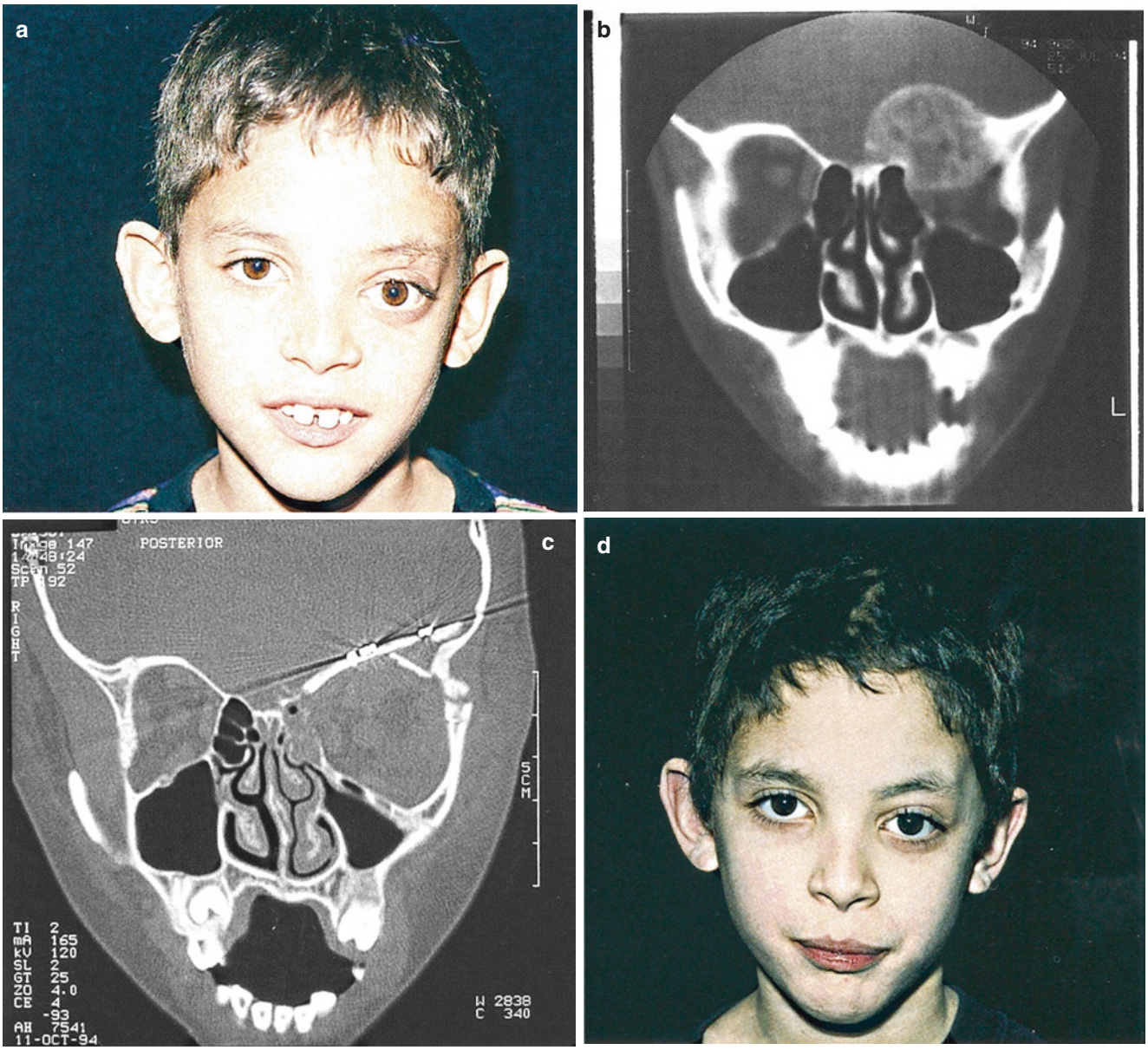


Fig. 40.36 Fibrous dysplasia correction. (**a**, **b**) A-P photograph and CT scan of extensive fibrous dysplasia of the orbital roof leading to dystopia and proptosis. (**c**) Coronal CT following resection and bone graft reconstruction. (**d**) Patient seen 6 months following surgical resection and reconstruction

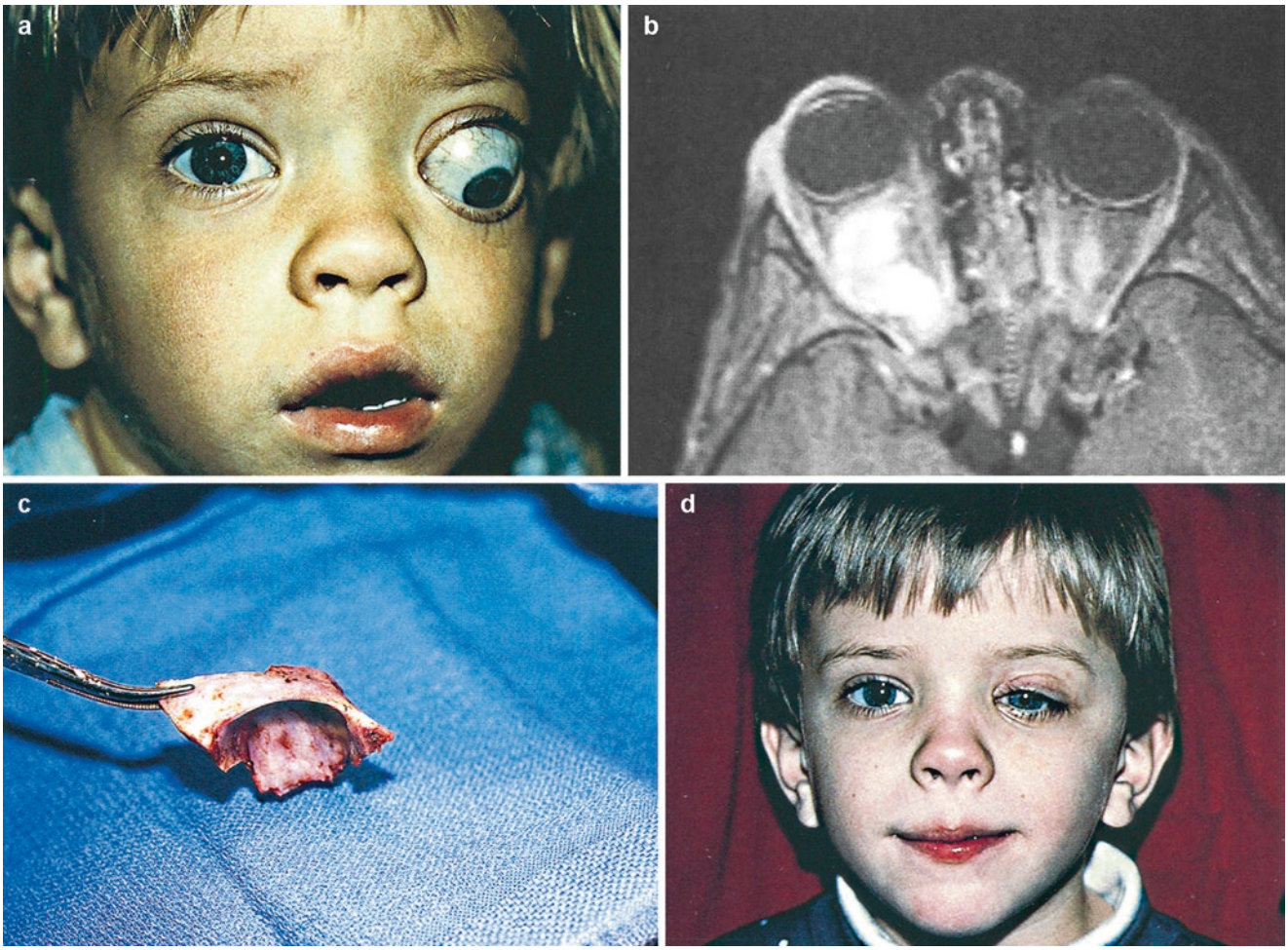


Fig. 40.37 Optic nerve glioma. (**a**) Optic nerve glioma leading to progressive proptosis of the ocular globe. (**b**) Involvement of the optic nerve at the apex is demonstrated in this MRI scan. (**c**) Osteotomized segments of the supraorbital bar shown intraoperatively. This was preceded by a frontal craniotomy and was followed by transcranial combined resection of the orbital components of the tumor. Replacement of osteotomized segments and bone grafting of any gaps was subsequently completed. (**d**) The patient 6 months postoperatively

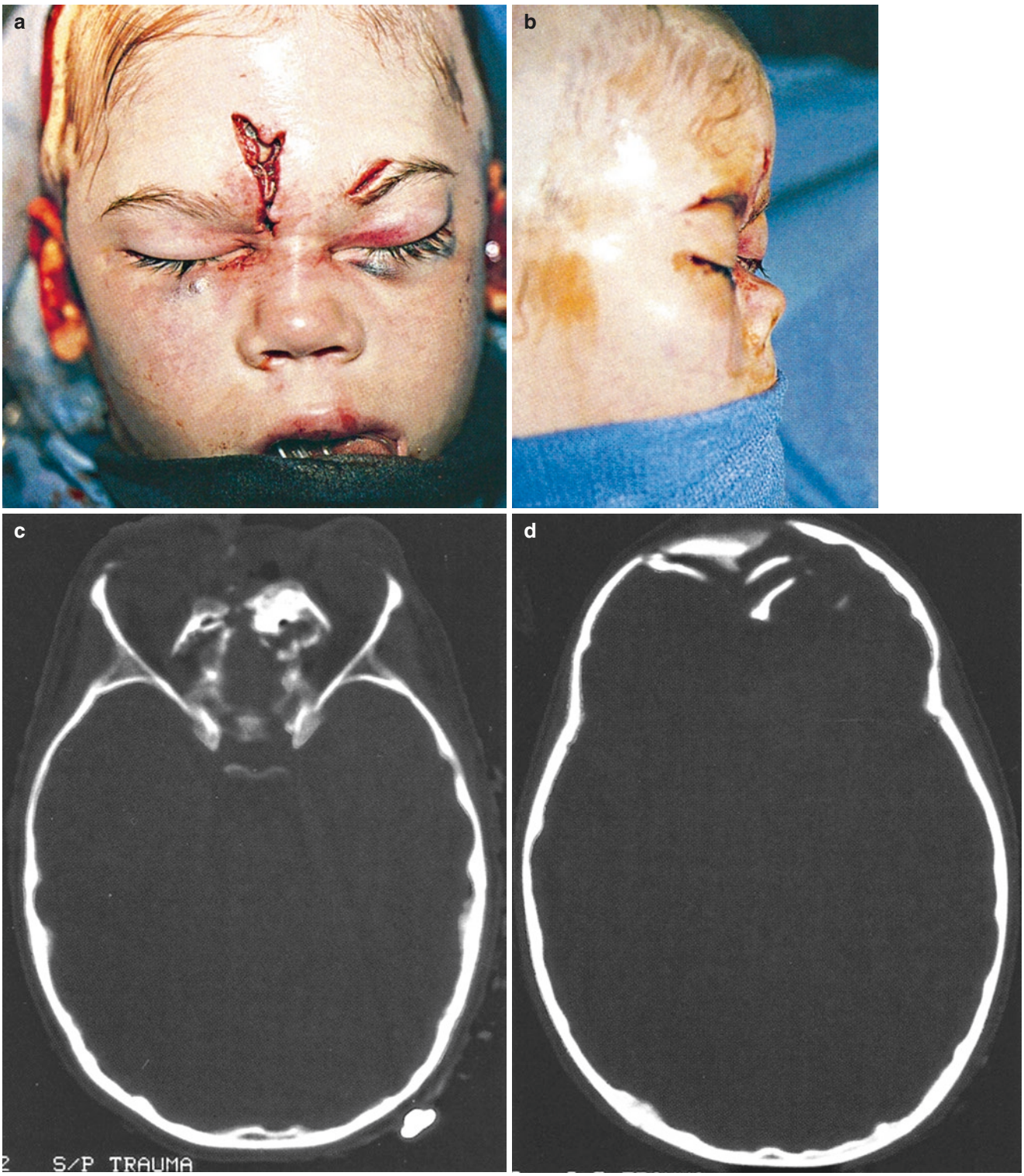


Fig. 40.38 Fronto-orbito-ethmoid trauma. (**a**, **b**) Severe fronto-orbito-ethmoid trauma in this 6-year-old child has caused displacement of the entire orbito-ethmoid skeleton posteriorly with traumatic telecanthus. (**c**, **d**) CT scan demonstrating compaction and frontal bone/cranial base injury.



Fig. 40.38 (continued) (**e**, **f**) Patient seen 9 months following repair with a stable facial skeleton. Injuries such as this may have long-term implications of growth, and continued follow-up and reassessment are mandated. Frequently, secondary augmentation or osteotomy and repositioning may be required later in life

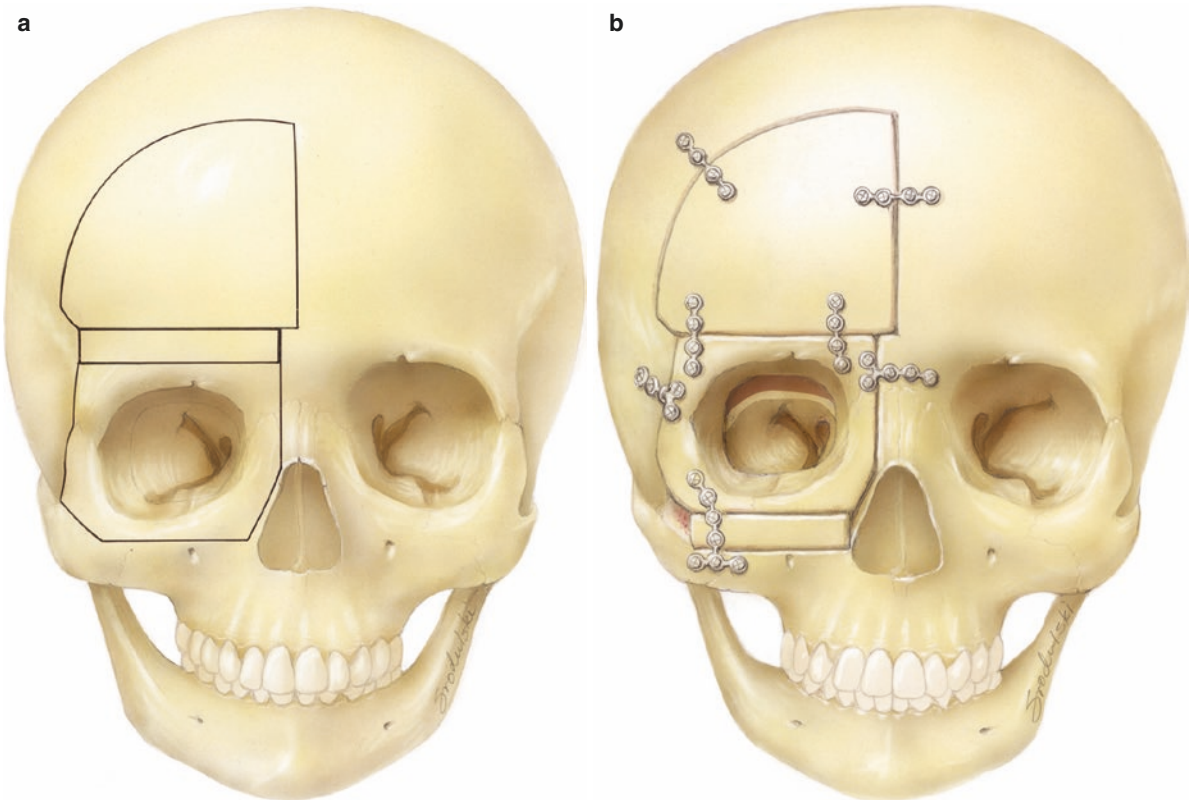


Fig. 40.39 Surgical correction of orbital dystopias. (**a**) Surgical correction of isolated orbital dystopias involves a 360° orbital osteotomy with translocation of the orbit and its contents superiorly. (**b**) The bone graft taken out superiorly is typically used to support the advanced orbit inferiorly followed by stabilization with screws and plates or wires

Complications

As in any surgical intervention, craniofacial surgery is not risk-free [94]. Despite the major types of interventions, death and blindness are rare. In our own personal series of nearly 3500 transcranial pediatric procedures, there has been one death and two significant neural injuries. With improved techniques, infection rate is 3% and is highest in those cases that are performed secondarily and in whom the primary deformity is severe. Most reported infection rates range from 3% to 5%, and the offending agent is usually skin flora [95, 96]. As mentioned previously, there have been reports of hardware translocation over time, and so we have evolved from using metal plates and screws and wires in the younger patients. Dural tears and resulting CSF leak is also a potential complication. If intraoperatively there is a known dural tear, this will usually be repaired directly. In some cases, spinal drains may be required for a period of 5–7 days. Perhaps the most common postoperative complication is failure of bone growth at the gaps created during the remodeling surgery. In our experience, the extent of these persistent skull defects is unpredictable. We no longer leave any bone defects in our craniofacial reconstructions. We advocate the use of bone scrapings from the inner table of the elevated bone flaps to fill any spaces prior to scalp closure. Other complications include extraocular muscle dysfunction, ptosis, nasolacrimal obstruction, malocclusion, and the like [95, 97]. With increased experience, these complications should decrease to less than 10%. The dreaded complication of blindness is an extremely rare one but one that should remain at the forefront of the surgeon's mind. Periodic evaluation of the globe and pupil during the procedure is paramount, especially after any traction is placed on the optic nerve.

Long-Term Results of Craniofacial Surgery

Since many of these procedures are performed in infants and young children, as opposed to adults, a fundamental difference is apparent: surgery done in infancy and childhood may be compromised by subsequent facial growth. Not only do many of the syndromes have inherent growth deficiency, but the surgical intervention itself, with subsequent scarring, devascularization, and the like, may also influence the final outcome. When operations are performed in infancy, it is imperative that the operating surgeon and craniofacial team continue to follow these patients for the long term, so that appropriate secondary interventions may be performed in a timely fashion to optimize the functional and the aesthetic results. There is a battle between operating early enough to prevent long-term neurocognitive deficits as a result of the underlying pathology and operating late enough to ensure greater longevity of the correction [98, 99]. Our experience has been one of the corrections that have held up well over time, with a low revision rate [99].

References

1. Tessier P, Guiot G, Rougerie J, Delbet J, Pastoriza J. Osteotomies cranio-nasoorbito-faciales hypertelorism. Ann Chir Plast. 1967;12:103–9.
2. Tessier P. Osteotomies totales de la face: syndrome de Crouzon, syndrome d'Apert, oxycephalies, scaphocephalies, turricephalies. Ann Chir Plast. 1967;12:273–8.
3. Tessier P. Dysostoses cranio-faciales: osteotomies totales de la face. In: Transactions of the fourth international congress of plastic and reconstructive surgery. Amsterdam: Excerpta Medica; 1969.
4. Shillito J, Matson D. Craniosynostosis: a review of 519 surgical patients. Pediatrics. 1968;4:829–35.
5. Jackson I. Management of craniofacial tumors. In: Caronni E, editor. Journal of Craniofacial Surgery. Boston: Little Brown; 1982. p. 315–28.
6. Hardesty R, Coffey J Jr. Secondary cranio-maxillo-facial deformities: current principles of management. Clin Plast Surg. 1992;19:275–81.
7. Thaller S, Kawamoto H. Surgical correction of exophthalmos secondary to Grave's disease. Plast Reconstr Surg. 1990;86:411–5.
8. Whitaker L, Morales L, Farkas L. Aesthetic surgery of the supraorbital ridge and forehead structures. Plast Reconstr Surg. 1986;78:23–6.
9. Gorlin R, Cohen M, Levin S. Syndromes of the head and neck. 3rd ed. New York: Oxford University Press; 1990.
10. Whitaker L, Pashayan H, Reichman J. A proposed new classification of craniofacial anomalies. Cleft Palate J. 1981;18:161–4.
11. Marsh J, Vannier M. Computer-assisted imaging in the diagnosis, management and study of dysmorphic patients. In: Vig K, Burdi A, editors. Craniofacial morphogenesis and dysmorphogenesis. Ann Arbor: University of Michigan; 1988. p. 109–26.
12. Mansfield P, Morris P. NMR imaging in biomedicine. New York: Academic; 1982.
13. Pertschuk M, Whitaker L. Social and psychological effects of craniofacial deformity and surgical reconstruction. Clin Plast Surg. 1982;9:297–301.
14. Fearon JA, Weinthal J. The use of recombinant erythropoietin in the reduction of blood transfusion rates in cranio- synostosis repair in infants and children. Plast Reconstr Surg. 2002;109:2190–6.
15. Krajewski K, Ashley RK, Pung N, et al. Successful blood conservation during craniosynostotic correction with dual therapy using procrit and cell saver. J Craniofac Surg. 2008;19:101–5.
16. Naran S, Cladis F, Fearon J, et al. Safety of preoperative erythropoietin in surgical calvarial remodeling: an 8-year retrospective review and analysis. Plast Reconstr Surg. 2012;130:305–310e.
17. Cladis FP, Bykowski M, Schmitt E. Postoperative hyponatremia following calvarial vault remodeling in craniosynostosis. Paediatr Anaesth. 2011;21:1020–5.
18. Whitaker L, Salyer K, Munro I, Jackson I. Atlas of craniomaxillofacial surgery. St. Louis: Mosby; 1982.
19. Fuente del Campo A. Rigid fixation and osteotomy design in frontal orbital advancement osteotomies. Clin Plast Surg. 1989;16:187–91.
20. Beals S, Munro I. The use of mini-plates in craniomaxillofacial surgery. Plast Reconstr Surg. 1987;79:33–8.

21. Goldberg D, Bartlett S, Yu J, Hunter J, Whitaker L. Critical review of microfixation in pediatric craniofacial surgery. J Craniofac Surg. 1995;6:301–7.
22. Yu J, Bartlett S, Goldberg D, et al. An experimental study of the effects of craniofacial growth on the long-term positional stability of microfixation. J Craniofac Surg. 1996;7:64–71.
23. Zins J, Whitaker L. Membranous versus endochondral bone autografts: implications for craniofacial reconstruction. Surg Forum. 1979;30:521–3.
24. Wolfe S. Autogenous bone grafting of orbitocranial defects versus the use of alloplastic materials. In: Caronni E, editor. Journal of Craniofacial Surgery. Boston: Little Brown; 1982. p. 476–89.
25. Tessier P. Anatomical classification of facial, craniofacial and laterofacial clefts. J Maxillofac Surg. 1976;4:69–76.
26. Kawamoto H. The kaleidoscopic world of rare craniofacial clefts: order out of chaos (Tessier classification). Clin Plast Surg. 1976;3:529–36.
27. Galante G, Dado D. The Tessier no. 5 cleft: a report of two cases and a review of the literature. Plast Reconstr Surg. 1991;88:131–6.
28. Resnick J, Kawamoto H. Rare craniofacial clefts: Tessier no. 4 clefts. Plast Reconstr Surg. 1990;85:843–8.
29. Fuente-del-Campo A. Surgical correction of Tessier no. 8 cleft. Plast Reconstr Surg. 1990:658–64.
30. Franschetti A, Klein D. Mandibulo-facial dysostosis: a new hereditary syndrome. Acta Ophthalmol. 1949;27:144–52.
31. Collins E. Cases with symmetrical congenital notches in the outer part of each lid and defective development of the malar bones. Trans Ophthalmol Soc UK. 1900;20:190.
32. Plomp RG, Lieshout M, Joosten K, et al. Teacher Collins syndrome: a systematic review of evidence-based treatment and recommendations. Plast Reconstr Surg. 2016;137(1):191–204.
33. Kadakia S, Helman SN, et al. Treacher Collins syndrome: the genetics of a craniofacial disease. Int J Pediatr Otorhinolaryngol. 2014;78(6):893–8.
34. Rogers B. Berry–Treacher–Collin's syndrome: a review of 200 cases. Br J Plast Surg. 1964;17:109–18.
35. Rogers B, McCarthy J, Converse J. Plastic surgical reconstruction of Treacher–Collin's syndrome. In: Converse J, McCarthy J, Wood-Smith D, editors. Symposium on diagnosis and treatment of craniofacial anomalies. St. Louis: Mosby; 1979.
36. McCarthy J, Cutting C, Shaw W. Vascularized calvarial flaps. Clin Plast Surg. 1987;74:10–20.
37. Jackson I. Reconstruction of the lower eyelid defect in Treacher–Collin's syndrome. Plast Reconstr Surg. 1981;67:365–72.
38. McCarthy J. Lengthening the human mandible by gradual distraction. Plast Reconstr Surg. 1992;89:1–10.
39. McCarthy JG, Stelnicki EJ, Mehrara BJ, et al. Distraction osteogenesis of the craniofacial skeleton. Plast Reconstr Surg. 2001;107:1812–27.
40. Persing J, Jane J, Shaffrey M. Virchow and the pathogenesis of craniosynostosis: a translation of his original work. Plast Reconstr Surg. 1989;83:738–46.
41. Moss M. The pathogenesis of premature cranial synostosis in man. Acta Anat (Basel). 1959;37:351–70.
42. Latham R. Growth and development of the craniofacial skeleton. In: Serafin D, Georgiade N, editors. Pediatric plastic surgery. St. Louis: Mosby; 1984. p. 216–29.
43. Lannelongue M. De la craniectomie dans la microcephalic. CR Acad Sci. 1890;110:1382–91.
44. Lane L. Pioneer craniectomy for relief of mental inmbecility due to premature sutural closure and microcephalus. JAMA. 1982;18:29–33.
45. Whitaker L, Bartlett S, Schut L, Bruce D. Craniosynostosis: an analysis of the timing, treatment, and complications in 164 consecutive patients. Plast Reconstr Surg. 1987;80:195–206.
46. Hoffman H, Kestle J. Craniofacial surgery. In: Cheek W, editor. Pediatric neurosurgery: surgery of the developing nervous system. Philadelphia: WB Saunders; 1994. p. 124–38.
47. Thompson D, Malcolm G, Jones B, et al. Intracranial pressure in single-suture craniosynostosis. Pediatr Neurosurg. 1995;22:235–40.
48. Wall SA, Thomas GP, Johnson D, et al. The preoperative incidence of raised intracranial pressure in nonsyndromic sagittal craniosynostosis is underestimated in the literature. J Neurosurg Pediatr. 2014;14(6):674–81.
49. Gault D, Renier D, Marchac D, et al. Intracranial pressure and intracranial volume in children with craniosynostosis. Plast Reconstr Surg. 1992;90:337–45.
50. Marchac D, Renier D, Broumand S. Timing of treatment for craniosynostosis and fascio-craniosynostosis: a 20 year experience. Br J Plast Surg. 1994;4:211–22.
51. Resnick D, Pollack I, Albright A. Surgical management of the cloverleaf skull deformity. Pediatr Neurosurg. 1995;22:29–37.
52. Thompson D, Haywood R, Harkness W, et al. Lessons from a case of Kleeblatschädel. J Neurosurg. 1995;82:1071–4.
53. Manjila S, et al. History of Kleeblattschadel deformity: origin of concepts and evolution of management in the past 50 years. Neurosurg Focus. 2010;29(6):E7.
54. Siddiqi S, Posnick J, Bancic R, et al. The detection and management of intracranial hypertension after initial suture release and decompression for craniofacial dysostosis syndromes. Neurosurgery. 1995;36:703–8.
55. Tuite G, Chong W, Evanson J, et al. The effectiveness of papilledema as an indicator of intracranial pressure in children with craniosynostosis. Neurosurgery. 1996;38:272–8.
56. Katz D, Trobe J, Muraszko K, et al. Shunt failure without ventriculomegaly proclaimed by ophthalmic findings. J Neurosurg. 1994;81:721–5.
57. Sutton L, Bartlett S, Duhaime A, et al. Total cranial vault reconstruction for the older child with scaphocephaly. Pediatr Neurosurg. 1993;19:63–72.
58. Bhadkamkar MA, Albright SB, Wolfswinkel EM, Bolio R, Buchanan EP. Posterior cranial vault distraction in the treatment of shunt-induced craniosynostosis. J Craniofac Surg. 2015;26(1):e70–2.
59. Heuze Y, et al. Closing the gap: genetic and genomic continuum from syndromic to nonsyndromic craniosynostoses. Curr Genet Med Rep. 2014;2(3):135–45.
60. Soh N, et al. Gradual distraction fronto-orbital advancement with 'floating forehead' for patients with syndromic craniosynostosis. J Craniofacial Surg. 2006;17(3):497–505.
61. Sameep K, et al. Carpenter syndrome: a review for the craniofacial surgeon. J Craniofacial Surg. 2014;25(5):1653–7.
62. Howard TD, Paznekas WA, Green ED, et al. Mutations in TWIST, a basic helix-loop-helix transcription factor, in Saethre–Chotzen syndrome. Nat Genet. 1997;15:36–41.
63. Tahiri Y, Bastidas N, McDonald-McGinn D, Birgfeld C, Zackai E, Taylor J, Bartlett S. New pattern of sutural synostosis associated with TWIST gene mutation and Saethre-Chotzen syndrome: peace sign stenosis. J Craniofac Surg. 2015;26(5):1564–7.
64. Stein S, Schut L. Management of scaphocephaly. Surg Neurol. 1977;7:153–5.
65. Hoffman H, Mohr G. Lateral canthal advancement of the supraorbital margin: a new corrective technique in the treatment of coronal synostosis. J Neurosurg. 1976;45:376–81.

66. Whitaker L, Bartlett S. The craniofacial dysostoses: guidelines for management of the symmetric and asymmetric deformities. Clin Plast Surg. 1987;14:73–81.
67. Salkind G, Sutton L, Bruce D, et al. Management of trigonocephaly. Surg Neurol. 1986;25:159–62.
68. Marchac D. Radical forehead remodeling for craniostenosis. Plast Reconstr Surg. 1978;61:823–30.
69. Whitaker L, Schut L, Kerr L. Early surgery for isolated craniofacial dysostosis. Plast Reconstr Surg. 1977;60:575–82.
70. Marchac D, Renier D. Lefront flottant, traitement precote de faciocraniostenosoes. Ann Chir Plast. 1979;24:121–8.
71. Persing J, Edgerton M, Park T, et al. Barrel stave osteotomy for correction of turribrachycephaly craniosynostosis deformity. Ann Plast Surg. 1987;18:488–93.
72. Bartlett S, Whitaker L, Marchac D. The operative treatment of isolated craniofacial dysostosis (plagiocephaly): a comparison of the unilateral and bilateral techniques. Plast Reconstr Surg. 1990;85:677–83.
73. Whitaker L, Katowitz J, Jacobs W. Ocular adnexal problems in craniofacial deformities. J Maxillofac Surg. 1979;7:55–62.
74. Greig D. Hypertelorism: a hitherto undifferentiated congenital craniofacial deformity. Edinburg Med J. 1924;31:560–9.
75. Vander Meulen J, Vaandrager J. Surgery related to the correction of hypertelorism. Plast Reconstr Surg. 1983;71:6–13.
76. Ortiz Monasterio F, Medina O, Musolas A. Geometrical planning for the correction of orbital hypertelorism. Plast Reconstr Surg. 1990;86:650–6.
77. Archambault L, Fromm W. Progressive facial hemiatrophy. Arch Neurol Psychiatr. 1932;27:529–39.
78. Aydin H, Yologlu Z, et al. Parry-Romberg syndrome: physical, clinical and imaging features. Neurosciences. 2015;20(4):368–71.
79. Bucher F, Fricke J, Neugebauer A, Cursiefen C, Heindl LM. Ophthalmological manifestations of Parry-Romberg syndrome. Surv Ophthalmol. 2016;61(6):693–701.
80. Upton J, Mulliken J, Hicks P, Murray J. Restoration of facial contour using free vascularized omental transfer. Plast Reconstr Surg. 1980;66:560–8.
81. Marra KG, Rubin JP. The potential of adipose-derived stem cells in craniofacial repair and regeneration. Birth Defect Res C Embryo Today. 2012;96:95–7.
82. Cohen S, Bartlett S, Whitaker L. Reconstruction of late craniofacial deformities after irradiation of the head and face during childhood. Plast Reconstr Surg. 1990;86:229–36.
83. Bardakjian T, Weiss A and Schneider A. Microphthalmia/anophthalmia/coloboma spectrum. GeneReviews. 2015.
84. Buchman S, Bartlett S, Wornom I III, Whitaker L. The role of pressure on the regulation of craniofacial bone growth. J Craniofac Surg. 1994;5:2–8.
85. Elisevich K, Bite U, Colcleugh R. Micro-orbitalism: a technique for orbital rim expansion. Plast Reconstr Surg. 1991;88:609–15.
86. Moore A, Buncic J, Munro I. Fibrous dysplasia of the orbit in childhood: clinical features and management. Ophthalmology. 1985;92:12–20.
87. McCune D. Osteitis fibrosa cystica: the case of a nine year old girl who also exhibits precocious puberty. Am J dis Child. 1936;52:743–7.
88. Boyce AM and Collins MT. Fibrous dysplasia/McCune-Albright syndrome. GeneReviews 2015.
89. Agopiantz M, Journeau P, Lebon-Labich B, Sorlin A, Cuny T, Weryha G, Leheup B. McCune-Albright syndrome, natural history and multidisciplinary management in a series of 14 pediatric cases. Ann Endocrinol. 2016;77(1):7–13.
90. Chen Y, Nordhof M. Treatment of craniomaxillofacial fibrous dysplasia: how early and how extensive. Plast Reconstr Surg. 1990;86:835–42.
91. Bartlett S, DeLozier J. Controversies in the management of pediatric facial fractures. Clin Plast Surg. 1992;19:245–54.
92. Barisic I, et al. Meckel-Gruber syndrome: a population-based study on prevalence, prenatal diagnosis, clinical features, and survival in Europe. Eur J Hum Genet. 2015;23(6):746–52.
93. Gross J, Wolfe S. Correction of vertical orbital dystopia. In: Ortiz-Monasterio F, editor. Craniofacial surgery 5. Bologna: Monduzzi; 1994. p. 257–8.
94. Whitaker L, Munro I, Salyer K, et al. Combined report of problems and complications in 793 craniofacial operations. Plast Reconstr Surg. 1979;64:198–206.
95. Poole M. Complications in craniofacial surgery. Br J Plast Surg. 1988;41:608–14.
96. Fearon JA, Yu J, Bartlett SP, et al. Infections in craniofacial surgery: a combined report of 567 procedures from two centers. Plast Reconstr Surg. 1997;100:862–8.
97. Goodrich JT. Craniofacial surgery: complications and their prevention. Semin Pediatr Neurol. 2004;11:288–300.
98. Patel A, Yang JF, Hashim PW, et al. The impact of age at surgery on long-term neuropsychological outcomes in sagittal craniosynostosis. Plast Reconstr Surg. 2014;4:608–617e.
99. Wes A, Paliga JT, Goldstein JA. An evaluation of complications, revisions, and long-term aesthetic outcomes in nonsyndromic metopic craniosynostosis. Plast Reconstr Surg. 2014;133:1453–63.

Pediatric Enucleation, Evisceration, and Exenteration Techniques

41

Femida Kherani, Sonul Mehta, and James A. Katowitz

Replacing lost orbital volume after surgical removal of an eye in a child is essential to maintain normal bony growth. Without an ocular implant of sufficient size, orbital and facial hypoplasia will be the result. A variety of ocular implants have been devised as replacements for this loss of orbital volume.

Implants: Past and Present

A vast array of materials has been used as ocular implant materials to restore the orbital volume after the loss of an eye. Hollow glass and gold spheres were initially used as ocular implants. In the late 1800s and early part of the 1900s, some ophthalmologists felt that the glass and gold implants were not optimally tolerated by the periocular tissues and began experimenting with other materials. Implants made of rubber, silver, platinum, aluminum, Vitallium, paraffin, agar, peat, sponge, cotton, wool, silk, asbestos, cork, ivory, and catgut were all tried. Others sought a more "natural" approach and tried fat, bone, and cartilage. Even transplantation of rabbit eyes into humans was tried. This was first reported by Chibret in 1885 and continued well into the 1900s, but the search for a better implant continued.

F. Kherani
Department of Surgery, University of Calgary, Calgary, Canada

Department of Ophthalmology, University of British Columbia, Vancouver, BC, Canada

S. Mehta (✉)
Division of Oculo-Facial Plastic and Reconstructive Surgery, Department of Ophthalmology, Hospital of the University of Pennsylvania, Philadelphia, PA, USA
e-mail: sonulmehta@gmail.com

J.A. Katowitz, MD, FACS
The Children's Hospital of Philadelphia and The Edwin and Fannie Gray Hall Center for Human Appearance, University of Pennsylvania, Philadelphia, PA, USA
e-mail: katowitz@email.chop.edu

The years following World War II saw the introduction of a wide array of new implant materials, shapes, and techniques. Polymerized methyl methacrylate (acrylic) was developed and marketed around 1937. This new plastic compound allowed for the development of a tremendous number of implant shapes and the combination of different materials. Prior to 1941, all the implants were completely buried. In 1941, Ruedemann introduced a new era of implants, the exposed-integrated implants (motility implants) [1]. His first implant was a combined ocular implant and prosthesis. Because of numerous difficulties with prosthesis alignment, extrusion, and the custom nature of the implant, it was abandoned. But the concept of an implant that was attached to both the extraocular muscles and prosthesis remained. Integrating the muscles with the implant improved prosthesis mobility, as did the direct coupling of the prosthesis to the implant. Following the Ruedemann implant, a wide assortment of integrated implants were developed [2]. In the mid-1940s, acrylic implants covered with tantalum mesh were introduced. The tantalum mesh provided a means of attaching the muscles directly to the implant. A whole series of "peg" implants evolved. These had a hole on the anterior surface of the implant that was left exposed. A peg was then placed on the posterior surface of the prosthesis which inserted into the implant. Chronic infections with purulent discharge, recurrent granulomas, and eventual extrusion caused these implants to fall into disuse.

Around the same time, buried, integrated implants were also being designed. The hope was to avoid the infections and extrusions associated with the exposed surface while maintaining good prosthetic motion. This was accomplished by constructing a means to attach the muscles to the implant either by a meshwork or by tunnels, completely burying the implant within the muscle cone and modifying the shape of the surface of the implant, so the posterior surface of the prosthesis would "fit" over the surface contours without being directly coupled to it. In 1945, a "basket" implant was designed. This was a buried implant in which the muscles were passed through tunnels in the implant, imparting motion

© Springer International Publishing AG 2018

J.A. Katowitz, W.R. Katowitz (eds.), *Pediatric Oculoplastic Surgery*, https://doi.org/10.1007/978-3-319-60814-3_41

to the implant. The prosthesis had a central raised area on the posterior surface that matched the impression (the "basket") of the underlying implant, thus transmitting the motion to the prosthesis. Numerous other variations followed. A novel design concept was produced by Troutman in 1949. Both the implant and prosthesis had a magnet incorporated into them, essentially coupling the two together [3]. In 1957, modifying an earlier implant, Allen developed an implant that has become a classic. Four projections were placed on the anterior surface. Tenon's and conjunctiva layers were closed over these projections, creating four mounds of tissue. The ocular prosthesis had corresponding depressions on its posterior surface, coupling the two. A later version, the Iowa implant, first used in 1957, and a still later modification, the Universal implant, are both still in use today [4–6].

Silicone was introduced during the mid-1950s. Because of its soft, pliable nature, a new series of implants was created. A very light, hollow sphere with a silicone mesh surface was designed by Uribe in 1966. In 1967, Iliff devised an inflatable silicone implant. This was followed by Soil, who used an inflatable implant. The implant volume could be increased postoperatively in the office by injecting a solution into the implant. Over time, most of these designs were abandoned. A few of the reasons for this were pressure point erosion through the conjunctiva, implant displacement due to the weight of the implant or shape, and extrusion due to infection of the exposed implant variety (50–80%) [7–9].

The classic spherical shape has persisted as an effective implant with minimal complications. Acrylic and silicone spheres are still probably the two most common materials in use. Modifications in the surgical implantation technique have significantly reduced extrusion rates with these two materials [10].

Porous Implants

Two new materials recently entered the ocular implant market: hydroxyapatite (HA) and porous polyethylene (PPE) (Fig. 41.1). The hydroxyapatite implant was introduced in 1985 by Perry (Bio-eye, Integrated Orbital Implants, San Diego, CA), and the porous polyethylene was introduced in the mid- to late 1980s (Porex Surgical, College Park, GA) [11]. The design advantage of both these implants is their porous nature. There is actual fibrovascular ingrowth into the implant, thus truly integrating the implant into the orbital tissues [12]. The ingrowth of the fibrovascular tissue is thought to make these implants more resistant to migration, extrusion, and infection.

The HA implant may be inserted wrapped or unwrapped. The unwrapped HA implants, however, have a much higher surface exposure rate. The cause of the erosion is likely due to multiple factors, but one of the reasons is the rough surface of the HA implant, which causes it to erode through the thin conjunctiva and Tenon's layers [13–16]. Thus, most surgeons wrap the HA implant prior to insertion.

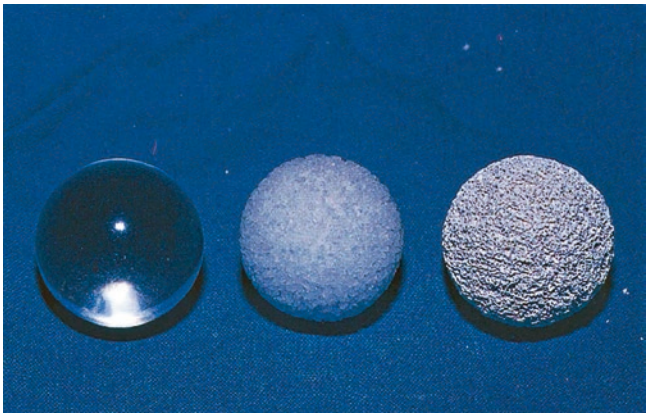


Fig. 41.1 Ocular implants. Acrylic, porous polyethylene, hydroxyapatite (from *right* to *left*)

Hydroxyapatite appears to be biocompatible, nonallergenic, nontoxic, and nonbiodegradable [17–21]. When implanted into soft tissue, the porous HA matrix is infiltrated by host fibrovascular tissue [22–24]. The extraocular muscles can be directly attached to the wrapping material of the implant, producing very good implant movement. Following complete vascularization of the implant, a hole can be drilled into the implant and a motility peg placed, directly coupling the implant to the prosthesis, thus maximizing the prosthetic motility.

The porous polyethylene implant also has the advantage of allowing fibrovascular ingrowth of the implant [23, 24]. It, too, can be inserted either wrapped or unwrapped, but there has not appeared to be an increased exposure rate in the unwrapped state. Thus, an advantage of the PPE implant is that wrapping the implant is not required. The material is soft enough to allow direct suturing of the muscle onto the surface of the implant, producing excellent implant motility. A system that utilizes a titanium peg that can be placed into the anterior surface of the implant and couples the implant and prosthesis has recently been developed, and this system further improves prosthetic motility. The PPE appears to be biocompatible, nonallergenic, nontoxic, and nonbiodegradable.

Early results with both of these implants are very encouraging, but it takes many years to accurately assess the success and failure rates of a new design. A recent report utilizing a synthetic bioceramic implant wrapped in polyglactin mesh has also been promising (FCI, Cedex, France) [25]. More anterior placement of the rectus muscles also appears to reduce exposure problems with the mesh. There have also been concerns regarding the transmission of HIV virus or even prions from sclera or dura [26–30].

Dermis-Fat Grafts

Dermis-fat grafts (DFG) are often not thought of as ocular implants, but in children, a DFG is an excellent primary choice to consider. The extraocular muscles can be sutured directly to the graft, increasing its motility. The significant graft atrophy that is sometimes seen in adults' sockets following DFG placement is unusual in the pediatric socket. There have even been cases where the DFG has grown too much in the pediatric socket and has later needed to be debulked [31]. As one can see in the in the following list of "ideal" implant characteristics, the DFG demonstrates many of these properties.

The "Ideal" Implant

With 110 years of experience and a plethora of materials that have been implanted in the orbit, the "ideal" implant should offer the following:

1. It should be easy to use and readily available.
2. It should compensate for the volume loss of the eye in a manner that imitates the natural condition as closely as possible.
3. The implant should become incorporated within the orbital tissues and have a direct attachment to the extraocular muscles.
4. It should allow for maximum movement of the prosthesis, thus maximizing the rehabilitation potential of the patient.
5. The implant should be biocompatible and should not cause any inflammatory, rejection, allergic, or carcinogenic reactions by the tissues.
6. The material should not be biodegradable.
7. It should not cause a fibrotic reaction that could lead to a contracted socket.
8. Complications related to the implant should not occur. No extrusions, exposures, infections, or displacements of the implant should result.
9. It should provide maximal stimulus for growth of the bony orbit and facial structures.

The Reconstructive Plan

Orbital Growth

The early growth of the face and orbital area in the child is rapid. At 3 months of age, the face is only about 40% of that of an adult. But at 2 years it has reached approximately 70% of the adult dimensions and by 5.5 years attains 80% of its adult size. An anophthalmic orbit or an orbit with a severely microphthalmic eye can have devastating effects on the bony orbital growth and affect the overall facial development. Orbital soft tissue volume is a critical factor in orbital bone development. Therefore, replacing the orbital soft tissue volume is essential in continued orbital bone growth. This should be kept in mind when choosing an implant. For example, in a 6-month-old child who is being enucleated, a solid or porous implant would have to be relatively small because the orbit is small. Such a small implant will have an adverse effect on the overall orbital growth. To compensate for a small implant and to provide adequate orbital volume, an increasingly larger prosthetic shell will be required. This anteriorly placed shell will not have the same stimulatory effect as an appropriate-size implant, and the larger prosthesis will ultimately produce another set of problems, such as reduced motility, increased lower lid laxity, and increased discharge due to a suboptimal fit.

Ocular Implants in Younger Children

Patients younger than 5 years of age have typically received a nonporous implant as this has facilitated easier replacement with a larger porous implant later in childhood or adolescence. In children 3 years of age and under who undergo an enucleation, most of the oculoplastic contributors in this text prefer dermis-fat grafts as the primary ocular implant. At less than 3 years of age, the orbit still needs to undergo significant growth. Autogenous dermis-fat grafts have been shown to stimulate orbital growth in infants and children, often resulting in near normal orbitofacial development [32]. The grafts tend to grow as the child grows and in many cases obviate the need for additional volume augmentation when the child is older. The DFG seems to simulate the forces that were provided by the globe. Therefore, in children 3 years of age or less who need an implant (due to retinoblastoma, trauma, congenital problems, etc.), a dermis-fat graft is an excellent choice.

Between 3 and 6 years of age, recommendations vary as to which is the best implant to use. The orbit still has a significant amount of growth to undergo. A DFG offers all the previously mentioned advantages and is an excellent implant choice in this age group. However, the orbit is bigger and can accommodate a larger implant, so some surgeons prefer to insert a spherical implant. Some authors prefer a spherical nonporous implant for children less than 5 years of age preferably wrapped nonporous sphere implant (PMMA, silicone), at least 16–18 mm diameter centered within the muscle cone [33–35]. There has, however, recently been a reported use of hydroxyapatite porous sphere implants used in children as young as 4 months. Based on this study of over 531 children treated with HA implants following enucleation, the ideal HA

implant size for a patient less than 4 months was 16 mm, 4 months to 1 year was 18 mm, 1–2 years of age was 18–20 mm, and greater than 2 years of age was 20 mm [36].

This brings up another concern, however, that in this younger age group, there is the distinct possibility that additional surgery may be required at a later date. Depending on the original problem, this may be due to tumor recurrence or the need to replace a small implant with a larger implant for volume considerations. If a porous or solid implant is used in a young child, the problem, as mentioned previously, involves the need to place the maximum size implant that can fit into a small, developing orbit. A small implant may not provide sufficient stimulation for orbital growth or in later years become a volume deficiency problem. A porous implant can also be very difficult to remove because of the fibrovascular ingrowth into the implant. The surgeon may want to consider the porous implant better as a permanent implant and, if additional surgery is a future possibility, recognize that either a DFG or a nonporous implant would be considerably less damaging to the orbital contents if additional surgery was in fact required.

In considering the possibility that additional orbital volume augmentation might be required in the future, a secondary implant can be placed in a socket that has had a DFG placed previously. In the infant or child, the DFG usually provides all the volume augmentation needed, as previously mentioned, and in some instances has even required debulking [31]. If, in a rare situation, there is still a need for volume augmentation, then after the graft has had time to completely heal, the DFG can be split open and a secondary implant of the desired size inserted behind the graft. The dermis is then sutured closed. An alternative is to place hydroxyapatite or other materials through a subperiosteal incision to increase mass behind the DFG [21]. With the advent of hydrogel expanders, however, the solution to the problem is even simpler, since a much smaller incision can be made in the dermis to allow a small, dehydrated spherical expander to be placed deep intraconally. The wound is then secured with 2 sutures of 5–0 Vicryl. The spheres range in hydrated volume from 2 to 5 mL which expands from a 5 to 8 mm diameter range dehydrated to from 16 to 22 mm when hydrated.

Tissue Expanders

In cases of early childhood enucleation, tissue expanders have been used to stimulate orbital bony growth. In the past inflatable expanders were used, but our preference today, again, is for osmotic hydrogel expanders if there is significant orbital and fissure asymmetry that requires intervention (see Chap. 39 for more details).

Ocular Implants in Older Children

In children older than 6 years of age, the orbit has reached 80% or more of its adult dimensions. Porous implants offer particular advantages to this age group. An adult-size implant can be used, and the advantages of the porous implants over the solid implants have been discussed. Dermis-fat grafts can still be used in this group, but orbital growth is less of a concern [32].

Special Situations

Solid implants, acrylic and silicone, are still used by many surgeons and have a consistent success rate [10]. They do not offer the theoretical advantages that the porous implants offer, but in trauma settings or conditions that may require implant removal in the future, the solid implants (acrylic and silicone) have their own advantages. Their smooth surface makes them easy to insert, and the lack of fibrovascular ingrowth makes them easy to remove if necessary. In the trauma setting where additional orbital reconstructive surgery may be needed, the surgeon should consider the ease of implantation and removal of these implants, should this be necessary. In the severely traumatized orbit, future volume augmentation may be required, bony reconstruction may be needed, and significant scarring and tissue contraction may occur. All these forces can cause an implant to become displaced or to extrude. Porous implants can be very difficult to remove, requiring sharp dissection.

Thus, the type of implant chosen should take all the abovementioned factors into consideration. Throughout the years, numerous authors have published their results using differing implant types and techniques, often with confusing and conflicting results. There are always multiple factors contributing to the success of any surgery. Besides the type of implant used, the surgical technique, the use of a wrapping material, and the type of material used all are extremely important. Studies examining the techniques and materials need to be continued to help us advance our technology. The DFG and the porous ceramic implants have yielded excellent results for the authors of this chapter.

Specific Procedures

Enucleation

One must be meticulous in identifying the correct eye for enucleation. It is recommended that numerous check systems be employed to eliminate the devastating event of removing the wrong eye. One suggestion is to employ a system that checks which eye is to be removed at several different stages.

First, the nurse in the preoperative staging area asks the patient or parents which eye is to be removed and reviews the operative consent. If both the consent and patient are in agreement, the nurse places a small mark with a skin-marking pen above the brow of the eye to be enucleated. When the patient is brought back to the operating suite, the anesthesiologist again asks the patient which eye is to be removed. The circulating nurse witnesses this, checks for the correct location of the skin mark, and checks the operative consent. The final check is by the surgeon, reviewing the medical record and checking for the correct location of the skin mark over the eye to be enucleated. The patient is then examined. In cases of trauma, it is often obvious which eye is to be removed. However, in cases involving a retinoblastoma, for example, it may not be obvious. In such cases only the eye with the tumor is dilated, and indirect ophthalmoscopy is performed for tumor identification. Once the tumor is identified, the eye to be removed is then marked. Such a system of numerous checks guards against wrongful removal of a nondiseased eye.

The enucleation procedure is a relatively standard technique with the incorporation of minor personal variations. In prepping and draping the patient, the entire midface is exposed in the surgical field. This is very useful when soft tissue or eyelid work also needs to be performed, as in trauma cases. A plastic eye shield is placed in the nondiseased eye for protection. Traction sutures are placed at the lid margins of the operative eye. The superior and inferior fornices are preserved by the placement of a double-armed silk suture passed from the conjunctival surface full thickness through the lid and tied externally. A 360° conjunctival peritomy is made around the limbus. The medial and lateral rectus muscles are hooked, tagged with a double-armed 5–0 Vicryl suture, and severed from the globe with the Bovie cautery (using the Colorado Needle tip) (Fig. 41.2). A traction suture is placed on the globe at the stump of the insertion of both the medial and lateral recti. The inferior rectus and superior rectus are located, tagged, and severed from the globe. The inferior oblique and superior oblique are located and severed from the globe. These can also be tagged with a suture for attachment to the implant if desired.

Once all the muscles have been removed from the eye, the optic nerve is cut and the eye is removed. Various methods

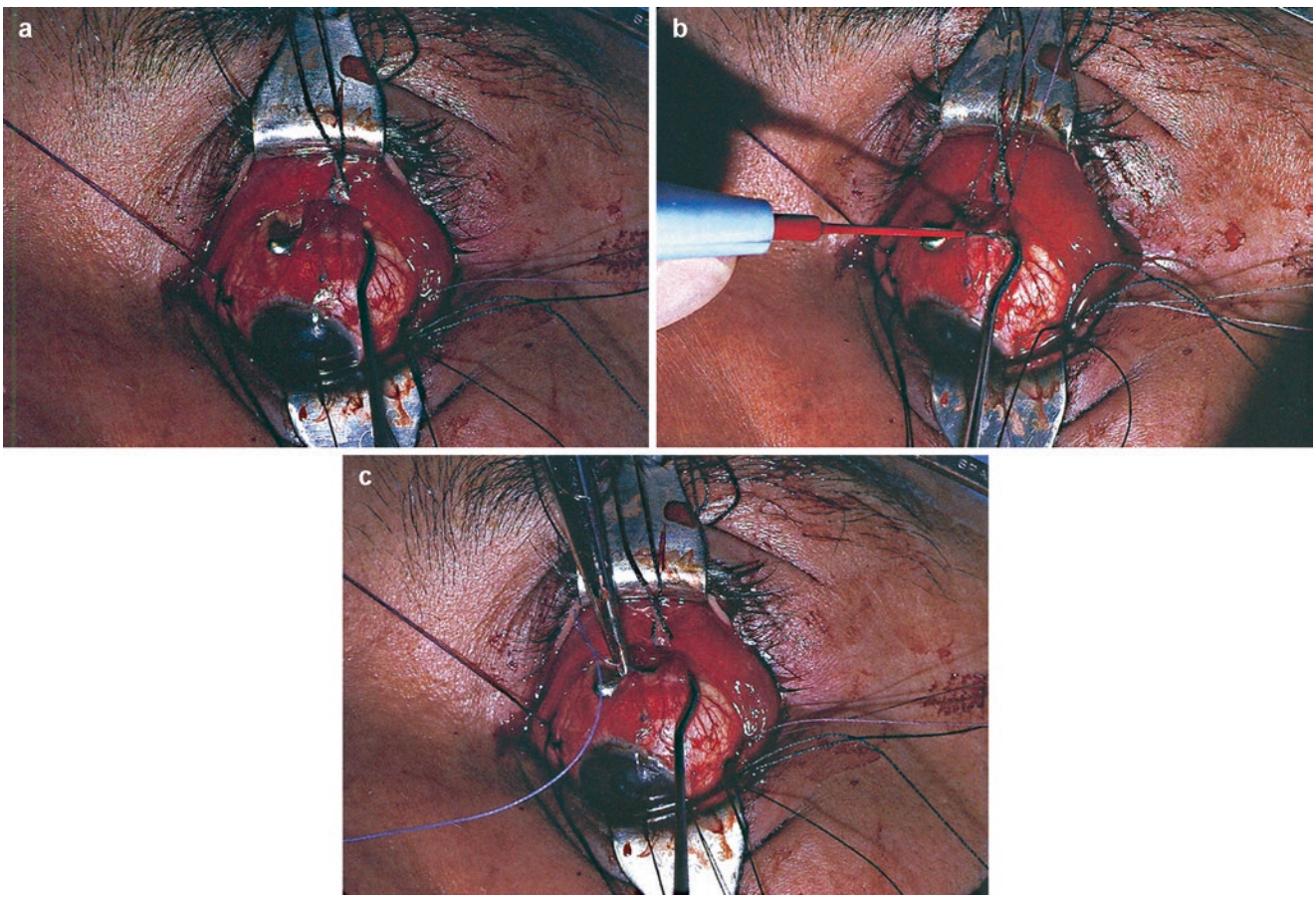


Fig. 41.2 Enucleation procedure. (**a**) Superior rectus muscle is isolated on the muscle hook. (**b**) The muscle is tagged with a 5–0 Vicryl suture. (**c**) The muscle is severed from the globe with a monopolar cautery using the Colorado needle tip

can be used to control bleeding from the cutting of the optic nerve. The nerve can be clamped for several minutes prior to cutting it. This technique should be avoided in situations involving an intraocular tumor, such as a retinoblastoma, where malignant cells may be pushed farther down the nerve. Another technique is to pack the socket with iced gauze pads immediately following the removal of the eye and apply pressure for 5 min. The gauze pads are gently removed, and the socket is examined for any signs of bleeding. If bleeding is present, the socket is again packed with iced gauze pads for 5 min. If bleeding is still present, which is unusual, the bleeding sites are located and cauterized with the bipolar cautery. Cautery is kept to a minimum to avoid extensive tissue damage and, if the optic nerve stump is cauterized, to avoid proximal nerve tissue injury. Additionally, gel foam soaked in thrombin can also be placed over the severed optic nerve to aid in hemostasis and left in the orbit.



Fig. 41.4 Dermis-fat graft. The epithelium has been removed from the surface of the graft area

Dermis-Fat Grafts

Harvesting

Even in the infant, a dermis-fat graft can be harvested. An accessible site is the lateral buttock area, which usually provides ample tissue even in the slimmest or youngest of patients (Fig. 41.3). Once the donor site is determined, the epithelium needs to be removed. This can be done by sharply dissecting the epidermis off exposing the dermal tissue, or various methods of dermabrasion can be employed, yielding pinpoint bleeding of the abraded dermis (Fig. 41.4). A 1- to 2-cm plug of dermal tissue with attached fat is desired. After the epidermis is removed, a scalpel blade is used to make a full-thickness dermal incision. The fatty tissue is bluntly and sharply dissected until the desired amount of fat is obtained. A larger diameter of fat is generally removed around the dermis graft. Care is taken to minimize the trauma to the graft. Excessive trauma to the graft will increase the amount of graft atrophy. To help stabilize the fat cell membranes, one author soaks the DFG in 50 units of regular insulin in 100 mL of normal saline. Once the graft is removed, the wound is closed primarily in layers. Deep, interrupted 3–0 polyglycolic acid sutures are used to close the deep layer. A 4–0 polyglycolic acid suture is used as either a running subcuticular stitch or as an interrupted horizontal mattress as the next layer to remove tension from the skin closure. Absorbable skin sutures are very useful in children. The skin is closed with a 5–0 fast absorbing gut suture. An alternative is a running subcuticular 4–0 Prolene or nylon suture, which is left in place for 10–14 days and then removed.



Fig. 41.3 Dermis-fat graft. The patient is positioned for harvesting a graft from the lateral buttock area

Implantation

After the enucleation has been completed, the DFG can be placed into the socket (Fig. 41.5). The volume of the DFG should be slightly more than the tissue removed. The four replaced recti muscle sutures are now secured to the appropriate positions at the edge of the dermis. The two oblique muscles can also be attached to the graft if desired. Tenon's and conjunctival tissue are attached to the edge of the dermis using a running or interrupted 5–0 Vicryl suture. The conjunctiva need not be closed over the entire dermal plug. The conjunctival tissue will epithelialize over the dermis. This is very useful in situations where there is a shortage of conjunctiva. The fat will continue to prolapse until the conjunctiva is completely closed. However, excessive pressure should not be placed on the graft, and excess fat should be trimmed from the graft prior to complete closure of the conjunctiva (Fig. 41.6). An appropriate-size conformer is then placed in the socket. The conformer should not be so large as to place tension on the wound edges. A pressure dressing is applied (Fig. 41.7).



Fig. 41.5 Dermis-fat graft. An oversized graft has been obtained and is ready to be sculpted to the correct size and implanted in the socket

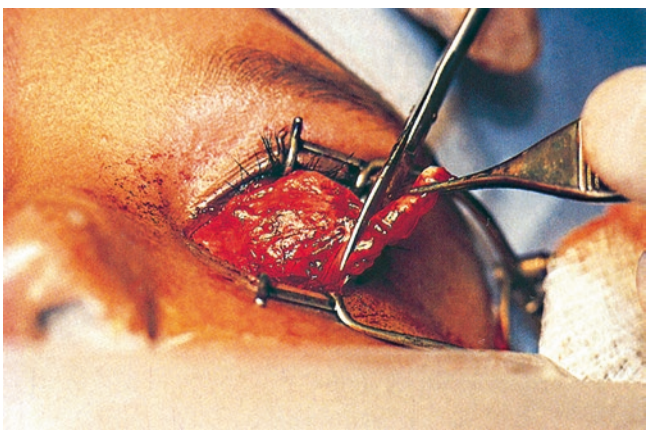


Fig. 41.6 Dermis-fat graft. Excess fat is being trimmed off of the graft prior to final closure of the conjunctiva

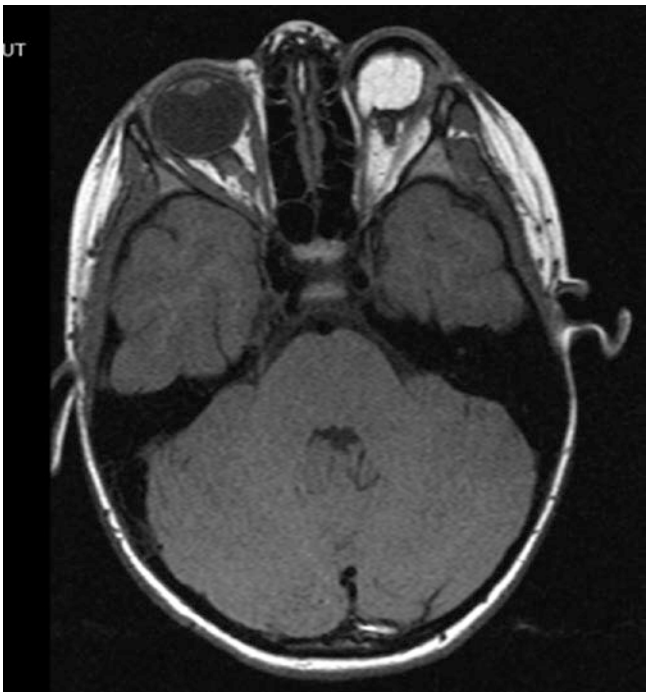


Fig. 41.7 Dermis-fat graft appearance in left orbit on MRI scan; black line over graft represents conformer shell

Porous Implant Preparation

Once the eye has been enucleated and no bleeding is present in the orbit, the chosen implant is ready to be inserted. Sizing spheres can be used to determine the most appropriate implant size on an individual basis. If the implant is wrapped, the wrapping increases the overall implant diameter by approximately 2 mm. As previously mentioned, the porous polyethylene ocular implants may be inserted unwrapped with no increased risk of implant exposure. The hydroxyapatite ocular implant should be wrapped prior to insertion to avoid the significant risk of implant exposure associated with the unwrapped HA implants. Our preference is for autogenous fascia lata as the wrapping material, when possible. If for some reason donor tissue is required, we prefer irradiated fascia lata over donor sclera for several reasons, including a reduced risk of disease transmission [34, 35].

Wrapping the HA Implant with Autogenous Fascia Lata

Autogenous fascia has several advantages over sclera [35]. It is easy to harvest, it is readily available, there is no risk of

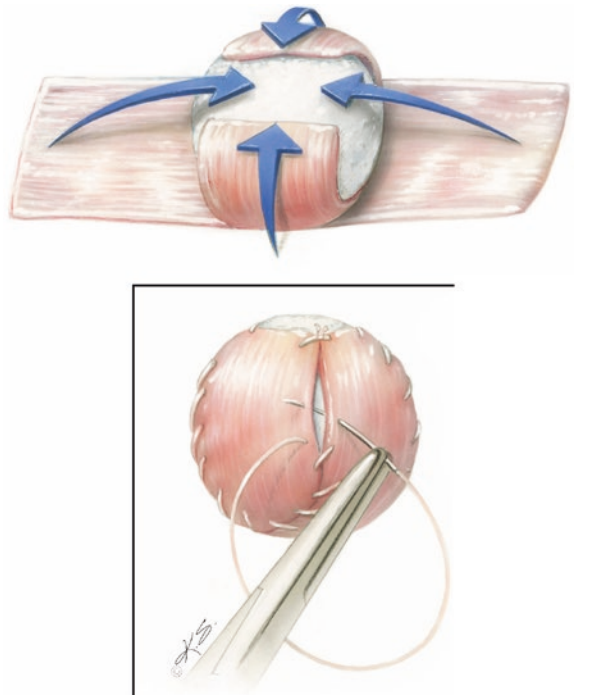


Fig. 41.8 Wrapping a hydroxyapatite implant using the crisscross technique



Fig. 41.9 A completed HA implant wrapped using the crisscross technique. Windows in the fascia have been cut for the attachment of the extraocular muscles

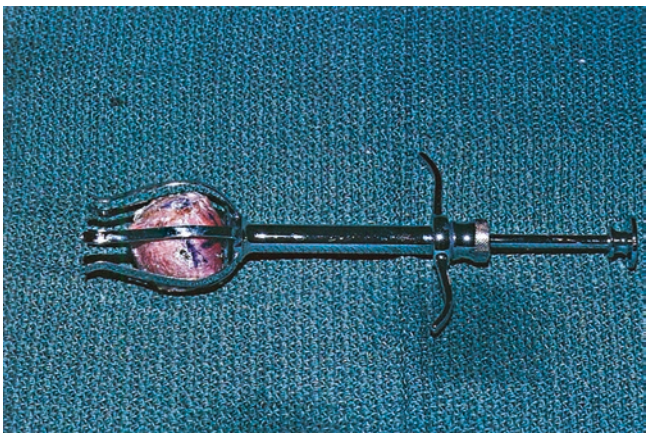


Fig. 41.10 Carter sphere inserter and a wrapped HA implant ready for implantation

acquired infection, it does not appear to resorb as donor sclera does, and it is stronger than sclera. It also offers the theoretical advantage of transplanting additional living tissue into the socket. The socket is an ideal recipient site for fascia lata, since it is grafted into the area of Tenon's tissue, which is also fascia [35].

Some authors prefer the crisscross technique when wrapping the implant with autogenous fascia [34, 35]. This technique involves using two 2 × 6-cm strips of fascia. One of the fascia strips is placed on top of the other strip, perpendicular in orientation. The implant is placed in the center of the crossed portion of the strips. The four flaps of fascia are then draped over the HA implant. The fascia is secured into position by suturing the fascia strips together with a running 4–0 Vicryl suture on the two opposite sides of the implant in a "baseball" fashion (Fig. 41.8). Windows are cut into the fascia where the recti muscles are to be inserted. The anterior surface of the implant now has a double layer of fascia covering it, adding an additional barrier to guard against implant exposure. Posteriorly, the implant is exposed to accelerate the vascularization rate, and the recti muscles will be in direct contact to the implant, enhancing the motility of the implant and optimizing the rate of vascularization (Fig. 41.9).

Recently, safer, processed fascia and processed sclera have become available as implant wrapping material (Tutoplast Fascia and Sclera, IOP, Inc., Costa Mesa CA). This donor material has been treated both chemically and with gamma irradiation. It is another option if wrapping material is desired but the patient is too young or the family is concerned about autogenous tissue harvesting.

Other options for wrapping material include Vicryl mesh or polyglactin mesh. Using a synthetic material to wrap the orbital implant decreases operating time and theoretically eliminates the potential of immunologic reaction or transmission of infectious organisms [28–30].

Implant Insertion

Any number of standard maneuvers to place the implant in the orbit can be used. The following technique is very useful. The opening in posterior Tenon's tissue is enlarged by using a blunt scissors and stretching the tissue by opening the blades. This allows the implant to be placed slightly more posteriorly in the orbit. Because of the rough surface of the porous implants, tissue adheres very readily to their surface, making implantation difficult. The Carter sphere introducer (Storz E5652) is very easy and quick to use and gives ideal implant

placement with the initial insertion nearly every time. It can be used with wrapped or unwrapped implants. The implant is loaded into the basket of the sphere introducer, and the implant is positioned in the proper orientation within the basket. The basket is placed into the orbit at the desired depth and stabilized, and then the implant is "injected" into the socket (Fig. 41.10). The implant is at the desired depth and in the correct orientation (muscle windows are oriented in the proper vertical and horizontal locations). Another method that aids in the insertion of the porous implants uses a portion of a plastic surgical drape. The implant is covered with two thin strips of the plastic drape and inserted into the socket. The plastic keeps the implant from prematurely attaching to the orbital tissue on insertion. When the implant is at the desired depth, the plastic covering is removed.

The four recti muscles (and the obliques, if desired) are now attached to the implant. The preplaced Vicryl sutures are placed through the inner surface of the anterior portion of the fascial window in wrapped implants or sewn directly to the implant in PPE implants. The muscle is then brought up into direct contact with the implant and the sutures are tied. Tenon's tissue and conjunctiva are closed as separate layers with a 5–0 running Vicryl suture. The appropriate-size conformer is placed in the socket so that there is no tension on the wound with the lids closed, and a pressure dressing is applied.

Pegging of a Porous Orbital Implant

The pegging of porous orbital implant is usually not considered appropriate for children and if desired later is deferred until the patient is old enough to care for the prosthesis and maintain regular follow-up visits as this is needed for a healthy peg. Furthermore, there has not been conclusive evidence that prosthetic motility improves with pegged implant [35].

Postoperative Management

The pressure dressing can be left in place for several days (2–5 days) and then removed. During this time, the patient is usually given oral antibiotics. When the dressing is removed, antibiotic eye ointment is applied in the socket 2–3 times a day. The socket can be fit for a prosthesis as soon as the socket heals, the sutures dissolve, and the edema subsides. The average is approximately 6 weeks but can range from 3 to 12 weeks.

Care of the prosthesis is usually minimal and depends on the amount of secretions the individual is experiencing. If the discharge is minimal or nonexistent, the prosthesis may need to be removed and cleaned only weekly or monthly. More frequent cleaning may be required if discharge is a greater problem. Contact lens cleaner can be used to clean the surface of the prosthesis and minimize the protein buildup.

Evisceration

An evisceration in a child is usually not recommended for a number of reasons. In many of the cases involving children, such as intraocular tumors, congenital microphthalmia, and anophthalmia, an evisceration is not an option. In the few cases where it may appear to be an option, the surgeon must consider the factors mentioned regarding orbital growth. This usually has involved severe trauma to the globe in an older child. The eviscerated scleral shell in a young child will be able to accommodate only a very small implant. This again can lead to a marked volume deficiency and decreased orbital growth.

Exenteration

An exenteration procedure involves removal of the entire contents of the orbit. This somewhat radical procedure becomes necessary when a malignant tumor involves the orbital tissues, such as may be needed, for example, when there is an orbital recurrence following a previously enucleated retinoblastoma.

There are several variations of the procedure that range from a complete excision of the eyelids to preservation of the lids and conjunctiva if possible [37]. If the eyelid tissue is not involved, the eyelid skin can be used in the reconstruction. This has been termed as an eyelid- sparing form of exenteration, but, in fact, this is really a misnomer as the lid margin and eyelashes are actually excised. The lid is split into its anterior and posterior lamellae (Fig. 41.11). Dissection is continued in this plane until the orbital rim is reached (Fig. 41.12). The periosteum is incised, and the dissection is directed posteriorly in the subperiosteal plane until the orbital apex is reached (Fig. 41.13). If the eyelid

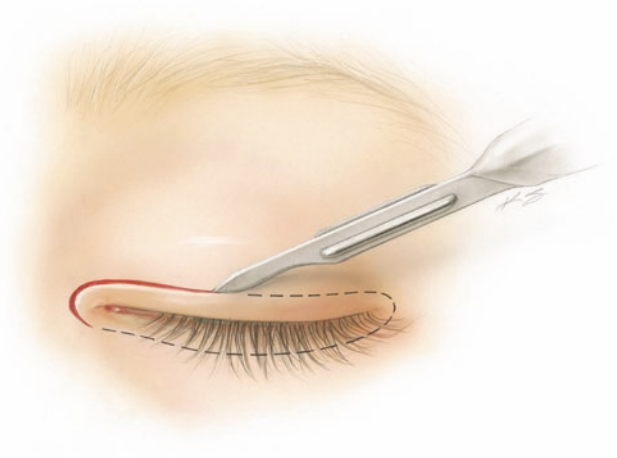


Fig. 41.11 Exenteration: lid-sparing technique. The entire eyelid margin, including the eyelashes, is excised

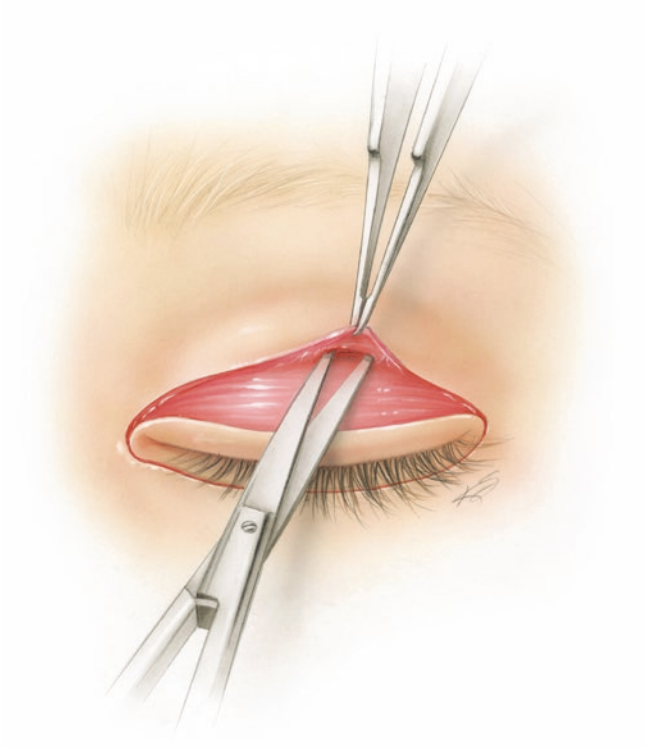


Fig. 41.12 Exenteration: lid-sparing technique. The suborbicularis plane is entered. Dissection is carried to the orbital rim for the entire orbital area

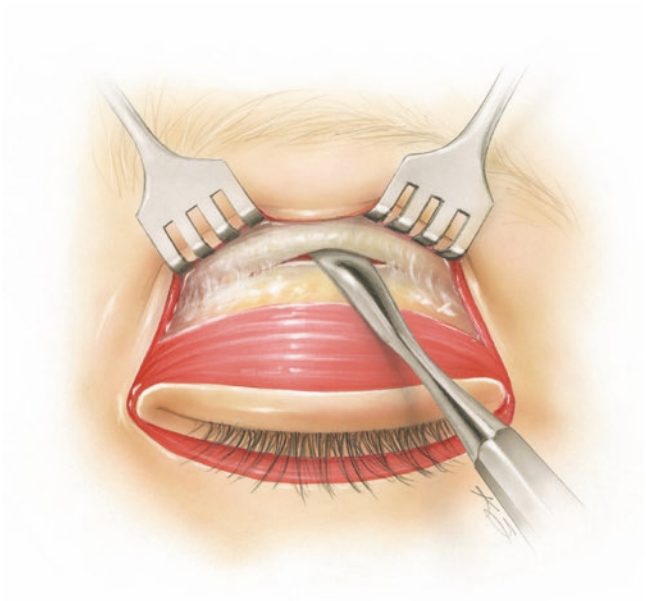


Fig. 41.13 Exenteration: lid-sparing technique. When the orbital rim is reached, the periosteum is incised, and dissection is continued posteriorly in the subperiosteal plane

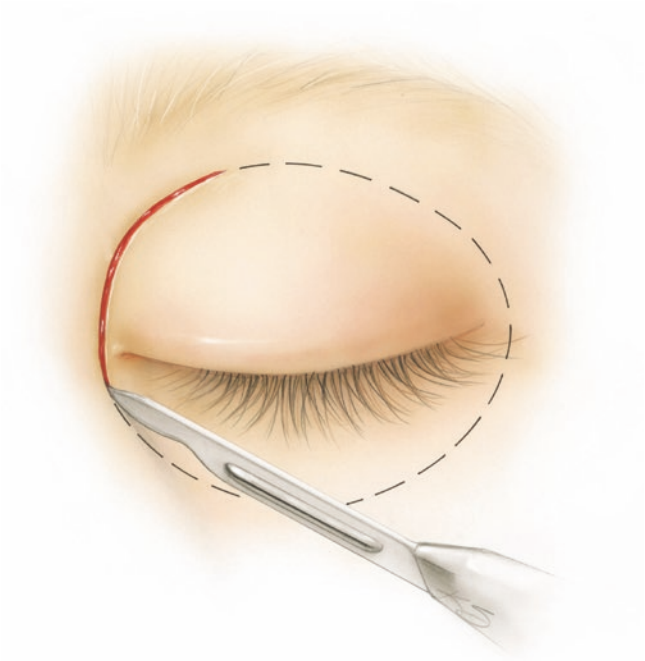


Fig. 41.14 Exenteration: lid-sacrificing technique. A full-thickness incision is made directly over the orbital rim until the periosteum is reached

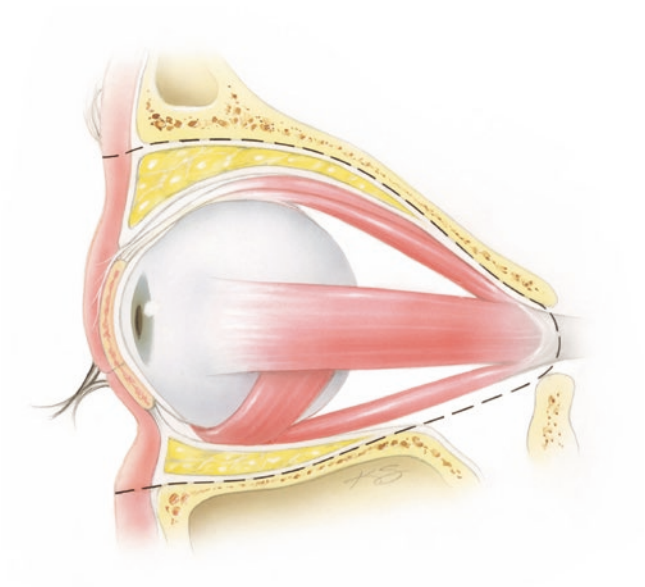


Fig. 41.15 Exenteration: the plane of dissection for removal of the entire orbital contents

skin is involved in the malignant process, the entire eyelid area will need to be sacrificed. In this scenario, the incisions must be full thickness along the orbital rim area (Fig. 41.14). A cutting cautery unit can be used. Typical areas of resistance include the medial and lateral canthal tendons, trochlea, and origin of the inferior oblique. When the orbital contents are dissected free, a clamp is placed across the apical tissues. An enucleation scissors is used to cut across the tissue and the entire contents of the orbit are removed (Fig. 41.15). Bleeding is usually brisk. The orbit should be immediately packed with iced gauze and pressure



Fig. 41.16 Left orbit after exenteration and healing by spontaneous granulation

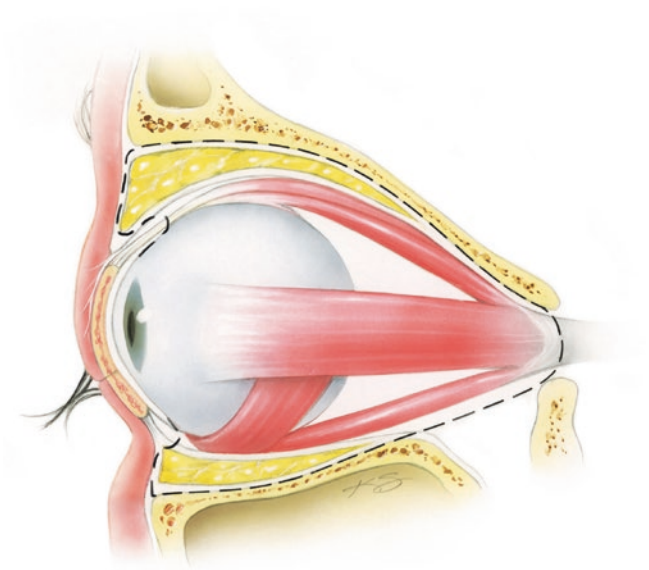


Fig. 41.17 Lid and conjunctiva-sparing exenteration. Dotted outline shows path of excision following a 360-degree limbal peritomy and stripping of periorbita to permit exenteration with retention of all eyelid structures as well as the bulbar conjunctiva and cul-de-sacs

applied. Using suction, the bleeding vessels are located and clamped, tied, or cauterized. Thrombin-soaked gel foam can also be very useful in hemostasis. It can be placed and left in the orbit.

After the bleeding has been completely controlled, a meshed, split-thickness skin graft can be placed into the orbit. It is sutured to the eyelid skin. The orbit is packed with petrolatum gauze, and a pressure dressing is applied. As an alternative, the eyelid skin can be sutured together and allowed to retract into the orbit. The orbit will granulate in (Fig. 41.16), but this can require a prolonged period of time. Reconstructive options are the same for both techniques. Temporalis muscle flaps can be used to fill in the vacant orbit on occasion. This can be done as a primary or secondary procedure. If the exenteration is due to a malignant process, it is advisable to monitor the orbit for recurrence for a period of time. If there is no recurrence, a secondary temporalis muscle transfer can then be performed at a later date. Further examples of various reconstructive and prosthetic options are discussed in detail in Chap. 8.

More recently, there have been reports of successful preservation of the eyelid margins and conjunctival lining so that a more normal prosthetic appearance can be achieved. This technique is possible only when the malignant involvement in the orbit is more posterior so that these anterior structures can be preserved without significant risk of recurrence of the malignant process [38, 39]. In our experience, the ability to wear a cosmetically acceptable ocular prosthesis afforded by this lid margin and conjunctiva-sparing technique has proven invaluable from both a functional as well as a psychosocial perspective. It is our recommendation that the lid margin and conjunctiva-sparing technique as presented here be strongly considered for similar patient profiles with posterior or intraocular malignant orbital tumors. This technique was first described in 1998 [31, 40].

The technique involves placement of a large dermis-fat graft taken from the buttock to provide volume after removal of the orbital contents. After exposing the globe with a lid speculum or lid traction sutures, a 360-degree conjunctival peritomy is performed at the corneal limbus with sharp scissors. Dissection is done in a subconjunctival plane with release of Tenon's capsule. The rectus muscles are isolated and secured with silk sutures for traction. The levator aponeurosis and Muller's muscle are resected from their posterior attachment at the border of the tarsus. Correspondingly, the lower lid retractors are also released. Dissection is then carried into a pre-septal plane and the orbital rim exposed. A fine tip monopolar cutting cautery is used to incise the periosteum circumferentially at the orbital rim. An elevator is used to enter the subperiosteal plane and strip the periorbita from the bony walls. Dissection progresses posteriorly from the orbital rim to the apex permitting removal of the orbital contents.

Hemostasis is achieved with cautery as needed (Fig. 41.17). The remaining surgical margins can be sampled as needed to rule out any residual disease. Figure 41.18 demonstrates this technique in a patient with sudden proptosis due to a rapidly growing tumor behind the left globe. A 13-month-old female child presented to CHOP with left proptosis and edema. An orbital biopsy was performed, and the pathology confirmed the diagnosis of a central primitive neuroectodermal tumor (PNET). The child underwent an eyelid margin and conjunctiva-sparing exenteration with immediate dermis-fat graft placement. Subsequent chemotherapy included vincristine, VP16, Cytoxan, and cisplatin. The child was able to successfully wear an ocular prosthesis with minimal psychosocial problems no different from that for any patient following a routine enucleation at an early age.

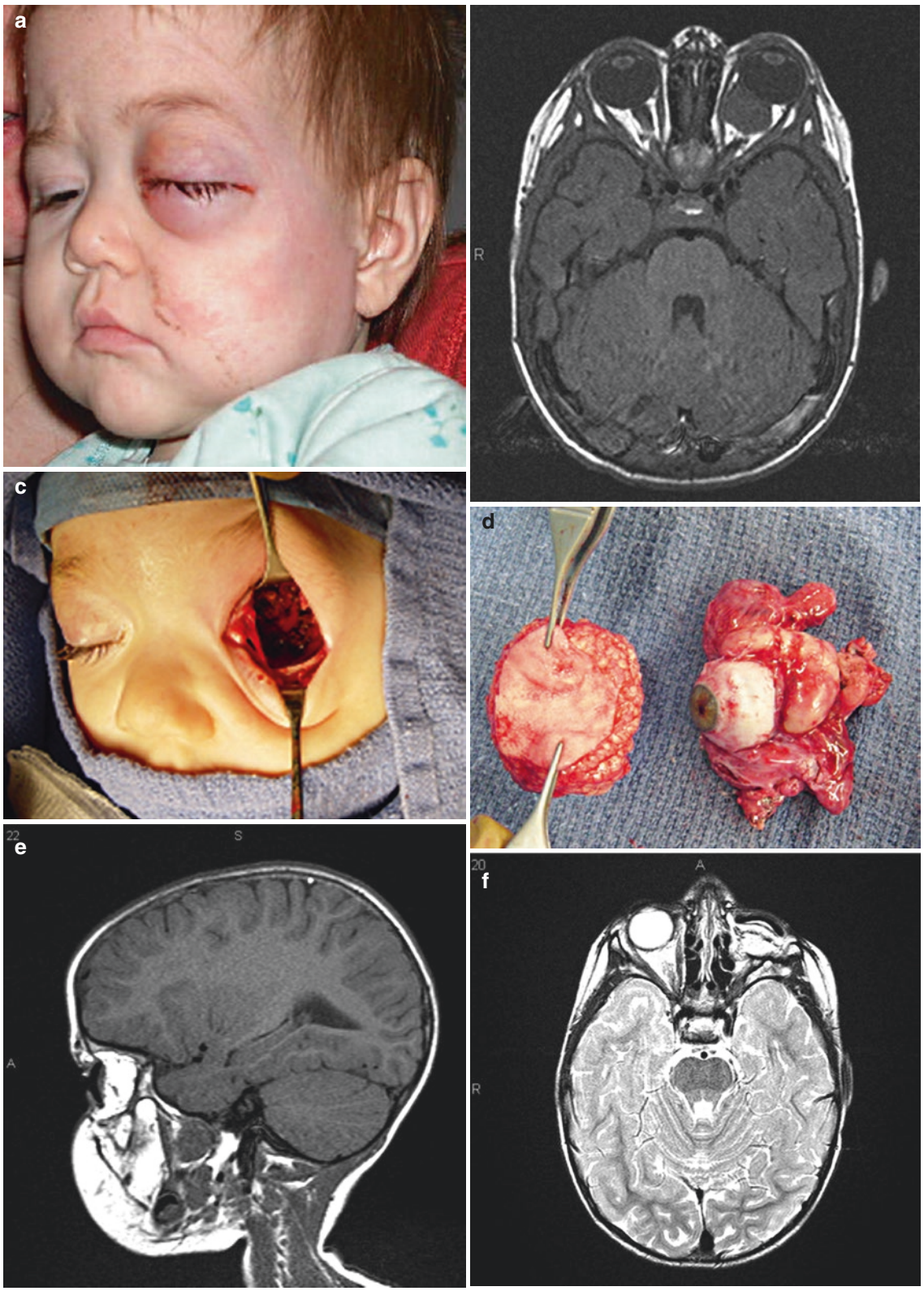


Fig. 41.18 Lid margin and conjunctiva-sparing exenteration for a 13-month-old child with a central primitive neuroectodermal tumor (PNET). (**a**) A 3-week history of left proptosis. (**b**) Retrobulbar intraconal mass on MRI. (**c**) Orbit immediately following lid margin and conjunctiva-sparing exenteration. (**d**) Orbital contents with dermis-fat graft (DFG) for immediate socket reconstruction. (**e**) Sagittal MRI scan 18 months post-op and 12 months post-chemo Rx (VP16, Cytoxan, cisplatin, vincristine) and stem cell transplant. (**f**) Axial scan 18 months post-op with no evidence of recurrence.

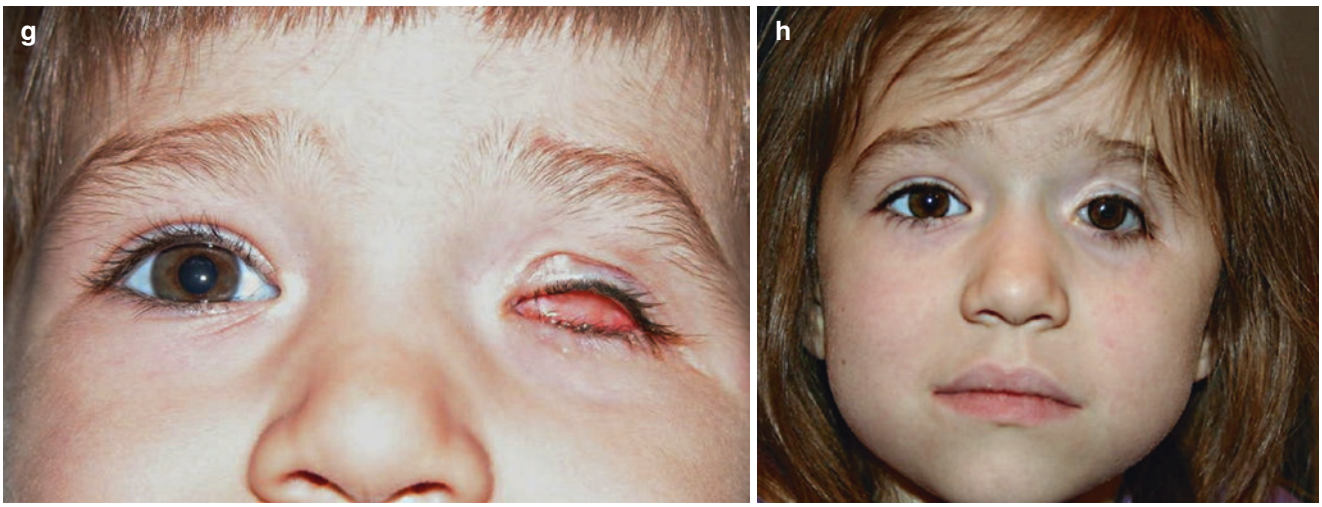


Fig. 41.18 (continued) (**g**) 18 months post-op chemotherapy and peripheral stem cell transplant; healthy DFG with normal development and neurological exam for her age at 2 1/2 years. (**h**) 4 years post-op lid margin and conjunctiva-sparing exenteration. Happy well-adjusted child with obvious psychosocial benefit from more normal appearance with this technique

The Anophthalmic Socket and Secondary Reconstruction

Despite appropriate reconstructive efforts at the time of enucleation, over time a deficiency of adequate orbital volume may develop. This often compromises the fit of the ocular prosthesis and requires additional reconstruction. If the enucleation was done at a very young age and a very small implant was placed in the socket, exchanging this implant for a larger implant may be all that is required. Dermis-fat grafts can also be used as secondary implants to augment the orbital volume either alone or in conjunction with a porous ocular implant. If a synthetic implant is already in place and is the appropriate size, a DFG can be placed over the preexisting implant. If a DFG is already in place and has healed appropriately, but the orbital volume is still inadequate, the DFG can be incised either through the center of the graft or by opening a sufficient space at the junction of the conjunctiva and Tenon's capsule with the edge of the DFG. A porous implant is then inserted posterior to the DFG for additional volume augmentation. If, despite the above measures, the orbital soft tissue is still insufficient, one can make the orbital dimensions smaller by the placement of subperiosteal implants. A subperiosteal implant, especially if placed posteriorly, will decrease the orbital dimensions; thus, the existing orbital soft tissue contents will have less space to occupy and will be shifted forward. Solid subperiosteal implants of silicone and porous polyethylene can be placed along the floor of the orbit using the surgical approach one would use in repairing an orbital floor fracture. The implant should be placed as far posteriorly as possible to decrease the anterior-posterior dimension of the orbit and shift the orbital soft tissue contents anteriorly. An alternative to the solid subperiosteal implant is the use of granular hydroxyapatite [21]. The subperiosteal space of the orbital floor is entered as in the use of the solid implants, but the granular HA can be packed into the posterior areas more readily. The desired amount of HA is placed to get the appropriate volume correction, and the periosteum is closed.

Complications

Contraction of the conjunctival cul-de-sacs can occur from trauma either pre- or postoperatively in association with loss of an eye. This can also occur if a conformer is not kept in place postoperatively before prosthetic fitting. Grafting of oral mucus membrane or use of amniotic membrane grafts may be helpful in more complex contraction, but too often are less than satisfactory.

The most common complication is extrusion of an ocular implant. Primary repair is usually insufficient, and the use of a dermis graft over the exposed implant has proven most effective in retaining a prosthesis. Removal of a porous implant can be difficult, and grinding down the exposed portion before covering it with dermis is helpful. Glass or silicone implants are easily removed if necessary, and the use of a dermis-fat graft is a useful replacement at that point.

Conclusion

The pediatric socket presents a number of issues that are not present when working with the adult socket. Both dermis-fat grafts and the porous ocular implants fulfill many of the criteria of the "ideal" reconstructive implant. Both have their advantages and disadvantages in the reconstruction of children, and both have yielded excellent results. The decision of which type of implant to use will be based on the child's age and factors discussed in

this chapter. The main issue when dealing with children is that the loss of the eye affects not just the orbital growth but the growth pattern of the entire face. The resulting facial deformity can be quite severe. Thus, the decision to remove an eye and the techniques of reconstruction are of major importance, because these choices will affect the child for the rest of his or her life.

References

1. Ruedeman AD. Plastic eye implant. Am J Ophthalmol. 1946;29: 947–52.
2. Danz W. Motility implants: a review. In: Bosniak SL, Smith BC, editors. Advances in ophthalmic plastic and reconstructive surgery: the anophthalmic socket, vol. 8. New York: Pergamon; 1990. p. 46–52.
3. Troutman RC. Five year survey on the use of a magnetic implant for improving cosmetic results of enucleation. Arch Ophthalmol. 1954:531–58.
4. Allen L, Spivey BE, Burns CA. A larger Iowa implant. Am J Ophthalmol. 1969;68:397–400.
5. Fan JT, Robertson DM. Long-term follow-up of the Allen implant: 1967–1991. Ophthalmology. 1995;102:510–6.
6. Anderson RL, Thiese SM, Nerad JN, et al. The universal orbital implant: indication and methods. In: Bosniak SL, Smith BC, editors. Advances in ophthalmic plastic and reconstructive surgery: the anophthalmic socket, vol. 8. New York: Pergamon; 1990. p. 88–99.
7. Choyce DP. Orbital implants: review of the results obtained at the Moorfields branch of the Moorfields, Westminster, and Central Eye Hospitals, London. Br J Ophthalmol. 1952;36:123–30.
8. Castrin JA. Experiences with different orbital implants after enucleation. Acta Ophthalmol. 1963;41:435–44.
9. Gougelmann HP. The evolution of the ocular motility implant. Int Ophthalmol Clin. 1970:689–733.
10. Nunery WR, Cepela MA, Heinz GW, et al. Extrusion rate of silicone spherical anophthalmic socket implants. Ophthalmic Plast Reconstr Surg. 1993;9:90–5.
11. Perry AC. Advances in enucleation. Ophthalmol Clin N Am. 1991;8:75–81.
12. Perry AC. Integrated orbital implants. In: Bosniak SL, Smith BC, editors. Advances in ophthalmic plastic and reconstructive surgery: the anophthalmic socket, vol. 8. New York: Pergamon; 1990. p. 75–87.
13. Nunery WR, Heinz GW, Bonnin JM, et al. Exposure rate of hydroxyapatite spheres in the anophthalmic socket: histopathologic correlation and comparison with silicone sphere implants. Ophthal Plastic Reconstr Surg. 1993;9:96–14.
14. Lin CW, Liao SL. Long-term complications of different porous orbital implants: a 21-year review. Br J Ophthalmol. 2017;101(5):681–685. pii: bjophthalmol-2016-308932. doi:10.1136/bjophthalmol-2016-308932.
15. Schellini S, Jorge E, Sousa R, Burroughs J, El-Dib R. Porous and nonporous orbital implants for treating the anophthalmic socket: a meta-analysis of case series studies. Orbit. 2016;35(2):78–86. doi: 10.3109/01676830.2016.1139591. Epub 2016 Feb 29
16. Mourits DL, Moll AC, Bosscha MI, Tan HS, Hartong DT. Orbital implants in retinoblastoma patients: 23 years of experience and a review of the literature. Acta Ophthalmol. 2016;94(2):165–74. doi:10.1111/aos.12915. Epub 2015 Nov 25. Review
17. Drobesk HP, Rothstein SS, Gumaer KI, et al. Histologic observation of soft tissue responses to implants, multifaceted particles and discs of hydroxyapatite. J Oral Maxillofac Surg. 1984;42:143–9.
18. Roses HM, McFarland MM. The biological behavior of hydroxyapatite implanted into the maxillofacial skeleton. Plast Reconstr Surg. 1990;85:718–23.
19. Piecuch JF. Extraskeletal implantation of a porous hydroxyapatite ceramic. J Dent Res. 1982;61:1458–60.
20. Chao SY, Poon CK. Histologic study of tissue response to implanted hydroxyapatite in two patients. J Oral Maxillofac Surg. 1987;45:359–62.
21. Kazim M, Katowitz JA, Fallon M, Piest KL. Evaluation of a collagen/hydroxyapatite implant for orbital reconstructive surgery. Ophthalmic Plast Reconstr Surg. 1992;8:94–108.
22. Ferrone PJ, Dutton JJ. Rate of vascularization of coralline hydroxyapatite ocular implants. Ophthalmology. 1992;99:376–9.
23. Rubin PA, Popham JK, Bilyk JW, Shore JW. Comparison of fibrovascular ingrowth into hydroxyapatite and porous polyethylene orbital implants. Ophthalmic Plast Reconstr Surg. 1994;10:96–103.
24. Tambe K, Pushpoth S, Mudhar HS, Sandramouli S. A histopathologic study of orbital implant vascularization. Orbit. 2009;28(1):50–7.
25. Jordan DR, Bawazer A. Experience with 120 synthetic hydroxyapatite implants (FCl3). Ophthalmic Plast Reconstr Surg. 2001;17(3):184–90.
26. Perry AC. Eradication of HIV from HIV impregnated sclera. Presented at the Annual Meeting of the American Society of Ophthalmic Plastic and Reconstructive Surgery, San Francisco, California, 29 October 1994.
27. Guidelines for preventing transmission of human immunodeficiency virus through transplantation of human tissue and organs. U.S. Department of Health and Human Services, Centers for Disease Control, Atlanta, Georgia, 20 May 1994.
28. Bedrossian EH. HIV and banked fascia lata. Ophthalmic Plast Reconstr Surg. 1991;7:284–8.
29. Michel RG, Patterson CN. Evaluation of sclera as a homograft in facial plastic and reconstructive surgery. Facial Plast Surg. 1978;86:206–13.
30. Bodian M. Repair of ptosis using human sclera. Am J Ophthalmol. 1968;65:352–8.
31. Heher K, Katowitz J, Low J. Unilateral dermis-fat implantation in the pediatric orbit. Ophthalmic Plast Reconstr Surg. 1998;14(2):81–8.
32. Katowitz JA. Orbital expansion with dermis-fat grafts in the pediatric age group. Presented at the Annual Meeting of the American Academy of Ophthalmology, Anaheim, California, 14 October 1991.
33. Crawford JS, Doucet TW. Uses of fascia in ophthalmology and the benefits of autogenous sources. J Pediatr Ophthalmol Strabismus. 1982;19:21–5.
34. Jordon DR, Anderson RL. Obtaining fascia lata. Arch Ophthalmol. 1987;105:1139–40.
35. Jordan DR, Klapper SR. Chapter 14: controversies in enucleation technique and implant selection: whether to wrap, attach muscles, and peg? In: Guthoff R, Katowitz J, editors. Essentials of ophthalmology, Orbit, vol. 3. Berlin: Springer; 2008. p. 195–201.
36. Shah SU, Shields CL, Lally SE, Shields JA. Hydroxyapatite orbital implant in children following enucleation: analysis of 531 sockets. Ophthal Plast Reconstr Surg. 2015;31(2):108–14.
37. Small RG. Exenteration of the orbit: indications and techniques. In: Smith BC, Della Rocca RC, Nesi FA, Lisman RD, editors. Ophthalmic plastic and reconstructive surgery. St. Louis: Mosby; 1987. p. 1151–64.
38. Kherani F and Katowitz J Pediatric eyelid and conjunctival sparing orbital exenteration. Canadian Academy of Ophthalmology Annual Meeting, 2005.
39. Looi A, Kazim M, Cortes M, Rootman J. Orbital reconstruction and eyelid- and conjunctiva-sparing orbital exenteration. Ophthal Plast Reconstr Surg. 2006;22:1–6. Heher KL, Katowitz JA, Low JE. Unilateral dermis-fat graft implantation in the pediatric orbit. Ophthal Plast Reconstr Surg. 1998;14(2): 81–8.
40. Handler LF, Heher KL, Katowitz JA. Chapter 30 Management of the microphthalmic orbit. In: Katowitz JA, editor. Pediatric oculoplastic surgery. Berlin: Springer; 2002. p. 576–8.

Pediatric Orbital Trauma

42

Jordan E. Hollsten, Patrick A. Gerety, Jesse A. Taylor, and Donald A. Hollsten

The pediatric age group is not immune to trauma containing enough energy to fracture the bones of the orbit and damage the adjacent soft tissue. The mechanisms are often unique (Fig. 42.1). Management of pediatric orbital trauma utilizes most of the concepts and techniques learned in the management of adult orbital trauma, but differences do exist. The facial skeleton of a child is less mature and differs in proportion from the adult facial skeleton. The paranasal sinuses are incompletely developed. The very young child who has been seriously injured can be very difficult to examine, so an accurate assessment of the visual system is more difficult to obtain. Finally, any visual compromise risks the development of amblyopia. These factors combine to make management of orbital trauma in the pediatric population particularly challenging.

Following preservation of life, preservation of vision should be the foremost in managing the severely injured child. Injury to the facial skeleton can result in a variety of sight-threatening injuries involving the orbit. Early and appropriate intervention can positively influence the final visual outcome. The purpose of this chapter is to familiarize the physician with the evaluation of the injured orbit and management of those injuries.



Fig. 42.1 Screen door handle impaled left lower lid. The handle of a screen door is impaled in the lower lid and orbit of this 6-year-old male. The handle passed under the globe, through the orbital floor into the maxillary sinus, and through the posterior wall of the sinus

Ocular Exam

The history of the injury usually provides a substantial number of details to assist with management decisions when the orbit has been traumatized. The cause of the injury and character of any projectile or blunt object that struck the orbit should be determined, if possible. The extent of injury created by the trauma is directly proportional to the force; the amount of penetration, if any; and the adjacent tissue damage caused by the penetrating object. A sharp object will cause less surrounding damage than a blunt, penetrating object, for example. This information can be used to guide clinical judgment concerning the extent of damage and any treatment required. A vital piece of information to obtain in the history is the status of the vision immediately after the injury. This cannot be overemphasized. Was there vision loss? If so, was the loss gradual or sudden? Was the loss total or incomplete? The pediatric patient's injuries and age may prevent accurate history taking. However, parents or older siblings are often witnesses to the injury and can provide helpful information.

J.E. Hollsten (✉)
Ophthalmology, Plastic and Reconstructive Surgery, University of Texas Health Science Center at San Antonio, San Antonio, TX, USA
e-mail: jhollsten@gmail.com

P.A. Gerety
Department of Surgery, University of Indiana and Riley Hospital for Children, Indianapolis, IN, USA

J.A. Taylor
Plastic Surgery and Craniofacial Surgery, Department of Surgery, Children's Hospital of Philadelphia, Philadelphia, PA, USA

D.A. Hollsten
Ophthalmology, Plastic and Reconstructive Surgery, University of Texas Health Science Center at San Antonio, San Antonio, TX, USA

© Springer International Publishing AG 2018

J.A. Katowitz, W.R. Katowitz (eds.), *Pediatric Oculoplastic Surgery*, https://doi.org/10.1007/978-3-319-60814-3_42

A brief ocular exam is essential. As a minimum, the exam should attempt to determine the visual acuity, status of the pupils, and ocular motility. A standard visual acuity with an eye chart or near vision card is preferable. A 2009 article found that visually asymptomatic patients do not have ocular injuries requiring emergent evaluation [1]. There is evidence, however, that 50% of pediatric patients with orbital fractures have associated ocular injuries, so it is still necessary to perform as complete an ophthalmic examination as is safely possible in the acute situation [2]. It may be necessary to manually separate the lids to obtain a visual acuity, but if there is any concern regarding globe rupture, extreme caution is wise and may dictate the use of local or general anesthesia. A lid retractor is often helpful for separating the eyelids. A bent paper clip or Desmarres retractor can also be used. In the younger pediatric patient, the ability to fixate on and follow a target is ascertained, if possible. The response of the pupils to light should be determined. The presence of an afferent pupillary defect indicates optic nerve or diffuse retinal damage. The injured child may be unable to cooperate adequately for the determination of an accurate visual acuity. In this circumstance, the pupillary response is the best indicator of the visual status.

An external exam of the lids and adnexa is performed quickly, providing valuable information. The integrity of the eyelids, including the position of the medial and lateral canthal tendons, is determined. Gentle manipulation of the soft tissue with cotton-tipped applicators is usually possible. Lacerations are examined closely. Lacerations penetrating the orbital septum usually have orbital fat in the wound, which should alert the examiner to the possibility of deeper, more severe trauma. This may involve retained foreign bodies deeper in the orbit, penetration of the globe, or even neurosurgical damage with penetration into the anterior cranial fossa via the orbital roof or into the middle cranial fossa via the deep lateral wall of the orbit and superior orbital fissure.

After the lids are separated, a brief assessment of the integrity of the globe can be made. A shallow anterior chamber indicates anterior globe rupture or penetration. A deep anterior chamber indicates a loss of globe integrity posteriorly. The motion of the globe can be quickly assessed if the patient is alert and cooperative. If the child's level of consciousness does not allow for direct evaluation of globe motility, forced ductions are necessary. In the pediatric patient, it is usually not possible to perform this test in the office, but it can be done if the child is placed under general anesthesia for any reason. Forced ductions are contraindicated if there is suspicion of a ruptured globe. A positive result indicates either severe orbital edema or entrapment of orbital soft tissue.

Imaging the injured orbit is essential to adequately assess the integrity of the globe and surrounding structures. The ready availability of computed topographic (CT) scans has largely replaced plain film x-rays in evaluating orbital trauma [3]. Magnetic resonance imaging (MRI) is also readily available and offers some advantages over CT scans. The orbital soft tissue is shown in much greater detail. Furthermore, nonmagnetic foreign bodies are revealed more easily with MRI scanning [4]. CT scans are still superior for the evaluation of orbital bone damage, localization of magnetic foreign bodies, and localization of nonmetallic but still radio-opaque objects. When evaluating orbital trauma, it is recommended that CT scans be obtained first, to reveal the presence of any fractures. If greater soft tissue details are needed, an MRI scan of the orbit can then be obtained (see Chap. 32). The younger pediatric patient will require some level of sedation to undergo these exams.

The traumatized orbit is best imaged with thin axial and direct coronal CT scans through the orbit [5]. The spiral CT scan is rapid enough that it may not be necessary to sedate the pediatric patient [6]. These patients are frequently immobilized for C-spine safety, however, and it is often not possible to obtain direct coronal views. It has been suggested that the best protocol is to obtain thin-section axial CT scans, 0.625–1.25 mm. A multiplanar reformation can then provide different views. A three-dimensional reformation is a useful tool when an orbital fracture is present [5].

Close communication between the physician managing orbital trauma and the radiologist is essential. Routine scans of the brain, face, or sinuses do not provide enough data to enable the physician to make proper clinical decisions when managing orbital trauma. The physician should insist that the proper views and scans, as described above, be obtained as the initial study. In this way, unnecessary returns to the CT scanning suite and delays in initiating therapy can be avoided.

Penetrating Orbital Injuries

Penetration of the orbital soft tissues with a foreign body has very serious potential complications. Not only is the integrity of the globe threatened, but it is also possible to penetrate the cranial vault through the orbit. It is, therefore, safest to assume that an intracranial injury is present with all penetrating orbital injuries until proven otherwise. The energy and size of the penetrating object will determine the severity of the damage [7]. A sharp object or a minute particle, such as a sliver of metal generated by metal-on-metal pounding, may penetrate the orbit and globe with minimal disruption of the immediately surrounding tissue, thus creating little collateral damage and leaving a reasonable possibility of repair with preservation of vision. In contrast, blunt objects or high-velocity projectiles, such as a bullet, can blind the eye without directly contacting the globe.

Dividing penetrating orbital trauma into low-energy trauma versus high-energy trauma is a clinically useful concept. Since not all penetrating objects are associated with significant collateral damage, therapeutic options and expectations are different. Penetrating objects that are small in size or of relatively slow speed cause less surrounding damage. In this category would be most projectiles propelled by the human hand, BBs, pellet gun projectiles, and particles small enough to lack sufficient energy to visibly disrupt the globe

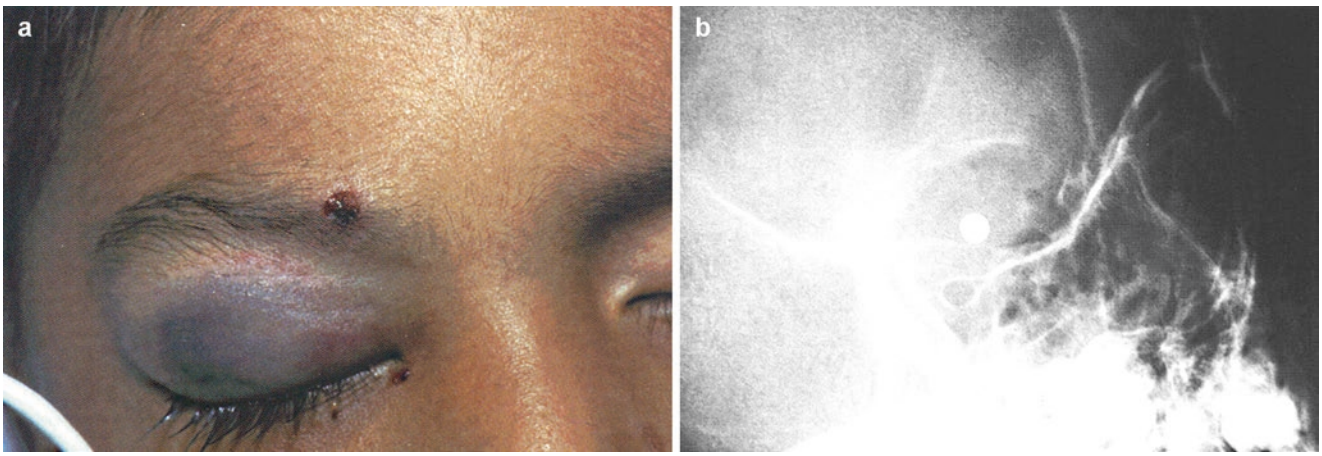


Fig. 42.2 Penetrating pellet in right orbit. (**a**) Entrance site of pellet which penetrated into the right orbit of this 5-year-old male. (**b**) Plain film x-rays confirmed the presence of the orbital foreign body but do not assist with its localization

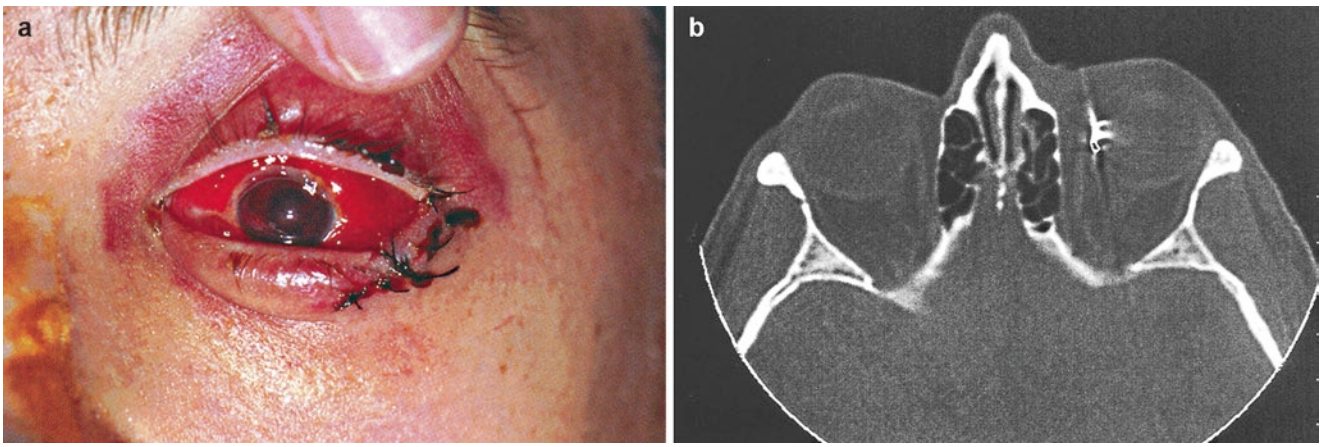


Fig. 42.3 Penetration of small metallic object. (**a**) Clinical photo of injury caused by penetration of small metallic foreign body. (**b**) CT shows location of the foreign body. The eye became phthisical from the injury and surgery

(Fig. 42.2). Injuries in this category are also unlikely to result in significant orbital fractures. There may be bony defects at the site of penetration, but significant displacement of the orbital bones is unlikely to occur. The orbital bones may deflect or block further penetration of the foreign body. A small chip fracture may be present at this point. The damage suffered by orbital soft tissue structures will be from direct injury by the projectile. This may involve cutting or tearing of the extraocular muscles, severing of the motor nerve(s) with subsequent deficits in the activity of one or more extraocular muscles, orbital hemorrhage from severing an artery within the orbit, globe penetration with possible intraocular hemorrhage or retinal damage, or any combination of the above. Seemingly innocuous and well-tolerated penetration can result in sudden and complete blindness if the optic nerve is impaled or severed by the penetrating object.

On the other hand, orbital trauma caused by high energy can be devastating. Examples of such trauma include gunshot wounds, blunt trauma from a fall or accident, assault with a club of some kind, and concussion from a blast injury. With this mechanism of injury, the damage is caused not only by the actual penetration but by the shock wave as well. Such a blow can disrupt orbital structures and easily cause rupture of the globe. The injury can be far more extensive than is initially apparent, based solely on the location of the penetration. High-energy trauma is far more likely to penetrate the cranial vault, creating injuries with neurosurgical consequences.

Creating a distinction between high- and low-energy penetrating trauma is not intended to minimize the potential consequence to the visual system of globe penetration with a small fragment. A small metal fragment that would represent a mere nuisance anywhere else in the body can be blinding if it strikes and penetrates the eye (Fig. 42.3). Appropriate and timely intervention by an ophthalmologist experienced in posterior segment trauma can maximize the potential outcome.

Penetrating injuries mandate an imaging study. An orbital CT scan is the most appropriate first choice. This will usually localize any radio-opaque intraorbital or intraocular foreign body [8]. It is not foolproof, however. A foreign body lodged immediately adjacent to the sclera may present a confusing picture (Fig. 42.4). The distinction between intraocular and

extraocular location can be difficult. Communication with the radiologist is very helpful in this situation. The gain and contrast on the CT can be manipulated to minimize scatter from metallic foreign bodies. This will also enhance one's ability to determine the exact location with respect to the globe. Clinical correlation may be necessary. As stated earlier, an MRI offers advantages over CT scans when the penetrating object is a plant foreign matter of some kind (Fig. 42.5). Although plain film x-rays are often suggested as a screening tool, they do not localize foreign bodies within the orbit with the same precision afforded by CT scanning and will not image foreign bodies that are not opaque to x-rays.

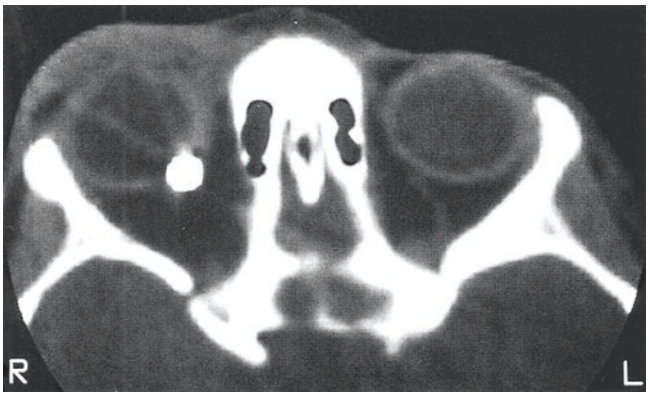


Fig. 42.4 CT scan of retained pellet in the right orbit. Clinical correlation determined that the pellet was extrascleral

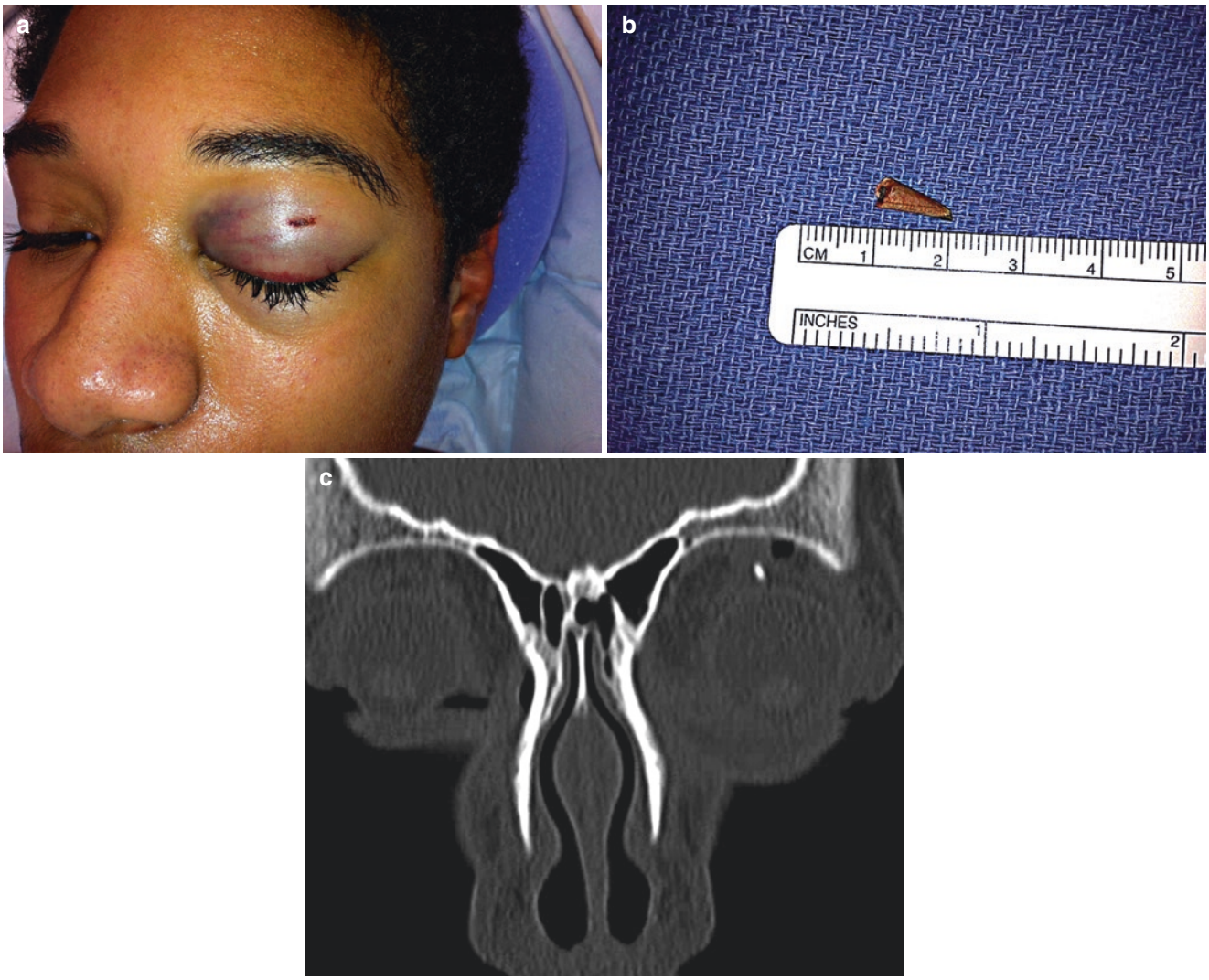


Fig. 42.5 Penetrating foreign body. The patient was hit by a backpack at school and presented with an upper eyelid puncture wound (**a**) Surgical exploration revealed the tip of a pencil adjacent to the globe (**b**) The coronal CT highlights the lead of the pencil (**c**)

Management of Penetrating Orbital Injuries

The initial management consists of the diagnosis of the injury, extent of the penetration, assessment of damage to the bones and soft tissue, as well as determining if there is a retained foreign body, as discussed above. Nonsurgical management consists of preventing infection and reducing inflammation. The child's inoculation history should be obtained to insure that the tetanus immunization is up to date. Parenteral antibiotics should be started. At a minimum, a single dose of a broad-spectrum antibiotic such as ceftriaxone should be given. Ceftriaxone has the advantage of a long half-life and can be administered once daily. The duration of antibiotic therapy must be determined by the type of injury. For example, retained foreign bodies that are potentially contaminated, such as wood or plant material, require prolonged therapy because of the high potential for infection. If a longer course of antibiotics is considered necessary, a home health agency may be of assistance, to avoid unnecessary hospitalization. If a purulent discharge does develop, cultures must be obtained to guide accurate antibiotic selection. Topical therapy of intraocular injury should be initiated, if appropriate. Pain medication should not be neglected. Liquid preparations that include codeine are available for the pediatric age group and should be used if appropriate.

Surgical removal of retained orbital foreign bodies is indicated for the following reasons:

1. Penetration of the globe
2. Foreign bodies of wood or plant material (Fig. 42.5)
3. Partial penetration of the orbit with an exposed foreign body (Fig. 42.6)
4. Foreign bodies that traverse the orbit into the cranial vault (Fig. 42.7)
5. Large foreign bodies
6. Foreign bodies that cause continued harm or pain by their presence
7. Superficial foreign bodies that are readily accessible

It is not mandatory to remove all orbital foreign bodies; clinical judgment is certainly necessary. If removing the foreign body will do more harm than leaving it in place, then removal is not indicated. Removal of small foreign bodies from the orbit is never as easy as it may appear clinically or on a scan. Foreign bodies that can be left in place are usually small and relatively inert, such as glass or small fragments of metal. The composition of the metal fragment may assume importance if it can degenerate and be absorbed with potential systemic consequences (e.g., copper) [8]. It has also been shown that loss of vision is almost always the result of the initial trauma rather than the subsequent management [8].

One of the more common foreign bodies in the pediatric age group is the BB or pellet from a CO_2-powered pellet gun. These pellets are usually composed of metal alloy, which may include copper. If left alone, they will quickly become encapsulated by scar tissue. This sequesters the foreign body from the systemic circulation. Despite containing some copper, the authors are not aware of any harm done by leaving these foreign bodies in place. The initial penetration causes the problem in these instances, and this type of foreign body can be left in place without long-term sequelae (Fig. 42.8).

If the foreign body is one that requires removal, the surgeon should insure that the preoperative localization of the foreign body is quantified as accurately as possible. This requires imaging tests as described above. The surgical approach to the orbit will be dictated by the location of the foreign body. The anterior orbit can be entered easily by utilizing the lid crease incision in the upper lid or the fornix in the lower lid (see Chap. 37). This will minimize postoperative scarring. The lateral orbit can be approached with a lateral orbitotomy. Depending on the location of the foreign

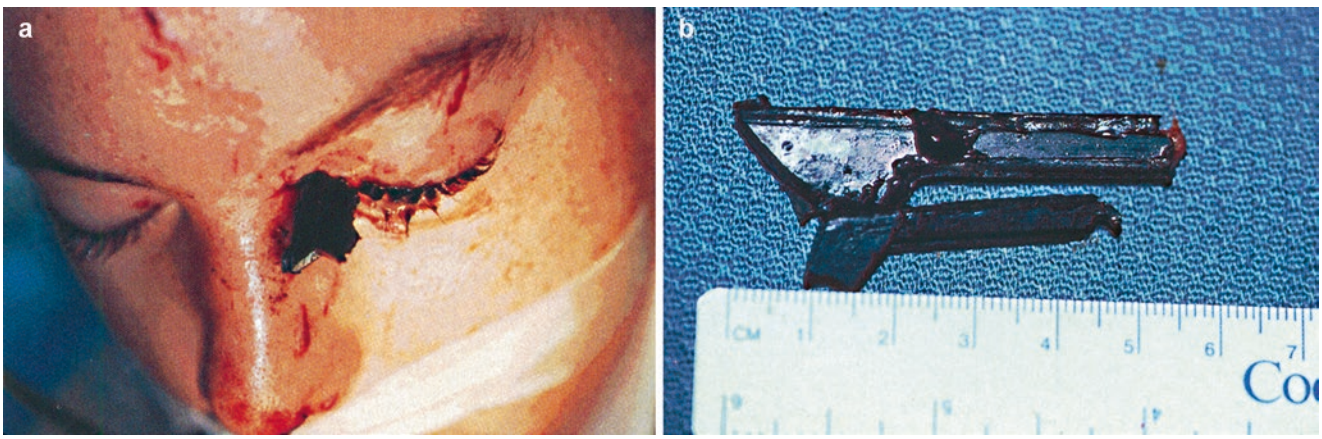


Fig. 42.6 Foreign body from auto accident. (**a**) Orbital foreign body from an auto accident penetrating the medial aspect of the left orbit. (**b**) Size of the foreign body apparent after removal

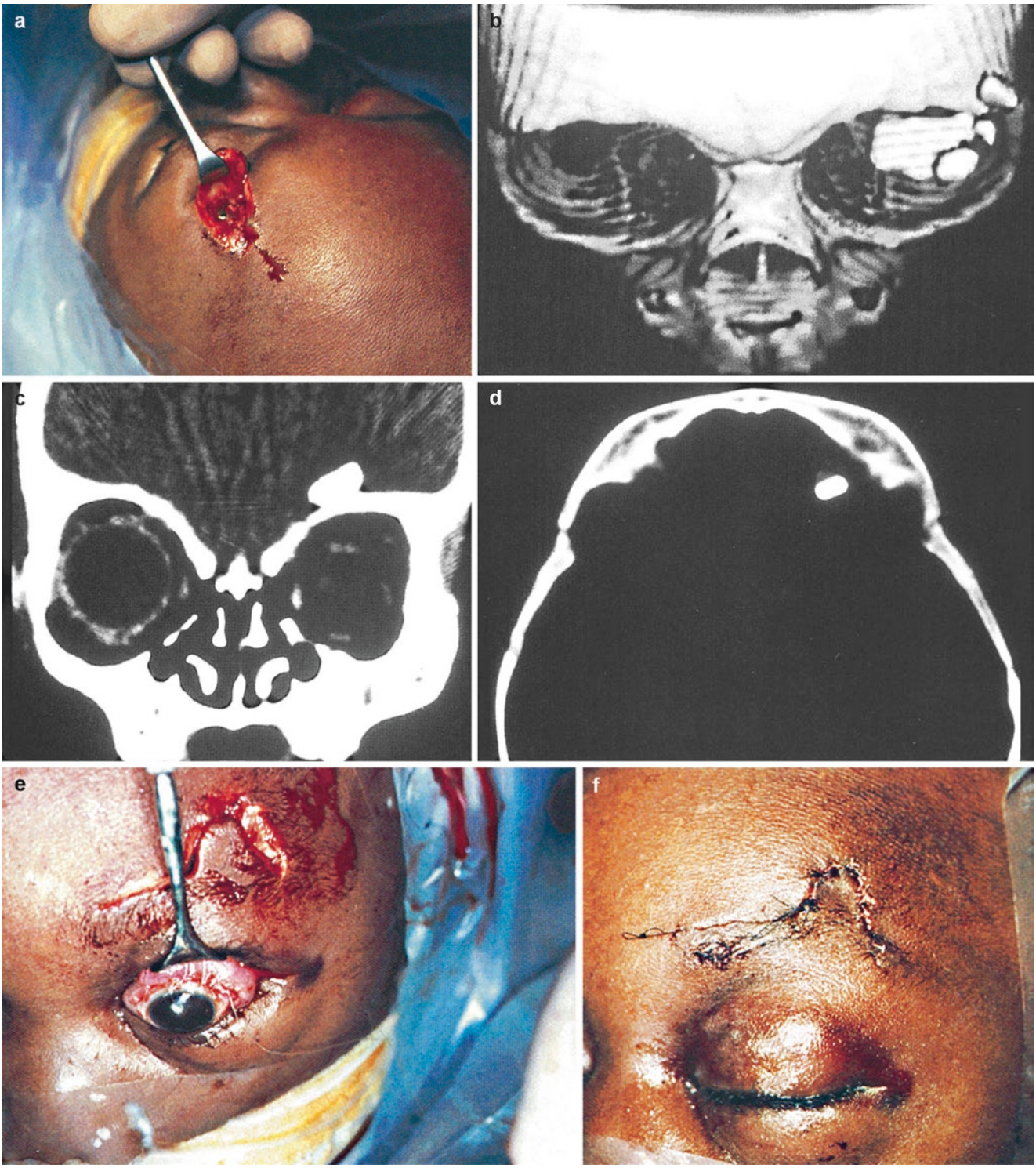


Fig. 42.7 Glass foreign bodies. (**a**) Infant fell out of high chair onto a glass bottle. (**b**) 3D CT of glass foreign bodies that penetrated the anterior cranial fossa. (**c**) Coronal CT scan shows foreign body above orbital roof. (**d**) Axial CT shows foreign body in frontal lobe. (**e**) Repair of scleral laceration with uveal prolapse caused by penetrating glass fragment. (**f**) Repair of brow laceration after coronal flap repositioned

body and the damage that has occurred, it may be necessary to enlist the assistance of those in other disciplines, such as the otolaryngologist for concomitant sinus damage or the neurosurgeon for deep posterior foreign bodies which require a transcranial approach (Fig. 42.9). Once it has been decided to remove the foreign body, it is critical to remove the entire object, if at all possible (Fig. 42.10). This can be a clinical challenge with multiple small foreign bodies. Plant material,

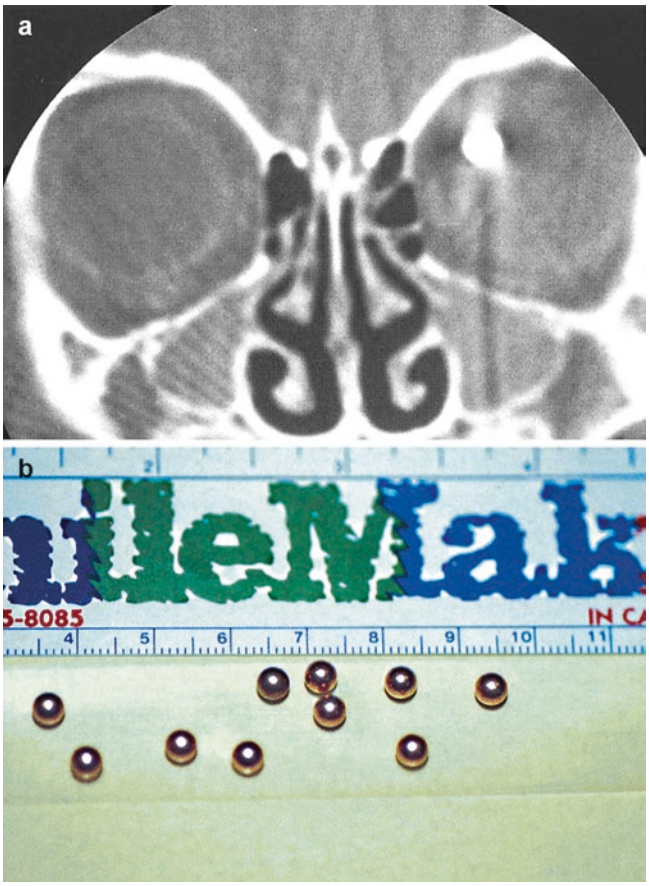


Fig. 42.8 Pellets. (**a**) CT scan of pellet retained in the right orbit (clinical photograph in Fig. 42.2a. The pellet was intraconal and extraocular. It was left in place. The ptosis and soft tissue swelling resolved completely. (**b**) Pellets identical to the one seen on the CT scan. These were removed from the pellet gun that fired that pellet

such as a tree branch, that penetrates the orbit is also difficult to remove in its entirety. Wood or other plant material that is retained will usually develop into chronic orbital-cutaneous fistula. The development of a chronic draining fistula following blunt orbital trauma is a sensitive sign indicating retained orbital foreign material. It may even be unsuspected prior to the development of the fistula (Fig. 42.11).

Blast injuries can occur in the pediatric age group. These are usually related to exploding fireworks. They can be devastating, destroying the globe and lids. Milder injuries that result in retained corneal or intraocular foreign bodies are more commonly seen. Timing of removal depends on the material retained and surrounding damage. A safe general rule is to remove foreign bodies from the globe as soon as the patient can tolerate the procedure. Lid foreign bodies should be removed at the time of repair of the lid damage.

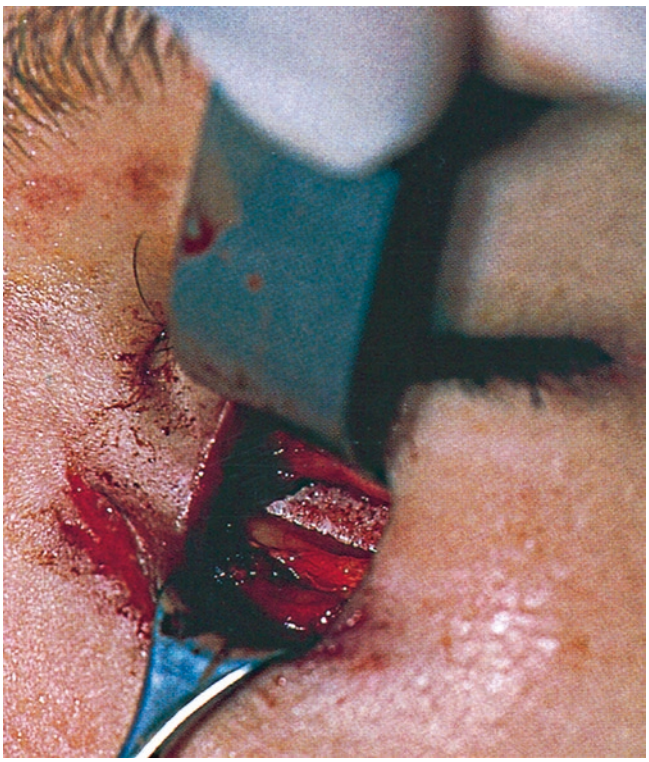


Fig. 42.9 Intraoperative appearance of child in Fig. 42.1. Removal of the foreign body was performed in conjunction with an ENT specialist. A Caldwell-Luc incision was used to view the handle in the sinus, and at the same time, the orbital floor was exposed through the lid defect. MEDPOR is seen covering the orbital floor defect



Fig. 42.10 Immediate postoperative appearance of the patient in Fig. 42.6a. The vision returned to 20/20 and the medial rectus was not damaged

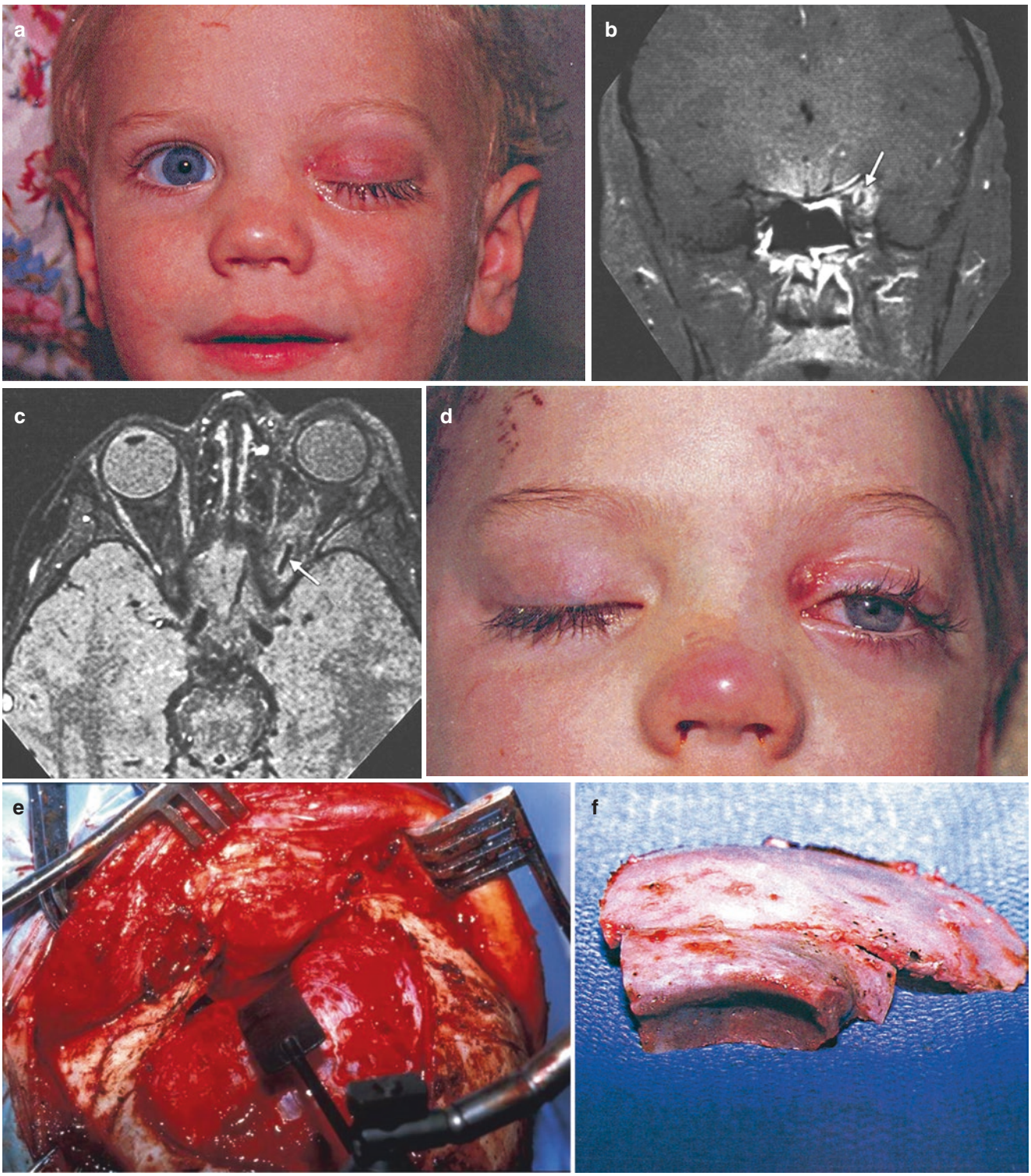


Fig. 42.11 Wood foreign body in orbit. (**a**) Appearance of child after falling onto cut grass stubble. (**b**) MRI demonstrates foreign body penetrating through orbit into the cavernous sinus (*arrow*). (**c**) Location of foreign body in posterior orbit and proximity of this to carotid artery in cavernous sinus were major concerns regarding neurosurgical intervention. (**d**) Chronic fistula persists despite multiple attempts to explore, track, and remove anterior fragments of foreign body. (**e**) Because of intermittent fistulas and proptosis, a decision was made to proceed with transcranial approach to orbit via craniotomy and removal of orbital rim and roof. Brain retractor is just above the annulus of Zinn. (**f**) Orbital rim, roof, and cranial bone.

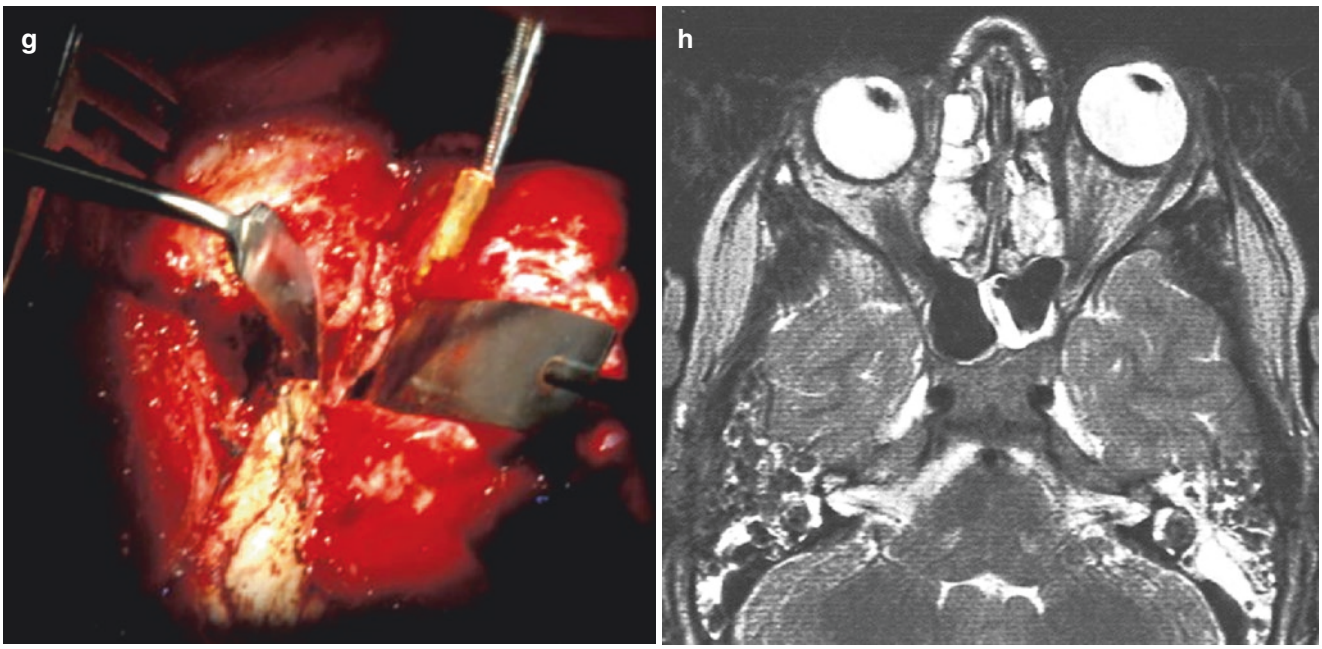


Fig. 42.11 (continued) (**g**) After careful palpation, an incision was made in periorbita, medial to the annulus of Zinn; a 15-mm wood foreign body was located and removed with forceps. (**h**) MRI of orbit 1 year postoperative shows the absence of inflammation

Management of Orbital Hemorrhage

Acute intraorbital hemorrhage that causes decreased visual acuity, acute proptosis, and increased intraocular pressure is a true ophthalmic emergency requiring immediate intervention. The buildup of orbital pressure may be faster than the globe and optic nerve can tolerate, leading to a pressure higher than that in the central retinal artery. This can cause an occlusion of this vascular structure. A brief occlusion may be tolerated by the retina without long-term sequelae, but occlusions lasting longer than 90 min in animal models have demonstrated permanent ischemic necrosis of the inner layer of the retina and permanent loss of visual function [9]. Blunt or penetrating trauma of any type can cause a severe orbital hemorrhage. Children with hemophilia, bone marrow disorders, and severe malnutrition with its associated vitamin deficiencies are predisposed to the development of orbital hemorrhage with even trivial trauma.

Orbital hemorrhage may produce severe proptosis compromising coverage of the cornea, optic nerve dysfunction accompanied by an afferent pupillary defect caused by stretching or compression, or vascular compromise caused by the buildup of orbital pressure. Orbital imaging, either CT or MRI, will confirm the presence of orbital hemorrhage as well as pinpoint its location. Treatment of the hemorrhage is indicated whenever visual function is threatened.

If treatment is indicated, the progression of surgical intervention is as follows:

1. Lateral canthotomy, splitting the lateral canthal tendon horizontally into an upper and lower section down to the orbital rim (Fig. 42.12a).
2. Cantholysis of the inferior arm of the lateral canthal tendon, severing all attachments of the lower lid to the orbital rim. This is best accomplished by a vertical inferior cut close to the orbital rim, which also releases the orbital septal attachments (Fig. 42.12b).
3. Limbal peritomy, opening Tenon's fascia between the lateral and inferior rectus muscle, spreading the orbital fat with blunt-tipped scissors, permitting egress of the orbital hemorrhage. This is required only in very extreme circumstances.

The canthotomy and cantholysis may be performed in an emergency room setting, even in a pediatric patient. Local infiltration of anesthesia is followed immediately by the procedure. Canthotomy with cantholysis is usually effective in relieving the pressure of the hemorrhage [10]. If this is ineffective, however, then a limbal peritomy or deeper orbital exploration must be performed. This requires general anesthesia in children and the use of operating room facilities.

All procedures for the relief of orbital hemorrhage require that the patient be watched closely to insure that the vision does not decrease. If this does occur, the orbit should be examined immediately, utilizing CT scanning with narrow axial cuts to insure that anterior movement of the globe has not placed the optic nerve on stretch. Release of the lids, on rare occasion, has allowed for enough anterior displacement of the globe to stretch and compromise the optic nerve. Should this happen, an emergent orbital decompression is then indicated.

Blunt trauma may also cause an orbital hemorrhage in a subperiosteal location (Fig. 42.13). This type of hemorrhage will tend to be more localized and less likely to cause severe

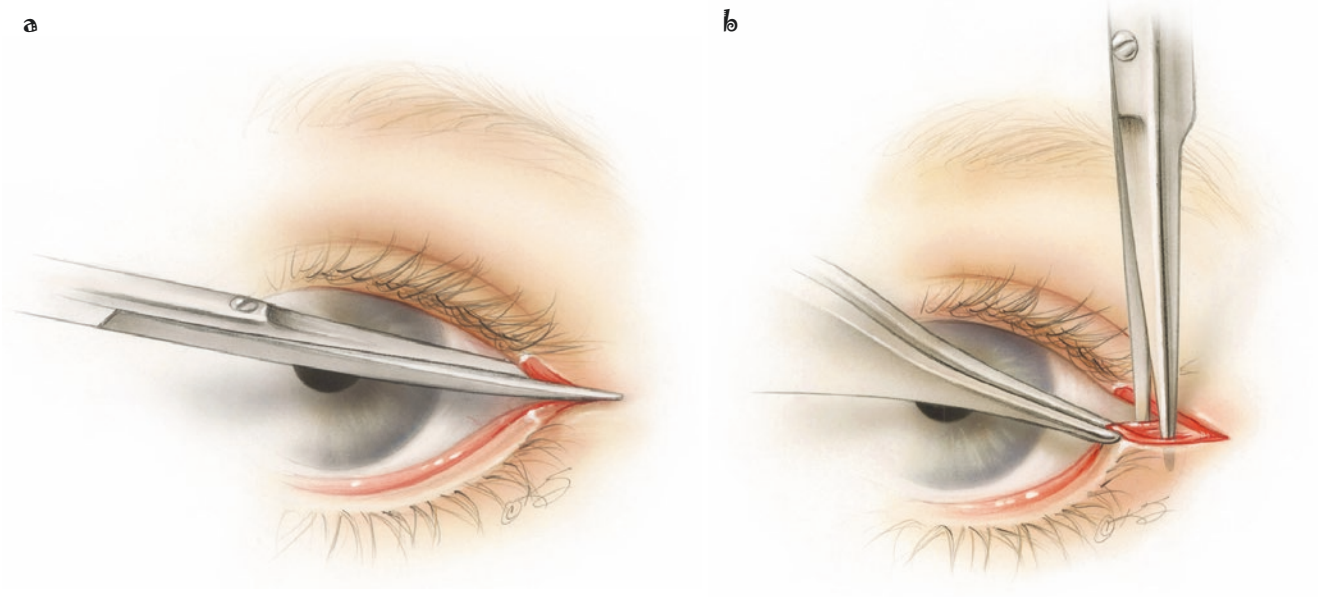


Fig. 42.12 Canthotomy and cantholysis successfully removed foreign body. (**a**) Lateral canthotomy splits the lateral canthal tendon in two down to the orbital rim. (**b**) A cantholysis of the inferior arm of the lateral canthal tendon detaches the lower lid, further decompressing the orbit anteriorly

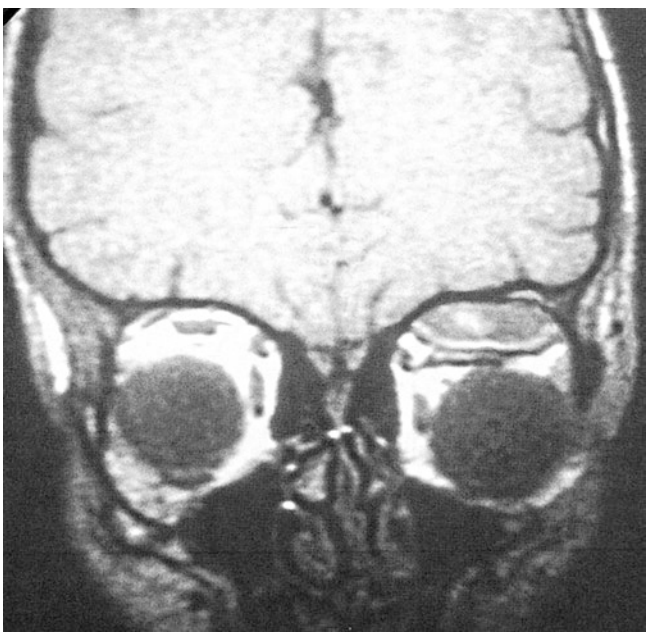


Fig. 42.13 MRI of subperiosteal hematoma of the left orbit. The localization of the hematoma is excellent with MR imaging

proptosis. This is obviously not accessible to the limbal approach for emergent drainage. The subperiosteal hemorrhage must be drained when it is considered responsible for visual compromise. This will be determined by the clinical exam, based on visual function, and the results of orbital imaging, defining the size and location of the hemorrhage. Subperiosteal hemorrhages are usually located superiorly or nasally. Either location may be approached through the lid crease.

A question that frequently arises is why the release of orbital pressure itself does not cause more hemorrhaging to occur, thus worsening the clinical situation. The most likely explanation, in our opinion, is that by the time the patient has been brought to the emergency room or physician's office and the proper diagnosis made, blood clots have already sealed the site of the hemorrhage. Treatment of the hemorrhage, then, releases the pressure without inducing further bleeding. Severe proptosis caused by the lateral canthal tendon release is an indication of the severe orbital pressure elevation that has been present and only rarely indicates continued hemorrhage.

Orbital Fractures

Orbital Blowout Fracture

While blowout fractures in the pediatric age group share much in common with adult blowout fractures, there are differences. First, the sinuses are developing in the pediatric patient. The ethmoid sinuses are the first to appear, developing at age 2 years. The maxillary sinus is next, beginning at age 4 years. A true blowout fracture cannot occur until the maxillary sinus has developed.

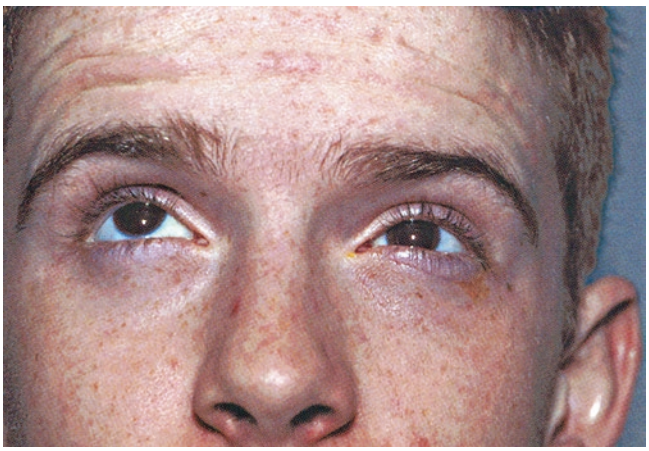


Fig. 42.14 Vertical gaze restriction left eye. Vertical gaze restriction from entrapment of the inferior rectus muscle following blunt trauma to the left orbit

Secondly, pediatric patients are the recipients of unique forms of injury causing blowout fractures. We have managed pediatric blowout fractures caused by a knee striking the orbit during a cannonball dive into the swimming pool, by blunt trauma suffered during the collapse of a cheerleader pyramid, by a horse rolling over the patient during a barrel race, and by a thrown softball, among others. This contrasts with the more frequent findings of assault, falls, and motor vehicle accidents in an older patient population.

Blowout fractures of the orbital floor are a frequent sequela of blunt facial and head trauma. The most common cause of pediatric orbital fractures is sports injuries, assault, and motor vehicle accidents [2]. Two mechanisms have been attributed to the cause of orbital floor fractures. An acute increase in pressure within the orbit represents the hydraulic mechanism. The buckling theory suggests a pressure wave transmission through the bones in the orbit, fracturing the weakest point. Multiple studies have proven that it is a combination of the two causes the fractures [11, 12]. Orbital floor fractures frequently cause diplopia, usually vertical (Fig. 42.14). This is secondary to either frank entrapment of the inferior orbital tissue in the fracture site or stiffness of the muscle from a contusion or hematoma. Thus, upgaze of the involved eye is restricted and a hypotropia or vertical gaze restriction results. The restriction can occur without entrapment of the inferior rectus muscle. The orbital soft tissue is interlaced with fibrous orbital septa [13]. Entrapment of these septa in the fracture site may be sufficient to cause tethering of the globe with attempted upgaze.

The presence of entrapment is most accurately determined by forced duction testing. This test is difficult to perform on pediatric patients and usually requires general anesthesia. When performed, inferior tethering is evaluated by grasping the insertion of the inferior rectus (−7.0 mm below the limbus at the 6 o'clock position). Superior traction applied to the inferior rectus will then reveal the presence or absence of tethering. Alternatively, one can grasp the globe at the 3 and 9 o'clock position to apply superior traction. This eliminates the risk of scratching the cornea should the instrument slip. In an older or otherwise cooperative child, use of a cotton-tipped pad applicator after instillation of topical anesthesia may give some indication of restriction (see Chap. 11).

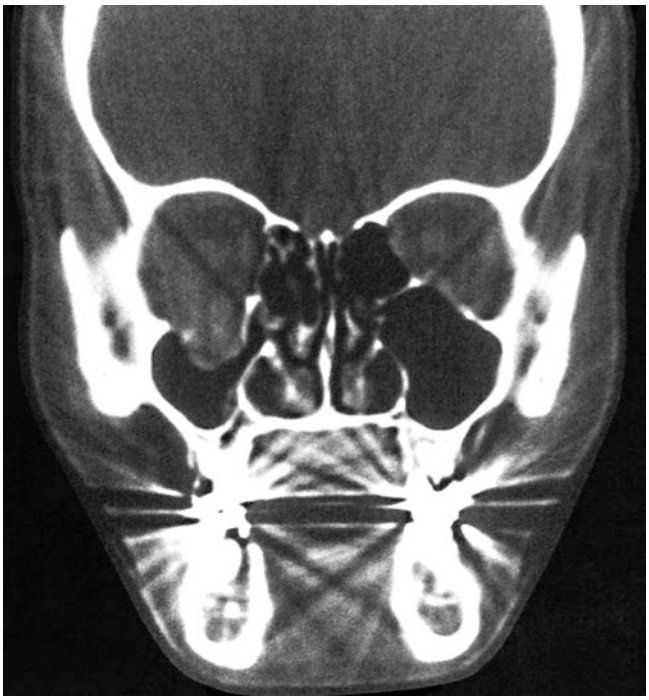


Fig. 42.15 CT scan of a 13-year-old patient with a large orbital floor fracture and soft tissue prolapse indicating likely severe right enophthalmos

The other serious sequela of an orbital floor fracture is enophthalmos caused by a significant increase in the orbital volume. This is secondary to a traumatic decompression of orbital soft tissues into the maxillary sinus, ethmoid sinus, or both. Fractures large enough to cause enophthalmos will often not entrap the inferior orbital tissue because the bone fragments are widely spread and no trapdoor capable of pinching tissue exists. A large fracture of the orbital floor should be suspected when the acutely injured patient is enophthalmic at the time of the initial exam (Fig. 42.15).

It is important to obtain CT scans of the orbit whenever blunt trauma has occurred. If the patient does not complain of diplopia, a fracture of the orbital floor may not be obvious and could be missed if not properly evaluated (Fig. 42.16). Three-millimeter-thick direct coronal views of the orbit are most commonly used to investigate the presence and size of a blowout fracture. Thin-section axial CT scans, 0.625–1.25 mm with multiplanar reformation, can help if the condition of the patient does not allow for direct coronals. Enhancement of the soft tissue with IV contrast does not contribute to the evaluation of a blowout fracture and is not essential [5, 6].

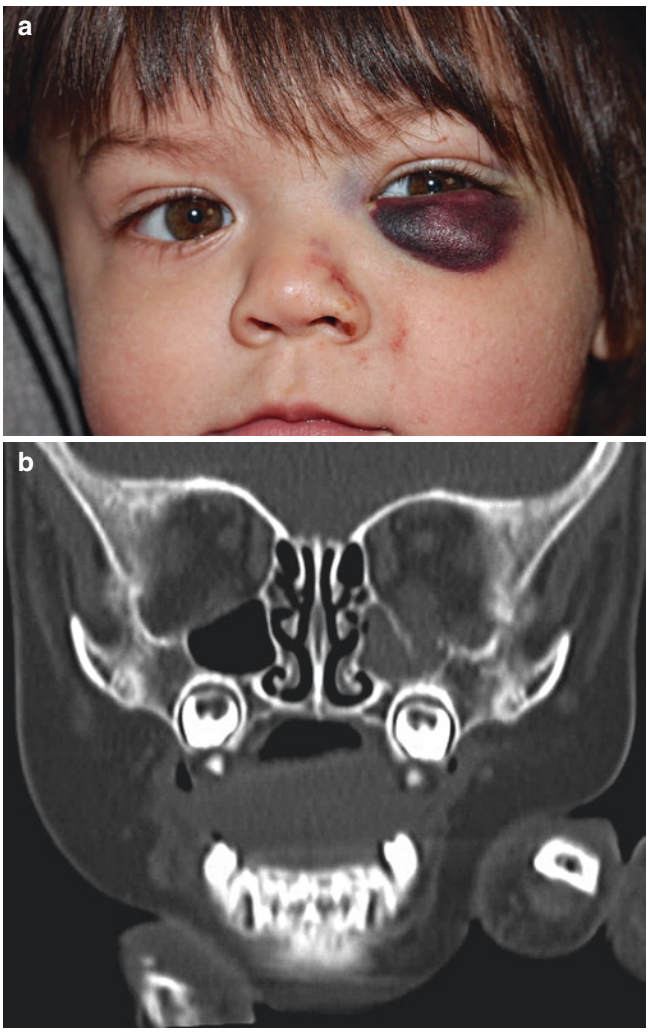


Fig. 42.16 A large lower eyelid hematoma with hyperglobus (**a**). The CT scan demonstrates a large orbital floor fracture (**b**)

There are two indications for surgical repair of the orbital floor. The first indication is the presence of symptomatic double vision caused by tethering of the inferior rectus muscle. The definition of "symptomatic" double vision is a function of the visual requirements, lifestyle, and occupational demands of the patient but most commonly is within 30° of primary gaze. Second, repair should be performed when the fracture is large and likely to result in postoperative enophthalmos after the hemorrhage and edema resolve. Fractures in this category usually involve more than 50% of the orbital floor [2].

These patients may present with enophthalmos at the time of the initial exam. However, orbital soft tissue swelling from the injury may initially mask the enophthalmos (Fig. 42.17). Clinically, it can be challenging to judge when the fracture involves more than 50% of the orbital floor. Orbital CT scans provide critical information needed to make this decision. The authors have found it useful to diagnose the fracture as large and requiring repair if it measures 20 mm or more from the anterior edge of visible fracture to posterior extent of the fracture. The fracture is also considered large if it measures 15 mm or more from front to back and has been depressed 10 mm or more into the maxillary sinus. Finally, a floor fracture combined with a medial wall fracture into the ethmoid sinus almost always requires repair. These clinical guidelines are subjectively modified in the very young pediatric patient because of the altered orbital size.



Fig. 42.17 Horizontal restriction. Horizontal restriction of the left eye caused by a left medial wall fracture

Indications for repair of a medial wall blowout fracture differ. Anatomically, the medial wall and the optic nerve converge in the posterior orbit. The traction required to expose medial wall fractures can stretch the optic nerve. This makes medial wall blowout repair more hazardous. Repair is warranted if the medial rectus is trapped in the fracture site, causing horizontal diplopia (Fig. 42.17). Very large fractures are unusual because of the honeycomb-like structure of the ethmoid air cells. Individual cells will break, but it is unusual for a large expanse of the medial wall to be fractured. When a large medial wall fracture does occur, it is usually accompanied by decompression of orbital fat through a periorbital tear into the ethmoid sinus (Fig. 42.18). This can also produce significant enophthalmos and require repair.

The surgical technique for repair of an orbital floor blowout fracture is straightforward. The orbital floor is exposed, the orbital soft tissues are freed and returned to their normal anatomic position, and a barrier of some kind is placed to prevent the future prolapse and/or entrapment of orbital tissue. The orbital floor can be approached via a conjunctival route, via a subciliary incision, or via a Caldwell-Luc approach through the maxillary sinus. The conjunctival route is preferred by most ophthalmic plastic surgeons and is easily used in the pediatric patient with excellent results (Fig. 42.19).

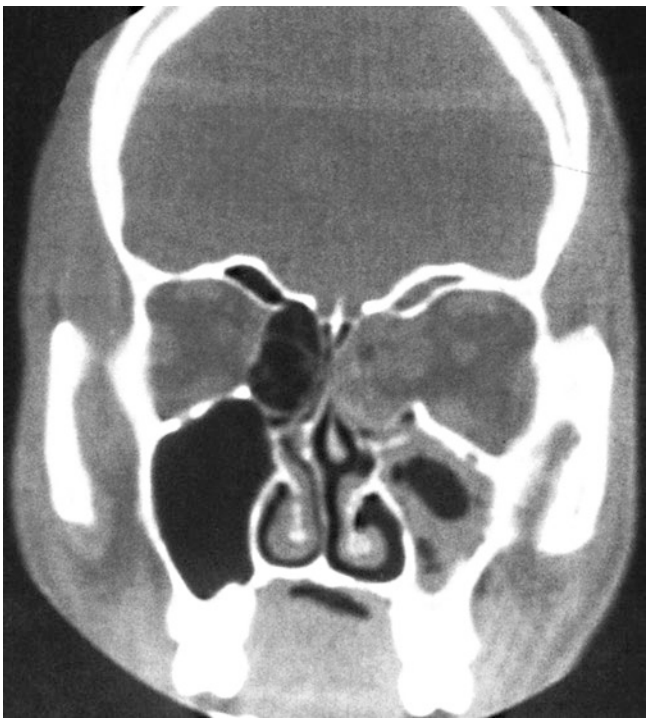


Fig. 42.18 Example of large left medial wall fracture requiring repair

After general anesthesia has been induced, the lower lid is injected to the orbital rim with local anesthesia containing epinephrine (e.g., 0.25% bupivacaine with 1:100,000 epinephrine). This assists with hemostasis during surgery and pain control postoperatively. A globe protector covers the eye. The lower lid is placed on stretch inferiorly and the conjunctiva incised at the lower edge of the tarsal plate. Needle-tipped cutting cautery is very useful during this step. A suture for traction is placed in the edge of the conjunctiva and the conjunctiva stretched superiorly. This helps separate the tissue in the lower lid and aids with dissection. The surgical plane is carried down the anterior surface of the orbital septum to the orbital rim, and the periosteum is incised just outside of the orbit. Care is required to avoid making a buttonhole incision in the skin of the lower lid. A periosteal elevator lifts the periosteum from the bone. This dissection is carried around the orbital rim onto the floor of the orbit. The fracture is usually easily identified and is most frequently nasal in location, although temporal fractures of the floor can occur. The preoperative CT will determine the location of the fracture and help prevent intraoperative surprises. The infraorbital groove is frequently the lateral edge of the fracture. The key to repositioning the orbital soft tissue is to remove

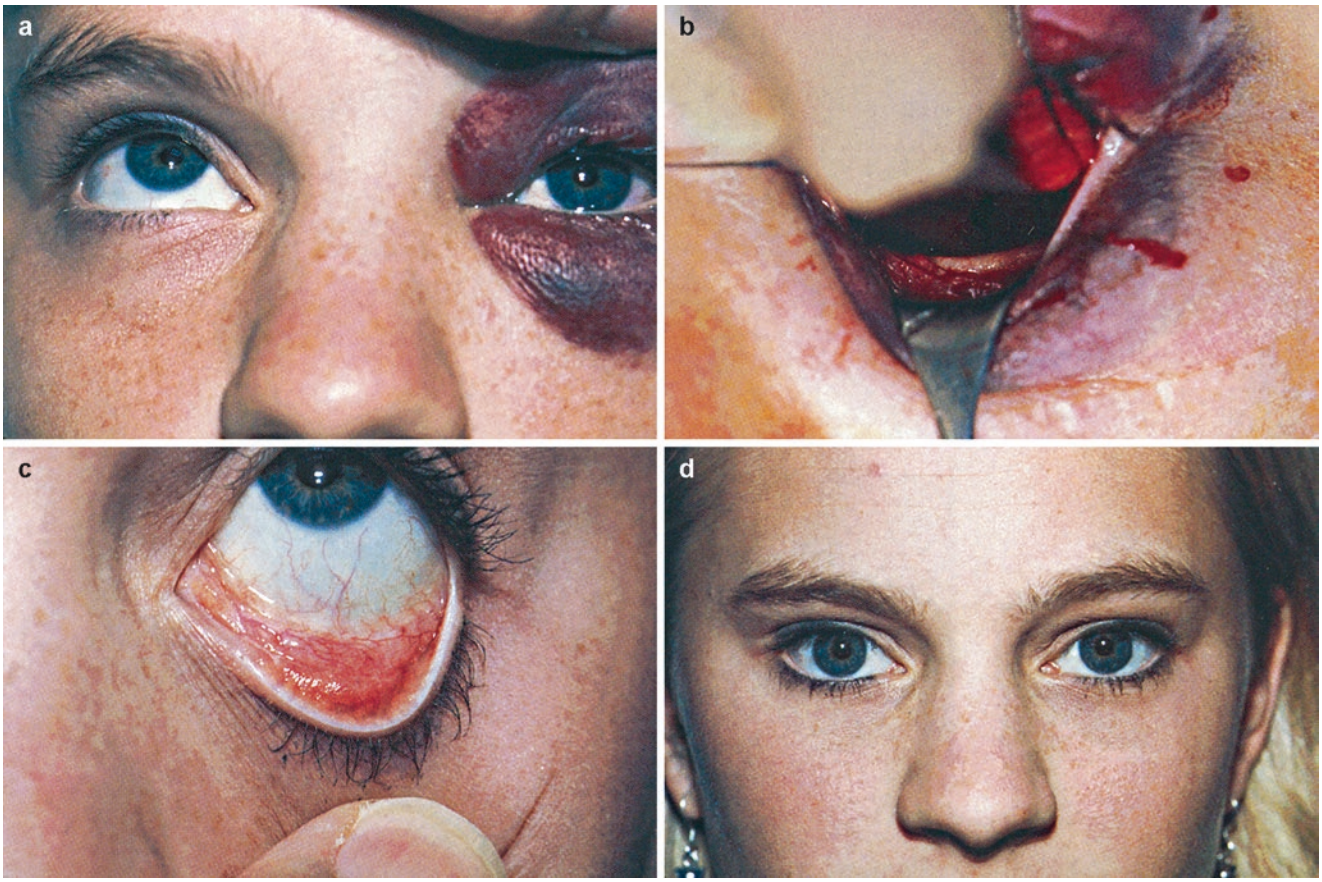


Fig. 42.19 Orbital floor fracture. (**a**) Preoperative appearance of patient with left orbital floor fracture and entrapment. (**b**) Intraoperative view of the fracture site through a conjunctival incision. A lateral cantholysis was not performed. (**c**) Appearance of the conjunctival scar 2 months after surgery. (**d**) Final clinical appearance after repair of the left orbital floor blowout fracture through a conjunctival incision

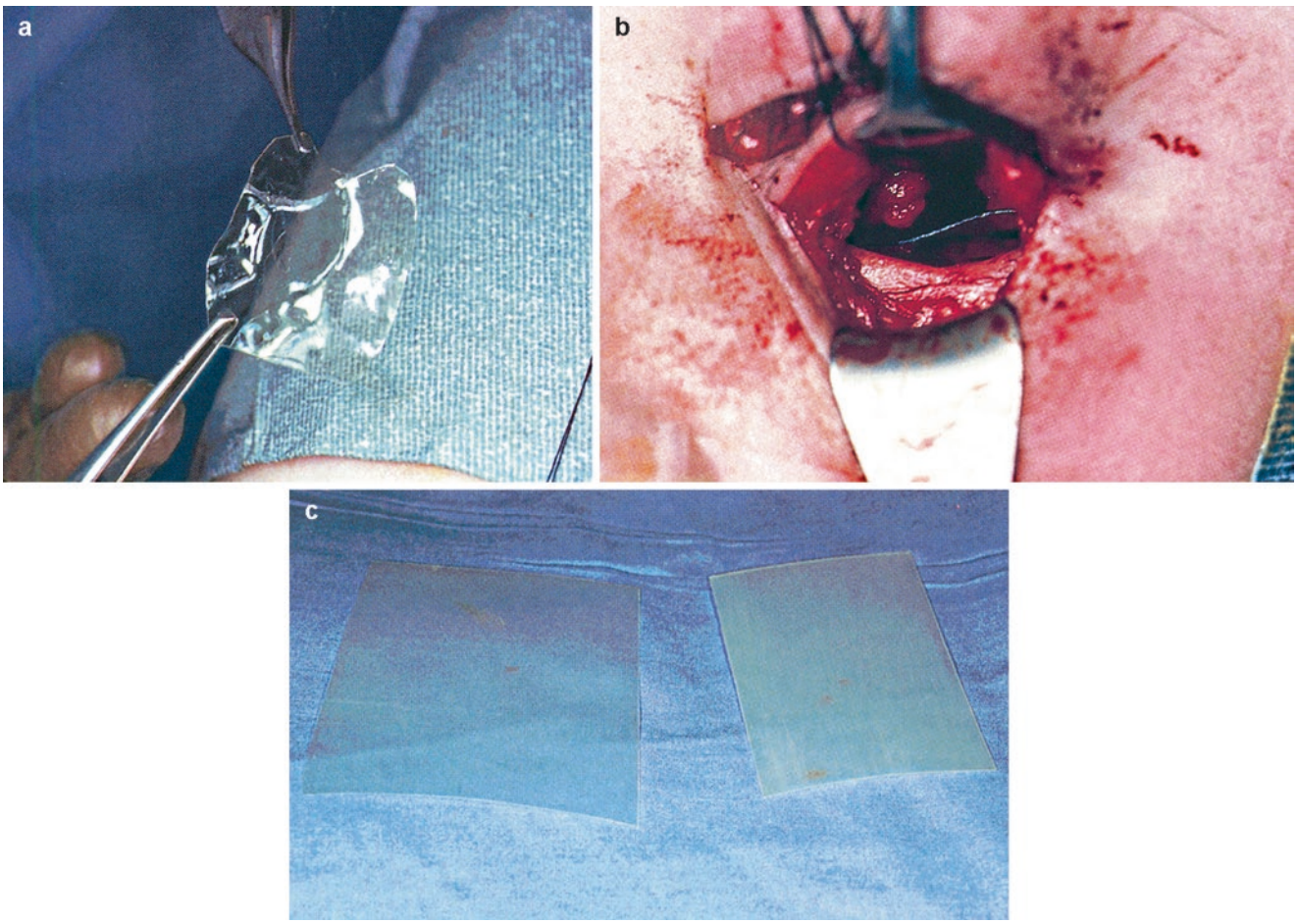


Fig. 42.20 Floor implants. (**a**) Gelfilm can be used to cover a small crack in the orbital floor. (**b**) Most small defects can be covered with a thin 0.3 mm supramid foil implant. (**c**) These are examples of 0.3 and 0.4 mm supramid sheet for floor fracture repair

the periosteum still attached to the orbital contents from the bone fragments depressed into the maxillary sinus. Once the soft tissue has been mobilized and returned to the orbit, the defect in the orbital floor is covered.

The material used to provide the barrier against future prolapse of orbital tissue depends on the experience and desires of the surgeon. Many options are available. Small fractures that return to a normal position after the orbital soft tissue has been repositioned can be covered with gelfilm (Fig. 42.20). Larger defects require the use of other material such as Silastic or Supramid sheets. MEDPOR (Porex Surgical, College Park, GA) is another option, providing greater rigidity and a porous composition for better stability (Fig. 42.21). Other options include the use of autologous bone, either rib or split thickness cranial bone, as well as a variety of titanium or Vitallium plates designed for use in the orbit with miniplating systems.

Should it be necessary to repair a medial wall fracture, it can be approached in several ways. An incision in the skin at the superior nasal orbital rim can be used. nasal portion of the lid crease can be used (Fig. 42.21). Another method involves an incision through the nasal portion of the conjunctiva at the caruncle. The concept is the same as for the floor fracture outlined above. The soft tissue is repositioned into the orbit and a barrier placed to prevent its prolapse into the fracture site after surgery. The surgical space is often too small for bone to be used as the barrier in the medial wall repair. Gelfilm, thin Silastic sheeting, Supramid, or a thin MEDPOR sheet are possible barrier materials. On rare occasions, autologous bone can be used, particularly in late enophthalmos associated with a large medial wall defect.

Timing of surgical repair in the pediatric age group is critical. True entrapment is most likely to occur in this group of patients because the bones are more pliable and therefore

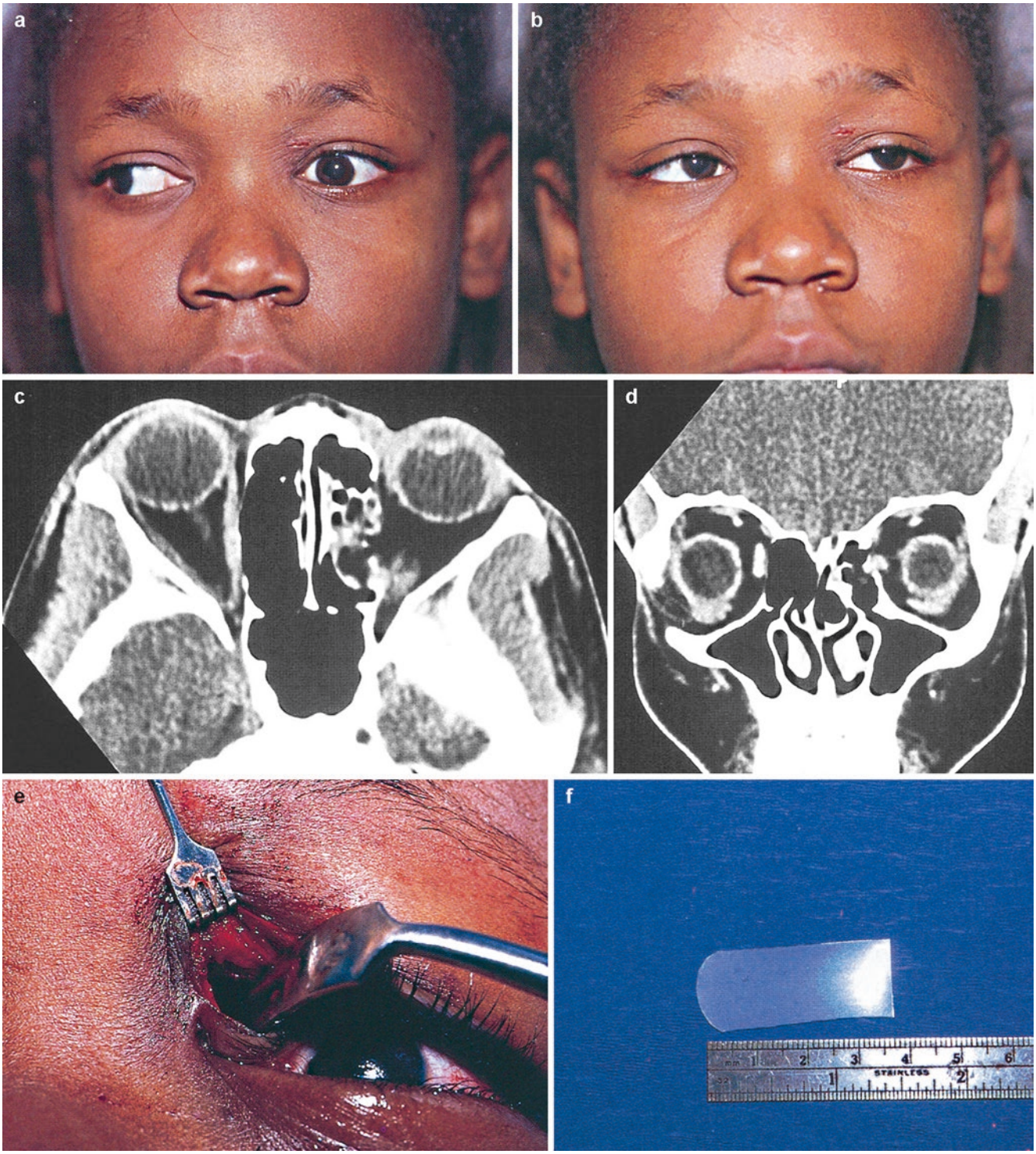


Fig. 42.21 Lid crease incision for medial wall fracture repair. (**a**) Patient's left orbit struck by elbow; limitation of gaze right. (**b**) Limitation of gaze left. (**c**) Axial view of wall fracture with bone fragments in ethmoid sinus. (**d**) Coronal view shows entrapped medial rectus muscle. (**e**) Upper lid crease incision gains access to medial orbital wall after incising periorbita; retractor used to carefully free medial rectus muscle. (**f**) 0.3 mm supramid foil cut and shaped.

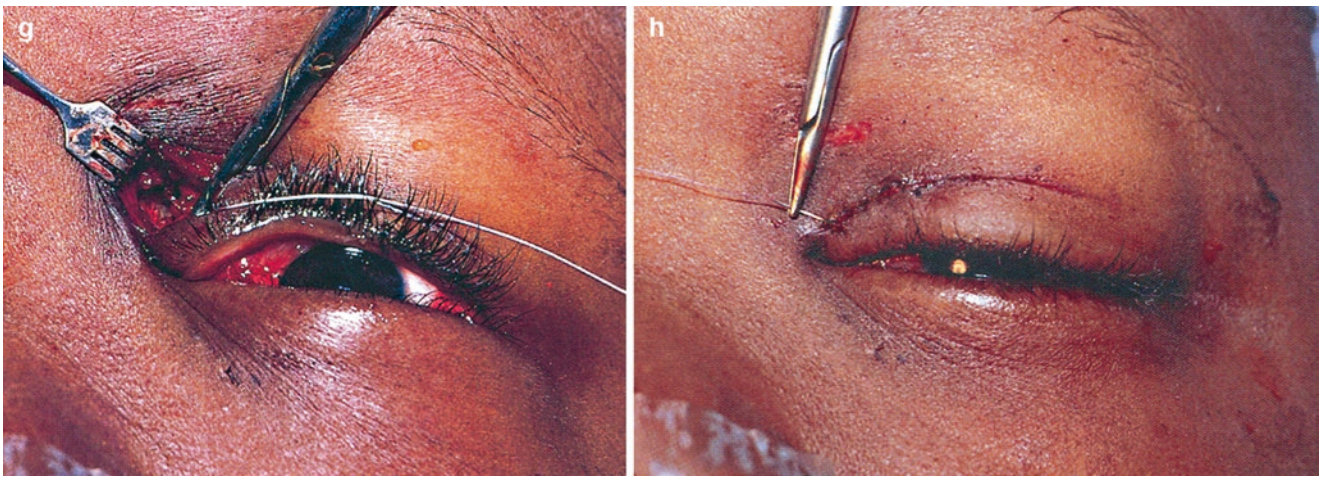


Fig. 42.21 (continued) (**g**) After foil inserted and trimmed, forced ductions show no restriction. Periorbita closed with 4-0 Vicryl suture on P-2 needle. (**h**) Lid crease incision closed with (Ethicon) 6-0 fast absorbing catgut

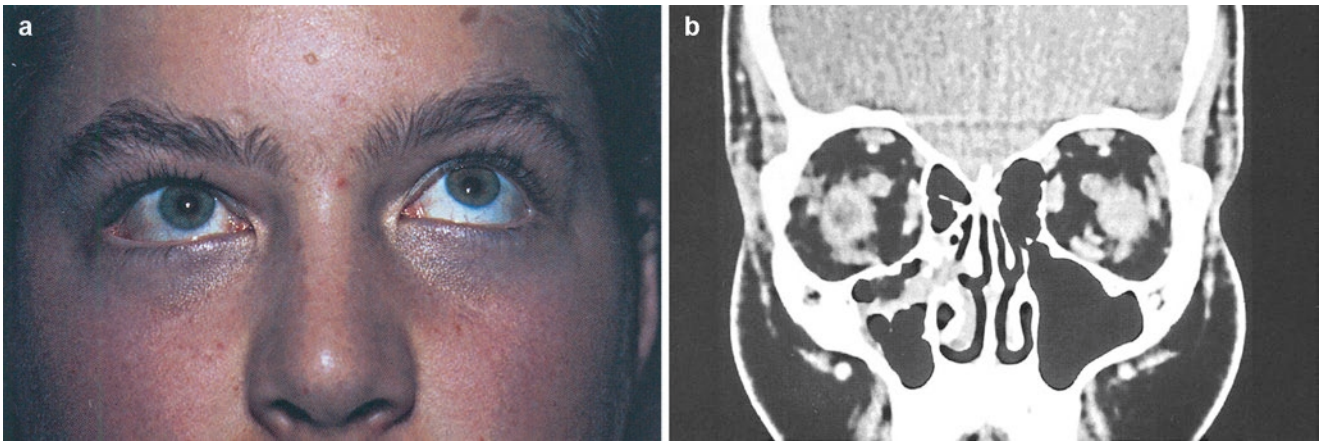


Fig. 42.22 Orbital floor trapdoor fracture. (**a**) A 14-year-old male had a right orbital floor trapdoor fracture with true entrapment of the inferior rectus repair 10 days after the injury. Intense inflammation of the inferior orbital soft tissue was encountered. Vertical gaze restriction (not paresis) persisted despite normal intraoperative forced ductions. (**b**) CT scan of the orbital floor fracture

more likely to break as a greenstick fracture, causing entrapment of the inferior rectus muscle. In this scenario, if the inferior rectus muscle is damaged, an intense inflammatory response may ensue, causing cicatrization in the inferior orbit, which in turn leads to a significant restriction in gaze up or down with symptomatic vertical diplopia (Fig. 42.22). We have witnessed this clinical scenario in the pediatric population and, because of this, consider true entrapment of the inferior rectus muscle to be a surgical emergency, requiring intervention at the earliest possible opportunity. Immediate intervention can release the trapped inferior rectus muscle before the inflammatory response has been stimulated, preventing the formation of scar tissue and the ensuing vertical gaze restriction. Other indications for immediate repair are nonresolving oculocardiac reflex and early enophthalmos [14]. Larger fractures, on the other hand, do not pinch the inferior rectus muscle. An intense inflammatory response in the inferior orbit does not develop and it may be desirable to wait for the orbital edema induced by the injury to subside. A wait of 1–2 weeks after injury, allowing resolution of the tissue edema, is acceptable [14]. If the inferior rectus muscle itself is not entrapped, but only Tenon's capsule or surrounding soft tissue caught in the trapdoor, it may be possible to delay surgical intervention, but it is sometimes difficult to be sure on imaging that the inferior rectus muscle itself is not pinched and damaged. The resolution of diplopia is associated with both the cause of the injury and the fracture location. The younger the patient, the longer the recovery from the diplopia after surgery [15].

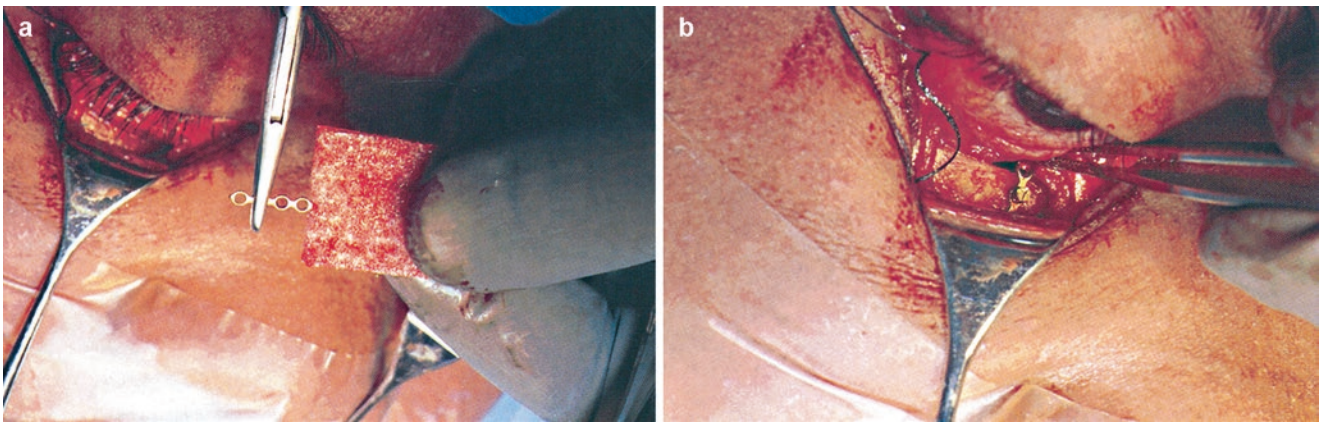


Fig. 42.23 MEDPOR channeled implant. (**a**) Miniplate passed into channel of MEDPOR implant. (**b**) Miniplate bent over orbital rim and secured with 4-mm screw

A long-term complication of the unrepaired blowout fracture is enophthalmos. More than 2 mm of enophthalmos, as measured by an exophthalmometer, usually represents a cosmetic and functional problem. Ptosis with an associated superior sulcus deformity usually results. This may be due not only to an orbital decompression effect but also to actual fat atrophy secondary to the trauma. In severe cases, the globe may settle inferiorly, causing a visible hypo-ophthalmia. The most effective therapy is to prevent this complication by repairing the large orbital blowout fracture early. Late therapy for enophthalmos involves exposing the displaced orbital floor and returning the orbital contents to their normal position. There are many options available to accomplish this. A thick implant of MEDPOR or other material can be fashioned and placed. The use of hydroxyapatite in block or granule form has been advocated. MEDPOR channel implants can be used, with miniplates inserted into the channels to secure them in place in the orbital floor, utilizing orbital rim screws for fixation (Fig. 42.23). MEDPOR is now also manufactured in an implant shaped specifically for placement into the inferior subperiosteal space. Autologous cranial bone can also be utilized for secondary enophthalmos repair. One advantage of autologous bone is that it is not a foreign body and, therefore, has less risk for chronic infection over an open sinus. Over time, however, a fibrous capsule usually surrounds most implants, and in the case of MEDPOR, there is the advantage of vascularization into the implant, which theoretically reduces the chance of infection. This quality could be a disadvantage, however, if removal should become necessary. The porous nature with fibrovascular ingrowth might make removal more difficult, although this is rarely required.

Orbital Roof Fracture

Superior orbital rim and orbital roof fractures are relatively rare in all age groups. These fractures illustrate the difference in injury patterns between adults and children. In adults the frontal sinuses have pneumatized and the frontal bone is thick and fracture resistant. In general high-energy trauma is required to fracture the frontal bones and superior orbit [2, 16]. By contrast, pediatric patients have thinner cranial bone and non-pneumatized frontal sinuses which makes a fracture here more likely. In both cases, however fracture of the rim and/or roof requires a large amount of energy such as a fall, high-velocity impact (MVC), assault, or penetrating trauma. These fractures are most often discovered on a craniofacial CT scan on workup for polytrauma or craniofacial injury [17]. Pretest suspicion may be elevated if there is obvious suprabrow trauma including a laceration or ecchymoses. Extension to the cranial base and cribriform plate may cause CSF rhinorrhea or anosmia. These signs are often noted well after a workup has been done in a trauma patient. The risk of orbital roof/rim fractures in children seems to decrease after the age of 7–10 years because of substantial frontal pneumatization and bone thickening [18].

Life-threatening injuries are prioritized in patients with orbital rim and roof fractures. In the very young pediatric patients, an important consideration about orbital rim and frontal bone fractures is the potential for dural injury and the described phenomenon of a *growing skull fracture* [19]. This includes an expanding CSF-containing cyst that ultimately may create a large full-thickness frontal bone defect but may also exert downward force on the entire bony orbit causing an inferiorly positioned orbit (vertical orbital dystopia) and facial asymmetry. In pediatric patients with

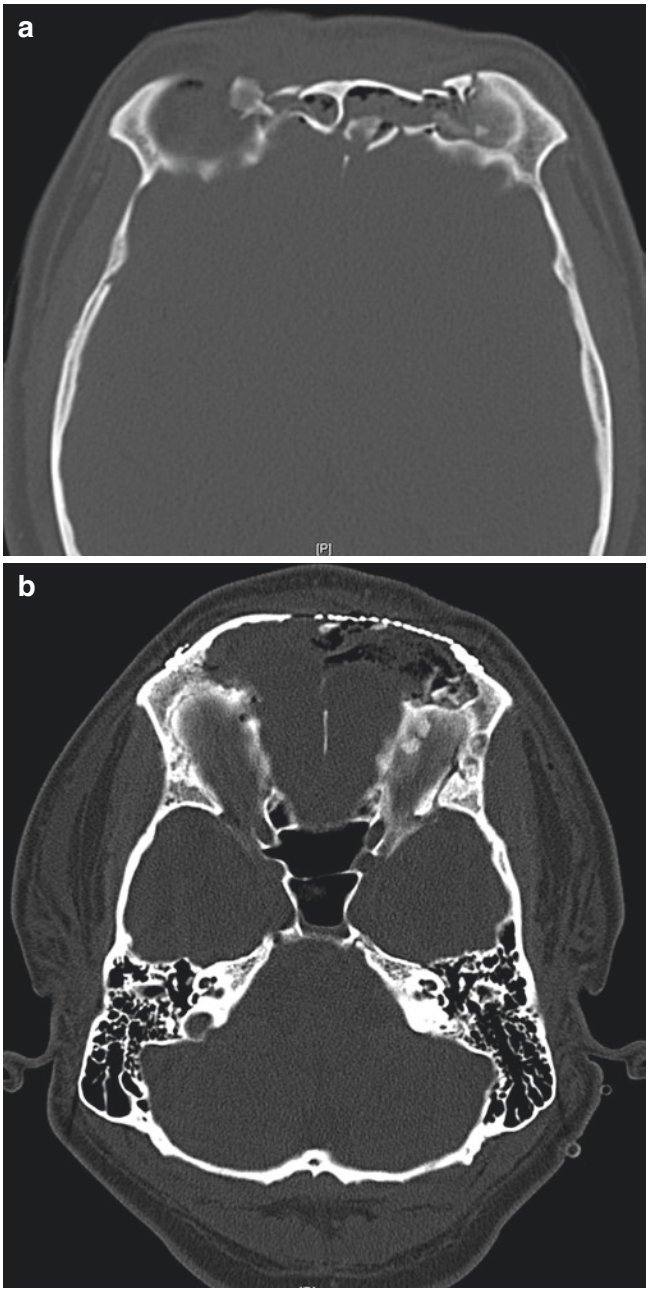


Fig. 42.24 Orbital roof fracture. (**a**) This significant injury can be seen to impact the pneumatized frontal sinus which must be treated as well. (**b**) The orbital roof and frontal bone have been reduced and fixated. The frontal sinus has been cranialized

pneumatized frontal sinuses, the well-descried frontal bone fracture pathway for adults should be followed. In brief nondisplaced fractures with no evidence of dural injury are treated expectantly. Anterior table fractures with displacement are treated with open reduction and internal fixation after obliteration of the frontal sinus (removal/destruction of sinus mucosa, obstruction of frontonasal duct with bone graft). Posterior table fractures with dural injury are treated with open reduction, internal fixation, and frontal sinus cranialization after repair of the dural injury. Therefore in pediatric patients, a critical aspect of reviewing CT scans is looking for frontal sinus pneumatization and involvement (see Fig. 42.24).

There are three fundamental approaches to the orbital roof and rim – the upper lid, a bicoronal incision, and through traumatic lacerations. In general the upper blepharoplasty incision provides limited ability to treat only minimally displaced orbital rim fractures. Facial lacerations often provide access to some bony injuries during repair. Comminuted orbital roof fractures, complex rim fractures, and posterior table frontal bone fractures must be approached with a bicoronal incision. These incisions are well tolerated because of postoperative coverage with hair. The reconstruction of the orbital roof, particularly in the pediatric population, may have important consequences. Herniation of anterior cranial fossa and middle cranial fossa brain contents through the orbital roof or large sphenoid wing defects is well-documented in neurofibromatosis patients to cause slow, incipient changes in orbital anatomy ultimately resulting in significant orbital dystopia and vision changes. These fractures also illustrate the role of new technology in improving the accuracy of reconstruction. The orbital roof is a complex, saddle-like structure that even via an anterior craniotomy is difficult to visualize because of the presence of the frontal bones. CT scans with 3D reconstructions are now used to produce both stereolithographic models that may be brought sterile to the operating room as well as to manufacture patient-specific implants. In children many surgeons have begun to take into account the potential growth effect and long-term consequences of permanent hardware. These injuries are rare and reconstruction is even rarer. The reality is that these fractures are typically non-operative. In the cases

that there is an operative indication, it is often a persistent CSF leak. The approach to these gravely injured patients is multidisciplinary with ophthalmology, neurosurgery, craniofacial surgery, and intensivists. Comminution of the orbital roof has likely led to concomitant devastating brain injury.

The current approach of two authors (PAG, JAT) in children under the age of 5 years is to bend a resorbable mesh to the shape of the orbital roof using CAD/CAM technology. Morsellized bone graft shavings from the cranium are placed onto the comminuted orbital roof, and the roof is then covered with this mesh to create a rigid environment. This resorbable material retains mechanical strength for approximately 3 months and resorbs completely in 2 years. It is fixated to surrounding bone with resorbable screws. In older children and adults in a trauma setting, this reconstruction would typically be done in a similar fashion but with titanium mesh.

Zygomatic Fractures

The zygoma represents a large and prominent bone of the face making it prone to direct trauma. Injury to the zygoma may be to the main body or to the zygomatic arch. The zygomatic body has a complex three-dimensional structure with four important articulations: maxillary, frontal, arch, and greater wing of the sphenoid within the orbit [20]. There are anatomic and behavioral reasons that make zygomatic fractures less common in young children. Facial projection in the very young child is relatively greater in the frontal bone than in the facial bones making a direct blow to the zygomatic body less likely. In addition, the maxilla is filled with unerupted teeth, and the maxillary sinuses have not yet pneumatized making fracture less likely. Young pediatric patients are also more likely to suffer "greenstick" (unicortical) fractures with no displacement. That observation has been challenged by some large series, however. In a series of 912 pediatric patients, one group found that approximately 24% of patients had zygomatic fractures. Of these 70% were treated operatively either with minimally invasive reduction or with open reduction and internal fixation [21].

Signs that may suggest the presence of a zygomatic fracture include laceration/abrasion/ecchymosis over the zygoma, high-energy trauma with other facial injuries, and numbness in the upper lip and territory of the inferior alveolar nerve. 3D CT scan confirms the presence of a fracture, degree of displacement, and the presence of bony comminution. Displaced zygomatic fractures can decrease facial projection and width leading to poor aesthetic results if not addressed. The displaced zygoma can also interfere with mandibular coronoid translation. Because it contributes to the orbit, zygoma fractures from high-energy trauma have also been observed to cause vision changes and blindness.

The surgical approach to zygomatic body fractures when they are isolated is often through multiple incisions: extended upper lid blepharoplasty incision, transconjunctival incision, and upper buccal sulcus incision. The upper lid blepharoplasty incision allows visualization and fixation of the zygomaticofrontal suture (ZF), which is often kept in preliminary reduction with wire fixation. The lower lid incision allows examination and treatment of the inferior orbital rim and if present the orbital floor. The upper buccal sulcus incision allows access for plate fixation of the zygomaticomaxillary junction. In general after preliminary ZF reduction, the zygoma is reduced at the ZM and in the orbit at its junction with the greater wing of the sphenoid. If a subciliary incision (skin-muscle flap) is used to access the inferior orbital rim, it is critical to resuspend the soft tissue to the bone (see Fig. 42.25). A lateral canthopexy through the upper lid incision may also be advisable. Displaced arch fractures may be treated through a temporal incision (Gillies approach) minimally (Fig. 42.26). A small transverse incision is designed 2–3 cm anterior and superior to the helical rim. This incision is directly above the zygomatic arch. The incision is carried down to the deep temporal fascia. The fascia is incised and an elevator is passed into the fascia above the temporalis muscle. The elevator is positioned medial to the arch fragment and used to reduce the fragment.

Complex Facial Fractures

Complex facial fractures include a number of other facial fractures including Le Fort (LF) patterns of facial fractures, naso-orbital-ethmoid fractures, and pan facial fractures.

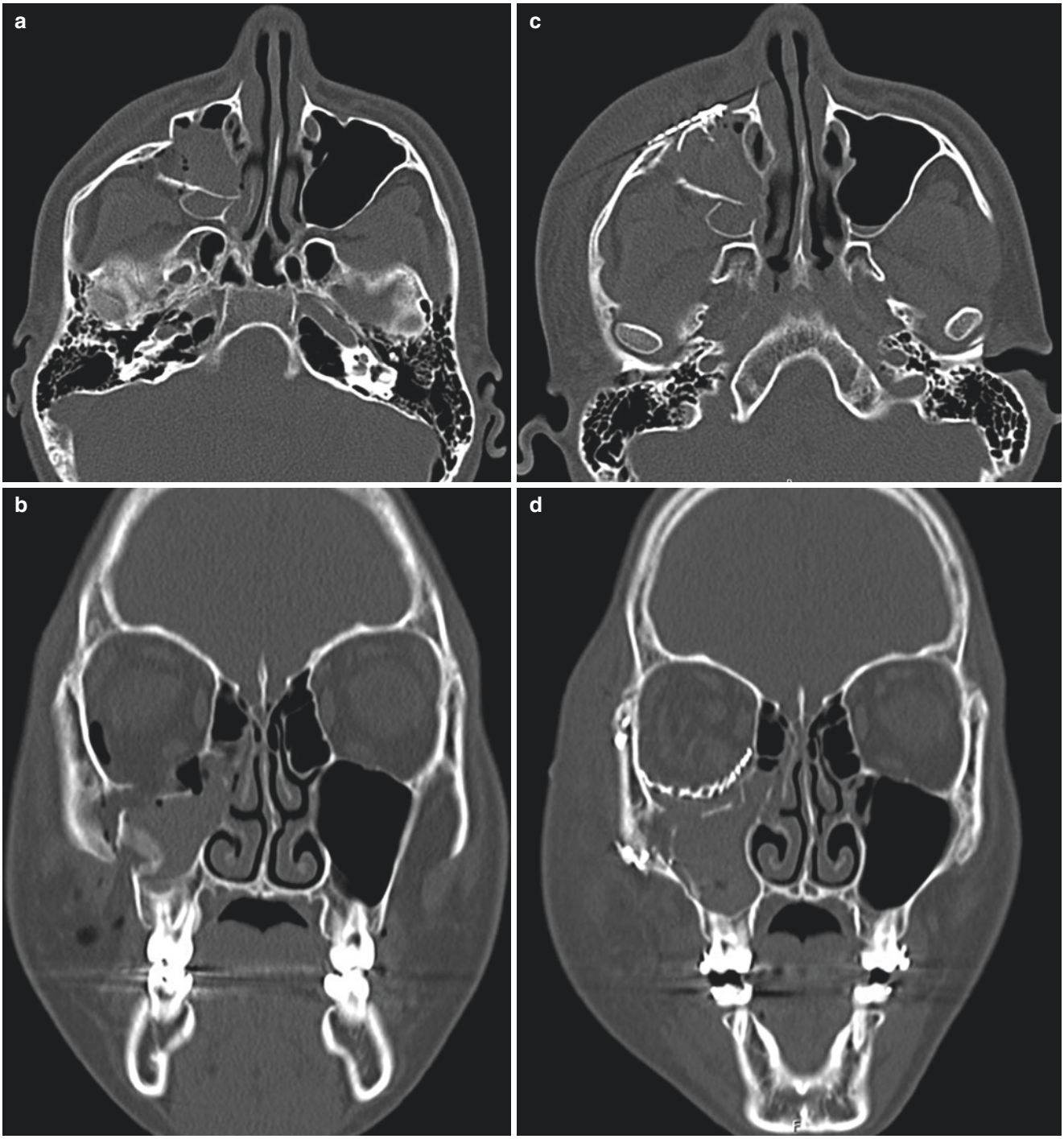


Fig. 42.25 Zygoma fracture. (**a**, **b**) This patient has a displaced and comminuted right zygoma fracture. (**c**, **d**) The zygoma is reduced and fixated, and the orbital floor is treated simultaneously

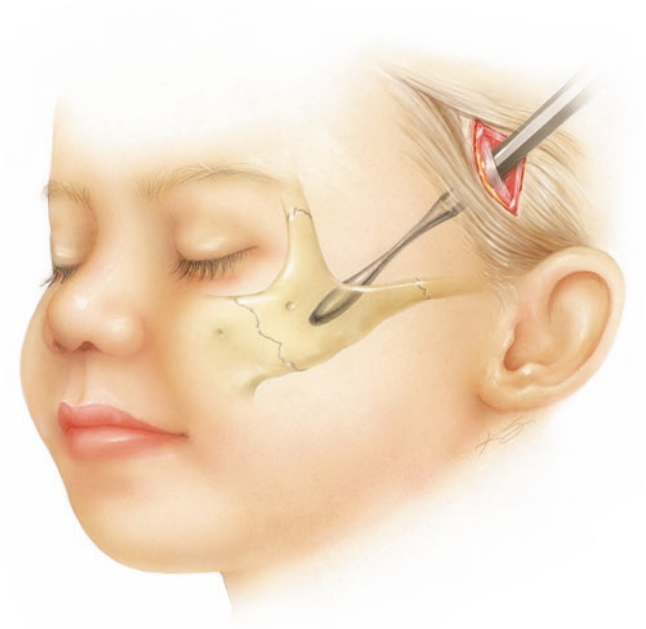


Fig. 42.26 The Gillies temporal approach to reduction of a zygomatic arch fracture

Critical aspects of managing these complex facial fractures include airway management, coordinating care of the facial fractures with that of concomitant injuries, and timing of repairs in the critically ill patient.

Nasoorbitoethmoid (NOE) Fractures

NOE fractures are complex fractures that often result in depressed/collapsed nasal dorsum as well as lateral displacement of the media canthi (telecanthus). They are often associated with other injuries and facial fractures. In the course of repairing NOE, it may also be necessary to repair medial orbital, orbital rim, and frontal bone fractures. NOE fractures can be diagnosed with physical exam, but definitive anatomic diagnosis is made with CT scan preferably with 3D reconstructions. The critical goals of treating NOE fractures are to reduce and fixate the bony fragments while simultaneously returning the medial canthus to an anatomic position. This can be challenging to estimate if the patient has bilateral NOE fractures. The Manson-Markowitz classification is a simple system for describing the level of comminution: Type 1, medial canthus attached to large bony fragment; Type 2, medial canthus attached to small bony fragment; and Type 3, medial canthus completely avulsed [22] (Fig. 42.27). A type 1 injury may allow canthal reposition by ORIF, but the Types 2 and 3 often require transnasal wiring with a judgment about canthal positioning made in the OR.

The surgical approach to the NOE fracture is typically via lower lid and bicoronal incisions. An upper buccal sulcus incision may also be useful. Some patients will present with a laceration that can be used for direct exposure also. Minimally comminuted fractures with Type 1 NOE can be reduced and fixated. Severely comminuted fractures with Type 2 and 3 NOE fractures are much more challenging (Fig. 42.28). This often requires fixation as best possible and subsequent transnasal wiring of the medical canthus. The critical teaching is a superior and posterior vector of pull for the medial canthus to avoid undercorrection and correction positioning. The superior aspect of the lacrimal fossa is typically the aiming point. Xeroform or other bolsters are often placed after transnasal wires to ensure close skin apposition to the canthus – these are typically kept in place for 1–2 weeks. Long-term complications of NOE fractures are largely related to inadequate correction of dorsal collapse, medial canthal malposition, and medial canthal soft tissue swelling/cicatrix [23]. High rates (50%) of lacrimal drainage dysfunction have been observed [24]. The nasal airway may also be obstructed.

Le Fort Fractures

The pattern of these maxillary fractures was described after a series of cadaver experiments in 1901 by Rene Le Fort [25]. In more recent history his fracture patterns have been translated into surgical procedures to correct malocclusive states and craniofacial abnormalities. It is important to recognize that these fractures occur after high-energy trauma and are often accompanied by additional facial bone fractures (see *Panfacial Fractures*). Additionally, while the levels that Le Fort described allow for easy to remember classification, the actual fracture patterns may be asymmetric (i.e., left fracture different than right) and/or combined. There are three commonly recognized Le Fort fracture patterns. Completeness of all three levels of fractures depends upon dysjunction at the pterygomaxillary level (retromolar area). Le Fort I (LF1) is also known as the "horizontal" fracture. This fracture occurs transversely through the

maxilla below the zygoma. Le Fort II (LF2) or the "pyramidal" fracture is fracture dislocation of the nasofrontal junction and the zygomaticomaxillary suture (across the inferior orbital rim and up through the medial orbital wall). Le Fort III (LF3) is called the "transverse" fracture and is upper face separation. The fracture occurs transversely across the face with separation of the zygomatic arch, zygomaticofrontal suture (ZF), and nasofrontal (NF) junction (Fig. 42.29).

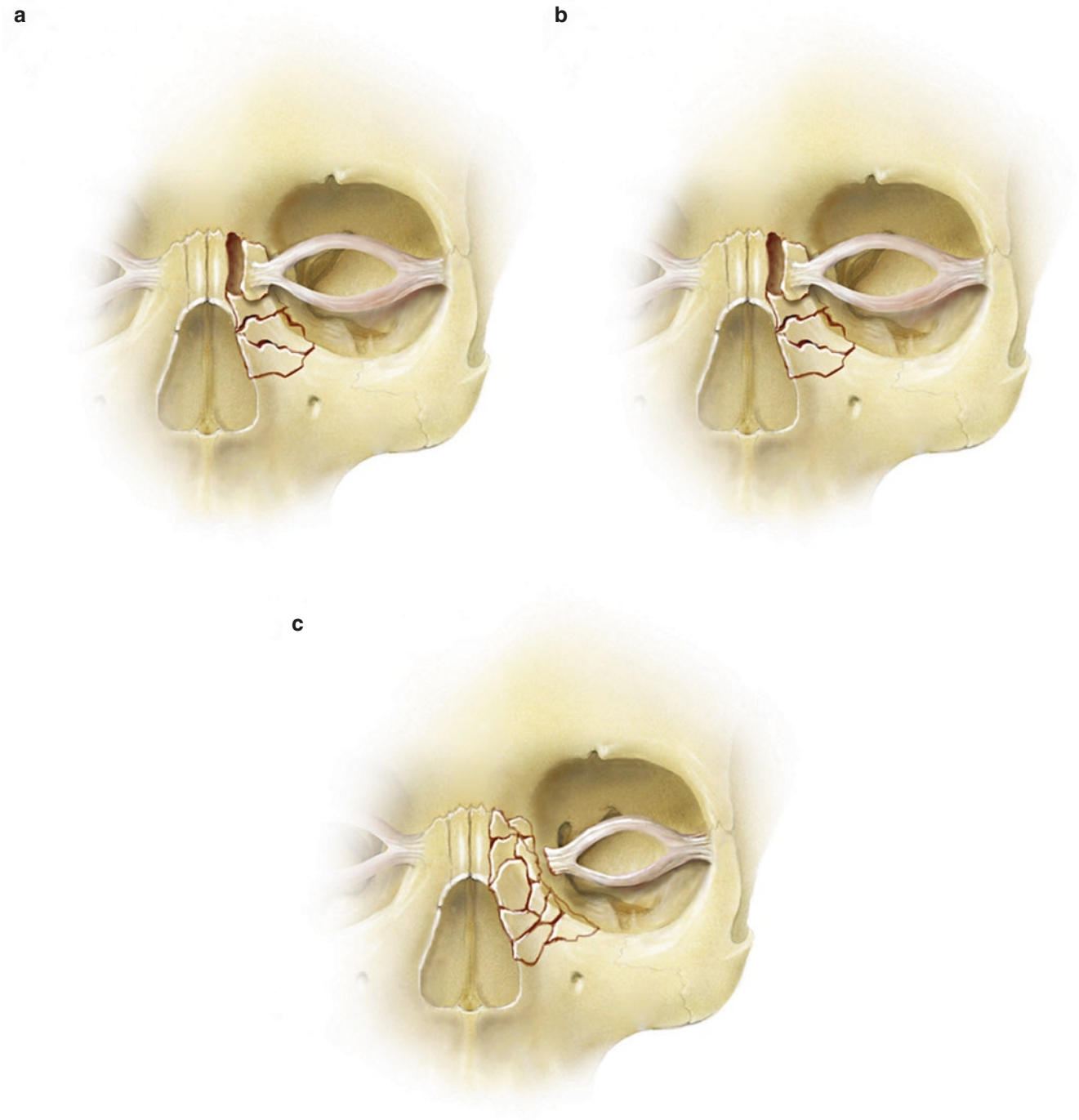


Fig. 42.27 Manson-Markowitz classification for NOE fractures. (**a**) Type 1 – medial canthus attached to large bony fragment. (**b**) Type 2 – medial canthus attached to small bony fragment. (**c**) Type 3 – medial canthus completely avulsed

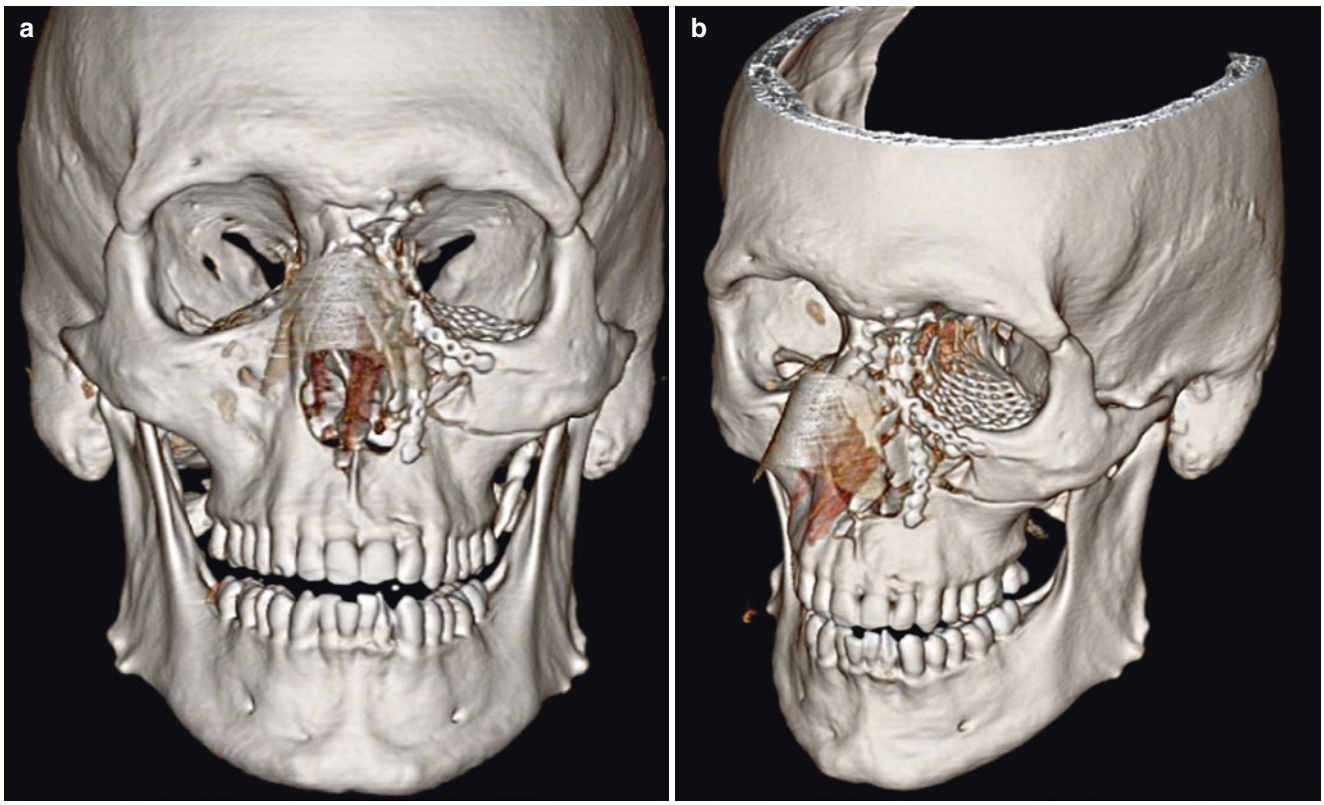


Fig. 42.28 Type 2 NOE fracture. (**a**, **b**) Postoperative changes demonstrating reduction and fixation of the NOE as well as the orbital floor, and orbital rim. The Le Fort 1 fracture was incomplete and stable and thus not fixated

A key feature of these fractures is malocclusion, which is a main aim of surgical correction. LF1 fractures by definition do not impact the orbit. LF2 and LF3 fractures impact the orbit, and in reconstructing them, it is important to recognize whether the orbital floor (inferior or medial) needs reconstruction or augmentation. Surgical approaches to LF fractures depend upon the level. Most important is recreation of the premorbid occlusion. Occlusion is maintained intraoperatively using maxillomandibular fixation. LF1 fractures are approached through an upper buccal sulcus incision. The nasomaxillary (medial) and zygomaticomaxillary (lateral) buttresses are reduced and fixated. Treatment of LF2 fractures typically requires the addition of a transconjunctival lower lid incision for rim reduction and fixation. LF3 fractures typically require the use of a bicoronal incision to access the NF and the zygomatic arch in addition to the upper buccal sulcus incision.

Pan Facial Fractures

Pan facial fractures as the name implies generally describe massive bony facial injury. The challenge is generally twofold: (1) a high number of fractures to expose, reduce, and fixate and (2) loss of stable relationships upon which to base bony reduction. Additionally these patients may be complicated by other life-threatening bodily injuries, intracranial injury, and significant facial soft tissue injury [26].

The critical first steps in treating a pan facial fracture patient are securing a stable airway and a proper trauma assessment to identify all injuries. Classically, patients underwent a tracheostomy in preparation for repair of fractures. Now many argue for less permanent airway such as a submentally placed endotracheal tube that allows establishment of occlusion but otherwise acts as a normal temporary tube [27]. The philosophical approaches to these have been developed to address this lack of stable reference. There is considerable disagreement about the sequence of fracture treatment in these patients – different groups have argued for top down, bottom up, inside out, and outside in fracture reduction [28, 29]. This appears to be a matter of surgeon preference. As with the other fractures discussed above, the orbit may be variably affected but must always be assessed. Fig. 42.30.

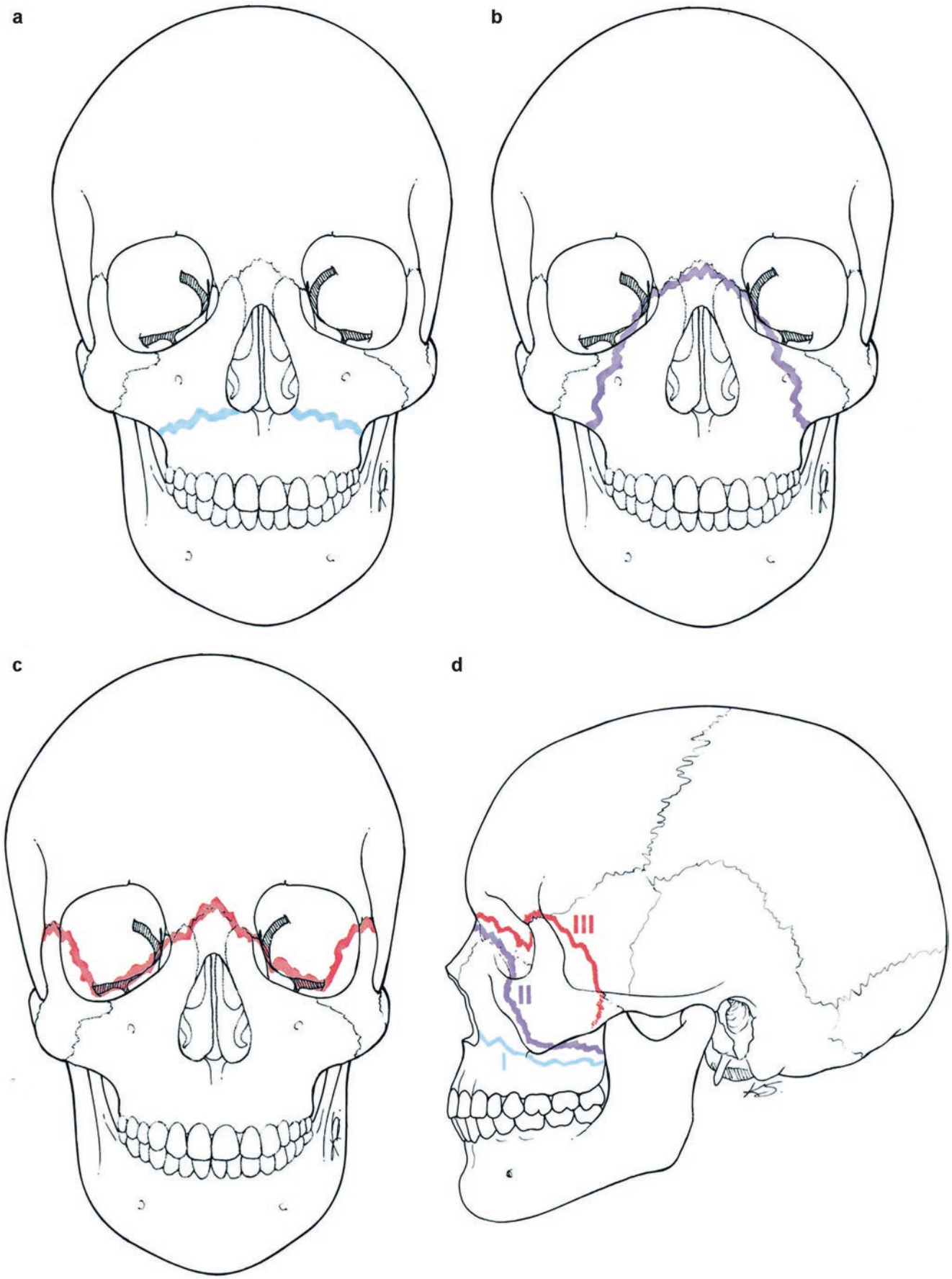


Fig. 42.29 Le Fort fractures. (**a**) Le Fort I fracture. (**b**) Le Fort II fracture. (**c**) Le Fort III fracture. (**d**) Lateral view demonstrating fracture lines for each type of Le Fort fracture



Fig. 42.30 Complex fracture repair. (**a**) Seventeen-year-old patient following motor vehicle injury. (**b**) CT demonstrating fractures of orbital rim, floor, maxilla, and zygoma. (**c**) Coronal flap used to expose complex fracture involving the superior orbital rim fixation plates in place. (**d**) Transantral approach used to wire fragments of maxillary bone. (**e**) Transconjunctival approach used to expose inferior orbital rim and floor. Rim fragments wired in place; A 0.3 mm supramid sheet was placed on floor. (**f**) Appearance of patient 6 months postoperative

Orbital Plating Systems

In adult craniofacial trauma, titanium hardware remains the mainstay for rigid fixation. Pediatric patients present a challenge in that treatment will occur in the presence of ongoing growth and in the setting of a long future life span. Many attempts have been made to avoid using permanent hardware in pediatric patients. There is a long history of using cranial bone for a craniofacial reconstruction in pediatric trauma patients. In the modern paradigm, cranial bone graft (typically the inner table split from the outer table) is used left often. There are circumstances including isolated orbital floor or medial orbital wall fractures in which this entails a fairly morbid donor sites. Harvest requires part or all of a bicoronal incision and may cause a cranial irregularity at the donor site as well as putting the patient at risk for harvest-related complications. Split calvarial bone graft remains a key component of augmenting complex craniofacial reconstruction particularly in pediatric patients. The most important reason that it is not used solely is that significant degree of resorption has been noted by surgeons making the reconstruction somewhat unpredictable [30].

Titanium mesh and miniplates remain the most popular rigid reconstructive option. Plates for orbital floor reconstruction have been designed to mimic the normal contours of the floor. It may be tempting to view these plates as "plug and play," but they are almost always tailored by the surgeon to the specific patient. Titanium hardware has many advantages including strength, infection-resistance, conformability, and simplicity. Many surgeons have begun to advocate for removing the hardware after bony healing is adequate in the growing pediatric patient (less than 10 years of age) [31]. A variety of nonmetallic alloplastic materials exist for treating orbital fractures. The most notable and popular one is porous polyethylene known commonly by its trade name MEDPOR (Stryker Corporation, Kalamazoo, Michigan, USA). This material has been used for reconstructive and cosmetic facial implants. Its pores and material properties promote soft tissue ingrowth and partial vascularization. There has been hope that this would enhance resistance to microbe colonization and infection. However there have been many reports of infected porous polyethylene being removed. Porous polyethylene and titanium are now commonly used as a combination orbital floor plate [32].

Resorbable plates, meshes, and screws hold a great deal of appeal in pediatric patients. Resorbable materials have the potential to mitigate long-term growth restriction, avoid long-term infectious complications, and remove the need for later anesthetic and surgery to remove existing hardware. A number of different resorbing polymers have been brought to market. PLLA (poly L-lactide) has had some late resorption-related inflammation. Resorbable mesh currently in use is made of 85:15 poly L-lactide-co-glycolide (Synthes, Johnson & Johnson) (Fig. 42.31). This material is resorbed through hydrolysis. Full resorption typically takes 12–18 months. Small series using this material have demonstrated comparable rates of enophthalmos in the long term [33, 34]. The challenges of using resorbable hardware include less robust implantation with resorbable screws, more fatigability of the plates, less structural rigidity, and high cost [35]. Table 42.1.

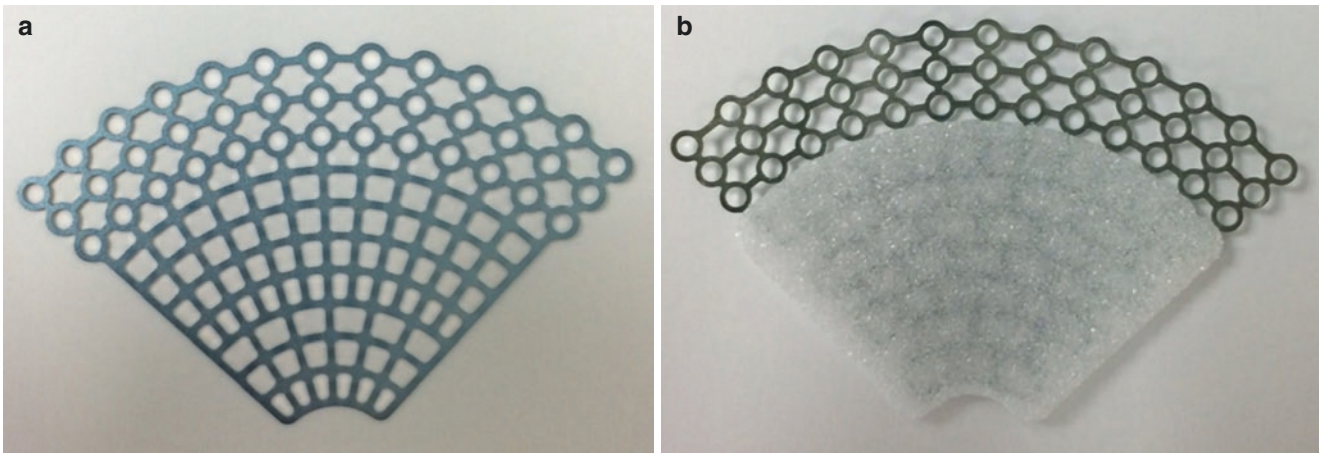


Fig. 42.31 Additional examples of typical orbital floor repair material. (**a**) Titanium mesh. (**b**) MEDPOR with titanium reinforced.

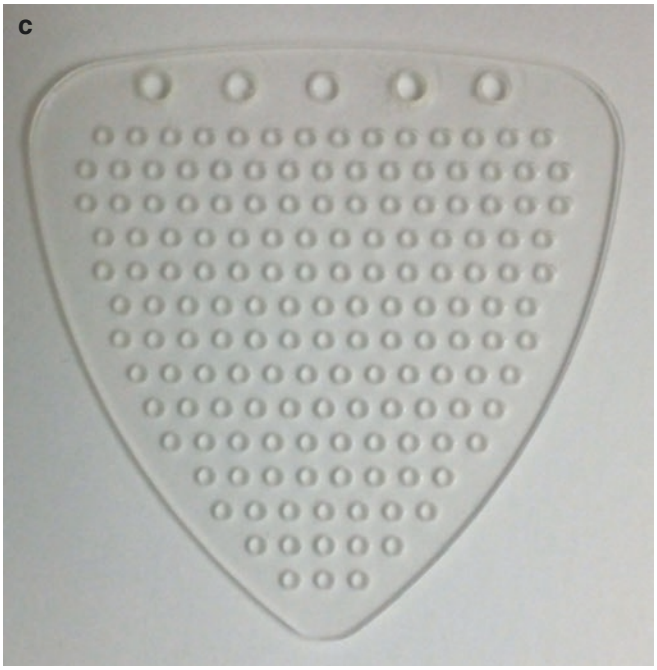


Fig. 42.31 (continued) (**c**) Resorbable mesh (85:15 poly (L-lactide-co-glycolide)

Table 42.1 Commonly available plating systems for orbital floor and facial fractures

Manufacturer	Orbital floor material	Screw diameter (mm)	Comments
DePuy Synthes CMF West Chester, PA	Titanium Mesh Synpor (porous polyethylene) sheet Synpor (porous polyethylene) titanium reinforced resorbable	1.0, 1.3	Thickness 0.2, 0.3, and 0.4 mm; anatomic variant available Thickness 0.45–3.0 mm, some stack for enophthalmos correction Thickness 0.5 mm
KLS Martin LP Jacksonville, FL	Titanium mesh	1.0, 1.5, 2.0	
Stryker CMF Kalamazoo, MI	Titanium mesh MEDPOR (porous polyethylene) sheet MEDPOR (porous polyethylene) titanium reinforced	1.2	Thickness 0.25–3.0 mm, ultrathick semi-custom variant for enophthalmos Available in nonporous form on one or both sides
Biomet Jacksonville, FL	Titanium mesh	1.5, 1.8	Thickness 0.2, 0.3 mm

3D Computer-Aided Surgical Planning

Computer-assisted surgical planning (CASP) has become commonplace in a number of areas in craniomaxillofacial reconstruction. Those areas include post-oncologic reconstruction with fibula free flaps and orthognathic surgery (see Chap. 9). CASP has not found a need in the repair of acute fractures because one of its most powerful features is precise planning of osteotomies – unnecessary in that setting. CASP has been used for late reconstruction of maxillofacial fracture malunion [36].

Traumatic Optic Neuropathy

Blunt trauma of the head, even if not of sufficient severity to cause a fracture, can injure the optic nerve [37]. Traumatic optic neuropathy is a frequently overlooked cause of post-trauma morbidity.

The mechanism of injury involves blunt trauma, usually in the area of the brow. An instantaneous deformation of the bony orbit will result. This deformation need not cause a fracture. This deformation is accompanied by sudden movement of the orbital soft tissue, caused by the impact of the injury. The optic nerve is subjected to massive mechanical forces caused by the deformation and the soft tissue shifting. The portion of the optic nerve within the optic canal, which is firmly anchored to the periosteum, can be damaged by this mechanism. Canal deformation can crush the nerve within the canal, or the nerve can be damaged by a shear injury within the canal. The net result is the same: damage to the optic nerve.

The presence of traumatic optic neuropathy should be suspected with any type of head trauma (Fig. 42.32). The diagnosis is made by documenting decreased vision, as well as signs of optic nerve dysfunction, such as a Marcus Gunn pupil (afferent pupillary defect). The diagnosis can be difficult to confirm clinically. The patient's level of consciousness may not allow for an accurate visual acuity. The pediatric patient often is unable to cooperate adequately for the practitioner to obtain an accurate visual acuity. The pupil may be difficult to examine because of surrounding soft tissue swelling, because the pupil has been pharmacologically altered by narcotics prior to consulting the ophthalmologist, or because the pupil itself was injured by the blunt trauma. In these situations, the clinician will have to use clinical judgment to determine appropriate therapy.

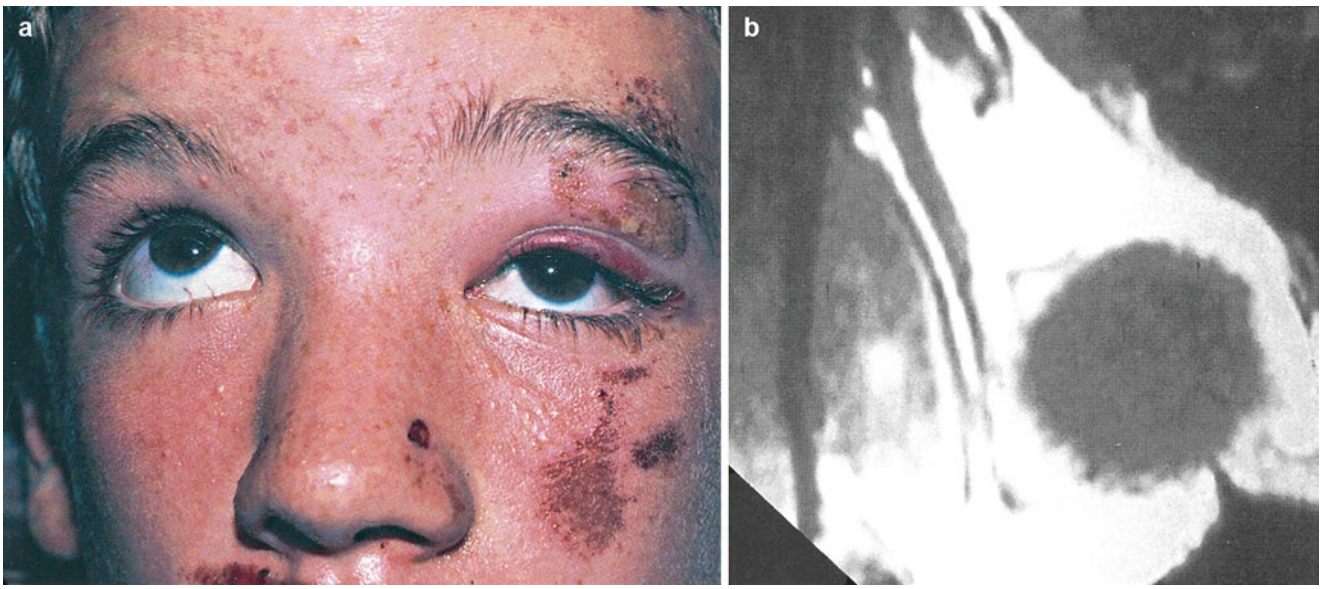


Fig. 42.32 Traumatic optic neuropathy. (**a**) A 13-year-old male fell while skateboarding, striking left brow. Vision in the left eye was count fingers with an obvious afferent pupillary defect present when he was first examined in the emergency room. Restriction of upgaze due to mass effect of hematoma. (**b**) Sagittal view of MRI shows large subperiosteal hematoma. Coronal view is shown in Fig. 42.13

The most important step in managing traumatic optic neuropathy is to consider it. It is imperative that the diagnosis be entertained in any patient with head trauma. An accurate visual acuity should be obtained at the earliest possible opportunity. The first reliable visual acuity obtained will be the one used to guide appropriate therapy. While the visual acuity is best evaluated by having the patient read a Snellen acuity chart at 20 ft, this is usually not a practical consideration. A near vision card held at 13 inches will work. If not available, have the patient try to read anything available in an attempt to assess the visual acuity. Next, the pupil is tested for an afferent defect by using the swinging flashlight test.

Once the diagnosis is established by the presence of decreased vision and optic nerve dysfunction or suspected by the severity of the trauma, the orbit must be evaluated with CT scans. Narrow cuts provide the most detail and are preferable. Axial CT scans of the orbits 1.5 mm in thickness with coronal and possibly sagittal reconstructions should be ordered. Direct coronal views of the orbit, while highly desirable, often cannot be obtained in the trauma patient because of cervical spine precautions. While an orbital CT scan is essential to evaluate the possibility of bone fragments compressing the optic nerve, the diagnosis of traumatic optic neuropathy does not require the presence of a visible fracture.

As soon as the diagnosis is made, medical management can be initiated. This can start even prior to imaging the orbit. The management of this condition is not entirely clear, but much anecdotal evidence supports the use of high-dose steroids [38, 39]. The initial dose is either 30 mg/kg of methylprednisolone followed by 5.4 mg/kg/h or 2–3 mg/kg of Decadron in the first 24 h. This involves using 3–4 mg/kg of Decadron to load followed by 1–2 mg/kg every 6 h for 24 h. Medical management beyond the first 24 h depends on the clinical response. If vision is poor and there is no improvement, steroid use can be rapidly tapered in 1–3 days. Improvement in the visual acuity of any kind requires a slower taper with frequent checks of the vision to insure the response is maintained.

Surgery does have a place in the management of this condition, however. If CT scans reveal bone fragments compressing the optic nerve, surgical removal of the fragments is indicated. Our preference is for an endoscopic approach for decompression of the optic canal in conjunction with our otolaryngology colleagues (see Chap. 9). Another situation where surgical therapy is indicated involves the patient who responds well to steroids initially but loses the response as the steroid dose is tapered. A corollary of this is the patient who responds initially to steroids only to deteriorate while still on the same steroid

dose. Despite both medical and surgical management, many patients who present with a traumatic optic neuropathy do not improve. A 1996 study found that there was no clear benefit for either corticosteroid therapy or optic canal decompression; thus management may be determined on an individual patient basis [38].

It is critical to recognize that this condition is a dynamic one. Frequent visual acuity checks are necessary. Medical management should start as soon as the diagnosis is made. The natural history of traumatic optic neuropathy in many individuals is to improve. Anecdotal evidence strongly supports the use of high-dose steroids for this condition; however treatment is best determined on an individual patient basis.

Summary

Trauma of the periorbital area and globe can cause severe morbidity if not properly treated. While maintenance of life certainly takes priority in managing trauma, it is vital that ocular trauma be recognized and appropriately managed to prevent or minimize the associated morbidity. Recognition and management of injury to the globe, optic nerve, and surrounding bones and soft tissues require the early and active management of an ophthalmologist who is comfortable with the management of trauma. Early medical and surgical intervention of these injuries will insure that the best possible outcome is realized. This is best handled with a multidisciplinary team approach.

Textbooks often, out of necessity, treat pediatric diseases as discrete and separate entities. This approach has shortcomings when dealing with pediatric trauma. A severely injured child often requires the expertise of multiple specialists for appropriate management. This is especially true of the severe head injury in the child. Appropriate management may require input from a neurosurgeon, craniofacial surgeon, general surgeon, oromaxillofacial surgeon, otorhinolaryngologist, ophthalmologist, and pediatrician. It is important that each of these specialists appreciates and respects the expertise brought to the management of head trauma by the others. The team approach is in the patient's best interest, with frequent discussion between specialists to insure that care is coordinated and applied in the proper sequence. No single specialist can manage all the possible conditions created by severe head trauma.

References

1. Mellema PA, Dewan MA, Lee MS, Smith SD, Harrison AR. Incidence of ocular injury in visually asymptomatic orbital fractures. Ophthal Plast Reconstr Surg. 2009;25(4):306–8.
2. Hatton M, Watkins L, Rubin P. Orbital fractures in children. Ophthal Plast Reconstr Surg. 2001;17(3):174–9.
3. Caranci F, Cicala D, Cappabianca S, Briganti F. Orbital fractures: role of imaging. Semin Ultrasound CT MR. 2012;33(5):385–91.
4. Green B, Kraft S, Carter K, Buncic J, Nerad J. Intraorbital wood: detection by magnetic resonance imaging. Ophthalmology. 1990;97(5):608–11.
5. Kubal W. Imaging of Orbital Trauma 1. Radiographics. 2008;28(6):1729–39.
6. Mitchell A, Louik C, Lacouture P, Slone D. Risks to children from computed tomographic scan premedication. JAMA. 1982;247(17):2385–8.
7. Ordog G, Rosenthal M. Management of gunshot wounds. In: Ordog G, editor. Management of Gunshot Wounds. New York: Elsevier; 1988.
8. Fulcher T, McNab A, Sullivan T. Clinical features and management of intraorbital foreign bodies. Ophthalmology. 2002;109(3):494–500.
9. Hayreh S, Kolder H, Weingeist T. Central retinal artery occlusion and retinal tolerance time. Ophthalmology. 1980;87(1):75–8.
10. Lima V, Burt B, Leibovitch I, Prabhakaran V. Orbital compartment syndrome: the ophthalmic surgical emergency. Surv Ophthalmol. 2009;54(4):441–9.
11. Ahmad F, Kirkpatrick N, Lyne J. Buckling and hydraulic mechanisms in orbital blowout fractures: fact or fiction? J Craniofac Surg. 2006;17(3):438–41.
12. Warwar R, Bullock J, Ballal D. Mechanisms of orbital floor fractures: a clinical, experimental, and theoretical study. Ophthal Plast Reconstr Surg. 2000;16(3):188–200.
13. Koornneef L. Orbital septa: anatomy and function. Ophthalmology. 1979;86:876.
14. Katowitz J, Welsh M, Bersani T. Lid crease approach for medial wall fracture repair. Ophthalmic Surg. 1987;18(4):288–90.
15. Su Y, Shen Q, Lin M, Fan X. Diplopia of pediatric orbital blowout fractures: a retrospective study of 83 patients classified by age groups. Medicine (Baltimore). 2015;94(4):e477.
16. Losee J, Afifi A, Jiang S. Pediatric orbital fractures: classification, management, and early follow-up. Plast Reconstr Surg. 2008;122(3):886–97.
17. Haug R, Van SJ, Jenkins W. Demographics and treatment options for orbital roof fractures. Oral Surg Oral med Oral Pathol Oral Radiol Endod. 2002;93(3):238–46.
18. Koltai PJ, Amjad I, Meyer D, Feustel PJ. Orbital fractures in children. Arch Otolaryngol Head Neck Surg. 1995;121(12):1375–9.
19. Havlik R, Sutton L, Bartlett S. Growing skull fractures and their craniofacial equivalents. J Craniofac Surg. 1995;6(2):103–10; discussion 111–2.
20. Alcalá-Galiano A, Arribas-García I. Pediatric facial fractures: children are not just small adults 1. Radiographics. 2008;28(2):441–61; quiz 618.
21. Ferreira PC, Amarante JM, Silva PN, et al. Retrospective study of 1251 maxillofacial fractures in children and adolescents. Plast Reconstr Surg. 2005;115(6):1500–8.

22. Markowitz BL, Manson PN, Sargent L, et al. Management of the medial canthal tendon in nasoethmoid orbital fractures: the importance of the central fragment in classification and treatment. Plast Reconstr Surg. 1991;87(5):843–53.
23. Herford A, Ying T, Brown B. Outcomes of severely comminuted (type III) nasoorbitoethmoid fractures. J Oral Maxillofac Surg. 2005;63(9):1266–77.
24. Becelli R, Renzi G, Mannino G, Cerulli G. Posttraumatic obstruction of lacrimal pathways: a retrospective analysis of 58 consecutive naso-orbitoethmoid fractures. J Craniofac Surg. 2004;15(1):29–33.
25. Gartshore L. A brief account of the life of René Le Fort. Br J Oral Maxillofac Surg. 2010;48(3):173–5.
26. Follmar K, DeBruijn M, Baccarani A. Concomitant injuries in patients with panfacial fractures. J Trauma. 2007;63(4):831–5.
27. Caron G, Paquin R, Lessard M. Submental endotracheal intubation: an alternative to tracheotomy in patients with midfacial and panfacial fractures. J Trauma. 2000;48(2):235–40.
28. Markowitz B, Manson P. Panfacial fractures: organization of treatment. Clin Plast Surg. 1989;16(1):105–14.
29. Kelly K, Manson P, Kolk C. Vander. Sequencing LeFort fracture treatment (Organization of treatment for a panfacial fracture). J Craniofac Surg. 1990;1(4):168–78.
30. Rogers G, Greene A. Autogenous bone graft: basic science and clinical implications. J Craniofac Surg. 2012;23(1):323–7.
31. Nagase D. Plate removal in traumatic facial fractures: 13-year practice review. Ann Plast Surg. 2005;55(6):608–11.
32. Villarreal PM, Monje F, Morillo AJ, Junquera LM, González C, Barbón JJ. Porous polyethylene implants in orbital floor reconstruction. Plast Reconstr Surg. 2002;109(3):877–85; discussion 886–887.
33. Eppley B. Use of resorbable plates and screws in pediatric facial fractures. J Oral Maxillofac Surg. 2005;63(3):385–91.
34. Tuncer S, Yavuzer R, Kandal S. Reconstruction of traumatic orbital floor fractures with resorbable mesh plate. J Craniofac Surg. 2007;18(3):598–605.
35. Bell R, Kindsfater C. The use of biodegradable plates and screws to stabilize facial fractures. J Oral Maxillofac Surg. 2006;64(1):31–9.
36. Tepper O, Sorice S, Hershman G, Saadeh P. Use of virtual 3-dimensional surgery in post-traumatic craniomaxillofacial reconstruction. J Oral Maxillofac Surg. 2011;69(3):733–41.
37. Lessell S. Indirect optic nerve trauma. Arch Ophthalmol. 1989;107(3):382–6.
38. Cook M, Levin L, Joseph M. Traumatic optic neuropathy: a meta-analysis. Arch Otolaryngol Head Neck Surg. 1996;122(4):389–92.
39. Ford R, Lee V, Xing W, Bunce C. A 2-year prospective surveillance of pediatric traumatic optic neuropathy in the United Kingdom. J AAPOS. 2012;16(5):413–7.

Index

A
Abducens nerve, 243
Abrasions, 463–464
Abscess, 623, 624, 629, . *See also Specific types of abscess*
Accessory lacrimal gland, 32
Acetylcholine receptor (AChR), 237, 238
Acetylcholinesterase inhibitors, 239
Acquired immunodeficiency syndrome (AIDS), 449
Acrobrachycephaly, 806, 807
Acrocephalosyndactyly. *See* Apert syndrome
Acrylic conformer, 851
Acuity testing
  quantitative methods of, 184–188
  recognition, 187
Acute intraorbital hemorrhage, 935
Acute lymphoblastic leukemia (ALL), 230
Acute myeloid leukemia (AML), 230, 755
Acute sinusitis, orbital complications, 634
ADC. *See* Apparent diffusion coefficient (ADC)
Adenoid cystic carcinoma, 754
Adhesion molecule, 46
Adnexa
  anatomy, 29–36
  problems, 868
Adnexal trauma, eyelids
  abrasions, 463
  burns, 464
  canalicular laceration, 459
  evaluation, 455
  hemorrhage, 463
  management, 457
  puncture wound, 464
  types, 453
Advancement flap, 77
Agenesis
  canalicular, 521
  punctal, 521
Airway management, 89
  face mask, 89
  laryngeal mask airway, 89–90
  tracheal intubation, 90
Albright syndrome, 177
Alcohol syndrome, 3
Allergic mycotic sinusitis, 576
Allergies, 82
Alloderm, 316
α-smooth muscle actin, 47
Alveolar rhabdomyosarcoma (aRMS), 266, 274, 746–750
Alveolar soft part sarcoma, 751, 752
Amblyopia, 183, 185, 188, 190, 820, 822
American Cleft Palate-Craniofacial Association (ACPA), 875
American College of Radiology, 555, 557, 558
American College of Rheumatology, 655
Amniotic band syndrome, 117, 118, 818, 819
Amniotic membrane, 841–843
  grafts, 925
Amniotic rupture malformation sequence, 117
Amniotoceles, 482
Anesthesia, examination under, 94
Anesthetic induction techniques, 86–88
Aneuploidy, 14
Aneurysmal bone cyst, 618, 731
Angelman syndrome, 14
Angiogenes, 47
Angiographic interventional neuroradiology, 547
Angiosarcoma, 752
Angiotensin converting enzyme (ACE), 649
Anisometropic (astigmatic) amblyopia, 125
Ankyloblepharon, 333
Annulus of Zinn, 789
Anophthalmia, 316–320, 831, 832
  adnexal problems, 868–870
  bony orbital expansion, 848–850
  cosmetic considerations in, 285
  craniofacial reconstruction, 870
  DFG, 858
  etiology, 832–833
  eyelid fissures, 840
  family resources, 872–873
  fetal MRI, 559
  imaging techniques, 835
  incidence, 833
  inflatable orbital implants, 850
  ocularist role, 837
  oculoplastic evaluation, 834
  orbital sphere implantation, 850
  orbital volume expansion, socket management, 867
  osmotic orbital expanders, 853
  with neuroglial malformation, 570–571
  socket, 840
  ultrsound, 837
Anophthalmic socket, 925
Anterior idiopathic orbital inflammation (IOI), 645
Anti-muscle-specific kinase (anti-MuSK) antibodies, 238
Anti-neutrophil cytoplasmic antibodies (ANCA), 651, 652
Antinuclear antibody (ANA), SLE, 655
Anxiety, during induction, 86
Apert syndrome, 807, 808, 887, 897
Apical idiopathic orbital inflammation (IOI), 645, 647
Aponeurotic ptosis, 364, 383
Apparent diffusion coefficient (ADC), 553, 588
Appearance satisfaction, 293
Apraclonidine testing, 240
Argon laser, 699
Arruga trephine, 505
Arterial aneurysms, 133

© Springer International Publishing AG 2018

J.A. Katowitz, W.R. Katowitz (eds.), *Pediatric Oculoplastic Surgery*, https://doi.org/10.1007/978-3-319-60814-3

Arteriography, 123
Arteriovenous malformations, 133–134
Asian eyelid, 402–403
Aspergillosis, 637
  CT, 590
  paranasal sinuses, 589
Asymmetric bilateral ptosis, 386
Asymptomatic ONGs, 248
Atrophy, hypoplasia, 902
Autogenous fascia, HA implant, 919
Autologous tissue reconstruction, 147
Autosomal dominant inheritance, 6, 7
Autosomal recessive inheritance, 7–11
Avulsions, 454
Azathioprine (AZA), 660

B
Balloon catheter, 488
  DCR, 514, 516
Basal cell carcinoma (BCC), 107, 108, 445, 449
Basal cell nevus syndrome, 113–116, 448, 449
Baseline tear secretion test (BTST), 372
B-cell lymphomas, 756
Benign cephalic histiocytosis, 113
Benign orbital tumors, 544, 547
Benign tumors, 177
  mucoceles and, 176
Benign variants, 5
Beta-blockers, 108, 282
  therapy for infantile hemangiomas, 125–127
Bias
  evaluating, 303
  information bias, 302
  preventing bias, 303
  selection bias, 302
Bicanalicular silastic intubation, 528
Bicanalicular silicone intubation, 497
Bicanalicular stents, 493
  complications, 495–497
  extruding, 497
  fixation of tubing, 494
  insertion, 493–494
  postoperative management, 495
  silicone intubation, failure of, 498
  silicone tubing, removal of, 497–498
Bilateral double elevator palsy, 573
Bilateral granulomas, 407
Biologic agents, IOI
  rituximab, 661
  TNF, 661
Birbeck granule, 760, 762
Blau syndrome, 112
Blepharophimosis, 357, 361, 382
Blepharophimosis, ptosis, and epicanthus inversus syndrome (BPES), 353, 361
Blowout fractures, orbit, 936
Blunt trauma, 454, 455, 463
  head, 953
  orbital hemorrhage, 935
Body image, 293–294
Bone bending, 879
Bone grafts, 879, 881
Bone harvesting, 880
Bony abnormalities, 691
Bony defects, 672
Bony lesions, 548
Bony optic nerve canal, 786, 789
Bony orbital expansion, 848, 871, 902
Brachycephaly, 806
Brachyturricephaly, 894
BRAF gene, 105
Branchial arches, 18
Brooke's tumor, 449
B-scan ultrasonography, 694, 709, 713
  infantile orbital hemorrhage, 714
  Schwannomas, 729
Bulbar transconjunctival orbitotomy, 778, 779
Buphthalmos, 560
Burkitt's lymphoma, 213, 234, 756, 757
Burns, 464

C
Caldwell–Luc approach, 631
Camouflage facial defects, 289
Canal deformation, 953
Canalicular agenesis, 523, 524
Canalicular atresia, 521–522
  preexisting patent canaliculus, 523
  single patent canaliculus, 522
Canalicular laceration, 459
  avulsion repair, 460–461
  involvement, 459
  repair of, 462
Canalicular meningiomas, 721, 722
Canalicular stenosis, 525, 526
Canalicular trephine, 524
Canaliculitis, 526–527
Canaliculodacryocystorhinostomy (CLDCR), 524, 525, 529, 532. *See also* Dacryocystorhinostomy (DCR)
  canaliculus repair with, 530
  closed approach, 533–535
  complication, 538
  indications, 529–532
  minimally invasive approach, 537
  open approach, 535–537
  postoperative management, 537–538
  surgical technique, 532–533
Canaliculus, 519
  abnormalities, 521
Cancer, hallmarks of, 274
Cancer stem cells (CSCs), 273
Canthal dystopias, 331–333, 825
Canthal tendon, 32
Cantholysis, 777, 935, 936
Canthotomy, 777, 935, 936
Capillary hemangioma, 582, 584–591, 596, 597
Capillary vascular malformations, 129–131
Capsulopalpebral fascia, 35, 203, 314
Carboplatin, 275
Cardiff Visual Ability Questionnaire for Children (CVAQC), 293
Carpenter syndrome, 811, 897
Cartilage grafts, ear, 75
Cartilaginous neurocranium, 23
Cautery, 319
Cavernous hemangioma, 714
Cavernous sinus, 572
Cavernous sinus thrombosis, 242, 243, 629, 630
Ceftriaxone, 931
Cell adhesion molecules, 52
Cell sorting, 263

CellCept®, 659–660
Cellular degradation, 46
Cellular mediators, 50
Cellulitis
  herpes simplex, 634
  orbital, 626, 627, 635, 636
  preseptal, 623, 624, 626
Central nervous system (CNS) abnormalities, 808
Central neurofibromatosis, 422
Centurion syndrome, 349
Cephaloceles, 687–691
CFEOM. *See* Congenital fibrosis of extraocular muscles (CFEOM)
Chalazion, 439–441
CHARGE syndrome, 320
Chemotherapy, 223–225, 227, 232
  cytotoxic, 225
  gender-based side effects of, 234
  retinoblastoma, 766
Chiasm tumors, 248
Chiasmal lesions, 543
Children's Hospital of Philadelphia (CHOP), 460, 727, 744, 851, 858
  hydrogel expansion, 856
Children's Oncology Group Neuroblastoma Risk Stratification System, 759
Children's Visual Function Questionnaire (CVFQ), 293
Choristoma, 680
Chromic gut, 319
Chromosomal disorders, 3
Chromosomal microarray analysis, 15
Chromosome, 3, 6, 14, 16
  deletions, duplications, and rearrangements, 14–15
  sex, 9
Chronic progressive external ophthalmoplegia (CPEO), 242, 362
Cicatricial retraction, 464
Cidofovir, 215
Clefting syndromes, 194, 195, 811, 815
  amniotic band syndrome, 818
  oculo-auriculo-vertebral spectrum, 817–818
  Treacher Collins syndrome, 815–816
Clinical research, 305–308
  bias, 302–303
  blinding (masking), 299
  case-control study, 299
  case reports and series, 298
  causation vs. association, 305
  chance and p-value, 302
  cohort study, 298–299
  confidence intervals, 305
  confounding, 303–304
  data analysis, 301–302
  data collection, 300
  electronic medical record data, 301
  levels of evidence, 299–300
  odds ratios, 304
  organizing, 297
  paper
    reading, 307–308
    writing, 305–307
  prospective vs. retrospective, 299
  randomized controlled trial, 299
  research question, 297–298
  sample size, 300
  study designs, 298
  subjects, 300
Cloverleaf skull, 810
Cloverleaf synostosis, 823
Coagulopathy, 96
Cocaine, 240
Cogan lid twitch, 238
CO_2 laser resurfacing, 54
Collagen, 51
Coloboma, 114, 320
  MRI, 563
  location of, 322
  optic nerve, 562
  repair of lower colobomas, 326
  repair of upper colobomas, 322
Colobomatous cyst, 683, 832, 848, 849
Color Doppler flow ultrasonography, 546
Color vision, 189
Common canaliculus (CC), 502, 516
Complex facial fractures, 945, 947, 949, 951
Computed tomography (CT), 552, 556
  abnormal globe, 559
  anophthalmia, 835
  buphthalmos, 560
  cephaloceles, 689
  contrast agents, 554
  cryptophthalmos, 560
  dermoid cyst, 424, 561
  developmental anomalies, 558–562, 564, 565
  epidermoid cysts, 561
  extraocular muscles, abnormalities, 565
  fibrous dysplasia, 616
  foreign body, 581
  glial–neural hamartomas, 564
  infantile hemangioma, 413
  infections, 573
  IOI, 577, 640, 642
  LCH, 616
  meningiomas, 608
  metastatic tumors, 613
  microphthalmia, 835
  mucoceles, 684
  mucormycosis, 635
  nasolacrimal duct obstruction, 475
  OLM, 591
  optic hypoplasia, 560
  optic nerve glioma, 593–606
  optic neuritis, 579
  orbital cellulitis, 630
  orbital disorders, 546
  orbital teratomas, 562
  orbital traumatic lesions, 569
  penetrating injuries, 929, 930
  plexiform neurofibromas, 606
  preseptal cellulitis, 624
  radiation exposure, 555
  retinoblastoma, 593
  rhabdomyosarcoma, 608
  sino-orbital aspergillosis, 590
  traumatic optic neuropathy, 954
  vascular lesions, 581, 584
Computer-assisted surgical planning (CASP), 953
Confidence interval (CI), 305
Confounding
  dealing, 303
  measurement, 303–304
Congenital abnormalities, 479
Congenital anophthalmia and microphthalmia (A/M), 316
Congenital craniofacial deformities, 498
Congenital craniofacial disorders, 801, 803, 827

Congenital divided nevus, 105
Congenital eyelid, 361
  retraction, 343
Congenital fibrosis of extraocular muscles (CFEOM), 242, 362
Congenital fibrosis syndromes, 242
Congenital giant hairy nevus, 447, 448
Congenital glaucoma, 561
Congenital Horner syndrome, 365
Congenital kissing nevus, cosmetic considerations, 286
Congenital lacrimal fistula, 519
Congenital masses, 175
Congenital melanocytic nevus, 105–106
Congenital microphthalmos, 285
Congenital myasthenic syndromes, 239
Congenital nasolacrimal duct obstruction (CNLDO), 475, 479
Congenital nevi, 134–135
Congenital nevomelanocytic nevus (CNN), 447
Congenital orbital fibrosis syndrome, 362, 382, 383, 574
Congenital ptosis, 280
  simultaneous vs. sequential, 386
  surgery, 404–408
  repair cosmetic considerations in, 279
Congenital supernumerary (anlage) ducts, 519
Congenital third-nerve palsies, 365
Conjunctiva, 32, 33, 394, 546, 777
Conjunctival biopsy, 213
Conjunctival malignancies, 207–215
Conjunctival melanoma, 209
Conjunctival nevus, 209–211, 286
Conjunctival rhabdomyosarcoma, 211
Contrast agents, 554–555
Contrast enhancement, 747
Contrast material, 573
Contrast-induced nephrotoxicity (CIN), 554
Corneal anesthesia, 161
Corneal integrity, 822
Corneal reflection test, 189
Coronal sections, 494
Corticosteroids (CS)
  infantile hemangioma, 417
  IOI, 644
Cosmetic considerations
  camouflage facial defects, 289
  congenital kissing nevus, 286
  in congenital microphthalmos, 285
  in congenital ptosis repair, 279–282
  conjunctival nevus, 286
  in infantile hemangiomas, 282–285
  limbal dermoids, 286–287
  lipodermoids, 286
  in management of scar formation, 289–290
  periocular soft tissue volume augmentation, 287–289
  posttraumatic scar, 288–289
  in surgically induced anophthalmos, 285
  surgical treatment, 285–286
  vision-threatening hemangiomas, 284
Cover testing, 189
Cox tube, 533, 536, 538
CPEO. *See* Chronic progressive external ophthalmoplegia (CPEO)
Cranial base cartilage, 804
Craniofacial abnormalities, 815, 817, 818, 820–827, 875, 888, 894, . *See also* Craniofacial surgery
  atrophy and hypoplasia, 900
  Carpenter syndrome, 811
  clefting syndromes, 811
    amniotic band syndrome, 818
    OAV spectrum, 817
    Treacher Collins syndrome, 815
  conditions, 904–910
  craniosynostosis, 806–811, 887, 888
    nonsyndromic synostoses, 888
    syndromic synostoses, 894
  embryology of human skull, 801
  eye examination sheet, 820
  hyperplasia, 902
  hypertrophy, 902–904
  neoplasia, 902
  OHT, 898
  ophthalmic examination and surgical considerations
    baseline exam, 820
    exophthalmos, 821
    eyelids, 822
    globe, 822
    nasolacrimal system, 822
    vision and alignment, 820–822
  ophthalmic/oculoplastic surgical considerations, 823
    canthal dystopias, 825
    corneal exposure, 823–825
    nasolacrimal anomalies, 825–826
    ptosis, 827
    strabismus, 827
  rare craniofacial clefts, 881
  regional classification of cleft, 812, 814, 815
  team approach, 818–819
  Treacher Collins syndrome, 884–887
Craniofacial and orbital procedures
  anesthetic emergence and postoperative recovery, 96–97
  anesthetic induction and monitoring, 95
  complications, 96
  intraoperative fluid management, 95–96
  intraoperative maintenance, 95
  preoperative evaluation, 94
  temperature, 96
Craniofacial clefts
  eyelids cleft, 815
  lateral canthal cleft, 815
  medial canthal and nasolacrimal clefts, 814
  midline facial clefts, 814
Craniofacial deformity. *See also* Craniofacial surgery
  approaches, 876
  classification, 875–876
  repair, 531
Craniofacial disorders, 194
Craniofacial implants, 149, 152, 153
  osseointegrated, 151
  titanium, 151
Craniofacial morphogenesis, 18
Craniofacial surgery, 870–872
  complications, 910
  long-term results, 910–912
  preoperative evaluations, 876–881
  preparation, 876
Craniofacial syndrome, 81, 82, 527, 529, 532, 888
Craniofacial team, 876
Craniomaxillofacial reconstruction, 953
Cranio-orbital teratoma, 569
Cranio-orbitotomy, 786
Craniosynostoses, 23, 194, 805, 806, 887
  Apert syndrome, 807
  Carpenter syndrome, 811
  Crouzon syndrome, 806
  Muenke syndrome, 810
  nonsyndromic synostoses, 888
  Pfeiffer syndrome, 809

Saethre–Chotzen syndrome, 810
sagittal, 889
skull deformities arising, 806
syndromic synostoses, 894
Craniotomy, 895
bifrontal, 879, 888, 891, 894, 895
unilateral frontal, 888
with osteotomy, 891, 902
Crawford bicanalicular system, 459
Crawford double-rhomboid technique, 399
Crawford tubes, 516
Crisscross technique, 920
Crohn disease, 656
Crouzon syndrome, 806, 807, 887, 895
Cryptophthalmos, 24, 314–316, 560, 561, 565
CT angiography (CTA), 552
Cushingoid appearance, 644
Custom-designed orbital expander, 853
Cutaneous melanoma, 447
Cyclophosphamide (CYC), 660, 757
Cycloplegic retinoscopy, 372
Cyclosporine (CsA), 660
Cystic lesions, 106, 546, 547
Cysts
dermoid, 106, 135
epidermal, 107
Cytogenesis, 17
Cytokines, 53
Cytoplasmic-ANCA (c-ANCA), 652
Cytotoxic chemotherapy, 225

D
Dacryoadenitis, 649
Dacryoceles, 482–483, 501, 562, 568, 687-688
Dacryocystectomy, 652
Dacryocystitis, 483, 533, 538
Dacryocystocele, 482–483, 501, 562, 568, 687-688
Dacryocystogram, 476
Dacryocystography (DCG), 475, 476, 521, 527
Dacryocystorhinostomy (DCR), 94, 501, 503–509, 521, 523, 652, . *See also* Canaliculodacryocystorhinostomy (CLDCR)
anatomical considerations, 501–502
complication, 513–514
endoscopic, 503, 509–513
external, 503, 507
children, 503–509
incisions, 504
failure, 514–518
nasal opening, 515
postoperative care, 509, 513
preoperative evaluation, 502–503
silicone stents, 503
with Silastic intubation, 530
Dacryolith stones, 527
Dacryoscintigraphy (DSG), 476–477
Dacryostenosis, 479, 480, 487, 488
conservative/surgical management for, 480–482
failed probing, treatment for, 487
intubation materials, 488–489
management of dacryoceles, 482
monocanalicular stents, 489
nasolacrimal duct
balloon dilation of, 487–488
silicone intubation of, 488
neonatal dacryocystitis, 483
probing and irrigation under general anesthesia, 483
De Sanctis-Cacchione syndrome, 214
Death-associated protein kinase gene (DAPK), 274
Deformity
craniofacial
approaches, 876
classification, 875–876
repair, 531
dog-ear, 78–80
foot deformity, 808
Demyelination, T2 FLAIR, 553
Dendritic cell (DC) disorders, 656
Dental abscess, 626
Dental anomalies, 808
Dermabrader, 862
Dermabrasion, 105
Dermis fat graft (DFG), 76, 77, 841, 849, 857, 858, 860–864, 871, 872, 915, 918, 919
anophthalmic socket, 925
harvesting, 918
implantation, 918–919
orbital implant, 858–867
Dermoid cyst, 106, 107, 135, 561, 566, 567, 667, 669, 671
CT, 424
deep, 672
DWI, 568
eyelids, 420, 422
medial, 674
paraorbital, preseptal, 566
recurrent, 677
temporal, 673
Dermolipoma, 676, 678
Developmental anomalies of the orbits, 194
Difficult airway, 81, 87
algorithm, 91, 92
Diffuse cutaneous mastocytosis, 108
Diffuse idiopathic orbital inflammation (IOI), 645
Diffusion-weighted imaging (DWI), 553
dermoid cyst, 568
ischemic papillitis, 594–595
rhabdomyosarcoma, 610, 614
subperiosteal abscess, 588
Dificult airway management, 91
DiGeorge syndrome, 3
Digital subtraction MDCG, 475
Diplopia, 242
Discharge criteria
after day surgery, 97
medically fit for, 97
Disease-modifying antirheumatic drug (DMARD), 659
Distal canalicular system, 524–525
Distal nasolacrimal lacrimal system, 22
Distichiasis, 333–336
Distraction osteogenesis, 885, 886
Divided nevus, 105
DNA, 6
inheritance, mitochondrial, 11
nucleotides in, 6
Dog bite injury, 454, 457, 463
Dog-ear deformity, 78–80
Donor dominance, 140
Dorsal neural crest cells, 801
Down syndrome, 3, 14, 527
DSG. *See* Dacryoscintigraphy (DSG)
Duane's retraction syndrome, 832
Ductions movement, 189
Dumbbell-type dermoid cyst, 669
DWI. *See* Diffusion-weighted imaging (DWI)

Dye disappearance test (DDT), 475
Dysplasia, 618
  fibrous (*see* Fibrous dysplasia)
  septo-optic, 564
Dystrophic epidermolysis bullosa, 115

E
Ear cartilage grafts, 75
EB. *See* Epidermolysis bullosa (EB)
Ectomesenchymoma, 751
Ectrodactyly-ectodermal dysplasia-clefting (EEC) syndrome, 521
Ectropion, 341–342
Ehlers-Danlos syndrome, 51
Electronic medical record (EMR) data, 301
Electrophysiologic testing, 834
Electroretinogram (ERG), 315
Electroretinographic testing, 189
Embryological development, 17, 24
  craniofacial morphogenesis, 18
  cytogenesis and morphogenesis, 17–18
  facial development, 19
  pharyngeal arches, 18
  skull development, 23–24
Embryology, human skull, 801–804
Emergence delirium (ED), 99
Encephaloceles, 690, 904
Endoscopic dacryocystorhinostomy (enDCR), 503, 509, 512
Endothelial cells, 47
Enophthalmos, 936, 937, 943
Entropion, 336
Enucleation, 150, 217, 916–918
  bilateral, 151
  defects, 150
  orbital, 154
  with retinoblastoma, 217
Eosinophilic granuloma, 450. *See also* Unifocal LCH
Epiblepharon, 336–339
Epibulbar tumors, 207
Epicanthal folds, 30, 350, 355, 356
Epidermal nevus syndrome, 114
Epidermoid cyst, 107, 425, 561, 566, 567, 669
Epidermolysis bullosa (EB), 114–115
Epigenetics, 12
Epiphora, 472, 473, 477, 527, 529, 532
  laceration, 528
  surgical injury, 527
  thermal/chemical/radiation therapy burns, 527
  traumatic/iatrogenic causes, 527, 528
Epistaxis, 180–181
Epithelial cell, 52
Epstein-Barr virus (EBV), 234, 756
Erdheim-Chester disease (ECD), 275
Erythema multiforme major. *See* Stevens-Johnson syndrome
Esthesioneuroblastomas, 176, 766–770
Ethmoid air cells, 501, 502
Ethmoid bone, 26
Ethmoidectomy, 179, 780
Euryblepharon syndrome, 349, 350
Eversion, 341
Evisceration, 921
Ewing sarcoma (ES), 226, 275, 763
  clinical presentation, 225
  diagnosis, 225
  epidemiology, 224–225
  evaluation, 225
  risk groups and prognosis, 225
  treatment, 225–226
Ewing sarcoma family tumors (EWFT), 763
Exenteration, 921–925
Exophthalmos, 558, 578, 611, 793, 821–823
External dacryocystorhinostomy, 503, 507
  in children, 503
  incisions, 504
  postoperative care, 509
Extracellular signal-related kinase (ERK) hyperactivation, 616
Extraocular muscle, 39
  abnormalities, 199, 565–569
  complex, 193
  dysfunction, 193, 194
Eyebrow
  hair transplantation for, 140
  reconstruction, 138
Eyelash
  hair transplantation for, 140
  irritation from, 527
  reconstruction, 138
Eyelids, 322–329, 332, 445, 447–449, 453–464
  abnormalities, 832
  abnormal lashes, 336
  and adnexal trauma
    abrasions, 463
    burns, 464
    canalicular laceration, 459–463
    evaluation, 455–457
    hemorrhage, 463
    management, 457–458
    puncture wound, 464
    types, 453–455
  anatomy, 29, 30, 32, 35, 313
  ankyloblepharon, 333
  arterial arcades of, 41
  arterial supply, 40–42
  basal cell carcinoma, 445
  bilateral lower eyelid entropion, 340
  blepharophimosis, 357
  BPES, 353–354
  canthal dystopias, 331
  canthal tendon plication, 354
  chalazion, 439–441
  clefts, 815
  coloboma repair, 320–322, 816, 825, 826
    lower colobomas, 326–329
    upper colobomas, 322–326, 332
  congenital anophthalmia and microphthalmia, 316
  congenital eyelid retraction, 343–349
  corneal exposure, 348
  cryptophthalmos, 314, 315
  cutaneous melanoma, 447
  dermoid cyst, 420, 422
  development, 24
  differential diagnosis of, 344
  distichiasis and trichiasis, 333
  ectropion and eversion, 341
  embryologic formation of, 311
  epiblepharon and entropion, 336
  epicanthal folds, 350–353, 355, 356
  Euryblepharon and Centurion syndrome, 349–350
  facial processes, 312
  fissures, 840–841
  formation, 311
  granuloma annulare, 442, 443

granulomas, 407
hard plate mucosal grafts, 319
infantile hemangioma, 411–413
juvenile xanthogranuloma, 438, 439
laceration, 454, 456–458, 463
lateral canthoplasty, 327
lymphangioma, 419, 420
malignancies with systemic conditions, 449, 450
malposition, 202–205, 527
margin, 31
margin abnormalities, 527
margin annealing tarsorrhaphy, 348
Merkel cell tumors, 451
neurofibroma, 430–432
neurofibromatosis, 422
nevus, 434–436
ophthalmic examination and surgical considerations, 822
pilomatrixoma, 436
plexiform neurofibroma, 422, 426, 429
premalignant lesions, 447
basal cell nevus syndrome, 448
CNN, 447
linear nevus sebaceous syndrome, 449
xeroderma pigmentosum, 448
primary mesenchymal chondrosarcoma, 451
primary mucinous carcinomas, 451
ptosis, 237
retraction, 343
rhabdomyosarcoma, 451
sebaceous cell carcinoma, 446
skin cancers on (*see* Skin cancer)
squamous cell carcinoma, 446
stages of development, 312
surgical considerations, 312–314
telecanthus, 354–357
thyroid eye disease, 344
timing of surgical intervention, 433, 434
transnasal wiring, 355
transposition flaps, 329
upper eyelid entropion, 340, 341
vascular lesion, 411
vascular malformation, 417
venous drainage from, 42–43

F
Facial bipartition, 900
Facial clefting, 811
eyelids, 815
lateral canthal cleft, 815
medial canthal and nasolacrimal clefts, 814
median, 811, 814
regional classification, 813–815
syndromes, 453
Facial defect, 146
Facial development, 19–23
Facial milia, 107
Facial nerve, and musculature, 36
Family history, 3, 7, 15
Fasanella-Servat procedure, 375, 841
Fascia lata grafts, 72–73
Fatigability, 238
FC. *See* Flow cytometry (FC)
Fetal fibroblasts, 50
Fetal immune system, 50
Fetal skin, 48–50
Fetal wound contraction, 52–53
Fetal wound healing, 48, 50–52
cellular level
fetal fibroblast, 50
hemostatic plug and platelet function, 50
inflammatory phase and cellular mediators, 50
macrophages, 50
extracellular level
collagen, 51
fibromodulin, 51–52
hyaluronic acid, 51
Fibroblast, 47
Fibroblast contraction in collagen lattices (FPCL), 53
Fibroblast growth factor receptor 2 gene (FGFR2), 806, 809
Fibromodulin, 51
Fibronectin, 52
Fibro-osseous lesions, 178
Fibrotic myopathy, 544
Fibrous dysplasia, 616–619, 733, 902
correction, 906
nasoethmoid region, 905
Fibrous histiocytoma, 735
Fibula flap, 158
FISH. *See* Fluorescence in situ hybridization (FISH)
Fissures, 26
Fixation preference, 183, 184
Flaps, 77
Flow cytometry (FC), 262
applications, 263
limitations, 265
scatter plots, 264
single-cell suspension, 263
Fluid-attenuated inversion recovery (FLAIR), 553
Fluorescence in situ hybridization (FISH), 15
applications, 265
FOXO1 gene, 266
limitations, 266
method, 265
Foot deformity, 808
Forced duction testing, 544
Foreign body (FB), 623, 624, 630, 658
from auto accident, 931
on CT, 581
glass, 932
in lacrimal sac, 455
metallic orbital, 578
occult wooden, 658
penetrating injuries, 930, 931
posterior orbit, 580
right orbit, 581
superior extraconic space, 579
wood, 934–935
FOXO1 gene, 266
Fractures, orbit
blowout, 936
complex facial fractures, 945, 947, 949, 951
roof, 943–945
zygoma, 945–947
Franceschetti–Klein syndrome, 815
Fraser syndrome, 24, 320, 565
Free fibula osteocutaneous flap, 158
Free tissue transfer, 156
Freer elevator, 511
Fresh frozen plasma (FFP), 96
Frontal bone, 28
Frontal sinus, 173, 177

Frontalis muscle, 359
Frontalis suspension surgery, 280, 379–381
Frontoethmoidal mucoceles, 684
Fronto-orbito-ethmoid trauma, 908–909
Functional residual capacity (FRC), 91
Fungal infections of orbit
  aspergillosis, 637
  mucormycosis, 634
Fungal sinusitis, 174
Fusiform excision, 70

G
GA. *See* Granuloma annulare (GA)
Gadolinium, MRI, 555
Gamma-aminobutyric acid (GABAA) receptors, 84
Gaze, cardinal positions of, 189
Gene, 4, 6
  and environmental influences, 5
  mutated, 5
  suppressor, 5
  X-linked, 11
Gene sequencing, 15
General anesthesia, 483–487
Genetic disorders, 3–5
Genetic resources, 16
Genetic testing options, 15
Genetics, 265–269
Genodermatoses, 113
Genomic imprinting, 12–14
Genomics, 265
Genotype, 5
Gillies temporal approach, zygomatic fractures, 947
Glial–neural hamartomas, 564
Gliomas
  optic nerve, 243, 593–606, 715–721, 907
  visual pathway, 593, 595, 604, 605
Glue tarsorrhaphy, 856, 857, 864
Goldenhar syndrome, 320, 321, 324, 817, 818
Goldmann perimeter, 198
Gorlin syndrome. *See* Basal cell nevus syndrome
Gorlin-Goltz syndrome. *See* Basal cell nevus syndrome
GPA. *See* Granulomatosis with polyangiitis (GPA)
Grafts, 71
  fascia lata, 72
  hard palate mucosa, 74
  oral mucous membrane, 73
  skin, 71
Granuloma annulare (GA), 111, 112
  eyelid, 442, 443
Granulomas, 514
  pyogenic, 128
Granulomatosis with polyangiitis (GPA), 651–653
Granulomatous lesions, 111–112
Graves disease, 237
Growth factors, 53
Guibor probe, 506

H
HA. *See* Hyaluronic acid (HA)
Hamartomas, glial neural, 564, 565, 570
Hand-Schuller-Christian disease, 450, 657
Hard palate mucosa grafts, 74, 75
Hasner valve, 38
Healing process, 842, 843. *See also Specific types of healing*
Health-related quality of life (HRQOL), 292
Hemangiomas, 108, 121, 124, 125, 127
  cavernous, 714
  clinical course, 124
  history, 122
  of infancy (*see* infantile hemangioma)
  lab and imaging studies, 123–124
  lobular capillary, 128
  periorbital
    laser therapy for, 127
    nonoperative treatment of, 124–125
    operative therapy for, 127
  physical examination, 123
  segmental, 693
Hematoma, subperiosteal, 575–576
Hemifacial microsomia, 162, 817
Hemi-hang-back procedure (HHB), 202
Hemorrhage
  cystic hygroma, 598
  DCR, 503
  orbital, 935–936
  treatment, 935
  VLM with, 706
Hemostasis, 46, 64, 65
Hepatosplenomegaly, 762
Hering's law, 371
Herpes simplex cellulitis, 634
Heterochromia, 365
Histiocytic disorders, 112, 113, 656–658
  LCH, 656–658
  RDD, 658
Histiocytic lesions, 548
Histiocytosis, 213
Hodgkin's lymphoma (HL), 233, 234
Horner syndrome, 239–241, 365, 385, 616, 758, 759
Hospital for Sick Children in Toronto, 754
Human genome, 6
Hyalinosis cutis et mucosae. *See* Lipoid proteinosis
Hyaluronic acid (HA), 51
Hydrocephalus, neurosurgical shunt for, 824
Hydrogel expansion, 853, 854
  CHOP, 856
Hydrogel implants, 856–860
Hydroxyamphetamine, 240
Hydroxyapatite (HA) implant, 914
  with autogenous fascia lata, 919–920
Hyperplasia, 902
Hypertelorism, 195
Hypertrophic scars, 69
Hypertrophy, 902
Hypoplasia, 320, 900
  optic nerves, 560

I
Iatrogenic complications, 179–180
Idiopathic granulomatous orbital inflammation, 651
Idiopathic orbital inflammation (IOI), 577, 578, 591, 639, 641, 644, 659–661
  anterior, 645
  apical, 645, 647
  classification, 645, 648, 649
  CT, 640
  diffuse, 645
  etiology, 639
  evaluation, 642

lacrimal gland, 649
MRI, 640
orbital imaging, 640
orbital myositis, 648
pharmacotherapy, 659–662
biologic agents, 661
conventional immunomodulatory agents, 659, 660
posterior scleritis, 592
presentation, 640
recurrent, 592
sclerosing, 645
signs and symptoms, 642
tissue biopsy, 643
treatment, 643, 645
corticosteroids, 644
radiation, 644
IHC. *See* Immunohistochemistry (IHC)
Imaging modalities, 835
Immunoglobulin G4-related disease (IgG4-RD), 654
Immunohistochemistry (IHC)
applications, 261
direct and indirect IHC methods, 262
Glut-1 IHC, 263
limitations, 262
stains, 262
Immunomodulatory (IMT) agents, 645, 651, 655, 659
Immunomodulatory agents, IOI
azathioprine, 660
cyclophosphamide, 660
cyclosporine, 660
MTX, 659
mycophenolate mofetil, 659
Implants, 913, 914, 918, 919
DFG (*see* Dermis fat graft (DFG))
ideal, 915
insertion, 920–921
ocular, 914–916
porous, 914, 919, 921
Imprinted disorders, 3
Infantile hemangioma, 667, 693–701, . *See also* Capillary hemangioma
beta blocker therapy for, 125
CO2 laser debulking, 418
corticosteroid treatment, 417
cosmetic considerations in, 282
CT, 413
eyelids, 411–413
inpatient admission protocol, 415
management, 413
MRI, 411, 414
radiation therapy, 416
ultrasound, 414
Infantile orbital hemorrhage, 714
Infections, 573–577
Infectious/inflammatory lesions, 547
Inferior oblique muscle, 202
Inferior orbitotomy, 784, 785
Inferior rectus, 203
Inflammatory disorders, 194, 196
Inflammatory phlegmon, 582
Inflatable device extrusion, 855
Inflatable orbital implants, 850–853
Inflation tubing, 850
Infliximab (IFX), 661
Information bias, 302
Infranuclear disease, 193
Inhalation anesthetics, 87
Inheritance
autosomal dominant, 6
autosomal recessive, 7
mitochondrial DNA, 11
modes of, 6
patterns of, 9
X-linked, 12, 13
Inpatient admission protocol, 415–416
Intercanthal distance (IC), 354
Intergroup Rhabdomyosarcoma Study (IRS), 746, 747
Intergroup rhabdomyosarcoma study group (IRSG)
staging system, 750
surgical-pathologic grouping system, 750
Interleukin, 53
International Society for Clinical Electrophysiology of Vision (ISCEV), 187
International Society for the Study of Vascular Anomalies (ISSVA), 581, 692, 700
Intra-arterial chemotherapy, retinoblastoma, 601
Intracellular messengers, 17
Intraconal abscess, 629
Intraconal orbital tissue expander, 852
Intracranial abscess, 632
Intracranial pressure (ICP), 94, 887
Intralesional steroid, 125
Intralesional therapy, 125
Intramuscular neostigmine, 239
Intranasal cyst, 484, 501
Intraocular malignancies, 215–219
Intraoperative fluid management, 95
Intraoperative techniques
complications
airway fire, 93
laryngospasm, 93
local anesthetic systemic toxicity, 93
oculocardiac reflex, 93
dissection, 64
eye protection, 64
hemostasis, 64
incision creation, 64
incision location, 63
instruments
blades, 61
forceps and skin hooks, 60–61
needle drivers, 61
scissors, 61
suture materials, 63
suture needles, 61–63
marking, 63–64
traction and countertraction, 64
wound closure, 65–67
Intraorbital abscess, 629, 632
Intraorbital hemorrhage, 935
Intravenous anesthetics, 87–88
Intravenous antiemetic medications, 98
Intravenous chemoreduction, 215
Intravenous contrast (IVC), 554
Intravenous edrophonium, 239
IOI. *See* Idiopathic orbital inflammation (IOI)
Ionizing radiation, 551, 555–558, 606
Iris heterochromia, 240
Ischemic papillitis, 594–595
Isopters, 198

J
Jones dye tests, 474
Jones tube, 532, 533, 536, 537
Junctional epidermolysis bullosa, 115
Juvenile angiofibromas, 176
Juvenile myasthenia gravis, 237, 238
Juvenile nasopharyngeal angiofibroma, 178
Juvenile ossifying fibroma, 731, 732
Juvenile xanthogranuloma (JXG), 112, 113, 275
  eyelids, 437–439

K
Kaplan-Meier analysis, 208
Kaposi sarcoma (KS), 449, 450
Kasabach–Merritt syndrome, 694
Kearns-Sayre Syndrome (KSS), 242, 362
Keloids, 69
Kerrison rongeurs, 503, 505, 509, 512, 788, 793–795
Kindler syndrome, 115
Krause glands, 32
Krause valve, 38
KSS. *See* Kearns-Sayre Syndrome (KSS)
KTP laser, 511, 514–516

L
Lacerations, 454, 928
  adnexal, 462
  brow and non-marginal lid, 457
  canalicular, 459
  deep brow, 457
  eyelid, 454, 456–458, 463
  lid, 454
  sub-/supra-brow, 457
LacriCATH, 488
Lacrimal bone, 26, 502
Lacrimal drainage system, 469–471, 519
  dysfunction, 947
Lacrimal gland, 32, 38
  IOI, 649
  tumor, 754
Lacrimal mucocele, 689
Lacrimal outflow system, 469
Lacrimal problems, 498–499
Lacrimal pump, 470–472, 475, 477
Lacrimal sac, 26, 37, 470, 471, 474, 498
Lacrimal scintigram, 476
Lacrimo-auriculo-dento-digital (LADD) syndrome, 521
Lagophthalmos, 361, 372, 406
Lambdoid synostosis, 888
Lamina papyracea, 26
Langerhans cell histiocytosis (LCH), 213, 214, 450, 451, 617, 656–658
  clinical classification, 760
  CT, 616
  MRI, 616
  multisystem disease, 761
  orbital malignancy, 760–763
Laryngeal mask, 485
Laryngeal mask airway (LMA), 89, 483
Laryngeal mask anesthesia, 200
Laryngospasm, 93
Laser photocoagulation, 129
Laser therapy
  CNN, 448
  for periorbital hemangiomas, 127
LAST. *See* Local anesthetic systemic toxicity (LAST)
Lateral canthal tendon, 936
Lateral orbitotomy, 781–784
Lateral rhinotomy, 179
Latissimus dorsi flap, 149
LCH. *See* Langerhans cell histiocytosis (LCH)
Le Fort (LF) fractures, 947–950
Legius syndrome, 115, 116
Letterer-Siwe disease, 450, 657
Leukemia, 212, 213, 743, 750, 754
  clinical presentation, 230–231
  diagnosis, 231
  epidemiology, 230
  intraocular involvement, 756
  prognosis, 233
  treatment, 232–233
Leukocoria, 593, 599
Levator aponeurosis, 35, 360, 391–393
Levator muscle, 360
Levator palpebrae muscle, 35
Levator resection, 392
Levator surgery, 377–379
Levy-Hollister syndrome. *See* Lacrimo-auriculo-dento-digital (LADD) syndrome
Lid hematoma, 454
Lid hemorrhage, 463
Lid lag, 372
Lid masses, 423
Lid trauma, 463–465
Lid-sparing technique, 921, 922
Life-threatening injuries, 943
Light microscopy, 759
  rhabdomyosarcoma, 746
Limbal dermoids, cosmetic considerations, 286
Linear nevus sebaceous syndrome, 449
Lipodermoid cysts, 669
Lipodermoids, cosmetic considerations, 286
Lipoid proteinosis, 115
Liquid malignancies, 230–235
LMA. *See* Laryngeal mask airway (LMA)
Lobular capillary hemangiomas, 128
Local anesthesia, 319
Local anesthetic systemic toxicity (LAST), 93
Lockwood ligament, 35
Lower lid retractor complex, 36
Lumbar puncture, 733
LV Prasad-Functional Vision Questionnaire (LVP-FVQ), 293
Lymphangioma, 385, 692, 700, 704
  eyelids, 419, 420
Lymphatic malformations, 132
Lymphatic-venous malformation (LVM), 417, 419, 420
Lymphedema distichiasis syndrome (LDS), 333
Lymphoma, 212
  clinical presentation, 234
  diagnosis, 234
  epidemiology, 233–234
  prognosis, 235
  treatment, 234–235
Lynch incision, medial orbitotomy, 780, 781
Lyon hypothesis, 9

M
MAC. *See* Minimum alveolar concentration (MAC)
Macrodacryocystography (MDCG), 475
Macrophage-derived growth factor, 47

Macrophages, 50
Magnetic resonance imaging (MRI), 552–554
  abnormal globe, 559
  anophthalmia, 559, 835
  bilateral colobomas, 563
  buphthalmos, 560
  contrast agents, 554
  cryptophthalmos, 560
  dermoid and epidermoid cysts, 561
  developmental anomalies, 558–562, 564, 565
  extraocular muscles, abnormalities, 565
  fibrous dysplasia, 616
  gadolinium, 555
  glial–neural hamartomas, 564
  hyperintense on, 553
  infantile hemangioma, 411, 414
  infections, 573
  IOI, 577, 642
  LCH, 616
  meningiomas, 608
  metastatic tumors, 613
  microphthalmia, 835
  microphthalmos, 560
  mucoceles, 684
  nasolacrimal duct obstruction, 475
  OLM, 591
  optic hypoplasia, 560
  optic nerve glioma, 593
  optic neuritis, 579
  orbital disorders, 546
  orbital growth, 836
  orbital teratomas, 562
  orbital trauma, 928
  orbital traumatic lesions, 569
  plexiform neurofibromas, 606
  retinoblastoma, 593
  rhabdomyosarcoma, 608
  subperiosteal hematoma, 936
  superonasal cyst, 420–421
  vascular lesions, 581, 584
  VLM, 703
Malar Ewing's sarcoma, 164
Malignant hyperthermia (MH), 83
Malignant neoplasms, 176–177
Malignant orbital tumors, 544, 546, 548
Malignant rhabdoid tumor, 753
Malignant tumors, 178
Mandibulofacial dysostosis. *See* Treacher Collins syndrome
Mandibulofacial dysostosis (MFD), 22, 23
Manson-Markowitz classification, 948
Marcus Gunn jaw-winking ptosis, 365, 383
Marcus Gunn pupil, 953
Margin reflex distance (MRD_1), 370, 371
Masterka monocanalicular stent, 489, 492
Mastocytosis, 108–109
Matrix synthesis, 47
Maxilla-lacrimal suture (MLS), 502
McCune–Albright syndrome, 618, 733, 902
Mechanical ptosis, 367, 385
Meckel–Gruber syndrome, 904
Medial canthal anatomy, 456
Medial orbitotomy, 780
  Lynch incision, 780
  transconjunctival incision, 781
Medial wall fracture, 938–942, 952
Median craniofacial dysraphia, 814
Medical tattooing, 138
MEDPOR, 940, 943, 952
Medpor implant, 784
Medulloepithelioma, 219
Melanocytosis
  ocular, 207
  oculodermal, 208
Melanoma
  conjunctival, 209
  cutaneous, 447
  ocular, 106
  uveal, 218, 219
Melanosis, ocular, 207
Mendelian disorders, 3
Meningeal infiltration, 756
Meningioma, 176, 250, 608, 721–724
  orbital roof, 724–725
Meningoencephalocele, 688
Merkel cell tumors, 451
Mesenchymal chondrosarcoma, 752
Mesenchymal stem cells (MSCs), 274
Metastatic lesions, 219
Metastatic tumors, 613–616
Methicillin-resistant *Staphylococcus aureus* (MRSA), 82, 583, 624, 631
Methotrexate (MTX), IOI, 659
Meticulous hemostasis, 64
Microdebrider (Medtronic, Mansfield, MA), 483, 484, 509, 687
Microdrill instrument, 509
Microphthalmia, 15, 189, 316, 318, 560, 563, 564, 831–833, 840, 902
  adnexal problems, 868
  bony orbital expansion, 848
  with chronic retinal detachment, 559
  colobomatous cyst, 848, 849
  correction with prosthesis, 839
  craniofacial reconstruction, 870
  CT, 835
  current therapies, 836
  custom saline-filled anterior expander, 853–854
  with cyst, 681–683
  DFG, 858
  etiology, 832
  evaluation, 833–834
  eyelid fissures, 840
  facial maturation, 835
  family resources, 872
  with fronto-nasal dysplasia, 870
  hydrogel expansion, CHOP, 856–858
  imaging techniques, 835–836
  incidence, 833
  inflatable orbital implants, 850
  MRI, 560, 835
  neonates born, 833
  ocularist role, 837
  oculoplastic evaluation, 834–835
  ophthalmic examination, 834
  orbital hypoplasia, 835
  orbital sphere implantation, 850
  orbital volume expansion, socket management, 867
  osmotic orbital expanders, 853
  socket, 840–848, 872
  treatment, 681
  ultrasound, 833
  unilateral, 832
Micropigmentation, 138, 140
Microvascular free flap, 156, 872
Midfacial degloving, 179
Milia, 107
Minimal residual disease (MRD), 233

Minimally invasive approach, CLDCR, 537
Mini-Monoka device, 459, 462
Minimum alveolar concentration (MAC), 87
Missense mutation, 16
Mitochondrial DNA (mtDNA), 11
  inheritance, 11–12
MMD. *See* Myotonic muscular dystrophy (MMD)
Modified Fasanella-Servat procedure, 375, 376, 390
Modified Hotz technique, 336, 337
Molecular biology
  FC, 262
  FISH, 265
  IHC, 261
  NGS, 268
  PCR, 267
Molluscum contagiosum, 116, 117
Moniliform blepharosis, 115
Monocanalicular stents
  dacryostenosis, 489
  pulled, 489–491
  pushed, 492–493
Monoka monocanalicular tubing, 489, 491
Monosomy, 14, 16
Monostotic fibrous dysplasia, 176
Morphogenesis, 17
  craniofacial, 18
Motility assessment, 189–190
Moyamoya disease, 719
mtDNA. *See* Mitochondrial DNA (mtDNA)
Mucoceles, 177, 482, 683–688, 690
  and benign tumors, 176–177
Mucormycosis, 634–637
Mucosa, 317, 319
  flaps, 506, 508
Mucous membrane graft, 62, 73
  corneal protective cover, 848
  cul-du-sac reconstruction, 842–843
Muenke syndrome, 810–811
Müller's muscle, 35, 359, 374
  surgery, 375–377
Müller's superior tarsal muscle, 314
Müllerectomy, 373, 374
Multifactorial disorders, 3
Multiple pilomatricomas, 110
Multiplex ligation-dependent probe amplification (MPLA), 15
Muscle relaxants, 88
Musculature, 36
Myasthenia gravis, 237–239, 365
Mycophenolate mofetil (MMF), 659–660
Mycoplasma-associated mucositis, 118
Myectomy, 202
Myofibroblast, 47, 52
Myogenic ptosis, 361–364, 374, 375
  with associated superior rectus muscle weakness, 381–382
Myositis, 648
  noninfectious, 196
Myotomy, 202
Myotonic dystrophy, 364
Myotonic muscular dystrophy (MMD), 242

N
Nasal endoscopy, 533
Nasal fat pad, 772, 791, 793
Nasal fossa and sinuses, 471
Nasal glioma, 109
Nasal scarring, 538
Nasal septum, 804
Nasolacrimal drainage system, 37, 529
Nasolacrimal duct, 36–38, 469, 470, 472, 473, 822
  formation, 22
  obstruction, 94, 475, 501
  outflow, ancillary tests, 475, 476
Nasolacrimal duct cyst, 483
Nasolacrimal stents, 503
Naso-ocular clefts, 814
Nasoorbitoethmoid (NOE) fractures, 947–949
Necrotizing fasciitis, 625
Neonatal dacryocystitis, 485
Neoplasia, 902
Neoplasms
  meningiomas, 608
  metastatic tumors, 613
  optic nerve glioma, 593
  plexiform neurofibromas, 606–608
  retinoblastoma, 593
  rhabdomyosarcoma, 608
Neostigmine, 367
Nephrogenic systemic fibrosis (NSF), 554, 555
Nerve fiber layer, 546
Neural crest cell migration, 18
Neurilemmomas. *See* Schwannomas
Neuroblastoma, 757–760
  clinical presentation, 228
  epidemiology, 228
  evaluation, 228–230
  risk group classification, 230
  treatment, 230
Neurofibromas, 253, 724–729
  eyelids, 430–432
Neurofibromatosis, 115, 116, 275, 606, 608, 724
  ectopic orbital meningioma, 611
  eyelid, 422
  type 1, 595, 598, 602, 715, 716
  type 2, 607
  visual pathway glioma, 604
Neurofibromatosis type 1 (NF1), 115, 116, 247, 248, 253
Neurofibromatosis type 2 (NF2), 250, 252
Neurogenic lesions, 547
Neurogenic ptosis, 365
  Horner syndrome, 385
  Marcus Gunn jaw-winking ptosis, 383–384
  third-nerve palsy, 384
Neuroglial malformation, anophthalmos, 570–571
Neuroimaging, orbital disorders, 546
Neuromuscular relaxants, 88
Neuronal tumors
  meningiomas, 721
  neurilemmomas, 729
  neurofibromatosis, 724
  optic nerve gliomas, 715
Neurotoxicity, 84
Neutrophils, 46
Nevoid basal cell carcinoma. *See* Basal cell nevus syndrome
Nevus, 434–436
Nevus of ota, 106
Nevus sebaceous syndrome, 114
Next-generation sequencing (NGS), 269
  applications, 268
  limitations, 269
  method, 268
9p–syndrome, 14

N-methyl-D-aspartate (NMDA) glutamate receptors, 84
Non-accidental trauma (NAT), 457
Non-Hodgkin's lymphoma (NHL), 233, 234
Noninfectious myositis, 196
Non-rhabdomyosarcoma, 751
Nonsteroidal anti-inflammatory agents (NSAIDS), 98
Nonsyndromic synostoses, craniosynostosis, 888–898
Non-thyroid-associated proptosis, 798
Nose, embryology/anatomy, 169–171
NPO, 99
NRAS gene, 105

O
OAV spectrum. *See* Oculo-auriculo-vertebral (OAV) spectrum
Occlusion therapy, 372
Ocular globe, 40
Ocular implants, 914
Ocular lymphoproliferative disorders, 212
Ocular melanocytosis, 207
Ocular melanoma, 106
Ocular melanosis, 207
Ocular motility, 197, 237, 238, 544
Ocular myasthenia gravis, 237, 238
Ocular prostheses, 150
Ocularist role, 837–840
Oculo-auriculo-vertebral (OAV) spectrum, 817, 832
Oculocardiac reflex, 93
Oculodermal melanocytosis, 106, 208, 436
Oculomotor nerve palsy, 241
Oculomotor nerves, 3D–CISS images, 554
Oculomotor schwannoma, 571
Oculomotor system abnormalities, 193
Oculopharyngeal muscular dystrophy, 364
Oculoplastic disorders, 194
  genetic causes of, 13, 14, 16
  treatment, 199
Oculoplastics, 217
  enucleation skills, 217
  surgeon, 837
Odds ratio (OR), 304–305
O-defects, 77–79
OLM. *See* Orbital lymphaticovenous malformation (OLM)
ONSM. *See* Optic nerve sheath meningiomas (ONSM)
Operating room environment, 88–89
Operculum of the middle turbinate (OMT), 502
OPGs. *See* optic pathway gliomas (OPGs)
Ophthalmic trauma, 456
Opioids, 99
OPPN. *See* Orbitotemporal plexiform neurofibromas (OPPN)
Optic gliomas, 116
Optic nerve, 39, 40, 543, 782
  and chiasm, 605
  colobomas, 561, 562
  edema, 546
  etiology, 807
  function, 545
  meningioma, 722
  orbital AML, 755
  sarcoid, 595, 651
  sheath, 546
Optic nerve gliomas, 243, 275, 593–606, 717, 719, 720, 907
  clinical presentation, 248
  diagnostic imaging, 248
  epidemiology, 247, 248
  future directions, 250
  neuronal tumors, 715
  pathology, 248
  treatment considerations, 248–250
Optic nerve hypoplasia, 560
Optic nerve sheath decompression, 779
Optic nerve sheath meningioma (ONSM), 721
  clinical presentation, 250
  diagnostic imaging, 250
  epidemiology, 250
  future directions, 252
  pathology, 250–252
  treatment, 252
  vision loss in, 252
Optic neuritis, 593
  CT, 579–581
  MRI, 579–581
Optic neuropathy, 616, 729, 953, 954
Optic pathway gliomas (OPGs), 247, 715
Optic placodes, 24
Optical coherence tomography (OCT), 547
Oral acetylcholinesterase inhibitors, 239
Oral mucous membrane graft, 73, 74, 842, 843
Oral steroid therapy, 125
Orbicularis oculi, 31, 32, 238, 312
Orbit
  arterial supply, 40
  development, 24–26
  nerve, 39–40
  venous drainage from, 42
Orbital abscess, 574, 584, 629, 630
  subperiosteal (*see* Subperiosteal abscess)
Orbital adnexa, clefts affect, 812–815
Orbital bones, 26–29
  decompression, 793
Orbital cellulitis, 584, 626–636
  antibiotic treatment, 634
  superior ophthalmic vein thrombophlebitis, 589
Orbital complications management, 180
Orbital deformities, 166
Orbital dermoids, 658
Orbital disorders
  classification, 547–549
  history, 544
  neuroimaging, 546–547
  neuro-ophthalmic localization, 543–544
  physical examination, 544–546
Orbital dystopias, surgical correction, 909
Orbital evisceration, 154
Orbital exenteration defect, 146
Orbital expansion
  bony, 848, 871
  custom-designed, 853
  osmotic, 853
Orbital extraocular muscles, 195
Orbital fascia, 38–39
Orbital fat, 33–34
  decompression, 791, 792
Orbital fibrosis, 574
Orbital floor fracture, 938–940, 942, 952, 953
Orbital fungal infections
  aspergillosis, 637
  mucormycosis, 634
Orbital granulocytic sarcoma, 756
Orbital growth, 915
Orbital hypertelorism (OHT), 898–900

Orbital imaging, 558. *See also* Computed tomography (CT). *See also* Magnetic resonance imaging (MRI)
Orbital implant, DFG, 858
Orbital infection, 171
Orbital inflammatory disease, 633, 639, 643
  GPA, 651
  IgG4-RD, 654
  sarcoidosis, 649
  SLE, 655
  SS, 655
  TED, 653
Orbital lesions, 543, 544, 546, 547
  cavernous hemangioma, 714
  cephaloceles, 687
  choristomas, 680–681
  dermoid/epidermoid cysts, 669–676
  dermolipomas, 676–679
  fibrous, 733–735
  infantile hemangioma, 693
  infantile orbital hemorrhage, 714
  microphthalmos with cyst, 681–683
  mucocele, 683–685
  phakomatous choristoma, 680
  teratoma, 685–687
  varices, 712
  vascular, 691–693
  VLM, 700
Orbital lymphaticovenous malformation (OLM), 591, 598, 599
Orbital malignancy, 743, 744
  adenoid cystic carcinoma, 754
  ectomesenchymoma, 751
  ES, 763
  esthesioneuroblastoma, 766
  LCH, 760
  leukemic/lymphomatous disorders, 754–757
  metastatic, 754–764
  neuroblastoma, 757
  PNET, 764
  primary, 744–754
  retinoblastoma, 764
  rhabdomyosarcoma, 744
  secondary, 764–770
  soft tissue sarcomas, 751–754
Orbital myositis, 648
Orbital prostheses, 149
Orbital rhabdomyosarcoma, 224, 225, 255
Orbital roof, 786, 788–791, 793
  fracture, 579
  meningioma, 724–725
Orbital septum, 33, 314, 359, 394, 773, 784
Orbital sphere implantation, 850
Orbital surgery, 771–778
  anterior approaches, 772, 773
    subciliary lower eyelid approach, 774–778
    upper eyelid skin approach, 772–774
  bulbar transconjunctival approach, 778
  inferior approach, 784, 785
  lateral approach, 781–783
  medial approach, 780, 781
  orbital bone decompression, 793–795
  orbital fat decompression, 791–793
  posterior approach, 780
  superior approach, 785, 786
  transcranial approach, 787, 788
Orbital teratomas, 562–564, 686, 688
Orbital tissue expansion, 851
Orbital trauma
  blowout fractures, 936–943
  CASP, 953
  complex facial fractures, 945–947, 949, 951
  hemorrhage, 935
  lesions, 569
  ocular exam, 927–928
  orbital plating systems, 952
  penetrating orbital injuries, 928, 931
  roof fractures, 943–945
  traumatic optic neuropathy, 953–955
  zygomatic fractures, 945–947
Orbital traumatic lesions, 569
Orbital tumors, clinical management of, 247
Orbital volume expansion, socket management, 867
Orbitofacial neurofibromatosis, 728
Orbitotemporal plexiform neurofibromas (OPPN), 425
  debulking, 433
  diagnostic imaging, 253
  epidemiology, 252
  future directions, 253
  pathology, 253
  surgical management concerns, 433
  timing of surgical intervention, 433
  treatment, 253
Osmotic orbital expanders, 853–854
Osseointegrated craniofacial implants, 151
Osseous lesions, 176
Ossifying fibromas, 177, 731
Ossifying lesions
  aneurysmal bone cysts, 731
  ossifying fibromas, 731
  osteoblastoma, 730
  osteomas, 729
  osteopetrosis, 731
Osteoblastoma, 730–731
Osteomas, 729–730
Osteopetrosis, 731–733
Osteosarcoma
  clinical presentation, 227
  epidemiology, 227
  evaluation, 227
  risk group and prognosis, 227
  treatment, 227–228
Osteotomy, 505, 782, 783, 879, 888, 903
Ostiomeatal complex (OMC), 171
Ostium enlargement, 505
Otolaryngology, 169, 175
Oxycephaly, 806, 807
Oxymetazoline, 486

P
Packed red blood cells (PRBCs), 95
Paediatric orbital tumours, 273–277
Pain assessment, 98
Palatine bone, 27
Palpebral conjunctiva, 32
Pan facial fractures, 949–952
Papilledema, 807–809, 822, 888
Papillitis, 593–595
Paralytic strabismus, 193, 195–197
Parameningeal rhabdomyosarcoma, 255–257, 746
Paranasal sinuses, 501
  embryology and anatomy, 169
Parental presence at induction (PPIA), 86

Parkes–Weber syndrome, 133
Pathogenic variants, 5
Patient-controlled analgesia (PCA), 99
Pattern visual evoked potential (PVEP), 187
PCR. *See* Polymerase chain reaction (PCR)
Pediatric acute rhinosinusitis, 171
Pediatric airway
  airway evaluation, 94–95
  anatomy and physiology, 91
  dificult airway management, 91–93
Pediatric anesthesia, 81
Pediatric epistaxis, 175
Pediatric Eye Disease Investigator Group (PEDIG), 479
Pediatric orbit. *See* Orbit
Pediatric Psychosocial Preventative Health Model (PPPHM)
  clinical families, 292
  targeted families, 292
  universal families, 291
Pediatric Quality of Life Inventory, 293
Pediatric uveal melanoma, 218
Pedigree, 3, 8
  nomenclature, 6
Pellets, 929, 933
Penetrance, 5
Penetrating injuries, 464, 928–931
  management, 931–933
Percutaneous sclerotherapy, 707–708
Periocular soft tissue volume augmentation, 287
Periodic acid-Schiff (PAS), 745, 752
Periorbita, 137, 138, 140–143, 782
  abscess, 173, 174
  reconstructive strategies in
    eyebrow and eyelash reconstruction, 138
    hair transplantation for eyebrow and eyelash, 140–143
    micropigmentation, 138
    skin coverage, 137–138
Periorbital cellulitis
  diagnosis, 171–172
  medical management, 172
  surgical management, 172
Periorbital defects, 145
Periorbital hemangiomas, 138
  laser therapy for, 127
  nonoperative treatment of, 124
  operative therapy for, 127–128
Periorbital milia, 107
Periorbital reconstruction, 145, 158
Periorbital tumors, 247
Peripheral nerve sheath tumors, 176
Peripheral primitive neuroectodermal tumor (pPNET), 764, 765
Pfeiffer syndrome, 809, 810, 897
PHACE syndrome, 123, 411, 693–695
Phakomatose syndrome, 449
Phakomatous choristoma, 680
Pharyngeal arches, 18, 19
Phenotype, 3, 5, 14, 15
Phenylephrine test, 372
Philadelphia chromosome (Ph), 265
Phleboliths, 713
Pigmented lesions, 105–106
Pilomatrixoma, 109, 110, 436, 437
Plagiocephaly, 806
Plain film radiography, 734
Plastic surgical techniques
  contouring, 160–161
  ocular prostheses, 150–154
  orbital prostheses, 149–150
  periorbital reconstruction, 158–160
  prosthetic considerations, 147–149
  reanimation and sensory restoration, 161–166
  reconstructive considerations, 145–147
  reconstructive options, 154–155
  socket preparation, 156–158
Platelet-derived growth factor (PDGF), 53
Platelets, 46, 50
Pleomorphic rhabdomyosarcoma, 746
Plexiform neurofibroma (PN), 116, 252, 385, 606, 607, 667, 724–727
  eyelid, 422, 426, 429
  management, 726
  surgical excision, 728
Plus lenses, 838
Polymerase chain reaction (PCR)
  applications, 267
  limitations, 268
  method, 267
  negative PCR, 268
Polymerized methyl methacrylate, 913
Polymorphisms, 5
Polyostotic disease, 902
Polyostotic fibrous dysplasia, 177
Polyps, 178
PONV. *See* Postoperative nausea and vomiting (PONV)
Porous implants, 914, 921
  preparation, 919
Positional plagiocephaly, 888, 890
Posterior scleritis, 645, 646
Postoperative nausea and vomiting (PONV), 97–98
Postoperative pain management, 98
  emergence delirium (ED), 99–100
  inpatients, 99
  outpatients, 98–99
  pain assessment, 98
Prader-Willi syndrome, 3, 12
Preoperative assessment and preparation, 81, 85, 86
  age, weight, height, and vital signs, 83
  allergies, 82–83
  anxiety during induction, 86
  family history, 83
  medications, 82
  neurotoxicity, 84–85
  parental presence, 86
  past medical history, 81
  past surgical and anesthetic history, 81–82
  physical examination, 83–84
  preoperative fasting, 85
    clear liquids, 85
    milk and formula, 86
    solids, 86
  preoperative preparation, 84
  preoperative sedation, 86
  preoperative testing, 84
  review of system, 83
  risks of anesthesia, 84
Preoperative considerations, 59
  consent, 60
  history, 59
  patient and family expectations, 59
  physical exam, 60
  preoperative planning, 60
Preseptal cellulitis, 538, 623–626
Pretarsal orbicularis, 359
Primary hypertelorism, 195

Primary mesenchymal chondrosarcoma, 451
Primary mucinous carcinomas, 451
Primitive neuroectodermal tumors (PNET), 216, 275, 764
Pro-inflammatory cytokines, 639
Projectile trauma, 454, 455
Prokera rings, 843–847
Prolene suture, 462
Proptosis, 710, 711, 716, 775, 776, 783, 791, 793
  colobomatous cyst, 683
  non-thyroid-associated, 798
  surgical treatment, 285
  thyroid eye disease, 796, 797
Prostigmin, 367
Protein, 4, 5
Protein expression, 261–265
Proteinase antibodies, 652
Proteoglycans, 51
Pseudo inferior oblique overaction, 200
Pseudoptosis, 369
Pseudorheumatoid nodules. *See* Granuloma annulare (GA)
Pseudotumor, 639
Psychosocial Assessment Tool (PAT), 292
Psychosocial risk assessment, 291–292
Psychosocial support, 294–295
Ptosis, 359, 394, 397–399, 827
  acquired Horner Syndrome, 366
  aponeurotic ptosis, 364, 365, 383
  Asian eyelid, 402–403
  asymmetric bilateral ptosis, 386
  autogenous fascia lata sling, 400–402
  bilateral autogenous fascia lata sling repair, 402
  bilateral ptosis, 386
  bilateral silicone sling frontalis suspension, 380
  blepharophimosis, 382
  choice of operation, 373–374
  classification, 370
  congenital Horner syndrome, 366
  congenital orbital fibrosis syndrome, 382–383
  congenital ptosis, 361, 373, 404–409
  conjunctival-Müllerectomy, 377
  CPEO, 362, 363
  deprivation amblyopia, 385
  etiology of, 361
  external examination, 370
  eyelid anatomy, 360
  eyelid fold, 407
  eyelid margin, 407
  eye-popping reflex, 370
  frontalis suspension, 379–380
    crawford double-rhomboid technique, 399
    double-triangle technique with tied silicone knot technique, 397–399
    single rhomboid technique with silicone, 394
  harvesting autogenous fascia lata, 399, 400
  history, 369
  intermarginal suture technique, 405
  left upper lid infantile hemangioma, 367
  levator aponeurosis advancement, 391–392
  levator function, 371
  levator resection, 378, 392–394
  levator surgery, 377–379
  lid fold, 408
  Marcus Gunn jaw, 384
  Marcus Gunn jaw-winking ptosis, 365
  mechanical ptosis, 367, 385
  modified Fasanella-Servat procedure, 390–391
  myogenic ptosis, 361–364, 374–383
  neurogenic ptosis, 365–367, 383–385
  observation, 369
  physical examination, 369–373
  postsurgical management, 403–404
  Putterman's conjunctivo-Müllerectomy, 386–388
  recurrent ptosis, 408
  repair, 374, 378
  simple congenital ptosis, 361
  simultaneous *vs.* sequential congenital ptosis, 386
  surgical anatomy of upper lid, 359–361
  synthetic materials vs. preserved fascia lata, 380–381
  third-nerve palsy, 365
  traumatic ptosis, 367, 368, 385
  unilateral fascia lata sling repair, 402
  unilateral silicone sling frontalis suspension, 381
  upper lid section, 360
  Werb procedure, 388
Ptosis repair, 94
Punctae, 37
Punctal agenesis, 521, 524
Punctal granuloma, 514
Punctal stenosis, 526
Punctoplasty, 526
Punctum, 519, 521–523
Puncture wounds, 464
Putterman's conjunctivo-Müllerectomy, 386, 387
Putterman's procedure, 375
Putterman-Plus procedure, 377
Pyogenic granuloma, 110, 128, 129, 496, 538
Pyrex tube, 505, 529, 530, 532, 534, 536, 537, 826

Q
Qualitative PCR (qPCR), 267
Quality of life (QOL), 292–293

R
Radial forearm flap, 157
Radiation, 233, 234
  exposure in CT, 555–558
  IOI, 644
  microphthalmic sockets, 872
  therapy, 225, 226, 230
Radiation oncology, 224
Radiotherapy
  infantile hemangioma, 416
  ONSM, 723
  retinoblastoma, 766
  visual pathway gliomas, 718, 719
Randomized controlled trial (RCT), 299
Rare craniofacial clefts, 881–884
RASopathy disorder, 114
RDD. *See* Rosai-Dorfman disease (RDD)
Recognition acuity, 186–188
Reconstructive plan
  ocular implants, 915, 916
  orbital growth, 915
  tissue expanders, 916
Rectus muscle, 574, 575
  weakness, 381–382
Rectus myocutaneous flap, 147
Refractive error, 190, 807, 808, 816
Relaxed skin tension lines (RSTL), 63
Resolution acuity techniques, 184–186

Retinal function, 189
Retinoblastoma, 215, 216, 615, 764–766
  CT, 593
  intra-arterial chemotherapy, 601
  MRI, 593
  with restricted diffusion, 600
  with retinal detachment, 600
Retrocaruncular incision, medial orbitotomy, 781
Rhabdomyosarcoma (RMS), 163, 178, 274, 275, 451, 612–614, 694, 745
  alveolar, 750
  clinical presentation, 223
  conjunctival, 211
  CT, 608–613
  epidemiology, 223
  evaluation, 223
  histopathologic risk classification, 750
  light microscopy, 746
  MRI, 608
  orbital and parameningeal
    diagnostic imaging, 255
    epidemiology, 255
    future directions, 257
    pathology, 255
    presentation, 255
    treatment, 255–257
  orbital malignancy, 744–750
  presumed, 748–749
  risk group classification, 223–224
  treatment, 224
Rhinosinusitis, 171
Rhinotomy, 179
Ring-Adair-Elwyn (RAE) tube, 90
Risks of anesthesia, 84
Ritleng intubation, 490
Rituximab (RTX), 661
Rollet Rugine, 505
Romberg disease, 900, 901
Roof fractures, orbit, 943–945
Rosai-Dorfman disease (RDD), 275, 441, 443, 658
Rosenmulle valve, 38
Rotation and transposition flaps, 77

S
Saccharin taste tests, 474
Saethre–Chotzen syndrome, 809, 810, 897
Saphenous vein graft, 156
Sarcoidosis, 112, 649, 650
Sarcomas
  alveolar soft part, 751, 752
  angiosarcoma, 752
  Ewing sarcoma, 226, 275, 763
    clinical presentation, 225
    diagnosis, 225
    epidemiology, 224–225
    evaluation, 225
    risk groups and prognosis, 225
    treatment, 225–226
  Kaposi sarcoma, 449, 450
  soft tissue, 751–754
Scaphoid skull, 805
Scapular flap, 161
Scar revision, 69–70
  fusiform, 70
  W-plasty, 71
  Z-plasty, 70–71
Scarless repair
  fetal sheep eyelid, 49
  fetal skin, 52
  lip wound, 49
Scarring, 48
Scars, 54
  formation, 45, 48, 52, 53, 289
  prevention and treatment
    CO_2 laser resurfacing, 54
    miscellaneous agents, 54
SCC. *See* Squamous cell carcinoma (SCC)
Schimmelpenning syndrome. *See* Linear nevus sebaceous syndrome
Schwannoma, 729
  oculomotor, 571
Scleritis, 592
Sclerosing idiopathic orbital inflammation (IOI), 645
Sclerotherapy, 676, 705–709, 713
Sebaceous cell carcinoma, 446, 447
Segmental hemangiomas, 693
Selection bias, 302
Selfish spermatogonial selection, 808
Self-threading monocanalicular stent, 507
Sensory testing, 190
Septo-optic dysplasia, 564
Serial conformer expansion, 851, 857, 867, 870
Serpentine tarsorrhaphy, 347
Serum anti-ACh receptor antibody titer, 367
Sex chromosomes, 9–11
Sharp trauma, 454, 463
Silicone, 914
  sling set, 397
  stents, 503, 507
Single binocular vision (SBV), 198
Single-fiber EMG, 239
Single-gene disorders, 3
Sinuses, 43
Sinusitis
  fungal, 174
  ophthalmic complications of, 171
Sisler trephine, 516, 517
Sjögren syndrome (SS), 655, 656
Skin cancer, 445–451
  eyelids, 445
    basal cell carcinoma, 445–446
    basal cell nevus syndrome, 448
    CNN, 447
    cutaneous melanoma, 447
    KS, 449
    LCH, 450
    linear nevus sebaceous syndrome, 449
    Merkel cell tumors, 451
    primary mesenchymal chondrosarcoma, 451
    primary mucinous carcinomas, 451
    rhabdomyosarcoma, 451
    sebaceous cell carcinoma, 446
    squamous cell carcinoma, 446
    xeroderma pigmentosum, 448
Skin fistulization, 675
Skin grafts, 71, 72, 148
Skin marker, 397
Skull development, 23
Sleeve technique, 394–396
Sliding flap, 77
Small interstitial leucine-rich proteoglycans (SLRP), 51
2-Snip procedure, 526

Socket
expansion, 840
management after orbital volume expansion, 867–868
microphthalmic, 872
surgical expansion, 841
Soft tissues
flaps, 159
OPPN, 433
sarcomas, 751–754
Solid tumors, 223–224
Solitary mastocytomas, 108
Solitary neurofibroma, 426–427
Sonopet®, 509–512
SPECC1L gene, 16
Sphenoid sinuses, 169
Spider angioma, 131
Sporadic lesions, 248
Squamous cell carcinoma (SCC), 110, 214, 215, 446
Stephens scissors, 784
Stereotactic fractionated radiotherapy, 252
Stevens-Johnson syndrome, 118, 474
Strabismic amblyopia, 185
Strabismus, 190, 194, 565, 807, 810, 827
diagnostic technique, 196–199
primary, 195–196
repair, 94, 386
secondary, 194–195
surgical techniques, 200–202
treatment, 199–200
Sturge–Weber syndrome, 122, 129
Sub-brow incision, 786, 787
Subconjunctival abscess, 636
Subdural empyema, restricted diffusion from, 586–587
Subperiosteal abscess, 627–631, 780, 781, 784
DWI and ADC, 588
inflammatory phlegmon *vs.*, 582
orbital cellulitis and, 584
with intracranial extension, 585
Subperiosteal effusion, 627, 628
Subperiosteal hematoma, 575, 576, 936
Subperiosteal hemorrhages, 936
Subperiosteal implant, 925
Subperiosteal orbital abscess
diagnosis, 171
medical management, 172
surgical management, 172–174
Subperiosteal plane, 778
Superficial dermoids, 669, 670, 676
Superficial hemangioma, 693, 703
Superior ophthalmic vein (SOV), 576, 589
Superior orbitotomy, 785–787
Supernumerary duct repair, 519–521
Superonasal cyst, MRI, 420–421
Surface squamous cell neoplasia (SCCA), 214, 215
Surgically induced anophthalmos, 285
Suspected Child Abuse and Neglect (SCAN), 457
Suture closure, 894
Suture granuloma, 406
Suture tarsorrhaphy, 347
Syringomas, 111
Systemic lupus erythematosus (SLE), 655

T
Tarsal eversion, 405
Tarsectomy, 374
Tarsorrhaphy, 825, 854, 856, 859, 860, 864
Tarsus, 32, 359
Tattoo, 138, 140
Tear breakup time (TBUT), 372
Tearing, 530
Tearing in children, 469
congenital nasolacrimal duct obstruction, 475
DCG, 475
DSG, 476
examination, 474
history, 472–474
in-office tests, 474–475
lacrimal drainage pump, 471
lacrimal drainage system, 469
TED. *See* Thyroid eye disease (TED)
Tegaderm dressings, 68
Telecanthus, 354–356
Teller acuity card procedure, 185–187
Tenascin, 52
Tenectomy, 202
Tenotomy, 202
Tensilon test, 367
Tension-relieving sutures, 67
Teratomas, 562, 569, 686, 688
Tessier's clockface system, 812
Third-nerve palsy, 241, 365, 384
Three-dimensional (3-D) ultrasound, 835, 836
Three-dimensional constructive interference in steady state (3D CISS), 553
Thrombophlebitis, 589
Thrombosis, cavernous sinus, 242
Thymic hyperplasia, 237
Thyroid eye disease (TED), 364, 653, 654, 791, 793, 795–797
Thyroid ophthalmopathy, 203
Tissue biopsy, IOI, 643
Tissue expanders, 916
Titanium
craniofacial implant, 151
orbital plating systems, 952–953
Tobradex ointment, 509
Tolosa-Hunt syndrome, 648
Total intravenous anesthesia (TIVA), 88
Tracheal intubation, 90
Traction suture, 778
Transconjunctival incision, medial orbitotomy, 781
Transcranial orbital osteotomy, 878, 899
Transcranial orbitotomy, 787–791
Transforming growth factor-beta (TGF-β), 47, 50, 53
early paradoxical effects, 53
expression, 53
isoforms, 53
transcription, 50
Transfusion, 81, 95, 96
Transillumination, 681
Transposition flaps, 329–331
Trauma, 195, 241, 457, 927. *See also Specific types of trauma*
orbit (*see* Orbital trauma)
types, 453
Traumatic optic neuropathy, 953, 954
Traumatic orbital lesions, 569–573
Traumatic ptosis, 367–369, 385
Treacher Collins syndrome, 22, 162, 320, 321, 330, 331, 815, 816, 884
Trichiasis, 333, 527
Trichoepitheliomas, 111, 449
Trigonocephaly, 891–893

Trisomy, 16
Tukel syndrome, 242
Tumor, 107–111
  types and anatomical location, 176
Tumor necrosis factor (TNF), 661
Tumor necrosis factor-alpha (TNFα), 661
Turricephaly, 894
22q11.2 deletion syndrome, 3

U
Ultrasonic bone aspirator (UBA), 503, 509, 510
Ultrasound
  anophthalmia, 837
  infantile hemangioma, 414
  orbital disorders, 546
Uncinate process (UP), 502
Unicoronal synostosis, 890–892
Unifocal LCH, 657
Unilateral coronal synostosis, 888
Unilateral fibrosis syndrome, 195
Unilateral microphthalmia, 189
Unilateral osteotomy, 891
Upper lid, surgical anatomy of, 359
Upper respiratory infection (URI), 83
Urbach-Wiethe syndrome. *See* Lipoid proteinosis
Urticaria pigmentosa, 108, 109
Uveal melanoma, 218, 219

V
Valsalva maneuvers, 689, 694, 712
Valve of Hasner, 470, 473
Valve of Rosenmuller, 470
Vancomycin, 82
Varices, 709–714
Vascular lesions, 128–135, 548, 581–584, 691
  capillary hemangioma, 584
  eyelid, 411
  OLM, 591–593
Vascular malformations, 121
  capillary, 129
  eyelid, 417
  venolymphatic, 133
  venous, 131, 132
Vascular tumors, 121
Venolymphatic malformation (VLM), 132, 385, 700–709
  hemorrhage with, 706
  treatment, 709–710
Venolymphatic vascular malformation, 133
Venous stasis, 212
Venous vascular malformations, 131, 132
Ventriculomegaly, 808
VEP. *See* Visual evoked potential (VEP)
Versions movement, 189
Vertical fissure height (VFH), 370, 371
Vicryl suture, 319
Vincristine, 275
Vision loss, 745, 807, 820
  VLM with, 705–706
Vision-threatening hemangiomas, 416
Visual acuity, 954, 955
  clinical examination, 183
Visual disability, 291
Visual evoked potential (VEP), 187, 316
Visual evoked response (VER), 732, 733
Visual field, 188
Visual function assessment, 183, 188, 189
Visual loss, source of, 734
Visual pathway gliomas, 593, 595, 604, 605, 715. *See also* Optic nerve glioma
  clinical signs and symptoms, 716
  radiotherapy, 718, 719
  treatment, 717
Vitrectomy light pipe, 511
VLM. *See* Venolymphatic malformation (VLM)
von Recklinghausen's disease, 422

W
Warts, 117
Werb procedure, 376, 388–390
Westcott scissor, 781
Wet eye, 474
White-eyed blowout fracture (WEBOF), 558, 570, 576, 577
Whitnall's ligament, 35, 314, 360, 772
Wound care, 68
Wound closure, 65
  closing deep tissue, 65–66
  closing skin, 66
  tarsorrhaphy sutures, 66
  traction sutures, 66–67
Wound healing, 47, 68
  contraction phase, 69
  fibroblastic phase, 69
  inflammatory phase, 69
  modulators in postnatal, 53–54
  postnatal and adult, 46–48
  scar maturation phase, 69
Wound, puncture, 464
W-plasty, 71

X
Xanthelasma, 111
Xanthoma disseminatum, 113
Xanthoma palpebrarum, 111
X chromosome, 3, 4, 9, 12
Xeroderma pigmentosum (XP), 214, 445, 446, 448
X-linked gene, 11
X-linked inheritance, 12, 13
X-linked recessive disorders, 10

Y
Y chromosome, 4

Z
Z-plasty, 70, 71, 290
Zygoma, 27, 28
Zygomatic fractures, 945–947